ISSN 1007-9327 (print)
ISSN 2219-2840 (online)

World Journal of *Gastroenterology*

World J Gastroenterol 2018 March 7; 24(9): 957-1062

Published by Baishideng Publishing Group Inc

World Journal of Gastroenterology

Contents

Weekly Volume 24 Number 9 March 7, 2018

CASE REPORT

Contents

World Journal of Gastroenterology
Volume 24 Number 9 March 7, 2018

ABOUT COVER

Editorial board member of *World Journal of Gastroenterology*, Sang Chul Lee, MD, PhD, Chief Doctor, Full Professor, Professor, Surgeon, Surgical Oncologist, Division of Colorectal Surgery, Department of General Surgery, Catholic University of Korea, Daejeon St. Mary's Hospital, Daejeon 34943, South Korea

AIMS AND SCOPE

World Journal of Gastroenterology (*World J Gastroenterol*, *WJG*, print ISSN 1007-9327, online ISSN 2219-2840, DOI: 10.3748) is a peer-reviewed open access journal. *WJG* was established on October 1, 1995. It is published weekly on the 7th, 14th, 21st, and 28th each month. The *WJG* Editorial Board consists of 642 experts in gastroenterology and hepatology from 59 countries.

The primary task of *WJG* is to rapidly publish high-quality original articles, reviews, and commentaries in the fields of gastroenterology, hepatology, gastrointestinal endoscopy, gastrointestinal surgery, hepatobiliary surgery, gastrointestinal oncology, gastrointestinal radiation oncology, gastrointestinal imaging, gastrointestinal interventional therapy, gastrointestinal infectious diseases, gastrointestinal pharmacology, gastrointestinal pathophysiology, gastrointestinal pathology, evidence-based medicine in gastroenterology, pancreatology, gastrointestinal laboratory medicine, gastrointestinal molecular biology, gastrointestinal immunology, gastrointestinal microbiology, gastrointestinal genetics, gastrointestinal translational medicine, gastrointestinal diagnostics, and gastrointestinal therapeutics. *WJG* is dedicated to become an influential and prestigious journal in gastroenterology and hepatology, to promote the development of above disciplines, and to improve the diagnostic and therapeutic skill and expertise of clinicians.

INDEXING/ABSTRACTING

World Journal of Gastroenterology (*WJG*) is now indexed in Current Contents®/Clinical Medicine, Science Citation Index Expanded (also known as SciSearch®), Journal Citation Reports®, Index Medicus, MEDLINE, PubMed, PubMed Central and Directory of Open Access Journals. The 2017 edition of Journal Citation Reports® cites the 2016 impact factor for *WJG* as 3.365 (5-year impact factor: 3.176), ranking *WJG* as 29th among 79 journals in gastroenterology and hepatology (quartile in category Q2).

NAME OF JOURNAL
World Journal of Gastroenterology

ISSN
ISSN 1007-9327 (print)
ISSN 2219-2840 (online)

LAUNCH DATE
October 1, 1995

FREQUENCY
Weekly

EDITORIAL OFFICE
Ze-Mao Gong, Director
World Journal of Gastroenterology
Baishideng Publishing Group Inc
7901 Stoneridge Drive, Suite 501,
Pleasanton, CA 94588, USA
Telephone: +1-925-2238242
Fax: +1-925-2238243
E-mail: editorialoffice@wjgnet.com
Help Desk: http://www.f6publishing.com/helpdesk
http://www.wjgnet.com

PUBLISHER
Baishideng Publishing Group Inc
7901 Stoneridge Drive, Suite 501,
Pleasanton, CA 94588, USA
Telephone: +1-925-2238242
Fax: +1-925-2238243
E-mail: bpgoffice@wjgnet.com
Help Desk: http://www.f6publishing.com/helpdesk
http://www.wjgnet.com

PUBLICATION DATE
March 7, 2018

INSTRUCTIONS TO AUTHORS
Full instructions are available online at http://www.wjgnet.com/bpg/gerinfo/204

ONLINE SUBMISSION
http://www.f6publishing.com

World Journal of Gastroenterology

Submit a Manuscript: http://www.f6publishing.com

World J Gastroenterol 2018 March 7; 24(9): 957-970

DOI: 10.3748/wjg.v24.i9.957

ISSN 1007-9327 (print) ISSN 2219-2840 (online)

REVIEW

Quantitative and noninvasive assessment of chronic liver diseases using two-dimensional shear wave elastography

Li-Ting Xie, Chun-Hong Yan, Qi-Yu Zhao, Meng-Na He, Tian-An Jiang

Li-Ting Xie, Chun-Hong Yan, Qi-Yu Zhao, Meng-Na He, Tian-An Jiang, Department of Ultrasound, The First Affiliated Hospital, College of Medicine, Zhejiang University, Hangzhou 310003, Zhejiang Province, China

ORCID number: Li-Ting Xie (0000-0002-0498-193X); Chun-Hong Yan (0000-0001-8084-4155); Qi-Yu Zhao (0000-0002-8732-8564); Meng-Na He (0000-0002-8178-3531); Tian-An Jiang (0000-0002-7672-8394).

Author contributions: Xie LT, Yan CH, Zhao QY, He MN and Jiang TA contributed to the research, and to drafting and editing of the manuscript; all authors approved the final draft submitted.

Conflict-of-interest statement: Authors declare no conflict of interests for this article.

Manuscript source: Unsolicited manuscript

Correspondence to: Tian-An Jiang, MD, PhD, Professor, Surgeon, Department of Ultrasound, The First Affiliated Hospital, College of Medicine, Zhejiang University, Qingchun Road, No.79, Hangzhou 310003, Zhejiang Province, China. tiananjiang@zju.edu.cn
Telephone: +86-18857127666

Received: December 28, 2017
Peer-review started: December 29, 2017
First decision: January 17, 2018
Revised: February 1, 2018
Accepted: February 9, 2018
Article in press: February 9, 2018
Published online: March 7, 2018

Abstract

Two-dimensional shear wave elastography (2D-SWE) is a rapid, simple and novel noninvasive method that has been proposed for assessing hepatic fibrosis in patients with chronic liver diseases (CLDs) based on measurements of liver stiffness. 2D-SWE can be performed easily at the bedside or in an outpatient clinic and yields immediate results with good reproducibility. Furthermore, 2D-SWE was an efficient method for evaluating liver fibrosis in small to moderately sized clinical trials. However, the quality criteria for the staging of liver fibrosis are not yet well defined. Liver fibrosis is the main pathological basis of liver stiffness and a key step in the progression from CLD to cirrhosis; thus, the management of CLD largely depends on the extent and progression of liver fibrosis. 2D-SWE appears to be an excellent tool for the early detection of cirrhosis and may have prognostic value in this context. Because 2D-SWE has high patient acceptance, it could be useful for monitoring fibrosis progression and regression in individual cases. However, multicenter data are needed to support its use. This study reviews the current status and future perspectives of 2D-SWE for assessments of liver fibrosis and discusses the technical advantages and limitations that impact its effective and rational clinical use.

Key words: Elastography; Shear wave; Chronic liver disease; Liver fibrosis

Core tip: There has been considerable research in recent years dedicated to the development of noninvasive methods of chronic liver diseases (CLDs). These include novel elastography methods. In this review, we outline the current state and future perspectives of the commonly used two-dimensional

shear wave elastography (2D-SWE) in CLDs. In particular, we discuss the applications and problems in chronic viral hepatitis, nonalcoholic fatty liver disease, alcoholic liver disease, liver transplantation, focal liver lesions, and autoimmune liver disease to synthesize existing evidence for the reader. This is the first full and complete review to assess various CLDs using 2D-SWE.

Xie LT, Yan CH, Zhao QY, He MN, Jiang TA. Quantitative and noninvasive assessment of chronic liver diseases using two-dimensional shear wave elastography. *World J Gastroenterol* 2018; 24(9): 957-970 Available from: URL: http://www.wjgnet.com/1007-9327/full/v24/i9/957.htm DOI: http://dx.doi.org/10.3748/wjg.v24.i9.957

INTRODUCTION

Liver fibrosis results from repetitive or sustained liver inflammation caused by chronic liver diseases (CLDs) and has serious long-term consequences in terms of patient morbidity and mortality due to the progression to cirrhosis. Patients with cirrhosis are at a higher risk of developing complications, including esophageal varices, ascites, liver failure and hepatocellular carcinoma (HCC), than healthy individuals[1,2]. Liver fibrosis is an important factor in the development of various CLDs and is mainly mediated by chronic liver injury, which leads to liver fibrosis characterized by increased extracellular matrix production by fibroblast-like cells and increased liver stiffness (LS)[3]. The precise assessment of the severity of liver fibrosis and reliable diagnosis of cirrhosis are vital steps in the management of CLDs, as they provide information that impacts therapeutic decisions[4,5].

Liver biopsy remains the reference standard for the staging of liver fibrosis, despite its limitations, including its invasivity and the pain experienced by patients, high cost, risk of bleeding and poor reproducibility, and contraindications, such as cases of massive ascites[6,7]. Furthermore, the accuracy of liver biopsy is influenced by several factors, including intra- and interobserver variability and sampling error[8,9]. Given these limitations, liver biopsy is not an ideal method for repeated assessments of disease progression as well.

The noninvasive assessment of liver fibrosis has recently become a research focus, leading to the introduction of new technologies. In particular, shear wave elastography (SWE), which is based on ultrasound (US) technology, has been widely applied and has gained acceptance. The latest guidelines on the clinical use of liver US elastography of the European Federation of Societies for Ultrasound in Medicine and Biology (EFSUMB)[10] and the guidelines on the evaluation of liver disease severity and prognosis of the European Association for the Study of the Liver- Asociación Latinoamericana para el Estudio del Hígado state that two-dimension (2D)-SWE is a valid and promising technique for noninvasive staging of liver fibrosis in viral hepatitis and seems to be at least equivalent to transient elastography (TE) and point SWE (pSWE)/acoustic radiation force impulse (ARFI)[11].

THE BASICS OF 2D-SWE

Comparison of elastography methods

Several elasticity imaging techniques have recently been developed for assessing the mechanical properties of liver tissues and staging the fibrosis level using different imaging modalities. In accordance with the Guidelines for the Basic Principles and Technology of EFSUMB[12], the available US-based elastography techniques include strain elastography (SE) and SWE; SWE can be further subdivided into three techniques - TE, pSWE and 2D-SWE - in addition to radiology-based magnetic resonance elastography (MRE).

Among these, TE is the most widely used elastography method. However, in a study of 13369 CLD patients over a 5-year period of using TE, unreliable results were obtained in 15.8% of cases[13]. The limitations of TE, such as the difficulty in measuring obese patients and patients with narrow intercostal spaces, the variations in operator experience, and the fact that it is not applicable in patients with ascites, were the primary factors contributing to these unreliable results. Importantly, the issue of obesity has been partially addressed by the introduction of specially designed XL probes that measure LS deeper than the standard M probes. It has also been reported that TE and ARFI elastography are inaccurate in the detection of early and intermediate fibrosis[14,15].

MRE can be used to quantitatively diagnose liver fibrosis with high accuracy and is mainly used for the diagnosis of advanced liver fibrosis and cirrhosis. The diagnostic accuracy of MRE increased when the liver fibrosis was getting serious, whereas the level of early fibrosis detected by MRE is inaccurate[16,17]. 2D-SWE is the latest elastography technology and can assess the elasticity of liver tissue easily and quickly, thus reflecting the degree of liver fibrosis. Table 1 demonstrates the comparison of currently available noninvasive methods in patients with CLD.

Principles of 2D-SWE

2D-SWE is a novel noninvasive method that has been proposed for assessing LS by measuring the velocity of elastic shear waves in the liver parenchyma[18]. In SWE, shear waves are created by US-generated pulses of an acoustic radiation force (Figure 1). The velocity of the shear wave is then estimated by a Doppler-like effect over a region of interest (ROI) and is related to the stiffness or elasticity of the medium[19]. This shear wave velocity can be used to calculate the tissue stiffness by the formula $E = \rho c^2$, where E is tissue elasticity (Young's modulus, kPa), ρ is tissue density (kg/m^3), and c is shear wave velocity (m/s)[20,21].

Table 1 Comparison of currently available noninvasive methods in patients with chronic liver disease

Content	Methods			
	TE	pSWE	2D-SWE	MRE
Technical principle	TE was the first commercially available elastography method developed for measuring liver stiffness using a dedicated device that includes an amplitude modulation (A) mode image for organ localization	pSWE can be implemented on a common ultrasound diagnostic system. It uses a regular ultrasonic probe to emit a single impulse of acoustic radiation force and generates a shear wave to detect the shear wave propagation velocity	2D-SWE is the combination of a radiation force applied to the tissues by focused ultrasonic beams and a very high frame rate US imaging sequence, which is able to capture the propagation of resulting the shear waves in real time	MRE enables the measurement of liver stiffness with an MRI-compatible generator; mechanical shear waves are delivered to the tissue and displayed as elastograms using phase-contrast image sequences
Reference point	▪Young's modulus (kPa)	▪Shear wave speed (m/s) ▪Young's modulus (kPa)	▪Shear wave speed (m/s) ▪Young's modulus (kPa)	▪Shear wave speed (m/s) ▪Young's modulus (kPa)
Selected example	▪FibroScan (Echosens, France)	▪VTQ using ARFI imaging (Siemens Healthcare, Germany) ▪ElastPQ (Philips Healthcare, Netherlands) ▪Shear Wave Measurement (Hitachi Aloka Medical, Japan)	▪SWE (SuperSonic Imagine, France) ▪Virtual Touch IQ (Siemens Healthcare, Germany) ▪Logiq E9 (GE Healthcare, United Kingdom) ▪Aplio 500 (Toshiba Medical Systems, United Kingdom)	▪MR Touch (GE Healthcare, United Kingdom) ▪MRE (Philips Healthcare, Netherlands; Siemens Healthcare, Germany)
Advantages	▪Most widely used and validated technique ▪Quality criteria well defined ▪ User friendly, rapid, easy to measure at the bedside ▪Good reproducibility ▪Good performance for noninvasive assessments of liver fibrosis staging ▪Excellent diagnostic accuracy for excluding liver cirrhosis ▪Prognostic value in cirrhosis	▪Can be performed using a regular US machine ▪ The ROI can be positioned under B-mode visualization ▪Higher applicability than TE (not limited by ascites or obesity) ▪pSWE is equal to the performance of TE for significant fibrosis and cirrhosis	▪Can be performed using a regular US machine ▪ Simple and fast to use ▪ The ROI can be positioned under B-mode visualization ▪ A larger ROI than that of TE and pSWE ▪Good applicability (not limited by ascites or obesity) ▪Good stability and reproducibility ▪Generates a real-time quantitative map of liver tissue stiffness ▪Can avoid large vessels and the gallbladder ▪ High performance for cirrhosis	▪Can be performed using a regular MRI machine ▪ Good stability and reproducibility ▪Scans the whole liver ▪Higher applicability than TE (not limited by ascites or obesity) ▪Excellent diagnostic accuracy for noninvasive staging of liver fibrosis and cirrhosis
Disadvantages	▪Requires a special device and probe ▪ ROI size is rather small and cannot be chosen ▪Lack of applicability (limited by ascites, severe obesity) ▪No B-mode orientation ▪ Cannot avoid large vessels or the gallbladder ▪Unable to distinguish between intermediate stages of liver fibrosis	▪ROI size is smaller than that of TE and cannot be modified ▪Quality criteria not yet well defined ▪Narrow range of values ▪Unable to distinguish between intermediate stages of liver fibrosis	▪Quality criteria not well defined ▪ No further prospective studies published ▪ Many factors cause failed measurements in clinical practice ▪Unable to distinguish between intermediate stages of liver fibrosis	▪Time-consuming ▪Even more costly than SWE and TE ▪ Failure can occur due to claustrophobia and iron overload ▪Affected by respiratory movement ▪ Hepatic MRE signal may be so low that waves cannot be adequately visualized with a gradient-echo based MRE sequence

2D-SWE: Two-dimensional shear wave elastography; MRE: Magnetic resonance elastography; MRI: Magnetic resonance imaging; pSWE: Point shear wave elastography; ROI: Region of interest; TE: Transient elastography; US: Ultrasound; VTQ: Virtual touch tissue quantification.

Elasticity is shown on a color-coded image displayed on a B-mode image. Then, with the ROI on the elasticity image, the mean, maximal and minimal LS values within the ROI can be visualized on a screen, along with the standard deviation (SD) of the measured elasticity[19,22]. The size and position of the ROI can be modified by the operator based on the specific goals of each liver assessment (Figure 2). In general, red areas indicate larger Young's modulus of stiffer tissues, while blue areas indicate smaller Young's modulus of softer tissues.

Examination technique

2D-SWE examination of the liver is performed by using convex US probes with integrated technological solutions allowing elasticity imaging and measurements, according to the World Federation for Ultrasound in Medicine and Biology[22,23] and the EFSUMB Guidelines for the Clinical Use of US Elastography[10,12], as well as the Society of Radiologists in Ultrasound Consensus Conference Statement regarding the assessment of liver fibrosis by elastography[24]. The proper examination procedure is described in Table 2, and the precautions

Table 2 Procedures of two-dimensional shear wave elastography

Key points	Procedures
Adequate preparation	▪ Fast and rest before the exam ▪ Perform in a supine position ▪ Train the patients on breathing
Accurate positioning	▪ Scan the 6/7/8 intercostal spaces of the right liver ▪ Acquire stable and high-quality images ▪ Instruct the patient to hold the breath for 3-5 s
Stable measurement	▪ Switch to SWE mode ▪ Freeze the image and adjust the position of the ROI ▪ Calculate the LS automatically ▪ Average the repeated measurement values

LS: Liver stiffness; ROI: Region of interest; SWE: Shear wave elastography.

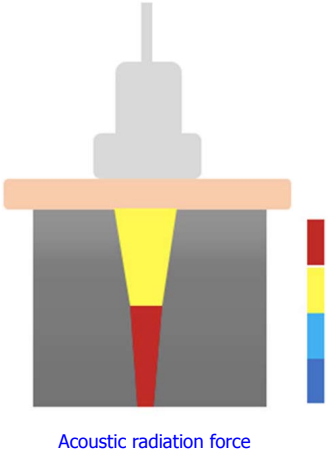

Figure 1 The principle of two-dimensional shear wave elastography. 2D-SWE is created by ultrasound-generated pulses from an acoustic radiation force that produce plane shear waves, and the propagation of the resulting shear waves can be captured in real time. 2D-SWE: Two-dimensional shear wave elastography.

and techniques of 2D-SWE in Table 3.

Normal value

"Normal" LS values have recently been studied in healthy subjects who have undergone a professional check-up and who have no overt causes of liver disease, with normal liver enzymes. Various results for normal LS values are shown in Table 4.

CLINICAL APPLICATIONS OF 2D-SWE

Diagnosis of chronic viral hepatitis

Viral hepatitis is a global public health issue, with approximately 248 million and 185 million people worldwide suffering from chronic hepatitis B (CHB) and hepatitis C (CHC), respectively[25-27]. Patients with advanced liver fibrosis from chronic viral hepatitis have a high risk of developing liver cancer and related complications, including portal hypertension (PH), esophageal and gastric variceal bleeding (EGVB), and liver failure. In these cases, prognosis and treatment are mainly affected by the degree of fibrosis, and the primary aim of treatment is controlling the progression of liver fibrosis[28,29]. The clinical practice guidelines for the management of CHB and CHC of the European Association for the Study of the Liver (EASL)[30,31], as well as the World Health Organization Guidelines for the Prevention, Care and Treatment of Persons with Chronic Hepatitis B Infection[32], recommend elastography as a routine method for clinically evaluating liver fibrosis to avoid the need for liver biopsy in some patients.

Recent studies performed worldwide have focused on 2D-SWE for determining the role of viral hepatitis in liver fibrosis. In one study, 454 CHB patients were examined by 2D-SWE and TE[33]. The results showed that 2D-SWE provided a more accurate correlation of liver elasticity with liver fibrosis stage than TE, especially for the identification of significant fibrosis (≥ F2). Bavu *et al*[18] examined 113 CHC patients and found that SWE performed better diagnostically for early, intermediate and advanced predicted levels of fibrosis than TE. Ferraioli *et al*[20] used biopsy as a reference to assess the accuracy of SWE and TE in 121 CHC patients; they found that real-time SWE was more accurate than TE for assessing significant fibrosis (≥ F2). These results were strongly supported by three meta-analyses published by other authors[34-36]. In addition, a recent large-sample meta-analysis concluded that SWE was more accurate for advanced fibrosis (≥ F3) and cirrhosis (F4)[37]. What's more, Grgurevic *et al*[38] evaluated the performance of real-time 2D-SWE for quantitatively assessing liver and spleen stiffness in patients with chronic viral hepatitis. They showed that real-time 2D-SWE can accurately identify various degrees of liver fibrosis and cirrhosis and demonstrated that liver and spleen stiffness continue to increase even after cirrhosis has developed. In fact, they noticed that spleen and liver stiffness tended to converge in more advanced stages of liver cirrhosis. This is an important study showing that 2D-SWE can be used to study the evolution of liver disease beyond cirrhosis.

As described above, SWE has high accuracy and specificity for assessing liver fibrosis due to chronic viral hepatitis, which makes it convenient for the real-time clinical monitoring of liver fibrosis. SWE technology is expected to replace biopsy, thereby eliminating the invasiveness and poor reproducibility of the latter technique. However, the quality criteria for the staging of liver fibrosis are not yet well defined. In addition, 2D-SWE has shown different diagnostic accuracies for liver fibrosis in patients with CHB and CHC. We suppose that this is probably due to the different etiologies of hepatitis B virus (HBV) and hepatitis C virus that lead to different tissue patterns and distributions of fibrosis development. Specifically, cirrhosis patients with HBV tend to produce larger regenerative nodules, which may result in different LS measurements if the ROI is placed in such an area. These findings suggest that assessments of the degree of liver fibrosis in different liver diseases cannot be based on the same diagnostic criteria, leading to

Table 3 Precautions and techniques of two-dimensional shear wave elastography

Key points	Precautions and techniques
Fasting and resting	▪ Patients should fast for a minimum of 2 h and rest for a minimum of 10 min before undergoing liver stiffness measurement with SWE
Position	▪ Measurement of liver stiffness by 2D-SWE should be performed in a supine position with the right arm maximally extended; this position ensures the best possible access for assessing the right liver lobe ▪ The transducer is placed in a right intercostal space to visualize the right liver lobe in B mode
Breathing train	▪ Instruct the patient not to breathe in or breathe out deeply in order to eliminate unreliable measurements induced by breathing movements ▪ It has been suggested that a breath hold for a few seconds during quiet breathing may lead to the best results
Clear 2D-US images	▪ Adequate B-mode liver image is a prerequisite for 2D-SWE measurements ▪ Must avoid the ribs, gas and other factors of routine ultrasound ▪ The appropriate pressure can be applied with the ultrasound probe to broaden the intercostal space and, thus, acquiring clear images. Contrary to the ordinary suggestion, this does not increase the liver's stiffness, as the intervening tissues prevent distortion of the liver surface
Scale	▪ Generally, the Young's modulus scale should not be less than 30 kPa and preferably not higher than 150 kPa
Depth	▪ Liver stiffness measured by 2D-SWE should be performed at least 10 mm under the liver capsule ▪ Measurements should not be performed too deep or too close, in order to avoid reverberation artifacts, insufficient penetration and acoustic shadow, as these factors will lead to incorrect results
Sampling frame	▪ The sampling frame should be placed in a well-visualized area of the right liver lobe, free of large vessels, the gallbladder, the liver capsule, and any other hollow organs ▪ In addition, the sampling frame should be placed in the center of the image
ROI	▪ For valid measurement quality of 2D-SWE, the ROI should be placed at a minimum of 1-2 cm and a maximum of 6 cm beneath the liver capsule ▪ The SWE acquisition is continued for 4-5 s once a stable SWE image is obtained ▪ The operator freezes the image, and the ROI should be placed in the most homogeneously colored area of the SWE ROI
Penetration mode	▪ When measuring patients with thick subcutaneous fat, fatty liver or advanced cirrhosis, SWE can be adjusted to "Pen" mode to improve the measurement success rate ▪ In 2D-SWE, if the signal is weak or unstable, the penetration mode can be activated

2D-SWE: Two-dimensional shear wave elastography; 2D-US: Two-dimensional ultrasound; Pen: Penetration; ROI: Region of interest; SWE: Shear wave elastography.

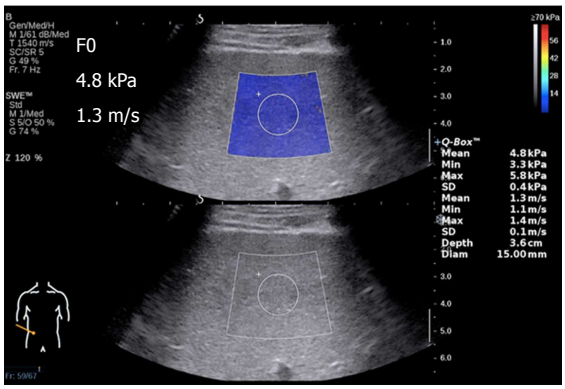

Figure 2 Example of two-dimensional shear wave elastography of the liver implemented using the Aixplorer US system (SuperSonic Imaging, France), which can be displayed simultaneously with the B-mode image. A 2D-SWE image from a 42-year-old male who had normal liver function with liver biopsy-proven fibrosis at METAVIR stage F0. The rectangular box is the area of view where the shear wave measurements were made and color-coded. The round circle is the ROI where the measurements were obtained. The system provides the mean, Max, Min, SD and Diam of the stiffness measurements within the ROI. For this case, the following measurements were made: Young's modulus: Mean = 4.8 kPa, Min = 3.3 kPa, Max = 5.8 kPa, SD = 0.4 kPa; shear wave velocity: Mean = 1.3 m/s, Min = 1.1 m/s, Max = 5.8 m/s, SD = 0.1 m/s, Depth = 3.6 cm, and Diam = 15.0 mm. 2D-SWE: Two-dimensional shear wave elastography; Diam: Diameter; Max: Maximum; Min: Minimum; ROI: Region of interest; SD: Standard deviation; US: Ultrasound.

the issue of how to establish diagnostic criteria for patients with multiple CLDs, *e.g.*, HBV patients with nonalcoholic fatty liver disease (NAFLD).

In the future, diagnosis and treatment in such situations will require personalization. The lack of specific criteria may also be due to the paucity of studies, small sample sizes, and diverse research areas; future developments will require more evidence-based medical data from large-scale, multicenter studies. Table 5 includes the cut-off values of LS assessed by 2D-SWE in various studies. Figure 3 shows 2D-SWE of liver fibrosis at METAVIR stages F1 through F4. Note that the LS gradually increases, and the color of the sampling frame gradually changes in the initial stages and incrementally increases in the later stages of fibrosis.

Diagnosis of NAFLD

NAFLD is the most prevalent CLD, representing a spectrum ranging from simple fatty liver (SFL) to nonalcoholic steatohepatitis (NASH)[39,40]. NAFLD has become a global health problem, with a prevalence comparable to the rates of metabolic syndrome, obesity, type 2 diabetes mellitus and dyslipidemia[41,42]. The morbidity and mortality of patients with NAFLD are related to the development of NASH, which may progress to fibrosis and cirrhosis, even resulting in an increased risk of HCC[43]. A meta-analysis[44] demonstrated that even SFL may result in fibrosis development, and fibrosis development was observed in approximately 30% of patients with SFL, as well as in patients with NASH. Liver fibrosis, but no other histological features, has been demonstrated as the

Table 4 Summary of the literature for two-dimensional shear wave elastography normal values

Ref.	Year	Country	Number	Mean age	Sex, female/male	Mean SWE, standard deviation, range	Remarks
Muller *et al*[19]	2009	France	15	NA	NA	2.6-6.2 kPa	No data available regarding age or sex of normal subjects
Ferraioli *et al*[79]	2012	Italy	42	34.8	13/29	4.92-5.39 kPa	
Sirli *et al*[82]	2013	Romania	82	26	56/26	6.0 ± 1.4 kPa	Female: 5.7 ± 1.3 kPa Male: 6.6 ± 1.5 kPa BMI ⩾ 25 kg/m²: 6.5 ± 1.5 kPa BMI < 25 kg/m²: 5.8 ± 1.3 kPa
Hudson *et al*[83]	2013	Canada	15	27	5/10	5.55 ± 0.74 kPa	
Wang *et al*[84]	2014	China	30	36.1 ± 14.7	14/16	4.29 kPa	
Suh *et al*[73]	2014	South Korea	196	29.2 ± 9.2	66/130	2.6-6.2 kPa	
Huang *et al*[85]	2014	China	502	37.9	310/192	5.10 ± 1.02 kPa	Female: 5.45 ± 1.02 kPa Male: 4.89 ± 0.96 kPa
Yoon *et al*[86]	2014	South Korea	122	NA	NA	5.12 ± 1.46 kPa (session Ⅰ) 4.95 ± 1.40 kPa (session Ⅱ)	No data available regarding age or sex of normal subjects
Leung *et al*[33]	2013	China	171	40.6 ± 10.8	103/68	5.5 ± 0.7 kPa	Female: 5.7 ± 0.5 kPa Male: 5.4 ± 0.7 kPa
Franchi-Abella *et al*[87]	2016	France	51	0-15	26/25	6.53 ± 1.38 kPa	No significant differences were observed between male and female patients, right and left lobes, or different breathing conditions

NA: Not available.

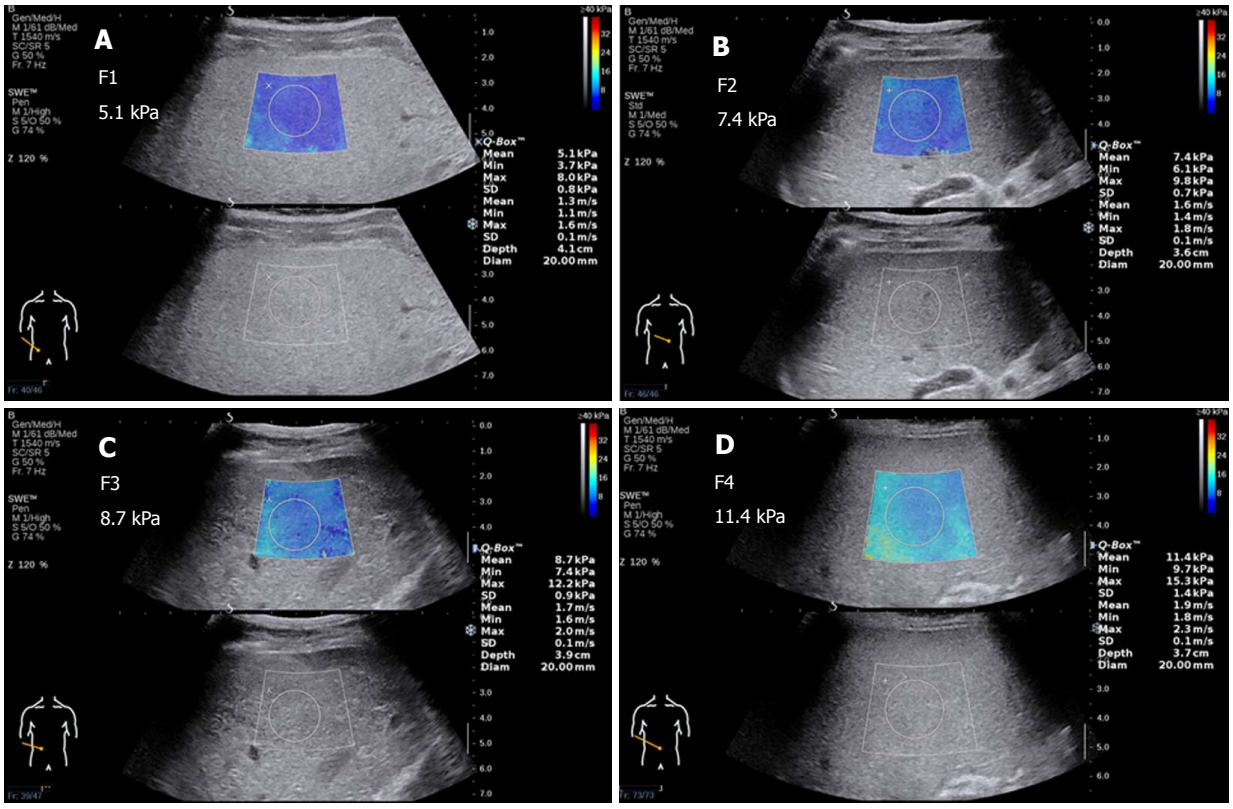

Figure 3 Two-dimensional shear wave elastography (Aixplorer US system, SuperSonic Imaging, France) of the liver in chronic hepatitis B patients with liver biopsy-proven fibrosis at METAVIR stages F1 through F4. A: F1 stage, mean Young's modulus = 5.1 kPa, mean shear wave velocity = 1.3 m/s; B: F2 stage, mean Young's modulus = 7.4 kPa, mean shear wave velocity = 1.4 m/s; C: F3 stage, mean Young's modulus = 8.7 kPa, mean shear wave velocity = 1.7 m/s; D: F4 stage, mean Young's modulus = 11.4 kPa, mean shear wave velocity = 1.9 m/s. Note the liver stiffness gradually increases, and the color of the sampling frame gradually changes in the initial stages and incrementally increases in the later stages of fibrosis. 2D-SWE: Two-dimensional shear wave elastography; US: Ultrasound.

single most crucial histological feature associated with the risk of liver-related complications and death in patients with NAFLD[45]. Therefore, the most important issue for patients with NAFLD is recognizing and assessing the stage of liver fibrosis, which is possible by using US elastography.

Table 5 Cut-off values of liver stiffness assessed with two-dimensional shear wave elastography in various studies

Ref.	Etiologies	Year	Country	Patients, *n*	⩾ F1 (fibrosis)		⩾ F2 (significant fibrosis)		⩾ F3 (severe fibrosis)		F4 (cirrhosis)	
					Cut-off, kPa	AUROC, %	Cut-off, kPa	AUROC, %	Cut-off, kPa	AUROC, %	Cut-off, kPa	AUROC, %
Leung *et al*[33]	HBV	2013	China	454	6.5	86	7.1	88	7.9	93	10.1	98
Herrmann *et al*[37]	HBV	2017	Germany	206	NA	NA	7.1	91	8.1	91	11.5	96
Zeng *et al*[29]	HBV	2014	China	303	NA	NA	7.2	92	9.7	95	11.7	95
Bavu *et al*[18]	HCV	2011	France	113	NA	NA	9.1	95	10.1	96	13.3	97
Ferraioli *et al*[20]	HCV	2012	Italy	121	NA	NA	7.1	92	8.7	98	10.4	98
Grgurevic *et al*[38]	CVH	2015	Croatia	123	NA	NA	8.1	99	NA	NA	10.8	95
Cassinotto *et al*[46]	NAFLD	2014	France	108	NA	NA	6.3	86	8.3	89	10.5	88
Garcovich *et al*[47]	NAFLD	2016	Italy	78	5.1	92	6.7	96	NA	NA	NA	NA
Thiele *et al*[51]	ALD	2016	Denmark	199	NA	NA	10.2	94	NA	NA	16.4	95

2D-SWE: Two-dimensional shear wave elastography; ALD: Alcoholic liver disease; AUROC: Area under the receiver operating characteristic curve; CVH: Chronic viral hepatitis; HBV: Hepatitis B virus; HCV: Hepatitis C virus; LS: Liver stiffness; NA: Not available; NAFLD: Nonalcoholic fatty liver disease.

Cassinotto *et al*[46] enrolled 291 patients with NAFLD and compared the performance of 2D-SWE, TE and Virtual Touch Quantification using liver biopsy as the reference method. They found that although obesity was related to an increased rate of failed LS measurements, these techniques, especially SWE, were valuable for diagnosing liver fibrosis in patients with NAFLD. The diagnostic performances of 2D-SWE for assessing liver fibrosis are as follows. For a sensitivity of at least 90% for diagnosing significant fibrosis (⩾ F2), severe fibrosis (⩾ F3) and cirrhosis (F4), the specificity is approximately 60%-70%; for a specificity of at least 90%, the sensitivity is approximately 50%-70%. 2D-SWE had areas under the receiver operating characteristic curves of 86%, 89% and 88% for the diagnosis of ⩾ F2, ⩾ F3 and F4, respectively. Furthermore, LS was mainly related to the fibrosis stage, and steatosis, inflammation and hepatocyte ballooning did not have significant influences on LS. Some NASH patients may have no fibrosis, and SWE may not be useful for the diagnosis of early-stage NASH without fibrosis. Hence, the next question became whether SWE can differentiate NASH from SFL, especially in the early stages of fibrosis. Probably not, and this is an area that relies on biochemical methods. Solutions to these problems will require multifaceted, prospective clinical studies to establish cut-off values for fibrosis staging.

In a study using SWE to identify the diagnostic accuracy of different degrees of fibrosis in 78 pediatric patients with biopsy-proven NASH[47], SWE was shown to be able to accurately evaluate significant liver fibrosis and, less efficiently, mild liver fibrosis in pediatric NAFLD patients. The study suggested that SWE can be used to assess liver fibrosis not only in adults but also in children and adolescents. However, few studies have focused on children; although fibrosis can be detected in children, the stage of fibrosis cannot yet be fully resolved, especially for fibrosis due to fatty liver. Consequently, the technique should be extended to all ages to further demonstrate the stability and reliability of the results.

Diagnosis of alcoholic liver disease

Alcoholic liver disease (ALD) is the most common liver disease in the Western world. Chronic and excessive alcohol consumption is responsible for the progression of alcoholic steatosis, hepatitis, fibrosis and cirrhosis. Complete therapy requires abstention from alcohol. Moreover, liver transplantation (LT) remains a life-saving treatment for patients with advanced ALD[48,49]. The EASL published clinical practice guidelines for the management of ALD in 2012[50]. The guidelines noted that elastography is a notable method for the early diagnosis of alcoholic cirrhosis.

A recent prospective study of 199 alcohol-overusing individuals with varying degrees of alcoholic liver fibrosis evaluated two elastography methods for the diagnosis of alcoholic fibrosis and cirrhosis, using liver biopsy as a reference[51]. The study found that 2D-SWE has a high accuracy (area under the curve ⩾ 0.92) for identifying subjects with significant fibrosis and cirrhosis, and the 2D-SWE cut-off values for optimal identification of significant fibrosis and cirrhosis were 10.2 kPa and 16.4 kPa. 2D-SWE was an extremely useful tool for diagnosing alcoholic fibrosis and, furthermore, was more appropriate for diagnosing early cirrhosis than for distinguishing

between early and advanced cirrhosis. However, the threshold values that will allow the accurate diagnosis of cirrhosis by SWE and obviate the need for liver biopsy in adults with ALD remain to be determined.

Patients with advanced ALD ultimately experience life-threatening complications, such as PH and ascites. These may lead to EGVB, which is among the most important causes of high mortality in patients with cirrhosis[52]. Therefore, assessing the severity of PH during follow-up is essential in patients with cirrhosis. The hepatic venous pressure gradient (HVPG) has been used to assess PH, but it is rarely used in clinical practice because of its invasiveness. A recent study found that LS measured by SWE is an independent predictor of the presence of HCC and esophageal and gastric varices in patients with CLD[53]. Another study demonstrated that SWE, as a promising tool to diagnose PH, has outstanding diagnostic accuracy, with a specificity and sensitivity ranging around 80%, and showed it to be superior to TE[54]; however, more than 30% of the clinically significant PH patients could not be conclusively diagnosed or ruled disease-free because their SWE values were between the cut-offs. Several recent studies have reported that LS measured by SWE in connection with HVPG is important for predicting clinically significant PH in patients with cirrhosis[55,56]. Thus, although 2D-SWE has exceptional clinical value for assessing HCC patients with PH and EGVB, it still cannot replace digestive endoscopy[52].

Assessment of end-stage liver disease after LT

LT is the only therapy for many patients who eventually progress to end-stage liver disease. However, LT is associated with a high rate of complications, which are difficult to identify in the early stages. One study reported a right lobe liver transplant recipient who experienced anastomotic stenosis of the right hepatic vein. SWE was quantitatively used to evaluate stiffness. The results suggested that SWE may be a noninvasive tool for assessing alterations in LS secondary to hepatic venous congestion after LT[57]. Another study showed that SWE may be useful during follow-up after LT. Liver rejection or hepatitis can be predicted at > 4 wk based on liver grafts that are stiffer than normal[58]. In a more recent study, SWE was successfully utilized to monitor the therapeutic effects of direct-acting antivirals in hepatitis C recurrence after LT; the median LS values decreased dramatically after treatment ($P < 0.001$). The study suggested that SWE is a valid diagnostic tool to follow-up hepatitis C patients undergoing LT[59].

From this study, we observed that SWE aids in the clinical diagnosis and detection of complications after LT, which represents great progress in SWE technology from diagnosis to monitoring. However, few studies have examined elastography in LT. This study represents the first step, although there is great potential for future research opportunities. Moreover, US elastography should be applied more for monitoring and predicting the complications of LT, particularly for assessing disease progression and prognosis.

Assessment of focal liver lesions

Focal liver lesions (FLLs) represent novel lesions for the field of US elastography and include those found in hemangioma, HCC, focal nodular hyperplasia (FNH), metastatic cancer and adenoma. Several studies have reported that 2D-SWE is a useful method for distinguishing FLLs, although it does not completely distinguish benign from malignant lesions[60-64]. The stiffness of lesions in liver malignancies is significantly higher than that of the liver parenchyma and is also higher than that of benign lesions[60,61] (Figure 4 shows HCC images of 2D-SWE). In malignant tumors, the hardness values of metastases were significantly higher than those found in HCC and cholangiocarcinoma[62]. In benign lesions, 2D-SWE has been regarded as a practical tool for distinguishing FNH from adenoma[63].

A recent study demonstrated the correct differentiation between benign and malignant FLLs by using real-time 2D-SWE in 96.1% of patients (area under the curve = 0.98)[64]. They used three elastography parameters, the mean stiffness of the FLL, the ratio between the minimal and maximum lesion stiffness, and the ratio between the stiffness of the FLL and the surrounding liver parenchyma to construct a new Liver Elastography Malignancy Prediction score based on a regression analysis. A simpler approach considering only mean lesion stiffness in a dichotomized fashion could be used to diagnose or rule-out malignancy with cut-off values of 14 kPa and 32.5 kPa, respectively.

Nonetheless, conclusions based on the current literature remain unclear. When 2D US and Doppler US suggest that a lesion is a benign tumor but elastography suggests malignancy, the lesion cannot therefore be diagnosed as malignant. Several technical limitations still exist. In situations in which the lesion is smaller than the ROI or located deep or near the heart, the shear wave propagation and imaging stability will be affected. Furthermore, lesion areas with necrotic liquefaction or calcification are not representative of the true lesion stiffness, which often leads to misdiagnosis.

Assessment of autoimmune liver disease

Autoimmune liver disease (AILDs) are intricate disorders resulting from the effects of multiple genes in association with environmental factors. The three major AILDs are primary biliary cirrhosis, primary sclerosing cholangitis and autoimmune hepatitis[65]. As they progress, these diseases may ultimately lead to chronic liver damage, liver fibrosis and cirrhosis. Zeng *et al*[66] used liver biopsy as the reference standard for determining the diagnostic accuracy of 2D-SWE for noninvasively assessing liver fibrosis in patients with AILD. Their results indicated that the optimal cut-off values for significant fibrosis (≥ F2), severe fibrosis (≥ F3) and cirrhosis (F4) were 9.7

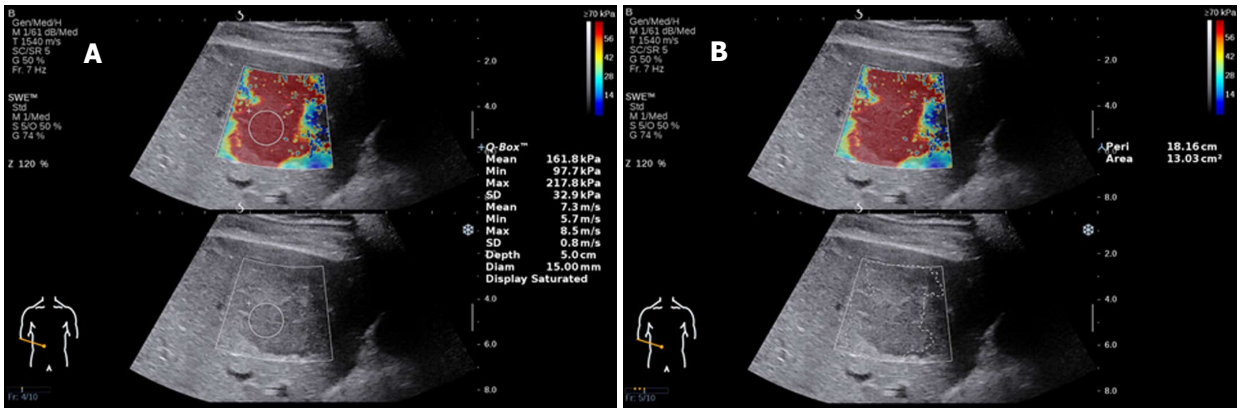

Figure 4 Two-dimensional shear wave elastography (Aixplorer US system, SuperSonic Imaging, France) images of a 69-year-old male with hepatocellular carcinoma based on the cirrhosis caused by hepatitis B virus. A: The mean Young's modulus is 161.8 kPa and the mean shear wave velocity is 7.3 m/s, which is obviously higher than the benign lesion; B: The area of the tumor is 13.03 cm^2. 2D-SWE: Two-dimensional shear wave elastography; HBV: Hepatitis B virus; HCC: Hepatocellular carcinoma; US: Ultrasound.

kPa, 13.2 kPa and 16.3 kPa, respectively. Moreover, the sensitivity and specificity ranged from 75% to 87% for all fibrosis stages. As these data show, SWE has high cut-off values in patients with AILD. The critical cut-off value was obviously higher than that for CHB/CHC. Therefore, different diseases have different thresholds, representing different developmental processes. AILD is relatively rare, and the current study was small; thus, further confirmation is necessary.

These results of LT, FLLs and AILD based on SWE cannot yet be clinically translated, as the research published to date is insufficient to definitively establish diagnostic criteria. However, elastography has shown promise for use in many research and development opportunities and future applications.

Future perspectives

Although there is evidence that 2D-SWE could become a crucial tool in end-stage liver disease, additional research and development are necessary. Additional work should focus on the role of SWE not only in cross-sectional diagnosis but also in longitudinal studies considering disease progression, regression and clinical outcomes[67]. Priority should be given to multicenter, large-scale verification research. Indeed, the longitudinal monitoring of fibrosis in patients with CLD may be a highly practical application for SWE. Preliminary research has revealed a remarkable decrease in LS values in patients with chronic viral hepatitis after continued antiviral treatment[68,69]. Given its high patient acceptance and good accessibility, SWE may also become a convenient tool for identifying patients with liver disease and a promising avenue for future research. However, several issues warrant further consideration.

The basic problem

1. Although alternative techniques, such as pSWE/ARFI or 2D-SWE, seem to overcome the limitations of TE, their quality criteria for the staging of liver fibrosis are not yet well defined.
   a. It remains unclear whether the shear wave Young's modulus or shear wave velocity is more representative.
   b. It remains unknown whether multiple measurements in one location are necessary when satisfactory measures of stiffness are obtained. Or, whether measurements in more than one location are needed.
   c. There is currently no agreement on objective quality criteria regarding what constitutes a valid measurement and what is an invalid measurement.
2. It remains unknown whether a simple semi-quantitative fibrosis score can adequately reflect the complexity of the pathophysiological process.

The clinical questions

1. In the era of promotion of precision medicine, can 2D-SWE accurately guide clinical work to aid in the design of an antiviral therapy for hepatitis B patients?
2. Can 2D-SWE be a reliable measurement of the prognosis of liver fibrosis?
3. Does a greater Young's modulus indicate more serious disease progression? Does a reduced Young's modulus indicate disease remission or effective treatment?
4. How do we diagnose the mixed types of liver disease?
5. In adult patients with NAFLD, what SWE LS cut-off value allows us to accurately diagnose the presence of cirrhosis and eliminate the need for liver biopsy?
6. In compensated cirrhosis of adult CLD, what 2D-SWE liver stiffness cut-off value allows us to avoid the need for gastroscopy?
7. Focal lesions can lead to erroneous results. How should these be resolved?

Patient follow-up questions

1. During follow-up monitoring, are there any definite cut-off values to weigh the progression, regression and outcome of liver disease?
2. What is a minimal time span for measuring LS over time? How often should measurements be performed?
3. How should elastography be used to predict the risk for HCC in patients with cirrhosis, regardless of etiology?

Here, we will address the first clinical issue. On the basis of the current study, we believe that SWE can guide clinical work to help develop a reasonable treatment strategy for patients with CLDs by measuring the degree of LS, which reflects the degree of liver fibrosis, and by monitoring the progress of the disease in real time. According to the EASL guidelines, it is of particular significance to identify patients with cirrhosis, as their treatment regimen and posttreatment surveillance must be adapted[27]. The latest report[70] from a European, 10-center, cohort study of 1951 adult Caucasian CHB patients found that HCC incidence distinctly dropped after the first 5 years of therapy, particularly in those with compensated cirrhosis. Furthermore, multivariable analysis showed that a LS $\geqslant$ 12 kPa at year 5 was related to greater HCC development after year 5, which likely represents valuable indirect markers of the severity of liver disease. Consequently, we believe that SWE can reflect liver fibrosis and guide therapy, thus decreasing the risk of HCC and remarkably improving the prognosis. This represents a major advancement in the treatment of CLD.

2D-SWE is known to be a multifactorial technique that factors in the anatomy of the liver, the physical characteristics and the underlying illness of the patient, the experience of the examiner, and differences in equipment. The following details include the factors associated with SWE reliability and ways to improve its performance in liver applications.

Anatomy of the liver

The liver is located in the upper abdomen, near the heart, lungs and gastrointestinal tract, and is particularly affected by respiratory movements as well as the heartbeat and gas in the gastrointestinal tract[71]. Measurements of the left liver lobe yield markedly higher values and are more variable than the right lobe; thus, LSM in the left liver lobe should be avoided whenever possible[72]. During the examination, the patient needs to cooperate by holding their breath (neither in the expiratory phase nor in the aspirated phase) to stabilize the 2D image measurement because stable 2D imaging is the basis of successful results[24].

Physical characteristics and underlying illness of the patient

Previous studies have reported that SWE measurements are not affected by a high body mass index, ascites or fatty liver[20,73], while in clinical practice, high measurement failure rates are due to obesity or ascites causing poor penetration[4]. Obese patients often have a fatty liver with a thick layer of subcutaneous fat and echo attenuation throughout the liver, which is not conducive to clear 2D imaging. In some very thin patients with a narrow intercostal space, especially patients who have entered the end-stage of liver cirrhosis, the right liver has been severely reduced to the extent that it affects elasticity measurements[33].

Using current methods, according to the patient's liver, the depth should be dropped, and the image should be appropriately enlarged while the areas of the sampling frame and ROI are adjusted to the shrinking liver. In addition, some factors influence the LS measured by elastography, leading to an overestimation of liver fibrosis[71,74-78]. Such factors include excessive alcohol intake, elevated central venous pressure, cardiac failure, intra- or extrahepatic cholestasis, alanine aminotransferase flare in acute or chronic hepatitis, and histological necroinflammation activity.

Operator experience

LS measurements by 2D-SWE should be made by an expert operator. It has been reported that experienced examiners have higher reproducibility of measurements than novice examiners[79,80]. It is advised that at least 50 supervised 2D-SWE measurements should be performed by beginners in order to acquire reliable results[79]. This issue therefore necessitates strict prejob training for operators to reduce the error caused by lack of experience and to improve the stability of clinical implementations (Figure 5 shows an analysis of failed measurements).

Differences in manufacturer equipment

There may be significant variation in the frequency of acoustic radiation forces used across manufacturers, although variations can even be observed across different equipment from the same manufacturer or due to different settings applied using the same equipment. Large differences among the measurements provided by different settings create obstacles to the clinical application of SWE that need be addressed in the future[81]. In summary, these techniques need to be performed using a standardized protocol with critically interpreted results, taking confounding factors into account.

CONCLUSION

In conclusion, 2D-SWE appears to be a valid, simple, rapid and reproducible method for the noninvasive assessment of liver fibrosis, with advantages including its low cost and widespread availability. As liver biopsies cannot be performed frequently, SWE can be used to regularly monitor liver fibrosis over the long term. SWE is a promising technology with potential clinical applications, including accurate quantification and therapeutic monitoring. We believe that with the popularity of US elastography, the noninvasive assessment of liver fibrosis will be further promoted. Most importantly, in the future, SWE may become a routine method of screening for patients with CLDs. Finally, large-scale, multicenter, multifield clinical studies are needed to explore the applications of SWE, as there may be variability in terms of demographics, disease and liver cancer incidence predictions. We are

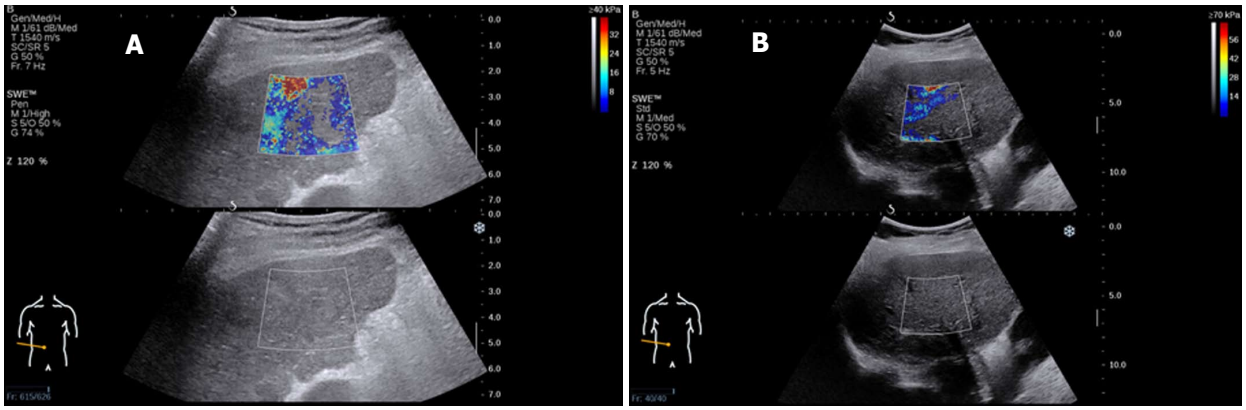

Figure 5 Analysis of failed measurements. A: A 69-year-old female who had right heart failure and could not hold her breath, causing the failed liver stiffness measurement; B: An image acquired by an inexperienced operator who did not set the standard parameters.

hopeful that SWE will continue to evolve and attain a utility equal to that of Doppler as a new mode of US imaging.

REFERENCES

1 **Singh S**, Muir AJ, Dieterich DT, Falck-Ytter YT. American Gastroenterological Association Institute Technical Review on the Role of Elastography in Chronic Liver Diseases. *Gastroenterology* 2017; **152**: 1544-1577 [PMID: 28442120 DOI: 10.1053/j.gastro.2017.03.016]

2 **GBD 2013 Mortality and Causes of Death Collaborators**. Global, regional, and national age-sex specific all-cause and cause-specific mortality for 240 causes of death, 1990-2013: a systematic analysis for the Global Burden of Disease Study 2013. *Lancet* 2015; **385**: 117-171 [PMID: 25530442 DOI: 10.1016/s0140-6736(14)61682-2]

3 **Lee YA**, Wallace MC, Friedman SL. Pathobiology of liver fibrosis: a translational success story. *Gut* 2015; **64**: 830-841 [PMID: 25681399 DOI: 10.1136/gutjnl-2014-306842]

4 **Friedrich-Rust M**, Poynard T, Castera L. Critical comparison of elastography methods to assess chronic liver disease. *Nat Rev Gastroenterol Hepatol* 2016; **13**: 402-411 [PMID: 27273167 DOI: 10.1038/nrgastro.2016.86]

5 **Stasi C**, Milani S. Non-invasive assessment of liver fibrosis: Between prediction/prevention of outcomes and cost-effectiveness. *World J Gastroenterol* 2016; **22**: 1711-1720 [PMID: 26819535 DOI: 10.3748/wjg.v22.i4.1711]

6 **Sharma S**, Khalili K, Nguyen GC. Non-invasive diagnosis of advanced fibrosis and cirrhosis. *World J Gastroenterol* 2014; **20**: 16820-16830 [PMID: 25492996 DOI: 10.3748/wjg.v20.i45.16820]

7 **Seeff LB**, Everson GT, Morgan TR, Curto TM, Lee WM, Ghany MG, Shiffman ML, Fontana RJ, Di Bisceglie AM, Bonkovsky HL, Dienstag JL; HALT-C Trial Group. Complication rate of percutaneous liver biopsies among persons with advanced chronic liver disease in the HALT-C trial. *Clin Gastroenterol Hepatol* 2010; **8**: 877-883 [PMID: 20362695 DOI: 10.1016/j.cgh.2010.03.025]

8 **Schiavon Lde L**, Narciso-Schiavon JL, de Carvalho-Filho RJ. Non-invasive diagnosis of liver fibrosis in chronic hepatitis C. *World J Gastroenterol* 2014; **20**: 2854-2866 [PMID: 24659877 DOI: 10.3748/wjg.v20.i11.2854]

9 **Cassinotto C**, Lapuyade B, Mouries A, Hiriart JB, Vergniol J, Gaye D, Castain C, Le Bail B, Chermak F, Foucher J, Laurent F, Montaudon M, De Ledinghen V. Non-invasive assessment of liver fibrosis with impulse elastography: comparison of Supersonic Shear Imaging with ARFI and FibroScan®. *J Hepatol* 2014; **61**: 550-557 [PMID: 24815876 DOI: 10.1016/j.jhep.2014.04.044]

10 **Dietrich CF**, Bamber J, Berzigotti A, Bota S, Cantisani V, Castera L, Cosgrove D, Ferraioli G, Friedrich-Rust M, Gilja OH, Goertz RS, Karlas T, de Knegt R, de Ledinghen V, Piscaglia F, Procopet B, Saftoiu A, Sidhu PS, Sporea I, Thiele M. EFSUMB Guidelines and Recommendations on the Clinical Use of Liver Ultrasound Elastography, Update 2017 (Long Version). *Ultraschall Med* 2017; **38**: e16-e47 [PMID: 28407655 DOI: 10.1055/s-0043-103952]

11 **European Association for Study of Liver**; Asociacion Latinoamericana para el Estudio del Higado. EASL-ALEH Clinical Practice Guidelines: Non-invasive tests for evaluation of liver disease severity and prognosis. *J Hepatol* 2015; **63**: 237-264 [PMID: 25911335 DOI: 10.1016/j.jhep.2015.04.006]

12 **Bamber J**, Cosgrove D, Dietrich CF, Fromageau J, Bojunga J, Calliada F, Cantisani V, Correas JM, D'Onofrio M, Drakonaki EE, Fink M, Friedrich-Rust M, Gilja OH, Havre RF, Jenssen C, Klauser AS, Ohlinger R, Saftoiu A, Schaefer F, Sporea I, Piscaglia F. EFSUMB guidelines and recommendations on the clinical use of ultrasound elastography. Part 1: Basic principles and technology. *Ultraschall Med* 2013; **34**: 169-184 [PMID: 23558397 DOI: 10.1055/s-0033-1335205]

13 **Castéra L**, Foucher J, Bernard PH, Carvalho F, Allaix D, Merrouche W, Couzigou P, de Lédinghen V. Pitfalls of liver stiffness measurement: a 5-year prospective study of 13,369 examinations. *Hepatology* 2010; **51**: 828-835 [PMID: 20063276 DOI: 10.1002/hep.23425]

14 **Friedrich-Rust M**, Ong MF, Martens S, Sarrazin C, Bojunga J, Zeuzem S, Herrmann E. Performance of transient elastography for the staging of liver fibrosis: a meta-analysis. *Gastroenterology* 2008; **134**: 960-974 [PMID: 18395077 DOI: 10.1053/j.gastro.2008.01.034]

15 **Haque M**, Robinson C, Owen D, Yoshida EM, Harris A. Comparison of acoustic radiation force impulse imaging (ARFI) to liver biopsy histologic scores in the evaluation of chronic liver disease: A pilot study. *Ann Hepatol* 2010; **9**: 289-293 [PMID: 20720270]

16 **Singh S**, Venkatesh SK, Wang Z, Miller FH, Motosugi U, Low RN, Hassanein T, Asbach P, Godfrey EM, Yin M, Chen J, Keaveny AP, Bridges M, Bohte A, Murad MH, Lomas DJ, Talwalkar JA, Ehman RL. Diagnostic performance of magnetic resonance elastography in staging liver fibrosis: a systematic review and meta-analysis of individual participant data. *Clin Gastroenterol Hepatol* 2015; **13**: 440-451.e6 [PMID: 25305349 DOI: 10.1016/j.cgh.2014.09.046]

17 **Huwart L**, Sempoux C, Vicaut E, Salameh N, Annet L, Danse E, Peeters F, ter Beek LC, Rahier J, Sinkus R, Horsmans Y, Van Beers BE. Magnetic resonance elastography for the noninvasive staging of liver fibrosis. *Gastroenterology* 2008; **135**: 32-40 [PMID: 18471441 DOI: 10.1053/j.gastro.2008.03.076]

18 **Bavu E**, Gennisson JL, Couade M, Bercoff J, Mallet V, Fink M, Badel A, Vallet-Pichard A, Nalpas B, Tanter M, Pol S. Noninvasive in vivo liver fibrosis evaluation using supersonic shear imaging: a clinical study on 113 hepatitis C virus patients. *Ultrasound Med*

Biol 2011; **37**: 1361-1373 [PMID: 21775051 DOI: 10.1016/j.ultrasmedbio.2011.05.016]
19 **Muller M**, Gennisson JL, Deffieux T, Tanter M, Fink M. Quantitative viscoelasticity mapping of human liver using supersonic shear imaging: preliminary in vivo feasibility study. *Ultrasound Med Biol* 2009; **35**: 219-229 [PMID: 19081665 DOI: 10.1016/j.ultrasmedbio.2008.08.018]
20 **Ferraioli G**, Tinelli C, Dal Bello B, Zicchetti M, Filice G, Filice C; Liver Fibrosis Study Group. Accuracy of real-time shear wave elastography for assessing liver fibrosis in chronic hepatitis C: a pilot study. *Hepatology* 2012; **56**: 2125-2133 [PMID: 22767302 DOI: 10.1002/hep.25936]
21 **Poynard T**, Munteanu M, Luckina E, Perazzo H, Ngo Y, Royer L, Fedchuk L, Sattonnet F, Pais R, Lebray P, Rudler M, Thabut D, Ratziu V. Liver fibrosis evaluation using real-time shear wave elastography: applicability and diagnostic performance using methods without a gold standard. *J Hepatol* 2013; **58**: 928-935 [PMID: 23321316 DOI: 10.1016/j.jhep.2012.12.021]
22 **Shiina T**, Nightingale KR, Palmeri ML, Hall TJ, Bamber JC, Barr RG, Castera L, Choi BI, Chou YH, Cosgrove D, Dietrich CF, Ding H, Amy D, Farrokh A, Ferraioli G, Filice C, Friedrich-Rust M, Nakashima K, Schafer F, Sporea I, Suzuki S, Wilson S, Kudo M. WFUMB guidelines and recommendations for clinical use of ultrasound elastography: Part 1: basic principles and terminology. *Ultrasound Med Biol* 2015; **41**: 1126-1147 [PMID: 25805059 DOI: 10.1016/j.ultrasmedbio.2015.03.009]
23 **Ferraioli G**, Filice C, Castera L, Choi BI, Sporea I, Wilson SR, Cosgrove D, Dietrich CF, Amy D, Bamber JC, Barr R, Chou YH, Ding H, Farrokh A, Friedrich-Rust M, Hall TJ, Nakashima K, Nightingale KR, Palmeri ML, Schafer F, Shiina T, Suzuki S, Kudo M. WFUMB guidelines and recommendations for clinical use of ultrasound elastography: Part 3: liver. *Ultrasound Med Biol* 2015; **41**: 1161-1179 [PMID: 25800942 DOI: 10.1016/j.ultrasmedbio.2015.03.007]
24 **Barr RG**, Ferraioli G, Palmeri ML, Goodman ZD, Garcia-Tsao G, Rubin J, Garra B, Myers RP, Wilson SR, Rubens D, Levine D. Elastography Assessment of Liver Fibrosis: Society of Radiologists in Ultrasound Consensus Conference Statement. *Radiology* 2015; **276**: 845-861 [PMID: 26079489 DOI: 10.1148/radiol.2015150619]
25 **Schweitzer A**, Horn J, Mikolajczyk RT, Krause G, Ott JJ. Estimations of worldwide prevalence of chronic hepatitis B virus infection: a systematic review of data published between 1965 and 2013. *Lancet* 2015; **386**: 1546-1555 [PMID: 26231459 DOI: 10.1016/s0140-6736(15)61412-x]
26 **Petruzziello A**, Marigliano S, Loquercio G, Cozzolino A, Cacciapuoti C. Global epidemiology of hepatitis C virus infection: An up-date of the distribution and circulation of hepatitis C virus genotypes. *World J Gastroenterol* 2016; **22**: 7824-7840 [PMID: 27678366 DOI: 10.3748/wjg.v22.i34.7824]
27 **European Association for the Study of the Liver**. Electronic address: easloffice@easloffice.eu.; European Association for the Study of the Liver. EASL 2017 Clinical Practice Guidelines on the management of hepatitis B virus infection. *J Hepatol* 2017; **67**: 370-398 [PMID: 28427875 DOI: 10.1016/j.jhep.2017.03.021]
28 **Rockey DC**. Noninvasive assessment of liver fibrosis and portal hypertension with transient elastography. *Gastroenterology* 2008; **134**: 8-14 [PMID: 18166342 DOI: 10.1053/j.gastro.2007.11.053]
29 **Zeng J**, Liu GJ, Huang ZP, Zheng J, Wu T, Zheng RQ, Lu MD. Diagnostic accuracy of two-dimensional shear wave elastography for the non-invasive staging of hepatic fibrosis in chronic hepatitis B: a cohort study with internal validation. *Eur Radiol* 2014; **24**: 2572-2581 [PMID: 25027837 DOI: 10.1007/s00330-014-3292-9]
30 **European Association For The Study Of The Liver**. EASL clinical practice guidelines: Management of chronic hepatitis B virus infection. *J Hepatol* 2012; **57**: 167-185 [PMID: 22436845 DOI: 10.1016/j.jhep.2012.02.010]
31 **European Association for Study of Liver**. EASL Clinical Practice Guidelines: management of hepatitis C virus infection. *J Hepatol* 2014; **60**: 392-420 [PMID: 24331294 DOI: 10.1016/j.jhep.2013.11.003]
32 **WHO Guidelines Approved by the Guidelines Review Committee**. Guidelines for the Prevention, Care and Treatment of Persons with Chronic Hepatitis B Infection. Geneva: World Health Organization Copyright (c) World Health Organization 2015, 2015
33 **Leung VY**, Shen J, Wong VW, Abrigo J, Wong GL, Chim AM, Chu SH, Chan AW, Choi PC, Ahuja AT, Chan HL, Chu WC. Quantitative elastography of liver fibrosis and spleen stiffness in chronic hepatitis B carriers: comparison of shear-wave elastography and transient elastography with liver biopsy correlation. *Radiology* 2013; **269**: 910-918 [PMID: 23912619 DOI: 10.1148/radiol.13130128]
34 **Feng JC**, Li J, Wu XW, Peng XY. Diagnostic Accuracy of SuperSonic Shear Imaging for Staging of Liver Fibrosis: A Meta-analysis. *J Ultrasound Med* 2016; **35**: 329-339 [PMID: 26795041 DOI: 10.7863/ultra.15.03032]
35 **Li C**, Zhang C, Li J, Huo H, Song D. Diagnostic Accuracy of Real-Time Shear Wave Elastography for Staging of Liver Fibrosis: A Meta-Analysis. *Med Sci Monit* 2016; **22**: 1349-1359 [PMID: 27102449 DOI: 10.12659/msm.895662]
36 **Jiang T**, Tian G, Zhao Q, Kong D, Cheng C, Zhong L, Li L. Diagnostic Accuracy of 2D-Shear Wave Elastography for Liver Fibrosis Severity: A Meta-Analysis. *PLoS One* 2016; **11**: e0157219 [PMID: 27300569 DOI: 10.1371/journal.pone.0157219]
37 **Herrmann E**, de Lédinghen V, Cassinotto C, Chu WC, Leung VY, Ferraioli G, Filice C, Castera L, Vilgrain V, Ronot M, Dumortier J, Guibal A, Pol S, Trebicka J, Jansen C, Strassburg C, Zheng R, Zheng J, Francque S, Vanwolleghem T, Vonghia L, Manesis EK, Zoumpoulis P, Sporea I, Thiele M, Krag A, Cohen-Bacrie C, Criton A, Gay J, Deffieux T, Friedrich-Rust M. Assessment of biopsy-proven liver fibrosis by two-dimensional shear wave elastography: An individual patient data-based meta-analysis. *Hepatology* 2018; **67**: 260-272 [PMID: 28370257 DOI: 10.1002/hep.29179]
38 **Grgurevic I**, Puljiz Z, Brnic D, Bokun T, Heinzl R, Lukic A, Luksic B, Kujundzic M, Brkljacic B. Liver and spleen stiffness and their ratio assessed by real-time two dimensional-shear wave elastography in patients with liver fibrosis and cirrhosis due to chronic viral hepatitis. *Eur Radiol* 2015; **25**: 3214-3221 [PMID: 25903706 DOI: 10.1007/s00330-015-3728-x]
39 **Haga Y**, Kanda T, Sasaki R, Nakamura M, Nakamoto S, Yokosuka O. Nonalcoholic fatty liver disease and hepatic cirrhosis: Comparison with viral hepatitis-associated steatosis. *World J Gastroenterol* 2015; **21**: 12989-12995 [PMID: 26675364 DOI: 10.3748/wjg.v21.i46.12989]
40 **Younossi ZM**, Koenig AB, Abdelatif D, Fazel Y, Henry L, Wymer M. Global epidemiology of nonalcoholic fatty liver disease-Meta-analytic assessment of prevalence, incidence, and outcomes. *Hepatology* 2016; **64**: 73-84 [PMID: 26707365 DOI: 10.1002/hep.28431]
41 **Williams CD**, Stengel J, Asike MI, Torres DM, Shaw J, Contreras M, Landt CL, Harrison SA. Prevalence of nonalcoholic fatty liver disease and nonalcoholic steatohepatitis among a largely middle-aged population utilizing ultrasound and liver biopsy: a prospective study. *Gastroenterology* 2011; **140**: 124-131 [PMID: 20858492 DOI: 10.1053/j.gastro.2010.09.038]
42 **Sanyal AJ**, Brunt EM, Kleiner DE, Kowdley KV, Chalasani N, Lavine JE, Ratziu V, McCullough A. Endpoints and clinical trial design for nonalcoholic steatohepatitis. *Hepatology* 2011; **54**: 344-353 [PMID: 21520200 DOI: 10.1002/hep.24376]
43 **Vernon G**, Baranova A, Younossi ZM. Systematic review: the epidemiology and natural history of non-alcoholic fatty liver disease and non-alcoholic steatohepatitis in adults. *Aliment Pharmacol Ther* 2011; **34**: 274-285 [PMID: 21623852 DOI: 10.1111/j.1365-2036.2011.04724.x]
44 **Singh S**, Allen AM, Wang Z, Prokop LJ, Murad MH, Loomba R. Fibrosis progression in nonalcoholic fatty liver vs nonalcoholic steatohepatitis: a systematic review and meta-analysis of paired-biopsy studies. *Clin Gastroenterol Hepatol* 2015; **13**: 643-54.e1-9; quiz e39-40 [PMID: 24768810 DOI: 10.1016/j.cgh.2014.04.014]
45 **Angulo P**, Kleiner DE, Dam-Larsen S, Adams LA, Bjornsson ES, Charatcharoenwitthaya P, Mills PR, Keach JC, Lafferty HD,

Stahler A, Haflidadottir S, Bendtsen F. Liver Fibrosis, but No Other Histologic Features, Is Associated With Long-term Outcomes of Patients With Nonalcoholic Fatty Liver Disease. *Gastroenterology* 2015; **149**: 389-97.e10 [PMID: 25935633 DOI: 10.1053/j.gastro.2015.04.043]

46 **Cassinotto C**, Boursier J, de Lédinghen V, Lebigot J, Lapuyade B, Cales P, Hiriart JB, Michalak S, Bail BL, Cartier V, Mouries A, Oberti F, Fouchard-Hubert I, Vergniol J, Aubé C. Liver stiffness in nonalcoholic fatty liver disease: A comparison of supersonic shear imaging, FibroScan, and ARFI with liver biopsy. *Hepatology* 2016; **63**: 1817-1827 [PMID: 26659452 DOI: 10.1002/hep.28394]

47 **Garcovich M**, Veraldi S, Di Stasio E, Zocco MA, Monti L, Tomà P, Pompili M, Gasbarrini A, Nobili V. Liver Stiffness in Pediatric Patients with Fatty Liver Disease: Diagnostic Accuracy and Reproducibility of Shear-Wave Elastography. *Radiology* 2017; **283**: 820-827 [PMID: 27982761 DOI: 10.1148/radiol.2016161002]

48 **Rehm J**, Samokhvalov AV, Shield KD. Global burden of alcoholic liver diseases. *J Hepatol* 2013; **59**: 160-168 [PMID: 23511777 DOI: 10.1016/j.jhep.2013.03.007]

49 **Mueller S**, Seitz HK, Rausch V. Non-invasive diagnosis of alcoholic liver disease. *World J Gastroenterol* 2014; **20**: 14626-14641 [PMID: 25356026 DOI: 10.3748/wjg.v20.i40.14626]

50 **European Association for the Study of Liver**. EASL clinical practical guidelines: management of alcoholic liver disease. *J Hepatol* 2012; **57**: 399-420 [PMID: 22633836 DOI: 10.1016/j.jhep.2012.04.004]

51 **Thiele M**, Detlefsen S, Sevelsted Møller L, Madsen BS, Fuglsang Hansen J, Fialla AD, Trebicka J, Krag A. Transient and 2-Dimensional Shear-Wave Elastography Provide Comparable Assessment of Alcoholic Liver Fibrosis and Cirrhosis. *Gastroenterology* 2016; **150**: 123-133 [PMID: 26435270 DOI: 10.1053/j.gastro.2015.09.040]

52 **Tripathi D**, Stanley AJ, Hayes PC, Patch D, Millson C, Mehrzad H, Austin A, Ferguson JW, Olliff SP, Hudson M, Christie JM; Clinical Services and Standards Committee of the British Society of Gastroenterology. U.K. guidelines on the management of variceal haemorrhage in cirrhotic patients. *Gut* 2015; **64**: 1680-1704 [PMID: 25887380 DOI: 10.1136/gutjnl-2015-309262]

53 **Kasai Y**, Moriyasu F, Saito K, Hara T, Kobayashi Y, Nakamura I, Sugimoto K. Value of shear wave elastography for predicting hepatocellular carcinoma and esophagogastric varices in patients with chronic liver disease. *J Med Ultrason (2001)* 2015; **42**: 349-355 [PMID: 26576786 DOI: 10.1007/s10396-014-0603-3]

54 **Jansen C**, Bogs C, Verlinden W, Thiele M, Möller P, Görtzen J, Lehmann J, Praktiknjo M, Chang J, Krag A, Strassburg CP, Francque S, Trebicka J. Algorithm to rule out clinically significant portal hypertension combining Shear-wave elastography of liver and spleen: a prospective multicentre study. *Gut* 2016; **65**: 1057-1058 [PMID: 26896458 DOI: 10.1136/gutjnl-2016-311536]

55 **Procopet B**, Berzigotti A, Abraldes JG, Turon F, Hernandez-Gea V, García-Pagán JC, Bosch J. Real-time shear-wave elastography: applicability, reliability and accuracy for clinically significant portal hypertension. *J Hepatol* 2015; **62**: 1068-1075 [PMID: 25514554 DOI: 10.1016/j.jhep.2014.12.007]

56 **Maruyama H**, Kobayashi K, Kiyono S, Sekimoto T, Kanda T, Yokosuka O. Two-dimensional shear wave elastography with propagation-based reliability assessment for grading hepatic fibrosis and portal hypertension. *J Hepatobiliary Pancreat Sci* 2016; **23**: 595-602 [PMID: 27440720 DOI: 10.1002/jhbp.379]

57 **Wang HK**, Lai YC, Tseng HS, Lee RC, Loong CC, Lin NC, Chou YH, Chiou HJ, Chang CY. Hepatic venous congestion after living donor liver transplantation: quantitative assessment of liver stiffness using shear wave elastography--a case report. *Transplant Proc* 2012; **44**: 814-816 [PMID: 22483503 DOI: 10.1016/j.transproceed.2012.01.035]

58 **Yoon JH**, Lee JY, Woo HS, Yu MH, Lee ES, Joo I, Lee KB, Yi NJ, Lee YJ, Han JK, Choi BI. Shear wave elastography in the evaluation of rejection or recurrent hepatitis after liver transplantation. *Eur Radiol* 2013; **23**: 1729-1737 [PMID: 23300037 DOI: 10.1007/s00330-012-2748-z]

59 **Korda D**, Lenard ZM, Gerlei Z, Jakab Z, Haboub-Sandil A, Wagner L, Varga M, Cseprekal O, Marton A, Horvathy D, Takacs S, Doros A, Mathe Z. Shear-wave elastography for the assessment of liver fibrosis in liver transplant recipients treated for hepatitis C virus recurrence. *Eur J Gastroenterol Hepatol* 2018; **30**: 27-32 [PMID: 29049126 DOI: 10.1097/MEG.0000000000001003]

60 **Conti CB**, Cavalcoli F, Fraquelli M, Conte D, Massironi S. Ultrasound elastographic techniques in focal liver lesions. *World J Gastroenterol* 2016; **22**: 2647-2656 [PMID: 26973405 DOI: 10.3748/wjg.v22.i9.2647]

61 **Park HS**, Kim YJ, Yu MH, Jung SI, Jeon HJ. Shear Wave Elastography of Focal Liver Lesion: Intraobserver Reproducibility and Elasticity Characterization. *Ultrasound Q* 2015; **31**: 262-271 [PMID: 26086459 DOI: 10.1097/RUQ.0000000000000175]

62 **Lu Q**, Ling W, Lu C, Li J, Ma L, Quan J, He D, Liu J, Yang J, Wen T, Wu H, Zhu H, Luo Y. Hepatocellular carcinoma: stiffness value and ratio to discriminate malignant from benign focal liver lesions. *Radiology* 2015; **275**: 880-888 [PMID: 25636031 DOI: 10.1148/radiol.14131164]

63 **Brunel T**, Guibal A, Boularan C, Ducerf C, Mabrut JY, Bancel B, Boussel L, Rode A. Focal nodular hyperplasia and hepatocellular adenoma: The value of shear wave elastography for differential diagnosis. *Eur J Radiol* 2015; **84**: 2059-2064 [PMID: 26299323 DOI: 10.1016/j.ejrad.2015.07.029]

64 **Grgurevic I**, Bokun T, Salkic NN, Brkljacic B, Vukelić-Markovic M, Stoos-Veic T, Aralica G, Rakic M, Filipec-Kanizaj T, Berzigotti A. Liver elastography malignancy prediction score for noninvasive characterization of focal liver lesions. *Liver Int* 2017; Epub ahead of print [PMID: 29028279 DOI: 10.1111/liv.13611]

65 **Carbone M**, Neuberger JM. Autoimmune liver disease, autoimmunity and liver transplantation. *J Hepatol* 2014; **60**: 210-223 [PMID: 24084655 DOI: 10.1016/j.jhep.2013.09.020]

66 **Zeng J**, Huang ZP, Zheng J, Wu T, Zheng RQ. Non-invasive assessment of liver fibrosis using two-dimensional shear wave elastography in patients with autoimmune liver diseases. *World J Gastroenterol* 2017; **23**: 4839-4846 [PMID: 28765706 DOI: 10.3748/wjg.v23.i26.4839]

67 **Grgurević I**, Bokun T, Mustapić S, Trkulja V, Heinzl R, Banić M, Puljiz Ž, Lukšić B, Kujundžić M. Real-time two-dimensional shear wave ultrasound elastography of the liver is a reliable predictor of clinical outcomes and the presence of esophageal varices in patients with compensated liver cirrhosis. *Croat Med J* 2015; **56**: 470-481 [PMID: 26526884 DOI: 10.3325/cmj.2015.56.470]

68 **Marcellin P**, Gane E, Buti M, Afdhal N, Sievert W, Jacobson IM, Washington MK, Germanidis G, Flaherty JF, Aguilar Schall R, Bornstein JD, Kitrinos KM, Subramanian GM, McHutchison JG, Heathcote EJ. Regression of cirrhosis during treatment with tenofovir disoproxil fumarate for chronic hepatitis B: a 5-year open-label follow-up study. *Lancet* 2013; **381**: 468-475 [PMID: 23234725 DOI: 10.1016/S0140-6736(12)61425-1]

69 **Hartl J**, Denzer U, Ehlken H, Zenouzi R, Peiseler M, Sebode M, Hübener S, Pannicke N, Weiler-Normann C, Quaas A, Lohse AW, Schramm C. Transient elastography in autoimmune hepatitis: Timing determines the impact of inflammation and fibrosis. *J Hepatol* 2016; **65**: 769-775 [PMID: 27238753 DOI: 10.1016/j.jhep.2016.05.023]

70 **Papatheodoridis GV**, Idilman R, Dalekos GN, Buti M, Chi H, van Boemmel F, Calleja JL, Sypsa V, Goulis J, Manolakopoulos S, Loglio A, Siakavellas S, Keskın O, Gatselis N, Hansen BE, Lehretz M, de la Revilla J, Savvidou S, Kourikou A, Vlachogiannakos I, Galanis K, Yurdaydin C, Berg T, Colombo M, Esteban R, Janssen HLA, Lampertico P. The risk of hepatocellular carcinoma decreases after the first 5 years of entecavir or tenofovir in Caucasians with chronic hepatitis B. *Hepatology* 2017; **66**: 1444-1453 [PMID: 28622419 DOI: 10.1002/hep.29320]

71 **Cosgrove D**, Piscaglia F, Bamber J, Bojunga J, Correas JM, Gilja OH, Klauser AS, Sporea I, Calliada F, Cantisani V, D'Onofrio M, Drakonaki EE, Fink M, Friedrich-Rust M, Fromageau J, Havre RF, Jenssen C, Ohlinger R, Săftoiu A, Schaefer F, Dietrich CF; EFSUMB. EFSUMB guidelines and recommendations

on the clinical use of ultrasound elastography. Part 2: Clinical applications. *Ultraschall Med* 2013; **34**: 238-253 [PMID: 23605169 DOI: 10.1055/s-0033-1335375]
72 **Karlas T**, Pfrepper C, Wiegand J, Wittekind C, Neuschulz M, Mössner J, Berg T, Tröltzsch M, Keim V. Acoustic radiation force impulse imaging (ARFI) for non-invasive detection of liver fibrosis: examination standards and evaluation of interlobe differences in healthy subjects and chronic liver disease. *Scand J Gastroenterol* 2011; **46**: 1458-1467 [PMID: 21916815 DOI: 10.3109/00365521.2011.610004]
73 **Suh CH**, Kim SY, Kim KW, Lim YS, Lee SJ, Lee MG, Lee J, Lee SG, Yu E. Determination of normal hepatic elasticity by using real-time shear-wave elastography. *Radiology* 2014; **271**: 895-900 [PMID: 24555633 DOI: 10.1148/radiol.14131251]
74 **Mueller S**, Millonig G, Sarovska L, Friedrich S, Reimann FM, Pritsch M, Eisele S, Stickel F, Longerich T, Schirmacher P, Seitz HK. Increased liver stiffness in alcoholic liver disease: differentiating fibrosis from steatohepatitis. *World J Gastroenterol* 2010; **16**: 966-972 [PMID: 20180235 DOI: 10.3748/wjg.v16.i8.966]
75 **Millonig G**, Friedrich S, Adolf S, Fonouni H, Golriz M, Mehrabi A, Stiefel P, Pöschl G, Büchler MW, Seitz HK, Mueller S. Liver stiffness is directly influenced by central venous pressure. *J Hepatol* 2010; **52**: 206-210 [PMID: 20022130 DOI: 10.1016/j.jhep.2009.11.018]
76 **Millonig G**, Reimann FM, Friedrich S, Fonouni H, Mehrabi A, Büchler MW, Seitz HK, Mueller S. Extrahepatic cholestasis increases liver stiffness (FibroScan) irrespective of fibrosis. *Hepatology* 2008; **48**: 1718-1723 [PMID: 18836992 DOI: 10.1002/hep.22577]
77 **Arena U**, Vizzutti F, Corti G, Ambu S, Stasi C, Bresci S, Moscarella S, Boddi V, Petrarca A, Laffi G, Marra F, Pinzani M. Acute viral hepatitis increases liver stiffness values measured by transient elastography. *Hepatology* 2008; **47**: 380-384 [PMID: 18095306 DOI: 10.1002/hep.22007]
78 **Fraquelli M**, Rigamonti C, Casazza G, Donato MF, Ronchi G, Conte D, Rumi M, Lampertico P, Colombo M. Etiology-related determinants of liver stiffness values in chronic viral hepatitis B or C. *J Hepatol* 2011; **54**: 621-628 [PMID: 21146243 DOI: 10.1016/j.jhep.2010.07.017]
79 **Ferraioli G**, Tinelli C, Zicchetti M, Above E, Poma G, Di Gregorio M, Filice C. Reproducibility of real-time shear wave elastography in the evaluation of liver elasticity. *Eur J Radiol* 2012; **81**: 3102-3106 [PMID: 22749107 DOI: 10.1016/j.ejrad.2012.05.030]
80 **Zhuang Y**, Ding H, Zhang Y, Sun H, Xu C, Wang W. Two-dimensional Shear-Wave Elastography Performance in the Noninvasive Evaluation of Liver Fibrosis in Patients with Chronic Hepatitis B: Comparison with Serum Fibrosis Indexes. *Radiology* 2017; **283**: 873-882 [PMID: 27982760 DOI: 10.1148/radiol.2016160131]
81 **Piscaglia F**, Salvatore V, Mulazzani L, Cantisani V, Colecchia A, Di Donato R, Felicani C, Ferrarini A, Gamal N, Grasso V, Marasco G, Mazzotta E, Ravaioli F, Ruggieri G, Serio I, Sitouok Nkamgho JF, Serra C, Festi D, Schiavone C, Bolondi L. Differences in liver stiffness values obtained with new ultrasound elastography machines and Fibroscan: A comparative study. *Dig Liver Dis* 2017; **49**: 802-808 [PMID: 28365330 DOI: 10.1016/j.dld.2017.03.001]
82 **Sirli R**, Bota S, Sporea I, Jurchis A, Popescu A, Gradinaru-Tascău O, Szilaski M. Liver stiffness measurements by means of supersonic shear imaging in patients without known liver pathology. *Ultrasound Med Biol* 2013; **39**: 1362-1367 [PMID: 23743106 DOI: 10.1016/j.ultrasmedbio.2013.03.021]
83 **Hudson JM**, Milot L, Parry C, Williams R, Burns PN. Inter- and intra-operator reliability and repeatability of shear wave elastography in the liver: a study in healthy volunteers. *Ultrasound Med Biol* 2013; **39**: 950-955 [PMID: 23453379 DOI: 10.1016/j.ultrasmedbio.2012.12.011]
84 **Wang CZ**, Zheng J, Huang ZP, Xiao Y, Song D, Zeng J, Zheng HR, Zheng RQ. Influence of measurement depth on the stiffness assessment of healthy liver with real-time shear wave elastography. *Ultrasound Med Biol* 2014; **40**: 461-469 [PMID: 24361224 DOI: 10.1016/j.ultrasmedbio.2013.10.021]
85 **Huang Z**, Zheng J, Zeng J, Wang X, Wu T, Zheng R. Normal liver stiffness in healthy adults assessed by real-time shear wave elastography and factors that influence this method. *Ultrasound Med Biol* 2014; **40**: 2549-2555 [PMID: 25282481 DOI: 10.1016/j.ultrasmedbio.2014.05.008]
86 **Yoon JH**, Lee JM, Han JK, Choi BI. Shear wave elastography for liver stiffness measurement in clinical sonographic examinations: evaluation of intraobserver reproducibility, technical failure, and unreliable stiffness measurements. *J Ultrasound Med* 2014; **33**: 437-447 [PMID: 24567455 DOI: 10.7863/ultra.33.3.437]
87 **Franchi-Abella S**, Corno L, Gonzales E, Antoni G, Fabre M, Ducot B, Pariente D, Gennisson JL, Tanter M, Corréas JM. Feasibility and Diagnostic Accuracy of Supersonic Shear-Wave Elastography for the Assessment of Liver Stiffness and Liver Fibrosis in Children: A Pilot Study of 96 Patients. *Radiology* 2016; **278**: 554-562 [PMID: 26305193 DOI: 10.1148/radiol.2015142815]

P- Reviewer: Grgurevic I, Tahiri M, Tantau M **S- Editor**: Gong ZM
L- Editor: Filipodia **E- Editor**: Huang Y

World Journal of Gastroenterology

Submit a Manuscript: http://www.f6publishing.com

World J Gastroenterol 2018 March 7; 24(9): 971-981

DOI: 10.3748/wjg.v24.i9.971

ISSN 1007-9327 (print) ISSN 2219-2840 (online)

ORIGINAL ARTICLE

Basic Study

Can bacterial virulence factors predict antibiotic resistant *Helicobacter pylori* infection?

Denise E Brennan, Colin Dowd, Colm O'Morain, Deirdre McNamara, Sinéad M Smith

Denise E Brennan, Colin Dowd, Colm O'Morain, Deirdre McNamara, Sinéad M Smith, Department of Clinical Medicine, School of Medicine, Trinity College Dublin, Dublin D2, Ireland

ORCID number: Denise E Brennan (0000-0001-8200-3181); Colin Dowd (0000-0003-0608-0585); Colm O'Morain (0000-0002-1847-6782); Deirdre McNamara (0000-0003-2324-3382); Sinéad M Smith (0000-0003-3460-3590).

Author contributions: McNamara D and Smith SM contributed equally to the study; McNamara D and Smith SM designed the study and coordinated the research; Brennan DE, Dowd C and Smith SM performed experiments and analysed data; O'Morain C and McNamara D recruited patients; Brennan DE, McNamara D and Smith SM wrote the paper; all authors provided critical input into the final manuscript.

Supported by the Health Research Board (HRA-POR-2014-526).

Institutional review board statement: The study was reviewed and approved by the Adelaide and Meath Hospital Research Ethics Committee.

Conflict-of-interest statement: None to declare.

Data sharing statement: There is no additional data to share.

Manuscript source: Invited manuscript

Correspondence to: Sinéad M Smith, PhD, Ussher Assistant Professor in Applied and Translational Medicine, Rm 1.46, Department of Clinical Medicine, Trinity Centre, Adelaide and Meath Hospital, Tallaght, Dublin D24, Ireland. smithsi@tcd.ie
Telephone: +353-1-8963844
Fax: +353-1-8962988

Received: January 10, 2018
Peer-review started: January 10, 2018
First decision: January 18, 2018
Revised: February 5, 2018
Accepted: February 8, 2018
Article in press: February 8, 2018
Published online: March 7, 2018

Abstract

AIM

To evaluate the association between virulence factor status and antibiotic resistance in *Helicobacter pylori* (*H. pylori*)-infected patients in Ireland.

METHODS

DNA was extracted from antral and corpus biopsies obtained from 165 *H. pylori*-infected patients. Genotyping for clarithromycin and fluoroquinolone-mediating mutations was performed using the Genotype HelicoDR assay. *cagA* and *vacA* genotypes were investigated using PCR.

RESULTS

Primary, secondary and overall resistance rates for clarithromycin were 50.5% (*n* = 53/105), 78.3% (*n* = 47/60) and 60.6% (*n* = 100/165), respectively. Primary, secondary and overall resistance rates for fluoroquinolones were 15.2% (*n* = 16/105) and 28.3% (*n* = 17/60) and 20% (*n* = 33/165), respectively. Resistance to both antibiotics was 12.4% (*n* = 13/105) in treatment-naïve patients, 25% (*n* = 15/60) in those previously treated and 17% (*n* = 28/165) overall. A *cagA*-positive genotype was detected in 22.4% (*n* = 37/165) of patient samples. The dominant *vacA* genotype was S1/M2 at 44.8% (*n* = 74/165), followed by S2/M2 at 26.7% (*n* = 44/165), S1/M1 at 23.6% (*n*

= 39/165) and S2/M1 at 4.8% (*n* = 8/165). Primary clarithromycin resistance was significantly lower in *cagA*-positive strains than in *cagA*-negative strains [32% (*n* = 8/25) *vs* 56.3% (*n* = 45/80); *P* = 0.03]. Similarly, in patients infected with more virulent *H. pylori* strains bearing the *vacA* s1 genotype, primary clarithromycin resistance was significantly lower than in those infected with less virulent strains bearing the *vacA* s2 genotype, [41% (*n* = 32/78) *vs* 77.8% (*n* = 21/27); *P* = 0.0001]. No statistically significant association was found between primary fluoroquinolone resistance and virulence factor status.

CONCLUSION

Genotypic *H. pylori* clarithromycin resistance is high and *cagA*-negative strains are dominant in our population. Less virulent (*cagA*-negative and *vacA* S2-containing) strains of *H. pylori* are associated with primary clarithromycin resistance.

Key words: *Helicobacter pylori*; Antibiotic resistance; Fluoroquinolone; Clarithromycin; Virulence factor; VacA; CagA

Core tip: The management of *Helicobacter pylori* (*H. pylori*) infection is challenging, largely due to the emergence of antibiotic resistance. A greater understanding of local antibiotic resistance rates is important in determining the most appropriate treatment regimen in a given population. Furthermore, insight into the virulence of the infecting strains and the association between virulence and antibiotic resistance could potentially be an avenue to explore in the effort to improve eradication rates. This study provides and update on the prevalence of clarithromycin and fluoroquinolone resistance in Ireland and demonstrates that less virulent strains of *H. pylori* are predictive of primary clarithromycin resistance.

Brennan DE, Dowd C, O'Morain C, McNamara D, Smith SM. Can bacterial virulence factors predict antibiotic resistant *Helicobacter pylori* infection? *World J Gastroenterol* 2018; 24(9): 971-981 Available from: URL: http://www.wjgnet.com/1007-9327/full/v24/i9/971.htm DOI: http://dx.doi.org/10.3748/wjg.v24.i9.971

INTRODUCTION

Helicobacter pylori (*H. pylori*) infection causes acute and chronic gastritis, gastric and duodenal ulcers, and in rare cases gastric adenocarcinoma and MALT (mucosa-associated lymphoid tissue) lymphoma[1]. While its prevalence in the developed world has generally decreased, it is still high in indigenous populations and the developing world[2]. The Maastricht consensus recommends that all symptomatic *H. pylori*-infected adults are treated[1]. There are many different treatment options available, however the most common treatment for first-line eradication of *H. pylori* is triple therapy, which consists of two antibiotics (clarithromycin and amoxicillin) and a proton pump inhibitor, taken for 7-14 d. An efficacious therapy for *H. pylori* eradication is one that achieves an eradication rate of over 80%[1]. However, in many countries, the eradication rate for standard triple therapy has fallen below 80%. Indeed in a recent study in Ireland, the eradication rates of standard seven-day triple therapy were just 56.8% and 61% by intention-to-treat and per-protocol analysis, respectively[3]. There are several factors that impact the efficacy of treatment for *H. pylori*; high bacterial load, high gastric acidity and poor patient compliance. However, undoubtedly the most important is the rapid emergence of antimicrobial resistant strains of *H. pylori*, particularly to clarithromycin[4-6]. Resistance to clarithromycin can decrease the success rate of clarithromycin-based triple therapy by up to 70%[7]. One study found that the presence of clarithromycin resistant strains in a patient infected with *H. pylori* predicted treatment failure almost perfectly[8].

H. pylori is a highly heterogeneous bacterium and its virulence varies geographically. Virulence factors not only contribute to the pathogenicity of the bacteria but may play a role in determining treatment outcome[9]. The most commonly studied virulence factors in *H. pylori* are encoded by the cytotoxin associated gene A (*cagA*) and the vacuolating associated gene A (*vacA*). There are at least 4 variable regions in the *vacA* gene; in the signal (s) region, of which one of two alleles can be present: s1 or s2, and in the middle (m) region, of which one of two alleles can be present; m1 or m2[10]. These variable regions display different levels of toxicity to host cells, with *vacA* s1/m1 being most cytotoxic, followed by s1/m2. The s2/m2 genotype has been found to induce little or no toxicity[11]. A possible relationship between virulence factors and antimicrobial resistance has been suggested. A study conducted in 2009 in Ireland reported that the absence of *cagA* may be a risk factor for developing metronidazole resistance[12]. This study aimed to provide an update on the prevalence of virulence factor genotypes and antibiotic resistance in Irish *H. pylori* strains and assess the relationship between clarithromycin and fluoroquinolone resistance with virulence factor status.

MATERIALS AND METHODS

Study design and ethics

A prospective study was carried out in a tertiary referral teaching hospital (Adelaide and Meath Hospital, Dublin, Ireland) affiliated with Trinity College Dublin. Patients who had been referred to the endoscopy clinic were included from August 2014 until June 2017. The study received ethical approval from the Adelaide and Meath

Table 1 Polymerase chain reaction primers used in this study

Primer	Primer sequence	Gene	Product size (bp)
CAGA-F	5′-GATAACAGGCAAGCTTTTGATG-3′	*cagA*	349
CAGA-R	5′-CTGCAAAAGATTGTTTGGCAGA-3′		
VA1-F	5′- ATGGAAATACAACAACAAACACAC-3′	*vacA* signal region	259/286 (s1/s2)
VA1-R	5′ – CTGCTTGAATGCGCCAAAC-3′		
VAG-F	5′ – CAATCTGTCCAATCAAGCGAG-3′	*vacA* middle region	567/642 (m1/m2)
VAG-R	5′- GCTTCAAAATAATTCCAAGG-3′		

Hospital Research Ethics Committee. Informed consent was obtained from all patients before enrolment.

Study population

Inclusion criteria were (1) ability and willingness to participate in the study and to provide informed consent, and (2) confirmed *H. pylori* infection as indicated by a positive rapid urease test (TRI-MED Distributors, PTY LTD, Washington, United States) at 30 min and by histology.

Exclusion criteria were (1) age less than 18 years, (2) pregnancy or lactation, (3) severe inter-current illness, (4) current PPI use or recent antibiotic use (within 4 wk); and (5) bleeding problems or use of blood thinning drugs.

Sample collection

A single corpus and antrum biopsy from each patient were placed into collection tubes and stored at -20 ℃ until processed for genomic DNA isolation using the QIAamp DNA Mini Kit (Qiagen GmbH, Hilden, Germany) according to manufacturer's instructions. All isolated DNA was stored -20 ℃ until genotyping was performed.

Antimicrobial susceptibility genotyping

Genotyping for clarithromycin and fluoroquinolone-mediating mutations was performed using the Genotype HelicoDR assay (Hain Lifescience GmbH, Nehren, Germany) according to the manufacturer's instructions. Briefly, multiplex amplification of DNA regions of interest was performed using biotinylated primers supplied in the GenoType HelicoDR kit and the Hotstart Taq DNA polymerase kit (Qiagen). PCR products were reverse hybridised to DNA strips containing probes for gene regions of interest, developed and interpreted according to the manufacturers' instructions[13].

Virulence factor genotyping

To determine virulence factor genotype, PCR was performed as previously described by Taneike *et al*[12] using the primers described in Table 1. C*agA* and *vacA* genotypes were evaluated by performing gel electrophoresis on the PCR products using 1% agarose gel.

Statistical analysis

Statistical analysis was carried out using GraphPad Prism (GraphPad Software Inc., CA, United States). Continuous variables are presented as arithmetic mean and SD. *P* values for continuous variables were calculated and compared using the two-tailed independent *t*-test. *P* values for categorical variables were calculated using the Fisher's exact test/Pearson χ^2-test. In all cases, a *P* value less than 0.05 was considered significant.

RESULTS

Prevalence of genotypic antimicrobial resistance

Samples from a total of 165 *H. pylori*-infected patients were analysed in the study. Patient demographics and clinical characteristics are shown in Table 2. 63.6% (*n* = 105) of patients had not been treated for *H. pylori* infection previously, while 36.4% (*n* = 60) had undergone at least one eradication treatment regimen (Table 2).

Primary resistance rates for clarithromycin and fluoroquinolones were 50.5% (*n* = 53/105; Table 3) and 15.2% (*n* = 16/105; Table 4), respectively. In those previously treated for *H. pylori* infection, the resistance rates for both clarithromycin and fluoroquinolones were higher at 78.3% (*n* = 47/60; Table 3) and 28.3% (*n* = 17/60; Table 4), respectively. Overall resistance rates, regardless of treatment history, were 60.6% (*n* = 100/165; Table 3) and 20% (*n* = 33/165; Table 4) for clarithromycin and fluoroquinolones, respectively. Among patients infected with a clarithromycin-resistant strain, the most common point mutation was A2147G, at 78% (*n* = 78/100; Table 3). The most common point mutation conferring resistance to fluoroquinolones in resistant patients was *gyr*91 D91Y, at 54.5% (*n* = 18/33; Table 4).

Dual resistance rates for clarithromycin and fluoroquinolones were 12.4% (*n* = 13/105) in the treatment naïve, 25% (*n* = 15/60) in those previously treated and 17% (*n* = 28/165) in all patients included (Table 5). The overall rate of dual susceptibility among the patients was 36.4% (*n* = 60/165; Table 5). Dual susceptibility was significantly higher in treatment-naïve patients versus those previously treated (46.6%, *n* = 49/105 versus 18.3%, *n* = 11/60; $P < 0.05$; Fisher's exact test).

Distribution of H. pylori virulence-factor genotype

Table 6 illustrates the distribution of *H. pylori* virulence factor genotype in infected patients. Overall, 22.4% (*n*

Table 2 Demographic and clinical characteristics of *Helicobacter pylori*-infected patients included in the study

	Number of gastric biopsy specimens *n* (%)		
	All patients 165 (100)	Treatment Naïve 105 (63.6)	Previously treated 60 (36.4)
Gender			
Female	69 (41.8)	31 (29.5)	38 (63.3)
Male	96 (58.2)	74 (70.5)	22 (36.7)
Age			
mean ± SD	49.2 ± 15.8	50.3 ± 16.3	47.4 ± 14.7
Histology findings			
Chronic gastritis	130 (78.8)	78 (74.3)	52 (86.7)
Intestinal metaplasia	23 (13.9)	16 (15.2)	7 (11.7)
No data available	11 (6.7)	10 (9.5)	1 (1.7)
Normal mucosa	1 (0.6)	1 (1.0)	0 (0.0)
Endoscopic findings			
Gastritis	92 (55.8)	57 (54.3)	35 (58.3)
Normal	32 (19.4)	19 (18.1)	13 (21.7)
Gastric/duodenal ulcer	21 (12.7)	15 (14.3)	6 (10.0)
No data available	17 (10.3)	11 (10.5)	6 (10.0)
Atrophic mucosa	1 (0.6)	1 (1.0)	0 (0.0)
Other[1]	2 (1.2)	2 (1.9)	0 (0.0)

[1]Other endoscopic findings: 1 intestinal metaplasia and erosion: 1 portal hypertensive gastropathy.

Table 3 Clarithromycin resistance rates and the distribution of resistance-mediating mutations

Genotype	Number of gastric biopsy specimens *n* (%)			*P* value[1]
	All patients 165 (100)	Treatment Naïve 105 (63.6)	Previously treated 60 (36.4)	
Clarithromycin^S (WT)	65 (39.4)	52 (49.5)	13 (21.7)	< 0.001
Clarithromycin^R	100 (60.6)	53 (50.5)	47 (78.3)	
Point mutations				
A2147G	78 (78)	44 (83)	34 (72.3)	NS
A2146G	8 (8)	3 (5.7)	5 (10.6)	NS
A2146C	6 (6)	3 (5.7)	3 (6.4)	NS
A2146C + A2147G	5 (5)	3 (5.7)	2 (4.3)	NS
A2146G + A2147G	2 (2)	0 (0)	2 (4.3)	NS
A2146G + A2146C	1 (1)	0 (0)	1 (2.1)	NS

[1]Treatment-naïve versus previously treated patients (Fisher's exact test). Clarithromycin^S: Sensitive to clarithromycin; Clarithromycin^R: Resistant to clarithromycin.

= 37/165) of patients were infected with strains that were *cagA* positive and 77.6% (*n* = 128/165) that were *cagA* negative. The most prevalent *vacA* allele was S1/M2 at 44.8% (*n* = 74/165), followed by S2/M2, S1/M1 and S2/M1 at 26.7% (*n* = 44/165), 23.6% (*n* = 39/165) and 4.8% (*n* = 8/165), respectively (Table 6). Interestingly, the frequency of the *vacA* S1 genotype (the more virulent S region genotype) was significantly lower in those previously treated than the treatment-naïve group [58.3% (*n* = 35/60) *vs* 74.3% (*n* = 78/105) respectively; *P* < 0.05; Fisher's exact test]. Additionally, the frequency of the S2/M2 genotype (the least virulent genotype) was significantly higher in those patients who have been treated previously [36.7% (*n* = 22/60) *vs* 21% (*n* = 22/105) respectively; *P* < 0.05; Fisher's exact test; Table 6].

Less virulent strains of H. pylori are associated with primary clarithromycin resistance

Next, the relationship between antibiotic resistance and virulence factor genotype was assessed. Analysis of all recruited patients revealed that genotypic resistance to clarithromycin was significantly lower in *cagA*-positive strains than in *cagA*-negative strains [40.5% (*n* = 15/37) *vs* 66.4% (*n* = 85/128); χ^2 = 8.04; *P* = 0.004; Pearson χ^2 test; Figure 1A]. When patients were sub-grouped into treatment-naïve (Figure 1B) and those previously treated (Figure 1C), clarithromycin resistance was also lower in *cagA*-positive strains compared to *cagA*-negative strains, although this only reached statistical significance in the treatment-naïve cohort [32% (*n* = 8/25) *vs* 56.3% (*n* = 45/80); χ^2 = 4.5; *P* = 0.03; Pearson χ^2 test; Figure 1B]. Similarly, in patients infected with more virulent *H. pylori* strains bearing the *vacA* s1 genotype, clarithromycin resistance was significantly lower than in those infected with less virulent strains bearing the *vacA* s2 genotype, when all patients were included [52.2% (*n* = 59/113) *vs* 78.8% (*n* = 41/52); χ^2 = 10.6; *P* = 0.001; Pearson χ^2 test; Figure 2A] and in those that were treatment-naïve [41% (*n* = 32/78) *vs* 77.8% (*n* = 21/27); χ^2 = 10.8; *P* = 0.0001; Pearson χ^2 test; Figure 2B], but not in patients that were previously treated (Figure 2C).

Table 4 Fluoroquinolone resistance rates and the distribution of resistance-mediating mutations

Genotype	Number of gastric biopsy specimens *n* (%)			*P* value[1]
	All patients 165 (100)	Treatment Naïve 105 (63.6)	Previously treated 60 (36.4)	
Fluoroquinolone^{S} (WT)	132 (80.0)	89 (84.8)	43 (71.7)	
Fluoroquinolone^{R}	33 (20.0)	16 (15.2)	17 (28.3)	NS
Point mutations				
*gyr*91 D91Y	18 (54.5)	10 (62.5)	8 (47.1)	NS
*gyr*91 D91N	6 (18.2)	2 (12.5)	4 (23.5)	NS
*gyr*91 D91G	2 (6.1)	0 (0.0)	2 (11.8)	NS
*gyr*91 D91N + *gyr*91 D91G	2 (6.1)	1 (6.3)	1 (5.9)	NS
*gyr*91 D91N +*gyr*91 D91Y	2 (6.1)	1 (6.3)	1 (5.9)	NS
*gyr*87 N87K	1 (3.0)	1 (6.3)	0 (0.0)	NS
*gyr*87 N87K + *gyr*91 D91N + *gyr*91 D91G	1 (3.0)	0 (0.0)	1 (5.9)	NS
*gyr*87 N87K + *gyr*91 D91N + *gyr*91 D91G + *gyr*91 D91Y	1 (3.0)	1 (6.3)	0 (0.0)	NS

[1]Treatment-naïve versus previously treated patients (Fisher's exact test). Fluoroquinolone^{S}: Sensitive to fluoroquinolones; Fluoroquinolone^{R}: Resistant to fluoroquinolones.

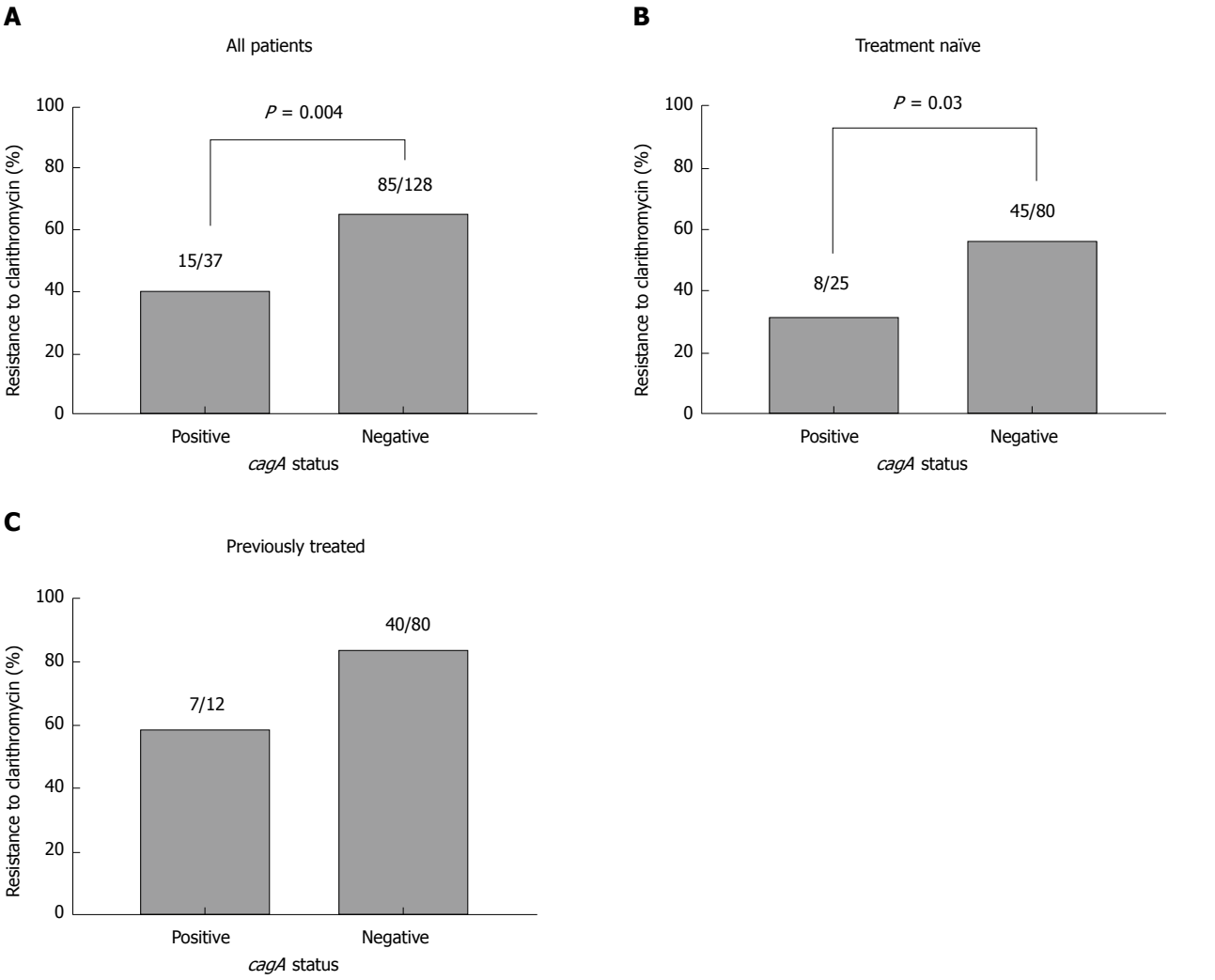

Figure 1 Prevalence of clarithromycin-resistance according to *cagA* genotype. A: All patients; B: Treatment naïve patients; C: Previously treated patients.

The frequency of resistance to fluoroquinolones in each virulence factor genotype was also examined. *CagA* status was not significantly associated with fluoroquinolone resistance when all patients were analysed (Figure 3A) or when the patients were sub-divided into those with primary infections (Figure 3B) and those previously treated (Figure 3C). While there was a significant association between the less virulent *vacA* s2 genotype and fluoroquinolone resistance when all patients were included [15% (*n* = 17/113) *vs* 30.8% (*n* = 16/52); χ^2 = 5.5; *P* = 0.02; Pearson χ^2 test; Figure 4A], this did not reach statistical

Table 5 Antimicrobial susceptibility results for both clarithromycin and fluoroquinolone

Genotype	Number of gastric biopsy specimens *n* (%)			*P* value[1]
	All patients 165 (100)	Treatment Naïve 105 (63.6)	Previously treated 60 (36.4)	
Susceptible (to both)	60 (36.4)	49 (46.6)	11 (18.3)	< 0.05
Resistant (to at least one)	105 (63.6)	56 (53.3)	49 (81.6)	
Susceptible/resistant to one	137 (83.0)	92 (87.6)	45 (75.0)	
Resistant to both	28 (17.0)	13 (12.4)	15 (25.0)	0.05

[1]Treatment-naïve versus previously treated patients (Fisher's exact test).

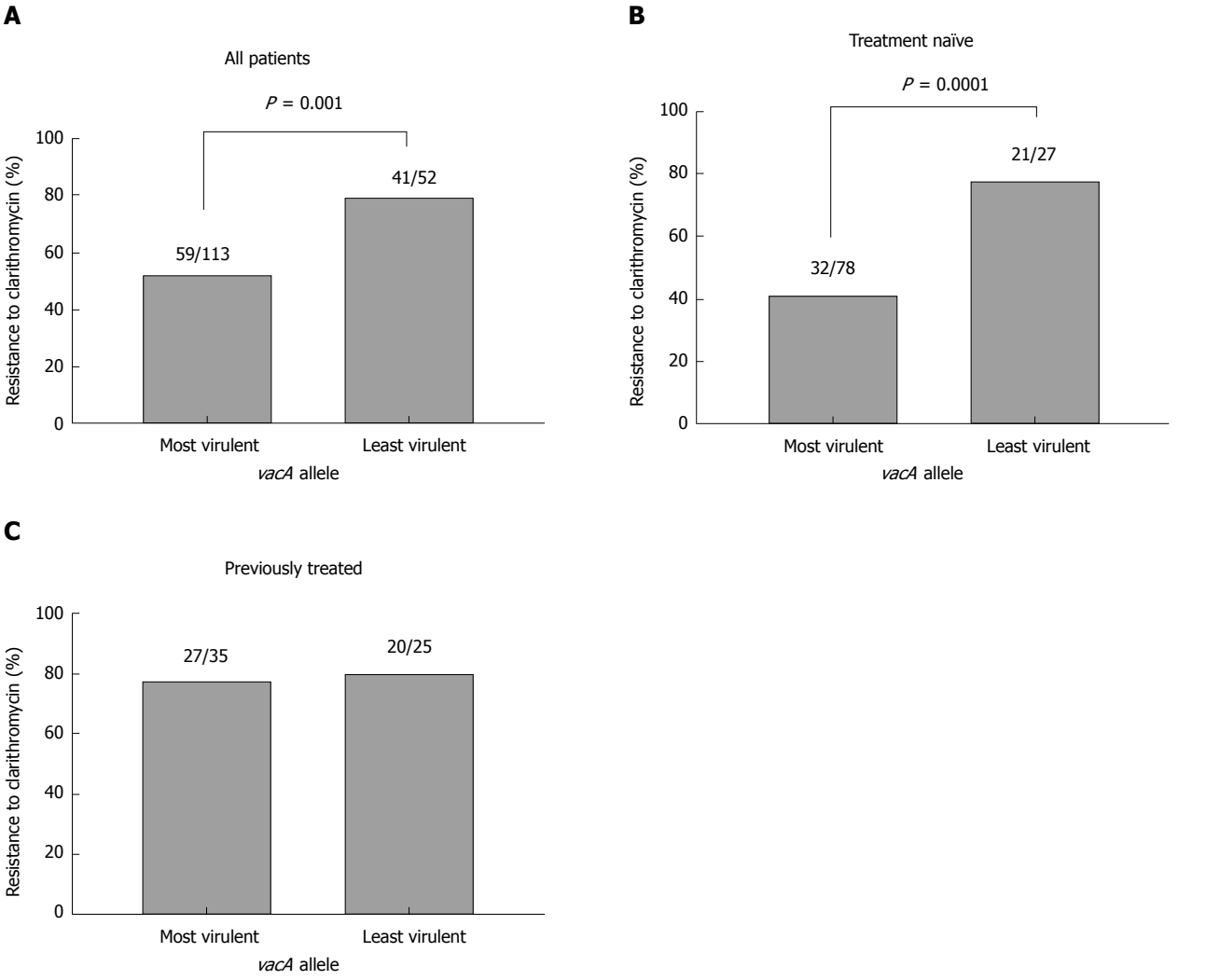

Figure 2 Prevalence of clarithromycin resistance according to *vacA* genotype. A: All patients; B: Treatment naïve patients; C: Previously treated patients. Most virulent: S1/M1, S1/M2; Least virulent: S2/M1; S2/M2.

significance in treatment naïve patients (Figure 4B) or those previously treated (Figure 4C).

Taken together, these findings indicate that the absence of *cagA* and the less virulent *vacA* genotypes (S2/M1 and S2/M2) may be predictors of primary clarithromycin resistance in treatment-naïve patients.

DISCUSSION

This study aimed to provide an update on the prevalence of antibiotic resistance and distribution of virulence factor genotypes in *H. pylori* strains in Ireland. In addition we investigated whether virulence factor genotypes are associated with antibiotic susceptibility. Primary clarithromycin resistance among our patients was high at 50.5% and even higher in those previously treated at 78%. Among patients infected with a resistant strain, the most common point mutation conferring clarithromycin resistance was A2147G, in keeping with other studies[14-19]. Our primary clarithromycin resistance rate is high compared to rates reported in Europe, Asia Pacific and other countries[5,19-21]. Variations

Table 6 Distribution of *Helicobacter pylori* virulence-factor genotypes among infected patients in Ireland *n* (%)

Genotype	Overall (*n* = 165)	Treatment naïve (*n* = 105)	Previous treatment (*n* = 60)	*P* value[1]
cagA status				
Positive	37 (22.4)	25 (23.8)	12 (20)	NS
Negative	128 (77.6)	80 (76.2)	48 (80)	
vacA allele				
S1	113 (68.5)	78 (74.3)	35 (58.3)	
S2	52 (31.5)	27 (25.7)	25 (41.7)	< 0.05
M1	47 (28.5)	31 (29.5)	16 (26.7)	
M2	118 (71.5)	74 (70.5)	44 (73.3)	NS
S1/M1	39 (23.6)	26 (24.8)	13 (21.7)	NS
S1/M2	74 (44.8)	52 (49.5)	22 (36.7)	NS
S2/M1	8 (4.8)	5 (4.8)	3 (5.0)	NS
S2/M2	44 (26.7)	22 (21.0)	22 (36.7)	< 0.05

[1]Treatment-naïve versus previously treated patients (Fisher's exact test).

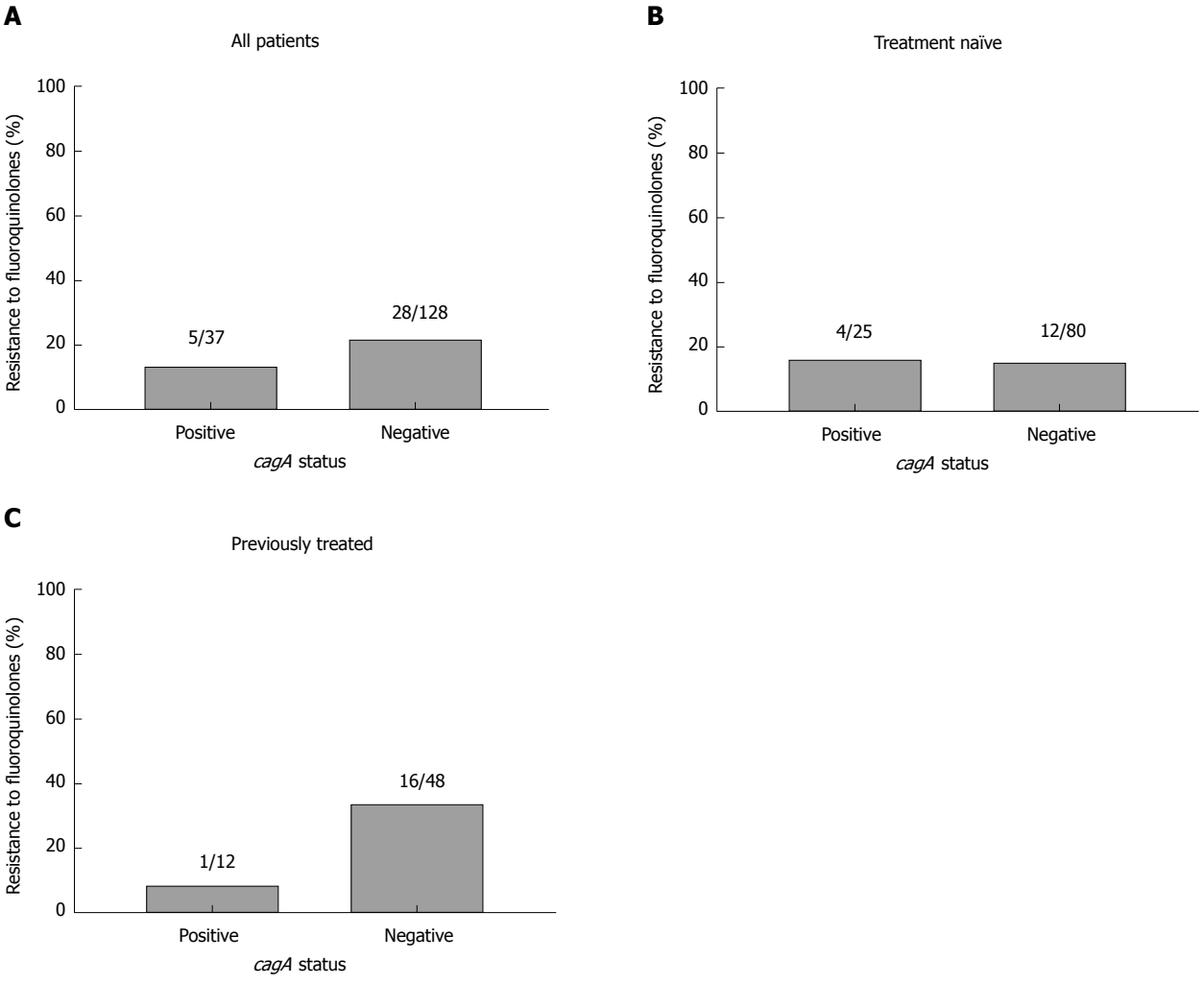

Figure 3 Prevalence of fluoroquinolone-resistance according to *cagA* genotype. A: All patients; B: Treatment naïve patients; C: Previously treated patients.

in *H. pylori* antibiotic resistance rates among different populations are influenced by previous antibiotic use, with studies demonstrating that previous exposure to macrolides increases the risk of clarithromycin resistant *H. pylori* infection[5,22]. The sharp increase in primary clarithromycin resistance from 3.9% in 1997 to 9.3% in 2008[23], to the current rate of 50.5% in 2017 is a cause for concern and is reflected in the poor eradication rate (56.8% ITT) for 7 days clarithromycin-based triple therapy recently reported from our centre[3]. In an effort to address increasing antibiotic resistance and falling eradication rates, the Irish *H. pylori* Working Group

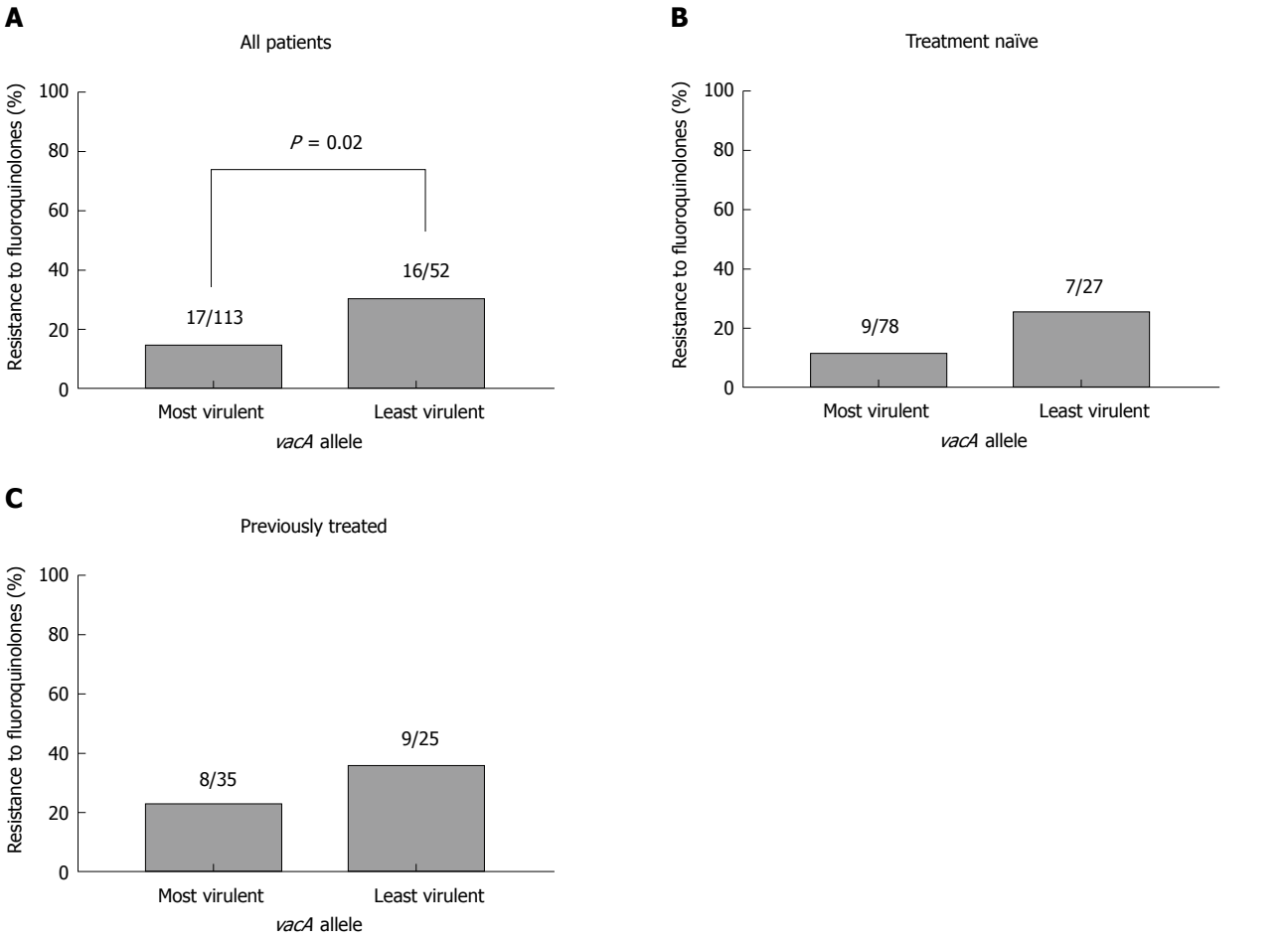

Figure 4 Prevalence of fluoroquinolone-resistance according to *vacA* genotype. A: All patients; B: Treatment naïve patients; C: Previously treated patients. Most virulent: S1/M1, S1/M2; Least virulent: S2/M1; S2/M2.

have recently highlighted the need for more widespread antibiotic resistance surveillance and extended *H. pylori* treatment durations[24]. It should be noted that antibiotic resistance was determined at the genetic level in the current study compared to culture and Etests in the earlier Irish surveys.

The primary and secondary rates of fluoroquinolone resistance were 15.2% and 28.3%, respectively. The primary rate of levofloxacin resistance has only risen slightly since the last Irish survey in 2008-2009, which reported a rate of 12%[25], and is in keeping with the 14.1% rate reported in Europe[5]. The most common point mutation conferring resistance to fluoroquinolones in our patients was *gyr91* D91Y. This contrasts with other studies in which *gyr91* D91N and *gyr87* N87K mutations were reported with highest frequency[14,16-18].

In our cohort, the overall frequency of *H. pylori* infections with strains containing the *cagA* gene was 22.4%. This has decreased since the distribution of the *cagA* genotype was last investigated in Ireland in 2009, with a frequency of 68% reported[12]. It is also lower than distributions reported in Cuba and Iran[26,27]. There is a well-known association between *cagA*-positive strains of *H. pylori* and peptic ulcer disease[28,29]. This relatively low frequency of *cagA*-positive genotype is not surprising given that the prevalence of peptic ulcer disease was also low in our cohort at 12.7% (Table 2), which is a decrease on the prevalence of peptic ulcer disease reported in the previous Irish study (17%[12]). The most prevalent *vacA* genotype in our cohort was S1/M2, followed by S2/M2, S1/M1 and S2/M1. This pattern is similar to the pattern reported in Ireland in 2009 as well as the studies mentioned above[12,26,27].

Interestingly, the frequency of the more virulent S1 genotype was significantly lower in those previously treated than the treatment-naïve group (58.3% *vs* 74.3%). Additionally, the frequency of the least virulent S2/M2 genotype was significantly higher in those previously treated previously (36.7% *vs* 21%). This is in accordance with a hypothesis described previously which suggests that more virulent strains elicit a stronger inflammatory response, enabling increased blood flow to the site of infection, therefore enhancing delivery of antibiotics and the potential for successful eradication[30]. Another potential explanation is that a more virulent strain of *H. pylori* may replicate faster and is therefore more susceptible to antibiotics, whose mechanisms of action are to inhibit bacterial replication[31].

We found an inverse relationship between the

virulence of the infecting strain and the presence of clarithromycin resistance: the absence of *cagA,* and the less virulent *vacA* genotypes (S2/M1 and S2/M2), may be indicators of clarithromycin resistance, in particular in treatment-naïve patients. The association between virulence factors and antibiotic resistance in *H. pylori* has been evaluated in other studies, with controversial results. Absence of *cagA* was found to be a risk factor for metronidazole resistance[12] and other studies have found an association between clarithromycin resistance mutations and the less virulent *vacA* genotypes[32,33]. Another report revealed that *cagE* and *vacA* S1 correlated with clarithromycin and metronidazole resistance[34], while others found that neither *cagA* nor *vacA* was associated with resistance[29,35-37]. There may be no direct causation involving the presence of less virulent strains of *H. pylori* and antibiotic resistance. Rather, the presence or absence of virulence factors may cause physiological effects which create an environment in which antibiotic resistant strains of *H. pylori* can flourish as outlined above[31]. As less virulent strains are less immunogenic, an inadequate delivery of antibiotics may reach infected areas in the stomach and as a result, antimicrobial resistant strains may be selected for in the population of less virulent strains. It has been shown that a *cagA*- strain may tend to acquire drug resistance *in vitro*[12]. Indeed, studies have shown that virulence factor genotype may also influence treatment outcome. A number of studies have reported the presence or absence of *cagA* and *vacA* as predictors of eradication of *H. pylori*[36,38-40]. Wang *et al*[39] conducted a meta-analysis of 25 studies and found that infection with *cagA* positive, *vacA* S1 strains were associated with *H. pylori* eradication.

In conclusion, this study found that the *cagA* negative and *vacA* S1/M2 genotypes were the most dominant in *H. pylori* strains in Ireland. A surprisingly high rate of primary genotypic clarithromycin resistance was observed (50.5%), with a primary genotypic fluoroquinolone resistance rate of 15.2%. It was also found that there is a relationship between the less virulent strains of *H. pylori* (*cagA*-negative and *vacA* S2) and primary clarithromycin resistance. It is well known that the prevalence of antibiotic resistance is increasing worldwide while eradication rates of *H. pylori* are decreasing. The relationship between less virulent strains of *H. pylori* and presence of antibiotic resistance found herein could potentially be an avenue to explore in the effort to improve eradication rates.

ARTICLE HIGHLIGHTS

Research background

Helicobacter pylori (H. pylori) causes chronic gastritis, gastric and duodenal ulcers, gastric adenocarcinoma and mucosa-associated lymphoid tissue lymphoma. Disease outcome is related to both host and bacterial factors. Eradication is recommended in all symptomatic patients and those at risk of gastric cancer. However, eradication rates for current therapies are falling due to the emergence of antibiotic resistant *H. pylori* strains. *H. pylori* is a highly heterogeneous bacterium and its virulence varies geographically. Virulence factors contribute to the pathogenicity of the bacteria and have been suggested to influence treatment outcome.

Research motivation

In response to the increasing problem of *H. pylori* antibiotic resistance, local antibiotic resistance surveillance is recommended to guide clinicians in their choice of *H. pylori* therapy. Knowledge of local antimicrobial resistance rates and the prevalence of virulent infections will influence strategies for optimising the management of *H. pylori* infection.

Research objectives

This study aimed to provide an update on the prevalence of antibiotic resistance in Ireland, in particular for the antibiotics clarithromycin and fluoroquinolones. The virulence of the infecting strains was assessed by investigating *cagA* and *vacA* status. In addition the relationship between virulence factor status and antibiotic resistance was evaluated.

Research methods

DNA was extracted from antral and corpus biopsies obtained from *H. pylori*-infected patients. Genotyping for clarithromycin and fluoroquinolone-mediating mutations was performed using the Genotype HelicoDR assay. *CagA* and *vacA* genotypes were investigated using PCR and agarose gel electrophoresis.

Research results

Primary resistance to clarithromycin was high at 50.5%. Primary resistance to fluoroquinolones was 15.2%. Primary resistance to both antibiotics was 12.4%. A *cagA*-positive genotype was detected in 22.4% of patient samples. The dominant *vacA* genotype was S1/M2 at 44.8%, followed by S2/M2 at 26.7%, S1/M1 at 23.6% and S2/M1 at 4.8%. Primary clarithromycin resistance was significantly lower in *cagA*-positive strains than in *cagA*-negative strains (32% *vs* 56.3%). Similarly, in patients infected with more virulent *H. pylori* strains bearing the *vacA* s1 genotype, primary clarithromycin resistance was significantly lower than in those infected with less virulent strains bearing the *vacA* s2 genotype, (41% *vs* 77.8%). In summary, genotypic *H. pylori* clarithromycin resistance is high and *cagA*-negative strains are dominant in our population. Less virulent (*cagA*-negative and *vacA* S2-containing) strains of *H. pylori* are associated with primary clarithromycin resistance.

Research perspectives

Given the high rate of primary clarithromycin resistance detected in our study, the use of alternatives to clarithromycin-based triple therapy should be considered for first line *H. pylori* treatment in our cohort. In order to validate the association between less virulent strains and clarithromycin resistance, the influence of virulence factor genotype on treatment outcome should be assessed.

ACKNOWLEDGMENTS

The authors would like to acknowledge Mark Feighery, Ciara Treacy and Edwin Fahy for technical assistance.

REFERENCES

1 **Malfertheiner P**, Megraud F, O'Morain CA, Gisbert JP, Kuipers EJ, Axon AT, Bazzoli F, Gasbarrini A, Atherton J, Graham DY, Hunt R, Moayyedi P, Rokkas T, Rugge M, Selgrad M, Suerbaum S, Sugano K, El-Omar EM; European Helicobacter and Microbiota Study Group and Consensus panel. Management of Helicobacter pylori infection-the Maastricht V/Florence Consensus Report. *Gut* 2017; **66**: 6-30 [PMID: 27707777 DOI: 10.1136/gutjnl-2016-312288]

2 **Leja M**, Axon A, Brenner H. Epidemiology of Helicobacter pylori infection. *Helicobacter* 2016; **21** Suppl 1: 3-7 [PMID: 27531531 DOI: 10.1111/hel.12332]

3 **Haider RB**, Brennan DE, Omorogbe J, Holleran G, Hall B, O'Morain C, Breslin N, O'Connor HJ, Smith SM, McNamara

D. A randomized-controlled study to compare the efficacy of sequential therapy with standard triple therapy for Helicobacter pylori eradication in an Irish population. *Eur J Gastroenterol Hepatol* 2015; **27**: 1265-1269 [PMID: 26287955 DOI: 10.1097/MEG.0000000000000457]

4 **Graham DY**, Fischbach L. Helicobacter pylori treatment in the era of increasing antibiotic resistance. *Gut* 2010; **59**: 1143-1153 [PMID: 20525969 DOI: 10.1136/gut.2009.192757]

5 **Megraud F**, Coenen S, Versporten A, Kist M, Lopez-Brea M, Hirschl AM, Andersen LP, Goossens H, Glupczynski Y; Study Group participants. Helicobacter pylori resistance to antibiotics in Europe and its relationship to antibiotic consumption. *Gut* 2013; **62**: 34-42 [PMID: 22580412 DOI: 10.1136/gutjnl-2012-302254]

6 **Smith SM**, O'Morain C, McNamara D. Antimicrobial susceptibility testing for Helicobacter pylori in times of increasing antibiotic resistance. *World J Gastroenterol* 2014; **20**: 9912-9921 [PMID: 25110421 DOI: 10.3748/wjg.v20.i29.9912]

7 **Fischbach L**, Evans EL. Meta-analysis: the effect of antibiotic resistance status on the efficacy of triple and quadruple first-line therapies for Helicobacter pylori. *Aliment Pharmacol Ther* 2007; **26**: 343-357 [PMID: 17635369 DOI: 10.1111/j.1365-2036.2007.03386.x]

8 **Broutet N**, Tchamgoué S, Pereira E, Lamouliatte H, Salamon R, Mégraud F. Risk factors for failure of Helicobacter pylori therapy--results of an individual data analysis of 2751 patients. *Aliment Pharmacol Ther* 2003; **17**: 99-109 [PMID: 12492738 DOI: 10.1046/j.1365-2036.2003.01396.x]

9 **Uotani T**, Miftahussurur M, Yamaoka Y. Effect of bacterial and host factors on Helicobacter pylori eradication therapy. *Expert Opin Ther Targets* 2015; **19**: 1637-1650 [PMID: 26245678 DOI: 10.1517/14728222.2015.1073261]

10 **Atherton JC**, Cao P, Peek RM Jr, Tummuru MK, Blaser MJ, Cover TL. Mosaicism in vacuolating cytotoxin alleles of Helicobacter pylori. Association of specific vacA types with cytotoxin production and peptic ulceration. *J Biol Chem* 1995; **270**: 17771-17777 [PMID: 7629077 DOI: 10.1074/jbc.270.30.17771]

11 **Rhead JL**, Letley DP, Mohammadi M, Hussein N, Mohagheghi MA, Eshagh Hosseini M, Atherton JC. A new Helicobacter pylori vacuolating cytotoxin determinant, the intermediate region, is associated with gastric cancer. *Gastroenterology* 2007; **133**: 926-936 [PMID: 17854597 DOI: 10.1053/j.gastro.2007.06.056]

12 **Taneike I**, Nami A, O'Connor A, Fitzgerald N, Murphy P, Qasim A, O'Connor H, O'Morain C. Analysis of drug resistance and virulence-factor genotype of Irish Helicobacter pylori strains: is there any relationship between resistance to metronidazole and cagA status? *Aliment Pharmacol Ther* 2009; **30**: 784-790 [PMID: 19604178 DOI: 10.1111/j.1365-2036.2009.04095.x]

13 **Brennan DE**, Omorogbe J, Hussey M, Tighe D, Holleran G, O'Morain C, Smith SM, McNamara D. Molecular detection of Helicobacter pylori antibiotic resistance in stool vs biopsy samples. *World J Gastroenterol* 2016; **22**: 9214-9221 [PMID: 27895408 DOI: 10.3748/wjg.v22.i41.9214]

14 **Pastukh N**, Binyamin D, On A, Paritsky M, Peretz A. GenoType ® HelicoDR test in comparison with histology and culture for Helicobacter pylori detection and identification of resistance mutations to clarithromycin and fluoroquinolones. *Helicobacter* 2017; **22** [PMID: 29058343 DOI: 10.1111/hel.12447]

15 **Cambau E**, Allerheiligen V, Coulon C, Corbel C, Lascols C, Deforges L, Soussy CJ, Delchier JC, Megraud F. Evaluation of a new test, genotype HelicoDR, for molecular detection of antibiotic resistance in Helicobacter pylori. *J Clin Microbiol* 2009; **47**: 3600-3607 [PMID: 19759218 DOI: 10.1128/JCM.00744-09]

16 **Lee JW**, Kim N, Nam RH, Park JH, Choi YJ, Kim JM, Kim JS, Jung HC. GenoType HelicoDR test in the determination of antimicrobial resistance of Helicobacter pylori in Korea. *Scand J Gastroenterol* 2014; **49**: 1058-1067 [PMID: 24957849 DOI: 10.3109/00365521.2014.894117]

17 **Miendje Deyi VY**, Burette A, Bentatou Z, Maaroufi Y, Bontems P, Lepage P, Reynders M. Practical use of GenoType® HelicoDR, a molecular test for Helicobacter pylori detection and susceptibility testing. *Diagn Microbiol Infect Dis* 2011; **70**: 557-560 [PMID: 21696906 DOI: 10.1016/j.diagmicrobio.2011.05.002]

18 **Sanches BS**, Martins GM, Lima K, Cota B, Moretzsohn LD, Ribeiro LT, Breyer HP, Maguilnik I, Maia AB, Rezende-Filho J, Meira AC, Pinto H, Alves E, Mascarenhas R, Passos R, de Souza JD, Trindade OR, Coelho LG. Detection of Helicobacter pylori resistance to clarithromycin and fluoroquinolones in Brazil: A national survey. *World J Gastroenterol* 2016; **22**: 7587-7594 [PMID: 27672279 DOI: 10.3748/wjg.v22.i33.7587]

19 **Tanih NF**, Ndip RN. Molecular Detection of Antibiotic Resistance in South African Isolates of Helicobacter pylori. *Gastroenterol Res Pract* 2013; **2013**: 259457 [PMID: 23710166 DOI: 10.1155/2013/259457]

20 **Macías-García F**, Llovo-Taboada J, Díaz-López M, Bastón-Rey I, Domínguez-Muñoz JE. High primary antibiotic resistance of Helicobacter Pylori strains isolated from dyspeptic patients: A prevalence cross-sectional study in Spain. *Helicobacter* 2017; **22** [PMID: 28913872 DOI: 10.1111/hel.12440]

21 **Kuo YT**, Liou JM, El-Omar EM, Wu JY, Leow AHR, Goh KL, Das R, Lu H, Lin JT, Tu YK, Yamaoka Y, Wu MS; Asian Pacific Alliance on Helicobacter and Microbiota. Primary antibiotic resistance in Helicobacter pylori in the Asia-Pacific region: a systematic review and meta-analysis. *Lancet Gastroenterol Hepatol* 2017; **2**: 707-715 [PMID: 28781119 DOI: 10.1016/S2468-1253(17)30219-4]

22 **McNulty CA**, Lasseter G, Shaw I, Nichols T, D'Arcy S, Lawson AJ, Glocker E. Is Helicobacter pylori antibiotic resistance surveillance needed and how can it be delivered? *Aliment Pharmacol Ther* 2012; **35**: 1221-1230 [PMID: 22469191 DOI: 10.1111/j.1365-2036.2012.05083.x]

23 **O'Connor A**, Taneike I, Nami A, Fitzgerald N, Murphy P, Ryan B, O'Connor H, Qasim A, Breslin N, O'Moráin C. Helicobacter pylori resistance to metronidazole and clarithromycin in Ireland. *Eur J Gastroenterol Hepatol* 2010; **22**: 1123-1127 [PMID: 20354442 DOI: 10.1097/MEG.0b013e328338e43d]

24 **Smith S**, Boyle B, Brennan D, Buckley M, Crotty P, Doyle M, Farrell R, Hussey M, Kevans D, Malfertheiner P, Megraud F, Nugent S, O'Connor A, O'Morain C, Weston S, McNamara D. The Irish Helicobacter pylori Working Group consensus for the diagnosis and treatment of H. pylori infection in adult patients in Ireland. *Eur J Gastroenterol Hepatol* 2017; **29**: 552-559 [PMID: 28350745 DOI: 10.1097/MEG.0000000000000822]

25 **O'Connor A**, Taneike I, Nami A, Fitzgerald N, Ryan B, Breslin N, O'Connor H, McNamara D, Murphy P, O'Morain C. Helicobacter pylori resistance rates for levofloxacin, tetracycline and rifabutin among Irish isolates at a reference centre. *Ir J Med Sci* 2013; **182**: 693-695 [PMID: 23625165 DOI: 10.1007/s11845-013-0957-3]

26 **Feliciano O**, Gutierrez O, Valdés L, Fragoso T, Calderin AM, Valdes AE, Llanes R. Prevalence of Helicobacter pylori vacA, cagA, and iceA Genotypes in Cuban Patients with Upper Gastrointestinal Diseases. *Biomed Res Int* 2015; **2015**: 753710 [PMID: 25945344 DOI: 10.1155/2015/753710]

27 **Pajavand H**, Alvandi A, Mohajeri P, Bakhtyari S, Bashiri H, Kalali B, Gerhard M, Najafi F, Abiri R. High Frequency of vacA s1m2 Genotypes Among Helicobacter pylori Isolates From Patients With Gastroduodenal Disorders in Kermanshah, Iran. *Jundishapur J Microbiol* 2015; **8**: e25425 [PMID: 26862378 DOI: 10.5812/jjm.25425]

28 **van Doorn LJ**, Schneeberger PM, Nouhan N, Plaisier AP, Quint WG, de Boer WA. Importance of Helicobacter pylori cagA and vacA status for the efficacy of antibiotic treatment. *Gut* 2000; **46**: 321-326 [PMID: 10673291 DOI: 10.1136/gut.46.3.321]

29 **Godoy AP**, Ribeiro ML, Benvengo YH, Vitiello L, Miranda Mde C, Mendonça S, Pedrazzoli J Jr. Analysis of antimicrobial susceptibility and virulence factors in Helicobacter pylori clinical isolates. *BMC Gastroenterol* 2003; **3**: 20 [PMID: 12911839 DOI: 10.1186/1471-230X-3-20]

30 **Khan A**, Farooqui A, Manzoor H, Akhtar SS, Quraishy MS, Kazmi SU. Antibiotic resistance and cagA gene correlation: a looming crisis of Helicobacter pylori. *World J Gastroenterol* 2012; **18**: 2245-2252 [PMID: 22611319 DOI: 10.3748/wjg.v18.i18.2245]

31 **Sugimoto M**, Yamaoka Y. Virulence factor genotypes of Helicobacter pylori affect cure rates of eradication therapy. *Arch Immunol Ther Exp* (Warsz) 2009; **57**: 45-56 [PMID: 19219527 DOI: 10.1007/s00005-009-0007-z]

32 **Boyanova L**, Markovska R, Yordanov D, Gergova G, Mitov I. Clarithromycin Resistance Mutations in Helicobacter pylori in Association with Virulence Factors and Antibiotic Susceptibility of the Strains. *Microb Drug Resist* 2016; **22**: 227-232 [PMID: 26618567 DOI: 10.1089/mdr.2015.0199]

33 **Elviss NC**, Owen RJ, Xerry J, Walker AM, Davies K. Helicobacter pylori antibiotic resistance patterns and genotypes in adult dyspeptic patients from a regional population in North Wales. *J Antimicrob Chemother* 2004; **54**: 435-440 [PMID: 15243025 DOI: 10.1093/jac/dkh343]

34 **Karabiber H**, Selimoglu MA, Otlu B, Yildirim O, Ozer A. Virulence factors and antibiotic resistance in children with Helicobacter pylori gastritis. *J Pediatr Gastroenterol Nutr* 2014; **58**: 608-612 [PMID: 24792628 DOI: 10.1097/MPG.0000000000000273]

35 **López-Brea M**, Martínez MJ, Domingo D, Sánchez I, Alarcón T. Metronidazole resistance and virulence factors in Helicobacter pylori as markers for treatment failure in a paediatric population. *FEMS Immunol Med Microbiol* 1999; **24**: 183-188 [PMID: 10378418 DOI: 10.1111/j.1574-695X.1999.tb01280.x]

36 **Liou JM**, Chang CY, Chen MJ, Chen CC, Fang YJ, Lee JY, Wu JY, Luo JC, Liou TC, Chang WH, Tseng CH, Wu CY, Yang TH, Chang CC, Wang HP, Sheu BS, Lin JT, Bair MJ, Wu MS; Taiwan Gastrointestinal Disease and Helicobacter Consortium. The Primary Resistance of Helicobacter pylori in Taiwan after the National Policy to Restrict Antibiotic Consumption and Its Relation to Virulence Factors-A Nationwide Study. *PLoS One* 2015; **10**: e0124199 [PMID: 25942450 DOI: 10.1371/journal.pone.0124199]

37 **van Doorn LJ**, Glupczynski Y, Kusters JG, Mégraud F, Midolo P, Maggi-Solcà N, Queiroz DM, Nouhan N, Stet E, Quint WG. Accurate prediction of macrolide resistance in Helicobacter pylori by a PCR line probe assay for detection of mutations in the 23S rRNA gene: multicenter validation study. *Antimicrob Agents Chemother* 2001; **45**: 1500-1504 [PMID: 11302817 DOI: 10.1128/AAC.45.5.1500-1504.2001]

38 **Suzuki T**, Matsuo K, Sawaki A, Ito H, Hirose K, Wakai K, Sato S, Nakamura T, Yamao K, Ueda R, Tajima K. Systematic review and meta-analysis: importance of CagA status for successful eradication of Helicobacter pylori infection. *Aliment Pharmacol Ther* 2006; **24**: 273-280 [PMID: 16842453 DOI: 10.1111/j.1365-2036.2006.02994.x]

39 **Wang D**, Li Q, Gong Y, Yuan Y. The association between vacA or cagA status and eradication outcome of Helicobacter pylori infection: A meta-analysis. *PLoS One* 2017; **12**: e0177455 [PMID: 28493953 DOI: 10.1371/journal.pone.0177455]

40 **Figura N**, Moretti E, Vaglio L, Langone F, Vernillo R, Vindigni C, Giordano N. Factors modulating the outcome of treatment for the eradication of Helicobacter pylori infection. *New Microbiol* 2012; **35**: 335-340 [PMID: 22842603]

P- Reviewer: Chiba T, Rodrigo L, Sugimoto M **S- Editor**: Wang XJ
L- Editor: A **E- Editor**: Huang Y

World Journal of Gastroenterology

Submit a Manuscript: http://www.f6publishing.com

World J Gastroenterol 2018 March 7; 24(9): 982-991

DOI: 10.3748/wjg.v24.i9.982

ISSN 1007-9327 (print) ISSN 2219-2840 (online)

ORIGINAL ARTICLE

Basic Study

Dysregulation of PARP1 is involved in development of Barrett's esophagus

Chao Zhang, Teng Ma, Tao Luo, Ang Li, Xiang Gao, Zhong-Gao Wang, Fei Li

Chao Zhang, Tao Luo, Ang Li, Xiang Gao, Zhong-Gao Wang, Fei Li, Department of General Surgery, Xuanwu Hospital, Capital Medical University, Beijing 100053, China

Teng Ma, Beijing Institute of Radiation Medicine, Beijing 100053, China

Zhong-Gao Wang, Department of Gastroesophageal Reflux Disease, Second Artillery General Hospital of Chinese People's Liberation Army, Beijing 100088, China

ORCID number: Chao Zhang (0000-0002-1825-0097); Teng Ma (0000-0002-8360-1543); Tao Luo (0000-0002-4641-0027); Ang Li (0000-0003-4795-8374); Xiang Gao (0000-0003-2297-903X); Zhong-Gao Wang (0000-0003-4436-3770); Fei Li (0000-0002-1713-967X).

Author contributions: Zhang C, Ma T and Luo T are co-first authors; Zhang C, Ma T, Luo T and Li F designed and performed the research; Ma T, Li A and Gao X contributed the analytical tools; Zhang C and Luo T analyzed the data; Zhang C and Ma T wrote the manuscript; Luo T and Li F revised the manuscript; all authors read and approved the final manuscript.

Supported by the National Natural Science Foundation of China, No. 81470587; and Beijing Municipal Natural Science Foundation of China, No. 7162076.

Institutional review board statement: The study was reviewed and approved by the Second Artillery General Hospital of Chinese People's Liberation Army and the Xuanwu Hospital Institutional Review Boards.

Institutional animal care and use committee statement: Approval from the animal care and use committee of Xuanwu Hospital was obtained for this study.

Conflict-of-interest statement: The authors declare that they have no conflicts of interest.

Data sharing statement: There are no additional data available.

ARRIVE guidelines statement: This study meets the requirements of the ARRIVE guidelines.

Manuscript source: Unsolicited manuscript

Correspondence to: Fei Li, MD, PhD, Chief Doctor, Professor, Department of General Surgery, Xuanwu Hospital of Capital Medical University, No. 45, Changchun Street, Xicheng District, Beijing 100053, China. feili35@126.com
Telephone: +86-10-83198731
Fax: +86-10-83198868

Received: December 9, 2017
Peer-review started: December 9, 2017
First decision: December 20, 2017
Revised: December 26, 2017
Accepted: January 23, 2018
Article in press: January 23, 2018
Published online: March 7, 2018

Abstract

AIM

To investigate the potential role of poly(ADP-ribose) polymerase 1 (PARP1) in the development of Barrett's esophagus (BE).

METHODS

A BE mouse model was established to examine the esophageal morphological changes and molecular changes. Microarray analysis was performed to compare the gene expression profiles between BE patients and healthy controls. qPCR was used to examine the PARP1 expression in cell lines after treatment with H_2O_2 and

bile acids (pH 4). Immunofluorescence staining, comet assay, and annexin V staining were used to evaluate the impact of PARP1 activity on cell survival and DNA damage response after oxidative stress.

RESULTS

The gene expression profile in normal and BE esophageal epithelial cells showed that PARP1, the major poly(ADP-ribose) polymerase, was overexpressed in BE. In the mouse model of BE, positive staining for NF-κB, γH2AX, and poly(ADP-ribose) (PAR) was observed. H_2O_2 and bile acids (pH 4) increased the PARP1 mRNA expression level in normal esophageal epithelial cells. Using shRNA-PARP1 to suppress PARP1 activity decreased the cell viability after treatment with H_2O_2 and bile acids (pH 4), and increased the oxidative damage as demonstrated by an increase in the levels of H_2O_2, intracellular reactive oxygen species (ROS), oxidative DNA damage, double-strand breaks, and apoptosis ($P < 0.01$).

CONCLUSION

The dysfunction of PARP1 in esophageal epithelial cells increases the levels of ROS and oxidative DNA damage, which could be common risk factors for BE and esophageal adenocarcinoma.

Key words: PARP1; Barrett's esophagus; DNA repair; Oxidative damage; Bile acids

Core tip: In this study, we compared the gene expression profile in normal esophagus and Barrett's esophagus (BE), and found that poly(ADP-ribose) polymerase 1 (PARP1) was overexpressed in BE. In a BE model, positive staining for NF-κB, γH2AX, and PAR was observed. H_2O_2 and bile acids (pH 4) increased the PARP1 mRNA expression level in normal esophageal epithelial cells. PARP1 inhibition could decrease the cell viability after bile acids treatment, and increased the oxidative damage, double-strand breaks, and apoptosis. Thus, our study demonstrates a novel molecular mechanism for the role of PARP1 in the process of Barrett's metaplasia, which sheds a potential therapeutic role for PARP1 inhibitor in BE.

Zhang C, Ma T, Luo T, Li A, Gao X, Wang ZG, Li F. Dysregulation of PARP1 is involved in development of Barrett's esophagus. *World J Gastroenterol* 2018; 24(9): 982-991 Available from: URL: http://www.wjgnet.com/1007-9327/full/v24/i9/982.htm DOI: http://dx.doi.org/10.3748/wjg.v24.i9.982

INTRODUCTION

Gastro-esophageal reflux disease (GERD) is known as reflux of gastric acid, usually mixed with bile acids, into the lower esophagus[1-3]. GERD-associated chronic mucosal injury and inflammation are major risk factors for the development of Barrett's esophagus (BE), a premalignant condition closely associated with the development of esophageal adenocarcinoma. BE is present in 10%-20% of patients with GERD[4,5]. Although the leading cause of BE is formerly considered a chronic inflammation, increasing evidence suggests that oxidative stress-induced DNA damage induces the apoptosis of esophageal epithelial cells during the pathogenesis of BE. However, it is unclear why esophageal epithelial cells are sensitive to oxidative damage.

Oxidative DNA damage is usually induced by reactive oxygen species (ROS) primarily generated from normal intracellular metabolism in mitochondria and peroxisomes[6,7]. A number of external hazards such as ionizing radiation, chemicals, and solar ultraviolet light can also trigger ROS production. These active free radicals attack double-strand DNA, inducing various types of DNA lesions, including DNA single-strand breaks (SSBs) and DNA double-strand breaks (DSBs), which may lead to genomic instability[6,8]. To cope with these threats, cells have evolved DNA damage response systems to detect and repair DNA lesions. As one of the earliest alarm systems and regulators in DNA damage response, poly(ADP-ribose) (PAR) participates in the repair of numerous types of DNA damage including SSBs and DSBs[9]. Thus, the cellular metabolism of PAR is critical for DNA damage response and genomic stability. The reaction of poly(ADP-ribosyl)ation (PARylation) is catalyzed by a group of PAR polymerases (PARPs). Using NAD+ as the substrate, PARPs covalently adds ADP-ribose to the side chains of arginine, aspartic acid, and glutamic acid residues in target proteins. After catalyzing the first ADP-ribose onto the proteins, other ADP-riboses can be covalently linked and the continuous reactions produce both linear and branched polymers known as PAR[10]. The structure of PAR has been well characterized: the ADP-ribose unit in the polymer is linked by glycosidic ribose-ribose 1'-2' bonds. The chain length is heterogeneous and can reach around 200 units with 20-50 units in each branch[11].

Although PARylation has been examined both *in vivo* and *in vitro*, the function of PARP1 in esophageal epithelial cells remains elusive. In this study, we hypothesized that PARP1 may be involved in the oxidative damage in the development of BE. We aimed to investigate the potential role of PARP1 and PARylation-related DNA damage in the process of BE in GERD through using a BE mouse model and BE cell lines. Elucidating the role of PARP1 in BE will provide a novel therapeutic strategy for this condition.

MATERIALS AND METHODS

GERD model preparation and BE verification

Experiments in 20 male C57Bl/6 mice with a mean weight of 29 g (27-31 g) were performed. All

Table 1 Baseline patient characteristics

Patient characteristic	*n* = 20
Age (mean ± SD), yr	56.0 ± 12.5
Gender, male, *n* (%)	16 (80)
Body mass index (mean ± SD), kg/m^2	26.5 ± 3.1
Barrett's length (median, IQR), cm	4.7 (3.8-5.5)
Circumferential extent (C)	100%

mice adapted to the environment 7 d to 10 d after purchase, and then water was banned for 24 h before the operation. Chloral hydrate (10%; 3 mL/kg) was administered intraperitoneally for anesthesia. The lower end of the esophagus was separated and a longitudinal cut (about 1-1.5 cm) was performed at the gastroesophageal junction without vascular region. The anti-reflux barrier of the gastroesophageal junction was damaged by the operation.

Hematoxylin and eosin staining and immunohistochemical staining

Animals were sacrificed 3 mo after surgery. Samples were taken in the operating room of the animal facility immediately after the animal sacrifice. The entire stomach and esophagus were removed and immediately fixed in formalin for at least 24 h. Subsequently, samples were processed for paraffin embedding and 7 μmol/L sections were obtained through a microtome and put on positive charged slides. Sections of the lower esophagus were then stained with HE following a standardized protocol and observed under a light microscope. The same samples were subjected for immunohistochemistry. For immunohistochemical staining, sections were placed on polylysine-coated slides. After deparaffinization in xylene and rehydration through graded alcohol, each section was treated with 1% hydrogen peroxide for 20 min, and then blocking serum was applied for 20 min. The slides were incubated overnight with the primary antibody (γH2AX and NF-κB at 1:300 and PAR at 1:500) at 4 ℃ in a closed chamber. Immunohistochemical staining was performed by the streptoavidin-biotin-peroxidase complex technique (Histofine SAB-PO(M) Kit; Nichirei Corp., Tokyo, Japan). Staining was done with 3,3′-diaminobenzidine followed by light counterstaining with methyl green and dehydration.

Cell isolation and culture

Immortalised BE cell lines BAR-T and CP-A (American Type Culture Collection, ATCC, Manassas, VA, United States) were cultured with epithelial cell medium 2 (ScienCell, Carlsbad, CA, United States), supplemented with 5% fetal bovine serum and antibiotics on primaria plates and flasks (BD Biosciences, Bedford, MA, United States). The immortalised human esophageal epithelia cell lines HET1A and EPC2 were obtained from ATCC. HET1A cell line was cultured in Dulbecco's modified Eagle's medium (DMEM) supplemented with 10% fetal bovine serum and antibiotics (Invitrogen). EPC2 cells were grown in keratinocyte SFM medium supplemented with 40 mg/mL bovine pituitary extract and 1.0 ng/mL epidermal growth factor (Invitrogen, Carlsbad, California, United States). All cell lines were grown at 37 ℃ in 5% carbon dioxide.

Patients

Tissue samples of the lower esophagus from 39 individuals, consisting of esophageal squamous epithelia from 19 healthy subjects and 20 specimens from patients with BE, were obtained from the pathological center of the Xuanwu Hospital or the Second Artillery General Hospital of Chinese People's Liberation Army in China. The baseline characteristics of patients are shown in Table 1. Gene expression was examined by whole-human-genome microarrays (Affymetrix, Santa Clara, CA, United States). Normal healthy esophageal biopsies were collected from patients with esophageal pain but diagnosed with normal squamous epithelia without pathological changes.

All samples were snap-frozen in liquid nitrogen and stored at -80 ℃. We obtained tissue specimens from all subjects with informed written consent (approved by the local ethics committees of the Xuanwu Hospital and the Second Artillery General Hospital of Chinese People's Liberation Army. Each single specimen included in this study was histopathologically approved according to grading and staging results by an experienced pathologist.

Microarray

Preparation of labeled cRNA and hybridization were done using the gene chip hybridization, wash, and stain kit (Affymetrix, Santa Clara, CA, United States). Two cycle labeling was applied to all samples. In total, 28 chip data were collected using Gene Chip Operation Software (GCOS, Affymetrix, United States). The 39 specimens analyzed consisted of 20 BE and 19 normal esophageal samples. To obtain the relative gene expression measurements, probe set-level data extraction was performed with the GCRMA (Robust Multiarray Average) normalization algorithm implemented in GeneSpring GX10.2 (Agilent). All data were log2 transformed.

RNA extraction and qRT-PCR

RNA extraction was carried out using the RNeasy Mini Kit (Qiagen, Valencia, CA, United States). Total RNA quality and yield were assessed using a bioanalyzer system (Agilent 2100 Bioanalyzer; Agilent Technologies, CA, United States) and a spectrophotometer (NanoDrop ND-1000; NanoDrop Technologies, DE, United States). Only RNA with an RNA integrity number > 9.0 was used for microarray analysis.

For quantification of mRNA expression, qRT-PCR was performed for three genes plus one control, using pre-designed gene-specific TaqMan probes and primer

sets purchased from Applied Biosystems.

Comet assays

Single-cell gel electrophoretic comet assays were performed under alkaline conditions. Briefly, cells were treated with 100 μmol/L H_2O_2 at 37 ℃. For cellular lysis, the slides were immersed in the alkaline lysis solution overnight in the dark. Next, the slides were subjected to electrophoresis at 20 V (0.6 V/cm) for 25 min and stained in 2.5 mg/mL propidium iodide for 20 min. All images were taken with a fluorescence microscope and analyzed with Comet Assay IV software.

Immunofluorescence staining

After treatment with H_2O_2, cells were fixed in 3% paraformaldehyde and permeabilized in 0.5% Triton X-100 for 30 min at room temperature. Samples were blocked with 5% goat serum and then incubated in primary antibody for 1 h. Samples were then washed with PBS three times and incubated with secondary antibody for 30 min. After PBS washing, the nuclei were stained with Hoechst 33258. The signals were visualized by fluorescence microscopy. We calculated the number of γH2AX foci per nucleus, and for quantitative analysis, 15 nuclear foci were selected to count in each group. For the immunofluorescence assay of anti-8-oxoguanine (8-OXOG), cells were exposed to bile acids cocktail (0.1 mmol/L; pH 4) for 60 min. Cells were then incubated with primary antibody against 8-OXOG (mouse, 1:200; Millipore) overnight at 48 ℃, followed by incubation with secondary goat anti-mouse antibody conjugated with TRITC (1:1000) at room temperature for 45 min. The slides were mounted using Vectashield with DAPI (Vector Laboratories, Burlingame, CA, United States) and viewed under a fluorescence microscope.

Western blot analysis

Cells were harvested and lysed with 100 μL of NETN 300 lysis buffer unless otherwise specified. Soluble fractions were subjected to Western blot analysis.

Statistical analysis

All experiments were performed in triplicate unless indicated otherwise. Student's *t*-test was used for statistical analyses, and $P < 0.05$ was considered statistically significant.

RESULTS

Increased DNA damage response and inflammation in the mouse BE model

During the surgical operation, the mortality rate of mice was 10%, the perioperative mortality rate was 15%, and 1 wk later, the mortality rate was 10%. The lower esophagus from the BE mouse model was processed for staining for γH2AX, NF-κB, and PAR. In the mouse BE model, esophagitis with esophageal erosions and squamous epithelial thickening with basal cell layer hyperplasia were seen. Esophagitis was accompanied by the development of papillary hyperplasia of the squamous epithelia (Figure 1A). Columnar intestinal-type metaplasia resembling that of human BE was seen with erosive esophagitis. No adenocarcinoma or squamous cell carcinoma was seen. In the immunohistochemistry staining, more positive staining for γH2AX, NF-κB, and PAR was observed, suggesting the DNA damage response and inflammation in the BE epithelium.

PARP1 expression is upregulated in the esophageal epithelial cells of BE

To investigate the gene expression changes during the development of BE, samples from BE patients and normal esophagus controls were subjected to microarray analysis. 20 BE lesions for microarray analysis were resected from 20 patients with a mean age of 56 ± 12 years between February 2013 and January 2016. Main patient characteristics are presented in Table 1.

As shown in Figure 2A, PARP1 was one of the up-regulated genes. Representative expression profile of PARP1 between the BE patients and normal controls was also showed in Figure 2B. Besides, PARP1 expression in normal esophageal epithelial cell lines (HET1A and EPC2) and BE epithelial cell lines (CP-A and BAR-T) was also examined. PAPR1 was increased in CP-A and BAR-T cell lines.

To investigate whether PARP1 expression levels can be upregulated by exposure to H_2O_2 and acidic bile acids, we exposed HET1A cells to H_2O_2 (100 μmol/L) and bile acids (0.1 mmol/L; pH 4) for 30 min. Following this exposure, cells were washed in PBS and cultured in regular medium for 30 min, 1 h, 2 h, 4 h, or 8 h, and mRNA levels were measured by RT-PCR. In response to this treatment, significant upregulation of the mRNA levels of PARP1 was observed at 2 h for H_2O_2 and at 4 h and 8 h for both H_2O_2 and bile acids (Figure 2C).

PARP1 protects the epithelial cells of BE from H_2O_2-induced oxidative stress

We next tested the protective effect of PARP1 against H_2O_2-induced oxidative stress. The knockdown of PARP1 in BAR-T cells (Figure 3A) led to a significantly lower cell viability following exposure to H_2O_2, compared with controls ($P < 0.01$ for 100 μmol/L, 200 μmol/L, and 400 μmol/L H_2O_2; Figure 3B), suggesting that the downregulation of endogenous PARP1 sensitized the BAR-T cells to H_2O_2-induced oxidative stress. To further examine the oxidative DNA damage effect after H_2O_2 treatment, we performed comet assay analysis. As shown in Figure 3C, BAR-T cells with PARP1 knockdown displayed a significantly severe DNA damage signal upon exposure to 200 μmol/L H_2O_2 for 2 h (4.3 ± 0.8 *vs*

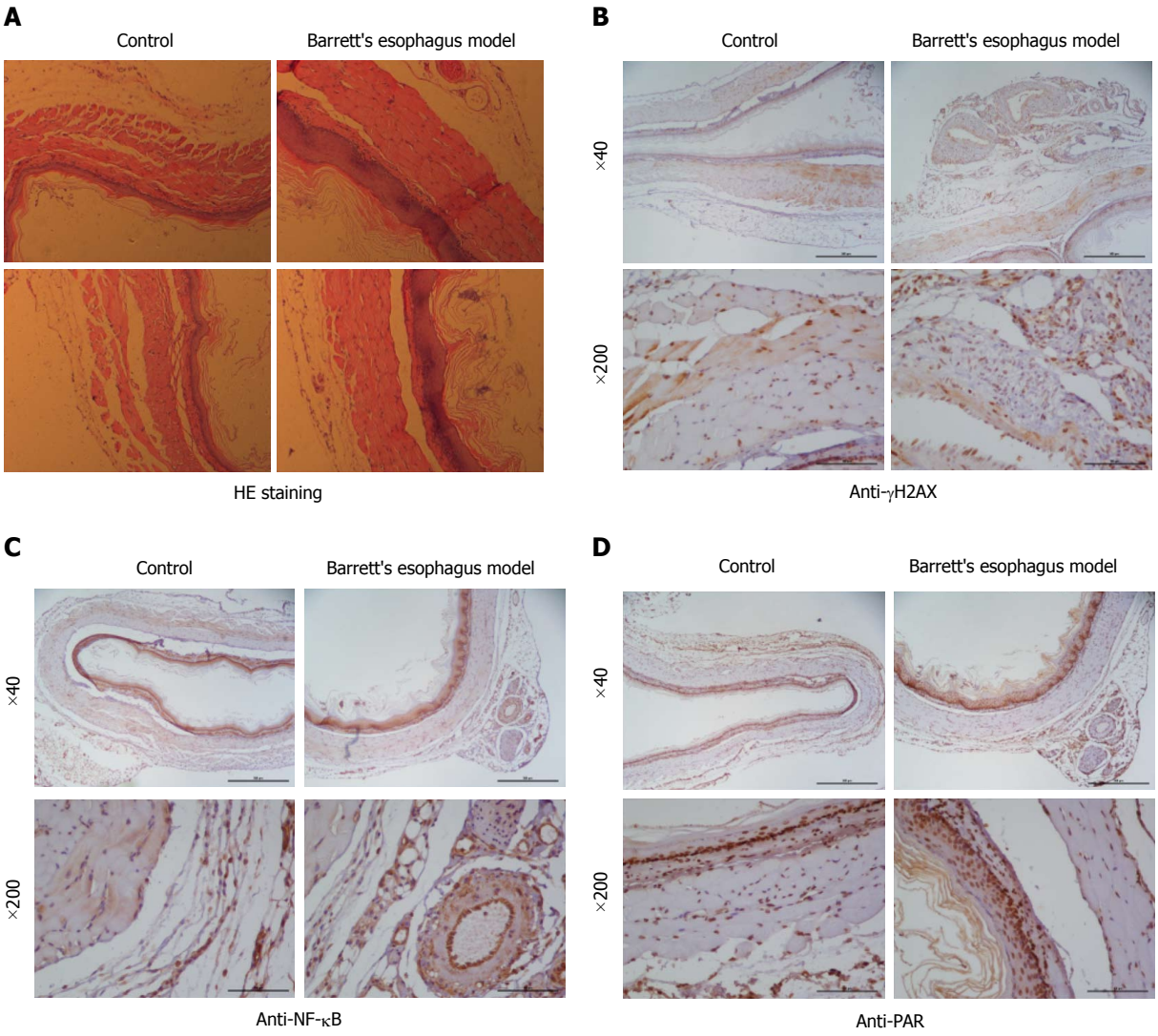

Figure 1 Establishment of a Barrett's esophagus mouse model. A: HE staining; B: γH2AX staining; C: NF-κB staining; D: Poly(ADP-ribose) staining.

8.6 ± 1.4, $P < 0.01$).

PARP1 knockdown leads to increased acidic bile acid-induced H_2O_2 level

We exposed BE epithelial cells to a bile acids cocktail adjusted to pH 4 and performed the Amplex UltraRed H_2O_2 assay to measure H_2O_2 levels. BAR-T cells with knockdown of endogenous PARP1 displayed higher H_2O_2 levels than control cells transfected with scrambled shRNA (Figure 4A).

PARP1 protects the epithelial cells of BE from acidic bile acid-induced oxidative DNA damage

We used immunofluorescence staining for 8-OXOG, one of the most identified oxidative DNA damage sites. On exposure of BAR-T cells with PARP1 knockdown to bile acids (pH 4), more oxidative DNA damage was observed than control cells exposed to acidic bile acids (Figure 4B).

PARP1 protects esophageal epithelial cells from acidic bile acid-induced DNA damage

Gastric acid, particularly in combination with bile acids, has been shown to induce DSBs in esophageal epithelial cells. The immunocytochemical staining for γH2AX, a reliable marker for DSBs, demonstrated significantly high levels of positive γH2AX sites following knockdown of PARP1 in BAR-T cells (19.8% ± 0.3% *vs* 42.6% ± 7.2%, $P < 0.01$, Figure 4C) than in control cells.

PARP1 protects esophageal epithelial cells from acidic bile acid-induced apoptosis

Because PARP1 expression protected cells from acidic bile acid-induced DNA damage, it may protect the epithelial cells of BE from acidic bile acid-induced apoptosis. BAR-T cells were treated with bile acids (pH 4) for 10 min or 30 min, followed by replacement with a regular culture medium for 24 h. The ATP-Glo cell

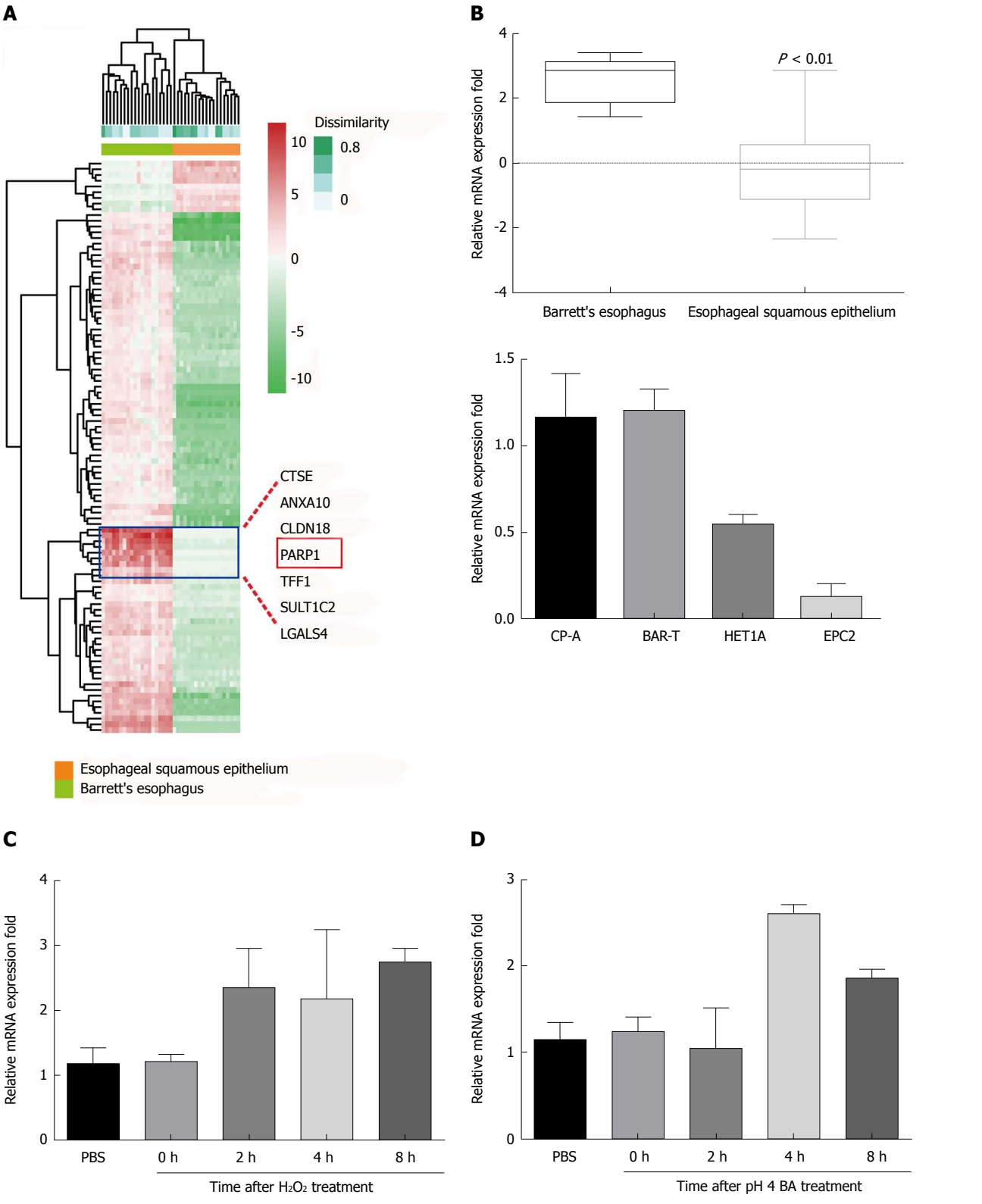

Figure 2 PARP1 is aberrantly expressed in Barrett's esophagus. A: Microarray profiling of gene expression between esophageal squamous epithelium and Barrett's esophagus; B: PARP1 is overexpressed in Barrett's esophagus and Barrett's esophagus cell lines; C: H_2O_2 increased PARP1 expression; D: BAs (pH 4) increased PARP1 expression.

viability assay was then used to determine cell viability at this 24 h time point. As shown in Figure 4D, the short-term exposure (10 min) did not change the cell viability at 24 h. However, the exposure for 30 min demonstrated a significant reduction in cell viability in BAR-T cells lacking PARP1 (82.5% ± 2.2% *vs* 63.0% ± 1.6%, $P < 0.05$). Consistent with this finding, the cells with PARP1 knockdown displayed significantly more

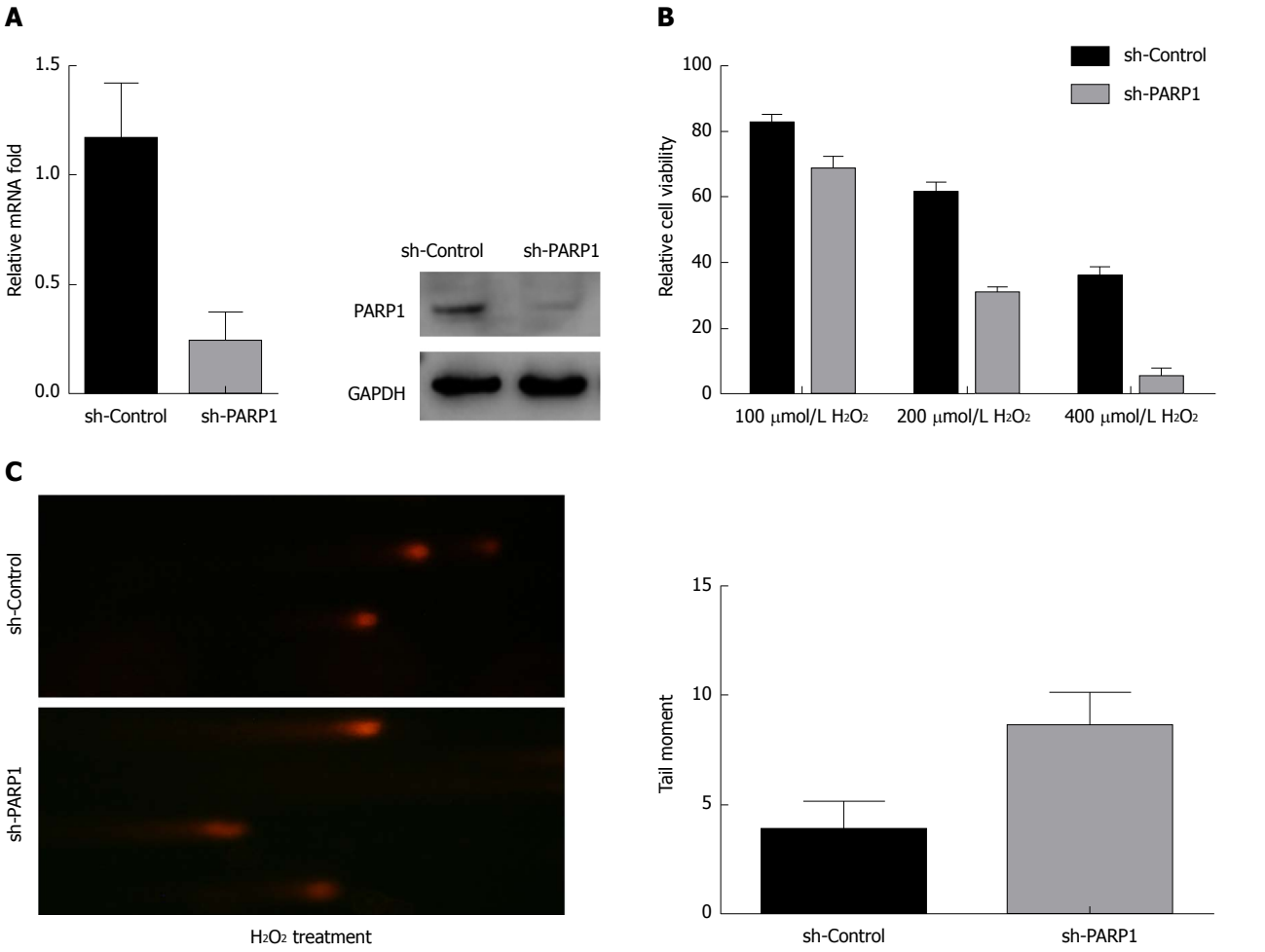

Figure 3 PARP1 protects Barrett's esophagus cells from H_2O_2-induced oxidative damage. A: Knockdown of PARP1 in BAR-T cells; B: BAR-T cells were more sensitive to H_2O_2-induced cell death after PARP1 knockdown; C: BAR-T cells were more sensitive to H_2O_2-induced DNA damage after PARP1 knockdown.

apoptosis after acidic bile acid exposure as indicated by annexin V assay ($P < 0.05$, 10 min: 2.1 ± 0.2 *vs* 6.3 ± 0.8; 30 min: 2.3 ± 0.1 *vs* 8.5 ± 1.2, Figure 4E).

DISCUSSION

During pathological events such as excessive and unrepairable oxidant DNA damage, highly activated PARPs synthesize large amounts of PAR in a few seconds. Our results showed that excessive PARP1 expression may probably a resistance factor of BE epithelial cells to H_2O_2 or bile acid-induced oxidative damage and cell death. In recent years, PARP1 inhibitors have shown promising therapeutic effects on ovarian cancer, breast cancer[12], and neurological diseases[13], and this effect is mainly associated with the induction of DSBs. Interestingly, pharmacological inhibition of PARP1 provides significant benefits in animal models of cardiovascular disorders[14]. It is also reported that PARP1 was identified as a direct target gene of miR-223, which is overexpressed in BE-associated esophageal adenocarcinoma[15]. Here, we demonstrated that PARP1 contributes to genomic stability and oxidative stress injury, and positively regulates the viability of esophageal epithelial cells, which reveals a potential therapeutic strategy for BE.

GERD is a chronic inflammation of the esophagus stimulated by repeated acid/bile acids. Esophagitis, of course, is clinically the major pathological manifestation as the result from GERD, which is also characterized with BE[16]. It is known that metaplasia is a pathological condition that commonly occurs in the presence of chronic inflammation[17], including typical Barrett's metaplasia[18]. In our mouse BE model, esophagitis and papillary hyperplasia of the squamous epithelia was observed, suggesting that the manifestation of GERD occurred. Furthermore, chronic inflammation is likely to carry an increased risk of cancer via oxidative damage pathways[19]. Thus, there is a strong association between GERD-induced ROS accumulation, chronic inflammatory infiltration, and BE formation.

Moreover, the BE mouse model also showed increased positivity for NF-κB, which is a transcription factor that has been established to play an active role in inflammation[20], and there is evidence that it serves as a key determinant of mucosal inflammation

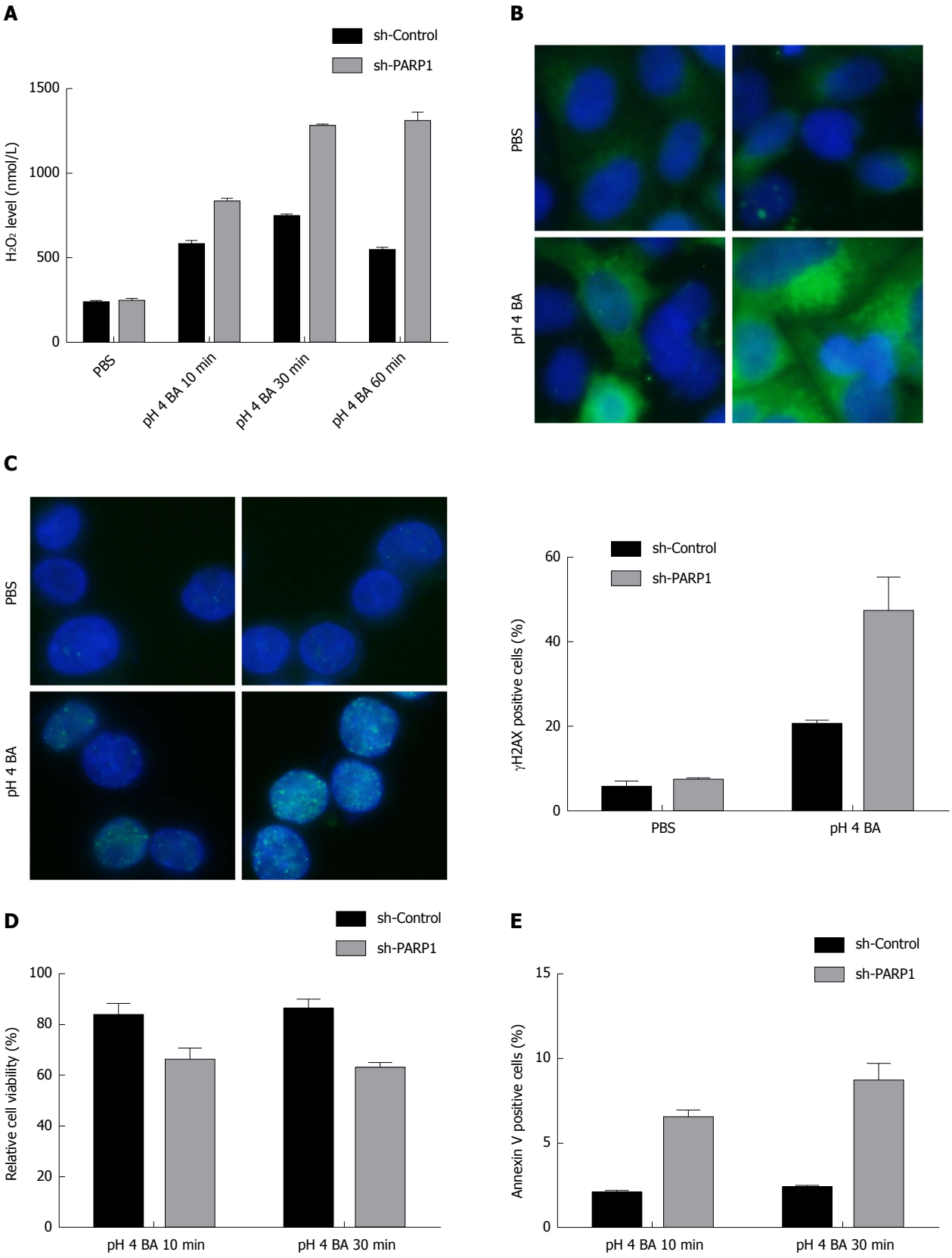

Figure 4 PARP1 protects Barrett's esophagus cells from BA (pH 4)-induced oxidative damage. A: H_2O_2 levels in PARP1-depleted BAR-T cells; B: 8-OXOG staining in PARP1-depleted BAR-T cells; C: γH2AX staining in PARP1- depleted BAR-T cells; D and E: Decreased cell viability in PARP1-depleted BAR-T cells.

and protection[21]. In particular, NF-κB expression has been found in 40%-60% of biopsy specimens of Barrett metaplasia and in 61%-80% of Barrett's adenocarcinomas, but in only 13% of reflux-injured squamous epithelia[22,23]. The level of NF-κB activation is correlated with the process from Barrett's mucosal

metaplasia to carcinogenesis, and indirectly proves that an inflammatory response might contribute to carcinogenesis[23]. This suggests the possibility that inflammation-mediated activation of the NF-κB pathway in a portion of cells, which may regulate the expression of NF-κB downstream proteins to replace the normal squamous cells for metaplasia and carcinogenesis.

Both the immunohistochemistry staining results and cell line results demonstrated that elevated expression of PARP1 is involved in the pathogenesis of BE. More importantly, PARP1 is known to be a co-activator of NF-κB and play a key role in pro-inflammation to contribute to inflammatory processes through the regulation of transcription factors[24,25]: NF-κB is one of the first mediators of inflammation to be identified as a target for PARP activity, which was proved to be a binding partner and also to be PARylated by PARP1. Further, NF-κB activity was greatly abrogated independent of upstream activation of NF-κB in PARP-/- mice and cell lines[26], and PARP1 inhibition reduced the extent of inflammation by modulating oxidative stress and impairing the activation of NF-κB and activator protein-1 in an inflammation model[27]. Both PAR and NF-κB staining increased in the BE mouse model, indicating the possible correlation between PARP1 activity and NF-κB. Further molecular mechanistic study in cells could clarify whether PARP1 regulates NF-κB activity in the oxidative damage-induced BE.

In conclusion, our study suggests that a high level of endogenous PARP1 in esophageal epithelial cells impairs oxidative DNA damage repair, inducing the death of esophageal epithelial cells during the process of BE formation. PARP inhibition treatment suppresses PARP activity and facilitates DNA damage repair in esophageal epithelial cells by prolonging PARylation. Thus, PARP1 acts as a mediator of esophageal disease, and PARylation may play a pivotal protective role as an antioxidant defense mechanism by maintaining esophageal epithelial cell function under pathological conditions of oxidative stress. Hence, PARP inhibitors may provide a novel clinical treatment for suppressing BE caused by oxidative damage.

ARTICLE HIGHLIGHTS

Research background

Barrett's esophagus is a major complication of gastro-esophageal reflux disease (GERD) and an important precursor lesion for the development of esophageal adenocarcinoma. However, the cellular and molecular mechanisms of Barrett's metaplasia remain unclear. It has been demonstrated that poly(ADP-ribose) polymerases (PARPs)-associated ADP-ribosylation plays an important role in DNA damage and inflammatory response. Although PARP1-associated ADP-ribosylation has been examined both *in vivo* and *in vitro*, the function of PARP1 in esophageal epithelial cells and Barrett's esophagus has not been illustrated.

Research motivation

In this study, the potential role of PARP1 and PARP1-related oxidative damage in Barrett's esophagus was investigated.

Research objectives

The study investigated the potential role of PARP1 in oxidative damage in Barrett's esophagus, which is urgent and essential for developing therapeutic targets.

Research methods

Expression of PARP1 gene was analyzed using microarray analysis in patient esophageal tissue samples. A Barrett's esophagus mouse model was established to examine the esophageal morphological changes and molecular changes. qPCR was used to examine the PARP1 expression in cell lines after treatment with H_2O_2 and bile acids (pH 4). To evaluate the impact of PARP1 activity on cell survival and DNA damage response after oxidative stress, immunofluorescence staining, comet assay, and annexin V staining were used.

Research results

High expression of PARP1 was associated with Barrett's esophagus. Positive staining for NF-κB, γH2AX, and poly(ADP-ribose) was observed in the mouse model of Barrett's esophagus. Knockdown of PARP1 decreased the cell viability following treatment with H_2O_2 and bile acids (pH 4). We further demonstrated that PARP1 inhibition could increase the oxidative damage as demonstrated by an increase in the levels of H_2O_2, intracellular reactive oxygen species, oxidative DNA damage, double-strand breaks, and apoptosis.

Research conclusions

The dysfunction of PARP1 in esophageal epithelial cells increases the levels of reactive oxygen species and oxidative DNA damage, and downregulation of PARP1 or PARP1 inhibitor may be a potential therapeutic strategy for Barrett's esophagus.

Research perspectives

This study will provide an example for investigating the relationship between the oxidative DNA damage and Barrett's metaplasia, and the underlying role of the PARP1 in Barrett's esophagus. The direction of the future research is to provide more evidence for developing novel strategies by targeting PARP1 in Barrett's esophagus. In our future research, the PARP1-related downstream signaling pathway (inflammation or DNA damage) will be tested in Barrett's esophagus epithelial cells or animal models to observe the inhibitory effect of PARP1.

REFERENCES

1 **Nehra D**, Howell P, Williams CP, Pye JK, Beynon J. Toxic bile acids in gastro-oesophageal reflux disease: influence of gastric acidity. *Gut* 1999; **44**: 598-602 [PMID: 10205192 DOI: 10.1136/gut.44.5.598]

2 **Herregods TV**, Bredenoord AJ, Smout AJ. Pathophysiology of gastroesophageal reflux disease: new understanding in a new era. *Neurogastroenterol Motil* 2015; **27**: 1202-1213 [PMID: 26053301 DOI: 10.1111/nmo.12611]

3 **Tack J**, Pandolfino JE. Pathophysiology of Gastroesophageal Reflux Disease. *Gastroenterology* 2018; **154**: 277-288 [PMID: 29037470 DOI: 10.1053/j.gastro.2017.09.047]

4 **Eluri S**, Shaheen NJ. Barrett's esophagus: diagnosis and management. *Gastrointest Endosc* 2017; **85**: 889-903 [PMID: 28109913 DOI: 10.1016/j.gie.2017.01.007]

5 **Shaheen NJ**. New Directions in Barrett's Esophagus. *Gastrointest Endosc Clin N Am* 2017; **27**: xv-xvi [PMID: 28577775 DOI: 10.1016/j.giec.2017.04.001]

6 **Cadet J**, Wagner JR. Oxidatively generated base damage to cellular DNA by hydroxyl radical and one-electron oxidants: similarities and differences. *Arch Biochem Biophys* 2014; **557**: 47-54 [PMID: 24820329 DOI: 10.1016/j.abb.2014.05.001]

7 **Finkel T**, Holbrook NJ. Oxidants, oxidative stress and the biology of ageing. *Nature* 2000; **408**: 239-247 [PMID: 11089981 DOI: 10.1038/35041687]

8 **Olinski R**, Gackowski D, Foksinski M, Rozalski R, Roszkowski

K, Jaruga P. Oxidative DNA damage: assessment of the role in carcinogenesis, atherosclerosis, and acquired immunodeficiency syndrome. *Free Radic Biol Med* 2002; **33**: 192-200 [PMID: 12106815 DOI: 10.1016/S0891-5849(02)00878-X]

9 **Li M**, Yu X. Function of BRCA1 in the DNA damage response is mediated by ADP-ribosylation. *Cancer Cell* 2013; **23**: 693-704 [PMID: 23680151 DOI: 10.1016/j.ccr.2013.03.025]

10 **Schreiber V**, Dantzer F, Ame JC, de Murcia G. Poly(ADP-ribose): novel functions for an old molecule. *Nat Rev Mol Cell Biol* 2006; **7**: 517-528 [PMID: 16829982 DOI: 10.1038/nrm1963]

11 **Kim MY**, Zhang T, Kraus WL. Poly(ADP-ribosyl)ation by PARP-1: 'PAR-laying' NAD+ into a nuclear signal. *Genes Dev* 2005; **19**: 1951-1967 [PMID: 16140981 DOI: 10.1101/gad.1331805]

12 **Lesueur P**, Chevalier F, Austry JB, Waissi W, Burckel H, Noël G, Habrand JL, Saintigny Y, Joly F. Poly-(ADP-ribose)-polymerase inhibitors as radiosensitizers: a systematic review of pre-clinical and clinical human studies. *Oncotarget* 2017; **8**: 69105-69124 [PMID: 28978184 DOI: 10.18632/oncotarget.19079]

13 **Sriram CS**, Jangra A, Kasala ER, Bodduluru LN, Bezbaruah BK. Targeting poly(ADP-ribose)polymerase1 in neurological diseases: A promising trove for new pharmacological interventions to enter clinical translation. *Neurochem Int* 2014; **76**: 70-81 [PMID: 25049175 DOI: 10.1016/j.neuint.2014.07.001]

14 **Xu S**, Bai P, Little PJ, Liu P. Poly(ADP-ribose) polymerase 1 (PARP1) in atherosclerosis: from molecular mechanisms to therapeutic implications. *Med Res Rev* 2014; **34**: 644-675 [PMID: 24002940 DOI: 10.1002/med.21300]

15 **Streppel MM**, Pai S, Campbell NR, Hu C, Yabuuchi S, Canto MI, Wang JS, Montgomery EA, Maitra A. MicroRNA 223 is upregulated in the multistep progression of Barrett's esophagus and modulates sensitivity to chemotherapy by targeting PARP1. *Clin Cancer Res* 2013; **19**: 4067-4078 [PMID: 23757351 DOI: 10.1158/1078-0432.CCR-13-0601]

16 **Vaezi MF**, Richter JE. Role of acid and duodenogastroesophageal reflux in gastroesophageal reflux disease. *Gastroenterology* 1996; **111**: 1192-1199 [PMID: 8898632 DOI: 10.1053/gast.1996.v111.pm8898632]

17 **V. Kumar AKA,** N Fausto, R Mitchell. Robbins Basic Pathology. 8th ed: Elsevier Saunders, 2007

18 **Colleypriest BJ**, Palmer RM, Ward SG, Tosh D. Cdx genes, inflammation and the pathogenesis of Barrett's metaplasia. *Trends Mol Med* 2009; **15**: 313-322 [PMID: 19564133 DOI: 10.1016/j.molmed.2009.05.001]

19 **Farinati F**, Piciocchi M, Lavezzo E, Bortolami M, Cardin R. Oxidative stress and inducible nitric oxide synthase induction in carcinogenesis. *Dig Dis* 2010; **28**: 579-584 [PMID: 21088405 DOI: 10.1159/000320052]

20 **Baeuerle PA**. IkappaB-NF-kappaB structures: at the interface of inflammation control. *Cell* 1998; **95**: 729-731 [PMID: 9865689 DOI: 10.1016/S0092-8674(00)81694-3]

21 **Jobin C**, Sartor RB. The I kappa B/NF-kappa B system: a key determinant of mucosalinflammation and protection. *Am J Physiol Cell Physiol* 2000; **278**: C451-C462 [PMID: 10712233 DOI: 10.1152/ajpcell.2000.278.3.C451]

22 **Abdel-Latif MM**, O'Riordan J, Windle HJ, Carton E, Ravi N, Kelleher D, Reynolds JV. NF-kappaB activation in esophageal adenocarcinoma: relationship to Barrett's metaplasia, survival, and response to neoadjuvant chemoradiotherapy. *Ann Surg* 2004; **239**: 491-500 [PMID: 15024310 DOI: 10.1097/01.sla.0000118751.95179.c6]

23 **O'Riordan JM**, Abdel-latif MM, Ravi N, McNamara D, Byrne PJ, McDonald GS, Keeling PW, Kelleher D, Reynolds JV. Proinflammatory cytokine and nuclear factor kappa-B expression along the inflammation-metaplasia-dysplasia-adenocarcinoma sequence in the esophagus. *Am J Gastroenterol* 2005; **100**: 1257-1264 [PMID: 15929754 DOI: 10.1111/j.1572-0241.2005.41338.x]

24 **Hassa PO**, Hottiger MO. A role of poly (ADP-ribose) polymerase in NF-kappaB transcriptional activation. *Biol Chem* 1999; **380**: 953-959 [PMID: 10494847 DOI: 10.1515/bc.1999.118]

25 **Liu L**, Ke Y, Jiang X, He F, Pan L, Xu L, Zeng X, Ba X. Lipopolysaccharide activates ERK-PARP-1-RelA pathway and promotes nuclear factor-κB transcription in murine macrophages. *Hum Immunol* 2012; **73**: 439-447 [PMID: 22391342 DOI: 10.1016/j.humimm.2012.02.002]

26 **Oliver FJ**, Ménissier-de Murcia J, Nacci C, Decker P, Andriantsitohaina R, Muller S, de la Rubia G, Stoclet JC, de Murcia G. Resistance to endotoxic shock as a consequence of defective NF-kappaB activation in poly (ADP-ribose) polymerase-1 deficient mice. *EMBO J* 1999; **18**: 4446-4454 [PMID: 10449410 DOI: 10.1093/emboj/18.16.4446]

27 **Brunyánszki A**, Hegedus C, Szántó M, Erdélyi K, Kovács K, Schreiber V, Gergely S, Kiss B, Szabó E, Virág L, Bai P. Genetic ablation of PARP-1 protects against oxazolone-induced contact hypersensitivity by modulating oxidative stress. *J Invest Dermatol* 2010; **130**: 2629-2637 [PMID: 20613774 DOI: 10.1038/jid.2010.190]

P- Reviewer: Zhao JB **S- Editor**: Wang JL
L- Editor: Wang TQ **E- Editor**: Huang Y

World Journal of Gastroenterology

Submit a Manuscript: http://www.f6publishing.com

World J Gastroenterol 2018 March 7; 24(9): 992-1003

DOI: 10.3748/wjg.v24.i9.992

ISSN 1007-9327 (print) ISSN 2219-2840 (online)

ORIGINAL ARTICLE

Basic Study

Autophagy activation by Jiang Zhi Granule protects against metabolic stress-induced hepatocyte injury

Yi-Yuan Zheng, Miao Wang, Xiang-Bing Shu, Pei-Yong Zheng, Guang Ji

Yi-Yuan Zheng, Miao Wang, Xiang-Bing Shu, Pei-Yong Zheng, Guang Ji, Institute of Digestive Disease, Longhua Hospital, Shanghai University of Traditional Chinese Medicine, Shanghai 200032, China

ORCID number: Yi-Yuan Zheng (0000-0001-9487-3766); Miao Wang (0000-0002-0344-7575); Xiang-Bing Shu (0000-0002-4096-8281); Pei-Yong Zheng (0000-0003-1084-5317); Guang Ji (0000-0003-0842-3676).

Author contributions: Zheng YY and Wang M contributed equally as co-first authors; Zheng YY and Wang M performed the majority of experiments and drafted the article; Shu XB established the animal model; Zheng PY analyzed the data; Ji G designed the research; all authors approved the final version of the article to be published.

Supported by the National Natural Science Foundation of China, No. 81370092.

Institutional review board statement: This study was reviewed and approved by the Institutional Review Board of Institute of Digestive Disease, Shanghai University of Traditional Chinese Medicine, Shanghai, China.

Institutional animal care and use committee statement: All procedures involving animals were reviewed and approved by the Institutional Animal Care and Use Committee of Shanghai University of Traditional Chinese Medicine (IACUC protocol number Approval number: SZY201508004).

Conflict-of-interest statement: All authors declare that they have no conflicts of interest.

Data sharing statement: No additional data are available.

Manuscript source: Unsolicited manuscript

Correspondence to: Guang Ji, PhD, Chief Doctor, Professor, Institute of Digestive Disease, Longhua Hospital, Shanghai University of Traditional Chinese Medicine, No. 725 South Wanping Road, Shanghai 200032, China. jiliver@vip.sina.com
Telephone: +86-21-64385700
Fax: +86-21-64385700

Received: November 9, 2017
Peer-review started: November 10, 2017
First decision: December 13, 2017
Revised: December 22, 2017
Accepted: January 1, 2018
Article in press: January 1, 2018
Published online: March 7, 2018

Abstract

AIM

To elucidate the potential role of autophagy and the protective effects of Jiang Zhi Granule (JZG) in metabolic stress-induced hepatocyte injury.

METHODS

An *in vitro* and *in vivo* approach was used in this study. HepG2 cells were incubated in culture medium containing palmitate (PA; 0, 0.1, 0.2, 0.3, 0.4 or 0.5 mmol/L) and treated with or without JZG (100 μg/mL) for 24 h or 48 h, and the progression of autophagy was visualized by stable fluorescence-expressing cell lines LC3 and p62. Western blot analyses were performed to examine the expression of LC3-Ⅱ/LC3-Ⅰ, p62, mTOR and PI3K, while mitochondrial integrity and oxidative stress were observed by fluorescence staining of JC-1 and reactive oxygen species. C57BL/6 mice

were divided into three groups: control group (n = 10), high fat (HF) group (n = 13) and JZG group (n = 13); and, histological staining was carried out to detect inflammation and lipid content in the liver.

RESULTS

The cell trauma induced by PA was aggravated in a dose- and time-dependent manner, and hepatic function was improved by JZG. PA had dual effects on autophagy by activating autophagy induction and blocking autophagic flux. The PI3K-AKT-mTOR signaling pathway and the fusion of isolated hepatic autophagosomes and lysosomes were critically involved in this process. JZG activated autophagy progression by either induction of autophagosomes or co-localization of autophagosomes and lysosomes as well as degradation of autolysosomes to protect against PA-induced hepatocyte injury, and protected mitochondrial integrity against oxidative stress in PA-induced mitochondrial dysfunction. In addition, JZG ameliorated lipid droplets and inflammation induced by HF diet *in vivo*, leading to improved metabolic disorder and associated liver injury in a mouse model of non-alcoholic fatty liver disease (NAFLD).

CONCLUSION

Metabolic stress-induced hepatocyte injury exhibited dual effects on autophagy and JZG activated the entire process, resulting in beneficial effects in NAFLD.

Key words: Autophagy; PI3K-AKT-mTOR signaling pathway; Autophagic flux; Oxidative stress; Hepatocyte injury; Non-alcoholic fatty liver disease

Core tip: Non-alcoholic fatty liver disease (NAFLD), which is mainly characterized by the accumulation of lipids and energy metabolism dysfunction, is now one of the most common risk factors worldwide. As studies have demonstrated that autophagy is important in the maintenance of normal hepatocyte function and in the response to pathogenic changes, we examined the potential role of autophagy in metabolic stress-induced hepatocyte injury. The results showed that metabolic stress had dual effects on autophagy, resulting in autophagy induction and autophagic flux inhibition. The Chinese herbal formula Jiang Zhi Granule activated the autophagy process to protect against metabolic stress-induced hepatocyte injury in NAFLD.

Zheng YY, Wang M, Shu XB, Zheng PY, Ji G. Autophagy activation by Jiang Zhi Granule protects against metabolic stress-induced hepatocyte injury. *World J Gastroenterol* 2018; 24(9): 992-1003 Available from: URL: http://www.wjgnet.com/1007-9327/full/v24/i9/992.htm DOI: http://dx.doi.org/10.3748/wjg.v24.i9.992

INTRODUCTION

Fatty liver disease (FLD), which is mainly characterized by the accumulation of lipids in hepatocytes and energy metabolism dysfunction, is clinically classified into two broad categories: alcoholic (A)FLD and non-alcoholic (NA)FLD[1]. NAFLD is currently much more prevalent than AFLD, which accounts for 75% of all chronic liver diseases, and is increasingly recognized as one of the most common risk factors worldwide[2]. NAFLD has a wide clinical pathological spectrum, ranging from simple steatosis non-alcoholic fatty liver to non-alcoholic steatohepatitis, which includes fibrosis and cirrhosis[3]. And, in the meantime, it often occurs with other metabolic diseases, such as obesity and diabetes[4].

The pathogenesis of NAFLD is still unknown; however, the "two hits" hypothesis is now widely accepted[5]. A disturbance in metabolic homeostasis is one of the key events during the occurrence of NAFLD and typical pathological features, including steatosis, inflammation, fibrosis and cirrhosis, are considered to be related to oxidative stress resulting from lipid accumulation and reactive oxygen species (ROS) generation[6].

Oxidative stress is a stimulus for autophagy, which is important for metabolic homeostasis in the liver[7], as it can prompt nutrient recycling, remove abnormal organelles and toxic protein aggregates and alter the level of metabolic factors, thus contributing to the maintenance of normal hepatocyte function and the response to pathogenic changes in the liver[8,9]. Hepatic autophagy occurs at a basal level and can be elevated under stress conditions[10], such as oxidative stress.

Studies have shown that autophagy is a highly selective process and can modulate cellular energy stores, such as carbohydrates and lipids[11,12], and recent research has demonstrated that autophagy assists in the degradation of triglycerides in the liver[13]. Autophagy regulators, such as rapamycin and carbamazepine, have been proven effective to improve hepatic function[14]. However, no effective therapeutic approach has been accepted as the standard option for NAFLD and its complications. Thus, new treatments are still urgently needed to prevent or delay the onset as well as the progression of NAFLD.

Jiang Zhi Granule (JZG), which is composed of *Herba gynostemmatis, Radix salviae, Rhizoma polygoni cuspidati, Herba artemisiae scopariae* and *Folium nelumbinis*, is a clinically used herbal formula designed to treat patients with NAFLD[15]. JZG had a positive drug safety evaluation and has been approved for clinical trials by the State Food and Drug Administration (SFDA; Authorization Number: Z10960082). Our preliminary studies indicated that JZG had beneficial effects in improving hepatic fat accumulation in both cell lines and animals[16], and the efficacy of JZG in patients with

NAFLD was also confirmed[17]. As previous studies on JZG have indicated its antisteatotic effect, we conducted this study to determine the underlying mechanism of JZG.

MATERIALS AND METHODS

Animal models

Male C57BL/6 mice aged 6 wk were purchased from SLAC Animal Laboratories (Shanghai, China). After 1-wk acclimatization, the mice were divided into three groups: the control group (n = 10) received a 12-wk standard diet (STD); the high fat (HF) group (n = 13) received a HF diet (HFD; consisting of 10% lard oil, 2% cholesterol and 88% STD) supplemented with 1% DSS (MP Biomedicals, Solon, OH, United States) in drinking water; and, the JZG group (n = 13) also received a HF-DSS diet, but were also given JZG which had been dissolved in saline and was administered daily by oral gavage at a dose of 994 mg/kg daily (approximately 12 times that of the standard dose used in clinical practice). DSS was given in cycles; each cycle consisted of 7 d DSS administration followed by a 10-d interval with normal drinking water[18]. At the end of the experimental period, blood samples were drawn from the heart, while the mice were under anesthesia, livers were excised, and samples were either immediately snap-frozen in liquid nitrogen or fixed in 4% PFA.

Cell culture

HepG2 cells were obtained from the Cell Bank of the Chinese Academy of Sciences (Shanghai, China), and were cultured in DMEM supplemented with 10% fetal bovine serum, 100 U/mL penicillin and 100 μg/mL streptomycin. Saturated palmitic acid (PA) and JZG were used in this study. HepG2 cells were incubated in culture medium containing PA (0, 0.1, 0.2, 0.3, 0.4 or 0.5 mmol/L) and treated with or without JZG (100 μg/mL) for 24 h or 48 h, as described previously[16].

Western blot

Western blot analyses were performed as described previously[19]. Rabbit antibodies against LC3 (monoclonal ab192890), SQSTM1/p62 (monoclonal ab109012), p-mTOR (phosphor-S2481) (monoclonal ab137133), mTOR (monoclonal ab87540), p-PI3K (phosphor-Y607) (polyclonal ab182651), PI3K (monoclonal ab40755) and actin (polyclonal ab8227) were purchased from Abcam (Cambridge, MA, United States).

Establishment of stable fluorescence-expressing cell lines

HepG2 cells were cultured according to the above protocol and infected with mRFP-GFP-LC3 lentivirus at an MOI of 10 for 48 h to establish a stable mRFP-GFP-LC3-expressing HepG2 cell line, and then infected with mCherry-p62 lentivirus at an MOI of 10 for 48 h to establish a stable mCherry-p62-expressing HepG2 cell line.

Fluorescence staining

Mitochondria and lysosomes were detected using the MitoTracker Green FM and LysoTracker Deep Red staining kit, respectively (Thermo Fisher Scientific, Waltham, MA, United States). Intracellular ROS generation was detected using the DCFH-DA fluorescent probe. Mitochondrial membrane potential was determined by the mitochondrial membrane potential assay kit (JC-1). Pretreated cells in 6-well plates were processed following the protocols and were observed immediately under a fluorescence microscope at an excitation wavelength of 488 nm and emission wavelength of 525 nm.

Histological staining

Histological staining was performed as described previously[20]. Liver samples were fixed, processed, and embedded in paraffin blocks, and then hematoxylin and eosin (H&E) staining was performed. Frozen liver sections were fixed and stained with oil Red O. Images were acquired on an Olympus BX-50 microscope.

Statistical analysis

All data were expressed as the mean ± SEM. Statistical analyses were performed using GraphPad Prism (GraphPad Software, La Jolla, CA, United States). The differences between groups were analyzed by Student's t-test or ANOVA, as appropriate, and $P < 0.05$ was considered statistically significant.

RESULTS

Autophagy was activated by JZG to protect against injury in PA-treated cells

To determine whether autophagy was involved in the progression of NAFLD, HepG2 cells were treated with PA - a main type of saturated free fatty acid which is elevated in obese subjects and can induce NAFLD[21] - at various concentrations and for different time periods. Results showed that the expression of alanine aminotransferase (ALT) increased in a dose- and time-dependent manner and JZG significantly reduced high ALT levels (Figure 1A and B), suggesting that cell trauma was induced by PA and JZG improved hepatic function. These results also indicated that the dose of 0.4 mmol/L may be an appropriate concentration in subsequent experiments and the time points should include 24 h and 48 h.

Western blot analyses showed that PA increased LC3-Ⅱ/actin expression (Figure 1C), indicating the activation of autophagy. However, the expression of LC3-Ⅱ/LC3-Ⅰ was not increased accordingly after long-term PA stimulation (Figure 1C). In the meantime, the expression of p62 was also increased (Figure 1C), suggesting the restriction of autophagic flux. Thus, it was proposed that PA exhibited dual effects on

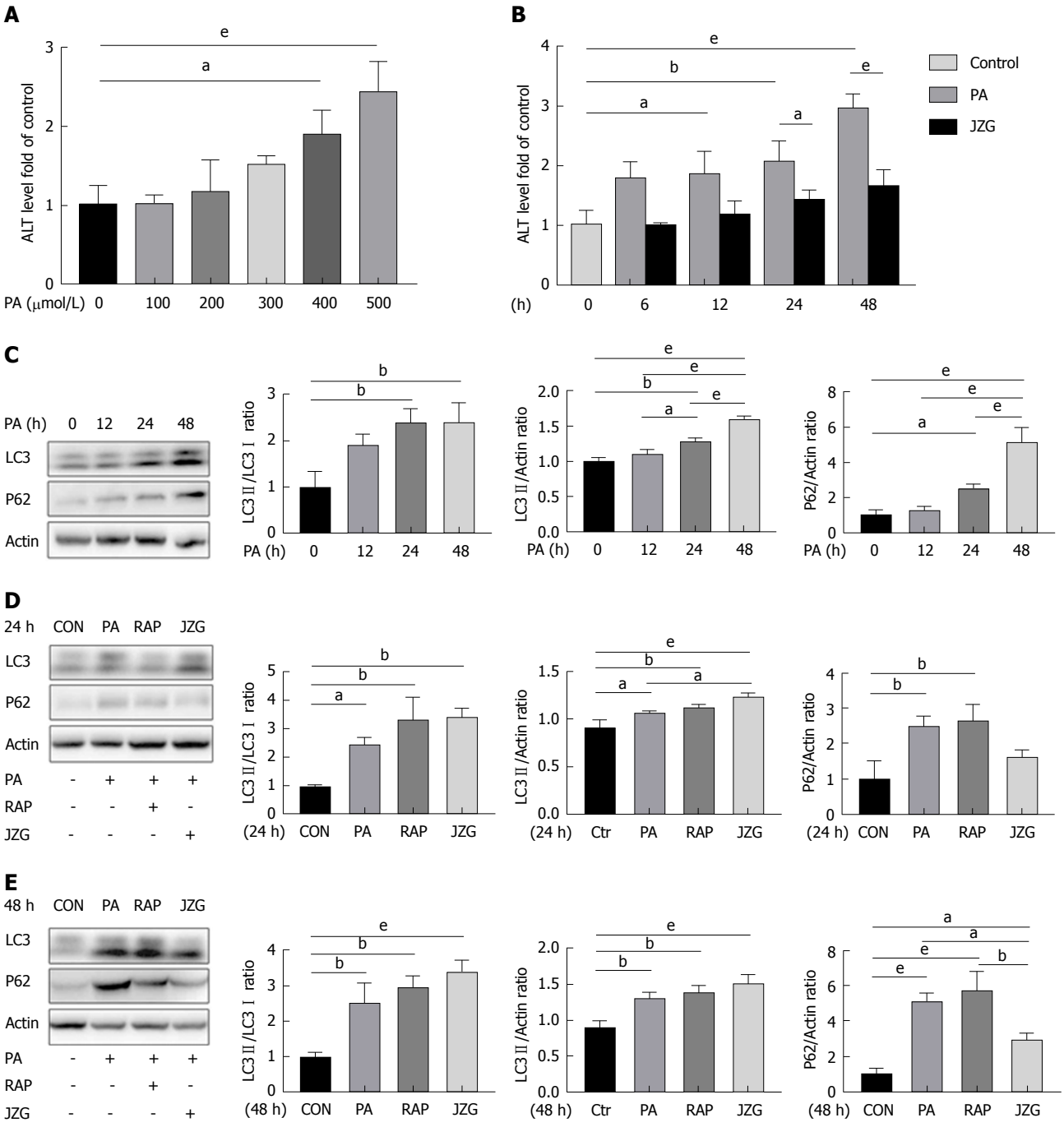

Figure 1 Autophagy was activated by JZG to protect against injury in palmitate-treated cells. A: The expression of ALT in the supernatants of cell cultures was determined by ELISA. HepG2 cells were incubated in culture medium containing PA (0, 0.1, 0.2, 0.3, 0.4 or 0.5 mmol/L); B: The expression of ALT in the supernatants of cell cultures was determined by ELISA. HepG2 cells were treated with 0.4 mmol/L PA with or without JZG (100 μg/mL) for different time periods (0, 6, 12, 24 or 48 h); C: HepG2 cells were treated with 0.4 mmol/L PA for different time periods (0, 12, 24 or 48 h); D: HepG2 cells were treated with 0.4 mmol/L PA and rapamycin (2 μmol/L) or JZG (100 μg/mL) for 24 h; E: HepG2 cells were treated with 0.4 mmol/L PA and rapamycin (2 μmol/L) or JZG (100 μg/mL) for 48 h. Data are expressed as mean ± SEM. $^{a}P < 0.05$, $^{b}P < 0.01$, $^{e}P < 0.001$. ALT: Alanine aminotransferase; ELISA: Enzyme-linked immunosorbent assay; JZG: Jiang Zhi Granule; PA: Palmitate.

autophagy.

A recent study showed that mitochondrial dysfunction caused by elevated mitochondrial stress may block autophagic flux[18]; thus, rapamycin was used in the present study to enhance autophagy at different time points. The outcomes displayed that the expression of LC3-Ⅱ/actin and p62 were both increased but the expression of LC3-Ⅱ/LC3-Ⅰ was not, confirming the dual effects of PA on autophagy (Figure 1D and E).

An increase in LC3-Ⅱ/LC3-Ⅰ expression and a reduction in p62 expression were observed following treatment with JZG for two different time periods (Figure 1D and E), indicating that JZG activated autophagy to protect against PA-induced cell injury.

PI3K-AKT-mTOR pathway was involved in autophagy in JZG-treated cells

As the activation of autophagy can occur due to an

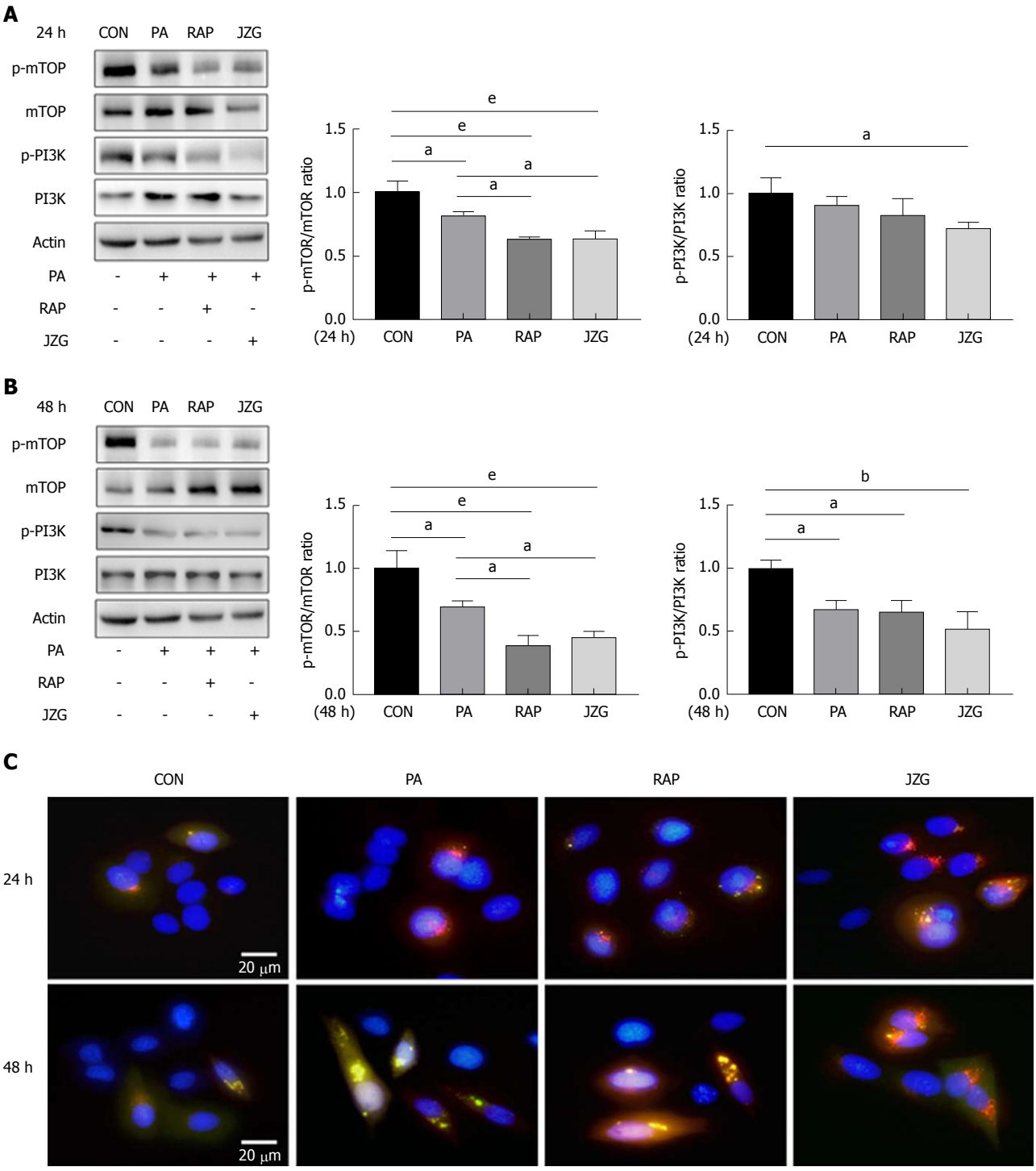

Figure 2 PI3K-AKT-mTOR pathway was involved in autophagy in Jiang Zhi Granule-treated cells. A: HepG2 cells were treated with 0.4 mmol/L PA and rapamycin (2 μmol/L) or JZG (100 μg/mL) for 24 h; B: HepG2 cells were treated with 0.4 mmol/L PA and rapamycin (2 μmol/L) or JZG (100 μg/mL) for 48 h; C: HepG2 cells stably expressing mRFP-GFP-LC3 were pretreated with 0.4 mmol/L PA and rapamycin (2 μmol/L) or JZG (100 μg/mL) for 24 h and 48 h, and then analyzed by fluorescence microscopy. Data are expressed as mean ± SEM. $^{a}P < 0.05$, $^{b}P < 0.01$, $^{e}P < 0.001$. JZG: Jiang Zhi Granule; PA: Palmitate.

increase in autophagy induction and autophagic flux, we first investigated the pathway involved in autophagy induction in JZG-treated cells. The PI3K-AKT-mTOR pathway, a classic signaling pathway that has been identified to be important in autophagy induction, was examined in this study. Western blot analyses revealed that the phosphorylation signaling processes of mTOR and PI3K were inhibited in PA-treated cells, and these results were further confirmed by the addition of rapamycin (Figure 2A and B). As an inhibitor of mTOR, rapamycin did not further depress the phosphorylation of PI3K. Conversely, an additional restraint on both phosphorylation signaling processes was observed in JZG-treated cells (Figure 2A and B), suggesting that

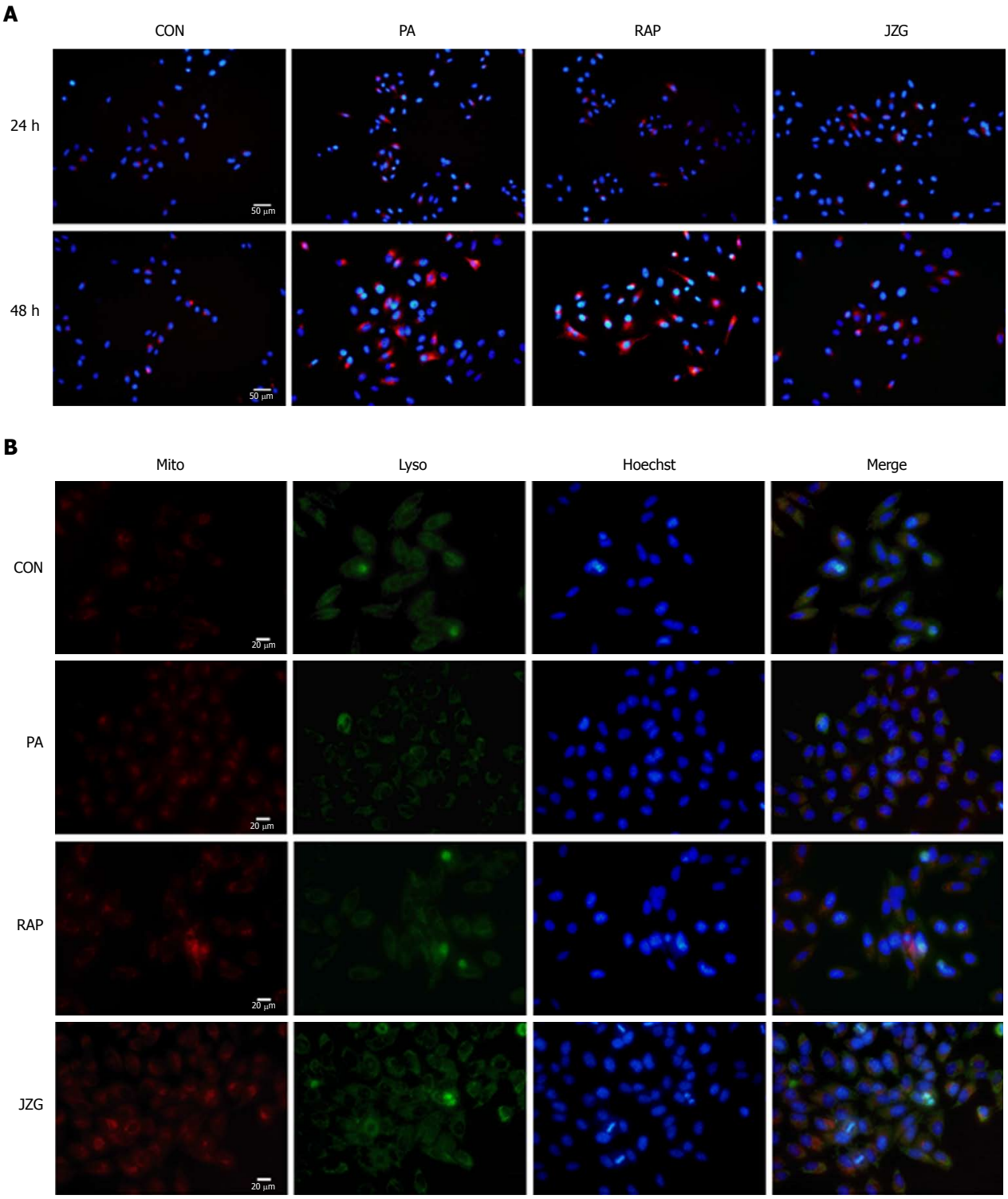

Figure 3 Effects of Jiang Zhi Granule on autophagic flux in palmitate-treated cells. A: HepG2 cells stably expressing mCherry-p62 were pretreated with 0.4 mmol/L PA and rapamycin (2 μmol/L) or JZG (100 μg/mL) for 24 h and 48 h, and then analyzed by fluorescence microscopy; B: HepG2 cells were treated with 0.4 mmol/L PA and rapamycin (2 μmol/L) or JZG (100 μg/mL) for 48 h, and then analyzed by fluorescence microscopy. JZG: Jiang Zhi Granule; PA: Palmitate.

the PI3K-AKT-mTOR pathway is critically involved in autophagy induction in response to PA challenge.

As LC3 is the major constituent of autophagosomes, a stable mRFP-GFP-LC3-expressing HepG2 cell line was established to visualize the progression of autophagosome formation in real time in liver cells. Diffuse cytoplasmic localization of mRFP-GFP-LC3 was observed in the control group, whereas punctate fluorescence was observed in PA-treated cells (Figure 2C), indicating that cytoplasmic LC3 was processed and recruited to autophagosomes. Rapamycin and JZG advanced this process, indicating increased autophagy induction, which confirmed that JZG induced the formation of autophagosomes.

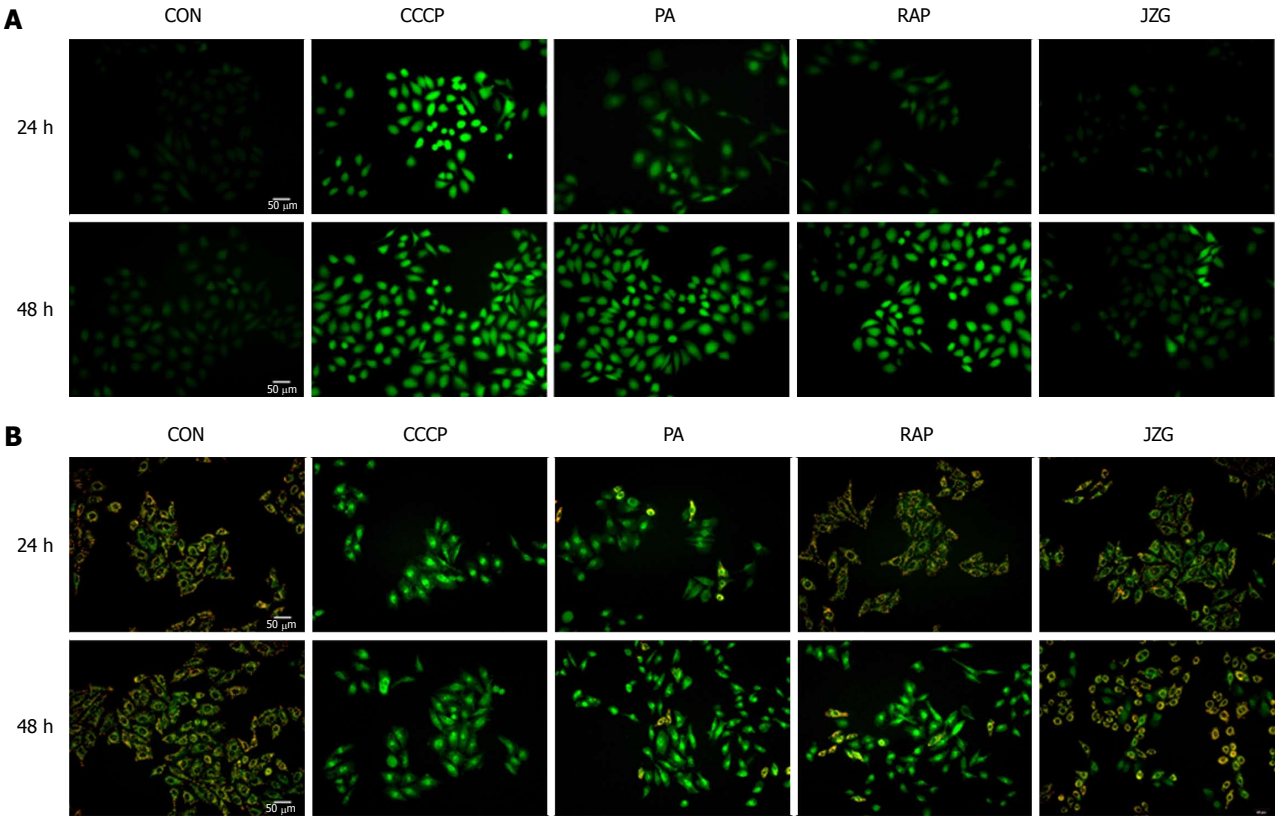

Figure 4 Jiang Zhi Granule protected mitochondrial integrity against oxidative stress. A: The ROS-sensitive fluorescent probe DCFH-DA was used to monitor mitochondrial membrane potential in HepG2 cells pretreated with 0.4 mmol/L PA and rapamycin (2 μmol/L) or JZG (100 μg/mL) for 24 h and 48 h, and the cells were then analyzed by fluorescence microscopy; B: JC-1 was used to monitor mitochondrial membrane potential in HepG2 cells pretreated with 0.4 mmol/L PA and rapamycin (2 μmol/L) or JZG (100 μg/mL) for 24 h and 48 h, and the cells were then analyzed by fluorescence microscopy. JZG: Jiang Zhi Granule; PA: Palmitate; ROS: Reactive oxygen species.

Effects of JZG on autophagic flux in PA-treated cells

To determine the effect of JZG on autophagic flux in PA-treated cells, we first observed this effect in mRFP-GFP-LC3-expressing HepG2 cells. We found that yellow fluorescence - indicating that GFP was not degraded by lysosomal enzymes - was largely seen in HepG2 cells treated with PA for 48 h, whereas red fluorescence was very rare (Figure 2C). These results led us to propose that the colocalization of autophagosomes and lysosomes was prevented and the autophagosomal degradation was blocked. Yellow punctate fluorescence was reduced in JZG-treated cells and red diffuse fluorescence was increased (Figure 2C), suggesting that JZG promoted colocalization.

To confirm these findings, we established another stable mCherry-p62-expressing HepG2 cell line to visualize the cellular expression levels of p62, which inversely correlated with autophagic flux *via* selective incorporation into autophagosomes to be efficiently degraded by autophagy. We found that punctate fluorescence was enhanced in HepG2 cells treated with PA for 48 h and was weak in JZG-treated cells (Figure 3A), confirming the previous findings.

As it has been shown that mitochondrial dysfunction may block autophagic flux[22], we next examined whether the mitochondrial integrity was affected in PA-treated cells. MitoTracker and LysoTracker were used to stain the mitochondria and lysosomes, respectively. The results showed that mitochondrial dysfunction was much more serious in PA-treated cells than in control cells (Figure 3B). A protective effect of JZG on mitochondrial integrity was demonstrated and the colocalization of mitochondria and lysosomes in JZG-treated cells showed that the mitochondrial integrity was related to activation of autophagic flux. Together, these findings suggested that JZG increased the formation of both autophagosomes and autolysosomes and protected against PA-induced mitochondrial dysfunction by activating autophagy.

JZG protected mitochondrial integrity against oxidative stress

As the protective effect of JZG on mitochondrial integrity was demonstrated, we then examined whether oxidative stress was involved in this process. The ROS-sensitive fluorescent probe DCFH-DA was used to monitor cellular oxidative stress. We found that the accumulation of intracellular ROS was considerably increased in PA-treated cells, and JZG significantly reduced the PA-induced increase in ROS production

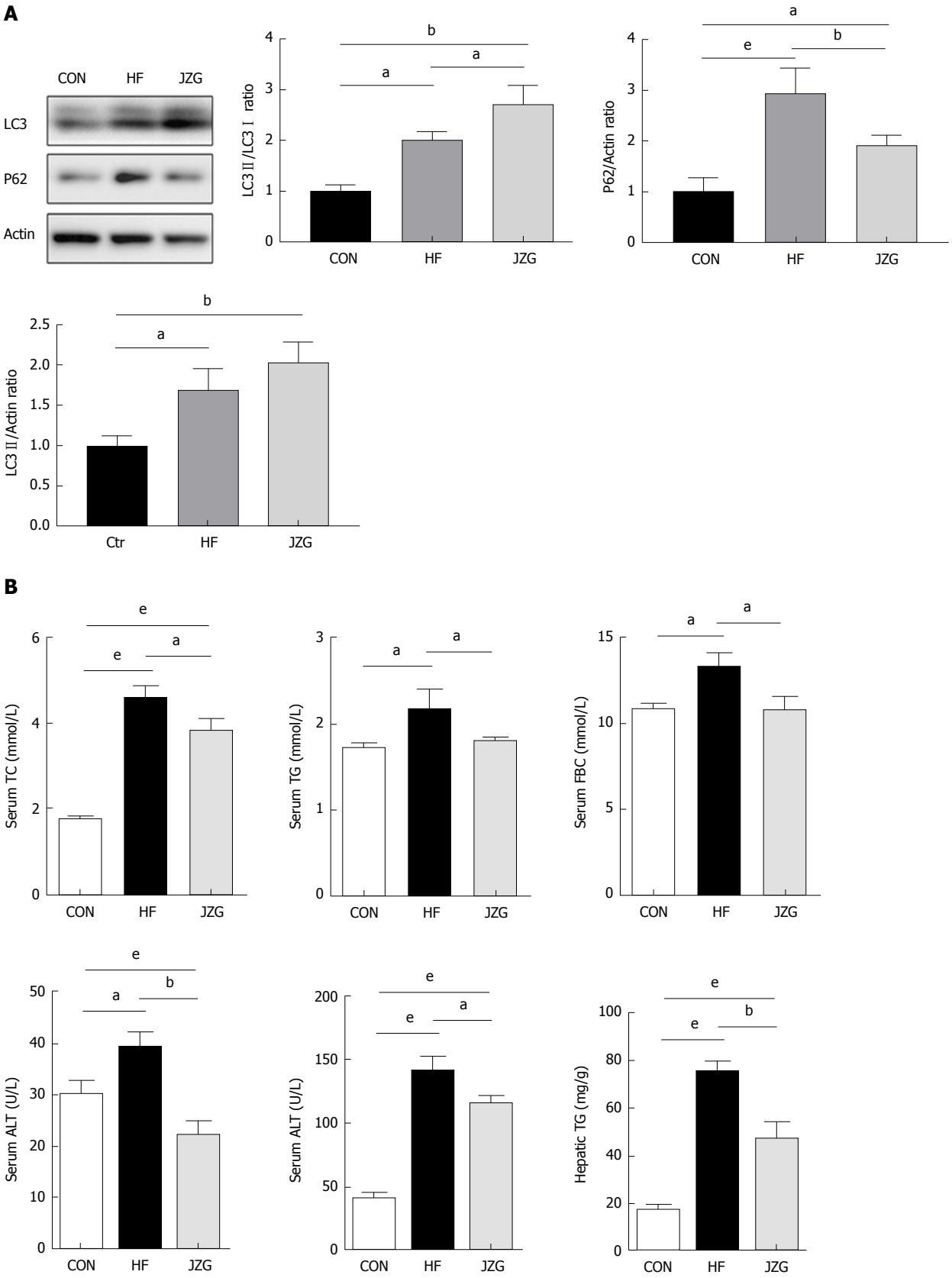
A
CON
HF
JZG
LC3
P62
Actin
LC3 II/LC3 I ratio
P62/Actin ratio
LC3 II/Actin ratio
Ctr
B
Serum TC (mmol/L)
Serum TG (mmol/L)
Serum FBC (mmol/L)
Serum ALT (U/L)
Serum ALT (U/L)
Hepatic TG (mg/g)

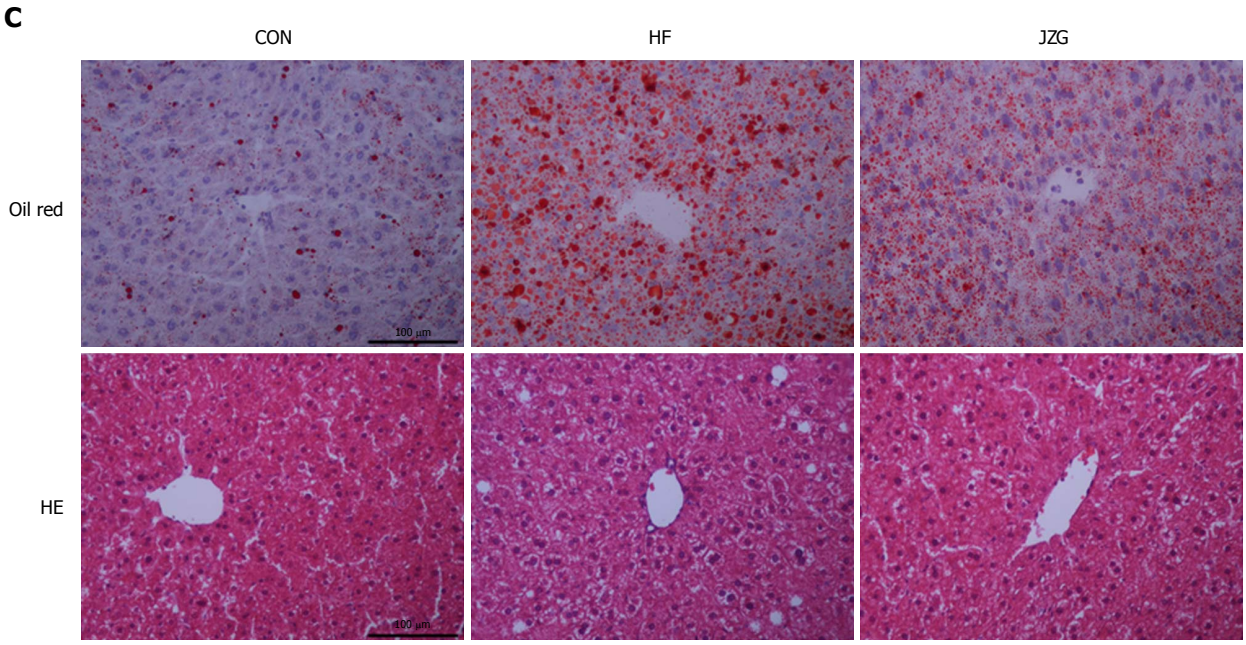

Figure 5 Autophagy was activated by Jiang Zhi Granule to improve non-alcoholic fatty liver disease *in vivo*. A: Autophagy of liver tissue was examined by western blot analyses; B: Biochemical analysis of TG, TC, ALT, AST and FBG using an automatic blood chemistry analyzer; C: Inflammation and lipid content in the liver was detected by HE staining and oil Red O staining. Data are expressed as mean ± SEM. $^{a}P < 0.05$, $^{b}P < 0.01$, $^{e}P < 0.001$. ALT: Alanine aminotransferase; AST: Aspartate aminotransferase; HE: Hematoxylin and eosin; JZG: Jiang Zhi Granule; PA: Palmitate; TC: Total cholesterol; TG: Triglycerides.

(Figure 4A), indicating the potential role of oxidative stress in mitochondrial dysfunction. We also monitored mitochondrial membrane potential with JC-1 to evaluate oxidative damage, and the results revealed a reduction in mitochondrial membrane potential in PA-treated cells, and JZG prevented this PA-induced reduction (Figure 4B), confirming that JZG protected mitochondrial integrity against oxidative stress in PA-induced mitochondrial dysfunction.

Autophagy was activated by JZG to improve NAFLD in vivo

A murine model of NAFLD induced by HFD was employed to assess the potential role of autophagy in metabolic stress-induced liver injury and inflammation. As expected, the HFD increased both the expression of LC3-Ⅱ/actin and p62 (Figure 5A), suggesting the activation of autophagy induction and inhibition of autophagic flux. JZG treatment induced an increase in LC3-Ⅱ/LC3-Ⅰ expression and led to a decrease in p62 expression (Figure 5A), indicating up-regulation of the autophagy pathway in JZG-treated mice.

Biochemical analyses showed that HFD elevated the expression of circulating ALT, aspartate aminotransferase, total cholesterol, triglycerides and fasting blood glucose as well as hepatic triglycerides, and JZG improved the metabolic disorder and associated liver injury (Figure 5B). The results of HE and oil red O staining demonstrated that lipid droplets and inflammation were induced by HFD and JZG ameliorated these conditions (Figure 5C). Together, these findings suggested that JZG had beneficial effects in improving NAFLD *in vivo*.

DISCUSSION

NAFLD, as the leading cause of chronic liver disease, could result in serious liver-related complications and an increase in overall mortality. In previous research, we demonstrated that the Chinese herbal formula, JZG, had beneficial effects in improving hepatic fat accumulation, and in this study, we showed that autophagy is critically involved in this process.

Autophagy occurs when autophagosomes are formed and autophagy induction is attributed to various origins, such as the endoplasmic reticulum, the Golgi apparatus, the mitochondria or the plasma membrane[23,24]. The autophagosomes then become autolysosomes by fusing with lysosomes and degrading the components in cytosols[25,26]. Thus, the upstream event of autophagy induction was presented by LC3-Ⅱ/actin expression in this study, and the downstream event of autophagic flux was presented by the expression of LC3-Ⅱ/LC3-Ⅰ. Stable fluorescence-expressing cell lines of LC3 were established to visualize the whole progression of autophagic flux. Results showed that metabolic stress-induced hepatocyte injury exhibited dual effects on autophagy by activating autophagy induction and blocking autophagic flux.

A series of signaling pathways and regulators which regulate autophagy have been identified in the past decade. In this research, a classic signaling pathway, the PI3K-AKT-mTOR signaling pathway[27], was confirmed to be important in response to PA challenge. As the

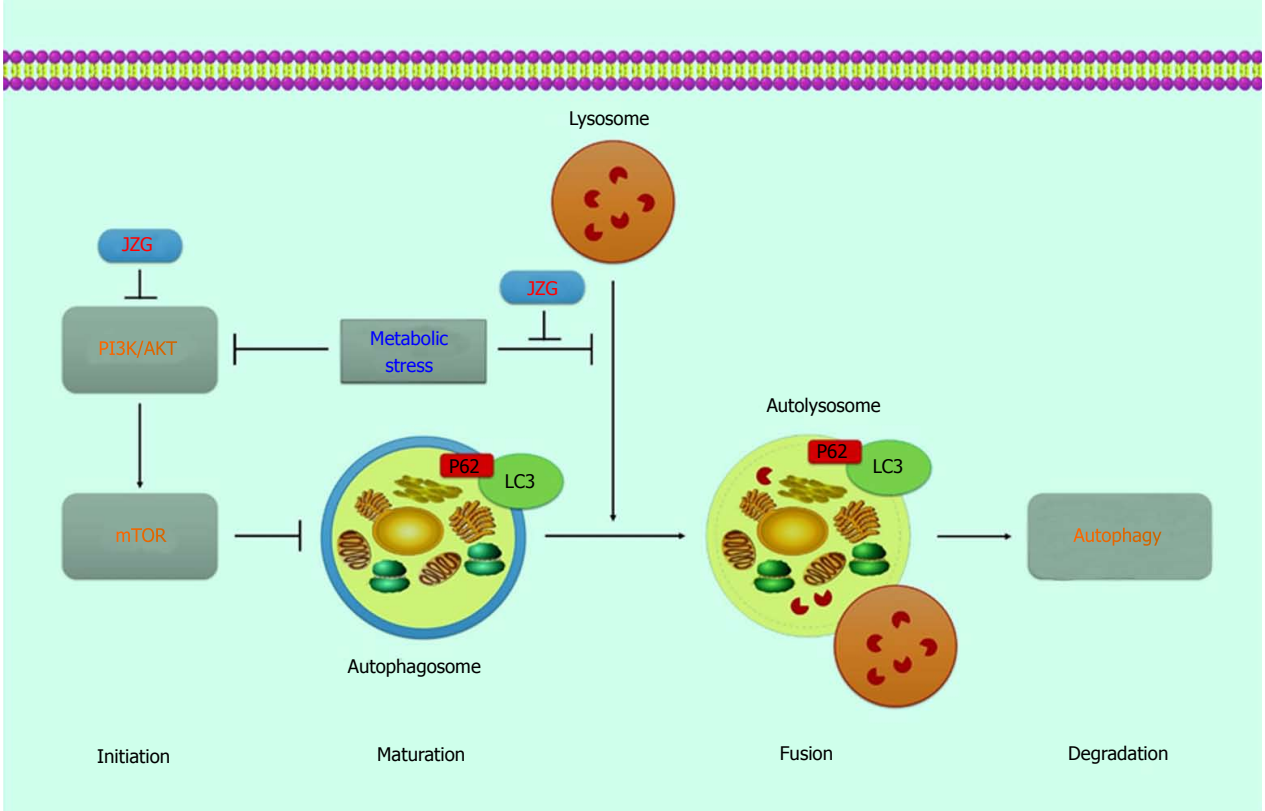

Figure 6 The potential role of autophagy in metabolic stress-induced hepatocyte injury and the protective mechanism of JZG in this process. JZG: Jiang Zhi Granule.

core target in this signaling pathway, mTOR, a master regulator of cellular metabolism, can be stimulated by multiple stimulants, such as nutritional status, hormonal factors and oxygen concentrations[28]. Under these conditions, mTOR complex 1 (mTORC1) will inhibit the ULK complex by phosphorylating Atg13 and ULK1/2, which results in autophagy suppression[29]. However, restraints on both phosphorylation signaling processes of PI3K and mTOR were observed in JZG-treated cells, indicating that the PI3K-AKT-mTOR pathway was involved in autophagy in the JZG-treated cells.

Subsequent studies have shown that SQSTM1/p62 accumulation is correlated with NAFLD and the fusion of isolated hepatic autophagosomes and lysosomes is different in NAFLD patients[30], which suggests that an excessive amount of lipids may contribute to SQSTM1/p62 accumulation by suppressing autophagosomes/lysosome fusion[31,32]. Thus, we examined the SQSTM1/p62 accumulation and the results confirmed previous findings.

Fluorescence staining was performed to connect the mitochondrial integrity with oxidative stress induced by PA. We also found that JZG could activate the autophagy process by either induction of autophagosomes or colocalization of autophagosomes and lysosomes as well as degradation of autolysosomes to protect against metabolic stress-induced hepatocyte injury in NAFLD (Figure 6).

Limitations should be acknowledged. The complex compounds contained in this prescription may have led to multitarget effects, and a series of signaling pathways and regulators were not examined. Beyond that, as p62 could also be degraded by proteasome, further studies on this aspect should be continually conducted to confirm the findings in the future. However, as the current epidemic of obesity and obesity-related NAFLD continues to increase, new approaches for prevention and treatment are urgently needed, and traditional Chinese medicine, as an alternative and complementary medicine, may be an effective addition to the current standardized intervention strategy.

ARTICLE HIGHLIGHTS

Research background

Non-alcoholic fatty liver disease (NAFLD), as the leading cause of chronic liver disease, can result in serious liver-related complications and an increase in overall mortality. However, the pathogenesis of NAFLD is still unknown and no effective therapeutic strategy has been accepted as the standard treatment option. In previous studies, the authors found that JZG had beneficial effects in improving hepatic fat accumulation, metabolic disorder and associated liver injury, and its efficacy in patients with NAFLD was also confirmed.

Research motivation

Autophagy is important in liver diseases, and research has demonstrated that autophagy regulators can improve hepatic function. However, no effective therapeutic strategy has been accepted as the standard option for NAFLD and

its complications. Thus, novel treatments are still urgently needed to prevent or delay the onset as well as the progression of NAFLD.

Research objectives

NAFLD, as the leading cause of chronic liver disease, could result in serious liver-related complications and an increase in overall mortality. And traditional Chinese medicine, as an alternative and complementary medicine, may be an effective addition to the current standardized intervention strategy.

Research methods

The process of autophagy was detected by the expressions of LC3 and SQSTM1/p62. The upstream event of autophagy induction was presented by LC3-Ⅱ/actin expression and the downstream event of autophagic flux was presented by the expressions of LC3-Ⅱ/LC3-Ⅰ and SQSTM1/p62. Stable fluorescence-expressing cell lines were established with mRFP-GFP-LC3 and mCherry-p62 lentivirus to visualize the whole progression of autophagic flux.

Research results

In previous research, the authors had demonstrated that the Chinese herbal formula JZG had beneficial effects in improving hepatic fat accumulation. In this study, autophagy was demonstrated to be critically involved in this process.

Research conclusions

The authors confirmed that metabolic stress-induced hepatocyte injury exhibited dual effects on autophagy, while JZG activated the whole process to provide beneficial effects in NAFLD.

Research perspectives

The exact compounds contained in this prescription are still unknown and the complex compounds might have led to multitarget effects. A systems pharmacology approach to determine the active compounds and action mechanisms might be a good method for the future research.

REFERENCES

1 **Bellentani S**, Marino M. Epidemiology and natural history of non-alcoholic fatty liver disease (NAFLD). *Ann Hepatol* 2009; **8** Suppl 1: S4-S8 [PMID: 19381118]
2 **López-Velázquez JA**, Silva-Vidal KV, Ponciano-Rodríguez G, Chávez-Tapia NC, Arrese M, Uribe M, Méndez-Sánchez N. The prevalence of nonalcoholic fatty liver disease in the Americas. *Ann Hepatol* 2014; **13**: 166-178 [PMID: 24552858]
3 **Wree A**, Broderick L, Canbay A, Hoffman HM, Feldstein AE. From NAFLD to NASH to cirrhosis-new insights into disease mechanisms. *Nat Rev Gastroenterol Hepatol* 2013; **10**: 627-636 [PMID: 23958599 DOI: 10.1038/nrgastro.2013.149]
4 **Tiniakos DG**, Vos MB, Brunt EM. Nonalcoholic fatty liver disease: pathology and pathogenesis. *Annu Rev Pathol* 2010; **5**: 145-171 [PMID: 20078219 DOI: 10.1146/annurev-pathol-121808-102132]
5 **Reiniers MJ**, van Golen RF, van Gulik TM, Heger M. Reactive oxygen and nitrogen species in steatotic hepatocytes: a molecular perspective on the pathophysiology of ischemia-reperfusion injury in the fatty liver. *Antioxid Redox Signal* 2014; **21**: 1119-1142 [PMID: 24294945 DOI: 10.1089/ars.2013.5486]
6 **Jung UJ**, Choi MS. Obesity and its metabolic complications: the role of adipokines and the relationship between obesity, inflammation, insulin resistance, dyslipidemia and nonalcoholic fatty liver disease. *Int J Mol Sci* 2014; **15**: 6184-6223 [PMID: 24733068 DOI: 10.3390/ijms15046184]
7 **Yin XM**, Ding WX, Gao W. Autophagy in the liver. *Hepatology* 2008; **47**: 1773-1785 [PMID: 18393362 DOI: 10.1002/hep.22146]
8 **Cheng Y**, Ren X, Hait WN, Yang JM. Therapeutic targeting of autophagy in disease: biology and pharmacology. *Pharmacol Rev* 2013; **65**: 1162-1197 [PMID: 23943849 DOI: 10.1124/pr.112.007120]
9 **Kim KH**, Lee MS. Autophagy--a key player in cellular and body metabolism. *Nat Rev Endocrinol* 2014; **10**: 322-337 [PMID: 24663220 DOI: 10.1038/nrendo.2014.35]
10 **Johansen T**, Lamark T. Selective autophagy mediated by autophagic adapter proteins. *Autophagy* 2011; **7**: 279-296 [PMID: 21189453]
11 **Stolz A**, Ernst A, Dikic I. Cargo recognition and trafficking in selective autophagy. *Nat Cell Biol* 2014; **16**: 495-501 [PMID: 24875736 DOI: 10.1038/ncb2979]
12 **Christian P**, Sacco J, Adeli K. Autophagy: Emerging roles in lipid homeostasis and metabolic control. *Biochim Biophys Acta* 2013; **1831**: 819-824 [PMID: 23274236 DOI: 10.1016/j.bbalip.2012.12.009]
13 **Singh R**, Kaushik S, Wang Y, Xiang Y, Novak I, Komatsu M, Tanaka K, Cuervo AM, Czaja MJ. Autophagy regulates lipid metabolism. *Nature* 2009; **458**: 1131-1135 [PMID: 19339967 DOI: 10.1038/nature07976]
14 **Lin CW**, Zhang H, Li M, Xiong X, Chen X, Chen X, Dong XC, Yin XM. Pharmacological promotion of autophagy alleviates steatosis and injury in alcoholic and non-alcoholic fatty liver conditions in mice. *J Hepatol* 2013; **58**: 993-999 [PMID: 23339953 DOI: 10.1124/10.1016/j.jhep.2013.01.011]
15 **Song HY**, Zhang L, Pan JL, Yang LL, Ji G. Bioactivity of five components of Chinese herbal formula Jiangzhi granules against hepatocellular steatosis. *J Integr Med* 2013; **11**: 262-268 [PMID: 23867244 DOI: 10.3736/jintegrmed2013034]
16 **Wang M**, Sun S, Wu T, Zhang L, Song H, Hao W, Zheng P, Xing L, Ji G. Inhibition of LXRα/SREBP-1c-Mediated Hepatic Steatosis by Jiang-Zhi Granule. *Evid Based Complement Alternat Med* 2013; **2013**: 584634 [PMID: 23762146 DOI: 10.1155/2013/584634]
17 **Pan J**, Wang M, Song H, Wang L, Ji G. The efficacy and safety of traditional chinese medicine (jiang zhi granule) for nonalcoholic Fatty liver: a multicenter, randomized, placebo-controlled study. *Evid Based Complement Alternat Med* 2013; **2013**: 965723 [PMID: 24369486 DOI: 10.1155/2013/965723]
18 **Matsushita N**, Osaka T, Haruta I, Ueshiba H, Yanagisawa N, Omori-Miyake M, Hashimoto E, Shibata N, Tokushige K, Saito K, Tsuneda S, Yagi J. Effect of Lipopolysaccharide on the Progression of Non-Alcoholic Fatty Liver Disease in High Caloric Diet-Fed Mice. *Scand J Immunol* 2016; **83**: 109-118 [PMID: 26524607 DOI: 10.1111/sji.12397]
19 **Cui W**, Wang M, Maegawa H, Teranishi Y, Kawada N. Inhibition of the activation of hepatic stellate cells by arundic acid via the induction of cytoglobin. *Biochem Biophys Res Commun* 2012; **425**: 642-648 [PMID: 22850540 DOI: 10.1016/j.bbrc.2012.07.126]
20 **Shu X**, Wang M, Xu H, Liu Y, Huang J, Yao Z, Zhang L. Extracts of Salvia-Nelumbinis Naturalis Ameliorate Nonalcoholic Steatohepatitis via Inhibiting Gut-Derived Endotoxin Mediated TLR4/NF-κB Activation. *Evid Based Complement Alternat Med* 2017; **2017**: 9208314 [PMID: 28831287 DOI: 10.1155/2017/9208314]
21 **Kamikubo R**, Kai K, Tsuji-Naito K, Akagawa M. β-Caryophyllene attenuates palmitate-induced lipid accumulation through AMPK signaling by activating CB2 receptor in human HepG2 hepatocytes. *Mol Nutr Food Res* 2016; **60**: 2228-2242 [PMID: 27234712 DOI: 10.1002/mnfr.201600197]
22 **Ruan L**, Zhou C, Jin E, Kucharavy A, Zhang Y, Wen Z, Florens L, Li R. Cytosolic proteostasis through importing of misfolded proteins into mitochondria. *Nature* 2017; **543**: 443-446 [PMID: 28241148 DOI: 10.1038/nature21695]
23 **Hamasaki M**, Shibutani ST, Yoshimori T. Up-to-date membrane biogenesis in the autophagosome formation. *Curr Opin Cell Biol* 2013; **25**: 455-460 [PMID: 23578367 DOI: 10.1016/j.ceb.2013.03.004]
24 **Lamb CA**, Yoshimori T, Tooze SA. The autophagosome: origins unknown, biogenesis complex. *Nat Rev Mol Cell Biol* 2013; **14**: 759-774 [PMID: 24201109 DOI: 10.1038/nrm3696]
25 **Kaur J**, Debnath J. Autophagy at the crossroads of catabolism and anabolism. *Nat Rev Mol Cell Biol* 2015; **16**: 461-472 [PMID: 26177004 DOI: 10.1038/nrm4024]
26 **Madrigal-Matute J**, Cuervo AM. Regulation of Liver Metabolism by Autophagy. *Gastroenterology* 2016; **150**: 328-339 [PMID: 26453774 DOI: 10.1053/j.gastro.2015.09.042]

27 **Liu HY**, Han J, Cao SY, Hong T, Zhuo D, Shi J, Liu Z, Cao W. Hepatic autophagy is suppressed in the presence of insulin resistance and hyperinsulinemia: inhibition of FoxO1-dependent expression of key autophagy genes by insulin. *J Biol Chem* 2009; **284**: 31484-31492 [PMID: 19758991 DOI: 10.1074/jbc.M109.033936]

28 **Levine B**, Kroemer G. Autophagy in the pathogenesis of disease. *Cell* 2008; **132**: 27-42 [PMID: 18191218 DOI: 10.1016/j.cell.2007.12.018]

29 **Kim YC**, Guan KL. mTOR: a pharmacologic target for autophagy regulation. *J Clin Invest* 2015; **125**: 25-32 [PMID: 25654547 DOI: 10.1172/JCI73939]

30 **Fukuo Y**, Yamashina S, Sonoue H, Arakawa A, Nakadera E, Aoyama T, Uchiyama A, Kon K, Ikejima K, Watanabe S. Abnormality of autophagic function and cathepsin expression in the liver from patients with non-alcoholic fatty liver disease. *Hepatol Res* 2014; **44**: 1026-1036 [PMID: 24299564 DOI: 10.1111/hepr.12282]

31 **Koga H**, Kaushik S, Cuervo AM. Altered lipid content inhibits autophagic vesicular fusion. *FASEB J* 2010; **24**: 3052-3065 [PMID: 20375270 DOI: 10.1096/fj.09-144519]

32 **Inami Y**, Yamashina S, Izumi K, Ueno T, Tanida I, Ikejima K, Watanabe S. Hepatic steatosis inhibits autophagic proteolysis via impairment of autophagosomal acidification and cathepsin expression. *Biochem Biophys Res Commun* 2011; **412**: 618-625 [PMID: 21856284 DOI: 10.1016/j.bbrc.2011.08.012]

P- Reviewer: Demonacos C, Marcos R, Osna NA
S- Editor: Gong ZM **L- Editor**: Filipodia **E- Editor**: Huang Y

World Journal of Gastroenterology

Submit a Manuscript: http://www.f6publishing.com

World J Gastroenterol 2018 March 7; 24(9): 1004-1012

DOI: 10.3748/wjg.v24.i9.1004

ISSN 1007-9327 (print) ISSN 2219-2840 (online)

ORIGINAL ARTICLE

Basic Study

Long noncoding RNA RP4 functions as a competing endogenous RNA through miR-7-5p sponge activity in colorectal cancer

Mu-Lin Liu, Qiao Zhang, Xiao Yuan, Long Jin, Li-Li Wang, Tao-Tao Fang, Wen-Bin Wang

Mu-Lin Liu, Long Jin, Li-Li Wang, Tao-Tao Fang, Department of Gastrointestinal Surgery, the First Affiliated Hospital of Bengbu Medical College, Bengbu 233004, Anhui Province, China

Qiao Zhang, Department of General Surgery, the First Affiliated Hospital of Xinxiang Medical University, Xinxiang 453100, Henan Province, China

Xiao Yuan, Wen-Bin Wang, Department of General Surgery, the Fourth Affiliated Hospital of Anhui Medical University, Hefei 230022, Anhui Province, China

ORCID number: Mu-Lin Liu (0000-0003-3930-678X); Qiao Zhang (0000-0001-5413-4547); Xiao Yuan (0000-0002-4299-7377); Long Jin (0000-0002-7765-4091); Li-Li Wang (0000-0003-0439-8119); Tao-Tao Fang (0000-0002-1831-1937); Wen-Bin Wang (0000-0002-9023-6855).

Author contributions: Liu ML, Zhang Q and Yuan X contributed equally to this work; Liu ML and Zhang Q conceived the study and participated in its design and coordination; Yuan X drafted and revised the manuscript; Jin L helped with the statistical analysis; Wang LL and Fang TT performed the experiments; Wang WB conceived the study and revised the manuscript; all authors read and approved the final manuscript.

Supported by Scientific Research Foundation of Anhui Education Department, No. KJ2017A219 to Liu ML; Scientific Research Foundation of Academic Leader of Anhui Province, No. 2016H105 to Liu ML; Education Talent Foundation of Universities of Anhui Education Department, No. gxbjZD2016070 to Liu ML; National Natural Science Foundation of China, No. 81500373 to Wang WB; and Natural Science Foundation of Anhui Province, No. 1608085MH193 to Wang WB.

Institutional review board statement: The study was reviewed and approved by the Ethics Committee of the First Affiliated Hospital of Bengbu Medical College.

Institutional animal care and use committee statement: All procedures involving animals were reviewed and approved by the Institutional Animal Care and Use Committee of SHRM.

Conflict-of-interest statement: The authors declare that there is no conflict of interest related to this study.

Data sharing statement: The datasets supporting the conclusions of this article are included within the article.

Manuscript source: Unsolicited manuscript

Correspondence to: Wen-Bin Wang, PhD, Doctor, Professor, Department of General Surgery, the Fourth Affiliated Hospital of Anhui Medical University, No. 372, Tunxi Road, Hefei 230022, Anhui Province, China. surdoctor@163.com
Telephone: +86-551-62879386
Fax:+86-552-3070260

Received: November 15, 2017
Peer-review started: November 16, 2017
First decision: December 20, 2017
Revised: December 26, 2017
Accepted: January 16, 2018
Article in press: January 16, 2018
Published online: March 7, 2018

Abstract

AIM

To investigate the role of long noncoding RNA (lncRNA) RP4 in colorectal cancer.

METHODS
Lentivirus-mediated lncRNA RP4 overexpression and knockdown were performed in the colorectal cancer cell line SW480. Cell proliferation, tumor growth, and early apoptosis were evaluated by a cell counting kit-8 assay, an *in vivo* xenograft tumor model, and annexin V/propidium iodide staining, respectively. Analysis of the lncRNA RP4 mechanism involved assessment of the association of its expression with miR-7-5p and the *SH3GLB1* gene. Western blot analysis was also performed to assess the effect of lncRNA RP4 on the autophagy-mediated cell death pathway and phosphatidylinositol-3-kinase (PI3K)/Akt signaling.

RESULTS
Cell proliferation, tumor growth, and early apoptosis in SW480 cells were negatively regulated by lncRNA RP4. Functional experiments indicated that lncRNA RP4 directly upregulated *SH3GLB1* expression by acting as a competing endogenous RNA (ceRNA) for miR-7-5p. This interaction led to activation of the autophagy-mediated cell death pathway and de-repression of PI3K and Akt phosphorylation in colorectal cancer cells *in vivo*.

CONCLUSION
Our results demonstrated that lncRNA RP4 is a ceRNA that plays an important role in the pathogenesis of colorectal cancer, and could be a potential therapeutic target for colorectal cancer treatment.

Key words: Colorectal cancer; Long noncoding RNA RP4; SH3GLB1; miR-7-5p; Competing endogenous RNA

Core tip: In the present study, we investigated the role of long noncoding RNA (lncRNA) RP4 in colorectal cancer using an *in vivo* cell model and an *in vivo* xenograft model. Mechanistic analysis suggested that lncRNA RP4 functions in colorectal cancer pathogenesis as a competing endogenous RNA that regulates SH3GLB1 expression by acting as a sponge for miR-7-5p. It could also serve as a potential therapeutic target for colorectal cancer treatment.

Liu ML, Zhang Q, Yuan X, Jin L, Wang LL, Fang TT, Wang WB. Long noncoding RNA RP4 functions as a competing endogenous RNA through miR-7-5p sponge activity in colorectal cancer. *World J Gastroenterol* 2018; 24(9): 1004-1012 Available from: URL: http://www.wjgnet.com/1007-9327/full/v24/i9/1004.htm DOI: http://dx.doi.org/10.3748/wjg.v24.i9.1004

INTRODUCTION

Colorectal cancer is the fourth most common cancer and the fifth most common cause of cancer-related death in China, with an estimated 331300 newly diagnosed patients and 159300 deaths in 2012[1]. Surgical resection followed by adjuvant chemotherapy is the most commonly used strategy for colorectal cancer management. However, although the overall 5-year survival rate of colorectal cancer has improved to 65%, the 5-year survival rate was only 15% in patients presenting with distant metastasis[2], reflecting the poor treatment response in some patients. Therefore, it is necessary to identify effective therapeutic targets to improve treatment and prognosis.

Long noncoding RNAs (lncRNAs), > 200 nucleotides in length, are a recently discovered novel class of genes with regulatory functions but lacking protein-coding ability. Several studies have identified important roles for lncRNAs in a wide range of cellular processes, including X chromosome inactivation, splicing, imprinting, epigenetic control, and gene transcription regulation[3-5]. Moreover, the dysregulated expression of lncRNAs is present in various human diseases, especially in cancers including breast cancer, lung cancer, gastric cancer, and colorectal cancer[6-8]. Indeed, several recent pieces of evidence suggest that lncRNAs are involved in the development and progression of human colorectal cancer and may serve as novel therapeutic targets[9-11]. However, the role of lncRNAs in colorectal cancer is largely unknown.

The dysregulation of lncRNA RP4 has previously been shown by expression profile analysis of a transcriptome microarray. Therefore, the present study investigated the role of lncRNA RP4 in colorectal cancer using an *in vitro* cell model and an *in vivo* xenograft model. Mechanistic analysis suggested that lncRNA RP4 functions in colorectal cancer pathogenesis as a competing endogenous RNA (ceRNA) that regulates *SH3GLB1* expression by acting as a sponge for the microRNA (miRNA) miR-7-5p. It could also serve as a potential therapeutic target for colorectal cancer treatment.

MATERIALS AND METHODS

Ethics statement

This study was conducted in accordance with the ethical standards, the Declaration of Helsinki, and national and international guidelines, and was approved by the authors' institutional review board, which adheres to generally accepted international guidelines for animal experimentation.

Cell culture

The human colorectal cancer cell line SW480 was obtained from the American Type Culture Collection. Cells were maintained as monolayers in cell culture flasks with RPMI1640 medium containing 10% (v/v) fetal bovine serum and 1% antibiotics. They were cultured at 37 ℃ in a humidified atmosphere with 5% CO_2. All cell culture media and additives were purchased from Invitrogen (CA, United States).

Lentiviral short hairpin (sh)RNA particles

Recombinant lentiviral particles expressing lncRNA RP4

Table 1 Sequences of the primers used

Gene	Forward primer (5′-3′)	Reverse primer (5′-3′)
ENST00000565575	ATCCGTTCCAAATCCTGTCGT	TTCAAGCAGAGGCTGTATCGTG
SH3GLB1	CGCTGTCTGAATGACTTTGT	CCTTTCTGCTGCCACTACAC
β-actin	GTGGCCGAGGACTTTGATTG	CCTGTAACAACGCATCTCATATT

or lncRNA RP4 small interfering (si)RNA were obtained from GenePharm Co., Ltd. (Shanghai, China). Cells were grown to approximately 40% confluence and infected with lentiviral particles in complete medium for 48 h. To increase the infection efficiency, cells were co-treated with the cationic polymer polybrene (8 μg/mL in water). Neither shRNA nor polybrene affected cell viability. siRNA and shRNA had no off-target effects, and did not affect cell adherence, shape, or viability at the indicated multiplicity of infection.

Real-time quantitative reverse transcription polymerase chain reaction

Total RNA was extracted from SW480 cells using TRIzol reagent (Invitrogen). RT-PCR was carried out using a One Step SYBR PrimeScript RT-PCR kit (Takara, Dalian, China) and an iQ5 Real-time PCR Detection system (Bio-Rad, Hercules, CA, United States) for evaluation of the expression of lncRNA RP4. The miRNA miR-7-5p was obtained using the PureLink miRNA Isolation Kit (Invitrogen), and the quantification of miRNA expression was performed with a TaqMan MicroRNA Assay Kit (Applied Biosystems, Foster City, CA, United States). The expression of β-actin and *U6* snRNA genes was assessed simultaneously in all samples as an internal control for lncRNA/mRNA and miRNA expression, respectively. Relative gene expression was determined by the $2^{-\Delta\Delta CT}$ method[12]. Oligonucleotide primers specific for lncRNA RP4, *SH3GLB1*, and β-actin are listed in Table 1.

Western blot analysis

Cells were lysed in RIPA buffer, centrifuged at high speed, and then underwent protein quantification using a bicinchoninic acid assay. Cellular proteins were separated by sodium dodecyl sulfate polyacrylamide gel electrophoresis and transferred onto polyvinylidene difluoride membranes. After blocking, the membranes were incubated with anti-total- or -phosphor-PI3K, phospho-Akt, LC3A/B, Bax, and caspase 3 monoclonal primary antibodies (Cell Signaling Technology, Cambridge, MA, United States). β-actin (Santa Cruz Biotechnology, Santa Cruz, CA, United States) was used as the loading control. Appropriate horseradish peroxidase-conjugated secondary antibodies were applied to detect labeled proteins. The protein bands were developed with SuperSignal Ultra Chemiluminescent Substrate (Pierce, Rockford, IL, United States) on X-ray films (Kodak, Tokyo, Japan).

Cell proliferation

SW480 cells (3×10^3 cells) were seeded in 96-well plates in complete medium and infected with lncRNA RP4, lncRNA RP4 siRNA, or control lentivirus particles. Two days later, cell proliferation was evaluated by the cell counting kit-8 method according to the manufacturer's instructions using a microplate reader (Molecular Devices, Sunnyvale, CA, United States) to measure the absorbance.

Nude mouse model of ectopic tumors

Athymic nude (nu/nu) mice at 6 wk old were purchased from Shanghai SLAC Laboratory Animal Co., Ltd. Tumors were generated by the subcutaneous injection of 2×10^6 SW480 cells infected with lncRNA RP4, lncRNA RP4 siRNA, or control lentivirus particles and suspended in 50 μL of PBS into the dorsal region near the thigh. Mice were then weighed and assessed for tumor size every 7 wk by measuring the tumor length and width.

Cell apoptosis analysis

SW480 cells (3×10^5 cells) were seeded in 6-well plates in complete medium and infected with lncRNA RP4, lncRNA RP4 siRNA, or control lentivirus particles. Two days later, cell proliferation was evaluated by flow cytometry (FACScalibur; BD Biosciences, CA, United States) after annexin V/propidium iodide staining (Beyotime institution, Nantong, China).

Statistical analysis

All statistical analyses were carried out using SPSS v18 software (SPSS, Chicago, IL, United States). Data are presented as the mean ± SD. The Student's *t*-test or one-way analysis of variance were used to examine differences between two or multiple groups. Correlation analyses of the expression levels of lncRNA RP4, *SH3GLB1*, and miR-7-5p were performed using Pearson's correlation coefficient. A P-value < 0.05 was considered statistically significant.

RESULTS

lncRNA RP4 regulates proliferation, tumor growth, and early apoptosis in colorectal cancer cells

To investigate the role of lncRNA RP4 in the pathogenesis of colorectal cancer, we performed lentivirus-mediated overexpression and knockdown. As shown in Figure 1A, SW480 cell proliferation was negatively regulated by lncRNA RP4, while early apoptosis was positively regulated by lncRNA RP4 (Figure 1C and D). These results suggested that lncRNA RP4 exerts a negative regulatory role in colorectal cancer cell

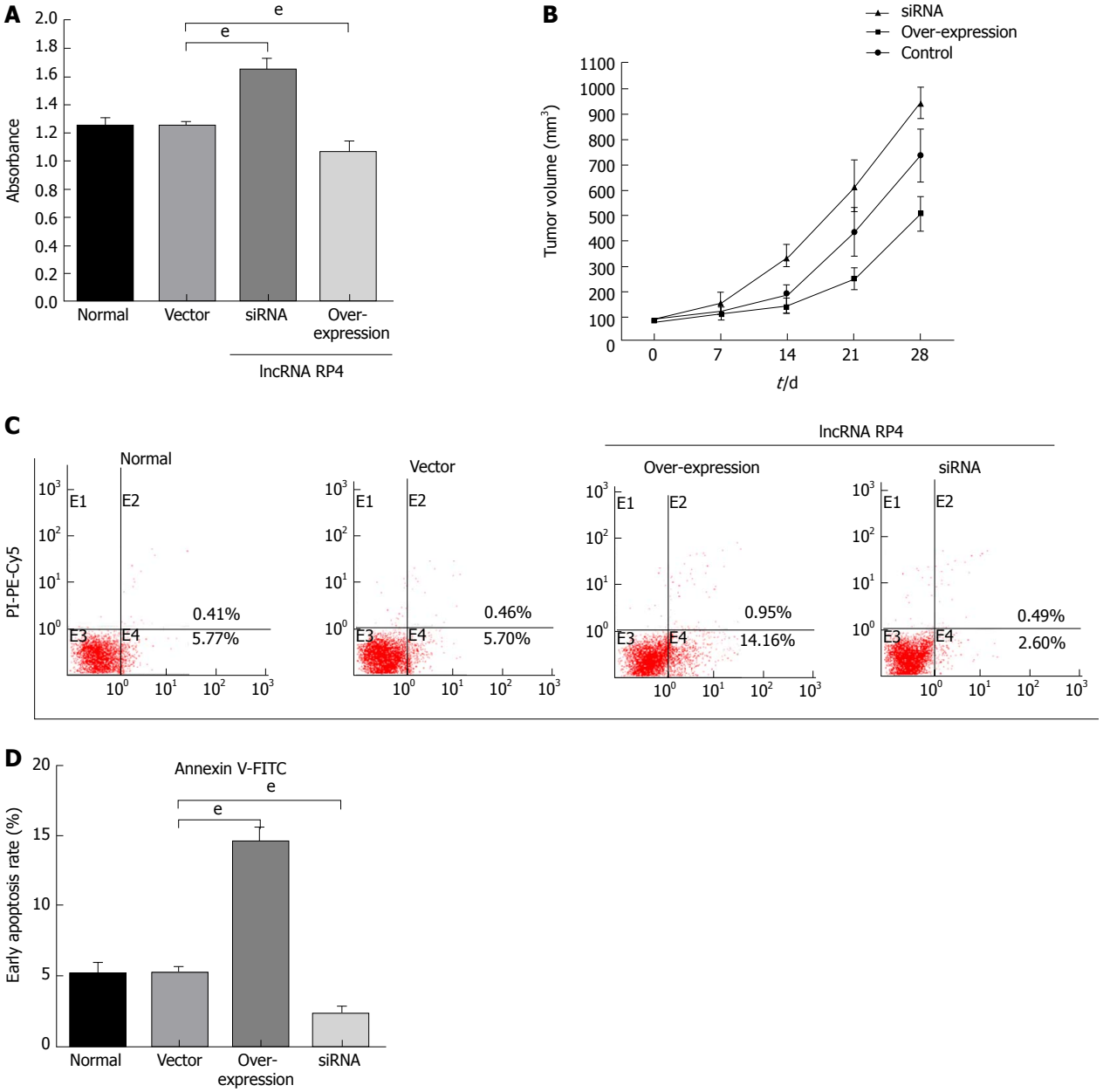

Figure 1 lncRNA RP4 regulates proliferation, tumor growth, and early apoptosis in colorectal cancer cells. Lentivirus-mediated lncRNA RP4 overexpression and knockdown were performed in the colorectal cancer line SW480, and cell proliferation, tumor growth, and early apoptosis were examined. A: Cell proliferation was examined by the CCK-8 assay. lncRNA RP4 overexpression and knockdown were shown to decrease and increase cell proliferation, respectively. B: Tumor growth was evaluated by tumor volume change. lncRNA RP4 overexpression and knockdown were shown to significantly decrease and increase tumor volume, respectively, at weeks 14, 21, and 28. C: Flow cytometry assessment of early apoptosis. lncRNA RP4 overexpression and knockdown increased and decreased early apoptosis, respectively, in colorectal cancer. D: Early apoptosis quantification. $^{e}P < 0.001$ for between-group comparisons.

proliferation and a positive regulatory role in early apoptosis of colorectal cancer cells.

lncRNA RP4 inhibits the growth of colorectal cancer on mice

Compared with the control group, colorectal cancer with lncRNA RP4 siRNA showed a bigger volume, while there was a smaller volume in the group with lncRNA RP4 overexpression (Figure 1B). Consistent with the results in cell line, the results *in vivo* also suggested that lncRNA RP4 plays an inhibitory role in colorectal cell growth.

lncRNA RP4 inhibits the growth of colorectal cancer cells by regulating SH3GLB1

To explore the mechanism of lncRNA RP4-mediated effects in colorectal cancer cells, we examined *SH3GLB1* expression in SW480 cells following lncRNA RP4 overexpression and knockdown. lncRNA RP4 was found to positively regulate *SH3GLB1* expression, and correlation analyses further confirmed the existence of a significant correlation between lncRNA RP4 and

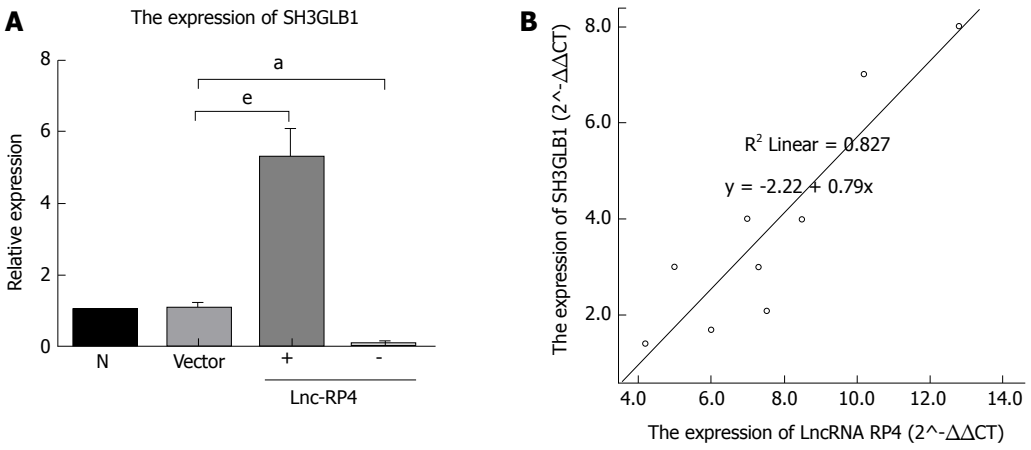

Figure 2 lncRNA RP4 affects the expression of *SH3GLB1* in colorectal cancer cells. Lentivirus-mediated lncRNA RP4 overexpression and knockdown were performed in *SW480* cells, and *SH3GLB1* expression was evaluated by real-time quantitative PCR, followed by association analyses between *SH3GLB1* and lncRNA RP4 levels. A: LncRNA RP4 overexpression and knockdown, respectively, increased and decreased *SH3GLB1* expression in SW480 cells. B: Correlation analyses revealed a linear association between the expression of *SH3GLB1* and lncRNA RP4, with an r^2 value of 0.827. $^aP < 0.05$ and $^eP < 0.001$ for between-group comparisons.

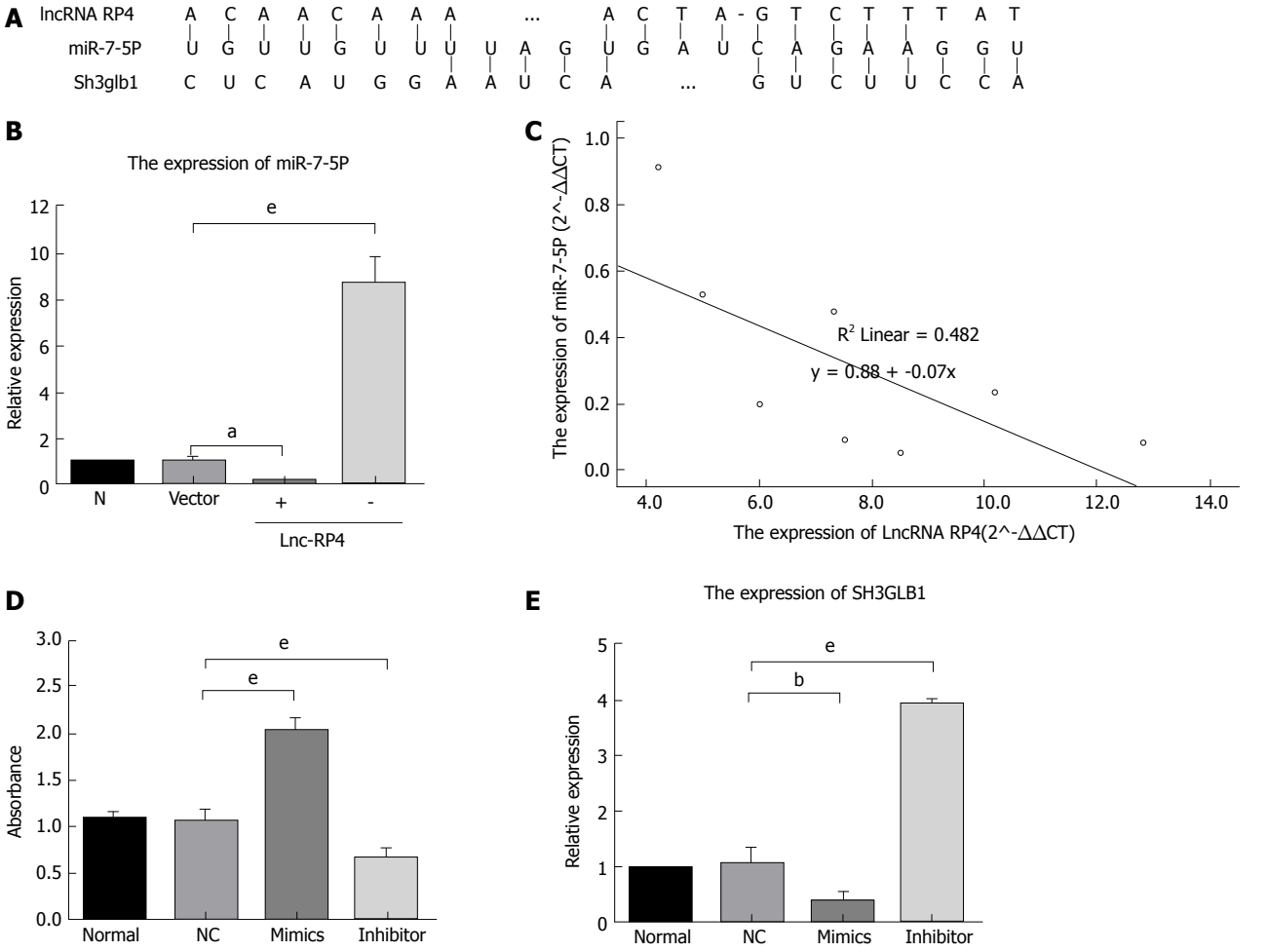

Figure 3 lncRNA RP4 functions as an miR-7-5p decoy in colorectal cancer cells. A: The predicted miR-7-5p binding sites on the *SH3GLB1* and lncRNA RP4 transcript. B: LncRNA RP4 overexpression and knockdown, respectively, decreased and increased the expression of miR-7-5p in SW480 cells. C: Correlation analyses revealed a linear association between the expression of lncRNA RP4 and miR-7-5p, with an r^2 value of 0.482. D: *SW480* cells were transfected with an miR-7-5p mimic and inhibitor, and cell proliferation was evaluated by the CCK-8 assay. miR-7-5p overexpression and knockdown increased and decreased cell proliferation, respectively. E. Real-time quantitative PCR showed that miR-7-5p overexpression and knockdown, respectively, decreased and increased *SH3GLB1* expression level in SW480 colorectal cancer cells. $^aP < 0.05$, $^bP < 0.01$, and $^eP < 0.001$ for between-group comparisons.

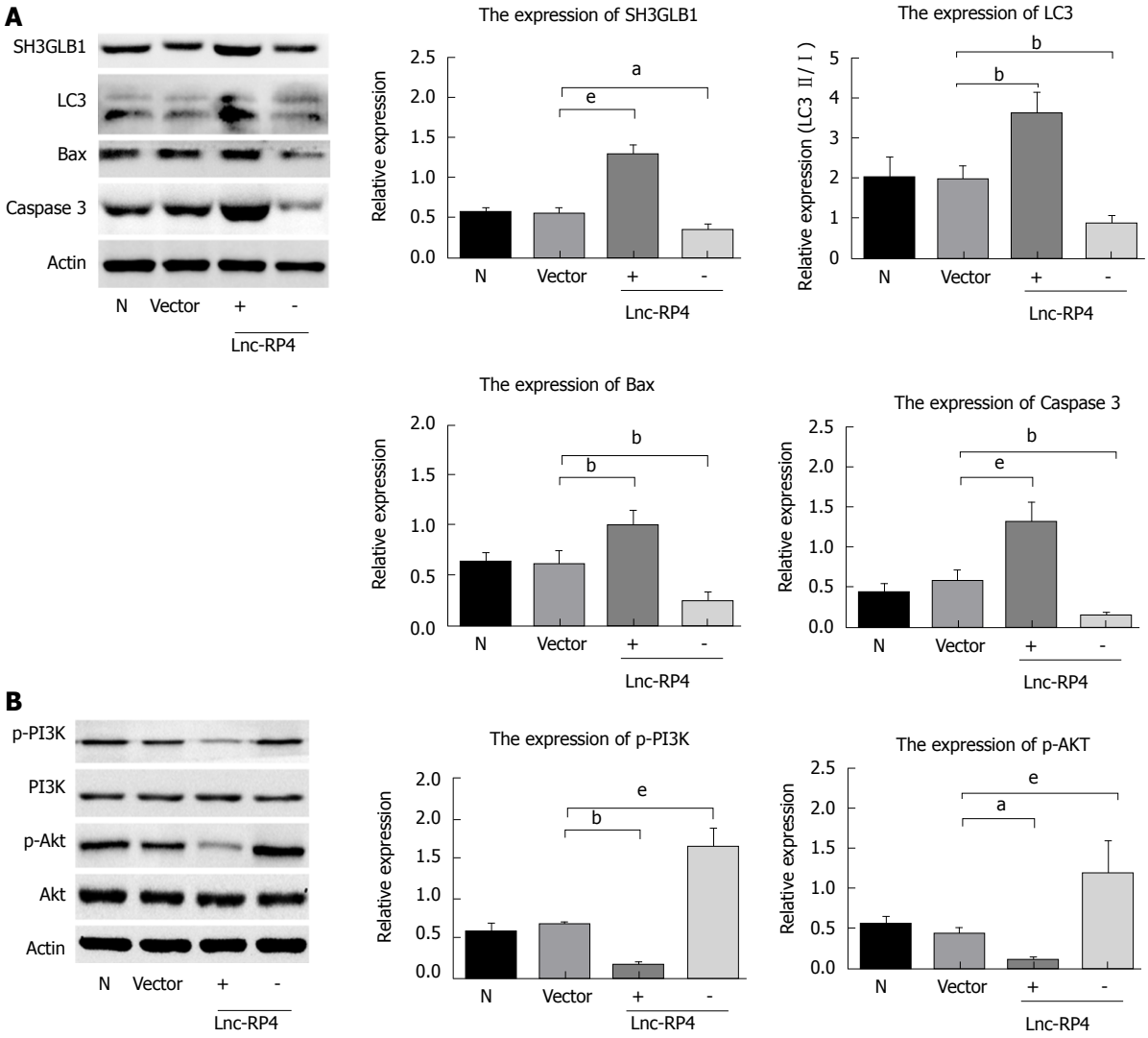

Figure 4 Involvement of the autophagy-mediated cell death pathway and PI3K/Akt signaling pathway in lncRNA RP4-mediated effects in colorectal cancer cells. A: LncRNA RP4 overexpression and knockdown, respectively, decreased and increased expression of the autophagy marker LC3, and apoptosis-related proteins Bax and caspase 3 in SW480 cells, suggesting that it positively regulates autophagy-mediated cell death in colorectal cancer cells. B: LncRNA RP4 overexpression and knockdown, respectively, decreased and increased PI3K and Akt phosphorylation in SW480 cells, indicating that it negatively regulates PI3K/Akt in colorectal cancer cells. C: Schematic of lncRNA RP4 functioning as a decoy by competitively binding miR-7-5p, upregulating the specific repressor SH3GLB1, activating autophagy-mediated cell death, and inhibiting the PI3K/Akt signaling pathway, thereby suppressing colorectal carcinogenesis. $^{a}P < 0.05$, $^{b}P < 0.01$, and $^{e}P < 0.001$ for between-group comparisons.

SH3GLB1 expression (Figure 2).

lncRNA RP4 functions as an miR-7-5p decoy in the regulation of SH3GLB1

Because no direct interaction exists between lncRNA RP4 and *SH3GLB1*, we further analyzed the potential functional mechanism by the introduction of miRNA. lncRNAs were recently reported to act as decoys that sequester miRNAs and prevent them from binding to targets, hence modulating many functional mRNA targets through translation. Bioinformatics analysis (webserver lnCeDB; http://gyanxet-beta.com/lncedb/) predicted potential interactions between lncRNA RP4 and miR-7-5p (Figure 3A), which was confirmed by correlation analysis (Figure 3B and C). We also observed a positive regulatory effect of miR-7-5p on cell proliferation *via* the negative regulation of *SH3GLB1* (Figure 3D and E). These results suggested that lncRNA RP4 functions as an miR-7-5p decoy in colorectal cancer cells.

Involvement of the autophagy-mediated cell death pathway and PI3K/Akt signaling pathway in lncRNA-RP4 mediated effects in colorectal cancer cells

According to previous findings[13,14], autophagy-mediated cell death is involved in the early apoptosis of cancer, while the PI3K/Akt signaling pathway plays a role in cancer cell proliferation and growth[15,16]. Analysis of the effects of lncRNA-RP4 on intracellular signaling revealed that lncRNA-RP4 overexpression and knockdown, respectively, upregulated and downregulated expression levels of the autophagy marker LC3 and apoptosis-related molecules Bax and caspase 3 (Figure 4A). We also observed the negative regulation of PI3K and Akt phosphorylation by lncRNA-RP4 in colorectal cancer cells (Figure 4B). Taken together, we propose a schematic whereby lncRNA RP4 functions as a decoy that competitively binds miR-7-5p, upregulating the specific repressor *SH3GLB1*, activating autophagy-mediated cell death, and inhibiting PI3K/Akt signaling, thereby suppressing colorectal carcinogenesis (Figure 4C).

DISCUSSION

Noncoding regions account for more than 90% of the entire human genome, and are thought to play a critical role in the regulation of physiological function given that only 9% of human genes are protein-coding. As a representative of noncoding regions, approximately 18% of lncRNAs are associated with human tumors and have been shown to act as major contributors in the development and progression of human cancers[17]. Multiple mechanisms have been suggested for the regulatory role of lncRNAs in physiological functions, including trans- and cis-regulatory mechanisms. In a trans-regulatory mechanism, lncRNAs (such as HOTAIR) could affect the transcription of specific genes through their interaction with chromatin-remodeling complexes and complex recruitment to genomic DNA sequences[18]. Some lncRNAs (such as lincRNA-21) also act as cis-regulators by exerting their function on nearby transcripts[19]. Growing evidence has shown that lncRNAs may act as ceRNAs *via* their miRNA response elements for specific miRNA targets, thus blocking the target binding ability of a single miRNA or multiple miRNAs[20,21]. Several lncRNAs have been suggested to function as ceRNAs, including PTENP1[22], H19[23], and CCAT1[24].

In the present study, we investigated the potential role of lncRNA RP4 as a ceRNA of *SH3GLB1* that competes for miRNA-7-5p binding sites, thereby regulating the expression of *SH3GLB1* mRNA targeted by miRNA-7-5p. The overexpression of lncRNA RP4 inhibited colorectal cancer cell proliferation and tumor growth both *in vitro* and *in vivo*, and increased early apoptosis. These findings suggest that lncRNA RP4 plays a critical role in the modulation of colorectal cancer progression.

To further elucidate the role of lncRNA RP4 in colorectal cancer, we analyzed its regulatory mechanism as a ceRNA by bioinformatics analysis and experimental verification. qRT-PCR analysis showed that lncRNA RP4 overexpression downregulated miR-7-5p expression in colorectal cancer cells, while an inverse correlation was detected between lncRNA RP4 and miR-7-5p expression. Additional functional experiments confirmed that miR-7-5p overexpression promoted cell proliferation, while an inverse correlation was detected between miR-7-5p and *SH3GLB1* expression. Consistent with these findings, miR-7-5p has been found to affect cell proliferation, anchorage-independent growth, migration and invasion, apoptosis, and chemosensitivity by targeting specific oncogenic genes in various types of tumor[25-27].

SH3GLB1, a membrane curvature-inducing protein, interacts with BECN1 though UVRAG and regulates the post-Golgi trafficking of membrane-integrated ATG9A during autophagy[28]. In the present study, we found that lncRNA RP4 overexpression upregulated autophagy. Recently, Takahashi *et al*[29] reported that SH3GLB1 is a haploinsufficient tumor suppressor that functions to prevent the acquisition of apoptosis resistance and malignant transformation during *Myc*-driven lymphomagenesis. Our data supported the tumor suppressor role of SH3GLB1 in colorectal cancer. During tumor development and progression, protein interactions between SH3GLB1 and BAX resulted in the activation of caspase 3, thereby inducing apoptosis[30]. Similarly, we showed that lncRP4-induced *SH3GLB1* upregulation increased levels of BAX and caspase 3 in colorectal cancer cells.

Previous studies observed that dysregulated PI3K/Akt signaling in human colorectal cancer is associated with the growth and proliferation pattern of cancer cells[15,16], while the PI3K/Akt pathway negatively regulates autophagy[31,32]. Consistent with this, we

detected reduced PI3K and Akt phosphorylation in lncRP4-overexpressing colorectal cancer cells.

The present study has a number of limitations. First, because of a lack of colorectal cancer tissue, we could not evaluate the expression pattern of lncRNA RP4, miR-7-5p, or *SH3GLB1* in carcinoma tissues and were thus unable to elucidate the clinical significance of lncRP4 in colorectal cancer. The collection of more colorectal cancer tissue will be necessary to overcome this. Second, we did not use small inhibitors of different signaling pathways, yet it is conceivable that the mechanism of lncRNA RP4 involves multiple modalities.

Taken together, our results demonstrate that lncRNA RP4 plays an important role in the progression of human colorectal cancer by functioning as a ceRNA to regulate the expression of *SH3GLB1* through miR-7-5p sponge activity. The pleiotropic effects of lncRNA RP4 on colorectal cancer pathogenesis suggest that is has the potential to be a therapeutic target for colorectal cancer.

ARTICLE HIGHLIGHTS

Research background

Colorectal cancer is the fourth most common cancer and the fifth most common cause of cancer-related death in China. Surgical resection followed by adjuvant chemotherapy, the most commonly used strategy for colorectal cancer management, has poor treatment response in some patients. Therefore, it is necessary to identify effective therapeutic targets to improve treatment and prognosis.

Research motivation

Long noncoding RNAs (lncRNAs), which may serve as novel therapeutic targets, are involved in the development and progression of human colorectal cancer. In our previous study, lncRNA RP4 was found to be dysregulated in colorectal cancer *via* microarray analysis. This indicated that this lncRNA may play an important role in colorectal cancer. Thus, in the present study, lncRNA RP4 was investigated to find out its role in colorectal cancer progression through an *in vitro* cell model and an *in vivo* xenograft model. Besides, the possible mechanisms in the regulation of lncRNA RP4 had not been well described.

Research objectives

To investigate the role of long noncoding (lnc)RNA RP4 in colorectal cancer, and to find out the possible mechanisms of the regulation.

Research methods

Cell counting kit-8 assay *in vitro* and xenograft tumor model *in vivo* were performed to evaluate the role of lncRNA RP4 in the regulation of proliferation. Annexin V/propidium iodide staining was performed to detect the role of lncRNA RP4 in apoptosis. qPCR and Western blot were performed to identify the relationship between lncRNA RP4 and SH3GLB1. And then, Western blot was done to analyse PI3K/Akt signaling pathway and autophagy pathway in the regulation.

Research results

Both cell counting kit-8 assay *in vitro* and xenograft tumor model *in vivo* showed that lncRNA RP4 could inhibit the proliferation and growth of colorectal cancer cells. lncRNA RP4 could promote early apoptosis. lncRNA RP4 was found to positively regulate SH3GLB1 expression, and correlation analyses further confirmed the existence of a significant correlation between lncRNA RP4 and SH3GLB1 expression. We also observed a positive regulatory effect of miR-7-5p on cell proliferation *via* the negative regulation of SH3GLB1.

Research conclusions

Our results demonstrate that lncRNA RP4 plays an important role in the progression of human colorectal cancer by functioning as a ceRNA to regulate the expression of SH3GLB1 through miR-7-5p sponge activity. The pleiotropic effects of lncRNA RP4 on colorectal cancer pathogenesis suggest that is has the potential to be a therapeutic target for colorectal cancer.

Research perspectives

This study suggests that the lncRNA intervention may be a promising treatment strategy for colorectal cancer. The future study might focus on the specific regulatory role of lncRNA RP4 in colorectal cancer *in vivo*, and the therapeutic effect of lncRNA RP4 needs to be validated in clinical practice.

REFERENCES

1 **Chen W**, Zheng R, Zuo T, Zeng H, Zhang S, He J. National cancer incidence and mortality in China, 2012. *Chin J Cancer Res* 2016; **28**: 1-11 [PMID: 27041922 DOI: 10.3978/j.issn.1000-9604.2016.02.08]

2 **Siegel RL**, Miller KD, Jemal A. Cancer statistics, 2016. *CA Cancer J Clin* 2016; **66**: 7-30 [PMID: 26742998 DOI: 10.3322/caac.21332]

3 **Yue M**, Charles Richard JL, Ogawa Y. Dynamic interplay and function of multiple noncoding genes governing X chromosome inactivation. *Biochim Biophys Acta* 2016; **1859**: 112-120 [PMID: 26260844 DOI: 10.1016/j.bbagrm.2015.07.015]

4 **Butler AA**, Webb WM, Lubin FD. Regulatory RNAs and control of epigenetic mechanisms: expectations for cognition and cognitive dysfunction. *Epigenomics* 2016; **8**: 135-151 [PMID: 26366811 DOI: 10.2217/epi.15.79]

5 **Kanduri C**. Long noncoding RNAs: Lessons from genomic imprinting. *Biochim Biophys Acta* 2016; **1859**: 102-111 [PMID: 26004516 DOI: 10.1016/j.bbagrm.2015.05.006]

6 **Tordonato C**, Di Fiore PP, Nicassio F. The role of non-coding RNAs in the regulation of stem cells and progenitors in the normal mammary gland and in breast tumors. *Front Genet* 2015; **6**: 72 [PMID: 25774169 DOI: 10.3389/fgene.2015.00072]

7 **Prensner JR**, Iyer MK, Balbin OA, Dhanasekaran SM, Cao Q, Brenner JC, Laxman B, Asangani IA, Grasso CS, Kominsky HD, Cao X, Jing X, Wang X, Siddiqui J, Wei JT, Robinson D, Iyer HK, Palanisamy N, Maher CA, Chinnaiyan AM. Transcriptome sequencing across a prostate cancer cohort identifies PCAT-1, an unannotated lincRNA implicated in disease progression. *Nat Biotechnol* 2011; **29**: 742-749 [PMID: 21804560 DOI: 10.1038/nbt.1914]

8 **Li W**, Zheng J, Deng J, You Y, Wu H, Li N, Lu J, Zhou Y. Increased levels of the long intergenic non-protein coding RNA POU3F3 promote DNA methylation in esophageal squamous cell carcinoma cells. *Gastroenterology* 2014; **146**: 1714-1726.e5 [PMID: 24631494 DOI: 10.1053/j.gastro.2014.03.002]

9 **Yin D**, He X, Zhang E, Kong R, De W, Zhang Z. Long noncoding RNA GAS5 affects cell proliferation and predicts a poor prognosis in patients with colorectal cancer. *Med Oncol* 2014; **31**: 253 [PMID: 25326054 DOI: 10.1007/s12032-014-0253-8]

10 **Han Y**, Yang YN, Yuan HH, Zhang TT, Sui H, Wei XL, Liu L, Huang P, Zhang WJ, Bai YX. UCA1, a long non-coding RNA up-regulated in colorectal cancer influences cell proliferation, apoptosis and cell cycle distribution. *Pathology* 2014; **46**: 396-401 [PMID: 24977734 DOI: 10.1097/PAT.0000000000000125]

11 **Ding J**, Lu B, Wang J, Wang J, Shi Y, Lian Y, Zhu Y, Wang J, Fan Y, Wang Z, De W, Wang K. Long non-coding RNA Loc554202 induces apoptosis in colorectal cancer cells via the caspase cleavage cascades. *J Exp Clin Cancer Res* 2015; **34**: 100 [PMID: 26362196 DOI: 10.1186/s13046-015-0217-7]

12 **Ji Y**, Strawn TL, Grunz EA, Stevenson MJ, Lohman AW, Lawrence DA, Fay WP. Multifaceted role of plasminogen activator inhibitor-1 in regulating early remodeling of vein bypass grafts.

Arterioscler Thromb Vasc Biol 2011; **31**: 1781-1787 [PMID: 21571686 DOI: 10.1161/ATVBAHA.111.228767]
13 **Santoni M**, Amantini C, Morelli MB, Farfariello V, Nabissi M, Liberati S, Bonfili L, Mozzicafreddo M, Eleuteri AM, Burattini L, Berardi R, Cascinu S, Santoni G. ifferent effects of sunitinib, sorafenib, and pazopanib on inducing cancer cell death: The role of autophagy. *J Clin Oncol* 2013; **6** suppl: 270 [DOI: 10.1200/jco.2013.31.6_suppl.270]
14 **Fulda S**. Autophagy in Cancer Therapy. *Front Oncol* 2017; **7**: 128 [PMID: 28674677 DOI: 10.3389/fonc.2017.00128]
15 **Liu X**, Gomez-Pinillos A, Shah P, Lavilla C, Ferrari AC. Effect of inhibition of the PI3K/Akt/mTOR pathway on AR splicing and downstream targets. *J Clin Oncol* 2013; **6** suppl: 101 [DOI: 10.1200/jco.2013.31.6_suppl.101]
16 **Jeon YW**, Ahn YE, Chung WS, Choi HJ, Suh YJ. Synergistic effect between celecoxib and luteolin is dependent on estrogen receptor in human breast cancer cells. *Tumour Biol* 2015; **36**: 6349-6359 [PMID: 25851346 DOI: 10.1007/s13277-015-3322-5]
17 **Khachane AN**, Harrison PM. Mining mammalian transcript data for functional long non-coding RNAs. *PLoS One* 2010; **5**: e10316 [PMID: 20428234 DOI: 10.1371/journal.pone.0010316]
18 **Bhan A**, Mandal SS. LncRNA HOTAIR: A master regulator of chromatin dynamics and cancer. *Biochim Biophys Acta* 2015; **1856**: 151-164 [PMID: 26208723 DOI: 10.1016/j.bbcan.2015.07.001]
19 **Dimitrova N**, Zamudio JR, Jong RM, Soukup D, Resnick R, Sarma K, Ward AJ, Raj A, Lee JT, Sharp PA, Jacks T. LincRNA-p21 activates p21 in cis to promote Polycomb target gene expression and to enforce the G1/S checkpoint. *Mol Cell* 2014; **54**: 777-790 [PMID: 24857549 DOI: 10.1016/j.molcel.2014.04.025]
20 **Wang K**, Long B, Zhou LY, Liu F, Zhou QY, Liu CY, Fan YY, Li PF. CARL lncRNA inhibits anoxia-induced mitochondrial fission and apoptosis in cardiomyocytes by impairing miR-539-dependent PHB2 downregulation. *Nat Commun* 2014; **5**: 3596 [PMID: 24710105 DOI: 10.1038/ncomms4596]
21 **Tay Y**, Rinn J, Pandolfi PP. The multilayered complexity of ceRNA crosstalk and competition. *Nature* 2014; **505**: 344-352 [PMID: 24429633 DOI: 10.1038/nature12986]
22 **Yu G**, Yao W, Gumireddy K, Li A, Wang J, Xiao W, Chen K, Xiao H, Li H, Tang K, Ye Z, Huang Q, Xu H. Pseudogene PTENP1 functions as a competing endogenous RNA to suppress clear-cell renal cell carcinoma progression. *Mol Cancer Ther* 2014; **13**: 3086-3097 [PMID: 25249556 DOI: 10.1158/1535-7163.MCT-14-0245]
23 **Kallen AN**, Zhou XB, Xu J, Qiao C, Ma J, Yan L, Lu L, Liu C, Yi JS, Zhang H, Min W, Bennett AM, Gregory RI, Ding Y, Huang Y. The imprinted H19 lncRNA antagonizes let-7 microRNAs. *Mol Cell* 2013; **52**: 101-112 [PMID: 24055342 DOI: 10.1016/j.molcel.2013.08.027]
24 **Ma MZ**, Chu BF, Zhang Y, Weng MZ, Qin YY, Gong W, Quan ZW. Long non-coding RNA CCAT1 promotes gallbladder cancer development via negative modulation of miRNA-218-5p. *Cell Death Dis* 2015; **6**: e1583 [PMID: 25569100 DOI: 10.1038/cddis.2014.541]
25 **Kalinowski FC**, Brown RA, Ganda C, Giles KM, Epis MR, Horsham J, Leedman PJ. microRNA-7: a tumor suppressor miRNA with therapeutic potential. *Int J Biochem Cell Biol* 2014; **54**: 312-317 [PMID: 24907395 DOI: 10.1016/j.biocel.2014.05.040]
26 **Kalinowski FC**, Giles KM, Candy PA, Ali A, Ganda C, Epis MR, Webster RJ, Leedman PJ. Regulation of epidermal growth factor receptor signaling and erlotinib sensitivity in head and neck cancer cells by miR-7. *PLoS One* 2012; **7**: e47067 [PMID: 23115635 DOI: 10.1371/journal.pone.0047067]
27 **Giles KM**, Brown RA, Ganda C, Podgorny MJ, Candy PA, Wintle LC, Richardson KL, Kalinowski FC, Stuart LM, Epis MR, Haass NK, Herlyn M, Leedman PJ. microRNA-7-5p inhibits melanoma cell proliferation and metastasis by suppressing RelA/NF-κB. *Oncotarget* 2016; **7**: 31663-31680 [PMID: 27203220 DOI: 10.18632/oncotarget.9421]
28 **Takahashi Y**, Young MM, Serfass JM, Hori T, Wang HG. Sh3glb1/Bif-1 and mitophagy: acquisition of apoptosis resistance during Myc-driven lymphomagenesis. *Autophagy* 2013; **9**: 1107-1109 [PMID: 23680845 DOI: 10.4161/auto.24817]
29 **Takahashi Y**, Hori T, Cooper TK, Liao J, Desai N, Serfass JM, Young MM, Park S, Izu Y, Wang HG. Bif-1 haploinsufficiency promotes chromosomal instability and accelerates Myc-driven lymphomagenesis via suppression of mitophagy. *Blood* 2013; **121**: 1622-1632 [PMID: 23287860 DOI: 10.1182/blood-2012-10-459826]
30 **Fino KK**, Yang L, Silveyra P, Hu S, Umstead TM, DiAngelo S, Halstead ES, Cooper TK, Abraham T, Takahashi Y, Zhou Z, Wang HG, Chroneos ZC. SH3GLB2/endophilin B2 regulates lung homeostasis and recovery from severe influenza A virus infection. *Sci Rep* 2017; **7**: 7262 [PMID: 28779131 DOI: 10.1038/s41598-017-07724-5]
31 **Mans LA**, Querol Cano L, van Pelt J, Giardoglou P, Keune WJ, Haramis AG. The tumor suppressor LKB1 regulates starvation-induced autophagy under systemic metabolic stress. *Sci Rep* 2017; **7**: 7327 [PMID: 28779098 DOI: 10.1038/s41598-017-07116-9]
32 **Wang S**, Li J, Du Y, Xu Y, Wang Y, Zhang Z, Xu Z, Zeng Y, Mao X, Cao B. The Class I PI3K inhibitor S14161 induces autophagy in malignant blood cells by modulating the Beclin 1/Vps34 complex. *J Pharmacol Sci* 2017; **134**: 197-202 [PMID: 28779993 DOI: 10.1016/j.jphs.2017.07.001]

P- Reviewer: Luchini C **S- Editor**: Gong ZM **L- Editor**: Wang TQ
E- Editor: Ma YJ

World Journal of Gastroenterology

Submit a Manuscript: http://www.f6publishing.com

World J Gastroenterol 2018 March 7; 24(9): 1013-1021

DOI: 10.3748/wjg.v24.i9.1013

ISSN 1007-9327 (print) ISSN 2219-2840 (online)

ORIGINAL ARTICLE

Retrospective Study

Quality indicators in pediatric colonoscopy in a low-volume center: Implications for training

Way-Seah Lee, Chun-Wei Tee, Zhong-Lin Koay, Tat-Seng Wong, Fatimah Zahraq, Hee-Wei Foo, Sik-Yong Ong, Shin-Yee Wong, Ruey-Terng Ng

Way-Seah Lee, Chun-Wei Tee, Zhong-Lin Koay, Tat-Seng Wong, Fatimah Zahraq, Hee-Wei Foo, Sik-Yong Ong, Shin-Yee Wong, Ruey-Terng Ng, Department of Paediatrics, University Malaya Medical Centre, Kuala Lumpur 59100, Malaysia

Way-Seah Lee, Paediatric and Child Health Research Group, University Malaya, Kuala Lumpur 50603, Malaysia

ORCID number: Way-Seah Lee (0000-0001-9163-2828); Chun-Wei Tee (0000-0002-1119-2971); Zhong-Lin Koay (0000-0002-8724-9903); Tat-Seng Wong (0000-0002-3076-228X); Fatimah Zahraq (0000-0002-2658-1945); Hee-Wei Foo (0000-0001-7761-0550); Sik-Yong Ong (0000-0001-9647-5788); Shin-Yee Wong (0000-0002-7486-0594); Ruey-Terng Ng (0000-0003-1656-5797).

Author contributions: Lee WS conceived the idea of the research; Lee WS, Ng RT, Ong SY and Foo HW provided the clinical data; Tee CW, Koay ZL, Wong TS and Zahraq F collected the data; Wong SY performed the statistical analysis; Lee WS and Tee CW analyzed the data; Lee WS wrote the first draft; All authors contributed equally to writing of the final draft; All authors authorized the final version of the manuscript.

Supported by Research grant from Ministry of Higher Education, Malaysia, No. UM.C/625/HIR/MOHE/CHAN/13/1.

Institutional review board statement: This study was reviewed and approved by the Ethics Committee of the University Malaya Medical Centre (MEC reference: 902.15).

Informed consent statement: Patients were not required to give informed consent to the study because the analysis performed used anonymous clinical data that were obtained after each patient agreed to treatment by written consent.

Conflict-of-interest statement: All authors declare no conflicts-of-interest related to this article.

Data sharing statement: No additional data are available.

Manuscript source: Unsolicited manuscript

Correspondence to: Way-Seah Lee, MBBS, FRCPCH, MD, Professor, Department of Paediatrics, Level 9, Women's and Children's Block, University Malaya Medical Center, Kuala Lumpur 59100, Malaysia. leews@ummc.edu.my
Telephone: +60-3-79492065
Fax: +60-3-79494704

Received: November 24, 2017
Peer-review started: November 25, 2017
First decision: December 27, 2017
Revised: January 15, 2018
Accepted: January 19, 2018
Article in press: January 19, 2018
Published online: March 7, 2018

Abstract

AIM

To study implications of measuring quality indicators on training and trainees' performance in pediatric colonoscopy in a low-volume training center.

METHODS

We reviewed retrospectively the performance of pediatric colonoscopies in a training center in Malaysia over 5 years (January 2010-December 2015), benchmarked against five quality indicators: appropriateness of indications, bowel preparations, cecum and ileal

examination rates, and complications. The European Society of Gastrointestinal Endoscopy guideline for pediatric endoscopy and North American Society for Pediatric Gastroenterology, Hepatology and Nutrition training guidelines were used as benchmarks.

RESULTS

Median (± SD) age of 121 children [males = 74 (61.2%)] who had 177 colonoscopies was 7.0 (± 4.6) years. On average, 30 colonoscopies were performed each year (range: 19-58). Except for investigations of abdominal pain (21/177, 17%), indications for colonoscopies were appropriate in the remaining 83%. Bowel preparation was good in 87%. One patient (0.6%) with severe Crohn's disease had bowel perforation. Cecum examination and ileal intubation rate was 95% and 68.1%. Ileal intubation rate was significantly higher in diagnosing or assessing inflammatory bowel disease (IBD) than non-IBD (72.9% *vs* 50.0%; P = 0.016). Performance of four trainees was consistent throughout the study period. Average cecum and ileal examination rate among trainees were 97% and 77%.

CONCLUSION

Benchmarking against established guidelines helps units with a low-volume of colonoscopies to identify area for further improvement.

Key words: Pediatric colonoscopies; Quality indicators; Performance

Core tip: Competency in colonoscopy is an essential component in the training for pediatric gastroenterology worldwide. We measured the performance of pediatric colonoscopy from a low-volume training center on quality indicators against established guidelines. The unit, which performed an average of 30 colonoscopies each year, performed well in clear indication for colonoscopy, good bowel preparation, safety and high rate of cecal examination (95%) but needs improvement for ileal intubation (at 68%). Benchmarking against established guidelines helps units with a low volume of colonoscopies to identify area for improvement.

Lee WS, Tee CW, Koay ZL, Wong TS, Zahraq F, Foo HW, Ong SY, Wong SY, Ng RT. Quality indicators in pediatric colonoscopy in a low-volume center: Implications for training. *World J Gastroenterol* 2018; 24(9): 1013-1021 Available from: URL: http://www.wjgnet.com/1007-9327/full/v24/i9/1013.htm DOI: http://dx.doi.org/10.3748/wjg.v24.i9.1013

INTRODUCTION

Colonoscopy is an essential diagnostic procedure for the evaluation and treatment of lower gastrointestinal pathologies in children[1-4]. Major indications for colonoscopy in children include rectal bleeding, investigation of diarrhea, failure to thrive and perianal lesions, and as initial diagnostic evaluation for inflammatory bowel disease (IBD)[5-10].

Approximately 20%-30% of IBD patients have onset of disease in childhood[11]. A study from Australia showed that IBD was the diagnosis in 58% of children who had initial diagnostic colonoscopy[5]. The percentage is much lower in Asia, ranging from 10.9% in Taiwanese children[8] to 19.6% in Korean children[7]. The incidence of IBD is increasing worldwide[12,13]. The incidence in Asia, including Malaysia, is increasing as well, although it is still relatively uncommon as compared to North America and Western Europe[13,14].

Competency in colonoscopy has become an essential component in the training syllabus for both adult and pediatric gastroenterology worldwide[15,16]. In adult colonoscopy, cecal intubation and detection for adenoma are considered as standard quality measures[15]. In children, however, routine screening for adenomas is generally not recommended[15]. On the other hand, ileal intubation is essential for accurate diagnosis of IBD, particularly Crohn's disease (CD)[17]. Thus, appropriate indication for colonoscopy, complete examination including inspection of cecum and terminal ileum, adequate bowel preparation and free of complications are all important quality indicators in pediatric colonoscopy[16].

In areas where the prevalence of IBD is low, such as Malaysia, the volume of pediatric colonoscopies performed may be limited[7-10,18]. The reported cecum examination and ileal intubation rates vary. In Hong Kong, the cecal and ileal intubation rates were 97.6% and 75.6%[10]. In Taiwan, the ileal intubation rate was 77.5%[8]. In Australia, where the incidence of IBD is high, Singh *et al*[5] reported that the cecal and ileal intubation rates were 96.3% and 92.4%, respectively.

A study on quality indicators published previously showed that performance benchmarked against quality indicators varies in different centers[16]. To the best of our knowledge, however, no study on performance benchmarked against quality indicators from low-volume centers has been published previously.

We aimed to ascertain the performance of our unit when benchmarked against established quality indicators in pediatric colonoscopy covering the following areas: indications, quality of bowel preparation, safety and complications, cecal examination and terminal ileum intubation rates. We also assessed the implications of our performance to ascertain opportunities for improvements to the training program in this training center.

MATERIALS AND METHODS

This was a retrospective review on all pediatric colonoscopies performed between January 2010 and

December 2015 at the Paediatric Gastroenterology Unit, University Malaya Medical Centre (UMMC), Malaysia. The present study was approved by the institutional ethics review committee (MEC reference: 902.15). During the study period, the unit was staffed by one full-time consultant and a part-time visiting consultant. They were assisted by fellows-in-training, who spent the first 18 mo of a 3-year fellowship training program in the unit.

Data collection

Cases were retrieved from hospital and the unit database. The following data were collected: demographics and clinical features; indications for colonoscopy; laboratory data; degree of bowel preparation; extent of colonoscopic examination; and complications. Colonoscopic and pathological diagnoses were ascertained. Cases were excluded if the data were incomplete.

Quality indicators

The following areas were used as quality indicators: (1) appropriateness of indications; (2) quality of bowel preparation and extent of colonoscopic examination, including (3) cecum examination and (4) ileal intubation; and (5) safety (including anesthesia and sedation) and complications. Factors affecting extent of examination and the performances of trainees were also analyzed.

Indications and preparations for colonoscopy

In our unit, each referral for colonoscopy was screened and decided by a consultant. Generally, the indications for colonoscopy followed the established guidelines[3,4], and has been reported previously[18]. For the purpose of the present study, the European Society of Gastrointestinal Endoscopy (ESGE) guideline for pediatric endoscopy was used as a benchmark[4].

Sedation and anesthesia

In our unit, colonoscopies were usually performed under general anesthesia. In adolescents, sedation (generally a combination of midazolam and pethidine) was used occasionally at the discretion of the anesthetist.

Bowel preparation

Bowel preparation has been standardized throughout the study period. Two days prior to colonoscopy, each patient was allowed a low residue diet. On the night before the procedure, each patient had bowel cleansing with polyethylene glycol solution and glycerin rectal enema. The degree of bowel preparation observed during colonoscopy was not standardized. It was judged by the endoscopist as poor, fair, good or excellent[6].

Extent of colonoscopy

The extent of the colonoscopy was confirmed by visual identification of the colonic wall appearance, and the anatomy the cecum and terminal ileum. The biopsy of the terminal ileum was also used as an additional confirmation. The recommendation by North American Society for Pediatric Gastroenterology, Hepatology and Nutrition (NASPGHAN) guidelines for training in pediatric gastroenterology was used as a benchmark[19]. The NASPGHAN guidelines recommends a cecum and ileal examination rate of between 90%-95%[19].

Performance

For the purpose of the present study, analysis on performance was confined to colonoscopies where an inspection of ileum was intended. This included cases where intubation of terminal ileum was indicated (*i.e.,* in diagnosing or assessing IBD), feasible (acceptable quality of bowel preparation where full examination was feasible) or safe (benefit of ileal intubation outweighs the risk of full examination, such as bowel perforation).

Performance by trainees

Analysis on the performance by trainees was confined to trainees who had completed a minimum of 12 mo training in the unit during the study period. Number of colonoscopies performed, cecum examination and ileal intubation rates were noted. In colonoscopies where trainees encountered technical difficulties during the procedure and were subsequently taken over by the consultant, the procedures were logged as performed by the consultant.

Statistical analysis

Data were collected and managed by using a statistical software program (SPSS version 20.0; SPSS Inc., IBM Corp., Armonk, NY, United States). Descriptive data were described in percentage, mean and median. Categorical data were analyzed using a two-tailed χ^2 test.

RESULTS

During the 6-year study period, 194 colonoscopies were performed in the unit. Data on 17 procedures were incomplete and were excluded from analysis. Of the remaining 177 colonoscopies, 56 were repeated procedures. Thus, 121 patients who had 177 colonoscopies were analyzed. The results are presented in two parts: (1) indications, colonoscopic findings and diagnosis of 121 patients who had first colonoscopy; and (2) quality indicators of 177 colonoscopies performed.

Volume of procedures

There was a steady increase in the number of colonoscopies performed each year during the study period (Figure 1). On average, 30 colonoscopies were performed each year during the study period, ranging from 19 procedures per year in the first 2 years to 58 procedures in 2015. Among the procedures, 15% (27/177) were logged as performed by consultants, while the remaining 85% (150/177) were performed

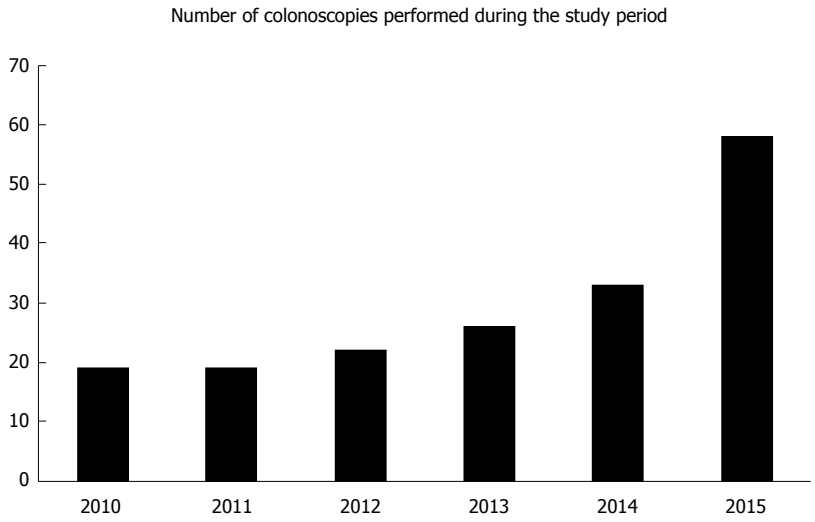

Figure 1 Number of colonoscopies performed each year during the study period.

by trainees supervised by a consultant.

Epidemiology, demographic features in 121 patients

There was a male preponderance (males = 74, 61%) in the 121 patients who had first colonoscopy (Table 1). The median (± SD) age was 7.5 (± 4.5) years. Eighty-one (67%) patients also had concomitant esophago-gastro-duodenoscopy (EGDS).

Indications for first colonoscopy in 121 patients

The most common indication was confirming the diagnosis of IBD (36/121, 30%; Table 1). Others were investigation of anemia or rectal bleeding (25/121, 21%). Investigation of abdominal pain was the indication in 17% (21/121). Most of the repeat colonoscopies were for disease assessment in IBD.

Colonoscopic findings in 121 patients

A positive finding was noted in 68 (56.2%) colonoscopies, while the remaining 53 (43.8%) had a normal colonoscopic finding. Indications for colonoscopy for the 53 patients with a negative finding were: excluding IBD (n = 18); disease assessment of pre-existing IBD (n = 4); assessment of abdominal pain (n = 8); ascertainment of lower gastrointestinal bleeding (n = 10); and, miscellaneous (n = 13).

Diagnosis in 121 patients

In addition to 16 patients who had colonoscopic assessment of preexisting IBD, a new clinical diagnosis or institution of new therapeutic measures was made in another 87 patients following colonoscopy. Thus, a total of 103 patients had a positive diagnosis. The diagnostic yield was 85%.

The colonoscopic diagnoses are shown in Table 1. Overall, 50 (41%) patients had a diagnosis of IBD (newly diagnosed, n = 34; diagnosis confirmed elsewhere, n = 16; Figure 2). Of these, 30 patients had CD and 20 had ulcerative colitis, respectively. Another 22 (18%) patients had focal inflammation of the rectum (IBD-unclassified) or solitary rectal ulcer syndrome.

Trend for diagnosis of IBD in 121 patients

The number of new cases of IBD seen in the unit during the study period is shown in Figure 2. There was an increasing trend in the number of new IBD cases, especially for CD.

Sedation and anesthesia in 177 colonoscopies

Vast majority (165/177, 93.2%) of the procedures were performed under general anesthesia. The remaining 12 procedures (6.8%) were performed under sedation, being administered by anesthetist. No major events related to anesthesia or sedation were observed during the study period.

Bowel preparation in 177 colonoscopies

Bowel preparation was judged to be good by the endoscopist in 87% (155/177) of the patients, moderate in 0.6% (1/177) and bad in 12% (21/177) patients.

Cecum and terminal ileum intubation in 177 colonoscopies

Information on the extent of colonoscopy was available in all 177 procedures (Table 1). The overall ileal intubation rate was 54.2% (96/177). Cecum was examined in an additional 22.0% (39/177). Thus, the cecum was reached in 76.3% (135/177) of patients. The extents of colonoscopy of the remaining 42 procedures are shown in Table 1.

In 36 patients, full colonoscopic examination and ileal intubation were not intended. They were not indicated in 18 cases, including those for confirmation or surveillance of graft-versus-host disease (n = 10), confirmation of rectal metastasis (n = 2), tissue biopsy for malabsorption (1 each for food protein-induced

Table 1 Indications, diagnoses and quality indicators in 121 children who had 177 colonoscopies

	n	%
Sex, males	74	61
Age in yr, median ± SD	7.5 ± 4.5	
Concomitant esophagogastroduodenoscopy	81	67
Indications, *n* = 121[1]		
Suspected of inflammatory bowel disease, new patients	36	30
Per rectal bleeding/investigations of anemia	25	21
Investigation of gastrointestinal symptoms	21	17
Assessment of inflammatory bowel disease, diagnosed elsewhere	16	13
Suspected of colonic polyps	7	6
Exclusion of graft-versus-host disease or colonic malignancies	7	6
Assessment of failure to thrive/malabsorption	4	3.3
Others	10	8
Colonoscopic diagnosis, *n* = 121		
Crohn's disease	30	25
Ulcerative colitis	20	17
Non-specific colitis or solitary rectal ulcer syndrome	22	18
Infective colitis	9	7
Colonic polyps	8	7
Graft-versus-host disease	5	4
Malabsorption	2	2
Allergic colitis	2	2
Miscellaneous diagnosis	5	4
No diagnosis	18	15
Extent of colonoscopic examination, 177 colonoscopies		
Terminal ileum	96	54
Cecum	38	21
Ascending colon	9	5
Transverse colon	13	7
Descending colon	12	7
Sigmoid colon	7	4
Rectum	1	0.6
Reached cecum but no terminal ileum intubation	134	76
Ileal intubation not intended, 177 colonoscopies[2]	36	
Not indicated	18	
Distorted anatomy due to previous surgery	1	
External stricture	2	
Previous colostomy in Crohn's disease	4	
Large polyp at rectum	2	
Risk of perforation outweighs benefit of full examination due to Severe colitis	5	
Poor bowel preparation	4	
Full colonoscopic examination intended, 177 colonoscopies[2]	141	
Ileal intubation	96	68
Cecum examination	134	95

[1]Some patients had more than one indication; [2]Not intended include not indicated, not feasible or the risks of full examination outweigh the benefit of full examination.

enterocolitis syndrome and autoimmune enteropathy), trichuriasis (*n* = 2), and assessment of previously confirmed solitary rectal ulcer syndrome (*n* = 2). Risk of perforation was judged to outweigh benefit of full examination in 5 patients. All had IBD with severe colitis and friable mucosal wall (ulcerative colitis, *n* = 3; CD, *n* = 2). Poor bowel preparation prevented a complete examination in 4 patients. A large rectal polyp obstructing the lumen (*n* = 1) and excessive bleeding in a patient with a large rectal polyp (*n* = 1) prevented a complete colonoscopy in 2 patients.

Of the remaining 141 patients in whom inspection of the terminal ileum was intended, the cecum examination and ileal intubation rates were 95.0% (134/141) and 68.1% (96/141), respectively. Overall, 45.8% of colonoscopies did not include an inspection of terminal ileum, and 31.9% did not reach terminal ileum when it was intended. Similarly, 24.3% of the procedures did not reach the cecum, and 5.0% failed to reach cecum when it was intended.

Factors affecting complete examination

Rate of complete examination was not significantly affected by the age of patients [ileal intubation rate; < 5 years (35/141) *vs* ⩾ 5 years (106/141) = 62.9% *vs* 69.8%; *P* = 0.44]. However, the ileal intubation rate was significantly higher when the indication for the colonoscopy was for the diagnosis or assessment of

Table 2 Colonoscopic performance by trainees

	Trainee A	Trainee	Trainee C	Trainee D	Average
Duration of training in mo	18	18	24	18	19.5
Number of colonoscopies performed during training period	19	17	44	36	29
Number of colonoscopies where intubation of terminal ileum was intended	16	13	39	28	24
Intubation of terminal ileum	12 (75)	10 (77)	34 (87)	18 (64)	77%
Examination of cecum and terminal ileum	16 (100)	13 (100)	38 (97)	26 (93)	97%

Data are presented as *n* or *n* (%), unless otherwise indicated. Note: In colonoscopies where trainees encountered technical difficulties during the procedure and were subsequently taken over by the consultant, the procedures were logged as performed by the consultant.

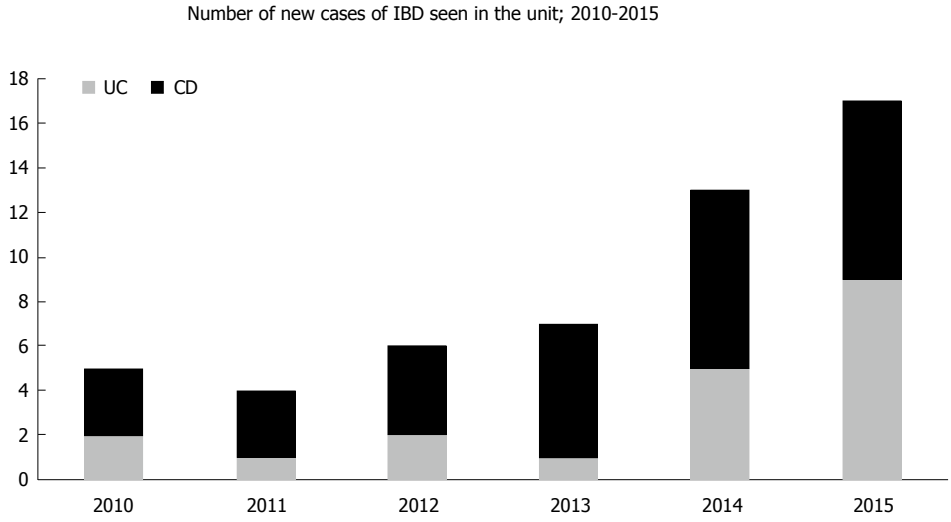

Figure 2 Number of new cases of pediatric inflammatory bowel disease seen in the unit during the study period. CD: Crohn's disease; IBD: Inflammatory bowel disease; UC: Ulcerative colitis.

IBD (73.0% *vs* 50%; $P = 0.016$).

Performance by trainees

During the study period, four trainees completed a minimum of 12-mo training in pediatric colonoscopy in the unit (Table 2). Part of the training period of another three trainees fell outside the study period and were not included in the analysis. The average number of colonoscopies performed was 29. The overall cecum examination rate was 97%, while the overall ileal intubation rate was 77%. There was a consistent performance by the trainees (Table 2).

Complications in 177 colonoscopies

A 7-year-old boy with CD who had gross delay in referral, severe malnutrition and severe mucosal ulcerations had iatrogenic perforation of the colon during the procedure. The patient had an uneventful recovery after colostomy and repair. Another patient with rectal polyp developed bleeding while it was removed during colonoscopy. The bleeding stopped after cauterization. No blood transfusion was required. No other complications were noted in the remaining 175 procedures, either associated with the procedure, anesthesia or sedation.

DISCUSSION

To the best of our knowledge, the present study is the first of its kind on performance benchmarked against established quality indicators in pediatric colonoscopy from a center where the volume of colonoscopy is low. During the study period, the number of colonoscopies performed in the center each year ranged from 19 to 58, with an average of 30. It was conducted in a setting with a low but rapidly increasing incidence of IBD.

Our results reveal that of the five quality indicators which were benchmarked against, the performance was high in four indicators. Most of the indications for colonoscopy performed in the unit were appropriate, following the recommendations of ESGE guidelines. Performances were good in bowel preparation, patient safety and complications. The cecum examination rate reached the expected rate at 95% by NASPGHAN, but was somewhat limited in ileal intubation rate at 68.1%. The performance of all trainees was consistently good in cecum examination but variable in ileal intubation.

There are several important implications on the results of the present study. Firstly, the indications for colonoscopies in the present study were mostly appropriate according to established guidelines[4]. The overall diagnostic yield was 85%. Previously, we observed that 99.7% of all EGDS and colonoscopies performed in the unit were appropriate[18]. The most common indications for colonoscopy were diagnosing or assessing IBD and ascertaining the cause of anemia. There was an increasing trend in the number of newly-diagnosed IBD cases during the study period. Investigation of abdominal symptoms, mainly abdominal pain, was the indication in only 17% of the patients[4].

In adult colonoscopy, screening for colon cancer is the main quality indicator[19]. Surrogate measures, such as colonic adenoma detection and complete examination of the colon, have been found to correlate with high-quality colonoscopy[20]. Pediatric colonoscopy, on the other hand, is fundamentally a different procedure with different indications, technical requirement, and different quality indicators[21]. The most important difference between adult and pediatric colonoscopies are the size of the patients and indications[21].

Screening for IBD is an important indication in pediatric colonoscopy. Differentiating between ulcerative colitis and CD is important in the diagnosis of IBD. Thus, examination of the cecum and terminal ileum are important quality indicators in pediatric colonoscopy[22]. In particular, intubation of the terminal ileum and sampling biopsy is essential for confirming the diagnosis of CD[23,24]. Pediatric endoscopy training guidelines suggest the cecal intubation rate to be at least 90% to 95%, with a comparable terminal ileum intubation rate[16,19].

Based on these quality indicators, the performances of centers vary. In Australia where screening for IBD was the major indication for colonoscopy, the reported cecum and ileal examination rates were 96.3% and 92.4%, respectively[5]. In Taiwan, the reported ileal intubation rate was 77.5%, while in China it was 81.7%[8,9]. The ileal intubation rates in the multicenter consortium review from the United States ranged from 30% to 90%[16].

After excluding procedures where either complete colonoscopy was not indicated, unsafe or not feasible, the cecum examination and ileal intubation rates in the present study were 95% and 68.1%, respectively. The cecum examination was comparable to the NASPGHAN pediatric gastroenterology training guidelines[19], but the ileal intubation rate was somewhat lower. Nevertheless, these figures were comparable with those reported in the region and the United States multicenter consortium study[8,16].

Bowel preparation was noted to be good in the majority of the cases (87%). Colonic perforation was observed in 1 patient who had severe long-standing CD prior to referral. The perforation rate was 0.5%. We reported two perforations in 66 colonoscopies previously[18].

The present study showed that all the trainees have a satisfactory cecum intubation rate, although the ileal intubation rate needs to be improved. To achieve cecal intubation examination and ileal intubation rate of 90%-95%, NASPGHAN guidelines for training in pediatric gastroenterology recommended 120 colonoscopies for pediatric trainees[19]. In this center, each trainee performed about 12-20 colonoscopies in children each year during their training. Before starting pediatric colonoscopy under supervision, the trainees were required to undergo training in adult colonoscopy, performing at least 50 colonoscopies in adult patients.

The implication of this is that the trainees would not have adequate training opportunity of reaching the recommended 120 colonoscopies in pediatric colonoscopy if the entire training was spent in this unit alone. Trainees spent between 18 mo to 24 mo of training in this center. The trainees usually start the training in endoscopic procedures with the adult gastroenterologists before being allowed to perform pediatric colonoscopy. The final year of the training is usually spent in a center of excellence for training in Australia or United Kingdom, where there is abundant opportunity for pediatric colonoscopy. Thus, even though the ileal intubation rate of the trainees noted in the present study did not reach the intended goal suggested by the NASPGHAN training guidelines[19], it is expected that their performance will be enhanced further once the oversea training is completed.

Another potential way to enhance colonoscopic skills is simulated colonoscopy training[25]. Studies involving trainees in adult colonoscopy showed improved performances during patient-based colonoscopy[25]. However, to date, no such study has been published involving training in pediatric colonoscopy.

Other important quality indicators which were not included in the present study were documentation of American Society of Anesthesiologist Physical Status Classification System (ASA) risk assessment and procedure duration. ASA risk assessment was routinely checked by the anesthetist. It was documented separately but was not captured in the present study. Additional potential measures of high-quality pediatric colonoscopy which have been mentioned but not included in this study are minimization of air insufflation, ease of patient sedation, duration of procedure, performance of mucosal biopsy sampling, patient recovery time and ongoing procedural competency assessment[22].

An obvious limitation to this study is its retrospective nature. The data was only collected from one center. However, our center is the only training center for pediatric gastroenterology in the whole country; we are unable to benchmark our performance against other centers. Nevertheless, with the exception of a somewhat lower ileal intubation rate, the performance in other quality indicators is excellent.

In conclusion, there is an increasing trend in the number of colonoscopies performed each year in this center. This is due to the increasing number of newly-diagnosed IBD cases during the study period. The performance of pediatric colonoscopy in this center was excellent in four of the five quality indicators benchmarked. The ileal intubation rate needs to be improved. A period of training in a center with a large volume of IBD will enhance the skills and performance of colonoscopy among the trainees of pediatric gastroenterology in Malaysia.

ARTICLE HIGHLIGHTS

Research background

The incidence of inflammatory bowel disease is on the rise worldwide, including in Asia. The gold standard for the diagnosis of inflammatory bowel disease is histologic confirmation from tissue biopsies obtained during esophago-gastro-duodenoscopy and colonoscopy. In particular, differentiating Crohn' s disease from ulcerative colitis is dependent upon inspection and biopsy of the terminal ileum. Thus, intubation of the terminal ileum is considered as an important quality indicator in pediatric colonoscopy. Current guidelines by the North American Society of Pediatric Gastroenterology, Hepatology and Nutrition recommend the cecum examination and terminal ileum of 95%. This target should be used by pediatric gastroenterology centers worldwide to benchmark their performance.

Research motivation

Current literature showed that reported ileal intubation rate in pediatric colonoscopy from centers around Asia ranged from 75.6% to 77.5%. The performance of our unit, from an area where the incidence of inflammatory bowel disease is currently low but is on the rise, is unknown. Thus, we were motivated to benchmark our performance against current recommendation to identify areas for improvement to enhance the quality of our training program.

Research objectives

The main objective was to benchmark the performance of our unit, in particular the completeness of colonoscopic examination, *i.e.* cecal examination and ileal intubation, against current recommended guidelines. We also evaluated other indicators such as appropriateness of indications, level of bowel preparation, as well as safety and complications of the procedures encountered.

Research methods

We conducted a retrospective analysis on all the pediatric colonoscopies performed in a pediatric gastroenterology training center in Malaysia over a period of 6 years. We included the following indicators: appropriateness of indications; quality of bowel preparation; safety and complications; as well as cecal examination and terminal ileum intubation rates. The performances of trainees in the cecal and ileal examination rates were ascertained separately.

Research results

We found that of the 177 colonoscopies performed, the diagnostic yield was 85%, quality of bowel preparation was good in 87%, while one of 177 procedures was complicated by perforation during the procedure. The overall cecum examination rate was 76.3% and ileal intubation rate was 54.2%. After excluding colonoscopy where full colonoscopic examination was either not indicated, not feasible because of poor bowel preparation or unsafe (severe colitis), the cecum examination rate was 95.0% and ileal intubation rate was 68.1%. Among four trainees who completed a minimum of 12 mo training, the overall cecum rate was 97% while the overall ileal intubation rate was 77%. The performance of all trainees was consistent. Thus, the cecum examination rate of our unit was satisfactory but the rate of terminal ileum intubation needs further improvement. To improve the rate of ileal intubation, the trainees would spend part of their training program in a center of excellence with adequate volume of pediatric colonoscopy.

Research conclusions

The present study was the first attempt by a pediatric gastroenterology unit in Asia to benchmark its performance in pediatric colonoscopy against established international guidelines. Our study suggests that such a benchmark is both applicable and desirable. The study allows our unit to identify areas for further improvement. Trainees from our unit now routinely spend part of their training in a center of excellence to enhance their skills in colonoscopy.

Research perspectives

Benchmarking against established guidelines has been adopted as part of quality assurance of our unit. We plan to conduct a prospective study to include other indicators of good practice not included in this retrospective review. These include anesthetic risk assessment, duration of procedure, ease of sedation, quality of mucosal biopsy sampling and patient recovery time.

REFERENCES

1 **Teague RH**, Salmon PR, Read AE. Fibreoptic examination of the colon: a review of 255 cases. *Gut* 1973; **14**: 139-142 [PMID: 4540492]

2 **Hassall E**, Barclay GN, Ament ME. Colonoscopy in childhood. *Pediatrics* 1984; **73**: 594-599 [PMID: 6718114]

3 **ASGE Standards of Practice Committee**, Lightdale JR, Acosta R, Shergill AK, Chandrasekhara V, Chathadi K, Early D, Evans JA, Fanelli RD, Fisher DA, Fonkalsrud L, Hwang JH, Kashab M, Muthusamy VR, Pasha S, Saltzman JR, Cash BD; American Society for Gastrointestinal Endoscopy. Modifications in endoscopic practice for pediatric patients. *Gastrointest Endosc* 2014; **79**: 699-710 [PMID: 24593951 DOI: 10.1016/j.gie.2013.08.014]

4 **Thomson M**, Tringali A, Dumonceau JM, Tavares M, Tabbers MM, Furlano R, Spaander M, Hassan C, Tzvinikos C, Ijsselstijn H, Viala J, Dall'Oglio L, Benninga M, Orel R, Vandenplas Y, Keil R, Romano C, Brownstone E, Hlava Š, Gerner P, Dolak W, Landi R, Huber WD, Everett S, Vecsei A, Aabakken L, Amil-Dias J, Zambelli A. Paediatric Gastrointestinal Endoscopy: European Society for Paediatric Gastroenterology Hepatology and Nutrition and European Society of Gastrointestinal Endoscopy Guidelines. *J Pediatr Gastroenterol Nutr* 2017; **64**: 133-153 [PMID: 27622898 DOI: 10.1097/MPG.0000000000001408]

5 **Singh HK**, Withers GD, Ee LC. Quality indicators in pediatric colonoscopy: an Australian tertiary center experience. *Scand J Gastroenterol* 2017; **52**: 1453-1456 [PMID: 28936881 DOI: 10.1080/00365521.2017.1380224]

6 **Wahid AM**, Devarajan K, Ross A, Zilbauer M, Heuschkel R. Paediatric gastrointestinal endoscopy: a qualitative study. *Eur J Gastroenterol Hepatol* 2016; **28**: 25-29 [PMID: 26473298 DOI: 10.1097/MEG.0000000000000488]

7 **Lee YW**, Chung WC, Sung HJ, Kang YG, Hong SL, Cho KW, Kang D, Lee IH, Jeon EJ. Current status and clinical impact of pediatric endoscopy in Korea. *Korean J Gastroenterol* 2014; **64**: 333-339 [PMID: 25530584]

8 **Wu CT**, Chen CA, Yang YJ. Characteristics and Diagnostic Yield of Pediatric Colonoscopy in Taiwan. *Pediatr Neonatol* 2015; **56**: 334-338 [PMID: 25850637 DOI: 10.1016/j.pedneo.2015.01.005]

9 **Lei P**, Gu F, Hong L, Sun Y, Li M, Wang H, Zhong B, Chen M, Cui Y, Zhang S. Pediatric colonoscopy in South China: a 12-year experience in a tertiary center. *PLoS One* 2014; **9**: e95933 [PMID: 24759776 DOI: 10.1371/journal.pone.0095933]

10 **Tam YH**, Lee KH, Chan KW, Sihoe JD, Cheung ST, Mou JW. Colonoscopy in Hong Kong Chinese children. *World J Gastroenterol* 2010; **16**: 1119-1122 [PMID: 20205284 DOI: 10.3748/wjg.v16.i9.1119]

11 **Ruel J**, Ruane D, Mehandru S, Gower-Rousseau C, Colombel JF. IBD across the age spectrum: is it the same disease? *Nat Rev*

Gastroenterol Hepatol 2014; **11**: 88-98 [PMID: 24345891 DOI: 10.1038/nrgastro.2013.240]

12 **Ng SC**, Tang W, Ching JY, Wong M, Chow CM, Hui AJ, Wong TC, Leung VK, Tsang SW, Yu HH, Li MF, Ng KK, Kamm MA, Studd C, Bell S, Leong R, de Silva HJ, Kasturiratne A, Mufeena MN, Ling KL, Ooi CJ, Tan PS, Ong D, Goh KL, Hilmi I, Pisespongsa P, Manatsathit S, Rerknimitr R, Aniwan S, Wang YF, Ouyang Q, Zeng Z, Zhu Z, Chen MH, Hu PJ, Wu K, Wang X, Simadibrata M, Abdullah M, Wu JC, Sung JJ, Chan FK; Asia–Pacific Crohn's and Colitis Epidemiologic Study (ACCESS) Study Group. Incidence and phenotype of inflammatory bowel disease based on results from the Asia-pacific Crohn's and colitis epidemiology study. *Gastroenterology* 2013; **145**: 158-165.e2 [PMID: 23583432 DOI: 10.1053/j.gastro.2013.04.007]

13 **Malmborg P**, Hildebrand H. The emerging global epidemic of paediatric inflammatory bowel disease--causes and consequences. *J Intern Med* 2016; **279**: 241-258 [PMID: 26355194 DOI: 10.1111/joim.12413]

14 **Hilmi I**, Jaya F, Chua A, Heng WC, Singh H, Goh KL. A first study on the incidence and prevalence of IBD in Malaysia--results from the Kinta Valley IBD Epidemiology Study. *J Crohns Colitis* 2015; **9**: 404-409 [PMID: 25744112 DOI: 10.1093/ecco-jcc/jjv039]

15 **Walsh CM**, Ling SC, Mamula P, Lightdale JR, Walters TD, Yu JJ, Carnahan H. The gastrointestinal endoscopy competency assessment tool for pediatric colonoscopy. *J Pediatr Gastroenterol Nutr* 2015; **60**: 474-480 [PMID: 25564819 DOI: 10.1097/MPG.0000000000000686]

16 **Thakkar K**, Holub JL, Gilger MA, Shub MD, McOmber M, Tsou M, Fishman DS. Quality indicators for pediatric colonoscopy: results from a multicenter consortium. *Gastrointest Endosc* 2016; **83**: 533-541 [PMID: 26253014 DOI: 10.1016/j.gie.2015.06.028]

17 **Levine A**, Koletzko S, Turner D, Escher JC, Cucchiara S, de Ridder L, Kolho KL, Veres G, Russell RK, Paerregaard A, Buderus S, Greer ML, Dias JA, Veereman-Wauters G, Lionetti P, Sladek M, Martin de Carpi J, Staiano A, Ruemmele FM, Wilson DC; European Society of Pediatric Gastroenterology, Hepatology, and Nutrition. ESPGHAN revised porto criteria for the diagnosis of inflammatory bowel disease in children and adolescents. *J Pediatr Gastroenterol Nutr* 2014; **58**: 795-806 [PMID: 24231644 DOI: 10.1097/MPG.0000000000000239]

18 **Lee WS**, Zainuddin H, Boey CC, Chai PF. Appropriateness, endoscopic findings and contributive yield of pediatric gastrointestinal endoscopy. *World J Gastroenterol* 2013; **19**: 9077-9083 [PMID: 24379634 DOI: 10.3748/wjg.v19.i47.9077]

19 **Leichtner AM**, Gillis LA, Gupta S, Heubi J, Kay M, Narkewicz MR, Rider EA, Rufo PA, Sferra TJ, Teitelbaum J; NASPGHAN Training Committee; North American Society for Pediatric Gastroenterology. NASPGHAN guidelines for training in pediatric gastroenterology. *J Pediatr Gastroenterol Nutr* 2013; **56** Suppl 1: S1-S8 [PMID: 23263531 DOI: 10.1097/MPG.0b013e31827a78d6]

20 **Rex DK**. Quality in colonoscopy: cecal intubation first, then what? *Am J Gastroenterol* 2006; **101**: 732-734 [PMID: 16635220 DOI: 10.1111/j.1572-0241.2006.00483.x]

21 **Rex DK**. Colonoscopy. *Gastrointest Endosc* 2013; **78**: 444-449 [PMID: 23948194 DOI: 10.1016/j.gie.2013.06.025]

22 **Kay M**, Wyllie R. It's all about the loop: quality indicators in pediatric colonoscopy. *Gastrointest Endosc* 2016; **83**: 542-544 [PMID: 26897046 DOI: 10.1016/j.gie.2015.08.058]

23 **Sawczenko A**, Sandhu BK. Presenting features of inflammatory bowel disease in Great Britain and Ireland. *Arch Dis Child* 2003; **88**: 995-1000 [PMID: 14612366]

24 **Batres LA**, Maller ES, Ruchelli E, Mahboubi S, Baldassano RN. Terminal ileum intubation in pediatric colonoscopy and diagnostic value of conventional small bowel contrast radiography in pediatric inflammatory bowel disease. *J Pediatr Gastroenterol Nutr* 2002; **35**: 320-323 [PMID: 12352520]

P- Reviewer: Choi YS **S- Editor**: Gong ZM **L- Editor**: Filipodia **E- Editor**: Huang Y

World Journal of Gastroenterology

Submit a Manuscript: http://www.f6publishing.com

World J Gastroenterol 2018 March 7; 24(9): 1022-1034

DOI: 10.3748/wjg.v24.i9.1022

ISSN 1007-9327 (print) ISSN 2219-2840 (online)

ORIGINAL ARTICLE

Retrospective Study

Prognostic value of lymph nodes count on survival of patients with distal cholangiocarcinomas

Hua-Peng Lin, Sheng-Wei Li, Ye Liu, Shi-Ji Zhou

Hua-Peng Lin, Sheng-Wei Li, Department of Hepatobiliary Surgery, The Second Affiliated Hospital of Chongqing Medical University, Chongqing 400010, China

Ye Liu, Department of Neonatal, Children's Hospital Chongqing Medical University, Chongqing 400016, China

Shi-Ji Zhou, Department of Gastrointestinal Surgery, The Second Affiliated Hospital of Chongqing Medical University, Chongqing 400010, China

ORCID number: Hua-Peng Lin (0000-0002-8632-0069); Sheng-Wei Li (0000-0002-9748-8190); Ye Liu (0000-0002-8077-2961); Shi-Ji Zhou (0000-0002-2145-0786).

Author contributions: Zhou SJ and Lin HP conducted the analyses and wrote the manuscript; all other authors contributed to the idea of the manuscript and approved the final version.

Supported by the National Natural Science Foundation of China, No. 81301975; and the Chongqing Natural Science Foundation, No. cstc2016jcyjA016.

Institutional review board statement: This article does not contain any studies with human participants or animals performed by any of the authors.

Informed consent statement: As this study is based on a publicly available database without identifying patient information, informed consent was not needed.

Conflict-of-interest statement: All authors declare no conflicts-of-interest related to this article.

Data sharing statement: No additional data are available.

Manuscript source: Unsolicited manuscript

Correspondence to: Shi-Ji Zhou, MD, PhD, Doctor, Surgeon, Surgical Oncologist, Department of Gastrointestinal Surgery, The Second Affiliated Hospital of Chongqing Medical University, 74 Linjiang Road, Yuzhong District, Chongqing 400010, China. zhoushiji@hospital.cqmu.edu.cn
Telephone: +86-23-63693626
Fax: +86-23-63693533

Received: December 23, 2017
Peer-review started: December 23, 2017
First decision: January 17, 2018
Revised: January 30, 2018
Accepted: February 8, 2018
Article in press: February 8, 2018
Published online: March 7, 2018

Abstract

AIM

To evaluate the prognostic value of the number of retrieved lymph nodes (LNs) and other prognostic factors for patients with distal cholangiocarcinomas, and to determine the optimal retrieved LNs cut-off number.

METHODS

The Surveillance, Epidemiology and End Results database was used to screen for patients with distal cholangiocarcinoma. Patients with different numbers of retrieved LNs were divided into three groups by the X-tile program. X-tile from Yale University is a useful tool for outcome-based cut-point optimization. The Kaplan-Meier method and Cox regression analysis were utilized for survival analysis.

RESULTS

A total of 449 patients with distal cholangiocarcinoma met the inclusion criteria. The Kaplan-Meier survival analysis for all patients and for N1 patients revealed no significant differences among patients with different retrieved LN counts in terms of overall and cancer-specific survival. In patients with node-negative distal cholangiocarcinoma, patients with four to nine retrieved LNs had a significantly better overall (P = 0.026) and cancer-specific survival (P = 0.039) than others. In the subsequent multivariate analysis, the number of retrieved LNs was evaluated to be independently associated with survival. Additionally, patients with four to nine retrieved LNs had a significantly lower overall mortality risk [hazard ratio (HR) = 0.39; 95% confidence interval (CI): 0.20-0.74] and cancer cause-specific mortality risk (HR = 0.32; 95%CI: 0.15-0.66) than other patients. Additionally, stratified survival analyses showed persistently better overall and cancer-specific survival when retrieving four to nine LNs in patients with any T stage of tumor, a tumor between 20 and 50 mm in diameter, or a poorly differentiated or undifferentiated tumor, and in patients who were $\leqslant$ 70-years-old.

CONCLUSION

The number of retrieved LNs was an important independent prognostic factor for patients with node-negative distal cholangiocarcinoma. Additionally, patients with four to nine retrieved LNs had better overall and cancer-specific survival rates than others, but the reason and mechanism were unclear. This conclusion should be validated in future studies.

Key words: Distal cholangiocarcinomas; Lymph node count; Survival analysis; SEER

Core tip: The prognostic value of retrieved lymph node (LN) counts is still under debate for patients with distal cholangiocarcinomas. The aim of the present study was to evaluate the prognostic value of the number of retrieved lymph nodes and other prognostic factors for patients with distal cholangiocarcinomas and to determine the optimal retrieved LNs cut-off number. A total of 449 patients with distal cholangiocarcinoma were included in this study. The univariate and multivariate analyses revealed that the number of retrieved LNs was independently associated with survival. And, patients with four to nine retrieved LNs had a better overall and cancer-specific survival rate than others.

Lin HP, Li SW, Liu Y, Zhou SJ. Prognostic value of lymph nodes count on survival of patients with distal cholangiocarcinomas. *World J Gastroenterol* 2018; 24(9): 1022-1034 Available from: URL: http://www.wjgnet.com/1007-9327/full/v24/i9/1022.htm
DOI: http://dx.doi.org/10.3748/wjg.v24.i9.1022

INTRODUCTION

Cholangiocarcinoma constitutes approximately 15% of hepatobiliary tumors and 3% of gastrointestinal tumors[1]. According to its anatomic location, cholangiocarcinoma is classified as intrahepatic, perihilar or distal malignancy. Distal cholangiocarcinoma comprise approximately 30% of all cholangiocarcinoma; it is a relatively uncommon disease. The only optimal treatment for distal cholangiocarcinoma is surgical resection, as a result of the insensitivity of cholangiocarcinoma to radiation and chemotherapy[2]. Additionally, complete tumor resection of distal cholangiocarcinoma always relies on pancreaticoduodenectomy, which is a complicated operation with high morbidity and mortality[3]. Hence, the postoperative prognosis of patients with distal cholangiocarcinoma has attracted great interest in several studies[4,5]. Lymph node (LN) status was determined to be a strong predictor for the prognosis of patients with distal cholangiocarcinoma[6]. Patients without LN metastasis had a better prognosis than those with LN involvement. Thus, an adequate number of retrieved LNs is vital to distinguish N0 patients from N1 ones. The appropriate cut-off of retrieved LNs counts should be determined.

Currently, the number of LNs that should be retrieved is still under debate. Several studies evaluated the prognostic value of retrieved LN counts and tried to determine the benchmark number of examined LNs[6-9]. Nevertheless, most of them were designed retrospectively with a small sample size, and cases that met their inclusion criteria comprised both perihilar and distal cholangiocarcinomas. The differences in biological and pathological features, as well as surgical strategies and prognoses, between perihilar and distal cholangiocarcinomas lead to a different influence of retrieving LN counts on survival.

The American Joint Committee on Cancer (AJCC) staging system suggested a different appropriate number of retrieved LNs for perihilar and distal cholangiocarcinomas. For distal cholangiocarcinoma, the number that AJCC suggested was 12. However, this suggestion lacks verification because the retrieved LN counts in most previous studies did not reach 12. Additionally, in the study of Kawai *et al*[10], patients with more than 12 retrieved LNs only had a moderately better survival rate than patients with a smaller number of retrieved LNs in a univariate analysis, not a multivariate analysis. A subgroup study of Kiriyama *et al*[11], using a cohort of N0 patients, found that patients with more than 10 retrieved LNs had a better survival. This subgroup analysis was based on a small sample

size with a univariate analysis, and the cancers of the involved cases were all stages Ⅰ and Ⅱ. Therefore, the appropriate cut-off number of retrieved LNs is still unconfirmed.

Our study was performed to evaluate the interactions between the number of retrieved LNs and the prognosis of patients with distal cholangiocarcinoma; additionally, this study determined the appropriate retrieved LN cut-off number. To obtain a larger sample size, the Surveillance, Epidemiology and End Results (SEER) database was used for the selection of patients with at least one retrieved LN.

MATERIALS AND METHODS

Data source

SEER is a public dataset that collects survival and incidence data of various types of cancers and covers more than 25% of the United States' population. SEER data include tumor characteristics such as primary tumor site, TNM staging of tumor, tumor size, type of treatment and cause of death, and demographic characteristics such as race of patients, age of diagnosis, sex, *etc*. Our study used the latest 11 years' data from SEER (from 2004-2014). We downloaded the data from SEER with SEER*Stat Software (version 8.3.4; https://seer.cancer.gov/seerstat/).

Patients

Our study was designed to be a retrospective study. The inclusion criteria were (1) patients greater than 20 years in age; (2) patients diagnosed with distal cholangiocarcinoma according to the term "006-BileDuctsDistal" of "CS SCHEMA v0204+"; (3) patients with histology code of 8010, 8020, 8070, 8140, 8144, 8160, 8162, 8163, 8260, 8480, 8490 or 8560; (4) patients with diagnoses that were not confirmed by a death certificate or autopsy; (5) patients with active follow-up; (6) patients from a time span of 2004 to 2014 according to the term "year of diagnosis"; (7) patients with only one tumor who had survived more than 1 mo; (8) patients without distant metastasis (the M0 patients); (9) patients who received intent surgery in terms of the combination of "Surg Prim Site" and "Reason no cancer-directed surgery"; (10) patients who did not receive preoperative radiotherapy according to the terms of "Radiation" and "Surg/Rad Seq"; and (11) patients with at least one retrieved LN according to the terms "Regional Nodes Examined". Demographics of patients such as race, age at diagnosis and marital status, and tumor characteristics such as tumor size, laterality of tumor, grade and stage of tumor were all extracted for subsequent analysis. The terms "SEER cause-specific death classification" and "SEER other cause of death classification" were used to distinguish our two endpoints: all-cause mortality and cancer cause-specific mortality.

Statistical analysis

Statistical analyses were conducted with SPSS (version 23.0; IBM Corp., Armonk, NY, United States). The demographic data of patients were compared by *t* tests (for continuous variables) and chi-square tests (for proportion variables). A *P*-value of < 0.05 was defined to be statistically significant. Patients with different numbers of retrieved LNs were divided into three groups.

The cut-off number of retrieved LNs for grouping was determined by the X-tile program (http://www.tissuearray.org/rimmlab/). X-tile from Yale University is a useful tool for outcome-based cut-point optimization. The strategies of the X-tile program for grouping included that it would try each number between the range of the retrieved LN counts as the cut-off; then, the χ^2 score and *P*-value were calculated with this number as the cut-off[12,13]. Eventually, the number with a maximum χ^2 score and a minimum *P*-value would be suggested to be the final cut-off.

The Kaplan-Meier method (univariate analysis) with log-rank tests and Cox regression analysis (multivariate analysis) were utilized for survival analysis. The overall survival and cancer-specific survival were compared between patients with the different categories of retrieved LNs counts. Then, we performed stratified survival analyses for the number of retrieved LNs, in terms of the confounders that were evaluated to be independently associated with survival in the multivariate analysis.

RESULTS

Patient and demographics details

A total of 449 patients with distal cholangiocarcinoma (2004-2014) met the inclusion criteria for this research. The majority of them were white and male. The distributions of age and the diagnosis year were averaged. Nearly 70% of the patients were married. The size of the tumor was less than 50 mm in most patients. Patient and tumor characteristics are shown in Table 1.

The retrieved LN counts ranged from one to sixty-three. More than half of the patients had > 10 LNs retrieved, and 22.7% of patients had > 20 LNs retrieved. There were 226 N0 patients and 223 N1 patients. Most patients underwent extensive surgery and postoperative chemotherapy; the number of patients who received adjuvant radiotherapy was less.

Impact of the number of retrieved LNs on survival rates

We divided patients with different numbers of retrieved LNs into three groups, by use of the X-tile program. Then, the retrieved LN count was converted from continuous variables into categorical variables to study its impact on survival. As shown in Figure 1, the cut-off numbers for grouping in all patients were 3 and 6, the

Table 1 Characteristics of patients and tumors

Variable	No. of patients, *n* (%) of *n* = 449
Race	
White	321 (71.5)
Black	35 (7.8)
Other	93 (20.7)
Sex	
Male	286 (63.7)
Female	163 (36.3)
Age at diagnosis, in yr	
⩽ 60	128 (28.5)
60-70	171 (38.1)
> 70	150 (33.4)
Marital status	
Married	302 (67.3)
Divorced	33 (7.3)
Separated or single	58 (12.9)
Widowed	40 (8.9)
Unknown	16 (3.6)
Year of diagnosis	
2004-2010	110 (24.5)
2011-2012	160 (35.6)
2013-2014	179 (39.9)
Tumor size, in mm	
⩽ 20	203 (45.2)
20-50	191(42.5)
> 50	15 (3.3)
Unknown	40 (8.9)
Grade	
Well differentiated	54 (12.0)
Moderately differentiated	204 (45.4)
Poorly differentiated	158 (35.2)
Undifferentiated	3 (0.7)
Unknown	30 (6.7)
Stage	
Ⅰ A	44 (9.8)
Ⅰ B	60 (13.7)
Ⅱ A	89 (19.8)
Ⅱ B	161 (35.9)
Ⅲ	95 (21.2)
T stage	
T1	49 (10.9)
T2	85 (18.9)
T3	220 (49.0)
T4	95 (21.2)
pN stage	
pN0	226 (50.3)
pN1	223 (49.7)
Surgery type	
Local excision	102 (22.7)
Extensive surgery	347 (77.3)
Adjuvant radiotherapy	
No/Unknown radiotherapy	298 (66.3)
Beam radiation	151 (33.7)
Adjuvant chemotherapy	
No/Unknown chemotherapy	204 (45.4)
Chemotherapy performed	245 (54.6)
No. of LNs retrieved	
1-10	196 (43.7)
11-20	151 (33.6)
> 20	102 (22.7)

LNs: Lymph nodes.

cut-off numbers for N0 patients were 4 and 9, and the cut-off numbers for N1 patients were 4 and 16.

In the Kaplan-Meier survival analysis, no significant difference was observed among the three categories of retrieved LN counts for all and N1 patients with distal cholangiocarcinomas. For patients with node-negative distal cholangiocarcinomas, there was a significantly better overall and cancer-specific survival in patients with 4-9 retrieved LNs than in patients with 1-3 or > 9 retrieved LNs. Additionally, we compared overall and cancer-specific survival among each number of retrieved LNs. Because of space limitations, we could only put part of the results into the table (Table 2).

There was a similar trend of survival rate as the retrieved LN count increased in all, N0 and N1 patients; patients with seven retrieved LNs had the best survival rate compared with the others. In N0 patients, patients with seven or nine retrieved LNs had a significantly higher survival rate compared with other patients; this result was confirmed in analysis regarding retrieved LN counts as categorical variables.

Survival analyses in all patients and patients with node-negative distal cholangiocarcinoma

The results of survival analysis for all patients in the present study were similar to previous studies. As shown in Figure 1 and Table 3, retrieved LN counts were not associated with survival in all patients (P = 0.233). Factors such as tumor size and T and N stages that were significant in univariate analysis were entered into a multivariate model. N stage was shown to be independently associated with overall survival [hazard ratio (HR) = 1.40; 95% confidence interval (CI): 1.05-1.86]. In terms of cancer-specific survival, T stage [(HR = 1.45; 95%CI: 1.02-2.07)] was shown to be an independent risk factor of survival, along with N stage (HR = 1.42; 95%CI: 1.05-1.92).

For N0 patients, univariate analysis showed that retrieved LN counts, age at diagnosis, and grade of tumor were associated with overall survival. After those factors were entered into multivariate analysis, retrieved LN counts and grade of tumor were determined to be independent risk factors of overall survival. Patients with four to nine retrieved LNs had a significantly lower all-cause mortality risk than other patients (HR = 0.39; 95%CI: 0.20-0.74). In terms of cancer-specific survival, tumor size, grade of tumor, T stage and retrieved LN counts were evaluated to be associated with survival in both univariate and multivariate analyses. There was a significant decrease in terms of cancer cause-specific mortality risk (HR = 0.32; 95%CI: 0.15-0.66) for patients with four to nine retrieved LNs (Table 4).

Stratified analyses for the number of retrieved LNs in patients with node-negative distal cholangiocarcinoma

To further study the interactions between retrieved LN counts and prognoses of patients with node-negative distal cholangiocarcinoma, we performed survival analysis stratified by size, grade, T stage of tumor and age of patients. For patients ⩽ 70-years-old, retrieving four to nine LNs resulted in a significantly

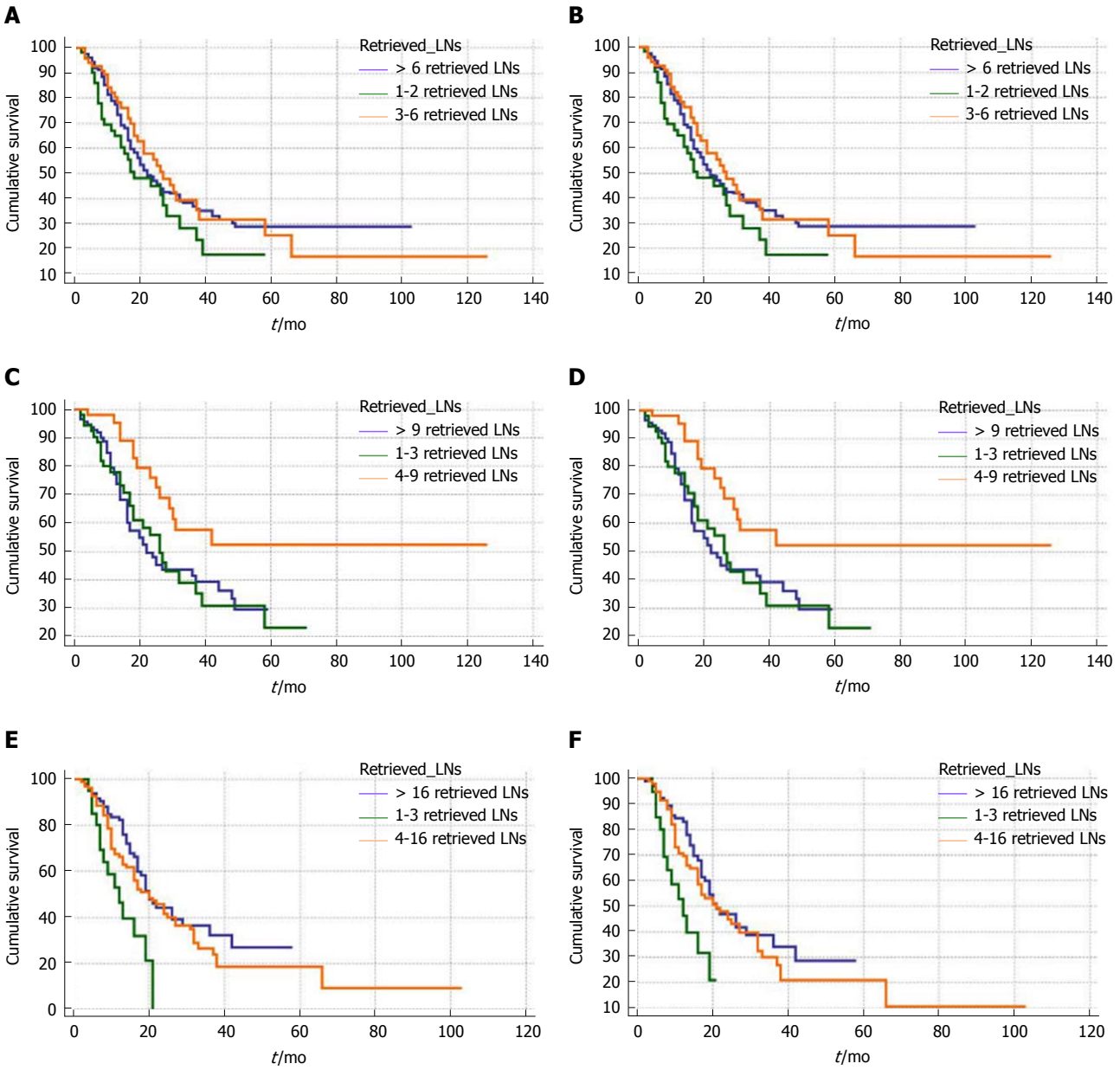

Figure 1 Kaplan-Meier survival curves of all patients in terms of (A) overall survival and (B) cancer-specific survival. There was no significant difference in terms of overall survival (P = 0.233) and cancer-specific survival (P = 0.141) among the three groups. Kaplan-Meier survival curves of patients with node-negative distal cholangiocarcinoma in terms of (C) overall survival and (D) cancer-specific survival. Patients with four to nine retrieved LNs had a better overall (P = 0.026) and cancer-specific (P = 0.008) survival than patients with one to three retrieved LNs and patients with more than nine retrieved LNs. Kaplan-Meier survival curves of N1 patients in terms of (E) overall survival and (F) cancer-specific survival. There was no significant difference in terms of overall survival (P = 0.053) and cancer-specific survival (P = 0.0564) among the three groups. LNs: Lymph nodes.

better survival rate than retrieving one to three LNs in terms of overall survival (Figure 2A) and cancer-specific survival (Figure 3A). Additionally, no significant difference between patients with one to three retrieved LNs and > 9 retrieved LNs in terms of overall and cancer-specific survival was observed.

Subsequently, the above results were confirmed in multivariate survival analyses after adjusting for all confounders (Table 5). As shown in Figures 2 and 3 and Table 5, similar results were found for patients with any T stage of tumor, tumor size between 20 and 50 mm, and tumors that were poorly defined or undifferentiated. The prognostic effect of retrieved LN counts was not present when analyses were limited to well or moderately differentiated tumors, tumors $\leqslant$ 20 mm, and patients greater than 70 years in age.

DISCUSSION

Nodal status is a well-studied indicator for the prognosis of patients with distal cholangiocarcinoma. In addition to the stage of LNs, the prognostic value of positive node counts and lymph node ratios has been evaluated in several studies[6,10,11]. While the prognostic value of the number of retrieved LNs is still under debate, the optimal cut-off number of retrieved LNs

Table 2 Impact of the number of retrieved LNs on survival rates

Retrieved LNs counts	No.	3-yr OS	95%CI	3-yr CSS	95%CI
For all patients					
1	26	29.51%	10.90-51.07	29.51%	10.90-51.07
3	23	35.33%	13.50-58.23	43.64%	18.10-66.88
5	18	46.55%	16.40-72.36	51.20%	17.95-77.03
7	22	63.31%	35.24-81.81	63.31%	35.24-81.84
9	16	57.29%	27.94-78.40	66.20%	32.37-86.00
11	16	37.09%	11.27-63.72	40.46%	12.19-67.77
13	11	28.41%	4.52-59.96	28.41%	4.52-59.96
15	13	16.46%	0.90-50.11	16.46%	0.90-50.11
17	15	15.80%	0.82-49.22	17.01%	0.84-51.90
19	9	34.29%	4.81-68.55	34.29%	4.81-68.55
21	12	47.62%	19.35-71.52	47.62%	19.35-71.52
23	5	33.86%	5.73-66.35	33.86%	5.73-66.35
25	15	37.50%	9.37-66.61	37.50%	9.37-66.61
For N0 patients					
1	17	40.38%	14.15-65.68	40.38%	14.15-65.68
3	18	43.65%	17.20-67.68	47.01%	18.51-71.34
5	11	30.00%	1.23-71.92	37.50%	1.10-80.80
7	16	76.15%	42.67-91.65	76.15%	42.67-91.65
9	5	66.67%	5.41-94.52	66.67%	5.41-94.52
11	9	50.79%	15.67-78.07	59.26%	18.59-84.95
13	4	37.50%	1.10-80.80	37.50%	1.10-80.80
15	6	26.67%	0.97-68.61	26.67%	0.97-68.61
17	4	-	-	-	-
19	2	-	-	-	-
21	6	55.56%	7.34-87.61	55.56%	7.34-87.61
23	1	-	-	-	-
25	7	42.00%	7.01-75.34	52.50%	8.42-84.55
For N1 patients					
1	9	14.29%	0.71-46.49	14.29%	0.71-46.49
3	5	33.33%	0.90-77.41	33.33%	0.90-77.41
5	7	53.57%	13.20-82.50	53.57%	13.20-82.50
7	6	55.56%	7.34-87.61	55.56%	7.34-87.61
9	11	45.00%	13.88-72.41	58.33%	18.02-84.41
11	7	25.00%	1.23-64.59	25.00%	1.23-64.59
13	7	41.67%	5.60-76.65	41.67%	5.60-76.65
15	7	35.71%	1.41-77.98	35.71%	1.41-77.98
17	11	17.05%	0.84-51.92	18.94%	0.87-55.82
19	7	26.67%	0.97-68.61	26.67%	0.97-68.61
21	6	43.64%	11.29-72.96	43.64%	11.29-72.96
23	4	-	-	-	-
25	8	28.57%	4.11-61.15	28.57%	4.11-61.15

CI: Confidence interval; CSS: Cancer-specific survival; LNs: Lymph nodes; OS: Overall survival.

is also unconfirmed. Several studies of other diseases revealed the difference in retrieved LNs' influence on survival between N0 and N1 patients[8,14,15]. Nevertheless, for N0 patients, more LNs retrieved significantly improved survival. Therefore, studies of distal cholangiocarcinoma on retrieved LN counts should be performed in a cohort of N0 patients for whom the prognostic value of retrieved LN counts has never been systematically studied.

Our study screened 449 patients with distal cholangiocarcinoma in a population-based database; a total of 226 patients with node-negative distal cholangiocarcinoma were among them. Retrieved LN counts did not show its prognostic value in the whole cohort and N1 patients. However, in patients with node-negative distal cholangiocarcinoma, patients with four to nine retrieved LNs were determined to have a significantly better prognosis than patients with $\leqslant$ 3 retrieved LNs in terms of overall and cancer-specific survivals. Additionally, tumor size, grade and T stage of tumor were evaluated to be independent risk factors of cancer-specific survival. Therefore, retrieving at least four LNs would be optimal for patients with node-negative distal cholangiocarcinoma.

More retrieved LNs could promote the accuracy of LNs staging to avoid the under-staging effect, thus to improve survival of patients with distal cholangiocarcinoma. Studies on cholangiocarcinoma demonstrated there were micrometastases in approximately 5% of LNs which were diagnosed as negative nodes[16]. The more LNs that were resected and retrieved meant less micrometastases were left, therefore the survival of patients with more retrieved LNs counts could be improved. Additionally, more retrieved LNs represented adequate surgical, pathological and institutional care[17]. What's more, anatomic studies determined that more

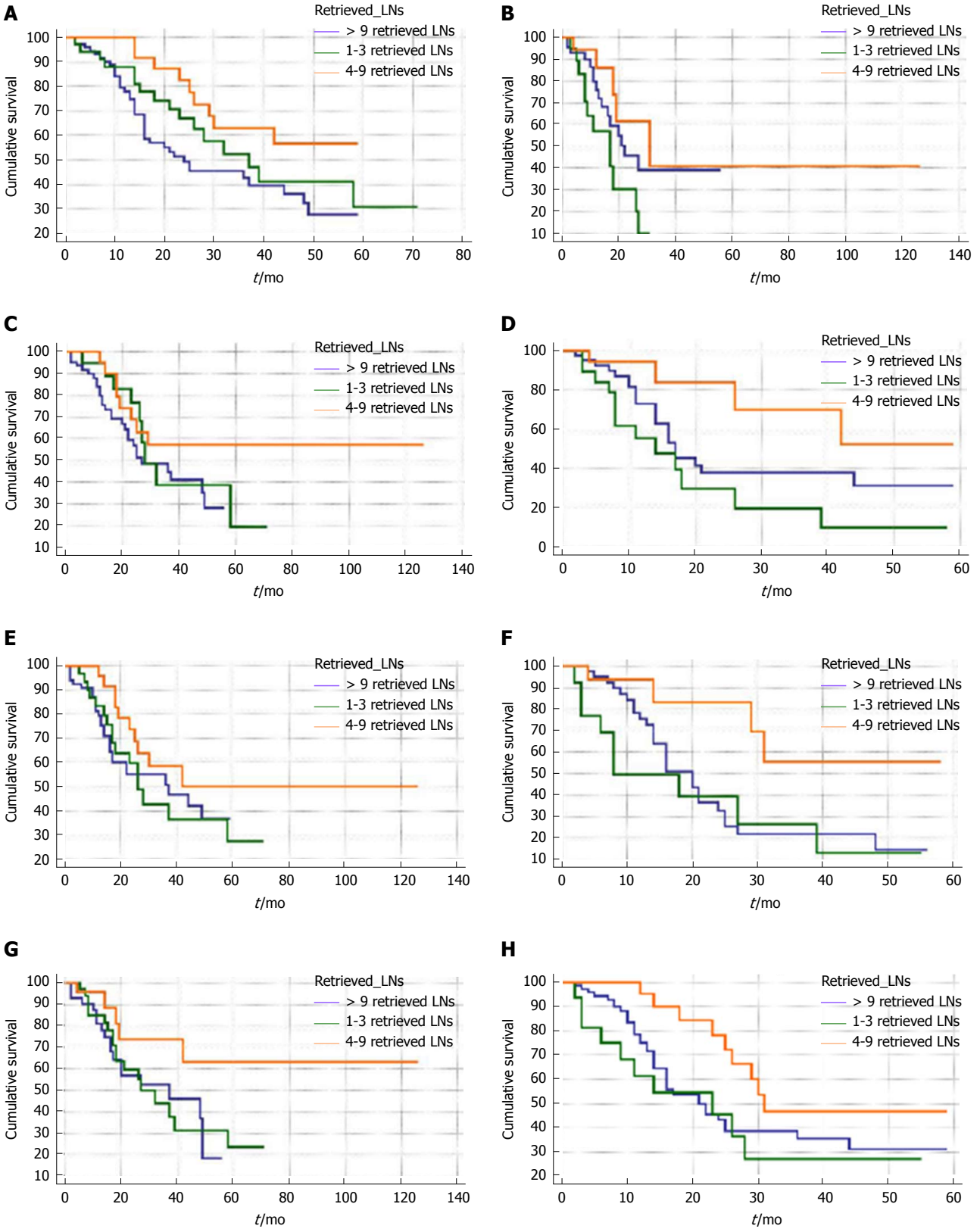

Figure 2 Kaplan-Meier survival curves of stratified analyses in (A) patients ⩽ 70-years-old, (B) > 70-years-old, (C) with tumors of ⩽ 20 mm, (D) with tumors of 20 to 50 mm, (E) with tumors defined as well or moderately differentiated, (F) with tumors defined as poorly or undifferentiated, (G) with tumors of T1/T2 stage, and (H) with tumors of T3/T4 stage in terms of overall survival. Patients with four to nine retrieved LNs had a significantly better overall survival than patients with one to three retrieved LNs and patients with more than nine retrieved LNs in the group of patients ⩽ 70-years-old (P = 0.029), with tumors of 20 to 50 mm (P = 0.018), with tumors defined as poorly or undifferentiated (P = 0.030), and with tumors of T3/T4 stage (P = 0.041). LNs: Lymph nodes.

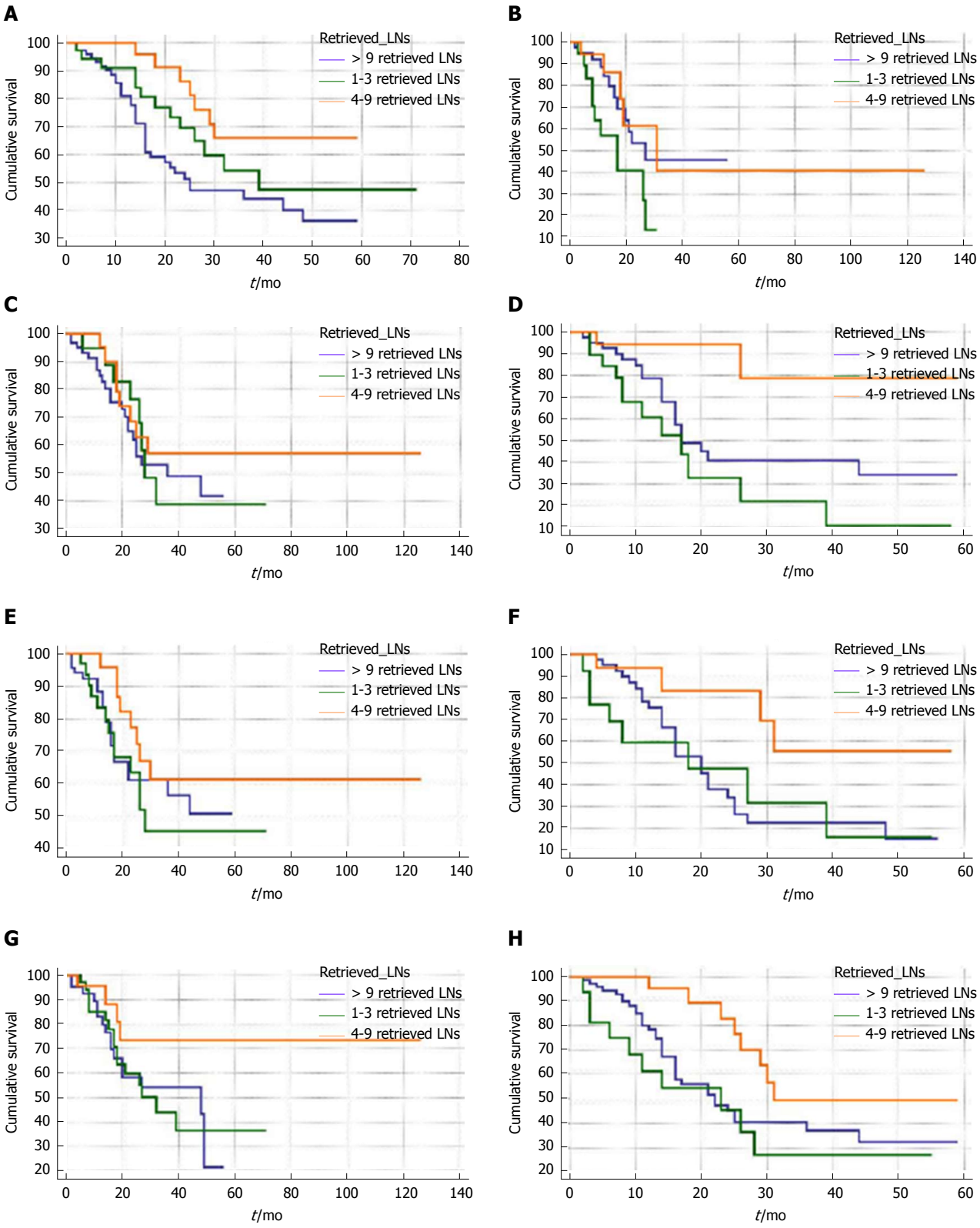

Figure 3 Kaplan-Meier survival curves of stratified analyses in (A) patients ⩽ 70-years-old, (B) > 70-years-old, (C) with tumors of ⩽ 20 mm, (D) with tumors of 20 to 50 mm, (E) with tumors defined as well or moderately differentiated, (F) with tumors defined as poorly or undifferentiated, (G) with tumors of T1/T2 stage, and (H) with tumors of T3/T4 stage in terms of cancer-specific survival. Patients with four to nine retrieved LNs had a significantly better cancer-specific survival than patients with one to three retrieved LNs and patients with more than nine retrieved LNs in the group of patients ⩽ 70-years-old (P = 0.025), with tumors of 20 to 50 mm (P = 0.0.006), with tumors defined as poorly or undifferentiated (P = 0.049), and with tumors of T3/T4 stage (P = 0.041). LNs: Lymph nodes.

Table 3 Univariate and multivariate survival analyses of factors associated with overall and cancer-specific survival of all patients with distal cholangiocarcinoma

Variables	Overall survival					Cancer-specific survival				
	Univariate analysis			Multivariate analysis		Univariate analysis			Multivariate analysis	
	3-yr OS	χ^2	*P* value	HR (95%CI)	*P* value	3-yr OS	χ^2	*P* value	HR (95%CI)	*P* value
Race		2.22	0.329				1.95	0.377		
White	33.3%					36.1%				
Black	34.8%					36.9%				
Other	38.9%					42.1%				
Sex		0.44	0.507				0.54	0.463		
Male	35.3%					38.3%				
Female	37.7%					40.9%				
Age at diagnosis, in yr		1.89	0.387				0.48	0.783		
⩽ 60	31.2%					35.8%				
60-70	39.1%					41.4%				
> 70	30.7%					36.8%				
Marital status		5.02	0.285				5.98	0.201		
Married	37.3%					39.6%				
Divorced	-					-				
Separated or single	31.4%					35.3%				
Widowed	34.1%					-				
Unknown	-									
Year of diagnosis		1.82	0.402				3.25	0.197		
2004-2010	37.3%					41.4%				
2011-2012	30.9%					33.2%				
2013-2014	-					-				
Tumor size, in mm		8.04	0.045		0.230		8.76	0.032		0.249
⩽ 20	40.8%			Reference		44.0%			Reference	
20-50	29.9%			1.25 (0.94-1.67)		33.2%			1.23 (0.91-1.68)	
> 50	0.0%			1.67 (0.86-3.23)		0.0%			1.76 (0.91-3.43)	
Unknown	37.7%			0.95 (0.57-1.58)		46.3%			0.96 (0.56-1.65)	
Grade		6.77	0.079				6.92	0.074		
Well differentiated	48.6%					52.4%				
Moderately differentiated	32.6%					38.9%				
Poorly or undifferentiated	30.3%					32.6%				
Unknown	43.2%					43.2%				
T stage		5.57	0.018		0.270		11.16	< 0.001		0.037
T1/T2	44.3%			Reference		51.6%			Reference	
T3/T4	29.6%			1.19 (0.87-1.64)		32.6%			1.45 (1.02-2.07)	
N stage		10.64	0.001		0.020		12.27	< 0.001		0.022
N0	44.5%			Reference		47.4%			Reference	
N1	26.9%			1.40 (1.05-1.86)		30.3%			1.42 (1.05-1.92)	
Surgery type		1.20	0.272				0.73	0.393		
Local excision	44.0%					45.3%				
Extensive surgery	34.4%					37.9%				
Adjuvant radiotherapy		0.16	0.683				0.79	0.372		
No/Unknown radiotherapy	39.9%					44.3%				
Beam radiation	29.5%					30.5%				
Adjuvant chemotherapy		1.10	0.293				2.92	0.087		
No/Unknown chemotherapy	41.2%					47.5%				
Chemotherapy performed	32.2%					33.3%				
No. of LNs retrieved		2.91	0.233				3.90	0.141		
1-2	23.6%					29.9%				
3-6	35.6%					39.4%				
> 6	36.0%					39.0%				

CI: Confidence interval; HR: Hazard ratio; LNs: Lymph nodes; OS: Overall survival.

resected LNs could improve the underlying tumor-host interactions and reset the immunological balance to improve survival[18].

The AJCC system suggested the optimal number of retrieved LNs of patients with distal cholangiocarcinoma should be 12. Whereas study of Sasaki *et al*[6] demonstrated there was no difference between patients with ⩾ 12 retrieved LNs and < 12 retrieved LNs in terms of overall survival. A subgroup analysis in the study of Kiriyama *et al*[11] revealed that patients with stage Ⅰ or Ⅱ tumors who had more than 10 LNs retrieved had a better survival rate than others. While 83.2% of patients in their study retrieved more than 12 LNs, the number of patients with < 10 retrieved LNs was very small (n = 22), and their results were based on a univariate analysis. Therefore, selection

Table 4 Univariate and multivariate survival analyses of factors associated with overall and cancer-specific survival of patients with node-negative distal cholangiocarcinoma

Variable	Overall survival					Cancer-specific survival				
	Univariate analysis			Multivariate analysis		Univariate analysis			Multivariate analysis	
	3-yr OS	χ^2	*P* value	HR (95%CI)	*P* value	3-yr OS	χ^2	*P* value	HR (95%CI)	*P* value
Race		0.82	0.663				0.13	0.939		
White	44.3%					46.8%				
Black	49.4%					49.4%				
Other	40.4%					44.0%				
Sex		1.32	0.250				0.77	0.377		
Male	39.5%					46.0%				
Female	47.0%					49.8%				
Age at diagnosis, in yr		3.85	0.049		0.056		2.73	0.097		
≤ 70	49.8%			Reference		51.8%				
> 70	31.4%			1.51 (0.98-2.33)		35.7%				
Marital status		6.30	0.177				6.52	0.163		
Married	42.9%					48.5%				
Divorced	-					-				
Separated or single	31.8%					39.6%				
Widowed	46.9%					46.9%				
Unknown	-					-				
Year of diagnosis		3.41	0.181				4.05	0.131		
2004-2010	50.0%					52.1%				
2011-2012	36.5%					41.4%				
2013-2014	48.8%					54.0%				
Tumor size, in mm		7.47	0.058				9.11	0.027		0.036
≤ 20	47.3%					49.6%			Reference	
20-50	36.9%					40.0%			1.57 (0.98-2.53)	
> 50	0.0%					0.0%			3.08 (1.16-8.21)	
Unknown	46.8%					60.8%			0.72 (0.30-1.71)	
Grade		9.65	0.021		0.014		12.56	0.005		0.003
Well differentiated	56.8%			Reference		63.3%			Reference	
Moderately differentiated	43.5%			1.59 (0.84-2.99)		51.8%			1.44 (0.70-2.97)	
Poorly or undifferentiated	26.0%			2.35 (1.24-4.46)		30.5%			2.90 (1.43-5.88)	
Unknown	57.0%			0.76 (0.27-2.16)		57.0%			1.14 (0.37-3.50)	
T stage		1.35	0.244				4.63	0.031		0.030
T1/T2	48.7%					58.4%			Reference	
T3/T4	37.1%					38.7%			1.69 (1.05-2.71)	
Surgery type		0.10	0.748				0.23	0.631		
Local excision	45.7%					48.2%				
Extensive surgery	44.1%					47.0%				
Adjuvant radiotherapy		1.64	0.199				1.53	0.215		
No/Unknown radiotherapy	48.2%					53.2%				
Beam radiation	35.5%					37.2%				
Adjuvant chemotherapy		1.31	0.251				1.48	0.222		
No/Unknown chemotherapy	46.3%					53.8%				
Chemotherapy performed	38.5%					42.1%				
No. of LNs retrieved		7.24	0.026		0.013		6.47	0.039		0.008
1-3	35.1%			Reference		40.9%			Reference	
4-9	52.3%			0.39 (0.20-0.74)		60.0%			0.32 (0.15-0.66)	
> 9	39.3%			0.85 (0.53-1.36)		44.9%			0.62 (0.36-1.07)	

CI: Confidence interval; CSS: Cancer-specific survival; HR: Hazard ratio; LNs: Lymph nodes; OS: Overall survival.

bias should be kept in mind when interpreting their results. The fact that retrieving more than 10 or 12 LNs is an indicator of better prognosis is still disputable.

The present study denoted that retrieving more than nine LNs did not indicate a better prognosis in patients with node-negative distal cholangiocarcinoma, but an increase in terms of all-cause mortality risk and cancer cause-specific mortality risk was observed compared with retrieving four to nine LNs. For patients with distal cholangiocarcinoma, retrieving too many LNs did not obtain better outcomes. This result was contrary to the prevailing dogma that a better prognosis was always associated with higher retrieved LN counts.

There were several hypotheses for the reason why more retrieved LNs represented a worse prognosis. Necrosis represented an aggressive biology of tumor and a decreased survival rate; it had a close association with LN hyperplasia. LN hyperplasia always resulted in increases in the size and number of detectable LNs; therefore, more retrieved LNs (detectable LNs) were related to a worse prognosis[19-21]. The other hypothesis was that there might be a difference at the molecular level between tumors with more and less detectable LNs. Tumors with more detectable LNs, *i.e.*

Table 5 Stratified analyses of overall and cancer-specific survival according to the number of retrieved LNs for N0 patients

Variable	4-9 retrieved LNs (1-3 retrieved LNs as the reference)				> 9 retrieved LNs (1-3 retrieved LNs as the reference)			
	Overall survival		Cancer-specific survival		Overall survival		Cancer-specific survival	
	HR (95%CI)	*P* value	HR (95%CI)	*P* value	HR (95%CI)	*P* value	HR (95%CI)	*P* value
Age, in yr								
≤ 70	0.33 (0.13-0.86)	0.023	0.34 (0.13-0.89)	0.030	1.02 (0.49-2.14)	0.940	0.93 (0.46-1.88)	0.848
> 70	0.32 (0.11-0.98)	0.047	0.33 (0.11-1.04)	0.059	0.63 (0.26-1.49)	0.294	0.40 (1.55-1.04)	0.059
Tumor size, in mm								
≤ 20	0.55 (0.21-1.46)	0.232	0.61 (0.22-1.68)	0.340	1.34 (0.60-2.97)	0.472	0.96 (0.41-2.23)	0.921
20-50	0.22 (0.07-0.69)	0.010	0.12 (0.03-0.55)	0.007	0.54 (0.24-1.21)	0.134	0.48 (0.21-1.12)	0.090
> 50	-	-	-	-	-	-	-	-
Grade								
Well or moderately differentiated	0.56 (0.24-1.30)	0.180	0.47 (0.18-1.20)	0.114	0.99 (0.49-2.01)	0.994	0.74 (0.34-1.62)	0.454
Poorly or undifferentiated	0.23 (0.07-0.79)	0.020	0.26 (0.07-0.89)	0.032	0.69 (0.31-1.58)	0.389	0.75 (0.32-1.78)	0.514
T stage								
T1/T2	0.30 (0.11-0.85)	0.024	0.30 (0.09-0.94)	0.039	0.79 (0.39-1.59)	0.501	0.76 (0.36-1.59)	0.467
T3/T4	0.34 (0.13-0.85)	0.022	0.31 (0.12-0.79)	0.016	0.66 (0.31-1.41)	0.285	0.65 (0.30-1.39)	0.267

CI: Confidence interval; HR: Hazard ratio; LNs: Lymph nodes.

more retrieved LNs, might belong to another subset of distal cholangiocarcinoma that acts biologically more aggressively[19]. Additionally, routine histologic techniques for retrieving LNs may ignore the micrometastases, leading to the under-staging of LNs. Hence, without the application of immunohistochemical techniques that was determined to increase the detection rate of micrometastases, more retrieved LNs could not promote the accuracy of LN staging or improve patient survival. And, we wanted to know if more retrieved LNs reflected extended lymphadenectomy that may result in increasing postoperative complications. However, because of the limitation of the SEER database, we could not compare the background data in the > 9 retrieved LNs group with that in four to nine retrieved LN groups.

There were several limitations in our study. First, although a population-based database was utilized to screen patients, the total number of patients involved in our study was still not large enough compared with congener studies for other diseases. Second, information for adjuvant chemotherapy and radiotherapy in survival analysis did not contain the details of the protocols, and the SEER database did not provide data. Third, disease-free survival could not be calculated because of the lack of information about local recurrence in the SEER. Fourth, patients who received preoperative radiation were excluded. There might be patients who received radiation in some other centers that were not recorded in the SEER, so the down-staging effect of radiation could not be entirely ruled out. Fifth, the number of lymph nodes retrieved may depend upon the type of surgical procedures. And, the lymph nodes distant from the lesion (for example, nodes from Whipple's procedure) may not have the same predicting value as these from local or limited resection specimen. However, the detailed operation methods were unknown because of the limitation of the SEER, *i.e.* we could not know how many patients underwent pancreatoduodenectomy or segmental bile duct resection. Sixth, the number of lymph nodes retrieved may rely on lymph node dissection skill in each individual institution (grossing by resident *vs* practicing pathologists or pathologist assistant). But, the SEER database only provided the information of the region where the patients were from, and the classes of hospital were unknown. Therefore, such institution bias should be taken into consideration when interpreting our results. Seventh, we could only compare survival among the groups of patients with four to nine lymph nodes and others based upon pathological stage and not clinical stage due to the limitation of SEER (the SEER database only provided the information of pathological stage for patients with resectable distal cholangiocarcinomas). Eighth, the AJCC staging system utilized in the present study was the 6th edition, which was not the most commonly used one nowadays (due to limitations of SEER). Finally, we could not get the data referring to the surgical margin status in SEER; surgical margin status was an important prognostic factor in patients with resected distal cholangiocarcinoma.

In conclusion, the number of retrieved LNs did not show its prognostic value in the whole group of patients (a mixture of N0 and N1 patients) and N1 patients. However, the number of retrieved LNs was an independent prognostic factor of overall and cancer-specific survival for patients with node-negative distal cholangiocarcinoma. Patients with four to nine retrieved LNs had better overall and cancer-specific survival rates than others, but the reason and mechanism were unclear. The future studies should consider more operation- and adjuvant therapy-related parameters into their analysis to evaluate our results.

ARTICLE HIGHLIGHTS

Research background

Lymph node (LN) status was determined to be a strong predictor for the prognosis of patients with distal cholangiocarcinoma. However, the prognostic

value of the retrieved LNs counts in distal cholangiocarcinoma is still under debate.

Research motivation

The benchmark number of retrieved LNs has been determined in many gastrointestinal carcinomas, in addition to the distal cholangiocarcinomas. Previous studies regarding the retrieved LNs counts in distal cholangiocarcinomas were limited by their small sample size, and the patients in those studies comprised both perihilar and distal cholangiocarcinomas. The present study tried to determine the interactions between the retrieved LNs counts and the prognosis in patients with only distal cholangiocarcinomas, and a population-based database was used for patients' selection that provided a sufficient sample size.

Research objectives

We aimed to evaluate the prognostic value of the number of retrieved LNs for patients with distal cholangiocarcinomas and to determine the optimal retrieved LNs cut-off number.

Research methods

The Surveillance, Epidemiology and End Results (SEER) database was used to screen for patients with distal cholangiocarcinoma. The retrieved LNs counts were transformed from continuous variables to categorical variables, and the cut-off was defined by the X-tile program. The overall and cancer-specific survival was compared between the different categories of retrieved LNs counts by the means of the Kaplan-Meier method and Cox regression analysis. Then, we performed stratified analyses by the clinical factors that were evaluated to be independently associated with survival in the Cox regression analysis, among patients within the different LNs groups.

Research results

A total of 449 patients with distal cholangiocarcinoma were included in the present study. The Kaplan-Meier survival analysis for all patients and for N1 patients revealed no significant differences among patients with different retrieved LN counts in terms of overall and cancer-specific survivals. In patients with node-negative distal cholangiocarcinoma, patients with four to nine retrieved LNs had a significantly better overall (P = 0.026) and cancer-specific (P = 0.039) survival than others. In the subsequent multivariate analysis, the number of retrieved LNs was evaluated to be independently associated with survival. Additionally, patients with four to nine retrieved LNs had a significantly lower overall mortality risk (hazard ratio (HR): 0.39; 95% confidence interval (CI): 0.20-0.74) and cancer cause-specific mortality risk (HR: 0.32; 95%CI: 0.15-0.66) than other patients. Additionally, stratified survival analyses showed persistent better overall and cancer-specific survival when retrieving four to nine LNs in patients with any T stage of tumor, a tumor between 20 and 50 mm in diameter, or a poorly differentiated or undifferentiated tumor and in patients who were $\leqslant$ 70-years-old.

Research conclusions

The number of retrieved LNs was an important independent prognostic factor for patients with node-negative distal cholangiocarcinoma. Additionally, patients with four to nine retrieved LNs had a better overall and cancer-specific survival rate than patients with less than four or more than nine retrieved LNs.

Research perspectives

Although our study revealed retrieving four to nine LNs in patients with node-negative distal cholangiocarcinoma had better overall and cancer-specific survival rates than others, the reason and mechanism for that were unclear. The future studies should consider more operation- and adjuvant therapy-related parameters into their analysis to evaluate our results.

REFERENCES

1 **Siegel R**, Naishadham D, Jemal A. Cancer statistics, 2012. *CA Cancer J Clin* 2012; **62**: 10-29 [PMID: 22237781 DOI: 10.3322/caac.20138]

2 **Komaya K**, Ebata T, Shirai K, Ohira S, Morofuji N, Akutagawa A, Yamaguchi R, Nagino M; Nagoya Surgical Oncology Group. Recurrence after resection with curative intent for distal cholangiocarcinoma. *Br J Surg* 2017; **104**: 426-433 [PMID: 28138968 DOI: 10.1002/bjs.10452]

3 **Gouma DJ**, van Geenen RC, van Gulik TM, de Haan RJ, de Wit LT, Busch OR, Obertop H. Rates of complications and death after pancreaticoduodenectomy: risk factors and the impact of hospital volume. *Ann Surg* 2000; **232**: 786-795 [PMID: 11088073 DOI: 10.1097/00000658-200012000-00007]

4 **Murakami Y**, Uemura K, Hayashidani Y, Sudo T, Hashimoto Y, Ohge H, Sueda T. Prognostic significance of lymph node metastasis and surgical margin status for distal cholangiocarcinoma. *J Surg Oncol* 2007; **95**: 207-212 [PMID: 17278119 DOI: 10.1002/jso.20668]

5 **Murakami Y**, Uemura K, Sudo T, Hashimoto Y, Nakashima A, Kondo N, Sakabe R, Ohge H, Sueda T. Prognostic factors after surgical resection for intrahepatic, hilar, and distal cholangiocarcinoma. *Ann Surg Oncol* 2011; **18**: 651-658 [PMID: 20945107 DOI: 10.1245/s10434-010-1325-4]

6 **Oshiro Y**, Sasaki R, Kobayashi A, Murata S, Fukunaga K, Kondo T, Oda T, Ohkohchi N. Prognostic relevance of the lymph node ratio in surgical patients with extrahepatic cholangiocarcinoma. *Eur J Surg Oncol* 2011; **37**: 60-64 [PMID: 21094016 DOI: 10.1016/j.ejso.2010.10.011]

7 **Schwarz RE**, Smith DD. Lymph node dissection impact on staging and survival of extrahepatic cholangiocarcinomas, based on U.S. population data. *J Gastrointest Surg* 2007; **11**: 158-165 [PMID: 17390167 DOI: 10.1007/s11605-006-0018-6]

8 **Ito K**, Ito H, Allen PJ, Gonen M, Klimstra D, D'Angelica MI, Fong Y, DeMatteo RP, Brennan MF, Blumgart LH, Jarnagin WR. Adequate lymph node assessment for extrahepatic bile duct adenocarcinoma. *Ann Surg* 2010; **251**: 675-681 [PMID: 20224368 DOI: 10.1097/SLA.0b013e3181d3d2b2]

9 **Pomianowska E**, Westgaard A, Mathisen Ø, Clausen OP, Gladhaug IP. Prognostic relevance of number and ratio of metastatic lymph nodes in resected pancreatic, ampullary, and distal bile duct carcinomas. *Ann Surg Oncol* 2013; **20**: 233-241 [PMID: 22893118 DOI: 10.1245/s10434-012-2592-z]

10 **Kawai M**, Tani M, Kobayashi Y, Tsuji T, Tabuse K, Horiuchi T, Oka M, Yamaguchi K, Sakata Y, Shimomura T, Yamaue H. The ratio between metastatic and examined lymph nodes is an independent prognostic factor for patients with resectable middle and distal bile duct carcinoma. *Am J Surg* 2010; **199**: 447-452 [PMID: 19596119 DOI: 10.1016/j.amjsurg.2009.01.019]

11 **Kiriyama M**, Ebata T, Aoba T, Kaneoka Y, Arai T, Shimizu Y, Nagino M; Nagoya Surgical Oncology Group. Prognostic impact of lymph node metastasis in distal cholangiocarcinoma. *Br J Surg* 2015; **102**: 399-406 [PMID: 25611179 DOI: 10.1002/bjs.9752]

12 **Xiao J**, Ye ZS, Wei SH, Zeng Y, Lin ZM, Wang Y, Teng WH, Chen LC. Prognostic significance of pretreatment serum carcinoembryonic antigen levels in gastric cancer with pathological lymph node-negative: A large sample single-center retrospective study. *World J Gastroenterol* 2017; **23**: 8562-8569 [PMID: 29358864 DOI: 10.3748/wjg.v23.i48.8562]

13 **Qureshi YA**, Sarker SJ, Walker RC, Hughes SF. Proximal Resection Margin in Ivor-Lewis Oesophagectomy for Cancer. *Ann Surg Oncol* 2017; **24**: 569-577 [PMID: 27573522 DOI: 10.1245/s10434-016-5510-y]

14 **Bagante F**, Tran T, Spolverato G, Ruzzenente A, Buttner S, Ethun CG, Groot Koerkamp B, Conci S, Idrees K, Isom CA, Fields RC, Krasnick B, Weber SM, Salem A, Martin RC, Scoggins C, Shen P, Mogal HD, Schmidt C, Beal E, Hatzaras I, Vitiello G, IJzermans JN, Maithel SK, Poultsides G, Guglielmi A, Pawlik TM. Perihilar Cholangiocarcinoma: Number of Nodes Examined and Optimal Lymph Node Prognostic Scheme. *J Am Coll Surg* 2016; **222**: 750-759.e2 [PMID: 27113512 DOI: 10.1016/j.jamcollsurg.2016.02.012]

15 **Mao K**, Liu J, Sun J, Zhang J, Chen J, Pawlik TM, Jacobs LK, Xiao Z, Wang J. Patterns and prognostic value of lymph node dissection for resected perihilar cholangiocarcinoma. *J Gastroenterol Hepatol* 2016; **31**: 417-426 [PMID: 26250532 DOI:

10.1111/jgh.13072]
16 **Mantel HT**, Wiggers JK, Verheij J, Doff JJ, Sieders E, van Gulik TM, Gouw AS, Porte RJ. Lymph Node Micrometastases are Associated with Worse Survival in Patients with Otherwise Node-Negative Hilar Cholangiocarcinoma. *Ann Surg Oncol* 2015; **22** Suppl 3: S1107-S1115 [PMID: 26178761 DOI: 10.1245/s10434-015-4723-9]
17 **Johnson PM**, Porter GA, Ricciardi R, Baxter NN. Increasing negative lymph node count is independently associated with improved long-term survival in stage IIIB and IIIC colon cancer. *J Clin Oncol* 2006; **24**: 3570-3575 [PMID: 16877723 DOI: 10.1200/jco.2006.06.8866]
18 **Zheng WF**, Ji TT, Lin Y, Li RZ. The prognostic value of lymph nodes count on survival of patients with node-negative gastric cancer. *Oncotarget* 2016; **7**: 43680-43688 [PMID: 27270656 DOI: 10.18632/oncotarget.9845]
19 **Mersin H**, Yildirim E, Bulut H, Berberoğlu U. The prognostic significance of total lymph node number in patients with axillary lymph node-negative breast cancer. *Eur J Surg Oncol* 2003; **29**: 132-138 [PMID: 12633555 DOI: 10.1053/ejso.2002.1285]
20 **Camp RL**, Rimm EB, Rimm DL. A high number of tumor free axillary lymph nodes from patients with lymph node negative breast carcinoma is associated with poor outcome. *Cancer* 2000; **88**: 108-113 [PMID: 10618612]
21 **Moorman PG**, Hamza A, Marks JR, Olson JA. Prognostic significance of the number of lymph nodes examined in patients with lymph node-negative breast carcinoma. *Cancer* 2001; **91**: 2258-2262 [PMID: 11413513]

P- Reviewer: Antonini F, Nah YW, Xu RL **S- Editor**: Wang XJ
L- Editor: Filipodia **E- Editor**: Huang Y

World Journal of Gastroenterology

Submit a Manuscript: http://www.f6publishing.com

World J Gastroenterol 2018 March 7; 24(9): 1035-1045

DOI: 10.3748/wjg.v24.i9.1035

ISSN 1007-9327 (print) ISSN 2219-2840 (online)

ORIGINAL ARTICLE

Clinical Practice Study

Phenotypic and genotypic characterization of inflammatory bowel disease in children under six years of age in China

You-Hong Fang, You-You Luo, Jin-Dan Yu, Jin-Gan Lou, Jie Chen

You-Hong Fang, You-You Luo, Jin-Dan Yu, Jin-Gan Lou, Jie Chen, Department of Gastroenterology, Children's Hospital, Zhejiang University School of Medicine, Hangzhou 310052, Zhejiang Province, China

ORCID number: You-Hong Fang (0000-0003-3686-1016); You-You Luo (0000-0002-0185-1371); Jin-Dan Yu (0000-0002-3390-1660); Jin-Gan Lou (0000-0001-9142-5378); Jie Chen (0000-0002-3603-3213).

Author contributions: Chen J, Fang YH and Luo YY designed the research; Fang YH, Luo YY, Yu JD, Lou JG and Chen J performed the research; Fang YH analyzed the data; Fang YH and Chen J wrote the paper.

Supported by Zhejiang Province Medical Platform Backbone, No. 2017KY436.

Institutional review board statement: This study was reviewed and approved by the Ethics Committee of the Children's Hospital of Zhejiang University School of Medicine.

Conflict-of-interest statement: The authors have no financial relationships to disclose.

Data sharing statement: No additional data are available.

Manuscript source: Unsolicited manuscript

Correspondence to: Jie Chen, MD, Attending Doctor, Chief Doctor, Department of Gastroenterology, Children's Hospital, Zhejiang University School of Medicine, 3333 Bin Sheng Road, Hangzhou 310052, Zhejiang Province, China. hzcjie@zju.edu.cn

Telephone: +86-571-87061007

Received: December 12, 2017
Peer-review started: December 12, 2017
First decision: January 18, 2018
Revised: January 31, 2018
Accepted: February 8, 2018
Article in press: February 8, 2018
Published online: March 7, 2018

Abstract

AIM

To analyze clinical differences between monogenic and nonmonogenic very-early-onset inflammatory bowel disease (VEO-IBD) and to characterize monogenic IBD phenotypically and genotypically *via* genetic testing.

METHODS

A retrospective analysis of children aged 0 to 6 years diagnosed with VEO-IBD in a tertiary hospital in southern China from 2005 to 2017 was performed. Clinical data for VEO-IBD patients were collected, and genetic characteristics were analyzed using whole exome sequencing or target gene panel sequencing.

RESULTS

A total of 54 VEO-IBD patients were included in this study. A diagnosis of Crohn's disease (CD) or CD-like intestinal manifestations accounted for 72.2% of the VEO-IBD cases. Nine patients (16.7%) were identified by genetic testing as having monogenic IBD. The median age of diagnosis in the monogenic group was younger than that of the nonmonogenic IBD group, at 18 mo (interquartile range (IQR): 4 to 78) and 43.5 mo (IQR: 3 to 173), respectively; the *P*-value was 0.021. The incidence of perianal disease in the monogenic group was higher than that in the

nonmonogenic group (P = 0.001). However, there were no significant differences between weight-for-age and height-for-age Z-scores between the two groups, and similar laboratory results were obtained for the two groups. Five patients were found to have *IL10* receptor mutation, two patients had chronic granulomatous disease, one patient had common variable immunodeficiency disease, and one patient had X-linked inhibitor of apoptosis protein deficiency.

CONCLUSION

A high proportion of monogenic IBD was observed in the VEO-IBD group, especially with disease onset before the age of 6 mo. Monogenic IBD and nonmonogenic IBD exhibited similar clinical features. Furthermore, next-generation sequencing played an important role in the diagnosis of monogenic IBD, and *IL10* receptor mutation was predominant in this cohort.

Key words: Monogenic; Very-early-onset inflammatory bowel disease; Primary immunodeficiency diseases; *IL10*; *IL10R*

Core tip: This study is the largest study to analyze clinical differences between monogenic and non-monogenic very-early-onset inflammatory bowel disease (VEO-IBD) in China. Moreover, we characterized monogenic IBD phenotypically and genotypically through genetic testing (whole exome sequencing and targeted gene panel sequencing). We found a high proportion of monogenic IBD in the VEO-IBD group, with the most common monogenic IBD being *IL10R* mutation. Monogenic IBD and nonmonogenic IBD showed similar clinical features. Next-generation sequencing played an important role in the diagnosis of monogenic IBD.

Fang YH, Luo YY, Yu JD, Lou JG, Chen J. Phenotypic and genotypic characterization of inflammatory bowel disease in children under six years of age in China. *World J Gastroenterol* 2018; 24(9): 1035-1045 Available from: URL: http://www.wjgnet.com/1007-9327/full/v24/i9/1035.htm DOI: http://dx.doi.org/10.3748/wjg.v24.i9.1035

INTRODUCTION

Very-early-onset inflammatory bowel disease (VEO-IBD) refers to an IBD diagnosis established before the 6th year of life, including a subset of patients with disease onset before the age of 2 years, known as infantile-onset IBD (IO-IBD)[1]. VEO-IBD is rare, with an estimated incidence of 4.37 and a prevalence of 14 per 100000 children[2-4]. These patients present with abdominal pain, intestinal bleeding, diarrhea and malnutrition, similar to adults with IBD. In addition, growth failure is often observed[5,6]. However, VEO-IBD is considered to be a unique entity, and compared to adults with IBD, VEO-IBD children are more likely to present with extensive and treatment-resistant disease.

These patients may require the combined use of immunosuppressant and biologic agents and even early intestinal surgery. Although the IBD classification was recently modified to address the younger age group, this step may not be sufficient to accommodate the heterogeneous phenotypes of VEO-IBD[7]. The etiology of IBD is related to genetic and environmental factors as well as to the intestinal microbiome. Furthermore, VEO-IBD, especially IO-IBD, presents with IBD-like intestinal inflammation and shows a close association with primary immunodeficiency diseases (PIDs), defined as monogenic IBD[3].

More than 50 VEO-IBD-related genes have been reported to date, including those associated with *IL10* and *IL10* receptor mutation, immune dysregulation, polyendocrinopathy, enteropathy X-linked (IPEX) syndrome and X-linked inhibitor of apoptosis (XIAP) deficiency[3]. Nonetheless, the exact incidence of monogenic IBD remains unknown[8] due to variations in the genetic background of this disease. Most reports regarding monogenic IBD are based on small populations or case reports, with only a small number of genes investigated. To the best of our knowledge, this study reports the largest cohort of genetically screened patients with VEO-IBD from China.

MATERIALS AND METHODS

Study subjects

This study was approved by the Ethics Committee of the Children's Hospital of Zhejiang University School of Medicine. A total of 54 pediatric patients diagnosed with VEO-IBD in the Gastroenterology Department of Children's Hospital of Zhejiang University School of Medicine from October 2005 to May 2017 were included in this study. According to Porto criteria[9], Crohn's disease (CD) and CD-like intestinal inflammation present as noncontiguous aphthous or linear ulcers, primarily in the ileum or colon. Histologically, the disease is characterized by chronic focal inflammation with or without granulomas and perianal or fistulating disease. Ulcerative colitis (UC) or UC-like intestinal inflammation presents as continuous mucosal inflammation of the colon starting from the rectum, without small bowel involvement and without CD features. Patients with a definitive diagnosis of IBD with inflammation limited to the colon but without the typical features of UC and CD are classified as IBD of an unclassified type (IBDU).

The clinical characteristics of the pediatric patients, including sex, first symptom(s), time of onset of symptom(s), clinical features, surgical history, medication

history and family history, were collected from medical records.

The following were criteria for genetic testing: (1) patients with disease onset before 6 mo of age; (2) patients with disease onset beyond 6 mo accompanied with severe perianal disease, severe malnutrition or growth failure, or resistance to treatment.

Whole exome sequencing and targeted gene panel sequencing

Genomic DNA was isolated from peripheral blood of the patients. For whole exome sequencing (WES), whole exome library preparation was based on modifications of a protocol using the Agilent SureSelect XT Human All Exon Kit. Sequencing was performed using the Illumina HiSeq 2500 platform.

For targeted gene panel sequencing (TGPS), target sequences were enriched using customized capture probe chips (SureSelect Inherited Disease Panel; Agilent Technologies), which included 4,503 genes known to cause inherited disorders. DNA probes were designed for exons and flanking 10 bp intronic sequences. Briefly, 1 μg of genomic DNA was fragmented into 200-300 bp lengths by the Covaris Acoustics system. The DNA fragments were subsequently processed by end-repairing, A-tailing and adaptor ligation, 4-cycle pre-capture polymerase chain reaction (PCR) amplification, and targeted sequence capture. The captured DNA fragments were eluted and amplified by 15-cycle postcapture PCR. The final products were sequenced with 150-bp paired-end reads using the Illumina HiSeq X Ten platform according to the standard manual.

Raw data were processed by the Illumina pipeline (version 1.3.4) for image analysis, error estimation, base calling and generating the primary sequence data. For quality control, Cutadapt (https://pypi.python.org/pypi/cutadapt) and FastQC (https://www.bioinformatics.babraham.ac.uk/projects/fastqc/) were used to remove 3′-/5′- adapters and low-quality reads, respectively. Clean short reads were mapped to the human genome (hg19) using Burrows Wheeler Aligner software (http://sourceforge.net/projects/bio-bwa/). SOAPsnp software (http: //soap.genomics.org.cn/) and SAM tools Pileup software (http://sourceforge.net/projects/samtools/) were used to detect single-nucleotide polymorphisms and small insertions and deletions.

Variants were annotated using ANNOVAR software (http://www.openbioinformatics.org/annovar/), which includes function implications (gene region, functional effect, mRNA GenBank accession number, amino acid change, cytoband) and allele frequencies in dbSNP, 1000 genomes (http://www.1000genomes.org), ESP6500 (http://evs.gs.washington.edu/EVS/) and ExAc (http://exac.broadinstitute.org/). Damaging missense mutations were predicted by SIFT (http://sift.bii.a-star.edu.sg/), PolyPhen-2 (http://genetics.bwh.harvard.edu/pph2/) and MutationTaster (http://www.mutationtaster.org/). Interpretation of variants was based on recommended standards from the American College of Medical Genetics and Genomics[1,2], and all variants were categorized as pathogenic, likely pathogenic, variants of unknown significance, likely benign or benign.

To validate the variants based on next-generation sequencing (NGS) and WES, PCR amplification and Sanger sequencing were performed for the sequence centers on variant genes.

Statistical analysis

The categorical variables were presented as number (percentage). The continuous variables of normal distribution were presented as mean ± SD, otherwise as median ± interquartile range (IQR). The normality test was performed by Shapiro-Wilk test. The difference in variables with normal/abnormal distribution between nonmonogenic and monogenic IBD were estimated by Student's *t*-test and Mann-Whitney test, respectively. The differences in categorical variables between non-monogenic and monogenic IBD were assessed using the chi-square test; however, if total sample size was less than 40 or the number in one cell was less than 5, Fisher's exact test was used for testing the difference. $P < 0.05$ was considered to be a statistically significant difference. All statistical analyses were conducted with SPSS 22.0 statistical software (SPSS Inc., IBM Corp., Armonk, NY, United States).

RESULTS

General characteristics of VEO-IBD patients

From October 2005 to May 2017, 136 pediatric patients were diagnosed with IBD at our hospital, among which 54 were diagnosed with VEO-IBD; thus, VEO-IBD patients accounted for 39.7% of pediatric IBD patients in our cohort. Among the 54 VEO-IBD patients, 37 were males and 17 females, for a male to female ratio of 2.18:1. Thirty-one VEO-IBD patients (57.4%) had disease onset before the age of 2 years.

Of the 54 patients with VEO-IBD, 72.2% had a diagnosis of CD or CD-like intestinal manifestations, 7.4% had a diagnosis of UC or UC-like intestinal manifestations, and 20.4% had a diagnosis of IBDU. Only one patient was the offspring of a consanguineous union, and his older sister also had similar symptoms during the neonatal period, though without a definitive diagnosis. None of the remaining patients had a positive family history of IBD or PID.

The median age of disease onset was 14 mo (IQR: 0 to 72 mo), and the median age of diagnosis was 35.5 mo (IQR: 3 to 173 mo). The median time to diagnosis was 9 mo (IQR: 0.4 to 104 mo). The Z-scores for median weight-for-age, height-for-age and body mass index -for-age were -1.69 (IQR: -4.69 to 2.2), -1.41 (IQR: -6.43 to 2.51) ($n = 51$) and 14 (IQR: 0 to 72) respectively.

Mortality

The overall mortality rate was 11.1% (6/54). The

Table 1 Clinical features of dead very-early-onset inflammatory bowel disease patients

Patient	Sex	Age of disease onset	Chief complaints	Perianal diseases	EIMs	Colonoscopy features	Disease cause death	Genetic diagnosis
1	M	Neonate	Diarrhea	Perianal abscess and fistula	Arthritis, oral ulcers	Pancolitis, ulcers and hyperplasia	Lymphoma	NA
2	M	2 mo	Diarrhea, bloody stools	None	None	Proctitis, linear and aphthous ulcers	Suspension of treatment	NA
3	M	1 yr 5 mo	Diarrhea, bloody stools	Perianal abscess	None	Pancolitis and terminal ilium ulcers and hyperplasia	Suspension of treatment	NA
4	F	3 yr 10 mo	Abdominal pain	None	None	Pancolitis, ulcers and cobble stone appearance of colon	Sepsis, multiple organ failure	NA
5	M	4 yr 11 mo	Diarrhea, bloody stools, fever, malnutrition	None	Rash, oral erosion	Pancolitis, erosion, ulcers and multiple hyperplasia lesions	Intestinal bleeding	NA
6	M	2 mo 13 d	Diarrhea, fever	Perianal abscess	None	Proctitis, longitudinal ulcer	Sepsis and shock	CGD

EIMs: Extraintestinal manifestations.

Table 2 General data of very-early-onset inflammatory bowel disease patients

	Monogenic IBD	Nonmonogenic IBD	*P* value
Patients	9	45	
Sex, M/F	8/1	28/17	
Median age of disease onset, in mo	1 (0, 72)	19.5 (0, 72)	0.008[a]
Median age of disease diagnosis, in mo	18 (4, 78)	43.5 (3, 173)	0.021[a]
Duration before diagnosis, in mo	6 (2, 29)	9 (0, 104)	0.668

[a]$P < 0.05$. IBD: Inflammatory bowel disease.

clinical conditions of these 6 patients are listed in Table 1. Among the 6 patients, 4 had a diagnosis of CD and 2 a diagnosis of IBDU. Moreover, 2 of the patients had disease onset before 2 years of age.

Clinical characteristics

Nine patients (16.7%) were diagnosed with monogenic IBD; among them, 6 were diagnosed with CD and 3 with IBDU. We also compared the clinical manifestations of monogenic and nonmonogenic IBD patients. The monogenic group was predominately male, with a male to female ratio of 8:1. Four patients had disease onset during the neonatal period, and two patients presented with symptoms before 1 year of age. The median age of disease onset for the monogenic patients was earlier than that for the nonmonogenic patients at 1 mo (IQR: 0 to 72) and 19.5 mo (IQR: 0 to 72) respectively (P = 0.008). Similarly, the median age of diagnosis for the monogenic group was earlier than that for the nonmonogenic group, at 18 mo (IQR: 4 to 78) and 43.5 mo (IQR: 3 to 17) respectively (P = 0.021). However, there was no significant difference in the median time from disease onset to diagnosis between the two groups (P = 0.668; Table 2).

The incidence of perianal disease in the monogenic group was higher than that in the nonmonogenic group (P = 0.001); when comparing weight-for-age and height-for-age Z-scores, no significant differences between the two groups were found. Moreover, laboratory findings were similar between the two groups. Mesalazine was more commonly used in the monogenic than in the nonmonogenic group (P = 0.009). A greater number of patients underwent intestinal surgery in the monogenic group than in the nonmonogenic group; however, this difference was not statistically significant at P = 0.050. To date, more patients in the nonmonogenic group have died compared to the monogenic group (P = 0.000; Table 3).

Genetics

A total of 16 patients underwent WES or TGPS, 6 and 12 respectively (2 patients were tested by both WES and TGPS). Two patients underwent genetic testing (*IL10RA*) at another hospital. Nine patients were diagnosed with monogenic IBD. Seven of these patients were diagnosed by TGPS, and two were diagnosed by both methods. Five patients were diagnosed with *IL10R* mutation, two patients were diagnosed with chronic granulomatous disease (CGD) with *CYBB* mutation, and one patient was diagnosed with XIAP deficiency. One patient was diagnosed with common variable immune deficiency (CVID) with *TNFRSF13B* mutation. The clinical information for the 9 monogenic patients are listed in Table 4, and the genetic phenotypes of the 18 patients are provided in Table 5.

IL10 and IL10R mutations

Patient 1 was a male offspring from a consanguineous union, with disease onset during the neonatal period. The first manifestation was a perianal abscess followed by recurrent fever, bloody stools, anal fistula and anal abscess formation, and skin infections. Colonoscopic findings included strictures of the colon near the splenic flexure, extensive polypoid hyperplasia, irregular ulcers,

Table 3 Comparison of clinical features of monogenic and nonmonogenic inflammatory bowel disease groups

	Nonmonogenic IBD	Monogenic IBD	*P* value
Diagnosis			
CD, %	75.0	50.0	
IBD-U, %	18.2	40.0	
UC, %	6.8	10.0	
Abdominal pain, *n*	25	2	0.142
Diarrhea, *n*	36	8	1.000
Bloody stools, *n*	26	8	0.131
Malnutrition, *n*	19	5	0.489
Growth failure, *n*	14	4	0.461
Oral ulcers, *n*	3	1	0.529
Persistent fever, *n*	3	0	1.000
Perianal diseases, *n*	9	7	0.001[a]
Body weight Z-score	-1.54 (-4.69, 2.20)	-2.04 (-3.66, 0.96)	0.303
Height Z-score	-1.38 (-6.43, 2.51)	-1.76 (-4.92, 0.46)	0.597
WBC, as $^{a}10^{9}$	15.04 ± 1.72	12.53 ± 1.72	0.382
HGB, in g/L	103.02 ± 2.57	106.67 ± 5.00	0.496
PLT, as $^{a}10^{12}$	454.60 ± 28.40	421.89 ± 54.97	0.632
CRP, in mg/L	51.16 ± 8.43	20.22 ± 2.43	0.668
ESR, in mm/h	29.22 ± 4.70	21.00 ± 4.56	0.923
ALB, in g/L	33.80 ± 1.10	36.60 ± 1.77	0.283
Steroid, *n*	36	6	0.399
Antibiotics, *n*	29	7	0.484
Mesalazine, *n*	32	2	0.009[a]
Immunosuppressants, *n*	25	8	0.075
Nutrition, *n*	33	5	0.425
Infliximab, *n*	14	4	0.461
Surgery, *n*	6	4	0.050
Death, *n*	5	1	0.000[a]

[a]$P < 0.05$. IBD: Inflammatory bowel disease.

and inflammatory tags. Esophagogastroduodenoscopy was normal. Preliminary immune tests and the serum IL10 level were normal. The patient underwent a colostomy at the age of 1 year and 1 mo due to recurrent diarrhea and perianal abscesses. At 2 years and 5 mo of age, he underwent transverse partial colectomy, small bowel internal fistula resection and anastomosis. The pathological evaluation revealed transmural inflammatory infiltrate and linear serpentine ulcerations. The patient also underwent incision, drainage and seton placement for multiple abscesses. He was resistant to treatment with antibiotics, steroids, total parenteral nutrition (TPN), enteral nutrition (EN) and infliximab. At the time of writing this manuscript, he is in clinical remission on a combination treatment of azathioprine and thalidomide. Genetic testing by both TGS and WES revealed the following homozygous *IL10RB* mutation: Chr21:34660499: c.737G>A, p.W246X. This mutation has not been reported in HGMDpro.

Patient 2 was a female with VEO-IBD of neonatal onset, with first symptoms of recurrent watery diarrhea and blood and mucous in stools followed by a perianal abscess, fistula formation and recurrent fever. The patient was initially treated with elemental formula due to suspected cow's milk allergy. She had her first colostomy at 1 year and 11 mo of age. Colonoscopy showed a cobble stone appearance and linear ulcerations in the colon. The pathological evaluation revealed classic CD features (strictures, transmural inflammatory infiltrate, linear serpentine ulcerations and noncaseating granulomas). Preliminary immune tests were normal, and the serum IL10 level was slightly elevated. She was resistant to treatment with steroids, mesalazine, antibiotics, immunosuppressants and infliximab. At 3 years and 1 mo of age, she underwent repair for a small bowel perforation, pancolectomy and ileal pouch-anal anastomosis. TGPS revealed the following compound heterozygous *IL10RA* mutations: Chr11:117864125: c.537G>A, p.T179T and Chr11:117860269: c.301C>T, p.R101W. The two mutations were derived from the mother and father, respectively. Both mutations are reported in HGMDpro[10,11].

Patient 3 was a male with disease onset at 1 mo of age. The patient had symptoms of recurrent diarrhea with mucous and blood, oral ulcers, anal fistula, obvious malnutrition and growth failure. Initial immune tests were normal, and the IL10 level was elevated at 85.5 pg/mL (normal range from 2.6 to 4.9 pg/mL). Colonoscopy showed deep ulcers in the rectum. The pathology evaluation showed nonspecific inflammation of the colon. The traditional treatments of antibiotics, TPN, EN and steroids were unsuccessful. Genetic testing at an outside hospital detected the following compound heterozygous *IL10RA* mutations: Chr11:117860269, c.301C>T, p.R101W, Chr11:117993268: c.470A>G, p.Y157C. The two mutations were from his mother and father, respectively. His older sister is a hereditary carrier.

Table 4 Clinical characteristics of monogenic very-early-onset inflammatory bowel disease patients

Patient	Sex	Disease onset	Z-score of height	Z-score of body weight	Chief complaints	Others	Disease locations and behavior	Clinical and genetic diagnosis	Intestinal surgery	Treatment	Prognosis
1	M	< 1 mo	0.22	-1.18	Diarrhea, bloody stools	Pyoderma	L2, P, B2B3	CD, IL10RB mutation	Colostomy	Steroid, IFX, thalidomide, 6-MP/MTX/AZA	Remission
2	F	4 mo	-1.76	-0.96	Diarrhea, bloody stools	Pyoderma	L2,L4b, P, B2B3	CD, IL10RA mutation	Intestinal perforation repair, colostomy and J-POUCH	Steroid, mesalazine, IFX, MTX/CsA	Remission
3	M	1 mo+	-0.79	-2.21	Diarrhea, bloody stools	Elevation of ALT	L2, P, B2	CD, IL10RA mutation	None	None	Waiting HSCT
4	M	1 mo+	-3.11	-3.66	Diarrhea, bloody stools	None	L2, P, B1	IBDU, IL10RA mutation	None	Antibiotics	Give up
5	M	11 d	-4.92	-3.38	Diarrhea, bloody stools	NEC	L2,L4b, P, B1	CD, IL10RA mutation	None	Steroids, AZA	Give up
6	M	< 1 mo	0.46	-1.08	Diarrhea, bloody stools	Epilepsy	L2, P, B1	IBDU, CGD	None	None	Remission
7	M	< 1 mo	-0.84	-2.04	Persistent fever	Intestinal malrotation, elevation of ALT	L2, P, B1	IBDU, CGD	None	None	Dead
8	M	9 mo	-4.63	-2.95	Diarrhea, bloody stools	Hepatosplenomegaly	L2, B1	CD, CVID	Intestinal resection and anastomosis	Steroid, 6MP, mesalazine, thalidomide	Partial remission
9	M	5 yr 11 mo	-2.2	-1.57	Abdominal pain, diarrhea, bloody stools	None	L2, L4b	CD, XIAP deficiency	None	DXM, IFX, 6MP/AZA	Remission

6-MP: 6-mercaptopurine; ALT: Alanine aminotransferase; AZA: Azathioprine; CGD: Chronic granulomatous disease; CsA: Cyclosporin A; CVID: Common variable immunodeficiency; HSCT: Hematopoietic stem cell transplantation; IFX: Infliximab; IL10R: Interleukin 10 receptor; MTX: Methotrexate; XIAP: X-linked inhibitor of apoptosis protein.

At the time of this writing, he is awaiting hematopoietic stem cell transplantation (HSCT). The pathogenic mutation c.301C>T is reported in HGMDpro[10], and c.470A>G was predicted by software mentioned in the methods section to be the likely pathogenic gene.

Patient 4 was a male with first symptoms of recurrent perianal abscess followed by watery diarrhea with scant fresh blood, rash and severe malnutrition. Immune tests were normal, and the IL10 level was 47.2 pg/mL. Colonoscopy showed multiple irregular ulcers at the sigmoid colon and rectum with polypoid hyperplasia and ulcers of the anus. Pathological examination revealed nonspecific findings. TGPS revealed the following homozygous mutation of *IL10RA*: Chr11:117860269: c.301C>T, p.R101W. The mutation was verified in his mother. The mutation is reported in HGMDpro to be pathogenic[10].

Patient 5 was a male with disease onset during the neonatal period. He initially presented with bloody diarrhea and was diagnosed with necrotizing enterocolitis; however, his symptoms persisted after surgery. This patient subsequently presented with a perianal fistula and severe malnutrition. Colonoscopy showed polypoid hyperplasia at the colon and ulcers at the rectum. This patient was treated with mesalazine and enemas. Genetic testing at an outside hospital revealed the following compound heterozygous *IL10RA* mutations: Chr11:117860269: c.301C>T, p.R101W, c.350G>A, p.R117H. The two mutations are reported in the literature to be pathogenic[10,12].

CGD

Patient 6 was a male with disease onset during the neonatal period. He presented with recurrent diarrhea, bloody stools and a perianal abscess. Preliminary immune tests were normal. Colonoscopy showed pancolitis and a perianal abscess. TGPS revealed the following hemizygotic mutation of *CYBB*: ChrX:37658209: c.676C>T, p.R226X. The mutation originates from his mother and is reported in HGMDpro to be pathogenic. The mutation is a termination mutation, which can alter the function of the encoded protein[13].

Patient 7 was a male diagnosed with intestinal malrotation during the neonatal period. He presented with pneumonia, perianal abscess and liver dysfunction; he developed diarrhea and fever during hospitalization. The immunoglobulin level and CD3 (46.81%), CD4 (29.86%), natural killer cell (7.79%), CD4/CD8 (1.86) levels were normal. Colonoscopy showed a longitudinal ulcer at the rectum. Soon thereafter, the patient developed multiple organ failure due to severe infection. TGPS

Table 5 Genetic testing of very-early-onset inflammatory bowel disease patients

Patient	Sex	Age of disease onset	WES/TGPS	Genetic mutation	Location of mutation	Mutation of parents	Homo/Heterozygote	SIFT score/ prediction	Polyphen2 score/ prediction	MutationTaster score/ prediction
1	M	Neonate	Both	*IL10RB*	Chr21:34660499 c.737G>A p.W246X	Heterozygotic mutation of parents c.737G>A	Homozygote	-	-	6/D
2	F	4 mo	TGPS	*IL10RA*	Chr11:117860269 c.301C>T p.R101W	Heterozygotic mutation of father c.301C>T	Compound heterozygote	0/D	1/D	101/D
					Chr11:117864125 c.537G>A p.T179T	mother c.537G>A		1/T	-	-
3	M	1 mo+	TGPS	IL10RA	Chr11:117860269 c.301C>T p.R101W	Heterozygotic mutation of father c.301C>T	Compound heterozygote	0/D	1/D	101/D
					Chr11:117864058 c.470A>G p.Y157C (rs1027503096)	mother c.470A>G		0.001/D	1/D	194/N
4	M	1 mo+	TGPS	IL10RA	Chr11:117860269 c.301C>T p.R101W	Heterozygotic mutation of parents c.301C>T	Homozygote	0/D	1/D	101/D
5	M	Neonate	TGPS	IL10RA	Chr11:117860269 c.301C>T p.R101W	Heterozygotic mutation of father c.301C>T	Compound heterozygote	0/D	1/D	101/D
					c.350G>A p.R117H (rs199989396)	mother c.350G>A		0.011/D	1/D	29/D
6	M	Neonate	TGPS	CYBB	ChrX:37658209 c.676C>T p.R226X (rs137854592)	Heterozygotic mutation of mother c.676C>T	Hemizygotic mutation	-	-	6/D
7	M	Neonate	TGPS	CYBB	ChrX:37642741 c.142-2A>G splicing	Heterozygotic mutation of mother c.142-2A>G	Hemizygotic mutation	-	-	-
8	M	9 mo	Both	TNFRSF13B	Chr17:16843819 c.452C>T p.P151L (rs200037919)	Heterozygotic mutation of father c.452C>T	Compound heterozygote	0.568/T	0.005/B	98/N
					Chr17:16852132 c.365G>A p.R122Q (rs755343222)	mother c.365G>A		0.485/T	0.136/B	43/N
9	M	5 yr 11 mo	TGPS	XIAP	ChrX:123022501 c.910G>T p.G304X	No mutation in parents	Hemizygotic mutation	-	-	6/D
10	F	5 yr 9 mo	TGPS	IL10RB	Chr21:34652146 c.421G>A p.E141K (rs387907326)	Heterozygotic mutation in father c.421G>A	Heterozygote	0.026/D	0.946/D	56/D
11	F	4 mo	WES	-						
12	M	8 mo	WES	-						
13	F	3 yr 3 mo	TGPS	-						
14	F	4 yr	TGPS	-						
15	M	1 yr 10 mo	WES	-						
16	F	4 yr 8 mo	WES	-						

TGPS: Targeted gene panel sequencing; WES: Whole exome sequencing.

revealed the following hemizygotic mutation of *CYBB*: ChrX:37642741: c.142-2A>G splicing. The mutation is reported as pathogenic in HGMDpro[14].

CVID

Patient 8 was a male who presented with jaundice and recurrent respiratory infections during the neonatal period. Immunoglobulin (Ig)G and IgM levels were below normal. He was treated with antibiotics and intravenous immunoglobulin. He gradually developed splenomegaly. At the age of 9 mo, this patient presented with recurrent bloody stools. Colonoscopy showed ulcers and polypoid hyperplasia, which eventually spread to involve the entire colon. Pathological examination of the intestinal biopsy showed nonspecific inflammatory changes. The patient underwent laparotomy, which revealed intestinal swelling and with fissure ulcers, and ulcers involving the tunica muscularis. Treatments with steroids, TPN, EN, mesalazine, infliximab and multiple immunosuppressants were unsuccessful. Both WES and TGPS showed the following compound heterozygous mutations in *TNFRSF13B*: Chr17:16843819: c.452C>T, p.P151L and Chr17:16852132:c.365G>A, p.R122Q. These mutations are reported to be associated with CVID, though they have not been reported in HGMDpro. Further tests are required to determine the effects of these mutations.

XIAP deficiency

Patient 9 was a male, aged 5 years and 11 mo, who presented with recurrent bloody stools, fever and abdominal pain. He had been diagnosed with hemophagocytic syndrome at 4 years of age. Colonoscopy showed blunting and flattening of villi at the terminal ileum. The entire colon showed irregular deep ulcers and aphthous ulcers. Capsule endoscopy revealed sporadic jejunal ulcers. Immune tests were normal. He did not respond to exclusive enteral nutrition therapy and oral steroids. He was treated with infliximab and 6-Mercaptopurine and is currently in clinical remission. His colonoscopy findings have also improved. TGPS revealed the following mutation associated with XIAP deficiency: ChrX:123022501: c.910G>T, p.G304X. The mutation was not acquired from his parents. This mutation has not been reported in HGMDpro.

DISCUSSION

VEO-IBD children are generally recognized as having more severe clinical symptoms, more extensive intestinal inflammation, higher rates of treatment resistances and rapid disease progression compared to patients with adolescence- or adult-onset IBD[15-17]. In contrast, several studies have reported that VEO-IBD patients are not prone to a more severe clinical course compared to those with adolescence-onset IBD[18]. However, geographic and/or ethnic differences can affect genetic background and therefore cause conflicting results among studies. Monogenic IBD typically presents early, with severe clinical features and is resistant to traditional therapy; a portion of VEO-IBD patients even require HSCT[19].

In the study by Jochen Kammermeier *et al*[16], a high rate of IBDU (71%) in patients younger than 2-years-old was observed, among whom 29% were offspring from consanguineous unions, 18% had a positive family history of IBD in a first-degree relative, and 31% were diagnosed with monogenic IBD. In that study, high rates of consanguineous unions and positive family history of IBD resulted in high rates of monogenic IBD, exhibiting a more severe clinical course than traditional IBD[16]. Abdulrahman Al-Hussaini *et al*[20] analyzed 352 IBD patients in Saudi Arabia and found that 21.6% were diagnosed with IBD before the age of 6 years and 9% before the age of 3 years, and the consanguinity rate was significantly higher in the infantile or toddler-onset CD subgroup (57.1%).

In our study, the percentage of VEO-IBD patients among cases of pediatric IBD was similar to that reported by Oren Ledder *et al*[17]. Monogenic IBD patients showed earlier disease onset than nonmonogenic IBD patients, and CD was the predominant diagnosis in both groups. Nonetheless, IBDU was more common in the monogenic group, which suggests that most of the monogenic IBD patients had disease limited to the colon. The results of laboratory tests were similar between the two groups. Moreover, patients in the monogenic group did not show a propensity to be prescribed infliximab and immunosuppressants earlier than those in the nonmonogenic group.

According to the diagnostic guidelines for pediatric IBD by the European Society of Paediatric Gastroenterology, Hepatology and Nutrition[9], CD is likely to be the diagnosis when colonoscopy shows classic or nonclassic CD features with small bowel involvement or the presence of fistula/perianal disease. IBDU classification is reserved for patients with inflammation limited to the colon, in the absence of features suggestive of either UC or CD. If the initial immune work-up is normal, further investigation may be considered by physicians to be unnecessary. However, monogenic IBD, including IL10/R and XIAP deficiencies, CGD, and IPEX syndrome, presents with such features as perianal/fistulating disease, linear serpentine ulcerations, and even non-caseating granulomas[21-23], and these patients are likely to be diagnosed with IBDU or CD. It is recognized that onset of disease before 6 mo of age, growth stunting (height-for-age Z-score < 3), extensive disease and epithelial abnormalities are significantly more prevalent in monogenic IBD[16], which may indicate the need for immune tests and even genetic screening in this group of patients[3].

PID can present as IBD-like symptoms with intestinal manifestations and can be diagnosed by immune tests. CGD is characterized by genetic defects in components of the phagocyte reduced nicotinamide

adenine dinucleotide phosphate (NADPH) oxidase (phox) complex, which can be detected by the neutrophil oxidative burst assay. High levels of IgG may indicate FOXP3 deficiency[16,24]. However, Wiskott-Aldrich syndrome, hyper-IgE syndrome and *IL10* or *IL10R* mutations are not detected by basic immunodeficiency screening tests and require specific functional analyses. Defects in gene *IL10RA* and *IL10RB* can be detected by assays that determine whether exogenous IL10 will suppress lipopolysaccharide-induced peripheral blood mononuclear cell cytokine secretion or IL10-induced STAT3 phosphorylation[22]. Flow cytometry can detect functional defects in muramyl dipeptide signaling in patients with XIAP deficiency[25].

Given the large number of potential candidate genes and overlapping phenotypes, single-gene sequencing and immune tests are becoming less appropriate in children with suspected monogenic IBD. NGS techniques have significantly improved in recent years, with lower cost and diagnosis time. Although WES is suitable for novel gene discovery, it offers less reliable gene coverage in the diagnostic setting compared to TGPS[8]. TGPS and WES were both used in our study, with 16 VEO-IBD patients with suspected immune deficiency undergoing WES and/or TGPS, which revealed 9 cases of monogenic IBD (*IL10RA, IL10RB, XIAP* and *CYBB*). Among the 9 patients, 4 had disease onset during the neonatal period, and 4 had symptoms within 1 year of age. The phenotypes of the patients were in accordance with the genotypes. SIFT, Polyphen2 and MutationTaster were used to predict the innocuousness of the mutated genes.

There were limitations in this study. First, we did not perform functional analyses of novel mutations, and such studies should be performed to confirm the results. However, the novel mutations were all predicted to be pathogenic and likely pathogenic by SIFT, PolyPhen-2 and MutationTaster. Second, not all of the VEO-IBD patients were assessed by genetic testing. In cases in which immune deficiency disease was strongly suspected but could not be diagnosed by initial immune tests, genetic testing was recommended. At our hospital, the identification of monogenic IBD and genetic testing in VEO-IBD patients have only been performed during the last 5 years. Several IO-IBD patients diagnosed in early years who met the criteria for genetic testing had died, and their blood samples were not collected. For this reason, more cases of monogenetic IBD might have been present in our cohort.

In the present study, we identified monogenic IBD in 9 patients, predominantly with *IL10R* mutation; five patients were diagnosed with *IL10R* mutation. Among them, 1 patient was the offspring of a consanguineous union, with a homozygous mutation of *IL10R* which has not been reported in the literature. All remaining patients had compound heterozygous mutations of *IL10R*. *IL10* and *IL10R* mutations have been reported previously. Patients with *IL10* signaling defects primarily present with IBD symptoms within 3 mo of life, with severe perianal disease (abscess, fistula formation, fissure, tags) and susceptibility to infections. In addition, they are usually resistant to traditional therapies, though HSCT can induce sustained remission of intestinal inflammation[19,26,27]. Defects in *IL10* signaling are associated with extraintestinal inflammation, such as folliculitis and arthritis, as well as a predisposition toward B-cell lymphoma[28].

In the report of Zhiheng Huang *et al*[27], 42 IO-IBD patients among the Han population in China had *IL10R* mutations, 41 patients had *IL10RA* mutations, and only 1 patient had an *IL10RB* mutation; thus, *IL10RA* was predominant in the Han population. In another report from China, Xiao *et al*[19] described 4 patients with *IL10RA* mutation and 1 with *IL10RB* mutation among 13 VEO-IBD patients. In the present study and in other studies from Asia[26], monogenic IBD is predominately due to mutations in *IL10R* and *XIAP* and CGD, whereas mutations in *EPCAM, TTC37, SKIV2LLRBA* and *TTC7A* have been reported in Western countries[16]. These findings suggest that *IL10R* mutation is the most common cause of monogenic IBD in the Han population. Further multicenter studies are warranted.

The genetic background of VEO-IBD patients is not clear, especially among different ethnicities. Due to the heterogeneity of VEO-IBD with overlapping phenotypes between different genotypes, TGSP is appropriate for rapid recognition of monogenic IBD in VEO-IBD patients with the signs and features of monogenic IBD. This approach may help guide a more appropriate treatment strategy. For example, sustained remission after HSCT can be achieved with *IL10R*/*IL10* mutation[12], XIAP deficiency[29] and FOXP3 deficiency[30].

In conclusion, using WES and TGPS, we identified underlying PID gene mutations in pediatric patients with VEO-IBD in a Chinese population. There was a high proportion of monogenic IBD in the VEO-IBD group, especially with disease onset before 6 mo of age. *IL10R* mutation was predominant in our cohort.

ARTICLE HIGHLIGHTS

Research background

Very-early-onset inflammatory bowel disease (VEO-IBD) patients show a close association with primary immunodeficiency diseases, defined as monogenic IBD. More than 50 VEO-IBD related genes have been reported to date. Nonetheless, the incidence of monogenic IBD in Chinese population remains unknown.

Research motivation

Most reports regarding monogenic IBD were based on small population or case report, with only a small number of genes investigated. This study reports the largest cohort of genetically screened patients with VEO-IBD from China.

Research objectives

The objective of this research is to characterize monogenic IBD phenotypically and genotypically *via* genetic testing and to analyze clinical differences between

monogenic and nonmonogenic VEO-IBD patients.

Research methods

A retrospective analysis of children aged 0 to 6 years diagnosed with VEO-IBD in a tertiary hospital in southern China from 2005 to 2017 was performed. Clinical data for VEO-IBD patients were collected, and their genetic characteristics were analyzed using whole exome sequencing or target gene panel sequencing.

Research results

Nine patients (16.7%) were identified to have monogenic IBD by genetic testing. Five patients were shown to have *IL10R* mutation, two patients had chronic granulomatous disease, one patient had common variable immunodeficiency disease, and one patient had X-linked inhibitor of apoptosis deficiency.

Research conclusions

A high proportion of monogenic IBD was observed among the VEO-IBD group, especially with disease onset before the age of 6 mo. *IL10RA* was the predominant mutation in this cohort. Monogenic IBD and nonmonogenic IBD demonstrated similar clinical features. Next-generation sequencing played an important role in the diagnosis of monogenic IBD.

Research perspectives

Next-generation sequencing revealed a high proportion of monogenic IBD in our VEO-IBD cohort. Multicenter prospective studies are expected to determine the incidence of monogenic IBD in the Chinese VEO-IBD population and to investigate the genetic characteristics of monogenic IBD in China.

REFERENCES

1 **Muise AM**, Snapper SB, Kugathasan S. The age of gene discovery in very early onset inflammatory bowel disease. *Gastroenterology* 2012; **143**: 285-288 [PMID: 22727850 DOI: 10.1053/j.gastro.2012.06.025]

2 **Benchimol EI**, Fortinsky KJ, Gozdyra P, Van den Heuvel M, Van Limbergen J, Griffiths AM. Epidemiology of pediatric inflammatory bowel disease: a systematic review of international trends. *Inflamm Bowel Dis* 2011; **17**: 423-439 [PMID: 20564651 DOI: 10.1002/ibd.21349]

3 **Uhlig HH**, Schwerd T, Koletzko S, Shah N, Kammermeier J, Elkadri A, Ouahed J, Wilson DC, Travis SP, Turner D, Klein C, Snapper SB, Muise AM; COLORS in IBD Study Group and NEOPICS. The diagnostic approach to monogenic very early onset inflammatory bowel disease. *Gastroenterology* 2014; **147**: 990-1007.e3 [PMID: 25058236 DOI: 10.1053/j.gastro.2014.07.023]

4 **Heyman MB**, Kirschner BS, Gold BD, Ferry G, Baldassano R, Cohen SA, Winter HS, Fain P, King C, Smith T, El-Serag HB. Children with early-onset inflammatory bowel disease (IBD): analysis of a pediatric IBD consortium registry. *J Pediatr* 2005; **146**: 35-40 [PMID: 15644819 DOI: 10.1016/j.jpeds.2004.08.043]

5 **Moeeni V**, Day AS. Impact of Inflammatory Bowel Disease upon Growth in Children and Adolescents. *ISRN Pediatr* 2011; **2011**: 365712 [PMID: 22389775 DOI: 10.5402/2011/365712]

6 **Kim S**, Koh H. Nutritional aspect of pediatric inflammatory bowel disease: its clinical importance. *Korean J Pediatr* 2015; **58**: 363-368 [PMID: 26576179 DOI: 10.3345/kjp.2015.58.10.363]

7 **Levine A**, Griffiths A, Markowitz J, Wilson DC, Turner D, Russell RK, Fell J, Ruemmele FM, Walters T, Sherlock M, Dubinsky M, Hyams JS. Pediatric modification of the Montreal classification for inflammatory bowel disease: the Paris classification. *Inflamm Bowel Dis* 2011; **17**: 1314-1321 [PMID: 21560194 DOI: 10.1002/ibd.21493]

8 **Kammermeier J**, Drury S, James CT, Dziubak R, Ocaka L, Elawad M, Beales P, Lench N, Uhlig HH, Bacchelli C, Shah N. Targeted gene panel sequencing in children with very early onset inflammatory bowel disease--evaluation and prospective analysis. *J Med Genet* 2014; **51**: 748-755 [PMID: 25194001 DOI: 10.1136/jmedgenet-2014-102624]

9 **Levine A**, Koletzko S, Turner D, Escher JC, Cucchiara S, de Ridder L, Kolho KL, Veres G, Russell RK, Paerregaard A, Buderus S, Greer ML, Dias JA, Veereman-Wauters G, Lionetti P, Sladek M, Martin de Carpi J, Staiano A, Ruemmele FM, Wilson DC; European Society of Pediatric Gastroenterology, Hepatology, and Nutrition. ESPGHAN revised porto criteria for the diagnosis of inflammatory bowel disease in children and adolescents. *J Pediatr Gastroenterol Nutr* 2014; **58**: 795-806 [PMID: 24231644 DOI: 10.1097/MPG.0000000000000239]

10 **Mao H**, Yang W, Lee PP, Ho MH, Yang J, Zeng S, Chong CY, Lee TL, Tu W, Lau YL. Exome sequencing identifies novel compound heterozygous mutations of IL-10 receptor 1 in neonatal-onset Crohn's disease. *Genes Immun* 2012; **13**: 437-442 [PMID: 22476154 DOI: 10.1038/gene.2012.8]

11 **Yanagi T**, Mizuochi T, Takaki Y, Eda K, Mitsuyama K, Ishimura M, Takada H, Shouval DS, Griffith AE, Snapper SB, Yamashita Y, Yamamoto K. Novel exonic mutation inducing aberrant splicing in the IL10RA gene and resulting in infantile-onset inflammatory bowel disease: a case report. *BMC Gastroenterol* 2016; **16**: 10 [PMID: 26822028 DOI: 10.1186/s12876-016-0424-5]

12 **Engelhardt KR**, Shah N, Faizura-Yeop I, Kocacik Uygun DF, Frede N, Muise AM, Shteyer E, Filiz S, Chee R, Elawad M, Hartmann B, Arkwright PD, Dvorak C, Klein C, Puck JM, Grimbacher B, Glocker EO. Clinical outcome in IL-10- and IL-10 receptor-deficient patients with or without hematopoietic stem cell transplantation. *J Allergy Clin Immunol* 2013; **131**: 825-830 [PMID: 23158016 DOI: 10.1016/j.jaci.2012.09.025]

13 **Curnutte JT**, Hopkins PJ, Kuhl W, Beutler E. Studying X inactivation. *Lancet* 1992; **339**: 749 [PMID: 1347621]

14 **Roos D**. The genetic basis of chronic granulomatous disease. *Immunol Rev* 1994; **138**: 121-157 [PMID: 8070813]

15 **Ruel J**, Ruane D, Mehandru S, Gower-Rousseau C, Colombel JF. IBD across the age spectrum: is it the same disease? *Nat Rev Gastroenterol Hepatol* 2014; **11**: 88-98 [PMID: 24345891 DOI: 10.1038/nrgastro.2013.240]

16 **Kammermeier J**, Dziubak R, Pescarin M, Drury S, Godwin H, Reeve K, Chadokufa S, Huggett B, Sider S, James C, Acton N, Cernat E, Gasparetto M, Noble-Jamieson G, Kiparissi F, Elawad M, Beales PL, Sebire NJ, Gilmour K, Uhlig HH, Bacchelli C, Shah N. Phenotypic and Genotypic Characterisation of Inflammatory Bowel Disease Presenting Before the Age of 2 years. *J Crohns Colitis* 2017; **11**: 60-69 [PMID: 27302973 DOI: 10.1093/ecco-jcc/jjw118]

17 **Ledder O**, Catto-Smith AG, Oliver MR, Alex G, Cameron DJ, Hardikar W. Clinical patterns and outcome of early-onset inflammatory bowel disease. *J Pediatr Gastroenterol Nutr* 2014; **59**: 562-564 [PMID: 24979317 DOI: 10.1097/MPG.0000000000000465]

18 **Gupta N**, Bostrom AG, Kirschner BS, Cohen SA, Abramson O, Ferry GD, Gold BD, Winter HS, Baldassano RN, Smith T, Heyman MB. Presentation and disease course in early- compared to later-onset pediatric Crohn's disease. *Am J Gastroenterol* 2008; **103**: 2092-2098 [PMID: 18796101 DOI: 10.1111/j.1572-0241.2008.02000.x]

19 **Xiao Y**, Wang XQ, Yu Y, Guo Y, Xu X, Gong L, Zhou T, Li XQ, Xu CD. Comprehensive mutation screening for 10 genes in Chinese patients suffering very early onset inflammatory bowel disease. *World J Gastroenterol* 2016; **22**: 5578-5588 [PMID: 27350736 DOI: 10.3748/wjg.v22.i24.5578]

20 **Al-Hussaini A**, El Mouzan M, Hasosah M, Al-Mehaidib A, ALSaleem K, Saadah OI, Al-Edreesi M. Clinical Pattern of Early-Onset Inflammatory Bowel Disease in Saudi Arabia: A Multicenter National Study. *Inflamm Bowel Dis* 2016; **22**: 1961-1970 [PMID: 27104817 DOI: 10.1097/MIB.0000000000000796]

21 **Marciano BE**, Rosenzweig SD, Kleiner DE, Anderson VL, Darnell DN, Anaya-O'Brien S, Hilligoss DM, Malech HL, Gallin JI, Holland SM. Gastrointestinal involvement in chronic granulomatous disease. *Pediatrics* 2004; **114**: 462-468 [PMID: 15286231]

22 **Glocker EO**, Kotlarz D, Boztug K, Gertz EM, Schäffer AA, Noyan F, Perro M, Diestelhorst J, Allroth A, Murugan D, Hätscher

N, Pfeifer D, Sykora KW, Sauer M, Kreipe H, Lacher M, Nustede R, Woellner C, Baumann U, Salzer U, Koletzko S, Shah N, Segal AW, Sauerbrey A, Buderus S, Snapper SB, Grimbacher B, Klein C. Inflammatory bowel disease and mutations affecting the interleukin-10 receptor. *N Engl J Med* 2009; **361**: 2033-2045 [PMID: 19890111 DOI: 10.1056/NEJMoa0907206]

23 **Worthey EA**, Mayer AN, Syverson GD, Helbling D, Bonacci BB, Decker B, Serpe JM, Dasu T, Tschannen MR, Veith RL, Basehore MJ, Broeckel U, Tomita-Mitchell A, Arca MJ, Casper JT, Margolis DA, Bick DP, Hessner MJ, Routes JM, Verbsky JW, Jacob HJ, Dimmock DP. Making a definitive diagnosis: successful clinical application of whole exome sequencing in a child with intractable inflammatory bowel disease. *Genet Med* 2011; **13**: 255-262 [PMID: 21173700 DOI: 10.1097/GIM.0b013e3182088158]

24 **Uzel G**, Sampaio EP, Lawrence MG, Hsu AP, Hackett M, Dorsey MJ, Noel RJ, Verbsky JW, Freeman AF, Janssen E, Bonilla FA, Pechacek J, Chandrasekaran P, Browne SK, Agharahimi A, Gharib AM, Mannurita SC, Yim JJ, Gambineri E, Torgerson T, Tran DQ, Milner JD, Holland SM. Dominant gain-of-function STAT1 mutations in FOXP3 wild-type immune dysregulation-polyendocrinopathy-enteropathy-X-linked-like syndrome. *J Allergy Clin Immunol* 2013; **131**: 1611-1623 [PMID: 23534974 DOI: 10.1016/j.jaci.2012.11.054]

25 **Ammann S**, Elling R, Gyrd-Hansen M, Dückers G, Bredius R, Burns SO, Edgar JD, Worth A, Brandau H, Warnatz K, Zur Stadt U, Hasselblatt P, Schwarz K, Ehl S, Speckmann C. A new functional assay for the diagnosis of X-linked inhibitor of apoptosis (XIAP) deficiency. *Clin Exp Immunol* 2014; **176**: 394-400 [PMID: 24611904 DOI: 10.1111/cei.12306]

26 **Suzuki T**, Sasahara Y, Kikuchi A, Kakuta H, Kashiwabara T, Ishige T, Nakayama Y, Tanaka M, Hoshino A, Kanegane H, Abukawa D, Kure S. Targeted Sequencing and Immunological Analysis Reveal the Involvement of Primary Immunodeficiency Genes in Pediatric IBD: a Japanese Multicenter Study. *J Clin Immunol* 2017; **37**: 67-79 [PMID: 27747465 DOI: 10.1007/s10875-016-0339-5]

27 **Huang Z**, Peng K, Li X, Zhao R, You J, Cheng X, Wang Z, Wang Y, Wu B, Wang H, Zeng H, Yu Z, Zheng C, Wang Y, Huang Y. Mutations in Interleukin-10 Receptor and Clinical Phenotypes in Patients with Very Early Onset Inflammatory Bowel Disease: A Chinese VEO-IBD Collaboration Group Survey. *Inflamm Bowel Dis* 2017; **23**: 578-590 [PMID: 28267044 DOI: 10.1097/MIB.0000000000001058]

28 **Neven B**, Mamessier E, Bruneau J, Kaltenbach S, Kotlarz D, Suarez F, Masliah-Planchon J, Billot K, Canioni D, Frange P, Radford-Weiss I, Asnafi V, Murugan D, Bole C, Nitschke P, Goulet O, Casanova JL, Blanche S, Picard C, Hermine O, Rieux-Laucat F, Brousse N, Davi F, Baud V, Klein C, Nadel B, Ruemmele F, Fischer A. A Mendelian predisposition to B-cell lymphoma caused by IL-10R deficiency. *Blood* 2013; **122**: 3713-3722 [PMID: 24089328 DOI: 10.1182/blood-2013-06-508267]

29 **Marsh RA**, Rao K, Satwani P, Lehmberg K, Müller I, Li D, Kim MO, Fischer A, Latour S, Sedlacek P, Barlogis V, Hamamoto K, Kanegane H, Milanovich S, Margolis DA, Dimmock D, Casper J, Douglas DN, Amrolia PJ, Veys P, Kumar AR, Jordan MB, Bleesing JJ, Filipovich AH. Allogeneic hematopoietic cell transplantation for XIAP deficiency: an international survey reveals poor outcomes. *Blood* 2013; **121**: 877-883 [PMID: 23131490 DOI: 10.1182/blood-2012-06-432500]

30 **Barzaghi F**, Passerini L, Bacchetta R. Immune dysregulation, polyendocrinopathy, enteropathy, x-linked syndrome: a paradigm of immunodeficiency with autoimmunity. *Front Immunol* 2012; **3**: 211 [PMID: 23060872 DOI: 10.3389/fimmu.2012.00211]

P- Reviewer: Ishige T, Sandberg KC **S- Editor**: Wang XJ
L- Editor: Filipodia **E- Editor**: Huang Y

World Journal of Gastroenterology

Submit a Manuscript: http://www.f6publishing.com

World J Gastroenterol 2018 March 7; 24(9): 1046-1055

DOI: 10.3748/wjg.v24.i9.1046

ISSN 1007-9327 (print) ISSN 2219-2840 (online)

ORIGINAL ARTICLE

Randomized Controlled Trial

Effect of polyglycolic acid sheet plus esophageal stent placement in preventing esophageal stricture after endoscopic submucosal dissection in patients with early-stage esophageal cancer: A randomized, controlled trial

Ning-Li Chai, Jia Feng, Long-Song Li, Sheng-Zhen Liu, Chen Du, Qi Zhang, En-Qiang Linghu

Ning-Li Chai, Jia Feng, Long-Song Li, Sheng-Zhen Liu, Chen Du, Qi Zhang, En-Qiang Linghu, Department of Gastroenterology, Chinese PLA General Hospital, Beijing 100853, China

ORCID number: Ning-Li Chai (0000-0003-0583-4189); Jia Feng (0000-0001-6839-3531); Long-Song Li (0000-0003-4593-7668); Sheng-Zhen Liu (0000-0001-6495-2818); Chen Du (0000-0003-4790-6056); Qi Zhang (0000-0002-6550-9217); En-Qiang Linghu (0000-0002-6311-5265).

Author contributions: Chai NL and Feng J contributed equally to this article; Linghu EQ contributed to study conception and design; Chai NL and Feng J contributed to data acquisition, analysis, and interpretation; Li LS and Liu SZ drafted the manuscript; Du C and Zhang Q contributed to editing and revising the article; all authors read and approved the manuscript.

Institutional review board statement: The study was reviewed and approved by the Ethics Committee of Chinese PLA General Hospital.

Clinical trial registration statement: This study is registered on http:// www.chictr.org.cn (No. chictr-inr-16008709).

Informed consent statement: All study participants provided written informed consent prior to study enrolment.

Conflict-of-interest statement: The authors have no conflicts of interest to disclose.

Data sharing statement: No additional data are available.

Manuscript source: Unsolicited manuscript

Correspondence to: En-Qiang Linghu, MD, PhD, Chief Doctor, Department of Gastroenterology, Chinese PLA General Hospital, 28 Fuxing Road, Beijing 100853, China. 0572013@fudan.edu.cn
Telephone: +86-10-55499292
Fax: +86-10-55499292

Received: September 20, 2017
Peer-review started: September 21, 2017
First decision: September 27, 2017
Revised: January 2, 2018
Accepted: January 16, 2018
Article in press: January 16, 2018
Published online: March 7, 2018

Abstract

AIM

To assess the effect of polyglycolic acid (PGA) plus stent placement compared with stent placement alone in the prevention of post-endoscopic submucosal dissection (ESD) esophageal stricture in early-stage esophageal cancer (EC) patients.

METHODS

Seventy EC patients undergoing ESD were enrolled in this randomized, controlled study. Patients were allocated randomly at a 1:1 ratio into two groups as follows: (1) PGA plus stent group (PGA sheet-coated stent placement was performed); and (2) Stent group (only stent placement was performed). This study was

registered on http://www.chictr.org.cn (No. chictr-inr-16008709).

RESULTS

The occurrence rate of esophageal stricture in the PGA plus stent group was 20.5% (n = 7), which was lower than that in the stent group (46.9%, n = 15) (P = 0.024). The mean value of esophageal stricture time was 59.6 ± 16.1 d and 70.7 ± 28.6 d in the PGA plus stent group and stent group (P = 0.174), respectively. Times of balloon dilatation in the PGA plus stent group were less than those in the stent group [4 (2-5) *vs* 6 (1-14), P = 0.007]. The length (P = 0.080) and diameter (P = 0.061) of esophageal strictures were numerically decreased in the PGA plus stent group, whereas no difference in location (P = 0.232) between the two groups was found. Multivariate logistic analysis suggested that PGA plus stent placement (P = 0.026) was an independent predictive factor for a lower risk of esophageal stricture, while location in the middle third (P = 0.034) and circumferential range = 1/1 (P = 0.028) could independently predict a higher risk of esophageal stricture in EC patients after ESD.

CONCLUSION

PGA plus stent placement is more effective in preventing post-ESD esophageal stricture compared with stent placement alone in EC patients with early-stage disease.

Key words: Esophageal cancer; Endoscopic submucosal dissection; Polyglycolic acid plus stent placement; Esophageal stricture

Core tip: This study determines the effect of polyglycolic acid (PGA) plus stent placement compared with stent placement alone in the prevention of post-endoscopic submucosal dissection (ESD) esophageal stricture in early-stage esophageal cancer (EC) patients. Our findings confirm that PGA plus stent placement is more effective in preventing post-ESD esophageal stricture compared with stent placement alone in EC patients with early-stage disease.

Chai NL, Feng J, Li LS, Liu SZ, Du C, Zhang Q, Linghu EQ. Effect of polyglycolic acid sheet plus esophageal stent placement in preventing esophageal stricture after endoscopic submucosal dissection in patients with early-stage esophageal cancer: A randomized, controlled trial. *World J Gastroenterol* 2018; 24(9): 1046-1055 Available from: URL: http://www.wjgnet.com/1007-9327/full/v24/i9/1046.htm DOI: http://dx.doi.org/10.3748/wjg.v24.i9.1046

INTRODUCTION

Esophageal cancer (EC) is one of the most common carcinomas with high mortality and has been identified as the sixth leading cause of cancer-related death worldwide[1]. Based on 2015 global cancer statistics, an estimated 455800 new EC cases and 400200 deaths occurred in 2012. In the United States, approximately 16940 new EC cases and 15690 deaths will be seen in 2017[2,3]. Endoscopic submucosal dissection (ESD), performed as an endoscopic resection technique, has been widely utilized in the treatment of EC patients with early-stage disease, due to its minimal invasiveness and high rate of *en bloc* resection[4,5]. However, more than 30% of EC patients after ESD still experience postoperative esophageal stricture, which is characterized by dysphagia, dramatically decreasing the quality of life[6,7].

To prevent post-ESD esophageal stricture, various treatments have been implemented, such as polyglycolic acid (PGA) sheet, stent placement, and esophageal balloon dilatation[8]. Among these, PGA sheet, a biodegradable suture material, could be used to prevent post-ESD esophageal stricture because of its advantages of reinforcing suture and minimal scar contracture, although the limitation of instability between the PGA sheet and wound surface after long-term pasting still exists[9-11]. Another popular method is stent placement, which is frequently used with covered self-expandable metal material, and has been verified to have curative effects on refractory stricture to some extent, although its complications, such as translocation and promotion of granulation tissue proliferation, still affect its clinical outcomes in EC patients[12,13].

Although some studies on the applications of combinations of two or three treatments in the prevention of esophageal stricture after ESD have been performed, no study has explored the effect of the combination of PGA and stent placement in the prevention of post-ESD esophageal stricture[9,14]. Therefore, the aim of this study was to assess the effect of PGA plus stent placement compared with stent placement alone in the prevention of post-ESD esophageal stricture in early-stage EC patients.

MATERIALS AND METHODS

Patients

A total of 70 early-stage EC patients receiving ESD at Department of Gastroenterology, China PLA General Hospital from July 2016 to May 2017 were consecutively enrolled in this randomized controlled study. The inclusion criteria were as follows: (1) Circumferential range above 3/4; (2) Longitudinal length above 3 cm; (3) Lesion depth no more than M2; and (4) Tumor lesion could be completely removed. The exclusion criteria were as follows: (1) Patients with coagulative dysfunction, hepatic failure, renal failure, or cardiopulmonary dysfunction; (2) Patients complicated with malignant hematological disease or other solid tumors; (3) Patients who had a previous history of esophagectomy or radiation therapy; (4) Patients

who were unable to complete the ESD operation; (5) Pregnant or lactating women; (6) Patients who could not be followed regularly; and (7) Patients who refused to participate in this study.

This study was approved by the Ethics Committee of China PLA General Hospital (approval No. S2016-059-01), and all participants provided written informed consent. This study was registered on http://www.chictr.org.cn (Chinese Clinical Trial Registry conducted by World Health Organization; registration No. chictr-inr-16008709).

Randomization

The randomization code was generated by a statistician using the blocked randomization method with block length set as four because of the need for allocation balance between the two groups (1:1 ratio). The documents were subsequently sent and kept in Shanghai Qeejen Bio-tech Company (a medical and statistical service company). After screening, when a patient was eligible for the study, a call was made to the Qeejen Company, and a unique subject identification number was provided from the randomized module.

Treatment

After the randomization, patients were allocated to the PGA plus stent treatment group or stent treatment group at a 1:1 ratio. In the PGA plus stent group, the patients received PGA sheet-coated stent placement to prevent esophageal stricture post ESD operation; in the stent group, the patients received only stent placement to prevent esophageal stricture post ESD operation.

ESD procedure

After intravenous anesthesia, patients with tracheal intubation and oropharyngeal tube placement underwent endoscope (Olympus, Japan) insertion to the area of the tumor lesion. Subsequently, the lesion margins were stained with iodine, and the submucosa was labeled. Then, the lesion dissections were performed, and endoscopic submucosal tunnel dissection was used for lesion stripping, followed by hemostasis.

Combination of PGA membrane and stent

According to the ESD wound length (Figure 1A), the length of stent (Derman Science, China, 1.7 cm of diameter, stainless steel, silicone rubber membrane) was selected (Figure 1B), followed by PGA sheet selection (NEOVEIL, Japan, 100 mm × 100 mm × 0.15 mm) (Figure 1C). Subsequently, the stent was coated with the PGA sheet (Figure 1D), and the covered place was designed to the ESD wound site after stent release. Then, this stent covered with a PGA sheet was mounted on the conveyer for the esophageal stent ring supporter (Figure 1E and F) and inserted under endoscopic observation (Figure 1G).

Stent placement

The length of the ESD wound was measured, and then the appropriate length of metal coated stent was selected (Derman Science, China, 1.7 cm of diameter, stainless steel, silicone rubber membrane), which was beyond the top and bottom edge of the lesion by more than 2 cm. Subsequently, the guide wire was placed under the endoscope, and then the endoscope was pulled out and the conveyer was inserted for the esophageal stent ring supporter along with the guide wire for the stent placement. After stent placement, the endoscope was inserted again to observe the stent position. A chest X-ray was performed after the stent placement, and the stent position was recorded.

Stent removal

In the PGA plus stent group, the stent was removed by endoscopy at 4 wk, whereas in the stent group, the stent was removed at 8 wk after operation. Endoscopic evaluation of the ESD wound was performed (Figure 2A-C). The time to remove the stent between the two groups was different because PGA is a biodegradable suture material, which would be degraded after a period of time. According to a preliminary study with a small sample size, we found that when PGA plus stent placement was used to prevent post-ESD esophageal stricture in early-stage EC patients, the PGA was degraded at approximately 3 or 4 wk after ESD, and therefore, the previous clinical experiences suggested that removing PGA plus stent placement at 4 wk might be a good choice in EC patients.

Assessment

The primary endpoint was esophageal stricture occurrence after ESD operation, which was defined as diameter of stricture section below 1 cm (endoscopy could not pass through) under endoscopy. The secondary endpoints were as follows: time to esophageal stricture; location, length, and diameter of esophageal stricture; and balloon dilatation times for the esophageal stricture.

Follow-up

All patients were followed through clinic visits or telephone interviews. Each patient was asked if dysphagia or other symptoms occurred at each visit or call, and if distinct dysphagia was determined, endoscopy was performed to examine the esophageal stricture. Chest X-ray examination was performed every 2 wk to monitor the position of esophageal stent, and if a stent shifted more than 2 cm, endoscopy was performed to adjust the stent to the original place.

Balloon dilatation

All patients with esophageal stricture received endoscopic balloon dilation treatment (balloon diameter: 8 mm/10 mm/12 mm/15 mm, Boston Scientific, United States). The esophageal stricture section was repeatedly

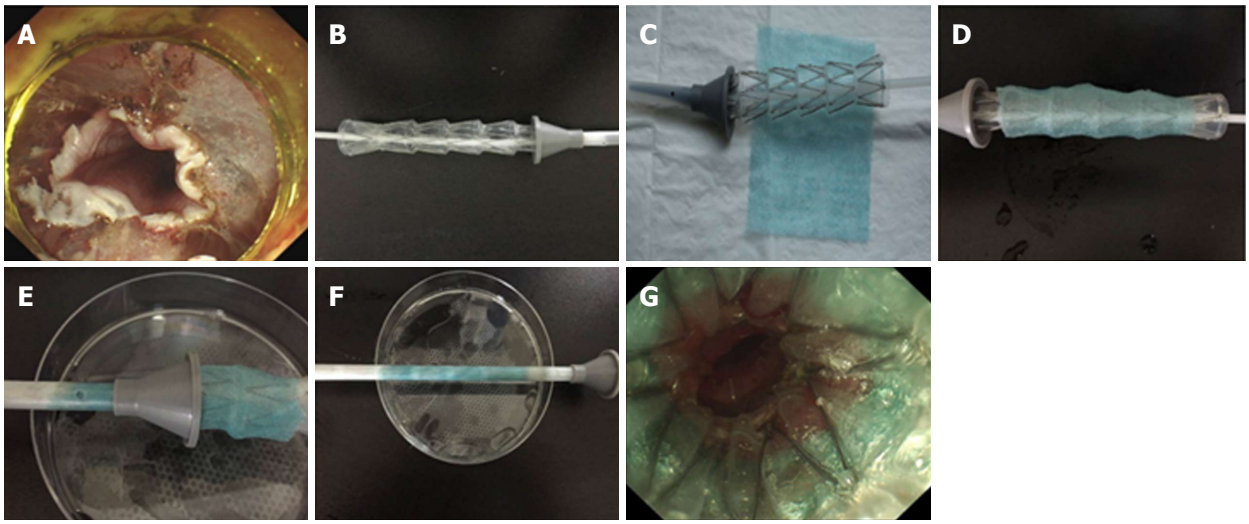

Figure 1 Combination of polyglycolic acid sheet and stent. A: Measurement of endoscopic submucosal dissection wound length; B: Adjustment of stent length; C: Polyglycolic acid sheet selection based on lesion length; D: Stent coating with polyglycolic acid (PGA) sheet; E-F: Stent covered with PGA sheet mounted on the stent support; G: Insertion of stent covered with PGA sheet under endoscopic observation.

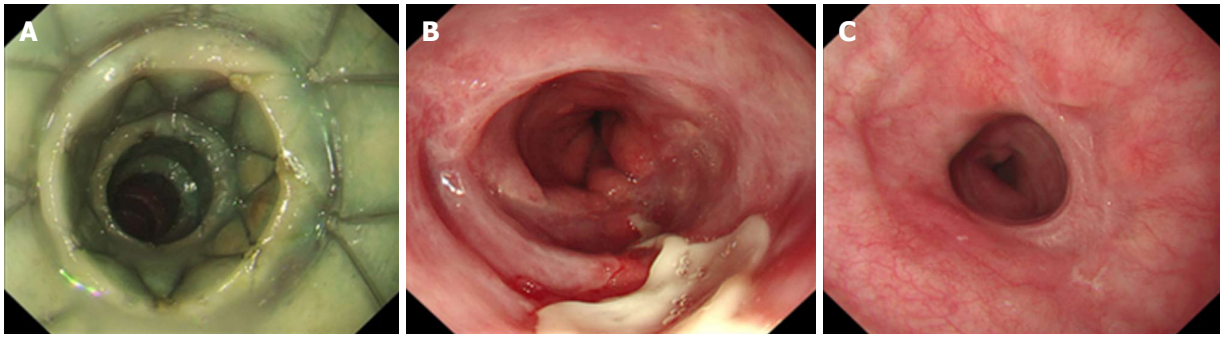

Figure 2 The management of one of the study patients. A: Stent covered with polyglycolic acid sheet inserted after 1 wk; B: Stent removed after 4 wk with a portion of wound not healed; C: No formation of esophageal stricture observed after 2 mo.

dilated until the endoscope could successfully pass through at each endoscopic examination, and balloon dilation was performed every week until the endoscope could pass through the section before dilation.

Statistical analysis

Statistical analyses were performed using SPSS 22.0 (IBM, United States) and OFFICE 2010 (Microsoft, United States). Data are mainly presented as mean value ± SD, median value (range), or count (percentage). The comparison between two groups was determined by *t*-test, Chi-square test, or Wilcoxon rank sum test. Factors affecting esophageal stricture occurrence were evaluated by univariate logistic regression analysis, and all factors with a *P*-value below 0.1 were further detected by multivariate logistic regression analysis. $P < 0.05$ was considered significant.

RESULTS

Study flow

In the current study, 109 EC patients were screened for eligibility, while 39 cases were excluded as follows: 21 patients for exclusions and 10 patients who refused to participate in this study (Figure 3). Subsequently, the remaining 70 patients were randomized at a 1:1 ratio into two groups as follows: PGA plus stent group and stent group. In the PGA plus stent group, one case withdrew during the study due to a lesion depth > M2 post-ESD operation, and 34 (97%) cases completed the entire study. In the stent group, there were three total withdrawals; three patients with lesion depth more than M2 after ESD operation withdrew, and 32 (91%) cases completed the entire study. Ultimately, a total of 66 EC patients completed the final analysis. After the operation, the stent was removed by endoscopy at 4 wk in the PGA plus stent group, and it was removed at 8 wk in the stent group. During the study, stent displacement was adjusted by endoscopy. Chest X-ray examination was performed every 2 wk. Endoscopy was performed to check the esophageal stricture. All patients with esophageal stricture received endoscopic balloon dilation treatment.

Baseline characteristics

As shown in Table 1, no difference in patients'

Table 1 Baseline characteristics *n* (%)

Parameter	PGA + stent group (*n* = 34)	Stent group (*n* = 32)	*P* value
Patients characteristic			
Age (yr)	62.74 ± 8.38	59.91 ± 8.80	0.186
Gender (Male/Female)	22/12	18/14	0.482
Tumor lesion feature			
Location			0.145
Upper third	0 (0)	0 (0)	
Middle third	12 (35)	17 (53)	
Lower third	22 (65)	15 (47)	
Tissue depth			0.331
M1	20 (59)	15 (47)	
M2	14 (41)	17 (53)	
Longitudinal length (cm)	5.97 ± 2.68	6.06 ± 2.12	0.878
Circumferential range			0.684
3/4	12 (35)	14 (44)	
4/5	8 (24)	8 (25)	
1/1	14 (41)	10 (31)	

Data are presented as mean ± SD or count (with or without percentage). Comparison was performed by *t*-test or Chi-square test. $P < 0.05$ was considered significant. PGA: Polyglycolic acid.

Table 2 Comparison of esophageal stricture features in polyglycolic acid + stent and stent groups

Parameter	PGA + stent group (*n* = 7)	Stent group (*n* = 15)	*P* value
Length (cm)	0.97 + 0.59	1.47 + 0.59	0.080
Diameter (cm)	0.37 + 0.17	0.51 + 0.14	0.061
Location (distance from the incisors, cm)	31.71 + 3.20	29.07 + 5.20	0.232
Balloon dilatation times	4 (2-5)	6 (1-14)	0.007

Data are presented as mean ± SD or median (range). Comparison was performed by *t*-test or Wilcoxon rank sum test. $P < 0.05$ was considered significant. PGA: Polyglycolic acid.

characteristics and tumor lesion features between the PGA plus stent group and stent group were observed ($P > 0.05$ for all). The numbers of patients with tumor location at the upper, middle, and lower third were 0 (0%), 12 (35%), and 22 (65%), respectively, in the PGA plus stent group, while 0 (0%), 17 (53%), and 15 (47%) in the stent group ($P = 0.145$). In terms of tissue depth ($P = 0.331$), there were 20 (59%) patients with M1 and 14 (41%) patients with M2 in the PGA plus stent group and 15 (47%) patients with M1 and 17 (53%) patients with M2 were in the stent group. The mean value of longitudinal length was 5.97 ± 2.68 cm in the PGA plus stent group and 6.06 ± 2.12 cm in the stent group ($P = 0.878$). Other baseline characteristics are presented in Table 1.

Comparison of post-ESD stricture in the two groups

The occurrence rate of patients with esophageal stricture in the PGA plus stent group was 20.5% ($n = 7$), which was lower than that in the stent group (46.9%, $n = 15$) ($P = 0.024$, Figure 4A). Regarding time to esophageal stricture, the mean value was 59.6 ± 16.1 d and 70.7 ± 28.6 d in the PGA plus stent group and stent groups, respectively ($P = 0.174$, Figure 4B).

Comparison of esophageal stricture features in the two groups

T-test or Wilcoxon rank sum test was used to compare esophageal stricture features between the PGA plus stent and stent groups (Table 2). The balloon dilatation times for esophageal stricture in the PGA plus stent group were less than those in the stent group [4 (2-5) *vs* 6 (1-14), $P = 0.007$]. Length ($P = 0.080$) and diameter ($P = 0.061$) of esophageal stricture were numerically decreased in the PGA plus stent group compared with the stent group, whereas there was no difference in location ($P = 0.232$) between the two groups (Table 2).

Comparison of tumor lesion features in patients with esophageal stricture

As presented Table 3, comparison of tumor lesion features in patients with esophageal stricture between the PGA plus stent and stent groups was performed. No difference was observed in location ($P = 0.899$), tissue depth ($P = 0.823$), longitudinal length ($P = 0.360$), or circumferential range ($P = 0.181$) in patients with

Table 3 Comparison of tumor lesion features in patients with esophageal stricture *n* (%)

Parameter	PGA + stent group (*n* = 7)	Stent group (*n* = 15)	*P* value
Location			0.899
Upper third	0 (0)	0 (0)	
Middle third	4 (57)	9 (60)	
Lower third	3 (43)	6 (40)	
Tissue depth			0.823
M1	2 (29)	5 (33)	
M2	5 (71)	10 (67)	
Longitudinal length (cm)	7.71 + 3.50	6.60 + 2.10	0.360
Circumferential range			0.181
3/4	0 (0)	4 (27)	
4/5	1 (14)	4 (27)	
1/1	6 (86)	7 (47)	

Data are presented as mean ± SD or count (percentage). Comparison was determined by *t*-test or Chi-square test. $P < 0.05$ was considered significant. PGA: Polyglycolic acid.

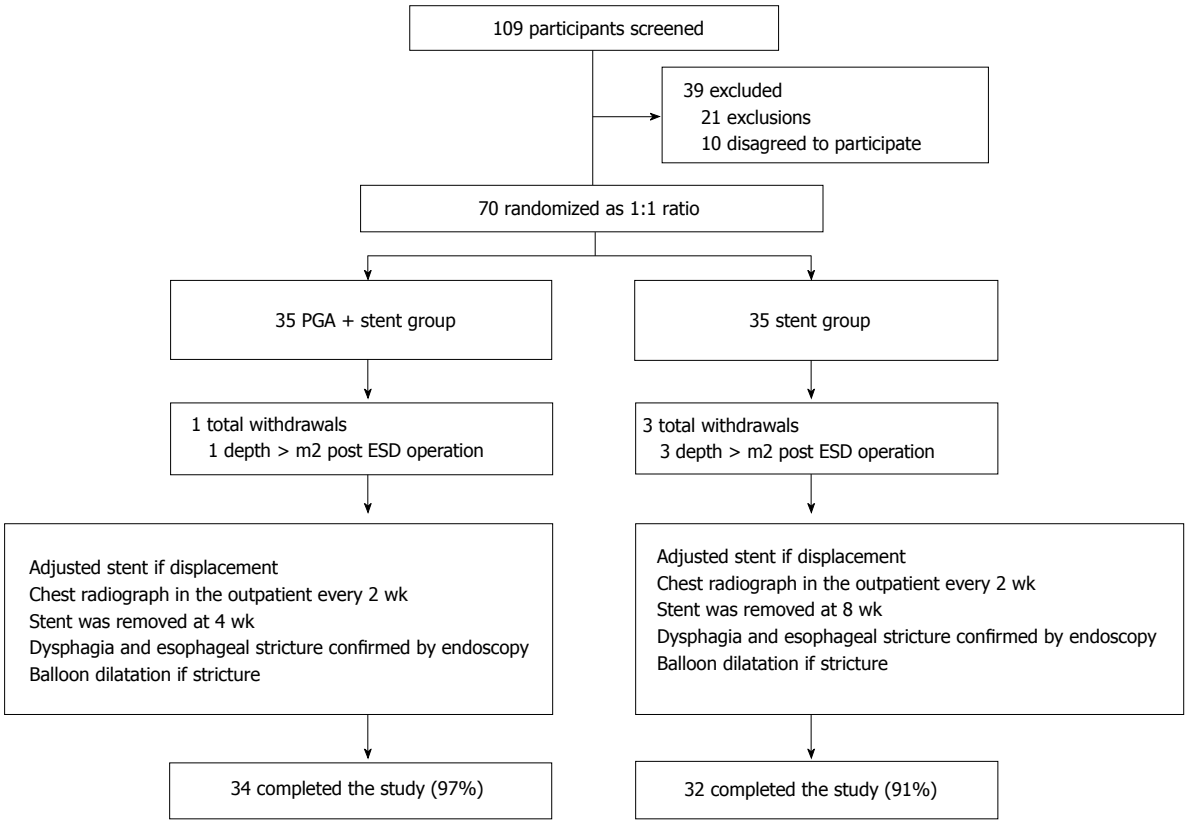

Figure 3 Study flow. ESD: Endoscopic submucosal dissection.

esophageal stricture between the two groups (Table 3).

Analysis of factors affecting esophageal stricture occurrence

Factors affecting esophageal stricture occurrence were determined by univariate logistic regression analysis (Table 4). PGA plus stent placement ($P = 0.027$) was correlated with a lower possibility of esophageal stricture occurrence, whereas circumferential range = 1/1 ($P = 0.008$) and tissue depth M2 ($P = 0.017$) were associated with a higher probability of esophageal stricture occurrence. Location in the middle third ($P = 0.083$) and longitudinal length ⩾ 6 cm ($P = 0.059$) were two factors that appeared to be correlated with a higher risk of esophageal stricture but without statistical significance. All factors with a *P*-value not above 0.1 were further detected by multivariate logistic regression analysis. PGA plus stent placement ($P = 0.026$) was an independent predictive factor for a lower risk of esophageal stricture, whereas location in the middle third ($P = 0.034$) and circumferential range = 1/1 ($P = 0.028$) could independently predict a

Table 4 Logistic analysis of factors affecting esophageal stricture occurrence

Parameter	Univariate logistic regression				Multivariate logistic regression			
	P value	OR	95%CI		*P* value	OR	95%CI	
			Lower	Higher			Lower	Higher
PGA + stent (*vs* stent alone)	0.027	0.294	0.099	0.868	0.026	0.197	0.047	0.820
Age ⩾ 62 yr	0.298	1.733	0.615	4.887	-	-	-	-
Location - middle third (*vs* lower third)	0.083	2.528	0.886	7.214	0.034	5.148	1.135	23.344
Longitudinal length ⩾ 6 cm	0.059	2.779	0.963	8.019	0.092	3.826	0.801	18.270
Circumferential range = 1/1 (*vs* others)	0.008	4.333	1.457	12.888	0.028	5.113	1.194	21.892
Tissue depth M2 (*vs* M1)	0.017	3.750	1.264	11.123	0.069	3.284	0.912	11.822

Data are presented as *P*-value, OR (odds ratio), and 95%CI. Factors affecting esophageal stricture occurrence were determined by univariate logistic regression analysis, while all factors with a *P*-value less than 0.1 were further detected by multivariate logistic regression analysis. *P*-value < 0.05 was considered significant. PGA: Polyglycolic acid.

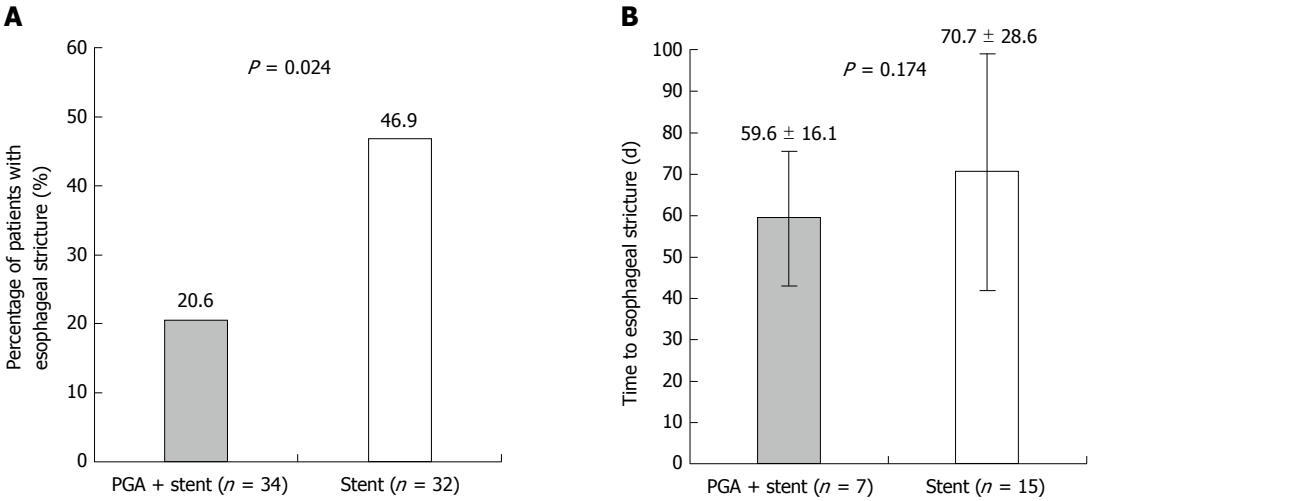

Figure 4 Comparison of post-endoscopic submucosal dissection stricture in polyglycolic acid plus stent and stent groups. A: Patients in the polyglycolic acid (PGA) plus stent group had a lower occurrence rate of esophageal stricture than that in the stent group; B: No difference in time to esophageal stricture was observed between the PGA plus stent and stent groups. Comparison of post-endoscopic submucosal dissection stricture in the PGA plus stent and stent groups was performed by *t*-test. *P* < 0.05 was considered significant.

higher risk of esophageal stricture in EC patients after ESD.

DISCUSSION

In the current study, we found that: (1) the occurrence rate of esophageal stricture in the PGA plus stent group was lower compared with the stent group, and the balloon dilatation times of esophageal stricture in the PGA plus stent group were less compared with the stent group; and (2) PGA plus stent placement could independently predict a lower occurrence rate of esophageal stricture, while location in the middle third and circumferential range = 1/1 were independent predictive factors for a higher possibility of post-ESD esophageal stricture occurrence in EC patients.

ESD, which is considered an effective method to completely resect mucosal lesions, has been popularly applied in EC patients with early-stage disease, although due to the physiological characteristics of the esophageal cavity, esophageal stricture frequently occurs after ESD[4,15,16]. Recent data indicate that the appearance of several fibroblasts and the shrinking of the natural muscle layer are present in the formation of post-ESD esophageal stricture, which suggests that fiber proliferation, scar formation, and wound contracture might contribute to the formation of post-ESD esophageal stricture[17].

Stenting has been regarded as a useful way to prevent post-ESD esophageal stricture, although a high recurrence rate still exists in most patients after removing the stent, and some patients with long-term stent placement experience several complications, such as displacement and granulation tissue hyperplasia[18,19]. In clinical practice, stent insertion has been reported to decrease the dysphagia score and the mean diameter of esophageal stricture[20]. PGA sheet, a polymer with a fiber mesh structure, could: (1) provide abundant cytoskeletons to support cell crawling during the repair process, and inhibit rejection reaction by its strong degradative function, thereby leading to a decreased risk of scar germination and stricture formation; and (2) carry cells and medicines to promote cell repair and wound healing. An interesting study revealed that

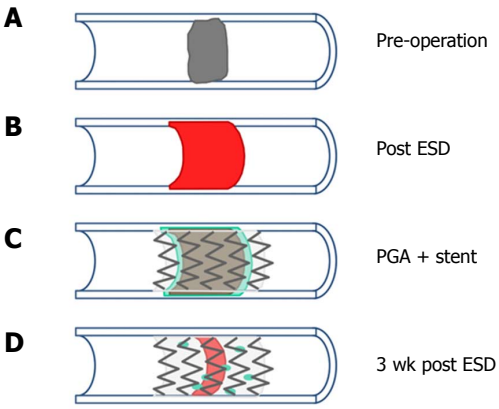

Figure 5 The endoscopic submucosal dissection wound before and after the polyglycolic acid sheet plus stent placement. A: The esophageal lesion before endoscopic submucosal dissection (ESD); B: The mucosal defect after ESD; C: The ESD wound after the PGA sheet plus stent placement; D: The PGA sheet plus stent placement was inserted after 3 wk.

PGA sheets could shield mucosal defects and prevent scarring, reducing postoperative adverse events in patients with colorectal ESD[21]. However, some limitations of PGA sheets still exist, which are easy to fall off for long-term utilization[9,10]. Therefore, both stents and PGA can decrease the risk of esophageal stricture to some extent. However, there remain several limitations. No study on the effects of the combined application of PGA and stent has been reported. Our study compared the occurrence rate of post-ESD esophageal stricture between the PGA plus stent and stent groups and indicated that the percentage of post-ESD esophageal stricture in the PGA plus stent group was lower compared with the stent group. Balloon dilatation, which is one of the most common treatments for esophageal stricture, has been identified to have good short-term efficacy, whereas the long-term curative effect is still far from satisfactory. A previous study suggested that the average usage rate of balloon dilatation is estimated to be 16 times for post-ESD esophageal stricture[22]. The results of our study also found that the balloon dilatation times for esophageal stricture in the PGA plus stent group were less than those in the stent group [4 (2-5) *vs* 6 (1-14) times]. Therefore, these findings indicated that PGA plus stent placement could decrease the risk of esophageal stricture and the balloon dilatation times for esophageal stricture compared with stent placement alone. Possible explanations might be as follows: (1) The stent could provide radial force to fix the PGA sheet, thereby preventing the defluvium of the PGA sheet[18,19]; and (2) The PGA sheet could increase the friction between the stent and wound surface, reducing stent displacement, and also provide cytoskeleton and carry medicine to accelerate cell repair and wound healing. Therefore, the interaction of the PGA sheet with the stent could decrease the occurrence rate of post-ESD esophageal stricture[9,11]. However, seven patients still reported the formation of esophageal stricture in the PGA plus stent group. This occurrence might be explained by the fact that during the process of wound repair, epithelial cells usually crawl from the edge of the wound to the central area. Because of the long-term repair, the PGA sheet might be degraded to result in frameless support, leading to its defluvium and increasing the occurrence rate of esophageal stricture in the central area (Figure 5A-D). As to the predictive value, the results of the present study showed that PGA plus stent placement could be an independent factor to predict a lower possibility of esophageal stricture occurrence. The possible reasons are that the stent contributes to fixing the PGA sheet and the PGA sheet increases the friction to reduce stent displacement, thereby preventing the occurrence of post-ESD esophageal stricture[9,11,18,19]. Although there is no report on the effects of PGA plus stent in the prevention of post-ESD esophageal stricture in EC patients, further studies investigating other combined treatments, such as PGA plus stent plus corticosteroids, are greatly needed. Furthermore, the results of our study also found that shorter length (P = 0.080) and diameter (P = 0.061) were observed in the PGA plus stent group compared with the stent group, which suggests that the interaction of PGA and stent might decrease the severity of the degree of esophageal stricture.

In clinical practice, glucocorticoids have established their value in inhibiting the inflammatory response, repressing collagen synthesis, and promoting collagen decomposition, thereby preventing the formation of post-ESD esophageal stricture[23,24]. Although glucocorticoid injection is a good way to decrease the occurrence of systemic adverse reactions, it still leads to several complications in EC patients after ESD, including perforation, bleeding, and mediastinal abscess[23,25]. Therefore, a PGA sheet infiltrated with a glucocorticoid (triamcinolone acetonide) might decrease the occurrence of post-ESD esophageal stricture while reducing adverse reactions. Furthermore, to optimize the methods to prevent esophageal stricture, we explored the combined application of PGA, stent, and glucocorticoid in three EC patients after ESD (Figure 6A-C). After stent removal, no formation of esophageal stricture occurred and good effectiveness was achieved during a 3 mo follow-up (Figure 6D and E). However, further study with a larger sample size and a longer follow-up period is necessary.

One limitation in the present study was that the total number of recruited EC patients was relatively small, which might cause lower statistical efficiency compared with a study with a large sample size. Therefore, a study with a larger sample size is needed to further confirm the efficacy of PGA plus stent placement in preventing esophageal stricture.

In conclusion, PGA plus stent placement is more effective in preventing post-ESD esophageal stricture compared with stent placement alone in EC patients

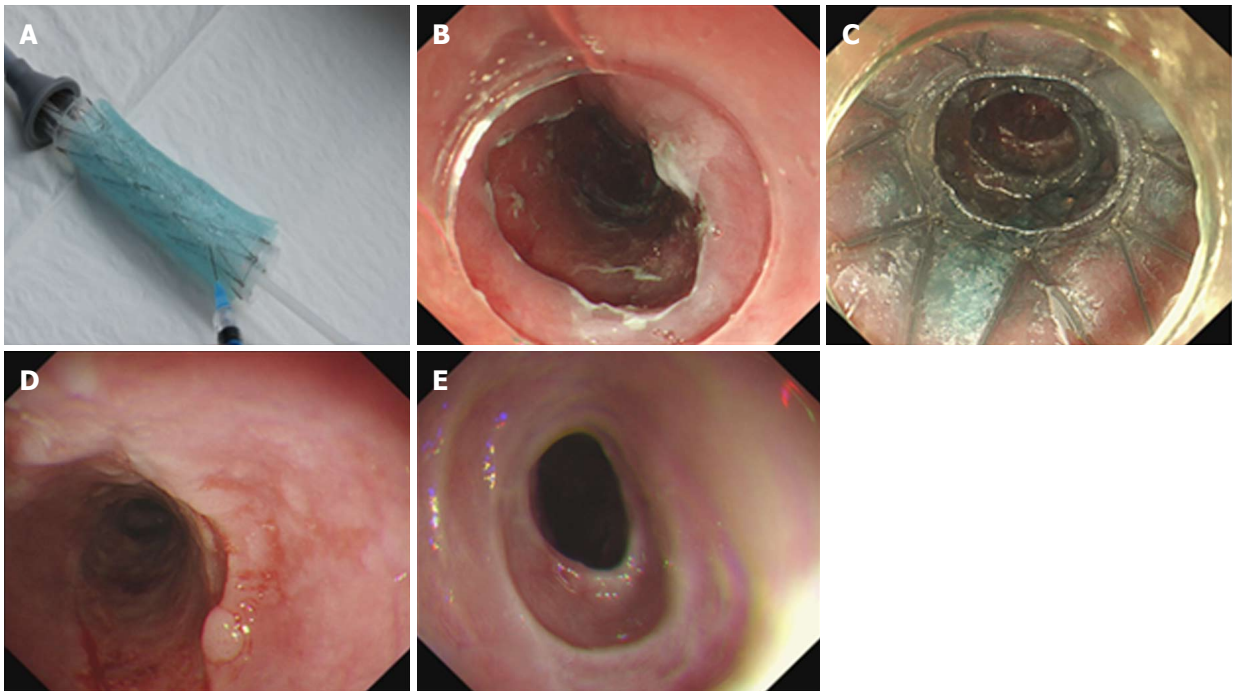

Figure 6 The management of one of the study patients. A: Stent covered with polyglycolic acid (PGA) sheet was injected with glucocorticoid before insertion; B: The mucosal defect after endoscopic submucosal dissection (ESD); C: The combination of PGA, stent, and glucocorticoid was applied after 1 wk; D: The endoscopic appearance of the esophagus 4 wk after ESD; E: The endoscopic appearance of the esophagus 3 mo after ESD.

with early-stage disease.

ARTICLE HIGHLIGHTS

Research background

Esophageal cancer (EC) is one of the most common carcinomas with high mortality, and more than 30% of EC patients after endoscopic submucosal dissection (ESD) still experience postoperative esophageal stricture, which dramatically decreases the quality of life.

Research motivation

The applications of combinations of two or three treatments in the prevention of esophageal stricture after ESD have been investigated in some studies. However, no study explored the effect of the combination of PGA and stent placement in the prevention of post-ESD esophageal stricture.

Research objectives

This study aimed to assess the effect of PGA plus stent placement *vs* stent placement alone in the prevention of post-ESD esophageal stricture in early-stage EC patients.

Research methods

About 70 EC patients undergoing ESD were enrolled in this study. Patients were allocated randomly at a 1:1 ratio into a PGA plus stent group (PGA sheet-coated stent placement was performed) and a stent group (only stent placement was performed). All patients were followed, and if dysphagia or other symptoms occurred, endoscopy was performed to examine the esophageal stricture.

Research results

The occurrence rate of esophageal stricture in the PGA plus stent group was lower than that in the stent group. Times of balloon dilatation in the PGA plus stent group were less than those in the stent group. Multivariate logistic analysis suggested that PGA plus stent placement was an independent predictive factor for a lower risk of esophageal stricture, while location in the middle third and circumferential range = 1/1 could independently predict a higher risk of esophageal stricture in EC patients after ESD.

Research conclusions

PGA plus stent placement is more effective in preventing post-ESD esophageal stricture *vs* stent placement alone in early-stage EC patients.

Research perspectives

The total number of recruited EC patients in the present study was relatively small. And a study with a larger sample size is needed to further confirm the efficacy of PGA plus stent placement in preventing esophageal stricture.

REFERENCES

1 **Mohammed F**. Esophageal cancer. *N Engl J Med* 2004; **350**: 1363-1364; author reply 1363-1364 [PMID: 15044652 DOI: 10.1056/NEJMc033106]
2 **Torre LA**, Bray F, Siegel RL, Ferlay J, Lortet-Tieulent J, Jemal A. Global cancer statistics, 2012. *CA Cancer J Clin* 2015; **65**: 87-108 [PMID: 25651787 DOI: 10.3322/caac.21262]
3 **Scott DL**, Wolfe F, Huizinga TW. Rheumatoid arthritis. *Lancet* 2010; **376**: 1094-1108 [PMID: 20870100 DOI: 10.1016/S0140-6736(10)60826-4]
4 **Ning B**, Abdelfatah MM, Othman MO. Endoscopic submucosal dissection and endoscopic mucosal resection for early stage esophageal cancer. *Ann Cardiothorac Surg* 2017; **6**: 88-98 [PMID: 28446997 DOI: 10.21037/acs.2017.03.15]
5 **Yu JP**, Liu YJ, Tao YL, Ruan RW, Cui Z, Zhu SW, Shi W. Prevention of Esophageal Stricture After Endoscopic Submucosal Dissection: A Systematic Review. *World J Surg* 2015; **39**: 2955-2964 [PMID: 26335901 DOI: 10.1007/s00268-015-3193-3]
6 **Shi KD**, Ji F. Prophylactic stenting for esophageal stricture prevention after endoscopic submucosal dissection. *World J Gastroenterol* 2017; **23**: 931-934 [PMID: 28246466 DOI: 10.3748/wjg.v23.i6.931]
7 **Jain D**, Singhal S. Esophageal Stricture Prevention after Endoscopic Submucosal Dissection. *Clin Endosc* 2016; **49**: 241-256 [PMID: 26949124 DOI: 10.5946/ce.2015.099]

8 **ASGE Technology Committee.**, Maple JT, Abu Dayyeh BK, Chauhan SS, Hwang JH, Komanduri S, Manfredi M, Konda V, Murad FM, Siddiqui UD, Banerjee S. Endoscopic submucosal dissection. *Gastrointest Endosc* 2015; **81**: 1311-1325 [PMID: 25796422 DOI: 10.1016/j.gie.2014.12.010]

9 **Sakaguchi Y**, Tsuji Y, Ono S, Saito I, Kataoka Y, Takahashi Y, Nakayama C, Shichijo S, Matsuda R, Minatsuki C, Asada-Hirayama I, Niimi K, Kodashima S, Yamamichi N, Fujishiro M, Koike K. Polyglycolic acid sheets with fibrin glue can prevent esophageal stricture after endoscopic submucosal dissection. *Endoscopy* 2015; **47**: 336-340 [PMID: 25314328 DOI: 10.1055/s-0034-1390787]

10 **Kim YJ**, Park JC, Chung H, Shin SK, Lee SK, Lee YC. Polyglycolic acid sheet application to prevent esophageal stricture after endoscopic submucosal dissection for recurrent esophageal cancer. *Endoscopy* 2016; **48**: E319-E320 [PMID: 27706540 DOI: 10.1055/s-0042-117224]

11 **Iizuka T**, Kikuchi D, Yamada A, Hoteya S, Kajiyama Y, Kaise M. Polyglycolic acid sheet application to prevent esophageal stricture after endoscopic submucosal dissection for esophageal squamous cell carcinoma. *Endoscopy* 2015; **47**: 341-344 [PMID: 25412087 DOI: 10.1055/s-0034-1390770]

12 **Yamasaki T**, Tomita T, Takimoto M, Ohda Y, Oshima T, Fukui H, Watari J, Miwa H. Esophageal stricture after endoscopic submucosal dissection treated successfully by temporary stent placement. *Clin J Gastroenterol* 2016; **9**: 337-340 [PMID: 27687827 DOI: 10.1007/s12328-016-0685-0]

13 **Vleggaar FP**. Stent placement in esophageal cancer as a bridge to surgery. *Gastrointest Endosc* 2009; **70**: 620-622 [PMID: 19788979 DOI: 10.1016/j.gie.2009.03.025]

14 **Nagami Y**, Shiba M, Tominaga K, Ominami M, Fukunaga S, Sugimori S, Tanaka F, Kamata N, Tanigawa T, Yamagami H, Watanabe T, Fujiwara Y, Arakawa T. Hybrid therapy with locoregional steroid injection and polyglycolic acid sheets to prevent stricture after esophageal endoscopic submucosal dissection. *Endosc Int Open* 2016; **4**: E1017-E1022 [PMID: 27652294 DOI: 10.1055/s-0042-111906]

15 **Nagami Y**, Ominami M, Shiba M, Minamino H, Fukunaga S, Kameda N, Sugimori S, Machida H, Tanigawa T, Yamagami H, Watanabe T, Tominaga K, Fujiwara Y, Arakawa T. The five-year survival rate after endoscopic submucosal dissection for superficial esophageal squamous cell neoplasia. *Dig Liver Dis* 2017; **49**: 427-433 [PMID: 28096057 DOI: 10.1016/j.dld.2016.12.009]

16 **Kanai N**, Yamato M, Ohki T, Yamamoto M, Okano T. Fabricated autologous epidermal cell sheets for the prevention of esophageal stricture after circumferential ESD in a porcine model. *Gastrointest Endosc* 2012; **76**: 873-881 [PMID: 22867446 DOI: 10.1016/j.gie.2012.06.017]

17 **Nonaka K**, Miyazawa M, Ban S, Aikawa M, Akimoto N, Koyama I, Kita H. Different healing process of esophageal large mucosal defects by endoscopic mucosal dissection between with and without steroid injection in an animal model. *BMC Gastroenterol* 2013; **13**: 72 [PMID: 23617935 DOI: 10.1186/1471-230X-13-72]

18 **Wagh MS**, Forsmark CE, Chauhan S, Draganov PV. Efficacy and safety of a fully covered esophageal stent: a prospective study. *Gastrointest Endosc* 2012; **75**: 678-682 [PMID: 22243830 DOI: 10.1016/j.gie.2011.10.006]

19 **Shah MB**, Jajoo K. Endoscopic retrieval of a migrated esophageal stent in the cecum. *Endoscopy* 2010; **42** Suppl 2: E245-E246 [PMID: 20931463 DOI: 10.1055/s-0030-1255604]

20 **Cheng YS**, Li MH, Chen WX, Chen NW, Zhuang QX, Shang KZ. Temporary partially-covered metal stent insertion in benign esophageal stricture. *World J Gastroenterol* 2003; **9**: 2359-2361 [PMID: 14562413 DOI: 10.3748/wjg.v9.i10.2359]

21 **Tsuji Y**, Ohata K, Gunji T, Shozushima M, Hamanaka J, Ohno A, Ito T, Yamamichi N, Fujishiro M, Matsuhashi N, Koike K. Endoscopic tissue shielding method with polyglycolic acid sheets and fibrin glue to cover wounds after colorectal endoscopic submucosal dissection (with video). *Gastrointest Endosc* 2014; **79**: 151-155 [PMID: 24140128 DOI: 10.1016/j.gie.2013.08.041]

22 **Yamaguchi N**, Isomoto H, Nakayama T, Hayashi T, Nishiyama H, Ohnita K, Takeshima F, Shikuwa S, Kohno S, Nakao K. Usefulness of oral prednisolone in the treatment of esophageal stricture after endoscopic submucosal dissection for superficial esophageal squamous cell carcinoma. *Gastrointest Endosc* 2011; **73**: 1115-1121 [PMID: 21492854 DOI: 10.1016/j.gie.2011.02.005]

23 **Hanaoka N**, Ishihara R, Takeuchi Y, Uedo N, Higashino K, Ohta T, Kanzaki H, Hanafusa M, Nagai K, Matsui F, Iishi H, Tatsuta M, Ito Y. Intralesional steroid injection to prevent stricture after endoscopic submucosal dissection for esophageal cancer: a controlled prospective study. *Endoscopy* 2012; **44**: 1007-1011 [PMID: 22930171 DOI: 10.1055/s-0032-1310107]

24 **Nagami Y**, Shiba M, Tominaga K, Minamino H, Ominami M, Fukunaga S, Sugimori S, Tanigawa T, Yamagami H, Watanabe K, Watanabe T, Fujiwara Y, Arakawa T. Locoregional steroid injection prevents stricture formation after endoscopic submucosal dissection for esophageal cancer: a propensity score matching analysis. *Surg Endosc* 2016; **30**: 1441-1449 [PMID: 26123341 DOI: 10.1007/s00464-015-4348-x]

25 **Hashimoto S**, Kobayashi M, Takeuchi M, Sato Y, Narisawa R, Aoyagi Y. The efficacy of endoscopic triamcinolone injection for the prevention of esophageal stricture after endoscopic submucosal dissection. *Gastrointest Endosc* 2011; **74**: 1389-1393 [PMID: 22136782 DOI: 10.1016/j.gie.2011.07.070]

P- Reviewer: Sato Y, Rodrigo L **S- Editor**: Wang JL
L- Editor: Wang TQ **E- Editor**: Huang Y

World Journal of Gastroenterology

Submit a Manuscript: http://www.f6publishing.com

World J Gastroenterol 2018 March 7; 24(9): 1056-1062

DOI: 10.3748/wjg.v24.i9.1056

ISSN 1007-9327 (print) ISSN 2219-2840 (online)

CASE REPORT

Four cancer cases after esophageal atresia repair: Time to start screening the upper gastrointestinal tract

Floor WT Vergouwe, Madeleine Gottrand, Bas PL Wijnhoven, Hanneke IJsselstijn, Guillaume Piessen, Marco J Bruno, René MH Wijnen, Manon CW Spaander

Floor WT Vergouwe, Marco J Bruno, Manon CW Spaander, Department of Gastroenterology and Hepatology, Erasmus MC University Medical Center, Rotterdam 3000 CA, Netherlands

Floor WT Vergouwe, Hanneke IJsselstijn, René MH Wijnen, Department of Pediatric Surgery, Erasmus MC University Medical Center - Sophia Children's Hospital, Rotterdam 3000 CB, Netherlands

Madeleine Gottrand, Department of Pediatrics, Jeanne de Flandre Children's Hospital - Univ. Lille, CHU Lille, Lille 59000, France

Bas PL Wijnhoven, Department of Surgery, Erasmus MC University Medical Center, Rotterdam 3000 CA, Netherlands

Guillaume Piessen, Department of Digestive and Oncological Surgery, Claude Huriez Hospital - Univ. Lille, CHU Lille, Lille 59000, France

ORCID number: Floor WT Vergouwe (0000-0002-8599-4264); Madeleine Gottrand (0000-0002-2908-6931); Bas PL Wijnhoven (0000-0003-4738-3697); Hanneke IJsselstijn (0000-0001-5824-3492); Guillaume Piessen (0000-0001-8243-8310); Marco J Bruno (0000-0001-9181-5499); René MH Wijnen (0000-0001-7266-9713); Manon CW Spaander (0000-0002-9103-9757).

Author contributions: Vergouwe FWT, Gottrand M, Wijnhoven BPL and Piessen G collected clinical data; Vergouwe FWT, IJsselstijn H and Spaander MCW designed the manuscript; Vergouwe FWT, IJsselstijn H and Spaander MCW interpreted the data and drafted the manuscript; Gottrand M, Wijnhoven BPL, Piessen G, Bruno MJ and Wijnen RMH interpreted the data and critically revised the manuscript; all authors gave their final approval of the version of the article to be published.

Informed consent statement: Informed consent was waived since all handling to the subjects was part of standard clinical care.

Conflict-of-interest statement: All authors have no conflicts of interest to declare.

Manuscript source: Unsolicited manuscript

Correspondence to: Manon CW Spaander, MD, PhD, Associate Professor, Department of Gastroenterology and Hepatology, Erasmus MC University Medical Center, P.O. Box 2040, Rotterdam 3000 CA, Netherlands. v.spaander@erasmusmc.nl
Telephone: +31-10-7035643
Fax: +31-10-7035172

Received: October 26, 2017
Peer-review started: October 28, 2017
First decision: November 22, 2017
Revised: December 4, 2017
Accepted: January 24, 2018
Article in press: January 24, 2018
Published online: March 7, 2018

Abstract

Esophageal atresia (EA) is one of the most common congenital digestive malformations and requires surgical correction early in life. Dedicated centers have reported survival rates up to 95%. The most frequent comorbidities after EA repair are dysphagia (72%) and gastroesophageal reflux (GER) (67%). Chronic GER after EA repair might lead to mucosal damage, esophageal stricturing, Barrett's esophagus and eventually esophageal adenocarcinoma. Several long-term follow-up studies found an increased risk of

Barrett's esophagus and esophageal carcinoma in EA patients, both at a relatively young age. Given these findings, the recent ESPGHAN-NASPGHAN guideline recommends routine endoscopy in adults born with EA. We report a series of four EA patients who developed a carcinoma of the gastrointestinal tract: three esophageal carcinoma and one colorectal carcinoma in a colonic interposition. These cases emphasize the importance of lifelong screening of the upper gastrointestinal tract in EA patients.

Key words: Adenocarcinoma; Esophageal atresia; Esophageal cancer; Screening; Barrett's esophagus; Squamous cell carcinoma

Core tip: Esophageal atresia (EA) is a common congenital malformation that requires surgical correction early in life. Improved perioperative care and surgical techniques have increased the survival rate. Gastroesophageal reflux and stasis are common after surgical repair and may be associated with an increased esophageal cancer risk. However, data on incidence and risk factors for esophageal carcinogenesis after EA repair are scarce. The recent ESPGHAN-NASPGHAN guideline recommends routine endoscopy in adults born with EA. Here we report four cancer cases at a relatively young age after EA repair: three esophageal carcinoma and one colorectal carcinoma in a colonic interposition.

Vergouwe FW, Gottrand M, Wijnhoven BP, IJsselstijn H, Piessen G, Bruno MJ, Wijnen RM, Spaander MC. Four cancer cases after esophageal atresia repair: Time to start screening the upper gastrointestinal tract. *World J Gastroenterol* 2018; 24(9): 1056-1062 Available from: URL: http://www.wjgnet.com/1007-9327/full/v24/i9/1056.htm DOI: http://dx.doi.org/10.3748/wjg.v24.i9.1056

INTRODUCTION

With a prevalence of 2.43 per 10000 births, esophageal atresia (EA) with or without a tracheoesophageal fistula (TEF) is one of the most common congenital digestive malformations[1]. Surgical correction needs to be performed shortly after birth. Due to advanced surgical techniques and improved perioperative care, survival rate has increased up to 95% in dedicated centers[2,3]. Follow-up studies have shown that most EA patients have a favourable long-term outcome despite persistant digestive and respiratory problems. Common gastrointestinal symptoms after EA repair are dysphagia and gastroesophageal reflux (GER) in up to 72% and 67% of the patients, respectively[4,5]. Chronic GER after EA repair might lead to mucosal damage, esophageal stricturing, Barrett's esophagus and eventually esophageal adenocarcinoma (EAC)[5-8]. Data on incidence and risk factors for esophageal carcinogenesis after EA repair are scarce[8-10]. The recent ESPGHAN-NASPGHAN guideline recommends routine endoscopy in adults born with EA[11]. Until now, eight cases of esophageal cancer in young EA patients have been described: five esophageal squamous cell carcinoma (ESCC) and three EAC[10,12-15]. Here we report four EA patients who developed a carcinoma of the gastrointestinal tract: three esophageal carcinoma and one colorectal carcinoma in a colonic interposition. These cases emphasize the importance of lifelong screening and surveillance of the upper gastrointestinal tract in EA patients.

CASE REPORT

Case 1

Patient A presented for the first time with esophageal carcinoma at age 45 years. He was born with EA Gross type C (with a distal TEF) which was surgically repaired with closing of the fistula and end-to-end anastomosis of the esophagus. In childhood he had undergone a number of esophageal dilations to treat an anastomotic stricture.

At the age of 37 years he developed progressive dysphagia. Upper endoscopy showed proximal esophagitis and a stenotic anastomosis, which then was dilated. No biopsies were taken. Eight years later, dysphagia for solid foods reoccurred with complaints of heartburn and weight loss of 6 kg in six months (BMI 21.6 kg/m^2). He was a tobacco smoker (at least 27 pack years) and used 3-4 alcoholic beverages per day. Upper endoscopy showed a non-stenotic anastomosis at 30 cm from the incisors with a ¾ circular growing easily bleeding lesion from 33-42 cm from the incisors. Biopsies showed chronic inflammation. A chest CT scan revealed a stenotic esophagus extending from the aortic arch to the cardia with a malignant appearance and mediastinal lymph nodes (pre- and subcarinal). Due to the strong suspicion of esophageal cancer an esophageal resection with gastric tube reconstruction was performed. Pathology results confirmed the diagnosis of a squamous cell carcinoma (SCC) of the distal esophagus (pT2N0M0) which did not need further treatment.

Fifteen years later, at the age of 60 years, he again developed dysphagia and odynophagia with 7 kg weight loss (BMI 23.2 kg/m^2). Endoscopy revealed a circular tumor (17-21 cm from incisors) in the remaining cervical native esophagus eroding the constructed gastric tube and trachea. Biopsies showed a well-differentiated SCC. One suspicious supraclavicular and two mediastinal FDG-positive lymph nodes were seen on PET-CT scan images and tumor invasion in the left thyroid gland was suspected (Figure 1). Given the long interval between the two malignancies, this new

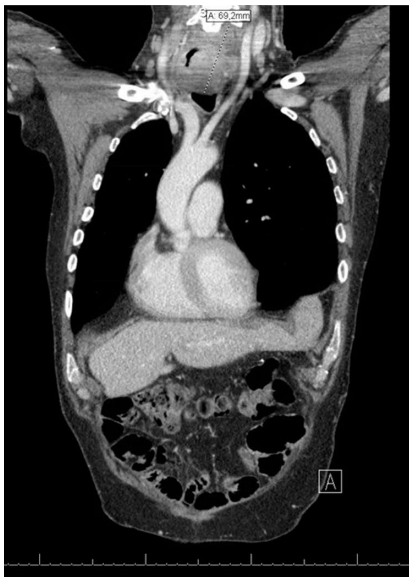

Figure 1 Chest computed tomography scan (CT scan) (case 1, tumor 2) demonstrating a tumor mass in the cervical native esophagus with suspected tumor invasion in the left thyroid gland.

tumor (T4bN2M0) was most likely a second primary tumor in the remaining cervical esophagus. In a multidisciplinary team discussion it was decided to treat with induction chemotherapy (carboplatin/paclitaxel). Initially the tumor responded well, but four months later he suffered from progressive disease with fistula formation to the trachea which was a contraindication for additional radiotherapy. An esophageal stent was placed to manage progressive dysphagia and palliative radiotherapy (13 × 3 Gy) was started to manage neuropathic pain caused by tumor invasion with imminent spinal cord compression. He died two days later.

Case 2

Patient B was a 42-year old man born with VACTERL association (acronym: vertebral anomalies, anal atresia, cardiac anomalies, TEF, renal anomalies, and limb defects)[16] including EA Gross type A (long gap without TEF), anorectal malformation, coccyx agenesis and vertebral anomalies. Continuity of the esophagus was restored with a delayed end-to-end anastomosis.

At 37 years of age he presented with dysphagia. Upper endoscopy revealed a stenotic anastomosis at 30 cm from the incisors, which could be easily dilated. In the next two years he underwent another three esophageal dilation procedures because of recurrent dysphagia. Biopsies revealed chronic and active inflammation with presence of hyphae. At the age of 42 years he presented with progressive dysphagia, without weight loss (BMI 17.6 kg/m^2). He smoked tobacco and drank alcoholic beverages only in the weekend. This time upper endoscopy revealed a circular stenotic ulcerative ESCC in the proximal esophagus (22-29 cm, anastomosis not visible) (Figure 2A). Endoscopic ultrasound findings were suspicious for tumor invasion in the trachea and several potentially malignant regional lymph nodes (T4N2M0). The tumor was considered unresectable due to invasion of surrounding vital structures (cT4b) (Figure 2B), lymph node metastases, previous thoracotomies (both sides) and intra-mediastinal surgery. Induction chemotherapy (paclitaxel/carboplatin) was started to which the tumor evidently had responded after 2 mo. Concomitant chemoradiotherapy was given (28 × 1.8 Gy) with curative intent. Six years after treatment he shows no signs of recurrent or metastatic disease.

Case 3

Patient C presented at the age of 36 years. She was born with an EA Gross type A which was surgically repaired with an end-to-end anastomosis using Livaditis elongation procedure at one month of age. At one year of age she underwent a Nissen fundoplication for severe GER. At the age of 3 years, an anastomotic stricture developed which was treated with repeated esophageal dilations. At the age of 22 years she presented with chronic respiratory symptoms, severe pneumonia, persistent GER, and dysphagia complaints. Upper endoscopy with esophageal biopsies showed no abnormality. In view of the respiratory and gastrointestinal symptoms a duodenal diversion procedure (partial antrectomy with Roux-en-Y gastrojejunal anastomosis) was performed at the age of 23 years.

At 36 years of age she presented with food impaction and weight loss of 4 kg (BMI 14.9 kg/m^2). She did not smoke tobacco and did not drink alcoholic beverages. Upper endoscopy revealed a stenotic ulcerative tumor in the distal esophagus with proximal dilation of the esophagus (25-32 cm from the incisors, gastroesophageal junction at 34 cm, anastomosis not visible). Biopsies revealed a well differentiated SCC. PET-CT scan (Figure 3) and bronchoscopy did not reveal any metastasis. She underwent a subtotal esophagectomy with total gastrectomy and a colonic interposition (pT1bN0M0). Within the following month she required reoperation for a cervical fistula and mediastinitis and underwent two endoscopic dilations of an anastomotic stricture without any evidence of tumor recurrence. Twelve months after surgery she was diagnosed with pleural and bone metastases for which she recently has started palliative chemotherapy.

Case 4

Patient D presented at the age of 47 years. He was born with VACTERL association[16](EA Gross type C, anorectal malformation, congenital urethral valves with bilateral vesicoureteral reflux and hydronephrosis left kidney). At day 5 after birth a thoracotomy was performed with TEF closure, gastrostomy and cervical esophagostomy placement. In addition the

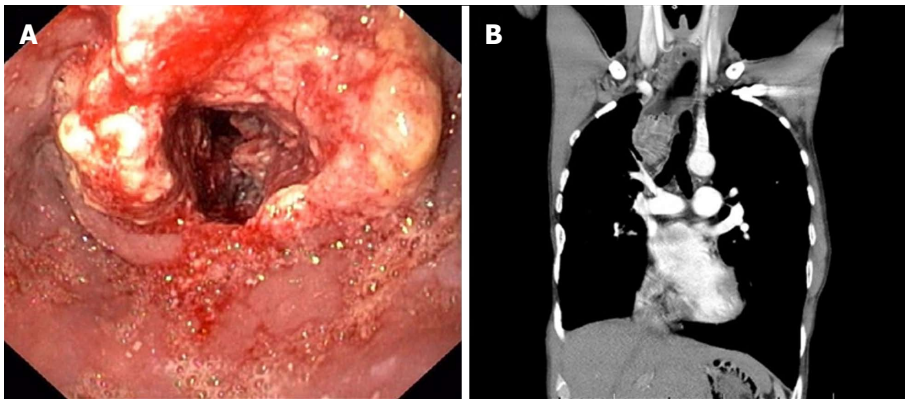

Figure 2 Findings at upper endoscopy and chest computed tomography scan (CT scan) (case 2). A: Upper endoscopy revealing a stenotic ulcerative tumor in the proximal esophagus, 22-29 cm from incisors. Histological examination of esophageal biopsies confirmed the diagnosis esophageal squamous cell carcinoma. B: Chest CT scan showing a tumor mass in the proximal esophagus with suspected tumor invasion in the trachea.

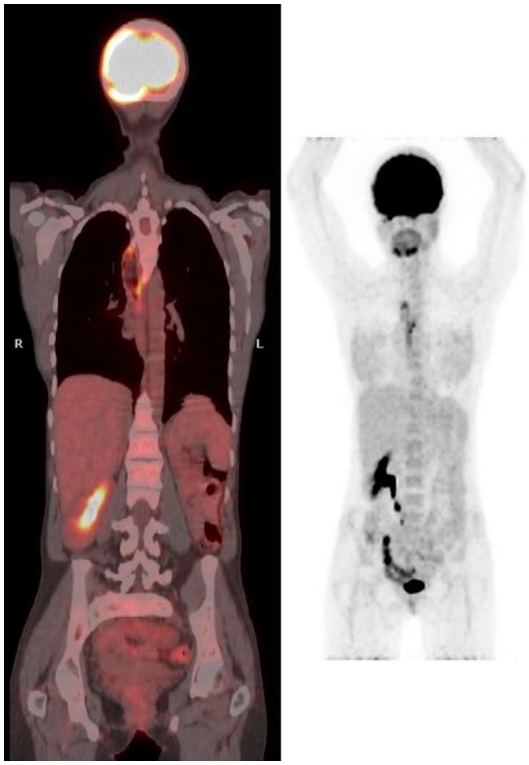

Figure 3 Initial findings at positron emission tomography-computed tomography scan (PET-CT scan) (case 3), showing PET-positive lesion in the distal esophagus without metastasis.

anorectal malformation was corrected. Nine days later a recurrent TEF was ligated. At day 29 the distal esophagus was ligated directly above the stomach and after 7 mo a colonic interposition was constructed. The spleen was congested and therefore resected during this surgery. Revision was needed because of leakage of the proximal anastomosis 19 days later. At 2.5 year of age the gastrostomy was closed. Other medical history included asthmatic bronchitis, bilateral orchidopexy, transurethral resection of urethral valves and nephrectomy of an afunctional infected left kidney.

At presentation the patient suffered from pneumonia with a density in the lower lobe of the right lung. Subsequent PET-scan revealed a PET-positive thickening in the colonic interposition for which he had been referred to our center. He complained about progressive dysphagia without any weight loss (BMI 18.6 kg/m^2). He was a cannabis smoker (2 joints/wk), had quit tobacco smoking just before presentation (a few cigarettes per day) and only sporadically drank alcoholic beverages. Upper endoscopy revealed the proximal and distal anastomosis of the colonic interposition at, respectively, 21 and 47 cm from incisors. From 26-30 cm from incisors a tumor was visible in the colon interposition which could be easily passed with the scope. Histology revealed a moderately differentiated adenocarcinoma. No abnormalities were found at colonoscopy. PET-CT scan showed circumferential thickening of the colonic interposition over a length of 10 cm, not clearly separated from the thyroid and left brachiocephalic vein, a small lesion in the lower right lobe of the lung (PET-negative) and a few locoregional lymph nodes ($\leqslant$ 1 cm, PET-negative) (Figure 4 A and B).

Patient D was treated with induction chemotherapy (capecitabine/oxaliplatin) to enable maximum tumor regression. After six treatments, the colonic interposition was resected and an esophagostomy and jejunal fistula for feeding were created. Pathological examination confirmed the diagnosis of colonic adenocarcinoma with a maximum diameter of 4.1 cm, tumor free resection margins ($\geqslant$ 1 cm) and one of 19 lymph nodes positive for metastasis (ypT2N1). Family history was negative for Lynch Syndrome. Both pentaplex microsatellite instability testing and mismatch repair gene expression analysis for MLH1, MSH2, MSH6 and PMS2 were normal.

After 4 mo continuity was restored by a subcutaneous gastric tube pull-up. At oncological follow-up one year after resection of the colonic interposition patient D did not experience any dysphagia, weight was stable (BMI 19.7 kg/m^2) and ultrasound of the liver and

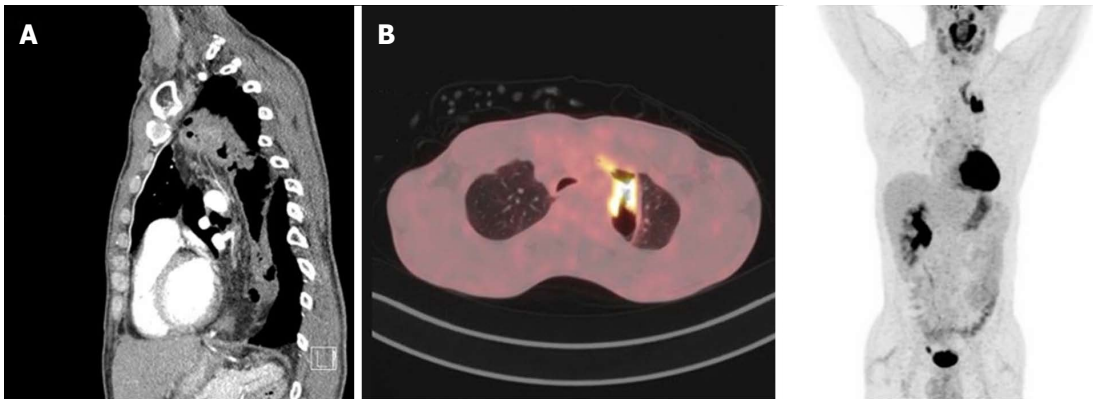

Figure 4 Initial findings at positron emission tomography-computed tomography scan (PET-CT scan) (case 4). A: Chest CT scan image with a circumferential wall thickening of the thoracic colonic interposition over a length of 10 cm, not clearly separated from the thyroid and left brachiocephalic vein. Locoregional suspected lymph nodes (< 1 cm). B: PET-CT scan showing a PET-positive lesion in the thoracic colonic interposition. No PET-positive lesions or lymph nodes.

CEA were normal (2.72 μg/L).

DISCUSSION

We presented four cases of gastrointestinal cancer that have developed more than 30 years after surgical treatment of EA: three esophageal carcinoma and one unusual presentation of colorectal carcinoma in a colonic interposition. These patients' relatively young age, the fact that only few carcinogenic factors were identified and the high incidence of cancer development in a low prevalence disease suggest that EA carries an increased risk for esophageal cancer development and therefore screening and surveillance may be warranted, as recommended in the ESPGHAN-NASPGHAN guideline[11].

Esophageal cancer is the 8th most common cancer worldwide, with an incidence rate of 6.4 and 1.2 per 100000 males and females respectively in developed countries and 10.1 and 4.1 per 100000 males and females, respectively, in less developed countries[17]. ESCC and EAC have different etiologies. ESCC arrises from dysplastic squamous epithelium and is associated with a low socioeconomic status, use of tobacco or alcohol, several dietary factors, and human papilloma virus[18,19]. The main risk factors for EAC are GER, use of tobacco, obesity, and hiatal hernia[18]. Chronic GER might lead to gastric and intestinal metaplasia of the squamous epithelium in the esophagus, known as Barrett's esophagus, which predisposes to dysplasia and EAC. GER is present in up to 67% of the adult EA patients and is likely to contribute to EAC development[5]. However, in literature - and also in our case series - ESCC is more common than EAC in EA patients[10,12-15]. The reason for this high risk of ESCC development has not yet been established. The pathogenesis might be the same as in achalasia, where ESCC is thought to result from stasis, causing bacterial overgrowth with nitrosamine production and subsequent esophageal inflammation, dysplasia and cancer[20,21]. Most of the ESCC in EA patients were found near or at the anastomosis (mid-distal esophagus). It has been suggested, therefore, that frequent dilation procedures with associated mucosal tears, scarring and inflammation may lead to development of ESCC in this patient group[10,12]. Mitomycin-C, an antifibrotic applicant used to prevent recurrence of strictures, may be an additional risk factor for ESCC, but this was not used in any of the patients in present case series[22]. Moreover, genetic predisposition may contribute to esophageal cancer in EA patients and is subject to future studies.

Endoscopic surveillance of EA patients is advocated to detect lesions at an early stage[11]. Those treated with a colonic interposition should not be excluded from surveillance, as carcinoma could arise in the cervical native esophagus or thoracic colon. More data on the actual incidence of esophageal cancer development in adulthood will hopefully become available soon when surveillance programs have been implemented. Together with the identification of risk factors this will help to optimize surveillance strategies in EA patients. Until then, pediatric surgeons and gastroenterologists who are involved in treatment of EA patients should be made aware of the cancer risk and be encouraged to reach consensus on optimal surveillance. When EA patients reach adulthood, they should be transferred to a gastroenterologist for endoscopic surveillance.

ARTICLE HIGHLIGHTS

Case characteristics

At presentation (age 36-47 years) all four patients born with esophageal atresia (EA) complained of progressive dysphagia, and two of them had lost weight.

Clinical diagnosis

Clinical diagnosis was made by upper endoscopy, revealing a for potentially malignant circular stenotic lesion in the esophagus in three cases and a tumor in the colonic interposition in one case.

Differential diagnosis

The differential diagnosis included severe ulcerative esophagitis, benign stenotic anastomosis, and motility disorder.

Laboratory diagnosis

Carcinoembryonic antigen (CEA) was measured (normal) in the patient with a colonic adenocarcinoma in the colonic interposition.

Imaging diagnosis

In addition to upper endoscopy a positron emission tomography-computed tomography scan (PET-CT scan) - in combination with endoscopic ultrasound in one case - was performed, which revealed a stenotic esophagus in three cases; a circumferential thickening of the colonic interposition in one case; potentially malignant lymph nodes in three cases; and suspected tumor invasion in two cases.

Pathological diagnosis

Histology and immunohistochemistry results confirmed the diagnosis of squamous cell carcinoma of the esophagus in three cases and adenocarcinoma of the colonic interposition in one case, in the latter case pentaplex microsatellite instability testing and mismatch repair gene expression analysis for MLH1, MSH2, MSH6 and PMS2 were normal.

Treatment

The esophageal cancer patients underwent (sub)total esophagectomy with reconstruction (curative intent); received induction chemotherapy (paclitaxel/carboplatin) followed by chemoradiotherapy (curative intent); or received palliative radiotherapy or chemotherapy. The patient with colon cancer was treated with induction chemotherapy (capecitabine/oxaliplatin) followed by resection of the colonic interposition with construction of an esophagostoma and jejunal fistula for feeding.

Related reports

Up to two-thirds of EA patients suffer from gastroesophageal reflux, which in the long-term might lead to mucosal damage including Barrett's esophagus and esophageal adenocarcinoma. As dysphagia is common (up to 72%) after EA repair, this symptom may be neglected as an early warning symptom of esophageal cancer in these patients. Up till now, eight esophageal cancer cases have been described in young EA patients.

Term explanation

EA with or without tracheoesophageal fistula (TEF) is a common congenital malformation and requires surgical correction early in life. The Gross classification divides five types of EA: type A (isolated EA), type B (EA with proximal TEF), type C (EA with distal TEF), type D (EA with dual TEF's) or type E (isolated TEF).

VACTERL is an acronym that describes a nonrandom association of birth defects: Vertebral anomalies, Anal atresia, Cardiac anomalies, TEF, Renal anomalies, and Limb defects.

Experiences and lessons

These patients' relatively young age, the fact that only few carcinogenic factors were identified and the high incidence of cancer development in a low prevalence disease suggest that EA carries an increased risk for esophageal cancer development. This emphasizes the importance of lifelong screening and surveillance of the upper gastrointestinal tract in EA patients.

REFERENCES

1 **Pedersen RN**, Calzolari E, Husby S, Garne E; EUROCAT Working group. Oesophageal atresia: prevalence, prenatal diagnosis and associated anomalies in 23 European regions. *Arch Dis Child* 2012; **97**: 227-232 [PMID: 22247246 DOI: 10.1136/archdischild-2011-300597]

2 **Wang B**, Tashiro J, Allan BJ, Sola JE, Parikh PP, Hogan AR, Neville HL, Perez EA. A nationwide analysis of clinical outcomes among newborns with esophageal atresia and tracheoesophageal fistulas in the United States. *J Surg Res* 2014; **190**: 604-612 [PMID: 24881472 DOI: S0022-4804(14)00433-8]

3 **Sulkowski JP**, Cooper JN, Lopez JJ, Jadcherla Y, Cuenot A, Mattei P, Deans KJ, Minneci PC. Morbidity and mortality in patients with esophageal atresia. *Surgery* 2014; **156**: 483-491 [PMID: 24947650 DOI: S0039-6060(14)00109-3]

4 **Rintala RJ**, Pakarinen MP. Long-term outcome of esophageal anastomosis. *Eur J Pediatr Surg* 2013; **23**: 219-225 [PMID: 23737132 DOI: 10.1055/s-0033-1347912]

5 **Vergouwe FW**, IJsselstijn H, Wijnen RM, Bruno MJ, Spaander MC. Screening and Surveillance in Esophageal Atresia Patients: Current Knowledge and Future Perspectives. *Eur J Pediatr Surg* 2015; **25**: 345-352 [PMID: 26302062 DOI: 10.1055/s-0035-1559817]

6 **Huynh Trudeau V**, Maynard S, Terzic T, Soucy G, Bouin M. Dysphagia among adult patients who underwent surgery for esophageal atresia at birth. *Can J Gastroenterol Hepatol* 2015; **29**: 91-94 [PMID: 25803019]

7 **Taylor AC**, Breen KJ, Auldist A, Catto-Smith A, Clarnette T, Crameri J, Taylor R, Nagarajah S, Brady J, Stokes K. Gastroesophageal reflux and related pathology in adults who were born with esophageal atresia: a long-term follow-up study. *Clin Gastroenterol Hepatol* 2007; **5**: 702-706 [PMID: 17544997 DOI: S1542-3565(07)00285-6]

8 **Sistonen SJ**, Koivusalo A, Nieminen U, Lindahl H, Lohi J, Kero M, Kärkkäinen PA, Färkkilä MA, Sarna S, Rintala RJ, Pakarinen MP. Esophageal morbidity and function in adults with repaired esophageal atresia with tracheoesophageal fistula: a population-based long-term follow-up. *Ann Surg* 2010; **251**: 1167-1173 [PMID: 20485152 DOI: 10.1097/SLA.0b013e3181c9b613]

9 **Sistonen SJ**, Koivusalo A, Lindahl H, Pukkala E, Rintala RJ, Pakarinen MP. Cancer after repair of esophageal atresia: population-based long-term follow-up. *J Pediatr Surg* 2008; **43**: 602-605 [PMID: 18405703 DOI: S0022-3468(07)00982-7]

10 **Jayasekera CS**, Desmond PV, Holmes JA, Kitson M, Taylor AC. Cluster of 4 cases of esophageal squamous cell cancer developing in adults with surgically corrected esophageal atresia--time for screening to start. *J Pediatr Surg* 2012; **47**: 646-651 [PMID: 22498376 DOI: S0022-3468(11)00837-2]

11 **Krishnan U**, Mousa H, Dall'Oglio L, Homaira N, Rosen R, Faure C, Gottrand F. ESPGHAN-NASPGHAN Guidelines for the Evaluation and Treatment of Gastrointestinal and Nutritional Complications in Children With Esophageal Atresia-Tracheoesophageal Fistula. *J Pediatr Gastroenterol Nutr* 2016; **63**: 550-570 [PMID: 27579697 DOI: 10.1097/MPG.0000000000001401]

12 **Deurloo JA**, van Lanschot JJ, Drillenburg P, Aronson DC. Esophageal squamous cell carcinoma 38 years after primary repair of esophageal atresia. *J Pediatr Surg* 2001; **36**: 629-630 [PMID: 11283893 DOI: S0022-3468(01)36587-9]

13 **Adzick NS**, Fisher JH, Winter HS, Sandler RH, Hendren WH. Esophageal adenocarcinoma 20 years after esophageal atresia repair. *J Pediatr Surg* 1989; **24**: 741-744 [PMID: 2769539 DOI: S0022346889002757]

14 **Alfaro L**, Bermas H, Fenoglio M, Parker R, Janik JS. Are patients who have had a tracheoesophageal fistula repair during infancy at risk for esophageal adenocarcinoma during adulthood? *J Pediatr Surg* 2005; **40**: 719-720 [PMID: 15852288 DOI: S0022346805000217]

15 **Pultrum BB**, Bijleveld CM, de Langen ZJ, Plukker JT. Development of an adenocarcinoma of the esophagus 22 years after primary repair of a congenital atresia. *J Pediatr Surg* 2005; **40**: e1-e4 [PMID: 16338286 DOI: S0022-3468(05)00647-0]

16 **Solomon BD**, Baker LA, Bear KA, Cunningham BK, Giampietro PF, Hadigan C, Hadley DW, Harrison S, Levitt MA, Niforatos N, Paul SM, Raggio C, Reutter H, Warren-Mora N. An approach to the identification of anomalies and etiologies in neonates with identified or suspected VACTERL (vertebral defects, anal atresia, tracheo-esophageal fistula with esophageal atresia, cardiac anomalies, renal

anomalies, and limb anomalies) association. *J Pediatr* 2014; **164**: 451-457.e1 [PMID: 24332453 DOI: 10.1016/j.jpeds.2013.10.086]

17 **Torre LA**, Bray F, Siegel RL, Ferlay J, Lortet-Tieulent J, Jemal A. Global cancer statistics, 2012. *CA Cancer J Clin* 2015; **65**: 87-108 [PMID: 25651787 DOI: 10.3322/caac.21262]

18 **Kamangar F**, Chow WH, Abnet CC, Dawsey SM. Environmental causes of esophageal cancer. *Gastroenterol Clin North Am* 2009; **38**: 27-57, vii [PMID: 19327566 DOI: S0889-8553(09)00006-5]

19 **Zhang SK**, Guo LW, Chen Q, Zhang M, Liu SZ, Quan PL, Lu JB, Sun XB. The association between human papillomavirus 16 and esophageal cancer in Chinese population: a meta-analysis. *BMC Cancer* 2015; **15**: 1096 [PMID: 25777422 DOI: 10.1186/s12885-015-1096-1]

20 **Sandler RS**, Nyrén O, Ekbom A, Eisen GM, Yuen J, Josefsson S. The risk of esophageal cancer in patients with achalasia. A population-based study. *JAMA* 1995; **274**: 1359-1362 [PMID: 7563560]

21 **Pajecki D**, Zilberstein B, Cecconello I, Dos Santos MA, Yagi OK, Gama-Rodrigues JJ. Larger amounts of nitrite and nitrate-reducing bacteria in megaesophagus of Chagas' disease than in controls. *J Gastrointest Surg* 2007; **11**: 199-203 [PMID: 17390173 DOI: 10.1007/s11605-006-0066-y]

22 **Chapuy L**, Pomerleau M, Faure C. Topical mitomycin-C application in recurrent esophageal strictures after surgical repair of esophageal atresia. *J Pediatr Gastroenterol Nutr* 2014; **59**: 608-611 [PMID: 24590215 DOI: 10.1097/MPG.0000000000000352]

P- Reviewer: De Lusong MAA, Thota PN, Wani HU
S- Editor: Gong ZM **L- Editor**: A **E- Editor**: Huang Y

Published by **Baishideng Publishing Group Inc**
7901 Stoneridge Drive, Suite 501, Pleasanton, CA 94588, USA
Telephone: +1-925-223-8242
Fax: +1-925-223-8243
E-mail: bpgoffice@wjgnet.com
Help Desk: http://www.f6publishing.com/helpdesk
http://www.wjgnet.com

ISSN 1007-9327

ISSN 1007-9327 (print)
ISSN 2219-2840 (online)

World Journal of *Gastroenterology*

World J Gastroenterol 2018 March 14; 24(10): 1063-1180

Published by Baishideng Publishing Group Inc

World Journal of Gastroenterology

Contents

Weekly Volume 24 Number 10 March 14, 2018

MINIREVIEWS

ORIGINAL ARTICLE

Basic Study

Retrospective Cohort Study

Retrospective Study

ABOUT COVER

Editorial board member of *World Journal of Gastroenterology*, Georgios Tsoulfas, MD, PhD, Associate Professor, Department of Surgery, Aristotle University of Thessaloniki, 66 Tsimiski St, Thessaloniki 54622, Greece

AIMS AND SCOPE

World Journal of Gastroenterology (*World J Gastroenterol*, *WJG*, print ISSN 1007-9327, online ISSN 2219-2840, DOI: 10.3748) is a peer-reviewed open access journal. *WJG* was established on October 1, 1995. It is published weekly on the 7th, 14th, 21st, and 28th each month. The *WJG* Editorial Board consists of 642 experts in gastroenterology and hepatology from 59 countries.

The primary task of *WJG* is to rapidly publish high-quality original articles, reviews, and commentaries in the fields of gastroenterology, hepatology, gastrointestinal endoscopy, gastrointestinal surgery, hepatobiliary surgery, gastrointestinal oncology, gastrointestinal radiation oncology, gastrointestinal imaging, gastrointestinal interventional therapy, gastrointestinal infectious diseases, gastrointestinal pharmacology, gastrointestinal pathophysiology, gastrointestinal pathology, evidence-based medicine in gastroenterology, pancreatology, gastrointestinal laboratory medicine, gastrointestinal molecular biology, gastrointestinal immunology, gastrointestinal microbiology, gastrointestinal genetics, gastrointestinal translational medicine, gastrointestinal diagnostics, and gastrointestinal therapeutics. *WJG* is dedicated to become an influential and prestigious journal in gastroenterology and hepatology, to promote the development of above disciplines, and to improve the diagnostic and therapeutic skill and expertise of clinicians.

INDEXING/ABSTRACTING

World Journal of Gastroenterology (*WJG*) is now indexed in Current Contents®/Clinical Medicine, Science Citation Index Expanded (also known as SciSearch®), Journal Citation Reports®, Index Medicus, MEDLINE, PubMed, PubMed Central and Directory of Open Access Journals. The 2018 edition of Journal Citation Reports® cites the 2016 impact factor for *WJG* as 3.365 (5-year impact factor: 3.176), ranking *WJG* as 29th among 79 journals in gastroenterology and hepatology (quartile in category Q2).

NAME OF JOURNAL
World Journal of Gastroenterology

ISSN
ISSN 1007-9327 (print)
ISSN 2219-2840 (online)

LAUNCH DATE
October 1, 1995

FREQUENCY
Weekly

EDITORIAL OFFICE
Ze-Mao Gong, Director
World Journal of Gastroenterology
Baishideng Publishing Group Inc
7901 Stoneridge Drive, Suite 501,
Pleasanton, CA 94588, USA
Telephone: +1-925-2238242
Fax: +1-925-2238243
E-mail: editorialoffice@wjgnet.com
Help Desk: http://www.f6publishing.com/helpdesk
http://www.wjgnet.com

PUBLISHER
Baishideng Publishing Group Inc
7901 Stoneridge Drive, Suite 501,
Pleasanton, CA 94588, USA
Telephone: +1-925-2238242
Fax: +1-925-2238243
E-mail: bpgoffice@wjgnet.com
Help Desk: http://www.f6publishing.com/helpdesk
http://www.wjgnet.com

PUBLICATION DATE
March 14, 2018

INSTRUCTIONS TO AUTHORS
Full instructions are available online at http://www.wjgnet.com/bpg/gerinfo/204

ONLINE SUBMISSION
http://www.f6publishing.com

World Journal of Gastroenterology

Submit a Manuscript: http://www.f6publishing.com

World J Gastroenterol 2018 March 14; 24(10): 1063-1071

DOI: 10.3748/wjg.v24.i10.1063

ISSN 1007-9327 (print) ISSN 2219-2840 (online)

MINIREVIEWS

Inflammatory bowel disease registries for collection of patient iron parameters in Europe

Jonas Halfvarson, Fraser Cummings, Olof Grip, Guillaume Savoye

Jonas Halfvarson, Department of Gastroenterology, Faculty of Medicine and Health, Örebro University, Örebro SE 70182, Sweden

Fraser Cummings, Department of Gastroenterology, Southampton University Hospital NHS Foundation Trust, Southampton, Hampshire SO16 6YD, United Kingdom

Olof Grip, Department of Gastroenterology, Skåne University Hospital, Malmö S-20502, Sweden

Guillaume Savoye, Service d'hépato-gastroentérologie, CHU de Rouen-Hôpital Charles Nicolle, Rouen 76031, France

ORCID number: Jonas Halfvarson (0000-0003-0122-7234); Fraser Cummings (0000-0002-9659-3247); Olof Grip (0000-0001-5033-7451); Guillaume Savoye (0000-0002-9200-2067).

Author contributions: All authors contributed equally to the conception and topics for this review and to revising the article critically for intellectual content; all authors approved the final version of the manuscript for submission.

Conflict-of-interest statement: Halfvarson J has received honoraria/grants from Abbvie, Celgene, Hospira, Janssen, Medivir, MSD, Pfizer, Sandoz, Takeda, Tillotts Pharma, and Vifor Pharma; Cummings F has received honoraria/grants from Biogen, Abbvie, Ferring, Hospira, Janssen, Pfizer, MSD, Napp, Pharmacosmos, Shield Therapeutics, Takeda, and Vifor Pharma; Grip O has received honoraria from Abbvie, Ferring, Janssen, Takeda, and Vifor Pharma; and Savoye G has received honoraria from HAC Pharma France, Pharmacosmos, and Vifor Pharma.

Manuscript source: Unsolicited manuscript

Correspondence to: Jonas Halfvarson, MD, PhD, Associate Professor, Department of Gastroenterology, Faculty of Medicine and Health, Örebro University, Örebro SE 70182, Sweden. jonas.halfvarson@regionorebrolan.se
Telephone: +46-19-303000
Fax: +46-19-6021774

Received: December 14, 2017
Peer-review started: December 15, 2017
First decision: December 27, 2017
Revised: February 2, 2018
Accepted: February 9, 2018
Article in press: February 9, 2018
Published online: March 14, 2018

Abstract

Iron deficiency without anemia and iron deficiency anemia are common and frequently overlooked complications of inflammatory bowel disease. Despite the frequency and impact of iron deficiency in inflammatory bowel disease, there are gaps in our understanding about its incidence, prevalence and natural history and, consequently, patients may be undertreated. Medical registries have a key role in collecting data on the disease's natural history, the safety and effectiveness of drugs in routine clinical practice, and the quality of care delivered by healthcare services. Even though iron deficiency impacts inflammatory bowel disease patients and healthcare systems substantially, none of the established European inflammatory bowel disease registries systematically collects information on iron parameters and related outcomes. Collection of robust iron parameter data from patient registries is one way to heighten awareness about the importance of iron deficiency in this disease and to generate data to improve the quality of patient care, patient outcomes, and thus quality of life. This objective could be achieved through collection of specific laboratory, clinical, and patient-

reported measurements that could be incorporated into existing registries. This review describes the status of current European inflammatory bowel disease registries and the data they generate, in order to highlight their potential role in collecting iron data, to discuss how such information gathering could contribute to our understanding of iron deficiency anemia, and to provide practical information in regard to the incorporation of accumulated iron parameter data into registries.

Key words: Anemia; Iron deficiency; Registries; Inflammatory bowel disease; Patient care

Core tip: Despite its prevalence, iron deficiency is often overlooked in inflammatory bowel disease (IBD). More data are required to fully understand the epidemiology, treatment, and quality of care around iron deficiency in IBD. We suggest that IBD registries are ideally positioned to collect these data from routine clinical practice. We discuss the laboratory, clinical, and patient-reported data that could be collected, and review how best to incorporate collection of these data into existing registries.

Halfvarson J, Cummings F, Grip O, Savoye G. Inflammatory bowel disease registries for collection of patient iron parameters in Europe. *World J Gastroenterol* 2018; 24(10): 1063-1071 Available from: URL: http://www.wjgnet.com/1007-9327/full/v24/i10/1063.htm DOI: http://dx.doi.org/10.3748/wjg.v24.i10.1063

INTRODUCTION

The current healthcare landscape relies heavily on controlled trials to generate evidence to support regulatory approval of new drugs and inform treatment of patients[1-4]. While scientifically rigorous, the applicability to everyday clinical situations might be questionable, since it does not necessarily include a cohort that is representative of the real-world patient population[5]. In contrast, registries have a key role in acquiring, maintaining, analyzing and, ultimately, publishing data that reveal how drugs are used in routine clinical practice. Medical registries can survey the demographics of patients with a particular medical condition, collect data on the use of a particular pharmaceutical product, class of products or use of a particular medical device, or be used to evaluate the quality of care delivered. Consequently, the use of national registries to generate real-world data is of great value, particularly in complex diseases such as inflammatory bowel disease (IBD), namely Crohn's disease and ulcerative colitis.

Iron deficiency anemia (IDA) is ranked as one of the world's ten leading causes of years lived with disability[6] and can manifest in a broad range of symptoms, including chronic fatigue, increased susceptibility to infection, tachycardia, sleep disturbance, impaired cognitive function, hair loss, and changes to skin and nails[7]. Iron deficiency without anemia (ID) and IDA are two of the most common systemic complications of IBD; estimates of prevalence indicate that ID occurs in 60%-80% of people with IBD, with the prevalence of anemia ranging from 16% to 74%[8].

For patients with IBD, IDA can be caused by a variety of factors[8] and affect a range of physical, personal, and social parameters, impairing work productivity and ultimately compounding the diminished quality of life (QoL) associated with IBD alone[9]. The economic burden of IBD is elevated by the presence of IDA; a retrospective review of healthcare claims data in the US estimated the direct treatment costs for each IBD patient to be substantially higher for those with anemia versus those without[10].

The natural history of IDA in IBD is not fully understood and its occurrence remains underestimated[11], so patients are potentially undertreated. The gaps in our understanding require comprehensive longitudinal data collection-an important source of which may be the collection of iron parameter data from patient registries. The objectives of this review article are to describe the status of current European IBD registries and the data they generate, to highlight the potential role of IBD registries in collecting IDA data and contributing to our understanding of IDA, and to provide practical information in regard to the incorporation of collated iron parameter data into IBD registries.

EXISTING REGISTRIES

Registry searches

A literature search was conducted to identify IBD registries that are currently collecting data in Europe, using the PubMed online database and internet searches. The search term "inflammatory bowel disease registry" was used and results were reviewed to identify articles meeting the inclusion criteria. The reference lists of any article meeting the inclusion criteria were reviewed manually to identify additional relevant publications. Where articles were identified, the name of the registry was used as a search term in the Google internet search engine in an attempt to find further relevant information. Where a web page did not provide information in English, translation software was used to determine if the information was relevant. For inclusion in this review, studies were required to have met the following criteria, in regard to the registry: (1) Being disease-specific with information on IBD; (2) being located in a European country; and (3) currently collecting data. Registries that were specific to treatment, and not disease, were excluded. Details of the registries identified are shown in Table 1. Note

Table 1 Examples of active inflammatory bowel disease registries in Europe

Name	Country	Year established	Description and aim	IBD Study population	Data collected
Competence Network IBD Registry[27]	Germany	2015	Scientists, physicians, clinics, research institutes, and industry with an interest in research to improve the care of patients with IBD	Approximately 50000 (anticipated)	IBD frequency and course; comorbidity incidence; efficacy of treatment; predictive parameters; subgroup characterization; outpatient vs inpatient costing; guideline implementation; service delivery
ENEIDA[28,29]	Spain	2006	Promotion of clinical and genetic studies in IBD, epidemiology of IBD, clinical outcomes, and drug safety in IBD treatment	> 11000	Patient demographics, disease classification, treatment outcomes and safety, phenotype, and family history of IBD
EPIMAD[18,30-34]	Northern France	1988	To provide reliable data on the epidemiology of IBD to healthcare authorities, provide data to search for a cause of disease, and describe in a population-based setting the natural history and real-life management of IBD	All IBD patients in region (approximately 20000 patients)	Patient demographics and disease data
SWIBREG[35]	Sweden	2005	To serve as a decision support tool in everyday life, assessing disease activity and quality of life	> 40000 (adult and pediatric)	Patient demographics and disease data, drug history, treatment and disease outcomes, surgical interventions, patient-reported outcomes. Capacity to enter information about comorbidities
SIBDC[12]	Switzerland	2005	To build understanding of the consequences of IBD on the physical, mental, and social conditions of IBD patients	Voluntary national database of > 2500 patients	Patient demographics, disease and treatment information. Patient blood samples are kept in a biobank providing a databank of genetic and disease information
UK IBD Registry[13]	United Kingdom	2013	To drive improvement in patient care and access to care across the United Kingdom, inform commissioning and service design, improve understanding of long, term outcomes in IBD, provide local, regional, and national data in order to better define the pattern of ulcerative colitis and Crohn's disease, and support IBD research	Approximately 20000 (adult and pediatric)	Patient demographics, disease data, any surgical interventions, drug history, treatment and disease outcomes, disease activity scores and patient-reported outcomes
Pediatric registries					
CEDATA[36]	Austria and Germany	2004	Developed and operated by the working group of chronic inflammatory bowel diseases of the Society for Pediatric Gastroenterology and Nutrition; aims to improve the care of children and adolescents with IBD.	Approximately 1000	Patient demographics, disease and treatment data
SPIRIT-IBD[37]	Spain	1996	To understand the incidence and prevalence of IBD in pediatric patients	Approximately 2000	Patient demographics, disease and treatment data
EUROKIDS[38,39]	Europe and Israel	2004	To audit the diagnostic workup of pediatric IBD patients and to accurately describe disease in newly diagnosed pediatric IBD patients	Approximately 4000	Patient demographics, disease and treatment data

IBD: Inflammatory bowel disease; IDA: Iron deficiency anemia.

that the list of identified registries presented here may not be exhaustive, as small local or regional registries may not be visible to such a search, and this work is not intended to be a complete systematic review.

Data collected by European registries on IBD

Items common to the IBD registries include: number of patients with IBD in the region covered, information on clinical characteristics, medication, treatment effectiveness,

Table 2 Suggested iron deficiency anemia-related parameters to collect in an inflammatory bowel disease registry

Laboratory measurements
Hemoglobin level
Serum ferritin level
Transferrin saturation level
Soluble transferrin receptor level
Hepcidin
Mean corpuscular volume
Mean corpuscular hemoglobin
C-reactive protein level
Clinical observations
Identification of ID/IDA-related symptoms
Duration of possible ID/IDA-related symptoms
Number of, duration of, and reasons for healthcare visits
Medication usage
Patient-reported outcomes
Quality-of-life questionnaires
Fatigue questionnaires
Work productivity and activity questionnaires
Treatment decisions
Iron supplement (oral or IV)
IBD medication
Surgical procedures

IBD: Inflammatory bowel disease; IDA: Iron deficiency anemia.

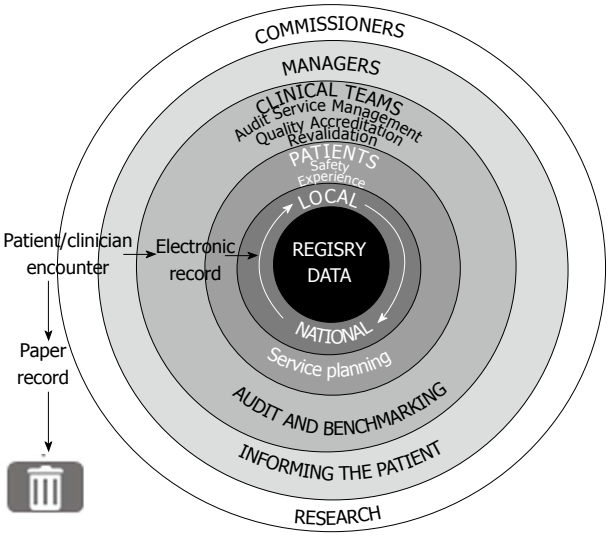

Figure 1 Data recorded at the point of care on an electronic system can be used to achieve a wide range of local and national objectives.

and service delivery. Some information is registry specific, such as biobanking of blood samples for genotyping, as within the Swiss cohort[12]. It is notable that, despite the prevalence of ID/IDA among IBD patients, none of the registries identified explicitly were collecting information on iron parameters and related outcomes in a systematic manner at the time of this review.

The approach to data collection and verification varies among registries. For example, in EPIMAD (Registre des Maladies Inflammatoires Chroniques de l'Intestin du Nord Ouest de la France), data are collected by interviewer practitioners when possible cases of IBD are identified, and a diagnosis of IBD is verified by two expert practitioners. Each patient can be followed, if necessary, for 2 years until a final diagnosis is confirmed. In contrast, the UK IBD Registry utilizes electronic data-entry systems, such that data are collected in real time at the point of care (Figure 1). Some of the data-entry tools allow for the upload of laboratory data directly into the system, such that, after negotiations with the relevant providers, iron parameters could be added to the data collected with relative ease[13]. Similarly, the Swedish Quality Registry for Inflammatory Bowel Disease (SWIBREG) - which is notable in being well established and in covering half of the Swedish IBD population-can be linked to other national registers to evaluate etiology, prognosis, and outcomes of different treatment modalities[14].

Despite the coverage of these registries, the initial research questions used, the configuration of data-collection systems, and available resources (both financial and personnel) all impose limits on the data they can gather. Information about medications to treat conditions concomitant to IBD, such as ID and IDA, may not be captured. Similarly, the collection and inclusion of patient-reported outcome (PRO) data in existing IBD registries is not a trivial undertaking. Given the importance of ID-related symptoms, the collection and analysis of PRO questionnaires is important and should be considered.

HOW SHOULD IDA-RELATED DATA BE COLLECTED IN IBD REGISTRIES?

Although national healthcare databases collect and store data from blood tests on anemias, ID, and the drugs used in their treatment, they do not seem to be an appropriate way to collect data on IDA in IBD. In general, such databases are optimized to collect high-level administrative data, and do not describe IBD patients adequately to offer the level of medical detail needed to research the natural history of disease. This is also the case for databases owned by agencies involved in reimbursement of medical treatment. From this, a clear need for prospective and specific collection of iron parameter data can be established, which may be achieved through the adaptation of existing IBD registries.

Even though IDA and ID are common in IBD, and exert a substantial burden on patients and healthcare systems[8-10], none of the established European IBD registries systematically collects information on iron parameters and related outcomes. Addressing this shortfall in data collection requires examination of the primary objectives of the registries in question, and consideration of parameters that could answer further research questions around this objective. The parameters collected would be determined by the type of registry (condition-, product-, or service-based) and should serve its primary research objective; suggestions

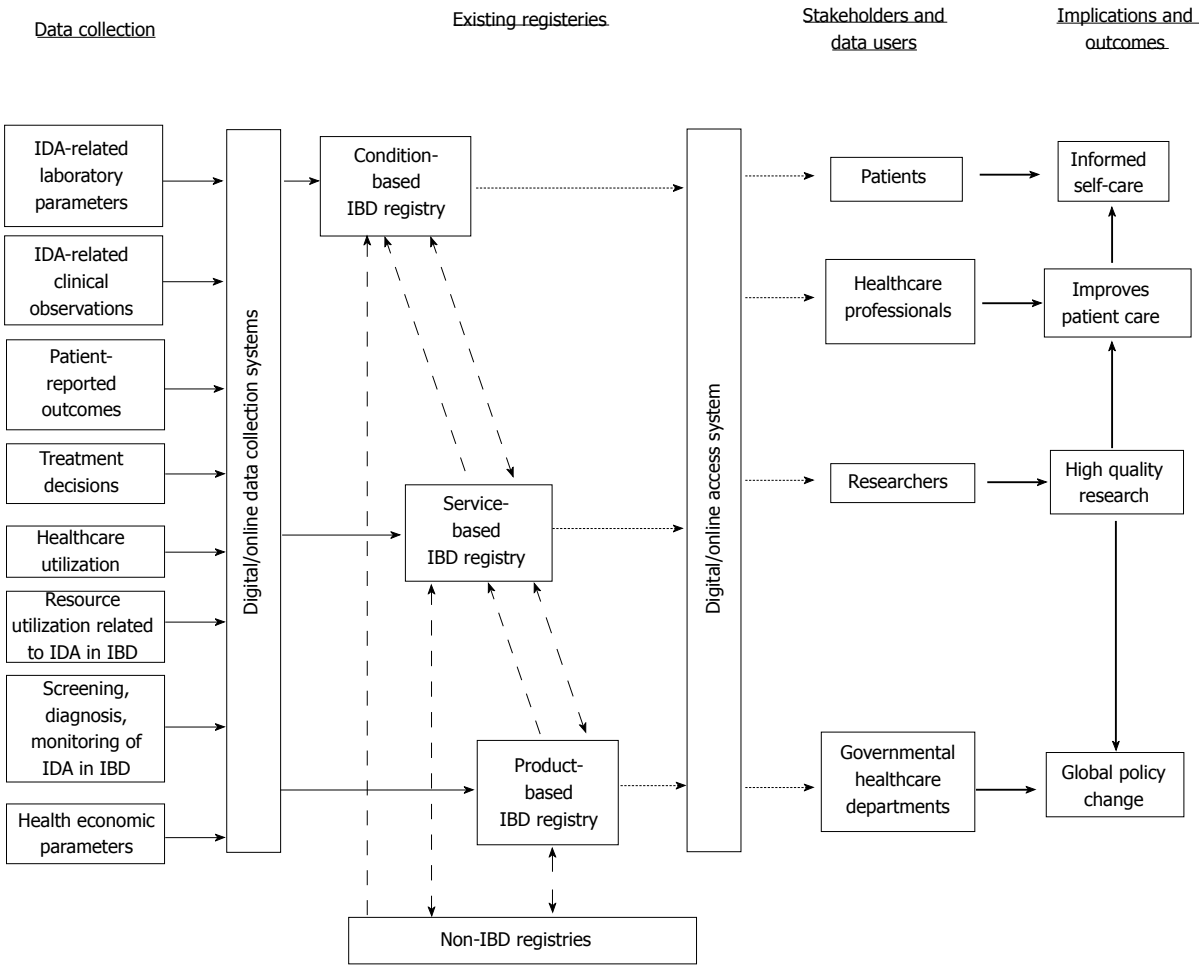

Figure 2 Collection and flow of data between existing healthcare registries to support various outcomes for multiple stakeholders. Solid line: flow of patient-level data; dashed line: flow of pseudo-anonymized data; dash-dot line: flow of aggregated anonymized data; block arrows, overall and relationships between implications. IBD: Inflammatory bowel disease; IDA: Iron deficiency anemia.

are listed in Table 2.

A condition-based registry designed to monitor epidemiology of IBD could also collect data to provide snapshots of the prevalence and severity of IDA. Longitudinal analyses of IDA duration and disease course, with the potential to identify commonly associated factors-including ID-related burden occurring during pregnancy-could also be included. To chronicle the natural history of IDA, it is necessary to collect longitudinal information on clinical, biochemical and endoscopic disease activity; data from imaging techniques such as magnetic resonance imaging should ideally be included. In line with the current European Crohn's and Colitis Organisation (ECCO) consensus on the diagnosis and management of ID with and without anemias in IBD[15], a basic dataset may comprise hemoglobin levels, transferrin saturation and serum ferritin levels, and perhaps mean corpuscular volume and mean corpuscular hemoglobin. Measuring C-reactive protein would inform the interpretation of serum ferritin levels, which may be elevated by inflammation. Recording the levels of individual iron parameters (rather than a diagnosis of anemia) would offer a more detailed view of ID and the capacity to investigate concepts such as absolute and functional ID[15]. To further understand the impact that ID and IDA have on disease course and its influence on the response to treatment the registry would need to collect medication history and validated disease activity scores/PROs that evaluate fatigue, QoL, and impaired productivity. Fatigue is a key symptom of ID (and of IBD) and can be quantified using a validated scoring system such as the functional assessment of chronic illness therapy-fatigue (FACIT-F)-Fatigue questionnaire[16]. There are several tools available to measure QoL in patients with IBD or, more recently, disability[17,18], although these do not necessarily distinguish between the burden of ID/IDA and IBD.

A product-based registry (focused on IBD treatment) could be used to monitor use of iron supplements. Information on prescribed iron replacement therapy, including doses, may be recorded as either oral or intravenous, to illustrate any impact of a different choice of iron administration route.

A service-based registry would typically have a different dataset, including information on the use of healthcare (including hospitalizations and surgery),

and the resource utilization attributable to ID and IDA in IBD. Collection of data on screening, diagnosis, and monitoring of ID and IDA in IBD could offer a perspective on aspects of quality of care, with reference to the recommendations of the European Consensus on the Diagnosis and Management of Iron Deficiency and Anaemia in Inflammatory Bowel Diseases[15]. If an economic perspective is deemed valuable, observations on impaired work productivity and activity can be collected, as well as information on absences from work or full-time education, healthcare attendance, need for surgery, and medication adherence and persistence.

A registry would ideally use appropriate digital and online technologies to make it easier for sites to contribute data, including enabling data entry at point of care and a facility for patients to submit disease-related information. Incentives for teams to use these technologies might include the opportunity to deliver data-driven care to patients. Patients may also be given access to presentations of these data to facilitate supported self-management, and improve patient participation and empowerment. An example of success in this area is Improve Care Now-a network of people from 95 care centers in the United States, Qatar, and United Kingdom that has the objective of improving the health, care, and costs for children and adolescents with IBD[19]. The centers involved in this initiative collect data about treatment and performance in a standardized format; the tools for best practice in the treatment of these patients, with the related evidence, is shared within the network, leading to substantial improvements in patient outcomes and better patient safety[20].

Cross-registry interoperability and integration, to facilitate sharing of data with existing healthcare systems and resources, would be highly beneficial; Figure 2 illustrates a potential model for how data could move between registries and shows the potential outcomes for stakeholders. Collection and incorporation of unique pseudoanonymized national personal identifiers of patients enables connections to be made between registries. IDA is prevalent in patients with renal disease, heart disease, and cancer, and can affect cognitive development/function and resistance to infection[21,22]. Correlation between disease registries in IBD, oncology, heart failure, and mental health could offer completely new perspectives on improving the multidisciplinary care of patients with ID. Further connections could be made with drug prescription databases with the intention of correlating disease outcomes with specific treatment information. Linkage of an IBD registry with national service-based registries could show the frequency of outpatient visits, inpatient care, surgery, and co-existing disease, based on the international classification of disease codes. Linkage with mortality databases would provide an additional view of disease outcomes. A potential barrier to sharing of data is the governance issues around information. Any such sharing should comply with the registry's ethical requirements and national laws covering data protection. If there are restrictions on exporting personal data from the country, steps must be taken to anonymize and aggregate the information. It is also important to understand exactly what is of interest to a collaborating registry, and to identify and characterize all variables collected, as these may vary between registries[14].

HOW CAN EXISTING IBD REGISTRIES BE ADAPTED TO COLLECT IDA-RELATED PARAMETERS?

The current IBD registries are positioned well to collect iron parameter data and link these with IBD-specific data. Although it is beyond the scope of this article to provide detailed guidance on adapting a registry to collect a new set of variables, there are several factors that should be considered, in regard to the prospective collection of iron parameters in an IBD registry. Initially, it is important to consider the change in scope of a registry, in terms of its expected redefined purpose, objectives, and overall outputs. While it may be tempting to maximize the opportunities for data collection, this must be balanced against the importance of collecting high-quality, reliable data with no significant increased burden associated with their entry to the database. Limiting the scope of a registry ensures that specific objectives and well-defined research questions can be established in order to specify what outputs should be sought. Defining and confirming the scope of any changes with all stakeholders will optimize the work needed as the changes to the registry are implemented. When the objectives have been clearly established, the data to be collected can then be determined. The data collection method should suit the data type. The practicalities of incorporating collection of iron parameters into an existing IBD registry could present a challenge, as it would depend on the healthcare system in which the registry operates. Ideally, the addition of new parameters to a registry should not generate substantially more work for sites contributing to the registry. With the introduction of electronic medical records and network integration it is theoretically possible for iron parameter data from medical laboratories to be automatically added to a medical record and uploaded to a registry database. This would greatly minimize the resources needed for data entry, avoiding the review and entry of information from unstructured case notes, and circumventing double entry of data. However, there are currently barriers to this approach. Firstly, retrieval of data from laboratory service providers requires negotiation, financial commitment, and often improvement of IT facilities. This problem is magnified if a country has multiple service providers, each of which is presenting data in a proprietary format, thus requiring a large amount of interface development work. Secondly, the use of electronic medical records is still not widely used, and standards of interoperability are yet to be

established. The functioning of a registry could be complicated if data source inputs present information in a range of formats that have to be interpreted before they can be used. Many commercial providers offer digital and online interfaces to facilitate data capture in a registry; however, there can be great variation between them in terms of financial cost, ease-of-use, and features (not all of which may be necessary or relevant to an individual registry)[23]. Indeed, the quality and capabilities of different software used to manage data in clinical studies and registries can vary greatly, raising barriers in interoperability and evaluation of data across studies[24]. Open-source software offers an alternative that is both low-cost and can be modified by researchers to suit specific requirements[24]. A key role for national and international registries would be to define data submission frameworks that enable the entry of data from a range of different sources.

The rise in health technologies that are accessible from personal mobile devices is likely to have an important role in collection of PROs. Electronic PRO data collection has many advantages relating to easy, accurate, and complete collection of data that is potentially of great value to investigators and healthcare systems[25]. In the context of a registry, as opposed to a clinical trial, it may make sense for a patient to be able to complete PRO information using their own mobile device, rather than attending an appointment. Although this adds a level of convenience for both patient and healthcare team, a number of barriers still remain including data security, patient compliance with data collection, and what to do if a patient does not possess a suitable device[25]. Nevertheless, ePROs show promise; indeed, pilot studies of an electronic data submission method implemented by the SWIBREG registry have proved successful and its launch is imminent in some regions in Sweden. A UK study to collect ePROs in an elective orthopedic setting showed great promise, gathering reliable data but also highlighting that the ePRO system may not be adequate for some patients[26].

The incorporation of iron parameter data into European IBD registries offers great opportunities to improve the care of IBD patients. Firstly, highlighting the prevalence of IDA in the IBD population would show the unmet need in this patient group in countries across Europe. It is notable that the ECCO guidelines for diagnosis and management of ID and IDA in IBD recommend that all patients with IBD should be assessed for the presence of anemia[15]. Robust data are necessary to heighten awareness of the importance of IDA in IBD and to lobby healthcare systems to improve access to the full range of iron supplementation therapies. Secondly, longitudinal analysis of iron parameters and treatment could offer a perspective to assess some aspects of the quality of care that patients receive, including the management of IDA and ID, as well as the numbers of patients who receive optimal treatment. Thirdly, the inclusion of QoL information and PROs would offer perspectives on how optimal treatment could change the burden of IDA on the patient, as well as potentially providing economic arguments for the use of iron supplementation. Finally, the information collected could inform service planning at the local and national level, including on how resources should be managed to provide improved access to nursing support or access to infusion suites. Periodic assessment of the data collected in national registries would also provide information needed for clinical audits and quality improvement programs.

Beyond the local and national level, the collection and comparison of iron parameters by multiple registries would allow the relationship between IBD and IDA to be examined from different perspectives, stemming from each registry's specific remit, leading to the generation of new research questions and ultimately improving patient care. A further possibility would be the pooling of data between national registries to identify and study any differences in patterns of disease, and to compare practices in healthcare service delivery. A very large dataset should also able to highlight any rare effects that might not be evident from a single national registry. This initiative would, of course, require agreement on the collection of a basic dataset and standardization of methodologies, as well as addressing how data should be anonymized and aggregated to comply with the legal aspects of sharing data across national borders.

CONCLUSION

Iron deficiency and IDA are common and often overlooked complications of IBD. Historically, ID and IDA have been accepted as part of IBD, and not as an issue to be addressed and treated independently. The prevailing attitude was that treatment of IBD would lead to the resolution of anemia, so organized research efforts to understand ID in patients with IBD were minimal. In recent years, however, opinion has shifted, with a growing acknowledgement that ID/IDA is an issue to be managed concomitantly with IBD. A recent consensus statement provides up-to-date guidance on the diagnosis, treatment and prevention of ID/IDA in IBD[15]. Despite the frequency and impact of ID and IDA in IBD, there are gaps in our understanding about its incidence, prevalence, natural history, and particularly its impact on patients. Due to similarities between symptoms of IBD and ID/IDA, the identification of ID/IDA-specific symptoms in the IBD population is necessary. There is, therefore, a clear need to collect robust, structured data around ID/IDA in IBD, its treatment, and on related service delivery. Despite potential limitations (possible selection bias and potential variability in data quality), it has been suggested that 'real-world' data have a greater applicability to the routine clinical setting than the findings of controlled trials[5]. Current digital technologies and networking capabilities raise the prospect of an acquisition and analysis of real-world

data that is (and should be) easier than ever before. With appropriate planning, information governance structures, adaptation, and negotiation, registries are ideally placed to collect this information in a routine clinical practice setting. The direct input by patients of self-reported data can capture and quantify symptoms such as fatigue and cognitive impairment, which can otherwise be difficult to evaluate. If multiple registries were to commence collection of ID/IDA data in IBD as a standard, there would be an opportunity to compare and pool data collected from multiple sources. Although this endeavor would be challenging, the ultimate benefit to the care of patients with IBD would be substantial.

ACKNOWLEDGEMENTS

Vifor Pharma provided funding for an initial meeting of authors at which the content of this article was discussed. Under the direction of the authors, AXON Communications provided writing and editorial, assistance in formatting, proofreading, copy editing and fact checking, funded by Vifor Pharma.

REFERENCES

1 **Gionchetti P**, Dignass A, Danese S, Magro Dias FJ, Rogler G, Lakatos PL, Adamina M, Ardizzone S, Buskens CJ, Sebastian S, Laureti S, Sampietro GM, Vucelic B, van der Woude CJ, Barreiro-de Acosta M, Maaser C, Portela F, Vavricka SR, Gomollón F; ECCO. 3rd European Evidence-based Consensus on the Diagnosis and Management of Crohn's Disease 2016: Part 2: Surgical Management and Special Situations. *J Crohns Colitis* 2017; **11**: 135-149 [PMID: 27660342 DOI: 10.1093/ecco-jcc/jjw169]

2 **Gomollón F**, Dignass A, Annese V, Tilg H, Van Assche G, Lindsay JO, Peyrin-Biroulet L, Cullen GJ, Daperno M, Kucharzik T, Rieder F, Almer S, Armuzzi A, Harbord M, Langhorst J, Sans M, Chowers Y, Fiorino G, Juillerat P, Mantzaris GJ, Rizzello F, Vavricka S, Gionchetti P; ECCO. 3rd European Evidence-based Consensus on the Diagnosis and Management of Crohn's Disease 2016: Part 1: Diagnosis and Medical Management. *J Crohns Colitis* 2017; **11**: 3-25 [PMID: 27660341 DOI: 10.1093/ecco-jcc/jjw168]

3 **Harbord M**, Eliakim R, Bettenworth D, Karmiris K, Katsanos K, Kopylov U, Kucharzik T, Molnár T, Raine T, Sebastian S, de Sousa HT, Dignass A, Carbonnel F; European Crohn's and Colitis Organisation [ECCO]. Third European Evidence-based Consensus on Diagnosis and Management of Ulcerative Colitis. Part 2: Current Management. *J Crohns Colitis* 2017; **11**: 769-784 [PMID: 28513805 DOI: 10.1093/ecco-jcc/jjx009]

4 **Magro F**, Gionchetti P, Eliakim R, Ardizzone S, Armuzzi A, Barreiro-de Acosta M, Burisch J, Gecse KB, Hart AL, Hindryckx P, Langner C, Limdi JK, Pellino G, Zagórowicz E, Raine T, Harbord M, Rieder F; European Crohn's and Colitis Organisation [ECCO]. Third European Evidence-based Consensus on Diagnosis and Management of Ulcerative Colitis. Part 1: Definitions, Diagnosis, Extra-intestinal Manifestations, Pregnancy, Cancer Surveillance, Surgery, and Ileo-anal Pouch Disorders. *J Crohns Colitis* 2017; **11**: 649-670 [PMID: 28158501 DOI: 10.1093/ecco-jcc/jjx008]

5 **Silverman SL**. From randomized controlled trials to observational studies. *Am J Med* 2009; **122**: 114-120 [PMID: 19185083 DOI: 10.1016/j.amjmed.2008.09.030]

6 **GBD 2015 Disease and Injury Incidence and Prevalence Collaborators**. Global, regional, and national incidence, prevalence, and years lived with disability for 310 diseases and injuries, 1990-2015: a systematic analysis for the Global Burden of Disease Study 2015. *Lancet* 2016; **388**: 1545-1602 [PMID: 27733282 DOI: 10.1016/S0140-6736(16)31678-6]

7 **Ghosh K**. Non haematological effects of iron deficiency - a perspective. *Indian J Med Sci* 2006; **60**: 30-37 [PMID: 16444088 DOI: 10.4103/0019-5359.19676]

8 **Stein J**, Dignass AU. Management of iron deficiency anemia in inflammatory bowel disease - a practical approach. *Ann Gastroenterol* 2013; **26**: 104-113 [PMID: 24714874]

9 **Danese S**, Hoffman C, Vel S, Greco M, Szabo H, Wilson B, Avedano L. Anaemia from a patient perspective in inflammatory bowel disease: results from the European Federation of Crohn's and Ulcerative Colitis Association's online survey. *Eur J Gastroenterol Hepatol* 2014; **26**: 1385-1391 [PMID: 25264983 DOI: 10.1097/MEG.0000000000000200]

10 **Ershler WB**, Chen K, Reyes EB, Dubois R. Economic burden of patients with anemia in selected diseases. *Value Health* 2005; **8**: 629-638 [PMID: 16283863 DOI: 10.1111/j.1524-4733.2005.00058.x]

11 **Stein J**, Bager P, Befrits R, Gasche C, Gudehus M, Lerebours E, Magro F, Mearin F, Mitchell D, Oldenburg B, Danese S. Anaemia management in patients with inflammatory bowel disease: routine practice across nine European countries. *Eur J Gastroenterol Hepatol* 2013; **25**: 1456-1463 [PMID: 24100539 DOI: 10.1097/MEG.0b013e328365ca7f]

12 **Swiss IBD Cohort (SIBDC)**. Zurich: Department of Gastroenterology and Hepatology, Department of Internal Medicine, University Hospital of Zurich. [cited July 31, 2017]. 2017 Available from: URL: http://www.ibdcohort.ch/

13 **The UK IBD Registry**. London: British Society of Gastroenterology; 2017 [cited July 31, 2017]. Available from: URL: http://ibdregistry.org.uk/

14 **Brooke H**, Holzmann M, Olén O, Talbäck M, Feychting M, Berglund A, Ludvigsson J, Ljung R. Enhancing evidence based medicine: Twelve tips for conducting register-based research. *MedEdPublish* 2016; **5**: 43 [DOI: 10.15694/mep.2016.000071]

15 **Dignass AU**, Gasche C, Bettenworth D, Birgegård G, Danese S, Gisbert JP, Gomollon F, Iqbal T, Katsanos K, Koutroubakis I, Magro F, Savoye G, Stein J, Vavricka S; European Crohn's and Colitis Organisation [ECCO]. European consensus on the diagnosis and management of iron deficiency and anaemia in inflammatory bowel diseases. *J Crohns Colitis* 2015; **9**: 211-222 [PMID: 25518052 DOI: 10.1093/ecco-jcc/jju009]

16 **Tinsley A**, Macklin EA, Korzenik JR, Sands BE. Validation of the functional assessment of chronic illness therapy-fatigue (FACIT-F) in patients with inflammatory bowel disease. *Aliment Pharmacol Ther* 2011; **34**: 1328-1336 [PMID: 21999576 DOI: 10.1111/j.1365-2036.2011.04871.x]

17 **Alrubaiy L**, Rikaby I, Dodds P, Hutchings HA, Williams JG. Systematic review of health-related quality of life measures for inflammatory bowel disease. *J Crohns Colitis* 2015; **9**: 284-292 [PMID: 25576752 DOI: 10.1093/ecco-jcc/jjv002]

18 **Gower-Rousseau C**, Sarter H, Savoye G, Tavernier N, Fumery M, Sandborn WJ, Feagan BG, Duhamel A, Guillon-Dellac N, Colombel JF, Peyrin-Biroulet L; and the International Programme to Develop New Indexes for Crohn's Disease (IPNIC) group; International Programme to Develop New Indexes for Crohn's Disease (IPNIC) group. Validation of the Inflammatory Bowel Disease Disability Index in a population-based cohort. *Gut* 2017; **66**: 588-596 [PMID: 26646934 DOI: 10.1136/gutjnl-2015-310151]

19 **Improve Care Now [internet]**; 2017 [cited July 31, 2017]. Available from: URL: http://www.improvecarenow.org/

20 **Crandall WV**, Margolis PA, Kappelman MD, King EC, Pratt JM, Boyle BM, Duffy LF, Grunow JE, Kim SC, Leibowitz I, Schoen BT, Colletti RB; ImproveCareNow Collaborative. Improved outcomes in a quality improvement collaborative for pediatric inflammatory bowel disease. *Pediatrics* 2012; **129**: e1030-e1041 [PMID: 22412030 DOI: 10.1542/peds.2011-1700]

21 **Abbaspour N**, Hurrell R, Kelishadi R. Review on iron and its importance for human health. *J Res Med Sci* 2014; **19**: 164-174 [PMID: 24778671]

22 **Peyrin-Biroulet L**, Williet N, Cacoub P. Guidelines on the diagnosis and treatment of iron deficiency across indications: a

systematic review. *Am J Clin Nutr* 2015; **102**: 1585-1594 [PMID: 26561626 DOI: 10.3945/ajcn.114.103366]
23 **Shah J**, Rajgor D, Pradhan S, McCready M, Zaveri A, Pietrobon R. Electronic Data Capture for Registries and Clinical Trials in Orthopaedic Surgery: Open Source versus Commercial Systems. *Clin Orthop Relat Res* 2010; **468**: 2664-2671 [PMID: 20635174 DOI: 10.1007/s11999-010-1469-3]
24 **Müller J**, Heiss KI, Oberhoffer R. Implementation of an open adoption research data management system for clinical studies. *BMC Res Notes* 2017; **10**: 252 [PMID: 28683771 DOI: 10.1186/s13104-017-2566-0]
25 **Coons SJ**, Eremenco S, Lundy JJ, O'Donohoe P, O'Gorman H, Malizia W. Capturing Patient-Reported Outcome (PRO) Data Electronically: The Past, Present, and Promise of ePRO Measurement in Clinical Trials. *Patient* 2015; **8**: 301-309 [PMID: 25300613 DOI: 10.1007/s40271-014-0090-z]
26 **Malhotra K**, Buraimoh O, Thornton J, Cullen N, Singh D, Goldberg AJ. Electronic capture of patient-reported and clinician-reported outcome measures in an elective orthopaedic setting: a retrospective cohort analysis. *BMJ Open* 2016; **6**: e011975 [PMID: 27324718 DOI: 10.1136/bmjopen-2016-011975]
27 **Competence Network Inflammatory Bowel Disease**. Call for tenders for the Project: Long-term Observation of Patients with Chronic Inflammatory Bowel Disease: Establishment of a Registry [information document]. [cited July 31, 2017]. Kiel: Competence Network Inflammatory Bowel Disease, 2013 Available from: URL: http://www.kompetenznetz-ced.de/Aktuelle_Meldung/items/ausschreibung-zur-einrichtung-eines-nationalen-ced-registers-91.html?file=tl_files/Downloads/PDF/Presse/2014/Ausschreibung_Langzeitregister_KN%20CED.pdf
28 Grupo Espanol de Trabajo en Enfermdad de Crohn y Colitis Ulcerosa [Internet]. Bilbao: Grupo Espanol de Trabajo en Enfermdad de Crohn y Colitis Ulcerosa [internet]; 2016 Características y objetivos de ENEIDA [Features and objectives of ENEIDA]. [cited July 31, 2017]. Available from: URL: http://geteccu.org/eneida/caracteristicas-y-objetivos-de-eneida
29 **Andreu M**, Márquez L, Domènech E, Gisbert JP, García V, Marín-Jiménez I, Peñalva M, Gomollón F, Calvet X, Merino O, Garcia-Planella E, Vázquez-Romero N, Esteve M, Nos P, Gutiérrez A, Vera I, Cabriada JL, Martín MD, Cañas-Ventura A, Panés J; Spanish GETECCU group (ENEIDA project). Disease severity in familial cases of IBD. *J Crohns Colitis* 2014; **8**: 234-239 [PMID: 24016462 DOI: 10.1016/j.crohns.2013.08.010]
30 **Charpentier C**, Salleron J, Savoye G, Fumery M, Merle V, Laberenne JE, Vasseur F, Dupas JL, Cortot A, Dauchet L, Peyrin-Biroulet L, Lerebours E, Colombel JF, Gower-Rousseau C. Natural history of elderly-onset inflammatory bowel disease: a population-based cohort study. *Gut* 2014; **63**: 423-432 [PMID: 23408350 DOI: 10.1136/gutjnl-2012-303864]
31 **Chouraki V**, Savoye G, Dauchet L, Vernier-Massouille G, Dupas JL, Merle V, Laberenne JE, Salomez JL, Lerebours E, Turck D, Cortot A, Gower-Rousseau C, Colombel JF. The changing pattern of Crohn's disease incidence in northern France: a continuing increase in the 10- to 19-year-old age bracket (1988-2007). *Aliment Pharmacol Ther* 2011; **33**: 1133-1142 [PMID: 21488915 DOI: 10.1111/j.1365-2036.2011.04628.x]
32 **Gower-Rousseau C**, Savoye G, Colombel JF, Peyrin-Biroulet L. Are we improving disease outcomes in IBD? A view from the epidemiology side. *Gut* 2014; **63**: 1529-1530 [PMID: 24287275 DOI: 10.1136/gutjnl-2013-306045]
33 **Gower-Rousseau C**, Vasseur F, Fumery M, Savoye G, Salleron J, Dauchet L, Turck D, Cortot A, Peyrin-Biroulet L, Colombel JF. Epidemiology of inflammatory bowel diseases: new insights from a French population-based registry (EPIMAD). *Dig Liver Dis* 2013; **45**: 89-94 [PMID: 23107487 DOI: 10.1016/j.dld.2012.09.005]
34 **Penninck E**, Fumery M, Armengol-Debeir L, Sarter H, Savoye G, Turck D, Pineton de Chambrun G, Vasseur F, Dupas JL, Lerebours E, Colombel JF, Peyrin-Biroulet L, Gower-Rousseau C; EPIMAD Group. Postoperative Complications in Pediatric Inflammatory Bowel Disease: A Population-based Study. *Inflamm Bowel Dis* 2016; **22**: 127-133 [PMID: 26355466 DOI: 10.1097/mib.0000000000000576]
35 **Jakobsson GL**, Sternegård E, Olén O, Myrelid P, Ljung R, Strid H, Halfvarson J, Ludvigsson JF. Validating inflammatory bowel disease (IBD) in the Swedish National Patient Register and the Swedish Quality Register for IBD (SWIBREG). *Scand J Gastroenterol* 2016; **52**: 216-221 [PMID: 27797278 DOI: 10.1080/00365521.2016.1246605]
36 Gesellschaft für Pädiatrische Gastroenterologie und Ernährung[internet]. Berlin: Gesellschaft für Pädiatrische Gastroenterologie und Ernährung; 2017 CEDATA-GPGE. [cited July 31, 2017]. Available from: URL: http://www.gpge.de/cedata-gpge/
37 **Martín-de-Carpi J**, Rodríguez A, Ramos E, Jiménez S, Martínez-Gómez MJ, Medina E; SPIRIT-IBD Working Group of Sociedad Española de Gastroenterología, Hepatología y Nutricion Pediátrica. Increasing incidence of pediatric inflammatory bowel disease in Spain (1996-2009): the SPIRIT Registry. *Inflamm Bowel Dis* 2013; **19**: 73-80 [PMID: 22535573 DOI: 10.1002/ibd.22980]
38 European Society for Paediatric Gastroenterology, Hepatology and Nutrition[internet]. 2017 Paediatric and adolescent inflammatory bowel diseases [cited July 31, 2017] Available from: URL: http://www.espghan.org/about-espghan/committees/gastroenterology/working-groups/paediatric-and-adolescent-ibd/
39 **de Bie C**. Pediatric Inflammatory Bowel Disease: from diagnosis to transition. PhD thesis, Erasmus Universiteit Rotterdam [internet];. 2012 [cited July 31, 2017] Available from: URL: https://repub.eur.nl/pub/37166/120907_Bie,%20Charlotte%20Irene%20de.pdf

P- Reviewer: Gassler N, Gazouli M, Sergi CM **S- Editor**: Gong ZM
L- Editor:A **E- Editor**: Ma YJ

World Journal of Gastroenterology

Submit a Manuscript: http://www.f6publishing.com

World J Gastroenterol 2018 March 14; 24(10): 1072-1083

DOI: 10.3748/wjg.v24.i10.1072

ISSN 1007-9327 (print) ISSN 2219-2840 (online)

ORIGINAL ARTICLE

Basic Study

Narrow line between benefit and harm: Additivity of hyperthermia to cisplatin cytotoxicity in different gastrointestinal cancer cells

Vaidotas Cesna, Arturas Sukovas, Aldona Jasukaitiene, Rima Naginiene, Giedrius Barauskas, Zilvinas Dambrauskas, Saulius Paskauskas, Antanas Gulbinas

Vaidotas Cesna, Giedrius Barauskas, Department of Surgery, Lithuanian University of Health Sciences, Kaunas LT-50161, Lithuania

Arturas Sukovas, Saulius Paskauskas, Department of Obstetrics and Gynecology, Lithuanian University of Health Sciences, Kaunas LT-50161, Lithuania

Aldona Jasukaitiene, Zilvinas Dambrauskas, Antanas Gulbinas, Institute for Digestive Research, Lithuanian University of Health Sciences, Kaunas LT-50161, Lithuania

Rima Naginiene, Neuroscience Institute, Lithuanian University of Health Sciences, Kaunas LT-50161, Lithuania

ORCID number: Vaidotas Cesna (0000-0003-4719-8483); Arturas Sukovas (0000-0001-7007-3959); Aldona Jasukaitiene (0000-0002-4606-1963); Rima Naginiene (0000-0001-5770-2618); Giedrius Barauskas (0000-0002-4321-7280); Zilvinas Dambrauskas (0000-0003-2173-1294); Saulius Paskauskas (0000-0001-9930-4124); Antanas Gulbinas (0000-0002-6683-1339).

Author contributions: Cesna V, Sukovas A analyzed the data and drafted the manuscript; Jasukaitiene A performed most of experiments; intracellular cisplatin concentration analysis was performed by Naginiene R; Barauskas G, Paskauskas S and Gulbinas A designed and coordinated the research; Gulbinas A and Dambrauskas Z revised the manuscript for important intellectual content; all authors have read and approved the final version to be published.

Supported by the Research Council of Lithuania, No. SEN-01/2015.

Institutional review board statement: The study was reviewed and approved by the Kaunas Regional Biomedical Research Ethics Committee.

Conflict-of-interest statement: All authors have nothing to disclose.

Data sharing statement: No additional data are available.

Manuscript source: Unsolicited manuscript

Correspondence to: Zilvinas Dambrauskas, MD, PhD, Lecturer, Professor, Surgeon, Lithuanian University of Health Sciences, Institute for Digestive Research, Eiveniu str., 4, Kaunas LT-50161, Lithuania. zilvinas.dambrauskas@lsmuni.lt
Telephone: +370-68-669255
Fax: +370-37-326179

Received: December 2, 2017
Peer-review started: December 2, 2017
First decision: December 27, 2017
Revised: January 2, 2018
Accepted: January 16, 2018
Article in press: January 16, 2018
Published online: March 14, 2018

Abstract

AIM

To investigate the response to hyperthermia and chemotherapy, analyzing apoptosis, cytotoxicity, and cisplatin concentration in different digestive system cancer cells.

METHODS

AGS (gastric cancer cell line), Caco-2 (colon cancer cell line) and T3M4 (pancreatic cancer cell line) were

treated by cisplatin and different temperature setting (37 ℃ to 45 ℃) either in isolation, or in combination. Treatment lasted for one hour. 48 h after the treatment viability was evaluated by MTT, cell apoptosis by Annexin V-PE and 7ADD flow cytometry. Intracellular cisplatin concentration was measured immediately after the treatment, using mass spectrometry. Isobologram analysis was performed to evaluate the mathematical combined effect of temperature and cisplatin.

RESULTS

AGS cells were the most sensitive to isolated application of hyperthermia. Hyperthermia, in addition to cisplatin treatment, did not provoke a synergistic effect at intervals from 37 ℃ to 41 ℃ in neither cancer cell line. However, a temperature of 43 ℃ enhanced cisplatin cytotoxicity for Caco-2 cells. Moreover, isobologram analysis revealed mathematical antagonistic effects of cisplatin and temperature combined treatment in AGS cells; variations between synergistic, additive, and antagonistic effects in Caco-2 cells; and additive and antagonistic effects in T3M4 cells. Combined treatment enhanced initiation of cell apoptosis in AGS, Caco-2, and T3M4 cells by 61%, 20%, and 19% respectively. The increase of intracellular cisplatin concentration was observed at 43 ℃ by 30%, 20%, and 18% in AGS, Caco-2, and T3M4 cells, respectively.

CONCLUSION

In addition to cisplatin, hyperthermia up to 43 ℃ does not affect the viability of cancer cells in a synergistic manner.

Key words: Hyperthermal intraperitoneal chemotherapy; Cisplatin; Hyperthermia; Isobolograms; Gastric cancer; Pancreatic cancer; Colon cancer

Core tip: Hyperthermal intraperitoneal chemotherapy is widely used as a standard treatment option for peritoneum invading gastrointestinal cancer. Our *in vitro* results suggest that optimal temperature has to be taken into consideration for achieving optimal therapeutic effect. In addition to cisplatin, hyperthermia up to 43 ℃ does not affect the viability of AGS, Caco-2, and T3M4 cells in a synergistic manner. However, some regimens of hyperthermia and cisplatin treatment are beneficial regarding an increase in intracellular cisplatin concentration and enhancement apoptosis of gastrointestinal cancer cells.

Cesna V, Sukovas A, Jasukaitiene A, Naginiene R, Barauskas G, Dambrauskas Z, Paskauskas S, Gulbinas A. Narrow line between benefit and harm: Additivity of hyperthermia to cisplatin cytotoxicity in different gastrointestinal cancer cells. *World J Gastroenterol* 2018; 24(10): 1072-1083 Available from: URL: http://www.wjgnet.com/1007-9327/full/v24/i10/1072.htm DOI: http://dx.doi.org/10.3748/wjg.v24.i10.1072

INTRODUCTION

For the past two decades, hyperthermal intraperitoneal chemotherapy (HIPEC) has been considered as a treatment option for peritoneum invading gastrointestinal cancers[1]. Various studies have demonstrated improved survival rates for gastric[2] and colorectal cancers[3-5]. The clinical application of hyperthermia is based on the assumption that it may enhance the effect of the chemotherapy, especially cisplatin-based treatments[6-8]. There are some experimental studies providing evidence that hyperthermia can affect cell membranes, cytoskeletons, synthesis of macromolecules, increase drug-induced DNA damage, and inhibit the repair of drug-induced DNA damage[9]. Hyperthermia may provide higher local cisplatin concentrations in tissues, indicating the pharmacokinetic advantage of its use and reduction of systemic toxicity[10]. Hyperthermia-induced PARP blockade can increase chemotherapy-induced damage in BRCA-competent cells of ovarian and colon cancer[11].

However, the results of available studies on the synergy of hyperthermia and cisplatin chemotoxicity, initiation of apoptosis, and intracellular accumulation of cisplatin in different gastrointestinal cancer cells are controversial. The opposite effect of hyperthermia on cisplatin sensitivity was observed in mismatch repair deficiency and mismatch repair proficiency in colon cancer cell lines[12]. Isolated hyperthermia only temporarily inhibited cell proliferation without cytotoxic effects on gastric cancer cell lines. However, a synergistic effect of hyperthermia and chemotherapy on inhibiting proliferation and induction of cell death via the apoptotic pathway was reported[13]. Interestingly, the hyperthermia-mediated increase of cellular accumulation of cisplatin and persistent DNA damage in gastric cancer cells was observed only with the addition of tumor necrosis factor[14]. The expression of heat shock genes and proteins provides an adaptive mechanism for stress tolerance, allowing cells to survive non-physiologic conditions. However, the same adaptive mechanism can ultimately favor malignant transformation by interfering with pathways that regulate cell growth and apoptosis. Cytoprotection and thermotolerance raised the concern that heat-treated tumor cells might also be resistant to attack by immune effector mechanisms[15]. Data on the additive effect of hyperthermia in terms of enhanced chemo-cytotoxicity in cancer cells of pancreatic origin are scarce.

Therefore, the aim of this study was to analyze the additivity of hyperthermia to cisplatin effects in gastric, pancreatic, and colorectal cancer cell lines evaluating cell cytotoxicity, apoptosis, and intracellular cisplatin concentration.

MATERIALS AND METHODS

Human cancer cell lines

The AGS and Caco-2 cell lines were purchased from

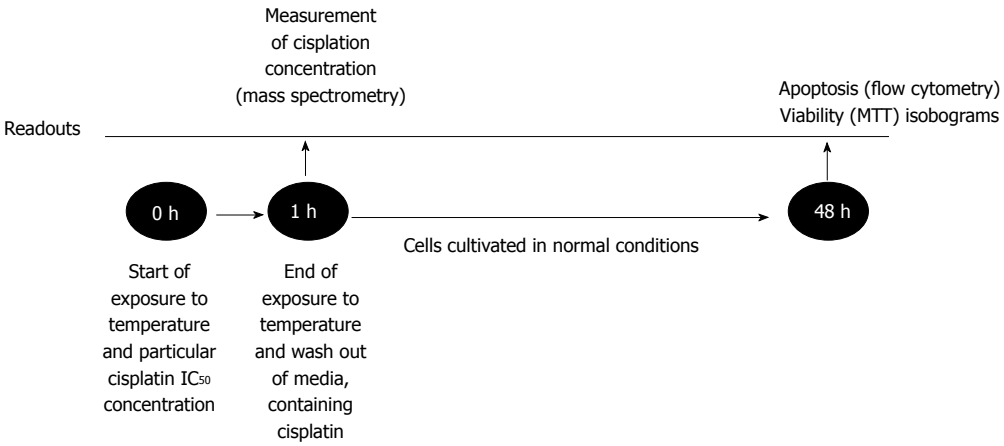

Figure 1 Design of experiment.

American Type Cell Culture (ATCC Manassas, VA, United States). AGS cell line is derived from a gastric adenocarcinoma of the stomach of a 54 year-old Caucasian female with no prior anti-cancer treatment. Caco-2 cells were isolated from a primary colonic tumor in a 72-year-old Caucasian male using the explant culture technique. Forms moderately well differentiated adenocarcinomas consistent with colonic primary grade Ⅱ, in nude mice. T3M4 cell line was obtained as a gift from the European Pancreas Center (Heidelberg, Germany). This cell line was derived from a lymph node metastasis of the Japanese male patient, diagnosed with pancreatic ductal adenocarcinoma. It is characterized as pancreatic adenocarcinoma producing CEA, K-ras activated, and with slow cell growth. Cells were grown in RPMI medium (Gibco/Invitrogen, Carlsbad, CA, United States) with the addition of 10% fetal bovine serum (Gibco/Invitrogen) and 1% penicillin/streptomycin solution (Gibco/Invitrogen). Flasks with cells were cultured in a humid incubator with a CO_2 level of 5% and temperature of 37 ℃.

Design of experiment

Cancer cells were cultivated for 24 h in the conditions described above. Afterwards, cells were treated by one of two separate factors: temperature (37 ℃, 38 ℃, 39 ℃, 40 ℃, 41 ℃, 42 ℃, 43 ℃, 44 ℃, 45 ℃) or IC_{50} dose of cisplatin, which was specifically determined for each cell line. Moreover, the combination of hyperthermia and cisplatin treatment was applied (Figure 1). The duration of treatment was 1 h as it reflected the treatment time under the clinical conditions of HIPEC. Cells were heated in humid incubators at particular temperature regimens. When temperature of the media reached desired level, we started the countdown of one hour exposure. Medium temperature was controlled by the electronic thermometer. Following the treatment, the medium was changed, and cells were cultivated for 48 h under the conditions as previously described. Afterwards, MTT and flow cytometry were performed (see "MTT assay" and "Cell apoptosis"). All experiments were repeated at least three times.

MTT assay

Cytotoxicity of cisplatin or/and hyperthermia was determined by MTT [3-(4, 5-dimethylthiazol-2-Yl)-2, 5-diphenyltetrazolium bromide] (Gibco/Invitrogen) assay. The plate was incubated for 4 h at 37 ℃ after 5 mg/mL of the MTT reagent was added to the wells. Then the supernatant was removed, and DMSO (dimethyl sulfoxide) (Carl Roth GmbH, Karlsruhe, Germany) was added to solubilize the resulting formazan crystals. Absorbance measurements were made at 570 nm on the Sunrise spectrophotometer (Tecan GmbH, Grodig, Austria).

Cell apoptosis

The changes in apoptosis were evaluated after treatment of the cells by hyperthermia (43 ℃) and the previously determined IC_{50} of cisplatin (specific for particular cell line). Untreated cisplatin cells and normothermia (37 ℃) cultivated cells were defined as controls. Forty-eight hours after the experiment (Figure 1), the rate of apoptosis was determined by flow cytometer Guava Nexin Annexin V Assay (Merck, Millipore United States and Canada). All the procedures were performed according to the manufacturer's instructions. Samples were measured using a Guava Personal Cell Analysis (PCA) Flow Cytometer (Merck, Millipore) and CytoSoft software.

Intracellular concentration of cisplatin

Immediately after the experiment, the cell lysate samples were diluted ten times with high purity deionized water. Concentration of total intracellular cisplatin was analyzed by inductively coupled plasma mass spectrometer (ICP-MS) NexION™ 300D (PerkinElmer, United States) equipped with nickel cones and a quartz cyclonic spray chamber as a sample introduction system and using collision mode kinetic energy discrimination (KED) with helium gas (purity ⩾ 99.999%) to remove polyatomic interferences.

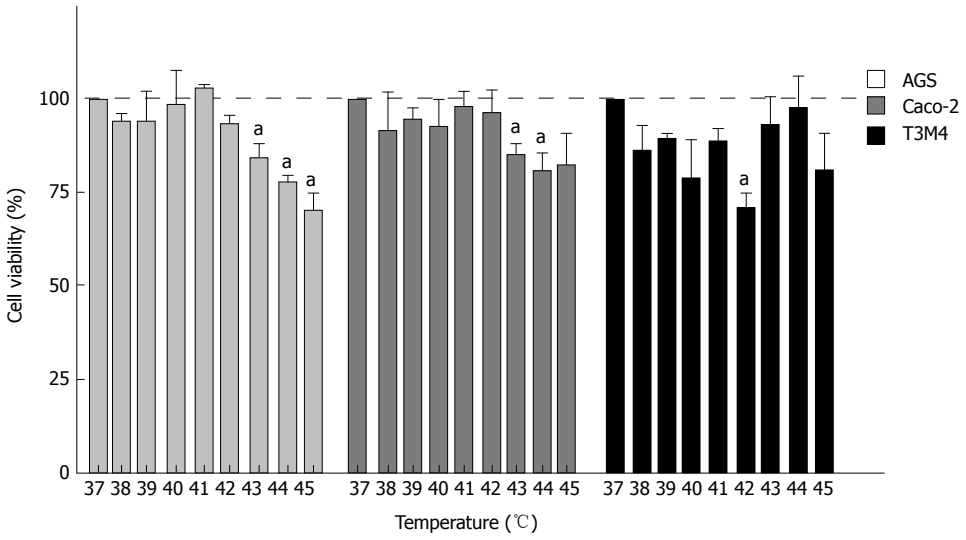

Figure 2 The different effect of the temperature on cancer cell viability. Following a one-hour exposure of AGS, Caco-2, and T3M4 cells to temperatures ranging from 37 ℃ to 42 ℃, there were no significant viability changes. Starting at 43 ℃, viability gradually decreased in AGS and Caco-2 cells. Activation of viability was evident in T3M4 cells at temperatures of 43 ℃ and 44 ℃. All data were compared with a control group (viability of cells at temperature of 37 ℃ set as 100%). Statistical analysis was performed using the Mann-Whitney *U* test comparing selected groups to the control. $^{a}P < 0.05$ *vs* control.

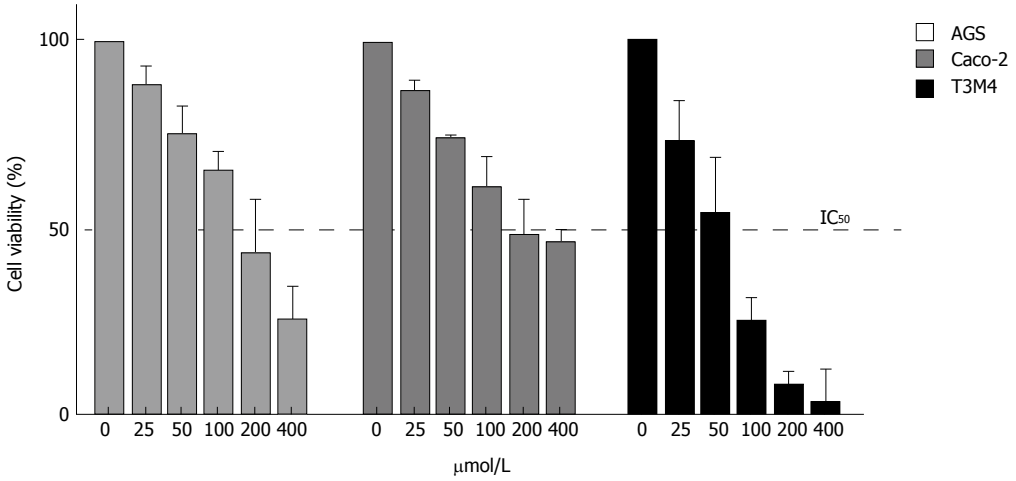

Figure 3 The influence of different cisplatin doses on cancer cell viability. Exposure to gradually increasing doses of cisplatin resulted in a linear decrease of viability in all cancer cell lines. T3M4 cells were the most sensitive to cisplatin, followed by Caco-2 and AGS cells. All data were compared with the control group (viability of cells at 37 ℃ set as 100%). Data are presented as the mean ± SE from ≥ 3 replicates.

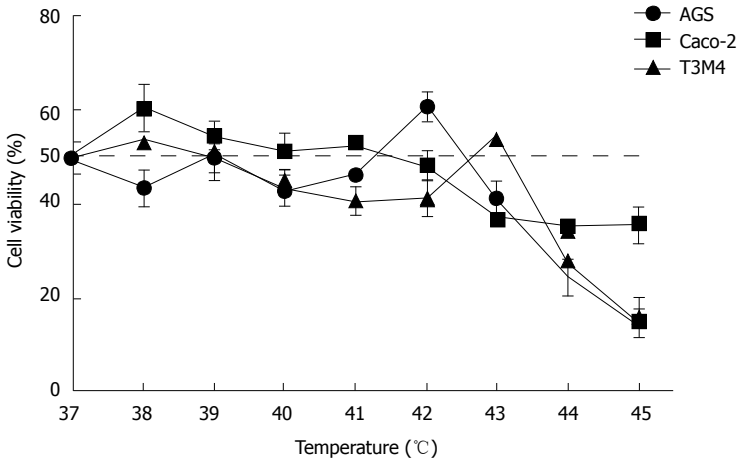

Figure 4 Effect of temperature and cisplatin (IC_{50}) combinations on cancer cell viability. The increase of temperature had no significant additional effect on cancer cell viability with the exception of extreme hyperthermia (44 ℃-45 ℃). Peaks of enhanced viability were observed in AGS and T3M4 cells at temperatures of 42 ℃ and 43 ℃. Data are equalized to control (untreated cells) as 100% and shown in percentages. Dashed line shows IC_{50}.

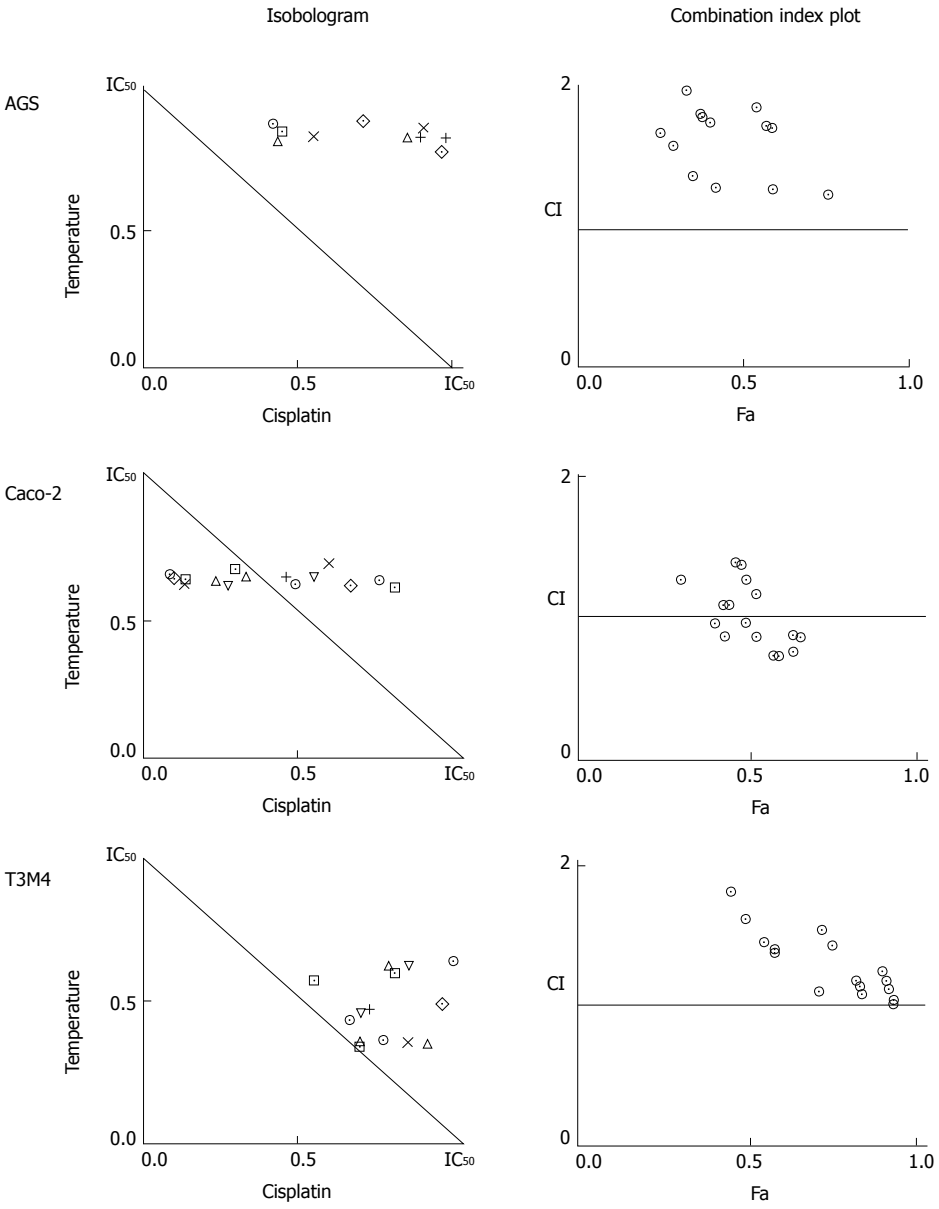

Figure 5 Interaction of temperature and cisplatin using the isobologram method for cancer cell viability. Mathematically revealed combined effects of hyperthermia and cisplatin differ in AGS, Caco-2, and T3M4 cell lines. The isobologram represents the interaction between cisplatin and temperature resulting in inhibition of cancer cell growth. The solid line in the diagram (Combination Index = 1) indicates the alignment of theoretical values of an additive interaction between two effectors and represents calculated conditions required to inhibit cell growth by 50%. Mathematically calculated IC_{50} for AGS cells: temperature 51 ℃, cisplatin 159 μmol/L; Caco-2 cells: temperature 66 ℃, cisplatin 328 μmol/L; T3M4 cells: temperature 61 ℃, cisplatin 0 μmol/L. Treatment combination points falling above the line indicate mathematical antagonism (below synergism, on the line additivity). Combination points that are distant from the line are not shown. Tables on the right represent the CI of selected combinations.

The calibration graphs for determination of Platinum by ICP-MS were prepared in the range of 0-50 ng/mL using Pure Plus 10 mg/L Multi-Element calibration standard 4 (PerkinElmer, United States). The working conditions of the spectrometer were optimized daily in order to obtain the maximal sensitivity and stability.

Isobologram analysis

To identify the confidence limits for the additive action of hyperthermia and cisplatin, isobologram analysis was applied. Data for analysis was obtained from the MTT test (Figure 4). Temperature data points of 38 ℃, 39 ℃, 40 ℃, 41 ℃, 42 ℃, 43 ℃, 44 ℃, and 45 ℃, and cisplatin concentration data points of 25 μmol/L, 50 μmol/L, 100 μmol/L, 200 μmol/L, and 400 μmol/L were used to define the dose effect curve for temperature and cisplatin, respectively. For combined treatment analysis, the following combinations of factors were used: 39 ℃ + 50 μmol/L; 39 ℃ + 100 μmol/L; 39 ℃ + 200 μmol/L; 40 ℃ + 50 μmol/L; 40 ℃ + 100 μmol/L; 40 ℃ + 200 μmol/L; 41 ℃ + 50 μmol/L; 41 ℃ + 100 μmol/L; 41 ℃ + 200 μmol/L; 42 ℃ + 50 μmol/L; 42 ℃ + 100 μmol/L; 42 ℃ + 200 μmol/L; 43 ℃ + 50 μmol/L; 43 ℃ + 100 μmol/L; 43 ℃ + 200 μmol/L; 44 ℃ + 50 μmol/L; 44 ℃ + 100 μmol/L; 44 ℃ + 200 μmol/L. The Chou median effect equation was used[16]. It provides

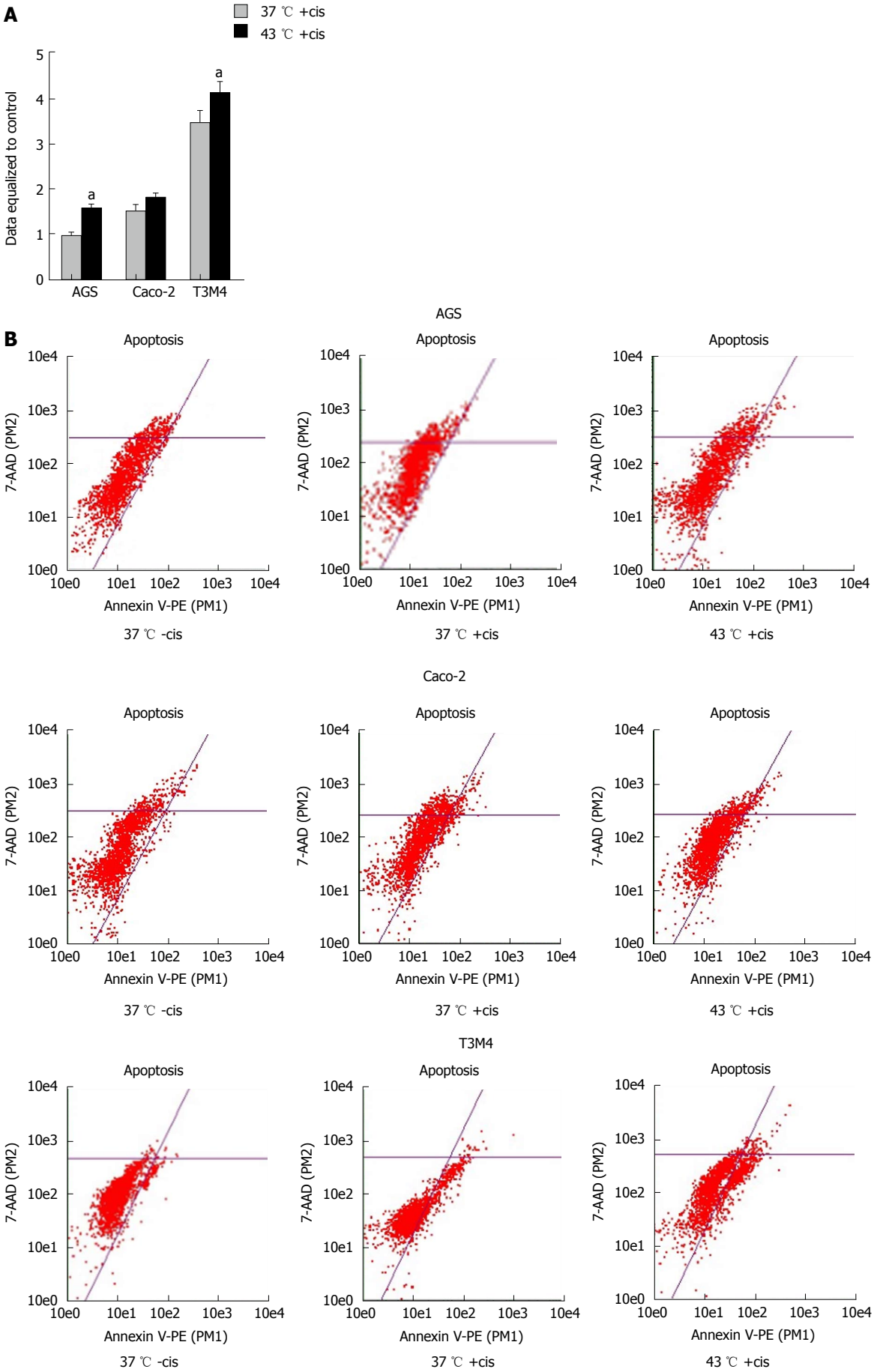

Figure 6 Apoptotic effect of temperature and cisplatin in cancer cells. A: Early apoptosis was significantly induced by hyperthermia in cisplatin-treated cells, with the exception of Caco-2 cells, where temperature had no significant role. The dashed line represents control rates of apoptosis in untreated cells. Statistical analysis was performed using the Mann-Whitney *U* test. $^{a}P < 0.05$. B: Dot plots presenting change of apoptosis in cisplatin untreated/treated cells and cultivated in hyperthermia. "-cis": Cisplatin untreated cells; "+cis": Cisplatin treated cells.

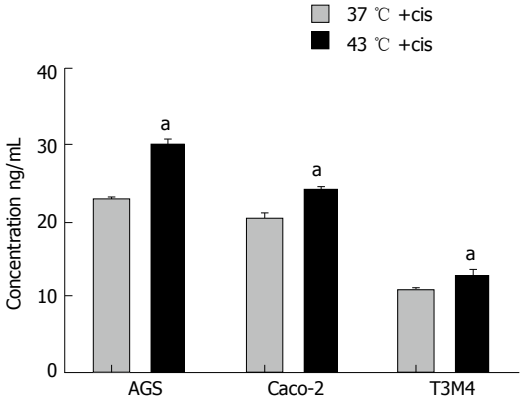

Figure 7 The change of the intracellular cisplatin concentration. Temperature of 43 ℃ significantly increased the intracellular concentration of cisplatin in all analyzed cell lines. Data are shown as concentrations of ng/mL. Statistical analysis was performed using the Mann-Whitney *U* test. $^{a}P < 0.05$. "+cis": Cisplatin treated cells.

the theoretical basis for the combination index (CI), which enabled quantification of drug interaction affects defining synergism (CI < 1), additivity (CI = 1), or antagonism (CI > 1). The CompuSyn software (CompuSyn, Inc., Paramus, NJ, United States) was used for calculations.

RESULTS

Different cell lines have specific responses to hyperthermia

To evaluate the effect of hyperthermia *per se* on different cancer cells *in vitro*, we examined the response of the AGS, Caco-2, and T3M4 cell lines to temperature using a stepwise increase of one degree ranging from 37 ℃ to 45 ℃. Cell viability was determined by MTT assay. Every cell line demonstrated a different pattern of response to hyperthermia (Figure 2). AGS cells were the most sensitive one to hyperthermia, where a temperature rise from 41 ℃ to 45 ℃ gradually decreased its viability by 30%. In the 37 ℃ to 41 ℃ interval, the viability stayed constant. Cells affected by 43 ℃, 44 ℃, and 45 ℃ dropped their viability rate by 16%, 22 ℃, and 30%, respectively, as compared to the control (37 ℃). A temperature increase from 37 ℃ to 42 ℃ had no significant effect on Caco-2 cells, but at 43 ℃ and 44 ℃, its viability dropped by 14% and 20%, respectively, but stayed constant at higher temperatures. The response of T3M4 cells to the changes of temperature was different. Temperatures from 37 ℃ to 42 ℃ decreased its viability by 30%. At 43 ℃, the viability of T3M4 cells sharply increased by 20% and stayed at this level in higher temperatures. Overall, only the AGS cell line responded to hyperthermia as implied, with gradual inhibition of cell viability.

Different cell lines respond to cisplatin in a comparable linear pattern but with specific sensitivity

Cisplatin induced a dose-dependent suppressor effect on cancer cell viability, with a similar linear response in the AGS, Caco-2, and T3M4 cell lines. Pancreatic cancer cells (T3M4) were the most sensitive, revealing cisplatin IC_{50} at 48 μmol/L. The IC_{50} for Caco-2 was 194 μmol/L, and for AGS, it was 182 μmol/L (Figure 3).

Insufficient temperature regimens can be detrimental in combined hyperthermic chemotherapy

Previously determined IC_{50} doses of cisplatin were used for particular cell lines during this experiment. Simultaneous exposure of cells to hyperthermic conditions and cisplatin triggered different response in AGS, Caco-2, and T3M4 cells (Figure 4). Overall, temperatures ranging from 37 ℃ to 41 ℃ had no detectable additive effect to cisplatin cytotoxicity. Interestingly, we observed peaks of viability in AGS (42 ℃, increase by 33%) and T3M4 (43 ℃, increase by 32%) cells. Higher temperatures, in addition to cisplatin exposure, inhibited cell growth dramatically; AGS viability dropped by 70% and T3M4 dropped by 76% at 45 ℃. Application of hyperthermia in addition to cisplatin in the Caco-2 cell line gradually improved the cytotoxic effect and decreased the viability of cells by one-fourth from 43 ℃ to 45 ℃. In summary, application of hyperthermia (43 ℃ and higher) in addition to cisplatin might enhance its cytotoxic effect in the Caco-2 cell line. However, lower (*e.g.*, < 43 ℃) temperature regimens may even promote cell proliferation and worsen expected hyperthermal chemotherapy effects in AGS and T3M4 cell lines.

Isobologram analysis: Unpredictable response of the cells to hyperthermia and cisplatin

We constructed isobolograms to reveal if the combined application of hyperthermia and cisplatin had synergistic, antagonistic, or additive effects. Combination of temperature and cisplatin was strongly antagonistic for AGS cells in all studied data points. Combined application of hyperthermia and cisplatin was tripled in Caco-2 cells: synergistic (at 40 ℃ with 50 μmol/L and 100 μmol/L of cisplatin, at 43 ℃ with 50 μmol/L, 100 μmol/L, and 200 μmol/L cisplatin, at 44 ℃ with 50 μmol/L , 100 μmol/L, and 200 μmol/L of cisplatin), additive (at 39 ℃ with 100 μmol/L of cisplatin, at 41 ℃ with 100 μmol/L cisplatin, and at 42 ℃ with 50 μmol/L and 100 μmol/L of cisplatin), and antagonistic (at 39 ℃ with 200 μmol/L of cisplatin, at 40 ℃ with 200 μmol/L cisplatin, at 41 ℃ with 50 μmol/L and 200 μmol/L cisplatin, and at 42 ℃ with 200 μmol/L of cisplatin). Combined treatment of T3M4 at 41 ℃ with 200 μmol/L cisplatin, at 42 ℃ with 50 μmol/L cisplatin, and at 44 ℃ with 100 μmol/L and 200 μmol/L of cisplatin had an additive effect. The remaining combinations were antagonistic (Figure 5).

Hyperthermia addition to cisplatin enhances rates of early apoptosis

Annexin V-PE flow cytometry analysis was performed to evaluate rates of early apoptosis. Cisplatin induced early

Table 1 Overview of results

Cell line	Effect of temperature at 43 ℃ on cancer cells viability	IC_{50} dose of cisplatin	Combined effect of temperature, at 43 ℃ and IC_{50} dose of cisplatin on cancer cells viability	Effect of temperature in addition to IC_{50} dose of cisplatin on cancer cell apoptosis	Effect of temperature on intracellular cisplatin concentration
AGS	↓↓	182	↓	↑	↑↑↑
Caco-2	↓	194	↓↓	-	↑↑
T3M4	-	48	-	↑	↑

The number of the arrows represents strength of effect.

apoptosis in Caco-2 and T3M4 cells 1.5-fold and 3.4-fold, respectively. The number of dead/late apoptotic cells was insignificant in the following groups: 0.5% of Caco-2 cells and 2.9% of T3M4 cells. Hyperthermia of 43 ℃ in addition to cisplatin induced early apoptosis as compared to cells treated in normothermia by 20% in Caco-2 (1% of dead cells) and 19% (3.9% dead cells) in T3M4, respectively. Interestingly, early apoptosis was not significantly induced by isolated cisplatin treatment in AGS cells. Rates of AGS early apoptosis were not significantly induced by an isolated cisplatin treatment. However, application of combined treatment with hyperthermia and cisplatin increased early apoptosis by 61% (0.4% dead cells) (Figure 6).

Hyperthermia increases intracellular cisplatin concentration

Hypothesizing that hyperthermia promotes delivery of cisplatin to cancer cells, we aimed to measure intracellular cisplatin concentrations. Analysis was performed immediately following a one-hour exposure to the IC_{50} of cisplatin at 37 ℃ and 43 ℃. Overall, 43 ℃ promoted an increase of intracellular cisplatin concentration. The concentration was significantly increased in AGS, Caco-2, and T3M4 cells by 30%, 20%, and 18%, respectively (Figure 7).

DISCUSSION

Hyperthermal intraperitoneal chemotherapy has been applied to treat peritoneal carcinomatosis for gastric[17-19], colorectal[20], ovarian[21], and peritoneal mesothelioma[22] and has aided in prolonged long-term survival in selected patients[23-26]. In HIPEC, intraperitoneal free cancer cells and the serous surface of the bowel and peritoneum are exposed to high concentrations of chemotherapy agents. Hyperthermia itself may affect cell cytoskeletons, cell membranes, synthesis of macromolecules, and DNA repair mechanisms[9].

As the origin, genotypes, and phenotypes of free cancer cells may be quite different, it seems unreasonable to treat all peritoneal metastases the same way. Until now, basic information regarding the contribution of hyperthermia to intraperitoneal chemotherapeutic agents in different gastrointestinal cancers is poor and controversial. In this *in vitro* study, we have applied hyperthermia and chemotherapy for 1 h in order to mimic clinical conditions. We have performed our aimed readouts at 48 h following the experiment as the earlier readouts have not proven any changes.

We have chosen three most common peritoneum invading GI cancers in our study, selecting one cancer cell line per cancer type. It is known that various cancer cells of same cancer type are different in the manner of apoptosis, biomarker expression etc [27]. This study is an overview, which leads to a better knowledge of gastric, pancreatic and colorectal cancer cell response to simultaneous hyperthermia and cisplatin treatment.

Until now, our analyzed cells are well examined in various aspects. AGS cells in 516 analyzed genes, have 40 mutations, like KRAS, WNK1 and WNK2[28]. Overexpression of HER-2, EGFR, VEGF, Bcl-2 biomarkers was investigated in gastric cancer cells[29]. Mutations of *SMAD4* and *TP53* genes and overexpression of *ILF3*, *TIMP3* genes are present in Caco-2 cells[30-32] . T3M4 are the least examined cells. No known gene mutations were found[33] and they are known to overexpress growth factors as FGFR4[34].

Our experiments revealed the differences of cell viability in response to isolated hyperthermia. We even observed positive effects of isolated hyperthermia on the viability of pancreatic cancer cells. We hypothesize that this effect could be related to the activation of the cytoprotective heat shock proteins (HSP), an effect described in other studies[35]. It is known that higher temperatures can enhance thermotolerance by activating HSPs[36]. However, gastric cancer cells (AGS) and colon cancer cells (Caco-2) responded to hyperthermia with a significant drop of viability at 43 ℃. One study demonstrated that hyperthermia alone can significantly reduce viability of the Colon 26 cancer cells[37]. The investigation of the effect of local heat used for ablation of tumor nodules showed that exposing cultured Caco-2 cells to 48 ℃ for 2 h resulted in an approximately 80% reduction of cell viability[38]. However, in our study, the viability of Caco-2 cells decreased only by 14% after exposure to 43 ℃ for 1 h.

Hyperthermia may enhance the effect of chemotherapy, especially cisplatin-based treatments[6-8]. Ferraro *et al*[39] studied the effects of hyperthermia and cisplatin on model protein hen eggs and revealed that increased temperature enhanced cisplatin cytotoxicity.

Tang *et al*[13] have shown a synergistic effect of hyperthermia and chemotherapy inhibiting

proliferation in six gastric cancer cell lines, including AGS, in a certain range of chemoagent (cisplatin) concentration. Moreover, hyperthermia, in addition to chemotherapy, induced cell apoptosis as the major type of death. MicroRNA-218 upregulation and increased chemosensitivity were observed in gastric cancer cells after exposing them to hyperthermal conditions[40]. However, in our study, only temperatures higher than 43 ℃ in addition to cisplatin exposure inhibited cell growth. In the isobologram analysis, the combination of temperature and cisplatin was antagonistic for AGS cells. On the contrary, AGS cells showed an increased viability of 33% at 42 ℃. This is an important observation as it may highlight the possibility that technically incorrect temperature regimens may activate metabolism of cancer cells and increase their resistance to chemotherapy. Interestingly, we observed that application of cisplatin to gastric cancer (AGS) cells for one h had no significant impact on cell apoptosis. However, the combination of cisplatin and hyperthermia (43 ℃) increased the affect by 61%. Our results suggest that temperature and cisplatin are not always acting in synergy as was shown by isobolograms.

Previous *in vitro* investigations have revealed that the response of the colon cancer cells to hyperthermia and chemotherapeutic drug differ by cell type. Some authors have shown that hyperthermia alone significantly decreased the viability of the Colon 26 cancer cells[37], and the cytotoxic effect of cisplatin[41] was enhanced at hyperthermal conditions. After exposure to 43 ℃, the activity of oxaliplatin markedly and rapidly increased, indicating its inhibiting potential in Colon 26 cells[42]. Significant synergy of hyperthermia and chemotherapy was detected in CX-1 cells[43] in similar experimental conditions (42 ℃ for 1 h). Some authors described similar results in HCT116+ch2 (MMR-) cells that were resistant to heat treatment at temperatures of 41 ℃ and 42 ℃[12]. The exposition of the colon carcinoma cell lines CX-1 and HTC 116 to 42 ℃ for 1 h revealed no change in cell viability[13,43]. Moreover, HCT116+ch2 (MMR-) cells exposed to a mild heat were 1.42-fold more resistant to cisplatin[12]. We observed that the addition of hyperthermia to cisplatin treatment had a slight positive influence on Caco-2 cell viability. At 43 ℃, cisplatin had an insignificant effect regarding apoptosis, whereas intracellular cisplatin concentration was elevated by 26% as compared to the control. Isobologram analysis showed approximately 50% of selected cisplatin and temperature treatment combinations acted in a synergistic manner, indicating that some of hyperthermic chemotherapy regimens might be useful.

Recent studies reported that hyperthermia increased sensitivity to gemcitabine[44] and enhanced gemcitabine-related apoptotic cell death in pancreatic cancer cells[45]. Moreover, the improved drug delivery and antitumor effects in combination with mild hyperthermia were reported [46].

The combined cytotoxic effect of cisplatin and hyperthermia in T3M4 cells was evident only when the temperature was higher than 43 ℃. These cells were the most sensitive to cisplatin with the lowest IC_{50}. Cisplatin amplified apoptosis by 3.4-fold and hyperthermia increased the effect by 19%; however, it was 3-fold less in the gastric cancer cell line. Similar to AGS cells, T3M4 isobologram analysis revealed that the combination of treatments acted in an antagonistic manner in most of the selected combinations; however, in few of them, the additive effect of the two agents was revealed. An extremely limited increase of intracellular cisplatin concentration in hyperthermia could be observed in pancreatic cancer cells. Our experiments elucidated that the response of T3M4 cells differs from other studied gastrointestinal cancer cells (AGS and Caco-2). A review by Loggie *et al*[47] postulated that hyperthermia combined with chemotherapy is probably beneficial for less aggressive tumors and should be the standard of care for appendiceal and colorectal cancers.

Caco-2 cell results varied from the other cells in our study. In some cases, they acted in unpredictable manner. One of the possible explanations for this discrepancy, would be that Caco-2 cells can differentiate their phenotype prior to post-confluence stage, and lead to the change of morphology, degree of differentiation etc[48].

In summary, we have proven that the role of hyperthermia in addition to cisplatin is different in gastric, colonic, and pancreatic cancer cells. The overview of the basic results is shown in Table 1. Different cancer cells respond to combined treatments in different manners, and temperature-induced apoptosis is initiated by various pathways[49].

In conclusion, hyperthermia up to 43 ℃ in addition to cisplatin does not influence AGS, Caco-2, and T3M4 cell viability in a synergistic manner. However, some regimens of hyperthermia and cisplatin treatment are beneficial regarding the apoptotic response and an increase of intracellular cisplatin concentration.

ARTICLE HIGHLIGHTS

Research background

Hyperthermal intraperitoneal chemotherapy is an option to treat peritoneum invading gastrointestinal cancer. Until now the results of hyperthermal intraperitoneal chemotherapy (HIPEC) treatment are controversy, needing unification in selected parameters of the treatment. In different cancer centers, the procedure varies in time setting, hyperthermia level and different chemotherapy drugs are used.

Research motivation

As HIPEC is widely used in clinical practice, still there is a lack of studies, analyzing the impact of hyperthermia and cisplatin to cancer cells. The cellular response to the treatment is still not clear. There is no clear data defining optimal timing and temperature of the procedure.

Research objectives

Our objective was to analyze gastric, pancreatic and colorectal cancer cells response to hyperthermia and cisplatin treatment regarding viability, change of intracellular cisplatin concentration and apoptosis rate.

Research methods

We used AGS (gastric cancer), T3M4 (pancreatic cancer) and Caco-2 (colorectal cancer) cells. Mimicking HIPEC procedure, cells were treated with specific to each cell line IC_{50} dose of cisplatin at the temperature regimens ranging from 37 ℃ to 45 ℃. Treatment lasted for one hour. Later cells were harvested in normothermia, changing cisplatin containing media to fresh one. Immediately after experiment, intracellular cisplatin concentration was measured, using mass spectrometer analysis. For other readouts cells were harvested for 48 hours in normal conditions. MTT test was performed for cellular viability evaluation and isobologram analysis. We used flow cytometry to determine apoptosis change of hyperthermia and cisplatin treatment.

Research results

Cells responded to hyperthermia (ranging from 38 ℃ to 45 ℃) in a different manner. Viability of AGS cells was the most hyperthermia-dependent, decreasing by 30% (from 41 ℃ to 45 ℃). Caco-2 cell viability had no change in the interval from 38 ℃ to 42 ℃. Higher temperature regimens dropped its viability rate by 14%-20%. T3M4 cells reacted differently. Viability dropped until 42 ℃, but at higher temperature regimens, we observed increase of viability. While in simultaneous hyperthermia and cisplatin treatment, we observed no change of viability until 41 ℃ in all cancer cells. Higher temperatures inhibited cell growth. Interestingly, we observed peaks of viability in AGS (42 ℃, increase by 33%) and T3M4 (43 ℃, increase by 32%) cells. Putting all MTT data to isobologram analysis, we observed synergistic, antagonistic, or additive effects of combined treatment. Hyperthermia and cisplatin treatment was strongly antagonistic in AGS cells. In Caco-2 cells we observed synergistic, additive and antagonistic effects of simultaneous treatment. Few combined treatment regimens were additive for T3M4 cells, and remaining antagonistic. Cisplatin induced early apoptosis in Caco-2 and T3M4 cells 1.5-fold and 3.4-fold, respectively. Hyperthermia of 43 ℃ in addition to cisplatin induced early apoptosis as compared to cells treated in normothermia by 20% in Caco-2 and 19% in T3M4, respectively. Hyperthermia strongly decreased intracellular cisplatin concentration in AGS, Caco-2, and T3M4 cells by 30%, 20%, and 18%, respectively.

Research conclusions

Our data suggest that HIPEC conditions have to be cancer type dependent and well revised. Particular temperature regimens can do more harm, than benefit, by activating cell division and growth.

Research perspectives

To get better knowledge of hyperthermia and cisplatin treatment effects, future studies should include more cancer cell lines per cancer type. Also, *in vivo* vehicle should be established.

REFERENCES

1 **Glehen O**, Mohamed F, Gilly FN. Peritoneal carcinomatosis from digestive tract cancer: new management by cytoreductive surgery and intraperitoneal chemohyperthermia. *Lancet Oncol* 2004; **5**: 219-228 [PMID: 15050953 DOI: 10.1016/S1470-2045(04)01425-1]

2 **Coccolini F**, Cotte E, Glehen O, Lotti M, Poiasina E, Catena F, Yonemura Y, Ansaloni L. Intraperitoneal chemotherapy in advanced gastric cancer. Meta-analysis of randomized trials. *Eur J Surg Oncol* 2014; **40**: 12-26 [PMID: 24290371 DOI: 10.1016/j.ejso.2013.10.019]

3 **Bloemendaal AL**, Verwaal VJ, van Ruth S, Boot H, Zoetmulder FA. Conventional surgery and systemic chemotherapy for peritoneal carcinomatosis of colorectal origin: a prospective study. *Eur J Surg Oncol* 2005; **31**: 1145-1151 [PMID: 16084051 DOI: 10.1016/j.ejso.2005.06.002]

4 **Glehen O**, Cotte E, Schreiber V, Sayag-Beaujard AC, Vignal J, Gilly FN. Intraperitoneal chemohyperthermia and attempted cytoreductive surgery in patients with peritoneal carcinomatosis of colorectal origin. *Br J Surg* 2004; **91**: 747-754 [PMID: 15164446 DOI: 10.1002/bjs.4473]

5 **Chua TC**, Esquivel J, Pelz JO, Morris DL. Summary of current therapeutic options for peritoneal metastases from colorectal cancer. *J Surg Oncol* 2013; **107**: 566-573 [PMID: 22688776 DOI: 10.1002/jso.23189]

6 **Bergs JW**, Franken NA, Haveman J, Geijsen ED, Crezee J, van Bree C. Hyperthermia, cisplatin and radiation trimodality treatment: a promising cancer treatment? A review from preclinical studies to clinical application. *Int J Hyperthermia* 2007; **23**: 329-341 [PMID: 17558732 DOI: 10.1080/02656730701378684]

7 **Alvarez-Berríos MP**, Castillo A, Mendéz J, Soto O, Rinaldi C, Torres-Lugo M. Hyperthermic potentiation of cisplatin by magnetic nanoparticle heaters is correlated with an increase in cell membrane fluidity. *Int J Nanomedicine* 2013; **8**: 1003-1013 [PMID: 23493492 DOI: 10.2147/IJN.S38842]

8 **Gabano E**, Colangelo D, Ghezzi AR, Osella D. The influence of temperature on antiproliferative effects, cellular uptake and DNA platination of the clinically employed Pt(II)-drugs. *J Inorg Biochem* 2008; **102**: 629-635 [PMID: 18037490 DOI: 10.1016/j.jinorgbio.2007.10.006]

9 **van de Vaart PJ**, van der Vange N, Zoetmulder FA, van Goethem AR, van Tellingen O, ten Bokkel Huinink WW, Beijnen JH, Bartelink H, Begg AC. Intraperitoneal cisplatin with regional hyperthermia in advanced ovarian cancer: pharmacokinetics and cisplatin-DNA adduct formation in patients and ovarian cancer cell lines. *Eur J Cancer* 1998; **34**: 148-154 [PMID: 9624250 DOI: 10.1016/S0959-8049(97)00370-5]

10 **Ried M**, Potzger T, Braune N, Diez C, Neu R, Sziklavari Z, Schalke B, Hofmann HS. Local and systemic exposure of cisplatin during hyperthermic intrathoracic chemotherapy perfusion after pleurectomy and decortication for treatment of pleural malignancies. *J Surg Oncol* 2013; **107**: 735-740 [PMID: 23386426 DOI: 10.1002/jso.23321]

11 **Schaaf L**, Schwab M, Ulmer C, Heine S, Mürdter TE, Schmid JO, Sauer G, Aulitzky WE, van der Kuip H. Hyperthermia Synergizes with Chemotherapy by Inhibiting PARP1-Dependent DNA Replication Arrest. *Cancer Res* 2016; **76**: 2868-2875 [PMID: 27013194 DOI: 10.1158/0008-5472.CAN-15-2908]

12 **Sottile ML**, Losinno AD, Fanelli MA, Cuello-Carrión FD, Montt-Guevara MM, Vargas-Roig LM, Nadin SB. Hyperthermia effects on Hsp27 and Hsp72 associations with mismatch repair (MMR) proteins and cisplatin toxicity in MMR-deficient/proficient colon cancer cell lines. *Int J Hyperthermia* 2015; **31**: 464-475 [PMID: 26043026 DOI: 10.3109/02656736.2015.1026848]

13 **Tang R**, Zhu ZG, Qu Y, Li JF, Ji YB, Cai Q, Liu BY, Yan M, Yin HR, Lin YZ. The impact of hyperthermic chemotherapy on human gastric cancer cell lines: preliminary results. *Oncol Rep* 2006; **16**: 631-641 [PMID: 16865266 DOI: 10.3892/or.16.3.631]

14 **Buell JF**, Reed E, Lee KB, Parker RJ, Venzon DJ, Amikura K, Arnold S, Fraker DL, Alexander HR. Synergistic effect and possible mechanisms of tumor necrosis factor and cisplatin cytotoxicity under moderate hyperthermia against gastric cancer cells. *Ann Surg Oncol* 1997; **4**: 141-148 [PMID: 9084851 DOI: 10.1007/BF02303797]

15 **Milani V**, Noessner E. Effects of thermal stress on tumor antigenicity and recognition by immune effector cells. *Cancer Immunol Immunother* 2006; **55**: 312-319 [PMID: 16151807 DOI: 10.1007/s00262-005-0052-3]

16 **Chou TC**. Theoretical basis, experimental design, and computerized simulation of synergism and antagonism in drug combination studies. *Pharmacol Rev* 2006; **58**: 621-681 [PMID: 16968952 DOI: 10.1124/pr.58.3.10]

17 **Seshadri RA**, Glehen O. Cytoreductive surgery and hyperthermic intraperitoneal chemotherapy in gastric cancer. *World J Gastroenterol* 2016; **22**: 1114-1130 [PMID: 26811651 DOI: 10.3748/wjg.v22.i3.1114]

18 **Yonemura Y**, Canbay E, Li Y, Coccolini F, Glehen O, Sugarbaker PH, Morris D, Moran B, Gonzaletz-Moreno S, Deraco M, Piso P, Elias D, Batlett D, Ishibashi H, Mizumoto A, Verwaal V, Mahtem H. A comprehensive treatment for peritoneal metastases from gastric cancer with curative intent. *Eur J Surg Oncol* 2016; **42**: 1123-1131 [PMID: 27160355 DOI: 10.1016/j.ejso.2016.03.016]

19 **Yuan M**, Wang Z, Hu G, Yang Y, Lv W, Lu F, Zhong H. A retrospective analysis of hyperthermic intraperitoneal chemotherapy for gastric cancer with peritoneal metastasis. *Mol Clin Oncol* 2016; **5**: 395-399 [PMID: 27446587 DOI: 10.3892/mco.2016.918]

20 **Simkens GA**, van Oudheusden TR, Braam HJ, Wiezer MJ, Nienhuijs SW, Rutten HJ, van Ramshorst B, de Hingh IH. Cytoreductive surgery and HIPEC offers similar outcomes in patients with rectal peritoneal metastases compared to colon cancer patients: a matched case control study. *J Surg Oncol* 2016; **113**: 548-553 [PMID: 27110701 DOI: 10.1002/jso.24169]

21 **Spiliotis J**, Halkia E, Lianos E, Kalantzi N, Grivas A, Efstathiou E, Giassas S. Cytoreductive surgery and HIPEC in recurrent epithelial ovarian cancer: a prospective randomized phase III study. *Ann Surg Oncol* 2015; **22**: 1570-1575 [PMID: 25391263 DOI: 10.1245/s10434-014-4157-9]

22 **Kepenekian V**, Elias D, Passot G, Mery E, Goere D, Delroeux D, Quenet F, Ferron G, Pezet D, Guilloit JM, Meeus P, Pocard M, Bereder JM, Abboud K, Arvieux C, Brigand C, Marchal F, Classe JM, Lorimier G, De Chaisemartin C, Guyon F, Mariani P, Ortega-Deballon P, Isaac S, Maurice C, Gilly FN, Glehen O; French Network for Rare Peritoneal Malignancies (RENAPE). Diffuse malignant peritoneal mesothelioma: Evaluation of systemic chemotherapy with comprehensive treatment through the RENAPE Database: Multi-Institutional Retrospective Study. *Eur J Cancer* 2016; **65**: 69-79 [PMID: 27472649 DOI: 10.1016/j.ejca.2016.06.002]

23 **Michalakis J**, Georgatos SD, de Bree E, Polioudaki H, Romanos J, Georgoulias V, Tsiftsis DD, Theodoropoulos PA. Short-term exposure of cancer cells to micromolar doses of paclitaxel, with or without hyperthermia, induces long-term inhibition of cell proliferation and cell death in vitro. *Ann Surg Oncol* 2007; **14**: 1220-1228 [PMID: 17206477 DOI: 10.1245/s10434-006-9305-4]

24 **Zhang XL**, Hu AB, Cui SZ, Wei HB. Thermotherapy enhances oxaliplatin-induced cytotoxicity in human colon carcinoma cells. *World J Gastroenterol* 2012; **18**: 646-653 [PMID: 22363135 DOI: 10.3748/wjg.v18.i7.646]

25 **Steel GG**, Peckham MJ. Exploitable mechanisms in combined radiotherapy-chemotherapy: the concept of additivity. *Int J Radiat Oncol Biol Phys* 1979; **5**: 85-91 [PMID: 422420 DOI: 10.1016/0360-3016(79)90044-0]

26 **Verwaal VJ**, van Ruth S, de Bree E, van Sloothen GW, van Tinteren H, Boot H, Zoetmulder FA. Randomized trial of cytoreduction and hyperthermic intraperitoneal chemotherapy versus systemic chemotherapy and palliative surgery in patients with peritoneal carcinomatosis of colorectal cancer. *J Clin Oncol* 2003; **21**: 3737-3743 [PMID: 14551293 DOI: 10.1200/JCO.2003.04.187]

27 **Li Q**, Wennborg A, Aurell E, Dekel E, Zou JZ, Xu Y, Huang S, Ernberg I. Dynamics inside the cancer cell attractor reveal cell heterogeneity, limits of stability, and escape. *Proc Natl Acad Sci USA* 2016; **113**: 2672-2677 [PMID: 26929366 DOI: 10.1073/pnas.1519210113]

28 **Zang ZJ**, Ong CK, Cutcutache I, Yu W, Zhang SL, Huang D, Ler LD, Dykema K, Gan A, Tao J, Lim S, Liu Y, Futreal PA, Grabsch H, Furge KA, Goh LK, Rozen S, Teh BT, Tan P. Genetic and structural variation in the gastric cancer kinome revealed through targeted deep sequencing. *Cancer Res* 2011; **71**: 29-39 [PMID: 21097718 DOI: 10.1158/0008-5472.CAN-10-1749]

29 **Jin Z**, Jiang W, Wang L. Biomarkers for gastric cancer: Progression in early diagnosis and prognosis (Review). *Oncol Lett* 2015; **9**: 1502-1508 [PMID: 25788990 DOI: 10.3892/ol.2015.2959]

30 **Fleming NI**, Jorissen RN, Mouradov D, Christie M, Sakthianandeswaren A, Palmieri M, Day F, Li S, Tsui C, Lipton L, Desai J, Jones IT, McLaughlin S, Ward RL, Hawkins NJ, Ruszkiewicz AR, Moore J, Zhu HJ, Mariadason JM, Burgess AW, Busam D, Zhao Q, Strausberg RL, Gibbs P, Sieber OM. SMAD2, SMAD3 and SMAD4 mutations in colorectal cancer. *Cancer Res* 2013; **73**: 725-735 [PMID: 23139211 DOI: 10.1158/0008-5472.CAN-12-2706]

31 **Ahmed D**, Eide PW, Eilertsen IA, Danielsen SA, Eknæs M, Hektoen M, Lind GE, Lothe RA. Epigenetic and genetic features of 24 colon cancer cell lines. *Oncogenesis* 2013; **2**: e71 [PMID: 24042735 DOI: 10.1038/oncsis.2013.35]

32 **Tremblay E**, Auclair J, Delvin E, Levy E, Ménard D, Pshezhetsky AV, Rivard N, Seidman EG, Sinnett D, Vachon PH, Beaulieu JF. Gene expression profiles of normal proliferating and differentiating human intestinal epithelial cells: a comparison with the Caco-2 cell model. *J Cell Biochem* 2006; **99**: 1175-1186 [PMID: 16795037 DOI: 10.1002/jcb.21015]

33 **Moore PS**, Sipos B, Orlandini S, Sorio C, Real FX, Lemoine NR, Gress T, Bassi C, Klöppel G, Kalthoff H, Ungefroren H, Löhr M, Scarpa A. Genetic profile of 22 pancreatic carcinoma cell lines. Analysis of K-ras, p53, p16 and DPC4/Smad4. *Virchows Arch* 2001; **439**: 798-802 [PMID: 11787853 DOI: 10.1007/s004280100474]

34 **Shah RN**, Ibbitt JC, Alitalo K, Hurst HC. FGFR4 overexpression in pancreatic cancer is mediated by an intronic enhancer activated by HNF1alpha. *Oncogene* 2002; **21**: 8251-8261 [PMID: 12447688 DOI: 10.1038/sj.onc.1206020]

35 **Guo Y**, Ziesch A, Hocke S, Kampmann E, Ochs S, De Toni EN, Göke B, Gallmeier E. Overexpression of heat shock protein 27 (HSP27) increases gemcitabine sensitivity in pancreatic cancer cells through S-phase arrest and apoptosis. *J Cell Mol Med* 2015; **19**: 340-350 [PMID: 25331547 DOI: 10.1111/jcmm.12444]

36 **Liu T**, Ye YW, Zhu AL, Yang Z, Fu Y, Wei CQ, Liu Q, Zhao CL, Wang GJ, Zhang XF. Hyperthermia combined with 5-fluorouracil promoted apoptosis and enhanced thermotolerance in human gastric cancer cell line SGC-7901. *Onco Targets Ther* 2015; **8**: 1265-1270 [PMID: 26064061 DOI: 10.2147/OTT.S78514]

37 **Kudo M**, Asao T, Hashimoto S, Kuwano H. Closed continuous hyperthermic peritoneal perfusion model in mice with peritoneal dissemination of colon 26. *Int J Hyperthermia* 2004; **20**: 441-450 [PMID: 15204523 DOI: 10.1080/02656730310001637352]

38 **Kirstein MN**, Root SA, Moore MM, Wieman KM, Williams BW, Jacobson PA, Marker PH, Tuttle TM. Exposure-response relationships for oxaliplatin-treated colon cancer cells. *Anticancer Drugs* 2008; **19**: 37-44 [PMID: 18043128 DOI: 10.1097/CAD.0b013e3282f07791]

39 **Ferraro G**, Pica A, Russo Krauss I, Pane F, Amoresano A, Merlino A. Effect of temperature on the interaction of cisplatin with the model protein hen egg white lysozyme. *J Biol Inorg Chem* 2016; **21**: 433-442 [PMID: 27040953 DOI: 10.1007/s00775-016-1352-0]

40 **Zhang XL**, Shi HJ, Wang JP, Tang HS, Wu YB, Fang ZY, Cui SZ, Wang LT. MicroRNA-218 is upregulated in gastric cancer after cytoreductive surgery and hyperthermic intraperitoneal chemotherapy and increases chemosensitivity to cisplatin. *World J Gastroenterol* 2014; **20**: 11347-11355 [PMID: 25170221 DOI: 10.3748/wjg.v20.i32.11347]

41 **Muenyi CS**, States VA, Masters JH, Fan TW, Helm CW, States JC. Sodium arsenite and hyperthermia modulate cisplatin-DNA damage responses and enhance platinum accumulation in murine metastatic ovarian cancer xenograft after hyperthermic intraperitoneal chemotherapy (HIPEC). *J Ovarian Res* 2011; **4**: 9 [PMID: 21696631 DOI: 10.1186/1757-2215-4-9]

42 **Okayama T**, Kokura S, Ishikawa T, Adachi S, Hattori T, Takagi T, Handa O, Naito Y, Yoshikawa T. Antitumor effect of pretreatment for colon cancer cells with hyperthermia plus geranylgeranylacetone in experimental metastasis models and a subcutaneous tumor model of colon cancer in mice. *Int J Hyperthermia* 2009; **25**: 141-149 [PMID: 19337914 DOI: 10.1080/02656730802631783]

43 **Yoo J**, Lee YJ. Effect of hyperthermia and chemotherapeutic agents on TRAIL-induced cell death in human colon cancer cells. *J Cell Biochem* 2008; **103**: 98-109 [PMID: 17520700 DOI: 10.1002/jcb.21389]

44 **Vertrees RA**, Das GC, Popov VL, Coscio AM, Goodwin TJ, Logrono R, Zwischenberger JB, Boor PJ. Synergistic interaction of hyperthermia and Gemcitabine in lung cancer. *Cancer Biol Ther* 2005; **4**: 1144-1153 [PMID: 16138007 DOI: 10.4161/cbt.4.10.2074]

45 **Adachi S**, Kokura S, Okayama T, Ishikawa T, Takagi T, Handa O, Naito Y, Yoshikawa T. Effect of hyperthermia combined with

gemcitabine on apoptotic cell death in cultured human pancreatic cancer cell lines. *Int J Hyperthermia* 2009; **25**: 210-219 [PMID: 19437237 DOI: 10.1080/02656730802657036]

46 **Kirui DK**, Celia C, Molinaro R, Bansal SS, Cosco D, Fresta M, Shen H, Ferrari M. Mild hyperthermia enhances transport of liposomal gemcitabine and improves in vivo therapeutic response. *Adv Healthc Mater* 2015; **4**: 1092-1103 [PMID: 25721343 DOI: 10.1002/adhm.201400738]

47 **Loggie BW**, Thomas P. Gastrointestinal Cancers With Peritoneal Carcinomatosis: Surgery and Hyperthermic Intraperitoneal Chemotherapy. *Oncology* (Williston Park) 2015; **29**: 515-521 [PMID: 26178339]

48 **Ferraretto A**, Gravaghi C, Donetti E, Cosentino S, Donida BM, Bedoni M, Lombardi G, Fiorilli A, Tettamanti G. New methodological approach to induce a differentiation phenotype in Caco-2 cells prior to post-confluence stage. *Anticancer Res* 2007; **27**: 3919-3925 [PMID: 18225551]

49 **Ahmed K**, Tabuchi Y, Kondo T. Hyperthermia: an effective strategy to induce apoptosis in cancer cells. *Apoptosis* 2015; **20**: 1411-1419 [PMID: 26354715 DOI: 10.1007/s10495-015-1168-3]

P- Reviewer: Caboclo JL, Zhu YL **S- Editor**:Gong ZM
L- Editor: A **E- Editor**: Ma YJ

World Journal of Gastroenterology

Submit a Manuscript: http://www.f6publishing.com

World J Gastroenterol 2018 March 14; 24(10): 1084-1092

DOI: 10.3748/wjg.v24.i10.1084

ISSN 1007-9327 (print) ISSN 2219-2840 (online)

ORIGINAL ARTICLE

Basic Study

Sex disparity in viral load, inflammation and liver damage in transgenic mice carrying full hepatitis B virus genome with the W4P mutation in the preS1 region

Seoung-Ae Lee, So-Young Lee, Yu-Min Choi, Hong Kim, Bum-Joon Kim

Seoung-Ae Lee, So-Young Lee, Yu-Min Choi, Hong Kim, Bum-Joon Kim, Department of Microbiology and Immunology, Biomedical Sciences, Liver Research Institute and Cancer Research Institute, Seoul National University, College of Medicine, Seoul 110799, South Korea

ORCID number: Seoung-Ae Lee (0000-0002-4451-8165); So-Young Lee (0000-0002-9638-893X); Yu-Min Choi (0000-0003-4709-3155); Hong Kim (0000-0003-1383-6803); Bum-Joon Kim (0000-0003-0085-6709).

Author contributions: Kim BJ conceived this research and participated in its design and coordination; Lee SA performed the experiments; Lee SY, Choi YM and Kim H analyzed and interpreted the data; Kim BJ contributed the reagents, materials and analysis tools.

Supported by the Korea Health Technology R&D Project through the Korea Health Industry Development Institute and the Ministry of Health and Welfare, South Korea, No. HI14C0955.

Conflict-of-interest statement: There was no conflict of interest.

Data sharing statement: No additional data are available.

Manuscript source: Unsolicited manuscript

Correspondence to: Bum-Joon Kim, PhD, Professor, Department of Biomedical Sciences, Microbiology and Immunology, and Liver Research Institute, Seoul National University College of Medicine, 103, Daehak-ro, Jongno-gu, Seoul 110799, South Korea. kbumjoon@snu.ac.kr
Telephone: +82-2-7408316
Fax: +82-2-7430881

Received: January 11, 2018
Peer-review started: January 11, 2018
First decision: January 25, 2018
Revised: January 31, 2018
Accepted: February 9, 2018
Article in press: February 9, 2018
Published online: March 14, 2018

Abstract

AIM

To study sex disparity in susceptibility to hepatocellular carcinoma (HCC), we created a transgenic mouse model that expressed the full hepatitis B virus (HBV) genome with the W4P mutation.

METHODS

Transgenic mice were generated by transferring the pHY92-1.1x-HBV-full genome plasmid (genotype A2) into C57Bl/6N mice. We compared serum levels of hepatitis B surface antigen (HBsAg), interleukin (IL)-6, and the liver enzymes alanine aminotransferase (ALT) and aspartate transaminase (AST), as well as liver histopathological features in male and female transgenic (W4P TG) mice and in nontransgenic littermates of 10 mo of age.

RESULTS

W4P TG males exhibited more pronounced hepatomegaly, significantly increased granule generation in liver tissue, elevated HBsAg expression in the liver and serum, and higher serum ALT and IL-6 levels compared

to W4P TG females or littermate control groups.

CONCLUSION

Together, our data indicate that the W4P mutation in preS1 may contribute to sex disparity in susceptibility to HCC by causing increased HBV virion replication and enhanced IL-6-mediated inflammation in male individuals. Additionally, our transgenic mouse model that expresses full HBV genome with the W4P mutation in preS1 could be effectively used for the studies of the progression of liver diseases, including HCC.

Key words: Hepatitis B virus; W4P mutation of preS1; Transgenic mice; Hepatocellular carcinoma

Core tip: With the development of hepatitis B virus (HBV) vaccine, the rate of chronic HBV infection has dramatically declined worldwide. However, the incidence of hepatocellular carcinoma (HCC), which is characterized by poor prognosis and low survival rate, is on the rise. Predominance in males is a representative global epidemiological characteristic of HCC. Recently, we introduced the novel W4P substitution into the preS1 region, which associated with HCC and notably occurred exclusively in male patients. Our study in the nude mouse xenograft model indicated that the W4P mutation likely contributed to IL-6-dependent HCC progression, particularly in male individuals. Here, to gain further insight into the role of this mutation in HBV-induced liver inflammation, we created transgenic mice carrying the full HBV genome with this mutation. Of note, our data showed that W4P transgene males of 10 mo of age, but not W4P transgene females, spontaneously developed liver damage due to IL-6-mediated liver inflammation, further supporting the previous finding regarding the contribution of the W4P mutation to sex disparity in susceptibility to HCC. Furthermore, our results prove the utility of the developed W4P transgene mouse model for research into the mechanisms of HBV-caused liver diseases.

Lee SA, Lee SY, Choi YM, Kim H, Kim BJ. Sex disparity in viral load, inflammation and liver damage in transgenic mice carrying full hepatitis B virus genome with the W4P mutation in the preS1 region. *World J Gastroenterol* 2018; 24(10): 1084-1092 Available from: URL: http://www.wjgnet.com/1007-9327/full/v24/i10/1084.htm DOI: http://dx.doi.org/10.3748/wjg.v24.i10.1084

INTRODUCTION

Hepatitis B virus (HBV) infection causes a wide range of chronic infectious diseases, including chronic hepatitis, liver cirrhosis and hepatocellular carcinoma (HCC). In 2010, the number of patients in which HBV infection was the main cause of death was reported to be 786000 worldwide[1,2].

The incidence of chronic HBV infection in children has been considerably decreased by the successful development of antiHBV vaccine[3-5]. Nevertheless, the high risk of liver cirrhosis (LC) and HCC is still a problem in adult HBV carriers. The five-year cumulative risk of HCC progression is approximately 10%-17% in LC patients, and disease progression from chronic hepatitis B to LC is expected in 12%-20% of patients in 5 years[6-8]. HBV genotype C2, which is predominant in Asia, is associated with a particularly significant risk of HCC compared to that conferred by HBVs of other genotypes[9-11]. The correlation between HBV infection and sex disparity in susceptibility to HCC has been well documented. However, the mechanism by which HBV causes cancer development is still unresolved. Premature termination of HBV X protein (HBx), which results in truncated hepatitis B surface antigen (HBsAg), or mutations, particularly deletions, in the preS region of large-surface proteins (LHBs) have been reported to be associated with HCC progression[12-15].

Prevalence in males is one of the remarkable global epidemiological characteristics of HCC, as approximately 3-5 times more cases of HCC are observed in men than in women[16-18]. The sex disparity is more prominent in HBV-related HCC than in hepatitis C virus-related HCC, suggesting the presence of an HBV infection-related factor that determines HCC male predominance[19,20]. It has been reported that high expression levels of both androgen and active androgen receptor gene alleles increase the risk of HCC in male patients with chronic hepatitis B due to the interaction between HBx and androgen axis[21-23].

HCC development is likely affected not only by the HBx-androgen axis interactions but also by a tumor-protective effect of estrogen. In particular, it has been suggested that taking contraceptives or postmenopausal hormone therapy associated with long-term exposure to estrogen reduces the risk of HCC in female patients[24]. In addition, it has been reported that estrogen receptor α-mediated inhibition of interleukin (IL)-6 production had an essential role in inhibiting carcinogenesis in a mouse model of HCC induced chemically by diethylnitrosamine[25,26].

On the basis of differential time courses of HCC development and disease severity in wild-type (WT) individuals and in individuals with LHB mutations, it has been proposed that mutated LHBs lead to carcinogenesis by inducing endoplasmic reticulum stress pathway or by altering transactivating capacity of hepatocytes[27-29].

In a molecular epidemiological study, we have previously found that the W4P mutation in the preS1 start region is associated with HCC development in male but not female patients[30]. In addition, our further cell-based and nude mouse xenograft model studies supported the notion that the W4P mutation likely induced HCC progression in an IL-6-dependent manner

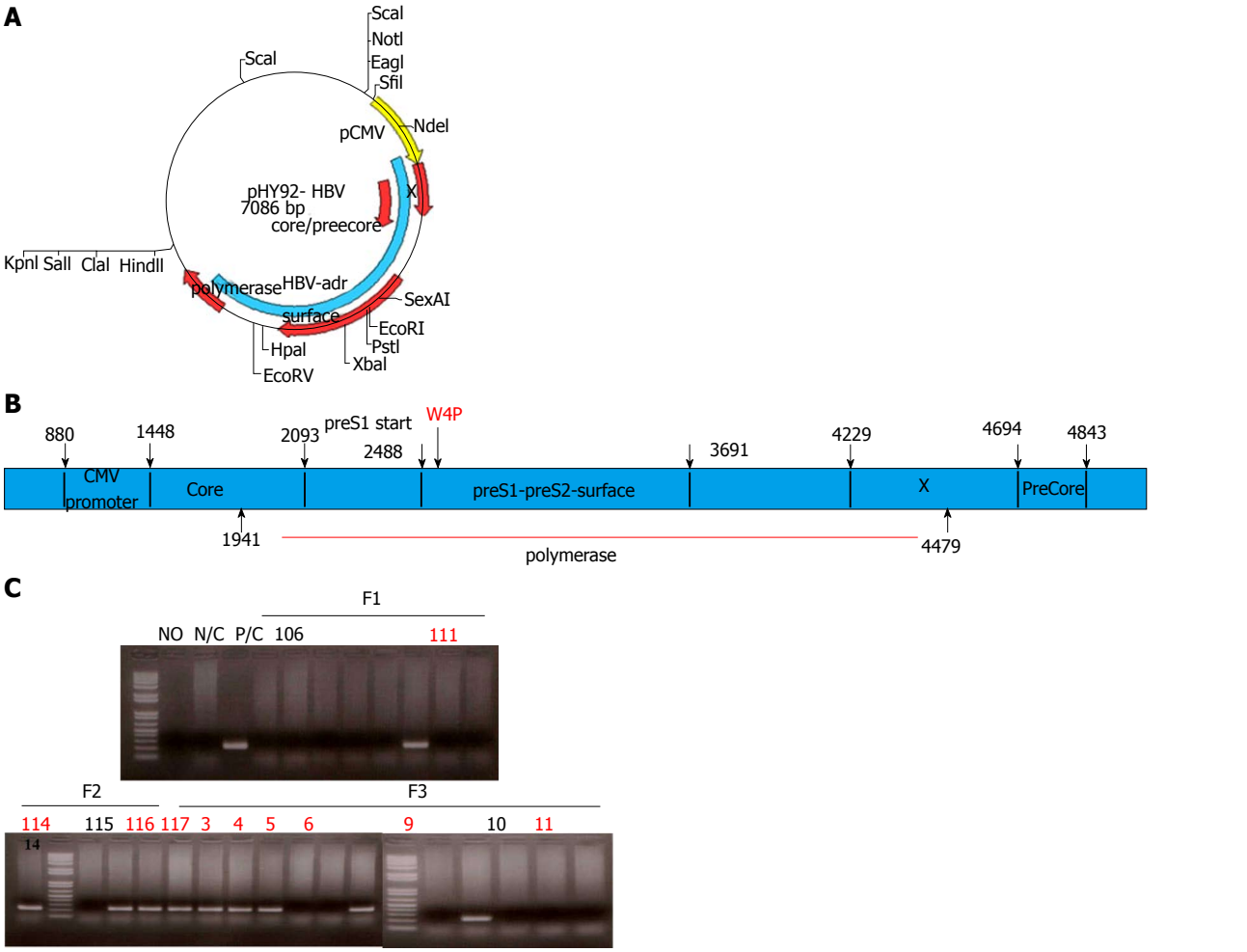

Figure 1 Construction of the W4P TG mice expressing pHY92-1.1x the HBV full genome with the preS1 W4P mutation and the screening of the constructed W4P TG mice. A: A plasmid map of pHY92 vector containing a copy of the 1.1x-unit length HBV genome under the control of a CMV promoter; B: The HBV full genome construct with a W4P missense mutation in the preS1 region; C: Screening of the constructed W4P TG mice by PCR targeting the preS1 region. CMV: Cytomegalovirus; HBV: Hepatitis B virus.

in male patients[31]. Here, to gain further insight into the role of this mutation in the sex disparity of HBV-induced liver inflammation, we created transgenic (TG) mice carrying the full HBV genome with the W4P mutation and evaluated HBV virion replication and IL-6-mediated inflammation in male and female TG and WT individuals.

MATERIALS AND METHODS

Generation of the full-length HBV genome construct with the prS1 W4P mutation using site-directed mutagenesis

The mutant full-length HBV genome construct carrying the W4P mutation in the preS1 region (hereafter, pHY92-W4P) was generated by site-directed mutagenesis of the WT pHBV-1.1x vector (hereafter, pHY92-WT) (Genotype A, GenBank No. AF305422), which was kindly provided by Yang *et al*[32]. The mutagenesis was performed using the forward primer W4P-F (5'- AACAAGAGCTACGCATGGGAGGTCCGT CATCAAAACCTC-3') and the reverse primer W4P-R (5'-GAGGTTTTGATGACGGACCT CCCATGCTGTAGCTCTTGTT-3') located from 2473 bp and 2513 bp. Site-directed mutagenesis of the full HBV genome was performed as described[33].

TG mice

To generate W4P TG mice, fertilized C57BL/6N embryos and HBV full genome with the W4P mutation were co-microinjected into one-cell embryo in accordance with the standard microinjection procedures for TG mouse production (Macrogen, Seoul, Korea). Genotyping of TG mice was conducted by PCR and viral DNA samples obtained from tail vein bleeds were screened using the primers PreS-F (5'-GGGTCACCATATTCTTGGGAA-3') and PreS-R (5'-CGAATGCTCCCRCTCCTAC-3). The mice were housed in a specific pathogen-free laboratory animal center. The TG mice were crossed with B6D2F1/J mice (The Jackson Laboratory, Bar Harbor, ME, United States) and the HBV-expressing offspring mice, as well as their littermates, were used in this study. All animal experiments were conducted following United States' National Institutes of Health guidelines for housing and care of laboratory animals

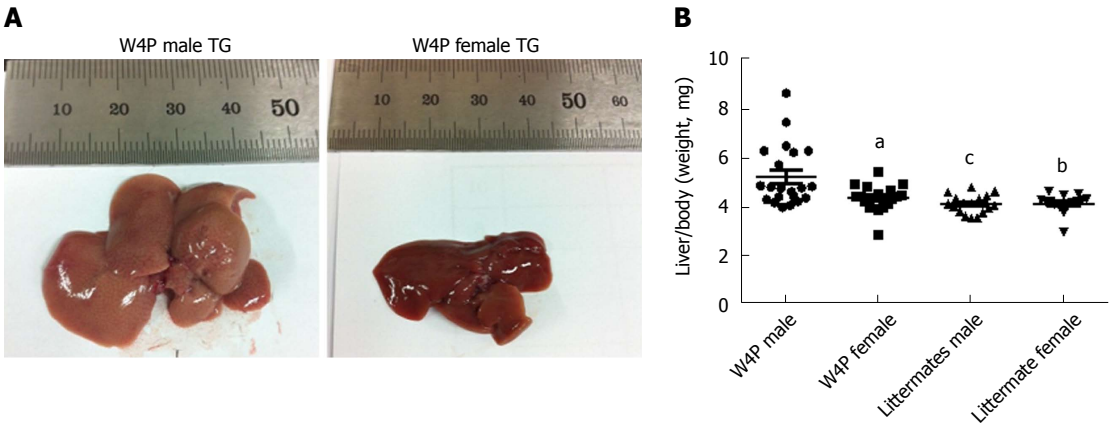

Figure 2 Increased hepatomegaly in the W4P male TG mice. A: *In situ* view of liver of W4P TG male mice and W4P TG female mice at 10 mo of age; B: Liver weight ratio against the total body weight (mg) in W4P mutant mice (males: 24 mice; females: 18 mice) and nonTG littermates (males: 17 mice; females: 15 mice) at 10 mo of age ($^{a}P < 0.05$, $^{b}P < 0.01$, and $^{c}P < 0.001$ *vs* W4P male, one-way ANOVA.

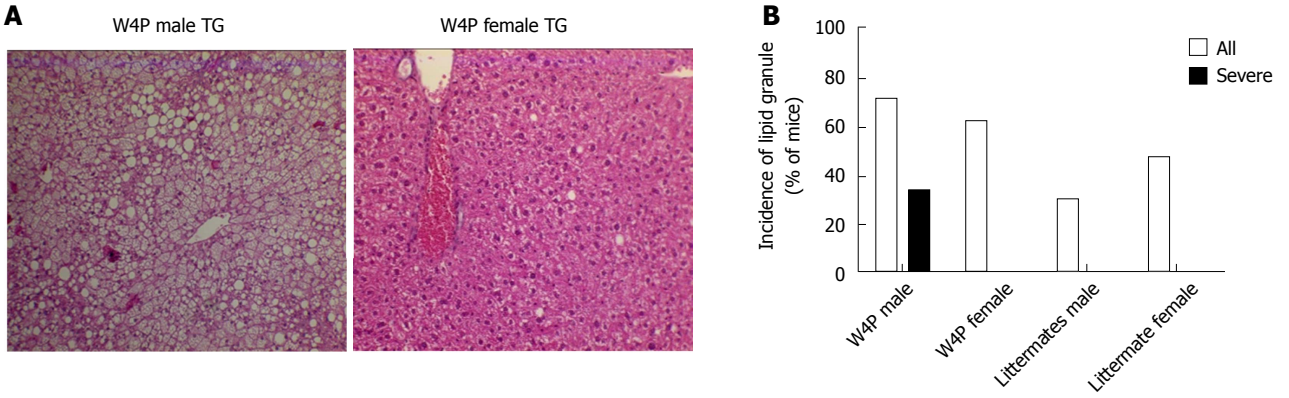

Figure 3 Increased generation of lipid droplets in W4P male TG mice. A: Comparison of generated lipid droplets in the liver section by hematoxylin-eosin staining (× 200); B: Incidence of lipid droplets in W4P mutant mice (males: 24 mice; females: 18 mice) and non TG littermates (males: 17 mice; females: 15 mice) at 10 mo of age.

and in accordance with the protocol approved by the Institutional Animal Care and Use Committee (IAUAC) of the Seoul National University College of Medicine (Protocol No. SNU-111025).

Enzyme-linked immunosorbent assay

Serum HBsAg levels in male and female W4P TG mice and their WT littermates were determined by enzyme-linked immunosorbent assay (ELISA) using a commercial Bioelisa HBsAg color kit (Biokit, Barcelona, Spain) according to the procedures provided by the manufacturer. The amount of secreted IL-6 was determined by a mIL-6 ELISA kit (eBioscience, San Diego, CA, United States). Serum levels of alanine aminotransferase (ALT) and aspartate transaminase (AST) were determined at the Seoul National University Hospital Biomedical Research Institute facility.

Hematoxylin and eosin staining and immunohistochemistry

Liver samples were fixed with 4% paraformaldehyde in phosphate-buffered saline and embedded in paraffin. Tissue sections were stained with hematoxylin and eosin at the Seoul National University Hospital Biomedical Research Institute facility. Immunohistochemical staining with an anti-preS1 monoclonal antibody (Aprogen, Daejeon, South Korea) was also performed. Deparaffinized sections were heated in citrate buffer (Zytomed, Berlin, Germany) to accomplish antigen retrieval. Endogenous peroxidase was blocked with peroxidase blocking solution (Zytomed). An anti-preS1 antibody was applied as the primary antibody followed by the application of the avidin-biotin complex method to detect the primary antibody. Peroxidase activity was visualized by a 3,3'-diaminobenzidine substrate kit (Zytomed) with hematoxylin (Wako, Osaka, Japan) as counterstain.

Statistical analysis

All ELISA assays in this study were repeated at least three times, and the results were expressed as the mean percentage ± standard deviation, or as the median (± range). For continuous variables, separate one-way analyses of variance were used to determine

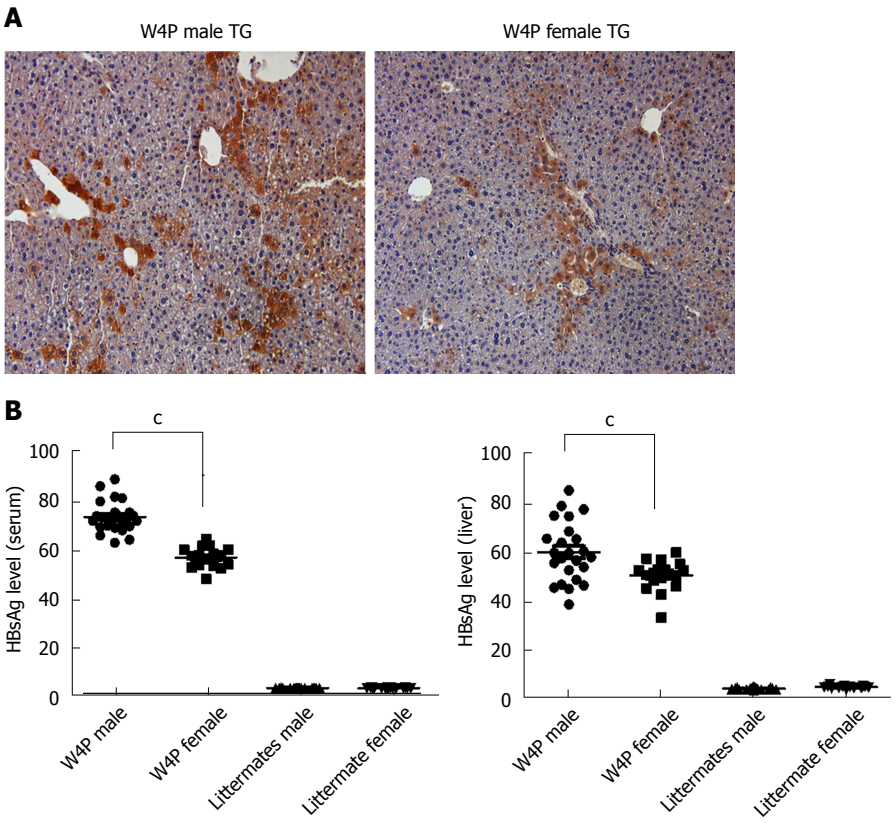

Figure 4 Increased secreted HBsAg level and liver LHBs in W4P male TG mice. A: Comparison of LHBs level in liver section by IHC analysis using anti-preS1 antibodies between W4P TG male and female mice (× 200); B: Comparison of HBsAg level in the liver and serum from W4P mutant mice (males: 24 mice; females: 18 mice) and nonTG littermates (males: 17 mice; females: 15 mice) at 10 mo of age ($^{c}P < 0.001$ *vs* W4P male, one-way ANOVA). HBsAg: Hepatitis B surface antigen; IHC: Immunohistochemistry; LHBs: Large-surface proteins.

if there was a significant difference by using the Bartlett's test. All statistical analyses were conducted with a significance level of $\alpha = 0.05$ ($P < 0.05$).

RESULTS

Construction of TG mice harboring full HBV genome with the W4P mutation in preS1

TG mice generated on B6D2F1/J background expressed the full-length HBV genome with the W4P mutation in preS1 under the control of the cytomegalovirus (CMV) promoter. For this purpose, we used site-directed mutagenesis of the pHY92 vector containing a copy of the 1.1x-unit length HBV genome under the control of the CMV promoter (genotype A, serotype adw, HBV strain identical to GenBank AF305422), which was provided by Yang *et al*[32], and generated a missense mutation, changing tryptophan to proline (TGG to CCG) at the fourth codon of preS1 (Figure 1A). Comparison of WT and W4P mutant LHB region sequences is shown in Supplementary Figure 1.

To confirm whether TG mice harbored the full HBV genome, the presence of virion DNA and secreted HBsAg in the serum or liver was checked by PCR and ELISA, respectively (Figure 1A).

Increased hepatomegaly and lipid granule content in male W4P TG mice

To check whether there was sex disparity in hepatomegaly, we examined the ratio of the liver weight to total body weight between W4P TG mice (24 males, 18 females) and their nonTG littermates (17 males, 15 females) at 10 mo of age. W4P TG male mice showed a significantly higher liver to total body weight ratio compared to that in mice of the three other groups, including W4P TG female mice and nonTG littermates (male and female mice) (Figure 2). Examination of histological samples stained with hematoxylin and eosin revealed that the incidence of mice generating lipid granules was higher in W4P male mice compared to that in W4P TG female mice and nonTG littermates (Figure 3).

Higher serum levels of HBsAg and increased amounts of LHBs in the livers of male W4P TG mice

Next, to check whether there was sex disparity in HBV production, we determined HBsAg levels in the serum and LHB levels in the livers of W4P TG mice (24 males, 18 females) and their nonTG littermates (17 males, 15 females) at 10 mo of age. W4P TG male mice showed a significantly higher level of HBsAg in the serum

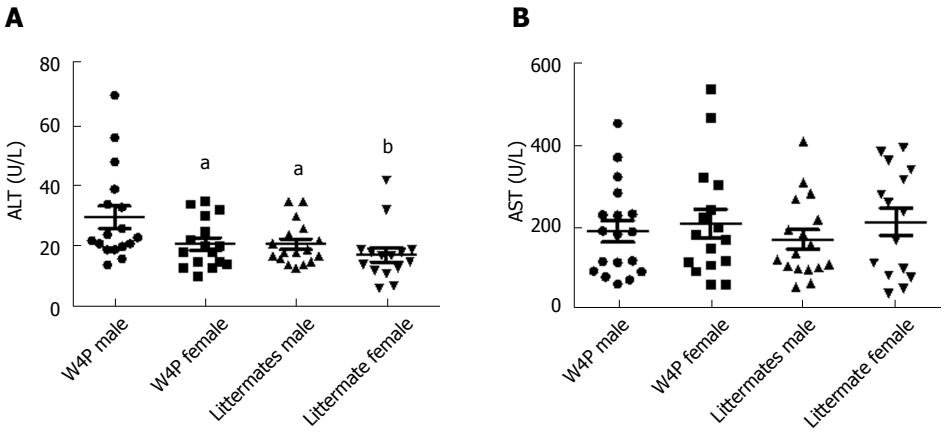

Figure 5 Serum alanine aminotransferase (A) and aspartate transaminase (B) levels in W4P TG mice (males: 24 mice; females: 18 mice) and nonTG littermates (males: 17 mice; females: 15 mice) at 10 mo of age. [a]*P* < 0.05, and [b]*P* < 0.01, *vs* W4P male, one-way ANOVA. ALT: Alanine aminotransferase; AST: Aspartate transaminase.

compared to that in mice from the other three groups. Immunohistochemical staining of the liver samples using an anti-preS1 antibody also showed increased LHB production in W4P TG male mice (Figure 4).

Increased serum levels of ALT and IL-6 in male W4P TG mice

It has been reported previously that the presence of the W4P mutation in the preS1 region sex-dependently affected IL-6 production in the xenograft nude mouse model system, which could be one of the reasons for increased male susceptibility to HCC[31]. Thus, to check whether there was sex disparity in the induction of IL-6-mediated inflammation, we next examined serum IL-6 levels in W4P TG mice (24 males, 18 females) and their nonTG littermates (17 males, 15 females) at 10 mo of age. W4P TG male mice showed significantly higher serum IL-6 levels than did mice of the other three groups (Figure 5). We also checked the levels of liver enzymes in the serum as indicators of liver damage in the four groups of mice. We found that W4P TG male mice had significantly higher serum levels of ALT than mice from the other three groups. However, serum AST levels were not significantly different in the four groups of mice (Figure 6).

DISCUSSION

Increasing evidence has shown sex disparity in the incidence of HBV-associated HCC in a sex hormone-dependent manner. Sex hormones, including androgen and estrogen, likely affect the progression of HBV infection and development of HBV-related HCC *via* their actions on receptor-mediated cell signaling[24-26]. To date, of all HBV proteins, HBx has been most extensively studied as the predominant virus interactor with host cell sex hormone-mediated signaling[22,23]. However, in our recent molecular epidemiologic and cell-based studies, we have demonstrated that LHB harboring the W4P mutation in preS1 could also contribute to the sex disparity of HBV-associated HCC in an IL-6-dependent manner[30,31]. In the present study, we constructed W4P TG mice that expressed the full HBV genome, which can help us to study sex disparity of the progression of liver diseases, including chronic hepatitis, steatohepatitis, cirrhosis and HCC, following chronic HBV infection.

We identified three noteworthy findings supporting the contribution of the W4P mutation in preS1 to liver disease progression in male patients. First, by using the W4P TG mouse model of chronic HBV infection, we found that male W4P TG mice exhibited higher levels of secreted HBsAg and liver LHBs, which was indicative of higher HBV replication than in female W4P TG mice (Figure 4) and is one of the known HCC risk factors[34]. Second, we found that male W4P TG mice showed increased incidence of hepatomegaly and lipid droplets (Figure 3), reflecting the imbalance of metabolic liver homeostasis, which could drive liver pathogenesis, including fatty liver and steatohepatitis, and further promote tumorigenesis. Third, we found that male W4P TG mice had increased IL-6-related liver inflammation and higher serum ALT levels (Figure 5), which were indications of liver damage, compared to those seen in female W4P TG mice.

IL-6 is one of the core stimulators that lead to persistent HBV infection and development of HBV-related HCC. It is also a key cytokine that may be a link to preferential male susceptibility to HCC[25,31]. A previous study that used diethylnitrosamine to evoke HCC showed that estrogen prevented HCC generation in female mice by inhibiting IL-6 production in a Myd88-dependent manner. That observation suggested that inhibition of IL-6 production in liver Kupffer cells by estrogen and estrogen receptor-mediated signaling pathways could be a major molecular mechanism that underlies sex disparity in HBV-associated liver diseases, including HCC[25,26]. Furthermore, increased hepatic IL-6 production also likely plays a pivotal role in the development of nonalcoholic fatty liver disease, nonalcoholic steatohepatitis, and insulin

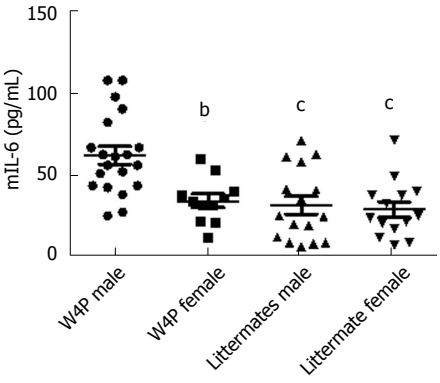

Figure 6 Secreted interleukin-6 levels in the W4P TG mice (males: 24 mice; females: 18 mice) and nonTG littermates (males: 17 mice; females: 15 mice) at 10 mo of age. ($^{a}P < 0.05$, $^{b}P < 0.01$, and $^{c}P < 0.001$ *vs* W4P_male, one-way ANOVA). ALT: Alanine aminotransferase; AST: Aspartate transaminase; IL: Interleukin.

resistance, which are the leading causes of HCC[35-40]. Thus, our W4P TG model showing increased hepatic IL-6 production could provide a novel insight into the relationships between IL-6 production due to an infection caused by an HBV variant on the one hand, and development of nonalcoholic steatohepatitis, type 2 diabetes or HCC on the other hand.

Our study had some limitations. Unfortunately, we did not prove predominant carcinogenesis in males in our W4P TG mice. Therefore, further studies are necessary to demonstrate higher male susceptibility to liver carcinogenesis in our W4P TG mouse model and clarify its mechanism in the future. In addition, the relationships between increased hepatic production of IL-6 in mice expressing HBV genome with the W4P mutation and fat accumulation, increased liver weight and HCC development also remain to be elucidated in the future.

The phenotypes of male W4P TG mice, namely higher levels of IL-6 and ALT in the serum, could provide a technical advantage in drug screening protocols, as it will be possible to analyze not only the inhibition of HBV replication but also the antiinflammatory activity. To the best of our knowledge, this possibility is currently not available in other related TG mouse models.

In conclusion, we created W4P TG mice that constitutively express the full HBV genome with the W4P mutation in preS1 in the present study. Our data using W4P TG mice indicate that this mutation likely contributes to sex disparity in the susceptibility to liver disease, including HCC, leading to increased HBV virion replication and enhanced IL-6-mediated inflammation in male individuals. Additionally, the developed TG mouse model system carrying the full HBV genome with the W4P mutation in preS1 could be effectively used not only in basic research into the mechanisms of liver disease progression in HCC but also for the screening of antiHBV or antiinflammatory drugs.

ARTICLE HIGHLIGHTS

Research background

A remarkable global epidemiological feature of hepatocellular carcinoma (HCC) is its higher incidence in males. Recently, we identified the novel W4P substitution in the preS1 region of hepatitis B virus (HBV) related to HCC that occurs exclusively in male patients. We have also shown that the W4P mutation likely contributed to HCC development, particularly in male patients, in an interleukin (IL)-6-dependent manner.

Research motivation

Studies of sex disparity in the susceptibility to HCC *in vivo* have mainly utilized the chemical agent diethylnitrosamine to induce HCC in mice. However, no transgenic (TG) mouse model system expressing the full HBV genome has yet been available for the study of sex disparity in HBV-related liver diseases.

Research objectives

To gain further insight into the role of the W4P mutation in the preS1 region of HBV on sex disparity of HBV-induced liver inflammatory manifestations, we created a TG mouse that carried the full HBV genome with this mutation and evaluated HBV virion replication and IL-6-mediated inflammation in mutant and wild-type (WT) mice of both sexes.

Research methods

TG mice were generated by transferring the pHY92-1.1x-HBV-full genome plasmid (genotype A2) into C57Bl/6N mice. We compared serum levels of hepatitis B surface antigen (HBsAg), IL-6, and the liver enzymes alanine aminotransferase (ALT) and aspartate transaminase (AST), as well as liver histopathology features in male and female W4P TG mice and their WT littermates.

Research results

Our data showed significantly increased hepatomegaly, enhanced granule generation in liver tissue, higher HBsAg expression in the liver and serum, and higher serum ALT and IL-6 levels in W4P TG males compared to the values of these parameters in W4P TG females or littermate control groups.

Research conclusions

This is the first study that used TG mice to uncover the role of the W4P mutation in HBV preS1 in sex disparity of liver disease progression due to concomitantly increased HBV virion replication and greater IL-6-mediated inflammation in male individuals.

Research perspectives

The obtained results suggest that W4P TG mice developed in this study could be effectively used not only for the basic research into the mechanisms of HBV-associated liver diseases, including HCC, but also for screening antiHBV and antiinflammatory drugs.

REFERENCES

1 **Lee WM**. Hepatitis B virus infection. *N Engl J Med* 1997; **337**: 1733-1745 [PMID: 9392700 DOI: 10.1056/NEJM199712113372406]

2 **Lozano R**, Naghavi M, Foreman K, Lim S, Shibuya K, Aboyans V, Abraham J, Adair T, Aggarwal R, Ahn SY, Alvarado M, Anderson HR, Anderson LM, Andrews KG, Atkinson C, Baddour LM, Barker-Collo S, Bartels DH, Bell ML, Benjamin EJ, Bennett D, Bhalla K, Bikbov B, Bin Abdulhak A, Birbeck G, Blyth F, Bolliger I, Boufous S, Bucello C, Burch M, Burney P, Carapetis J, Chen H, Chou D, Chugh SS, Coffeng LE, Colan SD, Colquhoun S, Colson KE, Condon J, Connor MD, Cooper LT, Corriere M, Cortinovis M, de Vaccaro KC, Couser W, Cowie BC, Criqui MH, Cross M, Dabhadkar KC, Dahodwala N, De Leo D, Degenhardt

L, Delossantos A, Denenberg J, Des Jarlais DC, Dharmaratne SD, Dorsey ER, Driscoll T, Duber H, Ebel B, Erwin PJ, Espindola P, Ezzati M, Feigin V, Flaxman AD, Forouzanfar MH, Fowkes FG, Franklin R, Fransen M, Freeman MK, Gabriel SE, Gakidou E, Gaspari F, Gillum RF, Gonzalez-Medina D, Halasa YA, Haring D, Harrison JE, Havmoeller R, Hay RJ, Hoen B, Hotez PJ, Hoy D, Jacobsen KH, James SL, Jasrasaria R, Jayaraman S, Johns N, Karthikeyan G, Kassebaum N, Keren A, Khoo JP, Knowlton LM, Kobusingye O, Koranteng A, Krishnamurthi R, Lipnick M, Lipshultz SE, Ohno SL, Mabweijano J, MacIntyre MF, Mallinger L, March L, Marks GB, Marks R, Matsumori A, Matzopoulos R, Mayosi BM, McAnulty JH, McDermott MM, McGrath J, Mensah GA, Merriman TR, Michaud C, Miller M, Miller TR, Mock C, Mocumbi AO, Mokdad AA, Moran A, Mulholland K, Nair MN, Naldi L, Narayan KM, Nasseri K, Norman P, O'Donnell M, Omer SB, Ortblad K, Osborne R, Ozgediz D, Pahari B, Pandian JD, Rivero AP, Padilla RP, Perez-Ruiz F, Perico N, Phillips D, Pierce K, Pope CA 3rd, Porrini E, Pourmalek F, Raju M, Ranganathan D, Rehm JT, Rein DB, Remuzzi G, Rivara FP, Roberts T, De León FR, Rosenfeld LC, Rushton L, Sacco RL, Salomon JA, Sampson U, Sanman E, Schwebel DC, Segui-Gomez M, Shepard DS, Singh D, Singleton J, Sliwa K, Smith E, Steer A, Taylor JA, Thomas B, Tleyjeh IM, Towbin JA, Truelsen T, Undurraga EA, Venketasubramanian N, Vijayakumar L, Vos T, Wagner GR, Wang M, Wang W, Watt K, Weinstock MA, Weintraub R, Wilkinson JD, Woolf AD, Wulf S, Yeh PH, Yip P, Zabetian A, Zheng ZJ, Lopez AD, Murray CJ, AlMazroa MA, Memish ZA. Global and regional mortality from 235 causes of death for 20 age groups in 1990 and 2010: a systematic analysis for the Global Burden of Disease Study 2010. *Lancet* 2012; **380**: 2095-2128 [PMID: 23245604 DOI: 10.1016/S0140-6736(12)61728-0]

3 **Chang MH**, Chen TH, Hsu HM, Wu TC, Kong MS, Liang DC, Ni YH, Chen CJ, Chen DS; Taiwan Childhood HCC Study Group. Prevention of hepatocellular carcinoma by universal vaccination against hepatitis B virus: the effect and problems. *Clin Cancer Res* 2005; **11**: 7953-7957 [PMID: 16278421 DOI: 10.1158/1078-0432.CCR-05-1095]

4 **Lavanchy D**. Worldwide epidemiology of HBV infection, disease burden, and vaccine prevention. *J Clin Virol* 2005; **34** Suppl 1: S1-S3 [PMID: 16461208 DOI: 10.1016/S1386-6532(05)00384-7]

5 **Liang X**, Bi S, Yang W, Wang L, Cui G, Cui F, Zhang Y, Liu J, Gong X, Chen Y, Wang F, Zheng H, Wang F, Guo J, Jia Z, Ma J, Wang H, Luo H, Li L, Jin S, Hadler SC, Wang Y. Reprint of: Epidemiological serosurvey of Hepatitis B in China--declining HBV prevalence due to Hepatitis B vaccination. *Vaccine* 2013; **31** Suppl 9: J21-J28 [PMID: 23948229 DOI: 10.1016/j.vaccine.2013.08.012]

6 **Lavanchy D**. Hepatitis B virus epidemiology, disease burden, treatment, and current and emerging prevention and control measures. *J Viral Hepat* 2004; **11**: 97-107 [PMID: 14996343 DOI: 10.1046/j.1365-2893.2003.00487.x]

7 **Hui CK**, Leung N, Yuen ST, Zhang HY, Leung KW, Lu L, Cheung SK, Wong WM, Lau GK; Hong Kong Liver Fibrosis Study Group. Natural history and disease progression in Chinese chronic hepatitis B patients in immune-tolerant phase. *Hepatology* 2007; **46**: 395-401 [PMID: 17628874 DOI: 10.1002/hep.21724]

8 **Liaw YF**, Chu CM. Hepatitis B virus infection. *Lancet* 2009; **373**: 582-592 [PMID: 19217993 DOI: 10.1016/S0140-6736(09)60207-5]

9 **McMahon BJ**. The influence of hepatitis B virus genotype and subgenotype on the natural history of chronic hepatitis B. *Hepatol Int* 2009; **3**: 334-342 [PMID: 19669359 DOI: 10.1007/s12072-008-9112-z]

10 **Schaefer S**. Hepatitis B virus taxonomy and hepatitis B virus genotypes. *World J Gastroenterol* 2007; **13**: 14-21 [PMID: 17206751 DOI:10.3748/wjg.v13.i1.14]

11 **Croagh CM**, Desmond PV, Bell SJ. Genotypes and viral variants in chronic hepatitis B: A review of epidemiology and clinical relevance. *World J Hepatol* 2015; **7**: 289-303 [PMID: 25848459 DOI: 10.4254/wjh.v7.i3.289]

12 **Wang C**, Teng Z, Zhu Y, Zhao AZ, Sun C. Associations between pre-S deletion mutation of hepatitis B virus and risk of hepatocellular carcinoma in the Asian population: a meta-analysis. *Med Sci Monit* 2015; **21**: 1072-1077 [PMID: 25868851 DOI: 10.12659/MSM.894058]

13 **Mun HS**, Lee SA, Jee Y, Kim H, Park JH, Song BC, Yoon JH, Kim YJ, Lee HS, Hyun JW, Hwang ES, Kook YH, Kim BJ. The prevalence of hepatitis B virus preS deletions occurring naturally in Korean patients infected chronically with genotype C. *J Med Virol* 2008; **80**: 1189-1194 [PMID: 18461612 DOI: 10.1002/jmv.21208]

14 **Pollicino T**, Cacciola I, Saffioti F, Raimondo G. Hepatitis B virus PreS/S gene variants: pathobiology and clinical implications. *J Hepatol* 2014; **61**: 408-417 [PMID: 24801416 DOI: 10.1016/j.jhep.2014.04.041]

15 **Iwamoto M**, Watashi K, Tsukuda S, Aly HH, Fukasawa M, Fujimoto A, Suzuki R, Aizaki H, Ito T, Koiwai O, Kusuhara H, Wakita T. Evaluation and identification of hepatitis B virus entry inhibitors using HepG2 cells overexpressing a membrane transporter NTCP. *Biochem Biophys Res Commun* 2014; **443**: 808-813 [PMID: 24342612 DOI: 10.1016/j.bbrc.2013.12.052]

16 **Jemal A**, Bray F, Center MM, Ferlay J, Ward E, Forman D. Global cancer statistics. *CA Cancer J Clin* 2011; **61**: 69-90 [PMID: 21296855 DOI: 10.3322/caac.20107]

17 **Prieto J**. Inflammation, HCC and sex: IL-6 in the centre of the triangle. *J Hepatol* 2008; **48**: 380-381 [PMID: 18093689 DOI: 10.1016/j.jhep.2007.11.007]

18 **Mittal S**, El-Serag HB. Epidemiology of hepatocellular carcinoma: consider the population. *J Clin Gastroenterol* 2013; **47** Suppl: S2-S6 [PMID: 23632345 DOI: 10.1097/MCG.0b013e3182872f29]

19 **Liu WC**, Liu QY. Molecular mechanisms of gender disparity in hepatitis B virus-associated hepatocellular carcinoma. *World J Gastroenterol* 2014; **20**: 6252-6261 [PMID: 24876746 DOI: 10.3748/wjg.v20.i20.6252]

20 **Wang SH**, Chen PJ, Yeh SH. Gender disparity in chronic hepatitis B: Mechanisms of sex hormones. *J Gastroenterol Hepatol* 2015; **30**: 1237-1245 [PMID: 25708186 DOI: 10.1111/jgh.12934]

21 **Yu MW**, Yang YC, Yang SY, Cheng SW, Liaw YF, Lin SM, Chen CJ. Hormonal markers and hepatitis B virus-related hepatocellular carcinoma risk: a nested case-control study among men. *J Natl Cancer Inst* 2001; **93**: 1644-1651 [PMID: 11698569 DOI: 10.1093/jnci/93.21.1644]

22 **Chiu CM**, Yeh SH, Chen PJ, Kuo TJ, Chang CJ, Chen PJ, Yang WJ, Chen DS. Hepatitis B virus X protein enhances androgen receptor-responsive gene expression depending on androgen level. *Proc Natl Acad Sci* 2007; **104**: 2571-2578 [PMID: 17259306 DOI: 10.1073/pnas.0609498104]

23 **Bouchard MJ**, Wang L, Schneider RJ. Activation of focal adhesion kinase by hepatitis B virus HBx protein: multiple functions in viral replication. *J Virol* 2006; **80**: 4406-4414 [PMID: 16611900 DOI: 10.1128/JVI.80.9.4406-4414.2006]

24 **Lam CM**, Yong JL, Chan AO, Ng KK, Poon RT, Liu CL, Lo CM, Fan ST. Better survival in female patients with hepatocellular carcinoma: oral contraceptive pills related? *J Clin Gastroenterol* 2005; **39**: 533-539 [PMID: 15942442 DOI: 10.1097/01.mcg.0000165670.25272.46]

25 **Naugler WE**, Sakurai T, Kim S, Maeda S, Kim K, Elsharkawy AM, Karin M. Gender disparity in liver cancer due to sex differences in MyD88-dependent IL-6 production. *Science* 2007; **317**: 121-124 [PMID: 17615358 DOI: 10.1126/science.1140485]

26 **Yeh SH**, Chen PJ. Gender disparity of hepatocellular carcinoma: the roles of sex hormones. *Oncology* 2010; **78** Suppl 1: 172-179 [PMID: 20616601 DOI: 10.1159/000315247]

27 **Wang HC**, Huang W, Lai MD, Su IJ. Hepatitis B virus pre-S mutants, endoplasmic reticulum stress and hepatocarcinogenesis. *Cancer Sci* 2006; **97**: 683-688 [PMID: 16863502 DOI: 10.1111/j.1349-7006.2006.00235.x]

28 **Hsieh YH**, Su IJ, Wang HC, Chang WW, Lei HY, Lai MD, Chang WT, Huang W. Pre-S mutant surface antigens in chronic

hepatitis B virus infection induce oxidative stress and DNA damage. *Carcinogenesis* 2004; **25**: 2023-2032 [PMID: 15180947 DOI: 10.1093/carcin/bgh207]

29 **Caselmann WH**, Meyer M, Kekulé AS, Lauer U, Hofschneider PH, Koshy R. A trans-activator function is generated by integration of hepatitis B virus preS/S sequences in human hepatocellular carcinoma DNA. *Proc Natl Acad Sci* 1990; **87**: 2970-2974 [PMID: 2158099 DOI: 10.1073/pnas.87.8.2970]

30 **Lee SA**, Kim KJ, Kim DW, Kim BJ. Male-specific W4P/R mutation in the pre-S1 region of hepatitis B virus, increasing the risk of progression of liver diseases in chronic patients. *J Clin Microbiol* 2013; **51**: 3928-3936 [PMID: 24025913 DOI: 10.1128/JCM.01505-13]

31 **Lee SA**, Kim H, Won YS, Seok SH, Na Y, Shin HB, Inn KS, Kim BJ. Male-specific hepatitis B virus large surface protein variant W4P potentiates tumorigenicity and induces gender disparity. *Mol Cancer* 2015; **14**: 23 [PMID: 25645622 DOI: 10.1186/s12943-015-0303-7]

32 **Yang H**, Westland C, Xiong S, Delaney WE 4th. In vitro antiviral susceptibility of full-length clinical hepatitis B virus isolates cloned with a novel expression vector. *Antiviral Res* 2004; **61**: 27-36 [PMID: 14670591 DOI: 10.1016/j.antiviral.2003.07.003]

33 **Zheng L**, Baumann U, Reymond JL. An efficient one-step site-directed and site-saturation mutagenesis protocol. *Nucleic Acids Res* 2004; **32**: e115 [PMID: 15304544 DOI: 10.1093/nar/gnh110]

34 **Fattovich G**, Stroffolini T, Zagni I, Donato F. Hepatocellular carcinoma in cirrhosis: incidence and risk factors. *Gastroenterology* 2004; **127**: S35-S50 [PMID: 15508101 DOI: 10.1053/j.gastro.2004.09.014]

35 **Haukeland JW**, Damås JK, Konopski Z, Løberg EM, Haaland T, Goverud I, Torjesen PA, Birkeland K, Bjøro K, Aukrust P. Systemic inflammation in nonalcoholic fatty liver disease is characterized by elevated levels of CCL2. *J Hepatol* 2006; **44**: 1167-1174 [PMID: 16618517 DOI: 10.1016/j.jhep.2006.02.011]

36 **Abiru S**, Migita K, Maeda Y, Daikoku M, Ito M, Ohata K, Nagaoka S, Matsumoto T, Takii Y, Kusumoto K, Nakamura M, Komori A, Yano K, Yatsuhashi H, Eguchi K, Ishibashi H. Serum cytokine and soluble cytokine receptor levels in patients with non-alcoholic steatohepatitis. *Liver Int* 2006; **26**: 39-45 [PMID: 16420507 DOI: 10.1111/j.1478-3231.2005.01191.x]

37 **Abdelmalek MF**, Diehl AM. Nonalcoholic fatty liver disease as a complication of insulin resistance. *Med Clin North Am* 2007; **91**: 1125-1149, ix [PMID: 17964913 DOI: 10.1016/j.mcna.2007.06.001]

38 **Grivennikov SI**, Karin M. Inflammatory cytokines in cancer: tumour necrosis factor and interleukin 6 take the stage. *Ann Rheum Dis* 2011; **70** Suppl 1: i104-i108 [PMID: 21339211 DOI: 10.1136/ard.2010.140145]

39 **Michelotti GA**, Machado MV, Diehl AM. NAFLD, NASH and liver cancer. *Nat Rev Gastroenterol Hepatol* 2013; **10**: 656-665 [PMID: 24080776 DOI: 10.1038/nrgastro.2013.183]

40 **Scalera A**, Tarantino G. Could metabolic syndrome lead to hepatocarcinoma via non-alcoholic fatty liver disease? *World J Gastroenterol* 2014; **20**: 9217-9228 [PMID: 25071314 DOI: 10.3748/wjg.v20.i28.9217]

:

P- Reviewer: Bramhall S, Huang C, Kai K, Tarantino G, Tomizawa M

S- Editor: Wang XJ **L- Editor**: Filipodia **E- Editor**: Ma YJ

World Journal of Gastroenterology

Submit a Manuscript: http://www.f6publishing.com

World J Gastroenterol 2018 March 14; 24(10): 1093-1106

DOI: 10.3748/wjg.v24.i10.1093

ISSN 1007-9327 (print) ISSN 2219-2840 (online)

ORIGINAL ARTICLE

Basic Study

Determination of the mitigating effect of colon-specific bioreversible codrugs of mycophenolic acid and aminosugars in an experimental colitis model in Wistar rats

Shakuntala Santosh Chopade, Suneela Sunil Dhaneshwar

Shakuntala Santosh Chopade, Suneela Sunil Dhaneshwar, Department of Pharmaceutical Chemistry, Poona College of Pharmacy, Bharati Vidyapeeth University, Pune 411038, India

ORCID number: Shakuntala Santosh Chopade (0000-0002-3886-6577); Suneela Sunil Dhaneshwar (0000-00c01-7646-642X).

Author contributions: Chopade SS and Dhaneshwar SS equally contributed to the conception and design of the study, acquisition, analysis and interpretation of data, drafted the article and made revisions related to the intellectual content of the manuscript.

Supported by Women Scientist Scheme-A (DST), No. SR/WOS-A/LS-1115/2014.

Institutional animal care and use committee statement: All animal experimentation was approved by the Institutional Animal Ethics Committee (IAEC-approval number: CPCSEA/PCH/15/2014-15) of Poona College of Pharmacy, Bharati Vidyapeeth University, Erandwane, Pune 411038, India.

Conflict-of-interest statement: The authors wish to declare no conflict of interest.

Data sharing statement: There are no additional data available in relation to this manuscript.

ARRIVE guidelines statement: The authors have read the ARRIVE guidelines, and the manuscript was prepared and revised according to the guidelines.

Manuscript source: Invited manuscript

Correspondence to: Suneela Sunil Dhaneshwar, BPharm, PhD, Professor, Department of Pharmaceutical Chemistry, Poona College of Pharmacy, Bharati Vidyapeeth University, Pune 411038, India. suneeladhaneshwar@rediffmail.com
Telephone:+91-20-25437237
Fax: +91-20-25439382

Received: December 11, 2017
Peer-review started: December 12, 2017
First decision: December 27, 2017
Revised: December 31, 2017
Accepted: January 24, 2018
Article in press: January 24, 2018
Published online: March 14, 2018

Abstract

AIM

To design colon-targeted codrugs of mycophenolic acid (MPA) and aminosugars as a safer option to mycophenolate mofetil (MMF) in the management of inflammatory bowel disease.

METHODS

Codrugs were synthesized by coupling MPA with aminosugars (D-glucosamine and D-galactosamine) using EDCI coupling. The structures were confirmed by infrared radiation, nuclear magnetic resonance, mass spectroscopy and elemental analysis. The release profile of codrugs was extensively studied in aqueous buffers, upper gastrointestinal homogenates, faecal matter and caecal homogenates (*in vitro*) and rat blood (*in vitro*). Anti-colitic activity was assessed in 2,4,6-trinitrobezenesulfonic acid-induced colitis in Wistar rats by the estimation of various demarcating parameters. Statistical evaluation was performed by applying one-way and two-way ANOVA when compared with the disease control.

RESULTS

The prodrugs resisted activation in HCl buffer (pH 1.2) and stomach homogenates of rats with negligible hydrolysis in phosphate buffer (pH 7.4) and intestinal homogenates. Incubation with colon homogenates (*in vitro*) produced 76% to 89% release of MPA emphasizing colon-specific activation of codrugs and the release of MPA and aminosugars at the site of action. In the *in vitro* studies, the prodrug of MPA with D-glucosamine (MGLS) was selected which resulted in 68% release of MPA in blood. *in vitro* studies on MGLS revealed its colon-specific activation after a lag time of 8 h which could be ascribed to the hydrolytic action of N-acyl amidases found in the colon. The synthesized codrugs markedly diminished disease activity score and revived the disrupted architecture of the colon that was comparable to MMF but superior to MPA.

CONCLUSION

The significant attenuating effect of prodrugs and individual aminosugars on colonic inflammation proved that the rationale of the codrug approach is valid.

Key words: Mycophenolic acid; Mutual prodrug; Inflammatory bowel disease; Mycophenolate mofetil

Core tip: Mycophenolic acid (MPA), an immunosuppressant and its morpholinoethyl ester prodrug: mycophenolate mofetil are under investigation for the treatment of inflammatory bowel disease (IBD). Diarrhea and local gut toxicity are their major setbacks. The present work focused on the synthesis of colon-targeted prodrugs wherein MPA was bio-reversibly linked with aminosugars to mask the carboxyl group of MPA responsible for gastrointestinal side effects. The synthesized prodrugs exhibited a significant mitigating effect on 2,4,6-trinitrobezenesulfonic acid-induced colitis in Wistar rats compared to MPA. The absence of pancreatitis, hepatitis and the gastro-sparing nature of the prodrugs emphasize their potential which could be investigated further for the management of IBD.

Choapade SS, Dhaneshwar SS. Determination of the mitigating effect of colon-specific bioreversible codrugs of mycophenolic acid and aminosugars in an experimental colitis model in Wistar rats. *World J Gastroenterol* 2018; 24(10): 1093-1106 Available from: URL: http://www.wjgnet.com/1007-9327/full/v24/i10/1093.htm DOI: http://dx.doi.org/10.3748/wjg.v24.i10.1093

INTRODUCTION

Mycophenolic acid (MPA) was synthesized as a fermentation product of *Penicillium stoloniferum* cultures by Gosio in 1896. Since its discovery, MPA has been the subject of intensive *in vivo* and *in vitro* screening for antifungal[1], antibacterial[2,3] and immunosuppressive activities[4-8]. Currently it is under investigation for the treatment of inflammatory bowel disease (IBD) and rheumatoid arthritis (RA). MPA is a potent, non-competitive, reversible inhibitor of eukaryotic inosine monophosphate dehydrogenase which is necessary for the growth of T cells and B cells. Due to its local gastric irritant side effect, it is being marketed in two forms *i.e.* mycophenolate mofetil (MMF) and mycophenolate sodium (enteric coated) to improve its gastrointestinal tolerance[7] and enhance bioavailability. MMF is an immunosuppressant of choice due to its multifaceted spectrum of activities and the apparent advantage of enhanced oral bioavailability. However, MMF-induced diarrhoea and local gut toxicity lead to poor patient compliance. It is under investigation for the treatment of IBD patients refractory or intolerant to steroids.

Since the isolation of MPA, it has been shown to possess a broad spectrum of activities due to which continuous attempts were made to improve its specificity by replacement of the lactone ring, modification of aromatic substituents, ester or amide derivatization, but these failed to show any benefits in most cases. Various derivatives of MPA, their synthesis and uses in the treatment of autoimmune diseases, psoriasis, inflammatory diseases including IBD, RA, tumors, virus and allograft rejection are described in many United States Patents[9-12]. Hydroxamic acid derivatives of MPA as histone deacetylases at the cellular level have been reported by Batovska *et al*[9]. 4 and 6-substituted derivatives of MPA[10], 5-hexanoic acid side chain derivatives of MPA[11] and a parenteral formulation of MPA, a salt or prodrug[12] thereof have been filed in the last two decades. Recently, Iwaszkiewicz-Grzes *et al*[13] in search of new immunosuppressants, synthesized amino acid derivatives of MPA as methyl esters using EDCI as the coupling reagent. With the exception of MMF, the morpholinoethyl ester prodrug of MPA, there are no reports of any prodrugs in the literature that are designed with the objective of enhancing its efficacy, reducing its effective dose or rendering a gastro-sparing effect.

The routine drug therapy of IBD involves the use of 5-aminosalicylic acid (5-ASA), sulfasalazine, corticosteroids (hydrocortisone, prednisolone, betamethasone, beclometasone and budesonide) and immunosuppressive agents (6-mercaptopurine, azathioprine, methotrexate and cyclosporine), whereas 4-ASA, broad-spectrum antibiotics, MMF, metronidazole, nicotine and thalidomide are other choices available for the treatment of disease or its secondary effects. Short chain fatty acids such as butyric acid are presently under investigation as treatment options for the safer management of IBD. Alternative treatments for IBD involve the use of colestyramine, sodium cromoglycate, bismuth and arsenical salts, methotrexate, lidocaine (lignocaine), sucralfate, new steroid entities, cytoprotective agents, fish oils and human growth hormone. During the last

decade, a huge number of biological agents against tumor necrosis factor-α, as well as many biochemical substances, have been developed for the effective treatment of patients with IBD. Among the new biologic agents, natalizumab is currently in regular use in the United States. Several nutritional deficiencies have been indicated in IBD and there are reports of improvement in the symptoms by taking daily supplements of nutraceuticals like vitamin A and carotenoids, vitamin E, vitamin C, vitamin K, folic acid, calcium, iron, selenium, zinc, magnesium and copper. Patients with active ulcerative colitis (UC) have a reduction in the amounts of obligate anaerobes, facultative organisms and micro-aerobes, when compared to UC patients in remission. Supplementation with probiotics is considered an effective option in UC. Leukocytapheresis has shown satisfactory results in steroid-refractory patients with UC. Unfractionated heparin and low molecular weight heparins (LMWH) have been used in patients with active UC with encouraging results. Microbes and microbial products including eggs of helminths seem to reduce disease activity in patients with UC or Crohn's disease[14].

5-ASA and its colon-targeted prodrug sulphasalazine, are associated with various serious side effects including ulcerogenicity, hypersensitivity, skin rash, blood disorders, pancreatitis and hepatitis. Corticosteroids and immunosuppressants are also known to produce many serious side effects so there is an urgent need for steroid-sparing, non-nephrotoxic, safe anti-inflammatory agents to treat inflammatory diseases such as IBD, RA, psoriasis and organ transplantations[14-18].

The present work was focused on exploring colon-targeting prodrugs of MPA for their possible application in the management of IBD. For the study, aminosugars such as D-galactosamine and D-glucosamine were selected as promoieties. An extensive literature review revealed that aminosugars play a vital role in resisting chemical attack and improving the tenacity of colon mucus. Moreover, glucosamine is involved in the biosynthesis of glucosaminoglycans and intestinal mucus. Colonic mucus is distinguished from mucus in the proximal intestine not only by its greater sialylation but also by its marked degree of sulphation[19]. The mucin molecule bristles with oligosaccharide side chains, the initial sugar of which is always N-acetyl galactosamine O-linked onto serine or threonine in the protein core. Onto this initial galactosamine may be attached up to 10 or more sugar moieties which can include N-acetyl glucosamine, galactose, N-acetyl galactosamine, fucose or the acid sugar sialic acid (usually as N-acetyl neuraminic acid). Alterations in sialylation and sulphation of mucins and O-acetylation of the mucin sialic acids could all have important effects on the resistance of mucus to bacterial enzymatic attack leading to colorectal cancer and IBD. Clamp and colleagues demonstrated that in UC and Crohn's disease, the oligosaccharide side chain of mucin is greatly shortened[20]. Therefore, we thought of linking glucosamine and galactosamine with MPA which when released in the colon would help to retain the architecture of mucin and form a protective layer on the colon mucosa. In addition to this, the polyhydroxy nature of these aminosugars would increase the hydrophilicity of MPA to such an extent that absorption of the intact prodrug in the upper gastrointestinal tract (GIT) would be minimized assuring efficient delivery to the site of action.

In the present study, we synthesized colon-specific mutual prodrugs involving the formation of a covalent amide linkage between MPA and aminosugars (glucosamine and galactosamine) in such a manner that upon oral administration the linkage remains intact in the upper GIT, but releases MPA in the colon through enzymatic activation[14,21]. Site-specific drug delivery through site-specific prodrug activation may be accomplished by the utilization of specific enzymes secreted by the colonic microflora such as N-acyl amidases. The present work was aimed at the rational design, pharmacokinetic and pharmacodynamic comparison of colon-targeting, mutual prodrugs of MPA with the marketed prodrug MMF.

MATERIALS AND METHODS

Mycophenolate sodium was generously gifted by Emcure Pharmaceuticals Pvt. Ltd., Pune, India. D-(+)-glucosamine hydrochloride and D-(+)-galactosamine hydrochloride were purchased from Sigma-Aldrich, St. Louis, United States and Himedia Laboratories Pvt. Ltd., Nashik, India, respectively. All other chemicals used in the synthesis were purchased from Merck Speciality Pvt. Ltd., Mumbai, India. The reactions were monitored on TLC, which was performed on pre-coated silica gel plates-60 F264 (Merck). Nuclear magnetic resonance (NMR) spectra were recorded on a NMR Varian Mercury 400 MHz at SAIF, Panjab University, Chandigarh, India. The IR spectra were recorded on a Jasco, V-530 FTIR in potassium bromide (anhydrous IR grade). A Jasco V530, UV-Visible double-beam spectrophotometer was used for determination of aqueous solubility and partition coefficient. The partition coefficient was determined in n-octanol/distilled water, whereas aqueous solubility was determined in distilled water at room temperature (25 ± 1 ℃). *In vitro* and *in vivo* studies were carried out using HPLC. Before analysis, the mobile phase was filtered through a 0.45 μm membrane filter and degassed using a sonicator. Sample solutions were also filtered through the same system. The HPLC system consisted of a pump (Jasco PU-1580, Serial No. B179460677), with an autosampler injector (Jasco AS-1555) and a UV/VIS detector (Jasco UV 1575, Serial No. A083360681). Data were incorporated using Jasco Borwin version 1.5. The Waters Xterra RP 18 (4.6 mm I.D. × 150 mmL; Part No. 186000442) column along with a Hypersil guard column were used in the reversed phase partition chromatographic condition. The system was used in an air-conditioned HPLC laboratory atmosphere (20 ±

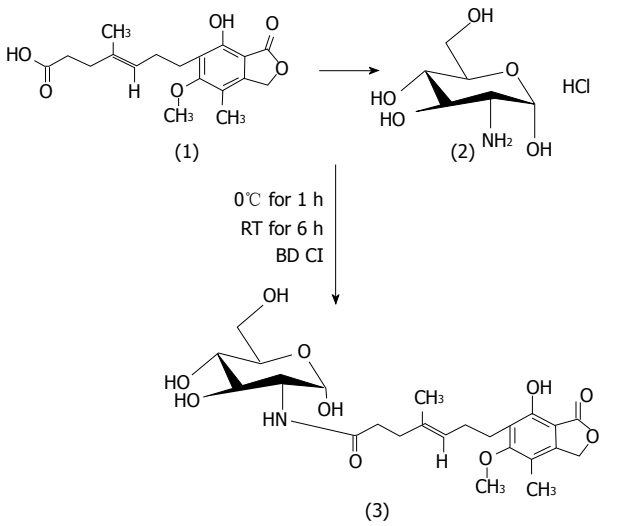

Figure 1 Scheme of synthesis. (1) Mycophenolic acid: (2) D-glucosamine and (3) Prodrug of mycophenolic acid and D-glucosamine.

1 ℃). The column was monitored for UV absorbance at a detection wavelength of 225 nm for estimation of both prodrugs. All kinetic studies were carried out in triplicate. The K values from the plots were calculated separately and the average K and SD values were determined. Histopathological studies of the colon, liver and pancreas were carried out at PRADO Pathology Laboratory, Pune. The pathologist was unaware of the experimental protocols. The histopathological sections were stained with haematoxylin and eosin. Colour microphotographs of the sections were captured on a Nikon optical microscope, Eclipse E-200, with resolution 10 × 40 ×, and a trinocular camera at Poona College of Pharmacy, Pune.

Synthesis

MPA (1 mol) in DMF was reacted with EDCI (2 mol) at 0 ℃. The reaction was continued for 1 h until the MPA-EDCI activated complex was formed. Then in a separate beaker, the aminosugar (1.2 mol/L) in methanol was mixed with 2 drops of triethylamine until basic to litmus and the resulting solution was added to the MPA-EDCI activated complex and stirred at room temperature for 6 h. After completion of the reaction, the solution was poured into 15 mL of cold water and extracted with ethyl acetate. The organic layer was separated and dried with sodium sulphate, filtered and concentrated. The crude product was purified by preparative chromatography using chloroform:methanol:glacial acetic acid (90 V:9 V:1 V). The structures of the synthesized prodrugs (MPA with D-glucosamine: MGLS and MPA with D-galactosamine: MGAS) were established by spectroscopic methods. The scheme of synthesis[13] is presented in Figure 1.

In vitro stability and release studies

In vitro release profiling of the synthesized prodrugs was carried out in aqueous buffers (0.05 mol/L HCl buffer pH 1.2 and 0.05 mol/L phosphate buffer pH 7.4), faecal matter and tissue homogenates of the upper GIT and colon of male Wistar rats by a validated HPLC method. The R_t values for MPA, MGAS and MGLS were 5.9, 9.7 and 11.6, respectively. Concentrations of the parent drug and prodrugs were calculated by equations generated from their respective calibration curves. All the kinetic studies were carried out in triplicate and their standard deviation was calculated.

Aqueous buffers

Prodrug (50 mg) was introduced into 100 mL of HCl buffer in a flask which was kept in a constant temperature bath at 37 ± 1 ℃ under continuous stirring and 2 mL aliquots were withdrawn at different time intervals (0-180 min), each time reloading with an equal volume of fresh buffer. The aliquots were filtered through a membrane filter (0.45 μm) and directly estimated by HPLC at 225 nm using phosphate buffer (pH 4.5):acetonitrile (40 V:60 V) as mobile phase. The same procedure as described above was followed to study the release kinetics of prodrugs in 0.05 mol/L phosphate buffer pH 7.4.

Upper GIT homogenates

Wistar rats (250 g) were anesthetized by ether, sacrificed and then midline incisions were made. Sections of stomach, small intestine and colon were collected separately, homogenized using a Remi overhead homogenizer and diluted to half concentration with isotonic HCl buffer (pH 1.2) for stomach homogenates and with isotonic phosphate buffer (pH 7.4) for small intestinal homogenates and colon homogenates. To each Eppendorf tube, 0.8 mL of prodrug solution (1 mg/mL) and 0.2 mL of homogenate solution were added and incubated at 37 ± 1 ℃. Subsequently, at 15 min intervals for the first 1 h and then hourly for the next 3 h (stomach homogenates), 7 h (small intestinal homogenates) and 10 h (colon homogenates), the Eppendorf tubes were withdrawn and mixed in a vortex mixer, centrifuged at 10000 rpm for 10 min and the supernatants were filtered through a membrane filter (0.45 μm). The filtrate (20 μL) was injected into the HPLC system and the amount of MPA released estimated by the UV detector using the same mobile phase as above at 225 nm.

Faecal matter and caecal homogenate

To a 0.1 mL suspension of fresh rat faecal matter and caecal homogenate (homogenised and diluted with phosphate buffer pH 7.4), prodrug solution (0.9 mL) was added and the tubes were incubated at 37 ± 1 ℃. The samples were removed from the incubator at predetermined time intervals over a period of 13 h and the same procedure was followed for analysis as mentioned in the above section.

Table 1 Doses of test and standard compounds

Groups	Dose[1] (mg/kg)
HC	0.9% saline (1 mL)
MPA	18.5
MMF	25.0
MGLS	28.5
MGAS	28.5
D- Glucosamine	12.4
D- Galactosamine	12.4
MPA + GL	18.5 + 12.4
MPA + GA	18.5 + 12.4

[1]All doses were calculated on an equimolar basis to the dose of MPA. HC: Healthy control; MPA: Mycophenolic acid; MMF: Mycophenolate mofetil; MGLS: Prodrug of MPA and D-glucosamine; MGAS: Prodrug of MPA and D-galactosamine; MPA + GL: Physical mixture of MPA and D-glucosamine; MPA + GA: Physical mixture of MPA and D-galactosamine.

In vivo pharmacokinetics

Of the two prodrugs, MGLS was selected for *in vivo* study. All the experimental procedures and protocols used for the *in vivo* release studies were reviewed and approved by the Institutional Animal Ethical Committee (IAEC) of Poona College of Pharmacy, Pune (CPCSEA/PCH/15/2014-15) and were in accordance with the guidelines of the Committee for the purpose of Control and Supervision of Experiment on Animals (CPCSEA), Government of India.

Male Wistar rats fasted for 24 h (average weight 200-230 g; 12-15 wk; *n* = 6/group) were provided with only water *ad libitum*. The retro-orbital bleeding technique was used to withdraw blood from the rats (1 mL) and this was considered the zero hour reading. Then an oral dose of MGLS prodrug (28.53 mg/kg) in 1.0 mL of physiological saline was administered and blood samples were collected in EDTA tubes at 15 min intervals for 1 h and then on an hourly basis until the 11th hour and finally at the 24th hour. The EDTA tubes were centrifuged at 5000 rpm at 0-5 ℃ for 10 min. The supernatant solution of centrifuged blood was added to the Eppendorf tube and 0.9 mL of methanol was added for immediate plasma precipitation. All the solutions were then vortexed for 2 min, centrifuged at 10000 rpm for 5 min at 0-5 ℃, filtered through a membrane filter and analysed by HPLC.

Faeces and urine were collected from metabolic cages, pooled together as 24 h samples, diluted 100- and 10-fold, respectively, with isotonic phosphate buffer solution pH (7.4) and then the same procedure was followed as described above.

Pharmacological evaluation

Induction of colitis: To induce inflammation in rat colon, all the groups except the healthy control group were catheterized using a rubber cannula (8 cm intra-rectal) and 0.25 mL of 2,4,6-trinitrobezenesulfonic acid (TNBS) (100 mg/kg of body weight in 50% v/v ethanol solution) was administered after light narcotizing with ether. The animals were then maintained in a vertical position for 30 s and returned to their cages. The rats were housed without treatment for 3 d to maintain the development of a full inflammatory bowel disease model. The animals received standard and test compounds orally, once daily for five continuous days. The doses of prodrugs were calculated on an equimolar basis to MPA and are shown in Table 1. The healthy control and colitis control groups were given only saline instead of free drug or prodrug[22].

During the course of 11 d, three parameters were observed; weight loss, stool consistency and rectal bleeding. Anti-colitic activity was estimated by assessment of the disease activity score rate[23] (Table 3). As previously applied by Krawisz *et al*[24], the disease activity score was determined by calculating the average of the above three parameters for each group on each day in the range of 0 (healthy) to 4 (maximal activity of colitis). On the 11th day the animals were sacrificed by isoflurane anaesthesia and their colon/body weight ratio was calculated using dissected sections of colon. Anti-colitic activity of the prodrugs was compared with MPA and MMF as standards. Rat stomach, colon, liver and pancreas were dissected. Gastric ulcers were scanned and the ulcer index was calculated by scoring the ulcers as per the method reported by Cioli *et al*[25] (1979). Specimens of colon, liver and pancreas were fixed in formalin for histopathological analysis.

Statistical analysis

All data were expressed as mean ± SEM; (*n* refers to the number of animals in each group). For the disease activity score rate, statistical differences between groups were calculated by two-way ANOVA followed by Bonferroni's test, whereas statistical analysis of ulcerogenic activity was carried out using one-way ANOVA followed by the Dunnett's *post- hoc* test. Differences were considered significant at $P < 0.001$-0.05.

RESULTS

Aqueous solubility and partition coefficient

The aqueous solubility was determined experimentally and was found to be 0.42 mg/mL and 0.21 mg/mL for MGLS and MGAS, respectively. Log *P* in n-octanol/distilled water was found to be 2.1 and 2.3, respectively.

Spectral analysis

Structures of the synthesized prodrugs were confirmed by IR, NMR, mass spectroscopy and elemental analysis.

Amide prodrug of MPA and D-glucosamine

MGLS: (E)-N-((2S, 3R, 4R, 5S)-tetrahydro-2,4,5-trihydroxy-6-(hydroxymethyl)-2H-pyran-3-yl)-7-1,3-dihydro-7-hydroxy-5-methoxy-4-methyl-1-oxoiso-benzofuran-6-yl)-4-methylhept-4-enamide, M.P: 78 ℃ (uncorrected), R_f 0.42; chloroform: methanol: glacial acetic acid (90:9:1; v/v/v), Aq. sol.: 0.42 mg/mL,

Table 2 Results of in vitro release in different incubation media

Prodrug	Incubation media							
	Aqueous buffers pH 1.2 and pH 7.4	Stomach and intestinal homogenates	Colon homogenate				Faecal matter	
			K ± SD (min^{-1})[1]	$t_{1/2}$ (min)	% Prodrug hydrolysed	% MPA released	% Prodrug hydrolysed	% MPA released
MGLS	Stable	1.30%	0.0025 ± 0.000978	275	92.6	86.7	63	54
MGAS	Stable	14-19%	0.000108 ± 0.00001	305	79.15	76.4	47	52

[1]Average of six readings, follows first-order kinetics. MGLS: Prodrug of mycophenolic acid and D-glucosamine; MGAS: Prodrug of mycophenolic acid and D-galactosamine.

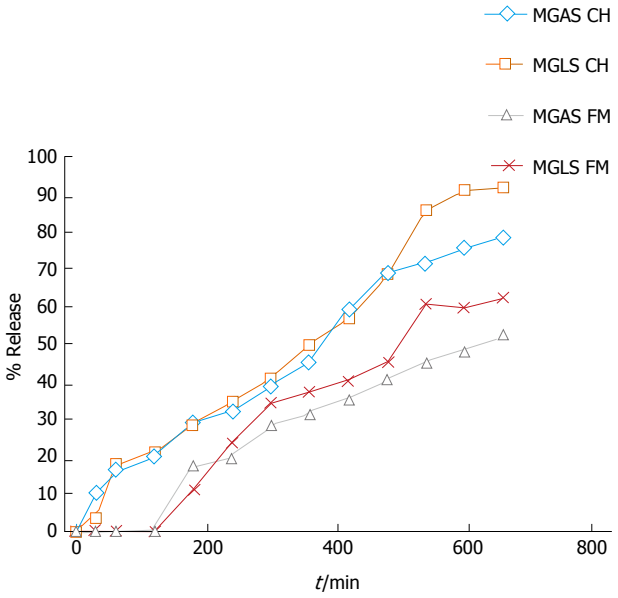

Figure 2 *In vitro* release of mycophenolic acid from prodrugs in different incubation media. MPA: Mycophenolic acid; MGLS: Prodrug of MPA and D-glucosamine; CH: Colon homogenate; FM: Faecal matter.

Log P_{oct}: 2.1, FTIR (anhydrous KBr; cm^{-1}): 3530 (OH stretch), 3284 (NH stretch sec. amide), 3048 (C=C stretch aromatic ring), 1765 (C=O stretch ester), 1698 (C=O stretch sec. amide), 1536 (C=C bend aromatic ring), 1133 (C-O stretch ester), ^{1}H NMR ($CDCl_3$; 400MHz) MPA backbone : δ 1.71 [s,3H] C-CH_3 , 1.80-1.89 [t, 2H] C-CH_2, 2.33-2.38 [q, 2H]-CH_2, 2.50 [s, 3H] -CH_3 Ar-H, 2.59-2.63 [m, 4H] O=C-CH_2 and Ar-CH_2, 3.71 [t, 3H] -OCH_3, 3.77-3.78 [d, H] = CH, 5.20 [s, 2H] lactone ring, 5.26 [s, H] -OH glucosamine backbone: 2.1 [s, 2H] -OH tetrahydropyran, 2.17-2.22 [t, 2H] -OH group tetrahydropyran, 3.06-3.36 [m, 5H]-CH, 3.79-3.82 [d, H]-CH2-OH, 9.2 [s, H] -NH sec. amide, ^{13}C NMR (400 MHz, $CDCl_3$): δ 11.00, 11.40, 14.42, 16.06, 22.34, 25.74, 34.09, 60.41, 68.65, 78.31, 78.64, 78.84, 78.97, 106.63, 115.71, 122.16, 122.82, 123.14, 133.29, 145.03, 162.60, 170.53, Mass: m/z M+1: 496. 99, (molecular weight: 495.52), Elemental analysis: calculated for $C_{24}H_{33}NO_{10}$; C, 58.17; H, 6.71; N, 2.83. Found: C, 58.24; H, 6.72; N, 2.82.

Amide prodrug of MPA and D-galactosamine

MGAS: (E)-N-((2S, 3R, 4R, 5R)-tetrahydro-2,4,5-trihydroxy-6-(hydroxymethyl)-2H-pyran-3-yl)-7-(1,3-dihydro-7-hydroxy-5-methoxy-4-methyl-1-oxoisobenzofuran-6-yl)-4-methylhept-4-enamide. M.P: 80 ℃ (uncorrected), R_f 0.41; chloroform: methanol: glacial acetic acid (90:9:1; v/v/v), Aq. sol.: 0.21 mg/mL, Log P_{oct}: 2.3, FTIR (anhydrous KBr ; cm^{-1}): 3652 (OH stretch) , 3284 (NH stretch sec. amide group), 2997 (C=C stretch aromatic), 1765 (C=O stretch ester), 1698 (C=O stretch sec. amide), 1536 (C=C bend aromatic), 1132 (C-O stretch ester), ^{1}H NMR ($CDCl_3$; 400MHz) MPA backbone : δ 1.88 [s, 3H] =C-CH_3, 2.09 [s, 3H] Ar-CH_3 , 2.17-2.20 [m, 4H]-CH_2-CH_2-, 2.29-2.36 [q, 2H]=C-CH_2, 2.59-2.70 [t, 2H]Ar-CH_2, 3.1 6[s, 3H] -OCH_3 , 5.13 [t, 1H] =C-H, 5.14 [s, 2H] lactone ring, 5.29 [s, 1H] OH group, galactosamine backbone: 1.79 [s, 1H] -OH tetrahydropyran, 2.50-2.52 [s, 3H] -OH tetrahydropyran , 3.20-3.38 [m, 7H] C-H tetrahydropyran ring, 9.1 [s, 1H] -NH sec. amide, ^{13}C NMR (400 MHz, $CDCl_3$, δ ppm): 11.01, 14.46, 15.82, 22.35, 32.15, 34.09, 34.80, 51.02, 60.49, 60.93, 68.59, 78.53, 78.86, 79.19, 106.81, 115.83, 122.21, 123.05, 133.06, 145.46, 152.73, 162.54, 170.24, 172.75, Mass: m/z M+2 497. 09, (molecular weight: 495.52), Elemental analysis: calculated for $C_{24}H_{33}NO_{10}$; C, 58.17; H, 6.71; N, 2.83. Found: C, 58.21; H, 6.72; N, 2.82.

In vitro stability study

In vitro release kinetics are an important tool in understanding the behaviour of prodrugs with respect to their stability and ability to release drugs under *in vitro* conditions that simulate those in the body with respect to pH and enzymes. For the *in vitro* study, prodrugs were incubated at 37 ℃ in aqueous buffers at pH 1.2 and 7.4 representing the pH of stomach and small intestine, respectively. The prodrugs were also incubated with homogenates of stomach and small intestine at 37 ℃ and the release of MPA was studied. Approximately 1%-3% and 14%-19% release of MPA was observed in homogenates of stomach and small intestine, respectively, suggesting negligible hydrolysis by peptidases in the upper GIT. MGLS and MGAS showed 63% and 52% release of MPA in rat faecal matter, respectively, and 87% and 76% release in colon homogenate, respectively (Figure 2). The half-lives of MGLS and MGAS were found to be 275 min and 305

Table 3 Disease activity score rate

Groups	Days										
	1	2	3	4	5	6	7	8	9	10	11
HC	0	0	0	0	0	0	0	0	0	0	0
DC	0	0.67 ± 1.15	0.87 ± 1.50	2.53 ± 0.50	2.63 ± 0.65	2.63 ± 0.65	2.97 ± 0.85	3.12 ± 1.80	3.22 ± 1.70	3.23 ± 2.00	3.30 ± 2.0
MMF	0	0.33 ± 0.58	0.67 ± 1.15	1.07 ± 1.29	1.53 ± 0.50	2.53 ± 0.0	2.10 ± 0.85	1.07 ± 0.51	0.73 ± 0.81	0.23 ± 0.68	0[c]
MPA	0	0.43 ± 0.75	0.67 ± 1.15	2.50 ± 0.17	2.63 ± 0.35	2.63 ± 0.35	2.33 ± 0.58	1.97 ± 0.65	1.63 ± 0.91	0.97 ± 0.85	0.77 ± 0.68[c]
MGLS	0	0.33 ± 0.58	0.33 ± 0.58	1.77 ± 0.40	1.97 ± 0.65	2.53 ± 1.08	1.73 ± 1.03	1.06 ± 0.50	0.63 ± 0.65	0.33 ± 0.17	0[c]
MGAS	0	0.33 ± 0.58	0.43 ± 0.75	1.53 ± 0.81	2.10 ± 0.17	2.33 ± 0.58	1.73 ± 1.03	0.93 ± 0.58	0.73 ± 0.81	0.50 ± 0.35	0.30 ± 0.1[c]
GL	0	0.33 ± 0.58	0.67 ± 1.15	2.1 ± 0.85	2.3 ± 0.89	2.53 ± 0.50	2.1 ± 0.85	1.73 ± 0.75	1.40 ± 0.17	1.20 ± 0.40	1.02 ± 0.2[b]
GA	0	0.43 ± 0.75	0.67 ± 1.15	2.17 ± 0.75	2.53 ± 0.50	2.53 ± 0.52	2.33 ± 0.58	2.10 ± 0.85	1.50 ± 1.01	1.39 ± 1.00	1.30 ± 0.4[b]
GL + MPA	0	0.33 ± 0.58	0.33 ± 0.58	1.83 ± 0.68	2.17 ± 0.75	2.17 ± 0.75	1.87 ± 0.51	1.30 ± 0.70	0.93 ± 0.58	0.53 ± 0.50	0.40 ± 0.35[c]
GA + MPA	0	0.33 ± 0.58	0.667 ± 1.15	1.97 ± 0.65	1.97 ± 0.654	2.3 ± 0.89	1.77 ± 0.51	1.17 ± 0.51	0.73 ± 0.23	0.53 ± 0.50	0.40 ± 0.35[c]

Average of six readings; two-way ANOVA followed by Bonferroni's Test, statistical significance considered at [c]$P < 0.001$ *vs* Disease control. HC: Healthy control; DC: Disease control; MMF: Mycophenolate mofetil; MPA: Mycophenolic acid; MGLS: Prodrug of MPA and D-glucosamine; MGAS: Prodrug of MPA and D-galactosamine; GL: D-glucosamine; GA: D-galactosamine; GL+MPA: Physical mixture of D-glucosamine and MPA; GA + MPA oral: Physical mixture of D-galactosamine and MPA.

min in rat colon homogenates and 523 min and 641 min in rat faecal matter following first order kinetics (Table 2).

In vivo kinetics

MGLS was selected as a representative of the two synthesized prodrugs to study *in vivo* behaviour which was compared with standard MPA. The study was carried out by oral administration of 28.53 mg/kg MGLS and 18.5 mg/kg plain MPA in male Wistar rats housed in metabolic cages. The blood samples were withdrawn by retro-orbital puncture at pre-set time intervals. Urine/faeces samples were collected at various time intervals and pooled together over a period of 24 h. The release pattern of the prodrug was determined by injecting these biological samples into the HPLC system using the newly developed and validated method. After oral administration, MPA appeared in the blood after 1 h, reached a maximum at 7 h (68%) and then gradually declined with disappearance at 24 h. After administration of MGLS, neither MPA nor intact prodrug was observed until 6 h. At 7 h, MGLS was observed in the blood. MGLS showed 70% concentration at 10 h. MPA was observed in the blood at 10 h and reached 68% at 13 h. The concentration of MPA and MGLS started to decline in the blood and was negligible at 24 h (Figure 3).

Pharmacological evaluation

The TNBS model efficiently imitates both acute and chronic colitis resembling human UC[26]. All animals in each group were examined for stool consistency, rectal bleeding and weight loss for 11 d to determine the disease activity score. On the 11th day, all animals were sacrificed and the colon/body weight ratio was calculated to quantify inflammation (Figure 5). The mitigating effect of synthesized prodrugs as well as standards was evaluated for disease activity score rate and colon/body weight ratio in the TNBS-induced experimental colitis model in Wistar rats[24,27]. The results for disease activity score, colon/body weight ratio and ulcerogenic activity are shown in Table 3, Figures 5 and 6, respectively, while photomicrographs of rat colon, pancreas, and liver are shown in Figures 7-9, respectively.

DISCUSSION

Aqueous solubility and partition coefficient

Two mutual latentiated amide derivatives (MGLS and MGAS) of MPA were synthesized with aminosugars D-glucosamine and D-galactosamine, respectively. As anticipated, the outcomes of physico-chemical characterisation revealed that the aqueous solubility of MPA (practically insoluble in water) was significantly improved with

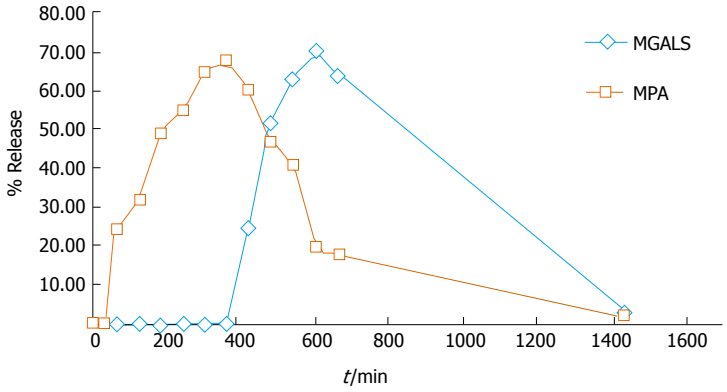

Figure 3 ***In vivo*** **kinetics.** MPA: Mycophenolic acid; MGLS: Prodrug of MPA and D-glucosamine.

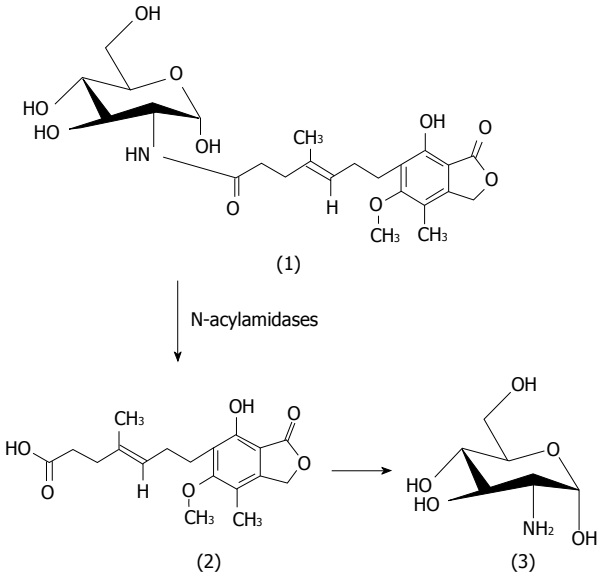

Figure 4 Mode of activation of mycophenolic acid and D-glucosamine prodrug. (1) MGLS prodrug; (2) Mycophenolic acid; and (3) D-glucosamine. MPA: Mycophenolic acid; MGLS: Prodrug of MPA and D-glucosamine.

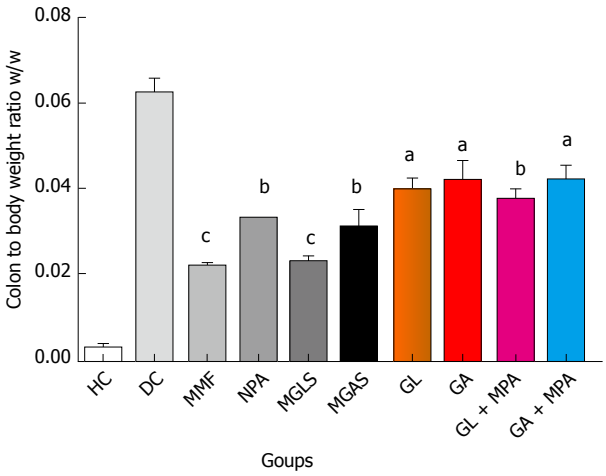

Figure 5 Colon to body weight ratio. Average of six readings; One-way ANOVA followed by Dunnett's Multiple Comparison Test, statistical significance considered at $^{a}P < 0.05$, $^{b}P < 0.01$, $^{c}P < 0.001$ *vs* Disease control. HC: Healthy control; DC: Disease control; MMF: Mycophenolate mofetil; MPA: Mycophenolic acid; MGLS: Prodrug of MPA and D-glucosamine; MGAS: Prodrug of MPA and D-galactosamine; GL: D-glucosamine; GA: D-galactosamine; GL + MPA: Physical mixture of D-glucosamine and MPA; GA + MPA oral: Physical mixture of D-galactosamine and MPA.

a corresponding decrease in the partition coefficient (2.8) in prodrugs. This feature would minimize trans-cellular absorption of prodrugs, thus facilitating their passage directly to the colon. Increased aqueous solubility was attributed to the polyhydroxy nature of the aminosugars.

Spectral study

The IR spectra showed characteristic 2 amide stretches at 3284 and 3283 and C=O stretches of amide at 1698 and 1700 cm^{-1}. ^{1}H NMR of both prodrugs showed characteristic chemical shifts for protons of amide between δ 5 to 8. ^{13}C NMR showed all the relevant chemical shifts as per number of anticipated carbon atoms present in the prodrugs. Disappearance of C=O stretch and OH stretch of carboxylic acid confirmed the formation of an amide bond between MPA and the aminosugars.

The outcomes of ^{1}H NMR and ^{13}C NMR spectral

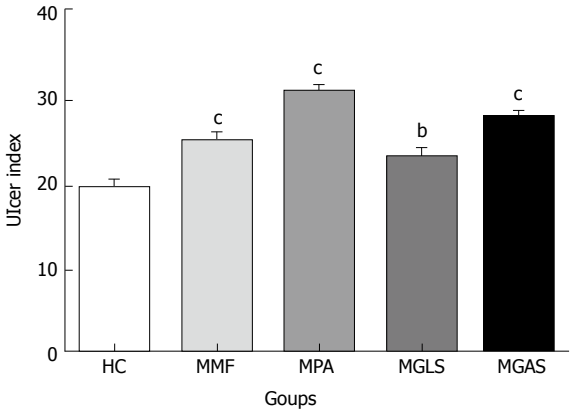

Figure 6 Results of ulcerogenic activity. Average of six readings; One-way ANOVA followed by Dunnett's Multiple Comparison Test, statistical significance considered at $^{b}P < 0.01$, $^{c}P < 0.001$ *vs* Healthy control. HC: Healthy control; MMF: Mycophenolate mofetil; MPA: Mycophenolic acid; MGLS: Prodrug of MPA and D-glucosamine; MGAS: Prodrug of MPA and D-galactosamine.

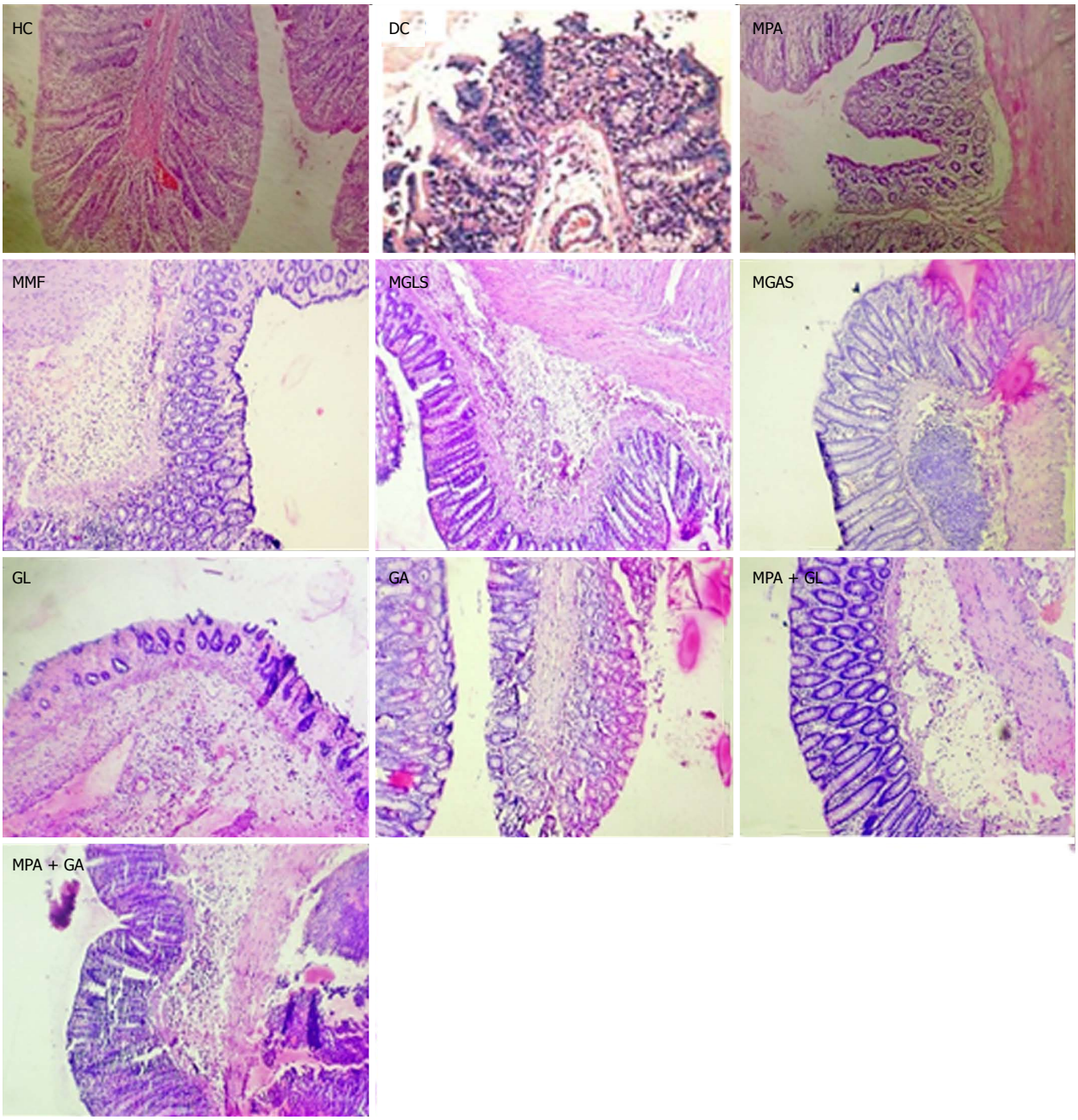

Figure 7 Photomicrographs of colon. HC: Healthy control showing normal architecture of colon mucosa; DC: Disease control showing severe haemorrhage in submucosa with infiltration of inflammatory cells; MPA: MPA showing mild infiltration of inflammatory cells and mild degeneration of epithelium lining; MMF: Showing mild infiltration of inflammatory cells and mild degeneration of epithelium lining; MGLS: Prodrug of MPA and D-glucosamine; MGAS: Prodrug of MPA and D-galactosamine showing mild infiltration of inflammatory cells; GL: D-glucosamine showing mild infiltration of inflammatory cells; GA: D-galactosamine showing mild infiltration of inflammatory cells; MPA + GL: Physical mixture of D-glucosamine and MPA showing mild infiltration of inflammatory cells; MPA + GA: Physical mixture of D-galactosamine and MPA showing mild infiltration of inflammatory cells and mild degeneration of epithelium lining.

studies supported the formation of MGLS and MGAS prodrugs. The results of elemental analysis and mass spectroscopy revealed that the calculated molecular weights of the prodrugs were in accordance with their predicted molecular weights.

In vitro stability study

The aim of the present work was to achieve colon-targeted drug delivery of MPA through its site-specific activation in the colon by resident microflora. The *in vitro* studies showed that the prodrugs were stable in aqueous buffers at pH 1.2 and 7.4 over a period of 3 h and 7 h, respectively, confirming that the prodrugs were not released in the upper GIT. Further studies revealed that both prodrugs exhibited faster activation in colon homogenates as compared to faecal content which was attributed to greater microbial populations in the colon than in faeces. The release of MPA from prodrugs in rat colon homogenates and faecal matter confirmed their colon-specific activation.

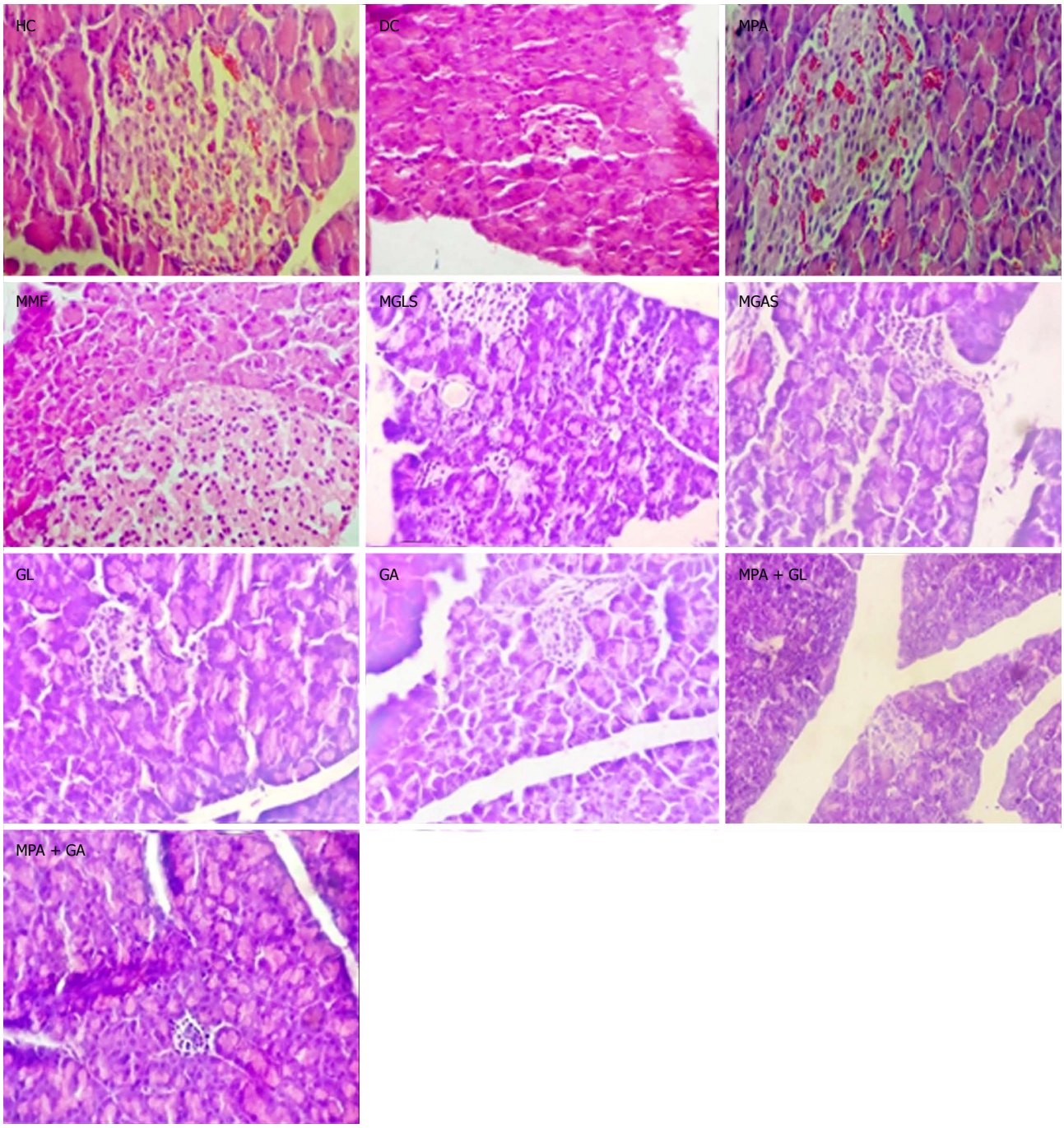

Figure 8 Photomicrographs of pancreas. HC: Healthy control; DC: Disease control; MMF: Mycophenolate mofetil; MPA: Mycophenolic acid; MGLS: Prodrug of MPA and D-glucosamine; MGAS: Prodrug of MPA and D-galactosamine; GL: D-glucosamine; GA: D-galactosamine; GL + MPA: Physical mixture of D-glucosamine and MPA; GA + MPA oral: Physical mixture of D-galactosamine and MPA. DC group showing reduced number and size of islets of Langerhans while all other groups showed normal pancreas architecture without evidence of pancreatitis.

In vivo kinetic study

The *in vivo* study indicated quick absorption of MPA in the upper GIT. In contrast, when MGLS was administered, neither MPA nor intact prodrug was observed until 6 h indicating that prodrug was not absorbed from the stomach and remained intact there. MGLS was observed in the blood at 7 h indicating minimal absorption through the small intestine. The concentration of MGLS consistently increased in the blood reaching a maximum of 70% at 10 h indicating its absorption from the large intestine (colonic mucosa) into the systemic circulation. MPA was observed in the blood at 10 h indicating hydrolysis of MGLS to MPA in the large intestine which was due to its high lipophilicity and it may have transversed the colonic mucosa into the systemic circulation. MPA concentration reached 68% at 13 h. The concentration of MPA and MGLS started to decline in the blood and was negligible at 24 h (Figure 3). The *in vivo* release profile clearly indicated that activation of the prodrug was pH-

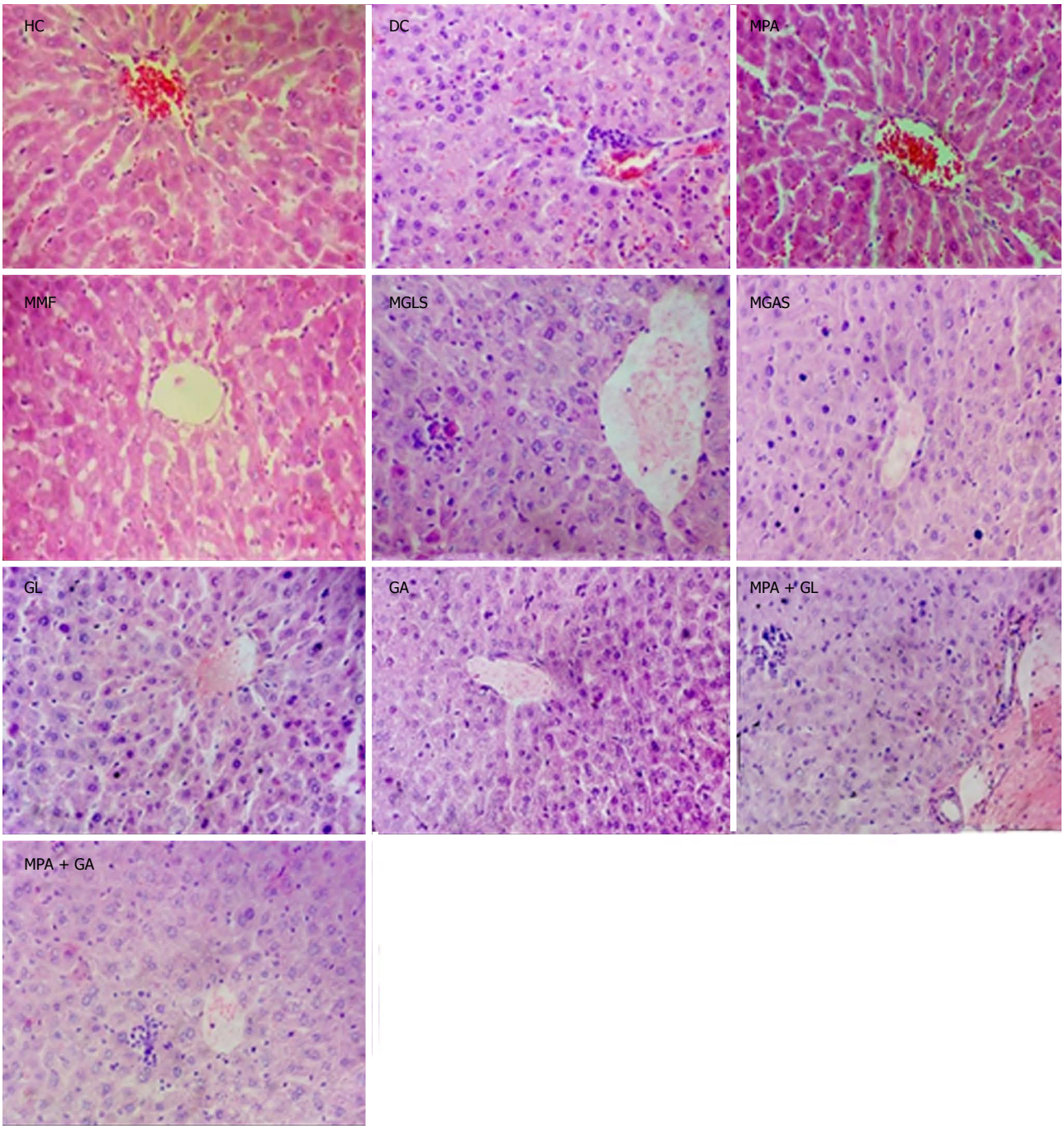

Figure 9 Photomicrographs of liver. HC: Healthy control; DC: Disease control showing minimal degeneration of hepatocytes and congestion of blood vessels; MPA: MPA showing normal liver architecture; MMF: MMF Showing normal liver architecture; MGLS: Prodrug of MPA and D-glucosamine showing minimal infiltration of inflammatory cells; MGAS: Prodrug of MPA and D-galactosamine showing mild infiltration of inflammatory cells; GL: D-Glucosamine showing minimal infiltration of inflammatory cells; GA: D-galactosamine showing minimal infiltration of inflammatory cells; MPA + GL: Physical mixture of D-glucosamine and MPA showing minimal infiltration of inflammatory cells; MPA + GA: Physical mixture of D-galactosamine and MPA showing mild infiltration of inflammatory cells.

dependent (pH 7.4) and by N-acyl amidase present in the colon (Figure 4). The 24 h pooled faeces and urine samples also showed peaks of prodrug and MPA, which confirmed that the prodrug passed through the entire length of the GIT and hence appeared in the faeces; thus, the objective of targeting MPA to the colon was achieved. Moreover, the systemic availability of MPA at high concentration at 13 h revealed that MGLS can be used effectively for the treatment of inflammatory diseases associated with the circadian rhythm such as rheumatoid arthritis.

Pharmacological evaluation

An approximately 11 d TNBS-induced colitis model was used for the pharmacological evaluation. The anti-colitic activity of prodrugs was compared with MMF and MPA. Up to the 5th day the disease activity score increased rapidly and consistently for all TNBS-treated groups

(Table 3). From day 6 to day 10, standard MMF and MPA, prodrugs, carriers and physical mixtures were administered orally to the animals. Full-blown colonic inflammation was demonstrated by the high disease activity score (3.30 ± 2.0) in the colitis control group. Prodrug-treated groups showed a marked decrease in disease activity score rate (99%-100%) that was comparable with the MMF-treated groups. The results of the animal study showed that the disease activity-lowering effect of both prodrugs was significantly superior to MPA (77%), individual carriers (61%-69%) and physical mixtures (88%). Overall, the maximum decrease in colon/body weight ratio was observed in the prodrug-treated groups indicating their significant protective effect on colon inflammation, which was significantly better than MMF and MPA. The lowering effect of carriers and physical mixtures was also better than that of both standards.

Microscopic characterisation of a colon section was performed by considering the following four important parameters, mucosal distortion, inflammation, fibrosis and cryptitis (Figure 7). The colitis control showed severe erosion with absence of the mucosal layer, goblet cell depletion, distorted crypt architecture, lymphocytic infiltration, and thickening of the muscularis mucosa. The lamina propria was also infiltrated with leukocytes. Due to the destruction of crypts, normal mucosal architecture was totally lost. Treatment with the synthesized prodrugs resulted in a marked decrease in the extent and severity of colonic damage (Figure 7) with normal morphology and mild lymphocytic infiltration, which may have been due to activation of T lymphocytes triggered by immune-stimulation of D-glucosamine as well as D-galactosamine as reported by Sadeghi *et al*[28], while the colon of animals treated with a physical mixture of MPA and aminosugars, appeared congested with ulcerated mucosa. MGLS and MGAS proved to be better than the physical mixtures as they were able to release MPA and aminosugars locally in the colon in effective concentrations, thus having a protective effect, while MPA and aminosugars administered orally were unable to reach the colon in required concentrations to mitigate colonic inflammation.

All groups except DC exhibited normal pancreas morphology (Figure 8). Mild infiltration of inflammatory cells in the liver was observed in the groups treated orally with prodrugs and physical mixtures (Figure 9).

The synthesized prodrugs resulted in substantial lowering of ulcer indices as compared to MMF and MPA (Figure 6). These results were consistent with their stability in upper GIT homogenates.

In conclusion, in the present study carrier-linked codrug platforms were successfully designed for efficient colon-specific transport of MPA in order to investigate their potential in mitigating local inflammation in the colon induced by TNBS. Tethering aminosugars to MPA as promoieties resulted in a significant outcome in terms of a marked protective effect compared to MPA without the perpetual diarrhoea observed with MMF therapy. The gastro-sparing nature of the prodrugs and the absence of adverse effects on the pancreas and liver make them promising candidates which should be exploited further as mainstream therapy in the management of IBD.

ARTICLE HIGHLIGHTS

Research background

Defects in the innate immune system are key factors in the pathogenesis of inflammatory bowel disease (IBD). The most commonly used immunomodulators are azathioprine (AZA) or 6-mercaptopurine; however, approximately 10% of patients exhibit intolerance to these drugs, resulting in either withdrawal or prescription of an alternative immunomodulator. Discovered by Gosio in 1893, mycophenolic acid (MPA) was the first antibiotic to be synthesized in a pure and crystalline form. It was used as an immunosuppressant to prevent rejection in organ transplantation, but poor oral bioavailability of MPA was an issue of serious concern. To overcome this setback, mycophenolate mofetil (MMF), the only marketed prodrug of MPA was introduced in 1995 (Trade name: Cellcept) which was used in the treatment of refractory Crohn's disease. Unfortunately MMF also induced GI side effects such as diarrhoea and local gut toxicity leading to poor patient compliance. The role of MMF as an immunomodulator in managing IBD is yet to be fully defined. It is reported in the literature that it may represent a promising treatment for inducing and maintaining remission in IBD patients intolerant of thiopurines. It may be of more value and relevance in ulcerative colitis, as few alternative proven therapies are available.

Hence, it is necessary to design novel colon-targeted prodrugs of MPA with improved bioavailability, lower gastrointestinal (GI) side effects and enhanced efficacy. Many derivatives of MPA have been patented but none has cleared the clinical trials. Therefore, in the present study, colon-specific mutual prodrugs were synthesized by the formation of a covalent amide linkage between MPA and aminosugars. To confirm attainment of an effective concentration of MPA in the colon, *in vivo* pharmacokinetic studies were performed. A 2,4,6-trinitrobezenesulfonic acid (TNBS)-induced colitis model in Wistar rats was used for biological screening of prodrugs and to confirm their mitigating effect on colonic inflammation. The present study underlines the potential of colon-targeting co-therapy of IBD using a novel strategy of delivering MPA with aminosugars simultaneously at the site of action without causing the GIT distress associated with MMF therapy.

Research motivation

Immunosuppressants such as AZA are an inherent constituent of therapy for 50% of patients with Crohn's disease (CD) who develop steroid-dependent or refractory disease. MMF is of proven efficacy and safety in transplantation and in some autoimmune disorders. It has been reported that both AZA and MMF are effective in inducing remission, but AZA seems to be more effective in maintaining remission while onset of the therapeutic effect is delayed less under MMF treatment. Both drugs have steroid-sparing potential, which is delayed under AZA. It seems that AZA is still the immunosuppressant of choice in chronic active CD, but MMF is a reasonable alternative in patients who do not tolerate AZA. One of the major side effects of MMF is gastric distress and diarrhoea that may worsen the symptoms of IBD. The morpholino moiety in MMF is implicated in these side effects. This particular observation inspired us to design codrugs of MPA; replacing the morpholino moiety of MMF with aminosugars which could help to maintain the integrity of the colonic mucosal wall. It was envisaged that these prodrugs might find applicability in those cases of CD which are intolerant to AZA.

Research objectives

The main objectives of this work were to minimize gastric discomfort caused by MMF, and improve the bioavailability and efficacy of MPA in the management of IBD. As gastric side effects are known to be caused by the morpholino moiety of MMF, replacing this moiety with nontoxic aminosugars may have a mitigating effect on inflammation, a stabilizing effect on the colonic mucosal layer and the requisite hydrophilic nature that would impart the desired aqueous solubility to MPA ensuring its efficient delivery to the colon. As anticipate,

effective targeting of MPA to the colon using glucosamine and galactosamine as carriers was achieved due to enhanced aqueous solubility of the prodrugs and a resistant amide linkage between MPA and the aminosugars. MMF-related diarrhoea was not evident in the prodrug-treated groups, which was one of the important objectives of the present study. Site-specific delivery of MPA resulted in improved bioavailability of MPA. Future research should be directed at investigating the potential of these prodrugs on refractory CD and for inducing and maintaining remission in IBD patients intolerant of thiopurines.

Research methods

A clean, single step synthesis of target codrugs was achieved through optimization of the EDCI coupling reaction to avoid complex purification procedures. The synthesized compounds were extensively characterized by spectral analysis. New HPLC methods were developed and validated for simultaneous estimation of MPA and aminosugars in the presence of intact codrugs in order to study the release profiles of codrugs in buffers of various pH, homogenates of gastro-intestinal tract, faecal matter, rat blood, urine and faeces. The TNBS-induced experimental colitis model was optimized to investigate the mitigating effect of codrugs of MPA and aminosugars in comparison to standard drugs (MPA and MMF) and physical mixtures (MPA plus aminosugars) to prove the codrug hypothesis. All data were analysed using relevant statistical tests.

Research results

Colon-targeted release of MPA, absence of gastric distress, diarrhoea, maintenance of the integrity of colonic mucosa by released aminosugars and a significant marked amelioration of TNBS-induced colitis in Wistar rats as compared to MPA were the promising outcomes of this study. These codrugs should be explored further as an alternative to MMF for inducing and maintaining remission in IBD patients, those intolerant to thiopurines as well as those with refractory CD.

A comparative analysis of efficacy of these codrugs against the established anticolitics such as aminosalicylates and corticosteroids is required. In addition, screening of combinations of these prodrugs with established therapies would help to prove their potential in the management of IBD. Acute toxicity and estimation of various pro-inflammatory mediators such as interleukins, tumour necrosis factor-α and myeloperoxidase enzyme are several studies which are underway.

Research conclusions

In the present work, the morpholino moiety of MMF was replaced by novel aminosugars which were tethered with MPA as a literature review revealed that glucosamine and galactosamine play a vital role in resisting chemical attack and improving the tenacity of colon mucus. The novel strategy of codrug therapy proved to be beneficial in terms of lowering the disease activity, colon to body weight ratio and markedly improving the degenerated colon morphology induced by TNBS. MMF-related gut toxicity and diarrhoea were not evident with these codrugs, which was a very promising outcome. This study underlined the utility of aminosugars in maintaining the integrity of colonic mucosa and supported the significant role of an abnormal immune response in the pathophysiology of IBD. These codrugs have the potential to be screened further to determine their efficacy in refractory CD and in the induction and maintenance of IBD remission in patients who are intolerant to thiopurines or MMF.

Research perspectives

A mutual prodrug approach was proven to be superior to physical mixtures of two active drugs *i.e.*, MPA and aminosugars in this study as the efficacy of the codrugs was found to be significantly better than physical mixtures. There is a scope to explore the possibility of conjugation of other nontoxic, biocompatible carrier moieties and established drugs with MPA for a synergistic advantage over administering them in the form of a physical combination.

ACKNOWLEDGEMENTS

The authors are grateful to Department of Science and Technology, New Delhi (DST- WOS-A) for financial assistance to carry out this project and Emcure Pharmaceuticals Pvt. Ltd. Pune, Maharashtra for providing a gift sample of mycophenolate sodium. The authors would like to thank Dr. K.R. Mahadik, Principal, Poona College of Pharmacy, Pune for providing the necessary facilities to carry out the work.

REFERENCES

1 **Hohenleutner U**, Mohr VD, Michel S, Landthaler M. Mycophenolate mofetil and cyclosporin treatment for recalcitrant pyoderma gangrenosum. *Lancet* 1997; **350**: 1748 [PMID: 9413469 DOI: 10.1016/S0140-6736(05)63571-4]

2 **Wilkins WH**. Investigation into the production of bacteriostatic substances by fungi; preliminary examination of the fifth 100 species, all basidiomycetes, mostly of the wood-destroying type. *Br J Exp Pathol* 1946; **27**: 140-142 [PMID: 20995642]

3 **Abraham EP.** The Antibiotics. In: Florkin M, Stotz EH. Comprehensive Biochemistry. Oxford: Sir William Dunn School of Pathology, University of Oxford (Great Britain), **1963**: 181-224 [DOI: 10.1016/B978-1-4831-9711-1.50022-3]

4 **Wilasrusmee C**, Da Silva M, Singh B, Siddiqui J, Bruch D, Kittur S, Wilasrusmee S, Kittur DS. Morphological and biochemical effects of immunosuppressive drugs in a capillary tube assay for endothelial dysfunction. *Clin Transplant* 2003; **17** Suppl 9: 6-12 [PMID: 12795661 DOI: 10.1034/j.1399-0012.17.s9.1.x]

5 **Mitsui A**, Suzuki S. Immunosuppressive effect of mycophenolic acid. *J Antibiot* (Tokyo) 1969; **22**: 358-363 [PMID: 5345678 DOI: 10.7164/antibiotics.22.358]

6 **Eugui EM**, Almquist SJ, Muller CD, Allison AC. Lymphocyte-selective cytostatic and immunosuppressive effects of mycophenolic acid in vitro: role of deoxyguanosine nucleotide depletion. *Scand J Immunol* 1991; **33**: 161-173 [PMID: 1826793 DOI: 10.1111/j.1365-3083.1991.tb03746.x]

7 **Eugui EM**, Mirkovich A, Allison AC. Lymphocyte-selective antiproliferative and immunosuppressive effects of mycophenolic acid in mice. *Scand J Immunol* 1991; **33**: 175-183 [PMID: 2017655 DOI: 10.1111/j.1365-3083.1991.tb03746.x]

8 **Cioli V**, Putzolu S, Rossi V, Corradino C. A toxicological and pharmacological study of ibuprofen guaiacol ester (AF 2259) in the rat. *Toxicol Appl Pharmacol* 1980; **54**: 332-339 [PMID: 6968463 DOI: 10.1016/0041-008X(80)90203-3]

9 **Batovska DI**, Kim DH, Mitsuhashi S, Cho YS, Kwon HJ, Ubukata M. Hydroxamic acid derivatives of mycophenolic acid inhibit histone deacetylase at the cellular level. *Biosci Biotechnol Biochem* 2008; **72**: 2623-2631 [PMID: 18838793 DOI: 10.1271/bbb.80303]

10 **Patterson JW,** inventor. Syntex (USA) Inc., assignee. 4 and 6-substituted derivatives of MPA. United States patent No.5,554,612. 1996

11 **Morgans J,** inventor. Syntex (USA) Inc., assignee. 5-hexanoic acid side chain derivatives of MPA. United States patent No. 5,633,279. 1997

12 **Ahlheim M,** inventor**.** Parenteral formulation of mycophenolic acid, a salt or prodrug thereof. United States Patent No. 20060189683 A1. 2006

13 **Iwaszkiewicz-Grzes D**, Cholewinski G, Kot-Wasik A, Trzonkowski P, Dzierzbicka K. Synthesis and biological activity of mycophenolic acid-amino acid derivatives. *Eur J Med Chem* 2013; **69**: 863-871 [PMID: 24121309 DOI: 10.1016/j.ejmech.2013.09.026]

14 **Dhaneshwar SS**, Vadnerkar G. Rational design and development of colon-specific prodrugs. *Curr Top Med Chem* 2011; **11**: 2318-2345 [PMID: 21671865 DOI: 10.2174/156802611797183249]

15 **Jung YJ**, Lee JS, Kim YM. Synthesis and in vitro/in vivo evaluation of 5-aminosalicyl-glycine as a colon-specific prodrug of 5-aminosalicylic acid. *J Pharm Sci* 2000; **89**: 594-602 [PMID: 10756325 DOI: 10.1002/(SICI)1520-

6017(200005)89:53.0.CO;2-8]
16 **Jung YJ**, Kim HH, Kong HS, Kim YM. Synthesis and properties of 5-aminosalicyl-taurine as a colon-specific prodrug of 5-aminosalicylic acid. *Arch Pharm Res* 2003; **26**: 264-269 [PMID: 12735682 DOI: 10.1007/BF02976953]
17 **Kim H**, Huh J, Jeon H, Choi D, Han J, Kim Y, Jung Y. N,N'-Bis(5-aminosalicyl)-L-cystine is a potential colon-specific 5-aminosalicylic acid prodrug with dual therapeutic effects in experimental colitis. *J Pharm Sci* 2009; **98**: 159-168 [PMID: 18399548 DOI: 10.1002/jps.21404]
18 **Nagpal D,** Singh R, Gairola, N, Bodhankar SL, Dhaneshwar SS. Mutual azo prodrug of 5-aminosalicylic acid for colon targeted drug delivery: synthesis, kinetic studies and pharmacological evaluation. *Ind J Pharm Sci* 2006; **68**: 171-178 [DOI: 10.4103/0250-474X.25710]
19 **Rhodes JM**. Colonic mucus and mucosal glycoproteins: the key to colitis and cancer? *Gut* 1989; **30**: 1660-1666 [PMID: 2693227 DOI: 10.1136/gut.30.12.1660]
20 **Clamp JR**, Fraser G, Read AE. Study of the carbohydrate content of mucus glycoproteins from normal and diseased colons. *Clin Sci* (Lond) 1981; **61**: 229-234 [PMID: 7261546 DOI: 10.1042/cs0610229]
21 **Dhaneshwar S**, Gautam H. Exploring novel colon-targeting antihistaminic prodrug for colitis. *J Physiol Pharmacol* 2012; **63**: 327-337 [PMID: 23070081]
22 **Yamada Y**, Marshall S, Specian RD, Grisham MB. A comparative analysis of two models of colitis in rats. *Gastroenterology* 1992; **102**: 1524-1534 [PMID: 1314749 DOI: 10.1016/0016-5085(92)91710-L]
23 **Hartmann G**, Bidlingmaier C, Siegmund B, Albrich S, Schulze J, Tschoep K, Eigler A, Lehr HA, Endres S. Specific type IV phosphodiesterase inhibitor rolipram mitigates experimental colitis in mice. *J Pharmacol Exp Ther* 2000; **292**: 22-30 [PMID: 10604928]
24 **Krawisz JE**, Sharon P, Stenson WF. Quantitative assay for acute intestinal inflammation based on myeloperoxidase activity. Assessment of inflammation in rat and hamster models. *Gastroenterology* 1984; **87**: 1344-1350 [PMID: 6092199]
25 **Cioli V**, Putzolu S, Rossi V, Scorza Barcellona P, Corradino C. The role of direct tissue contact in the production of gastrointestinal ulcers by anti-inflammatory drugs in rats. *Toxicol Appl Pharmacol* 1979; **50**: 283-289 [PMID: 505458 DOI: 10.1016/0041-008X(79)90153-4]
26 **Ajuebor MN**, Hogaboam CM, Kunkel SL, Proudfoot AE, Wallace JL. The chemokine RANTES is a crucial mediator of the progression from acute to chronic colitis in the rat. *J Immunol* 2001; **166**: 552-558 [PMID: 11123336 DOI: 10.4049/jimmunol.166.1.552]
27 **Barbier M**, Cherbut C, Aubé AC, Blottière HM, Galmiche JP. Elevated plasma leptin concentrations in early stages of experimental intestinal inflammation in rats. *Gut* 1998; **43**: 783-790 [PMID: 9824605 DOI: 10.1136/gut.43.6.783]
28 **Sadeghi B**, Hagglund H, Remberger M, Al-Hashmi S, Hassan Z, Abedi-Valugerdi M, Hassan M. Glucosamine Activates T Lymphocytes in Healthy Individuals and may Induce GVHD/GVL in Stem Cell Transplanted Recipients. *Open Transplant J* 2011; **5**: 1-7 [DOI: 10.2174/18744184011050.10001]

P- Reviewer: Gassler N, Mijandrusic-Sincic B, Sergi CM
S- Editor: Wang JL **L- Editor**: Webster JR **E- Editor**: Ma YJ

World Journal of Gastroenterology

Submit a Manuscript: http://www.f6publishing.com

World J Gastroenterol 2018 March 14; 24(10): 1107-1119

DOI: 10.3748/wjg.v24.i10.1107

ISSN 1007-9327 (print) ISSN 2219-2840 (online)

ORIGINAL ARTICLE

Basic Study

Maturity of associating liver partition and portal vein ligation for staged hepatectomy-derived liver regeneration in a rat model

Yi-Fan Tong, Ning Meng, Miao-Qin Chen, Han-Ning Ying, Ming Xu, Billy Lu, Jun-Jie Hong, Yi-Fan Wang, Xiu-Jun Cai

Yi-Fan Tong, Ning Meng, Han-Ning Ying, Ming Xu, Jun-Jie Hong, Yi-Fan Wang, Xiu-Jun Cai, Department of General Surgery, Sir Run Run Shaw Hospital, School of Medicine, Zhejiang University, Hangzhou 310000, Zhejiang Province, China

Ning Meng, Department of General Surgery, Second Hospital, School of Medicine, Hangzhou Normal University, Hangzhou 310000, Zhejiang Province, China

Miao-Qin Chen, Department of Biological Treatment Research Center, Sir Run Run Shaw Hospital, School of Medicine, Zhejiang University, Hangzhou 310000, Zhejiang Province, China

Billy Lu, National Center for Advancing Translational Science/ National Institutes of Health (NIH), Rickville 20850, American Samoa

ORCID number: Yi-Fan Tong (0000-0001-9028-5756); Ning Meng (0000-0001-8334-1801); Miao-Qin Chen (0000-0001-9479-3574); Han-Ning Ying (0000-0001-6026-580X); Ming Xu (0000-0003-0339-3332); Billy Lu (0000-0001-8369-8157); Jun-Jie Hong (0000-0002-6286-415X); Yi-Fan Wang (0000-0002-8828-4268); Xiu-Jun Cai (0000-0002-3615-4680).

Author contributions: Tong YF, Meng N, Chen MQ, Ying HN and Xu M contributed equally to this work; Cai XJ, Wang YF and Tong YF designed research; Tong YF, Chen MQ and Xu M performed research; Meng N and Ying HN contributed new reagents or analytic tools; Tong YF and Chen MQ analyzed data; Tong YF and Meng N wrote the paper; Lu B, Hong JJ and Cai XJ revised and supervised the study and revised the paper; all authors have read and approved the final version to be published.

Supported by the Major Scientific and Technological Project of Zhejiang Province, China, No. 2015C03026.

Institutional review board statement: This study was reviewed and approved by the Ethical Committees for Human Subjects at Zhejiang University, China, Institutional Review Board.

Institutional animal care and use committee statement: All animal experiments were conducted in accordance with policies of Institutional Animal Care and Use Committee (IACUC) of the School of Medicine, Zhejiang University, China. Specific protocols used in this study were approved by School of Medicine, Zhejiang University IACUC.

Conflict-of-interest statement: The authors declared no conflicts of interest was included in the study.

Data sharing statement: Technical appendix, statistical code, and dataset available from the corresponding author at srrsh_cxj@zju.edu.cn. Participants gave informed consent for data sharing.

ARRIVE guidelines statement: The authors have read the ARRIVE guidelines, and the manuscript was prepared and revised according to the ARRIVE guidelines.

Manuscript source: Unsolicited manuscript

Corresponding to: Xiu-Jun Cai, FRSC, MD, Professor, Surgeon, Department of General Surgery, Sir Run Run Shaw Hospital, School of Medicine, Zhejiang University, Qingchun East Road No.3, Hangzhou 310016, Zhejiang Province, China. srrsh_cxj@zju.edu.cn
Telephone: +86-571-86006605
Fax: +86-571-86006605

Received: December 28, 2017

Peer-review started: December 29, 2017
First decision: January 17, 2018
Revised: February 4, 2018
Accepted: February 9, 2018
Article in press: February 9, 2018
Published online: March 14, 2018

Abstract

AIM

To establish a rat model for evaluating the maturity of liver regeneration derived from associating liver partition and portal vein ligation for staged hepatectomy (ALPPS).

METHODS

In the present study, ALPPS, partial hepatecotmy (PHx), and sham rat models were established initially, which were validated by significant increase of proliferative markers including Ki-67, proliferating cell nuclear antigen, and cyclin D1. In the setting of accelerated proliferation in volume at the second and fifth day after ALPPS, the characteristics of newborn hepatocytes, as well as specific markers of progenitor hepatic cell, were identified. Afterwards, the detection of liver function followed by cluster analysis of functional gene expression were performed to evaluate the maturity.

RESULTS

Compared with PHx and sham groups, the proliferation of FLR was significantly higher in ALPPS group (P = 0.023 and 0.001 at second day, P = 0.034 and P < 0.001 at fifth day after stage I). Meanwhile, the increased expression of proliferative markers including Ki-67, proliferating cell nuclear antigen, and cyclin D1 verified the accelerated liver regeneration derived from ALPPS procedure. However, ALPPS-induced Sox9 positive hepatocytes significantly increased beyond the portal triad, which indicated the progenitor hepatic cell was potentially involved. And the characteristics of ALPPS-induced hepatocytes indicated the lower expression of hepatocyte nuclear factor 4 and anti-tryptase in early proliferative stage. Both suggested the immaturity of ALPPS-derived liver regeneration. Additionally, the detection of liver function and functional genes expression confirmed the immaturity of renascent hepatocytes derived in early stage of ALPPS-derived liver regeneration.

CONCLUSION

Our study revealed the immaturity of ALPPS-derived proliferation in early regenerative response, which indicated that the volumetric assessment overestimated the functional proliferation. This could be convincing evidence that the stage Ⅱ of ALPPS should be performed prudently in patients with marginally adequate FLR, as the ALPPS-derived proliferation in volume lags behind the functional regeneration.

Key words: Associating liver partition and portal vein ligation for staged hepatectomy; Liver regeneration; Hepatic progenitor cell; Function; Immature

Core tip: Despite the rapid proliferation of future liver remnant induced by associating liver partition and portal vein ligation for staged hepatectomy (ALPPS), the high mortality and morbidity rates have remained alarming. A plausible reason was the functional proliferation lagged behind the increase in volume. In this study, a rat model was established to evaluate the maturity of ALPPS-derived hepatocytes. Through the identification of hepatic characteristics, detection of liver function, and analysis of functional gene expression, we revealed the immaturity of ALPPS-derived proliferation in early regenerative response, which indicated that the volumetric assessment overestimated the functional proliferation. And clinically, the stage Ⅱ of ALPPS should be performed prudently in patients with marginally adequate FLR, as the ALPPS-derived proliferation in volume lags behind the functional regeneration.

Tong YF, Meng N, Chen MQ, Ying HN, Xu M, Lu B, Hong JJ, Wang YF, Cai XJ. Maturity of associating liver partition and portal vein ligation for staged hepatectomy-derived liver regeneration in a rat model. *World J Gastroenterol* 2018; 24(10): 1107-1119 Available from: URL: http://www.wjgnet.com/1007-9327/full/v24/i10/1107.htm DOI: http://dx.doi.org/10.3748/wjg.v24.i10.1107

INTRODUCTION

Given its increasing incidence, liver tumor is one of the most life-threatening diseases worldwide[1]. Despite the development in a variety of therapies based on the property of tumor (*e.g.,* transcatheter arterial chemoembolization, chemotherapy, molecular targeting therapy, *etc.*) in recent decades, surgery remains the only curative treatment for patients with primary or metastatic hepatic malignancies[2,3]. Although the remarkable regenerative capacity of the liver permits the extended hepatectomy in clinic, postoperative liver failure caused by small-for-size syndrome (SFSS) represents the most common cause of death after hepatectomy[4]. To address this issue, a novel innovation called associating liver partition and portal vein ligation for staged hepatectomy (ALPPS) has been invented. This technique induces the accelerated growth of future liver remnant (FLR) within transient period through integrating the portal vein occlusion and parenchymal transection[5-8].

However, some experts caution the feasibility and safety of such procedure, and the initial enthusiasm for ALPPS also was tempered because of high morbidity and mortality[9-12]. The improvement of technology and accumulation of experience has decreased the mortality rate to less than 10%, but this remains too high[8].

A rational possibility is that volumetric assessment overestimates the functional proliferation. Given the development of induced pluripotent stem cell technique and the illustration of the roadmap determining the fate of diverse cells, the mechanism of hepatocyte differentiation has been elucidated gradually through the lineage tracing method[13]. Basic research has elucidated that it takes about 8 to 10 d for a hepatoblast to mature into a hepatocyte[14]. In this setting, within a short interval period of ALPPS procedure, the maturity of induced hepatocytes has to be queried. Clinically, the interval time between two stages of ALPPS is usual one or two weeks. Additionally, several studies also have shown that there is a distinct delay in functional gain compared to volumetric increase in ALPPS[15,16]. Therefore, the functional quality of hypertrophic response derived from ALPPS procedure, not just volumetric assessment of the FLR, should be performed to time the stage Ⅱ.

Despite the establishment of several ALPPS animal studies with remarkable growth in volume, none of models were dedicated to evaluating functional proliferation. Thus, the aim of study was to establish a rat model mimicking ALPPS procedure to assess the maturity of ALPPS-derived liver regeneration functionally and volumetrically. This might be of great value in timing the stage Ⅱ of ALPPS and improving its safety clinically.

MATERIALS AND METHODS

Study design

The protocol of this study was reviewed and approved by the animal ethics committee of the Zhejiang University, Hangzhou, China. All experiments were performed in accordance with relevant approved guidelines and regulations. In the present study, male Sprague-Dawley rats, weighing 180 to 230 g from experimental animal center of Zhejiang province, Hangzhou, China, were used. All the rats were housed in a restricted access room with controlled temperature (23 ℃) and a light/dark (12 h:12 h) cycle, and had free access to food and water before and after treatment. Initially, a preliminary study was simply performed to screen the feasible models (n = 5, each group). The sham group was adopted as negative control and the appropriate PHx model was regarded as a positive control. Then, the volumetric and functional liver regeneration of three groups, ALPPS group, PHx group, and sham group were compared in this study.

Definition of different groups

According to the results of preliminary study, the ALPPS, PHx, and sham groups were defined as experimental, positive, and negative control groups in this study. ALPPS group: ligation of the portal vein belonging to left lateral, right, caudate lobes, and transection of parenchyma of middle lobe. PHx group: removal of left lateral, right and caudate lobes. Sham group: Open and close the abdominal cavity.

Surgical procedure

All rats were fasted 8 h before operation. Under the general anesthesia with 8% of chloral hydrate (5.0 mL/kg) by intra-abdominal injection, the abdominal transverse incision was adopted. For the ALPPS procedure, dissection of the left lateral lobe followed by ligation of the portal vein supplying the corresponding lobe with 5-0 silk were performed while artery and biliary duct branches were maintained. Then, the same procedure was conducted in the portal branches of the right and caudate lobes, respectively. The parenchyma was partitioned by 5-0 silks along with the ischemic demarcation line of the middle lobe. Five days after stage Ⅰ, the stage Ⅱ was performed, in which the deportalization lobes were removed (n = 5). For the PHx model, the left lateral, right, and caudate lobes were removed after corresponding hepatic pedicle were ligated with 3-0 silks. And for sham group, opening followed by closing the abdominal cavity was performed (Figure 1A).

Previously, several studies indicated the ALPPS procedure was divided into early (1-3 d after stage Ⅰ) and later stage (4-7 d after stage Ⅰ) generally[17-21]. Therefore in our study, the rats were sacrificed on the second and fifth day after operation. The specimen was collected for subsequent research. Each group at different time points contained six rats. Half of them were used for evaluating the efficiency of proliferation, and the other three rats were used for primary hepatocyte isolation and subsequent detection of hepatic function.

RNA extraction, reverse transcription, quantitative real-time PCR

For RNA extraction, total RNA was extracted from 50 mg of liver specimen by TRIzol reagent (CWBIO, China). 5 μg of RNA were reverse-transcribed by the HiFiScript cDNA Synthesis Kit (CWBIO, China), yielding the complementary DNA template. The quantitative real-time PCR amplification was performed by the ROCHE Light Cycler 480 Ⅱ. The expression of mRNA was shown as fold induction. The primer sequences were listed in Supplement Table 1.

Western blotting

The detection of proteins was performed by standard western blot assays according to the steps below[22]. Total proteins from liver tissues were extracted with RIPA buffer containing protease inhibitors (Beyotime, China) and quantified using the Pierce BCA Protein Assay Kit (Thermo Scientific, United States). About 40 μg of total protein was separated by 10% SDS-PAGE. Samples were transferred to PVDF membranes

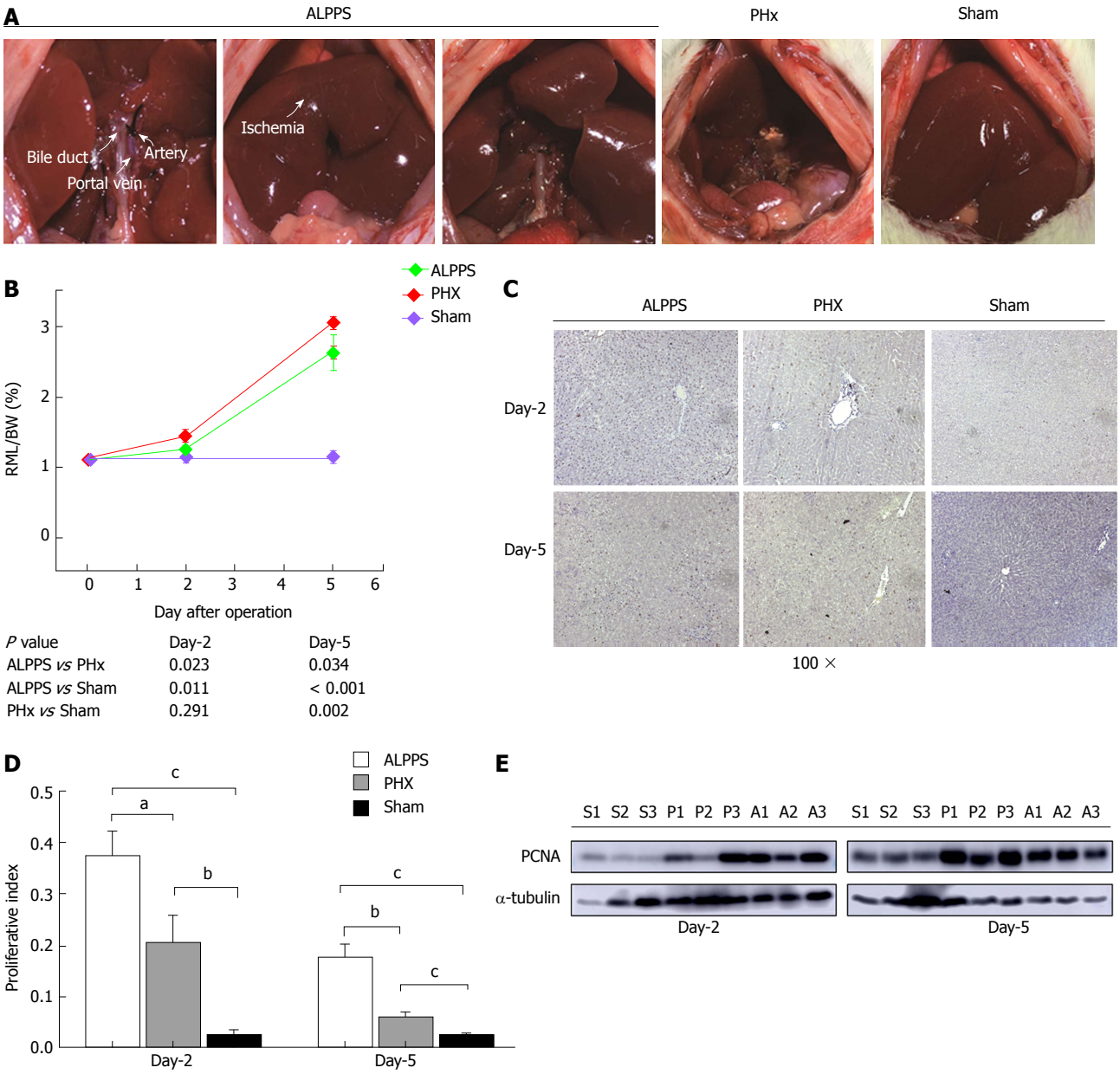

P value	Day-2	Day-5
ALPPS *vs* PHx	0.023	0.034
ALPPS *vs* Sham	0.011	< 0.001
PHx *vs* Sham	0.291	0.002

Figure 1 Establishment of ALPPS model. A: Pictures of ALPPS, PHx, and sham models; B: Proliferation of ALPPS, PHx, and sham models. The X axis represented the day after operation while the Y axis represents the RML/WB (%); C: Representative image (100 ×) of Ki-67 stain by immunohistochemistry of each group at day 2 and 5, respectively; D: Proliferative index of different models, which was calculated by the mean of percentage of Ki-67 positive particle in four random visual fields (200 ×) of IHC stain. $^{a}P < 0.05$, $^{b}P < 0.01$, $^{c}P < 0.001$; E: Protein level of represent expression of PCNA of each group. A: ALPPS; P/PHx: Partial hepatectomy; S: Sham; PCNA: Proliferating cell nuclear antigen; IHC: Immunohistochemistry; RML: Right middle lobe; WB: Body weight.

(Millipore, United States) and incubated overnight at 4 degrees with primary antibodies. The blots were incubated with horseradish peroxidase (HRP)-conjugated secondary antibodies and visualized using the ECL system (Thermo Fisher Scientific, Rochester, NY, United States).

Histological examination

The liver tissues were immersion fixed in 4% formaldehyde overnight. Then, they were embedded, sectioned, dehydrated in ethanol and xylene before being stained with hematoxylin-eosin (HE) immunohistochemistry (IHC). Through the IHC stain, the number of Ki-67 positive hepatocytes were calculated randomly in four visual fields (× 400) and analyzed by Image Pro plus 5.1 (Media Cybernetics, United States), which was presented as the proliferation index. With respect to immunofluorescence, the primary antibody to Sox9 (ab185230) and Albumin (ab106582) were produced from Abcam. The experimental procedure was according to the standard protocol.

Primary hepatocyte isolation and function detection

The protocol for isolation of primary hepatocytes was

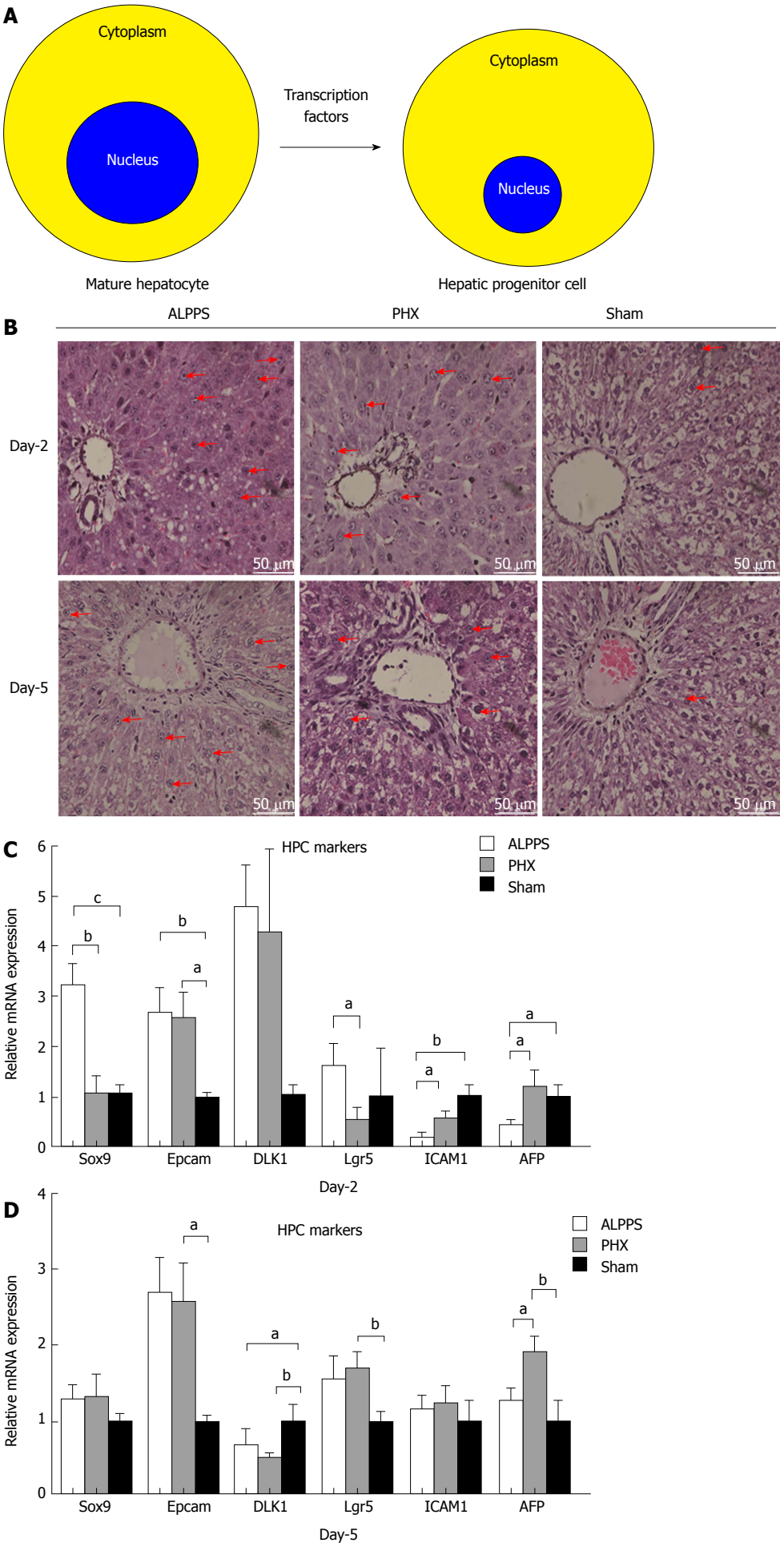
A
Cytoplasm
Nucleus
Transcription factors
Cytoplasm
Nucleus
Mature hepatocyte
Hepatic progenitor cell
B
ALPPS
PHX
Sham
Day-2
Day-5
50 μm
C
HPC markers
ALPPS
PHX
Sham
Relative mRNA expression
Sox9
Epcam
DLK1
Lgr5
ICAM1
AFP
Day-2
D
HPC markers
ALPPS
PHX
Sham
Relative mRNA expression
Sox9
Epcam
DLK1
Lgr5
ICAM1
AFP
Day-5

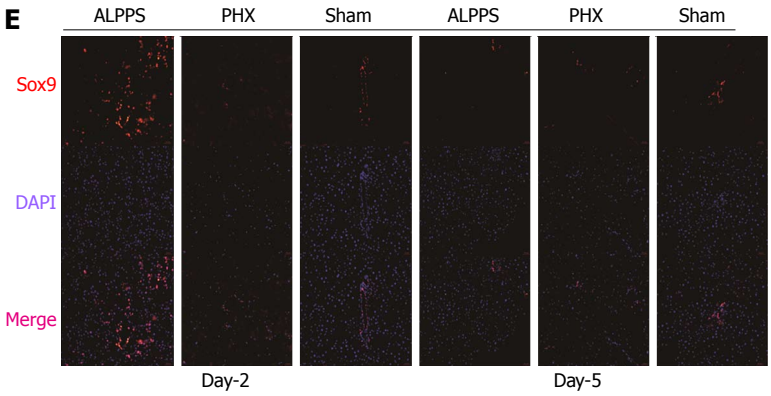

Figure 2 The role of hepatic progenitor cell in associating liver partition and portal vein ligation for staged hepatectomy. A: The schematic of differentiation from hepatic progenitor cell to mature hepatocyte; B: Representative image (400 ×) of HE stain of each group at day 2 and 5, respectively; C: Relative mRNA expression of hepatic progenitor cell markers of each group; D: Immunofluorescence for expression of Sox9 in different groups. $^{a}P < 0.05$, $^{b}P < 0.01$, $^{c}P < 0.001$.

according to three-step collagenase perfusion. Briefly, the liver was perfused through the suprahepatic inferior vena cava with calcium-free buffer (0.5 mmol/L EGTA, 1 × EBSS without Ca^{2+} and Mg^{2+}), followed by the calcium-bearing buffer (10 mmol/L HEPES, 1 × EBSS with Ca^{2+} and Mg^{2+}), and then irrigated with collagenase [0.2 mg/mL collagenase type Ⅳ (Yeasen, China)]. Subsequently, parenchymal cells were purified by 90% Percoll buffer (Sigma) at low speed centrifugation (1000 rpm, 10 min). After the cells were cultured in DMEM medium with 10% FBS for 8 h, PAS stain, OilRed stain, and detection of urea nitrogen were performed following the manufacturer's instructions (Solarbio, China). In the indocyanine green (ICG) uptake assay, hepatocytes were cultured with 1 mg/mL ICG (Tianyi, China) at 37 ℃ for 90 min and washed with PBS three times.

Statistical analysis

The data were expressed as a mean with standard deviation or a percentage. Correspondingly, Student *t*-test or χ^2 test was used to analyze the difference. Significance was considered when a two-tailed *P* value was less than 0.05. Statistical analysis was performed using SPSS, version 22.0 for Windows (IBM Corporation, Armonk, NY, United States).

RESULTS

Establishment of rat models

To establish a feasible positive control model, various PHx models with different extensions of hepatectomy were compared (Supplement Figure 1). The mortality of extended PHx group (removal of left lateral, left middle, right and caudate lobes, $n = 5$), which presented the same extension of stage Ⅱ of ALPPS, was 80%. Compared with extended PHx model (removal left lateral, left middle, right and caudate lobes) and minor PHx model (only removal left lateral), the medium PHx group (removal of left lateral, right and caudate lobes) presented an acceptable mortality (20%) and triggered a remarkable proliferation of FLR. It was therefore determined as positive control group in this study.

Compared with extended PHx group, no rat in ALPPS group which induces rapid hepatic proliferation (removal of left lateral, left middle, right and caudate lobes) died both in stage Ⅳ and Ⅱ. (0% *vs* 80%, $P = 0.053$). As the preservation of portal vein of right middle lobe (RLM) in each group, the liver regeneration was assessed by the ratio of RLM weight to body weight (BW). The mean RML/BW of ALPPS, PHx, sham groups were 1.44% ± 0.04%, 1.24% ± 0.09%, 1.14% ± 0.11% on the second day after operation, and 3.06% ± 0.11%, 2.63% ± 0.39%, 1.13% ± 0.10% on the fifth day after operation, respectively (Figure 1B). Compared with sham group, the proliferation of PHx group was remarkably induced in later stage ($P = 0.002$). However, in the ALPPS group, the hypertrophic response was more active than that of the PHx groups in whole course ($P = 0.023$ and $P = 0.034$). To further confirm the regenerative response, the staining of Ki-67 followed by the calculation of proliferation index of different groups were compared (Figure 1C and D). The expression of PCNA, a classical marker for cell proliferation, was detected by western blotting. Apparently, up-regulated expression of PCNA in the ALPPS group appeared earlier than that in PHx group (Figure 1E).

Thus, these results indicated PHx procedure could trigger liver regeneration, but a stronger regenerative response was activated by ALPPS procedure.

The characteristics of induced hepatocytes

As suggested by previous studies showing that the progenitor hepatic cell (HPC) differentiated into mature hepatocyte by the regulation of hepatic transcription factors (Figure 2A), we found that the hepatocytes in ALPPS and PHx presented a larger nucleus around the portal triad in both early and late stages (Figure 2B). These special hepatoctyes, we suspected, might be immature HPC. To verify this hypothesis, classical markers of hepatic progenitor cell were detected (Figure 2C). Compared with sham group, several markers, including Sox9 and Epcam were significantly increased at mRNA level ($P < 0.001$ and $P = 0.002$), especially in early proliferative stage. Furthermore, we checked

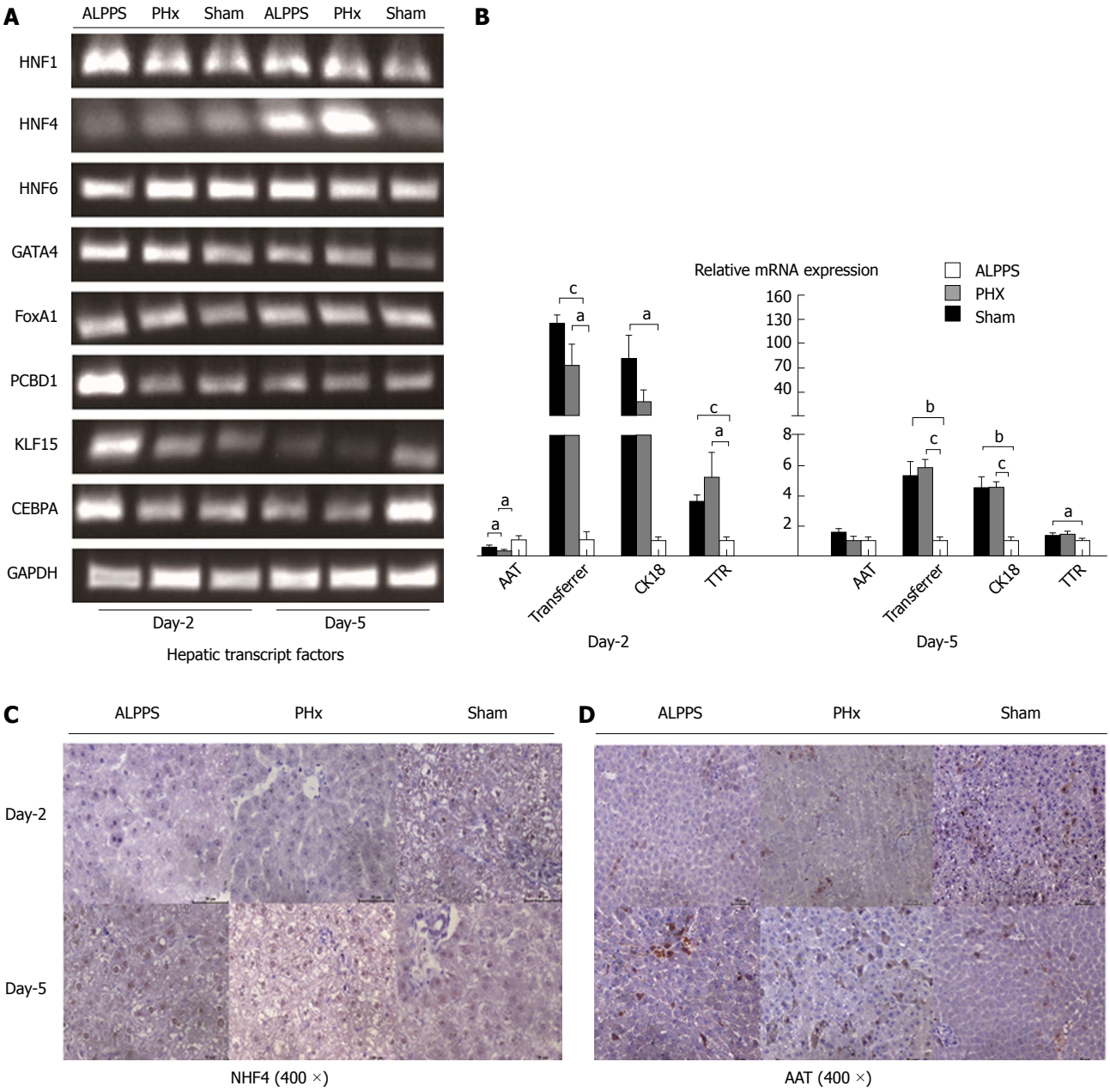

Figure 3 Characteristics of induced hepatocytes. A: The expression of hepatic transcription factors in different groups at each time point at RNA level; B: Relative mRNA expression of mature hepatocyte markers; C: Detection of HNF4 and AAT content by immunohistochemistry procedure of each group at day 2 and 5, respectively. $^{a}P < 0.05$, $^{b}P < 0.01$, $^{c}P < 0.001$.

the expression of Sox9 at protein level, and found it remarkable that the Sox9-positive hepatocytes were widespread beyond the portal traid on second day after ALPPS procedure (Figure 2D). These might imply the activation of HPC in early regenerative response, which was in accordance with the powerful regenerative capacity of HPC from literature reports[23]. As suggested by expression of HPC special markers, the maturity of induced liver hypertrophy either by ALPPS or conventional PHx procedure seemed comparable in later stage of proliferation. And thereby, we inferred the ALPPS-derived liver regeneration might be not completely mature in early phase. Meanwhile, a delay of functional proliferation was indicated in comparison of PHx-derived liver regeneration.

To clarify the above-mentioned inference from the other side, we detected the expression of well-known markers of mature hepatocytes (Figure 3A). Several transcription factors (*e.g.*, HNF1, HNF4, GATA4, FoxA1, *etc*) had been demonstrated to regulate the lineage reprogramming of fibroblasts into hepatocytes *in vitro*[24]. In this study, the HNF4 was delayed up-regulation on the fifth day of ALPPS and PHx groups, suggesting the process of differentiation of hepatocyte remained activated even in later phase. To measure the expression of HNF4 at protein level, the IHC stain was performed, which presented a negative result in early stage but a positive result in later stage of hypertrophic

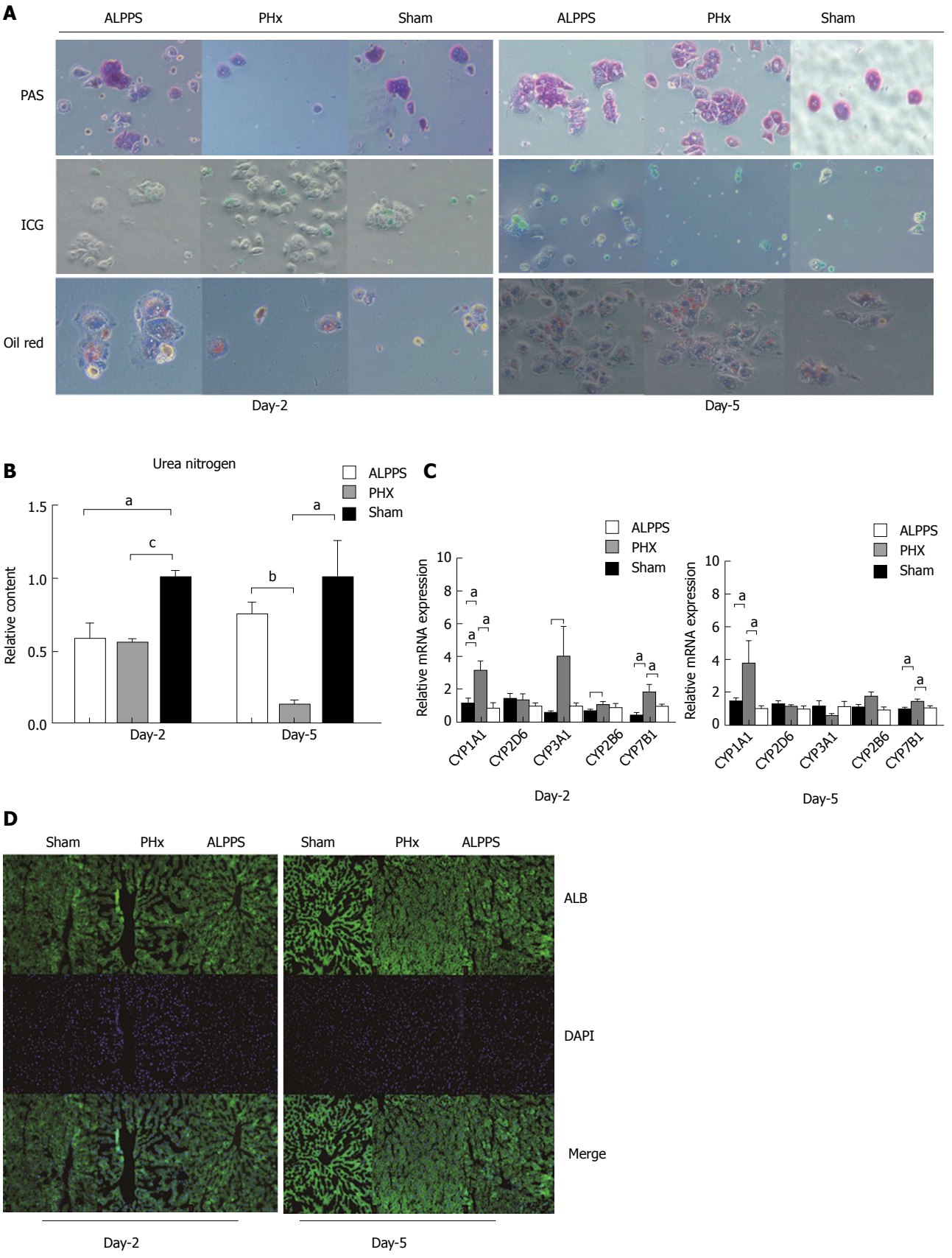

Figure 4 Hepatocytes function. A: Glycogen storage was assayed by PAS staining; Fat storage was assayed by OilRed staining; ICG uptake in cells of different groups (green staining); B: P450Y enzymes expression at RNA level; C: The synthesis of Urea nitrogen of ALPPS, PHx, sham groups at each time point; D: The protein level of albumin expression was measured by Immunofluorescence. A: ALPPS; P/PHx: Partial hepatectomy; S: Sham. $^{a}P < 0.05$, $^{b}P < 0.01$, $^{c}P < 0.001$.

response (Figure 3C). Similarly, functional proteins in the cytoplasm were detected. We found that in the initial

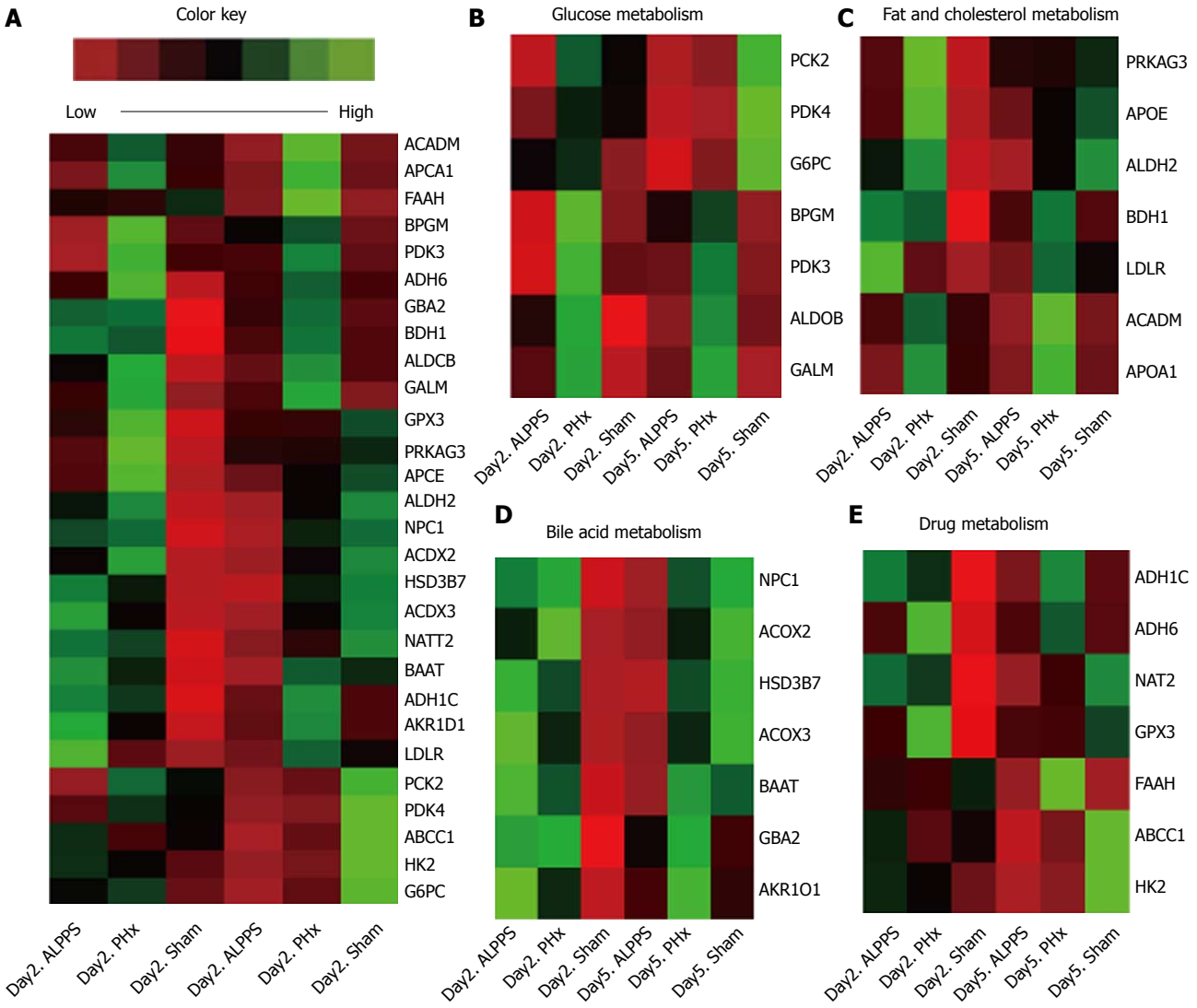

Figure 5 Cluster analysis of different expression of functional genes. The color key represented the abundance expression of indicated genes (Compared with corresponding sham group at each time point). A: The overall cluster analysis of expression of functional genes; B: Glucose metabolism associated functional genes; C: Fat and cholesterol metabolism associated functional genes; D: Bile acid metabolism associated functional genes; E: Drug metabolism associated functional genes.

process of regeneration, the expression of anti-tryptase (AAT) was relatively reduced even in the setting of the increase in amount of hepatocytes (Figure 3B and D).

Taken together, compared with intrinsic hepatocyte in sham group, the immaturity of newborn hepatocytes in early proliferative response of ALPPS and PHx group were elucidated. Among, the differentiation of hepatocyte in ALPPS group appeared to be more prolonged than that in PHx group through the analysis of characteristics of induced hepatocyte.

Detection of hepatocyte function

Given the proliferation in volume and the immaturity of the induced hepatocyte, the functional regeneration had to be naturally questioned. Despite the complexity of induced liver regeneration, an elaborate detection of hepatocyte function was performed as shown below. By primary hepatocyte isolation, the PAS stain, OilRed stain, ICG stain, and synthesis of urea nitrogen of each group in early and later stages were conducted (Figure 4A). As a result, a comparable capacity of glycogen synthesis and fat metabolism was presented between groups, even in the early stage of proliferation. Nevertheless, compared with sham group on the second day after operation, the PHx group had a decreased capability of ICG up-take. Furthermore, the ALPPS group showed a more inferior capacity of ingestion of ICG. Moreover, an insufficiency of urea nitrogen synthesis of hypertrophic groups existed in the whole course of liver regeneration (Figure 4B). With respect to the metabolism, the P450Y enzyme system was the most representative substance. In comparison of PHx group, the expression of CYP3A1 and CYP2B6 in ALPPS group was suppressed on the second day and the expression of CYP1A1 and CYP7B1 was down-regulated in both stages (Figure 4C). But in terms of expression of albumin, no inter-group discrepancy was clarified (Figure 4D).

In this section, we found that the ALPPS-derived

liver regeneration postponed the functional maturity in aspects of ICG up-take, synthesis of urea nitrogen, and expression of P450Y enzyme in the early stage of proliferation.

Cluster analysis of different expression of functional genes

As seen from above, because the ALPPS-derived liver regeneration might be not completely mature in early stage, cluster analysis of different expression of functional genes was therefore performed. All expression of functional genes were summarized in Figure 5A and Supplement Table 2. In the initial stage of liver regeneration, almost all functional genes were up-regulated and were accompanied by an increase in the amount of hepatocyte, which either was induced by ALPPS or PHx procedure. Intriguingly, although the PAS stain showed comparable capacity of synthesis of glycogen in ALPPS and PHx groups, the cluster analysis indicated a relatively low expression of genes in regard to glycogen metabolism. Until the later stage of proliferation, almost all genes had relatively lower expression in the ALPPS group (Figure 5B-E).

Together, these results suggested the expression of functional genes in hepatocytes derived from ALPPS procedure were relatively lower, even in the later stage of proliferation.

DISCUSSION

Based on the first ALPPS Consensus Meeting held in Hamburg in February 2015, the timing of stage Ⅱ was recommended until the FLR reached 40% in liver with cirrhosis or 25% to 30% in normal liver[25,26]. Nevertheless, the incidence of postoperative hepatic failure remains up to 31% even when sufficient FLR volumes were achieved[27]. A rational explanation is the fact that rapid increase in volume derived from ALPPS lags behind the functional proliferation. And thereby, the timing of stage Ⅱ could be better addressed and the rate of mortality could be minimized more efficiently on the basis of functional evaluation. Till now, several technologies including ICG disappearance rate, fluorodeoxyglucose imaging, and 99mTc-mebrofenin hepatobiliary scintigraphy (HBS) had been established[28,29]. Among them, the widespread application of HBS is of great help in the assessment of functional maturity before and after hepatectomy, even in the ALPPS procedure[8]. However, the functional maturity in the process of liver regeneration is too complicated to be determined by merely the uptake and excretory function. For instance, the synthesis of urea nitrogen and albumin, vitality of P450Y enzyme, and fat metabolism are vital parameters in the assessment of liver function. Clinically, it is quite difficult to recruit adequate recipients to fulfill the study of functional detection in ALPPS procedure. Thus, we conducted a rat model mimicking ALPPS procedure to evaluate the functional proliferation, which could be of great help in clinical decision-making.

As suggested by previous results presenting that the volumetric proliferation of FLR could be induced in patients who underwent ALPPS procedure, it was remarkable that the right middle lobe in our rat model was rapidly hypertrophic through the same manipulation. Nonetheless, we found that the newborn hepatocytes for liver restoration remained poorly characterized. First of all, our study revealed that in ALPPS and PHx models, of the majority of cells with a large ratio of nucleus to cytoplasm appeared enriched around the portal vein. In addition, a significant up-regulation of Sox9 on the second day after ALPPS and subsequent decrease in the later stage indicated the potential role of HPC in triggering the activation of regeneration[30]. Based on previous reports, the HPC, a stem-like cell around the portal triads, presented a dramatic capacity to restore liver function and replenish liver mass in liver regeneration[31-33]. Thus, we inferred that the activity of HPC promoted the accelerated liver restoration. To clarify the immaturity of newborn hepatocyte, we detected several transcription factors associated with the destiny of hepatocytes, and found that the peak of HNF4, which plays a critical role in regulating the expression of differentiation-related genes and maintenance of liver function in mammals, was postponed[34-36]. Meanwhile, the inferior expression of AAT was manifested on the second day of ALPPS and PHx groups, which supported the immaturity of hepatocytes. To sum up, the induced hepatocytes were still in the process of differentiation, which suggested the induced-hepatocytes were defective functionally in early regenerative response.

To further evaluate the maturity of neonatal hepatocytes, function detection was performed. In this section, a mild inefficiency of ICG uptake capacity was presented in ALPPS group in early stage. And the insufficient synthesis of P450Y enzymes indicated a deficient capacity of ALPPS-derived hepatocyte in early stage. As seen from the above, the metabolic function is not recovered in early stage of ALPPS procedure. Hence, for patients with biliary obstruction or disorder of renal function, the accumulation of detrimental substances always aggravates the burden of detoxification, and thereby induces the hepatic failure theoretically. Correspondingly, the patients with hilar cholangiocarcinoma or gallbladder cancer, always combined with biliary obstruction, presented a higher mortality and morbidity clinically. Intriguingly, the cluster analysis of different genes expression revealed a paradoxical result. The lower abundance of functional genes relevant to glycogen metabolism presented an insufficiency of synthesis in the ALPPS group, even though the PAS stain presented a comparable capacity in terms of glycogen synthesis. Moreover, relatively low expression of genes in regards to fat, cholesterol, bile acid, and drugs in later stage reminded us that liver

function of hepatocytes derived from ALPPS procedure lagged behind the increase in liver volume. Taken together, the assessment of ICG clearance and hepatic metabolites could improve the comprehensiveness of liver functional evaluation, avoiding the process by which the volumetric increase overestimates the functional gain in liver.

In the present study, we demonstrated that the liver regeneration derived from ALPPS was not completely mature in early stage, but the functional proliferation was mainly completed on the fifth day after ALPPS. Besides, the 0% of mortality after stage Ⅱ indirectly clarified both volumetric and functional regeneration were achieved. Nevertheless, whether the results could be generalized to clinical patients are warranted definitely. To begin with, a majority of ALPPS procedure are performed in patients with diseased liver (*e.g.,* fibrosis, non-alcoholic steatohepatitis, post-chemotherapy, *etc*). Given that the capacity of liver regeneration was attenuated in the diseased liver, the maturity has to be queried subsequently. In this setting, the timing of stage Ⅱ should be prolonged as well. Additionally, the rate of metabolism is apparently faster in rats than in humans. The optimal time to perform stage Ⅱ in human is still controversial, despite that extended hepatecotmy was performed smoothly with an interval time of five days in rat. Theoretically, the species-specific characteristics and inconsecutive observation point time could contribute to a confounding effect on the conclusion.

Given the mechanism of ALPPS-derived liver regeneration is scarce, our follow-up work will verify the hypothesis that the dramatic capacity of regeneration is derived from HPC by lineage tracing method (Sox9-Cre-GFP mouse)[32]. Despite these limitations, our study revealed the immaturity of ALPPS-derived proliferation in early regenerative response, which indicated the volumetric assessment overestimated the functional proliferation. This could be a convincing evidence that the stage Ⅱ of ALPPS should be performed prudently in patients with marginally adequate FLR, as the ALPPS-derived proliferation in volume lags behind the functional regeneration.

ARTICLE HIGHLIGHTS

Research background

Associating liver partition and portal vein ligation for staged hepatectomy (ALPPS) has been increasingly popular worldwide recently. However, the high mortality makes surgeons reconsider the difference between functional and volumetric proliferation in ALPPS-derived liver regeneration. In this study, we therefore establish a rat model to mimic the ALPPS, exploring whether the functional proliferation lags behind the hypertrophy in volume.

Research motivation

This was a preliminary study with regard to the maturity of ALPPS-derived liver regeneration. On the basis of developing a rat model, we found the volumetric assessment overestimated the functional proliferation in ALPPS procedure, which indicated the stage II of ALPPS should be performed prudently in patients with marginally adequate future liver remnant.

Research objectives

This study was to evaluate the maturity of ALPPS-derived liver regeneration. In our rat model, the postponed maturity in function might be an important reason for high mortality of ALPPS even when the adequate future liver remnant was achieved before stage II of ALPPS. Likewise, the functional proliferation should be performed to time the stage II of ALPPS clinically.

Research methods

In this study, ALPPS, partial hepatectomy (PHx) and sham models were conducted. The ratio of right middle lobe to body weight as well as proliferative markers were used for assessing the liver regeneration. Morphological changes by HE stain and detection of specific markers of progenitor or mature hepatocytes were adopted to identify the characteristics of newborn hepatocytes. Eventually, the liver function in vivo and vitro was measured, followed by the cluster analysis of expression of functional genes to detect the maturity of liver regeneration from different models.

Research results

By establishment of ALPPS, PHx and sham models, we demonstrated that ALPPS could induce an accelerated proliferative response. However, the characteristics of newborn hepatocytes seemed to be not mature completely. Sox9 positive hepatocyte, as well as different expression of other specific markers, indicated the potential role of progenitor hepatic cell in ALPPS-derived regeneration. Parts of limited liver function and different expression of functional genes supported the above-mentioned immaturity in ALPPS-induced proliferation.

Research conclusions

As the mortality remains unsatisfactory even in patients with adequate future liver remnant after stage I of ALPPS, this study presented the immaturity of ALPPS-derived proliferation in early regenerative response, which indicated that the volumetric assessment overestimated the functional proliferation. To the best of our knowledge, this is the first study to evaluate the maturity of ALPPS-derived liver regeneration in a rat model. Meanwhile, Sox9 positive hepatocyte indicated the potential role of hepatic progenitor cell in the ALPPS rather than conventional PHx model. Therefore, a more detailed research about the hepatic progenitor cell promotes the ALPPS-derived liver regeneration and its mechanism would be done in our next work.

Research perspectives

The stage II of ALPPS should be performed prudently in patients with marginally adequate future liver remnant, as the ALPPS-derived proliferation in volume lags behind the functional regeneration. By the way, as the hepatic progenitor cell might be an important role in ALPPS-derived liver regeneration, our future work is to further demonstrate the fate of Sox9 positive hepatocyte with ALPPS procedure and its underlying mechanism by lineage tracing method.

ACKNOWLEDGEMENTS

Thanks to Professor Li-jian Hui, PhD, Laboratory of Molecular Cell Biology, Institute of Biochemistry and Cell Biology, Shanghai Institutes for Biological Sciences, Chinese Academy for Sciences, for guidance of primary hepatocyte isolation.

REFERENCES

1 **Torre LA**, Bray F, Siegel RL, Ferlay J, Lortet-Tieulent J, Jemal A. Global cancer statistics, 2012. *CA Cancer J Clin* 2015; **65**: 87-108 [PMID: 25651787 DOI: 10.3322/caac.21262]

2 **Zhong BY**, Ni CF, Chen L, Zhu HD, Teng GJ. Early Sorafenib-related Biomarkers for Combination Treatment with Transarterial Chemoembolization and Sorafenib in Patients with Hepatocellular Carcinoma. *Radiology* 2017; **284**: 583-592 [PMID: 28263701 DOI: 10.1148/radiol.2017161975]

3 **Tong Y**, Li Z, Liang Y, Yu H, Liang X, Liu H, Cai X. Postoperative adjuvant TACE for patients of hepatocellular carcinoma in AJCC stage I: friend or foe? a propensity score analysis. *Oncotarget* 2017; **8**: 26671-26678 [PMID: 28460456 DOI: 10.18632/oncotarget.15793]

4 **Langiewicz M**, Schlegel A, Saponara E, Linecker M, Borger P, Graf R, Humar B, Clavien PA. Hedgehog pathway mediates early acceleration of liver regeneration induced by a novel two-staged hepatectomy in mice. *J Hepatol* 2017; **66**: 560-570 [PMID: 27771454 DOI: 10.1016/j.jhep.2016.10.014]

5 **Olthof PB**, Coelen RJS, Wiggers JK, Groot Koerkamp B, Malago M, Hernandez-Alejandro R, Topp SA, Vivarelli M, Aldrighetti LA, Robles Campos R, Oldhafer KJ, Jarnagin WR, van Gulik TM. High mortality after ALPPS for perihilar cholangiocarcinoma: case-control analysis including the first series from the international ALPPS registry. *HPB* (Oxford) 2017; **19**: 381-387 [PMID: 28279621 DOI: 10.1016/j.hpb.2016.10.008]

6 **Lang H**, de Santibanes E, Clavien PA. Outcome of ALPPS for perihilar cholangiocarcinoma: case-control analysis including the first series from the international ALPPS registry. *HPB* (Oxford) 2017; **19**: 379-380 [PMID: 28262523 DOI: 10.1016/j.hpb.2017.01.024]

7 **Chan ACY**, Chok K, Dai JWC, Lo CM. Impact of split completeness on future liver remnant hypertrophy in associating liver partition and portal vein ligation for staged hepatectomy (ALPPS) in hepatocellular carcinoma: Complete-ALPPS versus partial-ALPPS. *Surgery* 2017; **161**: 357-364 [PMID: 27596751 DOI: 10.1016/j.surg.2016.07.029]

8 **Linecker M**, Björnsson B, Stavrou GA, Oldhafer KJ, Lurje G, Neumann U, Adam R, Pruvot FR, Topp SA, Li J, Capobianco I, Nadalin S, Machado MA, Voskanyan S, Balci D, Hernandez-Alejandro R, Alvarez FA, De Santibañes E, Robles-Campos R, Malagó M, de Oliveira ML, Lesurtel M, Clavien PA, Petrowsky H. Risk Adjustment in ALPPS Is Associated With a Dramatic Decrease in Early Mortality and Morbidity. *Ann Surg* 2017; **266**: 779-786 [PMID: 28806301 DOI: 10.1097/SLA.0000000000002446]

9 **Olthof PB**, Huiskens J, Wicherts DA, Huespe PE, Ardiles V, Robles-Campos R, Adam R, Linecker M, Clavien PA, Koopman M, Verhoef C, Punt CJ, van Gulik TM, de Santibanes E. Survival after associating liver partition and portal vein ligation for staged hepatectomy (ALPPS) for advanced colorectal liver metastases: A case-matched comparison with palliative systemic therapy. *Surgery* 2017; **161**: 909-919 [PMID: 28038862 DOI: 10.1016/j.surg.2016.10.032]

10 **Sun Z**, Tang W, Sakamoto Y, Hasegawa K, Kokudo N. A systematic review and meta-analysis of feasibility, safety and efficacy of associating liver partition and portal vein ligation for staged hepatectomy (ALPPS) versus two-stage hepatectomy (TSH). *Biosci Trends* 2015; **9**: 284-288 [PMID: 26559020 DOI: 10.5582/bst.2015.01139]

11 **Bertens KA**, Hawel J, Lung K, Buac S, Pineda-Solis K, Hernandez-Alejandro R. ALPPS: challenging the concept of unresectability--a systematic review. *Int J Surg* 2015; **13**: 280-287 [PMID: 25496851 DOI: 10.1016/j.ijsu.2014.12.008]

12 **Schadde E**, Schnitzbauer AA, Tschuor C, Raptis DA, Bechstein WO, Clavien PA. Systematic review and meta-analysis of feasibility, safety, and efficacy of a novel procedure: associating liver partition and portal vein ligation for staged hepatectomy. *Ann Surg Oncol* 2015; **22**: 3109-3120 [PMID: 25448799 DOI: 10.1245/s10434-014-4213-5]

13 **Han X**, Yu H, Huang D, Xu Y, Saadatpour A, Li X, Wang L, Yu J, Pinello L, Lai S, Jiang M, Tian X, Zhang F, Cen Y, Fujiwara Y, Zhu W, Zhou B, Zhou T, Ouyang H, Wang J, Yuan GC, Duan S, Orkin SH, Guo G. A molecular roadmap for induced multi-lineage trans-differentiation of fibroblasts by chemical combinations. *Cell Res* 2017; **27**: 386-401 [PMID: 28128194 DOI: 10.1038/cr.2017.17]

14 **Chaudhari P**, Tian L, Deshmukh A, Jang YY. Expression kinetics of hepatic progenitor markers in cellular models of human liver development recapitulating hepatocyte and biliary cell fate commitment. *Exp Biol Med* (Maywood) 2016; **241**: 1653-1662 [PMID: 27390263 DOI: 10.1177/1535370216657901]

15 **Truant S**, Baillet C, Deshorgue AC, El Amrani M, Huglo D, Pruvot FR. Contribution of hepatobiliary scintigraphy in assessing ALPPS most suited timing. *Updates Surg* 2017; **69**: 411-419 [PMID: 28795384 DOI: 10.1007/s13304-017-0481-5]

16 **Stockmann M**, Bednarsch J, Malinowski M, Blüthner E, Pratschke J, Seehofer D, Jara M. Functional considerations in ALPPS - consequences for clinical management. *HPB* (Oxford) 2017; **19**: 1016-1025 [PMID: 28844397 DOI: 10.1016/j.hpb.2017.07.010]

17 **Shi H**, Yang G, Zheng T, Wang J, Li L, Liang Y, Xie C, Yin D, Sun B, Sun J, Wang H, Pan S, Jiang H, Lau W, Liu L. A preliminary study of ALPPS procedure in a rat model. *Sci Rep* 2015; **5**: 17567 [PMID: 26631552 DOI: 10.1038/srep17567]

18 **Wei W**, Zhang T, Zafarnia S, Schenk A, Xie C, Kan C, Dirsch O, Settmacher U, Dahmen U. Establishment of a rat model: Associating liver partition with portal vein ligation for staged hepatectomy. *Surgery* 2016; **159**: 1299-1307 [PMID: 26879073 DOI: 10.1016/j.surg.2015.12.005]

19 **Schlegel A**, Lesurtel M, Melloul E, Limani P, Tschuor C, Graf R, Humar B, Clavien PA. ALPPS: from human to mice highlighting accelerated and novel mechanisms of liver regeneration. *Ann Surg* 2014; **260**: 839-846; discussion 846-847 [PMID: 25379855 DOI: 10.1097/SLA.0000000000000949]

20 **Linecker M**, Kambakamba P, Reiner CS, Linh Nguyen-Kim TD, Stavrou GA, Jenner RM, Oldhafer KJ, Björnsson B, Schlegel A, Györi G, Schneider MA, Lesurtel M, Clavien PA, Petrowsky H. How much liver needs to be transected in ALPPS? A translational study investigating the concept of less invasiveness. *Surgery* 2017; **161**: 453-464 [PMID: 27814957 DOI: 10.1016/j.surg.2016.08.004]

21 **Almau Trenard HM**, Moulin LE, Padín JM, Stringa P, Gondolesi GE, Barros Schelotto P. Development of an experimental model of portal vein ligation associated with parenchymal transection (ALPPS) in rats. *Cir Esp* 2014; **92**: 676-681 [PMID: 25064517 DOI: 10.1016/j.ciresp.2013.11.005]

22 **Wang Y**, Zhou Y, Tao F, Chai S, Xu X, Yang Y, Yang Y, Xu H, Wang K. N-myc downstream regulated gene 1(NDRG1) promotes the stem-like properties of lung cancer cells through stabilized c-Myc. *Cancer Lett* 2017; **401**: 53-62 [PMID: 28456659 DOI: 10.1016/j.canlet.2017.04.031]

23 **Huang P**, He Z, Ji S, Sun H, Xiang D, Liu C, Hu Y, Wang X, Hui L. Induction of functional hepatocyte-like cells from mouse fibroblasts by defined factors. *Nature* 2011; **475**: 386-389 [PMID: 21562492 DOI: 10.1038/nature10116]

24 **Nishikawa T**, Bell A, Brooks JM, Setoyama K, Melis M, Han B, Fukumitsu K, Handa K, Tian J, Kaestner KH, Vodovotz Y, Locker J, Soto-Gutierrez A, Fox IJ. Resetting the transcription factor network reverses terminal chronic hepatic failure. *J Clin Invest* 2015; **125**: 1533-1544 [PMID: 25774505 DOI: 10.1172/JCI73137]

25 **Oldhafer KJ**, Stavrou GA, van Gulik TM; Core Group. ALPPS--Where Do We Stand, Where Do We Go?: Eight Recommendations From the First International Expert Meeting. *Ann Surg* 2016; **263**: 839-841 [PMID: 26756771 DOI: 10.1097/SLA.0000000000001633]

26 **Cai X**, Tong Y, Yu H, Liang X, Wang Y, Liang Y, Li Z, Peng S, Lau WY. The ALPPS in the Treatment of Hepatitis B-Related Hepatocellular Carcinoma With Cirrhosis: A Single-Center Study and Literature Review. *Surg Innov* 2017; **24**: 358-364 [PMID: 28689487 DOI: 10.1177/1553350617697187]

27 **Schadde E**, Raptis DA, Schnitzbauer AA, Ardiles V, Tschuor C, Lesurtel M, Abdalla EK, Hernandez-Alejandro R, Jovine E, Machado M, Malago M, Robles-Campos R, Petrowsky H, Santibanes ED, Clavien PA. Prediction of Mortality After ALPPS Stage-1: An Analysis of 320 Patients From the International ALPPS Registry. *Ann Surg* 2015; **262**: 780-785; discussion 785-786 [PMID: 26583666 DOI: 10.1097/SLA.0000000000001450]

28 **Olthof PB**, Coelen RJS, Bennink RJ, Heger M, Lam MF, Besselink MG, Busch OR, van Lienden KP, van Gulik TM. 99mTc-mebrofenin hepatobiliary scintigraphy predicts liver failure following major liver resection for perihilar cholangiocarcinoma. *HPB* (Oxford) 2017; **19**: 850-858 [PMID: 28687148 DOI:

10.1016/j.hpb.2017.05.007]
29 **Serenari M**, Collaud C, Alvarez FA, de Santibañes M, Giunta D, Pekolj J, Ardiles V, de Santibañes E. Interstage Assessment of Remnant Liver Function in ALPPS Using Hepatobiliary Scintigraphy: Prediction of Posthepatectomy Liver Failure and Introduction of the HIBA Index. *Ann Surg* 2017; Epub ahead of print [PMID: 28121683 DOI: 10.1097/SLA.0000000000002150]
30 **Itoh T**. Stem/progenitor cells in liver regeneration. *Hepatology* 2016; **64**: 663-668 [PMID: 27227904 DOI: 10.1002/hep.28661]
31 **Li D**, Li W, Hui L. Hybrid hepatocyte: A newly identified player for regeneration in hepatic injuries. *Hepatology* 2016; **64**: 2244-2246 [PMID: 27641691 DOI: 10.1002/hep.28837]
32 **Font-Burgada J**, Shalapour S, Ramaswamy S, Hsueh B, Rossell D, Umemura A, Taniguchi K, Nakagawa H, Valasek MA, Ye L, Kopp JL, Sander M, Carter H, Deisseroth K, Verma IM, Karin M. Hybrid Periportal Hepatocytes Regenerate the Injured Liver without Giving Rise to Cancer. *Cell* 2015; **162**: 766-779 [PMID: 26276631 DOI: 10.1016/j.cell.2015.07.026]
33 **Iacob R**, Rüdrich U, Rothe M, Kirsch S, Maasoumy B, Narain N, Verfaillie CM, Sancho-Bru P, Iken M, Popescu I, Schambach A, Manns MP, Bock M. Induction of a mature hepatocyte phenotype in adult liver derived progenitor cells by ectopic expression of transcription factors. *Stem Cell Res* 2011; **6**: 251-261 [PMID: 21474405 DOI: 10.1016/j.scr.2011.02.002]
34 **Zhu S**, Rezvani M, Harbell J, Mattis AN, Wolfe AR, Benet LZ, Willenbring H, Ding S. Mouse liver repopulation with hepatocytes generated from human fibroblasts. *Nature* 2014; **508**: 93-97 [PMID: 24572354 DOI: 10.1038/nature13020]
35 **Mederacke I**, Hsu CC, Troeger JS, Huebener P, Mu X, Dapito DH, Pradere JP, Schwabe RF. Fate tracing reveals hepatic stellate cells as dominant contributors to liver fibrosis independent of its aetiology. *Nat Commun* 2013; **4**: 2823 [PMID: 24264436 DOI: 10.1038/ncomms3823]
36 **Friedman SL**, Sheppard D, Duffield JS, Violette S. Therapy for fibrotic diseases: nearing the starting line. *Sci Transl Med* 2013; **5**: 167sr1 [PMID: 23303606 DOI: 10.1126/scitranslmed.3004700]

P- Reviewer: Campos RR, Starlinger P **S- Editor**: Gong ZM
L- Editor: A **E- Editor**: Ma YJ

World Journal of Gastroenterology

Submit a Manuscript: http://www.f6publishing.com

World J Gastroenterol 2018 March 14; 24(10): 1120-1133

DOI: 10.3748/wjg.v24.i10.1120

ISSN 1007-9327 (print) ISSN 2219-2840 (online)

ORIGINAL ARTICLE

Basic Study

Proteinase-activated receptor 2 promotes tumor cell proliferation and metastasis by inducing epithelial-mesenchymal transition and predicts poor prognosis in hepatocellular carcinoma

Liang Sun, Pi-Bao Li, Yan-Fen Yao, Ai-Yuan Xiu, Zhi Peng, Yu-Huan Bai, Yan-Jing Gao

Liang Sun, Qilu Hospital of Shandong University, Jinan 250012, Shandong Province, China

Liang Sun, Pi-Bao Li, Yan-Fen Yao, Department of Critical Care Medicine, Shandong Traffic Hospital, Jinan 250000, Shandong Province, China

Ai-Yuan Xiu, Zhi Peng, Yu-Huan Bai, Yan-Jing Gao, Department of Gastroenterology, Qilu Hospital of Shandong University, Jinan 250012, Shandong Province, China

ORCID number: Liang Sun (0000-0003-0308-8426); Pi-Bao Li (0000-0003-3944-5106); Yan-Fen Yao (0000-0002-5633-9172); Ai-Yuan Xiu (0000-0002-5009-8961); Zhi Peng (0000-0002-9612-5064); Yu-Huan Bai (0000-0002-2848-4639); Yan-Jing Gao (0000-0001-8153-3754).

Author contributions: Sun L and Gao YJ designed the research; Sun L, Xiu AY and Peng Z performed the research; Li PB and Bai YH contributed new reagents or analytic tools; Sun L and Yao YF analyzed the data; Sun L wrote the paper.

Supported by Jinan College Innovation Plan, No. 26010105081333; and Shandong Social Development Plan, No. 26010104011343.

Institutional animal care and use committee statement: The use and care of experimental animals were approved by the Institutional Animal Care and Use Committee, Qilu Hospital of Shandong University.

Conflict-of-interest statement: The authors declare that they have no competing interests.

Data sharing statement: No additional data are available.

Manuscript source: Unsolicited manuscript

Correspondence to: Yan-Jing Gao, PhD, Chief Doctor, Professor, Department of Gastroenterology, Qilu Hospital of Shandong University, No. 107, West Wenhua Road, Jinan 250012, Shandong Province, China. gaoyanjing@sdu.edu.cn
Telephone: +86-531-86927544

Received: December 8, 2017
Peer-review started: December 8, 2017
First decision: December 20, 2017
Revised: December 29, 2017
Accepted: January 24, 2018
Article in press: January 24, 2018
Published online: March 14, 2018

Abstract

AIM

To clarify the role of proteinase-activated receptor 2 (PAR2) in hepatocellular carcinoma, especially in the process of metastasis.

METHODS

PAR2 expression levels were assessed by qRT-PCR and immunohistochemistry (IHC) in patient tissues and in hepatocellular carcinoma cell lines SMMC-7721 and HepG2. Cell proliferation and metastasis were assessed both *in vitro* and *in vitro*. Immunoblotting was carried out to monitor the levels of mitogen-activated protein kinase (MAPK) and epithelial-mesenchymal transition

markers.

RESULTS

The prognosis was significantly poorer in patients with high PAR2 levels than in those with low PAR2 levels. Patients with high PAR2 levels had advanced tumor stage (P = 0.001, chi-square test), larger tumor size (P = 0.032, chi-square test), and high microvascular invasion rate (P = 0.037, chi-square test). The proliferation and metastasis ability of SMMC-7721 and HepG2 cells was increased after PAR2 overexpression, while knockdown of PAR2 decreased the proliferation and metastasis ability of SMMC-7721 and HepG2 cells. Knockdown of PAR2 also inhibited hepatocellular carcinoma tumor cell growth and liver metastasis in nude mice. Mechanistically, PAR2 increased the proliferation ability of SMMC-7721 and HepG2 cells *via* ERK activation. Activated ERK further promoted the epithelial-mesenchymal transition of these cells, which endowed them with enhanced migration and invasion ability.

CONCLUSION

These data suggest that PAR2 plays an important role in the proliferation and metastasis of hepatocellular carcinoma. Therefore, targeting PAR2 may present a favorable target for treatment of this malignancy.

Key words: Hepatocellular carcinoma; Proteinase-activated receptor 2; Epithelial-mesenchymal transition

Core tip: The role of proteinase-activated receptor 2 (PAR2) in tumor progression especially metastasis of hepatocellular carcinoma and how it is regulated are still unclear. In this study, we found that PAR2 was upregulated in hepatocellular carcinoma (HCC) tumor tissues and related with poor prognosis in HCC patients. In addition, we proved that PAR2 could not only promote the proliferation and metastasis ability of SMMC-7721 and HepG2 cells *in vitro*, but also promoted xenograft tumor growth and HCC cell liver metastasis *in vivo*. These effects were mediated by the activation of ERK, which further induced epithelial-mesenchymal transition of HCC cells.

Sun L, Li PB, Yao YF, Xiu AY, Peng Z, Bai YH, Gao YJ. Proteinase-activated receptor 2 promotes tumor cell proliferation and metastasis by inducing epithelial-mesenchymal transition and predicts poor prognosis in hepatocellular carcinoma. *World J Gastroenterol* 2018; 24(10): 1120-1133 Available from: URL: http://www.wjgnet.com/1007-9327/full/v24/i10/1120.htm DOI: http://dx.doi.org/10.3748/wjg.v24.i10.1120

INTRODUCTION

Hepatocellular carcinoma (HCC) is one of the most common malignancies worldwide[1,2]. Surgical resection is the main strategy for treating this deadly malignancy[3]. Unfortunately, intrahepatic and extrahepatic metastases often occur in progressive and recurrent patients, thus leading to a poor prognosis[4]. Metastasis is a comprehensive process that facilitates cancer cell transition from a primary lesion to a metastatic focus. Many intrinsic cellular characteristics and extrinsic microenvironmental factors influence the metastatic potential of HCC cells[5]. However, the underlying mechanisms that facilitate this process remain largely unknown, therefore, it is critical to identify new targets for these patients to improve their prognosis.

Proteinase-activated receptor 2 (PAR2) is a member of the G-protein coupled receptor 1 family[6]. PAR2 downstream signaling is mediated through several signaling pathways such as intracellular calcium, phospholipase C (PLC), mitogen-activated protein kinase (MAPK), Rho, and I-kappaB kinase/NF-kappaB[7,8]. It is also transactivated by cleaved F2R/PAR1[9]. PAR2 is known to regulate physiological responses such as vasoregulation, cell growth, inflammation, and nociception[10,11]. However, there is growing evidence that PAR2 also has an important role in tumors, especially in tumors of epithelial origin[12-15]. PAR2 is expressed in HCC tissues and multiple HCC cell lines, where it promotes cancer cell migration and invasion through different signaling pathways including $[Ca^{2+}]_i$ mobilization, Src, Met, and p42/p44 MAPK[16,17]. PAR2 also participates in tumor initiation, self-renewal, and metastasis by regulating $CD47^+$ HCC stem cells[18]. Moreover, PAR2 in hepatic stellate cells (HSCs) plays an important role in promoting HCC growth through mediating migration and secretion of pro-angiogenic and pro-mitotic factors[19]. In addition, TF/VIIa/PAR2 signaling is involved in mTOR mediated autophagy in HCC[20]. Collectively, these data suggest an important role for PAR2 in HCC progression. However, the role of PAR2 in HCC metastasis and the underlying mechanism are poorly understood.

Epithelial-mesenchymal transition (EMT) and its intermediate states have been identified as crucial drivers of organ fibrosis and tumor progression[21,22]. EMT is thought to be activated in cancer cells to allow for dissociation from the primary tumor and intravasation into blood vessels[23,24]. However, the impact of PAR2-associated EMT in cancer metastasis is still poorly understood. Based on these findings, we sought to investigate the relationship between PAR2 expression and HCC prognosis and the underlying mechanisms of the EMT in HCC.

MATERIALS AND METHODS

Patients

Cancer tissue sections were obtained with informed consent from 60 HCC patients undergoing radical resection between 2010 and 2012 at Qilu Hospital of Shandong University. Ethical consent was granted from

the Institutional Ethics Committee, Qilu Hospital of Shandong University.

Immunohistochemistry and evaluation of PAR2 expression

Immunohistochemistry (IHC) was performed using a standard immunoperoxidase staining method. Rabbit anti-PAR2 antibody (#6976) was purchased from Cell Signaling Technology (Danvers, United States). PAR2 expression in HCC tissues was evaluated using a method described previously[25]. The scoring of PAR2 immunohistochemical staining was performed as follows: the degree of staining [yellow (1) and brown (2)] and the percentage of area staining positive [< 50% (1) and > 50% (2)]. The final score was the product of the two parameters, and the samples were grouped as high (2-4 point) or low PAR2 expression (1). Two experienced pathologists evaluated the staining for PAR2.

Cell culture

HepG2 and SMMC-7721 cells were cultured at 37 ℃ in a humidified atmosphere containing 5% CO_2. Cells were cultured in DMEM (Gibco, NY, United States) supplemented with 10% fetal bovine serum (FBS; Gibco, NY, United States), 100 U/mL penicillin, and 100 μg/mL streptomycin (Hyclone, UT, United States).

Cell proliferation analysis

The cell counting kit 8 (CCK8) assay (Tongren Chemical Research Institute, Kyushu, Japan) was used to measure cell proliferation. HepG2 and SMMC-7721 cells in the exponential growth phase were seeded into a 96-well plate at 1000 cells per well with five replicates. DMEM medium containing 10% FBS was used to culture the cells. At 6, 24, 48, 72, 96, or 120 h after plating the cells, 100 μL of DMEM containing 10 μL of CCK-8 solution was added into each well. The wells were then incubated for 2 h at 37 ℃, and the absorbance was measured at 450 nm. The absorbance at 6 h of each group was designated as baseline.

Colony formation assay

Cells were seeded in 6-well plates (500 cells per well) and cultured for 2 wk. The generated colonies were fixed with 4% paraformaldehyde and then stained with 5% crystal violet dye (Sigma, MO, United States). The total number of colonies in each well was manually counted.

Cell invasion and migration assays

Cell invasion and migration assays were carried out using a 24-well plate and 8-μm polyethylene terephthalate membrane filters (Costar, MA, United States). Serum-free medium (200 μL) containing 3 × 10^4 HepG2 and SMMC-7721 cells was added to the upper chambers, which contained either uncoated (for migration assay) or matrigel coated (for invasion assay) membranes. Each inferior chamber was filled with 600 μL of medium containing 10% FBS. After 16 h of incubation, the filters were taken out, fixed with 4% paraformaldehyde for 30 min, and stained with crystal violet dye for 30 min. Then, the remaining cells on the upper sides of the filters were removed using cotton swabs. Migrated or invaded cells in four randomly chosen fields (× 100 magnification) per well were counted.

Wound healing assay

HepG2 and SMMC-7721 cells were seeded into 6-well plates and grown to 90% confluence. Then, the confluent cell monolayers were scraped with a 10 μL pipette tip to create wounds. The cellular debris was removed and cells were cultured in FBS-free medium. Pictures were taken under a microscope (Leica) at 0, 24, and 48 h. The difference in wound width represents the migration ability.

Plasmid construction and transfection

The coding region of PAR2 was cloned into a pcDNA3.1(+) plasmid at *EcoR* I and *Xho* I sites; this is referred to as pcDNA3.1-PAR2. Empty control and pcDNA3.1-PAR2 vectors were transfected into HepG2 and SMMC-7721 cells using Lipofectamine 2000 (Thermo, United States) according to the manufacturer's instructions. Primer sequences for vector construction were as follows: forward, 5′-GGAATTCTCGGGGCTTCCAGGAGGA-3′ and reverse, 5′-CCGCTCGAGTTCCCATCTGAGGACCTGG-3′.

Lentivirus-mediated RNA interference

pLKO.1 vector encoding shRNA targeting human PAR2 was purchased from Sigma (MISSION shRNA lentivirus-mediated transduction system, SHCLNG-NM_005242). To generate lentivirus that expressed shRNA, HEK293T cells were cultured in DMEM (Gibco, NY, United States) supplemented with 10% FBS (Gibco, NY, United States). Using polyethyleneimine, we transfected cells transiently with pLKO.1-derived plasmids combined with pRev, pEnv-VSV-G, and pMDLg. Retrovirus particles were collected from the media after 12, 24, and 48 h[19]. HepG2 and SMMC-7721 cells were infected three times with the retrovirus particles with 8.0 μg/mL polybrene. At 48 h after the transduction, transduced cells were selected using 2.0 μg/mL puromycin for one week. The efficiency of the shRNA knockdown was measured *via* quantitative real-time RT-PCR and immunoblot analysis.

RNA extraction and quantitative real-time PCR

Total RNA was extracted from cultured cells using Trizol reagent (Takara, Japan). cDNA was synthesized from at most 1 μg of total RNA (Takara, Japan). RNA expression was measured by qRT-PCR using SYBR-Green (Takara, Japan) according to the manufacturer's guidelines. Primers for PAR2 were: forward, 5′-GATGGCACATCCCACGTCACT-3′ and reverse, 5′-TTGGCAAACCCACCACAAACAC-3′. GAPDH was used as

Table 1 Immunohistochemical score for proteinase-activated receptor 2 in hepatocellular carcinoma

Score	Patient number
1	22
2	15
4	23

an endogenous control.

Immunoblot analysis

Rabbit anti-PAR2, anti-ERK, anti-phospho-ERK, anti-E-cadherin, anti-N-cadherin, and anti-GAPDH antibodies were obtained from Cell Signaling Technology (Danvers, United States). Cell lysates were prepared in RIPA buffer (Sigma-Aldrich, MO, United States) where equal quantities of cellular proteins were separated by sodium dodecyl sulfate-polyacrylamide gel electrophoresis and transferred onto polyvinylidene difluoride membranes. The membranes were blocked with skimmed milk, incubated with a primary antibody, washed with TBST three times, and then incubated with a secondary antibody (Cell Signaling Technology, GA, United States). After the secondary antibody incubation, the membranes were washed three more times with TBST, and the proteins were visualized by enhanced chemiluminescence (Millipore, MA, United States). GADPH was used as the internal loading control.

Experimental animals

Male Balb/c nude mice (aged 4 wk with an initial body weight of 20 ± 2 g) were purchased from Shanghai SLAC Laboratory Animal Co., Ltd. (Shanghai, China). The mice were housed at a temperature of 25 ± 2 ℃ and a relative humidity of 70% ± 5% under natural light/dark conditions for 1 wk and allowed free access to food and water. The animal experiments were performed in strict accordance with international ethical guidelines and the National Institutes of Health Guide for the Care and Use of Laboratory Animals. The protocols were approved by the Institutional Animal Care and Use Committee, Qilu Hospital of Shandong University.

Tumor xenograft model

HepG2 or SMMC-7721 cells (2×10^6) suspended in 100 μL of normal saline were subcutaneously injected into the axillae of the nude mice (4 wk). Tumor growth was monitored every week and tumor volume was calculated as follows: tumor volume = $4\pi/3 \times (\text{width}/2)^2 \times (\text{length}/2)$, in which the length and width are the longest and shortest diameters, respectively. Four weeks after injection, the mice were sacrificed and the tumors were dissected and weighed.

Tumor metastasis model

HepG2 and SMMC-7721 cells (2×10^6) suspended in 100 μL of normal saline were injected into the spleen of nude mice (4 wk) followed by a splenectomy 3 min later; the mice were monitored every 3 d after the procedure. After the 4th week, the mice were sacrificed and their livers were dissected. The liver tumor was weighed and tumor number on each liver was counted.

Table 2 Clinicopathological characteristics of hepatocellular carcinoma patients according to proteinase-activated receptor 2 expression

Clinicopathological variable	PAR2 expression		
	Low	High	*P* value
All cases	22	38	
Gender			
Male	16	28	0.832
Female	6	10	
Age (yr)			
< 60	10	22	0.352
⩾ 60	12	16	
TNM stage			
Early (Ⅰ-Ⅱ)	16	12	0.001[a]
Late (Ⅲ-Ⅳ)	6	26	
Tumor size (cm)			
Small (⩽ 5)	15	15	0.032[a]
Large (> 5)	7	23	
Microvascular invasion			
Present	5	21	0.037[a]
Absent	17	17	
HBsAg			
Negative	3	7	0.632
Positive	19	31	
Serum AFP level (ng/mL)			
< 400	18	25	0.154
⩾ 400	4	13	

[a]*P* < 0.05. PAR2: Proteinase-activated receptor 2; HBsAg: Hepatitis B surface antigen; AFP: Alpha-fetoprotein.

Statistical analysis

All assays were done in triplicate. The data are shown as mean ± SD. To compare the mean values between the two groups, the independent Student's *t*-test was used. To compare the mean values among more than two groups, two-way ANOVA was used. Fisher's exact test was used to compare tumor metastatic rate in the two groups. A Pearson χ^2 test was adopted to analyze the clinicopathological variables according to PAR2 expression. For survival analysis, Kaplan-Meier method and log-rank test were used. $P < 0.05$ was considered statistically significant.

RESULTS

The expression level of PAR2 correlates with TNM stage, tumor size, microvascular invasion, and patients' overall survival and disease-free survival

To determine whether PAR2 plays an important role in HCC progression, the expression level of PAR2 in patients' tumor tissues was detected by IHC. PAR2 was mainly located on the plasma membrane (Figure 1A). The patient distribution of PAR2 IHC score is shown in Table 1. Patients were divided into PAR2 high and PAR2 low groups according to the IHC score (Figure

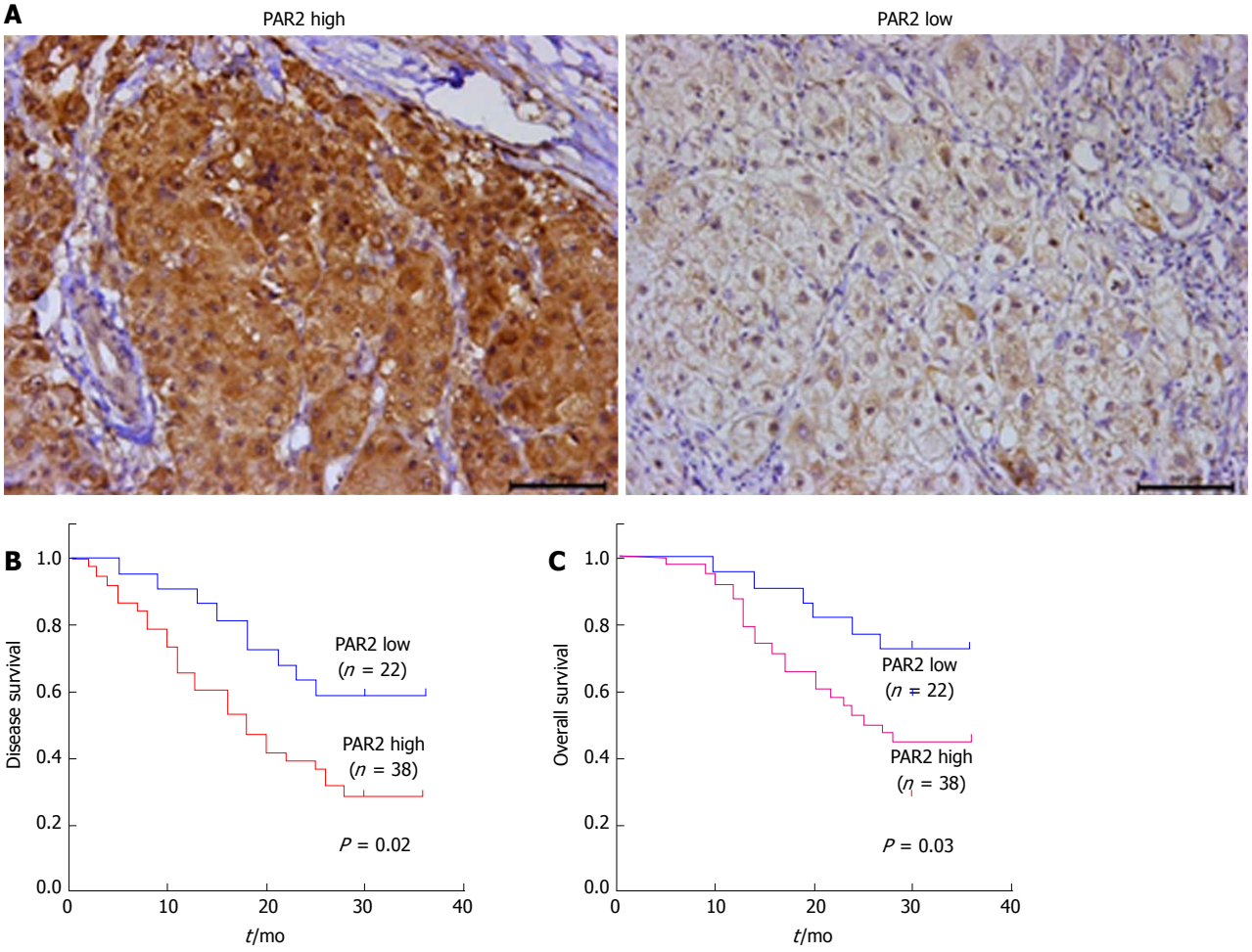

Figure 1 The expression level of proteinase-activated receptor 2 predicts overall survival and disease-free survival in hepatocellular carcinoma patients. A: Immunohistochemical staining for proteinase-activated receptor 2 (PAR2) in hepatocellular carcinoma (HCC) tissues, and the expression level of PAR2 was divided into high (left) and low (right); B: Disease-free survival in HCC patients correlated with PAR2 expression; C: Overall survival in HCC patients correlated with PAR2 expression.

1A). Patients with high PAR2 levels had advanced tumor stage (P = 0.001, chi-square test), larger tumor size (P = 0.032, chi-square test), and high microvascular invasion rate (P = 0.037, chi-square test; Table 2). Patients with high PAR2 expression levels had significantly shorter overall survival (OS) and disease-free survival (DFS) than those with low PAR2 expression levels (P = 0.02 and P = 0.03, respectively; Figure 1B and C). Multivariate Cox regression analysis further revealed that PAR2 was an independent prognostic marker for the OS of HCC patients (hazard ratio = 1.814; P = 0.041) (Table 3). These data suggest that PAR2 is associated with tumor growth and invasion; it can also predict the prognosis of HCC patients.

PAR2 is stably knocked down by lentiviral-mediated RNAi and transiently overexpressed by plasmid transfection

To determine whether PAR2 is essential for HCC carcinogenesis, the expression of PAR2 was stably knocked down using lentiviral-mediated shRNA in HepG2 and SMMC-7721 cells. The PAR2 knockdown is referred to as shPAR2, while the negative control is referred to as shNC. The PAR2 RNA and protein levels both decreased in shPAR2 knockdown cells (Figure 2A and B). To overexpress PAR2, its coding region was amplified and inserted into the pcDNA3.1 (+) plasmid. After transfecting cells with empty pcDNA3.1 or pcDNA3.1-PAR2 using Lipofectamine 2000, PAR2 was transiently overexpressed in pcDNA3.1-PAR2 cells (Figure 2C and D).

PAR2 promotes proliferation of HCC cells

CCK8 and colony formation assays were used to uncover the role of PAR2 in promoting HCC cell proliferation. Cell viability and proliferation were dramatically reduced after PAR2 knockdown (Figure 3A and B), but increased after PAR2 overexpression (Figure 3C and D). The same results were also observed using a colony formation assay (Figure 3E and F). These results demonstrate that PAR2 could promote the proliferation

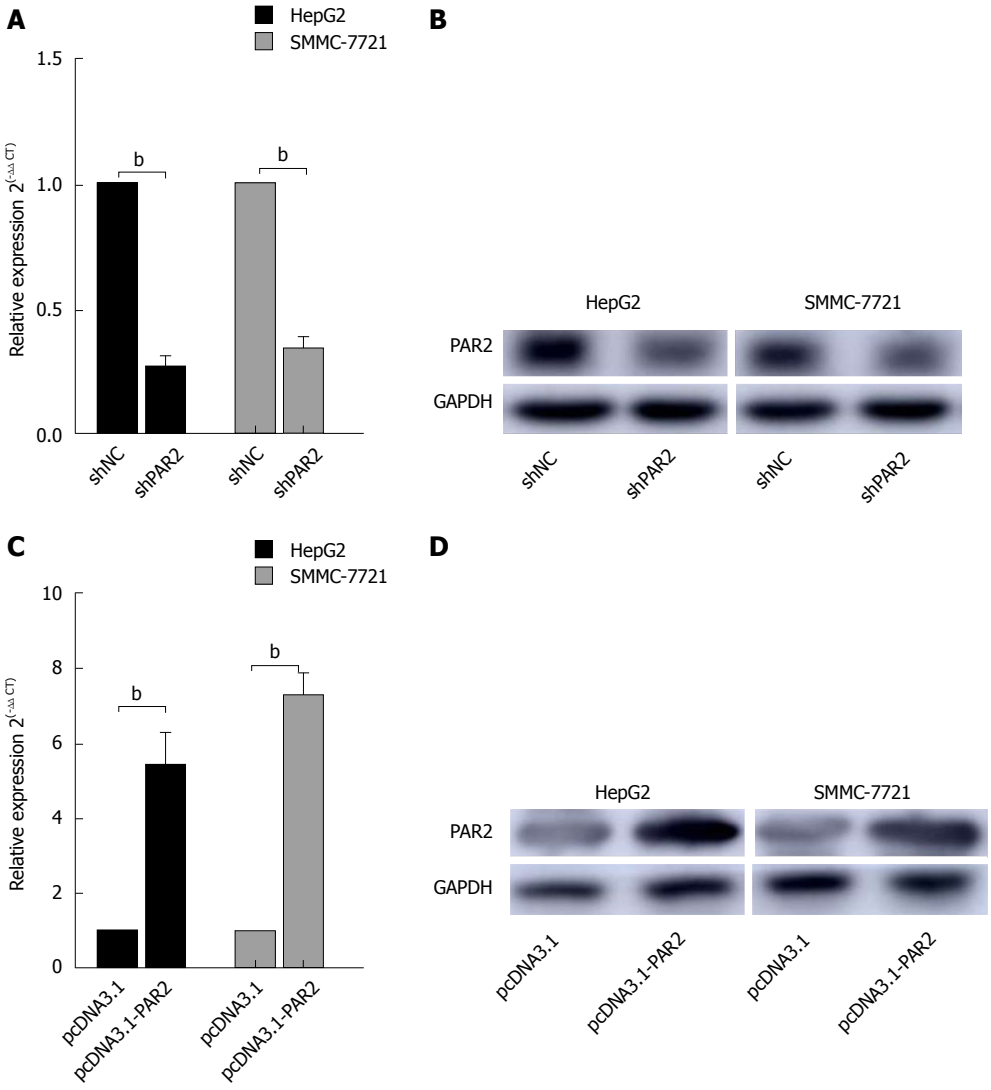

Figure 2 Proteinase-activated receptor 2 knockdown and overexpression. A: qRT-PCR analysis of the proteinase-activated receptor 2 (PAR2) mRNA expression levels in HepG2 and SMMC-7721 cells with PAR2 knockdown; B: Immunoblot analysis of the protein levels of PAR2 in HepG2 and SMMC-7721 cells with PAR2 knockdown; C: The RNA expression levels of PAR2 in HepG2 and SMMC-7721 cells with PAR2 overexpression were measured by qRT-PCR; D: The protein levels of PAR2 in HepG2 and SMMC-7721 cells with PAR2 overexpression were measured by immunoblot analysis. $^{b}P < 0.01$.

Table 3 Multivariate analysis of the association of prognosis with clinicopathological variables and proteinase-activated receptor 2 expression in hepatocellular carcinoma patients

Clinicopathological variable	Hazard ratio	*P* value
Gender (male *vs* female)	0.214	0.672
Age (< 60 *vs* ⩾ 60)	0.126	0.763
TNM stage (Ⅰ-Ⅱ *vs* Ⅲ-Ⅳ)	4.292	0.016[a]
Tumor size (⩽ 5 cm *vs* >5 cm)	2.193	0.034[a]
Microvascular invasion (present vs absent)	2.499	0.029[a]
HBsAg (negative *vs* positive)	1.072	0.092
Serum AFP level (< 400 ng/mL *vs* ⩾ 400 ng/mL)	3.688	0.023[a]
PAR2 expression (high *vs* low)	1.814	0.041[a]

[a]$P < 0.05$. HBsAg: Hepatitis B surface antigen; AFP: Alpha-fetoprotein; PAR2: Proteinase-activated receptor 2.

ability of HCC cells.

PAR2 promotes HCC cell invasion and migration

Metastasis often occurs in HCC patients and the results shown in Table 1 suggest that PAR2 is associated with tumor microvascular invasion. To determine whether PAR2 could promote HCC cell migration and invasion, transwells with or without matrigel coating were used to measure cell migration *in vitro*. As shown in Figure 4A and B, the migration and invasion abilities of HepG2 and SMMC-7721 cells were reduced after PAR2 knockdown, but increased after overexpression. These results were also verified using a wound healing assay (Figure 4C and D). The wound healing assay showed that the migration rate of shPAR2 cells was significantly slower than that of the control shNC cells. Also, the migration rate of pcDNA3.1-PAR2 cells was faster than that of the control pcDNA3.1 cells. These data suggest that PAR2 can influence the process of HCC cell invasion and migration.

PAR2 knockdown inhibits tumor growth in nude mice

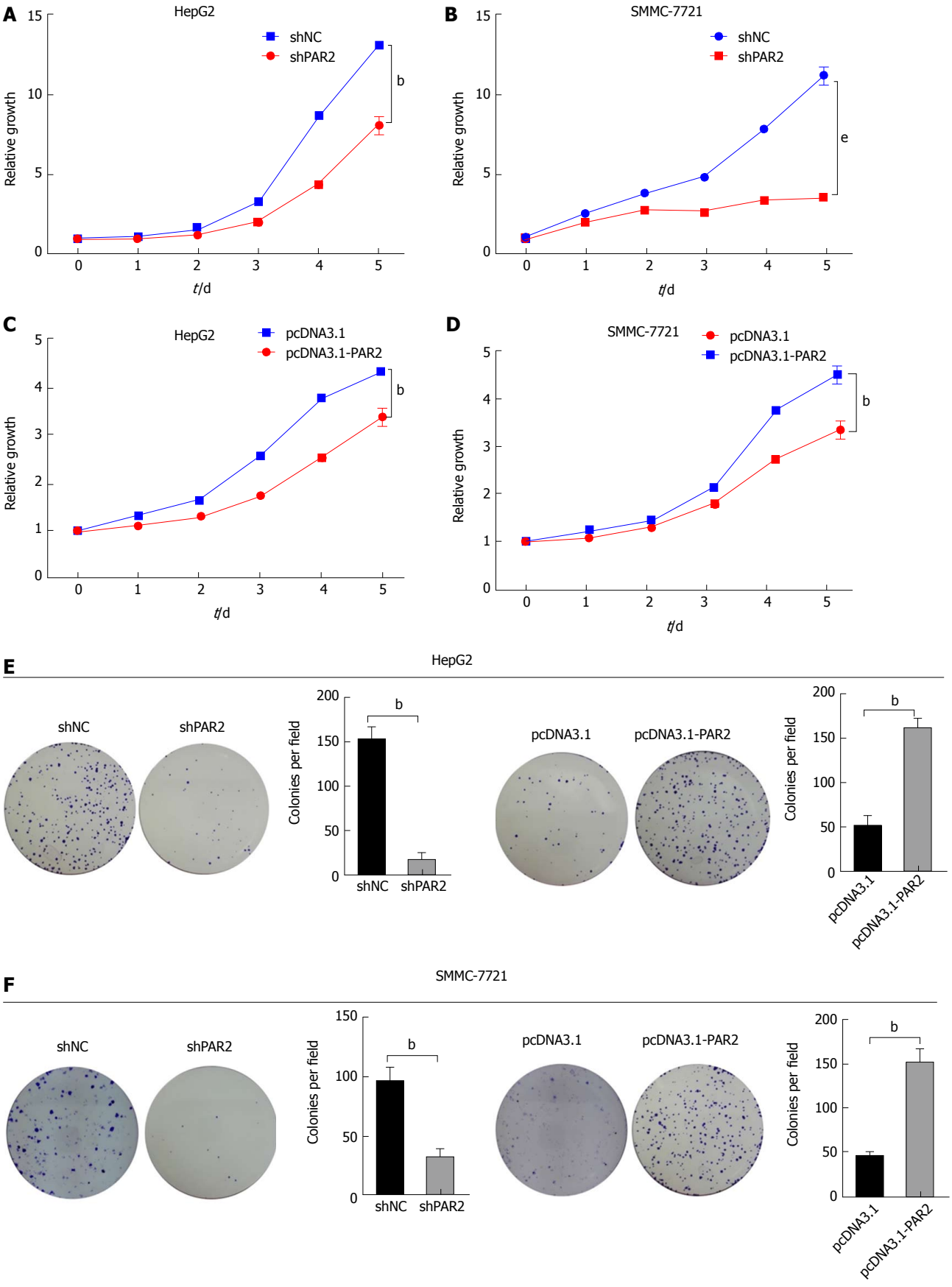

Figure 3 Proteinase-activated receptor 2 promotes proliferation of hepatocellular carcinoma cells. A-D: CCK8 assay in HepG2 and SMMC-7721 cells; E and F: Colony formation assay in HepG2 and SMMC-7721 cells. The colony number in each field was counted. $^{b}P < 0.01$, $^{e}P < 0.001$.

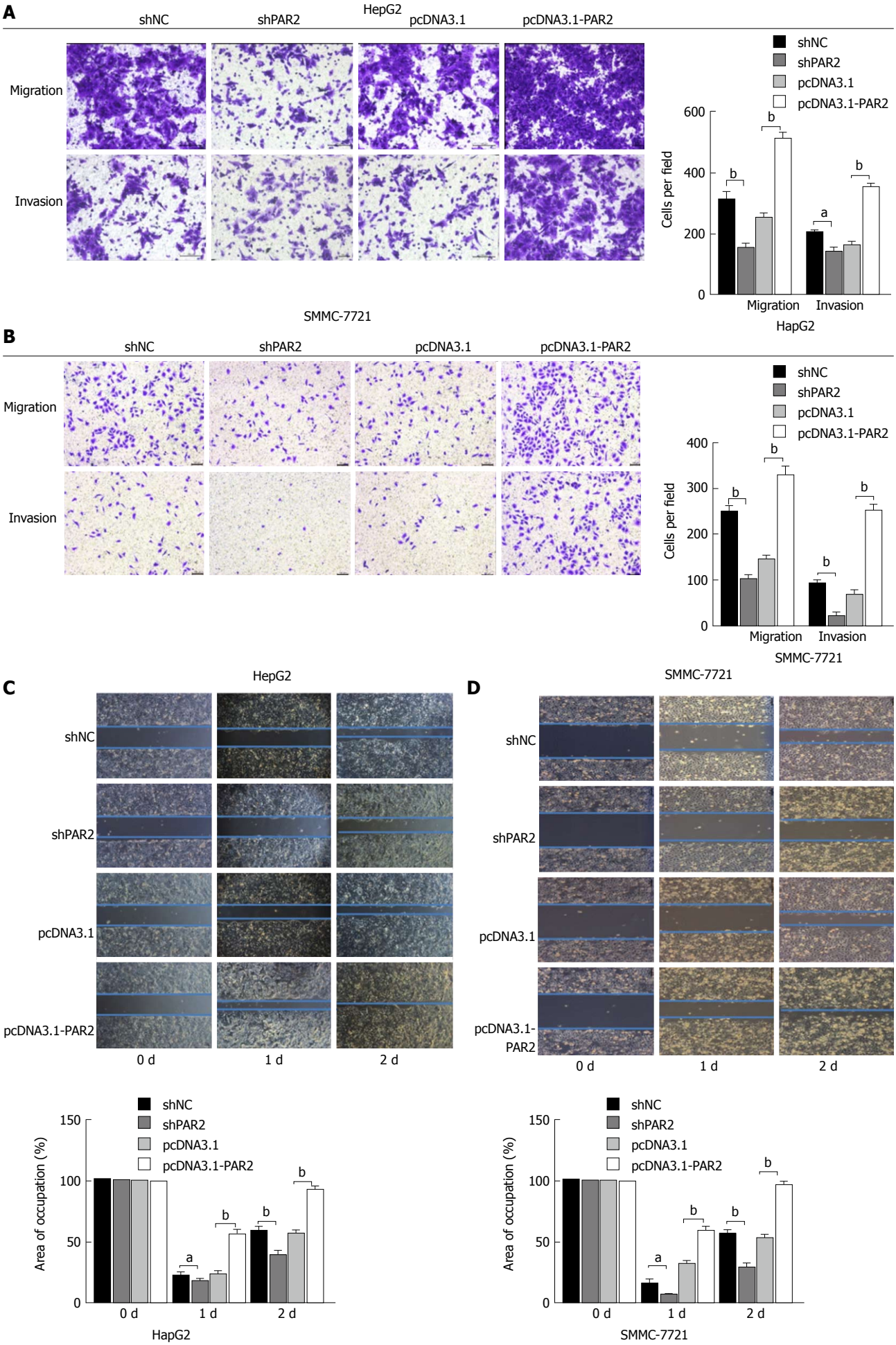
A
HepG2
shNC
shPAR2
pcDNA3.1
pcDNA3.1-PAR2
Migration
Invasion
Cells per field
600
400
200
0
b
a
Migration
Invasion
HapG2
SMMC-7721
B
shNC
shPAR2
pcDNA3.1
pcDNA3.1-PAR2
Migration
Invasion
Cells per field
400
300
200
100
0
SMMC-7721
C
HepG2
shNC
shPAR2
pcDNA3.1
pcDNA3.1-PAR2
0 d
1 d
2 d
Area of occupation (%)
150
100
50
0
HapG2
D
SMMC-7721
shNC
shPAR2
pcDNA3.1
pcDNA3.1-PAR2
0 d
1 d
2 d
Area of occupation (%)
SMMC-7721

Figure 4 Proteinase-activated receptor 2 promotes hepatocellular carcinoma cell invasion and migration *in vitro*. A and B: Transwell assays with or without matrigel coating were performed in HepG2 and SMMC-7721 cells. Cell number in each field was counted; C and D: Wound healing assays were performed in HepG2 and SMMC-7721 cells and the pictures were taken every 24 h ($^{a}P < 0.05$, $^{b}P < 0.01$).

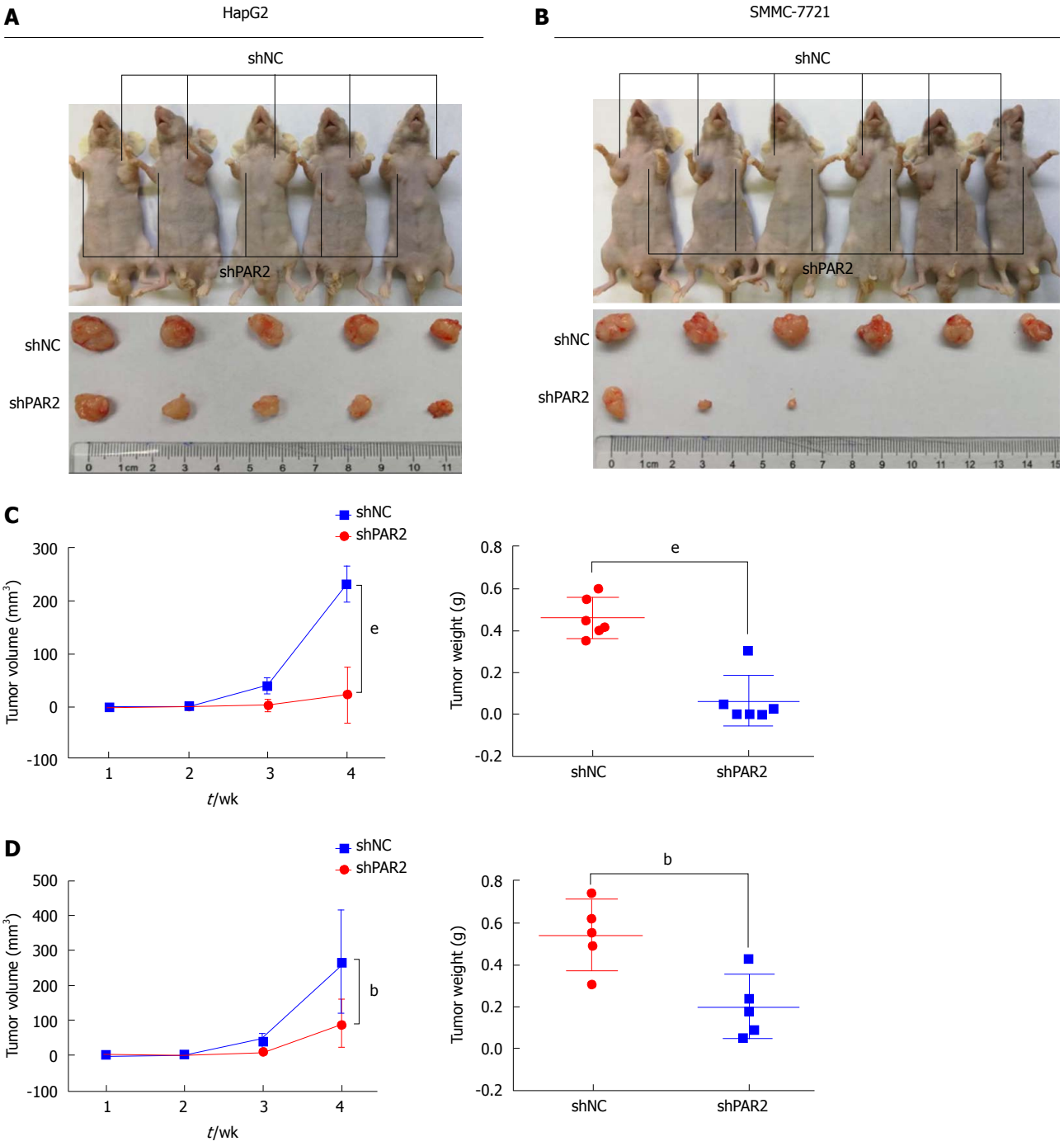

Figure 5 Proteinase-activated receptor 2 knockdown inhibits tumor growth in nude mice. A and B: Subcutaneous xenografts of HepG2 and SMMC-7721 cells in nude mice growing for 4 wk; C and D: Tumor volumes were measured every week and tumor weights were tested at the end. $^{b}P < 0.01$, $^{e}P < 0.001$.

To further confirm the role of PAR2 in promoting cell proliferation *in vivo*, HepG2 and SMMC-7721 cells with stable knockdown of either PAR2 or NC were subcutaneously injected into nude mice to make tumor xenografts. After 4 wk, tumors from the NC groups were much larger than those from the shPAR2 groups for both HepG2 and SMMC-7721 cells (Figure 5A and B). Tumor weights from the NC groups were much greater than those of the shPAR2 groups (Figure 5C and D). These data suggest that PAR2 knockdown could dramatically inhibit tumor growth *in vivo*.

PAR2 knockdown inhibits tumor metastasis in nude mice

Intrahepatic metastasis is the most common mode of HCC metastasis[26]. To determine whether PAR2 could

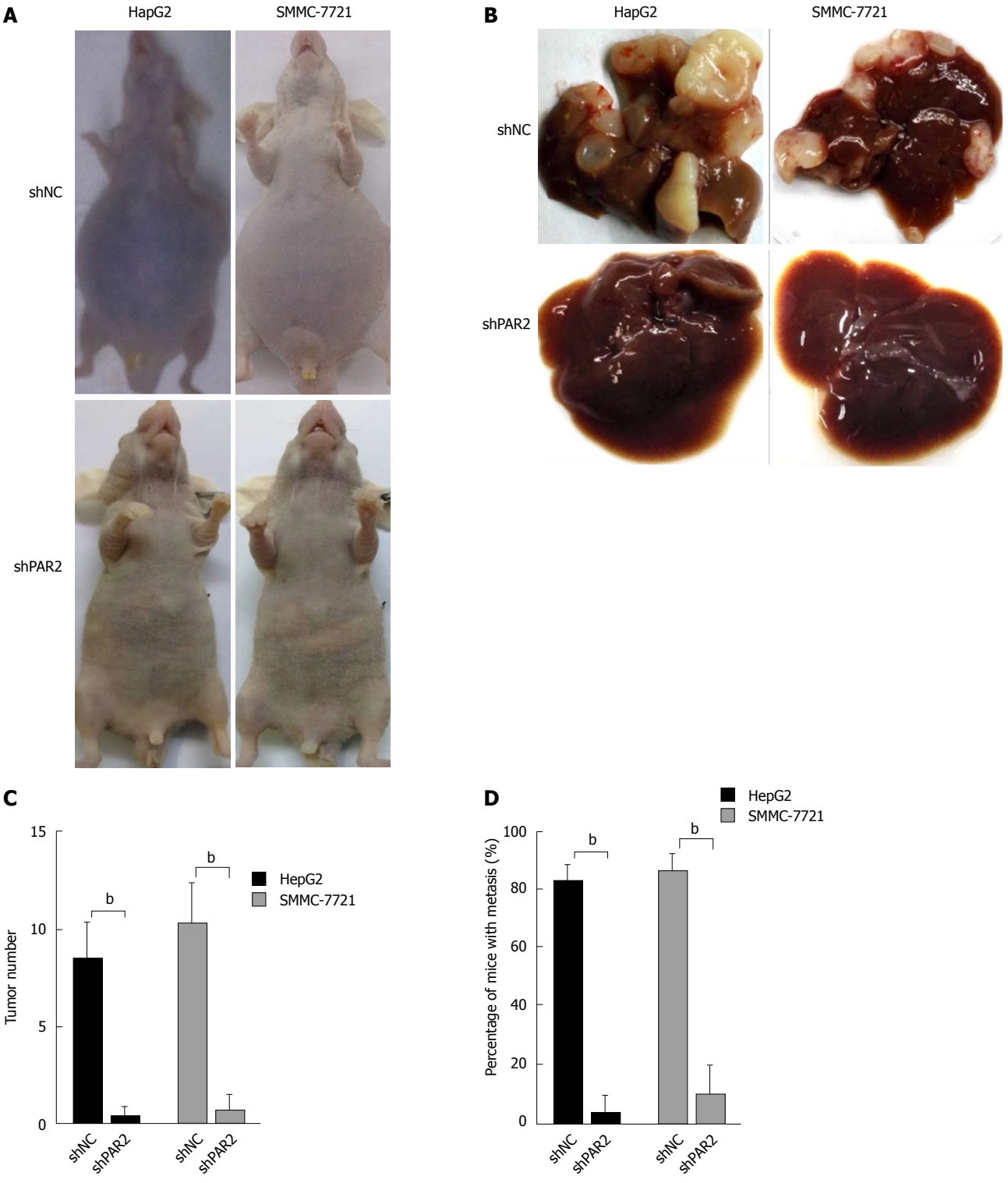

Figure 6 Proteinase-activated receptor 2 knockdown inhibits tumor metastasis in nude mice. A: HepG2 and SMMC-7721 cells were injected into the spleen of nude mice to form liver metastases. The appearance of mice after 4 wk is shown; B: Tumors grown on the liver; C: Tumor number on each liver was counted; D: Percentage of mice with liver metastases (n = 10 per group). $^{b}P < 0.01$.

facilitate tumor metastasis *in vivo*, a mouse model was established that mimics the process of tumor metastasis to the liver. HepG2 and SMMC-7721 cells stably expressing shPAR2 or shNC were injected into the spleen of nude mice, and then a splenectomy was performed. This allows the tumor cells to circulate into the liver through the portal vein, thus forming liver metastases. After 4 wk, ascites and liver tumors grew in the mice of the shNC groups (Figure 6A), the maximum body weight that increased due to ascites was no more than 10% of the body weight in age-matched shPAR2 group. The mice in both groups were sacrificed and

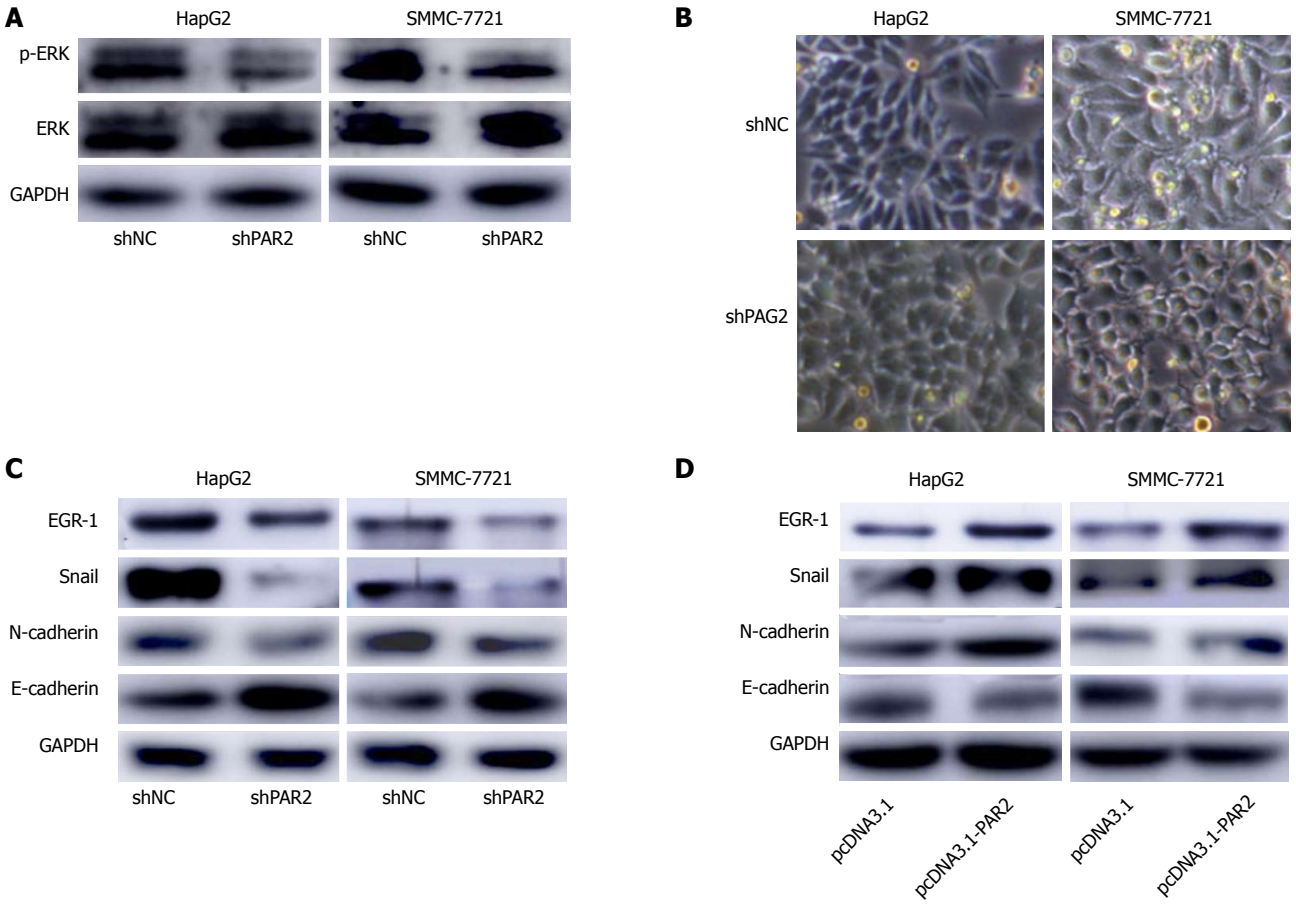

Figure 7 Proteinase-activated receptor 2 mediates the activation of ERK and further induces epithelial-mesenchymal transition. A: The protein levels of ERK and p-ERK in HepG2 and SMMC-7721 cells; B: The morphological changes in HepG2 and SMMC-7721 cells after proteinase-activated receptor 2 knockdown; C and D: The protein levels of EGR-1, Snail, E-cadherin, and N-cadherin in HepG2 and SMMC-7721 cells. GAPDH was selected as an endogenous control.

the tumor volumes of the shNC groups were much larger than those in the shPAR2 groups (Figure 6B). Livers in the shNC group also had a higher number of tumors compared to the shPAR2 groups (Figure 6C). There was almost no liver metastasis observed in the shPAR2 groups (Figure 6D). From this metastasis model, it appears that PAR2 is necessary for HCC intrahepatic metastasis. PAR2 knockdown could inhibit the colonization of HCC cells on the liver.

PAR2 mediates the activation of ERK to promote cell proliferation and induces EMT to promote metastasis

PAR2 is reported to activate ERK to promote HCC cell proliferation[16]; these results were confirmed in HepG2 and SMMC-7721 cells (Figure 7A), but the downstream mechanisms that facilitate metastasis are unclear. EMT is a common mechanism of cancer metastasis, and it is reported that activated ERK can activate EGR-1[27]. As a transcription factor, EGR-1 induces Snail expression to inhibit E-cadherin expression, thus inducing EMT[27-29]. Interestingly, after knockdown of PAR2, HepG2 and SMMC-7721 cells showed obvious morphological changes toward an epithelial phenotype (Figure 7B). Therefore, we measured EGR-1, Snail, and the EMT markers E-cadherin and N-cadherin expression in shNC and shPAR2 cells through immunoblot analysis. As shown in Figure 7C, the epithelial marker E-cadherin was upregulated while EGR-1, Snail, and the mesenchymal marker N-cadherin were downregulated when PAR2 was knocked down. After transient overexpression of PAR2, E-cadherin was downregulated, and EGR-1, Snail, and N-cadherin were upregulated (Figure 7D). These results demonstrate that PAR2 participates in the process of EMT and promotes HCC cell metastasis.

DISCUSSION

HCC is one of the most lethal malignancies worldwide, especially in China[4]. Although many genes and signaling pathways have been found to participate in HCC carcinogenesis[30-33], the prognosis of the patients is still unsatisfactory, therefore it is urgent to uncover more genes responsible for the development of HCC. The focus of this work was PAR2, which is evident for its important role in the development of tumors, especially of epithelial origin[12-15]. PAR2 is known to promote proliferation, migration, and invasion of HCC cells. Unfortunately, the underlying mechanism of PAR2 activity in HCC metastasis is unclear and few *in*

vivo studies have been carried out elucidating its role in tumor development. Additionally, the association between PAR2 and clinicopathological variables of HCC patients has not been analyzed; this work addressed those questions.

In the clinical association study, expression levels of PAR2 were analyzed in 60 HCC patients by immunohistochemistry. Patients with high PAR2 expression levels tended to have advanced tumor stage, larger tumor size, and high microvascular invasion rate, indicating that PAR2 plays an important role in the development of HCC. Additionally, patients with high PAR2 expression levels had shorter OS and DFS, implying that PAR2 could serve as a biomarker to predict the prognosis of HCC patients.

Because PAR2 is associated with tumor size and microvascular invasion, the role of PAR2 in HCC proliferation and invasion was investigated. PAR2 was stably knocked down using shRNA or transiently overexpressed in HepG2 and SMMC-7721 cells. CCK8 and colony forming assays were used to measure *in vitro* cell proliferation. These assays showed that PAR2 knockdown inhibited cell proliferation and colony formation ability, while overexpression of PAR2 presented adverse effects. From transwell and wound healing assays, PAR2 was shown to promote tumor cell migration and invasion. These *in vitro* experiments indicated that PAR2 plays an important role in tumorigenesis and the development of HCC cells.

Two mouse models were used to explore the role of PAR2 in HCC progression *in vivo*. From a subcutaneous xenograft model, it was determined that knockdown of PAR2 could inhibit tumor growth to a great extent. From the liver metastasis model, PAR2 was shown to help HCC cells plant onto the liver and form metastatic foci. These *in vivo* data provide solid evidence that PAR2 promotes HCC cell proliferation, invasion, and migration.

After knockdown of PAR2, morphological changes toward an epithelial phenotype were observed in HepG2 and SMMC-7721 cells. EMT is an important step in tumor progression and plays a critical role during cancer invasion and metastasis. During EMT, cells lose their epithelial qualities and acquire mesenchymal features[21] such as increased expression of mesenchymal-related markers (such as N-cadherin), and reduced expression of epithelial-related markers (such as E-cadherin)[28]. It is reported that the function of PAR2 is mediated by activating MAPK proteins such as ERK[16]; ERK activation by PAR2 was verified in this study. Interestingly, it is reported that activated ERK can induce EMT through EGR-1 and Snail[28,29], therefore the expression levels of EGR-1, Snail, E-cadherin, and N-cadherin were monitored through immunoblot analysis in HepG2 and SMMC-7721 cells. PAR2 knockdown resulted in higher levels of E-cadherin and lower levels of N-cadherin, while overexpression of PAR2 reduced the levels of E-cadherin and increased the levels of N-cadherin. This implies that PAR2 can promote EMT in HCC cells through activating ERK, at least in part. As we all know, PAR2 is activated *via* its N-terminal cleavage by several proteases such as serine proteases[34], but which protease is responsible for PAR2 activation in HCC is still not clear. This is a very interesting direction in the following study. Recently, some growth factors such as HGF were reported to be responsible for EMT in HCC. Whether HGF participates in PAR2-induced EMT could be further investigated based on this study[27,35].

Collectively, this study comprehensively investigated the role of PAR2 in HCC progression *in vitro*, *in vivo,* and in clinical samples for the first time. PAR2 could promote HCC cell proliferation, invasion, and migration by activating ERK and thus inducing EMT. These findings highlight the potential role of PAR2 in directing the diagnosis, treatment, and prognosis of HCC.

ARTICLE HIGHLIGHTS

Research background

Hepatocellular carcinoma (HCC) is one of the most common malignancies worldwide. Metastasis often occurs in HCC patients, thus leading to a poor prognosis. It is urgent for us to find out molecules that are responsible for HCC metastasis to improve the prognosis of HCC patients.

Research motivation

Proteinase-activated receptor 2 (PAR2) is reported to be responsible for HCC development, but the underlying mechanism is unclear. Figuring out the detailed mechanisms for PAR2-induced metastasis of HCC could give us more options for HCC treatment.

Research objectives

Although the role of PAR2 in HCC has been reported, the underlying mechanism for PAR2-induced metastasis is more important. Therefore, we aimed to find out the downstream signaling for PAR2-induced HCC metastasis. This could help us to find targets for HCC treatment.

Research methods

PAR2 expression levels were assessed by qRT-PCR and immunohistochemistry in patient tissues. Cell proliferation was investigated by CCK8 and colony formation assays *in vitro* and tumor xenograft *in vivo*. HCC cell metastasis was assessed by transwell and wound healing assays *in vitro* and intrasplenic injection of HCC cells in mice *in vivo*. Immunoblotting was carried out to monitor the levels of mitogen-activated protein kinases and epithelial-mesenchymal transition (EMT) markers to figure out the underlying mechanisms for PAR2. This is the first time to analyze the correlation between PAR2 expression and HCC clinicopathological characteristics. Also, it is the first for us to investigate the underlying mechanism for PAR2-mediated HCC metastasis. What's more, we proved the role of PAR2 in HCC proliferation and metastasis using an animal model.

Research results

The prognosis of patients with high PAR2 levels was poorer than those with low PAR2 levels. Patients with high PAR2 levels had advanced tumor stage, larger tumor size, and high microvascular invasion rate. The proliferation and metastasis ability of SMMC-7721 and HepG2 cells was increased after PAR2 overexpression, while knockdown of PAR2 decreased the proliferation and metastasis ability of SMMC-7721 and HepG2 cells. Knockdown of PAR2 also inhibited HCC tumor cell growth and liver metastasis in nude mice. Mechanistically, PAR2 increased the proliferation ability of SMMC-7721 and HepG2 cells *via* ERK activation. Activated ERK further promoted the epithelial-mesenchymal transition of these cells with the help of EGR-1 and Snail, which endowed them with enhanced migration and invasion ability.

Research conclusions

In this study, we found that PAR2 was upregulated in HCC tumor tissues and related with poor prognosis in HCC patients. In addition, we proved that PAR2 could not only promote the proliferation and metastasis ability of SMMC-7721 and HepG2 cells *in vitro*, but also promoted xenograft tumor growth and HCC cell liver metastasis *in vivo*. These effects were mediated by the activation of ERK, which further induced EMT by EGR-1 and Snail of HCC cells. Therefore, targeting PAR2 may present a favorable anticancer target for treatment.

Research perspectives

As we all know, PAR2 is activated *via* its N-terminal cleavage by several proteases such as serine proteases, but which protease is responsible for PAR2 activation in HCC is still not clear. This is a very interesting direction in the following study. Recently, some growth factors such as HGF were reported to be responsible for EMT in HCC. Whether HGF participates in PAR2-induced EMT could be further investigated based on this study.

REFERENCES

1 **Bruix J**, Reig M, Sherman M. Evidence-Based Diagnosis, Staging, and Treatment of Patients with Hepatocellular Carcinoma. *Gastroenterology* 2016; **150**: 835-853 [PMID: 26795574 DOI: 10.1053/j.gastro.2015.12.041]

2 **Ye JZ**, Chen JZ, Li ZH, Bai T, Chen J, Zhu SL, Li LQ, Wu FX. Efficacy of postoperative adjuvant transcatheter arterial chemoembolization in hepatocellular carcinoma patients with microvascular invasion. *World J Gastroenterol* 2017; **23**: 7415-7424 [PMID: 29151695 DOI: 10.3748/wjg.v23.i41.7415]

3 **Feng LH**, Dong H, Lau WY, Yu H, Zhu YY, Zhao Y, Lin YX, Chen J, Wu MC, Cong WM. Novel microvascular invasion-based prognostic nomograms to predict survival outcomes in patients after R0 resection for hepatocellular carcinoma. *J Cancer Res Clin Oncol* 2017; **143**: 293-303 [PMID: 27743138 DOI: 10.1007/s00432-016-2286-1]

4 **Chan SL**, Wong VW, Qin S, Chan HL. Infection and Cancer: The Case of Hepatitis B. *J Clin Oncol* 2016; **34**: 83-90 [PMID: 26578611 DOI: 10.1200/JCO.2015.61.5724]

5 **Fidler IJ**. The pathogenesis of cancer metastasis: the 'seed and soil' hypothesis revisited. *Nat Rev Cancer* 2003; **3**: 453-458 [PMID: 12778135 DOI: 10.1038/nrc1098]

6 **Nystedt S**, Emilsson K, Wahlestedt C, Sundelin J. Molecular cloning of a potential proteinase activated receptor. *Proc Natl Acad Sci USA* 1994; **91**: 9208-9212 [PMID: 7937743 DOI: 10.1073/pnas.91.20.9208]

7 **Ossovskaya VS**, Bunnett NW. Protease-activated receptors: contribution to physiology and disease. *Physiol Rev* 2004; **84**: 579-621 [PMID: 15044683 DOI: 10.1152/physrev.00028.2003]

8 **Grab DJ**, Garcia-Garcia JC, Nikolskaia OV, Kim YV, Brown A, Pardo CA, Zhang Y, Becker KG, Wilson BA, de A Lima AP, Scharfstein J, Dumler JS. Protease activated receptor signaling is required for African trypanosome traversal of human brain microvascular endothelial cells. *PLoS Negl Trop Dis* 2009; **3**: e479 [PMID: 19621073 DOI: 10.1371/journal.pntd.0000479]

9 **Lin H**, Trejo J. Transactivation of the PAR1-PAR2 heterodimer by thrombin elicits β-arrestin-mediated endosomal signaling. *J Biol Chem* 2013; **288**: 11203-11215 [PMID: 23476015 DOI: 10.1074/jbc.M112.439950]

10 **Weithauser A**, Rauch U. Role of protease-activated receptors for the innate immune response of the heart. *Trends Cardiovasc Med* 2014; **24**: 249-255 [PMID: 25066486 DOI: 10.1016/j.tcm.2014.06.004]

11 **Weithauser A**, Bobbert P, Antoniak S, Böhm A, Rauch BH, Klingel K, Savvatis K, Kroemer HK, Tschope C, Stroux A, Zeichhardt H, Poller W, Mackman N, Schultheiss HP, Rauch U. Protease-activated receptor-2 regulates the innate immune response to viral infection in a coxsackievirus B3-induced myocarditis. *J Am Coll Cardiol* 2013; **62**: 1737-1745 [PMID: 23871888 DOI: 10.1016/j.jacc.2013.05.076]

12 **Kanemaru A**, Yamamoto K, Kawaguchi M, Fukushima T, Lin CY, Johnson MD, Camerer E, Kataoka H. Deregulated matriptase activity in oral squamous cell carcinoma promotes the infiltration of cancer-associated fibroblasts by paracrine activation of protease-activated receptor 2. *Int J Cancer* 2017; **140**: 130-141 [PMID: 27615543 DOI: 10.1002/ijc.30426]

13 **Quanjun D**, Qingyu Z, Qiliang Z, Liqun X, Jinmei C, Ziquan L, Shike H. Effect and mechanism of PAR-2 on the proliferation of esophageal cancer cells. *Eur Rev Med Pharmacol Sci* 2016; **20**: 4688-4696 [PMID: 27906434]

14 **Zeeh F**, Witte D, Gädeken T, Rauch BH, Grage-Griebenow E, Leinung N, Fromm SJ, Stölting S, Mihara K, Kaufmann R, Settmacher U, Lehnert H, Hollenberg MD, Ungefroren H. Proteinase-activated receptor 2 promotes TGF-β-dependent cell motility in pancreatic cancer cells by sustaining expression of the TGF-β type I receptor ALK5. *Oncotarget* 2016; **7**: 41095-41109 [PMID: 27248167 DOI: 10.18632/oncotarget.9600]

15 **Schaffner F**, Versteeg HH, Schillert A, Yokota N, Petersen LC, Mueller BM, Ruf W. Cooperation of tissue factor cytoplasmic domain and PAR2 signaling in breast cancer development. *Blood* 2010; **116**: 6106-6113 [PMID: 20861457 DOI: 10.1182/blood-2010-06-289314]

16 **Kaufmann R**, Oettel C, Horn A, Halbhuber KJ, Eitner A, Krieg R, Katenkamp K, Henklein P, Westermann M, Böhmer FD, Ramachandran R, Saifeddine M, Hollenberg MD, Settmacher U. Met receptor tyrosine kinase transactivation is involved in proteinase-activated receptor-2-mediated hepatocellular carcinoma cell invasion. *Carcinogenesis* 2009; **30**: 1487-1496 [PMID: 19546160 DOI: 10.1093/carcin/bgp153]

17 **Kaufmann R**, Mussbach F, Henklein P, Settmacher U. Proteinase-activated receptor 2-mediated calcium signaling in hepatocellular carcinoma cells. *J Cancer Res Clin Oncol* 2011; **137**: 965-973 [PMID: 21125404 DOI: 10.1007/s00432-010-0961-1]

18 **Lee TK**, Cheung VC, Lu P, Lau EY, Ma S, Tang KH, Tong M, Lo J, Ng IO. Blockade of CD47-mediated cathepsin S/protease-activated receptor 2 signaling provides a therapeutic target for hepatocellular carcinoma. *Hepatology* 2014; **60**: 179-191 [PMID: 24523067 DOI: 10.1002/hep.27070]

19 **Mußbach F**, Ungefroren H, Günther B, Katenkamp K, Henklein P, Westermann M, Settmacher U, Lenk L, Sebens S, Müller JP, Böhmer FD, Kaufmann R. Proteinase-activated receptor 2 (PAR2) in hepatic stellate cells - evidence for a role in hepatocellular carcinoma growth in vivo. *Mol Cancer* 2016; **15**: 54 [PMID: 27473374 DOI: 10.1186/s12943-016-0538-y]

20 **Chen KD**, Wang CC, Tsai MC, Wu CH, Yang HJ, Chen LY, Nakano T, Goto S, Huang KT, Hu TH, Chen CL, Lin CC. Interconnections between autophagy and the coagulation cascade in hepatocellular carcinoma. *Cell Death Dis* 2014; **5**: e1244 [PMID: 24853422 DOI: 10.1038/cddis.2014.212]

21 **Nieto MA**, Huang RY, Jackson RA, Thiery JP. EMT: 2016. *Cell* 2016; **166**: 21-45 [PMID: 27368099 DOI: 10.1016/j.cell.2016.06.028]

22 **Lamouille S**, Xu J, Derynck R. Molecular mechanisms of epithelial-mesenchymal transition. *Nat Rev Mol Cell Biol* 2014; **15**: 178-196 [PMID: 24556840 DOI: 10.1038/nrm3758]

23 **De Craene B**, Berx G. Regulatory networks defining EMT during cancer initiation and progression. *Nat Rev Cancer* 2013; **13**: 97-110 [PMID: 23344542 DOI: 10.1038/nrc3447]

24 **Chua KN**, Poon KL, Lim J, Sim WJ, Huang RY, Thiery JP. Target cell movement in tumor and cardiovascular diseases based on the epithelial-mesenchymal transition concept. *Adv Drug Deliv Rev* 2011; **63**: 558-567 [PMID: 21335038 DOI: 10.1016/j.addr.2011.02.003]

25 **Pinheiro C**, Longatto-Filho A, Scapulatempo C, Ferreira L, Martins S, Pellerin L, Rodrigues M, Alves VA, Schmitt F, Baltazar F. Increased expression of monocarboxylate transporters 1, 2, and 4 in colorectal carcinomas. *Virchows Arch* 2008; **452**: 139-146 [PMID: 18188595 DOI: 10.1007/s00428-007-0558-5]

26 **Kudo M**. Early detection and curative treatment of early-stage hepatocellular carcinoma. *Clin Gastroenterol Hepatol* 2005; **3**: S144-S148 [PMID: 16234064 DOI: 10.1016/S1542-3565(05)00712-3]

27 **Grotegut S**, von Schweinitz D, Christofori G, Lehembre F. Hepatocyte growth factor induces cell scattering through

MAPK/Egr-1-mediated upregulation of Snail. *EMBO J* 2006; **25**: 3534-3545 [PMID: 16858414 DOI: 10.1038/sj.emboj.7601213]

28 **Waerner T**, Alacakaptan M, Tamir I, Oberauer R, Gal A, Brabletz T, Schreiber M, Jechlinger M, Beug H. ILEI: a cytokine essential for EMT, tumor formation, and late events in metastasis in epithelial cells. *Cancer Cell* 2006; **10**: 227-239 [PMID: 16959614 DOI: 10.1016/j.ccr.2006.07.020]

29 **Cai L**, Ye Y, Jiang Q, Chen Y, Lyu X, Li J, Wang S, Liu T, Cai H, Yao K, Li JL, Li X. Epstein-Barr virus-encoded microRNA BART1 induces tumour metastasis by regulating PTEN-dependent pathways in nasopharyngeal carcinoma. *Nat Commun* 2015; **6**: 7353 [PMID: 26135619 DOI: 10.1038/ncomms8353]

30 **Weiler SME**, Pinna F, Wolf T, Lutz T, Geldiyev A, Sticht C, Knaub M, Thomann S, Bissinger M, Wan S, Rössler S, Becker D, Gretz N, Lang H, Bergmann F, Ustiyan V, Kalin TV, Singer S, Lee JS, Marquardt JU, Schirmacher P, Kalinichenko VV, Breuhahn K. Induction of Chromosome Instability by Activation of Yes-Associated Protein and Forkhead Box M1 in Liver Cancer. *Gastroenterology* 2017; **152**: 2037-2051.e22 [PMID: 28249813 DOI: 10.1053/j.gastro.2017.02.018]

31 **Nakagawa H**, Mizukoshi E, Kobayashi E, Tamai T, Hamana H, Ozawa T, Kishi H, Kitahara M, Yamashita T, Arai K, Terashima T, Iida N, Fushimi K, Muraguchi A, Kaneko S. Association Between High-Avidity T-Cell Receptors, Induced by α-Fetoprotein-Derived Peptides, and Anti-Tumor Effects in Patients With Hepatocellular Carcinoma. *Gastroenterology* 2017; **152**: 1395-1406.e10 [PMID: 28188748 DOI: 10.1053/j.gastro.2017.02.001]

32 **Schneider AT**, Gautheron J, Feoktistova M, Roderburg C, Loosen SH, Roy S, Benz F, Schemmer P, Büchler MW, Nachbur U, Neumann UP, Tolba R, Luedde M, Zucman-Rossi J, Panayotova-Dimitrova D, Leverkus M, Preisinger C, Tacke F, Trautwein C, Longerich T, Vucur M, Luedde T. RIPK1 Suppresses a TRAF2-Dependent Pathway to Liver Cancer. *Cancer Cell* 2017; **31**: 94-109 [PMID: 28017612 DOI: 10.1016/j.ccell.2016.11.009]

33 **Fortin J**, Mak TW. Targeting PI3K Signaling in Cancer: A Cautionary Tale of Two AKTs. *Cancer Cell* 2016; **29**: 429-431 [PMID: 27070694 DOI: 10.1016/j.ccell.2016.03.020]

34 **Cattaruzza F**, Amadesi S, Carlsson JF, Murphy JE, Lyo V, Kirkwood K, Cottrell GS, Bogyo M, Knecht W, Bunnett NW. Serine proteases and protease-activated receptor 2 mediate the proinflammatory and algesic actions of diverse stimulants. *Br J Pharmacol* 2014; **171**: 3814-3826 [PMID: 24749982 DOI: 10.1111/bph.12738]

35 **Gui Y**, Khan MGM, Bobbala D, Dubois C, Ramanathan S, Saucier C, Ilangumaran S. Attenuation of MET-mediated migration and invasion in hepatocellular carcinoma cells by SOCS1. *World J Gastroenterol* 2017; **23**: 6639-6649 [PMID: 29085209 DOI: 10.3748/wjg.v23.i36.6639]

P- Reviewer: Midorikawa Y, Vij M, Ilangumaran S, Sakaguchi T
S- Editor: Gong ZM **L- Editor**: Wang TQ **E- Editor**: Ma YJ

World Journal of Gastroenterology

Submit a Manuscript: http://www.f6publishing.com

World J Gastroenterol 2018 March 14; 24(10): 1134-1143

DOI: 10.3748/wjg.v24.i10.1134

ISSN 1007-9327 (print) ISSN 2219-2840 (online)

ORIGINAL ARTICLE

Retrospective Cohort Study

Budd-Chiari syndrome in China: A 30-year retrospective study on survival from a single center

Wei Zhang, Qiao-Zheng Wang, Xiao-Wei Chen, Hong-Shan Zhong, Xi-Tong Zhang, Xu-Dong Chen, Ke Xu

Wei Zhang, Xu-Dong Chen, Department of Interventional Radiology, Shenzhen People's Hospital, the Second Affiliated Hospital of Jinan University, Shenzhen 518020, Guangdong Province, China

Wei Zhang, Qiao-Zheng Wang, Xiao-Wei Chen, Hong-Shan Zhong, Xi-Tong Zhang, Ke Xu, Department of Radiology, The First Affiliated Hospital of China Medical University, Shenyang 110001, Liaoning Province, China

Wei Zhang, Xiao-Wei Chen, Hong-Shan Zhong, Ke Xu, Key Laboratory of Diagnostic Imaging and Interventional Radiology of Liaoning Province, The First Affiliated Hospital of China Medical University, Shenyang 110001, Liaoning Province, China

ORCID number: Wei Zhang (0000-0003-2179-6821); Qiao-Zheng Wang (0000-0003-3512-3118); Xiao-Wei Chen (0000-0002-7839-7584); Hong-Shan Zhong (0000-0002-6150-6115); Xi-Tong Zhang (0000-0003-2519-9047); Xu-Dong Chen (0000-0002-3789-0495); Ke Xu (0000-0001-7587-822X).

Author contributions: Zhang W, Xu K and Chen XD designed the research; Xu K, Zhang XD and Zhong HS performed the research; Zhang W, Wang QZ and Chen XW analyzed the data; Zhang W wrote the paper; Wang QZ, Chen XW, Zhong HS, Zhang XT, Chen XD and Xu K critically revised the manuscript for important intellectual content.

Institutional review board statement: This study was reviewed and approved by the Research Ethics Committee of Faculty of Medicine, The First Affiliated Hospital of China Medical University Institutional Review Board.

Informed consent statement: All study participants provided written informed consent for personal and medical data collection prior to study enrollment and each patient agreed to management *via* written consent.

Conflict-of-interest statement: The authors declare that there are no conflicts of interest regarding the publication of this paper.

Data sharing statement: The technical appendix, statistical code, and dataset are available from the corresponding author at kexu@vip.sina.com. The participants gave informed consent for the data sharing.

STROBE statement: The authors have read the STROBE Statement-checklist of items, and the manuscript was prepared and revised according to the STROBE Statement-checklist of items.

Manuscript source: Unsolicited manuscript

Correspondence to: Ke Xu, MD, PhD, Professor, Department of Radiology and Key Laboratory of Diagnostic Imaging and Interventional Radiology of Liaoning Province, the First Affiliated Hospital of China Medical University, 155 Nanjing Bei Street, Shenyang 110001, Liaoning Province, China. kexu@vip.sina.com
Telephone: +86-24-83282730
Fax: +86-24-83282629

Received: December 8, 2017
Peer-review started: December 8, 2017
First decision: December 20, 2017
Revised: January 2, 2018
Accepted: January 24, 2018
Article in press: January 24, 2018
Published online: March 14, 2018

Abstract

AIM

To investigate 30-year treatment outcomes associated with Budd-Chiari syndrome (BCS) at a tertiary hospital in China.

METHODS
A total of 256 patients diagnosed with primary BCS at our tertiary hospital between November 1983 and September 2013 were followed and retrospectively studied. Cumulative survival rates and cumulative mortality rates of major causes were calculated by Kaplan-Meier analysis, and the independent predictors of survival were identified using a Cox regression model.

RESULTS
Thirty-four patients were untreated; however, 222 patients were treated by medicine, surgery, or interventional radiology. Forty-four patients were lost to follow-up; however, 212 patients were followed, 67 of whom died. The symptom remission rates of treated and untreated patients were 81.1% (107/132) and 46.2% (6/13), respectively (P = 0.009). The cumulative 1-, 5-, 10-, 20-, and 30-year survival rates of the treated patients were 93.5%, 81.6%, 75.2%, 64.7%, and 58.2%, respectively; however, the 1-, 5-, 10-, 20-, and 30-year survival rates of the untreated patients were 70.8%, 70.8%, 53.1%, 0%, and unavailable, respectively (P = 0.007). Independent predictors of survival for treated patients were gastroesophageal variceal bleeding (HR = 3.043, 95%CI: 1.363-6.791, P = 0.007) and restenosis (HR = 4.610, 95%CI: 1.916-11.091, P = 0.001). The cumulative 1-, 5-, 10-, 20-, and 30-year mortality rates for hepatocellular carcinoma were 0%, 2.6%, 3.5%, 8%, and 17.4%, respectively.

CONCLUSION
Long-term survival is satisfactory for treated Chinese patients with BCS. Hepatocellular carcinoma is a chronic complication and should be monitored with long-term follow-up.

Key words: Budd-Chiari syndrome; Chinese; Survival; Interventional radiology

Core tip: This is the first study to evaluate interventional treatment outcomes of Chinese Budd-Chiari syndrome (BCS) patients with more than 20-year follow-up, and the cumulative 20-year survival rate was 69.5% for patients treated by interventional radiological procedures. The cumulative 1-, 5-, 10-, and 20-year survival rates for untreated BCS patients were 70.8%, 70.8%, 53.1%, and 0%, respectively. Restenosis and gastroesophageal variceal bleeding were critical factors for predicting long-term survival. Long-term follow-up to monitor the chronic complications of BCS should not be less than 10 years, and deaths greatly increase after 10-year follow-up, especially those of patients who died from hepatocellular carcinoma.

Zhang W, Wang QZ, Chen XW, Zhong HS, Zhang XT, Chen XD, Xu K. Budd-Chiari syndrome in China: A 30-year retrospective study on survival from a single center. *World J Gastroenterol* 2018; 24(10): 1134-1143 Available from: URL: http://www.wjgnet.com/1007-9327/full/v24/i10/1134.htm DOI: http://dx.doi.org/10.3748/wjg.v24.i10.1134

INTRODUCTION

Budd-Chiari syndrome (BCS) is a rare disease defined as hepatic venous outflow tract obstruction at any level from small hepatic veins (HVs) to the junction of the inferior vena cava (IVC) and right atrium in the absence of right heart failure or constrictive pericarditis[1]. An obstruction that originates from endoluminal lesions (*i.e.*, thrombosis, webs, and endophlebitis) is considered primary BCS[2]. Western and Asian patients exhibit different characteristics regarding the nature and level of obstructive lesions; therefore, clinical presentations and treatment strategies are also different in these groups[3]. In Western countries, where hepatic thrombosis is the major obstructive lesion of BCS, a step-wise therapeutic strategy aimed at minimizing invasiveness has been advocated and proven to be effective[4,5]. The most widely used treatment modalities are anticoagulation and trans-jugular intra-hepatic porto-systemic shunt (TIPS)[5,6]. However, for Asian patients, especially Chinese patients, the predominant obstructive lesions are membranous and segmental obstructions of the supra-hepatic or retro-hepatic portion of the IVC, and the most used treatment modalities are interventional re-canalization and surgery[7-11].

Till the year 2014, more than 20000 cases of BCS have been published in China[12], since the first Chinese case was reported in 1957[13]. According to a recent literature survey study, interventional radiological procedures (mainly percutaneous re-canalization) have become the most common treatment option[14], and their outcomes are good or excellent[10,15,16]. However, outcomes from more than 10-year follow-up are scarcely reported[10,15-20]. Ten years may not be long enough for long-term outcome observations in Chinese patients with BCS characterized by insidious onset and chronic development[21,22]. The aim of this study was to retrospectively analyze the 30-year follow-up outcomes of BCS patients at our center and to evaluate their long-term survival and its related predictors.

MATERIALS AND METHODS

Study design and case selection

This retrospective case series study was approved by the ethics committee of our hospital. All patients were informed about the benefits and related risks before treatment, and they provided written informed consent. Medical records of 410 patients treated between November 1983 and September 2013 with an admission diagnosis of BCS were identified in

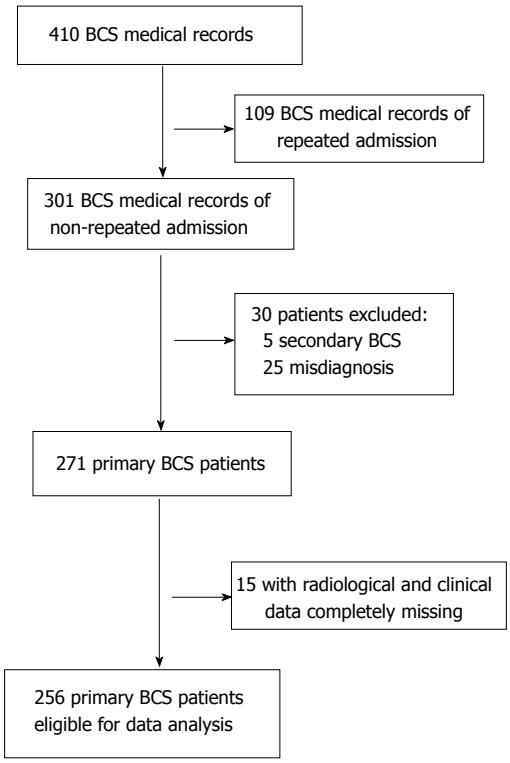

Figure 1 Flow chart of case selection. BCS: Budd-Chiari syndrome.

our hospitalization register system. There were 172 records from 63 patients that represented repeated hospitalizations; only the primary hospitalization medical records were enrolled. Thirty records were excluded, including 5 for secondary BCS and 25 for misdiagnoses of BCS. For the remaining 271 primary BCS records, 15 were not qualified for statistical analysis due to missing laboratory and imaging investigation data. Finally, 256 patients were eligible for our study. A flow chart of case selection is shown in Figure 1.

Diagnosis and classification

BCS was diagnosed by color Doppler ultrasonography, computed tomography, magnetic resonance imaging, and/or venography of HVs and the IVC. BCS patients were classified into three groups according to the obstruction site of the hepatic venous outflow tract: (1) IVC type, manifesting as obstruction of the IVC with at least one patent HV; (2) HV type, manifesting as obstruction of the three main HVs; and (3) combined type, manifesting as obstruction of both the IVC and three main HVs[10]. Patients were considered symptomatic when they had any one of the following manifestations: abdominal pain, abdominal distention, ascites, esophageal and gastric varicose bleeding, encephalopathy, or lower-extremity edema.

Treatment

In this case series, 34 patients were untreated (did not receive any regular treatments) due to technical contraindications (n = 9), poverty (n = 10), or relatively mild symptoms (n = 15), and 222 patients received treatment. Treatment modalities used for BCS patients included medical treatments, surgical operations, and interventional radiological procedures. Medical treatments included anticoagulation, diuretics, paracentesis and reinfusion of ascites, and albumin infusion. Surgical operations included cavoatrial shunting, radical resection, meso-cavo-atrial shunting, splenopneumopexy, and splenocaval shunting and were performed as described in a previous study[23]. Interventional radiological procedures included percutaneous intravascular catheter-directed thrombolysis, percutaneous transluminal angioplasty (PTA) with or without stent implantation, and TIPS, and the techniques were described in our previous studies[10,24]. Technical success of the interventional radiological procedures (mostly percutaneous recanalization) was defined as the recanalization of hepatic venous outflow tract obstruction as demonstrated by venography[10].

Data collection and follow-up

Baseline data were extracted from the medical records before treatment, including demographic data, clinical presentations, laboratory test results, and imaging data. Patients were followed until death, the end of this study (December 31, 2014), or the last outpatient visit date if the patient was lost to follow-up. Symptom remission was defined as complete remission or substantial partial remission of the main symptoms that the patients complained about most urgently. Patients were examined by color Doppler ultrasonography, computed tomography, or magnetic resonance imaging at their local hospitals for restenosis evaluation, and the results were confirmed by venography at our hospital. Follow-up data were obtained from medical records or by telephone interview of the patients themselves or their family members.

Statistical analysis

Categorical variables are expressed as absolute numbers (or frequencies, if indicated) and were compared using the chi-square or Fisher's exact test. Continuous variables are summarized as medians and ranges and were compared by using the independent sample t-test or one-way analysis of variance. Cumulative survival rates and cumulative mortalities associated with major causes were analyzed using Kaplan-Meier curves and compared by the log-rank test. The Cox regression model was employed for the analysis of factors related to survival. Variables reaching statistical significance ($P < 0.05$) in the univariate analysis were incorporated into a multivariate analysis as covariates. Two-tailed P-values less than 0.05 were considered statistically significant. All statistical calculations were performed using SPSS 21.0 package (SPSS Inc, Chicago, IL, United States).

RESULTS

Characteristics of patients

Two hundred and fifty-six patients with confirmed diagnoses of primary BCS were analyzed, including 153 males and 103 females with a median age of 41 (range,

Table 1 Baseline characteristics of the 256 patients

	Medicine	Surgery	Intervention	Untreated
Total number	30	14	178	34
Demographic data				
Sex				
Male	16	4	109	24
Female	14	10	69	10
Age (yr)[1]	36 (7-74)	35 (24-47)	41 (14-80)	44.5 (14-66)
Duration of symptoms				
≤ 1 mo	5	0	28	7
1-6 mo	7	2	35	12
≥ 6 mo	18	12	115	15
Clinical manifestations				
Abdominal distention	24	12	82	15
Abdominal wall varicosis	12	13	105	16
Lower-extremity edema	17	13	104	17
Gastroesophageal variceal bleeding	8	3	26	4
Hepatic encephalopathy	0	0	0	2
Laboratory tests[1,2]				
Hemoglobin level (g/L)	133 (64-172)	149 (101-176)	130.5 (30-180)	134 (80-180)
Platelet count (× 10^9/L)	130 (49-479)	92 (47-160)	108.5 (33-603)	139.5 (50-341)
Alanine transaminase level (× ULN)	0.6 (0.2-7.6)	0.6 (0.3-1.6)	0.6 (0.2-28)	0.7 (0.3-3.6)
Albumin level (g/L)	34.5 (13.1-54)	36 (22-41)	37.4 (16.7-57.7)	35 (16-58)
Total bilirubin level (μmol/L)	26.2 (6-146.2)	28.6 (17.1-68.4)	26 (7-292)	24.9 (6.1-168)
International normalized ratio	1.4 (0.9-1.9)	1.3 (1.1-1.7)	1.3 (0.9-2.9)	1.3 (0.9-1.8)
Creatinine level (μmol/L)	106.3 (85-341)	74 (71-77)	74.1 (30-254)	75 (29.6-146)
Blood urea nitrogen level (mmol/L)	5.3 (1.8-26.6)	5.1 (2.5-18.6)	5.3 (2.5-39.1)	5.6 (3.6-11.8)
Imaging features				
Type of obstruction				
HV	9	0	25	10
IVC	3	2	41	9
Com	18	12	112	15
Pattern of IVC obstruction				
No obstruction	7	0	25	10
Membranous	14	8	108	15
Segmental	8	4	36	4
Long segmental	1	2	9	5
Ascites	17	9	85	14
AHV compensation	1	3	34	4
IVC thrombosis	11	5	57	14
Portal vein thrombosis	1	0	3	3
Prognostic index				
Child-Pugh score[1,2]	7 (5-9)	6 (5-7)	7 (5-12)	6 (5-11)
Child-Pugh class[2]				
A	3	1	59	6
B	6	1	61	4
C	0	0	6	1

[1]Data are shown as median with range in parentheses; [2]Data are incomplete because some laboratory tests were not performed prior to the year 2000. Except where indicated, data are shown as number of patients. ULN: Upper limit of normal; HV: Hepatic vein; IVC: Inferior vena cava; Com: Combination; AHV: Accessory hepatic vein.

7-80) years. The baseline characteristics of the 256 patients are shown in Table 1 according to treatment modality. Furthermore, the patients were divided into two groups according to whether they received treatment or not, and their baseline characteristics were compared. The treated and untreated groups had statistically significant differences in the presentation of hepatic encephalopathy (P = 0.017), the pattern of IVC obstruction (P = 0.016), and portal vein thrombosis (P = 0.047).

Treatment

Except for 34 untreated patients, 222 patients received treatment, including 30 treated by medicine, 14 by surgery, and 178 by interventional radiology. Detailed information is presented in Table 2 for the 14 patients treated by surgical operations and the 178 patients treated by interventional procedures. For the patients treated by interventional radiology, the procedures were successful in 172 (96.6%) patients and failed in 6 patients due to diffuse HV obstruction (n = 4) and long segments (more than 5 cm) of IVC obstruction (n = 2). For the patients who experienced procedure-related complications, one died of disseminated intravascular coagulation 6 h after PTA, one died of severe hemoptysis of bronchiectasis 72 h after thrombolysis, one had stent fracture and was treated by implantation of an additional stent, and the other patients were

Table 2 Detailed information on surgical operations and interventional procedures

Department	Operations/procedures	No.	Complications
Surgery	Cavoatrial shunt	10	Hemorrhagic shock (n = 1)
	Radical resection	1	
	Meso-cavo-atrial shunt	1	Acute hepatic failure (n = 1)
	Splenopneumopexy	1	
	Splenocaval shunt	1	
Interventional radiology	Technic failure	6	
	PTA	96	Abdominal pain (n = 4), DIC (n = 1)
	PTA combined with stent	69	Abdominal pain (n = 2), Stent fracture (n = 1), Supraventricular tachycardia (n = 2)
	TIPS	7	
	Catheter directed thrombolysis	19[1]	Hematuria (n = 2), Hemoptysis (n = 1)

[1]The total number of patients treated by interventional procedures was 178, and the 19 patients treated by catheter directed thrombolysis were repeatedly counted among the patients treated by PTA (n = 5) and PTA combined with stent implantation (n = 14). PTA: Percutaneous transluminal angioplasty; TIPS: Transjugular intrahepatic portosystemic shunt; DIC: Disseminated intravascular coagulation.

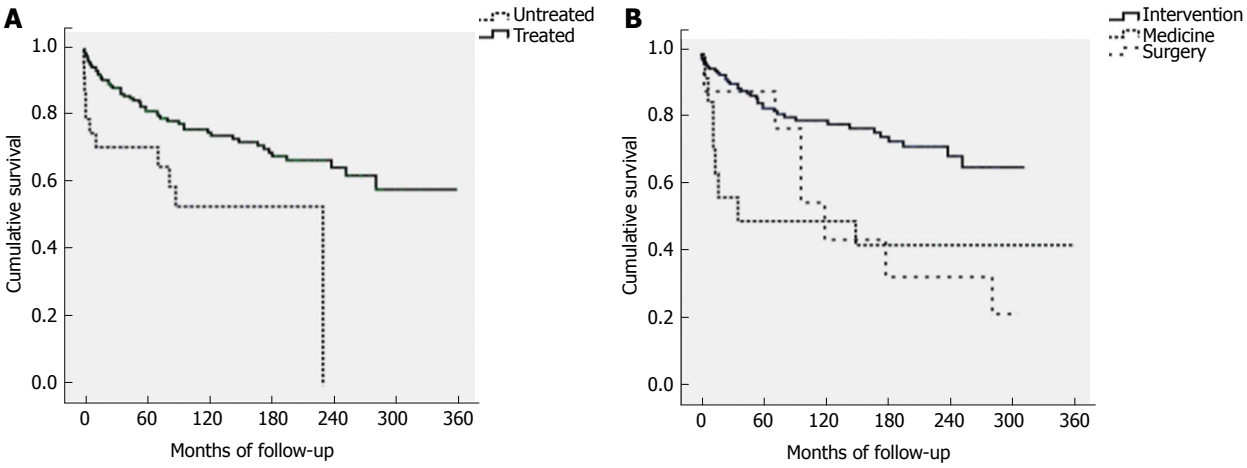

Figure 2 Survival rates of Budd-Chiari syndrome patients. A: Comparison of cumulative survival rates of Budd-Chiari syndrome (BCS) between the 188 treated patients and 24 untreated patients. Treated patients had significantly better long-term survival than untreated patients (P = 0.007); B: Comparison of cumulative survival rates of BCS among different treatment modalities. Patients treated by interventional radiology had significantly better long-term survival than patients treated by medicine or surgery (P = 0.002).

given symptomatic treatment.

Follow-up

Forty-four patients were lost to follow-up, and 212 patients were followed with a median period of 89 (0.2-360) mo; 67 of the followed patients died, with a median follow-up period of 28 (0.2-289) mo. The deaths of five patients who suffered from intracranial hemorrhage induced by hypertension (n = 1), cholangiocarcinoma (n = 1), disseminated intravascular coagulation (n = 1), accidental death (n = 1), and hemoptysis (n = 1) were not considered to be related to BCS. Detailed follow-up information is shown in Table 3. Regarding the remission of symptoms, symptoms were relieved in 107 out of 132 living patients in the treated group, and the overall remission rate was 81.1%; for the untreated group, 6 out of the 13 living patients were relieved of symptoms, and the remission rate was 46.2%. The difference between these two groups was statistically significant (P = 0.009). Furthermore, the comparison of loss rates between these two groups was not significantly different (P = 0.052). It was notable that the loss rate of the untreated group was 29.4% (10/34), which was higher than 20%.

Survival

The cumulative 1-, 5-, 10-, 20-, and 30-year survival rates of the 188 treated patients were 93.5%, 81.6%, 75.2%, 64.7%, and 58.2%, respectively; for the 24 untreated patients, the 1-, 5-, 10-, 20-, and 30-year survival rates were 70.8%, 70.8%, 53.1%, 0%, and unavailable, respectively. The difference in cumulative survival rates between these two groups was statistically significant (P = 0.007) (Figure 2A). Regarding the different treatment modalities, the cumulative 1-, 5-, 10-, 20-, and 30-year survival rates of patients treated by interventional radiology were 95.7%, 85.3%, 80.2%, 69.5%, and unavailable, respectively; the 1-, 5-, 10-, 20-, and 30-year rates of patients treated by medicine were 85.7%, 50%, 50%, 50%, and 50%, respectively; and the 1-, 5-, 10-, 20-, and 30-year rates of patients treated by surgery were 88.9%, 88.9%, 44.4%, 33.3%, and unavailable, respectively. The difference in cumulative survival rates among these three treatment

Table 3 Follow-up results of 256 Budd-Chiari syndrome patients

Treatment	Total	Lost	Death	Remission	Non-remission/progression
Medicine	30	16	Variceal bleeding (n = 4), liver or multiple organ failure (n = 3), and hepatocellular carcinoma (n = 1)	3	Abdominal distention (n = 3)
Surgery	14	5	Liver or multiple organ failure (n = 3), hepatocellular carcinoma (n = 1), variceal bleeding (n = 1), anastomotic infection (n = 1), and hepatic encephalopathy (n = 1)	1	Abdominal distention (n = 1)
Interventional radiology					
Technic failure	6	0	Liver or multiple organ failure (n = 3)	1	Abdominal distention (n = 1) and lower-extremity edema (n = 1)
PTA	96	6	Liver or multiple organ failure (n = 8), hepatocellular carcinoma (n = 5), variceal bleeding (n = 3), cholangiocarcinoma (n = 1), intracranial hemorrhage induced by hypertension (n = 1), DIC (n = 1), and accidental death (n = 1)	57	Abdominal distention (n = 7), lower-extremity edema (n = 4), and lower-extremity varix (n = 2)
PTA combined with stent placement	69	5	Liver or multiple organ failure (n = 7), hepatocellular carcinoma (n = 3), variceal bleeding (n = 2), hepatic encephalopathy (n = 2), and hemoptysis (n = 1)	44	Abdominal distention (n = 3), lower-extremity edema (n = 1), and muscle wasting (n = 1)
TIPS	7	2	Liver or multiple organ failure (n = 2), and variceal bleeding (n = 1)	1	Jaundice (n = 1)
Untreated	34	10	Liver or multiple organ failure (n = 7), variceal bleeding (n = 1), hepatocellular carcinoma (n = 1), hepatic encephalopathy (n = 1), and chronic leukemia (n = 1)	6	Abdominal distention (n = 4), muscle wasting (n = 2), and lower-extremity edema (n = 1)

PTA: Percutaneous transluminal angioplasty; TIPS: Transjugular intrahepatic portosystemic shunt; DIC: Disseminated intravascular coagulation.

modalities was statistically significant (P = 0.002) (Figure 2B). The factors related to survival, excluding the five deaths unrelated to BCS, were analyzed in the treated patients. In univariate analysis, the predictors of survival included gastroesophageal variceal bleeding, a high level of alanine transaminase, ascites, and restenosis. In multivariate analysis, the independent predictors of survival were gastroesophageal variceal bleeding (HR = 3.043, 95%CI: 1.363-6.791, P = 0.007) and restenosis (HR = 4.610, 95%CI: 1.916-11.091, P = 0.001) (Table 4).

Cumulative mortalities of major causes

For the treated patients, the major causes of death were liver or multiple organ failure (n = 26), gastroesophageal variceal bleeding (n = 11), and hepatocellular carcinoma (HCC) (n = 10), which accounted for more than 80% of the total deaths (83.9%). The median survival time was 37.5 (1-239) mo for patients who died of liver or multiple organ failure, 48 (4-150) mo for patients who died of gastroesophageal variceal bleeding, and 122.5 (14-282) mo for patients who died of HCC. The difference in survival times across these three groups was statistically significant (P = 0.016). The cumulative 1-, 5-, 10-, 20-, and 30-year mortality rates for liver or multiple organ failure were 4.4%, 10.1%, 14.5%, 20.5%, and 20.5%, respectively (Figure 3A); the 1-, 5-, 10-, 20-, and 30-year mortality rates for gastroesophageal variceal bleeding were 0.5%, 5.3%, 7.3%, 8.5%, and 8.5%, respectively (Figure 3B); and the 1-, 5-, 10-, 20-, and 30-year mortality rates for HCC were 0%, 2.6%, 3.5%, 8%, and 17.4%, respectively (Figure 3C).

DISCUSSION

To the best of our knowledge, the present study is the first large case series that evaluated interventional treatment outcomes of Chinese BCS patients with more than 20-year follow-up. We assume that most Chinese BCS patients are characterized by insidious onset and chronic development[22,25,26]; therefore, a relatively long time is needed to observe long-term outcomes. However, the follow-up time span that can be defined as "long-term follow-up" is still debatable. According to our study, we found that deaths greatly increased after 10-year follow-up, especially those of patients who died of HCC. Therefore, we suggest that the long-term follow-up span should not be less than 10 years for Chinese BCS patients.

In the present study, patients were retrospectively divided into a treated group and an untreated group according to whether the patients received treatment or not. Less than half of the patients who did not receive any regular treatments (medicine, surgery, or interventional radiology) had intermittent, spontaneous relief of clinical symptoms, and none survived for more than 20 years. These findings were very interesting because the follow-up results might reflect the natural outcomes of Chinese BCS patients. According to our

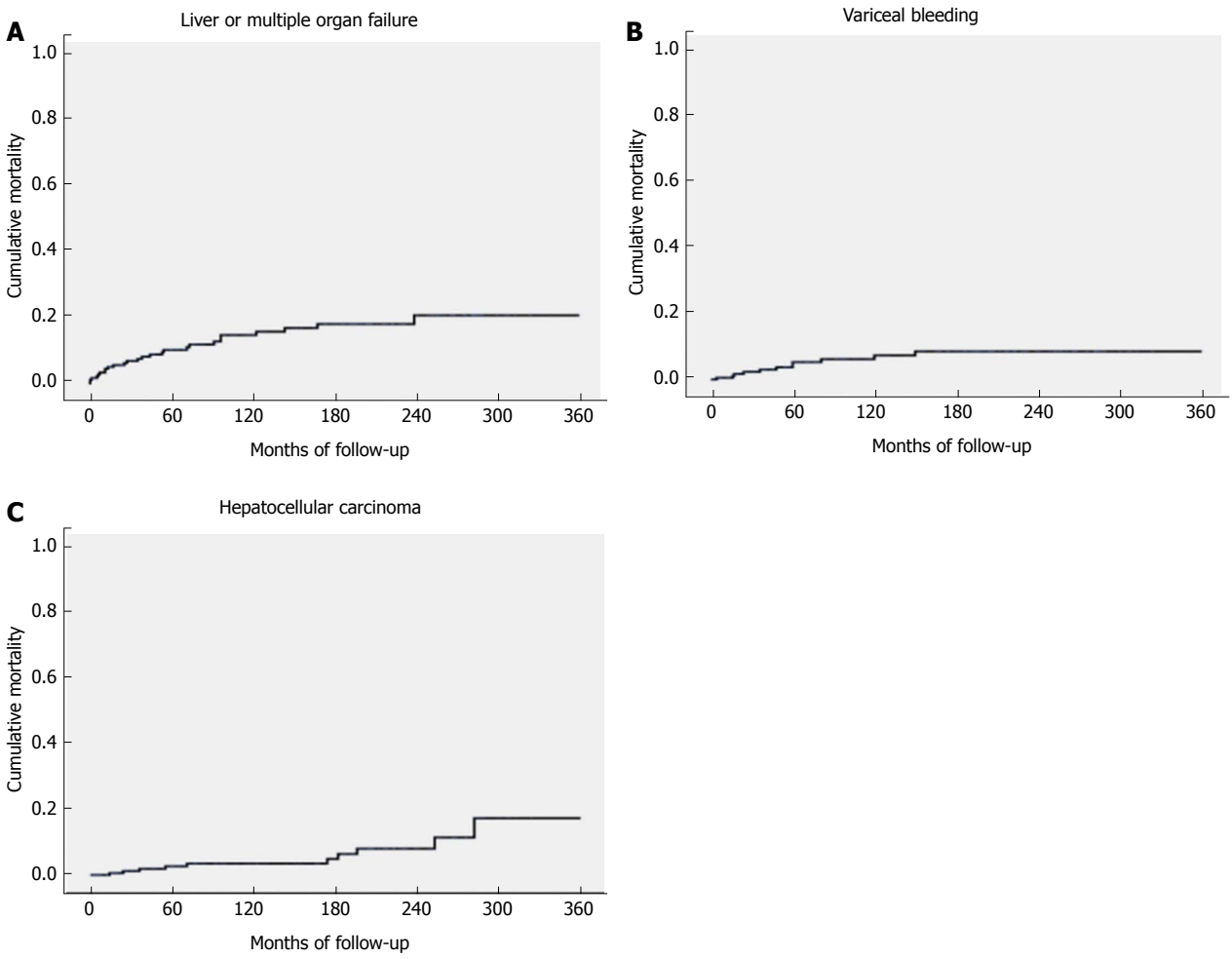

Figure 3 Cumulative mortality rates of Budd-Chiari syndrome. A: Cumulative mortality rates of Budd-Chiari syndrome (BCS) patients who died of liver or multiple organ failure; B: Cumulative mortality rates of BCS patients who died of gastroesophageal variceal bleeding; C: Cumulative mortality rates of BCS patients who died of hepatocellular carcinoma.

results, the natural survival of Chinese BCS patients seemed to be better than that of Western patients, for whom it was estimated that 90% of untreated patients would die within 3 years[2,27]. The follow-up results also suggested that timely intervention was crucial for the survival of BCS patients, even if their symptoms could be spontaneously intermittently relieved. It was noteworthy that the loss rate was higher than 20% for untreated patients; therefore, the findings that reflected the natural outcomes of Chinese BCS patients should be carefully interpreted.

The cumulative survival rates of the treated group were better than those of the untreated group. However, some baseline characteristics between these two groups were different (the presentation of hepatic encephalopathy and portal vein thrombosis was higher in the untreated group than in the treated group, indicating a more serious condition). For the patients treated by interventional radiology, the cumulative 1-, 5-, 10-, and 20-year survival rates were 95.7%, 85.3%, 80.2%, and 69.5%, respectively. The cumulative 1-, 5-, and 10-year survival rates were excellent and comparable to the results recently reported from a systematic review, which found that the median 1-, 5-, and 10-year survival rates were 93%, 83%, and 73% after interventional radiological treatments, respectively[28]. The cumulative 20-year survival rate of patients treated by intervention radiology was significantly better than that of patients treated by medicine or surgery (69.5% *vs* 50% or 33.3%, respectively), which supported wide future use of interventional radiological procedures as a treatment modality. Furthermore, the cumulative 20- and 30-year survival rates of the treated patients were 64.7% and 58.2%, which were satisfying for such a rare disease with chronic history. Of note, the actual survival rates of patients treated by medicine and surgery in our study were influenced by the high ratio of patients lost to follow-up (more than 50%) and should be cautiously interpreted.

According to previous studies, the causes of death of BCS patients mainly included liver failure, gastroesophageal bleeding, HCC, hepatic encephalopathy, and chronic leukemia[5,10,29]. The present study demonstrated that the major cause of death was liver or multiple organ failure, which accounted for 46% (26/56) of the total deaths of treated patients,

Table 4 Univariate and multivariate analyses of the predictors of survival for treated patients

Variable	Univariate analysis			Multivariate analysis		
	HR	95%CI	*P* value	HR	95%CI	*P* value
Sex (Male/Female)	0.558	0.297-1.050	0.071			
Age	0.992	0.968-1. 017	0.550			
History of BCS since first presentation	0.994	0.987-1.000	0.055			
Abdominal distention (Yes/No)	0.943	0.531-1.643	0.813			
Abdominal wall varicosis (Yes/No)	0.819	0.461-1.457	0.497			
Gastroesophageal variceal bleeding (Yes/No)	2.928	1.647-5.270	< 0.001	3.043	1.363-6.791	0.007
Lower-extremity edema (Yes/No)	1.318	0.757-2.294	0.330			
Hemoglobin level	0.994	0.983-1.005	0.311			
Platelet count	1.002	0.998-1.006	0.308			
Alanine transaminase level	1.003	1.001-1.005	0.005	1.002	0.999-1.005	0.274
Albumin level	0.975	0.928-1.024	0.307			
Total bilirubin level	1.007	0.997-1.017	0.183			
INR	1.280	0.367-4.468	0.699			
Creatinine level	1.005	0.991-1.019	0.489			
Blood urea nitrogen level	1.049	0.971-1.133	0.225			
Ascites (Yes/No)	2.108	1.205-3.686	0.009	1.849	0.812-4.213	0.143
Accessory hepatic vein (Yes/No)	2.126	0.842-5.366	0.110			
Associated IVC thrombosis (Yes/No)	1.000	0.553-1.809	0.999			
Restenosis (Yes/No)	5.309	2.378-11.852	< 0.001	4.610	1.916-11.091	0.001
Child-Pugh score	1.108	0.852-1.440	0.444			

HR: Hazard ratio; BCS: Budd-Chiari syndrome; INR: International normalized ratio; IVC: Inferior vena cava.

and this proportion was relatively high compared with results from previous studies[5,6,10]. We explored the possible reasons for this relatively higher occurrence of liver or multiple organ failure by further calculating its cumulative mortality and found that liver or multiple organ failure occurred more frequently within 5 years after primary treatments, which was longer than the 2-year time-frame reported in a previous study[5]. One possible explanation is that for Chinese BCS patients, the chronic development course may allow formation of HV collateral circulation or accessory HV compensation, which might slow down the occurrence of liver failure but simultaneously increases the number of patients who are prone to liver failure.

Another major cause of death that we focused on was HCC. It occurred in 10 of the 188 treated patients, and the median time of survival was 122.5 (14-282) mo, which indicated that it was a chronic complication of BCS. This result agreed with previous studies and demonstrated that HCC was a chronic complication of BCS and mostly occurred over a relatively long time[30-32]. A recent study demonstrated that the cumulative incidence of HCC was 3.5% at 10 years, and the risk factors related to HCC development were liver cirrhosis, combined IVC and HV block, and long-segment IVC block. The authors found that association of these three events with occurrence of HCC would indicate that degree and extent of outflow obstruction, and presence of advanced degree of fibrosis suggesting prolonged hepatic congestion with resultant parenchymal loss were associated with HCC development[33].

In our study, 10 patients experienced HCC and died during 30-year follow-up, and this incidence was higher than that in the above mentioned study (8 out of 413 patients during 20-year follow-up). In addition, we further calculated the cumulative mortality of HCC and found that the cumulative 1-, 5-, 10-, 20-, and 30-year mortality rates were 0%, 2.6%, 3.5%, 8%, and 17.4%, respectively. This result also demonstrated that the incidence and number of patients who died of HCC progressively increased over time, which is consistent with the results of the above mentioned study.

One major limitation of our study was its retrospective nature. Some of the earlier original data (especially before the year 2000) were not recorded or lost. In addition, although a regular follow-up schedule was established and we tried our best to stay in contact with all BCS patients, approximately 17% (44/256) of the total patients were lost to follow-up, and this proportion was even higher (more than 50%) in patients treated by medicine or surgery. One possible explanation is that most of the lost patients were admitted in a relatively early period (before 2002) when follow-up was very difficult, especially for patients in poverty or remote regions. Another limitation was that the baseline data of patients treated by different modalities were inhomogeneous; thus, subgroup analysis was inappropriate.

In conclusion, the long-term survival of Chinese BCS patients was satisfactory for treated patients, especially for patients treated by interventional procedures. Restenosis and gastroesophageal variceal bleeding were critical factors for predicting long-term survival. Long-term follow-up should not be less than 10 years to monitor the chronic complications of HCC.

ARTICLE HIGHLIGHTS

Research background

Budd-Chiari syndrome (BCS) is a rare disease. For Asian patients, especially Chinese patients, the predominant obstructive lesions are membranous and

segmental obstructions of the supra-hepatic or retro-hepatic portion of the inferior vena cava. Till the year 2014, more than 20000 cases of BCS have been published in China, and interventional radiological procedures (mainly percutaneous re-canalization) have become the most common treatment option. However, outcomes from more than 10-year follow-up are scarcely reported for Chinese BCS patients.

Research motivation

As Chinese BCS patients are characterized by insidious onset and chronic development, ten years may not be long enough for long-term outcome observations. We want to find the 20-year and 30-year survival rates at our single center, which may represent the Chinese BCS population to a certain extent. Furthermore, for the chronic complications, such as hepatocellular carcinoma, the incidence and mortality of Chinese BCS patients are still unknown, and we are very interested in these issues.

Research objectives

The objectives were to analyze a 30-year follow-up outcome Chinese BCS patients in a single Chinese center, specifically, to find the 20-year and 30-year cumulative survival rates for the different treatment modalities applied in our center; to find the factors related to long-term survival; and to calculate the cumulative mortalities of major causes.

Research methods

We retrospectively analyzed a 30-year follow-up outcome of BCS patients at our center. Medical records of 410 patients treated between November 1983 and September 2013 with an admission diagnosis of BCS were identified in our hospitalization register system. Only the primary hospitalization medical records were enrolled. Finally, 256 patients were eligible for our study. In this case series, 34 patients were untreated (did not receive any regular treatments) and 222 patients received treatment, including 30 treated by medicine, 14 by surgery, and 178 by interventional radiology. Patients were followed until the end of this study (December 31, 2014). Symptom remission was defined as complete remission or substantial partial remission of the main symptoms that the patients complained about most urgently. Patients were examined by color Doppler ultrasonography, computed tomography, or magnetic resonance imaging for restenosis evaluation, and the results were confirmed by venography at our hospital. Cumulative survival rates and cumulative mortalities associated with major causes were analyzed. The Cox regression model was employed for the analysis of factors related to survival. Variables reaching statistical significance in the univariate analysis were incorporated into a multivariate analysis as covariates. $P < 0.05$ was considered statistically significant.

Research results

About 212 patients (44 were lost to follow-up) were followed with a median time of 89 (0.2-360) mo; 67 of the followed patients died, with a median follow-up period of 28 (0.2-289) mo. A statistically significant difference was found in cumulative survival rates between these two groups. A statistically significant difference was also found in cumulative survival rates among these three treatment modalities. The independent predictors of survival were gastroesophageal variceal bleeding and restenosis. For the treated patients, the major causes of death were liver or multiple organ failure, gastroesophageal variceal bleeding, and hepatocellular carcinoma (HCC), which accounted for more than 80% of the total deaths.

Research conclusions

The present study is the first large case series that evaluated interventional treatment outcomes of Chinese BCS patients with more than 20-year follow-up, to the best of our knowledge. We suggest that the long-term follow-up span should not be less than 10 years for Chinese BCS patients. Less than half of the patients had intermittent, spontaneous relief of clinical symptoms, and none survived for more than 20 years. Restenosis and gastroesophageal variceal bleeding were critical factors for predicting the long-term survival. To monitor the chronic complications of BCS such as HCC, long-term follow-up should not be less than 10 years.

Research perspectives

In future studies, prospective and multi-center research should be encouraged to overcome the high rate of loss and to do the subgroup analysis.

REFERENCES

1 **European Association for the Study of the Liver**. EASL Clinical Practice Guidelines: Vascular diseases of the liver. *J Hepatol* 2016; **64**: 179-202 [PMID: 26516032 DOI: 10.1016/j.jhep.2015.07.040]

2 **Valla DC**. Primary Budd-Chiari syndrome. *J Hepatol* 2009; **50**: 195-203 [PMID: 19012988 DOI: 10.1016/j.jhep.2008.10.007]

3 **Valla DC**. Hepatic venous outflow tract obstruction etiopathogenesis: Asia versus the West. *J Gastroenterol Hepatol* 2004; **19**: S204-S211 [DOI: 10.1111/j.1440-1746.2004.03642.x]

4 **Plessier A**, Sibert A, Consigny Y, Hakime A, Zappa M, Denninger MH, Condat B, Farges O, Chagneau C, de Ledinghen V, Francoz C, Sauvanet A, Vilgrain V, Belghiti J, Durand F, Valla D. Aiming at minimal invasiveness as a therapeutic strategy for Budd-Chiari syndrome. *Hepatology* 2006; **44**: 1308-1316 [PMID: 17058215 DOI: 10.1002/hep.21354]

5 **Seijo S**, Plessier A, Hoekstra J, Dell'era A, Mandair D, Rifai K, Trebicka J, Morard I, Lasser L, Abraldes JG, Darwish Murad S, Heller J, Hadengue A, Primignani M, Elias E, Janssen HL, Valla DC, Garcia-Pagan JC; European Network for Vascular Disorders of the Liver. Good long-term outcome of Budd-Chiari syndrome with a step-wise management. *Hepatology* 2013; **57**:1962-1968 [PMID: 23389867 DOI: 10.1002/hep.26306]

6 **Darwish Murad S**, Plessier A, Hernandez-Guerra M, Fabris F, Eapen CE, Bahr MJ, Trebicka J, Morard I, Lasser L, Heller J, Hadengue A, Langlet P, Miranda H, Primignani M, Elias E, Leebeek FW, Rosendaal FR, Garcia-Pagan JC, Valla DC, Janssen HL; EN-Vie (European Network for Vascular Disorders of the Liver). Etiology, management, and outcome of the Budd-Chiari syndrome. *Ann Intern Med* 2009; **151**: 167-175 [PMID: 19652186 DOI: 10.7326/0003-4819-151-3-200908040-00004]

7 **Okuda K**, Kage M, Shrestha SM. Proposal of a new nomenclature for Budd-Chiari syndrome: hepatic vein thrombosis versus thrombosis of the inferior vena cava at its hepatic portion. *Hepatology* 1998; **28**: 1191-1198 [PMID: 9794901 DOI: 10.1002/hep.510280505]

8 **Wang ZG**, Zhang FJ, Yi MQ, Qiang LX. Evolution of management for Budd-Chiari syndrome: a team's view from 2564 patients. *ANZ J Surg* 2005; **75**: 55-63 [PMID: 15740519 DOI: 10.1111/j.1445-2197.2005.03135.x]

9 **Dilawari JB**, Bambery P, Chawla Y, Kaur U, Bhusnurmath SR, Malhotra HS, Sood GK, Mitra SK, Khanna SK, Walia BS. Hepatic outflow obstruction (Budd-Chiari syndrome). Experience with 177 patients and a review of the literature. *Medicine* (Baltimore) 1994; **73**: 21-36 [PMID: 8309360]

10 **Han G**, Qi X, Zhang W, He C, Yin Z, Wang J, Xia J, Xu K, Guo W, Niu J, Wu K, Fan D. Percutaneous recanalization for Budd-Chiari syndrome: an 11-year retrospective study on patency and survival in 177 Chinese patients from a single center. *Radiology* 2013; **266**: 657-667 [PMID: 23143028 DOI: 10.1148/radiol.12120856]

11 **Rathod K**, Deshmukh H, Shukla A, Popat B, Pandey A, Gupte A, Gupta DK, Bhatia SJ. Endovascular treatment of Budd-Chiari syndrome: Single center experience. *J Gastroenterol Hepatol* 2017; **32**: 237-243 [PMID: 27218672 DOI: 10.1111/jgh.13456]

12 **Zhang W**, Qi X, Zhang X, Su H, Zhong H, Shi J, Xu K. Budd-Chiari Syndrome in China: A Systematic Analysis of Epidemiological Features Based on the Chinese Literature Survey. *Gastroenterol Res Pract* 2015; **2015**: 738548 [PMID: 26504461 DOI: 10.1155/2015/738548]

13 **Shenyang Branch of Internal Medicine Institute of Chinese Medical Association and Department of Pathology of Shenyang Medical College**. Discussion of clinical pathology: case No. 32. *Zhonghua Nei Ke Za Zhi* 1957; **5**: 166-169

14 **Qi XS**, Ren WR, Fan DM, Han GH. Selection of treatment modalities for Budd-Chiari Syndrome in China: a preliminary

survey of published literature. *World J Gastroenterol* 2014; **20**: 10628-10636 [PMID: 25132785 DOI: 10.3748/wjg.v20.i30.10628]
15 **Tripathi D**, Sunderraj L, Vemala V, Mehrzad H, Zia Z, Mangat K, West R, Chen F, Elias E, Olliff SP. Long-term outcomes following percutaneous hepatic vein recanalization for Budd-Chiari syndrome. *Liver Int* 2017; **37**: 111-120 [PMID: 27254473 DOI: 10.1111/liv.13180]
16 **Zhang QQ**, Xu H, Zu MH, Gu YM, Shen B, Wei N, Xu W, Liu HT, Wang WL, Gao ZK. Strategy and long-term outcomes of endovascular treatment for Budd-Chiari syndrome complicated by inferior vena caval thrombosis. *Eur J Vasc Endovasc Surg* 2014; **47**: 550-557 [PMID: 24560649 DOI: 10.1016/j.ejvs.2014.01.014]
17 **Zhang CQ**, Fu LN, Xu L, Zhang GQ, Jia T, Liu JY, Qin CY, Zhu JR. Long-term effect of stent placement in 115 patients with Budd-Chiari syndrome. *World J Gastroenterol* 2003; **9**: 2587-2591 [PMID: 14606103 DOI: 10.3748/wjg.v9.i11.2587]
18 **Qiao T**, Liu CJ, Liu C, Chen K, Zhang XB, Zu MH. Interventional endovascular treatment for Budd-Chiari syndrome with long-term follow-up. *Swiss Med Wkly* 2005; **135**: 318-326 [PMID: 16034686 DOI: 2005/21/smw-10947]
19 **Meng X**, Lv Y, Zhang B, He C, Guo W, Luo B, Yin Z, Fan D, Han G. Endovascular Management of Budd-Chiari Syndrome with Inferior Vena Cava Thrombosis: A 14-Year Single-Center Retrospective Report of 55 Patients. *J Vasc Interv Radiol* 2016; **27**: 1592-1603 [PMID: 27397618 DOI: 10.1016/j.jvir.2016.04.019]
20 **Ding PX,** Li Z, Zhang SJ, Han XW, Wu Y, Wang ZG, Fu MT. Outcome of the Z-expandable metallic stent for Budd-Chiari syndrome and segmental obstruction of the inferior vena cava. *Eur J Gastroenterol Hepatol* 2016; **28**: 972-979 [PMID: 27172449 DOI: 10.1097/MEG.0000000000000640]
21 **Zhang XM**, Li QL. Etiology, treatment, and classification of Budd-Chiari syndrome. *Chin Med J* (Engl) 2007; **120**: 159-161[PMID: 17335663]
22 **Cheng D**, Xu H, Lu ZJ, Hua R, Qiu H, Du H, Xu X, Zhang J. Clinical features and etiology of Budd-Chiari syndrome in Chinese patients: a single-center study. *J Gastroenterol Hepatol* 2013; **28**: 1061-1067 [PMID: 23425079 DOI: 10.1111/jgh.12140]
23 **Wang ZG**, Jones RS. Budd-Chiari syndrome. *Curr Probl Surg* 1996; **33**: 83-211 [PMID: 8595784 DOI: 10.1016/S0011-3840(96)80001-3]
24 **Xu K**, Feng B, Zhong H, Zhang X, Su H, Li H, Zhao Z, Zhang H. Clinical application of interventional techniques in the treatment of Budd-Chiari syndrome. *Chin Med J* (Engl) 2003; **116**: 609-615 [PMID: 12875733]
25 **Dang X**, Li L, Xu P. Research status of Budd-Chiari syndrome in China. *Int J Clin Exp Med* 2014; **7**: 4646-4652 [PMID: 25663961]
26 **Fan JG**, Wang FS. Difference of Budd-Chiari syndrome between West and China. *Hepatology* 2014; **62**: 657 [PMID: 25476406 DOI: 10.1002/hep.27627]
27 **Tavill AS**, Wood EJ, Kreel L, Jones EA, Gregory M, Sherlock S. The Budd-Chiari syndrome: correlation between hepatic scintigraphy and the clinical, radiological, and pathological findings in nineteen cases of hepatic venous outflow obstruction. *Gastroenterology* 1975; **68**: 509-518 [PMID: 1112452]
28 **Qi X**, Ren W, Wang Y, Guo X, Fan D. Survival and prognostic indicators of Budd-Chiari syndrome: a systematic review of 79 studies. *Expert Rev Gastroenterol Hepatol* 2015; **9**: 865-875 [PMID: 25754880 DOI: 10.1586/17474124.2015.1024224]
29 **Eapen CE**, Velissaris D, Heydtmann M, Gunson B, Olliff S, Elias E. Favourable medium term outcome following hepatic vein recanalisation and/or transjugular intrahepatic portosystemic shunt for Budd Chiari syndrome. *Gut* 2006; **55**: 878-884 [PMID: 16174658 DOI: 10.1136/gut.2005.071423]
30 **Moucari R**, Rautou PE, Cazals-Hatem D, Geara A, Bureau C, Consigny Y, Francoz C, Denninger MH, Vilgrain V, Belghiti J, Durand F, Valla D, Plessier A. Hepatocellular carcinoma in Budd-Chiari syndrome: characteristics and risk factors. *Gut* 2008; **57**: 828-835 [PMID: 18218675 DOI: 10.1136/gut.2007.139477]
31 **Ren W**, Qi X, Yang Z, Han G, Fan D. Prevalence and risk factors of hepatocellular carcinoma in Budd-Chiari syndrome: a systematic review. *Eur J Gastroenterol Hepatol* 2013; **25**: 830-841 [PMID: 23411869 DOI: 10.1097/MEG.0b013e32835eb8d4]
32 **Sakr M**, Abdelhakam SM, Dabbous H, Hamed A, Hefny Z, Abdelmoaty W, Shaker M, El-Gharib M, Eldorry A. Characteristics of hepatocellular carcinoma in Egyptian patients with primary Budd-Chiari syndrome. *Liver Int* 2017; **37**: 415-422 [PMID: 27507647 DOI: 10.1111/liv.13219]
33 **Paul SB**, Shalimar, Sreenivas V, Gamanagatti SR, Sharma H, Dhamija E, Acharya SK. Incidence and risk factors of hepatocellular carcinoma in patients with hepatic venous outflow tract obstruction. *Aliment Pharmacol Ther* 2015; **41**: 961-971 [PMID: 25809735 DOI: 10.1111/apt.13173]

P- Reviewer: Elsiesy H, Gad EH, Garbuzenko DV, Tahiri MJT
S- Editor: Wang JL **L- Editor**: Wang TQ **E- Editor**: Ma YJ

World Journal of Gastroenterology

Submit a Manuscript: http://www.f6publishing.com

World J Gastroenterol 2018 March 14; 24(10): 1144-1151

DOI: 10.3748/wjg.v24.i10.1144

ISSN 1007-9327 (print) ISSN 2219-2840 (online)

ORIGINAL ARTICLE

Retrospective Study

Risk factors of electrocoagulation syndrome after esophageal endoscopic submucosal dissection

Dae Won Ma, Young Hoon Youn, Da Hyun Jung, Jae Jun Park, Jie-Hyun Kim, Hyojin Park

Dae Won Ma, Young Hoon Youn, Da Hyun Jung, Jae Jun Park, Jie-Hyun Kim, Hyojin Park, Department of Internal Medicine, Gangnam Severance Hospital, Yonsei University College of Medicine, Seoul 06273, South Korea

ORCID number: Dae Won Ma (0000-0002-0321-1140); Young Hoon Youn (0000-0002-0071-229X); Da Hyun Jung (0000-0001-6668-3113); Jae Jun Park (0000-0001-5297-5414); Jie-Hyun Kim (0000-0002-9198-3326); Hyojin Park (0000-0002-5759-5135).

Author contributions: All authors helped to perform their research; Ma DW substantial contributions to conception and design, or analysis and interpretation of data and drafting the article or revising it critically for important intellectual content; Youn YH substantial contributions to conception and design, final approval of the version to be published and agreement to be accountable for all aspects of the work; Jung DH, Park JJ, Kim JH and Park H revising the article critically for important intellectual content.

Supported by Basic Science Research Program through the National Research Foundation of Korea (NRF) funded by the Ministry of Science and ICT, No. NRF-2015R1C1A1A01054352.

Institutional review board statement: The Institutional Review Board of Gangnam Severance Hospital approved this study (3-2017-0163).

Informed consent statement: Patients were not required to give informed consent the study because the analysis used anonymous clinical data that were obtained after each patient agreed to treatment by written consent.

Conflict-of-interest statement: All authors declare no conflicts-of-interest related to this article.

Manuscript source: Unsolicited manuscript

Correspondence to: Young Hoon Youn, MD, PhD, Professor, Department of Internal Medicine, Gangnam Severance Hospital, Yonsei University College of Medicine, 211 Eonjuro, Gangnam-gu, Seoul 06273, South Korea. dryoun@yuhs.ac
Telephone: +82-2-20193453
Fax: +82-2-34633882

Received: January 15, 2018
Peer-review started: January 15, 2018
First decision: January 16, 2018
Revised: January 22, 2018
Accepted: January 29, 2018
Article in press: January 29, 2018
Published online: March 14, 2018

Abstract

AIM

To investigate post endoscopic submucosal dissection electrocoagulation syndrome (PEECS) of the esophagus.

METHODS

We analyzed 55 consecutive cases with esophageal endoscopic submucosal dissection for superficial esophageal squamous neoplasms at a tertiary referral hospital in South Korea. Esophageal PEECS was defined as "mild" meeting one of the following criteria without any obvious perforation: fever (≥ 37.8 ℃), leukocytosis (> 10800 cells/μL), or regional chest pain more than 5/10 points as rated on a numeric pain intensity scale. The grade of PEECS was determined as "severe" when meet two or more of above criteria.

RESULTS

We included 51 cases without obvious complications

in the analysis. The incidence of mild and severe esophageal PEECS was 47.1% and 17.6%, respectively. Risk factor analysis revealed that resected area, procedure time, and muscle layer exposure were significantly associated with PEECS. In multivariate analysis, a resected area larger than 6.0 cm^2 (OR = 4.995, 95%CI: 1.110-22.489, P = 0.036) and muscle layer exposure (OR = 5.661, 95%CI: 1.422-22.534, P = 0.014) were independent predictors of esophageal PEECS. All patients with PEECS had favorable outcomes with conservative management approaches, such as intravenous hydration or antibiotics.

CONCLUSION

Clinicians should consider the possibility of esophageal PEECS when the resected area exceeds 6.0 cm^2 or when the muscle layer exposure is noted.

Key words: Electrocoagulation; Endoscopic submucosal dissection; Esophageal neoplasm; Syndrome

Core tip: A number of patients experience fever, chest pain, and/or a systemic inflammatory response after esophageal endoscopic submucosal dissection, even in the absence of obvious perforation. Post endoscopic submucosal dissection electrocoagulation syndrome which is characterized by fever, leukocytosis, and chest pain has been found to be a relatively common condition after esophageal endoscopic submucosal dissection. It more frequently occurs when the resection area is wide (OR = 4.995) or when there is muscle layer damage (OR = 5.661), but it is restored without significant sequelae by conservative treatment.

Ma DW, Youn YH, Jung DH, Park JJ, Kim JH, Park H. Risk factors of electrocoagulation syndrome after esophageal endoscopic submucosal dissection. *World J Gastroenterol* 2018; 24(10): 1144-1151 Available from: URL: http://www.wjgnet.com/1007-9327/full/v24/i10/1144.htm DOI: http://dx.doi.org/10.3748/wjg.v24.i10.1144

INTRODUCTION

With the development of endoscopic imaging technology and the increase in early endoscopic surveillance, the incidence of superficial esophageal neoplasm (SEN) has increased substantially[1,2]. Endoscopic resection has been considered to be a feasible procedure for SEN because of its minimal invasiveness and the fact that it does not compromise organ function[3,4]. Endoscopic submucosal dissection (ESD) is an endoscopic resection method that enables high rates of en bloc resection regardless of tumor size and consequently reduces local recurrence[5,6]. However, esophageal ESD is a more difficult procedure to perform than gastric ESD. The technical resectability of the lesion is affected by various applied techniques, the expertise of the endoscopist, and the location and/or features of the lesion[1,6].

Well-known complications of esophageal ESD include perforation (0%-6.9%), bleeding (0%-5.2%), and post-procedural stricture (0%-17.2%)[1,4,7-10]. However, post ESD electrocoagulation syndrome (PEECS) can be also a common complication of ESD[11,12]. PEECS is characterized by localized abdominal pain, rebound tenderness, fever, and signs of peritoneal irritation without frank perforation after gastric or colorectal ESD. Several previous studies analyzed PEECS after gastric or colonic ESD, but PEECS after esophageal ESD has not been studied yet[12,13]. Actually, some patients demonstrate clinical signs of PEECS after esophageal ESD associated with fever, chest pain and leukocytosis, despite the absence of perforation. However, the possibility of PEECS in the esophagus has received little attention. As far as we know, no studies have yet been conducted on PEECS in the esophagus, and we tried to investigate this new study. Therefore, we aimed to evaluate the incidence and risk factors of PEECS in the esophagus.

MATERIALS AND METHODS

Patients and tumors

We retrospectively analyzed prospectively collected database of patients who underwent esophageal ESD for superficial esophageal squamous neoplasms between March 2009 and December 2016 at Gangnam Severance Hospital, Seoul, South Korea. The analyzed demographic data and clinicopathologic features included patient age, sex, comorbidities, smoking and alcohol history, gross appearance of the tumor, location of the tumor, histological type, invasion depth, circumferential extension of the tumor, area of resection, degree of exposure of the muscularis propria, procedure time, systemic inflammatory response markers (*e.g.*, leukocyte count and body temperature), administration of antibiotics, and hospitalization period. The gross appearance of the tumor was categorized according to the Paris classification system[14]. Tumor histology was assigned according to the Japanese Classification of Esophageal Carcinoma scheme[15]. Tumor location was classified according to the guidelines of the American Joint Committee on Cancer[16]. The resected specimen was assumed to have an elliptical shape. Therefore, the resected area was calculated using the major and minor specimen axes, both of which were measured by a pathologist. The procedure time for ESD was defined as the time from circumferential marking to the retrieval of the resected specimens by an endoscope. Proper muscle layer exposure was defined as when the fine texture of the muscle fibers of muscularis propria was clearly exposed and visible endoscopically due to deep submucosal dissection (Figure 1). Patients who underwent multiple esophageal ESD were excluded in this study.

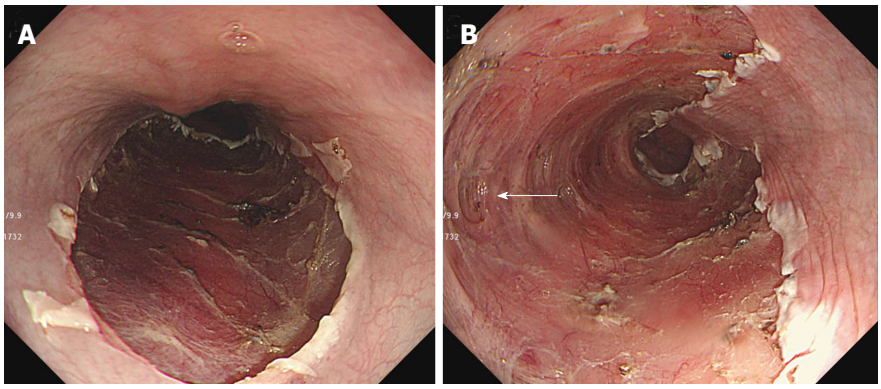

Figure 1 Proper muscle layer exposure during endoscopic submucosal dissection in esophagus. A: Absent; B: Present.

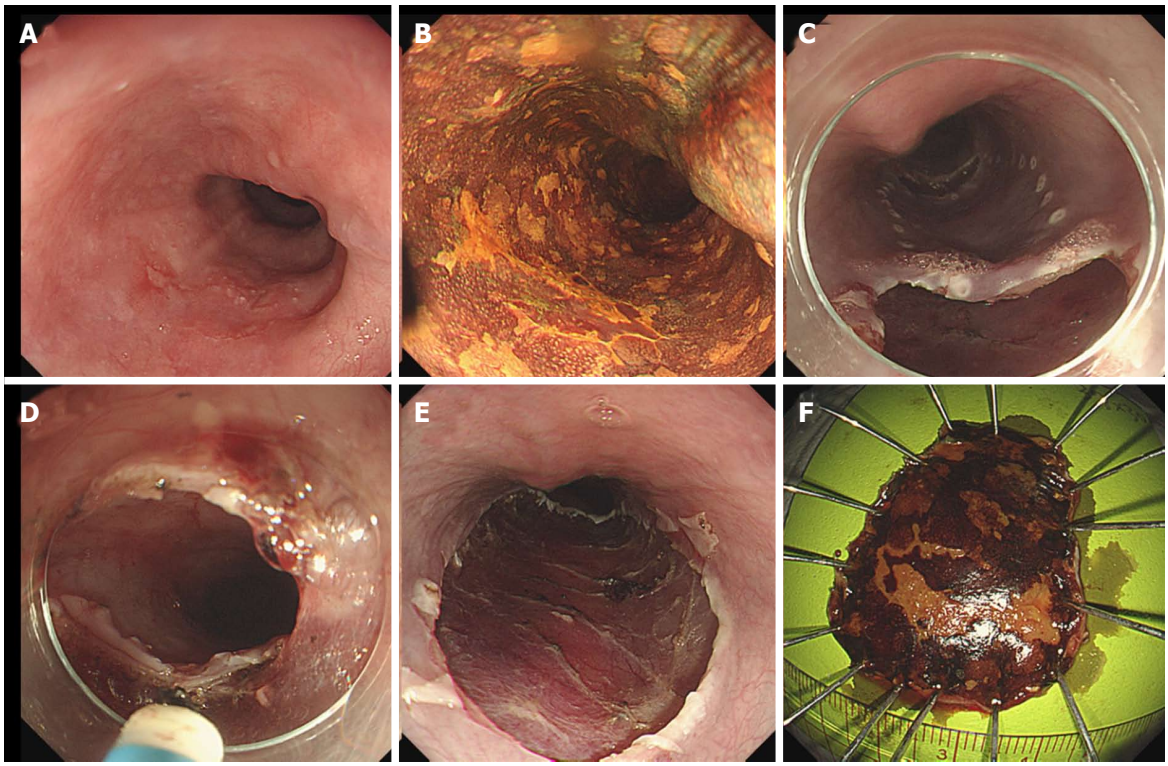

Figure 2 Endoscopic submucosal dissection of a superficial esophageal neoplasm. A and B: A flat erythematous lesion that is unstained with Lugol's solution; C and D: Endoscopic submucosal dissection is made with a dual-knife after local submucosal injection; E and F: The lesion is completely resected.

PEECS was defined as meeting following criteria: fever (≥ 37.8 ℃), leukocytosis (> 10800 counts/μL), or regional chest pain greater than 5/10 points as assessed on a numeric pain rating scale within 24 h after ESD[11,12]. Patients indicated the intensity of current, best, and worst pain levels on a scale of 0 (no pain) to 10 (worst pain imaginable)[17]. If one of the criteria was met, it was defined as mild PEECS and defined as severe PEECS if two or more criteria were met. Patients who had ESD complications such as overt perforation or bleeding were excluded from the analyses. Overt perforation was defined as radiographic evidence of free air, mediastinal emphysema, or subcutaneous emphysema after the procedure. Massive bleeding was defined as bleeding that led to the termination of the procedure. Patients with other defined infections such as pneumonia were also excluded. The Institutional Review Board (IRB) of Gangnam Severance Hospital approved this study (3-2017-0163). We received a consent exemption from the IRB. Patients records and information was anonymized

ESD procedures

All ESD procedures were performed by two expert ESD endoscopists (Y.Y.H. and J.K.). Patients were moderately sedated with midazolam and propofol while ESD was performed. A video endoscope with a water-jet function (GIF-HQ290, GIF-Q260J; Olympus, Tokyo, Japan) was used. A disposable distal transparent cap (D-201-11804; Olympus) was mounted on the tip of

Table 1 Baseline patient and tumor characteristics *n* (%)

Characteristic	Value (*n* = 51)
Number of patients	51
Sex	
Male	46 (90.2)
Female	5 (9.8)
Age, mean ± SD, yr	63.6 ± 9.4
Comorbidity	
Hypertension	21 (41.2)
Diabetes mellitus	7 (13.7)
Chronic kidney disease	1 (2.0)
Smoker	42 (82.4)
Alcohol consumption	40 (78.4)
Gross appearance of tumor	
Polypoid	1 (2.0)
Elevated	8 (15.7)
Flat	40 (78.4)
Depressed	2 (3.9)
Location of tumor	
Upper third of esophagus	3 (5.9)
Middle third of esophagus	20 (39.2)
Lower third of esophagus	24 (47.1)
Esophagogastric junction	4 (7.8)
Circumferential extension, median (IQR), %	40 (30-60)
Pathology of tumor	
Dysplasia	14 (27.5)
Squamous cell carcinoma	37 (72.5)
Invasion depth of tumor	
Mucosa	38 (74.5)
Submucosa	13 (25.5)
Resected area, median (IQR), cm^2	4.5 (2.9-8.2)
Procedure time, median (IQR), min	40 (27-69)
Muscle layer exposure	
Absent	27 (52.9)
Present	24 (47.1)
En bloc resection	51 (100)
Antibiotics use	23 (45.1)
Post procedure BT, mean ± SD, ℃	36.6 ± 0.5
Post procedure WBC, median (IQR), counts/μL	10800 (9340-12600)
Post procedure pain scale score, median (IQR)	5 (3-6)
Duration of hospitalization, median (IQR), d	4 (3-6)
Post ESD electrocoagulation syndrome	
Absent	18 (35.3)
Mild	24 (47.1)
Severe	9 (17.6)

SD: Standard deviation; IQR: Interquartile range; BT: Body temperature; WBC: White blood cell.

the endoscope in all cases. To identify the target lesion, chromoendoscopy with Lugol's stain or narrow band imaging with magnification was used. The area around the lesion was marked with electrical coagulation. A mixture of 10% glycerol solution and 0.005 mg/mL epinephrine was injected through a 25-gauge needle into the submucosal layer under the lesion. In some cases, hyaluronic acid (Endo-Mucoup; BMI Korea, Jeju, South Korea) was added to the mixture. An endoscopic carbon dioxide regulation unit (UCR, Olympus, Tokyo, Japan) was used for the insufflation. A dual knife (KD-650Q; Olympus) or an IT-knife 2 (KD-610L; Olympus) was used to perform the submucosal dissection with the Swift coagulation mode of an electrosurgical generator (VIO 300D; Erbe Elektromedizin GmbH, Tübingen, Germany). Hemostatic forceps (Coagrasper, FD-410LR; Olympus) with a soft coagulation mode (60-W output) were used to control bleeding during the procedure (Figure 2).

After ESD, the patients were closely observed to detect any adverse events. Intravenous proton pump inhibitors and oral sucralfate were administered to each patient to prevent procedure-related bleeding. Chest and abdominal X-rays were taken immediately at the end of the procedure and the following morning to identify any leakage of luminal air or pneumonic consolidation. On the day following the procedure, complete blood cell count was performed to evaluate the leukocytosis. If any aspiration or minute perforation was suspected during ESD, prophylactic antibiotics were administered to the patients. In the absence of evidence of complications such as bleeding or perforation, a clear liquid diet was served the following morning and the patient was discharged in two or three days.

Statistical analysis

Categorical data were analyzed using Fisher's exact test or the χ^2 test. Student's *t*-test or the Mann-Whitney *U* test was used for analysis of quantitative data. Receiver operating characteristic (ROC) curve analysis was performed to find the optimal cutoff values of quantitative data such as resected area and procedure time. In the univariate analysis to determine independent risk factors for PEECS, variables with $P < 0.05$ were considered statistically significant and were added to the multivariate logistic regression. All statistical analysis was performed using SPSS software, version 18.0 for Windows (SPSS, Chicago, IL, United States).

RESULTS

We obtained data from 55 consecutive patients with SEN treated by ESD at Gangnam Severance Hospital. Among them, 4 patients were excluded because of procedure-related complication (3 cases of perforation, 1 case of bleeding). Thus, 51 patients were enrolled in our study. Table 1 shows the patient and tumor baseline characteristics. Most of the patients were male (46, 90.2%), and the mean age was 63.6 years. According to the Paris classification scheme, the tumors of 40 patients (78.4%) had type 0-IIb gross appearance. There were 14 patients (27.5%) who had dysplasia and 37 patients (72.5%) who had squamous cell carcinoma. Regarding tumor invasion depth, 38 cases (74.5%) had mucosal invasion and 13 cases (25.5%) had submucosal invasion. More than half of the patients had no muscle fiber exposure after the procedure (52.9%). The median resected area was 4.5 cm^2 (range 0.8-17.6) and the median procedure time was 40 minutes (range 17-167). The median WBC after the procedure was 10800 cells/uL. There were 2 patients who had a fever (≥ 37.8 ℃) without any obvious evidence of infection. There were 8 patients (15.7%) who had severe pain (≥ 6 points) after ESD. As a result, 24 patients

Table 2 Univariate analysis of risk factors for post endoscopic submucosal dissection electrocoagulation syndrome *n* (%)

	No PEECS (*n* = 18)	PEECS (*n* = 33)	*P* value
Male sex,	17 (94.4)	29 (87.9)	0.451
Age, mean ± SD, yr	63.6 ± 11.2	63.6 ± 8.5	0.977
Comorbidity			0.769
Absent	9 (50.0)	19 (57.6)	
Present	9 (50.0)	14 (42.4)	
Gross appearance			0.933
Flat	14 (77.8)	26 (78.8)	
Non-flat	4 (22.2)	7 (21.2)	
Location			0.378
Upper and middle	10 (55.6)	13 (39.4)	
Lower and EGJ	8 (44.4)	20 (60.6)	
Circumferential extension, median (IQR), %	35 (30-42.5)	40 (30-60)	0.164
Pathology			0.487
Dysplasia	6 (33.3)	8 (24.2)	
Squamous cell carcinoma	12 (66.7)	25 (75.8)	
Invasion depth			0.082
Mucosa	16 (88.9)	22 (66.7)	
Submucosa	2 (11.1)	11 (33.3)	
Resected area			0.035
< 6.0 cm^2	15 (83.3)	17 (51.5)	
⩾ 6.0 cm^2	3 (16.7)	16 (48.5)	
Procedure time			0.026
< 25 min	7 (38.9)	4 (12.1)	
⩾ 25 min	11 (61.1)	29 (87.9)	
Muscle layer exposure			0.018
Absent	14 (77.8)	13 (39.4)	
Present	4 (22.2)	20 (60.6)	
Hospitalization period, mean (IQR), d	3.5 (3-4)	5 (4-6)	0.007
Antibiotics use			0.020
No	14 (77.8)	14 (42.4)	
Yes	4 (22.2)	19 (57.6)	

PEECS: Post endoscopic submucosal dissection electrocoagulation syndrome; SD: Standard deviation; EGJ: Esophagogastric junction; IQR: Interquartile range.

(47.1%) developed mild PEECS and 9 patients (17.6%) developed severe PEECS during the post-ESD period.

There were several significant differences between patients with *vs* patients without PEECS. Patients with PEECS had a relatively larger resection area, a longer mean procedure time, a more often incidence of proper muscle layer exposure, a more prolonged hospitalization period, and a more frequent administration of antibiotics. However, patient-related factors (sex, age, comorbidity) and tumor-related factors (gross appearance, tumor location, tumor histology, tumor invasion depth) were not significantly associated with the development of PEECS (Table 2). Also, ESD learning curve did not show statistically significant relationship with PEECS. The difference in PEECS incidence among the operators was not statistically significant (55.8% *vs* 50%, $P = 0.529$). Multivariate analysis revealed that a resection area larger than 6.0 cm^2 (OR = 4.995, 95%CI: 1.110-22.489, $P = 0.036$) and a present of muscle layer exposure (OR = 5.661, 95%CI: 1.422-22.534, $P = 0.014$) were independent risk factors for PEECS (Table 3). We did not include hospitalization period and antibiotics use in the multivariate analysis, because these factors are considered as consequence of the PEECS rather than cause. No patient diagnosed with PEECS required additional surgery and all patients diagnosed with PEECS spontaneously recovered with intravenous hydration and antibiotics.

DISCUSSION

While ESD is a feasible and effective method for the treatment of SEN, it is a technically difficult procedure and its complications remain a problem[18]. Pain, bleeding, and perforation are common acute complications after esophageal ESD[19]. In addition to major complications, various minor complications may accompany this procedure. These complications, such as chest discomfort, nausea, vomiting, and pyrexia, tend to occur frequently in the postesophageal ESD period. We define esophageal PEECS as a condition accompanied by fever, systemic inflammatory response and chest pain after ESD without such perforation. There have been previous studies on PEECS for Gastric ESD and Colonic ESD[13,20]. The present study is the first to focus on PEECS in the esophagus, which was characterized by fever, leukocytosis, or regional chest pain.

The incidence of esophageal PEECS in this study was higher (60.8%) than the incidence of PEECS in the colon in previous studies[11,12]. This relatively high incidence may have several explanations. Firstly, the esophagus lacks a serosal membrane, unlike other gastrointestinal

Table 3 Multivariate logistic regression analysis of risk factors for post endoscopic submucosal dissection electrocoagulation syndrome

Factor	OR (95%CI)	*P* value
Procedure time		0.379
≤ 25 min	Reference	
> 25 min	2.032 (0.419-9.868)	
Resected area		0.036
≤ 6.0 cm^2	Reference	
> 6.0 cm^2	4.995 (1.110-22.489)	
Muscle layer exposure		0.014
Absent	Reference	
Present	5.661 (1.422-22.534)	

tract organs. Instead of a serosal membrane, the esophagus has a unique structure called adventitia, which is composed of loose connective tissue. Due to the lack of a serosal layer in the esophageal wall, the esophagus might be more susceptible to PEECS than the colon. Moreover, many important organs surround the esophagus, such as the aorta and the bronchus. We propose that these anatomical differences may affect the development of esophageal PEECS. Secondly, although we proposed a definition of esophageal PEECS for this study, a definitive definition of PEECS has not yet been established. While the definition of post polypectomy coagulation syndrome was first published in the 1980s, the criteria were ambiguous and no exact value has been proposed[21]. Moreover, previous studies on gastric or colorectal PEECS also used slightly different definitions[11-13]. These discrepancies may affect relatively high incidence of the PEECS.

In this study, 2 risk factors - resection area and muscle layer exposure - were identified for PEECS in esophageal ESD. These findings are slightly different from previous studies. For instance, polyp size and location were found to be risk factors of post polypectomy electrocoagulation syndrome in the colon[22,23]. For colorectal PEECS, female sex, tumor location, piecemeal resection, tumor size, and procedure time have been identified as risk factors[11,12]. In gastric ESD, tumor size, location, and procedure time have been identified as risk factors for PEECS[13]. While sex differences might influence pain perception, most of the patients with SEN were male[6,17,18,24]. Therefore, it is difficult to identify differences in the incidence of PEECS due to sex based on the data in the present study. In colon ESD, PEECS has been shown to be more common in the right colon than the left colon because of anatomical differences[12,23]. However, unlike the colon, anatomical variation according to the location in the esophagus did not significantly affect the occurrence of PEECS.

PEECS occurred more often with wide resection areas, most likely because the wide area meant that more electric cauterization was required[11,12]. Also, the muscle layer exposure affected the development of PEECS in this study. In colon ESD, superficial damage of the muscularis propria does not significantly influence the spread of inflammation[11]. However, the esophagus does not have serosa membrane, and exposure of bare muscle fibers may have an effect on the propagation of inflammatory substances through muscularis propria. For complete resection of the tumor, clinicians usually attempt to dissect the submucosal layer as deeply as possible to the extent that it does not damage the muscular layers of the esophagus. Therefore, muscle layer exposure can occur frequently during the procedure, and it can be expected that it would have a significant impact on the occurrence of PEECS. The longer procedure time, the chance of fluid aspiration to the respiratory tract may increase substantially. Although longer procedure time was significantly associated with PEECS in univariate analysis, the multivariate analysis showed that longer procedure time was not an independent risk factor of esophageal PEECS. Kawata *et al*[25]. reported an incidence of bacteremia after esophageal ESD of 1%. Due to the rare incidence of bacteremia, they did not recommend prophylactic antibiotics for patients who undergo esophageal ESD. In our study, we used antibiotics only when patients were suspected to have complications. All patients with PEECS showed good outcomes without any severe complications. As a result, we suggest that esophageal PEECS is a systemic inflammatory response syndrome caused by electrical burns and transmural penetration of oro-esophageal secretion rather than true infection.

There are several limitations of our study. First, it was a small number and retrospective study that was performed at a single center. Thus, the cut off values we have established need external validation. Furthermore, there may be a recording bias because of retrospective design. Second, assessment of pain felt by patients after ESD may be subjective because pain tolerance can vary according to sex or age[17]. Third, we routinely perform chest and abdomen X-ray examinations after esophageal ESD. A computed tomography (CT) scan might be needed to detect micro perforations accurately after ESD. However, we performed a CT scan only when perforation was suspected on X-ray scans. Even if micro perforations were present, all patients in our study showed improvement with conservative treatment.

This is the first study of PEECS for esophageal lesions. PEECS is a common clinical syndrome characterized by chest pain, leukocytosis, or fever after esophageal ESD. It is another kind of clinical syndrome that is different from systemic inflammatory response syndrome. However, PEECS can be easily controlled by conservative management without surgical intervention when there is no obvious perforation. We found that the incidence of PEECS was high when the resected tumor area exceeded 6.0 cm^2 or when the muscle layer exposure was present. If these risk factors are accompanied, careful attention should be paid to the

potential occurrence of PEECS after esophageal ESD.

ARTICLE HIGHLIGHTS

Research background

A number of patients experience fever, chest pain, and/or a systemic inflammatory response after esophageal endoscopic submucosal dissection (ESD), even in the absence of obvious perforation.

Research motivation

Post ESD electrocoagulation syndrome (PEECS) is known as a common complication after colon ESD. However, there were no studies of PEECS after esophageal ESD.

Research objectives

We aimed to investigate the incidence and risk factors of PEECS in the esophagus.

Research methods

We retrospectively analyzed electronic medical database of patients who underwent esophageal ESD for superficial esophageal squamous neoplasms between March 2009 and December 2016 at single center in South Korea. PEECS was defined as meeting one of following criteria: fever (≥ 37.8 ℃), leukocytosis (> 10800 counts/μL), or regional chest pain greater than 5/10 points as assessed on a numeric pain rating scale within 24 h after ESD.

Research results

As a result, 24 patients (47.1%) developed mild PEECS and 9 patients (17.6%) developed severe PEECS during the post-ESD period. We identified that that a resection area larger than 6.0 cm^2 (OR = 4.995, 95%CI: 1.110-22.489, P = 0.036) and a present of muscle layer exposure (OR 5.661, 95%CI: 1.422-22.534, P = 0.014) were independent risk factors for PEECS. All patients diagnosed with PEECS fully recovered with conservative management, such as intravenous hydration and antibiotics.

Research conclusions

PEECS is not a rare clinical after esophageal ESD. However, PEECS can be easily controlled by conservative management without surgical intervention when there is no obvious perforation. We conclude that the incidence of PEECS is expected to be high when the resected tumor area exceeds 6.0 cm^2 or when the muscle layer exposure is present.

Research perspective

If these risk factors are accompanied, careful attention should be paid to the potential occurrence of PEECS after esophageal ESD. Further large-scale study is needed to validate our research.

REFERENCES

1 **Ono S**, Fujishiro M, Niimi K, Goto O, Kodashima S, Yamamichi N, Omata M. Long-term outcomes of endoscopic submucosal dissection for superficial esophageal squamous cell neoplasms. *Gastrointest Endosc* 2009; **70**: 860-866 [PMID: 19577748 DOI: 10.1016/j.gie.2009.04.044]

2 **Shimizu Y**, Takahashi M, Yoshida T, Ono S, Mabe K, Kato M, Asaka M, Sakamoto N. Endoscopic resection (endoscopic mucosal resection/ endoscopic submucosal dissection) for superficial esophageal squamous cell carcinoma: current status of various techniques. *Dig Endosc* 2013; **25** Suppl 1: 13-19 [PMID: 23480399 DOI: 10.1111/j.1443-1661.2012.01408.x]

3 **Das A**, Singh V, Fleischer DE, Sharma VK. A comparison of endoscopic treatment and surgery in early esophageal cancer: an analysis of surveillance epidemiology and end results data. *Am J Gastroenterol* 2008; **103**: 1340-1345 [PMID: 18510606 DOI: 10.1111/j.1572-0241.2008.01889.x]

4 **Takahashi H**, Arimura Y, Masao H, Okahara S, Tanuma T, Kodaira J, Kagaya H, Shimizu Y, Hokari K, Tsukagoshi H, Shinomura Y, Fujita M. Endoscopic submucosal dissection is superior to conventional endoscopic resection as a curative treatment for early squamous cell carcinoma of the esophagus (with video). *Gastrointest Endosc* 2010; **72**: 255-264, 264.e1-264.e2 [PMID: 20541198 DOI: 10.1016/j.gie.2010.02.040]

5 **Fujishiro M**. Perspective on the practical indications of endoscopic submucosal dissection of gastrointestinal neoplasms. *World J Gastroenterol* 2008; **14**: 4289-4295 [PMID: 18666315 DOI: 10.3748/wjg.14.4289]

6 **Tsujii Y**, Nishida T, Nishiyama O, Yamamoto K, Kawai N, Yamaguchi S, Yamada T, Yoshio T, Kitamura S, Nakamura T, Nishihara A, Ogiyama H, Nakahara M, Komori M, Kato M, Hayashi Y, Shinzaki S, Iijima H, Michida T, Tsujii M, Takehara T. Clinical outcomes of endoscopic submucosal dissection for superficial esophageal neoplasms: a multicenter retrospective cohort study. *Endoscopy* 2015; **47**: 775-783 [PMID: 25826277 DOI: 10.1055/s-0034-1391844]

7 **Hirasawa K**, Kokawa A, Oka H, Yahara S, Sasaki T, Nozawa A, Tanaka K. Superficial adenocarcinoma of the esophagogastric junction: long-term results of endoscopic submucosal dissection. *Gastrointest Endosc* 2010; **72**: 960-966 [PMID: 21034897 DOI: 10.1016/j.gie.2010.07.030]

8 **Ishihara R**, Iishi H, Uedo N, Takeuchi Y, Yamamoto S, Yamada T, Masuda E, Higashino K, Kato M, Narahara H, Tatsuta M. Comparison of EMR and endoscopic submucosal dissection for en bloc resection of early esophageal cancers in Japan. *Gastrointest Endosc* 2008; **68**: 1066-1072 [PMID: 18620345 DOI: 10.1016/j.gie.2008.03.1114]

9 **Kakushima N**, Yahagi N, Fujishiro M, Kodashima S, Nakamura M, Omata M. Efficacy and safety of endoscopic submucosal dissection for tumors of the esophagogastric junction. *Endoscopy* 2006; **38**: 170-174 [PMID: 16479425 DOI: 10.1055/s-2005-921039]

10 **Oyama T**, Tomori A, Hotta K, Morita S, Kominato K, Tanaka M, Miyata Y. Endoscopic submucosal dissection of early esophageal cancer. *Clin Gastroenterol Hepatol* 2005; **3**: S67-S70 [PMID: 16013002 DOI: 10.1016/S1542-3565(05)00291-0]

11 **Yamashina T**, Takeuchi Y, Uedo N, Hamada K, Aoi K, Yamasaki Y, Matsuura N, Kanesaka T, Akasaka T, Yamamoto S, Hanaoka N, Higashino K, Ishihara R, Iishi H. Features of electrocoagulation syndrome after endoscopic submucosal dissection for colorectal neoplasm. *J Gastroenterol Hepatol* 2016; **31**: 615-620 [PMID: 26202127 DOI: 10.1111/jgh.13052]

12 **Jung D**, Youn YH, Jahng J, Kim JH, Park H. Risk of electrocoagulation syndrome after endoscopic submucosal dissection in the colon and rectum. *Endoscopy* 2013; **45**: 714-717 [PMID: 23990482 DOI: 10.1055/s-0033-1344555]

13 **Lee H**, Cheoi KS, Chung H, Park JC, Shin SK, Lee SK, Lee YC. Clinical features and predictive factors of coagulation syndrome after endoscopic submucosal dissection for early gastric neoplasm. *Gastric Cancer* 2012; **15**: 83-90 [PMID: 21761134 DOI: 10.1007/s10120-011-0073-x]

14 . The Paris endoscopic classification of superficial neoplastic lesions: esophagus, stomach, and colon: November 30 to December 1, 2002. *Gastrointest Endosc* 2003; **58**: S33-S43 [PMID: 14652541 DOI: 10.1016/S0016-5107(03)02159-X]

15 **Shimoda T**. Japanese classification of esophageal cancer, the 10th edition--Pathological part. *Nihon Rinsho* 2011; **69** Suppl 6: 109-120 [PMID: 22471004]

16 **Rice TW**, Blackstone EH, Rusch VW. 7th edition of the AJCC Cancer Staging Manual: esophagus and esophagogastric junction. *Ann Surg Oncol* 2010; **17**: 1721-1724 [PMID: 20369299 DOI: 10.1245/s10434-010-1024-1]

17 Pain: clinical manual for nursing practice Pain: clinical manual for nursing practice Margo McCaffery Alexander Beebe Mosby Yearbook UK £17.25 0 7234 1992 2. *Nurs Stand* 1994; **9**: 55 [PMID: 27527475 DOI: 10.7748/ns.9.11.55.s69]

18 **Kim DH**, Jung HY, Gong EJ, Choi JY, Ahn JY, Kim MY, Choi KS, Lee JH, Choi KD, Song HJ, Lee GH, Kim JH, Park YS, Baek S. Endoscopic and Oncologic Outcomes of Endoscopic Resection

for Superficial Esophageal Neoplasm. *Gut Liver* 2015; **9**: 470-477 [PMID: 25473069 DOI: 10.5009/gnl13263]
19 **Isomoto H**, Yamaguchi N, Minami H, Nakao K. Management of complications associated with endoscopic submucosal dissection/endoscopic mucosal resection for esophageal cancer. *Dig Endosc* 2013; **25** Suppl 1: 29-38 [PMID: 23368404 DOI: 10.1111/j.1443-1661.2012.01388.x]
20 **Onogi F**, Araki H, Ibuka T, Manabe Y, Yamazaki K, Nishiwaki S, Moriwaki H. "Transmural air leak": a computed tomographic finding following endoscopic submucosal dissection of gastric tumors. *Endoscopy* 2010; **42**: 441-447 [PMID: 20432207 DOI: 10.1055/s-0029-1244013]
21 Selected papers from the Second International Congress on Colonoscopy and Diseases of the Large Bowel, March 6 to 8, 1980. *Gastrointest Endosc* 1981; **27**: 184-187 [PMID: 7297830 DOI: 10.1016/S0016-5107(81)73190-0]
22 **Cha JM**, Lim KS, Lee SH, Joo YE, Hong SP, Kim TI, Kim HG, Park DI, Kim SE, Yang DH, Shin JE. Clinical outcomes and risk factors of post-polypectomy coagulation syndrome: a multicenter, retrospective, case-control study. *Endoscopy* 2013; **45**: 202-207 [PMID: 23381948 DOI: 10.1055/s-0032-1326104]
23 **Choo WK**, Subhani J. Complication rates of colonic polypectomy in relation to polyp characteristics and techniques: a district hospital experience. *J Interv Gastroenterol* 2012; **2**: 8-11 [PMID: 22586542 DOI: 10.4161/jig.20126]
24 **Park JS**, Youn YH, Park JJ, Kim JH, Park H. Clinical Outcomes of Endoscopic Submucosal Dissection for Superficial Esophageal Squamous Neoplasms. *Clin Endosc* 2016; **49**: 168-175 [PMID: 26867548 DOI: 10.5946/ce.2015.080]
25 **Kawata N**, Tanaka M, Kakushima N, Takizawa K, Imai K, Hotta K, Matsubayashi H, Tsukahara M, Kawamura I, Kurai H, Ono H. The low incidence of bacteremia after esophageal endoscopic submucosal dissection (ESD) obviates the need for prophylactic antibiotics in esophageal ESD. *Surg Endosc* 2016; **30**: 5084-5090 [PMID: 26983438 DOI: 10.1007/s00464-016-4857-2]

P- Reviewer: Hashimoto N, Jani K, Jonaitis LV **S- Editor**: Ma YJ
L- Editor: A **E- Editor**: Ma YJ

World Journal of Gastroenterology

Submit a Manuscript: http://www.f6publishing.com

World J Gastroenterol 2018 March 14; 24(10): 1152-1166

DOI: 10.3748/wjg.v24.i10.1152

ISSN 1007-9327 (print) ISSN 2219-2840 (online)

ORIGINAL ARTICLE

Clinical Practice Study

Progesterone receptor membrane component 1 as a potential prognostic biomarker for hepatocellular carcinoma

Hung-Wen Tsai, Chung-Liang Ho, Shu-Wen Cheng, Yih-Jyh Lin, Chou-Cheng Chen, Pin-Nan Cheng, Chia-Jui Yen, Ting-Tsung Chang, Po-Min Chiang, Shih-Huang Chan, Cheng-Hsun Ho, Shu-Hui Chen, Yi-Wen Wang, Nan-Haw Chow, Jou-Chun Lin

Hung-Wen Tsai, Po-Min Chiang, Institute of Clinical Medicine, National Cheng Kung University Hospital, College of Medicine, National Cheng Kung University, Tainan 70403, Taiwan

Hung-Wen Tsai, Chung-Liang Ho, Shu-Wen Cheng, Yi-Wen Wang, Nan-Haw Chow, Jou-Chun Lin, Department of Pathology, National Cheng Kung University Hospital, College of Medicine, National Cheng Kung University, Tainan 70403, Taiwan

Hung-Wen Tsai, Chung-Liang Ho, Shu-Wen Cheng, Chou-Cheng Chen, Nan-Haw Chow, Jou-Chun Lin, Institute of Basic Medical Sciences, College of Medicine, National Cheng Kung University, Tainan 70403, Taiwan

Hung-Wen Tsai, Ting-Tsung Chang, Center of Infectious Disease and Signaling Research, College of Medicine, National Cheng Kung University, Tainan 70403, Taiwan

Yih-Jyh Lin, Department of Surgery, National Cheng Kung University Hospital, College of Medicine, National Cheng Kung University, Tainan 70403, Taiwan

Pin-Nan Cheng, Chia-Jui Yen, Ting-Tsung Chang, Cheng-Hsun Ho, Department of Internal Medicine, National Cheng Kung University Hospital, College of Medicine, National Cheng Kung University, Tainan 70403, Taiwan

Shih-Huang Chan, Department of Statistics, College of Management, National Cheng Kung University, Tainan 70403, Taiwan

Cheng-Hsun Ho, Research Center of Clinical Medicine, National Cheng Kung University Hospital, College of Medicine, National Cheng Kung University, Tainan 70403, Taiwan

Shu-Hui Chen, Department of Chemistry, College of Sciences, National Cheng Kung University, Tainan 70403, Taiwan

ORCID number: Hung-Wen Tsai (0000-0001-9223-2535); Chung-Liang Ho (0000-0002-4562-5122); Shu-Wen Cheng (0000-0002-8684-4428); Yih-Jyh Lin (0000-0003-0998-3229); Chou-Cheng Chen (0000-0002-4030-8849); Pin-Nan Cheng (0000-0001-9331-9018); Chia-Jui Yen (0000-0001-8744-6248); Ting-Tsung Chang (0000-0002-5073-2678); Po-Min Chiang (0000-0002-4950-9292); Shih-Huang Chan (0000-0002-3666-180X); Cheng-Hsun Ho (0000-0003-4451-2887); Shu-Hui Chen (0000-0003-1871-9366); Yi-Wen Wang (0000-0001-7863-727X); Nan-Haw Chow (0000-0002-0277-1947); Jou-Chun Lin (0000-0002-2358-3670).

Author contributions: Lin JC, Cheng SW, Wang YW and Tsai HW conducted the experiments in this study, analyzed the data, and prepared the manuscript; Tsai HW, Ho CL, Chiang PM and Chow NH performed the pathological analysis; Lin YJ, Cheng PN, Yen CJ and Chang TT provided and analyzed the clinical information; Chen CC performed the TCGA data analysis; Chan SH conducted the statistical analysis; Ho CH and Chen SH performed the mass spectrometry and data analysis; Tsai HW designed the study.

Supported by the Ministry of Science and Technology, No. NSC102-2320-B-006-011., No. MOST103-2320-B-006-021-MY2, and No. MOST105-2320-B-006-033 to Tsai HW; and National Cheng Kung University Hospital, Taiwan, No. NCKUH-10406002 and No. NCKUH-10509001 to Tsai HW.

Institutional review board statement: The study was conducted in accordance with the Declaration of Helsinki and approved by the Human Experiment and Ethics Committee of NCKUH (No. BR-100-117).

Conflict-of-interest statement: The authors declare that they have no competing interests.

Data sharing statement: Technical appendix and study data are available from the corresponding author at hungwen@mail.ncku.edu.tw with the permission of Hung-Wen Tsai. Consent was not obtained but the presented data are anonymized and the risk of identification is low. No additional data are available.

Manuscript source: Unsolicited manuscript

Correspondence to: Hung-Wen Tsai, MD, Associate Professor, Department of Pathology, National Cheng Kung University Hospital, College of Medicine, National Cheng Kung University, 138 Sheng-Li Road, Tainan 70403, Taiwan. hungwen@mail.ncku.edu.tw
Telephone: +886-6-2353535-2635
Fax: +886-6-2766195

Received: December 11, 2017
Peer-review started: December 12, 2017
First decision: December 27, 2017
Revised: January 16, 2018
Accepted: January 24, 2018
Article in press: January 24, 2018
Published online: March 14, 2018

Abstract

AIM

To investigate the clinicopathological significance of progesterone receptor membrane component 1 (PGRMC1) and PGRMC2 in hepatocellular carcinoma (HCC).

METHODS

We performed immunohistochemical staining to evaluate the estrogen receptor (ER), progesterone receptor (PR), PGRMC1, and PGRMC2 in a clinical cohort consisting of 89 paired HCC and non-tumor liver samples. We also analyzed HCC data (n = 373) from The Cancer Genome Atlas (TCGA). We correlated the expression status of PGRMC1 and PGRMC2 with clinicopathological indicators and the clinical outcomes of the HCC patients. We knocked down or overexpressed PGRMC1 in HCC cell lines to evaluate its biological significance in HCC cell proliferation, differentiation, migration, and invasion.

RESULTS

We found that few HCC cases expressed ER (5.6%) and PR (4.5%). In contrast, most HCC cases expressed PGRMC1 (89.9%) and PGRMC2 (100%). PGRMC1 and PGRMC2 exhibited significantly lower expression in tumor tissue than in non-tumor tissue (P < 0.001). Lower PGRMC1 expression in HCC was significantly associated with higher serum alpha-fetoprotein expression (P = 0.004), poorer tumor differentiation (P = 0.045) and liver capsule penetration (P = 0.038). Low PGRMC1 expression was an independent predictor for worse disease-free survival (P = 0.002, HR = 2.384, CI: 1.377-4.128) in our cases, as well as in the TCGA cohort (P < 0.001, HR = 2.857, CI: 1.781-4.584). The expression of PGRMC2 did not relate to patient outcome. PGRMC1 knockdown promoted a poorly differentiated phenotype and proliferation of HCC cells *in vitro*, while PGRMC1 overexpression caused the opposite effects.

CONCLUSION

PGRMC1 is a non-classical hormonal receptor that negatively regulates hepatocarcinogenesis. PGRMC1 down-regulation is associated with progression of HCC and is a poor prognostic indicator.

Key words: Progesterone receptor membrane component 1; Hormonal receptor; Proliferation; Hepatocellular carcinoma; Prognosis

Core tip: Neither estrogen receptor or progesterone receptor are commonly expressed in hepatocellular carcinoma (HCC), implying the existence of other hormone-related events in the pathogenesis of HCC. Most primary HCC cases expressed progesterone receptor membrane component 1 (PGRMC1) (89.9%) in our clinical cohort (n = 89). Down-regulation of PGRMC1 was associated with poor tumor differentiation and worse patient survival. The potential prognostic significance was independently validated by The Cancer Genome Atlas (TCGA) database (n = 373). Knockdown of PGRMC1 promoted proliferation and a poorly differentiated phenotype *in vitro*. Overexpression of PGRMC1 resulted in suppressed proliferation in response to progesterone treatment. PGRMC1 is a prognostic marker and a potential auxiliary therapeutic target for human HCC.

Tsai HW, Ho CL, Cheng SW, Lin YJ, Chen CC, Cheng PN, Yen CJ, Chang TT, Chiang PM, Chan SH, Ho CH, Chen SH, Wang YW, Chow NH, Lin JC. Progesterone receptor membrane component 1 as a potential prognostic biomarker for hepatocellular carcinoma. *World J Gastroenterol* 2018; 24(10): 1152-1166 Available from: URL: http://www.wjgnet.com/1007-9327/full/v24/i10/1152.htm DOI: http://dx.doi.org/10.3748/wjg.v24.i10.1152

INTRODUCTION

The major risk factors for hepatocellular carcinoma (HCC) are chronic liver diseases induced by hepatitis B (HBV) and hepatitis C (HCV), alcohol abuse, and non-alcoholic steatohepatitis. Regardless of etiology, the incidence of HCC is higher in males than in females, with a male to female ratio between 2:1 and 4:1[1]. However, the biological role of sex hormones and their receptors in HCC remains poorly understood. The androgen

receptor appears to contribute to HCC development by acting as a tumor promoter[2], whereas the estrogen receptor (ER) appears to act as a tumor suppressor[3]. Oophorectomy performed during premenopausal years has been found to be a risk factor for HCC[4]. The human liver is important in the metabolism of progesterone. Progesterone is known to inhibit autophagy and to augment epirubicin-induced apoptosis in hepatoma cells by increasing oxidative stress and upregulating Fas/FasL[5,6]. In a clinical trial, HCC patients with variant ERs had a significantly longer median survival if megestrol acetate was given[7], suggesting that progesterone is protective against HCC.

Progesterone receptor membrane component 1 (PGRMC1) and PGRMC2, which belong to the membrane-associated progesterone receptor (MAPR) family, have been suggested to be non-classical progesterone receptors[8,9]. These proteins contain a cytochrome b5-like heme/steroid-binding domain. Both PGRMC1 and PGRMC2 are derived from a single gene. The structure of PGRMC1 contains two SH2 target sequences, a SH3 target sequence, a tyrosine kinase target site, two acidophilic kinase (CK2, casein kinase 2) target sites, and binding sites for ERK1 and PDK1. PGRMC2 differs from PGRMC1 in the following aspects: First, the transmembrane domain and N-terminals are different, resulting in diverse interaction partners in the lumen of sub-cellular organelles or on the cell membrane surface. Second, the SH3 target sequence of PGRMC1 with its consensus CK2 site is absent in PGRMC2, suggesting that PGRMC2 may not interact with SH3-containing proteins. Third, PGRMC2 has a predicted PDGFR or EGFR target and an additional potential CK2 site[8]. Therefore, these two proteins may have different interacting partners in terms of connecting with the cellular membrane, organelles and cell signaling molecules.

In the case of tumorigenesis, PGRMC1 expression is associated with advanced-stage disease and poor prognoses in both breast and ovarian cancer[10,11]. However, several studies have shown that PGRMC1 mediates the anti-mitotic actions of progesterone in endometrial and ovarian cancer cells[12,13]. With regard to PGRMC2, copy number loss has been correlated with nodal metastasis in uterine cervical adenocarcinoma, suggesting that PGRMC2 can function as a metastasis suppressor[14]. PGRMC2 negatively affects SKOV-3 ovarian cell migration[15]. Therefore, PGRMC1 and PGRMC2 may have multiple biological functions related to metabolism and carcinogenesis. A proteomic study showed that PGRMC1 was expressed in HCC[16] but there is no information regarding PGRMC1 or PGRMC2 expression patterns in HCC or their clinical significance in this disease. To address this issue, we examined PGRMC1 and PGRMC2 expression in a clinical cohort of paired HCC and non-tumor tissue samples (n = 89). We analyzed an independent HCC cohort (n = 373) from The Cancer Genome Atlas (TCGA cohort) to validate our findings. We also investigated the significance of PGRMC1 in cell proliferation, differentiation, migration, and invasion *in vitro*.

MATERIALS AND METHODS

Patients and samples

Eighty-nine patients who underwent surgical resection for HCC at National Cheng Kung University Hospital (NCKUH) from January 1995 to September 2000 were included in this study. Frozen tissue, serum samples and archival paraffin blocks were retrieved from the Human Biobank at NCKUH. HCC differentiation was categorized according to the World Health Organization (WHO) system[17]. Six paraffin samples and four frozen liver samples were retrieved from six normal non-hepatitis patients who underwent surgery for cavernous hemangioma and acted as controls.

Bioinformatic TCGA dataset analysis

We analyzed the TCGA provisional dataset (TCGA dataset, https://tcga-data.nci.nih.gov/tcga/), which contained 373 HCC patients with mRNA expression data (RNA Seq V2 RSEM), clinicopathological indicators, and follow-up information. Of these patients, 50 had expression data pertaining to HCC and matched adjacent non-tumor tissue samples. Disease-free survival (DFS) and overall survival (OS) were calculated based on *PGRMC1* and *PGRMC2* expression. Expression levels greater than the median were classified as high expression; otherwise, they were classified as low expression.

Western blotting

Protein lysates were prepared from either frozen tissue samples or HCC cell lines. Equal amounts of protein (50 micrograms) were separated *via* 8% sodium dodecyl sulfate-polyacrylamide gel electrophoresis (SDS-PAGE) under reducing conditions. The proteins were then transferred to nitrocellulose membranes and stained with Ponceau S to assess transfer quality and ensure equal sample loading. The primary antibodies used were anti-PGRMC1 (Abnova Corporation, Walnut, CA, United States. PAB20135, 1:3000), anti-PGRMC2 (Abnova Corporation. H00010424-M04, 1:1000), anti-PR (Ventana Medical Systems, Inc. 790-2223, 1:100), anti-alpha-fetoprotein (Dako Cytomation, Inc., Carpinteria, CA, USA. A0008, 1:1000), anti-Glypican3 (BioMosaics, Burlington, VT, United States. 1G12, 1:1000) and anti-β-actin (GeneTex Inc. GTX109639, 1:10000). The indicated secondary antibodies (anti-rabbit and anti-mouse, IgG-HRP; Santa Cruz Biotechnology) were used to amplify the signals as appropriate.

Immunohistochemical staining and interpretation

Immunohistochemical staining was performed with primary antibodies against ER (Ventana Medical Systems, Inc., Arizona, United States), PR (Ventana

Medical Systems, Inc.), PGRMC1 (Abnova Corporation, Walnut, CA, United States. PAB20135) or PGRMC2 (Abnova Corporation. H00010424-M04). ER, PR, PGRMC1 and PGRMC2 expression was graded independently by two pathologists (Tsai HW and Ho CL) according to the percentages of stained hepatocytes or HCC cells. Because PGRMC1 is found in the cytosol and subcellular organelles[8], cytoplasmic staining was considered to be positive. High PGRMC expression was defined as more than two-thirds of the cells exhibited positive staining. In the case of ER and PR, nuclear staining was considered to be positive.

In-gel trypsin digestion and mass spectrometry

Fifty micrograms of tissue extracts were resolved using 12% SDS-PAGE and were stained using Coomassie brilliant blue r-250. The protein spot located between 20-28 kDa was excised and then in-gel digested using 20 ng/μL of trypsin (Promega, San Luis Obispo, CA, United States, sequencing grade) in 10 mmol/L NH_4HCO_3 with an enzyme-to-substrate ratio of 1:100 at 37 ℃ overnight. Peptides were extracted using 50% acetonitrile in 1% formic acid followed by sonication.

A nanoflow high-performance liquid chromatography system (LC Packings, Amsterdam, The Netherlands) equipped with a C18 nano-precolumn cartridge (*i.d.* = 300 μm × 1 mm, 5 μm C18, P/N160458; LC Packings) and a C18 column (*i.d.* = 75 μm, o.d. = 280 μm × 15 cm, 3 μm C18, LC Packings) was coupled online to a Q-TOF micro-instrument (Micromass, Manchester, United Kingdom). Mobile phase A was 0.1% formic acid in a 5% acetonitrile solution, and mobile phase B was 0.1% formic acid in 80% acetonitrile. A linear gradient from 5% to 90% B over 60 min at a flow rate of 250 nL/min was applied. A survey MS spectrum with a mass-to-charge ratio ranging from 400 to 1600 was followed by a MS/MS scan at a mass-to-charge ratio ranging from 50 to 2000. The threshold to switch from MS to MS/MS was 10 counts. Raw data were processed into peak lists, and then a Mascot search on a Swiss-Prot (human) protein database was conducted.

The mass tolerance was set at 0.2 Da for both the precursor and product ions. Dimethyl labeling of both the N-terminal and lysine residues was chosen for variable modifications; Carbamidomethyl (C) was chosen for fixed modification, and one miss cleavage on Arg-C was allowed. A cutoff value of 20 was set for the ion score to eliminate proteins with low matches. The default significance threshold for protein identification was set at $P < 0.05$.

Measurement of progesterone levels in sera and tissue

Tissue samples were minced and homogenized at a 1:10 (w:v) ratio with phosphate buffered saline at pH 7.4 using a homogenizer (PRO Scientific Inc., Oxford, CT, United States). The homogenates were centrifuged at 9000 × *g* at 4 ℃ for 30 min and the supernatants were immediately analyzed. The progesterone levels in the sera and tissue supernatants were analyzed using the Elecsys and Cobas e-immunoassay analyzer (Roche Diagnostics, Mannheim, Germany).

Cell lines

The HepG2 and Huh7 cell lines were maintained in Dulbecco's modified Eagle's medium (DMEM, Invitrogen Corp., Carlsbad, CA, United States) supplemented with 10% fetal bovine serum (FBS), penicillin (100 U/mL), and streptomycin (100 μg/mL) in a humidified incubator at 37 ℃ with 5% CO_2, whereas the PLC/PRF/5 and Hep3B cell lines were maintained in modified Eagle's medium (MEM, Invitrogen Corp.) supplemented with 10% FBS, penicillin (100 U/mL), and streptomycin (100 μg/mL) in a humidified incubator at 37 ℃ with 5% CO_2. Huh-7 cells were obtained from JCRB. Hep3B, HepG2 and PLC/PRF/5 cells were obtained from BCRC.

Knockdown and overexpression of PGRMC1

pLKO.1 plasmids expressing small hairpin RNA (shRNA) were purchased from the National RNAi Core Facility (Academia Sinica, Taipei, Taiwan). Lentivirus particles were obtained from RNAi Core of the Research Center of Clinical Medicine, NCKUH. The following shRNAs were used to knock down PGRMC1 expression in HepG2 and Hep3B cells: sh-1: TRCN0000311671, target sequence: 5'-ACTGTGTACTCAGATGAGGAA-3'; sh-2: TRCN0000363644, target sequence: 5'-CGCCGACCCAAGCGATCTGGA-3'; and sh-3: TRCN0000349346, target sequence: 5'-AGGATGAGTACGATGACCTTT -3'. A pLKO_TRC005 plasmid was used as a negative control. PGRMC1 knockdown was performed as described previously[15].

The pMSCVpuro (BD Clontech), pMSCV-PGRMC1, and pSUPERretro vectors were co-transfected into GP2-293T packaging cells along with VSV-G plasmids for 48 h using the calcium phosphate method. Either PLC/PRF/5 or Huh7 cells (1×10^6 cells/well) were seeded in a 6-cm dish and incubated overnight under 5% CO_2 at 37 ℃. The retroviral supernatant was treated with 8 ng/mL polybrene (Sigma, St. Louis, MO, United States) to infect the cells. Pooled PLC/PRF/5 or Huh7 cells expressing either pMSCVpuro or pMSCV-PGRMC1 were selected using 0.7 μg/mL puromycin (Sigma-Aldrich).

XTT proliferation assay

Stable pools were seeded in 24-well plates for 96 h. Triplicate wells were plated at each time point and examined at 24-h intervals over 4 d. The number of viable cells for each time point was determined using the XTT reagent, according to standard protocols (Roche Diagnostics GmbH, Vienna, Austria). To evaluate the impact of progesterone treatment, control cells and PGRMC1-overexpressing cells were cultured to 50% confluence and treated with progesterone (0, 10, 100, or 1000 nmol/L) for 48 h before the XTT assay.

In vitro migration and invasion assay

Transwell migration and invasion assays were performed using 24-well 8-micrometer pore Transwell plates,

Table 1 Prognostic significance of clinicopathological indicators, PGRMC1 and PGRMC2 for disease-free survival in the clinical cohort (*n* = 89)

Factor	DFS univariate				DFS multivariate		
	Group	HR	95%CI	*P* value	HR	95%CI	*P* value
Age, yr	< 60/≥ 60	0.997	0.609-1.632	0.989			
Sex	Male/female	1.014	0.599-1.715	0.960			
Viral infection				0.825			
	B/C	1.177	0.703-1.971				
	B/B + C	1.068	0.448-2.547				
Child-Pugh score	5/≥ 6	2.407	1.346-4.302	0.003[a]	2.005	(1.097-3.665)	0.024[a]
Cirrhosis	-/+	0.743	0.664-1.776	0.299			
Serum AFP	< 100/≥ 100 ng/ml	1.357	0.823-2.238	0.231			
Differentiation	W/M-P	1.682	0.943-2.999	0.078			
Multifocal tumor	-/+	0.985	0.514-1.888	0.965			
Satellite nodule	-/+	2.173	1.303-3.624	0.003[a]			NS
Tumor size	< 5/≥ 5 cm	2.446	1.486-4.028	< 0.001[a]			NS
Tumor capsular invasion	-/+	0.985	0.545-1.780	0.959			
Vascular invasion	-/+	2.551	1.553-4.190	< 0.001[a]			NS
Liver capsule penetration	-/+	2.235	1.010-4.945	0.047[a]			NS
Bile duct invasion	-/+	3.200	0.986-10.385	0.053			
Margin status, mm	≥ 1 /< 1	3.793	2.079-6.920	< 0.001[a]	4.720	(2.458-9.063)	< 0.001[a]
AJCC stage	I-II/ IIIA-C	2.907	1.738-4.861	< 0.001[a]	3.262	(1.895-5.617)	< 0.001[a]
PGRMC1	H/L	1.918	1.145-3.213	0.013[a]	2.384	(1.377-4.128)	0.002[a]
PGRMC2	H/L	1.377	0.798-2.379	0.251			
ER	-/+	0.528	0.128-2.173	0.376			
PR	-/+	0.777	0.243-2.484	0.670			

[a]*P* < 0.05. DFS: Disease-free survival; AFP: Alpha-fetoprotein; AJCC: American Joint Committee on Cancer; H: High expression; L: Low expression.

according to the manufacturer's instructions (Corning, New York, NY, United States). A total of 5 × 10^4 cells in serum-free DMEM medium were split onto the upper Transwell chamber, the membrane of which was coated with (for invasion) or without (for migration) Matrigel (BD Biosciences, San Diego, CA, United States). The lower chamber was filled with DMEM containing 10% FBS as a chemoattractant. After incubation for 24 h at 37 ℃, non-invading cells on the upper side of the chamber were removed from the surface of the membrane by scrubbing, and the membrane was fixed with 4% paraformaldehyde for 10 min. The cells on the membrane were stained using crystal violet solution and detected *via* microscopy. Mean cell numbers were calculated from five random fields.

Statistical analysis

The correlations between PGRMC1 expression, PGRMC2 expression, viral infection status, and clinicopathological indicators were assessed using the Wilcoxon rank sum test, the χ^2 test, or Fisher's exact test, as appropriate. Paired data were analyzed using paired Student's *t*-tests or the Wilcoxon signed-rank test. For the *in vitro* experiments, a Student's *t*-test was used for simple comparisons. Data are presented as the mean ± SEM. DFS and OS were calculated using the Kaplan-Meier method, and the log-rank test was used to assess the differences between groups. A Cox proportional hazards regression model was used to measure the independence of different factors. A Cox regression was performed *via* a forward stepwise analysis, and only the prognostic variables that were significant in the univariate analysis were included in the model. *P* values less than 0.05 were considered statistically significant.

RESULTS

Identification and analysis of PGRMC1 and progesterone expression in HCC

The HCC tissue extract was resolved using SDS-PAGE. The protein spot located between 20 to 28 kDa was in-gel trypsinized and subjected to mass spectrometry (MS). PGRMC1 was detected using MS (Supplementary Table 1). We subsequently examined the expression of PGRMC1 in 10 paired tumor and non-tumor liver samples (7 males and 3 females) using Western blotting. Another membrane-associated progesterone receptor family member, PGRMC2 was also examined for comparison. The age of the patients ranged from 57 to 77 years. Expression of PGRMC1 and PGRMC2 was lower in all HCC samples compared with the corresponding non-tumor liver samples (Figure 1A). Furthermore, both PGRMC1 and PGRMC2 were highly expressed in the normal liver as was the case in the non-tumor liver samples (Supplementary Figure 1A).

Progesterone expression was also evaluated in the HCC patients (*n* = 10). Serum progesterone levels (mean: 0.276 ng/mL for male patients and 0.167 ng/mL for female patients) were within the 5th-95th physical range in men (0.2-1.4 ng/mL) and postmenopausal women (0.1-0.8 ng/mL) (Figure 1D). However, progesterone levels in the HCC tissue were significantly lower than in the non-tumor liver tissue (*P* = 0.007, Figure 1B and C).

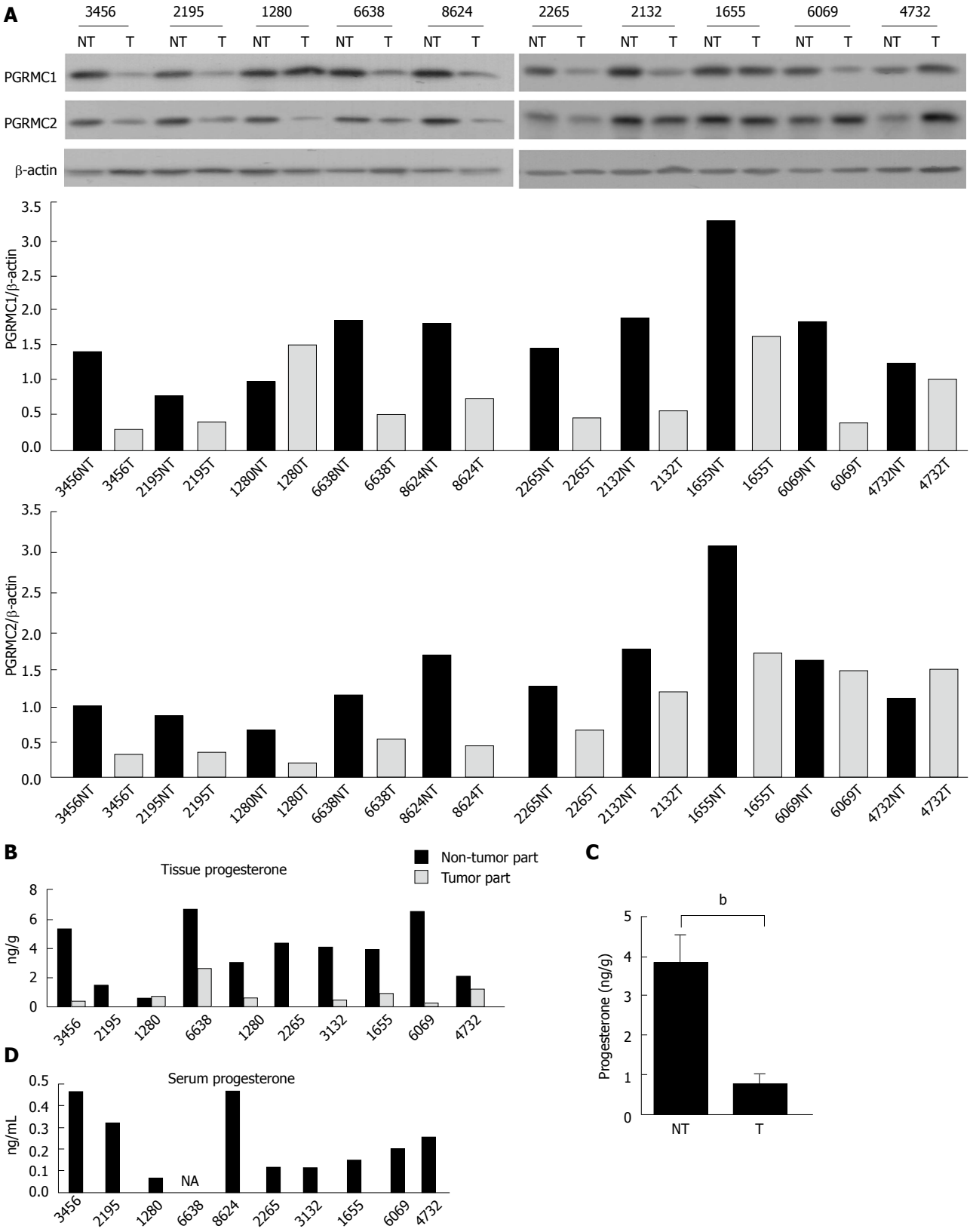

Figure 1 Western blot analysis of PGRMC1 and PGRMC2 expression in 10 paired hepatocellular carcinoma tumor (T)/non-tumor liver (NT) samples (A). B: Progesterone level in HCC tissue samples and non-tumor liver tissue; C: A comparison of progesterone levels in HCC (T) and non-tumor liver (NT) tissue samples; D: Serum progesterone level in the corresponding HCC patients. [b]$P < 0.01$.

Patient profiles

Immunohistochemical (IHC) staining for PGRMC1 and PGRMC2 was performed in the clinical cohort of 89 paired HCC and non-tumor liver samples. The profiles of the 89 patients are summarized in Supplementary Table 2. The patient population included 65 men and 24 women. The mean age was 55.2 years. The mean follow-up duration was 44.5 mo (range, 0.9-133.1

Table 2 Prognostic significance of clinicopathological indicators, *progesterone receptor membrane component 1* and *PGRMC2* for disease-free survival in The Cancer Genome Atlas cohort (*n* = 373)

Factor		DFS univariate			DFS multivariate		
	Group	HR	95%CI	*P* value	HR	95%CI	*P* value
Age, yr	< 60/≥ 60	1.019	0.756-1.373	0.903			
Sex	Male/female	1.157	0.845-1.585	0.364			
HCC risk factors				0.014[a]			< 0.001[a]
	B/NAFLD	1.433	0.601-3.414	0.417	2.903	(1.130-7.461)	0.027[a]
	B/Alcohol	1.449	0.948-2.217	0.087	1.002	(0.595-1.689)	0.993
	B/C	2.421	1.422-4.121	0.001[a]	3.368	(1.773-6.395)	< 0.001[a]
Child-Pugh score	A/B-C	1.332	0.709-2.504	0.372			
Cirrhosis	-/+	1.117	0.761-1.641	0.572			
Serum AFP, ng/ml	< 100/≥ 100	1.097	0.752-1.599	0.632			
Tumor grade	2/4/2001	1.330	0.868-2.038	0.191			
Vascular invasion	-/+	2.001	1.418-2.823	< 0.001[a]	3.040	(1.889-4.891)	< 0.001[a]
Residual tumor	-/+	1.733	0.938-3.200	0.079			
AJCC stage	Ⅰ-Ⅱ/Ⅲ-Ⅳ	2.354	1.693-3.272	< 0.001[a]	1.899	(1.107-3.255)	0.020[a]
PGRMC1	H/L	1.834	1.359-2.475	< 0.001[a]	2.857	(1.781-4.584)	< 0.001[a]
PGRMC2	H/L	1.242	0.923-1.671	0.152			

[a]*P* < 0.05. DFS: Disease-free survival; NAFLD: Non-alcoholic fatty liver disease; AFP: Alpha-fetoprotein; AJCC: American Joint Committee on Cancer; H: High expression; L: Low expression.

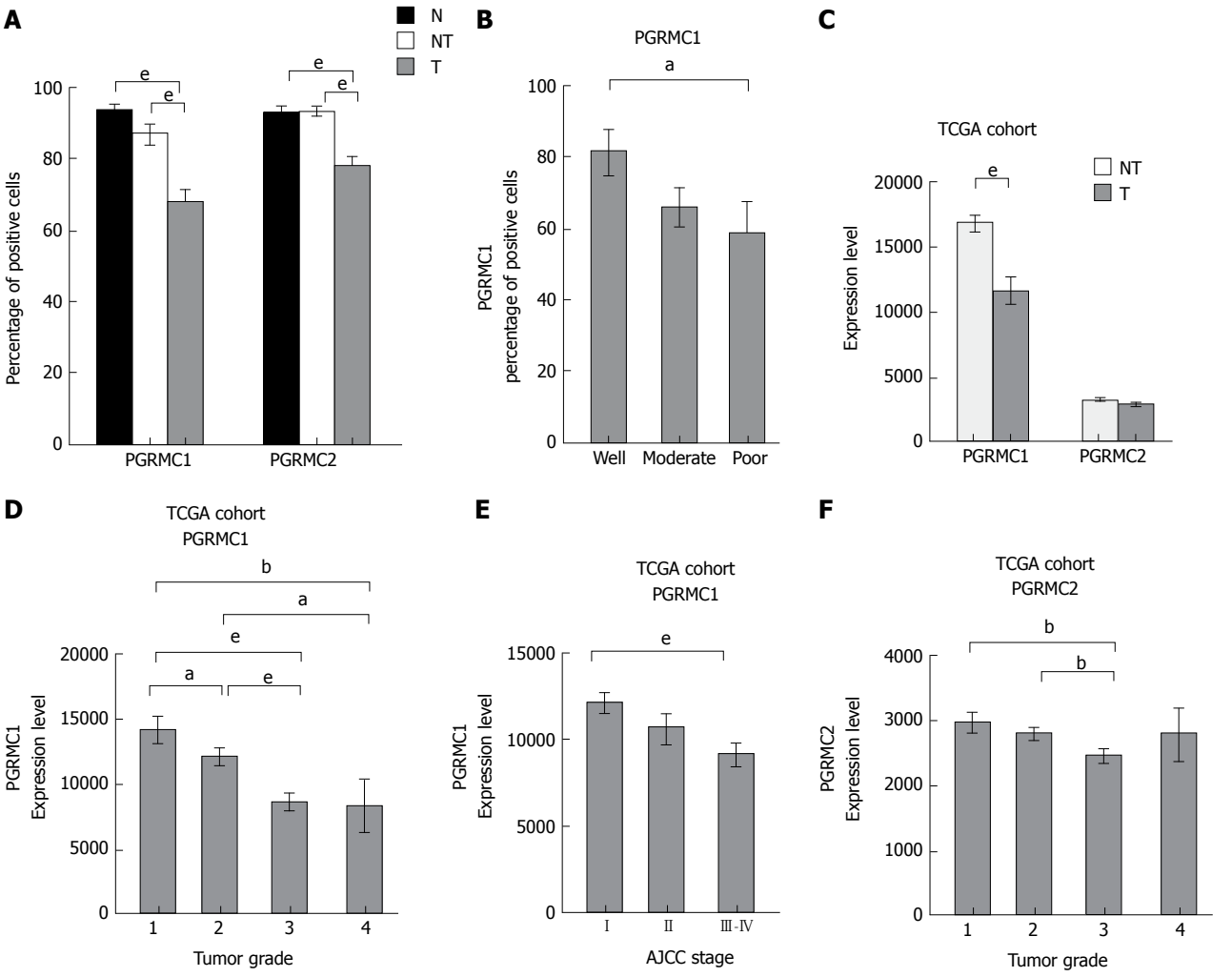

Figure 2 PGRMC1 and PGRMC2 expression levels, expressed as positive immunohistochemical staining percentages in the clinical cohort (A and B) and as normalized mRNA expression in the TCGA cohort (C-F). A: A comparison of PGRMC1 and PGRMC2 staining in HCC (T), non-tumor liver (NT) and normal liver (N) tissue samples; B: A comparison of PGRMC1 staining in HCC samples with different degrees of tumor differentiation; C: A comparison of PGRMC1 and PGRMC2 mRNA expression levels in HCC (T) and non-tumor liver (NT) samples; D: A comparison of PGRMC1 mRNA expression levels in HCC samples with different tumor grades; E: A comparison of PGRMC1 mRNA expression levels in HCC samples with different tumor stages; F: A comparison of PGRMC2 mRNA expression levels in HCC samples with different tumor grades. [a]*P* < 0.05, [b]*P* < 0.01, [e]*P* < 0.001.

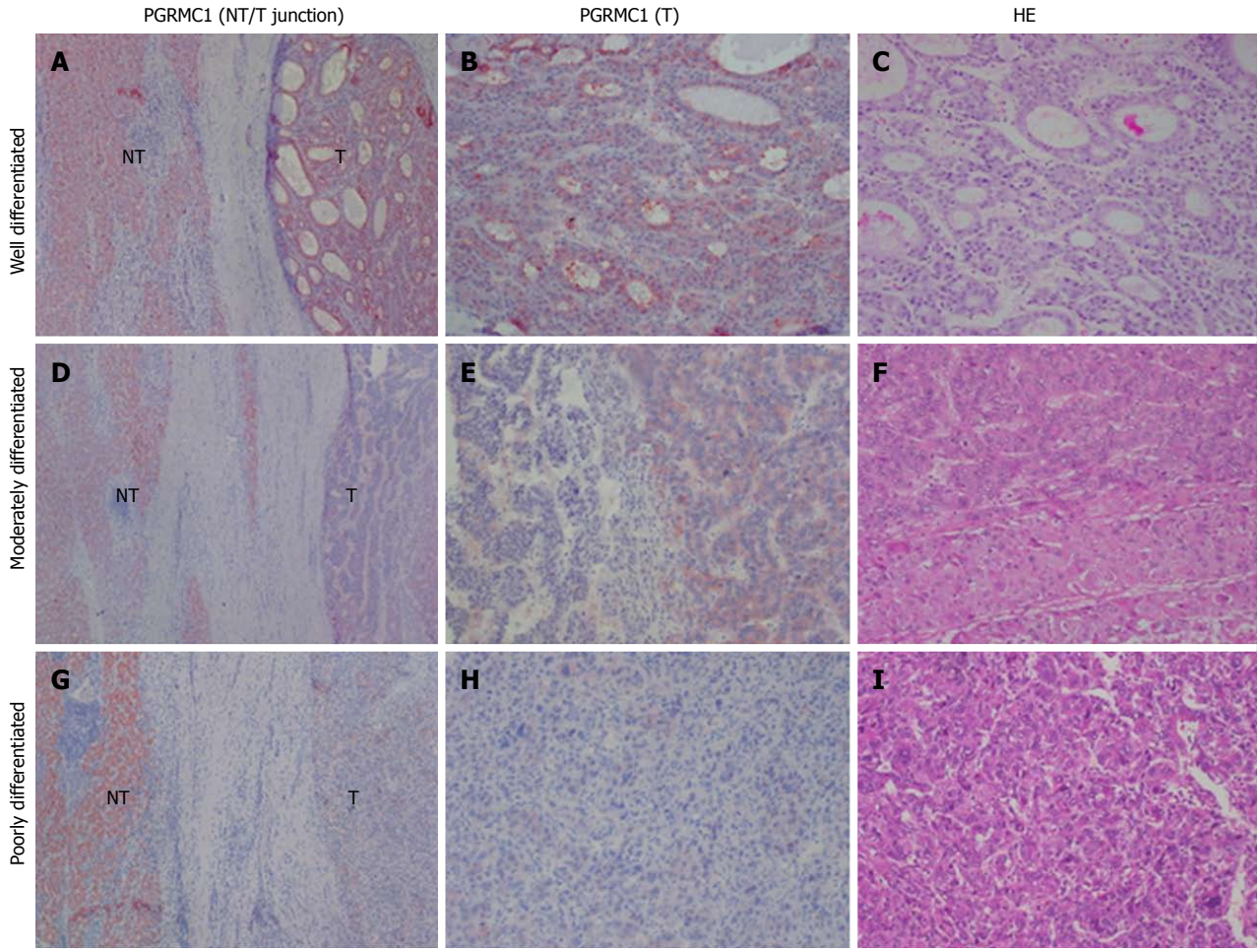

Figure 3 Representative images of PGRMC1 immunohistochemical staining in hepatocellular carcinoma. A-C: Well-differentiated HCC; D-F: Moderately differentiated HCC; G-I: Poorly differentiated HCC. Note that higher PGRMC1 expression was observed in non-tumor liver tissue samples (NT) as compared to HCC tissue samples (T) (A, D and G: 40 ×; B, C, E, F, H, and I: 100 ×).

mo). Sixty-seven patients (75.3%) developed local recurrence at a mean of 21.8 mo after surgery (range, 0.2-115.1 mo). A total of 45 patients (50.1%) died of HCC after having survived for a mean of 35.4 mo after surgery (range, 1.3-123.4 mo). The profiles of the 373 patients in the TCGA cohort are summarized in Supplementary Table 3.

The association of PGRMC1 and PGRMC2 expression with clinicopathological indicators

Few HCC cases expressed ER or PR (5.6% and 4.5%, respectively) (Supplementary Figure 2A-C). The mean cell percentage of ER expression was lower in the HCC tissue than in the non-tumor tissue (mean: 0.7% *vs* 12.4%, $P < 0.001$) (Supplementary Figure 2D). The mean cell percentage of PR expression was very low in the HCC tissue and non-tumor tissue (mean: 0.12% *vs* 0.01%, $P = 0.172$) (Supplementary Figure 2E). Positive IHC staining for PGRMC1 and PGRMC2 was observed in 80 (89.9%) and 89 (100%) cases of HCC, respectively. PGRMC1 (mean: 67.9% *vs* 86.9%, $P < 0.001$) and PGRMC2 (mean: 77.3% *vs* 92.6%, $P < 0.001$) were expressed at lower percentages in tumor cells than in non-tumor cells (Figure 2A, and 3, and Supplementary Figure 3). IHC expression of PGRMC1 and PGRMC2 in the normal liver tissue was not significantly different from that in the non-tumor liver samples, a result consistent with the Western blot experiment (Figure 2A and Supplementary Figure 1B and 1C). The PGRMC1 and PGRMC2 expression levels were compared among the normal livers of healthy persons, non-cirrhotic livers, and cirrhotic livers of HCC patients (Supplementary Figure 4A and B). There were no significant differences between the liver samples of healthy persons and those of HCC patients. In both non-cirrhotic patients and cirrhotic patients, the PGRMC1 and PGRMC2 expression levels were downregulated in the HCC tissue compared to non-tumor liver tissue (Supplementary Figure 4C-F). In the TCGA cohort, the HCC tissue samples exhibited lower *PGRMC1* mRNA expression levels than in the non-tumor tissue samples ($P < 0.001$), while *PGRMC2* levels between the HCC and non-tumor livers were not significantly different (Figure 2C).

Lower PGRMC1 expression in HCC was associated with poor HCC differentiation ($P = 0.045$) (Figure 2B

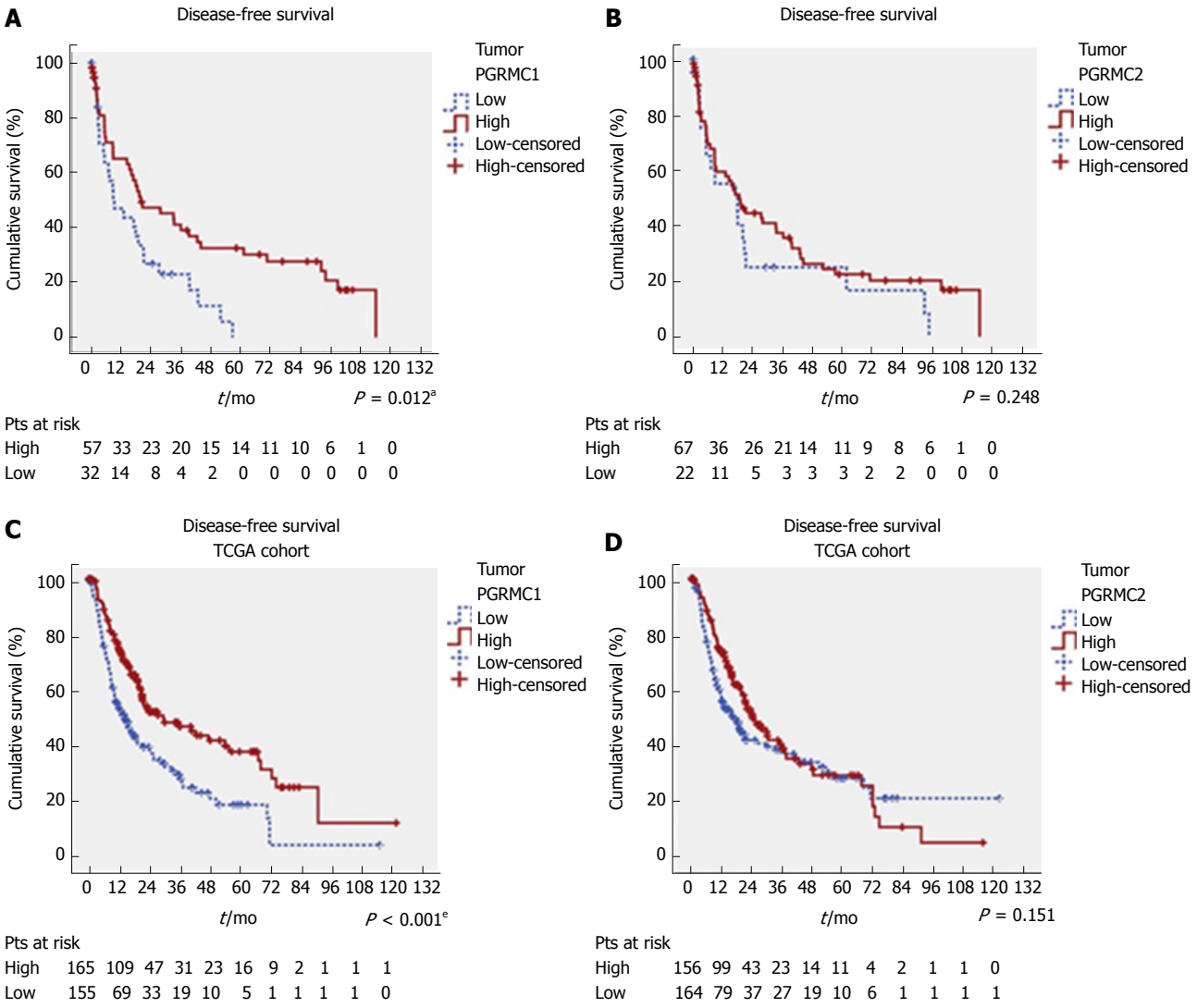

Figure 4 Kaplan-Meier analysis of the relationships of PGRMC1 and PGRMC2 expression with disease-free survival (DFS) in the clinical cohort (A-B) and TCGA cohort (C-D). [a]*P* < 0.05, [e]*P* < 0.001.

and Figure 3), younger age (*P* = 0.016), higher serum alpha-fetoprotein (AFP) levels (*P*=0.004), and liver capsule penetration (*P* = 0.038) (Supplementary Table 4). Lower PGRMC2 expression in HCC was significantly associated with tumor capsular invasion (*P* = 0.048), liver capsule penetration (*P* = 0.035), and bile duct invasion (*P* = 0.032) (Supplementary Table 4). In the TCGA cohort, lower *PGRMC1* expression in HCC was associated with higher tumor grade (*P* < 0.001) (Figure 2D), younger age (*P* = 0.014), female gender (*P* = 0.015), higher serum AFP expression (*P* < 0.001), vascular invasion (*P* = 0.007), and higher AJCC stage (Figure 2E) (*P* = 0.002) (Supplementary Table 5). Lower *PGRMC2* expression in HCC was significantly associated with higher tumor grade (*P* = 0.022) (Figure 2F) and younger age (*P* = 0.006) (Supplementary Table 5). Female patients exhibited higher baseline non-tumor liver tissue *PGRMC1* expression in the TCGA cohort (*P* < 0.001) (Supplementary Figure 5A-D). Using corresponding non-tumor liver tissue samples as a reference, it was determined that female HCC patients in the TCGA cohort exhibited greater *PGRMC1* down-regulation than male patients (Supplementary Figure 5E-H).

Prognostic significance of PGRMC1 and PGRMC2 in HCC

Low IHC PGRMC1 expression in HCC was significantly associated with worse DFS (*P* = 0.012) (Figure 4A), but was not significantly associated with OS (*P* = 0.395) (Supplementary Figure 6A). In contrast, PGRMC2 expression was not correlated with survival status (Figure 4B and Supplementary Figure 6B). The univariate analysis showed that the Child-Pugh scores (*P* = 0.003), satellite lesions (*P* = 0.003), tumor size (*P* < 0.001), vascular invasion (*P* < 0.001), liver capsule perforation (*P* = 0.047), insufficient surgical margins (*P* < 0.001), AJCC stage (*P* < 0.001), and low PGRMC1 expression (*P* = 0.013) were significant predictors of worse DFS (Table 1). The multivariate analysis showed that the Child-Pugh scores (*P* = 0.024, HR = 2.005, CI: 1.097-3.665), surgical margins (*P* < 0.001, HR =

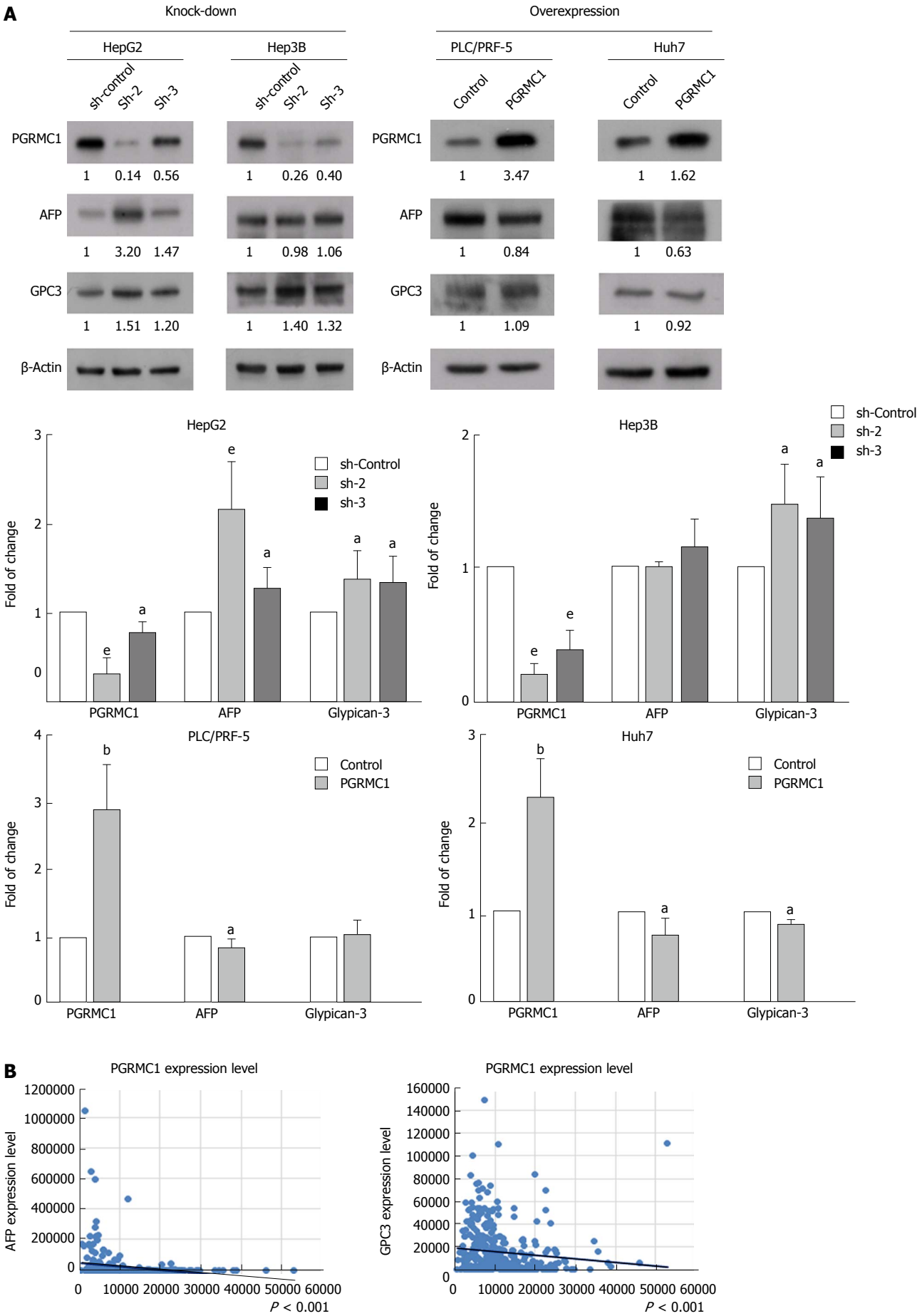
A
Knock-down
Overexpression
HepG2
Hep3B
PLC/PRF-5
Huh7
sh-control
Sh-2
Sh-3
Control
PGRMC1
PGRMC1
AFP
GPC3
β-Actin
1 0.14 0.56
1 0.26 0.40
1 3.47
1 1.62
1 3.20 1.47
1 0.98 1.06
1 0.84
1 0.63
1 1.51 1.20
1 1.40 1.32
1 1.09
1 0.92
HepG2
Hep3B
PLC/PRF-5
Huh7
sh-Control
sh-2
sh-3
Control
PGRMC1
Fold of change
PGRMC1
AFP
Glypican-3
B
PGRMC1 expression level
AFP expression level
GPC3 expression level
0 10000 20000 30000 40000 50000 60000
P < 0.001

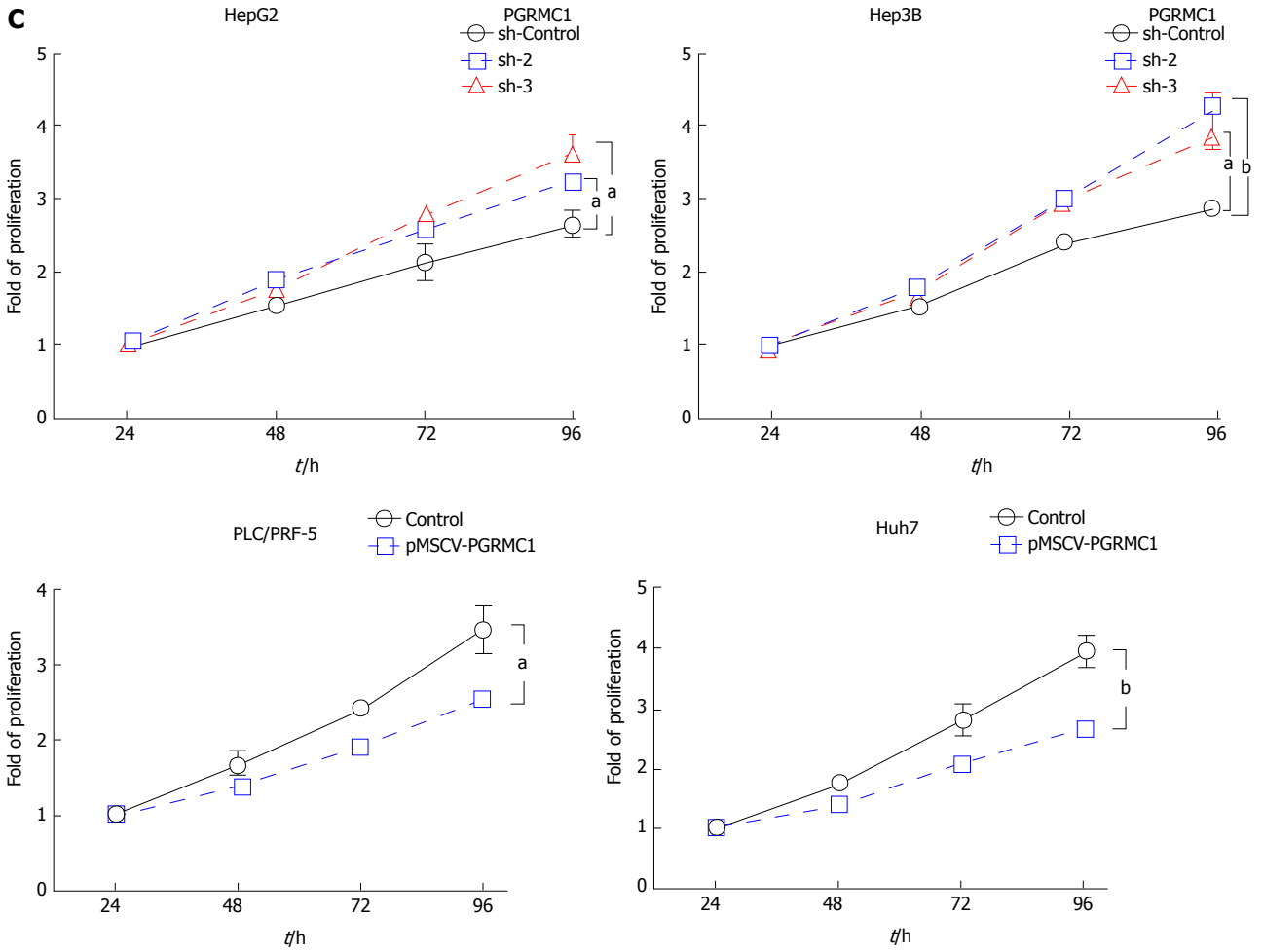

Figure 5 Alpha-fetoprotein and glypican-3 expression in PGRMC1-knockdown HepG2 and Hep3B cells and PGRMC1-overxpressing PLC/PRF/5 and Huh7 cells (A). B: The correlation of PGRMC1 with AFP and GPC3 in HCC tissue samples in the TCGA cohort; C: Cell proliferation assay (XTT) of PGRMC1-knockdown HepG2 and Hep3B cells and PGRMC1-overxpressing PLC/PRF/5 and Huh7 cells. The experiment was performed in triplicate. $^{a}P < 0.05$, $^{b}P < 0.01$, $^{e}P < 0.001$. AFP: Alpha-fetoprotein; GPC3: Glypican-3.

4.720, CI: 2.458-9.063), AJCC stage ($P < 0.001$, HR = 3.262, CI: 1.895-5.617), and low PGRMC1 expression ($P = 0.002$, HR = 2.384, CI: 1.377-4.128) were independently associated with DFS (Table 1).

To validate our findings, we analyzed the TCGA cohort data. Patients with low *PGRMC1* expression consistently exhibited worse DFS ($P < 0.001$) and OS than those with high *PGRMC1* expression ($P = 0.013$), as determined by the Kaplan-Meier and log-rank test analyses (Figure 4C and Supplementary Figure 6C). *PGRMC2* expression was not correlated with survival status (Figure 4D and Supplementary Figure 6D). The univariate analysis showed that HCC risk factors ($P = 0.014$), vascular invasion ($P < 0.001$), AJCC stage ($P < 0.001$), and low *PGRMC1* expression ($P < 0.001$) were significant predictors of worse DFS (Table 2), and that AJCC stage ($P < 0.001$) and low *PGRMC1* expression ($P = 0.014$) were significant predictors of worse OS (Supplementary Table 6). The multivariate analysis showed that low *PGRMC1* expression was an independent predictor of both worse DFS ($P < 0.001$, HR = 2.857, CI: 1.781-4.584) and worse OS ($P = 0.020$, HR = 1.556, CI: 1.072-2.260) (Table 2 and Supplementary Table 6).

Effects of PGRMC1 on proliferation, differentiation, migration and invasion of HCC cells

As PGRMC1 was significantly associated with HCC prognosis, we examined its biological significance *in vitro*. HepG2 and Hep3B cells exhibited higher PGRMC1 expression than PLC/PRF/5 and Huh7 cells. Therefore, we knocked down PGRMC1 in HepG2 and Hep3B cells and overexpressed PGRMC1 in PLC/PRF/5 and Huh7 cells (Figure 5A). Both AFP and glypican-3 (GPC3) are well-known oncofetal proteins in malignant transformation and dedifferentiation of HCC. Higher expression of these markers has been associated with poor differentiation of HCC[18,19]. Knockdown of PGRMC1 resulted in increased expression of AFP and GPC3 in HepG2 cells, while GPC3 expression was increased in Hep3B cells (Figure 5A). In contrast, overexpression of PGRMC1 suppressed expression of AFP in PLC/PRF/5 cells and suppressed expression of AFP and GPC3 in Huh7 cells (Figure 5A). In addition, PGRMC1

expression was inversely correlated with AFP and GPC3 expression in the HCC tissue samples (Figure 5B) and serum AFP levels (Supplementary Tables 4 and 5). PGRMC1 knockdown resulted in significantly increased proliferation of HepG2 and Hep3B cells (Figure 5C). In contrast, PGRMC1 overexpression resulted in decreased proliferation of PLC/PRF/5 and Huh7 cells (Figure 5C). PGRMC1 did not have significant effects on cell migration and invasion (Supplementary Figure 7).

As PGRMC1 was downregulated in HCC and it has been suggested that it mediates the anti-proliferative effects of progesterone[12,13], we assessed if overexpression of PGRMC1 in HCC cells could increase the anti-proliferative effect under progesterone treatment. PGRMC1 overexpression resulted in a significant decrease in the proliferation of PLC/PRF-5 cells and Huh7 cells in response to progesterone treatment (10^{-6} mol/L) (Supplementary Figure 8A and B). Expression of PR was not increased in these cells (Supplementary Figure 8C). On this basis, it is suggested that a more plausible explanation for the significant progesterone treatment effect on PGRMC1-overexpressing PLC/PRF-5 and Huh7 cells may be the overexpression of PGRMC1 *per se* rather than upregulated PR in these cells.

DISCUSSION

In this study, few HCC cases expressed ER and PR (5.6% and 4.5%, respectively), implying that an alternative hormone-related event may be involved in this sexually dimorphic malignancy. Both PGRMC1 and PGRMC2 were expressed in normal liver and non-tumor liver, but were down-regulated in HCC. In addition, the level of progesterone was lower in the HCC as compared to the non-tumor liver, suggesting that progesterone-related signaling is down-regulated in the pathogenesis of HCC. As down-regulated PGRMC1 and PGRMC2 were correlated with poorer differentiation and higher tumor grading, PGRMC down-regulation may play an important role in the progression of hepatocarcinogenesis. PGRMC1 differs from PGRMC2 in the transmembrane domain, N-terminals and SH3 target sequence, resulting in different interaction partners in terms of connecting with the cellular membrane, organelles and cell signaling molecules[8]. PGRMC1 has been proposed as a sigma-2 receptor with capability to inhibit tumor growth[20-22]. In our study, PGRMC1 was inversely associated with AFP and AJCC stage compared with PGRMC2. In multivariate analysis, PGRMC1 was an independent parameter in predicting better patient survival in two different cohorts. Therefore, only PGRMC1 was proved to be a prognostic biomarker in HCC. All of our patients had HBV and/or HCV infections, while more than half of the patients in the TCGA cohort had alcoholic and/or non-alcoholic fatty liver disease, suggesting that the findings of this investigation are universal. Together, PGRMCs, especially PGRMC1, may play a protective role in liver tumorigenesis.

Experiments *in vitro* demonstrated that PGRMC1 knockdown results in a poorly differentiated phenotype of HCC cells and increased proliferation. PGRMC1 contains two SH2 target sequences, an SH3 target sequence, a tyrosine kinase target site, two acidophilic kinase target sites, and ERK1 and PDK1 consensus binding sites[8]. A prior report showed that PGRMC1 can interact with beta-tubulin and inhibit mitosis by increasing mitotic spindle stability[13]. PGRMC1 protein has also been proposed as a sigma-2 receptor binding site[20], and activation of the sigma-2 receptor can inhibit tumor growth[21,22]. Thus, PGRMC1 is speculated to inhibit HCC progression through activation of hormone-independent signaling events.

PGRMC1 contains a motif common to heme-binding proteins, suggesting a role in oxidative metabolism[23]. Free heme, *i.e.,* heme not appropriately bound by hemoproteins or heme-binding proteins, is a powerful pro-oxidant agent and therefore potentially toxic[24]. Heme-binding proteins are required to maintain cellular stasis and to detoxify cells. Excessive heme iron has been reported to increase the risk of several types of cancer, such as colon cancer[25], gastric cancer[26], esophageal cancer[27], and HCC[28]. As a heme-binding protein, PGRMC1 has been reported to interact with P450 proteins and protect cells from DNA damage[29-31]. Therefore, PGRMC1 may protect hepatocytes from oxidative stress and suppress carcinogenesis by appropriate heme delivery or heme containment.

Most prior PGRMC1 studies have been focused on the female genital organs or female-related cancers. PGRMCs are involved in regulating the menstrual cycle and ovarian granulosa cell function by acting as progesterone receptors[9,32]. Endometrial expression of PGRMC1 in menstrual cycling is most abundant during the proliferative phase, while expression of PGRMC2 is highest during the secretory phase. These results highlight the differences between PGRMC1 and PGRMC2 in response to steroid hormones[32]. Previous reports showed that PGRMC1 mediates the anti-mitotic actions of progesterone in endometrial and ovarian cancer cells[12,13,33]. In immortalized granulosa cells, PGRMC1 suppresses cell cycle entry by binding to the GTPase activating protein binding protein 2[33]. PGRMC1 also suppresses the T-cell-specific transcription factor/lymphoid enhancer factor (Tcf/Lef) and its downstream c-myc activity in ovarian granulosa cells[9]. In this investigation, we provide evidence that overexpression of PGRMC1 may also activate the non-classical PR pathway in tumorigenesis. The potential of PGRMC1 being an alternative target for auxiliary anti-HCC treatment deserves further investigation.

Previous studies have shown that high levels of progesterone can be observed in patients with cirrhosis[34]. This is likely due to impairment of progesterone metabolism in the liver. It is controversial whether high levels of progesterone are associated with premalignant cirrhosis. Previous studies have shown that the occurrence of natural menopause at a younger

age or oophorectomy performed at age 50 or younger is associated with increased risk of HCC[4,35]. PR expression in HCC has been correlated with a better prognosis[36]. These findings suggest that progesterone may be protective against HCC. Furthermore, progesterone can serve as the precursor for the major steroid hormones (androgens, estrogens, and corticosteroids). The oncogenic effects of androgen and the protective effects of estrogen and progesterone in liver may also depend on the hormonal receptors expressed on hepatocytes or cancer cells[4].

Sex hormones can exert different tumorigenic properties depending on the tissue type. For example, contrary to their hypothetical protective role in liver cancer development, chronic exposure to estrogens favors carcinogenesis in the breast and uterus. Expression of PGRMC1 was shown to be upregulated in breast cancer and ovarian cancer and was found to be associated with advanced stage or poor prognosis[10,11]. Its expression was more often detected in ER-negative breast cancers[10], and it may act *via* cross-talk with nuclear or extranuclear ER receptors[37]. PGRMC1 has been localized in hypoxic areas of breast cancer[10] and demonstrated to activate the expression of vascular endothelial growth factor in glial cells[38]. A D120G mutant of PGRMC1 increased the susceptibility of breast cancer cells to doxorubicin and camptothecin treatment[39]. However, PGRMC1 has been reported to be associated with EGFR in lung cancer cells and to enhance susceptibility to the EGFR inhibitor, erlotinib[40]. Overexpression of PGRMC1 in the MCF-7 breast cancer cell line sensitizes cancer cells to hydrogen peroxide treatment with corresponding hyperphosphorylation of Akt and IkB proteins[29]. These findings suggest that PGRMC1 plays a plethora of biological roles in human cancers. In contrast to breast and ovarian cancer, PGRMC1 is downregulated in HCC. PGRMC1 is located on chromosome Xq22-q24. A prior genomic study found a frequent loss of heterozygosity of Xq (43%) in HCC[41] with a progressive increase in fractional allelic imbalance from cirrhotic nodules at progressive stages (11%-57%) to HCC, suggesting its involvement in hepatocarcinogenesis. Furthermore, let-7/miR-98 was reported to repress PGRMC1[42,43], and gradually elevated miR-98 has been associated with the progression of liver cancer[44]. Therefore, microRNA could be an alternative regulatory mechanism in suppression of PGRMC1 expression. Further study is needed to clarify the mechanisms of PGRMC downregulation in HCC.

Overall, men are two to four times more likely to develop HCC than women[1]. Estrogen has been shown to inhibit IL-6 production[45]. Foxa1/a2 may interact with either the ER or AR to activate different hepatocyte target genes[46]. HBx can increase AR N-terminal transactivation domain activation through c-Src kinase and enhance AR dimerization by inhibiting GSK-3 activity[47]. This information may explain, in part, the molecular mechanisms underlying gender differences in HCC development. Female patients in the current study exhibited higher baseline non-tumor liver tissue *PGRMC1* mRNA expression and greater HCC *PGRMC1* down-regulation than male patients, suggesting that greater PGRMC1 down-regulation is needed to induce HCC transformation in female patients, thus causing the gender disparities associated with HCC development.

In conclusion, expression of PGRMC1 and PGRMC2 was suppressed in HCC, and PGRMC1 down-regulation promoted HCC progression. PGRMC1 may play a protective role in hepatocarcinogenesis by inhibiting cell proliferation and tumor dedifferentiation. Further study is necessary to evaluate the potential of targeting PGRMC1 in HCC treatment.

ARTICLE HIGHLIGHTS

Research background

Hepatocellular carcinoma (HCC) is a sexually dimorphic disease with a significantly higher incidence in males than females. The androgen receptor appears to function as a tumor promoter, whereas the estrogen receptor appears to act as a tumor suppressor for HCC. Whether additional hormone-related events are implicated in the pathogenesis of HCC remain to be clarified.

Research motivation

The membrane-associated progesterone receptors, *i.e.* PGRMC1 and PGRMC2, have been investigated in female cancers of the breast, endometrium and ovary. PGRMC1 is thought to coordinate non-classical progesterone signaling. PGRMC1 was demonstrated to mediate the anti-mitotic actions of progesterone in endometrial and ovarian cancer cells. This study was performed to examine the significance of PGRMC1 and/or PGRMC2 in the progression of HCC.

Research objectives

The aim of this study was to clarify the potential significance of PGRMCs as prognostic biomarkers in HCC and their biological effects *in vitro*.

Research methods

Immunohistochemical staining of the estrogen receptor (ER), progesterone receptor (PR), PGRMC1 and PGRMC2 was performed in a clinical cohort consisting of 89 cases of paired HCC and non-tumor liver. The clinical implications of PGRMCs in HCC (n = 373) from The Cancer Genome Atlas (TCGA) database were *also analyzed*. The expression of PGRMC1 and PGRMC2 was correlated with clinicopathological indicators and the clinical outcome of HCC patients. The impact of PGRMC1 on the biological effects of HCC was investigated by knocking down its expression in HepG2 and Hep3B cell lines, and overexpressing in PLC/PRF-5 and Huh7 cell lines. The analyzed cellular functions included proliferation, differentiation, migration, and invasion.

Research results

Primary HCC demonstrated a high incidence of PGRMC1 (89.9%) and PGRMC2 (100%) expression, respectively. Down-regulated PGRMC1 was significantly associated with higher serum alpha-fetoprotein levels, poor tumor differentiation, liver capsule penetration, and the risk of recurrence. Low PGRMC1 expression was an independent indicator of worse disease-free survival. Knock-down of PGRMC1 promoted a poorly differentiated phenotype and proliferation of HCC *in vitro*, while over-expression of PGRMC1 suppressed cell proliferation.

Research conclusions

PGRMC1 is a prognostic marker for HCC. PGRMC1 may play a protective role in hepatocarcinogenesis by inhibiting cell proliferation and tumor

dedifferentiation.

Research perspectives

PGRMC1 could be a novel therapeutic target for human HCC, especially as a biotarget of chemoprevention.

ACKNOWLEDGEMENTS

We are grateful for the support from the Human Biobank, Research Center of Clinical Medicine and the Cancer Data Bank of National Cheng Kung University Hospital.

REFERENCES

1 **El-Serag HB**, Rudolph KL. Hepatocellular carcinoma: epidemiology and molecular carcinogenesis. *Gastroenterology* 2007; **132**: 2557-2576 [PMID: 17570226 DOI: 10.1053/j.gastro.2007.04.061]
2 **Ma WL**, Hsu CL, Yeh CC, Wu MH, Huang CK, Jeng LB, Hung YC, Lin TY, Yeh S, Chang C. Hepatic androgen receptor suppresses hepatocellular carcinoma metastasis through modulation of cell migration and anoikis. *Hepatology* 2012; **56**: 176-185 [PMID: 22318717 DOI: 10.1002/hep.25644]
3 **Keng VW**, Largaespada DA, Villanueva A. Why men are at higher risk for hepatocellular carcinoma? *J Hepatol* 2012; **57**: 453-454 [PMID: 22425699 DOI: 10.1016/j.jhep.2012.03.004]
4 **Yeh YT**, Chang CW, Wei RJ, Wang SN. Progesterone and related compounds in hepatocellular carcinoma: basic and clinical aspects. *Biomed Res Int* 2013; **2013**: 290575 [PMID: 23484104 DOI: 10.1155/2013/290575]
5 **Chang WT**, Hsieh BS, Cheng HL, Lee KT, Chang KL. Progesterone augments epirubicin-induced apoptosis in HA22T/VGH cells by increasing oxidative stress and upregulating Fas/FasL. *J Surg Res* 2014; **188**: 432-441 [PMID: 24594218 DOI: 10.1016/j.jss.2014.01.063]
6 **Chang WT**, Cheng HL, Hsieh BS, Chiu CC, Lee KT, Chang KL. Progesterone increases apoptosis and inversely decreases autophagy in human hepatoma HA22T/VGH cells treated with epirubicin. *ScientificWorldJournal* 2014; **2014**: 567148 [PMID: 24971383 DOI: 10.1155/2014/567148]
7 **Villa E**, Ferretti I, Grottola A, Buttafoco P, Buono MG, Giannini F, Manno M, Bertani H, Dugani A, Manenti F. Hormonal therapy with megestrol in inoperable hepatocellular carcinoma characterized by variant oestrogen receptors. *Br J Cancer* 2001; **84**: 881-885 [PMID: 11286465 DOI: 10.1054/bjoc.2000.1534]
8 **Cahill MA**. Progesterone receptor membrane component 1: an integrative review. *J Steroid Biochem Mol Biol* 2007; **105**: 16-36 [PMID: 17583495 DOI: 10.1016/j.jsbmb.2007.02.002]
9 **Peluso JJ**, Pru JK. Non-canonical progesterone signaling in granulosa cell function. *Reproduction* 2014; **147**: R169-R178 [PMID: 24516175 DOI: 10.1530/REP-13-0582]
10 **Neubauer H**, Clare SE, Wozny W, Schwall GP, Poznanovic S, Stegmann W, Vogel U, Sotlar K, Wallwiener D, Kurek R, Fehm T, Cahill MA. Breast cancer proteomics reveals correlation between estrogen receptor status and differential phosphorylation of PGRMC1. *Breast Cancer Res* 2008; **10**: R85 [PMID: 18922159 DOI: 10.1186/bcr2155]
11 **Peluso JJ**, Liu X, Saunders MM, Claffey KP, Phoenix K. Regulation of ovarian cancer cell viability and sensitivity to cisplatin by progesterone receptor membrane component-1. *J Clin Endocrinol Metab* 2008; **93**: 1592-1599 [PMID: 18319313 DOI: 10.1210/jc.2007-2771]
12 **Friel AM**, Zhang L, Pru CA, Clark NC, McCallum ML, Blok LJ, Shioda T, Peluso JJ, Rueda BR, Pru JK. Progesterone receptor membrane component 1 deficiency attenuates growth while promoting chemosensitivity of human endometrial xenograft tumors. *Cancer Lett* 2015; **356**: 434-442 [PMID: 25304370 DOI: 10.1016/j.canlet.2014.09.036]
13 **Lodde V**, Peluso JJ. A novel role for progesterone and progesterone receptor membrane component 1 in regulating spindle microtubule stability during rat and human ovarian cell mitosis. *Biol Reprod* 2011; **84**: 715-722 [PMID: 21148105 DOI: 10.1095/biolreprod.110.088385]
14 **Hirai Y**, Utsugi K, Takeshima N, Kawamata Y, Furuta R, Kitagawa T, Kawaguchi T, Hasumi K, Noda T. Putative gene loci associated with carcinogenesis and metastasis of endocervical adenocarcinomas of uterus determined by conventional and array-based CGH. *Am J Obstet Gynecol* 2004; **191**: 1173-1182 [PMID: 15507938 DOI: 10.1016/j.ajog.2004.04.015]
15 **Albrecht C**, Huck V, Wehling M, Wendler A. In vitro inhibition of SKOV-3 cell migration as a distinctive feature of progesterone receptor membrane component type 2 versus type 1. *Steroids* 2012; **77**: 1543-1550 [PMID: 23064006 DOI: 10.1016/j.steroids.2012.09.006]
16 **Lee NP**, Chen L, Lin MC, Tsang FH, Yeung C, Poon RT, Peng J, Leng X, Beretta L, Sun S, Day PJ, Luk JM. Proteomic expression signature distinguishes cancerous and nonmalignant tissues in hepatocellular carcinoma. *J Proteome Res* 2009; **8**: 1293-1303 [PMID: 19161326 DOI: 10.1021/pr800637z]
17 **Bosman FT**, Carneiro F, Hruban RH, Theise ND. WHO classification of Tumours of the Digestive System. Lyon: International Agency for Research on Cancer, 2010
18 **Shafizadeh N**, Ferrell LD, Kakar S. Utility and limitations of glypican-3 expression for the diagnosis of hepatocellular carcinoma at both ends of the differentiation spectrum. *Mod Pathol* 2008; **21**: 1011-1018 [PMID: 18536657 DOI: 10.1038/modpathol.2008.85]
19 **Liu C**, Xiao GQ, Yan LN, Li B, Jiang L, Wen TF, Wang WT, Xu MQ, Yang JY. Value of α-fetoprotein in association with clinicopathological features of hepatocellular carcinoma. *World J Gastroenterol* 2013; **19**: 1811-1819 [PMID: 23555170 DOI: 10.3748/wjg.v19.i11.1811]
20 **Xu J**, Zeng C, Chu W, Pan F, Rothfuss JM, Zhang F, Tu Z, Zhou D, Zeng D, Vangveravong S, Johnston F, Spitzer D, Chang KC, Hotchkiss RS, Hawkins WG, Wheeler KT, Mach RH. Identification of the PGRMC1 protein complex as the putative sigma-2 receptor binding site. *Nat Commun* 2011; **2**: 380 [PMID: 21730960 DOI: 10.1038/ncomms1386]
21 **Hornick JR**, Spitzer D, Goedegebuure P, Mach RH, Hawkins WG. Therapeutic targeting of pancreatic cancer utilizing sigma-2 ligands. *Surgery* 2012; **152**: S152-S156 [PMID: 22763259 DOI: 10.1016/j.surg.2012.05.014]
22 **Huang YS**, Lu HL, Zhang LJ, Wu Z. Sigma-2 receptor ligands and their perspectives in cancer diagnosis and therapy. *Med Res Rev* 2014; **34**: 532-566 [PMID: 23922215 DOI: 10.1002/med.21297]
23 **Mifsud W**, Bateman A. Membrane-bound progesterone receptors contain a cytochrome b5-like ligand-binding domain. *Genome Biol* 2002; **3**: RESEARCH0068 [PMID: 12537557]
24 **Correia MA**, Sinclair PR, De Matteis F. Cytochrome P450 regulation: the interplay between its heme and apoprotein moieties in synthesis, assembly, repair, and disposal. *Drug Metab Rev* 2011; **43**: 1-26 [PMID: 20860521 DOI: 10.3109/03602532.2010.515222]
25 **Bastide NM**, Pierre FH, Corpet DE. Heme iron from meat and risk of colorectal cancer: a meta-analysis and a review of the mechanisms involved. *Cancer Prev Res* (Phila) 2011; **4**: 177-184 [PMID: 21209396 DOI: 10.1158/1940-6207.CAPR-10-0113]
26 **Jakszyn P**, Agudo A, Lujan-Barroso L, Bueno-de-Mesquita HB, Jenab M, Navarro C, Palli D, Boeing H, Manjer J, Numans ME, Igali L, Boutron-Ruault MC, Clavel-Chapelon F, Morois S, Grioni S, Panico c, Tumino R, Sacerdote C, Quirós JR, Molina-Montes E, Huerta Castaño JM, Barricarte A, Amiano P, Khaw KT, Wareham N, Allen NE, Key TJ, Jeurnink SM, Peeters PH, Bamia C, Valanou E, Trichopoulou A, Kaaks R, Lukanova A, Bergmann MM, Lindkvist B, Stenling R, Johansson I, Dahm CC, Overvad K, Olsen A, Tjonneland A, Skeie G, Broderstad AR, Lund E, Michaud DS, Mouw T, Riboli E, González CA. Dietary intake of heme iron and risk of gastric cancer in the European prospective investigation into cancer and nutrition study. *Int J Cancer* 2012; **130**: 2654-2663

[PMID: 21717452 DOI: 10.1002/ijc.26263]
27 **Ward MH**, Cross AJ, Abnet CC, Sinha R, Markin RS, Weisenburger DD. Heme iron from meat and risk of adenocarcinoma of the esophagus and stomach. *Eur J Cancer Prev* 2012; **21**: 134-138 [PMID: 22044848 DOI: 10.1097/CEJ.0b013e32834c9b6c]
28 **Freedman ND**, Cross AJ, McGlynn KA, Abnet CC, Park Y, Hollenbeck AR, Schatzkin A, Everhart JE, Sinha R. Association of meat and fat intake with liver disease and hepatocellular carcinoma in the NIH-AARP cohort. *J Natl Cancer Inst* 2010; **102**: 1354-1365 [PMID: 20729477 DOI: 10.1093/jnci/djq301]
29 **Hand RA**, Craven RJ. Hpr6.6 protein mediates cell death from oxidative damage in MCF-7 human breast cancer cells. *J Cell Biochem* 2003; **90**: 534-547 [PMID: 14523988 DOI: 10.1002/jcb.10648]
30 **Hughes AL**, Powell DW, Bard M, Eckstein J, Barbuch R, Link AJ, Espenshade PJ. Dap1/PGRMC1 binds and regulates cytochrome P450 enzymes. *Cell Metab* 2007; **5**: 143-149 [PMID: 17276356 DOI: 10.1016/j.cmet.2006.12.009]
31 **Mallory JC**, Crudden G, Johnson BL, Mo C, Pierson CA, Bard M, Craven RJ. Dap1p, a heme-binding protein that regulates the cytochrome P450 protein Erg11p/Cyp51p in Saccharomyces cerevisiae. *Mol Cell Biol* 2005; **25**: 1669-1679 [PMID: 15713626 DOI: 10.1128/MCB.25.5.1669-1679.2005]
32 **Pru JK**, Clark NC. PGRMC1 and PGRMC2 in uterine physiology and disease. *Front Neurosci* 2013; **7**: 168 [PMID: 24065879 DOI: 10.3389/fnins.2013.00168]
33 **Peluso JJ**, Griffin D, Liu X, Horne M. Progesterone receptor membrane component-1 (PGRMC1) and PGRMC-2 interact to suppress entry into the cell cycle in spontaneously immortalized rat granulosa cells. *Biol Reprod* 2014; **91**: 104 [PMID: 25253729 DOI: 10.1095/biolreprod.114.122986]
34 **Farinati F**, De Maria N, Marafin C, Fagiuoli S, Della Libera G, Naccarato R. Hepatocellular carcinoma in alcoholic cirrhosis: is sex hormone imbalance a pathogenetic factor? *Eur J Gastroenterol Hepatol* 1995; **7**: 145-150 [PMID: 7712307]
35 **Yu MW**, Chang HC, Chang SC, Liaw YF, Lin SM, Liu CJ, Lee SD, Lin CL, Chen PJ, Lin SC, Chen CJ. Role of reproductive factors in hepatocellular carcinoma: Impact on hepatitis B- and C-related risk. *Hepatology* 2003; **38**: 1393-1400 [PMID: 14647050 DOI: 10.1016/j.hep.2003.09.041]
36 **Vizoso FJ**, Rodriguez M, Altadill A, González-Diéguez ML, Linares A, González LO, Junquera S, Fresno-Forcelledo F, Corte MD, Rodrigo L. Liver expression of steroid hormones and Apolipoprotein D receptors in hepatocellular carcinoma. *World J Gastroenterol* 2007; **13**: 3221-3227 [PMID: 17589901 DOI: 10.3748/wjg.v13.i23.3221]
37 **Schneck H**, Ruan X, Seeger H, Cahill MA, Fehm T, Mueck AO, Neubauer H. Membrane-receptor initiated proliferative effects of dienogest in human breast cancer cells. *Gynecol Endocrinol* 2013; **29**: 160-163 [PMID: 23116217 DOI: 10.3109/09513590.2012.730572]
38 **Swiatek-De Lange M**, Stampfl A, Hauck SM, Zischka H, Gloeckner CJ, Deeg CA, Ueffing M. Membrane-initiated effects of progesterone on calcium dependent signaling and activation of VEGF gene expression in retinal glial cells. *Glia* 2007; **55**: 1061-1073 [PMID: 17551930 DOI: 10.1002/glia.20523]
39 **Crudden G**, Chitti RE, Craven RJ. Hpr6 (heme-1 domain protein) regulates the susceptibility of cancer cells to chemotherapeutic drugs. *J Pharmacol Exp Ther* 2006; **316**: 448-455 [PMID: 16234411 DOI: 10.1124/jpet.105.094631]
40 **Ahmed IS**, Rohe HJ, Twist KE, Craven RJ. Pgrmc1 (progesterone receptor membrane component 1) associates with epidermal growth factor receptor and regulates erlotinib sensitivity. *J Biol Chem* 2010; **285**: 24775-24782 [PMID: 20538600 DOI: 10.1074/jbc.M110.134585]
41 **Yeh SH**, Chen PJ, Shau WY, Chen YW, Lee PH, Chen JT, Chen DS. Chromosomal allelic imbalance evolving from liver cirrhosis to hepatocellular carcinoma. *Gastroenterology* 2001; **121**: 699-709 [PMID: 11522754 DOI: 10.1053/gast.2001.27211]
42 **Panda H**, Chuang TD, Luo X, Chegini N. Endometrial miR-181a and miR-98 expression is altered during transition from normal into cancerous state and target PGR, PGRMC1, CYP19A1, DDX3X, and TIMP3. *J Clin Endocrinol Metab* 2012; **97**: E1316-E1326 [PMID: 22492871 DOI: 10.1210/jc.2012-1018]
43 **Wendler A**, Keller D, Albrecht C, Peluso JJ, Wehling M. Involvement of let-7/miR-98 microRNAs in the regulation of progesterone receptor membrane component 1 expression in ovarian cancer cells. *Oncol Rep* 2011; **25**: 273-279 [PMID: 21109987]
44 **Sukata T**, Sumida K, Kushida M, Ogata K, Miyata K, Yabushita S, Uwagawa S. Circulating microRNAs, possible indicators of progress of rat hepatocarcinogenesis from early stages. *Toxicol Lett* 2011; **200**: 46-52 [PMID: 21035526 DOI: 10.1016/j.toxlet.2010.10.013]
45 **Naugler WE**, Sakurai T, Kim S, Maeda S, Kim K, Elsharkawy AM, Karin M. Gender disparity in liver cancer due to sex differences in MyD88-dependent IL-6 production. *Science* 2007; **317**: 121-124 [PMID: 17615358 DOI: 10.1126/science.1140485]
46 **Li Z**, Tuteja G, Schug J, Kaestner KH. Foxa1 and Foxa2 are essential for sexual dimorphism in liver cancer. *Cell* 2012; **148**: 72-83 [PMID: 22265403 DOI: 10.1016/j.cell.2011.11.026]
47 **Yang WJ**, Chang CJ, Yeh SH, Lin WH, Wang SH, Tsai TF, Chen DS, Chen PJ. Hepatitis B virus X protein enhances the transcriptional activity of the androgen receptor through c-Src and glycogen synthase kinase-3beta kinase pathways. *Hepatology* 2009; **49**: 1515-1524 [PMID: 19205031 DOI: 10.1002/hep.22833]

P- Reviewer: Elalfy H, Guan YS, Hashimoto N **S- Editor**: Gong ZM
L- Editor: Webster JR **E- Editor**: Ma YJ

World Journal of Gastroenterology

Submit a Manuscript: http://www.f6publishing.com

World J Gastroenterol 2018 March 14; 24(10): 1167-1180

DOI: 10.3748/wjg.v24.i10.1167

ISSN 1007-9327 (print) ISSN 2219-2840 (online)

META-ANALYSIS

Colonic lesion characterization in inflammatory bowel disease: A systematic review and meta-analysis

Richard Lord, Nicholas E Burr, Noor Mohammed, Venkataraman Subramanian

Richard Lord, Nicholas E Burr, Noor Mohammed, Venkataraman Subramanian, Department of Gastroenterology, Leeds Teaching Hospitals NHS Trust, Leeds LS97TF, United Kingdom

Richard Lord, Nicholas E Burr, Venkataraman Subramanian, University of Leeds, Leeds Institute of Biomedical and Clinical Sciences, Leeds LS97TF, United Kingdom

ORCID number: Richard Lord (0000-0002-8356-7824); Nicholas E Burr (0000-0003-1988-2982); Noor Mohammed (0000-0003-0180-1080); Venkataraman Subramanian (0000-0003-3603-0861).

Author contributions: Subramanian V envisaged and designed the research; Subramanian V performed the statistical analysis; Lord R wrote the paper and did the information searching; Lord R and Burr NE performed the Selection of papers and data abstraction; Lord R and Mohammed N performed the study quality analysis; all authors have reviewed the manuscript.

Conflict-of-interest statement: The authors deny any conflict of interest.

PRISMA 2009 checklist statement: The authors have read the PRISMA 2009 Checklist, and the manuscript was prepared and revised according to the PRISMA 2009 Checklist.

Manuscript source: Invited manuscript

Correspondence to: Venkataraman Subramanian, CCST, MBBS, MD, MRCP, Assistant Professor, Department of gastroenterology, Leeds Teaching Hospitals NHS Trust, Beckett St, Leeds LS97TF, United Kingdom. v.subramanian@leeds.ac.uk

Telephone: +44-113-2068691
Fax: +44-113-2068688

Received: January 8, 2018
Peer-review started: January 9, 2018
First decision: February 5, 2018
Revised: February 18, 2018
Accepted: February 15, 2018
Article in press: February 15, 2018
Published online: March 14, 2018

Abstract

AIM

To perform a systematic review and meta-analysis for the diagnostic accuracy of *in vivo* lesion characterization in colonic inflammatory bowel disease (IBD), using optical imaging techniques, including virtual chromoendoscopy (VCE), dye-based chromoendoscopy (DBC), magnification endoscopy and confocal laser endomicroscopy (CLE).

METHODS

We searched Medline, Embase and the Cochrane library. We performed a bivariate meta-analysis to calculate the pooled estimate sensitivities, specificities, positive and negative likelihood ratios (+LHR, -LHR), diagnostic odds ratios (DOR), and area under the SROC curve (AUSROC) for each technology group. A subgroup analysis was performed to investigate differences in real-time non-magnified Kudo pit patterns (with VCE and DBC) and real-time CLE.

RESULTS

We included 22 studies [1491 patients; 4674 polyps, of which 539 (11.5%) were neoplastic]. Real-time CLE had a pooled sensitivity of 91% (95%CI: 66%-98%), specificity of 97% (95%CI: 94%-98%), and an AUSROC of 0.98 (95%CI: 0.97-0.99). Magnification endoscopy had a pooled sensitivity of 90% (95%CI: 77%-96%)

and specificity of 87% (95%CI: 81%-91%). VCE had a pooled sensitivity of 86% (95%CI: 62%-95%) and specificity of 87% (95%CI: 72%-95%). DBC had a pooled sensitivity of 67% (95%CI: 44%-84%) and specificity of 86% (95%CI: 72%-94%).

CONCLUSION
Real-time CLE is a highly accurate technology for differentiating neoplastic from non-neoplastic lesions in patients with colonic IBD. However, most CLE studies were performed by single expert users within tertiary centres, potentially confounding these results.

Key words: Inflammatory bowel disease dysplasia; Lesion characterization; Confocal laser endomicroscopy; Narrow band imaging; I-scan; Fujinon intelligence chromoendoscopy

Core tip: *In vivo* lesion characterization in colonic inflammatory bowel disease presents many challenges. Lesions tend to be morphologically different and potentially associated with surrounding/overlying inflammation, obscuring the pit pattern. The ability to accurately characterize lesions *in vivo* could reduce costs and complications by decreasing the need for polypectomies. Virtual chromoendoscopy (VCE) and dye-based chromoendoscopy currently cannot be recommended for lesion characterization. Confocal laser endomicroscopy is an accurate technology at differentiating neoplastic from non-neoplastic lesions but studies within this meta-analysis involved single expert center with single advanced endoscopic operators, reducing its generalizability. Larger studies are required specifically looking at lesion characterization, especially with rapid technological advancements in VCE (Narrow band imaging, i-scan, Fujinon intelligence chromoendoscopy).

Lord R, Burr NE, Mohammed N, Subramanian V. Colonic lesion characterization in inflammatory bowel disease: A systematic review and meta-analysis. *World J Gastroenterol* 2018; 24(10): 1167-1180 Available from: URL: http://www.wjgnet.com/1007-9327/full/v24/i10/1167.htm DOI: http://dx.doi.org/10.3748/wjg.v24.i10.1167

INTRODUCTION

The association between colonic inflammatory bowel disease (IBD) and colorectal cancer (CRC) has been acknowledged for almost 100 years[1]. Several meta-analyses have attempted to estimate this increased risk with varying results, reflecting the heterogeneity of studies included[2-4]. Nevertheless all agree that disease duration, disease activity and extent of IBD increase the risk for developing CRC. In response, surveillance colonoscopy is recommended by most gastroenterology societies worldwide. Yet, there is still disparity amongst the societies with regards timing of surveillance intervals.

Most CRC within IBD is thought to develop along the inflammation-dysplasia-cancer pathway; however in rare cases it may not always evolve in this stepwise fashion, and its rate of transition could potentially be accelerated in some lesions[5].

With advancements in endoscopic technology and recommendations for surveillance during inactive disease, most dysplasia is now believed to be visible[6]. Gastroenterological societies currently advocate targeted biopsies for detection of dysplasia, owing to the low yield from random biopsies, with evidence supporting dye-based chromoendoscopy (DBC) for enhancing lesion detection[6-8]. An international consensus group in 2015 recommended that dysplastic polypoid or non-polypoid lesions within a colitic segment should be treated as significant and that well circumscribed lesions with no endoscopic features of submucosal invasion can now be resected[6]. The risk for developing CRC following complete endoscopic resection is now thought to be lower than previous studies suggested[9].

Novel technologies, including narrow band imaging (NBI), fujinon intelligence chromoendoscopy (FICE), i-scan, magnification endoscopy and confocal laser endomicroscopy (CLE), have been studied to obtain an *in-vivo* optical diagnosis of colorectal lesions. DBC using contrast agents, such as indigo-carmine, or absorptive agents, like methylene blue, are customarily applied *via* a spray catheter to provide mucosal enhancement. Virtual chromoendoscopy (NBI, FICE, i-scan) are dye-less enhancement technologies that are built into the colonoscope or processor. NBI uses optical filter enhancement at the distal end of the endoscope, narrowing the light bandwidth, thereby improving visualization of the mucosa. FICE and i-scan use digital post-processing technology with spectral estimation to achieve mucosal enhancement. Magnification endoscopy possesses a variable lens, providing magnification up to 150-fold, permitting detailed examination of the mucosal pit patterns. Whilst CLE technology involves focusing laser light onto the mucosa and the reflected light is returned *via* a pinhole. This filters out non-focused light, giving a highly magnified, real-time histological diagnosis. CLE can either be integrated (iCLE) within the endoscope or *via* a probe (pCLE), which can be passed through the biopsy channel.

In patients without colitis, multiple studies have looked at *in-vivo* optical diagnosis of colorectal lesions using these technologies, allowing differentiation between neoplastic and non-neoplastic lesions. The hope that this would be cost-effective, reduce risk associated with polypectomy and provide instant determination of polyp surveillance intervals for the patient. A recent meta-analysis by the ASGE group looked at novel technologies to allow a "diagnose and leave" and "resect and discard" strategy[10]. To achieve

a "diagnose and leave" strategy, (a decision to leave in-situ diminutive rectosigmoid polyps), the technology had to achieve > 90% NPV for adenomatous histology. To achieve a "resect and discard" strategy, (remove diminutive adenomatous polyps without histological assessment), the technology should provide > 90% agreement in post-polypectomy surveillance intervals. The meta-analysis showed that this could only be achieved with NBI technology, in endoscopists that were experienced and that the assessment of the polyp was made with high confidence. Recently a large multicenter prospective study evaluated the use of NBI assisted optical diagnosis in non-expert endoscopists for small colonic polyps and was found to not achieve the above criteria[11].

The accuracy of these technologies during surveillance colonoscopy in colonic IBD is unclear with the majority of studies being small and assessed as secondary outcomes. With additional hurdles to overcome in patients with colitis, such as active inflammation and the fact that lesions tend to be morphologically different (flatter rather than polypoid), how precise are we at characterizing lesions in IBD with the current technologies available. Our objective was to perform the first systematic review and meta-analysis for the diagnostic accuracy of optical imaging techniques for *in-vivo* lesion characterization in colonic IBD. We aimed to calculate the pooled estimated sensitivities, specificities, positive and negative likelihood ratios (+LHR, -LHR), diagnostic odd ratios (DOR), and area under summary receiver-operator characteristic (AUSROC) curve for each technology type, with histopathology as the reference standard. We also planned to perform a subgroup analysis looking at the accuracy of studies using real-time non-magnified Kudo pit pattern (Kudo PP) and real-time CLE[12].

MATERIALS AND METHODS

Information sources and search strategy

We performed a meta-analysis in concordance with the preferred reporting items for systematic reviews and meta-analyses (PRISMA) guidelines[13]. RL searched Medline (from 1946 to May 2017) and Embase (from 1974 to May 2017), using the healthcare databases advanced search (HDAS) system. The search terms used included: ((((("high definition").ti,ab OR (HD).ti,ab OR ("white light").ti,ab OR (WL).ti,ab OR (chromoendoscop*).ti,ab OR (CE).ti,ab OR (NBI).ti,ab OR ("narrow band").ti,ab OR (FICE).ti,ab OR ("fujinon intelligent chromoendoscopy").ti,ab OR ("I-scan").ti,ab OR (AFI).ti,ab OR (autofluorescence).ti,ab OR (CLE).ti,ab OR ("confocal laser").ti,ab OR ("real time histology").ti,ab) AND ((("colon imag*").ti,ab OR ("intestinal imag*").ti,ab OR (colonoscop*).ti,ab)) AND (("inflammatory bowel disease").ti,ab OR (IBD).ti,ab OR (coliti*).ti,ab OR (uc).ti,ab OR ("ulcerative coliti*").ti,ab OR ("crohns coliti*").ti,ab OR ("crohn's coliti*").ti,ab)) AND ((lesion*).ti,ab OR (polyp*).ti,ab OR (dysplas*).ti,ab OR (neoplas*).ti,ab)". A Cochrane Library search for any systematic reviews relevant to this area was also performed. No language restrictions were used. The results for each database were combined and any duplicates removed.

Inclusion and exclusion criteria

Study inclusion and exclusion was determined by predefined criteria.

Inclusion criteria: (1) Studies using novel technologies to provide *in-vivo* optical characterization of lesions in patients with colonic IBD during colonoscopy; (2) characterized lesions into neoplastic and non-neoplastic using histology as the reference standard; (3) able to extract data to obtain a 2 × 2 contingency table to calculate the true positive (TP), false positive (FP), false negative (FN) and true negative (TN); and (4) Real-time characterization or retrospective image-review.

Exclusion criteria: (1) Case studies or case series; (2) studies not involving patients with colonic ibd; (3) inability to construct a 2 × 2 contingency table from the data given; (4) inability to differentiate detection from characterization studies; and (5) not used histology as reference standard (6) children (age < 16).

Study selection and data extraction

RL and NB identified study eligibility using the above inclusion and exclusion criteria. We searched the combined list of results for relevant studies, looking at the abstract or if supplementary information required, the full article. Reference lists of selected papers were also checked for potential missed articles. Abstract or articles for clinical trials or observational studies were eligible for inclusion if characterization of lesions by NBI, FICE, i-scan, DBC, magnification endoscopy or CLE, differentiated neoplastic from non-neoplastic lesions in colonic IBD, using histopathology as the gold standard. From this, data was extracted using a 2 × 2 contingency table. If exact figures for the true positive (TP), false positive (FP), false negative (FN) and true negative (TN) were not represented in the articles, it was calculated from the documented sensitivity, specificity, accuracy, positive predictive value (PPV) or negative predictive value (NPV). RL and VS performed data ascertainment and calculations. If TP, FP, FN and TN couldn't be calculated from the article data, attempts were made to contact relevant authors by email for clarification of figures.

Risk of study bias

As studies included were diagnostic, RL and NM used the QUADAS-2 (quality assessment of diagnostic accuracy studies) tool to independently assess the degree of study validity[14]. This looks at the risk of bias and applicability regarding four domains: patient

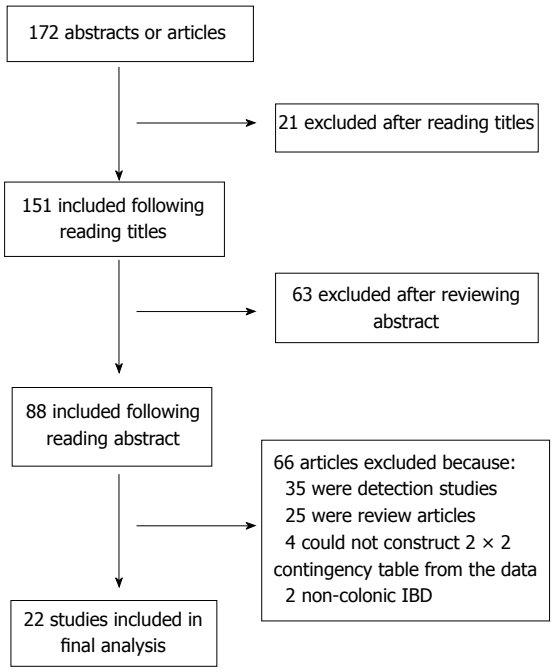

Figure 1 Study flow chart for studies eventually included into the meta-analysis. IBD: Inflammatory bowel disease.

selection, index test, reference standard, flow and timing. Risk of bias (involved all four domains) and applicability (involved three domains) is scored using low risk, high risk or unclear. Any indifference on determining risk between RL and NM was discussed and clarified with VS, who made the final decision.

Statistical analysis

In performing a systematic review for diagnostic studies, a bivariate meta-analysis using a random effects model was performed, allowing for the assumption of heterogeneity between the studies[15]. A random effects model was used in order to provide a more conservative result due to differences between study methods such as endoscopic expertise, classification model, study type and the population studied. We obtained summary estimates for sensitivity, specificity, +LHR, -LHR and DOR, with their 95% confidence intervals. A hierarchical summary receiver-operator characteristic (ROC) curve was plotted, with its summary point estimate, and a dashed line around representing its 95% confidence interval. The area under the SROC curve (AUROC) served as a marker of test accuracy. Forest plots were also calculated to demonstrate study sensitivity and specificity.

Heterogeneity between studies was assessed using the Cochrane *Q* and I^2 tests. Cochrane *Q* is established upon the chi-squared test, providing a weighted sum of the squared differences of each study estimate from the overall pooled estimate. *P* valves are given. I^2 describes the percentage of variation between studies that is due to heterogeneity rather than chance and is not dependent on the number of studies included. I^2 quantifies the impact of heterogeneity on the meta-analysis rather than just the extent of heterogeneity. Results range from 0-100%: 0% indicates there is no heterogeneity between the studies, whereas scores > 50% equate to moderate heterogeneity and > 75% high heterogeneity.

To help determine factors that may account for heterogeneity, we performed a subgroup analysis concentrating on real-time mucosal characterization, dividing into two groups: non-magnified Kudo PP (using VCE and DBC) and CLE. We also pooled results for all studies (real-time and retrospective image-capture) looking at non-magnified Kudo PP.

The Deeks *et al*[16] funnel plot assessed for publication bias. This uses regression of diagnostic log odds ratio against1/sqrt (effective sample size), weighting by sample size with a $P < 0.10$ for the slope coefficient as an indicator of substantial asymmetry.

All data analysis was done using Stata version 13 (Stata Corp, Texas, United States) using the user written command Midas (Dwamena, 2009)[17].

RESULTS

Study selection

One hundred and seventy-two abstracts and articles were obtained following the initial keyword search, following removal of duplicates (Figure 1). 21 studies were excluded following screening of the title, leaving 151 citations. A further 63 studies were excluded following review of the abstract, leaving 88 citations. 66 more studies were excluded following review of papers as a result of: 35 being detection studies, 25 were review articles, 2 involved patients without colonic IBD and 4 we were unable to construct a 2 × 2 contingency table.

Study characteristics

The characteristics of the 22 studies included are presented in Table 1[18-39]. Twenty-one studies included 1491 patients, with one study not reporting the number of patients included, and 4674 lesions, of which 539 (11.5%) were neoplastic.

The VCE group consisted of five studies, with one study looking at i-scan technology, two studies involved NBI and a further two used FICE. Three of the papers were abstracts and two being articles. All of these studies used endoscopic real-time diagnosis of lesions.

The DBC group entailed six studies, using either indigo-carmine (0.2%-0.4%) or methylene blue (0.1%) as the contrast agent. One of these studies performed endoscopic lesion diagnosis using a retrospective image-captured questionnaire, whilst the others used real-time diagnosis. Two were abstracts with the others being articles.

The CLE group comprised of nine studies; four studies used iCLE and five studies used pCLE. Three studies were retrospective image based, with the

Table 1 Study characteristics

Authors	Year	Abstract/ article	Technology	Number of endoscopists	Study design	Real time *vs* Image review	No. of Patients	No. of Polyps	Mucosal classification method
Virtual Chromoendoscopy									
Cassinotti *et al*[22]	2016	Abstract	i-scan HD	/	Single centre/prospective cohort Prospective cohort	Real time	40	287	Kudo PP + other endoscopic features
Efthymiou *et al*[21]	2013	Article	NBI HD	2	Single centre/prospective cohort	Real time	44	121	Kudo PP + low level magnification
Van den broek *et al*[23]	2011	Article	NBI HD	4	Single centre/randomized cross-over	Real time	48	153	Kudo PP
Cassinotti *et al*[24]	2015	Abstract	FICE HD	1	Single centre/randomized parallel	Real time	41	261	Kudo PP
Cassinotti *et al*[25]	2015	Abstract	FICE HD	1	Single centre/prospective cohort	Real time	59	205	Kudo PP
Dye-based Chromoendoscopy									
Carballal *et al*[26]	2016	Article	IC 0.4% SD/HD	15	Multi-centre/prospective cohort	Real time	350	595	Kudo PP + 10 other items
[1]Buchner *et al*[27]	2016	Abstract	MB 0.1% HD	/	Prospective cohort	Real time	22	21	/
[2]Wanders *et al*[20]	2016	Article	MB 0.1% SD	> 1	Multi-centre/prospective cohort	Real time	61	66	Kudo PP
Munoz *et al* [28]	2016	Abstract	IC 0.2%-0.4% HD	> 1	Multi-centre/retrospective cohort	Real time	243	953	Kudo PP
Wanders *et al*[29]	2015	Article	MB 0.1% or IC 0.3%	17	Multi-centre/retrospective questionnaire	Image review	/	30	/
[3]Hlavaty *et al* [18]	2011	Article	IC 0.4% SD	2	Single centre/prospective cohort	Real time	30	100	Kudo PP
Confocal Laser Endomicroscopy									
[2]Wanders *et al*[20]	2016	Article	iCLE	> 1	Multi-centre/prospective cohort	Real time	61	60	Mainz criteria
Dlugosz *et al*[30]	2016	Article	pCLE	1 endoscopist (2 reviewed images)	Single centre/retrospective cohort	Image review	69	644	Crypt + vessel architecture
[1]Buchner *et al*[27]	2016	Abstract	pCLE	/	Prospective cohort	Real time	22	20	Miami classification
Freire *et al*[31]	2014	Article	iCLE	1	Single centre/randomized trial	Real time	72	104	Mainz criteria
Rispo *et al*[32]	2012	Article	pCLE	1	Single centre/prospective cohort	Real time	51	15	De Palma classification
Shahid *et al*[33]	2011	Abstract	pCLE	3 reviewed images	Single centre/retrospective cohort	Image review	25	61	/
[3]Hlavaty *et al*[18]	2011	Article	iCLE	2	Single centre/prospective cohort	Real time	30	68	Mainz classification
[4]Van den broek *et al*[19]	2011	Article	pCLE	4 endoscopists (2 reviewing images)	Single centre/retrospective cohort	Image review	22	48	Crypt + vessel architecture
Keisslich *et al*[34]	2007	Article	iCLE	/	Single centre/randomized trial	Real time	80	134	Mainz classification
Magnification endoscopy									
Nishiyama *et al*[35]	2016	Article	NBI	5 reviewed images	Single centre/retrospective cohort	Image review	27	33	Surface + vessel patterns
[4]Van den broek *et al*[19]	2011	Article	NBI	4	Single centre/prospective cohort	Real time	22	48	Kudo PP + vascular patterns
Van den broek *et al*[36]	2008	Article	NBI	3	Single centre/randomized trial	Real time	50	98	Kudo PP
Matsumoto *et al*[37]	2007	Article	NBI	1	Single centre/prospective cohort	Real time	46	296	Surface structure
Keisslich *et al*[38]	2003	Article	MB 0.1%	1	Single centre/randomized trial	Real time	84	118	Kudo PP
Studies using combined technologies									
Bisschops *et al*[39]	2013	Abstract	Dye-based chromo/NBI	10 reviewed images	Multi-centre/retrospective cohort	Image review	27	50	Kudo PP

List of studies included in meta-analysis and displayed according to technology type. PP: Pit pattern; /: Data missing. [1]Two different technologies from same abstract; [2]Two different technologies from same article; [3]Two different technologies from same article; [4]Two different technologies from the same article.

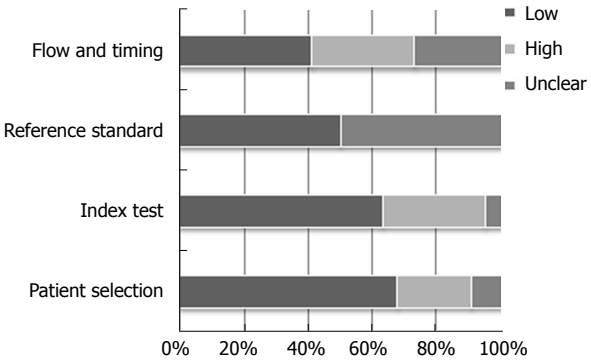

Figure 2 Stacked bar charts showing proportion of studies with low, high or unclear risks of bias. Vertical axis represents the four domains of the quality assessment of diagnostic accuracy studies 2.

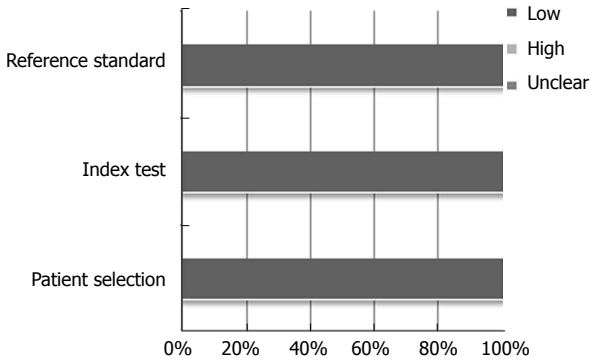

Figure 3 Stacked bar charts showing proportion of studies with low, high or unclear applicability. Vertical axis represents the three domains of the quality assessment of diagnostic accuracy studies 2.

remaining being real-time studies. Two were abstracts and the others being articles.

The magnification endoscopy group consisted of five studies, four of which being used in conjunction with NBI and one used with DBC. One study was retrospective image-based, with the others being real-time diagnosis. All were articles.

For the subgroup analysis, real-time non-magnified Kudo PP involved ten studies and real-time CLE involved six studies. The "all study" Kudo PP included twelve studies of which two were retrospective image-based abstracts.

Quality of assessment

The results for the study quality assessment using the QUADAS 2 tool are presented using stacked bar charts (Figure 2 and 3), displaying risk of bias and applicability. Individual study quality assessment can be seen in the supplementary table (Table 2). Results varied across the twenty-two studies. Abstracts predominantly scored "unclear" for domains associated with "risk of bias", due to lack of in-depth information within the abstract. However studies also scored "unclear" for "risk of bias" with regards "reference standard" if it did not clearly state if the histopathologist was blinded to the endoscopic diagnosis. Papers scoring "high" for "patient selection", "index test" and "flow and timing" for "risk of bias", were generally associated with retrospective image-captured studies which selected and reviewed only clear images of lesions, thereby introducing attrition bias. All studies scored "low" for all three domains with regards "applicability".

Pooled diagnostic accuracy results

A summary for the pooled diagnostic accuracy estimates for the different technologies and for the subgroup analysis is outlined in Table 3.

The meta-analysis for the five studies involving VCE showed it was fairly accurate at differentiating neoplastic from non-neoplastic lesions with a pooled sensitivity of 86% (95%CI: 62%-95%), specificity of 87% (95%CI: 72%-95%), and the area under the SROC curve was 0.93 (95%CI: 0.90-0.95).

Pooled results of the six studies for DBC revealed the least accurate results for lesion characterization, with a sensitivity of 67% (95%CI: 44%-84%), specificity of 86% (95%CI: 72%-94%) and an area under the SROC curve was 0.84 (95%CI: 0.81-0.87). Most of the studies within this group were multi-centre with more than one endoscopist.

Results of the five studies for magnification endoscopy showed a pooled sensitivity of 90% (95%CI: 77%-96%), specificity of 87% (95%CI: 81%-91%), and an area under the SROC curve was 0.93 (95%CI: 0.91-0.95). The results are similar to those of VCE; however these were mainly single centre, single expert endoscopist studies.

Meta-analysis of nine studies for CLE showed a sensitivity of 87% (95%CI: 71%-95%), specificity of 94% (95%CI: 87%-97%), with an area under the SROC curve of 0.96 (95%CI: 0.94-0.97). Again these mere all single centre, single expert endoscopist studies.

A subgroup analysis was performed involving studies using real-time endoscopic mucosal characterisation of lesions, divided into real-time non-magnified Kudo PP (with VCE and DBC) and real-time CLE. Both the forest plots and SROC curves for real-time non-magnified Kudo PP and real-time CLE are given in Figures 4 and 5. The subgroup for real-time Kudo PP included ten studies, with a pooled estimate sensitivity of 78% (95%CI: 57%-91%), specificity of 89% (95%CI: 80%-94%), with an area under the SROC of 0.91 (95%CI: 0.89-0.94). The subgroup analysis looking at real-time CLE included 6 studies. The pooled estimated sensitivity was 91% (95%CI: 66%-98%), specificity was 97% (95%CI: 94%-98%), and the area under the AUSROC was 0.98 (0.97-0.99).

A further subgroup analysis was performed looking at all (real-time and image review) non-magnified Kudo PP. This included twelve studies. The pooled estimate sensitivity was 78% (95%CI: 61%-88%), specificity of 86% (95%CI: 76%-92%), and an area under the

Table 2 quality assessment of diagnostic accuracy studies 2 for each study

	Cassinotti *et al*[22] 2016	Efthymiou *et al*[21] 2013	Van den broek *et al*[23] 2011	Cassinotti *et al*[24] 2015	Cassinotti *et al*[25] 2015	Carballel *et al*[26] 2016	Buchner *et al*[27] 2016	Wanders *et al*[20] 2016	Munoz *et al*[28] 2016	Wanders *et al*[29] 2015	Hlavaty *et al*[18] 2011	Dlugosz *et al*[30] 2016	Freire *et al*[31] 2014	Rispo *et al*[32] 2012	Shahid *et al*[33] 2011	Van den broek *et al*[19] 2011	Keisslich *et al*[34] 2007	Nishiyama *et al*[35] 2016	Van den Broek *et al*[36] 2008	Matsumoto *et al*[37] 2007	Keisslich *et al*[38] 2003	Bisschops *et al*[39] 2013
DOMAIN 1 Patient selection Risk of bias																						
Could selection of patients introduced bias?	L	L	L	L	L	L	U	L	L	H	U	L	L	L	H	H	L	H	L	L	L	H
Concerns regarding applicability																						
Concern included patients don't match review question?	L	L	L	L	L	L	L	L	L	L	L	L	L	L	L	L	L	L	L	L	L	L
DOMAIN 2 Index test Risk of bias																						
Conduct or interpretation of index test introduced bias?	L	L	L	L	L	L	L	L	U	H	H	H	L	L	H	H	L	H	L	L	L	H
Concerns regarding applicability																						
Concern index test, its conduct or interpretation differs from review question?	L	L	L	L	L	L	L	L	L	L	L	L	L	L	L	L	L	L	L	L	L	L

DOMAIN 3 Reference standard Risk of bias																						
Could reference standard, conduct or interpretation have introduced bias?	U	U	L	U	U	U	U	L	U	U	L	L	L	L	U	L	L	U	L	L	L	U
Concerns regarding applicability																						
Concern target condition as defined by reference standard not match review question?	L	L	L	L	L	L	L	L	L	L	L	L	L	L	L	L	L	L	L	L	L	L
DOMAIN 4 Flow and timing																						
Risk of bias																						
Could patient flow introduced bias?	U	L	H	U	U	L	U	L	U	H	H	U	L	L	H	H	L	H	L	L	L	H

L: Low risk; H: High risk; U: Unclear.

SROC of 0.89 (95%CI: 0.86-0.92).

Test for heterogeneity

I^2 and Cochrane Q were used to test for heterogeneity. Heterogeneity for VCE was moderate to high with an I^2 = 63% (95%CI: 16%-100%) and Q = 5.347 (P = 0.034). DBC showed extremely high levels of heterogeneity between studies with an I^2 = 89% (95%CI: 78%-100%) and Q = 18.573 (P = 0.00). Magnification [I^2 = 0 (95%CI: 0%-100%) and Q = 0.607 (P = 0.369)] and CLE [I^2 = 40% (95%CI: 0%-100%) and Q = 3.335 (P = 0.094)] represented low levels of heterogeneity between studies, however had very broad 95% confidence intervals.

Real-time non-magnified Kudo PP had an I^2 = 96% (95%CI: 92-99) and Q = 45.575 (P < 0.001) showing exceptionally high levels of heterogeneity. Real-time CLE studies had low levels of heterogeneity, with an I^2 = 0 (95%CI: 0-100%) and Q = 1.697 (P = 0.214).

Table 3 Accuracy of the different technologies

Analysis groups	No. of studies	Pooled estimates (95%CI)		Likelihood ratios (95%CI)		Diagnostic odds ratio (95%CI)	Area under SROC curve (95%CI)
		Sensitivity	Specificity	LHR+	LHR-	DOR	
All							
VCE	5	0.86 (0.62-0.95)	0.87 (0.72-0.95)	6.7 (2.6-17.8)	0.17 (0.05-0.53)	41 (6-297)	0.93 (0.90-0.95)
DBC	6	0.67 (0.44-0.84)	0.86 (0.72-0.94)	4.9 (2.1-11.3)	0.38 (0.20-0.73)	13 (3-48)	0.84 (0.81-0.87)
Magnification	5	0.90 (0.77-0.96)	0.87 (0.81-0.91)	7.0 (4.6-10.7)	0.11 (0.05-0.28)	62 (18-209)	0.93 (0.91-0.95)
CLE	9	0.87 (0.71-0.95)	0.94 (0.87-0.97)	14.0 (6.1-32.4)	0.14 (0.06-0.33)	101 (23-442)	0.96 (0.94-0.97)
Real-time							
Kudo PP	10	0.78 (0.57-0.91)	0.89 (0.80-0.94)	6.9 (3.5-13.5)	0.24 (0.11-0.55)	28 (7-110)	0.91 (0.89-0.94)
CLE	6	0.91 (0.66-0.98)	0.97 (0.94-0.98)	28.4 (13.6-59.1)	0.09 (0.02-0.43)	322 (41-2529)	0.98 (0.97-0.99)
All Kudo PP	12	0.78 (0.61-0.88)	0.86 (0.76-0.92)	5.5 (2.9-10.1)	0.26 (0.14-0.50)	21 (7-66)	0.89 (0.86-0.92)

All using both real-time and image based studies for the different technologies. Real-time, sub-group analysis with studies using only real time Kudo pit pattern (both VCE and DBC) and real-time CLE. All Kudo PP includes all studies using Kudo pit pattern (real-time and image-based). VCE: Virtual chromoendoscopy; DBC: Dye-based chromoendoscopy; CLE: Confocal laser endomicroscopy; Kudo PP: Kudo pit pattern; LHR+: Positive likelihood ratios; LHR-: Negative likelihood ratios; DOR: Diagnostic odd ratios.

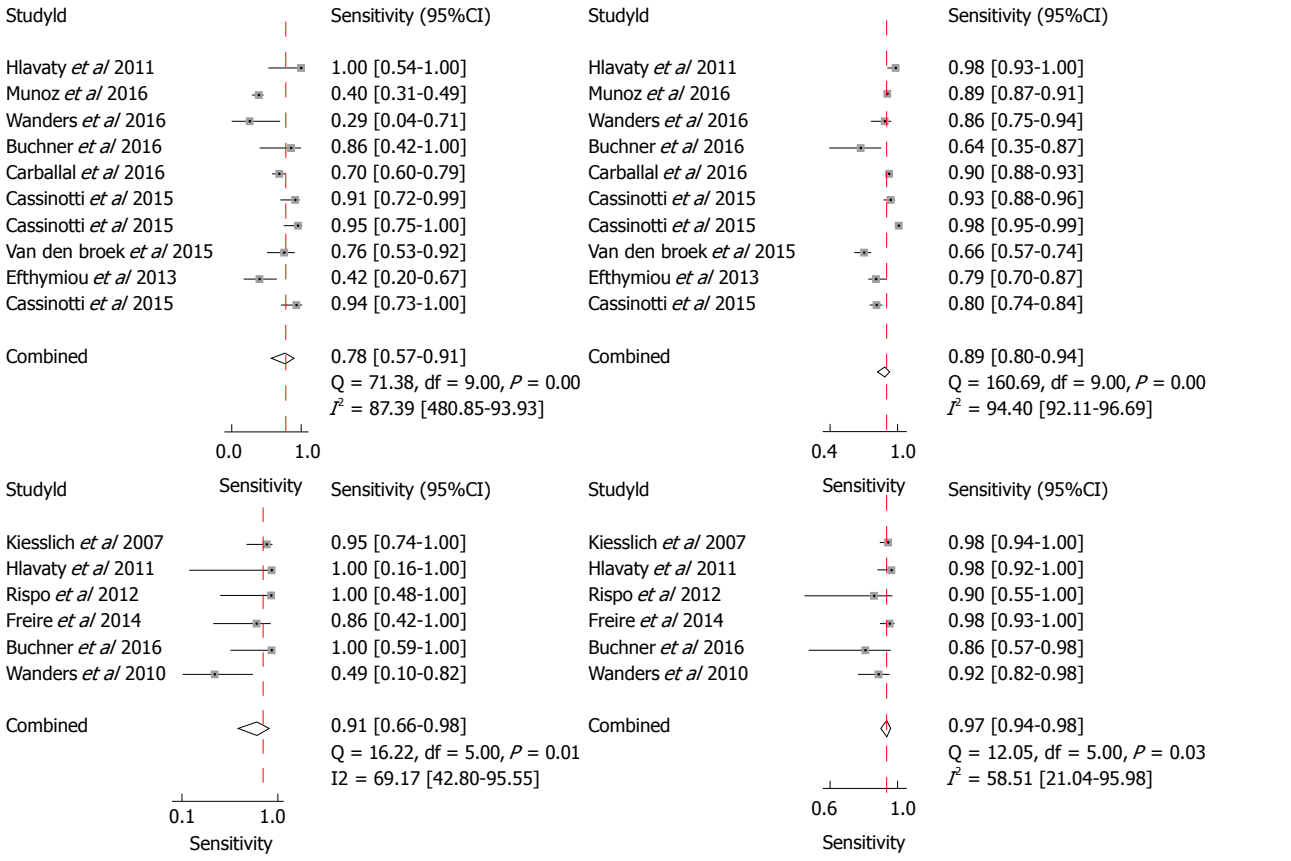

Figure 4 Forest plot for real-time Kudo pit pattern (A), and forest plot for real-time confocal laser endomicroscopy (B).

Publication bias

Deeks *et al*[15] funnel plot, seen in Figure 6, was used to assess publication bias. The funnel plot has slope coefficient of 9.84 (P = 0.194). The non-significant P valve would suggest a low likelihood of publication bias in this meta-analysis.

DISCUSSION

Our meta-analysis illustrates that real-time CLE currently appears to be the best technology in performing *in-vivo* lesion characterization in patients with colonic IBD, with an impressive AUSROC of 0.98 (95%CI: 0.97-0.99). It demonstrates an extremely high specificity, 97% (95%CI: 94%-98%), and sensitivity, 91% (95%CI: 66%-98%), in differentiating neoplastic from non-neoplastic lesions. Using all study types (real-time and image capture) CLE again out-performs the other technologies, with an area under SROC cure of 0.96 (95%CI: 0.94-0.97). Magnification and VCE technologies also show a good accuracy with a SROC of 0.93 (95%CI: 0.91-0.95) and 0.93 (95%CI: 0.90-0.95),

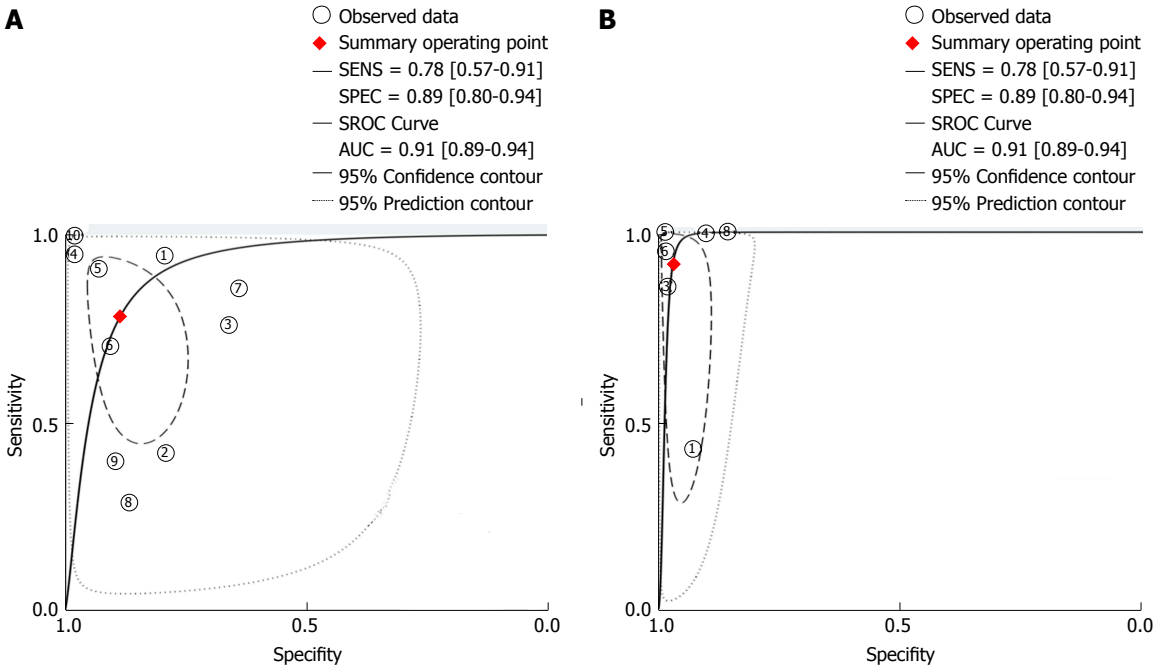

Figure 5 Area under SROC curve for real-time Kudo pit pattern (A) and area under SROC curve for real-time confocal laser endomicroscopy (B).

respectively.

Despite CLE being a highly accurate technology in lesion characterization, there are several concerns with regards applicability. Most of the studies in our meta-analysis for CLE involved a single endoscopy operator within a single-centre. They were vastly experienced in IBD surveillance endoscopy and in using CLE technology. Studies in which inexperienced operators used this technology, they themselves did not make real-time lesion diagnosis. Instead, people trained in the interpretation of the histology reviewed the images retrospectively. This is because CLE is not a routinely used modality. It requires expertise in handling, positioning of the colonoscope/probe onto the lesion and in analysing/interpreting *in-vivo* histology. Bowel preparation has to be meticulous, as any faecal material can interfere with image capture and lesion interrogation. This is unlikely to be achieved consistently during "real-life" surveillance lists. In one study, 32% of lesions were not accessible to CLE evaluation and a second study, 1.5% of lesions the histology was not visualised by CLE. These unclassified lesions aren't accounted for in the final results, contributing to attrition bias in the observed results. In addition, IV fluorescein injection is required before lesion analysis, further adding to procedure time. One study showed the mean additional time per procedure being 20 min. Adoption of this technology in throughout less experienced centres is doubtful. It would demand vast resources for training, education and require new guidance for endoscopic competence.

A further concern with CLE was equipment failure. In one multi-centre study, four of the five centres had to send the equipment back to the manufactures as the lens on the endomicroscope broke. Repair took the teams months to address, significantly affecting recruitment, resulting in the study being underpowered. With concerns over equipment failure, costs of purchasing the technology and repairs, CLE could in fact be a financial burden, negating any benefit obtained from the reduction in polypectomies and histological analysis. Therefore, questions still remain unanswered with regards practicalities and applicability for this technology.

VCE showed relatively good accuracy although fell short of reaching the 90% mark for sensitivity and specificity. One major limitation for this technology was the small number of studies for VCE technology. We therefore combined the NBI, FICE and i-scan to obtain pooled results. Although the technologies have been grouped as one, there are obvious differences in the way they achieve the modified image and the modes used with that technology. NBI endoscopes contain a rotating filter in front of the light source at the end of the endoscope, allowing a narrow wavelength of light to strike the mucosa resulting in image enhancement, whereas both FICE and i-scan use a post-processing technology built within the processer to provide a coloured-enhanced image. There were several other drawbacks with the VCE group analysis. One study in our meta-analysis used the first generation NBI technology, resulting in images being less bright, undoubtedly having an impact on lesion characterization when compared with newer generation technology. Three of the five studies for VCE were abstracts making critical analysis for the quality of these studies difficult to determine. From our results we cannot currently recommend using VCE solely as an accurate

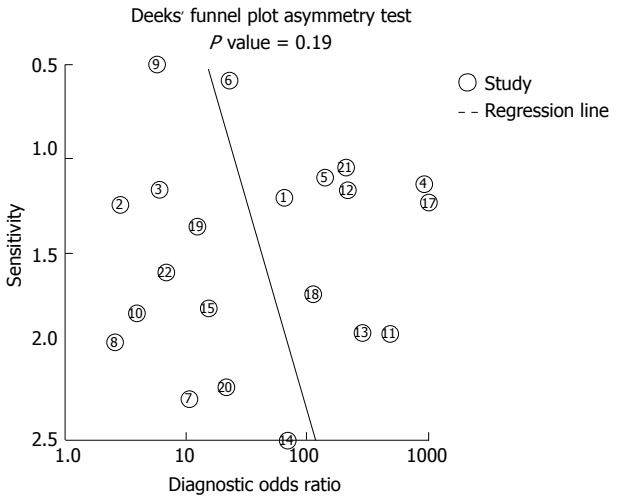

Figure 6 Funnel plot with superimposed regression line looking for publication bias.

technology for lesion characterization in IBD. However, with newer generation endoscopes, further evaluation is clearly warranted as these technologies continue to improve. In comparison with CLE, VCE is potentially less complicated to use, more robust, economical as they are almost universal in newer endoscope processors, and training is more likely to be attainable.

Magnification endoscopy achieves similar accuracy to VCE technology. However in the majority of these studies magnification was used in combination with NBI, predominantly using older NBI technology. This makes it challenging to differentiate the two technologies. With new colonoscopes delivering digital magnification, like "near focus" technology, it is questionable the additional information optical magnification will provide. A threshold may be reached at which further magnification provides no additional benefit for differentiating neoplastic from non-neoplastic pit patterns. However, this meta-analysis cannot necessarily address that question.

DBC pooled results were suboptimal for lesion characterization. However, more than half of the studies used standard-definition colonoscopies, reducing image resolution, and therefore impacting on lesion interpretation. With most centres now using high-definition colonoscopies accuracy is likely to improve. Another confounding factor was that the majority of the studies were multi-centred, with multiple operators, undoubtedly accounting for a diverse range of endoscopic experience and therefore skill at lesion classification.

A subgroup analysis was performed in order to look for potential sources of heterogeneity and to determine whether it was the type of mucosal classification used that influenced the accuracy rather than the technology. Real-time studies were used as this provided the most clinically authentic evaluation of lesions and minimises bias as a result of photographic selection and time for analysis. Most studies used Kudo PP or a variation on the Kudo PP (Kudo PP plus additional features) and therefore we pooled the results for both real-time VCE and DBC. Real-time Kudo PP had an area under the SROC curve of 0.91 (95%CI: 0.89-0.94), with a reasonable specificity of 89% (95%CI: 80%-94%) but a sensitivity of 78% (95%CI: 57%-91%). The poor sensitivity likely reflects inclusion of the DBC group with the majority involving standard-definition scopes. The use of Kudo PP and Kudo PP plus did not seem to influence the accuracy of lesion characterisation, independent of the technology. Caution however, has to be noted for combining DBC and VCE using Kudo PP as a mucosal classification system. Studies have shown a lack of pit pattern agreement between chromoendoscopy and NBI[40]. This has leading to the adoption of new classification systems, such as NICE for NBI[41]. Further mucosal classification systems may need to be studied, especially for i-scan and FICE. However, determining the ideal post-processing mode for these software systems could be challenging as these technologies have multiple combination options of modes.

Another important issue that wasn't clearly stated for studies in this meta-analysis was the degree of mucosal inflammation in which the lesions resided. Varying degrees of mucosal inflammation unquestionably contribute to difficulties in pit pattern and vasculature interpretation and therefore diagnostic accuracy. Future studies looking at *in-vivo* lesion diagnostic accuracy could stratify patients depending on the degree of inflammation surrounding the lesions.

As with any meta-analysis there are limitations. The number of studies for each technology group was fairly limited, except for the CLE group. Seven of the twenty-two studies were abstracts introducing concerns with regards data extraction and interrogation for study validity.

Despite an extensive literature review, no papers had direct head-to-head studies, comparing the different technologies against each other. However, this would require a very large cohort looking specifically at lesion characterisation and all endoscopists participating being familiar with the different technologies. Endoscopic familiarity with certain technologies in such a study could potentially confound the accuracy of lesion interpretation.

In the majority of studies, lesion characterization was a secondary outcome, therefore in some studies the number of lesions being characterised was small. Some studies didn't clearly state the TP, FP, FN and TN, therefore calculations had to be performed in order to achieve this.

There was also a large degree of heterogeneity within the VCE and DBC groups that was further increased when we performed real-time Kudo PP assessment. Further areas of subgroup classification that were not explored within this meta-analysis were the number of endoscopists performing the procedures in each study and also whether it was a single centre

or multi-centre study. This undoubtedly will have an impact on the accuracy of the technology being used. Single-centre, single endoscopist studies are more likely to achieve better results.

Suggested avenues to explore in future studies looking at *in-vivo* lesion characterization in colonic IBD include: accuracy according to varying endoscopic experience, accuracy dependent on the degree of surrounding mucosal inflammation, whether the endoscopist confidence (high or low) in lesion characterization impacts accuracy and exploring new mucosal lesion classification for different technologies.

CONCLUSION

Real-time CLE appears to be currently the best commercially available technology at differentiating neoplastic from non-neoplastic lesions in patients with colonic IBD, with an area under the SROC of 0.98 (95%CI: 97%-99%). However, most CLE studies were single centered with single expert users, which could significantly confound the results, and some studies not reporting non-interpretable images, contributing to attrition bias. Clinical applicability for this technology is likely to be a challenge. VCE technology performed well but currently cannot be recommended for *in-vivo* lesion characterization in such a high-risk group. However, with improved endoscopes and newer generation technologies further studies are required to assess their real-time performance in clinical settings with trained colonoscopists.

ARTICLE HIGHLIGHTS

Research background

Patients with inflammatory bowel disease (IBD) colitis are known to have an increased risk of colorectal cancer compared to that of non-colitic patients. This is thought to progress along the inflammation-dysplasia-carcinoma pathway. Many studies and meta-analyses have been performed for lesion detection in IBD but few studies have looked into *in-vivo* lesion characterization. This is the first meta-analysis on lesion characterization in colonic IBD.

Research motivation

Characterization of colonic lesions in IBD maybe more challenging because they tend to be flatter and their pit-pattern maybe obscured by inflammation. Some patients also have numerous pseudopolyps throughout the colon, making polypectomy impractical, time-consuming, costly and potentially associated with increased risk. If we are able to characterize these lesions with a high accuracy without needing to perform polypectomy, we could potentially circumvent these problems.

Research objectives

Our objective was to perform the first systematic review and meta-analysis for the diagnostic accuracy of optical imaging techniques for *in-vivo* lesion characterization in colonic IBD.

Research methods

We conducted a review of the current literature and included studies which characterized lesions *in-vivo* into neoplastic and non-neoplastic, using histology as the gold standard. Data was pooled for each technology using a bivariate meta-analysis with a random effects model to account for study differences. Sensitivities, specificities, positive and negative likelihood ratios, diagnostic odds ratio, and area under summary receiver-operator characteristic curve, were calculated for each technology type.

Research results

Confocal laser endomicroscopy (CLE) had the greatest accuracy for differentiating neoplastic from non-neoplastic lesions *in-vivo*. Magnification and virtual chromoendoscopy (VCE) performed well, whilst dye-based chromoendoscopy (DBC) had suboptimal accuracy.

Research conclusions

CLE is highly accurate at *in-vivo* lesion characterization but studies are within experienced centres with mainly single expert users limiting its generalizability.

Research perspectives

Future studies should look at newer generation virtual chromoendoscopic technology [narrow band imaging (NBI), i-scan, fujinon intelligence chromoendoscopy (FICE)] for lesion characterization. A standardised mucosal lesion classification system specific for lesions in IBD colitis accounting for the technology being used should be explored.

REFERENCES

1 **Crohn B,** Rosenberg H. The sigmoidoscopic picture of chronic ulcerative colitis (non- specific). *AM J MED SCI* 1925; **170**: 220-227 [DOI: 10.1097/00000441-192508010-00006]

2 **Eaden JA**, Abrams KR, Mayberry JF. The risk of colorectal cancer in ulcerative colitis: a meta-analysis. *Gut* 2001; **48**: 526-535 [PMID: 11247898 DOI: 10.1136/gut.48.4.526]

3 **Jess T**, Rungoe C, Peyrin-Biroulet L. Risk of colorectal cancer in patients with ulcerative colitis: a meta-analysis of population-based cohort studies. *Clin Gastroenterol Hepatol* 2012; **10**: 639-645 [PMID: 22289873 DOI: 10.1016/j.cgh.2012.01.010]

4 **Lutgens MW**, van Oijen MG, van der Heijden GJ, Vleggaar FP, Siersema PD, Oldenburg B. Declining risk of colorectal cancer in inflammatory bowel disease: an updated meta-analysis of population-based cohort studies. *Inflamm Bowel Dis* 2013; **19**: 789-799 [PMID: 23448792 DOI: 10.1097/MIB.0b013e31828029c0]

5 **Zisman TL**, Rubin DT. Colorectal cancer and dysplasia in inflammatory bowel disease. *World J Gastroenterol* 2008; **14**: 2662-2669 [PMID: 18461651 DOI 10.3748/wjg.14.2662]

6 **Laine L**, Kaltenbach T, Barkun A, McQuaid KR, Subramanian V, Soetikno R; SCENIC Guideline Development Panel. SCENIC international consensus statement on surveillance and management of dysplasia in inflammatory bowel disease. *Gastroenterology* 2015; **148**: 639-651.e28 [PMID: 25702852 DOI: 10.1053/j.gastro.2015.01.031]

7 **Cairns SR**, Scholefield JH, Steele RJ, Dunlop MG, Thomas HJ, Evans GD, Eaden JA, Rutter MD, Atkin WP, Saunders BP, Lucassen A, Jenkins P, Fairclough PD, Woodhouse CR; British Society of Gastroenterology; Association of Coloproctology for Great Britain and Ireland. Guidelines for colorectal cancer screening and surveillance in moderate and high risk groups (update from 2002). *Gut* 2010; **59**: 666-689 [PMID: 20427401 DOI: 10.1136/gut.2009.179804]

8 **Annese V**, Daperno M, Rutter MD, Amiot A, Bossuyt P, East J, Ferrante M, Götz M, Katsanos KH, Kießlich R, Ordás I, Repici A, Rosa B, Sebastian S, Kucharzik T, Eliakim R; European Crohn's and Colitis Organisation. European evidence based consensus for endoscopy in inflammatory bowel disease. *J Crohns Colitis* 2013; **7**: 982-1018 [PMID: 24184171 DOI: 10.1016/j.crohns.2013.09.016]

9 **Wanders LK**, Dekker E, Pullens B, Bassett P, Travis SP, East JE. Cancer risk after resection of polypoid dysplasia in patients with longstanding ulcerative colitis: a meta-analysis. *Clin Gastroenterol Hepatol* 2014; **12**: 756-764 [PMID: 23920032 DOI: 10.1016/j.cgh.2013.07.024]

10 **ASGE Technology Committee**, Abu Dayyeh BK, Thosani N, Konda V, Wallace MB, Rex DK, Chauhan SS, Hwang JH,

Komanduri S, Manfredi M, Maple JT, Murad FM, Siddiqui UD, Banerjee S. ASGE Technology Committee systematic review and meta-analysis assessing the ASGE PIVI thresholds for adopting real-time endoscopic assessment of the histology of diminutive colorectal polyps. *Gastrointest Endosc* 2015; **81**: 502.e1-502.e16 [PMID: 25597420 DOI: 10.1016/j.gie.2014.12.022]

11 **Rees CJ**, Rajasekhar PT, Wilson A, Close H, Rutter MD, Saunders BP, East JE, Maier R, Moorghen M, Muhammad U, Hancock H, Jayaprakash A, MacDonald C, Ramadas A, Dhar A, Mason JM. Narrow band imaging optical diagnosis of small colorectal polyps in routine clinical practice: the Detect Inspect Characterise Resect and Discard 2 (DISCARD 2) study. *Gut* 2017; **66**: 887-895 [PMID: 27196576 DOI: 10.1136/gutjnl-2015-310584]

12 **Kudo S**, Tamura S, Nakajima T, Yamano H, Kusaka H, Watanabe H. Diagnosis of colorectal tumorous lesions by magnifying endoscopy. *Gastrointest Endosc* 1996; **44**: 8-14 [PMID: 8836710 DOI: 10.1016/S0016-5107(96)70222-5]

13 **Liberati A**, Altman DG, Tetzlaff J, Mulrow C, Gøtzsche PC, Ioannidis JP, Clarke M, Devereaux PJ, Kleijnen J, Moher D. The PRISMA statement for reporting systematic reviews and meta-analyses of studies that evaluate healthcare interventions: explanation and elaboration. *BMJ* 2009; **339**: b2700 [PMID: 19622552 DOI: 10.1136/bmj.b2700]

14 **Whiting PF**, Rutjes AW, Westwood ME, Mallett S, Deeks JJ, Reitsma JB, Leeflang MM, Sterne JA, Bossuyt PM; QUADAS-2 Group. QUADAS-2: a revised tool for the quality assessment of diagnostic accuracy studies. *Ann Intern Med* 2011; **155**: 529-536 [PMID: 22007046 DOI: 10.7326/0003-4819-155-8-201110180-00009]

15 **Dwamena BA.** MIDAS: Stata module for meta-analytical integration of diagnostic test accuracy studies. Statistical Software Components S456880. Boston, MA: Boston College Department of Econonics. 2009

16 **Deeks JJ**, Macaskill P, Irwig L. The performance of tests of publication bias and other sample size effects in systematic reviews of diagnostic test accuracy was assessed. *J Clin Epidemiol* 2005; **58**: 882-893 [PMID: 16085191 DOI: 10.1016/j.jclinepi.2005.01.016]

17 **StataCorp.** 2013. Stata Statistical Software: Release 13. College Station, TX: StataCorp LP. 2013

18 **Hlavaty T**, Huorka M, Koller T, Zita P, Kresanova E, Rychly B, Toth J. Colorectal cancer screening in patients with ulcerative and Crohn's colitis with use of colonoscopy, chromoendoscopy and confocal endomicroscopy. *Eur J Gastroenterol Hepatol* 2011; **23**: 680-689 [PMID: 21602687 DOI: 10.1097/MEG.0b013e32834791b4]

19 **van den Broek FJ**, van Es JA, van Eeden S, Stokkers PC, Ponsioen CY, Reitsma JB, Fockens P, Dekker E. Pilot study of probe-based confocal laser endomicroscopy during colonoscopic surveillance of patients with longstanding ulcerative colitis. *Endoscopy* 2011; **43**: 116-122 [PMID: 21165821 DOI: 10.1055/s-0030-1255954]

20 **Wanders LK**, Kuiper T, Kiesslich R, Karstensen JG, Leong RW, Dekker E, Bisschops R. Limited applicability of chromoendoscopy-guided confocal laser endomicroscopy as daily-practice surveillance strategy in Crohn's disease. *Gastrointest Endosc* 2016; **83**: 966-971 [PMID: 26358329 DOI: 10.1016/j.gie.2015.09.001]

21 **Efthymiou M**, Allen PB, Taylor AC, Desmond PV, Jayasakera C, De Cruz P, Kamm MA. Chromoendoscopy versus narrow band imaging for colonic surveillance in inflammatory bowel disease. *Inflamm Bowel Dis* 2013; **19**: 2132-2138 [PMID: 23899540 DOI: 10.1097/MIB.0b013e31829637b9]

22 **Gordon H**, Langholz E. The EpiCom Survey-Registries Across Europe, Epidemiological Research and Beyond. *J Crohns Colitis* 2017; **11**: 1019-1021 [PMID: 28158624 DOI: 10.1093/ecco-jcc/jjx013]

23 **van den Broek FJ**, Fockens P, van Eeden S, Stokkers PC, Ponsioen CY, Reitsma JB, Dekker E. Narrow-band imaging versus high-definition endoscopy for the diagnosis of neoplasia in ulcerative colitis. *Endoscopy* 2011; **43**: 108-115 [PMID: 21165822 DOI: 10.1055/s-0030-1255956]

24 **Cassinotti A,** Ardizzone S, Buffoli F, Fociani P, Villanacci V, Nebuloni M, Fichera M, Salemme M, Lombardini M, Molteni P, Sampietro G, Furfaro F, Dell'Era A, Gambitta P, Foschi D, Duca P, De Franchis R, Maconi G. Virtual chromoendoscopy with FICE is superior to standard colonoscopic surveillaillance for flat visibile dysplasic lesions and raised lesions (polyps and pseudopolyps) evaluation in long-standing ulcerative colitis: a prospective, randomized, trial. *J CROHNS COLITIS* 2015; **9** Suppl 1: S1-S479

25 **Gordon H**, Langholz E. The EpiCom Survey-Registries Across Europe, Epidemiological Research and Beyond. *J Crohns Colitis* 2017; **11**: 1019-1021 [PMID: 28158624 DOI: 10.1093/ecco-jcc/jjx013]

26 **Carballal S**, Maisterra S, López-Serrano A, Gimeno-García AZ, Vera MI, Marín-Garbriel JC, Díaz-Tasende J, Márquez L, Álvarez MA, Hernández L, De Castro L, Gordillo J, Puig I, Vega P, Bustamante-Balén M, Acevedo J, Peñas B, López-Cerón M, Ricart E, Cuatrecasas M, Jimeno M, Pellisé M; EndoCAR group of the Spanish Gastroenterological Association and Spanish Digestive Endoscopy Society. Real-life chromoendoscopy for neoplasia detection and characterisation in long-standing IBD. *Gut* 2018; **67**: 70-78 [PMID: 27612488 DOI: 10.1136/gutjnl-2016-312332]

27 **Buchner AM,** Ma GK, Ginsberg GG, Lichtenstein GR, Kerner C. Chromoendoscopy-Guided Probe Based Confocal Laser Endomicroscopy: A Novel Approach for Dysplasia Evaluation in IBD Surveillance. *Gastroenterology* 2016; **150**: S627 [DOI: 10.1016/S0016-5085(16)32152-7]

28 **Muñoz J,** García M, Sicilia B, Sierra M, Fernandez N, Arias L, Barrio J, Velayos B, Hernandez-Villalba L. Results of dysplasia surveillance programme with chromoendoscopy for inflammatory bowel disease. *Journal of Crohn's and Colitis* 2016; **10** Suppl: 158

29 **Wanders LK**, Mooiweer E, Wang J, Bisschops R, Offerhaus GJ, Siersema PD, D'Haens GR, Oldenburg B, Dekker E. Low interobserver agreement among endoscopists in differentiating dysplastic from non-dysplastic lesions during inflammatory bowel disease colitis surveillance. *Scand J Gastroenterol* 2015; **50**: 1011-1017 [PMID: 25794268 DOI: 10.3109/00365521.2015.1016449]

30 **Dlugosz A**, Barakat AM, Björkström NK, Öst Å, Bergquist A. Diagnostic yield of endomicroscopy for dysplasia in primary sclerosing cholangitis associated inflammatory bowel disease: a feasibility study. *Endosc Int Open* 2016; **4**: E901-E911 [PMID: 27540581 DOI: 10.1055/s-0042-111203]

31 **Freire P**, Figueiredo P, Cardoso R, Donato MM, Ferreira M, Mendes S, Silva MR, Cipriano A, Ferreira AM, Vasconcelos H, Portela F, Sofia C. Surveillance in ulcerative colitis: is chromoendoscopy-guided endomicroscopy always better than conventional colonoscopy? A randomized trial. *Inflamm Bowel Dis* 2014; **20**: 2038-2045 [PMID: 25185683 DOI: 10.1097/MIB.0000000000000176]

32 **Rispo A**, Castiglione F, Staibano S, Esposito D, Maione F, Siano M, Salvatori F, Masone S, Persico M, De Palma GD. Diagnostic accuracy of confocal laser endomicroscopy in diagnosing dysplasia in patients affected by long-standing ulcerative colitis. *World J Gastrointest Endosc* 2012; **4**: 414-420 [PMID: 23125900 DOI: 10.4253/wjge.v4.i9.414]

33 **Shahid MW,** Wang YR, Cangemi JR, Wallace MB, Picco MF. The Role of Probe-Based Confocal Laser Endomicroscopy in Detection of Neoplasia in Polypoid Lesions in Ulcerative Colitis: An Exploratory Pilot Study. *Gastrointest Endosc* 2011; **73**: AB302-AB3 [DOI: 10.1016/j.gie.2011.03.608]

34 **Kiesslich R**, Goetz M, Lammersdorf K, Schneider C, Burg J, Stolte M, Vieth M, Nafe B, Galle PR, Neurath MF. Chromoscopy-guided endomicroscopy increases the diagnostic yield of intraepithelial neoplasia in ulcerative colitis. *Gastroenterology* 2007; **132**: 874-882 [PMID: 17383417 DOI: 10.1053/j.gastro.2007.01.048]

35 **Nishiyama S**, Oka S, Tanaka S, Sagami S, Hayashi R, Ueno Y, Arihiro K, Chayama K. Clinical usefulness of narrow band imaging magnifying colonoscopy for assessing ulcerative colitis-associated cancer/dysplasia. *Endosc Int Open* 2016; **4**: E1183-E1187 [PMID: 27853744 DOI: 10.1055/s-0042-116488]

36 **van den Broek FJ**, Fockens P, van Eeden S, Reitsma JB, Hardwick JC, Stokkers PC, Dekker E. Endoscopic tri-modal imaging for surveillance in ulcerative colitis: randomised comparison of high-resolution endoscopy and autofluorescence imaging for neoplasia detection; and evaluation of narrow-band imaging for classification of lesions. *Gut* 2008; **57**: 1083-1089 [PMID: 18367559 DOI: 10.1136/gut.2007.144097]
37 **Matsumoto T**, Kudo T, Jo Y, Esaki M, Yao T, Iida M. Magnifying colonoscopy with narrow band imaging system for the diagnosis of dysplasia in ulcerative colitis: a pilot study. *Gastrointest Endosc* 2007; **66**: 957-965 [PMID: 17826773 DOI: 10.1016/j.gie.2007.04.014]
38 **Kiesslich R**, Fritsch J, Holtmann M, Koehler HH, Stolte M, Kanzler S, Nafe B, Jung M, Galle PR, Neurath MF. Methylene blue-aided chromoendoscopy for the detection of intraepithelial neoplasia and colon cancer in ulcerative colitis. *Gastroenterology* 2003; **124**: 880-888 [PMID: 12671882 DOI: 10.1053/gast.2003.50146]
39 **Bisschops R,** Bessissow T, Bhandari P, Dekker E, East JE, Ignjatovic A, Parra-Blanco A, Ragunath K, Rutter MD, Schoon EJ, Baert FJ, Rutgeerts PJ, Ferrante M. Chromo-Endoscopy and NBI for Ruling out Neoplasia in Ulcerative Colitis: an International Multicenter Interobserver Study. *Gastrointest Endosc* 2013; **77**: AB444-AB455 [DOI: 10.1016/j.gie.2013.03.356]
40 **East JE**, Suzuki N, Saunders BP. Comparison of magnified pit pattern interpretation with narrow band imaging versus chromoendoscopy for diminutive colonic polyps: a pilot study. *Gastrointest Endosc* 2007; **66**: 310-316 [PMID: 17643705 DOI: 10.1016/j.gie.2007.02.026]
41 **Hewett DG**, Kaltenbach T, Sano Y, Tanaka S, Saunders BP, Ponchon T, Soetikno R, Rex DK. Validation of a simple classification system for endoscopic diagnosis of small colorectal polyps using narrow-band imaging. *Gastroenterology* 2012; **143**: 599-607.e1 [PMID: 22609383 DOI: 10.1053/j.gastro.2012.05.006]

P- Reviewer: Espinel J, Guerra IG, Tang ST **S- Editor**: Wang XJ
L- Editor: A **E- Editor**: Ma YJ

Published by **Baishideng Publishing Group Inc**
7901 Stoneridge Drive, Suite 501, Pleasanton, CA 94588, USA
Telephone: +1-925-223-8242
Fax: +1-925-223-8243
E-mail: bpgoffice@wjgnet.com
Help Desk: http://www.f6publishing.com/helpdesk
http://www.wjgnet.com

ISSN 1007-9327

ISSN 1007-9327 (print)
ISSN 2219-2840 (online)

World Journal of *Gastroenterology*

World J Gastroenterol 2018 March 21; 24(11): 1181-1284

Published by Baishideng Publishing Group Inc

World Journal of Gastroenterology

Contents

Weekly Volume 24 Number 11 March 21, 2018

Prospective Study

ABOUT COVER

Editorial board member of *World Journal of Gastroenterology*, Chang Moo Kang, MD, PhD, Associate Professor, Division of Hepatobiliary and Pancreatic Surgery, Department of Surgery, Yonsei University, Pancreaticobiliary Cancer Clinic, Yonsei Cancer Center, Severance Hospital, Seoul 120-752, South Korea

AIMS AND SCOPE

World Journal of Gastroenterology (*World J Gastroenterol*, *WJG*, print ISSN 1007-9327, online ISSN 2219-2840, DOI: 10.3748) is a peer-reviewed open access journal. *WJG* was established on October 1, 1995. It is published weekly on the 7th, 14th, 21st, and 28th each month. The *WJG* Editorial Board consists of 642 experts in gastroenterology and hepatology from 59 countries.

The primary task of *WJG* is to rapidly publish high-quality original articles, reviews, and commentaries in the fields of gastroenterology, hepatology, gastrointestinal endoscopy, gastrointestinal surgery, hepatobiliary surgery, gastrointestinal oncology, gastrointestinal radiation oncology, gastrointestinal imaging, gastrointestinal interventional therapy, gastrointestinal infectious diseases, gastrointestinal pharmacology, gastrointestinal pathophysiology, gastrointestinal pathology, evidence-based medicine in gastroenterology, pancreatology, gastrointestinal laboratory medicine, gastrointestinal molecular biology, gastrointestinal immunology, gastrointestinal microbiology, gastrointestinal genetics, gastrointestinal translational medicine, gastrointestinal diagnostics, and gastrointestinal therapeutics. *WJG* is dedicated to become an influential and prestigious journal in gastroenterology and hepatology, to promote the development of above disciplines, and to improve the diagnostic and therapeutic skill and expertise of clinicians.

INDEXING/ABSTRACTING

World Journal of Gastroenterology (*WJG*) is now indexed in Current Contents®/Clinical Medicine, Science Citation Index Expanded (also known as SciSearch®), Journal Citation Reports®, Index Medicus, MEDLINE, PubMed, PubMed Central and Directory of Open Access Journals. The 2017 edition of Journal Citation Reports® cites the 2016 impact factor for *WJG* as 3.365 (5-year impact factor: 3.176), ranking *WJG* as 29th among 79 journals in gastroenterology and hepatology (quartile in category Q2).

NAME OF JOURNAL
World Journal of Gastroenterology

ISSN
ISSN 1007-9327 (print)
ISSN 2219-2840 (online)

LAUNCH DATE
October 1, 1995

FREQUENCY
Weekly

EDITORIAL OFFICE
Ze-Mao Gong, Director
World Journal of Gastroenterology
Baishideng Publishing Group Inc
7901 Stoneridge Drive, Suite 501,
Pleasanton, CA 94588, USA
Telephone: +1-925-2238242
Fax: +1-925-2238243
E-mail: editorialoffice@wjgnet.com
Help Desk: http://www.f6publishing.com/helpdesk
http://www.wjgnet.com

PUBLISHER
Baishideng Publishing Group Inc
7901 Stoneridge Drive, Suite 501,
Pleasanton, CA 94588, USA
Telephone: +1-925-2238242
Fax: +1-925-2238243
E-mail: bpgoffice@wjgnet.com
Help Desk: http://www.f6publishing.com/helpdesk
http://www.wjgnet.com

PUBLICATION DATE
March 21, 2018

INSTRUCTIONS TO AUTHORS
Full instructions are available online at http://www.wjgnet.com/bpg/gerinfo/204

ONLINE SUBMISSION
http://www.f6publishing.com

World Journal of Gastroenterology

Submit a Manuscript: http://www.f6publishing.com

World J Gastroenterol 2018 March 21; 24(11): 1181-1195

DOI: 10.3748/wjg.v24.i11.1181

ISSN 1007-9327 (print) ISSN 2219-2840 (online)

REVIEW

Functional macrophages and gastrointestinal disorders

Yue-Hong Liu, Yue Ding, Chen-Chen Gao, Li-Sheng Li, Yue-Xiu Wang, Jing-Dong Xu

Yue-Hong Liu, Yue Ding, School of Basic Medical Science, Beijing Capital Medical University, Beijing 100069, China

Chen-Chen Gao, Jing-Dong Xu, Department of Physiology and Pathophysiology, School of Basic Medical Science, Capital Medical University, Beijing 100069, China

Li-Sheng Li, Function Platform Center, School of Basic Medical Science, Capital Medical University, Beijing 100069, China

Yue-Xiu Wang, Beijing Institute for Brain Disorders, Capital Medical University, Beijing 100069, China

ORCID number: Yue-Hong Liu (0000-0002-6618-3511); Yue Ding (0000-0001-6291-6848); Chen-Chen Gao (0000-0002-3730-0272); Li-Sheng Li (0000-0002-7255-6863); Yue-Xiu Wang (0000-0002-3243-3092); Jing-Dong Xu (0000-0003-4546-563X).

Author contributions: Liu YH and Ding Y contributed equally to the writing of this manuscript; Liu YH, Ding Y and Xu JD wrote the manuscript; Liu YH and Gao CC designed the illustrations; Li LS and Wang YX analyzed the data; Xu JD revised the manuscript.

Supported by National Natural Science Foundation of China, No. 81274173, No. 81673671 and No. 81270443; Beijing National Science Foundation, No. 7122017.

Conflict-of-interest statement: The authors do not have any relevant conflicts of interest (including relevant financial interests, activities, relationships and/or affiliations).

Manuscript source: Unsolicited manuscript

Correspondence to: Jing-Dong Xu, PhD, Assistant Professor, Department of Physiology and Pathophysiology, School of Basic Medical Science, Capital Medical University, No. 10, Xitoutiao, You An Menwai, Fengtai District, Beijing 100069, China. xujingdong@163.com
Telephone: +86-10-83911469
Fax: +86-10-83911469

Received: January 27, 2018
Peer-review started: January 28, 2018
First decision: February 10, 2018
Revised: February 12, 2018
Accepted: February 25, 2018
Article in press: February 25, 2018
Published online: March 21, 2018

Abstract

Macrophages (MΦ) differentiate from blood monocytes and participate in innate and adaptive immunity. Because of their abilities to recognize pathogens and activate bactericidal activities, MΦ are always discovered at the site of immune defense. MΦ in the intestine are unique, such that in the healthy intestine, they possess complex mechanisms to protect the gut from inflammation. In these complex mechanisms, they produce anti-inflammatory cytokines, such as interleukin-10 and transforming growth factor-β, and inhibit the inflammatory pathways mediated by Toll-like receptors. It has been demonstrated that resident MΦ play a crucial role in maintaining intestinal homeostasis, and they can be recognized by their unique markers. Nonetheless, in the inflamed intestine, the function of MΦ will change because of environmental variation, which may be one of the mechanisms of inflammatory bowel disease (IBD). We provide further explanation about these mechanisms in our review. In addition, we review recent discoveries that MΦ may be involved in the development of gastrointestinal tumors. We will highlight the possible therapeutic targets for the management of IBD and gastrointestinal tumors, and we also discuss why more details are needed to fully

understand all other effects of intestinal MΦ.

Key words: Macrophages; Homeostasis; Inflammatory bowel disease; Gastrointestinal tumors; Therapeutic targets

Core tip: The manuscript involves three components. First, after briefly describing the origin of macrophages (MΦ), it summarizes their general biologic features and common functions. The second component reveals the differences between resident MΦ in the intestine and those in other tissues. Notably, we depicted how resident MΦ participate in maintaining intestinal homeostasis and why they can maintain intestinal health by comparison between each of these distinct features. The third part discusses how the deficiency of this anti-inflammatory system leads to autoimmune diseases. However, we also discuss the many details of why intestinal MΦ and the underlying mechanism of inflammatory bowel disease and gut tumors remain obscure.

Liu YH, Ding Y, Gao CC, Li LS, Wang YX, Xu JD. Functional macrophages and gastrointestinal disorders. *World J Gastroenterol* 2018; 24(11): 1181-1195 Available from: URL: http://www.wjgnet.com/1007-9327/full/v24/i11/1181.htm DOI: http://dx.doi.org/10.3748/wjg.v24.i11.1181

INTRODUCTION

The intestine is organized into distinct specialized and functional tissues, such as the epithelium and lamina propria (LP). As the major site of bacterial colonization (10^2 cfu/mL in the duodenum, 10^2 cfu/mL in the jejunum, 10^3 cfu/mL in the proximal ileum, 10^7-10^8 cfu/mL in the distal ileum, and 10^{11}-10^{12} cfu/mL in the colon[1]), it is crucial to maintain intestinal homeostasis in which the intestinal immune system contributes to such maintenance under physiological conditions. Meanwhile, both commensal bacteria and their products play important roles[2].

The mammalian intestine is considered the largest immune organ in the body. It is estimated that 65%-80% of the immune cells, such as macrophages (MΦ), dendritic cells (DCs), T cells and B cells[3], exist in the intestine. There are many lymphocytes and natural killer (NK) cells in the region of the epithelial base[4,5]. Most of the intraepithelial lymphocytes are T cells, and they express CD3, CD8[6], TCRαβ[5] or TCRγδ[7] (mainly in mice). Goblet cells of the intestinal epithelium secrete net-like MUC2 mucins that compose the surface mucus layer, which can filter out microbes[8,9]. Both the intestinal epithelium and mucus layer constitute the double-protective barrier to maintain homeostasis at the entrance where pathogens invade. With the background described above, it seems that MΦ are insignificant in the intestinal immune system. In fact, they play a unique supporting role in maintaining the balance of intestinal immunity, and they are by no means as simple as we thought.

MΦ are one of the nonhematopoietic cells in all mammalian species that are distributed throughout the tissues of individuals. Their origin is relatively clear, and their biologic features have long been explored. In terms of immune defense, their name reveals their function: phagocytosis. They participate in innate immune responses and adaptive immune responses, especially in the intestine, which is the largest pool of MΦ and commensal bacteria. They can be considered as regulators instead of inflammation propellants (see below).

Emerging evidence suggests that intestinal resident MΦ contribute to maintaining intestinal homeostasis by several mechanisms (see below), and the production of immunosuppressive cytokines and their inhibitory biologic behavior suppress cascaded inflammatory responses. This is beneficial to the host because they protect the intestine from over-responding to commensal bacteria, resulting in severe tissue damage. Thus, they have attracted increasing attention in research on intestinal homeostasis and the correlative mechanisms of intestinal autoimmune diseases, represented by inflammatory bowel disease (IBD).

IBD includes two types of diseases: ulcerative colitis (UC) and Crohn's disease (CD). IBD has long been considered a typical autoimmune disease. Several reports have confirmed that multiple factors, for example, epithelial defects, disturbance of commensal or pathogenic bacteria and destruction of the mucus layer, lead to the development of IBD. In addition, intestinal MΦ highlight the defects of their protective function in IBD.

In addition, we propose some promising targets for the studies and treatments of IBD and gastrointestinal tumors. These comprehensive descriptions and findings of MΦ above have been summarized in figures of our manuscript to make the unique function of intestinal MΦ more understandable.

MACROPHAGES: DIFFERENTIATION AND BIOLOGY

Macrophages differentiate from blood monocytes

In 1884, Ilya Ilyich Mechnikov, an immunologist and pathologist in Russia, identified MΦ. Hereafter, the exploration of this cell type has never waned. Regarding the origin of MΦ, the mononuclear phagocyte system arises from hematopoietic stem cells in the bone marrow and from progenitors in the embryonic yolk sac[10], as well as from fetal liver during early development. As early as 1980, it was verified by using

the Chediak-Higashi marker that both interstitial and intraalveolar MΦ of the lung are derived from bone marrow precursor cells[11]. The family of mononuclear phagocytes consists of monocytes (Mo), MΦ, osteoclasts and DCs.

Granulocyte-macrophage colony stimulating factor (GM-CSF) is a major factor that can promote hematopoietic stem cell differentiation into granulocyte-monocyte cells, promonocytes and Mo[12,13]. Thereafter, Mo circulate in the blood stream in different types of tissues (the environment with different types of tissues controls the differentiation and maturation of resident MΦ by several molecular mechanisms[14-19]), a part of the blood MΦ undergo maturation, adapt to their local microenvironment and turn into various resident MΦ. Resident MΦ may remain as relatively long-life span cells, although they usually cease to proliferate[20]. The remaining blood Mo differentiate into free MΦ, migrating between diverse tissues like amoebae.

To be more rigorous, some researchers further showed that Mo in the bone marrow can be classified as $Ly6C^{hi}$ Mo and $Ly6C^{lo}$ Mo by their expression of Ly6C/Gr1, CCR2 and CX3CR1. $Ly6C^{hi}$ Mo express high levels of Ly6C/Gr-1, CCR2 and CD62L, but low levels of CX3CR1. CCR2 is a chemokine receptor, which is essential for $Ly6C^{+}Gr1^{+}CX3CL1^{-}$ Mo to enter the circulation. $Ly6C^{lo}$ Mo express low levels of Ly6C/Gr1, CCR2 and CD62L but high levels of CX3CR1[21]. $Ly6C^{lo}$ Mo are proposed to be the precursors of resident MΦ[4,22], but there are some conflicts about this hypothesis if the Mo entering the blood stream rely on expressing CCR2, and there is no abundant evidence to support this conclusion. Moreover, MΦ differentiate from blood Mo, a finding that has been challenged recently. Some researchers have suggested that blood Mo contribute little to MΦ in the steady state, and emerging evidence indicates that resident MΦ can undergo self-renewal[23]. However, other researchers demonstrated that blood $Ly6C^{hi}$ Mo are responsible for turning into resident MΦ because they convert into $Ly6C^{lo}$ Mo and can return to the bone marrow, differentiating into $Ly6C^{lo}$ Mo[21]. This explanation may be helpful to understand the origin of resident MΦ.

Biologic features and common functions of macrophages

The volume of MΦ is 5-10 times that of Mo, and they have more organelles (especially lysosomes), folds and pseudopodia. Resident MΦ are widely distributed throughout the body with distinctive phenotypes - for example, dust cells in lung, Langerhans cells in skin, histiocytes in connective tissue, Kupffer cells in the liver, mesangial cells in the kidney and microglial cells in the central nervous system.

A considerable amount of MΦ exists in the intestine, and specific markers expressed by MΦ can be used to study the heterogeneity. For instance, the F4/80[24] antigen and macrosialin in mice are proven to be useful markers in most of the tissues to define the distribution of MΦ, while several antigens such as sialoadhesin, a lectin-like receptor for sialylated glycoconjugates, are particularly strongly present in populations of MΦ in lymphoid organs that do not express F4/80 or CD68. In humans, the CD68 antigen (the human homolog of macrosialin) is widely found in MΦ expressing EMR2 (the human homolog of F4/80)[20].

Presently, many promising markers are awaiting identification, and some detected materials have already generated new hypotheses. For example, matrix metalloproteinase-9, produced by MΦ in the early phase of mouse peritonitis, may be used as an inflammatory marker[25]. In addition, the protein dehydrogenase/reductase-9 was identified as a specific and stable marker of human regulatory MΦ (Mregs)[26], which contributed greatly to the existing body of knowledge on immunosuppressive therapy.

MΦ can be classified as M_1 and M_2, functionally within the Mregs. M_1 MΦ produce high interleukin (IL)-12 and low IL-10, while M_2 MΦ show the opposite trend. Additionally, M_2 MΦ express IL-13α1, but M_1 MΦ do not[27]. A recent study has shown that a novel marker, MS4A4A (a member of the membrane-spanning 4A gene family), is only expressed in M_2 MΦ - that is, MS4A4A might be a surface marker of M_2 MΦ[28]. M_2 MΦ were largely mysterious in the past, while the importance of M_1 MΦ in mucosal biology has been appreciated for decades; the immune regulatory function of M_2 MΦ has only begun to be understood in the last few years. Additionally, their differentiation, as well as their differences from M_1 MΦ in cell biology, will become clearer in the future. Thus, regarding Mregs, it is also important that they are activated by different pathways and play diverse roles in the immune system, which will be described below.

MΦ, "big eaters", are named after their major function: phagocytosis, involving the uptake of particulate materials (> 5.0 μm) by opsonic (Fc receptors and C3b receptors) or non-opsonic receptors such as mannose receptors, scavenger receptors, formyl-methionine-leucyl-phenylalanine, and pattern recognition receptors (PRRs), especially the Toll-like receptors (TLRs). With the existence of these receptors, MΦ can participate in innate immunity and adaptive immunity (Figure 1).

MΦ dispose of approximately 2×10^{11} erythrocytes a day and clear damaged or dying cells[20]. Activated MΦ can recognize microorganisms that break into the epithelial or mucosal barriers with their special/nonspecial receptors and stretch the pseudopodia to swallow these microbes, followed by their digestion by oxygen-dependent/-independent pathways in phagolysosomes. Beyond that, MΦ can be activated by IL-8 and release chemotactic factors and mediators of inflammation (IL-1, IL-6, IL-12 and tumor necrosis factor (TNF)-α, which recruit neutrophils to the inflammatory site.

The neutrophils produce bactericidal compounds,

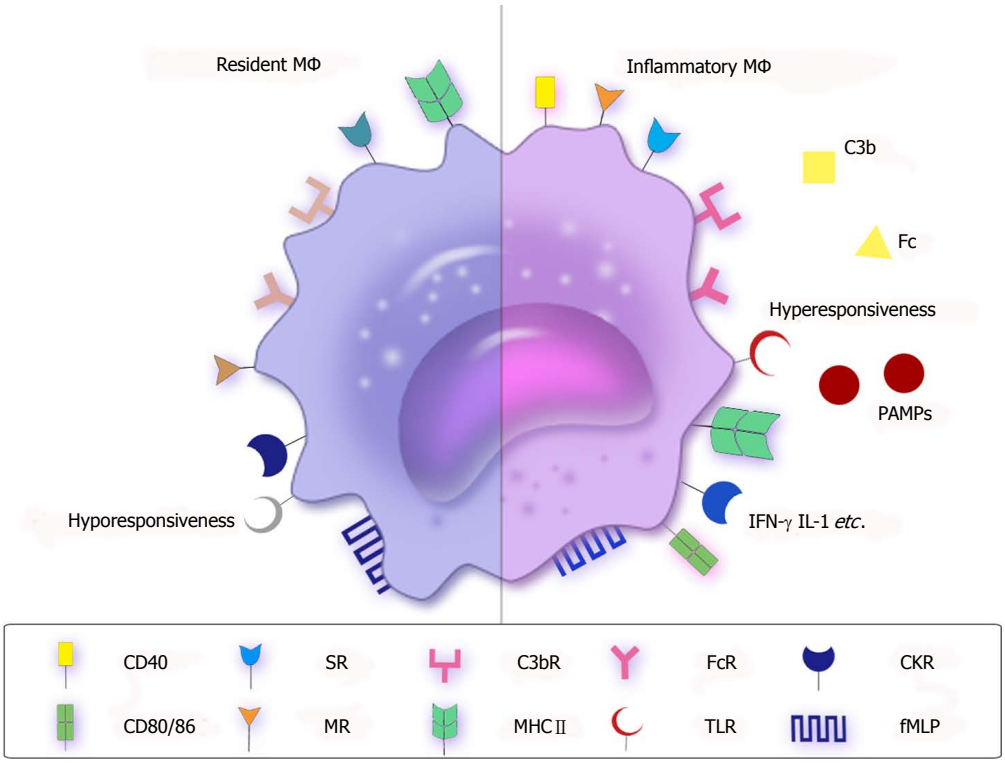

Figure 1 Receptors or molecules of resident and inflammatory macrophages. MΦ express opsonic (FcR and C3bR) or nonopsonic receptors, such as CKRs, MRs, SRs, fMLP and TLRs, as well as express high levels of MHC Ⅱ. However, there are some differences between resident MΦ and inflammatory MΦ. Resident MΦ (left side) do not express high levels of costimulatory molecules such as CD40, CD80 and CD86, and present hyporesponsiveness to TLRs to suppress inflammation. However, inflammatory MΦ (right side) show the opposite trend. The PAMPs lead to inflammation by connecting with hyperresponsive TLRs. CKR: Cytokine receptor; fMLP: Formyl-methionine-leucyl-phenylalanine; MR: Mannose receptor; MΦ: Macrophages; PAMP: Pathogen-associated molecular pattern; SR: Scavenger receptor; TLR: Toll-like receptor.

causing the liquefaction of tissue and formation of pus to eliminate the invading as well as missing pathogens. To complement MΦ, neutrophils secrete several preformed proteins stored in the granules, such as lactoferrin, lipocalin, lysozyme, IL-37, defensins and myeloperoxidase (converts H_2O_2 to hypochlorous acid)[20]. However, MΦ are not so bellicose. To maintain homeostasis of innate immunity, several self-regulative mechanisms restrain inflammation. NK cells inhibit the activation of MΦ by releasing IFN-γ or reducing the number of overactive MΦ by cytotoxicity. IL-1β, IL-10 and transforming growth factor (TGF)-β, produced by MΦ, are responsible for down-regulating the innate immune response. Moreover, the dead neutrophils are phagocytosed by mononuclear phagocytes, and lipoxins, protectins and resolvins contribute to the restoration of normal function[20].

In adaptive immunity, MΦ are an antigen-presenting cell type, like DCs. In the marginal sinus of a lymphoid organ, after digestion, MΦ present fragments at the cell surface on MHCII molecules. Indeed, MΦ are less effective than DCs in antigen presentation to naïve T cells because they only express appropriate costimulatory molecules (*e.g*., CD40, CD80 and CD86) following infection or contact with microbial productions. However, DCs express high levels of MHCII molecules as well as costimulatory molecules. In fact, several microbial productions promote the expression of MHCII molecules and costimulatory molecules in MΦ, which probably enhance the autoimmune response[29].

Gut-associated lymphoid tissues, including dispersed and aggregative tissues, are the primary part of the intestinal immune system[30-32]. The latter type is represented by Peyer's patches (PPs), settled in the LP of the appendix and small intestine, and the solitary lymphoid follicles, widely distributed in the intestinal LP[33,34]. The PPs look like an arch, and they are covered by follicle-associated epithelium, which involves special cells named microfold/membranous cells (M cells)[34,35]. T cells, B cells[36], DCs and MΦ exist in a pocket-like structure outside the base of M cells. M cells efficiently uptake antigens. However, instead of processing and presenting antigens, they are only responsible for transporting antigens and communicating with the resident B cells in the center of PPs.

Most PP cells are B cells, and only a few are T cells, which has been explored in mature mice. The B cells located in the germinal centers of PPs can produce IgA[37-40] (ingredient of sIgA) to participate in pathogen defense. In addition, M cells transport antigens to epithelial cells or antigen presenting cells (DCs and MΦ) to induce the adaptive immune response. It has been certified that the cell-bound antigen transportation can affect mucosal tolerance with the participation of

regional lymph nodes[41].

M_1 MΦ or classically activated MΦ develop in cell-mediated immune responses, which are mainly driven by interferon (IFN)-γ and TNF. IFN-γ can be produced in innate immunity and adaptive immunity. In the former, NK cells are important, but the production of IFN-γ in NK cells is too transient for the persistence of this population of MΦ. Consequently, it is necessary to depend on the adaptive immune response; T helper (Th)1 cells release sustainable IFN-γ and induce classical activated MΦ to kill the microbes indiscriminately[42].

Endogenously produced IFN-β is another factor that can replace IFN-γ to activate classically activated MΦ[43]. M_1 MΦ are the major component of host defense. They produce pro-inflammatory cytokines (*e.g.*, IL-1, IL-6 and IL-23) and associate with Th cells, but it has been reported that their connection with Th17 cells, which produce IL-17, results in serious tissue damage. Thus, their over-activation may be the cause of autoimmune diseases[42].

M_2 MΦ or alternatively-activated MΦ are produced during the innate or adaptive immune response. Basophils and mast cells produce innate IL-4, one of the first innate signals released during tissue injury, and IL-4 turns the resident MΦ into this population of cells to promote wound healing. IL-4 can also be released in adaptive immune responses that can be thought as particularly important pathways to develop and persist the alternatively-activated MΦ[42]. In addition, the Th2-type immune responses have been documented to work at the intestinal mucosal surface to respond to the disturbances by cytokines, such as IL-4 and IL-13[44]. However, compared with M_1 MΦ, there is no sufficient evidence to show that M_2 MΦ directly participate in the bactericidal activities, but they do have indirect regulatory effects[45], which may explain why it is hotly debated in the field of neoplasms[46-56], fibrosis[57-60], metabolic syndrome (might relate to insulin resistance)[61-65] and intestinal autoimmune diseases.

Mregs are a type of immunosuppressive cells, which have been illustrated comprehensively by Mosser *et al*[42]. Those authors summarized the mechanisms of producing Mregs in innate and adaptive immune responses and the stimuli of these processes. In addition, they mentioned that Mregs produce IL-10 and decrease the production of IL-12 to dampen inflammation. However, their helpful antiinflammatory function might be exploited by parasites to safely survive in the host's defense, which is an interesting point and powerful evidence to confirm the role of Mregs in the immune system.

To summarize, MΦ are extraordinarily complicated in their structure and functions. On the one hand, they are pioneers of pathogen defense *in vivo*, and one of the regulators that control the immune responses. On the other hand, they can be considered a bridge between innate immunity and adaptive immunity. It has been proven that they are very important in diseases such as asthma[66-70], atherosclerosis[71-76], retinopathy[77-80], neoplasm and autoimmune diseases.

MΦ PLAY A FUNCTIONAL ROLE IN INTESTINAL HOMEOSTASIS

General characteristics of intestinal MΦ

The differentiation of intestinal MΦ rely on intestinal epithelial cells, which have been proven by an extracorporeal three-dimensional coculture model[81]. MΦ are found in the intestinal tract of all mammals, both in the mucosa and deeper layers[82]. They are found mostly frequently in the LP and produce PGF2 to replenish deficient epithelial cells[23]. Several studies have summarized a rule about the quantity of intestinal MΦ, as follows: in different parts of the intestine, the numbers of MΦ correlate with the quantity of bacteria. An experiment provided the supporting evidence by recording the weight of each mouse organ or tissue and calculating their F4/80 antigen levels. The total F4/80 antigen levels in the small bowel were 1.3×10^7, and 1.4×10^7 in the large bowel. In the intestine of germ-free mice, the numbers of MΦ are decreased[24], likely indicating that the pathogen defense should also be the basic function of intestinal MΦ.

The general markers of MΦ have been mentioned above. Regarding intestinal MΦ, they can be recognized by their unique markers. Resident MΦ in the healthy mouse colon are F4/80^{hi}, class Ⅱ MHC^{hi} (also found in humans[83]), CX3CR1^{hi}, CD11c$^+$, CD103$^-$ and Siglec F$^-$[82]. Unlike resident MΦ in other tissues, the highly expressed CX3CR1 is unique. Furthermore, the intestinal MΦ express CD13[84], CD14 and CD70, and they can be subdivided according to their size[85]. Previously, it was difficult to distinguish between intestinal DCs and MΦ; however, a small population of mucosal MΦ has recently been found to express CD11c, which is a specific marker of DCs. The F4/80$^+$, CD11b$^+$, and CD68$^+$ cells are more likely to be MΦ rather than DCs. They do not present antigens to naïve T cells, and only the CD103$^+$CX3CR1$^-$ cells are classical DCs[82,86-90]. These findings resolved a few puzzles concerning intestinal DCs and MΦ-like cells with the emergence of a possible hypothesis about the relationship between intestinal MΦ and DCs.

Differences between macrophages in the intestine and other tissues are illustrated in Figure 1. Unlike MΦ in other tissues, resident MΦ[91] in the healthy intestine do not express high levels of costimulatory molecules, such as CD40, CD80 and CD86[83], and they do not up-regulate costimulatory molecules or induce a respiratory burst to exterminate microbes[92-94]. Additionally, their responses to TLR ligands are unexpected[83,95]. TLRs are membrane glycoproteins located at the cell surface or within endosomes. They have an extracellular region to bind ligand and an ectoplasmic domain to trigger the

intracellular signaling cascade. They can form hetero- or homodimers with each other, or complex with other receptors to recognize a wide range of microbes.

In general, with the TLRs, MΦ can be activated through many pathways mediated by MyD88, TRIF and NF-κB[20]. It is widely accepted that TLRs are the most characteristic PRRs. However, the intestinal resident MΦ do not respond to TLR ligands and produce proinflammatory cytokines or chemokines, such as IL-1, IL-6, IL-12, IL-23, TNF-α and CXCL10[82,91], which can be considered the inertia of mucosal MΦ. It has been conjectured that such is likely due to the absence of TLRs and other receptors (NOD-1/NOD-2) or malfunction of signaling pathways (*via* inhibitors or other mechanisms[96])[82,97,98]. However, this does not mean that the intestinal resident MΦ do not express TLRs or that TLRs are not necessary. In fact, they are essential to protect the intestinal epithelium under pathological circumstances[97,99,100].

These differences between intestinal mucosal MΦ and their homogeneity in other tissues reveal that they are more likely to control inflammation and maintain homeostasis in healthy individuals. However, what will occur if the balance has become broken?

Intestinal MΦ change dramatically under different situations

It is less rigorous to use the word "change[101]" in the subtitle because there is little detail to describe that the intestinal resident MΦ change into inflammatory MΦ (classical MΦ) under pathological circumstances with the changes in the environment, or that these two types of MΦ coexist in healthy intestine, working respectively. Nonetheless, there is another possibility. A credible concept has been explained[21] involving $CD14^{hi}CD16^{-}$ Mo, which can be considered to enter the intestinal LP only in a CCR2-dependent[102] manner and turn into the resident $CD14^{lo}$ $MHCII^{hi}CD163^{hi}CD64^{+}$ MΦ or inflammatory $CD14^{hi}MHCII^{hi}CD163^{lo}CD64^{+}$ MΦ in different circumstances. However, confusion concerning the relationship between $CD14^{hi}CD16^{-}$ Mo and $Ly6C^{hi}$/ $Ly6C^{lo}$ Mo has emerged and remains to be directly described.

It is clear that intestinal resident MΦ produce antiinflammatory cytokines, especially IL-10 and TGF-β[4,84,103-111], whereas inflammatory MΦ work at the inflammatory site and have strong bactericidal activity, as explained above. In healthy intestine, IL-10 is produced by mucosal MΦ themselves and is a component of T cells[112]. Vasoactive intestinal peptide (VIP) and pituitary adenylate cyclase-activating polypeptide increase the production of IL-10 by mucosal MΦ *in vitro* and *in vivo*[113]. IL-10 prevents the NF-κB pathway, and inhibiting the autocrine/paracrine production of IL-10 reverses TLR unresponsiveness in MΦ[82]. Maintaining Foxp3 expression of regulatory T cells (Tregs) has been reported as one of the important functions of IL-10 produced by MΦ[114]. $CD4^{+}Foxp3^{+}$ Tregs greatly contribute to the immune regulatory networks with the complement of other T cells and B cells, maintaining intestinal homeostasis[115]. Recently, research[107] on *Citrobacter rodentium*-infected mice with cell type-specific deletion of Il-10 demonstrated that IL-10 prevents excessive inflammation in acute bacterial infection by controlling IL-23[116,117] production to limit innate immunity. Another study indicated that the deficiency of IL-10 results in stable chromatin alterations in intestinal MΦ[118]. These results showed that IL-10 indeed plays a critical role in limiting inflammation.

Another factor for antiinflammation is TGF-β. Intestinal resident MΦ express high levels of TGF-β receptors and show constitutively-active TGF-β signaling[82]. TGF-β also connects with Foxp3, expressed by Tregs, and $CD4^{+}Foxp3^{+}$ Tregs decrease the ability of mucosal MΦ to activate and translocate NF-κB[115]. Intestinal resident MΦ do not respond to TLR ligands with the existence of TGF-β[82]. In contrast to IL-10, their production in murine MΦ is inhibited by VIP[111]. Moreover, the expression of Smad7 (a member of the Smad family that mediates a pathway for TGF-β and BMP-2 signal transduction) interrupts TGF-β signaling and activates inflammatory MΦ, a finding that was demonstrated in an experiment of necrotizing enterocolitis MΦ[110].

Currently, the study of CD200 for antiinflammation has received less attention. CD200L is a member of the protective system, with the ability to restrain the activity of MΦ. Inhibitory signaling of CD200L is triggered by the interaction with CD200 in nonhematopoietic cells as well as MΦ[20]. This process protects tissues from severe damage. A study reported that knock-out of CD200 or CD200R1 produces MΦ hyperactivity and autoimmune diseases[119]. Enlightened by this, it is possible to assume CD200 maintains intestinal homeostasis. There are some relevant studies in the respiratory system[120], but the existing evidence in the intestine remains insufficient.

The enteric nervous system (ENS) plays a crucial role in controlling gastrointestinal physiology and interacting with microbes and immune cells, functions that have been explored for decades. Accumulating evidence indicates they closely contact MΦ. The development of $CX3CR1^{hi}MHCII^{hi}$ $CD11b^{+}CD11c^{lo}CD103^{-}$ muscularis MΦ (MMs) requires CSF1, and enteric neurons selectively express bone morphogenetic protein (BMP; expressed by MMs) receptor 2, which produces CSF1. By contrast, the expression of BMP2 activates enteric neurons. The correlation of MMs and ENS contributes to gut motility[121]. Additionally, MMs have been found to express tissue-protective and wound-healing genes resembling M_2 MΦ, reacting in intestinal infection[122].

More importantly, neurotransmitters are essential for neuronal immune control. VIP is known to exhibit

antiinflammatory effects, depending on promoting the production of IL-10. Nitric oxide is well known for its antimicrobe ability in the respiratory burst. However, it suppresses excitability in neurons[121] and influences ENS during intestinal inflammation[91]. Interestingly, serotonin (5-HT), which was considered a trigger of inflammation, has been demonstrated to act, indirectly, on MMs by 5-HT_4 receptors in neurons and to stimulate an antiinflammatory cascade in MΦ. It has been indicated that 5-HT_2 and 5-HT_7 are related to the development of M_1 and M_2 MΦ[91]. In addition, γ-amino butyric acid has been suggested to have an immunosuppressive effect on resident MΦ of the central nervous system[91]. However, in the intestine, it remains unclear. It is worth investigating the functions of ENS and how they act on MΦ to understand the gut immune system and associated disease treatments in the future.

Current views about intestinal MΦ

First, Kennichi *et al*[123] provided an exhaustive experimental result concerning LP-resident $CD169^+$ MΦ that mainly persist in secondary lymphoid organs. They indicate that $CD169^+$ MΦ reside at the bottom-end of the LP microenvironment, far away from the epithelium-LP border. Most importantly, the $CD169^+$ MΦ recruit inflammatory monocytes by producing CCL8, selective depletion of $CD169^+$ MΦ and anti-CCL8 antibody promotion of dextran sulfate sodium-induced colitis in mice. The comparison of $CD109^-$ and $CD109^+$ MΦ led to an interesting hypothesis. Unlike $CD109^-$ MΦ, $CD109^+$ MΦ are located in a region distant from the perimeter where they can be interrupted by commensal bacteria and dead epithelial cells, and they can directly release CCL8 into the systemic circulation in the vascular-rich environment. $CD109^+$ MΦ probably respond to the collapse of the frontline defense - *i.e.* they can be considered as a "conservation corps" in the intestine (Figure 2).

Second, M_2 MΦ struggle for attention. As another regulative population, M_2 MΦ produce IL-10 and express CD163 and CD206 lectin receptors. They do not produce proinflammatory mediators with signals of stimulation. Certainly, they produce tissue-repairing factors, such as vascular endothelial growth factor (VEGF), actin and metalloproteinases, due to their function in wound healing. M_2 MΦ are $MHCII^+$, which may be helpful in exploring their potential in bactericidal activities[82,83,124,125]. Unlike M_2 MΦ, Mregs express high levels of costimulatory molecules, such as CD40, CD80 and CD86, to submit antigens to T cells more effectively[42], highlighting the hypothesis that the regulation of M_2 MΦ in the intestine might be different from that of Mregs. However, the antiinflammatory function of Mregs mentioned above has not been directly verified in the intestine. Therefore, we are unsure about the role of Mregs in intestinal homeostasis, and some questions remain concerning the meaning of the difference between M_2 MΦ and Mregs (Figure 2).

Finally, a novel finding[126] concerning GPBAR1 (a G protein-coupled receptor for secondary bile acids) suggests that GPBAR1 is essential to maintain intestinal immune homeostasis by regulating M_1/M_2 MΦ. BAR501 (a small-molecule stimulus of GPBAR1) contributes to this regulatory process, depending on the production control of IL-10. Absence of the GPBAR1 gene causes the recruitment of M_1 macrophages and severe inflammation in the colon. Exposure to BAR501 leads to the increased expression of IL-10 and TGF-β mRNA, and percentage of $CD4^+/Foxp3^+$ cells. Based on this study, GPBAR1 deserves attention for its potential to protect intestinal health (Figure 2).

MΦ AND GASTROINTESTINAL DISORDERS

MΦ and IBD

According to the mechanisms of intestinal MΦ in maintaining homeostasis, any defect of the antiinflammation system may bring the reduction of immune tolerance, resulting in IBD. In 1998, it was found that intestinal MΦ displayed low expression of class Ⅱ MHC molecules in mouse colitis[127]. A hypothesis arose from this study that there could be dysfunction of MΦ participating in adaptive immune responses when inflammation occurs.

From the origin of MΦ, emerging evidence suggests that GM-CSF plays a central role and has a protective effect in human CD and acute colitis by activating specific Mo[128,129]. Classical $CD14^{hi}CD16^-$ Mo differentiate into large numbers of inflammatory MΦ in the inflamed mucosa of patients with CD[21]. $CD14^+$ Mo in the mucosa from IBD patients increase the production of TNF-α[130,131], IL-1β and IL-6, and enhance respiratory burst activity[21]. Moreover, IL-10 knock-out mice develop spontaneous IBD[82]. An intrinsic resistance to TGF-β receptor signaling has been shown in the mucosa from patients with CD[132]. $CD4^+Foxp3^+$ T cells fail to protect the intestine from chronic inflammation without IL-10- and TGF-β-dependent mechanisms[115]. M_2 MΦ have been certified to be activated by the Wnt signaling pathway, which is associated with UC[133]. These studies showed that intestinal MΦ are of great value for IBD. Following this result, promising treatments for IBD, such as $CD109^+$ MΦ Tregs and GPBAR1, can be considered new therapeutic targets.

MΦ are clearly associated with IBD, but there remain a few puzzles regarding some details. The first study[134] observed that $RoRγ^+$ innate lymphoid cells (ILCs; the primary source of GM-CSF in the gut) promote MΦ to respond to the microbial signals and produce IL-1β, which enhances inflammation. By contrast, another study[135] discovered that with the regulation of $RoRγ^+$ ILCs, MΦ promote a negative feedback

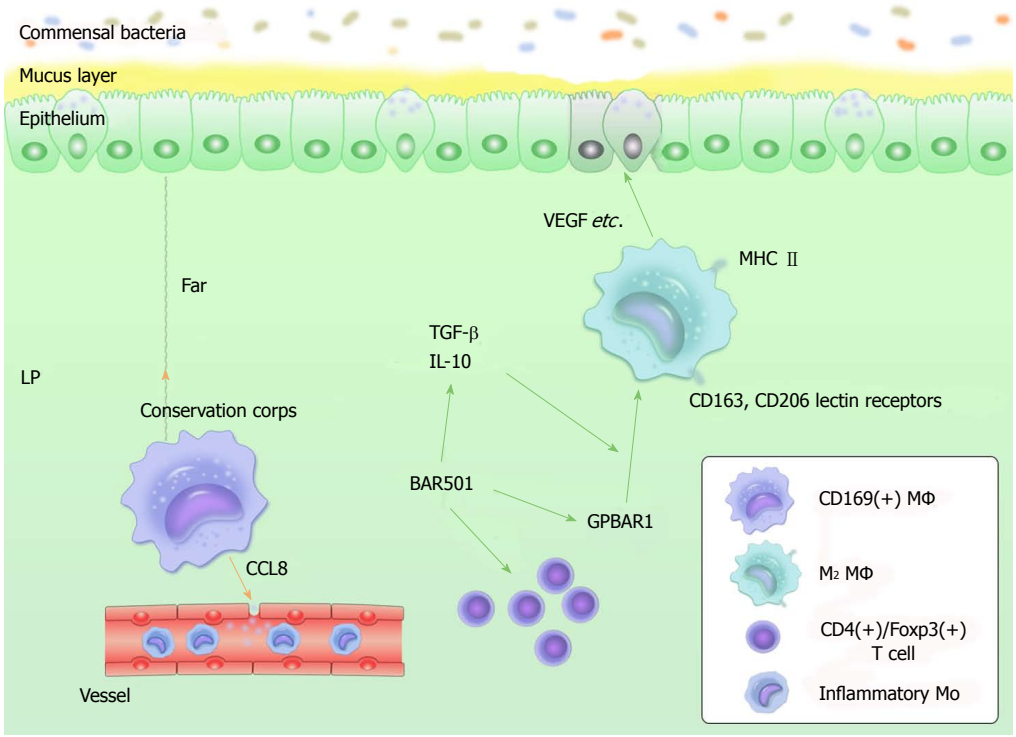

Figure 2 Current views about intestinal macrophages. 1. LP-resident CD169$^+$ MΦ reside at the bottom-end of the LP microenvironment, far away from the epithelium-LP border. CD169$^+$ MΦ recruit inflammatory monocytes by producing CCL8. CD109$^+$ MΦ can be considered as a "conservation corps" in the intestine because they likely respond to the collapse of frontline defense. 2. M_2 MΦ are MHC Ⅱ$^+$, producing IL-10 and expressing CD163, CD206 and lectin receptors. They do not produce proinflammatory mediators with signals of stimulation. In addition, they produce tissue-repairing factors, such as VEGF, actin and metalloproteinases. 3. GPBAR1 is essential to maintain intestinal immune homeostasis by regulating M_1/M_2 MΦ. BAR501 is a small-molecule stimulus for GPBAR1. It contributes to this regulative process, depending on the production control of IL-10. Exposure to BAR501 leads to increased expression of IL-10, TGF-β mRNA and the percentage of CD4$^+$/Foxp3$^+$ cells. IL: Interleukin; LP: Lamina propria; MΦ: Macrophages; TGF: Tumor growth factor; VEGF: Vascular endothelial growth factor.

pathway through the activation of IL-22 production, which might be protective. Indeed, the quantity of RoRγ$^+$ ILCs could increase in human CD. This finding inspires the question of whether the possibility exists that a portion of MΦ still tries to restore intestinal homeostasis when the intestine is trapped in a vicious cycle for inflammatory macrophages. The second item concerns CD200/CD200R1 mentioned above. Knock-out of CD200 results in MΦ hyperactivity *in vitro*, but CD200R1 knock-out mice have normal intestinal MΦ populations, and they neither develop spontaneous IBD nor become more susceptible to colitis induced by the dextran sulfate sodium model[82]. This indicates that CD200R1 may not be as important as we had previously considered, but the reasons remain unclear.

MΦ and gastrointestinal tumors

Since the end of the last century, many studies have certified the connection between MΦ and tumors in various systems. There are considerable numbers of investigations concerning tumor-associated macrophages (TAMs). They promote immunosuppression, tumor immune evasion[136], tumorigenesis, tumor metastasis and angiogenesis as well as invasion by releasing various cytokines and inflammatory mediators, such as IL-6, IL-10, TFG-β, CCL2, CCL17, VEGF and cathepsins[137]. However, different populations of TAM have different functions. M_1 MΦ have been confirmed to recognize and clear tumor cells, a function that is beneficial to health. By contrast, the development and movement of tumors benefit from M_2 MΦ. TAMs are one of the promising targets of tumor therapy, especially M_2 MΦ. Gut tumors are also included. We provide more details about TAMs and references in Box 4 to further illustrate the relationship between TAMs and tumors.

Similar to other MΦ, TAMs arise from hemato-poietic stem cells in the bone marrow and from progenitors in the embryonic yolk sac. With different environmental signals, Mo differentiate into distinctive macrophages[137,138]. Tumor signals contribute to the development of TAMs. Mantovani *et al*[139] summarized the signals associated with TAMs. For example, lactic acid, CCL2, CSF1, VEGF and TGF-1 from tumor cells, IL-1β from tumor-associated fibroblasts, and IL-10 from Tregs, all can drive TAMs into tumor-promoting MΦ. Moreover, they also list the products of TAMs which have different functions. For instance, IL-6, MFG-E8 and osteopontin from TAMs can active tumor stem cells; TAMs produce epidermal growth factor to promote tumor growth, invasion and metastasis. Nitric oxide and reactive oxygen species can be released to destroy tumor cells. However, they might

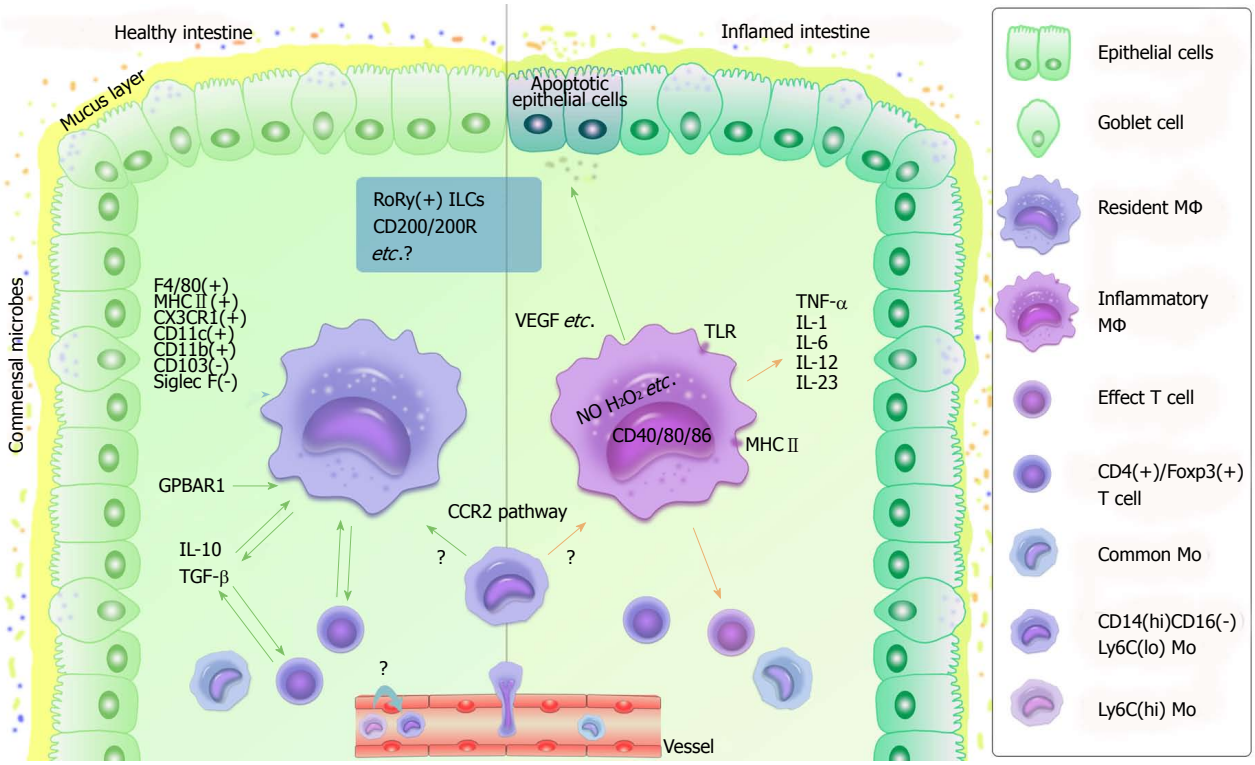

Figure 3 Functional role of macrophages in healthy or inflamed intestine. MΦ differentiate from blood Mo. Ly6c^{lo} Mo are proposed to be the precursors of resident MΦ. CD14^{hi}CD16^{-} Mo turn into resident or inflammatory MΦ according to different circumstances *via* the CCR2 pathway. In healthy intestine (left side), resident MΦ are F4/80^{hi}, class Ⅱ MHC^{hi} CX3CR1^{hi}, CD11c^{+}, CD103^{-} and Siglec F^{-}. They do not express high levels of costimulatory molecules such as CD40, CD80 and CD86. Their connections with CD4^{+}/Foxp3^{+} T cells, IL-10 and TGF-β are helpful to maintain intestinal homeostasis (green arrows). GPBAR1 is essential to maintain intestinal immune homeostasis by regulating M1/M2 MΦ. In inflamed intestine (right side), Mo change into inflammatory MΦ, which produce TNF-β, IL-1, IL-6, IL-12, and IL-23, and activate effective T cells with several specific receptors, such as TLR, as well as induce respiratory burst (*e.g.*, NO and H_2O_2 production), leading to inflammation (orange arrows). In addition, M2 MΦ produce tissue-repairing factors such as VEGF, which shows a positive effect in individuals during inflammation (green arrow). Regarding MΦ and intestinal immunity, many details remain unclear - for instance, the functions of RoRγ^{+} ILCs and CD200/200R (in blue rectangle) as well as that of Ly6C$^{hi/lo}$ Mo. IL: Interleukin; ILC: Innate lymphoid cell; Mo: Monocytes; MΦ: Macrophages; NO: Nitric oxide; TGF: Tumor growth factor; TLR: Toll-like receptor; TNF: Tumor necrosis factor; VEGF: Vascular endothelial growth factor.

result in genetic instability, causing tumor formation. Nevertheless, further studies have indicated that not all the macrophages that have emerged into the tumor microenvironment are tumor promoting.

M1 MΦ (having antitumor function) can recognize tumors and kill tumor cells by the cytotoxic effect, representing a double-edged sword. They have been verified as an independent predictor of survival time in patients with non-small cell lung cancer[140]. M2 MΦ have a protumor function. They promote the metastasis of K7M2 wild-type osteosarcoma cells in mice. Additionally, all-trans retinoic acid dampens the profunction of M2 MΦ by suppressing the production of IL-13 or IL-14 (from M2 m MΦ) to inhibit the metastasis of osteosarcoma[141]. CHI3L1, a protein secreted by M2 MΦ, promotes the metastasis of gastric and breast cancer cells[55]. In addition, it was confirmed that patients with peritoneal dissemination in gastric cancer have more M2 MΦ and low expression of M1-related messengers[142]. MFG-E8, a powerful angiogenic factor, is induced by bone marrow-derived mesenchymal stromal cells in mice. Attenuated tumor growth and the decreasing function of M2 MΦ can be found in MFG-E8-deficient mice[143], which represent M2 MΦ that contribute to tumor angiogenesis; whether the correlation of M2 MΦ and MFG-E8 is parallel or antiparallel should be further clarified.

Above all, TAMs have advantages and disadvantages to both human physiology and tumors. They are members of our defensive line, but they are also tumor helpers. Compared with the favorable contributions of TAMs, such as M1 MΦ in tumor resistance, the promising therapeutic targets they provide might be more useful. In the 1990s, some scientists systematically revealed that TAMs were worth exploring for antitumor therapy[144], and more and more findings were uncovered during the last 50 years. On the one hand, TAMs are hopeful antitumor targets; on the other hand, as Mantovani and Allavena[139] illustrated, the mechanisms of TAMs in tumor development and antitumor processes are intricate, which limits researchers' ability to find the antitumor target precisely. This phenomenon is the yin-yang of antitumor therapy and the challenge[145] of future antitumor studies.

Several studies have presented recent research progress in gastrointestinal tumors. First, tumor angiogenesis and survival in intestinal-type gastric cancer is closely associated with the infiltration of thymidine

phosphorylase-positive MΦ[146]. Therefore, thymidine phosphorylase could be a useful marker for tumor angiogenesis, and the prognosis of intestinal-type gastric cancer. Second, there is a hotspot induced by M_2 MΦ. A portion of M_2 MΦ, cooperating with TNF, were shown to be recruited to tumors[56,147]. The macromolecular contrast agent PG-Gd-NIR813 shows a dual magneto-optical imaging probe of tumor-associated M_2 MΦ[50], and a few new factors have been evaluated as mediators of the development of gastrointestinal tumors, such as M_2 MΦ-secreted CHI3L1 protein[55] and monocyte chemoattractant protein-1[148]. All are likely to become novel approaches for antitumor therapy.

CONCLUSION

In summary (Figure 3), MΦ with their various receptors act as sentinels in innate immunity and adaptive immunity. In healthy intestinal mucosa, they are indispensable to suppress inflammation and play an essential role in maintaining homeostasis by producing many inhibitors, such as IL-10 and TGF-β. However, they show strong bactericidal activities. Intestinal resident MΦ create a harmonious environment for commensal bacteria and their host. Any defect in keeping this balance can reduce immune tolerance, causing acute tissue damage or chronic autoimmune diseases, explaining their close association with IBD. New findings concerning intestinal MΦ and IBD, as well as tumors, can be very helpful for studies and disease treatments. Meanwhile, there are many details awaiting clarification as well as many unresolved issues.

ACKNOWLEDGMENTS

We wish to thank Prof. Zhang Min (School of Biological Engineering, Capital Medical University) for her contribution in polishing the language of this manuscript.

REFERENCES

1 **Sartor RB**. Microbial influences in inflammatory bowel diseases. *Gastroenterology* 2008; **134**: 577-594 [PMID: 18242222 DOI: 10.1053/j.gastro.2007.11.059]
2 **Macpherson AJ**, Harris NL. Interactions between commensal intestinal bacteria and the immune system. *Nat Rev Immunol* 2004; **4**: 478-485 [PMID: 15173836 DOI: 10.1038/nri1373]
3 **Tang L**, Cheng CY, Sun X, Pedicone AJ, Mohamadzadeh M, Cheng SX. The Extracellular Calcium-Sensing Receptor in the Intestine: Evidence for Regulation of Colonic Absorption, Secretion, Motility, and Immunity. *Front Physiol* 2016; **7**: 245 [PMID: 27458380 DOI: 10.3389/fphys.2016.00245]
4 **Bain CC**, Mowat AM. Macrophages in intestinal homeostasis and inflammation. *Immunol Rev* 2014; **260**: 102-117 [PMID: 24942685 DOI: 10.1111/imr.12192]
5 **Altmeyer S**, Zentek J, Vahjen W, Scharek-Tedin L. The expression of NKG2D on porcine IEL and its possible relation to the adaptive intestinal immune system. *Vet Immunol Immunopathol* 2017; **187**: 89-95 [PMID: 28494934 DOI: 10.1016/j.vetimm.2017.03.005]
6 **Goodyear AW**, Kumar A, Dow S, Ryan EP. Optimization of murine small intestine leukocyte isolation for global immune phenotype analysis. *J Immunol Methods* 2014; **405**: 97-108 [PMID: 24508527 DOI: 10.1016/j.jim.2014.01.014]
7 **Weitkamp JH**, Rosen MJ, Zhao Z, Koyama T, Geem D, Denning TL, Rock MT, Moore DJ, Halpern MD, Matta P, Denning PW. Small intestinal intraepithelial TCRγδ+ T lymphocytes are present in the premature intestine but selectively reduced in surgical necrotizing enterocolitis. *PLoS One* 2014; **9**: e99042 [PMID: 24905458 DOI: 10.1371/journal.pone.0099042]
8 **Kim YS**, Ho SB. Intestinal goblet cells and mucins in health and disease: recent insights and progress. *Curr Gastroenterol Rep* 2010; **12**: 319-330 [PMID: 20703838 DOI: 10.1007/s11894-010-0131-2]
9 **Johansson ME**, Hansson GC. Mucus and the goblet cell. *Dig Dis* 2013; **31**: 305-309 [PMID: 24246979 DOI: 10.1159/000354683]
10 **Takata K**, Kozaki T, Lee CZW, Thion MS, Otsuka M, Lim S, Utami KH, Fidan K, Park DS, Malleret B, Chakarov S, See P, Low D, Low G, Garcia-Miralles M, Zeng R, Zhang J, Goh CC, Gul A, Hubert S, Lee B, Chen J, Low I, Shadan NB, Lum J, Wei TS, Mok E, Kawanishi S, Kitamura Y, Larbi A, Poidinger M, Renia L, Ng LG, Wolf Y, Jung S, Önder T, Newell E, Huber T, Ashihara E, Garel S, Pouladi MA, Ginhoux F. Induced-Pluripotent-Stem-Cell-Derived Primitive Macrophages Provide a Platform for Modeling Tissue-Resident Macrophage Differentiation and Function. *Immunity* 2017; **47**: 183-198.e6 [PMID: 28723550 DOI: 10.1016/j.immuni.2017.06.017]
11 **Johnson KJ**, Ward PA, Striker G, Kunkel R. A study of the origin of pulmonary macrophages using the Chédiak-Higashi marker. *Am J Pathol* 1980; **101**: 365-374 [PMID: 7001909]
12 **Fuad MB**, Robert MN. Allergy and Immunology of the Upper Airway. In: Flint PW Haughey BH, Lund V, Niparko JK, Robbins KT, Thomas JR, Lesperance MM, editor Cummings Otolaryngology. 6th ed. Philadelphia, PA, US: Elsevier Saunders, 2015: 593-625
13 **MacDonald KP**, Palmer JS, Cronau S, Seppanen E, Olver S, Raffelt NC, Kuns R, Pettit AR, Clouston A, Wainwright B, Branstetter D, Smith J, Paxton RJ, Cerretti DP, Bonham L, Hill GR, Hume DA. An antibody against the colony-stimulating factor 1 receptor depletes the resident subset of monocytes and tissue- and tumor-associated macrophages but does not inhibit inflammation. *Blood* 2010; **116**: 3955-3963 [PMID: 20682855 DOI: 10.1182/blood-2010-02-266296]
14 **Dubertret L**, Breton-Gorius J, Fosse M, Touraine R. A cytochemical marker for epidermal differentiation, Langerhans cells, skin resident macrophages and mitochondria. *Br J Dermatol* 1982; **107** Suppl 23: 96-100 [PMID: 7138784]
15 **Hoefsmit EC**, Schadee-Eestermans IL, Beelen RH. The development of the resident pattern of endogenous peroxidatic activity in mouse peritoneal macrophages coincides with the expression of the differentiation antigen F4/80. A combined method for immunoperoxidase labeling and endogenous peroxidase cytochemistry. *J Histochem Cytochem* 1986; **34**: 633-640 [PMID: 3517147 DOI: 10.1177/34.5.3517147]
16 **Iwama A**, Wang MH, Yamaguchi N, Ohno N, Okano K, Sudo T, Takeya M, Gervais F, Morissette C, Leonard EJ, Suda T. Terminal differentiation of murine resident peritoneal macrophages is characterized by expression of the STK protein tyrosine kinase, a receptor for macrophage-stimulating protein. *Blood* 1995; **86**: 3394-3403 [PMID: 7579443]
17 **Satoh T**, Kidoya H, Naito H, Yamamoto M, Takemura N, Nakagawa K, Yoshioka Y, Morii E, Takakura N, Takeuchi O, Akira S. Critical role of Trib1 in differentiation of tissue-resident M2-like macrophages. *Nature* 2013; **495**: 524-528 [PMID: 23515163 DOI: 10.1038/nature11930]
18 **Meireles AM**, Shiau CE, Guenther CA, Sidik H, Kingsley DM, Talbot WS. The phosphate exporter xpr1b is required for differentiation of tissue-resident macrophages. *Cell Rep* 2014; **8**: 1659-1667 [PMID: 25220463 DOI: 10.1016/j.celrep.2014.08.018]
19 **Wang Y**, Colonna M. Interkeukin-34, a cytokine crucial for the differentiation and maintenance of tissue resident macrophages and Langerhans cells. *Eur J Immunol* 2014; **44**: 1575-1581 [PMID: 24737461 DOI: 10.1002/eji.201344365]
20 **David M**, Jonathan B, David BR, Ivan MR. Mononuclear

Phagocytes in Immune Defense. In: David M, Jonathan B, David BR, Ivan MR, editor Immunology. 8 ed. Philadelphia, PA, US: Elsevier Saunders 2013: 125-126
21 **Gren ST**, Grip O. Role of Monocytes and Intestinal Macrophages in Crohn's Disease and Ulcerative Colitis. *Inflamm Bowel Dis* 2016; **22**: 1992-1998 [PMID: 27243595 DOI: 10.1097/MIB.0000000000000824]
22 **Geissmann F**, Jung S, Littman DR. Blood monocytes consist of two principal subsets with distinct migratory properties. *Immunity* 2003; **19**: 71-82 [PMID: 12871640]
23 **Bain CC**, Mowat AM. Intestinal macrophages - specialised adaptation to a unique environment. *Eur J Immunol* 2011; **41**: 2494-2498 [PMID: 21952804 DOI: 10.1002/eji.201141714]
24 **Lee SH**, Starkey PM, Gordon S. Quantitative analysis of total macrophage content in adult mouse tissues. Immunochemical studies with monoclonal antibody F4/80. *J Exp Med* 1985; **161**: 475-489 [PMID: 3973536]
25 **Kolaczkowska E**, Arnold B, Opdenakker G. Gelatinase B/MMP-9 as an inflammatory marker enzyme in mouse zymosan peritonitis: comparison of phase-specific and cell-specific production by mast cells, macrophages and neutrophils. *Immunobiology* 2008; **213**: 109-124 [PMID: 18241695 DOI: 10.1016/j.imbio.2007.07.005]
26 **Riquelme P**, Amodio G, Macedo C, Moreau A, Obermajer N, Brochhausen C, Ahrens N, Kekarainen T, Fändrich F, Cuturi C, Gregori S, Metes D, Schlitt HJ, Thomson AW, Geissler EK, Hutchinson JA. DHRS9 Is a Stable Marker of Human Regulatory Macrophages. *Transplantation* 2017; **101**: 2731-2738 [PMID: 28594751 DOI: 10.1097/TP.0000000000001814]
27 **Dhakal M**, Hardaway JC, Guloglu FB, Miller MM, Hoeman CM, Zaghouani AA, Wan X, Rowland LM, Cascio JA, Sherman MP, Zaghouani H. IL-13Rα1 is a surface marker for M2 macrophages influencing their differentiation and function. *Eur J Immunol* 2014; **44**: 842-855 [PMID: 24281978 DOI: 10.1002/eji.201343755]
28 **Sanyal R**, Polyak MJ, Zuccolo J, Puri M, Deng L, Roberts L, Zuba A, Storek J, Luider JM, Sundberg EM, Mansoor A, Baigorri E, Chu MP, Belch AR, Pilarski LM, Deans JP. MS4A4A: a novel cell surface marker for M2 macrophages and plasma cells. *Immunol Cell Biol* 2017; **95**: 611-619 [PMID: 28303902 DOI: 10.1038/icb.2017.18]
29 **David M**, Jonathan B, David BR, Ivan MR. Antigen Presentation. Immunology. 8 ed. Philadelphia, PA, US: Elsevier Saunders, 2013: 143-153
30 **Gerber HA**, Morris B, Trevella W. The role of gut-associated lymphoid tissues in the generation of immunoglobulin-bearing lymphocytes in sheep. *Aust J Exp Biol Med Sci* 1986; **64** (Pt 3): 201-213 [PMID: 3767761]
31 **Forchielli ML**, Walker WA. The role of gut-associated lymphoid tissues and mucosal defence. *Br J Nutr* 2005; **93** Suppl 1: S41-S48 [PMID: 15877894]
32 **Donaldson DS**, Else KJ, Mabbott NA. The Gut-Associated Lymphoid Tissues in the Small Intestine, Not the Large Intestine, Play a Major Role in Oral Prion Disease Pathogenesis. *J Virol* 2015; **89**: 9532-9547 [PMID: 26157121 DOI: 10.1128/JVI.01544-15]
33 **Doe WF**. The intestinal immune system. *Gut* 1989; **30**: 1679-1685 [PMID: 2693229]
34 **Kajiwara E**, Shigeta A, Horiuchi H, Matsuda H, Furusawa S. Development of Peyer's patch and cecal tonsil in gut-associated lymphoid tissues in the chicken embryo. *J Vet Med Sci* 2003; **65**: 607-614 [PMID: 12808213]
35 **Roy MJ**, Varvayanis M. Development of dome epithelium in gut-associated lymphoid tissues: association of IgA with M cells. *Cell Tissue Res* 1987; **248**: 645-651 [PMID: 3300998]
36 **Ratcliffe MJ**. B cell development in gut associated lymphoid tissues. *Vet Immunol Immunopathol* 2002; **87**: 337-340 [PMID: 12072255]
37 **Kawanishi H**, Saltzman L, Strober W. Mechanisms regulating IgA class-specific immunoglobulin production in murine gut-associated lymphoid tissues. II. Terminal differentiation of postswitch sIgA-bearing Peyer's patch B cells. *J Exp Med* 1983; **158**: 649-669 [PMID: 6604126]
38 **Kawanishi H**, Strober W. T cell regulation of IgA immunoglobulin production in gut-associated lymphoid tissues. *Mol Immunol* 1983; **20**: 917-930 [PMID: 6606114]
39 **Weisz-Carrington P**, Grimes SR Jr, Lamm ME. Gut-associated lymphoid tissue as source of an IgA immune response in respiratory tissues after oral immunization and intrabronchial challenge. *Cell Immunol* 1987; **106**: 132-138 [PMID: 3568143]
40 **Moro I**, Komiyama K, Kusama K, Iwase T, Asano M, Takenouchi N. [Molecular aspects of secretory IgA (S-IgA) in gut-associated lymphoid tissues]. *Nihon Rinsho* 1996; **54**: 1155-1161 [PMID: 8920690]
41 **Pabst O**, Bernhardt G, Förster R. The impact of cell-bound antigen transport on mucosal tolerance induction. *J Leukoc Biol* 2007; **82**: 795-800 [PMID: 17565048 DOI: 10.1189/jlb.0307144]
42 **Mosser DM**, Edwards JP. Exploring the full spectrum of macrophage activation. *Nat Rev Immunol* 2008; **8**: 958-969 [PMID: 19029990 DOI: 10.1038/nri2448]
43 **Yamamoto M**, Sato S, Hemmi H, Hoshino K, Kaisho T, Sanjo H, Takeuchi O, Sugiyama M, Okabe M, Takeda K, Akira S. Role of adaptor TRIF in the MyD88-independent toll-like receptor signaling pathway. *Science* 2003; **301**: 640-643 [PMID: 12855817 DOI: 10.1126/science.1087262]
44 **Edwards JP**, Zhang X, Frauwirth KA, Mosser DM. Biochemical and functional characterization of three activated macrophage populations. *J Leukoc Biol* 2006; **80**: 1298-1307 [PMID: 16905575 DOI: 10.1189/jlb.0406249]
45 **Cordeiro-da-Silva A**, Tavares J, Araújo N, Cerqueira F, Tomás A, Kong Thoo Lin P, Ouaissi A. Immunological alterations induced by polyamine derivatives on murine splenocytes and human mononuclear cells. *Int Immunopharmacol* 2004; **4**: 547-556 [PMID: 15099532 DOI: 10.1016/j.intimp.2004.02.009]
46 **Mantovani A**, Sozzani S, Locati M, Allavena P, Sica A. Macrophage polarization: tumor-associated macrophages as a paradigm for polarized M2 mononuclear phagocytes. *Trends Immunol* 2002; **23**: 549-555 [PMID: 12401408]
47 **Sun S**, Cui Y, Ren K, Quan M, Song Z, Zou H, Li D, Zheng Y, Cao J. 8-bromo-7-methoxychrysin Reversed M2 Polarization of Tumor-associated Macrophages Induced by Liver Cancer Stem-like Cells. *Anticancer Agents Med Chem* 2017; **17**: 286-293 [PMID: 26845136]
48 **Simões RL**, De-Brito NM, Cunha-Costa H, Morandi V, Fierro IM, Roitt IM, Barja-Fidalgo C. Lipoxin A4 selectively programs the profile of M2 tumor-associated macrophages which favour control of tumor progression. *Int J Cancer* 2017; **140**: 346-357 [PMID: 27615282 DOI: 10.1002/ijc.30424]
49 **Kimura Y**, Sumiyoshi M, Baba K. Antitumor and Antimetastatic Activity of Synthetic Hydroxystilbenes Through Inhibition of Lymphangiogenesis and M2 Macrophage Differentiation of Tumor-associated Macrophages. *Anticancer Res* 2016; **36**: 137-148 [PMID: 26722037]
50 **Melancon MP**, Lu W, Huang Q, Thapa P, Zhou D, Ng C, Li C. Targeted imaging of tumor-associated M2 macrophages using a macromolecular contrast agent PG-Gd-NIR813. *Biomaterials* 2010; **31**: 6567-6573 [PMID: 20537382 DOI: 10.1016/j.biomaterials.2010.05.001]
51 **Umemura N**, Saio M, Suwa T, Kitoh Y, Bai J, Nonaka K, Ouyang GF, Okada M, Balazs M, Adany R, Shibata T, Takami T. Tumor-infiltrating myeloid-derived suppressor cells are pleiotropic-inflamed monocytes/macrophages that bear M1- and M2-type characteristics. *J Leukoc Biol* 2008; **83**: 1136-1144 [PMID: 18285406 DOI: 10.1189/jlb.0907611]
52 **Van Ginderachter JA**, Meerschaut S, Liu Y, Brys L, De Groeve K, Hassanzadeh Ghassabeh G, Raes G, De Baetselier P. Peroxisome proliferator-activated receptor gamma (PPARgamma) ligands reverse CTL suppression by alternatively activated (M2) macrophages in cancer. *Blood* 2006; **108**: 525-535 [PMID: 16527895 DOI: 10.1182/blood-2005-09-3777]
53 **Sica A**, Schioppa T, Mantovani A, Allavena P. Tumour-associated macrophages are a distinct M2 polarised population promoting

tumour progression: potential targets of anti-cancer therapy. *Eur J Cancer* 2006; **42**: 717-727 [PMID: 16520032 DOI: 10.1016/j.ejca.2006.01.003]

54 **Mantovani A**, Sozzani S, Locati M, Schioppa T, Saccani A, Allavena P, Sica A. Infiltration of tumours by macrophages and dendritic cells: tumour-associated macrophages as a paradigm for polarized M2 mononuclear phagocytes. *Novartis Found Symp* 2004; **256**: 137-145; discussion 146-148, 259-269 [PMID: 15027487]

55 **Chen Y**, Zhang S, Wang Q, Zhang X. Tumor-recruited M2 macrophages promote gastric and breast cancer metastasis via M2 macrophage-secreted CHI3L1 protein. *J Hematol Oncol* 2017; **10**: 36 [PMID: 28143526 DOI: 10.1186/s13045-017-0408-0]

56 **Beider K**, Bitner H, Leiba M, Gutwein O, Koren-Michowitz M, Ostrovsky O, Abraham M, Wald H, Galun E, Peled A, Nagler A. Multiple myeloma cells recruit tumor-supportive macrophages through the CXCR4/CXCL12 axis and promote their polarization toward the M2 phenotype. *Oncotarget* 2014; **5**: 11283-11296 [PMID: 25526031 DOI: 10.18632/oncotarget.2207]

57 **Maier C**, Ramming A, Bergmann C, Weinkam R, Kittan N, Schett G, Distler JHW, Beyer C. Inhibition of phosphodiesterase 4 (PDE4) reduces dermal fibrosis by interfering with the release of interleukin-6 from M2 macrophages. *Ann Rheum Dis* 2017; **76**: 1133-1141 [PMID: 28209630 DOI: 10.1136/annrheumdis-2016-210189]

58 **Vannella KM**, Barron L, Borthwick LA, Kindrachuk KN, Narasimhan PB, Hart KM, Thompson RW, White S, Cheever AW, Ramalingam TR, Wynn TA. Incomplete deletion of IL-4Rα by LysM(Cre) reveals distinct subsets of M2 macrophages controlling inflammation and fibrosis in chronic schistosomiasis. *PLoS Pathog* 2014; **10**: e1004372 [PMID: 25211233 DOI: 10.1371/journal.ppat.1004372]

59 **Bility MT**, Cheng L, Zhang Z, Luan Y, Li F, Chi L, Zhang L, Tu Z, Gao Y, Fu Y, Niu J, Wang F, Su L. Hepatitis B virus infection and immunopathogenesis in a humanized mouse model: induction of human-specific liver fibrosis and M2-like macrophages. *PLoS Pathog* 2014; **10**: e1004032 [PMID: 24651854 DOI: 10.1371/journal.ppat.1004032]

60 **Braga TT**, Correa-Costa M, Guise YF, Castoldi A, de Oliveira CD, Hyane MI, Cenedeze MA, Teixeira SA, Muscara MN, Perez KR, Cuccovia IM, Pacheco-Silva A, Gonçalves GM, Camara NO. MyD88 signaling pathway is involved in renal fibrosis by favoring a TH2 immune response and activating alternative M2 macrophages. *Mol Med* 2012; **18**: 1231-1239 [PMID: 22777483 DOI: 10.2119/molmed.2012.00131]

61 **Braune J**, Weyer U, Hobusch C, Mauer J, Brüning JC, Bechmann I, Gericke M. IL-6 Regulates M2 Polarization and Local Proliferation of Adipose Tissue Macrophages in Obesity. *J Immunol* 2017; **198**: 2927-2934 [PMID: 28193830 DOI: 10.4049/jimmunol.1600476]

62 **Camell C**, Smith CW. Dietary oleic acid increases m2 macrophages in the mesenteric adipose tissue. *PLoS One* 2013; **8**: e75147 [PMID: 24098682 DOI: 10.1371/journal.pone.0075147]

63 **Shaul ME**, Bennett G, Strissel KJ, Greenberg AS, Obin MS. Dynamic, M2-like remodeling phenotypes of CD11c+ adipose tissue macrophages during high-fat diet--induced obesity in mice. *Diabetes* 2010; **59**: 1171-1181 [PMID: 20185806 DOI: 10.2337/db09-1402]

64 **Fujisaka S**, Usui I, Bukhari A, Ikutani M, Oya T, Kanatani Y, Tsuneyama K, Nagai Y, Takatsu K, Urakaze M, Kobayashi M, Tobe K. Regulatory mechanisms for adipose tissue M1 and M2 macrophages in diet-induced obese mice. *Diabetes* 2009; **58**: 2574-2582 [PMID: 19690061 DOI: 10.2337/db08-1475]

65 **Aron-Wisnewsky J**, Tordjman J, Poitou C, Darakhshan F, Hugol D, Basdevant A, Aissat A, Guerre-Millo M, Clément K. Human adipose tissue macrophages: m1 and m2 cell surface markers in subcutaneous and omental depots and after weight loss. *J Clin Endocrinol Metab* 2009; **94**: 4619-4623 [PMID: 19837929 DOI: 10.1210/jc.2009-0925]

66 **Zaslona Z**, Przybranowski S, Wilke C, van Rooijen N, Teitz-Tennenbaum S, Osterholzer JJ, Wilkinson JE, Moore BB, Peters-Golden M. Resident alveolar macrophages suppress, whereas recruited monocytes promote, allergic lung inflammation in murine models of asthma. *J Immunol* 2014; **193**: 4245-4253 [PMID: 25225663 DOI: 10.4049/jimmunol.1400580]

67 **Madore AM**, Perron S, Turmel V, Laviolette M, Bissonnette EY, Laprise C. Alveolar macrophages in allergic asthma: an expression signature characterized by heat shock protein pathways. *Hum Immunol* 2010; **71**: 144-150 [PMID: 19913588 DOI: 10.1016/j.humimm.2009.11.005]

68 **Vissers JL**, van Esch BC, Hofman GA, van Oosterhout AJ. Macrophages induce an allergen-specific and long-term suppression in a mouse asthma model. *Eur Respir J* 2005; **26**: 1040-1046 [PMID: 16319333 DOI: 10.1183/09031936.05.00089304]

69 **Lee TH**, Poston R, Godard P, Bousquet J. Macrophages and allergic asthma. *Clin Exp Allergy* 1991; **21** Suppl 1: 22-23 [PMID: 2032150]

70 **Godard P**, Damon M, Chanez P, Michel FB. Releasability of airway macrophages in bronchial asthma. *Int Arch Allergy Appl Immunol* 1991; **95**: 97-101 [PMID: 1937933]

71 **Cochain C**, Zernecke A. Macrophages in vascular inflammation and atherosclerosis. *Pflugers Arch* 2017; **469**: 485-499 [PMID: 28168325 DOI: 10.1007/s00424-017-1941-y]

72 **Neele AE**, Van den Bossche J, Hoeksema MA, de Winther MP. Epigenetic pathways in macrophages emerge as novel targets in atherosclerosis. *Eur J Pharmacol* 2015; **763**: 79-89 [PMID: 26004034 DOI: 10.1016/j.ejphar.2015.03.101]

73 **Moore KJ**, Tabas I. Macrophages in the pathogenesis of atherosclerosis. *Cell* 2011; **145**: 341-355 [PMID: 21529710 DOI: 10.1016/j.cell.2011.04.005]

74 **Lucas AD**, Greaves DR. Atherosclerosis: role of chemokines and macrophages. *Expert Rev Mol Med* 2001; **3**: 1-18 [PMID: 14585150 DOI: 10.1017/S1462399401003696]

75 **Daoud AS**, Fritz KE, Jarmolych J, Frank AS. Role of macrophages in regression of atherosclerosis. *Ann N Y Acad Sci* 1985; **454**: 101-114 [PMID: 3865603]

76 **Wolman M**, Gaton E. [Macrophages and smooth muscle cells in the pathogenesis of atherosclerosis]. *Harefuah* 1976; **90**: 400-402 [PMID: 939449]

77 **Portillo JC**, Lopez Corcino Y, Miao Y, Tang J, Sheibani N, Kern TS, Dubyak GR, Subauste CS. CD40 in Retinal Müller Cells Induces P2X7-Dependent Cytokine Expression in Macrophages/Microglia in Diabetic Mice and Development of Early Experimental Diabetic Retinopathy. *Diabetes* 2017; **66**: 483-493 [PMID: 27474370 DOI: 10.2337/db16-0051]

78 **Davies MH**, Eubanks JP, Powers MR. Microglia and macrophages are increased in response to ischemia-induced retinopathy in the mouse retina. *Mol Vis* 2006; **12**: 467-477 [PMID: 16710171]

79 **Naug HL**, Browning J, Gole GA, Gobé G. Vitreal macrophages express vascular endothelial growth factor in oxygen-induced retinopathy. *Clin Exp Ophthalmol* 2000; **28**: 48-52 [PMID: 11345346]

80 **Esser P**, Heimann K, Wiedemann P. Macrophages in proliferative vitreoretinopathy and proliferative diabetic retinopathy: differentiation of subpopulations. *Br J Ophthalmol* 1993; **77**: 731-733 [PMID: 8280690]

81 **Spoettl T**, Hausmann M, Menzel K, Piberger H, Herfarth H, Schoelmerich J, Bataille F, Rogler G. Role of soluble factors and three-dimensional culture in in vitro differentiation of intestinal macrophages. *World J Gastroenterol* 2007; **13**: 1032-1041 [PMID: 17373737 DOI: 10.3748/wjg.v13.i7.1032]

82 **Mowat AM**, Bain CC. Mucosal macrophages in intestinal homeostasis and inflammation. *J Innate Immun* 2011; **3**: 550-564 [PMID: 22025201 DOI: 10.1159/000329099]

83 **Smith PD**, Smythies LE, Shen R, Greenwell-Wild T, Gliozzi M, Wahl SM. Intestinal macrophages and response to microbial encroachment. *Mucosal Immunol* 2011; **4**: 31-42 [PMID: 20962772 DOI: 10.1038/mi.2010.66]

84 **Sheikh SZ**, Plevy SE. The role of the macrophage in sentinel responses in intestinal immunity. *Curr Opin Gastroenterol* 2010; **26**: 578-582 [PMID: 20717022 DOI: 10.1097/MOG.0b013e32833d4b71]

85 **Bar-On L**, Zigmond E, Jung S. Management of gut inflammation through the manipulation of intestinal dendritic cells and macrophages? *Semin Immunol* 2011; **23**: 58-64 [PMID: 21292502 DOI: 10.1016/j.smim.2011.01.002]

86 **Cerovic V**, Houston SA, Scott CL, Aumeunier A, Yrlid U, Mowat AM, Milling SW. Intestinal CD103(-) dendritic cells migrate in lymph and prime effector T cells. *Mucosal Immunol* 2013; **6**: 104-113 [PMID: 22718260 DOI: 10.1038/mi.2012.53]

87 **Schulz O**, Jaensson E, Persson EK, Liu X, Worbs T, Agace WW, Pabst O. Intestinal CD103+, but not CX3CR1+, antigen sampling cells migrate in lymph and serve classical dendritic cell functions. *J Exp Med* 2009; **206**: 3101-3114 [PMID: 20008524 DOI: 10.1084/jem.20091925]

88 **Kelsall B**. Recent progress in understanding the phenotype and function of intestinal dendritic cells and macrophages. *Mucosal Immunol* 2008; **1**: 460-469 [PMID: 19079213 DOI: 10.1038/mi.2008.61]

89 **Pabst O**, Bernhardt G. The puzzle of intestinal lamina propria dendritic cells and macrophages. *Eur J Immunol* 2010; **40**: 2107-2111 [PMID: 20853495 DOI: 10.1002/eji.201040557]

90 **Cerovic V**, Bain CC, Mowat AM, Milling SW. Intestinal macrophages and dendritic cells: what's the difference? *Trends Immunol* 2014; **35**: 270-277 [PMID: 24794393 DOI: 10.1016/j.it.2014.04.003]

91 **Wehner S**, Engel DR. Resident macrophages in the healthy and inflamed intestinal muscularis externa. *Pflugers Arch* 2017; **469**: 541-552 [PMID: 28236119 DOI: 10.1007/s00424-017-1948-4]

92 **Mahida YR**, Wu KC, Jewell DP. Respiratory burst activity of intestinal macrophages in normal and inflammatory bowel disease. *Gut* 1989; **30**: 1362-1370 [PMID: 2511088]

93 **Rugtveit J**, Haraldsen G, Høgåsen AK, Bakka A, Brandtzaeg P, Scott H. Respiratory burst of intestinal macrophages in inflammatory bowel disease is mainly caused by CD14+L1+ monocyte derived cells. *Gut* 1995; **37**: 367-373 [PMID: 7590432]

94 **Goode EC**, Warburton RC, Gelson WT, Watson AJ. Activated intestinal macrophages in patients with cirrhosis release NO and IL-6 that may disrupt intestinal barrier function. *Gastroenterology* 2013; **145**: 1481-1484 [PMID: 24409494]

95 **Platt AM**, Bain CC, Bordon Y, Sester DP, Mowat AM. An independent subset of TLR expressing CCR2-dependent macrophages promotes colonic inflammation. *J Immunol* 2010; **184**: 6843-6854 [PMID: 20483766 DOI: 10.4049/jimmunol.0903987]

96 **Kang GD**, Kim DH. Poncirin and its metabolite ponciretin attenuate colitis in mice by inhibiting LPS binding on TLR4 of macrophages and correcting Th17/Treg imbalance. *J Ethnopharmacol* 2016; **189**: 175-185 [PMID: 27224242 DOI: 10.1016/j.jep.2016.05.044]

97 **Lee IA**, Park YJ, Joh EH, Kim DH. Soyasaponin Ab ameliorates colitis by inhibiting the binding of lipopolysaccharide (LPS) to Toll-like receptor (TLR)4 on macrophages. *J Agric Food Chem* 2011; **59**: 13165-13172 [PMID: 22060784 DOI: 10.1021/jf2033818]

98 **Qian Z**, Wu Z, Huang L, Qiu H, Wang L, Li L, Yao L, Kang K, Qu J, Wu Y, Luo J, Liu JJ, Yang Y, Yang W, Gou D. Mulberry fruit prevents LPS-induced NF-κB/pERK/MAPK signals in macrophages and suppresses acute colitis and colorectal tumorigenesis in mice. *Sci Rep* 2015; **5**: 17348 [PMID: 26615818 DOI: 10.1038/srep17348]

99 **Regan T**, Nally K, Carmody R, Houston A, Shanahan F, Macsharry J, Brint E. Identification of TLR10 as a key mediator of the inflammatory response to Listeria monocytogenes in intestinal epithelial cells and macrophages. *J Immunol* 2013; **191**: 6084-6092 [PMID: 24198280 DOI: 10.4049/jimmunol.1203245]

100 **Wehner S**, Buchholz BM, Schuchtrup S, Rocke A, Schaefer N, Lysson M, Hirner A, Kalff JC. Mechanical strain and TLR4 synergistically induce cell-specific inflammatory gene expression in intestinal smooth muscle cells and peritoneal macrophages. *Am J Physiol Gastrointest Liver Physiol* 2010; **299**: G1187-G1197 [PMID: 20829523 DOI: 10.1152/ajpgi.00452.2009]

101 **Little MC**, Hurst RJ, Else KJ. Dynamic changes in macrophage activation and proliferation during the development and resolution of intestinal inflammation. *J Immunol* 2014; **193**: 4684-4695 [PMID: 25261482 DOI: 10.4049/jimmunol.1400502]

102 **Seo SU**, Kuffa P, Kitamoto S, Nagao-Kitamoto H, Rousseau J, Kim YG, Núñez G, Kamada N. Intestinal macrophages arising from CCR2(+) monocytes control pathogen infection by activating innate lymphoid cells. *Nat Commun* 2015; **6**: 8010 [PMID: 26269452 DOI: 10.1038/ncomms9010]

103 **Smith P**, Mangan NE, Walsh CM, Fallon RE, McKenzie AN, van Rooijen N, Fallon PG. Infection with a helminth parasite prevents experimental colitis via a macrophage-mediated mechanism. *J Immunol* 2007; **178**: 4557-4566 [PMID: 17372014]

104 **Hayashi A**, Sato T, Kamada N, Mikami Y, Matsuoka K, Hisamatsu T, Hibi T, Roers A, Yagita H, Ohteki T, Yoshimura A, Kanai T. A single strain of Clostridium butyricum induces intestinal IL-10-producing macrophages to suppress acute experimental colitis in mice. *Cell Host Microbe* 2013; **13**: 711-722 [PMID: 23768495 DOI: 10.1016/j.chom.2013.05.013]

105 **Jamontt J**, Petit S, Clark N, Parkinson SJ, Smith P. Nucleotide-binding oligomerization domain 2 signaling promotes hyperresponsive macrophages and colitis in IL-10-deficient mice. *J Immunol* 2013; **190**: 2948-2958 [PMID: 23396949 DOI: 10.4049/jimmunol.1201332]

106 **Leung G**, Wang A, Fernando M, Phan VC, McKay DM. Bone marrow-derived alternatively activated macrophages reduce colitis without promoting fibrosis: participation of IL-10. *Am J Physiol Gastrointest Liver Physiol* 2013; **304**: G781-G792 [PMID: 23494123 DOI: 10.1152/ajpgi.00055.2013]

107 **Krause P**, Morris V, Greenbaum JA, Park Y, Bjoerheden U, Mikulski Z, Muffley T, Shui JW, Kim G, Cheroutre H, Liu YC, Peters B, Kronenberg M, Murai M. IL-10-producing intestinal macrophages prevent excessive antibacterial innate immunity by limiting IL-23 synthesis. *Nat Commun* 2015; **6**: 7055 [PMID: 25959063 DOI: 10.1038/ncomms8055]

108 **Li B**, Gurung P, Malireddi RK, Vogel P, Kanneganti TD, Geiger TL. IL-10 engages macrophages to shift Th17 cytokine dependency and pathogenicity during T-cell-mediated colitis. *Nat Commun* 2015; **6**: 6131 [PMID: 25607885 DOI: 10.1038/ncomms7131]

109 **Liu W**, Zhang S, Gu S, Sang L, Dai C. Mesenchymal stem cells recruit macrophages to alleviate experimental colitis through TGFβ1. *Cell Physiol Biochem* 2015; **35**: 858-865 [PMID: 25632987 DOI: 10.1159/000369743]

110 **MohanKumar K**, Namachivayam K, Chapalamadugu KC, Garzon SA, Premkumar MH, Tipparaju SM, Maheshwari A. Smad7 interrupts TGF-β signaling in intestinal macrophages and promotes inflammatory activation of these cells during necrotizing enterocolitis. *Pediatr Res* 2016; **79**: 951-961 [PMID: 26859364 DOI: 10.1038/pr.2016.18]

111 **Sun W**, Tadmori I, Yang L, Delgado M, Ganea D. Vasoactive intestinal peptide (VIP) inhibits TGF-beta1 production in murine macrophages. *J Neuroimmunol* 2000; **107**: 88-99 [PMID: 10808055]

112 **Kamanaka M**, Kim ST, Wan YY, Sutterwala FS, Lara-Tejero M, Galán JE, Harhaj E, Flavell RA. Expression of interleukin-10 in intestinal lymphocytes detected by an interleukin-10 reporter knockin tiger mouse. *Immunity* 2006; **25**: 941-952 [PMID: 17137799 DOI: 10.1016/j.immuni.2006.09.013]

113 **Delgado M**, Munoz-Elias EJ, Gomariz RP, Ganea D. Vasoactive intestinal peptide and pituitary adenylate cyclase-activating polypeptide enhance IL-10 production by murine macrophages: in vitro and in vivo studies. *J Immunol* 1999; **162**: 1707-1716 [PMID: 9973433]

114 **Weinhage T**, Däbritz J, Brockhausen A, Wirth T, Brückner M, Belz M, Foell D, Varga G. Granulocyte Macrophage Colony-Stimulating Factor-Activated CD39+/CD73+ Murine Monocytes Modulate Intestinal Inflammation via Induction of Regulatory T Cells. *Cell Mol Gastroenterol Hepatol* 2015; **1**: 433-449.e1 [PMID: 28210690 DOI: 10.1016/j.jcmgh.2015.04.005]

115 **Izcue A**, Coombes JL, Powrie F. Regulatory lymphocytes and intestinal inflammation. *Annu Rev Immunol* 2009; **27**: 313-338 [PMID: 19302043 DOI: 10.1146/annurev.immunol.021908.132657]

116 **Kamada N**, Hisamatsu T, Okamoto S, Chinen H, Kobayashi T, Sato T, Sakuraba A, Kitazume MT, Sugita A, Koganei K, Akagawa KS, Hibi T. Unique CD14 intestinal macrophages contribute to the pathogenesis of Crohn disease via IL-23/IFN-gamma axis. *J Clin Invest* 2008; **118**: 2269-2280 [PMID: 18497880 DOI: 10.1172/JCI34610]

117 **Arnold IC**, Mathisen S, Schulthess J, Danne C, Hegazy AN, Powrie F. CD11c(+) monocyte/macrophages promote chronic Helicobacter hepaticus-induced intestinal inflammation through the production of IL-23. *Mucosal Immunol* 2016; **9**: 352-363 [PMID: 26242598 DOI: 10.1038/mi.2015.65]

118 **Simon JM**, Davis JP, Lee SE, Schaner MR, Gipson GR, Weiser M, Sartor RB, Herfarth HH, Rahbar R, Sadiq TS, Koruda MJ, McGovern DP, Lieb JD, Mohlke KL, Furey TS, Sheikh SZ. Alterations to chromatin in intestinal macrophages link IL-10 deficiency to inappropriate inflammatory responses. *Eur J Immunol* 2016; **46**: 1912-1925 [PMID: 27159132 DOI: 10.1002/eji.201546237]

119 **Boudakov I**, Liu J, Fan N, Gulay P, Wong K, Gorczynski RM. Mice lacking CD200R1 show absence of suppression of lipopolysaccharide-induced tumor necrosis factor-alpha and mixed leukocyte culture responses by CD200. *Transplantation* 2007; **84**: 251-257 [PMID: 17667818 DOI: 10.1097/01.tp.0000269795.04592.cc]

120 **Snelgrove RJ**, Goulding J, Didierlaurent AM, Lyonga D, Vekaria S, Edwards L, Gwyer E, Sedgwick JD, Barclay AN, Hussell T. A critical function for CD200 in lung immune homeostasis and the severity of influenza infection. *Nat Immunol* 2008; **9**: 1074-1083 [PMID: 18660812 DOI: 10.1038/ni.1637]

121 **Cipriani G**, Gibbons SJ, Kashyap PC, Farrugia G. Intrinsic Gastrointestinal Macrophages: Their Phenotype and Role in Gastrointestinal Motility. *Cell Mol Gastroenterol Hepatol* 2016; **2**: 120-130.e1 [PMID: 27047989 DOI: 10.1016/j.jcmgh.2016.01.003]

122 **Obata Y**, Pachnis V. The Effect of Microbiota and the Immune System on the Development and Organization of the Enteric Nervous System. *Gastroenterology* 2016; **151**: 836-844 [PMID: 27521479 DOI: 10.1053/j.gastro.2016.07.044]

123 **Asano K**, Takahashi N, Ushiki M, Monya M, Aihara F, Kuboki E, Moriyama S, Iida M, Kitamura H, Qiu CH, Watanabe T, Tanaka M. Intestinal CD169(+) macrophages initiate mucosal inflammation by secreting CCL8 that recruits inflammatory monocytes. *Nat Commun* 2015; **6**: 7802 [PMID: 26193821 DOI: 10.1038/ncomms8802]

124 **Geissmann F**, Manz MG, Jung S, Sieweke MH, Merad M, Ley K. Development of monocytes, macrophages, and dendritic cells. *Science* 2010; **327**: 656-661 [PMID: 20133564 DOI: 10.1126/science.1178331]

125 **Haribhai D**, Ziegelbauer J, Jia S, Upchurch K, Yan K, Schmitt EG, Salzman NH, Simpson P, Hessner MJ, Chatila TA, Williams CB. Alternatively Activated Macrophages Boost Induced Regulatory T and Th17 Cell Responses during Immunotherapy for Colitis. *J Immunol* 2016; **196**: 3305-3317 [PMID: 26927797 DOI: 10.4049/jimmunol.1501956]

126 **Biagioli M**, Carino A, Cipriani S, Francisci D, Marchianò S, Scarpelli P, Sorcini D, Zampella A, Fiorucci S. The Bile Acid Receptor GPBAR1 Regulates the M1/M2 Phenotype of Intestinal Macrophages and Activation of GPBAR1 Rescues Mice from Murine Colitis. *J Immunol* 2017; **199**: 718-733 [PMID: 28607110 DOI: 10.4049/jimmunol.1700183]

127 **Rogler G**, Hausmann M, Vogl D, Aschenbrenner E, Andus T, Falk W, Andreesen R, Schölmerich J, Gross V. Isolation and phenotypic characterization of colonic macrophages. *Clin Exp Immunol* 1998; **112**: 205-215 [PMID: 9649182]

128 **Däbritz J**. Granulocyte macrophage colony-stimulating factor and the intestinal innate immune cell homeostasis in Crohn's disease. *Am J Physiol Gastrointest Liver Physiol* 2014; **306**: G455-G465 [PMID: 24503766 DOI: 10.1152/ajpgi.00409.2013]

129 **Meshkibaf S**, Martins AJ, Henry GT, Kim SO. Protective role of G-CSF in dextran sulfate sodium-induced acute colitis through generating gut-homing macrophages. *Cytokine* 2016; **78**: 69-78 [PMID: 26687628 DOI: 10.1016/j.cyto.2015.11.025]

130 **Nakata K**, Inagawa H, Nishizawa T, Honda T, Kohchi C, Tonomoto Y, Yoshimura H, Nagasue N, Natori S, Terada H, Soma G. Inherent potential for production of tumor necrosis factor-alpha by human intestinal macrophages. *Int J Colorectal Dis* 2006; **21**: 339-347 [PMID: 16091914 DOI: 10.1007/s00384-005-0021-5]

131 **Khalil M**, Babes A, Lakra R, Försch S, Reeh PW, Wirtz S, Becker C, Neurath MF, Engel MA. Transient receptor potential melastatin 8 ion channel in macrophages modulates colitis through a balance-shift in TNF-alpha and interleukin-10 production. *Mucosal Immunol* 2016; **9**: 1500-1513 [PMID: 26982596 DOI: 10.1038/mi.2016.16]

132 **Monteleone G**, Boirivant M, Pallone F, MacDonald TT. TGF-beta1 and Smad7 in the regulation of IBD. *Mucosal Immunol* 2008; **1** Suppl 1: S50-S53 [PMID: 19079231 DOI: 10.1038/mi.2008.55]

133 **Cosín-Roger J**, Ortiz-Masiá D, Calatayud S, Hernández C, Alvarez A, Hinojosa J, Esplugues JV, Barrachina MD. M2 macrophages activate WNT signaling pathway in epithelial cells: relevance in ulcerative colitis. *PLoS One* 2013; **8**: e78128 [PMID: 24167598 DOI: 10.1371/journal.pone.0078128]

134 **Mortha A**, Chudnovskiy A, Hashimoto D, Bogunovic M, Spencer SP, Belkaid Y, Merad M. Microbiota-dependent crosstalk between macrophages and ILC3 promotes intestinal homeostasis. *Science* 2014; **343**: 1249288 [PMID: 24625929 DOI: 10.1126/science.1249288]

135 **Mizuno S**, Mikami Y, Kamada N, Handa T, Hayashi A, Sato T, Matsuoka K, Matano M, Ohta Y, Sugita A, Koganei K, Sahara R, Takazoe M, Hisamatsu T, Kanai T. Cross-talk between RORγt+ innate lymphoid cells and intestinal macrophages induces mucosal IL-22 production in Crohn's disease. *Inflamm Bowel Dis* 2014; **20**: 1426-1434 [PMID: 24991784 DOI: 10.1097/MIB.0000000000000105]

136 **Che F**, Heng X, Zhang H, Su Q, Zhang B, Chen Y, Zhang Z, Du Y, Wang L. Novel B7-H4-mediated crosstalk between human non-Hodgkin lymphoma cells and tumor-associated macrophages leads to immune evasion via secretion of IL-6 and IL-10. *Cancer Immunol Immunother* 2017; **66**: 717-729 [PMID: 28246881 DOI: 10.1007/s00262-017-1961-7]

137 **Petty AJ**, Yang Y. Tumor-associated macrophages: implications in cancer immunotherapy. *Immunotherapy* 2017; **9**: 289-302 [PMID: 28231720 DOI: 10.2217/imt-2016-0135]

138 **Gieryng A**, Pszczolkowska D, Walentynowicz KA, Rajan WD, Kaminska B. Immune microenvironment of gliomas. *Lab Invest* 2017; **97**: 498-518 [PMID: 28287634 DOI: 10.1038/labinvest.2017.19]

139 **Mantovani A**, Allavena P. The interaction of anticancer therapies with tumor-associated macrophages. *J Exp Med* 2015; **212**: 435-445 [PMID: 25753580 DOI: 10.1084/jem.20150295]

140 **Ma J**, Liu L, Che G, Yu N, Dai F, You Z. The M1 form of tumor-associated macrophages in non-small cell lung cancer is positively associated with survival time. *BMC Cancer* 2010; **10**: 112 [PMID: 20338029 DOI: 10.1186/1471-2407-10-112]

141 **Zhou Q**, Xian M, Xiang S, Xiang D, Shao X, Wang J, Cao J, Yang X, Yang B, Ying M, He Q. All-Trans Retinoic Acid Prevents Osteosarcoma Metastasis by Inhibiting M2 Polarization of Tumor-Associated Macrophages. *Cancer Immunol Res* 2017; **5**: 547-559 [PMID: 28515123 DOI: 10.1158/2326-6066.CIR-16-0259]

142 **Yamaguchi T**, Fushida S, Yamamoto Y, Tsukada T, Kinoshita J, Oyama K, Miyashita T, Tajima H, Ninomiya I, Munesue S, Harashima A, Harada S, Yamamoto H, Ohta T. Tumor-associated macrophages of the M2 phenotype contribute to progression in gastric cancer with peritoneal dissemination. *Gastric Cancer* 2016; **19**: 1052-1065 [PMID: 26621525 DOI: 10.1007/s10120-015-0579-8]

143 **Yamada K**, Uchiyama A, Uehara A, Perera B, Ogino S, Yokoyama Y, Takeuchi Y, Udey MC, Ishikawa O, Motegi S. MFG-E8 Drives Melanoma Growth by Stimulating Mesenchymal Stromal Cell-Induced Angiogenesis and M2 Polarization of Tumor-Associated Macrophages. *Cancer Res* 2016; **76**: 4283-4292 [PMID: 27197197 DOI: 10.1158/0008-5472.CAN-15-2812]

144 **Wahl LM**, Kleinman HK. Tumor-associated macrophages as targets for cancer therapy. *J Natl Cancer Inst* 1998; **90**: 1583-1584 [PMID: 9811301]
145 **Andón FT**, Digifico E, Maeda A, Erreni M, Mantovani A, Alonso MJ, Allavena P. Targeting tumor associated macrophages: The new challenge for nanomedicine. *Semin Immunol* 2017; **34**: 103-113 [PMID: 28941641 DOI: 10.1016/j.smim.2017.09.004]
146 **Kawahara A**, Hattori S, Akiba J, Nakashima K, Taira T, Watari K, Hosoi F, Uba M, Basaki Y, Koufuji K, Shirouzu K, Akiyama S, Kuwano M, Kage M, Ono M. Infiltration of thymidine phosphorylase-positive macrophages is closely associated with tumor angiogenesis and survival in intestinal type gastric cancer. *Oncol Rep* 2010; **24**: 405-415 [PMID: 20596627]
147 **Kratochvill F**, Neale G, Haverkamp JM, Van de Velde LA, Smith AM, Kawauchi D, McEvoy J, Roussel MF, Dyer MA, Qualls JE, Murray PJ. TNF Counterbalances the Emergence of M2 Tumor Macrophages. *Cell Rep* 2015; **12**: 1902-1914 [PMID: 26365184 DOI: 10.1016/j.celrep.2015.08.033]
148 **McClellan JL**, Davis JM, Steiner JL, Enos RT, Jung SH, Carson JA, Pena MM, Carnevale KA, Berger FG, Murphy EA. Linking tumor-associated macrophages, inflammation, and intestinal tumorigenesis: role of MCP-1. *Am J Physiol Gastrointest Liver Physiol* 2012; **303**: G1087-G1095 [PMID: 23019193 DOI: 10.1152/ajpgi.00252.2012]

P- Reviewer: Caboclo JL, Contini S, Grizzi F **S- Editor**: Gong ZM
L- Editor: Filipodia **E- Editor**: Huang Y

World Journal of Gastroenterology

Submit a Manuscript: http://www.f6publishing.com

World J Gastroenterol 2018 March 21; 24(11): 1196-1205

DOI: 10.3748/wjg.v24.i11.1196

ISSN 1007-9327 (print) ISSN 2219-2840 (online)

ORIGINAL ARTICLE

Basic Study

NOD2- and disease-specific gene expression profiles of peripheral blood mononuclear cells from Crohn's disease patients

Holger Schäffler, Maria Rohde, Sarah Rohde, Astrid Huth, Nicole Gittel, Hannes Hollborn, Dirk Koczan, Änne Glass, Georg Lamprecht, Robert Jaster

Holger Schäffler, Maria Rohde, Sarah Rohde, Astrid Huth, Nicole Gittel, Hannes Hollborn, Georg Lamprecht, Robert Jaster, Department of Medicine II, Division of Gastroenterology, Rostock University Medical Center, Rostock 18057, Germany

Dirk Koczan, Institute of Immunology, Rostock University Medical Center, Rostock 18057, Germany

Änne Glass, Institute for Biostatistics and Informatics in Medicine and Ageing Research, Rostock 18057, Germany

ORCID number: Holger Schäffler (0000-0002-8475-3741); Maria Rohde (0000-0001-8924-3292); Sarah Rohde (0000-0002-6892-1565); Astrid Huth (0000-0002-0858-7948); Nicole Gittel (0000-0002-7134-069X); Hannes Hollborn (0000-0002-2366-4390); Dirk Koczan (0000-0002-3183-998X); Änne Glass (0000-0002-7715-9058); Georg Lamprecht (0000-0003-0997-3135); Robert Jaster (0000-0002-8220-4570).

Author contributions: Schäffler H, Rohde S and Jaster R designed the study; Huth A, Schäffler H and Lamprecht G took responsibility for patient care and follow-up; Rohde M, Rohde S, Hollborn H, Jaster R and Koczan D (microarray studies) performed the experiments; Gittel N, Huth A and Schäffler H collected the samples and performed the clinical characterization of the patients; Glass Ä performed the biostatistics; all authors analyzed the data; and Schäffler H and Jaster R wrote the manuscript.

Supported by a grant from the Damp-Foundation (2016-04) to Schäffler H and Rohde S.

Institutional review board statement: The study was approved by the ethics board of the Medical Faculty of the University of Rostock (A 2015-0042). Written informed consent was obtained from each participant prior to enrollment.

Conflict-of-interest statement: The authors declare that there is no conflict of interest.

Data sharing statement: No additional data are available.

Manuscript source: Unsolicited manuscript

Correspondence to: Robert Jaster, MD, Academic Research, Professor, Senior Scientist, Department of Medicine II, Division of Gastroenterology, Rostock University Medical Center, E.-Heydemann-Str. 6, Rostock 18057, Germany. robert.jaster@med.uni-rostock.de
Telephone: +49-381-4947349
Fax: +49-381-4947482

Received: December 21, 2017
Peer-review started: December 21, 2017
First decision: January 18, 2018
Revised: January 29, 2018
Accepted: February 1, 2018
Article in press: February 1, 2018
Published online: March 21, 2018

Abstract

AIM

To investigate disease-specific gene expression profiles of peripheral blood mononuclear cells (PBMCs) from Crohn's disease (CD) patients in clinical remission.

METHODS
Patients with CD in clinical remission or with very low disease activity according to the Crohn's disease activity index were genotyped regarding nucleotide-binding oligomerization domain 2 (*NOD2*), and PBMCs from wild-type (WT)-*NOD2* patients, patients with homozygous or heterozygous *NOD2* mutations and healthy donors were isolated for further analysis. The cells were cultured with vitamin D, peptidoglycan (PGN) and lipopolysaccharide (LPS) for defined periods of time before RNA was isolated and subjected to microarray analysis using Clariom S assays and quantitative real-time PCR. *NOD2*- and disease-specific gene expression profiles were evaluated with repeated measure ANOVA by a general linear model.

RESULTS
Employing microarray assays, a total of 267 genes were identified that were significantly up- or downregulated in PBMCs of WT-*NOD2* patients, compared to healthy donors after challenge with vitamin D and/or a combination of LPS and PGN ($P < 0.05$; threshold: ≥ 2-fold change). For further analysis by real-time PCR, genes with known impact on inflammation and immunity were selected that fulfilled predefined expression criteria. In a larger cohort of patients and controls, a disease-associated expression pattern, with higher transcript levels in vitamin D-treated PBMCs from patients, was observed for three of these genes, *CLEC5A* ($P < 0.030$), *lysozyme* (*LYZ*; $P < 0.047$) and *TREM1* ($P < 0.023$). Six genes were found to be expressed in a *NOD2*-dependent manner (*CD101*, $P < 0.002$; *CLEC5A*, $P < 0.020$; *CXCL5*, $P < 0.009$; *IL-24*, $P < 0.044$; *ITGB2*, $P < 0.041$; *LYZ*, $P < 0.042$). Interestingly, the highest transcript levels were observed in patients with heterozygous *NOD2* mutations.

CONCLUSION
Our data identify *CLEC5A* and *LYZ* as CD- and *NOD2*-associated genes of PBMCs and encourage further studies on their pathomechanistic roles.

Key words: Peripheral blood mononuclear cells; Gene expression; *NOD2*; *Lysozyme*; Crohn's disease; *CLEC5A*

Core tip: Peripheral blood mononuclear cells (PBMCs) are a useful tool to study peculiarities of the immune response in the context of Crohn's disease (CD). Here, we investigated whether PBMCs from patients with CD, even at the stage of clinical remission, exhibit altered gene expression profiles after challenge with pathogen-associated molecular patterns and vitamin D. For *TREM1*, *lysozyme* and *CLEC5A*, disease-associated expression patterns, with higher transcript levels in patient-derived PBMCs, were observed. The two latter genes, along with four other transcripts, also showed *NOD2*-dependent expression profiles. *TREM1* and *CLEC5A* may act with *NOD2* in a regulatory network with a pathophysiological role in CD.

Schäffler H, Rohde M, Rohde S, Huth A, Gittel N, Hollborn H, Koczan D, Glass Ä, Lamprecht G, Jaster R. *NOD2*- and disease-specific gene expression profiles of peripheral blood mononuclear cells from Crohn's disease patients. *World J Gastroenterol* 2018; 24(11): 1196-1205 Available from: URL: http://www.wjgnet.com/1007-9327/full/v24/i11/1196.htm DOI: http://dx.doi.org/10.3748/wjg.v24.i11.1196

INTRODUCTION

Inflammatory bowel diseases (IBD) are chronic intestinal disorders and mainly consist of the two entities Crohn's disease (CD) and ulcerative colitis (UC)[1,2]. The clinical course of IBD is characterized by intermittent periods of relapses and remission, which are unpredictable in clinical practice. The pathogenesis of IBD is multifactorial, including genetic and environmental factors, and involves an inappropriate activation of the mucosal immune system, which is triggered by the intestinal microbiota in genetically predisposed individuals[1-5]. In Caucasian populations, nucleotide-binding oligomerization domain 2 (*NOD2*) has emerged as one of the main susceptibility genes for CD[6-8]. NOD2 is an intracellular pattern recognition receptor sensing muramyl dipeptide (MDP)[9,10], a fragment of peptidoglycan (PGN), but also PGN by itself[11,12] and, upon ligand binding, induces activation of the transcription factor NF-κB[13]. However, NOD2 activation via PGN is dependent on a TLR2 co-stimulatory signal[14].

In addition, the environment, *e.g.*, vitamin D deficiency, also affects the development and clinical course of IBD[15-17]. Vitamin D deficiency has a high prevalence in IBD patients[17,18]. We have recently shown that clinical factors, *e.g.*, the use of tumor necrosis factor (TNF)-α inhibitor, are associated with significant changes in vitamin D levels[19]. Vitamin D was originally mainly implicated in bone health, regulating calcium and phosphate metabolism[20,21], but recent evidence has shown that vitamin D also profoundly impacts the innate and adaptive immune system[22-24]. Underscoring its role in the pathogenesis of CD, vitamin D was shown to be an inductor of *NOD2* gene expression[25]. Using peripheral blood mononuclear cells (PBMCs) and dendritic cells, Dionne *et al*[26] showed that 1, 25-vitamin D acts as a modulator of the innate immune system. However, little is known about the effects of vitamin D and the presence of *NOD2* mutations on different gene expression levels in CD. The aim of our study was therefore to further characterize different gene expression profiles in CD patients and healthy controls correlating to *NOD2* mutation status and vitamin D pretreatment. We identified different genes associated with the presence of CD and mutations in the *NOD2*

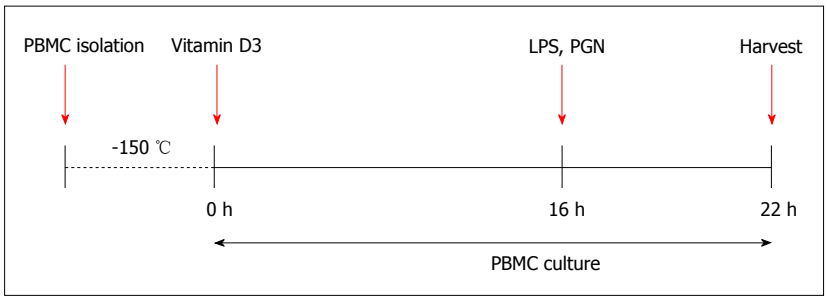

Figure 1 Protocol of peripheral blood mononuclear cells treatment.

gene. Follow-up studies on these genes may provide novel insights into the pathogenesis of CD and could contribute to the establishment of biomarkers to better predict the clinical course of the disease.

MATERIALS AND METHODS

Patients and controls

Sixteen patients with CD were recruited from the Rostock University Medical Center. The disease activity was determined via the Crohn's disease activity index (CDAI)[27]. Furthermore, all patients were classified according to the Montreal classification[28], and age, gender and disease-specific medication were recorded. Six healthy volunteers without immune-mediated gastrointestinal or other autoimmune disorders served as controls. EDTA blood samples were drawn from all participants for genotyping studies and isolation of PBMCs. Plasma levels of vitamin D and C-reactive protein (CRP) were determined using routine laboratory methods.

The study was approved by the ethics board of the University of Rostock (A-2015-0042). Written informed consent was obtained from each participant prior to enrollment.

Isolation, culture and treatment of PBMCs

PBMCs were isolated from EDTA venous blood using density-gradient centrifugation over Pancoll (PAN-Biotech, Aidenbach, Germany). Immediately after isolation, PBMCs were resuspended in cryopreservation medium [fetal calf serum (FCS) supplemented with 10% dimethyl sulfoxide (DMSO)] and stored at -150 ℃ until required. After thawing, the cells were cultured in RPMI-1640 medium supplemented with 10% FCS and 1% penicillin/streptomycin (all reagents from Biochrom/Merck, Berlin, Germany), and exposed to 1α,25-dihydroxyvitamin D3 (Santa Cruz Biotechnology, Dallas, TX, United States) at 40 nmol/L as indicated. After an incubation period of 20 h at 37 ℃ in a 5% CO_2 humidified atmosphere, lipopolysaccharide (LPS; 1 μg/mL; Sigma-Aldrich, Deisenhofen, Germany) and peptidoglycan (PGN; 10 μg/mL; Sigma-Aldrich) were added to the cells as indicated, and incubation continued for another 6 h (Figure 1). Subsequently, the cells were lysed in RTL Plus buffer, which was included in the RNeasy Plus Kit (Qiagen, Hilden, Germany), and subjected to RNA isolation (see below).

NOD2 genotyping

DNA was isolated from whole blood using a QIAamp DNA Blood Mini Kit (Qiagen) according to the manufacturer's protocol. All patients and controls were genotyped with respect to the three major mutations in the *NOD2* gene (SNP 8; R702W, NCBI reference SNP ID: rs2066844, SNP 12; G908R, NCBI reference SNP ID: rs2066845 and SNP 13; 1007fs, NCBI reference SNP ID: rs2066847). The corresponding regions of the *NOD2* gene were amplified by PCR using a Taq PCR Master Mix Kit (Qiagen) and primers as specified in Table 1. The following PCR conditions were used: 5 min, 94 ℃; 1 min, 94/60/72 ℃ (45 cycles); 7 min, 72 ℃; 4 ℃. After Sanger sequencing (Seqlab, Göttingen, Germany), the data were analyzed using the software Chromas, version 2.6. Individuals with no SNP mutations were considered wild-type (WT) for *NOD2*.

Microarray analysis of RNA expression profiles

RNA was extracted employing an RNeasy Plus Kit according to the manufacturer's protocol. Total RNA samples were quantified with a spectrophotometer (NanoDrop 1000, Thermo Fisher Scientific, Waltham, MA, United States), and their integrity was confirmed using the Agilent Bioanalyzer 2100 with an RNA Nano chip kit (both from Agilent Technologies, Waldbronn, Germany).

Expression profiling was performed using 200 ng RNA and the Affymetrix Human Clariom S Assay (Affymetrix/Thermo Fisher Scientific), which interrogates over 20000 well-annotated genes. Therefore, the so-called Whole Transcriptome protocol was employed. T7 promoter tags were introduced into all RNA molecules by using N6 3'-ends for DNA strand synthesis, before RNA strand replacement according to Eberwine[29] was conducted. Non-labeled aRNA was produced by *in vitro* transcription. All RNA molecules were amplified in a linear manner, avoiding a 3' bias. Using purified aRNA as a template, a new strand-identical single-strand DNA was produced by adding random primers and dNTPs (including dUTP, which replaced a limited

Table 1 Primer for *NOD2*-genotyping

SNP	Primer
8	Forward: 5′CCTCTTCAATTGTGGCAGGC-3′
	Reverse: 5′-CTCCTGCATCTCGTACAGGC-3′
12	Forward: 5′-ATGGAGGCAGGTCCACTTTG-3′
	Reverse: 5′-TTACCTGAGCCACCTCAAGC-3′
13	Forward: 5′-GATGGTACTGAGCCTTTGTTGA-3′
	Reverse: 5′-CAGACTTCCAGGATGGTGTCAT -3′

amount of dTTP). After digestion with RNase H, endpoint fragmentation was performed with uracil-DNA-glycosylase in combination with apurinic/apyrimidinic endonuclease 1, and biotinylated dNTPs were added to the 3′-ends of the single-stranded DNA fragments with deoxynucleotidyl transferase. Subsequently, hybridization of the microarrays was performed at 45 ℃ in a GeneChip® Hybridization Oven 645 (Affymetrix/Thermo Fisher Scientific). After overnight incubation, the microarrays were scanned using the GeneChip Scanner 3000 (Affymetrix/Thermo Fisher Scientific) at 0.7 μm resolution.

Primary data analysis was performed with the Affymetrix Transcriptome Analysis Console software version 3.1.0.5 including the Robust Multiarray Average module for normalization. Gene expression data were log-transformed. A change was considered significant when the ANOVA *P*-value met the criterion $P < 0.05$ at fold changes >|2|, *i.e.*, expression increments or declines larger than two. Along with the publication of the manuscript, our complete microarray data will be available in the Gene Expression Omnibus database (GEO accession number: GSE110186).

Quantitative reverse transcriptase-PCR using real-time TaqMan™ technology

Unless indicated otherwise, reagents from Thermo Fisher Scientific were used in all subsequent steps. Cellular RNA prepared as described above was treated with a DNA-free kit to remove traces of genomic DNA, and 250 ng of RNA per sample was reverse transcribed into cDNA using TaqMan™ Reverse Transcription Reagents and random priming. Using a ViiA 7 sequence detection system (Thermo Fisher Scientific), target cDNA levels were quantified by real-time PCR. Therefore, qPCR MasterMix (Eurogentec, Seraing, Liège, Belgium) and the following human-specific TaqMan™ gene expression assays with fluorescently labeled MGB probes were used: Hs00355476_m1 (*CCL20*), Hs00188627_m1 (*CD101*), Hs00370621_m1 (*CLEC12A*), Hs04398399_m1 (*CLEC5A*), Hs01902549_s1 (*CLEC7A*), Hs01099660_g1 (*CXCL5*), Hs01114274_m1 (*IL24*), Hs00167304_m1 (*ITGAM*), Hs00164957_m1 (*ITGB2*), Hs00426232_m1 (*LYZ*), Hs00234007_m1 (*MSR1*), Hs01065279_m1 (*PECAM1*), Hs00218624_m1 (*TREM1*), and Hs99999905_m1 (*GAPDH*). PCR conditions were as follows: 95 ℃ for 10 min, followed by 40 cycles of 15 s at 95 ℃/ 1 min at 60 ℃. Relative amounts of target mRNA in PBMCs were expressed as $2^{-(\Delta Ct)}$ values.

Statistical analysis

Real-time PCR data were analyzed with repeated-measures ANOVA. Mean group differences were compared for "disease" (patients with CD *vs* controls) and "*NOD2*-status" (WT, heterozygote, homozygote), as well as for (within-subject factors) "vitamin D application" (yes *vs* no) and "stimulation" (LPS, PGN, LPS + PGN, controls), employing a *general linear model* for repeated measurements. Age was considered a covariate in the disease model because disease groups were not balanced by age, and *NOD2* groups were tested post hoc by LSD. Normal distribution of measurements was assessed using the Kolmogorov-Smirnov test. $P < 0.05$ was considered statistically significant. All data were processed using IBM® SPSS® Advanced Statistics 22.0.

RESULTS

PBMCs provide an easily accessible tool to investigate disease-associated peculiarities of the antipathogenic immune response of patients with CD. To study transcripts in an unbiased manner, we initially chose a microarray approach. Therefore, PBMCs from healthy individuals and patients with CD in remission ($n = 3$ each; all of them *NOD2*-WT) were pretreated with vitamin D3 for 20 h before they were challenged simultaneously with LPS and PGN for 6 h. Subsequently, global gene expression was analyzed employing Clariom S assays, and data were compared with those of untreated controls. Table 2 gives an overview of the significant differences between patients with CD and controls under identical conditions of PBMC treatment.

Under basal conditions and any treatment regimen, genes upregulated in patients with CD exceeded downregulated genes both in number and maximum change. Complete lists of the 267 genes are presented as Supplementary Table 1.

Many of the differentially expressed genes are well-known modulators of immune cell functions in the context of innate and adaptive immunity, and unsurprisingly, some of them have previously been implicated in the pathogenesis of CD, including several immune cell receptors, cytokines/chemokines and their cognate receptors and the antimicrobial peptide lysozyme[30-36]. The latter transcript was found to be upregulated in PBMCs of patients with CD in response to LPS/PGN treatment, independent of the presence or absence of vitamin D3. Intriguingly, expression of various genes was synchronously up- or downregulated under different conditions, suggesting a robustness of the expression profile against external perturbations.

For in-depth analysis, we selected a panel of 11 genes from the list of candidates shown in Table 2 that fulfilled the following criteria: (1) differential expression in PBMCs from patients with CD and controls under basal conditions and/or under at least two

Table 2 Numbers and maximum changes of up- and downregulated genes in peripheral blood mononuclear cells from Crohn's disease patient *vs* identically treated controls

Treatment of PBMCs	Upregulated genes	Downregulated genes
Untreated	85 (59-fold)	39 (39-fold)
Vitamin D3	25 (21-fold)	12 (9-fold)
LPS/PGN	54 (6-fold)	15 (5-fold)
Vitamin D3 + LPS/PGN	29 (15-fold)	8 (5-fold)

$P < 0.05$; Threshold: ⩾ 2-fold change. PBMCs: Peripheral blood mononuclear cells; LPS: Lipopolysaccharide; PGN: Peptidoglycan.

Table 3 Genes selected for real-time PCR studies

Transcript	Fold changes: patients *vs* controls				Details on function/ reasons to study
	Basal	+D, -L/P	-D, +L/P	+D, +L/P	
MSR1	9.56	13.19		14.72	macrophage scavenger receptor[49]; differentially expressed in 3 of 4 groups
CD101	2.66				expressed on various immune cells; inhibits expansion of colitogenic T cells[30]
CLEC5A		2.82		3.11	C-type lectin member 5A, pattern recognition receptor; involved in antibacterial/ antiviral defense[43]
CLEC7A	4.53			3.94	C-type lectin member 7A, pattern recognition receptor; control of fungal infections[50]
CLEC12A	6.04	4.52			C-type lectin member 12A, pattern recognition receptor, inhibits cell death-induced inflammation[51]
ITGAM	2.18				CD11b; integrin αM; expressed by many immune cells; polymorphisms linked to autoimmunity[52]
LYZ			3.51	2.03	antimicrobial enzyme; essential role in innate immunity; increased production linked to CD[31]
PECAM1	3.15				CD31; implicated in transendothelial leukocyte migration in experimental colitis[32]
CCL20	-2.33		-5.08		chemokine expressed by neutrophils, enterocytes, B-cells and dendritic cell; IBD predilection gene[33]
CXCL5	-38.89		-5.32		regulates neutrophil homeostasis and chemotaxis; increased serum levels in IBD patients reported[34]
IL-24			-3.49	-4.82	Involved in host defence against bacteria and fungi; increased expression in patients with active IBD[35]
TREM1					amplifier of antimicrobial immune responses and inflammation in experimental colitis and IBD[36]

$P < 0.05$; Threshold: ⩾ 2-fold change. Positive values refer to genes upregulated and negative values to genes downregulated in CD patients. LPS: Lipopolysaccharide; PGN: Peptidoglycan; PBMCs: Peripheral blood mononuclear cells. CD: Crohn's disease; IBD: Inflammatory bowel diseases.

treatment regimens (vitamin D3, LPS+PGN and their combination, respectively) and (2) an established or potential role in inflammation and/or regulation of the immune response. Table 3 shows details regarding all selected genes as well as a twelfth gene, *TREM1*, that was included as a control as an established vitamin D-responsive gene with immunomodulatory function[37]. Interestingly, three pro-inflammatory mediators, *CCL20*, *CXCL5* and *IL-24*, displayed lower expression levels in patients with CD, which might be a consequence of their disease-specific medication (see below).

The expression profiles of the selected genes were subsequently studied by real-time PCR. In addition to WT-*NOD2* patients and healthy controls (n = 6 each, including the samples previously analyzed by microarray technology), we also included patients with heterozygous and homozygous mutations of *NOD2* (n = 5 each). Furthermore, we refined the protocol of PBMC treatment using LPS and PGN both in combination and as individual factors (Supplementary Table 2).

The clinical characteristics, laboratory findings and the medication of all 16 patients are shown in Table 4. Except for one person with a slightly increased CDAI of 166, all patients presented with a CDAI of < 150, indicating disease remission[27]. The CRP-values of 13 patients were in the normal range (below 5 mg/L). In the remaining three patients, modestly elevated CRP-values (all below 14 mg/L) were detected. Disease activity in all patients could still be considered low. All but two patients presented with vitamin D levels below 75 nmol/L, suggesting an insufficiency or even deficiency (levels below 50 nmol/L). This finding was not unexpected, as all of the samples were collected during the European winter season. As a consequence, a vitamin D substitution therapy was initiated, if appropriate. Three of the patients were on steroids (> 10 mg prednisolone/d) at the time of the study, 7 received azathioprine, and 12 were treated with anti-TFN-α antibodies. Healthy controls consisted of 3 males and 3 females with an age range from 25 to 53 years.

For statistical data analysis, a general linear model repeated measure was chosen to assess mean differ-

Table 4 Characteristics of the patients –nucleotide-binding oligomerization domain 2 status, classification and activity of the disease, C-reactive protein and vitamin D levels, and medication at the time of the study

No.	Sex	Age	NOD2	Montreal classification	CDAI	CRP (mg/L)	Vitamin D (nmol/L)	Prednisolon (> 10 mg/d)	Azathio-prine	Anti-TNF-α
1	M	24	WT[1]	A2 L3 L4 B1	121	2.58	104.0	Yes	No	Yes
2	M	28	WT[1]	A2 L3 B3p	46	< 1.0	62.9	No	No	Yes
3	M	64	WT[1]	A3 L3 B2p	111	4.58	27.0	Yes	No	Yes
4	F	60	WT	A2 L3 B2	100	2.27	72.5	No	No	Yes
5	F	62	WT	A3 L3 B3p	82	< 1.0	58.2	Yes	Yes	Yes
6	M	46	WT	A2 L3 L4 B2p	110	4.97	32.9	No	No	Yes
7	M	38	HO	A2 L3 B3p	92	13.30	40.2	No	Yes	No
8	M	64	HO	A3 L3 B1	34	< 1.0	53.0	No	No	Yes
9	F	48	HO[2]	A2 L3 B2	54	< 1.0	67.6	No	No	Yes
10	M	54	HO	A2 L3 B2p	103	1.63	51.9	No	Yes	No
11	M	26	HO	A1 L3 B2p	120	7.86	31.0	No	Yes	Yes
12	M	27	HT	A2 L3 B1	106	1.41	47.2	No	No	Yes
13	M	37	HT	A2 L3 B2p	166	4.56	37.9	No	Yes	No
14	F	48	HT	A2 L1 B3p	115	1.01	55.2	No	Yes	Yes
15	M	57	HT	A1 L3 B2p	132	12.30	52.3	No	No	Yes
16	M	47	HT	A2 L3 B3	60	2.62	92.0	No	Yes	No

[1]Patients who were also included into microarray analysis; [2]SNP8 mutation. All other HO/HT mutations refer to SNP13. NOD2: Nucleotide-binding oligomerization domain 2; CDAI: Crohn's disease activity index; CRP: C-reactive protein; TNF : Tumor necrosis factor; WT: Wild-type; HO: Homozygous mutation; HT: Heterozygous mutation.

Table 5 differentially expressed transcripts in vitamin D-pretreated peripheral blood mononuclear cells from Crohn's disease patients and controls (with and without additional stimulation with lipopolysaccharide and peptidoglycan, respectively, age adjusted)

Gene	*P* value	Upregulated in
CLEC5A	0.030	CD patients
LYZ	0.047	CD patients
TREM1	0.023	CD patients

CD: Crohn's disease.

ences between groups. Comparing controls to CD patients, no significant differences were detected when samples with and without vitamin D incubation were considered conjointly, due to the strong overlaying effect of vitamin D. However, focusing on the subgroup of vitamin D treated samples, disease-related differences were observed (no. 5-8 in Supplementary Table 2). Here, with age adjustment, three genes displayed a disease-dependent expression pattern (Table 5): consistent with the microarray data, significantly higher *CLEC5A* and *LYZ* transcript levels were observed in PBMCs of patients with CD. The same finding was observed for *TREM1*, which was included due to its vitamin D-dependent expression pattern but not because of the microarray results. Together, these findings suggest that CD-associated changes in gene expression could be attributed to treatment protocols that include vitamin D, as analyses in the remaining subgroup (w/o vitamin D) did not show any differences (all $P > 0.20$).

We also analyzed the influence of *NOD2* mutations on the expression of the gene panel described above. Considering all treated and untreated samples (Supplementary Table 2), a significant effect of the *NOD2* status was observed for 5 of these genes, including *CLEC5A* and *LYZ*, and one additional gene from Table 2, integrin subunit beta *2* (*ITGB2*) (Table 6). With a *P*-value of 0.053, *TREM1* just missed statistical significance.

Unexpectedly, heterozygous CD patients displayed the highest expression levels for all of the genes, whereas no statistically significant differences between persons with WT-*NOD2* (patients and controls) and homozygous *NOD2* mutations were detected. The phenomenon is apparently unrelated to medication, which was very similar in the groups of patients with heterozygous and homozygous *NOD2* mutations (Table 4). This conclusion is also supported by statistical evaluations, which did not show any significant association between treatment with prednisolone, azathioprine or anti-TNF-α and expression of *CLEC5A*, *LYZ* and *TREM1* in PBMCs of patients with CD.

DISCUSSION

Many studies have shown that numerous risk genes of CD code for molecules involved in host defense against pathogens, such as nucleotide-binding oligomerization domain 2 (*NOD2*), *ATG16L1*, and those implicated in the T helper type 17 (Th17) pathway[38-43]. Here, we tested the hypothesis that PBMCs of patients with CD, even at the stage of clinical remission, exhibit an

Table 6 Transcripts with a *NOD2*-dependent expression pattern

Gene	*P* value	Highest levels
CD101	0.002	Heterozygotes
CLEC5A	0.020	Heterozygotes
CXCL5	0.009	Heterozygotes
IL-24	0.044	Heterozygotes
ITGB2	0.041	Heterozygotes
LYZ	0.042	Heterozygotes

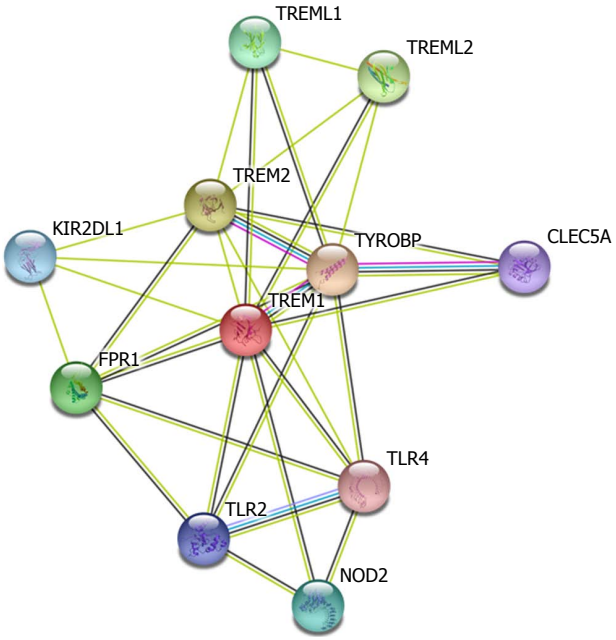

Figure 2 Network analysis using the STRING database[48]. The network was derived employing human TREM1 as the search term (https://string-db.org/cgi/network.pl?taskId=PmXpOD7RMwaM).

altered gene expression profile upon challenge with pathogen-associated molecular patterns (PAMPs) and/or the immunomodulatory hormone vitamin D, which has previously been shown to exert differential effects on the expression of NOD2- and TLR-induced cytokines in the context of CD[26].

Initial microarray experiments identified more than 200 genes with different expression patterns among patients with CD and controls. Based on predefined expression criteria, genes with roles in inflammation and immunity were selected for in-depth analysis by real-time PCR. A disease-associated expression pattern was identified for *CLEC5A*, *lysozyme* and *TREM1*. Six genes, including *CLEC5A* and *lysozyme*, displayed a *NOD2*-dependent expression pattern. With respect to lysozyme and TREM1, our findings are consistent with previous reports, which found that increased levels of both proteins in serum were implicated in the pathophysiology of IBD[44,45]. To the best of our knowledge, however, this is the first report of an association between *CLEC5A* expression and CD. CLEC5A has most recently been identified as an important receptor in innate immunity by neutrophil trap formation and secretion of different proinflammatory cytokines after stimulation with *Listeria monocytogenes*[43]. This finding is especially interesting, as defective bacterial clearance was shown to play a crucial role in the pathogenesis of CD[46,47]. Of note, both CLEC5A and TREM1 proteins can be linked to the product of the best-established CD risk gene, *NOD2*, by the STRING database[48] (Figure 2).

In conclusion, we found that PBMCs of patients with CD display alterations in their response to vitamin D and PAMPs. Disease-associated and *NOD2*-dependent gene expression profiles are preserved even at the stage of clinical remission. Our data identify *CLEC5A*, *LYZ* and *TREM1* as genes of particular interest for follow-up studies. We hypothesize that these genes may act in a common network relevant to CD pathogenesis. Establishment of biomarkers to better predict the clinical course of the disease remains a long-term goal of our studies.

ARTICLE HIGHLIGHTS

Research background

In Crohn's disease (CD), the interplay of genetic and environmental factors converges at the level of an altered antipathogenic immune response, which is incompletely understood. Peripheral blood mononuclear cells (PBMCs) provide a useful tool to study elements of the immunopathogenesis of the disease *in vitro*.

Research motivation

Currently, there is a lack of biomarkers to predict the clinical course of CD. Furthermore, the development of specific therapies would benefit from an improved mechanistic understanding of the pathogenesis of the disease.

Research objectives

The aim of this study was to identify disease-specific gene expression profiles of PBMCs from patients with CD in clinical remission. Specifically, we were interested in alterations of the gene expression profile after challenging PBMCs with pathogen-associated molecular patterns (PAMPs) and the immunomodulatory hormone vitamin D.

Research methods

PBMCs from patients with CD and healthy donors were cultured with vitamin D, peptidoglycan (PGN) and lipopolysaccharide (LPS), before RNA was isolated and subjected to microarray analysis and quantitative real-time PCR. Disease-specific gene expression profiles were evaluated by *general linear model repeated measure* analysis, paying particular attention to the well-established CD risk gene *NOD2*.

Research results

Microarray experiments yielded a total of 267 genes that were significantly up- or downregulated in PBMCs of patients with CD, compared to healthy donors, after challenge with vitamin D and/or a combination of LPS and PGN. For further analysis by real-time PCR, genes with roles in inflammation and immunity were selected. For three of these genes, *CLEC5A*, *lysozyme* and *TREM1*, a disease-associated expression pattern was validated. Six genes, including *CLEC5A* and *lysozyme*, were found to be expressed in a *NOD2*-dependent manner.

Research conclusions

PBMCs of patients with CD display alterations of their response to vitamin D and PAMPs that are preserved even at the stage of clinical remission. *CLEC5A*, *TREM1* and *NOD2* may act in a common network relevant to CD pathogenesis.

Research perspectives

Follow-up studies on alterations of the antipathogenic immune response may provide novel insights into the pathogenesis of CD and may also help to establish biomarkers to better predict the clinical course of the disease.

ACKNOWLEDGMENTS

We thank Mrs. Katja Bergmann for expert technical assistance.

REFERENCES

1 **Abraham C**, Cho JH. Inflammatory bowel disease. *N Engl J Med* 2009; **361**: 2066-2078 [PMID: 19923578 DOI: 10.1056/NEJMra0804647]

2 **Baumgart DC**, Sandborn WJ. Crohn's disease. *Lancet* 2012; **380**: 1590-1605 [PMID: 22914295 DOI: 10.1016/S0140-6736(12)60026-9]

3 **Mayer L**. Evolving paradigms in the pathogenesis of IBD. *J Gastroenterol* 2010; **45**: 9-16 [PMID: 19960355 DOI: 10.1007/s00535-009-0138-3]

4 **Sartor RB**. Microbial influences in inflammatory bowel diseases. *Gastroenterology* 2008; **134**: 577-594 [PMID: 18242222 DOI: 10.1053/j.gastro.2007.11.059]

5 **Naser SA**, Arce M, Khaja A, Fernandez M, Naser N, Elwasila S, Thanigachalam S. Role of ATG16L, NOD2 and IL23R in Crohn 's disease pathogenesis. *World J Gastroenterol* 2012; **18**: 412-424 [PMID: 22346247 DOI: 10.3748/wjg.v18.i5.412]

6 **Hugot JP**, Chamaillard M, Zouali H, Lesage S, Cézard JP, Belaiche J, Almer S, Tysk C, O'Morain CA, Gassull M, Binder V, Finkel Y, Cortot A, Modigliani R, Laurent-Puig P, Gower-Rousseau C, Macry J, Colombel JF, Sahbatou M, Thomas G. Association of NOD2 leucine-rich repeat variants with susceptibility to Crohn 's disease. *Nature* 2001; **411**: 599-603 [PMID: 11385576 DOI: 10.1038/35079107]

7 **Ogura Y**, Bonen DK, Inohara N, Nicolae DL, Chen FF, Ramos R, Britton H, Moran T, Karaliuskas R, Duerr RH, Achkar JP, Brant SR, Bayless TM, Kirschner BS, Hanauer SB, Nuñez G, Cho JH. A frameshift mutation in NOD2 associated with susceptibility to Crohn's disease. *Nature* 2001; **411**: 603-606 [PMID: 11385577 DOI: 10.1038/35079114]

8 **Cho JH**. The genetics and immunopathogenesis of inflammatory bowel disease. *Nat Rev Immunol* 2008; **8**: 458-466 [PMID: 18500230 DOI: 10.1038/nri2340]

9 **Girardin SE**, Boneca IG, Viala J, Chamaillard M, Labigne A, Thomas G, Philpott DJ, Sansonetti PJ. Nod2 is a general sensor of peptidoglycan through muramyl dipeptide (MDP) detection. *J Biol Chem* 2003; **278**: 8869-8872 [PMID: 12527755 DOI: 10.1074/jbc.C200651200]

10 **Inohara N**, Ogura Y, Fontalba A, Gutierrez O, Pons F, Crespo J, Fukase K, Inamura S, Kusumoto S, Hashimoto M, Foster SJ, Moran AP, Fernandez-Luna JL, Nuñez G. Host recognition of bacterial muramyl dipeptide mediated through NOD2. Implications for Crohn's disease. *J Biol Chem* 2003; **278**: 5509-5512 [PMID: 12514169 DOI: 10.1074/jbc.C200673200]

11 **Natsuka M**, Uehara A, Yang S, Echigo S, Takada H. A polymer-type water-soluble peptidoglycan exhibited both Toll-like receptor 2- and NOD2-agonistic activities, resulting in synergistic activation of human monocytic cells. *Innate Immun* 2008; **14**: 298-308 [PMID: 18809654 DOI: 10.1177/1753425908096518]

12 **Iyer JK**, Coggeshall KM. Cutting edge: primary innate immune cells respond efficiently to polymeric peptidoglycan, but not to peptidoglycan monomers. *J Immunol* 2011; **186**: 3841-3845 [PMID: 21357534 DOI: 10.4049/jimmunol.1004058]

13 **Strober W**, Murray PJ, Kitani A, Watanabe T. Signalling pathways and molecular interactions of NOD1 and NOD2. *Nat Rev Immunol* 2006; **6**: 9-20 [PMID: 16493424 DOI: 10.1038/nri1747]

14 **Schäffler H**, Demircioglu DD, Kühner D, Menz S, Bender A, Autenrieth IB, Bodammer P, Lamprecht G, Götz F, Frick JS. NOD2 stimulation by Staphylococcus aureus-derived peptidoglycan is boosted by Toll-like receptor 2 costimulation with lipoproteins in dendritic cells. *Infect Immun* 2014; **82**: 4681-4688 [PMID: 25156723 DOI: 10.1128/IAI.02043-14]

15 **Rebouças PC**, Netinho JG, Cunrath GS, Ronchi LS, de Melo MM, Gonçalves Filho Fde A, Muniz RC, Martins AT, de Oliveira RA, Costa Junior RM. Association between vitamin D serum levels and disease activity markers in patients with Crohn's Disease. *Int J Colorectal Dis* 2016; **31**: 1495-1496 [PMID: 26971347 DOI: 10.1007/s00384-016-2555-0]

16 **Ananthakrishnan AN**, Khalili H, Higuchi LM, Bao Y, Korzenik JR, Giovannucci EL, Richter JM, Fuchs CS, Chan AT. Higher predicted vitamin D status is associated with reduced risk of Crohn 's disease. *Gastroenterology* 2012; **142**: 482-489 [PMID: 22155183 DOI: 10.1053/j.gastro.2011.11.040]

17 **Ulitsky A**, Ananthakrishnan AN, Naik A, Skaros S, Zadvornova Y, Binion DG, Issa M. Vitamin D deficiency in patients with inflammatory bowel disease: association with disease activity and quality of life. *JPEN J Parenter Enteral Nutr* 2011; **35**: 308-316 [PMID: 21527593 DOI: 10.1177/0148607110381267]

18 **Leslie WD**, Miller N, Rogala L, Bernstein CN. Vitamin D status and bone density in recently diagnosed inflammatory bowel disease: the Manitoba IBD Cohort Study. *Am J Gastroenterol* 2008; **103**: 1451-1459 [PMID: 18422819 DOI: 10.1111/j.1572-0241.2007.01753.x]

19 **Schäffler H**, Schmidt M, Huth A, Reiner J, Glass Ä, Lamprecht G. Clinical factors are associated with vitamin D levels in IBD patients: A retrospective analysis. *J Dig Dis* 2018; **19**: 24-32 [PMID: 29232067 DOI: 10.1111/1751-2980.12565]

20 **DeLuca HF**. Overview of general physiologic features and functions of vitamin D. *Am J Clin Nutr* 2004; **80**: 1689S-1696S [PMID: 15585789]

21 **Holick MF**. Optimal vitamin D status for the prevention and treatment of osteoporosis. *Drugs Aging* 2007; **24**: 1017-1029 [PMID: 18020534]

22 **Cantorna MT**, Zhu Y, Froicu M, Wittke A. Vitamin D status, 1,25-dihydroxyvitamin D3, and the immune system. *Am J Clin Nutr* 2004; **80**: 1717S-1720S [PMID: 15585793]

23 **Olliver M**, Spelmink L, Hiew J, Meyer-Hoffert U, Henriques-Normark B, Bergman P. Immunomodulatory effects of vitamin D on innate and adaptive immune responses to Streptococcus pneumoniae. *J Infect Dis* 2013; **208**: 1474-1481 [PMID: 23922371 DOI: 10.1093/infdis/jit355]

24 **Zhao H**, Zhang H, Wu H, Li H, Liu L, Guo J, Li C, Shih DQ, Zhang X. Protective role of 1,25(OH)2 vitamin D3 in the mucosal injury and epithelial barrier disruption in DSS-induced acute colitis in mice. *BMC Gastroenterol* 2012; **12**: 57 [PMID: 22647055 DOI: 10.1186/1471-230X-12-57]

25 **Wang TT**, Dabbas B, Laperriere D, Bitton AJ, Soualhine H, Tavera-Mendoza LE, Dionne S, Servant MJ, Bitton A, Seidman EG, Mader S, Behr MA, White JH. Direct and indirect induction by 1,25-dihydroxyvitamin D3 of the NOD2/CARD15-defensin beta2 innate immune pathway defective in Crohn disease. *J Biol Chem* 2010; **285**: 2227-2231 [PMID: 19948723 DOI: 10.1074/jbc.C109.071225]

26 **Dionne S**, Calderon MR, White JH, Memari B, Elimrani I, Adelson B, Piccirillo C, Seidman EG. Differential effect of vitamin D on NOD2- and TLR-induced cytokines in Crohn's disease. *Mucosal Immunol* 2014; **7**: 1405-1415 [PMID: 24781050 DOI: 10.1038/mi.2014.30]

27 **Best WR**, Becktel JM, Singleton JW, Kern F Jr. Development of a Crohn's disease activity index. National Cooperative Crohn 's Disease Study. *Gastroenterology* 1976; **70**: 439-444 [PMID: 1248701]

28 **Silverberg MS**, Satsangi J, Ahmad T, Arnott ID, Bernstein CN, Brant SR, Caprilli R, Colombel JF, Gasche C, Geboes K, Jewell DP, Karban A, Loftus EV Jr, Peña AS, Riddell RH, Sachar DB, Schreiber S, Steinhart AH, Targan SR, Vermeire S, Warren BF. Toward an integrated clinical, molecular and serological classification of inflammatory bowel disease: report of a Working

Party of the 2005 Montreal World Congress of Gastroenterology. *Can J Gastroenterol* 2005; **19** Suppl A: 5A-36A [PMID: 16151544]
29 **Van Gelder RN**, von Zastrow ME, Yool A, Dement WC, Barchas JD, Eberwine JH. Amplified RNA synthesized from limited quantities of heterogeneous cDNA. *Proc Natl Acad Sci USA* 1990; **87**: 1663-1667 [PMID: 1689846]
30 **Schey R**, Dornhoff H, Baier JL, Purtak M, Opoka R, Koller AK, Atreya R, Rau TT, Daniel C, Amann K, Bogdan C, Mattner J. CD101 inhibits the expansion of colitogenic T cells. *Mucosal Immunol* 2016; **9**: 1205-1217 [PMID: 26813346 DOI: 10.1038/mi.2015.139]
31 **Rubio CA**. Increased Production of Lysozyme Associated with Bacterial Proliferation in Barrett's Esophagitis, Chronic Gastritis, Gluten-induced Atrophic Duodenitis (Celiac Disease), Lymphocytic Colitis, Collagenous Colitis, Ulcerative Colitis and Crohn's Colitis. *Anticancer Res* 2015; **35**: 6365-6372 [PMID: 26637845]
32 **Rijcken E**, Mennigen RB, Schaefer SD, Laukoetter MG, Anthoni C, Spiegel HU, Bruewer M, Senninger N, Krieglstein CF. PECAM-1 (CD 31) mediates transendothelial leukocyte migration in experimental colitis. *Am J Physiol Gastrointest Liver Physiol* 2007; **293**: G446-G452 [PMID: 17510197 DOI: 10.1152/ajpgi.00097.2007]
33 **Liu JZ**, van Sommeren S, Huang H, Ng SC, Alberts R, Takahashi A, Ripke S, Lee JC, Jostins L, Shah T, Abedian S, Cheon JH, Cho J, Dayani NE, Franke L, Fuyuno Y, Hart A, Juyal RC, Juyal G, Kim WH, Morris AP, Poustchi H, Newman WG, Midha V, Orchard TR, Vahedi H, Sood A, Sung JY, Malekzadeh R, Westra HJ, Yamazaki K, Yang SK; International Multiple Sclerosis Genetics Consortium; International IBD Genetics Consortium, Barrett JC, Alizadeh BZ, Parkes M, Bk T, Daly MJ, Kubo M, Anderson CA, Weersma RK. Association analyses identify 38 susceptibility loci for inflammatory bowel disease and highlight shared genetic risk across populations. *Nat Genet* 2015; **47**: 979-986 [PMID: 26192919 DOI: 10.1038/ng.3359]
34 **Singh UP**, Singh NP, Murphy EA, Price RL, Fayad R, Nagarkatti M, Nagarkatti PS. Chemokine and cytokine levels in inflammatory bowel disease patients. *Cytokine* 2016; **77**: 44-49 [PMID: 26520877 DOI: 10.1016/j.cyto.2015.10.008]
35 **Fonseca-Camarillo G**, Furuzawa-Carballeda J, Granados J, Yamamoto-Furusho JK. Expression of interleukin (IL)-19 and IL-24 in inflammatory bowel disease patients: a cross-sectional study. *Clin Exp Immunol* 2014; **177**: 64-75 [PMID: 24527982 DOI: 10.1111/cei.12285]
36 **Schenk M**, Bouchon A, Seibold F, Mueller C. TREM-1--expressing intestinal macrophages crucially amplify chronic inflammation in experimental colitis and inflammatory bowel diseases. *J Clin Invest* 2007; **117**: 3097-3106 [PMID: 17853946 DOI: 10.1172/JCI30602]
37 **Kim TH**, Lee B, Kwon E, Choi SJ, Lee YH, Song GG, Sohn J, Ji JD. Regulation of TREM-1 expression by 1,25-dihydroxyvitamin D3 in human monocytes/macrophages. *Immunol Lett* 2013; **154**: 80-85 [PMID: 24012964 DOI: 10.1016/j.imlet.2013.08.012]
38 **Saleh M**, Elson CO. Experimental inflammatory bowel disease: insights into the host-microbiota dialog. *Immunity* 2011; **34**: 293-302 [PMID: 21435584 DOI: 10.1016/j.immuni.2011.03.008]
39 **Rai E**, Wakeland EK. Genetic predisposition to autoimmunity--what have we learned? *Semin Immunol* 2011; **23**: 67-83 [PMID: 21288738 DOI: 10.1016/j.smim.2011.01.015]
40 **Jostins L**, Ripke S, Weersma RK, Duerr RH, McGovern DP, Hui KY, Lee JC, Schumm LP, Sharma Y, Anderson CA, Essers J, Mitrovic M, Ning K, Cleynen I, Theatre E, Spain SL, Raychaudhuri S, Goyette P, Wei Z, Abraham C, Achkar JP, Ahmad T, Amininejad L, Ananthakrishnan AN, Andersen V, Andrews JM, Baidoo L, Balschun T, Bampton PA, Bitton A, Boucher G, Brand S, Büning C, Cohain A, Cichon S, D'Amato M, De Jong D, Devaney KL, Dubinsky M, Edwards C, Ellinghaus D, Ferguson LR, Franchimont D, Fransen K, Gearry R, Georges M, Gieger C, Glas J, Haritunians T, Hart A, Hawkey C, Hedl M, Hu X, Karlsen TH, Kupcinskas L, Kugathasan S, Latiano A, Laukens D, Lawrance IC, Lees CW, Louis E, Mahy G, Mansfield J, Morgan AR, Mowat C, Newman W, Palmieri O, Ponsioen CY, Potocnik U, Prescott NJ, Regueiro M, Rotter JI, Russell RK, Sanderson JD, Sans M, Satsangi J, Schreiber S, Simms LA, Sventoraityte J, Targan SR, Taylor KD, Tremelling M, Verspaget HW, De Vos M, Wijmenga C, Wilson DC, Winkelmann J, Xavier RJ, Zeissig S, Zhang B, Zhang CK, Zhao H; International IBD Genetics Consortium (IIBDGC), Silverberg MS, Annese V, Hakonarson H, Brant SR, Radford-Smith G, Mathew CG, Rioux JD, Schadt EE, Daly MJ, Franke A, Parkes M, Vermeire S, Barrett JC, Cho JH. Host-microbe interactions have shaped the genetic architecture of inflammatory bowel disease. *Nature* 2012; **491**: 119-124 [PMID: 23128233 DOI: 10.1038/nature11582]
41 **Franke A**, McGovern DP, Barrett JC, Wang K, Radford-Smith GL, Ahmad T, Lees CW, Balschun T, Lee J, Roberts R, Anderson CA, Bis JC, Bumpstead S, Ellinghaus D, Festen EM, Georges M, Green T, Haritunians T, Jostins L, Latiano A, Mathew CG, Montgomery GW, Prescott NJ, Raychaudhuri S, Rotter JI, Schumm P, Sharma Y, Simms LA, Taylor KD, Whiteman D, Wijmenga C, Baldassano RN, Barclay M, Bayless TM, Brand S, Büning C, Cohen A, Colombel JF, Cottone M, Stronati L, Denson T, De Vos M, D'Inca R, Dubinsky M, Edwards C, Florin T, Franchimont D, Gearry R, Glas J, Van Gossum A, Guthery SL, Halfvarson J, Verspaget HW, Hugot JP, Karban A, Laukens D, Lawrance I, Lemann M, Levine A, Libioulle C, Louis E, Mowat C, Newman W, Panés J, Phillips A, Proctor DD, Regueiro M, Russell R, Rutgeerts P, Sanderson J, Sans M, Seibold F, Steinhart AH, Stokkers PC, Torkvist L, Kullak-Ublick G, Wilson D, Walters T, Targan SR, Brant SR, Rioux JD, D'Amato M, Weersma RK, Kugathasan S, Griffiths AM, Mansfield JC, Vermeire S, Duerr RH, Silverberg MS, Satsangi J, Schreiber S, Cho JH, Annese V, Hakonarson H, Daly MJ, Parkes M. Genome-wide meta-analysis increases to 71 the number of confirmed Crohn's disease susceptibility loci. *Nat Genet* 2010; **42**: 1118-1125 [PMID: 21102463 DOI: 10.1038/ng.717]
42 **Khor B**, Gardet A, Xavier RJ. Genetics and pathogenesis of inflammatory bowel disease. *Nature* 2011; **474**: 307-317 [PMID: 21677747 DOI: 10.1038/nature10209]
43 **Chen ST**, Li FJ, Hsu TY, Liang SM, Yeh YC, Liao WY, Chou TY, Chen NJ, Hsiao M, Yang WB, Hsieh SL. CLEC5A is a critical receptor in innate immunity against Listeria infection. *Nat Commun* 2017; **8**: 299 [PMID: 28824166 DOI: 10.1038/s41467-017-00356-3]
44 **Park JJ**, Cheon JH, Kim BY, Kim DH, Kim ES, Kim TI, Lee KR, Kim WH. Correlation of serum-soluble triggering receptor expressed on myeloid cells-1 with clinical disease activity in inflammatory bowel disease. *Dig Dis Sci* 2009; **54**: 1525-1531 [PMID: 18975078 DOI: 10.1007/s10620-008-0514-5]
45 **Fixa B**, Komárková O, Procházková J. Serum lysozyme in inflammatory gastric and enteric diseases and in functional dyspepsia. *Scand J Gastroenterol* 1983; **18**: 349-352 [PMID: 6673061 DOI: 10.1080/00365510600898263]
46 **Cooney R**, Baker J, Brain O, Danis B, Pichulik T, Allan P, Ferguson DJ, Campbell BJ, Jewell D, Simmons A. NOD2 stimulation induces autophagy in dendritic cells influencing bacterial handling and antigen presentation. *Nat Med* 2010; **16**: 90-97 [PMID: 19966812 DOI: 10.1038/nm.2069]
47 **Travassos LH**, Carneiro LA, Ramjeet M, Hussey S, Kim YG, Magalhães JG, Yuan L, Soares F, Chea E, Le Bourhis L, Boneca IG, Allaoui A, Jones NL, Nuñez G, Girardin SE, Philpott DJ. Nod1 and Nod2 direct autophagy by recruiting ATG16L1 to the plasma membrane at the site of bacterial entry. *Nat Immunol* 2010; **11**: 55-62 [PMID: 19898471 DOI: 10.1038/ni.1823]
48 **Szklarczyk D**, Morris JH, Cook H, Kuhn M, Wyder S, Simonovic M, Santos A, Doncheva NT, Roth A, Bork P, Jensen LJ, von Mering C. The STRING database in 2017: quality-controlled protein-protein association networks, made broadly accessible. *Nucleic Acids Res* 2017; **45**: D362-D368 [PMID: 27924014 DOI: 10.1093/nar/gkw937]
49 **Platt N**, Haworth R, Darley L, Gordon S. The many roles of the class A macrophage scavenger receptor. *Int Rev Cytol* 2002; **212**:

1-40 [PMID: 11804035]
50 **Taylor PR**, Tsoni SV, Willment JA, Dennehy KM, Rosas M, Findon H, Haynes K, Steele C, Botto M, Gordon S, Brown GD. Dectin-1 is required for beta-glucan recognition and control of fungal infection. *Nat Immunol* 2007; **8**: 31-38 [PMID: 17159984 DOI: 10.1038/ni1408]
51 **Neumann K**, Castiñeiras-Vilariño M, Höckendorf U, Hannesschläger N, Lemeer S, Kupka D, Meyermann S, Lech M, Anders HJ, Kuster B, Busch DH, Gewies A, Naumann R, Groß O, Ruland J. Clec12a is an inhibitory receptor for uric acid crystals that regulates inflammation in response to cell death. *Immunity* 2014; **40**: 389-399 [PMID: 24631154 DOI: 10.1016/j.immuni.2013.12.015]
52 **Rosetti F**, Mayadas TN. The many faces of Mac-1 in autoimmune disease. *Immunol Rev* 2016; **269**: 175-193 [PMID: 26683153 DOI: 10.1111/imr.12373]

P- Reviewer: Day AS, Liu F, Macedo G **S- Editor**: Wang XJ
L- Editor: A **E- Editor**: Huang Y

World Journal of Gastroenterology

Submit a Manuscript: http://www.f6publishing.com

World J Gastroenterol 2018 March 21; 24(11): 1206-1215

DOI: 10.3748/wjg.v24.i11.1206

ISSN 1007-9327 (print) ISSN 2219-2840 (online)

ORIGINAL ARTICLE

Basic Study

Three-microRNA signature identified by bioinformatics analysis predicts prognosis of gastric cancer patients

Cheng Zhang, Chun-Dong Zhang, Ming-Hui Ma, Dong-Qiu Dai

Cheng Zhang, Chun-Dong Zhang, Ming-Hui Ma, Dong-Qiu Dai, Department of Gastroenterological Surgery, the Fourth Affiliated Hospital of China Medical University, Shenyang 110032, Liaoning Province, China

ORCID number: Cheng Zhang (0000-0001-5317-8775); Chun-Dong Zhang (0000-0002-5274-5210); Ming-Hui Ma (0000-0002-2566-0932); Dong-Qiu Dai (0000-0002-1154-3276).

Author contributions: Dai DQ designed this study; Zhang C, Zhang CD, and Ma MH conducted the data analysis; Zhang C wrote the article.

Supported by National Natural Science Foundation of China, No. 30572162; and Natural Science Foundation of Liaoning Province, No. 201602817.

Conflict-of-interest statement: The authors declare that there is no conflict of interest related to this study.

Data sharing statement: No additional data are available.

Manuscript source: Unsolicited manuscript

Correspondence to: Dong-Qiu Dai, PhD, Chief Doctor, Professor, Surgical Oncologist, Department of Gastroenterological Surgery, the Fourth Affiliated Hospital of China Medical University, 4 Chongshan Road, Shenyang 110032, Liaoning Province, China. daidq63@163.com
Telephone: +86-24-62043110
Fax: +86-24-62043110

Received: December 9, 2017
Peer-review started: December 10, 2017
First decision: December 21, 2017
Revised: December 25, 2017
Accepted: January 16, 2018
Article in press: January 16, 2018
Published online: March 21, 2018

Abstract

AIM

To identify multiple microRNAs (miRNAs) for predicting the prognosis of gastric cancer (GC) patients by bioinformatics analysis.

METHODS

The original microarray dataset GSE93415, which included 20 GC and 20 tumor adjacent normal gastric mucosal tissues, was downloaded from the Gene Expression Omnibus database and used for screening differentially expressed miRNAs (DEMs). The cut-off criteria were $P < 0.05$ and fold change > 2.0. In addition, we acquired the miRNA expression profiles and clinical information of 361 GC patients from The Cancer Genome Atlas database to assess the prognostic role of the DEMs. The target genes of miRNAs were predicted using TargetScan, miRDB, miRWalk, and DIANA, and then the common target genes were selected for functional enrichment analysis.

RESULTS

A total of 110 DEMs including 19 up-regulated and 91 down-regulated miRNAs were identified between 20 pairs of GC and tumor adjacent normal tissues, and the Kaplan-Meier survival analysis found that a three-miRNA signature (miR-145-3p, miR-125b-5p, and miR-99a-5p) had an obvious correlation with the survival of GC patients. Furthermore, univariate and multivariate Cox regression analyses indicated that the three-

miRNA signature could be a significant prognostic marker in GC patients. The common target genes of the three miRNAs are added up to 108 and used for Gene Functional Enrichment analysis. Biological Process and Molecular Function analyses showed that the target genes are involved in cell recognition, gene silencing and nucleic acid binding, transcription factor activity, and transmembrane receptor activity. Cellular Component analysis revealed that the genes are portion of nucleus, chromatin silencing complex, and TORC1/2 complex. Biological Pathway analysis indicated that the genes participate in several cancer-related pathways, such as the focal adhesion, PI3K, and mTOR signaling pathways.

CONCLUSION

This study justified that a three-miRNA signature could play a role in predicting the survival of GC patients.

Key words: Gene functional enrichment; Prognosis; Bioinformatic analysis; Differentially expressed miRNAs; Gastric cancer

Core tip: We identified 110 differentially expressed miRNAs through mining the datasets of Gene Expression Omnibus database and acquired the miRNA expression profiles and clinical information of 361 gastric cancer (GC) patients from The Cancer Genome Atlas database. Multiple miRNAs together acting as biomarkers may have a stronger reliability in survival prediction. Our study found that a novel three-miRNA signature could be used for predicting the prognosis of GC patients.

Zhang C, Zhang CD, Ma MH, Dai DQ. Three-microRNA signature identified by bioinformatics analysis predicts prognosis of gastric cancer patients. *World J Gastroenterol* 2018; 24(11): 1206-1215 Available from: URL: http://www.wjgnet.com/1007-9327/full/v24/i11/1206.htm DOI: http://dx.doi.org/10.3748/wjg.v24.i11.1206

INTRODUCTION

Gastric cancer (GC) is the fourth most common cancer in incidence and the second in mortality among all cancers worldwide[1]. In 2008, a total of 989600 individuals were newly diagnosed with GC and 738,000 deaths occurred, therefore, this disease is a serious public health issue worldwide[2]. Research studies that explore the cellular and molecular mechanisms of GC development and the validation of novel biomarkers are urgently needed to achieve early diagnosis and treatment.

MicroRNAs (miRNAs), which are endogenous small noncoding RNAs (20-22 nt), have been identified as the key regulators of genes at the post-transcriptional level[3]. Increasing studies have found that miRNAs are associated with the development and progression of GC, and can act as important biomarkers in diagnosis[4,5], therapy[6], and prognosis[7,8]. Thus, the identification of differentially expressed miRNAs (DEMs) may contribute to the early diagnosis and the prediction of survival prognosis in GC.

Several studies have found that a number of miRNAs are differentially expressed in GC and are associated with survival prognosis. However, these studies lack a large sample size or an appropriate proportion of samples. A reliable survival prediction requires large-scale samples that include detailed clinical characteristics. The Gene Expression Omnibus (GEO) database is a public functional genomics data repository that includes array- and sequence-based data and allows users to query and download experiments or curated gene expression profiles[9]. The Cancer Genome Atlas (TCGA, http://cancergenome.nih.gov) project is one of the most useful cancer genomics programs and has generated, analyzed, and made available genomic sequence, expression, methylation, and copy number variation data on over 11,000 individuals who represent over 30 different types of cancer[10]. In the present study, we identified DEMs between GC and adjacent normal tissues by analyzing the miRNA data of GSE93415 from GEO. In addition, the associations between DEMs and survival prognosis were analyzed using the expression profiles and clinical features downloaded from TCGA.

MATERIALS AND METHODS

Microarray data processing and DEMs identification

The microarray data of GSE93415 were downloaded from the GEO database (https://www.ncbi.nlm.nih.gov/geo/) and the miRNA expression data were processed with the limma package in R. Statistically significant DEMs between GC and adjacent normal samples were identified with the cut-off criterion $P < 0.05$ and fold change > 2.0.

Association analysis between DEMs and GC patients' survival

TCGA (https://cancergenome.nih.gov/) stomach adenocarcinoma and adjacent normal tissue miRNA sequencing data and clinical information were downloaded for analysis. The inclusion criteria included: (1) samples with completed data for analysis; (2) patients had not received preoperative chemoradiation; and (3) overall survival time less than 80 mo. Consequently, 361 GC samples were included in the present study. The Kaplan-Meier method and log-rank test were conducted to test the prognostic value of DEMs. When $P < 0.05$, miRNAs were considered significantly associated with

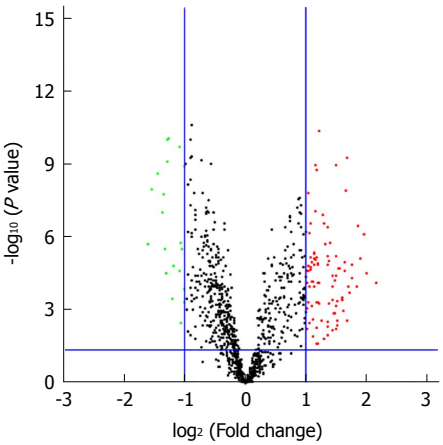

Figure 1 The volcano plot of the differentially expressed miRNAs. A total of 110 DEMs were identified between 20 pairs of GC patients and adjacent normal tissues (cut-off criteria are $P < 0.05$ and fold change > 2.0). The green and red spots represent downregulated and upregulated miRNAs, respectively. DEMs: Differentially expressed miRNAs; GC: Gastric cancer.

the prognosis of patients. Then, we ranked prognosis-related miRNAs according to the median expression level. Subsequently, we scored each GC patient in accordance with a high or low level of expression, and a risk grade was defined by the total scores. Finally, GC patients were sorted into high and low risk groups by the risk-score rank. The prognosis-related miRNA signature was used to analyze overall survival between high and low risk group patients using a Kaplan-Meier curve.

Target genes prediction of prognostic DEMs

We used four online tools to predict the potential target genes of the prognostic related DEMs, including TargetScan (http://www.targetscan.org/vert_71/), miRDB (http://www.mirdb.org/), miRWalk (http://zmf.umm.uni-heidelberg.de/apps/zmf/mirwalk2/index.html), and DIANA (http://www.microrna.gr/microT-CDS). In order to obtain the more reliable target genes, the Venn plot was performed to acquire the consensus genes of the four online tools.

Function analysis of target genes

FunRich [Functional Enrichment analysis tool (http://www.funrich.org/)] is a stand-alone software used for functional enrichment and interaction network analysis of genes and proteins[11]. Enrichment analysis was conducted on the consensus genes using the FunRich tool in the following categories: Biological Process, Cellular Component, Molecular Function, and Biological Pathways. $P < 0.05$ was considered statistically significant.

Statistical analysis

The data of miRNA expression in GC and adjacent normal samples were performed by unpaired t-test. The association between DEMs expression and clinical characteristics was analyzed by the chi-square and *t*-tests. Kaplan-Meier survival analysis and the univariate/multivariate Cox regression analysis were used to assess the expression levels of DEMs and prognostic features. All the statistical analyses were performed with IBM SPSS version 19.0 and $P < 0.05$ was considered statistically significant.

RESULTS

Identification of DEMs in GC

The microarray data of GSE93415, including 20 pairs of GC and adjacent normal tissue samples, were obtained from the NCBI-GEO database. After applying cut-off criteria of $P < 0.05$ and fold change > 2.0, a total of 110 DEMs were identified between GC and adjacent normal tissues (Table 1). The results of 19 downregulated miRNAs and 91 upregulated miRNAs are displayed in the volcano plot (Figure 1). A heat map of hierarchic cluster analysis showed that DEMs could be discriminated between GC and normal tissues (Figure 2).

Identification of DEMs related with overall survival in GC

To identify the DEMs which could be used to predict the overall survival of GC patients, we collected 361 samples from TCGA to assess the relationship between DEMs and the overall survival of GC patients. The patients' clinical characteristics including age at diagnosis, gender, race, TNM stage, and histologic grade are shown in Table 2. By using a log-rank test and Kaplan-Meier curve, we found that three DEMs (miR-145-3p, miR-125b-5p, and miR-99a-5p) were negatively associated with overall survival (Figure 3). The association analysis between the three DEMs and clinical characteristics indicated that miR-145-3p, miR-125b-5p, and miR-99a-5p were all significantly associated with histologic grade ($P < 0.05$). The detailed results are shown in Table 3.

Prognostic role of a three-DEM signature in GC patients

We ranked the three DEMs by the median of expression and then scored each GC patient in accordance with high or low-level expression. A risk grade was defined by the total scores. As a result, all the 361 GC patients were sorted into a high or low risk group. A survival analysis with the Kaplan-Meier method and log-rank test was conducted. The results indicated that the overall survival between the high risk and low risk groups was significantly different ($P = 0.045$). Interestingly, compared to patients in the high risk group, the low risk patients tended to have a better prognosis (Figure 4). Furthermore, we performed univariate and multivariate Cox regression analyses to verify the prognostic role of the three-DEM signature according to clinical features. The univariate analysis showed that pathologic stage (HR = 1.825, $P < 0.001$), T stage (HR = 1.864, $P = 0.006$), N stage (HR = 2.005, $P = 0.001$), and the three-DEM signature (HR = 1.422,

Table 1 The differentially expressed miRNAs identified between gastric cancer and adjacent normal tissues

Upregulated DEMs[1]	*P* value	Downregulated DEMs	*P* value
hsa-miR-199a-3p/hsa-miR-199b-3p	7.10E-05	hsa-miR-652-5p	0.000135
hsa-miR-125b-5p	2.99E-05	hsa-miR-1269b	1.13E-09
hsa-miR-199a-5p	7.65E-07	hsa-miR-665	2.86E-06
hsa-miR-223-3p	7.49E-06	hsa-miR-375	0.003304
hsa-miR-196a-5p	3.22E-07	hsa-miR-4501	1.64E-06
hsa-miR-27a-3p	0.000112	hsa-miR-4279	1.94E-10
hsa-miR-23b-3p	4.71E-05	hsa-miR-943	2.46E-05
hsa-miR-21-5p	1.36E-05	hsa-miR-148a-3p	1.53E-05
hsa-miR-100-5p	0.000197	hsa-miR-1275	0.000349
hsa-miR-20a-5p	0.000102	hsa-miR-4290	8.91E-11
hsa-miR-23a-3p	5.15E-10	hsa-miR-4268	9.16E-11
hsa-miR-1	0.002694	hsa-miR-891a	7.29E-10
hsa-miR-214-3p	1.23E-08	hsa-miR-4795-3p	3.07E-05
hsa-miR-10a-5p	2.33E-05	hsa-miR-1298	3.00E-06
hsa-miR-135b-5p	1.04E-05	hsa-miR-660-3p	1.75E-08
hsa-miR-99a-5p	0.001109	hsa-miR-4661-5p	9.22E-08
hsa-miR-20b-5p	0.000365	hsa-miR-4539	2.37E-09
hsa-miR-199b-5p	0.000291	hsa-let-7d-3p	1.10E-08
hsa-miR-10b-5p	1.83E-05	hsa-miR-4636	1.94E-06
hsa-miR-27b-3p	1.95E-05		
hsa-miR-126-3p	0.004079		
hsa-miR-130a-3p	0.000442		
hsa-miR-142-3p	0.002661		
hsa-miR-4291	1.12E-09		
hsa-miR-24-3p	6.14E-06		
hsa-let-7a-5p	0.0059		
hsa-miR-145-5p	0.00066		
hsa-miR-17-5p	3.84E-05		
hsa-miR-143-5p	6.07E-05		
hsa-let-7f-5p	0.001364		
hsa-miR-4328	0.001281		
hsa-miR-4324	3.91E-05		
hsa-miR-145-3p	0.000389		
hsa-miR-143-3p	0.006402		
hsa-miR-95	0.000106		

[1]Upregulated DEMs are listed according to the rank of fold changes. DEMs: Differentially expressed miRNAs.

P = 0.039) were significantly associated with the prognostic outcome of GC patients. The multivariate analysis revealed that T stage (HR = 1.623, *P* = 0.044) and the three-DEM signature (HR = 1.451, *P* = 0.032) were all independent factors in predicting the prognosis of GC patients (Table 4).

Target prediction of three DEMs and gene function analysis

The online target prediction tools TargetScan, miRDB, miRWalk, and DIANA were used to predict the targets genes of miR-145-3p, miR-125b-5p, and miR-99a-5p. We then obtained the consensus genes of each DEM from the four online predictions (Figure 5). As a result, we identified a 108 consensus target genes. Furthermore, we conducted gene enrichment analysis to identify the biological function of common target genes (Figure 6). The Biological Process analysis indicated that the genes were mostly enriched in cell recognition, regulation of nucleic acid, and gene silencing. Cellular Component analysis indicated that genes were enriched in the nucleus, RNA-induced silencing complex, chromatin silencing complex, and phosphoinositide 3-kinase complex. Molecular Function analysis showed that genes were enriched in transmembrane receptor, transcription regulator, and transcription factor activity. Biological Pathways were mainly enriched in the VEGFR, PI3K/Akt, and mTOR signaling pathways.

DISCUSSION

Due to the reduction in chronic *Helicobacter pylori* infection and improvement of sanitation, the incidence and mortality rates of GC have declined in recent years[12]. However, there are still almost 460,000 new GC cases and 350000 GC deaths each year in China[13]. The prognosis of GC patients is poor and the five-year survival rate is 5%-20% despite advances in GC therapy[14]. Thus, to improve the clinical treatment and management of GC patients, it is urgent to identify reliable prognostic biomarkers. In this study, we identified a total of 110 DEMs by analyzing the GSE93415 data and discovered that three miRNAs (miR-145-3p, miR-125b-5p, and miR-99a-5p) were

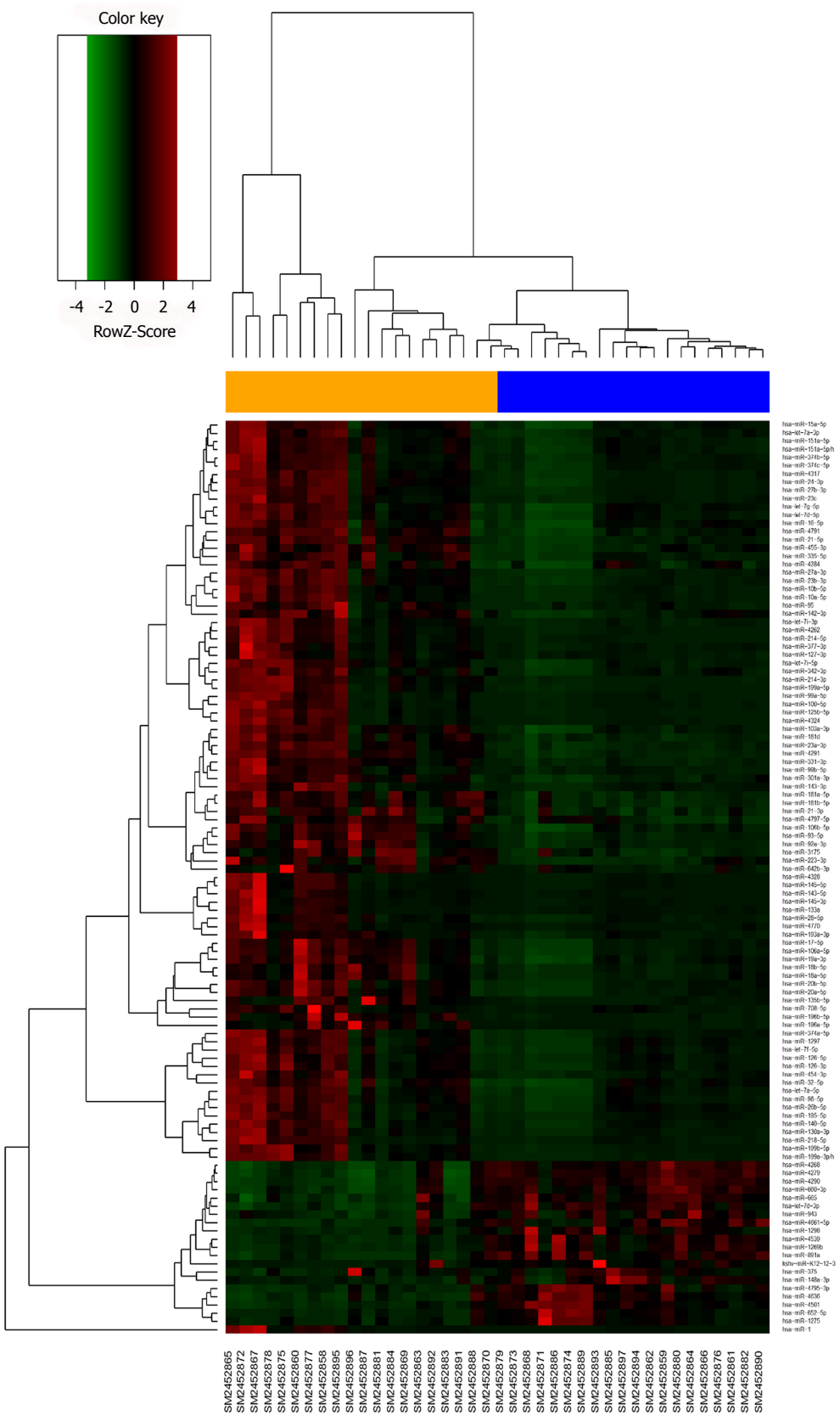

Figure 2 Hierarchical clustering analysis of the differentially expressed miRNAs between 20 pairs of gastric cancer and adjacent normal sample. Each row represents the expression of an miRNA and each column represents a sample: orange color for gastric cancer, blue for normal.

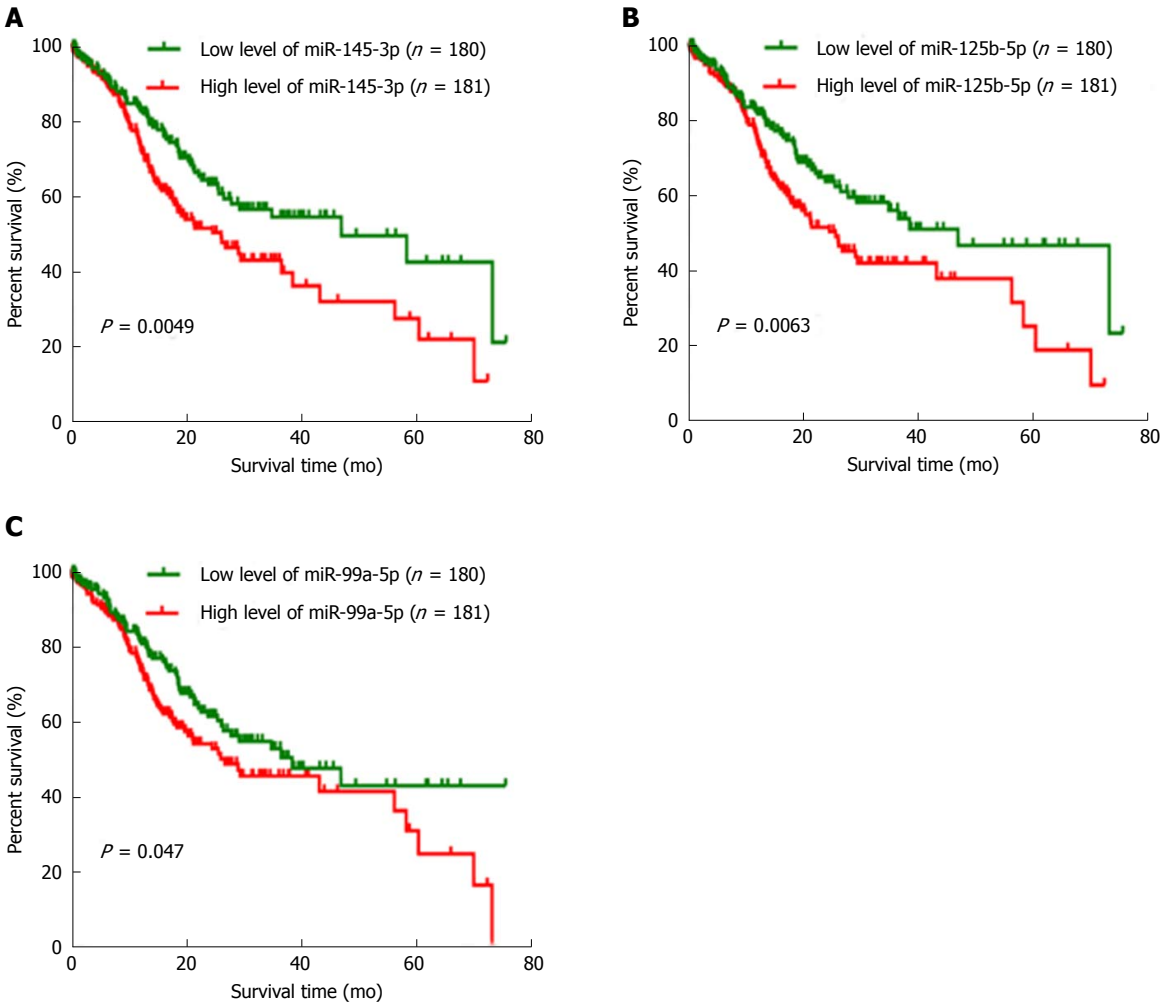

Figure 3 Three differentially expressed miRNAs are negatively associated with overall survival in gastric cancer. A: Patients with a high level of miR-145-3p (n = 180) had a poorer prognosis than those with a low level of miR-145-3p (n = 181) (P = 0.0049). B: Patients with a high level of miR-125b-5p (n = 180) had a poorer prognosis than those with a low level of miR-125b-5p (n = 181) (P = 0.0063). C: Patients with a high level of miR-99a-5p (n = 180) had a poorer prognosis than those with a low level of miR-99a-5p (n = 181) (P = 0.047).

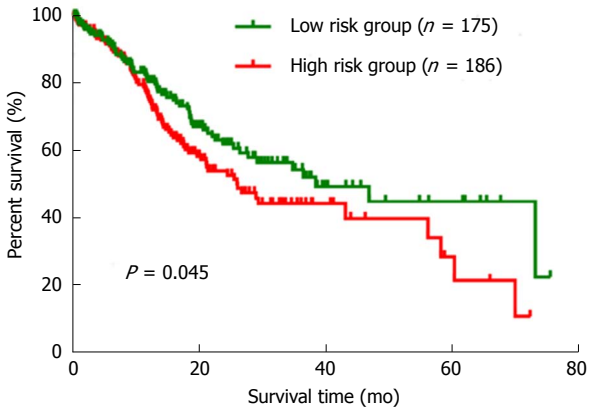

Figure 4 The Kaplan-Meier curve for the three-miRNA signature in gastric cancer. The three differentially expressed miRNAs were ranked by the median of expression and then scored for each gastric cancer patient in accordance with high or low-level expression. The low risk group (n = 175) and high risk group (n = 186) were defined by the total scores. Compared to the low risk group, patients in the high risk group had a poorer prognosis (P = 0.045).

negatively associated with overall survival. Additionally, we constructed a three-miRNA signature to predict the prognosis of GC patients.

For decades, a large number of studies have reported that miRNAs can play oncogenic or tumor-suppressing roles in regulating cell biological behavior of cells[15-18]. At present, several miRNAs are known to be useful in the early diagnosis of cancers, including miR-21[19], miR-486[20], miR-24[21], and miR-125a-5p[22]. In addition, miR-191[23], miR-1908[24], miR-200c[25], and miR-217[26] were found to be potential prognostic indictors in cancer. However, these studies only used a single indictor or a limited number of patients for survival analysis. In this study, we identified DEMs by analyzing the array data from the GEO database and found that three highly expressed miRNAs (miR-145-3p, miR-125b-5p, and miR-99a-5p) may be potential prognostic indictors in GC. Kaplan-Meier and Log-rank test survival analysis indicated that the three-miRNA

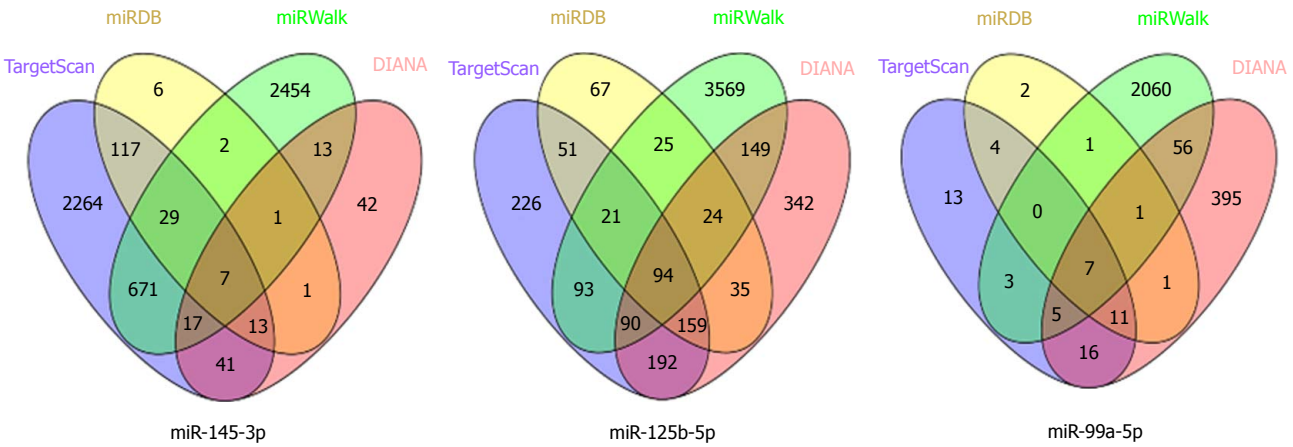

Figure 5 The consensus target genes of each differentially expressed miRNA. The target genes of the three miRNAs were predicted with four online tools (TargetScan, miRDB, miRWalk, and DIANA).

Table 2 Clinical features of gastric cancer patients

Variables	Case, *n* (%)
Age at diagnosis (yr)	
< 60	113 (31.3)
⩾ 60	248 (68.7)
Gender	
Male	241 (66.8)
Female	120 (33.2)
T stage	
T1 + T2	88 (24.4)
T3 + T4	273 (75.6)
Histologic grade	
G1 + G2	134 (37.1)
G3 + G4	227 (62.9)
Race	
White	234 (64.8)
Asian	83 (23.0)
Black or African American	12 (3.3)
NA	32 (8.9)
Pathologic stage	
Ⅰ	44 (12.2)
Ⅱ	117 (32.4)
Ⅲ	162 (44.9)
Ⅳ	30 (8.3)
NA	8 (2.2)
Node status	
N0	111 (30.7)
N1-3	249 (69.0)
NA	1 (0.3)
Metastasis	
M0	325 (90.0)
M1	22 (6.1)
Mx	14 (3.9)

NA: Not available.

signature can be used to predict the prognosis of GC patients.

We then searched present publications online to compare and test our findings. Chang *et al*[27] showed that miR-125b-5p was overexpressed in GC patients and promoted invasion and metastasis of GC by targeting *STARD13* and *NEU1*. It was also indicated that miR-125b-5p could be a potential biomarker for predicting prognoses and clinical outcomes in patients with HER2-positive GC that receive trastuzumab treatment[28]. Wu *et al*[29] found that miR-125b-5p promotes cell migration and invasion by targeting PPP1CA-Rb signal pathways and acts as an independent prognostic factor in GC. Furthermore, Zhang *et al*[30] demonstrated that miR-99a-5p might function as a novel molecule to regulate cisplatin resistance by directly targeting the calpain small subunit 1 (CAPNS1)-associated pathway in GC. Interestingly, there are no studies describing relations between miR-145-3p and GC. However, in non-small cell lung cancer, miR-145-3p was found to inhibit cancer cell migration and invasion by targeting *PDK1 via* the mTOR signaling pathway[31]. Moreover, miR-145-3p was also identified to be down-regulated in metastatic castration-resistant prostate cancer and target four molecules which can significantly predict survival in prostate cancer[32]. These results may suggest that miR-145-3p has a complicated effect in different cancers and, in future research, we will investigate the role of miR-145-3p in GC.

Dysregulated genes may participate in tumorigenesis and progression by aberrant signaling pathways. In this study, we predicted the target genes of the three miRNAs and performed gene functional enrichment analysis. The results showed that these target genes were associated with the process of gene silencing and cell recognition, as well as focal adhesion, EGFR, PI3K/Akt, and mTOR signaling pathways. Xu *et al*[33] suggested that the EGFR-Akt signaling pathway regulates drug resistance in GC patients. The PI3K/Akt pathway was demonstrated to be associated with poor prognosis, tumor progression, and resistance to systematic therapy in many cancers including GC[34,35]. In addition, the PI3K/Akt/mTOR pathway is a key signaling pathway that is reported to be involved in GC[36]. Thus, the results of our functional enrichment analysis are in accordance with present studies.

Above all, we identified a three-miRNA signature for predicting the prognosis of patients with GC and

Table 3 Association between the three differentially expressed miRNAs and clinical features

Variables	miR-145-3p expression		*P* value	miR-125b-5p expression		*P* value	miR-99a-5p expression		*P* value
	Low	High		Low	High		Low	High	
Age at diagnosis (yr)									
< 60	51	62	0.225	42	71	0.001[a]	49	64	0.096
⩾ 60	129	119		138	110		131	117	
T stage									
T1 + T2	40	48	0.342	51	37	0.081	46	42	0.603
T3 + T4	140	133		129	144		134	139	
N stage									
N0	58	53	0.567	57	54	0.731	57	54	0.731
N1-3	119	124		120	123		120	123	
M stage									
M0	163	162	0.670	165	160	0.191	164	161	0.386
M1	10	12		8	14		9	13	
Histologic grade									
G1 + G2	77	57	0.026[a]	87	47	< 0.001[a]	80	54	0.004[a]
G3 + G4	103	124		93	134		100	127	
Pathologic stage									
Ⅰ + Ⅱ	81	80	0.876	86	75	0.221	80	81	0.954
Ⅲ + Ⅳ	95	97		90	102		96	96	

[a]$P < 0.05$, statistically significant.

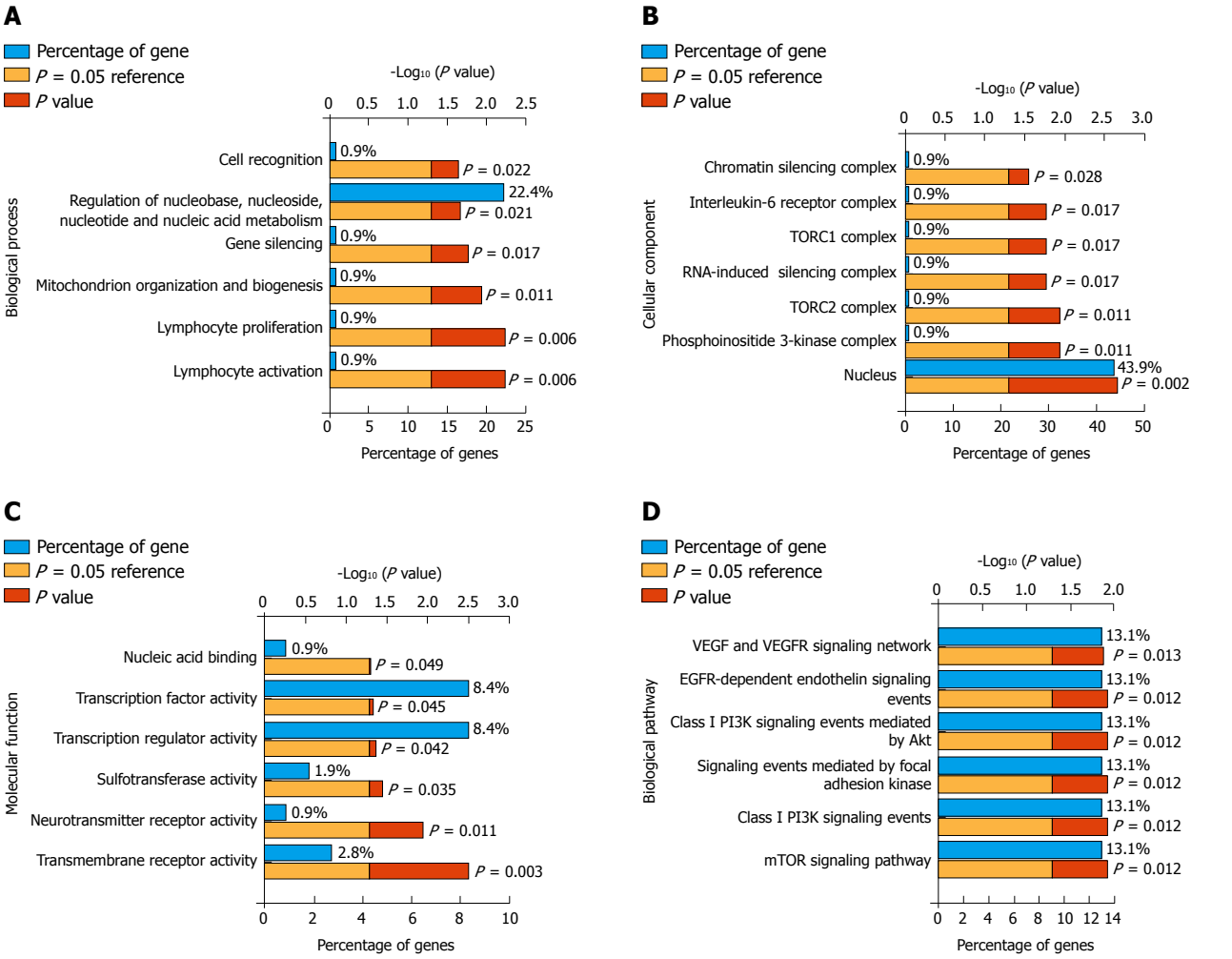

Figure 6 Genetic functional enrichment analysis. A total of 108 consensus genes were used for functional enrichment analysis with the tool of FunRich. A: Biological process analysis showed that the genes are involved in cell recognition and gene silencing; B: Cellular component analysis indicated that the genes are portion of nucleus, chromatin silencing complex, and TORC1/2 complex; C: Molecular function results showed that the genes are involved in nucleic acid binding, transcription factor activity, and transmembrane receptor activity; D: Biological pathway analysis indicated that the genes participate in focal adhesion, PI3K, and mTOR cancer-related signaling pathways. TORC1/2: Target of rapamycin 1/2; PI3K: Phosphatidylinositide 3-kinase; mTOR: Mammalian target of rapamycin.

Table 4 Univariate and multivariate Cox regression analyses of the association between the three differentially expressed miRNAs and clinical features

Variables	Univariate analysis		Multivariate analysis	
	HR (95%CI)	*P* value	HR (95%CI)	*P* value
Age at diagnosis (≥ 60 *vs* < 60)	1.373 (0.948-1.988)	0.094	1.642 (1.122-2.401)	0.011[a]
Pathologic stage (Ⅲ + Ⅳ *vs* Ⅰ + Ⅱ)	1.825 (1.332-2.499)	< 0.001[a]	1.252 (0.812-1.929)	0.309
T stage (T3 + T4 *vs* T1 + T2)	1.864 (1.197-2.902)	0.006[a]	1.623 (1.012-2.603)	0.044[a]
N stage (N1-2 *vs* N0)	2.005 (1.328-3.026)	0.001[a]	1.602 (0.935-2.744)	0.086
M stage (M1 *vs* M0)	1.368 (0.964-1.941)	0.080	1.313 (0.919-1.875)	0.134
Three-DEM signature (high *vs* low risk)	1.442 (1.018-1.988)	0.039[a]	1.451 (1.033-2.040)	0.032[a]

[a]$P < 0.05$, statistically significant. DEMs: Differentially expressed miRNAs.

analyzed potential signaling pathways in the development and progression of GC. However, to determine the genesis and development mechanism of GC, more large-scale and systematic investigations are required.

ARTICLE HIGHLIGHTS

Research background

Increasing studies have reported that microRNAs (miRNAs) play an important role in the development and progression of cancers, including gastric cancer (GC). Furthermore, miRNAs can also act as accurate biomarkers in diagnosis and prognosis prediction. In this study, we found that a three-miRNA signature could be used for predicting the prognosis of GC patients and multiple miRNAs together acting as biomarkers may have a stronger reliability in survival prediction.

Research motivation

The worldwide incidence and mortality rates of GC are fairly high. Most of GC patients have been in the advanced stage when diagnosed and endure a poor prognosis. Identifying accurate biomarkers in predicting prognosis of patients is an urgent issue to be solved, so that patients could have an individualized treatment and an improvement in prognosis.

Research objectives

We aimed to identify multiple miRNAs for predicting the prognosis of patients with gastric cancer. In the present study, we found that a three-miRNA (miR-145-3p, miR-125b-5p, and miR-99a-5p) signature could be used for predicting the prognosis of patients with gastric cancer. This objective could be applied to clinical practice and have a guidance role in improving the prognosis of patients with gastric cancer.

Research methods

We obtained the differentially expressed miRNAs by analyzing a microarray dataset from the Gene Expression Omnibus database with the limma package in R. The Kaplan-Meier method and log-rank test were used for describing the survival curve. The target genes of the three miRNAs (miR-145-3p, miR-125b-5p, and miR-99a-5p) were predicted with the online tools of TargetScan, miRDB, miRWalk, and DIANA. Venn plot was performed to obtain the common target genes from these four online tools. Enrichment analysis was conducted on the consensus genes using the FunRich tool.

Research results

In the present study, we found that a three-miRNA (miR-145-3p, miR-125b-5p, and miR-99a-5p) signature could be used for predicting the prognosis of patients with gastric cancer. Multiple miRNAs together acting as prognosis-related biomarkers may have a stronger reliability and this finding could be useful in clinical treatment according to gastric cancer patients with different prognoses. However, the role of miR-145-3p in the tumorigenesis and progression of gastric cancer remains unclear. Thus, this problem remains to be solved in our future study.

Research conclusions

Our study identified that the three miRNAs (miR-145-3p, miR-125b-5p, and miR-99a-5p) were up-regulated in gastric cancer patients by analyzing a microarray dataset. Besides, the novel three-miRNA signature could be used for predicting the prognosis of patients with gastric cancer. Multiple miRNAs together acting as prognosis-related biomarkers may have a stronger reliability, so that our finding could be useful in clinical treatment according to gastric cancer patients with different prognoses.

Research perspectives

This study provides us with a new insight that multiple miRNAs can be together used for predicting the prognosis of patients with gastric cancer. In order to further confirm the prognostic value of the three-miRNA signature, our future research may focus on exploring the relation between miR-145-3p and gastric cancer.

REFERENCES

1 **Piazuelo MB**, Correa P. Gastric cáncer: Overview. *Colomb Med* (Cali) 2013; **44**: 192-201 [PMID: 24892619]

2 **Jemal A**, Bray F, Center MM, Ferlay J, Ward E, Forman D. Global cancer statistics. *CA Cancer J Clin* 2011; **61**: 69-90 [PMID: 21296855 DOI: 10.3322/caac.20107]

3 **Filipowicz W**, Bhattacharyya SN, Sonenberg N. Mechanisms of post-transcriptional regulation by microRNAs: are the answers in sight? *Nat Rev Genet* 2008; **9**: 102-114 [PMID: 18197166 DOI: 10.1038/nrg2290]

4 **Wang D**, Fan Z, Liu F, Zuo J. Hsa-miR-21 and Hsa-miR-29 in Tissue as Potential Diagnostic and Prognostic Biomarkers for Gastric Cancer. *Cell Physiol Biochem* 2015; **37**: 1454-1462 [PMID: 26509997 DOI: 10.1159/000438514]

5 **Liu X**, Kwong A, Sihoe A, Chu KM. Plasma miR-940 may serve as a novel biomarker for gastric cancer. *Tumour Biol* 2016; **37**: 3589-3597 [PMID: 26456959 DOI: 10.1007/s13277-015-4019-5]

6 **Merhautova J**, Demlova R, Slaby O. MicroRNA-Based Therapy in Animal Models of Selected Gastrointestinal Cancers. *Front Pharmacol* 2016; **7**: 329 [PMID: 27729862 DOI: 10.3389/fphar.2016.00329]

7 **Hou CG**, Luo XY, Li G. Diagnostic and Prognostic Value of Serum MicroRNA-206 in Patients with Gastric Cancer. *Cell Physiol Biochem* 2016; **39**: 1512-1520 [PMID: 27614739 DOI: 10.1159/000447854]

8 **Zhang L**, Huang Z, Zhang H, Zhu M, Zhu W, Zhou X, Liu P. Prognostic value of candidate microRNAs in gastric cancer: A validation study. *Cancer Biomark* 2017; **18**: 221-230 [PMID: 27983528 DOI: 10.3233/CBM-160091]

9 **Barrett T**, Wilhite SE, Ledoux P, Evangelista C, Kim IF, Tomashevsky M, Marshall KA, Phillippy KH, Sherman PM, Holko M, Yefanov A, Lee H, Zhang N, Robertson CL, Serova N, Davis

S, Soboleva A. NCBI GEO: archive for functional genomics data sets--update. *Nucleic Acids Res* 2013; **41**: D991-D995 [PMID: 23193258 DOI: 10.1093/nar/gks1193]

10 **Wang Z**, Jensen MA, Zenklusen JC. A Practical Guide to The Cancer Genome Atlas (TCGA). *Methods Mol Biol* 2016; **1418**: 111-141 [PMID: 27008012 DOI: 10.1007/978-1-4939-3578-9_6]

11 **Pathan M**, Keerthikumar S, Ang CS, Gangoda L, Quek CY, Williamson NA, Mouradov D, Sieber OM, Simpson RJ, Salim A, Bacic A, Hill AF, Stroud DA, Ryan MT, Agbinya JI, Mariadason JM, Burgess AW, Mathivanan S. FunRich: An open access standalone functional enrichment and interaction network analysis tool. *Proteomics* 2015; **15**: 2597-2601 [PMID: 25921073 DOI: 10.1002/pmic.201400515]

12 **Parkin DM**. The global health burden of infection-associated cancers in the year 2002. *Int J Cancer* 2006; **118**: 3030-3044 [PMID: 16404738 DOI: 10.1002/ijc.21731]

13 **Chen W**, Zheng R, Zhang S, Zhao P, Li G, Wu L, He J. Report of incidence and mortality in China cancer registries, 2009. *Chin J Cancer Res* 2013; **25**: 10-21 [PMID: 23372337 DOI: 10.3978/j.issn.1000-9604.2012.12.04]

14 **Wang Z**, Cai Q, Jiang Z, Liu B, Zhu Z, Li C. Prognostic role of microRNA-21 in gastric cancer: a meta-analysis. *Med Sci Monit* 2014; **20**: 1668-1674 [PMID: 25230738 DOI: 10.12659/MSM.892096]

15 **Zhang B**, Pan X, Cobb GP, Anderson TA. microRNAs as oncogenes and tumor suppressors. *Dev Biol* 2007; **302**: 1-12 [PMID: 16989803 DOI: 10.1016/j.ydbio.2006.08.028]

16 **Nohata N**, Hanazawa T, Kinoshita T, Okamoto Y, Seki N. MicroRNAs function as tumor suppressors or oncogenes: aberrant expression of microRNAs in head and neck squamous cell carcinoma. *Auris Nasus Larynx* 2013; **40**: 143-149 [PMID: 22831895 DOI: 10.1016/j.anl.2012.07.001]

17 **Chen Y**, Fu LL, Wen X, Liu B, Huang J, Wang JH, Wei YQ. Oncogenic and tumor suppressive roles of microRNAs in apoptosis and autophagy. *Apoptosis* 2014; **19**: 1177-1189 [PMID: 24850099 DOI: 10.1007/s10495-014-0999-7]

18 **Babashah S**, Soleimani M. The oncogenic and tumour suppressive roles of microRNAs in cancer and apoptosis. *Eur J Cancer* 2011; **47**: 1127-1137 [PMID: 21402473 DOI: 10.1016/j.ejca.2011.02.008]

19 **Zeng Z**, Wang J, Zhao L, Hu P, Zhang H, Tang X, He D, Tang S, Zeng Z. Potential role of microRNA-21 in the diagnosis of gastric cancer: a meta-analysis. *PLoS One* 2013; **8**: e73278 [PMID: 24023850 DOI: 10.1371/journal.pone.0073278]

20 **Li W**, Wang Y, Zhang Q, Tang L, Liu X, Dai Y, Xiao L, Huang S, Chen L, Guo Z, Lu J, Yuan K. MicroRNA-486 as a Biomarker for Early Diagnosis and Recurrence of Non-Small Cell Lung Cancer. *PLoS One* 2015; **10**: e0134220 [PMID: 26237047 DOI: 10.1371/journal.pone.0134220]

21 **Fang Z**, Tang J, Bai Y, Lin H, You H, Jin H, Lin L, You P, Li J, Dai Z, Liang X, Su Y, Hu Q, Wang F, Zhang ZY. Plasma levels of microRNA-24, microRNA-320a, and microRNA-423-5p are potential biomarkers for colorectal carcinoma. *J Exp Clin Cancer Res* 2015; **34**: 86 [PMID: 26297223 DOI: 10.1186/s13046-015-0198-6]

22 **Wang P**, Yang D, Zhang H, Wei X, Ma T, Cheng Z, Hong Q, Hu J, Zhuo H, Song Y, Jia C, Jing F, Jin Q, Bai C, Mao H, Zhao J. Early Detection of Lung Cancer in Serum by a Panel of MicroRNA Biomarkers. *Clin Lung Cancer* 2015; **16**: 313-319.e1 [PMID: 25639977 DOI: 10.1016/j.cllc.2014.12.006]

23 **Gao X**, Xie Z, Wang Z, Cheng K, Liang K, Song Z. Overexpression of miR-191 Predicts Poor Prognosis and Promotes Proliferation and Invasion in Esophageal Squamous Cell Carcinoma. *Yonsei Med J* 2017; **58**: 1101-1110 [PMID: 29047233 DOI: 10.3349/ymj.2017.58.6.1101]

24 **Teng C**, Zheng H. Low expression of microRNA-1908 predicts a poor prognosis for patients with ovarian cancer. *Oncol Lett* 2017; **14**: 4277-4281 [PMID: 28943939 DOI: 10.3892/ol.2017.6714]

25 **Si L**, Tian H, Yue W, Li L, Li S, Gao C, Qi L. Potential use of microRNA-200c as a prognostic marker in non-small cell lung cancer. *Oncol Lett* 2017; **14**: 4325-4330 [PMID: 28943946 DOI: 10.3892/ol.2017.6667]

26 **Yang J**, Zhang HF, Qin CF. MicroRNA-217 functions as a prognosis predictor and inhibits pancreatic cancer cell proliferation and invasion via targeting E2F3. *Eur Rev Med Pharmacol Sci* 2017; **21**: 4050-4057 [PMID: 29028097]

27 **Chang S**, He S, Qiu G, Lu J, Wang J, Liu J, Fan L, Zhao W, Che X. MicroRNA-125b promotes invasion and metastasis of gastric cancer by targeting STARD13 and NEU1. *Tumour Biol* 2016; **37**: 12141-12151 [PMID: 27220320 DOI: 10.1007/s13277-016-5094-y]

28 **Sui M**, Jiao A, Zhai H, Wang Y, Wang Y, Sun D, Li P. Upregulation of miR-125b is associated with poor prognosis and trastuzumab resistance in HER2-positive gastric cancer. *Exp Ther Med* 2017; **14**: 657-663 [PMID: 28672982 DOI: 10.3892/etm.2017.4548]

29 **Wu JG**, Wang JJ, Jiang X, Lan JP, He XJ, Wang HJ, Ma YY, Xia YJ, Ru GQ, Ma J, Zhao ZS, Zhou R. MiR-125b promotes cell migration and invasion by targeting PPP1CA-Rb signal pathways in gastric cancer, resulting in a poor prognosis. *Gastric Cancer* 2015; **18**: 729-739 [PMID: 25240408 DOI: 10.1007/s10120-014-0421-8]

30 **Zhang Y**, Xu W, Ni P, Li A, Zhou J, Xu S. MiR-99a and MiR-491 Regulate Cisplatin Resistance in Human Gastric Cancer Cells by Targeting CAPNS1. *Int J Biol Sci* 2016; **12**: 1437-1447 [PMID: 27994509 DOI: 10.7150/ijbs.16529]

31 **Chen GM**, Zheng AJ, Cai J, Han P, Ji HB, Wang LL. microRNA-145-3p inhibits non-small cell lung cancer cell migration and invasion by targeting PDK1 via the mTOR signaling pathway. *J Cell Biochem* 2018; **119**: 885-895 [PMID: 28661070 DOI: 10.1002/jcb.26252]

32 **Goto Y**, Kurozumi A, Arai T, Nohata N, Kojima S, Okato A, Kato M, Yamazaki K, Ishida Y, Naya Y, Ichikawa T, Seki N. Impact of novel miR-145-3p regulatory networks on survival in patients with castration-resistant prostate cancer. *Br J Cancer* 2017; **117**: 409-420 [PMID: 28641312 DOI: 10.1038/bjc.2017.191]

33 **Xu H**, Miao ZF, Wang ZN, Zhao TT, Xu YY, Song YX, Huang JY, Zhang JY, Liu XY, Wu JH, Xu HM. HCRP1 downregulation confers poor prognosis and induces chemoresistance through regulation of EGFR-AKT pathway in human gastric cancer. *Virchows Arch* 2017; **471**: 743-751 [PMID: 28963677 DOI: 10.1007/s00428-017-2237-5]

34 **Lin HL**, Yang MH, Wu CW, Chen PM, Yang YP, Chu YR, Kao CL, Ku HH, Lo JF, Liou JP, Chi CW, Chiou SH. 2-Methoxyestradiol attenuates phosphatidylinositol 3-kinase/Akt pathway-mediated metastasis of gastric cancer. *Int J Cancer* 2007; **121**: 2547-2555 [PMID: 17680560 DOI: 10.1002/ijc.22963]

35 **Altomare DA**, Testa JR. Perturbations of the AKT signaling pathway in human cancer. *Oncogene* 2005; **24**: 7455-7464 [PMID: 16288292 DOI: 10.1038/sj.onc.1209085]

36 **Liu M**, Li CM, Chen ZF, Ji R, Guo QH, Li Q, Zhang HL, Zhou YN. Celecoxib regulates apoptosis and autophagy via the PI3K/Akt signaling pathway in SGC-7901 gastric cancer cells. *Int J Mol Med* 2014; **33**: 1451-1458 [PMID: 24676394 DOI: 10.3892/ijmm.2014.1713]

P- Reviewer: Kimura A, Matowicka-Karna J **S- Editor**: Gong ZM
L- Editor: Wang TQ **E- Editor**: Huang Y

World Journal of Gastroenterology

Submit a Manuscript: http://www.f6publishing.com

World J Gastroenterol 2018 March 21; 24(11): 1216-1227

DOI: 10.3748/wjg.v24.i11.1216

ISSN 1007-9327 (print) ISSN 2219-2840 (online)

ORIGINAL ARTICLE

Retrospective Cohort Study

Differing profiles of people diagnosed with acute and chronic hepatitis B virus infection in British Columbia, Canada

Mawuena Binka, Zahid A Butt, Stanley Wong, Mei Chong, Jane A Buxton, Nuria Chapinal, Amanda Yu, Maria Alvarez, Maryam Darvishian, Jason Wong, Gina McGowan, Mikhail Torban, Mark Gilbert, Mark Tyndall, Mel Krajden, Naveed Z Janjua

Mawuena Binka, Zahid A Butt, Stanley Wong, Mei Chong, Jane A Buxton, Nuria Chapinal, Amanda Yu, Maria Alvarez, Maryam Darvishian, Jason Wong, Mark Gilbert, Mark Tyndall, Mel Krajden, Naveed Z Janjua, British Columbia Centre for Disease Control, Vancouver BC V5Z4R4, Canada

Mawuena Binka, Zahid A Butt, Stanley Wong, Jane A Buxton, Maryam Darvishian, Jason Wong, Mark Gilbert, Mark Tyndall, Naveed Z Janjua, School of Population and Public Health, University of British Columbia, Vancouver BC V6T1Z3, Canada

Gina McGowan, Mikhail Torban, Division of Population and Public Health, Ministry of Health, Victoria BC V8W9P1, Canada

Mel Krajden, Department of Pathology and Laboratory Medicine, University of British Columbia, Vancouver BC V6T1Z2, Canada

ORCID number: Mawuena Binka (0000-0002-9370-1708); Zahid A Butt (0000-0002-2486-4781); Stanley Wong (0000-0003-0886-9889); Mei Chong (0000-0002-6397-4385); Jane A Buxton (0000-0003-2295-393X); Nuria Chapinal (0000-0001-7489-6389); Amanda Yu (0000-0002-7871-8122); Maria Alvarez (0000-0002-1248-2559); Maryam Darvishian (0000-0002-2238-0564); Jason Wong (0000-0002-7681-7573); Gina McGowan (0000-0003-2144-4156); Mikhail Torban (0000-0002-5377-8428); Mark Gilbert (0000-0001-5978-6843); Mark Tyndall (0000-0003-4450-5679); Mel Krajden (0000-0002-3477-8748); Naveed Z Janjua (0000-0001-5681-719X).

Author contributions: Janjua NZ conceptualized the study; Janjua NZ, Chong M and Wong S contributed to study design; Binka M and Janjua NZ contributed to data analysis and interpretation, and writing of article; Butt ZA, Wong S, Chong M, Chapinal N, Yu A, Alvarez M, McGowan G, Torban M, Darvishian M and Janjua NZ contributed to data acquisition; Butt ZA, Buxton JA, Wong J, McGowan G, Torban M, Gilbert M, Tyndall M, Krajden M and Janjua NZ contributed to editing, reviewing and final approval of article.

Supported by the BC Centre for Disease Control and the Canadian Institutes of Health Research, No. NHC–142832 and No. PHE-141773.

Institutional review board statement: The Behavioral Research Ethics Board of the University of British Columbia approved this study (H14-01649).

Conflict-of-interest statement: Mel Krajden reports receiving grant funding via his institution from Roche Molecular Systems, Boehringer Ingelheim, Merck, Siemens Healthcare Diagnostics and Hologic Inc. No other authors have conflicts of interest to declare.

Data sharing statement: Data are available from the BC Centre for Disease Control Institutional Data Access for researchers who meet the criteria for access to confidential data.

STROBE statement: The manuscript was prepared according to the STROBE Statement.

Manuscript source: Invited manuscript

Correspondence to: Naveed Z Janjua, MBBS, MSc, DrPH, BC Centre for Disease Control, 655 West 12th Avenue, Vancouver BCV5ZR4, Canada. naveed.janjua@bccdc.ca
Telephone: +1-604-7072514
Fax: +1-604-7072401

Received: January 13, 2018
Peer-review started: January 13, 2018
First decision: February 5, 2018
Revised: February 21, 2018
Accepted: March 3, 2018
Article in press: March 3, 2018
Published online: March 21, 2018

Abstract

AIM

To describe the characteristics of people diagnosed with acute and chronic hepatitis B virus (HBV) infection in British Columbia (BC).

METHODS

We used data from the BC Hepatitis Testers Cohort (BC-HTC), which includes all individuals tested for hepatitis C virus (HCV) or human immunodeficiency virus (HIV) or those diagnosed with HBV or active tuberculosis in BC since 1990. These data were integrated with prescription drug, medical visit, hospitalization and mortality data. HBV cases were classified as acute or chronic according to provincial guidelines. We compared characteristics of individuals by HBV infection group (acute, chronic and negative). Factors associated with acute or chronic HBV infection were assessed with multinomial logistic regression models in comparison to the HBV negative group.

RESULTS

46498 of the 1058056 eligible BC-HTC participants were diagnosed with HBV infection. 4.3% of HBV positive individuals were diagnosed with acute HBV infections while 95.7% had chronic infections. Problematic alcohol use, injection drug use, and HIV or HCV co-infection were more common among individuals diagnosed with acute HBV compared to those with chronic infections and HBV negative individuals. In multivariable multinomial logistic regression models, we observed significant associations between acute or chronic HBV diagnosis and being male, age at HBV diagnosis or birth cohort, South and East Asian ethnicity, HCV or HIV infection, and injection drug use. The odds of acute HBV decreased with increasing age among people who inject drugs, while the opposite was true for chronic HBV. Persons with acute HBV were predominantly White (78%) while those with chronic HBV were mostly East Asian (60%). Relative to Whites, East Asians had 12 times greater odds of being diagnosed with chronic HBV infection. These odds increased with increasing socioeconomic deprivation.

CONCLUSION

Differences in the profiles of people diagnosed with acute and chronic HBV infection necessitate differentiated screening, prevention, care and treatment programs.

Key words: Hepatitis B virus; Ethnicity; Drug use; Acute hepatitis B; BC Hepatitis Testers Cohort; North America

Core tip: Substance use, major mental illness and hepatitis C virus or human immunodeficiency virus co-infection were more common among individuals with acute HBV compared with those diagnosed with chronic hepatitis B virus (HBV). Acute HBV was mainly diagnosed in the White population, while chronic HBV was mostly diagnosed among people with East Asian ethnicity. The risk of acute HBV was highest among the younger population who injected drugs, while the risk of chronic HBV infection was highest among East Asian people with lower socioeconomic status. Differences in the profiles of people diagnosed with acute and chronic HBV suggest the need for different interventions for both population groups.

Binka M, Butt ZA, Wong S, Chong M, Buxton JA, Chapinal N, Yu A, Alvarez M, Darvishian M, Wong J, McGowan G, Torban M, Gilbert M, Tyndall M, Krajden M, Janjua NZ. Differing profiles of people diagnosed with acute and chronic hepatitis B virus infection in British Columbia, Canada. *World J Gastroenterol* 2018; 24(11): 1216-1227 Available from: URL: http://www.wjgnet.com/1007-9327/full/v24/i11/1216.htm DOI: http://dx.doi.org/10.3748/wjg.v24.i11.1216

INTRODUCTION

Hepatitis B virus (HBV) affects 257 million people worldwide, including approximately 200000 Canadians[1-4]. Chronic HBV infection is associated with 66% of the 1.34 million viral hepatitis-related deaths reported worldwide and is responsible for a substantial disease burden from liver cancer and end-stage liver disease[2].

HBV vaccination is highly effective in preventing infection[1,3,5]. Mother to child transmission during childbirth is the most common mode of infection in HBV-endemic countries, while infection typically occurs through sexual transmission and injection drug use in Canada and other developed countries[1,3,5]. Over 90% of children and 50% of adults display no symptoms with acute infection[1,3,5]. The asymptomatic nature of this disease makes diagnosis difficult, leading to chronic illness in 5% of infected adults, 30% to 50% of children, and 90% of infected neonates[1,3,5]. Childhood vaccination programs have led to a dramatic reduction in the occurrence of acute infections in developed countries, including Canada and the United States[1,3,6]. The record low number of reported acute HBV infections in British Columbia (BC) in 2015 have been attributed to successful vaccination programs[7]. However, certain high risk groups, including men who have sex with men (MSM) and people who inject drugs (PWID),

continue to acquire and transmit HBV infection[8,9]. As HBV infection is mostly asymptomatic, identifying the factors associated with acute and chronic infection could determine avenues for closing gaps in screening, vaccination and other prevention programs.

In many developed countries, a relatively larger number of people are diagnosed with chronic HBV, compared with acute HBV, each year[5,10-13]. Data from Canada, the United States and other developed countries indicate that most chronic HBV infections are diagnosed among immigrants from HBV-endemic Asia-Pacific countries[10,12-14]. Our previous work suggests that 49% of persons with chronic HBV and decompensated cirrhosis and 46% of those with HCC in BC were diagnosed late in the course of their infections[15]. The rate of late diagnosis has declined but is still substantially higher for HBV compared to hepatitis C virus (HCV)[15]. Therefore, establishing the characteristics of individuals who are more likely to be infected with HBV could enhance the planning of screening programs to further reduce late diagnoses within the province.

Individuals diagnosed with acute and chronic HBV infections may differ with regards to demographics and risk behavior[1,5]. These distinctions may have implications for interventions targeted at either population. Analyses based on these differences could also identify areas for the optimal integration of such HBV programs with currently available health services. We are unaware of any study comparing large population level data for both acute and chronic HBV. Previous studies have mainly focused on chronic HBV epidemiology, with limited data on acute HBV, or acute HBV only[10,11,16-18]. In this study, we describe the characteristics of individuals with acute and chronic HBV infections and identify the factors associated with HBV infection within the BC Hepatitis Testers Cohort (BC-HTC).

MATERIALS AND METHODS

The cohort

The BC-HTC includes over 1.7 million individuals tested for hepatitis C virus (HCV) or human immunodeficiency virus (HIV) at the BC Centre for Disease Control Public Health Laboratory, or reported to BC public health as a confirmed case of HCV, HBV, HIV/AIDS or active tuberculosis (TB) since 1990[19]. Cohort data are integrated with data on medical visits, hospitalizations, prescription drugs, cancers and deaths[19]. Details of cohort creation and epidemiological characteristics have been reported previously and are summarized in Supplementary Table 1[19]. This analysis is based on data collected between April 1, 1990 and December 31, 2015.

Study population

BC-HTC participants who were included in the provincial registry of reported HBV cases, those who tested positive for HBV DNA or HBeAg, and those who were recorded as having received treatment for HBV were considered as cases of HBV. HBV cases recorded in the BC provincial registry with an acute diagnosis were classified as acute HBV infections, while the remainder were designated as having chronic HBV (Supplementary Table 2). Individuals who were not diagnosed with HBV but were tested for HBsAg or anti HBV core total were denoted as being HBV negative.

Definitions and covariates

We assessed potential risk factors at HBV diagnosis or at the last negative test, including age, birth cohort, sex, infection with HIV, HCV or TB, problematic alcohol use, illicit drug use, major mental illness, and material and social deprivation. HIV, HCV or TB diagnoses were based on laboratory confirmation or being reported as a confirmed case in the public health reportable disease database. Assessment of problematic alcohol and illicit drug use, and major mental illness was based on associated diagnostic codes in administrative health datasets evaluated across the entire dataset prior to the first positive or the last negative test (Supplementary Table 2).

Ethnicity classification was based on the validated name recognition software Onomap[20,21]. Onomap sensitivity and specificity relative to self-identified ethnicity, determined on a subset of the BC-HTC (n = 5962), was 93% and 98.6% for South Asians, and 67% and 99.5% for East Asians. Race/ethnicity was grouped as White, South Asian (Pakistani, Indians, Bangladeshis, Nepalese and Sri Lankans), East Asian (Chinese, Filipinos, Japanese, Korean and South-East Asians), and Others (Black, Central Asian, Latin American, Pacific Islander and West Asian individuals). Socioeconomic status was assessed using the Quebec Material and Social deprivation Index[22].

Statistical analysis

We compared characteristics of individuals by HBV infection group (acute, chronic and negative) with Pearson's chi-square tests for categorical variables and Kruskal Wallis tests for median age. Factors associated with acute or chronic HBV infection were assessed with multivariable multinomial logistic regression models in comparison with the HBV negative group.

RESULTS

1058056 individuals were eligible for inclusion in this analysis. Of these, 46498 individuals were diagnosed with HBV infection while 1011558 were HBV negative. 4.3% of HBV positive individuals were diagnosed with acute HBV infections while 95.7% had chronic infections (Table 1).

Characteristics of acute, chronic and hepatitis B negative individuals

About two-thirds of acute infections (70.7%) and half

Table 1 Characteristics of hepatitis B testers in the British Columbia Hepatitis Testers Cohort by hepatitis B diagnosis, 1990-2015 *n* (%)

	HBV positive			HBV negative	
	Acute	Chronic	All positive		*P* value
	n = 2015	*n* = 44483	*n* = 46498	*n* = 1011558	
Sex					
Female	590 (29.3)	20094 (45.2)	20684 (44.5)	563440 (55.7)	0.000
Male	1425 (70.7)	24387 (54.8)	25812 (55.5)	448072 (44.3)	
Unknown	0 (0.0)	2 (0.0)	2 (0.0)	44 (0.0)	
Birth Cohort					
< 1945	204 (10.1)	5385 (12.1)	5589 (12.0)	103498 (10.2)	0.000
1945-1964	1001 (49.7)	20316 (45.7)	21317 (45.8)	297768 (29.4)	
1965-1974	577 (28.6)	9852 (22.1)	10429 (22.4)	199121 (19.7)	
> 1974	233 (11.6)	8930 (20.1)	9163 (19.7)	411171 (40.6)	
Age group at HBV diagnosis (yr)					
< 25	306 (15.2)	5163 (11.6)	5469 (11.8)	137379 (13.6)	0.000
25-34	653 (32.4)	9963 (22.4)	10616 (22.8)	264809 (26.2)	
35-44	552 (27.4)	11835 (26.6)	12387 (26.6)	220745 (21.8)	
45-54	317 (15.7)	9202 (20.7)	9519 (20.5)	165884 (16.4)	
55-64	115 (5.7)	4954 (11.1)	5069 (10.9)	117550 (11.6)	
> 64	72 (3.6)	3366 (7.6)	3438 (7.4)	105191 (10.4)	
Median [IQR]	35 [28-45]	41 [31-51]	40 [31-50]	39 [29-53]	0.000
Year of HBV diagnosis					
1990-1999	1388 (68.9)	14068 (31.6)	15456 (33.2)	47343 (4.7)	0.000
2000-2004	362 (18.0)	11246 (25.3)	11608 (25.0)	126715 (12.5)	
2005-2009	196 (9.7)	8968 (20.2)	9164 (19.7)	219195 (21.7)	
2010-2015	69 (3.4)	10201 (22.9)	10270 (22.1)	618305 (61.1)	
Ethnicity					
East Asian	278 (13.8)	26578 (59.7)	26856 (57.8)	139306 (13.8)	0.000
Other	35 (1.7)	1651 (3.7)	1686 (3.6)	41452 (4.1)	
South Asian	125 (6.2)	1420 (3.2)	1545 (3.3)	83200 (8.2)	
White	1577 (78.3)	14834 (33.3)	16411 (35.3)	747600 (73.9)	
HCV					
Negative	1296 (64.3)	39575 (89.0)	40871 (87.9)	964780 (95.4)	0.000
Positive	719 (35.7)	4908 (11.0)	5627 (12.1)	46778 (4.6)	
HIV					
Negative	1888 (93.7)	43370 (97.5)	45258 (97.3)	1006511 (99.5)	0.000
Positive	127 (6.3)	1113 (2.5)	1240 (2.7)	5047 (0.5)	
HCV and HIV					
Positive	82 (4.1)	712 (1.6)	794 (1.7)	1768 (0.2)	0.000
Active tuberculosis					
Negative	2004 (99.5)	44101 (99.1)	46105 (99.2)	1008555 (99.7)	0.000
Positive	11 (0.5)	382 (0.9)	393 (0.8)	3003 (0.3)	
Problematic alcohol use					
No	1807 (89.7)	42544 (95.6)	44531 (95.8)	959326 (94.8)	0.000
Yes	208 (10.3)	1939 (4.4)	2147 (4.6)	52232 (5.2)	
Illicit drug use					
No	1617 (80.2)	41558 (93.4)	43175 (92.9)	944910 (93.4)	0.000
Yes	398 (19.8)	2925 (6.6)	3323 (7.1)	66648 (6.6)	
Injection drug use					
No	1718 (85.3)	42040 (94.5)	43758 (94.1)	960849 (95.0)	0.000
Yes	297 (14.7)	2443 (5.5)	2740 (5.9)	50709 (5.0)	
Major mental illness					
No	1788 (88.7)	41410 (93.1)	43198 (92.9)	874387 (86.4)	0.000
Yes	227 (11.3)	3073 (6.9)	3300 (7.1)	137171 (13.6)	
Material deprivation quintile					
Q1 (most privileged)	320 (15.9)	7076 (15.9)	7396 (15.9)	228694 (22.6)	0.000
Q2	303 (15.0)	6753 (15.2)	7056 (15.2)	189225 (18.7)	
Q3	320 (15.9)	7797 (17.5)	8117 (17.5)	189823 (18.8)	
Q4	425 (21.1)	9564 (21.5)	9989 (21.5)	198263 (19.6)	
Q5 (most deprived)	585 (29.0)	12226 (27.5)	12811 (27.6)	185193 (18.3)	
Unknown	62 (3.1)	1067 (2.4)	1129 (2.4)	20360 (2.0)	
Social deprivation quintile					
Q1 (most privileged)	247 (12.3)	9952 (22.4)	10199 (21.9)	184233 (18.2)	0.000
Q2	267 (13.3)	9032 (20.3)	9299 (20.0)	180059 (17.8)	
Q3	314 (15.6)	7574 (17.0)	7888 (17.0)	173461 (17.1)	
Q4	383 (19.0)	7336 (16.5)	7719 (16.6)	199229 (19.7)	
Q5 (most deprived)	742 (36.8)	9522 (21.4)	10264 (22.1)	254216 (25.1)	
Unknown	62 (3.1)	1067 (2.4)	1129 (2.4)	20360 (2.0)	

Data collected at baseline (date of diagnosis for HBV positive or last negative test for HBV negative) unless otherwise indicated. HIV: Human immunodeficiency virus; HCV: Hepatitis C virus; HBV: Hepatitis B virus; IDU: Injection drug use; OST: Opioid substitution therapy; Q: Quintile.

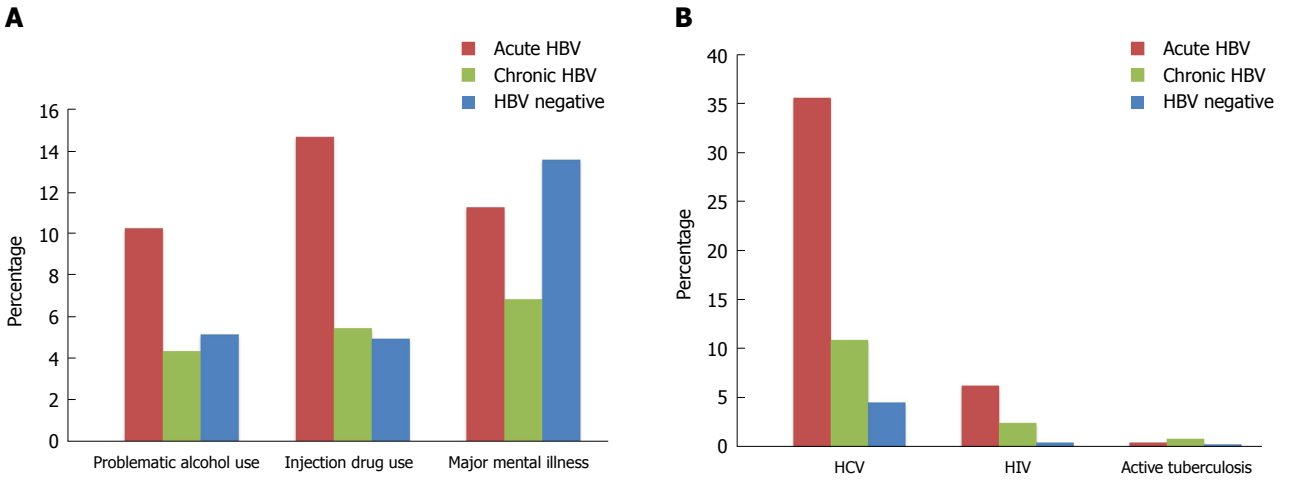

Figure 1 Comorbidities and co-infections in the British Columbia Hepatitis Testers Cohort, 1990-2015. A: Distribution of problematic alcohol use, injection drug use, and major mental illness by hepatitis B diagnosis; B: Distribution of co-infections by HBV diagnosis. HBV: Hepatitis B virus; HCV: Hepatitis C virus; HIV: Human immunodeficiency virus.

of chronic HBV infections (54.8%) were diagnosed among males. In contrast, HBV negative individuals were predominantly female (55.7%). The 1945-1964 birth cohort formed the majority of persons with either acute or chronic HBV infections (acute: 49.7%; chronic: 45.7%) but represented a smaller proportion of the HBV negative group (29.4%). Age at HBV testing or diagnosis was significantly lower among persons with acute HBV compared to those with chronic infections and HBV negative individuals (median age: 35 *vs* 41 and 39 years; $P < 0.001$). Additionally, females were more likely to be tested or diagnosed at a younger age compared to males (median age: 37 *vs* 41 years, $P < 0.001$).

The majority of HBV negative individuals (73.9%) and those with acute HBV (78.3%) were White. Chronic HBV infections, however, were more frequently diagnosed among East Asians (59.7%). Material deprivation was more common among HBV positive individuals than among HBV negative persons [Q5 (most deprived): acute HBV: 29.0%; chronic HBV: 27.5%; HBV negative: 18.3%]. In contrast, social deprivation was predominant within each HBV group, though highest among individuals with acute HBV [Q5 (most deprived): acute HBV: 36.8%; chronic HBV: 21.4%; HBV negative: 25.1%] (Table 1).

A larger proportion of persons with acute HBV experienced problematic alcohol use, illicit drug use, and injection drug use relative to those with chronic infections and HBV negative individuals (problematic alcohol use: 10.3%, 4.4%, 5.2%, $P < 0.001$; illicit drug use: 19.8%, 6.6%, 6.6%, $P < 0.001$; injection drug use: 14.7%, 5.5%, 5.0%, $P < 0.001$) (Figure 1A, Table 1). Conversely, major mental illness was most prevalent among HBV negative individuals (HBV negative: 13.6%; acute HBV: 11.3%, chronic HBV: 6.9%; $P < 0.001$).

HCV and HIV co-infections were more common among people diagnosed with acute HBV than among persons with chronic HBV and HBV negative individuals (HCV: 35.7%, 11.0%, 4.6%, $P < 0.001$; HIV: 6.3%, 2.5%, 0.5%, $P < 0.001$) (Figure 1B, Table 1). Active TB was less prevalent in the cohort, but more common among those with chronic HBV relative to HBV negative individuals and those with acute HBV (0.9%, 0.3%, 0.5%; $P < 0.001$). The cohort also consisted of 749 persons with HBV/HCV/HIV triple infection, who mostly had acute HBV infections (acute HBV: 4.1%, chronic HBV: 1.6%; HBV negative: 0.2%, $P < 0.001$) (Table 1).

Factors associated with acute and chronic HBV infection

In multivariable multinomial logistic regression models, we observed significant associations between acute or chronic HBV diagnosis and being male, age at HBV diagnosis or birth cohort, South and East Asian ethnicity, HCV or HIV infection, and injection drug use (Table 2 and Supplementary Table 3). However, the magnitude and direction of association for various variables differed for acute and chronic HBV.

South and East Asians had higher odds of acute or chronic HBV compared to Whites, with East Asians having 12 times greater odds of chronic HBV (ORacute: East Asian: 1.76, 95%CI: 1.53-2.02; South Asian: 1.66, 95%CI: 1.37-2.02; ORchronic: East Asian: 12.45, 95%CI: 12.15-12.77; South Asian: 1.26, 95%CI: 1.19-1.33) (Table 2).

Individuals with HCV or HIV infection had 5 times the odds acute HBV infection compared to their HBV negative counterparts (OR: HIV: 5.29, 95%CI: 4.30-6.51; HCV: 5.23, 95%CI: 4.65-5.87). For chronic infections, however, the odds of infection were slightly elevated among people with HIV co-infection (OR: 5.73, 95%CI: 5.29-6.20), but much lower among those infected with HCV (OR: 2.89, 95%CI: 2.77-3.01) (Table 2).

Injection drug use was associated with increased odds of both acute and chronic HBV (ORacute: 1.84, 95%CI: 1.57-2.17; ORchronic: 1.67, 95%CI: 1.58-1.77). In contrast, individuals with major mental

Table 2 Multivariable multinomial regression model for factors associated with acute or chronic hepatitis B virus in the British Columbia Hepatitis Testers Cohort, 1990-2015

	Adjusted OR (95%CI)	
	Acute HBV	Chronic HBV
Sex		
Male	2.28 (2.06-2.52)	1.43 (1.40-1.46)
Female	1.00	1.00
Age at HBV diagnosis (yr)		
< 25	2.38 (1.97-2.87)	0.89 (0.85-0.92)
25-34	2.62 (2.21-3.09)	1.09 (1.05-1.13)
35-44	1.82 (1.53-2.16)	1.19 (1.15-1.23)
45-54	1.49 (1.23-1.79)	1.22 (1.18-1.27)
55 +	1.00	1.00
Ethnicity		
East Asian	1.76 (1.53-2.02)	12.45 (12.15-12.77)
Other	0.88 (0.63-1.24)	3.06 (2.90-3.23)
South Asian	1.66 (1.37-2.02)	1.26 (1.19-1.33)
White	1.00	1.00
HCV		
Positive	5.23 (4.65-5.87)	2.89 (2.77-3.01)
Negative	1.00	1.00
HIV		
Positive	5.29 (4.30-6.51)	5.73 (5.29-6.20)
Negative	1.00	1.00
Active tuberculosis		
Yes	0.59 (0.32-1.09)	0.97 (0.85-1.10)
No	1.00	1.00
Problematic alcohol use		
Yes	0.87 (0.74-1.04)	1.02 (0.96-1.08)
No	1.00	1.00
Injection drug use		
Yes	1.84 (1.57-2.17)	1.67 (1.58-1.77)
No	1.00	1.00
Major mental illness		
Yes	0.73 (0.62-0.85)	0.74 (0.71-0.78)
No	1.00	1.00
Material deprivation quintile		
Q1 (most privileged)	1.00	1.00
Q2-4	1.06 (0.94 -1.21)	1.10 (1.06-1.13)
Q5 (most deprived)	1.35 (1.17 -1.55)	1.35 (1.30-1.39)
Social deprivation quintile		
Q1 (most privileged)	1.00	1.00
Q2-4	1.20 (1.04-1.39)	0.97 (0.95-1.00)
Q5 (most deprived)	1.56 (1.34-1.82)	1.00 (0.97-1.03)
Year of HBV diagnosis		
1990-1999	1.00	1.00
2000-2004	0.10 (0.09-0.12)	0.27 (0.26-0.28)
2005-2009	0.03 (0.03-0.04)	0.14 (0.13-0.14)
2010-2015	0.00 (0.00-0.01)	0.05 (0.05-0.06)

HIV: Human immunodeficiency virus; HCV: Hepatitis C virus; HBV: Hepatitis B virus; Q: Quintile.

illness had lower odds of either infection (ORacute: 0.73, 95%CI: 0.62-0.85; ORchronic: 0.74, 95%CI: 0.71-0.78). Material deprivation was also associated with increased odds of acute and chronic HBV infection (Q5: ORacute: 1.35, 95%CI: 1.17-1.55; ORchronic: 1.35, 95%CI: 1.30-1.39) (Table 2). Although social deprivation was associated with higher odds of acute HBV infection (ORacute: 1.56, 95%CI: 1.34-1.82), it was not significantly associated with a chronic infection (ORchronic: 1.00, 95%CI: 0.97-1.03).

In an additional model, composite variables (age at HBV diagnosis and injection drug use, and race/ethnicity and material deprivation) were used to determine joint effects on HBV infection (Figure 2, Table 3). In this model, there was a graded decrease in the odds of acute HBV with increasing age at diagnosis among PWID (OR: < 25 years: 7.55, 95%CI: 5.13-11.10; 25-34 years: 5.32, 95%CI: 4.08-6.94; 35-44 years: 2.98, 95%CI: 2.26-3.9; 45-54 years: 1.77, 95%CI: 1.19-2.62; 55 + years: 1.56, 95%CI: 0.78-3.10) (Figure 2A, Table 3). The opposite pattern was observed for chronic HBV infections, as the odds of chronic HBV increased with age at diagnosis (OR: < 25 years: 1.43, 95%CI: 1.18-1.73; 25-34 years: 1.72, 95%CI:

Table 3 Multivariable multinomial regression model (with interaction terms) for factors associated with acute or chronic hepatitis B virus in the British Columbia Hepatitis Testers Cohort, 1990-2015

	Adjusted OR (95% CI)	
	Acute HBV	Chronic HBV
Sex		
Male	2.30 (2.08-2.54)	1.43 (1.4-1.46)
Female	1.00	1.00
HCV		
Positive	5.22 (4.65-5.86)	2.88 (2.77-3.00)
Negative	1.00	1.00
HIV		
Positive	5.25 (4.26-6.47)	5.75 (5.31-6.22)
Negative	1.00	1.00
Active tuberculosis		
Yes	0.58 (0.31-1.08)	0.97 (0.86-1.10)
No	1.00	1.00
Problematic alcohol use		
Yes	0.90 (0.75-1.07)	1.01 (0.95-1.07)
No	1.00	1.00
Major mental illness		
Yes	0.72 (0.61-0.84)	0.75 (0.71-0.78)
No	1.00	1.00
Social deprivation quintile		
Q2-Q4	1.21 (1.05-1.40)	0.97 (0.94-1.00)
Q5 (most deprived)	1.58 (1.36-1.84)	0.99 (0.96-1.03)
Q1 (most privileged)	1.00	1.00
IDU*Age at HBV diagnosis (yr)		
IDU* < 25	7.55 (5.13-11.10)	1.43 (1.18-1.73)
IDU*25-34	5.32 (4.08-6.94)	1.72 (1.55-1.91)
IDU*35-44	2.98 (2.26-3.93)	1.87 (1.71-2.05)
IDU*45-54	1.77 (1.19-2.62)	2.06 (1.87-2.28)
IDU*55+	1.56 (0.78-3.10)	2.34 (2.05-2.65)
No IDU* < 25	2.23 (1.84-2.71)	0.90 (0.86-0.93)
No IDU*25-34	2.53 (2.13-3.01)	1.11 (1.07-1.15)
No IDU*35-44	1.84 (1.54-2.19)	1.21 (1.17-1.25)
No IDU*45-54	1.57 (1.30-1.90)	1.24 (1.20-1.28)
No IDU*55+	1.00	1.00
Ethnicity*Material Deprivation quintile		
East Asian*Material deprivation Q2-Q4	1.71 (1.37-2.12)	13.39 (12.82-13.98)
East Asian*Material deprivation Q5	2.61 (2.06-3.32)	15.98 (15.23-16.77)
East Asian*Material deprivation Q1	2.05 (1.49-2.81)	11.69 (11.07-12.33)
Other*Material deprivation Q2-Q4	0.97 (0.60-1.57)	3.32 (3.07-3.60)
Other*Material deprivation Q5	1.15 (0.59-2.26)	4.23 (3.78-4.74)
Other*Material deprivation Q1	0.89 (0.44-1.81)	2.62 (2.32-2.95)
South Asian*Material deprivation Q2-Q4	1.81 (1.35-2.42)	1.42 (1.30-1.54)
South Asian*Material deprivation Q5	2.44 (1.81-3.30)	1.41 (1.28-1.56)
South Asian*Material deprivation Q1	1.02 (0.48-2.19)	1.55 (1.32-1.82)
White*Material deprivation Q2-Q4	1.08 (0.94-1.25)	1.03 (0.98-1.08)
White*Material deprivation Q5	1.33 (1.13-1.56)	1.36 (1.29-1.43)
White*Material deprivation Q1	1.00	1.00
Year of HBV diagnosis		
1990-1999	1.00	1.00
2000-2004	0.10 (0.09-0.12)	0.27 (0.26-0.28)
2005-2009	0.03 (0.03-0.04)	0.14 (0.13-0.14)
2010-2015	0.00 (0.00-0.01)	0.05 (0.05-0.06)

IDU: Injection drug use; HIV: Human immunodeficiency virus; HCV: Hepatitis C virus; HBV: Hepatitis B virus; Q: Quintile.

1.55-1.91; 35-44 years: 1.87, 95%CI: 1.71-2.05; 45-54 years: 2.06, 95%CI: 1.87-2.28; 55 + years: 2.34, 95%CI: 2.05-2.65) (Figure 2B, Table 3). This model also demonstrated that the relatively high odds of chronic HBV among East Asians increased further with worsening material deprivation [OR: Material deprivation, Q1 (most privileged): 11.69, 95%CI: 11.07-12.33; Q2-Q4: 13.39, 95%CI: 12.82-13.98; Q5 (most deprived): 15.98, 95%CI: 15.23-16.77) (Figure 2B, Table 3).

DISCUSSION

In this large population based cohort study, we assessed over 1 million individuals for risk factors associated with acute and chronic HBV infection in British Columbia. This

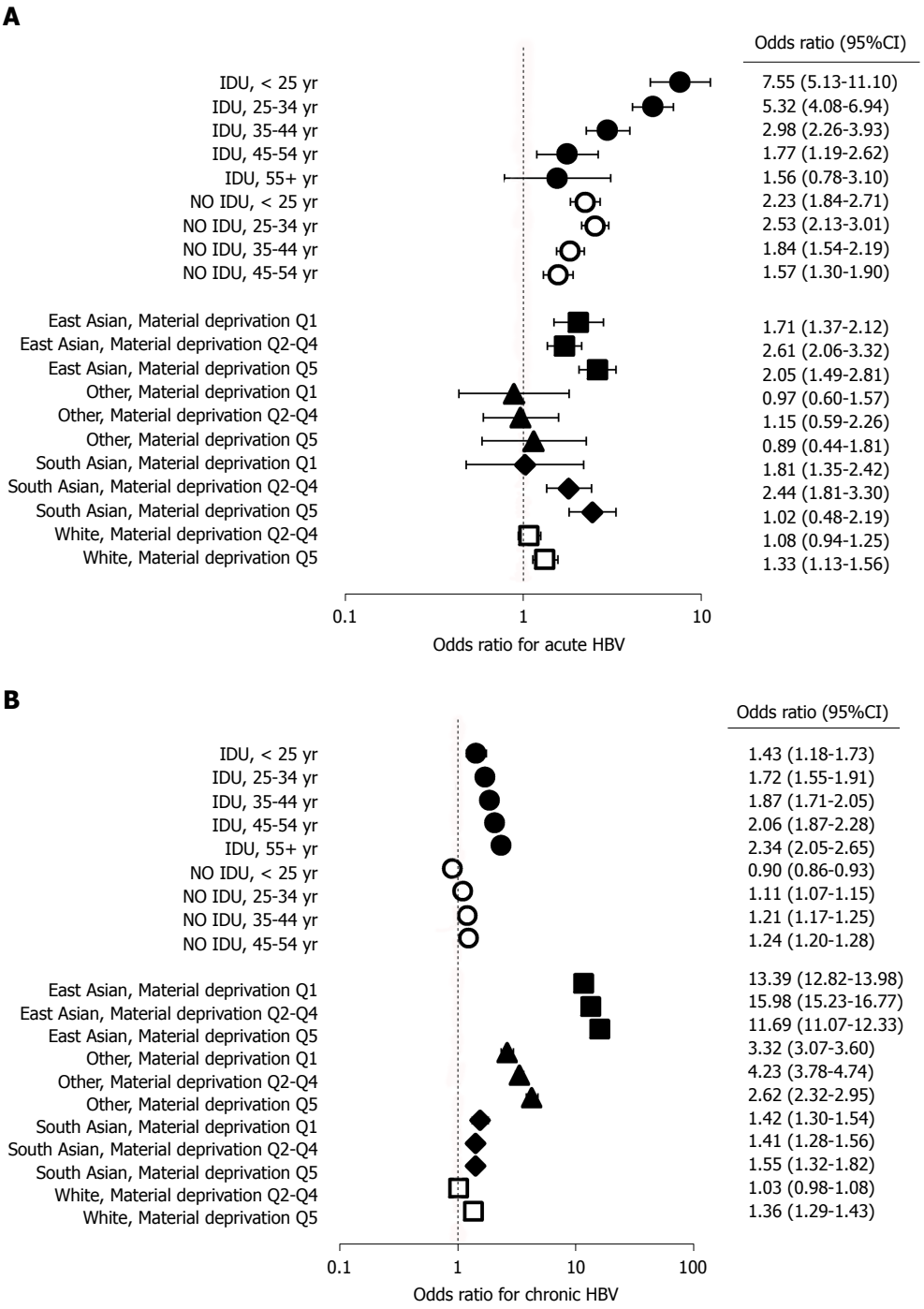

Figure 2 Odds ratios for interactions of factors associated with hepatitis B infection in the British Columbia Hepatitis Testers Cohort, 1990-2015. A: Acute hepatitis B infection; B: Chronic hepatitis B infection.

study shows two distinct patterns of risk factors among people diagnosed with acute and chronic infections. Acute HBV infections, indicative of new transmission events, occurred predominantly among males, persons aged between 25 and 34 years, White individuals, and socioeconomically disadvantaged persons. Problematic alcohol use, injection drug use, HIV and HCV co-infection were also common within this group. Individuals diagnosed with chronic HBV infection had similar characteristics, but were predominantly older, that is, aged between 35 to 44 years, and East Asian. Additionally, substance use and HIV or HCV co-infection were relatively low within this group. These findings highlight distinct risk patterns for individuals with acute and chronic HBV infections within the province and underscore the need for different strategies to prevent, diagnose and treat HBV within these groups.

Persons with acute and chronic infections had distinct co-infections and concurrent social condition profiles. Problematic alcohol use, illicit drug use and major mental illness were more common among individuals diagnosed with acute HBV than among

those with chronic HBV. Similarly, HBV/HCV, HBV/HIV and HBV/HCV/HIV co-infection occurred 3 times more frequently among individuals diagnosed with acute infections. These findings are consistent with those of studies in the United States and with observations made among seroconverters and chronically infected HCV positive individuals in the BC-HTC[17,18,23]. The HBV vaccination rate in BC is high and the incidence of acute HBV infections gradually declined to just 6 reported cases in 2015[7,24]. However, the current opioid epidemic may lead to localized HBV transmission among unvaccinated PWID, as was seen in suburban United States[18,25]. In our study, the odds of acute HBV were highest among younger persons and these age-dependent odds were greatly elevated by injection drug use among younger age groups. Younger PWID had 8-fold greater odds of being diagnosed with acute HBV than older non-PWID and up to 3 times the odds of their non-PWID of identical age. These findings demonstrate the interconnected nature of HBV, HCV and HIV infection, mental illness and alcohol/drug addiction and, therefore, highlight the need for a syndemic approach to significantly reducing new HBV infections. As the incidence of vaccine preventable HBV infection typically occurs among populations that are already affected by many social conditions and infections, such an approach should involve the integration of HBV prevention, screening and treatment programs with those of HIV, HCV, mental health and addiction programs.

Ethnicity was the most distinguishing factor between individuals diagnosed with acute and chronic HBV in BC. While over 75% of persons with acute HBV in the BC-HTC were White, 60% of chronically infected persons were East Asian. East Asian individuals had 12-fold greater odds of being diagnosed with chronic HBV than White persons, which worsened with declining socioeconomic status. Recent studies from the US on acute HBV infection also indicated that 57%-89% of acute infections were among the White population, while the majority of prevalent HBV infections were among people from the Asia-Pacific region[12,13,17,18]. Similarly, most individuals with chronic HBV in Australia in 2011 (38%) were born in the Asia-Pacific region[10]. These results mirror those observed in Canada (2007-2011), where rates of chronic HBV among foreign-born and non-White Canadians were estimated to be 4 and 5 times the national rates, respectively[4]. Low socioeconomic status within the East Asian community may act as a double-edged sword; increasing their risk of chronic HBV, while acting as a barrier to accessing health care. East Asian immigrants may also face additional barriers to health care, including language and cultural barriers, and insufficient information to make full use of the health care system[26-28]. Lack of awareness about HBV and its effects on health, a large proportion of unvaccinated individuals and low awareness of vaccination status may also affect HBV screening and treatment within this population[28,29]. In general, the asymptomatic nature of HBV infection leads to late diagnosis after complications have developed[1]. Studies have shown that immigrants in Canada are disproportionately affected by HCC and decompensated cirrhosis and have up to 5 times greater risk of death from these causes than their Canadian-born counterparts[14,30,31]. Therefore, screening for HBV within the East Asian population is vital for early diagnosis. As the East Asian population in BC faces the additional challenge of a high burden of TB, the integration of HBV screening with TB screening and treatment programs should create additional avenues for the identification of undiagnosed HBV carriers within the East Asian population in BC[32]. The ethnicity-related differences in acute and chronic HBV and related comorbidities and social conditions emphasize the need for differentiated programing for prevention, diagnosis and treatment by ethnicity.

The differences in HBV risk factor patterns among individuals diagnosed with acute and chronic HBV infection in BC are also mirrored by the distinct patterns of circulating HBV genotypes in both populations[33]. Between 2006 and 2012, genotype C viruses were predominantly isolated from individuals with chronic HBV, while genotype D viruses were prevalent among persons diagnosed with acute HBV in Canada[33]. As a high rate of chronic HBV diagnoses in Canada occur among immigrants form HBV endemic countries, these distinctions in circulating HBV genotypes may be related to the primary circulating strains in their home countries as well as to differing modes of acquisition[4,33]. In contrast to developed countries, major risk factors for HBV acquisition in HBV endemic developing countries include unsafe medical practices, for example, during circumcision and dental procedures[34,35]. These variations in circulating genotypes may have serious implications for disease progression and treatment outcomes among individuals diagnosed with either acute or chronic HBV in Canada[33,36]. Indeed, the elevated risk of HCC among African, Asian and Alaskan populations may be linked to circulating HBV genotypes[36]. This reinforces the need for ethnicity-based screening programs that go beyond the ongoing prenatal screening, and neonatal/preadolescent vaccination programs for immigrants originating from HBV endemic countries in certain parts of Canada[37].

The findings of this study should be interpreted in the light of following methodological considerations. As inclusion in the BC-HTC is dependent on either testing for HCV or HIV at the public health laboratory or being reported as confirmed cases of HIV, HCV, HBV or TB, individuals who test negative for HBV and do not meet any of the aforementioned criteria were excluded from our dataset. However, given the large number of HBV negative individuals in the study, we do not expect any major impact on our findings. Data on vaccination status, household contacts, sexual transmission and orientation were not available, which could have further enhanced our understanding of HBV epidemiology within the province. Additionally, ethnicity classifications

in our analysis may be affected by the variable sensitivity of Onomap in assigning Asian ethnicities[20]. Onomap was validated on a subset of the BC-HTC and showed low sensitivity for Filipinos. This may have resulted in the misclassification of East Asians from the Philippines as Whites and in the underestimation of the HBV in East Asian population. Previous studies have shown that foreign-born and Indigenous Canadians have a higher prevalence of chronic HBV relative to Canadian-born and non-Indigenous Canadians, respectively[5,30,38]. Similar findings have been reported in Australia and the United States[10,39]. Therefore, future analyses incorporating Indigenous and immigration status would provide additional insights for more tailored prevention and screening programs.

In summary, our findings show distinct characteristics of people diagnosed with acute and chronic infection in BC. Persons diagnosed with acute infection had a high level of substance use, co-infection with HIV or HCV, and were predominantly young White males. As acute HBV infection co-occurs with other infections and social conditions, a syndemic approach, where HBV prevention, screening, and treatment programs are integrated with those of other sexually transmitted and blood-borne infections as well as with mental health and addiction care would be an optimal approach for further reducing the incidence of acute HBV in the province and providing care to those diagnosed with acute HBV.

In contrast, the majority of chronic HBV infections in BC were diagnosed among East and South Asian individuals, who had very low levels of illicit drug and problem alcohol use, major mental illness and co-infection with HIV or HCV. Since traditional risk behavior and viral co-infection are less common among persons with chronic HBV infections, risk-based screening and prevention programs may impact only a fraction of such individuals. Given the asymptomatic nature of the disease and the grave health-related consequences of untreated HBV infection, organized screening programs are urgently needed to facilitate early diagnosis within the immigrant population in BC. Therefore, HBV screening and treatment programs focusing specifically on foreign-born East and South Asian population within BC would be necessary to have a significant impact on HBV-related disease burden within the province.

ARTICLE HIGHLIGHTS

Research background

Hepatitis B virus (HBV) affects approximately 200000 Canadians and 257 million people worldwide. In many developed countries, a relatively larger number of people are diagnosed with chronic HBV compared to acute HBV, each year. Chronic HBV infection is associated with 66% of the 1.34 million viral hepatitis-related deaths reported worldwide. It is responsible for a substantial disease burden from liver cancer and end-stage liver disease.

Research motivation

Data from Canada, the United States and other developed countries indicate that most chronic HBV infections are diagnosed among immigrants from HBV-endemic Asia-Pacific countries, while acute infections are predominant among White individuals. Persons diagnosed with acute and chronic HBV infections may differ with respect to demographics and risk behavior. These distinctions may have implications for interventions targeted at either population. Additionally, 49% of persons with chronic HBV and decompensated cirrhosis and 46% of those with HCC in British Columbia (BC) were diagnosed late in the course of their infections. Therefore, establishing the characteristics of individuals who are more likely to be infected with HBV could enhance the planning of prevention and screening programs to further reduce late diagnoses within the province.

Research objectives

In this study, we describe the characteristics of individuals diagnosed with acute and chronic HBV infections and identify the factors associated with HBV infection within the BC Hepatitis Testers Cohort (BC-HTC). We are unaware of any study comparing large population level data for both acute and chronic HBV. Study findings should inform prevention and screening programs within BC.

Research methods

We used data from the BC Hepatitis Testers Cohort (BC-HTC), which includes all individuals tested for HCV or HIV and those diagnosed with HBV or TB in BC since 1990. These data were integrated with prescription drug, medical visit, hospitalization and mortality data. HBV cases were classified as acute or chronic in accordance with provincial guidelines. We compared characteristics of individuals by HBV infection group (acute, chronic and negative). Factors associated with acute or chronic HBV infection were assessed with multivariable multinomial logistic regression models in comparison with the HBV negative group.

Research results

46498 of the 1058056 eligible BC-HTC participants were diagnosed with HBV infection; 95.7% with chronic infections at HBV diagnosis. Acute HBV infections, indicative of new transmission events, were diagnosed predominantly among males, persons aged between 25 and 34 years, White individuals, and socioeconomically disadvantaged persons. Problematic alcohol use, injection drug use, HIV and HCV co-infection were also common within this group. Individuals diagnosed with chronic HBV infection were predominantly older and East Asian. Additionally, substance use and HIV or HCV co-infection were relatively low within this group. Relative to Whites, East Asians had 12 times greater odds of being diagnosed with chronic HBV infection. These odds increased with increasing socioeconomic deprivation.

Research conclusions

These findings highlight distinct risk patterns for individuals with acute and chronic HBV infections and underscore the need for different strategies to prevent, diagnose and treat HBV within these groups. Optimal care for acute HBV would require the integration of HBV prevention, screening, and treatment programs with programs for mental health, addiction and other blood-borne infections. Managing chronic HBV, on the other hand, may require screening programs focusing on at-risk ethnic groups, including foreign-born East and South Asians with low prevalence of traditional risk factors, for early diagnosis and treatment initiation.

Research perspectives

We found clear differences in the characteristics of individuals diagnosed with acute and chronic HBV in BC. Consequently, we propose two distinct interventions for the management of acute and chronic HBV in the province: the integration of HBV-related public health programs with those of blood borne infection programs and mental health services to provide optimal care for populations at risk for acquiring acute HBV, and the implementation of targeted screening programs for early diagnosis among ethnic groups at risk for chronic HBV.

ACKNOWLEDGMENTS

We acknowledge the assistance of BCCDC, PHSA Performance measurement and reporting, Information

Analysts, Ministry of Health Data Access, Research and Stewardship, and MSP, DAD and Medical Beneficiary and Pharmaceutical Services programme areas, BC Ministry of Health, and BC Cancer Agency and their staff involved in data access and procurement, and data management.

All inferences, opinions, and conclusions drawn in this publication are those of the authors, and do not necessarily reflect the opinions or policies of the (British Columbia) Ministry of Health.

REFERENCES

1 **Centers for Disease Control and Prevention**. Chapter 10: Hepatitis B. Jennifer Hamborsky, Kroger A, Wolfe C, editors. Epidemiology and prevention of vaccine preventable diseases. 13th ed. Washington, DC: Public Health Foundation; 2015

2 **World Health Organization**. Global hepatitis report, 2017. 2017; Available from: URL: http://www.who.int/hepatitis/publications/global-hepatitis-report2017/en/

3 **Public Health Agency of Canada**. Hepatitis B infection in Canada: Brief report; 2011. Available from: URL: http://www.phac-aspc.gc.ca/id-mi/hepatitisBCan-hepatiteBCan-eng.php

4 **Rotermann M**, Langlois K, Andonov A, Trubnikov M. Seroprevalence of hepatitis B and C virus infections: Results from the 2007 to 2009 and 2009 to 2011 Canadian Health Measures Survey. *Health Rep* 2013; **24**: 3-13 [PMID: 24259199]

5 **Public Health Agency of Canada**. Report on hepatitis B and C in Canada: 2013. 2016; Available from: URL: https://www.canada.ca/en/public-health/services/publications/diseases-conditions/report-hepatitis-b-c-canada-2013.html

6 **Meireles LC**, Marinho RT, Van Damme P. Three decades of hepatitis B control with vaccination. *World J Hepatol* 2015; **7**: 2127-2132 [PMID: 26328023 DOI: 10.4254/wjh.v7.i18.2127]

7 **British Columbia Centre for Disease Control**. British Columbia annual summary of reportable diseases, 2015. 2016; Available from: URL: http://www.bccdc.ca/resourcegallery/Documents/Statistics%20and%20Research/Statistics%20and%20Reports/Epid/Annual%20Reports/2015CDAnnualReportFinal.pdf

8 **McGuiness L**. BCCDC Enhanced Hepatitis Strain Surveillance System (EHSSS) site report, 2000-2011. 2014; Available from: URL: http://www.bccdc.ca/resourcegallery/Documents/Statistics%20and%20Research/Statistics%20and%20Reports/Hepatitis/EHSSS_BCCDC_Site_Report_200011Final_forWeb.ppt

9 **Fang L**, Yu A, Buxton JA. Identification of acute vaccine-preventable hepatitis in individuals with chronic hepatitis in British Columbia between 1991 and 2007. *Can J Infect Dis Med Microbiol* 2011; **22**: 10-14 [PMID: 22379482]

10 **MacLachlan JH**, Allard N, Towell V, Cowie BC. The burden of chronic hepatitis B virus infection in Australia, 2011. *Aust N Z J Public Health* 2013; **37**: 416-422 [PMID: 24090323 DOI: 10.1111/1753-6405.12049]

11 **Wallace L**, Yeung A, Trayner K, Cullen B, Templeton K, Aitken C. Surveillance report: Hepatitis B infection in Scotland: 2015. *Health Prot Scotl* 2017; **51**: 17-36

12 **Tsang CA**, Granseth G, Dudek J, Thomas J, Woodward P, Tran S. 2016 viral hepatitis epidemiologic profile for Arizona. Arizona Department of Health Services 2016. Available from: URL: http://www.azdhs.gov/documents/preparedness/epidemiology-disease-control/hepatitis/arizona-2016-viral-hepatitis-profile.pdf

13 **Centers for Disease Control and Prevention**. Viral hepatitis surveillance United States, 2015. 2017; Available from: URL: https://www.cdc.gov/hepatitis/statistics/2015surveillance/pdfs/2015HepSurveillanceRpt.pdf

14 **Pottie K**, Greenaway C, Feightner J, Welch V, Swinkels H, Rashid M, Narasiah L, Kirmayer LJ, Ueffing E, MacDonald NE, Hassan G, McNally M, Khan K, Buhrmann R, Dunn S, Dominic A, McCarthy AE, Gagnon AJ, Rousseau C, Tugwell P; coauthors of the Canadian Collaboration for Immigrant and Refugee Health. Evidence-based clinical guidelines for immigrants and refugees. *CMAJ* 2011; **183**: E824-E925 [PMID: 20530168 DOI: 10.1503/cmaj.090313]

15 **Samji H**, Yu A, Kuo M, Alavi M, Woods R, Alvarez M, Dore GJ, Tyndall M, Krajden M, Janjua NZ; BC Hepatitis Testers Cohort Team. Late hepatitis B and C diagnosis in relation to disease decompensation and hepatocellular carcinoma development. *J Hepatol* 2017; **67**: 909-917 [PMID: 28684103 DOI: 10.1016/j.jhep.2017.06.025]

16 **Ghany MG**, Perrillo R, Li R, Belle SH, Janssen HL, Terrault NA, Shuhart MC, Lau DT, Kim WR, Fried MW, Sterling RK, Di Bisceglie AM, Han SH, Ganova-Raeva LM, Chang KM, Lok AS; Hepatitis B Research Network; Hepatitis B Research Network. Characteristics of adults in the hepatitis B research network in North America reflect their country of origin and hepatitis B virus genotype. *Clin Gastroenterol Hepatol* 2015; **13**: 183-192 [PMID: 25010003 DOI: 10.1016/j.cgh.2014.06.028]

17 **Iqbal K**, Klevens RM, Kainer MA, Baumgartner J, Gerard K, Poissant T, Sweet K, Vonderwahl C, Knickerbocker T, Khudyakov Y, Xia GL, Roberts H, Teshale E. Epidemiology of Acute Hepatitis B in the United States From Population-Based Surveillance, 2006-2011. *Clin Infect Dis* 2015; **61**: 584-592 [PMID: 25904365 DOI: 10.1093/cid/civ332]

18 **Harris AM**, Iqbal K, Schillie S, Britton J, Kainer MA, Tressler S, Vellozzi C. Increases in Acute Hepatitis B Virus Infections - Kentucky, Tennessee, and West Virginia, 2006-2013. *MMWR Morb Mortal Wkly Rep* 2016; **65**: 47-50 [PMID: 26821369 DOI: 10.15585/mmwr.mm6503a2]

19 **Janjua NZ**, Kuo M, Chong M, Yu A, Alvarez M, Cook D, Armour R, Aiken C, Li K, Mussavi Rizi SA, Woods R, Godfrey D, Wong J, Gilbert M, Tyndall MW, Krajden M. Assessing Hepatitis C Burden and Treatment Effectiveness through the British Columbia Hepatitis Testers Cohort (BC-HTC): Design and Characteristics of Linked and Unlinked Participants. *PLoS One* 2016; **11**: e0150176 [PMID: 26954020 DOI: 10.1371/journal.pone.0150176]

20 **Lakha F**, Gorman DR, Mateos P. Name analysis to classify populations by ethnicity in public health: validation of Onomap in Scotland. *Public Health* 2011; **125**: 688-696 [PMID: 21907365 DOI: 10.1016/j.puhe.2011.05.003]

21 **Ryan R**, Vernon S, Lawrence G, Wilson S. Use of name recognition software, census data and multiple imputation to predict missing data on ethnicity: application to cancer registry records. *BMC Med Inform Decis Mak* 2012; **12**: 3 [PMID: 22269985 DOI: 10.1186/1472-6947-12-3]

22 **Pampalon R**, Hamel D, Gamache P, Simpson A, Philibert MD. Validation of a deprivation index for public health: a complex exercise illustrated by the Quebec index. *Chronic Dis Inj Can* 2014; **34**: 12-22 [PMID: 24618377]

23 **Janjua NZ**, Yu A, Kuo M, Alvarez M, Cook D, Wong J, Tyndall MW, Krajden M. Twin epidemics of new and prevalent hepatitis C infections in Canada: BC Hepatitis Testers Cohort. *BMC Infect Dis* 2016; **16**: 334 [PMID: 27436414 DOI: 10.1186/s12879-016-1683-z]

24 **Public Health Agency of Canada**. Canadian immunization guide: Part 4-Active vaccines-Hepatitis B vaccine; 2017. Available from: URL: https://www.canada.ca/en/public-health/services/publications/healthy-living/canadian-immunization-guide-part-4-active-vaccines/page-7-hepatitis-b-vaccine.html

25 **The Canadian Press**. BC first in Canada to declare public health emergency after fentanyl overdoses. Maclean's. 14 Apr 2016. Available from: URL: http://www.macleans.ca/news/canada/b-c-first-in-canada-to-declare-public-health-emergency-after-fentanyl-overdoses/

26 **Kalich A**, Heinemann L, Ghahari S. A Scoping Review of Immigrant Experience of Health Care Access Barriers in Canada. *J Immigr Minor Health* 2016; **18**: 697-709 [PMID: 26093784 DOI: 10.1007/s10903-015-0237-6]

27 **Newbold KB**. Health care use and the Canadian immigrant population. *Int J Health Serv* 2009; **39**: 545-565 [PMID: 19771955 DOI: 10.2190/HS.39.3.g]

28 **Sherman M**, Bilodeau M, Cooper C, Mackie D, Depew W, Villeneuve JP. Liver disease in Canada: A crisis in the making. Canadian Liver Foundation 2013. Available from: URL: http://www.liver.ca/files/PDF/Liver_Disease_Report_2013/Liver_Disease_in_Canada_-_E.pdf

29 **Lin SY**, Chang ET, So SK. Why we should routinely screen Asian American adults for hepatitis B: a cross-sectional study of Asians in California. *Hepatology* 2007; **46**: 1034-1040 [PMID: 17654490 DOI: 10.1002/hep.21784]

30 **Ng E**, Myers RP, Manuel D, Sanmartin C. Hospital stays for hepatitis B or C virus infection or primary liver cancer among immigrants: a census-linked population-based cohort study. *CMAJ Open* 2016; **4**: E162-E168 [PMID: 27398359 DOI: 10.9778/cmajo.20150117]

31 **DesMeules M**, Gold J, McDermott S, Cao Z, Payne J, Lafrance B, Vissandjée B, Kliewer E, Mao Y. Disparities in mortality patterns among Canadian immigrants and refugees, 1980-1998: results of a national cohort study. *J Immigr Health* 2005; **7**: 221-232 [PMID: 19813288]

32 **British Columbia Centre for Disease Control**. TB in British Columbia: Annual report 2014; 2016. Available from: URL: http://www.bccdc.ca/resource-gallery/Documents/Statistics%20and%20Research/Statistics%20and%20Reports/TB/TB_Annual_Report_2014.pdf

33 **Osiowy C**, Giles E, Trubnikov M, Choudhri Y, Andonov A. Characterization of Acute and Chronic Hepatitis B Virus Genotypes in Canada. *PLoS One* 2015; **10**: e0136074 [PMID: 26406309 DOI: 10.1371/journal.pone.0136074]

34 **Olayinka AT**, Oyemakinde A, Balogun MS, Ajudua A, Nguku P, Aderinola M, Egwuenu-Oladejo A, Ajisegiri SW, Sha'aibu S, Musa BO, Gidado S, Nasidi A. Seroprevalence of Hepatitis B Infection in Nigeria: A National Survey. *Am J Trop Med Hyg* 2016; **95**: 902-907 [PMID: 27527630 DOI: 10.4269/ajtmh.15-0874]

35 **Mahtab MA**, Rahman S, Karim MF, Khan M, Foster G, Solaiman S, Afroz S. Epidemiology of hepatitis B virus in Bangladeshi general population. *Hepatobiliary Pancreat Dis Int* 2008; **7**: 595-600 [PMID: 19073404]

36 **Sherman M**, Bain V, Villeneuve JP, Myers RP, Cooper C, Martin S, Lowe C. The management of chronic viral hepatitis: a Canadian consensus conference 2004. *Can J Gastroenterol* 2004; **18**: 715-728 [PMID: 15605136]

37 **Villeneuve JP**. The natural history of chronic hepatitis B virus infection. *J Clin Virol* 2005; **34** Suppl 1: S139-S142 [PMID: 16461215]

38 **Rossi C**, Schwartzman K, Oxlade O, Klein MB, Greenaway C. Hepatitis B screening and vaccination strategies for newly arrived adult Canadian immigrants and refugees: a cost-effectiveness analysis. *PLoS One* 2013; **8**: e78548 [PMID: 24205255 DOI: 10.1371/journal.pone.0078548]

39 **Liu SJ**, Iqbal K, Shallow S, Speers S, Rizzo E, Gerard K, Poissant T, Klevens RM. Characterization of chronic hepatitis B cases among foreign-born persons in six population-based surveillance sites, United States 2001-2010. *J Immigr Minor Health* 2015; **17**: 7-12 [PMID: 24705737 DOI: 10.1007/s10903-014-0012-0]

P- Reviewer: Gong ZJ, Roohvand F **S- Editor**: Wang XJ
L- Editor: A **E- Editor**: Huang Y

World Journal of Gastroenterology

Submit a Manuscript: http://www.f6publishing.com

World J Gastroenterol 2018 March 21; 24(11): 1228-1238

DOI: 10.3748/wjg.v24.i11.1228

ISSN 1007-9327 (print) ISSN 2219-2840 (online)

ORIGINAL ARTICLE

Retrospective Cohort Study

Role of relevant immune-modulators and cytokines in hepatocellular carcinoma and premalignant hepatic lesions

Abdel-Rahman N Zekri, Somaya El Deeb, Abeer A Bahnassy, Abeer M Badr, Mona S Abdellateif, Gamal Esmat, Hosny Salama, Marwa Mohanad, Ahmed Esam El-dien, Shimaa Rabah, Assmaa Abd Elkader

Abdel-Rahman N Zekri, Molecular Virology and Immunology Unit, Department of Cancer Biology, National Cancer Institute, Cairo University, Cairo 11976, Egypt

Somaya El Deeb, Abeer M Badr, Ahmed Esam El-dien, Shimaa Rabah, Assmaa Abd Elkader, Department of Zoology, Faculty of Science, Cairo University, Giza 12613, Egypt

Abeer A Bahnassy, Department of Pathology, National Cancer Institute, Cairo University, Cairo 11976, Egypt

Mona S Abdellateif, Medical Biochemistry and Molecular Biology, Department of Cancer Biology, National Cancer Institute, Cairo University, Cairo 11976, Egypt

Gamal Esmat, Hosny Salama, Department of Hepatology and Tropical Medicine, Faculty of Medicine, Cairo University, Cairo 11441, Egypt

Marwa Mohanad, Department of Biochemistry, Misr University for Science and Technology, 6th October 12945, Giza Governorate, Egypt

ORCID number: Abdel-Rahman N Zekri (0000-0003-3939-0416); Somaya El Deeb (0000-0002-1826-1503); Abeer A Bahnassy (0000-0001-5454-6576); Abeer M Badr (0000-0003-3503-6639); Mona S Abdellateif (0000-0002-5510-4435); Gamal Esmat (0000-0001-8614-1629); Hosny Salama (0000-0003-0670-3770); Marwa Mohanad (0000-0002-3827-9647); Ahmed Esam El-dien (0000-0002-7357-3235); Shimaa Rabah (0000-0003-0477-8672); Assmaa Abd Elkader (0000-0001-7945-1610).

Author contributions: Zekri AN was the main supervisor, put forth the idea and planned of work, and performed data interpretation; El Deeb S supervised the biochemical work; Bahnassy AA supervised the flow cytometry work and revised the paper; Badr AM revised the paper; Abdellateif MS analyzed the data and wrote the paper; Esmat G and Salama H performed the medical care and the follow-up of patients; Mohanad M analyzed the data; El-dien AE performed the immunophenotyping; Rabah S and Abd Elkader A performed the ELISA work.

Institutional review board statement: The study was reviewed and approved for publication by our Institutional Reviewer.

Informed consent statement: All study participants or their legal guardian provided informed written consent about personal and medical data collection prior to study enrolment.

Conflict-of-interest statement: All the authors have no conflict of interest related to the manuscript.

Data sharing statement: The original anonymized dataset is available on request from the corresponding author at ncizekri@yahoo.com.

Manuscript source: Invited manuscript

Correspondence to: Abdel-Rahman N Zekri, MSc, PhD, Professor, Molecular Virology and Immunology Unit, Department of Cancer Biology, National Cancer Institute, Cairo University, Kasr Al-Aini Street, Fom El-Khaleeg, Cairo 11976, Egypt. ncizekri@yahoo.com
Telephone: +2-10-01413521
Fax: +2-202-23644720

Received: November 5, 2017
Peer-review started: November 6, 2017
First decision: November 27, 2017
Revised: December 24, 2017
Accepted: January 16, 2018

Article in press: January 16, 2018
Published online: March 21, 2018

Abstract

AIM

To assess the levels of different immune modulators in patients with hepatocellular carcinoma (HCC), in relation to other hepatic diseases.

METHODS

Eighty-eight patients were included in the current study and represented patients with HCC (20), liver cirrhosis (28) and chronic hepatitis (CH; 25), and normal controls (NC; 15). Peripheral blood was isolated for immunophenotyping of active myeloid dendritic cells (mDCs; CD1c and CD40), mature inactive myeloid cells (CD1c and HLA), active plasmacytoid cells (pDCs; CD303 and CD40), mature inactive pDCs (CD30 and HLA), active natural killer (NK) cells (CD56 and CD161), active NK cells (CD56 and CD314) and inactive NK cells (CD56 and CD158) was done by flow cytometry. Serum levels of interleukin (IL)-2, IL-10, IL-12, IL-1β, interferon (IFN)-α, IFN-γ and tumor necrosis factor (TNF)-αR2 were assessed by ELISA.

RESULTS

Active mDCs (CD1C+/CD40+) and inactive mDCs (CD1c+/HLA+) were significantly decreased in HCC patients in relation to NC ($P < 0.001$). CD40+ expression on active pDCs was decreased in HCC patients ($P < 0.001$), and its level was not significantly changed among other groups. Inactive pDCs (CD303+/HLA+), inactive NKs (CD56+/CD158+) and active NKs (CD56+/CD161+) were not statistically changed among the four groups studied; however, the latter was increased in CH ($P < 0.05$). NKG2D was statistically decreased in HCC, CH and cirrhosis ($P < 0.001$), and it was not expressed in 63% (12/20) of HCC patients. There was significant decrease of IL-2, IFN-α and IFN-γ ($P < 0.001$), and a significant increase in IL-10, IL-1β, and TNF-αR2 ($P < 0.01$, $P < 0.001$ and $P < 0.001$; respectively) in HCC patients. There was inverted correlation between IL-12 and IL-1β in HCC ($r = -0.565$, $P < 0.01$), with a strong correlation between pDCs (CD303+/CD40+) and NKs (CD56+/CD161+; $r = 0.512$, $P < 0.05$) as well as inactive mDCs (CD1c+/HLA+) and inactive NK cells (CD56+/CD158+; $r = 0.945$, $P < 0.001$).

CONCLUSION

NKG2D, CD40, IL-2 and IL-10 are important modulators in the development and progression of HCC.

Key words: Hepatocellular carcinoma; Hepatitis C virus; NKG2D; CD40; Interleukin-2; Interleukin-10; Myeloid dendritic cells; Plasmacytoid cells; Natural killer cell; Cytokines

Core tip: We assessed the levels of different immune modulatory cytokines and innate immune cells as natural killer (NK) cells and dendritic cells (DCs) in patients with disease progression of hepatocarcinogenesis. Our results showed significant down-regulation in active mDCs and pDCs expressing CD40 as well as NK cells expressing NKG2D. The expression of NKG2D on NKs was not expressed in 63% of hepatocellular carcinoma (HCC) patients. Also, there was significant decrease of interleukin (IL)-2, interferon-α and interferon-γ, and a significant increase in IL-10, IL-1β, and TNF-αR2 in HCC patients. These factors could be implicated in the pathogenesis of HCC, and represent attractive targets for therapy in chronic hepatitis C virus hepatitis and HCC.

Zekri AN, El Deeb S, Bahnassy AA, Badr AM, Abdellateif MS, Esmat G, Salama H, Mohanad M, El-dien AE, Rabah S, Abd Elkader A. Role of relevant immune-modulators and cytokines in hepatocellular carcinoma and premalignant hepatic lesions. *World J Gastroenterol* 2018; 24(11): 1228-1238 Available from: URL: http://www.wjgnet.com/1007-9327/full/v24/i11/1228.htm DOI: http://dx.doi.org/10.3748/wjg.v24.i11.1228

INTRODUCTION

Hepatocellular carcinoma (HCC) is a major health problem worldwide. It is the sixth most common cancer and the second leading cause of cancer-related death in the world[1]. In Egypt, HCC ranks the first among cancers in males (33.6%), and the 2nd in females after breast cancer (13.5%)[2]. This high incidence is attributed to the high prevalence of hepatitis C virus (HCV) infection, especially of genotype IV, in Egypt[3]. Despite advances in treatment modalities, sorafenib is still the only treatment approved by the Food and Drug Administration (FDA) for HCC; however, it extends the overall survival by 3 mo only. Hence, it is crucial to understand the underlying biological and immunological changes in HCC and to develop new treatment modalities based on these data[4,5].

The body's immune defense mechanism(s) plays an important role in the inhibition or progression of cancer. However, tumors can escape immune surveillance by producing a local and/or systemic immune-suppressive environment[6]. Although the underlying molecular mechanisms are not yet fully clear, recent studies show that the immune response in cancer patients is usually down-regulated by immunosuppressive cells, mainly T regulatory cells (Tregs) and myeloid-derived suppressor cells (MDSCs), which suppress the immune system and promote immunologic tolerance[7]. These inhibitory cells accumulate during advanced cancer stages. They are involved in chronic inflammation and tumor progression and they can inhibit many immune cells

(*e.g.*, CD4+, CD8+, natural killer (NK) cells)[8]. They also secrete many immune-suppressive cytokines, such as interleukin (IL)-6, IL-10, and transforming growth factor (TGF)-β, creating a tolerogenic and suppressive environment[9].

The NK cells represent 25%-30% of the human liver lymphocytes, compared to 10%-20% of the total peripheral blood lymphocytes[10]. They are the main effector cells of innate immunity, which play an important role in tumor surveillance. The NK cells achieve their functions through the release of cytolytic mediators, such as perforin and granzymes, or the induction of apoptosis *via* the expression of tumor necrosis factor (TNF) ligands and interferon (IFN)-γ[11]. Activation of NK cells is strictly regulated by a balance between activating and inhibitory signals, whereas the inhibitory signals are mainly induced by receptors for MHC class I molecules (KIRs, CD94/NKG2A). The activating signals are mainly achieved through NKG2D, a C-type lectin-like receptor which is expressed on NK cells, γδ T cells and CD8+ T cells[12,13]. NKG2D is responsible for detection and elimination of transformed cells *via* binding to MICA (MHC class I–related chain), MICB and the UL16-binding proteins[14]. Activation of NKG2D provides unique costimulation to antigen-specific CD8 T cells that is non-redundant to CD28 costimulation[15].

Dendritic cells (DCs) are the most professional antigen-presenting cells which respond rapidly to microenvironment signals. Upon maturation by tumor antigen, cross-priming to T and B lymphocytes occurs to produce antitumor adaptive immune responses[16]. There are two subsets of DCs: the myeloid dendritic cells (mDCs), which are characterized by their ability to produce IL-12; and, the plasmacytoid cells (pDCs), which are responsible for the production of over 95% of type-I IFNs in response to viral infection[17]. On activation, the CD8+ cytotoxic T cells (CTLs) eliminate tumor cells by the production of IFN-γ, whereas CD4+ T helper cells stimulate B cells to support the cytotoxic and humoral immune response[18].

IL-1β is a regulatory cytokine produced by tumor and immune cells, such as MDSCs. It also induces COX-2 expression, which prevents maturation and activation of antigen presenting cells at the tumor site[19].

In the current study, we assessed the role(s) of different immune regulatory cells and cytokines in the development and progression of chronic liver disease (chronic active hepatitis, cirrhosis and HCC) compared to the normal healthy volunteers. We believe that this could allow for better understanding of different pathways implicated in the development and progression of hepatocarcinogenesis, and could also help in designing new immune-therapeutic drugs.

MATERIALS AND METHODS

Patients

The current study included 88 patients who attended the medical oncology clinics of the National Cancer Institute (NCI), Cairo University during the period from 2014 to 2016. Patients were divided into four groups: HCC (20 patients - G1), liver cirrhosis (28 patients - G2), chronic hepatitis (CH; 25 patients - G3) and normal healthy volunteers as a control group (NC; 15 persons, matched for age and sex - G4). The Ethical Committee of the NCI, Egypt approved the study protocol and an informed consent was obtained from all participants before enrollment in the study.

Characterization of immune cells by flow cytometry

Peripheral blood samples were isolated from patients and healthy subjects for immunophenotyping of active mDCs (CD1c and CD40), mature inactive myeloid cells (CD1c and HLA), active pDCs (CD303 and CD40), mature inactive pDCs (CD303 and HLA), active NK cells (CD56 and CD161), active NK cells (CD56F CD314) and inactive NK cells (CD56 and CD158) using the specific monoclonal antibodies according to manufacturer's protocols (all monoclonal antibodies were purchased from Invitrogen, eBioscience, San Diego, CA, United States). Samples were then analyzed by flow cytometry (FACSCaliber; Becton and Dickenson, Franklin Lakes, NJ, United States).

Detection of cytokine levels by ELISA

Serum levels of IL-2, IL-10, IL-12, IL-1β, IFN-α, IFN-γ and TNF-αR2 were measured by the ELISA technique, according to manufacturer's instructions (Invitrogen, eBioscience), using ELISA reader (Sunrise; Tecan, Mannedorf, Switzerland).

Statistical analysis

Data were expressed as mean ± SE of mean for continuous variables. Comparison between cytokine levels and immune cells were performed using one-way analysis of variance followed by Tukeys' post hoc test. Pearson's correlation was used to assess the strength of correlation between different variables and a two-tailed *P*-value was determined. The *P*-value was considered significant at < 0.05. All statistical analyses were performed using SPSS, version 22 (IBM SPSS, Armonk, NY, United States).

RESULTS

Patients' characteristics

The mean age of the patients included in the current study was 57.1 ± 4.76 for HCC, patients, 51.29 ± 9.03 for liver cirrhosis patients, 49.64 ± 7.2 for CH patients and 42.9 ± 10.2 for NC (Table 1).

Flow cytometry data

There was a significant decrease in active mDCs (CD1C+/CD40+) and inactive mDCs (CD1c+/HLA+) in HCC patients compared to the NC group ($P < 0.001$), as well as in active mDCs (CD1C+/CD40+) in cirrhotic patients compared to CH patients ($P = 0.003$; Table

Table 1 Patient characteristics

	Normal	Chronic hepatitis	Cirrhosis	HCC
Sex				
Male	11 (73.3)	9 (36.0)	19 (67.9)	19 (95.0)
Female	4 (26.7)	16 (64.0)	9 (32.1)	1 (5.0)
Age, mean ± SD	42.9 ± 10.2	49.64 ± 7.2	51.29 ± 9.03	57.1 ± 4.76
HCV	+ve	+ve	+ve	+ve
Total	15	25	28	20

Data are presented as *n* (%), unless otherwise specified. HCC: Hepatocellular carcinoma; HCV: Hepatitis C virus.

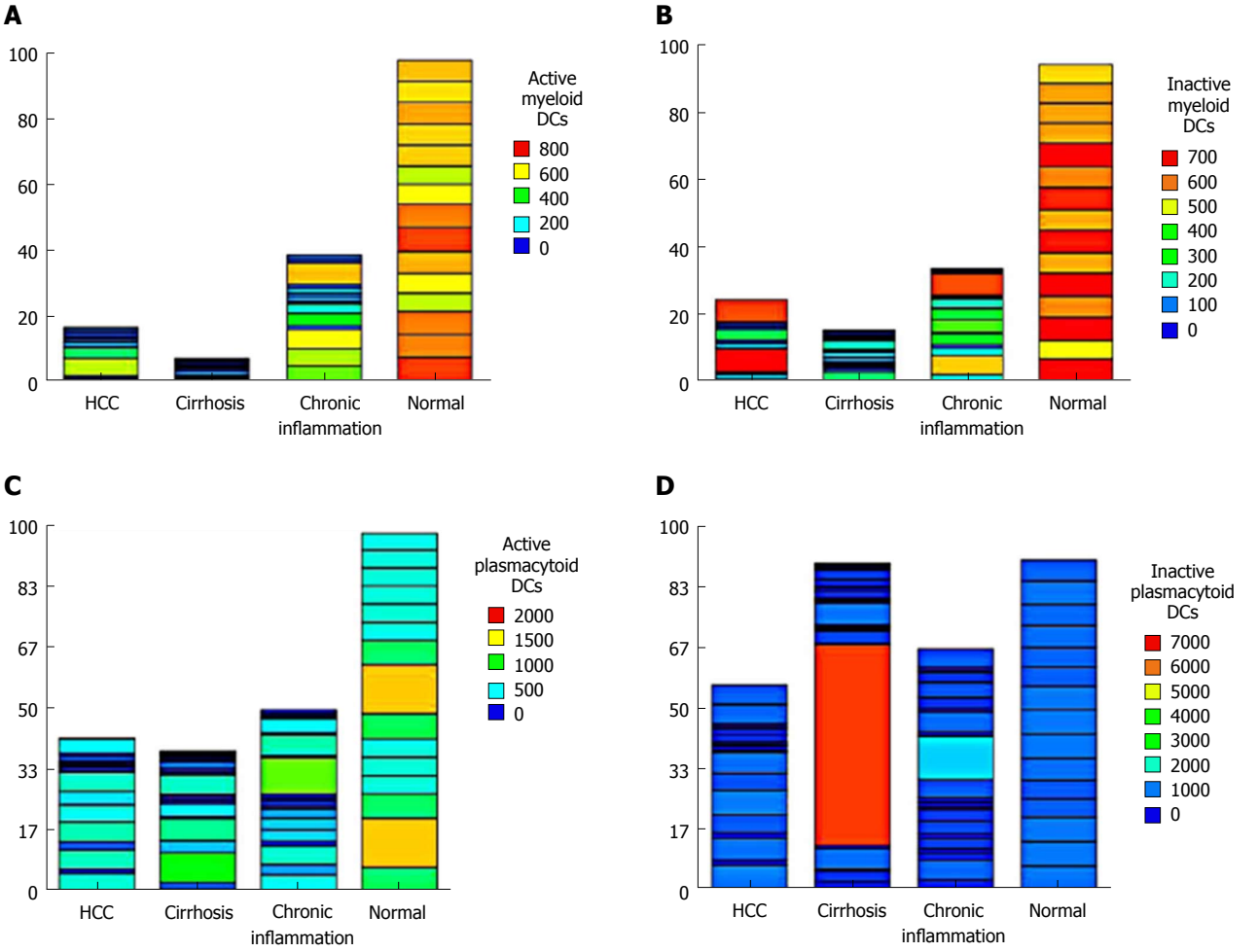

Figure 1 Heatmap of the differential levels of (A) active myeloid dendritic cells, (B) inactive myeloid dendritic cells, (C) active plasmacytoid cells, and (D) inactive plasmacytoid cells in the four groups studied. HCC: Hepatocellular carcinoma.

2). Also, the expression level of CD40+ on active pDCs (CD303+) was significantly decreased in HCC compared to the NC group ($P < 0.001$). However, there was no significant difference from the other groups (cirrhosis and CH). Meanwhile, the level of inactive pDCs (CD303+/HLA+) did not differ significantly between the four groups studied (Table 2, Figure 1).

The level of the nonactive NK cells (CD56+/CD158+) did not differ significantly among groups. However, the active NK cells (CD56+/CD161+) showed a significant increase in the CH group ($P < 0.05$), whereas the level of active NK cells (CD56+/CD314+) was statistically decreased in HCC, CH and cirrhotic patients compared to the NC group ($P < 0.001$), indicating an important role of these cells in the pathogenesis of HCC (Table 2). The expression of all cell types in each patient showed that active NK cells (CD56+/CD314+) were not expressed in 63% (12/20) of HCC patients. However, 2 patients showed unexplainable high variability (Figure 2).

We also found a significant decrease in the active NK cells (CD56+/CD314+; $P < 0.05$) and active pDCs (CD303+, CD40+; $P < 0.05$) compared to the inactive NK cells (CD56+/CD158+) and inactive pDCs (CD303+/HLA+) respectively in HCC. To the contrary,

Table 2 Differential counts of nature killer cells and dendritic cells among the studied groups

	Normal	Chronic hepatitis	Cirrhosis	HCC	*P* value
Active mDCs (CD1C+/CD40+)	652.4 ± 15.9^{A1}	154.1 ± 40.9^{B}	25.5 ± 4.3^{C}	82.8 ± 28.7^{BC}	< 0.001
Inactive mature mDCs (CD1c+/HLA+)	627.1 ± 14.8^{A}	134.4 ± 37.1^{B}	54.7 ± 12.3^{B}	121.8 ± 44.8^{B}	< 0.001
Active pDCs (CD303+/CD40+)	782.2 ± 89.6^{A}	237.8 ± 56.2^{B}	164.1 ± 45.9^{B}	251 ± 55.9^{B}	< 0.001
Inactive mature pDCs (CD303+/HLA+)	727.5 ± 18.7^{A}	318.5 ± 61.4^{A}	385.7 ± 233.3^{A}	339.2 ± 67.5^{A}	0.339
Active NK cells (CD56+/CD161+)	535 ± 83.4^{AB}	1166.3 ± 426.3^{B}	399.8 ± 139.8^{AB}	145.5 ± 30.2^{A}	< 0.05
Inactive NK cells (CD56+/CD158+)	710.3 ± 127.9^{A}	656.3 ± 235.7^{A}	462.6 ± 105.3^{A}	456.7 ± 218.1^{A}	0.708
Active NK cells (CD56+/CD314+)	585.5 ± 35.9^{A}	188.5 ± 69.4^{B}	123.5 ± 47.6^{B}	196 ± 110.8^{B}	< 0.001

Data are presented as mean ± SEM. [1]Groups having the same letters in the same variable are statistically insignificant. HCC: Hepatocellular carcinoma; mDCs: Myeloid dendritic cells; NK: Natural killer; pDCs: Plasmacytoid cells.

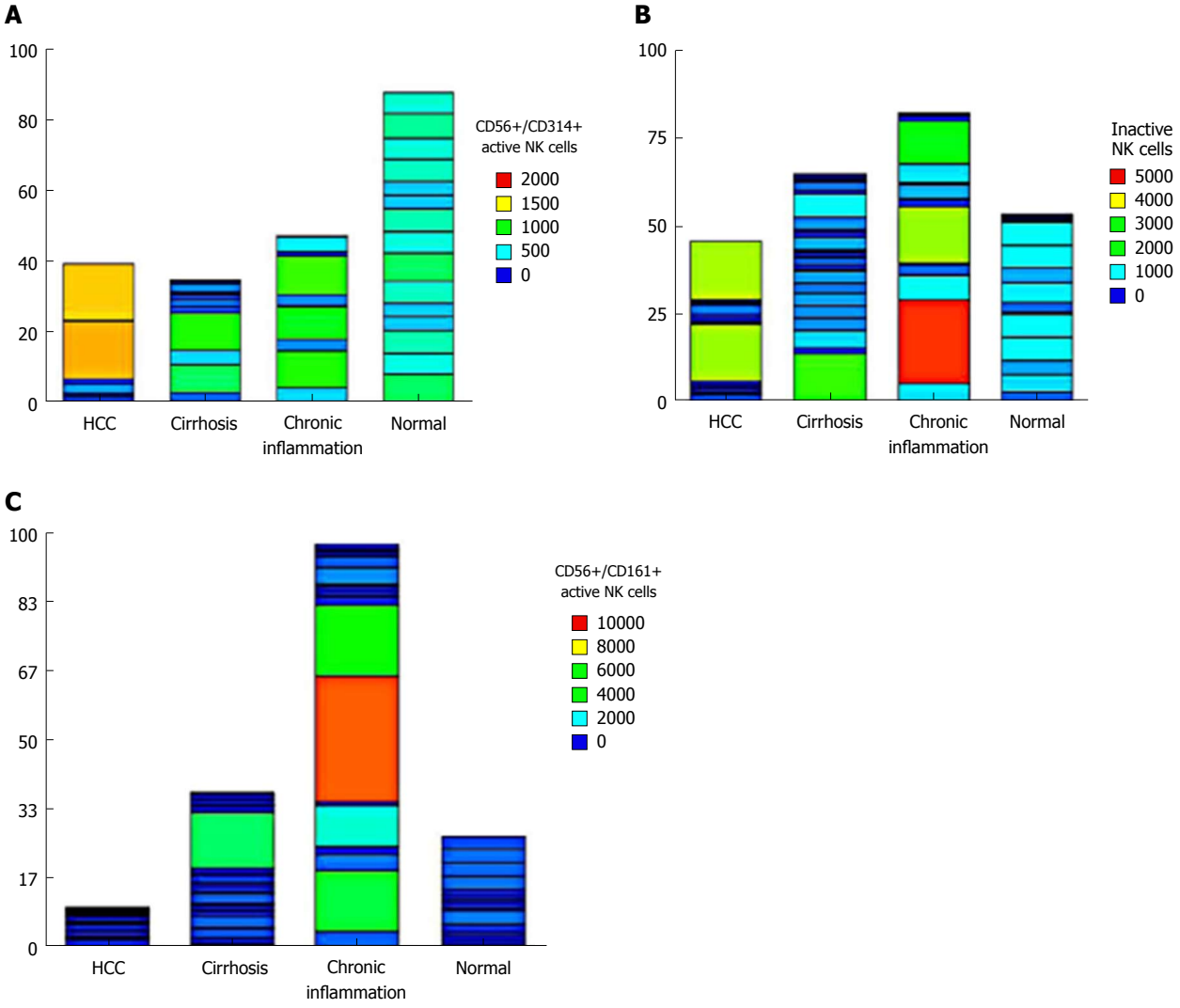

Figure 2 Heatmap of the differential levels of (A) active natural killer cells (CD56+/CD314+), (B) inactive natural killer cells (CD56+/CD158+), and (C) natural killer cells (CD56+/CD161+) in the four groups studied. HCC: Hepatocellular carcinoma.

the NK cells (CD56+/CD161+) and the mDCs did not differ significantly between groups (Figure 3).

Serum levels of cytokines

There was a significant decrease in serum levels of IL-2, IFN-α and IFN-γ in HCC patients compared to the NC group ($P < 0.001$), and a significant increase in serum levels of IL-10, IL-1β and TNF-αR2 in HCC compared to the NC group ($P < 0.01$, $P < 0.001$ and $P < 0.001$ respectively). However, there was no statistically significant change in the serum level of IL-12 ($P = 0.393$) among the four groups studied (Table 3, Figure 4).

Significant correlation was also reported in HCC patients between (1) serum level of IL-12 and IL-1β ($r = -0.565$, $P < 0.01$), (2) expression of CD40 on

Table 3 Levels of the studied cytokines among different studied groups

	Normal	Chronic hepatitis	Cirrhosis	HCC	*P* value
IL-2	22.13 ± 2.21^{A1}	16.28 ± 2.12^{B}	11.36 ± 0.95^{C}	10.24 ± 0.64^{C}	< 0.001
IL-10	74.8 1 ± 1.34^{A}	98.46 ± 4.01^{AB}	104.11 ± 9.35^{B}	132.1 ± 14.26^{C}	< 0.01
IL-12	0.06 ± 0.01^{A}	0.09 ± 0.01^{A}	0.15 ± 0.06^{A}	0.08 ± 0.01^{A}	0.393
IL-1β	3.46 ± 0.15^{A}	6.48 ± 0.58^{A}	6.71 ± 2.39^{A}	21.38 ± 4.88^{B}	< 0.001
IFN-α	31.20 ± 0.67^{A}	32.28 ± 1.44^{A}	21.31 ± 1.01^{B}	18.49 ± 1.37^{B}	< 0.001
IFN-γ	20.47 ± 0.49^{A}	29.75 ± 0.68^{B}	17.51 ± 1.18^{C}	10.46 ± 0.56^{D}	< 0.001
TNF-αR2	6.03 ± 0.07^{A}	13.25 ± 1.73^{A}	10.09 ± 0.97^{A}	47.42 ± 6.74^{B}	< 0.001

Data are presented as mean ± SEM. [1]Groups having the same letters in the same variable are statistically insignificant. HCC: Hepatocellular carcinoma; IFN: Interferon; IL: Interleukin; TNF: Tumor necrosis factor.

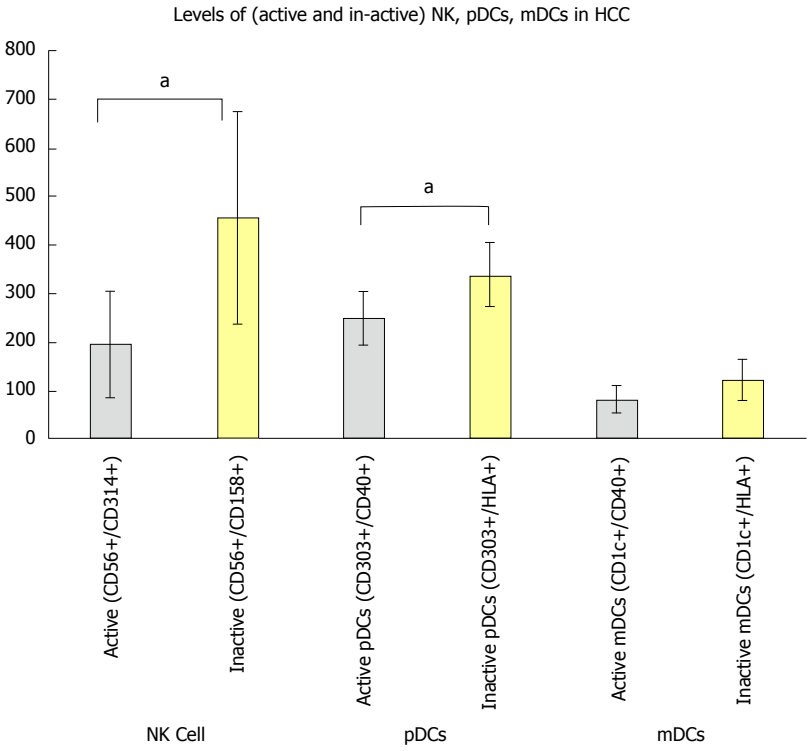

Figure 3 Balance between active and inactive natural killer cells, plasmacytoid cells, and myeloid dendritic cells in hepatocellular carcinoma patients in relation to the normal group. [a]*P* < 0.05. HCC: Hepatocellular carcinoma; mDCs: Myeloid dendritic cells; NK: Natural killer; pDCs: Plasmacytoid cells.

pDCs (CD303+, CD40+) and active NK cells (CD56+/CD161+; $r = 0.512$, $P < 0.05$), and (3) inactive mDCs (CD1c+/HLA+) and inactive NK cells (CD56+/CD158+; $r = 0.945$, $P < 0.001$) (Figure 5A-C).

Patients with chronic active hepatitis showed strong significant correlation between active NK cells (CD56+/CD161+) and both IL-2 and IL-12 ($r = 0.549$, $P = 0.004$ and $r = 0.660$, $P < 0.001$ respectively). Strong correlations were also reported between the expression of CD314 on NK cells and IL-2 ($r = 0.548$, $P < 0.01$) and active mDCs CD1c+/CD40+ ($r = 0.577$, $P = 0.003$). The level of IL-10 was strongly correlated with (1) increased inactive NK cells (CD56+/CD158+; $r = 0.604$, $P = 0.001$) and (2) inactive mDCs CD1c+/HLA+ ($r = 0.588$, $P = 0.002$; Table 4).

DISCUSSION

Identification of inflammatory mediators which promote or prevent the progression of cancer depends on the tumor microenvironment. Thus, this study was designed to assess the levels of different immune modulators and cytokines in patients with HCC, nonmalignant hepatic diseases (*e.g.*, CH and liver cirrhosis) compared to a normal group. This would enable us to study different pathways that help in identifying immune cells or biomarkers that may be implicated in hepatocellular carcinogenesis. This may also explain why liver disease progresses more rapidly in some patients than in others and provides additional therapeutic modalities for viral infections and HCC (immunotherapy).

One of the most powerful antigen presenting cells is the DC, which plays an important role in antitumor immune response. Our data revealed that active and inactive mDCs were significantly decreased in HCC patients compared to the NC group ($P < 0.001$); however, the level of active mDCs (CD1C+/CD40+) was significantly decreased in cirrhosis compared to CH

Table 4 Correlation between dendritic cell and nature killer cell count and the levels of studied cytokines in chronic active hepatitis

	IL-2	IL-12	IL-10	Active mDCs (CD1c+/CD40+)
Active NK cells (CD56+/CD161+)	$r = 0.549^{b}$ $P = 0.004$	$r = 0.660^{b}$ $P < 0.001$		
Active NK cells (CD56+/CD314+)	$r = 0.548^{a}$ $P = 0.005$			$r = 0.577^{b}$ $P = 0.003$
Inactive NK cells (CD56+/CD158+)			$r = 0.604^{b}$ $P = 0.001$	
Inactive mDCs (CD1c+/HLA+)			$r = 0.588^{b}$ $P = 0.002$	

$^{a}P < 0.05$ (2-tailed); $^{b}P < 0.01$ (2-tailed). IL: Interleukin; mDCs: Myeloid dendritic cells; NK: Natural killer.

patients ($P = 0.003$). These data are consistent with Obermajer *et al*[20], who reported that the inhibition of DC maturation in HCC may prove to be a critical feature of tumor escape, as well as with another two recent studies which reported numerical and functional defects in the peripheral DCs in hepatitis B- and C-associated HCC patients[21,22].

The pDC (CD303+, CD40+) represents the major cell responsible for antiviral immunity, and the main source of IFN-α in the body. Our data revealed that the expression level of CD40+ on active pDCs was significantly decreased in HCC patients compared to NC ($P < 0.001$). Meanwhile, inactive pDCs (CD303+/HLA+) did not change significantly among the four groups studied. This was also confirmed by the significant decrease of serum IFN-α, and the increase of IL-10 in HCC patients compared to the NC group ($P < 0.001$ and $P < 0.01$ respectively). This is in concordance with previous reports showing that IL-10 inhibits IFN-α production and promotes apoptosis of human pDCs[23,24]. Moreover, Gonzalez-Carmona *et al*[25] demonstrated that cancer patients had low CD40 expression on DCs or CD40L on T cells, which is associated with an impaired immune response, and Shurin *et al*[26] reported that the tumor-derived IL-10 inhibits CD40 expression on DCs and DC precursors and suppresses their maturation and function.

NK cells play an important role in controlling viral hepatitis, liver fibrosis and carcinogenesis. Their functions are modulated by different classes of receptors present on its surface[27]. Thus, it is essential to identify the roles of these cells in different stages of HCC development. Among these, we investigated the role of the killer cell immunoglobulin-like receptors (KIR; CD158), NKR-P1A (CD161) and NKG2D (CD314) in HCV CH patients, and in liver cirrhosis and its progression to HCC.

Our results revealed that the expression of the inhibitory KIR (CD158+) receptors and the activating NKR-P1A (CD161) on NK cells was not statistically changed between HCC and NC ($P = 0.827$ and $P = 0.788$ respectively). Thus, these two pathways may not be involved in the pathogenesis of HCC. However, the latter were statistically increased in CH ($P < 0.05$). This result was supported by our finding of a strong statistical correlation between the expression of CD161 on NK cells and IL-12 ($r = 0.77$, $P < 0.001$) in patients with HCV chronic active hepatitis. This illustrates the role of NK cells (CD56+/CD161+) in viral hepatitis.

On the other hand, the level of active NK cells expressing NKG2D were statistically decreased in HCC, CH and cirrhosis in relation to the NC group ($P < 0.001$), which could indicate the implication of these cells in the progression of HCC. This was clarified by representing its expression in each patient, it was not expressed in 63% (12/20) of HCC patients, emphasizing its important role in HCC development. These data were consistent with Lanier *et al*[28]. Yoon *et al*[29] reported that direct interaction between human NK cells and HCV-infected hepatoma cells down-regulates NK cell NKG2D expression and effector function with diminished IFN-γ production. Another study carried out by Kamiya *et al*[30] demonstrated that NKG2D was an important mediator of antiHCC activity. On the contrary, Oliviero *et al*[31] found a decreased percentage of NK cells expressing the inhibitory receptor KIR3DL1 and a concomitant increase in the proportion of $NKG2D^{+}$ NK cells in Italian patients with chronic HCV. This could be explained by racial and environmental differences with different viral genotypes, and also according to the clinical stage.

Our results regarding DCs and NK cells were supported by assessment of the cytokine serum levels in the four groups studied. We found that there was a significant increase in IL-1β ($P < 0.001$) in HCC patients compared to the NC group. However, there was no statistically significant change in the serum level of IL-12 ($P = 0.393$) among the four groups studied. Furthermore, we had a significant increase in the serum level of IL-10 in the cirrhosis and HCC groups compared to the NC group. This is consistent with Accapezzato *et al*[32]. IL-10 is important for allowing liver NK cells to maintain immune-tolerant states[33]. Its significant increase in HCC patients is responsible for the abnormal tolerant NK cells that cannot eliminate infected or transformed cells, which leads to immune evasion.

In the current study, there was a significant decrease of the serum levels of IFN-γ in chronic HCV hepatitis, cirrhosis and HCC patients in comparison to NC ($P < 0.001$). This is in agreement with Li *et al*[34],

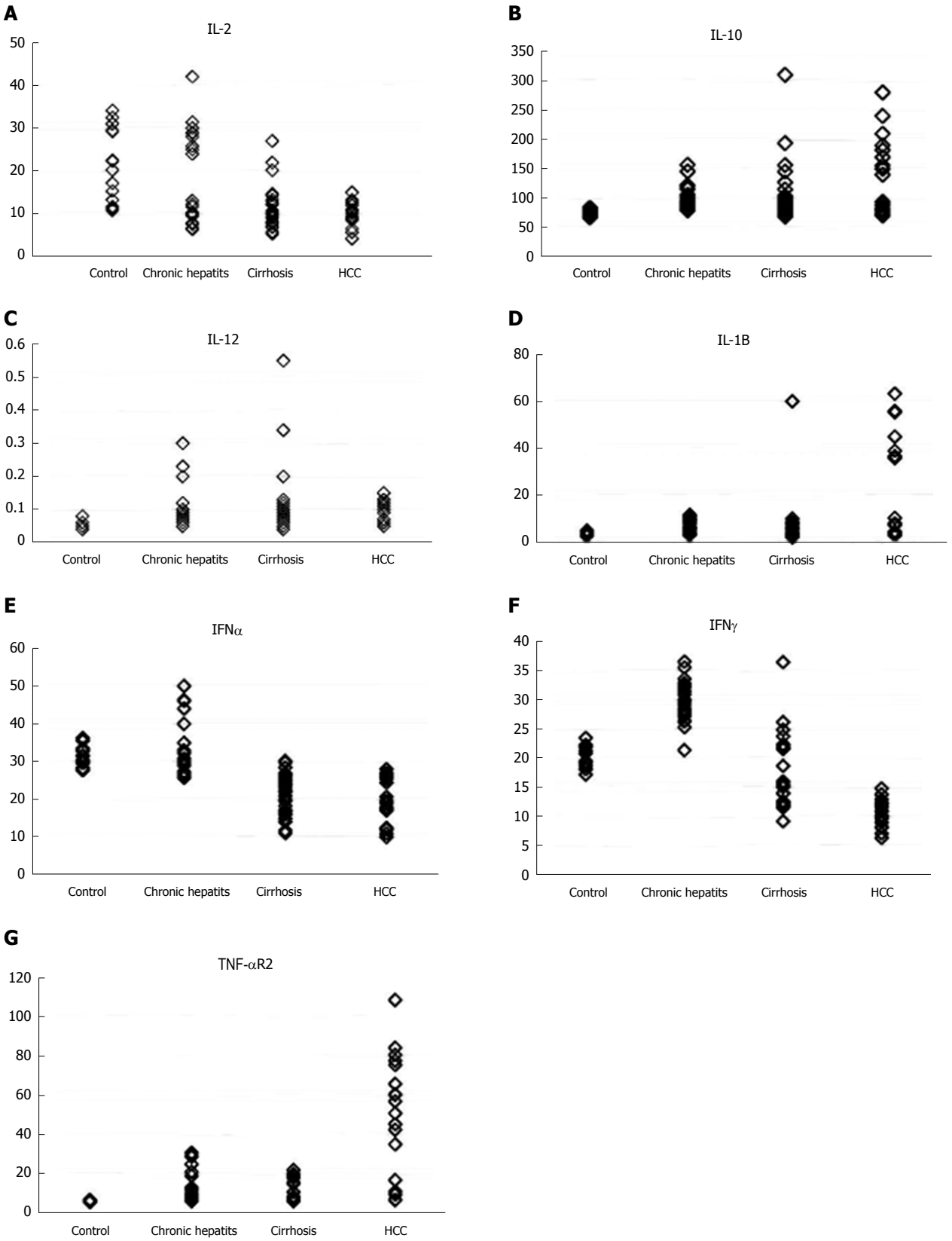

Figure 4 Different levels of serum cytokines in the four groups studied. A: IL-2; B: IL-10; C: IL-12; D: IL-1B; E: IFN-α; F: IFN-γ; G: TNF-αR2. IFN: Interferon; IL: Interleukin; TNF: Tumor necrosis factor.

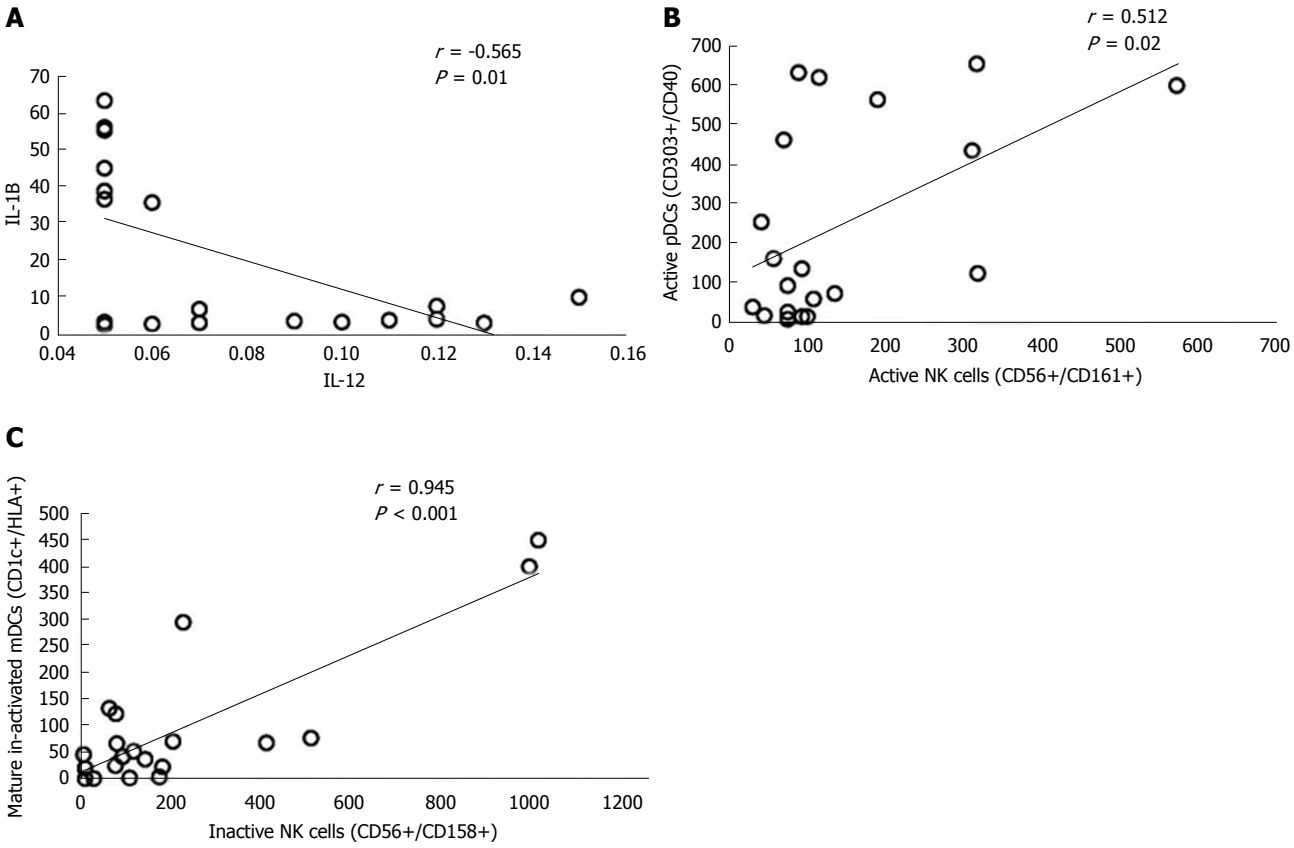

Figure 5 Correlation between immune cells and cytokine levels in hepatocellular carcinoma patients. IL: Interleukin; NK: Natural killer.

who found that NK cells cultured with cancer-associated fibroblasts from HCC (H-CAFs) down-regulate NKG2D and NKp46 and decrease expression of granzyme B, perforin and INF-γ. Later, another study showed that TGF-β and IL-10 in hepatic carcinoma patients induce the expression of microRNA (miR)-146a, which causes reduced IFN-γ production and cytotoxicity, resulting in a poorer prognosis[35]. Meanwhile, Zhang *et al*[36] found that MDSCs selectively suppressed the IFN-γ production deriving from NKT cells through membrane-bound TGF-β.

IL-2 plays a critical role in activation of the immune system, which could be used to eradicate cancer. It has been demonstrated as a monotherapy, and was approved for metastatic renal cell carcinoma and metastatic melanoma by the FDA[37]. Our results showed a significant increase in TNF-αR2 ($P < 0.001$) and significant decrease in IL-2 ($P < 0.001$) in HCC patients in relation to other groups, consistent with our previous results[38,39] that concluded the possible use of serum TNFR-II, IL-2Ra and IL-8 as combined biomarkers in HCV-infected patients at high risk of developing HCC.

Another important finding in the current study was that HCC patients had a significant decrease of active NK cells (CD56+/CD314+; $P < 0.05$) and active pDCs (CD303+, CD40+; $P < 0.05$) in comparison to inactive NK cells (CD56+/CD158+) and inactive pDCs (CD303+/HLA+) respectively. NK cells expressing CD56+/CD161+ and mDCs were not statistically affected. This revealed the importance of these two subsets of cells [active NK cells (CD56+/CD314+), and active pDCs (CD303+, CD40+)] in the pathogenesis of HCC, and allows for further research around the state of this imbalance that emerges in HCC patients.

We conclude that there are immunological changes occurring in HCC patients which could be possible candidate(s) for future immunotherapy for these patients. Among these are the NK cells expressing NKG2D and pDCs expressing CD40, IL-2 and IL-10. These factors could be implicated in the pathogenesis of HCC, and provide an attractive target for therapeutics in chronic HCV hepatitis and liver cancer.

ARTICLE HIGHLIGHTS

Research background

Hepatocellular carcinoma (HCC) is a major health problem worldwide and mainly in Egypt due to the high prevalence of hepatitis C virus (HCV) infection, especially of genotype IV. It ranks the first among cancers in males (33.6%), and the 2nd in females after breast cancer. Sorafenib is still the only treatment approved by the Food and Drug Administration for HCC; however, it extends the overall survival by 3 mo only. Hence, it is crucial to understand the underlying biological and immunological changes in HCC Egyptian patients, and to develop new treatment modalities based on these data.

Research motivation

The immune system plays an important role in suppression of cancer. However, tumors can escape immune surveillance by producing an immune-suppressive

environment, for which the underlying mechanisms are not fully clear. Recent studies show that the immune response in HCC patients is usually down-regulated by immunosuppressive cells (myeloid-derived suppressor cells and T regulatory cells) that are involved in chronic inflammation and tumor progression. Also, these inhibitory cells secrete many immune-suppressive cytokines, such as interleukin (IL)-6, IL-10 and transforming growth factor-β, creating a tolerogenic and suppressive environment[9].

Research objectives

The objective of this study was to assess the levels of different immune modulators and cytokines that may play a role in the pathogenesis of HCC and other hepatic diseases (*e.g.*, chronic hepatitis and liver cirrhosis) compared to a normal group. This would help in identifying additional therapeutic modalities for viral infections and HCC in the context of immunotherapy.

Research methods

This retrospective cohort study included 88 patients who attended the medical oncology clinics of the National Cancer Institute, Cairo University during the period from 2014 to 2016. Patients were divided into the HCC group (20 patients-G1), liver cirrhosis group (28 patients-G2), chronic hepatitis group (CH; 25 patients-G3) and normal healthy volunteers as a control group (NC; 15 persons). The immune system of the patients was assessed through immunophenotyping of CD1c and CD40, CD1c and HLA, CD303 and CD40, CD303 and HLA, CD56 and CD161, CD56 and CD314, and CD56 and CD158 by flow cytometry. On the other hand, serum levels of IL-2, IL-10, IL-12, IL-1β, interferon (IFN)-α, IFN-γ and tumor necrosis factor (TNF)-αR2 were measured by the ELISA technique, according to the manufacturer's instructions. Data were expressed as mean ± SE of mean, and statistical comparison between cytokine levels and immune cells were performed.

Research results

There was a significant decrease in active and inactive mDCs in HCC patients compared to the NC group, as well as active mDCs (CD1C+/CD40+) in cirrhotic patients compared to CH patients. The expression level of CD40+ on active pDCs (CD303+) was significantly decreased in HCC compared to the NC. However, there was no significant difference with the other groups (cirrhosis and CH). Meanwhile, the level of inactive pDCs (CD303+/HLA+) and inactive NK cells (CD56+/CD158+) did not differ significantly between the four groups studied.

The active NK cells (CD56+/CD161+) showed a significant increase in the CH group, whereas the level of active NK cells (CD56+/CD314+) was statistically decreased in HCC, CH and cirrhotic patients compared to the NC group, indicating an important role of these cells in the pathogenesis of HCC. The individual expression of each cell type in patients showed that active NK cells (CD56+/CD314+) were not expressed in 63% (12/20) of HCC patients.

There was a significant decrease in serum levels of IL-2, IFN-α and IFN-γ in HCC patients compared to the NC group, and a significant increase in serum levels of IL-10, IL-1β and TNF-αR2 in HCC compared to the NC group. However, there was no statistically significant change in the serum level of IL-12 among the four groups studied.

Research conclusions

We conclude that there are immunological changes occurring in HCC patients in relation to other liver diseases. The related immunological factors are NKG2D expressed on NK cells, and pDCs expressing CD40, IL-2 and IL-10. These factors could be implicated in the pathogenesis of HCC, and represent attractive targets for therapeutics in chronic HCV hepatitis and liver cancer.

Research perspectives

NKG2D, CD40, IL-2 and IL-10 could be a possible candidate for future immunotherapy for HCC patients. However, further studies are recommended regarding correlation of these factors and clincopathological features as well as the overall survival of the patients.

REFERENCES

1 **Ferlay J**, Soerjomataram I, Dikshit R, Eser S, Mathers C, Rebelo M, Parkin DM, Forman D, Bray F. Cancer incidence and mortality worldwide: sources, methods and major patterns in GLOBOCAN 2012. *Int J Cancer* 2015; **136**: E359-E386 [PMID: 25220842 DOI: 10.1002/ijc.29210]

2 **Ibrahim AS**, Khaled HM, Mikhail NN, Baraka H, Kamel H. Cancer incidence in egypt: results of the national population-based cancer registry program. *J Cancer Epidemiol* 2014; **2014**: 437971 [PMID: 25328522 DOI: 10.1155/2014/437971]

3 **Zekri AR**, Hafez MM, Bahnassy AA, Hassan ZK, Mansour T, Kamal MM, Khaled HM. Genetic profile of Egyptian hepatocellular-carcinoma associated with hepatitis C virus Genotype 4 by 15 K cDNA microarray: preliminary study. *BMC Res Notes* 2008; **1**: 106 [PMID: 18959789 DOI: 10.1186/1756-0500-1-106]

4 **Knudsen ES**, Gopal P, Singal AG. The changing landscape of hepatocellular carcinoma: etiology, genetics, and therapy. *Am J Pathol* 2014; **184**: 574-583 [PMID: 24388934 DOI: 10.1016/j.ajpath.2013.10.028]

5 **Llovet JM**, Villanueva A, Lachenmayer A, Finn RS. Advances in targeted therapies for hepatocellular carcinoma in the genomic era. *Nat Rev Clin Oncol* 2015; **12**: 408-424 [PMID: 26054909 DOI: 10.1038/nrclinonc.2015.103]

6 **Ostrand-Rosenberg S**. Tolerance and immune suppression in the tumor microenvironment. *Cell Immunol* 2016; **299**: 23-29 [PMID: 26435343 DOI: 10.1016/j.cellimm.2015.09.011]

7 **Gabrilovich DI**, Ostrand-Rosenberg S, Bronte V. Coordinated regulation of myeloid cells by tumours. *Nat Rev Immunol* 2012; **12**: 253-268 [PMID: 22437938 DOI: 10.1038/nri3175]

8 **Shrihari TG**. Dual role of inflammatory mediators in cancer. *Ecancermedicalscience* 2017; **11**: 721 [PMID: 28275390 DOI: 10.3332/ecancer.2017.721]

9 **Costa A**, Scholer-Dahirel A, Mechta-Grigoriou F. The role of reactive oxygen species and metabolism on cancer cells and their microenvironment. *Semin Cancer Biol* 2014; **25**: 23-32 [PMID: 24406211 DOI: 10.1016/j.semcancer.2013.12.007]

10 **Zeromski J**, Mozer-Lisewska I, Kaczmarek M, Kowala-Piaskowska A, Sikora J. NK cells prevalence, subsets and function in viral hepatitis C. *Arch Immunol Ther Exp* (Warsz) 2011; **59**: 449-455 [PMID: 21972016 DOI: 10.1007/s00005-011-0145-y]

11 **Zhong Z**, Sanchez-Lopez E, Karin M. Autophagy, Inflammation, and Immunity: A Troika Governing Cancer and Its Treatment. *Cell* 2016; **166**: 288-298 [PMID: 27419869 DOI: 10.1016/j.cell.2016.05.051]

12 **Lanier LL**. NK cell recognition. *Annu Rev Immunol* 2005; **23**: 225-274 [PMID: 15771571 DOI: 10.1146/annurev.immunol.23.021704.115526]

13 **Dai Z**, Turtle CJ, Booth GC, Riddell SR, Gooley TA, Stevens AM, Spies T, Groh V. Normally occurring NKG2D+CD4+ T cells are immunosuppressive and inversely correlated with disease activity in juvenile-onset lupus. *J Exp Med* 2009; **206**: 793-805 [PMID: 19289577 DOI: 10.1084/jem.20081648]

14 **Guerra N**, Tan YX, Joncker NT, Choy A, Gallardo F, Xiong N, Knoblaugh S, Cado D, Greenberg NM, Raulet DH. NKG2D-deficient mice are defective in tumor surveillance in models of spontaneous malignancy. *Immunity* 2008; **28**: 571-580 [PMID: 18394936 DOI: 10.1016/j.immuni.2008.02.016]

15 **Wu J**, Groh V, Spies T. T cell antigen receptor engagement and specificity in the recognition of stress-inducible MHC class I-related chains by human epithelial gamma delta T cells. *J Immunol* 2002; **169**: 1236-1240 [PMID: 12133944 DOI: 10.4049/jimmunol.169.3.1236]

16 **Burkholder B**, Huang RY, Burgess R, Luo S, Jones VS, Zhang W, Lv ZQ, Gao CY, Wang BL, Zhang YM, Huang RP. Tumor-induced perturbations of cytokines and immune cell networks. *Biochim Biophys Acta* 2014; **1845**: 182-201 [PMID: 24440852 DOI: 10.1016/j.bbcan.2014.01.004]

17 **Tel J**, van der Leun AM, Figdor CG, Torensma R, de Vries IJ. Harnessing human plasmacytoid dendritic cells as professional APCs. *Cancer Immunol Immunother* 2012; **61**: 1279-1288 [PMID: 22294456 DOI: 10.1007/s00262-012-1210-z]

18 **Korniluk A**, Koper O, Kemona H, Dymicka-Piekarska V. From

inflammation to cancer. *Ir J Med Sci* 2017; **186**: 57-62 [PMID: 27156054 DOI: 10.1007/s11845-016-1464-0]
19 **Kanterman J**, Sade-Feldman M, Baniyash M. New insights into chronic inflammation-induced immunosuppression. *Semin Cancer Biol* 2012; **22**: 307-318 [PMID: 22387003 DOI: 10.1016/j.semcancer.2012.02.008]
20 **Obermajer N**, Muthuswamy R, Lesnock J, Edwards RP, Kalinski P. Positive feedback between PGE2 and COX2 redirects the differentiation of human dendritic cells toward stable myeloid-derived suppressor cells. *Blood* 2011; **118**: 5498-5505 [PMID: 21972293 DOI: 10.1182/blood-2011-07-365825]
21 **Nakamoto Y**, Guidotti LG, Kuhlen CV, Fowler P, Chisari FV. Immune pathogenesis of hepatocellular carcinoma. *J Exp Med* 1998; **188**: 341-350 [PMID: 9670046 DOI: 10.1084/jem.188.2.341]
22 **Kakumu S**, Ito S, Ishikawa T, Mita Y, Tagaya T, Fukuzawa Y, Yoshioka K. Decreased function of peripheral blood dendritic cells in patients with hepatocellular carcinoma with hepatitis B and C virus infection. *J Gastroenterol Hepatol* 2000; **15**: 431-436 [PMID: 10824889 DOI: 10.1046/j.1440-1746.2000.02161.x]
23 **Dolganiuc A**, Chang S, Kodys K, Mandrekar P, Bakis G, Cormier M, Szabo G. Hepatitis C virus (HCV) core protein-induced, monocyte-mediated mechanisms of reduced IFN-alpha and plasmacytoid dendritic cell loss in chronic HCV infection. *J Immunol* 2006; **177**: 6758-6768 [PMID: 17082589 DOI: 10.4049/jimmunol.177.10.6758]
24 **Duramad O**, Fearon KL, Chan JH, Kanzler H, Marshall JD, Coffman RL, Barrat FJ. IL-10 regulates plasmacytoid dendritic cell response to CpG-containing immunostimulatory sequences. *Blood* 2003; **102**: 4487-4492 [PMID: 12946990 DOI: 10.1182/blood-2003-07-2465]
25 **Gonzalez-Carmona MA**, Lukacs-Kornek V, Timmerman A, Shabani S, Kornek M, Vogt A, Yildiz Y, Sievers E, Schmidt-Wolf IG, Caselmann WH, Sauerbruch T, Schmitz V. CD40ligand-expressing dendritic cells induce regression of hepatocellular carcinoma by activating innate and acquired immunity in vivo. *Hepatology* 2008; **48**: 157-168 [PMID: 18537185 DOI: 10.1002/hep.22296]
26 **Shurin MR**, Yurkovetsky ZR, Tourkova IL, Balkir L, Shurin GV. Inhibition of CD40 expression and CD40-mediated dendritic cell function by tumor-derived IL-10. *Int J Cancer* 2002; **101**: 61-68 [PMID: 12209589 DOI: 10.1002/ijc.10576]
27 **Tian Z**, Chen Y, Gao B. Natural killer cells in liver disease. *Hepatology* 2013; **57**: 1654-1662 [PMID: 23111952 DOI: 10.1002/hep.26115]
28 **Lanier LL**. NKG2D Receptor and Its Ligands in Host Defense. *Cancer Immunol Res* 2015; **3**: 575-582 [PMID: 26041808 DOI: 10.1158/2326-6066.CIR-15-0098]
29 **Yoon JC**, Lim JB, Park JH, Lee JM. Cell-to-cell contact with hepatitis C virus-infected cells reduces functional capacity of natural killer cells. *J Virol* 2011; **85**: 12557-12569 [PMID: 21937646 DOI: 10.1128/JVI.00838-11]
30 **Kamiya T**, Chang YH, Campana D. Expanded and Activated Natural Killer Cells for Immunotherapy of Hepatocellular Carcinoma. *Cancer Immunol Res* 2016; **4**: 574-581 [PMID: 27197065 DOI: 10.1158/2326-6066.CIR-15-0229]
31 **Oliviero B**, Varchetta S, Paudice E, Michelone G, Zaramella M, Mavilio D, De Filippi F, Bruno S, Mondelli MU. Natural killer cell functional dichotomy in chronic hepatitis B and chronic hepatitis C virus infections. *Gastroenterology* 2009; **137**: 1151-1160, 1160.e1-1160.e7 [PMID: 19470388 DOI: 10.1053/j.gastro.2009.05.047]
32 **Accapezzato D**, Francavilla V, Paroli M, Casciaro M, Chircu LV, Cividini A, Abrignani S, Mondelli MU, Barnaba V. Hepatic expansion of a virus-specific regulatory CD8(+) T cell population in chronic hepatitis C virus infection. *J Clin Invest* 2004; **113**: 963-972 [PMID: 15057302 DOI: 10.1172/JCI200420515]
33 **Wu Y**, Tian Z, Wei H. Developmental and Functional Control of Natural Killer Cells by Cytokines. *Front Immunol* 2017; **8**: 930 [PMID: 28824650 DOI: 10.3389/fimmu.2017.00930]
34 **Li T**, Yang Y, Hua X, Wang G, Liu W, Jia C, Tai Y, Zhang Q, Chen G. Hepatocellular carcinoma-associated fibroblasts trigger NK cell dysfunction via PGE2 and IDO. *Cancer Lett* 2012; **318**: 154-161 [PMID: 22182446 DOI: 10.1016/j.canlet.2011.12.020]
35 **Xu D**, Han Q, Hou Z, Zhang C, Zhang J. miR-146a negatively regulates NK cell functions via STAT1 signaling. *Cell Mol Immunol* 2017; **14**: 712-720 [PMID: 26996068 DOI: 10.1038/cmi.2015.113]
36 **Zhang H**, Li Z, Wang L, Tian G, Tian J, Yang Z, Cao G, Zhou H, Zhao L, Wu Z, Yin Z. Critical Role of Myeloid-Derived Suppressor Cells in Tumor-Induced Liver Immune Suppression through Inhibition of NKT Cell Function. *Front Immunol* 2017; **8**: 129 [PMID: 28243237 DOI: 10.3389/fimmu.2017.00129]
37 **Jiang T**, Zhou C, Ren S. Role of IL-2 in cancer immunotherapy. *Oncoimmunology* 2016; **5**: e1163462 [PMID: 27471638 DOI: 10.1080/2162402X.2016.1163462]
38 **Zekri AR**, Youssef AS, Bakr YM, Gabr RM, El-Rouby MN, Hammad I, Ahmed EA, Marzouk HA, Nabil MM, Hamed HA, Aly YH, Zachariah KS, Esmat G. Serum biomarkers for early detection of hepatocellular carcinoma associated with HCV infection in egyptian patients. *Asian Pac J Cancer Prev* 2015; **16**: 1281-1287 [PMID: 25735368 DOI: 10.7314/APJCP.2015.16.3.1281]
39 **Zekri AR**, Alam El-Din HM, Bahnassy AA, Zayed NA, Mohamed WS, El-Masry SH, Gouda SK, Esmat G. Serum levels of soluble Fas, soluble tumor necrosis factor-receptor II, interleukin-2 receptor and interleukin-8 as early predictors of hepatocellular carcinoma in Egyptian patients with hepatitis C virus genotype-4. *Comp Hepatol* 2010; **9**: 1 [PMID: 20051112 DOI: 10.1186/1476-5926-9-1]

P- Reviewer: Liu XL **S- Editor**: Wang JL **L- Editor**: Filipodia
E- Editor: Huang Y

World Journal of Gastroenterology

Submit a Manuscript: http://www.f6publishing.com

World J Gastroenterol 2018 March 21; 24(11): 1239-1249

DOI: 10.3748/wjg.v24.i11.1239

ISSN 1007-9327 (print) ISSN 2219-2840 (online)

ORIGINAL ARTICLE

Retrospective Study

Serum autotaxin levels are correlated with hepatic fibrosis and ballooning in patients with non-alcoholic fatty liver disease

Naoyuki Fujimori, Takeji Umemura, Takefumi Kimura, Naoki Tanaka, Ayumi Sugiura, Tomoo Yamazaki, Satoru Joshita, Michiharu Komatsu, Yoko Usami, Kenji Sano, Koji Igarashi, Akihiro Matsumoto, Eiji Tanaka

Naoyuki Fujimori, Takeji Umemura, Takefumi Kimura, Ayumi Sugiura, Tomoo Yamazaki, Satoru Joshita, Michiharu Komatsu, Akihiro Matsumoto, Eiji Tanaka, Department of Internal Medicine, Division of Gastroenterology, Shinshu University School of Medicine, Matsumoto 390-8621, Japan

Naoki Tanaka, Department of Metabolic Regulation, Shinshu University Graduate School of Medicine, Matsumoto, Japan, and Research Center for Agricultural Food Industry, Shinshu University, Matsumoto, 390-8621, Japan

Yoko Usami, Kenji Sano, Department of Laboratory Medicine, Shinshu University Hospital, Matsumoto 390-8621, Japan

Koji Igarashi, Bioscience Division, TOSOH Corporation, Kanagawa 252-1123, Japan

ORCID number: Naoyuki Fujimori (0000-0001-8744-8139); Takeji Umemura (0000-0001-7985-919X); Takefumi Kimura (0000-0002-1481-1029); Naoki Tanaka (0000-0002-0606-2101); Ayumi Sugiura (0000-0001-5427-7628); Tomoo Yamazaki (0000-0001-6958-1366); Satoru Joshita (0000-0002-6364-9654); Michiharu Komatsu (0000-0002-7860-2816); Yoko Usami (0000-0003-2230-5457); Kenji Sano (0000-0003-4312-2780); Koji Igarashi (0000-0002-5007-7079); Akihiro Matsumoto (0000-0001-6453-8529); Eiji Tanaka (0000-0002-0724-2104).

Author contributions: Umemura T designed the research; Kimura T, Sugiura A, Yamazaki T, Joshita S, Komatsu M and Matsumoto A treated the patients and collected materials and clinical data from patients; Usami Y and Igarashi K performed the assays; Sano K evaluated the histological findings, Fujimori N and Kimura T analyzed the data; Fujimori N, Kimura T and Tanaka N wrote the paper; Tanaka E supervised it.

Institutional review board statement: The study was reviewed and approved by the Committee for Medical Ethics of Shinshu University School of Medicine Institutional Review Board.

Informed consent statement: Written informed consent was obtained from all patients.

Conflict-of-interest statement: The authors declare that no conflict of interest exists.

Data sharing statement: No additional data are available.

Manuscript source: Invited manuscript

Correspondence to: Takefumi Kimura, MD, PhD, Doctor, Department of Internal Medicine, Division of Gastroenterology, Shinshu University School of Medicine, Asahi 3-1-1, Nagano, Matsumoto 390-8621, Japan. t_kimura@shinshu-u.ac.jp
Telephone: +81-263-372634
Fax: +81-263-329412

Received: January 17, 2018
Peer-review started: January 17, 2018
First decision: January 25, 2018
Revised: February 10, 2018
Accepted: March 3, 2018
Article in press: March 3, 2018
Published online: March 21, 2018

Abstract

AIM

To examine the relationship between serum autotaxin (ATX) concentrations and clinicopathological findings in non-alcoholic fatty liver disease (NAFLD) patients.

METHODS
One hundred eighty-six NAFLD patients who had undergone liver biopsy between 2008 and 2017 were retrospectively enrolled. Serum samples were collected at the time of biopsy and ATX was measured by enzyme immunoassays. Sera obtained from 160 healthy, non-obese individuals were used as controls. Histological findings were graded according to an NAFLD scoring system and correlations with serum ATX were calculated by Spearman's test. Diagnostic accuracy was evaluated using the area under the receiver operating characteristic curve (AUC). Cut-off values were identified by the Youden index, and the nearest clinically applicable value to the cutoff was considered the optimal threshold for clinical convenience.

RESULTS
Serum ATX levels were significantly higher in NAFLD patients than in controls (0.86 mg/L *vs* 0.76 mg/L, $P < 0.001$) and correlated significantly with ballooning score and fibrosis stage ($r = 0.36$, $P < 0.001$ and $r = 0.45$, $P < 0.001$, respectively). Such tendencies were stronger in female patients. There were no remarkable relationships between ATX and serum alanine aminotransferase, lipid profiles, or steatosis scores. The AUC values of ATX for predicting the presence of fibrosis (≥ F1), significant fibrosis (≥ F2), severe fibrosis (≥ F3), and cirrhosis (F4), were all more than 0.70 in respective analyses.

CONCLUSION
Serum ATX levels may at least partially reflect histological severity in NAFLD.

Key words: Autotaxin; Non-alcoholic fatty liver disease; Fibrosis; Ballooning

Core tip: Patients with non-alcoholic fatty liver disease (NAFLD) exhibited significantly higher serum levels of autotaxin (ATX) than did healthy subjects. Serum ATX levels correlated significantly with ballooning score and fibrosis stage in NAFLD patients and may therefore reflect histological severity in NAFLD.

Fujimori N, Umemura T, Kimura T, Tanaka N, Sugiura A, Yamazaki T, Joshita S, Komatsu M, Usami Y, Sano K, Igarashi K, Matsumoto A, Tanaka E. Serum autotaxin levels are correlated with hepatic fibrosis and ballooning in patients with non-alcoholic fatty liver disease. *World J Gastroenterol* 2018; 24(11): 1239-1249 Available from: URL: http://www.wjgnet.com/1007-9327/full/v24/i11/1239.htm DOI: http://dx.doi.org/10.3748/wjg.v24.i11.1239

INTRODUCTION

The prevalence of non-alcoholic fatty liver disease (NAFLD) is increasing worldwide[1,2]. NAFLD exhibits a wide spectrum, ranging from non-alcoholic fatty liver to non-alcoholic steatohepatitis (NASH) and ensuing cirrhosis and hepatocellular carcinoma[1-3]. Since the concept of NASH was developed using pathological characteristics, *i.e.*, the presence of hepatocyte ballooning and lobular inflammation in addition to macrovesicular steatosis, liver biopsy is currently considered the gold standard for evaluating NAFLD/NASH activity. However, general limitations of liver biopsy are the costs and invasiveness, but also sampling error and inter- and intra-observer variability[4]. So, simple, accurate, non-invasive, quantitative alternatives are needed. Several studies have attempted to estimate histological severity in NAFLD using various serum biomarkers[5-8], but the accuracy of these techniques remains unsatisfactory.

Autotaxin (ATX) was originally discovered in conditioned medium from human melanoma cell cultures[9]. The protein is encoded by ectonucleotide pyrophosphatase/phosphodiesterase family member 2 gene (*ENPP2*) and catalyzes the hydrolysis of lysophosphatidylcholine (LPC) to lysophosphatidic acid (LPA), which functions as a phospholipase[10,11]. Signaling *via* a family of six G-protein-coupled receptors (LPA_{1-6}) regulates the diverse cellular processes of ATX, including proliferation, migration, neurogenesis, angiogenesis, fibrogenesis, glucose homeostasis, insulin action, and cancer progression[12-18]. Disrupted LPC metabolism has been reported in murine NASH models[19,20].

ATX is synthesized by a variety of normal cells and tissues, secreted into the circulation as a glycoprotein, and later degraded by liver sinusoidal endothelial cells[21]. Serum ATX levels are reportedly increased during the progression of pregnancy[22] and in patients with idiopathic pulmonary fibrosis or some kinds of cancers[23-25]. Recently, elevated serum ATX has also been implicated in fibrosis progression in chronic hepatitis C[26,27], for which the retarded degradation of circulating ATX due to liver sinusoidal endothelial cell dysfunction from liver fibrosis was considered a main mechanism[28]. Perisinusoidal fibrosis is more frequently detected in alcoholic and non-alcoholic steatohepatitis than in viral hepatitis, with sinusoidal endothelial dysfunction also being reported in NAFLD[29].

Based on the above reports, we have hypothesized that serum ATX is increased in advanced stage NASH patients, but evidence is scarce on the relationship between circulating ATX concentration and histological severity in NAFLD. Accordingly, we measured serum ATX levels in 186 NAFLD patients who had undergone liver biopsy and examined for associations with clinicopathological findings.

MATERIALS AND METHODS

Patients and clinical examinations

This retrospective, cross-sectional study was approved by the Committee for Medical Ethics of Shinshu University School of Medicine (ID number: 3244) and performed

in accordance with the Helsinki declaration of 1975, 1983 revision. Informed consent was obtained from all patients. We enrolled 186 biopsy-proven Japanese NAFLD patients who were admitted to Shinshu University Hospital (Matsumoto, Japan) between November 2008 and May 2017. NAFLD was suspected based on the following criteria: (1) the presence of hepatorenal contrast and increased hepatic echogenicity on abdominal ultrasonography; (2) An average daily consumption of < 20 g/d of ethanol; And (3) the absence of other causes of liver dysfunction, such as viral hepatitis, drug-induced liver injury, autoimmune liver disease, primary sclerosing cholangitis, Wilson's disease, hereditary hemochromatosis, and citrin deficiency[30,31]. The diagnosis of NAFLD/NASH was confirmed with the histological findings of biopsied specimens. Body weight and height were measured before liver biopsy in a fasting state. All laboratory data were obtained in a fasting state on the day of liver biopsy. Homeostasis model assessment for insulin resistance (HOMA-IR), fibrosis-4 index (FIB-4), and aspartate aminotransferase (AST) to platelet ratio index (APRI) were calculated according to the following formulae: HOMA-IR = [fasting blood glucose (mg/dL) × fasting insulin (μU/mL)]/405[32,33], FIB-4 = [age (years) × AST (IU/L)]/[platelet count (10^9/L) × alanine aminotransferase (ALT) (IU/L)$^{1/2}$][34], and APRI = [AST/upper limit of normal; 28 (IU/L)] × [100/platelet count (10^9/L)][35]. One hundred sixty subjects (80 male and 80 female) whose liver function tests and body mass index (BMI) were within normal levels and having no past medical history of NAFLD were selected as healthy controls, with equal age distribution among the male and female individuals (twenties: 20 subjects, thirties: 20 subjects, forties: 20 subjects, fifties: 20 subjects). These healthy controls were same as our previous report[26]. Sera were obtained after overnight fasting on the day of the liver biopsy and stored at -80 ℃ until testing.

Measurement of ATX

Serum ATX concentrations were determined with a specific two-site enzyme immunoassay using the automated immunoassay analyzer AIA-2000 system (Tosoh Co., Tokyo, Japan), as described previously[36]. To prepare the 2-site immunoassay, R10.23 was digested with pepsin and the purified F(ab)$_2$ form using phenyl-5PW (Tosoh Co.) hydrophobic column chromatography in order to avoid the nonspecific binding of human antibodies against various animal IgG in human specimens, like human anti-mouse antibodies. Magnetic beads were coated with R10.23 F(ab)$_2$ and placed in the reaction cup, and 35 ng of alkaline phosphatase-labeled R10.21 in assay buffer (5% BSA, 5% sucrose, 10 mmol/L Tris-HCl, 10 mmol/L $MgCl_2$, pH 7.4) was added to the reaction cup. ATX assay reagent was prepared by immediate freeze-dry procedure of the reaction cup. The ATX assay reagent thus prepared can be used with AIA-system.

Histological findings

Liver specimens of at least 1.5 cm in length were obtained from segment 5 or 8 using 14-gauge needles, as described previously, and immediately fixed in 10% neutral formalin. Sections of 4 μm in thickness were cut and stained by means of the hematoxylin and eosin and Azan-Mallory methods. The histological activity of NAFLD was assessed by an independent expert pathologist (KS) in a blinded manner according to the NAFLD scoring system proposed by Kleiner *et al*[37]. Steatosis was graded as 0 to 3 based on the rate of steatotic hepatocytes (< 5%, 5%-33%, > 33-66%, and > 66%, respectively). Lobular inflammation was graded as 0 to 3 based on the overall assessment of all inflammatory foci (no foci, < 2 foci/200 × field, 2-4 foci/200× field, and > 4 foci/200× field, respectively). Ballooning grade was scored as 0-2 by the frequency of ballooned hepatocytes (none, few, and many, respectively). NAFLD activity score (NAS) was calculated as the sum of steatosis, lobular inflammation, and ballooning scores, and NASH was defined as the presence of macrovesicular steatosis (> 5% of hepatocytes affected) and hepatocyte ballooning with or without lobular inflammation and fibrosis. Fibrosis stage was scored as follows: F0, none; F1, perisinusoidal or periportal; F2, perisinusoidal and portal/periportal; F3, bridging fibrosis; and F4, cirrhosis.

Statistical analysis

Clinical data are expressed as the number (percentage) or median (interquartile range). Statistical analyses were performed using StatFlex Ver. 6.0 (Artech Co., Ltd., Osaka, Japan) and SPSS 24.0 (IBM, Chicago, IL, United States) software. The Mann-Whitney *U* test was used for comparisons between two groups. Bonferroni's correction test was performed for multiple comparisons. Correlation analysis was conducted by Spearman's test. Diagnostic accuracy was evaluated using the area under the receiver operating characteristic (ROC) curve (AUC). Cut-off values were identified by the Youden index, with the nearest clinically applicable value to the cutoff being considered as the optimal threshold for clinical convenience. All statistical tests were two-sided and evaluated at the 0.05 level of significance.

RESULTS

Serum ATX levels were higher in NAFLD patients

The clinicopathological features of the 186 NAFLD patients enrolled in this study are summarized in Table 1. Eighty (43%) were male, and median age was 56 years. The number of patients according to fibrosis stage F0, F1, F2, F3, and F4 was 35, 89, 19, 34, and 9, respectively. Comparisons between genders revealed

Table 1 Clinicopathological features of 186 patients with non-alcoholic fatty liver disease

	All (n = 186)	Male (n = 80)	Female (n = 106)	
	Median (IQR)/n	Median (IQR)/n	Median (IQR)/n	P value[1]
Age (yr)	56 (46-65)	50 (38-59)	61 (54-66)	< 0.001
BMI (kg/m^2)	26.2 (23.8-29.6)	26.1 (24.3-29.4)	26.5 (23.6-29.7)	NS
Laboratory data				
Albumin (g/dL)	4.5 (4.3-4.7)	4.6 (4.4-4.8)	4.4 (4.2-4.7)	< 0.001
T-bil (mg/dL)	0.87 (0.69-1.17)	0.94 (0.74-1.26)	0.81 (0.67-1.07)	< 0.05
AST (IU/L)	41 (30-65)	39 (30-62)	42 (30-69)	NS
ALT (IU/L)	63 (38-97)	68 (43-103)	53 (33-89)	NS
γ-GT (IU/L)	54 (35-92)	64 (43-99)	50 (32-81)	< 0.05
TG (mg/dL)	122 (92-159)	122 (91-159)	121 (95-159)	NS
LDL-C (mg/dL)	130 (107-151)	132 (105-154)	130 (109-149)	NS
HDL-C (mg/dL)	51 (44-60)	48 (44-56)	55 (47-63)	
Plt (× 10^4/μL)	23.1 (18.5-26.8)	23.0 (19.6-26.7)	23.3 (17.6-26.9)	NS
HbA1c (%)	5.9 (5.7-6.6)	5.9 (5.6-6.5)	5.9 (5.7-6.6)	NS
FBG (mg/dL)	108 (98-121)	108 (98-121)	108 (97-121)	NS
IRI (mU/L)	11.2 (7.2-16.7)	10.5 (6.8-16.3)	11.5 (7.4-17.2)	NS
HOMA-IR	3.0 (1.9-4.6)	2.9 (1.8-4.5)	3.2 (2.0-4.7)	NS
Fe (μg/dL)	111 (90-137)	120 (92-146)	104 (88-129)	< 0.05
Ferritin (ng/mL)	146 (79-274)	172 (126-293)	113 (58-236)	< 0.001
AFP (ng/mL)	3.2 (2.2-4.8)	2.8 (2.1-4.0)	3.4 (2.6-5.2)	< 0.01
Fibrosis markers				
HA (ng/mL)	51 (28-91)	41 (25-62)	63 (34-118)	< 0.001
4C7S (ng/mL)	4.6 (3.8-5.7)	4.5 (3.8-5.5)	4.7 (3.8-6.6)	NS
FIB-4	1.35 (0.94-2.18)	1.12 (0.77-1.88)	1.53 (1.13-2.51)	< 0.001
APRI	0.69 (0.46-1.13)	0.66 (0.44-1.03)	0.71 (0.46-1.25)	NS
Histological findings				
Steatosis (1/2/3)	57/90/39	24/41/15	33/49/24	NS
Lobular inflammation (0/1/2/3)	9/101/69/7	6/48/23/3	3/53/46/4	< 0.05
Ballooning (0/1/2)	43/98/45	22/44/14	21/54/31	NS
Fibrosis (0/1/2/3/4)	35/89/19/34/9	16/43/8/13/0	19/46/11/21/9	NS

[1]Comparison between male and female subjects. IQR: Interquartile range; BMI: Body mass index; T-bil: Total bilirubin; AST: Aspartate aminotransferase; ALT: Alanine aminotransferase; γ-GT: Gamma-glutamyltransferase; TG: Triglyceride; LDL-C: Low density lipoprotein cholesterol; HDL-C: High density lipoprotein cholesterol; Plt: Platelet; FBG: Fasting blood glucose; IRI: Immunoreactive insulin; HOMA-IR: Homeostasis model assessment of insulin resistance; AFP: Alpha-fetoprotein; HA: Hyaluronic acid; 4C7S: Type 4 collagen•7S; FIB-4: Fibrosis-4 index; APRI: AST to platelet ratio; NS: Not significant.

significant differences in fibrosis-related parameters, such as age, albumin, hyaluronic acid (HA), and FIB-4, but fibrosis stage distribution was comparable.

Median serum ATX levels were significantly higher in NAFLD patients than in healthy controls (0.86 *vs* 0.76 mg/L, $P < 0.001$) (Figure 1A). In agreement with a previous report demonstrating a gender difference in serum ATX levels[26], serum ATX levels were higher in female patients and controls than in their male counterparts (Figure 1B). The degree of a serum ATX concentration increase was significant in female NAFLD patients (Figure 1B).

Relationship between serum ATX levels and clinicopathological features in NAFLD patients

We observed significant but weak correlations between ATX and glucose metabolism, BMI, and iron status, but none with lipid profiles. ATX was significantly and positively correlated to the factors of age, AST, HA, type 4 collagen 7S (4C7S), FIB-4, and APRI and was significantly and negatively correlated to platelet count (Table 2), which supported an association with fibrosis stage in NAFLD[38]. Indeed, ATX was significantly and positively correlated with ballooning grade (r = 0.36, $P < 0.001$) and fibrosis stage (r = 0.45, $P < 0.001$) overall, with no significant relationships for steatosis grades (Table 2, Figure 2). These correlations were stronger for women than for men, as were the correlation coefficients for ballooning score and fibrosis stage (Table 2, Figure 3).

Performance of ATX for diagnosing fibrosis status

To assess the significance of ATX as a predictor of fibrosis stage, ROC analysis was performed. Cut off values, sensitivities, specificities, positive predictive values, negative predictive values, and accuracies for predicting the presence of fibrosis (≥ F1), significant fibrosis (≥ F2), severe fibrosis (≥ F3), and cirrhosis (F4) in overall, male, and female NAFLD patients are shown in Table 3, and these ROC curves are shown in Figure 4. The AUC values of ATX for predicting the presence of fibrosis (≥ F1), significant fibrosis (≥ F2), severe fibrosis (≥ F3), and cirrhosis (F4), were all more than 0.70 in respective analyses.

For comparison, ROC analysis of serum ATX and conventional fibrosis indicators (HA, 4C7S, APRI, and FIB-4) for determination of severe fibrosis (≥ F3) were performed (Table 4). Although sensitivity of ATX

Table 2 Correlation between autotaxin and clinicopathological findings

	All (n = 186)		Male (n = 80)		Female (n = 106)	
	r	P value	r	P value	r	P value
Age (yr)	0.48	< 0.001	0.45	< 0.001	0.28	< 0.01
BMI (kg/m^2)	0.18	< 0.05	0.06	NS	0.31	< 0.01
Platelet (× 10^4/μL)	-0.32	< 0.001	-0.28	< 0.05	-0.43	< 0.001
Albumin (g/dL)	-0.32	< 0.001	-0.10	NS	-0.31	< 0.01
AST (IU/L)	0.31	< 0.001	0.34	< 0.01	0.40	< 0.001
ALT (IU/L)	0.06	NS	0.14	NS	0.24	< 0.05
TG (mg/dL)	-0.09	NS	-0.14	NS	-0.08	NS
LDL-C (mg/dL)	-0.04	NS	-0.01	NS	-0.06	NS
HDL-C (mg/dL)	0.13	NS	-0.04	NS	-0.04	< 0.001
FBG (mg/dL)	0.22	< 0.01	0.36	0.001	0.21	< 0.05
IRI (mU/L)	0.20	< 0.01	0.15	NS	0.31	0.002
HOMA-IR	0.22	< 0.01	0.22	< 0.05	0.31	0.001
Fe (μg/dL)	0.09	NS	0.12	NS	0.35	< 0.001
Ferritin (ng/mL)	0.04	NS	0.22	NS	0.31	0.002
HA (ng/mL)	0.49	< 0.001	0.47	< 0.001	0.46	< 0.001
4C7S (ng/mL)	0.40	< 0.001	0.30	< 0.01	0.50	< 0.001
FIB-4	0.58	< 0.001	0.51	< 0.001	0.60	< 0.001
APRI	0.43	< 0.001	0.45	< 0.001	0.55	< 0.001
Histological findings						
Steatosis score	0.02	NS	0.12	NS	-0.03	NS
Lobular inflammation score	0.22	< 0.01	0.06	NS	0.25	< 0.01
Ballooning score	0.36	< 0.001	0.34	< 0.01	0.38	< 0.001
NAS	0.27	< 0.001	0.27	< 0.05	0.26	< 0.01
Fibrosis stage	0.45	< 0.001	0.44	< 0.001	0.53	< 0.001

Correlations were calculated using Spearman's test. ATX: Autotaxin; BMI: Body mass index; AST: Aspartate aminotransferase; ALT: Alanine aminotransferase; TG: Triglyceride; LDL-C: Low density lipoprotein cholesterol; HDL-C: High density lipoprotein cholesterol; FBG: Fasting blood glucose; IRI: Immunoreactive insulin; HOMA-IR: Homeostasis model assessment of insulin resistance; HA: Hyaluronic acid; 4C7S: Type 4 collagen•7S; FIB-4: Fibrosis-4 index; APRI: AST to platelet ratio; NAS: NAFLD activity score; NS: Not significant.

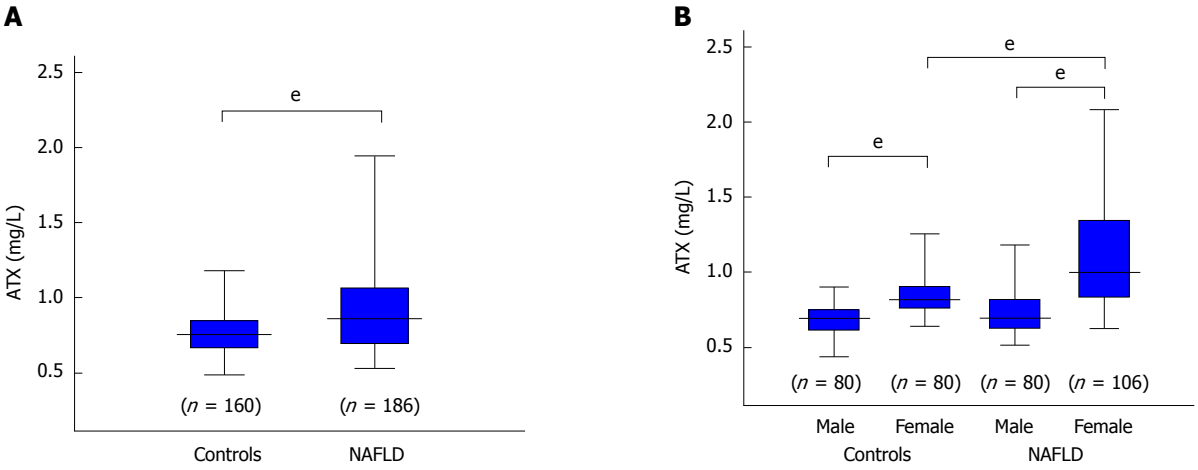

Figure 1 Comparison of autotaxin levels between controls and all patients with non-alcoholic fatty liver disease (A) and according to gender (B). The box plot shows the interquartile range, 95% confidence interval, and median. The difference between each group was tested with the Mann Whitney U test. ^eP < 0.001. ATX: Autotaxin; NAFLD: Non-alcoholic fatty liver disease.

is lower than those of HA, 4C7S, APRI, and FIB-4, specificity of ATX was highest (91%) compared to others.

DISCUSSION

Rachakonda *et al*[39] recently reported increased serum ATX levels in NAFLD patients. In severely obese and non-diabetic women, serum ATX was higher in those with NAFLD compared with those without NAFLD and positively correlated with insulin resistance. However, they did not assess liver pathology in their cohort of female subjects only. In this study, we compared serum ATX levels with clinicopathological background factors in biopsy-proven NAFLD patients and found that serum ATX levels were significantly related to hepatic fibrosis stage and ballooning score, implicating at least a partial reflection of histological severity in NAFLD.

Table 3 Diagnostic performance of autotaxin for predicting liver fibrosis stage in patients with non-alcoholic fatty liver disease

	Cut off	AUC	Sensitivity (%)	Specificity (%)	PPV (%)	NPV (%)	Accuracy (%)
All patients							
≥ F1	0.73	0.71	77	57	89	36	73
≥ F2	1.19	0.75	45	94	80	77	78
≥ F3	1.19	0.75	51	91	63	86	82
F4	1.20	0.87	78	85	21	99	84
Male							
≥ F1	0.70	0.73	58	94	97	36	65
≥ F2	0.71	0.75	81	68	47	91	71
F3	0.82	0.74	62	82	40	92	79
Female							
≥ F1	1.03	0.76	53	95	98	31	60
≥ F2	1.19	0.80	66	91	82	81	81
≥ F3	1.19	0.78	73	86	67	89	82
F4	1.20	0.78	78	74	22	97	75

ATX: Autotaxin; AUC: Area under the receiver operating characteristic curve; PPV: Positive predictive value; NPV: Negative predictive value.

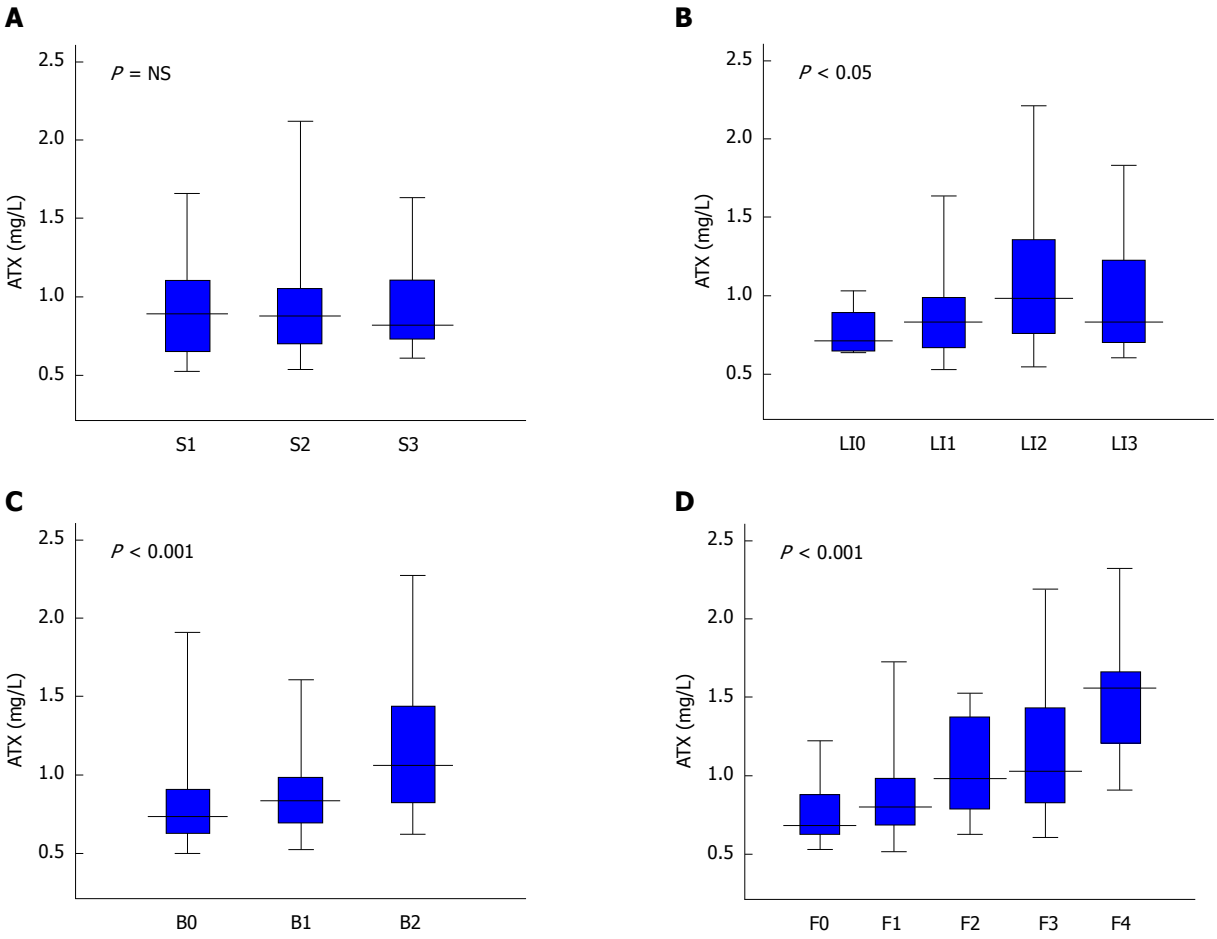

Figure 2 Relationship between autotaxin and histological grade in non-alcoholic fatty liver disease patients for steatosis (A), lobular inflammation (B), ballooning (C), and fibrosis (D). Table 1 presents the number of subjects for each histological stage. The Kruskal-Wallis test was used for multi-group simultaneous comparisons. *P* values are displayed in the upper left of each graph. ATX: Autotaxin; NAFLD: Non-alcoholic fatty liver disease; NS: Not significant.

The correlation between serum ATX levels and the severity of hepatic fibrosis has been explained by a mechanism of impaired circulating ATX degradation in damaged or impaired sinusoidal endothelial cells[28]. However, a recent study documented that ATX expression in hepatocytes activated hepatic stellate cells and amplified the fibrotic process, suggesting direct fibrosis-promoting properties of ATX[40]. Since ATX is a novel biomarker for hepatic fibrosis in chronic hepatitis C patients[26,27], we presumed similar results in NAFLD patients, but the correlation between ATX and fibrosis stage was comparatively weaker.

Table 4 Diagnostic performance of autotaxin and conventional fibrosis indicators for predicting severe fibrosis (≥ F3) in patients with non-alcoholic fatty liver disease

	AUC	Sensitivity (%)	Specificity (%)	PPV (%)	NPV (%)	Accuracy (%)
All patients						
ATX	0.75	51	91	63	86	82
HA	0.82	93	63	44	96	70
4C7S	0.87	75	88	64	92	85
APRI	0.82	60	89	62	88	82
FIB-4	0.85	79	74	48	92	75
Male						
ATX	0.74	62	82	40	92	79
HA	0.76	85	72	41	95	75
4C7S	0.81	69	89	56	94	86
APRI	0.74	77	64	29	93	66
FIB-4	0.81	92	75	41	98	78
Female						
ATX	0.78	73	86	67	89	82
HA	0.86	78	86	68	91	83
4C7S	0.89	78	90	75	92	87
APRI	0.86	63	95	83	87	86
FIB-4	0.85	80	75	56	90	76

AUC: Area under the receiver operating characteristic curve; PPV: Positive predictive value; NPV: Negative predictive value; ATX: Autotaxin; HA: Hyaluronic acid; 4C7S: Type 4 collagen•7S; APRI: AST to platelet ratio; FIB-4: Fibrosis-4 index.

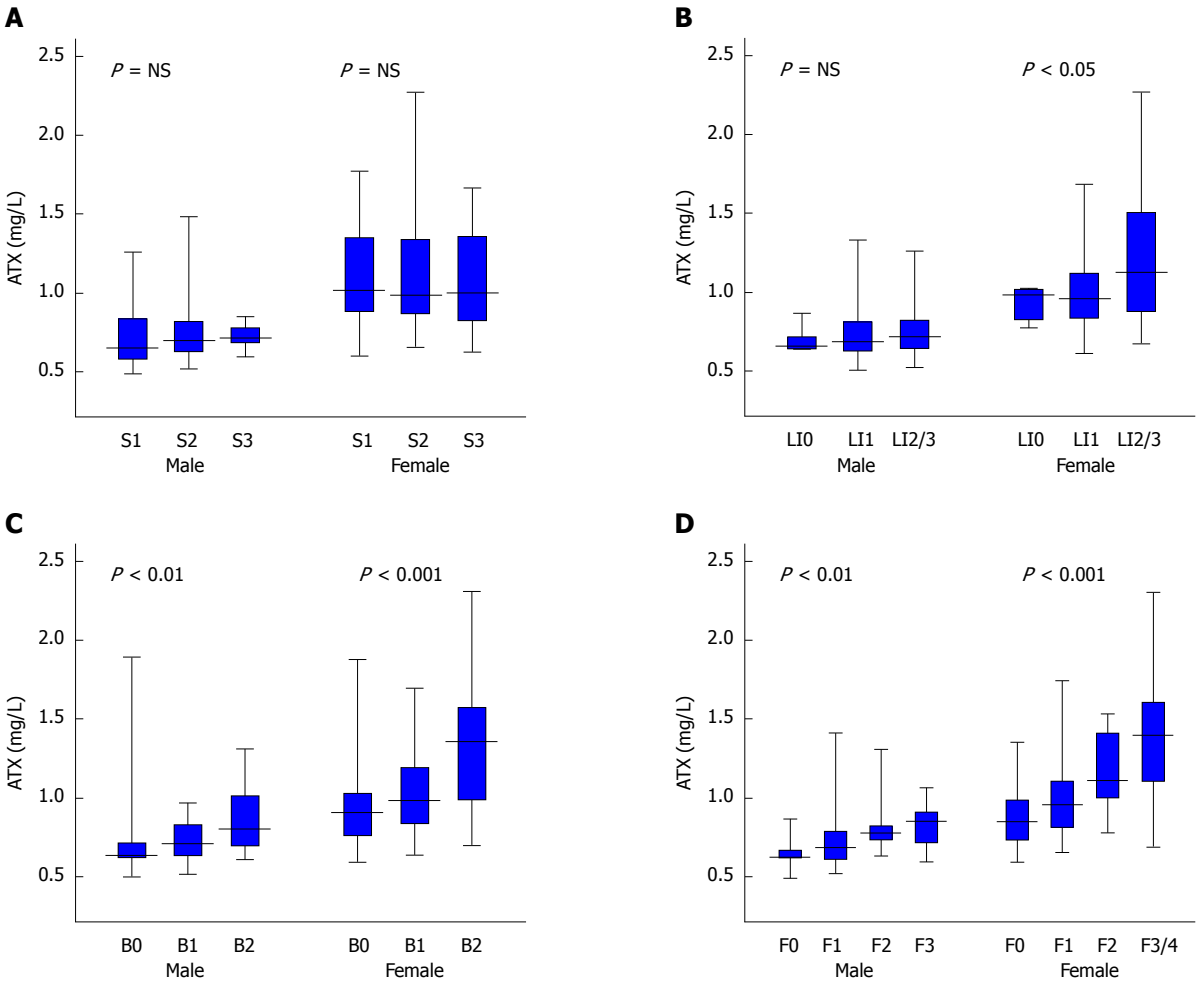

Figure 3 Relationship between autotaxin and histological grade in non-alcoholic fatty liver disease patients by gender for steatosis (A), lobular inflammation (B), ballooning (C), and fibrosis (D). Table 1 presents the number of subjects for each histological stage. The Kruskal-Wallis test was used for multi-group simultaneous comparisons. *P* values are displayed in the upper left of each graph. ATX: Autotaxin; NAFLD: Non-alcoholic fatty liver disease; NS: Not significant.

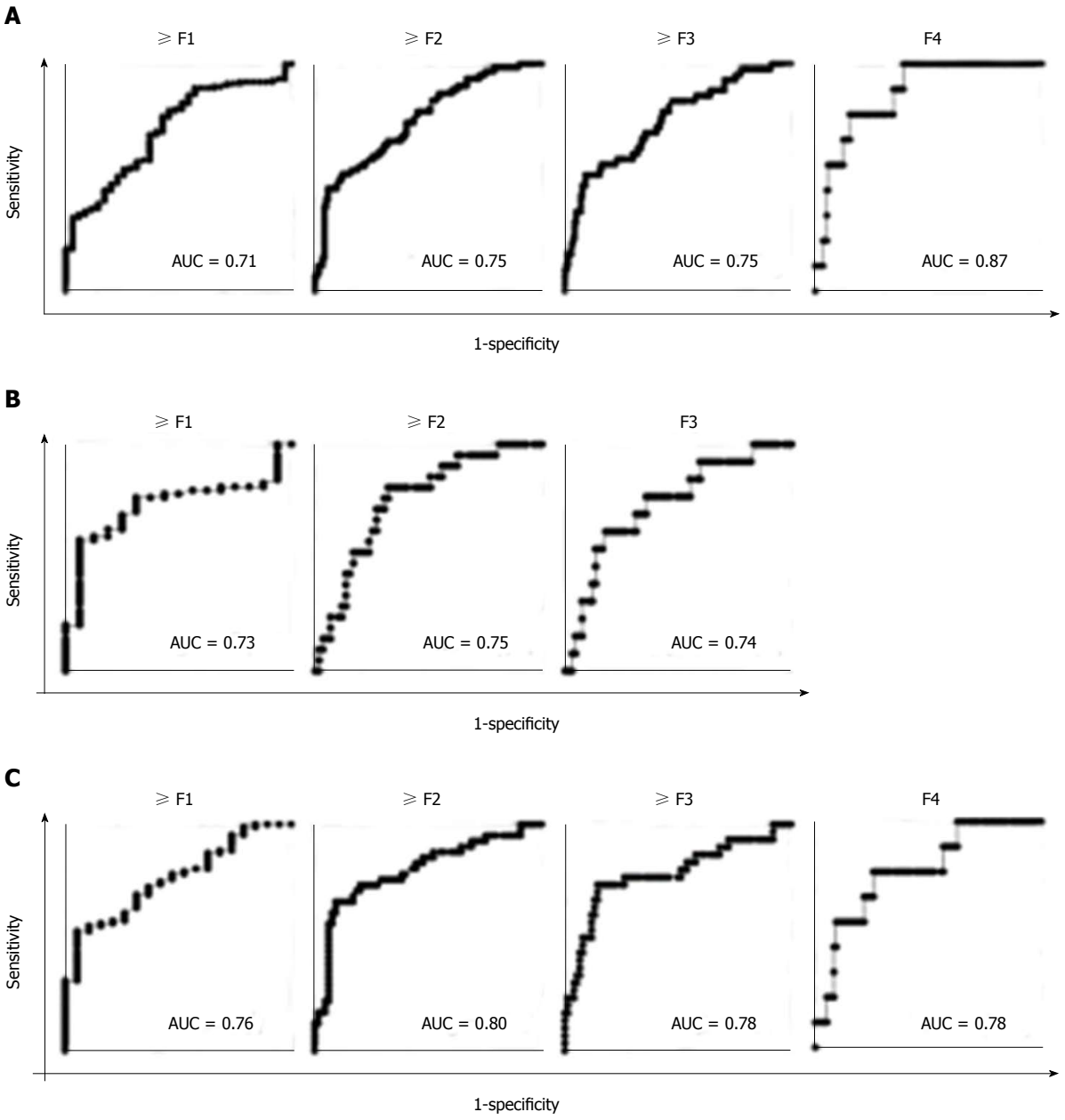

Figure 4 Receiver operating characteristic analysis of autotaxin for the estimation of the presence of fibrosis (≥ F1), significant fibrosis (≥ F2), severe fibrosis (≥ F3), and cirrhosis (F4) in all (A), male (B), and female (C) patients. The areas under the receiver operating characteristic curve are displayed in the lower right of each graph. AUC: Receiver operating characteristic curve; F: Fibrosis.

Thus, other mechanisms determining circulating ATX concentrations may exist as ATX is present in various tissues, such as white adipose tissue and the nervous system[41-43]. The importance of visceral fat has also been discussed[44], but in this study, we have not been able to examine waist circumference or waist-to-hip ratio, so this point is the limitation of this study.

In this study, we also conducted AUC analysis of ATX for determination of severe fibrosis (≥ F3) compared to conventional fibrosis indicators (HA, 4C7S, APRI, and FIB-4). AUC values and sensitivity of ATX was inferior to those other indicators[41], but specificity of ATX was highest among those other indicators. So ATX might be useful as a biomarker to exclude severe hepatic fibrosis.

Serum ATX levels were significantly associated with hepatocyte ballooning in our cohort, and a correlation was detected between fibrosis stage and ballooning grade (r = 0.56, P < 0.001). Ballooning degeneration is caused by an impaired intracellular cytoskeleton and resultant protein transport and appears after exposure to oxidative and endoplasmic reticulum stresses and during lipoapoptotic processes[45]. ATX expression was up-regulated by oxidative stress in microglia[46] and by LPC (18:1), an inducer of lipoapoptosis[47], in isolated hepatocytes[42]. Additionally, intravenous injection of LPC (18:1) into mice increased hepatic *Enpp2* mRNA expression and hepatocyte apoptosis[40]. These findings may explain how circulating ATX concentrations are

positively correlated with the prevalence of hepatocytes with ballooning degeneration.

In this study, we examined the relationship between NAFLD activity score as the severity of NAFLD/NASH and ATX, the correlation coefficient was significant but not high (r = 0.27, P < 0.001, Table 2). It seems difficult to predict the histological severity of NAFLD with ATX alone.

In conclusion, serum ATX levels were significantly higher in NAFLD patients over controls and correlated with ballooning score and fibrosis stage, especially in female patients. Further prospective research in larger cohorts is necessary for understanding the metabolism of circulating ATX in NAFLD.

ARTICLE HIGHLIGHTS

Research background

The prevalence of non-alcoholic fatty liver disease (NAFLD) is increasing worldwide. NAFLD exhibits a wide spectrum, ranging from non-alcoholic fatty liver to non-alcoholic steatohepatitis (NASH) and ensuing cirrhosis and hepatocellular carcinoma. Although the evaluation of NAFLD/NASH depends on the histological findings, there is a limitation and an alternative method is required.

Research motivation

Several studies have attempted to estimate histological severity in NAFLD using various serum biomarkers, but the accuracy of these techniques remains unsatisfactory.

Research objectives

Recently, elevated serum autotaxin (ATX) has been implicated in fibrosis progression in chronic liver disease, especially hepatitis C. So, we examine the relationship between serum ATX concentrations and clinicopathological findings in NAFLD patients.

Research methods

One hundred eighty-six NAFLD patients who had undergone liver biopsy between 2008 and 2017 were retrospectively enrolled. Serum samples were collected at the time of biopsy and ATX was measured by enzyme immunoassays. Sera obtained from 160 healthy, non-obese individuals were used as controls. Histological findings were graded according to an NAFLD scoring system and correlations with serum ATX were calculated by Spearman' s test. Diagnostic accuracy was evaluated using the area under the receiver operating characteristic curve (AUC). Cut-off values were identified by the Youden index, and the nearest clinically applicable value to the cutoff was considered the optimal threshold for clinical convenience.

Research results

Serum ATX levels were significantly higher in NAFLD patients than in controls (0.86 *vs* 0.76 mg/L, P < 0.001) and correlated significantly with ballooning score and fibrosis stage (r = 0.36, P < 0.001 and r = 0.45, P < 0.001, respectively). Such tendencies were stronger in female patients. There were no remarkable relationships between ATX and serum alanine aminotransferase, lipid profiles, or steatosis scores. The AUC values of ATX for predicting the presence of fibrosis (≥ F1), significant fibrosis (≥ F2), severe fibrosis (≥ F3), and cirrhosis (F4), were all more than 0.70 in respective analyses.

Research conclusions

Serum ATX levels may at least partially reflect histological severity in NAFLD.

Research perspectives

In order to evaluate the severity of NAFLD, it is considered that a method that can simultaneously evaluate activity and fibrosis is necessary.

REFERENCES

1 **Tanaka N**, Aoyama T, Kimura S, Gonzalez FJ. Targeting nuclear receptors for the treatment of fatty liver disease. *Pharmacol Ther* 2017; **179**: 142-157 [PMID: 28546081 DOI: 10.1016/j.pharmthera.2017.05.011]

2 **Bellentani S**. The epidemiology of non-alcoholic fatty liver disease. *Liver Int* 2017; **37** Suppl 1: 81-84 [PMID: 28052624 DOI: 10.1111/liv.13299]

3 **Cohen JC**, Horton JD, Hobbs HH. Human fatty liver disease: old questions and new insights. *Science* 2011; **332**: 1519-1523 [PMID: 21700865 DOI: 10.1126/science.1204265]

4 **Kobyliak N**, Abenavoli L. The role of liver biopsy to assess non-alcoholic fatty liver disease. *Rev Recent Clin Trials* 2014; **9**: 159-169 [PMID: 25514908]

5 **Sumida Y**, Nakajima A, Itoh Y. Limitations of liver biopsy and non-invasive diagnostic tests for the diagnosis of nonalcoholic fatty liver disease/nonalcoholic steatohepatitis. *World J Gastroenterol* 2014; **20**: 475-485 [PMID: 24574716 DOI: 10.3748/wjg.v20.i2.475]

6 **Giraudi PJ**, Gambaro SE, Ornelas Arroyo S, Chackelevicius CM, Giuricin M, Silvestri M, Macor D, Crocé LS, Bonazza D, Soardo G, de Manzini N, Zanconati F, Tiribelli C, Palmisano S, Rosso N. A simple in silico strategy identifies candidate biomarkers for the diagnosis of liver fibrosis in morbidly obese subjects. *Liver Int* 2018; **38**: 155-163 [PMID: 28650518 DOI: 10.1111/liv.13505]

7 **Tsutsui M**, Tanaka N, Kawakubo M, Sheena Y, Horiuchi A, Komatsu M, Nagaya T, Joshita S, Umemura T, Ichijo T, Matsumoto A, Yoshizawa K, Aoyama T, Tanaka E, Sano K. Serum fragmented cytokeratin 18 levels reflect the histologic activity score of nonalcoholic fatty liver disease more accurately than serum alanine aminotransferase levels. *J Clin Gastroenterol* 2010; **44**: 440-447 [PMID: 20104187 DOI: 10.1097/MCG.0b013e3181bdefe2]

8 **Kitabatake H**, Tanaka N, Fujimori N, Komatsu M, Okubo A, Kakegawa K, Kimura T, Sugiura A, Yamazaki T, Shibata S, Ichikawa Y, Joshita S, Umemura T, Matsumoto A, Koinuma M, Sano K, Aoyama T, Tanaka E. Association between endotoxemia and histological features of nonalcoholic fatty liver disease. *World J Gastroenterol* 2017; **23**: 712-722 [PMID: 28216979 DOI: 10.3748/wjg.v23.i4.712]

9 **Stracke ML**, Krutzsch HC, Unsworth EJ, Arestad A, Cioce V, Schiffmann E, Liotta LA. Identification, purification, and partial sequence analysis of autotaxin, a novel motility-stimulating protein. *J Biol Chem* 1992; **267**: 2524-2529 [PMID: 1733949]

10 **Nakanaga K**, Hama K, Aoki J. Autotaxin--an LPA producing enzyme with diverse functions. *J Biochem* 2010; **148**: 13-24 [PMID: 20495010 DOI: 10.1093/jb/mvq052]

11 **Umezu-Goto M**, Kishi Y, Taira A, Hama K, Dohmae N, Takio K, Yamori T, Mills GB, Inoue K, Aoki J, Arai H. Autotaxin has lysophospholipase D activity leading to tumor cell growth and motility by lysophosphatidic acid production. *J Cell Biol* 2002; **158**: 227-233 [PMID: 12119361 DOI: 10.1083/jcb.200204026]

12 **Moolenaar WH**. Lysophospholipids in the limelight: autotaxin takes center stage. *J Cell Biol* 2002; **158**: 197-199 [PMID: 12135981 DOI: 10.1083/jcb.200206094]

13 **van Meeteren LA**, Ruurs P, Stortelers C, Bouwman P, van Rooijen MA, Pradère JP, Pettit TR, Wakelam MJ, Saulnier-Blache JS, Mummery CL, Moolenaar WH, Jonkers J. Autotaxin, a secreted lysophospholipase D, is essential for blood vessel formation during development. *Mol Cell Biol* 2006; **26**: 5015-5022 [PMID: 16782887 DOI: 10.1128/MCB.02419-05]

14 **Pradère JP**, Tarnus E, Grès S, Valet P, Saulnier-Blache JS. Secretion and lysophospholipase D activity of autotaxin by adipocytes are controlled by N-glycosylation and signal peptidase. *Biochim Biophys Acta* 2007; **1771**: 93-102 [PMID: 17208043 DOI: 10.1016/j.bbalip.2006.11.010]

15 **Tager AM**, LaCamera P, Shea BS, Campanella GS, Selman M,

Zhao Z, Polosukhin V, Wain J, Karimi-Shah BA, Kim ND, Hart WK, Pardo A, Blackwell TS, Xu Y, Chun J, Luster AD. The lysophosphatidic acid receptor LPA1 links pulmonary fibrosis to lung injury by mediating fibroblast recruitment and vascular leak. *Nat Med* 2008; **14**: 45-54 [PMID: 18066075 DOI: 10.1038/nm1685]

16 **Castelino FV**, Seiders J, Bain G, Brooks SF, King CD, Swaney JS, Lorrain DS, Chun J, Luster AD, Tager AM. Amelioration of dermal fibrosis by genetic deletion or pharmacologic antagonism of lysophosphatidic acid receptor 1 in a mouse model of scleroderma. *Arthritis Rheum* 2011; **63**: 1405-1415 [PMID: 21305523 DOI: 10.1002/art.30262]

17 **Sakai N**, Chun J, Duffield JS, Wada T, Luster AD, Tager AM. LPA1-induced cytoskeleton reorganization drives fibrosis through CTGF-dependent fibroblast proliferation. *FASEB J* 2013; **27**: 1830-1846 [PMID: 23322166 DOI: 10.1096/fj.12-219378]

18 **Aikawa S**, Hashimoto T, Kano K, Aoki J. Lysophosphatidic acid as a lipid mediator with multiple biological actions. *J Biochem* 2015; **157**: 81-89 [PMID: 25500504 DOI: 10.1093/jb/mvu077]

19 **Tanaka N**, Matsubara T, Krausz KW, Patterson AD, Gonzalez FJ. Disruption of phospholipid and bile acid homeostasis in mice with nonalcoholic steatohepatitis. *Hepatology* 2012; **56**: 118-129 [PMID: 22290395 DOI: 10.1002/hep.25630]

20 **Tanaka N**, Takahashi S, Hu X, Lu Y, Fujimori N, Golla S, Fang ZZ, Aoyama T, Krausz KW, Gonzalez FJ. Growth arrest and DNA damage-inducible 45α protects against nonalcoholic steatohepatitis induced by methionine- and choline-deficient diet. *Biochim Biophys Acta* 2017; **1863**: 3170-3182 [PMID: 28844958 DOI: 10.1016/j.bbadis.2017.08.017]

21 **Jansen S**, Andries M, Vekemans K, Vanbilloen H, Verbruggen A, Bollen M. Rapid clearance of the circulating metastatic factor autotaxin by the scavenger receptors of liver sinusoidal endothelial cells. *Cancer Lett* 2009; **284**: 216-221 [PMID: 19482419 DOI: 10.1016/j.canlet.2009.04.029]

22 **Masuda A**, Fujii T, Iwasawa Y, Nakamura K, Ohkawa R, Igarashi K, Okudaira S, Ikeda H, Kozuma S, Aoki J, Yatomi Y. Serum autotaxin measurements in pregnant women: application for the differentiation of normal pregnancy and pregnancy-induced hypertension. *Clin Chim Acta* 2011; **412**: 1944-1950 [PMID: 21777571 DOI: 10.1016/j.cca.2011.06.039]

23 **Oikonomou N**, Mouratis MA, Tzouvelekis A, Kaffe E, Valavanis C, Vilaras G, Karameris A, Prestwich GD, Bouros D, Aidinis V. Pulmonary autotaxin expression contributes to the pathogenesis of pulmonary fibrosis. *Am J Respir Cell Mol Biol* 2012; **47**: 566-574 [PMID: 22744859 DOI: 10.1165/rcmb.2012-0004OC]

24 **Nakai Y**, Ikeda H, Nakamura K, Kume Y, Fujishiro M, Sasahira N, Hirano K, Isayama H, Tada M, Kawabe T, Komatsu Y, Omata M, Aoki J, Koike K, Yatomi Y. Specific increase in serum autotaxin activity in patients with pancreatic cancer. *Clin Biochem* 2011; **44**: 576-581 [PMID: 21439952 DOI: 10.1016/j.clinbiochem.2011.03.128]

25 **Xu A**, Ahsanul Kabir Khan M, Chen F, Zhong Z, Chen HC, Song Y. Overexpression of autotaxin is associated with human renal cell carcinoma and bladder carcinoma and their progression. *Med Oncol* 2016; **33**: 131 [PMID: 27757783 DOI: 10.1007/s12032-016-0836-7]

26 **Yamazaki T**, Joshita S, Umemura T, Usami Y, Sugiura A, Fujimori N, Shibata S, Ichikawa Y, Komatsu M, Matsumoto A, Igarashi K, Tanaka E. Association of Serum Autotaxin Levels with Liver Fibrosis in Patients with Chronic Hepatitis C. *Sci Rep* 2017; **7**: 46705 [PMID: 28425454 DOI: 10.1038/srep46705]

27 **Nakagawa H**, Ikeda H, Nakamura K, Ohkawa R, Masuzaki R, Tateishi R, Yoshida H, Watanabe N, Tejima K, Kume Y, Iwai T, Suzuki A, Tomiya T, Inoue Y, Nishikawa T, Ohtomo N, Tanoue Y, Omata M, Igarashi K, Aoki J, Koike K, Yatomi Y. Autotaxin as a novel serum marker of liver fibrosis. *Clin Chim Acta* 2011; **412**: 1201-1206 [PMID: 21419756 DOI: 10.1016/j.cca.2011.03.014]

28 **Ikeda H**, Yatomi Y. Autotaxin in liver fibrosis. *Clin Chim Acta* 2012; **413**: 1817-1821 [PMID: 22820036 DOI: 10.1016/j.cca.2012.07.014]

29 **Pasarín M**, La Mura V, Gracia-Sancho J, García-Calderó H, Rodríguez-Vilarrupla A, García-Pagán JC, Bosch J, Abraldes JG. Sinusoidal endothelial dysfunction precedes inflammation and fibrosis in a model of NAFLD. *PLoS One* 2012; **7**: e32785 [PMID: 22509248 DOI: 10.1371/journal.pone.0032785]

30 **Komatsu M**, Yazaki M, Tanaka N, Sano K, Hashimoto E, Takei Y, Song YZ, Tanaka E, Kiyosawa K, Saheki T, Aoyama T, Kobayashi K. Citrin deficiency as a cause of chronic liver disorder mimicking non-alcoholic fatty liver disease. *J Hepatol* 2008; **49**: 810-820 [PMID: 18620775 DOI: 10.1016/j.jhep.2008.05.016]

31 **Komatsu M**, Kimura T, Yazaki M, Tanaka N, Yang Y, Nakajima T, Horiuchi A, Fang ZZ, Joshita S, Matsumoto A, Umemura T, Tanaka E, Gonzalez FJ, Ikeda S, Aoyama T. Steatogenesis in adult-onset type II citrullinemia is associated with down-regulation of PPARα. *Biochim Biophys Acta* 2015; **1852**: 473-481 [PMID: 25533124 DOI: 10.1016/j.bbadis.2014.12.011]

32 **Matthews DR**, Hosker JP, Rudenski AS, Naylor BA, Treacher DF, Turner RC. Homeostasis model assessment: insulin resistance and beta-cell function from fasting plasma glucose and insulin concentrations in man. *Diabetologia* 1985; **28**: 412-419 [PMID: 3899825]

33 **Tanaka N**, Nagaya T, Komatsu M, Horiuchi A, Tsuruta G, Shirakawa H, Umemura T, Ichijo T, Matsumoto A, Yoshizawa K, Aoyama T, Kiyosawa K, Tanaka E. Insulin resistance and hepatitis C virus: a case-control study of non-obese, non-alcoholic and non-steatotic hepatitis virus carriers with persistently normal serum aminotransferase. *Liver Int* 2008; **28**: 1104-1111 [PMID: 18397231 DOI: 10.1111/j.1478-3231.2008.01737.x]

34 **Sterling RK**, Lissen E, Clumeck N, Sola R, Correa MC, Montaner J, S Sulkowski M, Torriani FJ, Dieterich DT, Thomas DL, Messinger D, Nelson M; APRICOT Clinical Investigators. Development of a simple noninvasive index to predict significant fibrosis in patients with HIV/HCV coinfection. *Hepatology* 2006; **43**: 1317-1325 [PMID: 16729309 DOI: 10.1002/hep.21178]

35 **Wai CT**, Greenson JK, Fontana RJ, Kalbfleisch JD, Marrero JA, Conjeevaram HS, Lok AS. A simple noninvasive index can predict both significant fibrosis and cirrhosis in patients with chronic hepatitis C. *Hepatology* 2003; **38**: 518-526 [PMID: 12883497 DOI: 10.1053/jhep.2003.50346]

36 **Nakamura K**, Igarashi K, Ide K, Ohkawa R, Okubo S, Yokota H, Masuda A, Oshima N, Takeuchi T, Nangaku M, Okudaira S, Arai H, Ikeda H, Aoki J, Yatomi Y. Validation of an autotaxin enzyme immunoassay in human serum samples and its application to hypoalbuminemia differentiation. *Clin Chim Acta* 2008; **388**: 51-58 [PMID: 17963703 DOI: 10.1016/j.cca.2007.10.005]

37 **Kleiner DE**, Brunt EM, Van Natta M, Behling C, Contos MJ, Cummings OW, Ferrell LD, Liu YC, Torbenson MS, Unalp-Arida A, Yeh M, McCullough AJ, Sanyal AJ; Nonalcoholic Steatohepatitis Clinical Research Network. Design and validation of a histological scoring system for nonalcoholic fatty liver disease. *Hepatology* 2005; **41**: 1313-1321 [PMID: 15915461 DOI: 10.1002/hep.20701]

38 **Nagaya T**, Tanaka N, Komatsu M, Ichijo T, Sano K, Horiuchi A, Joshita S, Umemura T, Matsumoto A, Yoshizawa K, Aoyama T, Kiyosawa K, Tanaka E. Development from simple steatosis to liver cirrhosis and hepatocellular carcinoma: a 27-year follow-up case. *Clin J Gastroenterol* 2008; **1**: 116-121 [PMID: 26193649 DOI: 10.1007/s12328-008-0017-0]

39 **Rachakonda VP**, Reeves VL, Aljammal J, Wills RC, Trybula JS, DeLany JP, Kienesberger PC, Kershaw EE. Serum autotaxin is independently associated with hepatic steatosis in women with severe obesity. *Obesity* (Silver Spring) 2015; **23**: 965-972 [PMID: 25865747 DOI: 10.1002/oby.20960]

40 **Kaffe E**, Katsifa A, Xylourgidis N, Ninou I, Zannikou M, Harokopos V, Foka P, Dimitriadis A, Evangelou K, Moulas AN, Georgopoulou U, Gorgoulis VG, Dalekos GN, Aidinis V. Hepatocyte autotaxin expression promotes liver fibrosis and cancer. *Hepatology* 2017; **65**: 1369-1383 [PMID: 27981605 DOI: 10.1002/hep.28973]

41 **Sumida Y**, Yoneda M, Hyogo H, Itoh Y, Ono M, Fujii H, Eguchi Y, Suzuki Y, Aoki N, Kanemasa K, Fujita K, Chayama K, Saibara T, Kawada N, Fujimoto K, Kohgo Y, Yoshikawa T, Okanoue T; Japan

Study Group of Nonalcoholic Fatty Liver Disease (JSG-NAFLD). Validation of the FIB4 index in a Japanese nonalcoholic fatty liver disease population. *BMC Gastroenterol* 2012; **12**: 2 [PMID: 22221544 DOI: 10.1186/1471-230X-12-2]

42 **D'Souza K**, Kane DA, Touaibia M, Kershaw EE, Pulinilkunnil T, Kienesberger PC. Autotaxin Is Regulated by Glucose and Insulin in Adipocytes. *Endocrinology* 2017; **158**: 791-803 [PMID: 28324037 DOI: 10.1210/en.2017-00035]

43 **Yuelling LM**, Fuss B. Autotaxin (ATX): a multi-functional and multi-modular protein possessing enzymatic lysoPLD activity and matricellular properties. *Biochim Biophys Acta* 2008; **1781**: 525-530 [PMID: 18485925 DOI: 10.1016/j.bbalip.2008.04.009]

44 **Finelli C**, Sommella L, Gioia S, La Sala N, Tarantino G. Should visceral fat be reduced to increase longevity? *Ageing Res Rev* 2013; **12**: 996-1004 [PMID: 23764746 DOI: 10.1016/j.arr.2013.05.007]

45 **Bedossa P**. Pathology of non-alcoholic fatty liver disease. *Liver Int* 2017; **37** Suppl 1: 85-89 [PMID: 28052629 DOI: 10.1111/liv.13301]

46 **Awada R**, Rondeau P, Grès S, Saulnier-Blache JS, Lefebvre d' Hellencourt C, Bourdon E. Autotaxin protects microglial cells against oxidative stress. *Free Radic Biol Med* 2012; **52**: 516-526 [PMID: 22155714 DOI: 10.1016/j.freeradbiomed.2011.11.014]

47 **Kakisaka K**, Cazanave SC, Fingas CD, Guicciardi ME, Bronk SF, Werneburg NW, Mott JL, Gores GJ. Mechanisms of lysophosphatidylcholine-induced hepatocyte lipoapoptosis. *Am J Physiol Gastrointest Liver Physiol* 2012; **302**: G77-G84 [PMID: 21995961 DOI: 10.1152/ajpgi.00301.2011]

P- Reviewer: Abenavoli L, Esmat S, Tarantino G **S- Editor**: Wang XJ
L- Editor: A **E- Editor**: Huang Y

World Journal of Gastroenterology

Submit a Manuscript: http://www.f6publishing.com

World J Gastroenterol 2018 March 21; 24(11): 1250-1258

DOI: 10.3748/wjg.v24.i11.1250

ISSN 1007-9327 (print) ISSN 2219-2840 (online)

ORIGINAL ARTICLE

Retrospective Study

Epidemiological features of chronic hepatitis C infection caused by remunerated blood donors: A nearly 27-year period survey

You-Wen Tan, Yan Tao, Long-Gen Liu, Yun Ye, Xin-Bei Zhou, Li Chen, Cong He

You-Wen Tan, Yan Tao, Yun Ye, Xin-Bei Zhou, Li Chen, Cong He, Department of Hepatology, The Third Hospital of Zhenjiang Affiliated Jiangsu University, Zhenjiang 212003, Jiangsu Province, China

Long-Gen Liu, Department of Hepatology, The Third People's Hospital of Changzhou, Changzhou 213001, Jiangsu Province, China

ORCID number: You-Wen Tan (0000-0002-5464-1407); Yan Tao (0000-0002-3502-6548); Long-Gen Liu (0000-0001-8652-2499); Yun Ye (0000-0002-0286-7359); Xin-Bei Zhou (0000-0002-8220-0377); Li Chen (0000-0002-9045-6292); Cong He (0000-0003-4085-5380).

Author contributions: Tan YW, Tao Y and Liu LG contributed equally to this work; Tan YW designed the research; Tao Y, Ye Y, Zhou XB, Chen L, He C and Liu LG collected and analyzed the data and drafted the manuscript; Tao Y and Ye Y performed the research; Ye Y and He C interpreted the data and revised the statistical analysis; Tan YW and Tao Y wrote and revised the article; all authors have read and approved the final version to be published.

Supported by the Preventive Medicine research projects of Jiangsu Province, No. Y2012016 and the Social Development Project of Zhenjiang City, No. SH2014060. The funders had no role in study design, data collection and analysis, nor decision to publish.

Institutional review board statement: The study was reviewed and approved for publication by our Institutional Reviewer.

Informed consent statement: All study participants or their legal guardian provided informed written consent about personal and medical data collection prior to study enrolment.

Conflict-of-interest statement: To the best of our knowledge, no conflict of interest exists.

Data sharing statement: The original anonymous dataset is available upon request from the corresponding author at tyw915@sina.com.

Manuscript source: Unsolicited manuscript

Correspondence to: You-Wen Tan, PhD, Attending Doctor, Chief Doctor, Department of Hepatology, The Third Hospital of Zhenjiang Affiliated Jiangsu University No. 300, Daijiamen, Runzhou Distinct, Zhenjiang 212003, Jiangsu Province, China. tyw915@sina.com
Telephone: +86-13914567088
Fax: +86-511-88970796

Received: January 9, 2018
Peer-review started: January 9, 2018
First decision: January 25, 2018
Revised: February 1, 2018
Accepted: February 9, 2018
Article in press: February 9, 2018
Published online: March 21, 2018

Abstract

AIM

To understand the prevalence of hepatitis C virus (HCV) infection in blood donors over a nearly 27-year interval and to explore the factors that affect the outcome of HCV infection.

METHODS

A retrospective and cross-sectional study was conducted. The participants, mostly plasma donors, were selected from three administrative villages in the Jiangsu province in Eastern China. A questionnaire was administered among the villagers who had a history of blood donation from the late 1980s to the early 1990s. All participants underwent physical examination, liver B-ultrasonography, and liver stiffness measurement. In addition, 10 mL of blood was collected from each participant to measure simple liver function parameters (albumin, alanine aminotransferase, aspirate aminotransferase), blood factors (platelet), and for hepatitis B surface antigen, antiHCV, and antihuman immunodeficiency virus detection. HCV RNA detection, HCV genotyping, and other tests were carried out in antiHCV-positive patients.

RESULTS

After a median of 27 years (25-31 years) from the last blood donation to the time of survey, a total of 1694 participants were investigated, and the antiHCV-positive individuals were categorized into three groups: blood donors (*n* = 12, 3.3%), plasma donors (*n* = 534, 68.5%), and mixed donors (*n* = 324, 58.8%). A total of 592 (68.05%) patients had detectable HCV RNA, and 91.9% had genotype 1b. A total of 161 (27.2%, 161/592) patients with chronic HCV were considered to have cirrhosis with a liver stiffness measurement level higher than 12 kPa. Multiple logistic (binary) regression analysis results showed that platelet and IgG levels were associated with cirrhosis.

CONCLUSION

The nearly 27-year interval investigation revealed that chronic hepatitis C infection is a very serious public health problem in Eastern China. Plasma donation and subsequent return of blood cells to the donor are the main causes of hepatitis C infection. The main HCV genotype is 1b. Nearly 28% of cases progressed to cirrhosis. Age, especially over 60 years, and regular drinking habits were risk factors associated with cirrhosis.

Key words: Blood donor; Hepatitis C; Cross-sectional study; Epidemiologic; China

Core tip: A retrospective and cross-sectional study was conducted. A total of 1694 participants were investigated and categorized into three groups: 2 (3.3%), 534 (68.5%), and 324 (58.8%) patients positive for anti-hepatitis C virus (HCV) in blood donor, single plasma donor, and mixed donor groups, respectively. A total of 592 (68.05%) cases had detectable HCV RNA, and genotype 1b accounted for 91.9%. A total of 161 (27.2%, 161/592) patients with chronic HCV were considered to have cirrhosis with a liver stiffness measurement level of more than 12 kPa. Multiple logistic (binary) regression analysis results showed that platelet and IgG levels were associated with cirrhosis.

Tan YW, Tao Y, Liu LG, Ye Y, Zhou XB, Chen L, He C. Epidemiological features of chronic hepatitis C infection caused by remunerated blood donors: A nearly 27-year period survey. *World J Gastroenterol* 2018; 24(11): 1250-1258 Available from: URL: http://www.wjgnet.com/1007-9327/full/v24/i11/1250.htm DOI: http://dx.doi.org/10.3748/wjg.v24.i11.1250

INTRODUCTION

Hepatitis C infection is a major global public health problem. The World Health Organization estimated that the global hepatitis C virus (HCV) infection rate is about 2.8% and that about 170 million people are infected with chronic HCV. Approximately 350000 people die each year from hepatitis C-related liver diseases[1,2]. However, because of the occult nature of HCV, most people who are infected have no knowledge of their HCV infection; thus, the global incidence of chronic hepatitis C (CHC) is not clear. A Serum Hepatitis C Epidemiology Survey carried out in 2006 in China showed that the general population aged 1-59 years has an antiHCV-carrying rate of 0.43% and in the global range, HCV infection has low prevalence in some areas[3].

HCV is mainly transmitted through contact with the blood of an infected person; thereby, blood donors, especially plasma donors, are high-risk groups for HCV infection[4]. A study in remunerated blood donors reported an increased HCV infection rate of 15.53%[5] due to the use of nonsterile medical devices and other reasons.

The phenomenon of remunerated blood donation has been reported to occur in underdeveloped rural areas with low economic status, from the late 1980s to the early 1990s. Moreover, most of these hepatitis C-infected individuals had no history of seeking any medical assistance and had no knowledge about their HCV status; although, a considerable proportion of infections among those who have progressed to cirrhosis or even to hepatocellular carcinoma (HCC) were found.

The natural history of HCV has not been as fully delineated as that of hepatitis B virus[6]. Some epidemiological studies suggest that an estimated nearly 55%-85% of the individuals infected with acute hepatitis C will develop CHC, and nearly 5%-15% of patients with CHC will progress to cirrhosis after 20 years[7]. However, the conclusions of these epidemiological studies differ widely and lack longer epidemiological surveys. The main reason is the lack of a relatively fixed CHC epidemiological population.

A CHC population infected through plasma apheresis donation has a relatively consistent infection time and place. Most of these patients with hepatitis C infection did not seek medical assistance. These characteristics have created a unique advantage for the study of the natural history of hepatitis C.

We, therefore, chose to study the natural administrative villages in Jiangsu, a province in Eastern China where most villagers are plasma donors, in order to further understand the prevalence and the prognosis of HCV infection over nearly 30 years and to explore the factors that affect the outcome of this infection.

MATERIALS AND METHODS

Ethics statement

The study was approved by the Medical Ethics Committee of the Third Hospital of Zhenjiang Affiliated Jiangsu University, and written informed consent was obtained from each patient prior to participation. The study was conducted in compliance with the Declaration of Helsinki.

Participation and methods

A retrospective and cross-sectional study was conducted. The research team was composed of a staff of more than 20 trained individuals, including specialist doctors, technicians, community doctors, nurses, epidemiological researchers, medical graduate students, *etc*. Before the survey, a formal survey plan was drafted in advance and a standard questionnaire formulated. Two weeks prior to the survey, a research representative informed participants about the questionnaire and their physical and ultrasound examinations, and provided information about any matter requiring attention. Signed informed consent was obtained before the study started in the community hospital at the appointed time.

Research participation: The participants were selected from three administrative villages in the Jiangsu province in Eastern China, where most people are plasma donors, and the questionnaires were carried out among the villagers who had a history of plasma extraction. The participants had signed written informed consent. The inclusion criteria were the following: (1) a history of remunerated blood donation from the late 1980s to the early 1990s; (2) age above 40 years; (3) voluntary provision of contact information; and (4) no HCV treatment performed. Qualified subjects participated in the health examination and questionnaire from March to May 2017.

Investigation methods: The researchers conducted a unified training. The questionnaire submitted to the patients included: social demographic characteristics; history of common diseases, viral hepatitis, family diseases, and remunerated blood donations; and blood transfusion methods. All participants underwent physical examination, liver B-ultrasound and liver stiffness measurement (LSM). In addition, 10 mL of blood were collected for simple liver function parameter analysis [albumin (ALB), alanine aminotransferase (ALT); aspartate aminotransferase (AST)], blood routine [platelet (PLT)], and hepatitis B surface antigen (HBsAg), antiHCV, and antihuman immunodeficiency virus (HIV) detection.

Detection for HCV RNA, HCV genotyping, and other tests were carried out in antiHCV-positive patients. HCV RNA from subjects' sera was quantified in fresh or well-preserved stored samples by commercial quantitative assays, such as real-time PCR (COBAS AmpliPrep/COBAS *Taq*Man HCV Test; Roche, DaAn Gene Co., Nanjing, China). The HCV genotype was assessed in all patients with detectable HCV RNA. We used a PCR assay based on reverse transcription of the HCV core region with genotype-specific primers, in accordance with the international classification (*i.e.* Ⅰa, Ⅰb, Ⅱa, Ⅱb, Ⅲ, Ⅳ, Ⅴ and Ⅵ) (DaAn Gene Co,). Antinuclear antibody (ANA) and smooth muscle actin (SMA) determination was carried out using indirect immunofluorescence.

LSM

LSM using transient elastography (TE) (FibroScan502®; Echosens, Paris, France) was performed with the 3.5 MHz standard probe operated by a skillful operator (experience: > 10000 measurements) in a blinded manner. As previously described, the examination was carried out with the patient lying down in a supine position with the right arm placed behind the head. The tip of the probe transducer was placed on the skin between the ribs at the level of the right lobe of the liver, exerting an adequate pressure on it. The results were expressed in kPa, and each LSM value corresponds to the median of 10 validated measurements[8]. An examination was considered successful and reliable if the interquartile range (IQR)/median for LSM was ⩽ 30% or the LSM was < 7.1 kPa when the IQR/median for LSM was > 30%[9]. For the diagnosis of liver cirrhosis, a cut-off value of 12 kPa was used.

Statistical analysis

Continuous variables are given as median (range) or mean ± SD and categorical variables as frequencies or percentages (%) of patients. All data of demographic and clinical features were analyzed using the Statistical Package for the Social Sciences (SPSS) Version 21.0 (IBM Corp., Armonk, NY, United States). Chi-squared and Fisher's exact tests were performed for categorical variables, while Student's *t*-test or one-way analysis of variance was used for group comparisons of parametric quantitative data. Multinomial (binary) logistic regression was performed to evaluate factors predicting CHC and cirrhosis. All *P* values were two-

Table 1 Demographic and clinical characteristics of remunerated blood donors

	Blood donors, *n* = 363	Single plasma donors, *n* = 780	Blood and plasma donors, *n* = 551	*P* value
Age in yr	56.8 ± 13.2	57.2 ± 11.3	57.1 ± 9.4	0.882[1]
⩾ 40, < 50	56 (15.4)	83 (10.6)	68 (12.3)	0.07
⩾ 50, < 60	203 (55.9)	501 (64.2)	336 (61.0)	
⩾ 60	104 (28.7)	196 (25.1)	147 (26.7)	
Sex				
Male	123 (33.92)	315 (36.5)	211 (38.3)	0.109[2]
Female	240 (66.1)	465 (63.5)	340 (61.5)	
BMI	25.52 ± 4.32	25.36 ± 4.11	25.45 ± 3.22	0.353[1]
< 25	178 (49)	395 (50.6)	294 (53.4)	0.167[2]
⩾ 25, < 28	130 (35.8)	284 (36.4)	169 (30.7)	
⩾ 28	55 (15.2)	101 (12.9)	88 (16)	
PLT as × 10^9/L	207.3 ± 64.8	161.8 ± 55.4	176.3 ± 63.1	< 0.001[1]
ALB in g/L	42.3 ± 3.5	41.4 ± 4.7	43.3 ± 4.5	0.513[1]
ALT in U/L	27.4 ± 6.5	63.2 ± 18.7	52.6 ± 15.4	< 0.001[1]
AST in U/L	23.5 ± 7.4	55.4 ± 12.9	44.5 ± 22.6	< 0.001[1]
Anti-HCV				
Positive	12 (3.3)	534 (68.5)	324 (58.8)	< 0.001[2]
Negative	351 (96.7)	246 (31.5)	227 (41.29)	
HBsAg				
Positive	2 (0.6)	3 (0.4)	1 (0.2)	0.643[3]
Negative	361 (99.4)	777 (99.6)	550 (99.8)	
LSM in kPa	5.56 ± 2.64	7.37 ± 3.62	6.54 ± 3.54	< 0.001[1]
⩾ 9	2 (0.6)	224 (28.7)	122 (22.1)	< 0.001[2]
< 9, ⩾ 6	20 (5.5)	313 (40.1)	287 (52.1)	
< 6	341 (93.9)	243 (31.2)	142 (25.8)	
Blood donated frequency times				
⩾ 10	212 (58.4)	245 (31.4)	187 (33.9)	< 0.001[2]
< 10, ⩾ 5	120 (33.1)	352 (45.1)	202 (36.7)	
< 5	31 (8.5)	183 (23.5)	162 (29.4)	
Interval time from last donated blood to survey in yr	27.56 ± 2.11	27.65 ± 3.02	27.84 ± 2.54	0.453[1]
Refused donated by elevated ALT				
Yes	37 (10.2)	317 (40.6)	195 (35.4)	< 0.001[2]
No	326 (89.8)	463 (59.4)	356 (64.6)	

Data are presented as *n* (%). The normal range of ALT and AST are 5-40 U/L, PLT is 100-300 × 10^9/L, ALB is 35-55 g/L. [1]One-way analysis; [2]Pearson Chi-Squared; [3]Fisher's exact test. ALB: Albumin; ALT: Alanine aminotransferase; AST: Aspartate aminotransferase; BMI: Body mass index; LSM: Liver stiffness measurement; PLT: Platelet.

sided.

RESULTS

Demographic and clinical characteristics of remunerated blood donors

In this survey, we investigated a total of 1694 participants after a median of 27 years (25-31 years) from the last blood donation to the moment of survey, including 363 blood donors, 780 plasma donors and 551 mixed blood donors. We detected 870 antiHCV-positive cases, 6 HBsAg-positive cases and no cases of HIV infection. As shown in Table 1, we analyzed age, sex, body mass index (BMI; < 25; ⩾ 25, < 28; ⩾ 28), PLT, ALB, ALT, AST, antiHCV (positive, negative), HBsAg (positive, negative), LSM (< 6; ⩾ 6, < 9; ⩾ 9), frequency of blood donation (< 5 ; ⩾ 5 < 10; ⩾ 10), and rejection of blood donation owing to elevated ALT (yes, no). The differences in PLT, ALT, AST, LSM, frequency of blood donation, and rejection of blood donation owing to elevated ALT were statistically significant ($P < 0.05$) among different blood donation mode groups. In particular, we observed 12 (3.3%), 534 (68.5%) and 324 (58.8%) antiHCV-positive patients in the blood donor, plasma donor and mixed donor groups, respectively.

Demographic and clinical characteristics of CHC

A total of 870 participants were antiHCV-positive; among them, 592 (68.05%) had detectable HCV RNA, were diagnosed with CHC and categorized to the CHC group, whereas 278 (31.95%) had undetectable HCV RNA and were categorized to the no CHC group. Table 2 shows an analysis of age, sex, BMI, (< 25; ⩾ 25, < 28; ⩾ 28), PLT, ALB, ALT, AST, SMA (positive, negative), ANA (positive, negative), immunoglobulin (IgG; normal, elevated), LSM (< 6; ⩾ 6, < 9; ⩾ 9), frequency of blood donation (< 5; ⩾ 5 < 10; ⩾ 10), and rejection of blood donation due to elevated ALT (yes, no). Differences in age, BMI, homeostatic model assessment of insulin resistance (HOMA-IR), ALT, AST, PLT and LSM were statistically significant ($P < 0.05$)

Table 2 Demographic and clinical characteristics of hepatitis C virus in remunerated blood donors and multiple logistic regression analysis of factors associated with hepatitis C virus

	CHC, *n* = 592	No CHC, *n* = 278	*P* value	Multivariate[4]			
				OR	95%CI	Wald	*P* value
Age in yr	55.4 ± 13.2	58.5 ± 9.4	< 0.001[1]	1.642	0.426-11.164	3.012	0.013
⩾ 40, < 50	121 (20.4)	35 (12.6)	0.003[2]		1		
⩾ 50, < 60	356 (60.1)	168 (60.4)		3.542	0.521-13.254	1.534	0.435
⩾ 60	115 (19.4)	75 (27.0)		11.226	0.065-137.53	5.322	0.004
Sex							
Male	277 (46.8)	111 (39.9)	0.058[2]		1		
Female	315 (53.2)	167 (60.1)		0.233	0.054-6.634	1.004	0.364
Alcohol consumption				0.532	0.147-1.647	0.853	0.547
Never	441 (74.5)	175 (62.9)	0.002[2]	0.436	0.124-1.006	1.075	0.443
Occasional	95 (16.0)	68 (24.5)		0.876	0.857-1.354	1.446	0.374
Often	56 (9.5)	35 (12.6)		1.231	0.843-1.556	0.667	0.432
BMI	24.12 ± 2.32	25.45 ± 3.22	< 0.001[1]	0.889	0.674-1.327	0.896	0.547
< 25	278 (47.0)	194 (69.8)	< 0.001[2]	1.216	0.536-1.625	0.034	0.646
⩾ 25, < 28	230 (38.9)	69 (24.8)		7.233	0.054-66.63	1.534	0.343
⩾ 28	84 (14.2)	15 (5.4)		4.365	0.643-22.534	1.543	0.113
HOMA-IR	1.53 ± 0.48	1.31 ± 0.52	< 0.001[1]	1.002	0.864-1.007	0.984	0.657
PLT as × 10^9/L	164.3 ± 64.8	196.3 ± 73.1	< 0.001[1]	3.112	1.475-121.153	16.886	< 0.001
ALB in g/L	42.3 ± 3.5	43.3 ± 4.5	0.513[1]	0.576	0.645-1.2147	0.543	0.674
ALT in U/L	67.4 ± 26.5	22.6 ± 15.4	< 0.001[1]	3.216	1.036-121.625	25.034	< 0.001
AST in U/L	53.5 ± 17.4	24.5 ± 10.6	< 0.001[1]	2.578	0.937-76.354	26.332	< 0.001
SMA							
Negative	517 (87.3)	262 (94.2)	0.002[2]		1		
Positive	75 (12.7)	16 (5.8)		1.146	0.545-1.654	0.543	0.653
ANA							
Negative	477 (80.6)	244 (87.8)	0.009[2]		1		
Positive	115 (19.4)	34 (12.2)		1.423	0.587-1.001	0.123	0.886
IgG							
Normal	271 (45.8)	261 (93.9)	< 0.001[2]		1		
Elevated	321(54.2)	17 (6.1)		6.001	0.957-12.353	6.075	< 0.001
LSM in kPa	7.67 ± 4.43	4.12 ± 2.25	< 0.001[1]	0.233	0.054-6.634	1.004	0.364
< 6	155 (26.2)	241 (86.7)	< 0.001[2]		1		
< 9, ⩾ 6	211 (35.6)	31 (11.2)		0.532	0.147-1.647	0.853	0.547
⩾ 9	226 (38.2)	6 (2.2)		2.436	0.124-11.776	7.075	< 0.001
Blood donated frequency times	8.67 ± 6.43	8.42 ± 6.25	0.107[1]	1.233	0.874-1.134	1.032	0.832
< 5	139 (23.5)	62 (22.3)	0.101[2]		1		
< 10, ⩾ 5	252 (42.6)	102 (36.7)		0.932	0.927-1.433	1.032	0.883
⩾ 10	201 (34.0)	114 (41.0)		0.247	0.257-1.754	1.054	0.664
Refused donated by elevated ALT							
No	377 (63.7)	148 (53.2)	0.003[3]		1		
Yes	215 (36.3)	130 (46.8)		1.668	1.061-3.143	4.804	0.027

Data are presented as *n* (%). Alcohol consumption: Often, the ethanol intake per week was more than 140 g in men (70 g in women) in the past 12 mo; Occasional, the ethanol intake per week was less than 140 g in men (70 g in women) in the past 12 mo. [1]One-way analysis; [2]Pearson's chi-square; [3]Fisher's exact test; [4]Binary logistic regression. ALB: Albumin; ALT: Alanine aminotransferase; ANA: Antinuclear antibody; AST: Aspartate aminotransferase; BMI: Body mass index; CI: Confidence interval; LSM: Liver stiffness measurement; OR: Odds ratio; SMA: Smooth muscle actin; PLT: Platelet.

between the HCV and no HCV groups. However, ALB, frequency of blood donation and refusal of donation by elevated ALT were not significantly different.

Demographic and clinical characteristics of cirrhosis caused by HCV infection and multiple logistic regression analysis associated with cirrhosis

A total of 161 (27.2%, 161/592) patients with CHC were diagnosed with cirrhosis, having an LSM value higher than 12 kPa. Among them, 431 patients were diagnosed with CHC. Table 3 shows an analysis of the age, sex, alcohol consumption (never, occasional, often), BMI (< 25; ⩾ 25, < 28; ⩾ 28), PLT, ALB, ALT, AST, HCV RNA (LgIU/mL, ⩾ 3,< 5; ⩾ 5), genotype (Ⅰ, Ⅱ, Ⅲ), frequency of blood donation (< 5 ; ⩾ 5 < 10; ⩾ 10), and rejection of blood donation due to elevated ALT (yes, no). Differences in age, alcohol consumption, PLT and IgG were statistically significant ($P < 0.05$) between the cirrhosis and CHC groups. However, sex, BMI, ALB, ALT, AST, SMA, ANA, HCV RNA, genotype, frequency of blood donation and rejection of blood donation due to elevated ALT were not significantly different. When the LSM level higher than 12 kPa was considered a binary dependent variable, multiple logistic (binary) regression analysis was used to assess factors associated with cirrhosis and CHC (Table 3).

Table 3 Demographic and clinical characteristics of cirrhosis by hepatitis C virus infection in remunerated blood donors and multiple logistic regression analysis of factors associated with cirrhosis

	Cirrhosis by HCV, *n* = 161	CHC, *n* = 431	*P* value	Multivariate[4]			
				OR	95%CI	Wald	*P* value
Age in yr	58.4 ± 13.2	56.5 ± 9.4	< 0.001[1]	2.143	0.553-6.453	4.543	0.002
⩾ 40, < 50	41 (25.43)	80 (18.6)	0.034[2]		1		
⩾ 50, < 60	82 (50.9)	270 (62.6)		2.443	0.242-7.345	1.423	0.065
⩾ 60	38 (23.6)	81 (18.8)		3.223	0.124-14.344	3.153	0.021
Sex							
Male	75 (46.6)	202 (46.9)	0.951[2]		1		
Female	86 (53.4)	229 (53.1)		1.223	0.112-6.765	0.653	0.445
Alcohol consumption							
Never	97 (60.2)	344 (79.8)	< 0.001[2]		1		
Occasional	40 (24.8)	55 (12.8)		0.879	0.647-2.654	2.753	0.152
Often	24 (14.9)	32 (7.4)		1.004	0.875-1.744	3.057	0.005
BMI	24.12 ± 2.32	25.45 ± 3.22	0.353[1]	0.647	0.465-1.632	4.135	0.432
< 25	78 (48.4)	200 (46.4)	0.108[2]		1		
⩾ 25, < 28	68 (42.2)	162 (37.6)		1.242	0.574-1.735	0.536	0.438
⩾ 28	15 (9.3)	69 (16)		0.665	0.426-1.645	0.476	0.537
HOMA-IR	1.53 ± 0.48	1.51 ± 0.52	0.556	0.023	0.772-1.423	0.365	0.221
PLT as × 10^9/L	147.3 ± 55.7	176.3 ± 84.2	< 0.001[1]	1.314	0.022-1.463	3.647	0.013
ALB in g/L	42.3 ± 3.5	43.3 ± 4.5	0.513[1]	0.864	0.707-1.364	1.557	0.675
ALT in U/L	67.4 ± 26.5	62.6 ± 25.4	0.113[1]	1.643	0.463-1.755	0.634	0.247
AST in U/L	53.5 ± 27.4	54.5 ± 22.6	0.201[1]	1.425	0.428-1.254	0.546	0.664
SMA							
Negative	144 (89.4)	373 (86.5)	0.346[2]		1		
Positive	17 (10.6)	58 (13.5)		0.526	0.537-1.843	1.034	0.536
ANA							
Negative	130 (80.7)	347 (80.5)	0.945[1]		1		
Positive	31 (19.3)	84 (19.5)		2.123	0.132-5.563	0.843	0.246
IgG							
Normal	60 (37.3)	205 (47.6)	0.025[2]		1		
Elevated	101 (62.7)	226 (52.4)		1.352	0.663-12.267	3.537	0.012
HCV RNA in LgIU/mL	7.12 ± 2.43	6.73 ± 2.533	0.067[1]	0.657	0.536-1.523	0.863	0.536
⩾ 3, < 5	22 (13.7)	51 (11.8)	0.546[2]		1		
⩾ 5	139 (86.3)	380 (88.2)		1.325	0.972-1.445	0.143	0.782
Genotype							
Ⅰ	152 (94.4)	390 (90.5)	0.310[2]		1		
Ⅱ	8 (5.0)	37 (8.6)		0.753	1.003-1.664	0.623	0.242
Ⅲ	1 (0.6)	4 (0.9)		1.862	1.182-1.635	0.845	0.118
Blood donated frequency times	8.67 ± 5.43	8.42 ± 6.25	0.107[1]	1.536	0.874-2.154	0.923	0.101
< 5	36 (22.4)	103 (23.9)	0.698[2]		1		
< 10, ⩾ 5	66 (41.0)	186 (43.2)		0.354	0.274-1.203	0.991	0.783
⩾ 10	59 (36.6)	142 (32.9)		1.024	0.154-2.163	0.332	0.224
Refused donated by elevated ALT							
No	94 (58.4)	243 (56.4)	0.661[2]		1		
Yes	67 (41.6)	188 (43.6)		0.012	0.037-1.002	0.682	0.563

Data are presented as *n* (%). Alcohol consumption: Often, the ethanol intake per week was more than 140 g in men (70 g in women) in the past 12 mo; Occasional, the ethanol intake per week was less than 140 g in men (70 g in women) in the past 12 mo. [1]One-way analysis; [2]Pearson's chi-square; [3]Fisher's exact test; [4]Binary logistic regression. ALB: Albumin; ALT: Alanine aminotransferase; ANA: Antinuclear antibody; AST: Aspirate aminotransferase; BMI: Body mass index; LSM: Liver stiffness measurement; SMA: Smooth muscle actin.

Using the "enter" method, the results suggested that age, alcohol consumption and PLT levels were associated with cirrhosis.

DISCUSSION

Hepatitis C is a blood-borne disease mainly transmitted by percutaneous exposure to contaminated blood and by unprotected sexual intercourse[10,11]. In the last century, from the late 1980s to the early 1990s, a large number of paid blood donors emerged in underdeveloped rural areas with a low economic status in Eastern China. Many blood donors were infected with HCV because of the use of contaminated medical devices. A total of 1694 participants were investigated, and 870 cases were positive for anti-HCV. In particular, we found 12 (3.3%), 534 (68.5%) and 324 (58.8%) patients positive against antiHCV in the blood donor, plasma donor and mixed donor groups, respectively.

The results showed that the blood donation method is the main cause of transmission of hepatitis C, and plasma donation in particular is the main causes of

hepatitis C infection. The rate of HCV infection in blood donors is 3.3%, quite similar to the average antiHCV-positivity rate of 3.2% in the general Chinese population according to the national epidemiological survey of HCV conducted from 1992 to 1995[12,13]. Some studies reported the transmission of hepatitis C in blood donors in the last decade in China[14-18]. However, this survey revealed that the blood donation method, in particular plasma apheresis, is the main cause of transmission of hepatitis C.

We also found that the frequency of blood donation in the plasma donor group was lower compared to the blood donor group, due to the more frequent rejection of blood donation in the plasma group because of elevated ALT. In other words, more plasma donors are likely to have been infected with HCV. The response of serum markers (ALT, AST and PLT) to liver damage in the plasma and mixed donor groups is higher than in the whole blood donor group. The HBsAg-positivity rate decreased because of the beginning of hepatitis B screening for blood donation.

HCV RNA was first detected in peripheral blood 1-3 wk after exposure to HCV[19]. Hepatitis C viremia not yet cleared 6 mo after exposure will progress to chronic infection. The hepatitis C chronicity rate is approximately 55%-85%[20-22]. Our survey interval of nearly 30 years shows that there are still 68% cases of detectable HCV RNA. Some studies have suggested that chronic predictive factors of HCV infection include male sex, age > 25 years, lack of symptoms after infection, race (African American), HIV infection, and immunosuppression[21]. The genetic background of the host may affect chronicity. IL-28B gene, human leukocyte antigen class 1 molecule HLA B57, and class Ⅱ molecules HLA DRB1 and DQBI allele polymorphism can affect HCV clearance[23-25]. For example, CC genotype at the rs12979860 site of the IL-28B gene leads to virus clearance, whereas TT is associated with a very low virus clearance[26,27].

In our study, age was a factor in the spontaneous clearance of the virus, but no sex-related differences in terms of HCV clearance were found. The increased levels of indicators of liver damage such as PLT, ALT, AST and LSM are considered the result of a chronic hepatitis C. Interestingly, blood donation due to elevated ALT reflects the activity of hepatitis C and indicates whether its current activity is beneficial to its spontaneous clearance.

HCV infection progresses slowly, up to 20 years after infection. The incidence of cirrhosis in children and young women is 2%-4%[28], in middle aged people infected due to blood transfusion 18%-30%[29], in plasma donors 1.4%-10.0%[7,30], and in the general population 5%-15%[26]. The factors that can promote disease progression include infection with HCV at age over 40 years, male sex, alcohol use (50 g/d or more in men, 70 g in women), HCV with HIV infection which leads to immune dysfunction[31,32], obesity, insulin resistance, hepatitis B virus infection, nonalcoholic fatty liver, high iron load in the liver, accompaniment of schistosomiasis infection, hepatotoxic drugs, and environmental pollution caused by toxic substances. Genetic factors can also promote disease progression[33,34].

Baseline liver tissue inflammation, necrosis and fibrosis stage are the best predictors of progression to cirrhosis. The incidence rate of cirrhosis of patients with CHC after a nearly 30-year interval is 27.2%, which was higher than in related studies[7,30]. Studying the incidence rate involved a long observation period, age, especially higher than 60 years, and regular drinking were risk factors for cirrhosis. Significantly increased levels of PLT and immunoglobulin are seen in cirrhosis.

HCV Ib and 2a genotypes were the most common in China, with genotype 1b (56.8%) being the highest, followed by genotypes 2 (24.1%) and 3 (9.1%). Genotypes 4 and 5 were not found, whereas genotype 6 (6.3%)[3] was found to be low. However, our study found that genotype 1b accounted for 91.9%, which shows heterogeneity in the distribution of hepatitis C genotypes in China.

In conclusion, this research over 27 years revealed that CHC infection remains a serious public health problem in Eastern China. Plasma donation is the main causes of hepatitis C infection. The main HCV genotype is 1b. After nearly 30 years of CHC, nearly 28% of cases progressed to cirrhosis. Age, especially greater than 60 years, and regular drinking habits were risk factors associated with cirrhosis.

ARTICLE HIGHLIGHTS

Research background

The natural history of hepatitis C virus (HCV) is still unclear. One of the main reasons why natural history is not clear is that the time of establishment of the infection is unclear. In this report, the authors followed many patients with HCV who can estimate the time of infection.

Research motivation

In the last century, from the late 1980s to the early 1990s, a large number of paid blood donors emerged in underdeveloped rural areas with a low economic status in Eastern China. Many blood donors were infected with HCV because of the use of contaminated medical devices.

Research objectives

The study aimed to understand the prevalence of HCV infection in blood donors over a nearly 27-year interval and to explore the factors that affect the outcome of HCV infection.

Research methods

A retrospective and cross-sectional study was conducted. The participants, mostly plasma donors, were selected from three administrative villages in the Jiangsu province in Eastern China. A questionnaire was administered among the villagers who had a history of blood donation from the late 1980s to the early 1990s. All participants underwent physical examination, liver B-ultrasonography, and liver stiffness measurement (LSM). In addition, 10 mL of blood was collected from each participant to measure simple liver function parameters [albumin (ALB), alanine aminotransferase (ALT), aspartate aminotransferase (AST)], blood factors [platelet (PLT)], and for hepatitis B surface antigen (HBsAg), antiHCV, and antihuman immunodeficiency virus

detection. HCV RNA detection, HCV genotyping, and other tests were carried out in antiHCV-positive patients.

Research results

After a median of 27 years (25-31 years) from the last blood donation to the time of survey, a total of 1694 participants were investigated, and the antiHCV-positive individuals were categorized into three groups: blood donors (*n* = 12, 3.3%), plasma donors (*n* = 534, 68.5%), and mixed donors (*n* = 324, 58.8%). A total of 592 (68.05%) patients had detectable HCV RNA, and 91.9% had genotype 1b. A total of 161 (27.2%, 161/592) patients with chronic hepatitis C (CHC) were considered to have cirrhosis, with an LSM level higher than 12 kPa. Multiple logistic (binary) regression analysis results showed that PLT and IgG levels were associated with cirrhosis.

Research conclusions

The nearly 27-year interval investigation revealed that CHC infection is a very serious public health problem in Eastern China. Plasma donation and subsequent return of blood cells to the donor are the main causes of hepatitis C infection. The main HCV genotype is 1b. Nearly 28% of cases progressed to cirrhosis. Age, especially over 60 years, and regular drinking habits were risk factors associated with cirrhosis.

Research perspectives

This research over 27 years revealed that CHC infection remains a serious public health problem in Eastern China. The epidemiological data in the present investigation may play an important role in focusing on the significance of public health in chronic HCV infection.

REFERENCES

1 **Petruzziello A**, Marigliano S, Loquercio G, Cozzolino A, Cacciapuoti C. Global epidemiology of hepatitis C virus infection: An up-date of the distribution and circulation of hepatitis C virus genotypes. *World J Gastroenterol* 2016; **22**: 7824-7840 [PMID: 27678366 DOI: 10.3748/wjg.v22.i34.7824]

2 **Zampino R**, Coppola N, Sagnelli C, Di Caprio G, Sagnelli E. Hepatitis C virus infection and prisoners: Epidemiology, outcome and treatment. *World J Hepatol* 2015; **7**: 2323-2330 [PMID: 26413221 DOI: 10.4254/wjh.v7.i21.2323]

3 **Chen YS**, Li L, Cui FQ, Xing WG, Wang L, Jia ZY, Zhou MG, Gong XH, Wang FZ, Zheng H, Luo HM, Bi SL, Wang N, Yang WZ, Liang XF. A sero-epidemiological study on hepatitis C in China. *Zhonghua Liu Xing Bing Xue Za Zhi* 2011; **32**: 888-891 [PMID: 22340876]

4 **Polaris Observatory HCV Collaborators.** Global prevalence and genotype distribution of hepatitis C virus infection in 2015: a modelling study. *Lancet Gastroenterol Hepatol* 2017; **2**: 161-176 [PMID: 28404132 DOI: 10.1016/S2468-1253(16)30181-9]

5 **Liu S**, Figueroa P, Rou K, Wu Z, Chen X, Detels R. Safety of the blood supply in a rural area of China. *J Acquir Immune Defic Syndr* 2010; **53** Suppl 1: S23-S26 [PMID: 20104105 DOI: 10.1097/QAI.0b013e3181c7d494]

6 **Foster GR**, Goldin RD, Thomas HC. Chronic hepatitis C virus infection causes a significant reduction in quality of life in the absence of cirrhosis. *Hepatology* 1998; **27**: 209-212 [PMID: 9425939 DOI: 10.1002/hep.510270132]

7 **Li JF**, Liu S, Ren F, Liu M, Wu HL, Chen Y, Zou HB, Bai L, Li Y, Zheng SJ, Duan ZP. Fibrosis progression in interferon treatment-naive Chinese plasma donors with chronic hepatitis C for 20 years: a cohort study. *Int J Infect Dis* 2014; **27**: 49-53 [PMID: 25168642 DOI: 10.1016/j.ijid.2014.07.003]

8 **Petta S**, Wong VW, Cammà C, Hiriart JB, Wong GL, Marra F, Vergniol J, Chan AW, Di Marco V, Merrouche W, Chan HL, Barbara M, Le-Bail B, Arena U, Craxì A, de Ledinghen V. Improved noninvasive prediction of liver fibrosis by liver stiffness measurement in patients with nonalcoholic fatty liver disease accounting for controlled attenuation parameter values. *Hepatology* 2017; **65**: 1145-1155 [PMID: 27639088 DOI: 10.1002/hep.28843]

9 **Cai YJ**, Dong JJ, Wang XD, Huang SS, Chen RC, Chen Y, Wang YQ, Song M, Chen YP, Li Z, Zhou MT, Shi KQ. A diagnostic algorithm for assessment of liver fibrosis by liver stiffness measurement in patients with chronic hepatitis B. *J Viral Hepat* 2017; **24**: 1005-1015 [PMID: 28419755 DOI: 10.1111/jvh.12715]

10 **Freeman AJ**, Law MG, Kaldor JM, Dore GJ. Predicting progression to cirrhosis in chronic hepatitis C virus infection. *J Viral Hepat* 2003; **10**: 285-293 [PMID: 12823595]

11 **Kanwal F**, Hoang T, Kramer JR, Asch SM, Goetz MB, Zeringue A, Richardson P, El-Serag HB. Increasing prevalence of HCC and cirrhosis in patients with chronic hepatitis C virus infection. *Gastroenterology* 2011; **140**: 1182-1188.e1 [PMID: 21184757 DOI: 10.1053/j.gastro.2010.12.032]

12 **Wang JT**, Wang TH, Lin JT, Lee CZ, Sheu JC, Chen DS. Effect of hepatitis C antibody screening in blood donors on post-transfusion hepatitis in Taiwan. *J Gastroenterol Hepatol* 1995; **10**: 454-458 [PMID: 8527713]

13 **Alter MJ**. Epidemiology of hepatitis C virus infection. *World J Gastroenterol* 2007; **13**: 2436-2441 [PMID: 17552026 DOI: 10.3748/wjg.v13.i17.2436]

14 **Gao X**, Cui Q, Shi X, Su J, Peng Z, Chen X, Lei N, Ding K, Wang L, Yu R, Wang N. Prevalence and trend of hepatitis C virus infection among blood donors in Chinese mainland: a systematic review and meta-analysis. *BMC Infect Dis* 2011; **11**: 88 [PMID: 21477324 DOI: 10.1186/1471-2334-11-88]

15 **Qiu Y**, Shi L, Wang Y, Zhang G, Zheng J, Gong X, Xia H, Zhang P, Ness P, Shan H. Risk factors for hepatitis C virus infection among blood donors in Beijing and implications for improving the pretesting donor screening process. *Transfusion* 2008; **48**: 1207-1212 [PMID: 18346015 DOI: 10.1111/j.1537-2995.2008.01673.x]

16 **Wang Y**, Tao QM, Zhao HY, Tsuda F, Nagayama R, Yamamoto K, Tanaka T, Tokita H, Okamoto H, Miyakawa Y. Hepatitis C virus RNA and antibodies among blood donors in Beijing. *J Hepatol* 1994; **21**: 634-640 [PMID: 7529274]

17 **Lin H**, Chen X, Zhu S, Mao P, Zhu S, Liu Y, Huang C, Sun J, Zhu J. Prevalence of Occult Hepatitis C Virus Infection among Blood Donors in Jiangsu, China. *Intervirology* 2016; **59**: 204-210 [PMID: 28208127 DOI: 10.1159/000455854]

18 **Zhuang W**, Ding X, Lyu C, Xiang L, Teng H, Li J. Hepatitis E virus seroprevalence among blood donors in Jiangsu Province, East China. *Int J Infect Dis* 2014; **26**: 9-11 [PMID: 24981426 DOI: 10.1016/j.ijid.2014.04.022]

19 **Farci P**, Alter HJ, Wong D, Miller RH, Shih JW, Jett B, Purcell RH. A long-term study of hepatitis C virus replication in non-A, non-B hepatitis. *N Engl J Med* 1991; **325**: 98-104 [PMID: 1646962 DOI: 10.1056/NEJM199107113250205]

20 **Corey KE**, Mendez-Navarro J, Gorospe EC, Zheng H, Chung RT. Early treatment improves outcomes in acute hepatitis C virus infection: a meta-analysis. *J Viral Hepat* 2010; **17**: 201-207 [PMID: 19674285 DOI: 10.1111/j.1365-2893.2009.01167.x]

21 **Chen SL**, Morgan TR. The natural history of hepatitis C virus (HCV) infection. *Int J Med Sci* 2006; **3**: 47-52 [PMID: 16614742]

22 **Vallet-Pichard A**, Pol S. Natural history and predictors of severity of chronic hepatitis C virus (HCV) and human immunodeficiency virus (HIV) co-infection. *J Hepatol* 2006; **44**: S28-S34 [PMID: 16343684 DOI: 10.1016/j.jhep.2005.11.008]

23 **Mizokami M**. Discovery of critical host factor, IL-28B, associated with response to hepatitis C virus treatment. *J Gastroenterol Hepatol* 2012; **27**: 425-429 [PMID: 22168813 DOI: 10.1111/j.1440-1746.2011.07054.x]

24 **Rangnekar AS**, Fontana RJ. Meta-analysis: IL-28B genotype and sustained viral clearance in HCV genotype 1 patients. *Aliment Pharmacol Ther* 2012; **36**: 104-114 [PMID: 22612303 DOI: 10.1111/j.1365-2036.2012.05145.x]

25 **Chuang WC**, Sarkodie F, Brown CJ, Owusu-Ofori S, Brown J, Li C, Navarrete C, Klenerman P, Allain JP. Protective effect of HLA-B57 on HCV genotype 2 infection in a West African population. *J Med Virol* 2007; **79**: 724-733 [PMID: 17546694 DOI: 10.1002/jmv.20848]

26 **Thursz M**, Yallop R, Goldin R, Trepo C, Thomas HC. Influence of MHC class II genotype on outcome of infection with hepatitis

C virus. The HENCORE group. Hepatitis C European Network for Cooperative Research. *Lancet* 1999; **354**: 2119-2124 [PMID: 10609818]
27 **Alric L**, Bonnet D, Fort M. Association between female sex, IL28B genotype, but also DQB1*0301 allele and the outcome of acute hepatitis C virus infection. *Hepatology* 2014; **60**: 2127 [PMID: 24715649 DOI: 10.1002/hep.27164]
28 **Kenny-Walsh E**. Clinical outcomes after hepatitis C infection from contaminated anti-D immune globulin. Irish Hepatology Research Group. *N Engl J Med* 1999; **340**: 1228-1233 [PMID: 10210705 DOI: 10.1056/NEJM199904223401602]
29 **Freeman AJ**, Dore GJ, Law MG, Thorpe M, Von Overbeck J, Lloyd AR, Marinos G, Kaldor JM. Estimating progression to cirrhosis in chronic hepatitis C virus infection. *Hepatology* 2001; **34**: 809-816 [PMID: 11584380 DOI: 10.1053/jhep.2001.27831]
30 **Rao HY**, Sun DG, Yang RF, Liu F, Wang J, Feng B, Wu N, Fang JL, Song GJ, Ma H, Guo F, Wang JH, Li XB, Jin Q, Qin H, Zhuang H, Wei L. Outcome of hepatitis C virus infection in Chinese paid plasma donors: a 12-19-year cohort study. *J Gastroenterol Hepatol* 2012; **27**: 526-532 [PMID: 21871021 DOI: 10.1111/j.1440-1746.2011.06880.x]
31 **Poynard T**, Bedossa P, Opolon P. Natural history of liver fibrosis progression in patients with chronic hepatitis C. The OBSVIRC, METAVIR, CLINIVIR, and DOSVIRC groups. *Lancet* 1997; **349**: 825-832 [PMID: 9121257]
32 **Barreiro P**, Pineda JA, Rallón N, Naggie S, Martín-Carbonero L, Neukam K, Rivero A, Benito JM, Caruz A, Vispo E, Camacho A, Medrano J, McHutchison J, Soriano V. Influence of interleukin-28B single-nucleotide polymorphisms on progression to liver cirrhosis in human immunodeficiency virus-hepatitis C virus-coinfected patients receiving antiretroviral therapy. *J Infect Dis* 2011; **203**: 1629-1636 [PMID: 21592993 DOI: 10.1093/infdis/jir113]
33 **Ohki T**, Tateishi R, Sato T, Masuzaki R, Imamura J, Goto T, Yamashiki N, Yoshida H, Kanai F, Kato N, Shiina S, Yoshida H, Kawabe T, Omata M. Obesity is an independent risk factor for hepatocellular carcinoma development in chronic hepatitis C patients. *Clin Gastroenterol Hepatol* 2008; **6**: 459-464 [PMID: 18387499 DOI: 10.1016/j.cgh.2008.02.012]
34 **Kamal SM**, Turner B, He Q, Rasenack J, Bianchi L, Al Tawil A, Nooman A, Massoud M, Koziel MJ, Afdhal NH. Progression of fibrosis in hepatitis C with and without schistosomiasis: correlation with serum markers of fibrosis. *Hepatology* 2006; **43**: 771-779 [PMID: 16557547 DOI: 10.1002/hep.21117]

P- Reviewer: Bock CT, He ST, Inoue K **S- Editor**: Wang XJ
L- Editor: Filipodia **E- Editor**: Huang Y

World Journal of Gastroenterology

Submit a Manuscript: http://www.f6publishing.com

World J Gastroenterol 2018 March 21; 24(11): 1259-1268

DOI: 10.3748/wjg.v24.i11.1259

ISSN 1007-9327 (print) ISSN 2219-2840 (online)

ORIGINAL ARTICLE

Clinical Trials Study

Low-FODMAP *vs* regular rye bread in irritable bowel syndrome: Randomized SmartPill® study

Laura Pirkola, Reijo Laatikainen, Jussi Loponen, Sanna-Maria Hongisto, Markku Hillilä, Anu Nuora, Baoru Yang, Kaisa M Linderborg, Riitta Freese

Laura Pirkola, Riitta Freese, Division of Nutrition, Department of Food and Environmental Sciences, University of Helsinki, Helsinki FI-00790, Finland

Laura Pirkola, Jussi Loponen, Sanna-Maria Hongisto, Fazer Group/ Fazer Bakeries Ltd, Vantaa FI-01230, Finland

Reijo Laatikainen, Medical Faculty, Pharmacology, Medical Nutrition Physiology, University of Helsinki, Helsinki FI-00290, Finland

Markku Hillilä, Clinic of Gastroenterology, University of Helsinki and Helsinki University, Hospital Jorvi, Espoo FI-02740, Finland

Anu Nuora, Baoru Yang, Kaisa M Linderborg, Food Chemistry and Food Development, Department of Biochemistry, University of Turku, Turku FI-20014, Finland

ORCID number: Laura Pirkola (0000-0002-1322-8544); Reijo Laatikainen (0000-0003-2907-0291); Jussi Loponen (0000-0002-6987-1627); Sanna-Maria Hongisto (0000-0002-9027-6451); Markku Hillilä (0000-0001-6836-7691); Anu Nuora (0000-0001-5896-9939); Baoru Yang (0000-0001-5561-514X); Kaisa M Linderborg (0000-0003-1977-7322); Riitta Freese (0000-0002-6833-2736).

Author contributions: Pirkola L, Freese R, Laatikainen R, Hongisto SM, Loponen J, Linderborg KM, and Hillilä M contributed to the design and practical implementation of the study; the research was performed by Pirkola L; the University of Turku team (Linderborg KM, Nuora A, and Yang B) provided the SmartPill equipment and related technical assistance; data analyses were performed by Pirkola L and Freese R. The manuscript was written by Laatikainen R, Pirkola L, and Freese R; all authors critically revised the manuscript; the authors had complete access to the data that supports the publication; all authors have approved the final version of the manuscript.

Clinical trial registration statement: ISRCTN registry (ISRCTN11005234).

Informed consent statement: All participants signed the informed consent form.

Conflict-of-interest statement: Laatikainen R has written a Finnish book on irritable bowel syndrome and diet; He is also founder and owner of Booston Ltd, which provides IBS-related dietetic services to IBS patients, healthcare professionals, and various organizations; Pirkola L, Hongisto SM, and Loponen J are employees of Fazer Bakeries; At the time of the research, Pirkola L was working at the University of Helsinki; Others have no personal interests to declare; Fazer Bakeries funded the study and provided the breads.

Data sharing statement: Patient-level data available upon request.

CONSORT 2010 statement: Aligned with CONSORT 2010.

Manuscript source: Unsolicited manuscript

Correspondence to: Laura Pirkola, MSc, Fazer Group/Fazer Bakeries Ltd, Fazerintie 6, Vantaa FI-01230, Finland. laura.pirkola@fazer.com
Telephone: +358-40-6564887

Received: January 11, 2018
Peer-review started: January 11, 2018
First decision: February 26, 2018
Revised: March 1, 2018
Accepted: March 3, 2018
Article in press: March 3, 2018
Published online: March 21, 2018

Abstract

AIM

To compare the effects of regular *vs* low-FODMAP rye bread on irritable bowel syndrome (IBS) symptoms and to study gastrointestinal conditions with SmartPill®.

METHODS

Our aim was to evaluate if rye bread low in FODMAPs would cause reduced hydrogen excretion, lower intraluminal pressure, higher colonic pH, different transit times, and fewer IBS symptoms than regular rye bread. The study was a randomized, double-blind, controlled cross-over meal study. Female IBS patients (n = 7) ate study breads at three consecutive meals during one day. The diet was similar for both study periods except for the FODMAP content of the bread consumed during the study day. Intraluminal pH, transit time, and pressure were measured by SmartPill, an indigestible motility capsule.

RESULTS

Hydrogen excretion (a marker of colonic fermentation) expressed as area under the curve (AUC)$_{(0\text{-}630\ min)}$ was [median (range)] 6300 (1785-10800) ppm·min for low-FODMAP rye bread and 10 635 (4215-13080) ppm·min for regular bread (P = 0.028). Mean scores of gastrointestinal symptoms showed no statistically significant differences but suggested less flatulence after low-FODMAP bread consumption (P = 0.063). Intraluminal pressure correlated significantly with total symptom score after regular rye bread (ρ = 0.786, P = 0.036) and nearly significantly after low-FODMAP bread consumption (ρ = 0.75, P = 0.052). We found no differences in pH, pressure, or transit times between the breads. Gastric residence of SmartPill was slower than expected. SmartPill left the stomach in less than 5 h only during one measurement (out of 14 measurements in total) and therefore did not follow on par with the rye bread bolus.

CONCLUSION

Low-FODMAP rye bread reduced colonic fermentation *vs* regular rye bread. No difference was found in median values of intraluminal conditions of the gastrointestinal tract.

Key words: Colonic pressure; FODMAP; Irritable bowel syndrome; Rye; Wireless motility capsule; Symptom severity

Core tip: Our study confirmed that low-FODMAP rye bread reduces colonic fermentation in irritable bowel syndrome (IBS) patients compared with regular rye bread. The observed correlation between increased intracolonic pressure and symptom severity underlines the central role of visceral sensitivity in IBS and suggests that some IBS symptoms might be exacerbated by any pathophysiological reason that leads to increased colonic pressure. The study also suggests that SmartPill might not be an optimal device to evaluate gastrointestinal circumstances during meal studies lasting less than 24 h, due to device's inability to measure effects of a singular food bolus in a timely manner.

Pirkola L, Laatikainen R, Loponen J, Hongisto SM, Hillilä M, Nuora A, Yang B, Linderborg KM, Freese R. Low-FODMAP *vs* regular rye bread in irritable bowel syndrome: Randomized SmartPill® study. *World J Gastroenterol* 2018; 24(11): 1259-1268 Available from: URL: http://www.wjgnet.com/1007-9327/full/v24/i11/1259.htm DOI: http://dx.doi.org/10.3748/wjg.v24.i11.1259

INTRODUCTION

Irritable bowel syndrome (IBS) is a common functional gastrointestinal disorder[1]. Symptoms include bloating, abdominal pain, flatulence, constipation, and diarrhea. Visceral sensitivity[2], low-grade inflammation[3], and impaired gas handling[4] contribute to the etiology of IBS.

Many patients consider food as a trigger of their symptoms[5,6] and half of IBS patients report postprandial exacerbation of symptoms[7]. FODMAPs (Fermentable Oligo-, Di-, Monosaccharides and Polyols) are poorly absorbable carbohydrates that are rapidly fermented in the proximal colon[8]. A low-FODMAP diet decreases colonic fermentation, which in turn parallels a reduction of IBS symptoms[9]. One of the major food groups excluded during a low-FODMAP diet is fiber-rich gluten-containing grain products[8]. Elimination of whole-grain products from the diet may, however, lead to decreased fiber intake and increase the risk of chronic diseases in the long term[10].

Rye, a widely-consumed grain in the Nordic countries, is very high in fiber that is mainly composed of arabinoxylan, lignin, cellulose, β-glucan, and fructans[11]. Fructans are classified as FODMAPs[8]. Typical rye bread contains more than 10% fiber and is the most important source of fiber (28%-35% of total intake) of Finnish adults[12]. Rye bread induces gastrointestinal symptoms in some individuals, possibly due to the high fructan content[13]. Therefore, IBS patients may avoid rye products.

Efforts are being made to develop grain products that are low in FODMAPs but high in other fibers[14]. In a recent study, an innovative low-FODMAP high-fiber (fiber > 10% of weight) rye bread caused less colonic fermentation and led to fewer IBS symptoms than regular rye bread[15]. The low-FODMAP rye bread was lower both in fructans and mannitol. Mannitol is a FODMAP compound that is formed during the rye sourdough breadmaking process.

A major challenge in the research of functional gastrointestinal disorders is the lack of objective markers of disease activity. Excretion of hydrogen and methane and colonic fermentation markers are among the rare easily available and objective markers of gastrointestinal circumstances during the consumption of FODMAPs or other poorly absorbable carbohydrates[16]. However, a recent study utilized a wireless motility capsule (SmartPill®) and demonstrated that pH in the colon of IBS patients is lower than in healthy subjects[17]. This may indicate more intensive fermentation in the colon of IBS patients. SmartPill measures intraluminal pH, temperature, motility, and pressure and might thus offer the means to gather objective data on gastrointestinal conditions in IBS patients. A combination of SmartPill data and measurements of perceived symptoms may improve our understanding on the etiology of IBS symptoms.

The aim of this pilot study was to compare a low-FODMAP rye bread and a regular rye bread with regards to postprandial abdominal symptoms, breath hydrogen concentration, and gastrointestinal transit times, pH, and pressure as measured by SmartPill. Our hypothesis was that a low-FODMAP rye bread would induce less hydrogen excretion, lower pressure, and increase pH in colon compared with regular rye bread, which would subsequently parallel with fewer IBS symptoms. The secondary objective was to evaluate the feasibility of the SmartPill capsule in associating IBS symptoms with physiologic responses in the gastrointestinal tract in a meal study.

MATERIALS AND METHODS

Study subjects

Patients with IBS were recruited from the Helsinki metropolitan area *via* the Internet. The eligibility inclusion criteria were the following: (1) female, (2) aged 18 to 65 years, (3) BMI 18.5-30 kg/m^2, and (4) IBS defined by the Rome III criteria[18]. The exclusion criteria were celiac disease, Crohn's disease, diverticulitis, severe dyspepsia, stomach bezoar, bowel obstruction, severe constipation, medication used in the management of intestinal motility, major abdominal surgery, dysphagia, pregnancy or breastfeeding, regular smoking, implanted medical device, and hormonal, renal, hepatic, or hematologic disease or participation in another clinical trial during the past two months.

The study candidates were pre-screened with questionnaires on health and diet and IBS diagnostic criteria. Candidates meeting the preliminary inclusion criteria received laboratory tests (blood count, sedimentation rate, thyroid function tests, transglutaminase antibodies and immunoglobulins for celiac disease, calprotectin, and gene test for lactose intolerance) and a clinical evaluation by a gastroenterologist. Weight and height were also measured. All participants signed an informed consent form. The study protocol was approved by the Ethics Committee of the Helsinki and Uusimaa Hospital District, Finland. The study was registered at ISRCTN registry (ISRCTN11005234).

Study design

This study was a randomized, double-blind, postprandial cross-over meal study. All participants attended on two occasions with a washout period of $\geqslant$ 2 wk between the study periods. Each study period consisted of a run-in period of 12 h (standardized dinner and overnight fast), a test day with study meals (breakfast, lunch, and dinner with low-FODMAP or regular rye bread) and a follow-up of 1 to 3 d depending on the transit time of the SmartPill capsule. The order of the interventions (low-FODMAP or regular rye bread) was randomized for each patient with a random number table. Both investigators and participants were blinded to the identity of the bread. The study events during the study period are detailed in Supplemental Table 1.

Study diets

The diet was standardized from the evening (-12 h) before the test breakfast (0 h) until the following morning (+24 h). The standardized diet consisted of regular grocery products and had a low FODMAP content (Supplemental Table 1). The diet was similar for both study periods except for the FODMAP content of the bread eaten during the study day. Participants kept a food diary from the day before the test day until the end of the study period.

On the morning of the test day, the volunteers ingested the SmartPill capsule with water and ate four slices (approximately 120 g) of bread with spread, cheese, vegetables, and coffee or tea. Lunch with two slices of the test bread was consumed six hours later and dinner with an additional two slices of bread 10-12 h after the breakfast. Thus, participants consumed a total of eight slices (approximately 240 g) of bread during each study period. Breads were developed and supplied by Fazer Bakeries (Vantaa, Finland). The low-FODMAP rye bread was prepared using a specific sourdough that contains unique lactobacilli that efficiently consume fructans and also results in low mannitol content. The control rye bread was prepared using a traditional rye sourdough. The breads were similar in appearance and taste.

The nutrient composition of the breads (Table 1) was analyzed by Eurofins scientific Finland, Raisio (Food and Agro), Finland. The dietary fiber content of the breads was determined by using the AOAC method 2011.25 that discriminates soluble and insoluble, low, and high molecular weight dietary fibers. The mannitol content was analyzed by the HPLC method used by Eurofins Food and Agro, Lidköping, Sweden. Fructan content was measured by using the AOAC 999.03 method (Megazyme assay kit K-FRUC, Megazyme

Table 1 Nutritional composition of the study breads

	Low-FODMAP rye bread		Regular rye bread	
	Per 100 g	Per slice (30 g)	Per 100 g	Per slice (30 g)
Energy (kJ/kcal)	1031/245	309/74	1037/246	311/74
Fat (g)	2.6	0.8	1.1	0.3
Protein (g)	7.5	2.3	7.5	2.3
Carbohydrates (g)	42.4	12.7	45.1	13.5
Dietary fiber (g)	10.8	3.2	12.8	3.8
Soluble fiber (g)	2.6	0.8	2.9	0.9
Insoluble fiber (g)	6.7	2.0	7.7	2.3
Fructans (g)	0.4	0.12	1.2	0.36
Mannitol (g)	0.09	0.03	0.26	0.08

international Ireland Ltd, Bray, Ireland).

SmartPill

SmartPill® (Given Imaging ltd, Yoqneam, Israel) is an indigestible wireless capsule that contains sensors for temperature, pH, and pressure. The capsule is 26.8 mm long and its diameter is 11.7 mm. The capsule sends the measured data to a receiver worn by the subject. Measurement data is uploaded to a computer and analyzed by MotiliGI® program. The program calculates mean pressure, median pH, contractions/min, and transit times based on changes in pH and temperature for the different parts of the gastrointestinal tract. In the present study, the capsule was swallowed with the test breakfast and the subject was prohibited from eating for six hours after the meal so the capsule would proceed to small intestine. Each study period ended when the capsule was defecated.

Breath hydrogen and IBS symptoms

Breath hydrogen was analyzed with Gastrolyzer® (Bedfont Scientific Ltd, Kent, England) before the test breakfast (0 min) and every 30 min for 11 h (660 min) on the test day and every three hours on the following days. Breath hydrogen was analyzed as a marker for colonic fermentation[19].

IBS symptoms during the study periods were collected with a visual analogue scale (VAS) questionnaire. We did not formally validate the questionnaire, but it follows the concept as described by Francis *et al*[20]. A similar scoring system has been used previously in other diet studies in IBS[21,22]. Symptoms were recorded once before the test breakfast (0 min) and every 30 min for 11 h on the test day and every 3 h on the following days. The questionnaire consisted of nine individual 100 mm VAS lines of the following different symptom classes: abdominal pain, abdominal cramps, bloating, flatulence, belly rumbling, nausea, heartburn, unpleasant sensation in the upper abdomen, and continuous urge to defecate. Additionally, participants kept a diary of defecation times and form of stool.

Missing values in gastrointestinal symptoms and hydrogen measurements were imputed with the mean value of the previous and following measurements. Two subjects failed to report the 660 min measurements for all symptoms and hydrogen concentration, and thus values were included only until 630 min for all subjects when calculating the outcome variables. The baseline (0 min) of symptoms was not included in outcome variables as this was measured before eating the test breakfast.

The outcome variables calculated from the symptom questionnaire scores were the following: mean of the scores for each symptom during the follow-up period (30-630 min), sum of total symptom scores at each time point, and the area under the curve (AUC) of the total symptom score during the follow up (30-630 min). AUC of breath hydrogen was calculated using the absolute breath hydrogen values (0-630 min). AUC values were calculated following trapezoidal rule[23] without respect to increase because symptom severity and hydrogen concentration may have a baseline value of zero. Symptom and H_2 measurements that were conducted after the test day were used to calculate the mean of total symptom score and mean of breath hydrogen content for different parts of the gastrointestinal tract.

Statistical analysis

Breath hydrogen was the primary outcome variable used in the study power calculations. Suitable previously published data was not available, and thus the study power was calculated based on a preliminary test performed in Fazer Bakeries in which healthy participants ate regular rye bread or low-FODMAP rye bread followed by analysis of breath hydrogen content during the six-hour postprandial period. The difference in breath hydrogen content (ppm) between fasting and at six hours was used to evaluate the number of subjects in the current study. Based on the power calculation, a sample size of eight would have 80% power to detect a 25-ppm difference in breath hydrogen using a paired *t*-test with a two-sided significance level of 0.05.

The patient characteristics and outcome variables are expressed as a median (range) and as number of cases for categorical variables. The difference in outcome variables between study periods was analyzed using the Wilcoxon signed-rank test for related samples. Correlations between mean symptom severity and

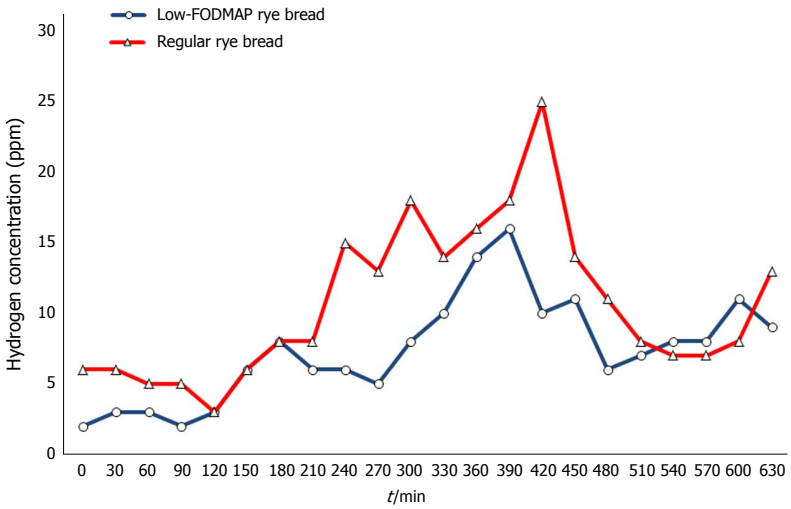

Figure 1 Medians of expired hydrogen concentration (ppm·min) during the test days.

mean breath hydrogen and between mean symptoms and SmartPill indices during the colonic phase were analyzed using the Spearman's rho. Statistical analysis was performed with IBM SPSS Statistics (Version 23, IBM Co., New York, United States) and Microsoft Office Excel 2013 (Microsoft Co., Washington, United States).

RESULTS

A total of nine female subjects (median age 39 years, range 29-51 years) with IBS were recruited into the study, of whom two withdrew during the study for personal reasons. The BMI of the subjects was [median (range)], 26.4 (19.5-30.4) kg/m^2. Three participants suffered from diarrhea-predominant IBS, two from constipation-predominant IBS and two from mixed type IBS. A flowchart of the recruitment process and the study is shown in Supplemental Figure 1.

Postprandial excretion of hydrogen expressed as $AUC_{(0\text{-}630\ min)}$ was [median (range)] 6300 (1785-10800) ppm·min for low-FODMAP rye bread and 10635 (4215-13080) ppm·min for regular bread. The two bread tests differed significantly (P = 0.028), indicating more intensive colonic fermentation after consumption of the regular rye bread. Median expired hydrogen concentrations are shown in Figure 1.

The means of the VAS measurements of individual gastrointestinal symptoms during the follow-up (30-630 min) did not reveal any statistically significant differences between the breads (Table 2). However, the flatulence severity was nearly significantly lower after low-FODMAP rye bread consumption (P = 0.06). Furthermore, there was a significant (P = 0.034) difference between the low-FODMAP bread (15 mm; range 5-34 mm) and the regular rye bread (34 mm; range 8-56 mm) in the maximum severity of flatulence (data for other maximum values not shown). Figure 2 shows the development of the total symptoms during the course of the test day. The difference in AUCs of total symptom score between low-FODMAP (23520 mm·min; range 6885-113610 mm·min) and regular rye breads (41130 mm·min; range 10785-83220 mm·min) was not statistically significant (P = 0.866).

All patients could swallow the SmartPill device without major challenges. In eight out of a total of 14 measurements the device stayed in the stomach for an unexpectedly long period (*i.e.*, > 10 h; in 6 measurements out of a total of 14 the device resided in the stomach > 15 h, data not shown). SmartPill left the stomach in less than five hours only during one measurement. Therefore, the devices did not follow on par with the rye bread bolus. All devices were defecated within three days of swallowing.

Transit times, median pH values, mean pressures, and contractions are shown in Table 3. SmartPill-derived transit times, pH values, mean pressure, or contractions/min in any part of the gastrointestinal tract did not differ between the bread tests. The association between colonic pressure and overall symptom severity during the time when the device was transiting the colon is shown in Figure 3. The correlation was significant after the participants had consumed regular rye bread (ρ = 0.786, P = 0.036) and was nearly significant after low-FODMAP bread consumption (ρ = 0.750, P = 0.052). The correlation coefficients between symptom severity and colonic contraction frequency were 0.775 (P = 0.041) and 0.786 (P = 0.036) after regular and low-FODMAP bread consumption, respectively. Colon pH and H_2 excretion were associated with symptom severity after regular bread (ρ = 0.821, P = 0.023 and ρ = 0.857, P = 0.014, respectively) but not after low-FODMAP bread (ρ = 0.342, P = 0.452 and ρ = 0.536, P = 0.215, respectively) consumption.

DISCUSSION

In this meal study, we demonstrated that consumption of low-FODMAP rye bread leads to reduced hydrogen

Table 2 Means (mm) of gastrointestinal symptoms from 30-630 min after the test meals median (range)

	Low-FODMAP rye	Regular rye bread	*P* value[1]
Abdominal pain	2.4 (0.0-28.2)	4.8 (0.1-21.9)	0.735
Cramps	1.2 (0.1-29.2)	3.0 (0.1-10.0)	0.917
Bloating	12.3 (1.0-48.4)	23.1 (1.1-37.8)	0.866
Flatulence	3.3 (0.5-7.6)	4.2 (0.5-28.2)	0.063
Belly rumbling	3.0 (0.1-6.6)	3.8 (1.4-11.4)	0.398
Nausea	1.0 (0.0-22.4)	2.1 (0.0-15.5)	1.000
Heartburn	1.4 (1.0-20.8)	1.8 (0.1-20.3)	1.000
Unpleasant sensation in the uppemen	7.4 (1.0-26.1)	11.8 (1.2-23.2)	0.310
Urge to defecate	1.5 (0.0-29.5)	2.1 (0.3-22.4)	0.735

[1]Wilcoxon signed-rank test.

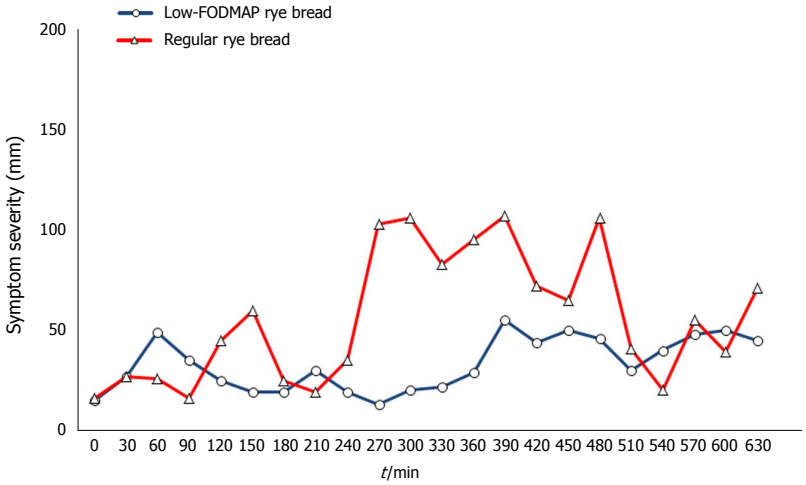

Figure 2 Medians of total symptom scores (mm) for both breads during the test days. The theoretical maximum of the symptom score sum is 900 mm.

expiration (a marker of colonic fermentation) when compared with regular rye bread consumption. Furthermore, the maximum flatulence severity was lower for the low-FODMAP rye bread compared with regular rye bread. No difference was found in other symptoms, pH, contractions, or total gastrointestinal tract pressure. Interestingly, intracolonic pressure and contraction frequency, rather than total gastrointestinal pressure, were associated with symptom severity during the colonic transition period of SmartPill. This finding suggests that the colon is most affected and is the origin of IBS symptoms. The exceedingly long gastric transit time measured by SmartPill was an unexpected finding.

Our finding of lower hydrogen excretion during the low-FODMAP rye bread test is consistent with previous studies; grain products that are high in fructans increase hydrogen excretion (*i.e.*, colonic fermentation) when compared with grain products low in fructans[15,24]. Additionally, the difference in the maximum flatulence value suggests a higher level of gas formation after regular rye bread consumption. There were no differences between the treatments in the perceived severity of other gastrointestinal symptoms, although the median values tended to favor the low-FODMAP rye bread. The perceived severity of symptoms was overall low. A larger sample size most likely would have been needed to reach statistical significance in symptom severity. The power calculation for the study was based on hydrogen excretion rather than change in symptoms.

A previous scintigraphy study has shown that after consumption of a medium-sized solid meal, 98%-99% of ingested food should leave the stomach within four hours and 84% within two hours[25]. The transition time of the SmartPill from stomach to small intestine varied from 4.5-22 h in the present study. These results are in contrast with previous studies[26,27], which have shown that gastric emptying of SmartPill takes place within five hours in most study subjects. On the other hand, sporadic prolonged gastric residence times of SmartPill in healthy volunteers have been previously reported[28,29]. SmartPill is a non-digestible capsule that presumably leaves the stomach during phase III of the migrating motor complex (MMC)[26]. The long gastric emptying times in the present study indicate that the six-hour lag time between the study breakfast and lunch was not long enough for the SmartPill to leave the stomach. The subsequent meal probably terminated the MMC cycle before the capsule was transported to the duodenum.

It is possible that gastric emptying times, at least

Table 3 SmartPill-derived transit times, pH values, mean pressure, and contractions/min median (range)

	Low-FODMAP rye bread	Regular rye bread	*P* value[1]
Transit time (h)			
Stomach	18.1 (5.3-22.3)	5.6 (4.5-18.0)	0.091
Small intestine	4.0 (2.1-5.6)	4.6 (3.2-6.6)	0.866
Colon	25.2 (12.2-50.0)	32.1 (14.7-47.6)	0.176
Whole GI tract	46.5 (22.6-73.5)	45.8 (24.3-70.4)	0.612
Median pH			
Stomach	1.5 (0.8-4.1)	1.5 (1.0-2.4)	0.671
Small intestine	7.5 (5.0-8.0)	7.6 (7.0-7.8)	0.915
Colon	7.2 (5.8-7.5)	6.5 (5.9-8.5)	0.612
Mean pressure (mmHg)			
Stomach	2.2 (1.9-2.7)	2.5 (2.0-3.0)	0.610
Small intestine	3.1 (1.6-8.6)	4.5 (2.4-7.0)	0.398
Colon	4.8 (3.2-6.3)	4.0 (2.0-6.7)	0.310
Contractions/min			
Stomach	1.2 (0.6-1.7)	1.0 (0.8-1.8)	0.553
Small intestine	3.2 (0.5-6.1)	4.9 (1.9-6.5)	0.176
Colon	1.7 (1.3-2.9)	1.7 (0.6-3.3)	0.495

[1]Wilcoxon signed-rank test.

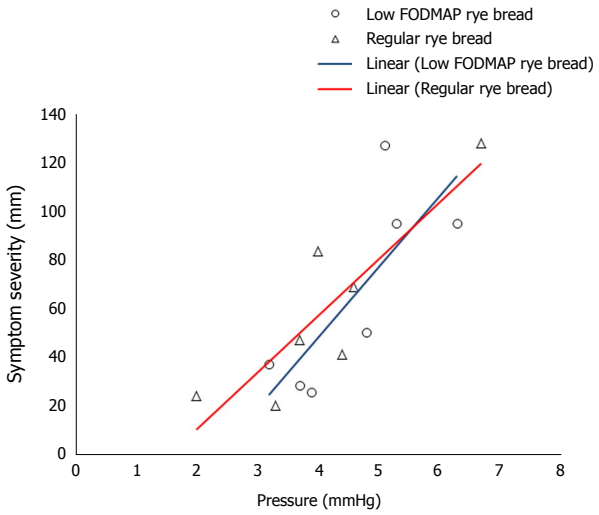

Figure 3 Association between intracolonic pressure and simultaneous total symptom score after consumption of test breads. The theoretical maximum symptom score sum is 900 mm.

those measured with SmartPill, are increased in IBS. Indeed, another study by Dupont *et al*[30] also reported gastric emptying times longer than 5 h in IBS patients. Furthermore, in study from Ringel-Kulka *et al*[17], patients with constipation-predominant IBS had prolonged gastric emptying times (mean 8 h). Although there were three bread meals during the study day, in many cases SmartPill followed the rye bolus with a delay of several hours. This is important information for future studies. SmartPill might fail to measure gastrointestinal circumstances in a timely manner, at least in patients with IBS. Based on our study, it is possible that SmartPill is more applicable for feeding studies lasting at least two days rather than one-day meal studies.

Due to the unexpectedly long residence of SmartPill in the stomach, the device was usually in the small intestine during the night. For this reason, we could not compare perceived symptoms and measured conditions in the small intestine. However, the residence time was longer in the large intestine, and thus we could link symptom ratings and conditions in the colon. Intracolonic pressure correlated with IBS symptom severity in our study. One of the key underlining reasons why IBS patients experience pain and discomfort is their lower threshold to sense pain and distension, a phenomenon called visceral hypersensitivity[2,31]. Therefore, any dietary or physio-anatomic factors that increase pressure in gut might worsen symptoms. Theoretically, intracolonic pressure might increase due to many factors, such as consumption of gas-forming FODMAPs, impaired handling of colonic gas, intestinal microbiota disturbances, fecal retention, difficulties in expelling gas or anatomical abnormalities that obstruct gas. However, with our methods we cannot explain the underlining cause of the increased intracolonic pressure. Nonetheless, hydrogen excretion did not correlate with intracolonic pressure in the present study, suggesting that other reasons such as intestinal abnormalities or microbiota disturbances might play a larger role. Intestinal abnormalities previously associated with IBS symptoms include small intestinal constriction, dilated transverse colon, and redundant colon[32,33]. Further research is warranted in the area of intracolonic pressure and its role in IBS symptoms. Interestingly, Rogers *et al*[34] have shown that intraluminal pressure was higher among subjects with IBS when compared with healthy subjects. These results, together with our findings, suggest that colonic gas amplitude may have a causal role in IBS symptom generation.

We also found a correlation between colonic contraction frequency and symptom severity during both bread periods. Previously, Hasler *et al*[35] demonstrated

in their SmartPill study that colonic motor activity (*i.e.*, colonic contraction frequency and duration of contractions) is increased in constipation-predominant IBS patients when compared with non-IBS subjects. Increased motoric activity might be one mechanism for how intracolonic pressure is increased in IBS. We also observed that pH and hydrogen excretion during the colonic phase were associated with symptom severity after consumption of regular rye bread; these findings might simply reflect the degree of colonic fermentation and act as surrogates of colonic pressure. Taken together, our findings with previous SmartPill-gathered data[17,35] provide further evidence for the role of intraluminal physiological conditions in triggering IBS symptoms. This observation is of relevance to clinicians as IBS is sometimes considered primarily as a psychosocial condition[36]. Interestingly, spasmolytics, such as peppermint oil capsules, relax smooth muscles of the intestinal wall and thus reduce colonic motility, which may explain the reductions in pain, discomfort, and feeling of bloating reported in several clinical trials[37]. Attempts to reduce intraluminal pressure and contractions might continue to be important therapeutic targets in IBS.

Our study has limitations. As stated previously, the number of subjects might have been too small to detect all true differences between the breads. The long residence of SmartPill in the stomach is a potential bias in our study. The observation period was rather short (630 min). On the basis of our experience in this study, we recommend longer studies when using SmartPill in diet-related research. The strengths of our study include the double-blind randomized setting and standardization of the evening snack before the trial and all food consumed during the first 24 h of the test period.

In conclusion, our meal study demonstrated that consumption of low-FODMAP rye bread led to reduced colonic fermentation and maximum flatulence values in IBS patients when compared with regular rye bread. No differences could be found in other symptoms, pH, colonic pressure, or gut contractions. Due to its inability to measure effects of a singular food bolus in a timely manner, this study also showed that SmartPill might not be an optimal device in evaluating gastrointestinal circumstances during meal studies lasting less than 24 h. The observed correlation between increased intracolonic pressure and symptom severity underlines the central role of visceral sensitivity in IBS. Further studies are needed to understand the role of intracolonic pressure formation in IBS.

ARTICLE HIGHLIGHTS

Research background

FODMAPs are rapidly fermentable carbohydrates shown to aggravate gastrointestinal symptoms in irritable bowel syndrome (IBS). A major challenge in the research of IBS is the lack of objective markers of disease activity. Excretion of hydrogen and methane and colonic fermentation markers are among the rare easily available and objective markers of gastrointestinal circumstances during the consumption of FODMAPs or other poorly absorbable carbohydrates. Grains are often considered as triggers of irritable bowel syndrome symptoms but less is known about the effects of grain products with differing content of FODMAPs on gastrointestinal transit times, pH and intraluminal pressure in patients with IBS.

Research motivation

SmartPill, a motility monitoring capsule, which measures intraluminal pH, transit time and pressure, and might thus offer the means to gather objective data on gastrointestinal conditions in IBS patients. A combination of SmartPill data and measurements of perceived symptoms may improve our understanding on the etiology of IBS symptoms when consuming grains high in FODMAPs.

Research objectives

Our aim was to evaluate if rye bread low in FODMAPs would cause less hydrogen excretion, lower intraluminal pressure, higher colonic pH and less IBS symptoms than regular rye bread.

Research methods

The study was conducted as a randomized double blind controlled cross-over meal study. Female IBS patients (n = 7) ate study breads on 3 consecutive meals. Intraluminal conditions were measured by SmartPill®, an indigestible motility capsule.

Research results

Postprandial hydrogen excretion, a marker of colonic fermentation, expressed as $AUC_{(0\text{-}630\ min)}$ was [median (range)] 6300 (1785-10800) for low-FODMAP rye bread and 10635 (4215-13080) ppm·min for regular bread (P = 0.028). The means of the visual analogue scale measurements of individual gastrointestinal symptoms did not show any statistically significant differences between the breads. Intraluminal pressure correlated significantly with total symptom score after regular rye bread (ρ = 0.786, P = 0.036) and nearly significantly after low-FODMAP bread consumption (ρ = 0.75, P = 0.052). We found no differences in pH, contractions or transit times between the breads. Gastric emptying of SmartPill was slower than expected on the basis of majority of research literature.

Research conclusions

Our meal study demonstrated that low-FODMAP rye bread reduces colonic fermentation but no difference was found in median values of symptoms, pH, colonic pressure of gastrointestinal tract when compared to regular rye bread. Our observation on the correlation between increased intra-colonic pressure and symptom severity warrants further studies in IBS.

Research perspectives

Our finding on the correlation of intracolonic pressure and symptom severity suggests that IBS symptoms might be worsened by any reason that leads to increased colonic pressure in IBS. Consequently, any therapeutic attempts to reduce intraluminal pressure and contractions might continue to be important therapeutic targets in IBS. The study also implied that SmartPill might not be an optimal device to evaluate the gastrointestinal circumstances during meal studies among IBS patients lasting less than 24 h, due to device's inability to measure effects of a singular food bolus in a timely manner. Observation and feeding periods longer than 38 h are recommended for future research utilizing SmartPill, especially among people with IBS.

REFERENCES

1 **Canavan C**, West J, Card T. The epidemiology of irritable bowel syndrome. *Clin Epidemiol* 2014; **6**: 71-80 [PMID: 24523597 DOI: 10.2147/CLEP.S40245]

2 **Simrén M**, Törnblom H, Palsson OS, van Tilburg MAL, Van Oudenhove L, Tack J, Whitehead WE. Visceral hypersensitivity is associated with GI symptom severity in functional GI disorders: consistent findings from five different patient cohorts. *Gut*.

2017; pii: gutjnl-2016-312361 [PMID: 28104632 DOI: 10.1136/gutjnl-2016-312361]
3 **Ford AC**, Talley NJ. Mucosal inflammation as a potential etiological factor in irritable bowel syndrome: a systematic review. *J Gastroenterol* 2011; **46**: 421-431 [PMID: 21331765 DOI: 10.1007/s00535-011-0379-9]
4 **Agrawal A**, Whorwell PJ. Review article: abdominal bloating and distension in functional gastrointestinal disorders--epidemiology and exploration of possible mechanisms. *Aliment Pharmacol Ther* 2008; **27**: 2-10 [PMID: 17931344 DOI: 10.1111/j.1365-2036.2007.03549.x]
5 **Jones VA**, McLaughlan P, Shorthouse M, Workman E, Hunter JO. Food intolerance: a major factor in the pathogenesis of irritable bowel syndrome. *Lancet* 1982; **2**: 1115-1117 [PMID: 6128447 DOI: 10.1016/S0140-6736(82)92782-9]
6 **Simrén M**, Månsson A, Langkilde AM, Svedlund J, Abrahamsson H, Bengtsson U, Björnsson ES. Food-related gastrointestinal symptoms in the irritable bowel syndrome. *Digestion* 2001; **63**: 108-115 [PMID: 11244249 DOI: 10.1159/000051878]
7 **Hayes PA**, Fraher MH, Quigley EM. Irritable bowel syndrome: the role of food in pathogenesis and management. *Gastroenterol Hepatol* 2014; **10**: 164-174 [PMID: 24829543]
8 **Gibson PR**, Shepherd SJ. Evidence-based dietary management of functional gastrointestinal symptoms: The FODMAP approach. *J Gastroenterol Hepatol* 2010; **25**: 252-258 [PMID: 20136989 DOI: 10.1111/j.1440-1746.2009.06149.x]
9 **Marsh A**, Eslick EM, Eslick GD. Does a diet low in FODMAPs reduce symptoms associated with functional gastrointestinal disorders? A comprehensive systematic review and meta-analysis. *Eur J Nutr* 2016; **55**: 897-906 [PMID: 25982757 DOI: 10.1007/s00394-015-0922-1]
10 **Liu L**, Wang S, Liu J. Fiber consumption and all-cause, cardiovascular, and cancer mortalities: a systematic review and meta-analysis of cohort studies. *Mol Nutr Food Res* 2015; **59**: 139-146 [PMID: 25382817 DOI: 10.1002/mnfr.201400449]
11 **Rakha A**, Åman P and Andersson R. Characterisation of dietary fibre components in rye products. *Food Chem* 2010; **119:** 859-867 [DOI: 10.1016/j.foodchem.2009.09.090]
12 **Helldán A**, Raulio S, Kosola M, Tapanainen H, Ovaskainen ML, Virtanen S. Finravinto 2012 tutkimus-The National FINDIET 2012 Survey. ISBN 978-952-245-950-3 (printed); 978-952-245-951-0 (pdf) THL. Raportti 16/2013, 187p. Helsinki, Finland, 2013
13 **Paajanen L**, Tuure T, Korpela R. Impaired tolerance of indigestible carbohydrates in adults with subjective milk intolerance *Scand J Nutr* 2004; **48**: 131-135
14 **Quigley EM**. Editorial: balancing fibre and FODMAPs in IBS - a 'rye' look at an old problem. *Aliment Pharmacol Ther* 2016; **44**: 1134-1135 [PMID: 27734545 DOI: 10.1111/apt.13805]
15 **Laatikainen R**, Koskenpato J, Hongisto SM, Loponen J, Poussa T, Hillilä M, Korpela R. Randomised clinical trial: low-FODMAP rye bread vs. regular rye bread to relieve the symptoms of irritable bowel syndrome. *Aliment Pharmacol Ther* 2016; **44**: 460-470 [PMID: 27417338 DOI: 10.1111/apt.13726]
16 **Marteau P**, Flourié B. Tolerance to low-digestible carbohydrates: symptomatology and methods. *Br J Nutr* 2001; **85** Suppl 1: S17-S21 [PMID: 11321024 DOI: 10.1079/BJN2000258]
17 **Ringel-Kulka T**, Choi CH, Temas D, Kim A, Maier DM, Scott K, Galanko JA, Ringel Y. Altered Colonic Bacterial Fermentation as a Potential Pathophysiological Factor in Irritable Bowel Syndrome. *Am J Gastroenterol* 2015; **110**: 1339-1346 [PMID: 26303129 DOI: 10.1038/ajg.2015.220]
18 Rome III Diagnostic Criteria for Functional Gastrointestinal Disorders. Available from: URL: http://www.romecriteria.org/assets/pdf/19_RomeIII_apA_885-898.pdf
19 **Levitt MD**. Production and excretion of hydrogen gas in man. *N Engl J Med* 1969; **281**: 122-127 [PMID: 5790483 DOI: 10.1056/NEJM196907172810303]
20 **Francis CY**, Morris J, Whorwell PJ. The irritable bowel severity scoring system: a simple method of monitoring irritable bowel syndrome and its progress. *Aliment Pharmacol Ther* 1997; **11**: 395-402 [PMID: 9146781 DOI: 10.1046/j.1365-2036.1997.142318000.x]
21 **Halmos EP**, Power VA, Shepherd SJ, Gibson PR, Muir JG. A diet low in FODMAPs reduces symptoms of irritable bowel syndrome. *Gastroenterology* 2014; **146**: 67-75.e5 [PMID: 24076059 DOI: 10.1053/j.gastro.2013.09.046]
22 **Biesiekierski JR**, Peters SL, Newnham ED, Rosella O, Muir JG, Gibson PR. No effects of gluten in patients with self-reported non-celiac gluten sensitivity after dietary reduction of fermentable, poorly absorbed, short-chain carbohydrates. *Gastroenterology* 2013; **145**: 320-328.e1-3 [PMID: 23648697 DOI: 10.1053/j.gastro.2013.04.051]
23 **Pruessner JC**, Kirschbaum C, Meinlschmid G, Hellhammer DH. Two formulas for computation of the area under the curve represent measures of total hormone concentration versus time-dependent change. *Psychoneuroendocrinology* 2003; **28**: 916-931 [PMID: 12892658 DOI: 10.1016/j.psyneuen.2003.10.002]
24 **Nilsson AC**, Ostman EM, Granfeldt Y, Björck IM. Effect of cereal test breakfasts differing in glycemic index and content of indigestible carbohydrates on daylong glucose tolerance in healthy subjects. *Am J Clin Nutr* 2008; **87**: 645-654 [PMID: 18326603]
25 **Vasavid P**, Chaiwatanarat T, Pusuwan P, Sritara C, Roysri K, Namwongprom S, Kuanrakcharoen P, Premprabha T, Chunlertrith K, Thongsawat S, Sirinthornpunya S, Ovartlarnporn B, Kachintorn U, Leelakusolvong S, Kositchaiwat C, Chakkaphak S, Gonlachanvit S. Normal Solid Gastric Emptying Values Measured by Scintigraphy Using Asian-style Meal:A Multicenter Study in Healthy Volunteers. *J Neurogastroenterol Motil* 2014; **20**: 371-378 [PMID: 24948129 DOI: 10.5056/jnm13114]
26 **Kuo B**, McCallum RW, Koch KL, Sitrin MD, Wo JM, Chey WD, Hasler WL, Lackner JM, Katz LA, Semler JR, Wilding GE, Parkman HP. Comparison of gastric emptying of a nondigestible capsule to a radio-labelled meal in healthy and gastroparetic subjects. *Aliment Pharmacol Ther* 2008; **27**: 186-196 [PMID: 17973643 DOI: 10.1111/j.1365-2036.2007.03564.x]
27 **Cassilly D**, Kantor S, Knight LC, Maurer AH, Fisher RS, Semler J, Parkman HP. Gastric emptying of a non-digestible solid: assessment with simultaneous SmartPill pH and pressure capsule, antroduodenal manometry, gastric emptying scintigraphy. *Neurogastroenterol Motil* 2008; **20**: 311-319 [PMID: 18194154 DOI: 10.1111/j.1365-2982.2007.01061.x]
28 **Timm D**, Willis H, Thomas W, Sanders L, Boileau T, Slavin J. The use of a wireless motility device (SmartPill®) for the measurement of gastrointestinal transit time after a dietary fibre intervention. *Br J Nutr* 2011; **105**: 1337-1342 [PMID: 21138605 DOI: 10.1017/S0007114510004988]
29 **Diaz Tartera HO**, Webb DL, Al-Saffar AK, Halim MA, Lindberg G, Sangfelt P, Hellström PM. Validation of SmartPill® wireless motility capsule for gastrointestinal transit time: Intra-subject variability, software accuracy and comparison with video capsule endoscopy. *Neurogastroenterol Motil* 2017; **29**: 1-9 [PMID: 28524600 DOI: 10.1111/nmo.13107]
30 **DuPont AW**, Jiang ZD, Harold SA, Snyder N, Galler GW, Garcia-Torres F, DuPont HL. Motility abnormalities in irritable bowel syndrome. *Digestion* 2014; **89**: 119-123 [PMID: 24503633 DOI: 10.1159/000356314]
31 **Major G**, Pritchard S, Murray K, Alappadan JP, Hoad CL, Marciani L, Gowland P, Spiller R. Colon Hypersensitivity to Distension, Rather Than Excessive Gas Production, Produces Carbohydrate-Related Symptoms in Individuals With Irritable Bowel Syndrome. *Gastroenterology* 2017; **152**: 124-133.e2 [PMID: 27746233 DOI: 10.1053/j.gastro.2016.09.062]
32 **Lam C**, Chaddock G, Marciani Laurea L, Costigan C, Cox E, Hoad C, Pritchard S, Gowland P, Spiller R. Distinct Abnormalities of Small Bowel and Regional Colonic Volumes in Subtypes of Irritable Bowel Syndrome Revealed by MRI. *Am J Gastroenterol* 2017; **112**: 346-355 [PMID: 27958282 DOI: 10.1038/ajg.2016.538]
33 **Raahave D**. Faecal retention: a common cause in functional bowel disorders, appendicitis and haemorrhoids--with medical and surgical therapy. *Dan Med J* 2015; **62**: pii: B5031 [PMID: 25748875]
34 **Rogers J**, Henry MM, Misiewicz JJ. Increased segmental activity

and intraluminal pressures in the sigmoid colon of patients with the irritable bowel syndrome. *Gut* 1989; **30**: 634-641 [PMID: 2731756]

35 **Hasler WL**, Saad RJ, Rao SS, Wilding GE, Parkman HP, Koch KL, McCallum RW, Kuo B, Sarosiek I, Sitrin MD, Semler JR, Chey WD. Heightened colon motor activity measured by a wireless capsule in patients with constipation: relation to colon transit and IBS. *Am J Physiol Gastrointest Liver Physiol* 2009; **297**: G1107-G1114 [PMID: 19808653 DOI: 10.1152/ajpgi.00136.2009]

36 **Lea R**, Whorwell PJ. New insights into the psychosocial aspects of irritable bowel syndrome. *Curr Gastroenterol Rep* 2003; **5**: 343-350 [PMID: 12864966 DOI: 10.1007/s11894-003-0073-z]

37 **Khanna R**, MacDonald JK, Levesque BG. Peppermint oil for the treatment of irritable bowel syndrome: a systematic review and meta-analysis. *J Clin Gastroenterol* 2014; **48**: 505-512 [PMID: 24100754 DOI: 10.1097/MCG.0b013e3182a88357]

P- Reviewer: Chiarioni G, Dumitrascu DL, Rostami K
S- Editor: Wang XJ **L- Editor**: A **E- Editor**: Huang Y

World Journal of Gastroenterology

Submit a Manuscript: http://www.f6publishing.com

World J Gastroenterol 2018 March 21; 24(11): 1269-1277

DOI: 10.3748/wjg.v24.i11.1269

ISSN 1007-9327 (print) ISSN 2219-2840 (online)

ORIGINAL ARTICLE

Prospective Study

Fatty liver in hepatitis C patients post-sustained virological response with direct-acting antivirals

Mazen Noureddin, Micaela M Wong, Tsuyoshi Todo, Shelly C Lu, Arun J Sanyal, Edward A Mena

Mazen Noureddin, Fatty Liver Program, Cedars-Sinai Medical Center, Los Angeles, CA 90048, United States

Mazen Noureddin, Division of Digestive and Liver Diseases, Cedars-Sinai Medical Center, Los Angeles, CA 90048, United States

Micaela M Wong, California Liver Research Institute, Pasadena, CA 91105, United States

Tsuyoshi Todo, Comprehensive Transplant Center, Department of Surgery, Cedars-Sinai Medical Center, Los Angeles, CA 90048, United States

Shelly C Lu, Division of Digestive and Liver Diseases, Cedars-Sinai Medical Center, Los Angeles, CA 90048, United States

Arun J Sanyal, Division of Gastroenterology, Hepatology and Nutrition, Department of Internal Medicine, School of Medicine, Virginia Commonwealth University, Richmond, VA 23298, United States

Edward A Mena, California Liver Research Institute, Pasadena, CA 91105, United States

ORCID number: Mazen Noureddin (0000-0003-2127-2040); Micaela M Wong (0000-0001-9912-2574); Tsuyoshi Todo (0000-0003-1264-9301); Shelly C Lu (0000-0003-2128-5407); Arun J Sanyal (0000-0001-8682-5748); Edward A Mena (0000-0003-0631-9525).

Author contributions: Noureddin M provided the study concept and design; Noureddin M, Wong MM and Mena EA contributed to acquisition of data; Noureddin M, Wong MM, Todo T, Lu SC and Sanyal AJ contributed to analysis and interpretation of data; Noureddin M drafted the manuscript; Noureddin M, Wong MM, Todo T, Lu SC, Sanyal AJ and Mena EA contributed to critical revision of the manuscript for important intellectual content; Noureddin M contributed to the statistical analysis; Noureddin M and Mena EA provided administrative and technical support and study supervision; Wong MM provided support for carrying out the study; all authors gave final approval of the version to be published and agree to be accountable for all aspects of the work in ensuring that questions related to the accuracy or integrity of any part of the work are appropriately investigated and resolved.

Institutional review board statement: This study was approved by the Central Institutional Review Board.

Informed consent statement: Informed voluntary consent was acquired from all the study participants.

Conflict-of-interest statement: Noureddin M has been on the advisory board or a speaker for EchoSens North America, OWL, Intercept and Abbott; Noureddin M has received research support from Gilead, Galmed, Galectin, Conatus, Zydus and Shire; Noureddin M is a minor shareholder of Anaetos; Sanyal AJ has been a consultant to Intercept, Galectin, BMS, Nitto Denko, Nimbus, Aredlyx, Vivelyx, and Tandeva; Sanyal AJ has received grants from Gilead, Intercept, Novartis, Merck, BMS, and Tobira; Sanyal AJ has stock or stock options in Genfit, Akarna, Tiziana, Natural Shield, Durect, and Exhalenz. Mena EA has received research support from Galmed, Conatus, Shire, Merck and Gilead; Mena EA has been a consultant and advisor to Gilead, Abbvie, Merck, Bayer, and Grifalos; Mena EA is a member of the speakers' bureaus for Gilead, Abbvie, Merck, Bayer, Echosens North America and Grifalos; Mena EA owns stocks in Gilead and Galectin; The other authors report no conflicts of interest.

Data sharing statement: The statistical code and dataset are available from the corresponding author at mazen.noureddin@cshs.org. Consent for data sharing was not obtained but the presented data are anonymized and risk of identification is low.

Manuscript source: Unsolicited manuscript

Correspondence to: Mazen Noureddin, MD, MHSc, Associate Professor, Division of Digestive and Liver Diseases,

Comprehensive Transplant Program, Cedars-Sinai Medical Center, 8900 Beverly Blvd, Suite 250, Los Angeles, CA 90048 United States. mazen.noureddin@cshs.org
Telephone: +1-310-4237088
Fax: +1-310-2488197

Received: December 3, 2017
Peer-review started: December 5, 2017
First decision: December 14, 2017
Revised: January 27, 2018
Accepted: March 3, 2018
Article in press: March 3, 2018
Published online: March 21, 2018

Abstract

AIM

To determine steatosis and fibrosis prevalence in hepatitis C patients after a sustained virological response achieved with direct-acting antivirals.

METHODS

Transient elastography with controlled attenuation parameter (CAP) was used to assess hepatic steatosis post-sustained virological response (SVR); the CAP technology was not available in the United States at study initiation. Liver stiffness/fibrosis was measured before and 47 wk after treatment completion. Patients with genotype 3 and patients with cirrhosis were excluded.

RESULTS

One hundred and one patients were included in the study. Post-SVR there were decreases from baseline in alanine aminotransferase (ALT) (63.1 to 17.8 U/L), aspartate aminotransferase (51.8 to 21.5 U/L) and fibrosis score (7.4 to 6.1 kPa) ($P < 0.05$). Post-SVR, 48 patients (47.5%) had steatosis on CAP; of these, 6.25% had advanced fibrosis. Patients with steatosis had higher body mass index (29.0 *vs* 26.1 kg/m^2), glucose (107.8 *vs* 96.6 mg/dL), ALT (20.4 *vs* 15.3 mg/dL), CAP score (296.3 *vs* 212.4 dB/m) and fibrosis score (7.0 *vs* 5.3 kPa); $P < 0.05$. Interestingly, compared to baseline, both patients with and without steatosis had change in fibrosis score post-SVR (7.7 kPa *vs* 7.0 kPa and 7.0 kPa *vs* 5.3 kPa); alternatively, ($P < 0.05$) and therefore patients with steatosis continued to have clinically significant stiffness ($\geqslant$ 7 kPa).

CONCLUSION

Fatty liver is very common in hepatitis C virus (HCV) patients post-SVR. These patients continue to have elevated mean fibrosis score ($\geqslant$ 7 kPa) compared to those without fatty liver; some have advanced fibrosis. Long term follow up is needed to assess steatosis and fibrosis in HCV patients post-SVR.

Key words: Nonalcoholic fatty liver disease; Hepatitis C; Fibrosis; Steatosis; Sustained virological response; Direct-acting antivirals

Core tip: This is the first prospective study to assess the prevalence of fatty liver in hepatitis C patients who have achieved a sustained virological response with direct-acting antivirals. The study's findings that fatty liver is present in 47.5% of these patients and that some steatotic patients have clinically significant fibrosis despite normal liver enzymes should raise awareness of the post-sustained virological response (SVR) prevalence of fatty liver and the importance of post-SVR assessment of steatosis and fibrosis and long-term follow up with these patients.

Noureddin M, Wong MM, Todo T, Lu SC, Sanyal AJ, Mena EA. Fatty liver in hepatitis C patients post-sustained virological response with direct-acting antivirals. *World J Gastroenterol* 2018; 24(11): 1269-1277 Available from: URL: http://www.wjgnet.com/1007-9327/full/v24/i11/1269.htm DOI: http://dx.doi.org/10.3748/wjg.v24.i11.1269

INTRODUCTION

With the growing epidemic of obesity and type 2 diabetes mellitus, nonalcoholic fatty liver disease (NAFLD) currently has a worldwide prevalence of 25.24% (approximately 1.8 billion people)[1], making it the most common cause of chronic liver disease (CLD), followed by chronic hepatitis B (CHB, 257 million people), and chronic hepatitis C (CHC, 71 million people)[2]. In the United States, NAFLD and CHC are the two most common CLD causes[3], and nonalcoholic steatohepatitis (NASH)-associated cirrhosis is the second leading indication for liver transplant (LT) after hepatitis C virus (HCV)-associated end-stage liver disease[4]. With the recent study that showed that between 2004 and 2013 the number of adult patients with NASH awaiting LTs almost tripled[4], combined with the rapidly expanding population of CHC patients achieving sustained virological responses (SVRs) with direct-acting antivirals (DAAs), it is thought that NASH may soon become the leading indication for LT. NAFLD prevalence is now estimated to be approximately 30% in the United States[5].

NAFLD is usually diagnosed by detecting steatosis after excluding other causes of liver disease. However, hepatic steatosis may occur in patients with other liver diseases, often in those with obesity and other metabolic factors typical of NAFLD, potentially creating an additive or synergistic combination of steatosis, oxidative damage, cellular impairment and other factors that may worsen liver injury[6]. Steatosis is known to escalate liver necroinflammatory activity and accelerate fibrosis in CHC patients[7]. The hepatic steatosis prevalence in

CHC patients has been reported to be approximately 50% (range 30%-70%)[8]. The mechanisms leading to steatosis in CHC have not been fully elucidated but may include host factors leading to insulin resistance and interactions between lipid metabolism pathways and the HCV core protein[9,10]. It has been proposed that HCV's effects on hepatic lipid metabolism may inhibit the export proteins needed for the assembly and secretion of very low density lipoproteins (VLDL), resulting in triglyceride accumulation in the liver[8]. Therefore, hepatic steatosis in HCV patients may result from some combination of viral and metabolic factors, other than in genotype 3 (GNT3) patients in which the steatosis may be due to direct effects of genotype 3 viral proteins[11].

Historically, an SVR with interferon was not associated with steatosis resolution except in GNT3 patients which has a different steatosis etiology[10]. In patients with an SVR achieved with DAAs steatosis prevalence is unknown. In this prospective, cross-sectional study, we assessed steatosis prevalence and degree of fibrosis in CHC patients who achieved an SVR through treatment with DAAs.

MATERIALS AND METHODS

Study design

This is a prospective, cross-sectional study of patients with CHC who achieved an SVR after treatment with DAAs. The patients in this cohort had been treated with a variety of direct-acting antiviral regimens: ledipasvir/sofosbuvir (Harvoni), 75 patients; elbasvir/grazoprevir (Zepatier), 1 patient; dasabuvir/ombitasvir/paritaprevir/ritonavir (Viekira), 7 patients; dasabuvir/ombitasvir/paritaprevir/ritonavir with ribavirin, 2 patients; sofosbuvir (Sovaldi) with ribavirin, 9 patients; sofosbuvir with daclatasvir (Daklinza), 1 patient; sofosbuvir with simeprevir (Olysio), 2 patients; sofosbuvir/velpatasvir (Epclusa), 4 patients. Between January 2016 and March 2017, 101 adult patients were enrolled, excluding patients with other liver diseases, secondary causes of steatosis (*e.g.*, medications, excessive alcohol), and GNT3 which has a different steatosis etiology. After achieving an SVR, patients were invited to undergo standardized history and anthropometric examination, laboratory testing, and transient elastography (TE) at the California Liver Research Institute in Los Angeles. This study received approval and was done under IRB protocol CLRI-01. Ethical guidelines for human research were followed. All patients signed informed consent.

Transient elastography

TE was performed using the FibroScan 502 Touch model (M Probe, XL Probe; Echosens, Paris, France) by an experienced TE-certified technician blinded to clinical data. Patients were asked to fast for at least 4 h prior to the examination. The procedure was performed in the supine position with the right arm adducted while holding the breath for 10 s. All patients were first scanned with the M probe (3.5 MHz) over the right liver lobe. If indicated by the machine, patients were re-evaluated using the XL probe (2.5 MHz). Ten measurements were made and the interquartile range was less than 30%. We defined test failure when no stiffness measurement was obtained or there were unreliable measurements (success rate < 60% or interquartile range/median > 30%)[12-14].

Liver stiffness/fibrosis scores were measured before and within one year after completion of HCV treatment with DAAs; the median time interval between treatment completion and post-SVR TE was 47 wk, with no significant difference between patients with and without steatosis. Simultaneous liver steatosis measurements were obtained using controlled attenuation parameter (CAP) values in dB/m only after SVR achievement as the technology was not available in the United States at the study's initiation. Based on the recent large patient data meta-analysis of studies containing histology-verified CAP data for grading of steatosis that determined optimal cut-offs for CAP[15], steatosis was defined as $\geqslant$ 248 dB/M. Clinically significant stiffness was defined as $\geqslant$ 7 kilopascal (kPa)[16,17].

Patients' specifications

We included patients if they were 18 years or older, were treated for CHC using DAAs and were able to provide informed consent. We excluded patients if they (1) had a history of significant alcohol intake within 2 years of recruitment (14 drinks/wk for men or 7 drinks/wk for women) as assessed by the hepatologist as well as the Alcohol Use Disorders Identification Test-Consumption (AUDIT-C) questionnaire; (2) had secondary causes of fatty liver such as medications (for example, methotrexate) or other infectious causes (for example, human immunodeficiency virus); (3) had evidence of liver diseases other than hepatitis C; (4) were HCV GNT3 as it is thought to have a different underlying etiology of steatosis related to the virus (viral steatosis) and we sought to investigate this genotype separately; or (5) had cirrhosis based on imaging or FibroScan. All the following information was collected: medical history, age, sex, height, weight, body mass index (BMI), ethnic background, and vital signs.

Laboratory measurements

The biochemical tests that were measured included aspartate aminotransferase (AST), alanine aminotransferase (ALT), alkaline phosphatase, total bilirubin, direct bilirubin, albumin, fasting glucose, hemoglobin A1c, triglycerides, total cholesterol, high-density lipoprotein, and low-density lipoprotein. Other measurements included platelets, prothrombin time, and international normalized ratio.

Statistical analysis

The chi-square test was used to compare between categorical variables, and a paired *t* test to compare

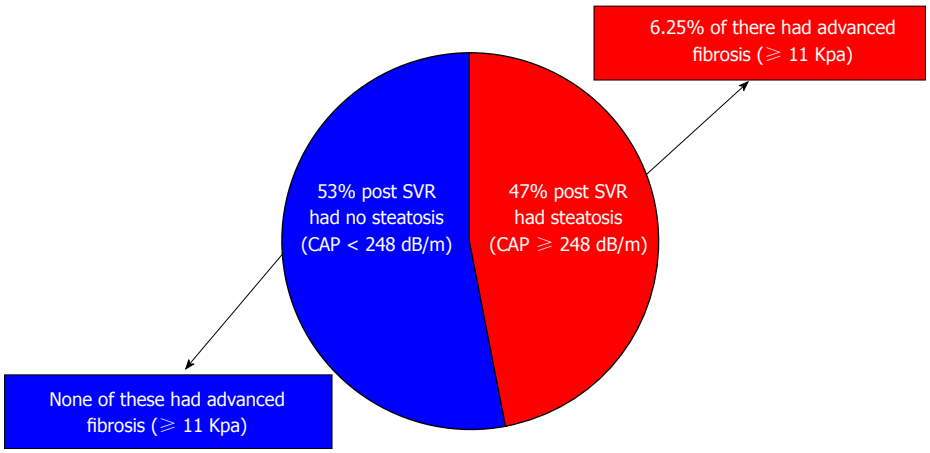

Figure 1 Post-sustained virological response steatosis prevalence in hepatitis C virus patients and advanced fibrosis prevalence in those with and without steatosis. SVR: Sustained virological response; CAP: Controlled attenuation parameter.

mean differences between continuous variables. Primary and secondary comparisons within groups were calculated with paired *t* tests, two-tailed, independent-sample *t* tests, or nonparametric tests including Wilcoxon signed-rank test as applicable. A two-tailed $P < 0.05$ was considered statistically significant. Statistical analyses were performed with SPSS 21.

RESULTS

Patient characteristics

Between January 2016 and March 2017, 101 adult CHC patients who achieved SVR were enrolled. At baseline the average age for the entire cohort was 60.3 ± 10.7 years and BMI was 27.6 ± 6.9 kg/m^2; 37% were Caucasian and 26% were Hispanic. The average fibrosis score was 7.4 ± 1.9 kPa. HCV genotypes were: GNT1 (85%), GNT2 (14%), and GNT4 (1%) (Table 1).

Changes post-SVR

Changes in the Entire Cohort: As expected, post-SVR HCV viral load was undetectable compared to prior baseline (prior to starting treatment) (0.0 ± 0.0 IU/m *vs* 6.2 ± 0.9 IU/m; $P < 0.0001$). ALT and AST decreased to normal levels post-SVR compared to baseline (17.8 ± 12.3 U/L *vs* 63.1 ± 62.6 U/L for ALT; $P < 0.0001$ and 21.5 ± 8.0 U/L *vs* 51.8 ± 41.1 U/L for AST; $P < 0.0001$). There was no change in BMI post-SVR compared to baseline (27.5 ± 6.9 kg/m^2 *vs* 27.6 ± 6.9 kg/m^2). In the overall cohort, post-SVR there was a significant decrease in fibrosis score on TE (7.4 ± 1.9 kPa to 6.1 ± 3.6 kPa; $P = 0.013$), a decline that is considered clinically significant.

Changes in patients with and without steatosis post-SVR: Post-SVR, 48 patients (47.5%) had steatosis with mean CAP score 296.3 ± 37.4 compared to a mean CAP score 212.4 ± 29.4 dB/m in patients without steatosis ($P < 0.0001$) (Figure 1). Patients with steatosis were more likely than patients without steatosis to have type 2 diabetes (18.7% *vs* 7.5%; $P = 0.04$), dyslipidemia (10.4% *vs* 5.7%; $P = 0.048$), higher body mass index (28.9 ± 6.6 kg/m^2 *vs* 26.1 ± 6.9 kg/m^2; $P = 0.049$), ALT (20.4 ± 16.5 U/L *vs* 15.3 ± 5.5 U/L; $P = 0.048$), fasting glucose (107.8 ± 30.5 mg/dL *vs* 96.5 ± 11.1 mg/dL; $P = 0.023$) and triglycerides (138.8 ± 77.9 mg/dL *vs* 109.7 ± 63.9 mg/dL; $P = 0.05$) (Table 2). None of the patients without steatosis had abnormal liver enzymes; only 6.25% of patients with steatosis had abnormal liver enzymes.

Changes in patients with and without steatosis between baseline and post-SVR: Interestingly, patients with steatosis continued to have clinically significant liver stiffness (mean baseline 7.7 ± 1.7 kPa; post-SVR 7.0 ± 4.8 kPa; $P = 0.037$) while patients without steatosis did not (mean baseline 7.1 ± 2.1; post-SVR 5.3 ± 1.5 kPa; $P < 0.0001$) (Table 3). Among patients with post-SVR steatosis, 6.25% had advanced fibrosis defined as ⩾ 11 kPa. No patients without steatosis had advanced fibrosis (Table 3).

Post-SVR, neither weight nor BMI changed while levels of transaminases and other liver enzymes dropped in patients both with and without steatosis, including ALT (55.6 ± 60.9 U/L to 15.3 ± 5.5 U/L in patients with steatosis, $P < 0.0001$, and 68.78 ± 52.8 U/L to 20.4 ± 16.5 U/L in patients without steatosis; $P < 0.0001$, respectively); AST (43.3 ± 35.6 U/L to 20.2 ± 5.4 U/L; $P < 0.0001$ and 61.3 ± 44.7 U/L to 22.9 ± 9.8 U/L; $P < 0.0001$, respectively); and alkaline phosphatase (78.5 ± 43.1 U/L to 70.8 ± 28.8 U/L; $P = 0.01$ and 75.5 ± 21.8 U/L to 71.3 ± 19.4 U/L; $P = 0.04$ (Table 3).

DISCUSSION

Since hepatic steatosis prevalence in CHC patients has previously been reported to be approximately 50%[8] our findings of a 47.5% prevalence post-SVR achieved with DAAs should perhaps not be surprising. However, this very high prevalence with continuing

Table 1 Demographic and clinical characteristics of the chronic hepatitis C patients prior to direct-acting antivirals treatment and after achieving sustained virological response 12 *n* (%)

	Prior to DAA treatment (baseline)	Post-SVR 12	*P*[1] value
Demographics			
Male	49 (48)	49 (48)	NS
Age (yr, mean ± SD)	60.3 ± 10.7	60.3 ± 10.7	NS
White	37 (37)	37 (37)	NS
Hispanic	26 (26)	26 (26)	NS
African American	13 (13)	13 (13)	NS
Asian	7 (7)	7 (7)	NS
Other	2 (2)	2 (2)	NS
Declined	16 (15)	16 (15)	NS
Clinical			
Hypertension	45 (43)	45 (43)	NS
Type 2 diabetes	13 (12.3)	13 (12.3)	NS
Dyslipidemia	8 (7.5)	8 (7.5)	NS
Anthropometric (mean ± SD)			
Body mass index (kg/m^2)	27.6 ± 6.9	27.5 ± 6.9	NS
Weight (Lbs.)	174.9 ± 46.9	172.7 ± 44.5	NS
Laboratory panel (mean ± SD)			
HCV vial load log$_{10}$ IU/mL	6.2 ± 0.9	0.0 ± 0.0	< 0.0001
HCV genotype			
Genotype 1	86 (85)		
Genotype 2	15 (14)		
Genotype 4	1 (1)		
AST (U/L)	51.8 ± 41.1	21.5 ± 8.0	< 0.0001
ALT (U/L)	63.1 ± 62.6	17.8 ± 12.3	< 0.0001
Alkaline phosphatase (U/L)	77.5 ± 34.0	71.0 ± 24.3	0.004
Albumin (g/dL)	4.3 ± 0.4	4.4 ± 0.4	NS
Bilirubin, total (mg/dL)	0.6 ± 0.2	0.6 ± 0.3	NS
Fasting glucose (mg/dL)	99.1 ± 30.1	102.1 ± 23.5	NS
FibroScan (mean ± SD)			
Fibrosis Score (kPa)	7.4 ± 1.9	6.1 ± 3.6	0.013
IQR (%)	12.6 ± 4.9	12.3 ± 5.5	NS

[1]*P* values (2-sided) determined from either a Fisher's exact test for categorical variables or *t*-test for continuous variables. DAA: Direct-acting antivirals; SVR: Sustained virological response; HCV: Hepatitis C virus; AST: Aspartate aminotransferase; ALT: Alanine aminotransferase; IQR: Interquartile range.

clinically significant fibrosis in the steatotic patients despite normal liver enzymes should be of concern to clinicians. The current European guidelines recommend assessing ALT and HCV RNA 48 wk post-treatment in non-cirrhotic patients with SVR, with no further follow up with normal ALT/undetectable HCV RNA[18]. The current United States guidelines for patients post-SVR recommend follow up only for those with advanced fibrosis; assessing other liver disease causes is only recommended in cases of persistently abnormal transaminases[19]. Importantly, we show that fatty liver may be present despite normal liver enzymes, confirming previous studies that have shown this[20]. Therefore, we recommend post-SVR assessment of steatosis and fibrosis in those with abnormal BMI or other risk factors typical of NAFLD. In patients found to have hepatic steatosis long-term follow up is warranted.

To our knowledge this is the first prospective study to assess the prevalence of fatty liver in HCV patients who achieved an SVR with DAAs. We hope that our study will raise awareness of the post-SVR prevalence of fatty liver and the need for screening and long-term follow up. Our study's strengths include the community-based hepatology setting, which likely accurately represents real life experience. In addition, we used TE, which is highly sensitive and specific, and is widely used and easy to perform. Although liver biopsy is still the gold standard to assess fatty liver and staging with MRI proton density fat fraction may be more accurate[21], biopsy is invasive and costly and many patients are reluctant to undergo the procedure because of concerns about pain and, although limited, possible complications. With biopsy there is also the possibility of inter-and intra-observer variability and sampling error[22]. MRI techniques are quite expensive. Neither of these is likely to be performed in post-SVR patients with normal liver enzymes. Thus, the use of TE with CAP is realistic in a real-world setting.

There is substantial data showing good sensitivity and specificity for the use of TE in determining either presence of advanced fibrosis or no fibrosis. In eight studies that compared the usefulness of TE and liver biopsy for assessment of liver fibrosis in NAFLD patients it was shown that TE is very good for diagnosis of F $\geqslant$ 3, with 84%-100% sensitivity and 83%-97% specificity[23-30]. Similar findings were reported in a recent large systematic review and meta-analysis that confirmed that TE was excellent for diagnosis of F $\geqslant$ 3 in NAFLD patients[31]. Although there is reduced accuracy using TE for distinguishing early fibrosis

Table 2 Characteristics of chronic hepatitis C patients after achieving sustained virological response 12 comparing those with and without steatosis *n* (%)

	Patients without steatosis (CAP < 248 dB/m) (*n* = 53)	Patients with steatosis (CAP ⩾ 248 dB/m) (*n* = 48)	*P*[1] value
Demographics			
Male	25 (47)	27 (56)	NS
Age (yr, mean ± SD)	59.4 ± 11.6	60.9 ± 9.4	NS
White	18 (34)	18 (38)	NS
Hispanic	14 (26)	12 (25)	NS
Clinical			
Hypertension	25 (47.2)	20 (41.7)	NS
Dyslipidemia	3 (5.7)	5 (10.4)	0.048
Type 2 diabetes	4 (7.5)	9 (18.7)	0.04
Anthropometric (mean ± SD)			
Body mass index (kg/m^2)	26.1 ± 6.9	28.9 ± 6.6	0.049
Weight (Lbs.)	161.0 ± 33.4	172.7 ± 44.5	0.005
Hepatology and viral hepatitis panel (mean ± SD)			
AST (U/L)	20.2 ± 5.4	22.9 ± 9.8	NS
ALT (U/L)	15.3 ± 5.5	20.4 ± 16.5	0.048
Alkaline phosphatase (U/L)	70.7 ± 28.2	71.3 ± 19.4	NS
Albumin (g/dL)	4.3 ± 0.2	4.5 ± 0.6	NS
Bilirubin, total (mg/dL)	0.6 ± 0.3	0.6 ± 0.2	NS
Other laboratory studies (mean ± SD)			
Total cholesterol (mg/dL)	184.8 ± 35.1	179 ± 37.2	NS
HDL cholesterol (mg/dL)	57.6 ± 18.6	50.8 ± 17.0	NS
LDL cholesterol (mg/dL)	102.6 ± 33.2	100.7 ± 31.5	NS
Triglycerides (mg/dL)	109.7 ± 63.9	138.9 ± 77.9	0.05
HbA1c (%)	5.7 ± 0.6	6.0 ± 0.9	NS
Fasting serum glucose (mg/dL)	96.5 ± 11.1	107.8 ± 30.5	0.023
FibroScan (mean ±SD)			
Fibrosis Score (kPa)	5.3 ± 1.6	7.0 ± 4.8	0.0013
CAP (dB/m)	212.4 ± 29.0	296.3 ± 37.4	< 0.0001
% of patient with fibrosis score of (⩾ 7 kPa)	0%	6.25%	0.066

[1]*P* values (2-sided) determined from either a Fisher's exact test for categorical variables or *t*-test for continuous variables. CAP: Controlled attenuation parameter; AST: Aspartate aminotransferase; ALT: Alanine aminotransferase; HDL: High density lipoprotein; LDL: Low density lipoprotein; CAP: Controlled attenuation parameter.

stages (F1-F2), in our study we were mainly comparing results in patients with and without advanced fibrosis. There is also substantial data showing good sensitivity and specificity of TE with CAP for assessing hepatic steatosis[32]. Although cutoff values for defining steatosis with CAP have not been fully formalized, we chose the value that defined steatosis (⩾ 248 dB/M) based on a very recent large (2735 patients) meta-analysis of studies containing histology-verified CAP data for grading of steatosis that determined optimal cut-offs for CAP[15].

Although until relatively recently, obesity (BMI > 30 kg/m^2) was associated with a reduced ability of TE to accurately determine fibrosis and steatosis, this problem has been largely addressed with the development of the obese-specific XL probe which we used in our study, confirmed in multiple studies to obtain reliable liver stiffness measurement in obese patients[33-35]. Another strength of our study is our inclusion of a detailed metabolic profile and alcohol questionnaire, with other causes carefully ruled out. It has been suggested that post-SVR some patients might feel free to indulge in alcohol consumption, with a resulting increase in liver stiffness measurements. Importantly, we ruled out increased alcohol intake through both medical records and use of the AUDIT-C at the time of the TE CAP assessment post-SVR.

Although our exclusion of HCV GNT3 patients means that our findings cannot be applied to the approximately 30.1% of HCV patients with this genotype[36], the exclusion is a strength of the study in other ways. Steatosis has been shown to correlate with intrahepatic viral replication in GNT3, with resolution of steatosis seen after effective antiviral treatment, suggesting a direct steatogenic effect of GNT3 virus[8]. In a study of patients treated with interferon, steatosis improvement post-SVR was seen in 91% of GNT3 patients *vs* 43% of patients with other genotypes ($P < 0.04$)[37]. In a study that compared the effects of interferon treatment in GNT1 and GNT3 patients, hepatic steatosis did not change in GNT1 patients, regardless of the treatment response, while steatosis was significantly reduced in GNT3 patients who achieved an SVR ($P < 0.001$) but not in patients who did not[38], again suggesting a direct steatogenic effect of GNT3 HCV. Thus, GNT3 patients represent a unique population in terms of steatosis that should be studied separately. Inclusion of these patients in our study could have substantially altered our findings regarding post-SVR steatosis, likely substantially reducing the prevalence due to steatosis reduction

Table 3 Comparison of pre-treatment *vs* post-sustained virological response characteristics in patients with and without post-sustained virological response steatosis

	Patients without steatosis n = 53			Patients with steatosis n = 48		
	Pretreatment	Post SVR	*P* value	Pretreatment	Post SVR	*P* value
Body mass index (kg/m^2)	25.5 ± 4.0	26.1 ± 6.9	NS	30.0 ± 8.5	29.0 ± 6.6	NS
Weight (Lbs.)	161.9 ± 32.6	161.0 ± 33.4	NS	187.3 ± 55.8	186.1 ± 51.3	NS
Laboratory panel (mean ± SD)						
HCV vial load log$_{10}$ IU/mL	6.1 ± 1.0	0.0 ± 0.0	< 0.0001	6.3 ± 0.8	0.0 ± 0.0	< 0.0001
AST (U/L)	43.3 ± 35.6	20.2 ± 5.4	< 0.0001	61.3 ± 44.7	22.9 ± 9.8	< 0.0001
ALT (U/L)	55.6 ± 60.9	15.3 ± 5.5	< 0.0001	68.78 ± 52.8	20.4 ± 16.5	< 0.0001
Alkaline phosphatase (U/L)	78.5 ± 43.1	70.8 ± 28.8	0.01	75.5 ± 21.8	71.3 ± 19.4	0.04
Albumin (g/dL)	4.2 ± 0.5	4.4 ± 0.3	0.006	4.3 ± 0.2	4.5 ± 0.6	0.006
Bilirubin total (mg/dL)	0.6 ± 0.2	0.6 ± 0.3	NS	0.6 ± 0.3	0.6 ± 0.2	NS
Fasting glucose (mg/dL)	95.6 ± 31.9	96.6 ± 11.1	NS	103.0 ± 27.5	107.8 ± 30.5	NS
FibroScan (mean ± SD)						
Fibrosis score (kPa)	7.1 ± 2.1	5.3 ± 1.5	< 0.0001	7.7 ± 1.7	7.0 ± 4.8	0.0037

SVR: Sustained virological response; HCV: Hepatitis C virus; AST: Aspartate aminotransferase; ALT: Alanine aminotransferase.

in GNT3 patients, resulting in an overall steatosis prevalence which would not be representative of the almost 70% of HCV patients with other genotypes[36].

A limitation of our study is that, because the CAP technology was not available in the United States at the time of study initiation, we were unable to estimate steatosis prevalence with CAP prior to the initiation of DAAs in order to determine treatment effect. However, regardless of baseline steatosis prevalence, there is real clinical value in assessing post-SVR prevalence so that appropriate long-term follow up can be recommended. Another limitation is the length of follow-up as the median time interval in our study is 47 wk between treatment completion and the post-SVR TE. Lengthier studies are definitely needed to assess NAFLD progression and steatosis and fibrosis changes over time in this population. However, by assessing patients at almost a year post-SVR we have at least provided a foundation upon which lengthier studies could expand. The sample size could be considered as a limitation; however, this is a proof of concept study that this is first of its kind and warrants larger studies. Finally, we excluded patients with cirrhosis. However, these patients are usually followed up closely post-SVR and steatosis has been found to be low when patients have advanced fibrosis[39].

In conclusion, our findings that 47.5% of HCV patients had steatosis post-SVR and that some steatotic patients had clinically significant fibrosis, despite normal liver enzymes, highlight the importance of post-SVR assessment of steatosis and fibrosis in these patients. We believe these patients should be followed longitudinally, both to provide appropriate patient care and to advance our understanding of the long-term consequences of hepatic steatosis in post-SVR patients. In addition, we note that despite SVR these steatotic CHC patients are excluded from most NAFLD clinical trials, predominantly because of the current guidelines' definition of NAFLD as a diagnosis of exclusion[40,41]. We propose revisiting this and implementing new definitions of those with concomitant liver diseases, including those with HCV SVRs, that might allow patients' participation in trials, an unmet need in the rising epidemic of NAFLD.

ARTICLE HIGHLIGHTS

Research background

It is known that the hepatic steatosis prevalence in hepatitis C patients who have achieved a sustained virological response with interferon is approximately 50%. However, the prevalence of fatty liver in hepatitis C patients who have achieved a sustained virological response with direct-acting antivirals has not previously been studied. Knowledge of this is important in order to direct appropriate long-term follow up for patients.

Research motivation

Post-sustained virological response (SVR), hepatitis C patients, many of whom have normal liver enzymes, are too often being discharged from their hepatologists' care with no further plans for follow up. The current European and United States guidelines only recommend long-term follow up in patients with elevated enzymes. In addition, many hepatitis C patients who have achieved an SVR are excluded from nonalcoholic fatty liver disease (NAFLD) clinical trials. We think it is important to determine the prevalence of NAFLD post-SVR and assess the severity of liver disease in these patients. Determining these things can provide a basis for future research aimed at determining the long-term natural history of the disease in these patients, and may prompt changes in both liver society guidelines for follow up and in clinical trial exclusion criteria.

Research objectives

The main objective, to determine the prevalence of fatty liver in hepatitis C patients who have achieved a sustained virological response with direct-acting antivirals, was achieved. This knowledge provides a basis for future research aimed at determining the long-term natural history of the disease in these patients.

Research methods

In this study we used transient elastography with controlled attenuation parameter to measure steatosis and fibrosis in hepatitis C patients post-SVR. This was the first study to measure both fibrosis and steatosis in hepatitis C patients using the FibroScan technology.

Research results

Our findings have added knowledge previously unknown in this field that may help to guide the need for long-term monitoring of hepatitis C patients post-SVR, with a particular focus on the possible occurrence of NAFLD in these

patients, whether or not there are elevated liver enzymes. The most important future research will be to carry out long-term follow up on hepatitis C patients post-SVR to determine the prevalence of fatty liver over time.

Research conclusions

This is the first prospective study to assess the prevalence of fatty liver in hepatitis C patients who have achieved a sustained virological response with direct-acting antivirals. The study's findings that fatty liver is present in 47.5% of these patients and that some steatotic patients have clinically significant fibrosis despite normal liver enzymes should raise awareness of the high post-SVR prevalence of fatty liver and the importance of post-SVR assessment of steatosis and fibrosis and long-term follow up with these patients. The study's findings raise concern that the recommendations found in the current U.S. and European guidelines for follow up of patients post-SVR could result in a lack of adequate long-term monitoring of these patients. In particular, the very high prevalence of fatty liver (47.5%) with continuing clinically significant fibrosis in the steatotic patients despite normal liver enzymes should be of concern to clinicians. Therefore, we recommend post-SVR assessment of steatosis and fibrosis in those with abnormal BMI or other risk factors typical of NAFLD. In patients found to have hepatic steatosis long-term follow up is clearly warranted.

Research perspectives

Our study's assessment of steatosis and fibrosis in hepatitis C patients at almost a year post-SVR has shown that long-term monitoring of these patients to assess the possibility of fatty liver and fibrosis is important. With this study, we have provided a foundation upon which lengthier and larger studies should expand, using regularly scheduled transient elastography with controlled attenuation parameter assessments in order to determine whether this high level of steatosis is still present multiple years post-SVR and the clinical ramifications for patients.

REFERENCES

1 **Younossi ZM**, Koenig AB, Abdelatif D, Fazel Y, Henry L, Wymer M. Global epidemiology of nonalcoholic fatty liver disease-Meta-analytic assessment of prevalence, incidence, and outcomes. *Hepatology* 2016; **64**: 73-84 [PMID: 26707365 DOI: 10.1002/hep.28431]

2 **World Health Organization**. Global hepatitis report 2017. Geneva, Switzerland: World Health Organization, 2017: 83

3 **Setiawan VW**, Stram DO, Porcel J, Lu SC, Le Marchand L, Noureddin M. Prevalence of chronic liver disease and cirrhosis by underlying cause in understudied ethnic groups: The multiethnic cohort. *Hepatology* 2016; **64**: 1969-1977 [PMID: 27301913 DOI: 10.1002/hep.28677]

4 **Wong RJ**, Aguilar M, Cheung R, Perumpail RB, Harrison SA, Younossi ZM, Ahmed A. Nonalcoholic steatohepatitis is the second leading etiology of liver disease among adults awaiting liver transplantation in the United States. *Gastroenterology* 2015; **148**: 547-555 [PMID: 25461851 DOI: 10.1053/j.gastro.2014.11.039]

5 **Vernon G**, Baranova A, Younossi ZM. Systematic review: the epidemiology and natural history of non-alcoholic fatty liver disease and non-alcoholic steatohepatitis in adults. *Aliment Pharmacol Ther* 2011; **34**: 274-285 [PMID: 21623852 DOI: 10.1111/j.1365-2036.2011.04724.x]

6 **Powell EE**, Jonsson JR, Clouston AD. Steatosis: co-factor in other liver diseases. *Hepatology* 2005; **42**: 5-13 [PMID: 15962320 DOI: 10.1002/hep.20750]

7 **Adinolfi LE**, Gambardella M, Andreana A, Tripodi MF, Utili R, Ruggiero G. Steatosis accelerates the progression of liver damage of chronic hepatitis C patients and correlates with specific HCV genotype and visceral obesity. *Hepatology* 2001; **33**: 1358-1364 [PMID: 11391523 DOI: 10.1053/jhep.2001.24432]

8 **Lonardo A**, Adinolfi LE, Loria P, Carulli N, Ruggiero G, Day CP. Steatosis and hepatitis C virus: mechanisms and significance for hepatic and extrahepatic disease. *Gastroenterology* 2004; **126**: 586-597 [PMID: 14762795]

9 **Castera L**. Steatosis, insulin resistance and fibrosis progression in chronic hepatitis C. *Minerva Gastroenterol Dietol* 2006; **52**: 125-134 [PMID: 16557184]

10 **Bondini S**, Younossi ZM. Non-alcoholic fatty liver disease and hepatitis C infection. *Minerva Gastroenterol Dietol* 2006; **52**: 135-143 [PMID: 16557185]

11 **Abenavoli L**, Masarone M, Peta V, Milic N, Kobyliak N, Rouabhia S, Persico M. Insulin resistance and liver steatosis in chronic hepatitis C infection genotype 3. *World J Gastroenterol* 2014; **20**: 15233-15240 [PMID: 25386071 DOI: 10.3748/wjg.v20.i41.15233]

12 **Castera L**, Forns X, Alberti A. Non-invasive evaluation of liver fibrosis using transient elastography. *J Hepatol* 2008; **48**: 835-847 [PMID: 18334275 DOI: 10.1016/j.jhep.2008.02.008]

13 **Han MA**, Saouaf R, Ayoub W, Todo T, Mena E, Noureddin M. Magnetic resonance imaging and transient elastography in the management of Nonalcoholic Fatty Liver Disease (NAFLD). *Expert Rev Clin Pharmacol* 2017; **10**: 379-390 [PMID: 28277807 DOI: 10.1080/17512433.2017.1299573]

14 **Rinella ME**, Sanyal AJ. Management of NAFLD: a stage-based approach. *Nat Rev Gastroenterol Hepatol* 2016; **13**: 196-205 [PMID: 26907882 DOI: 10.1038/nrgastro.2016.3]

15 **Karlas T**, Petroff D, Sasso M, Fan JG, Mi YQ, de Lédinghen V, Kumar M, Lupsor-Platon M, Han KH, Cardoso AC, Ferraioli G, Chan WK, Wong VW, Myers RP, Chayama K, Friedrich-Rust M, Beaugrand M, Shen F, Hiriart JB, Sarin SK, Badea R, Jung KS, Marcellin P, Filice C, Mahadeva S, Wong GL, Crotty P, Masaki K, Bojunga J, Bedossa P, Keim V, Wiegand J. Individual patient data meta-analysis of controlled attenuation parameter (CAP) technology for assessing steatosis. *J Hepatol* 2017; **66**: 1022-1030 [PMID: 28039099 DOI: 10.1016/j.jhep.2016.12.022]

16 **Park CC**, Nguyen P, Hernandez C, Bettencourt R, Ramirez K, Fortney L, Hooker J, Sy E, Savides MT, Alquiraish MH, Valasek MA, Rizo E, Richards L, Brenner D, Sirlin CB, Loomba R. Magnetic Resonance Elastography vs Transient Elastography in Detection of Fibrosis and Noninvasive Measurement of Steatosis in Patients With Biopsy-Proven Nonalcoholic Fatty Liver Disease. *Gastroenterology* 2017; **152**: 598-607 [PMID: 27911262 DOI: 10.1053/j.gastro.2016.10.026]

17 **Alkhouri N**, Feldstein AE. Noninvasive diagnosis of nonalcoholic fatty liver disease: Are we there yet? *Metabolism* 2016; **65**: 1087-1095 [PMID: 26972222 DOI: 10.1016/j.metabol.2016.01.013]

18 **European Association for the Study of the Liver**. EASL recommendations on treatment of hepatitis C 2016. *J Hepatol* 2017; **66**: 153-194 [PMID: 27667367 DOI: 10.1016/j.jhep.2016.09.001]

19 **American Association for the Study of Liver Diseases**, Infectious Diseases Society of America. Summary of the recommendations for monitoring patients who are starting HCV treatment, are on treatment, or have completed therapy. Available from: URL: https://www.hcvguidelines.org/evaluate/monitoring

20 **Browning JD**, Szczepaniak LS, Dobbins R, Nuremberg P, Horton JD, Cohen JC, Grundy SM, Hobbs HH. Prevalence of hepatic steatosis in an urban population in the United States: impact of ethnicity. *Hepatology* 2004; **40**: 1387-1395 [PMID: 15565570 DOI: 10.1002/hep.20466]

21 **Noureddin M**, Khoyilar C, Palmer SL. MRI, CT scan, and ultrasound in the diagnosis of nonalcoholic fatty liver disease. *J Clin Gastroenterol* 2015; **49**: 351-352 [PMID: 25551206 DOI: 10.1097/MCG.0000000000000281]

22 **Zeng DW**, Dong J, Liu YR, Jiang JJ, Zhu YY. Noninvasive models for assessment of liver fibrosis in patients with chronic hepatitis B virus infection. *World J Gastroenterol* 2016; **22**: 6663-6672 [PMID: 27547009 DOI: 10.3748/wjg.v22.i29.6663]

23 **Cassinotto C**, Boursier J, de Lédinghen V, Lebigot J, Lapuyade B, Cales P, Hiriart JB, Michalak S, Bail BL, Cartier V, Mouries A, Oberti F, Fouchard-Hubert I, Vergniol J, Aubé C. Liver stiffness in nonalcoholic fatty liver disease: A comparison of supersonic shear imaging, FibroScan, and ARFI with liver biopsy. *Hepatology* 2016; **63**: 1817-1827 [PMID: 26659452 DOI: 10.1002/hep.28394]

24 **Imajo K**, Kessoku T, Honda Y, Tomeno W, Ogawa Y, Mawatari H, Fujita K, Yoneda M, Taguri M, Hyogo H, Sumida Y, Ono

M, Eguchi Y, Inoue T, Yamanaka T, Wada K, Saito S, Nakajima A. Magnetic Resonance Imaging More Accurately Classifies Steatosis and Fibrosis in Patients With Nonalcoholic Fatty Liver Disease Than Transient Elastography. *Gastroenterology* 2016; **150**: 626-637 [PMID: 26677985 DOI: 10.1053/j.gastro.2015.11.048]

25 **Kumar R**, Rastogi A, Sharma MK, Bhatia V, Tyagi P, Sharma P, Garg H, Chandan Kumar KN, Bihari C, Sarin SK. Liver stiffness measurements in patients with different stages of nonalcoholic fatty liver disease: diagnostic performance and clinicopathological correlation. *Dig Dis Sci* 2013; **58**: 265-274 [PMID: 22790906 DOI: 10.1007/s10620-012-2306-1]

26 **Lupsor M**, Badea R, Stefanescu H, Grigorescu M, Serban A, Radu C, Crişan D, Sparchez Z, Iancu S, Maniu A. Performance of unidimensional transient elastography in staging non-alcoholic steatohepatitis. *J Gastrointestin Liver Dis* 2010; **19**: 53-60 [PMID: 20361076]

27 **Pathik P**, Ravindra S, Ajay C, Prasad B, Jatin P, Prabha S. Fibroscan versus simple noninvasive screening tools in predicting fibrosis in high-risk nonalcoholic fatty liver disease patients from Western India. *Ann Gastroenterol* 2015; **28**: 281-286 [PMID: 25830783]

28 **Wong VW**, Vergniol J, Wong GL, Foucher J, Chan HL, Le Bail B, Choi PC, Kowo M, Chan AW, Merrouche W, Sung JJ, de Lédinghen V. Diagnosis of fibrosis and cirrhosis using liver stiffness measurement in nonalcoholic fatty liver disease. *Hepatology* 2010; **51**: 454-462 [PMID: 20101745 DOI: 10.1002/hep.23312]

29 **Yoneda M**, Yoneda M, Fujita K, Inamori M, Tamano M, Hiriishi H, Nakajima A. Transient elastography in patients with non-alcoholic fatty liver disease (NAFLD). *Gut* 2007; **56**: 1330-1331 [PMID: 17470477 DOI: 10.1136/gut.2007.126417]

30 **Yoneda M**, Yoneda M, Mawatari H, Fujita K, Endo H, Iida H, Nozaki Y, Yonemitsu K, Higurashi T, Takahashi H, Kobayashi N, Kirikoshi H, Abe Y, Inamori M, Kubota K, Saito S, Tamano M, Hiraishi H, Maeyama S, Yamaguchi N, Togo S, Nakajima A. Noninvasive assessment of liver fibrosis by measurement of stiffness in patients with nonalcoholic fatty liver disease (NAFLD). *Dig Liver Dis* 2008; **40**: 371-378 [PMID: 18083083 DOI: 10.1016/j.dld.2007.10.019]

31 **Kwok R**, Tse YK, Wong GL, Ha Y, Lee AU, Ngu MC, Chan HL, Wong VW. Systematic review with meta-analysis: non-invasive assessment of non-alcoholic fatty liver disease--the role of transient elastography and plasma cytokeratin-18 fragments. *Aliment Pharmacol Ther* 2014; **39**: 254-269 [PMID: 24308774 DOI: 10.1111/apt.12569]

32 **Noureddin M**, Mato JM, Lu SC. Nonalcoholic fatty liver disease: update on pathogenesis, diagnosis, treatment and the role of S-adenosylmethionine. *Exp Biol Med* (Maywood) 2015; **240**: 809-820 [PMID: 25873078 DOI: 10.1177/1535370215579161]

33 **Mikolasevic I**, Orlic L, Franjic N, Hauser G, Stimac D, Milic S. Transient elastography (FibroScan(®)) with controlled attenuation parameter in the assessment of liver steatosis and fibrosis in patients with nonalcoholic fatty liver disease - Where do we stand? *World J Gastroenterol* 2016; **22**: 7236-7251 [PMID: 27621571 DOI: 10.3748/wjg.v22.i32.7236]

34 **Myers RP**, Pomier-Layrargues G, Kirsch R, Pollett A, Duarte-Rojo A, Wong D, Beaton M, Levstik M, Crotty P, Elkashab M. Feasibility and diagnostic performance of the FibroScan XL probe for liver stiffness measurement in overweight and obese patients. *Hepatology* 2012; **55**: 199-208 [PMID: 21898479 DOI: 10.1002/hep.24624]

35 **Sporea I**, Sirli R, Mare R, Popescu A, Ivascu SC. Feasibility of Transient Elastography with M and XL probes in real life. *Med Ultrason* 2016; **18**: 7-10 [PMID: 26962547 DOI: 10.11152/mu.2013.2066.181.xsi]

36 **Messina JP**, Humphreys I, Flaxman A, Brown A, Cooke GS, Pybus OG, Barnes E. Global distribution and prevalence of hepatitis C virus genotypes. *Hepatology* 2015; **61**: 77-87 [PMID: 25069599 DOI: 10.1002/hep.27259]

37 **Castéra L**, Hézode C, Roudot-Thoraval F, Lonjon I, Zafrani ES, Pawlotsky JM, Dhumeaux D. Effect of antiviral treatment on evolution of liver steatosis in patients with chronic hepatitis C: indirect evidence of a role of hepatitis C virus genotype 3 in steatosis. *Gut* 2004; **53**: 420-424 [PMID: 14960527]

38 **Kumar D**, Farrell GC, Fung C, George J. Hepatitis C virus genotype 3 is cytopathic to hepatocytes: Reversal of hepatic steatosis after sustained therapeutic response. *Hepatology* 2002; **36**: 1266-1272 [PMID: 12395339 DOI: 10.1053/jhep.2002.36370]

39 **Permutt Z**, Le TA, Peterson MR, Seki E, Brenner DA, Sirlin C, Loomba R. Correlation between liver histology and novel magnetic resonance imaging in adult patients with non-alcoholic fatty liver disease - MRI accurately quantifies hepatic steatosis in NAFLD. *Aliment Pharmacol Ther* 2012; **36**: 22-29 [PMID: 22554256 DOI: 10.1111/j.1365-2036.2012.05121.x]

40 **Chalasani N**, Younossi Z, Lavine JE, Diehl AM, Brunt EM, Cusi K, Charlton M, Sanyal AJ; American Gastroenterological Association; American Association for the Study of Liver Diseases; American College of Gastroenterologyh. The diagnosis and management of non-alcoholic fatty liver disease: practice guideline by the American Gastroenterological Association, American Association for the Study of Liver Diseases, and American College of Gastroenterology. *Gastroenterology* 2012; **142**: 1592-1609 [PMID: 22656328 DOI: 10.1053/j.gastro.2012.04.001]

41 **European Association for the Study of the Liver (EASL)**, European Association for the Study of Diabetes (EASD), European Association for the Study of Obesity (EASO). EASL-EASD-EASO Clinical Practice Guidelines for the management of non-alcoholic fatty liver disease. *J Hepatol* 2016; **64**: 1388-1402 [PMID: 27062661 DOI: 10.1016/j.jhep.2015.11.004]

P- Reviewer: Abenavoli L, Ho SB, Rodriguez-Frias F
S- Editor: Wang XJ **L- Editor**: A **E- Editor**: Huang Y

World Journal of Gastroenterology

Submit a Manuscript: http://www.f6publishing.com

World J Gastroenterol 2018 March 21; 24(11): 1278-1284

DOI: 10.3748/wjg.v24.i11.1278

ISSN 1007-9327 (print) ISSN 2219-2840 (online)

ORIGINAL ARTICLE

Prospective Study

Low-pressure pneumoperitoneum with abdominal wall lift in laparoscopic total mesorectal excision for rectal cancer: Initial experience

Ping-Tian Xia, Maimaiti Yusofu, Hai-Feng Han, Chun-Xiao Hu, San-Yuan Hu, Wen-Bin Yu, Shao-Zhuang Liu

Ping-Tian Xia, Maimaiti Yusofu, Hai-Feng Han, Chun-Xiao Hu, San-Yuan Hu, Wen-Bin Yu, Shao-Zhuang Liu, Department of General Surgery, Qilu Hospital of Shandong University, Jinan 250012, Shandong Province, China

ORCID number: Ping-Tian Xia (0000-0001-8032-8871); Maimaiti Yusofu (0000-0001-8762-5924); Hai-Feng Han (0000-0002-1417-9350); Chun-Xiao Hu (0000-0002-8015-4549); San-Yuan Hu (0000-0002-0546-9778); Wen-Bin Yu (0000-0002-9410-7188); Shao-Zhuang Liu (0000-0003-2052-0516).

Author contributions: Xia PT, Hu SY, Yu WB and Liu SZ designed the study, analyzed the data and wrote the paper; Yusofu M, Yu WB and Liu SZ performed the surgery and treated the patients; Han HF and Hu CX collected and analyzed the patient data; Hu SY and Liu SZ approved the final manuscript.

Supported by the Special Found for Taishan Scholar Project of Shandong Province, China.

Institutional review board statement: The study was reviewed and approved by the Ethics Committee of Scientific Research of Shandong University Qilu Hospital.

Informed consent statement: In this study, all involved participants or their legal guardian provided informed written consent before surgery.

Conflict-of-interest statement: No authors of this paper have conflicting interests.

Data sharing statement: No additional data are available.

CONSORT 2010 statement: The guidelines of the CONSORT 2010 Statement have been adopted.

Manuscript source: Unsolicited manuscript

Correspondence to: Shao-Zhuang Liu, MD, PhD, Attending Doctor, Postdoc, Department of General Surgery, Qilu Hospital of Shandong University, 107#, Wenhua Xi Road, Jinan 250012, Shandong Province, China. liushaozhuang@sdu.edu.cn
Telephone: +86-531-86920598
Fax: +86-531-86920598

Received: January 11, 2018
Peer-review started: January 11, 2018
First decision: January 25, 2018
Revised: January 30, 2018
Accepted: February 9, 2018
Article in press: February 9, 2018
Published online: March 21, 2018

Abstract

AIM

To evaluate the safety and feasibility of a new technology combining low-pressure pneumoperitoneum (LPP) and abdominal wall lift (AWL) in laparoscopic total mesorectal excision (TME) for rectal cancer.

METHODS

From November 2015 to July 2017, 26 patients underwent laparoscopic TME for rectal cancer using LPP (6-8 mmHg) with subcutaneous AWL in Qilu Hospital of Shandong University, Jinan, China. Clinical data regarding patients' demographics, intraoperative monitoring indices, operation-related indices and

pathological outcomes were prospectively collected.

RESULTS

Laparoscopic TME was performed in 26 cases (14 anterior resection and 12 abdominoperineal resection) successfully, without conversion to open or laparoscopic surgery with standard-pressure pneumoperitoneum. Intraoperative monitoring showed stable heart rate, blood pressure and paw airway pressure. The mean operative time was 194.29 ± 41.27 min (range: 125-270 min) and 200.41 ± 20.56 min (range: 170-230 min) for anterior resection and abdominoperineal resection, respectively. The mean number of lymph nodes harvested was 16.71 ± 5.06 (range: 7-27). There was no positive circumferential or distal resection margin. No local recurrence was observed during a median follow-up period of 11.96 ± 5.55 mo (range: 5-23 mo).

CONCLUSION

LPP combined with AWL is safe and feasible for laparoscopic TME. The technique can provide satisfactory exposure of the operative field and stable operative monitoring indices.

Key words: Laparoscopic surgery; Abdominal wall lift; Low-pressure pneumoperitoneum; Rectal cancer; Total mesorectal excision

Core tip: Low-pressure pneumoperitoneum (LPP) and abdominal wall lift (AWL) have been proposed as alternative approaches to standard-pressure pneumoperitoneum to avoid adverse cardiorespiratory effects. However, the operative field under these approaches is less optimal and accompanied by increased technical difficulties. We developed a new technique combining LPP and AWL, which improved exposure of the operative field that was compromised with LPP or AWL alone. We evaluated the safety and feasibility of this new technique in 26 cases of laparoscopic total mesorectal excision for rectal cancer. This technique can provide satisfactory exposure of the operative field and stable operative monitoring indices.

Xia PT, Yusofu M, Han HF, Hu CX, Hu SY, Yu WB, Liu SZ. Low-pressure pneumoperitoneum with abdominal wall lift in laparoscopic total mesorectal excision for rectal cancer: Initial experience. *World J Gastroenterol* 2018; 24(11): 1278-1284 Available from: URL: http://www.wjgnet.com/1007-9327/full/v24/i11/1278.htm DOI: http://dx.doi.org/10.3748/wjg.v24.i11.1278

INTRODUCTION

Pneumoperitoneum with carbon dioxide (CO_2) is the conventional method of creating a workspace in laparoscopic surgery. The application of pneumoperitoneum results in a variety of physiologic alterations, due to the systemic absorption of CO_2 and increased intra-abdominal pressure. CO_2 absorption across the peritoneum into the circulation can lead to hypercarbia and changes in blood gas parameters. Appropriate ventilator adjustment is usually required to eliminate the increased CO_2 load. Increased intraabdominal pressure by standard-pressure pneumoperitoneum (SPP; 12-15 mmHg) has been reported to result in lower respiratory compliance, increased paw airway pressure, enhanced venous stasis, reduced portal venous pressure and impaired cardiac function[1-5]. These alterations may be detrimental in high-risk patients with poor cardiopulmonary reserve, such as older and morbidly obese patients with American Society of Anesthesiologists (ASA) status Ⅲ and Ⅳ[6].

Low-pressure pneumoperitoneum (LPP), defined as 5-7 mmHg[7], has been proposed to reduce the adverse consequences of SPP, and is recommended in older and compromised patients. It was reported that LPP reduced the adverse effects on cardiopulmonary function without affecting laparoscopic feasibility[5,8]. It has also proved feasible and safe in cholecystectomy[5,9], Nissen fundoplication[10], hysterectomy[11], adrenalectomy[12] and donor nephrectomy[13]. Abdominal wall lift (AWL) is another alternative technique to SPP which avoids the destructive changes associated with CO_2 absorption and increased intraabdominal pressure. A variety of AWL systems have been developed and applied in a wide range of surgical procedures[14]. Compared with SPP, AWL results in more stable cardiopulmonary, hemodynamic and renal functions during laparoscopic procedures[15-17].

A frequent disadvantage during laparoscopic surgery with LPP or AWL is that the operative field is less optimal, which increases technical difficulties. In order to obtain adequate visualization, we combined LPP with AWL and initially used this technique in a case of laparoscopic single-site cholecystectomy[18]. In the present prospective pilot study, we aimed to evaluate the safety and feasibility of LPP with AWL in laparoscopic total mesorectal excision (TME) for rectal cancer.

MATERIALS AND METHODS

Clinical data

This was a prospective study, and the protocol was approved by the Ethics Committee of Scientific Research of Shandong University Qilu Hospital, Jinan, China. From November 2015 to May 2017, 26 patients underwent laparoscopic TME using LPP with AWL in Qilu Hospital of Shandong University, Jinan, China. Written informed consent was obtained from all patients. Rectal adenocarcinoma was diagnosed by colonoscopy and biopsy. Computed tomography scans of the abdomen and pelvis were used to determine tumor stage. Patients

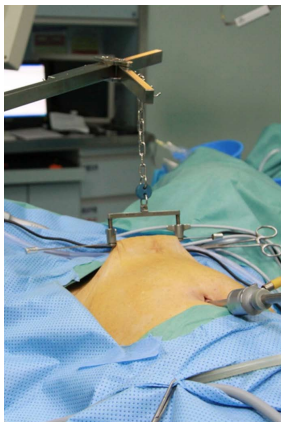

Figure 1 The subcutaneous abdominal wall lift system. The steel scaffold was fixed to the operating table. A sterilized needle was inserted through the subcutaneous tissue and drafted by a retractor to lift the abdominal wall.

without distant metastasis were eligible for enrollment in the study. All operations were performed by the same surgical group with considerable experience in advanced laparoscopic gastroenterological surgery.

Clinical data regarding patients' demographics [age, sex, body mass index (BMI)], ASA status, intraoperative monitoring indices (heart rate, blood pressure and paw airway pressure), operative time, blood loss, complications and pathological outcomes (tumor size, differentiation, depth of invasion, lymph nodes harvested, Dukes stage, completeness of TME, circumferential and distal margins) were obtained.

Instruments

The subcutaneous AWL system (Mizuho Medical Inc., Tokyo, Japan) was used in this study. It consisted of a sterilized steel scaffold with a lifting arm, retractors and steel needles. Other instruments included a harmonic scalpel (Ultracision; Ethicon Endosurgery, Cincinnati, OH, United States) and conventional laparoscopic instruments, such as a coagulation hook, dissector and grasper (Yida Medical Device Co., Ltd., Hangzhou, China). Hem-O-Lock clips (Weck Closure Systems, Triangle Park, NC, United States) were used to ligate vessels.

Surgical technique

The patients were placed in the lithotomy position under general anesthesia with a laryngeal mask airway. A 10-mm supraumbilical arc incision was made, and then a Veress needle was inserted to create the CO_2 pneumoperitoneum. The pressure was maintained at 6 mmHg with an insufflation rate of 10 L/min. The steel scaffold was fixed to the operating table. A sterilized needle was inserted through the subcutaneous tissue at 5 cm above the pubic level, then drafted by a retractor and the abdominal wall was slightly elevated to obtain additional exposure of the operative area (Figure 1).

The procedures were performed using 5 trocars. A careful exploration was performed to detect possible liver, peritoneal or pelvis metastases. The patient was then adjusted to the head-down position, which was about 20°-30° inclined to help move the small intestine for better exposure of the inferior mesenteric artery (IMA). The dissection began from the sigmoid mesocolon at the level of the sacral promontory, up to the origin of the IMA. The ascending left colic artery was preserved after a thorough clearance of the lymphatic and adipose tissues at the base of the IMA. The IMA was then ligated, and the inferior mesenteric vein was dissected and ligated at the level of the ligament of Treitz. The splenic flexure was mobilized routinely to achieve a tension-free anastomosis.

Exposure seemed inadequate during the above procedures, and an effort was made to achieve the optimal operative field. We developed and tested three methods. The first was to add a second needle in the supraumbilical area. This was abandoned due to frequent collisions of the instruments with the scaffold and lifting arms. We then tried the method reported by Park *et al*[19], where anchoring sutures were placed around the camera port and lifted up by an assistant to retract the abdominal wall for additional exposure. This method was successful and the workspace was improved. However, the view obtained from manual work was not stable. Therefore, we increased the pressure of the pneumoperitoneum to 8 mmHg. This method provided an adequate operative field for dissection of the IMA and inferior mesenteric vein and mobilization of the splenic flexure. These procedures were completed within approximately 20-30 min, and the pressure was then reduced to 6 mmHg.

TME was then started posteriorly after identification of the Holy Plane. Dissection was performed laterally and anteriorly down to the pelvic floor, until circumferential rectal mobilization was complete. The hypogastric nerves, inferior hypogastric plexuses, presacral nerves and ureters were carefully identified and preserved. For patients undergoing anterior resection, an endoscopic linear stapler was used to divide the rectum. The specimen was extracted through a protected incision at the left lower trocar site. After division of the proximal colon and introduction of the anvil of a circular stapler were complete, an intracorporeal end-to-end colorectal anastomosis was performed. A rectal decompression tube was placed and no diverting ileostomy was constructed. An abdominoperineal resection was performed if the tumor was located less than 5 cm from the anal verge, and perforation of the specimen was avoided with careful operation.

RESULTS

All 26 laparoscopic TME procedures, including 14 cases of anterior resection and 12 cases of abdominoperineal resection, were successfully completed without intraoperative complications. The patients' demographics, perioperative data and pathologic

Table 1 Patients' demographics and clinical characteristics

Variable	*n*/mean ± SD (range)
Age in yr	62.71 ± 8.71 (41- 82)
Sex	
Male	17
Female	9
BMI in kg/m^2	24.39 ± 2.68 (21.11-30.12)
ASA grade	
Ⅰ	1
Ⅱ	22
Ⅲ	3
Ⅳ	0
Procedure	
AR	14
APR	12
Operative time in min	
AR	194.29 ± 41.27 (125-270)
APR	200.41 ± 20.56 (170-230)
Estimated blood loss in mL	
AR	35.71 ± 16.35 (20-80)
APR	85.00 ± 26.61 (50-140)
Postoperative complications	
Shoulder pain	1
Pulmonary infection	1
Calf muscular venous thrombosis	2
Dysuria	4
Tumor size in cm	
Length	4.29 ± 1.19 (2-6.5)
Thickness	1.12 ± 0.45 (0.5-2)
Distal resection margin in cm	
AR	3.14 ± 1.34 (2-5)
APR	-
Differentiation	
Poorly	2
Moderate	19
Highly	5
Depth of invasion	
T1	1
T2	7
T3	1
T4	17
Lymph nodes harvested	16.71 ± 5.06 (7-27)
Dukes stage	
A	6
B	5
C	15
Follow-up in mo	11.96 ± 5.55 (5-23)

Data are number of cases (*n*) or mean ± SD. AR: Anterior resection; APR: Abdominoperineal resection; BMI: Body mass index; SD: Standard deviation.

outcomes are summarized in Table 1. LPP combined with AWL provided adequate exposure of the operating area. There were no conversions to open or laparoscopic surgery with SPP. Intraoperative monitoring resulted in stable curves of heart rate and blood pressure during surgery (Figure 2A). Peak and mean paw airway pressure increased when the pneumoperitoneum was created at the beginning of surgery, was stable throughout the laparoscopic stage, and then decreased after CO_2 was discharged at approximately 150-180 min (Figure 2B).

One patient had shoulder pain and pulmonary infection postoperatively. Dysuria occurred in 4 male patients after urethral catheters were removed. All 4 patients were diagnosed with benign prostatic hyperplasia preoperatively and the catheters were re-indwelt. All patients resumed free liquid diet 24 h after surgery. The rectal decompression tube was removed 3 d after surgery. There were no cases of adverse cardiovascular events, bleeding or anastomotic leakage observed after surgery.

The rectal specimens were thoroughly examined by the same group of colorectal pathologists. No positive circumferential or distal resection margins were found. No local recurrences were observed during a mean follow-up period of 11.96 mo (range: 5-23 mo).

DISCUSSION

LPP combined with AWL has been proposed as an alternative approach to SPP by the European Association for Endoscopic Surgery[7]. We initially used this method in a case of laparoscopic transumbilical single-site cholecystectomy which was converted from a gasless laparoscopic single-site procedure with AWL[18]. Due to the high BMI of the patient, a 6 mmHg pneumoperitoneum was created for better exposure of the operative field. In the present study, this technique was applied in laparoscopic TME for the first time.

Our preliminary experience indicated that LPP with AWL was safe and provided a satisfactory workspace for TME. The number of lymph nodes retrieved, the completeness of TME, the circumferential and mean distance to the distal margin were comparable with those reported in studies using SPP[20-23]. Another LPP (8 mmHg) and AWL technique was designed by Park *et al*[19] and proved feasible in laparoscopic colorectal surgery. In their study, anchoring sutures were placed around the camera port and lifted up by an assistant to retract the abdominal wall for additional exposure. Unlike this technique, we used the subcutaneous AWL system introduced by Nagai *et al*[24] and Hashimoto *et al*[25], in which a needle was inserted to retract the inferior abdominal wall rather than the periumbilical area. This technique provided a stable and superior operative field, although no strict comparison was performed between the two techniques.

The present study indicated that LPP combined with AWL resulted in stable heart rate, blood pressure and paw airway pressure monitored during laparoscopic TME. For rectal surgery which requires exposure of the lower abdomen, a head-down or Trendelenburg position is necessary. Pneumoperitoneum combined with this position contributes to pushing abdominal organs towards the chest for sufficient exposure of the IMA and mesocolon before dissection in TME. However, SPP combined with head-down or Trendelenburg position significantly reduces pulmonary compliance by more than 30% and leads to ventilation perfusion mismatch[7]. This should be avoided in patients with impaired cardiopulmonary function. Therefore, gasless

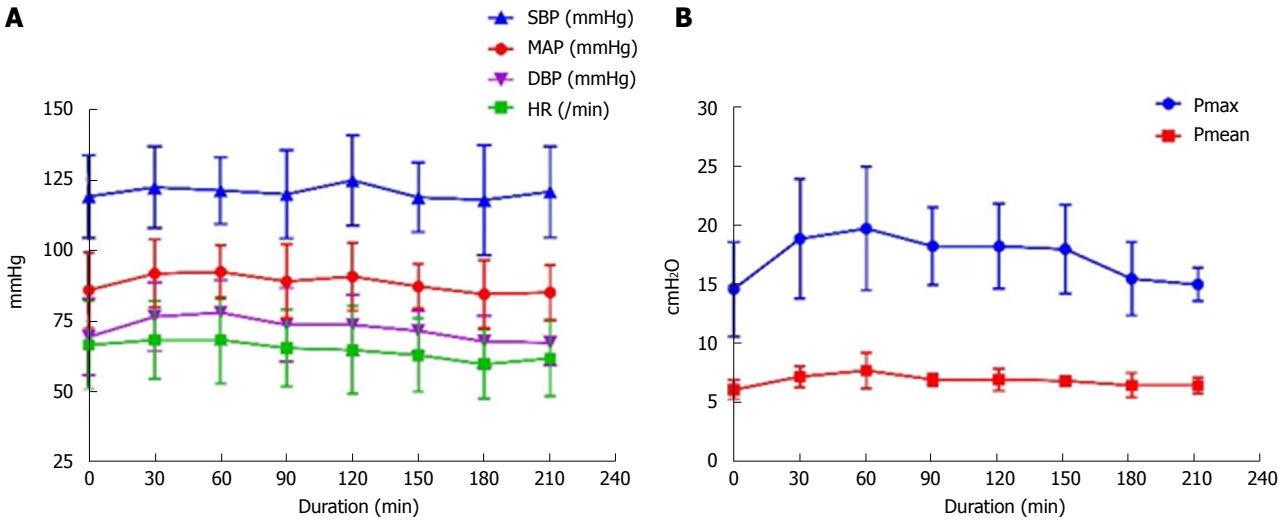

Figure 2 Intraoperative monitoring indexes. A: Heart rate (HR), systolic blood pressure (SBP), diastolic blood pressure (DBP) and mean arterial pressure (MAP); B: Peak and mean paw airway pressure (P_{max} and P_{mean}).

or LPP techniques should be recommended in these patients.

Gasless laparoscopic colorectal surgery was reported to be feasible in several studies[26,27]. However, studies of laparoscopic colorectal surgery with LPP are scant, which is possibly due to the restricted operative field. Compared with LPP or AWL alone, the combination of LPP and AWL may be a more appropriate technique with less adverse hemodynamic and respiratory alterations for laparoscopic TME. This was proved by the stable intraoperative monitoring indices, even in patients with ASA Ⅲ status, although the number of patients was small. In the present study, most of the patients were in ASA Ⅰ and Ⅱ status. Further studies are expected to confirm the superiority of this approach in patients with ASA Ⅲ and Ⅳ status.

The most obvious disadvantage of LPP and gasless techniques is limited exposure in the operative field. Based on our experience, the operative field provided by LPP combined with AWL was less optimal than that with SPP, but acceptable for laparoscopic TME in most patients. However, there were some difficulties in exposing and dissecting the IMA with a pneumoperitoneum of 6 mmHg, especially in obese patients. We increased the pressure to 8-10 mmHg and obtained better exposure of the IMA, and then decreased the pressure back to 6 mmHg after dissection.

Two alternative methods were used to improve exposure of the operative field in obese patients. A second needle was inserted 3 cm above the umbilical level. A better operative field was obtained, but surgery was more difficult due to frequent collisions of the laparoscopic instruments with the scaffold and lifting arms. We also used the method reported by Park *et al*[19], which was feasible, and exposure was improved when the camera port was lifted up. However, the operative field provided by the assistant was unstable. Therefore, we recommend that the pressure should be increased to 8-10 mmHg when there is difficulty in exposing and dissecting the IMA. No obvious changes in heart rate, blood pressure and paw airway pressure were observed during the short operating time.

Another major concern of LPP with AWL was the prolonged operative time and the accompanying increase in CO_2 absorption. Installation of the AWL device and inferior exposure of the operative field may result in longer operative time. During surgery, only approximately 5 min was needed to assemble the AWL system. The mean operative time was comparable to surgery with SPP[21,22]. The operative time may be longer for less skillful surgeons. However, CO_2 absorption will not increase due to slow absorption in the case of low pressure. It is possible that postoperative pain may increase due to the subcutaneous insertion of steel needles. However, our patients did not complain of pain at the insertion site, which may have been masked by pain from ports and the assisted incisions.

The major limitation of this study was that it was an observational study and restricted to a small number of patients. A large, well-controlled comparative study with open or standard-pressure laparoscopic TME would be helpful in providing stronger evidence. Another obvious limitation was that most patients in the present study were in ASA Ⅰ and Ⅱ status. Patients with compromised cardiopulmonary reserve should be enrolled in further studies to draw more convincing conclusions.

ARTICLE HIGHLIGHTS

Research background

Pneumoperitoneum with carbon dioxide (CO_2) is the conventional method of creating a workspace in laparoscopic surgery. Standard-pressure pneumoperitoneum (SPP; 12-15 mmHg) has been reported to result in lower respiratory compliance, increased paw airway pressure, enhanced venous stasis, reduced portal venous pressure and impaired cardiac function.

Low-pressure pneumoperitoneum (LPP) and abdominal wall lift (AWL)

have been proposed as alternative approaches to SPP to avoid adverse cardiopulmonary effects. However, the operative field with these techniques is less optimal with increased technical difficulties.

Research motivation

In order to obtain adequate visualization, we combined LPP with AWL and initially used this technique in a case of laparoscopic single-site cholecystectomy, and the surgery was performed successfully. For laparoscopic colorectal surgery which requires sufficient exposure of the lower abdomen, a head-down or Trendelenburg position is necessary. SPP combined with this kind of position significantly influences patients' cardiopulmonary function. Therefore, we decided to find out whether LPP with AWL technique can take the place of SPP in laparoscopic total mesorectal excision (TME) for rectal cancer.

Research objectives

In this study we designed and performed laparoscopic TME for rectal cancer using LPP with AWL, and evaluated the safety and feasibility. The outcomes of this study will guide the application of the new technique in laparoscopic TME and other surgeries in the future.

Research methods

From November 2015 to July 2017, 26 patients underwent laparoscopic TME for rectal cancer using LPP (6-8 mmHg) with subcutaneous AWL in Qilu Hospital of Shandong University, Jinan, China. Clinical data regarding patients' demographics, intraoperative monitoring indices, operation-related indices and pathological outcomes were prospectively collected and analyzed.

Research results

Laparoscopic TME was performed in 26 cases (14 anterior resection and 12 abdominoperineal resection) successfully without conversion to open or laparoscopic surgery with SPP. Intraoperative monitoring showed stable heart rate, blood pressure and paw airway pressure. The number of lymph nodes retrieved, the completeness of TME, and the circumferential and mean distance to the distal margin were comparable with those reported in studies using SPP. There was no positive circumferential or distal resection margin. No local recurrence was observed during a median follow-up period of 11.96 ± 5.55 mo (range: 5-23 mo). Our preliminary experience indicated that LPP with AWL was safe and provided a satisfactory workspace for TME.

Research conclusions

LPP combined with AWL is safe and feasible for laparoscopic TME. The technique can provide satisfactory exposure of the operative field and result in stable operative monitoring indexes. It should be considered as an alternative approach to SPP in patients undergoing laparoscopic TME.

Research perspectives

Further studies are required to confirm the superiority of LPP with AWL over SPP in preservation of cardiopulmonary function, especially in patients with American Society of Anesthesiologists Ⅲ and Ⅳ status. A prospective clinical trial study should be the best method for the future research.

REFERENCES

1 **Wirth S**, Biesemann A, Spaeth J, Schumann S. Pneumoperitoneum deteriorates intratidal respiratory system mechanics: an observational study in lung-healthy patients. *Surg Endosc* 2017; **31**: 753-760 [PMID: 27324326 DOI: 10.1007/s00464-016-5029-0]

2 **Nguyen NT**, Cronan M, Braley S, Rivers R, Wolfe BM. Duplex ultrasound assessment of femoral venous flow during laparoscopic and open gastric bypass. *Surg Endosc* 2003; **17**: 285-290 [PMID: 12364988 DOI: 10.1007/s00464-002-8812-z]

3 **Jakimowicz J**, Stultiëns G, Smulders F. Laparoscopic insufflation of the abdomen reduces portal venous flow. *Surg Endosc* 1998; **12**: 129-132 [PMID: 9479726]

4 **Meininger D**, Byhahn C, Bueck M, Binder J, Kramer W, Kessler P, Westphal K. Effects of prolonged pneumoperitoneum on hemodynamics and acid-base balance during totally endoscopic robot-assisted radical prostatectomies. *World J Surg* 2002; **26**: 1423-1427 [PMID: 12297911 DOI: 10.1007/s00268-002-6404-7]

5 **Dexter SP**, Vucevic M, Gibson J, McMahon MJ. Hemodynamic consequences of high- and low-pressure capnoperitoneum during laparoscopic cholecystectomy. *Surg Endosc* 1999; **13**: 376-381 [PMID: 10094751]

6 **Nguyen NT**, Wolfe BM. The physiologic effects of pneumoperitoneum in the morbidly obese. *Ann Surg* 2005; **241**: 219-226 [PMID: 15650630]

7 **Neudecker J**, Sauerland S, Neugebauer E, Bergamaschi R, Bonjer HJ, Cuschieri A, Fuchs KH, Jacobi Ch, Jansen FW, Koivusalo AM, Lacy A, McMahon MJ, Millat B, Schwenk W. The European Association for Endoscopic Surgery clinical practice guideline on the pneumoperitoneum for laparoscopic surgery. *Surg Endosc* 2002; **16**: 1121-1143 [PMID: 12015619 DOI: 10.1007/s00464-001-9166-7]

8 **Sroussi J**, Elies A, Rigouzzo A, Louvet N, Mezzadri M, Fazel A, Benifla JL. Low pressure gynecological laparoscopy (7mmHg) with AirSeal® System versus a standard insufflation (15mmHg): A pilot study in 60 patients. *J Gynecol Obstet Hum Reprod* 2017; **46**: 155-158 [PMID: 28403972 DOI: 10.1016/j.jogoh.2016.09.003]

9 **Sandhu T**, Yamada S, Ariyakachon V, Chakrabandhu T, Chongruksut W, Ko-iam W. Low-pressure pneumoperitoneum versus standard pneumoperitoneum in laparoscopic cholecystectomy, a prospective randomized clinical trial. *Surg Endosc* 2009; **23**: 1044-1047 [PMID: 18810547 DOI: 10.1007/s00464-008-0119-2]

10 **Schietroma M**, Carlei F, Cecilia EM, Piccione F, Sista F, De Vita F, Amicucci G. A prospective randomized study of systemic inflammation and immune response after laparoscopic nissen fundoplication performed with standard and low-pressure pneumoperitoneum. *Surg Laparosc Endosc Percutan Tech* 2013; **23**: 189-196 [PMID: 23579517 DOI: 10.1097/SLE.0b013e3182827e51]

11 **Madsen MV**, Istre O, Staehr-Rye AK, Springborg HH, Rosenberg J, Lund J, Gätke MR. Postoperative shoulder pain after laparoscopic hysterectomy with deep neuromuscular blockade and low-pressure pneumoperitoneum: A randomised controlled trial. *Eur J Anaesthesiol* 2016; **33**: 341-347 [PMID: 26479510 DOI: 10.1097/EJA.0000000000000360]

12 **Schietroma M**, Pessia B, Stifini D, Lancione L, Carlei F, Cecilia EM, Amicucci G. Effects of low and standard intra-abdominal pressure on systemic inflammation and immune response in laparoscopic adrenalectomy: A prospective randomised study. *J Minim Access Surg* 2016; **12**: 109-117 [PMID: 27073301 DOI: 10.4103/0972-9941.178513]

13 **Özdemir-van Brunschot DMD**, Scheffer GJ, van der Jagt M, Langenhuijsen H, Dahan A, Mulder JEEA, Willems S, Hilbrands LB, Donders R, van Laarhoven CJHM, d'Ancona FA, Warlé MC. Quality of Recovery After Low-Pressure Laparoscopic Donor Nephrectomy Facilitated by Deep Neuromuscular Blockade: A Randomized Controlled Study. *World J Surg* 2017; **41**: 2950-2958 [PMID: 28608013 DOI: 10.1007/s00268-017-4080-x]

14 **Alijani A**, Cuschieri A. Abdominal wall lift systems in laparoscopic surgery: gasless and low-pressure systems. *Semin Laparosc Surg* 2001; **8**: 53-62 [PMID: 11337737]

15 **Uemura N**, Nomura M, Inoue S, Endo J, Kishi S, Saito K, Ito S, Nakaya Y. Changes in hemodynamics and autonomic nervous activity in patients undergoing laparoscopic cholecystectomy: differences between the pneumoperitoneum and abdominal wall-lifting method. *Endoscopy* 2002; **34**: 643-650 [PMID: 12173086 DOI: 10.1055/s-2002-33252]

16 **Galizia G**, Prizio G, Lieto E, Castellano P, Pelosio L, Imperatore V, Ferrara A, Pignatelli C. Hemodynamic and pulmonary changes during open, carbon dioxide pneumoperitoneum and abdominal wall-lifting cholecystectomy. A prospective, randomized study. *Surg Endosc* 2001; **15**: 477-483 [PMID: 11353965 DOI: 10.1007/s004640000343]

17 **Chiu AW**, Chang LS, Birkett DH, Babayan RK. The impact of pneumoperitoneum, pneumoretroperitoneum, and gasless laparoscopy on the systemic and renal hemodynamics. *J Am Coll*

Surg 1995; **181**: 397-406 [PMID: 7582206]
18 **Zhang G**, Liu S, Yu W, Wang L, Liu N, Li F, Hu S. Gasless laparoendoscopic single-site surgery with abdominal wall lift in general surgery: initial experience. *Surg Endosc* 2011; **25**: 298-304 [PMID: 20607566 DOI: 10.1007/s00464-010-1177-9]
19 **Park IJ**, Kim SH, Joh YG, Hahn KY. Laparoscopic colorectal surgery using low-pressure pneumoperitoneum combined with abdominal wall lift by placement of anchoring sutures around the camera port. *Surg Endosc* 2006; **20**: 956-959 [PMID: 16738990 DOI: 10.1007/s00464-005-0459-0]
20 **Denost Q**, Adam JP, Pontallier A, Celerier B, Laurent C, Rullier E. Laparoscopic total mesorectal excision with coloanal anastomosis for rectal cancer. *Ann Surg* 2015; **261**: 138-143 [PMID: 25185482 DOI: 10.1097/SLA.0000000000000855]
21 **Liang JT**, Cheng JC, Huang KC, Lai HS, Sun CT. Comparison of tumor recurrence between laparoscopic total mesorectal excision with sphincter preservation and laparoscopic abdominoperineal resection for low rectal cancer. *Surg Endosc* 2013; **27**: 3452-3464 [PMID: 23508815 DOI: 10.1007/s00464-013-2898-3]
22 **Kim MJ**, Park SC, Park JW, Chang HJ, Kim DY, Nam BH, Sohn DK, Oh JH. Robot-assisted Versus Laparoscopic Surgery for Rectal Cancer: A Phase II Open Label Prospective Randomized Controlled Trial. *Ann Surg* 2018; **267**: 243-251 [PMID: 28549014 DOI: 10.1097/SLA.0000000000002321]
23 **Martínez-Pérez A**, Carra MC, Brunetti F, de'Angelis N. Pathologic Outcomes of Laparoscopic vs Open Mesorectal Excision for Rectal Cancer: A Systematic Review and Meta-analysis. *JAMA Surg* 2017; **152**: e165665 [PMID: 28196217 DOI: 10.1001/jamasurg.2016.5665]
24 **Nagai H**, Kondo Y, Yasuda T, Kasahara K, Kanazawa K. An abdominal wall-lift method of laparoscopic cholecystectomy without peritoneal insufflation. *Surg Laparosc Endosc* 1993; **3**: 175-179 [PMID: 8111552]
25 **Hashimoto D**, Nayeem SA, Kajiwara S, Hoshino T. Laparoscopic cholecystectomy: an approach without pneumoperitoneum. *Surg Endosc* 1993; **7**: 54-56 [PMID: 8424236]
26 **Jiang JK**, Chen WS, Yang SH, Lin TC, Lin JK. Gasless laparoscopy-assisted colorectal surgery. *Surg Endosc* 2001; **15**: 1093-1097 [PMID: 11727077 DOI: 10.1007/s004640080148]
27 **Kawamura YJ**, Sawada T, Sunami E, Saito Y, Watanabe T, Masaki T, Muto T. Gasless laparoscopically assisted colonic surgery. *Am J Surg* 1999; **177**: 515-517 [PMID: 10414705]

P- Reviewer: Goldaracena N, Snowdon VK, Yukihiko T
S- Editor: Wang XJ **L- Editor**: Filipodia **E- Editor**: Huang Y

Published by **Baishideng Publishing Group Inc**
7901 Stoneridge Drive, Suite 501, Pleasanton, CA 94588, USA
Telephone: +1-925-223-8242
Fax: +1-925-223-8243
E-mail: bpgoffice@wjgnet.com
Help Desk: http://www.f6publishing.com/helpdesk
http://www.wjgnet.com

ISSN 1007-9327

ISSN 1007-9327 (print)
ISSN 2219-2840 (online)

World Journal of *Gastroenterology*

World J Gastroenterol 2018 March 28; 24(12): 1285-1372

Published by Baishideng Publishing Group Inc

World Journal of Gastroenterology

Contents

Weekly Volume 24 Number 12 March 28, 2018

ABOUT COVER

Editorial board member of *World Journal of Gastroenterology*, José Manuel Ramia, MD, PhD, Associate Professor, Department of Surgery, Hospital Universitario de Guadalajara, Guadalajara 19002, Spain

AIMS AND SCOPE

World Journal of Gastroenterology (*World J Gastroenterol*, *WJG*, print ISSN 1007-9327, online ISSN 2219-2840, DOI: 10.3748) is a peer-reviewed open access journal. *WJG* was established on October 1, 1995. It is published weekly on the 7th, 14th, 21st, and 28th each month. The *WJG* Editorial Board consists of 642 experts in gastroenterology and hepatology from 59 countries.

The primary task of *WJG* is to rapidly publish high-quality original articles, reviews, and commentaries in the fields of gastroenterology, hepatology, gastrointestinal endoscopy, gastrointestinal surgery, hepatobiliary surgery, gastrointestinal oncology, gastrointestinal radiation oncology, gastrointestinal imaging, gastrointestinal interventional therapy, gastrointestinal infectious diseases, gastrointestinal pharmacology, gastrointestinal pathophysiology, gastrointestinal pathology, evidence-based medicine in gastroenterology, pancreatology, gastrointestinal laboratory medicine, gastrointestinal molecular biology, gastrointestinal immunology, gastrointestinal microbiology, gastrointestinal genetics, gastrointestinal translational medicine, gastrointestinal diagnostics, and gastrointestinal therapeutics. *WJG* is dedicated to become an influential and prestigious journal in gastroenterology and hepatology, to promote the development of above disciplines, and to improve the diagnostic and therapeutic skill and expertise of clinicians.

INDEXING/ABSTRACTING

World Journal of Gastroenterology (*WJG*) is now indexed in Current Contents®/Clinical Medicine, Science Citation Index Expanded (also known as SciSearch®), Journal Citation Reports®, Index Medicus, MEDLINE, PubMed, PubMed Central and Directory of Open Access Journals. The 2017 edition of Journal Citation Reports® cites the 2016 impact factor for *WJG* as 3.365 (5-year impact factor: 3.176), ranking *WJG* as 29th among 79 journals in gastroenterology and hepatology (quartile in category Q2).

NAME OF JOURNAL
World Journal of Gastroenterology

ISSN
ISSN 1007-9327 (print)
ISSN 2219-2840 (online)

LAUNCH DATE
October 1, 1995

FREQUENCY
Weekly

EDITORIAL OFFICE
Ze-Mao Gong, Director
World Journal of Gastroenterology
Baishideng Publishing Group Inc
7901 Stoneridge Drive, Suite 501,
Pleasanton, CA 94588, USA
Telephone: +1-925-2238242
Fax: +1-925-2238243
E-mail: editorialoffice@wjgnet.com
Help Desk: http://www.f6publishing.com/helpdesk
http://www.wjgnet.com

PUBLISHER
Baishideng Publishing Group Inc
7901 Stoneridge Drive, Suite 501,
Pleasanton, CA 94588, USA
Telephone: +1-925-2238242
Fax: +1-925-2238243
E-mail: bpgoffice@wjgnet.com
Help Desk: http://www.f6publishing.com/helpdesk
http://www.wjgnet.com

PUBLICATION DATE
March 28, 2018

INSTRUCTIONS TO AUTHORS
Full instructions are available online at http://www.wjgnet.com/bpg/gerinfo/204

ONLINE SUBMISSION
http://www.f6publishing.com

World Journal of Gastroenterology

Submit a Manuscript: http://www.f6publishing.com

World J Gastroenterol 2018 March 28; 24(12): 1285-1298

DOI: 10.3748/wjg.v24.i12.1285

ISSN 1007-9327 (print) ISSN 2219-2840 (online)

REVIEW

Review article: Update on current and emergent data on hepatopulmonary syndrome

Stergios Soulaidopoulos, Evangelos Cholongitas, George Giannakoulas, Maria Vlachou, Ioannis Goulis

Stergios Soulaidopoulos, Ioannis Goulis, Fourth Department of Internal Medicine, Hippokration General Hospital, Medical School of Aristotle University of Thessaloniki, Thessaloniki 54642, Greece

Evangelos Cholongitas, First Department of Internal Medicine, Laiko General Hospital, Medical School of National and Kapodistrian University of Athens, Athens 11527, Greece

George Giannakoulas, Maria Vlachou, Department of Cardiology, AHEPA University Hospital, Medical School of Aristotle University of Thessaloniki, Thessaloniki 54621, Greece

ORCID number: Stergios Soulaidopoulos (0000-0003-4150-5286); Evangelos Cholongitas (0000-0002-3645-582X); George Giannakoulas (0000-0002-2358-709X); Maria Vlachou (0000-0002-8004-2184); Ioannis Goulis (0000-0002-2765-4157).

Author contributions: Cholongitas E conceived of and designed the study; Soulaidopoulos S, Vlachou M and Giannakoulas G finished the data acquisition; Soulaidopoulos S and Vlachou M performed the data analysis and interpretation; Soulaidopoulos S and Cholongitas E drafted the manuscript; Goulis I, Cholongitas E, and Giannakoulas G made critical revision of the manuscript.

Conflict-of-interest statement: The authors have no financial or other conflicts of interest related to the submitted manuscript to declare.

Manuscript source: Invited manuscript

Correspondence to: Evangelos Cholongitas, MD, PhD, Associate Professor, First Department of Internal Medicine, Medical School of National & Kapodistrian University of Athens, Laiko General Hospital, Agiou Thoma 17, Athens 11527, Greece. cholongitas@yahoo.gr
Telephone: +30-6936-378903
Fax: +30-2310-992940

Received: January 9, 2018
Peer-review started: January 10, 2018
First decision: February 5, 2018
Revised: February 18, 2018
Accepted: March 7, 2018
Article in press: March 7, 2018
Published online: March 28, 2018

Abstract

Hepatopulmonary syndrome (HPS) is a frequent pulmonary complication of end-stage liver disease, characterized by impaired arterial oxygenation induced by intrapulmonary vascular dilatation. Its prevalence ranges from 4% to 47% in patients with cirrhosis due to the different diagnostic criteria applied among different studies. Nitric oxide overproduction and angiogenesis seem to be the hallmarks of a complicated pathogenetic mechanism, leading to intrapulmonary shunting and ventilation-perfusion mismatch. A classification of HPS according to the severity of hypoxemia has been suggested. Contrast-enhanced echocardiography represents the gold standard method for the detection of intrapulmonary vascular dilatations which is required, in combination with an elevated alveolar arterial gradient to set the diagnosis. The only effective treatment which can modify the syndrome's natural history is liver transplantation. Although it is usually asymptomatic, HPS imparts a high risk of pretransplantation mortality, independently of the severity of liver disease, while there is variable data concerning survival rates after liver transplantation. The potential of myocardial involvement in the setting of HPS has also gained increasing interest in recent research. The aim of this review is to critically approach the existing literature of HPS and emphasize

unclear points that remain to be unraveled by future research.

Key words: Hepatopulmonary syndrome; Liver cirrhosis; Liver transplantation; Portal hypertension; Contrast echocardiography

Core tip: Hepatopulmonary syndrome (HPS) constitutes a relatively frequent complication of end-stage liver disease, characterized by impairment of arterial oxygenation. The only effective treatment is liver transplantation, improving hypoxemia. While there are controversial data regarding HPS prognosis before and after liver transplantation, the question remains whether HPS constitutes an independent factor of morbidity, providing HPS patients priority for liver transplantation. Furthermore, possible associations with myocardial function, which could support the utility of echocardiographical parameters as markers of HPS, remain yet to be established.

Soulaidopoulos S, Cholongitas E, Giannakoulas G, Vlachou M, Goulis I. Review article: Update on current and emergent data on hepatopulmonary syndrome. *World J Gastroenterol* 2018; 24(12): 1285-1298 Available from: URL: http://www.wjgnet.com/1007-9327/full/v24/i12/1285.htm DOI: http://dx.doi.org/10.3748/wjg.v24.i12.1285

INTRODUCTION

Liver cirrhosis is often accompanied by complications from the pulmonary system. These include hepatic hydrothorax, portopulmonary hypertension and hepatopulmonary syndrome (HPS). Hepatic hydrothorax affects approximately 6%-10% of patients with end-stage liver disease and is the result of ascetic fluid passage to the pleural space through diaphragmatic defects[1]. Portopulmonary hypertension is characterized by pulmonary vasoconstriction and increased vascular resistance, developing in 2%-8.5% of patients with portal hypertension, combined with poor prognosis[2].

HPS constitutes a pulmonary disorder of chronic liver disease, characterized by poor arterial oxygenation and intrapulmonary vascular dilatations[3]. Although Fluckiger was the first to describe the syndrome in 1884, treating a woman with liver cirrhosis and cyanosis without any other obvious reason for pulmonary disease, the term "Hepatopulmonary Syndrome" was suggested in 1977 by Kennedy and Knudson[4]. Former autopsy studies had previously demonstrated the potential role of pulmonary vascular dilatations in the development of the syndrome[5,6].

The revised diagnostic criteria for HPS comprise the triad of chronic liver disease, pulmonary vascular dilatation and gas exchange abnormalities in the absence of other causes of impaired pulmonary function[7]. Except for chronic liver disease, HPS can coexist with acute or chronic hepatitis, portal hypertension without liver disease, alpha 1 antitrypsin deficiency, Wilson's disease and Abernathy malformation[8,9]. Defining gas exchange abnormalities, an increased alveolar-arterial oxygen gradient (> 15 mmHg or > 20 mmHg for age > 65 years) was suggested as a more sensitive marker of impaired pulmonary function in cirrhotic patients[3]. The presence of intrapulmonary dilatations can be assessed by several methods, but contrast-enhanced echocardiography with agitated saline is considered the gold standard technique[7].

The aim of this review is to provide a critical overview on prevalence, pathogenesis, diagnosis, clinical manifestations, treatment options and current data regarding prognosis before and after liver transplantation in patients with HPS. Upcoming data suggest remarkable associations between the presence of HPS and specific serum markers, clinical signs and echocardiographic parameters which are worthy of discussion.

SEARCH STRATEGY

A literature search was conducted using the online databases Medline, Embase and Scopus until January 2017 for original research papers and review articles concerning pathogenesis, clinical manifestations, diagnosis and management of HPS. Studies evaluating myocardial function in the setting of HPS were also included. The combination of the following terms was used to identify relevant publications: "liver cirrhosis" OR "prevalence" OR "diagnosis" OR "vasodilatation" OR "clinical features" OR "orthodeoxia" OR "platypnea" OR "treatment" OR "liver transplantation" OR "cardiac involvement" OR "myocardial function" AND "hepatopulmonary syndrome". The collected literature was examined for cited articles relevant to the subject to ensure that no important research data were missed. Articles that had been published as full journal articles in English were included. The above terms were used in ClinicalTrials.gov to search for recently completed or ongoing trials on HPS. Not accessible abstracts, conference proceedings or articles not translated in English were excluded.

PREVALENCE AND SEVERITY

Previous studies have used different criteria in terms of diagnostic methodology for HPS. More specifically, different thresholds for alveolar-arterial gradient and partial pressure of oxygen (PaO_2) have been used in order to define gas-exchange abnormalities, leading to a wide range of HPS prevalence rates[10]. Furthermore, different diagnostic methods have been performed to evaluate intrapulmonary dilatations. Based on

Table 1 Hepatopulmonary syndrome-diagnostic criteria

Presence of liver disease and/or portal hypertension AND
Partial pressure of oxygen < 80 mmHg or alveolar–arterial oxygen gradient [P(A-a)O_2 gradient] ⩾ 15 mmHg (or > 20 mmHg for patients > 65-years-old) while breathing ambient air AND
Documented intrapulmonary vascular dilatation by contrast-enhanced echocardiography or lung perfusion scanning with radioactive albumin

Table 2 Hepatopulmonary syndrome-severity classification

Mild	Alveolar-arterial oxygen gradient ⩾ 15 mmHg, partial pressure of oxygen ⩾ 80 mmHg
Moderate	Alveolar-arterial oxygen gradient ⩾ 15 mmHg, partial pressure of oxygen ⩾ 60 mmHg to < 80 mmHg
Severe	Alveolar-arterial oxygen gradient ⩾ 15 mmHg, partial pressure of oxygen ⩾ 50 mmHg to < 60 mmHg
Very severe	Alveolar–arterial oxygen gradient ⩾ 15 mmHg, partial pressure of oxygen < 50 mmHg

reports from several liver transplantation centers, the prevalence of HPS ranges from 4% to 47% in patients with liver cirrhosis[11-14]. The introduction of specific diagnostic criteria (Table 1), including the definition of impaired oxygenation, by the European Respiratory Society Task Force in 2004, provides the opportunity to obtain comparable results from recent studies[3]. The establishment of alveolar-arterial gradient as a more sensitive marker of pulmonary function as well as the screening of asymptomatic patients has led to higher rates of HPS diagnosis. Nevertheless, further well-designed, prospective, multicenter studies are needed for more accurate estimation of the syndrome's prevalence. Interestingly, intrapulmonary vascular dilatations can be detected in 13%-80% of liver transplantation candidates regardless of the development of arterial oxygenation abnormalities[15].

The evaluation of PaO_2 in the arterial blood is crucial for classification of the syndrome. According to arterial blood gas analysis, four severity stages of HPS can be distinguished while the patient is breathing ambient air (Table 2): mild (PaO_2 ⩾ 80 mmHg), moderate (PaO_2 ⩾ 60 and < 80 mmHg), severe (PaO_2 ⩾ 50 to < 60 mmHg), and very severe (PaO_2 < 50 mmHg)[2]. The existing data suggest that the majority of HPS patients are mild or moderate stage, while severe and very severe cases seem to be less common[16,17]. No associations have been demonstrated between the presence or severity of HPS and the severity of liver disease[18]. However, there is restricted data concerning HPS severity assessment, highlighting the need for well-designed HPS protocols in future studies.

PATHOGENESIS AND PATHOPHYSIOLOGY

Intrapulmonary capillary vasodilatations constitute the main anatomic disturbance of HPS leading to impaired arterial oxygenation through ventilation-perfusion mismatch[3,19]. The diameter of the dilated vessels may vary from 15-100 μm and in some cases to 500 μm when HPS is present, whereas normally it ranges between 8 μm and 15 μm[20,21]. Dilatation of pre-capillary and capillary vessels in combination with reduced or absent tone of pulmonary vasculature result in increased pulmonary blood flow, which is also boosted by hyperdynamic circulation in liver disease. In this way, there is an overperfusion of the alveolar capillary bed combined with a decrease in transit time of red blood cells, while ventilation remains unchanged. As a result, an excessive amount of blood passes through the pulmonary circulation without completing gas exchange, leading to increased alveolar arterial gradient and arterial hypoxemia[22], particularly during muscular activity[23].

Oxygen molecules have to cross a longer distance in less time to reach red blood cells in the center of the pulmonary capillaries due to vascular dilatation[24], while an increase in pulmonary capillary wall thickness has also been observed[21,25]. This alteration in oxygen diffusion contributes in the impaired oxygenation of HPS and could be correlated to the abnormal values of carbon monoxide diffusing capacity observed in these patients[14].

Intrapulmonary arteriovenous shunting constitutes another mechanism causing arterial hypoxia in HPS[6]. Mixed blood passes through pleural and pulmonary arteriovenous communications directly into the central circulation, without coming in touch with the alveoli. A few portopulmonary vascular communications can also be observed. The presence of more pronounced vascular dilatations and arteriovenous communications in lower lung zones, as it was suggested by thoracic computed tomography scans, may interpret the mechanism of orthodeoxia, *i.e.* reduction of PaO_2 from supine to upright patient position[26]. Gravitational pulmonary blood flow redistribution leads to overperfusion of these lower lung zones and increased intrapulmonary shunting, perhaps due to a more altered, maladjusted vascular tone[27].

It seems that the severity of arterial hypoxemia is related to the extent of ventilation-perfusion mismatch, intrapulmonary shunting and diffusion impairment[28]. Administration of 100% oxygen [⩾ 300 mmHg (40.0 kPa)] may improve hypoxia in some cases of HPS, as it provides enough pressure to partly overcome the diffusing limitation arising from the dilated pulmonary

vessels[29,30]. However, there is no effect in partial pressure of oxygen when hypoxia is the result of excessive arteriovenous blood shunting.

Pulmonary vasodilatation

Intrapulmonary vascular dilatations seem to be the result of an imbalance between several vasodilators and vasoconstrictors. Much of our knowledge arises from studies on rat experimental models, in which a common bile duct ligation has been performed in order to develop secondary biliary cirrhosis. The increased production of nitric oxide (NO) and carbon monoxide (CO), two pulmonary vasodilators, constitutes the key process for the development of pulmonary vasodilatation[31]. In common bile duct ligation animal models, the proliferation of cholangiocytes is followed by production and secretion of endothelin-1 (ET-1) after the stimulation by transforming growth factor beta-1 (TGFβ-1)[32,33]. The binding of endothelin-1 to its pulmonary receptor ET-1B triggers the activation of endothelial and inducible nitric oxide synthase (eNOS and iNOS) resulting in elevated NO production and NO-induced pulmonary vasodilatation[34,35]. The selective up-regulation of pulmonary ET-1B receptor in response to ET-1 biliary production in experimental portal hypertension has also been suggested[36]. In addition, levels of eNOS and iNOS protein are increased in HPS cirrhotic rats[37,38], while elevated levels of exhaled NO in HPS patients seem to return to normal after liver transplantation[39,40]. Furthermore, NO inhibition by methylene blue administration transiently improves oxygenation, whereas NG-nitro-L-arginine methylester, *via* iNOS inhibition, did not prove to affect hypoxemia of HPS[41-43]. Interestingly, a recent biopsy study comparing explanted livers from 76 patients with cirrhosis found that focal parenchyma extinction as well as vascular lesions, such as intrahepatic portal vein thrombosis, thickening or obstruction of centrilobular veins and sinusoidal proliferation, were more prevalent in those patients with HPS compared to those without, suggesting an association between liver ischemia and the production of proangiogentic and vasodilatation factors[44].

In patients with liver dysfunction, activation and massive accumulation of intravascular macrophages is observed as a result of intestinal bacterial translocation and endotoxemia[45-47]. These macrophages in the pulmonary vasculature produce proinflammatory cytokines, including tumor necrosis factor-alpha (TNF-α), contributing in the NO-mediated vasodilatation through iNOS activation. Furthermore, ET-1 seems to promote the accumulation of pulmonary monocytes[48]. In support of this theory, TNF-α inhibition by pentoxifylline administration has been shown to improve HPS in rat experimental models[49,50]. Norfloxacin also improved HPS through a reduction in intestinal bacterial load and bacterial translocation[51].

CO produced from the degradation of heme by heme oxygenase, may act as a vasodilator in HPS patients. The latter have elevated levels of arterial carboxyhemoglobin reflecting CO production[52]. Both bacterial accumulation and NO synthesis stimulate heme oxygenase expression[47,53]. Finally, administration of protoporphyrin IX, an inhibitor of heme oxygenase, seems to improve HPS hypoxemia[54].

Angiogenesis

Beside NO-mediated vasodilatation, angiogenesis is considered another crucial mechanism interpreting HPS pathogenesis. Intestinal bacterial translocation and the consequent endotoxemia due to liver dysfunction lead to the recruitment of monocytes and activated macrophages to the lung. These inflammatory cells together with circulating TNF-α stimulate the activation of vascular endothelial growth factor (VEGF) signaling pathways, which are related to angiogenesis[55,56]. The accumulation of CD68+ macrophages in the lungs of common bile duct ligation rats, expressing iNOS and VEGF, has been correlated to the presence of HPS[57]. Remarkably, increased endothelial tube formation and pulmonary artery smooth muscle cell proliferation in HPS plasma was observed. The depletion of CD68+ macrophages improved both histological and hemodynamic features of HPS, while iNOS inhibition disclosed exaggerated vasoconstrictor responses.

TNF-α neutralization in cirrhotic rats has been shown to decrease intrapulmonary shunt as well as alveolar-arterial O_2 gradient[49,58]. The role of specific chemokines, such as the circulating chemokine ligand 1(CX3CL1), in the activation of VEGF is also under investigation[59,60]. Anti-VEGF therapy with sorafenib administration, a kinase inhibitor, was found to improve HPS hypoxia and restrict VEGF-mediated angiogenesis and intrapulmonary shunting in rats with biliary cirrhosis[33,61,62]. Besides, it was recently demonstrated that HPS is independently associated with the presence of hepatocellular carcinoma, an entity also characterized by extensive angiogenesis and VEGF production[62]. Although it can be postulated that VEGF constitutes a regulator of angiogenesis with a possible role in the development of HPS, further studies with measurements of VEGF are needed to unravel the exact pathogenetic pathways. Figure 1 schematically summarizes the main events in HPS pathogenesis.

CLINICAL FEATURES

Progressive dyspnea is the most frequent symptom among HPS patients[63]. In a large cohort of patients listed for liver transplantation, it was found that dyspnea was significantly more frequent in patients with HPS than in those without HPS[64]. However, dyspnea is not specific for HPS, as it is common between patients with liver disease due to complications such as anemia, ascites, hydrothorax and muscular cachexia. Furthermore, HPS can also be asymptomatic, especially

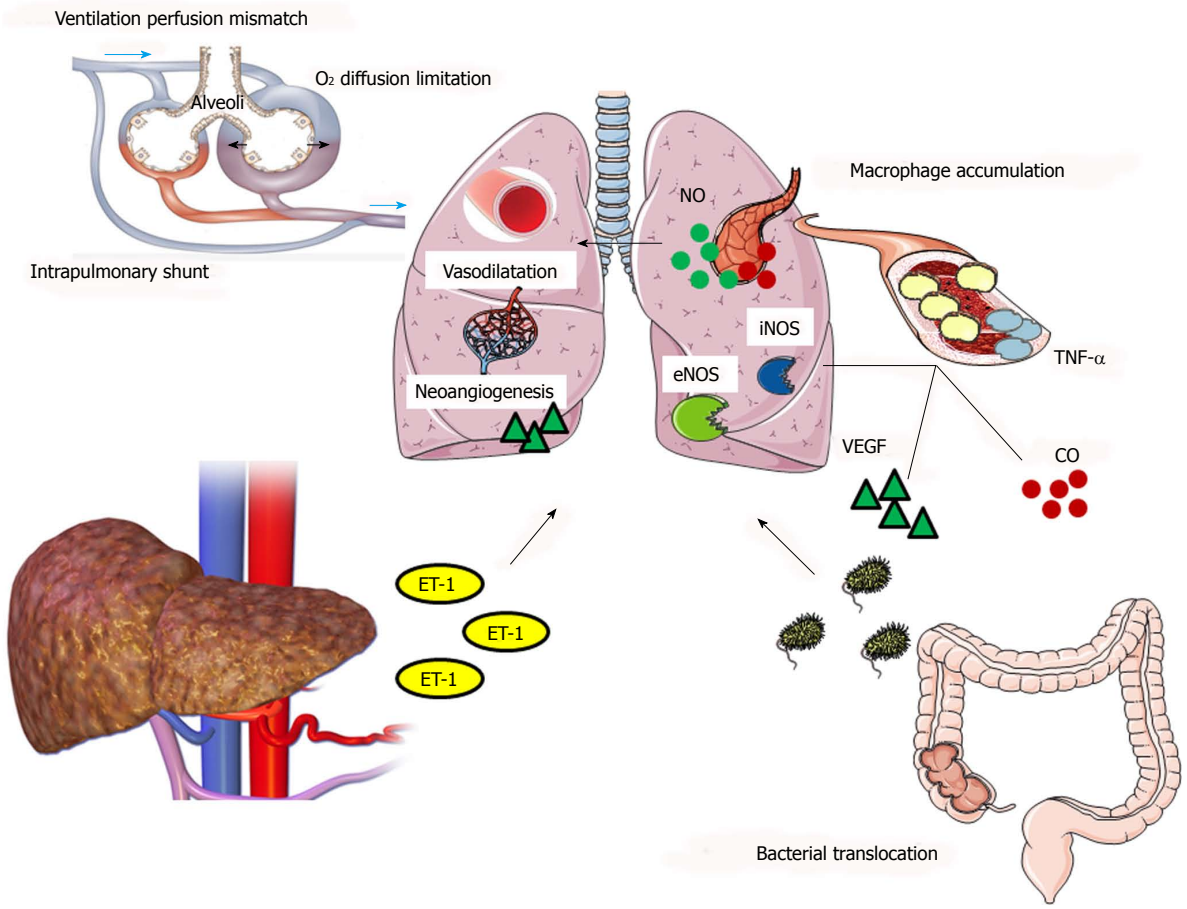

Figure 1 Schematic overview of the main pathways of the pathogenesis of hepatopulmonary syndrome. Liver cirrhosis and portal hypertension lead to endothelin-1 (ET-1) secretion. The binding of ET-1 to its receptor, activates pulmonary endothelial nitric oxide synthase (eNOS), leading to excessive production of nitric oxide (NO), a natural vasodilator. Bacterial translocation and the subsequent pulmonary macrophage accumulation result in the production of inflammatory cytokines, such as tumor necrosis factor-alpha (TNF-α), which contribute in NO-mediated vasodilatation through inducible nitric oxide synthase (iNOS)-enhanced expression. Carbon monoxide constitutes another pulmonary vasodilator produced by macrophage-induced heme oxygenase-1 (HO-1) increased expression. Pulmonary macrophage accumulation and TNF-α-increased circulation trigger vascular endothelial growth factor (VEGF) pathways, concluding in VEGF-mediated pulmonary angiogenesis. Mixed venous blood passes rapidly, due to hyperdynamic circulation observed in liver cirrhosis, through the dilated capillaries without completing gas exchange. An oxygen (O_2) diffusion limitation occurs, as O_2 molecules need to cross a longer distance to reach the center of dilated vasculature. As a result, there is an impairment of arterial oxygenation due to ventilation perfusion mismatch, also boosted by direct right-to-left shunt through arteriovenous communications.

in those with mild hypoxia and alveolar arterial gradient disturbance, with dyspnea observed more frequently in HPS patients with PaO_2 lower than 70 mmHg[10].

Another form of dyspnea, platypnea, is considered to be pathognomonic for HPS[65]. Platypnea is the condition of worsening dyspnea when patient moves from a supine to an upright position. It is the result of the decrease in PaO_2 in the arterial blood of $\geqslant$ 5% (or $\geqslant$ 4 mmHg) from supine to upright position due to increased perfusion of the basis of the lungs and elevated intrapulmonary shunting, a phenomenon called orthodeoxia[27]. Orthopnea, the worsening of dyspnea in lying position, has also been observed more frequently in patients with HPS[64].

Cyanosis, fatigue, spider naevi and digital clubbing are other clinical findings of HPS[63]. Spider angiomas have been suggested as cutaneous markers of HPS, possibly sharing the same pathogenetic mechanism with HPS, *i.e.* imbalance between vasoconstrictor and vasodilator substances[66]. In addition, digital clubbing has a positive predictive value of 75% in HPS diagnosis[67]. In the same study, dyspnea showed a negative predictive value of 75% in HPS diagnosis, whereas no correlation was found between HPS and splenomegaly, ascites, edema, jaundice, oliguria, and collateral veins. Oxygen desaturation during sleep was also correlated to the presence of HPS in another study[68].

Although none of the aforementioned clinical signs are considered to be specific for HPS and the majority of patients may not present any characteristic symptoms, HPS patients seem to have a worse quality of life and higher New York Heart Association functional class compared to patients without HPS[64]. Therefore, once again there is need for further larger studies to investigate thoroughly the exact clinical features that

may be related to HPS.

DIAGNOSIS

According to the European Respiratory Society Task Force in 2004, HPS diagnosis consists of the following criteria: (1) the presence of liver disease and/or portal hypertension; (2) elevated room air alveolar arterial oxygen gradient (≥ 15 mmHg or ≥ 20 mmHg in patients > 64-years-old; and (3) evidence of intrapulmonary vascular dilatations[3]. Diagnosis should be based on arterial blood gas analysis and alveolar arterial gradient calculation rather than a simple assessment of arterial hypoxemia. Several techniques have been developed for the evaluation of intrapulmonary vasodilatation, but contrast-enhanced echocardiography with agitated saline is considered the gold standard. Modern imaging techniques are also useful for the verification of pulmonary vascular dilatation and right-to-left communications as well as for the exclusion of other pulmonary complications associated with liver disease or lung disease that may coexist with HPS. Furthermore, pulmonary function tests are also valuable to detect abnormalities that may be indicative of HPS or helpful to unmask other underlying lung or cardiac diseases.

The fact that most HPS patients are asymptomatic or manifest nonspecific symptoms in combination with the application of different diagnostic criteria has led to an underestimation of the syndrome in the past. As there is lack of a reliable and simple screening method for diagnosis of HPS, liver transplantation centers should adopt strict diagnostic protocols using unified criteria in order to detect all HPS cases and export comparable results.

Intrapulmonary vascular dilatations

Contrast-enhanced transthoracic echocardiography with agitated saline is considered the cornerstone in the detection of pulmonary vascular dilatations[69]. Normal saline is shaken to produce microbubbles > 10 μm in diameter and is administered to a peripheral vein in the arm while a four-chamber transthoracic echocardiography is performed. Microbubbles are normally trapped in the pulmonary circulation and absorbed by the alveoli as they cannot pass through normal capillaries. However, in the presence of a dilated vascular bed and/or arteriovenous shunting, microbubbles elude pulmonary capture and reach the left cardiac chambers. Left atrial opacification with microbubbles between the fourth and sixth cardiac cycle after the repletion of the right atrial is indicative of intrapulmonary vasodilatation. Notably, the appearance of microbubbles in the left cardiac chambers within less than three cardiac cycles insinuates intracardial shunting and cannot be diagnostic for intrapulmonary vasodilatation[70].

Contrast-enhanced echocardiography constitutes a practical tool for HPS diagnosis. It is a minimally invasive, low-cost technique providing high sensitivity for the qualitative evaluation of intrapulmonary vascular dilatations and shunting. A positive test is not enough for HPS diagnosis, as the two other parameters of the HPS diagnostic triad must be fulfilled. Interestingly, a quantitative classification of intrapulmonary shunting based on the maximum number of microbubbles bypassing to the left ventricle in one still frame has been suggested[71,72]. According to this classification, severity of intrapulmonary shunting can be graded as stage 1 (< 30 microbubbles), 2 (30-100 microbubbles) or 3 (> 100 microbubbles) (Table 3). A possible correlation between this shunt grading and the proposed classification of HPS based on arterial PaO_2 remains to be verified in future studies.

Contrast transesophageal echocardiography is superior to transthoracic echocardiography concerning the sensitivity of the technique in the diagnosis of intrapulmonary vasodilatation[73]. However, it is not preferred for the assessment of HPS in cirrhotic patients due to the risk regarding possible trauma to esophageal varices.

Macroaggregated albumin lung perfusion is performed by injecting technetium-99m-labeled macroaggregated albumin followed by a lung and brain perfusion scanning. Brain uptake of the radionuclide higher or equal to 6% implies intrapulmonary or intracardiac shunting, as the large molecules of radiolabeled albumin are normally trapped in the pulmonary capillary bed[74]. Estimating the pathological retention of the radionuclide in the brain, this technique allows an indirect quantitative assessment of the intrapulmonary shunting. However, it is not as sensitive as contrast echocardiography, especially in early stages of HPS[75], while it cannot distinguish intrapulmonary from intracardial shunting.

Chest radiographs are only useful to exclude concomitant pulmonary disease as they rarely show evidence of dilated vasculature[3]. High resolution computed tomography may also identify large, dilated pulmonary vessels[76].

Pulmonary angiography provides a double contribution in HPS, diagnostic and therapeutic. Two types of HPS can be distinguished on the basis of angiographic findings[77]. Type 1 is characterized by minimally dilated vessels, and type 2 delineated by well-defined arteriovenous communications and resistance to 100% oxygen administration. The invasive character of pulmonary angiography makes it a less convenient method for the diagnosis of HPS.

Arterial oxygenation

Arterial blood gas analysis is required to detect all patients with HPS[78]. The calculation of the alveolar-arterial gradient is proposed as a better diagnostic parameter than the evaluation of the PaO_2 alone to identify those patients with impaired oxygenation. The sensitivity of this marker is attributed to the fact that the

Table 3 Intrapulmonary shunt quantitative classification

Contrast-enhanced echocardiography based on the number of microbubbles passing in the left ventricle	
No shunt	No detection of microbubbles
Stage 1	< 30 microbubbles
Stage 2	30-100 microbubbles
Stage 3	> 100 microbubbles
Macroaggregated albumin lung perfusion	
No shunt	< 6% brain uptake of radiolabeled albumin
Intrapulmonary shunt	⩾ 6% brain uptake of radiolabeled albumin

partial pressure of carbon dioxide ($PaCO_2$) is included to its calculation, so that lower values of $PaCO_2$ lead to an increased alveolar-arterial gradient, reflecting an elevated respiratory effort to maintain normal blood oxygenation, even before PaO_2 is affected. According to the European Respiratory Task Force, alveolar-arterial gradient greater than or equal to 15 mmHg (or ⩾ 20 mmHg in patients > 64-years-old) is indicative of impaired oxygenation, calculated at sea level while the patient is breathing ambient air at rest[3].

The potential role of pulse oximetry as a screening test for the presence of HPS has also been investigated. Lower values of oxygen saturation were measured in HPS patients compared to cirrhotic patients without HPS (96.8% *vs* 98.4%, $P = 0.02$)[79], while pulse oximetry values below 96% presented a sensitivity and specificity of 100% and 88% respectively for detecting patients with $PaO_2 < 60$ mmHg[80]. On the other hand, the utility of pulse oximetry in HPS diagnosis was not confirmed in children with cirrhosis[81]. The difference in oxygen saturation between supine and standing position was suggested as a method to detect HPS[82]. However, the use of low values of oxygen saturation (< 92%) as well as a decrease of ⩾ 4% after change from supine to upright position was unreliable as screening test for diagnosis of HPS. Notably, the majority of HPS patients present oxygen desaturation during sleep, proportional to the syndrome's severity[68]. Finally, the variation in oxygen saturation between supine and standing position was reported as a marker of possible intrapulmonary vascular dilatations[83].

A reduced diffusing capacity for carbon monoxide (DLCO) is the single most common defect among pulmonary function tests that has been correlated to the presence of HPS[14]. However, there is controversial data concerning DLCO as a diagnostic tool for HPS screening[84,85]. In contrast to ventilation-perfusion imbalance, which seems to resolve after liver transplantation, a restricted number of observational studies have suggested a persistence of low DLCO values after liver transplantation due to permanent liver-induced structural vascular changes in the pulmonary vasculature[86,87].

As pulse oximetry fails to detect mild and moderate HPS and the value of other screening markers remains undefined, alveolar-arterial gradient represents, as yet, the most remarkable method for HPS screening

TREATMENT

Liver transplantation constitutes the only established successful treatment that modifies the natural history of HPS, improving arterial hypoxemia within 6-12 mo[88]. The identification of HPS through established diagnostic protocols among liver transplantation candidates in combination with the model for end-stage liver disease (MELD) exception policy to facilitate liver transplantation may achieve an 88% 5-year posttransplantation survival for HPS patients[89]. Besides, oxygen therapy is recommended for those cases with severe hypoxemia[3]. Restricted data report improvement in liver function and oxygenation after 1 year of oxygen supplement[90].

Many pharmaceutical interventions have been studied both in humans and animal models, targeting the syndrome's pathogenetic pathways, without reaching encouraging outcomes. NO-mediated pulmonary vasodilatation and angiogenesis induced by proinflammatory cytokines, which represent the hallmarks of HPS pathogenesis, have constituted the main targets of medical intervention, in an effort to reverse the syndrome's evolutionary process and confirm the assumptions concerning the pathogenetic mechanisms.

Administration of octreotide, a somatostatin analogue inhibiting angiogenesis, failed to improve hypoxemia in patients with HPS[91]. Contrariwise, sorafenib improves experimental HPS by reducing VEGF-mediated angiogenesis and down-regulating eNOS activation through tyrosine kinase receptor inhibition[33,61]. Treatment with antibiotics, such as norfloxacin, in order to reduce endotoxemia and NO production triggered by bacterial translocation, did not improve gas exchange, in contrast to promising results in experimental models[92,93]. Single case reports suggest improvement of HPS after administration of cyclooxygenase inhibitors, such as indomethacin, and immunosuppressants, such as mycophenolate mofetil, but there are no randomized studies to investigate these findings[94-96].

Methylene blue is an oxidizing agent that restricts NO-mediated vasodilatation through blockage of soluble guanylate cyclase stimulation by NO[97]. Intravenous administration of methylene blue reduced intrapulmonary shunting and improved oxygenation

in experimental models and in a restricted number of patients with HPS[98,99].

There are conflicting results regarding the effect of pentoxifylline on HPS. Pentoxifylline is a TNF-α inhibitor that improves HPS in experimental models by reducing TNF-induced NO production through down-regulation of iNOS[50,58]. A dosage of 400 mg of pentoxifylline, three times per day for 3 mo significantly improved oxygenation and decreased TNF-α levels in 9 patients with symptomatic HPS[100]. Nevertheless, another pilot study enrolling 9 patients with advanced HPS reported no significant therapeutic response after pentoxifylline administration, while the drug was poorly tolerated due to gastrointestinal adverse events[101].

N(G)-nitro-L-arginine methylester, a nebulized inhibitor of NO synthesis, did not improve oxygenation in HPS patients, even if a reduction in exhaled NO was recorded[43,102]. Almitrine bismesylate, a potential vasoconstrictor, does not affect impaired oxygenation in HPS[103]. Finally, a few studies have demonstrated that garlic supplementation improves arterial oxygenation and symptoms in HPS[104]. A total reversal of HPS was observed in 14 of 21 patients after 9 mo of garlic treatment, compared to 1 of 20 HPS patients under placebo treatment[105].

Transjugular intrahepatic portosystemic shunting (commonly known as TIPS) was performed as a therapeutic maneuver in a limited number of patients with severe HPS, leading to variable results[106,107]. Although TIPS could be considered as a bridge towards transplantation, there is concern that persistent right-to-left shunting *via* TIPS prevents the reversal of intrapulmonary structural alterations[108]. Embolotherapy has also been performed to treat persistent hypoxemia of HPS, either before or after liver transplantation, in the presence of large arteriovenous communications[109,110].

Clearly, their poor outcomes as well as the small number of enrolled patients make the aforementioned studies insufficient to suggest effective therapeutic options for the management of HPS. In addition, these data underline the complexity of pathogenetic interactions in HPS and outline potential areas of interest and future research.

PROGNOSIS

Despite the relative high prevalence of HPS among cirrhotic patients, there is an inadequate number of prospective studies evaluating the syndrome's impact on overall morbidity and mortality. Once again, the use of varying thresholds, concerning arterial oxygenation, for the diagnosis of the syndrome, has led to ambiguous results about HPS prognosis. The main question remains whether the presence of HPS should be considered as an independent factor for morbidity, giving HPS patients priority to liver transplantation, and whether any correlations between the severity of HPS and the posttransplantation survival rates exist.

A retrospective analysis reported 41% mortality over an approximate 2.5-year period in 22 patients with HPS[77]. Comparing survival rates between cirrhotic patients with HPS and matched for the severity of liver disease by MELD and Child-Pugh score classification and age patients without HPS, who did not undergo liver transplantation, patients with HPS had a worse 5-year survival (23% *vs* 63%, $P = 0.0003$)[111]. Patients with PaO_2 less than 50 mmHg had significantly worse survival rates. Similar results were confirmed by a prospective study that reported lower median survival among HPS subjects compared to nonHPS cirrhotic patients (10.6 mo *vs* 40.8 mo, $P < 0.05$), while the mortality remained higher even after adjusting for age and liver disease severity[112]. Furthermore, HPS was associated with worse quality of life, assessed by the New York Heart Association classification, and higher risk of death compared to nonHPS matched for age, sex and MELD score cirrhotic subjects [hazard ratio = 2.41, 95% confidence interval (95%CI): 1.31-4.41, $P = 0.005$][64].On the other hand, no significant difference in overall survival between HPS and nonHPS transplantation candidates was demonstrated in a prospective study including 316 cirrhotic patients[16]. Notably, even in those studies that reported high HPS-related mortality, the causes of death were mainly attributed to liver dysfunction rather than pulmonary complications.

Liver transplantation is the only therapeutic intervention that reverses HPS between the first 6 to 12 mo, even for cases with severe preoperative hypoxemia[111]. The general policy is prioritizing patients with HPS and hypoxemia for liver transplantation, regardless of the severity of liver disease[113]. Beside poor prognosis of HPS, the progressive aggravation of hypoxemia, estimated at 5.2 mmHg per year, probably boosts the decision for a prompt management[111]. However, there is concern that through this organ allocation policy, HPS patients may be offered a pretransplantation survival advantage over nonHPS cirrhotic transplantation candidates, prompting the need for reassessment of the MELD exception criteria[114].

There is controversial data concerning posttransplantation mortality in HPS transplanted patients. A prospective study suggests higher 6-mo postoperative mortality rates in HPS patients compared to transplanted patients without HPS (33% *vs* 9.25%, $P = 0.0012$)[115]. A PaO_2 of 50 mmHg or less and a macroaggregated albumin shunt fraction > 20% are demonstrated as the most important predictors of mortality following transplantation, suggesting preoperative HPS staging to assess the risk of postoperative mortality[116]. Conversely, no difference in posttransplantation survival between patients with and without HPS was demonstrated in a large prospective study that enrolled 316 patients[16]. One-year posttransplantation survival may reach 93% in HPS patients[117], while the presence of HPS does not seem to affect duration of intensive care unit stay, duration of total hospital stay, rate of pulmonary complications or 3-mo survival after liver

transplantation[118]. Finally, there is a growing number of reports suggesting no differences in short- and long-term posttransplantation morbidity between patients with and without HPS, and no association between the severity of baseline hypoxia and survival after transplantation[17,119].

The discrepancies between the aforementioned studies can be attributed to different methodological approaches and HPS assessment protocols. The possibility of transplantation denial to patients with HPS and significant hypoxemia should always be considered as a confusing factor that may influence the comparison between different research outcomes[120].

HPS AND MYOCARDIAL FUNCTION

Liver cirrhosis is characterized by hyperdynamic circulation as a consequence of systematic vasodilatation[121] in order to preserve normal blood flow. Diastolic dysfunction and impaired cardiac contractile response to stress define cirrhotic cardiomyopathy, another cardiovascular complication strongly associated with chronic liver disease[122]. The possible association between specific markers of cardiac dysfunction and HPS remains an issue of debate.

Right ventricular diastolic dysfunction assessed by Doppler echocardiography was found to be more remarkable in the presence of HPS, in a study enrolling 46 cirrhotic patients, 10 of whom had HPS[123]. Significantly higher right ventricle and right atrial diameters as well as right ventricle wall thickness values were recorded in the HPS group. Moreover, patients with compared to those without HPS had higher estimated mean pulmonary artery pressure (48.9 ± 4.8 mmHg *vs* 40.6 ± 5.3 mmHg, $P < 0.05$) and higher pulmonary vascular resistance (3.97 ± 1.31 Wood's unit *vs* 3.25 ± 0.96 Wood's unit, $P < 0.05$).

Intrapulmonary shunting in the context of liver disease may aggravate hemodynamic imbalance, followed by further increase in cardiac output[124]. Reflecting hyperdynamic circulatory state, left atrial enlargement was associated with the presence of intrapulmonary vasodilatation, both in human and experimental studies[125]. Remarkably, left atrial volume equal or greater than 50 mL was suggested as a strong echocardiographic predictor of HPS in patients with liver cirrhosis (area under the receiver operating characteristic curve: 0.903, sensitivity 86.3%, specificity 81.2%)[126]. Left ventricular enlargement was also proposed as an independent, indirect echocardiographic marker of HPS[127]. In addition, higher systolic myocardial velocity of the mitral valve measured by tissue Doppler imaging technique was independently associated with HPS (odds ratio: 1.428, 95%CI: 1.049-1.943, $P = 0.026$), a finding implying left ventricular systolic dysfunction[127].

In contrast to the previous reports, Voiosu *et al*[128] found no correlations between HPS and echocardiographic markers of systolic or diastolic myocardial dysfunction in 74 patients with liver cirrhosis. Cirrhotic cardiomyopathy did not differentiate between patients with and without HPS, suggesting an independent pathogenetic nature of these complications. The methods and results of previous studies evaluating cardiac involvement in HPS are presented in Table 4.

While hyperdynamic circulation as a response to systemic vasodilatation in liver cirrhosis is well documented, the subsequent myocardial structural changes are not yet fully understood. Increased cardiac output seems to be the main pathogenetic event triggering systemic multifactorial, cellular, neuronal and humoral signaling mechanisms that induce cardiac contractile dysfunction, electrophysiological abnormalities and chronotropic incompetence in the setting of liver cirrhosis[129]. The most prevalent feature of this entity known as cirrhotic cardiomyopathy is silent diastolic dysfunction with impaired ventricular relaxation and ventricular filling, which may become overt after rapid increase in venous return after liver transplantation.

Currently, literature data cannot support an intimate association between cirrhotic cardiomyopathy and HPS[130]. A complicated interaction between different pathogenetic mechanisms is thought to involve myocardial function in the presence of intrapulmonary shunting. The available studies are not only restricted in number but also heterogenous concerning the assessed features of myocardial dysfunction and the evaluated parameters.

The hypothesis is that NO overproduction, which leads to intrapulmonary vasodilatation, is responsible for an intense hyperdynamic circulating state resulting in higher cardiac output and long-term left ventricle myocardial dysfunction. The potential structural myocardial alterations of the right ventricle in the presence of intrapulmonary vasodilatation as well as the effect of HPS hypoxemia on increased myocardial demands also remain to be clarified. Of great importance is to unravel the exact mechanisms affecting cardiac function that differentiate in patients with HPS. In order to extract more accurate results, the assessment tools of myocardial function should be independent of expanded plasma volume and bias correlated to the presence of ascites, diuretic treatment and sodium intake[131].

In this direction, novel promising echocardiographic techniques offering a more accurate assessment of cardiac structure as well as sensitive biomarkers of cardiac dysfunction need further evaluation in future research in order to elucidate possible interactions between pulmonary vasodilatation, hypoxemia and myocardial dysfunction in the context of chronic liver disease. Last but not least, the effect of possible HPS-related myocardial dysfunction on pre- and posttransplantation total survival is yet to be investigated.

CONCLUSION

HPS is a relatively common complication of chronic liver disease, with many of its aspects remaining still

Table 4 Hepatopulmonary syndrome and cardiac involvement

Study	Cirrhotic patients	Parameters assessed	Assessment tools	Associations
Karabulut *et al*[123]	36 without HPS	RV diastolic dysfunction	M-mode ECHO	RV diastolic dysfunction-HPS
	10 with HPS	PVR	TDI	HPS was associated with higher RV wall thickness (0.61 ± 0.13 cm *vs* 0.51 ± 0.10 cm) RVEDD (3.81 ± 0.38 cm *vs* 3.11 ± 0.94 cm)
		Systolic PAP		RA (3.96 ± 0.53 cm *vs* 3.58 ± 0.47 cm), systolic PAP (48.9 ± 4.8 mmHg *vs* 40.6 ± 5.3 mmHg)
				PVR (3.97 ± 1.31 Wood's unit *vs* 3.25 ± 0.96 Wood's unit)
Zamirian *et al*[124]	53 without IPS	LA dimension	M-mode ECHO	IPS was associated with higher LA dimension (4.58 ± 0.54 cm *vs* 3.87 ± 0.63 cm)
	39 with IPS	Cardiac output		Cardiac output (5.62 ± 0.83 L/min *vs* 4.75 ± 0.76 L/min)
Zamirian *et al*[126]	108 without HPS	LA volume	M-mode ECHO	Greater LA volume in HPS (55.1 ± 7.5 mL *vs* 37.1 ± 9.3 mL)
	41 with HPS			LA volume ⩾ 50 mL, AUC: 0.903, sensitivity: 86.3%, specificity: 81.2%
Pouriki *et al*[127]	67 without HPS	Markers of LV and RV diastolic and/or systolic cardiac function	M-mode ECHO	HPS was associated with higher LVEDD (OR = 1.230, 95%CI: 1.036-1.482; *P* = 0.019)
	12 with HPS		TDI	S wave at left lateral wall of MV (TDI) (OR = 1.428, 95%CI: 1.049-1.943; *P* = 0.026)
				S wave lateral ⩾ 13.5 cm/s, AUC: 0.736, sensitivity: 83.3%, specificity: 65.7%
				LVEDD ⩾ 50.5 mm, AUC: 0.724, sensitivity: 75%, specificity: 68.7%
Voiosu *et al*[128]	57 without HPS	Association between HPS and cirrhotic cardiomyopathy	M-mode ECHO	Higher RV wall width in HPS (3.8 ± 1.2 mm *vs* 3.4 ± 0.6 mm)
	17 with HPS		TDI	No association between HPS and cirrhotic cardiomyopathy
				No echocardiographic measurement predictive of HPS

AUC: Area under the curve; ECHO: Echocardiography; HPS: Hepatopulmonary syndrome; IPS: Intrapulmonary shunt; LA: Left atrial; LV: Left ventricle; LVEDD: Left ventricle end diastolic diameter; MV: Mitral valve; OR: Odds ratio; PVR: Pulmonary vascular resistance; PAP: Pulmonary artery pressure; RV: Right ventricle; RVEDD: Right ventricle end diastolic diameter; TDI: Tissue Doppler imaging.

largely unknown. HPS screening with the establishment of standardized protocols among patients with liver disease is crucial in the direction of achieving higher survival rates. Prospective studies evaluating long-term outcomes before and after liver transplantation in large patient cohorts will demonstrate the specific characteristics of HPS requiring management in priority. The precise events that trigger HPS pathogenesis as well as secondary clinical and subclinical vital organ interactions will constitute the field of future research.

REFERENCES

1 **Kiafar C**, Gilani N. Hepatic hydrothorax: current concepts of pathophysiology and treatment options. *Ann Hepatol* 2008; **7**: 313-320 [PMID: 19034230]

2 **Fussner LA**, Krowka MJ. Current Approach to the Diagnosis and Management of Portopulmonary Hypertension. *Curr Gastroenterol Rep* 2016; **18**: 29 [PMID: 27098816 DOI: 10.1007/s11894-016-0504-2]

3 **Rodríguez-Roisin R**, Krowka MJ, Hervé P, Fallon MB; ERS Task Force Pulmonary-Hepatic Vascular Disorders (PHD) Scientific Committee. Pulmonary-Hepatic vascular Disorders (PHD). *Eur Respir J* 2004; **24**: 861-880 [PMID: 15516683 DOI: 10.1183/09031936.04.00010904]

4 **Kennedy TC**, Knudson RJ. Exercise-aggravated hypoxemia and orthodeoxia in cirrhosis. *Chest* 1977; **72**: 305-309 [PMID: 891282]

5 **Hoffbauer FW**, Rydell R. Multiple pulmonary arteriovenous fistulas in juvenile cirrhosis. *Am J Med* 1956; **21**: 450-460 [PMID: 13354635]

6 **Berthelot P**, Walker JG, Sherlock S, Reid L. Arterial changes in the lungs in cirrhosis of the liver--lung spider nevi. *N Engl J Med* 1966; **274**: 291-298 [PMID: 5903210 DOI: 10.1056/NEJM196602102740601]

7 **Rodríguez-Roisin R**, Krowka MJ. Hepatopulmonary syndrome--a liver-induced lung vascular disorder. *N Engl J Med* 2008; **358**: 2378-2387 [PMID: 18509123 DOI: 10.1056/NEJMra0707185]

8 **Krowka MJ**. Hepatopulmonary syndrome: recent literature (1997 to 1999) and implications for liver transplantation. *Liver Transpl* 2000; **6**: S31-S35 [PMID: 10915189]

9 **Elias N**, Scirica CV, Hertl M. Liver transplantation for the Abernathy malformation. *N Engl J Med* 2008; **358**: 858 [PMID: 18287614 DOI: 10.1056/NEJMc0707762]

10 **Schenk P**, Fuhrmann V, Madl C, Funk G, Lehr S, Kandel O, Müller C. Hepatopulmonary syndrome: prevalence and predictive value of various cut offs for arterial oxygenation and their clinical consequences. *Gut* 2002; **51**: 853-859 [PMID: 12427789]

11 **Stoller JK**, Lange PA, Westveer MK, Carey WD, Vogt D, Henderson JM. Prevalence and reversibility of the hepatopulmonary syndrome after liver transplantation. The Cleveland Clinic experience. *West J Med* 1995; **163**: 133-138 [PMID: 7571560]

12 **Hopkins WE**, Waggoner AD, Barzilai B. Frequency and significance of intrapulmonary right-to-left shunting in end-stage hepatic disease. *Am J Cardiol* 1992; **70**: 516-519 [PMID: 1642191]

13 **Al-Harbi A**, Abdullah K, Al-Abdulkareem A, Alghamdi A, Al-Jahdali H. Prevalence, Severity, and Prognostic Effect of Hepatopulmonary Syndrome in Liver Transplant Candidates. *Ann Transplant* 2016; **21**: 180-184 [PMID: 27020907]

14 **Martínez GP**, Barberà JA, Visa J, Rimola A, Paré JC, Roca J, Navasa M, Rodés J, Rodriguez-Roisin R. Hepatopulmonary syndrome in candidates for liver transplantation. *J Hepatol* 2001; **34**: 651-657 [PMID: 11434610 DOI: 10.1016/S0168-8278(00)00108-2]

15 **Kim BJ**, Lee SC, Park SW, Choi MS, Koh KC, Paik SW, Lee SH, Hong KP, Park JE, Seo JD. Characteristics and prevalence of intrapulmonary shunt detected by contrast echocardiography with harmonic imaging in liver transplant candidates. *Am J Cardiol* 2004; **94**: 525-528 [PMID: 15325947 DOI: 10.1016/j.amjcard.2004.04.074]

16 **Pascasio JM**, Grilo I, López-Pardo FJ, Ortega-Ruiz F, Tirado JL, Sousa JM, Rodriguez-Puras MJ, Ferrer MT, Sayago M, Gómez-Bravo MA, Grilo A. Prevalence and severity of hepatopulmonary syndrome and its influence on survival in cirrhotic patients evaluated for liver transplantation. *Am J Transplant* 2014; **14**:

1391-1399 [PMID: 24730359 DOI: 10.1111/ajt.12713]
17 **Deberaldini M**, Arcanjo AB, Melo E, da Silva RF, Felício HC, Arroyo PC Jr, Duca WJ, Cordeiro JA, da Silva RC. Hepatopulmonary syndrome: morbidity and survival after liver transplantation. *Transplant Proc* 2008; **40**: 3512-3516 [PMID: 19100426 DOI: 10.1016/j.transproceed.2008.08.134]
18 **Krowka MJ**, Wiseman GA, Burnett OL, Spivey JR, Therneau T, Porayko MK, Wiesner RH. Hepatopulmonary syndrome: a prospective study of relationships between severity of liver disease, PaO(2) response to 100% oxygen, and brain uptake after (99m)Tc MAA lung scanning. *Chest* 2000; **118**: 615-624 [PMID: 10988181]
19 **Davis HH 2nd**, Schwartz DJ, Lefrak SS, Susman N, Schainker BA. Alveolar-capillary oxygen disequilibrium in hepatic cirrhosis. *Chest* 1978; **73**: 507-511 [PMID: 630968]
20 **Williams A**, Trewby P, Williams R, Reid L. Structural alterations to the pulmonary circulation in fulminant hepatic failure. *Thorax* 1979; **34**: 447-453 [PMID: 505339]
21 **Schraufnagel DE**, Kay JM. Structural and pathologic changes in the lung vasculature in chronic liver disease. *Clin Chest Med* 1996; **17**: 1-15 [PMID: 8665783 DOI: 10.1016/S0272-5231(05)70295-1]
22 **Rodriguez-Roisin R**, Roca J, Agusti AG, Mastai R, Wagner PD, Bosch J. Gas exchange and pulmonary vascular reactivity in patients with liver cirrhosis. *Am Rev Respir Dis* 1987; **135**: 1085-1092 [PMID: 3579008 DOI: 10.1164/arrd.1987.135.5.1085]
23 **Thorens JB**, Junod AF. Hypoxaemia and liver cirrhosis: a new argument in favour of a "diffusion-perfusion defect". *Eur Respir J* 1992; **5**: 754-756 [PMID: 1628734]
24 **Katsuta Y**, Zhang XJ, Ohsuga M, Akimoto T, Komeichi H, Shimizu S, Kato Y, Miyamoto A, Satomura K, Takano T. Arterial hypoxemia and intrapulmonary vasodilatation in rat models of portal hypertension. *J Gastroenterol* 2005; **40**: 811-819 [PMID: 16143886 DOI: 10.1007/s00535-005-1633-9]
25 **Stanley NN**, Williams AJ, Dewar CA, Blendis LM, Reid L. Hypoxia and hydrothoraces in a case of liver cirrhosis: correlation of physiological, radiographic, scintigraphic, and pathological findings. *Thorax* 1977; **32**: 457-471 [PMID: 929488]
26 **McAdams HP**, Erasmus J, Crockett R, Mitchell J, Godwin JD, McDermott VG. The hepatopulmonary syndrome: radiologic findings in 10 patients. *AJR Am J Roentgenol* 1996; **166**: 1379-1385 [PMID: 8633451 DOI: 10.2214/ajr.166.6.8633451]
27 **Gómez FP**, Martínez-Pallí G, Barberà JA, Roca J, Navasa M, Rodríguez-Roisin R. Gas exchange mechanism of orthodeoxia in hepatopulmonary syndrome. *Hepatology* 2004; **40**: 660-666 [PMID: 15349905 DOI: 10.1002/hep.20358]
28 **Edell ES**, Cortese DA, Krowka MJ, Rehder K. Severe hypoxemia and liver disease. *Am Rev Respir Dis* 1989; **140**: 1631-1635 [PMID: 2513764 DOI: 10.1164/ajrccm/140.6.1631]
29 **Castro M**, Krowka MJ. Hepatopulmonary syndrome. A pulmonary vascular complication of liver disease. *Clin Chest Med* 1996; **17**: 35-48 [PMID: 8665789]
30 **Genovesi MG**, Tierney DF, Taplin GV, Eisenberg H. An intravenous radionuclide method to evaluate hypoxemia caused by abnormal alveolar vessels. Limitation of conventional techniques. *Am Rev Respir Dis* 1976; **114**: 59-65 [PMID: 937842 DOI: 10.1164/arrd.1976.114.1.59]
31 **Cremona G**, Higenbottam TW, Mayoral V, Alexander G, Demoncheaux E, Borland C, Roe P, Jones GJ. Elevated exhaled nitric oxide in patients with hepatopulmonary syndrome. *Eur Respir J* 1995; **8**: 1883-1885 [PMID: 8620957]
32 **Fallon MB**, Abrams GA, McGrath JW, Hou Z, Luo B. Common bile duct ligation in the rat: a model of intrapulmonary vasodilatation and hepatopulmonary syndrome. *Am J Physiol* 1997; **272**: G779-G784 [PMID: 9142908]
33 **Yang W**, Zhang J, Hu B, Wu W, Venter J, Alpini G, Fallon MB. The role of receptor tyrosine kinase activation in cholangiocytes and pulmonary vascular endothelium in experimental hepatopulmonary syndrome. *Am J Physiol Gastrointest Liver Physiol* 2014; **306**: G72-G80 [PMID: 24200956 DOI: 10.1152/ajpgi.00178.2013]
34 **Zhang M**, Luo B, Chen SJ, Abrams GA, Fallon MB. Endothelin-1 stimulation of endothelial nitric oxide synthase in the pathogenesis of hepatopulmonary syndrome. *Am J Physiol* 1999; **277**: G944-G952 [PMID: 10564099]
35 **Ling Y**, Zhang J, Luo B, Song D, Liu L, Tang L, Stockard CR, Grizzle WE, Ku DD, Fallon MB. The role of endothelin-1 and the endothelin B receptor in the pathogenesis of hepatopulmonary syndrome in the rat. *Hepatology* 2004; **39**: 1593-1602 [PMID: 15185300 DOI: 10.1002/hep.20244]
36 **Luo B**, Liu L, Tang L, Zhang J, Stockard CR, Grizzle WE, Fallon MB. Increased pulmonary vascular endothelin B receptor expression and responsiveness to endothelin-1 in cirrhotic and portal hypertensive rats: a potential mechanism in experimental hepatopulmonary syndrome. *J Hepatol* 2003; **38**: 556-563 [PMID: 12713865]
37 **Nunes H**, Lebrec D, Mazmanian M, Capron F, Heller J, Tazi KA, Zerbib E, Dulmet E, Moreau R, Dinh-Xuan AT, Simonneau G, Hervé P. Role of nitric oxide in hepatopulmonary syndrome in cirrhotic rats. *Am J Respir Crit Care Med* 2001; **164**: 879-885 [PMID: 11549549 DOI: 10.1164/ajrccm.164.5.2009008]
38 **Zhang XJ**, Katsuta Y, Akimoto T, Ohsuga M, Aramaki T, Takano T. Intrapulmonary vascular dilatation and nitric oxide in hypoxemic rats with chronic bile duct ligation. *J Hepatol* 2003; **39**: 724-730 [PMID: 14568253]
39 **Rolla G**, Brussino L, Colagrande P, Dutto L, Polizzi S, Scappaticci E, Bergerone S, Morello M, Marzano A, Martinasso G, Salizzoni M, Bucca C. Exhaled nitric oxide and oxygenation abnormalities in hepatic cirrhosis. *Hepatology* 1997; **26**: 842-847 [PMID: 9328302 DOI: 10.1053/jhep.1997.v26.pm0009328302]
40 **Rolla G**, Brussino L, Colagrande P, Scappaticci E, Morello M, Bergerone S, Ottobrelli A, Cerutti E, Polizzi S, Bucca C. Exhaled nitric oxide and impaired oxygenation in cirrhotic patients before and after liver transplantation. *Ann Intern Med* 1998; **129**: 375-378 [PMID: 9735065]
41 **Schenk P**, Madl C, Rezaie-Majd S, Lehr S, Müller C. Methylene blue improves the hepatopulmonary syndrome. *Ann Intern Med* 2000; **133**: 701-706 [PMID: 11074903]
42 **Fallon MB**. Methylene blue and cirrhosis: pathophysiologic insights, therapeutic dilemmas. *Ann Intern Med* 2000; **133**: 738-740 [PMID: 11074907]
43 **Gómez FP**, Barberà JA, Roca J, Burgos F, Gistau C, Rodríguez-Roisin R. Effects of nebulized N(G)-nitro-L-arginine methyl ester in patients with hepatopulmonary syndrome. *Hepatology* 2006; **43**: 1084-1091 [PMID: 16628648 DOI: 10.1002/hep.21141]
44 **Lejealle C**, Paradis V, Francoz C, Soubrane O, Lebrec D, Valla D, Durand F, Rautou PE. Pathological Analysis of the Liver of Patients with Cirrhosis and Hepatopulmonary Syndrome Reveals a Vascular Pattern of Damages. *J Hepatol* 2016; **64**: S444 [DOI: 10.1016/S0168-8278(16)00734-0]
45 **Zhang HY**, Han DW, Wang XG, Zhao YC, Zhou X, Zhao HZ. Experimental study on the role of endotoxin in the development of hepatopulmonary syndrome. *World J Gastroenterol* 2005; **11**: 567-572 [PMID: 15641147 DOI: 10.3748/wjg.v11.i4.567]
46 **Sztrymf B**, Libert JM, Mougeot C, Lebrec D, Mazmanian M, Humbert M, Herve P. Cirrhotic rats with bacterial translocation have higher incidence and severity of hepatopulmonary syndrome. *J Gastroenterol Hepatol* 2005; **20**: 1538-1544 [PMID: 16174071 DOI: 10.1111/j.1440-1746.2005.03914.x]
47 **Schroeder RA**, Ewing CA, Sitzmann JV, Kuo PC. Pulmonary expression of iNOS and HO-1 protein is upregulated in a rat model of prehepatic portal hypertension. *Dig Dis Sci* 2000; **45**: 2405-2410 [PMID: 11258566]
48 **Luo B**, Tang L, Wang Z, Zhang J, Ling Y, Feng W, Sun JZ, Stockard CR, Frost AR, Chen YF, Grizzle WE, Fallon MB. Cholangiocyte endothelin 1 and transforming growth factor beta1 production in rat experimental hepatopulmonary syndrome. *Gastroenterology* 2005; **129**: 682-695 [PMID: 16083721 DOI: 10.1016/j.gastro.2005.05.050]
49 **Liu L**, Liu N, Zhao Z, Liu J, Feng Y, Jiang H, Han D. TNF-α neutralization improves experimental hepatopulmonary syndrome in rats. *Liver Int* 2012; **32**: 1018-1026 [PMID: 22672643 DOI:

10.1111/j.1478-3231.2012.02821.x]
50 **Sztrymf B**, Rabiller A, Nunes H, Savale L, Lebrec D, Le Pape A, de Montpreville V, Mazmanian M, Humbert M, Hervé P. Prevention of hepatopulmonary syndrome and hyperdynamic state by pentoxifylline in cirrhotic rats. *Eur Respir J* 2004; **23**: 752-758 [PMID: 15176692]
51 **Rabiller A**, Nunes H, Lebrec D, Tazi KA, Wartski M, Dulmet E, Libert JM, Mougeot C, Moreau R, Mazmanian M, Humbert M, Hervé P. Prevention of gram-negative translocation reduces the severity of hepatopulmonary syndrome. *Am J Respir Crit Care Med* 2002; **166**: 514-517 [PMID: 12186830 DOI: 10.1164/rccm.200201-027OC]
52 **Arguedas MR**, Drake BB, Kapoor A, Fallon MB. Carboxyhemoglobin levels in cirrhotic patients with and without hepatopulmonary syndrome. *Gastroenterology* 2005; **128**: 328-333 [PMID: 15685544]
53 **Carter EP**, Hartsfield CL, Miyazono M, Jakkula M, Morris KG Jr, McMurtry IF. Regulation of heme oxygenase-1 by nitric oxide during hepatopulmonary syndrome. *Am J Physiol Lung Cell Mol Physiol* 2002; **283**: L346-L353 [PMID: 12114196 DOI: 10.1152/ajplung.00385.2001]
54 **Zhang J**, Ling Y, Luo B, Tang L, Ryter SW, Stockard CR, Grizzle WE, Fallon MB. Analysis of pulmonary heme oxygenase-1 and nitric oxide synthase alterations in experimental hepatopulmonary syndrome. *Gastroenterology* 2003; **125**: 1441-1451 [PMID: 14598260]
55 **Bosch J**. Vascular deterioration in cirrhosis: the big picture. *J Clin Gastroenterol* 2007; **41** Suppl 3**:** S247-S253 [PMID: 17975472 DOI: 10.1097/MCG.0b013e3181572357]
56 **Zhang J**, Luo B, Tang L, Wang Y, Stockard CR, Kadish I, Van Groen T, Grizzle WE, Ponnazhagan S, Fallon MB. Pulmonary angiogenesis in a rat model of hepatopulmonary syndrome. *Gastroenterology* 2009; **136**: 1070-1080 [PMID: 19109954 DOI: 10.1053/j.gastro.2008.12.001]
57 **Thenappan T**, Goel A, Marsboom G, Fang YH, Toth PT, Zhang HJ, Kajimoto H, Hong Z, Paul J, Wietholt C, Pogoriler J, Piao L, Rehman J, Archer SL. A central role for CD68(+) macrophages in hepatopulmonary syndrome. Reversal by macrophage depletion. *Am J Respir Crit Care Med* 2011; **183**: 1080-1091 [PMID: 21148721 DOI: 10.1164/rccm.201008-1303OC]
58 **Zhang J**, Ling Y, Tang L, Luo B, Chacko BK, Patel RP, Fallon MB. Pentoxifylline attenuation of experimental hepatopulmonary syndrome. *J Appl Physiol* (1985) 2007; **102**: 949-955 [PMID: 17110505 DOI: 10.1152/japplphysiol.01048.2006]
59 **Zhang J**, Yang W, Luo B, Hu B, Maheshwari A, Fallon MB. The role of CX_3CL1/CX_3CR1 in pulmonary angiogenesis and intravascular monocyte accumulation in rat experimental hepatopulmonary syndrome. *J Hepatol* 2012; **57**: 752-758 [PMID: 22659346 DOI: 10.1016/j.jhep.2012.05.014]
60 **Zhang J**, Yang W, Hu B, Wu W, Fallon MB. Endothelin-1 activation of the endothelin B receptor modulates pulmonary endothelial CX3CL1 and contributes to pulmonary angiogenesis in experimental hepatopulmonary syndrome. *Am J Pathol* 2014; **184**: 1706-1714 [PMID: 24731444 DOI: 10.1016/j.ajpath.2014.02.027]
61 **Chang CC**, Chuang CL, Lee FY, Wang SS, Lin HC, Huang HC, Teng TH, Hsu SJ, Hsieh HG, Lee SD. Sorafenib treatment improves hepatopulmonary syndrome in rats with biliary cirrhosis. *Clin Sci* (Lond) 2013; **124**: 457-466 [PMID: 23043394 DOI: 10.1042/CS20120052]
62 **Soulaidopoulos S**, Goulis I, Giannakoulas G, Panagiotidis T, Doumtsis P, Karasmani A, Oikonomou T, Tzoumari T, Karvounis H, Cholongitas E. Hepatopulmonary syndrome is associated with the presence of hepatocellular carcinoma in patients with decompensated cirrhosis. *Ann Gastroenterol* 2017; **30**: 225-231 [PMID: 28243044 DOI: 10.20524/aog.2016.0117]
63 **Anand AC**, Mukherjee D, Rao KS, Seth AK. Hepatopulmonary syndrome: prevalence and clinical profile. *Indian J Gastroenterol* 2001; **20**: 24-27 [PMID: 11206870]
64 **Fallon MB**, Krowka MJ, Brown RS, Trotter JF, Zacks S, Roberts KE, Shah VH, Kaplowitz N, Forman L, Wille K, Kawut SM; Pulmonary Vascular Complications of Liver Disease Study Group. Impact of hepatopulmonary syndrome on quality of life and survival in liver transplant candidates. *Gastroenterology* 2008; **135**: 1168-1175 [PMID: 18644373 DOI: 10.1053/j.gastro.2008.06.038]
65 **Singh C**, Sager JS. Pulmonary complications of cirrhosis. *Med Clin North Am* 2009; **93**: 871-883, viii [PMID: 19577119 DOI: 10.1016/j.mcna.2009.03.006]
66 **Silvério Ade O**, Guimarães DC, Elias LF, Milanez EO, Naves S. Are the spider angiomas skin markers of hepatopulmonary syndrome? *Arq Gastroenterol* 2013; **50**: 175-179 [PMID: 24322187 DOI: 10.1590/S0004-28032013000200031]
67 **Mohammad Alizadeh AH**, Fatemi SR, Mirzaee V, Khoshbaten M, Talebipour B, Sharifian A, Khoram Z, Haj-sheikh-oleslami F, Gholamreza-shirazi M, Zali MR. Clinical features of hepatopulmonary syndrome in cirrhotic patients. *World J Gastroenterol* 2006; **12**: 1954-1956 [PMID: 16610006 DOI: 10.3748/wjg.v12.i12.1954]
68 **Palma DT**, Philips GM, Arguedas MR, Harding SM, Fallon MB. Oxygen desaturation during sleep in hepatopulmonary syndrome. *Hepatology* 2008; **47**: 1257-1263 [PMID: 18311748 DOI: 10.1002/hep.22143]
69 **Abrams GA**, Jaffe CC, Hoffer PB, Binder HJ, Fallon MB. Diagnostic utility of contrast echocardiography and lung perfusion scan in patients with hepatopulmonary syndrome. *Gastroenterology* 1995; **109**: 1283-1288 [PMID: 7557096]
70 **Soliman OI**, Geleijnse ML, Meijboom FJ, Nemes A, Kamp O, Nihoyannopoulos P, Masani N, Feinstein SB, Ten Cate FJ. The use of contrast echocardiography for the detection of cardiac shunts. *Eur J Echocardiogr* 2007; **8**: S2-12 [PMID: 17462958 DOI: 10.1016/j.euje.2007.03.006]
71 **Barzilai B**, Waggoner AD, Spessert C, Picus D, Goodenberger D. Two-dimensional contrast echocardiography in the detection and follow-up of congenital pulmonary arteriovenous malformations. *Am J Cardiol* 1991; **68**: 1507-1510 [PMID: 1746435]
72 **Velthuis S**, Buscarini E, Gossage JR, Snijder RJ, Mager JJ, Post MC. Clinical implications of pulmonary shunting on saline contrast echocardiography. *J Am Soc Echocardiogr* 2015; **28**: 255-263 [PMID: 25623000 DOI: 10.1016/j.echo.2014.12.008]
73 **Vedrinne JM**, Duperret S, Bizollon T, Magnin C, Motin J, Trepo C, Ducerf C. Comparison of transesophageal and transthoracic contrast echocardiography for detection of an intrapulmonary shunt in liver disease. *Chest* 1997; **111**: 1236-1240 [PMID: 9149575]
74 **Abrams GA**, Nanda NC, Dubovsky EV, Krowka MJ, Fallon MB. Use of macroaggregated albumin lung perfusion scan to diagnose hepatopulmonary syndrome: a new approach. *Gastroenterology* 1998; **114**: 305-310 [PMID: 9453490]
75 **Mimidis KP**, Vassilakos PI, Mastorakou AN, Spiropoulos KV, Lambropoulou-Karatza CA, Thomopoulos KC, Tepetes KN, Nikolopoulou VN. Evaluation of contrast echocardiography and lung perfusion scan in detecting intrapulmonary vascular dilatation in normoxemic patients with early liver cirrhosis. *Hepatogastroenterology* 1998; **45**: 2303-2307 [PMID: 9951913]
76 **Köksal D**, Kaçar S, Köksal AS, Tüfekçioğlu O, Küçükay F, Okten S, Saşmaz N, Arda K, Sahin B. Evaluation of intrapulmonary vascular dilatations with high-resolution computed thorax tomography in patients with hepatopulmonary syndrome. *J Clin Gastroenterol* 2006; **40**: 77-83 [PMID: 16340638]
77 **Krowka MJ**, Dickson ER, Cortese DA. Hepatopulmonary syndrome. Clinical observations and lack of therapeutic response to somatostatin analogue. *Chest* 1993; **104**: 515-521 [PMID: 8101797]
78 **Krowka MJ**, Fallon MB, Kawut SM, Fuhrmann V, Heimbach JK, Ramsay MA, Sitbon O, Sokol RJ. International Liver Transplant Society Practice Guidelines: Diagnosis and Management of Hepatopulmonary Syndrome and Portopulmonary Hypertension. *Transplantation* 2016; **100**: 1440-1452 [PMID: 27326810 DOI: 10.1097/TP.0000000000001229]
79 **Kochar R**, Tanikella R, Fallon MB. Serial pulse oximetry in hepatopulmonary syndrome. *Dig Dis Sci* 2011; **56**: 1862-1868 [PMID: 21327708 DOI: 10.1007/s10620-011-1600-7]

80 **Arguedas MR**, Singh H, Faulk DK, Fallon MB. Utility of pulse oximetry screening for hepatopulmonary syndrome. *Clin Gastroenterol Hepatol* 2007; **5**: 749-754 [PMID: 17392034 DOI: 10.1016/j.cgh.2006.12.003]

81 **Hoerning A**, Raub S, Neudorf U, Müntjes C, Kathemann S, Lainka E, Stehling F, Hoyer PF, Gerner P. Pulse oximetry is insufficient for timely diagnosis of hepatopulmonary syndrome in children with liver cirrhosis. *J Pediatr* 2014; **164**: 546-52.e1-2 [PMID: 24321540 DOI: 10.1016/j.jpeds.2013.10.070]

82 **Deibert P**, Allgaier HP, Loesch S, Müller C, Olschewski M, Hamm H, Maier KP, Blum HE. Hepatopulmonary syndrome in patients with chronic liver disease: role of pulse oximetry. *BMC Gastroenterol* 2006; **6**: 15 [PMID: 16638132 DOI: 10.1186/1471-230X-6-15]

83 **Voiosu A**, Voiosu T, Stănescu CM, Chirilă L, Băicuş C, Voiosu R. Novel predictors of intrapulmonary vascular dilatations in cirrhosis: extending the role of pulse oximetry and echocardiography. *Acta Gastroenterol Belg* 2013; **76**: 241-245 [PMID: 23898563]

84 **Hourani JM**, Bellamy PE, Tashkin DP, Batra P, Simmons MS. Pulmonary dysfunction in advanced liver disease: frequent occurrence of an abnormal diffusing capacity. *Am J Med* 1991; **90**: 693-700 [PMID: 1904192]

85 **Lima BL**, França AV, Pazin-Filho A, Araújo WM, Martinez JA, Maciel BC, Simões MV, Terra-Filho J, Martinelli AL. Frequency, clinical characteristics, and respiratory parameters of hepatopulmonary syndrome. *Mayo Clin Proc* 2004; **79**: 42-48 [PMID: 14708947 DOI: 10.4065/79.1.42]

86 **Martínez-Palli G**, Gómez FP, Barberà JA, Navasa M, Roca J, Rodríguez-Roisin R, Burgos F, Gistau C. Sustained low diffusing capacity in hepatopulmonary syndrome after liver transplantation. *World J Gastroenterol* 2006; **12**: 5878-5883 [PMID: 17007057 DOI: 10.3748/wjg.v12.i36.5878]

87 **Battaglia SE**, Pretto JJ, Irving LB, Jones RM, Angus PW. Resolution of gas exchange abnormalities and intrapulmonary shunting following liver transplantation. *Hepatology* 1997; **25**: 1228-1232 [PMID: 9141442 DOI: 10.1002/hep.510250527]

88 **Rodriguez-Roisin R**, Krowka MJ. Is severe arterial hypoxaemia due to hepatic disease an indication for liver transplantation? A new therapeutic approach. *Eur Respir J* 1994; **7**: 839-842 [PMID: 8050537]

89 **Iyer VN**, Swanson KL, Cartin-Ceba R, Dierkhising RA, Rosen CB, Heimbach JK, Wiesner RH, Krowka MJ. Hepatopulmonary syndrome: favorable outcomes in the MELD exception era. *Hepatology* 2013; **57**: 2427-2435 [PMID: 22996424 DOI: 10.1002/hep.26070]

90 **Fukushima KY**, Yatsuhashi H, Kinoshita A, Ueki T, Matsumoto T, Osumi M, Matsuoka Y. Two cases of hepatopulmonary syndrome with improved liver function following long-term oxygen therapy. *J Gastroenterol* 2007; **42**: 176-180 [PMID: 17351808 DOI: 10.1007/s00535-006-1965-0]

91 **Söderman C**, Juhlin-Dannfelt A, Lagerstrand L, Eriksson LS. Ventilation-perfusion relationships and central haemodynamics in patients with cirrhosis. Effects of a somatostatin analogue. *J Hepatol* 1994; **21**: 52-57 [PMID: 7963422]

92 **Añel RM**, Sheagren JN. Novel presentation and approach to management of hepatopulmonary syndrome with use of antimicrobial agents. *Clin Infect Dis* 2001; **32**: E131-E136 [PMID: 11317264 DOI: 10.1086/320149]

93 **Gupta S**, Faughnan ME, Lilly L, Hutchison S, Fowler R, Bayoumi AM. Norfloxacin therapy for hepatopulmonary syndrome: a pilot randomized controlled trial. *Clin Gastroenterol Hepatol* 2010; **8**: 1095-1098 [PMID: 20816858 DOI: 10.1016/j.cgh.2010.08.011]

94 **Song JY**, Choi JY, Ko JT, Bae EJ, Kim HS, Noh CI, Yoon YS. Long-term aspirin therapy for hepatopulmonary syndrome. *Pediatrics* 1996; **97**: 917-920 [PMID: 8657540]

95 **Shijo H**, Sasaki H, Yuh K, Sakaguchi S, Okumura M. Effects of indomethacin on hepatogenic pulmonary angiodysplasia. *Chest* 1991; **99**: 1027-1029 [PMID: 2009756]

96 **Moreira Silva H**, Reis G, Guedes M, Cleto E, Vizcaíno JR, Kelly D, Gennery AR, Santos Silva E. A case of hepatopulmonary syndrome solved by mycophenolate mofetil (an inhibitor of angiogenesis and nitric oxide production). *J Hepatol* 2013; **58**: 630-633 [PMID: 23104163 DOI: 10.1016/j.jhep.2012.10.021]

97 **Moncada S**, Palmer RM, Gryglewski RJ. Mechanism of action of some inhibitors of endothelium-derived relaxing factor. *Proc Natl Acad Sci USA* 1986; **83**: 9164-9168 [PMID: 3024168]

98 **Rolla G**, Bucca C, Brussino L. Methylene blue in the hepatopulmonary syndrome. *N Engl J Med* 1994; **331**: 1098 [PMID: 8090178 DOI: 10.1056/NEJM199410203311617]

99 **Miyamoto A**, Katsuta Y, Zhang XJ, Li HL, Ohsuga M, Komeichi H, Shimizu S, Akimoto T, Mizuno K. Effect of chronic methylene blue administration on hypoxemia in rats with common bile duct ligation. *Hepatol Res* 2010; **40**: 622-632 [PMID: 20412326 DOI: 10.1111/j.1872-034X.2010.00640.x]

100 **Gupta LB**, Kumar A, Jaiswal AK, Yusuf J, Mehta V, Tyagi S, Tempe DK, Sharma BC, Sarin SK. Pentoxifylline therapy for hepatopulmonary syndrome: a pilot study. *Arch Intern Med* 2008; **168**: 1820-1823 [PMID: 18779471 DOI: 10.1001/archinte.168.16.1820]

101 **Tanikella R**, Philips GM, Faulk DK, Kawut SM, Fallon MB. Pilot study of pentoxifylline in hepatopulmonary syndrome. *Liver Transpl* 2008; **14**: 1199-1203 [PMID: 18668653 DOI: 10.1002/lt.21482]

102 **Brussino L**, Bucca C, Morello M, Scappaticci E, Mauro M, Rolla G. Effect on dyspnoea and hypoxaemia of inhaled N(G)-nitro-L-arginine methyl ester in hepatopulmonary syndrome. *Lancet* 2003; **362**: 43-44 [PMID: 12853200 DOI: 10.1016/S0140-6736(03)13807-X]

103 **Krowka MJ**, Cortese DA. Severe hypoxemia associated with liver disease: Mayo Clinic experience and the experimental use of almitrine bismesylate. *Mayo Clin Proc* 1987; **62**: 164-173 [PMID: 3821178]

104 **Abrams GA**, Fallon MB. Treatment of hepatopulmonary syndrome with Allium sativum L. (garlic): a pilot trial. *J Clin Gastroenterol* 1998; **27**: 232-235 [PMID: 9802451]

105 **De BK**, Dutta D, Pal SK, Gangopadhyay S, Das Baksi S, Pani A. The role of garlic in hepatopulmonary syndrome: a randomized controlled trial. *Can J Gastroenterol* 2010; **24**: 183-188 [PMID: 20352147]

106 **Allgaier HP**, Haag K, Ochs A, Hauenstein KH, Jeserich M, Krause T, Heilmann C, Gerok W, Rössle M. Hepato-pulmonary syndrome: successful treatment by transjugular intrahepatic portosystemic stent-shunt (TIPS) *J Hepatol* 1995; **23**: 102 [PMID: 8530801]

107 **Paramesh AS**, Husain SZ, Shneider B, Guller J, Tokat I, Gondolesi GE, Moyer S, Emre S. Improvement of hepatopulmonary syndrome after transjugular intrahepatic portasystemic shunting: case report and review of literature. *Pediatr Transplant* 2003; **7**: 157-162 [PMID: 12654059]

108 **Benítez C**, Arrese M, Jorquera J, Godoy I, Contreras A, Loyola S, Domínguez P, Jarufe N, Martínez J, Pérez-Ayuso RM. Successful treatment of severe hepatopulmonary syndrome with a sequential use of TIPS placement and liver transplantation. *Ann Hepatol* 2009; **8**: 71-74 [PMID: 19221539]

109 **Poterucha JJ**, Krowka MJ, Dickson ER, Cortese DA, Stanson AW, Krom RA. Failure of hepatopulmonary syndrome to resolve after liver transplantation and successful treatment with embolotherapy. *Hepatology* 1995; **21**: 96-100 [PMID: 7806175]

110 **Lee HW**, Suh KS, Kim J, Shin WY, Yi NJ, Jae HJ, Chung JW, Oh SW, Kang KW, Lee KU. Pulmonary artery embolotherapy in a patient with type I hepatopulmonary syndrome after liver transplantation. *Korean J Radiol* 2010; **11**: 485-489 [PMID: 20592935 DOI: 10.3348/kjr.2010.11.4.485]

111 **Swanson KL**, Wiesner RH, Krowka MJ. Natural history of hepatopulmonary syndrome: Impact of liver transplantation. *Hepatology* 2005; **41**: 1122-1129 [PMID: 15828054 DOI: 10.1002/hep.20658]

112 **Schenk P**, Schöniger-Hekele M, Fuhrmann V, Madl C, Silberhumer G, Müller C. Prognostic significance of the hepatopulmonary syndrome in patients with cirrhosis. *Gastroenterology* 2003; **125**: 1042-1052 [PMID: 14517788]

113 **Mandell MS**. Hepatopulmonary syndrome and portopulmonary hypertension in the model for end-stage liver disease (MELD) era. *Liver Transpl* 2004; **10**: S54-S58 [PMID: 15382220 DOI: 10.1002/lt.20260]

114 **Goldberg DS**, Krok K, Batra S, Trotter JF, Kawut SM, Fallon MB. Impact of the hepatopulmonary syndrome MELD exception policy on outcomes of patients after liver transplantation: an analysis of the UNOS database. *Gastroenterology* 2014; **146**: 1256-65.e1 [PMID: 24412528 DOI: 10.1053/j.gastro.2014.01.005]

115 **Schiffer E**, Majno P, Mentha G, Giostra E, Burri H, Klopfenstein CE, Beaussier M, Morel P, Hadengue A, Pastor CM. Hepatopulmonary syndrome increases the postoperative mortality rate following liver transplantation: a prospective study in 90 patients. *Am J Transplant* 2006; **6**: 1430-1437 [PMID: 16686767 DOI: 10.1111/j.1600-6143.2006.01334.x]

116 **Arguedas MR**, Abrams GA, Krowka MJ, Fallon MB. Prospective evaluation of outcomes and predictors of mortality in patients with hepatopulmonary syndrome undergoing liver transplantation. *Hepatology* 2003; **37**: 192-197 [PMID: 12500204 DOI: 10.1053/jhep.2003.50023]

117 **Gupta S**, Castel H, Rao RV, Picard M, Lilly L, Faughnan ME, Pomier-Layrargues G. Improved survival after liver transplantation in patients with hepatopulmonary syndrome. *Am J Transplant* 2010; **10**: 354-363 [PMID: 19775311 DOI: 10.1111/j.1600-6143.2009.02822.x]

118 **Kim HY**, Choi MS, Lee SC, Park SW, Lee JH, Koh KC, Paik SW, Yoo BC, Rhee JC. Outcomes in patients with hepatopulmonary syndrome undergoing liver transplantation. *Transplant Proc* 2004; **36**: 2762-2763 [PMID: 15621142 DOI: 10.1016/j.transproceed.2004.10.002]

119 **Fussner LA**, Iyer VN, Cartin-Ceba R, Lin G, Watt KD, Krowka MJ. Intrapulmonary vascular dilatations are common in portopulmonary hypertension and may be associated with decreased survival. *Liver Transpl* 2015; **21**: 1355-1364 [PMID: 26077312 DOI: 10.1002/lt.24198]

120 **Krowka MJ**, Mandell MS, Ramsay MA, Kawut SM, Fallon MB, Manzarbeitia C, Pardo M Jr, Marotta P, Uemoto S, Stoffel MP, Benson JT. Hepatopulmonary syndrome and portopulmonary hypertension: a report of the multicenter liver transplant database. *Liver Transpl* 2004; **10**: 174-182 [PMID: 14762853 DOI: 10.1002/lt.20016]

121 **Groszmann RJ**. Hyperdynamic circulation of liver disease 40 years later: pathophysiology and clinical consequences. *Hepatology* 1994; **20**: 1359-1363 [PMID: 7927273 DOI: 10.1002/hep.1840200538]

122 **Ruiz-del-Árbol L**, Serradilla R. Cirrhotic cardiomyopathy. *World J Gastroenterol* 2015; **21**: 11502-11521 [PMID: 26556983 DOI: 10.3748/wjg.v21.i41.11502]

123 **Karabulut A**, Iltumur K, Yalcin K, Toprak N. Hepatopulmonary syndrome and right ventricular diastolic functions: an echocardiographic examination. *Echocardiography* 2006; **23**: 271-278 [PMID: 16640703 DOI: 10.1111/j.1540-8175.2006.00210.x]

124 **Zamirian M**, Aslani A, Sharifkazemi MB. Prediction of intrapulmonary right to left shunt with left atrial size in patients with liver cirrhosis. *Eur J Echocardiogr* 2008; **9**: 1-4 [PMID: 17140853 DOI: 10.1016/j.euje.2006.10.003]

125 **Niederberger M**, Martin PY, Ginès P, Morris K, Tsai P, Xu DL, McMurtry I, Schrier RW. Normalization of nitric oxide production corrects arterial vasodilation and hyperdynamic circulation in cirrhotic rats. *Gastroenterology* 1995; **109**: 1624-1630 [PMID: 7557147]

126 **Zamirian M**, Aslani A, Shahrzad S. Left atrial volume: a novel predictor of hepatopulmonary syndrome. *Am J Gastroenterol* 2007; **102**: 1392-1396 [PMID: 17433020 DOI: 10.1111/j.1572-0241.2007.01228.x]

127 **Pouriki S**, Alexopoulou A, Chrysochoou C, Raftopoulos L, Papatheodoridis G, Stefanadis C, Pectasides D. Left ventricle enlargement and increased systolic velocity in the mitral valve are indirect markers of the hepatopulmonary syndrome. *Liver Int* 2011; **31**: 1388-1394 [PMID: 21771264 DOI: 10.1111/j.1478-3231.2011.02591.x]

128 **Voiosu AM**, Daha IC, Voiosu TA, Mateescu BR, Dan GA, Băicuş CR, Voiosu MR, Diculescu MM. Prevalence and impact on survival of hepatopulmonary syndrome and cirrhotic cardiomyopathy in a cohort of cirrhotic patients. *Liver Int* 2015; **35**: 2547-2555 [PMID: 25974637 DOI: 10.1111/liv.12866]

129 **Gassanov N**, Caglayan E, Semmo N, Massenkeil G, Er F. Cirrhotic cardiomyopathy: a cardiologist's perspective. *World J Gastroenterol* 2014; **20**: 15492-15498 [PMID: 25400434 DOI: 10.3748/wjg.v20.i42.15492]

130 **Enache I**, Oswald-Mammosser M, Woehl-Jaegle ML, Habersetzer F, Di Marco P, Charloux A, Doutreleau S. Cirrhotic cardiomyopathy and hepatopulmonary syndrome: prevalence and prognosis in a series of patients. *Respir Med* 2013; **107**: 1030-1036 [PMID: 23615223 DOI: 10.1016/j.rmed.2013.03.010]

131 **Pozzi M**, Carugo S, Boari G, Pecci V, de Ceglia S, Maggiolini S, Bolla GB, Roffi L, Failla M, Grassi G, Giannattasio C, Mancia G. Evidence of functional and structural cardiac abnormalities in cirrhotic patients with and without ascites. *Hepatology* 1997; **26**: 1131-1137 [PMID: 9362352 DOI: 10.1002/hep.510260507]

P- Reviewer: Corrales FJ, Ruiz-Margain A **S- Editor**: Wang XJ
L- Editor: Filipodia **E- Editor**: Huang Y

World Journal of Gastroenterology

Submit a Manuscript: http://www.f6publishing.com

World J Gastroenterol 2018 March 28; 24(12): 1299-1311

DOI: 10.3748/wjg.v24.i12.1299

ISSN 1007-9327 (print) ISSN 2219-2840 (online)

ORIGINAL ARTICLE

Basic Study

Cell culture-adaptive mutations in hepatitis C virus promote viral production by enhancing viral replication and release

Qi Wang, Yue Li, Shun-Ai Liu, Wen Xie, Jun Cheng

Qi Wang, Wen Xie, Jun Cheng, Center of Liver Diseases, Beijing Ditan Hospital, Capital Medical University, Beijing 100015, China

Yue Li, Department of Pathology, Beijing Ditan Hospital, Capital Medical University, Beijing 100015, China

Shun-Ai Liu, Jun Cheng, Institute of Infectious Diseases, Beijing Ditan Hospital, Capital Medical University, Beijing 100015, China

Qi Wang, Shun-Ai Liu, Jun Cheng, Beijing Key Laboratory of Emerging Infectious Diseases, Beijing 100015, China

ORCID number: Qi Wang (0000-0002-0269-1568); Yue Li (0000-0002-7412-7632); Shun-Ai Liu (0000-0002-0004-3217); Wen Xie (0000-0002-7314-8175); Jun Cheng (0000-0001-5579-8353).

Author contributions: Wang Q and Li Y contributed equally to this work; Wang Q and Li Y performed the experiments and analyzed the data; Wang Q and Cheng J designed the research; Wang Q and Li Y wrote the manuscript; Xie W revised the manuscript; Liu SA provided vital reagents and analytical tools.

Supported by Beijing Natural Science Foundation, No. 7161006; and Beijing Municipal Administration of Hospitals' Youth Program, No. QML20161801 and No. QML20171801.

Institutional review board statement: This study did not involve any animal experiments or human specimens, and thus was exempted from ethical review according to the Human Research Management Stipulation of the Beijing Ditan Hospital Affiliated to the Capital University of Medical Sciences.

Conflict-of-interest statement: The authors declare that there are no conflicts of interest in this study.

Data sharing statement: Technical appendix, statistical code, and data set available from the corresponding author at chengj0817@ccmu.edu.cn. No additional data are available.

Manuscript source: Unsolicited manuscript

Correspondence to: Jun Cheng, MD, PhD, Professor, Center of Liver Diseases, Beijing Ditan Hospital, Capital Medical University, No. 8, Jingshun East Street, Chaoyang District, Beijing 100015, China. chengj0817@ccmu.edu.cn
Telephone: +86-10-84322006
Fax: +86-10-84397196

Received: December 1, 2017
Peer-review started: December 1, 2017
First decision: December 20, 2017
Revised: January 4, 2018
Accepted: January 17, 2018
Article in press: January 17, 2018
Published online: March 28, 2018

Abstract

AIM

To explore hepatitis C virus (HCV) adaptive mutations or combinations thereof responsible for enhanced viral production and investigate the underlying mechanisms.

METHODS

A series of plasmids with adaptive mutations were constructed. After the plasmids were transfected into Huh7.5 cells, we determined the infectious HCV particle titers by NS5A immunofluorescence assays, and detected HCV RNA replication by real-time PCR and protein expression by Western blot. Then we carried out immunoblotting of supernatants and cell

lysates with anti-NS3 to analyze the virus release level. In addition, co-localization of lipid droplets (LDs) with NS5A was measured using confocal laser scanning microscopy. The ratio between the p56 and p58 phosphoforms of NS5A was analyzed further.

RESULTS

The plasmids named JFH1-mE2, JFH1-mp7, JFH1-mNS4B, JFH1-mNS5A, JFH1-mE2/NS5A, JFH1-mp7/NS5A, JFH1-mNS4B/NS5A, JFH1-mE2/p7/NS5A, and mJFH1 were constructed successfully. This study generated infectious HCV particles with a robust titer of 1.61×10^6 focus-forming units (FFUs)/mL. All of the six adaptive mutations increased the HCV particle production at varying levels. The NS5A (C2274R, I2340T, and V2440L) and p7 (H781Y) were critical adaptive mutations. The effect of NS5A (C2274R, I2340T, and V2440L), p7 (H781Y), and NS4B (N1931S) on infectious HCV titers was investigated by measuring the HCV RNA replication, protein expression, and virion release. However, the six adaptive mutations were not required for the LD localization of NS5A proteins or the phosphorylation of NS5A.

CONCLUSION

In this study, we generated infectious HCV particles with a robust titer of 1.61×10^6 FFUs/mL, and found that the viral replication and release levels could be enhanced by some of the adaptive mutations.

Key words: Hepatitis C virus; JFH1; Adaptive mutation; RNA replication; Virion release; Lipid droplet localization

Core tip: In this study, we explored hepatitis C virus (HCV) adaptive mutations or combinations thereof responsible for enhanced viral production and investigated the underlying mechanisms. We generated infectious HCV particles with a robust titer of 1.61×10^6 focus-forming units (FFUs)/mL, and confirmed that the adaptive mutations could enhance viral replication and release. The results were established at the levels of infectious particle titers, HCV RNA, protein expression, virus release, lipid droplet, and NS5A co-localization, and further the ratio between p56 and p58 phosphoforms of NS5A.

Wang Q, Li Y, Liu SA, Xie W, Cheng J. Cell culture-adaptive mutations in hepatitis C virus promote viral production by enhancing viral replication and release. *World J Gastroenterol* 2018; 24(12): 1299-1311 Available from: URL: http://www.wjgnet.com/1007-9327/full/v24/i12/1299.htm DOI: http://dx.doi.org/10.3748/wjg.v24.i12.1299

INTRODUCTION

Hepatitis C virus (HCV) is a member of the flaviviridae family. HCV infection is a major public health challenge, with an estimated number of 130 to 170 million individuals infected worldwide[1,2]. HCV causes acute and chronic hepatitis, and also leads to permanent liver damage and hepatocellular carcinoma in a significant number of patients, *via* oxidative stress, insulin resistance, fibrosis, liver cirrhosis, and HCV-induced steatosis[3]. Interferon-α-based therapy, in combination with ribavirin, has limited efficacy in approximately 50% of patients and is associated with severe side effects[4]. Direct-acting antivirals (DAAs) targeting NS3/4A, NS5A, and NS5B proteins can lead to higher sustained virological responses than interferon-based regimens, have shorter treatment duration, are orally administered, and have fewer side effects[5].

HCV is an enveloped RNA virus whose replication occurs in the cytoplasm. It consists of a single-stranded 9.6-kb RNA genome of positive polarity with a 5′ internal ribosome entry site (IRES). IRES-driven HCV RNA produces a polyprotein of approximately 3000 amino acids localized to the rough endoplasmic reticulum (ER), where it is cleaved into at least four structural proteins (C, E1, E2, and p7) and six nonstructural proteins (NS2, NS3, NS4A, NS4B, NS5A, and NS5B) that play a key role in viral replication, assembly, and pathogenesis[6].

Elucidation of the viral structure and virus-host interaction is an important goal of anti-HCV drug discovery and vaccine development[7]. HCV replicon system has contributed to the study of HCV in the human hepatoma cell line Huh-7[8,9]. The infectious HCV JFH1 cell culture system represents a major advance in anti-HCV drug discovery research[7,10-12]. This model generates infectious viral particles in cell culture (HCVcc) and facilitates the study of HCV life cycle[7,11]. However, HCV JFH1 variant genome (genotype 2a) results in relatively low viral titers[7,13,14].

Several studies suggested that cell culture-adaptive mutations in HCV genomic RNA might potentially increase the production of infectious HCV particles[13,15-18]. Recently, an adaptive HCV JFH1 reporter isolate designated as JFH1-ΔV3-EGFP was identified[19], which produced higher titers (10^6 focus-forming units [FFUs]/mL) of HCV-EGFP reporter virus. Whole genome sequencing analysis showed that JFH1-ΔV3-EGFP included six mutations located in the E2, p7, NS4B, and NS5A regions as follows: D657G in E2; H781Y in p7; N1931S in NS4B; and C2274R, I2340T, and V2440L in NS5A. V2440L and H781Y improved the infectious HCV titers[20,21], while data pertaining to the other mutations are not available. In this study, we explored these mutations or combinations thereof responsible for enhanced viral production and investigated the underlying mechanisms.

MATERIALS AND METHODS

Cell culture

The human hepatoma cell line Huh7.5 was generously provided by Dr. Charles M. Rice[22] (Rockefeller

Table 1 Sequence of primers used for adaptive mutation plasmid construction

Primer	Sequence (5′-3′)
1340-F	CTGGCGTACGTGATGCG
m2310-R	TGTCCCTGTCCTCCAAGCCGCAGCGAT
m2310-F	ATCGCTGCGGCTTGGAGGACAGGGACA
3500-R	GCCCCGTCATACTCACCAC
m2681-R	TGATGTACCAAGCTGCCACGAAGAAG
m2681-F	CTTCTTCGTGGCAGCTTGGTACATCA
5249-F	AATGAGGTCACCCTCACACA
m6132-R	ACGTGGCTTCCTCTGGAAGCAAAGGCA
m6132-F	TGCCTTTGCTTCCAGAGGAAGCCACGT
7791-R	GATGTTGTACAGTACACCTTG
5249-F	AATGAGGTCACCCTCACACA
m7160-R	AGCATGCGCTCCGATGGTATTGAG
m7160-F	CTCAATACCATCGGAGCGCATGCT
m7359-R	TTCTGATGTGGTGCTCTCGCTCAG
m7359-F	CTGAGCGAGAGCACCACATCAGAA
m7658-R	GCACAGGGTGGTATCGTCCTCCT
m7658-F	AGGAGGACGATACCACCCTGTGC
7966-R	CTTGGATCTTGCAGAAT

Table 2 Primer combinations used in adaptive mutation plasmid construction

Fragment	Template	Primers	
		Sense	Anti-sense
mE2-1	JFH1	1340-F	m2310-R
mE2-2		m2310-F	3500-R
mp7-1		1340-F	m2681-R
mp7-2		m2681-F	3500-R
mNS4B-1		5249-F	m6132-R
mNS4B-2		m6132-F	7791-R
mNS5A-1		5249-F	m7160-R
mNS5A-2		m7160-F	m7359-R
mNS5A-3		m7359-F	m7658-R
mNS5A-4		m7658-F	7966-R
mNS4B/NS5A-1	JFH1-mNS5A	5249-F	m6132-R
mNS4B/NS5A-2		m6132-F	7791-R
mE2/p7 -1	JFH1-mp7/NS5A	1350-F	m2310-R
mE2/p7 -2		m2310-F	3500-R

University) and maintained in Dulbecco's modified Eagle's medium (DMEM) (Invitrogen) supplemented with 100 U/mL of penicillin, 100 μg/mL of streptomycin, non-essential amino acids, and 10% fetal bovine serum (Invitrogen) at 37 ℃ in 5% CO_2. All the experiments described in this study were performed using these cells.

Antibodies

The monoclonal antibody to NS5A protein (Abcam), the goat anti-mouse IgG conjugated with horseradish peroxidase (Sigma), and goat anti-mouse IgG conjugated with Alexa Fluor 594 (Invitrogen) were all obtained commercially.

Plasmid construction

Plasmid constructs were based on the consensus sequence of HCV pJFH1, which was kindly provided by Dr. Wakita[10]. JFH1-ΔV3-EGFP and JFH1-AM120 plasmids were kindly provided by Dr. C.H. Hagedorn and Shuang-Hu Liu[19]. The mutations located in HCV genomic RNA are shown in Figure 1. A series of primers for construction of adaptive variants of wild-type HCV JFH1 listed in Table 1 were designed using the pJFH1 sequence and mutations. The pJFH1 plasmid was used as a template for subsequent PCR with Phushion High-Fidelity PCR Master Mix with GC buffer (New England Biolabs) according to the manufacturer's instructions. The preliminary PCR products (mE2-1, mE2-2, mp7-1, mp7-2, mNS4B-1, mNS4B-2, mNS5A-1, mNS5A-2, mNS5A-3, and mNS5A-4) were analyzed by 1% agarose gel electrophoresis, and used for overlap PCR following the combination showed in Tables 2 and 3 to obtain adaptive mutation fragments. The above fragments (mE2, mp7, mNS4B, mNS5A, mE2/NS5A, mp7/NS5A, mNS4B/NS5A, and mE2/p7/NS5A) were sub-cloned into pJFH1 using the appropriate unique restriction enzyme sites such as *Bsi*w I, *Kpn* I, *Nsi* I, *Rsr* II, or *Bsr*G I, to produce JFH1-mE2, JFH1-mp7, JFH1-mNS4B, JFH1-mNS5A, JFH1-mE2/ NS5A, JFH1-mp7/NS5A, JFH1-mNS4B/NS5A, JFH1-mE2/p7/ NS5A, and also mJFH1, which contained all the six mutations. All new clones were sequenced using an ABI 3700-XL (Shanghai Sangon Biotech).

Transfection with HCV RNA

To generate the full-length genomic RNA, pJFH-1 and all plasmids were linearized with *Xba* I. The linearized plasmid DNA was purified and then used as a template for T7 *in vitro* transcription (MEGAscript; Ambion). The RNA genomes were detected by formaldehyde agarose gel electrophoresis as described previously[23], and transfected into cells by electroporation[13].

Immunofluorescence assay

Cells seeded on glass coverslips were infected with HCV. After 48 h, the slips were washed with PBS. Then, the cells were fixed with 4% paraformaldehyde, permeabilized with 0.2% Triton X-100, and blocked with 1% BSA and 1% normal goat serum. The NS5A in cells was detected with a monoclonal antibody and a secondary goat anti-mouse Alexa Fluor 594 antibody (Invitrogen) and visualized by fluorescence microscopy.

Virus titration

The titer of infectious HCV was determined by immunofluorescence assay[7]. Virus titers from supernatants and cell lysates as well were determined using FFUs.

Cell lysates were prepared as described previously[24]. Briefly, cell pellets harvested after trypsinization were washed with PBS, re-suspended in completed culture medium, and lysed in four freeze/thaw cycles at -80 ℃ and 37 ℃. The cell lysates were centrifuged at 4000 rpm for 5 min prior to inoculation into naïve Huh7.5 cells.

Virus titration analysis was conducted by serially diluting the cell supernatants or cell lysates 10-fold in DMEM. The supernatants were used to infect 1×10^4

Table 3 Primers and templates for overlap PCR

Fragment	Template	Primer	
		Upstream	Downstream
mE2	mE2-1 + mE2-2	1340-F	3500-R
mp7	mp7-1 + mp7-2	1340-F	3500-R
mNS4B	mNS4B-1 + mNS4B-2	5249 F	7791-R
mNS5A-3/4	mNS5A-3 + mNS5A-4	m7359-F	7966-R
mNS5A-2/3/4	mNS5A-2 + mNS5A-3/4	m7160-F	7966-R
mNS5A	mNS5A-1 + mNS5A-2/3/4	5249-F	7966-R
mNS4B/NS5A	mNS4B/NS5A-1 + mNS4B/NS5A-2	5249 F	7791-R
mE2/p7	mE2/p7 -1 + mE2/p7-2	1340-F	3500-R

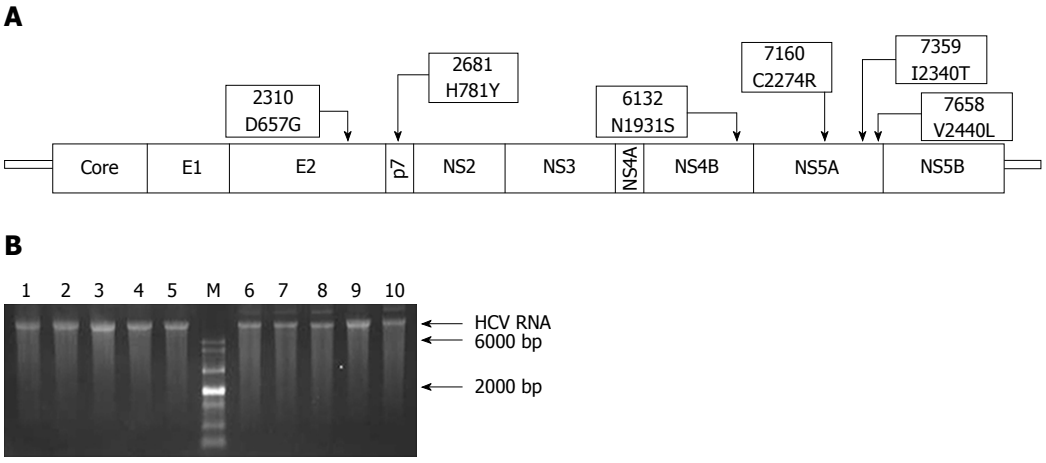

Figure 1 Schematic representation of adaptive mutations used in this study (A) and the electrophoresis results of each mutant virus RNA (B). A: Both nucleotide substitutions (2310, 2681, 6132, 7160, 7359, and 7658) and amino acid substitutions (D657G, H781Y, N1931S, C2274R, I2340T, and V2440L) are shown; B: HCV RNA (500 ng) was analyzed using formaldehyde agarose gel electrophoresis. Lane 1: JFH1; Lane 2: JFH1-mE2; Lane 3: JFH1-mP7; Lane 4: JFH1-mNS4B; Lane 5: JFH1-mNS5A; Lane 6: JFH1-mE2/NS5A; Lane 7: JFH1-mp7/NS5A; Lane 8: JFH1-mNS4B/NS5A; Lane 9: mJFH1; Lane 10: JFH1-mE2/p7/NS5A; M: RNA marker. HCV: hepatitis C virus.

naïve Huh7.5 cells in 96-well plates. The cells were incubated with virus for 2 h at 37 ℃, washed, and incubated with complete DMEM. The level of HCV infection was analyzed 3 and 9 d post-infection by immune- fluorescence staining for NS5A.

Western blot analysis

The Huh7.5 cells infected with HCV RNA were lysed in 50 mmol/L Tris-HCl (pH 7.5) containing 150 mmol/L sodium chloride, 1% Nonidet P40, 0.5% sodium deoxycholate, 0.1% SDS, and proteinase inhibitors (Complete Mini, Roche). Samples were separated by 10% SDS-PAGE and then transferred onto nitrocellulose membranes. The HCV NS5A (p56/p58) was analyzed as described previously[13].

Quantification of HCV RNA by qPCR

Total RNA was extracted with TRIzol (Invitrogen). HCV RNA was measured by qPCR analysis as described previously[25]. β-actin was used as the internal control. The relative quantity of HCV RNA in control and HCV samples was calculated by the comparative Ct (cycling threshold) method using LightCycler480.

Confocal laser scanning microscopy

Cells transfected with HCV RNA with adaptive mutations were seeded onto 24-well plates with cover slips. The cells were treated as previously described[13]. After 48 h, the cells were washed with PBS, fixed with 4% paraformaldehyde, and then permeabilized with 0.2% Triton X-100. Fixed cells were blocked with 1% bovine serum albumin and 1% normal goat serum in PBS. Next, HCV NS5A was analyzed in cells using a NS5A monoclonal antibody and a secondary goat anti-mouse IgG conjugated with Alexa 488 (Invitrogen, dilution of 1:1000). LipidTOX Deep Red (Invitrogen) was used to detect neutral lipids present in lipid droplets (LDs). The slides were counterstained using DAPI (Invitrogen), and examined using an Zeiss LSM 510 Meta confocal laser scanning microscope.

RESULTS

Effect of individual mutations or combinations of adaptive mutations on the production of infectious HCV

A previous study demonstrated that JFH-ΔV3-EGFP variant produces a higher titer of reporter virus[19]. The

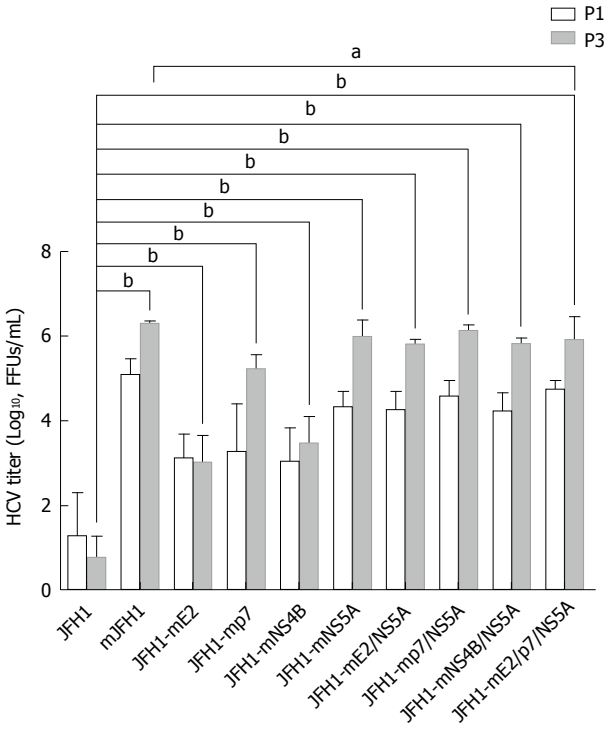

Figure 2 Generation of high titer cell culture-adaptive JFH1 virus. Hepatitis C virus RNA was electroporated into Huh7.5 cells to produce the recombinants of adapted virus in cell culture. The transfected cells were passaged every three days. The infectivity titers of the culture supernatants at day 3 (P1) and day 9 (P3) were measured. Viral titers are expressed as focus-forming units per milliliter (FFUs/mL). The data are presented as mean ± SD (n = 3). HCV: Hepatitis C virus. $^{a}P < 0.05$; $^{b}P < 0.01$.

six adaptive mutations in this variant were located in the E2 (D657G), p7 (H781Y), NS4B (N1931S), and NS5A (C2274R, I2340T, and V2440L) (Figure 1A), respectively. To determine the individual or synergistic combination of these mutations responsible for the increased viral production, recombinant JFH1 genomes containing only one of the selected mutations or four different combinations as shown in Figure 1A were constructed.

Next, ten *in vitro*-transcribed mutant JFH1 RNAs (Figure 1B) were electroporated into Huh7.5 cells to produce recombinants of adapted virus. The transfected cells were sub-cultured every three days. The infectivity titers of supernatants at day 3 (P1) and day 9 (P3) were measured (Figure 2). Viral titers are expressed as FFUs/mL and were assayed in duplicate, which was repeated three times. The data are presented as mean ± SD (n = 3). The HCV titers of wild type JFH1 (JFH1) were extremely low, with a typical titer of 10^2 FFUs/mL. The adaptive mutations in E2, p7, NS4B, and NS5A individually increased the production of infectious HCV titers 2- to 4-fold compared with the levels of JFH1. The NS5A mutations exhibited the greatest effect on the production of infectious HCV particles, with a titer of 1.30×10^6 FFUs/mL at P3. The p7 mutation followed closely, generating a titer of 2.10×10^5 FFUs/mL. Briefly, except for E2, the HCV titers of other variants at P3 were partially higher than those at P1.

To further determine any synergistic effect of the six adaptive mutations on HCV production, we focused on the recombinant viruses with adaptive mutations in different combinations. As shown in Figure 2, JFH1-mE2/NS5A, JFH1-mp7/NS5A, JFH1-mNS4B/NS5A, and JFH1-mE2/p7/NS5A remarkably enhanced the production of infectious HCV, and the mJFH1 produced infectious HCV particles with a robust titer of 1.61×10^6 FFUs/mL 9 d post-transfection.

These results suggest that all the six adaptive mutations increase the HCV particle production. NS5A (C2274R, I2340T, and V2440L) and p7 (H781Y) are the critical adaptive mutations.

HCV RNA replication and protein expression are up-regulated by adaptive mutations

HCV RNA genome replication and structural or non-structural protein expression are early steps in the HCV life cycle. To further confirm our speculation that the robust HCV titers and enhanced virion release were both related to up-regulated RNA replication and protein expression, we determined the relative HCV RNA, NS5A immunofluorescence, and NS3 protein levels in the RNA-transfected Huh7.5 cells on day 3 (P1) and day 9 (P3).

As shown in Figure 3, the expression of NS5A (Figure 3A) and NS3 (Figure 3B) in mutants was up-regulated at different levels during serial passages. The trend was extraordinary obvious in NS5A or p7 mutants. Anti-NS3 Western blot analysis, which was the most widely used for quantitative experiment, yielded consistent results.

As shown in Figure 3C, the RNA levels of all the mutants were increased compared with JFH1, and mJFH1 was increased 18.7-fold. Interestingly, the results indicated that JFH1-mNS4B expression increased 6.1-fold, and the combination of mutants showed a 7.4-16.8-fold increase.

Taken together, we confirmed that the effect of NS5A (C2274R, I2340T and V2440L), p7 (H781Y), and NS4B (N1931S) on infectious HCV titers was robust, and started with HCV RNA replication and protein expression, followed by virion release.

Adapted variants enhance the efficiency of virus release

Virion release is the last step of the HCV life cycle. To further explore the mechanism underlying the enhanced virus production, the role of adaptive mutations was examined. Ten HCV RNAs (JFH1, JFH1-mE2, JFH1-mP7, JFH1-mNS4B, JFH1-mNS5A, JFH1-mE2/NS5A, JFH1-mp7/NS5A, JFH1-mNS4B/NS5A, mJFH1, and JFH1-mE2/p7/NS5A) were electroporated into Huh7.5 cells. After 3 d, we collected the supernatants and cell lysates, and measured the HCV titers using NS5A immunofluorescence assays. Furthermore, to confirm the infectivity of virions, we carried out immunoblotting of supernatants and cell lysates with anti-NS3, which was extraordinarily consistent with the infectious HCV titers (Figure 4A). As shown in Figure 4B, we also calculated the proportion of extracellular (supernatant)

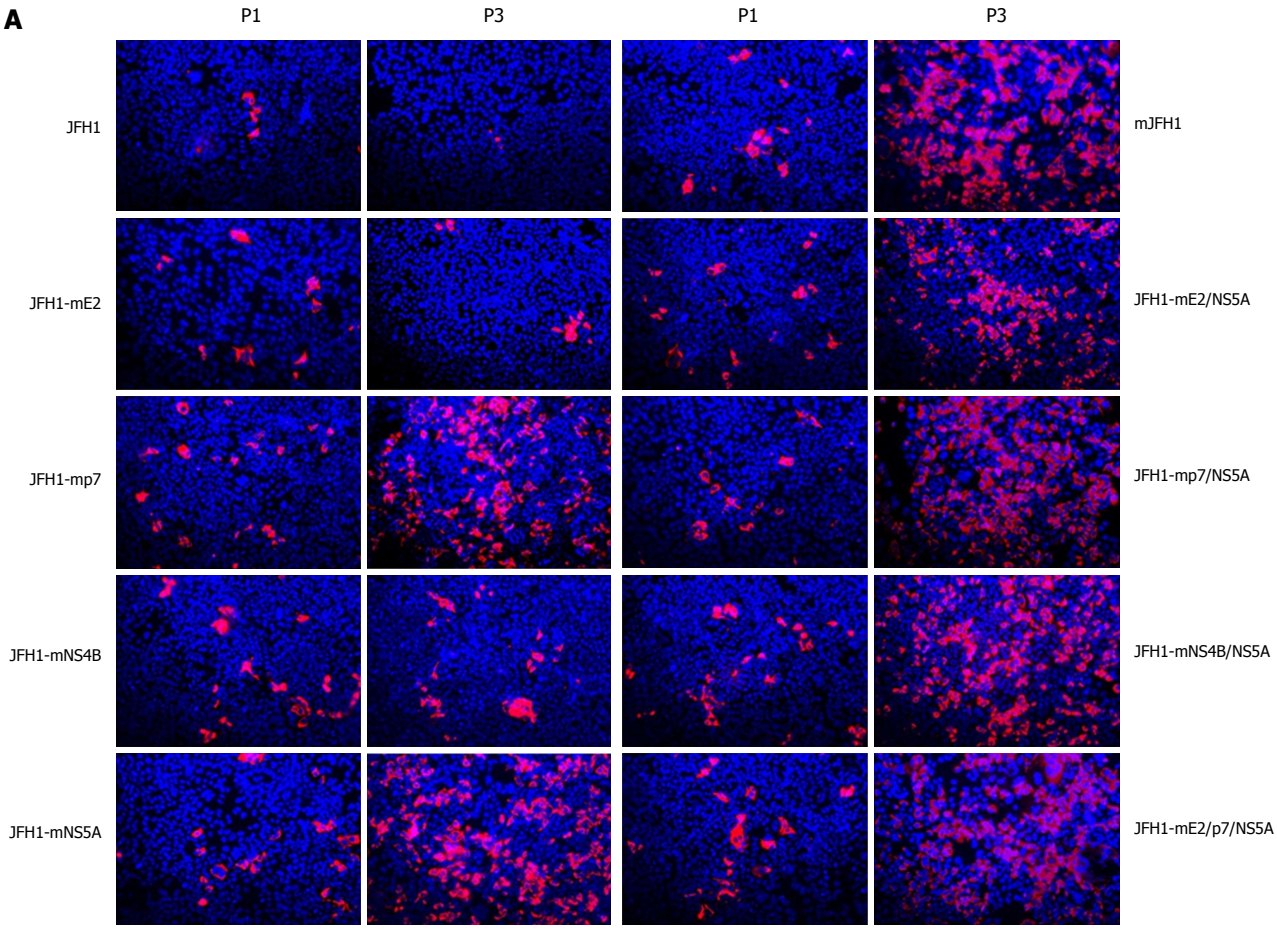
A
P1
P3
P1
P3
JFH1
mJFH1
JFH1-mE2
JFH1-mE2/NS5A
JFH1-mp7
JFH1-mp7/NS5A
JFH1-mNS4B
JFH1-mNS4B/NS5A
JFH1-mNS5A
JFH1-mE2/p7/NS5A

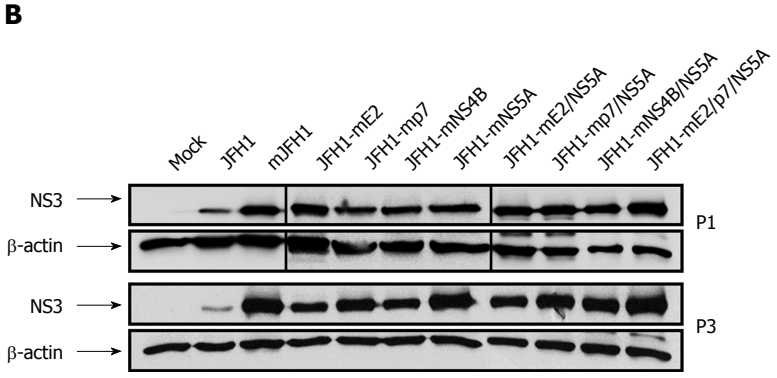
B
Mock
JFH1
mJFH1
JFH1-mE2
JFH1-mp7
JFH1-mNS4B
JFH1-mNS5A
JFH1-mE2/NS5A
JFH1-mp7/NS5A
JFH1-mNS4B/NS5A
JFH1-mE2/p7/NS5A
NS3
β-actin
NS3
β-actin
P1
P3

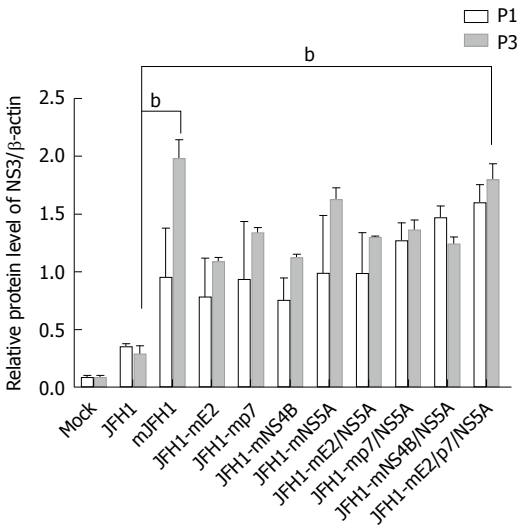
P1
P3
b
b
Relative protein level of NS3/β-actin
2.5
2.0
1.5
1.0
0.5
0.0
Mock
JFH1
mJFH1
JFH1-mE2
JFH1-mp7
JFH1-mNS4B
JFH1-mNS5A
JFH1-mE2/NS5A
JFH1-mp7/NS5A
JFH1-mNS4B/NS5A
JFH1-mE2/p7/NS5A

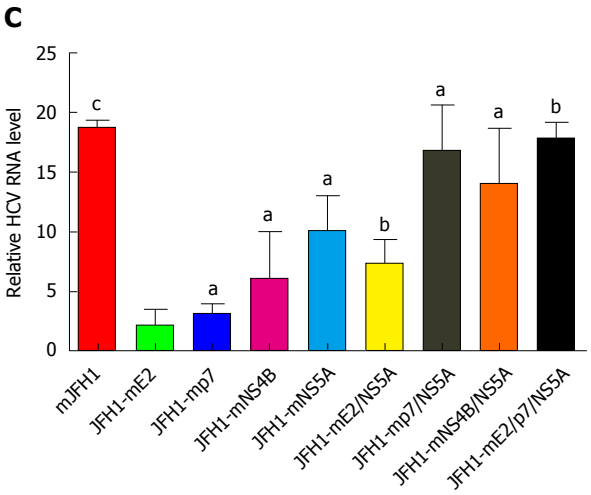

Figure 3 Effects of the adaptive mutations on the hepatitis C virus RNA replication. A: Hepatitis C virus (HCV) RNA was electroporated into Huh7.5 cells to produce the recombinants of adapted virus. The transfected cells were passaged every 3 d. Cells were fixed 48 h after passage and infected cells were identified by fluorescence immunostaining and microscopy. Nuclear DNA was stained with DAPI (blue); B: HCV RNA was electroporated into Huh7.5 cells to produce the recombinants of adapted virus in cell culture. The transfected cells were passaged every 3 d. Cells were lysed at 72 h after passage. The HCV NS3 protein levels were analysis by Western blot. $^{b}P < 0.01$; C: HCV RNA levels in cells 3 d after transfection. Intracellular HCV RNA levels were analyzed by quantitative RT-PCR. The mean ± SD for three independent experiments are presented (qPCR assays, $n = 3$). $^{a}P < 0.05$; $^{b}P < 0.01$; $^{c}P < 0.001$.

or intracellular (cell lysate) HCV titers using total titers as 100%. Typically, the supernatant and intracellular HCV titers of JFH1 were 76.31% and 23.69%, respectively, and those of mJFH1 were 94.00% and 6.00%, respectively. Taken together, these findings provide evidence suggesting that the ten variant viruses enhanced the virion release, and the high viral production was linked to the effective virion release. NS5A (C2274R, I2340T, and V2440L) and p7 (H781Y) showed the highest levels compared with the others.

Adaptive mutations are not essential for intracellular LD localization of the NS5A protein

LDs have been reported to play an important role in the HCV virion assembly process[26]. To determine if the six adaptive mutations increased the assembly of HCV at this step, LDs and NS5A were stained in JFH1 and mJFH1 transfected cells and the co-localization of LDs with NS5A was measured. As shown in Figure 5, the LDs were totally covered with NS5A in all cases. However, no significant difference was observed between JFH1 and mJFH1 groups using Image J software and Pearson's correlation coefficient analysis. These results indicated that the six adaptive mutations were not required for LD localization of the NS5A proteins.

Adapted mutations do not affect hyper-phosphorylation of NS5A

Previous studies showed that a ratio between the p56 and p58 phosphoforms of NS5A is required for optimal HCV RNA replication[13,27-29]. JFH1-AM120 is a robust adaptive mutant selected by Liu *et al*[13]. which displays significant switch of p56/p58. In this study, JFH1, JFH1-AM120, and mJFH1 RNA were transfected into Huh7.5 cells, and the total protein was used for Western blot analysis after 3 d (Figure 6). However, we observed no difference in p56 and p58 between the two groups. These results demonstrated that the phosphorylation level of NS5A was not affected by adaptive mutations.

DISCUSSION

Previous studies suggested that *in vitro* adaptive mutations enhance the production of infectious virus[13-17,20,21,30-34]. A high mutation rate in HCV RNA genome is a challenge for successful HCV treatment and vaccine research, although a method to obtain a robust clonal culture of HCV has been unavailable[13]. Liu *et al*[19] demonstrated that a JFH1-ΔV3-EGFP variant produced higher titer of reporter virus. The six adaptive mutations in this variant were located in the E2 (D657G), p7 (H781Y), NS4B (N1931S), and NS5A (C2274R, I2340T, and V2440L) (Figure 1A). However, the mutations responsible for enhanced viral production were not clear. The six mutations in this study were simultaneously located in JFH1-ΔV3-EGFP, which was a reporter EGFP gene chimera virus[19]. The mJFH1 refers to JFH1-ΔV3-EGFP that yielded a robust titer up to 1.61×10^6 FFUs/mL in this study, suggesting that the six mutations are effective adaptive mutations.

HCV is a single, positive-strand RNA virus. We focused on key life cycle events in the virus such as replication, expression, assembly, and release. Infectious virion release is the last step and the final objective of the JFH1 system. In our study, we detected variant virus titers initially. Consistent with previous reports[7,14], JFH1 only exhibited a decreased titer of 10^2 FFUs/mL. The other mutants showed increased titers with several orders of magnitude compared with JFH1. Synergistic enhancement of HCV titer was demonstrated obviously. Jiang *et al*[35] suggested that adaptive mutations enhance specific protein-protein interactions among viral proteins and promote the assembly of infectious HCV particles. We speculated that the six mutations involved

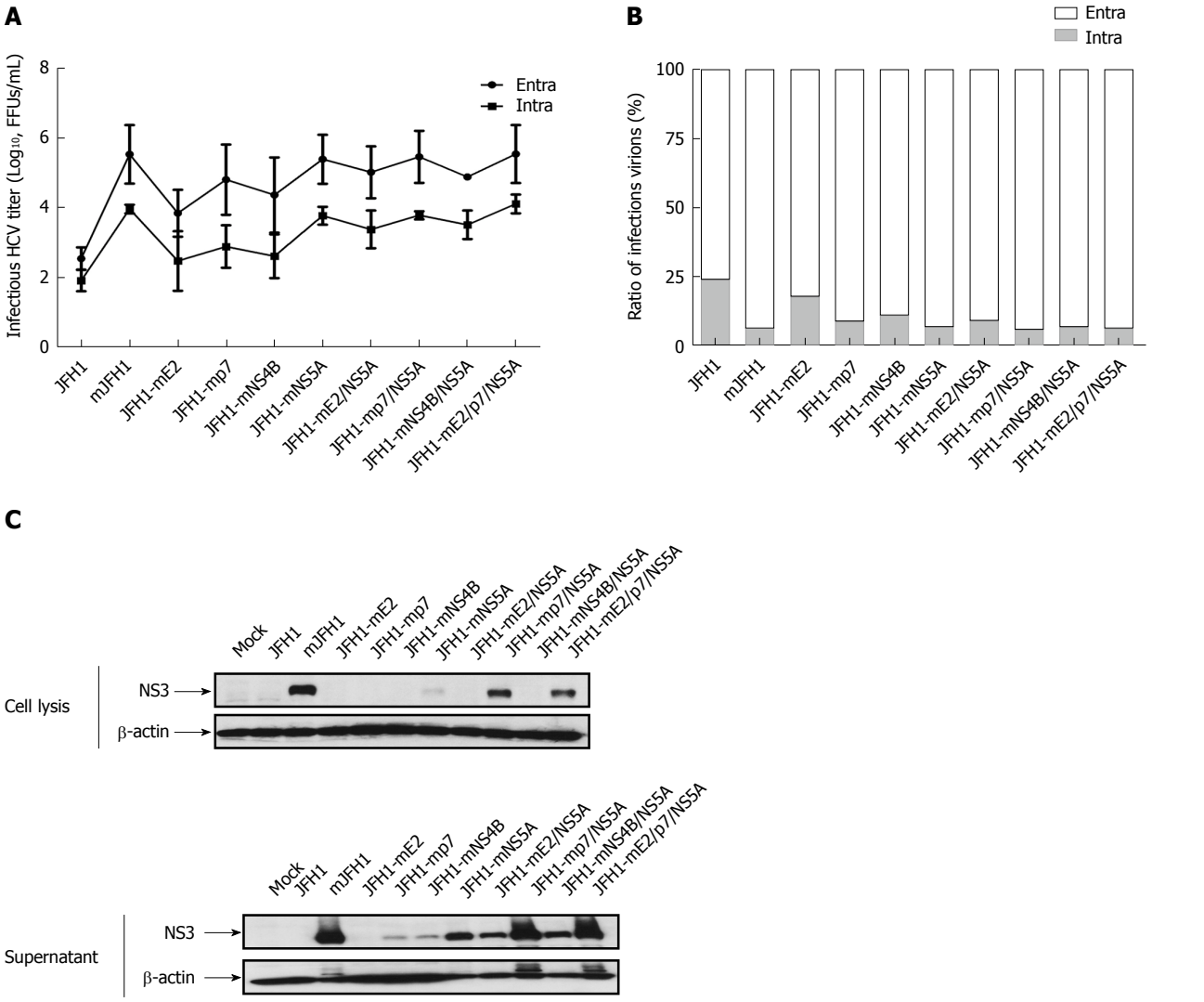

Figure 4 Effect of the adaptive mutations on the virion release. A: Hepatitis C virus (HCV) RNA was electroporated into Huh7.5 cells to produce the recombinants of adapted virus. At 72 h after transfection, the infectivity titers of the culture supernatants and cell lysates were measured. Viral titers are expressed as FFUs/mL. The data are presented as mean ± SD (n = 3); B: HCV RNA was electroporated into Huh7.5 cells to produce the recombinants of adapted virus. At 72 h after transfection, the infectivity titers of the culture media and cell lysates were measured. The extracellular and intracellular viral titers were measured. The relative ratios of infectious virions are shown. The results were from three independent experiments; C: The naive Huh7.5 cells were infected with the culture media and cell lysates. At 72 h after infection, cells were lysed with RIPA buffer, and analyzed by Western blot.

refer to unknown life cycle phases and mechanism as well. Therefore, we analyzed the effect of viral mutations on the distribution of virions in the supernatant and the cell lysate, co-localization of LDs and NS5A, HCV RNA level, NS3 expression, and p56/p58. We found that the adaptive mutations were associated with diverse effects on the life cycle events. The virion release and RNA genome replication were specifically associated with NS5A and p7 mutations.

The transmembrane domains of chimeric E1 and/or E2 HCV glycoproteins were modified to allow transport to and assembly at the cell surface[36]. E2 consisted of three critical domains: a receptor-binding domain (RBD; residues 384-661), the membrane proximal stem-like region of E2 (residues 675-699), and a hydrophobic heptad repeat linking the two domains[37]. Within the RBD, the E2 bound the cellular receptor CD81, leading to receptor-mediated endocytosis of virions[38,39]. Serial studies showed that the mutations in E2 play a role in the HCV life cycle *via* different mechanisms. Tao *et al*[30] demonstrated that the E2 (I414T) mutation had no significant effect on HCV RNA replication and viral entry. However, it enhanced the production of infectious viral particles and decreased the receptor-mediated viral entry. E2 (G451R) altered the relationship between particle density and infectivity, disrupted the co-receptor dependence, and increased virion sensitivity to receptor mimics[40]. The T563I mutation in the E2 protein increased virion viability at 37 ℃. Unfortunately, D657G in E2 improved the HCV titer *via* an unknown mechanism, without any effect on HCV RNA replication or virion release.

As a small membrane polypeptide, the HCV p7 channel plays multiple roles in virus life cycle and

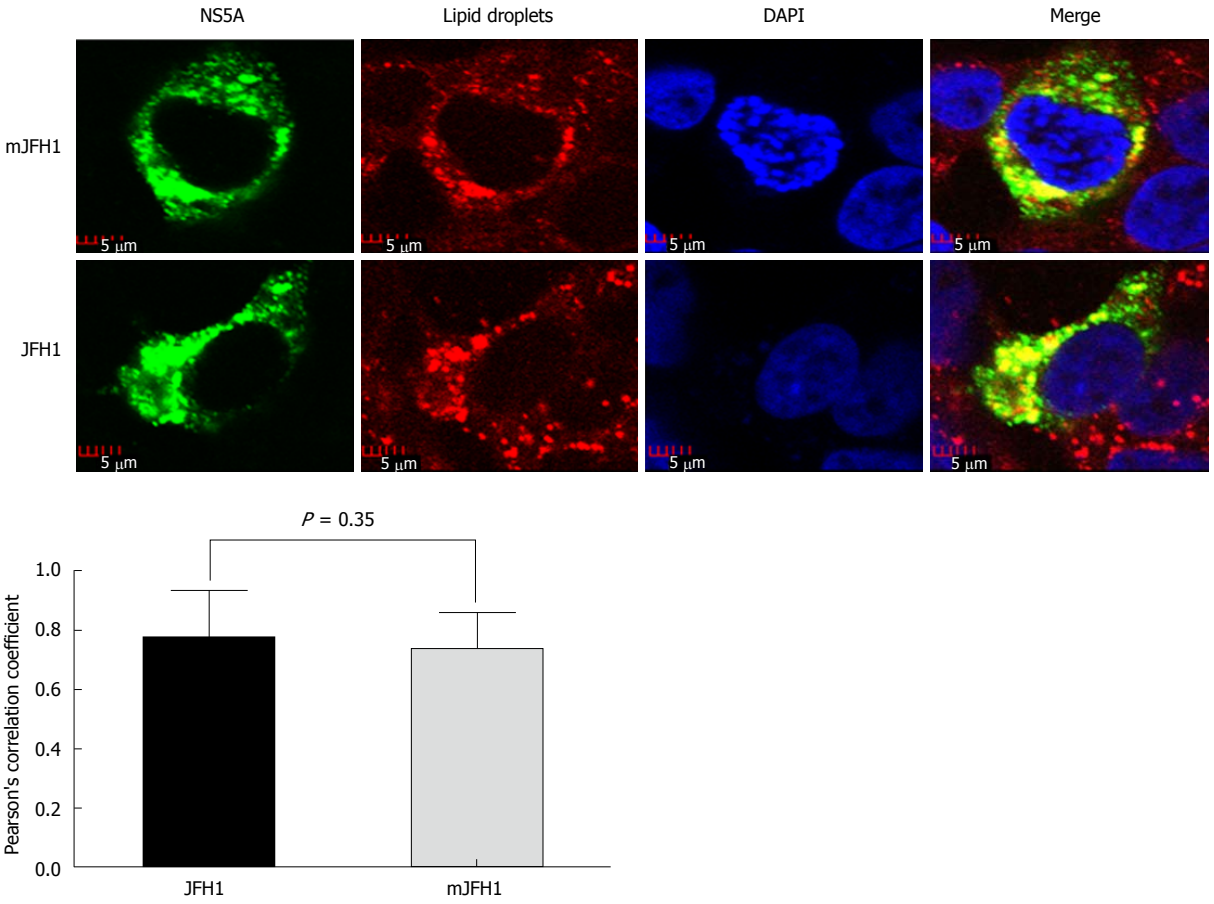

Figure 5 Colocalization analysis of lipid droplets and hepatitis C virus NS5A. JFH1 and mJFH1 RNA was electroporated into Huh7.5 cells to produce the recombinants of adapted virus. At 48 h after transfection, the cells were fixed. Lipid droplets were stained with LipidTOXRed (Red). The HCV NS5A was stained with anti-NS5A antibody (Green). The nucleus was stained with DAPI (Blue). Each triplicate sample of 25 cells was analyzed using Image J software. The degree of co-localization was quantified and compared using Pearson's correlation coefficients.

mediates several biological functions in HCV infection[41]. The p7 consists of six equivalent hydrophobic pockets between the peripheral and pore-forming helices[42]. Generally, p7 is not essential for HCV RNA replication, but required for virion assembly and release[43]. The adaptive mutation N765D in p7 influenced early stages of the HCV life cycle, and increased the infectious HCV titer[15]. Y781H enhances the level of HCV core in the supernatant three- to five-fold, and moderately increases virion assembly and release[21]. In our study, we found similar results, and Y781H enhanced HCV RNA replication 3.1-fold, suggesting its role as a critical initiating agent and a novel mechanism during the HCV life cycle.

HCV NS4B plays an important role in RNA genome replication and virion assembly[44]. NS4B triggers the formation of a viral replication complex[45] similar to the "sponge-like inclusions" observed in the liver of HCV-infected chimpanzee[46]. NS4B (K1846T) increased HCV RNA replication nearly 30-fold[47]. N1931S is located between helices 1 and 2 of the NS4B C-terminus, and was first determined by Li *et al*[48] during HCV RNA replication and virion assembly. Our data suggested that the N1931S increased HCV titer to 10^3 FFUs/mL, which was 10^3-fold compared with JFH1. It significantly enhanced HCV genome replication, and slightly improved virion release. N1931S is a novel mutation in the JFH1 system, and comprehensive studies investigating its role in HCV infection are needed.

HCV NS5A is a phosphoprotein existing in two different forms: a basic phosphorylated NS5A, p56, and a hyperphosphorylatedNS5A, p58. It appears to play an important role in viral replication, since most of the adaptive mutations determined so far are located within the region of NS5A[47]. The three domains in NS5A include: domain I (aa 28-213) coordinating a single zinc atom, and domains II (aa 250-342) and III (aa 356-447), which are less well characterized but are important in RNA replication and/or virion assembly[28]. A previous report suggested that V2440L was located at the NS5A-B cleavage site and decreased the cleavage kinetics[20]. Thus, the mutation C2274R is located in domain II, and the other mutations (I2340T and V2440L) occur in domain III. We analyzed the HCV RNA replication and protein expression. The results showed that the three mutations enhanced HCV RNA replication,

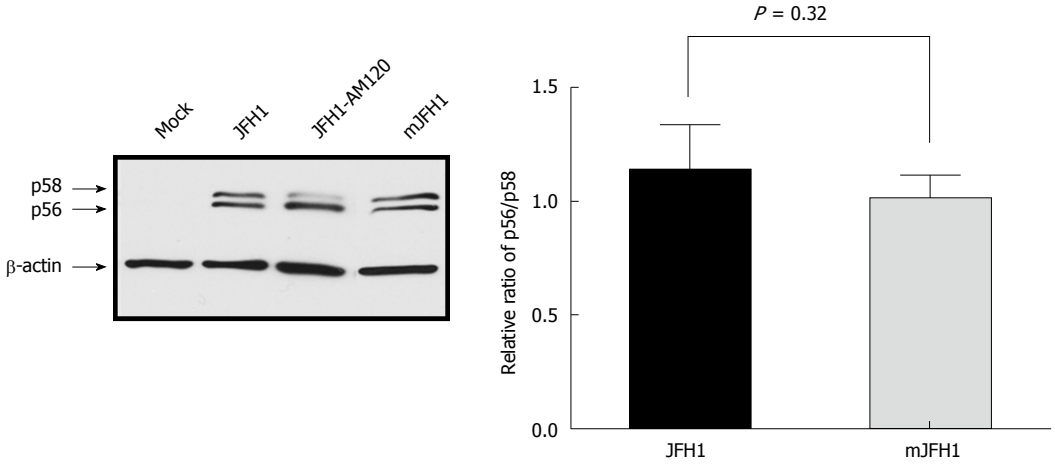

Figure 6 Phosphorylation of NS5A during JFH1 and mJFH1 replication. Huh7.5 cells were transfected with JFH1 or mJFH1 RNA. After three days of culture, cells were lysed for western blot using anti-NS5A and anti-β-actin antibodies. The quantity of p56 and p58 was determined using Image J software and the ratios of p56/p58 are shown. Data are presented as mean ± SD (n = 3). JFH1-AM120 was used as the positive control.

which is consistent with the structure.

A previous study demonstrated that HCV p7 promotes a late step of assembly and release of infectious virions[49] and NS5A plays a major role in regulating the release of infectious virus particles in cell culture[32]. In this study, there were three mutants (C2274R, I2340T, and V2440L) located in NS5A and one located (H781Y) in p7. Our results showed that these mutants obviously promoted the HCV viral particles release (Figure 4). HCV core is located on the cytosolic side of the ER membrane, assembly probably initiates in the cytosol before further maturation, and release occurs by transfer of nascent particles across the ER membrane to enable access to the secretory pathways in hepatocytes[50]. The amino acid changes induced by mutants in NS5A and P7 may be involved in these steps. The specific mechanism needs to be further studied in future.

Previous studies suggested that the up-regulation of p56/p58 ratio might be a critical factor for HCV titer[13] and increased HCV replication since specific mutations reduced NS5A hyper-phosphorylation activating RNA replication[27]. NS5A-p58 levels increased following overexpression of CKI-alpha, CKI-delta, and CKI-epsilon, whereas RNA interference of CKI-alpha alone reduced NS5A hyper-phosphorylation[51]. Here, we detected the status of p56/p58. However, there was no switch between the JFH1 and mJFH1 groups. The two viral proteins including the core and NS5A were localized to LDs, which play an important role in the intracellular assembly of HCV[24,26]. The recruitment of NS5A to LDs was a prerequisite for virion assembly in Huh7.5 cells[26]. Our analysis of the co-localization of NS5A and LDs showed no significant difference between mJFH1 and JFH1, suggesting that these adaptive mutations did not alter virion formation.

The life cycle of HCV is extremely complex, and several details remain unknown. Regulation of host gene expression[52,53], altered association between viral proteins and/or host-cell proteins, and changes in virus *per se*[54] represent obvious mechanisms. In our study, we confirmed that the adaptive mutations led to a robust infectious titer *via* enhanced viral replication and release. It is recommended that DAA regimens can be used for treatment of patients with hepatitis C rather than pegylated interferon/rabivirin[5]. Meanwhile, our study was limited by the reaction of DAAs to above adaptive mutations. Further studies investigating the underlying mechanisms of viral morphogenesis are needed.

In conclusion, we generated infectious HCV particles with a robust titer of 1.61 × 10^6 FFUs/mL in this study. All of the six adaptive mutations increased the HCV particle production at varying levels. The NS5A (C2274R, I2340T, and V2440L) and p7 (H781Y) were critical adaptive mutations. This study confirmed that the JFH1 is still a promising system to study the HCV life cycle. To use adaptive mutations is an effective means to establish a new system with higher infectious HCV virions titer. And the research on molecular mechanism of interaction between viral proteins and/or host-cell proteins should be carried out in depth.

ARTICLE HIGHLIGHTS

Research background

Hepatitis C virus (HCV) causes acute and chronic hepatitis, and leads to permanent liver damage and hepatocellular carcinoma. The infectious HCV JFH1 cell culture system represents a major advance in anti-HCV drug discovery research and facilitates the study of HCV life cycle. However, HCV JFH1 (genotype 2a) merely generates relatively low viral titers. JFH1-ΔV3-EGFP, which includes six mutations located in the E2, p7, NS4B, and NS5A regions, could produce higher titers of HCV-EGFP reporter virus. However, there were no data about which mutations or combinations thereof are responsible for enhanced viral production and the underlying mechanisms.

Research motivation

This JFH1 model generated infectious viral particles in cell culture and facilitated the study of the HCV life cycle, but the low infectious virion titer limits

its application range. Some previous studies have confirmed that adaptive mutations could enhance the virion titer, but the mechanism has not yet been fully elucidated. In this study, we focused on the positive effect of six adaptive mutations located in the E2, p7, NS4B, and NS5A regions, and found that the mechanism was different among them during the procession. These results gave us some new insights into the infectious HCV cell culture system and adaptive mutations.

Research objectives

The main objective of this study was to establish an infectious HCV cell culture system with a robust titer, and to discuss the underlying mechanisms of the adaptive mutations found in previous studies. The results of this study have supplied the researchers with a useful tool. We hope it will be used for the study of viral structure, virus-host interaction, anti-HCV drug discovery, and vaccine development.

Research methods

We investigated JFH1-mE2, JFH1-mp7, JFH1-mNS4B, JFH1-mNS5A, JFH1-mE2/NS5A, JFH1-mp7/NS5A, JFH1-mNS4B/NS5A, JFH1-mE2/p7/ NS5A, and mJFH1, carrying all the six mutations. We analyzed the infectious HCV titer, HCV RNA and NS3 protein levels, viral release capacity, assembly and hyper-phosphorylation of NS5A to determine the role of these mutations in the HCV life cycle. These methods were the routine ways adopted widely in virological and molecular biological research.

Research results

The main findings in this study were as follows: (1) we generated infectious HCV particles with a robust titer of 1.61×10^6 FFUs/mL; (2) The six adaptive mutations increased the HCV particle production at varying levels. The NS5A (C2274R, I2340T, and V2440L) and p7 (H781Y) are critical adaptive mutations. The effect of NS5A (C2274R, I2340T, and V2440L), p7 (H781Y), and NS4B (N1931S) on infectious HCV titers was investigated by measuring the HCV RNA replication, protein expression, and virion release; and (3) the six adaptive mutations were all not required for the lipid droplet localization of NS5A proteins or the phosphorylation of NS5A. To our knowledge, this is a new robust titer related to adaptive mutations from JFH1. The problems that remain to be solved in the future include: (1) how could the adaptive mutations be translated to clinical conditions? (2) are these mutation patterns observed *in vivo*? and (3) would these results be relevant to the resistance to direct-acting antivirals (DAAs)?

Research conclusions

First, this study generated infectious HCV particles with a robust titer of 1.61×10^6 FFUs/mL. Second, all of the six adaptive mutations increased the HCV particle production at varying levels. Third, the NS5A (C2274R, I2340T, and V2440L) and p7 (H781Y) were critical adaptive mutations, but they were not required for the LD localization of NS5A proteins or the phosphorylation of NS5A. Based on the new findings of this study, we proposed that more important adaptive mutations would be addressed in the future, and unknown mechanism of the HCV life cycle would be explained.

Research perspectives

This study re-confirmed that the JFH1 was still a promising system to study the HCV life cycle. To use adaptive mutations was an effective way to establish a new system with higher infectious HCV virion titer. In addition, we also re-confirmed that the molecular mechanism of interaction between viral proteins and/or host-cell proteins is more complex and important.

ACKNOWLEDGMENTS

We thank Dr. Wakita T for providing the plasmid containing the HCV JFH1 plasmid. We also thank Dr. Xu HT for providing Huh7.5 cells, and Dr. Hagedorn CH and Dr. Liu SH for providing JFH1-ΔV3-EGFP and JFH1-AM120 plasmids.

REFERENCES

1 **Li YP**, Ramirez S, Jensen SB, Purcell RH, Gottwein JM, Bukh J. Highly efficient full-length hepatitis C virus genotype 1 (strain TN) infectious culture system. *Proc Natl Acad Sci USA* 2012; **109**: 19757-19762 [PMID: 23151512 DOI: 10.1073/pnas.1218260109]
2 **Averhoff FM**, Glass N, Holtzman D. Global burden of hepatitis C: considerations for healthcare providers in the United States. *Clin Infect Dis* 2012; **55** Suppl 1: S10-S15 [PMID: 22715208 DOI: 10.1093/cid/cis361]
3 **Jahan S**, Ashfaq UA, Qasim M, Khaliq S, Saleem MJ, Afzal N. Hepatitis C virus to hepatocellular carcinoma. *Infect Agent Cancer* 2012; **7**: 2 [PMID: 22289144 DOI: 10.1186/1750-9378-7-2]
4 **Hoofnagle JH**, di Bisceglie AM. The treatment of chronic viral hepatitis. *N Engl J Med* 1997; **336**: 347-356 [PMID: 9011789 DOI: 10.1056/NEJM199701303360507]
5 **World Health Organization**. Guidelines for the Screening Care and Treatment of Persons with Chronic Hepatitis C Infection: Updated Version. Geneva: World Health Organization; 2016 [PMID: 27227200]
6 **Moradpour D**, Penin F. Hepatitis C virus proteins: from structure to function. *Curr Top Microbiol Immunol* 2013; **369**: 113-142 [PMID: 23463199 DOI: 10.1007/978-3-642-27340-7_5]
7 **Zhong J**, Gastaminza P, Cheng G, Kapadia S, Kato T, Burton DR, Wieland SF, Uprichard SL, Wakita T, Chisari FV. Robust hepatitis C virus infection in vitro. *Proc Natl Acad Sci USA* 2005; **102**: 9294-9299 [PMID: 15939869 DOI: 10.1073/pnas.0503596102]
8 **Lohmann V**, Körner F, Koch J, Herian U, Theilmann L, Bartenschlager R. Replication of subgenomic hepatitis C virus RNAs in a hepatoma cell line. *Science* 1999; **285**: 110-113 [PMID: 10390360]
9 **Blight KJ**, Kolykhalov AA, Rice CM. Efficient initiation of HCV RNA replication in cell culture. *Science* 2000; **290**: 1972-1974 [PMID: 11110665]
10 **Kato T**, Furusaka A, Miyamoto M, Date T, Yasui K, Hiramoto J, Nagayama K, Tanaka T, Wakita T. Sequence analysis of hepatitis C virus isolated from a fulminant hepatitis patient. *J Med Virol* 2001; **64**: 334-339 [PMID: 11424123]
11 **Wakita T**, Pietschmann T, Kato T, Date T, Miyamoto M, Zhao Z, Murthy K, Habermann A, Kräusslich HG, Mizokami M, Bartenschlager R, Liang TJ. Production of infectious hepatitis C virus in tissue culture from a cloned viral genome. *Nat Med* 2005; **11**: 791-796 [PMID: 15951748 DOI: 10.1038/nm1268]
12 **Lindenbach BD**, Evans MJ, Syder AJ, Wölk B, Tellinghuisen TL, Liu CC, Maruyama T, Hynes RO, Burton DR, McKeating JA, Rice CM. Complete replication of hepatitis C virus in cell culture. *Science* 2005; **309**: 623-626 [PMID: 15947137 DOI: 10.1126/science.1114016]
13 **Liu S**, Xiao L, Nelson C, Hagedorn CH. A cell culture adapted HCV JFH1 variant that increases viral titers and permits the production of high titer infectious chimeric reporter viruses. *PLoS One* 2012; **7**: e44965 [PMID: 23028707 DOI: 10.1371/journal.pone.0044965]
14 **Delgrange D**, Pillez A, Castelain S, Cocquerel L, Rouillé Y, Dubuisson J, Wakita T, Duverlie G, Wychowski C. Robust production of infectious viral particles in Huh-7 cells by introducing mutations in hepatitis C virus structural proteins. *J Gen Virol* 2007; **88**: 2495-2503 [PMID: 17698659 DOI: 10.1099/vir.0.82872-0]
15 **Kim CS**, Keum SJ, Jang SK. Generation of a cell culture-adapted hepatitis C virus with longer half life at physiological temperature. *PLoS One* 2011; **6**: e22808 [PMID: 21829654 DOI: 10.1371/journal.pone.0022808]
16 **Gorzin AA**, Ramsland PA, Tachedjian G, Gowans EJ. Identification of residues involved in NS2 homodimerization and elucidation of their impact on the HCV life cycle. *J Viral Hepat* 2012; **19**: 189-198 [PMID: 22329373 DOI: 10.1111/j.1365-2893.2011.01504.x]
17 **Chan K**, Robinson M, Yang H, Cornew S, Delaney Iv WE.

Development of a robust luciferase reporter 1b/2a hepatitis C virus (HCV) for characterization of early stage HCV life cycle inhibitors. *Antiviral Res* 2013; **98**: 85-92 [PMID: 23376631 DOI: 10.1016/j.antiviral.2013.01.005]

18 **Liu S**, Nelson CA, Xiao L, Lu L, Seth PP, Davis DR, Hagedorn CH. Measuring antiviral activity of benzimidazole molecules that alter IRES RNA structure with an infectious hepatitis C virus chimera expressing Renilla luciferase. *Antiviral Res* 2011; **89**: 54-63 [PMID: 21075143 DOI: 10.1016/j.antiviral.2010.11.004]

19 **Liu S**, Chen R, Hagedorn CH. Direct visualization of hepatitis C virus-infected Huh7.5 cells with a high titre of infectious chimeric JFH1-EGFP reporter virus in three-dimensional Matrigel cell cultures. *J Gen Virol* 2014; **95**: 423-433 [PMID: 24243732 DOI: 10.1099/vir.0.055772-0]

20 **Kaul A**, Woerz I, Meuleman P, Leroux-Roels G, Bartenschlager R. Cell culture adaptation of hepatitis C virus and in vivo viability of an adapted variant. *J Virol* 2007; **81**: 13168-13179 [PMID: 17881454 DOI: 10.1128/JVI.01362-07]

21 **Brohm C**, Steinmann E, Friesland M, Lorenz IC, Patel A, Penin F, Bartenschlager R, Pietschmann T. Characterization of determinants important for hepatitis C virus p7 function in morphogenesis by using trans-complementation. *J Virol* 2009; **83**: 11682-11693 [PMID: 19726506 DOI: 10.1128/JVI.00691-09]

22 **Blight KJ**, McKeating JA, Rice CM. Highly permissive cell lines for subgenomic and genomic hepatitis C virus RNA replication. *J Virol* 2002; **76**: 13001-13014 [PMID: 12438626]

23 **Bryant S**, Manning DL. Formaldehyde gel electrophoresis of total RNA. *Methods Mol Biol* 1998; **86**: 69-72 [PMID: 9664456 DOI: 10.1385/0-89603-494-1:69]

24 **Gastaminza P**, Kapadia SB, Chisari FV. Differential biophysical properties of infectious intracellular and secreted hepatitis C virus particles. *J Virol* 2006; **80**: 11074-11081 [PMID: 16956946 DOI: 10.1128/JVI.01150-06]

25 **Papic N**, Maxwell CI, Delker DA, Liu S, Heale BS, Hagedorn CH. RNA-sequencing analysis of 5' capped RNAs identifies many new differentially expressed genes in acute hepatitis C virus infection. *Viruses* 2012; **4**: 581-612 [PMID: 22590687 DOI: 10.3390/v4040581]

26 **Miyanari Y**, Atsuzawa K, Usuda N, Watashi K, Hishiki T, Zayas M, Bartenschlager R, Wakita T, Hijikata M, Shimotohno K. The lipid droplet is an important organelle for hepatitis C virus production. *Nat Cell Biol* 2007; **9**: 1089-1097 [PMID: 17721513 DOI: 10.1038/ncb1631]

27 **Tellinghuisen TL**, Foss KL, Treadaway J. Regulation of hepatitis C virion production via phosphorylation of the NS5A protein. *PLoS Pathog* 2008; **4**: e1000032 [PMID: 18369478 DOI: 10.1371/journal.ppat.1000032]

28 **Qiu D**, Lemm JA, O'Boyle DR 2nd, Sun JH, Nower PT, Nguyen V, Hamann LG, Snyder LB, Deon DH, Ruediger E, Meanwell NA, Belema M, Gao M, Fridell RA. The effects of NS5A inhibitors on NS5A phosphorylation, polyprotein processing and localization. *J Gen Virol* 2011; **92**: 2502-2511 [PMID: 21795470 DOI: 10.1099/vir.0.034801-0]

29 **Huang Y**, Staschke K, De Francesco R, Tan SL. Phosphorylation of hepatitis C virus NS5A nonstructural protein: a new paradigm for phosphorylation-dependent viral RNA replication? *Virology* 2007; **364**: 1-9 [PMID: 17400273 DOI: 10.1016/j.virol.2007.01.042]

30 **Tao W**, Xu C, Ding Q, Li R, Xiang Y, Chung J, Zhong J. A single point mutation in E2 enhances hepatitis C virus infectivity and alters lipoprotein association of viral particles. *Virology* 2009; **395**: 67-76 [PMID: 19793603 DOI: 10.1016/j.virol.2009.09.006]

31 **Kaul A**, Stauffer S, Berger C, Pertel T, Schmitt J, Kallis S, Zayas M, Lohmann V, Luban J, Bartenschlager R. Essential role of cyclophilin A for hepatitis C virus replication and virus production and possible link to polyprotein cleavage kinetics. *PLoS Pathog* 2009; **5**: e1000546 [PMID: 19680534 DOI: 10.1371/journal.ppat.1000546]

32 **Han Q**, Xu C, Wu C, Zhu W, Yang R, Chen X. Compensatory mutations in NS3 and NS5A proteins enhance the virus production capability of hepatitis C reporter virus. *Virus Res* 2009; **145**: 63-73 [PMID: 19540283 DOI: 10.1016/j.virusres.2009.06.005]

33 **Murayama A**, Sugiyama N, Suzuki R, Moriyama M, Nakamura N, Mochizuki H, Wakita T, Kato T. Amino Acid Mutations in the NS4A Region of Hepatitis C Virus Contribute to Viral Replication and Infectious Virus Production. *J Virol* 2017; **91**: pii: e02124-16 [PMID: 27928005 DOI: 10.1128/JVI.02124-16]

34 **Yan Y**, He Y, Boson B, Wang X, Cosset FL, Zhong J. A Point Mutation in the N-Terminal Amphipathic Helix α0 in NS3 Promotes Hepatitis C Virus Assembly by Altering Core Localization to the Endoplasmic Reticulum and Facilitating Virus Budding. *J Virol* 2017; **91**: pii: e02399-16 [PMID: 28053108 DOI: 10.1128/JVI.02399-16]

35 **Jiang J**, Luo G. Cell culture-adaptive mutations promote viral protein-protein interactions and morphogenesis of infectious hepatitis C virus. *J Virol* 2012; **86**: 8987-8997 [PMID: 22674987 DOI: 10.1128/JVI.00004-12]

36 **Bartosch B**, Vitelli A, Granier C, Goujon C, Dubuisson J, Pascale S, Scarselli E, Cortese R, Nicosia A, Cosset FL. Cell entry of hepatitis C virus requires a set of co-receptors that include the CD81 tetraspanin and the SR-B1 scavenger receptor. *J Biol Chem* 2003; **278**: 41624-41630 [PMID: 12913001 DOI: 10.1074/jbc.M305289200]

37 **Drummer HE**, Boo I, Maerz AL, Poumbourios P. A conserved Gly436-Trp-Leu-Ala-Gly-Leu-Phe-Tyr motif in hepatitis C virus glycoprotein E2 is a determinant of CD81 binding and viral entry. *J Virol* 2006; **80**: 7844-7853 [PMID: 16873241 DOI: 10.1128/JVI.00029-06]

38 **Pileri P**, Uematsu Y, Campagnoli S, Galli G, Falugi F, Petracca R, Weiner AJ, Houghton M, Rosa D, Grandi G, Abrignani S. Binding of hepatitis C virus to CD81. *Science* 1998; **282**: 938-941 [PMID: 9794763]

39 **Codran A**, Royer C, Jaeck D, Bastien-Valle M, Baumert TF, Kieny MP, Pereira CA, Martin JP. Entry of hepatitis C virus pseudotypes into primary human hepatocytes by clathrin-dependent endocytosis. *J Gen Virol* 2006; **87**: 2583-2593 [PMID: 16894197 DOI: 10.1099/vir.0.81710-0]

40 **Grove J**, Nielsen S, Zhong J, Bassendine MF, Drummer HE, Balfe P, McKeating JA. Identification of a residue in hepatitis C virus E2 glycoprotein that determines scavenger receptor BI and CD81 receptor dependency and sensitivity to neutralizing antibodies. *J Virol* 2008; **82**: 12020-12029 [PMID: 18829747 DOI: 10.1128/JVI.01569-08]

41 **Du QS**, Wang SQ, Chen D, Meng JZ, Huang RB. In depth analysis on the binding sites of adamantane derivatives in HCV (hepatitis C virus) p7 channel based on the NMR structure. *PLoS One* 2014; **9**: e93613 [PMID: 24714586 DOI: 10.1371/journal.pone.0093613]

42 **OuYang B**, Xie S, Berardi MJ, Zhao X, Dev J, Yu W, Sun B, Chou JJ. Unusual architecture of the p7 channel from hepatitis C virus. *Nature* 2013; **498**: 521-525 [PMID: 23739335 DOI: 10.1038/nature12283]

43 **Lohmann V**. Hepatitis C virus RNA replication. *Curr Top Microbiol Immunol* 2013; **369**: 167-198 [PMID: 23463201 DOI: 10.1007/978-3-642-27340-7_7]

44 **Jones DM**, Patel AH, Targett-Adams P, McLauchlan J. The hepatitis C virus NS4B protein can trans-complement viral RNA replication and modulates production of infectious virus. *J Virol* 2009; **83**: 2163-2177 [PMID: 19073716 DOI: 10.1128/JVI.01885-08]

45 **Gawlik K**, Baugh J, Chatterji U, Lim PJ, Bobardt MD, Gallay PA. HCV core residues critical for infectivity are also involved in core-NS5A complex formation. *PLoS One* 2014; **9**: e88866 [PMID: 24533158 DOI: 10.1371/journal.pone.0088866]

46 **Pfeifer U**, Thomssen R, Legler K, Böttcher U, Gerlich W, Weinmann E, Klinge O. Experimental non-A, non-B hepatitis: four types of cytoplasmic alteration in hepatocytes of infected chimpanzees. *Virchows Arch B Cell Pathol Incl Mol Pathol* 1980; **33**: 233-243 [PMID: 6110271]

47 **Lohmann V**, Hoffmann S, Herian U, Penin F, Bartenschlager R. Viral and cellular determinants of hepatitis C virus RNA replication in cell culture. *J Virol* 2003; **77**: 3007-3019 [PMID: 12584326]

48 **Li YP**, Ramirez S, Gottwein JM, Scheel TK, Mikkelsen L, Purcell RH, Bukh J. Robust full-length hepatitis C virus genotype 2a and 2b infectious cultures using mutations identified by a systematic approach applicable to patient strains. *Proc Natl Acad Sci U S A* 2012; **109**: E1101-E1110 [PMID: 22467829 DOI: 10.1073/pnas.1203829109]

49 **Steinmann E**, Penin F, Kallis S, Patel AH, Bartenschlager R, Pietschmann T. Hepatitis C virus p7 protein is crucial for assembly and release of infectious virions. *PLoS Pathog* 2007; **3**: e103 [PMID: 17658949 DOI: 10.1371/journal.ppat.0030103]

50 **Jones DM**, McLauchlan J. Hepatitis C virus: assembly and release of virus particles. *J Biol Chem* 2010; **285**: 22733-22739 [PMID: 20457608 DOI: 10.1074/jbc.R110.133017]

51 **Quintavalle M**, Sambucini S, Di Pietro C, De Francesco R, Neddermann P. The alpha isoform of protein kinase CKI is responsible for hepatitis C virus NS5A hyperphosphorylation. *J Virol* 2006; **80**: 11305-11312 [PMID: 16943283 DOI: 10.1128/JVI.01465-06]

52 **Ding Q**, Huang B, Lu J, Liu YJ, Zhong J. Hepatitis C virus NS3/4A protease blocks IL-28 production. *Eur J Immunol* 2012; **42**: 2374-2382 [PMID: 22685015 DOI: 10.1002/eji.201242388]

53 **Li X**, Jiang H, Qu L, Yao W, Cai H, Chen L, Peng T. Hepatocyte nuclear factor 4α and downstream secreted phospholipase A2 GXIIB regulate production of infectious hepatitis C virus. *J Virol* 2014; **88**: 612-627 [PMID: 24173221 DOI: 10.1128/JVI.02068-13]

54 **Alisi A**, Arciello M, Petrini S, Conti B, Missale G, Balsano C. Focal adhesion kinase (FAK) mediates the induction of pro-oncogenic and fibrogenic phenotypes in hepatitis C virus (HCV)-infected cells. *PLoS One* 2012; **7**: e44147 [PMID: 22937161 DOI: 10.1371/journal.pone.0044147]

P- Reviewer: Bock CT, Shi ZJ, Sipos F **S- Editor**: Wang JL
L- Editor: Wang TQ **E- Editor**: Huang Y

World Journal of Gastroenterology

Submit a Manuscript: http://www.f6publishing.com

World J Gastroenterol 2018 March 28; 24(12): 1312-1320

DOI: 10.3748/wjg.v24.i12.1312

ISSN 1007-9327 (print) ISSN 2219-2840 (online)

ORIGINAL ARTICLE

Case Control Study

Serum interleukin-34 level can be an indicator of liver fibrosis in patients with chronic hepatitis B virus infection

Yin-Qiu Wang, Wen-Jun Cao, Yu-Feng Gao, Jun Ye, Gui-Zhou Zou

Yin-Qiu Wang, Wen-Jun Cao, Yu-Feng Gao, Jun Ye, Gui-Zhou Zou, Department of Infectious Disease, The Second Affiliated Hospital of Anhui Medical University, Hefei 230601, Anhui Province, China

ORCID number: Yin-Qiu Wang (0000-0001-6069-1809); Wen-Jun Cao (0000-0003-1204-592X); Yu-Feng Gao (0000-0003-1822-8161); Jun Ye (0000-0003-4808-5608); Gui-Zhou Zou (0000-0002-4690-5580).

Author contributions: Wang YQ and Cao WJ contributed to the literature search and writing of the manuscript; Ye J, Zou GZ and Gao YF contributed to the original idea, as well as the polishing and final proof of the manuscript.

Supported by Natural Science Foundation of Anhui Province, No. 1608085MH164.

Institutional review board statement: This study was reviewed and approved by the Biomedical Ethics Committee of the Anhui Medical University.

Informed consent statement: All study participants, or their legal guardian, provided informed written consent prior to study enrollment.

Conflict-of-interest statement: The authors have no conflicts of interest to report.

Data sharing statement: Technical appendix, statistical code, and dataset available from the corresponding author at aygyf@126.com. Participants gave informed consent for data sharing.

STROBE statement: The guidelines of the STROBE Statement have been adopted.

Manuscript source: Unsolicited manuscript

Correspondence to: Yu-Feng Gao, MAMS, Professor, Department of Infectious Disease, Second Affiliated Hospital of Anhui Medical University, 678 Furong Road, Economic and Technological Development District, Hefei 230601, Anhui Province, China. aygyf@126.com
Telephone: +86-551-63869420
Fax: +86-551-63869400

Received: January 21, 2018
Peer-review started: January 22, 2018
First decision: February 3, 2018
Revised: February 11, 2018
Accepted: February 26, 2018
Article in press: February 26, 2018
Published online: March 28, 2018

Abstract

AIM

To investigate whether serum interleukin (IL)-34 levels are correlated with hepatic inflammation and fibrosis in patients with chronic hepatitis B virus (HBV) infection.

METHODS

In this study, serum IL-34 levels were assessed by enzyme-linked immunosorbent assay in 19 healthy controls and 175 patients with chronic HBV infection undergoing biopsy. The frequently used serological markers of liver fibrosis were based on laboratory indexes measured at the Clinical Laboratory of the Second Affiliated Hospital of Anhui Medical University. Liver stiffness was detected by transient elastography with FibroTouch. The relationships of non-invasive makers of liver fibrosis and IL-34 levels with inflammation and fibrosis were analyzed. The diagnostic value of IL-34 and other liver fibrosis makers were

evaluated using areas under the receiver operating characteristic curves, sensitivity and specificity.

RESULTS

Serum IL-34 levels were associated with inflammatory activity in the liver, and IL-34 levels differed among phases of chronic HBV infection (P = 0.001). By comparing serum IL-34 levels among patients with various stages of liver fibrosis determined by liver biopsy, we found that IL-34 levels ⩾ 15.83 pg/mL had a high sensitivity of 86.6% and a specificity of 78.7% for identifying severe fibrosis (S3-S4). Furthermore, we showed that IL-34 is superior to the fibrosis-4 score, one of the serum makers of liver fibrosis, in identifying severe liver fibrosis and early cirrhosis in patients with HBV-related liver fibrosis in China.

CONCLUSION

Our results indicate that IL-34, a cytokine involved in the induction of activation of profibrogenic macrophages, can be an indicator of liver inflammation and fibrosis in patients with chronic HBV infection.

Key words: Interleukin 34; Hepatitis B virus; Liver fibrosis; Diagnosis

Core tip: Interleukin (IL)-34 is a cytokine involved in the induction of activation of profibrogenic macrophages, which is associated with the severity of liver fibrosis and inflammation. Numerous studies have shown that it has the potential to be a serological indicator of liver fibrosis and inflammation. We investigated the serum IL-34 levels in patients with chronic hepatitis B virus infection, and found the significance of serum levels of IL-34 as a serum target of liver fibrosis associated with chronic hepatitis B virus infection.

Wang YQ, Cao WJ, Gao YF, Ye J, Zou GZ. Serum interleukin-34 level can be an indicator of liver fibrosis in patients with chronic hepatitis B virus infection. *World J Gastroenterol* 2018; 24(12): 1312-1320 Available from: URL: http://www.wjgnet.com/1007-9327/full/v24/i12/1312.htm DOI: http://dx.doi.org/10.3748/wjg.v24.i12.1312

INTRODUCTION

Liver fibrosis is a process accompanied by wound-healing responses caused by chronic injury and inflammation in the hepatic parenchyma, and it often results in serious complications, including portal hypertension and liver failure. It can lead to cirrhosis, which is identified as the final stage of liver fibrosis[1] and can even evolve into hepatocellular carcinoma. Liver fibrosis is often caused by viral infection, toxins and excess alcohol consumption, among others. Chronic hepatitis B virus (HBV) infection is the most common cause of liver fibrosis in China[2].

Chronic HBV infection is characterized by progressive hepatic fibrosis and inflammation. In addition to the key role of hepatic stellate cells, the progression of liver fibrosis depends on the recruitment and accumulation of inflammatory monocytes, which can locally differentiate into macrophages, to the liver[3]. These macrophages activate hepatic stellate cells and promote and perpetuate fibrosis[4,5]. It has already been confirmed that interleukin (IL)-34 is a kind of macrophage differentiation factor that signals *via* the M-CSF receptor (c-fms or CD115)[6,7] and that its serum levels are elevated in hepatitis C virus (HCV)-infected patients and nonalcoholic fatty liver disease patients with advanced liver fibrosis[3,8,9]. Although IL-34 has been identified as a profibrotic factor associated with chronic HCV infection-mediated fibrosis, data on the serum level and role of IL-34 in chronic HBV-infected patients are lacking.

The indication for antiviral therapy depends on HBV DNA levels, aminotransferase levels and/or the grade of inflammation and fibrosis determined by liver biopsy[10]. However, the extent of disease progression is often insufficiently reflected by aminotransferase levels; additionally, liver biopsy has substantial limitations because of the invasive nature of the process[11]. Up to 40% of patients are ineligible for liver biopsy[12]. Therefore, studies are investigating noninvasive methods for detecting fibrosis[13]. These methods rely on biomarkers that are easily determined using one or more serum indexes, such as aspartate transaminase (AST) to platelet ratio index (APRI), fibrosis-4 (FIB-4) score, and fibrosis index (FI)[14]. Although these methods demonstrate adequate diagnostic performance, they still have some limitations. Liver stiffness, measured *via* transient elastography using FibroTouch, can be reliably used to detect fibrosis in most patients; however, this method cannot be used in patients with ascites or obesity, and its performance varies with operator experience[15].

In this study, we assessed the serum level of IL-34 in 175 chronic HBV-infected patients undergoing biopsy. We also analyzed the correlation between IL-34 and other serum indexes that reflect the extent of liver injury and inflammation and evaluated the possibility of using IL-34 level as a marker of liver fibrosis in patients with chronic HBV infection by comparing it with other assessment methods for liver fibrosis.

MATERIALS AND METHODS

Selection of patients

In total, 175 treatment-naive chronic hepatitis B (CHB) patients who had undergone percutaneous liver biopsies at the Department of Infectious Diseases of the Second Affiliated Hospital of Anhui Medical University from January 2014 to March 2016 were

Table 1 Levels of interleukin-34 in patients with different stages of liver fibrosis

Stage	*n*	Median	95%CI
S0 patients and healthy subjects	34	10.05	9.28-11.27
S1-S2 patients	93	11.53	10.38-13.92
S3-S4 patients	67	19.84	17.34-20.63

CI: Confidence interval.

enrolled in this retrospective study. The inclusion criteria were age ⩾ 16 years, history of HBV infection of more than 6 mo and positivity for hepatitis B surface antigen. The exclusion criteria were concomitant infection with the HCV or human immunodeficiency virus, history of antiviral therapy, compensated or decompensated liver cirrhosis, presence of alcoholic liver disease, nonalcoholic fatty liver disease, autoimmune liver diseases, chronic liver diseases due to other causes and renal insufficiency, inadequate biopsy samples, and incomplete clinical data. Nineteen healthy subjects who gave blood on a voluntary basis served as controls, and written informed consent was obtained. This retrospective study was approved by the Ethics Committee of Anhui Medical University. The study was performed in accordance with the 1975 Declaration of Helsinki.

Cytokine quantification

Blood samples were collected at the time of patient presentation at our department, and serum was separated from blood samples by centrifugation. Serum IL-34 levels were quantified by enzyme-linked immunosorbent assay (R and D Systems, United States).

Liver biopsies and fibrosis staging

Percutaneous liver biopsies were obtained using ultrasound-guided biopsy needles. The specimens were then fixed, paraffin-embedded and stained with hematoxylin and eosin. All liver tissues samples were evaluated by board-certified pathologists who were unaware of the patients' clinical history. Liver fibrosis stages (S0-S4) were determined using the Scheuer's classification system. The lack of fibrosis was characterized as S0, mild fibrosis as S1, moderate fibrosis as S2, severe fibrosis as S3-S4 and cirrhosis as S4.

Other laboratory and virological parameters

Other laboratory parameters including AST, alanine transaminase (ALT), gamma-glutamyl transferase, alkaline phosphatase and bilirubin levels, platelet count and virological test results were routinely evaluated prior to liver biopsy at the Clinical Laboratory of the Second Affiliated Hospital of Anhui Medical University.

Transient elastography

Prior to liver biopsy, liver stiffness was determined using the FibroTouch instrument (Wuxi Hayes Kell Medical Technology Co. Ltd., China) operated by experienced technicians. Ten successful acquisitions were performed for each patient. The median value of the 10 measurements was used for analyses. Liver stiffness was expressed in kilopascals (kPa).

Statistical analysis

All statistical analyses were performed using MedCalc 15.8, GraphPad Prism 5.0 and SPSS 17.0. Differences between groups were tested using the Mann-Whitney *U*-test or Wilcoxon-Mann-Whitney test (for continuous variables and nonparametric analyses for independent samples, respectively). Correlation coefficients (*r*) were calculated with nonparametric Spearman's correlation analyses. Receiver operating characteristic (ROC) curves were generated for the assessment of scores predictive of stages of fibrosis. Area under the curve (AUC), sensitivity and specificity were calculated for each factor. The value with the best sensitivity and specificity in AUC analysis (Youden's index) was chosen as the best cut-off. AUCs were compared using the approach described by Hanley and McNeil. $P < 0.05$ (two-sided) was considered significant.

RESULTS

Serum levels of IL-34 among groups of patients with various fibrosis stages

By investigating the serum levels of IL-34 in 19 healthy controls and 175 patients, we found that IL-34 levels were significantly different among the no fibrosis group (S0 patients and healthy subjects), mild to moderate fibrosis group (S1-S2), and advanced fibrosis group (S3-S4) ($P = 0.000$, Kruskal-Wallis test, two-tailed). The median expression level of IL-34 in S0 patients and healthy subjects was 10.05 pg/mL. The mean expression level of IL-34 was 11.53 pg/mL in S1-S2 patients, and the median increased to 19.84 pg/mL in S3-S4 patients (Table 1). We also found a highly statistically significant difference ($P = 0.000$, Kruskal-Wallis test, two-tailed) among HBV patients with different inflammation grades (Figure 1A).

IL-34 levels in different phases of CHB infection

Based on HBV DNA levels, hepatitis B envelope antigen (HBeAg) status and serum aminotransferase levels, patients were classified into four groups according to the European Association for the Study of the Liver guidelines: immune-tolerant patients ($n = 26$), HBeAg-positive hepatitis patients ($n = 24$), HBeAg-negative

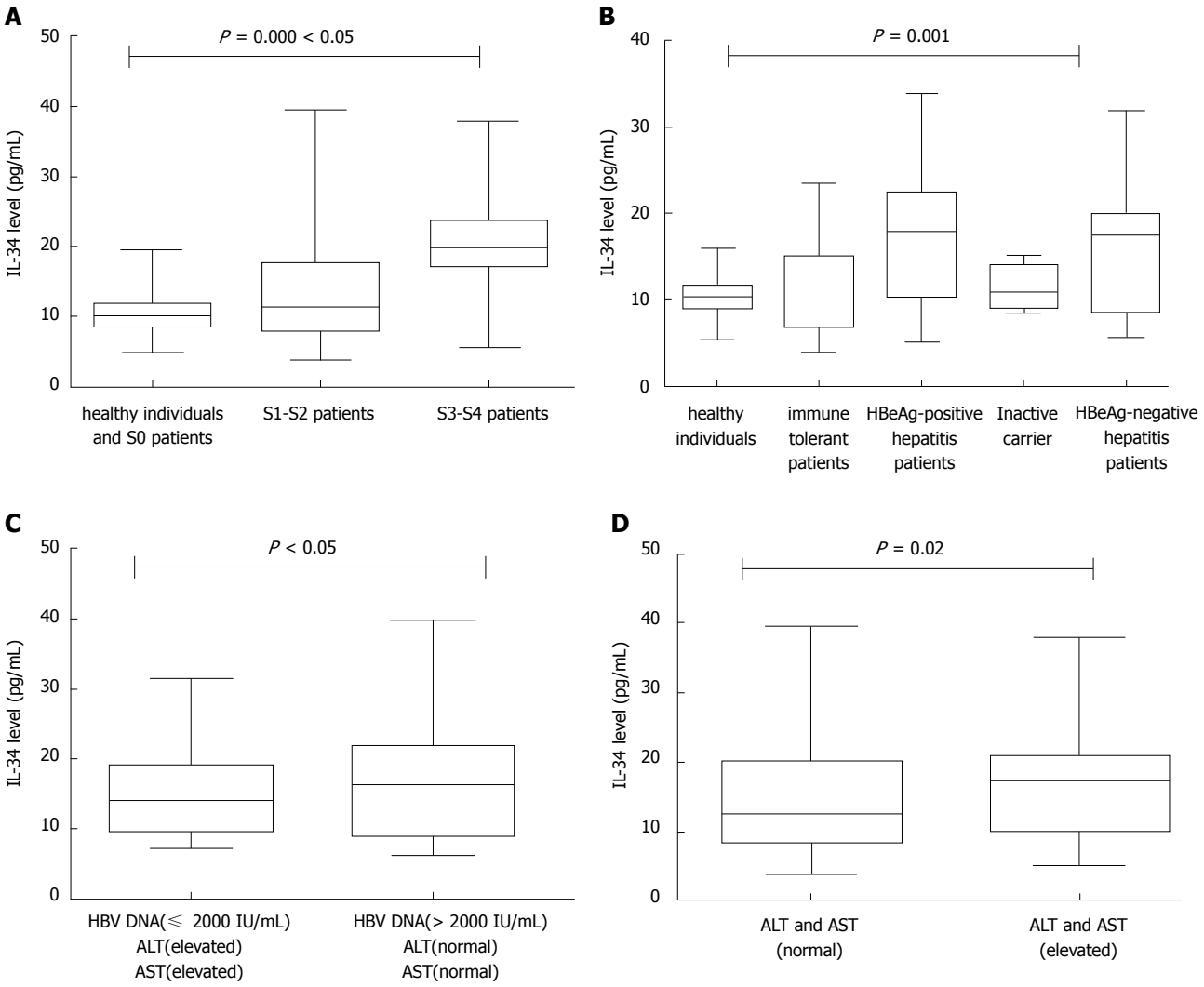

Figure 1 Box-and-whisker plots. A: IL-34 levels in groups of patients with various stages of fibrosis; B: IL-34 levels in groups of different phases of chronic hepatitis B infection; C: IL-34 levels in two groups of HBeAg-negative patients: low viral load (HBV DNA level ≤ 2000 IU/mL) and elevated aminotransferase level; high viral load (HBV DNA level > 2000 IU/mL) and normal aminotransferase level; D: IL-34 levels in group of patients with normal aminotransferase or elevated aminotransferase level. IL: Interleukin; HBeAg: Hepatitis B e antigen; HBV: Hepatitis B virus.

hepatitis patients (n = 40) and inactive carriers (n = 6)[10]. Furthermore, patients with HBeAg-negative status were stratified into two additional groups: patients with low-replicative hepatitis, characterized by low viral load (HBV DNA level ≤ 2000 IU/mL) and elevated aminotransferase levels (n = 13); and patients with high viral load (HBV DNA level > 2000 IU/mL) and normal aminotransferase levels (n = 26)[10].

Serum IL-34 levels were determined in patients and healthy individuals. Serum IL-34 concentrations ranged from 3.90 pg/mL to 39.56 pg/mL in HBV-infected patients and from 5.39 pg/mL to 15.78 pg/mL in healthy individuals. There were highly significant differences in serum IL-34 levels observed between these groups according to the Kruskal-Wallis test (P = 0.001) (Figure 1B). Patients with HBV infection had the highest IL-34 levels, followed by patients with HBeAg-negative or HBeAg-positive hepatitis. In contrast, inactive HBV carriers and immune-tolerant patients had the lowest IL-34 concentrations. Additionally, there were no differences in serum IL-34 levels among inactive HBV carriers, immune-tolerant patients and healthy individuals.

Correlation between IL-34 levels and other laboratory indexes

In patients with liver fibrosis (chronic HBV infection), there was a significant positive correlation between the serum levels of IL-34 and levels of ALT (r = 0.159, P = 0.036), AST (r = 0.257, P = 0.001), total bilirubin (r = 0.199, P = 0.008), indirect bilirubin (r = 0.225, P = 0.003), gamma-glutamyl transferase (r = 0.178, P = 0.018), alkaline phosphatase (r = 0.214, P = 0.004), and platelet count (r = -0.323, P = 0.000) (Figure 2). IL-34 levels were significantly higher in patients with elevated aminotransferase levels than in patients with

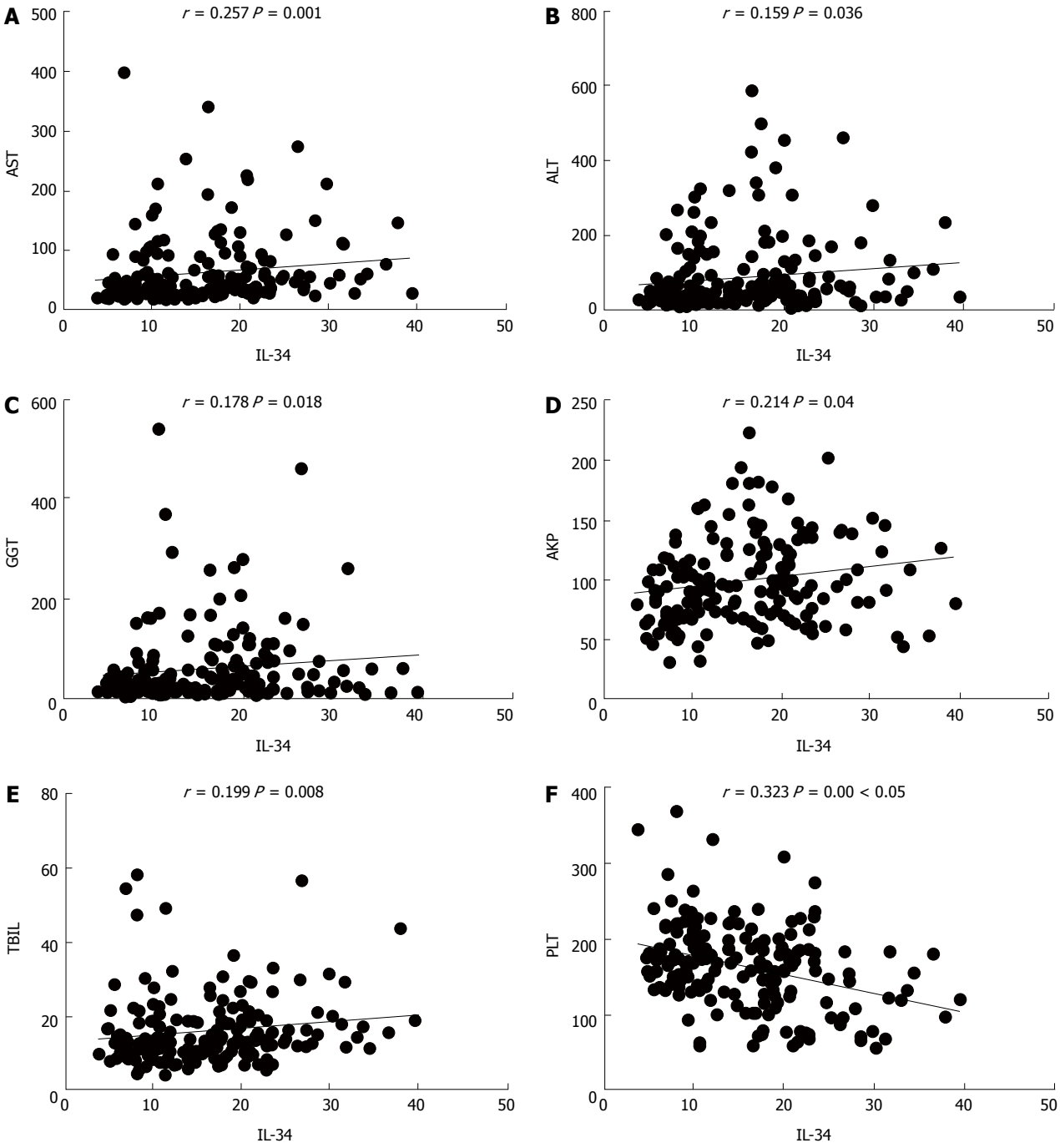

Figure 2 Correlation between IL-34 levels and other laboratory indexes. A: AST; B: ALT; C: GGT; D: AKP; E: TBIL; F: PLT. AKP: Alkaline phosphatase; ALT: Alanine aminotransferase; AST: Aspartate aminotransferase; GGT: Gamma-glutamyl transferase; PLT: Platelet; TBIL: Total bilirubin.

normal aminotransferase levels (P = 0.02) (Figure 1C).

Diagnostic value of IL-34 in predicting severe liver fibrosis

We aimed to determine whether severe liver fibrosis, defined as fibrosis at stages greater than or equal to S3 (S3-S4), in chronic HBV patients is critical for guiding the prognosis and treatment of patients with hepatitis B. Encouraged by our results showing that IL-34 may be a marker of fibrosis stage, we sought to determine whether IL-34 is a marker of severe liver fibrosis (S3-S4) and early cirrhosis (S4). ROC curve analysis resulted in AUCs of 0.829 and 0.836 for severe fibrosis (S3-S4) (Figure 3A) and early cirrhosis (S4) (Figure 3B), respectively. IL-34 levels predicted severe fibrosis (S3-S4) with a sensitivity of 86.6% and a specificity of 78.7%. When IL-34 level > 15.83 pg/mL was used as a cut-off to diagnose severe fibrosis. The sensitivity and specificity of IL-34 on predicting early cirrhosis (S4) are 100% and 64.9%, and the cut-off value is 15.83 pg/mL.

Comparison of IL-34 and several commonly used scores for diagnosing severe liver fibrosis and early cirrhosis

Different fibrosis scores (FIB-4, APRI, Forns and fibrosis-cirrhosis index) have been used to diagnose liver fibrosis or cirrhosis. We compared the performance

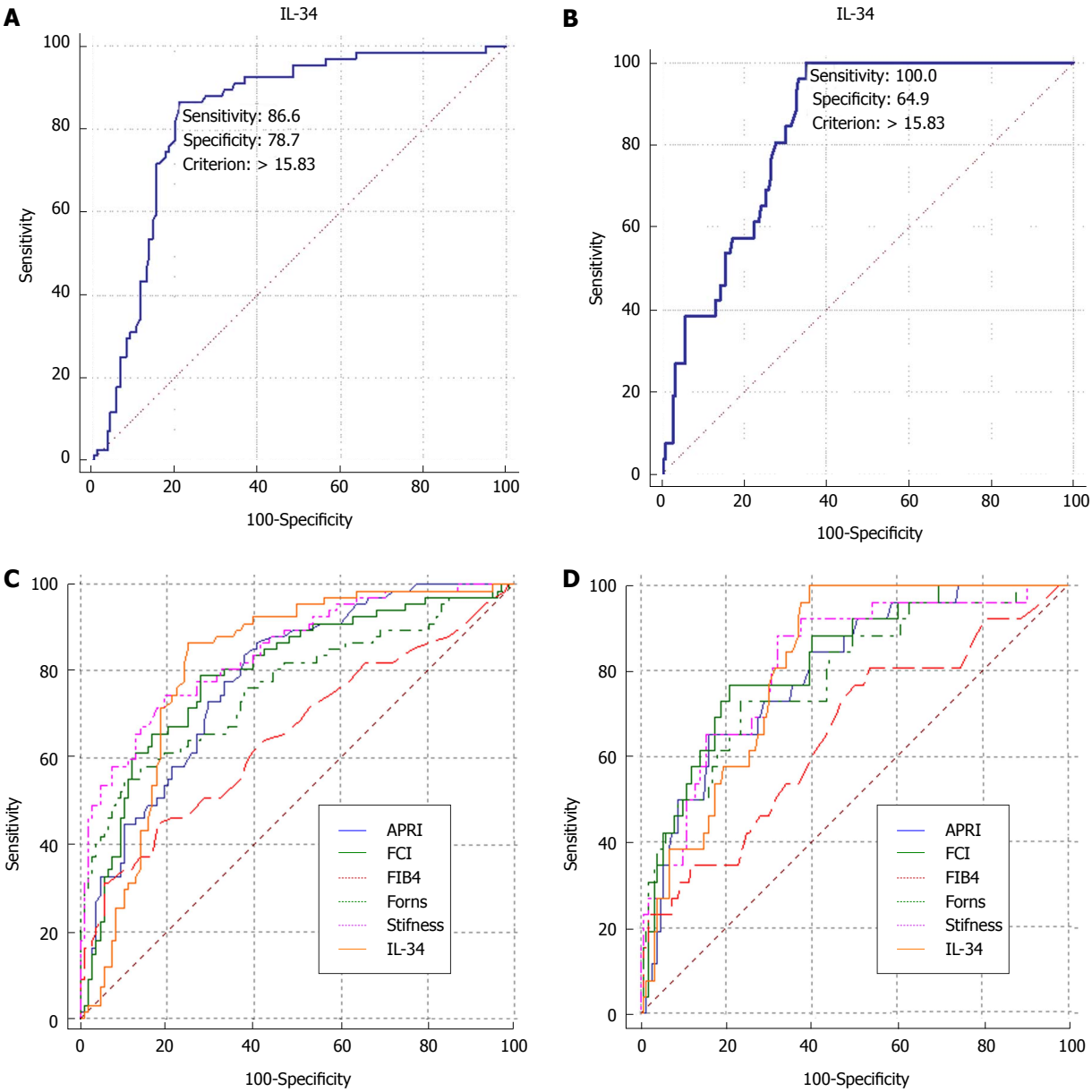

Figure 3 ROC curves, sensitivity and specificity. A: ROC curve analysis for severe fibrosis (S3-S4); B: ROC curve analysis for early cirrhosis (S4); C: AUC comparison of IL-34 level, liver stiffness and other scores for the diagnosis of severe fibrosis (S3-S4); D: AUC comparison of IL-34 level, liver stiffness and other scores for the diagnosis of early cirrhosis (S4). APRI: Aspartate aminotransferase to platelet ratio index; AUC: Area under the curve; FCI: Fibrosis-cirrhosis index; FIB-4: Fibrosis-4; ROC: Receiver operating characteristic.

of IL-34 to the performance of these serum fibrosis scores for the detection of severe liver fibrosis. We conducted a comparative ROC analysis for these scores for individually diagnosing severe liver fibrosis. There were significant differences in AUCs between IL-34 and the FIB-4 score (P = 0.005) in predicting severe fibrosis, indicating that IL-34 was superior to the FIB-4 score. IL-34 was also better than the FIB-4 score in diagnosing early cirrhosis (P = 0.0092). However, for both severe fibrosis and early cirrhosis, the diagnostic accuracy of IL-34 was similar to that of liver stiffness and other scores (Figure 3C and D, Table 2).

DISCUSSION

The correct staging of liver fibrosis is important for guiding the clinical treatment of chronic hepatitis. Liver biopsy, the gold standard for staging liver fibrosis, is invasive and has many limitations[13]. Other recognized noninvasive methods for determining the stage of liver fibrosis also have many disadvantages[16]. Therefore, an increasing number of scholars are investigating noninvasive methods for staging liver fibrosis. In this study, we found that serum IL-34 levels are elevated in HBV-infected patients with severe liver fibrosis (S3-S4) and that IL-34 may be potential marker for differentiating early-stage fibrosis (S0-S2) from late-stage fibrosis (S3-S4) in patients with HBV-related liver fibrosis in China.

This study also clearly demonstrates the diagnostic value of IL-34 as a noninvasive biomarker in the assessment of HBV-related liver fibrosis in patients in

Table 2 Area under the curves for different fibrosis scores for the various stages of fibrosis

	AUC (95%CI)		
	S0 *vs* S1-S4	S3-S4 *vs* S0-S2	S4 *vs* S0-S3
IL-34	0.753 (0.659-0.848)	0.809 (0.743-0.875)	0.815 (0.747-0.883)
APRI	0.714 (0.580-0.847)	0.783 (0.715-0.850)	0.797 (0.710-0.884)
FIB-4	0.577 (0.427-0.727)	0.651 (0.564-0.738)	0.651 (0.529-0.773)
Forns	0.529 (0.405-0.653)	0.762 (0.685-0.839)	0.788 (0.689-0.886)
FCI	0.580 (0.422-0.738)	0.793 (0.723-0.863)	0.822 (0.739-0.906)
Liver stiffness	0.684 (0.565-0.803)	0.844 (0.784-0.903)	0.815 (0.728-0.902)

APRI: Aspartate aminotransferase to platelet ratio index; AUC: Area under the curves; CI: Confidence interval; FCI: Fibrosis-cirrhosis index; FIB-4: Fibrosis-4; IL: Interleukin.

China. We were able to demonstrate IL-34 as predictor of severe liver fibrosis (S3-S4) and early cirrhosis (S4) in HBV-infected patients in China. The AUC of IL-34 was 0.829 for the detection of severe liver fibrosis (S3-S4) and 0.836 for the detection of early cirrhosis (S4). Especially for early cirrhosis (S4) patients, the sensitivity can be up to 100%. This means that it may be possible to avoid missed diagnosis of early cirrhosis. After all, the effective treatments are available to reverse the progress of disease[17]. And, regardless of the situation of ALT and HBeAg, as long as there is an objective basis for cirrhosis, active antiviral therapy is recommended[10].

Compared with other serological models, IL-34 was comparable to the FIB-4 score for the detection of severe liver fibrosis (S3-S4) and early cirrhosis (S4). Even for diagnosing S0 liver fibrosis, IL-34 was comparable to the FIB-4 score (data not shown). Most scholars consider transient elastography to be a promising noninvasive method for the detection of fibrosis in chronic HBV patients[18]. However, this technique is usually only available in specialized centers. Another limitation of transient elastography is that it has a failure rate of approximately 20%, especially in the case of obese individuals[14]. Although the AUC of IL-34 was not significantly different from that of liver stiffness or other fibrosis scores except for FIB-4, IL-34 may be used as a biomarker, as it is sufficient by itself and can be detected in simple-to-obtain samples compared with other established complex fibrosis scores. Perhaps we can also try to combine it with other indicators to improve the effectiveness of disease diagnosis?

Because of the different phases of chronic HBV infection, ranging from stable disease with minimal injury in inactive carriers to rapid cirrhosis development in patients with highly active HBV infection[10], investigations on the mechanisms of liver inflammation and fibrosis together with the establishment of reliable markers for different HBV phases are very meaningful. We showed that serum levels of IL-34, reflective of profibrogenic macrophage activation[3], differ with the phases of HBV infection and are correlated with hepatic inflammation and liver fibrosis.

One of features of hepatotoxic immune responses with increased inflammation and fibrosis in chronic viral hepatitis is the induction of profibrogenic macrophages[3,4]. In accordance with the important role of liver macrophages in HBV-mediated liver damage, we observed high IL-34 levels in patients with HBeAg-positive or HBeAg-negative hepatitis. Patients with HBeAg-positive or HBeAg-negative hepatitis have a high risk of disease progression and development of cirrhosis and hepatocellular carcinoma due to increased hepatic inflammation and fibrogenesis[10,19-21]. In contrast, IL-34 levels in inactive HBV carriers with HBV DNA levels $\leqslant$ 2000 U/mL and normal transaminase levels did not differ from those in healthy subjects, indicating that the low levels of activation of the innate immune system reflect good prognosis[10,19].

Although the IL-34 levels of immune-tolerant patients were markedly different from those of HBeAg-positive or HBeAg-negative hepatitis patients, immune-tolerant patients had comparable IL-34 levels to healthy subjects. This might indicate that if the human immune system fails to respond to HBV, the damage to the liver by the virus is minimal[22]. Liver biopsies in immune-tolerant patients generally show no signs of significant inflammation or fibrosis[23,24]. Given that serum IL-34 concentrations were strongly correlated with aminotransferase levels and could differentiate patients with extensive hepatic inflammation from subjects with reduced inflammatory activity, IL-34 may be used as a potential biomarker for hepatic inflammation.

In summary, IL-34 may aid in the staging of liver fibrosis and diagnosing different phases of HBV infection in China. These processes are critical for guiding the treatment of chronic HBV infection. IL-34 is known to regulate the profibrogenic functions of macrophages by binding to its receptor[3,6,7]. IL-34 and its receptor are highly expressed in hepatocytes in patients with liver fibrosis, mainly in hepatocytes located around fibrotic and inflammatory lesions[3,25]. We hypothesized that by preventing IL-34 from binding with its receptor, the progression of liver fibrosis can be delayed, and inflammation and necrosis of the liver can be prevented. Thus, apart from its above-mentioned function in diagnosis, IL-34 may also be investigated as a therapeutic target for reversing fibrosis.

ARTICLE HIGHLIGHTS

Research background

It is generally believed that the persistence of inflammation plays an important role in the progression of liver fibrosis. Previous studies have shown that interleukin (IL)-34 is an inflammatory cytokine involved in the induction of activation of profibrogenic macrophages, which is associated with the severity of liver fibrosis and inflammation in patients with chronic hepatitis C virus infection and nonalcoholic fatty liver disease.

Research motivation

In order to be helpful to demonstrate the mechanism of liver fibrosis from the perspective of inflammation and provide a new direction for the search of potential new serological diagnostic fibrosis indicators, we investigated the relationship between IL-34 and liver fibrosis in patients with chronic hepatitis B virus (HBV) infection.

Research objectives

This study aimed to investigate whether serum IL-34 levels are correlated with hepatic inflammation and fibrosis in patients with chronic HBV infection.

Research methods

In this study, serum IL-34 levels of 19 healthy controls and 175 patients with chronic HBV infection undergoing biopsy were analyzed.

Research results

We found that the serum IL-34 levels were different among phases of chronic HBV infection and stages of inflammation and fibrosis. We also thought that the serum IL-34 level has potential to diagnose liver fibrosis through comparative analysis of the diagnostic value of IL-34 and other diagnostic methods, except for pathological diagnosis.

Research conclusions

Serum IL-34 level has the potential to be a new indicator of liver inflammation and fibrosis in patients with chronic HBV infection.

Research perspectives

The diagnostic accuracy of serum IL-34 level is not ideal at present. Thus, we can try combining IL-34 with any of other scores and/or with any clinical variable in order to obtain a new "score" with enhanced diagnostic accuracy. Another approach is to increase the sample size for testing.

REFERENCES

1 **Pellicoro A**, Ramachandran P, Iredale JP, Fallowfield JA. Liver fibrosis and repair: immune regulation of wound healing in a solid organ. *Nat Rev Immunol* 2014; **14**: 181-194 [PMID: 24566915 DOI: 10.1038/nri3623]

2 **Liao B**, Wang Z, Lin S, Xu Y, Yi J, Xu M, Huang Z, Zhou Y, Zhang F, Hou J. Significant fibrosis is not rare in Chinese chronic hepatitis B patients with persistent normal ALT. *PLoS One* 2013; **8**: e78672 [PMID: 24205292 DOI: 10.1371/journal.pone.0078672]

3 **Preisser L**, Miot C, Le Guillou-Guillemette H, Beaumont E, Foucher ED, Garo E, Blanchard S, Frémaux I, Croué A, Fouchard I, Lunel-Fabiani F, Boursier J, Roingeard P, Calès P, Delneste Y, Jeannin P. IL-34 and macrophage colony-stimulating factor are overexpressed in hepatitis C virus fibrosis and induce profibrotic macrophages that promote collagen synthesis by hepatic stellate cells. *Hepatology* 2014; **60**: 1879-1890 [PMID: 25066464 DOI: 10.1002/hep.27328]

4 **Tacke F**. Functional role of intrahepatic monocyte subsets for the progression of liver inflammation and liver fibrosis in vivo. *Fibrogenesis Tissue Repair* 2012; **5**: S27 [PMID: 23259611 DOI: 10.1186/1755-1536-5-S1-S27]

5 **Koyama Y**, Brenner DA. Liver inflammation and fibrosis. *J Clin Invest* 2017; **127**: 55-64 [PMID: 28045404 DOI: 10.1172/JCI88881]

6 **Hume DA**, MacDonald KP. Therapeutic applications of macrophage colony-stimulating factor-1 (CSF-1) and antagonists of CSF-1 receptor (CSF-1R) signaling. *Blood* 2012; **119**: 1810-1820 [PMID: 22186992 DOI: 10.1182/blood-2011-09-379214]

7 **Nakamichi Y**, Udagawa N, Takahashi N. IL-34 and CSF-1: similarities and differences. *J Bone Miner Metab* 2013; **31**: 486-495 [PMID: 23740288 DOI: 10.1007/s00774-013-0476-3]

8 **Ma X**, Lin WY, Chen Y, Stawicki S, Mukhyala K, Wu Y, Martin F, Bazan JF, Starovasnik MA. Structural basis for the dual recognition of helical cytokines IL-34 and CSF-1 by CSF-1R. *Structure* 2012; **20**: 676-687 [PMID: 22483114 DOI: 10.1016/j.str.2012.02.010]

9 **Shoji H**, Yoshio S, Mano Y, Kumagai E, Sugiyama M, Korenaga M, Arai T, Itokawa N, Atsukawa M, Aikata H, Hyogo H, Chayama K, Ohashi T, Ito K, Yoneda M, Nozaki Y, Kawaguchi T, Torimura T, Abe M, Hiasa Y, Fukai M, Kamiyama T, Taketomi A, Mizokami M, Kanto T. Interleukin-34 as a fibroblast-derived marker of liver fibrosis in patients with non-alcoholic fatty liver disease. *Sci Rep* 2016; **6**: 28814 [PMID: 27363523 DOI: 10.1038/srep28814]

10 **European Association for the Study of the Liver**; European Association for the Study of the Liver. EASL 2017 Clinical Practice Guidelines on the management of hepatitis B virus infection. *J Hepatol* 2017; **67**: 370-398 [PMID: 28427875 DOI: 10.1016/j.jhep.2017.03.021]

11 **Afdhal NH**. Biopsy or biomarkers: is there a gold standard for diagnosis of liver fibrosis? *Clin Chem* 2004; **50**: 1299-1300 [PMID: 15277345 DOI: 10.1373/clinchem.2004.035899]

12 **Beinhardt S**, Staettermayer AF, Rutter K, Maresch J, Scherzer TM, Steindl-Munda P, Hofer H, Ferenci P. Treatment of chronic hepatitis C genotype 1 patients at an academic center in Europe involved in prospective, controlled trials: is there a selection bias? *Hepatology* 2012; **55**: 30-38 [PMID: 21932410 DOI: 10.1002/hep.24671]

13 **Sharma S**, Khalili K, Nguyen GC. Non-invasive diagnosis of advanced fibrosis and cirrhosis. *World J Gastroenterol* 2014; **20**: 16820-16830 [PMID: 25492996 DOI: 10.3748/wjg.v20.i45.16820]

14 **Castera L**. Noninvasive methods to assess liver disease in patients with hepatitis B or C. *Gastroenterology* 2012; **142**: 1293-1302.e4 [PMID: 22537436 DOI: 10.1053/j.gastro.2012.02.017]

15 **Degos F**, Perez P, Roche B, Mahmoudi A, Asselineau J, Voitot H, Bedossa P; FIBROSTIC study group. Diagnostic accuracy of FibroScan and comparison to liver fibrosis biomarkers in chronic viral hepatitis: a multicenter prospective study (the FIBROSTIC study). *J Hepatol* 2010; **53**: 1013-1021 [PMID: 20850886 DOI: 10.1016/j.jhep.2010.05.035]

16 **Motola DL**, Caravan P, Chung RT, Fuchs BC. Noninvasive Biomarkers of Liver Fibrosis: Clinical Applications and Future Directions. *Curr Pathobiol Rep* 2014; **2**: 245-256 [PMID: 25396099 DOI: 10.1007/s40139-014-0061-z]

17 **Chang TT**, Liaw YF, Wu SS, Schiff E, Han KH, Lai CL, Safadi R, Lee SS, Halota W, Goodman Z, Chi YC, Zhang H, Hindes R, Iloeje U, Beebe S, Kreter B. Long-term entecavir therapy results in the reversal of fibrosis/cirrhosis and continued histological improvement in patients with chronic hepatitis B. *Hepatology* 2010; **52**: 886-893 [PMID: 20683932 DOI: 10.1002/hep.23785]

18 **Chon YE**, Choi EH, Song KJ, Park JY, Kim DY, Han KH, Chon CY, Ahn SH, Kim SU. Performance of transient elastography for the staging of liver fibrosis in patients with chronic hepatitis B: a meta-analysis. *PLoS One* 2012; **7**: e44930 [PMID: 23049764 DOI: 10.1371/journal.pone.0044930]

19 **Fattovich G**, Bortolotti F, Donato F. Natural history of chronic hepatitis B: special emphasis on disease progression and prognostic factors. *J Hepatol* 2008; **48**: 335-352 [PMID: 18096267 DOI: 10.1016/j.jhep.2007.11.011]

20 **Villeneuve JP**. The natural history of chronic hepatitis B virus infection. *J Clin Virol* 2005; **34** Suppl 1: S139-S142 [PMID: 16461215 DOI: 10.1016/S1386-6532(05)80024-1]

21 **Fattovich G**, Boscaro S, Noventa F, Pornaro E, Stenico D, Alberti A, Ruol A, Realdi G. Influence of hepatitis delta virus infection on progression to cirrhosis in chronic hepatitis type B.

J Infect Dis 1987; **155**: 931-935 [PMID: 3559292 DOI: 10.1093/infdis/155.5.931]

22 **Hui CK**, Leung N, Yuen ST, Zhang HY, Leung KW, Lu L, Cheung SK, Wong WM, Lau GK; Hong Kong Liver Fibrosis Study Group. Natural history and disease progression in Chinese chronic hepatitis B patients in immune-tolerant phase. *Hepatology* 2007; **46**: 395-401 [PMID: 17628874 DOI: 10.1002/hep.21724]

23 **Mani H**, Kleiner DE. Liver biopsy findings in chronic hepatitis B. *Hepatology* 2009; **49**: S61-S71 [PMID: 19399798 DOI: 10.1002/hep.22930]

24 **Shao J**, Wei L, Wang H, Sun Y, Zhang LF, Li J, Dong JQ. Relationship between hepatitis B virus DNA levels and liver histology in patients with chronic hepatitis B. *World J Gastroenterol* 2007; **13**: 2104-2107 [PMID: 17465456 DOI: 10.3748/wjg.v13.i14.2104]

25 **Jia JB**, Wang WQ, Sun HC, Zhu XD, Liu L, Zhuang PY, Zhang JB, Zhang W, Xu HX, Kong LQ, Lu L, Wu WZ, Wang L, Tang ZY. High expression of macrophage colony-stimulating factor-1 receptor in peritumoral liver tissue is associated with poor outcome in hepatocellular carcinoma after curative resection. *Oncologist* 2010; **15**: 732-743 [PMID: 20551429 DOI: 10.1634/theoncologist.2009-0170]

P- Reviewer: Vespasiani-Gentilucci U **S- Editor**: Ma YJ
L- Editor: Filipodia **E- Editor**: Huang Y

World Journal of Gastroenterology

Submit a Manuscript: http://www.f6publishing.com

World J Gastroenterol 2018 March 28; 24(12): 1321-1331

DOI: 10.3748/wjg.v24.i12.1321

ISSN 1007-9327 (print) ISSN 2219-2840 (online)

ORIGINAL ARTICLE

Retrospective Cohort Study

Model combining pre-transplant tumor biomarkers and tumor size shows more utility in predicting hepatocellular carcinoma recurrence and survival than the BALAD models

Nicha Wongjarupong, Gabriela M Negron-Ocasio, Roongruedee Chaiteerakij, Benyam D Addissie, Essa A Mohamed, Kristin C Mara, William S Harmsen, J Paul Theobald, Brian E Peters, Joseph G Balsanek, Melissa M Ward, Nasra H Giama, Sudhakar K Venkatesh, Denise M Harnois, Michael R Charlton, Hiroyuki Yamada, Alicia Algeciras-Schimnich, Melissa R Snyder, Terry M Therneau, Lewis R Roberts

Nicha Wongjarupong, Gabriela M Negron-Ocasio, Benyam D Addissie, Essa A Mohamed, Nasra H Giama, Michael R Charlton, Lewis R Roberts, Division of Gastroenterology and Hepatology, Mayo Clinic, Rochester, MN 55905, United States

Gabriela M Negron-Ocasio, University of Puerto Rico Medical Sciences Campus, San Juan 00921, Puerto Rico

Nicha Wongjarupong, Roongruedee Chaiteerakij, Department of Medicine, Faculty of Medicine, Chulalongkorn University and King Chulalongkorn Memorial Hospital, Thai Red Cross Society, Bangkok 10400, Thailand

Kristin C Mara, William S Harmsen, Terry M Therneau, Division of Biomedical Statistics and Informatics, Mayo Clinic, Rochester, MN 55905, United States

J Paul Theobald, Brian E Peters, Joseph G Balsanek, Melissa M Ward, Alicia Algeciras-Schimnich, Melissa R Snyder, Division of Laboratory Medicine, Department of Laboratory Medicine and Pathology, Mayo Clinic College of Medicine, Rochester, MN 55905, United States

Sudhakar K Venkatesh, Department of Radiology, Mayo Clinic College of Medicine, Rochester, MN 55905, United States

Denise M Harnois, Department of Transplantation, Mayo Clinic Florida, Jacksonville, FL 32224, United States

Hiroyuki Yamada, Wako Life Sciences, Incorporated, Mountain View, CA 94043, United States

ORCID number: Nicha Wongjarupong (0000-0001-8676-413X); Gabriela M Negron-Ocasio (0000-0002-8484-8601); Roongruedee Chaiteerakij (0000-0002-7191-3881); Benyam D Addissie (0000-0001-8772-7074); Essa A Mohamed (0000-0002-0307-6241); Kristin C Mara (0000-0001-9824-6049); William S Harmsen (0000-0001-7134-5362); J Paul Theobald (0000-0002-5730-8925); Brian E Peters (0000-0003-2485-0766); Joseph G Balsanek (0000-0003-2929-2871); Mellisa M Ward (0000-0001-9784-9518); Nasra H Giama (0000-0003-2764-866X); Sudhakar K Venkatesh (0000-0002-7514-1030); Denise M Harnois (0000-0001-7307-2900); Michael R Charlton (0000-0002-8766-7494); Hiroyuki Yamada (0000-0002-1827-3758); Alicia Algeciras-Schimnich (0000-0002-4455-6217); Melissa R Snyder (0000-0002-5442-4699); Terry M Therneau (0000-0003-1490-6711); Lewis R Roberts (0000-0001-7885-8574).

Author contributions: Wongjarupong N, Chaiteerakij R and Roberts LR designed research; Wongjarupong N, Chaiteerakij R, Negron-Ocasio GM, Addissie BD, Mohamed EA, Giama NH, Venkatesh SK, Harnois DM and Charlton MR performed research; Theobald JP, Peters BE, Balsanek JG, Ward MM, Yamada H, Algeciras-Schimnich A and Synder MR contributed new reagents and analytic tools; Mara KC, Harmsen WS, Therneau TM analyzed data; Wongjarupong N, Negron-Ocasio GM, Roberts LR wrote the paper.

Supported by Mayo Clinic Center for Clinical and Translational Science (CCATS), No. NCATS 1UL1TR002377-01; Mayo Clinic Center for Cell Signaling in Gastroenterology, No. NIDDK P30DK084567-09; and Wako Life Sciences, Inc.

Institutional review board statement: This study was approved by Mayo Clinic Institutional Review Board (IRB 17-001912).

Informed consent statement: The IRB waived the requirement written informed consent for this minimal risk retrospective study.

Conflict-of-interest statement: Roberts LR has received grant funding from BTG, Gilead Sciences and Wako Life Sciences; Yamada H is an employee of Wako Life Sciences. There are no other potential conflicts of interest for the rest of the authors.

Manuscript source: Invited manuscript

Correspondence to: Lewis R Roberts, MB ChB, PhD, Professor of Medicine, Consultant, Division of Gastroenterology and Hepatology, Mayo Clinic Rochester, 200 First Street SW Rochester, MN 55905, United States. roberts.lewis@mayo.edu
Telephone: +1-507-2664720
Fax: +1-507-2840762

Received: December 3, 2017
Peer-review started: December 4, 2017
First decision: December 13, 2017
Revised: March 10, 2018
Accepted: March 18, 2018
Article in press: March 18, 2018
Published online: March 28, 2018

Abstract

AIM

To assess the performance of BALAD, BALAD-2 and their component biomarkers in predicting outcome of hepatocellular carcinoma (HCC) patients after liver transplant.

METHODS

BALAD score and BALAD-2 class are derived from bilirubin, albumin, alpha-fetoprotein (AFP), Lens culinaris agglutinin-reactive AFP (AFP-L3), and des-gamma-carboxyprothrombin (DCP). Pre-transplant AFP, AFP-L3 and DCP were measured in 113 patients transplanted for HCC from 2000 to 2008. Hazard ratios (HR) for recurrence and death were calculated. Univariate and multivariate regression analyses were conducted. C-statistics were used to compare biomarker-based to predictive models.

RESULTS

During a median follow-up of 12.2 years, 38 patients recurred and 87 died. The HRs for recurrence in patients with elevated AFP, AFP-L3, and DCP defined by BALAD cut-off values were 2.42 (1.18-5.00), 1.86 (0.98-3.52), and 2.83 (1.42-5.61), respectively. For BALAD, the HRs for recurrence and death per unit increased score were 1.48 (1.15-1.91) and 1.59 (1.28-1.97). For BALAD-2, the HRs for recurrence and death per unit increased class were 1.45 (1.06-1.98) and 1.38 (1.09-1.76). For recurrence prediction, the combination of three biomarkers had the highest c-statistic of 0.66 vs. 0.64, 0.61, 0.53, and 0.53 for BALAD, BALAD-2, Milan, and UCSF, respectively. Similarly, for death prediction, the combination of three biomarkers had the highest c-statistic of 0.66 *vs* 0.65, 0.61, 0.52, and 0.50 for BALAD, BALAD-2, Milan, and UCSF. A new model combining biomarkers with tumor size at the time of transplant (S-LAD) demonstrated the highest predictive capability with c-statistics of 0.71 and 0.69 for recurrence and death.

CONCLUSION

BALAD and BALAD-2 are valid in transplant HCC patients, but less predictive than the three biomarkers in combination or the three biomarkers in combination with maximal tumor diameter (S-LAD).

Key words: Alpha-fetoprotein; AFP-L3; Des-gamma-carboxyprothrombin; BALAD; BALAD-2; Hepatocellular carcinoma; Liver transplant; Recurrence; Outcome

Core tip: BALAD score and BALAD-2 class incorporating alpha-fetoprotein (AFP), AFP-L3, and des-gamma-carboxyprothrombin are used to predict survival of patients with hepatocellular carcinoma. However, there were limited numbers of patients who received liver transplant in previous cohorts in which performance of the BALAD was studied. Our study showed that pre-transplant BALAD score and BALAD-2 class are useful for predicting outcome of hepatocellular carcinoma patients receiving liver transplant. However, a more predictive model uses the combination of all three biomarkers using the cut-offs from the BALAD score along with maximum tumor size at the time of transplant.

Wongjarupong N, Negron-Ocasio GM, Chaiteerakij R, Addissie BD, Mohamed EA, Mara KC, Harmsen WS, Theobald JP, Peters BE, Balsanek JG, Ward MM, Giama NH, Venkatesh SK, Harnois DM, Charlton MR, Yamada H, Algeciras-Schimnich A, Snyder MR, Therneau TM, Roberts LR. Model combining pre-transplant tumor biomarkers and tumor size shows more utility in predicting hepatocellular carcinoma recurrence and survival than the BALAD models. *World J Gastroenterol* 2018; 24(12): 1321-1331 Available from: URL: http://www.wjgnet.com/1007-9327/full/v24/i12/1321.htm DOI: http://dx.doi.org/10.3748/wjg.v24.i12.1321

INTRODUCTION

The incidence of hepatocellular carcinoma (HCC) in the United States has increased 3-fold in the last 30 years[1]. Currently, liver cancer has also become the second leading cause of cancer-related deaths worldwide[2]. Liver transplant is one of the few curative treatments that can achieve a 5-year survival rate of 70% for some HCC patients. However, to be eligible for a liver transplant, patients with HCC have to meet a rigorous set of criteria. Despite these selection criteria, recurrence of cancer is seen in up to 20% of HCC patients that undergo liver transplantation[3].

This high proportion of recurrences calls into question the liver transplant guidelines used for patients with cancer. For patients with HCC, the Milan and UCSF criteria have been used as standards to determine the eligibility for liver transplant[4,5]. Although adherence to the Milan criteria has been associated with relatively lower recurrence rates after transplantation, it is still considered suboptimal because it relies primarily on tumor morphologic characteristics[6]. Other liver transplant guidelines have been proposed, but similar to the Milan and UCSF criteria, they fail to incorporate the biological behavior of the tumor[6,7].

To achieve more objective models for selection of HCC patients for liver transplant, several serum tumor biomarkers have been evaluated to assess the biological aggressiveness of HCC. Multiple studies suggest that high pre-transplant alpha fetoprotein (AFP), a widely known HCC biomarker, is associated with poor post-transplant outcomes[8] and the AFP model, combining alpha-fetoprotein (AFP) with the tumor number and tumor size, has been proposed and validated to predict HCC recurrence[9]. The BALAD score, a model that incorporates the use of 5 serum biomarkers, has been successful in predicting the survival and recurrence of patients with HCC[10]. In addition to assessing the remnant liver function via the Bilirubin and Albumin levels, the BALAD score incorporates 3 additional serum tumor biomarkers, namely AFP, Lens culinaris agglutinin-reactive AFP (AFP-L3), and des-gamma-carboxyprothrombin (DCP). However, previous studies, including a validation study, have only included a limited number of liver transplant patients[11-14].

The aim of this study was to assess the performance of the discontinuous BALAD and continuous BALAD-2 scores in patients who underwent liver transplant for HCC. In addition, we aimed to assess the utility of each component of the BALAD in predicting outcomes and to develop a more effective model for liver transplant patients.

MATERIALS AND METHODS

Study population and data abstraction

There were 299 patients with HCC who underwent liver transplant between January 2000 and December 2008. Of the 299 patients, 113 had available results of all five biomarkers within two days before the liver transplant. The HCC diagnosis criteria included (1) explanted liver pathology; or (2) a new liver mass with largest diameter of > 1 cm, arterial enhancement and portal venous washout on computed tomography or magnetic resonance imaging. Patients with warfarin use and congenital biliary disorder which could alter the bilirubin level, such as Gilbert disease, were excluded. The transplant selection criteria for the HCC patients during the study period were primarily based on the Milan criteria. Staging within the extended UCSF criteria was accepted in 17 patients based on provider selection and organ availability at the time of transplant. Most patients with intermediate stage disease beyond Milan criteria received locoregional treatment with transarterial chemoembolization prior to liver transplantation. For surveillance for post-transplant HCC recurrence, patients underwent CT scan of the abdomen and chest along with serum AFP at 4, 8, 12, 18, and 24 mo post-transplant.

Patient age, sex, race, etiology of liver disease, date of HCC diagnosis, date of liver transplant, baseline tumor characteristics at the time of diagnosis, and at the time of imaging closest to the transplant (diameter of the largest tumor, tumor number, macrovascular invasion), biomarker results, recurrence date, death date and last follow-up date were abstracted. The Child-Turcotte-Pugh (CTP) class and MELD score were calculated at the time closest to liver transplant in every patient regardless of cirrhosis status. Tumor size and tumor number were also determined from the most recent imaging study prior to the transplant. The Milan and UCSF criteria were also determined from the imaging prior to and closest to the transplant date. HCC recurrence was defined by the presence of new malignant masses seen on imaging, either intrahepatic or extrahepatic metastases, as assessed by the radiologist. The tumor response to treatment was assessed according to the modified Response Evaluation Criteria in Solid Tumors (mRECIST), version 1.0. The survival of patients who were lost to follow-up was obtained using the Accurint system.

BALAD score and BALAD-2 class were calculated based on five biomarkers including total bilirubin, albumin, AFP, AFP-L3, and DCP measured within the two days prior to transplant (Tables 1 and 2). The GALAD and GALAD-z scores were also calculated based on gender, age, and biomarkers within the same period (Table 3).

Measurement of biomarkers

Serum samples were collected and stored at -80 ℃. AFP, AFP-L3, and DCP were measured simultaneously using a liquid-phase binding assay on the μTASWako i30 instrument (Wako Life Sciences Inc., Mountain View, CA, United States). Details of the sample processing and biomarker results were previously published[15].

Statistical analysis

Baseline characteristics were reported as mean ± standard deviation (SD) or median and interquartile range for continuous variables, and percentage for categorical variables. Hazard ratios (HRs) for time to recurrence and death were calculated for each variable and each BALAD score and BALAD-2 class grouping. HRs were presented as HR (95%CI, *P* value). C statistics were used to compare different scores. All analyses were performed using SAS 9 (SAS Institute, Cary, NC, United States). $P < 0.05$ was considered as

Table 1 BALAD score calculation

	0 point	1 point	2 points	3 points
Bilirubin (mg/dL)	< 1.0	1.0-2.0	> 2.0	
Albumin (g/dL)	> 3.5	2.8-3.5	< 2.8	
Summation of these 2 points, then classified as A (0-1), B (2-3), C (4)				
Albumin-Bilirubin	A	B	C	-
No. of elevated markers[1]	0	1	2	3
Summation of these 2 points for BALAD score (0-5)				

[1]Defined by AFP > 400 ng/mL, AFP-L3 > 15%, and DCP > 100 ng/mL.

Table 2 BALAD-2 class calculation

Linear predictor = 0.02 × (AFP - 2.57) + 0.012 × [(AFP-L3) - 14.19] + 0.19 × [ln(DCP) - 1.93] + 0.17 × [(bilirubin)$^{1/2}$ - 4.50] - 0.09 × (albumin - 35.11)
AFP capped at 50000 units. AFP and DCP modeled as /1000 units.
Units: Bilirubin (μmol/L), albumin (g/L), AFP and DCP (ng/mL), AFP-L3 (%).
class 1 (≤ -1.74), class 2 (> -1.74 to -0.91), class 3 (> -0.91 to 0.24), class 4 (> 0.24)

Table 3 GALAD-z and GALAD score calculation

GALAD-z = -10.08 + 0.09 × (Age) + 1.67 × (sex) + 2.34 × log(AFP) + 0.04 × (AFP-L3) + 1.33 × log(DCP)
GALAD score = exp (GALAD-z)/[1 + exp(GALAD-z)]

Sex = 1 for male and 0 for female.

statistically significant.

RESULTS

Demographic characteristics

Of the 113 included patients, the majority were male (*n* = 86, 76%), with viral hepatitis C as the most common liver disease etiology (*n* = 66, 58%) as shown in Table 4. There were 104 (92%) patients with cirrhosis of whom 13 (12%), 76 (67%), and 24 (21%) patients had CTP class A, B, and C cirrhosis, respectively. There were 1 (1%), 39 (35%), 7 (6%), 40 (35%), and 26 (23%) patients with BCLC stage 0, A, B, C, and D HCC, respectively. There were no patients with portal or nodal invasion. BCLC stages C and D were assigned because of poor ECOG performance status and/or CTP class C cirrhosis. The median (range) of total bilirubin and albumin at the time of transplant were 2.3 (0.2-29.5) mg/dL and 3.2 (2.1-5.2) g/dL. For the tumor biomarkers, the median (range) of AFP, AFP-L3, and DCP were 25.3 (0.8-27800) ng/dL, 12 (1-86.5)%, and 1.2 (0.2-1480) ng/mL, respectively. The median waiting time for the included patients was 2.8 (range 0-20) mo.

Of the 113 included patients, 87 (77%) and 96 (85%) were within Milan and UCSF criteria at the time of diagnosis; and 88 (78%) and 105 (93%) were within Milan and UCSF criteria at the time of transplant, respectively. The AFP level was not included in the transplant selection criteria during the study period. Of the 113 patients, 111 patients received TACE, 1 received RFA and 1 received both TACE and RFA prior to liver transplant. Thirty-nine patients (35%) had available imaging for evaluating the locoregional therapy response. Sixty-nine patients had baseline imaging at the time of HCC diagnosis but did not have follow-up imaging after locoregional therapy as most of these patients underwent transplantation shortly after TACE. Another 5 patients had radiology reports in the medical record but did not have the images available for review as the imaging was performed outside Mayo Clinic. Of the 39 patients with imaging available for assessing the treatment response, 29 (74%) were responders (13 complete response and 16 partial response) and 10 (26%) were non-responders (8 stable disease and 2 progressive disease) according to the mRECIST criteria.

According to the explant pathology reports, there were 19, 53, 16, and 2 patients with well-, moderately-, poorly-, and undifferentiated tumors, respectively. There were 23 patients with no report of tumor differentiation. The correlations of the number of elevated tumor biomarkers according to the BALAD score cut-off with the BALAD score are shown in Supplementary Figure 1. There was no correlation between number of elevated tumor biomarkers (P = 0.34), or BALAD score (P = 0.28) with tumor differentiation.

Factors associated with HCC recurrence and death after liver transplant

During a median follow-up of 12.2 years, 38 patients had recurrence and 87 died. The median survival was 10.2 years. The 3-year and 5-year survivals were 74.3% (95%CI: 66.7%-82.8%) and 66.3% (95%CI:

Table 4 Baseline characteristics of 113 hepatocellular carcinoma patients who underwent liver transplant with available biomarker results *n* (%)

Variables	Value
Age, yr, mean ± SD	58.2 ± 8.3
Male sex	86 (76)
Race	
White	91 (80)
Asian	11 (10)
Others	7 (6)
Unknown	4 (4)
Etiology	
Hepatitis virus C	66 (58)
Hepatitis virus B	11 (10)
Alcohol	14 (12)
Non-alcoholic fatty liver disease or cryptogenic	14 (12)
Others	8 (7)
Cirrhosis	104 (92)
CTP class	
A	13 (12)
B	76 (67)
C	24 (21)
MELD score, median (range)	14.2 (6.4–38.6)
ECOG status	
0	57 (50)
1	34 (30)
2	19 (17)
3	3 (3)
Diameter of the largest tumor at the time of transplant by imaging, cm, mean ± SD	2.7 ± 1.6
Tumor number at the time of transplant	
1	73 (64.6)
2	26 (23.0)
3	7 (6.2)
⩾ 4	7 (6.2)
BCLC staging	
Stage 0	1 (1)
Stage A	39 (35)
Stage B	7 (6)
Stage C	40 (35)
Stage D	26 (23)
Within Milan criteria at diagnosis	87 (77)
Within UCSF criteria at diagnosis	96 (85)
Within Milan criteria at transplant	88 (78)
Within UCSF criteria at transplant	105 (93)
AFP model score > 2	26 (23)
Total bilirubin, mg/dL, median (range)	2.3 (0.2-29.5)
Albumin, g/dL, median (range)	3.2 (2.1-5.2)
AFP, ng/mL, median (range)	25.3 (0.8-27800)
AFP > 400 ng/mL	18 (16)
AFP-L3, %, median (range)	12 (1-86.5)
AFP-L3 > 15%	45 (40)
DCP, ng/mL, median (range)	1.2 (0.2-1480)
DCP > 1.2 ng/mL	56 (50)

AFP: Alpha-fetoprotein; AFP-L3: Lens culinaris agglutinin-reactive alpha-fetoprotein; CTP: Child-Turcotte-Pugh; DCP: Des-gamma-carboxyprothrombin.

58.1%-75.6%).

By Cox proportional hazard ratio, the diameter of the largest tumor at the time of transplant was associated with both transplant outcomes with HRs per centimeter of 1.27 (1.04-1.56, $P = 0.02$) for recurrence and 1.21 (1.03-1.41, $P = 0.02$) for death. A neutrophil-lymphocyte ratio of more than 4 also correlated with outcomes, with HRs of 2.24 (1.17-4.26, $P = 0.04$) for recurrence, and 1.66 (1.004-2.73, $P = 0.048$) for death. We did not find any significant increases in risk of recurrence or death for either tumor number or hypothyroidism (Table 5).

Levels of all three tumor biomarkers that exceeded the BALAD score cut-off were associated with increased recurrence and death outcomes in the transplant cohort, whereas albumin and bilirubin, the other components of the BALAD score, were not associated with either outcome. The HRs for recurrence of elevated AFP, AFP-L3, and DCP according to the BALAD score cut-off were 2.42 (1.18-5.00, $P = 0.02$), 1.86 (0.98-3.52, $P = 0.056$), and 2.83 (1.42-5.61, $P = 0.003$), respectively. Similarly, the HRs for death were 3.27 (1.84-5.80, $P < 0.001$), 1.88 (1.14-3.09, $P = 0.01$), and 2.40 (1.43-4.04, $P < 0.001$), respectively. The cumulative incidence of recurrence curve and Kaplan-Meyer survival curve by number of elevated biomarkers are shown in Figure 1A and B, respectively.

BALAD score and BALAD-2 class and risk of HCC recurrence and death

When classified by the BALAD score, there were 14, 31, 33, 23, 9, and 3 patients with BALAD scores of 0 to 5, respectively. By BALAD-2 class there were 29, 30, 34, and 20 patients in BALAD-2 classes 1 to 4, respectively.

For BALAD scores of 1, 2, 3, 4, and 5 *vs* 0, the HRs for recurrence were 0.70 (0.20-2.47), 1.18 (0.37-3.75), 1.99 (0.62-6.36), 2.97 (0.84-10.58), and 5.02 (0.92-27.54); and HRs for death were 1.14 (0.40-3.23), 2.01 (0.75-5.38), 2.73 (0.99-7.51), 4.68 (1.52-14.36), and 17.40 (3.81-79.47), respectively (Figure 2A and B). The HRs per each unit increase in BALAD score for recurrence and death were 1.48 (1.15-1.91) and 1.59 (1.28-1.97). For BALAD-2 classes 2, 3, and 4 *vs* 1, the HRs for recurrence were 0.41 (0.12-1.32), 1.53 (0.66-3.54), and 2.17 (0.90-5.25); and HRs for death were 1.07 (0.50-2.28), 1.76 (0.87-3.54), and 2.45 (1.16-5.17) (Figure 3A and B). The HRs per each unit increase in BALAD-2 class for recurrence and death were 1.45 (1.06-1.98) and 1.38 (1.09-1.76), respectively. A multivariate model of diameter of the largest tumor with BALAD and BALAD-2 was created (Tables 6 and 7). The risk of recurrence was 1.53 (1.17-2.01) per increase of 1 in the BALAD score and 1.42 (1.05-2.03) per increase of one BALAD-2 class. The risk of death was 1.57 (1.27-1.96) per increase of 1 in the BALAD score and 1.37 (1.07-1.76) per increase of 1 BALAD-2 class.

In addition, the HRs for early recurrence were also calculated. Early recurrence was defined as recurrence occurring within 36 mo after transplant. Of the 38 patients with any recurrence, 31 had early recurrence. The BALAD score had better performance for early than overall recurrence with a HR of 1.66 (1.24-2.22) per each unit increase of BALAD score, whereas the BALAD-2 class had similar performance for both recurrence outcomes with a HR of 1.46 (1.04-2.07) per

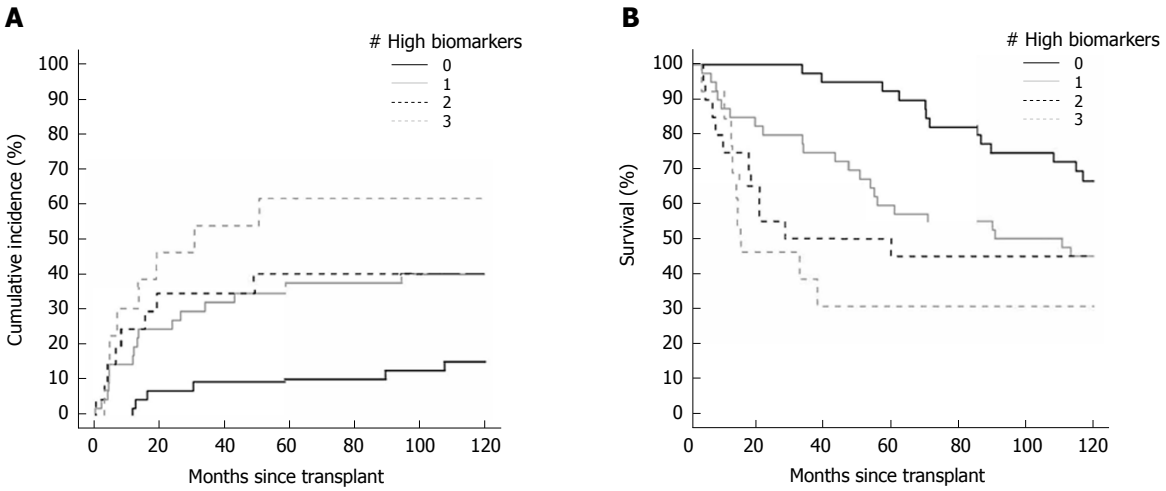

Figure 1 Cumulative incidence of recurrence curve (A) and Kaplan-Meyer survival curve (B) by number of elevated tumor biomarkers.

Table 5 Univariate models for recurrence and death outcome

Variable	Hazard ratio for recurrence		Hazard ratio for death	
	HR (95%CI)	*P* value	HR (95%CI)	*P* value
MELD score (per point)	1.03 (0.98-1.09)	0.26	1.05 (1.003-1.09)	0.04[a]
Diameter of the largest tumor at time of transplant (per cm)	1.27 (1.04-1.56)	0.02[a]	1.21 (1.03-1.41)	0.02
Tumor number at time of transplant	1.001 (0.73-1.37)	1.00	0.93 (0.72-1.20)	0.57
Neutrophil lymphocyte ratio > 4	2.24 (1.17-4.26)	0.02[a]	1.66 (1.004-2.73)	0.048[a]
Hypothyroidism	1.26 (0.55-2.85)	0.59	1.54 (0.82-2.90)	0.18
BALAD components				
Albumin (per g/dL)	0.75 (0.41-1.38)	0.36	0.69 (0.43-1.13)	0.14
Bilirubin (per mg/dL)	1.03 (0.98-1.09)	0.21	1.04 (0.995-1.08)	0.08
AFP: > 400 ng/mL	2.42 (1.18-5.00)	0.02[a]	3.27 (1.84-5.80)	< 0.001[b]
AFP-L3 > 15%	1.86 (0.98-3.52)	0.056	1.88 (1.14-3.09)	0.01[a]
DCP > 1.2 ng/mL	2.83 (1.42-5.61)	0.003[b]	2.40 (1.43-4.04)	< 0001[b]
BALAD Score				
0	Reference		Reference	
1	0.70 (0.20-2.47)	0.58	1.14 (0.40-3.23)	0.81
2	1.18 (0.37-3.75)	0.78	2.01 (0.75-5.38)	0.17
3	1.99 (0.62-6.36)	0.24	2.73 (0.99-7.51)	0.052
4	2.97 (0.84-10.58)	0.09	4.68 (1.52-14.36)	0.007[b]
5	5.02 (0.92-27.54)	0.06	17.40 (3.81-79.47)	< 0.001[b]
BALAD Score (per increase of 1)	1.48 (1.15-1.91)	0.002[b]	1.59 (1.28-1.97)	< 0.001[b]
BALAD-2 Score				
1	Reference		Reference	
2	0.41 (0.12-1.32)	0.13	1.07 (0.50-2.28)	0.86
3	1.53 (0.66-3.54)	0.32	1.76 (0.87-3.54)	0.11
4	2.17 (0.90-5.25)	0.09	2.45 (1.16-5.17)	0.02[a]
BALAD-2 Score (per increase of 1)	1.45 (1.06-1.98)	0.02[a]	1.38 (1.09-1.76)	0.008[b]
Within Milan criteria at diagnosis	1.69 (0.84-3.41)	0.14	2.17 (1.25-3.78)	0.006[b]
Within UCSF criteria at diagnosis	1.85 (0.85-4.05)	0.12	3.19 (1.75-5.84)	< 0.001[b]
Within Milan criteria at transplant	1.24 (0.59-2.62)	0.57	1.06 (0.57-1.95)	0.86
Within UCSF criteria at transplant	0.33 (0.05-2.43)	0.28	0.68 (0.21-2.17)	0.51
z-GALAD	1.12 (1.03-1.21)	0.006[b]	1.12 (1.06-1.19)	< 0.001[b]
GALAD score	3.01 (1.14-7.91)	0.03[a]	3.22 (1.48-7.00)	0.003[b]
AFP model cutoff > 2 (explant)	2.82 (1.47-5.41)	0.002[b]	2.83 (1.67-4.82)	< 0.001[b]
AFP model (per increase of 1, explant)	1.42 (1.20-1.68)	< 0.001[b]	1.34 (1.16-1.54)	< 0.001[b]

[a]$P < 0.05$, [b]$P < 0.01$, statistical difference. AFP: Alpha-fetoprotein; AFP-L3: Lens culinaris agglutinin-reactive alpha-fetoprotein; DCP: Des-gamma-carboxyprothrombin.

increase of 1 class (Supplementary Table 1).

Multivariate model of elevated tumor biomarkers combination with tumor size

Based on the results of the univariate analysis, we combined the elevated tumor biomarkers including AFP, AFP-L3, and DCP with diameter of the largest tumor per centimeter increase in diameter (Table 8). In this multivariate model, diameter of the largest tumor and elevated DCP remained significantly associated with recurrence and death, whereas elevated AFP was only associated with death but not with recurrence.

Table 6 Multivariate model for recurrence outcome with BALAD and BALAD-2

Variable	Hazard ratio with BALAD		Hazard ratio with BALAD-2	
	HR (95%CI)	*P* value	HR (95%CI)	*P* value
Diameter of the largest tumor at time of transplant (per cm)	1.33 (1.07-1.66)	0.02[b]	1.30 (1.05-1.59)	0.014[a]
Neutrophil-lymphocyte ratio	1.55 (0.78-3.14)	0.21	1.76 (0.90-3.49)	0.10
BALAD (per increase of 1)	1.53 (1.17-2.01)	0.002[b]	-	-
BALAD-2 (per increase of 1)	-	-	1.45 (1.05-2.03)	0.02[a]

[a]$P < 0.05$, [b]$P < 0.01$, statistical difference.

Table 7 Multivariate model for death outcome with BALAD and BALAD-2

Variable	Hazard ratio with BALAD		Hazard ratio with BALAD-2	
	HR (95%CI)	*P* value	HR (95%CI)	*P* value
Diameter of the largest tumor at time of transplant (per cm)	1.24 (1.04-1.48)	0.016[a]	1.20 (1.02-1.42)	0.03[a]
Neutrophil-lymphocyte ratio	1.13 (0.67-1.92)	0.64	1.31 (0.78-2.19)	0.31
BALAD (per increase of 1)	1.57 (1.27-1.96)	< 0.0001	-	-
BALAD-2 (per increase of 1)	-	-	1.37 (1.07-1.76)	0.013[a]

[a]$P < 0.05$, [b]$P < 0.01$, statistical difference.

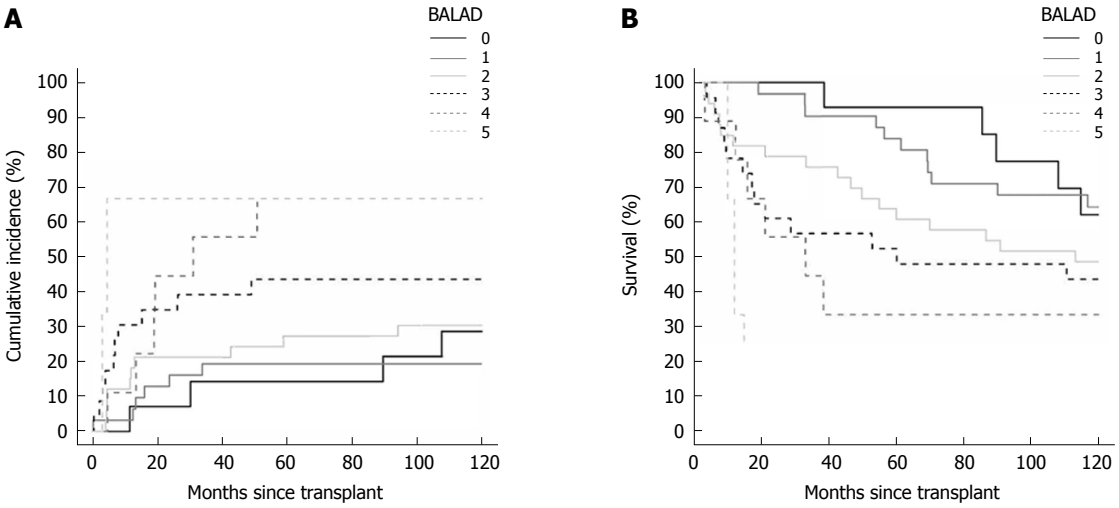

Figure 2 Cumulative incidence of recurrence curve (A) and Kaplan-Meyer survival curve (B) by BALAD score.

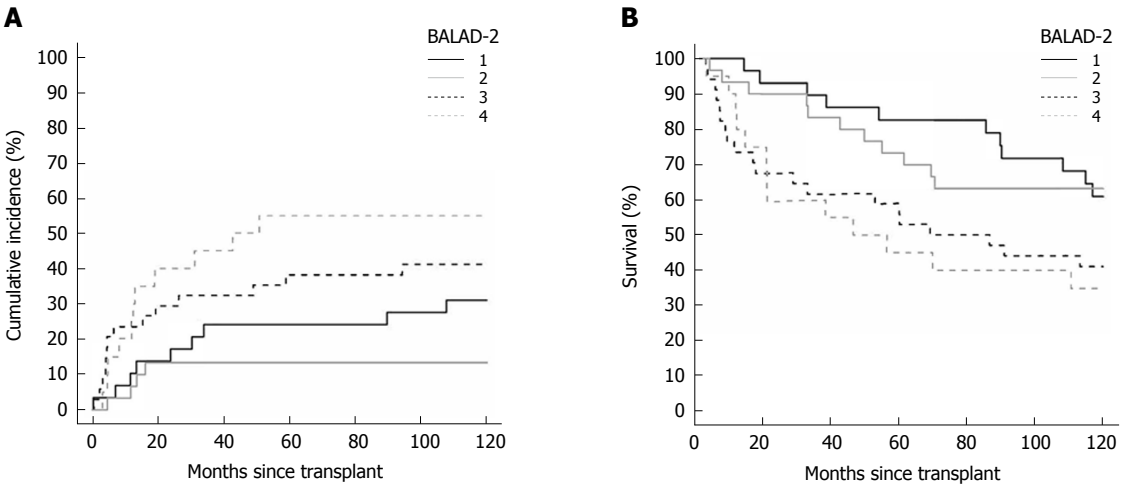

Figure 3 Cumulative incidence of recurrence curve (A) and Kaplan-Meyer survival curve (B) by BALAD-2 class.

Table 8 Multivariate model of biomarkers and tumor size at time of transplant (S-LAD)

Variable	Hazard ratio for recurrence		Hazard ratio for death	
	HR (95%CI)	*P* value	HR (95%CI)	*P* value
Diameter of the largest tumor at time of transplant (per cm)	1.30 (1.05-1.61)	0.02[a]	1.29 (1.08-1.55)	0.006[b]
AFP: > 400 ng/mL	1.63 (0.70-3.83)	0.26	2.40 (1.19-4.83)	0.02[a]
AFP-L3 > 15%	0.995 (0.46-2.18)	0.99	1.01 (0.54-1.88)	0.98
DCP > 1.2 ng/mL	2.69 (1.28-5.64)	0.009[b]	2.33 (1.31-4.13)	0.004[b]
c-statistic (95%CI)	0.71 (0.62-0.81)		0.69 (0.61-0.77)	

[a]$P < 0.05$, [b]$P < 0.01$, statistical difference. AFP: Alpha-fetoprotein; AFP-L3: Lens culinaris agglutinin-reactive alpha-fetoprotein; DCP: Des-gamma-carboxyprothrombin.

Table 9 Comparison of models to predict outcome of liver transplant patients

Variable	c-statistic (95%CI)	
	For recurrence	For death
Number of elevated biomarkers	0.66 (0.57-0.75)	0.66 (0.59-0.73)
BALAD Score (per increase of 1)	0.64 (0.55-0.73)	0.65 (0.58-0.73)
BALAD-2 Score (per increase of 1)	0.61 (0.52-0.70)	0.61 (0.54-0.68)
Within Milan criteria at diagnosis	0.56 (0.49-0.62)	0.58 (0.54-0.63)
Within UCSF criteria at diagnosis	0.55 (0.49-0.60)	0.59 (0.55-0.63)
Within Milan criteria at transplant	0.53 (0.46-0.59)	0.52 (0.47-0.57)
Within UCSF criteria at transplant	0.53 (0.48-0.58)	0.50 (0.47-0.54)
z-GALAD	0.63 (0.53-0.72)	0.64 (0.56-0.72)
GALAD score	0.63 (0.53-0.72)	0.64 (0.56-0.72)
AFP model (explant model)	0.59 (0.51-0.67)	0.58 (0.51-0.65)

AFP-L3 did not relate to either recurrence or death in this multivariate model. The c-statistics for the combined models were 0.71 (0.62-0.81) and 0.69 (0.61-0.77) for recurrence and death, respectively.

Comparisons to the currently used models

The c-statistic was used to compare models which predict outcome of liver transplant patients. A combination of elevated tumor biomarkers based on the BALAD score cut-offs demonstrated the highest c-statistic for prediction of both recurrence and death, with values of 0.66 (0.57-0.75) and 0.66 (0.59-0.73), respectively. For the outcome of recurrence, BALAD and BALAD-2 (per increase of 1 score/class) showed c-statistics of 0.64 (0.55-0.73) and 0.61 (0.52-0.70), respectively. For the outcome of death, BALAD and BALAD-2 showed c-statistics of 0.65 (0.58-0.73) and 0.61 (0.54-0.68). The c-statistics for the Milan and UCSF criteria at the time of diagnosis and prior to transplant, the GALAD, and AFP explant models are shown in Table 9.

DISCUSSION

The pre-transplant BALAD score and BALAD-2 class had a moderate capability to predict both recurrence and death in liver transplant HCC patients. The most predictive model was the combination of three tumor biomarkers using the cut-offs for the BALAD score. In addition, our study showed that large tumor size, high neutrophil-lymphocyte ratio, and elevated individual tumor biomarkers were associated with recurrence and mortality of patients with HCC who underwent transplant.

Tumor size was found to be significantly related to the outcomes in our cohort with HRs per centimeter of 1.27 for recurrence and 1.21 for death. This supports the use of the Milan and UCSF criteria which are based on tumor size, tumor number and vascular invasion[4,5]. The correlation of increased tumor size and elevated tumor biomarkers with outcomes has been shown in previous cohorts[16,17]. Accordingly, the biomarkers can potentially be used as more convenient predictors of patient outcome.

BALAD and BALAD-2 score contain two major components; the bilirubin-albumin score representing liver functional reserve and the three biomarkers representing tumor biology that independently reflect different characteristics of HCC progression[10]. In our study, by using the cut-off of the tumor markers according to the BALAD score, the three tumor biomarkers individually were predictive for recurrence and mortality. This is concordant with many previous studies of HCC patients receiving transplants[8,18]. High biomarker levels can reflect a poor prognosis, as a high DCP level is related to tumor vascular invasion and portal vein thrombosis[19], whereas a high AFP-L3 level has also been found to be related to vascular invasion and infiltrative growth[20].

The differences between the previous cohorts in which the predictive capability of the BALAD score was shown and our current study is the treatment received and the time of biomarker measurement. The nationwide study of HCC in the Japanese population found that the BALAD score was effective, regardless of the treatment[13]. However, this was concluded with a limited proportion of patients in the cohort receiving liver transplant as a treatment. In contrast to the previous studies of the BALAD score, we found that the c-statistic of the combination of the three biomarkers was the highest among all the tested models, including BALAD and BALAD-2. This finding could be explained by the almost immediate restoration of normal functioning of the liver after liver transplant, and thus consequently the less significant roles of bilirubin and albumin as predictors of outcomes after transplant[21].

By combining the three tumor biomarkers with tumor size, we created a model that is more predictive of both recurrence and survival (S-LAD model). A previous study from our group combined each of the biomarkers with the Milan criteria and found a significant improvement in the ability of the Milan criteria to predict recurrence[15]. In addition to this previous study, as HCC is considered a highly heterogeneous disease[22], the combination of the three biomarkers could further improve the predictive model. The GALAD score is another model that uses the combination of biomarkers with sex and age and which was originally developed for predicting risk of HCC in patients with cirrhosis[23]. Interestingly, the GALAD score also showed good performance in predicting both outcomes in our study. However, age and sex were not found to have any correlation with liver transplant outcomes in our study.

It is important to note that the proportion of recurrences after liver transplant in this study is higher than in previous studies in tertiary care centers[3]. Thirty-eight of the 113 patients (33.6%) with available serum had recurrence. However, when considering all HCC patients who underwent liver transplant during the same period, 43 of 299 patients (14.4%) had recurrence. Per report from the Mayo Clinic Transplant Biorepository, serum samples from patients with non-recurrent HCC were more frequently requested, which led to an unequal availability of the samples from patients with and without HCC recurrence. To control for the effect of the difference in sample availability on this study, we compared the characteristics and survival outcomes of non-recurrent patients without samples to those of patients with samples, finding no substantial differences in their baseline characteristics (Supplementary Table 2).

A major strength of this study is that we were able to assess the performance of BALAD, BALAD-2, and their component tumor biomarkers, and included the largest number of transplant HCC patients evaluated thus far. However, there are several limitations to our study. For most of the patients we did not have biomarker results at the time of diagnosis, as was used in the model development and most of the validation cohorts. Thus, the BALAD score and BALAD-2 class at the time of diagnosis were not available for our study. In addition, with the relatively small number of patients, further validation with a larger cohort is needed.

In conclusion, the combination of the three biomarkers used in the BALAD score along with maximal tumor diameter (S-LAD) was the most predictive model for recurrence and death outcomes for HCC patients receiving liver transplants. However, validation of this new S-LAD model is warranted. Unlike the performance for other HCC treatment modalities, the BALAD score and BALAD-2 class are less predictive for recurrence and death in HCC patients with liver transplant, presumably because liver function is restored after liver transplantation.

ARTICLE HIGHLIGHTS

Research background

Liver transplant is one of the curative treatments for hepatocellular carcinoma (HCC). However, with the limited availability of donor organs, it is essential to select patients who will derive the most benefit from transplant. The alpha-fetoprotein (AFP) model has been widely used for this purpose. In the development cohort of the BALAD model by Toyoda *et al*, liver transplant patients were excluded. In the validation cohort in four countries by Chan *et al*, there were only 21 transplant patients included, and in the Japan Nationwide study from Toyoda *et al*, an unknown number of transplant patients were classified in the other treatment group. There is therefore very limited data on the utility of the BALAD model in patients with liver transplant.

Research motivation

The BALAD model has been shown to be a promising predictor of outcome in hepatocellular carcinoma patients receiving most treatment modalities, but there is very limited data on its performance in hepatocellular carcinoma patients receiving liver transplants. The BALAD model incorporates three tumor biomarkers which represent the underlying biology of hepatocellular carcinomas, as well as the serum bilirubin and albumin, which reflect the extent of the underlying liver dysfunction in patients with chronic liver disease. Individually, the AFP, AFP-L3, and des-gamma-carboxyprothrombin (DCP) have been shown to predict the recurrence and survival of hepatocellular carcinoma patients receiving liver transplants. However, presumably due to replacement of the diseased liver during transplantation, it has been shown that the serum bilirubin and albumin are not predictive of patient outcomes post liver transplant.

Research objectives

We aimed to assess the performance of the discontinuous BALAD and continuous BALAD-2 scores in patients who underwent liver transplant for HCC. Further, we assessed the performance of each component of the BALAD in predicting outcomes and propose a more effective model for liver transplant patients.

Research methods

We included patients with hepatocellular carcinoma receiving liver transplants between 2000 and 2008 for whom blood samples were available to allow testing and calculation of the BALAD scores. Patient characteristics, the components of the BALAD model, BALAD score, and BALAD-2 class were analyzed to calculate hazard ratios for recurrence and death. Currently used predictive models including the Milan and UCSF criteria, GALAD score, and AFP model were compared with the BALAD models using c-statistics. A new multivariate model incorporating the three tumor markers and largest tumor diameter was created from these statistically significant variables. The long follow-up period allows assessment of the long term outcomes of the liver transplant patients.

Research results

113 patients were included in the study. The diameter of the largest tumor at the time of transplant, neutrophil-lymphocyte ratio of more than 4, elevated AFP, AFP-L3, and DCP by BALAD score cut-off were associated with both recurrence and death. The HRs per each unit increase in BALAD score for recurrence and death were 1.48 (1.15-1.91) and 1.59 (1.28-1.97). The HRs per each unit increase in BALAD class for recurrence and death were 1.45 (1.06-1.98) and 1.38 (1.09-1.76), respectively. By c-statistics, a model based on the combination of AFP, AFP-L3, and DCP using the BALAD score cut-off had a higher predictive performance than any of the prior models (0.66 for both recurrence and death). Further, a multivariate model incorporating the three biomarkers and the largest diameter of the tumor, designated the S-LAD model, showed a higher c-statistic than all other models (0.71 for recurrence and 0.69 for death). The main limitation of this study is the need for validation of the S-LAD model.

Research conclusions

BALAD and BALAD-2 are valid in transplant HCC patients, but less predictive than the three biomarkers in combination or the three biomarkers in combination

with largest tumor diameter (S-LAD).

Research perspectives

Due to the limited number of patients included, further cohort studies to assess the performance of the BALAD and S-LAD models in hepatocellular carcinoma patients receiving liver transplant are warranted.

REFERENCES

1 **Rahib L**, Smith BD, Aizenberg R, Rosenzweig AB, Fleshman JM, Matrisian LM. Projecting cancer incidence and deaths to 2030: the unexpected burden of thyroid, liver, and pancreas cancers in the United States. *Cancer Res* 2014; **74**: 2913-2921 [PMID: 24840647 DOI: 10.1158/0008-5472.can-14-0155]

2 **GBD 2013 Mortality and Causes of Death Collaborators**. Global, regional, and national age-sex specific all-cause and cause-specific mortality for 240 causes of death, 1990-2013: a systematic analysis for the Global Burden of Disease Study 2013. *Lancet* 2015; **385**: 117-171 [PMID: 25530442 DOI: 10.1016/s0140-6736(14)61682-2]

3 **Zimmerman MA**, Ghobrial RM, Tong MJ, Hiatt JR, Cameron AM, Hong J, Busuttil RW. Recurrence of hepatocellular carcinoma following liver transplantation: a review of preoperative and postoperative prognostic indicators. *Arch Surg* 2008; **143**: 182-8; discussion 188 [PMID: 18283144 DOI: 10.1001/archsurg.2007.39]

4 **Mazzaferro V**, Regalia E, Doci R, Andreola S, Pulvirenti A, Bozzetti F, Montalto F, Ammatuna M, Morabito A, Gennari L. Liver transplantation for the treatment of small hepatocellular carcinomas in patients with cirrhosis. *N Engl J Med* 1996; **334**: 693-699 [PMID: 8594428 DOI: 10.1056/nejm199603143341104]

5 **Yao FY**, Ferrell L, Bass NM, Watson JJ, Bacchetti P, Venook A, Ascher NL, Roberts JP. Liver transplantation for hepatocellular carcinoma: expansion of the tumor size limits does not adversely impact survival. *Hepatology* 2001; **33**: 1394-1403 [PMID: 11391528 DOI: 10.1053/jhep.2001.24563]

6 **Clavien PA**, Lesurtel M, Bossuyt PM, Gores GJ, Langer B, Perrier A; OLT for HCC Consensus Group. Recommendations for liver transplantation for hepatocellular carcinoma: an international consensus conference report. *Lancet Oncol* 2012; **13**: e11-e22 [PMID: 22047762 DOI: 10.1016/s1470-2045(11)70175-9]

7 **Mazzaferro V**, Bhoori S, Sposito C, Bongini M, Langer M, Miceli R, Mariani L. Milan criteria in liver transplantation for hepatocellular carcinoma: an evidence-based analysis of 15 years of experience. *Liver Transpl* 2011; **17** Suppl 2: S44-S57 [PMID: 21695773 DOI: 10.1002/lt.22365]

8 **Hakeem AR**, Young RS, Marangoni G, Lodge JP, Prasad KR. Systematic review: the prognostic role of alpha-fetoprotein following liver transplantation for hepatocellular carcinoma. *Aliment Pharmacol Ther* 2012; **35**: 987-999 [PMID: 22429190 DOI: 10.1111/j.1365-2036.2012.05060.x]

9 **Duvoux C**, Roudot-Thoraval F, Decaens T, Pessione F, Badran H, Piardi T, Francoz C, Compagnon P, Vanlemmens C, Dumortier J, Dharancy S, Gugenheim J, Bernard PH, Adam R, Radenne S, Muscari F, Conti F, Hardwigsen J, Pageaux GP, Chazouillères O, Salame E, Hilleret MN, Lebray P, Abergel A, Debette-Gratien M, Kluger MD, Mallat A, Azoulay D, Cherqui D; Liver Transplantation French Study Group. Liver transplantation for hepatocellular carcinoma: a model including α-fetoprotein improves the performance of Milan criteria. *Gastroenterology* 2012; **143**: 986-94.e3; quiz e14-5 [PMID: 22750200 DOI: 10.1053/j.gastro.2012.05.052]

10 **Toyoda H**, Kumada T, Osaki Y, Oka H, Urano F, Kudo M, Matsunaga T. Staging hepatocellular carcinoma by a novel scoring system (BALAD score) based on serum markers. *Clin Gastroenterol Hepatol* 2006; **4**: 1528-1536 [PMID: 17162244 DOI: 10.1016/j.cgh.2006.09.021]

11 **Kitai S**, Kudo M, Minami Y, Haji S, Osaki Y, Oka H, Seki T, Kasugai H, Sasaki Y, Matsunaga T. Validation of a new prognostic staging system for hepatocellular carcinoma: a comparison of the biomarker-combined Japan Integrated Staging Score, the conventional Japan Integrated Staging Score and the BALAD Score. *Oncology* 2008; **75** Suppl 1: 83-90 [PMID: 19092276 DOI: 10.1159/000173428]

12 **Chan SL**, Mo F, Johnson P, Li L, Tang N, Loong H, Chan AW, Koh J, Chan AT, Yeo W. Applicability of BALAD score in prognostication of hepatitis B-related hepatocellular carcinoma. *J Gastroenterol Hepatol* 2015; **30**: 1529-1535 [PMID: 25968302 DOI: 10.1111/jgh.13005]

13 **Toyoda H**, Tada T, Johnson PJ, Izumi N, Kadoya M, Kaneko S, Kokudo N, Ku Y, Kubo S, Kumada T, Matsuyama Y, Nakashima O, Sakamoto M, Takayama T, Kudo M; Liver Cancer Study Group of Japan. Validation of serological models for staging and prognostication of HCC in patients from a Japanese nationwide survey. *J Gastroenterol* 2017; **52**: 1112-1121 [PMID: 28224228 DOI: 10.1007/s00535-017-1321-6]

14 **Berhane S**, Toyoda H, Tada T, Kumada T, Kagebayashi C, Satomura S, Schweitzer N, Vogel A, Manns MP, Benckert J, Berg T, Ebker M, Best J, Dechêne A, Gerken G, Schlaak JF, Weinmann A, Wörns MA, Galle P, Yeo W, Mo F, Chan SL, Reeves H, Cox T, Johnson P. Role of the GALAD and BALAD-2 Serologic Models in Diagnosis of Hepatocellular Carcinoma and Prediction of Survival in Patients. *Clin Gastroenterol Hepatol* 2016; **14**: 875-886.e6 [PMID: 26775025 DOI: 10.1016/j.cgh.2015.12.042]

15 **Chaiteerakij R**, Zhang X, Addissie BD, Mohamed EA, Harmsen WS, Theobald PJ, Peters BE, Balsanek JG, Ward MM, Giama NH, Moser CD, Oseini AM, Umeda N, Venkatesh S, Harnois DM, Charlton MR, Yamada H, Satomura S, Algeciras-Schimnich A, Snyder MR, Therneau TM, Roberts LR. Combinations of biomarkers and Milan criteria for predicting hepatocellular carcinoma recurrence after liver transplantation. *Liver Transpl* 2015; **21**: 599-606 [PMID: 25789635 DOI: 10.1002/lt.24117]

16 **Toyoda H**, Kumada T, Tada T, Sone Y, Kaneoka Y, Maeda A. Tumor Markers for Hepatocellular Carcinoma: Simple and Significant Predictors of Outcome in Patients with HCC. *Liver Cancer* 2015; **4**: 126-136 [PMID: 26020034 DOI: 10.1159/000367735]

17 **Nakamura S**, Nouso K, Sakaguchi K, Ito YM, Ohashi Y, Kobayashi Y, Toshikuni N, Tanaka H, Miyake Y, Matsumoto E, Shiratori Y. Sensitivity and specificity of des-gamma-carboxy prothrombin for diagnosis of patients with hepatocellular carcinomas varies according to tumor size. *Am J Gastroenterol* 2006; **101**: 2038-2043 [PMID: 16848811 DOI: 10.1111/j.1572-0241.2006.00681.x]

18 **Taketomi A**, Sanefuji K, Soejima Y, Yoshizumi T, Uhciyama H, Ikegami T, Harada N, Yamashita Y, Sugimachi K, Kayashima H, Iguchi T, Maehara Y. Impact of des-gamma-carboxy prothrombin and tumor size on the recurrence of hepatocellular carcinoma after living donor liver transplantation. *Transplantation* 2009; **87**: 531-537 [PMID: 19307789 DOI: 10.1097/TP.0b013e3181943bee]

19 **Koike Y**, Shiratori Y, Sato S, Obi S, Teratani T, Imamura M, Yoshida H, Shiina S, Omata M. Des-gamma-carboxy prothrombin as a useful predisposing factor for the development of portal venous invasion in patients with hepatocellular carcinoma: a prospective analysis of 227 patients. *Cancer* 2001; **91**: 561-569 [PMID: 11169939]

20 **Tada T**, Kumada T, Toyoda H, Kiriyama S, Sone Y, Tanikawa M, Hisanaga Y, Kitabatake S, Kuzuya T, Nonogaki K, Shimizu J, Yamaguchi A, Isogai M, Kaneoka Y, Washizu J, Satomura S. Relationship between Lens culinaris agglutinin-reactive alpha-fetoprotein and pathologic features of hepatocellular carcinoma. *Liver Int* 2005; **25**: 848-853 [PMID: 15998436 DOI: 10.1111/j.1478-3231.2005.01111.x]

21 **Johnson PJ**, Berhane S, Kagebayashi C, Satomura S, Teng M, Reeves HL, O'Beirne J, Fox R, Skowronska A, Palmer D, Yeo W, Mo F, Lai P, Iñarrairaegui M, Chan SL, Sangro B, Miksad R, Tada T, Kumada T, Toyoda H. Assessment of liver function in patients with hepatocellular carcinoma: a new evidence-based approach-the ALBI grade. *J Clin Oncol* 2015; **33**: 550-558 [PMID: 25512453 DOI: 10.1200/jco.2014.57.9151]

22 **Jeng KS**, Chang CF, Jeng WJ, Sheen IS, Jeng CJ. Heterogeneity of hepatocellular carcinoma contributes to cancer progression. *Crit*

Rev Oncol Hematol 2015; **94**: 337-347 [PMID: 25680939 DOI: 10.1016/j.critrevonc.2015.01.009]

23 **Johnson PJ**, Pirrie SJ, Cox TF, Berhane S, Teng M, Palmer D, Morse J, Hull D, Patman G, Kagebayashi C, Hussain S, Graham J, Reeves H, Satomura S. The detection of hepatocellular carcinoma using a prospectively developed and validated model based on serological biomarkers. *Cancer Epidemiol Biomarkers Prev* 2014; **23**: 144-153 [PMID: 24220911 DOI: 10.1158/1055-9965.epi-13-0870]

P- Reviewer: Johnson P, Rodriguez-Peralvarez ML, Sugawara Y
S- Editor: Gong ZM **L- Editor**: A **E- Editor**: Huang Y

World Journal of Gastroenterology

Submit a Manuscript: http://www.f6publishing.com

World J Gastroenterol 2018 March 28; 24(12): 1332-1342

DOI: 10.3748/wjg.v24.i12.1332

ISSN 1007-9327 (print) ISSN 2219-2840 (online)

ORIGINAL ARTICLE

Retrospective Study

Intraoperative frozen section diagnosis of bile duct margin for extrahepatic cholangiocarcinoma

Takayuki Shiraki, Hajime Kuroda, Atsuko Takada, Yoshimasa Nakazato, Keiichi Kubota, Yasuo Imai

Takayuki Shiraki, Keiichi Kubota, Department of Gastroenterological Surgery, Dokkyo Medical University, Tochigi 321-0293, Japan

Hajime Kuroda, Atsuko Takada, Yoshimasa Nakazato, Yasuo Imai, Department of Diagnostic Pathology, Dokkyo Medical University, Tochigi 321-0293, Japan

ORCID number: Takayuki Shiraki (0000-0003-2935-6708); Hajime Kuroda (0000-0001-6546-5317); Atsuko Takada (0000-0001-7042-435X); Yoshimasa Nakazato (0000-0002-0325-9451); Keiichi Kubota (0000-0003-4484-7708); Yasuo Imai (0000-0002-1422-7789).

Author contributions: Shiraki T and Kuroda H contributed equally to this work; Shiraki T collected clinical information; Kuroda H and Imai Y reviewed the pathological diagnosis; Shiraki T, Kuroda H, and Imai Y analyzed the data and wrote the manuscript; Takada A and Nakazato Y made critical revisions of the manuscript; Kubota K and Imai Y designed the study; Imai Y gave the final approval of the manuscript for publication.

Supported by JSPS KAKENHI (No. JP16K08695) from the Ministry of Education, Culture, Sports, Science and Technology of Japan.

Institutional review board statement: This study protocol was approved by the ethical review board in the Dokkyo Medical University Hospital (DMUH: R-2-21).

Informed consent statement: Patients were not required to give informed consent to the study because the analysis used anonymous clinical data that were obtained after each patient agreed to treatment by written consent.

Conflict-of-interest statement: The authors declare no competing interests related to this study.

Manuscript source: Unsolicited manuscript

Correspondence to: Yasuo Imai, MD, PhD, Department of Diagnostic Pathology, Dokkyo Medical University, 880 Kitakobayashi, Mibu, Shimotsuga, Tochigi 321-0293, Japan. ya-imai@dokkyomed.ac.jp
Telephone: +81-282-872130
Fax: +81-282-861681

Received: February 13, 2018
Peer-review started: February 13, 2018
First decision: February 24, 2018
Revised: March 5, 2018
Accepted: March 7, 2018
Article in press: March 7, 2018
Published online: March 28, 2018

Abstract

AIM

To evaluate the usefulness of frozen section diagnosis (FSD) of bile duct margins during surgery for extrahepatic cholangiocarcinoma (CCA).

METHODS

We retrospectively analyzed 74 consecutive patients who underwent surgery for extrahepatic CCA from 2012 to 2017, during which FSD of bile duct margins was performed. They consisted of 40 distant and 34 perihilar CCAs (45 and 55 bile duct margins, respectively). The diagnosis was classified into three categories: negative, borderline (biliary intraepithelial neoplasia-1 and 2, and indefinite for neoplasia), or positive. FSD in the epithelial layer, subepithelial layer, and total layer was compared with corresponding permanent section diagnosis (PSD) postoperatively.

Then, association between FSD and local recurrence was analyzed with special reference to borderline.

RESULTS

Analysis of 100 duct margins revealed that concordance rate between FSD and PSD was 68.0% in the total layer, 69.0% in the epithelial layer, and 98.0% in the subepithelial layer. The extent of remaining biliary epithelium was comparable between FSD and PSD, and more than half of the margins lost > 50% of the entire epithelium, suggesting low quality of the samples. In FSD, the rate of negative margins decreased and that of borderline and positive margins increased according to the extent of the remaining epithelium. Diagnostic discordance between FSD and PSD was observed in 31 epithelial layers and two subepithelial layers. Alteration from borderline to negative was the most frequent (20 of the 31 epithelial layers). Patients with positive margin in the total and epithelial layers by FSD demonstrated a significantly worse local recurrence-free survival (RFS) compared with patients with borderline and negative margins, which revealed comparable local RFS. Patients with borderline and negative margins in the epithelial layer by PSD also revealed comparable local RFS. These results suggested that epithelial borderline might be regarded substantially as negative. When classifying the status of the epithelial layer either as negative or positive, concordance rates between FSD and PSD in the total, epithelial, and subepithelial layers were 95.0%, 93.0%, and 98.0%, respectively.

CONCLUSION

During intraoperative assessment of bile duct margin, borderline in the epithelial layer can be substantially regarded as negative, under which condition FSD is comparable to PSD.

Key words: Cholangiocarcinoma; Bile duct cancer; Frozen section diagnosis; Permanent section diagnosis; Bile duct margin; Biliary intraepithelial neoplasia; Dysplasia; Indefinite for neoplasia; Borderline lesion; Local recurrence

Core tip: Usefulness of intraoperative frozen section diagnosis (FSD) of bile duct margin for extrahepatic cholangiocarcinoma was investigated. The diagnosis was classified into negative, borderline (biliary intraepithelial neoplasia-1 and 2, and indefinite for neoplasia), or positive, and FSD was compared with permanent section diagnosis postoperatively. In contrast to previous studies, positive FSD in the epithelial layer was significantly associated with local recurrence. Furthermore, borderline FSD in the epithelial layer could be substantially regarded as negative, which could aid surgeons to determine the resection range of the bile duct. Finally, we demonstrated that FSD was reliable enough for pathological diagnosis.

Shiraki T, Kuroda H, Takada A, Nakazato Y, Kubota K, Imai Y. Intraoperative frozen section diagnosis of bile duct margin for extrahepatic cholangiocarcinoma. *World J Gastroenterol* 2018; 24(12): 1332-1342 Available from: URL: http://www.wjgnet.com/1007-9327/full/v24/i12/1332.htm DOI: http://dx.doi.org/10.3748/wjg.v24.i12.1332

INTRODUCTION

Bile duct cancer (cholangiocarcinoma: CCA) is a rare malignancy (incidence < 6 cases per 100000 people) in most countries[1], and approximately 8000 people in the United States are diagnosed with CCA annually[2]. It develops in any part of the bile duct system and it is classified into three types based on location: intrahepatic CCA, perihilar CCA (pCCA), and distal CCA (dCCA). The latter two types are grouped as extrahepatic CCA (eCCA). Taken together, CCAs represent the second most frequent liver cancer and up to 3% of all gastrointestinal cancers[1,3]. CCA is generally asymptomatic in the early stages, and a late diagnosis and anatomical complexity of the cancer location result in poor prognosis: Five-year survival rate of eCCA with American Joint Committee on Cancer tumor node metastasis (TNM) stage Ⅰ is 30%, stages Ⅱ and Ⅲ 24%, and stage Ⅳ 2%[2].

Most TNM stage 0, Ⅰ, and Ⅱ CCAs and some stage Ⅲ CCAs are potentially resectable, and complete surgical resection is the only treatment with the potential for cure. The status of the final ductal margin is strongly associated with prognosis of patients with resectable CCA[2,4]. Intraoperative frozen section diagnosis (FSD) of the bile duct margins has traditionally been used to guide the extent of operative resection, but the usefulness of FSD has been controversial until now[5-9]. Because of the rarity and locoregional anatomical complexity of CCA, few centers have substantial clinical experience of managing this disease, and few pathologists have expertise in characterizing resected specimens accurately. In addition, the greatest difficulty of FSD is the low quality of samples because of tissue degeneration and/or destruction during freezing and sectioning. Therefore, production of formalin-fixed and paraffin-embedded samples that reuses frozen samples, and comparison between FSD and permanent section diagnosis (PSD) are mandatory. As a result, alteration of diagnosis often occurs. The primary purpose of this study was to examine reliability of intraoperative FSD to evaluate the margin status. The secondary purpose was to clarify clinical relevance of borderline lesions that could not be definitely determined whether malignant or benign. Borderline in the present study included

Table 1 Clinicopathological characteristics of extrahepatic cholangiocarcinoma

	pCCA (n = 34)	dCCA (n = 40)
Age (yr), median (range)	71.5 (44-82)	72.5 (39-85)
Gender		
Male	23	6
Female	11	34
Preoperative biliary drainage		
Yes	33	38
No	1	2
Procedure		
PD	1	38
HH	27	1
PD + HH	5	0
Bile duct resection	0	1
Others	1	0
Total number of duct margins for frozen section	55	45
Number of duct margins for frozen section		
1	15	35
2	17	5
3	2	0
pT		
pT1/pT2	27	20
pT3/pT4	6	19
Unknown	1	1

dCCA: Distal cholangiocarcinoma; HH: Hemihepatectomy; pCCA: Perihilar cholangiocarcinoma; PD: Pancreaticoduodenectomy.

such lesions as low-grade and intermediate-grade dysplasia (biliary intraepithelial neoplasia (BilIN)-1 and BilIN-2)[10] and lesions indefinite for neoplasia that could not be determined as reactive or neoplastic. For these purposes, we analyzed postoperative local recurrence of eCCA according to the margin status of FSD.

MATERIALS AND METHODS

Patients

We analyzed 74 consecutive patients who underwent hemihepatectomy and/or pancreaticoduodenectomy for eCCA at the Department of Gastroenterological Surgery, Dokkyo Medical University from December 2012 to February 2017. There were 40 cases of dCCA (45 bile duct margins) and 34 of pCCA (55 bile duct margins). The histopathological diagnosis was reviewed by two experienced pathologists (HK and YI), and diagnostic inconsistency between the two pathologists was resolved by discussion. The clinicopathological information was retrospectively retrieved on the electronic medical chart system of the Dokkyo Medical University Hospital (Table 1).

Histopathological analysis

FSD of the resected bile duct margin was performed during the operation. The margin tissue was mounted in WHITE TISSUE-COAT (U.I. Kasei, Amagasaki, Hyogo, Japan), frozen in liquid nitrogen, and thin sections were cut from the frozen blocks using a cryostat. The sections were stained by hematoxylin and eosin and subjected to microscopic diagnosis. At least two, three or more as needed, pieces of frozen sections were examined for each margin. When FSD was positive for malignancy (positive) in the first submitted specimen, additional resection of the margin was performed to the maximal extent possible. Results of the last submitted specimens were analyzed in the present study. After FSD, the tissues were thawed, fixed in formalin, and embedded in paraffin. Thin sections were cut from paraffin-embedded blocks, stained, and observed with microscopy. FSD and PSD were compared with each other.

The surgical margins were diagnosed as either negative for malignancy (negative), borderline, or positive (Figure 1). Borderline included BilIN-1 and 2, and indefinite for neoplasia. We separately assessed the epithelial and subepithelial layers, and made a diagnosis based on both results. The epithelial layer tends to detach from the basement membrane during sample preparation for FSD. In relation to the entire circumference, we defined E1 as 0%-24% remaining epithelium, E2 as 25%-49% remaining epithelium, and E3 as 50%-100% remaining epithelium.

The concordance rate between FSD and PSD was investigated at the margin and patient levels, but survival analysis was performed solely at the patient level; for example, a patient with two negative margins and one positive margin was assigned to the positive group.

The presence or absence of postoperative local recurrence was detected by imaging studies including ultrasonography and computed tomography. The criteria for the local recurrence were defined as mass lesions within the resection field with or without clinical manifestation and/or elevated tumor markers. The

Table 2 Histopathological results of the biliary duct margins

	Negative (%)	Borderline (%)	Positive (%)	Total (%)	*P* value
Margin level					
Total layer					
FSD	41 (41.0)	39 (39.0)	20 (20.0)	100 (100)	0.039
PSD	56 (56.0)	23 (23.0)	21 (21.0)	100 (100)	
Epithelial layer					
FSD	44 (44.0)	41 (41.0)	15 (15.0)	100 (100)	0.078
PSD	59 (59.0)	27 (27.0)	14 (14.0)	100 (100)	
Subepithelial layer					
FSD	87 (87.0)	1 (1.0)	12 (11.0)	100 (100)	0.560
PSD	86 (86.0)	0 (0.0)	14 (14.0)	100 (100)	
Patient level					
Total layer					
FSD	26 (35.1)	31 (41.9)	17 (23.0)	74 (100)	0.134
PSD	36 (48.7)	20 (27.0)	18 (24.3)	74 (100)	

FSD: Frozen section diagnosis; PSD: Permanent section diagnosis.

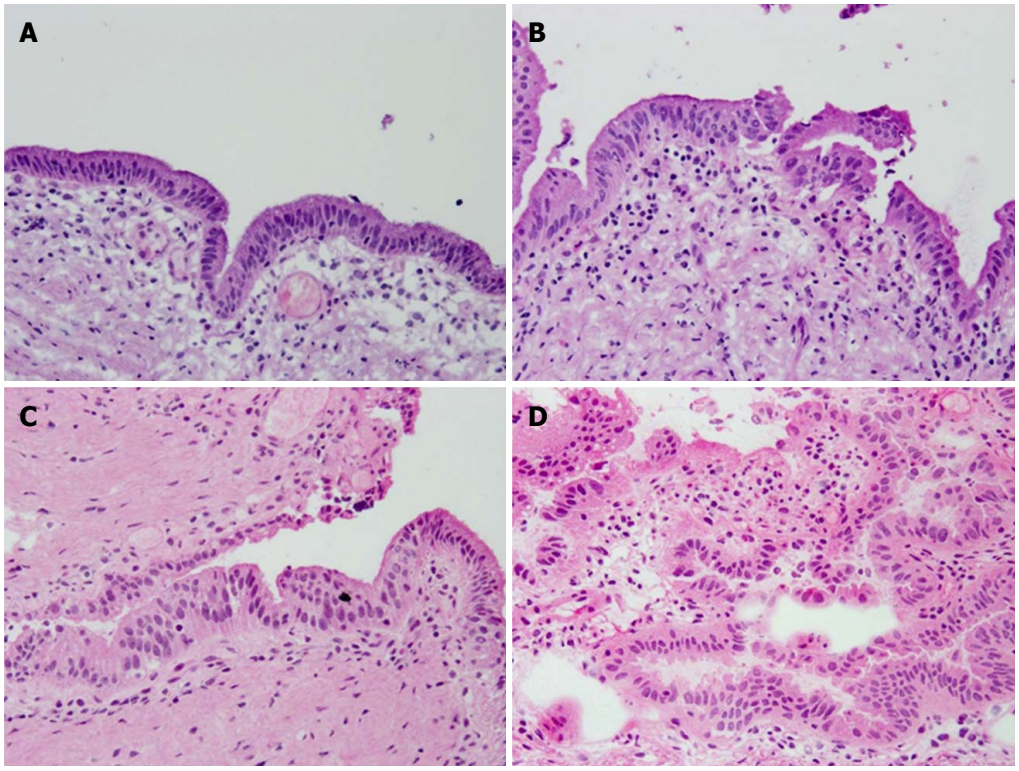

Figure 1 Representative histopathology of BilIN-1, 2, and 3 by frozen section diagnosis. A: Normal mucosa; B: Borderline (BilIN-1); (C) Borderline (BilIN-2); and D: Positive (BilIN-3) (hematoxylin and eosin, 20 ×). BilIN: Biliary intraepithelial neoplasia.

diagnosis of local recurrence was made by the surgeons in charge of each patient.

Statistical analysis

Comparison of categorical data sets between FSD and PSD was performed by the χ^2 test. Local recurrence-free survival (RFS) curves were depicted using the Kaplan-Meier method and analyzed by the log-rank test. $P < 0.05$ was considered significant. Statistical analysis was performed using IBM SPSS Statistics 24 (IBM, Armonk, NY, United States).

RESULTS

Concordance rate between FSD and PSD at the margin level

FSD revealed 41 (41.0%) negative, 20 (20.0%) positive, and 39 (39.0%) borderline out of 100 bile duct margins, while PSD revealed 56 (56.0%) negative, 21 (21.0%) positive, and 23 (23.0%) borderline margins (Table 2). The number of positive margins was similar between FSD and PSD, but the number of negative margins increased and that of borderline decreased

Table 3 Concordance rate between frozen section diagnosis and permanent section diagnosis

	Concordance rate (%)	Sensitivity (%)	Specificity (%)	Positive-predictive value (%)	Negative-predictive value (%)
Original diagnostic results					
Total layer	68.0	85.7	66.1	90.0	90.2
Epithelial layer	69.0	78.6	64.6	73.3	86.4
Subepithelial layer	98.0	85.7	100.0	100.0	98.9
Revised diagnostic results					
Total layer	95.0	85.7	97.5	90.0	97.5
Epithelial layer	93.0	70.0	95.6	73.3	96.5
Subepithelial layer	98.0	85.7	100.0	100.0	98.9

Table 4 Extent of the remaining epithelium and diagnostic results of the bile duct margin

	Extent of the remaining epithelium	Negative (%)	Borderline (%)	Positive (%)	Total (%)
FSD					
	E1 (0%-24%)	22 (66.6)	9 (27.3)	2 (6.1)	33 (100)
	E2 (25%-49%)	8 (38.1)	11 (52.4)	2 (9.5)	21 (100)
	E3 (50%-100%)	14 (30.4)	21 (45.7)	11 (23.9)	46 (100)
PSD					
	E1 (0%-24%)	22 (68.7)	7 (21.9)	3 (9.4)	32 (100)
	E2 (25%-49%)	9 (42.9)	9 (42.9)	3 (14.3)	21 (100)
	E3 (50%-100%)	28 (59.6)	11 (23.4)	8 (17.0)	47 (100)

FSD: Frozen section diagnosis; PSD: Permanent section diagnosis.

significantly in PSD (P = 0.039) (Table 2). The concordance rate between FSD and PSD is summarized in Table 3 as original diagnostic results.

We separately analyzed the status of the surgical margin in the epithelial and subepithelial layers. FSD in the epithelial layer revealed 44 (44.0%) negative, 15 (15.0%) positive, and 41 (41.0%) borderline margins, while PSD revealed 59 (59.0%) negative, 14 (14.0%) positive, and 27 (27.0%) borderline margins. The number of positive margins was similar between FSD and PSD, but the number of negative margins increased and that of borderline decreased in PSD with marginal significance (P = 0.078) (Table 2) (Figure 2A and B).

The extent of the remaining biliary epithelium lining the resected margin might represent the quality of samples especially in evaluating the epithelial layer. A total of 33 samples were E1, 21 were E2, and 46 were E3 in FSD, while a total of 32 samples were E1, 21 were E2, and 47 were E3 in PSD (Table 4). The rate of the remaining epithelium was almost identical between FSD and PSD. More than half of the total margins lacked > 50% of the entire biliary epithelium in FSD and PSD. The rate of negative margins decreased and the rate of borderline and positive margins increased in FSD according to the rate of the remaining epithelium. This suggested proportional sensitivity to the remaining rate and intrinsic difficulty in the assessment of the epithelial layer. The concordance rate between FSD and PSD in the evaluation of the epithelial layer is summarized in Table 3 as original diagnostic results.

In the subepithelial layer, FSD revealed 87 (87.0%) negative, 12 (12.0%) positive, and 1 (1.0%) borderline margins, while PSD revealed 86 (86.0%) negative and 14 (14.0%) positive margins. There was a nearly complete consistency between FSD and PSD (P = 0.560) (Table 2). The concordance rate between FSD and PSD in the evaluation of the subepithelial layer is summarized in Table 3 as original diagnostic results.

Analysis of diagnostic discordance between FSD and PSD

Diagnostic discordance between FSD and PSD was observed in 31 epithelial layers and two subepithelial layers (Table 5). The discordance rate in the epithelial layer was considerably high, while that in the subepithelial layer was very low. The discordance rate in the epithelial layer was somewhat higher in pCCA than dCCA, but there was no significant difference in the discordance rate between pCCA and dCCA in the epithelial layer and subepithelial layer (P = 0.128 and 1.000, respectively). Alteration from borderline to negative in the epithelial layer was the most frequent (20 margins). Less frequently, alterations from negative to borderline (4 margins) and positive to borderline (4 margins) were observed in the epithelial layer (Table 6). Regrettably, alteration from negative to positive was also noted in two margins (Figure 2C and D).

Concordance rate between FSD and PSD at the patient level

FSD revealed 26 (35.1%) negative, 17 (23.0%) positive, and 31 (41.9%) borderline margins in 74 patients with eCCA, while PSD revealed 36 (48.7%) negative, 18 (24.3%) positive, and 20 (27.0%) borderline margins. The number of positive margins was similar between FSD and PSD, but the number

Table 5 Diagnostic discordance between frozen section diagnosis and permanent section diagnosis

	Diagnostic discordance		Total (%)
	Yes (%)	No (%)	
Epithelial layer	31 (31.0)	69 (69.0)	100 (100)
pCCA	21 (38.2)	34 (61.8)	55 (100)
dCCA	10 (22.2)	35 (77.8)	45 (100)
Subepithelial layer	2 (2.0)	98 (98.0)	100 (100)
pCCA	1 (1.8)	54 (98.2)	55 (100)
dCCA	1 (2.2)	44 (97.8)	45 (100)
Total layer	28 (28.0)	72 (72.0)	100 (100)
pCCA	18 (32.7)	37 (67.3)	55 (100)
dCCA	10 (22.2)	35 (77.8)	45 (100)

pCCA: Perihilar cholangiocarcinoma; dCCA: Distal cholangiocarcinoma.

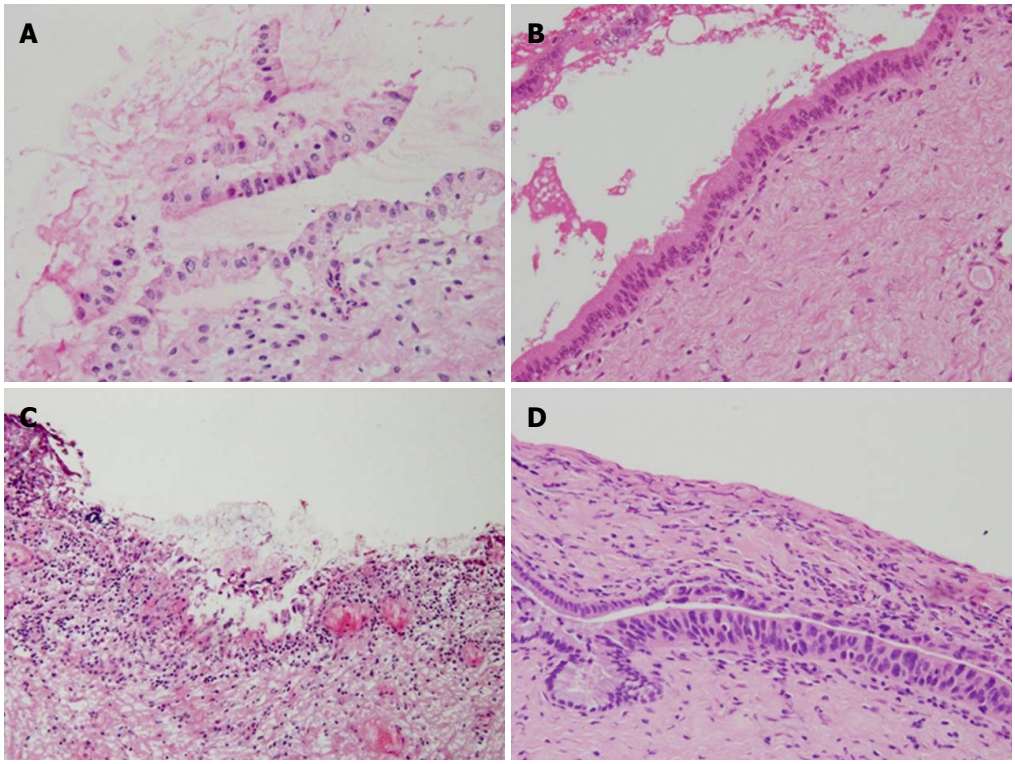

Figure 2 Discordance between frozen section diagnosis and permanent section diagnosis. Bile duct margin of Case 172 (dCCA) prepared for FSD (A) and PSD (B), and that of Case 157 (dCCA) prepared for FSD (C) and PSD (D) (hematoxylin and eosin, 20 ×). These two sets of figures represent the same region of the bile duct margin, respectively. Epithelium was detached from subepithelium, denatured, twisted, and FSD was borderline (BilIN-2) (A), while PSD was negative (B). Epithelium was severely denatured owing to artifacts and FSD was negative (C), while BilIN-3/carcinoma *in situ* appeared in different sections prepared for PSD (D). FSD: Frozen section diagnosis; PSD: Permanent section diagnosis; dCCA: Distal cholangiocarcinoma; BilIN: Biliary intraepithelial neoplasia.

of negative margins increased and that of borderline decreased slightly in PSD (P = 0.134) (Table 2).

Local RFS analysis

The overall follow-up period of the 74 patients from surgery to disease-related death or censoring were 4 to 2343 days (Median, 623 d).

We first performed local RFS analysis based on FSD of the bile duct margin in the total layer. Local RFS rates for 1, 3, and 5 years are listed in Table 7. Patients with positive margins demonstrated a significantly worse survival compared with those with negative or borderline margins (both P < 0.01). In contrast, patients with negative and borderline margins showed comparable prognoses (P = 0.906) (Figure 3A).

We then focused on the status of the epithelial layer, since we thought that diagnosis as borderline was the greatest issue for surgeons in deciding whether to perform additional resection. Patients with borderline and positive margins in the subepithelial layer were excluded from this analysis in order to investigate the pure effect of the status of the epithelial layer. Local RFS rates for 1, 3, and 5 years are listed in Table 7. Patients with positive margins demonstrated a significantly worse survival compared with those with negative or borderline margins (both P < 0.01). In contrast, patients with

Table 6 Details of diagnostic discordance between frozen section diagnosis and permanent section diagnosis

	Epithelial layer (pCCA:dCCA)	Subepithelial layer (pCCA:dCCA)
From negative to borderline	4 (2:2)	0 (0:0)
From negative to positive	1 (0:1)	1 (1:0)
From borderline to negative	20 (13:7)	0 (0:0)
From borderline to positive	2 (2:0)	1 (0:1)
From positive to borderline	4 (4:0)	0 (0:0)
Total	31 (21:10)	2 (1:1)

pCCA: Perihilar cholangiocarcinoma; dCCA: Distal cholangiocarcinoma.

Table 7 Local recurrence-free survival rates of patients according to the status of the bile duct margin evaluated by frozen section diagnosis

	Duration (yr)	Negative	Borderline	Positive
Total layer				
Number of cases		26	31	17
	1	0.916	0.918	0.518
	3	0.769	0.725	0.194
	5	0.769	0.725	0.194
[1]Epithelial layer				
Number of cases		26	30	6
	1	0.916	0.915	0.333
	3	0.769	0.722	0.000
	5	0.769	0.722	0.000

[1]Patients with borderline or positive subepithelial layer were excluded.

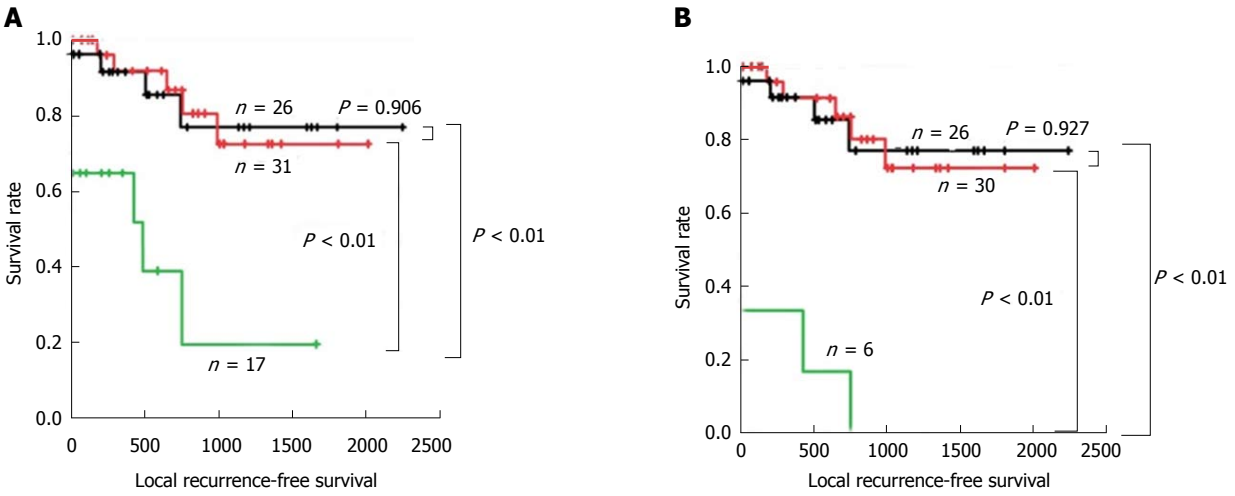

Figure 3 Local recurrence-free survival analysis according to the frozen section diagnosis status. The Kaplan-Meier curves of patients with eCCA according to the status of the bile duct margin evaluated by FSD in total layer (A) and epithelial layer (B). Patients with borderline or positive subepithelial layer were excluded from the analysis in the epithelial layer. Black line: negative; Red line: borderline; Green line: positive; eCCA: Extrahepatic cholangiocarcinoma; FSD: Frozen section diagnosis.

negative and borderline margins showed comparable prognoses (P = 0.927) (Figure 3B).

Local RFS analysis according to the epithelial and total status assessed by PSD demonstrated similar results (Figure 4 and Table 8). Patients with positive margins in the total and epithelial layers demonstrated significantly worse survival compared with those with negative or borderline margins (all P < 0.01). In contrast, patients with negative and borderline margins in the total and epithelial layers showed similar prognoses (both P = 0.896).

Based on the results of survival analysis, borderline margins in the epithelial layer were regarded substantially as negative. Histopathological diagnosis in the epithelial layer was reclassified into positive or negative, and the concordance rate between FSD and PSD was revised (Table 3). The concordance rates in the total, epithelial, and subepithelial layers were 95.0%, 93.0%,

Table 8 Local recurrence-free survival rates of patients according to the status of the bile duct margin evaluated by permanent section diagnosis

	Duration (yr)	Negative	Borderline	Positive
Total layer				
Number of cases		36	20	18
	1	0.940	0.862	0.667
	3	0.710	0.790	0.356
	5	0.710	ND	ND
[1]Epithelial layer				
Number of cases		36	20	6
	1	0.940	0.862	0.333
	3	0.710	0.790	0.167
	5	0.710	ND	ND

[1]Patients with borderline or positive subepithelial layer were excluded. ND: Not determined.

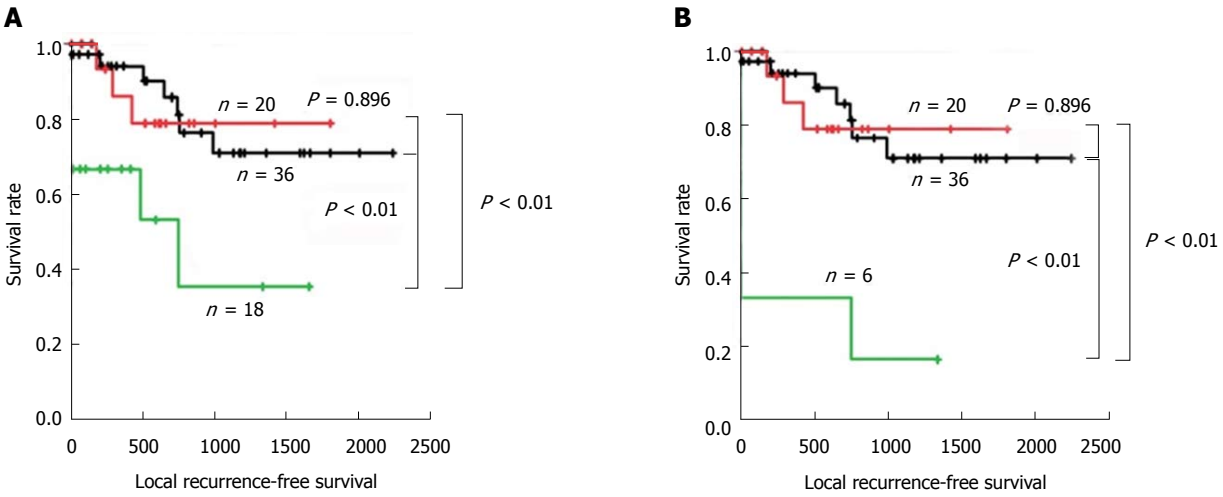

Figure 4 Local recurrence-free survival analysis according to the permanent section diagnosis status. The Kaplan-Meier curves of patients with eCCA according to the status of the bile duct margin evaluated by PSD in total layer (A) and epithelial layer (B). Patients with borderline or positive subepithelial layer were excluded from the analysis in the epithelial layer. Black line: negative; Red line: borderline; Green line: positive; eCCA: Extrahepatic cholangiocarcinoma; PSD: Permanent section diagnosis.

and 98.0%, respectively. These results suggest that FSD is a reliable method to evaluate margin status of the bile duct intraoperatively.

DISCUSSION

The status of the bile duct margin has been assessed by intraoperative FSD for complete resection of eCCA. However, the usefulness of FSD is controversial owing to the frequent discordance between FSD and PSD. Okazaki *et al*[5] reported that concordance rate between FSD and PSD was only 56.5%, and concluded that FSD should not be carried out for patients with a high risk of hepatic failure. Yamaguchi *et al*[7] reported that diagnosis of resected bile duct margin was altered from FSD to PSD in five of 20 patients with gall bladder or bile duct cancer who underwent surgical resection. Endo *et al*[9] reported that discrepancies between FSD and PSD were observed in 10 of 101 patients with pCCA who underwent surgery. In the present study, we experienced diagnostic discordance in 28 of 100 duct margins between FSD and PSD. This high discordance rate was probably due to the grouping method of histopathological results. The margin status was classified into either positive or negative by Yamaguchi *et al*[7] and either positive/suspicious or negative in the study by Endo *et al*[9], in which only invasive carcinoma was diagnosed as positive. In contrast, the margin status in the present study was grouped into three categories of positive, borderline, or negative. Diagnostic discordance in this study was only 2% if only invasive cancer was classified as positive.

Discordance between FSD and PSD was observed in 28 bile duct margins; 31 in the epithelial layer and two in the subepithelial layer. The most frequent alteration was borderline to negative in the epithelial layer. During frozen sample preparation, epithelium easily detaches from basement membrane, and becomes twisted, folded, and overlapped. The nuclei are often swollen because of rapid freezing, which

makes it difficult to discriminate the epithelium from dysplasia and/or carcinoma *in situ*. We assume that the low quality of the frozen section sample may have been the greatest cause of the discordance (Figure 2A and B). The low quality of the frozen section sample was also demonstrated by the low remaining rate of the epithelium for histopathological evaluation. In this study, more than half of the epithelium was lost during sample preparation, and this might have resulted in underdiagnosis in the epithelial layer. In light of the similar extent of the remaining epithelium between FSD and PSD, the epithelial layer might be lost during resection for intraoperative diagnosis by surgeons. We experienced two cases of alteration from negative to positive. These were caused by sampling different sections within the bile duct margin (Figure 2C and D). The cut-surface of the permanent histology was different from that of frozen section histology. We did not overlook cancer cells within frozen section samples. Marked stromal cell infiltration into the tumor is an inherent characteristic of CCA, which may fundamentally underlie inaccurate FSD. Mucosal inflammation caused by the catheter for preoperative biliary drainage may also mislead the frozen diagnosis[5,7]. It may cause regenerative atypia of normal mucosa with thick and multilayered atypical epithelial cells and immature mesenchymal cells, which may be misdiagnosed as malignant epithelium showing sarcomatous changes. In this study, the rate of borderline was significantly higher in the epithelial layer than in the subepithelial layer on FSD, and borderline epithelial margins significantly decreased but borderline subepithelial margins did not change on PSD. This may be partly explained by the fact that almost all patients underwent biliary drainage tube insertion preoperatively (Table 1).

In the present study, patients with negative margins by FSD demonstrated a significantly favorable local RFS compared with patients with positive margins, suggesting that FSD is useful for complete resectability and predicting good prognosis. Positive margins in this study included the presence of cancer cells in the epithelial and/or subepithelial layers, of the bile duct submitted for diagnosis. However, clinical significance of positive surgical margins of the bile duct is controversial. Some authors reported no correlation between positive margins and postoperative local recurrence of pCCA[11]. In contrast, a strong correlation has been reported by other authors[9,12-14]. For example, pCCA patients with positive bile duct margins by paraffin section histology demonstrated significantly worse disease-specific survival compared with those with negative bile duct margins[9]. Bile duct margin was evaluated as positive only when invasive cancer was confirmed histologically[9]. In addition, local recurrence of gall bladder and bile duct cancer was slightly associated with the margin status by paraffin section histology, that is, 4/7 positive patients *versus* 9/37 negative patients (P = 0.081)[7]. In the patients with positive margins, local recurrence occurred only when cancer cells were observed in the subepithelial layer[7]. In the study of middle and distal bile duct cancer, PSD of the hepatic-side duct margin predicted local recurrence with marginal significance, that is, 2 of 6 (33%) positive patients *versus* 4 of 45 (9%) negative patients (P = 0.08)[4]. Localization of cancer cells in the surgical margin was not described in that study[4].

It has been reported that the presence of epithelial dysplasia at the bile duct margin confirmed postoperatively is not associated with survival of patients who undergo R0 resection[9,12,13]. Yamaguchi *et al*[7] also reported that local recurrence occurred in neither of the two patients with carcinoma *in situ* of the bile duct margin by permanent histopathology. In the present study, local recurrence was observed in all six patients with positive margins in the epithelial layer by FSD, suggesting the need for accurate intraoperative diagnosis of BilIN-3/severe dysplasia/*in situ* carcinoma. However, FSD of the bile duct is often difficult even for experienced pathologists. In addition, there is some interobserver variation in the evaluation of the grade of biliary dysplasia. In contrast, diagnosis of invasive carcinoma in the subepithelial layer is easier, especially when there is perineural invasion. Analysis of a greater number of cases is awaited to clarify the significance of BilIN-3/*in situ* carcinoma in the bile duct margin.

One of the main purposes of this study was to determine the relevance of borderline lesions, consisting of BilIN-1 and 2 and indefinite for neoplasia, diagnosed intraoperatively. Approximately 40% of the epithelial layer was diagnosed as borderline, while only 1% of the subepithelial layer was diagnosed as borderline by FSD. We thought that the difference was due to the following reasons: (1) intrinsic borderline lesion, such as BilIN-1 and 2, is defined as a diagnostic category in the epithelial lesion; (2) epithelium is more vulnerable to artifacts than subepithelial stromal tissue is; and (3) impact of preoperative biliary drainage tube insertion. Because our patients had pCCA and dCCA, which are locoregionally different tumors, we investigated only local recurrence rate and not overall survival rate. By survival analysis, patients with borderline margins in the epithelial layer demonstrated a comparable local RFS compared with patients with negative margins. These data suggested that epithelial borderline lesions might be interpreted substantially as negative margins and that additional ductal resection might not be necessary in such institutions as having well-experienced pathologists.

On the other hand, it is quite likely that some borderline margins may ultimately turn out to be positive in a larger series with more diverse pathologist. Hence, if the first margin is borderline and additional margin can be safely obtained, additional ductal resection will be desirable to achieve negative margin as the local recurrence is very high in positives.

In the present study, four of 26 patients with negative frozen margins had local recurrence. PSD was also negative in all these patients. This may have

been because CCA sometimes shows discontinuous longitudinal spread or tumorigenesis from separate foci along the bile duct[14,15].

In conclusion, FSD of the bile duct margin was reliable enough to provide useful information for deciding the extent of resection of eCCA regardless of technical limitations in sample preparation. Positive margins in the epithelial layer was significantly associated with local recurrence, while the borderline margins demonstrated a similar local recurrence rate to that of negative margins. Although it is desirable to achieve negative margin if the first margin is borderline, epithelial borderline lesions could be regarded substantially as negative margins in such institutions as with well-experienced pathologists.

ARTICLE HIGHLIGHTS

Research background

Cholangiocarcinoma (CCA) is a rare malignancy with poor prognosis. Complete surgical resection is the only treatment with the potential for cure, and the status of the final ductal margin is strongly associated with prognosis. Intraoperative frozen section diagnosis (FSD) of the bile duct margins has traditionally been used to guide the extent of operative resection, but its usefulness has been controversial until now.

Research motivation

Because of the rarity and locoregional anatomical complexity of CCA, few centers have substantial clinical experience of managing this disease, and few pathologists have expertise in characterizing resected specimens accurately. In addition, quality of FSD samples is very low. Hence, discordance between FSD and permanent section diagnosis (PSD) that reuses frozen samples often occurs.

Research objectives

The primary purpose of this study was to examine reliability of intraoperative FSD to evaluate the margin status. The secondary purpose was to clarify clinical relevance of borderline lesions that could not be definitely determined whether malignant or benign. Borderline in the present study included such lesions as low-grade and intermediate-grade dysplasia [biliary intraepithelial neoplasia (BilIN)-1 and BilIN-2] and lesions indefinite for neoplasia.

Research methods

We retrospectively analyzed 74 consecutive patients who underwent surgery for extrahepatic CCA (eCCA) from 2012 to 2017, during which FSD of bile duct margins was performed. They consisted of 40 distant CCAs (dCCAs) and 34 perihilar CCAs (pCCAs) (45 and 55 bile duct margins, respectively). The diagnosis was classified into three categories: negative, borderline, or positive. FSD in the epithelial layer, subepithelial layer, and total layer was compared with corresponding PSD postoperatively. Then, association between FSD and local recurrence was analyzed. The concordance rate between FSD and PSD was investigated at the margin and patient levels, but survival analysis was performed solely at the patient level.

Research results

Analysis of 100 duct margins revealed that original concordance rate between FSD and PSD was 68.0% in the total layer, 69.0% in the epithelial layer, and 98.0% in the subepithelial layer. The extent of remaining biliary epithelium was comparable between FSD and PSD, and more than half of the margins lost > 50% of the entire epithelium, suggesting low quality of the samples. In FSD, the rate of negative margins decreased and that of borderline and positive margins increased according to the extent of the remaining epithelium, suggesting proportional sensitivity to the remaining rate and intrinsic difficulty in the assessment of the epithelial layer. Diagnostic discordance between FSD and PSD was observed in 31 epithelial layers and two subepithelial layers. Although the discordance rate in the epithelial layer was somewhat higher in pCCA than dCCA, there was no significant difference between them in the epithelial layer and subepithelial layer. Alteration from borderline to negative was the most frequent (20 of the 31 epithelial layers). Less frequently, alterations from negative to borderline (4 margins) and positive to borderline (4 margins) were observed in the epithelial layer. Although some authors reported no correlation between positive margins and postoperative local recurrence, in the present study patients with positive margin in the total and epithelial layers by FSD demonstrated a significantly worse local recurrence-free survival (RFS) compared with patients with borderline and negative margins. On the other hand, patients with borderline and negative margins in the total and epithelial layers by FSD revealed comparable local RFS. Patients with borderline and negative margins in the epithelial layer by PSD also revealed comparable local RFS. These results suggested that epithelial borderline might be regarded substantially as negative in such institutions as having well-experienced pathologists. However, if the first margin is borderline and additional margin can be safely obtained, additional ductal resection will be desirable to achieve negative margin, because it is quite likely that some borderline margins may ultimately turn out to be positive in a larger series with more diverse pathologist and the local recurrence is very high in positive margins. When classifying the status of the epithelial layer either as negative or positive, concordance rates between FSD and PSD in the total, epithelial, and subepithelial layers were 95.0%, 93.0%, and 98.0%, respectively. These results suggest that FSD is a reliable method to evaluate margin status of the bile duct intraoperatively.

Research conclusions

FSD of the bile duct margin was reliable enough to provide useful information for deciding the extent of resection of eCCA regardless of technical limitations in sample preparation. In contrast to the previous reports, positive margins in the epithelial layer was significantly associated with local recurrence, while the borderline margins demonstrated a similar local recurrence rate to that of negative margins. Although negative margin is desirable, epithelial borderline lesions could be regarded substantially as negative in such institutions as with well-experienced pathologists. These findings would aid surgeons to determine the resection range of the bile duct and better manage the patients with eCCA.

Research perspectives

Intraoperative FSD of the bile duct margins has traditionally been used to guide the extent of operative resection, but the usefulness of FSD has been controversial until now. In the present study, we clearly demonstrated that FSD was reliable enough for pathological diagnosis by comparing FSD and PSD and based on the results of survival analysis. In addition, in contrast to some previous reports, we demonstrated that positive FSD in the epithelial layer was significantly associated with local recurrence and that borderline FSD in the epithelial layer could be substantially regarded as negative. Our results may be partly due to a relatively large number of eCCA cases. This study also highlighted the need for precise and detailed histopathological diagnosis. In this respect, the future challenge is more objective differential diagnosis of BilIN-1, 2, and 3 by FSD. Development of morphometric analysis, special staining procedure, immunohistochemistry, and molecular diagnostics which can be available over a short time of intraoperative FSD are awaited. It will be also necessary to develop the training program of pathologists who can make a correct diagnosis of bile duct margin by intraoperative FSD.

REFERENCES

1 **Global Burden of Disease Cancer Collaboration**, Fitzmaurice C, Dicker D, Pain A, Hamavid H, Moradi-Lakeh M, MacIntyre MF, Allen C, Hansen G, Woodbrook R, Wolfe C, Hamadeh RR, Moore A, Werdecker A, Gessner BD, Te Ao B, McMahon B, Karimkhani C, Yu C, Cooke GS, Schwebel DC, Carpenter DO, Pereira DM, Nash D, Kazi DS, De Leo D, Plass D, Ukwaja KN, Thurston GD, Yun Jin K, Simard EP, Mills E, Park EK, Catalá-López F, deVeber G, Gotay C, Khan G, Hosgood HD 3rd, Santos IS, Leasher JL, Singh J, Leigh J, Jonas JB, Sanabria J, Beardsley J, Jacobsen KH, Takahashi K, Franklin RC, Ronfani L, Montico M, Naldi L, Tonelli M, Geleijnse J, Petzold M, Shrime MG, Younis M, Yonemoto N, Breitborde N, Yip P, Pourmalek F, Lotufo PA, Esteghamati A, Hankey GJ, Ali R, Lunevicius R, Malekzadeh R, Dellavalle R, Weintraub R, Lucas R, Hay R, Rojas-Rueda D, Westerman

R, Sepanlou SG, Nolte S, Patten S, Weichenthal S, Abera SF, Fereshtehnejad SM, Shiue I, Driscoll T, Vasankari T, Alsharif U, Rahimi-Movaghar V, Vlassov VV, Marcenes WS, Mekonnen W, Melaku YA, Yano Y, Artaman A, Campos I, MacLachlan J, Mueller U, Kim D, Trillini M, Eshrati B, Williams HC, Shibuya K, Dandona R, Murthy K, Cowie B, Amare AT, Antonio CA, Castañeda-Orjuela C, van Gool CH, Violante F, Oh IH, Deribe K, Soreide K, Knibbs L, Kereselidze M, Green M, Cardenas R, Roy N, Tillmann T, Li Y, Krueger H, Monasta L, Dey S, Sheikhbahaei S, Hafezi-Nejad N, Kumar GA, Sreeramareddy CT, Dandona L, Wang H, Vollset SE, Mokdad A, Salomon JA, Lozano R, Vos T, Forouzanfar M, Lopez A, Murray C, Naghavi M. The Global Burden of Cancer 2013. *JAMA Oncol* 2015; **1**: 505-527 [PMID: 26181261 DOI: 10.1001/jamaoncol.2015.0735]

2 **About Bile Duct Cancer**. American Cancer Society. Downloaded on October 30, 2017. Available from: URL: https://www.cancer.org/content/dam/CRC/PDF/Public/8552.00.pdf

3 **Banales JM**, Cardinale V, Carpino G, Marzioni M, Andersen JB, Invernizzi P, Lind GE, Folseraas T, Forbes SJ, Fouassier L, Geier A, Calvisi DF, Mertens JC, Trauner M, Benedetti A, Maroni L, Vaquero J, Macias RI, Raggi C, Perugorria MJ, Gaudio E, Boberg KM, Marin JJ, Alvaro D. Expert consensus document: Cholangiocarcinoma: current knowledge and future perspectives consensus statement from the European Network for the Study of Cholangiocarcinoma (ENS-CCA). *Nat Rev Gastroenterol Hepatol* 2016; **13**: 261-280 [PMID: 27095655 DOI: 10.1038/nrgastro.2016.51]

4 **Sakamoto Y**, Kosuge T, Shimada K, Sano T, Ojima H, Yamamoto J, Yamasaki S, Takayama T, Makuuchi M. Prognostic factors of surgical resection in middle and distal bile duct cancer: an analysis of 55 patients concerning the significance of ductal and radial margins. *Surgery* 2005; **137**: 396-402 [PMID: 15800484 DOI: 10.1016/j.surg.2004.10.008]

5 **Okazaki Y**, Horimi T, Kotaka M, Morita S, Takasaki M. Study of the intrahepatic surgical margin of hilar bile duct carcinoma. *Hepatogastroenterology* 2002; **49**: 625-627 [PMID: 12063955]

6 **Hirohashi K**, Uenishi T, Kubo S, Yamamoto T, Tanaka H, Shuto T, Yamasaki O, Horii K, Kinoshita H. Histologic bile duct invasion by a mass-forming intrahepatic cholangiocarcinoma. *J Hepatobiliary Pancreat Surg* 2002; **9**: 233-236 [PMID: 12140612 DOI: 10.1007/s005340200024]

7 **Yamaguchi K**, Shirahane K, Nakamura M, Su D, Konomi H, Motoyama K, Sugitani A, Mizumoto K, Tanaka M. Frozen section and permanent diagnoses of the bile duct margin in gallbladder and bile duct cancer. *HPB* (Oxford) 2005; **7**: 135-138 [PMID: 18333177 DOI: 10.1080/13651820510028873]

8 **Lechago J**. Frozen section examination of liver, gallbladder, and pancreas. *Arch Pathol Lab Med* 2005; **129**: 1610-1618 [PMID: 16329733]

9 **Endo I**, House MG, Klimstra DS, Gönen M, D'Angelica M, Dematteo RP, Fong Y, Blumgart LH, Jarnagin WR. Clinical significance of intraoperative bile duct margin assessment for hilar cholangiocarcinoma. *Ann Surg Oncol* 2008; **15**: 2104-2112 [PMID: 18543039 DOI: 10.1245/s10434-008-0003-2]

10 **Albores-Saavedra J**, Adsay NV, Crawford JM et al. Carcinoma of the gall bladder and extrahepatic bile ducts. In: Bosman FT, Carneiro F, Hruban RH, and Theise ND, eds. WHO classification of tumours of the digestive system, 4th ed. Lyon: IARC Press 2010: 266-273

11 **Bhuiya MR**, Nimura Y, Kamiya J, Kondo S, Nagino M, Hayakawa N. Clinicopathologic factors influencing survival of patients with bile duct carcinoma: multivariate statistical analysis. *World J Surg* 1993; **17**: 653-657 [PMID: 8273388 DOI: 10.1007/BF01659134]

12 **Sasaki R**, Takeda Y, Funato O, Nitta H, Kawamura H, Uesugi N, Sugai T, Wakabayashi G, Ohkohchi N. Significance of ductal margin status in patients undergoing surgical resection for extrahepatic cholangiocarcinoma. *World J Surg* 2007; **31**: 1788-1796 [PMID: 17647056 DOI: 10.1007/s00268-007-9102-7]

13 **Wakai T**, Shirai Y, Moroda T, Yokoyama N, Hatakeyama K. Impact of ductal resection margin status on long-term survival in patients undergoing resection for extrahepatic cholangiocarcinoma. *Cancer* 2005; **103**: 1210-1216 [PMID: 15685618 DOI: 10.1002/cncr.20906]

14 **Hayashi S**, Miyazaki M, Kondo Y, Nakajima N. Invasive growth patterns of hepatic hilar ductal carcinoma. A histologic analysis of 18 surgical cases. *Cancer* 1994; **73**: 2922-2929 [PMID: 8199989]

15 **Shimada H**, Niimoto S, Matsuba A, Nakagawara G, Kobayashi M, Tsuchiya S. Experience with intrahepatic cholangiojejunostomy for unresectable carcinoma of the hepatic hilus. *Int Surg* 1988; **73**: 1-5 [PMID: 3360569]

P- Reviewer: Bramhall S, Kapoor S, Lin J **S- Editor**: Gong ZM
L- Editor: A **E- Editor**: Huang Y

World Journal of Gastroenterology

Submit a Manuscript: http://www.f6publishing.com

World J Gastroenterol 2018 March 28; 24(12): 1343-1352

DOI: 10.3748/wjg.v24.i12.1343

ISSN 1007-9327 (print) ISSN 2219-2840 (online)

ORIGINAL ARTICLE

Clinical Trials Study

Correlation between serum vitamin B12 level and peripheral neuropathy in atrophic gastritis

Guo-Tao Yang, Hong-Ying Zhao, Yu Kong, Ning-Ning Sun, Ai-Qin Dong

Guo-Tao Yang, Hong-Ying Zhao, Yu Kong, Ning-Ning Sun, Ai-Qin Dong, Department of Third Neurology, Cangzhou Central Hospital, Cangzhou Clinical Medical School of Hebei Medical University, Cangzhou 061001, Hebei Province, China

Hong-Ying Zhao, Department of Elderly Internal Medicine, Cangzhou Central Hospital, Cangzhou Clinical Medical School of Hebei Medical University, Cangzhou 061001, Hebei Province, China

Yu Kong, Department of Second Digestion, Cangzhou Central Hospital, Cangzhou Clinical Medical School of Hebei Medical University, Cangzhou 061001, Hebei Province, China

Ning-Ning Sun, Department of First Digestion, Cangzhou Central Hospital, Cangzhou Clinical Medical School of Hebei Medical University, Cangzhou 061001, Hebei Province, China

ORCID number: Guo-Tao Yang (0000-0001-8760-1092); Hong-Ying Zhao (0000-0002-2313-8569); Yu Kong (0000-0002-7423-5051); Ning-Ning Sun (0000-0002-1711-6451); Ai-Qin Dong (0000-0002-1362-4520).

Author contributions: Yang GT, Zhao HY, Kong Y, Sun NN and Dong AQ designed the research; Yang GT, Zhao HY and Dong AQ performed the research; Yang GT, Zhao HY, Sun NN and Dong AQ contributed new reagents/analytic tools; Yang GT, Zhao HY and Dong AQ analyzed the data; and Yang GT and Dong AQ wrote the paper.

Supported by Cangzhou City Science and Technology Plan Projects, No. 151302138.

Institutional review board statement: The study was reviewed and approved by the Cangzhou Central Hospital, Cangzhou Clinical Medical School of Hebei Medical University Institutional Review Board.

Clinical trial registration statement: This study is registered with the Chinese Clinical Trial Registry, No. ChiCTR-ROC-17014051.

Informed consent statement: All study participants, or their legal guardian, provided informed written consent prior to study enrollment.

Conflict-of-interest statement: We declare that there are no conflicts of interest to disclose.

Manuscript source: Unsolicited manuscript

Correspondence to: Dr. Guo-Tao Yang, MD, Department of Third Neurology, Cangzhou Central Hospital, Cangzhou Clinical Medical School of Hebei Medical University, Gaojiao District, Cangzhou 061001, Hebei Province, China. yangguotao3815@cz_hospital.ac.cn
Telephone: +86-317-2179510
Fax: +86-317-2179510

Received: December 20, 2017
Peer-review started: December 20, 2017
First decision: January 4, 2018
Revised: February 7, 2018
Accepted: February 26, 2018
Article in press: February 26, 2018
Published online: March 28, 2018

Abstract

AIM

To explore the correlation between serum vitamin B12 level and peripheral neuropathy in patients with chronic atrophic gastritis (CAG).

METHODS

A total of 593 patients diagnosed with chronic gastritis by gastroscopy and pathological examination from

September 2013 to September 2016 were selected for this study. The age of these patients ranged within 18- to 75-years-old. Blood pressure, height and weight were measured in each patient, and the body mass index value was calculated. Furthermore, gastric acid, serum gastrin, serum vitamin and serum creatinine tests were performed, and peripheral nerve conduction velocity and *Helicobacter pylori* (*H. pylori*) were detected. In addition, the type of gastritis was determined by gastroscopy. The above factors were used as independent variables to analyze chronic gastritis with peripheral neuropathy and vitamin B12 deficiency risk factors, and to analyze the relationship between vitamin B12 levels and peripheral nerve conduction velocity. In addition, in the treatment of CAG on the basis of vitamin B12, patients with peripheral neuropathy were observed.

RESULTS

Age, *H. pylori* infection, CAG, vitamin B9 and vitamin B12 were risk factors for the occurrence of peripheral nerve degeneration. Furthermore, CAG and *H. pylori* infection were risk factors for chronic gastritis associated with vitamin B12 deficiency. Serum vitamin B12 level was positively correlated with sensory nerve conduction velocity in the tibial nerve (R = 0.463). After vitamin B12 supplementation, patients with peripheral neuropathy improved.

CONCLUSION

Serum vitamin B12 levels in patients with chronic gastritis significantly decreased, and the occurrence of peripheral neuropathy had a certain correlation. CAG and *H. pylori* infection are risk factors for vitamin B12 deficiency and peripheral neuropathy. When treating CAG, vitamin B12 supplementation can significantly reduce peripheral nervous system lesions. Therefore, the occurrence of peripheral neuropathy associated with vitamin B12 deficiency may be considered in patients with CAG. Furthermore, the timely supplementation of vitamin B12 during the clinical treatment of CAG can reduce or prevent peripheral nervous system lesions.

Key words: Chronic gastritis; Chronic atrophic gastritis; Vitamin B12; Peripheral neuropathy

Core tip: The general situation and peripheral nerve conduction velocity of 593 patients with chronic gastritis were compared. We found that serum vitamin B12 levels in patients with chronic gastritis significantly decreased, and the occurrence of peripheral neuropathy had a certain correlation. Vitamin B12 supplementation can significantly reduce peripheral nervous system lesions. The occurrence of peripheral neuropathy associated with vitamin B12 deficiency may be considered in patients with chronic atrophic gastritis. Timely supplementation of vitamin B12 during the clinical treatment of chronic atrophic gastritis can reduce or prevent peripheral nervous system lesions.

Yang GT, Zhao HY, Kong Y, Sun NN, Dong AQ. Correlation between serum vitamin B12 level and peripheral neuropathy in atrophic gastritis. *World J Gastroenterol* 2018; 24(12): 1343-1352 Available from: URL: http://www.wjgnet.com/1007-9327/full/v24/i12/1343.htm DOI: http://dx.doi.org/10.3748/wjg.v24.i12.1343

INTRODUCTION

Chronic atrophic gastritis (CAG) is a common chronic digestive system disease, and its main clinical manifestations include excessive abdominal pain, bloating and abdominal discomfort. Some patients may develop numbness and other neurological disease symptoms, and its pathological features are gastric mucosal and inherent glandular atrophy[1,2]. In addition, gastric mucosal and inherent glandular atrophy lead to gastric acid. Furthermore, internal factors, such as the insufficient secretion of substances, affect vitamin B12 (VitB12) absorption[3,4], which in turn leads to lack of VitB12 *in vivo*[5-9]. Related studies have shown that VitB12 and folic acid deficiency can affect homocysteine metabolism, which leads to impaired neurons, causing peripheral neuropathy[10-12]. Therefore, numbness and other neurological symptoms that may be related to VitB12 and folic acid deficiency should be considered in patients with CAG.

No clinical evidence published to date has confirmed the relationship between these two. Furthermore, no study has reported the supplementation of VitB12 during the occurrence and prognosis of peripheral neuropathy in patients with CAG. Moreover, the association of patients with CAG and peripheral neuropathy remains unclear. Therefore, in the present study, through the treatment of peripheral neuropathy in patients with chronic gastritis, the clinical characteristics were analyzed and the possible risk factors were screened out to identify viable preventive measures and interventions, thereby playing a guiding role in the clinical treatment of CAG. The details are reported as follows.

MATERIALS AND METHODS

Object of study

Outpatients diagnosed with chronic gastritis by gastroscopy and pathological examination in our hospital from September 2013 to September 2016 were selected for this study. Exclusion criteria: (1) patients < 18-years-old or > 75-years-old; (2) patients who received drugs to treat gastritis within the past 2 wk; (3) patients who received VitB12 supplements and folic acid drugs within the past 2 wk; (4) patients whose other

systems or organs are good, patients with malignant neoplasms, severe cardiovascular, cerebrovascular, liver or kidney disease, patients with primary disease of the hematopoietic system and patients with mental illness; (5) or patients who are pregnant and lactating. Finally, a total of 593 patients were included in the study. Among these patients, 295 were male and 298 were female. The average age of these patients was 46.5 ± 12.8 years, their mean blood pressure was 130.54 ± 19.96 mmHg/96.56 ± 9.70 mmHg, and their average body mass index (BMI) value was 21.16 ± 2.34. This research program and its experimental design were approved by the Ethics Committee of our institute. All patients provided signed informed consent.

Detection methods and groupings

Measurement of nerve conduction velocity: The Dantec Keypoint EMG/evoked potential (Denmark) was used at room temperature (25 ℃). The median nerve, ulnar nerve, tibial nerve and sural nerve sensory and motor nerve conduction velocity of patients were routinely detected. Nerve conduction velocity was lower than the average conduction velocity in healthy young people, and was less than three times the standard deviation, or the same nerve conduction velocity difference of > 10%; that is, peripheral nerve conduction velocity abnormality. These abnormalities were measured again. Hence, there were two results for the abnormal diagnosis for peripheral neuropathy. In our hospital, the motor nerve conduction velocity reference value was as follows: median nerve: 57.8 ± 6.2; ulnar nerve: 55.36 ± 4.65; tibial nerve: 44.96 ± 2.57; and sural nerve: 50.17 ± 3.62. The sensory nerve conduction velocity reference value was as follows: median nerve: 55.18 ± 4.26; ulnar nerve: 50.27 ± 4.53; tibial nerve: 52.43 ± 3.62; and sural nerve: 47.65 ± 6.47. These patients were divided into two groups, according to these results: peripheral neuropathy group, and no peripheral neuropathy group.

Determination of serum creatinine, serum gastrin and vitamin levels: 5 mL of venous blood was collected from all patients after 1 d of fasting. After anticoagulation, the collected samples were centrifuged. Then, after the serum was separated, the sample was frozen and stored in aliquots at -20 ℃ for testing. Serum creatinine and serum gastrin were detected using a Hitachi 7060 automatic biochemical analyzer (Japan), and serum vitamin was detected by immunoenzyme analysis. All related operations were performed by highly experienced personnel, in strict accordance with instrument instructions. The VitB12 normal reference value in our hospital was > 160 ng/L.

Gastric juice analysis: Patients were instructed to fast for 8-12 hr prior to their examination in the morning. The nasogastric tube was placed into the stomach through the nose, and overnight net pumping of fasting gastric juice was performed. Pentagastrin was subcutaneously injected to stimulate gastric acid secretion, and gastric juice suction was continued for 1 hr. Then, the maximum amount of gastric acid secreted by the patient was recorded.

Gastroscopy: Patients were instructed to fast for 6-8 hr prior to the examination. After the antifoaming agent was administered and pharyngeal anesthesia was performed, an Olympus GIF-XQ230 gastroscope (Japan) was used for the examination. For the endoscopy of each patient, two tissue samples were collected from the antrum and curvature of the gastric body, respectively. The specimens were immediately fixed in methanol after collection. After the specimens were conventionally fixed, the tissues were embedded, sliced, dyed and microscopically observed by experienced hospital laboratory personnel to identify the type of chronic gastritis.

***H. pylori* detection:** Each patient underwent the following tests for *H. pylori* detection: (1) rapid urease test; (2) 13C urea breath test; and (3) pathological examination. If the results revealed two or more signs of *H. pylori* positivity, the patient was diagnosed with *H. pylori* infection.

Intervention method

In addition to the conventional treatment of chronic gastritis, each patient was supplemented for vitamin deficiency according to their condition. The supplementation of VitB12 for CAG patients with peripheral neuropathy was based on the primary disease treatment and control of risk factors that lead to VitB12 deficiency.

Specific methods: In the treatment of CAG or the radical treatment of *H. pylori* on the basis of conventional medication, patients were intramuscularly injected with 0.5 mg of VitB12 once a week. Then, the VitB12 level and peripheral nerve conduction velocity (tibial nerve sensory nerve) of each patient were determined *in vivo* after diagnosis; that is, at the start of the medication, before the start of the medication, 1-3 mo after the medication, and 6 mo after the medication, respectively. The data were recorded and compared.

Statistical analysis

SPSS 19.0 was used for statistical analysis. The age and incidence of peripheral neuropathy in each group was used for count data, and analyzed by χ^2-test. Age, blood pressure, serum creatinine, gastric acid, serum gastrin and serum vitamin levels, and nerve conduction velocity measurement data were expressed as mean ± SD. *T*-test was used to compare between groups. The multivariate regression analysis of chronic gastritis with peripheral neuropathy was performed by logistic regression analysis. The correlation analysis between VitB12 and peripheral nerve conduction velocity

Table 1 Comparison of the peripheral nerve conduction velocity of patients with or without peripheral neuropathy

Item	Sensory nerve conduction velocity				Motor nerve conduction velocity			
	With peripheral nerve damage	Without peripheral nerve damage	*t*	*P* value	With peripheral nerve damage	Without peripheral nerve damage	*t*	*P* value
Median nerve	50.10 ± 7.80	52.30 ± 8.90	-2.733	0.006	54.20 ± 8.70	56.20 ± 10.70	-2.129	0.034
Ulnar nerve	49.40 ± 8.10	51.50 ± 9.20	-2.556	0.011	50.30 ± 9.40	51.30 ± 8.60	-1.230	0.219
Tibial nerve	38.30 ± 3.20	44.20 ± 7.60	-9.563	0.000	50.4 ± 8.70	55.60 ± 9.80	-5.931	0.000
Sural nerve	45.40 ± 5.00	50.80 ± 8.30	-7.622	0.000	46.70 ± 7.90	51.10 ± 9.00	-5.479	0.000

was analyzed by Pearson analysis. The multivariate regression analysis of chronic gastritis with VitB12 deficiency was performed using logistic regression analysis. The level of serum VitB12 and folic acid were compared using one-way ANOVA after 1-3 mo and 6 mo. $P < 0.05$ was considered statistically significant.

RESULTS

Groupings and the comparison of peripheral nerve conduction velocity between the two groups

A total of 593 patients with chronic gastritis were included in the present study. Among these patients, 162 had peripheral neuropathy (peripheral neuropathy group) and 431 had no peripheral neuropathy (no peripheral neuropathy group). The peripheral nerve conduction velocity in these two groups was compared. The ulnar-median nerve, tibial nerve and sural nerve sensory and motor nerve conduction velocity, and ulnar nerve sensory nerve conduction velocity were lower in patients with peripheral neuropathy, compared to patients without peripheral neuropathy, and the difference was statistically significant ($P < 0.05$). There was no significant difference in nerve conduction velocity between these two groups ($P > 0.05$; Table 1).

Comparison of the general situation of patients in the peripheral neuropathy and no peripheral neuropathy groups

In comparing the general information of patients in these two groups, it was revealed that age, *H. pylori* infection rate and the prevalence of CAG were higher in patients in the peripheral neuropathy group than in patients in the no peripheral neuropathy group, while BMI, serum vitamin A, vitamin B9 (folic acid) and VitB12 were lower than in patients in the no peripheral neuropathy group, and the differences were statistically significant ($P < 0.05$). Moreover, the difference in sex, blood pressure, serum creatinine, VitB1, VitB6 and VitE between these two groups were not statistically significant ($P > 0.05$; Table 2).

Peripheral neuropathy multivariate logistic regression analysis results

A further factorial analysis was performed on factors that were statistically significant in the univariate analysis. Age, BMI, *H. pylori* infection, endoscopic results (CAG), vitamin A, VitB9 (folic acid) and VitB12 were included in the analysis. The logistic regression analysis results revealed that BMI, gastric acid, serum gastrin and vitamin A had no significant effect on peripheral neuropathy, and the difference was not statistically significant ($P > 0.05$). On the contrary, age (P =0.037), *H. pylori* infection (P = 0.000), CAG (P = 0.000), VitB9 (P = 0.034) and VitB12 (P = 0.000) had a significant effect on peripheral neuropathy. Further analysis revealed that based on odds ratio (OR) values, the following factors effected peripheral neuropathy (arranged in descending order according to occurrence): VitB12, CAG, *H. pylori* infection, VitB9 and age (Table 3).

Correlation analysis of serum VitB12 levels and sensory nerve conduction velocity in the tibial nerve for patients with chronic gastritis

The correlation between serum VitB12 and peripheral nerve conduction velocity in patients with chronic gastritis was analyzed. Results are shown in Figure 1. There was a positive correlation between serum VitB12 levels and peripheral nerve conduction velocity (r = 0.631, P = 0.000).

Comparison of the general situation of patients with or without VitB12 deficiency

In comparing the general situation of chronic gastritis patients with VitB12 deficiency and normal VitB12 levels, it was found that age, *H. pylori* infection rate, the prevalence of CAG and serum gastrin levels were significantly higher in patients with VitB12 deficiency than in patients with normal VitB12 levels ($P < 0.05$), while BMI values and folic acid levels were low in patients with normal VitB12 levels; and, the difference was statistically significant ($P < 0.05$). However, the difference in sex, blood pressure and serum creatinine levels between both groups of patients was not statistically significant ($P > 0.05$; Table 4).

Multivariate logistic regression analysis results for chronic gastritis patients with VitB12 deficiency

Further factorial analysis was performed on factors that were statistically significant for the univariate analysis. Age, BMI value, *H. pylori* infection, endoscopy results (CAG), gastric acid and serum gastrin were included in the analysis. The logistic regression analysis results revealed that BMI values, gastric acid and serum gastrin had no significant effect on VitB12 deficiency,

Table 2 Comparison of the general situation of patients in the peripheral neuropathy and no peripheral neuropathy groups

Item	Peripheral neuropathy group	No peripheral neuropathy group	t/c^2	*P* value
Age in yr	50.50 ± 13.90	45.00 ± 12.40	4.653	0.000
Sex, % male	50.60	49.50	0.068	0.795
Systolic blood pressure in mmHg	130.17 ± 18.98	128.35 ± 20.32	0.989	0.323
Diastolic blood pressure in mmHg	75.34 ± 10.32	77.02 ± 9.45	-1.880	0.061
BMI in kg/m^2	19.26 ± 2.15	21.88 ± 2.27	-12.703	0.000
Gastroscopy results, % prevalence of chronic atrophic gastritis	76.50%	59.20%	15.418	0.000
Helicobacter pylori infection, %	86.40	56.40	46.452	0.000
Gastric acid in mmol	6.80 ± 3.70	17.80 ± 3.50	-33.570	0.000
Serum gastrin in pg/mL	532.42 ± 167.33	208.43 ± 44.12	36.968	0.000
Serum creatinine in μmol/L	78.60 ± 17.20	76.50 ± 12.40	1.643	0.101
VitA in ng/mL	0.267 ± 0.269	0.383 ± 0.336	-3.944	0.000
VitB1 in nmol/L	79.40 ± 20.70	82.60 ± 17.50	-1.884	0.060
VitB6 in mmol/L	30.90 ± 14.80	32.70 ± 15.60	-1.269	0.205
VitB9 in ng/mL	9.06 ± 3.81	10.60 ± 3.27	-2.495	0.013
VitB12 in pg/mL	170.20 ± 111.20	216.40 ± 149.80	-2.731	0.007
VitE in μmol/L	31.60 ± 5.48	33.20 ± 6.37	-1.346	0.181

BMI: Body mass index; Vit: Vitamin.

Table 3 Peripheral neuropathy multivariate logistic regression analysis results

Influencing factor	β	SE	Wald value	OR	95%CI		*P* value
Age	0.140	0.056	4.658	1.150	1.030	1.283	0.034
BMI	-0.139	2.321	3.097	0.871	0.009	82.261	0.089
Helicobacter pylori infection, infected = 1; uninfected = 0	1.541	0.124	7.816	4.670	3.662	5.955	0.000
Gastric acid	1.332	1.469	1.158	3.790	0.213	67.465	0.886
Serum gastrin	1.545	2.497	1.796	4.690	0.035	626.127	0.375
Endoscopy results, atrophic gastritis = 1; nonatrophic gastritis = 0	1.663	0.197	8.562	5.276	3.586	7.762	0.000
VitA	0.039	0.127	1.562	1.041	0.811	1.334	0.645
VitB9	0.871	0.359	4.162	2.390	1.183	4.830	0.037
VitB12	1.883	0.236	9.364	6.571	4.137	10.434	0.000

BMI: Body mass index; CI: Confidence interval; OR: Odds ratio; SE: Standard error; Vit: Vitamin.

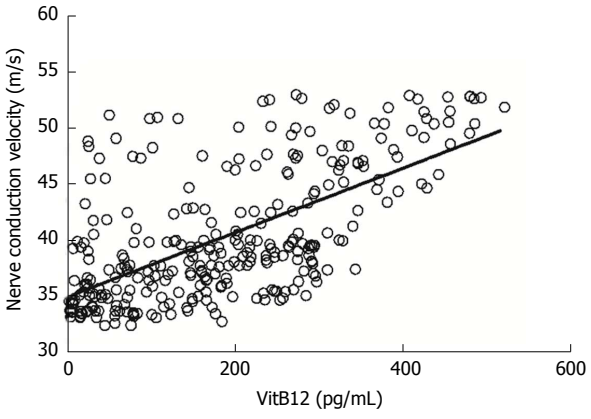

Figure 1 Correlation analysis of serum VitB12 level and sensory nerve conduction velocity in the tibial nerve of patients with chronic gastritis. Vit: Vitamin.

and the difference was not statistically significant ($P > 0.05$); while age ($P = 0.037$), *H. pylori* infection ($P = 0.000$) and CAG ($P = 0.000$) had a significant effect on VitB12 deficiency. Further analysis revealed that based on OR values, the following factors affected VitB12 deficiency (in descending order): CAG, *H. pylori* infection and age (Table 5).

Changes of serum VitB12 levels and nerve conduction velocity in patients after supplementation with VitB12

Chronic gastritis in patients with VitB12 deficiency occurred mainly due to slow atrophic gastritis and *H. pylori* infection. In the present study, atrophic gastritis and radical *H. pylori* infection were treated based on the supplementation of VitB12 in patients. These results revealed that compared with untreated patients, serum VitB12 levels gradually increased ($F = 5.241$, $P < 0.05$); and after 1 mo of treatment, the differences were statistically significant ($T = 4.647$, $P = 0.000$). Furthermore, nerve conduction velocity gradually accelerated ($F = 3.172$, $P < 0.05$; Table 6, Figures 2 and 3).

DISCUSSION

CAG is a common digestive system disease, which commonly causes *H. pylori* infection, bile reflux, vasoactive factors and cytokine changes. It has been generally accepted that CAG occurs under the joint action of

Table 4 Comparison of the general situation of patients with or without vitamin B12 deficiency

Item	VitB12 deficiency, n = 207	Normal VitB12 level, n = 386	t/c^2	P value
Age in yr	51.70 ± 14.70	44.3 ± 11.80	6.666	0.000
Sex, % male	51.60	48.80	0.481	0.488
Systolic blood pressure in mmHg	132.13 ± 19.37	129.35 ± 20.06	1.628	0.104
Diastolic blood pressure in mmHg	75.26 ± 11.44	76.31 ± 9.37	-1.202	0.230
BMI in kg/m^2	18.36 ± 3.22	22.45 ± 2.39	-17.529	0.000
Helicobacter pylori infection, %	87.6	74.8	12.949	0.000
Gastroscopy results, % prevalence of chronic atrophic gastritis	86.50	51.80	70.180	0.000
Serum creatinine in μmol/L	78.60 ± 17.20	76.5 ± 12.40	1.709	0.088
Gastric acid in mmol	7.90 ± 4.20	17.60 ± 3.50	-29.955	0.000
Serum gastrin in pg/mL	432.85 ± 137.62	219.49 ± 47.98	27.516	0.000

BMI: Body mass index; Vit: Vitamin.

Table 5 Multivariate logistic regression analysis of VitB12 deficiency

Influencing factor	β	SE	Wald value	OR	95%CI		P value
Age	0.519	0.149	4.865	1.680	1.255	2.250	0.023
BMI	1.477	1.325	0.004	4.380	0.326	58.795	0.957
Helicobacter pylori infection, positive = 1; negative = 0	1.730	0.279	7.218	5.640	3.264	9.745	0.000
Endoscopy results, atrophic gastritis = 1; nonatrophic gastritis = 0	2.145	0.364	9.645	8.546	4.187	17.442	0.000
Gastric acid	0.948	1.269	1.024	2.580	0.214	31.032	0.762
Serum gastrin	1.479	2.226	2.549	4.390	0.056	344.567	0.267

BMI: Body mass index; CI: Confidence interval; OR: Odds ratio; SE: Standard error; Vit: Vitamin.

Table 6 Changes in serum VitB12 levels and nerve conduction velocity in patients after half a year of VitB12 supplementation

Item	0 mo	1 mo	2 mo	3 mo	6 mo
VitB12 in pg/mL	158.70 ± 104.50	237.20 ± 156.40	481.50 ± 164.60	614.80 ± 186.70	635.20 ± 174.80
Nerve conduction velocity in m/s at 0 mo	40.10 ± 5.50	40.30 ± 4.70	41.60 ± 7.40	42.70 ± 5.90	45.80 ± 5.80

Vit: Vitamin.

various factors, and its development process is caused by the long evolution of multiple genes. Its main clinical manifestations include stomach pain, fullness, ruffian nausea, belching and acid reflux. Some patients may also experience numbness and present other nervous system symptoms. In the course of disease development, gastric mucosal and inherent gland atrophy, decreased gastric acid secretion and other serious effects may disrupt the absorption of nutrients[13-15].

VitB12 is one of the essential vitamins that can improve folic acid utilization, and in turn promote homocysteine metabolism[16-18]. Studies have shown that VitB12 and folic acid deficiency lead to homocysteine metabolism, and is inhibited by the role of axons and myelin in Schwann cells, leading to neuronal damage and peripheral neuropathy[19]. Another study revealed that VitB12 deficiency can lead to neuronal myelination[20-22]. However, at present, the relationship between these two has not been clinically confirmed. Furthermore, the effect of VitB12 on the occurrence and outcome of peripheral neuropathy in patients with CAG remains unclear.

In the present study, by comparing the effects of different factors on peripheral nerve conduction velocity and serum VitB12 levels, it was found that VitB12 deficiency may be a major risk factor for CAG patients with peripheral neuropathy, while CAG and *H. pylori* infection may be risk factors for chronic gastritis patients with VitB12 deficiency. Simultaneously, this study confirmed that treating the primary disease with the supplementation of VitB12 can significantly improve peripheral neuropathy symptoms, suggesting that the timely supplementation of VitB12 can prevent or improve CAG in patients with peripheral neuropathy symptoms.

Analysis of the influencing factors of peripheral neuropathy

In comparing the general situation of patients with or without peripheral neuropathy, it was found that age, *H. pylori* infection rate, CAG, BMI, serum vitamin A,

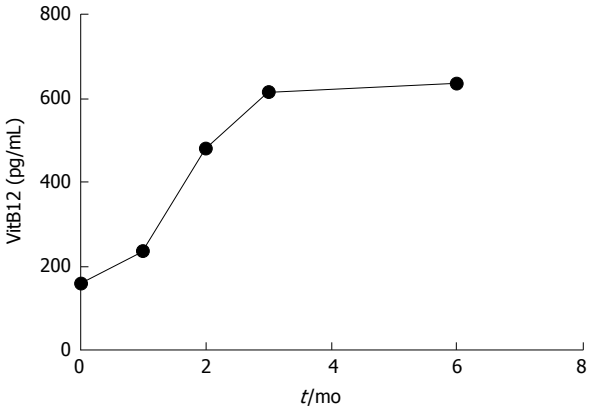

Figure 2 Trend changes in serum VitB12 level. Vit: Vitamin.

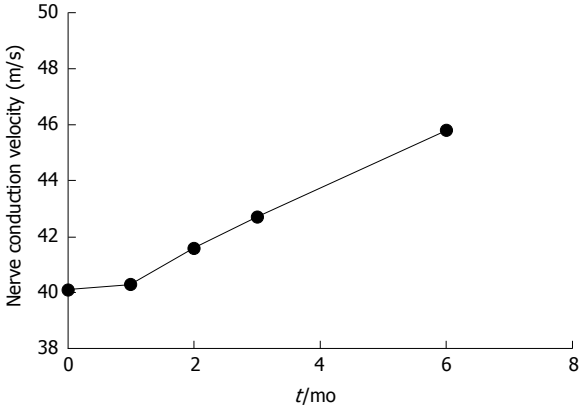

Figure 3 Trend changes in nerve conduction velocity.

vitamin B9 (folic acid) and VitB12 were the possible risk factors for peripheral neuropathy in patients with chronic gastritis. Based on further logistic multivariate regression analysis, it was found that age, *H. pylori* infection, CAG, VitB9 and VitB12 were risk factors for peripheral neurodegeneration. Among these factors, VitB12, *H. pylori* infection and CAG exhibited a higher relative risk. In addition, age is also one of the risk factors for CAG[23-28], which may be due to its long course; that is, pathogenic factors take a long period of time to become a risk factor for peripheral neuropathy.

Correlation between peripheral nerve conduction velocity and serum VitB12 level

In the assessment of peripheral nerve conduction velocity, it was found that this was more obvious in lower limb peripheral neuropathy, and was particularly evident in tibial nerve sensory nerves in the lower limb. Therefore, the correlation between serum VitB12 level and peripheral conduction velocity was analyzed by tibial nerve sensory nerve conduction velocity. The correlation analysis revealed that peripheral nerve conduction velocity was positively correlated with serum VitB12 levels (R = 0.463); that is, as serum VitB12 levels decreased, the degree of peripheral neuropathy gradually increased.

Analysis of influencing factors for VitB12 deficiency

The above studies show that serum VitB12 levels in patients with chronic gastritis were associated with the risk factors for peripheral neuropathy. In order to explore the etiology of VitB12 in patients with chronic gastritis in the present study, the general situations of chronic gastritis patients associated with VitB12 deficiency were compared. Based on further logistic multivariate regression analysis, it was found that *H. pylori* infection and CAG were independent risk factors for chronic gastritis with VitB12 deficiency. Among these factors, *H. pylori* infection can lead to VitB12 deficiency[29-31]. Furthermore, *H. pylori* infection is one of the common causes of CAG[32-40]. The possible cause for VitB12 deficiency is the damage induced by *H. pylori* infection on gastric mucosal cells[41,42], which reduces gastric acid secretion and affects the separation of VitB12 from food[43]. At the same time, the reduction in gastric mucosal secretion of vitamin C and stomach pH value is affected by the increased absorption of vitamin B[44,45].

Effects of VitB12 supplementation on peripheral neuropathy

Peripheral neuropathy can be treated by VitB12 supplementation. A large number of studies have shown that VitB12 can significantly improve nervous system diseases in patients, such as spinal cord subacute combined disease and reversible myelopathy[46-50]. In the present study, the management of VitB12 deficiency may be a risk factor (CAG and *H. pylori* infection). On this basis, by comparing patients with CAG on the basis of conventional treatment without VitB12 supplementation (0 mo), and after 1-3 mo and 6 mo of treatment, the serum VitB12 level and peripheral nerve conduction velocity trend revealed that serum VitB12 level and nerve conduction velocity gradually increased after treatment. As shown in Figures 2 and 3, it can be observed that the increase in peripheral nerve conduction velocity was faster than that of serum VitB12 levels. It can be speculated that the speed of peripheral nerve conduction was accelerated due to elevated serum VitB12 levels. Hence, VitB12 supplementation can improve peripheral neuropathy.

Limitations and outlook

In the present study, the subjects collected for the experiment all came from our hospital, which may give rise to some limitations. However, there were significant differences in VitB12 and nerve conduction velocity between these two groups. Hence, there can still be a certain degree of response to the relationship between these two. In subsequent studies, a multi-center and multi-region joint cooperation should be conducted to expand the sample size and improve the sample representation, in order to provide results with a higher

degree of confidence.

Summary

In summary, in the present study, we analyzed the risk factors of chronic gastritis with peripheral neuropathy. Furthermore, the correlation between serum VitB12 level and peripheral neuropathy was analyzed. The level of serum VitB12 in patients with chronic gastritis was a risk factor for peripheral neuropathy, and serum VitB12 levels and the severity of peripheral neuropathy were positively correlated. In addition, CAG and *H. pylori* infection were the major risk factors for VitB12 deficiency in patients with chronic gastritis.

By comparing the peripheral nerve conduction velocity after VitB12 supplementation, it was found that the treatment of CAG and the control of *H. pylori* infection while supplementing with VitB12 can significantly reduce peripheral neuropathy. This suggests that the timely supplementation of VitB12 may become a treatment or even prevent the occurrence of CAG in patients or the occurrence of peripheral neuropathy. However, it remains to be further studied whether this can be applied to this population.

ARTICLE HIGHLIGHTS

Research background

The main clinical manifestations of chronic atrophic gastritis are excessive abdominal pain, bloating and abdominal discomfort. It is known that the insufficient secretion of substances would affect vitamin B12 (VitB12) absorption. VitB12 and folic acid deficiency can affect homocysteine metabolism, which leads to peripheral neuropathy. Therefore, the occurrence of patients with chronic atrophic gastritis numbness and other nervous system symptoms may be related to VitB12 and folic acid deficiency

Research motivation

At present, there are no studies reporting the effect of VitB12 supplementation on the occurrence and outcome of peripheral neuropathy in patients with chronic atrophic gastritis. The causes of peripheral neuropathy in patients with chronic atrophic gastritis are also not clear. Therefore, it is necessary to explore the risk factors of peripheral neuropathy in patients with chronic atrophic gastritis.

Research objectives

This study aimed to explore the clinical features of peripheral neuropathy in patients with chronic atrophic gastritis and to screen out the possible risk factors in order to find out the feasible prevention and intervention measures for the clinical treatment of chronic atrophic gastritis

Research methods

In total, 593 patients diagnosed with chronic gastritis were involved and their gastric acid, serum gastrin, serum vitamin and serum creatinine tests, peripheral nerve conduction velocity and *Helicobacter pylori* (*H. pylori*) were detected. In addition, the type of gastritis was determined by gastroscopy. All detected results were used to analyze the relationship between VitB12 levels and peripheral nerve conduction velocity.

Research results

H. pylori infection and chronic atrophic gastritis were independent risk factors for chronic gastritis associated with VitB12 deficiency. The separation of VitB12 from food was affected because *H. pylori* infection in gastric mucosal cells damage gastric acid secretion (reducing it). This study also found that the serum VitB12 and nerve conduction velocity gradually increased after VitB12 supplement treatment, suggesting that VitB12 supplementation can improve peripheral neuropathy.

Research conclusions

This study found that serum VitB12 is a risk factor for peripheral neuropathy in patients with chronic gastritis, and serum vitamin B12 is positively correlated with the severity of peripheral neuropathy. Chronic atrophic gastritis and *H. pylori* infection are the main risk factors of VitB12 deficiency in patients with chronic gastritis. In addition, timely VitB12 supplementation may be an effective treatment and even a prevention method of peripheral neuropathy in patients with chronic atrophic gastritis.

Research perspectives

Although this study has demonstrated serum VitB12 level is related to peripheral neuropathy in patients with chronic atrophic gastritis, it is still limited since it's a single center study. Future research should be designed as a multicenter study, and a large sample size is needed to make the findings more credible.

REFERENCES

1 **Wei Y**, Ma LX, Yin SJ, An J, Wei Q, Yang JX. Huangqi Jianzhong Tang for Treatment of Chronic Gastritis: A Systematic Review of Randomized Clinical Trials. *Evid Based Complement Alternat Med* 2015; **2015**: 878164 [PMID: 26819622 DOI: 10.1155/2015/878164]

2 **Mescoli C**, Gallo Lopez A, Taxa Rojas L, Jove Oblitas W, Fassan M, Rugge M. Gastritis staging as a clinical priority. *Eur J Gastroenterol Hepatol* 2018; **30**: 125-129 [PMID: 29215433 DOI: 10.1097/MEG.0000000000001015]

3 **Nomura S**, Ida K, Terao S, Adachi K, Kato T, Watanabe H, Shimbo T; Research Group for Establishment of Endoscopic Diagnosis of Chronic Gastritis. Endoscopic diagnosis of gastric mucosal atrophy: multicenter prospective study. *Dig Endosc* 2014; **26**: 709-719 [PMID: 24698334 DOI: 10.1111/den.12286]

4 **Cavalcoli F**, Zilli A, Conte D, Massironi S. Micronutrient deficiencies in patients with chronic atrophic autoimmune gastritis: A review. *World J Gastroenterol* 2017; **23**: 563-572 [PMID: 28216963 DOI: 10.3748/wjg.v23.i4.563]

5 **Toh BH**, Chan J, Kyaw T, Alderuccio F. Cutting edge issues in autoimmune gastritis. *Clin Rev Allergy Immunol* 2012; **42**: 269-278 [PMID: 21174235 DOI: 10.1007/s12016-010-8218-y]

6 **Lahner E**, Gentile G, Purchiaroni F, Mora B, Simmaco M, Annibale B. Single nucleotide polymorphisms related to vitamin B12 serum levels in autoimmune gastritis patients with or without pernicious anaemia. *Dig Liver Dis* 2015; **47**: 285-290 [PMID: 25681243 DOI: 10.1016/j.dld.2015.01.147]

7 **Harakal J**, Rival C, Qiao H, Tung KS. Regulatory T Cells Control Th2-Dominant Murine Autoimmune Gastritis. *J Immunol* 2016; **197**: 27-41 [PMID: 27259856 DOI: 10.4049/jimmunol.1502344]

8 **Parsons BN**, Ijaz UZ, D'Amore R, Burkitt MD, Eccles R, Lenzi L, Duckworth CA, Moore AR, Tiszlavicz L, Varro A, Hall N, Pritchard DM. Comparison of the human gastric microbiota in hypochlorhydric states arising as a result of Helicobacter pylori-induced atrophic gastritis, autoimmune atrophic gastritis and proton pump inhibitor use. *PLoS Pathog* 2017; **13**: e1006653 [PMID: 29095917 DOI: 10.1371/journal.ppat.1006653]

9 **Kulnigg-Dabsch S**. Autoimmune gastritis. *Wien Med Wochenschr* 2016; **166**: 424-430 [PMID: 27671008 DOI: 10.1007/s10354-016-0515-5]

10 **Varbanova M**, Frauenschläger K, Malfertheiner P. Chronic gastritis - an update. *Best Pract Res Clin Gastroenterol* 2014; **28**: 1031-1042 [PMID: 25439069 DOI: 10.1016/j.bpg.2014.10.005]

11 **Dobson R**, Alvares D. The difficulties with vitamin B12. *Pract Neurol* 2016; **16**: 308-311 [PMID: 27009308 DOI: 10.1136/practneurol-2015-001344]

12 **Stredny CM**, Frosch O, Singhi S, Furutani E, Durbin AD, Grace RF, Ullrich NJ. Vitamin B12 Deficiency Presenting with Neurological Dysfunction in an Adolescent. *Pediatr Neurol* 2016; **62**: 66-70

[PMID: 27473652 DOI: 10.1016/j.pediatrneurol.2016.03.022]
13 **Wilmshurst JM**, Ouvrier R. Hereditary peripheral neuropathies of childhood: an overview for clinicians. *Neuromuscul Disord* 2011; **21**: 763-775 [PMID: 21741240 DOI: 10.1016/j.nmd.2011.05.013]
14 **Rohde C**, von Teeffelen-Heithoff A, Thiele AG, Arelin M, Mütze U, Kiener C, Gerloff J, Baerwald C, Schultz S, Heller C, Müller AS, Kiess W, Beblo S. PKU patients on a relaxed diet may be at risk for micronutrient deficiencies. *Eur J Clin Nutr* 2014; **68**: 119-124 [PMID: 24253763 DOI: 10.1038/ejcn.2013.218]
15 **Betesh AL**, Santa Ana CA, Cole JA, Fordtran JS. Is achlorhydria a cause of iron deficiency anemia? *Am J Clin Nutr* 2015; **102**: 9-19 [PMID: 25994564 DOI: 10.3945/ajcn.114.097394]
16 **Sipponen P**, Maaroos HI. Chronic gastritis. *Scand J Gastroenterol* 2015; **50**: 657-667 [PMID: 25901896 DOI: 10.3109/00365521.2015.1019918]
17 **Ni J**, Zhang L, Zhou T, Xu WJ, Xue JL, Cao N, Wang X. Association between the MTHFR C677T polymorphism, blood folate and vitamin B12 deficiency, and elevated serum total homocysteine in healthy individuals in Yunnan Province, China. *J Chin Med Assoc* 2017; **80**: 147-153 [PMID: 28094233 DOI: 10.1016/j.jcma.2016.07.005]
18 **Katsiki N**, Perez-Martinez P, Mikhailidis DP. Homocysteine and Non-Cardiac Vascular Disease. *Curr Pharm Des* 2017; **23**: 3224-3232 [PMID: 28317478 DOI: 10.2174/1381612823666170317124913]
19 **Shiran A**, Remer E, Asmer I, Karkabi B, Zittan E, Cassel A, Barak M, Rozenberg O, Karkabi K, Flugelman MY. Association of Vitamin B12 Deficiency with Homozygosity of the TT MTHFR C677T Genotype, Hyperhomocysteinemia, and Endothelial Cell Dysfunction. *Isr Med Assoc J* 2015; **17**: 288-292 [PMID: 26137654]
20 **Schroecksnadel K**, Leblhuber F, Fuchs D. Effect of L-dopa on plasma homocysteine in PD patients: relationship to B-vitamin status. *Neurology* 2004; **62**: 676; author reply 676-676; author reply 677 [PMID: 14994447]
21 **Hedera P**. Hereditary and metabolic myelopathies. *Handb Clin Neurol* 2016; **136**: 769-785 [PMID: 27430441 DOI: 10.1016/B978-0-444-53486-6.00038-7]
22 **Keenan A,** Whittam B, Rink R.Vitamin B12 deficiency in patients after enterocystoplasty. *J Pediatr Urol* 2015; **11**: 273.e1-273.e5 [DOI: 10.1016/j.jpurol.2015.04.026]
23 **Lindenbaum J**, Healton EB, Savage DG, Brust JC, Garrett TJ, Podell ER, Marcell PD, Stabler SP, Allen RH. Neuropsychiatric disorders caused by cobalamin deficiency in the absence of anemia or macrocytosis. *N Engl J Med* 1988; **318**: 1720-1728 [PMID: 3374544 DOI: 10.1056/NEJM198806303182604]
24 **Zhang Y**, Weck MN, Schöttker B, Rothenbacher D, Brenner H. Gastric parietal cell antibodies, Helicobacter pylori infection, and chronic atrophic gastritis: evidence from a large population-based study in Germany. *Cancer Epidemiol Biomarkers Prev* 2013; **22**: 821-826 [PMID: 23456556 DOI: 10.1158/1055-9965.EPI-12-1343]
25 **Namekata T**, Miki K, Kimmey M, Fritsche T, Hughes D, Moore D, Suzuki K. Chronic atrophic gastritis and Helicobacter pylori infection among Japanese Americans in Seattle. *Am J Epidemiol* 2000; **151**: 820-830 [PMID: 10965979]
26 **Brenner H**, Rothenbacher D, Weck MN. Epidemiologic findings on serologically defined chronic atrophic gastritis strongly depend on the choice of the cutoff-value. *Int J Cancer* 2007; **121**: 2782-2786 [PMID: 17691112 DOI: 10.1002/ijc.22992]
27 **Kohli Y**, Kato T, Suzuki K, Tada T, Fujiki N. Incidence of atrophic gastritis with age in Japan and Canada. *Jpn J Med* 1987; **26**: 158-161 [PMID: 3626154]
28 **Takase Y.** An endoscopie and bioptic Study on Chronic Gastrits (I) Atrophic Gastritis. *Nihon Shokakibyo Gakkai Zasshi* 2007; 99-106 [DOI: 10.11405/nisshoshi1964.70.99]
29 **Neumann WL**, Coss E, Rugge M, Genta RM. Autoimmune atrophic gastritis--pathogenesis, pathology and management. *Nat Rev Gastroenterol Hepatol* 2013; **10**: 529-541 [PMID: 23774773 DOI: 10.1038/nrgastro.2013.101]
30 **Stopeck A**. Links between Helicobacter pylori infection, cobalamin deficiency, and pernicious anemia. *Arch Intern Med* 2000; **160**: 1229-1230 [PMID: 10809024 DOI: 10.1001/archinte.160.9.1229]
31 **Kaptan K**, Beyan C, Ural AU, Cetin T, Avcu F, Gülşen M, Finci R, Yalçín A. Helicobacter pylori--is it a novel causative agent in Vitamin B12 deficiency? *Arch Intern Med* 2000; **160**: 1349-1353 [PMID: 10809040]
32 **Franceschi F**, Annalisa T, Teresa DR, Giovanna D, Ianiro G, Franco S, Viviana G, Valentina T, Riccardo LL, Antonio G. Role of Helicobacter pylori infection on nutrition and metabolism. *World J Gastroenterol* 2014; **20**: 12809-12817 [PMID: 25278679 DOI: 10.3748/wjg.v20.i36.12809]
33 **Sipponen P**. Chronic gastritis in former times and now. *Helicobacter* 2007; **12** Suppl 2: 16-21 [PMID: 17991172 DOI: 10.1111/j.1523-5378.2007.00561.x]
34 **Weck MN**, Brenner H. Association of Helicobacter pylori infection with chronic atrophic gastritis: Meta-analyses according to type of disease definition. *Int J Cancer* 2008; **123**: 874-881 [PMID: 18484586 DOI: 10.1002/ijc.23539]
35 **Chen XZ**, Schöttker B, Castro FA, Chen H, Zhang Y, Holleczek B, Brenner H. Association of helicobacter pylori infection and chronic atrophic gastritis with risk of colonic, pancreatic and gastric cancer: A ten-year follow-up of the ESTHER cohort study. *Oncotarget* 2016; **7**: 17182-17193 [PMID: 26958813 DOI: 10.18632/oncotarget.7946]
36 **Kobayashi S**, Ogura M, Suzawa N, Horiki N, Katsurahara M, Ogura T, Sakuma H. 18F-FDG uptake in the stomach on screening PET/CT: value for predicting Helicobacter pylori infection and chronic atrophic gastritis. *BMC Med Imaging* 2016; **16**: 58 [PMID: 27756255 DOI: 10.1186/s12880-016-0161-9]
37 **Roesler BM**, Rabelo-Gonçalves EM, Zeitune JM. Virulence Factors of Helicobacter pylori: A Review. *Clin Med Insights Gastroenterol* 2014; **7**: 9-17 [PMID: 24833944 DOI: 10.4137/CGast.S13760]
38 **Adamu MA**, Weck MN, Gao L, Brenner H. Incidence of chronic atrophic gastritis: systematic review and meta-analysis of follow-up studies. *Eur J Epidemiol* 2010; **25**: 439-448 [PMID: 20585973 DOI: 10.1007/s10654-010-9482-0]
39 **Reshetnyak VI**, Reshetnyak TM. Significance of dormant forms of Helicobacter pylori in ulcerogenesis. *World J Gastroenterol* 2017; **23**: 4867-4878 [PMID: 28785141 DOI: 10.3748/wjg.v23.i27.4867]
40 **Watari J**, Chen N, Amenta PS, Fukui H, Oshima T, Tomita T, Miwa H, Lim KJ, Das KM. Helicobacter pylori associated chronic gastritis, clinical syndromes, precancerous lesions, and pathogenesis of gastric cancer development. *World J Gastroenterol* 2014; **20**: 5461-5473 [PMID: 24833876 DOI: 10.3748/wjg.v20.i18.5461]
41 **Lee SY**. Endoscopic gastritis, serum pepsinogen assay, and Helicobacter pylori infection. *Korean J Intern Med* 2016; **31**: 835-844 [PMID: 27604795 DOI: 10.3904/kjim.2016.166]
42 **Yang YJ**, Sheu BS. Metabolic Interaction of Helicobacter pylori Infection and Gut Microbiota. *Microorganisms* 2016; **4**: [PMID: 27681909 DOI: 10.3390/microorganisms4010015]
43 **Annibale B**, Capurso G, Delle Fave G. Consequences of Helicobacter pylori infection on the absorption of micronutrients. *Dig Liver Dis* 2002; **34** Suppl 2: S72-S77 [PMID: 12408446 DOI: 10.1016/S1590-8658(02)80170-0]
44 **Claeys D**, Faller G, Appelmelk BJ, Negrini R, Kirchner T. The gastric H+,K+-ATPase is a major autoantigen in chronic Helicobacter pylori gastritis with body mucosa atrophy. *Gastroenterology* 1998; **115**: 340-347 [PMID: 9679039 DOI: 10.1016/S0016-5085(98)70200-8]
45 **Lahner E**, Persechino S, Annibale B. Micronutrients (Other than iron) and Helicobacter pylori infection: a systematic review. *Helicobacter* 2012; **17**: 1-15 [PMID: 22221610 DOI: 10.1111/j.1523-5378.2011.00892.x]
46 **Duque MA**, Kresak JL, Falchook A, Harris NS. Nitrous Oxide Abuse and Vitamin B12 Action in a 20-Year-Old Woman: A Case Report. *Lab Med* 2015; **46**: 312-315 [PMID: 26489675 DOI: 10.1309/LM0L9HAVXCHF1UQM]
47 **Chaugny C**, Simon J, Collin-Masson H, De Beauchêne M, Cabral D, Fagniez O, Veyssier-Belot C. [Vitamin B12 deficiency due to nitrous oxide use: unrecognized cause of combined spinal

cord degeneration]. *Rev Med Interne* 2014; **35**: 328-332 [PMID: 23773901 DOI: 10.1016/j.revmed.2013.04.018]
48 **Pugliese RS**, Slagle EJ, Oettinger GR, Neuburger KJ, Ambrose TM. Subacute combined degeneration of the spinal cord in a patient abusing nitrous oxide and self-medicating with cyanocobalamin. *Am J Health Syst Pharm* 2015; **72**: 952-957 [PMID: 25987690 DOI: 10.2146/ajhp140583]
49 **Kiasari AZ**, Firouzian A, Baradari AG, Nia HS, Kiasari SH. The Effect of Vitamin B12 Infusion on Prevention of Nitrous Oxide-induced Homocysteine Increase: A Double-blind Randomized Controlled Trial. *Oman Med J* 2014; **29**: 194-197 [PMID: 24936269 DOI: 10.5001/omj.2014.48]
50 **Safari A**, Emadi F, Jamali E, Borhani-Haghighi A. Clinical and MRI manifestations of nitrous oxide induced vitamin B12 deficiency: A case report. *Iran J Neurol* 2013; **12**: 111-113 [PMID: 24250916]

P- Reviewer: Gobejishvili L, Osuga T, Penaranda G **S- Editor**: Ma YJ
L- Editor: Filipodia **E- Editor**: Huang Y

World Journal of Gastroenterology

Submit a Manuscript: http://www.f6publishing.com

World J Gastroenterol 2018 March 28; 24(12): 1353-1360

DOI: 10.3748/wjg.v24.i12.1353

ISSN 1007-9327 (print) ISSN 2219-2840 (online)

ORIGINAL ARTICLE

Observational Study

Successful combination of direct antiviral agents in liver-transplanted patients with recurrent hepatitis C virus

Christian Rupp, Theresa Hippchen, Manuel Neuberger, Peter Sauer, Jan Pfeiffenberger, Wolfgang Stremmel, Daniel Nils Gotthardt, Arianeb Mehrabi, Karl-Heinz Weiss

Christian Rupp, Theresa Hippchen, Manuel Neuberger, Peter Sauer, Jan Pfeiffenberger, Wolfgang Stremmel, Daniel Nils Gotthardt, Karl-Heinz Weiss, Department of Internal Medicine IV, University Hospital of Heidelberg, Heidelberg 69120, Germany

Christian Rupp, Peter Sauer, Interdisciplinary Endoscopy Unit, University Hospital of Heidelberg, Heidelberg 69120, Germany

Arianeb Mehrabi, Department of General, Visceral and Transplantation Surgery, University Hospital of Heidelberg, Heidelberg 69120, Germany

ORCID number: Christian Rupp (0000-0003-2808-9230); Theresa Hippchen (0000-0002-0163-7084); Manuel Neuberger (0000-0003-4573-5134); Peter Sauer (0000-0003-2164-4035); Jan Pfeiffenberger (0000-0002-4741-3617); Wolfgang Stremmel (0000-0002-8545-1753); Daniel Nils Gotthardt (0000-0001-9978-9766); Arianeb Mehrabi (0000-0001-6163-1525); Karl-Heinz Weiss (0000-0002-6336-9935).

Author contributions: Rupp C, Hippchen T, Neuberger M, Sauer P, Gotthardt DN, Mehrabi A and Weiss KH contributed to the treatment and follow-up of patients; Rupp C, Hippchen T, Gotthardt DN and Weiss KH performed the statistical analyses; Rupp C, Sauer P, Stremmel W and Weiss KH conceived of the article and drafted the manuscript.

Supported by "Deutsche Forschungsgemeinschaft" to Rupp C and Gotthardt DN.

Institutional review board statement: This study was reviewed and approved for publication by the Institutional Review Board of the University Hospital of Heidelberg (Approval No. S-043/2011).

Informed consent statement: All study participants, or their legal guardian, provided written informed consent prior to study enrollment.

Conflict-of-interest statement: The authors declare no conflicts of interest.

Data sharing statement: The original anonymized dataset is available upon request from the Corresponding Author at: christian.rupp@med.uni-heidelberg.de.

STROBE statement: The authors have read the STROBE Statement - checklist of items, and the manuscript was prepared and revised according to the STROBE Statement - checklist of items.

Manuscript source: Invited manuscript

Correspondence to: Christian Rupp, MD, Department of Internal Medicine IV, University Hospital of Heidelberg, Im Neuenheimer Feld 410, Heidelberg 69120, Germany. christian_rupp@med.uni-heidelberg.de
Telephone: +49-6221-5636817
Fax: +49-6221-568904

Received: January 30, 2018
Peer-review started: January 31, 2018
First decision: February 24, 2018
Revised: March 2, 2018
Accepted: March 18, 2018
Article in press: March 18, 2018
Published online: March 28, 2018

Abstract

AIM

To analyze the safety and efficiency of direct-acting

antiviral (DAA) regimens in liver-transplanted patients with hepatitis C virus (HCV) reinfection.

METHODS

Between January 2014 and December 2016, 39 patients with HCV reinfection after liver transplantation were treated at our tertiary referral center with sofosbuvir (SOF)-based regimens, including various combinations with interferon (IFN), daclatasvir (DAC), simeprivir (SIM) and/or ledipasvir (LDV). Thirteen patients were treated with SOF + IFN ± RBV. Ten patients were treated with SOF + DAC ± RBV. Fiveteen patients were treated with fixed-dose combination of SOF + LDV ± RBV. One patient was treated with SOF + SIM + RBV. Three patients with relapse were retreated with SOF + LDV + RBV. The treatment duration was 12-24 wk in all cases. The decision about the HCV treatment was made by specialists at our transplant center, according to current available or recommended medications.

RESULTS

The majority of patients were IFN-experienced (29/39, 74.4%) and had a history of hepatocellular carcinoma (26/39, 66.7%) before liver transplantation. Sustained virological response at 12 wk (SVR12) was achieved in 10/13 (76.9%) of patients treated with SOF + IFN ± RBV. All patients with relapse were treated with fixed-dose combination of SOF + LDV + RBV. Patients treated with SOF + DAC + RBV or SOF + LDV + RBV achieved 100% SVR12. SVR rates after combination treatment with inhibitors of the HCV nonstructural protein (NS)5A and NS5B for 24 wk were significantly higher, as compared to all other therapy regimens (P = 0.007). Liver function was stable or even improved in the majority of patients during treatment. All antiviral therapies were safe and well-tolerated, without need of discontinuation of treatment or dose adjustment of immunosuppression. No serious adverse events or any harm to the liver graft became overt. No patient experienced acute cellular rejection during the study period.

CONCLUSION

Our cohort of liver-transplanted patients achieved high rates of SVR12 after a 24-wk course of treatment, especially with combination of NS5A and NS5B inhibitors.

Key words: Hepatitis C virus; Recurrence; Direct acting antivirals; Liver transplantation; Sustained virological response

Core tip: We examined the safety and efficiency of novel direct-acting antiviral agents (DAAs) in liver-transplanted patients with recurrence of hepatitis c virus (HCV) infection in a real-world cohort at our tertiary care center. In conclusion, DAAs are safe and very efficient in HCV patients after liver transplantation, even in case of recurrent cirrhosis or history of relapse after pegylated-interferon therapy. The high sustained virological response rates in our cohort, despite many patients with recurrent cirrhosis, may argue for a 24-wk therapy period in patients with risk factors for therapy failure in a posttransplant setting.

Rupp C, Hippchen T, Neuberger M, Sauer P, Pfeiffenberger J, Stremmel W, Gotthardt DN, Mehrabi A, Weiss KH. Successful combination of direct antiviral agents in liver-transplanted patients with recurrent hepatitis C virus. *World J Gastroenterol* 2018; 24(12): 1353-1360 Available from: URL: http://www.wjgnet.com/1007-9327/full/v24/i12/1353.htm DOI: http://dx.doi.org/10.3748/wjg.v24.i12.1353

INTRODUCTION

Recurrent infection with hepatitis C virus (HCV) following liver transplant (LT) treatment is the leading cause of liver graft loss and death in liver-transplanted patients infected with HCV[1]. In patients with detectable HCV RNA at the time of transplantation, HCV universally recurs. In such cases, HCV infection shows an accelerated course, with progression to advanced fibrosis within 5 years post LT in the majority of patients. Fundamental steps in understanding and deciphering the HCV replication system in the last 2 decades has opened up the way for development of highly effective new antiviral drugs[2-4].

Before introduction of the direct-acting antiviral (DAA) therapies, treatment options for recurrent HCV in liver-transplanted patients were limited, due to significant drug-drug interactions and severe side effects. The approval of DAAs has revolutionized HCV treatment. Nowadays, well-tolerated, interferon (IFN)-free and highly efficient treatment options are available for HCV-infected patients[5-8]. In most cases, DAA administration before liver transplantation prevents HCV recurrence[9].

Despite the growing number of successfully treated patients, HCV recurrence after orthotopic LT remains one of the most challenging clinical situations[10-12]. Thus, analysis of real-world cohorts of LT recipients may provide valuable insights into the safety and efficacy of DAA treatment in these cohorts[13-17]. Herein, we present the first experience of liver-transplanted patients with HCV recurrence at our tertiary care center.

MATERIALS AND METHODS

Study cohort

The study cohort comprised all liver-transplanted patients treated with a DAA regimen at the Heidelberg University Hospital. In total, 39 patients were included. The baseline characteristics are depicted in Table 1. All patients included in the study were treated with DAAs. All

Table 1 Baseline characteristics of study cohort *n* (%)

Characteristic		Data
Sex	Male	28 (71.8)
	Female	11 (28.2)
Age (yr)		58.6 (range: 45.8-72.3)
Immunosuppression	Cyclosporine	19 (48.7)
	Tacrolimus	18 (46.2)
	Sirolimus	1 (2.6)
	Everolimus	1 (2.6)
	Mycophenolate mofetil	21 (53.8)
Liver histology	F0-2	7 (17.9)
	F3	15 (38.5)
	F4	17 (43.6)
Liver function, CTP	A	17 (43.6)
	B	2 (5.1)
Risk factors	Interferon-experienced	29 (74.4)
	History of HCC	26 (66.7)
HCV genotype	1	24 (61.5)
	2	1 (2.6)
	3	13 (33.3)
	4	1 (2.6)

CTP: Child-turcotte-pugh; HCC: Hepatocellular carcinoma.

patients were at least 6-mo post LT before the antiviral therapy was started. In all patients, corticosteroids had been discontinued successfully, by tapering over a 3-mo to 6-mo period and immunosuppressive therapy reduced to a long-term dosage. Immunosuppression was achieved by cyclosporine in 19 (48.7%) patients, tacrolimus in 18 (46.2%) patients, and sirolimus 1 (2.6%) or everolimus in 1 (2.6%) patient, respectively. Comedication with mycophenolate mofetil was administered in 21 (53.8%) patients. Patients with a history of hepatocellular carcinoma (HCC) before liver transplantation accounted for 26 (66.7%). All patients with HCC before LT met the Milan-criteria. Three patients [3 (7.7%)] have been already retransplanted at least once. The study covered the period from January 2014 to December 2016. The outcomes of all patients in the study were followed until June 2017.

HCV treatment

HCV treatment was administered by the outpatient clinic at our tertiary center. The decision about the HCV treatment was made by specialists at our transplant center, according to current available or recommended medications. Patients were treated according to recommendations of available drugs that carried approval by the United States Food and Drug Administration and the European Medicines Evaluation Agency. As different drugs became approved during the course of this study, the therapy regimens were adapted. In the beginning, 400 mg sofosbuvir (SOF) was combined with pegylated (Peg)-IFN (180 μg once weekly, dosage modifications according manufacturers' recommendations) and ribavirin (RBV). After introduction of 60 mg daclatasvir (DAC), 150 mg simeprivir (SIM) and fixed-dose combination of 400 mg SOF with 90 mg ledipasvir (LDV), IFN-containing regimens were no longer perpetuated.

Statistical analysis

Calculations were carried out using PASW Statistics 22. Frequencies were compared using a χ^2 test or the Fisher's exact test, where appropriate. Continuous data were compared using the nonparametric Wilcoxon rank-sum test.

Ethic approval

Written informed consent was obtained from each patient included in the study. The study protocol conforms to the ethical guidelines of the 1975 Declaration of Helsinki, as reflected by the prior approval by the institution's human research committee. The study was approved by the local ethics committee of Heidelberg University as well.

RESULTS

Baseline characteristics

The baseline characteristics of the study cohort are presented in Table 1. The male to female ratio was 3:1. The median age at beginning of antiviral therapy was about 5 years above the median age of first liver transplantation (53.8 years; range: 23.4-68.4 years). Immunosuppression was achieved mainly by cyclosporine or tacrolimus, with only 2 of the patients receiving sirolimus or everolimus, respectively; half of the patients received comedication with mycophenolate mofetil.

Recurrent cirrhosis occurred in 17 (43.6%) patients, with the majority of cases having relatively low severity [Child-Turcotte-Pugh (CTP) score A] and 2 of the cases having mid-severity (CTP score B). Nearly two-thirds of the patients in the total study cohort were treatment experienced, with an IFN-containing regimen. 26 (66.7%) patients had a history of hepatocellular carcinoma (HCC) before liver transplantation. The median time since transplantation was 4.6 years, ranging from 5.5 mo to 22.7 years. The most common HCV genotypes were 1 and 3, respectively, with genotypes 2 and 4 being relatively rare. The median viral load before therapy was 1.43×10^6.

Therapy regimen

Nine patients were treated with SOF + RBV, five of who received the Peg-IFN combination therapy. In general, the treatment duration was 12 wk in cases of stable liver function and up to 24 wk in cases with known risk factors of therapy failure (*e.g.*, recurrent cirrhosis or treatment-experience). One patient received SOF + RBV for 48 wk, as she was awaiting liver transplantation. Eighteen patients were treated with the fixed-dose combination of SOF plus LDV, either with (n = 15) or without (n = 3) RBV for 24 wk.

Table 2 Hepatitis C virus treatment regimens

n	Therapy	SVR24
5	IFN + SOF + RBV	4/5 (80.0%)
8	SOF + RBV	6/8 (75.0%)
9	DAC +SOF + RBV	9/9 (100.0%)
1	DAC + SOF	1/1 (100.0%)
13	LDV + SOF + RBV	13/13 (100.0%)
2	LDV + SOF	2/2 (100.0%)
1	SIM + SOF + RBV	1/1 (100.0%)

DAC: Daclatasvir; IFN: Interferon; LDV: Ledipasvir; RBV: Ribavirin; SIM: Simeprevir; SOF: Sofosbuvir; SVR24: Sustained virological response at 24 wk.

Table 3 Viral load throughout treatment period

Time (wk)	Mean	Min	Max
T (0)	3268770	45600	25200000
T (4)	25812.1	0	771000
T (8)	22.8	0	268
T (12)	4.1	0	101
T (24)	0	0	0

Ten patients received SOF in combination with DAC, either with (n = 6) or without (n = 4) RBV for 24 wk. One patient was treated with a combination of SOF plus SIM and RBV for 24 wk (Table 2). Clinical and laboratory baseline characteristics were not different between the different regimen cohorts.

Safety

All patients completed antiviral treatment. No serious adverse events occurred that required hospitalization or discontinuation of therapy. No adaption of immunosuppression was necessary during the course of treatment. No patient experienced acute cellular rejection of the graft during the study period. Side effects attributable to the antiviral therapy were fatigue (14/39, 35.9%), anemia (11/39, 28.2%) and irritability (6/39, 15.4%). Side effects concerning blood cell count were attributable to concomitant therapy with RBV. In patients without RVB therapy, no anemia or thrombocytopenia occurred. All side effects disappeared after therapy was finished.

Sustained virological response

At the end of the study period, all patients had attained Sustained virological response (SVR) at 24 wk (SVR24). Of the thirty-nine patients, three patients experienced relapse after the first therapy with SOF + RBV, including those with (n = 1) or without (n = 2) the Peg-IFN for 24 wk. Relapse occurred within 4 wk after the end of therapy. All patients with relapse were retreated with fixed-dose combination of SOF + LDV and achieved SVR24.

The viral loads detected during therapy are shown in Table 3. In the majority of patients HCV was undetectable between weeks 4 through 8 of the antiviral therapy. Only 2 patients had detectable viral load after 12 wk of treatment. In both of these cases, no HCV was detectable after 24 wk of treatment and no relapse occurred. There was no association between viral load at the beginning or during the course of therapy and risk for relapse.

Liver function

The model for end-stage liver disease (MELD) score remained stable or improved in 20 (51.3%) patients until the end of therapy. At 12 wk after end of therapy, improved or stable MELD score was found in 21 (53.8%) patients. At 24 wk after end of therapy, the majority of patients (32/39, 82.1%) had at least stable or improved MELD score (Figure 1).

Risk factors for relapse

We assessed several clinical and laboratory risk factors associated with treatment failure. We found no association of sex, age, immunosuppression, HCV genotype, viral load, CTP score or MELD score with treatment failure. In addition, there was no association found for any of these factors with SVR. When comparing different therapy regimens, we were able to demonstrate superior rates of SVR at 12 wk (SVR12) for a combination of inhibitors of the HCV nonstructural protein (NS)5A and NS5B administered for 24 wk, as compared to all other regimens (29/29 *vs* 10/13; P = 0.007).

Overall graft and host survival rates and prevalence of HCC

During the study period, 1 patient underwent re-transplantation and 1 patient died because of progredient liver failure. Both had achieved SVR24 after successful antiviral therapy. During the study period, no HCC was detected in any patient, especially not in those who had had HCC before the LT. No other malignant disease became overt in our cohort during the study period.

DISCUSSION

The availability of new antiviral drugs poses new questions about the optimum timing and duration of treatment to prevent HCV recurrence after liver transplantation[18]. Facing good tolerance and low drug-drug interactions, antiviral treatment seems to be acceptable for both before and after transplantation[19-21]. Yet, antiviral therapy after liver transplantation remains challenging in this difficult-to-treat population[22,23]. On the one side, antiviral therapy should not interfere with immunosuppression; on the other side, stimulation of the immune system might compromise liver graft function. With the introduction of DAAs, a new era for treatment of HCV-infected patients has begun.

A growing amount of studies have confirmed the efficiency and safety of DAAs in LT recipients[24-26].

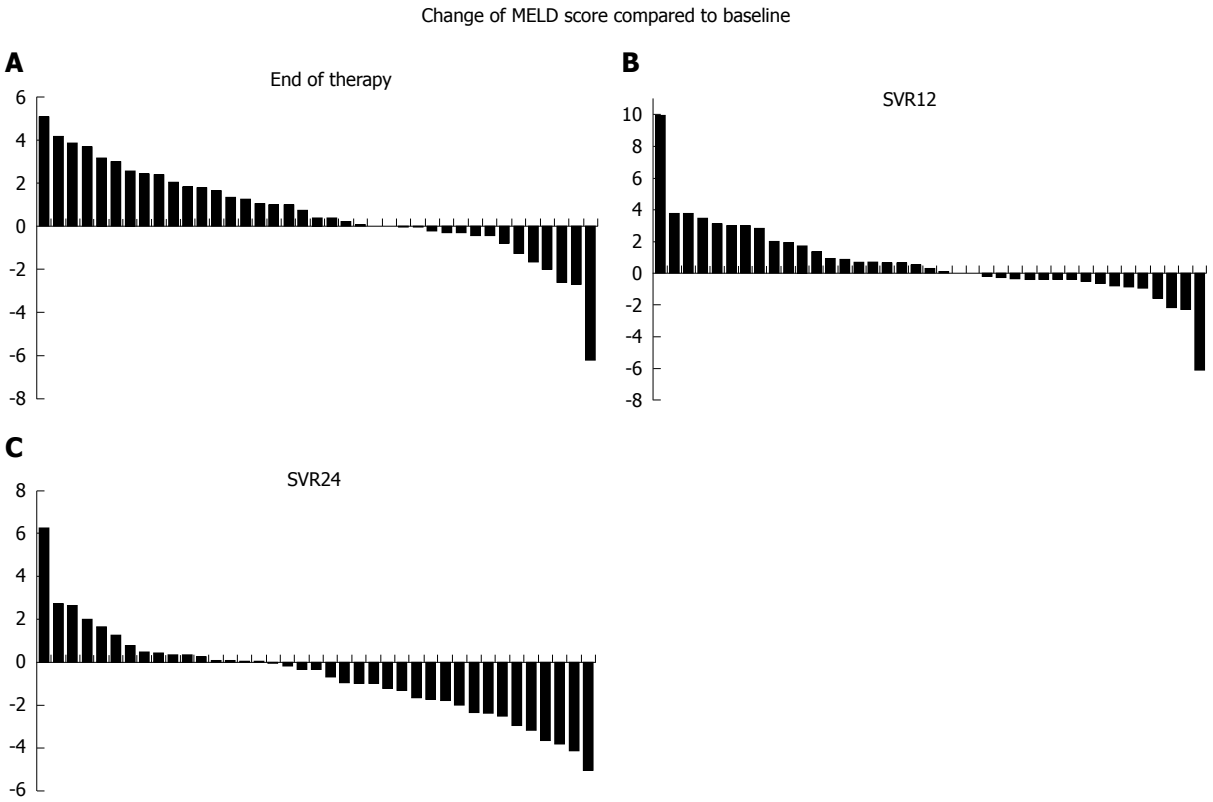

Figure 1 Model for end-stage liver disease score after the end of antiviral treatment. Differences in MELD score compared to baseline at A: the end of therapy; B: 12 wk after the end of treatment; C: and, 24 wk after the end of treatment. Each column indicates one patient. MELD: Model for end-stage liver disease.

Several therapy regimens have been successfully tested so far[14]. We report here about the first experiences with liver-transplanted patients and HCV reinfection at our tertiary care center. To the end of the study period, all patients had reached SVR12. In this study we showed also SVR24 rates, to rule out the possibility of delayed relapse in our patients, like rarely seen in patients treated with interferon and ribavirin. As all three relapses to DAA therapy appeared already within 4 wk after cessation of therapy we believe SVR12 is sufficient to determine successful HCV eradication. We had decided on a 24-wk treatment period for the majority of patients, as most patients had already relapsed or shown nonresponse with past administered IFN-containing HCV therapies. Furthermore, most patients had already developed recurrent cirrhosis, representing another risk factor for therapy failure[27].

HCV therapy was well tolerated in all our patients, and there was no case of therapy termination necessitated for any patient due to side effects or adverse events. In our cohort, most patients received RBV in addition to the DAA[28]. Side effects concerning affectation of the blood count might be attributable to the comedication with RBV. Importantly, we recognized no serious harmful effects on transplant function, as no patient experienced an episode of acute cellular rejection or required re-transplantation during or immediately after the antiviral therapy. Most patients showed improvement of liver function after the end of therapy, which might improve graft survival in the future[29].

One patient underwent re-transplantation at 1 year after successful antiviral therapy, and another patient died due to progredient liver failure after more than 2 years after reaching SVR12. Both patients had recurrent cirrhosis and were transplanted more than 5 years ago. These patients might represent a subgroup of patients that have reached a point of no return, as HCV infection has already caused severe damage to the liver graft, which cannot be reverted even by successful antiviral therapy[29-32].

Liver function remained stable in most patients during the course of therapy and improved within 24 wk after end of therapy in more than 80% of patients. This is in line with other studies of posttransplant patients and emphasizes the importance of antiviral therapy for liver graft protection. Importantly, there was no HCC recurrence despite a high number of patients with HCC prior to transplantation in our cohort[33-35].

We were not able to identify any potential risk factors for therapy failure according to the clinical or laboratory parameters used in our study. In particular, we found no correlation with successful antiviral therapy and viral load, genotype, age, immunosuppression or liver function. Additionally, we found no different outcome between patients treated with RBV or without, which might underline the advantage of an RBV-free regimen[28]. When comparing different therapy regimens, we were able to demonstrate superior SVR12 rates for a combination of NS5A and NS5B inhibitors at 24 wk, as compared to all other regimens. However, this study was not designed nor powered to answer this

question.

In conclusion, DAAs are safe and very efficient in HCV patients after liver transplantation, even in cases of recurrent cirrhosis or history of relapse after Peg-IFN therapy. The high SVR rates in our cohort, despite the many patients with recurrent cirrhosis, may argue for a 24-wk therapy period in patients with risk factors for therapy failure in a posttransplant setting.

ARTICLE HIGHLIGHTS

Research background

Recurrent infection with hepatitis C virus (HCV) following liver transplant (LT) treatment is the leading cause of liver graft loss and death in liver-transplanted patients infected with HCV. Before introduction of the direct-acting antiviral (DAA) therapies, treatment options for recurrent HCV in liver-transplanted patients were limited, due to significant drug-drug interactions and severe side effects. The approval of DAAs has revolutionized HCV treatment.

Research motivation

Despite the growing number of successfully treated patients, HCV recurrence after orthotopic LT remains one of the most challenging clinical situations. Thus, analysis of real-world cohorts of LT recipients may provide valuable insights into the safety and efficacy of DAA treatment in these cohorts.

Research objectives

To analyze the safety and efficiency of DAA regimens in liver-transplanted patients with HCV reinfection in a real-world cohort.

Research methods

The study cohort comprises all liver transplanted patients that were treated with direct acting antiviral regimen at the Heidelberg University Hospital from January 2014 to December 2016. In total 39 patients were included. Clinical and laboratory baseline characteristics were collected at entry into the study. All patients were at least six months liver transplanted before antiviral therapy was started. HCV treatment was administered by the outpatient clinic at our tertiary center. The decision about the HCV treatment was made by specialists at our transplant center, according to current available or recommended medication. Patients were treated according recommendations of available drugs after approval by FDA and EMEA. As different drugs were approved during the course of this study therapy regimen were adapted. In the beginning Sofosbuvir was combined with pegylated interferon (Peg-INF) and ribavirin. After introduction of Daclatasvir, Simeprivir and fixed-dose combination of Sofosbuvir with Ledipasvir interferon containing regimen were no longer perpetuated.

Research results

At the end of the study period, all thirty-nine patients had attained SVR at 24 wk (SVR24). Sustained virological response at 12 wk (SVR12) was achieved in 10/13 (76.9%) of patients treated with SOF + IFN ± RBV. All patients with relapse were treated with fixed-dose combination of SOF + LDV + RBV. Patients treated with SOF + DAC + RBV or SOF + LDV + RBV achieved 100% SVR12. SVR rates after combination treatment with inhibitors of the HCV nonstructural protein (NS)5A and NS5B for 24 wk were significantly higher, as compared to all other therapy regimens ($P = 0.007$). Liver function was stable or even improved in the majority of patients during treatment. All antiviral therapies were safe and well-tolerated, without need of discontinuation of treatment or dose adjustment of immunosuppression. No serious adverse events or any harm to the liver graft became overt. No patient experienced acute cellular rejection during the study period.

Research conclusions

In conclusion, DAAs are safe and very efficient in HCV patients after liver transplantation, even in cases of recurrent cirrhosis or history of relapse after Peg-IFN therapy. The high SVR rates in our cohort, despite the many patients with rrecurrent cirrhosis, may argue for a 24-wk therapy period in patients with risk factors for therapy failure in a posttransplant setting.

Research perspectives

HCV recurrence after orthotopic LT can be safely and efficiently treated with DAAs. Optimal timing and duration of antiviral therapy remains undetermined. Patients at risk for relapse need to be identified before initiation of therapy. Long-term effects of successful antiviral therapy, especially in patients with advanced recurrent cirrhosis, need to be analyzed in future.

REFERENCES

1 **Goldberg D**, Ditah IC, Saeian K, Lalehzari M, Aronsohn A, Gorospe EC, Charlton M. Changes in the Prevalence of Hepatitis C Virus Infection, Nonalcoholic Steatohepatitis, and Alcoholic Liver Disease Among Patients With Cirrhosis or Liver Failure on the Waitlist for Liver Transplantation. *Gastroenterology* 2017; **152**: 1090-1099.e1 [PMID: 28088461 DOI: 10.1053/j.gastro.2017.01.003]

2 **Lohmann V**, Körner F, Koch J, Herian U, Theilmann L, Bartenschlager R. Replication of subgenomic hepatitis C virus RNAs in a hepatoma cell line. *Science* 1999; **285**: 110-113 [PMID: 10390360]

3 **Bartenschlager R**, Lohmann V, Penin F. The molecular and structural basis of advanced antiviral therapy for hepatitis C virus infection. *Nat Rev Microbiol* 2013; **11**: 482-496 [PMID: 23748342 DOI: 10.1038/nrmicro3046]

4 **Lindenbach BD**, Meuleman P, Ploss A, Vanwolleghem T, Syder AJ, McKeating JA, Lanford RE, Feinstone SM, Major ME, Leroux-Roels G, Rice CM. Cell culture-grown hepatitis C virus is infectious in vivo and can be recultured in vitro. *Proc Natl Acad Sci* USA 2006; **103**: 3805-3809 [PMID: 16484368 DOI: 10.1073/pnas.0511218103]

5 **Weiler N**, Zeuzem S, Welker MW. Concise review: Interferon-free treatment of hepatitis C virus-associated cirrhosis and liver graft infection. *World J Gastroenterol* 2016; **22**: 9044-9056 [PMID: 27895394 DOI: 10.3748/wjg.v22.i41.9044]

6 **Kwo PY**, Mantry PS, Coakley E, Te HS, Vargas HE, Brown R Jr, Gordon F, Levitsky J, Terrault NA, Burton JR Jr, Xie W, Setze C, Badri P, Pilot-Matias T, Vilchez RA, Forns X. An interferon-free antiviral regimen for HCV after liver transplantation. *N Engl J Med* 2014; **371**: 2375-2382 [PMID: 25386767 DOI: 10.1056/NEJMoa1408921]

7 **Fontana RJ**, Hughes EA, Bifano M, Appelman H, Dimitrova D, Hindes R, Symonds WT. Sofosbuvir and daclatasvir combination therapy in a liver transplant recipient with severe recurrent cholestatic hepatitis C. *Am J Transplant* 2013; **13**: 1601-1605 [PMID: 23593993 DOI: 10.1111/ajt.12209]

8 **Forns X**, Charlton M, Denning J, McHutchison JG, Symonds WT, Brainard D, Brandt-Sarif T, Chang P, Kivett V, Castells L, Prieto M, Fontana RJ, Baumert TF, Coilly A, Londoño MC, Habersetzer F. Sofosbuvir compassionate use program for patients with severe recurrent hepatitis C after liver transplantation. *Hepatology* 2015; **61**: 1485-1494 [PMID: 25557906 DOI: 10.1002/hep.27681]

9 **Curry MP**, Forns X, Chung RT, Terrault NA, Brown R Jr, Fenkel JM, Gordon F, O'Leary J, Kuo A, Schiano T, Everson G, Schiff E, Befeler A, Gane E, Saab S, McHutchison JG, Subramanian GM, Symonds WT, Denning J, McNair L, Arterburn S, Svarovskaia E, Moonka D, Afdhal N. Sofosbuvir and ribavirin prevent recurrence of HCV infection after liver transplantation: an open-label study. *Gastroenterology* 2015; **148**: 100-107.e1 [PMID: 25261839 DOI: 10.1053/j.gastro.2014.09.023]

10 **Terrault NA**, Berenguer M, Strasser SI, Gadano A, Lilly L, Samuel D, Kwo PY, Agarwal K, Curry MP, Fagiuoli S, Fung JYY, Gane E, Brown KA, Burra P, Charlton M, Pessoa MG, McCaughan GW. International Liver Transplantation Society Consensus Statement on Hepatitis C Management in Liver Transplant Recipients. *Transplantation* 2017; **101**: 956-967 [PMID: 28437388 DOI: 10.1097/TP.0000000000001704]

11 **Fontana RJ**, Brown RS Jr, Moreno-Zamora A, Prieto M, Joshi S, Londoño MC, Herzer K, Chacko KR, Stauber RE, Knop V, Jafri SM, Castells L, Ferenci P, Torti C, Durand CM, Loiacono L, Lionetti R, Bahirwani R, Weiland O, Mubarak A, ElSharkawy AM, Stadler B, Montalbano M, Berg C, Pellicelli AM, Stenmark S, Vekeman F, Ionescu-Ittu R, Emond B, Reddy KR. Daclatasvir combined with sofosbuvir or simeprevir in liver transplant recipients with severe recurrent hepatitis C infection. *Liver Transpl* 2016; **22**: 446-458 [PMID: 26890629 DOI: 10.1002/lt.24416]

12 **Charlton M**, Gane E, Manns MP, Brown RS Jr, Curry MP, Kwo PY, Fontana RJ, Gilroy R, Teperman L, Muir AJ, McHutchison JG, Symonds WT, Brainard D, Kirby B, Dvory-Sobol H, Denning J, Arterburn S, Samuel D, Forns X, Terrault NA. Sofosbuvir and ribavirin for treatment of compensated recurrent hepatitis C virus infection after liver transplantation. *Gastroenterology* 2015; **148**: 108-117 [PMID: 25304641 DOI: 10.1053/j.gastro.2014.10.001]

13 **Herzer K**, Welzel TM, Spengler U, Hinrichsen H, Klinker H, Berg T, Ferenci P, Peck-Radosavljevic M, Inderson A, Zhao Y, Jimenez-Exposito MJ, Zeuzem S. Real-world experience with daclatasvir plus sofosbuvir ± ribavirin for post-liver transplant HCV recurrence and severe liver disease. *Transpl Int* 2017; **30**: 243-255 [PMID: 28012215 DOI: 10.1111/tri.12910]

14 **Kwok RM**, Ahn J, Schiano TD, Te HS, Potosky DR, Tierney A, Satoskar R, Robertazzi S, Rodigas C, Lee Sang M, Wiegel J, Patel N, Gripshover J, Hassan MA, Branch A, Smith CI. Sofosbuvir plus ledispasvir for recurrent hepatitis C in liver transplant recipients. *Liver Transpl* 2016; **22**: 1536-1543 [PMID: 27543748 DOI: 10.1002/lt.24614]

15 **Welzel TM**, Petersen J, Herzer K, Ferenci P, Gschwantler M, Wedemeyer H, Berg T, Spengler U, Weiland O, van der Valk M, Rockstroh J, Peck-Radosavljevic M, Zhao Y, Jimenez-Exposito MJ, Zeuzem S. Daclatasvir plus sofosbuvir, with or without ribavirin, achieved high sustained virological response rates in patients with HCV infection and advanced liver disease in a real-world cohort. *Gut* 2016; **65**: 1861-1870 [PMID: 27605539 DOI: 10.1136/gutjnl-2016-312444]

16 **Beinhardt S**, Peck-Radosavljevic M, Hofer H, Ferenci P. Interferon-free antiviral treatment of chronic hepatitis C in the transplant setting. *Transpl Int* 2015; **28**: 1011-1024 [PMID: 25864369 DOI: 10.1111/tri.12577]

17 **Chang CY**, Nguyen P, Le A, Zhao C, Ahmed A, Daugherty T, Garcia G, Lutchman G, Kumari R, Nguyen MH. Real-world experience with interferon-free, direct acting antiviral therapies in Asian Americans with chronic hepatitis C and advanced liver disease. *Medicine* (Baltimore) 2017; **96**: e6128 [PMID: 28178174 DOI: 10.1097/MD.0000000000006128]

18 **Fagiuoli S**, Ravasio R, Lucà MG, Baldan A, Pecere S, Vitale A, Pasulo L. Management of hepatitis C infection before and after liver transplantation. *World J Gastroenterol* 2015; **21**: 4447-4456 [PMID: 25914454 DOI: 10.3748/wjg.v21.i15.4447]

19 **Coilly A**, Roche B, Duclos-Vallée JC, Samuel D. Optimum timing of treatment for hepatitis C infection relative to liver transplantation. *Lancet Gastroenterol Hepatol* 2016; **1**: 165-172 [PMID: 28404073 DOI: 10.1016/S2468-1253(16)30008-5]

20 **Samur S**, Kues B, Ayer T, Roberts MS, Kanwal F, Hur C, Donnell DMS, Chung RT, Chhatwal J. Cost Effectiveness of Pre- vs Post-Liver Transplant Hepatitis C Treatment With Direct-Acting Antivirals. *Clin Gastroenterol Hepatol* 2018; **16**: 115-122.e10 [PMID: 28634131 DOI: 10.1016/j.cgh.2017.06.024]

21 **Levitsky J**, Verna EC, O'Leary JG, Bzowej NH, Moonka DK, Hyland RH, Arterburn S, Dvory-Sobol H, Brainard DM, McHutchison JG, Terrault NA. Perioperative Ledipasvir-Sofosbuvir for HCV in Liver-Transplant Recipients. *N Engl J Med* 2016; **375**: 2106-2108 [PMID: 27959735 DOI: 10.1056/NEJMc1611829]

22 **Younossi ZM**, Stepanova M, Charlton M, Curry MP, O'Leary JG, Brown RS, Hunt S. Patient-reported outcomes with sofosbuvir and velpatasvir with or without ribavirin for hepatitis C virus-related decompensated cirrhosis: an exploratory analysis from the randomised, open-label ASTRAL-4 phase 3 trial. *Lancet Gastroenterol Hepatol* 2016; **1**: 122-132 [PMID: 28404069 DOI: 10.1016/S2468-1253(16)30009-7]

23 **Ferenci P**. Treatment of hepatitis C in difficult-to-treat patients. *Nat Rev Gastroenterol Hepatol* 2015; **12**: 284-292 [PMID: 25895822 DOI: 10.1038/nrgastro.2015.53]

24 **Saxena V**, Khungar V, Verna EC, Levitsky J, Brown RS Jr, Hassan MA, Sulkowski MS, O'Leary JG, Koraishy F, Galati JS, Kuo AA, Vainorius M, Akushevich L, Nelson DR, Fried MW, Terrault N, Reddy KR. Safety and efficacy of current direct-acting antiviral regimens in kidney and liver transplant recipients with hepatitis C: Results from the HCV-TARGET study. *Hepatology* 2017; **66**: 1090-1101 [PMID: 28504842 DOI: 10.1002/hep.29258]

25 **Vukotic R**, Conti F, Fagiuoli S, Morelli MC, Pasulo L, Colpani M, Foschi FG, Berardi S, Pianta P, Mangano M, Donato MF, Malinverno F, Monico S, Tamè M, Mazzella G, Belli LS, Viganò R, Carrai P, Burra P, Russo FP, Lenci I, Toniutto P, Merli M, Loiacono L, Iemmolo R, Degli Antoni AM, Romano A, Picciotto A, Rendina M, Andreone P; AISF-SOFOLT Study group. Long-term outcomes of direct acting antivirals in post-transplant advanced hepatitis C virus recurrence and fibrosing cholestatic hepatitis. *J Viral Hepat* 2017; **24**: 858-864 [PMID: 28370880 DOI: 10.1111/jvh.12712]

26 **Belli LS**, Duvoux C, Berenguer M, Berg T, Coilly A, Colle I, Fagiuoli S, Khoo S, Pageaux GP, Puoti M, Samuel D, Strazzabosco M. ELITA consensus statements on the use of DAAs in liver transplant candidates and recipients. *J Hepatol* 2017; **67**: 585-602 [PMID: 28323126 DOI: 10.1016/j.jhep.2017.03.006]

27 **Ferenci P**, Kozbial K, Mandorfer M, Hofer H. HCV targeting of patients with cirrhosis. *J Hepatol* 2015; **63**: 1015-1022 [PMID: 26100497 DOI: 10.1016/j.jhep.2015.06.003]

28 **Pillai AA**, Maheshwari R, Vora R, Norvell JP, Ford R, Parekh S, Cheng N, Patel A, Young N, Spivey JR, Mgbemena O, Wedd JP. Treatment of HCV infection in liver transplant recipients with ledipasvir and sofosbuvir without ribavirin. *Aliment Pharmacol Ther* 2017; **45**: 1427-1432 [PMID: 28382751 DOI: 10.1111/apt.14059]

29 **Habib S**, Meister E, Habib S, Murakami T, Walker C, Rana A, Shaikh OS. Slower Fibrosis Progression Among Liver Transplant Recipients With Sustained Virological Response After Hepatitis C Treatment. *Gastroenterology Res* 2015; **8**: 237-246 [PMID: 27785303 DOI: 10.14740/gr686w]

30 **Young J**, Weis N, Hofer H, Irving W, Weiland O, Giostra E, Pascasio JM, Castells L, Prieto M, Postema R, Lefevre C, Evans D, Bucher HC, Calleja JL. The effectiveness of daclatasvir based therapy in European patients with chronic hepatitis C and advanced liver disease. *BMC Infect Dis* 2017; **17**: 45 [PMID: 28061762 DOI: 10.1186/s12879-016-2106-x]

31 **Vinaixa C**, Strasser SI, Berenguer M. Disease Reversibility in Patients With Post-Hepatitis C Cirrhosis: Is the Point of No Return the Same Before and After Liver Transplantation? A Review. *Transplantation* 2017; **101**: 916-923 [PMID: 28060241 DOI: 10.1097/TP.0000000000001633]

32 **Zanetto A**, Shalaby S, Vitale A, Mescoli C, Ferrarese A, Gambato M, Franceschet E, Germani G, Senzolo M, Romano A, Angeli P, Rugge M, Farinati F, Forton DM, Cillo U, Burra P, Russo FP. Dropout rate from the liver transplant waiting list because of hepatocellular carcinoma progression in hepatitis C virus-infected patients treated with direct-acting antivirals. *Liver Transpl* 2017; **23**: 1103-1112 [PMID: 28544587 DOI: 10.1002/lt.24790]

33 **Cabibbo G**, Petta S, Calvaruso V, Cacciola I, Cannavò MR, Madonia S, Distefano M, Larocca L, Prestileo T, Tinè F, Bertino G, Giannitrapani L, Benanti F, Licata A, Scalisi I, Mazzola G, Cartabellotta F, Alessi N, Barbàra M, Russello M, Scifo G, Squadrito G, Raimondo G, Craxì A, Di Marco V, Cammà C; Rete Sicilia Selezione Terapia - HCV (RESIST-HCV). Is early recurrence of hepatocellular carcinoma in HCV cirrhotic patients affected by treatment with direct-acting antivirals? A prospective multicentre study. *Aliment Pharmacol Ther* 2017; **46**: 688-695 [PMID: 28791711 DOI: 10.1111/apt.14256]

34 **Kanwal F**, Kramer J, Asch SM, Chayanupatkul M, Cao Y, El-

Serag HB. Risk of Hepatocellular Cancer in HCV Patients Treated With Direct-Acting Antiviral Agents. *Gastroenterology* 2017; **153**: 996-1005.e1 [PMID: 28642197 DOI: 10.1053/j.gastro.2017.06.012]

35 **Beste LA**, Green PK, Berry K, Kogut MJ, Allison SK, Ioannou GN. Effectiveness of hepatitis C antiviral treatment in a USA cohort of veteran patients with hepatocellular carcinoma. *J Hepatol* 2017; **67**: 32-39 [PMID: 28267622 DOI: 10.1016/j.jhep.2017.02.027]

P- Reviewer: Manolakopoulos S, Kanda T, Komatsu H, Sergi CM, Zhu X
S- Editor: Ma YJ **L- Editor**: A **E- Editor**: Huang Y

World Journal of Gastroenterology

Submit a Manuscript: http://www.f6publishing.com

World J Gastroenterol 2018 March 28; 24(12): 1361-1372

DOI: 10.3748/wjg.v24.i12.1361

ISSN 1007-9327 (print) ISSN 2219-2840 (online)

ORIGINAL ARTICLE

Randomized Clinical Trial

Daclatasvir plus asunaprevir in treatment-naïve patients with hepatitis C virus genotype 1b infection

Lai Wei, Fu-Sheng Wang, Ming-Xiang Zhang, Ji-Dong Jia, Alexey A Yakovlev, Wen Xie, Eduard Burnevich, Jun-Qi Niu, Yong Jin Jung, Xiang-Jun Jiang, Min Xu, Xin-Yue Chen, Qing Xie, Jun Li, Jin-Lin Hou, Hong Tang, Xiao-Guang Dou, Yash Gandhi, Wen-Hua Hu, Fiona McPhee, Stephanie Noviello, Michelle Treitel, Ling Mo, Jun Deng

Lai Wei, Peking University People's Hospital and Peking University Hepatology Institute, Beijing 100044, China

Fu-Sheng Wang, 302 Military Hospital of China, Beijing 100039, China

Ming-Xiang Zhang, the Sixth People's Hospital of Shenyang, Shenyang 110006, Liaoning Province, China

Ji-Dong Jia, Beijing Friendship Hospital, Capital Medical University, Beijing 100050, China

Alexey A Yakovlev, Saint-Petersburg State Healthcare Institution 'Clinical Infectious Hospital n.a. S.P. Botkin', Saint-Petersburg 191167, Russia

Wen Xie, Beijing Ditan Hospital, Capital Medical University, Beijing 100015, China

Eduard Burnevich, I.M. Sechenov First Moscow State Medical University, Moscow 119991, Russia

Jun-Qi Niu, The First Hospital of Jilin University, Jilin 1300021, Jilin Province, China

Yong Jin Jung, SMG-SNU Boramae Medical Center, Seoul 07061, South Korea

Xiang-Jun Jiang, Qingdao Municipal Hospital, Qingdao 266011, Shandong Province, China

Min Xu, Guangzhou No. 8 People's Hospital, Guangzhou 510060, Guangdong Province, China

Xin-Yue Chen, Beijing Youan Hospital, Capital Medical University, Beijing 100069, China

Qing Xie, Shanghai Ruijin Hospital, Jiaotong University School of Medicine, Shenyang 200025, Liaoning Province, China

Jun Li, TheFirst Affiliated Hospital with Nanjing Medical University, Nanjing 210029, Jiangsu Province, China

Jin-Lin Hou, Hepatology Unit, Nanfang Hospital, Southern Medical University, Guangzhou 510515, Guangdong Province, China

Hong Tang, West China Hospital, Sichuan University, Chengdu 610041, Sichuan Province, China

Xiao-Guang Dou, China Medical University, Shengjing Hospital, Shenyang 110004, Liaoning Province, China

Yash Gandhi, Wen-Hua Hu, Stephanie Noviello, Michelle Treitel, Bristol-Myers Squibb, Princeton, NJ 08540, United States

Fiona McPhee, Bristol-Myers Squibb, Wallingford, CT 06492, United States

Ling Mo, Jun Deng, Bristol-Myers Squibb, Shanghai 200040, China

ORCID number: Lai Wei (0000-0003-2326-1257); Fu-Sheng Wang (0000-0002-8043-6685); Ming-Xiang Zhang (0000-0001-6519-3497); Ji-Dong Jia (0000-0002-4673-8890); Alexey A Yakovlev (0000-0003-4163-5769); Wen Xie (0000-0002-7314-8175); Eduard Burnevich (0000-0002-7251-4284); Jun-Qi Niu (0000-0002-9857-6520); Yong Jin Jung (0000-0001-8785-2254); Xiang-Jun Jiang (0000-0001-8786-9654); Min Xu (0000-0003-0099-9101); Xin-Yue Chen (0000-0003-0099-2398); Qing Xie (0000-0002-2582-8803); Jun Li (0000-0002-1961-7188); Jin-Lin Hou (0000-0001-8230-8583); Hong Tang (0000-0002-9790-6225); Xiao-Guang Dou (0000-0002-5293-6009); Yash Gandhi (0000-0001-7637-9617); Wen-Hua Hu (0000-0002-8763-609X); Fiona McPhee (0000-0002-9321-4483); Stephanie Noviello (0000-0003-2705-1097);

Michelle Treitel (0000-0001-9488-7113); Ling Mo (0000-0001-8272-4210); Jun Deng (0000-0002-6390-7430).

Author contributions: Noviello S, Treitel M, Gandhi Y, Hu WH, Mo L, Deng J and McPhee F designed the research; Wang FS, Zhang MX, Jia JD, Yakovlev AA, Xie W, Burnevich EZ, Niu JQ, Jung YJ, Jiang XJ, Xu M, Chen XY, Xie Q, Li J, Hou JL, Tang H, Dou XG, Gandhi Y, Hu WH and McPhee F performed the research; Hu WH analyzed the data; Noviello S, Treitel M, Mo L and Deng J monitored the study conduct; All authors wrote the paper, had access to the study data and have reviewed and approved the final manuscript.

Supported by Bristol-Myers Squibb.

Institutional review board statement: The protocol was approved by the institutional review board/human research committee at each participating institution, and conformed to the ethical guidelines of the 2008 Declaration of Helsinki.

Clinical trial registration statement: This study is registered at ClinicalTrials.gov, registration number NCT02496078 (https://clinicaltrials.gov/ct2/show/NCT02496078).

Informed consent statement: All patients provided informed written consent prior to study enrollment.

Conflict-of-interest statement: All authors have no conflicts of interest for this manuscript.

Data sharing statement: Technical appendix, statistical code, and dataset available from the corresponding author. Patients gave informed consent regarding the relevant use and sharing of key-coded data.

CONSORT 2010 statement: The authors have read the CONSORT 2010 Statement, and the manuscript was prepared and revised according to the CONSORT 2010 Statement.

Manuscript source: Unsolicited manuscript

Correspondence to: Jun Deng, MD, Virology Clinical Research, Bristol-Myers Squibb, 55F Wheelock Square, 1717 West Nanjing Road, Shanghai 200040, China. daniel.deng@bms.com
Telephone: +86-21-23218405
Fax: +86-21-32303705

Received: December 22, 2017
Peer-review started: December 22, 2017
First decision: January 4, 2018
Revised: February 9, 2018
Accepted: February 26, 2018
Article in press: February 26, 2018
Published online: March 28, 2018

Abstract

AIM

To assess daclatasvir plus asunaprevir (DUAL) in treatment-naïve patients from mainland China, Russia and South Korea with hepatitis C virus (HCV) genotype 1b infection.

METHODS

Patients were randomly assigned (3:1) to receive 24 wk of treatment with DUAL (daclatasvir 60 mg once daily and asunaprevir 100 mg twice daily) beginning on day 1 of the treatment period (immediate treatment arm) or following 12 wk of matching placebo (placebo-deferred treatment arm). The primary endpoint was a comparison of sustained virologic response at posttreatment week 12 (SVR12) compared with the historical SVR rate for peg-interferon plus ribavirin (70%) among patients in the immediate treatment arm. The first 12 wk of the study were blinded. Safety was assessed in DUAL-treated patients compared with placebo patients during the first 12 wk (double-blind phase), and during 24 wk of DUAL in both arms combined.

RESULTS

In total, 207 patients were randomly assigned to immediate (n = 155) or placebo-deferred (n = 52) treatment. Most patients were Asian (86%), female (59%) and aged < 65 years (90%). Among them, 13% had cirrhosis, 32% had *IL28B* non-CC genotypes and 53% had baseline HCV RNA levels of ⩾ 6 million IU/mL. Among patients in the immediate treatment arm, SVR12 was achieved by 92% (95% confidence interval: 87.2-96.0), which was significantly higher than the historical comparator rate (70%). SVR12 was largely unaffected by cirrhosis (89%), age ⩾ 65 years (92%), male sex (90%), baseline HCV RNA ⩾ 6 million (89%) or *IL28B* non-CC genotypes (96%), although SVR12 was higher among patients without (96%) than among those with (53%) baseline NS5A resistance-associated polymorphisms (at L31 or Y93H). During the double-blind phase, aminotransferase elevations were more common among placebo recipients than among patients receiving DUAL. During 24 wk of DUAL therapy (combined arms), the most common adverse events (⩾ 10%) were elevated alanine aminotransferase and upper respiratory tract infection; emergent grade 3-4 laboratory abnormalities were infrequently observed, and all grade 3-4 aminotransferase abnormalities (alanine aminotransferase, n = 9; aspartate transaminase, n = 6) reversed within 8-11 d. Two patients discontinued DUAL treatment; one due to aminotransferase elevations, nausea, and jaundice and the other due to a fatal adverse event unrelated to treatment. There were no treatment-related deaths.

CONCLUSION

DUAL was well-tolerated during this phase 3 study, and SVR12 with DUAL treatment (92%) exceeded the

historical SVR rate for peg-interferon plus ribavirin of 70%.

Key words: Asunaprevir; Daclatasvir; Direct-acting antiviral; Chronic hepatitis C; Liver disease; NS3; NS5A; Genotype 1b

Core tip: This phase 3, placebo-controlled study assessed the efficacy and safety of daclatasvir (NS5A inhibitor) plus asunaprevir (NS3/4A protease inhibitor) in treatment-naïve patients from mainland China, Russia and South Korea with hepatitis C virus (HCV) genotype 1b infection. The rate of sustained virologic response at posttreatment week 12 among patients in the immediate treatment arm was 92%, which was significantly higher than the historical comparator rate (70%). The combination was well tolerated during 24 wk of treatment. These results demonstrate that for countries such as China, where interferon-based combinations are still widely used for the treatment of HCV genotype 1b, daclatasvir/asunaprevir offers a more efficacious and tolerable alternative with a shorter treatment duration.

Wei L, Wang FS, Zhang MX, Jia JD, Yakovlev AA, Xie W, Burnevich E, Niu JQ, Jung YJ, Jiang XJ, Xu M, Chen XY, Xie Q, Li J, Hou JL, Tang H, Dou XG, Gandhi Y, Hu WH, McPhee F, Noviello S, Treitel M, Mo L, Deng J. Daclatasvir plus asunaprevir in treatment-naïve patients with hepatitis C virus genotype 1b infection. *World J Gastroenterol* 2018; 24(12): 1361-1372 Available from: URL: http://www.wjgnet.com/1007-9327/full/v24/i12/1361.htm DOI: http://dx.doi.org/10.3748/wjg.v24.i12.1361

INTRODUCTION

Chronic hepatitis C virus (HCV) infection is a significant health burden across Asia[1], and affects 5-7 million people in China alone[2]. Without effective treatment, patients can develop severe complications, such as hepatocellular carcinoma (HCC)[3,4], for which HCV infection has become one of the most common causes in Asian and Western countries[5,6].

DUAL is an all-oral combination of daclatasvir (pan-genotypic NS5A inhibitor with *in vitro* activity against genotypes 1-6)[7,8] and asunaprevir (NS3 protease inhibitor with *in vitro* activity against genotypes 1 and 4-6)[9]. This regimen has demonstrated efficacy in several phase 3 studies of patients infected with HCV genotype 1b[10-13], the predominant genotype in East Asia[14-16], including those with characteristics known to attenuate response to interferon (IFN)-based treatment[17-19]. DUAL also has a superior safety profile compared with IFN-based combinations[20] and in April 2017 became the first all-oral, nonribavirin-containing combination for chronic HCV infection to gain approval in China[21].

In this study, we evaluated the efficacy and safety of DUAL in treatment-naïve patients from mainland China, South Korea and Russia with HCV genotype 1b infection.

MATERIALS AND METHODS

Study design and treatment

This was a phase 3, double-blind, placebo-controlled study (ClinicalTrials.gov number, NCT02496078) of DUAL, conducted between August 2015 and February 2017 in treatment-naïve patients from mainland China, South Korea and Russia with chronic HCV genotype 1b infection. Patients were randomly assigned (3:1) to receive DUAL (daclatasvir 60 mg tablet once daily and asunaprevir 100 mg soft capsule twice daily) for 24 wk either immediately (immediate treatment arm) or after 12 wk of matching placebo (placebo-deferred treatment arm) *via* an interactive voice-response system, and stratified according to the presence or absence of cirrhosis. Treatment was blinded to patients, investigators and the sponsor until week 12, and was open label thereafter.

The study was conducted according to local laws and regulatory requirements, and in accordance with Good Clinical Practice, as defined by the International Conference on Harmonization and the principles of the Declaration of Helsinki. Written informed consent was gained prior to study initiation.

Patients

The study population comprised male and female patients aged $\geqslant$ 18 years (body mass index: 18-35 kg/m^2) with chronic HCV genotype 1b infection (HCV RNA of $\geqslant$ 10000 IU/mL at screening) and no prior exposure to any IFN formulation, ribavirin or direct-acting antiviral agent for HCV. Patients with compensated cirrhosis were included (enrollment capped at approximately 25%). Cirrhosis status was defined by a hierarchical algorithm based on available biopsy, Fibroscan® or Fibrotest® (BioPredictive, Paris, France) and aspartate transaminase (AST):platelet ratio index (APRI) data. Patients were considered noncirrhotic if they met one of the following criteria: liver biopsy within 36 mo of screening showing absence of cirrhosis; Fibroscan® result of $\leqslant$ 9.6 kPa within 1 year of baseline/day 1; or FibroTest® score of $\leqslant$ 0.48 with APRI of $\leqslant$ 1 (performed during screening). Patients were considered cirrhotic if they met one of the following criteria: liver biopsy showing cirrhosis any time prior to screening; Fibroscan® showing cirrhosis or results of > 14.6 kPa within 1 year of baseline; or FibroTest® score of > 0.75 and an APRI of > 2 (at screening). Both sets of criteria are listed in decreasing hierarchical order.

Key exclusion criteria included: HCV infection other

than genotype 1b; evidence of a medical condition contributing to chronic liver disease other than HCV, or of decompensated liver disease (*e.g.,* history or presence of ascites, bleeding varices, or hepatic encephalopathy); diagnosed or suspected HCC or other malignancies; uncontrolled diabetes or hypertension; moderate to severe depression (well-controlled mild depression was permitted); total bilirubin ⩾ 34 μmol/L (or ⩾ 2 mg/dL) unless the patient had a documented history of Gilbert's disease; alanine aminotransferase (ALT) ⩾ 5 × the upper limit of normal; albumin < 3.5 g/dL; alpha-fetoprotein > 100 ng/mL (patients with alpha-fetoprotein 50-100 ng/mL required a liver ultrasound, and those with findings suspicious of HCC were excluded); hemoglobin < 8.5 g/dL; absolute neutrophil count < 0.5×10^9 cells/L; and, platelet count < 50×10^9 cells/L.

Study assessments

HCV RNA was quantified using the COBAS® *Taq*Man® assay v2.0 (Roche Molecular Diagnostics, Pleasanton, CA, United States) with a lower limit of quantitation (LLOQ) of 25 IU/mL. HCV genotype and subtype were determined using the RealTime HCV Genotype II assay (Abbott Molecular, Des Plaines, IL, United States); if the results were inconclusive, the Versant HCV Genotype 2.0 assay (Siemens, Erlangen, Germany) or population-based sequencing of the NS5A region was employed. *IL28B* rs12979860 single-nucleotide polymorphisms were identified using PCR amplification and sequencing (*Taq*Man assay; Applied Biosystems, Waltham, MA, United States).

Treatment failure comprised: virologic breakthrough, defined as any confirmed > 1 $\log_{10}$ increase in HCV RNA from nadir, or increase in HCV RNA ⩾ LLOQ after confirmed HCV RNA < LLOQ target detected or not detected (TD or TND) during treatment; HCV RNA < LLOQ but still detectable at end of treatment (EOT); or, relapse, defined as HCV RNA ⩾ LLOQ in any posttreatment window following HCV RNA < LLOQ TND at EOT.

Resistance testing was performed using population-based sequencing (threshold ⩾ 20% of a viral population) of the NS5A and NS3 regions on all available plasma samples at baseline, and on the samples of patients experiencing treatment failure with HCV RNA ⩾ 1000 IU/mL.

Safety was monitored based on incidence of adverse events (AEs) and abnormalities in clinical laboratory assessments, vital signs and physical examinations.

Study endpoints

The primary efficacy outcome was the proportion of patients, randomly assigned to the immediate treatment arm, achieving a sustained virologic response (HCV RNA < LLOQ, TD or TND) at posttreatment week 12 (SVR12), and the primary endpoint was comparison of this outcome against a historical SVR rate of 70% associated with peg-IFN plus ribavirin treatment.

SVR12 in the placebo-deferred treatment arm was a secondary endpoint. Safety-related secondary endpoints included the incidence of AEs, serious (S)AEs, discontinuations due to AEs, deaths, and grade 3-4 laboratory abnormalities observed during the 12-wk double-blind phase (DUAL *vs* placebo), and in both arms during 24 wk of treatment with DUAL. Efficacy-related secondary endpoints included SVR12 according to rs12979860 single-nucleotide polymorphisms in the *IL28B* gene; the proportion of patients achieving HCV RNA < LLOQ, TD or TND and TND only, in each treatment arm at on-treatment weeks 1, 2, 4, 6, 8, and 12, both on-treatment weeks 4 and 12, EOT, and post-treatment weeks 4 and 24.

Statistical analysis

The statistical methods used in this study were reviewed by the biometrics group at Bristol-Myers Squibb. The primary objective was to determine whether SVR12 among patients in the immediate treatment arm would be significantly higher than the historical 70% SVR rate associated with peg-IFN plus ribavirin. The lower bound of a two-sided 95% confidence interval (CI) for SVR12 was used to compare to the historical SVR rate; if it exceeded 70%, it was concluded that the primary objective was met and SVR12 for patients in the immediate treatment arm was significantly higher than the SVR rate associated with peg-IFN plus ribavirin. A sample size of approximately 150 patients would have provided a 95%CI with a lower bound exceeding 70% for a corresponding SVR12 rate of approximately 77.3% or higher, while an SVR12 rate of 90% would have provided a lower bound not less than 85%. Missing HCV RNA data at posttreatment week 12 were imputed using the next value carried backwards approach, where the next and closest available HCV RNA measurement after posttreatment week 12 was utilized instead.

RESULTS

Patient disposition

In total, 229 patients were enrolled, of whom 207 were randomly assigned to the immediate (*n* = 155) or placebo-deferred (*n* = 52) treatment arms.

Of 155 patients assigned to the immediate treatment arm, all completed the 12-wk double-blind phase, 148 completed 24 wk of treatment with DUAL, and 151 completed 24 wk of follow-up; seven discontinued treatment with DUAL due to lack of efficacy (*n* = 6) or AEs (*n* = 1), and four discontinued follow-up after posttreatment week 12 due to withdrawal of consent (*n* = 3) or inability to attend the visit due to an accident (*n* = 1).

Of 52 patients randomly assigned to placebo-deferred treatment, 51 completed the 12-wk double-blind phase, 44 completed 24 wk of treatment with DUAL, and 48 completed 24 wk of follow-up; one discontinued placebo due to an SAE (hepatitis E),

Table 1 Baseline demographics and disease characteristics *n* (%)[1]

Characteristic	Immediate treatment, *n* = 155[2]	Placebo-deferred treatment, *n* = 52	Overall, *n* = 207[2]
Age, median (range) years	49 (18-73)	49 (23-69)	49 (18-73)
< 65 yr	142 (92)	45 (87)	187 (90)
⩾ 65 yr	13 (8)	7 (14)	20 (10)
Male	61 (39)	23 (44)	84 (41)
Race			
Asian	132 (85)	45 (87)	177 (86)
White	23 (15)	7 (14)	30 (15)
Country			
Mainland China	119 (77)	42 (81)	161 (78)
Russia	23 (15)	7 (14)	30 (15)
South Korea	13 (8)	3 (6)	16 (8)
HCV RNA, median (range) $\log_{10}$ IU/mL	6.78 (3.1-7.6)	6.86 (5.6-7.6)	6.79 (3.1-7.6)
⩾ 6 million IU/mL	79 (51)	31 (60)	110 (53)
IL28B genotype			
CC	107 (69)	34 (65)	141 (68)
CT	43 (28)	17 (33)	60 (29)
TT	5 (3)	1 (2)	6 (3)
Cirrhosis	19 (12)	7 (14)	26 (13)

[1]Unless otherwise stated; [2]Includes one patient from mainland China who was subsequently reclassified as having HCV genotype 1a infection by phylogenetic analysis of the HCV NS5A sequence. HCV: Hepatitis C virus.

seven discontinued treatment with DUAL due to lack of efficacy (*n* = 6) or AEs (*n* = 1), and two discontinued follow-up after posttreatment week 12 due to withdrawal of consent (*n* = 1) or initiation of alternative HCV therapy (*n* = 1).

Baseline characteristics

The majority of patients were Chinese (77.8%) and female (60.6%); among them, 12.6% had compensated cirrhosis, 31.9% had *IL28B* non-CC genotypes, 53.1% had baseline HCV RNA ⩾ 6 million IU/mL and 9.7% were aged 65 years or older (Table 1). These data include six patients who were found not to meet the study enrollment criteria after treatment initiation; one of these patients, from mainland China, was reclassified as having genotype 1a infection, and five had received prior treatment with ribavirin and/or IFN regimens.

Efficacy endpoints

The study met its primary endpoint, with SVR12 achieved by 142 (91.6%, 95%CI: 87.2-96.0) patients in the immediate treatment arm (including the patient with HCV genotype 1a infection), significantly above the 70% historical comparator (Figure 1). SVR12 was comparable between patients from mainland China (110/119, 92.4%) and Russia (22/23, 95.7%), although lower among the smaller cohort of patients from South Korea (10/13, 76.9%). SVR12 in this arm was also comparable between patients with (17/19, 89.5%) and without (125/136, 91.9%) cirrhosis, with *IL28B* CC (96/107, 89.7%) and non-CC genotypes (46/48, 95.8%), aged < 65 (130/142, 91.5%) and ⩾ 65 (12/13, 92.3%) years, with baseline HCV RNA < 6 million (72/76, 94.7%) and ⩾ 6 million (70/79, 88.6%) IU/mL, and between male (55/61, 90.2%) and female (87/94, 92.6%) patients (Figure 2). HCV RNA declined rapidly from baseline, and by week 4 was undetectable in 140 (90.3%) patients.

SVR12 rates in the placebo-deferred treatment arm, overall and according to selected baseline characteristics, are provided in Figures 3 and 4.

Treatment failure

Thirteen (8.4%) patients in the immediate treatment arm failed to achieve SVR12. Six patients experienced virologic breakthrough [mainland China (*n* = 4), South Korea (*n* = 1), and Russia (*n* = 1)], one patient from mainland China had detectable HCV RNA at EOT, and six patients relapsed [mainland China (*n* = 4) and South Korea (*n* = 2)] (Figure 1).

Treatment failure in the placebo-deferred treatment arm is described in Figure 3.

Resistance analysis

Resistance analyses were conducted at baseline for 154 patients in the immediate treatment arm (excluding the patient with HCV genotype 1a infection) (Tables 2 and 3). Daclatasvir resistance-associated polymorphisms at NS5A amino acid positions L31 or Y93H preexisted in 17 (11.0%) patients, 9 of whom (52.9%) achieved SVR12. By contrast, SVR12 was achieved by 132 of 137 (96.4%) patients without baseline NS5A-L31 or NS5A-Y93H, and was comparably high among patients with (17/19, 89.5%) and without (115/118, 97.5%) cirrhosis who did not have baseline resistance-associated polymorphisms.

The asunaprevir resistance-associated polymorphism NS3-D168E preexisted in one (0.6%) patient who did not achieve SVR12; this patient also had NS5A-Y93H at baseline. Of the 13 patients in the immediate treatment

Table 2 SVR12 in hepatitis C virus genotype 1b-infected patients with and without resistance-associated polymorphisms at baseline (immediate treatment arm) *n* (%)

	All patients - immediate treatment arm							
	With RAPs at baseline				Without RAPs at baseline			
	Mainland China	Russia	South Korea	Overall	Mainland China	Russia	South Korea	Overall
NS5A-L31M/V	1/1 (100)	1/1(100)	0	2/2 (100)	108/117 (92.3)	21/22 (95.5)	10/13 (76.9)	139/152 (91.4)
Y93H	7/13(53.8)	0	0/2 (0)	7/15 (46.7)	102/105 (97.1)	22/23 (95.7)	10/11(90.9)	134/139 (96.4)
L31M/V or Y93H	8/14 (57.1)	1/1 (100)	0/2 (0)	9/17 (52.9)	101/104 (97.1)	21/22 (95.5)	10/11(90.9)	132/137 (96.4)
NS3-D168E	0/1 (0)	0	0	0/1 (0)	109/117 (93.2)	22/23 (95.7)	10/13 (76.9)	141/153 (92.2)

RAP: Resistance-associated polymorphism; SVR12: Sustained virologic response at posttreatment week 12.

Table 3 SVR12 in cirrhotic and non-cirrhotic hepatitis C virus genotype 1b-infected patients with and without resistance-associated polymorphisms at baseline (immediate treatment arm) *n* (%)

	Patients with cirrhosis - immediate treatment arm							
	With RAPs at baseline				Without RAPs at baseline			
	Mainland China	Russia	South Korea	Overall	Mainland China	Russia	South Korea	Overall
Patients with cirrhosis								
NS5A-L31M/V	0	0	0	0	15/16 (93.8)	0	2/3 (66.7)	17/19 (89.5)
Y93H	0	0	0	0	15/16 (93.8)	0	2/3 (66.7)	17/19 (89.5)
L31M/V or Y93H	0	0	0	0	15/16 (93.8)	0	2/3 (66.7)	17/19 (89.5)
NS3-D168E	0	0	0	0	15/16 (93.8)	0	2/3 (66.7)	17/19 (89.5)
Patients without cirrhosis								
NS5A-L31M/V	1/1 (100)	1/1 (100)	0	2/2 (100)	93/101 (92.1)	21/22 (95.5)	8/10 (80.0)	122/133 (91.7)
Y93H	7/13 (53.8)	0	0/2 (0)	7/15 (46.7)	87/89 (97.8)	22/23 (95.7)	8/8 (100)	117/120 (97.5)
L31M/V or Y93H	8/14 (57.1)	1/1 (100)	0/2 (0)	9/17 (52.9)	86/88 (97.7)	21/22 (95.5)	8/8 (100)	115/118 (97.5)
NS3-D168E	0/1 (0)	0	0	0/1 (0)	94/101 (93.1)	22/23 (95.7)	8/10 (80.0)	124/134 (92.5)

RAP: Resistance-associated polymorphism; SVR12: Sustained virologic response at posttreatment week 12.

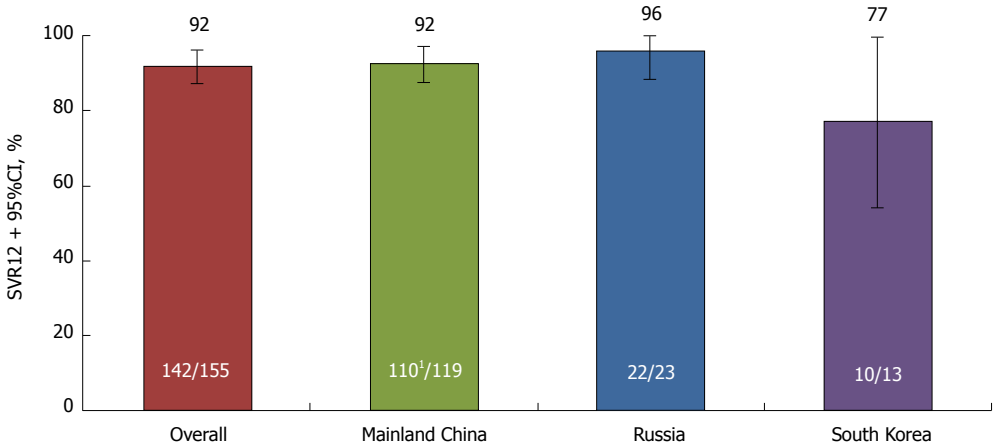

Figure 1 SVR12 in the immediate treatment arm. [1]Includes the patient with genotype 1a infection; [2]On-treatment HCV RNA ⩾ LLOQ after < LLOQ, or increased > 1 $\log_{10}$ over nadir; [3]Posttreatment HCV RNA ⩾ LLOQ after < LLOQ without detectable target at EOT. EOT: End of treatment; HCV: Hepatitis C virus; LLOQ: Lower limit of quantitation; SVR12: Sustained virologic response at post-treatment week 12.

arm who failed to achieve SVR12, 8 (61.5%) had the NS5A-Y93H polymorphism at baseline, including the patient who also had baseline NS3-D168E. At treatment failure, all 13 patients had emergent NS5A-L31 and/or NS5A-Y93H substitutions, while 10 of these patients also had emergent NS3-D168 substitutions (A/E/H/V/Y).

The impact of baseline resistance-associated polymorphisms on SVR12 in the placebo-deferred arm

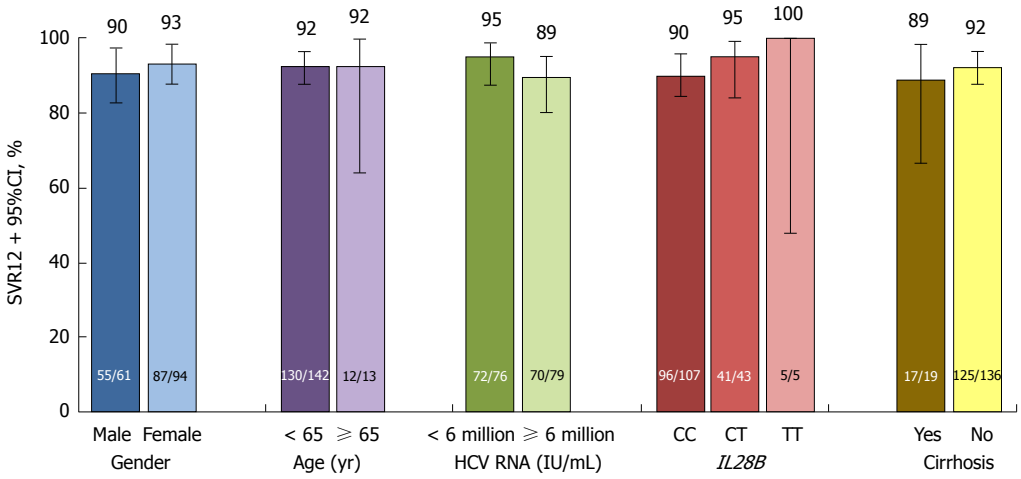

Figure 2 SVR12 according to selected baseline characteristics in the immediate treatment arm. HCV: Hepatitis C virus; SVR12: Sustained virologic response at posttreatment week 12.

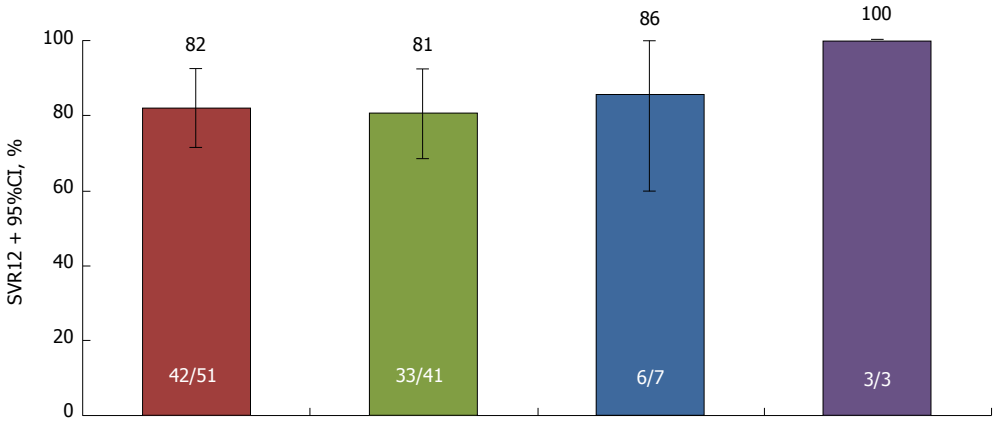

	Overall	Mainland China	Russia	South Korea
Virologic breakthrough, [1]*n*	7	7	0	0
Detectable HCV RNA at EOT, *n*	0	0	0	0
Relapse, [2]*n*	1	1	0	0
Other, [3]*n*	1	0	1[4]	0

Figure 3 SVR12 in the placebo-deferred treatment arm. [1]On-treatment HCV RNA ≥ LLOQ after < LLOQ, or increased >1 $\log_{10}$ over nadir; [2]HCV RNA < LLOQ (TND) at EOT followed by HCV RNA ≥ LLOQ at any follow-up visit; [3]Other nonresponders included patients who had HCV RNA < LLOQ (TND) at EOT, but with missing posttreatment week 12 data; [4]Death, not considered related to study therapy (stab wound). EOT: End of treatment; HCV: Hepatitis C virus; LLOQ: Lower limit of quantitation; SVR12, Sustained virologic response at post-treatment week 12.

is shown in Tables 4 and 5.

Safety and tolerability

The safety outcomes observed during the 12-wk double-blind phase are summarized in Table 6. Five (3.2%) patients in the immediate-treatment arm had SAEs considered related [study drug overdose (*n* = 2)] or unrelated to treatment [ventricular extra-systoles (*n* = 1), acute cholecystitis (*n* = 1) and intervertebral disc protrusion (*n* = 1)], and three (5.8%) patients in the placebo-deferred treatment arm had SAEs [ALT elevation (*n* = 1), coronary artery disease (*n* = 1), and hepatitis E virus infection plus liver injury (*n* = 1; leading to study discontinuation)] while receiving placebo. No treatment-related deaths were observed during the study.

The most common AEs (any grade) occurring in > 5% of patients in either arm during the initial 12-weeks of treatment with DUAL (immediate treatment arm) compared with placebo (placebo-deferred arm) were elevated ALT (3.2% *vs* 23.1%), elevated AST (1.3% *vs* 15.4%), hypertension (7.1% *vs* 7.7%), upper respiratory tract infection (6.5% *vs* 5.8%), platelet count decrease (1.9% *vs* 7.7%) and pyrexia (0.6% *vs* 5.8%). The most common grade 3-4 laboratory abnormalities during this period (DUAL *vs* placebo) were related to ALT (0.6% *vs* 9.6%), AST (0.6% *vs* 5.8%), total bilirubin (0.6% *vs* 0%) and hemoglobin (1.9% *vs* 0%).

The safety outcomes observed during 24 wk of

Table 4 SVR12 in hepatitis C virus genotype 1b-infected patients with and without resistance-associated polymorphisms at baseline (placebo-deferred treatment arm) *n* (%)

	All patients - placebo-deferred treatment arm							
	With RAPs at baseline				Without RAPs at baseline			
	Mainland China	Russia	South Korea	Overall	Mainland China	Russia	South Korea	Overall
NS5A-L31M/V	0	0	0	0	33/41 (80.5)	6/6 (100)	3/3 (100)	42/50 (84.0)
Y93H	2/8 (25.0)	0	0	2/8 (25.0)	31/33 (93.9)	6/6 (100)	3/3 (100)	40/42 (95.2)
L31M/V or Y93H	2/8 (25.0)	0	0	2/8 (25.0)	31/33 (93.9)	6/6 (100)	3/3 (100)	40/42 (95.2)
NS3-D168E	0	0	0	0	33/41 (80.5)	6/6 (100)	3/3 (100)	42/50 (84.0)

RAP: Resistance-associated polymorphism; SVR12: Sustained virologic response at posttreatment week 12.

Table 5 SVR12 in cirrhotic and noncirrhotic hepatitis C virus genotype-1b-infected patients with and without resistance-associated polymorphisms at baseline (placebo-deferred treatment arm) *n* (%)

	Patients with cirrhosis - placebo-deferred treatment arm							
	With RAPs at baseline				Without RAPs at baseline			
	Mainland China	Russia	South Korea	Overall	Mainland China	Russia	South Korea	Overall
Patients with cirrhosis								
NS5A-L31M/V	0	0	0	0	3/5 (60.0)	1/1 (100)	1/1 (100)	5/7 (71.4)
Y93H	1/3 (33.3)	0	0	1/3 (33.3)	2/2 (100)	1/1 (100)	1/1 (100)	4/4 (100)
L31M/V or Y93H	1/3 (33.3)	0	0	1/3 (33.3)	2/2 (100)	1/1 (100)	1/1 (100)	4/4 (100)
NS3-D168E	0	0	0	0	3/5 (60.0)	1/1 (100)	1/1 (100)	5/7 (71.4)
Patients without cirrhosis								
NS5A-L31M/V	0	0	0	0	30/36 (83.3)	5/5 (100)	2/2 (100)	37/43 (86.0)
Y93H	1/5 (20.0)	0	0	1/5 (20.0)	29/31 (93.5)	5/5 (100)	2/2 (100)	36/38 (94.7)
L31M/V or Y93H	1/5 (20.0)	0	0	1/5 (20.0)	29/31 (93.5)	5/5 (100)	2/2 (100)	36/38 (94.7)
NS3-D168E	0	0	0	0	30/36 (83.3)	5/5 (100)	2/2 (100)	37/43 (86.0)

RAP: Resistance-associated polymorphism; SVR12: Sustained virologic response at posttreatment week 12.

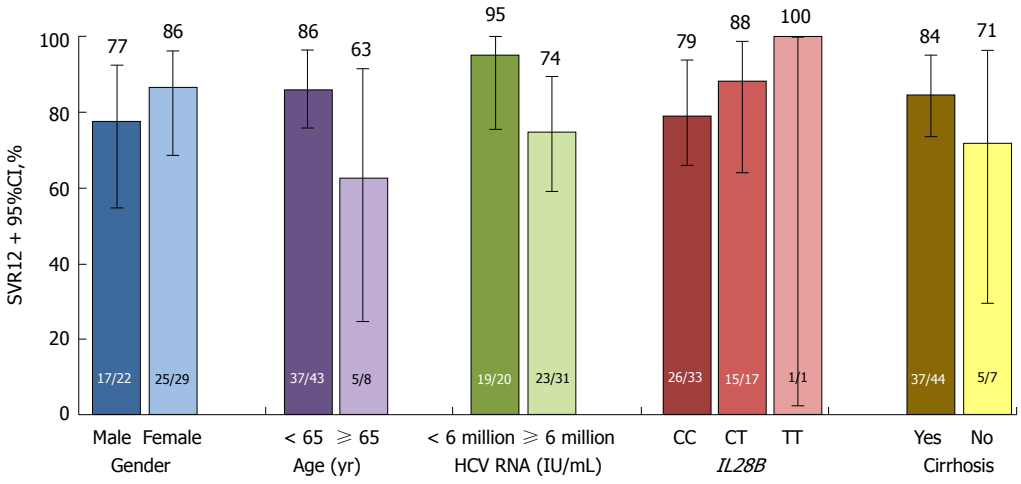

Figure 4 SVR12 according to selected baseline characteristics in the placebo-deferred treatment arm[1]. [1]Reasons for patients not achieving SVR12 included virologic breakthrough (*n* = 7), relapse (*n* = 1) or other (*n* = 1; death, not considered related to study therapy). HCV: Hepatitis C virus; SVR12: Sustained virologic response at post-treatment week 12.

DUAL treatment in either arm are summarized in Table 7. Two (1.3%) patients in the immediate treatment arm had SAEs deemed unrelated to treatment [appendicitis (*n* = 1) and retinal detachment (*n* = 1)] in addition to the five patients with SAEs during the 12-wk double-blind phase. One (2.0%) patient in the placebo-deferred treatment arm (excluding the patient who discontinued during the 12-wk double-blind phase) discontinued due to fatality unrelated to treatment (stab wound). One patient in the immediate treatment arm discontinued after twice meeting the biochemical criteria for Hy's law. On day 118, treatment was interrupted for this

Table 6 Safety during the 12-wk double-blind period *n* (%)

Parameter	Immediate treatment, *n* = 155	Placebo-deferred treatment, *n* = 52
AEs leading to discontinuation	0 (0)	1 (2)[1]
Serious AEs	5 (3)[2]	3 (6)[1,3]
AEs (any grade), ⩾ 5%		
ALT elevation	5 (3)	12 (23)
AST elevation	2 (1)	8 (15)
Hypertension	11 (7)	4 (8)
Upper respiratory tract infection	10 (6)	3 (6)
Platelet count decrease	3 (2)	4 (8)
Pyrexia	1 (1)	3 (6)
On-treatment grade 3-4 laboratory abnormalities		
ALT	1 (1)	5 (10)
AST	1 (1)	3 (6)
Total bilirubin	1 (1)	0 (0)
Hemoglobin	3 (2)	0 (0)

[1]Hepatitis E virus infection and liver injury (*n* = 1); [2]Treatment related: Study drug overdose (*n* = 2); Unrelated to treatment: Ventricular extrasystoles (*n* = 1), acute cholecystitis (*n* = 1) and intervertebral disc protrusion (*n* = 1); [3]ALT elevation (*n* = 1) and coronary artery disease (*n* = 1). AE: Adverse event; ALT: Alanine transaminase; AST: Aspartate transaminase.

Table 7 Safety during 24 wk of daclatasvir plus asunaprevir treatment in either arm *n* (%)

Parameter	Immediate treatment, *n* = 155	Placebo-deferred treatment, *n* = 51[1]	Overall, *n* = 206
AEs leading to discontinuation	1 (1)[2]	1 (2)[3]	2 (1)
Serious AEs	7 (5)[4,5]	1 (2)[3]	8 (4)
Deaths	0 (0)	1 (2)[3]	1 (< 1)
AEs (any grade), ⩾ 5%			
ALT elevation	17 (11)	5 (10)	22 (11)
Upper respiratory tract infection	13(8)	8(16)	21(10)
Hypertension	11 (7)	6 (12)	17 (8)
AST elevation	13 (8)	3 (6)	16 (8)
INR elevation6	11 (7)	2 (4)	13 (6)
Blood bilirubin elevation	12 (8)	0 (0)	12 (6)
Fatigue	5 (3)	6 (12)	11 (5)
On-treatment grade 3-4 laboratory abnormalities			
ALT	7 (5)[2]	2 (4)[7]	9 (4)
AST	5 (3)[2]	1 (2)[7]	6 (3)
Total bilirubin	1 (1)	0 (0)	1 (< 1)
Hemoglobin	3 (2)	0 (0)	3 (1)
Platelets	1 (1)	0 (0)	1 (< 1)
Absolute lymphocyte count	0 (0)	1 (2)	1 (< 1)
Absolute neutrophil count	1 (1)	0 (0)	1 (< 1)
Lipase	3 (2)	0 (0)	3 (1)

[1]Excludes the patient who discontinued during the double-blind phase; [2]Jaundice and nausea, which followed concomitant but reversible treatment-related ALT, AST and total bilirubin elevations (patient met the biochemical criteria for Hy's law; aminotransferases, jaundice and nausea resolved off-treatment and patient achieved SVR12); [3]Fatality (stab wound) unrelated to treatment; [4]Treatment related: Study drug overdose (*n* = 2); [5]Unrelated to treatment: Ventricular extrasystoles (*n* = 1), acute cholecystitis (*n* = 1), intervertebral disc protrusion (*n* = 1), retinal detachment (*n* = 1) and appendicitis (*n* = 1); [6]No grade 3-4 INR laboratory abnormalities were observed; [7]One patient experienced vomiting, decreased appetite and myalgia (all resolved), plus grade 3 ALT and AST abnormalities (both reversible), and interrupted DUAL treatment for 2 d (patient achieved SVR12). AE: Adverse event; ALT: Alanine transaminase; AST: Aspartate transaminase; INR: International normalized ratio.

patient until day 124 due to grade 3 ALT (320 U/L) and AST (237 U/L), grade 2 bilirubin (36.3 μmol/L), and grade 1 alkaline phosphatase (201 U/L). By day 133, the patient's AST level had improved to 195 U/L (grade 3), but levels of ALT (223 U/L) and blood bilirubin (37.6 μmol/L) remained elevated. On day 141, the patient's blood bilirubin and ALT levels had improved to 32.5 μmol/L (grade 2) and 155 U/L (grade 2), respectively; however, he was diagnosed with grade 2 AST (152 U/L) and grade 2 AEs of jaundice and nausea. Given this patient's already elevated levels of ALT, AST and alkaline phosphatase, he met the biochemical criteria for Hy's law for a second time and discontinued treatment the next day. All events resolved by day 152 and the patient achieved SVR12.

The most common AEs (any grade) occurring in > 5% of patients during 24 wk of treatment with DUAL in either treatment arm were elevated ALT (11%), upper respiratory tract infection (10%), hypertension (8%), elevated AST (8%), elevated international normalized

ratio (6%), elevated blood bilirubin (6%) and fatigue (5%). The most common grade 3-4 laboratory abnormalities were related to ALT (4%), AST (3%), hemoglobin (1%) or lipase (1%) (Table 7).

DISCUSSION

In this study, SVR12 was achieved by 91.6% of patients with HCV genotype 1b infection who were randomly assigned to receive immediate treatment with DUAL. With the lower bound of the corresponding 95%CI (87.2%) greater than the prespecified 70% threshold, the primary endpoint was met, confirming that DUAL is more efficacious than peg-IFN plus ribavirin in patients with HCV genotype 1b infection.

SVR12 was comparable between patients from mainland China (92.4%) and Russia (95.7%). By contrast, SVR12 was lower among patients from South Korea (76.9%); however, this was a small cohort and two of the three patients experiencing virologic failure had the NS5A-Y93H polymorphism at baseline, which has been shown to reduce SVR in patients with HCV genotype 1b infection receiving DUAL[18,22,23]. SVR12 was also lower among patients in the placebo-deferred arm following treatment with DUAL (42/51, 82.4%); however, again this was a small cohort and six of the eight patients with virologic failure had the NS5A-Y93H polymorphism at baseline. Nonetheless, consistent with the results of other phase 3 studies, SVR12 was high overall and largely unaffected by characteristics known to attenuate response to IFN, namely cirrhosis, *IL28B* non-CC genotypes, male sex, advanced age, and high baseline HCV RNA[10-13]. Virologic failure in the immediate treatment arm tended to coincide with the presence of baseline NS5A polymorphisms at L31M or Y93H, consistent with previous observations[18]. Although the prevalence of NS5A-L31 or NS5A-Y93H was relatively low in this study (11.0%), the observed SVR12 rates were, consistent with previous reports, higher among patients without these baseline polymorphisms (132/137, 96.4%), including those with cirrhosis (17/19, 89.5%), compared with cirrhotic patients with these baseline polymorphisms (9/17, 52.9%).

During the 12-wk double-blind phase, SAEs and AEs leading to discontinuation were infrequently observed in the immediate (5/155, 3.2% and none) and placebo-deferred (3/52, 5.8% and 1/52, 1.9%) treatment arms. However, although the AE profiles were broadly comparable between the two arms, elevations of ALT and AST were more common among patients receiving placebo (12/52, 23.1% and 8/52, 15.4%) compared with those receiving DUAL (5/155, 3.2% and 2/155, 1.3%). Consistent with this, grade 3-4 ALT and AST laboratory abnormalities during the blinded phase were more common among patients receiving placebo compared with those receiving DUAL. These elevations most likely reflected ongoing inflammation from untreated HCV infection; indeed, ALT and AST levels in most of these patients had begun to decrease by week 2 of open-label treatment with DUAL. One patient in the immediate treatment arm met the criteria for Hy's law during treatment with DUAL; however, following treatment discontinuation, the events resolved and the patient achieved SVR12.

DUAL was well tolerated during 24 wk of treatment in both arms, consistent with findings from other phase 3 studies[10-12,19]. SAEs (8/206, 3.9%) and AEs leading to discontinuation (2/206, 1.0%) were infrequently observed and, except for two cases of study drug overdose, no SAEs were deemed treatment related. Emergent grade 3-4 laboratory abnormalities were similarly uncommon. The most common grade 3-4 laboratory abnormalities were related to ALT (9/206, 4.4%) and AST (6/206, 2.9%), however these reversed rapidly (median reversal times: 11.0 and 8.5 d for ALT and AST abnormalities, respectively) during or after treatment, and their incidences were comparable with those observed in other studies[10,24-26].

A limitation of this study was the absence of a direct IFN-based comparator for the primary efficacy endpoint. However, despite the continuing importance of IFN-based treatment across much of Asia, it was felt that including an IFN-based treatment arm in the study design would have been unethical. Peg-IFN is associated with a high burden of systemic AEs that include "flu-like" symptoms, neutropenia and thrombocytopenia[27], while ribavirin is associated with hemolytic anemia, birth defects, nausea, rash, itching, coughing and hyperuricemia[28,29]. The result is a combination with poor treatment adherence and a high rate of study discontinuations due to AEs[30]. Comparing DUAL, an all-oral combination with superior efficacy and safety profiles, to peg-IFN plus ribavirin, a combination containing an injectable drug with inferior efficacy and safety profiles, would therefore have lacked clinical equipoise. We also acknowledge that some patients were denied access to DUAL for 12 wk during the double-blind phase; however, as liver disease progresses slowly in patients with HCV infection, we do not believe that giving placebo instead of active treatment for 12 wk in compensated, treatment-naïve patients posed any ethical concerns.

In conclusion, the findings of this study showed that the all-oral DUAL combination of daclatasvir plus asunaprevir was highly effective and well tolerated in treatment-naïve patients from mainland China, Russia and South Korea with HCV genotype 1b infection. For patients in China, where IFN-based combinations have been considered the standard of care for HCV infection, DUAL was the first all-oral, nonribavirin-containing combination to gain approval, providing patients with access to a more efficacious and tolerable alternative for the treatment of HCV genotype 1b infection, with an easier route of administration and shorter treatment duration. DUAL is also predicted to be a cost-effective treatment alternative for HCV genotype 1b in China[31]. In addition, in countries such as Japan, where all-

oral regimens are considered the standard of care for the treatment of HCV genotype 1b infection, DUAL is expected to be cost-saving compared with sofosbuvir/ledipasvir, with similar health outcomes[32].

ARTICLE HIGHLIGHTS

Research background

Chronic hepatitis C virus (HCV) infection is a significant health burden across Asia, and affects 5-7 million people in China alone. Without effective treatment, patients can develop severe complications, such as cirrhosis or hepatocellular carcinoma. Previous therapies for the treatment of chronic HCV infection have been based on a combination of peg-interferon and ribavirin, both of which are associated with a high burden of adverse events (AEs) that contribute to poor treatment adherence and high rates of treatment discontinuations.

Research motivation

Daclatasvir plus asunaprevir (DUAL) is an all-oral combination of daclatasvir, an HCV NS5A inhibitor, and asunaprevir, an NS3 protease inhibitor. This regimen has previously demonstrated efficacy in several phase 3 studies of patients infected with HCV genotype 1b, including those characteristics known to attenuate response to interferon-based therapies. In this study, we sought to evaluate the efficacy and safety of DUAL in treatment-naïve patients from mainland China, South Korea and Russia.

Research objectives

The primary efficacy objective of the study was to measure the rate of sustained virologic response at posttreatment week 12 (SVR12) and to determine if this rate was significantly higher than the historical rate of 70% associated with peg-interferon plus ribavirin. Safety was monitored based on incidence of AEs and abnormalities in clinical laboratory assessments, vital signs and physical examinations.

Research methods

This was a phase 3, double-blind, placebo-controlled study of DUAL in treatment-naïve patients from mainland China, South Korea and Russia with chronic HCV genotype 1b infection. Patients were randomly assigned (3:1) to receive DUAL (daclatasvir 60 mg tablet once daily and asunaprevir 100 mg soft capsule twice daily) for 24 wk either immediately (immediate treatment arm) or after 12 wk of matching placebo (placebo-deferred treatment arm).

Research results

An SVR12 rate of 91.6% (95% confidence interval: 87.2-96.0) was observed among patients in the immediate treatment arm, which was significantly higher than the historical comparator rate (70%). SVR12 was largely unaffected by cirrhosis (89%), age $\geqslant$ 65 years (92%), male sex (90%), baseline HCV RNA $\geqslant$ 6 million (89%), or *IL28B* non-CC genotypes (96%), although SVR12 was higher among patients without (96%) than among those with (53%) baseline NS5A resistance-associated polymorphisms (at L31 or Y93H). DUAL was well tolerated during 24 wk of therapy in this study; the most common AEs ($\geqslant$ 10% in the combined arms) were elevated alanine aminotransferase and upper respiratory tract infection. Two patients discontinued DUAL treatment; one due to aminotransferase elevations, nausea and jaundice and the other due to a fatality unrelated to treatment. There were no treatment-related deaths.

Research conclusions

This study demonstrates that the all-oral DUAL combination of daclatasvir plus asunaprevir was highly effective and well tolerated in treatment-naïve patients with HCV genotype 1b infection from mainland China, Russia and South Korea.

Research perspectives

These findings suggest that for patients in many Asian countries, such as China, where interferon-based combinations have been considered the standard of care for HCV infection, DUAL offers a more efficacious and tolerable alternative for the treatment of HCV genotype 1b infection, with an easier route of administration and shorter treatment duration.

ACKNOWLEDGMENTS

The authors would like to thank Phil Yin for support with the study. Editorial support was provided by Matthew Young of Articulate Science and was funded by Bristol-Myers Squibb.

REFERENCES

1 **Bennett H**, Waser N, Johnston K, Kao JH, Lim YS, Duan ZP, Lee YJ, Wei L, Chen CJ, Sievert W, Yuan Y, Li H. A review of the burden of hepatitis C virus infection in China, Japan, South Korea and Taiwan. *Hepatol Int* 2015; **9**: 378-390 [PMID: 26071238 DOI: 10.1007/s12072-015-9629-x]

2 **Sievert W**, Altraif I, Razavi HA, Abdo A, Ahmed EA, Alomair A, Amarapurkar D, Chen CH, Dou X, El Khayat H, Elshazly M, Esmat G, Guan R, Han KH, Koike K, Largen A, McCaughan G, Mogawer S, Monis A, Nawaz A, Piratvisuth T, Sanai FM, Sharara AI, Sibbel S, Sood A, Suh DJ, Wallace C, Young K, Negro F. A systematic review of hepatitis C virus epidemiology in Asia, Australia and Egypt. *Liver Int* 2011; **31** Suppl 2: 61-80 [PMID: 21651703 DOI: 10.1111/j.1478-3231.2011.02540.x]

3 **Mohd Hanafiah K**, Groeger J, Flaxman AD, Wiersma ST. Global epidemiology of hepatitis C virus infection: new estimates of age-specific antibody to HCV seroprevalence. *Hepatology* 2013; **57**: 1333-1342 [PMID: 23172780 DOI: 10.1002/hep.26141]

4 **Bandiera S**, Billie Bian C, Hoshida Y, Baumert TF, Zeisel MB. Chronic hepatitis C virus infection and pathogenesis of hepatocellular carcinoma. *Curr Opin Virol* 2016; **20**: 99-105 [PMID: 27741441 DOI: 10.1016/j.coviro.2016.09.010]

5 **Chinese Society of Hepatology**, Chinese Medical Association, Wei L; Chinese Society of Infectious Diseases, Chinese Medical Association, Hou JL. [The guideline of prevention and treatment for hepatitis C: a 2015 update]. *Zhonghua Gan Zang Bing Za Zhi* 2015; **23**: 906-923 [PMID: 26739465]

6 **Tsoulfas G**, Goulis I, Giakoustidis D, Akriviadis E, Agorastou P, Imvrios G, Papanikolaou V. Hepatitis C and liver transplantation. *Hippokratia* 2009; **13**: 211-215 [PMID: 20011084]

7 **Gao M**. Antiviral activity and resistance of HCV NS5A replication complex inhibitors. *Curr Opin Virol* 2013; **3**: 514-520 [PMID: 23896281 DOI: 10.1016/j.coviro.2013.06.014]

8 **Gao M**, Nettles RE, Belema M, Snyder LB, Nguyen VN, Fridell RA, Serrano-Wu MH, Langley DR, Sun JH, O'Boyle DR 2nd, Lemm JA, Wang C, Knipe JO, Chien C, Colonno RJ, Grasela DM, Meanwell NA, Hamann LG. Chemical genetics strategy identifies an HCV NS5A inhibitor with a potent clinical effect. *Nature* 2010; **465**: 96-100 [PMID: 20410884 DOI: 10.1038/nature08960]

9 **McPhee F**, Sheaffer AK, Friborg J, Hernandez D, Falk P, Zhai G, Levine S, Chaniewski S, Yu F, Barry D, Chen C, Lee MS, Mosure K, Sun LQ, Sinz M, Meanwell NA, Colonno RJ, Knipe J, Scola P. Preclinical Profile and Characterization of the Hepatitis C Virus NS3 Protease Inhibitor Asunaprevir (BMS-650032). *Antimicrob Agents Chemother* 2012; **56**: 5387-5396 [PMID: 22869577 DOI: 10.1128/AAC.01186-12]

10 **Kumada H**, Suzuki Y, Ikeda K, Toyota J, Karino Y, Chayama K, Kawakami Y, Ido A, Yamamoto K, Takaguchi K, Izumi N, Koike K, Takehara T, Kawada N, Sata M, Miyagoshi H, Eley T, McPhee F, Damokosh A, Ishikawa H, Hughes E. Daclatasvir plus asunaprevir for chronic HCV genotype 1b infection. *Hepatology* 2014; **59**: 2083-2091 [PMID: 24604476 DOI: 10.1002/hep.27113]

11 **Manns M**, Pol S, Jacobson IM, Marcellin P, Gordon SC, Peng CY, Chang TT, Everson GT, Heo J, Gerken G, Yoffe B, Towner WJ, Bourliere M, Metivier S, Chu CJ, Sievert W, Bronowicki JP, Thabut D, Lee YJ, Kao JH, McPhee F, Kopit J, Mendez P, Linaberry M, Hughes E, Noviello S; HALLMARK-DUAL Study Team. All-oral daclatasvir plus asunaprevir for hepatitis C virus

genotype 1b: a multinational, phase 3, multicohort study. *Lancet* 2014; **384**: 1597-1605 [PMID: 25078304 DOI: 10.1016/S0140-6736(14)61059-X]

12 **Wei L**, Zhang M, Xu M, Chuang WL, Lu W, Xie W, Jia Z, Gong G, Li Y, Bae SH, Yang YF, Xie Q, Lin S, Chen X, Niu J, Jia J, Garimella T, Torbeyns A, McPhee F, Treitel M, Yin PD, Mo L. A phase 3, open-label study of daclatasvir plus asunaprevir in Asian patients with chronic hepatitis C virus genotype 1b infection who are ineligible for or intolerant to interferon alfa therapies with or without ribavirin. *J Gastroenterol Hepatol* 2016; **31**: 1860-1867 [PMID: 27003037 DOI: 10.1111/jgh.13379]

13 **Kumada H**, Suzuki F, Suzuki Y, Toyota J, Karino Y, Chayama K, Kawakami Y, Fujiyama S, Ito T, Itoh Y, Tamura E, Ueki T, Ishikawa H, Hu W, McPhee F, Linaberry M, Hughes E. Randomized comparison of daclatasvir + asunaprevir versus telaprevir + peginterferon/ribavirin in Japanese hepatitis C virus patients. *J Gastroenterol Hepatol* 2016; **31**: 14-22 [PMID: 26252875 DOI: 10.1111/jgh.13073]

14 **Gower E**, Estes C, Blach S, Razavi-Shearer K, Razavi H. Global epidemiology and genotype distribution of the hepatitis C virus infection. *J Hepatol* 2014; **61**: S45-S57 [PMID: 25086286 DOI: 10.1016/j.jhep.2014.07.027]

15 **Zhang Y**, Chen LM, He M. Hepatitis C Virus in mainland China with an emphasis on genotype and subtype distribution. *Virol J* 2017; **14**: 41 [PMID: 28231805 DOI: 10.1186/s12985-017-0710-z]

16 **Dan YY**, Lim SG. Hepatitis C: An Eastern Perspective. *Gastroenterol Clin North Am* 2015; **44**: 793-805 [PMID: 26600220 DOI: 10.1016/j.gtc.2015.07.007]

17 **Kao JH**, Lee YJ, Heo J, Ahn SH, Lim YS, Peng CY, Chang TT, Torbeyns A, Hughes E, Bhore R, Noviello S. All-oral daclatasvir plus asunaprevir for chronic hepatitis C virus (HCV) genotype 1b infection: a sub-analysis in Asian patients from the HALLMARK DUAL study. *Liver Int* 2016; **36**: 1433-1441 [PMID: 27009831 DOI: 10.1111/liv.13128]

18 **McPhee F**, Suzuki Y, Toyota J, Karino Y, Chayama K, Kawakami Y, Yu ML, Ahn SH, Ishikawa H, Bhore R, Zhou N, Hernandez D, Mendez P, Kumada H. High Sustained Virologic Response to Daclatasvir Plus Asunaprevir in Elderly and Cirrhotic Patients with Hepatitis C Virus Genotype 1b Without Baseline NS5A Polymorphisms. *Adv Ther* 2015; **32**: 637-649 [PMID: 26155891 DOI: 10.1007/s12325-015-0221-5]

19 **Kao JH**, Jensen DM, Manns MP, Jacobson I, Kumada H, Toyota J, Heo J, Yoffe B, Sievert W, Bessone F, Peng CY, Roberts SK, Lee YJ, Bhore R, Mendez P, Hughes E, Noviello S. Daclatasvir plus asunaprevir for HCV genotype 1b infection in patients with or without compensated cirrhosis: a pooled analysis. *Liver Int* 2016; **36**: 954-962 [PMID: 26683763 DOI: 10.1111/liv.13049]

20 **Signorovitch JE**, Betts KA, Song Y, Sorg RA, Li J, Behl AS, Kalsekar A. Comparative efficacy and safety of daclatasvir/asunaprevir versus IFN-based regimens in genotype 1b hepatitis C virus infection. *J Comp Eff Res* 2015; **4**: 593-605 [PMID: 26159375 DOI: 10.2217/cer.15.33]

21 **Bristol-Myers Squibb.** China FDA approves country's first all-oral regimen for chronic hepatitis C, Daklinza® (daclatasvir) in combination with Sunvepra® (asunaprevir) (press release). [Internet]. [cited 2017 Jun 16]. Available from: URL: https://News.bms.com/press-release/bms/china-fda-approves-countrys-first-all-oral-regimen-chronic-hepatitis-c-daklinza-da

22 **Hernandez D**, Yu F, Huang X, Kirov S, Pant S, McPhee F. Impact of Pre-existing NS5A-L31 or -Y93H Minor Variants on Response Rates in Patients Infected with HCV Genotype-1b Treated with Daclatasvir/Asunaprevir. *Adv Ther* 2016; **33**: 1169-1179 [PMID: 27287851 DOI: 10.1007/s12325-016-0354-1]

23 **McPhee F**, Hernandez D, Zhou N, Yu F, Ueland J, Monikowski A, Chayama K, Toyota J, Izumi N, Yokosuka O, Kawada N, Osaki Y, Hughes EA, Watanabe H, Ishikawa H, Kumada H. Virological escape in HCV genotype-1-infected patients receiving daclatasvir plus ribavirin and peginterferon alfa-2a or alfa-2b. *Antivir Ther* 2014; **19**: 479-490 [PMID: 24448487 DOI: 10.3851/IMP2729]

24 **Lok AS**, Gardiner DF, Lawitz E, Martorell C, Everson GT, Ghalib R, Reindollar R, Rustgi V, McPhee F, Wind-Rotolo M, Persson A, Zhu K, Dimitrova DI, Eley T, Guo T, Grasela DM, Pasquinelli C. Preliminary study of two antiviral agents for hepatitis C genotype 1. *N Engl J Med* 2012; **366**: 216-224 [PMID: 22256805 DOI: 10.1056/NEJMoa1104430]

25 **Lok AS**, Gardiner DF, Hézode C, Lawitz EJ, Bourlière M, Everson GT, Marcellin P, Rodriguez-Torres M, Pol S, Serfaty L, Eley T, Huang SP, Li J, Wind-Rotolo M, Yu F, McPhee F, Grasela DM, Pasquinelli C. Randomized trial of daclatasvir and asunaprevir with or without PegIFN/RBV for hepatitis C virus genotype 1 null responders. *J Hepatol* 2014; **60**: 490-499 [PMID: 24444658 DOI: 10.1016/j.jhep.2013.10.019]

26 **Bronowicki JP**, Pol S, Thuluvath PJ, Larrey D, Martorell CT, Rustgi VK, Morris DW, Younes Z, Fried MW, Bourlière M, Hézode C, Reddy KR, Massoud O, Abrams GA, Ratziu V, He B, Eley T, Ahmad A, Cohen D, Hindes R, McPhee F, Reilly B, Mendez P, Hughes E. Randomized study of asunaprevir plus pegylated interferon-α and ribavirin for previously untreated genotype 1 chronic hepatitis C. *Antivir Ther* 2013; **18**: 885-893 [PMID: 23804631 DOI: 10.3851/IMP2660]

27 **Ferenci P**. Safety and efficacy of treatment for chronic hepatitis C with a focus on pegylated interferons: the backbone of therapy today and in the future. *Expert Opin Drug Saf* 2011; **10**: 529-544 [PMID: 21345149 DOI: 10.1517/14740338.2011.555079]

28 **Feld JJ**, Jacobson IM, Sulkowski MS, Poordad F, Tatsch F, Pawlotsky JM. Ribavirin revisited in the era of direct-acting antiviral therapy for hepatitis C virus infection. *Liver Int* 2017; **37**: 5-18 [PMID: 27473533 DOI: 10.1111/liv.13212]

29 **Dusheiko G**, Main J, Thomas H, Reichard O, Lee C, Dhillon A, Rassam S, Fryden A, Reesink H, Bassendine M, Norkrans G, Cuypers T, Lelie N, Telfer P, Watson J, Weegink C, Sillikens P, Weiland O. Ribavirin treatment for patients with chronic hepatitis C: results of a placebo-controlled study. *J Hepatol* 1996; **25**: 591-598 [PMID: 8938532]

30 **Younossi ZM**, Stepanova M, Henry L, Nader F, Younossi Y, Hunt S. Adherence to treatment of chronic hepatitis C: from interferon containing regimens to interferon and ribavirin free regimens. *Medicine* (Baltimore) 2016; **95**: e4151 [PMID: 27428205 DOI: 10.1097/MD.0000000000004151]

31 **Ward T,** Gordon J, Wygant G, Yan J, Wang F, McEwan P. Assessing the economic impact of the introduction of daclatasvir in combination with asunaprevir for the treatment of chronic hepatitis C in China. ISPOR 20th Annual European Congress. Abstract/Poster 247. Accessed January 20, 2018 Available from: URL: https://www.ispor.org/ScientificPresentationsDatabase/Presentation/78290?pdfid=51391

32 **Ward T**, Webster S, Mishina S, McEwan P, Wygant G, Wang F. Assessing the Budget Impact and Economic Outcomes of the Introduction of Daclatasvir + Asunaprevir and Sofosbuvir/Ledipasvir for the Treatment of Chronic Hepatitis C Virus Infection in Japan. *Value Health Reg Issues* 2017; **12**: 1-6 [PMID: 28648305 DOI: 10.1016/j.vhri.2016.10.002]

P- Reviewer: Köksal AS, Takahashi T **S- Editor**: Ma YJ
L- Editor: Filipodia **E- Editor**: Huang Y

Published by **Baishideng Publishing Group Inc**
7901 Stoneridge Drive, Suite 501, Pleasanton, CA 94588, USA
Telephone: +1-925-223-8242
Fax: +1-925-223-8243
E-mail: bpgoffice@wjgnet.com
Help Desk: http://www.f6publishing.com/helpdesk
http://www.wjgnet.com

ISSN 1007-9327

ISSN 1007-9327 (print)
ISSN 2219-2840 (online)

World Journal of *Gastroenterology*

World J Gastroenterol 2018 April 7; 24(13): 1373-1490

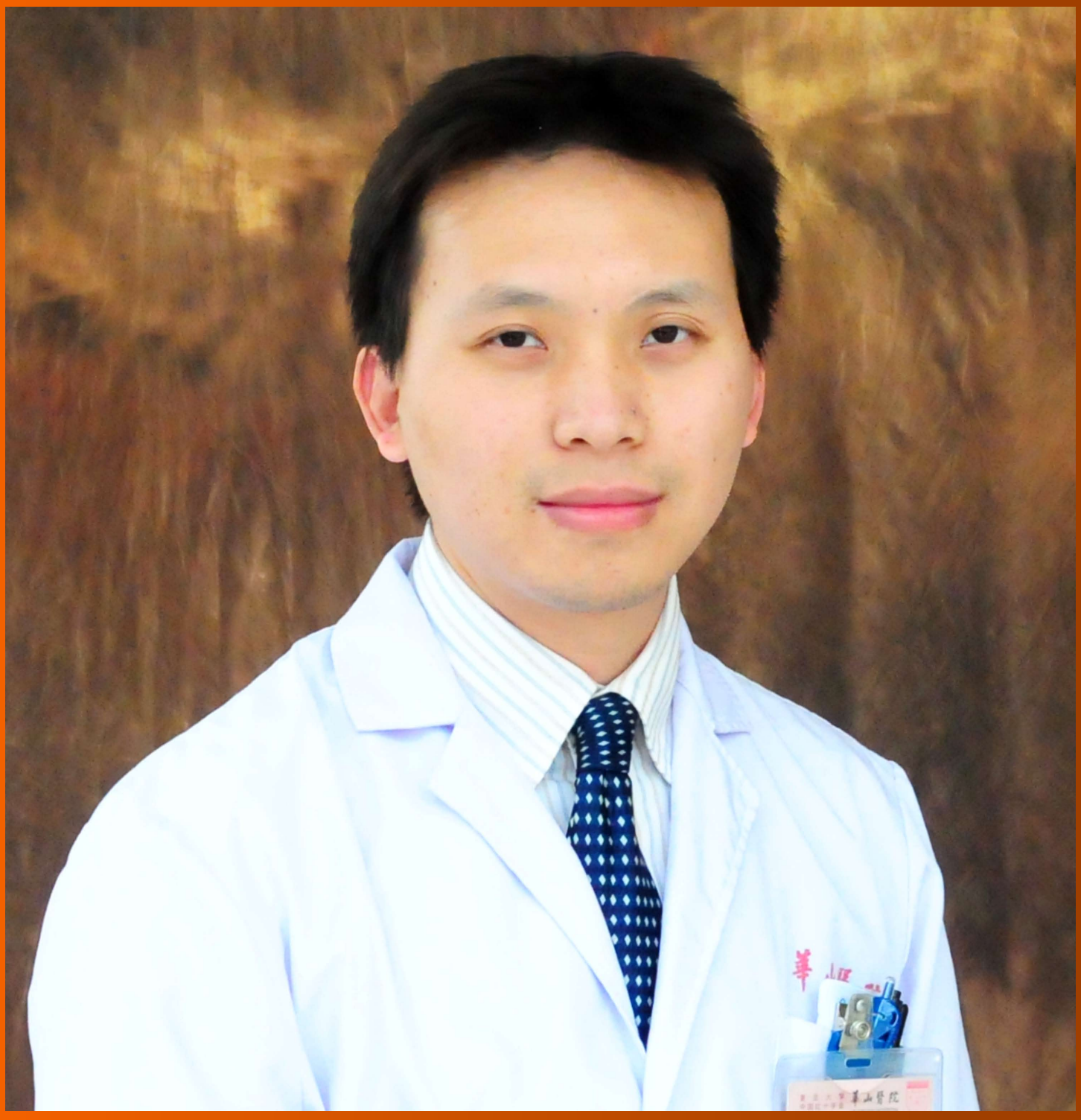

Published by Baishideng Publishing Group Inc

World Journal of Gastroenterology

Contents

Weekly Volume 24 Number 13 April 7, 2018

ABOUT COVER

Editorial board member of *World Journal of Gastroenterology*, Feng Yang, MD, PhD, Associate Professor, Doctor, Surgeon, Pancreatic Surgery, Huashan Hospital, Fudan University, Shanghai 200040, China

AIMS AND SCOPE

World Journal of Gastroenterology (*World J Gastroenterol*, *WJG*, print ISSN 1007-9327, online ISSN 2219-2840, DOI: 10.3748) is a peer-reviewed open access journal. *WJG* was established on October 1, 1995. It is published weekly on the 7th, 14th, 21st, and 28th each month. The *WJG* Editorial Board consists of 642 experts in gastroenterology and hepatology from 59 countries.

The primary task of *WJG* is to rapidly publish high-quality original articles, reviews, and commentaries in the fields of gastroenterology, hepatology, gastrointestinal endoscopy, gastrointestinal surgery, hepatobiliary surgery, gastrointestinal oncology, gastrointestinal radiation oncology, gastrointestinal imaging, gastrointestinal interventional therapy, gastrointestinal infectious diseases, gastrointestinal pharmacology, gastrointestinal pathophysiology, gastrointestinal pathology, evidence-based medicine in gastroenterology, pancreatology, gastrointestinal laboratory medicine, gastrointestinal molecular biology, gastrointestinal immunology, gastrointestinal microbiology, gastrointestinal genetics, gastrointestinal translational medicine, gastrointestinal diagnostics, and gastrointestinal therapeutics. *WJG* is dedicated to become an influential and prestigious journal in gastroenterology and hepatology, to promote the development of above disciplines, and to improve the diagnostic and therapeutic skill and expertise of clinicians.

INDEXING/ABSTRACTING

World Journal of Gastroenterology (*WJG*) is now indexed in Current Contents®/Clinical Medicine, Science Citation Index Expanded (also known as SciSearch®), Journal Citation Reports®, Index Medicus, MEDLINE, PubMed, PubMed Central and Directory of Open Access Journals. The 2017 edition of Journal Citation Reports® cites the 2016 impact factor for *WJG* as 3.365 (5-year impact factor: 3.176), ranking *WJG* as 29th among 79 journals in gastroenterology and hepatology (quartile in category Q2).

NAME OF JOURNAL
World Journal of Gastroenterology

ISSN
ISSN 1007-9327 (print)
ISSN 2219-2840 (online)

LAUNCH DATE
October 1, 1995

FREQUENCY
Weekly

EDITORIAL OFFICE
Ze-Mao Gong, Director
World Journal of Gastroenterology
Baishideng Publishing Group Inc
7901 Stoneridge Drive, Suite 501,
Pleasanton, CA 94588, USA
Telephone: +1-925-2238242
Fax: +1-925-2238243
E-mail: editorialoffice@wjgnet.com
Help Desk: http://www.f6publishing.com/helpdesk
http://www.wjgnet.com

PUBLISHER
Baishideng Publishing Group Inc
7901 Stoneridge Drive, Suite 501,
Pleasanton, CA 94588, USA
Telephone: +1-925-2238242
Fax: +1-925-2238243
E-mail: bpgoffice@wjgnet.com
Help Desk: http://www.f6publishing.com/helpdesk
http://www.wjgnet.com

PUBLICATION DATE
April 7, 2018

INSTRUCTIONS TO AUTHORS
Full instructions are available online at http://www.wjgnet.com/bpg/gerinfo/204

ONLINE SUBMISSION
http://www.f6publishing.com

World Journal of Gastroenterology

Submit a Manuscript: http://www.f6publishing.com

World J Gastroenterol 2018 April 7; 24(13): 1373-1385

DOI: 10.3748/wjg.v24.i13.1373

ISSN 1007-9327 (print) ISSN 2219-2840 (online)

REVIEW

Dissecting the molecular pathophysiology of drug-induced liver injury

Hui Ye, Leonard J Nelson, Manuel Gómez del Moral, Eduardo Martínez-Naves, Francisco Javier Cubero

Hui Ye, Eduardo Martínez-Naves, Francisco Javier Cubero, Department of Immunology, Ophtalmology and ORL, Complutense University School of Medicine, Madrid 28040, Spain

Hui Ye, Eduardo Martínez-Naves, Francisco Javier Cubero, 12 de Octubre Health Research Institute (imas12), Madrid 28041, Spain

Leonard J Nelson, Institute for BioEngineering (Human Liver Tissue Engineering, Faraday Building, The University of Edinburgh, The King Buildings, Mayfield Road, Edinburgh EH9 3 JL, Scotland, United Kingdom

Manuel Gómez del Moral, Department of Cell Biology, Complutense University School of Medicine, Madrid 28040, Spain

ORCID number: Hui Ye (0000-0002-7894-2992); Leonard J Nelson (0000-0002-4197-4843); Manuel Gómez del Moral (0000-0002-0642-8142); Eduardo Martínez-Naves (0000-0001-8136-9042); Francisco Javier Cubero (0000-0003-1499-650X).

Author contributions: Ye H and Cubero FJ outlined the review, wrote the manuscript and designed figures; Nelson LJ, Gómez del Moral M and Martínez-Naves E corrected the manuscript, checked English language and provided fundamental guidance.

Supported by the Spanish Ministerio de Economía y Competitividad (MINECO), No. RyC2014-15242 and No. SAF2016-78711 to Martinez-Naves E and Cubero FJ. Martinez-Naves E and Cubero FJ are part of the UCM group "Lymphocyte Immunobiology", Ref. 920631 (imas12-associated, Ref. IBL-6); Chinese Scholarship Council fellow to Ye H.

Conflict-of-interest statement: The authors declare that they have no conflicts of interest.

Manuscript source: Unsolicited manuscript

Correspondence to: Francisco Javier Cubero, BSc, MSc, PhD, Assistant Professor, Department of Immunology, Ophtalmology and ORL, Complutense University School of Medicine, Plaza de Ramón y Cajal s/n, Madrid 28040, Spain. fcubero@ucm.es
Telephone: +34-91-3941385
Fax: +34-91-3941641

Received: January 27, 2018
Peer-review started: January 28, 2018
First decision: February 10, 2018
Revised: February 16, 2018
Accepted: February 26, 2018
Article in press: February 26, 2018
Published online: April 7, 2018

Abstract

Drug-induced liver injury (DILI) has become a major topic in the field of Hepatology and Gastroenterology. DILI can be clinically divided into three phenotypes: hepatocytic, cholestatic and mixed. Although the clinical manifestations of DILI are variable and the pathogenesis complicated, recent insights using improved preclinical models, have allowed a better understanding of the mechanisms that trigger liver damage. In this review, we will discuss the pathophysiological mechanisms underlying DILI. The toxicity of the drug eventually induces hepatocellular damage through multiple molecular pathways, including direct hepatic toxicity and innate and adaptive immune responses. Drugs or their metabolites, such as the common analgesic, acetaminophen, can cause direct hepatic toxicity through accumulation of reactive oxygen species and mitochondrial dysfunction. The innate and adaptive immune responses play also a very important role in the occurrence of idiosyncratic DILI. Furthermore, we examine common forms of hepatocyte death and their association with the activation of specific signaling pathways.

Key words: Signaling pathways; Acetaminophen; Drug-

induced liver injury; Cell death; Reactive oxygen species

Core tip: Drug-induced liver injury (DILI) represents a broad spectrum of clinical manifestations, and is generally divided into two subtypes: intrinsic and idiosyncratic hepatotoxicity. Drugs and their reactive metabolites covalently bind to mitochondria and cause direct hepatic toxicity through accumulation of oxidative stress (ROS and RNS), endoplasmic reticulum stress and mitochondrial dysfunction, ultimately leading to cell death. The innate and adaptive immune responses also play an important role in the occurrence of idiosyncratic immunological reactions towards the drugs. In this review, we discuss the pathophysiological mechanisms underlying DILI, specific signaling pathways and the common forms of hepatocyte death.

Ye H, Nelson LJ, Gómez del Moral M, Martínez-Naves E, Cubero FJ. Dissecting the molecular pathophysiology of drug-induced liver injury. *World J Gastroenterol* 2018; 24(13): 1373-1385 Available from: URL: http://www.wjgnet.com/1007-9327/full/v24/i13/1373.htm DOI: http://dx.doi.org/10.3748/wjg.v24.i13.1373

INTRODUCTION

Drug-induced liver injury (DILI) is the most common cause of acute liver failure (ALF) in the United States and Europe[1], and is a leading reason for drug withdrawal and the high attrition rates in drug development (Table 1). In addition, the incidence of DILI has continued to rise and is therefore recognized as a major public health concern[2]. DILI is one of the most common and serious adverse drug reactions (ADRs)[3], and is defined as a chemical insult resulting in injury to the liver[4]. It can be triggered by the parent drug and/or its metabolites, or as a reaction of hypersensitivity to the compound. A wide variety of drugs can cause DILI, including anti-tumor chemotherapy drugs, anti-tuberculosis drugs, antipyretic analgesics, immunosuppressive agents, hypoglycaemic therapies, or anti-bacterial, anti-fungal and antiviral drugs. DILI leads to multiple presentations in the clinic, including elevated liver enzymes, hepatitis, hepatocellular necrosis, cholestasis, fatty liver and liver cirrhosis. Occasionally, the clinical symptoms are not specific and they are indistinguishable from other hepatic disorders. In some patients, liver injury is easily detected by blood tests. The wide range of clinical manifestation, the complication of aetiology and the lack of effective tests make its diagnosis and treatment particularly challenging.

DILI is generally divided into two subtypes according to the hepatotoxicity of the drug: "intrinsic" hepatotoxicity and "idiosyncratic" hepatotoxicity. The former refers to dose-dependent hepatotoxicity that is predictable in humans or animal models, while idiosyncratic DILI (iDILI) is an unpredictable injury that cannot be explained by the known pharmacological properties. Recently, the screening of new drugs has become more stringent and the monitoring of ADRs improved. Problems associated with DILI have become a major driver in the development of new medications, and for the withdrawal, restriction or project termination of existing drugs and drug compound candidates. In developed countries, iDILI is less common, occurring only very rarely among treated patients, while intrinsic hepatotoxicity is still a main cause of DILI[5,6]. The pathogenesis of DILI is a complex process that has recently attracted much attention. Some researchers recently proposed a new hypothesis, providing a clear framework and direction for the further study of DILI[7]. According to this hypothesis, drug-induced liver injury can be divided into three steps: an initial insulting stimulation causes the mitochondrial dysfunction, and ultimately leads to cell death. However, until now, the exact mechanism remains unclear. For the purpose of preventing DILI and improving clinical management, the study of the pathogenesis of DILI is particularly important. In this article, we will review and discuss recent progress towards understanding the underlying mechanisms triggering DILI.

DIRECT HEPATIC TOXICITY

The liver plays an important role in the metabolism of drugs or exogenous toxicants, and the majority of drugs are biologically transformed in the liver. The pathological state of the liver can affect drug metabolism, thus changing the efficacy and the ADRs, whilst the metabolic products of drugs can cause liver damage.

The cytochrome P450s (CYP) are a superfamily of iron porphyrin proteins, which are key factors involved in drug oxidative and reduction reactions. Through the P450s, drugs are metabolized and can form ions, oxygen free radicals and other active substances. The balance between toxic formation and detoxification is essential for DILI. Toxins are inactivated by the detoxification phase Ⅰ-Ⅲ pathways of the liver. However, once the amount of toxins exceeds the capacity of the hepatic detoxification function, drugs and their reactive metabolites impact cell function - leading to liver cell damage - eventually causing apoptotic or necrotic cell death. At present, the most frequently studied drug, which causes intrinsic DILI, is acetaminophen (APAP), which is also known as paracetamol[8].

Upon rapid absorption, APAP is mainly metabolized *via* Phase-Ⅰ reactions (sulfation or glucuronidation) and then excreted into the urine. APAP toxicity is caused mainly by the excess formation of the reactive intermediate, N-acetyl-p-benzoquinone imine (NAPQI)[9], as a result of CYP (predominately CYP2E1 and CYP1A2) metabolism. Under normal circumstances, NAPQI

Table 1 The incidence of drug-induced liver injury

Country	France	Iceland	South Korea	Spain	United Kingdom	United States	Sweden
DILI incidence (‰)	0.139	0.191	0.12	0.03	0.007-0.013	0.10-1.50	0.023

DILI: Drug-induced liver injury.

is detoxified by rapid conjugation with the hepatic glutathione (GSH) and excreted into the bile, thus, APAP usage is nontoxic. Following overdose, APAP saturates both the sulfation and the glucuronidation pathways[10], enhanced NAPQI production depletes mitochondrial GSH, and the excess NAPQI then reacts with sulfhydryl groups of proteins to form protein adducts[11]. The interaction of NAPQI with target DNA and proteins in the mitochondria and the formation of protein adducts is thought to be critical for the development of hepatic toxicity[12,13], leading to oxidative stress, mitochondrial dysfunction[14,15] and mitogen-activated protein kinase (MAPK) activation (Figure 1). Specific targets in the mitochondria, including glutathione peroxidase (GPx) and the alpha subunit of adenosine triphosphate (ATP) synthase, participate in adduct formation, which was identified using proteomic approaches[16]. Furthermore, some drugs lead to the obstruction of the bile duct and mediate inhibition of hepatobiliary transporter systems[17]. Bile salt export pump (BSEP) is an efflux transporter of bile acids (BAs) transport and responsible for the clearance of drugs from liver and the secretion of bile salts into bile. The inhibition of BSEP expression has profound effects on bile acid homeostasis[18]. The cytotoxic bile acids accumulating in the liver results in liver cell damage, and potentially cirrhosis[17].

Oxidative and nitrosative stress

Oxidative stress is the result of the generation of ROS, which are a by-product of normal metabolism and have roles in cell signaling and homeostasis. Some DILI-causing drugs increase ROS accumulation through a variety of mechanisms[19]. Iron overload also amplifies oxidative stress as a catalyst for ROS formation *via* the Fenton reaction, in which H_2O_2 splits into hydroxyl radicals ($OH^{\bullet}$) and hydroxide (OH^-) (Figure 2). Free radical metabolites participate in the redox process and are capable of inducing cell damage by covalently binding to macromolecules[20]. Moreover, radical species can oxidize essential cell components and result in mutations in genomic and mitochondrial DNA (p21, p53) and tumor generation.

The role of lipid peroxidation (LPO) remains controversial in APAP hepatoxicity, and is often considered to be involved in cell death[21]. However, APAP overdose causes severe liver damage but a minor increase in the levels of LPO in normal animals[22]. Thus it seems that lipid peroxidation is not a critical event in APAP-induced hepatotoxicity. The cell injury induced by LPO requires not only oxidant formation but also impairment of the antioxidant defense systems. Additionally, LPO can be a consequence of tissue injury rather than the cause[23].

Given a toxic dose of APAP, histological necrosis is evident in the liver at 4 h, and tyrosine nitration occurs, indicating peroxynitrite formation[24]. Enhanced production of superoxide radicals ($O_2^{\bullet-}$) reacts with nitric oxide (NO), produced by inducible nitric oxide synthase (iNOS), forming peroxynitrite ($ONOO^-$)[25]. Since the $O_2^{\bullet-}$ anion scarcely passes through the hepatocyte cell membrane, this process occurs exclusively within the mitochondria. The highly reactive and potent oxidant $ONOO^-$ also causes nitration of protein tyrosine residues[26] which induces damage to mitochondrial DNA and the opening of the mitochondrial membrane pore.

Mitochondrial oxidative stress alone is not sufficient to ultimately trigger mitochondrial membrane permeability transition (MPT) and induce cell death. A group of protein kinases known as the mitogen-activated protein kinases (MAPKs), one of the most actively studied kinases or signaling pathways, participates in this process. Conventional studies have shown that MAPK pathways include many proteins such as the extracellular signal-related kinases (ERK), c-Jun N-terminal kinases (JNKs) and p38[27]. The JNK genes, JNK1 and JNK2, are expressed in the liver. A dysregulation of JNK1 and JNK2 protein expression is characteristic in both human and murine models of DILI, and is a potential therapeutic target[28]. JNK activation occurs early after APAP overdose and is sustained during the process, inducing hepatocyte death. JNK activation has been found in both hepatocytes and infiltrating cells, and is mediated by MAP kinase kinases (MAP2K)[29], which in turn are phosphorylated and activated by MAP kinase kinase kinases (MAP3K). The apoptosis signal-regulating kinase-1 (ASK1) is involved in APAP-induced JNK elevation[30] and activated by the dissociation with thioredoxin-1(Trx-1). The mixed-lineage kinase-3 (MLK3), a member of serine/threonine protein kinases family, mediates the initial phase of JNK activation[31]. ASK1 and MLK belong to the MAP3K group and different MAP3K group members function cooperatively in the response to oxidative stress. The role of MAP3K in JNK regulation still requires to be further investigated; whilst the activation of JNK can also be influenced by the dose of APAP[32]. The fact that RIP3-deficiency prevented oxidant stress suggests that RIPK3 acted upstream of JNK activation[33]. After JNK activation and phosphorylation in the cytosol, JNK binds to the Sab protein on the outer mitochondrial membrane[34,35], leading to the inactivation of p-Src

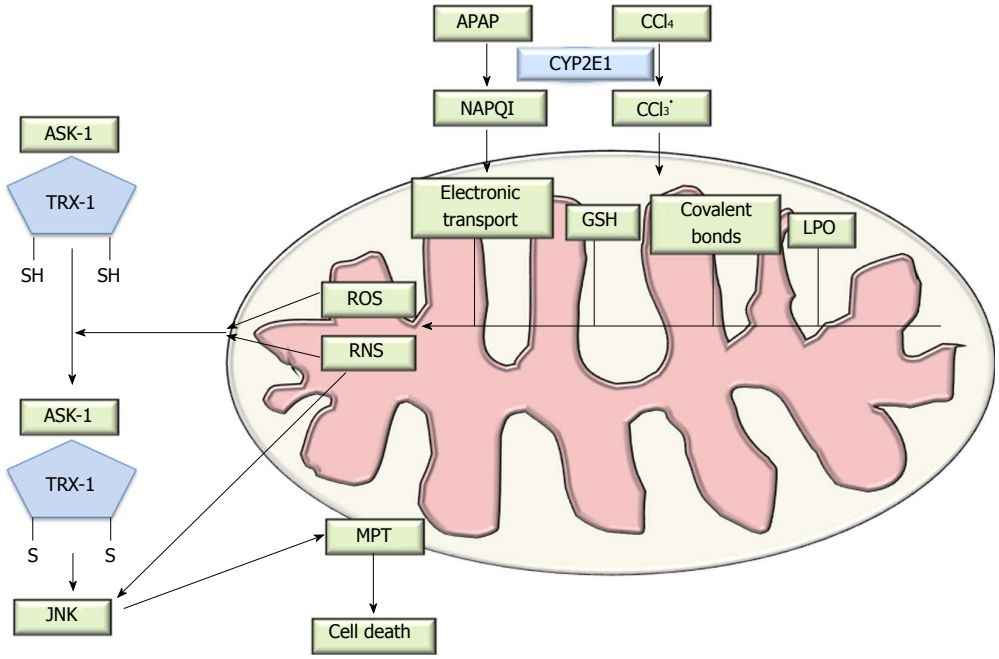

Figure 1 Pathophysiology of drug-induced liver injury. Schematic representation of paracetamol toxicology. Metabolism of acetaminophen (APAP) or carbon tetrachloride (CCl_4) catalyzed by CYP2E1 enzyme causes the generation of an intermediate reactive compound which causes covalent bonds, glutathione (GSH) depletion and increased in oxidative stress. Thioredoxin-1 (Trx-1) normally binds the N-terminal domain of Apoptosis signal-regulating kinase 1 (ASK1) and inhibits kinase activity. Reactive oxygen species (ROS) accumulation oxidizes and consequently removes Trx-1 from Trx-ASK1 complexes, leading to activation of ASK1 and subsequent apoptosis signalling cascade. Then c-Jun N-terminal kinases (JNK) translocates into the mitochondria and alters of the mitochondrial membrane potential, which triggers cell death. DILI: Drug-induced liver injury. MPT: Membrane permeability transition; LPO: Lipid peroxidation; NAPQI: N-acetyl-p-benzoquinone imine.

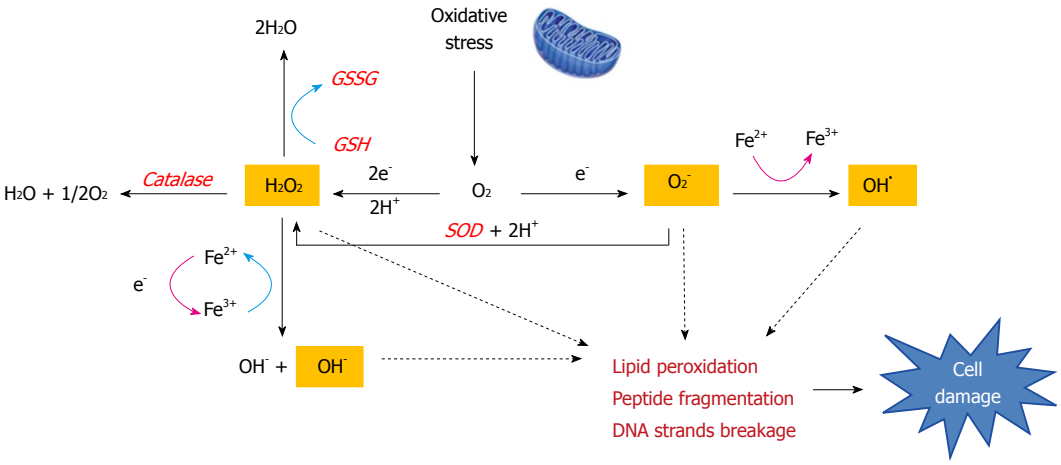

Figure 2 The Fenton reaction in liver disease. Oxidative stress produces large amounts of reactive compounds and cytotoxic free radicals (H_2O_2, $O_2^{\bullet-}$ and $OH^{\bullet}$). The Fenton reaction generates hydroxyl radicals ($OH^{\bullet}$) from hydrogen peroxide (H_2O_2) and superoxide ($O_2^{\bullet-}$) catalyzed by iron. This reaction occurs in cells and free radicals can attack the double bonds of non-saturated phospholipids in cell membranes which eventually degrade the structural integrity of cell membranes, impair enzymatic function and cause cross-linking of proteins or strand breaks in DNA. Cells also have an antioxidant enzyme system (catalase, GSH or SOD) is meant to neutralize free radicals and prevent damage.

on the inner mitochondrial membrane, which inhibits electron transport and increases ROS generation and further mitochondrial injury[36]. Ultimately, the pJNK translocates to the mitochondria and results in downstream signaling events[34].

Mitochondrial dysfunction

Mitochondrial dysfunction is the main cause of hepatocellular necrosis. The amplification of mitochondrial oxidative stress can reduce the synthesis of mitochondrial proteins and increase mitochondrial permeability transition. The induction of MPT increases mitochondrial membrane permeability allowing the exit of molecules less than 1500 Daltons[37], which causes mitochondria to become further depolarized, thus reducing the proton gradient leading to the collapse of the mitochondrial membrane potential (MMP). The mitochondria then swell, rupture and release proteins from the inter-

membrane space[38], a sequence implicated in cell death pathways such as apoptosis[39,40]. ROS are also produced because of the opening of the MPT pore, in turn, exaggerating oxidative stress and inducing DNA damage. Furthermore, the β-oxidation respiratory chain is compromised, and the process of ATP production is disrupted, resulting in reduced energy [41].

Endoplasmic reticulum stress

Various cellular stresses such as ROS or alteration in the cellular calcium (Ca^{2+}) concentration can impair protein folding and initiate the endoplasmic reticulum (ER) stress, which plays a critical role in APAP-induced hepatotoxicity[42]. Efficient protein folding in the ER requires tight coupling between the subunits of new proteins in the ER lumen and the ER folding capacity[43]. If the demand for protein folding increases, unfolded or misfolded proteins in the lumen also increase. ER stress is induced late after APAP intoxication (500 mg/kg) in murine models, and becomes significant 12 h following APAP administration[44]. The mechanisms by which APAP induces ER stress are poorly understood. One hypothesis is the alteration in the microsomes secondary to NAPQI generation. It has been reported that APAP induces an oxidative shift of the ER oxidoreductases, Erp72 and protein disulfide isomerase (PDI) in liver microsomes[45]. Furthermore, NAPQI can covalently bind to several microsomal proteins such as PDI and calreticulin, which have a significant role in protein folding in the ER, thus inducing ER stress. Another hypothesis suggests that ER stress might be due to ROS overproduction and mitochondrial dysfunction[46], including loss of the MMP and increase in intracellular Ca^{2+} concentration. Inhibition of BSEP results in not only cholestasis in some cases, but importantly, *via* bile acid retention, causes mitochondrial and ER stress, which may amplify injury or sensitize hepatocytes to other injury mechanisms[47].

iDILI

iDILI is a rare ADR[48], and occurs with a variable latency to onset, usually after several weeks or months of continuous treatment with the offending drug but, more importantly, it is unpredictable[49]. The incidence of iDILI ranges from 1/1000 to 1/200000[50], depending on the agent. The diagnosis of iDILI relies on the exclusion of other causes of liver injury and detailed medical history. The mechanisms of iDILI have not yet been elucidated. Although it is thought that iDILI is not dose-related, recent studies have supported the prediction of dose-response to some extent[51]. In general, it is associated with host condition, behavioural factors and drug exposure. Amongst behavioural factors, excessive alcohol consumption and smoking are very common triggers of iDILI. The host factors include genetic and non-genetic-derived iDILI. For example, genetically, it is considered that iDILI is caused by the deficiency or low activity of drug-metabolizing enzymes and an abnormal immune response. Non-genetic types include existing disease states, pregnancy, age and host gender. In some iDILI reactions, the same mechanisms of intrinsic DILI are involved: ROS, mitochondrial dysfunction and altered bile acid homeostasis. The typical drugs are tacrine and stavudine. Additionally, in some iDILI, after exposure to certain drugs, neoantigens are produced in the liver and can mobilize the immune cells and result in idiosyncratic immunological reactions towards the drugs.

The innate immune response

As a result of hepatocyte damage, iDILI triggers the inflammatory reaction, which involves the innate immune system. The innate immune system in the human liver is mainly composed of Kupffer cells (KCs), neutrophils, monocytes and natural killer cells/natural killer T cells (NK/NKT cells)[52,53]. In recent years, increasingly studies have confirmed that the innate immune system participates in the pathogenesis of iDILI, but the specific mechanism is still on the controversy. The main hypothesis is that neoantigen stimulates the cells of the innate immune system and creates inflammation by binding to Toll-like receptors (TLRs), scavenger receptors (SCRs) and mannitol receptors (MRs) of macrophages. In patients with iDILI, a large number of macrophages are mobilized in the blood and assemble around the damaged hepatocytes *via* adhesion factors. The proliferation of macrophages is also seen in the bone marrow[54]. The depletion of KC reduces the expression of IL-10, IL-6 and other mediators, and increases APAP-induced liver injury. Overall, the activation of KC is beneficial because the anti-inflammatory effects outweigh potential toxic effects[55]. Antigens derived from damage associated molecular patterns (DAMPs)[56] act as signals to activate innate immune cells. High mobility group box 1 protein (HMGB1) is one of the previously identified DAMPs. HMGB1 induces the infiltration of neutrophils, associates with TLRs and promotes the release of cytokines such as TNFα, IFNγ and IL-1, thereby activating the KC[57] and aggravating iDILI. In addition, the controversy surrounds the role of NK/NKT cells. Some researchers believe that NK/NKT cells ameliorate the liver injury caused by drugs through secreting IFNγ, IL-4 and other cytokines. However, some authors have reported no significant differences in the expression level of protective cytokines from the liver of NKT-cell-deficient mice[58]. In addition, the released cytokines and chemokines can enhance the adaptive immune response through a variety of mechanisms.

The adaptive immune response

The finding that the liver injury recurs promptly after

the iDILI patient is re-exposed to the offending drug, reflects the involvement of an adaptive immune response. This is in fact predictable, given that the antigen-specific immunocytes still remain in the body. During the process of drug metabolism, drug metabolite covalently binds to hepatic protein or modified proteins expressed on the surface of hepatocytes and form protein haptens (essentially an incomplete antigen). The hapten is released after hepatocyte death or damage and presented by antigen-presenting cells (APCs) in complex with major histocompatibility complex (MHC) class II molecules to cluster of differentiation 4 ($CD4^+$) T cells. When recognized as 'foreign' by T cells and following binding to T-cell receptors of $CD4^+$T cells, it then activates cluster of differentiation 8 ($CD8^+$) T cytotoxic cells *via* secretion of TNFα and IFNγ. $CD8^+$T cytotoxic cells mediate cytotoxic reactions though FasL or perforin and induce hepatocellular apoptosis. The anaesthetic drug Halothane exactly triggers this mechanism. Under normal conditions, hapten alone is not sufficient to activate the immune response, therefore activation of the adaptive immune system requires other cell/ tissue threatening events. This is termed the 'Hypothesis of danger signalling'. Indeed, it has been shown that the presence of an inflammatory background is associated with increased susceptibility to iDILI[59,60]. Infection and inflammation act as the danger signal and further augment the immune response by cell death or cytokine release[61]. However, the specific mechanisms still need further study.

The "hapten" hypothesis is a dominant mechanism proposed for the creation of neoantigens after drug exposure[62]. More recently, the 'pharmacological interaction' or 'p-i' model suggests a new hypothesis for activating T-cell-mediated immune responses[63]. The drug directly binds to either the T-cell receptor (TCR) or human leucocyte antigen (HLA) without intracellular antigen processing[64-66], and activates T cells in a peptide-independent manner[67]. This hypothesis might also explain the rapid reaction of T-cells after drug exposure *in vitro*, which is inconsistent with the time-course of antigen processing *in vivo*. Classic drugs that are considered to respond in this way are sulfamethoxazole, lamotrigine and carbamazepine.

The immune genetic polymorphism

A genome-wide association study (GWAS) proved that iDILI is associated with the HLA region on chromosome 6[68,69]. The HLA polymorphism results in the human body to be more prone to produce adaptive immune responses to certain drugs[70]. HLA genotyping of 75 amoxicillin-clavulanate hepatotoxicity cases in Spain has also demonstrated phenotype-specific HLA association[71]. Abacavir, a human immunodeficiency virus reverse transcriptase inhibitor, induces multi-organ toxicity exclusively in patients carrying the HLA-B*57:01 allele[72]. A GWAS on flucloxacillin hepatotoxicity (FLUX-DILI) has revealed a strong association with the HLA-B*57:01 allele[73]. Flucloxacillin is an effective antimicrobial drug against staphylococcal infections and widely used in Europe and Australia. The incidence of cholestatic hepatitis, which is induced by the use of flucloxacillin, is estimated to be 8.5 per 100000 in the first 1 to 45 d after start of treatment[74]. However, the incidence in the HLA-B*57:01 allele carriers raises more than 3-fold, indicating the HLA-B*57:01 have an added effect on FLUX-DILI[75].

Immune tolerance

Hepatocyte stress can be detected in the majority of individuals exposed to the insulting drug, especially at high concentrations. However, injury occurs in only a very small number of individuals. Although the liver is considered itself to be an immune-tolerant organ, the variation of susceptibility to the ensuing stress response(s) still exists; only in individuals with low tolerance, will DILI occur. The tolerance phenomenon due to liver immunity can be explained by: apoptosis of activated T cells, immune deviation and immune active suppression[53]. Antigen-specific $CD8^+$ T-cell populations accumulate transiently within the liver before apoptosis[76]. It is possible that the liver can induce apoptosis of activated T cells through toxic molecules or the deprivation of survival signals[77]. Hepatocytes can attract apoptotic T cells because specific markers are expressed in the membrane and are recognized by KCs or other cells in the liver. During the hepatic immune responses, there is immune deviation occurring. Klugewitz *et al*[78], reported that the liver sinusoidal endothelial cells (LSECs) can selectively inhibit T helper-1 (Th1) cells and reduce the production of INF-γ, but LSECs can also activate T helper-2 (Th2) cells leading to an increase in IL-4 secretion. The third mechanism is the result of the unique composition of tolerogenic APCs in the liver. The tolerogenic APCs within the liver include LSECs, KCs, and hepatic dendritic cells (DCs). Although recognized as APCs, these cells are incapable of stimulating antigen-specific T-cell responses[79]. On the contrary, they trap and interact with the inactive T cells in the liver sinusoid, thereby promoting tolerance. LSECs can act as APCs to some extent, but $CD4^+$ or $CD8^+$ T cells activated by them cannot further differentiate into Th1 cells or cytotoxic cells. Moreover, hepatic KCs can also suppress T-cell activation through the production of prostaglandins[80].

SIGNAL TRANSDUCTION AND HEPATOCYTE DEATH

The traditionally recognized forms of cell death are apoptosis and necrosis: apoptosis is a highly regulated and controlled cell death process that does not cause inflammation, while necrosis is a traumatic mode of

cell death that induces inflammation and can promote tissue fibrosis[81]. Recently, increasing evidence has shown that there is a specific subtype of necrosis, termed necroptosis[82]. Autophagy was first observed by Keith R Porter and his student in 1962[83] and has become a controversial topic in the occurrence of DILI, which is not only a protective pathway but also associated with cell death (discussed below).

Apoptosis

Apoptosis is a process of programmed cell death, which maintains physiological homeostasis in the normal human liver[84]. Characteristic apoptotic morphology includes cell shrinkage, nuclear fragmentation, chromatin condensation, chromosomal DNA fragmentation and global mRNA decay. Apoptosis can be initiated through two pathways: the intrinsic pathway (also called the mitochondrial pathway), and the extrinsic pathway. The intrinsic pathway is activated by intracellular signals generated when cells are stressed and depends on the release of proteins from the mitochondrial intermembrane space. The extrinsic pathway is activated by extracellular ligands binding to cell-surface death receptors (DRs). Both pathways induce cell death by activating executioner caspases (caspase 3 and 7) or enzymes that degrade protein (*e.g.*, non-caspases, cathepsins, calpains, granzymes, and the proteasome complex, also have roles in mediating and promoting cell death).

Death receptors belong to the TNF family, comprising TNF receptor (TNFR), FAS and TNF-related apoptosis-inducing ligand receptor (TRAIL-R)[85]. The most widely expressed on the hepatocellular membrane are CD95 (APO-1/FAS) and TNFR1 (CD120a). When DRs are engaged by their ligands, the death domains of the receptors are oligomerized and form a membrane-bound supramolecular structure termed death-inducing signaling complex (DISC), including TNFR-associated death domain (TRADD), receptor interacting protein kinase-1 (RIPK1), cellular inhibitor of apoptosis 1 and 2 (cIAP1 and 2) and TNFR-associated factor 2 (TRAF2) or TRAF5[86], thereby recruiting caspase-8[87], and transducing a downstream signal cascade resulting in apoptosis[88]. The intrinsic pathway is commonly triggered *via* Bid, a protein of the B-cell lymphoma 2 (Bcl-2) family. Caspase-8 mediates the cleavage of Bid and cleaved Bid (tBid) would translocate to mitochondria, lead to mitochondrial outer membrane permeabilization (MOMP) *via* Bax and Bak and induce cytochrome C release to the cytoplasm, which binds to Apaf-1, forming a complex with caspase-9. The activation of procaspase-9 initiates the caspase cascade, promoting cell death. Several intracellular factors can activate this pathway, including ER stress and P53 activation[89]. ER stress induces an intrinsic cell death pathway termed lipoapoptosis mediated by JNK activation, whereas p53 induces apoptosis though regulation of specific target genes such as Bax. In the liver, the extrinsic and intrinsic pathways are linked, because hepatocytes require mitochondrial amplification activating caspase-3 for cell death execution[90].

Necrosis

Conventionally necrosis is thought to be 'unprogrammed' cell death caused by factors external to the cell or tissue, such as infection, virus, toxins, drugs or trauma. This results in the loss of cell membrane integrity with an uncontrolled release of cellular constituents into the extracellular space, thus eliciting an inflammatory response in the surrounding tissue[91]. The typical features of necrosis include depletion of ATP, ion imbalance and mitochondrial dysfunction. Similar to the intrinsic pathway of apoptosis, mitochondrial injury is the key factor of early-stage necrosis. The change of cell size and the formation of membrane "blebs" are reversible, but once MPT is changed and cellular constituents are released, the cascade is irreversible, and leads to cell rupture. Hepatocellular necrosis also requires the participation of proteases, one of which is calpain-mediating necrosis. Furthermore, recent work has demonstrated that necrosis can be regulated by MPT inhibitor or caspase inhibitors[92]. RIPK3-mediated mitochondrial fission seems to be also a feature of APAP-induced hepatocyte necrosis. Drp1 translocates to the mitochondria mediated by RIPK3, polymerizes and constricts mitochondria to facilitate organelle division[33].

Necroptosis

Necroptosis is a "programmed" form of necrosis, which incorporates features of necrosis and apoptosis (Figure 3)[93]. Necroptosis shares the upstream pathway with apoptosis, and leads to cellular leakage, as seen in necrosis. Necroptosis can lead to cell death without the facilitation of caspase, in the presence of caspase inhibitors[93]. The typical signaling pathway of necroptosis is mediated by TNF super family member receptor. TNFα can stimulate its receptor TNFR1, and the TNFR-associated death protein TRADD signals to RIPK1 - which recruits RIPK3, to form the necrosome through the interaction of RIP-homology interaction motif (RHIM). RIPK3 then activates mixed lineage kinase domain like pseudokinase (MLKL) by phosphorylation, and p-MLKL subsequently drives oligomerization of MLKL, allowing MLKL to insert into and permeabilize plasma membranes and organelles[94]. The pro-inflammatory factors are then released and elicit immune responses ensue. The role of necroptosis in APAP-derived DILI is still controversial. Although TNF receptor signalling pathway is the best studied initiating event for necroptosis, there are multiple mechanisms to trigger this mode of cell death and further studies are needed to identify potential activators[95]. Many studies showed that Nec-1, an inhibitor of RIPK1, protects against APAP hepatotoxicity *in vivo* and *in vitro*[33,96]. However, RIPK3 and MLKL seem to be dispensable in APAP-derived DILI, whilst RIPK1 is essential for APAP

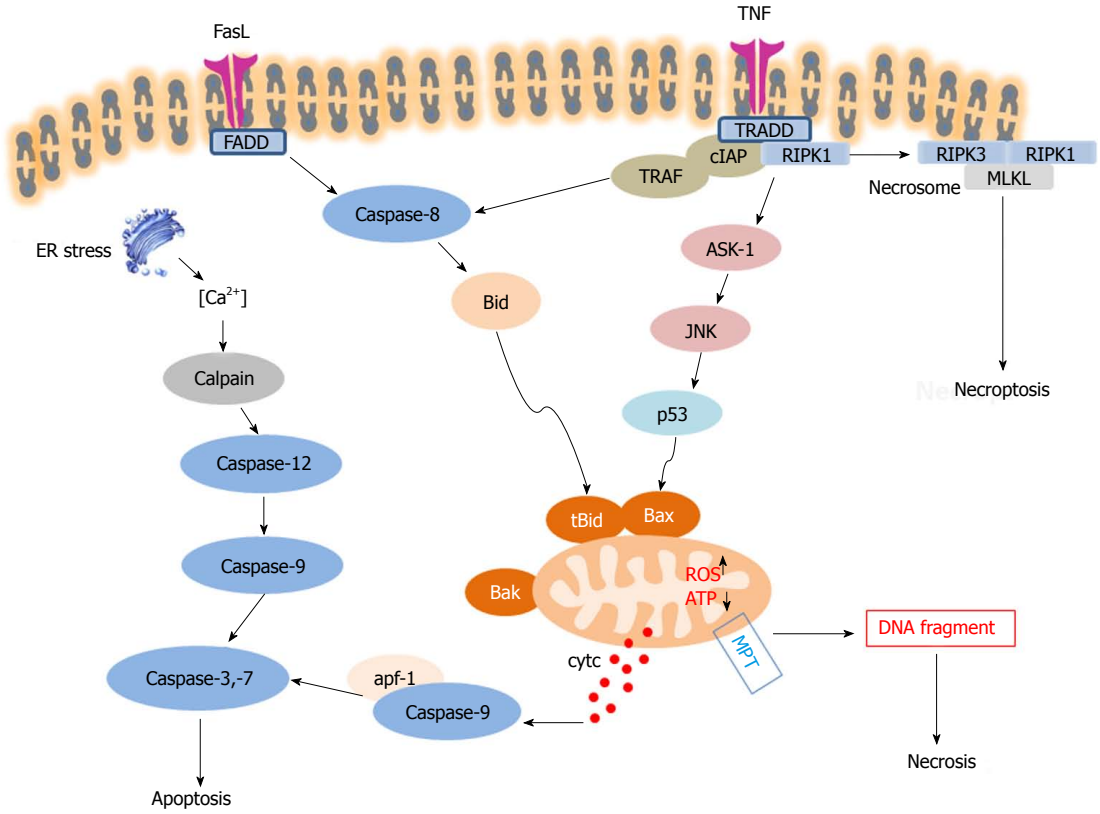

Figure 3 Schematic overview of three different modes of cell death: apoptosis, necrosis and necroptosis. When FasL or Tumor necrosis factor-alpha (TNF-α) bind to their death receptors (DRs), death domains of DRs are oligomerized and form death-inducing signalling complex (DISC), which recruits caspase-8. Active caspase 8 cleaves Bid into cleaved Bid (tBid), which translocates to mitochondria and cooperates with Bax. Meanwhile, JNKs are activated by Mitogen-activated protein kinases (MAPKs) and pJNK also translocates to the mitochondria *via* binding to the Sab protein. ROS accumulation and ATP depletion in the mitochondria aggravate mitochondrial damage and induce membrane permeability transition (MPT), resulting in release of cytochrome C, in turn promoting the activation of caspase-9 and caspase-3. Activated caspase-3 then leads to hepatocyte apoptosis. The extrinsic and intrinsic pathways of hepatocyte apoptosis are linked, because hepatocytes require mitochondrial amplification activating caspase-3 for cell death execution. The mitochondrial injury and MPT are also key factors in cascade of events leading to necrosis. Necroptosis shares the upstream pathway with apoptosis. When cellular inhibitors of apoptosis (cIAPs) are depleted, Receptor interacting protein kinase (RIPK)1 and RIPK3 interact with each other *via* membrane permeability transition (RHIM) domains to form the necrosome, and further recruit and phosphorylate MLKL to initiate necroptosis.

toxicity *via* JNK activation[97].

Autophagy

Autophagy functions in a wide variety of physiological and pathophysiological roles as a complex, destructive mechanism of the cell that disassembles unnecessary or dysfunctional components[98]. Lysosomes are responsible for intracellular autophagy and the degradation of the cell. Autophagy is observable with the formation of autophagosomes, which are double-membrane vesicles originating from rough ER and contain part of the cytoplasm, the organelles and the proteins need to be degraded. Then autophagosomes fuse with lysosomes and initiate the orderly degradation and recycling of cellular components[99]. In disease, autophagy is considered to be an adaptive response to stress, which promotes survival and plays a vital role in cellular reconstruction. Ni *et al*[100] found that autophagy is important for the regulation of APAP protein adducts levels in hepatocytes, and this selective autophagic removal is mediated by ubiquitin and p62[100,101]. It is thought that autophagy activated by 5'-adenosine monophosphate-activated protein kinase (AMPK), can lead to adiponectin accumulation, which, in turn, removes damaged mitochondria, thereby ameliorating oxidative stress and hepatotoxicity[102]. And Parkin-induced mitophagy is also a mechanism of protection against APAP-induced liver injury and necrosis by negatively regulating JNK activity[36,103] and Mcl-1 degradation and increasing hepatocyte proliferation[104]. However, chronic deletion and acute knockdown of Parkin have different regulation towards mitophagy and liver injury, the mechanism of which is still unidentified and need further study[104]. Autophagy has emerged as an exciting new field in DILI and warrants further investigation.

CLINICAL PERSPECTIVES

The clinical manifestations of DILI are usually non-specific. Many patients may have no significant symptoms and only present with elevations in the level of

hepatic biochemical indexes. For about the last half century, the traditional serum biomarkers for detecting DILI in clinics are alanine aminotransferase (ALT), aspartate aminotransferase (AST), alkaline phosphatase (ALP) and total bilirubin (TBIL). However, elevations in these biomarkers take place when hepatocyte injury has already occurred and cannot be used to identify a potential for DILI. In recent years, with the further understanding of the mechanisms of DILI, several new biomarkers have been reported, including apoptosis-related caspase cleaved keratin 18 (cCK18)[105], necrosis-related HMGB1[106,107] and microRNA (especially microRNA-122)[108,109], specific mitochondrial injury biomarker glutamate dehydrogenase (GLDH)[110], biomarkers reflecting cholestasis (*e.g.* BAs) as well as genetic biomarkers reflecting the susceptibility to DILI, such as the genetic polymorphisms of HLA, drug metabolizing enzymes and drug transport proteins[2]. MicroRNA-122 and GLDH have been proposed as more sensitive and specific biomarkers of liver injury than ALT[111]. APAP-protein adducts and NAPQI are specific biomarkers of APAP-mediated DILI[112]. And apolipoprotein-A1 and haptoglobin have significant predictive values for the prediction of recovery in DILI patients[113]. Some of these biomarkers are already being used in early clinical trials. Though current biomarker are not specific to DILI and their value for clinical use still needs to be widely verified, their addition to conventional measurements could soon transform DILI prediction and detection, thereby promoting earlier treatment.

CONCLUSION

The liver works as a central detoxifying organ towards xenobiotics and chemicals. However, during the process of biotransformation to less toxic substances, molecules that can induce liver injury through various pathways are produced. The pathogenesis of DILI is very complex, and the occurrence of DILI is the consequence of multiple factors. Generally, important mechanisms involved in drug-induced hepatic injury can be divided into: (1) reactive metabolite formation *via* metabolism; (2) covalent binding between cellular components with drug; (3) reactive oxygen species generation in the cells; (4) activation of signal transduction pathways that modulate cell death or survival; and (5) cellular mitochondrial damage[114]. The common forms of hepatocyte death include apoptosis, necrosis, necroptosis and autophagy. The clinical characteristics of DILI are variable, and no specific laboratory tests are predictable for DILI, thereby presenting a major challenge for clinical diagnosis and treatment. Research on the molecular mechanisms underlying DILI will contribute greatly to early-stage screening of new drugs, predicting hepatotoxicity, and the monitoring of drug side-effects, eventually reducing the incidence of DILI, but clinical translation of the numerous mechanisms remains a challenge, requiring a considerable investment.

REFERENCES

1 **Lee WM**. Drug-induced acute liver failure. *Clin Liver Dis* 2013; **17**: 575-586, viii [PMID: 24099019 DOI: 10.1016/j.cld.2013.07.001]

2 **Yu YC**, Mao YM, Chen CW, Chen JJ, Chen J, Cong WM, Ding Y, Duan ZP, Fu QC, Guo XY, Hu P, Hu XQ, Jia JD, Lai RT, Li DL, Liu YX, Lu LG, Ma SW, Ma X, Nan YM, Ren H, Shen T, Wang H, Wang JY, Wang TL, Wang XJ, Wei L, Xie Q, Xie W, Yang CQ, Yang DL, Yu YY, Zeng MD, Zhang L, Zhao XY, Zhuang H; Drug-induced Liver Injury (DILI) Study Group; Chinese Society of Hepatology (CSH); Chinese Medical Association (CMA). CSH guidelines for the diagnosis and treatment of drug-induced liver injury. *Hepatol Int* 2017; **11**: 221-241 [PMID: 28405790 DOI: 10.1007/s12072-017-9793-2]

3 **Miguel A**, Azevedo LF, Araújo M, Pereira AC. Frequency of adverse drug reactions in hospitalized patients: a systematic review and meta-analysis. *Pharmacoepidemiol Drug Saf* 2012; **21**: 1139-1154 [PMID: 22761169 DOI: 10.1002/pds.3309]

4 **Feldman M**, Friedman LS, Brandt LJ. Sleisenger and Fordtran's Gastrointestinal and Liver Disease. In: Chitturi S TN, Farrell GC, editor Hepatic drug metabolism and liver disease caused by drugs. Philadelphia, 2016

5 **Bell LN**, Chalasani N. Epidemiology of idiosyncratic drug-induced liver injury. *Semin Liver Dis* 2009; **29**: 337-347 [PMID: 19826967 DOI: 10.1055/s-0029-1240002]

6 **Chalasani NP**, Hayashi PH, Bonkovsky HL, Navarro VJ, Lee WM, Fontana RJ; Practice Parameters Committee of the American College of Gastroenterology. ACG Clinical Guideline: the diagnosis and management of idiosyncratic drug-induced liver injury. *Am J Gastroenterol* 2014; **109**: 950-66; quiz 967 [PMID: 24935270 DOI: 10.1038/ajg.2014.131]

7 **Vinken M**, Maes M, Vanhaecke T, Rogiers V. Drug-induced liver injury: mechanisms, types and biomarkers. *Curr Med Chem* 2013; **20**: 3011-3021 [PMID: 23746274]

8 **Park K**, Williams DP, Naisbitt DJ, Kitteringham NR, Pirmohamed M. Investigation of toxic metabolites during drug development. *Toxicol Appl Pharmacol* 2005; **207**: 425-434 [PMID: 15996699 DOI: 10.1016/j.taap.2005.02.029]

9 **Jaeschke H**, Knight TR, Bajt ML. The role of oxidant stress and reactive nitrogen species in acetaminophen hepatotoxicity. *Toxicol Lett* 2003; **144**: 279-288 [PMID: 12927346]

10 **Xie Y**, McGill MR, Cook SF, Sharpe MR, Winefield RD, Wilkins DG, Rollins DE, Jaeschke H. Time course of acetaminophen-protein adducts and acetaminophen metabolites in circulation of overdose patients and in HepaRG cells. *Xenobiotica* 2015; **45**: 921-929 [PMID: 25869248 DOI: 10.3109/00498254.2015.1026426]

11 **McGill MR**, Lebofsky M, Norris HR, Slawson MH, Bajt ML, Xie Y, Williams CD, Wilkins DG, Rollins DE, Jaeschke H. Plasma and liver acetaminophen-protein adduct levels in mice after acetaminophen treatment: dose-response, mechanisms, and clinical implications. *Toxicol Appl Pharmacol* 2013; **269**: 240-249 [PMID: 23571099 DOI: 10.1016/j.taap.2013.03.026]

12 **McGill MR**, Williams CD, Xie Y, Ramachandran A, Jaeschke H. Acetaminophen-induced liver injury in rats and mice: comparison of protein adducts, mitochondrial dysfunction, and oxidative stress in the mechanism of toxicity. *Toxicol Appl Pharmacol* 2012; **264**: 387-394 [PMID: 22980195 DOI: 10.1016/j.taap.2012.08.015]

13 **Hu J**, Ramshesh VK, McGill MR, Jaeschke H, Lemasters JJ. Low Dose Acetaminophen Induces Reversible Mitochondrial Dysfunction Associated with Transient c-Jun N-Terminal Kinase Activation in Mouse Liver. *Toxicol Sci* 2016; **150**: 204-215 [PMID: 26721299 DOI: 10.1093/toxsci/kfv319]

14 **Jaeschke H**, Williams CD, Ramachandran A, Bajt ML. Acetaminophen hepatotoxicity and repair: the role of sterile inflammation and innate immunity. *Liver Int* 2012; **32**: 8-20 [PMID: 21745276 DOI: 10.1111/j.1478-3231.2011.02501.x]

15 **Jaeschke H**, Xie Y, McGill MR. Acetaminophen-induced Liver Injury: from Animal Models to Humans. *J Clin Transl Hepatol* 2014; **2**: 153-161 [PMID: 26355817 DOI: 10.14218/JCTH.2014.00014]

16 **Qiu Y**, Benet LZ, Burlingame AL. Identification of the hepatic protein targets of reactive metabolites of acetaminophen in vivo in mice using two-dimensional gel electrophoresis and mass spectrometry. *J Biol Chem* 1998; **273**: 17940-17953 [PMID: 9651401]

17 **Pauli-Magnus C**, Meier PJ. Hepatobiliary transporters and drug-induced cholestasis. *Hepatology* 2006; **44**: 778-787 [PMID: 17006912 DOI: 10.1002/hep.21359]

18 **Qiu X**, Zhang Y, Liu T, Shen H, Xiao Y, Bourner MJ, Pratt JR, Thompson DC, Marathe P, Humphreys WG, Lai Y. Disruption of BSEP Function in HepaRG Cells Alters Bile Acid Disposition and Is a Susceptive Factor to Drug-Induced Cholestatic Injury. *Mol Pharm* 2016; **13**: 1206-1216 [PMID: 26910619 DOI: 10.1021/acs.molpharmaceut.5b00659]

19 **Gómez-Lechón MJ**, Tolosa L, Donato MT. Metabolic activation and drug-induced liver injury: in vitro approaches for the safety risk assessment of new drugs. *J Appl Toxicol* 2016; **36**: 752-768 [PMID: 26691983 DOI: 10.1002/jat.3277]

20 **Srivastava A**, Maggs JL, Antoine DJ, Williams DP, Smith DA, Park BK. Role of reactive metabolites in drug-induced hepatotoxicity. *Handb Exp Pharmacol* 2010; **196**: 165-194 [PMID: 20020263 DOI: 10.1007/978-3-642-00663-0_7]

21 **Negre-Salvayre A**, Auge N, Ayala V, Basaga H, Boada J, Brenke R, Chapple S, Cohen G, Feher J, Grune T, Lengyel G, Mann GE, Pamplona R, Poli G, Portero-Otin M, Riahi Y, Salvayre R, Sasson S, Serrano J, Shamni O, Siems W, Siow RC, Wiswedel I, Zarkovic K, Zarkovic N. Pathological aspects of lipid peroxidation. *Free Radic Res* 2010; **44**: 1125-1171 [PMID: 20836660 DOI: 10.3109/10715762.2010.498478]

22 **Knight TR**, Fariss MW, Farhood A, Jaeschke H. Role of lipid peroxidation as a mechanism of liver injury after acetaminophen overdose in mice. *Toxicol Sci* 2003; **76**: 229-236 [PMID: 12944590 DOI: 10.1093/toxsci/kfg220]

23 **Jaeschke H**, McGill MR, Ramachandran A. Oxidant stress, mitochondria, and cell death mechanisms in drug-induced liver injury: lessons learned from acetaminophen hepatotoxicity. *Drug Metab Rev* 2012; **44**: 88-106 [PMID: 22229890 DOI: 10.3109/03602532.2011.602688]

24 **Hinson JA**, Pike SL, Pumford NR, Mayeux PR. Nitrotyrosine-protein adducts in hepatic centrilobular areas following toxic doses of acetaminophen in mice. *Chem Res Toxicol* 1998; **11**: 604-607 [PMID: 9625727 DOI: 10.1021/tx9800349]

25 **Cover C**, Mansouri A, Knight TR, Bajt ML, Lemasters JJ, Pessayre D, Jaeschke H. Peroxynitrite-induced mitochondrial and endonuclease-mediated nuclear DNA damage in acetaminophen hepatotoxicity. *J Pharmacol Exp Ther* 2005; **315**: 879-887 [PMID: 16081675 DOI: 10.1124/jpet.105.088898]

26 **Radi R**, Peluffo G, Alvarez MN, Naviliat M, Cayota A. Unraveling peroxynitrite formation in biological systems. *Free Radic Biol Med* 2001; **30**: 463-488 [PMID: 11182518]

27 **Cargnello M**, Roux PP. Activation and function of the MAPKs and their substrates, the MAPK-activated protein kinases. *Microbiol Mol Biol Rev* 2011; **75**: 50-83 [PMID: 21372320 DOI: 10.1128/MMBR.00031-10]

28 **Cubero FJ**, Zoubek ME, Hu W, Peng J, Zhao G, Nevzorova YA, Al Masaoudi M, Bechmann LP, Boekschoten MV, Muller M, Preisinger C, Gassler N, Canbay AE, Luedde T, Davis RJ, Liedtke C, Trautwein C. Combined Activities of JNK1 and JNK2 in Hepatocytes Protect Against Toxic Liver Injury. *Gastroenterology* 2016; **150**: 968-981 [PMID: 26708719 DOI: 10.1053/j.gastro.2015.12.019]

29 **Tournier C**, Dong C, Turner TK, Jones SN, Flavell RA, Davis RJ. MKK7 is an essential component of the JNK signal transduction pathway activated by proinflammatory cytokines. *Genes Dev* 2001; **15**: 1419-1426 [PMID: 11390361 DOI: 10.1101/gad.888501]

30 **Nakagawa H**, Maeda S, Hikiba Y, Ohmae T, Shibata W, Yanai A, Sakamoto K, Ogura K, Noguchi T, Karin M, Ichijo H, Omata M. Deletion of apoptosis signal-regulating kinase 1 attenuates acetaminophen-induced liver injury by inhibiting c-Jun N-terminal kinase activation. *Gastroenterology* 2008; **135**: 1311-1321 [PMID: 18700144 DOI: 10.1053/j.gastro.2008.07.006]

31 **Sharma M**, Gadang V, Jaeschke A. Critical role for mixed-lineage kinase 3 in acetaminophen-induced hepatotoxicity. *Mol Pharmacol* 2012; **82**: 1001-1007 [PMID: 22918968 DOI: 10.1124/mol.112.079863]

32 **Xie Y**, Ramachandran A, Breckenridge DG, Liles JT, Lebofsky M, Farhood A, Jaeschke H. Inhibitor of apoptosis signal-regulating kinase 1 protects against acetaminophen-induced liver injury. *Toxicol Appl Pharmacol* 2015; **286**: 1-9 [PMID: 25818599 DOI: 10.1016/j.taap.2015.03.019]

33 **Ramachandran A**, McGill MR, Xie Y, Ni HM, Ding WX, Jaeschke H. Receptor interacting protein kinase 3 is a critical early mediator of acetaminophen-induced hepatocyte necrosis in mice. *Hepatology* 2013; **58**: 2099-2108 [PMID: 23744808 DOI: 10.1002/hep.26547]

34 **Hanawa N**, Shinohara M, Saberi B, Gaarde WA, Han D, Kaplowitz N. Role of JNK translocation to mitochondria leading to inhibition of mitochondria bioenergetics in acetaminophen-induced liver injury. *J Biol Chem* 2008; **283**: 13565-13577 [PMID: 18337250 DOI: 10.1074/jbc.M708916200]

35 **Win S**, Than TA, Han D, Petrovic LM, Kaplowitz N. c-Jun N-terminal kinase (JNK)-dependent acute liver injury from acetaminophen or tumor necrosis factor (TNF) requires mitochondrial Sab protein expression in mice. *J Biol Chem* 2011; **286**: 35071-35078 [PMID: 21844199 DOI: 10.1074/jbc.M111.276089]

36 **Saito C**, Lemasters JJ, Jaeschke H. c-Jun N-terminal kinase modulates oxidant stress and peroxynitrite formation independent of inducible nitric oxide synthase in acetaminophen hepatotoxicity. *Toxicol Appl Pharmacol* 2010; **246**: 8-17 [PMID: 20423716 DOI: 10.1016/j.taap.2010.04.015]

37 **Karch J**, Kwong JQ, Burr AR, Sargent MA, Elrod JW, Peixoto PM, Martinez-Caballero S, Osinska H, Cheng EH, Robbins J, Kinnally KW, Molkentin JD. Bax and Bak function as the outer membrane component of the mitochondrial permeability pore in regulating necrotic cell death in mice. *Elife* 2013; **2**: e00772 [PMID: 23991283 DOI: 10.7554/eLife.00772]

38 **Honda HM**, Korge P, Weiss JN. Mitochondria and ischemia/reperfusion injury. *Ann N Y Acad Sci* 2005; **1047**: 248-258 [PMID: 16093501 DOI: 10.1196/annals.1341.022]

39 **Masubuchi Y**, Suda C, Horie T. Involvement of mitochondrial permeability transition in acetaminophen-induced liver injury in mice. *J Hepatol* 2005; **42**: 110-116 [PMID: 15629515 DOI: 10.1016/j.jhep.2004.09.015]

40 **Ramachandran A**, Lebofsky M, Baines CP, Lemasters JJ, Jaeschke H. Cyclophilin D deficiency protects against acetaminophen-induced oxidant stress and liver injury. *Free Radic Res* 2011; **45**: 156-164 [PMID: 20942566 DOI: 10.3109/10715762.2010.520319]

41 **Will Y**, Dykens J. Mitochondrial toxicity assessment in industry--a decade of technology development and insight. *Expert Opin Drug Metab Toxicol* 2014; **10**: 1061-1067 [PMID: 25023361 DOI: 10.1517/17425255.2014.939628]

42 **Kalinec GM**, Thein P, Parsa A, Yorgason J, Luxford W, Urrutia R, Kalinec F. Acetaminophen and NAPQI are toxic to auditory cells via oxidative and endoplasmic reticulum stress-dependent pathways. *Hear Res* 2014; **313**: 26-37 [PMID: 24793116 DOI: 10.1016/j.heares.2014.04.007]

43 **Halperin L**, Jung J, Michalak M. The many functions of the endoplasmic reticulum chaperones and folding enzymes. *IUBMB Life* 2014; **66**: 318-326 [PMID: 24839203 DOI: 10.1002/iub.1272]

44 **Uzi D**, Barda L, Scaiewicz V, Mills M, Mueller T, Gonzalez-Rodriguez A, Valverde AM, Iwawaki T, Nahmias Y, Xavier R, Chung RT, Tirosh B, Shibolet O. CHOP is a critical regulator of acetaminophen-induced hepatotoxicity. *J Hepatol* 2013; **59**: 495-503 [PMID: 23665281 DOI: 10.1016/j.jhep.2013.04.024]

45 **Letelier ME**, López-Valladares M, Peredo-Silva L, Rojas-Sepúlveda D, Aracena P. Microsomal oxidative damage promoted by acetaminophen metabolism. *Toxicol In Vitro* 2011; **25**:

1310-1313 [PMID: 21569833 DOI: 10.1016/j.tiv.2011.04.022]
46 **Vineetha VP**, Soumya RS, Raghu KG. Phloretin ameliorates arsenic trioxide induced mitochondrial dysfunction in H9c2 cardiomyoblasts mediated via alterations in membrane permeability and ETC complexes. *Eur J Pharmacol* 2015; **754**: 162-172 [PMID: 25746422 DOI: 10.1016/j.ejphar.2015.02.036]
47 **Morgan RE**, Trauner M, van Staden CJ, Lee PH, Ramachandran B, Eschenberg M, Afshari CA, Qualls CW Jr, Lightfoot-Dunn R, Hamadeh HK. Interference with bile salt export pump function is a susceptibility factor for human liver injury in drug development. *Toxicol Sci* 2010; **118**: 485-500 [PMID: 20829430 DOI: 10.1093/toxsci/kfq269]
48 **Cosgrove BD**, Alexopoulos LG, Hang TC, Hendriks BS, Sorger PK, Griffith LG, Lauffenburger DA. Cytokine-associated drug toxicity in human hepatocytes is associated with signaling network dysregulation. *Mol Biosyst* 2010; **6**: 1195-1206 [PMID: 20361094 DOI: 10.1039/b926287c]
49 **Fontana RJ**, Hayashi PH, Gu J, Reddy KR, Barnhart H, Watkins PB, Serrano J, Lee WM, Chalasani N, Stolz A, Davern T, Talwakar JA; DILIN Network. Idiosyncratic drug-induced liver injury is associated with substantial morbidity and mortality within 6 months from onset. *Gastroenterology* 2014; **147**: 96-108.e4 [PMID: 24681128 DOI: 10.1053/j.gastro.2014.03.045]
50 **Goldman L**, Schafer AI. Goldman-Cecil medicine. In: WM L, editor 152-Toxin- and drug-induced liver disease. Philadelphia, 2012: 979-984
51 **Uetrecht J**, Naisbitt DJ. Idiosyncratic adverse drug reactions: current concepts. *Pharmacol Rev* 2013; **65**: 779-808 [PMID: 23476052 DOI: 10.1124/pr.113.007450]
52 **Tujios S**, Fontana RJ. Mechanisms of drug-induced liver injury: from bedside to bench. *Nat Rev Gastroenterol Hepatol* 2011; **8**: 202-211 [PMID: 21386809 DOI: 10.1038/nrgastro.2011.22]
53 **Ju C**, Reilly T. Role of immune reactions in drug-induced liver injury (DILI). *Drug Metab Rev* 2012; **44**: 107-115 [PMID: 22235834 DOI: 10.3109/03602532.2011.645579]
54 **Fisher JE**, McKenzie TJ, Lillegard JB, Yu Y, Juskewitch JE, Nedredal GI, Brunn GJ, Yi ES, Malhi H, Smyrk TC, Nyberg SL. Role of Kupffer cells and toll-like receptor 4 in acetaminophen-induced acute liver failure. *J Surg Res* 2013; **180**: 147-155 [PMID: 23260383 DOI: 10.1016/j.jss.2012.11.051]
55 **Jaeschke H**. Innate immunity and acetaminophen-induced liver injury: why so many controversies? *Hepatology* 2008; **48**: 699-701 [PMID: 18752320 DOI: 10.1002/hep.22556]
56 **Martin-Murphy BV**, Holt MP, Ju C. The role of damage associated molecular pattern molecules in acetaminophen-induced liver injury in mice. *Toxicol Lett* 2010; **192**: 387-394 [PMID: 19931603 DOI: 10.1016/j.toxlet.2009.11.016]
57 **Kubes P**, Mehal WZ. Sterile inflammation in the liver. *Gastroenterology* 2012; **143**: 1158-1172 [PMID: 22982943 DOI: 10.1053/j.gastro.2012.09.008]
58 **Martin-Murphy BV**, Kominsky DJ, Orlicky DJ, Donohue TM Jr, Ju C. Increased susceptibility of natural killer T-cell-deficient mice to acetaminophen-induced liver injury. *Hepatology* 2013; **57**: 1575-1584 [PMID: 23150232 DOI: 10.1002/hep.26134]
59 **Laverty HG**, Antoine DJ, Benson C, Chaponda M, Williams D, Kevin Park B. The potential of cytokines as safety biomarkers for drug-induced liver injury. *Eur J Clin Pharmacol* 2010; **66**: 961-976 [PMID: 20694460 DOI: 10.1007/s00228-010-0862-x]
60 **Maiuri AR**, Breier AB, Gora LF, Parkins RV, Ganey PE, Roth RA. Cytotoxic Synergy Between Cytokines and NSAIDs Associated With Idiosyncratic Hepatotoxicity Is Driven by Mitogen-Activated Protein Kinases. *Toxicol Sci* 2015; **146**: 265-280 [PMID: 25953702 DOI: 10.1093/toxsci/kfv091]
61 **Jiang J**, Mathijs K, Timmermans L, Claessen SM, Hecka A, Weusten J, Peters R, van Delft JH, Kleinjans JCS, Jennen DGJ, de Kok TM. Omics-based identification of the combined effects of idiosyncratic drugs and inflammatory cytokines on the development of drug-induced liver injury. *Toxicol Appl Pharmacol* 2017; **332**: 100-108 [PMID: 28733206 DOI: 10.1016/j.taap.2017.07.014]
62 **Tailor A**, Faulkner L, Naisbitt DJ, Park BK. The chemical, genetic and immunological basis of idiosyncratic drug-induced liver injury. *Hum Exp Toxicol* 2015; **34**: 1310-1317 [PMID: 26614821 DOI: 10.1177/0960327115606529]
63 **White KD**, Chung WH, Hung SI, Mallal S, Phillips EJ. Evolving models of the immunopathogenesis of T cell-mediated drug allergy: The role of host, pathogens, and drug response. *J Allergy Clin Immunol* 2015; **136**: 219-34; quiz 235 [PMID: 26254049 DOI: 10.1016/j.jaci.2015.05.050]
64 **Zanni MP**, von Greyerz S, Schnyder B, Brander KA, Frutig K, Hari Y, Valitutti S, Pichler WJ. HLA-restricted, processing- and metabolism-independent pathway of drug recognition by human alpha beta T lymphocytes. *J Clin Invest* 1998; **102**: 1591-1598 [PMID: 9788973 DOI: 10.1172/JCI3544]
65 **Zanni MP**, von Greyerz S, Schnyder B, Wendland T, Pichler WJ. Allele-unrestricted presentation of lidocaine by HLA-DR molecules to specific alphabeta+ T cell clones. *Int Immunol* 1998; **10**: 507-515 [PMID: 9620607]
66 **Schnyder B**, Mauri-Hellweg D, Zanni M, Bettens F, Pichler WJ. Direct, MHC-dependent presentation of the drug sulfamethoxazole to human alphabeta T cell clones. *J Clin Invest* 1997; **100**: 136-141 [PMID: 9202065 DOI: 10.1172/JCI119505]
67 **Schnyder B**, Burkhart C, Schnyder-Frutig K, von Greyerz S, Naisbitt DJ, Pirmohamed M, Park BK, Pichler WJ. Recognition of sulfamethoxazole and its reactive metabolites by drug-specific CD4+ T cells from allergic individuals. *J Immunol* 2000; **164**: 6647-6654 [PMID: 10843725]
68 **Spraggs CF**, Budde LR, Briley LP, Bing N, Cox CJ, King KS, Whittaker JC, Mooser VE, Preston AJ, Stein SH, Cardon LR. HLA-DQA1*02:01 is a major risk factor for lapatinib-induced hepatotoxicity in women with advanced breast cancer. *J Clin Oncol* 2011; **29**: 667-673 [PMID: 21245432 DOI: 10.1200/JCO.2010.31.3197]
69 **Lucena MI**, Molokhia M, Shen Y, Urban TJ, Aithal GP, Andrade RJ, Day CP, Ruiz-Cabello F, Donaldson PT, Stephens C, Pirmohamed M, Romero-Gomez M, Navarro JM, Fontana RJ, Miller M, Groome M, Bondon-Guitton E, Conforti A, Stricker BH, Carvajal A, Ibanez L, Yue QY, Eichelbaum M, Floratos A, Pe'er I, Daly MJ, Goldstein DB, Dillon JF, Nelson MR, Watkins PB, Daly AK; Spanish DILI Registry; EUDRAGENE; DILIN; DILIGEN; International SAEC. Susceptibility to amoxicillin-clavulanate-induced liver injury is influenced by multiple HLA class I and II alleles. *Gastroenterology* 2011; **141**: 338-347 [PMID: 21570397 DOI: 10.1053/j.gastro.2011.04.001]
70 **Alfirevic A**, Gonzalez-Galarza F, Bell C, Martinsson K, Platt V, Bretland G, Evely J, Lichtenfels M, Cederbrant K, French N, Naisbitt D, Park BK, Jones AR, Pirmohamed M. In silico analysis of HLA associations with drug-induced liver injury: use of a HLA-genotyped DNA archive from healthy volunteers. *Genome Med* 2012; **4**: 51 [PMID: 22732016 DOI: 10.1186/gm350]
71 **Stephens C**, López-Nevot MÁ, Ruiz-Cabello F, Ulzurrun E, Soriano G, Romero-Gómez M, Moreno-Casares A, Lucena MI, Andrade RJ. HLA alleles influence the clinical signature of amoxicillin-clavulanate hepatotoxicity. *PLoS One* 2013; **8**: e68111 [PMID: 23874514 DOI: 10.1371/journal.pone.0068111]
72 **Song B**, Aoki S, Liu C, Susukida T, Ito K. An animal model of abacavir-induced HLA-mediated liver injury. *Toxicol Sci* 2018; **162**: 713-723 [PMID: 29319822 DOI: 10.1093/toxsci/kfy001]
73 **Daly AK**, Donaldson PT, Bhatnagar P, Shen Y, Pe'er I, Floratos A, Daly MJ, Goldstein DB, John S, Nelson MR, Graham J, Park BK, Dillon JF, Bernal W, Cordell HJ, Pirmohamed M, Aithal GP, Day CP; DILIGEN Study; International SAE Consortium. HLA-B*5701 genotype is a major determinant of drug-induced liver injury due to flucloxacillin. *Nat Genet* 2009; **41**: 816-819 [PMID: 19483685 DOI: 10.1038/ng.379]
74 **Russmann S**, Kaye JA, Jick SS, Jick H. Risk of cholestatic liver disease associated with flucloxacillin and flucloxacillin prescribing habits in the UK: cohort study using data from the UK General Practice Research Database. *Br J Clin Pharmacol* 2005; **60**: 76-82 [PMID: 15963097 DOI: 10.1111/j.1365-2125.2005.02370.x]
75 **Andrews E**, Armstrong M, Tugwood J, Swan D, Glaves P,

Pirmohamed M, Aithal GP, Wright MC, Day CP, Daly AK. A role for the pregnane X receptor in flucloxacillin-induced liver injury. *Hepatology* 2010; **51**: 1656-1664 [PMID: 20222094 DOI: 10.1002/hep.23549]
76 **Holt MP**, Ju C. Mechanisms of drug-induced liver injury. *AAPS J* 2006; **8**: E48-E54 [PMID: 16584133 DOI: 10.1208/aapsj080106]
77 **Iwai Y**, Terawaki S, Ikegawa M, Okazaki T, Honjo T. PD-1 inhibits antiviral immunity at the effector phase in the liver. *J Exp Med* 2003; **198**: 39-50 [PMID: 12847136 DOI: 10.1084/jem.20022235]
78 **Klugewitz K**, Blumenthal-Barby F, Schrage A, Knolle PA, Hamann A, Crispe IN. Immunomodulatory effects of the liver: deletion of activated CD4+ effector cells and suppression of IFN-gamma-producing cells after intravenous protein immunization. *J Immunol* 2002; **169**: 2407-2413 [PMID: 12193708]
79 **Ju C**, McCoy JP, Chung CJ, Graf ML, Pohl LR. Tolerogenic role of Kupffer cells in allergic reactions. *Chem Res Toxicol* 2003; **16**: 1514-1519 [PMID: 14680364 DOI: 10.1021/tx0341761]
80 **You Q**, Cheng L, Kedl RM, Ju C. Mechanism of T cell tolerance induction by murine hepatic Kupffer cells. *Hepatology* 2008; **48**: 978-990 [PMID: 18712788 DOI: 10.1002/hep.22395]
81 **Danial NN**, Korsmeyer SJ. Cell death: critical control points. *Cell* 2004; **116**: 205-219 [PMID: 14744432]
82 **Linkermann A**, Green DR. Necroptosis. *N Engl J Med* 2014; **370**: 455-465 [PMID: 24476434 DOI: 10.1056/NEJMra1310050]
83 **Ashford TP**, Porter KR. Cytoplasmic components in hepatic cell lysosomes. *J Cell Biol* 1962; **12**: 198-202 [PMID: 13862833]
84 **Wang J**, Yuan L, Xiao H, Xiao C, Wang Y, Liu X. Momordin Ic induces HepG2 cell apoptosis through MAPK and PI3K/Akt-mediated mitochondrial pathways. *Apoptosis* 2013; **18**: 751-765 [PMID: 23417763 DOI: 10.1007/s10495-013-0820-z]
85 **Iorga A**, Dara L, Kaplowitz N. Drug-Induced Liver Injury: Cascade of Events Leading to Cell Death, Apoptosis or Necrosis. *Int J Mol Sci* 2017; **18**: pii: E1018 [PMID: 28486401 DOI: 10.3390/ijms18051018]
86 **Ashkenazi A**, Salvesen G. Regulated cell death: signaling and mechanisms. *Annu Rev Cell Dev Biol* 2014; **30**: 337-356 [PMID: 25150011 DOI: 10.1146/annurev-cellbio-100913-013226]
87 **Reinehr R**, Häussinger D. CD95 death receptor and epidermal growth factor receptor (EGFR) in liver cell apoptosis and regeneration. *Arch Biochem Biophys* 2012; **518**: 2-7 [PMID: 22182753 DOI: 10.1016/j.abb.2011.12.004]
88 **Micheau O**, Tschopp J. Induction of TNF receptor I-mediated apoptosis via two sequential signaling complexes. *Cell* 2003; **114**: 181-190 [PMID: 12887920]
89 **Shore GC**, Papa FR, Oakes SA. Signaling cell death from the endoplasmic reticulum stress response. *Curr Opin Cell Biol* 2011; **23**: 143-149 [PMID: 21146390 DOI: 10.1016/j.ceb.2010.11.003]
90 **Scaffidi C**, Fulda S, Srinivasan A, Friesen C, Li F, Tomaselli KJ, Debatin KM, Krammer PH, Peter ME. Two CD95 (APO-1/Fas) signaling pathways. *EMBO J* 1998; **17**: 1675-1687 [PMID: 9501089 DOI: 10.1093/emboj/17.6.1675]
91 **Festjens N**, Vanden Berghe T, Vandenabeele P. Necrosis, a well-orchestrated form of cell demise: signalling cascades, important mediators and concomitant immune response. *Biochim Biophys Acta* 2006; **1757**: 1371-1387 [PMID: 16950166 DOI: 10.1016/j.bbabio.2006.06.014]
92 **Schwab BL**, Guerini D, Didszun C, Bano D, Ferrando-May E, Fava E, Tam J, Xu D, Xanthoudakis S, Nicholson DW, Carafoli E, Nicotera P. Cleavage of plasma membrane calcium pumps by caspases: a link between apoptosis and necrosis. *Cell Death Differ* 2002; **9**: 818-831 [PMID: 12107825 DOI: 10.1038/sj.cdd.4401042]
93 **Vanden Berghe T**, Linkermann A, Jouan-Lanhouet S, Walczak H, Vandenabeele P. Regulated necrosis: the expanding network of non-apoptotic cell death pathways. *Nat Rev Mol Cell Biol* 2014; **15**: 135-147 [PMID: 24452471 DOI: 10.1038/nrm3737]
94 **Su L**, Quade B, Wang H, Sun L, Wang X, Rizo J. A plug release mechanism for membrane permeation by MLKL. *Structure* 2014; **22**: 1489-1500 [PMID: 25220470 DOI: 10.1016/j.str.2014.07.014]
95 **Vanlangenakker N**, Vanden Berghe T, Vandenabeele P. Many stimuli pull the necrotic trigger, an overview. *Cell Death Differ* 2012; **19**: 75-86 [PMID: 22075985 DOI: 10.1038/cdd.2011.164]
96 **Takemoto K**, Hatano E, Iwaisako K, Takeiri M, Noma N, Ohmae S, Toriguchi K, Tanabe K, Tanaka H, Seo S, Taura K, Machida K, Takeda N, Saji S, Uemoto S, Asagiri M. Necrostatin-1 protects against reactive oxygen species (ROS)-induced hepatotoxicity in acetaminophen-induced acute liver failure. *FEBS Open Bio* 2014; **4**: 777-787 [PMID: 25349782 DOI: 10.1016/j.fob.2014.08.007]
97 **Dara L**, Johnson H, Suda J, Win S, Gaarde W, Han D, Kaplowitz N. Receptor interacting protein kinase 1 mediates murine acetaminophen toxicity independent of the necrosome and not through necroptosis. *Hepatology* 2015; **62**: 1847-1857 [PMID: 26077809 DOI: 10.1002/hep.27939]
98 **Klionsky DJ**. Autophagy revisited: a conversation with Christian de Duve. *Autophagy* 2008; **4**: 740-743 [PMID: 18567941]
99 **Kobayashi S**. Choose Delicately and Reuse Adequately: The Newly Revealed Process of Autophagy. *Biol Pharm Bull* 2015; **38**: 1098-1103 [PMID: 26235572 DOI: 10.1248/bpb.b15-00096]
100 **Ni HM**, McGill MR, Chao X, Du K, Williams JA, Xie Y, Jaeschke H, Ding WX. Removal of acetaminophen protein adducts by autophagy protects against acetaminophen-induced liver injury in mice. *J Hepatol* 2016; **65**: 354-362 [PMID: 27151180 DOI: 10.1016/j.jhep.2016.04.025]
101 **Katsuragi Y**, Ichimura Y, Komatsu M. p62/SQSTM1 functions as a signaling hub and an autophagy adaptor. *FEBS J* 2015; **282**: 4672-4678 [PMID: 26432171 DOI: 10.1111/febs.13540]
102 **Lin Z**, Wu F, Lin S, Pan X, Jin L, Lu T, Shi L, Wang Y, Xu A, Li X. Adiponectin protects against acetaminophen-induced mitochondrial dysfunction and acute liver injury by promoting autophagy in mice. *J Hepatol* 2014; **61**: 825-831 [PMID: 24882054 DOI: 10.1016/j.jhep.2014.05.033]
103 **Gunawan BK**, Liu ZX, Han D, Hanawa N, Gaarde WA, Kaplowitz N. c-Jun N-terminal kinase plays a major role in murine acetaminophen hepatotoxicity. *Gastroenterology* 2006; **131**: 165-178 [PMID: 16831600 DOI: 10.1053/j.gastro.2006.03.045]
104 **Williams JA**, Ni HM, Haynes A, Manley S, Li Y, Jaeschke H, Ding WX. Chronic Deletion and Acute Knockdown of Parkin Have Differential Responses to Acetaminophen-induced Mitophagy and Liver Injury in Mice. *J Biol Chem* 2015; **290**: 10934-10946 [PMID: 25752611 DOI: 10.1074/jbc.M114.602284]
105 **Antoine DJ**, Williams DP, Kipar A, Jenkins RE, Regan SL, Sathish JG, Kitteringham NR, Park BK. High-mobility group box-1 protein and keratin-18, circulating serum proteins informative of acetaminophen-induced necrosis and apoptosis in vivo. *Toxicol Sci* 2009; **112**: 521-531 [PMID: 19783637 DOI: 10.1093/toxsci/kfp235]
106 **Antoine DJ**, Dear JW, Lewis PS, Platt V, Coyle J, Masson M, Thanacoody RH, Gray AJ, Webb DJ, Moggs JG, Bateman DN, Goldring CE, Park BK. Mechanistic biomarkers provide early and sensitive detection of acetaminophen-induced acute liver injury at first presentation to hospital. *Hepatology* 2013; **58**: 777-787 [PMID: 23390034 DOI: 10.1002/hep.26294]
107 **Antoine DJ**, Jenkins RE, Dear JW, Williams DP, McGill MR, Sharpe MR, Craig DG, Simpson KJ, Jaeschke H, Park BK. Molecular forms of HMGB1 and keratin-18 as mechanistic biomarkers for mode of cell death and prognosis during clinical acetaminophen hepatotoxicity. *J Hepatol* 2012; **56**: 1070-1079 [PMID: 22266604 DOI: 10.1016/j.jhep.2011.12.019]
108 **Wang K**, Zhang S, Marzolf B, Troisch P, Brightman A, Hu Z, Hood LE, Galas DJ. Circulating microRNAs, potential biomarkers for drug-induced liver injury. *Proc Natl Acad Sci USA* 2009; **106**: 4402-4407 [PMID: 19246379 DOI: 10.1073/pnas.0813371106]
109 **Dear JW**, Antoine DJ, Starkey-Lewis P, Goldring CE, Park BK. Early detection of paracetamol toxicity using circulating liver microRNA and markers of cell necrosis. *Br J Clin Pharmacol* 2014; **77**: 904-905 [PMID: 23879521 DOI: 10.1111/bcp.12214]
110 **McGill MR**, Sharpe MR, Williams CD, Taha M, Curry SC, Jaeschke H. The mechanism underlying acetaminophen-induced hepatotoxicity in humans and mice involves mitochondrial damage and nuclear DNA fragmentation. *J Clin Invest* 2012; **122**: 1574-1583 [PMID: 22378043 DOI: 10.1172/JCI59755]

111 **Church RJ**, Watkins PB. The transformation in biomarker detection and management of drug-induced liver injury. *Liver Int* 2017; **37**: 1582-1590 [PMID: 28386997 DOI: 10.1111/liv.13441]
112 **Fannin RD**, Russo M, O'Connell TM, Gerrish K, Winnike JH, Macdonald J, Newton J, Malik S, Sieber SO, Parker J, Shah R, Zhou T, Watkins PB, Paules RS. Acetaminophen dosing of humans results in blood transcriptome and metabolome changes consistent with impaired oxidative phosphorylation. *Hepatology* 2010; **51**: 227-236 [PMID: 19918972 DOI: 10.1002/hep.23330]
113 **Peta V**, Tse C, Perazzo H, Munteanu M, Ngo Y, Ngo A, Ramanujam N, Verglas L, Mallet M, Ratziu V, Thabut D, Rudler M, Thibault V, Schuppe-Koistinen I, Bonnefont-Rousselot D, Hainque B, Imbert-Bismut F, Merz M, Kullak-Ublick G, Andrade R, van Boemmel F, Schott E, Poynard T; Drug Induced Liver Injury- Groupe Hospitalier Pitié-Salpêtrière; Drug Induced Liver Group of the Injury Safer and Faster Evidence-based Translation consortium. Serum apolipoprotein A1 and haptoglobin, in patients with suspected drug-induced liver injury (DILI) as biomarkers of recovery. *PLoS One* 2017; **12**: e0189436 [PMID: 29287080 DOI: 10.1371/journal.pone.0189436]
114 **Han D**, Shinohara M, Ybanez MD, Saberi B, Kaplowitz N. Signal transduction pathways involved in drug-induced liver injury. *Handb Exp Pharmacol* 2010; **(196)**: 267-310 [PMID: 20020266 DOI: 10.1007/978-3-642-00663-0_10]

P- Reviewer: Higuera-de la Tijera F, Xiao J, Tanaka N
S- Editor: Gong ZM **L- Editor**: A **E- Editor**: Huang Y

World Journal of Gastroenterology

Submit a Manuscript: http://www.f6publishing.com

World J Gastroenterol 2018 April 7; 24(13): 1386-1397

DOI: 10.3748/wjg.v24.i13.1386

ISSN 1007-9327 (print) ISSN 2219-2840 (online)

MINIREVIEWS

Thrombocytopenia after liver transplantation: Should we care?

Kazuhiro Takahashi, Shunji Nagai, Mohamed Safwan, Chen Liang, Nobuhiro Ohkohchi

Kazuhiro Takahashi, Chen Liang, Nobuhiro Ohkohchi, Department of Surgery, Division of Gastroenterological and Hepatobiliary Surgery, and Organ Transplantation, University of Tsukuba, Tsukuba, Ibaraki 3058575, Japan

Shunji Nagai, Mohamed Safwan, Transplant and Hepatobiliary Surgery, Henry Ford Hospital, Detroit, ML 48202, United States

ORCID number: Kazuhiro Takahashi (0000-0003-1089-0644); Shunji Nagai (0000-0003-2612-8427); Mohamed Safwan (0000-0002-3299-9045); Chen Liang (0000-0002-4528-7303); Nobuhiro Ohkohchi (0000-0003-2779-1247).

Author contributions: Takahashi K, Nagai S, Safwan M, Liang C and Ohkohchi N contributed equally to this work; Takahashi K wrote the paper.

Conflict-of-interest statement: There is no conflict of interest associated with any of the senior author or other coauthors contributed their efforts in this manuscript.

Manuscript source: Invited manuscript

Correspondence to: Nobuhiro Ohkohchi, MD, PhD, Department of Surgery, Division of Gastroenterological and Hepatobiliary Surgery, and Organ Transplantation, University of Tsukuba, 1-1-1 Tennoudai, Tsukuba, Ibaraki 305-8575, Japan. nokochi3@md.tsukuba.ac.jp
Telephone: +81-29-8533221
Fax: +81-29-8533222

Received: January 30, 2018
Peer-review started: January 31, 2018
First decision: February 11, 2018
Revised: March 6, 2018
Accepted: March 18, 2018

Article in press: March 18, 2018
Published online: April 7, 2018

Abstract

Transient thrombocytopenia is a common phenomenon after liver transplantation. After liver transplantation (LT), platelet count decreases and reaches a nadir on postoperative days 3-5, with an average reduction in platelet counts of 60%; platelet count recovers to preoperative levels approximately two weeks after LT. The putative mechanisms include haemodilution, decreased platelet production, increased sequestration, medications, infections, thrombosis, or combination of these processes. However, the precise mechanisms remain unclear. The role of platelets in liver transplantation has been highlighted in recent years, and particular attention has been given to their effects beyond hemostasis and thrombosis. Previous studies have demonstrated that perioperative thrombocytopenia causes poor graft regeneration, increases the incidence of postoperative morbidity, and deteriorates the graft and decreases patient survival in both the short and long term after liver transplantation. Platelet therapies to increase perioperative platelet counts, such as thrombopoietin, thrombopoietin receptor agonist, platelet transfusion, splenectomy, and intravenous immunoglobulin treatment might have a potential for improving graft survival, however clinical trials are lacking. Further studies are warranted to detect direct evidence on whether thrombocytopenia is the cause or result of poor-graft function and postoperative complications, and to determine who needs platelet therapies in order to prevent postoperative complications and thus improve post-transplant outcomes.

Key words: Thrombocytopenia; Liver regeneration; Platelet therapy; Platelet; Thrombopoietin receptor agonist; Intravenous immunoglobulin treatment; Liver transplantation

Core tip: Transient thrombocytopenia is commonly seen after liver transplantation, and many studies have demonstrated that perioperative thrombocytopenia is associated with deterioration of the graft and decreased patient survival after liver transplantation. The role of platelets in liver transplantation has recently been highlighted, and particular attention has been given to their effects beyond hemostasis and thrombosis. Platelet therapies that increase platelet count, such as thrombopoietin, thrombopoietin receptor agonist, platelet transfusion, splenectomy, and intravenous immunoglobulin treatment, have a potential role for improving graft survival; however, clinical trials are still lacking, and further studies are warranted.

Takahashi K, Nagai S, Safwan M, Liang C, Ohkohchi N. Thrombocytopenia after liver transplantation: Should we care? *World J Gastroenterol* 2018; 24(13): 1386-1397 Available from: URL: http://www.wjgnet.com/1007-9327/full/v24/i13/1386.htm DOI: http://dx.doi.org/10.3748/wjg.v24.i13.1386

INTRODUCTION

Platelets are anucleate cytoplasmic discs derived from megakaryocytes in the bone marrow[1-3]. The normal life span of platelets is 8-10 d, and they are removed from circulation by sequestration in the spleen[4]. Platelets contain three types of secretory granules: alpha granules, dense granules, and lysosomal granules. Each granule contains growth factors and cytokines, such as platelet-derived growth factor, hepatocyte growth factor (HGF), insulin-like growth factor-1 (IGF-1), vascular endothelial growth factor (VEGF), serotonin, epidermal growth factor, and transforming growth factor-β[5,6]. Platelets have major roles in hemostasis, thrombosis, inflammation, and vascular biology and have recently been discovered to have additional functions in antimicrobial defense, angiogenesis, tissue repair and regeneration[7-10].

Orthotopic liver transplantation (LT) is the treatment of choice for patients with end-stage liver disease and hepatocellular carcinoma within the Milan criteria[11,12]. The short and long term outcomes of this procedure have dramatically improved as a result of innovations in both immune suppression and surgical techniques[11]. The total number of adult LTs performed in the world was 27759 in 2015, of which living donor LT (LDLT) accounted for 21%[13]. The number of transplant candidates on a waiting list has also steadily increased despite organ shortage being a worldwide issue. According to the 2015 annual report from the Scientific Registry of Transplant Recipients, the incidence of graft failure in the United States continues to decrease; in 2014, there were 6-mo graft failure rates of 7.8% and 12.5% and 1-year rates of 10.3% and 15.1% in deceased donor LT (DDLT) and in LDLT, respectively[14].

Post-transplant thrombocytopenia occurs in the majority of patients immediately after LT, with reported incidences of up to 90%[15,16]. After LT, platelet count decreases and reaches a nadir on postoperative days (PODs) 3-5, with an average reduction in platelet counts of 60%; platelet count recovers to preoperative levels approximately two weeks after LT[17]. Thrombocytopenia in the postoperative period is not simply an academic observation but can lead to catastrophic events, such as postoperative bleeding, cerebral hemorrhage, and infection, which eventually lead to graft failure and mortality. The putative mechanisms involved include decreased platelet production, increased platelet consumption, sequestration in the liver graft or spleen, dilution, medication, or a combination of these processes[18-22]. However, the precise mechanism is still unknown. In this review, we aimed to describe the clinical and experimental evidence of the role of platelets in LT. This review differs from previous reviews in the following three points. First, we describe the role of platelets in LT specifically with a focus on "post-transplant thrombocytopenia". Second, the involvement of platelets in DDLT and LDLT are described separately, since they are different in many aspects including the graft quality, the length of ischemia, and the recovery of portal hypertension after LT. Third, we delve into the potential mechanisms of post-transplant thrombocytopenia. We report previous evidence with consideration for future perspectives.

PLATELETS AND DDLT

Post-transplant thrombocytopenia after DDLT has been reported since the advent of liver transplantation and has been described in many articles. It was first reported by Hutchison *et al*[23] in 1968 (Table 1). They reviewed 8 LT recipients who received DDLT at the University of Colorado, which included 2 auxiliary and 6 orthotopic LT. An acute drop in platelet count to less than $10 \times 10^3/\mu L$ was observed in most patients within the first three postoperative days. To better comprehend this phenomenon, they performed experimental LT in dogs and found platelets located in the space of Disse along with Kupffer cells, some of which were ingesting the platelets. They concluded that post-transplant thrombocytopenia was primarily caused by the mechanical entrapment of platelets in the grafts, which were then destroyed by the Kupffer cells. The next report of this phenomenon came after a twenty year interval and was described by Plevak *et al*[16]. They observed that platelet counts dropped from preoperative levels of $137 \times 10^3/\mu L$ to $72 \times 10^3/\mu L$ on POD 3. Using ^{111}In-labeled platelets, they demonstrated that transplant recipients showed a delayed recovery of platelet counts after LT.

Since then, several consecutive reports have been

Table 1 Reports of postoperative thrombocytopenia after liver transplant

Author	Year	Type	Number of patients	Results
Hutchison *et al*[23]	1968	DDLT	8	Platelet count change from 200-400 × 10^3/μL to 67 × 10^3/μL on POD 3
Plevak *et al*[16]	1988	DDLT	76	Platelet count change from 137 × 10^3/μL to 72 × 10^3/μL on POD 3
Munoz *et al*[15]	1989	DDLT	3	Three patients with severe postoperative thrombocytopenia were successfully treated with high-dose gamma-globulin
McCaughan *et al*[17]	1992	DDLT	53	Patients who died during their hospital stay had lower postoperative platelet counts at the nadir, and the day of the nadir tended to be delayed
Chatzipetrou *et al*[24]	1999	DDLT	541	A platelet nadir of < 20 × 10^3/μL was associated with allograft dysfunction, graft rejection and poorer patient and graft survival
Chang *et al*[25]	2000	DDLT	50	Fungal infection was frequent in patients with a platelet nadir of < 30 × 10^3/μL
Ben Hamida *et al*[26]	2003	DDLT	161	Patients with a platelet count < 50 × 10^3/μL for three consecutive days showed a high mortality rate.
Nascimbene *et al*[19]	2007	DDLT	8	Infusion of high-dose gamma-globulins induced a prompt, complete and persistent resolution of postoperative severe thrombocytopenia in more than 70% of patients
Kim *et al*[47]	2010	LDLT	87	A total unit of platelet transfusion was significantly associated with graft regeneration
Lesurtel *et al*[28]	2014	DDLT	247	A platelet count of < 60 × 10^3/μL on POD 5 was related to poor graft survival within 90 d after LT
Sonny *et al*[27]	2015	DDLT	223	A preoperative platelet count of < 45 × 10^3/μL was related with short-term outcomes in patients ≥ 60 years old
Li *et al*[49]	2015	LDLT	234	Patients with an immediate postoperative platelet count of < 68 × 10^3/μL had a higher chance of developing EAD and severe complications
Takahashi *et al*[29]	2016	DDLT	975	A platelet count of < 72.5 × 10^3/μL on POD 5 was related to poor graft survival
Han *et al*[48]	2016	LDLT	441	An intraoperative platelet transfusion was also independently associated with enhanced graft regeneration at 14 ± 2 d after surgery
Pamecha *et al*[50]	2016	LDLT	120	A platelet count of < 30 × 10^3/μL on POD 3 was a strong predictor of complications and EAD
Gwiasda *et al*[31]	2017	DDLT	134	A higher preoperative platelet count was related to graft loss
Takahashi *et al*[30]	2017	DDLT	771	Persistent thrombocytopenia within 5 d after LT was related to progression of biliary anastomotic stricture
Akamatsu *et al*[51]	2017	LDLT	445	A Low platelet count on POD 3 was an independent predictor of grade Ⅲb/Ⅳ complications

LT: Liver transplant; DDLT: Deceased donor liver transplant; LDLT: Living donor liver transplant; POD: Postoperative day; EAD: Early allograft dysfunction.

published on this topic, and the majority of these studies indicate that postoperative thrombocytopenia may influence post-LT outcomes and have a negative impact on grafts and patient survival in the short and long term after LT[17,19,24-27]. McCaughan *et al*[17] reported a drop in postoperative platelet counts by 63%, which was the only independent predictor of short-term patient survival post-LT. In their analysis of a large cohort of 541 patients of DDLT in a single institute, Chatzipetrou *et al*[24] described that a post-transplant platelet count nadir of < 20 x 10^3/μL was associated with allograft dysfunction, graft rejection and poorer patient and graft survival. Chang *et al*[25] reported that the incidence of fungal infection was more frequent in patients with a platelet nadir of < 30 × 10^3/μL, leading to higher mortality rates. Sonny *et al*[27] focused on the elderly population and found that the length of intensive care unit (ICU) and hospital stays were longer in patients with preoperative platelet counts of < 45 × 10^3/μL. Factors such as low preoperative platelet counts, massive intraoperative platelet transfusions, retransplantation, and poor general preoperative conditions such as the need for dialysis, were found to be associated with post-transplant thrombocytopenia[24,26]. For the treatment of post-transplant thrombocytopenia, Munoz *et al*[15] and Nascimbene *et al*[19] separately reported that an infusion of high-dose gamma-globulins could induce resolution of severe postoperative thrombocytopenia However, they could not explain its mechanism of action.

Recently, some groups have focused on platelet counts particularly on POD 5, when platelet counts start to rise after the nadir. In 2014, Lesurtel *et al*[28] proposed the 60-5 criteria, in which a platelet count of < 60 × 10^3/μL on POD 5 was an independent risk factor associated for severe postoperative complications, early graft failure, and patient mortality in the short term after DDLT. Takahashi *et al*[29] focused on the long term impact after DDLT and noted that a platelet count of < 72.5 × 10^3/μL on POD 5 was a predictor for poor graft and patient survival. More recently, Takahashi *et al*[30] described that low perioperative platelet counts within 5 d after DDLT were associated with biliary anastomotic stricture (BAS) with duct-to-duct biliary reconstruction. They found that persistent postoperative thrombocytopenia, which

was defined as platelet counts of < 41 × 10^3/μL and < 53 × 10^3/μL on POD 3 and POD 5, respectively, was an independent risk factor for BAS.

In contrast, Gwiasda *et al*[31] stated that higher preoperative platelet count was associated with graft loss because platelets contribute to reperfusion injury after graft ischemia. Further, Eldeen *et al*[32] described that recipients who experienced early hepatic arterial thrombosis (HAT) had higher preoperative platelet counts, but this was not associated with the development of late HAT.

Clinical studies suggest that increasing postoperative platelet counts might improve graft and patient survival after DDLT[28-30]. This "protective effect of platelets" may be compatible with a study by Hisakura *et al*[33] who showed that thrombopoietin-mediated thrombocytosis protected the liver from damage after an extended hepatectomy in a pig model. However, transplant surgeons prefer relatively low postoperative platelet counts due to fear of HAT, and this preference has made it difficult to perform prospective trials.

PLATELETS AND LDLT

After LDLT, the liver undergoes two different processes, namely, liver regeneration and ischemia-reperfusion[34-36]. The liver regeneration process after LDLT has been divided into three phases[34]. The early phase is rapid regeneration, which occurs during the first two weeks and is associated with vascular engorgement and tissue edema. The second phase is volume decline, which may be attributed to the normalization of transient vascular engorgement or tissue edema at one to two months after hepatectomy. The third phase is a slow increase in volume, which occurs until the volume reaches a constant level[34]. Partial liver grafts need rapid regeneration to meet the functional demands of recipients; otherwise, liver failure would occur, and the short- and long-term outcomes would be affected. Liver regeneration is orchestrated by the interplay of various cells and mediators, and platelets are understood to have a role as well[37,38]. The role of platelets in accelerating liver regeneration after partial hepatectomy was first reported by Murata in 2004[39], and Lesurtel *et al*[40] reported platelet-derived serotonin-mediated liver regeneration using transgenic mice. Since then, many studies have been reported in this field, and it was implicated by a Japanese group that liver regeneration after partial hepatectomy is promoted by platelets through three different mechanisms: (1) a direct effect on hepatocytes; (2) a cooperative effect with liver sinusoidal endothelial cells; and (3) a collaborative effect with Kupffer cells[41-45]. On the other hand, in ischemia-reperfusion, platelets are generally considered to act in concert with activated Kupffer cells and leukocytes, and a triangular interaction between Kupffer cells, leukocytes, and platelets has been demonstrated to be the core mechanism of liver injury[46]. Thus, platelets have two ambivalent roles in LDLT.

Kim *et al*[47] were the first to report the positive role of platelets in LDLT in 2010 (Table 1). They investigated the relationships between clinical variables and liver graft regeneration rates in their study population of 87 recipients with adult-to-adult living donor recipients, all receiving right lobe grafts. They found that total units of platelet transfusion were significantly associated with graft regeneration. Han *et al*[48] studied the relationship between platelets and liver regeneration after LDLT. They described that intraoperative platelet transfusion was independently associated with enhanced graft regeneration at 14 ± 2 d after surgery without increasing morbidity and mortality rates. Furthermore, platelet count during the reperfusion phase was identified as a prognostic factor for graft regeneration. Li *et al*[49] focused on platelet count immediately after transplant and reported that patients with an immediate postoperative platelet count of < 68 × 10^3/μL had a higher chance of developing early allograft dysfunction and severe complications. Pamecha *et al*[50] demonstrated that a platelet count of < 30 × 10^3/μL on POD 3 was a strong predictor of major postoperative complications and was associated with early graft dysfunction, prolonged ascites, and sepsis. Akamatsu *et al*[51] also focused on POD 3 and described that a low platelet count on POD 3 was an independent predictor of grade ⅢIb/Ⅳ complications.

Only recently has post-transplant thrombocytopenia been reported to be associated with LDLT. Lower platelet counts lead to poor graft regeneration but lower incidences of ischemia-reperfusion injury in partial grafts. Overall higher platelets counts are beneficial because their impact on liver regeneration outweighs the associated risk of ischemia-reperfusion injury, most notably during the early post-LDLT period[52]. Animal experiments to explain this phenomenon are still lacking, and basic studies and prospective clinical trials are warranted.

PLATELET FUNCTION AND ANTIPLATELET THERAPY AFTER LT

In patients with end-stage liver disease (ESLD), platelet function is often reported to be compromised[53]. However, recent studies have demonstrated that platelet function in patients with ESLD was not as compromised as it was previously believed[54]. A few observational studies that evaluated platelet function after LT have been reported in the past, but these studies involved a small number of patients. Himmelreich *et al*[55] reported decreased platelet aggregation immediately after reperfusion in 10 patients after DDLT. The authors considered that a dysfunction in platelet aggregation may have been a major cause of intraoperative bleeding[55]. They also mentioned that administration of a small amount of University of Wisconsin (UW) solution into systemic circulation during reperfusion might further

decrease platelet function[56]. Jüttner *et al*[57] found marked depressed GPⅡb/Ⅲa and P-selectin expression in circulating platelets, and maximum aggregation of platelets was restored on the third day after reperfusion among patients with all types of underlying disease. Eyraud *et al*[58]. conducted platelet function testing with aggregometry using platelet-rich plasma obtained from 15 patients after DDLT. Compared with pre-transplant conditions, no significant difference was found in platelet function at 7 and 28 d after DDLT From these reports, platelet function is temporally impaired immediately after LT but recovers in 3-7 d.

Regarding the use of antiplatelet therapy, some studies have indicated favorable effects on LT, including a reduced incidence of post-transplant hepatic arterial thrombosis[59,60] and the prevention of progression of liver fibrosis after postoperative recurrence of hepatitis C[61]. Antiplatelet therapy has also been described to prevent the recurrence of hepatocellular carcinoma after curative hepatectomy[62] and to suppress hepatocellular carcinogenesis in patients with chronic hepatitis[63,64]. However, most of these studies were performed at a single institution or were retrospective in nature. A randomized clinical trial should be undertaken to analyze the risks and benefits of the use of post-transplant antiplatelet therapy.

MECHANISM OF POST-TRANSPLANT THROMBOCYTOPENIA

Thrombocytopenia, which is defined by a platelet count of < 150 × 10^3/μL, has been reported to occur in more than 70% of patients with cirrhosis[65-67]. This disorder is considered to be a result of reduced synthesis of thrombopoietin (TPO) and increased sequestration by hypersplenism[67]. In LT, post-transplantation thrombocytopenia can occur due to the following: hemodilution; decreased production of TPO; increased platelet sequestration in the liver graft or spleen; immunological reactions; platelet activation and consumption due to thrombosis, such as in disseminated intravascular coagulation (DIC), thrombotic microangiopathy, or venous thromboembolism; medication; infections; or a combination of these processes[18-22].

Hemodilution

Hemodilution due to intensive use of blood products, colloids and crystalloids during the transplant procedure may lead to a drop in the platelet count immediately after surgery, but the platelet nadir usually occurs on days 3-4, which does not validate hemodilution as a potential cause of postoperative thrombocytopenia.

Preservation solution

A correlation between lower post-transplant thrombocytopenia and the use of UW solution was implicated by Williams *et al*[68] However, their study was an observational study that consisted of a small number of recipients, and the level of evidence was low[69].

Sequestration in the spleen

Richards *et al*[20] described that patients in a hyposplenic state exhibit the same pattern of post-transplant thrombocytopenia as those with intact splenic function. Nascimbene *et al*[19] also noted that thrombocytopenia occurred regardless of the presence of hypersplenism. Thus, the spleen is not considered to be a major site of platelet consumption[20].

Consumption in the liver graft by Kupffer cells

Sindram *et al*[46] demonstrated that reperfusion of rat livers preserved for 24 h at a cold temperature resulted in rapid sequestration of platelets in the liver graft and platelet adherence to the sinusoidal lining, which induced apoptosis of the sinusoidal endothelial cells in concert with leukocytes and activated Kupffer cells. Cywes *et al*[18] detected significantly increased adherence of platelets to the hepatic endothelium after reperfusion of the liver graft. Porte *et al*[70] reported that thrombocytopenia started immediately after reperfusion, and sequestration of platelets was observed as platelets accumulated in the sinusoids and were phagocytized by Kupffer cells, which was similar to an earlier study. On the other hand, Takahashi *et al*[41] suggested that platelets that accumulate in the liver graft have with contact with Kupffer cells and release growth factors, such as HGF, IGF-1, and VEGF, that protect the liver graft and lead to improved graft survival in patients with higher platelet counts after DDLT[29].

Consumption at the liver graft with local thrombin generation

Richards *et al*[20] found that the levels of fibrin and fibrinogen degradation products are elevated postoperatively, which they speculated was due to endothelial damage in the liver graft during the preservation period, which lead to hepatic sequestration due to local thrombin generation. Nobuoka *et al*[71] focused on activity of a disintegrin-like and metalloproteinase with thrombospondin type-1 motifs member 13 (ADAMTS13), which is produced by stellate cells. ADAMTS13 is an enzyme that specifically cleaves multimetric von Willebrand factor (vWF), which mediates the adhesion of platelets to the site of vascular damage. They described that decreased activity of ADAMTS13 accompanied by elevated vWF levels was associated with thrombocytopenia 2 wk after LDLT. They considered that prolonged thrombocytopenia after LDLT was due to decreased production of ADAMTS13 in the graft with local thrombin generation and platelet aggregation. Nakanuma *et al*[72] found that platelet aggregation was mainly present at zone 3 in the liver graft as extravasated platelet aggregation (EPA), and peripheral platelet counts were lower after LDLT in the EPA-positive patients than the EPA-negative patients. They considered that EPA in the zone 3 caused the platelet consumption, activation, and degranulation, following the release of negative cytokines by platelets, and

might be involved in liver damage and poor outcomes after LDLT[72].

TPO production

Serum TPO concentration is inversely related to platelet concentration in patients with hematopoietic disorders characterized by deceased megakaryocytes in the bone marrow[5]. The level of expression of mRNA for TPO is high in the liver, indicating that the liver is the main source of TPO synthesis[73].

Richards *et al*[74] reported that thrombocytopenia following LT was accompanied by an increased rate of thrombopoiesis in the early period after transplantation, shown by increased reticulated platelets following the platelet nadir. Peck-Radosavljevic *et al*[75] observed that serum thrombopoietin levels increased significantly on the first day after LT, which preceded the increase in reticulated platelets by 3 d and in peripheral platelets by 5 d. This delayed rise in platelet count was compatible with the time lag between the appearance of reticulated platelets and peripheral platelets after *in vivo* administration of a recombinant human thrombopoietin analogue, and rules out the impaired production of TPO as a possible cause of post-transplant thrombocytopenia. Usui *et al*[76] reported the TPO levels in the prolonged thrombocytopenic group were significantly decreased. They considered that prolonged post-transplant thrombocytopenia was secondary to a decrease in TPO production suggesting graft dysfunction.

Medication

Immunosuppressive medications (*e.g.*, azathioprine, mycophenolate mofetil, cyclosporine and tacrolimus), heparin, anti-thymocyte globulin (ATG), antiviral drugs (ganciclovir and valganciclovir), trimethoprim sulfamethoxazole, *etc*., can cause thrombocytopenia after LT. Antimetabolites, such as azathioprine and mycophenolate mofetil, have myelosuppressive effects on the bone marrow in a dose-dependent manner[77,78]. Nascimbene *et al*[19] performed bone marrow aspirates during the early post-LT period and noticed marked megakaryocytic hyperplasia in all cases, ruling out drug-induced myelosuppression as a cause of post-transplant thrombocytopenia. Calcineurin inhibitors, such as cyclosporine and tacrolimus, may cause thrombocytopenia. The presentation is similar to thrombotic thrombocytopenic purpura (TTP), in which renal dysfunction is accompanied by thrombocytopenia[79-81]. Lee *et al*[79] described that the incidence of cyclosporine-induced TTP was low (incidence of 1%) and was seen only in the pediatric population, occurring at 2 to 30 wk after LT.

Heparin-induced thrombocytopenia (HIT) after LT has been reported in several articles[22,82-85]. Kaneko *et al*[22] demonstrated that the percentage of heparin-induced thrombocytopenia (HIT) antibody-positive patients was low (incidence of 5.6%), and none of the patients developed HIT. Bakchoul *et al*[82] also described that HIT was clinically suspected in 16% of recipients at a median of POD 6. However, only one of these patients was positive for anti-platelet factor 4/heparin IgG antibodies. ATG induces dose-dependent T-cell depletion by complement-dependent cytotoxicity, antibody-dependent cellular cytotoxicity, and apoptosis[86,87]. ATG-induced platelet aggregation is a specific reaction responsible for thrombocytopenia. Platelet surface antigen-CD32 has been suggested to play a crucial role in ATG-induced thrombocytopenia[88]. Ganciclovir and valganciclovir are suspected to have direct bone marrow toxicity. Gabardi *et al*[89] reported that the incidence of thrombocytopenia with low-dose valganciclovir, used as prophylaxis for cytomegalovirus (CMV) infections in post-transplant patients, was 24%. Trimethoprim sulfamethoxazole, when used as prophylaxis against *Pneumocystis jiroveci* pneumonia, causes drug-induced immune thrombocytopenia (ITP) by antibody formation[90].

ITP and infection

Viral infections, including CMV, Epstein-Barr virus (EBV), parvovirus B19, herpes zoster, human herpes virus 8, and some donor-derived viral infections, can induce ITP[91-97]. The early onset of ITP after LT occurs due to reactivation of CMV, EBV or varicella infection when patients are receiving high-dose immunosuppression. On the other hand, Taylor *et al*[21] reported 8 cases of ITP after LT (incidence of 0.7%), in which they could not find any evidence of infection. The majority of their patients developed ITP more than one year post-LT. Maar *et al*[98] described that recipients with CMV infection showed delayed thrombocytopenia, occurring later than 24 d after LT. They considered that CMV infection induced systemic endothelial activation with the expression of tissue factor on the endothelial cell surface and the release of vWF. These processes activate the clotting cascade and may augment platelet aggregation.

Considering that post-transplant thrombocytopenia mostly occurs during the early period after LT, sequestration in the new liver graft has the strongest potential to explain the temporal drop in platelet counts. However, the precise mechanism of sequestration is still unknown. Prolonged thrombocytopenia, which occurs more than one month after LT, may be attributed to other causes such as impaired TPO production due to graft dysfunction, viral infections, and medications.

PLATELETS AND TRANSFUSION

The median blood loss associated with LT has fallen dramatically with the development of surgical and anesthetic techniques. However, there are still a number of patients who require significant amounts of blood products perioperatively.

DDLT

In 1989, Miyata *et al*[99] described that there was positive correlation between the number of platelet

units transfused and endotoxin concentrations at the end of the anhepatic phase, which they considered to be the reason for increased pulmonary complications. de Boer *et al*[100] demonstrated that intraoperative platelet transfusion was an independent risk factor for one- and five-year survival after DDLT. A subsequent report from Pereboom *et al*[101] noted that platelet transfusion led to an increased one-year mortality from acute lung injury. More recently, Chin *et al*[102] reported that graft survival was reduced significantly in patients receiving intraoperative platelet transfusions at one year, but not at 90 d, and considered that intraoperative transfusion and not thrombocytopenia was associated with a poor outcome after LT. They found a relationship between intraoperative platelet transfusion and postoperative septicemia as a cause of death. Nacoti *et al*[103] focused on a pediatric population and found that platelet transfusion was an independent risk factor for developing major complications in the first year after DDLT. In contrast, Nixon *et al*[104] found that there was no substantiated effect of platelet transfusion on survival after LT, due to their use of plateletpheresis. They insisted on using single-donor platelet transfusions rather than random donor platelet preparations, along with leucocyte reduction strategies.

LDLT

Authors from two different institutes in South Korea described that platelet transfusion after LDLT was a protective factor for graft regeneration and survival[47,48]. Li *et al*[105] described that although massive red blood transfusion led to poor long-term survival, higher postoperative infection rates and prolonged ICU stays, platelet transfusion was not a risk factor for long-term graft survival.

Thromboelastography

With the hope of limiting the use of blood products, some transplant centers use thromboelastography (TEG) to monitor and detect coagulopathies[106]. TEG is a viscoelastic test that is performed on whole blood to analyze complete hemostasis, from platelet plug formation through coagulation and fibrinolysis. There is growing evidence to support the use of TEG as a technique to guide transfusion strategies for LT[107-109]. Kang *et al*[109] prospectively validated the use of TEG for reducing total blood product use. Lawson *et al*[107] described that the maximum amplitude measured preoperatively by TEG had high predictability for intraoperative massive transfusion. Krzanicki *et al*[110] performed a retrospective review of 124 DDLT recipients and found a higher incidence of a hypercoagulable state in patients with a background of cholestatic diseases and an intraoperative hypercoagulable state that was correlated with early HAT after LT. On the other hand, Wikkelsoe *et al*[111] performed a systemic review and meta-analysis including a sequential analysis of randomized clinical trials of a TEG/thromboelastometry-based algorithm compared with standard treatment in patients with cardiac surgery and LT, and found that the former had no impact on mortality, the amount of blood transfused, or the incidence of surgical reinterventions.

There was a significant difference in the impact of platelet transfusion between DDLT and LDLT, the former being negative, and the latter being positive. The reason for this difference could be due to graft type; partial grafts require postoperative liver regeneration. This result is compatible with a report from Matsuo *et al*[44] that transfusion of platelet-rich plasma accelerated liver regeneration, including liver/body weight ratio and hepatocyte Ki-67 labeling index during the early phase after hepatectomy in a rat model. However, it is still unknown how platelets interact with other cells when under ischemia-reperfusion conditions. The precise mechanisms need to be clarified by animal experiments. TEG may be a good option to stratify the risk of perioperative transfusions. However, it is still debated whether the use of TEG is realistically efficient for predicting the need for transfusions.

PLATELET, LT AND SPLENECTOMY

Splenectomy is currently one of the therapeutic procedures for avoiding small-for-size syndrome, and it is a choice for preventing postoperative thrombocytopenia in LDLT[112,113]. It has been indicated for the completion of post-transplant interferon therapy for hepatitis C virus (HCV) infection and ABO incompatible LT[113,114]. However, due to recent advances in interferon (INF)-free direct-acting antivirals for HCV infection and rituximab induction for ABO incompatible transplantation, the necessity for splenectomy is currently decreasing[114]. Partial splenic embolization is a minimally invasive treatment that can be performed as an additional treatment after LT; however, its efficacy may be insufficient, and serious complications, such as splenic abscess, splenic rupture, and venous thrombosis, have been reported[115]. On the other hand, simultaneous splenectomy in DDLT is not usually performed based on historical reports of septic complications after LT[116].

Marubashi *et al*[112] revealed that 7 patients who underwent a simultaneous splenectomy showed remarkable increases in platelet counts 2 wk after LDLT and found that graft size was positively associated with post-transplant thrombocytopenia. Morimoto *et al*[117] demonstrated that with simultaneous splenectomy, the platelet count increased to > 100 $\times$ $10^3/\mu L$ one month post-transplantation in recipients with HCV infection and achieved better sustained virological response after INF therapy. Additionally, a similar report by Chu *et al*[114] noted that patients with simultaneous splenectomy had significantly higher platelet counts at 1 and 6 mo after transplantation, with a higher HCV anti-therapy completion rate. On the other hand, Ito *et al*[116] observed that simultaneous splenectomy increased

platelet count more than 2 wk after LDLT but not during the early postoperative period. In addition, the incidence of reoperation for postoperative hemorrhage increased within the first week. The authors further demonstrated that simultaneous splenectomy was an independent predictor for postoperative lethal infectious complications. On the other hand, Takahashi *et al*[118] described the usefulness of pre-transplant splenectomy in pediatric recipients suffering from biliary atresia. After splenectomy, the platelet count was significantly elevated, with an improvement in the PT-INR and Model for End-Stage Liver Disease score. However, the complication rate for this procedure was relatively high.

The effect of splenectomy on restoring postoperative platelet counts during the early post-LT period may be delayed from the time when a higher platelet count is necessary. This issue may be resolved by pre-transplant splenectomy, which can elevate preoperative platelet counts. However, the decision to perform pre-transplant splenectomy should be given much care and consideration due to the poor general condition of the patients and their bleeding tendencies.

FUTURE PERSPECTIVES

TPO[33,43,45,119,120], TPO receptor agonists[121], artificial platelets[122,123], and freeze-dried platelets[124] are developing and beginning to be utilized in various clinical settings, and the importance of platelets is becoming more obvious. Additionally, the infusion of high-dose immunoglobulins may provide a safe, prompt, complete, and persistent resolution of severe post-transplant thrombocytopenia[15,19]. These platelet therapies, splenectomy and intravenous immunoglobulin treatment may have potential as therapeutic strategies to resolve post-transplant thrombocytopenia, leading to improved graft and patient survival after LT. In particular in LDLT, these strategies may be able to prevent small-for-size syndrome by promoting liver regeneration[47,48,112,118]. However, decreases in platelet count are sometimes falsely overestimated by automatic analyzers due to platelet aggregation. Therefore, manual counting to confirm a platelet reduction before initiating platelet therapies and monitoring precise platelet counts after therapy are necessary.

LIMITATIONS

We acknowledge there are limitations to this review. First, most studies are based on small retrospective series from single institutions. The reason for this is there is still no consensus regarding the role of platelets in LT (*i.e.*, "Are platelets a friend or foe in LT?"). This fact has led to difficulty in conducting multi-institutional prospective trials to clarify the role of platelets in LT. Second, it is still difficult to prove whether thrombocytopenia is a "result" or a "cause" of postoperative complications. Many studies describe post-transplant thrombocytopenia as a phenomenon, but there has been no direct evidence that show whether thrombocytopenia is a cause or a result of poor graft function or complications. It is necessary to clarify this important point with basic animal experiments. Third, since thrombocytopenia is common after LT, it is still unclear how to determine which patients need platelet therapies to prevent postoperative complications and yield better outcomes. By conducting multi-institutional prospective trials, it is important to generate a standardized cut-off value to specify the target patients for platelet therapies.

CONCLUSION

We described convincing evidence of post-transplant thrombocytopenia and the role of platelets in LT and discussed future perspectives. The mechanisms of thrombocytopenia and its effect on postoperative outcomes are still not completely understood. Since platelets have both beneficial and detrimental effects on liver grafts, therapeutic strategies to increase perioperative platelet counts, such as the use of thrombopoietin, thrombopoietin receptor agonist, platelet transfusion, splenectomy, and intravenous immunoglobulin treatment, could be targeted to enhance the beneficial effects while minimizing potential detrimental effects.

REFERENCES

1 **Holinstat M**. Normal platelet function. *Cancer Metastasis Rev* 2017; **36**: 195-198 [PMID: 28667366 DOI: 10.1007/s10555-017-9677-x]
2 **Broos K**, Feys HB, De Meyer SF, Vanhoorelbeke K, Deckmyn H. Platelets at work in primary hemostasis. *Blood Rev* 2011; **25**: 155-167 [PMID: 21496978 DOI: 10.1016/j.blre.2011.03.002]
3 **Broos K**, De Meyer SF, Feys HB, Vanhoorelbeke K, Deckmyn H. Blood platelet biochemistry. *Thromb Res* 2012; **129**: 245-249 [PMID: 22119499 DOI: 10.1016/j.thromres.2011.11.002]
4 **Holmsen H**. Platelet metabolism and activation. *Semin Hematol* 1985; **22**: 219-240 [PMID: 2994234]
5 **McNicol A**, Israels SJ. Platelet dense granules: structure, function and implications for haemostasis. *Thromb Res* 1999; **95**: 1-18 [PMID: 10403682]
6 **Polasek J**. Platelet secretory granules or secretory lysosomes? *Platelets* 2005; **16**: 500-501 [PMID: 16287618 DOI: 10.1080/09537100500169926]
7 **Elzey BD**, Sprague DL, Ratliff TL. The emerging role of platelets in adaptive immunity. *Cell Immunol* 2005; **238**: 1-9 [PMID: 16442516 DOI: 10.1016/j.cellimm.2005.12.005]
8 **Yamaguchi R**, Terashima H, Yoneyama S, Tadano S, Ohkohchi N. Effects of platelet-rich plasma on intestinal anastomotic healing in rats: PRP concentration is a key factor. *J Surg Res* 2012; **173**: 258-266 [PMID: 21074782 DOI: 10.1016/j.jss.2010.10.001]
9 **Mehta P**. Potential role of platelets in the pathogenesis of tumor metastasis. *Blood* 1984; **63**: 55-63 [PMID: 6360248]
10 **Xu XR**, Zhang D, Oswald BE, Carrim N, Wang X, Hou Y, Zhang Q, Lavalle C, McKeown T, Marshall AH, Ni H. Platelets are versatile cells: New discoveries in hemostasis, thrombosis, immune responses, tumor metastasis and beyond. *Crit Rev Clin Lab Sci* 2016; **53**: 409-430 [PMID: 27282765 DOI: 10.1080/10408363.2016.1200008]
11 **Meirelles Júnior RF**, Salvalaggio P, Rezende MB, Evangelista

AS, Guardia BD, Matielo CE, Neves DB, Pandullo FL, Felga GE, Alves JA, Curvelo LA, Diaz LG, Rusi MB, Viveiros Mde M, Almeida MD, Pedroso PT, Rocco RA, Meira Filho SP. Liver transplantation: history, outcomes and perspectives. *Einstein (Sao Paulo)* 2015; **13**: 149-152 [PMID: 25993082 DOI: 10.1590/S1679-45082015RW3164]

12 **Abbasoglu O**. Liver transplantation: yesterday, today and tomorrow. *World J Gastroenterol* 2008; **14**: 3117-3122 [PMID: 18506914 DOI: 10.3748/wjg.14.3117]

13 **Carmona M,** Álvarez M, Marco J, Mahíllo B. Organ Donation and Transplantation Activities 2015 Report. Global Obsevatory on Donation and Transplantation World Health Organization, 2017

14 **Kim WR**, Lake JR, Smith JM, Skeans MA, Schladt DP, Edwards EB, Harper AM, Wainright JL, Snyder JJ, Israni AK, Kasiske BL. OPTN/SRTR 2015 Annual Data Report: Liver. *Am J Transplant* 2017; **17** Suppl 1: 174-251 [PMID: 28052604 DOI: 10.1111/ajt.14126]

15 **Munoz SJ**, Carabasi AR, Moritz MJ, Jarrell BE, Maddrey WC. Postoperative thrombocytopenia in liver transplant recipients: prognostic implications and treatment with high dose of gamma-globulin. *Transplant Proc* 1989; **21**: 3545-3546 [PMID: 2662521]

16 **Plevak DJ**, Halma GA, Forstrom LA, Dewanjee MK, O'Connor MK, Moore SB, Krom RA, Rettke SR. Thrombocytopenia after liver transplantation. *Transplant Proc* 1988; **20**: 630-633 [PMID: 3279654]

17 **McCaughan GW**, Herkes R, Powers B, Rickard K, Gallagher ND, Thompson JF, Sheil AG. Thrombocytopenia post liver transplantation. Correlations with pre-operative platelet count, blood transfusion requirements, allograft function and outcome. *J Hepatol* 1992; **16**: 16-22 [PMID: 1484150]

18 **Cywes R**, Mullen JB, Stratis MA, Greig PD, Levy GA, Harvey PR, Strasberg SM. Prediction of the outcome of transplantation in man by platelet adherence in donor liver allografts. Evidence of the importance of prepreservation injury. *Transplantation* 1993; **56**: 316-323 [PMID: 7689257]

19 **Nascimbene A**, Iannacone M, Brando B, De Gasperi A. Acute thrombocytopenia after liver transplant: role of platelet activation, thrombopoietin deficiency and response to high dose intravenous IgG treatment. *J Hepatol* 2007; **47**: 651-657 [PMID: 17716776 DOI: 10.1016/j.jhep.2007.06.012]

20 **Richards EM**, Alexander GJ, Calne RY, Baglin TP. Thrombocytopenia following liver transplantation is associated with platelet consumption and thrombin generation. *Br J Haematol* 1997; **98**: 315-321 [PMID: 9266927]

21 **Taylor RM**, Bockenstedt P, Su GL, Marrero JA, Pellitier SM, Fontana RJ. Immune thrombocytopenic purpura following liver transplantation: a case series and review of the literature. *Liver Transpl* 2006; **12**: 781-791 [PMID: 16628698 DOI: 10.1002/lt.20715]

22 **Kaneko J**, Sugawara Y, Tamura S, Togashi J, Matsui Y, Makuuchi M. Heparin-induced thrombocytopenia after liver transplantation. *Transplant Proc* 2008; **40**: 1518-1521 [PMID: 18589141 DOI: 10.1016/j.transproceed.2008.01.069]

23 **Hutchison DE**, Genton E, Porter KA, Daloze PM, Huguet C, Brettschneider L, Groth CG, Starzl TE. Platelet changes following clinical and experimental hepatic homotransplantation. *Arch Surg* 1968; **97**: 27-33 [PMID: 4232038]

24 **Chatzipetrou MA**, Tsaroucha AK, Weppler D, Pappas PA, Kenyon NS, Nery JR, Khan MF, Kato T, Pinna AD, O'Brien C, Viciana A, Ricordi C, Tzakis AG. Thrombocytopenia after liver transplantation. *Transplantation* 1999; **67**: 702-706 [PMID: 10096525]

25 **Chang FY**, Singh N, Gayowski T, Wagener MM, Mietzner SM, Stout JE, Marino IR. Thrombocytopenia in liver transplant recipients: predictors, impact on fungal infections, and role of endogenous thrombopoietin. *Transplantation* 2000; **69**: 70-75 [PMID: 10653383]

26 **Ben Hamida C**, Lauzet JY, Rézaiguia-Delclaux S, Duvoux C, Cherqui D, Duvaldestin P, Stéphan F. Effect of severe thrombocytopenia on patient outcome after liver transplantation. *Intensive Care Med* 2003; **29**: 756-762 [PMID: 12677370 DOI: 10.1007/s00134-003-1727-x]

27 **Sonny A**, Kelly D, Hammel JP, Albeldawi M, Zein N, Cywinski JB. Predictors of poor outcome among older liver transplant recipients. *Clin Transplant* 2015; **29**: 197-203 [PMID: 25528882 DOI: 10.1111/ctr.12500]

28 **Lesurtel M**, Raptis DA, Melloul E, Schlegel A, Oberkofler C, El-Badry AM, Weber A, Mueller N, Dutkowski P, Clavien PA. Low platelet counts after liver transplantation predict early posttransplant survival: the 60-5 criterion. *Liver Transpl* 2014; **20**: 147-155 [PMID: 24123804 DOI: 10.1002/lt.23759]

29 **Takahashi K**, Nagai S, Putchakayala KG, Safwan M, Li AY, Kane WJ, Singh PL, Collins KM, Rizzari MD, Yoshida A, Schnickel GT, Abouljoud MS. Prognostic impact of postoperative low platelet count after liver transplantation. *Clin Transplant* 2017; **31**: [PMID: 27992667 DOI: 10.1111/ctr.12891]

30 **Takahashi K**, Nagai S, Putchakayala KG, Safwan M, Gosho M, Li AY, Kane WJ, Singh PL, Rizzari MD, Collins KM, Yoshida A, Abouljoud MS, Schnickel GT. Prediction of biliary anastomotic stricture after deceased donor liver transplantation: the impact of platelet counts - a retrospective study. *Transpl Int* 2017; **30**: 1032-1040 [PMID: 28605573 DOI: 10.1111/tri.12996]

31 **Gwiasda J**, Schrem H, Klempnauer J, Kaltenborn A. Identifying independent risk factors for graft loss after primary liver transplantation. *Langenbecks Arch Surg* 2017; **402**: 757-766 [PMID: 28573420 DOI: 10.1007/s00423-017-1594-5]

32 **Zahr Eldeen F**, Roll GR, Derosas C, Rao R, Khan MS, Gunson BK, Hodson J, Mergental H, Ferraz-Neto BH, Isaac J, Muiesan P, Mirza DF, Iqbal A, Perera MT. Preoperative Thromboelastography as a Sensitive Tool Predicting Those at Risk of Developing Early Hepatic Artery Thrombosis After Adult Liver Transplantation. *Transplantation* 2016; **100**: 2382-2390 [PMID: 27780186 DOI: 10.1097/TP.0000000000001395]

33 **Hisakura K**, Murata S, Fukunaga K, Myronovych A, Tadano S, Kawasaki T, Kohno K, Ikeda O, Pak S, Ikeda N, Nakano Y, Matsuo R, Konno K, Kobayashi E, Saito T, Yasue H, Ohkohchi N. Platelets prevent acute liver damage after extended hepatectomy in pigs. *J Hepatobiliary Pancreat Sci* 2010; **17**: 855-864 [PMID: 20734209 DOI: 10.1007/s00534-010-0276-2]

34 **Taki-Eldin A**, Zhou L, Xie HY, Zheng SS. Liver regeneration after liver transplantation. *Eur Surg Res* 2012; **48**: 139-153 [PMID: 22572792 DOI: 10.1159/000337865]

35 **Hua ZY**, Song J, Cheng F, Yu Y, Gao Y, Yao A, Wang X. The effect of hepatocyte growth factor on the initiation phase of liver regeneration after cold ischemia in a rat model of small-for-size liver transplantation. *Hepatogastroenterology* 2012; **59**: 1548-1552 [PMID: 22683971 DOI: 10.5754/hge10485]

36 **Haga J**, Shimazu M, Wakabayashi G, Tanabe M, Kawachi S, Fuchimoto Y, Hoshino K, Morikawa Y, Kitajima M, Kitagawa Y. Liver regeneration in donors and adult recipients after living donor liver transplantation. *Liver Transpl* 2008; **14**: 1718-1724 [PMID: 19025926 DOI: 10.1002/lt.21622]

37 **Michalopoulos GK**. Liver regeneration. *J Cell Physiol* 2007; **213**: 286-300 [PMID: 17559071 DOI: 10.1002/jcp.21172]

38 **Fausto N**, Campbell JS, Riehle KJ. Liver regeneration. *J Hepatol* 2012; **57**: 692-694 [PMID: 22613006 DOI: 10.1016/j.jhep.2012.04.016]

39 **Murata S,** Ohkohchi N, Abe T, Enomoto Y, Doi H, Samomi S. Platelets promote G1-S progression of liver regeneration after hepatectomy. Congress of the European Society for Surgical Research 2004; 107-112

40 **Lesurtel M**, Graf R, Aleil B, Walther DJ, Tian Y, Jochum W, Gachet C, Bader M, Clavien PA. Platelet-derived serotonin mediates liver regeneration. *Science* 2006; **312**: 104-107 [PMID: 16601191 DOI: 10.1126/science.1123842]

41 **Takahashi K**, Kozuma Y, Suzuki H, Tamura T, Maruyama T, Fukunaga K, Murata S, Ohkohchi N. Human platelets promote liver regeneration with Kupffer cells in SCID mice. *J Surg Res* 2013; **180**: 62-72 [PMID: 23260232 DOI: 10.1016/j.jss.2012.11.030]

42 **Kawasaki T**, Murata S, Takahashi K, Nozaki R, Ohshiro Y, Ikeda

N, Pak S, Myronovych A, Hisakura K, Fukunaga K, Oda T, Sasaki R, Ohkohchi N. Activation of human liver sinusoidal endothelial cell by human platelets induces hepatocyte proliferation. *J Hepatol* 2010; **53**: 648-654 [PMID: 20615569 DOI: 10.1016/j.jhep.2010.04.021]

43 **Murata S**, Ohkohchi N, Matsuo R, Ikeda O, Myronovych A, Hoshi R. Platelets promote liver regeneration in early period after hepatectomy in mice. *World J Surg* 2007; **31**: 808-816 [PMID: 17354025 DOI: 10.1007/s00268-006-0772-3]

44 **Matsuo R**, Nakano Y, Ohkohchi N. Platelet administration via the portal vein promotes liver regeneration in rats after 70% hepatectomy. *Ann Surg* 2011; **253**: 759-763 [PMID: 21475016 DOI: 10.1097/SLA.0b013e318211caf8]

45 **Myronovych A**, Murata S, Chiba M, Matsuo R, Ikeda O, Watanabe M, Hisakura K, Nakano Y, Kohno K, Kawasaki T, Hashimoto I, Shibasaki Y, Yasue H, Ohkohchi N. Role of platelets on liver regeneration after 90% hepatectomy in mice. *J Hepatol* 2008; **49**: 363-372 [PMID: 18602717 DOI: 10.1016/j.jhep.2008.04.019]

46 **Sindram D**, Porte RJ, Hoffman MR, Bentley RC, Clavien PA. Synergism between platelets and leukocytes in inducing endothelial cell apoptosis in the cold ischemic rat liver: a Kupffer cell-mediated injury. *FASEB J* 2001; **15**: 1230-1232 [PMID: 11344097]

47 **Kim J**, Yi NJ, Shin WY, Kim T, Lee KU, Suh KS. Platelet transfusion can be related to liver regeneration after living donor liver transplantation. *World J Surg* 2010; **34**: 1052-1058 [PMID: 20151125 DOI: 10.1007/s00268-010-0464-x]

48 **Han S**, Park HW, Song JH, Gwak MS, Lee WJ, Kim G, Lee SK, Ko JS. Association Between Intraoperative Platelet Transfusion and Early Graft Regeneration in Living Donor Liver Transplantation. *Ann Surg* 2016; **264**: 1065-1072 [PMID: 26720430 DOI: 10.1097/SLA.0000000000001526]

49 **Li L**, Wang H, Yang J, Jiang L, Yang J, Wang W, Yan L, Wen T, Li B, Xu M. Immediate Postoperative Low Platelet Counts After Living Donor Liver Transplantation Predict Early Allograft Dysfunction. *Medicine* (Baltimore) 2015; **94**: e1373 [PMID: 26313775 DOI: 10.1097/MD.0000000000001373]

50 **Pamecha V**, Mahansaria SS, Kumar S, Bharathy KG, Sasturkar SV, Sinha PK, Kumar N, Kumar V. Association of thrombocytopenia with outcome following adult living donor liver transplantation. *Transpl Int* 2016; **29**: 1126-1135 [PMID: 27429066 DOI: 10.1111/tri.12819]

51 **Akamatsu N**, Sugawara Y, Kanako J, Arita J, Sakamoto Y, Hasegawa K, Kokudo N. Low Platelet Counts and Prolonged Prothrombin Time Early After Operation Predict the 90 Days Morbidity and Mortality in Living-donor Liver Transplantation. *Ann Surg* 2017; **265**: 166-172 [PMID: 28009742 DOI: 10.1097/SLA.0000000000001634]

52 **Takahashi K**, Kurokawa T, Oshiro Y, Fukunaga K, Sakashita S, Ohkohchi N. Postoperative Decrease in Platelet Counts Is Associated with Delayed Liver Function Recovery and Complications after Partial Hepatectomy. *Tohoku J Exp Med* 2016; **239**: 47-55 [PMID: 27181573 DOI: 10.1620/tjem.239.47]

53 **Lisman T**, Leebeek FW, de Groot PG. Haemostatic abnormalities in patients with liver disease. *J Hepatol* 2002; **37**: 280-287 [PMID: 12127437]

54 **Lisman T**, Adelmeijer J, de Groot PG, Janssen HL, Leebeek FW. No evidence for an intrinsic platelet defect in patients with liver cirrhosis--studies under flow conditions. *J Thromb Haemost* 2006; **4**: 2070-2072 [PMID: 16836657 DOI: 10.1111/j.1538-7836.2006.02122.x]

55 **Himmelreich G**, Hundt K, Neuhaus P, Roissant R, Riess H. Decreased platelet aggregation after reperfusion in orthotopic liver transplantation. *Transplantation* 1992; **53**: 582-586 [PMID: 1549850]

56 **Himmelreich G**, Hundt K, Isenberg C, Bechstein WO, Neuhaus P, Riess H. Thrombocytopenia and platelet dysfunction in orthotopic liver transplantation. *Semin Thromb Hemost* 1993; **19**: 209-212 [PMID: 8362249 DOI: 10.1055/s-2007-994027]

57 **Jüttner B**, Brock J, Weissig A, Becker T, Studzinski A, Osthaus WA, Bornscheuer A, Scheinichen D. Dependence of platelet function on underlying liver disease in orthotopic liver transplantation. *Thromb Res* 2009; **124**: 433-438 [PMID: 19616824 DOI: 10.1016/j.thromres.2009.06.011]

58 **Eyraud D,** Gostian O, Gossem P. Does liver transplantation affect platelet function? *Euro J Anaesth* 2011; **28**: 87-88

59 **Vivarelli M**, La Barba G, Cucchetti A, Lauro A, Del Gaudio M, Ravaioli M, Grazi GL, Pinna AD. Can antiplatelet prophylaxis reduce the incidence of hepatic artery thrombosis after liver transplantation? *Liver Transpl* 2007; **13**: 651-654 [PMID: 17457885 DOI: 10.1002/lt.21028]

60 **Shay R**, Taber D, Pilch N, Meadows H, Tischer S, McGillicuddy J, Bratton C, Baliga P, Chavin K. Early aspirin therapy may reduce hepatic artery thrombosis in liver transplantation. *Transplant Proc* 2013; **45**: 330-334 [PMID: 23267805 DOI: 10.1016/j.transproceed.2012.05.075]

61 **Poujol-Robert A**, Boëlle PY, Conti F, Durand F, Duvoux C, Wendum D, Paradis V, Mackiewicz V, Chazouillères O, Corpechot C, Poupon R. Aspirin may reduce liver fibrosis progression: Evidence from a multicenter retrospective study of recurrent hepatitis C after liver transplantation. *Clin Res Hepatol Gastroenterol* 2014; **38**: 570-576 [PMID: 25130796 DOI: 10.1016/j.clinre.2014.07.004]

62 **Lee PC**, Yeh CM, Hu YW, Chen CC, Liu CJ, Su CW, Huo TI, Huang YH, Chao Y, Chen TJ, Lin HC, Wu JC. Antiplatelet Therapy is Associated with a Better Prognosis for Patients with Hepatitis B Virus-Related Hepatocellular Carcinoma after Liver Resection. *Ann Surg Oncol* 2016; **23**: 874-883 [PMID: 27541812 DOI: 10.1245/s10434-016-5520-9]

63 **Sitia G**, Aiolfi R, Di Lucia P, Mainetti M, Fiocchi A, Mingozzi F, Esposito A, Ruggeri ZM, Chisari FV, Iannacone M, Guidotti LG. Antiplatelet therapy prevents hepatocellular carcinoma and improves survival in a mouse model of chronic hepatitis B. *Proc Natl Acad Sci USA* 2012; **109**: E2165-E2172 [PMID: 22753481 DOI: 10.1073/pnas.1209182109]

64 **Sahasrabuddhe VV**, Gunja MZ, Graubard BI, Trabert B, Schwartz LM, Park Y, Hollenbeck AR, Freedman ND, McGlynn KA. Nonsteroidal anti-inflammatory drug use, chronic liver disease, and hepatocellular carcinoma. *J Natl Cancer Inst* 2012; **104**: 1808-1814 [PMID: 23197492 DOI: 10.1093/jnci/djs452]

65 **Giannini EG**. Review article: thrombocytopenia in chronic liver disease and pharmacologic treatment options. *Aliment Pharmacol Ther* 2006; **23**: 1055-1065 [PMID: 16611265 DOI: 10.1111/j.1365-2036.2006.02889.x]

66 **Afdhal N**, McHutchison J, Brown R, Jacobson I, Manns M, Poordad F, Weksler B, Esteban R. Thrombocytopenia associated with chronic liver disease. *J Hepatol* 2008; **48**: 1000-1007 [PMID: 18433919 DOI: 10.1016/j.jhep.2008.03.009]

67 **Peck-Radosavljevic M**. Thrombocytopenia in chronic liver disease. *Liver Int* 2017; **37**: 778-793 [PMID: 27860293 DOI: 10.1111/liv.13317]

68 **Williams R**, O'Grady JG. Liver transplantation: results, advances and problems. *J Gastroenterol Hepatol* 1990; **5** Suppl 1: 110-126 [PMID: 2103420]

69 **Kalayoglu M**, Sollinger HW, Stratta RJ, D'Alessandro AM, Hoffmann RM, Pirsch JD, Belzer FO. Extended preservation of the liver for clinical transplantation. *Lancet* 1988; **1**: 617-619 [PMID: 2894550]

70 **Porte RJ**, Blauw E, Knot EA, de Maat MP, de Ruiter C, Minke Bakker C, Terpstra OT. Role of the donor liver in the origin of platelet disorders and hyperfibrinolysis in liver transplantation. *J Hepatol* 1994; **21**: 592-600 [PMID: 7814807]

71 **Nobuoka Y**, Wada H, Mizuno S, Kishiwada M, Usui M, Sakurai H, Tabata M, Kobayashi T, Nobori T, Uemoto S, Isaji S. Prolonged thrombocytopenia after living donor liver transplantation is a strong prognostic predictor irrespective of splenectomy: the significance of ADAMTS13 and graft function [corrected]. *Int J Hematol* 2014; **99**: 418-428 [PMID: 24595551 DOI: 10.1007/s12185-014-1543-9]

72 **Nakanuma S**, Miyashita T, Hayashi H, Tajima H, Takamura H, Tsukada T, Okamoto K, Sakai S, Makino I, Kinoshita J, Nakamura K, Oyama K, Inokuchi M, Nakagawara H, Ninomiya I, Kitagawa H,

Fushida S, Fujimura T, Ohta T. Extravasated platelet aggregation in liver zone 3 may correlate with the progression of sinusoidal obstruction syndrome following living donor liver transplantation: A case report. *Exp Ther Med* 2015; **9**: 1119-1124 [PMID: 25780397 DOI: 10.3892/etm.2015.2245]

73 **Shimada Y**, Kato T, Ogami K, Horie K, Kokubo A, Kudo Y, Maeda E, Sohma Y, Akahori H, Kawamura K. Production of thrombopoietin (TPO) by rat hepatocytes and hepatoma cell lines. *Exp Hematol* 1995; **23**: 1388-1396 [PMID: 7498368]

74 **Richards EM**, Alexander GJ, Nichol JL, Baglin TP. Serum thrombopoietin levels following orthotopic liver transplantation. *Thromb Haemost* 1997; **78**: 1420-1421 [PMID: 9408033]

75 **Peck-Radosavljevic M**, Wichlas M, Zacherl J, Stiegler G, Stohlawetz P, Fuchsjäger M, Kreil A, Metz-Schimmerl S, Panzer S, Steininger R, Mühlbacher F, Ferenci P, Pidlich J, Gangl A. Thrombopoietin induces rapid resolution of thrombocytopenia after orthotopic liver transplantation through increased platelet production. *Blood* 2000; **95**: 795-801 [PMID: 10648388]

76 **Usui M,** Wada H, Mizuno S, Isaji S. Platelet activation and liver transplantation. *J Liver* 2017; 6 [DOI: 10.4172/2167-0889.1000210]

77 **Tredger JM**, Brown NW, Adams J, Gonde CE, Dhawan A, Rela M, Heaton N. Monitoring mycophenolate in liver transplant recipients: toward a therapeutic range. *Liver Transpl* 2004; **10**: 492-502 [PMID: 15048791 DOI: 10.1002/lt.20124]

78 **Danesi R**, Del Tacca M. Hematologic toxicity of immunosuppressive treatment. *Transplant Proc* 2004; **36**: 703-704 [PMID: 15110637 DOI: 10.1016/j.transproceed.2004.03.016]

79 **Lee CH**, Chen CL, Lin CC, Yang CH, Cheng YF, Wang MC, Eng HL, Liu PP, Chuang FR. Plasma exchange therapy for thrombotic thrombocytopenic purpura in pediatric patients with liver transplantation. *Transplant Proc* 2008; **40**: 2554-2556 [PMID: 18929799 DOI: 10.1016/j.transproceed.2008.07.011]

80 **Nwaba A**, MacQuillan G, Adams LA, Garas G, Delriviere L, Augustson B, DeBoer B, Moody H, Jeffrey GP. Tacrolimus-induced thrombotic microangiopathy in orthotopic liver transplant patients: case series of four patients. *Intern Med J* 2013; **43**: 328-333 [PMID: 23441660 DOI: 10.1111/imj.12048]

81 **Rerolle JP**, Akposso K, Lerolle N, Mougenot B, Ponnelle T, Rondeau E, Sraer JD. Tacrolimus-induced hemolytic uremic syndrome and end-stage renal failure after liver transplantation. *Clin Transplant* 2000; **14**: 262-265 [PMID: 10831087]

82 **Bakchoul T**, Assfalg V, Zöllner H, Evert M, Novotny A, Matevossian E, Friess H, Hartmann D, Hron G, Althaus K, Greinacher A, Hüser N. Anti-platelet factor 4/heparin antibodies in patients with impaired graft function after liver transplantation. *J Thromb Haemost* 2014; **12**: 871-878 [PMID: 24655935 DOI: 10.1111/jth.12569]

83 **Bachmann R**, Bachmann J, Lange J, Nadalin S, Königsrainer A, Ladurner R. Incidence of heparin-induced thrombocytopenia type II and postoperative recovery of platelet count in liver graft recipients: a retrospective cohort analysis. *J Surg Res* 2014; **186**: 429-435 [PMID: 24100055 DOI: 10.1016/j.jss.2013.08.034]

84 **Pannicke N**, Pollok JM, Kluge S, Petzoldt M. Heparin-induced thrombocytopenia associated with acute liver graft failure. *BMJ Case Rep* 2012; **2012**: [PMID: 23188860 DOI: 10.1136/bcr-2012-007323]

85 **Hüser N**, Aßfalg V, Reim D, Novotny A, Thorban S, Cheng Z, Kornberg A, Friess H, Büchler P, Matevossian E. Heparin-induced thrombocytopenia (HIT II) in liver transplant recipients: a retrospective multivariate analysis of prognostic factors. *Transpl Int* 2012; **25**: 739-747 [PMID: 22548256 DOI: 10.1111/j.1432-2277.2012.01486.x]

86 **Moicean AD**, Popp AM, Sinescu I. Thymoglobulin--new approaches to optimal outcomes. *J Med Life* 2009; **2**: 319-324 [PMID: 20112478]

87 **Lazarchick J**, Russell R, Horn B. Anti-thymocyte globulin induced thrombocytopenia. *Ann Clin Lab Sci* 1990; **20**: 373-378 [PMID: 2073086]

88 **Ankersmit HJ**, Roth GA, Moser B, Zuckermann A, Brunner M, Rosin C, Buchta C, Bielek E, Schmid W, Jensen-Jarolim E, Wolner E, Boltz-Nitulescu G, Volf I. CD32-mediated platelet aggregation in vitro by anti-thymocyte globulin: implication of therapy-induced in vivo thrombocytopenia. *Am J Transplant* 2003; **3**: 754-759 [PMID: 12780568]

89 **Gabardi S**, Magee CC, Baroletti SA, Powelson JA, Cina JL, Chandraker AK. Efficacy and safety of low-dose valganciclovir for prevention of cytomegalovirus disease in renal transplant recipients: a single-center, retrospective analysis. *Pharmacotherapy* 2004; **24**: 1323-1330 [PMID: 15628830]

90 **Hayashi M**, Strouse JJ, Veltri MA, Curtis BR, Takemoto CM. Immune thrombocytopenia due to Trimethoprim-Sulfamethoxazole; under-recognized adverse drug reaction in children? *Pediatr Blood Cancer* 2015; **62**: 922-923 [PMID: 25683320 DOI: 10.1002/pbc.25430]

91 **Piano S**, Gatta A, Angeli P. Immune thrombocytopenic purpura and Kaposi's sarcoma in a liver transplant recipient. *Transpl Int* 2012; **25**: e50-e52 [PMID: 22417011 DOI: 10.1111/j.1432-2277.2011.01424.x]

92 **Rosoff PM**, Tuttle-Newhall E, Treem WR. Successful treatment of immune thrombocytopenic purpura with anti-D antibody following a cadaveric liver transplant for hepatoblastoma. *Med Pediatr Oncol* 2003; **40**: 402-404 [PMID: 12692815 DOI: 10.1002/mpo.10243]

93 **Assy N**, Rosenthal E, Hazani A, Etzioni A, Baruch Y. Human parvovirus B19 infection associated with idiopathic thrombocytopenic purpura in a child following liver transplantation. *J Hepatol* 1997; **27**: 934-936 [PMID: 9382984]

94 **Singh N**, Gayowski T, Yu VL. Herpes zoster-associated idiopathic thrombocytopenic purpura in a liver transplant recipient: a case report and overview. *Transpl Int* 1995; **8**: 58-60 [PMID: 7888054]

95 **Takatsuki M**, Uemoto S, Kurokawa T, Koshiba T, Inomata Y, Tanaka K. Idiopathic thrombocytopenic purpura after a living-related liver transplantation. *Transplantation* 1999; **67**: 479-481 [PMID: 10030298]

96 **Gupta RK**, Gupta G, Chorasiya VK, Bag P, Shandil R, Bhatia V, Wadhawan M, Vij V, Kumar A. Dengue Virus Transmission from Living Donor to Recipient in Liver Transplantation: A Case Report. *J Clin Exp Hepatol* 2016; **6**: 59-61 [PMID: 27194898 DOI: 10.1016/j.jceh.2016.01.005]

97 **Arnold JC**, Heilig B, Otto G, Kommerell B, Theilmann L. Cytomegalovirus-induced severe thrombocytopenia after liver transplantation. *Transplantation* 1993; **56**: 1286-1288 [PMID: 8249141]

98 **Maar E,** Porte R, Harmsen M, Son W, Berg A, Slooff MJ, Nijsten M. Decreased platelet count precedes CMV antigenemia after liver transplantation. University of Groningen 2003; 129-138

99 **Miyata T**, Yokoyama I, Todo S, Tzakis A, Selby R, Starzl TE. Endotoxaemia, pulmonary complications, and thrombocytopenia in liver transplantation. *Lancet* 1989; **2**: 189-191 [PMID: 2568522]

100 **de Boer MT**, Christensen MC, Asmussen M, van der Hilst CS, Hendriks HG, Slooff MJ, Porte RJ. The impact of intraoperative transfusion of platelets and red blood cells on survival after liver transplantation. *Anesth Analg* 2008; **106**: 32-44, table of contents [PMID: 18165548 DOI: 10.1213/01.ane.0000289638.26666.ed]

101 **Pereboom IT**, de Boer MT, Haagsma EB, Hendriks HG, Lisman T, Porte RJ. Platelet transfusion during liver transplantation is associated with increased postoperative mortality due to acute lung injury. *Anesth Analg* 2009; **108**: 1083-1091 [PMID: 19299765 DOI: 10.1213/ane.0b013e3181948a59]

102 **Chin JL**, Hisamuddin SH, O'Sullivan A, Chan G, McCormick PA. Thrombocytopenia, Platelet Transfusion, and Outcome Following Liver Transplantation. *Clin Appl Thromb Hemost* 2016; **22**: 351-360 [PMID: 25430936 DOI: 10.1177/1076029614559771]

103 **Nacoti M**, Cazzaniga S, Colombo G, Corbella D, Fazzi F, Fochi O, Gattoni C, Zambelli M, Colledan M, Bonanomi E. Postoperative complications in cirrhotic pediatric deceased donor liver transplantation: Focus on transfusion therapy. *Pediatr Transplant* 2017; **21** [PMID: 28681471 DOI: 10.1111/petr.13020]

104 **Nixon C**, Gunn K, Main T, Young Y, McCall J. Platelets and survival after liver transplantation. *Anesth Analg* 2009; **108**: 1354-1355; author reply 1355 [PMID: 19299817 DOI: 10.1213/ane.0b013e318197c7c7]

105 **Li C**, Mi K, Wen TF, Yan LN, Li B, Wei YG, Yang JY, Xu MQ, Wang WT. Risk factors and outcomes of massive red blood cell transfusion following living donor liver transplantation. *J Dig Dis* 2012; **13**: 161-167 [PMID: 22356311 DOI: 10.1111/j.1751-2980.2011.00570.x]

106 **Nogami K**. The utility of thromboelastography in inherited and acquired bleeding disorders. *Br J Haematol* 2016; **174**: 503-514 [PMID: 27264484 DOI: 10.1111/bjh.14148]

107 **Lawson PJ**, Moore HB, Moore EE, Stettler GR, Pshak TJ, Kam I, Silliman CC, Nydam TL. Preoperative thrombelastography maximum amplitude predicts massive transfusion in liver transplantation. *J Surg Res* 2017; **220**: 171-175 [PMID: 29180179 DOI: 10.1016/j.jss.2017.05.115]

108 **Trautman CL**, Palmer WC, Taner CB, Canabal JM, Getz T, Goldman A, Heckman MG, Diehl NN, Lee DD, Stancampiano FF. Thromboelastography as a Predictor of Outcomes Following Liver Transplantation. *Transplant Proc* 2017; **49**: 2110-2116 [PMID: 29149970 DOI: 10.1016/j.transproceed.2017.07.015]

109 **Kang YG**, Martin DJ, Marquez J, Lewis JH, Bontempo FA, Shaw BW Jr, Starzl TE, Winter PM. Intraoperative changes in blood coagulation and thrombelastographic monitoring in liver transplantation. *Anesth Analg* 1985; **64**: 888-896 [PMID: 3896028]

110 **Krzanicki D**, Sugavanam A, Mallett S. Intraoperative hypercoagulability during liver transplantation as demonstrated by thromboelastography. *Liver Transpl* 2013; **19**: 852-861 [PMID: 23696318 DOI: 10.1002/lt.23668]

111 **Wikkelsoe AJ**, Afshari A, Wetterslev J, Brok J, Moeller AM. Monitoring patients at risk of massive transfusion with Thrombelastography or Thromboelastometry: a systematic review. *Acta Anaesthesiol Scand* 2011; **55**: 1174-1189 [PMID: 22092122 DOI: 10.1111/j.1399-6576.2011.02534.x]

112 **Marubashi S**, Dono K, Miyamoto A, Takeda Y, Nagano H, Umeshita K, Monden M. Impact of graft size on postoperative thrombocytopenia in living donor liver transplant. *Arch Surg* 2007; **142**: 1054-1058 [PMID: 18025333 DOI: 10.1001/archsurg.142.11.1054]

113 **Li DW**, Du CY, Fan B, Huang P, Luo SQ, He Q. Impact of simultaneous splenectomy and orthotopic liver transplantation in patients with end-stage liver diseases and splenic hyperfunction. *Hepatobiliary Pancreat Dis Int* 2012; **11**: 489-493 [PMID: 23060393]

114 **Chu HC**, Hsieh CB, Hsu KF, Fan HL, Hsieh TY, Chen TW. Simultaneous splenectomy during liver transplantation augments anti-viral therapy in patients infected with hepatitis C virus. *Am J Surg* 2015; **209**: 180-186 [PMID: 24928331 DOI: 10.1016/j.amjsurg.2014.03.004]

115 **Rysmakhanov M**, Doskali M, Taganova A, Kulmagambetov A, Smagulov A, Seidakhmetov A, Baigenzhin A, Doskaliyev Z. Splenic Artery Embolization in Patients After Orthotopic Liver Transplant. *Exp Clin Transplant* 2015; **13** Suppl 3: 52-54 [PMID: 26640912 DOI: 10.6002/ect.tdtd2015.O43]

116 **Ito K**, Akamatsu N, Ichida A, Ito D, Kaneko J, Arita J, Sakamoto Y, Hasegawa K, Kokudo N. Splenectomy is not indicated in living donor liver transplantation. *Liver Transpl* 2016; **22**: 1526-1535 [PMID: 27253521 DOI: 10.1002/lt.24489]

117 **Morimoto H**, Ishiyama K, Ishifuro M, Ohira M, Ide K, Tanaka Y, Tahara H, Teraoka Y, Yamashita M, Abe T, Hashimoto S, Hirata F, Tanimine N, Saeki Y, Shimizu S, Sakai H, Yano T, Tashiro H, Ohdan H. Clinical efficacy of simultaneous splenectomy in liver transplant recipients with hepatitis C virus. *Transplant Proc* 2014; **46**: 770-773 [PMID: 24767345 DOI: 10.1016/j.transproceed.2013.12.034]

118 **Takahashi Y**, Matsuura T, Yanagi Y, Yoshimaru K, Taguchi T. The role of splenectomy before liver transplantation in biliary atresia patients. *J Pediatr Surg* 2016; **51**: 2095-2098 [PMID: 27720430 DOI: 10.1016/j.jpedsurg.2016.09.048]

119 **Murata S**, Hashimoto I, Nakano Y, Myronovych A, Watanabe M, Ohkohchi N. Single administration of thrombopoietin prevents progression of liver fibrosis and promotes liver regeneration after partial hepatectomy in cirrhotic rats. *Ann Surg* 2008; **248**: 821-828 [PMID: 18948810 DOI: 10.1097/SLA.0b013e31818584c7]

120 **Watanabe M**, Murata S, Hashimoto I, Nakano Y, Ikeda O, Aoyagi Y, Matsuo R, Fukunaga K, Yasue H, Ohkohchi N. Platelets contribute to the reduction of liver fibrosis in mice. *J Gastroenterol Hepatol* 2009; **24**: 78-89 [PMID: 18624898 DOI: 10.1111/j.1440-1746.2008.05497.x]

121 **Schipperus M**, Fijnheer R. New therapeutic options for immune thrombocytopenia. *Neth J Med* 2011; **69**: 480-485 [PMID: 22173361]

122 **Bode AP**, Fischer TH. Lyophilized platelets: fifty years in the making. *Artif Cells Blood Substit Immobil Biotechnol* 2007; **35**: 125-133 [PMID: 17364477 DOI: 10.1080/10731190600974962]

123 **Okamura Y**, Takeoka S, Eto K, Maekawa I, Fujie T, Maruyama H, Ikeda Y, Handa M. Development of fibrinogen gamma-chain peptide-coated, adenosine diphosphate-encapsulated liposomes as a synthetic platelet substitute. *J Thromb Haemost* 2009; **7**: 470-477 [PMID: 19143920 DOI: 10.1111/j.1538-7836.2008.03269.x]

124 **Hoshi R**, Murata S, Matsuo R, Myronovych A, Hashimoto I, Ikeda H, Ohkohchi N. Freeze-dried platelets promote hepatocyte proliferation in mice. *Cryobiology* 2007; **55**: 255-260 [PMID: 17936259 DOI: 10.1016/j.cryobiol.2007.08.007]

P- Reviewer: Rodriguez-Peralvarez ML, Stanciu C **S- Editor**: Ma YJ
L- Editor: A **E- Editor**: Huang Y

World Journal of Gastroenterology

Submit a Manuscript: http://www.f6publishing.com

World J Gastroenterol 2018 April 7; 24(13): 1398-1409

DOI: 10.3748/wjg.v24.i13.1398

ISSN 1007-9327 (print) ISSN 2219-2840 (online)

ORIGINAL ARTICLE

Basic Study

Systems pharmacology approach reveals the antiinflammatory effects of *Ampelopsis grossedentata* on dextran sodium sulfate-induced colitis

You-Lan Chen, Ya-Li Zhang, Yan-Cheng Dai, Zhi-Peng Tang

You-Lan Chen, Ya-Li Zhang, Zhi-Peng Tang, Institute of Digestive Disease, Longhua Hospital, Shanghai University of Traditional Chinese Medicine, Shanghai 200032, China

You-Lan Chen, Yan-Cheng Dai, Zhi-Peng Tang, Department of Gastroenterology, Longhua Hospital Affiliated to Shanghai University of Traditional Chinese Medicine, Shanghai 200032, China

ORCID number: You-Lan Chen (0000-0002-4304-5693); Ya-Li Zhang (0000-0002-3538-9832); Yan-Cheng Dai (0000-0001-9919-4033); Zhi-Peng Tang (0000-0001-5695-8072).

Author contributions: Chen YL performed the majority of experiments and drafted the paper; Zhang YL participated in the treatment of animals; Dai YC analyzed the data; Tang ZP designed and coordinated the research; all authors have approved the final version of the article to be published.

Institutional review board statement: This study was reviewed and approved by the Institutional Review Board of Institute of Digestive Disease, Longhua Hospital, Shanghai University of Traditional Chinese Medicine, Shanghai, China.

Institutional animal care and use committee statement: All procedures involving animals were reviewed and approved by the Institutional Animal Care and Use Committee of Shanghai University of Traditional Chinese Medicine (IACUC Protocol Approval Number: SZY201710004).

Conflict-of-interest statement: The authors declare that there are no conflicts of interest related to this study.

Data sharing statement: Supplementary data accompanying this paper are included in the Supplementary information file.

Manuscript source: Unsolicited manuscript

Correspondence to: Zhi-Peng Tang, MD, PhD, Professor, Director, Institute of Digestive Disease, Longhua Hospital, Shanghai University of Traditional Chinese Medicine, No. 725 South Wanping Road, Shanghai 200032, China. zhipengtang@sohu.com
Telephone:+86-21-64385700
Fax: +86-21-64385700

Received: January 27, 2018
Peer-review started: January 28, 2018
First decision: February 10, 2018
Revised: February 12, 2018
Accepted: March 3, 2018
Article in press: March 3, 2018
Published online: April 7, 2018

Abstract

AIM

To investigate the protective effects of *Ampelopsis grossedentata* (AMP) on dextran sulfate sodium (DSS)-induced colitis in mice based on systems pharmacology approach.

METHODS

Systems pharmacology approach was used to predict the active ingredients, candidate targets and the efficacy of AMP on ulcerative colitis (UC) using a holistic process of active compound screening, target fishing, network construction and analysis. A DSS-induced colitis model in C57BL/6 mice (n = 10/group) was constructed and treated with 5-aminosalicylic acid (100 mg/kg/d) and AMP (400 mg/kg/d) to confirm

the underlying mechanisms and effects of AMP on UC with western blot analyses, polymerase chain reaction, histological staining and immunohistochemistry.

RESULTS

The therapeutic effects of AMP against DSS-induced colitis were determined in the beginning, and the results showed that AMP significantly improved the disease in general observations and histopathology analysis. Subsequent systems pharmacology predicted 89 corresponding targets for the four candidate compounds of AMP, as well as 123 candidate targets of UC, and protein-protein interaction networks were constructed for the interaction of putative targets of AMP against UC. Enrichment analyses on TNF-α and RANKL/RANK, a receptor activator of NF-κB signaling pathways, were then carried out. Experimental validation revealed that inflammation-related signaling pathways were activated in the DSS group, and AMP significantly suppressed DSS-induced high expression of IRAK1, TRAF6, IκB and NF-κB, and inhibited the elevated expression levels of TNF-α, IL-1β, IL-6 and IL-8.

CONCLUSION

AMP could exert protective effects on UC *via* suppressing the IRAK1/TRAF6/NF-κB-mediated inflammatory signaling pathways.

Key words: Ulcerative colitis; *Ampelopsis grossedentata*; Traditional Chinese medicine; Systems pharmacology; Inflammation

Core tip: Ulcerative colitis (UC), as one of the major forms of inflammatory bowel disease, could lead to various intestinal and extra-intestinal manifestations, which brings a huge challenge to the health care system. Given studies have confirmed that the flavonoid bioactive compounds contained in *Ampelopsis grossedentata* (AMP) possess strong antiinflammatory activity, we examined the potential therapeutic effects of AMP on UC based on systems pharmacology. Results showed that AMP could suppress the inflammation-related signaling pathways in dextran sulfate sodium-induced colitis, indicating protective effects on UC, which might provide an effective natural therapy for the treatment and prevention of UC.

Chen YL, Zhang YL, Dai YC, Tang ZP. Systems pharmacology approach reveals the antiinflammatory effects of *Ampelopsis grossedentata* on dextran sodium sulfate-induced colitis. *World J Gastroenterol* 2018; 24(13): 1398-1409 Available from: URL: http://www.wjgnet.com/1007-9327/full/v24/i13/1398.htm DOI: http://dx.doi.org/10.3748/wjg.v24.i13.1398

INTRODUCTION

Ulcerative colitis (UC), which is primarily characterized by recurrent abdominal pain, diarrhea and bloody purulent stools[1], is a chronic inflammatory condition of the intestine, with mucosal inflammation beginning in the rectum and extending continuously to part of or the entire colon. Inflammation in UC can lead to the occurrence of multifocal ulcers on the wall of the large intestine, causing nausea, cramps, diarrhea, pus, bleeding and fatigue. In general, patients with UC may develop varying degrees of extra-intestinal manifestations, which are attributed to the inflammatory cascade in the colorectum, including skin, mucosal, joint, ocular, hepatic and pulmonary disorders[2,3]. Meanwhile, the increasing prevalence of UC brings a considerable challenge to health care systems worldwide[4].

Given that UC is a kind of long-term disease with uncertain etiology, the aim of therapy is to induce and maintain clinical remission, defined as control of symptoms, endoscopic mucosal healing and avoidance of complications[1,5]. In addition to dietary control, the available pharmacologic treatments include 5-aminosalicylates, steroids, thiopurines and biological agents[6]. However, the routine medical treatments for UC are not fully curative, and investigations have shown that compared with standard care, the elevated cost-utility ratios of biologics reached up to $456979 (in United States' dollars)[7]. In addition, as UC mostly affects young people and takes a lifelong treatment, as well as has a low mortality[8,9] that is not different from that in the healthy population, the disease poses an enormous economic burden on individuals, families and society. Thus, promising and novel therapeutic tactics are urgently needed to be explored and developed for UC.

Complementary and alternative medicine, especially Chinese herbal medicine, is widely used among UC patients. Recent investigations revealed that many natural compounds have significant protective efficacies in UC patients[10]. *Ampelopsis grossedentata* (AMP), which contains a large amount of flavonoid active ingredients, has been widely consumed as a functional beverage and may be used consecutively as a supplementary option to the current standard treatment of UC. Dihydromyricetin, a major compound of AMP, has been reported to be highly distributed in the intestinal tract[11], and has hepatoprotective[12], insulin resistant[13], antioxidation[14], anticancer[15] and antiinflammatory activities, which are produced by suppression of nuclear factor kappa-B (NF-κB) activation[16,17]. However, few researchers have investigated the underlying mechanisms of the potential protective effects of AMP against UC, although AMP contains much more flavonoids and deserves further study.

Considering the complex combination and multi-target interactions of Chinese herbal plants, it is quite difficult to conduct a systematic study of the effects of AMP on diseases using conventional methods. Whereas, systems pharmacology, an emerging systems-oriented approach which has been reported to reveal the

mechanism of a disease and link it to the chemical network of a drug[18,19], provides new perspectives to predict the active ingredients and candidate targets through a holistic process of active compound screening, target fishing, network construction and analysis[20,21]. To further investigate the potential mechanisms and effects of AMP on UC, a systems pharmacology analysis and animal experiments were conducted in this study.

MATERIALS AND METHODS

Systems pharmacology

The active compounds and their corresponding putative targets of AMP were identified by the Traditional Chinese Medicine Systems Pharmacology (TCMSP) database. Known UC-related targets were obtained from the Genetic Association database, Therapeutic Target database and Online Mendelian Inheritance in Man database. Protein-protein interaction (PPI) networks were constructed for the interaction of putative targets of AMP against UC based on BisoGenet, and the degree centrality (DC) value, which represents the topological importance of a node in the intersection network, was used to filter the candidate targets. Finally, enrichment analysis was conducted using ClueGO, a Cytoscape plugin.

Animals

Male C57BL/6 mice aged 6 weeks were obtained from the SLAC Animal Laboratories (Shanghai, China). All mice were raised under standard conditions (room temperature, 24 ± 2 ℃; humidity, 50%-60%; light, 12-h light/12-h dark cycle).

Colitis model construction and treatment

Experimental colitis was induced by administration of 3.5% (w/v) dextran sulfate sodium (DSS, 36-50 kDa; MP Biomedicals, United States) in drinking water provided ad libitum for 7 d. The DSS solution was changed every day. For each experiment, the mice were randomly divided into four groups (n = 10/group): the control group was given normal water only; the DSS group, 5-aminosalicylic acid (5-ASA) group and AMP group received a 3.5% DSS solution for 7 d, respectively. For treatment experiment, the control group and DSS group were administered normal saline intragastrically daily. The 5-ASA group was given 5-ASA solution (100 mg/kg/d) and the AMP group were administered AMP solution (400 mg/kg/d) intragastrically. The severity of colitis was calculated daily using the disease activity index[22]; the disease activity index scores are shown in Supplementary Table 1. After treatment, blood was extracted by cardiac puncture under anesthesia. Intestinal tissues were fixed in 4% buffered formalin for hematoxylin & eosin/immunohistochemistry and the other tissues were snap-frozen for western blot/RT-PCR.

Histopathology and immunohistochemistry

Paraffin-embedded colon samples were stained with HE for histological evaluation, as well as were immunostained with anti-NF-κB, anti-tumor necrosis factor-alpha (TNF-α) and anti-interleukin-1 beta (IL-1β) for protein expression in intestinal tissues after being cut into 4 μm sections.

Western blot analysis

Protein extracts were separated using sodium dodecyl sulfate-polyacrylamide gel electrophoresis and then transferred to polyvinylidene fluoride membranes (Millipore, Germany). Protein expression was detected by western blot analysis. Primary antibodies used were rabbit monoclonal anti-NF-κB, anti-inhibitor of NF-κB (IκB), anti-p-IκB, anti-IL-1 receptor associated kinase (IRAK1), anti-TNF receptor-associated factor 2 (TRAF2) and anti-TNF receptor-associated factor 6 (TRAF6). All antibodies were purchased from Cell Signaling Technology (United States).

RNA isolation and quantitative RT-PCR

Total RNA was extracted using TRIzol reagent (Invitrogen, United States). RT-PCR was carried out using SYBR Green PCR Master Mix (Toyobo, Japan) in an Eppendorf PCR system. The data were analyzed by the $^{\Delta\Delta}$Ct method and samples were normalized to β-actin. Primer sequences are shown in Supplementary Table 2.

Enzyme-linked immunosorbent assay

The levels of inflammation-related cytokines (TNF-α, IL-1β, IL-6 and IL-8) were detected using mouse-specific ELISA kits (Dakewe Bio-engineering Co. Ltd., China), following the manufacturer's instructions.

Statistical analysis

All data are presented as the mean ± SD. Statistical analyses were performed using the Student's t-test or one-way ANOVA for group comparisons, and $P < 0.05$ was considered statistically significant.

RESULTS

AMP improved the DSS-induced inflammatory response in acute colitis mice

As the flavonoid bioactive compound extracted from AMP could inhibit inflammatory response *in vitro* and *in vivo*[16], the protective effects of AMP in DSS-induced colitis were examined in this study. Results presented a reduction of body weight together with an elevation of disease activity index scores under DSS stimulation (Figure 1A and B); meanwhile, treatment with 5-ASA and AMP prominently improved the body weight as well as the length of colon, with significant difference (Figure 1A and C). Additionally, histological analyses revealed more neutrophil infiltration, increased ulceration and

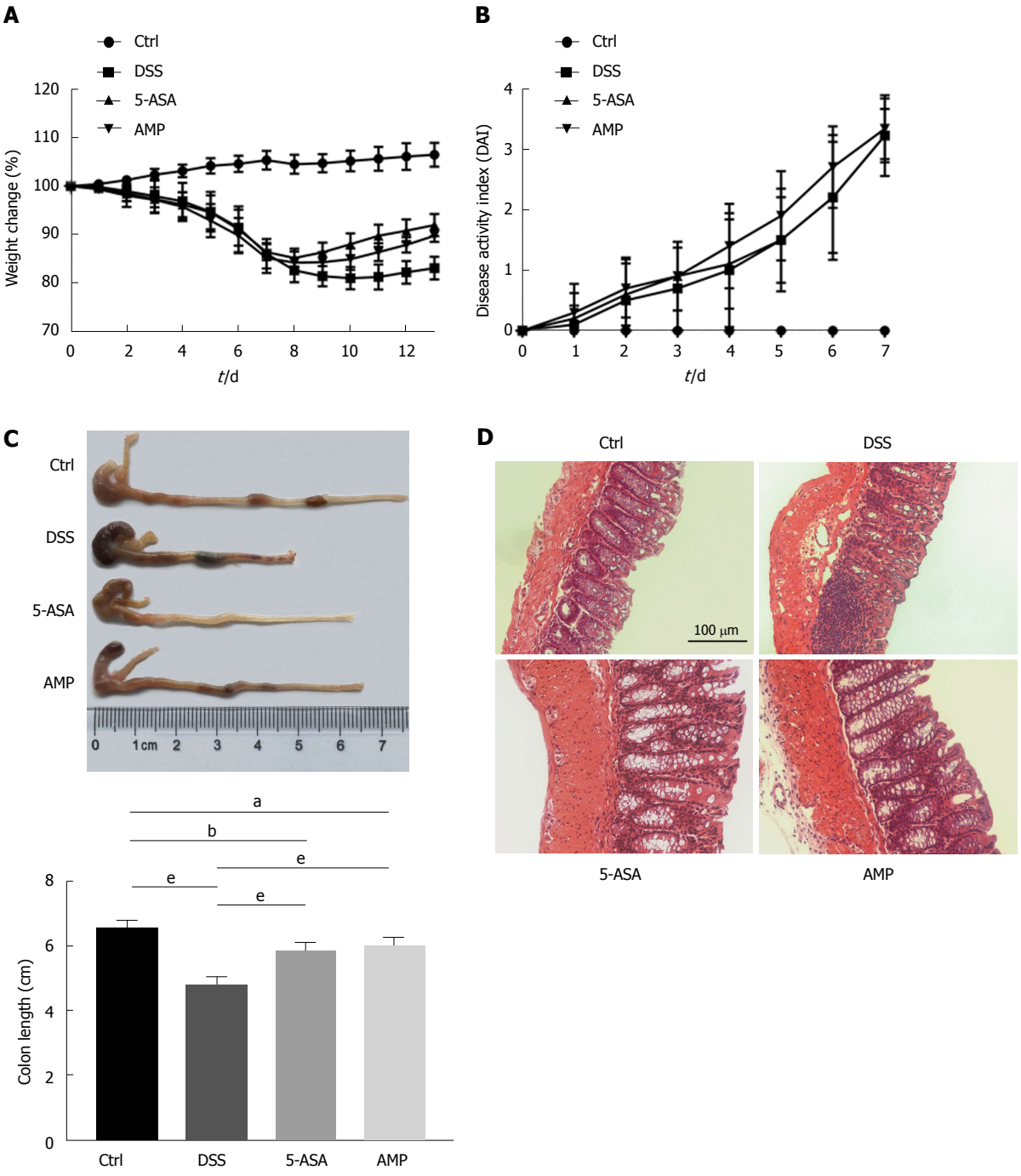

Figure 1 ***Ampelopsis grossedentata*** **improved dextran sulfate sodium-induced inflammatory response in acute colitis mice.** A: Body weight was measured every day; B: Disease activity index under DSS stimulation in mice; C: Length of colons and statistical graph; D: HE staining of colons. Data are presented as mean ± SD. $^{a}P < 0.05$, $^{b}P < 0.01$, $^{e}P < 0.001$. 5-ASA: 5-aminosalicylic acid; AMP: *Ampelopsis grossedentata*; DSS: Dextran sulfate sodium.

crypt loss in the colon in the DSS group compared with the control and treatment groups (Figure 1D), indicating a protective effect of AMP on experimental colitis.

Potential pharmacological mechanisms of AMP

Candidate compound screening and putative target prediction for AMP: Four candidate compounds of AMP were obtained from the TCMSP database, including dihydromyricetin, myricetin, quercetin and taxifolin (Figure 2A and Supplementary Table 3). Since recent research studies have demonstrated strong antiinflammatory activities for all the selected compounds[16,23-25], which may be crucially involved in the improvement of UC, putative target prediction was subsequently performed to confirm this hypothesis. Given that the comprehensive biological and pharmacological effects of Chinese herbal plants rely upon their complex compounds and multitarget interactions, a compound-target network was built based on massive open-source initiatives and free web-based tools. A total of 156 potential targets were collected from TCMSP, and 89 targets were ultimately

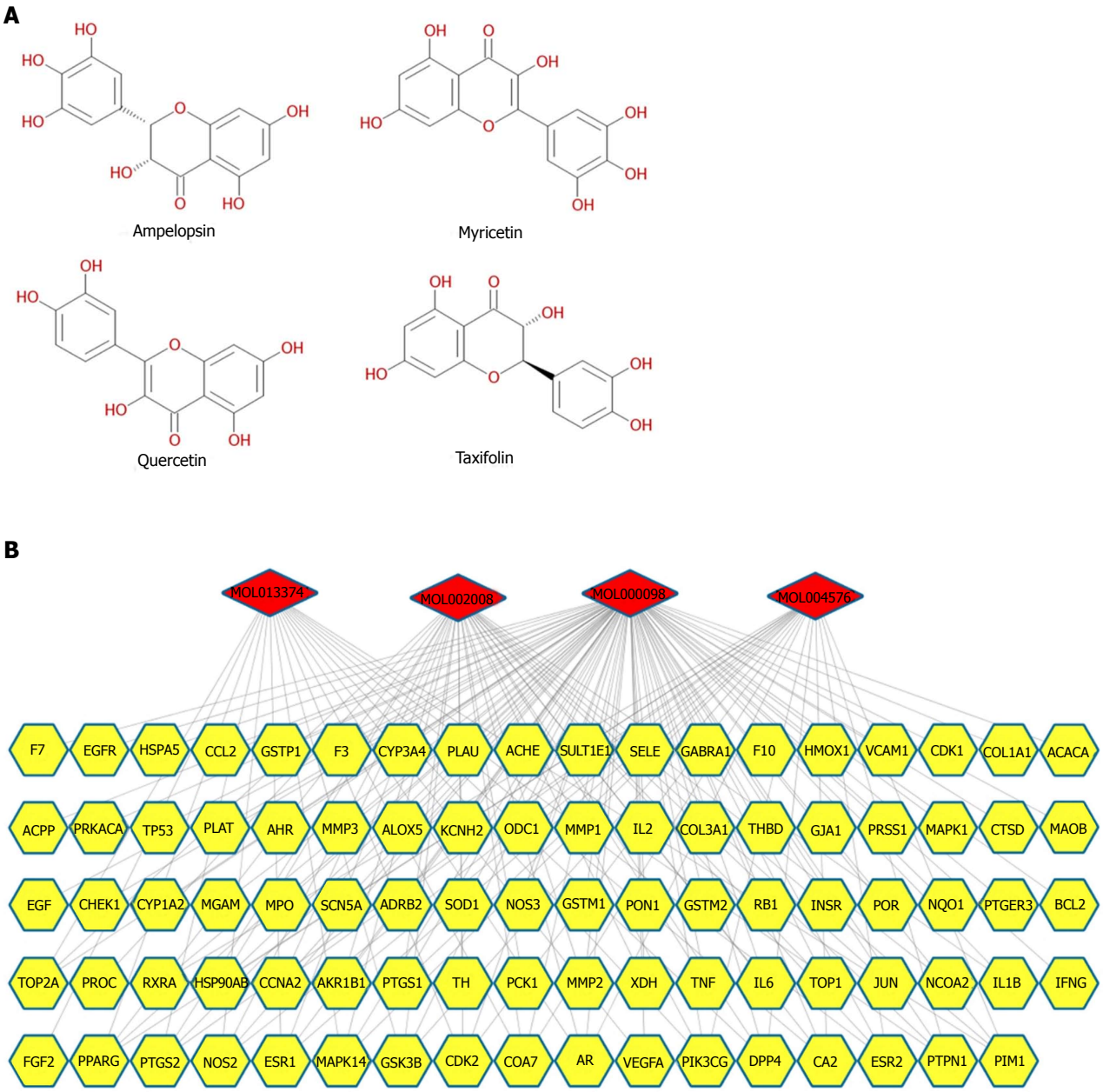

Figure 2 Candidate compound screening and putative target prediction for *ampelopsis grossedentata*. A: Chemical structures of active compounds for AMP; B: Compound-target network for AMP. AMP: *Ampelopsis grossedentata*.

included after filtering (Figure 2B and Supplementary Tables 4 and 5). Moreover, 67 targets overlapped in the 4 compounds, which indicated that most of the compounds of AMP hit multitargets to exert multifarious therapeutic effects.

PPI network constitution and identification of candidate targets for AMP against UC: To better understand the mechanisms of AMP in the treatment of UC, 123 candidate targets of UC were obtained from Genetic Association database, Therapeutic Target database and Online Mendelian Inheritance in Man database (Supplementary Table 6). As PPI maps represented physical interactions on a molecular level[19], a putative-target network (4998 nodes and 126594 edges) and a known UC-related target network (3824 nodes and 91207 edges) were constructed based on PPI database (Figure 3A and B). Subsequently, to confirm the candidate targets of AMP against UC, an intersection of the above networks was conducted, which consisted of 2543 nodes and 70816 edges, and the DC values of 35 and 70 were computed by CytoNCA to identify the putative targets during the process (Figure 3C).

In order to further elucidate the possible effects of AMP on UC, the biological processes and signaling pathways were determined through Cytoscape software. The results showed that the biological processes were largely related to the nucleic acid metabolic process, positive regulation of macromolecule metabolic process, positive regulation of response to stimulus and regu-

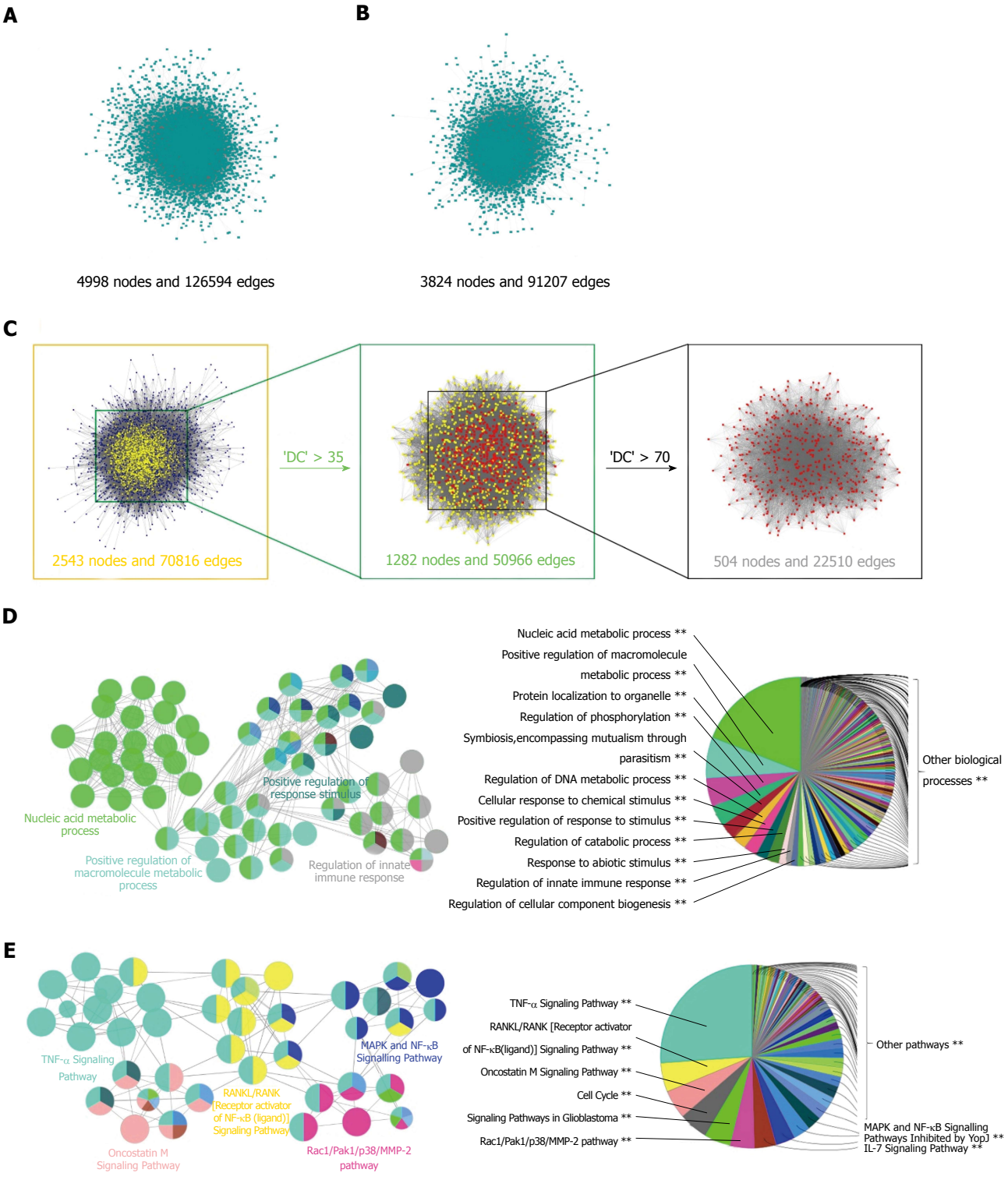

Figure 3 Protein-protein interaction network constitution and identification of candidate targets for *ampelopsis grossedentata* against ulcerative colitis. A: PPI network was constructed for the putative targets of AMP; B: PPI network was constructed for the known UC-related targets; C: Intersection networks for AMP against UC; D: Enrichment analysis of biological processes for AMP against UC; E: Enrichment analysis of signaling pathways for AMP against UC. AMP: *Ampelopsis grossedentata*; PPI: Protein-protein interaction; UC: Ulcerative colitis.

lation of the innate immune response (Figure 3D), and the signaling pathways were mainly involved with the TNF-α signaling pathway, RANKL/RANK (receptor activator of NF-κB) signaling pathway, oncostatin M pathway, Rac1/Pak1/p38/MMP-2 pathway and MAPK/NF-κB signaling pathway (Figure 3E). Based on these data, we proposed a hypothesis that the protective mechanisms of AMP on UC were possibly related to inflammatory signaling pathways.

Experimental validation

AMP could suppress the inflammation-related signaling pathways in DSS-induced colitis: Since systems pharmacology demonstrated that TNF-α and

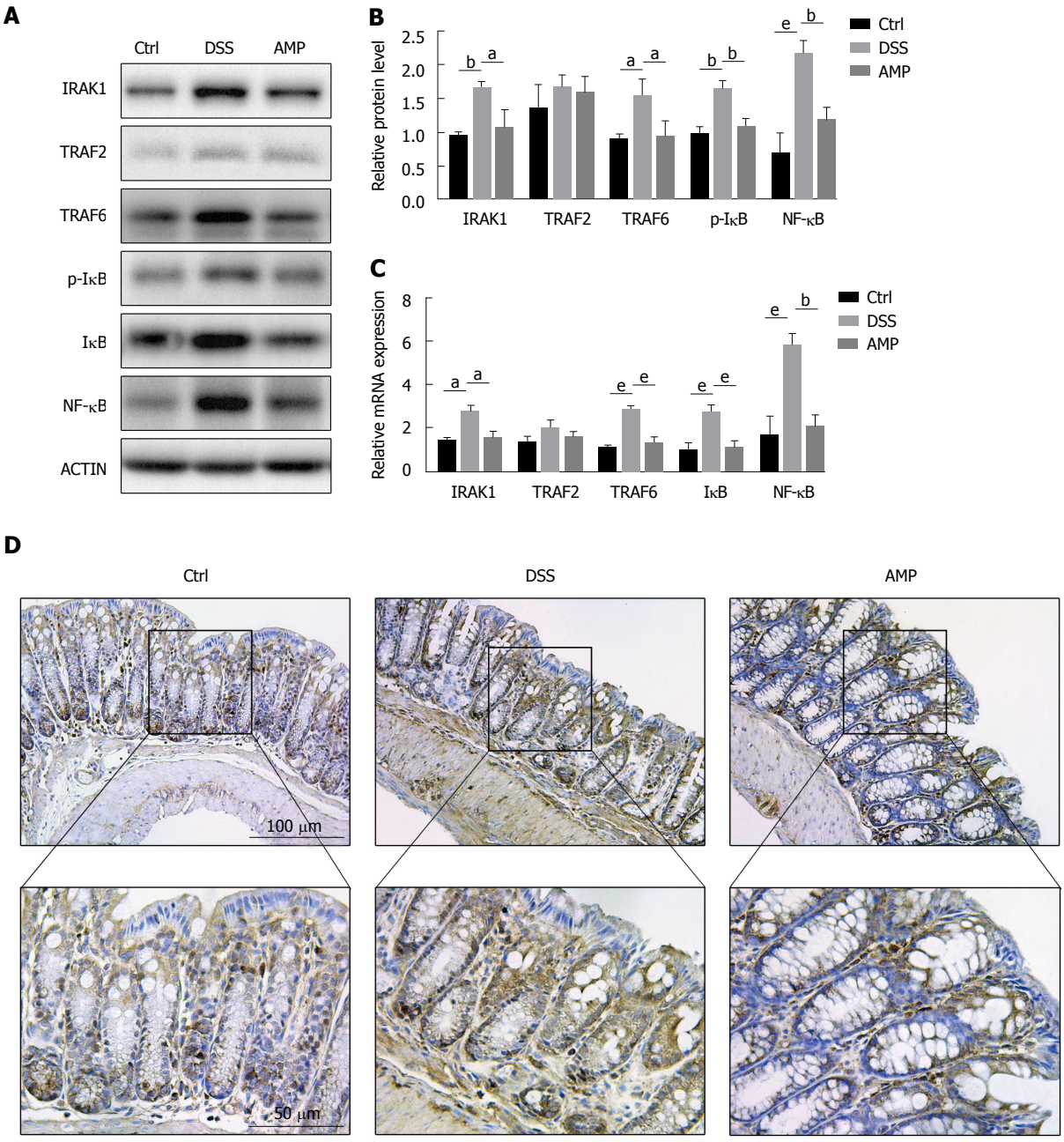

Figure 4 ***Ampelopsis grossedentata*** **could suppress the inflammation-related signaling pathways in dextran sulfate sodium-induced colitis.** A: Representative western blot analyses of inflammation-related proteins in colon tissues; B: Statistical graph of western blot analyses, relative protein levels of IRAK1, TRAF2, TRAF6 and NF-κB were determined by normalization to actin, and relative p-IκB level was determined by normalization to IκB; C: mRNA expression of inflammation-related genes in colon tissues, relative mRNA expression levels of IRAK1, TRAF2, TRAF6, IκB and NF-κB were determined by normalization to actin; D: Representative images of anti-NF-κB immunohistochemistry. Data are presented as mean ± SD. $^{a}P < 0.05$, $^{b}P < 0.01$, $^{e}P < 0.001$. AMP: *Ampelopsis grossedentata*; DSS: Dextran sulfate sodium.

RANKL/RANK (receptor activator of NF-κB) signaling pathways were involved in the therapeutic effects of AMP on UC, western blot analyses were performed to evaluate TRAF2 and TRAF6, the downstream events of TNFR and RANK. Interestingly, outcomes presented a significant increase of TRAF6 expression in the DSS group as well as a mild increase of TRAF2 expression, compared with the control group, and AMP could improve this condition (Figure 4A and B). Thus, the upstream indicator of TRAF6, IRAK1 was determined next to investigate the further mechanisms in the TRAF6-mediated inflammatory signaling pathway, and results showed a marked elevation in the DSS group and that AMP could alleviate this situation, suggesting that IL-1-mediated proinflammatory signaling might be involved in the antiinflammatory action of AMP in UC. Accordingly, the mRNA expression of TRAF6 and IRAK1 was enhanced, whereas the expression of TRAF2 was not (Figure 4C), indicating that AMP might exert antiinflammatory effects *via* IRAK1/TRAF6-mediated signaling pathway.

Given IκB was the shared core downstream event

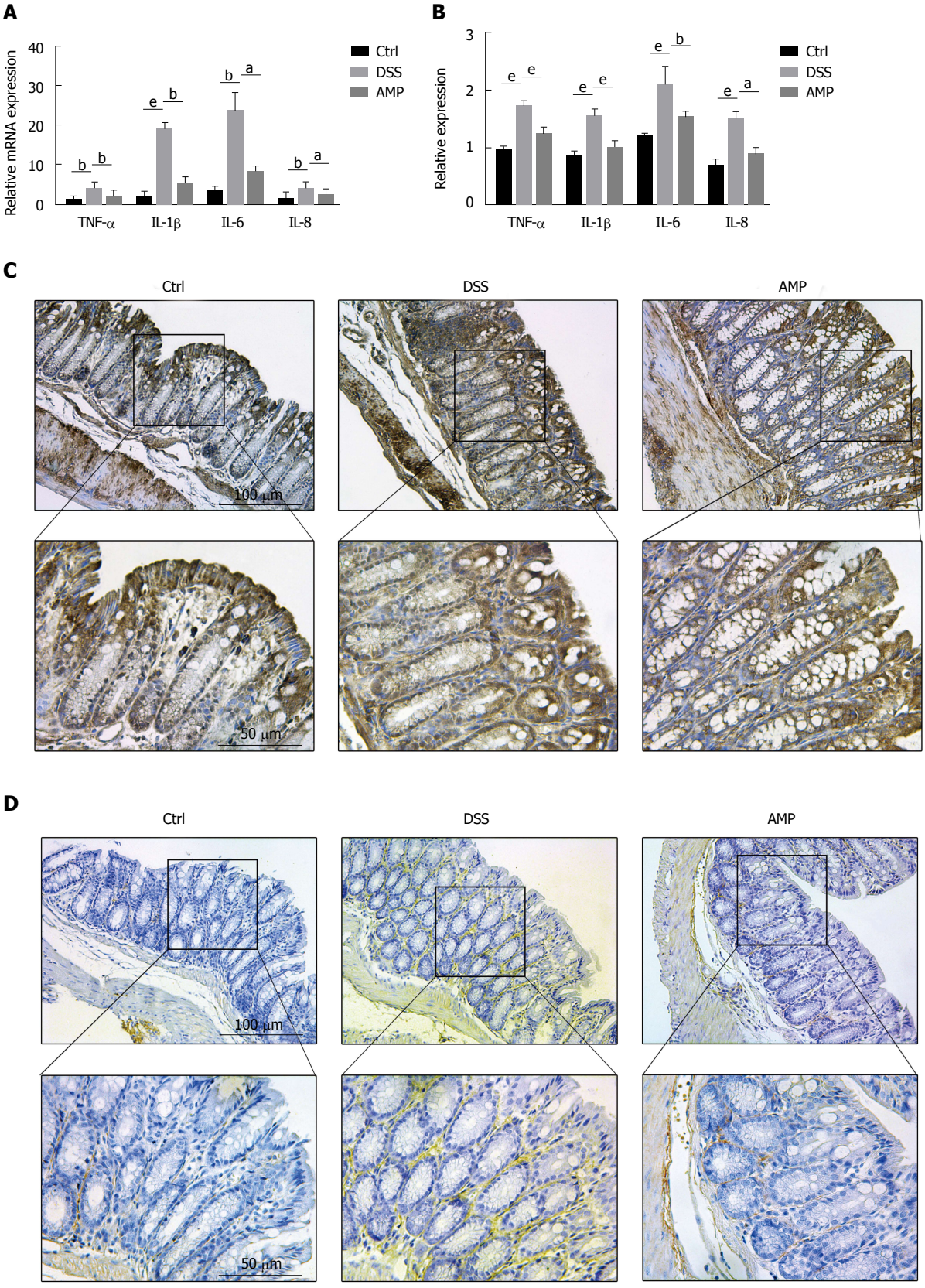

Figure 5 ***Ampelopsis grossedentata*** **has protective effects on ulcerative colitis by inhibiting inflammation.** A: mRNA expression of inflammation-related cytokines in colon tissues, with actin used as loading control; B: Relative expression levels of inflammation-related cytokines in serum examined by enzyme-linked immunosorbent assay; C: Representative images of anti-TNF-α immunohistochemistry; D: Representative images of anti-IL-1β immunohistochemistry. Data are presented as mean ± SD. $^{a}P < 0.05$, $^{b}P < 0.01$, $^{e}P < 0.001$. AMP: *Ampelopsis grossedentata*; DSS: Dextran sulfate sodium; UC: Ulcerative colitis.

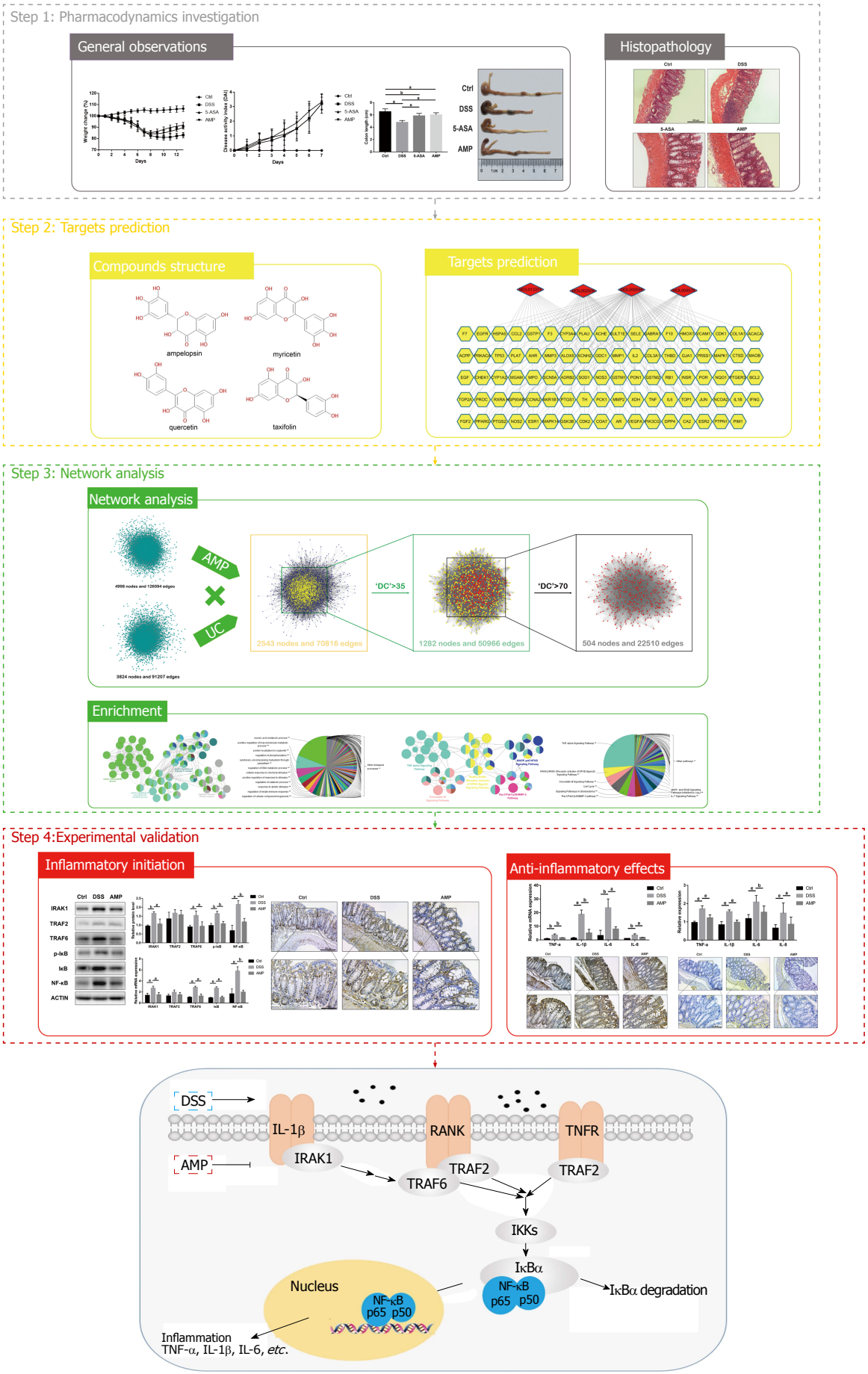

Figure 6 Schematic diagram of the research methodology and the proposed model of *ampelopsis grossedentata* acting on ulcerative colitis.

of TRAF2/6 and IRAK1, and phosphorylation of IκB could release NF-κB into the nucleus thus initiating the gene transcription of relevant proinflammatory signals to result in inflammatory responses in intestine, we determined the levels of p-IκB and NF-κB consequently. Western blot analyses manifested significant differences in p-IκB/IκB and NF-κB between the AMP group and the DSS group, and these changes were also significant compared with the control group (Figure 4A and B). Meanwhile, parallel changes were seen with the PCR analyses (Figure 4C), suggesting that NF-κB was activated in the DSS-induced colitis and was inhibited by AMP. Additionally, immunohistochemical estimation revealed that the protein expression of NF-κB in inflamed colon tissue was significantly increased in the DSS group and was prevented in the AMP group (Figure 4D), confirming the previous findings.

AMP has protective effects on UC by inhibiting inflammation: As NF-κB was tightly associated with a great deal of inflammation-related genes, which could release a series of proinflammatory cytokines, including TNF-α and IL-1β, thus activating the whole inflammatory feedback cycle process[26,27], we measured the relative expression levels of TNF-α, IL-1β, IL-6 and IL-8 with PCR and ELISA. Results presented that all the indicators were distinctly elevated under DSS stimulation, being alleviated with AMP treatment (Figure 5A and B). Furthermore, immunohistochemical estimation showed that the expression of secretory proteins TNF-α and IL-1β were both prominently increased in the DSS group and were improved in the AMP group (Figure 5C and D). Taken together, all the findings indicated that AMP might exert protective effects on UC *via* suppressing the IRAK1/TRAF6/NF-κB-mediated inflammatory signaling pathway.

DISCUSSION

UC, as one of the major forms of inflammatory bowel disease, represents an increased risk for progressing colorectal cancer[28]. Recent investigations have confirmed that flavonoid bioactive compounds isolated from the edible herb AMP have strong antiinflammatory activities in macrophages[16], and may provide effective natural therapies for the treatment and prevention of UC. Thus, a systems pharmacology approach was conducted in this study to explore the underlying pharmacological mechanisms of AMP on UC. The schematic diagram of the research methodology and the proposed model of AMP acting on UC was shown in Figure 6.

A DSS-induced experimental colitis model was constructed to verify the therapeutic effects, and results showed that AMP could significantly improve the general observations and histopathology analysis. Thus, systems pharmacology was performed subsequently to identify the active compounds and their corresponding targets, and results showed that four candidate compounds obtained from the TCMSP database were ultimately included in this study. Meanwhile, another four compounds, including ambrein, apiin, ampeloptin and myricomplanoside, were obtained from the National Scientific Data Sharing Platform database and Traditional Chinese Medicine Database @Taiwan, but were excluded due to rare corresponding targets. Finally, a compound-target network was constructed for the four selected compounds and their corresponding targets, indicating synergistic as well as multifarious effects for each compound of AMP.

PPI maps were next constructed for the functional analysis, on the basis of putative-target networks of AMP and UC. Enrichment analyses presented a series of biological processes and signaling pathways, and a large number of those were supposed to be tightly associated with the inflammatory response, including the nucleic acid metabolic process, positive regulation of macromolecule metabolic process, positive regulation of response to stimulus and the regulation of innate immune response, together with the TNF-α signaling pathway, RANKL/RANK (receptor activator of NF-κB) signaling pathway, oncostatin M pathway, Rac1/Pak1/p38/MMP-2 pathway and MAPK/NF-κB signaling pathway. Thus, we proposed that the NF-κB-related inflammatory signaling pathway, which was highly involved in all the above findings, might be a pivotal target in the treatment of AMP on UC.

NF-κB, as a central transcription factor of inflammatory mediators and a key participant in innate and adaptive immune responses involved in the perpetuation of inflammatory cascade[29], has been considered as the central molecular pathway for UC incidence[27]. Recent investigations revealed that the activation of proinflammatory cytokines, such as TNF-α and IL-1β, could induce the translocation of NF-κB from the cytoplasm to the nucleus, leading to the expression of a variety of inflammatory genes[30]. Given that inflammation was a major factor for the progression of UC[31], we performed the experimental validation to verify the above assumption.

The TNF-α signaling pathway and RANKL/RANK (receptor activator of NF-κB) signaling pathway were the most important parts in the signaling pathways obtained from enrichment analyses. TRAF2 and TRAF6, the downstream events of TNFR and RANK, were detected firstly, and results presented a significant response on TRAF6 but an insignificant response on TRAF2, suggesting the activation of TRAF6 in DSS-induced colitis. IRAK1, a protein kinase which is partially responsible for IL1-induced up-regulation of NF-κB by combining with TRAF6 and was also detected in previous enrichment analyses[32], was determined next to further explore the potential antiinflammatory mechanisms of AMP on UC. Outcomes presented a high expression of IRAK1 under DSS stimulation, indicating that IRAK1/TRAF6-mediated proinflammatory signaling might be participated in the antiinflammatory action of AMP on UC.

Thus, we validated the downstream proinflammatory signaling and the therapeutic effects, and results showed the activation of NF-κB under DSS stimulation as well as the protective effects of AMP against UC in mice. Interestingly, in the DSS group compared with the control group, there was an increased expression of proinflammatory signaling pathways and also of the levels of IκB; however, the increased expression of IκB detected by PCR was in accordance with the western blot analyses and the p-IκB/IκB ratio was elevated ultimately, which might be due to the feedback regulation of activated NF-κB. Together, all the findings revealed that AMP could exert protective effects on UC *via* suppressing the IRAK1/TRAF6/NF-κB-mediated inflammatory signaling pathway.

Limitations should be acknowledged in regards to the fact that research studies on AMP have been rare, resulting in a lack of retrieved compounds, so that the active compounds of AMP might not be fully predicted. Furthermore, some selected compounds were also rejected for the absence of efficient corresponding targets, which might be due to the relevant databases still not being well-developed. Besides, since UC is a chronic inflammatory condition of the intestine combined with a great deal of other biological processes, which have also been detected in this study, further studies are necessary to explore the systematic effects of AMP on UC.

ARTICLE HIGHLIGHTS

Research background

Ulcerative colitis (UC), as a recurrent chronic inflammatory disease, greatly affects the quality of life of patients, which brings an enormous challenge for both individuals and society worldwide. However, the etiology of UC is still unknown and conventional medical treatments for UC are not fully curative. Thus, promising and novel therapeutic strategies are imperatively needed and should be explored for UC.

Research motivation

Inflammation is a major factor for the progression of UC, and studies have confirmed that a great deal of natural medicines are intended for inhibition of various chronic inflammation-associated diseases, such as *Ampelopsis grossedentata* (AMP). Thus, we explored the mechanisms of therapeutic effects of AMP on UC, and provided a valid complementary treatment to the standard therapy.

Research objectives

To investigate the underlying mechanisms of protective effects of AMP on dextran sulfate sodium (DSS)-induced colitis.

Research methods

As an emerging approach, systems pharmacology was performed in this study to explore the systematic effects of AMP on DSS-induced colitis by active compound screening, target fishing, network construction and analysis.

Research results

The study revealed an antiinflammatory effect of AMP against DSS-induced colitis based on systems pharmacology and animal experiments.

Research conclusions

AMP could exert beneficial effects on DSS-induced colitis *via* suppressing inflammation-related signaling pathways.

Research perspectives

Since UC is an inflammatory condition combined with a large amount of other biological processes, we determined the inflammatory-related signaling pathways in this study. Other biological processes and signaling pathways as well as the systematic effects of AMP on UC were still unknown and need to be explored in further studies.

REFERENCES

1 **McDowell C**, Bhimji SS. Bowel, Inflammatory Disease (IBD). 2017 [PMID: 29262182]
2 **Olpin JD**, Sjoberg BP, Stilwill SE, Jensen LE, Rezvani M, Shaaban AM. Beyond the Bowel: Extraintestinal Manifestations of Inflammatory Bowel Disease. *Radiographics* 2017; **37**: 1135-1160 [PMID: 28548906 DOI: 10.1148/rg.2017160121]
3 **Ott C**, Schölmerich J. Extraintestinal manifestations and complications in IBD. *Nat Rev Gastroenterol Hepatol* 2013; **10**: 585-595 [PMID: 23835489 DOI: 10.1038/nrgastro.2013.117]
4 **M'Koma AE**. Inflammatory bowel disease: an expanding global health problem. *Clin Med Insights Gastroenterol* 2013; **6**: 33-47 [PMID: 24833941 DOI: 10.4137/CGast.S12731]
5 **Reinisch W**, Van Assche G, Befrits R, Connell W, D'Haens G, Ghosh S, Michetti P, Ochsenkühn T, Panaccione R, Schreiber S, Silverberg MS, Sorrentino D, van der Woude CJ, Vermeire S, Panes J. Recommendations for the treatment of ulcerative colitis with infliximab: a gastroenterology expert group consensus. *J Crohns Colitis* 2012; **6**: 248-258 [PMID: 22325181 DOI: 10.1016/j.crohns.2011.11.001]
6 **Bressler B**, Marshall JK, Bernstein CN, Bitton A, Jones J, Leontiadis GI, Panaccione R, Steinhart AH, Tse F, Feagan B; Toronto Ulcerative Colitis Consensus Group. Clinical practice guidelines for the medical management of nonhospitalized ulcerative colitis: the Toronto consensus. *Gastroenterology* 2015; **148**: 1035-1058.e3 [PMID: 25747596 DOI: 10.1053/j.gastro.2015.03.001]
7 **Stawowczyk E**, Kawalec P. A Systematic Review of the Cost-Effectiveness of Biologics for Ulcerative Colitis. *Pharmacoeconomics* 2017; **36**: 419-434 [PMID: 29260508 DOI: 10.1007/s40273-017-0601-6]
8 **Bernstein CN**, Ng SC, Lakatos PL, Moum B, Loftus EV Jr; Epidemiology and Natural History Task Force of the International Organization of the Study of Inflammatory Bowel Disease. A review of mortality and surgery in ulcerative colitis: milestones of the seriousness of the disease. *Inflamm Bowel Dis* 2013; **19**: 2001-2010 [PMID: 23624887 DOI: 10.1097/MIB.0b013e318281f3bb]
9 **Ordás I**, Eckmann L, Talamini M, Baumgart DC, Sandborn WJ. Ulcerative colitis. *Lancet* 2012; **380**: 1606-1619 [PMID: 22914296 DOI: 10.1016/s0140-6736(12)60150-0]
10 **Zhao L**, Zhang S, He P. Mechanistic Understanding of Herbal Therapy in Inflammatory Bowel Disease. *Curr Pharm Des* 2017; **23**: 5173-5179 [PMID: 29032748 DOI: 10.2174/1381612823666171010124414]
11 **Fan L**, Tong Q, Dong W, Yang G, Hou X, Xiong W, Shi C, Fang J, Wang W. Tissue Distribution, Excretion, and Metabolic Profile of Dihydromyricetin, a Flavonoid from Vine Tea (Ampelopsis grossedentata) after Oral Administration in Rats. *J Agric Food Chem* 2017; **65**: 4597-4604 [PMID: 28534405 DOI: 10.1021/acs.jafc.7b01155]
12 **Zeng X**, Yang J, Hu O, Huang J, Ran L, Chen M, Zhang Y, Zhou X, Zhu J, Zhang Q, Yi L, Mi M. Dihydromyricetin Ameliorates Nonalcoholic Fatty Liver Disease by Improving Mitochondrial Respiratory Capacity and Redox Homeostasis Through Modulation of SIRT3 Signaling. *Antioxid Redox Signal* 2018; Epub ahead of print [PMID: 29310441 DOI: 10.1089/ars.2017.7172]
13 **Le L**, Jiang B, Wan W, Zhai W, Xu L, Hu K, Xiao P. Metabolomics reveals the protective of Dihydromyricetin on glucose homeostasis by enhancing insulin sensitivity. *Sci Rep* 2016; **6**: 36184 [PMID:

27796348 DOI: 10.1038/srep36184]
14 **Wang Y**, Wang W, Qiu E. Protection of oxidative stress induced apoptosis in osteosarcoma cells by dihydromyricetin through down-regulation of caspase activation and up-regulation of BcL-2. *Saudi J Biol Sci* 2017; **24**: 837-842 [PMID: 28490955 DOI: 10.1016/j.sjbs.2016.12.004]
15 **Wang Z**, Sun X, Feng Y, Liu X, Zhou L, Sui H, Ji Q, E Q, Chen J, Wu L, Li Q. Dihydromyricetin reverses MRP2-mediated MDR and enhances anticancer activity induced by oxaliplatin in colorectal cancer cells. *Anticancer Drugs* 2017; **28**: 281-288 [PMID: 27997436 DOI: 10.1097/cad.0000000000000459]
16 **Wang R**, Pi J, Su X, Liu J, Zeng X, Wong I, Huang L, Zhou H, Cai J, Li T, Liu L. Dihydromyricetin suppresses inflammatory responses in vitro and in vivo through inhibition of IKKβ activity in macrophages. *Scanning* 2016; **38**: 901-912 [PMID: 27487564 DOI: 10.1002/sca.21339]
17 **Tang N**, Ma J, Wang KS, Mi C, Lv Y, Piao LX, Xu GH, Li X, Lee JJ, Jin X. Dihydromyricetin suppresses TNF-α-induced NF-κB activation and target gene expression. *Mol Cell Biochem* 2016; **422**: 11-20 [PMID: 27686451 DOI: 10.1007/s11010-016-2799-6]
18 **Fotis C**, Antoranz A, Hatziavramidis D, Sakellaropoulos T, Alexopoulos LG. Network-based technologies for early drug discovery. *Drug Discov Today* 2017; **23**: 626-635 [PMID: 29294361 DOI: 10.1016/j.drudis.2017.12.001]
19 **Bloomingdale P**, Nguyen VA, Niu J, Mager DE. Boolean network modeling in systems pharmacology. *J Pharmacokinet Pharmacodyn* 2018; **45**: 159-180 [PMID: 29307099 DOI: 10.1007/s10928-017-9567-4]
20 **Pei F**, Li H, Henderson MJ, Titus SA, Jadhav A, Simeonov A, Cobanoglu MC, Mousavi SH, Shun T, McDermott L, Iyer P, Fioravanti M, Carlisle D, Friedlander RM, Bahar I, Taylor DL, Lezon TR, Stern AM, Schurdak ME. Connecting Neuronal Cell Protective Pathways and Drug Combinations in a Huntington's Disease Model through the Application of Quantitative Systems Pharmacology. *Sci Rep* 2017; **7**: 17803 [PMID: 29259176 DOI: 10.1038/s41598-017-17378-y]
21 **Suh SY**, An WG. Systems Pharmacological Approach to the Effect of Bulsu-san Promoting Parturition. *Evid Based Complement Alternat Med* 2017; **2017**: 7236436 [PMID: 29234425 DOI: 10.1155/2017/7236436]
22 **Chaudhary G**, Mahajan UB, Goyal SN, Ojha S, Patil CR, Subramanya SB. Protective effect of Lagerstroemia speciosa against dextran sulfate sodium induced ulcerative colitis in C57BL/6 mice. *Am J Transl Res* 2017; **9**: 1792-1800 [PMID: 28469784]
23 **Zhang MJ**, Su H, Yan JY, Li N, Song ZY, Wang HJ, Huo LG, Wang F, Ji WS, Qu XJ, Qu MH. Chemopreventive effect of Myricetin, a natural occurring compound, on colonic chronic inflammation and inflammation-driven tumorigenesis in mice. *Biomed Pharmacother* 2018; **97**: 1131-1137 [PMID: 29136951 DOI: 10.1016/j.biopha.2017.11.018]
24 **Zhu M**, Zhou X, Zhao J. Quercetin prevents alcohol-induced liver injury through targeting of PI3K/Akt/nuclear factor-κB and STAT3 signaling pathway. *Exp Ther Med* 2017; **14**: 6169-6175 [PMID: 29285175 DOI: 10.3892/etm.2017.5329]
25 **Kim A**, Nam YJ, Lee CS. Taxifolin reduces the cholesterol oxidation product-induced neuronal apoptosis by suppressing the Akt and NF-κB activation-mediated cell death. *Brain Res Bull* 2017; **134**: 63-71 [PMID: 28710022 DOI: 10.1016/j.brainresbull.2017.07.008]
26 **Vlantis K**, Wullaert A, Polykratis A, Kondylis V, Dannappel M, Schwarzer R, Welz P, Corona T, Walczak H, Weih F, Klein U, Kelliher M, Pasparakis M. NEMO Prevents RIP Kinase 1-Mediated Epithelial Cell Death and Chronic Intestinal Inflammation by NF-κB-Dependent and -Independent Functions. *Immunity* 2016; **44**: 553-567 [PMID: 26982364 DOI: 10.1016/j.immuni.2016.02.020]
27 **Eissa N**, Hussein H, Kermarrec L, Elgazzar O, Metz-Boutigue MH, Bernstein CN, Ghia JE. Chromofungin (CHR: CHGA47-66) is downregulated in persons with active ulcerative colitis and suppresses pro-inflammatory macrophage function through the inhibition of NF-κB signaling. *Biochem Pharmacol* 2017; **145**: 102-113 [PMID: 28827109 DOI: 10.1016/j.bcp.2017.08.013]
28 **Ullman TA**, Itzkowitz SH. Intestinal inflammation and cancer. *Gastroenterology* 2011; **140**: 1807-1816 [PMID: 21530747 DOI: 10.1053/j.gastro.2011.01.057]
29 **DiDonato JA**, Mercurio F, Karin M. NF-κB and the link between inflammation and cancer. *Immunol Rev* 2012; **246**: 379-400 [PMID: 22435567 DOI: 10.1111/j.1600-065X.2012.01099.x]
30 **Matsuhisa K**, Watari A, Iwamoto K, Kondoh M, Yagi K. Lignosulfonic acid attenuates NF-κB activation and intestinal epithelial barrier dysfunction induced by TNF-α/IFN-γ in Caco-2 cells. *J Nat Med* 2017; **72**: 448-455 [PMID: 29275476 DOI: 10.1007/s11418-017-1167-5]
31 **Arulselvan P**, Fard MT, Tan WS, Gothai S, Fakurazi S, Norhaizan ME, Kumar SS. Role of Antioxidants and Natural Products in Inflammation. *Oxid Med Cell Longev* 2016; **2016**: 5276130 [PMID: 27803762]
32 **Hui B**, Zhang L, Zhou Q, Hui L. Pristimerin Inhibits LPS-Triggered Neurotoxicity in BV-2 Microglia Cells Through Modulating IRAK1/TRAF6/TAK1-Mediated NF-κB and AP-1 Signaling Pathways In Vitro. *Neurotox Res* 2018; **33**: 268-283 [PMID: 29119451 DOI: 10.1007/s12640-017-9837-3]

P- Reviewer: Zouiten-Mekki L **S- Editor**: Gong ZM
L- Editor: Filipodia **E- Editor**: Huang Y

World Journal of Gastroenterology

Submit a Manuscript: http://www.f6publishing.com

World J Gastroenterol 2018 April 7; 24(13): 1410-1418

DOI: 10.3748/wjg.v24.i13.1410

ISSN 1007-9327 (print) ISSN 2219-2840 (online)

ORIGINAL ARTICLE

Retrospective Cohort Study

Potential triggering factors of acute liver failure as a first manifestation of autoimmune hepatitis-a single center experience of 52 adult patients

Matthias Buechter, Paul Manka, Falko Markus Heinemann, Monika Lindemann, Hideo Andreas Baba, Martin Schlattjan, Ali Canbay, Guido Gerken, Alisan Kahraman

Matthias Buechter, Paul Manka, Guido Gerken, Alisan Kahraman, Department of Gastroenterology and Hepatology, University Clinic of Essen, Essen 45147, Germany

Paul Manka, Division of Transplantation Immunology and Mucosal Biology, King's College, London SE59RJ, United Kingdom

Falko Markus Heinemann, Monika Lindemann, Institute of Transfusion Medicine, University Clinic of Essen, Essen 45147, Germany

Hideo Andreas Baba, Martin Schlattjan, Institute of Pathology, University Clinic of Essen, Essen 45147, Germany

Ali Canbay, Department of Gastroenterology, Hepatology, and Infectious Diseases, Otto-von-Guericke University, Magdeburg 39120, Germany

ORCID number: Matthias Buechter (0000-0003-3394-5492); Paul Manka (0000-0001-8589-7280); Falko Markus Heinemann (0000-0002-9642-1154); Monika Lindemann (0000-0001-6708-4390); Hideo Andreas Baba (0000-0002-1750-5318); Martin Schlattjan (0000-0001-6639-5568); Ali Canbay (0000-0001-6069-7899); Guido Gerken (0000-0001-6734-5001); Alisan Kahraman (0000-0002-2823-6774).

Author contributions: Buechter M analyzed the data and wrote the manuscript; Manka P analyzed the data and performed the statistics; Heinemann FM and Lindemann M performed the HLA-typing; Baba HA and Schlattjan M evaluated the histological specimens; Canbay A and Gerken G treated the patients; Kahraman A treated the patients and designed the study.

Institutional review board statement: This study was reviewed and approved by the ethics committee of the University Clinic of Essen.

Informed consent statement: All patients gave their written informed consent prior to study inclusion.

Conflict-of-interest statement: All authors have nothing to declare.

Data sharing statement: No additional data are available.

Manuscript source: Unsolicited manuscript

Correspondence to: Kahraman Alisan, MD, Associate Professor, Department of Gastroenterology and Hepatology, University Hospital of Essen, Hufelandstr 55, Essen 45122, Germany. alisan.kahraman@uk-essen.de
Telephone: +49-201-72384797
Fax: +49-201-7235655

Received: December 6, 2017
Peer-review started: December 6, 2017
First decision: January 18, 2018
Revised: February 21, 2018
Accepted: March 3, 2018
Article in press: March 3, 2018
Published online: April 7, 2018

Abstract

AIM

To investigate potential triggering factors leading to acute liver failure (ALF) as the initial presentation of autoimmune hepatitis (AIH).

METHODS

A total of 565 patients treated at our Department between 2005 and 2017 for histologically-proven AIH were retrospectively analyzed. However, 52 patients (9.2%) fulfilled the criteria for ALF defined by the "American Association for the Study of the Liver (AASLD)". According to this definition, patients with "acute-on-chronic" or "acute-on-cirrhosis" liver failure were excluded. Following parameters with focus on potential triggering factors were evaluated: Patients' demographics, causation of liver failure, laboratory data (liver enzymes, MELD-score, autoimmune markers, virus serology), liver histology, immunosuppressive regime, and finally, outcome of our patients.

RESULTS

The majority of patients with ALF were female (84.6%) and mean age was 43.6 ± 14.9 years. Interestingly, none of the patients with ALF was positive for anti-liver kidney microsomal antibody (LKM). We could identify potential triggering factors in 26/52 (50.0%) of previously healthy patients presenting ALF as their first manifestation of AIH. These were drug-induced ALF (57.7%), virus-induced ALF (30.8%), and preceding surgery in general anesthesia (11.5%), respectively. Unfortunately, 6 out of 52 patients (11.5%) did not survive ALF and 3 patients (5.7%) underwent liver transplantation (LT). Comparing data of survivors and patients with non-recovery following treatment, MELD-score ($P < 0.001$), age ($P < 0.05$), creatinine ($P < 0.01$), and finally, ALT-values ($P < 0.05$) reached statistical significance.

CONCLUSION

Drugs, viral infections, and previous surgery may trigger ALF as the initial presentation of AIH. Advanced age and high MELD-score were associated with lethal outcome.

Key words: Acute liver failure; Autoimmune hepatitis; Drug-induced liver injury; Triggering factors; MELD-score

Core tip: Autoimmune hepatitis is considered to manifest as a chronic disease. In few cases, the clinician is challenged with patients revealing acute liver failure as their first manifestation of autoimmune hepatitis (AIH). The aim of our study was to investigate features of especially these patients with focus on potential triggering factors. We identified triggering factors in half of our patients (26 out of 52 patients with acute liver failure within a total cohort of 565 AIH patients). These were drugs, viral infections, and surgery. Advanced age and high MELD-score were associated with lethal outcome. Consequently, the clinician would be well-advised to document these underlying conditions.

Buechter M, Manka P, Heinemann FM, Lindemann M, Baba HA, Schlattjan M, Canbay A, Gerken G, Kahraman A. Potential triggering factors of acute liver failure as a first manifestation of autoimmune hepatitis-a single center experience of 52 adult patients. *World J Gastroenterol* 2018; 24(13): 1410-1418 Available from: URL: http://www.wjgnet.com/1007-9327/full/v24/i13/1410.htm DOI: http://dx.doi.org/10.3748/wjg.v24.i13.1410

INTRODUCTION

Autoimmune hepatitis (AIH) is a complex disease characterized by immune-mediated destruction of hepatic parenchyma, female gender bias, presence of auto-antibodies, hypergammaglobulinaemia, association with other autoimmune conditions, and excellent response to immunosuppressive therapy[1]. Since its first description by Waldenström in the early 1950's, AIH was considered to manifest as a chronic liver disease and its fulminant presentation was not commonly reported[2-4]. Over the last decades, it has become apparent that AIH can occur with diverse clinical phenotypes and its classical perception of a chronic inflammatory liver disease that affects mainly young Caucasian women has been expanded[5-8].

However, approximately 20%-30% of the patients reveal an acute presentation which may be induced by a triggering agent such as previous viral infections, toxic injury or treatment with immune-modifying drugs. Infectious triggers are commonly indicated as being involved in the induction of autoimmune diseases, with Epstein-Barr (EBV) or Cytomegalovirus (CMV) being implicated in several autoimmune liver disorders, such as type Ⅰ autoimmune hepatitis or primary biliary cholangitis (PBC)[9]. A remarkable proportion of patients with acute manifestation can develop acute liver failure (ALF), particularly in case of delayed diagnosis and treatment[4,10,11].

ALF is characterized by a rapid onset of severe hepatocyte injury without prior liver disease that is associated with significant morbidity and mortality[12,13]. The most widely accepted definition of ALF includes evidence of coagulation abnormality, usually an INR $\geqslant$ 1.5, and any degree of mental alteration (hepatic encephalopathy) in a patient without pre-existing chronic liver disease with an illness of < 26 wk duration[14].

Patients with AIH-induced ALF are frequently difficult to diagnose due to absence of serological markers including anti-nuclear (ANA), anti-smooth muscle (SMA), anti-liver kidney microsomal (LKM) antibodies, and normal immunoglobulin G (IgG)-levels in numerous cases[15,16]. In this setting, determination of major histocompatibility complex HLA-loci (*e.g.*, HLA-DR3 and -DR4), which are reported to have a strong association with AIH, might be helpful additional diagnostic tools[1,8,17].

In the daily clinical setting, the hepatologist is frequently faced with patients having unknown elevations of their liver enzymes for years or even decades. Most of these asymptomatic patients present only marginal increased liver enzymes with normal liver

function. Routine work-up of these cases leads finally to the diagnosis of underlying AIH and - following steroid therapy - transaminases often return to normal ranges. However, in few cases, one is challenged with patients previously being healthy without any signs of hepatopathy but rapidly demonstrating a life-threatening acute liver failure as their first manifestation of AIH with the necessity of urgent organ transplantation. Therefore, the aim of our study was to investigate demographic characteristics and clinical course of especially these patients presented with ALF as their initial presentation of AIH with special focus on potential triggering factors which may activate the "autoimmune machinery" leading to onset of the disease.

MATERIALS AND METHODS

Patients' characteristics, data collection and ethical considerations

In this retrospective study between 01/2005 and 04/2017, a total of 565 patients with histologically-proven AIH were analyzed, from whom 52 previously healthy patients suffered from ALF as their initial presentation of autoimmune hepatitis. According to the criteria defined by the "American Association for the Study of the Liver (AASLD)", ALF was diagnosed by elevation of liver enzymes in combination with hepatic encephalopathy (HE) and coagulopathy (INR > 1.5) in the absence of a pre-existing chronic liver disease[14]. AIH was diagnosed according to the "Diagnostic Scoring System of the International Autoimmune Hepatitis Group" including analysis of auto-antibodies, IgG-levels, histological features, and exclusion of viral markers[18,19]. Liver histology was available for the whole study population and was obtained either by percutaneous- or laparoscopy-guided biopsy (Figure 1A and B). Only adult patients (age ⩾ 18 years) were included in the study. The University Clinic of Essen ethics committee approved the retrospective, anonymous analysis of the data and the study was conducted according to the principles expressed in the Declaration of Helsinki. All patients gave their written informed consent prior to study inclusion.

Laboratory parameters

At initial presentation, alanine-aminotransferase (ALT), total bilirubin, serum creatinine, INR, IgG, IgM, γ-globulins, antibody profile (ANA, AMA, ANCA, SMA, LKM, SLA), and finally, HLA-loci (HLA- A1, -B8, -DR3, and -DR4) were analyzed. Each patient was also tested for viral markers (anti-HAV IgM, HBs-Ag, anti-HBc IgM, HBeAg, anti-HBe, anti-HBs, anti-HCV, anti-HDV-EIA, anti-HEV IgM, and PCR's for HBV, HCV, HEV, HSV, CMV, EBV), transferrin-saturation, ceruloplasmin, copper in serum, soluble interleukin-II receptor, α1-antitrypsin, and finally, GLDH. In suspected cases of Wilson's disease, additional examinations were performed (Kayser-Fleischer ring, copper in urine, parameters of hemolysis, and also determination of cupper in the liver biopsy).

RUCAM instrument

The appropriate diagnosis of drug-induced liver injury (DILI) *vs* DILI-AIH involves the collection of historical and laboratory data, including the latency in onset, the rate of resolution after discontinuing treatment, and exclusion of other reasonable causes of liver injury. The advantage of the RUCAM instrument is that it is systematic, thorough, and objective. We therefore used this instrument in our study population as - at present - it is considered the best method for assessing causality in DILI.

Liver histology

Liver biopsy was performed in all patients with evidence of typical histopathological features of AIH, namely presence of interface hepatitis, lymphoplasmacytic cell infiltration exceeding the borders of the portal tract, emperipolesis, and rosette formations, respectively. Differentiating between drug-induced ALF and AIH-induced ALF is difficult on the basis of histology alone. In both cases plasma cell rich inflammation with interface hepatitis can be present. In order to differentiate DILI from AIH clinical, historical, and laboratory data have to be considered. If EBV, CMV or HEV infection was suspected, viral detection by means of immunohistochemistry, in situ hybridization, and PCR was also performed.

Immunosuppressive therapy and definition of non-recovery

After diagnosis of AIH-induced ALF, each patient received standard steroid therapy (1 mg per kg body weight/d) intravenously with consecutive down-tapering to a maintenance dose of 7.5 mg daily. Non-recovery was defined as death or liver transplantation (LT) within 28 d despite steroid treatment and initiation of immunosuppressive therapy with azathioprine.

Statistical analysis

Statistical analysis was performed with GraphPad Prism, version 6.00 for MacOsX (GraphPad Software, San Diego, CA, United States). For descriptive statistics medians and IQR were determined. All variables were tested for normal distribution with the Kolmogorov-Smirnov test, the Shapiro-Wilk test, and calculation of skew and kurtosis. The Mann-Whitney *U* test was used to compare differences between independent groups. Categorical data were tested with the chi-square test and the Kruskal-Wallis test was used for multiple comparisons. $P < 0.05$ was considered statistically significant. The whiskers used in the graphs extend down to the 5th percentile and up to the 95th percentile.

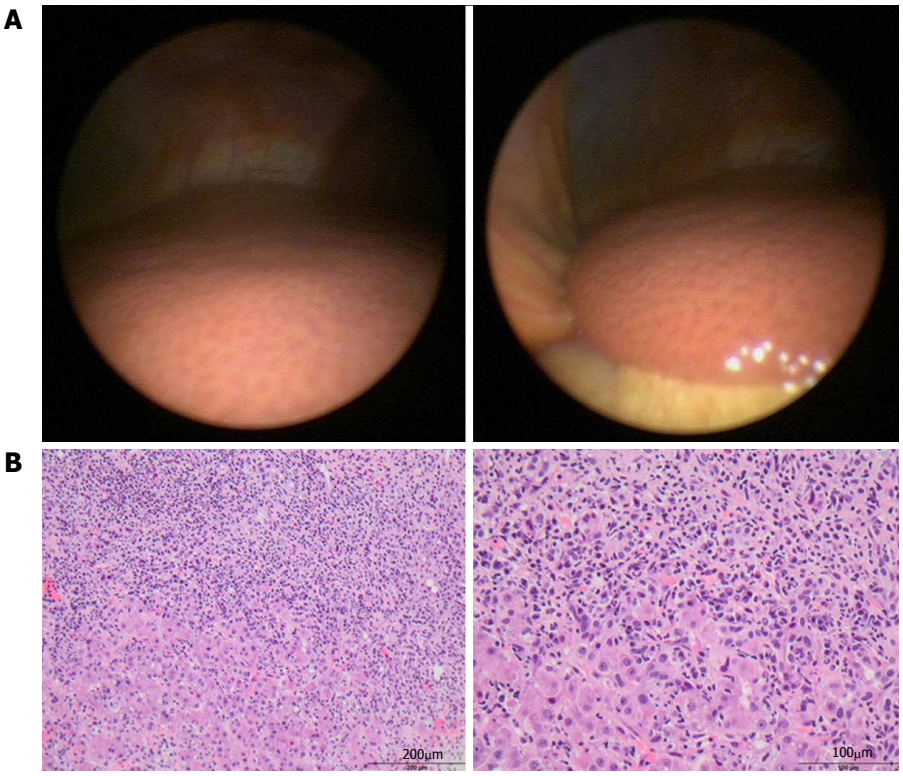

Figure 1 Mini-laparoscopy of a patient with acute liver failure due to newly diagnosed autoimmune hepatitis exemplarily showing the right liver lobe with diffuse capsular swelling, regenerative nodules, and rounded lower margin (upper panel) (A), and liver histology of the same patient with AIH-induced ALF (B). Left panel demonstrating severe inflammation with interface hepatitis (original magnification 200 ×) and the right panel with higher magnification (400 ×) revealing numerous plasma cells extending from the portal tract into the adjacent parenchyma (lower panel).

RESULTS

Patients' demographics, laboratory data, and immunosuppressive regime

Fifty-two out of 565 patients with AIH suffered from ALF as their initial presentation (9.2%) (Figure 1A and B) and were included in the study. Mean age of the study population was 43.6 ± 14.9 (19-76) years while the majority was of female gender (44/52, 84.6%). Laboratory parameters with median values on admission were as follows: ALT: 1391.0 (843.5-2154.5) U/L, total bilirubin: 14.3 (11.7-18.7) mg/dL, serum creatinine: 0.76 (0.55-0.95) mg/dL, INR: 1.78 (1.64-2.00), immunoglobulin G: 17.2 (13.1-22.8) g/L, and finally, γ-globulin-fraction: 24.5% (19.5%-29.3%). Calculated median labMELD-score was 24 (22-26) points. All patients with AIH-induced ALF received a pulse therapy with steroids starting with 1 mg/kg body weight intravenously. A total of 30 patients (57.7%) continued steroids in a daily dose of 7.5 mg to maintain remission. Azathioprine (in 27 patients, 51.9%) and also cyclosporine A (in 7 patients, 13.5%) were also used to maintain remission. Hepatic encephalopathy (HE) was classified using the West Haven criteria. We found HE grade Ⅰ in 46 of our 52 patients (88.4%), HE grade Ⅱ in 2 patients, HE grade Ⅲ in 2 patients, and finally, HE grade Ⅳ in 2 further patients, respectively. Unfortunately, patients with HE grade Ⅳ had poor prognosis and died of acute liver failure. We found no correlation between grade of HE and antibody or HLA-profiles. Moreover, we also did not found a correlation between the triggering factors with severity of HE (data nor shown). Patients' demographics and laboratory data are summarized in Table 1.

HLA-typing and auto-antibody profiles

Thirty-six out of 52 patients were positive for ANA (69.2%), 6/52 for AMA (11.5%), 4/52 for SMA (7.7%), and 2/52 for SLA (3.8%), respectively. Interestingly, none of the adult patients with acute liver failure was either positive for ANCA or LKM. Data on HLA-loci were available for 34 patients (65.4%) showing the following results: HLA-A1 positivity in 15/34 (44.1%), HLA-B8 in 6/34 (17.6%), HLA-DR3 in 8/34 (23.5%), and HLA-DR4 in 11/34 patients (32.4%). HLA- and antibody profiles of our study population are demonstrated in Figure 2A and B.

Potential triggering factors for ALF in patients with first manifestation of AIH

We could identify potential triggering factors for ALF in patients with their first manifestation of AIH in 26/52 patients (50.0%). These triggers were predominantly drugs [15/26 (57.7%), namely non-steroidal anti-inflammatory drugs (NSAID) (n = 8), antibiotics (n = 5),

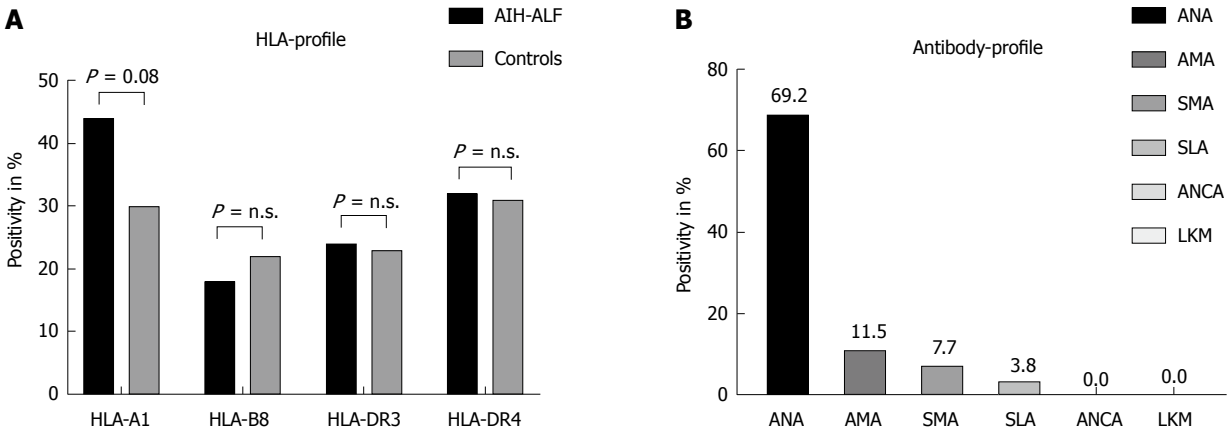

Figure 2 HLA-profile of the study population (*n* = 34) investigating HLA-A1, -B8, -DR3, and -DR4 status (A), and antibody-profile of the study population (*n* = 52) demonstrating positivity for ANA-, AMA-, SMA-, SLA-, ANCA-, and LKM-titers (B). ANA: Anti-nuclear; SMA: Anti-smooth muscle; LKM: Anti-liver kidney microsomal.

Table 1 Patients' demographics and laboratory with *n* = 52 demonstrating autoimmune hepatitis-induced acute liver failure (9.2%)

Study population (*n* = 52) with AIH-induced ALF	
Mean age (yr)	43.6 ± 14.9 (19-76)
Male	8 (15.4%)
Female	44 (84.6%)
Hepatic encephalopathy	Grade Ⅰ: 46/52 (88.4%)
	Grade Ⅱ: 2/52 (3.8%)
	Grade Ⅲ: 2/52 (3.8%)
	Grade Ⅳ: 2/52 (3.8%)
Immunosuppressive therapy	Steroid induction: 52/52 (100%)
	Steroid maintenance: 30/52 (57.7%)
	Steroid withdrawal: 20/52 (42.3%)
	Azathioprine: 27/52 (51.9%)
	Cyclosporine A: 7/52 (13.5%)
ALT (U/L)	1391.0 (843.5-2154.5)
Total bilirubin (mg/dL)	14.3 (11.7-18.7)
Creatinine (mg/dL)	0.76 (0.55-0.95)
INR	1.78 (1.64-2.00)
LabMELD-score	24 (22-26)
Immunoglobulin G (g/L)	17.2(13.1-22.8)
γ-globulin-fraction (%)	24.5 (19.5-29.3)

Data represents median and IQR. AIH: Autoimmune hepatitis; ALF: Acute liver failure; ALT: Alanine-aminotransferase.

ipilimumab (*n* = 1), and rivaroxaban (*n* = 1)] followed by previous acute viral infections [8/26 (30.8%), namely Epstein-Barr virus (*n* = 4), Cytomegalovirus (*n* = 3), and hepatitis E virus (*n* = 1)]. Finally, the remaining 3 patients underwent previous surgery in general anesthesia (11.5%) (Figure 3).

Higher age, creatinine, and MELD-score were associated with lethal outcome or need for liver transplantation, while elevated liver enzymes indicated recovery

Unfortunately, 6 out of 52 patients did not receive an organ offer and died due to ALF while 3 further patients underwent liver transplantation (non-recovery group). When comparing data of these patients with patients who responded to steroids and survived ALF (recovery group), statistical analysis revealed significant differences in terms of age [median age: 40.0 (28.0-52.0) years for the recovery group *vs* median age: 49.0 (44.0-62.5) years, for the non-recovery group, *P* = 0.031], serum creatinine [median for the recovery group: 0.72 (0.51-0.92) mg/dL *vs* median for the non-recovery group: 0.98 (0.77-1.61) mg/dL, *P* = 0.0069], labMELD-score [median for the recovery group: 23 (22-25) *vs* median for the non-recovery group: 27 (25-30), *P* = 0.0007, and finally, median ALT-values for the recovery group 1512 (904-2276) U/L *vs* median for the non-recovery group: 711 (324-1391) U/L, *P* = 0.0157) (Table 2 and Figure 4A-D). None of the remaining AIH patients of our cohort (*n* = 513 patients) developed acute liver failure under therapy with corticosteroids and/or immunosuppressive therapy. However, no significance was found for markedly increased bilirubin levels comparing both groups.

DISCUSSION

The etiology of autoimmune hepatitis (AIH) is uncertain but - in some cases - the disease can be triggered by external factors such as viruses or drugs. AIH usually develops in individuals with genetic background. Many drugs have been linked to AIH phenotypes, which sometimes persist after drug discontinuation, suggesting that they awaken latent autoimmunity. Growing information on the relationship of drugs and AIH is being available, being drugs and biologic agents more frequently involved in cases allowing to establish a causal relationship[20-23]. According to current literature, the frequency of patients with drug-induced AIH (DILI-AIH) is reported to range from 9%-17% in overall patients diagnosed with AIH[24,25].

Drug-induced liver injury (DILI) is the most common cause of acute liver failure (ALF) and responsible for approximately 50% of the cases in the United States and Western Europe. DILI may be dose-dependent and predictable (*e.g.*, acetaminophen-induced hepatotoxicity)

Table 2 Patients' data stratified by recovery and non-recovery (*n* = 52)

	Recovery (*n* = 43)	Non-recovery (*n* = 9)	*P* value
Age (yr)	40.0 (28.0-52.0)	49.0 (44.0-62.5)	0.031
Male/female	7/36	1/8	NS
ALT (U/L)	1512 (904-2276)	711 (324-1391)	0.0157
Total bilirubin (mg/dL)	14.0 (11.3-18.7)	16.1 (11.8-23.6)	NS
Creatinine (mg/dL)	0.72 (0.51-0.92)	0.98 (0.77-1.61)	0.0069
INR	1.76 (1.63-1.98)	1.96 (1.75-2.79)	0.0644
LabMELD-score	23 (22-25)	27 (25-30)	0.0007

Data represents median and IQR. ALF: Acute liver failure.

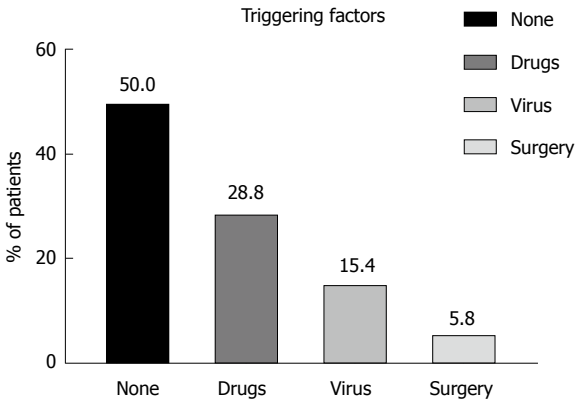

Figure 3 Potential triggering factors for acute liver failure in patients with their first manifestation of autoimmune hepatitis (*n* = 52).

or idiosyncratic, unpredictable, and probably independent of dose[12,26]. Autoimmune hepatitis - on the contrary - is a relatively rare cause of ALF in developed countries with an incidence of approximately 5%[27]. According to the "Acute Liver Failure Study Group (ALFSG)" registry, including 2436 patients between 1998 and 2016 in the United States, 163 (6.7%) were diagnosed with ALF due to AIH[28]. In our cohort 9.2% of AIH patients presented ALF. DILI is reported to have a phenotype of autoimmunity similar to AIH and distinguishing these entities still remains a challenge[29]. However, immune-mediated DILI nearly always resolves or becomes quiescent when drugs are withdrawn[24,30]. In contrast, in patients with drug-induced AIH, it can be assumed that predisposition for AIH existed before, but the disease was quiescent and remained undiagnosed until this drug triggered the autoimmune process. Recently, Licata and colleagues reported 12 patients from a series of 136 subjects with DILI that were diagnosed as drug-induced AIH (9%)[31]. Accordingly, Kuzu *et al*[32] described 82 DILI patients from whom five (6%) were diagnosed with DILI-AIH.

AIH - in its classical perception - commonly presents as a chronic hepatopathy. On the one hand, the majority of patients with AIH are diagnosed due to accidentally and repeatedly elevated liver enzymes in routine check-up examinations without having symptoms. On the other hand, AIH can lead to fulminant acute liver failure which is associated with high morbidity and mortality. The most important genetic risk factor is human leukocyte antigen, especially HLA-DR, whereas the role of environmental factors is not completely understood. Immunologically, disruption of the immune tolerance to autologous liver antigens may be a trigger of AIH. According to current data, triggering agents which may lead to this disruption are mainly unknown, but may include viral infections, environmental toxins, drugs, and vaccinations. There is growing evidence for a loss of immune tolerance to self-antigens playing a part in the development of this condition[33-38]. Genetic risk association studies have identified HLA loci for the development of disease and providing prognostic information[38,39]. Interestingly, when compared to published allele frequencies in healthy controls, HLA genotypes of our cohort did not reach statistical significance while only HLA-A1 status revealed a positive trend[40]. Moreover, none of our adult patients included in the analyses was diagnosed with LKM-positive AIH type 2. This observation matches with current literature: Kessler and colleagues, who analyzed 30 patients with fulminant hepatic failure as the initial presentation of acute AIH, found that only 3% were LKM-positive[3]. Likewise, di Giorgio *et al*[41] described 46 children with fulminant hepatic failure of autoimmune etiology, none was LKM-positive.

In this study, we aimed to check potential triggering factors which may lead to ALF as the initial presentation of AIH. However, in 50% of the patients, triggering factors for ALF as the initial presentation of AIH were suspected. These were predominantly drugs (*e.g.*, NSAID and antibiotics), followed by previous viral infections, and surgery in general anesthesia, respectively. Non-recovery - defined as death or liver transplantation within 28 d - was found among 9/52 patients (17.3%). Reviewing current literature, results of non-recovery in patients with ALF due to AIH differ significantly and range from 10%-60%[3,41,42]. Risk factors for non-recovery among our patients were increase in age, MELD-score, and creatinine levels, while higher liver enzymes (ALT-values) were associated with improved spontaneous recovery. Our center previously demonstrated that high ammonia, low albumin, and low ALT-levels were associated with worse outcome in childhood acute liver failure[43]. From our long-time clinical experience in patients with acute

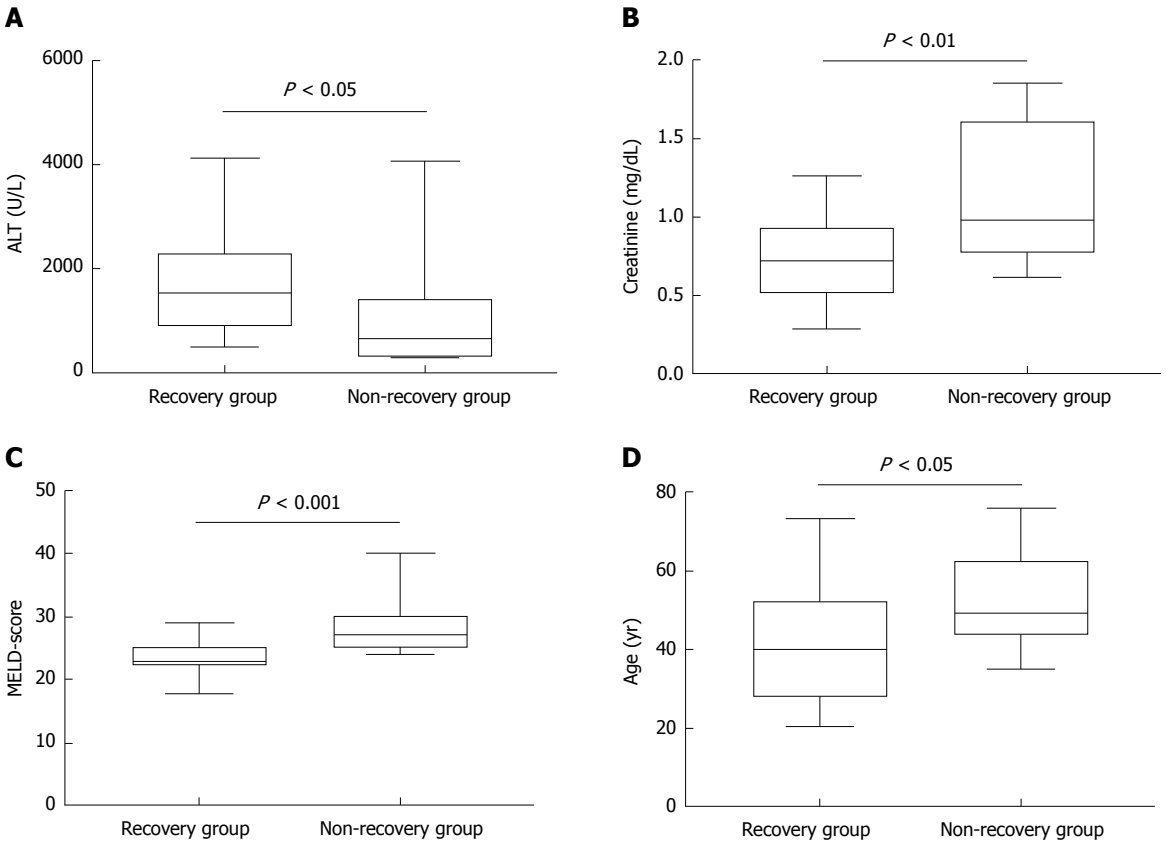

Figure 4 Higher age, creatinine, and MELD-score were associated with lethal outcome. A: Median alanine-aminotransferase (ALT)-values of patients with recovery as compared to the non-recovery group, $P < 0.05$; B: Median serum creatinine levels of patients with recovery and non-recovery, $P < 0.01$; C: Median labMELD-score of patients with recovery and non-recovery, $P < 0.001$; D: Median age of patients with recovery and non-recovery, $P < 0.05$.

liver failure, we observed that patients with high ALT-values recovered better than their counterparts with low ALT-values indicating that there is still functioning liver parenchyma despite the fact of acute liver injury. On the one hand, extreme inflammation may reflect less grade of already existing hepatic necrosis and higher proportion of vital hepatocytes while on the other hand, inflammation may increase the probability of response to immunosuppressive treatment.

In summary, approximately 9% of our patients were diagnosed with acute liver failure as their initial presentation of autoimmune hepatitis which may be potentially induced by drugs, viral infections, and surgery in general anesthesia. Consequently, the clinician would be well-advised to accurately document these underlying conditions. Increases of age, MELD-score, and creatinine levels may be risk factors for lethal outcome or need for urgent liver transplantation, while higher levels of transaminases come along with improved spontaneous recovery.

ARTICLE HIGHLIGHTS

Research background

Autoimmune hepatitis (AIH) is generally considered to manifest as a chronic liver disease. So far, only limited data are available investigating patients presenting a fulminant acute liver failure as a first manifestation of this autoimmune disorder. The significance of our study was therefore to investigate the circumstances leading to acute liver failure and onset of autoimmune hepatitis.

Research motivation

In the daily clinical setting, the hepatologist is frequently faced with patients demonstrating only a mild elevation of their liver enzymes. Routine work-up of these cases leads finally to the diagnosis of underlying AIH. However, in few cases, one is challenged with patients without any signs of hepatopathy but rapidly developing a life-threatening acute liver failure (ALF) as their first manifestation of AIH. We here presented potential triggering factors which may activate the "autoimmune machinery" leading to ALF.

Research objectives

The main objective of the present study was to gather more information with focus on potential triggering factors leading to acute presentation of AIH with consecutive liver failure. The clinician would be well-advised to accurately document these underlying conditions.

Research methods

In our retrospective cohort study we investigated patients with histologically-proven AIH and further analyzed the patients who presented acute liver failure. Patients' demographics, laboratory data, immunosuppressive regime, histology, and outcome were documented and studied.

Research results

We were able to identify potential triggering factors in 26/52 (50.0%) of our previously healthy patients presenting ALF as their first manifestation of AIH. These were drug-induced (*e.g.,* non-steroidal anti-inflammatory drugs and antibiotics) ALF (57.7%), virus-induced (Epstein-Barr, Cytomegalovirus and

HEV) ALF (30.8%), and surgery in general anesthesia (11.5%), respectively.

Research conclusions

Approximately 9% of our patients were diagnosed with ALF as their initial presentation of AIH which may be potentially induced by drugs, viral infections, and surgery in general anesthesia. Consequently, the clinician would be well-advised to ask his patients for hepato-toxic drugs and accurately document these underlying conditions. Increases of age, MELD-score, and creatinine levels were associated with lethal outcome or need for urgent liver transplantation.

Research perspectives

With our study and findings we hope to further attract the physician's attention especially in cases of acute liver failure induced by autoimmune hepatitis. In some cases, these disorders may be triggered by drugs and hepato-tropic viruses. We hope that more studies investigating acute liver failure as a first manifestation of AIH will be available in future.

ACKNOWLEDGMENTS

We thank Professor Dr. Gregory Gores from the Division of Gastroenterology and Hepatology, Mayo Clinic Rochester (Minnesota, United States) for his valuable contribution and his permanent support. We also thank the anonymous Reviewers for his/her thoughtful and constructive examination of our manuscript.

REFERENCES

1 **Wang Q**, Yang F, Miao Q, Krawitt EL, Gershwin ME, Ma X. The clinical phenotypes of autoimmune hepatitis: A comprehensive review. *J Autoimmun* 2016; **66**: 98-107 [PMID: 26614611 DOI: 10.1016/j.jaut.2015.10.006]
2 **WALDENSTROM J**. Liver, blood proteins and nutritive protein. *Dtsch Z Verdau Stoffwechselkr* 1953; **9**: 113-119 [PMID: 13150939]
3 **Kessler WR**, Cummings OW, Eckert G, Chalasani N, Lumeng L, Kwo PY. Fulminant hepatic failure as the initial presentation of acute autoimmune hepatitis. *Clin Gastroenterol Hepatol* 2004; **2**: 625-631 [PMID: 15224287]
4 **Mendizabal M**, Marciano S, Videla MG, Anders M, Zerega A, Balderramo DC, Tisi Baña MR, Barrabino M, Gil O, Mastai R, Yantorno S, Gadano A, Silva MO. Fulminant presentation of autoimmune hepatitis: clinical features and early predictors of corticosteroid treatment failure. *Eur J Gastroenterol Hepatol* 2015; **27**: 644-648 [PMID: 25923939 DOI: 10.1097/MEG.0000000000000353]
5 **Czaja AJ**. Diagnosis and Management of Autoimmune Hepatitis: Current Status and Future Directions. *Gut Liver* 2016; **10**: 177-203 [PMID: 26934884 DOI: 10.5009/gnl15352]
6 **European Association for the Study of the Liver**. EASL Clinical Practice Guidelines: Autoimmune hepatitis. *J Hepatol* 2015; **63**: 971-1004 [PMID: 26341719 DOI: 10.1016/j.jhep.2015.06.030]
7 **Lammert C**, Loy VM, Oshima K, Gawrieh S. Management of Difficult Cases of Autoimmune Hepatitis. *Curr Gastroenterol Rep* 2016; **18**: 9 [PMID: 26780632 DOI: 10.1007/s11894-015-0484-7]
8 **Heneghan MA**, Yeoman AD, Verma S, Smith AD, Longhi MS. Autoimmune hepatitis. *Lancet* 2013; **382**: 1433-1444 [PMID: 23768844 DOI: 10.1016/S0140-6736(12)62163-1]
9 **Rigopoulou EI**, Smyk DS, Matthews CE, Billinis C, Burroughs AK, Lenzi M, Bogdanos DP. Epstein-barr virus as a trigger of autoimmune liver diseases. *Adv Virol* 2012; **2012**: 987471 [PMID: 22693505 DOI: 10.1155/2012/987471]
10 **Dhawan A**. Acute liver failure in children and adolescents. *Clin Res Hepatol Gastroenterol* 2012; **36**: 278-283 [PMID: 22521555 DOI: 10.1016/j.clinre.2012.03.022]
11 **Sonthalia N**, Rathi PM, Jain SS, Surude RG, Mohite AR, Pawar SV, Contractor Q. Natural History and Treatment Outcomes of Severe Autoimmune Hepatitis. *J Clin Gastroenterol* 2017; **51**: 548-556 [PMID: 28272079 DOI: 10.1097/MCG.0000000000000805]
12 **Bernal W**, Wendon J. Acute liver failure. *N Engl J Med* 2013; **369**: 2525-2534 [PMID: 24369077 DOI: 10.1056/NEJMra1208937]
13 **Reddy KR**, Ellerbe C, Schilsky M, Stravitz RT, Fontana RJ, Durkalski V, Lee WM; Acute Liver Failure Study Group. Determinants of outcome among patients with acute liver failure listed for liver transplantation in the United States. *Liver Transpl* 2016; **22**: 505-515 [PMID: 26421889 DOI: 10.1002/lt.24347]
14 **Polson J**, Lee WM; American Association for the Study of Liver Disease. AASLD position paper: the management of acute liver failure. *Hepatology* 2005; **41**: 1179-1197 [PMID: 15841455 DOI: 10.1002/hep.20703]
15 **Czaja AJ**. Autoantibodies as prognostic markers in autoimmune liver disease. *Dig Dis Sci* 2010; **55**: 2144-2161 [PMID: 20464491 DOI: 10.1007/s10620-010-1268-4]
16 **Bernal W**, Ma Y, Smith HM, Portmann B, Wendon J, Vergani D. The significance of autoantibodies and immunoglobulins in acute liver failure: a cohort study. *J Hepatol* 2007; **47**: 664-670 [PMID: 17602781 DOI: 10.1016/j.jhep.2007.05.011]
17 **Zachou K**, Muratori P, Koukoulis GK, Granito A, Gatselis N, Fabbri A, Dalekos GN, Muratori L. Review article: autoimmune hepatitis -- current management and challenges. *Aliment Pharmacol Ther* 2013; **38**: 887-913 [PMID: 24010812 DOI: 10.1111/apt.12470]
18 **Czaja AJ**. Performance parameters of the diagnostic scoring systems for autoimmune hepatitis. *Hepatology* 2008; **48**: 1540-1548 [PMID: 18924244 DOI: 10.1002/hep.22513]
19 **Hennes EM**, Zeniya M, Czaja AJ, Parés A, Dalekos GN, Krawitt EL, Bittencourt PL, Porta G, Boberg KM, Hofer H, Bianchi FB, Shibata M, Schramm C, Eisenmann de Torres B, Galle PR, McFarlane I, Dienes HP, Lohse AW; International Autoimmune Hepatitis Group. Simplified criteria for the diagnosis of autoimmune hepatitis. *Hepatology* 2008; **48**: 169-176 [PMID: 18537184 DOI: 10.1002/hep.22322]
20 **Castiella A**, Zapata E, Lucena MI, Andrade RJ. Drug-induced autoimmune liver disease: A diagnostic dilemma of an increasingly reported disease. *World J Hepatol* 2014; **6**: 160-168 [PMID: 24799984 DOI: 10.4254/wjh.v6.i4.160]
21 **Watkins PB**, Seeff LB. Drug-induced liver injury: summary of a single topic clinical research conference. *Hepatology* 2006; **43**: 618-631 [PMID: 16496329 DOI: 10.1002/hep.21095]
22 **Alla V**, Abraham J, Siddiqui J, Raina D, Wu GY, Chalasani NP, Bonkovsky HL. Autoimmune hepatitis triggered by statins. *J Clin Gastroenterol* 2006; **40**: 757-761 [PMID: 16940892]
23 **Grasset L**, Guy C, Ollagnier M. Cyclines and acne: pay attention to adverse drug reactions! A recent literature review. *Rev Med Interne* 2003; **24**: 305-316 [PMID: 12763176]
24 **Björnsson E**, Talwalkar J, Treeprasertsuk S, Kamath PS, Takahashi N, Sanderson S, Neuhauser M, Lindor K. Drug-induced autoimmune hepatitis: clinical characteristics and prognosis. *Hepatology* 2010; **51**: 2040-2048 [PMID: 20512992 DOI: 10.1002/hep.23588]
25 **Castiella A**, Lucena MI, Zapata EM, Otazua P, Andrade RJ. Drug-induced autoimmune-like hepatitis: a diagnostic challenge. *Dig Dis Sci* 2011; **56**: 2501-2502; author reply 2502-2503 [PMID: 21674172 DOI: 10.1007/s10620-011-1787-7]
26 **Reuben A**, Koch DG, Lee WM; Acute Liver Failure Study Group. Drug-induced acute liver failure: results of a U.S. multicenter, prospective study. *Hepatology* 2010; **52**: 2065-2076 [PMID: 20949552 DOI: 10.1002/hep.23937]
27 **Lee WM**, Squires RH Jr, Nyberg SL, Doo E, Hoofnagle JH. Acute liver failure: Summary of a workshop. *Hepatology* 2008; **47**: 1401-1415 [PMID: 18318440 DOI: 10.1002/hep.22177]
28 **Tujios SR**, Lee WM. Acute liver failure induced by idiosyncratic reaction to drugs: Challenges in diagnosis and therapy. *Liver Int* 2018; **38**: 6-14 [PMID: 28771932 DOI: 10.1111/liv.13535]
29 **de Boer YS**, Kosinski AS, Urban TJ, Zhao Z, Long N, Chalasani N, Kleiner DE, Hoofnagle JH; Drug-Induced Liver Injury Network. Features of Autoimmune Hepatitis in Patients With Drug-induced Liver Injury. *Clin Gastroenterol Hepatol* 2017; **15**: 103-112.e2

[PMID: 27311619 DOI: 10.1016/j.cgh.2016.05.043]
30 **Liu ZX**, Kaplowitz N. Immune-mediated drug-induced liver disease. *Clin Liver Dis* 2002; **6**: 755-774 [PMID: 12362579]
31 **Licata A**, Maida M, Cabibi D, Butera G, Macaluso FS, Alessi N, Caruso C, Craxì A, Almasio PL. Clinical features and outcomes of patients with drug-induced autoimmune hepatitis: a retrospective cohort study. *Dig Liver Dis* 2014; **46**: 1116-1120 [PMID: 25224696 DOI: 10.1016/j.dld.2014.08.040]
32 **Kuzu UB**, Öztaş E, Turhan N, Saygili F, Suna N, Yildiz H, Kaplan M, Akpinar MY, Akdoğan M, Kaçar S, Kiliç ZM, Köksal AŞ, Ödemiş B, Kayaçetin E. Clinical and histological features of idiosyncratic liver injury: Dilemma in diagnosis of autoimmune hepatitis. *Hepatol Res* 2016; **46**: 277-291 [PMID: 25926402 DOI: 10.1111/hepr.12530]
33 **Aizawa Y**, Hokari A. Autoimmune hepatitis: current challenges and future prospects. *Clin Exp Gastroenterol* 2017; **10**: 9-18 [PMID: 28176894 DOI: 10.2147/CEG.S101440]
34 **Maggiore G**, Nastasio S, Sciveres M. Juvenile autoimmune hepatitis: Spectrum of the disease. *World J Hepatol* 2014; **6**: 464-476 [PMID: 25067998 DOI: 10.4254/wjh.v6.i7.464]
35 **Pischke S**, Iking-Konert C. Hepatitis E infections in rheumatology. A previously underestimated infectious disease? *Z Rheumatol* 2015; **74**: 731-736 [PMID: 26450437 DOI: 10.1007/s00393-015-1631-0]
36 **Lauletta G**, Russi S, Pavone F, Marzullo A, Tampoia M, Sansonno D, Dammacco F. Autoimmune Hepatitis: Factors Involved in Initiation and Methods of Diagnosis and Treatment. *Crit Rev Immunol* 2016; **36**: 407-428 [PMID: 28605347 DOI: 10.1615/CritRevImmunol.2017017868]
37 **van Gemeren MA**, van Wijngaarden P, Doukas M, de Man RA. Vaccine-related autoimmune hepatitis: the same disease as idiopathic autoimmune hepatitis? Two clinical reports and review. *Scand J Gastroenterol* 2017; **52**: 18-22 [PMID: 27565372 DOI: 10.1080/00365521.2016.1224379]
38 **Arndtz K**, Hirschfield GM. The Pathogenesis of Autoimmune Liver Disease. *Dig Dis* 2016; **34**: 327-333 [PMID: 27170385 DOI: 10.1159/000444471]
39 **Webb GJ**, Hirschfield GM. Using GWAS to identify genetic predisposition in hepatic autoimmunity. *J Autoimmun* 2016; **66**: 25-39 [PMID: 26347073 DOI: 10.1016/j.jaut.2015.08.016]
40 **Maiers M**, Gragert L, Madbouly A, Steiner D, Marsh SG, Gourraud PA, Oudshoorn M, van der Zanden H, Schmidt AH, Pingel J, Hofmann J, Müller C, Eberhard HP. 16(th) IHIW: global analysis of registry HLA haplotypes from 20 million individuals: report from the IHIW Registry Diversity Group. *Int J Immunogenet* 2013; **40**: 66-71 [PMID: 23280139 DOI: 10.1111/iji.12031]
41 **Di Giorgio A**, Bravi M, Bonanomi E, Alessio G, Sonzogni A, Zen Y, Colledan M, D'Antiga L. Fulminant hepatic failure of autoimmune aetiology in children. *J Pediatr Gastroenterol Nutr* 2015; **60**: 159-164 [PMID: 25304891 DOI: 10.1097/MPG.0000000000000593]
42 **Yeoman AD**, Westbrook RH, Zen Y, Bernal W, Al-Chalabi T, Wendon JA, O'Grady JG, Heneghan MA. Prognosis of acute severe autoimmune hepatitis (AS-AIH): the role of corticosteroids in modifying outcome. *J Hepatol* 2014; **61**: 876-882 [PMID: 24842305 DOI: 10.1016/j.jhep.2014.05.021]
43 **Kathemann S**, Bechmann LP, Sowa JP, Manka P, Dechêne A, Gerner P, Lainka E, Hoyer PF, Feldstein AE, Canbay A. Etiology, outcome and prognostic factors of childhood acute liver failure in a German Single Center. *Ann Hepatol* 2015; **14**: 722-728 [PMID: 26256901]

P- Reviewer: Eshraghian A, Lei YC, McMillin MA
S- Editor: Wang XJ **L- Editor**: A **E- Editor**: Huang Y

World Journal of Gastroenterology

Submit a Manuscript: http://www.f6publishing.com

World J Gastroenterol 2018 April 7; 24(13): 1419-1428

DOI: 10.3748/wjg.v24.i13.1419

ISSN 1007-9327 (print) ISSN 2219-2840 (online)

ORIGINAL ARTICLE

Retrospective Cohort Study

Helicobacter pylori infection in subjects negative for high titer serum antibody

Osamu Toyoshima, Toshihiro Nishizawa, Masahide Arita, Yosuke Kataoka, Kosuke Sakitani, Shuntaro Yoshida, Hiroharu Yamashita, Keisuke Hata, Hidenobu Watanabe, Hidekazu Suzuki

Osamu Toyoshima, Toshihiro Nishizawa, Masahide Arita, Yosuke Kataoka, Kosuke Sakitani, Shuntaro Yoshida, Hiroharu Yamashita, Keisuke Hata, Department of Gastroenterology, Toyoshima Endoscopy Clinic, Tokyo 1570066, Japan

Hidenobu Watanabe, Department of Pathology, Pathology and Cytology Laboratory Japan, Tokyo 1660003, Japan

Hidekazu Suzuki, Medical Education Center, Keio University School of Medicine, Tokyo 1608582, Japan

ORCID number: Osamu Toyoshima (0000-0002-6953-6079); Toshihiro Nishizawa (0000-0003-4876-3384); Masahide Arita (0000-0003-1952-8086); Yosuke Kataoka (0000-0002-8374-6558); Kosuke Sakitani (0000-0002-4537-6023); Shuntaro Yoshida (0000-0002-9437-9132); Hiroharu Yamashita (0000-0002-9468-3716); Keisuke Hata (0000-0003-4064-8701); Hidenobu Watanabe (0000-0002-7871-4738); Hidekazu Suzuki (0000-0002-3855-3140).

Author contributions: All authors were involved in designing the study; Toyoshima O, Nishizawa T and Suzuki H prepared the manuscript; Watanabe H was involved with histological diagnoses; Toyoshima O contributed to statistical analyses.

Institutional review board statement: This retrospective study was approved by the Ethical Review Committee of Hattori Clinic on September 7, 2017.

Informed consent statement: Written informed consents were obtained from the participants.

Conflict-of-interest statement: During the last five years, Toyoshima O received personal fees from Otsuka Pharmaceutical Co., Ltd. and Takeda Pharmaceutical Co., Ltd. outside of the submitted work; Suzuki H received scholarship funds for the research from Astellas Pharma Inc., Astra-Zeneca K.K., Otsuka Pharmaceutical Co., Ltd., Takeda Pharmaceutical Co., Ltd., and Zeria Pharmaceutical Co., Ltd. and received service honoraria from Astellas Pharma, Inc., Astra-Zeneca K.K., Otsuka Pharmaceutical Co., Ltd., Takeda Pharmaceutical Co., Ltd., and Zeria Pharmaceutical Co., Ltd.

STROBE statement: The authors have read the STROBE Statement-checklist of items, and the manuscript was prepared and revised according to the STROBE Statement-checklist of items.

Manuscript source: Unsolicited manuscript

Correspondence to: Osamu Toyoshima, MD, Director, Department of Gastroenterology, Toyoshima Endoscopy Clinic, 6-17-5 Seijo, Setagaya-ku, Tokyo 1570066, Japan. t@ichou.com
Telephone: +81-3-54299555
Fax: +81-3-54299511

Received: February 25, 2018
Peer-review started: February 25, 2018
First decision: March 9, 2018
Revised: March 13, 2018
Accepted: March 18, 2018
Article in press: March 18, 2018
Published online: April 7, 2018

Abstract

AIM

To investigate the clinicopathological features of the patients testing negative for high titer serum anti-*Helicobacter pylori* (*H. pylori*) antibody.

METHODS

The antibody titers were measured using antigens

derived from Japanese individuals. ^{13}C-urea breath test-positive individuals were defined as having *H. pylori* infection. We investigated the demographic characteristics, laboratory data, endoscopic findings including Kyoto classification of gastritis, and histology in negative-high titer patients without *H. pylori* eradication therapy. Kyoto classification consisted of scores for gastric atrophy, intestinal metaplasia, enlarged folds, nodularity, and redness.

RESULTS

Of the 136 subjects enrolled, 23 (17%) had *H. pylori* infection. Kyoto classification had an excellent area under the receiver operating characteristics curve (0.886, 95% confidence interval: 0.803-0.968, $P = 3.7 \times 10^{-20}$) for predicting *H. pylori* infection with a cut-off value of 2. Further, Kyoto classification, *H. pylori* density, and neutrophil activity had high accuracies (89.7%, 96.3%, and 94.1%, respectively). Kyoto classification was independent of the demographic and laboratory parameters in multivariate analysis.

CONCLUSION

Endoscopic Kyoto classification of gastritis is a useful predictor of *H. pylori* infection in negative-high titer antibody patients.

Key words: Kyoto classification; Gastritis; *Helicobacter pylori*; Antibody; Endoscopy

Core tip: Compared with negative-low titer (< 3 U/mL on E-plate Eiken kit), negative-high titer (3-9.9 U/mL) have been reported to be at higher risk for intestinal gastric cancer. *Helicobacter pylori* (*H. pylori*)-infected patients accounted for 94% of gastric cancer patients with an antibody titer of < 10 U/mL. Seventeen percent of subjects with negative-high titer serum anti-*H. pylori* antibody tested positive for *H. pylori* infection. Endoscopic Kyoto classification of gastritis was an excellent predictor of *H. pylori* infection with large area under the receiver operating characteristics curve (0.886), cut-off value of 2, and high accuracy (89.7%), indicating its high confidence.

Toyoshima O, Nishizawa T, Arita M, Kataoka Y, Sakitani K, Yoshida S, Yamashita H, Hata K, Watanabe H, Suzuki H. *Helicobacter pylori* infection in subjects negative for high titer serum antibody. *World J Gastroenterol* 2018; 24(13): 1419-1428 Available from: URL: http://www.wjgnet.com/1007-9327/full/v24/i13/1419.htm DOI: http://dx.doi.org/10.3748/wjg.v24.i13.1419

INTRODUCTION

Helicobacter pylori (*H. pylori*) is a group 1 carcinogen for gastric cancer. Therefore, the International Agency for Research on Cancer has recommended screening for and eradication of *H. pylori* for preventing gastric cancer[1]. The main non-invasive methods for diagnosing *H. pylori* infection are the serum immunoglobulin G antibody test, ^{13}C-urea breath test (UBT), and stool antigen test. Endoscopy, histology, culture, and rapid urease test have been used as the main invasive methods. The Maastricht V/Florence consensus report states that the urea breath test using ^{13}C-urea is the best test to diagnose *H. pylori* infection[2,3]. However, some of the available serum antibody kits including E-plate Eiken are excellent kits, with sensitivity and specificity above 90%[4,5]. Serology is hardly affected by the changes in the stomach that result in a low bacterial load, including gastrointestinal bleeding, atrophic gastritis, gastric mucosa-associated lymphoid tissue lymphoma, and gastric carcinoma[2,6]. Additionally, proton pump inhibitors and antibiotics have little influence on serological tests as well[7]. A serological test, with levels of serum anti-*H. pylori* antibody and pepsinogen I and II, is useful for identifying patients at increased risk of gastric cancer[2,8,9]. These are some of the merits of serological testing. However, subjects with an E-plate antibody titer of < 10 U/mL include patients with spontaneous disappearance of *H. pylori* from the gastric mucosa, who are known to have extremely severe gastritis and high risk for gastric cancer[10].

In clinical practice, in addition to evaluating the results of *H. pylori* serology as a categorical variable (*i.e.*, positive or negative), it is also important to consider the titer of *H. pylori* antibodies because there is a relationship between the antibody titer and the risk of gastric cancer. We mainly use the E-plate Eiken kit as an anti-*H. pylori* antibody test in Japan. The cut-off titer of this kit for diagnosing *H. pylori* infection is ≥ 10 U/mL, while the lower sensitivity limit of this kit is 3 U/mL. Previous reports have defined the titer between 3 and 9.9 U/mL as negative-high titer, and the titer < 3 U/mL as a negative-low titer. Compared with the negative-low titer, the negative-high titer has been reported to carry a higher risk, especially for intestinal gastric cancer in subjects with gastric atrophy[10-12].

There are some false negative results when screening for current *H. pylori* infection in patients with an E-plate antibody titer of < 10 U/mL. *H. pylori*-infected patients accounted for 94% of patients with gastric cancer with an E-plate antibody titer of < 10 U/mL. Additionally, in patients with gastric cancer with an E-plate antibody titer of < 10 U/mL, *H. pylori* infection was associated with higher titers of antibodies[13].

Thus, seronegative-high titer antibody is associated with gastric cancer. However, the clinicopathological characteristics of negative-high titer patients, including the prevalence of *H. pylori* infection, have not been studied extensively. This study focused on serum negative-high titer antibody subjects without history

of *H. pylori* eradication therapy and investigated the features of *H. pylori*-infected patients in the category.

MATERIALS AND METHODS

Subjects

We conducted this retrospective case-control study in patients with negative-high titer serum anti-*H. pylori* antibodies, who underwent esophagogastroduodenoscopy (EGD) and histological evaluation based on the updated Sydney system at Toyoshima Endoscopy Clinic between September 2016 to May 2017. EGDs were performed for screening, surveillance for gastrointestinal diseases, and investigation of some symptoms or abnormal results of the other assessments. We did not include subjects with history of gastric cancer, gastrectomy, *H. pylori* eradication therapy, and severe concomitant illnesses, and those who did not consent to this study. The following demographic characteristics were collected from the medical records: age, sex, body mass index (BMI), first-degree family history of gastric cancer, smoking history, and habitual drinking[14]. A score of at least 400 on the Brinkman index was defined as positive smoking history. Consumption of at least one drink of alcohol per day was defined as habitual.

This retrospective study was approved by the Ethical Review Committee of Hattori Clinic on September 7, 2017. Written informed consents were obtained from the participants. All clinical investigations were conducted according to the ethical guidelines of the Declaration of Helsinki.

Diagnosis of H. pylori and related findings

The *H. pylori* antibody titer was measured in the blood samples obtained at the time of the first visit or EGD. The antibody titer was measured using an enzyme immunoassay kit using antigens derived from Japanese individuals (E-plate Eiken *H. pylori* antibody II; Eiken Chemical, Tokyo, Japan). A negative-high titer was defined as 3-9.9 U/mL of anti-*H. pylori* antibodies.

UBT-positive individuals were defined as subjects with *H. pylori* infection[2,15,16]. We performed UBT using a 100 mg ^{13}C-urea tablet (Pylonic; Sumitomo Dainippon Pharma, Osaka, Japan) after at least 2 wk of cessation of proton pump inhibitors or antibiotics. The result was declared negative if it was lower than 3 per mil.

Kyoto classification of gastritis is based on the sum of scores of the following five endoscopic findings, which are scored from 0 to 8: atrophy, intestinal metaplasia (IM), enlarged folds, nodularity, and redness. A high score represents increased risk for gastric cancer[13,17]. Gastric atrophy was classified according to the extent of mucosal atrophy as described by Kimura and Takemoto[14,18,19]. C-II and C-III of Kimura-Takemoto classification were scored as 1, and O-Ⅰ to O-Ⅲ as 2. IM is observed as grayish-whitish and slightly opalescent patches. IM within the antrum was scored as 1, and IM extending into the corpus as 2. The presence of folds enlarged over 5 mm or more was scored as 1. Nodularity is characterized by the appearance of multiple whitish elevated lesions mainly in the pyloric gland mucosa. The presence of nodularity was scored as 1. Diffuse redness refers to uniform redness involving the entire fundic gland mucosa. The presence of redness with regular arrangements of collecting venules was scored as 1, and that without regular arrangement of collecting venules as 2. We also considered the presence of gastric sticky mucus and gastroduodenal ulcer as positive findings of *H. pylori* infection. On the contrary, gastroesophageal reflux disease, hiatal hernia, and fundic gland polyp were considered as findings of absence of *H. pylori* infection. Sticky mucus refers to grayish or yellowish mucus that adheres to the mucosal surface prior to washing with water. Gastroduodenal ulcer scars were included in the positive group. Grade A or more severe of Los Angeles classification in gastroesophageal reflux disease was defined as positive. We defined hiatal hernia of 2 cm or more as positive. Figure 1A-F shows the representative endoscopic findings related to *H. pylori* infection in negative-high titer patients of this study.

EGDs were performed by 14 expert physicians using Olympus Evis Lucera Elite system with endoscope: GIF-HQ290 or GIF-H290Z (Olympus Corporation, Tokyo, Japan). We carried out EGDs under conscious sedation with midazolam and/or pethidine hydrochloride. The EGD images were retrospectively reviewed by the chief investigator (OT). Any disagreements were resolved by consulting a third reviewer (TN). Discrepancies in diagnoses between the two sets of physicians were resolved through discussions.

Pathological findings were evaluated using the updated Sydney system score, including *H. pylori* density, neutrophil activity, chronic inflammation, IM, and glandular atrophy, with hematoxylin and eosin stains[20-22]. The biopsy samples were collected from the greater curvature of the corpus and antrum. We defined one or more score in either of the two points as present. The histological diagnosis was performed by an expert gastrointestinal pathologist, who was not an endoscopist, and was from another organization.

Statistical analysis

First, we evaluated the effects of age, sex, BMI, family history of gastric cancer, smoking, habitual drinking, serum anti-*H. pylori* antibody titer, endoscopic findings, and histological findings on *H. pylori* infection in univariate analysis using Fisher's exact test or Cochran-Armitage test for categorical variables and Mann-Whitney *U* test for quantitative variables. Next,

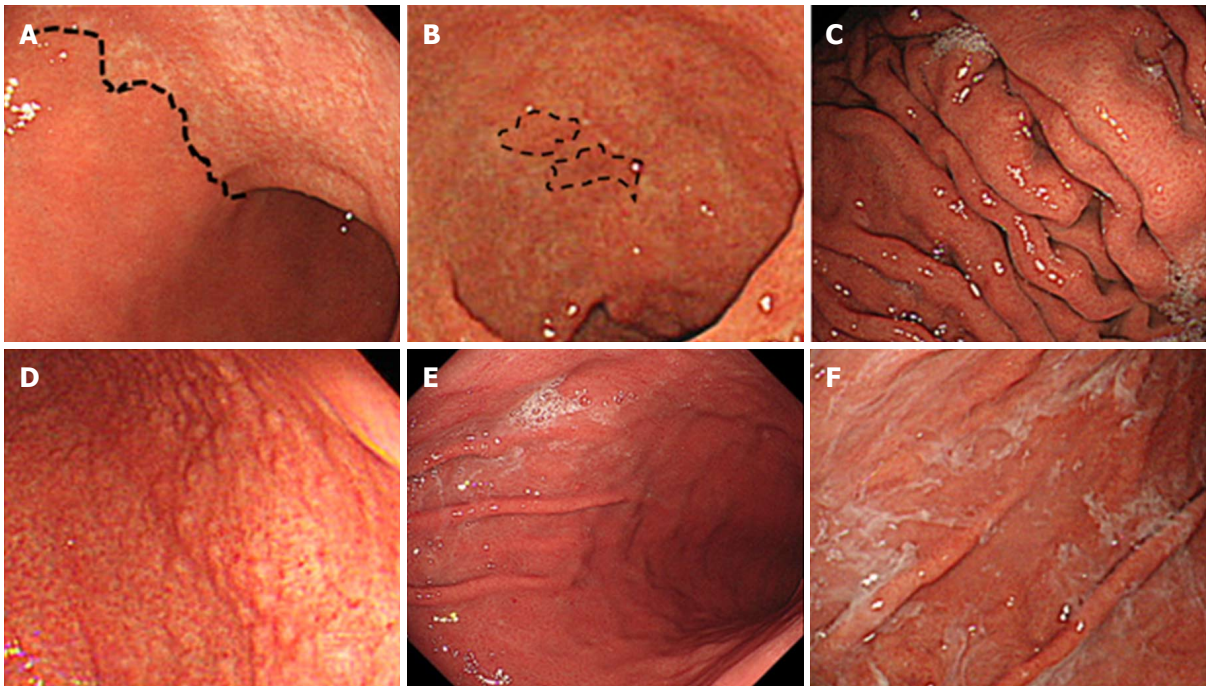

Figure 1 Endoscopic findings related to *Helicobacter pylori* infection. A: Atrophy is diagnosed based on the vascular pattern and rugal atrophy. The dotted line indicates an atrophic border in the anterior wall of the body (43-year-old woman; antibody titer: 4.3 U/mL; UBT: 55.3 per mil; Kyoto classification score: 2); B: Intestinal metaplasia is visible as grayish-whitish, slightly opalescent patches. The dotted line indicates the extent of the lesions in the lesser curvature of the antrum (81-year-old woman; antibody titer: 4.7 U/mL; UBT: 7.3 per mil; Kyoto classification score: 5); C: An enlarged fold is defined as that which is 5 mm or more in diameter. Enlarged folds are present in the greater curvature of the body (56-year-old man; antibody titer: 3.8 U/mL; UBT: 7.0 per mil; Kyoto classification score: 3); D: Nodularity is characterized by the appearance of multiple whitish elevated lesions mainly in the pyloric gland mucosa. Nodularity is present in the antrum (28-year-old man; antibody titer: 9.4 U/mL; UBT: 3.6 per mil; Kyoto classification score: 2); E: Redness refers to uniform redness involving the entire fundic gland mucosa. Redness is visible in the greater curvature of the body (44-year-old man; antibody titer: 8.7 U/mL; UBT: 26.5 per mil; Kyoto classification score: 3); F: Sticky mucus refers to grayish or yellowish mucus adhering to the mucosal surface. There is sticky mucus in the greater curvature of the body (70-year-old woman; antibody titer: 6.5 U/mL; UBT: 26.4 per mil; Kyoto classification score: 4). UBT: Urea breath test.

the values of the area under the receiver operating characteristic curve (AUC) for predicting *H. pylori* infection were compared with the value of 0.5 using the chi-squared test. The cut-off values for predicting *H. pylori* infection were estimated using the Youden index, which is the farthest point on the receiver operating characteristic curve from the positive diagonal[23]. We compared AUC values with the use of a chi-square test. Then, the performances of the endoscopic and histological findings for *H. pylori* infection, including accuracy, sensitivity, specificity, positive predictive value (PPV), and negative predictive value (NPV) were investigated. The predictors associated with *H. pylori* infection were subsequently assessed using multiple logistic regression analysis to distinguish the independent factors from other demographic and laboratory variables. A two-sided *P* value less than 0.05 was considered as significant. The data were analyzed using Ekuseru-Toukei 2015 software (Social Survey Research Information, Tokyo, Japan).

RESULTS

The characteristics of the participants of the present study are shown in Table 1. A total of 136 subjects were enrolled. The median age of the subjects was 45 (range: 17-82, interquartile range: 37-56) years, and 39% were males. The median titer of *H. pylori* antibody was 4.7 (interquartile range, 3.7-6.6) U/mL. Seventeen percent (n = 23) were diagnosed as *H. pylori*-infected based on UBT.

On comparing *H. pylori*-infected and -uninfected patients regarding the demographic characteristics and laboratory data, *H. pylori*-infected patients were older (53 years *vs* 42 years, P = 0.0057), and had higher BMI (22.7 kg/m^2 *vs* 21.2 kg/m^2, P = 0.028) and serum antibody titer (5.4 U/mL *vs* 4.7 U/mL, P = 0.048). No significant differences due to sex, family history of gastric cancer, habitual smoking, or habitual drinking were demonstrated. Regarding endoscopic findings, we found significant differences between them in Kyoto classification of gastritis score ($P = 3.8 \times 10^{-13}$), gastric sticky mucus (P = 0.013), and fundic gland polyp (P = 0.0022). Histologically, *H. pylori* density ($P = 2.8 \times 10^{-18}$), chronic inflammation ($P = 4.5 \times 10^{-10}$), and neutrophil activity ($P = 1.4 \times 10^{-14}$) were significantly different between the two groups (Table 1).

Then, we analyzed AUC for predicting *H. pylori* infection based on the variables that had significant differences between *H. pylori*-infected and -uninfected

Table 1 Characteristics of enrolled subjects

	Total	*H. pylori* infected[1]	*H. pylori* uninfected	*P* value[3]
n (%)	136	23 (17)	113 (83)	
Demographic characteristics				
Age median (IQR), yr	45 (37-56)	53 (44-68)	42 (35-53)	0.0057
Male sex (%)	53 (39)	7 (30)	46 (41)	0.48
Body mass index median (IQR), kg/m^2	21.2 (19.6-23.7)	22.7 (20.4-25.6)	21.2 (19.5-23.3)	0.028
Family history of gastric cancer, present/absent	12/124	3/20	9/104	0.43
Smoking, present/absent	4/132	0/23	4/109	1.0
Drinking, present/absent	25/111	4/19	21/92	1.0
Laboratory data				
Anti-*H. pylori* antibody median (IQR), U/mL	4.7 (3.7-6.6)	5.4 (4.2-7.9)	4.7 (3.7-6.4)	0.048
^{13}C-urea breath test result median (IQR), per mil	0.3 (0.1-0.8)	19.3 (9.3-26.3)	0.3 (0.1-0.4)	3.6×10^{-14}
Endoscopic findings				
Kyoto classification of gastritis[4], 5/4/3/2/1/0	1/3/14/9/13/96	1/3/8/6/2/3	0/0/6/3/11/93	3.8×10^{-13}
Atrophy, 2/1/0	15/20/101	10/4/2009	6/10/97	5.8×10^{-12}
Intestinal metaplasia, 1/0	14/122	9/14	5/108	2.9×10^{-5}
Enlarged folds, 1/0	5/131	4/19	1/112	0.0029
Nodularity, 1/0	2/134	2/21	0/113	0.028
Redness, 1/0	19/117	12/11	7/106	7.3×10^{-7}
Gastric sticky mucus, present/absent	22/114	8/15	14/99	0.013
Gastric ulcer, present/absent	1/135	1/22	0/113	0.17
Duodenal ulcer, present/absent	3/133	1/22	2/111	0.43
Gastroesophageal reflux disease, present/absent	20/116	2/21	18/95	0.53
Hiatal hernia, present/absent	18/118	2/21	16/97	0.74
Fundic gland polyp, present/absent	41/95	1/22	40/73	0.0022
Histological findings[5]				
H. pylori density, present/absent	18/118	18/5	0/113	2.8×10^{-18}
Chronic inflammation, present/absent	46/90	21/2	25/88	4.5×10^{-10}
Neutrophil activity, present/absent	15/121	15/8	0/113	1.4×10^{-14}
Intestinal metaplasia, present/absent	4/132	1/22	3/110	0.53
Glandular atrophy, present/absent	4/132	1/22	3/110	0.53

[1] [13]C-urea breath test-positive subjects were defined as *H. pylori*-infected patients; [3]Fisher's exact test, Cochran-Armitage test, or Mann-Whitney *U* test was used as appropriate; [4]Kyoto classification of gastritis was estimated by gastric atrophy, intestinal metaplasia, enlarged folds, nodularity, and redness[13]; [5]We defined one or more score classified by the updated Sydney system in either the great curvature of the corpus or the antrum as present. *H. pylori*: *Helicobacter pylori*; IQR: Interquartile range.

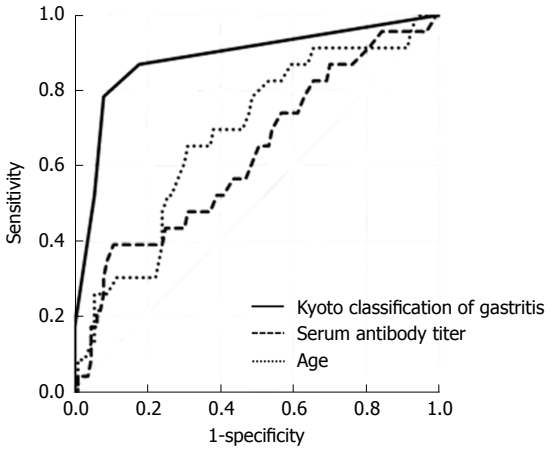

Figure 2 Receiver operating characteristics curves for predicting *Helicobacter pylori* infection. Receiver operating characteristics curves were based on endoscopic Kyoto classification of gastritis score, serum antibody titer, and age in 136 patients with negative-high titer antibody. Positive UBT was defined as *H. pylori* infection. UBT: Urea breath test.

patients (Table 2). AUC of *H. pylori* density (0.891, 95%CI: 0.805-0.977, $P = 5.6 \times 10^{-19}$) was the largest followed by those of Kyoto classification (0.886, 95%CI: 0.803-0.968, $P = 3.7 \times 10^{-20}$) and endoscopic atrophy (0.848, 95%CI: 0.760-0.936, $P = 7.7 \times 10^{-15}$). There was no significant difference between the three AUC values. The cut-off value of Kyoto classification of gastritis score for correlation with *H. pylori* infection was 2 and that of endoscopic atrophy was 1. The receiver operating characteristic curves based on Kyoto endoscopic classification, serum antibody titer, and age in 136 patients with negative-high titer antibody are shown in Figure 2.

The performances of endoscopic and histological findings for *H. pylori* infection are shown in Table 3. The highest accuracy was found in histological *H. pylori* density (96.3%), and its specificity and PPV were 100%. *H. pylori* density also had the second highest NPV (95.8%). The second highest accuracy was in neutrophil activity (94.1%), and its specificity and PPV were 100%. With regards to endoscopic findings, Kyoto classification of gastritis showed the highest accuracy (89.7%). The accuracies of redness, IM, atrophy (1 or more score as positive), enlarged folds, and nodularity followed that of Kyoto classification in order. The highest sensitivity (91.3%) and highest

Table 2 Area under the receiver operating characteristic curve for predicting *Helicobacter pylori* infection

	AUC	95%CI	*P* value
Age	0.684	0.564-0.804	0.0027
Body mass index	0.646	0.518-0.774	0.026
Serum antibody titer	0.631	0.500-0.763	0.051
Kyoto classification of gastritis	0.886	0.803-0.968	3.7×10^{-20}
Endoscopic atrophy	0.848	0.760-0.936	7.7×10^{-15}
Endoscopic intestinal metaplasia	0.674	0.570-0.777	0.0010
Enlarged fold	0.583	0.503-0.662	0.042
Nodularity	0.543	0.485-0.602	0.15
Redness	0.730	0.623-0.837	2.4×10^{-5}
Gastric sticky mucus	0.612	0.508-0.716	0.035
Fundic gland polyp	0.655	0.594-0.717	7.4×10^{-7}
H. pylori density	0.891	0.805-0.977	5.6×10^{-19}
Chronic inflammation	0.846	0.776-0.916	5.3×10^{-22}
Neutrophil activity	0.826	0.727-0.926	1.3×10^{-10}

Positive urea breath test was defined as *H. pylori* infection. The values of the AUC were compared with the value of 0.5 using the chi-square test. AUC: Area under the receiver operating characteristics curve; CI: Confidence interval; *H. pylori*: *Helicobacter pylori*.

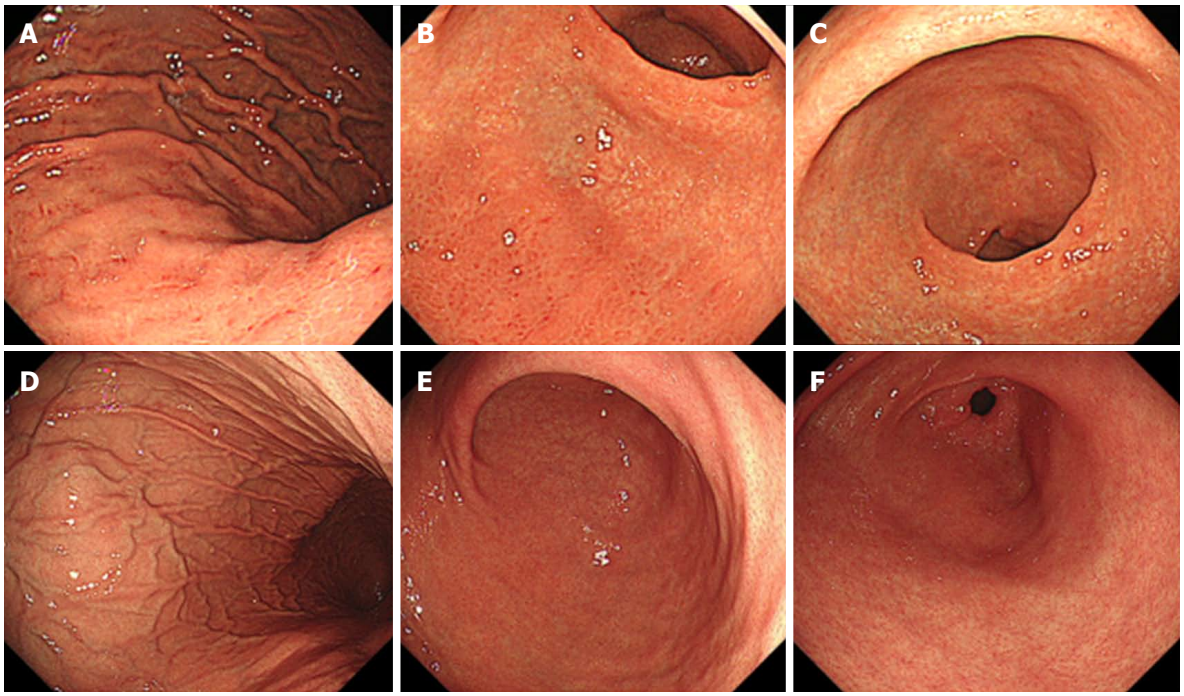

Figure 3 Representative endoscopic findings of negative-high titer antibody cases. A case with *Helicobacter pylori* infection; 81-year-old woman with antibody titer of 4.7 U/mL, UBT of 7.3 per mil, and Kyoto classification score of 5 (A-C). A: Greater curvature of the body of the stomach. Enlarged folds and redness are present; B: Lower body of the stomach. Endoscopic atrophic border lies in the anterior wall and greater curvature. Redness is present in the greater curvature; C: Antrum. Intestinal metaplasia is present in the lesser curvature. The mucosa is atrophic. A case without *H. pylori* infection; 31-year-old man with antibody titer of 5.7 U/mL, UBT of 1.2 per mil, and Kyoto classification score of 0 (D-F); D: The greater curvature of the body of the stomach. Regular arrangement of collecting venules and fundic gland polyps are present; E: Lower body of the stomach. Atrophy and redness are absent; F: Antrum. Intestinal metaplasia and atrophy are absent. UBT: Urea breath test.

NPV (97.8%) were shown with histological chronic inflammation.

Lastly, Kyoto classification was assessed using multivariate logistic regression analysis to identify any association with the variables such as age, BMI, and serum antibody titer. Kyoto classification was identified as an independent predictor of *H. pylori* infection ($P = 2.2 \times 10^{-6}$, Table 4).

Representative endoscopic findings of negative-high titer cases with or without *H. pylori* infection are demonstrated in Figure 3A-F.

DISCUSSION

We found that 17% of subjects with negative-high titer serum anti-*H. pylori* antibody were positive for *H.*

Table 3 Performance of endoscopic and histological findings for *Helicobacter pylori* infection

	Accuracy	Sensitivity	Specificity	PPV	NPV
Endoscopic findings					
Kyoto classification of gastritis[1]	89.7	78.3	92.0	66.7	95.4
Atrophy[2]	85.3	82.6	85.8	54.3	96.0
Intestinal metaplasia	86.0	39.1	95.6	64.3	88.5
Enlarged folds	85.3	17.4	99.1	80.0	85.5
Nodularity	84.6	8.7	100	100	84.3
Redness	86.8	52.2	93.8	63.2	90.6
Gastric sticky mucus	78.7	34.8	87.6	36.4	86.8
Gastric ulcer	83.8	4.3	100	50.0	83.7
Duodenal ulcer	82.4	4.3	98.2	33.3	83.5
Gastroesophageal reflux disease	71.3	8.7	84.1	10.0	81.9
Hiatal hernia	72.8	8.7	85.8	11.1	82.2
Fundic gland polyp	54.4	4.3	64.6	2.4	76.8
Histological findings					
H. pylori density	96.3	78.3	100	100	95.8
Chronic inflammation	80.1	91.3	77.9	45.7	97.8
Neutrophil activity	94.1	65.2	100	100	93.4
Intestinal metaplasia	81.6	4.3	97.3	25.0	83.3
Glandular atrophy	81.6	4.3	97.3	25.0	83.3

[1]A score of 2 or more was defined as positive; [2]A score of 1 or more was defined as positive. The data are presented as %. Positive urea breath test was defined as *H. pylori* infection. PPV: Positive predictive value; NPV: Negative predictive value; *H. pylori*: *Helicobacter pylori*.

Table 4 Multivariate analysis for independent predictors of *Helicobacter pylori* infection

	Odds ratio	95%CI	*P* value
Age	0.98	0.93-1.03	0.49
Body mass index	1.06	0.90-1.24	0.50
Serum antibody titer	1.21	0.87-1.68	0.26
Kyoto classification of gastritis	4.23	2.33-7.67	2.2×10^{-6}

pylori infection. Higher bacterial counts induce intense immune responses, resulting in subsequent higher antibody titers, while genetic differences between human hosts may affect the antibody levels in response to pathogens[24]. Precise diagnosis in patients with seronegativity is necessary to reduce the false negative estimation of gastric cancer risk[13]. We should identify *H. pylori*-infected cases in negative-high titer patients and carefully examine them.

Endoscopic Kyoto classification of gastritis proved to be an excellent predictor of *H. pylori* infection with large AUC (0.886), cut-off value of 2, high accuracy (89.7%), and was comparable to histological *H. pylori* density, indicating its high confidence. Kyoto classification also demonstrated to be independent of demographic and laboratory data. These results show that Kyoto classification is useful in the diagnosis of *H. pylori* infection among negative high-titer serum antibody patients. Endoscopic atrophy and nodularity have been attributed to *H. pylori* infection consistently, as was also seen with our results[25-28].

Kyoto classification score is believed to provide an estimate of the risk of gastric cancer. Sugimoto *et al*[29] showed that the mean Kyoto classification score in gastric cancer group was 4.6 ± 1.2, which was significantly higher than in gastritis-alone group (3.8 ± 1.1; $P < 0.001$). In subgroup analysis within the cancer group, the mean Kyoto classification score in the *H. pylori*-uneradicated subgroup was 4.8 ± 1.1, which was significantly higher than that in the eradicated subgroup (4.2 ± 1.2; $P < 0.001$). Our study showed that Kyoto classification score might be useful for not only estimating the risk of gastric cancer but also the prediction of *H. pylori* infection in negative-high titer patients.

Cases with negative-high titer antibodies with negative UBT could include not only subjects who have never been infected but also patients in whom infections resolved spontaneously[10,30]. Patients with spontaneous resolution are known to be at very high risk for gastric cancer. In this study, nine patients with Kyoto classification score 2 or more had negative results with UBT. These cases might be after spontaneous disappearance of *H. pylori* infection. Such patients would need careful surveillance.

Histological *H. pylori* density was the strongest contributing factor to *H. pylori* infection with the largest AUC and highest accuracy (96.3%). Neutrophil activity had the second highest accuracy (94.1%). Several investigators have inferred significant associations of anti-*H. pylori* antibody titers with *H. pylori* density and neutrophil activity[25,31-33]. Our findings are in accordance with their reports. Chronic inflammation had the highest sensitivity and NPV. Chronic inflammation has been reported to progress in parallel with increases in serum anti-*H. pylori* antibodies, and our results are consistent with this observation[25,28,32].

H. pylori-infected patients were older than the uninfected patients among negative-high titer antibody

participants. Kiso *et al*[13] reported that in serum *H. pylori* antibody-negative subjects, those with *H. pylori* infection and gastric cancer were older than those with gastric cancer but without the infection. Our results were concordant with their results. In this study, the BMI of *H. pylori*-infected patients was higher than that of -uninfected patients. Our results are in agreement with the results of a report that concluded a positive association between being overweight and serum *H. pylori* antibody[34].

There are some limitations to this study. We used UBT as the gold standard for *H. pylori* infection; however, its accuracy is not 100%. Better performance in serological screening depends on the use of the appropriate antigens and adjustment of cut-off values[35]. As we used antibodies against the Japanese strain, further investigation of the other antibodies is needed. Non-*H. pylori Helicobacter* species, including *H. suis* and *H. felis*, could provoke serum anti-*H. pylori* antibody positivity[36], and anti-*H. pylori* antibody correlates with the presence of cytotoxin associated gene A-positive strains[37]; however, we did not assess them. Furthermore, we did not analyze the long-term outcomes in 17% of the patients with negative-high titer anti-*H. pylori* antibodies without history of eradication therapy who had *H. pylori* infection. Further studies should be performed to analyze the long-term outcomes and the association between the presence of CagA positive *H. pylori* infection and Kyoto classification.

In conclusion, 17% of the patients with negative-high titer serum anti-*H. pylori* antibodies without history of eradication therapy had *H. pylori* infection. Endoscopic Kyoto classification of gastritis with a score of 2 or more could predict *H. pylori* infection in negative high-titer patients. Further examination including UBT should be considered in these patients with Kyoto classification score 2 or more.

ARTICLE HIGHLIGHTS

Research background

Patients who test negative but in the negative-high titer range of serum anti-*Helicobacter pylori* (*H. pylori*) antibodies are at a high risk for gastric cancer, especially the intestinal type, and sometimes have *H. pylori* infection. Patients with negative-high titers with *H. pylori* infection have higher risk for gastric cancer than do those without *H. pylori* infection.

Research motivation

The clinicopathological features including *H. pylori* infection rate in the negative-high titer patients are unclear.

Research objectives

The objective of this research was to elucidate the clinicopathological features of the negative-high titer patients.

Research methods

The antibody titers were measured using antigens derived from Japanese individuals, E-plate Eiken. ^{13}C-urea breath test (UBT)-positive individuals were defined as having *H. pylori* infection. We investigated the demographic characteristics, laboratory data, endoscopic findings including Kyoto classification of gastritis, and histology in negative-high titer patients without history of *H. pylori* eradication therapy.

Research results

Of the 136 subjects enrolled, 23 (17%) had *H. pylori* infection. Kyoto classification had an excellent area under the receiver operating characteristics curve (0.886) for predicting *H. pylori* infection, with a cut-off value of 2. Further, Kyoto classification had high accuracy (89.7%). Kyoto classification was independent of the demographic and laboratory parameters in multivariate analysis.

Research conclusions

In this study, 17% of patients with negative-high titer had *H. pylori* infection. Endoscopic Kyoto classification of gastritis with a score of 2 or more could predict *H. pylori* infection in negative high-titer patients. Further investigations including UBT should be considered in these patients.

Research perspectives

Long-term prospective studies are expected to investigate the role of serum antibody titer and Kyoto classification of gastritis in predicting not only *H. pylori* infection but also the risk of gastric cancer.

ACKNOWLEDGEMENTS

We would also like to thank Kanazawa T, Matsumoto S, Isomura Y, Arano T, Kinoshita H, Ohki D, Fukagawa K, and Sekiba K for performing esophagogastroduodenoscopy and Sugita K, Sakurai C, and Yamakawa T for collecting data.

REFERENCES

1 **Cancer IAfRo**. Helicobacter pylori eradication as a strategy for preventing gastric cancer. IARC Working Group Reports. Volume 8
2 **Malfertheiner P**, Megraud F, O'Morain CA, Gisbert JP, Kuipers EJ, Axon AT, Bazzoli F, Gasbarrini A, Atherton J, Graham DY, Hunt R, Moayyedi P, Rokkas T, Rugge M, Selgrad M, Suerbaum S, Sugano K, El-Omar EM; European Helicobacter and Microbiota Study Group and Consensus panel. Management of Helicobacter pylori infection-the Maastricht V/Florence Consensus Report. *Gut* 2017; **66**: 6-30 [PMID: 27707777 DOI: 10.1136/gutjnl-2016-312288]
3 **Nishizawa T,** Suzuki H, Fujimoto A, Kinoshita H, Yoshida S, Isomura Y, Toyoshima A, Kanai T, Yahagi N, Toyoshima O. Effects of patient age and choice of antisecretory agent on success of eradication therapy for *Helicobacter pylori* infection. *J Clin Biochem Nutr* 2017; **60**: 208-210 [PMID: 28584402 DOI: 10.3164/jcbn.16-86]
4 **Burucoa C**, Delchier JC, Courillon-Mallet A, de Korwin JD, Mégraud F, Zerbib F, Raymond J, Fauchère JL. Comparative evaluation of 29 commercial Helicobacter pylori serological kits. *Helicobacter* 2013; **18**: 169-179 [PMID: 23316886 DOI: 10.1111/hel.12030]
5 **Ueda J,** Okuda M, Nishiyama T, Lin Y, Fukuda Y, Kikuchi S. Diagnostic accuracy of the E-plate serum antibody test kit in detecting Helicobacter pylori infection among Japanese children. *J Epidemiol* 2014; **24**: 47-51 [PMID: 24240631]
6 **Tonkic A**, Tonkic M, Lehours P, Mégraud F. Epidemiology and diagnosis of Helicobacter pylori infection. *Helicobacter* 2012; **17** Suppl 1: 1-8 [PMID: 22958148 DOI: 10.1111/j.1523-5378.2012.00975.x]
7 **Parente F,** Sainaghi M, Sangaletti O, Imbesi V, Maconi G, Anderloni A, Bianchi Porro G. Different effects of short-term omeprazole, lansoprazole or pantoprazole on the accuracy of the

13C-urea breath test. *Aliment Pharmacol Ther* 2002; **16**: 553-557 [DOI: 10.1046/j.1365-2036.2002.01192.x]
8 **Sugano K**, Tack J, Kuipers EJ, Graham DY, El-Omar EM, Miura S, Haruma K, Asaka M, Uemura N, Malfertheiner P; faculty members of Kyoto Global Consensus Conference. Kyoto global consensus report on Helicobacter pylori gastritis. *Gut* 2015; **64**: 1353-1367 [PMID: 26187502 DOI: 10.1136/gutjnl-2015-309252]
9 **Yamaji Y**, Mitsushima T, Ikuma H, Okamoto M, Yoshida H, Kawabe T, Shiratori Y, Saito K, Yokouchi K, Omata M. Inverse background of Helicobacter pylori antibody and pepsinogen in reflux oesophagitis compared with gastric cancer: analysis of 5732 Japanese subjects. *Gut* 2001; **49**: 335-340 [PMID: 11511553]
10 **Kishikawa H**, Kimura K, Takarabe S, Kaida S, Nishida J. Helicobacter pylori Antibody Titer and Gastric Cancer Screening. *Dis Markers* 2015; **2015**: 156719 [PMID: 26494936 DOI: 10.1155/2015/156719]
11 **Yamaji Y**, Mitsushima T, Ikuma H, Okamoto M, Yoshida H, Kawabe T, Shiratori Y, Saito K, Yokouchi K, Omata M. Weak response of helicobacter pylori antibody is high risk for gastric cancer: a cross-sectional study of 10,234 endoscoped Japanese. *Scand J Gastroenterol* 2002; **37**: 148-153 [PMID: 11843049]
12 **Tatemichi M**, Sasazuki S, Inoue M, Tsugane S; JPHC Study Group. Clinical significance of IgG antibody titer against Helicobacter pylori. *Helicobacter* 2009; **14**: 231-236 [PMID: 19702853 DOI: 10.1111/j.1523-5378.2009.00681.x]
13 **Kiso M**, Yoshihara M, Ito M, Inoue K, Kato K, Nakajima S, Mabe K, Kobayashi M, Uemura N, Yada T, Oka M, Kawai T, Boda T, Kotachi T, Masuda K, Tanaka S, Chayama K. Characteristics of gastric cancer in negative test of serum anti-Helicobacter pylori antibody and pepsinogen test: a multicenter study. *Gastric Cancer* 2017; **20**: 764-771 [PMID: 28025702 DOI: 10.1007/s10120-016-0682-5]
14 **Nishizawa T,** Suzuki H, Sakitani K, Yamashita H, Yoshida S, Hata K, Kanazawa T, Fujiwara N, Kanai T, Yahagi N, Toyoshima O. Family history is an independent risk factor for the progression of gastric atrophy among patients with Helicobacter pylori infection. *United European Gastroenterol J* 2017; **5**: 32-36 [PMID: 28405319 DOI: 10.1177/2050640616642341]
15 **Gisbert JP,** Calvet X. Helicobacter Pylori "Test-and-Treat" Strategy for Management of Dyspepsia: A Comprehensive Review. *Clin Transl Gastroenterol* 2013; **4**: e32 [PMID: 23535826 DOI: 10.1038/ctg.2013.3]
16 **Ferwana M**, Abdulmajeed I, Alhajiahmed A, Madani W, Firwana B, Hasan R, Altayar O, Limburg PJ, Murad MH, Knawy B. Accuracy of urea breath test in Helicobacter pylori infection: meta-analysis. *World J Gastroenterol* 2015; **21**: 1305-1314 [PMID: 25632206 DOI: 10.3748/wjg.v21.i4.1305]
17 **Shichijo S**, Hirata Y, Niikura R, Hayakawa Y, Yamada A, Koike K. Association between gastric cancer and the Kyoto classification of gastritis. *J Gastroenterol Hepatol* 2017; **32**: 1581-1586 [PMID: 28217843 DOI: 10.1111/jgh.13764]
18 **Kimura K,** Takemoto T. An endoscopic recognition of the atrophic border and its significance in chronic gastritis. *Endoscopy* 1969; **3**: 87-97
19 **Toyoshima O,** Yamaji Y, Yoshida S, Matsumoto S, Yamashita H, Kanazawa T, Hata K. Endoscopic gastric atrophy is strongly associated with gastric cancer development after Helicobacter pylori eradication. *Surg Endosc* 2017; **31**: 2140-2148 [PMID: 27604367 DOI: 10.1007/s00464-016-5211-4]
20 **Dixon MF**, Genta RM, Yardley JH, Correa P. Classification and grading of gastritis. The updated Sydney System. International Workshop on the Histopathology of Gastritis, Houston 1994. *Am J Surg Pathol* 1996; **20**: 1161-1181 [PMID: 8827022]
21 **Uemura N**, Okamoto S, Yamamoto S, Matsumura N, Yamaguchi S, Yamakido M, Taniyama K, Sasaki N, Schlemper RJ. Helicobacter pylori infection and the development of gastric cancer. *N Engl J Med* 2001; **345**: 784-789 [PMID: 11556297 DOI: 10.1056/NEJMoa001999]
22 **Toyoshima O,** Tanikawa C, Yamamoto R, Watanabe H, Yamashita H, Sakitani K, Yoshida S, Kubo M, Matsuo K, Ito H, Koike K, Seto Y, Matsuda K. Decrease in PSCA expression caused by Helicobacter pylori infection may promote progression to severe gastritis. *Oncotarget* 2017; **9**: 3936-3945 [PMID: 29423095 DOI: 10.18632/oncotarget.23278]
23 **Perkins NJ**, Schisterman EF. The inconsistency of "optimal" cutpoints obtained using two criteria based on the receiver operating characteristic curve. *Am J Epidemiol* 2006; **163**: 670-675 [PMID: 16410346 DOI: 10.1093/aje/kwj063]
24 **Rubicz R,** Leach CT, Kraig E, Dhurandhar NV, Duggirala R, Blangero J, Yolken R, Göring HH. Genetic factors influence serological measures of common infections. *Hum Hered* 2011; **72**: 133-141 [PMID: 21996708 DOI: 10.1159/000331220]
25 **Kamada T**, Sugiu K, Hata J, Kusunoki H, Hamada H, Kido S, Nagashima Y, Kawamura Y, Tanaka S, Chayama K, Haruma K. Evaluation of endoscopic and histological findings in Helicobacter pylori-positive Japanese young adults. *J Gastroenterol Hepatol* 2006; **21**: 258-261 [PMID: 16460483 DOI: 10.1111/j.1440-1746.2006.04128.x]
26 **Adachi K**, Mishiro T, Tanaka S, Kinoshita Y. Analysis of negative result in serum anti-H. pylori IgG antibody test in cases with gastric mucosal atrophy. *J Clin Biochem Nutr* 2016; **59**: 145-148 [PMID: 27698543 DOI: 10.3164/jcbn.16-13]
27 **Watanabe M**, Kato J, Inoue I, Yoshimura N, Yoshida T, Mukoubayashi C, Deguchi H, Enomoto S, Ueda K, Maekita T, Iguchi M, Tamai H, Utsunomiya H, Yamamichi N, Fujishiro M, Iwane M, Tekeshita T, Mohara O, Ushijima T, Ichinose M. Development of gastric cancer in nonatrophic stomach with highly active inflammation identified by serum levels of pepsinogen and Helicobacter pylori antibody together with endoscopic rugal hyperplastic gastritis. *Int J Cancer* 2012; **131**: 2632-2642 [PMID: 22383377 DOI: 10.1002/ijc.27514]
28 **Bruden DL**, Bruce MG, Miernyk KM, Morris J, Hurlburt D, Hennessy TW, Peters H, Sacco F, Parkinson AJ, McMahon BJ. Diagnostic accuracy of tests for Helicobacter pylori in an Alaska Native population. *World J Gastroenterol* 2011; **17**: 4682-4688 [PMID: 22180710 DOI: 10.3748/wjg.v17.i42.4682]
29 **Sugimoto M**, Ban H, Ichikawa H, Sahara S, Otsuka T, Inatomi O, Bamba S, Furuta T, Andoh A. Efficacy of the Kyoto Classification of Gastritis in Identifying Patients at High Risk for Gastric Cancer. *Intern Med* 2017; **56**: 579-586 [PMID: 28321054 DOI: 10.2169/internalmedicine.56.7775]
30 **Bergey B,** Marchildon P, Peacock J, Mégraud F. What is the role of serology in assessing Helicobacter pylori eradication? *Aliment Pharmacol Ther* 2003; **18**: 635-639 [DOI: 10.1046/j.1365-2036.2003.01716.x]
31 **Kreuning J,** Lindeman J, Biemond I, Lamers CB. Relation between IgG and IgA antibody titres against Helicobacter pylori in serum and severity of gastritis in asymptomatic subjects. *J Clin Pathol* 1994; **47**: 227-231 [PMID: 8163693]
32 **Sheu BS**, Shiesh SC, Yang HB, Su IJ, Chen CY, Lin XZ. Implications of Helicobacter pylori serological titer for the histological severity of antral gastritis. *Endoscopy* 1997; **29**: 27-30 [PMID: 9083733 DOI: 10.1055/s-2007-1004057]
33 **Park CH**, Kim EH, Jung DH, Chung H, Park JC, Shin SK, Lee SK, Lee YC. The new modified ABCD method for gastric neoplasm screening. *Gastric Cancer* 2016; **19**: 128-135 [PMID: 25663259 DOI: 10.1007/s10120-015-0473-4]
34 **Thjodleifsson B**, Olafsson I, Gislason D, Gislason T, Jögi R, Janson C. Infections and obesity: A multinational epidemiological study. *Scand J Infect Dis* 2008; **40**: 381-386 [PMID: 17943636 DOI: 10.1080/00365540701708293]
35 **Hoang TT**, Wheeldon TU, Bengtsson C, Phung DC, Sörberg M, Granström M. Enzyme-linked immunosorbent assay for Helicobacter pylori needs adjustment for the population

investigated. *J Clin Microbiol* 2004; **42**: 627-630 [PMID: 14766827]

36 **Flahou B,** Haesebrouck F, Smet A, Yonezawa H, Osaki T, Kamiya S. Gastric and enterohepatic non-Helicobacter pylori Helicobacters. *Helicobacter* 2013; **18** Suppl 1: 66-72 [PMID: 24011248 DOI: 10.1111/hel.12072]

37 **Loffeld RJ**, Werdmuller BF, Kusters JG, Kuipers EJ. IgG antibody titer against Helicobacter pylori correlates with presence of cytotoxin associated gene A-positive H. pylori strains. *FEMS Immunol Med Microbiol* 2000; **28**: 139-141 [PMID: 10799804]

P- Reviewer: Engin AB, Papamichail K, Park WS
S- Editor: Wang XJ **L- Editor**: A **E- Editor**: Huang Y

World Journal of Gastroenterology

Submit a Manuscript: http://www.f6publishing.com

World J Gastroenterol 2018 April 7; 24(13): 1429-1439

DOI: 10.3748/wjg.v24.i13.1429

ISSN 1007-9327 (print) ISSN 2219-2840 (online)

ORIGINAL ARTICLE

Retrospective Study

Impact of postoperative TNM stages after neoadjuvant therapy on prognosis of adenocarcinoma of the gastro-oesophageal junction tumours

Michael Thomaschewski, Richard Hummel, Ekaterina Petrova, Juliana Knief, Ulrich Friedrich Wellner, Tobias Keck, Dirk Bausch

Michael Thomaschewski, Richard Hummel, Ekaterina Petrova, Ulrich Friedrich Wellner, Tobias Keck, Dirk Bausch, Department of Surgery, University Medical Center Schleswig-Holstein, Campus Lübeck, Lübeck 23538, Germany

Juliana Knief, Department of Pathology, University Medical Center Schleswig-Holstein, Campus Lübeck, Lübeck 23538, Germany

ORCID number: Michael Thomaschewski (0000-0002-5405-9716); Richard Hummel (0000-0001-5671-5222); Ekaterina Petrova (0000-0001-7740-6410); Juliana Knief (0000-0002-5036-3817); Ulrich Friedrich Wellner (0000-0002-8632-166X); Tobias Keck (0000-0001-7651-6183); Dirk Bausch (0000-0001-6511-1535).

Author contributions: Thomaschewski M, Hummel R and Bausch D drafted the original manuscript, contributed to design of the study, performance of statistical analyses and interpretation of the results; Petrova E collected the data; Wellner UF performed, reviewed and approved the statistical analyses; Keck T contributed to the design of the study and critically revised the manuscript for important intellectual content; all authors read and approved the final manuscript.

Supported by Land Schleswig-Holstein within the funding programme Open Access Publikationsfonds.

Institutional review board statement: The study was reviewed and approved by the institutional ethics committee (Ethik-Kommission Universität zu Lübeck/Aktenzeichen: 17-379A).

Conflict-of-interest statement: All authors declare no conflict-of-interest related to this article.

Data sharing statement: Consent for data sharing was not obtained and the data are not available.

Manuscript source: Unsolicited manuscript

Correspondence to: Michael Thomaschewski, MD, Doctor, Department of Surgery, University Medical Center Schleswig-Holstein, Campus Lübeck, Ratzeburger Allee 160, 23538 Lübeck, Germany. michael.thomaschewski@uksh.de
Telephone: +49-451-50040220
Fax: +49-451-5002069

Received: January 22, 2018
Peer-review started: January 22, 2018
First decision: February24, 2018
Revised: March 6, 2018
Accepted: March 10, 2018
Article in press: March 10, 2018
Published online: April 7, 2018

Abstract

AIM

To compare prognostic relevance of postoperative tumour/node/metastasis (TMN) stages between patients with and without neoadjuvant treatment.

METHODS

Data from patients with adenocarcinoma of the gastro-oesophageal junction (AEG) who had undergone surgical resection at a single German university centre were retrospectively analysed. Patients with or without neoadjuvant preoperative treatment were selected by exact matching based on preoperative staging. Standard assessment of preoperative (c)TNM stage was based on endoscopic ultrasound and computed tomography of the thorax and abdomen, according to the American Joint Committee on Cancer/Union

for International Cancer Control classification system. Patients with cT1cN0cM0 and cT2cN0cM0 stages were excluded from the study, as these patients are generally not recommended for pretreatment. Long-term survival among the various postoperative TNM stages was compared between the groups of patients with or without neoadjuvant treatment. For statistical assessments, a *P*-value of $\leqslant$ 0.05 was considered significant.

RESULTS

The study included a total of 174 patients. The group of patients who had received preoperative neoadjuvant treatment included more cases of AEG (Siewert) type 1 carcinoma ($P < 0.001$), and consequently oesophagectomy was performed more frequently among these patients ($P < 0.001$). The two groups (with or without preoperative neoadjuvant treatment) had comparable preoperative T stages, but the group of patients with preoperative neoadjuvant treatment presented a higher rate of preoperative N-positive disease ($P = 0.020$). Overall long-term survival was not different between the two groups of patients according to tumours of different AEG classifications, receipt of oesophagectomy or gastrectomy, nor between patients with similar postoperative TNM stage, resection margin and grading. However, an improvement of long-term survival was found for patients with nodal down-staging after neoadjuvant therapy ($P = 0.053$).

CONCLUSION

The prognostic relevance of postoperative TNM stages is similar for AEG in patients with or without neoadjuvant preoperative treatment, but treatment-related nodal down-staging prognosticates longer-term survival.

Key words: Adenocarcinoma of the gastro-oesophageal junction; American Joint Committee on Cancer/Union for International Cancer Control; TNM system; Neoadjuvant therapy; Oesophageal cancer

Core tip: Neoadjuvant therapy is the standard treatment for locally advanced adenocarcinoma of the gastro-oesophageal junction (AEG). Prognosis of AEG is based mainly on postoperative tumour/node/metastasis (TNM) stages, using the American Joint Committee on Cancer/Union for International Cancer Control classification system. Yet, whether prognostication based on postoperative TNM stage is affected by preoperative neoadjuvant therapy is unclear. Retrospective analysis of 174 patients showed that the prognostic relevance of postoperative TNM stage is independent of preoperative neoadjuvant therapy. However, nodal down-stage response following neoadjuvant therapy was found to result in improvement of survival.

Thomaschewski M, Hummel R, Petrova E, Knief J, Wellner UF, Keck T, Bausch D. Impact of postoperative TNM stages after neoadjuvant therapy on prognosis of adenocarcinoma of the gastro-oesophageal junction tumours. *World J Gastroenterol* 2018; 24(13): 1429-1439 Available from: URL: http://www.wjgnet.com/1007-9327/full/v24/i13/1429.htm DOI: http://dx.doi.org/10.3748/wjg.v24.i13.1429

INTRODUCTION

Adenocarcinoma of the gastro-oesophageal junction (AEG) is one of the most common cancers worldwide, with a global incidence of 0.7 per 100000[1,2]. It represents an aggressive disease with poor prognosis, and diagnosis is often delayed due to a lack of early disease-specific symptoms. Moreover, these tumours tend to spread to (local) lymph nodes even in early stages[3,4].

Today, curative treatment options involve multidisciplinary approaches including endoscopy, surgery, chemotherapy and radiotherapy. These treatments have led to improvements in clinical management and patient outcome over the last years[4,5]. In particular, effective neoadjuvant chemotherapy and/or radiotherapy approaches have been established for patients with locally advanced adenocarcinoma of the distal oesophagus and the gastro-oesophageal junction. When applied prior to surgery, these pretreatments provide a survival benefit, improve the potential for down-staging of the primary tumour and/or lymph node metastasis, and yield higher rates of complete tumour resection (R0) in contrast to a surgery-alone approach[6-10]. However, whether a patient benefits from neoadjuvant therapy depends on tumour biology, individual patient-related risk factors and stage of disease[6,8,9].

The American Joint Committee on Cancer (AJCC) and the Union for International Cancer Control (UICC) tumour/node/metastasis (TNM) system has been established as an international standard of classification of local, regional and distant extension/spread for many solid tumours, including AEG, and proven a powerful tool for prediction of prognosis of cancer patients[10-14].

For the first time, the recently published 8th edition of AJCC staging of cancers of the oesophagus and oesophago-gastric junction introduced the post-neoadjuvant (yp)TNM stage groupings in addition to the clinical (c)TNM and pathological (p)TNM stagings[12]. Whereas the separate definitions from the previous 7th AJCC/UICC edition for depth of wall infiltration by the primary tumour (the T staging), lymph node involvement (the N staging) and presence of distant metastases (the M staging) of AEG were not changed, stage grouping for neoadjuvant categories (*i.e.,* ypTNM) was newly classified with separate stage grouping for squamous cell carcinoma and adenocarcinoma, to account for the different prognostic implications

between ypTNM (postneoadjuvant) and pTNM cancer categories[12,13].

Based on data derived from the Worldwide Esophageal Cancer Collaboration (WECC), involving 7723 patients from different countries and continents, survival for neoadjuvant groups (ypTNM patients) differed from that for equivalent-stage patients that underwent surgery alone (pTNM patients)[13]. In detail, survival for node-negative (ypN0) patients and early-stage disease (ypTNM groups Ⅰ and Ⅱ) patients is significantly lower than for equivalently categorised patients that underwent surgery alone (pTNM)[13,15]. However, two other retrospective analyses showed that the prognostic relevance of postoperative AJCC/UICC TNM staging is similar for patients with or without neoadjuvant treatment[16,17].

In summary, the data available on the actual prognostic relevance of postoperative TNM stages of AEG patients who underwent neoadjuvant treatment are still limited and heterogeneous. The objective of this study, therefore, was to retrospectively analyse data from our University Cancer Center to compare the prognostic relevance of postoperative TMN stages between patients with and without preoperative neoadjuvant treatment, following surgery for tumours of the gastro-oesophageal junction.

MATERIALS AND METHODS

Patient selection and study parameters

Between 1996 and 2014, a total of 254 consecutive patients underwent curative surgery for AEG at the University Medical Center Schleswig-Holstein, Campus Lübeck. Data of all these patients were obtained from the institutional database and selected according to the following inclusion criteria: age > 18 years; histological confirmation of AEG (Siewert types Ⅰ to Ⅲ) on the basis of postoperative resection specimen analysis; curative intent of surgery/treatment; and, formal eligibility for neoadjuvant/perioperative treatment based on preoperative cTNM stages (according to AJCC Classification 8th edition[12]; for details, please see the "Neoadjuvant/perioperative treatment" section below). Exclusion criteria were in-hospital death (as we aimed to analyse long-term outcome) and early-stage cancers (cT1cN0cM0 and cT2cN0cM0). After identification of eligible patients, we applied exact matching techniques to select the final retrospective study population of patients for the "neoadjuvant treatment" and "no neoadjuvant treatment" groups. Local ethics board approval was obtained (Ethik-Kommission Universität zu Lübeck/Aktenzeichen: 17-379A).

Study parameters included sex, age, AEG (Siewert) classification[18], surgical procedure (see below), preoperative staging (including cT, cN and cM categories according to the AJCC Cancer Staging Manual 8th edition[12]), postoperative staging [including T, N and M categories according to the AJCC/UICC Cancer Staging Manual 7th edition[11], grade of differentiation (G) and resection margin status (R)], long-term survival (defined as time in months from the day of hospital discharge) and pathologic down-staging/response in T and N stages after neoadjuvant therapy. For this study, we defined any pathologic down-staging/improvement in T and N stages after neoadjuvant therapy as 'down-staged', in contrast to 'unchanged' or 'up-staged' T and N stages.

Preoperative and postoperative tumour staging

Standard assessment of diagnosis and preoperative TNM stage (cTNM) was based on findings from endoscopy with biopsy, including endoscopic ultrasound and computed tomography of the thorax and abdomen. The postoperative staging was based on the resection specimen (according to the AJCC/UICC Cancer Staging Manual 7th edition[11] and including G and R parameters). In this context, the resected specimens were re-evaluated by an independent pathologist for the purpose of this study.

Neoadjuvant / perioperative treatment

From the year 2005 onward, neoadjuvant chemotherapy has been used as standard treatment in the context of a multidisciplinary approach for locally advanced cancers. Our local standard protocol for neoadjuvant/perioperative tretment is based on the German National Guidelines for Diagnostics and Treatment of Adenocarcinomas of the Stomach and the Gastroesophageal Junction (http://www.awmf.org/uploads/tx_szleitlinien/ 032009l_S3_Magenkarzinom_Diagnostik_Therapie_Adenokarzinome_oesophagogastraler_Uebergang_2012abgelaufen.pdf). Generally, patients are deemed eligible for neoadjuvant/perioperative treatment if the tumour is locally advanced. In detail, we recommend neoadjuvant/perioperative treatment for patients with locally advanced tumour stages (cT2 node-positive disease as well as cT3/4), and patients with cT1 cN0 cM0 or cT2 cN0 cM0 are not recommended for pretreatment. Prior to 2005, patients received neoadjuvant/perioperative treatment on an individual basis based on recommendations of the local interdisciplinary tumour board. Neoadjuvant/perioperative therapy mainly consisted of cisplatin and fluorouracil (5-FU)-based regimens and included, over the time, different protocols such as cisplatin/5-FU, ECX, FLOT or ECF. For better presentation of results, neoadjuvant/perioperative treatment is referred to as 'neoadjuvant treatment' throughout the rest of the manuscript. In 26 cases, patients without neoadjuvant pretreatment had received adjuvant therapy (if recommended according to the local interdisciplinary tumor board). The decision was based on postoperative tumour stages and individual patient-specific risk factors.

Surgical procedures

The type of surgical resection for the AEG tumours was selected in accordance with tumour location and extent, and was chosen from among either oesophagectomy

Table 1 Demographics of the study population

	All, *n* = 174	No neoadjuvant tx	Neoadjuvant tx	*P* value
Male sex	85.1%	81.7	87.4	0.387
Age, median	61.5	64	58	0.043
Siewert stage				< 0.001
I	35.1%	16.9	47.6	
II	51.7%	67.6	40.8	
III	13.2%	15.5	11.7	
cT stage				0.9
T2	7.5%	8.5	6.8	
T3	74.7%	74.6	74.8	
T4	17.8%	16.9	18.4	
cN stage				0.02
Negative	17.2%	28.2	9.7	
Positive	82.8%	72.8	90.3	
Surgery				< 0.001
Oesophagectomy	54.0%	26.8	72.8	
Gastrectomy	46.0%	73.2	27.2	
pT stage				
T0	11%	-	20.0	
T1/2	26%	21.4	30.0	
T3/4	63%	78.6	50.0	
pN stage				
N0	37%	24.3	48.8	
N1	17%	18.6	15	
N2	21%	20	21.2	
N3	25%	37.1	15	
pM stage				
M0	94%	94.3	93.8	
M1	6%	5.7	6.2	

Data represent the entire study population ("All"), and the subgroups of patients with ("Neoadjuvant tx") or without ("No neoadjuvant tx") neoadjuvant pretreatment. Tx: Treatment.

techniques (open/hybrid/totally minimally invasive oesophagectomies), gastrectomy techniques (transhiatal extended gastrectomy) or combined oesophagectomy-and-total-gastrectomy techniques. For the purpose of this study, patients treated with the combined oesophagectomy-and-total-gastrectomy technique were included in the oesophagectomy group. The standard surgical procedure in our hospital included two-field lymphadenectomy for oesophagectomies and D2-lymphadenectomy for gastrectomies.

Follow-up

The Department of Surgery includes an Outpatient Cancer Clinic for follow up of cancer patients. Most of the cancer patients in our study are receiving their follow-up care in this outpatient clinic. However, for those patients who requested follow up with their general practitioner (*e.g.*, based on the location of their residence), we obtained their follow-up information *via* telephone and entered the respective information into our database.

Statistical analysis

Statistical analyses were performed using SPSS software (version 22; IBM Corp., Armonk, NY, United States). For analysis of categorical variables [sex, age, AEG (Siewert) classification, surgical procedure and pre-operative staging (cTNM)], Pearson's chisquare and Fisher´s exact tests were used. Long-term survival was analysed using the Kaplan-Meier method. Log-rank test was used for statistical comparison. For all statistical analyses, a *P*-value of $\leqslant$ 0.05 was considered significant.

RESULTS

Demographics and overall survival

Following the exact matching patient selection, we identified 174 out of the 254 patients for study inclusion. Table 1 presents an overview of the two study groups: "neoadjuvant treatment (tx)" *vs* "no neoadjuvant tx". The patients who underwent neoadjuvant treatment were significantly younger than their nontreated counterparts (58 years *vs* 64 years, P = 0.043) and presented significantly more often with Siewert type 1 AEG tumours (P < 0.001) mandating oesophagectomy rather than gastrectomy (P < 0.001). While patients in both groups presented comparable preoperative T stages, patients in the neoadjuvant treatment group presented higher preoperative rates of N-positive disease (P = 0.02). Rates of N-positive disease were 90% for neoadjuvant tx and 73% for no neoadjuvant tx. Analysis of overall survival of the entire patient population based on postoperative T and N

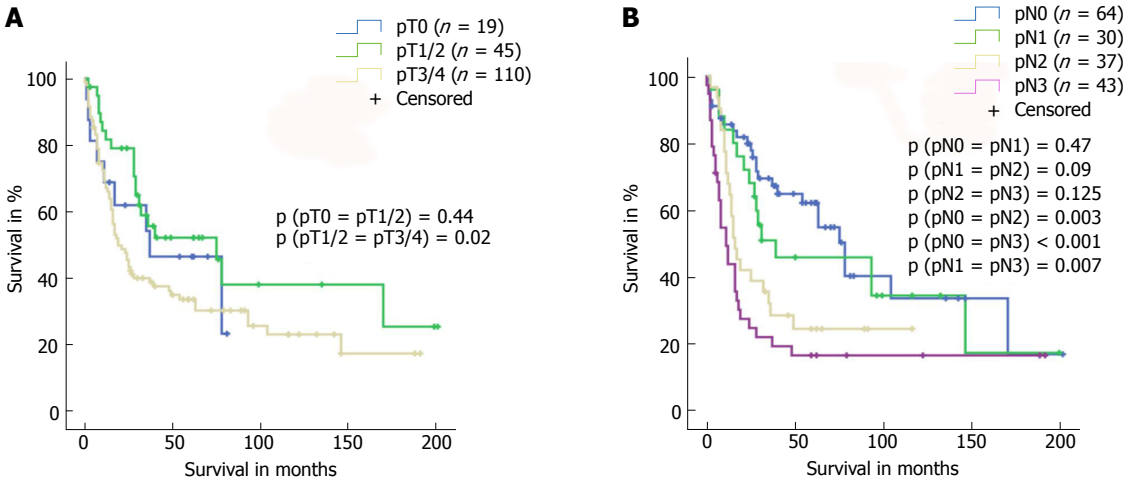

Figure 1 Overall survival. The graphs present an overview of the long-term survival of the entire study cohort based on tumour (A) and nodal (B) stages.

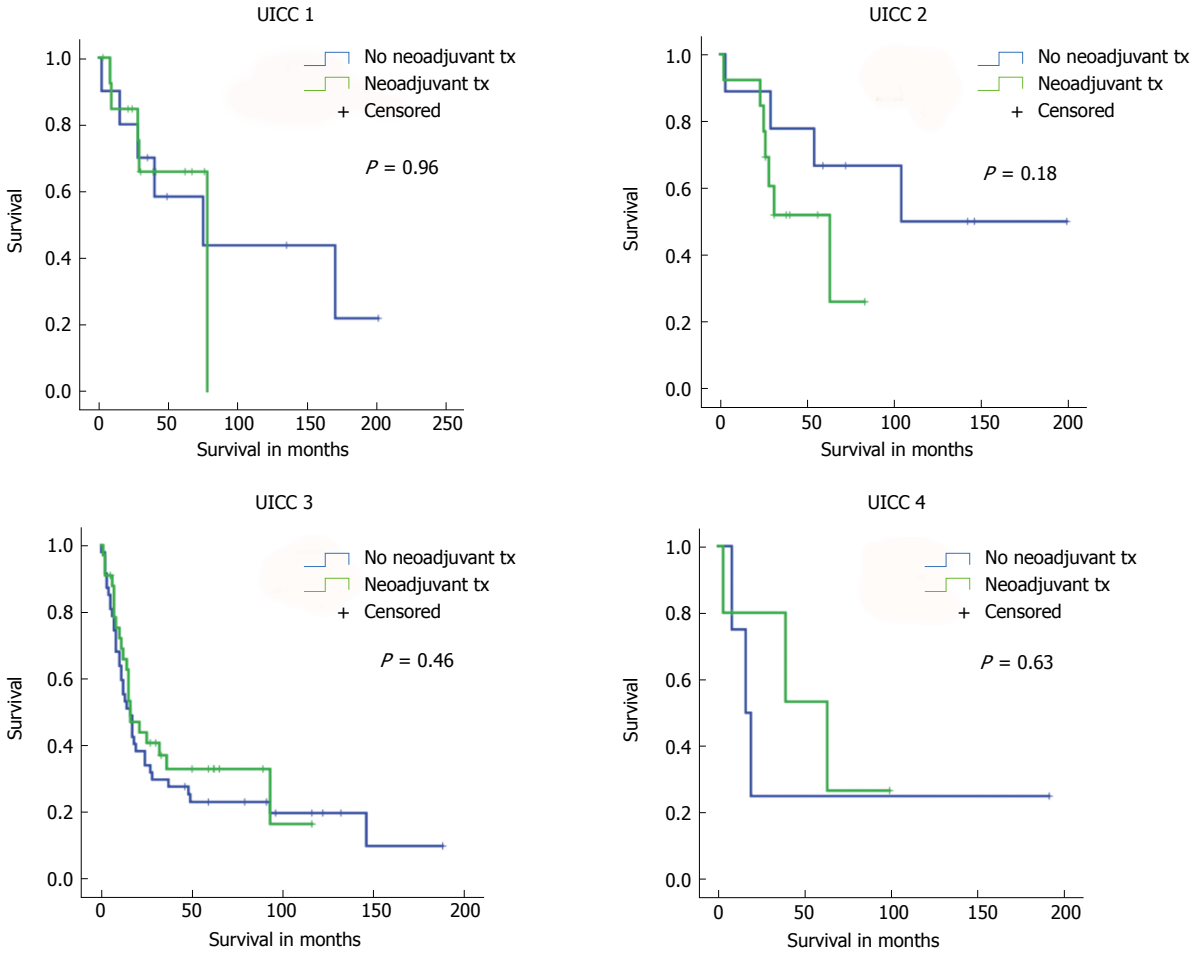

Figure 2 Impact of American Joint Committee on Cancer/Union for International Cancer Control stage on survival of patients with or without neoadjuvant pretreatment. The graphs show the long-term survival of patients with or without neoadjuvant pretreatment and with the same postoperative UICC stage. Tx: treatment; UICC: Union for International Cancer Control.

stages confirmed that long-term survival depended on disease stages (Figure 1).

Survival of patients with or without neoadjuvant treatment who had equivalent postoperative TNM stages

First, we compared long-term survival between groups of patients with or without neoadjuvant treatment who had equivalent postoperative AJCC/UICC TNM stages (stages Ⅰ-Ⅳ according to the 7th edition AJCC/UICC staging). We found no significant differences in long-term survival according to receipt of neoadjuvant treatment for the four AJCC/UICC stage subgroups (Figure 2).

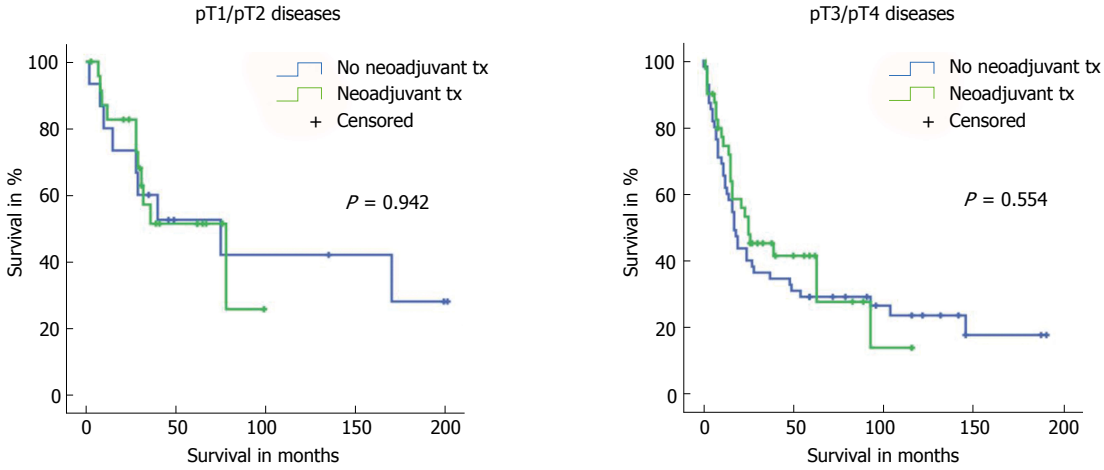

Figure 3 Impact of tumour stage on survival of patients with or without neoadjuvant pretreatment. The graphs present the long-term survival of patients with or without neoadjuvant pretreatment and with similar postoperative tumour stages (early stage cancers: pT1/2; advanced stage cancers: pT3/4). Tx: Treatment.

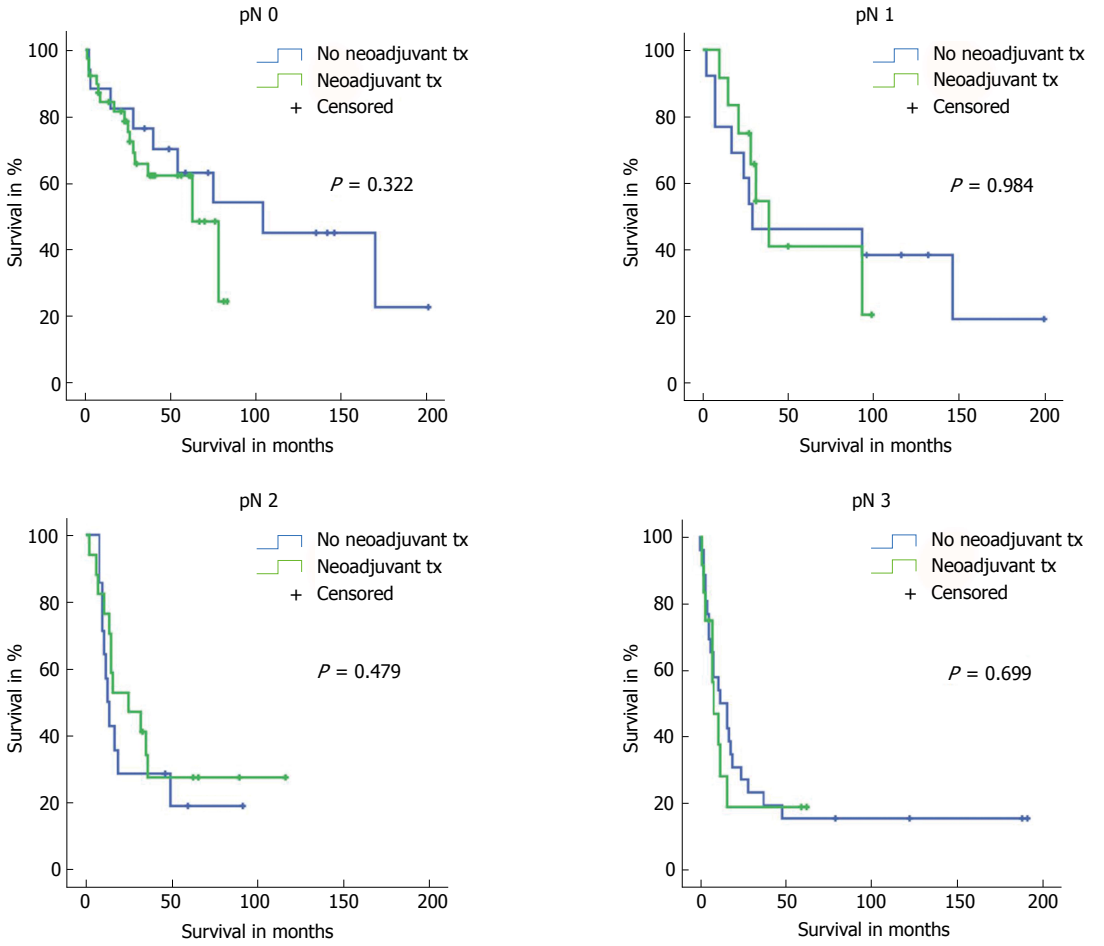

Figure 4 Impact of nodal stage on survival of patients with or without neoadjuvant pretreatment. The graphs show the long-term survival of patients with or without neoadjuvant pretreatment and with the same postoperative nodal stages (pN0/pN1/pN2/pN3). Tx: Treatment.

Furthermore, analysis of patients with either pT1/pT2 diseases or advanced pT3/pT4 diseases showed no significant difference in long-term survival related to receipt (or no receipt) of neoadjuvant pretreatment (Figure 3).

Subgroup analyses on all tumour (pT) stages separately showed that only neoadjuvant-pretreated patients with pT1 stage had slightly better long-term survival ($P = 0.046$). However, the statistical comparison of these groups included only 8 *vs* 5 patients. With regards to postoperative N stages (pN), we did not find any differences in outcome between patients with or

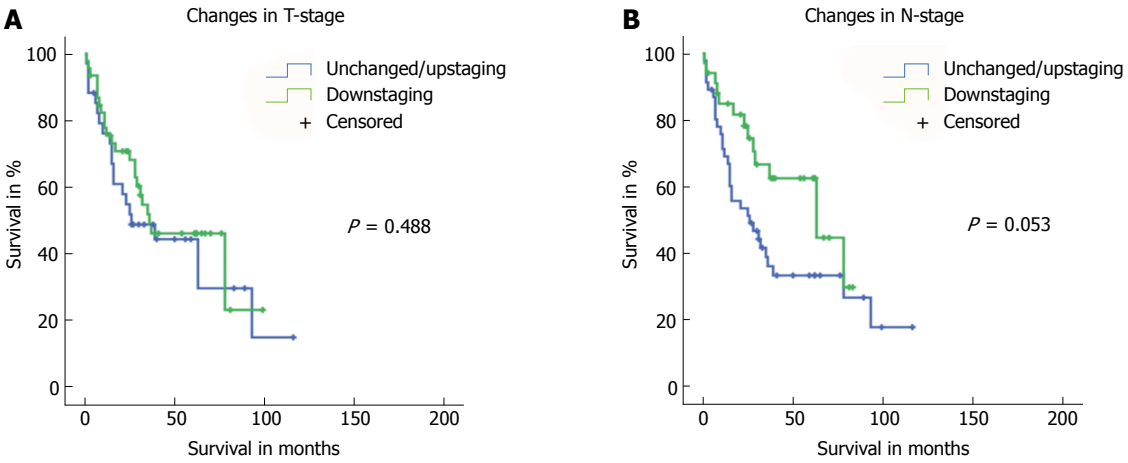

Figure 5 Impact of T and N down-staging on outcome after neoadjuvant treatment. A: The long-term survival of patients with either T "down-staging" or "unchanged/up-staging" after neoadjuvant treatment; B: The long-term survival of patients with either N "down-staging" or "unchanged/up-staging" after neoadjuvant treatment. N: Nodal; T: Tumour; Tx: Treatment.

without neoadjuvant therapy who represented the same postoperative pN stages (Figure 4).

Further subgroup analyses investigating effects of surgical procedure, postoperative G, positive/negative R and Siewert type Ⅰ/Ⅱ/Ⅲ AEG tumours on outcome showed that long-term survival rates were comparable between patients with the same G stage or R stage regardless of neoadjuvant pretreatment (G2: $P = 0.580$; G3: $P = 0.417$; R0: $P = 0.389$; R1: $P = 0.825$). With regards to the Siewert classification, only patients with pT1 tumours in Siewert type 2 AEG showed a better survival after neoadjuvant therapy ($P = 0.017$; 7 patients with neoadjuvant tx *vs* 3 patients with no neoadjuvant tx); otherwise, the location of the tumour classified by Siewert classification did not impact outcome of patients with or without neoadjuvant pretreatment. Similarly, patients with pT1 tumours who received gastrectomy showed a significantly better survival rate after neoadjuvant therapy ($P = 0.020$; 3 patients with neoadjuvant tx *vs* 4 patients with no neoadjuvant tx); otherwise, surgical procedures (oesophagectomy *vs* gastrectomy) did not impact outcome.

Effect of T and N down-staging after neoadjuvant therapy on long-term survival

Finally, we analysed if T or N down-staging after neoadjuvant treatment impacted outcome by comparing preoperative and postoperative T and N stages only for those patients that underwent neoadjuvant pretreatment. We found that T down-staging after neoadjuvant therapy did not affect long-term survival ($P = 0.488$; Figure 5). Subgroup analysis on patients with either unchanged or up-staged disease showed a trend towards worse survival for patients with up-staged T stage ($P = 0.628$; Supplementary Figure 1). However, these results are limited by the very low number of patients included ($n = 30$ *vs* $n = 4$). In contrast, N down-staging after neoadjuvant treatment resulted in borderline significant improvement in long-term survival ($P = 0.053$) (Figure 5).

DISCUSSION

The development of new therapeutic approaches and strategies for AEG within recent years has led to a multidisciplinary approach involving neoadjuvant/perioperative chemotherapy and/or radiotherapy. In contrast to the surgery-alone approaches, the multidisciplinary approaches have resulted in a relevant overall survival benefit to patients[7,19-22] and have become part of standard treatment for AEG tumours. In addition to a survival benefit, neoadjuvant pretreatment further showed potential for down-staging of the primary tumour and/or lymph node metastasis, and finally in improving rates of complete tumour resection (R0)[7,19-22]. While there is a broad consensus that neoadjuvant treatment affects outcome and prognosis of patients with AEG tumours, data are scarce on the exact prognostic relevance of postoperative AJCC/UICC TNM staging in the era of neoadjuvant treatment.

With this current study, we showed that there were no significant differences in the overall long-term survival of patients with or without neoadjuvant treatment, if they presented similar postoperative AJCC/UICC stages (stages Ⅰ-Ⅳ, according to the 7th edition AJCC/UICC), T stages (early pT1/2 and advanced pT3/4 cancers) or N stages (pN0/pN1/pN2/pN3). Furthermore, we could show that surgical procedure, postoperative G, positive/negative R and location (Siewert classification of AEG the tumour) did not affect outcome between patients with or without neoadjuvant treatment, except in some cases of patients with pT1 tumours.

In summary, in our opinion, these results provide an interesting contribution towards answering the question of whether the AJCC TNM staging system can predict or estimate individual prognosis of patients with AEG tumours, regardless of whether they received

neoadjuvant pretreatment or not. Oesophageal cancer staging in the 7th edition AJCC/UICC TNM is based on pTNM of patients that had undergone surgery alone[11,14]. Our data provide evidence that this system might also be applicable to patients who receive neoadjuvant treatment, and that prognosis of patients with similar T and N stages might indeed be comparable regardless of neoadjuvant treatment.

However, Rice *et al*[12,13] recently published the 8th edition of AJCC TNM, which includes, for the first time, neoadjuvant pretreatment stage groupings (*i.e.* ypTNM). A retrospective comparison of actual WECC survival data of patients with neoadjuvant treatment (ypTNM from the 8th edition) with data of patients who underwent surgery-alone (pTNM from the previous 7th edition) indicated that survival for the neoadjuvant-treated patients (ypTNM data) was lower than that found for patients of equivalent pathological staging that underwent surgery alone (pTNM data)[13,15]. However, these data only partly contradict our results, as Rice *et al*[13,15] described a worse prognosis of neoadjuvant categories (ypTNM) for adenocarcinoma patients compared to corresponding pTNM data alone for early-stage disease (stages Ⅰ and Ⅱ); advanced stage adenocarcinoma patients (stages Ⅲ-Ⅳ) showed no differences in survival[13,15].

We did not find any significant difference in survival for either early or advanced stage disease, apart from limited pT1 cases as discussed below. Our data are further supported by a retrospective analysis published by Davies *et al*[16] that showed prognostic relevance of postoperative pTNM stage was similar between patients with or without neoadjuvant pretreatment. Similarly, in another series, Swisher *et al*[17] demonstrated that pTNM-specific survival was similar for patients with down-staged disease but not for those with unchanged disease. We must acknowledge in this context that our study did not include analysis of patients with complete tumour regression (ypT0N0), as this subgroup of patients did not exist among the patients without neoadjuvant treatment. This caveat might impact our results for early-stage cancer patients and might lead to differences in results compared to the data of Rice *et al*[13]. On the other hand, WECC data represents a fairly heterogeneous patient population as well as of different treatment standards in different countries and continents, which is reflected in the heterogeneous survival rate[13]. In contrast, the patient population in our study might be more homogenous since all data were collected from a single cancer centre. Of note, in our study cohort, patients with ypT0N0 showed long-term survival similar to that of patients with pT1N0 (data not shown).

We found that T down-staging did not affect long-term outcome, whereas N down-staging appeared to improve survival (borderline significance; $P = 0.053$). This observation is supported by the fact that N involvement is one of the most important and strongest prognostic factors of AEG tumours. Recent data, for example, show that lymph node involvement is more important than regional anatomic location for prognosis[23,24]. The 7th edition AJCC TNM has already heralded the era of data-driven cancer staging and the incorporation of nonanatomic cancer characteristics[25]. And, indeed, factors beyond those included in the AJCC TNM system (*e.g.*, down-staging of the primary tumour and/or lymph node metastasis after neoadjuvant treatment) have been shown to represent independent prognostic factors for overall survival[7,16,17,19-22,26]. However, for prognostication, T or/and N down-staging were still not considered in the currently used 8th AJCC TNM edition[12].

In order to improve prognostication, some authors have suggested modification of the pTNM staging system to incorporate the extent of pathologic response following neoadjuvant treatment, rather than developing separate ypTNM stages[17]. This idea is supported by our data, which indicate that it might be necessary to include information on T or/and N down-staging in the AJCC TNM staging system in order to improve prognostic assessment of patients with AEG tumours.

There are, however, a number of aspects and limitations of the current study that must be considered for proper interpretation of the presented data. First, and most importantly, our study embodies all the known disadvantages of a retrospective study, including potential inhomogeneity of data acquisition and quality, single-centre data, changes of treatment protocols over time, *etc*. Second, we have to acknowledge that the patients without neoadjuvant treatment had been mainly recruited from the years 1996 to 2004, and patients with neoadjuvant treatment were from the year 2005 onward. This is based on the development and introduction of neoadjuvant treatment protocols into daily clinical practice since 2005. We are fully aware that inclusion of historical cohorts of patients might impact outcome of the respective groups[27]; however, it will be very difficult to recruit a significant number of patients in the current era who qualify for but do not receive any neoadjuvant treatment, as this treatment is part of standard protocols nowadays in most parts of the world.

It is also important to note that our two study groups (neoadjuvant tx *vs* no neoadjuvant tx) are not completely homogenous. In fact, there are significant differences between the groups in regards to age, location (Siewert classification), N involvement and surgical technique. This fact is based on the use of the method of exact matching that allowed for us to include different numbers of patients into both groups as long as the selected parameters (preoperative TNM stages) were identical. However, the aim of this study was to analyse if similar postoperative T and N stages indicate similar prognosis in patients with or without neoadjuvant pretreatment; such a question might not be highly affected by this selection of patients. We

found in our analyses that patients with postoperative T1 stages showed differences in survival between groups in limited cases. This observation, in our opinion, needs very careful interpretation, as the number of patients with pT1 stage in our study cohort was extremely low (n = 24 patients in total). These findings warrant further confirmation, and clinical relevance remains unclear. Furthermore, in our study, 26 patients without neoadjuvant pretreatment received adjuvant therapy; yet, subgroup analysis excluding this patient cohort produced no difference in the results (data not shown).

A number of studies have found that prognosis and tumour biology differs between AEG tumours at different locations according to the Siewert classification (types Ⅰ to Ⅲ), supporting the concept that Siewert type Ⅲ carcinoma represents true gastric adenocarcinoma, having a worse prognosis than Siewert types Ⅰ and Ⅱ carcinoma[28,29]. Interestingly, the 7th edition AJCC/UICC TNM classification did not include Siewert classification for prognostication, and instead classified all tumours within 5 cm of the gastro-oesophageal junction as oesophageal carcinoma.

Based on the discrepancy of available data, we performed subgroup analyses with regards to outcome of tumours in different locations according to the Siewert classification. Our data showed that, in general, location of the tumour classified by Siewert classification did not impact outcome of patients with or without neoadjuvant pretreatment. Only patients with pT1 tumours in Siewert type 2 AEG tumours showed a better survival after neoadjuvant therapy (P = 0.017), but this analysis was based on only 7 *vs* 3 patients, casting suspicion on the final significance of these findings. We can only hypothesize that our study might be underpowered for answering the question of whether location of tumours impacts outcome. Further studies are needed to elucidate this specific and highly relevant question in more detail.

In summary, our retrospective analysis of patients with AEG tumours demonstrated that there were no significant differences in the overall long-term survival of patients with or without neoadjuvant treatment, if they presented similar postoperative AJCC/UICC stages (stages Ⅰ-Ⅳ), T stages (early pT1/2 and advanced pT3/4 cancers) or N stages (pN0/pN1/pN2/pN3). Furthermore, we showed that N down-staging, especially, affected long-term survival of patients undergoing neoadjuvant treatment. Collectively, our data indicate that the pTNM staging system is reliable for assessment of individual prognosis for patients with AEG tumours, regardless of whether neoadjuvant treatment has been received or not. Furthermore, our data support the inclusion of T and/or N down-staging information, rather than separate pTNM and ypTNM stages, as independent risk factors for survival in the next edition of the AJCC TNM staging system.

ARTICLE HIGHLIGHTS

Research background

Adenocarcinoma of the gastro-oesophageal junction (AEG) has a poor prognosis. Neoadjuvant chemotherapy and radiotherapy have significantly improved clinical management and outcome of patients, leading to a major evolution in treatment of oesophageal cancer. Neoadjuvant therapy provides a survival benefit to patients with AEG, through its elimination of micrometastatic disease and potential for down-staging of the primary tumour and/or lymph node metastasis, ultimately leading to higher rates of complete resections (R0). For prediction of prognosis of cancer patients, the American Joint Committee on Cancer (AJCC) and the Union for International Cancer Control (UICC) system has been established. The 8th edition of AJCC staging of cancers of the oesophagus and oesophagogastric junction includes, for the first time, postneoadjuvant tumour/node/metastasis (ypTNM) stage groupings; the previous editions only referred to patients that underwent surgery alone. This raises the question of whether prognosis according to the postoperative pTNM/ypTNM stages is similar between patients that receive neoadjuvant pretreatment (ypTNM) or patients that undergo surgery alone (pTNM). According to the 8th edition AJCC, there are different prognostic implications between postneoadjuvant (ypTNM) and pathologic (pTNM) AEG categories. In detail, prognosis of node-negative (ypN0) and early-stage diseases (ypTNM groups Ⅰ and Ⅱ) is worse compared to patients with similar stages who underwent surgery alone. In contrast, for advanced stage AEG, there is no difference of prognosis among patients with identical pTNM/ypTNM stages. Other studies, however, have shown contradictory results. In these studies, the prognostic relevance of postoperative AJCC/UICC TNM staging did not differ between patients with or without neoadjuvant pretreatment.

Research motivation

Due to limited and heterogeneous data, the prognostic relevance of postoperative TNM staging in the era of neoadjuvant therapy of AEG remains unclear. However, due to the generally poor prognosis of AEG and the relevant risk of recurrence, an exact assessment of prognosis according to the TNM staging system is extremely important for the individual patient and for further treatment decision-making.

Research objectives

The main objective of this study was to compare the prognostic relevance of similar postoperative TNM stages between patients with or without neoadjuvant pretreatment. The results were expected to clarify the need of a separate postneoadjuvant stage grouping (ypTNM) for prognostication of AEG patients. Furthermore, in the era of neoadjuvant treatment, other prognostic factors may be relevant for prognostication of survival of patients with AEG.

Research methods

We conducted a retrospective study analysing 254 patients that underwent curative surgical treatment at our University Medical Center Schleswig-Holstein, Campus Lübeck. After excluding patients with preoperative tumour stages that preclude neoadjuvant pretreatment (cT1cN0cM0 and cT2cN0cM0), we performed exact matching to identify patients with or without neoadjuvant pretreatment who would be eligible for the study. Additionally, in-hospital deaths were excluded since we aimed to analyse long-term survival. Study parameters included sex, age, AEG (Siewert) classification, surgical procedure, preoperative staging (including cT, cN and cM categories according to the AJCC Cancer Staging Manual 8th edition), postoperative staging (including T, N and M categories according to the AJCC/UICC Cancer Staging Manual 7th edition, grade of differentiation (G) and resection margin status (R)), long-term survival (defined as time in months as from the day of hospital discharge) and pathologic down-staging/response in tumour (T) and nodal (N) stages after neoadjuvant therapy. Pearson's chi-square and Fisher´s exact tests were used for statistical analyses of categorical variables (sex, age, AEG (Siewert) classification, surgical procedure and preoperative staging (cTNM)). Long-term survival was analysed using the Kaplan-Meier method. For statistical comparisons, log-rank test was used. A P-value of $\leqslant$ 0.05 was considered

significant for all statistical analyses.

Research results

After patient selection and exact matching, 174 of the 254 patients were included in the study. Regarding demographics of both groups (no neoadjuvant treatment *vs* neoadjuvant treatment), patients who received neoadjuvant treatment were significantly younger (58 years *vs* 64 years, $P = 0.043$) and presented Siewert type I AEG tumours significantly more often ($P < 0.001$), resulting in significantly more oesophagectomies than gastrectomies ($P < 0.001$) for surgical treatment in this group. Patients who received neoadjuvant treatment presented higher preoperative rates of lymph node-positive disease ($P = 0.020$). Regarding overall survival of the entire study cohort, survival worsened at advanced postoperative AJCC/UICC TNM stages. Comparing long-term survival between patients with or without neoadjuvant pretreatment with identical postoperative TNM stages, no difference could be found. In addition, no difference was found in long-term survival of patients with or without neoadjuvant pretreatment for identical pT, pN or pM stages, G or R. Investigation of other prognostic markers for patients who received neoadjuvant pretreatment involved analysis of the effect of T and N down-staging on long-term survival. Here, we found that T down-staging did not have an impact on long-term survival ($P = 0.488$), while N down-staging after neoadjuvant treatment provided a significant but borderline improvement in long-term survival ($P = 0.053$).

Research conclusions

Our retrospective study demonstrated that the prognostic relevance of equivalent postoperative AJCC/UICC TNM stages is similar between patients with or without neoadjuvant pretreatment. Our data provide evidence that the pTNM staging system can be applied for assessment of individual prognosis of patients with AEG, regardless of whether or not they received neoadjuvant treatment. Furthermore, our study showed that N down-staging following neoadjuvant treatment positively affects long-term outcome, emphasizing the need of novel markers for prognostication in the era of neoadjuvant therapy.

Research perspectives

Our data support the idea of modifying the pTNM staging system by incorporating the extent of pathologic response following neoadjuvant treatment, rather than developing separate ypTNM stages. Prognostic factors or markers that reflect tumour biology, rather than the anatomical extent of growth, are promising for the development of new assessments for prognostication of survival of patients with AEG.

REFERENCES

1 **Arnold M**, Soerjomataram I, Ferlay J, Forman D. Global incidence of oesophageal cancer by histological subtype in 2012. *Gut* 2015; **64**: 381-387 [PMID: 25320104 DOI: 10.1136/gutjnl-2014-308124]

2 **Ferlay J**, Shin HR, Bray F, Forman D, Mathers C, Parkin DM. Estimates of worldwide burden of cancer in 2008: GLOBOCAN 2008. *Int J Cancer* 2010; **127**: 2893-2917 [PMID: 21351269 DOI: 10.1002/ijc.25516]

3 **Pennathur A**, Farkas A, Krasinskas AM, Ferson PF, Gooding WE, Gibson MK, Schuchert MJ, Landreneau RJ, Luketich JD. Esophagectomy for T1 esophageal cancer: outcomes in 100 patients and implications for endoscopic therapy. *Ann Thorac Surg* 2009; **87**: 1048-54; discussion 1054-5 [PMID: 19324126 DOI: 10.1016/j.athoracsur.2008.12.060]

4 **Pennathur A**, Gibson MK, Jobe BA, Luketich JD. Oesophageal carcinoma. *Lancet* 2013; **381**: 400-412 [PMID: 23374478 DOI: 10.1016/S0140-6736(12)60643-6]

5 **Enzinger PC**, Mayer RJ. Esophageal cancer. *N Engl J Med* 2003; **349**: 2241-2252 [PMID: 14657432 DOI: 10.1056/NEJMra035010]

6 **Li B**, Li J, Xu WW, Guan XY, Qin YR, Zhang LY, Law S, Tsao SW, Cheung AL. Suppression of esophageal tumor growth and chemoresistance by directly targeting the PI3K/AKT pathway. *Oncotarget* 2014; **5**: 11576-11587 [PMID: 25344912 DOI: 10.18632/oncotarget.2596]

7 **van Hagen P**, Hulshof MC, van Lanschot JJ, Steyerberg EW, van Berge Henegouwen MI, Wijnhoven BP, Richel DJ, Nieuwenhuijzen GA, Hospers GA, Bonenkamp JJ, Cuesta MA, Blaisse RJ, Busch OR, ten Kate FJ, Creemers GJ, Punt CJ, Plukker JT, Verheul HM, Spillenaar Bilgen EJ, van Dekken H, van der Sangen MJ, Rozema T, Biermann K, Beukema JC, Piet AH, van Rij CM, Reinders JG, Tilanus HW, van der Gaast A; CROSS Group. Preoperative chemoradiotherapy for esophageal or junctional cancer. *N Engl J Med* 2012; **366**: 2074-2084 [PMID: 22646630 DOI: 10.1056/NEJMoa1112088]

8 **Forde PM**, Kelly RJ. Genomic alterations in advanced esophageal cancer may lead to subtype-specific therapies. *Oncologist* 2013; **18**: 823-832 [PMID: 23853247 DOI: 10.1634/theoncologist.2013-0130]

9 **Findlay JM**, Middleton MR, Tomlinson I. A systematic review and meta-analysis of somatic and germline DNA sequence biomarkers of esophageal cancer survival, therapy response and stage. *Ann Oncol* 2015; **26**: 624-644 [PMID: 25214541 DOI: 10.1093/annonc/mdu449]

10 **Edge SB**, Compton CC. The American Joint Committee on Cancer: the 7th edition of the AJCC cancer staging manual and the future of TNM. *Ann Surg Oncol* 2010; **17**: 1471-1474 [PMID: 20180029 DOI: 10.1245/s10434-010-0985-4]

11 **Rice TW**, Blackstone EH, Rusch VW. 7th edition of the AJCC Cancer Staging Manual: esophagus and esophagogastric junction. *Ann Surg Oncol* 2010; **17**: 1721-1724 [PMID: 20369299 DOI: 10.1245/s10434-010-1024-1]

12 **Rice TW**, Patil DT, Blackstone EH. 8th edition AJCC/UICC staging of cancers of the esophagus and esophagogastric junction: application to clinical practice. *Ann Cardiothorac Surg* 2017; **6**: 119-130 [PMID: 28447000 DOI: 10.21037/acs.2017.03.14]

13 **Rice TW**, Lerut TE, Orringer MB, Chen LQ, Hofstetter WL, Smithers BM, Rusch VW, van Lanschot J, Chen KN, Davies AR, D'Journo XB, Kesler KA, Luketich JD, Ferguson MK, Räsänen JV, van Hillegersberg R, Fang W, Durand L, Allum WH, Cecconello I, Cerfolio RJ, Pera M, Griffin SM, Burger R, Liu JF, Allen MS, Law S, Watson TJ, Darling GE, Scott WJ, Duranceau A, Denlinger CE, Schipper PH, Ishwaran H, Apperson-Hansen C, DiPaola LM, Semple ME, Blackstone EH. Worldwide Esophageal Cancer Collaboration: neoadjuvant pathologic staging data. *Dis Esophagus* 2016; **29**: 715-723 [PMID: 27731548 DOI: 10.1111/dote.12513]

14 **Rice TW**, Rusch VW, Ishwaran H, Blackstone EH; Worldwide Esophageal Cancer Collaboration. Cancer of the esophagus and esophagogastric junction: data-driven staging for the seventh edition of the American Joint Committee on Cancer/International Union Against Cancer Cancer Staging Manuals. *Cancer* 2010; **116**: 3763-3773 [PMID: 20564099 DOI: 10.1002/cncr.25146]

15 **Rice TW**, Ishwaran H, Kelsen DP, Hofstetter WL, Apperson-Hansen C, Blackstone EH; Worldwide Esophageal Cancer Collaboration Investigators. Recommendations for neoadjuvant pathologic staging (ypTNM) of cancer of the esophagus and esophagogastric junction for the 8th edition AJCC/UICC staging manuals. *Dis Esophagus* 2016; **29**: 906-912 [PMID: 27905170 DOI: 10.1111/dote.12538]

16 **Davies AR**, Gossage JA, Zylstra J, Mattsson F, Lagergren J, Maisey N, Smyth EC, Cunningham D, Allum WH, Mason RC. Tumor stage after neoadjuvant chemotherapy determines survival after surgery for adenocarcinoma of the esophagus and esophagogastric junction. *J Clin Oncol* 2014; **32**: 2983-2990 [PMID: 25071104 DOI: 10.1200/JCO.2014.55.9070]

17 **Swisher SG**, Hofstetter W, Wu TT, Correa AM, Ajani JA, Komaki RR, Chirieac L, Hunt KK, Liao Z, Phan A, Rice DC, Vaporciyan AA, Walsh GL, Roth JA. Proposed revision of the esophageal cancer staging system to accommodate pathologic response (pP) following preoperative chemoradiation (CRT). *Ann Surg* 2005; **241**: 810-7; discussion 817-20 [PMID: 15849517]

18 **Siewert JR**, Stein HJ. Classification of adenocarcinoma of the oesophagogastric junction. *Br J Surg* 1998; **85**: 1457-1459 [PMID: 9823902 DOI: 10.1046/j.1365-2168.1998.00940.x]

19 **Kelsen DP**, Ginsberg R, Pajak TF, Sheahan DG, Gunderson L, Mortimer J, Estes N, Haller DG, Ajani J, Kocha W, Minsky

BD, Roth JA. Chemotherapy followed by surgery compared with surgery alone for localized esophageal cancer. *N Engl J Med* 1998; **339**: 1979-1984 [PMID: 9869669 DOI: 10.1056/NEJM199812313392704]
20 **Urba SG**, Orringer MB, Turrisi A, Iannettoni M, Forastiere A, Strawderman M. Randomized trial of preoperative chemoradiation versus surgery alone in patients with locoregional esophageal carcinoma. *J Clin Oncol* 2001; **19**: 305-313 [PMID: 11208820 DOI: 10.1200/JCO.2001.19.2.305]
21 **Arnott SJ**, Duncan W, Gignoux M, Hansen HS, Launois B, Nygaard K, Parmar MK, Rousell A, Spilopoulos G, Stewart G, Tierney JF, Wang M, Rhugang Z; Oeosphageal Cancer Collaborative Group. Preoperative radiotherapy for esophageal carcinoma. *Cochrane Database Syst Rev* 2005; **19**: CD001799 [PMID: 16235286 DOI: 10.1002/14651858.CD001799.pub2]
22 **Cunningham D**, Allum WH, Stenning SP, Thompson JN, Van de Velde CJ, Nicolson M, Scarffe JH, Lofts FJ, Falk SJ, Iveson TJ, Smith DB, Langley RE, Verma M, Weeden S, Chua YJ, MAGIC Trial Participants. Perioperative chemotherapy versus surgery alone for resectable gastroesophageal cancer. *N Engl J Med* 2006; **355**: 11-20 [PMID: 16822992 DOI: 10.1056/NEJMoa055531]
23 **Mariette C**, Piessen G, Briez N, Triboulet JP. The number of metastatic lymph nodes and the ratio between metastatic and examined lymph nodes are independent prognostic factors in esophageal cancer regardless of neoadjuvant chemoradiation or lymphadenectomy extent. *Ann Surg* 2008; **247**: 365-371 [PMID: 18216546 DOI: 10.1097/SLA.0b013e31815aaadf]
24 **DaVee T**, Ajani JA, Lee JH. Is endoscopic ultrasound examination necessary in the management of esophageal cancer? *World J Gastroenterol* 2017; **23**: 751-762 [PMID: 28223720 DOI: 10.3748/wjg.v23.i5.751]
25 **Rusch VW**, Rice TW, Crowley J, Blackstone EH, Rami-Porta R, Goldstraw P. The seventh edition of the American Joint Committee on Cancer/International Union Against Cancer Staging Manuals: the new era of data-driven revisions. *J Thorac Cardiovasc Surg* 2010; **139**: 819-821 [PMID: 20304130 DOI: 10.1016/j.jtcvs.2010.02.013]
26 **Ronellenfitsch U**, Schwarzbach M, Hofheinz R, Kienle P, Kieser M, Slanger TE, Jensen K; GE Adenocarcinoma Meta - analysis Group. Perioperative chemo(radio)therapy versus primary surgery for resectable adenocarcinoma of the stomach, gastroesophageal junction, and lower esophagus. *Cochrane Database Syst Rev* 2013; **31**: CD008107 [PMID: 23728671 DOI: 10.1002/14651858.CD008107.pub2]
27 **Cooke DT**, Calhoun RF, Kuderer V, David EA. A Defined Esophagectomy Perioperative Clinical Care Process Can Improve Outcomes and Costs. *Am Surg* 2017; **83**: 103-111 [PMID: 28234134]
28 **Curtis NJ**, Noble F, Bailey IS, Kelly JJ, Byrne JP, Underwood TJ. The relevance of the Siewert classification in the era of multimodal therapy for adenocarcinoma of the gastro-oesophageal junction. *J Surg Oncol* 2014; **109**: 202-207 [PMID: 24243140 DOI: 10.1002/jso.23484]
29 **Kulig P**, Sierzega M, Pach R, Kolodziejczyk P, Kulig J; Polish Gastric Cancer Study Group. Differences in prognosis of Siewert II and III oesophagogastric junction cancers are determined by the baseline tumour staging but not its anatomical location. *Eur J Surg Oncol* 2016; **42**: 1215-1221 [PMID: 27241921 DOI: 10.1016/j.ejso.2016.04.061]

P- Reviewer: Herbella F, Nishida T, Tsoulfas G **S- Editor**: Gong ZM
L- Editor: A **E- Editor**: Huang Y

World Journal of Gastroenterology

Submit a Manuscript: http://www.f6publishing.com

World J Gastroenterol 2018 April 7; 24(13): 1440-1450

DOI: 10.3748/wjg.v24.i13.1440

ISSN 1007-9327 (print) ISSN 2219-2840 (online)

ORIGINAL ARTICLE

Retrospective Study

Mild drinking habit is a risk factor for hepatocarcinogenesis in non-alcoholic fatty liver disease with advanced fibrosis

Takefumi Kimura, Naoki Tanaka, Naoyuki Fujimori, Ayumi Sugiura, Tomoo Yamazaki, Satoru Joshita, Michiharu Komatsu, Takeji Umemura, Akihiro Matsumoto, Eiji Tanaka

Takefumi Kimura, Naoyuki Fujimori, Ayumi Sugiura, Tomoo Yamazaki, Satoru Joshita, Michiharu Komatsu, Takeji Umemura, Akihiro Matsumoto, Eiji Tanaka, Department of Internal Medicine, Division of Gastroenterology, Shinshu University School of Medicine, Matsumoto 390-8621, Japan

Naoki Tanaka, Department of Metabolic Regulation, Shinshu University Graduate School of Medicine, Matsumoto 390-8621, Japan

Naoki Tanaka, Research Center for Agricultural Food Industry, Shinshu University, Matsumoto 390-8621, Japan

ORCID number: Takefumi Kimura (0000-0002-1481-1029); Naoki Tanaka (0000-0002-0606-2101); Naoyuki Fujimori (0000-0001-8744-8139); Ayumi Sugiura (0000-0001-5427-7628); Tomoo Yamazaki (0000-0001-6958-1366); Satoru Joshita (0000-0002-6364-9654); Michiharu Komatsu (0000-0002-7860 -2816); Takeji Umemura (0000-0001-7985-919X); Akihiro Matsumoto (0000-0001-6453-8529); Eiji Tanaka (0000-0002-0724-2104).

Author contributions: Kimura T and Tanaka N designed the research; Fujimori N, Sugiura A, Yamazaki T, Joshita S, Komatsu M, Umemura T, and Matsumoto A treated the patients and collected materials and clinical data; Kimura T analyzed the data; Kimura T and Tanaka N wrote the paper; Tanaka E supervised the research.

Institutional review board statement: The study was reviewed and approved by the Committee for Medical Ethics of Shinshu University School of Medicine Institutional Review Board.

Informed consent statement: Informed written consent was obtained from all patients.

Conflict-of-interest statement: The authors declare that no conflict of interest exists.

Data sharing statement: No additional data are available.

Manuscript source: Invited manuscript

Correspondence to: Naoki Tanaka, MD, PhD, Associate Professor, Doctor, Department of Metabolic Regulation, Shinshu University Graduate School of Medicine and Research Center for Agricultural Food Industry, Shinshu University, 3-1-1 Asahi, Matsumoto 390-8621, Japan. naopi@shinshu-u.ac.jp
Telephone: +81-263-372634
Fax: +81-263-329412

Received: January 31, 2018
Peer-review started: January 31, 2018
First decision: February 26, 2015
Revised: March 3, 2015
Accepted: March 10, 2018
Article in press: March 10, 2018
Published online: April 7, 2018

Abstract

AIM

The impact of mild drinking habit (less than 20 g/d of ethanol) on the clinical course of non-alcoholic fatty liver disease (NAFLD) has not been determined. We examined the influence of a mild drinking habit on liver carcinogenesis from NAFLD.

METHODS

A total of 301 patients who had been diagnosed as having NAFLD by liver biopsy between 2003 and 2016 [median age: 56 years, 45% male, 56% with non-alcoholic steatohepatitis, 26% with advanced fibrosis (F3-4)] were divided into the mild drinking group with

ethanol consumption of less than 20 g/d (mild drinking group, *n* = 93) and the non-drinking group (*n* = 208). Clinicopathological features at the time of liver biopsy and factors related to hepatocellular carcinoma (HCC) occurrence were compared between the groups.

RESULTS

We observed significant differences in male prevalence (*P* = 0.01), platelet count (*P* = 0.04), and gamma-glutamyl transpeptidase (*P* = 0.02) between the test groups. Over 6 years of observation, the HCC appearance rate was significantly higher in the mild drinking group (6.5% *vs* 1.4%, *P* = 0.02). Multivariate survival analysis using Cox's regression model revealed that hepatic advanced fibrosis (F3-4) (*P* < 0.01, risk ratio: 11.60), diabetes mellitus (*P* < 0.01, risk ratio: 89.50), and serum triglyceride (*P* = 0.04, risk ratio: 0.98) were factors significantly related to HCC in all NAFLD patients, while the effect of a drinking habit was marginal (*P* = 0.07, risk ratio: 4.43). In patients with advanced fibrosis (F3-4), however, a drinking habit (*P* = 0.04, risk ratio: 4.83), alpha-fetoprotein (*P* = 0.01, risk ratio: 1.23), and diabetes mellitus (*P* = 0.03, risk ratio: 12.00) were identified as significant contributors to HCC occurrence.

CONCLUSION

A mild drinking habit appears to be a risk factor for hepatocarcinogenesis in NAFLD patients, especially those with advanced fibrosis.

Key words: Non-alcoholic fatty liver disease; Ethanol; Hepatocellular carcinoma; Risk factor

Core tip: This study focused on the impact of a mild drinking habit on liver carcinogenesis in 301 biopsy-proven non-alcoholic fatty liver disease (NAFLD) patients. Multivariate analysis revealed that mild drinking of < 20 g/d might increase the risk of hepatocellular carcinoma in NAFLD patients, particularly those with advanced fibrosis (F3-4). NAFLD patients with severe fibrosis should abstain from even small amounts of regular alcohol consumption.

Kimura T, Tanaka N, Fujimori N, Sugiura A, Yamazaki T, Joshita S, Komatsu M, Umemura T, Matsumoto A, Tanaka E. Mild drinking habit is a risk factor for hepatocarcinogenesis in non-alcoholic fatty liver disease with advanced fibrosis. *World J Gastroenterol* 2018; 24(13): 1440-1450 Available from: URL: http://www.wjgnet.com/1007-9327/full/v24/i13/1440.htm DOI: http://dx.doi.org/10.3748/wjg.v24.i13.1440

INTRODUCTION

Over the past several decades, it has become clear that non-alcoholic fatty liver disease (NAFLD) and its advanced form non-alcoholic steatohepatitis (NASH) are major chronic liver diseases worldwide[1,2]. The prevalence rate of NAFLD has doubled during the last 20 years, while those of other chronic liver conditions have remained stable or even decreased[3]. Recent evidence has confirmed that NAFLD and NASH incidence is increasing in Japan as well[4].

The etiology of NAFLD/NASH has not been fully elucidated. The most widely accepted theory involves insulin resistance as an important mechanism leading to liver steatosis and perhaps steatohepatitis[5]. Others have proposed that "multiple hits" of additional oxidative stress and lipotoxicity are necessary for the necro-inflammatory component of steatohepatitis and carcinogenesis[6]. Liver iron, leptin, anti-oxidant deficiency, and intestinal microbiota have also been suggested as potential factors in the progression from steatosis to steatohepatitis[6-9]. However, research on NAFLD/NASH pathogenesis and carcinogenesis is ongoing.

Although it is widely accepted that more than 60 g/d of ethanol consumption may lead to alcoholic liver disease and steatosis, steatohepatitis, and hepatic fibrosis[10], there is in uncertainty on the influence of a mild drinking habit (< 20 g/d of ethanol) on human health. For example, mild habitual drinking improved insulin resistance and hepatic steatosis but either worsened or improved hepatic fibrosis[11-14]. Since NAFLD/NASH is defined as fatty liver disease with average ethanol intake of less than 20 g daily[10], some NAFLD patients may habitually consume small amounts of ethanol while others abstain completely. There are no reports to date investigating the influence of a mild drinking habit on NAFLD/NASH patients despite a growing number of reports on hepatocellular carcinoma (HCC). To investigate the influence of a mild drinking habit on liver carcinogenesis from NAFLD, we compared clinicopathological features and outcomes between NAFLD patients with a mild drinking habit and the non-drinking NAFLD patients.

MATERIALS AND METHODS

Ethics

This study was carried out in accordance with the World Medical Association Helsinki Declaration and was approved by the ethics committee of Shinshu University School of Medicine (approval ID: 2802).

Patients

We enrolled 301 patients who were diagnosed as having NAFLD by liver biopsy between 2003 and 2016 [median age: 56 years, 45% male, 56% with NASH, 26% with advanced fibrosis (F3-4)] at Shinshu University Hospital in Matsumoto, Nagano, Japan. These patients originally referred to our department from local hospitals in Nagano prefecture to confirm the diagnosis by liver biopsy.

The diagnosis of NAFLD was based on the criteria of: (1) the presence of hepato-renal contrast and increased hepatic echogenicity on abdominal ultrasonography (US), (2) an average daily consumption of < 20 g of ethanol, and (3) the absence of other causes of liver dysfunction, such as viral hepatitis, drug-induced liver injury, autoimmune liver diseases, primary sclerosing cholangitis, Wilson's disease, hereditary hemochromatosis, and citrin deficiency[15,16]. The diagnosis of NAFLD was confirmed based on histological findings of biopsied specimens. Pathology details are described below.

All patients were followed by US or computed tomography with measurements of serum alpha-fetoprotein every 6 mo. HCC was identified radiologically in all affected patients (n = 9). The radiological diagnosis of HCC was based on the American Association for the Study of Liver Diseases practice guidelines on the management of HCC as either: (1) the presence of a hepatic lesion > 2 cm in diameter with typical vascular pattern for HCC on one dynamic imaging technique or alpha-fetoprotein > 200 ng/mL; or (2) the presence of a lesion 1-2 cm in diameter with typical vascular pattern for HCC on two dynamic imaging techniques[17]. Follow-up time was defined as the number of days from biopsy to HCC diagnosis or from biopsy to the last follow-up visit when protocol surveillance confirmed no HCC. Patient drinking habits were confirmed as remaining unchanged during follow-up.

Clinical data collection

All laboratory data in a fasting state on the day of liver biopsy were obtained from our medical database. Past and current drinking habit data were collected by self-reported questionnaires and interviews with doctors performing the liver biopsy. We divided the subjects into two groups: the mild drinking group with ethanol consumption of less than 20 g/d (mild drinking group, n = 93) and the non-drinking group (n = 208). Patients were considered to be hypertensive if their systolic/diastolic pressure was > 140/90 mmHg or if they were taking anti-hypertensive drugs[18]. Patients were judged as having hyperlipidemia if their fasting serum levels of cholesterol or triglyceride were ⩾ 220 mg/dL or ⩾ 150 mg/dL, respectively, or if they were taking lipid-lowering drugs[19]. Patients were considered to be diabetic if they had a fasting glucose level of ⩾ 126 mg/dL or hemoglobin A1c (HbA1c) was ⩾ 6.5%, or if they were taking insulin or oral hypoglycemic agents[19].

Histological findings

Liver specimens of at least 1.5 cm in length were obtained from segment 5 or 8 using a 14-gauge needle, as described previously, and immediately fixed in 10% neutral formalin[20]. Sections of 4 μm in thickness were stained by means of the hematoxylin and eosin and Azan-Mallory methods. The histological activity of NAFLD was assessed by an independent expert pathologist in a blinded manner according to the NAFLD scoring system proposed by Kleiner *et al*[21]. Steatosis grade was scored as 0 to 3 by the fat degeneration rate of hepatocytes (< 5%, 5%-33%, 33%-66%, and > 66%, respectively). Lobular inflammation grade was also scored as 0 to 3 by overall assessment of all inflammatory foci (none, < 2 foci/200 × field, 2-4 foci/200 × field, and > 4 foci/200 × field, respectively). Ballooning grade was determined by the number of degenerating hepatocytes as 0 to 2, corresponding to none, few, and many, respectively. NAFLD activity score was the total of steatosis, lobular inflammation, and ballooning scores. Fibrosis was staged as 0 to 4 depending on the degree of fibrosis (F0, none; F1, perisinusoidal or periportal; F2, perisinusoidal and portal/periportal; F3, bridging fibrosis; and F4, cirrhosis)[21].

Statistical analysis

Clinical and histological data were expressed as a number (percentage) or median (range). Chi-square and Mann-Whitney U tests were used for comparisons between the groups. Kaplan-Meier analysis was performed to estimate HCC cumulative incidence from the time of liver biopsy, and plots of cumulative events *vs* years of follow-up were constructed. Receiver operating characteristic curves were plotted, and optimal cut-off points were determined as the values showing maximum sensitivity plus specificity. In order to assess which factors were associated with the development of HCC after liver biopsy, univariate and multivariate Cox's proportional hazard regression analysis was employed. Variables revealed as significant by univariate analysis were further tested by multivariate analysis. P < 0.05 was considered to be statistically significant. Data were analyzed using a statistical software package (SPSS for Windows, SPSS Inc., Chicago, IL, United States).

RESULTS

Overall HCC occurrence rate

HCC appeared in 9 subjects (3%) within a median of 6 years of follow-up from liver biopsy. Kaplan-Mayer analysis revealed the HCC occurrence rate in our cohort to be 0.9/2.6/6.0% in 3/5/10 years, respectively (Figure 1).

Comparison of clinicopathological features at the time of biopsy between the mild drinking and non-drinking groups

Comparisons of clinicopathological features at the time of biopsy between the mild drinking and non-drinking groups revealed significant differences for male prevalence (P = 0.01), platelet count (P = 0.04), and gamma-glutamyl transpeptidase (P = 0.02) (Table 1). No differences were observed between the groups for co-existing disease rate, serum albumin, bilirubin, or alpha-fetoprotein, HbA1c, or pathological features, such as grades for steatosis, lobular inflammation, ballooning, or NAFLD activity score (Table 1). The

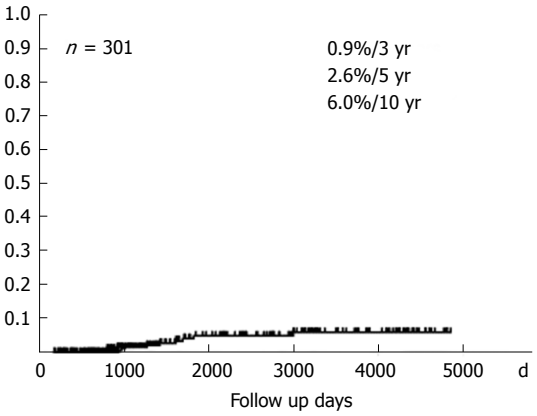

Figure 1 Cumulative incidence rate of hepatocellular carcinoma by Kaplan Meier analysis. The horizontal and vertical axes show days from liver biopsy and cumulative incidence rate of hepatocellular carcinoma, respectively.

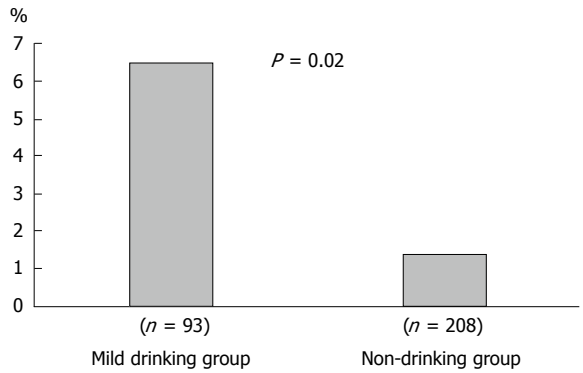

Figure 2 Comparison of incidence rates of hepatocellular carcinoma between mild drinking and non-drinking groups. The vertical axis shows incidence rate (percentage) of hepatocellular carcinoma during follow-up time.

prevalence of liver cirrhosis (F4) was higher in the mild drinking group compared to non-drinking groups (9 *vs* 8 cases: 10% *vs* 4%, $P = 0.04$) (Table 1), while the rate of hepatic advanced fibrosis (F3-4) was not different between the groups. Interestingly, the HCC appearance rate was higher in the mild drinking group (6 *vs* 3 cases: 6.5% *vs* 1.4%, $P = 0.02$) (Figure 2).

Comparison of clinicopathological features at the time of biopsy between the HCC and non-HCC groups

In comparisons of clinicopathological features at the time of biopsy between HCC and non-HCC patients (Table 2), those with HCC had significantly higher age ($P < 0.01$), higher prevalence of a drinking habit ($P = 0.02$), diabetes mellitus ($P < 0.01$), and hypertension ($P < 0.01$), higher HbA1c ($P = 0.01$), type Ⅳ collagen 7S ($P = 0.03$), and alpha-fetoprotein ($P < 0.01$), and lower albumin ($P < 0.01$), cholinesterase ($P < 0.01$), total cholesterol ($P = 0.02$), triglyceride ($P = 0.02$), and platelet count ($P < 0.01$) (Table 2). In pathological findings, the HCC group had a lower steatosis score ($P = 0.01$) and significantly higher fibrosis stage ($P < 0.01$) (Table 2).

Kaplan-Meier analysis was carried out for the HCC and non-HCC groups (Figure 3). Factors associated with higher HCC occurrence included age ⩾ 63 years at the time of biopsy ($P = 0.04$, Figure 3A), a mild drinking habit ($P < 0.01$, Figure 3B), diabetes mellitus ($P < 0.01$, Figure 3C), hypertension ($P < 0.01$, Figure 3D), albumin ≤ 4.0 g/dL ($P < 0.01$, Figure 3E), HbA1c ⩾ 6.6% ($P = 0.01$, Figure 3G), triglyceride < 133 mg/dL ($P = 0.02$, Figure 3I), platelet count < 13.3 × 10^4/μL ($P < 0.01$, Figure 3J), type Ⅳ collagen 7S ⩾ 5.0 ng/mL ($P = 0.01$, Figure 3K), alpha-fetoprotein ⩾ 6.0 ng/mL ($P < 0.01$, Figure 3L), steatosis grade 1 ($P = 0.01$, Figure 3M), and F3-4 ($P < 0.01$, Figure 3N).

Multivariate survival analysis using Cox's regression model revealed that hepatic advanced fibrosis (F3-4) ($P < 0.01$, risk ratio: 11.60), diabetes mellitus ($P < 0.01$, risk ratio: 89.50), and serum triglyceride ($P = 0.04$, risk ratio: 0.98) were factors significantly related to HCC, while a mild drinking habit appeared to be marginally related ($P = 0.07$, risk ratio: 4.43) (Table 3).

The result of all HCC patients having advanced hepatic fibrosis (F3-4) at the time of biopsy corroborated the close association between HCC and hepatic fibrosis. To elucidate the additional impact of mild drinking on HCC development in the HCC high-risk group, we evaluated the clinicopathological features of the HCC and non-HCC groups in NAFLD patients with advanced fibrosis (Table 4). Compared with the non-HCC group ($n = 68$), the HCC group ($n = 9$) had a significantly higher rate of a drinking habit ($P = 0.03$), diabetes mellitus ($P = 0.02$), and hypertension ($P = 0.01$), higher alpha-fetoprotein ($P = 0.04$), and lower cholinesterase ($P = 0.02$), triglyceride ($P = 0.02$), and platelet count ($P < 0.01$) (Table 4). There were no differences in pathological findings between the groups (Table 4).

In NAFLD cases with advanced fibrosis, multivariate survival analysis using Cox's regression model revealed that a mild drinking habit ($P = 0.04$, risk ratio: 4.83), alpha-fetoprotein ($P = 0.01$, risk ratio: 1.23), and diabetes mellitus ($P = 0.03$, risk ratio: 12.00) were factors significantly associated with HCC (Table 5). Accordingly, a mild drinking habit appeared to be a risk factor for hepatocarcinogenesis in NAFLD patients with advanced fibrosis.

DISCUSSION

Although continuous and excessive ethanol consumption is harmful to the liver, a mild drinking habit reportedly improves insulin sensitivity and decreases cardiovascular mortality in the general population[22]. One question arises on whether mild drinking is similarly beneficial for NAFLD patients, but there are few studies on NAFLD regarding the impact of light ethanol consumption. This study demonstrated that a mild drinking habit may be associated with HCC occurrence in NAFLD patients with advanced fibrosis. We therefore propose the abstinence

Table 1 Comparison of clinicopathological features at the time of biopsy between mild drinking and non-drinking groups

	Mild drinking group (n = 93)	Non-drinking group (n = 208)	P value
Age (yr)	55 (19-77)	56 (10-84)	0.50
Male	52 (56)	84 (40)	0.01
Body mass index (kg/m^2)	26.5 (18.3-40.0)	26.2 (17.8-41.0)	0.53
Co-existing disease			
Diabetes mellitus	32 (34)	78 (38)	0.57
Hypertension	41 (44)	81 (39)	0.44
Hyperlipidemia	55 (59)	135 (66)	0.29
Laboratory data			
Albumin (mg/dL)	4.5 (3.2-5.4)	4.5 (3.0-5.2)	0.48
Total bilirubin (mg/dL)	0.91 (0.40-2.20)	0.86 (0.38-2.64)	0.12
Aspartate aminotransferase (IU/L)	44 (20-175)	47 (13-263)	0.80
Alanine aminotransferase (IU/L)	68 (22-237)	67 (13-522)	0.74
Gamma-glutamyl transpeptidase (IU/L)	69 (19-400)	54 (7-544)	0.02
Cholinesterase (IU/L)	363 (171-586)	384 (189-591)	0.05
Fasting blood sugar (mg/dL)	106 (84-215)	108 (77-221)	0.63
HOMA-IR	3.4 (1.0-42.6)	3.3 (0.3-24.5)	0.58
HbA1c (%)	5.9 (5.1-9.8)	6.0 (4.9-12.3)	0.21
Total cholesterol (mg/dL)	205 (138-336)	208 (70-295)	0.68
Triglyceride (mg/dL)	115 (42-404)	133 (32-801)	0.14
Platelet (×10^4/μL)	21.1 (5.3-45.4)	22.1 (7.2-40.7)	0.04
Hyaluronic acid (ng/mL)	43 (12-320)	49 (9-1611)	0.57
Type Ⅳ collagen 7s (ng/mL)	4.3 (2-20)	4.5 (2-11)	0.93
Alpha-fetoprotein (ng/mL)	3.3 (0.7-13.5)	3.0 (0.7-20.3)	0.41
Pathology			
Steatosis			0.86
1	33 (36)	64 (31)	
2	36 (39)	90 (43)	
3	24 (26)	54 (26)	
Lobular inflammation			0.14
0	5 (5)	8 (4)	
1	47 (51)	83 (40)	
2	37 (40)	95 (46)	
3	4 (4)	22 (11)	
Ballooning			0.82
0	18 (19)	41 (20)	
1	50 (54)	118 (57)	
2	25 (27)	49 (24)	
NAFLD activity score			0.79
1	4 (4)	5 (2)	
2	8 (9)	16 (8)	
3	16 (17)	34 (16)	
4	17 (18)	32 (15)	
5	25 (27)	62 (30)	
6	14 (15)	36 (17)	
7	9 (10)	18 (9)	
8	0 (0)	5 (2)	
Fibrosis			0.39
0	17 (18)	40 (19)	
1	39 (42)	93 (45)	
2	10 (11)	25 (12)	
3	18 (19)	42 (20)	
4	9 (10)	8 (4)	
Fibrosis 3-4 (Advanced fibrosis)	27 (29)	50 (24)	0.36
Fibrosis 4 (Cirrhosis)	9 (10)	8 (4)	0.04

Data are expressed as median (range) or n (%). HbA1c: Hemoglobin A1c; HOMA-IR: Homeostasis model assessment for insulin resistance.

of ethanol, even in small amounts, in such individuals.

Mild to moderate alcohol consumption has been shown to decrease insulin resistance and improve components of metabolic syndrome[23]. Dunn *et al*[12] and Kwon *et al*[13] reported a positive association between moderate alcohol intake and decreased steatosis/ballooning and fibrosis grades in NAFLD patients, which might explain the protective effects of moderate alcohol intake on preventing histological injury. In our cohort, however, the mild and non-drinking groups did not differ with regard to steatosis/ballooning grade and the rate of liver cirrhosis was higher in the mild drinking group. The reason for these discrepancies is unknown, along with why there were no significant reductions in body mass index or homeostasis model assessment for insulin resistance score between our

Table 2 Comparison of clinicopathological features at the time of biopsy between hepatocellular carcinoma and non- hepatocellular carcinoma groups

	HCC group (n = 9)	Non-HCC group (n = 292)	P value
Age (yr)	65 (56-84)	55 (10-81)	< 0.01
Male	3 (33)	133 (46)	0.52
Body mass index (kg/m^2)	26.0 (18.3-28.7)	26.2 (17.8-41.0)	0.23
Drinking habit	6 (67)	87 (30)	0.02
Co-existing disease			
Diabetes mellitus	8 (89)	102 (35)	< 0.01
Hypertension	9 (100)	113 (39)	< 0.01
Hyperlipidemia	3 (33)	187 (65)	0.06
Laboratory data			
Albumin (mg/dL)	4.0 (3.7-4.6)	4.5 (3.0-5.4)	< 0.01
Total bilirubin (mg/dL)	0.91 (0.44-1.61)	0.88 (0.38-2.64)	0.75
Aspartate aminotransferase (IU/L)	52 (32-95)	46 (13-263)	0.71
Alanine aminotransferase (IU/L)	53 (16-132)	68 (13-522)	0.11
Gamma-glutamyl transpeptidase (IU/L)	65 (28-192)	56 (7-544)	0.48
Cholinesterase (IU/L)	249 (190-434)	380 (171-591)	< 0.01
Fasting blood sugar (mg/dL)	133 (84-172)	106 (77-221)	0.13
HOMA-IR	5.8 (1.2-9.8)	3.3 (0.3-42.6)	0.18
HbA1c (%)	6.6 (6.0-7.0)	5.9 (4.9-12.3)	0.01
Total cholesterol (mg/dL)	176 (153-264)	208 (70-336)	0.02
Triglyceride (mg/dL)	85 (64-140)	130 (32-801)	0.02
Platelet (×10^4/μL)	11.0 (6.4-18.6)	22.0 (5.3-45.4)	< 0.01
Hyaluronic acid (ng/mL)	42 (17-263)	42 (9-1180)	0.96
Type Ⅳ collagen 7s (ng/mL)	5.6 (4.7-8.4)	4.4 (2.0-20.0)	0.03
Alpha-fetoprotein (ng/mL)	6.0 (3.7-20.3)	3.0 (0.7-13.2)	< 0.01
Pathology			
Steatosis			0.01
1	7 (78)	90 (31)	
2	2 (22)	124 (43)	
3	0 (0)	78 (27)	
Lobular inflammation			0.21
0	0 (0)	13 (4)	
1	2 (22)	128 (44)	
2	7 (78)	125 (43)	
3	0 (0)	26 (9)	
Ballooning			0.76
0	1 (11)	58 (20)	
1	6 (67)	162 (56)	
2	2 (22)	72 (25)	
NAFLD activity score			0.53
1	0 (0)	9 (3)	
2	0 (0)	24 (8)	
3	3 (33)	47 (16)	
4	2 (22)	47 (16)	
5	4 (44)	83 (28)	
6	0 (0)	50 (17)	
7	0 (0)	27 (9)	
8	0 (0)	5 (2)	
Fibrosis			< 0.01
0	0 (0)	57 (20)	
1	0 (0)	132 (45)	
2	0 (0)	35 (12)	
3	4 (44)	56 (19)	
4	5 (56)	12 (4)	

Data are expressed as median (range) or n (%). HCC: Hepatocellular carcinoma; HOMA-IR: Homeostasis model assessment for insulin resistance; HbA1c: Hemoglobin A1c; NAFLD: Non-alcoholic fatty liver disease.

test groups. We presume that ethnic differences may account for differences in ethanol consumption effects on steatosis, ballooning, and fibrosis.

In 2010, Ascha *et al*[24] described that a mild drinking habit was associated with an increased risk of carcinogenesis in a NASH-associated cirrhosis cohort. Here, we focused on the impact of a mild drinking habit on liver carcinogenesis originating from NAFLD. All HCC-developing patients (n = 9) had advanced fibrosis (F3-4). Among all NAFLD patients, multivariate analysis revealed that fibrosis, diabetes mellitus, and serum triglyceride were factors significantly related to

Table 3 Factors related to hepatic carcinogenesis by multivariate survival analysis using Cox's regression model for all patients

	P value	Relative risk	95%CI
Fibrosis	< 0.01	11.6	2.36-56.9
Diabetes mellitus	< 0.01	89.5	6.01-1331.2
Triglyceride	0.04	0.98	0.95-0.99
Drinking habit	0.07	4.43	0.88-22.4

Table 4 Comparison of clinicopathological features at the time of biopsy between hepatocellular carcinoma and non- hepatocellular carcinoma groups in non-alcoholic fatty liver disease patients with advanced fibrosis (F3-4)

	HCC group (*n* = 9)	Non-HCC group (*n* = 68)	*P* value
Age (yr)	65 (56-84)	64 (30-81)	0.32
Male	3 (33)	14 (21)	0.39
Body mass index (kg/m^2)	26.0 (18.3-28.7)	27.7 (20.1-41.0)	0.05
Drinking habit	6 (67)	21 (31)	0.03
Co-existing disease			
Diabetes mellitus	8 (89)	32 (47)	0.02
Hypertension	9 (100)	38 (56)	0.01
Hyperlipidemia	3 (33)	35 (52)	0.31
Laboratory data			
Albumin (mg/dL)	4.0 (3.7-4.6)	4.3 (3.2-5.0)	0.07
Total bilirubin (mg/dL)	0.91 (0.44-1.61)	0.91 (0.48-2.15)	0.99
Aspartate aminotransferase (IU/L)	52 (32-95)	63 (20-200)	0.13
Alanine aminotransferase (IU/L)	53 (16-132)	71 (19-298)	0.09
Gamma-glutamyl transpeptidase (IU/L)	65 (28-192)	65 (25-205)	0.75
Cholinesterase (IU/L)	249 (190-434)	345 (171-467)	0.02
Fasting blood sugar (mg/dL)	133 (84-172)	110 (82-215)	0.30
HOMA-IR	5.8 (1.2-9.8)	4.3 (1.1-15.6)	0.54
HbA1c (%)	6.6 (6.0-7.0)	6.1 (5.0-10.9)	0.14
Total cholesterol (mg/dL)	176 (153-264)	201 (131-294)	0.10
Triglyceride (mg/dL)	85 (64-140)	119 (42-351)	0.03
Platelet (×10^4/μL)	11.0 (6.4-18.6)	16.6 (5.3-32.6)	< 0.01
Hyaluronic acid (ng/mL)	42 (17-263)	59 (11-1180)	0.45
Type Ⅳ collagen 7s (ng/mL)	5.6 (4.7-8.4)	6.8 (3.5-20.0)	0.61
Alpha-fetoprotein (ng/mL)	6.0 (3.7-20.3)	5.0 (1.1-11.3)	0.04
Pathology			
Steatosis			0.07
1	7 (78)	26 (38)	
2	2 (22)	32 (47)	
3	0 (0)	10 (15)	
Lobular inflammation			0.45
0	0 (0)	1 (2)	
1	2 (22)	17 (25)	
2	7 (78)	37 (54)	
3	0 (0)	13 (19)	
Ballooning			0.76
0	1 (11)	1 (2)	
1	6 (67)	34 (50)	
2	2 (22)	33 (49)	
NAFLD activity score			0.25
1	0 (0)	1 (2)	
2	0 (0)	1 (2)	
3	3 (33)	5 (7)	
4	2 (22)	10 (15)	
5	4 (44)	26 (38)	
6	0 (0)	16 (24)	
7	0 (0)	8 (12)	
8	0 (0)	1 (2)	

Data are expressed as median (range) or *n* (%). HCC: Hepatocellular carcinoma; HOMA-IR: Homeostasis model assessment for insulin resistance; HbA1c: Hemoglobin A1c; NAFLD: Non-alcoholic fatty liver disease.

HCC, while a mild drinking habit appeared to be only marginally related to carcinogenesis. On the other hand, in NAFLD cases with F3-4, multivariate survival analysis showed a mild drinking habit, alpha-fetoprotein, and diabetes mellitus to be factors significantly associated with HCC. Our results indicated that mild drinking may

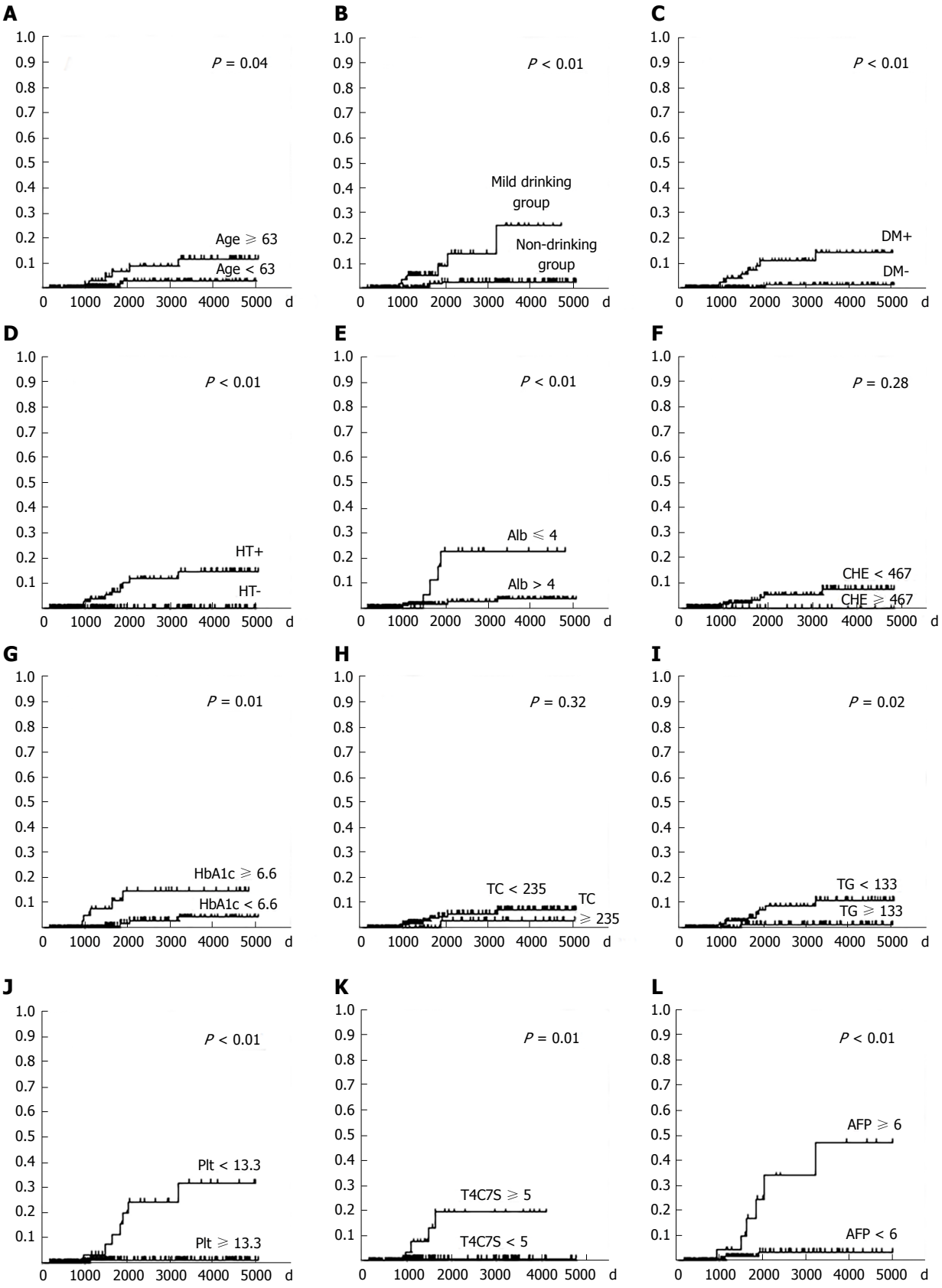
A
P = 0.04
Age ⩾ 63
Age < 63
B
P < 0.01
Mild drinking group
Non-drinking group
C
P < 0.01
DM+
DM-
D
P < 0.01
HT+
HT-
E
P < 0.01
Alb ⩽ 4
Alb > 4
F
P = 0.28
CHE < 467
CHE ⩾ 467
G
P = 0.01
HbA1c ⩾ 6.6
HbA1c < 6.6
H
P = 0.32
TC < 235
TC ⩾ 235
I
P = 0.02
TG < 133
TG ⩾ 133
J
P < 0.01
Plt < 13.3
Plt ⩾ 13.3
K
P = 0.01
T4C7S ⩾ 5
T4C7S < 5
L
P < 0.01
AFP ⩾ 6
AFP < 6
0 1000 2000 3000 4000 5000 d

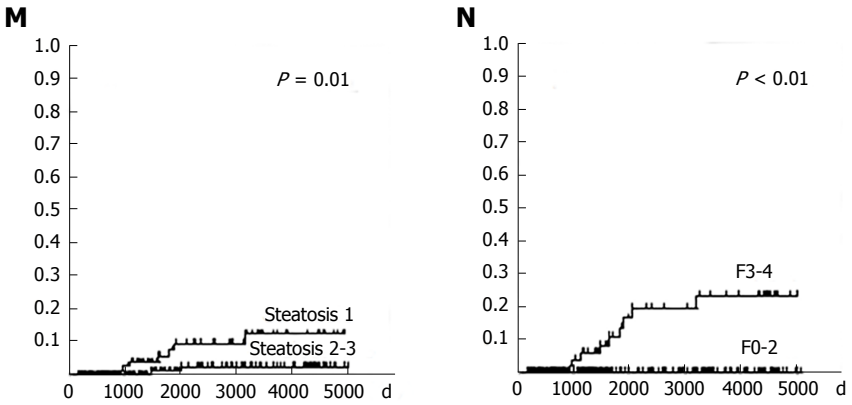

Figure 3 Cumulative incidence rate of hepatocellular carcinoma based on data at the time of liver biopsy. A: Age; B: Drinking habit; C: Diabetes mellitus; D: Hypertension; E: Albumin; F: Cholinesterase; G: HbA1c, H: Total cholesterol; I: Triglyceride; J: Platelet; K: Type Ⅳ collagen 7S; L: Alpha-fetoprotein; M: Steatosis; N: Fibrosis. The horizontal and vertical axes show days from liver biopsy and cumulative incidence rate of hepatocellular carcinoma, respectively. DM: Diabetes mellitus; HT: Hypertension; Alb: Albumin; CHE: Cholinesterase; TC: Total cholesterol; TG: Triglyceride; Plt: Platelet; T4C7S: Type Ⅳ collagen 7S; AFP: Alpha-fetoprotein; F: Fibrosis.

Table 5 Factors related to hepatic carcinogenesis by multivariate survival analysis using Cox's regression model for patients with advanced fibrosis (F3-4)

	P value	Relative risk	95%CI
Drinking habit	0.04	4.83	1.01-23.00
Alpha-fetoprotein	0.01	1.23	1.04-1.44
Diabetes mellitus	0.03	12.00	1.20-119.66

increase the risk of HCC in NAFLD patients with not only cirrhosis (F4), but also advanced fibrosis.

The International Agency for Cancer Research (WHO) has certified that alcohol intake is carcinogenic for humans[25]. Indeed, alcohol consumption has been associated with increased risks of head and neck, oral cavity, pharynx, larynx, esophagus, bowel, breast, and liver cancers[25]. Ethanol is metabolized into acetaldehyde by alcohol dehydrogenase and cytochrome P450 2E1 (CYP2E1) in the liver, which is then oxidized to acetate by aldehyde dehydrogenase (ALDH)[26]. Although the underlying causes of cancers related to ethanol consumption are not yet clear, various factors have been proposed as key contributors of hepatocarcinogenesis, including the direct genotoxicity of ethanol and its metabolite acetaldehyde, malnutrition, chronic inflammation, oxidative stress, interactions with retinoids, methylation level alterations, immunological surveillance, and angiogenesis[27]. Ethanol also reduces the levels of glutathione S-transferase, a detoxifier of oxidative stress, and increases the expression of CYP2E1, a generator of oxidative stress[28-32]. The net increases in oxidative stress by long-term ethanol consumption may lead to hepatocarcinogenesis in the presence of steatosis, while it is undetermined which factor is most affecting this oncogenic process[33-36]. The impact of ethanol per hepatocyte might be greater in cirrhotic patients because of the decreases in the number and function of hepatocytes. Actually, Vidal *et al*[37] reported that ALDH activity was significantly reduced in patients with advanced liver fibrosis compared with those having mild fibrosis. Therefore, we presume that increased acetaldehyde and resultant DNA damage may induce pro-carcinogenic gene mutations and/or epigenetic changes, even with mild drinking, in NAFLD patients with advanced fibrosis.

Based on the results of the present study, mild ethanol consumption should be abandoned for NAFLD patients, especially those with advanced fibrosis, due to the possible risk of liver tumorigenesis. The main limitation of this study was its retrospective design; there remains a need for future large-scale longitudinal studies that evaluate the outcomes of NAFLD patients with mild ethanol intake. Prospective studies investigating the effect of ethanol cession in NAFLD patients with a mild drinking habit are also required to confirm the impact of mild drinking on the clinical course of NAFLD.

In conclusion, in NAFLD patients, especially those with advanced fibrosis, a mild drinking habit is a risk factor for hepatocarcinogenesis that should be discouraged.

ARTICLE HIGHLIGHTS

Research background

The prevalence rate of non-alcoholic fatty liver disease (NAFLD) has doubled during the last 20 years.

Research motivation

The impact of mild drinking habit (less than 20 g/d of ethanol) on the clinical

course of NAFLD has not been determined. We examined the influence of a mild drinking habit on liver carcinogenesis from NAFLD.

Research objectives

A total of 301 patients who had been diagnosed as having NAFLD by liver biopsy between 2003 and 2016 (median age: 56 years, 45% male, 56% with non-alcoholic steatohepatitis, 26% with advanced fibrosis (F3-4) were divided into the mild drinking group with ethanol consumption of less than 20 g/d (mild drinking group, n = 93) and the non-drinking group (n = 208).

Research methods

Clinicopathological features at the time of liver biopsy and factors related to hepatocellular carcinoma (HCC) occurrence were compared between the groups.

Research results

We observed significant differences in male prevalence (P = 0.01), platelet count (P = 0.04), and gamma-glutamyl transpeptidase (P = 0.02) between the test groups. Over 6 years of observation, the HCC appearance rate was significantly higher in the mild drinking group (6.5% *vs* 1.4%, P = 0.02). Multivariate survival analysis using Cox's regression model revealed that hepatic advanced fibrosis (F3-4) (P < 0.01, risk ratio: 11.60), diabetes mellitus (P < 0.01, risk ratio: 89.50), and serum triglyceride (P = 0.04, risk ratio: 0.98) were factors significantly related to HCC in all NAFLD patients, while the effect of a drinking habit was marginal (P = 0.07, risk ratio: 4.43). In patients with advanced fibrosis (F3-4), however, a drinking habit (P = 0.04, risk ratio: 4.83), alpha-fetoprotein (P = 0.01, risk ratio: 1.23), and diabetes mellitus (P = 0.03, risk ratio: 12.00) were identified as significant contributors to HCC occurrence.

Research conclusions

A mild drinking habit appears to be a risk factor for hepatocarcinogenesis in NAFLD patients, especially those with advanced fibrosis.

Research perspectives

Prospective studies investigating the effect of ethanol cession in NAFLD patients with a mild drinking habit are also required to confirm the impact of mild drinking on the clinical course of NAFLD.

REFERENCES

1 **NCD Risk Factor Collaboration (NCD-RisC).** Trends in adult body-mass index in 200 countries from 1975 to 2014: a pooled analysis of 1698 population-based measurement studies with 19·2 million participants. *Lancet* 2016; **387**: 1377-1396 [PMID: 27115820 DOI: 10.1016/S0140-6736(16)30054-X]

2 **Vernon G**, Baranova A, Younossi ZM. Systematic review: the epidemiology and natural history of non-alcoholic fatty liver disease and non-alcoholic steatohepatitis in adults. *Aliment Pharmacol Ther* 2011; **34**: 274-285 [PMID: 21623852 DOI: 10.1111/j.1365-2036.2011.04724.x]

3 **Younossi ZM**, Koenig AB, Abdelatif D, Fazel Y, Henry L, Wymer M. Global epidemiology of nonalcoholic fatty liver disease-Meta-analytic assessment of prevalence, incidence, and outcomes. *Hepatology* 2016; **64**: 73-84 [PMID: 26707365 DOI: 10.1002/hep.28431]

4 **Eguchi Y**, Hyogo H, Ono M, Mizuta T, Ono N, Fujimoto K, Chayama K, Saibara T; JSG-NAFLD. Prevalence and associated metabolic factors of nonalcoholic fatty liver disease in the general population from 2009 to 2010 in Japan: a multicenter large retrospective study. *J Gastroenterol* 2012; **47**: 586-595 [PMID: 22328022 DOI: 10.1007/s00535-012-0533-z]

5 **Sanyal AJ**, Campbell-Sargent C, Mirshahi F, Rizzo WB, Contos MJ, Sterling RK, Luketic VA, Shiffman ML, Clore JN. Nonalcoholic steatohepatitis: association of insulin resistance and mitochondrial abnormalities. *Gastroenterology* 2001; **120**: 1183-1192 [PMID: 11266382 DOI: 10.1053/gast.2001.23256]

6 **Duvnjak M**, Lerotić I, Barsić N, Tomasić V, Virović Jukić L, Velagić V. Pathogenesis and management issues for non-alcoholic fatty liver disease. *World J Gastroenterol* 2007; **13**: 4539-4550 [PMID: 17729403]

7 **Tanaka N**, Aoyama T, Kimura S, Gonzalez FJ. Targeting nuclear receptors for the treatment of fatty liver disease. *Pharmacol Ther* 2017; **179**: 142-157 [PMID: 28546081 DOI: 10.1016/j.pharmthera.2017.05.011]

8 **Tanaka N**, Takahashi S, Hu X, Lu Y, Fujimori N, Golla S, Fang ZZ, Aoyama T, Krausz KW, Gonzalez FJ. Growth arrest and DNA damage-inducible 45α protects against nonalcoholic steatohepatitis induced by methionine- and choline-deficient diet. *Biochim Biophys Acta* 2017; **1863**: 3170-3182 [PMID: 28844958 DOI: 10.1016/j.bbadis.2017.08.017]

9 **Kitabatake H**, Tanaka N, Fujimori N, Komatsu M, Okubo A, Kakegawa K, Kimura T, Sugiura A, Yamazaki T, Shibata S, Ichikawa Y, Joshita S, Umemura T, Matsumoto A, Koinuma M, Sano K, Aoyama T, Tanaka E. Association between endotoxemia and histological features of nonalcoholic fatty liver disease. *World J Gastroenterol* 2017; **23**: 712-722 [PMID: 28216979 DOI: 10.3748/wjg.v23.i4.712]

10 **Kimura T**, Kobayashi A, Tanaka N, Sano K, Komatsu M, Fujimori N, Yamazaki T, Shibata S, Ichikawa Y, Joshita S, Umemura T, Matsumoto A, Horiuchi A, Mori H, Wada S, Kiyosawa K, Miyagawa SI, Tanaka E. Clinicopathological characteristics of non-B non-C hepatocellular carcinoma without past hepatitis B virus infection. *Hepatol Res* 2017; **47**: 405-418 [PMID: 27288988 DOI: 10.1111/hepr.12762]

11 **Bell RA**, Mayer-Davis EJ, Martin MA, D'Agostino RB Jr, Haffner SM. Associations between alcohol consumption and insulin sensitivity and cardiovascular disease risk factors: the Insulin Resistance and Atherosclerosis Study. *Diabetes Care* 2000; **23**: 1630-1636 [PMID: 11092284]

12 **Dunn W**, Sanyal AJ, Brunt EM, Unalp-Arida A, Donohue M, McCullough AJ, Schwimmer JB. Modest alcohol consumption is associated with decreased prevalence of steatohepatitis in patients with non-alcoholic fatty liver disease (NAFLD). *J Hepatol* 2012; **57**: 384-391 [PMID: 22521357 DOI: 10.1016/j.jhep.2012.03.024]

13 **Kwon HK**, Greenson JK, Conjeevaram HS. Effect of lifetime alcohol consumption on the histological severity of non-alcoholic fatty liver disease. *Liver Int* 2014; **34**: 129-135 [PMID: 23809459 DOI: 10.1111/liv.12230]

14 **Ajmera VH**, Terrault NA, Harrison SA. Is moderate alcohol use in nonalcoholic fatty liver disease good or bad? A critical review. *Hepatology* 2017; **65**: 2090-2099 [PMID: 28100008 DOI: 10.1002/hep.29055]

15 **Fujimori N**, Tanaka N, Shibata S, Sano K, Yamazaki T, Sekiguchi T, Kitabatake H, Ichikawa Y, Kimura T, Komatsu M, Umemura T, Matsumoto A, Tanaka E. Controlled attenuation parameter is correlated with actual hepatic fat content in patients with non-alcoholic fatty liver disease with none-to-mild obesity and liver fibrosis. *Hepatol Res* 2016; **46**: 1019-1027 [PMID: 27183219 DOI: 10.1111/hepr.12649]

16 **Komatsu M**, Kimura T, Yazaki M, Tanaka N, Yang Y, Nakajima T, Horiuchi A, Fang ZZ, Joshita S, Matsumoto A, Umemura T, Tanaka E, Gonzalez FJ, Ikeda S, Aoyama T. Steatogenesis in adult-onset type II citrullinemia is associated with down-regulation of PPARα. *Biochim Biophys Acta* 2015; **1852**: 473-481 [PMID: 25533124 DOI: 10.1016/j.bbadis.2014.12.011]

17 **Bruix J**, Sherman M; American Association for the Study of Liver Diseases. Management of hepatocellular carcinoma: an update. *Hepatology* 2011; **53**: 1020-1022 [PMID: 21374666 DOI: 10.1002/hep.24199]

18 **Kimura T**, Shinji A, Tanaka N, Koinuma M, Yamaura M, Nagaya T, Joshita S, Komatsu M, Umemura T, Horiuchi A, Wada S, Tanaka E. Association between lower air pressure and the onset of ischemic colitis: a case-control study. *Eur J Gastroenterol Hepatol* 2017; **29**: 1071-1078 [PMID: 28562393 DOI: 10.1097/MEG.0000000000000913]

19 **Kimura T**, Shinji A, Horiuchi A, Tanaka N, Nagaya T, Shigeno T, Nakamura N, Komatsu M, Umemura T, Arakura N, Matsumoto A,

Tanaka E. Clinical characteristics of young-onset ischemic colitis. *Dig Dis Sci* 2012; **57**: 1652-1659 [PMID: 22383082 DOI: 10.1007/s10620-012-2088-5]
20 **Umemura T**, Joshita S, Sekiguchi T, Usami Y, Shibata S, Kimura T, Komatsu M, Matsumoto A, Ota M, Tanaka E. Serum Wisteria floribunda Agglutinin-Positive Mac-2-Binding Protein Level Predicts Liver Fibrosis and Prognosis in Primary Biliary Cirrhosis. *Am J Gastroenterol* 2015; **110**: 857-864 [PMID: 25916223 DOI: 10.1038/ajg.2015.118]
21 **Kleiner DE**, Brunt EM, Van Natta M, Behling C, Contos MJ, Cummings OW, Ferrell LD, Liu YC, Torbenson MS, Unalp-Arida A, Yeh M, McCullough AJ, Sanyal AJ; Nonalcoholic Steatohepatitis Clinical Research Network. Design and validation of a histological scoring system for nonalcoholic fatty liver disease. *Hepatology* 2005; **41**: 1313-1321 [PMID: 15915461 DOI: 10.1002/hep.20701]
22 **Thun MJ**, Peto R, Lopez AD, Monaco JH, Henley SJ, Heath CW Jr, Doll R. Alcohol consumption and mortality among middle-aged and elderly U.S. adults. *N Engl J Med* 1997; **337**: 1705-1714 [PMID: 9392695 DOI: 10.1056/NEJM199712113372401]
23 **Alkerwi A**, Boutsen M, Vaillant M, Barre J, Lair ML, Albert A, Guillaume M, Dramaix M. Alcohol consumption and the prevalence of metabolic syndrome: a meta-analysis of observational studies. *Atherosclerosis* 2009; **204**: 624-635 [PMID: 19084839 DOI: 10.1016/j.atherosclerosis.2008.10.036]
24 **Ascha MS**, Hanouneh IA, Lopez R, Tamimi TA, Feldstein AF, Zein NN. The incidence and risk factors of hepatocellular carcinoma in patients with nonalcoholic steatohepatitis. *Hepatology* 2010; **51**: 1972-1978 [PMID: 20209604 DOI: 10.1002/hep.23527]
25 **Boffetta P**, Hashibe M. Alcohol and cancer. *Lancet Oncol* 2006; **7**: 149-156 [PMID: 16455479 DOI: 10.1016/S1470-2045(06)70577-0]
26 **Zakhari S**. Overview: how is alcohol metabolized by the body? *Alcohol Res Health* 2006; **29**: 245-254 [PMID: 17718403]
27 **Testino G**, Leone S, Borro P. Alcohol and hepatocellular carcinoma: a review and a point of view. *World J Gastroenterol* 2014; **20**: 15943-15954 [PMID: 25473148 DOI: 10.3748/wjg.v20.i43.15943]
28 **Tsutsumi T**, Suzuki T, Moriya K, Shintani Y, Fujie H, Miyoshi H, Matsuura Y, Koike K, Miyamura T. Hepatitis C virus core protein activates ERK and p38 MAPK in cooperation with ethanol in transgenic mice. *Hepatology* 2003; **38**: 820-828 [PMID: 14512869 DOI: 10.1053/jhep.2003.50399]
29 **Lu Y**, Cederbaum AI. CYP2E1 and oxidative liver injury by alcohol. *Free Radic Biol Med* 2008; **44**: 723-738 [PMID: 18078827 DOI: 10.1016/j.freeradbiomed.2007.11.004]
30 **Kanbe H**, Kamijo Y, Nakajima T, Tanaka N, Sugiyama E, Wang L, Fang ZZ, Hara A, Gonzalez FJ, Aoyama T. Chronic ethanol consumption decreases serum sulfatide levels by suppressing hepatic cerebroside sulfotransferase expression in mice. *Arch Toxicol* 2014; **88**: 367-379 [PMID: 24065054 DOI: 10.1007/s00204-013-1132-3]
31 **Okiyama W**, Tanaka N, Nakajima T, Tanaka E, Kiyosawa K, Gonzalez FJ, Aoyama T. Polyenephosphatidylcholine prevents alcoholic liver disease in PPARalpha-null mice through attenuation of increases in oxidative stress. *J Hepatol* 2009; **50**: 1236-1246 [PMID: 19398233 DOI: 10.1016/j.jhep.2009.01.025]
32 **Nakajima T**, Kamijo Y, Tanaka N, Sugiyama E, Tanaka E, Kiyosawa K, Fukushima Y, Peters JM, Gonzalez FJ, Aoyama T. Peroxisome proliferator-activated receptor alpha protects against alcohol-induced liver damage. *Hepatology* 2004; **40**: 972-980 [PMID: 15382117 DOI: 10.1002/hep.20399]
33 **Mantena SK**, King AL, Andringa KK, Eccleston HB, Bailey SM. Mitochondrial dysfunction and oxidative stress in the pathogenesis of alcohol- and obesity-induced fatty liver diseases. *Free Radic Biol Med* 2008; **44**: 1259-1272 [PMID: 18242193 DOI: 10.1016/j.freeradbiomed.2007.12.029]
34 **Moriya K**, Nakagawa K, Santa T, Shintani Y, Fujie H, Miyoshi H, Tsutsumi T, Miyazawa T, Ishibashi K, Horie T, Imai K, Todoroki T, Kimura S, Koike K. Oxidative stress in the absence of inflammation in a mouse model for hepatitis C virus-associated hepatocarcinogenesis. *Cancer Res* 2001; **61**: 4365-4370 [PMID: 11389061]
35 **Ramadori P**, Cubero FJ, Liedtke C, Trautwein C, Nevzorova YA. Alcohol and Hepatocellular Carcinoma: Adding Fuel to the Flame. *Cancers* (Basel) 2017; **9**: [PMID: 28946672 DOI: 10.3390/cancers9100130]
36 **Ambade A**, Satishchandran A, Gyongyosi B, Lowe P, Szabo G. Adult mouse model of early hepatocellular carcinoma promoted by alcoholic liver disease. *World J Gastroenterol* 2016; **22**: 4091-4108 [PMID: 27122661 DOI: 10.3748/wjg.v22.i16.4091]
37 **Vidal F**, Toda R, Gutiérrez C, Broch M, Fernández-Muixí F, Lorenzo A, Richart C. Influence of chronic alcohol abuse and liver disease on hepatic aldehyde dehydrogenase activity. *Alcohol* 1998; **15**: 3-8 [PMID: 9426831]

P- Reviewer: Peltec A, Sharafi H, Sanal MG **S- Editor**: Wang XJ
L- Editor: A **E- Editor**: Huang Y

World Journal of Gastroenterology

Submit a Manuscript: http://www.f6publishing.com

World J Gastroenterol 2018 April 7; 24(13): 1451-1463

DOI: 10.3748/wjg.v24.i13.1451

ISSN 1007-9327 (print) ISSN 2219-2840 (online)

ORIGINAL ARTICLE

Retrospective Study

Prognostic significance of combined preoperative fibrinogen and CA199 in gallbladder cancer patients

Wei-Yu Xu, Hao-Hai Zhang, Xiao-Bo Yang, Yi Bai, Jian-Zhen Lin, Jun-Yu Long, Jian-Ping Xiong, Jun-Wei Zhang, Xin-Ting Sang, Hai-Tao Zhao

Wei-Yu Xu, Hao-Hai Zhang, Xiao-Bo Yang, Yi Bai, Jian-Zhen Lin, Jun-Yu Long, Jian-Ping Xiong, Jun-Wei Zhang, Xin-Ting Sang, Hai-Tao Zhao, Department of Liver Surgery, Peking Union Medical College Hospital, Chinese Academy of Medical Sciences and Peking Union Medical College, Beijing 100730, China

ORCID number: Wei-Yu Xu (0000-0002-2101-4829); Hao-Hai Zhang (0000-0002-5292-6505); Xiao-Bo Yang (0000-0003-1929-8866); Yi Bai (0000-0002-1179-3734); Jian-Zhen Lin (0000-0002-4767-8834); Jun-Yu Long (0000-0001-5745-7165); Jian-Ping Xiong (0000-0002-6163-2621); Jun-Wei Zhang (0000-0002-2833-0090); Xin-Ting Sang (0000-0003-1952-0527); Hai-Tao Zhao (0000-0002-3444-8044).

Author contributions: Xu WY, Zhang HH and Yang XB contributed equally to this work. Xu WY conceived, designed and wrote the manuscript that led to the submission; Xu WY, Yang XB, Bai Y and Zhang JW collected the clinical data and followed up the patients; Lin JZ, Long JY and Xiong JP helped to analyze the data, Bai Y revised the manuscript, Sang XT and Zhao HT provided financial support for this work; Sang XT and Zhao HT are co-corresponding authors, and contributed equally to this work; all authors read and approved the final manuscript.

Supported by National Key Project Research and Development Projects, No. S2016G9012; International Science and Technology Cooperation Projects, No. 2015DFA30650; and The Capital Special Research Project for Clinical Application, No. Z151100004015170.

Institutional review board statement: The publication of this manuscript has been reviewed and approved by the PUMCH institutional review board.

Informed consent statement: All patients and their families signed informed consent statements before surgery, and the type of surgical procedure was performed according to the approved guidelines.

Conflict-of-interest statement: We declare that the authors have no conflict of interest.

Data sharing statement: No additional data are available.

Manuscript source: Unsolicited manuscript

Correspondence to: Hai-Tao Zhao, MD, Professor, Department of Liver Surgery, Peking Union Medical College Hospital, Chinese Academy of Medical Sciences and Peking Union Medical College, 1 Shuaifuyuan, Wangfujing, Beijing 100730, China. zhaoht@pumch.cn
Telephone: +86-10-69156042
Fax: +86-10-69156042

Received: January 26, 2018
Peer-review started: January 26, 2018
First decision: February 10, 2018
Revised: March 7, 2018
Accepted: March 10, 2018
Article in press: March 10, 2018
Published online: April 7, 2018

Abstract

AIM

To investigate the prognostic value of the combination of preoperative plasma fibrinogen and CA199 in patients with gallbladder carcinoma (GBC).

METHODS

The clinicopathological data of 154 GBC patients were retrospectively reviewed after surgery. A receiver

operating characteristic (ROC) curve was plotted to verify the optimum cut-off values for plasma fibrinogen and CA199. Univariate and multivariate survival analyses were performed to identify the factors associated with GBC prognosis. Based on the HRs calculated *via* multivariate survival analyses, patients with elevated plasma fibrinogen and CA199 levels were allocated a score of 2.1; those with an elevated plasma fibrinogen level only were allocated a score of 1, those with an elevated CA199 level only were allocated a score of 1.1, and those with neither of these abnormalities were allocated a score of 0.

RESULTS

ROC curve analysis showed that the optimum cut-off values for preoperative plasma fibrinogen and CA199 were 3.47 g/L and 25.45 U/mL, respectively. Multivariate analysis indicated that elevated preoperative plasma fibrinogen and CA199 levels were significantly correlated with worse overall survival (OS) (HR = 1.711, 95%CI: 1.114-2.627, P = 0.014, and HR = 1.842, 95%CI: 1.111-3.056, P = 0.018). When we combined these two parameters, the area under the ROC curve increased from 0.735 (for preoperative plasma fibrinogen only) and 0.729 (for preoperative CA199 only) to 0.765. When this combined variable was added to the multivariate analysis, the combination of plasma fibrinogen and CA199 (P < 0.001), resection margin (P < 0.001) and TNM stage (P = 0.010) were independent prognostic factors for GBC.

CONCLUSION

The combination of plasma fibrinogen and CA199 may serve as a more efficient independent prognostic biomarker for postoperative GBC patients than either parameter alone.

Key words: Prognostic factor; Plasma fibrinogen; CA199; Survival; Gallbladder cancer

Core tip: Elevated plasma fibrinogen and CA199 levels are associated with poor prognosis in patients with gallbladder carcinoma (GBC). The prognostic value of the combination of plasma fibrinogen and CA199 for GBC has not been reported. The most important finding in this study was that the combination of preoperative plasma fibrinogen and CA199 levels was a better independent prognostic indicator for GBC than either parameter alone.

Xu WY, Zhang HH, Yang XB, Bai Y, Lin JZ, Long JY, Xiong JP, Zhang JW, Sang XT, Zhao HT. Prognostic significance of combined preoperative fibrinogen and CA199 in gallbladder cancer patients. *World J Gastroenterol* 2018; 24(13): 1451-1463 Available from: URL: http://www.wjgnet.com/1007-9327/full/v24/i13/1451.htm DOI: http://dx.doi.org/10.3748/wjg.v24.i13.1451

INTRODUCTION

Primary gallbladder carcinoma (GBC) is relatively rare worldwide, but is the most common malignancy of the biliary tract system[1]. GBC is the seventh most common gastrointestinal cancer[2] and is attributable to approximately 1% of all cancer cases in China[3]. The incidence of this malignancy was recently reported to be approximately 2.5 per 100000 persons[4]. The prognosis of GBC is still typically poor due to nonspecific symptoms, late diagnosis, lack of treatment options, and the absence of effective prognostic markers. According to epidemiological studies, the overall survival (OS) of GBC patients is 6 mo, with a 5-year survival rate of less than 10%[1,5-7]. Therefore, investigations on the prognostic factors of GBC are especially important.

The association between hemostasis and cancer, and the influence of hemostatic factors on cancer development, growth, and metastasis are evident[8,9]. Fibrinogen is a 340-kDa plasma glycoprotein that is upregulated during systemic inflammation and tissue injury. Fibrinogen is synthesized in the liver and transformed into fibrin through the activity of activated thrombin, which is a key coagulation factor in platelet aggregation, clot formation, wound healing, and coagulation[10-12]. A number of studies have shown that plasma fibrinogen levels are upregulated in various cancer types, such as respiratory system tumors[13,14], digestive system tumors[15-18], gynecological tumors[19-22], head and neck cancer[23,24] and genitourinary tumors[25,26], and may indicate cancer progression, metastasis and recurrence[17,22,27-29]. However, to our knowledge, studies on the prognostic value of plasma fibrinogen levels in GBC are very rare[30].

In addition, CA199 has been traditionally used for the diagnosis and prognosis of GBC[31]; however, the reported results on its prognostic value in GBC patients are inconsistent and controversial[30,32,33]. Therefore, we hypothesized that the combination of plasma fibrinogen and CA199 levels may avoid inconsistent results and increase the prognostic accuracy for GBC.

Hence, the aim of the current study was to investigate the prognostic value of the combination of plasma fibrinogen and CA199 levels in patients with GBC. Additionally, we aimed to determine whether the combination of plasma fibrinogen and CA199 levels can serve as a more efficient predictive factor than either parameter alone in patients with GBC.

MATERIALS AND METHODS

Study population

From January 2005 to May 2017, a retrospective analysis of 154 GBC patients was conducted following surgery in the Department of Liver Surgery at the Peking Union Medical College Hospital of the Chinese Academy of Medical Sciences and Peking Union Medical College (CAMS & PUMC). The patients included in the analysis

met the following criteria: (1) GBC diagnosis confirmed by histopathology and cancer stage determined in accordance with the American Joint Committee on Cancer staging system, 8th Edition (AJCC-8), and the histopathologic postoperative pathologic tumor-node-metastasis (pTNM) categorization system (International Union against Cancer Staging Manual, 7th Edition; UICC-7); and (2) no adjuvant chemotherapy and/or radiotherapy before gallbladder resection surgery. Patients with the following characteristics were excluded: (1) other tumors; (2) inflammatory conditions, including infections, collagen diseases, anemia, other diseases concerning the hematological system, and absolute cardiovascular and cerebrovascular disorders; (3) liver disease; (4) oral administration of anticoagulants or acetylsalicylic acids within 3 mo before surgery; (5) lack of adequate clinical data or loss to follow-up. This study was approved by the Medical Ethics Committee of the Peking Union Medical College Hospital of the CAMS & PUMC, and all participants signed written informed consent forms.

Data collection

Patient characteristics were obtained *via* a retrospective medical record review using a standardized data collection form. Based on the medical records, the following data were collected for each patient: age, gender, plasma fibrinogen concentration, CA199 level, tumor size (defined as the longest diameter of the general postoperative pathological specimens), gallstone history, jaundice, comorbidity (diabetes), resection margin, tumor differentiation (categorized as poorly differentiated, moderately differentiated and well differentiated), T stage, N stage, M stage, pTNM stage (as defined by AJCC-8), pathological type and other miscellaneous characteristics.

Plasma fibrinogen concentration and CA199 level

The plasma fibrinogen concentration and CA199 level were measured within 3 d before surgery as part of a routine workup in these patients. The fibrinogen concentration was measured based on the Clauss method as previously described[34], and the CA199 level was determined *via* an electrochemiluminescence immunoassay at the Department of Liver Surgery of the Peking Union Medical Hospital affiliated to Peking Union Medical College, Beijing, China. According to the assay protocols, the normal reference values were as follows: serum fibrinogen concentration $\leqslant$ 4.0 g/L and CA199 level $\leqslant$ 39 U/mL.

Clinical treatment and follow-up assessments

All patients were treated by modified radical cholecystectomy or radical cholecystectomy and received systemic therapy in the adjuvant setting. All patients were followed *via* telephone interviews. The patients were carefully followed at 3-mo intervals for the first 2 years after surgery, at 6-mo intervals during the third year, and at 1-year intervals thereafter. The date of surgery marked the beginning of the follow-up period, which ended at the last follow-up visit (December 2017) or death.

Statistical analysis

Continuous variables are expressed as means ± standard deviation for normally distributed variables (Kolmogorov-Smirnov test, $P > 0.05$) or as medians (range) for non-normally distributed variables, and categorical variables were expressed as frequencies and percentages. OS was defined as the time from surgery to death from any cause or the last follow-up. A receiver operating characteristic (ROC) curve for OS prediction was constructed to estimate the optimal cut-off value for plasma fibrinogen, which allowed us to treat this parameter as a binary variable. The optimal cut-off value was determined as the point on the ROC curve that maximizes the Youden index. The area under the ROC curve (AUC) was used to calculate discrimination ability. The associations between clinicopathological variables and pretreatment plasma fibrinogen levels were assessed using either the chi-square test or the trend version of the chi-square test, as appropriate. Survival curves were generated using the Kaplan-Meier method, and the log-rank test was used to evaluate survival differences between groups. A univariate analysis using the log-rank test was performed to screen variables that could potentially predict prognosis. The statistically significantly predictive variables were then included in a multivariate Cox regression model to determine the independent prognostic risk factors. Statistical analysis of the data was performed using Statistical Package for the Social Sciences (SPSS®, version 24.0; IBM Corp., Armonk, NY, United States). Statistical significance was defined as a two-sided $P < 0.05$.

RESULTS

Patient characteristics

The detailed baseline clinicopathological characteristics of the 154 GBC patients are displayed in Table 1. There were 91 (59.1%) women and 63 (40.9%) men, and 98 (63.6%) of the patients were > 60 years old. The median age at diagnosis was 64 years (range: 29-85 years). There were 75 (48.7%) patients with a history of gallstones before surgery. Thirty-eight (24.7%) patients had diabetes before surgery. The entire cohort comprised 150 (97.4%) adenocarcinoma carcinoma patients, 3 (1.9%) adenosquamous carcinoma patients and 1 (0.6%) papillary carcinoma patient. The majority of patients had moderately or well differentiated cancer [94 (61.0%) patients with moderately or well differentiated cancer, 60 (39.0%) patients with poorly differentiated cancer]. Fifty-eight (37.7%) patients had a positive resection margin. Tumor invasion depths of Tis-T1a, T1b-T2b, T3, and T4 were observed in 10 (6.5%), 29 (18.8%), 103 (66.9%), and 12 (7.8%) patients, respectively. In terms of lymph node metastasis, 98 (63.6%) patients were N0, 47 (30.5%)

Table 1 Baseline characteristics of 154 patients who underwent potential curative cholecystectomy *n* (%)

Characteristic	Patients (*n* = 154)
Age (yr)	64 (29-85)
≤ 60	56 (36.4)
> 60	98 (63.6)
Sex	
Male	63 (40.9)
Female	91 (59.1)
Cholecystolithiasis	
Absent	79 (51.3)
Present	75 (48.7)
Diabetes	
Absent	116 (75.3)
Present	38 (24.7)
Jaundice	
Absent	129 (83.8)
Present	25 (8.9)
Blood groups	
A	43 (27.9)
B	56 (36.4)
AB	9 (5.8)
O	46 (29.9)
Pathological types	
Adenosquamous carcinoma	3 (1.9)
Adenocarcinoma	150 (97.4)
Papillocarcinoma	1 (0.6)
Degree of differentiation	
Poor	60 (39.0)
Moderate-well	94 (61.0)
Resection margin status	
Negative	96 (62.3)
Positive	58 (37.7)
Maximum tumor diameter (cm)	3 (0.2-13)
≤ 2.45	68 (44.2)
> 2.45	86 (55.8)
T stage	
Tis-T1a	10 (6.5)
T1b-T2b	29 (18.8)
T3	103 (66.9)
T4	12 (7.8)
N stage	
0	98 (63.6)
1	47 (30.5)
2	9 (5.8)
Distant metastasis	
Absent	142 (92.2)
Present	12 (7.8)
TNM stage	
0-Ⅰ stage	16 (10.4)
ⅡA-ⅡB stage	16 (10.4)
ⅢA-ⅢB stage	92 (59.7)
ⅣA-ⅣB stage	30 (19.5)
CA199 (U/mL)	69.3 (0.6-10524)
≤ 25.45	57 (37.0)
> 25.45	97 (63.0)
Fibrinogen concentration (g/L)	3.54 (1.71-7.47)
≤ 3.47	75 (48.7)
> 3.47	79 (51.3)

patients were N1 (1-3 positive lymph nodes), and 9 (5.8%) patients were N2 (≥ 4 positive lymph nodes). The majority [142 (92.2%)] of patients did not have distant metastasis. Of the 154 patients, 16 (10.4%) had stage 0-Ⅰ disease, 16 (10.4%) had stage ⅡA-ⅡB, 92 (59.7%) had stage ⅢA-ⅢB, and 30 (19.5%) had stage ⅣA-ⅣB.

Association between plasma fibrinogen levels and patient clinicopathological characteristics

The median plasma fibrinogen concentration in all patients was 3.54 g/L (range: 1.71-7.47 g/L). The optimum cut-off value for plasma fibrinogen according to the ROC curve was 3.47 g/L, with a sensitivity of 0.709 and a specificity of 0.721 (Figure 1A); the AUC was 0.735 (95%CI: 0.654-0.816). The entire cohort was stratified into 2 groups for further analysis: group A, with a plasma fibrinogen concentration > 3.47 g/L, included 79 patients (51.3%); group B, with a plasma fibrinogen concentration ≤ 3.47 g/L, included 75 patients (48.7%) (Table 1). As shown in Table 2, an elevated plasma fibrinogen level was significantly correlated with resection margin (P = 0.003), degree of differentiation (P = 0.048), jaundice (P = 0.003), T stage (P < 0.001), CA199 level (P = 0.003) and TNM stage (P = 0.011), but was not significantly correlated with gender, age, gallstone history, comorbidity (diabetes), pathological type, N stage, distant metastasis, ABO blood group, or tumor size (P > 0.05).

Association between CA199 levels and patient clinicopathological characteristics

The median CA199 level in all patients was 69.3 U/mL (range: 0.6-10524 U/mL). The optimum cut-off value for CA199 according to the ROC curve was 25.45 U/mL, with a sensitivity of 0.791 and a specificity of 0.574 (Figure 1B); the AUC was 0.729 (95%CI: 0.650-0.808). The entire cohort was stratified into 2 groups for further analysis: group A, with a CA199 level > 25.45 U/mL, included 97 patients (63.0%); group B, with a CA199 level ≤ 25.45 U/mL, included 57 patients (37.0%) (Table 1). As shown in Table 3, an elevated CA199 level was significantly correlated with resection margin (P = 0.001), jaundice (P = 0.022), T stage (P < 0.001), plasma fibrinogen concentration (P = 0.003) and TNM stage (P < 0.001), but was not significantly correlated with other factors (P > 0.05).

Analysis of factors influencing prognosis

The median follow-up time was 17 mo. One hundred and three patients died during the follow-up period, with an estimated median OS duration of 14.5 mo (range: 0.5-153.0 mo). The 1-year and 2-year survival rates were 55.8% and 35.7%, respectively.

A Cox univariate analysis of OS showed that resection margin (HR: 3.683, 95%CI: 2.468-5.496, P < 0.001), distant metastasis (HR = 2.550, 95%CI: 1.388-4.684, P = 0.003), jaundice (HR = 2.598, 95%CI: 1.644-4.106, P < 0.001), CA199 level (HR = 3.570, 95%CI: 2.213-5.760, P < 0.001), lymph node metastasis (P < 0.001), degree of differentiation (HR = 1.527, 95%CI: 1.031-2.261, P = 0.035), T stage (P < 0.001), TNM stage (P < 0.001), and plasma fibrinogen level (HR = 2.795, 95%CI: 1.853-4.214, P < 0.001) were significantly associated with unfavorable OS (Table 4). The OS curve stratified by plasma fibrinogen level

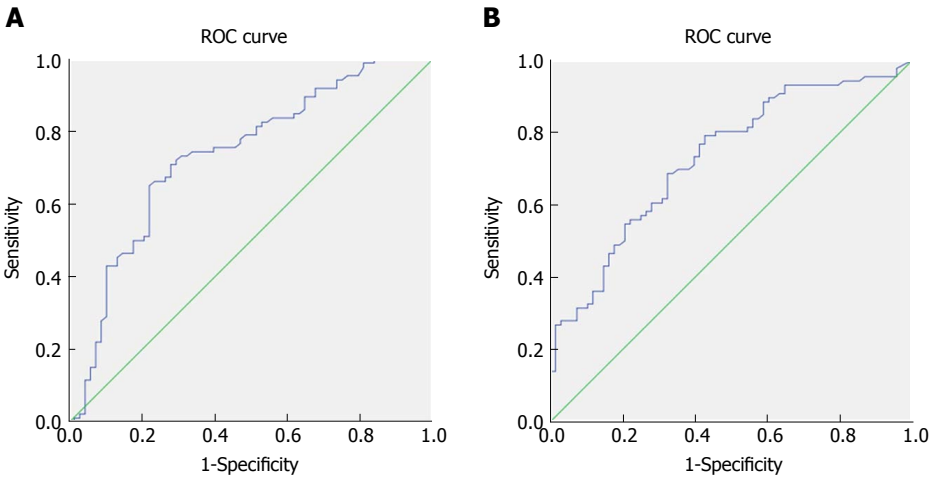

Figure 1 Receiver operating characteristic curve analysis based on fibrinogen for overall survival. A: The area under the ROC curve (AUC) indicates the diagnostic power of preoperative plasma fibrinogen concentration. In this model, the optimum cut-off point for fibrinogen concentration was 3.47 g/L, AUC was 0.735 (95%CI: 0.654-0.816), with a sensitivity of 0.709 and a specificity of 0.721 by the Youden index. B: AUC indicates the diagnostic power of preoperative CA199 level. In this model, the optimum cut-off point for CA199 level was 25.45 U/mL, AUC was 0.729 (95%CI: 0.650-0.808), with a sensitivity of 0.791 and a specificity of 0.574 by the Youden index. AUC: Area under curve. ROC: Receiver operating characteristic curve.

showed that GBC patients with a plasma fibrinogen level ⩽ 3.47 g/L had longer OS durations than those with a plasma fibrinogen level > 3.47 g/L (Figure 2A). In addition, the OS curve stratified by CA199 showed that GBC patients with a CA199 level ⩽ 25.45 U/mL had longer OS durations than those with a CA199 level > 25.45 U/mL (Figure 2B). Next, we selected the risk factors identified by the univariate analysis described above for multivariate Cox regression analysis of survival. Resection margin (HR = 1.971, 95%CI: 1.288-3.017, P = 0.002), TNM stage (P = 0.003), CA199 level (HR = 1.842, 95%CI: 1.111-3.056, P = 0.018) and plasma fibrinogen level (HR = 1.711, 95%CI: 1.114-2.627, P = 0.014) were identified as independent prognostic factors for GBC patient survival (Table 5).

Prognostic significance of the combination of plasma fibrinogen and CA199 in predicting the long-term survival of GBC patients

As shown by the above results of multivariate analysis, plasma fibrinogen and CA199 were independent prognostic biomarkers in GBC patients, but whether the combination of plasma fibrinogen and CA199 had the same efficacy remained unclear. As the HR for CA199/the HR for plasma fibrinogen = 1.842/1.711 approximately 1.10, patients with elevated plasma fibrinogen and CA199 levels were allocated a score of 2.1, those with an elevated plasma fibrinogen level only were allocated a score of 1, those with an elevated CA199 level only were allocated a score of 1.1, and those with neither of these abnormalities were allocated a score of 0. We then used the Kaplan-Meier method and a Cox regression model to investigate the prognostic significance of the combination of plasma fibrinogen and CA199 in these GBC patients.

Both the univariate and multivariate Cox regression analyses of survival revealed that the combination of plasma fibrinogen and CA199 was an independent prognostic factor for survival in GBC patients following surgery (Table 6). The results of the OS curve are presented in Figure 3. Finally, a ROC curve was generated to assess the prognostic accuracy of the combination of plasma fibrinogen and CA199. The results showed that for OS, the AUC of the combination of plasma fibrinogen and CA199 was 0.765 (95%CI: 0.688-0.841) (Figure 4), which was higher than that of plasma fibrinogen (0.735, 95%CI: 0.654-0.816) (Figure 1A) and that of CA199 (0.729, 95%CI: 0.650-0.808) (Figure 1B). These results indicated that the combination of plasma fibrinogen and CA199 may serve as a significant prognostic biomarker that is superior to either plasma fibrinogen or CA199 alone.

DISCUSSION

The incidence of GBC appears to be increasing worldwide, creating an enormous public health and economic burden. Due to a lack of effective prognostic biomarkers, the prognosis of GBC is typically poor. In the present study, we investigated the correlations between biomarkers, clinicopathological characteristics, and survival in patients with GBC undergoing surgical resection. Our results showed that plasma fibrinogen, CA199, resection margin and TNM stage were independent prognostic factors associated with OS in patients with GBC. Elevated plasma fibrinogen and CA199 levels were significantly correlated with worse OS. Moreover, to the best of our knowledge, the current study indicated for the first time that the combination of plasma fibrinogen and CA199 was more efficient than plasma fibrinogen or CA199 alone in predicting the prognosis of GBC patients who have undergone surgical resection.

Table 2 Correlation between fibrinogen concentration and clinicopathological characteristics in gallbladder carcinoma patients *n* (%)

Characteristics	Fibrinogen concentration		*P* value
	≤ 3.47 g/L (*n* = 75)	> 3.47 g/L (*n* = 79)	
Age (yr)			
≤ 60	31 (20.1)	25 (16.2)	0.243
> 60	44 (28.6)	54 (35.1)	
Sex			
Male	33 (21.4)	30 (19.5)	0.513
Female	42 (27.3)	49 (31.8)	
Cholecystolithiasis			
Absent	38 (24.7)	41 (26.6)	0.878
Present	37 (24.0)	38 (24.7)	
Diabetes			
Absent	57 (37.0)	59 (38.3)	0.850
Present	18 (11.7)	20 (13.0)	
Jaundice			
Absent	68 (44.2)	61 (39.6)	0.029
Present	7 (4.5)	18 (11.7)	
Blood groups			
A	19 (12.3)	24 (15.6)	0.145
B	33 (21.4)	23 (14.9)	
AB	2 (1.3)	7 (4.5)	
O	21 (13.6)	25 (16.2)	
Pathological types			
Adenosquamous carcinoma	0 (0)	3 (1.9)	0.142
Adenocarcinoma	75 (48.7)	75 (48.7)	
Papillocarcinoma	0 (0)	1 (0.6)	
Degree of differentiation			
Poor	23 (14.9)	37 (24.0)	0.048
Moderate-well	52 (33.8)	42 (27.3)	
Resection margin status			
Negative	56 (36.4)	40 (26.4)	0.003
Positive	19 (12.3)	39 (25.3)	
Maximum tumor diameter (cm)			
≤ 2.45	34 (22.1)	34 (22.1)	0.871
> 2.45	41 (26.6)	45 (29.2)	
T stage			
Tis-T1a	8 (5.2)	2 (1.3)	< 0.001
T1b-T2b	22 (14.3)	7 (4.5)	
T3	43 (27.9)	60 (39.0)	
T4	2 (1.3)	10 (6.5)	
N stage			
N0	50 (32.5)	48 (31.2)	0.748
N1	21 (13.6)	26 (16.9)	
N2	4 (2.6)	5 (3.2)	
Distant metastasis			
Absent	69 (44.8)	73 (47.4)	0.925
Present	6 (3.9)	6 (3.9)	
TNM stage			
0- Ⅰ stage	12 (7.8)	4 (2.6)	0.011
ⅡA-ⅡB stage	12 (7.8)	4 (2.6)	
ⅢA-ⅢB stage	39 (25.3)	53 (34.4)	
ⅣA-ⅣB stage	12 (7.8)	18 (11.7)	
CA199 (U/mL)			
≤ 25.45	37 (24.0)	20 (13.0)	0.003
> 25.45	38 (24.7)	59 (38.3)	

Due to the low incidence of GBC, few studies have examined the correlations between inflammation-related factors and GBC prognosis. The inflammation-related factors explored in previous studies include platelet count (PLT)[35], platelet to lymphocyte ratio (PLR)[32,33], neutrophil to lymphocyte ratio (NLR)[36,37] and plasma fibrinogen level[30].

Wang *et al*[35] showed that a PLT > 178 × 10^9/L was significantly correlated with worse prognosis of GBC (HR = 1.541, 95%CI: 1.038-2.287, *P* = 0.032) and identified 178 × 10^9/L as the optimal cut-off value (AUC = 0.798, 95%CI: 0.737-0.858, sensitivity: 0.746, specificity: 0.722). The prognostic accuracy of PLT for GBC was higher than that of plasma fibrinogen in our study (AUC = 0.735, 95%CI: 0.654-0.816, sensitivity: 0.709, specificity: 0.721). However, Pang *et al*[32] and Zhang *et al*[33] indicated that PLT was not associated with the prognosis of GBC (HR = 1.013,

Table 3 Correlation between CA199 level and clinicopathological characteristics in gallbladder carcinoma patients *n* (%)

Characteristics	CA199 level		*P* value
	≤ 25.45 U/mL (*n* = 57)	> 25.45 U/mL (*n* = 97)	
Age (yr)			
≤ 60	24 (15.6)	32 (20.8)	0.299
> 60	33 (21.4)	65 (42.2)	
Sex			
Male	23 (14.9)	40 (26.0)	0.914
Female	34 (21.1)	57 (37.0)	
Cholecystolithiasis			
Absent	32 (20.8)	47 (30.5)	0.406
Present	25 (16.2)	50 (32.5)	
Diabetes			
Absent	45 (29.2)	71 (46.1)	0.447
Present	12 (7.8)	26 (16.9)	
Jaundice			
Absent	53 (34.4)	76 (49.4)	0.022
Present	4 (2.6)	21 (13.6)	
Blood groups			
A	19 (12.3)	24 (15.6)	0.303
B	21 (13.6)	35 (22.7)	
AB	1 (0.6)	8 (5.2)	
O	16 (10.4)	30 (19.5)	
Pathological types			
Adenosquamous carcinoma	0 (0)	3 (1.9)	0.299
Adenocarcinoma	57 (37.0)	93 (60.4)	
Papillocarcinoma	0 (0)	1 (0.6)	
Degree of differentiation			
Poor	33 (21.4)	61 (39.6)	0.069
Moderate-well	24 (15.6)	36 (23.4)	
Resection margin status			
Negative	45 (29.2)	51 (33.1)	0.001
Positive	12 (7.8)	46 (29.9)	
Maximum tumor diameter (cm)			
≤ 2.45	30 (19.5)	38 (24.7)	0.131
> 2.45	27 (17.5)	59 (38.3)	
T stage			
Tis-T1a	7 (4.5)	3 (1.9)	< 0.001
T1b-T2b	18 (11.7)	11 (7.1)	
T3	32 (20.8)	71 (46.1)	
T4	0 (0.0)	12 (7.8)	
N stage			
N0	43 (27.9)	55 (35.7)	0.056
N1	11 (7.1)	36 (23.4)	
N2	3 (1.9)	6 (3.9)	
Distant metastasis			
Absent	53 (34.4)	89 (57.8)	0.783
Present	4 (2.6)	8 (5.2)	
TNM stage			
0-Ⅰ stage	11 (7.1)	5 (3.2)	< 0.001
ⅡA-ⅡB stage	12 (7.8)	4 (2.6)	
ⅢA-ⅢB stage	27 (17.5)	65 (42.2)	
ⅣA-ⅣB stage	7 (4.5)	23 (14.9)	
Fibrinogen concentration (g/L)			
≤ 3.47	37 (24.0)	38 (24.7)	0.003
> 3.47	20 (13.0)	59 (38.3)	

95%CI: 0.647-1.594, *P* = 0.956, and HR = 1.172, 95%CI: 0.794-1.731, *P* = 0.423). These results may be related to the different cut-off values chosen (300 × 10^9/L and 200 × 10^9/L) and different sample sizes (316 patients and 145 patients). Therefore, the prognostic significance of PLT in GBC patients requires further validation.

Zhang *et al*[33] and Zhang *et al*[36] demonstrated that NLR was significantly associated with an unfavorable prognosis of GBC (HR = 2.059, 95%CI: 1.253-3.384, *P* = 0.004, and HR = 1.65, *P* < 0.001), but the prognostic accuracy of NLR for GBC according to Lingqiang Zhang *et al*[36] (AUC = 0.637, 95%CI: 0.556-0.718, sensitivity: 0.713, specificity: 0.565) was not higher than that of plasma fibrinogen in our study (AUC = 0.735, 95%CI: 0.654-0.816, sensitivity: 0.709, specificity: 0.721).

Pang *et al*[32] showed that PLR was a negative

Table 4 Univariate analysis of overall survival in gallbladder cancer patients

Characteristics	HR (95%CI)	*P* value
Age (yr)	1.473 (0.973-2.230)	0.067
≤ 60		
> 60		
Sex	0.995 (0.670-1.477)	0.981
Male		
Female		
Cholecystolithiasis	1.198 (0.814-1.764)	0.360
Absent		
Present		
Diabetes	1.028 (0.651-1.623)	0.906
Absent		
Present		
Jaundice	2.598 (1.644-4.106)	< 0.001
Absent		
Present		
Blood groups	-	0.113
A		
B		
AB		
O		
Pathological types	-	0.165
Adenosquamous carcinoma		
Adenocarcinoma		
Papillocarcinoma		
Degree of differentiation	1.527 (1.031-2.261)	0.035
Poor		
Moderate-well		
Resection margin status	3.683 (2.468-5.496)	< 0.001
Negative		
Positive		
Maximum tumor diameter (cm)	1.101 (0.744-1.630)	0.631
≤ 2.45		
> 2.45		
T stage	-	< 0.001
Tis-T1a		
T1b-T2b		
T3		
T4		
N stage	-	< 0.001
N0		
N1		
N2		
Distant metastasis	2.550 (1.388-4.684)	< 0.003
Absent		
Present		
TNM stage	-	< 0.001
0- Ⅰ stage		
ⅡA-ⅡB stage		
ⅢA-ⅢB stage		
ⅣA-ⅣB stage		
CA199 (U/mL)	3.570 (2.213-5.760)	< 0.001
≤ 25.45		
> 25.45		
Fibrinogen concentration (g/L)	2.790 (1.853-4.214)	< 0.001
≤ 3.47		
> 3.47		

prognostic factor for GBC patients (HR = 2.02, 95%CI: 1.24-3.28, $P < 0.001$), although the prognostic accuracy of PLR for GBC (AUC = 0.620, 95%CI: 0.542-0.698, $P = 0.040$, sensitivity: 0.736, specificity: 0.532) was not superior to that of plasma fibrinogen in our study (AUC = 0.735, 95%CI: 0.654-0.816, sensitivity: 0.709, specificity: 0.721). However, Zhang *et al*[33] showed that PLR was not associated with the prognosis of patients with GBC. Therefore, the prognostic significance of PLR in GBC patients requires further validation.

To date, the only study to explore the prognostic significance of plasma fibrinogen in GBC patients was conducted by Shu *et al*[30]. Consistent with the results of our study, their results indicated that an elevated preoperative plasma fibrinogen level, poorer margin

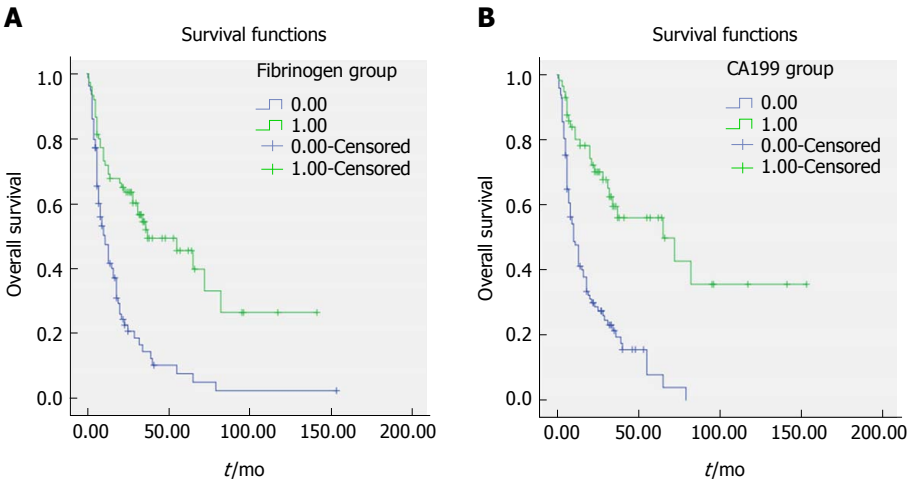

Figure 2 Survival curve according to the preoperative fibrinogen concentration (A) and CA199 level (B). A: Data compares fibrinogen concentration > 3.47 g/L *vs* ≤ 3.47 g/L group ($P < 0.05$). The number 1 for ≤ 3.47 g/L group, number 2 for > 3.47 g/L group. B: Data compares CA199 level > 25.45 U/mL *vs* ≤ 25.45 U/mL ($P < 0.05$). The number 1 for ≤ 25.45 U/mL group, number 2 for > 25.45 U/mL group.

Table 5 Multivariate analysis of overall survival in gallbladder cancer patients

Characteristics	HR (95%CI)	Wald	*P* value
Resection margin status	1.971 (1.288-3.017)		0.002
Negative			
Positive			
TNM stage		11.299	0.003
ⅡA-ⅡB stage/0-1 stage	1.336 (0.317-5.627)	0.156	0.693
ⅢA-ⅢB stage/0-1 stage	3.831 (1.167-12.571)	4.907	0.027
ⅣA-ⅣB stage/0-1 stage	5.204 (1.497-18.093)	6.730	0.009
Fibrinogen concentration (g/L)	1.711 (1.114-2.627)		0.014
≤ 3.47			
> 3.47			
CA199 (U/mL)	1.842 (1.111-3.056)		0.018
≤ 25.45			
> 25.45			

Table 6 Univariate and multivariate analysis of overall survival in gallbladder cancer patients according to the combination of fibrinogen and CA199

Characteristics	HR (95%CI)	Wald	*P* value
Univariate analysis			
Combined fibrinogen and CA199	-		< 0.001
0			
1			
1.1			
2.1			
Multivariate analysis			
Resection margin status	1.973 (1.289-3.020)		0.002
Negative			
Positive			
TNM stage	11.299		0.011
ⅡA-ⅡB stage/0-1 stage	1.342 (0.318-5.659)	0.160	0.689
ⅢA-ⅢB stage/0-1 stage	3.812 (1.158-12.545)	4.848	0.028
ⅣA-ⅣB stage/0-1 stage	5.189 (1.491-18.055)	6.699	0.010
Combined fibrinogen and CA199	14.218		0.003
1/0	1.784 (0.775-4.104)	1.854	0.173
1.1/0	1.895 (0.943-3.806)	3.222	0.073
2.1/0	3.195 (1.676-6.090)	12.454	0.000

The number 0 for fibrinogen concentration > 3.47g/L with CA199 level > 25.45 U/mL group, number 1 for fibrinogen concentration > 3.47 g/L with CA199 level ≤ 25.45 U/mL group, number 1.1 for fibrinogen concentration ≤ 3.47g/L with CA199 level > 25.45 U/mL group, and number 2.1 for fibrinogen concentration ≤ 3.47 g/L with CA199 level ≤ 25.45 U/mL group.

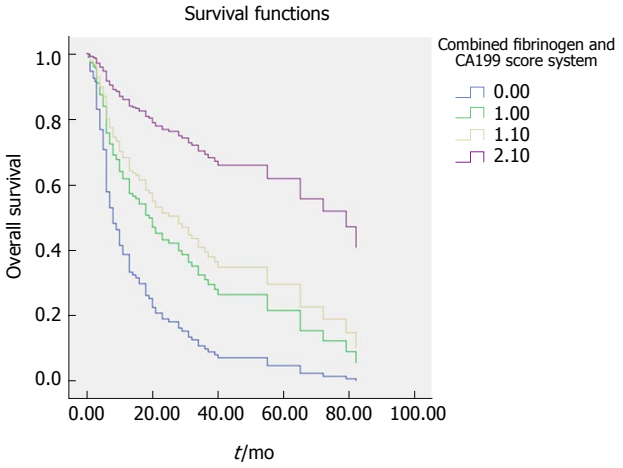

Figure 3 Survival curve according to the combined fibrinogen and CA199 scoring system. Data compares the fibrinogen concentration > 3.47 g/L with CA199 level > 25.45 U/mA group, fibrinogen concentration > 3.47 g/L with CA199 level ⩽ 25.45 U/mL group, fibrinogen concentration ⩽ 3.47 g/L with CA199 level > 25.45 U/mL group and fibrinogen concentration ⩽ 3.47 g/L with CA199 level ⩽ 25.45 U/mL group. The number 0 for fibrinogen concentration > 3.47 g/L with CA199 level > 25.45 U/mL group, number 1 for fibrinogen concentration > 3.47g/L with CA199 level ⩽ 25.45 U/mL group, number 1.1 for fibrinogen concentration ⩽ 3.47 g/L with CA199 level > 25.45 U/mL group, number 2.1 for fibrinogen concentration ⩽ 3.47 g/L with CA199 level ⩽ 25.45 U/mL group.

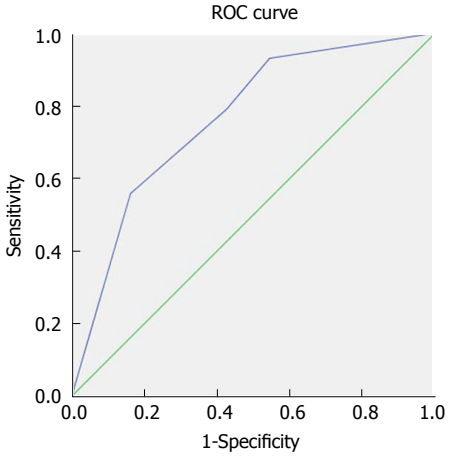

Figure 4 Receiver operating characteristic curve analysis based on the combination of fibrinogen and CA199 for overall survival. AUC indicates the diagnostic power of the combination of fibrinogen and CA199. In this model, AUC was 0.765 (95%CI: 0.688-0.841). AUC: Area under curve.

status and higher TNM stage were independently associated with worse OS. They also showed that lymphatic metastasis was a negative prognostic factor for GBC, but in our study, lymphatic metastasis was not identified as a prognostic factor. This difference may be related to the TNM stage classification standard used in the present study. The newly published AJCC-8 indicated that the number of positive lymph nodes rather than the location of lymph node metastasis is closely related to the prognosis of GBC. The new N stage defined 1-3 positive lymph nodes as N1, 4 or more positive lymph nodes as N2, and no positive lymph nodes as N0.

The prognostic significance of plasma fibrinogen in the study conducted by Shu *et al*[30] (AUR = 0.751, 95%CI: 0.653-0.848) was slightly superior to that observed in our study (AUC = 0.735, 95%CI: 0.654-0.816, sensitivity: 0.709, specificity: 0.721) and had a positive predictive value of 92.73%. This difference may be related to the different optimal cut-off values between the two studies (4.02 g/L and 3.47 g/L) and the different methods used to determine the optimal cut-off values. In their study, the dichotomous variable that was used to determine the optimal cut-off value on the ROC curve was TNM stage, whereas the dichotomous variable used in our study was OS. Our method is accepted by most researchers. Nonetheless, the results of their study support the conclusion reached in our study that the prognostic accuracy of the combination of plasma fibrinogen and CA199 (AUC = 0.765, 95%CI: 0.688-0.841) is higher than that of plasma fibrinogen alone (AUR = 0.751, 95%CI: 0.653-0.848).

Many recent studies have demonstrated that an elevated plasma fibrinogen level, as a marker of coagulation and fibrinolytic activation, is a strong predictor of poor prognosis for various malignant tumors[13,15,19,23,25]. Additionally, it was found that fibrinogen synthesis is significantly upregulated by inflammation[38]. However, the molecular mechanisms underlying the association between plasma fibrinogen and cancer prognosis is still uncertain. In an *in vitro* study, Shu *et al*[30] found that plasma fibrinogen at a high concentration induced epithelial-mesenchymal transition (EMT), thus increasing the migration, invasion, and metastatic capacity of co-cultured GBC cells by increasing the expression of vimentin (a mesenchymal marker) and reducing the expression of E-cadherin (an epithelial marker). EMT is known to confer migration, invasion, and metastatic capacity and multidrug resistance to cells[38,39]. However, this explanation needs to be verified through basic research in the future.

One of the methodological innovations of our study is that we assigned different scores to patients according to the HR for elevated plasma fibrinogen levels and elevated CA199 levels, instead of assigning all patients a score of 1 as in the previous scoring system. This new scoring method further distinguished the difference in prognostic efficiency between plasma fibrinogen and CA199, rather than simply assigning a score of 1 to each parameter, considering that the HRs for the two parameters are not the same (CA199: 1.842, plasma fibrinogen: 1.711). From the OS curve (Figure 3) and ROC curve (Figure 4), we observed that the new scoring system effectively improved the prognostic accuracy of the biomarkers.

This study is the first to investigate the prognostic significance of the combination of plasma fibrinogen

and CA199 in GBC patients. Inevitably, our study has some limitations that should be acknowledged. First, this study was performed using a retrospective design. Second, although this new scoring method distinguished the prognostic value of different biomarkers and improved prognostic accuracy, the validity and predictive value of this scoring method still require further verification. Third, the data were obtained from a single institution and the sample size was relatively small, which may have influenced the final conclusions. Fourth, to obtain more data, we did not distinguish between patients who underwent radical surgery and those who received palliative cholecystectomy or extended resection. Therefore, our results should be validated by prospective, multicenter studies with a large sample size.

In conclusion, elevated preoperative levels of both plasma fibrinogen and CA199 are independent prognostic factors for GBC. Additionally, the combination of plasma fibrinogen and CA199 showed superior prognostic accuracy compared with either parameter alone. Therefore, the combination of plasma fibrinogen and CA199 can facilitate the identification of GBC patients with poorer survival prognosis before surgery. We hypothesize that the combination of plasma fibrinogen and CA199 could be used as an inexpensive, simple, reliable and reproducible method to determine GBC prognosis in clinical practice.

ARTICLE HIGHLIGHTS

Research background

Gallbladder cancer is a rare hepatobiliary tumor with a relatively low incidence. Due to the lack of significant specific symptoms at the early stage, the prognosis of gallbladder cancer is poor and can be fatal. Therefore, determining a convenient and cost-effective prognostic biomarker is urgently required for patients with gallbladder cancer. Elevated fibrinogen has been demonstrated to be associated with poor prognosis in multiple malignancies, while CA199 is considered a widely accepted diagnostic and prognostic marker of gallbladder cancer. There have been very few studies on the role of fibrinogen in the prognosis of patients with gallbladder cancer. To date, studies on the combined use of fibrinogen and CA199 to predict the prognosis of patients with gallbladder cancer have not been conducted. The combined use of fibrinogen and CA199 avoids inconsistencies caused by the use of a single indicator and enhances predictive efficacy.

Research motivation

The main aim of this study was to validate and identify a convenient and inexpensive combination of biomarkers with a higher prognostic value for patients with gallbladder cancer. From our research, we found that the combination of preoperative plasma fibrinogen and CA199 was a more efficient prognostic factor than either parameter alone in patients with gallbladder cancer. Due to this finding, we can screen potential high-risk candidates for gallbladder cancer and provide prognostic guidance for surgical patients with gallbladder cancer. In addition, this study also provides clinical evidence and preconditions for the future study of how fibrinogen promotes the proliferation and metastasis of malignant tumor cells.

Research objectives

The main objective of this study was to identify a convenient and more efficient prognostic biomarker for gallbladder cancer patients. From this study, we found that both elevated fibrinogen and elevated CA199 were independent risk factors for gallbladder cancer patients. Furthermore, the combination of preoperative plasma fibrinogen and CA199 was a more efficient prognostic factor than either parameter alone in patients with gallbladder cancer. These findings not only provide a further example which proves the relationship between hemostasis and tumor, but also provide powerful clinical evidence for related basic research in the future.

Research methods

We used an Excel table to organize research-related clinical data, and imported these variables into SPSS 24.0 statistical software. We then assigned the different types of variables appropriately. We determined the optimal cut-off values for fibrinogen and CA199 by plotting ROC curves, and then determined the association of fibrinogen and CA199 with other clinicopathological variables using the R × C table. Finally, univariate and multivariate analyses were performed to determine the independent prognostic factors in patients with gallbladder cancer.

Given the different HRs of the two parameters (CA199: 1.842, plasma fibrinogen: 1.711), one methodological innovation of this study was that we assigned different scores to elevated plasma fibrinogen levels and elevated CA199 levels, instead of assigning the same score as in the previous scoring system. This scoring approach further differentiates the difference in the prognostic efficiency between plasma fibrinogen and CA199, rather than simply assigning each parameter with 1 point. Based on the overall survival curve (Figure 3) and the ROC curve (Figure 4) in the text, we observed that the new scoring system effectively improved the prognostic accuracy of the biomarkers.

Research results

Our study demonstrated that the best cut-off values for pretreatment fibrinogen and CA199 were 3.47 g/L and 25.45 U/mL, respectively, in patients with gallbladder cancer. After single factor and multivariate analysis, it was shown that elevated pretreatment fibrinogen, elevated pretreatment CA199, resection margin and TNM stage were independent risk factors for gallbladder cancer patients. When the elevated pretreatment fibrinogen and elevated pretreatment CA199 were combined with different assigned scores according to their different HRs, the prognostic accuracy and power was significantly improved (the AUROC increased to 0.765, a relatively high value). These research findings confirm the relationship between hemostatic factors and cancer, in this case gallbladder cancer. How does the hemostatic factor fibrinogen influence the development, growth, and metastasis of gallbladder cancer cells? The underlying mechanism is still unknown, and further studies are required to identify and confirm the mechanism involved.

Research conclusions

In the present study, we found that the combination of preoperative plasma fibrinogen and CA199 is a more efficient prognostic factor than either parameter alone in patients with gallbladder cancer. We proposed that the combination of hemostatic factor and specific oncology markers can better predict the prognosis of gallbladder cancer, as hemostatic and oncology markers can compensate for each other's inconsistency in predicting tumor prognosis and thus enhance overall prognostic efficacy. Fibrinogen is associated with the development, growth, and metastasis of cancer cells, and CA199 is a product of tumor cell growth and metabolism. However, from our study findings, we observed that they had different prognostic efficacy (as they had different HRs) in gallbladder cancer patients; therefore, we assigned different scores to them which differed from the previous traditional scoring system. Using this new method, the prognostic efficacy of these two prognostic biomarkers combined was significantly improved, and this combination was used to screen potential high-risk gallbladder cancer candidates, identify appropriate surgical patients, and adopt the best follow-up strategy.

Research perspectives

In this study, we found that the combination of a hemostatic factor and oncology factor could compensate for each other's inconsistency in predicting tumor prognosis and improve the overall prognostic efficacy. The combination of these factors was more efficient than either parameter alone in predicting the prognosis of gallbladder cancer patients. These factors are inexpensive, easy-to-use and highly accurate for determining the prognosis of gallbladder cancer

patients. Further large-scale, well-designed and prospective studies to verify the findings and conclusions of this investigation are required.

REFERENCES

1 **Hundal R**, Shaffer EA. Gallbladder cancer: epidemiology and outcome. *Clin Epidemiol* 2014; **6**: 99-109 [PMID: 24634588 DOI: 10.2147/CLEP.S37357]

2 **Wu XS**, Shi LB, Li ML, Ding Q, Weng H, Wu WG, Cao Y, Bao RF, Shu YJ, Ding QC, Mu JS, Gu J, Dong P, Liu YB. Evaluation of two inflammation-based prognostic scores in patients with resectable gallbladder carcinoma. *Ann Surg Oncol* 2014; **21**: 449-457 [PMID: 24081806 DOI: 10.1245/s10434-013-3292-z]

3 **Liu YB**, He XW, Wang JW, Li JT, Li KQ, Liu FB, Xue JF, Zhu JH, Li B, Peng SY. [Establishment of liver metastasis model of human gallbladder cancer and isolation of the subpopulation with high metastatic potential]. *Zhonghua Yi Xue Za Zhi* 2006; **86**: 2117-2121 [PMID: 17064616]

4 **Boutros C**, Gary M, Baldwin K, Somasundar P. Gallbladder cancer: past, present and an uncertain future. *Surg Oncol* 2012; **21**: e183-e191 [PMID: 23025910 DOI: 10.1016/j.suronc.2012.08.002]

5 **Srivastava K**, Srivastava A, Mittal B. Potential biomarkers in gallbladder cancer: present status and future directions. *Biomarkers* 2013; **18**: 1-9 [PMID: 22931385 DOI: 10.3109/1354750X.2012.717105]

6 **Choi SB**, Han HJ, Kim CY, Kim WB, Song TJ, Suh SO, Kim YC, Choi SY. Fourteen year surgical experience of gallbladder cancer: validity of curative resection affecting survival. *Hepatogastroenterology* 2012; **59**: 36-41 [PMID: 22251521 DOI: 10.5754/hge10297]

7 **Wang RT**, Xu XS, Liu J, Liu C. Gallbladder carcinoma: analysis of prognostic factors in 132 cases. *Asian Pac J Cancer Prev* 2012; **13**: 2511-2514 [PMID: 22938413]

8 **Balkwill F**, Mantovani A. Inflammation and cancer: back to Virchow? *Lancet* 2001; **357**: 539-545 [PMID: 11229684 DOI: 10.1016/S0140-6736(00)04046-0]

9 **Wang X**, Wang E, Kavanagh JJ, Freedman RS. Ovarian cancer, the coagulation pathway, and inflammation. *J Transl Med* 2005; **3**: 25 [PMID: 15969748 DOI: 10.1186/1479-5876-3-25]

10 **Lawrence SO**, Simpson-Haidaris PJ. Regulated de novo biosynthesis of fibrinogen in extrahepatic epithelial cells in response to inflammation. *Thromb Haemost* 2004; **92**: 234-243 [PMID: 15269818 DOI: 10.1160/TH04-01-0024]

11 **Collen D**, Tytgat GN, Claeys H, Piessens R. Metabolism and distribution of fibrinogen. I. Fibrinogen turnover in physiological conditions in humans. *Br J Haematol* 1972; **22**: 681-700 [PMID: 5064500]

12 **Koenig W**. Fibrin (ogen) in cardiovascular disease: an update. *Thromb Haemost* 2003; **89**: 601-609 [PMID: 12669113]

13 **Kim KH**, Park TY, Lee JY, Lee SM, Yim JJ, Yoo CG, Kim YW, Han SK, Yang SC. Prognostic significance of initial platelet counts and fibrinogen level in advanced non-small cell lung cancer. *J Korean Med Sci* 2014; **29**: 507-511 [PMID: 24753697 DOI: 10.3346/jkms.2014.29.4.507]

14 **Ghanim B**, Hoda MA, Klikovits T, Winter MP, Alimohammadi A, Grusch M, Dome B, Arns M, Schenk P, Jakopovic M, Samarzija M, Brcic L, Filipits M, Laszlo V, Klepetko W, Berger W, Hegedus B. Circulating fibrinogen is a prognostic and predictive biomarker in malignant pleural mesothelioma. *Br J Cancer* 2014; **110**: 984-990 [PMID: 24434429 DOI: 10.1038/bjc.2013.815]

15 **Zhang SS**, Lei YY, Cai XL, Yang H, Xia X, Luo KJ, Su CH, Zou JY, Zeng B, Hu Y, Luo HH. Preoperative serum fibrinogen is an independent prognostic factor in operable esophageal cancer. *Oncotarget* 2016; **7**: 25461-25469 [PMID: 27009857 DOI: 10.18632/oncotarget.8171]

16 **Wang GY**, Jiang N, Yi HM, Wang GS, Zhang JW, Li H, Zhang J, Zhang Q, Yang Y, Chen GH. Pretransplant Elevated Plasma Fibrinogen Level is a Novel Prognostic Predictor for Hepatocellular Carcinoma Recurrence and Patient Survival Following Liver Transplantation. *Ann Transplant* 2016; **21**: 125-130 [PMID: 26903139]

17 **Yamamoto M**, Kurokawa Y, Miyazaki Y, Makino T, Takahashi T, Yamasaki M, Nakajima K, Takiguchi S, Mori M, Doki Y. Usefulness of Preoperative Plasma Fibrinogen Versus Other Prognostic Markers for Predicting Gastric Cancer Recurrence. *World J Surg* 2016; **40**: 1904-1909 [PMID: 26969673 DOI: 10.1007/s00268-016-3474-5]

18 **Hong T**, Shen D, Chen X, Wu X, Hua D. Preoperative plasma fibrinogen, but not D-dimer might represent a prognostic factor in non-metastatic colorectal cancer: A prospective cohort study. *Cancer Biomark* 2017; **19**: 103-111 [PMID: 28269756 DOI: 10.3233/CBM-160510]

19 **Zhao K**, Deng H, Qin Y, Liao W, Liang W. Prognostic significance of pretreatment plasma fibrinogen and platelet levels in patients with early-stage cervical cancer. *Gynecol Obstet Invest* 2015; **79**: 25-33 [PMID: 25278089 DOI: 10.1159/000365477]

20 **Seebacher V**, Polterauer S, Grimm C, Husslein H, Leipold H, Hefler-Frischmuth K, Tempfer C, Reinthaller A, Hefler L. The prognostic value of plasma fibrinogen levels in patients with endometrial cancer: a multi-centre trial. *Br J Cancer* 2010; **102**: 952-956 [PMID: 20160724 DOI: 10.1038/sj.bjc.6605547]

21 **Bekos C**, Grimm C, Brodowicz T, Petru E, Hefler L, Reimer D, Koch H, Reinthaller A, Polterauer S, Polterauer M. Prognostic role of plasma fibrinogen in patients with uterine leiomyosarcoma - a multicenter study. *Sci Rep* 2017; **7**: 14474 [PMID: 29101329 DOI: 10.1038/s41598-017-13934-8]

22 **Mei Y**, Zhao S, Lu X, Liu H, Li X, Ma R. Clinical and Prognostic Significance of Preoperative Plasma Fibrinogen Levels in Patients with Operable Breast Cancer. *PLoS One* 2016; **11**: e0146233 [PMID: 26799214 DOI: 10.1371/journal.pone.0146233]

23 **Selzer E**, Grah A, Heiduschka G, Kornek G, Thurnher D. Pre-therapeutic fibrinogen levels are of prognostic significance in locally advanced head and neck cancer. *Wien Klin Wochenschr* 2016; **128**: 320-328 [PMID: 26919854 DOI: 10.1007/s00508-016-0963-3]

24 **Holzinger D**, Danilovic I, Seemann R, Kornek G, Engelmann J, Pillerstorff R, Holawe S, Psyrri A, Erovic BM, Farwell G, Perisanidis C. Prognostic Impact of Pretreatment Plasma Fibrinogen in Patients with Locally Advanced Oral and Oropharyngeal Cancer. *PLoS One* 2016; **11**: e0158697 [PMID: 27362659 DOI: 10.1371/journal.pone.0158697]

25 **Zhang B**, Song Y, Jin J, Zhou LQ, He ZS, Shen C, He Q, Li J, Liu LB, Wang C, Chen XY, Fan Y, Hu S, Zhang L, Yu W, Han WK. Preoperative Plasma Fibrinogen Level Represents an Independent Prognostic Factor in a Chinese Cohort of Patients with Upper Tract Urothelial Carcinoma. *PLoS One* 2016; **11**: e0150193 [PMID: 26930207 DOI: 10.1371/journal.pone.0150193]

26 **Ma C**, Zhou Y, Zhou S, Zhao K, Lu B, Sun E. Preoperative peripheral plasma fibrinogen level is an independent prognostic marker in penile cancer. *Oncotarget* 2017; **8**: 12355-12363 [PMID: 27738342 DOI: 10.18632/oncotarget.12563]

27 **Troppan KT**, Melchardt T, Wenzl K, Schlick K, Deutsch A, Bullock MD, Reitz D, Beham-Schmid C, Weiss L, Neureiter D, Tränkenschuh W, Greil R, Neumeister P, Egle A, Pichler M. The clinical significance of fibrinogen plasma levels in patients with diffuse large B cell lymphoma. *J Clin Pathol* 2016; **69**: 326-330 [PMID: 26644520 DOI: 10.1136/jclinpath-2015-203356]

28 **Zhang D**, Zhou X, Bao W, Chen Y, Cheng L, Qiu G, Sheng L, Ji Y, Du X. Plasma fibrinogen levels are correlated with postoperative distant metastasis and prognosis in esophageal squamous cell carcinoma. *Oncotarget* 2015; **6**: 38410-38420 [PMID: 26334098 DOI: 10.18632/oncotarget.4800]

29 **Zhu LR**, Li J, Chen P, Jiang Q, Tang XP. Clinical significance of plasma fibrinogen and D-dimer in predicting the chemotherapy efficacy and prognosis for small cell lung cancer patients. *Clin Transl Oncol* 2016; **18**: 178-188 [PMID: 26184726 DOI: 10.1007/s12094-015-1350-7]

30 **Shu YJ**, Weng H, Bao RF, Wu XS, Ding Q, Cao Y, Wang XA, Zhang F, Xiang SS, Li HF, Li ML, Mu JS, Wu WG, Liu YB. Clinical and prognostic significance of preoperative plasma hyperfibrinogenemia in gallbladder cancer patients following surgical resection: a retrospective and in vitro study. *BMC Cancer*

2014; **14**: 566 [PMID: 25096189 DOI: 10.1186/1471-2407-14-566]
31 **Wang YF**, Feng FL, Zhao XH, Ye ZX, Zeng HP, Li Z, Jiang XQ, Peng ZH. Combined detection tumor markers for diagnosis and prognosis of gallbladder cancer. *World J Gastroenterol* 2014; **20**: 4085-4092 [PMID: 24744600 DOI: 10.3748/wjg.v20.i14.4085]
32 **Pang Q**, Zhang LQ, Wang RT, Bi JB, Zhang JY, Qu K, Liu SS, Song SD, Xu XS, Wang ZX, Liu C. Platelet to lymphocyte ratio as a novel prognostic tool for gallbladder carcinoma. *World J Gastroenterol* 2015; **21**: 6675-6683 [PMID: 26074706 DOI: 10.3748/wjg.v21.i21.6675]
33 **Zhang Y**, Jiang C, Li J, Sun J, Qu X. Prognostic significance of preoperative neutrophil/lymphocyte ratio and platelet/lymphocyte ratio in patients with gallbladder carcinoma. *Clin Transl Oncol* 2015; **17**: 810-818 [PMID: 26077119 DOI: 10.1007/s12094-015-1310-2]
34 **Cl A**. [Rapid physiological coagulation method in determination of fibrinogen]. *Acta Haematol* 1957; **17**: 237-246 [PMID: 13434757 DOI: 10.1159/000205234]
35 **Wang RT**, Zhang LQ, Mu YP, Li JB, Xu XS, Pang Q, Sun LK, Zhang X, Dong SB, Wang L, Liu C. Prognostic significance of preoperative platelet count in patients with gallbladder cancer. *World J Gastroenterol* 2015; **21**: 5303-5310 [PMID: 25954104 DOI: 10.3748/wjg.v21.i17.5303]
36 **Zhang L**, Wang R, Chen W, Xu X, Dong S, Fan H, Liu C. Prognostic significance of neutrophil to lymphocyte ratio in patients with gallbladder carcinoma. *HPB* (Oxford) 2016; **18**: 600-607 [PMID: 27346141 DOI: 10.1016/j.hpb.2016.03.608]
37 **Whelton SP**, Narla V, Blaha MJ, Nasir K, Blumenthal RS, Jenny NS, Al-Mallah MH, Michos ED. Association between resting heart rate and inflammatory biomarkers (high-sensitivity C-reactive protein, interleukin-6, and fibrinogen) (from the Multi-Ethnic Study of Atherosclerosis). *Am J Cardiol* 2014; **113**: 644-649 [PMID: 24393259 DOI: 10.1016/j.amjcard.2013.11.009]
38 **Romano S**, Staibano S, Greco A, Brunetti A, Nappo G, Ilardi G, Martinelli R, Sorrentino A, Di Pace A, Mascolo M, Bisogni R, Scalvenzi M, Alfano B, Romano MF. FK506 binding protein 51 positively regulates melanoma stemness and metastatic potential. *Cell Death Dis* 2013; **4**: e578 [PMID: 23559012 DOI: 10.1038/cddis.2013.109]
39 **He L**, Zhou X, Qu C, Hu L, Tang Y, Zhang Q, Liang M, Hong J. Musashi2 predicts poor prognosis and invasion in hepatocellular carcinoma by driving epithelial-mesenchymal transition. *J Cell Mol Med* 2014; **18**: 49-58 [PMID: 24305552 DOI: 10.1111/jcmm.12158]

P- Reviewer: Armellini E, Osuga T, Tokunaga Y **S- Editor**: Gong ZM
L- Editor: Webster JR **E- Editor**: Huang Y

World Journal of Gastroenterology

Submit a Manuscript: http://www.f6publishing.com

World J Gastroenterol 2018 April 7; 24(13): 1464-1477

DOI: 10.3748/wjg.v24.i13.1464

ISSN 1007-9327 (print) ISSN 2219-2840 (online)

ORIGINAL ARTICLE

Retrospective Study

Fecal microbial dysbiosis in Chinese patients with inflammatory bowel disease

Hai-Qin Ma, Ting-Ting Yu, Xiao-Jing Zhao, Yi Zhang, Hong-Jie Zhang

Hai-Qin Ma, Ting-Ting Yu, Xiao-Jing Zhao, Yi Zhang, Hong-Jie Zhang, Department of Gastroenterology, First Affiliated Hospital of Nanjing Medical University, Nanjing 210029, Jiangsu Province, China

ORCID number: Hai-Qin Ma (0000-0002-2900-5994); Ting-Ting Yu (0000-0003-3433-9013); Xiao-Jing Zhao (0000-0001-5156-3864); Yi Zhang (0000-0002-3072-6043); Hong-Jie Zhang (0000-0003-4497-0503).

Author contributions: Ma HQ and Zhang HJ conceived the study; Ma HQ and Yu TT performed the research; Zhao XJ and Zhang Y analyzed the data; Ma HQ wrote this manuscript; Zhang HJ supervised the report.

Supported by the National Natural Science Foundation of China, No. 81470827.

Institutional review board statement: This study was reviewed and approved by the Ethics Committee of the First Affiliated Hospital of Nanjing Medical University.

Informed consent statement: All study participants provided informed written consent prior to study enrollment.

Conflict-of-interest statement: All authors declare no conflicts of interest related to this article.

Data sharing statement: No additional data are available.

Manuscript source: Unsolicited manuscript

Correspondence to: Hong-Jie Zhang, MD, PhD, Professor, Department of Gastroenterology, First Affiliated Hospital of Nanjing Medical University, 300 Guangzhou Road, Nanjing 210029, Jiangsu Province, China. hjzhang06@163.com
Telephone: +86-25-83718836-6920
Fax: +86-25-83674636

Received: January 10, 2018
Peer-review started: January 10, 2018
First decision: February 5, 2018
Revised: March 5, 2018
Accepted: March 7, 2018
Article in press: March 7, 2018
Published online: April 7, 2018

Abstract

AIM

To analyze the alterations of fecal microbiota in Chinese patients with inflammatory bowel disease (IBD).

METHODS

Fecal samples from 15 patients with Crohn's disease (CD) (11 active CD, 4 inactive CD), 14 patients with active ulcerative colitis (UC) and 13 healthy individuals were collected and subjected to 16S ribosomal DNA (rDNA) gene sequencing. The V4 hypervariable regions of 16S rDNA gene were amplified from all samples and sequenced by the Illumina MiSeq platform. Quality control and operational taxonomic units classification of reads were calculated with QIIME software. Alpha diversity and beta diversity were displayed with R software.

RESULTS

Community richness (chao) and microbial structure in both CD and UC were significantly different from those in normal controls. At the phyla level, analysis of the microbial compositions revealed a significantly greater abundance of *Proteobacteria* in IBD as compared to

that in controls. At the genera level, 8 genera in CD and 23 genera in UC (in particular, the *Escherichia* genus) showed significantly greater abundance as compared to that in normal controls. The relative abundance of *Bacteroidetes* in the active CD group was markedly lower than that in the inactive CD group. The abundance of *Proteobacteria* in patients with active CD was nominally higher than that in patients with inactive CD; however, the difference was not statistically significant after correction. Furthermore, the relative abundance of *Bacteroidetes* showed a negative correlation with the CD activity index scores.

CONCLUSION

Our study profiles specific characteristics and microbial dysbiosis in the gut of Chinese patients with IBD. *Bacteroidetes* may have a negative impact on inflammatory development.

Key words: Crohn's disease; Ulcerative colitis; Chinese; Microbial dysbiosis; 16S ribosomal DNA

Core tip: Intestinal microbiota plays an important role in the pathogenesis of inflammatory bowel disease. However, there are few data on global alteration of microbiota in Chinese patients. In this study, fecal samples were subjected to 16S ribosomal DNA sequencing. Community richness and microbial structure in inflammatory bowel disease were significantly different from those in normal controls. The relative abundance of *Bacteroidetes* in the active Crohn's disease group was significantly lower than that in the inactive Crohn's disease group, and it showed a negative correlation with Crohn's disease activity index, which indicates that *Bacteroidetes* may have a negative impact on inflammatory development.

Ma HQ, Yu TT, Zhao XJ, Zhang Y, Zhang HJ. Fecal microbial dysbiosis in Chinese patients with inflammatory bowel disease. *World J Gastroenterol* 2018; 24(13): 1464-1477 Available from: URL: http://www.wjgnet.com/1007-9327/full/v24/i13/1464.htm DOI: http://dx.doi.org/10.3748/wjg.v24.i13.1464

INTRODUCTION

Inflammatory bowel disease (IBD) is characterized by chronic relapsing inflammation of the gastrointestinal tract and includes two main clinical phenotypes: Crohn's disease (CD) and ulcerative colitis (UC). The etiopathogenesis of IBD is not completely understood. Several disease susceptibility genes, such as *NOD2*, *ATG16L1* and *IRGM*, have been implicated in its pathogenesis[1]. However, the rapid increase in the incidence of IBD cannot be explained by genetic factors alone; an accumulating body of evidence indicates that environmental factors play a key role in the development of IBD by triggering intestinal microbiota dysbiosis[2].

Currently available data from experimental models and clinical studies suggest that intestinal microbiota plays an important role in the pathogenesis of IBD[3]. The alterations in intestinal microbiota related to IBD include decrease in *Bacteroides, Firmicutes, Clostridia, Ruminococcaceae, Bifidobacterium, Lactobacillus*, and *Faecalibacterium prausnitzii,* but increase in *Gamma Proteobacteria* and presence of *Fusobacterium* and *Escherichia coli*, especially *adherent-invasive E. coli* (AIEC). In addition, IBD is also associated with alterations in the microbial metabolic functions, including decrease of short-chain fatty acids (SCFAs) and amino acid biosynthesis, and increase of auxotrophy, amino acid and sulfate transport, oxidative stress, and type II secretion system[4-7].

With respect to changes (increase or decrease) in intestinal microbiota in IBD patients, some conflicting findings have been reported for several bacteria, including *Bifidobacterium, Clostridiales, Clostridium difficile, Campylobacter, Helicobacter* and *Faecalibacterium prausnitzii*[8]. For example, the levels of *F. prausnitzii* in IBD patients were found to be reduced in several studies[9-11]. However, one study of *de novo* pediatric IBD revealed an increase in *F. prausnitzii* in CD, but not in UC[12]. Another study of twins showed an increase in *F. prausnitzii* in patients with colonic CD, but a decrease of *F. prausnitzii* in patients with ileal CD[13].

The intestinal microbiota of Western IBD patients has been extensively studied. However, the intestinal microbial profiles of Chinese IBD patients are not well characterized[14]. In the present study, we profiled and compared the fecal microbial community of IBD patients at different disease stages and healthy controls by using 16S rDNA amplicon-based analysis.

MATERIALS AND METHODS

Study population

Twenty-nine IBD patients (11 active CD, 4 inactive CD and 14 active UC patients) who regularly visited the First Affiliated Hospital of Nanjing Medical University (Jiangsu, China) from 2014 to 2016 were recruited to the study. The diagnosis of IBD was based on standard clinical, endoscopic, radiological and histological criteria[15]. The control group consisted of sex- and age-matched healthy subjects. Patients with IBD who met any of the following criteria were excluded: (1) use of antibiotics, probiotics or prebiotics in the 3-mo period immediately preceding the sampling time point; (2) current infectious diarrhea; and (3) malignancy. UC activity was evaluated using the Mayo score[16]; active UC was defined as UC disease activity index > 2. Activity of CD was scored by Crohn's disease activity

index (CDAI)[17]; active CD was defined as a CDAI > 150. Written informed consent was obtained from all subjects prior to their enrollment and the study was approved by the Ethics Committee at the First Affiliated Hospital of Nanjing Medical University, Jiangsu, China.

Fecal sample collection and extraction of genomic DNA

Fecal samples were collected from all subjects and subsequently stored at -80 ℃ within 2 h to prevent exposure of anaerobic bacteria to oxygen and to avoid bacterial overgrowth prior to DNA extraction. Genomic DNA was extracted from fecal samples using the QIAamp DNA Stool Mini Kit (Qiagen, Hilden, Germany) according to the manufacturer's instructions. Feces (200 mg) was added to a 2-mL screw cap vial containing 300 mg of 0.1-mm glass beads (Sigma, St. Louis, MO, United States) which was maintained on ice. The samples were added of 1.4 mL ASL buffer and then subjected to bead beating (45 s, speed 6.5) twice using a FastPrep-24 machine (MP Biomedicals, Solon, OH, United States) before the initial incubation for heat and chemical lysis at 95 ℃ for 5 min. Subsequent DNA extraction was performed following the QIAamp kit protocol for pathogen detection.

Sequencing

16S rDNA genes of V4 regions were amplified using specific primer with the barcode. All PCR reactions were carried out with Phusion® High-Fidelity PCR Master Mix (New England Biolabs, Ipswich, MA, United States). The same volume of 1 × loading buffer (containing SYB green) was mixed with PCR products and electrophoresis on 2% agarose gel was carried out for detection. Samples with the bright main band between 400-450 bp were chosen for further experiments. PCR products were mixed in equidensity ratios. The mixture of PCR products was subsequently purified with Qiagen Gel Extraction Kit. Sequencing libraries were generated using TruSeq®DNA PCR-Free Sample Preparation Kit (Illumina, San Diego, CA, United States) following manufacturer's recommendations, and index codes were added. The library quality was assessed on the Qubit@ 2.0 Fluorometer (Thermo Scientific, Waltham, MA, United States) and Agilent Bioanalyzer 2100 system. Finally, the library was sequenced on an Illumina MiSeq platform and 250 bp paired-end reads were generated.

Data analysis

Paired-end reads were assigned to samples based on their unique barcode and truncated by cutting off the barcode and primer sequence. Paired-end reads were merged using FLASH (V1.2.7, http://ccb.jhu.edu/software/FLASH/)[18], which was designed to merge paired-end reads when at least some of the reads overlapped the read generated from the opposite end of the same DNA fragment, and the splicing sequences were called raw tags. Quality filtering of the raw tags was performed under specific filtering conditions to obtain high-quality clean tags[19] according to the QIIME (V1.7.0, http://qiime.org/index.html)[20] quality controlled process. The tags were compared with the reference database (Gold database, http://drive5.com/uchime/uchime_download.html) using UCHIME algorithm (UCHIME Algorithm, http://www.drive5.com/usearch/manual/uchime_algo.html)[21] to detect chimera sequences, and then the chimera sequences were removed[22]. Finally, the effective tags were obtained. Analysis of sequences was performed with Uparse software (Uparse v7.0.1001, http://drive5.com/uparse/)[23]. Sequences with ⩾ 97% similarity were assigned to the same operational taxonomic units (OTUs). Representative sequence for each OTU was screened for further annotation. For each representative sequence, the GreenGene Database (http://greengenes.lbl.gov/cgi-bin/nph-index.cgi)[24] was used based on the RDP classifier (version 2.2, http://sourceforge.net/projects/rdp-classifier/)[25] algorithm to annotate taxonomic information.

In order to study the phylogenetic relationship of different OTUs, and the difference of the dominant species in different samples (groups), multiple sequence alignment was conducted using the MUSCLE software (version 3.8.31, http://www.drive5.com/muscle/)[26]. OTUs' abundance information was normalized using a standard sequence number corresponding to the sample with the least sequences. Subsequent analysis of alpha diversity and beta diversity were all performed based on this output normalized data. Alpha diversity and beta diversity were calculated with QIIME (version 1.7.0) and displayed with R software (version 2.15.3).

Statistical analysis was performed using Statistical Package for Social Sciences version 19.0 (SPSS Inc., Chicago, IL, United States). The microbiota data and community estimates were analyzed by Kruskal-Wallis one-way analysis of variance to compare median values of microbiota data between CD, UC and controls. Spearman correlation analysis was used to analyze the correlation between intestinal bacterial abundance and intestinal inflammatory status. *P* values were corrected for multiple comparisons using false discovery rate (FDR); $P < 0.05$ was considered statistically significant.

RESULTS

Patients' characteristics and sequencing data

Fecal samples from patients with active CD (n = 11), inactive CD (n = 4), active UC (n = 14), and 13 healthy individuals were analyzed in the current study. The median disease duration in patients with CD and UC was 10 mo (range: 3-48 mo) and 30 mo (range: 2-93 mo), respectively. Detailed clinical characteristics of the study subjects are presented in Table 1.

Paired-end reads were generated with the Illumina MiSeq platform. The reads with sequencing adapters,

Table 1 Clinical characteristics of enrolled patients

	CD	UC	Control
n	15	14	13
Age, mean ± SD, yr	37.7 ± 13.0	37.5 ± 17.1	39.8 ± 14.3
Sex, male/female	11/4	7/7	10/3
Disease duration in months, median (range)	10 (3-48)	30 (2-93)	-
Smoking habits	4 (26.7)	1 (7.1)	2 (15.4)
Abdominal surgery	4 (26.7)	0	0
Montreal A (age of onset)			
A1 (< 17)	1 (6.7)	-	-
A2 (17-40)	7 (46.7)	-	-
A3 (> 40)	7 (46.7)	-	-
Montreal L (location)			
L1 (ileal)	8 (53.3)	-	-
L2 (colonic)	1 (6.7)	-	-
L3 (ileocolonic)	6 (40)	-	-
L4 (upper gastrointestinal tract)	0	-	-
Montreal B (behavior)			
B1(nonstricturing, nonpenetrating)	8 (53.3)	-	-
B2 (stricturing)	6 (40)	-	-
B3 (penetrating)	1 (6.7)	-	-
p (perianal disease)	4 (26.7)	-	-
Montreal			
E1 ulcerative proctitis	-	4 (28.6)	-
E2 left sided ulcerative colitis	-	5 (35.7)	-
E3 extensive ulcerative colitis	-	5 (35.7)	-
CDAI score			
< 150	4 (26.7)	-	-
150-220	5 (33.3)	-	-
221-450	6 (40)	-	-
> 450	0	-	-
Mayo score			
0-2	-	0	-
3-5	-	7 (50.0)	-
6-10	-	5 (35.7)	-
11-12	-	2 (14.3)	-
Therapy			
5-ASA	14 (93.3)	14 (100)	-
Azathioprine	2 (13.3)	0	-
Steroids	1 (6.7)	6 (42.9)	-
Infliximab	0	0	-

Data are presented as *n* (%). 5-ASA: 5-aminosalicylic acid; CD: Crohn's disease; CDAI: CD activity index; SD: Standard deviation; UC: Ulcerative colitis.

N base, poly base, and low quality were filtered out with default parameters. High quality paired-end reads were combined to tags based on overlaps. A total of 1747775 tags were obtained with an average of 41613 tags per sample; the average length was 252 bp. Filtered tags were clustered into OTUs at 97% similarity and a total of 878 OTUs were generated from 42 samples (see Supplementary File 1).

Characteristics of the microbial community in IBD patients and controls

When comparing bacterial alpha diversity, including community richness (observed species, chao, and ace) and diversity (Shannon and Simpson) between CD, UC and control groups, we found overall differences with respect to each diversity index (Figure 1). Significant differences ($P < 0.05$) with respect to community richness (chao) were observed both between CD and controls and between UC and controls. The observed species and ace indices of CD patients were lower than those of controls; however, the differences were not statistically significant ($P > 0.05$). Moreover, the pattern of richness was found to be similar in CD and UC. When considering the species diversity of microbiota (Shannon and Simpson), the differences between each group were not statistically significant.

We subsequently surveyed the alpha diversity in IBD patients at different disease stages (see Supplementary Figure 1). Generally, the richness indices in IBD patients showed a decreasing trend (controls > inactive CD > active CD), but the between-group differences were not statistically significant. However, the diversity indices in IBD patients were not significantly different from those in controls.

Microbial community structures in IBD are distinct from those in normal controls

We used principal component analysis (PCA) to investigate the community structure of microbiota in CD, UC and controls. We found that samples tended to cluster together

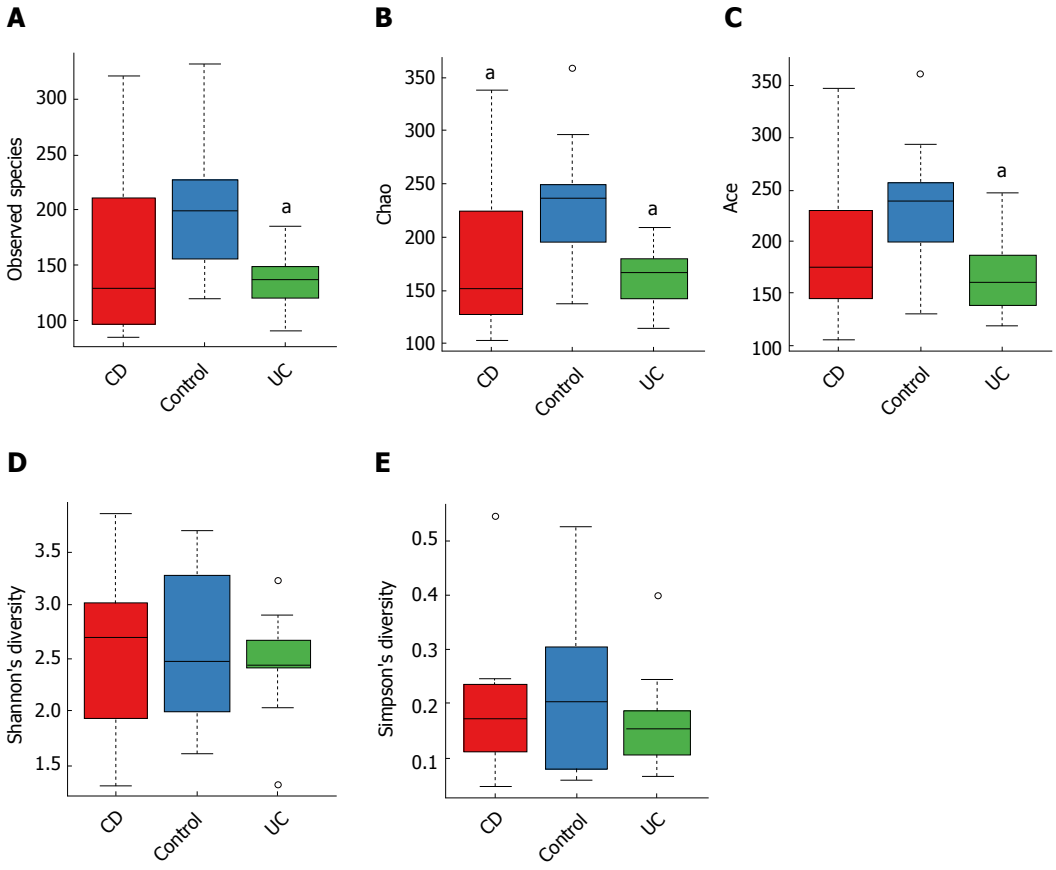

Figure 1 Alpha diversity indices boxplot, including community richness (observed species, chao, ace) and diversity (Shannon, Simpson) varied among each group. A: Observed species; B: Chao; C: Ace; D: Shannon; E: Simpson. [a]*P* < 0.05 *vs* control. CD: Crohn's disease; UC: Ulcerative colitis.

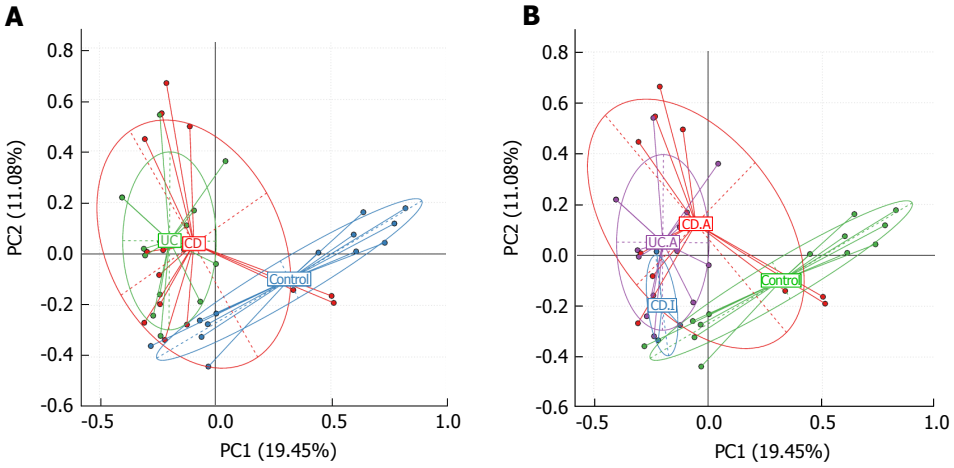

Figure 2 Principal component analysis based on the overall structure of the fecal microbiota in the entire study population. Each data point represents an individual sample. A: Disease phenotype group; B: Stages of disease group. CD: Crohn's disease; CD.A: Active CD; CD.I: Inactive CD; UC: Ulcerative colitis; UC.A: Active UC.

based on disease; however, to a certain extent, there was an overlap between all groups. IBD samples were mostly distinct from those of normal controls, which indicated differences with respect to community structure of the microbiota between IBD and controls (Anosim: CD *vs* control, $P = 0.02$; UC *vs* control, $P = 0.001$). However, samples of CD and UC were located closely, which suggested a similar bacterial community structure in the context of both CD and UC (Anosim: $P = 0.133$) (Figure 2A).

Next, we visualized the PCA to compare the microbial structure in patients at different disease stages (Figure 2B). The results showed that samples could be well separated between active CD and controls

Table 2 Significant differences in microbial distribution of taxa (phylum and genus) in patients with inflammatory bowel disease

	CD	UC	CD/UC	CD.A/CD.I	CD.A/UC.A
Firmicutes					
Abiotrophia[1]	↑c				
Butyricicoccus	↓c		c[3]		
RFN20[1]	↑c		c[2]		
Pseudoramibacter_Eubacterium[1]	↑b		c[2]		
Holdemania[1]		↓c			c[2]
02d06		↓c	c[2]		c[2]
Lachnobacterium		↓c			
Megamonas		↓c			
Mitsuokella	↓c	↓c			
Granulicatella		↑b			
Peptostreptococcus		↑b			
Schwartzia[1]		↑b			
Moryella[1]			c[3]		
Staphylococcus[1]			c[3]		c[3]
Epulopiscium					c[2]
Sarcina					c[2]
Bacteroidetes				b[3]	
Alistipes		↓c			
Butyricimonas		↓c			
Capnocytophaga[1]		↑c	c[3]		c[3]
Prevotella		↓c			
Proteobacteria	↑b	↑b			
Escherichia	↑c	↑b			
Haemophilus	↓c		b[3]		b[3]
Desulfovibrio		↓c	b[2]		c[2]
Oxalobacte[1]		↓c			
Janthinobacterium[1]		↑b	b[3]		
Campylobacter		↑b			
Cardiobacterium[1]			c[3]		
Lautropia[1]			c[3]		
Lupinus[1]			c[3]		
Shewanella[1]			b[3]		
Actinobacteria					
Actinomyces		↑c			
Eggerthella[1]		↑b			
Corynebacterium[1]		↑b	c[3]		b[3]
Slackia[1]			b[2]		c[2]
Synergistetes					
Pyramidobacter[1]		↓c			
Synergistes[1]		↓c			
TG5[1]			c[3]		
Spirochaetes		↑c			c[3]
Lentisphaerae		↓c			c[2]
Victivallis[1]	↓c	↓c			

↑ and ↓ relative to controls; [1]Relative abundance of genera < 0.01%; [2]Increase in value; [3]Decrease in value. [a]$P < 0.05$; [b]$P < 0.01$; [c]$P < 0.001$. CD: Crohn's disease; CD.A: Active CD; CD.I: Inactive CD; IBD: Inflammatory bowel disease; UC: Ulcerative colitis; UC.A: Active UC.

(Anosim: $P = 0.016$) as well as between active CD and active UC (Anosim: $P = 0.01$). However, there were no distinct microbiota structural patterns apparent between active CD and inactive CD groups, although the samples seemed to be clearly separated (Anosim: $P = 0.719$). There was also no separation between inactive CD and controls (Anosim: $P = 0.564$) based on the PCA. Our results indicated that the bacterial community structure in active CD was different from that in active UC; however, there was no difference with respect to the alterations of bacterial community structure in fecal samples of the total UC and CD patients.

Overall taxonomic analysis of IBD patients and controls

Taxonomic composition distribution histograms of each sample were summarized at the phyla level (Figure 3A). The dominant sequences belonged to four bacterial phyla (*Bacteroidetes*, *Firmicutes*, *Proteobacteria* and *Fusobacteria),* which accounted for over 97% of taxonomy generally (Figure 3B). Among all the relatively abundant dominant strains in IBD and normal controls, *Bacteroidetes* was, as a rule, the most abundant bacterial phylum.

Phylum-level analysis (Figure 3B, Table 2) revealed a nominal decrease in the relative abundance of *Bacteroidetes* in both CD and UC patients (CD *vs* control, 47.49% *vs* 66.85%, $P = 0.015$; UC *vs* control, 48.94% *vs* 66.85%, $P = 0.019$); however, these differences were not significant after adopting the FDR. On the contrary, *Proteobacteria* was significantly

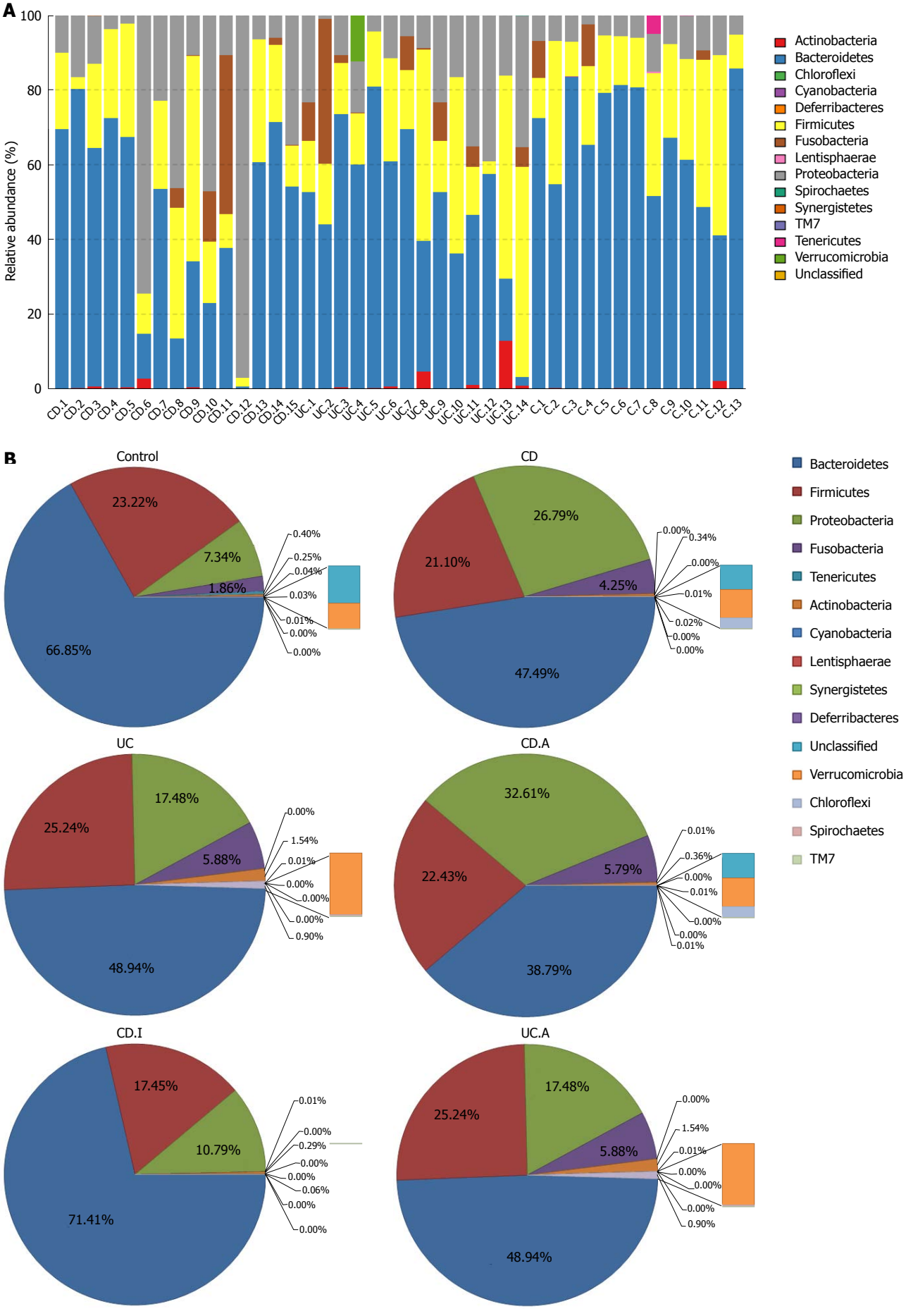

Figure 3 Taxonomic composition distribution in samples of phylum level. A: Individually; B: Integrally. CD: Crohn's disease; CD.A: Active CD; CD.I: Inactive CD; UC: Ulcerative colitis; UC.A: Active UC.

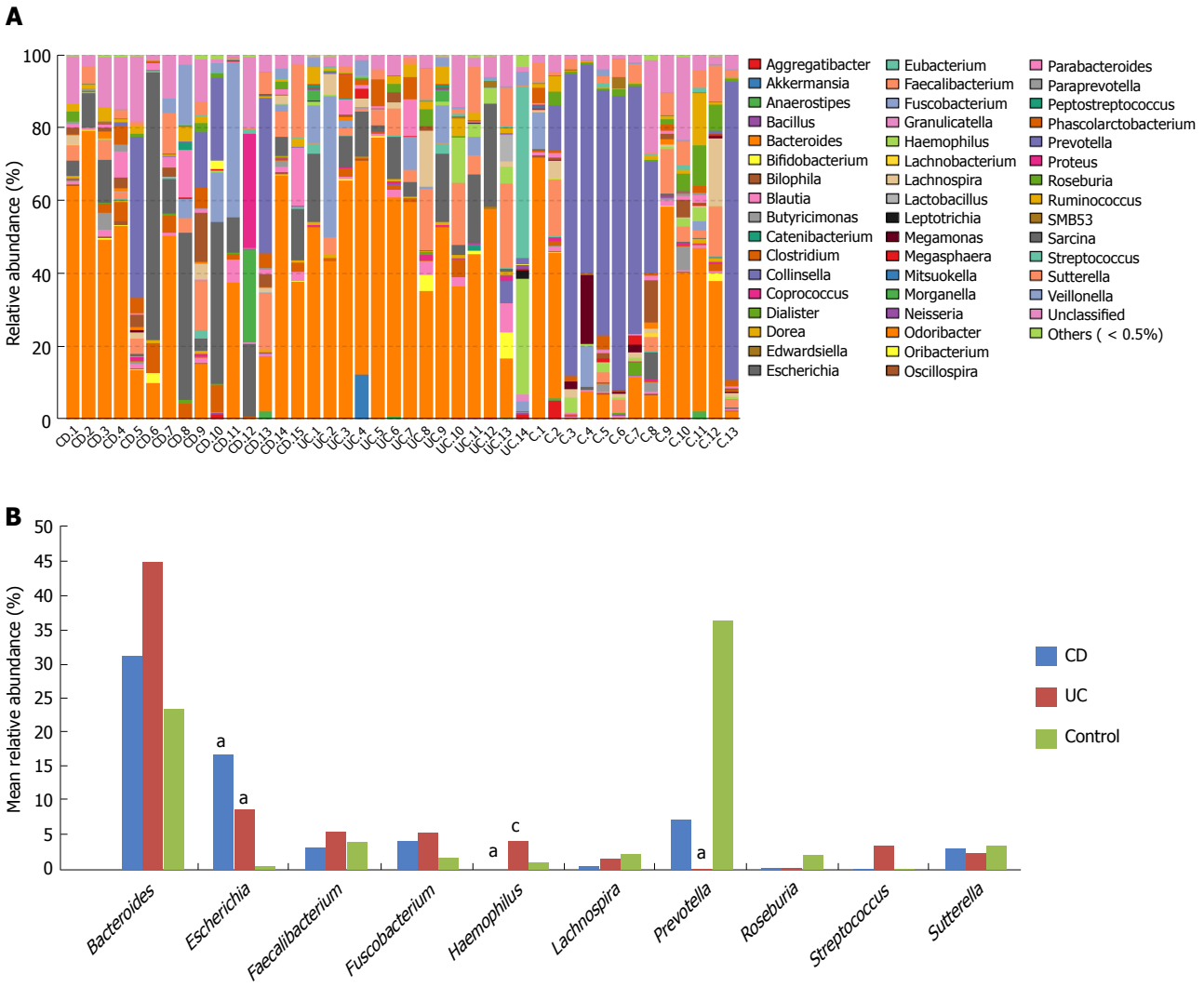

Figure 4 A: The taxonomic composition distribution in samples of genus level; B: Genera shown represent the 10 most abundant genera of CD, UC and control. $^{a}P < 0.05$ *vs* control, $^{c}P < 0.05$ *vs* CD. CD: Crohn's disease; UC: Ulcerative colitis.

increased in both CD and UC, as compared to that in controls (CD *vs* control, 26.79% *vs* 7.34%, $P = 0.002$; UC *vs* control, 17.48% *vs* 7.34%, $P = 0.005$). In addition, no *Spirochaetes* phylum was detected in CD and controls but it was observed in UC (0.015%). Similarly, *Lentisphaerae* phylum was found in the control group (accounting for 0.031%), but almost none was found in patients with IBD.

At the genus level, the relative abundance of all genera varied between different samples (Figure 4A). The top 10 abundant genera in UC, CD and controls were *Bacteroides*, *Escherichia*, *Faecalibacterium*, *Fusobacterium*, *Haemophilus*, *Lachnospira*, *Prevotella*, *Roseburia*, *Streptococcus*, and *Sutterella* (Figure 4B). Among these, the relative abundance of *Escherichia* in CD and UC was significantly higher than that in controls. In addition, abundance of Haemophilus in CD and Prevotella in UC patients were both markedly lower than that in normal controls. Moreover, the abundance of *Haemophilus* in CD was dramatically lower than that in UC. Besides the top 10 abundant genera, the relative abundance of remaining genera was comparable between IBD patients and normal controls (Table 2). The abundance of 12 genera, *Butyricicoccus*, *Mitsuokella, 02d06*, *Actinomyces*, *Alistipes*, *Butyricimonas*, *Campylobacter*, *Desulfovibrio*, *Granulicatella*, *Lachnobacterium*, *Megamonas* and *Peptostreptococcus*, was significantly different after correction among each group within the community; the sequence percentages for each of these 12 genera were more than 0.01%.

Taxonomic comparisons in IBD patients at different disease stages

On analysis of the alterations at the phyla level between active CD and inactive CD, we found that the dominant bacterial phyla were the same as described earlier (accounting for over 99% of taxonomy), with the exception that *Fusobacteria* was replaced by *Actinobacteria* in inactive CD (Figure 3B, Table 2). However, the abundance of *Bacteroidetes* was dramatically decreased in active CD group, as compared to that in the inactive CD group (CD.A

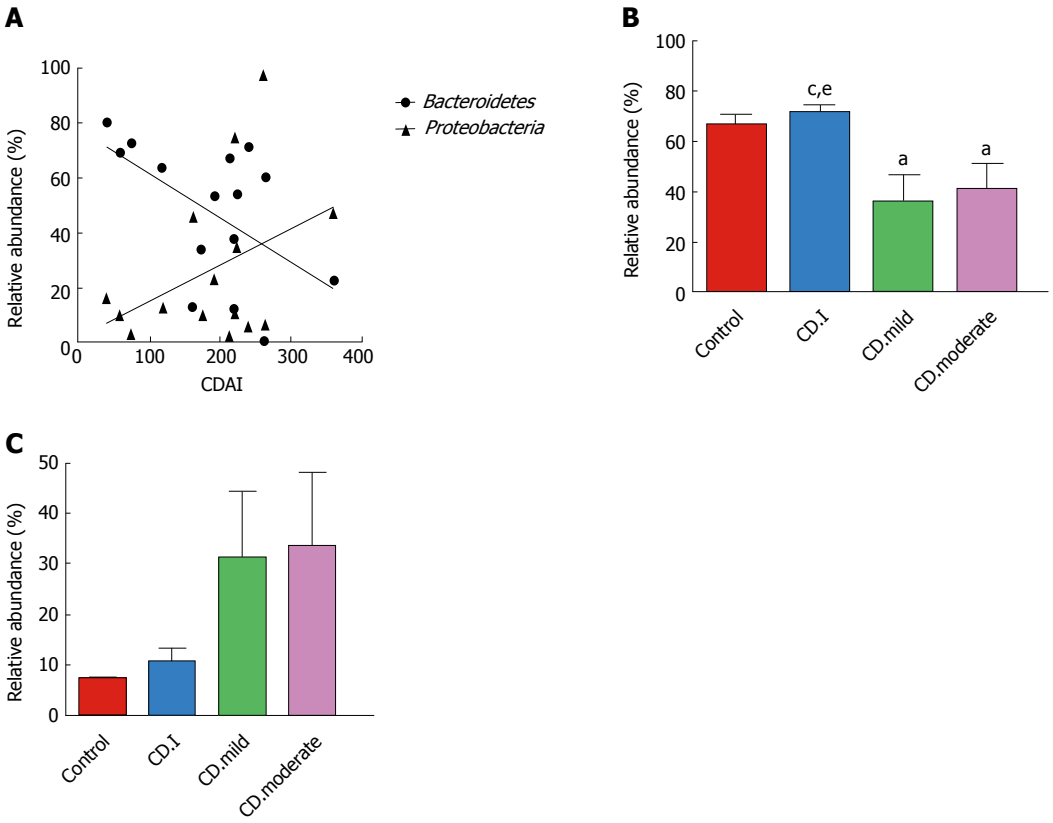

Figure 5 Correlation of the relative abundance of *Bacteroidetes* and *Proteobacteria* with Crohn's disease activity index scores (A). *Bacteroidetes* (r = -0.538, P = 0.039); *Proteobacteria* (r = 0.250, P = 0.369); B: Microbial composition of *Bacteroidetes* in patients with inactive/mild/moderate CD and in control; C: Microbial composition of *Proteobacteria* in patients with inactive/mild/moderate CD and in controls. $^{a}P < 0.05$ *vs* control; $^{c}P < 0.05$ *vs* CD.mild; $^{e}P < 0.05$ *vs* CD.moderate. CDAI: CD activity index; CD.I: Inactive CD; CD.mild: Mild CD; CD.moderate: Moderate CD.

vs CD.I, 38.79% *vs* 71.41%, P = 0.001). The abundance of *Proteobacteria* was just nominally increased in active CD, as compared to that in inactive CD (P = 0.023), which did not hold significance after correction. Similarly, no differences were detected with respect to the remaining dominant bacteria between active CD and inactive CD. Microbiota in active CD and active UC were found to be similar at the phyla level.

We then investigated the genera with percentages of sequences > 0.01% of community in different phases of IBD and found that the abundance of *Bacteroides* and *Prevotella* in active CD were only nominally different from that in inactive CD. However, *Desulfovibrio*, *02d06*, *Epulopiscium*, and *Sarcina* detected in active CD were markedly higher than that in active UC, while *Haemophilus* was markedly lower than that in active UC (Table 2).

Association between the inflammatory index of CD patients and microbiome

We assessed the correlation between the relative abundance of *Bacteroidetes* and CDAI scores of each CD patient; surprisingly, we found a negative correlation between the two (r = -0.538, P = 0.039) (Figure 5A). On the contrary, there was a trend of positive correlation between the abundance of *Proteobacteria* and CDAI (r = 0.250, P = 0.369); however, the correlation was not statistically significant.

Next, we analyzed the correlation between microbial composition and disease severity. Patients with mild and moderate CD had notably decreased levels of *Bacteroidetes* as compared to that in patients with inactive CD; however, no significant difference in this respect was noted between patients with mild and moderate CD (Figure 5B). Interestingly, *Proteobacteria* exhibited a noteworthy trend (controls < inactive CD < mild CD < moderate CD); however, the trend did not attain statistical significance (Figure 5C).

Effect of age and sex on intestinal microbial compositions

Although IBD mostly occurs in young adults (20- to 30-years-old), it can happen at any age. In the present research, no correlation was observed between microbial composition and age (see Supplementary Figure 2). Considering that most participants in our study (with the exception of one patient aged 14 years with UC) were adults, we divided the participants into two groups: age < 40 years and age > 40 years. However, no significant difference in microbial compositions was observed between the two groups (see Supplementary Table 1). On subgroup analysis based on sex, no notable

differences were observed between male and female patients in either subject subgroup (see Supplementary Table 2).

DISCUSSION

IBD is one of the most frequently studied human diseases linked to the gut microbiota. Distinctive microbial composition and its interaction with the host immunological response are believed to play a critical role in the pathogenesis of IBD[27,28]; however, several aspects of the relationship are not well-characterized. In this study, we demonstrated differences with respect to fecal microbiota between Chinese IBD patients and healthy controls based on 16S rDNA sequencing analysis.

The dominant dysbiosis pattern unraveled by the present study was the decrease in community abundance of fecal microbiota both in CD and UC patients; while microbial diversity in CD patients was lower than that in controls, the difference was not statistically significant. Previous studies have shown reduced diversity of fecal microbiota in both Western[29,30] and Chinese patients with IBD[14], as compared to that in healthy controls. These inconsistencies are likely attributable to differences with respect to study design, stage of disease, or technique employed to survey the gut microbiota. The reasons for the changes of diversity in these conditions are still not known. Indeed, despite general trends such as a reduction in diversity, the response to IBD may, to some extent, be subject-specific.

We analyzed the bacterial community structure of microbiota in IBD patients and healthy individuals. The results showed distinct differences both in CD and UC, as compared to controls; however, the microbiota were similar within CD and UC groups or within active CD and inactive CD groups, which were not structurally distinguishable according to PCA. These data were also consistent with the previous studies conducted in Chinese and Western populations[14,31]. However, Forbes *et al*[32] found a difference in the structure of microbiota between CD and UC. This result differed from those of other studies, as this study involved analysis of intestinal mucosa, while other studies were based on fecal analysis.

Detailed compositional alterations in fecal microbiota in IBD patients were detected at distinct taxonomic levels. The principle finding in our study was that the phylum *Proteobacteria* was significantly increased in IBD patients, which was in agreement with a consistent finding across published literature[33,34]. The genus *Escherichia*, especially *Escherichia coli* (data not shown), was also found to be notably higher in IBD patients, as compared to that in normal controls. *Escherichia coli*, particularly AIEC, as an important pathobiont that may play a role in IBD development, has been isolated from ileal CD biopsy specimens[35]. The initial lesions in the colon mucosa can be aggravated by alpha-hemolysin secreted by *Escherichia coli*, which can damage host cell membranes and epithelial barrier[36].

Moreover, both *E. coli* and *Campylobacter* (affiliated with *Proteobacteria*) are known to release cytolethal distending toxins, which leads to cell cycle arrest, chromatin fragmentation and apoptosis, all of which are involved in the pathogenesis of IBD[37].

In the present study, patients with IBD exhibited relatively less number of *Bacteroidetes* compared to that in controls. The lower proportion of *Bacteroidetes* was mainly attributable to notably reduced abundance of *Prevotella* genus. The results were largely similar to those of another study which employed 16S rDNA sequencing analysis[38]. Actually, alterations in *Bacteroidetes* in CD still remain controversial. Rehman *et al*[39] reported increased *Bacteroidetes* in CD patients and even demonstrated a notable increase in transcriptional activity, as compared to that in controls. Further studies are needed to clarify this issue. To minimize potential confounding factors, future studies should define gut dysbiosis in detail. Moreover, prospective cohort studies on newly diagnosed treatment-naïve patients will provide more definitive evidence in this respect.

In the present study, we documented increased abundance of *Haemophilus* and decreased *Desulfovibrio* (affiliated with *Proteobacteria*) in patients with UC. These findings were not observed in a previous study on fecal microbiota dysbiosis conducted by Chen *et al*[14] in Chinese patients with IBD. Recently, *Haemophilus* has been reported to contribute to oral dysbiosis in patients with IBD[40] and *Haemophilus* spp., like the *Enterobacteriaceae*, are well adapted to survive under conditions of increased oxidative stress[41]. To our knowledge, Rowan *et al*[42] demonstrated an increase of *Desulfovibrio* (sulfate-reducing bacteria) in patients with UC. *In vitro* studies have shown that 5-aminosalicylic acid (5-ASA) inhibits fecal sulfide production and fecal samples from patients not treated with this drug revealed higher levels of sulfide[43]. It is conceivable that all participants in the present study were treated with 5-ASA, which may have contributed to the opposite phenomenon.

In addition, the study found an abundance of *Butyricicoccus*, *Mitsuokella*, *02d06*, *Lachnobacterium* and *Megamonas* (all affiliated with *Clostridia* class, *Firmicutes* phylum), which are obligate anaerobes. These were found significantly decreased in IBD patients in the current study. Dysanaerobiosis in patients with UC was observed recently[44] and there seems to be a shift from anaerobiosis in healthy state to dysanaerobiosis in IBD, with an elevated oxygen level in the gut[45]. Furthermore, studies conducted on experimental colitis models showed decrease in obligate anaerobes of *Firmicutes* and increase in facultative anaerobes of *Proteobacteria*, which indicates a role of oxygen in gut dysbiosis[46]. In fact, both *Butyricicoccus* (affiliated

with *Ruminococcaceae* family) and *Lachnobacterium* (affiliated with *Lachnospiraceae* family) produce SCFAs, which are known as the primary energy source for colonic epithelial cells[47] and were shown to induce the expansion of colonic regulatory T cells[48]. These alterations in microbial composition suggested that reduction in beneficial microbiota (*Clostridia* class and SCFA-producing bacteria) is more associated with IBD patients compared to the increment of pathobionts (*Escherichia* and *Campylobacter*).

When analyzing the fecal microbiota at different disease stages of IBD, only the abundance of *Bacteroidetes* was dramatically decreased in active CD, as compared to that in inactive CD. About the relationship between microbiome and disease activity, we also found a negative correlation between the relative abundance of *Bacteroidetes* and CDAI in the present study. The relative abundance of *Bacteroidetes* in active CD patients was lower than that in inactive CD or controls, but the relative abundance of *Bacteroidetes* was similar between mild and moderate CD. All these findings suggest that *Bacteroidetes* may have a negative impact on inflammatory development.

Potential links between age or sex and microbial compositions have been suggested recently[49]. Gut microbiota vary in different age groups: infants, adults or the elderly. The microbiota in infants is often affected by the birth route, feeding patterns and illness history[50]. Not until adulthood does the microbiota become stable, complex and shows improved resilience against perturbations[51]. Then, the stability decreases in the elderly ($\geqslant$ 65 years of age)[52]. However, we did not find the effect of age and sex on microbiota in the current study. So, a different role for the microbiota in disease initiation and progression should be researched.

Our study faces several limitations. First of all, due to the small sample number and relatively high variability of microbial composition in each group, some of the relative abundances of specific bacteria between groups could not reach statistical significance after adopting the FDR. Secondly, 16S rDNA sequencing mainly focuses on the taxonomic profiling rather than providing greater insight into the function of the intestinal microbiota in disease[53,54]. Thirdly, the nature and extent of difference between the fecal microbiota and mucosa-associated microbiota in IBD remains unclear. Controversy still exists between them because of different techniques used in separate studies[55]. Several studies indicated that the fecal microbiota and mucosa-associated microbiota were similar[13,56,57]. However, some studies have found a significant difference between them[14,58,59]. It seems that the fecal microbiota represents a combination of a separate nonadherent luminal population and shed mucosal bacteria[59]. Further study with a large population is required to confirm our data and mucosa-associated microbiota needs to be researched in Chinese patients with IBD.

In conclusion, we presented a comprehensive analysis of fecal microbiota in Chinese patients with IBD. Significant differences in microbial composition of patients with IBD and controls were observed. Additionally, the negative correlation between *Bacteroidetes* and CDAI suggested that *Bacteroidetes* might have a negative impact on development of inflammation.

ARTICLE HIGHLIGHTS

Research background

Inflammatory bowel disease (IBD) is generally defined by two nonspecific inflammatory disorders, Crohn's disease (CD) and ulcerative colitis (UC), which are characterized by chronic persistent inflammation of the intestinal mucosa lining the intestinal tract. Recently, distinctive microbial composition and its interaction with the host immunological response are believed to play critical roles in the pathogenesis of IBD. Although the intestinal microbial composition of Western IBD patients has been extensively studied, there are conflicting reports about changes of the bacterial abundance. What's more, the intestinal microbial profiles of Chinese IBD patients are not well characterized. In the present study, we use 16S rDNA amplicon-based analysis to analyze the alterations of fecal microbiota in Chinese patients with IBD.

Research motivation

Although the microbial community is gaining increasing attention for its influence on IBD, there is a lack of data on global alteration of microbiota in Chinese patients and the relationship is poorly understood. This study would characterize the important differences of fecal microbiota between Chinese IBD patients and healthy controls based on a 16S rDNA sequencing analysis, hoping to explore which kinds of the microbiota could be involved in the pathogenesis of IBD or providing important references for diagnosis or treatment of IBD.

Research objectives

The research aimed to investigate the differences in quantity, diversity and similarity of the fecal bacterial population taken from Chinese IBD patients at different stages of disease and healthy individuals.

Research methods

Twenty-nine IBD patients (11 active CD, 4 inactive CD and 14 active UC patients) from the First Affiliated Hospital of Nanjing Medical University (Jiangsu, China) and 13 sex and age well-matched healthy individuals were enrolled in the study. 16S rDNA amplicon-based sequencing was used to analyze the fecal microbiota of each sample.

Research results

In this study, community richness (chao) and microbial structure in IBD were significantly different from those in normal controls. The relative abundance of *Bacteroidetes* in the active CD group was significantly lower than that in the inactive CD group, and it showed a negative correlation with Crohn's disease activity index (CDAI). At the phyla level, the abundance of *Proteobacteria* was significantly higher in IBD than in controls. At the genera level, 8 genera in CD and 23 genera in UC (in particular, the Escherichia genus) showed significantly greater abundance as compared to that in normal controls.

Research conclusions

Our study presented a comprehensive analysis of fecal microbiota in the gut of Chinese patients with IBD. Significant differences in microbial composition of patients with IBD and controls were observed. Additionally, the negative correlation between *Bacteroidetes* and CDAI suggested that *Bacteroidetes* might have a negative impact on development of inflammation.

Research perspectives

Fecal microbial examination is noninvasive and easily collected compared

with the mucosal biopsy, which may increase the risk of unexpected bleeding. However, the mucosa-associated microbiota is believed to directly affect epithelial and mucosal function. In the future, both the fecal and mucosa-associated microbiota should be investigated together to better understand the role of the intestinal microbiota in health and disease.

ACKNOWLEDGMENTS

The authors appreciate technical and statistical supports of BGI Tech Solutions Co., Ltd (Shenzhen, China) and would like to express thanks.

REFERENCES

1 **Khor B**, Gardet A, Xavier RJ. Genetics and pathogenesis of inflammatory bowel disease. *Nature* 2011; **474**: 307-317 [PMID: 21677747 DOI: 10.1038/nature10209]

2 **Molodecky NA**, Soon IS, Rabi DM, Ghali WA, Ferris M, Chernoff G, Benchimol EI, Panaccione R, Ghosh S, Barkema HW, Kaplan GG. Increasing incidence and prevalence of the inflammatory bowel diseases with time, based on systematic review. *Gastroenterology* 2012; **142**: 46-54.e42; quiz e30 [PMID: 22001864 DOI: 10.1053/j.gastro.2011.10.001]

3 **Knights D**, Lassen KG, Xavier RJ. Advances in inflammatory bowel disease pathogenesis: linking host genetics and the microbiome. *Gut* 2013; **62**: 1505-1510 [PMID: 24037875 DOI: 10.1136/gutjnl-2012-303954]

4 **Kostic AD**, Xavier RJ, Gevers D. The microbiome in inflammatory bowel disease: current status and the future ahead. *Gastroenterology* 2014; **146**: 1489-1499 [PMID: 24560869 DOI: 10.1053/j.gastro.2014.02.009]

5 **Krause DO**, Little AC, Dowd SE, Bernstein CN. Complete genome sequence of adherent invasive Escherichia coli UM146 isolated from Ileal Crohn's disease biopsy tissue. *J Bacteriol* 2011; **193**: 583 [PMID: 21075930 DOI: 10.1128/JB.01290-10]

6 **Kang S**, Denman SE, Morrison M, Yu Z, Dore J, Leclerc M, McSweeney CS. Dysbiosis of fecal microbiota in Crohn's disease patients as revealed by a custom phylogenetic microarray. *Inflamm Bowel Dis* 2010; **16**: 2034-2042 [PMID: 20848492 DOI: 10.1002/ibd.21319]

7 **Morgan XC**, Tickle TL, Sokol H, Gevers D, Devaney KL, Ward DV, Reyes JA, Shah SA, LeLeiko N, Snapper SB, Bousvaros A, Korzenik J, Sands BE, Xavier RJ, Huttenhower C. Dysfunction of the intestinal microbiome in inflammatory bowel disease and treatment. *Genome Biol* 2012; **13**: R79 [PMID: 23013615 DOI: 10.1186/gb-2012-13-9-r79]

8 **Li J**, Butcher J, Mack D, Stintzi A. Functional impacts of the intestinal microbiome in the pathogenesis of inflammatory bowel disease. *Inflamm Bowel Dis* 2015; **21**: 139-153 [PMID: 25248007 DOI: 10.1097/MIB.0000000000000215]

9 **Willing B**, Halfvarson J, Dicksved J, Rosenquist M, Järnerot G, Engstrand L, Tysk C, Jansson JK. Twin studies reveal specific imbalances in the mucosa-associated microbiota of patients with ileal Crohn's disease. *Inflamm Bowel Dis* 2009; **15**: 653-660 [PMID: 19023901 DOI: 10.1002/ibd.20783]

10 **Machiels K**, Joossens M, Sabino J, De Preter V, Arijs I, Eeckhaut V, Ballet V, Claes K, Van Immerseel F, Verbeke K, Ferrante M, Verhaegen J, Rutgeerts P, Vermeire S. A decrease of the butyrate-producing species Roseburia hominis and Faecalibacterium prausnitzii defines dysbiosis in patients with ulcerative colitis. *Gut* 2014; **63**: 1275-1283 [PMID: 24021287 DOI: 10.1136/gutjnl-2013-304833]

11 **Sokol H**, Pigneur B, Watterlot L, Lakhdari O, Bermúdez-Humarán LG, Gratadoux JJ, Blugeon S, Bridonneau C, Furet JP, Corthier G, Grangette C, Vasquez N, Pochart P, Trugnan G, Thomas G, Blottière HM, Doré J, Marteau P, Seksik P, Langella P. Faecalibacterium prausnitzii is an anti-inflammatory commensal bacterium identified by gut microbiota analysis of Crohn disease patients. *Proc Natl Acad Sci USA* 2008; **105**: 16731-16736 [PMID: 18936492 DOI: 10.1073/pnas.0804812105]

12 **Hansen R**, Russell RK, Reiff C, Louis P, McIntosh F, Berry SH, Mukhopadhya I, Bisset WM, Barclay AR, Bishop J, Flynn DM, McGrogan P, Loganathan S, Mahdi G, Flint HJ, El-Omar EM, Hold GL. Microbiota of de-novo pediatric IBD: increased Faecalibacterium prausnitzii and reduced bacterial diversity in Crohn's but not in ulcerative colitis. *Am J Gastroenterol* 2012; **107**: 1913-1922 [PMID: 23044767 DOI: 10.1038/ajg.2012.335]

13 **Willing BP**, Dicksved J, Halfvarson J, Andersson AF, Lucio M, Zheng Z, Järnerot G, Tysk C, Jansson JK, Engstrand L. A pyrosequencing study in twins shows that gastrointestinal microbial profiles vary with inflammatory bowel disease phenotypes. *Gastroenterology* 2010; **139**: 1844-1854.e1 [PMID: 20816835 DOI: 10.1053/j.gastro.2010.08.049]

14 **Chen L**, Wang W, Zhou R, Ng SC, Li J, Huang M, Zhou F, Wang X, Shen B, A Kamm M, Wu K, Xia B. Characteristics of fecal and mucosa-associated microbiota in Chinese patients with inflammatory bowel disease. *Medicine* (Baltimore) 2014; **93**: e51 [PMID: 25121355 DOI: 10.1097/MD.0000000000000051]

15 **Ouyang Q**, Tandon R, Goh KL, Pan GZ, Fock KM, Fiocchi C, Lam SK, Xiao SD. Management consensus of inflammatory bowel disease for the Asia-Pacific region. *J Gastroenterol Hepatol* 2006; **21**: 1772-1782 [PMID: 17074013 DOI: 10.1111/j.1440-1746.2006.04674.x]

16 **D'Haens G**, Sandborn WJ, Feagan BG, Geboes K, Hanauer SB, Irvine EJ, Lémann M, Marteau P, Rutgeerts P, Schölmerich J, Sutherland LR. A review of activity indices and efficacy end points for clinical trials of medical therapy in adults with ulcerative colitis. *Gastroenterology* 2007; **132**: 763-786 [PMID: 17258735 DOI: 10.1053/j.gastro.2006.12.038]

17 **Best WR**, Becktel JM, Singleton JW, Kern F Jr. Development of a Crohn's disease activity index. National Cooperative Crohn's Disease Study. *Gastroenterology* 1976; **70**: 439-444 [PMID: 1248701]

18 **Magoč T**, Salzberg SL. FLASH: fast length adjustment of short reads to improve genome assemblies. *Bioinformatics* 2011; **27**: 2957-2963 [PMID: 21903629 DOI: 10.1093/bioinformatics/btr507]

19 **Bokulich NA**, Subramanian S, Faith JJ, Gevers D, Gordon JI, Knight R, Mills DA, Caporaso JG. Quality-filtering vastly improves diversity estimates from Illumina amplicon sequencing. *Nat Methods* 2013; **10**: 57-59 [PMID: 23202435 DOI: 10.1038/nmeth.2276]

20 **Caporaso JG**, Kuczynski J, Stombaugh J, Bittinger K, Bushman FD, Costello EK, Fierer N, Peña AG, Goodrich JK, Gordon JI, Huttley GA, Kelley ST, Knights D, Koenig JE, Ley RE, Lozupone CA, McDonald D, Muegge BD, Pirrung M, Reeder J, Sevinsky JR, Turnbaugh PJ, Walters WA, Widmann J, Yatsunenko T, Zaneveld J, Knight R. QIIME allows analysis of high-throughput community sequencing data. *Nat Methods* 2010; **7**: 335-336 [PMID: 20383131 DOI: 10.1038/nmeth.f.303]

21 **Edgar RC**, Haas BJ, Clemente JC, Quince C, Knight R. UCHIME improves sensitivity and speed of chimera detection. *Bioinformatics* 2011; **27**: 2194-2200 [PMID: 21700674 DOI: 10.1093/bioinformatics/btr381]

22 **Haas BJ**, Gevers D, Earl AM, Feldgarden M, Ward DV, Giannoukos G, Ciulla D, Tabbaa D, Highlander SK, Sodergren E, Methé B, DeSantis TZ; Human Microbiome Consortium, Petrosino JF, Knight R, Birren BW. Chimeric 16S rRNA sequence formation and detection in Sanger and 454-pyrosequenced PCR amplicons. *Genome Res* 2011; **21**: 494-504 [PMID: 21212162 DOI: 10.1101/gr.112730.110]

23 **Edgar RC**. UPARSE: highly accurate OTU sequences from microbial amplicon reads. *Nat Methods* 2013; **10**: 996-998 [PMID: 23955772 DOI: 10.1038/nmeth.2604]

24 **DeSantis TZ**, Hugenholtz P, Larsen N, Rojas M, Brodie EL, Keller K, Huber T, Dalevi D, Hu P, Andersen GL. Greengenes, a chimera-checked 16S rRNA gene database and workbench compatible with ARB. *Appl Environ Microbiol* 2006; **72**: 5069-5072 [PMID: 16820507 DOI: 10.1128/aem.03006-05]

25 **Wang Q**, Garrity GM, Tiedje JM, Cole JR. Naive Bayesian classifier for rapid assignment of rRNA sequences into the new bacterial taxonomy. *Appl Environ Microbiol* 2007; **73**: 5261-5267 [PMID: 17586664 DOI: 10.1128/aem.00062-07]

26 **Edgar RC**. MUSCLE: multiple sequence alignment with high accuracy and high throughput. *Nucleic Acids Res* 2004; **32**: 1792-1797 [PMID: 15034147 DOI: 10.1093/nar/gkh340]

27 **Sartor RB**. Microbial influences in inflammatory bowel diseases. *Gastroenterology* 2008; **134**: 577-594 [PMID: 18242222 DOI: 10.1053/j.gastro.2007.11.059]

28 **Swidsinski A**, Ladhoff A, Pernthaler A, Swidsinski S, Loening-Baucke V, Ortner M, Weber J, Hoffmann U, Schreiber S, Dietel M, Lochs H. Mucosal flora in inflammatory bowel disease. *Gastroenterology* 2002; **122**: 44-54 [PMID: 11781279]

29 **Manichanh C**, Rigottier-Gois L, Bonnaud E, Gloux K, Pelletier E, Frangeul L, Nalin R, Jarrin C, Chardon P, Marteau P, Roca J, Dore J. Reduced diversity of faecal microbiota in Crohn's disease revealed by a metagenomic approach. *Gut* 2006; **55**: 205-211 [PMID: 16188921 DOI: 10.1136/gut.2005.073817]

30 **Ott SJ**, Musfeldt M, Wenderoth DF, Hampe J, Brant O, Fölsch UR, Timmis KN, Schreiber S. Reduction in diversity of the colonic mucosa associated bacterial microflora in patients with active inflammatory bowel disease. *Gut* 2004; **53**: 685-693 [PMID: 15082587]

31 **Andoh A**, Imaeda H, Aomatsu T, Inatomi O, Bamba S, Sasaki M, Saito Y, Tsujikawa T, Fujiyama Y. Comparison of the fecal microbiota profiles between ulcerative colitis and Crohn's disease using terminal restriction fragment length polymorphism analysis. *J Gastroenterol* 2011; **46**: 479-486 [PMID: 21253779 DOI: 10.1007/s00535-010-0368-4]

32 **Forbes JD**, Van Domselaar G, Bernstein CN. Microbiome Survey of the Inflamed and Noninflamed Gut at Different Compartments Within the Gastrointestinal Tract of Inflammatory Bowel Disease Patients. *Inflamm Bowel Dis* 2016; **22**: 817-825 [PMID: 26937623 DOI: 10.1097/MIB.0000000000000684]

33 **Man SM**, Kaakoush NO, Mitchell HM. The role of bacteria and pattern-recognition receptors in Crohn's disease. *Nat Rev Gastroenterol Hepatol* 2011; **8**: 152-168 [PMID: 21304476 DOI: 10.1038/nrgastro.2011.3]

34 **Sokol H**, Lepage P, Seksik P, Doré J, Marteau P. Temperature gradient gel electrophoresis of fecal 16S rRNA reveals active Escherichia coli in the microbiota of patients with ulcerative colitis. *J Clin Microbiol* 2006; **44**: 3172-3177 [PMID: 16954244 DOI: 10.1128/jcm.02600-05]

35 **Darfeuille-Michaud A**, Boudeau J, Bulois P, Neut C, Glasser AL, Barnich N, Bringer MA, Swidsinski A, Beaugerie L, Colombel JF. High prevalence of adherent-invasive Escherichia coli associated with ileal mucosa in Crohn's disease. *Gastroenterology* 2004; **127**: 412-421 [PMID: 15300573]

36 **Bücker R**, Schulz E, Günzel D, Bojarski C, Lee IF, John LJ, Wiegand S, Janßen T, Wieler LH, Dobrindt U, Beutin L, Ewers C, Fromm M, Siegmund B, Troeger H, Schulzke JD. α-Haemolysin of Escherichia coli in IBD: a potentiator of inflammatory activity in the colon. *Gut* 2014; **63**: 1893-1901 [PMID: 24534723 DOI: 10.1136/gutjnl-2013-306099]

37 **Smith JL**, Bayles DO. The contribution of cytolethal distending toxin to bacterial pathogenesis. *Crit Rev Microbiol* 2006; **32**: 227-248 [PMID: 17123907 DOI: 10.1080/10408410601023557]

38 **Lepage P**, Häsler R, Spehlmann ME, Rehman A, Zvirbliene A, Begun A, Ott S, Kupcinskas L, Doré J, Raedler A, Schreiber S. Twin study indicates loss of interaction between microbiota and mucosa of patients with ulcerative colitis. *Gastroenterology* 2011; **141**: 227-236 [PMID: 21621540 DOI: 10.1053/j.gastro.2011.04.011]

39 **Rehman A**, Lepage P, Nolte A, Hellmig S, Schreiber S, Ott SJ. Transcriptional activity of the dominant gut mucosal microbiota in chronic inflammatory bowel disease patients. *J Med Microbiol* 2010; **59**: 1114-1122 [PMID: 20522625 DOI: 10.1099/jmm.0.021170-0]

40 **Said HS**, Suda W, Nakagome S, Chinen H, Oshima K, Kim S, Kimura R, Iraha A, Ishida H, Fujita J, Mano S, Morita H, Dohi T, Oota H, Hattori M. Dysbiosis of salivary microbiota in inflammatory bowel disease and its association with oral immunological biomarkers. *DNA Res* 2014; **21**: 15-25 [PMID: 24013298 DOI: 10.1093/dnares/dst037]

41 **Harrison A**, Bakaletz LO, Munson RS Jr. Haemophilus influenzae and oxidative stress. *Front Cell Infect Microbiol* 2012; **2**: 40 [PMID: 22919631 DOI: 10.3389/fcimb.2012.00040]

42 **Rowan F**, Docherty NG, Murphy M, Murphy B, Calvin Coffey J, O'Connell PR. Desulfovibrio bacterial species are increased in ulcerative colitis. *Dis Colon Rectum* 2010; **53**: 1530-1536 [PMID: 20940602 DOI: 10.1007/DCR.0b013e3181f1e620]

43 **Pitcher MC**, Beatty ER, Cummings JH. The contribution of sulphate reducing bacteria and 5-aminosalicylic acid to faecal sulphide in patients with ulcerative colitis. *Gut* 2000; **46**: 64-72 [PMID: 10601057]

44 **Walujkar SA**, Dhotre DP, Marathe NP, Lawate PS, Bharadwaj RS, Shouche YS. Characterization of bacterial community shift in human Ulcerative Colitis patients revealed by Illumina based 16S rRNA gene amplicon sequencing. *Gut Pathog* 2014; **6**: 22 [PMID: 25018784 DOI: 10.1186/1757-4749-6-22]

45 **Rigottier-Gois L**. Dysbiosis in inflammatory bowel diseases: the oxygen hypothesis. *ISME J* 2013; **7**: 1256-1261 [PMID: 23677008 DOI: 10.1038/ismej.2013.80]

46 **Podolsky DK**. Inflammatory bowel disease (1) *N Engl J Med* 1991; **325**: 928-937 [PMID: 1881418 DOI: 10.1056/nejm199109263251306]

47 **Ahmad MS**, Krishnan S, Ramakrishna BS, Mathan M, Pulimood AB, Murthy SN. Butyrate and glucose metabolism by colonocytes in experimental colitis in mice. *Gut* 2000; **46**: 493-499 [PMID: 10716678]

48 **Smith PM**, Howitt MR, Panikov N, Michaud M, Gallini CA, Bohlooly-Y M, Glickman JN, Garrett WS. The microbial metabolites, short-chain fatty acids, regulate colonic Treg cell homeostasis. *Science* 2013; **341**: 569-573 [PMID: 23828891 DOI: 10.1126/science.1241165]

49 **Blaser MJ**, Falkow S. What are the consequences of the disappearing human microbiota? *Nat Rev Microbiol* 2009; **7**: 887-894 [PMID: 19898491 DOI: 10.1038/nrmicro2245]

50 **Dominguez-Bello MG**, Blaser MJ, Ley RE, Knight R. Development of the human gastrointestinal microbiota and insights from high-throughput sequencing. *Gastroenterology* 2011; **140**: 1713-1719 [PMID: 21530737 DOI: 10.1053/j.gastro.2011.02.011]

51 **Lozupone CA**, Stombaugh JI, Gordon JI, Jansson JK, Knight R. Diversity, stability and resilience of the human gut microbiota. *Nature* 2012; **489**: 220-230 [PMID: 22972295 DOI: 10.1038/nature11550]

52 **Claesson MJ**, Cusack S, O'Sullivan O, Greene-Diniz R, de Weerd H, Flannery E, Marchesi JR, Falush D, Dinan T, Fitzgerald G, Stanton C, van Sinderen D, O'Connor M, Harnedy N, O'Connor K, Henry C, O'Mahony D, Fitzgerald AP, Shanahan F, Twomey C, Hill C, Ross RP, O'Toole PW. Composition, variability, and temporal stability of the intestinal microbiota of the elderly. *Proc Natl Acad Sci U S A* 2011; **108** Suppl 1: 4586-4591 [PMID: 20571116 DOI: 10.1073/pnas.1000097107]

53 **Meyer F**, Trimble WL, Chang EB, Handley KM. Functional predictions from inference and observation in sequence-based inflammatory bowel disease research. *Genome Biol* 2012; **13**: 169 [PMID: 23013527 DOI: 10.1186/gb4042]

54 **Presley LL**, Ye J, Li X, Leblanc J, Zhang Z, Ruegger PM, Allard J, McGovern D, Ippoliti A, Roth B, Cui X, Jeske DR, Elashoff D, Goodglick L, Braun J, Borneman J. Host-microbe relationships in inflammatory bowel disease detected by bacterial and metaproteomic analysis of the mucosal-luminal interface. *Inflamm Bowel Dis* 2012; **18**: 409-417 [PMID: 21698720 DOI: 10.1002/ibd.21793]

55 **De Cruz P**, Prideaux L, Wagner J, Ng SC, McSweeney C, Kirkwood C, Morrison M, Kamm MA. Characterization of the gastrointestinal microbiota in health and inflammatory bowel disease. *Inflamm Bowel Dis* 2012; **18**: 372-390 [PMID: 21604329 DOI: 10.1002/ibd.21751]

56 **van der Waaij LA**, Harmsen HJ, Madjipour M, Kroese FG, Zwiers M, van Dullemen HM, de Boer NK, Welling GW, Jansen PL.

Bacterial population analysis of human colon and terminal ileum biopsies with 16S rRNA-based fluorescent probes: commensal bacteria live in suspension and have no direct contact with epithelial cells. *Inflamm Bowel Dis* 2005; **11**: 865-871 [PMID: 16189415]

57 **Bibiloni R**, Tandon P, Vargas-Voracka F, Barreto-Zuniga R, Lupian-Sanchez A, Rico-Hinojosa MA, Guban J, Fedorak R, Tannock GW. Differential clustering of bowel biopsy-associated bacterial profiles of specimens collected in Mexico and Canada: what do these profiles represent? *J Med Microbiol* 2008; **57**: 111-117 [PMID: 18065676 DOI: 10.1099/jmm.0.47321-0]

58 **Durbán A**, Abellán JJ, Jiménez-Hernández N, Ponce M, Ponce J, Sala T, D'Auria G, Latorre A, Moya A. Assessing gut microbial diversity from feces and rectal mucosa. *Microb Ecol* 2011; **61**: 123-133 [PMID: 20734040 DOI: 10.1007/s00248-010-9738-y]

59 **Eckburg PB**, Bik EM, Bernstein CN, Purdom E, Dethlefsen L, Sargent M, Gill SR, Nelson KE, Relman DA. Diversity of the human intestinal microbial flora. *Science* 2005; **308**: 1635-1638 [PMID: 15831718 DOI: 10.1126/science.1110591]

P- Reviewer: Naito Y, Zouiten-Mekki L **S- Editor**: Gong ZM
L- Editor: Filipodia **E- Editor**: Huang Y

World Journal of Gastroenterology

Submit a Manuscript: http://www.f6publishing.com

World J Gastroenterol 2018 April 7; 24(13): 1478-1485

DOI: 10.3748/wjg.v24.i13.1478

ISSN 1007-9327 (print) ISSN 2219-2840 (online)

ORIGINAL ARTICLE

Prospective Study

Hepatocellular carcinoma or interferon-based therapy history attenuates sofosbuvir/ribavirin for Japanese genotype 2 hepatitis C virus

Masayoshi Yada, Masayuki Miyazaki, Kosuke Tanaka, Akihide Masumoto, Kenta Motomura

Masayoshi Yada, Masayuki Miyazaki, Kosuke Tanaka, Akihide Masumoto, Kenta Motomura, Department of Hepatology, Iizuka Hospital, Iizuka, Fukuoka 820-8505, Japan

ORCID number: Masayoshi Yada (0000-0002-1129-5380); Masayuki Miyazaki (0000-0002-4192-8150); Kosuke Tanaka (0000-0003-1472-0597); Akihide Masumoto (0000-0003-4929-6271); Kenta Motomura (0000-0002-7515-099X).

Author contributions: Yada M and Motomura K wrote the paper; Yada M, Miyazaki M, Tanaka K, and Motomura K analyzed the data; Masumoto A supervised writing of the paper; all authors contributed to the manuscript.

Institutional review board statement: The study protocol conformed to the ethical guidelines of the 1975 Declaration of Helsinki, as reflected in a priori approval by the Ethics Committee of Iizuka Hospital (Approve No. 26282).

Informed consent statement: Written informed consent was obtained from all patients.

Conflict-of-interest statement: The authors have no disclosures to report.

Data sharing statement: No additional data are available.

Manuscript source: Unsolicited manuscript

Correspondence to: Masayoshi Yada, MD, PhD, Doctor, Department of Hepatology, Iizuka Hospital, 3-83 Yoshio-machi, Iizuka, Fukuoka 820-8505, Japan. myadah1@aih-net.com

Telephone: +81-948-223800
Fax: +81-948-295744

Received: February 5, 2018
Peer-review started: February 5, 2018
First decision: February 26, 2018
Revised: February 26, 2018
Accepted: March 7, 2018
Article in press: March 7, 2018
Published online: April 7, 2018

Abstract

AIM

To investigate the real-world efficacy and safety of sofosbuvir/ribavirin (SOF/RBV) therapy for Japanese patients with genotype 2 hepatitis C virus (GT2-HCV).

METHODS

A total of 182 patients with GT2-HCV infection who received SOF/RBV therapy for 12 wk at our hospital were enrolled. The patients comprised 122 men and 60 women (age range: 17-84 years; mean age ± SD: 60.1 ± 12.1 years). Relationships between virological response and clinical data were examined by logistic regression analyses.

RESULTS

The proportions of patients with liver cirrhosis and history of hepatocellular carcinoma (HCC) were 29.0% and 17.3%, respectively. The proportion of patients with prior interferon (IFN)-based therapy was 25.6%. SOF/RBV therapy rapidly decreased HCV RNA levels. Several patients required RBV dose reduction because of anemia or fatigue. Four patients discontinued the therapy. The rates of sustained virological response at 12 wk after the end of treatment were 87.9% (intention

to treat: 160/182) and 94.1% (per protocol: 159/169). Multivariate analyses showed that history of HCC or IFN-based therapy independently reduced the efficacy of SOF/RBV therapy.

CONCLUSION

SOF/RBV therapy for GT2-HCV is safe, highly tolerated, and effective. History of HCC or IFN-based therapy independently reduces the efficacy of this treatment.

Key words: Sofosbuvir; Ribavirin; Genotype 2; Hepatitis C virus; Interferon-based therapy; Hepatocellular carcinoma

Core tip: The real-world efficacy of sofosbuvir/ribavirin therapy for genotype 2 hepatitis C virus infection in Japan is high. Sofosbuvir/ribavirin therapy is safe and highly tolerated. History of hepatocellular carcinoma or interferon-based therapy independently reduces the efficacy of sofosbuvir/ribavirin therapy. Progressive liver fibrosis may attenuate the antiviral effect of sofosbuvir/ribavirin therapy.

Yada M, Miyazaki M, Tanaka K, Masumoto A, Motomura K. Hepatocellular carcinoma or interferon-based therapy history attenuates sofosbuvir/ribavirin for Japanese genotype 2 hepatitis C virus. *World J Gastroenterol* 2018; 24(13): 1478-1485 Available from: URL: http://www.wjgnet.com/1007-9327/full/v24/i13/1478.htm DOI: http://dx.doi.org/10.3748/wjg.v24.i13.1478

INTRODUCTION

Hepatitis C virus (HCV) infection is a leading cause of chronic hepatitis, liver cirrhosis (LC), and hepatocellular carcinoma (HCC). In Global hepatitis report 2017[1], World Health Organization (WHO) described that 71 million persons were living with chronic HCV infection in 2015 (the global prevalence of HCV infection was 1.0%). Approximately 399000 people died each year from HCV, mostly from LC and HCC. In 2011, Japanese estimated number of persons with chronic HCV infection was 1.25 million containing 64% with genotype 1B and 35% with genotype 2, respectively[2]. WHO targets 80% of persons with HCV will be treated by 2030[1]. Combination therapy with peg-interferon (PEG-IFN) and ribavirin (RBV) was the first-line therapy for genotype 2 HCV (GT2-HCV) infection, but only 80% of patients achieved elimination of HCV with this treatment[3]. The introduction of direct-acting antiviral agents has drastically improved the efficacy of treatments for chronic HCV infection. In Japan, telaprevir (TVR), a first-generation NS3/4A protease inhibitor for GT2-HCV, was approved for clinical use in 2013. Patients received TVR (750 mg, every 8 h) for 12 wk and PEG-IFN/RBV for 24 wk. The sustained virological response (SVR) rate in patients receiving triple therapy (TVR/PEG-IFN/RBV) was reported to be 85%[4].

Subsequently, combination therapy with NS5B RNA-dependent RNA polymerase inhibitor sofosbuvir (SOF) and RBV for patients with GT2-HCV infection was approved for clinical use in June 2015. This therapy showed improved efficacy and was well tolerated in a phase 3 trial[5]. We conducted a prospective study to investigate the efficacy and safety of SOF/RBV therapy for Japanese patients with GT2-HCV infection in a real-world clinical setting.

MATERIALS AND METHODS

Patients

A total of 182 patients with chronic GT2-HCV infection who received SOF/RBV therapy at Iizuka Hospital from September 2015 to January 2017 were enrolled. The patients comprised 122 men and 60 women with an age range of 17-86 years (mean ± SD: 60.1 ± 14.1 years). HCV genotype was determined by sequencing the NS5B region of the HCV genome. The results revealed 109 patients with genotype 2A and 70 patients with genotype 2B. Genotype was not determined in 3 patients. Presence of resistance-associated substitution (RAS) was analyzed by sequence determination around S282 in the NS5B region of the HCV genome. Two single nucleotide polymorphisms (SNPs), rs8099917 in the *interleukin-28B* (*IL28B*) locus associated with interferon (IFN) therapy[6] and rs1127354 in the *inosine triphosphate pyrophosphatase* (*ITPA*) locus associated with RBV-induced hemolytic anemia[7-9], were analyzed. fibrosis (FIB)-4 index was calculated as a noninvasive marker of liver fibrosis: FIB-4 index = age (years) × aspartate aminotransferase (IU/L)/[platelet count × 10^9/L × (alanine aminotransferase IU/L)$^{1/2}$]. FIB-4 index of > 3.25 was defined as progressive fibrosis, based on a previous report[10].

Treatment regimen

SOF (Sovaldi®, Gilead Sciences Inc., Durham, NC, United States) was administered orally at a dose of 400 mg once daily, and RBV (Rebetol®, MSD, Tokyo, Japan or Copegus®, Chugai, Shizuoka, Japan) was administered orally at a dose of 200-1000 mg for 12 wk. The starting RBV dose was determined by body weight (600 mg for < 60 kg; 800 mg for 60-80 kg; 1000 mg for > 80 kg) (Figure 1).

Evaluation of virological response

HCV RNA levels were measured by a COBAS TaqMan test (Roche Diagnostics, Tokyo, Japan) with a lower limit of quantitation of 1.2 logIU/mL. HCV RNA was measured at screening, at day 1 and weeks 4, 8, and 12 of treatment, and at 12 wk after the end of

Table 1 Pretreatment characteristics of the patients (n = 182)

Pretreatment characteristics	Values
Age[1], yr	60.1 ± 14.1
Age ⩾ 70 yr	27.40%
Sex, M : F	122:60
Body height[1], cm	163.0 ± 8.9
Body weight[1], kg	62.3 ± 12.1
Liver cirrhosis	26.60%
History of HCC	15.90%
FIB-4 index[2]	2.63 (0.45-19.03)
FIB-4 index > 3.25	40.70%
Wisteria floribunda agglutinin+-Mac-2 binding protein[2]	1.94 (0.20-18.51)
Hyaluronic acid[2], ng/mL	97.4 (10.0-2750.0)
History of IFN-based therapy	23.60%
IL28B-SNP rs8099917 TT/non TT	136/38/8
ITPA-SNP rs1127354 CC	129/45/8
HCV genotype 2A/2B/ND	109/70/3
HCV RNA[2], logIU/mL	6.1 (1.2-7.6)
HCV RNA > 6 logIU/mL	58.80%
White blood cell count[2], /mm^3	4575 (1700-12010)
Hemoglobin[2], g/dL	13.7 (10.1-17.6)
Platelet count[2], /mm^3	165 (38-389) × 10^3
Aspartate aminotransferase[2], IU/L	41 (14-336)
Alanine aminotransferase[2], IU/L	40 (5-391)
Albumin[2], g/dL	4.0 (2.6-5.0)
Total bilirubin[2], mg/dL	0.8 (0.3-3.0)
Blood urea nitrogen[2], mg/dL	13 (5-28)
Creatinine[2], mg/dL	0.71 (0.32-1.23)
Estimated glomerular filtration rate[2], mL/min/1.73 m^2	78.9 (42.6-164.2)

[1]Mean ± SD; [2]Median (range). M: Male; F: Female; HCC: Hepatocellular carcinoma; FIB: Fibrosis; *IL28B*: *Interleukin-28B*; SNP: Single nucleotide polymorphisms; *ITPA*: *Inosine triphosphate pyrophosphatase*; HCV: Hepatitis C virus.

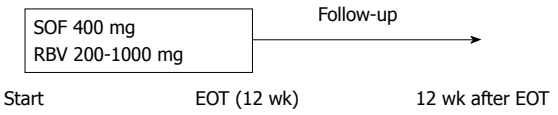

Figure 1 Treatment regimen of sofosbuvir and ribavirin. SOF: Sofosbuvir; RBV: Ribavirin; EOT: End of treatment.

treatment. The primary endpoint was the rate of SVR at 12 wk after the end of treatment (SVR12), defined as undetectable serum HCV RNA at this time point. Relapse and breakthrough were defined based on the guidelines of the American Association for the Study of Liver Diseases[11].

Safety assessments

Safety evaluations included reported adverse events and serious adverse events, clinical laboratory tests, and physical examinations.

Statistical analysis

Statistical analyses were performed using JMP software version 8.0.2 (SAS Institute Inc., Cary, NC, United States). Hemoglobin levels and estimated glomerular filtration rate were compared by the Tukey honestly significant difference test. Categorical data were compared by Chi-squared test. To identify independent factors predicting non-SVR, sex, age, liver cirrhosis, and variables with values of $P < 0.05$ in univariate analyses were entered into a multiple logistic regression analysis. Values of $P < 0.05$ were considered statistically significant.

RESULTS

Patient characteristics

The pretreatment characteristics of all patients enrolled in the study are presented in Table 1. There were 48 patients (26.4%) with LC, 43 (23.7%) with history of IFN-based therapy, and 28 (15.4%) with history of HCC. Presence of the SNPs in *IL28B* (rs8099917) and *ITPA* (rs1127354) was examined in 174 of 182 patients. HCV RAS of S282 in the NS5B domain was not detected in the 138 patients examined by the RAS test.

Treatment outcomes

Of the 182 patients, 178 (97.8%) completed the treatment. The causes of treatment discontinuation were fatigue (n = 1; 0.5%) and self-withdrawal (n = 3; 1.6%). The rates of SVR12 were 87.9% [intention to treat (ITT): 160/182] and 94.1% [per protocol (PP): 159/169]. SVR12 was not evaluated in 12 patients (6.7%) because of dropout from the study (Figure 2).

Hemoglobin levels during the treatment period were significantly reduced until 4 wk after the start of administration (Figure 3A). CC of the *ITPA* allele strongly contributed to anemia (Figure 3B). Twenty-nine (15.9%) of 182 patients needed RBV dose reduction because of anemia, but no patients discontinued the treatment for this reason. Although SOF and RBV cannot be used in patients with decreased renal function and we were concerned about SOF/RBV therapy decreasing the renal function of our patients, the estimated glomerular filtration rate did not change significantly during the treatment period (Figure 3C).

Factors contributing to SVR in the PP analysis

In the PP analysis, 13 of 182 patients who discontinued treatment and/or were not evaluated for SVR12 were excluded (Figure 2A). One hundred twenty three of 169 patients (72.8%) achieved rapid virological response (RVR), defined as undetectable serum HCV RNA after 4 wk of treatment. In univariate analyses, history of IFN-based therapy, LC, and history of HCC reduced the virological response, while age (⩾ 70 years), sex, FIB-4 index, *IL28B* SNP, *ITPA* SNP, HCV genotype, pretreatment viral load, RBV dose reduction, and RVR had no effect on the treatment efficacy (Figures 4 and 5). The SNPs of *IL28B* and *ITPA* were determined for 161 patients in the PP analysis. The HCV viral genotype was determined in 166 patients. Multivariate analysis showed that history of HCC or IFN-based therapy was independently related to non-

Table 2 Factors contributing to sustained virological response in the per protocol analysis

	Univariate			Multivariate		
	Odds ratio	95%CI	*P* value	Odds ratio	95%CI	*P* value
Age, ⩾ 70 yr	2.61	0.70, 9.82	0.1494			
Sex, male	4.76	0.85, 88.89	0.0781			
History of IFN-based therapy	5.12	1.39, 20.98	0.0147[a]	7.05	1.65, 36.08	0.0084[a]
Liver cirrhosis	6.72	1.78, 32.29	0.0048[a]	2.13	0.31, 14.34	0.4315
FIB-4 index, > 3.25	2.11	0.58, 8.54	0.2546			
History of HCC	8.87	2.36, 37.04	0.0015[a]	7.67	1.30, 60.30	0.0233[a]
IL28B-SNP, non TT	1.21	0.17, 5.55	0.8214			
ITPA-SNP, non CC	0.45	0.02, 2.63	0.4177			
HCV genotype, 2A	2.78	0.67, 18.84	0.1687			
Viral load, ⩾ 6 logIU/mL	1.53	0.41, 7.31	0.5478			
RBV dose reduction	2.29	0.47, 8.89	0.2757			
Rapid virological response	0.86	0.22, 4.15	0.8401			

[a]$P < 0.05$, significant difference. IFN: Interferon; FIB: Fibrosis; HCC: Hepatocellular carcinoma; *IL28B*: *Interleukin-28B*; SNP: Single nucleotide polymorphisms; *ITPA*: *Inosine triphosphate pyrophosphatase*; HCV: Hepatitis C virus; RBV: Ribavirin.

Table 3 Assessment of patients with history of hepatitis C virus

	SVR (*n* = 23)	Non SVR (*n* = 6)	*P* value
Alpha fetoprotein	9.6 (1.7-348.9)	5.3 (2.6-65.7)	0.2815
Latest treatment for HCC			0.2558
Surgical resection or Radiofrequency ablation	73.9% (17)	66.6% (6)	
Transcatheter arterial chemoembolization	26.1% (6)	16.7% (1)	
Radiation for bone metastasis	0% (0)	16.7% (1)	
Recurrent HCC within 1 yr from the end of SOF/RBV	65. 2% (15)	83.3% (5)	0.6328

SVR: Sustained virological response; HCC: Hepatocellular carcinoma; SOF/RBV: Sofosbuvir/ribavirin.

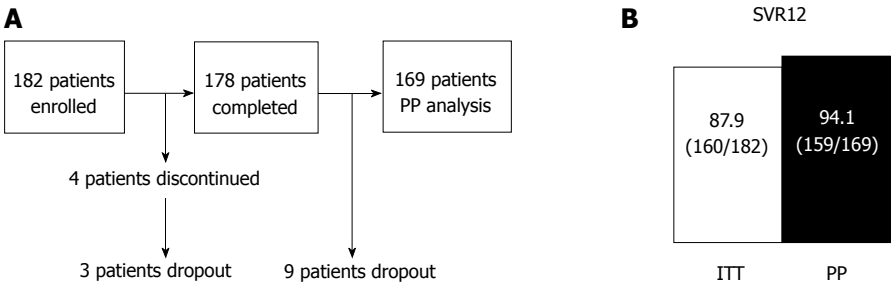

Figure 2 Flow sheet of this study (A) and virological response rates for combination therapy with sofosbuvir and ribavirin (B). The rates of sustained virological response at 12 wk after the end of treatment are shown for intention to treat and per protocol analyses. PP: Per protocol; ITT: Intention to treat; SVR12: Sustained virological response at 12 wk after the end of treatment.

SVR (Table 2).

Assessment of patients with history of HCC

We assessed 29 patients with history of HCC. We ascertained that their HCC was not detected by dynamic computed tomography or dynamic magnetic resonance imaging before initiation of SOF/RBV therapy. We compared alpha fetoprotein (AFP), latest therapy for HCC, and HCC recurrence within 1 year after the end of SOF/RBV therapy according to SVR or non-SVR (Table 3). The AFP level did not differ significantly between the two groups. Patients achieving SVR tended to be treated by surgical resection or radiofrequency ablation, and also tended to have no HCC recurrence.

DISCUSSION

Combination therapy with SOF/RBV was the first IFN-free therapy for GT2-HCV infection approved for clinical use in Japan. In a phase 3 trial, 97% of patients achieved SVR12 and no patients discontinued the treatment[5]. Thus, we expected high efficacy and tolerability, and conducted a prospective study in a real-world clinical practice setting to investigate the efficacy and safety of this combination therapy for Japanese patients with GT2-HCV infection.

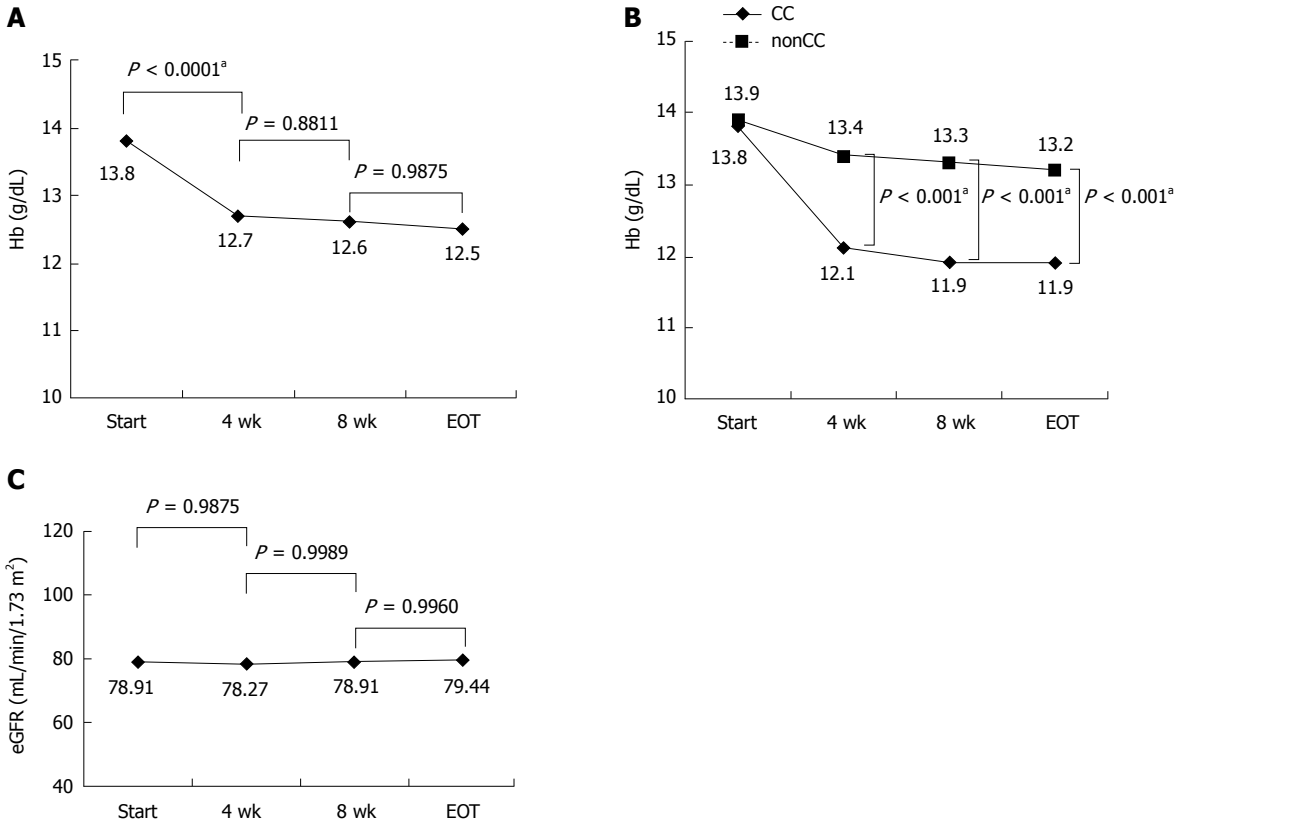

Figure 3 Hemoglobin levels in all patients during combination therapy with sofosbuvir and ribavirin (A), hemoglobin levels in 175 patients categorized by *inosine triphosphate pyrophosphatase* single nucleotide polymorphism rs1127354 (CC or non CC) (B), and estimated glomerular filtration rate levels in all patients during sofosbuvir/ribavirin therapy (C). Hb: Hemoglobin; EOT: End of treatment; eGFR: Estimated glomerular filtration rate. [a]*P* < 0.05, significant difference.

Hemoglobin levels rapidly reduced until 4 wk after the start of treatment. *ITPA* CC allele significantly contributed to anemia in this therapy, similar to the case for combination therapy of PEG-IFN and RBV[7-9]. Therefore, patients with the *ITPA* CC allele should be monitored frequently for their hemoglobin levels until 4 wk after the start of treatment. Despite our concern that SOF and RBV may decrease renal function of the patients, renal function degeneration was not observed in any of the patients. Many elderly patients (27.4% were aged ⩾ 70 years) and cirrhotic patients (26.6% had liver cirrhosis) were enrolled in this study. Thus, the present findings demonstrate that SOF/RBV therapy is safe and highly tolerated regardless of age and LC.

The ITT rate in this study was low compared with the rates in phase 3 clinical trials of SOF/RBV for Japanese[5] and European[12] patients with GT2-HCV infection. The reason for the difference was that SVR12 could not be evaluated in 12 patients (6.7%) because of dropout from the study. It is important to monitor carcinogenesis after virus elimination, and it is therefore necessary to provide patients with instructions that promote periodic examinations. Meanwhile, the PP rate was almost equal to the rates in the phase 3 clinical trial of SOF/RBV for Japanese patients with GT2-HCV infection[5] and in real-world cohorts in North America and Europe[13]. This finding shows that SOF/RBV therapy for Japanese patients with GT2-HCV infection is highly effective in real-world clinical practice.

In a meta-analysis, Rangnekar *et al*[14] reported that *IL28B* SNP was predictor of SVR in Caucasian patients with GT2-HCV infection receiving PEG-IFN/RBV for 24 wk. In contrast, *IL28B* SNP was not associated with SVR in Asian patients with GT2-HCV infection. This study also showed Japanese *IL28B* SNP had no relation to efficacy of SOF/RBV for GT2-HCV infection. Morisco *et al*[15] reported RVR was the only independent predictive factor of SVR in triple therapy (TVR/PEG-IFN/RBV) regardless of LC. In the present study, RVR did not affect efficacy of SOF/RBV for GT2-HCV infection. The multivariate regression analysis showed that history of HCC or IFN-based therapy was independently related to non-SVR. LC also reduced the efficacy in univariate analyses. It was previously reported that the efficacy of IFN-based therapy was inferior in LC patients[16,17]. Furthermore, it was reported that patients with progressive liver fibrosis have a high probability of hepatocellular carcinogenesis[18-21]. Prenner *et al*[22] reported that presence of active HCC at the start of direct acting antivirals, including SOF/RBV therapy, decreased the SVR rate. In our study, the proportion of non-SVR patients treated by surgical resection or radiofrequency ablation tended to be lower than the

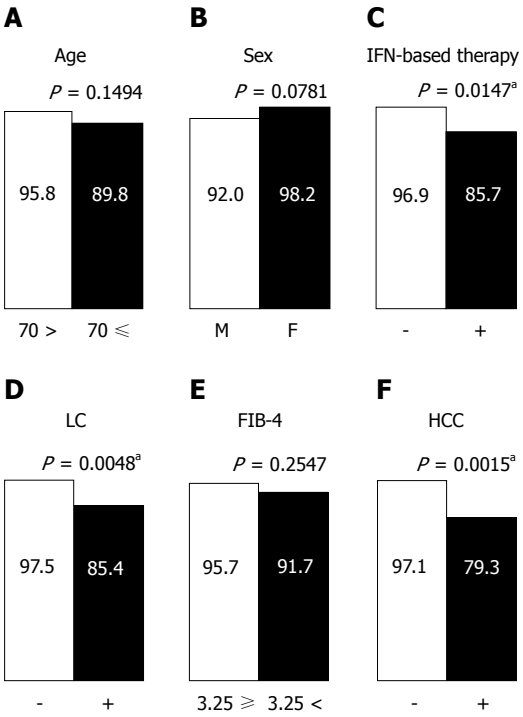

Figure 4 Virological response in patients with sofosbuvir and ribavirin (SOF/RBV) combination therapy categorized by patient characteristics. A: Age (< 70 or ⩾ 70 yr); B: Sex (male or female); C: History of interferon-based therapy (− or +); D: Liver cirrhosis (− or +); E: Fibrosis-4 index (⩽ 3.25 or > 3.25); F: History of hepatocellular carcinoma (− or +). $^{a}P < 0.05$: Significant difference. M: Male; F: Female; IFN: Interferon; LC: Liver cirrhosis; FIB: Fibrosis; HCC: Hepatocellular carcinoma.

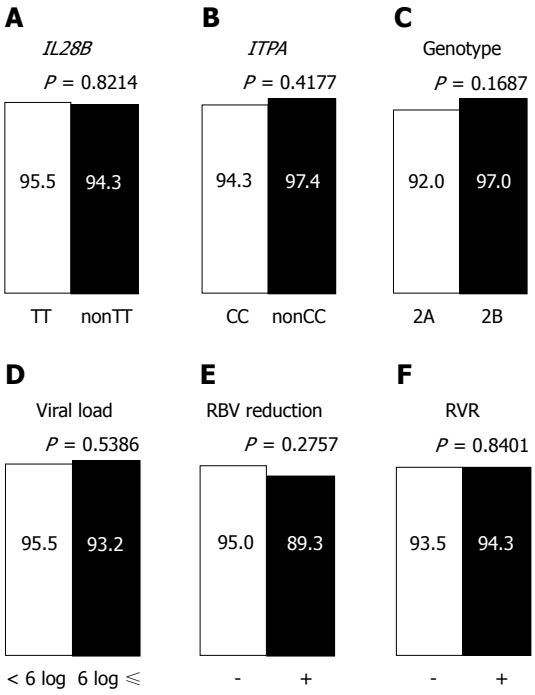

Figure 5 Virological response in patients with sofosbuvir and ribavirin combination therapy categorized by single nucleotide polymorphisms related to anti-hepatitis C virus therapy, pretreatment viral status, ribavirin dose, and rapid virological response. A: *IL28B* single nucleotide polymorphisms rs8099917 (TT or non TT); B: *ITPA* single nucleotide polymorphisms rs1127354 (CC or non CC); C: Hepatitis C virus genotype (2A or 2B); D: Pretreatment viral load (< 6 logIU/mL or ≥ 6 logIU/mL); E: Ribavirin dose reduction (− or +); F: Rapid virological response (− or +). $^{a}P < 0.05$: Significant difference. *IL28B: Interleukin-28B*; *ITPA*: *Inosine triphosphate pyrophosphatase*; RBV: Ribavirin; RVR: Rapid virological response.

proportion of non-SVR patients treated by transcatheter arterial chemoembolization or radiation for bone metastasis. Meanwhile, the rate of HCC recurrence within 1 year tended to be higher in non-SVR patients than that in SVR patients. These findings show a high probability that active HCC was not detected by dynamic computed tomography or dynamic magnetic resonance imaging at the start of SOF/RBV therapy. Prenner *et al*[22] discussed that a putative biological explanation could be inadequate drug delivery by decreased blood flow or local fibrosis arising from HCC treatment. The present results suggested that liver fibrosis attenuated the antiviral effect of SOF/RBV in patients with history of IFN-based therapy or HCC. Although the FIB-4 index, a fibrosis marker[10], had no effect on efficacy in the present study, the reason was unclear. History of IFN-based therapy and LC had no significant effect on SOF/RBV therapy in the phase 3 clinical trial for European patients with GT2-HCV infection[12]. However, it was reported that LC and lower serum albumin decreased the SVR rate in the real-world cohorts in North America and Europe[13]. Treatment-experienced patients tended to have ineffective outcomes in that study. These findings were similar to those in the present study. The real-world studies included larger populations of LC (26.6% in the present study and 26.8% in the North American and European study) than the phase 3 trials (11% in the Japanese trial[5] and 15% in the European trial[12]. Our study also enrolled patients with history of HCC (15.9%) and elderly patients aged ⩾ 70 years (27.4%). It is suggested that the real-world studies enrolled more patients with severe fibrosis than the phase 3 clinical trials. As viral breakthrough did not occur in any of the non-SVR patients and all of these patients had relapses, it is suggested that SOF/RBV therapy was not ineffective for these patients. Extension of the treatment period for patients with history of IFN-based therapy, HCC, or LC should be considered to increase the efficacy of the therapy. As active HCC not detected by imaging was probably related to non-SVR, monitoring is required for carcinogenesis and recurrence of HCC after the end of SOF/RBV therapy, especially in non-SVR patients.

In conclusion, SOF/RBV therapy for Japanese patients with GT2-HCV infection is safe, highly tolerated, and effective. History of HCC or IFN-based therapy independently reduces the efficacy of the treatment.

ARTICLE HIGHLIGHTS

Research background

Combination therapy with peg-interferon (PEG-IFN) and ribavirin (RBV) was the first-line therapy for genotype 2 hepatitis C virus (HCV) infection, but only 80% of patients achieved elimination of HCV with this treatment. The introduction of direct-acting antiviral agents has drastically improved the efficacy of treatments

for chronic HCV infection. Combination therapy with NS5B RNA-dependent RNA polymerase inhibitor sofosbuvir (SOF) and RBV for patients with genotype 2 hepatitis C virus (GT2-HCV) infection was approved for clinical use in June 2015.

Research motivation

This therapy showed improved efficacy and was well tolerated in a phase 3 trial. However, predictive factor of sustained virological response (SVR) is not unclear.

Research objectives

We conducted a prospective study to investigate the efficacy and safety of sofosbuvir/ribavirin (SOF/RBV) therapy for Japanese patients with GT2-HCV infection in a real-world clinical setting.

Research methods

A total of 182 patients with GT2-HCV infection who received SOF/RBV therapy for 12 wk at our hospital were enrolled. The patients comprised 122 men and 60 women (age range: 17-84 years; mean age ± SD: 60.1 ± 12.1 years). One hundred sixty nine of 182 patients completed 12 wk treatment and were examined their virological response. To investigate predictive factors of SVR, we examined the relationships between virological response and clinical data by logistic regression analyses.

Research results

The rates of SVR at 12 wk after the end of treatment were 87.9% (intention to treat: 160/182) and 94.1% (per protocol: 159/169). Multivariate analyses showed that history of hepatocellular carcinoma (HCC) or IFN-based therapy independently reduced the efficacy of SOF/RBV therapy.

Research conclusions

This study showed Japanese *IL28B* single nucleotide polymorphisms had no relation to efficacy of SOF/RBV for GT2-HCV infection. Morisco *et al*[15] reported rapid virological response (RVR) was the only independent predictive factor of SVR in triple therapy (Telaprevir/PEG-IFN/RBV) regardless of cirrhosis. In the present study, RVR did not affect efficacy of SOF/RBV for GT2-HCV infection. The multivariate regression analysis showed that history of HCC or IFN-based therapy was independently related to non-SVR. In our study, the proportion of non-SVR patients treated by surgical resection or radiofrequency ablation tended to be lower than the proportion of non-SVR patients treated by transcatheter arterial chemoembolization or radiation for bone metastasis. Meanwhile, the rate of HCC recurrence within 1 year tended to be higher in non-SVR patients than that in SVR patients.

Research perspectives

Prenner *et al* reported that presence of active HCC at the start of direct acting antivirals, including SOF/RBV therapy, decreased the SVR rate. As active HCC not detected by imaging was probably related to non-SVR, monitoring is required for carcinogenesis and recurrence of HCC after the end of SOF/RBV therapy, especially in non-SVR patients.

ACKNOWLEDGMENTS

We are grateful to Ishibashi Y for assistance with manuscript preparation.

REFERENCES

1 **World Health Organization.** Global hepatitis report, 2017. 2017 Available from: URL: http://www.who.int/hepatitis/publications/global-hepatitis-report2017/en/

2 **Liakina V**, Hamid S, Tanaka J, Olafsson S, Sharara AI, Alavian SM, Gheorghe L, El Hassan ES, Abaalkhail F, Abbas Z, Abdou A, Abourached A, Al Braiki F, Al Hosani F, Al Jaberi K, Al Khatry M, Al Mulla MA, Al Quraishi H, Al Rifai A, Al Serkal Y, Alam A, Alashgar HI, Alawadhi S, Al-Dabal L, Aldins P, Alfaleh FZ, Alghamdi AS, Al-Hakeem R, Aljumah AA, Almessabi A, Alqutub AN, Alswat KA, Altraif I, Alzaabi M, Andrea N, Assiri AM, Babatin MA, Baqir A, Barakat MT, Bergmann OM, Bizri AR, Blach S, Chaudhry A, Choi MS, Diab T, Djauzi S, El Khoury S, Estes C, Fakhry S, Farooqi JI, Fridjonsdottir H, Gani RA, Ghafoor Khan A, Goldis A, Gottfredsson M, Gregorcic S, Hajarizadeh B, Han KH, Hasan I, Hashim A, Horvath G, Hunyady B, Husni R, Jafri W, Jeruma A, Jonasson JG, Karlsdottir B, Kim DY, Kim YS, Koutoubi Z, Lesmana LA, Lim YS, Löve A, Maimets M, Makara M, Malekzadeh R, Matičič M, Memon MS, Merat S, Mokhbat JE, Mourad FH, Muljono DH, Nawaz A, Nugrahini N, Priohutomo S, Qureshi H, Rassam P, Razavi H, Razavi-Shearer D, Razavi-Shearer K, Rozentale B, Sadik M, Saeed K, Salamat A, Salupere R, Sanai FM, Sanityoso Sulaiman A, Sayegh RA, Schmelzer JD, Sibley A, Siddiq M, Siddiqui AM, Sigmundsdottir G, Sigurdardottir B, Speiciene D, Sulaiman A, Sultan MA, Taha M, Tarifi H, Tayyab G, Tolmane I, Ud Din M, Umar M, Valantinas J, Videčnik-Zorman J, Yaghi C, Yunihastuti E, Yusuf MA, Zuberi BF, Gunter J. Historical epidemiology of hepatitis C virus (HCV) in select countries - volume 3. *J Viral Hepat* 2015; **22** Suppl 4: 4-20 [PMID: 26513445 DOI: 10.1111/jvh.12475]

3 **Sato K**, Hashizume H, Yamazaki Y, Horiguchi N, Kakizaki S, Takagi H, Mori M; Gunma Liver Study Group. Response-guided peginterferon-alpha-2b plus ribavirin therapy for chronic hepatitis C patients with genotype 2 and high viral loads. *Hepatol Res* 2012; **42**: 854-863 [PMID: 22487210 DOI: 10.1111/j.1872-034X.2012.00997.x]

4 **Kumada H**, Sato K, Takehara T, Nakamuta M, Ishigami M, Chayama K, Toyota J, Suzuki F, Nakayasu Y, Ochi M, Yamada I, Okanoue T. Efficacy of telaprevir-based therapy for difficult-to-treat patients with genotype 2 chronic hepatitis C in Japan. *Hepatol Res* 2015; **45**: 745-754 [PMID: 25196718 DOI: 10.1111/hepr.12416]

5 **Omata M**, Nishiguchi S, Ueno Y, Mochizuki H, Izumi N, Ikeda F, Toyoda H, Yokosuka O, Nirei K, Genda T, Umemura T, Takehara T, Sakamoto N, Nishigaki Y, Nakane K, Toda N, Ide T, Yanase M, Hino K, Gao B, Garrison KL, Dvory-Sobol H, Ishizaki A, Omote M, Brainard D, Knox S, Symonds WT, McHutchison JG, Yatsuhashi H, Mizokami M. Sofosbuvir plus ribavirin in Japanese patients with chronic genotype 2 HCV infection: an open-label, phase 3 trial. *J Viral Hepat* 2014; **21**: 762-768 [PMID: 25196837 DOI: 10.1111/jvh.12312]

6 **Tanaka Y**, Nishida N, Sugiyama M, Kurosaki M, Matsuura K, Sakamoto N, Nakagawa M, Korenaga M, Hino K, Hige S, Ito Y, Mita E, Tanaka E, Mochida S, Murawaki Y, Honda M, Sakai A, Hiasa Y, Nishiguchi S, Koike A, Sakaida I, Imamura M, Ito K, Yano K, Masaki N, Sugauchi F, Izumi N, Tokunaga K, Mizokami M. Genome-wide association of IL28B with response to pegylated interferon-alpha and ribavirin therapy for chronic hepatitis C. *Nat Genet* 2009; **41**: 1105-1109 [PMID: 19749757 DOI: 10.1038/ng.449]

7 **Fellay J**, Thompson AJ, Ge D, Gumbs CE, Urban TJ, Shianna KV, Little LD, Qiu P, Bertelsen AH, Watson M, Warner A, Muir AJ, Brass C, Albrecht J, Sulkowski M, McHutchison JG, Goldstein DB. ITPA gene variants protect against anaemia in patients treated for chronic hepatitis C. *Nature* 2010; **464**: 405-408 [PMID: 20173735 DOI: 10.1038/nature08825]

8 **Ochi H**, Maekawa T, Abe H, Hayashida Y, Nakano R, Kubo M, Tsunoda T, Hayes CN, Kumada H, Nakamura Y, Chayama K. ITPA polymorphism affects ribavirin-induced anemia and outcomes of therapy--a genome-wide study of Japanese HCV virus patients. *Gastroenterology* 2010; **139**: 1190-1197 [PMID: 20637204 DOI: 10.1053/j.gastro.2010.06.071]

9 **Thompson AJ**, Fellay J, Patel K, Tillmann HL, Naggie S, Ge D, Urban TJ, Shianna KV, Muir AJ, Fried MW, Afdhal NH, Goldstein DB, McHutchison JG. Variants in the ITPA gene protect against ribavirin-induced hemolytic anemia and decrease the need for ribavirin dose reduction. *Gastroenterology* 2010; **139**: 1181-1189 [PMID: 20547162 DOI: 10.1053/j.gastro.2010.06.016]

10 **Sterling RK**, Lissen E, Clumeck N, Sola R, Correa MC, Montaner J, S Sulkowski M, Torriani FJ, Dieterich DT, Thomas

DL, Messinger D, Nelson M; APRICOT Clinical Investigators. Development of a simple noninvasive index to predict significant fibrosis in patients with HIV/HCV coinfection. *Hepatology* 2006; **43**: 1317-1325 [PMID: 16729309 DOI: 10.1002/hep.21178]

11 **Ghany MG**, Strader DB, Thomas DL, Seeff LB; American Association for the Study of Liver Diseases. Diagnosis, management, and treatment of hepatitis C: an update. *Hepatology* 2009; **49**: 1335-1374 [PMID: 19330875 DOI: 10.1002/hep.22759]

12 **Zeuzem S**, Dusheiko GM, Salupere R, Mangia A, Flisiak R, Hyland RH, Illeperuma A, Svarovskaia E, Brainard DM, Symonds WT, Subramanian GM, McHutchison JG, Weiland O, Reesink HW, Ferenci P, Hézode C, Esteban R; VALENCE Investigators. Sofosbuvir and ribavirin in HCV genotypes 2 and 3. *N Engl J Med* 2014; **370**: 1993-2001 [PMID: 24795201 DOI: 10.1056/NEJMoa1316145]

13 **Welzel TM**, Nelson DR, Morelli G, Di Bisceglie A, Reddy RK, Kuo A, Lim JK, Darling J, Pockros P, Galati JS, Frazier LM, Alqahtani S, Sulkowski MS, Vainorius M, Akushevich L, Fried MW, Zeuzem S; HCV-TARGET Study Group. Effectiveness and safety of sofosbuvir plus ribavirin for the treatment of HCV genotype 2 infection: results of the real-world, clinical practice HCV-TARGET study. *Gut* 2017; **66**: 1844-1852 [PMID: 27418632 DOI: 10.1136/gutjnl-2016-311609]

14 **Rangnekar AS**, Fontana RJ. IL-28B polymorphisms and the response to antiviral therapy in HCV genotype 2 and 3 varies by ethnicity: a meta-analysis. *J Viral Hepat* 2013; **20**: 377-384 [PMID: 23647954 DOI: 10.1111/jvh.12039]

15 **Morisco F**, Masarone M, Rosato V, Camera S, Granata R, Tartaglione MT, Coppola C, Coppola N, Salomone-Megna A, Gentile I, De Luna A, Federico A, Precone D, Claar E, Abenavoli L, Persico M. Impact of Telaprevir in HCV Patients with Cirrhosis and RVR: Real-Life Data from Boceprevir or Telaprevir based "Triple Therapy" Experience in Southern Italy. *Rev Recent Clin Trials* 2016; **11**: 306-316 [PMID: 26672601]

16 **Kaserer K**, Fiedler R, Steindl P, Müller CH, Wrba F, Ferenci P. Liver biopsy is a useful predictor of response to interferon therapy in chronic hepatitis C. *Histopathology* 1998; **32**: 454-461 [PMID: 9639122]

17 **Akuta N**, Suzuki F, Kawamura Y, Yatsuji H, Sezaki H, Suzuki Y, Hosaka T, Kobayashi M, Kobayashi M, Arase Y, Ikeda K, Kumada H. Predictors of viral kinetics to peginterferon plus ribavirin combination therapy in Japanese patients infected with hepatitis C virus genotype 1b. *J Med Virol* 2007; **79**: 1686-1695 [PMID: 17854035 DOI: 10.1002/jmv.20979]

18 **Zaman SN**, Melia WM, Johnson RD, Portmann BC, Johnson PJ, Williams R. Risk factors in development of hepatocellular carcinoma in cirrhosis: prospective study of 613 patients. *Lancet* 1985; **1**: 1357-1360 [PMID: 2861313]

19 **Shiffman ML**. Natural history and risk factors for progression of hepatitis C virus disease and development of hepatocellular cancer before liver transplantation. *Liver Transpl* 2003; **9**: S14-S20 [PMID: 14586890 DOI: 10.1053/jlts.2003.50254]

20 **Ikeda M**, Fujiyama S, Tanaka M, Sata M, Ide T, Yatsuhashi H, Watanabe H. Risk factors for development of hepatocellular carcinoma in patients with chronic hepatitis C after sustained response to interferon. *J Gastroenterol* 2005; **40**: 148-156 [PMID: 15770398 DOI: 10.1007/s00535-004-1519-2]

21 **Tokita H**, Fukui H, Tanaka A, Kamitsukasa H, Yagura M, Harada H, Okamoto H. Risk factors for the development of hepatocellular carcinoma among patients with chronic hepatitis C who achieved a sustained virological response to interferon therapy. *J Gastroenterol Hepatol* 2005; **20**: 752-758 [PMID: 15853990 DOI: 10.1111/j.1440-1746.2005.03800.x]

22 **Prenner SB**, VanWagner LB, Flamm SL, Salem R, Lewandowski RJ, Kulik L. Hepatocellular carcinoma decreases the chance of successful hepatitis C virus therapy with direct-acting antivirals. *J Hepatol* 2017; **66**: 1173-1181 [PMID: 28161470 DOI: 10.1016/j.jhep.2017.01.020]

P- Reviewer: Abenavoli L, Dogan UB, El-Shabrawi MHF, Esmat S, Waheed Y **S- Editor**: Wang XJ **L- Editor**: A **E- Editor**: Huang Y

World Journal of Gastroenterology

Submit a Manuscript: http://www.f6publishing.com

World J Gastroenterol 2018 April 7; 24(13): 1486-1490

DOI: 10.3748/wjg.v24.i13.1486

ISSN 1007-9327 (print) ISSN 2219-2840 (online)

CASE REPORT

Gilbert syndrome combined with prolonged jaundice caused by contrast agent: Case report

Jian-Dan Qian, Feng-Qin Hou, Tai-Ling Wang, Chen Shao, Gui-Qiang Wang

Jian-Dan Qian, Feng-Qin Hou, Gui-Qiang Wang, Department of Infectious Diseases and the Center for Liver Diseases, Peking University First Hospital, Beijing 100034, China

Tai-Ling Wang, Department of Pathology, China-Japan Friendship Hospital, Beijing 100029, China

Chen Shao, Department of Pathology, Beijing YouAn Hospital Capital Medical University, Beijing 100069, China

Gui-Qiang Wang, The Collaborative Innovation Center for Diagnosis and Treatment of Infectious Diseases, Zhejiang University, Hangzhou 310003, Zhejiang Province, China

Gui-Qiang Wang, Peking University International Hospital, Beijing 102206, China

ORCID number: Jian-Dan Qian (0000-0002-0112-7500); Feng-Qin Hou (0000-0002-4771-0478); Tai-Ling Wang (0000-0003-2006-0978); Chen Shao (0000-0002-7914-5493); Gui-Qiang Wang (0000-0003-0515-7974).

Author contributions: Qian JD designed and wrote the report; Hou FQ reviewed the manuscript for its intellectual content and revised the entire work; Wang TL and Shao C performed the histological assessments and evaluations; Wang GQ reviewed the manuscript for its intellectual content.

Supported by National Natural Science Foundation of China, No. 81470849.

Informed consent statement: The patient involved in this study gave written informed consent authorizing the use and disclosure of his protected health information.

Conflict-of-interest statement: The authors of this manuscript have no conflicts of interest to disclose.

Manuscript source: Unsolicited manuscript

Correspondence to: Gui-Qiang Wang, MD, PhD, Professor, Department of Infectious Diseases and the Center for Liver Diseases, Peking University First Hospital, 8 Xishiku Dajie, Xicheng District, Beijing 100034, China. 04486@pkufh.com
Fax: +86-10-66551680

Received: January 19, 2018
Peer-review started: January 20, 2018
First decision: February 3, 2018
Revised: February 7, 2018
Accepted: February 26, 2018
Article in press: February 26, 2018
Published online: April 7, 2018

Abstract

This case highlights a patient with Gilbert syndrome who underwent endoscopic retrograde cholangiopancreatography (ERCP) with removal of bile duct stones, who then experienced an unexplained increase in bilirubin, with total bilirubin (TBIL) levels increasing from 159.5 μmol/L to 396.2 μmol/L and to a maximum of 502.8 μmol/L after 9 d. Following the decrease in the TBIL level, enhanced magnetic resonance cholangiopancreatography (MRCP) was performed to exclude any possible remaining choledocholithiasis. Nevertheless, the serum bilirubin level increased again, with TBIL levels rising from 455.7 μmol/L to 594.8 μmol/L and a maximum level of 660.3 μmol/L with no remaining bile duct stones. A liver biopsy showed severe bile duct cholestasis with no inflammation. Based on the exclusion of other potential causes of hyperbilirubinemia and the fact that both instances of increased bilirubin occurred after ERCP and MRCP, the contrast agents iopromide and gadoterate meglumine were suspected to be the causes of the hyperbilirubinemia. As of the writing of this report, the patient's bilirubin levels have spontaneously returned to baseline levels. In summary,

ERCP and MRCP utilizing the contrast agents iopromide and gadoterate meglumine may possibly induce prolonged hyperbilirubinemia.

Key words: Contrast agent; Iopromide; Gadoterate meglumine; Gilbert syndrome; Jaundice

Core tip: Over the past years, only few cases of prolonged postendoscopic retrograde cholangiopancreatography jaundice caused by toxicity of the contrast agent iobitridol have been reported in the world. Up to now, no case of postenhanced magnetic resonance cholangiopancreatography-related jaundice has been reported. Persistent jaundice affects the patient's quality of life, even seriously to life-threatening. Because of the high rarity, treatment experience is not sufficient and more cases need to be accumulated for further analysis.

Qian JD, Hou FQ, Wang TL, Shao C, Wang GQ. Gilbert syndrome combined with prolonged jaundice caused by contrast agent: Case report. *World J Gastroenterol* 2018; 24(13): 1486-1490 Available from: URL: http://www.wjgnet.com/1007-9327/full/v24/i13/1486.htm DOI: http://dx.doi.org/10.3748/wjg.v24.i13.1486

INTRODUCTION

Gilbert syndrome is a liver disorder caused by a genetic mutation of the bilirubin UDP-glucuronosyltransferase (UGT1A1) gene, which results in elevated levels of unconjugated bilirubin. The elevation of serum bilirubin is usually mild, typically less than 102.6 μmol/L. Most cases of Gilbert syndrome are detected due to mild jaundice after pubescence or a mild elevation of unconjugated bilirubin found by chance during a blood examination[1].

Both endoscopic retrograde cholangiopancreatography (ERCP) and magnetic resonance cholangiopancreatography (MRCP) can be used for the diagnosis of cholelithiasis. The major complications related to ERCP involve acute pancreatitis, bleeding, sepsis and perforation. Prolonged postERCP jaundice has been described as a rare postERCP complication due to the known toxicity of the contrast agent iobitridol[2]. However, no cases of postenhanced MRCP-related jaundice have been reported. We report here a case of postERCP and postenhanced-MRCP prolonged hyperbilirubinemia due to toxicity from the contrast agents iopromide and gadoterate meglumine.

CASE REPORT

A 35-year-old man presented with intermittent upper abdominal pain associated with eating greasy food for more than 4 mo. His eyes became yellow, and he reported dark urine and generalized itching for more than 1 mo. The liver test results at the onset of the disease were as follows: total bilirubin (TBIL) 268.7 μmol/L, direct bilirubin (DBIL) 114.4 μmol/L, alanine aminotransferase (ALT) 155 IU/L, aspartate aminotransferase (AST) 71 IU/L, alkaline phosphatase (ALP) 172 IU/L, and gamma-glutamyl transpeptidase (GGT) 424 IU/L. Abdominal computed tomography showed the presence of cholecystolithiasis with features of cholecystitis and dilation of the common bile duct (CBD) and intrahepatic ducts, due to a distal CBD obstruction. MRCP showed a low signal of the distal CBD and bile duct expansion.

The patient had undergone ERCP with sphincterotomy and extraction of a CBD stone 2 wk before presenting to our hospital, and the contrast agent used was iopromide (370 mg/mL). After ERCP, the patient's ALT and GGT levels had significantly decreased and quickly returned to normal; although, the bilirubin levels had increased markedly, with the TBIL level increasing from 159.5 μmol/L to 396.2 μmol/L and the DBIL level increasing from 94.2 μmol/L to 186.9 μmol/L, and with the ALP level increasing markedly from 135.6 IU/L to 192 IU/L (Figures 1 and 2). The amylase and lipase levels had been normal. Ursodeoxycholic acid (UDCA) had been prescribed at a dose of 250 mg three times daily, but the bilirubin levels continued to increase, resulting in levels of TBIL up to 442.5 μmol/L and DBIL up to 334.9 μmol/L. Prednisolone (30 mg daily) had been added, although the hyperbilirubinemia did not improve, at which point the patient presented to our hospital for further diagnosis and treatment.

On the day the patient presented to our hospital, his TBIL level was 502.8 μmol/L and his DBIL level was 295.51 μmol/L. Prednisolone was continued at a dose of 30 mg daily. The fourth day after he presented to our hospital, his bilirubin level decreased slightly, with the TBIL level decreasing from 502.8 μmol/L to 455.7 μmol/L and the DBIL level decreasing from 295.51 μmol/L to 277.44 μmol/L. Once his bilirubin levels decreased, he underwent enhanced-MRCP with gadoterate meglumine as the contrast agent to exclude the possibility of any remaining choledocholithiasis. However, after the enhanced-MRCP, the patient's bilirubin levels increased again, with the TBIL level increasing from 455.7 μmol/L to 594.8 μmol/L and finally to a maximum of 660.3 μmol/L; meanwhile, the patient's DBIL level increased from 277.44 μmol/L to 359.63 μmol/L and then to a maximum of 396.46 μmol/L (Figure 1). The enhanced-MRCP did not show any positive findings.

The markers of infection for hepatitis A, B and C, and other viruses (cytomegalovirus, Epstein-Barr virus) were all negative. Immunological tests for antinuclear antibody, smooth muscle antibody, antimitochondrial antibodies, anti-M2 and antibody to liver kidney microsomal antigen were also negative, with the exception of an increase in IgG-4 values (110 mg/dL). The patient's ferritin level, complete blood count and

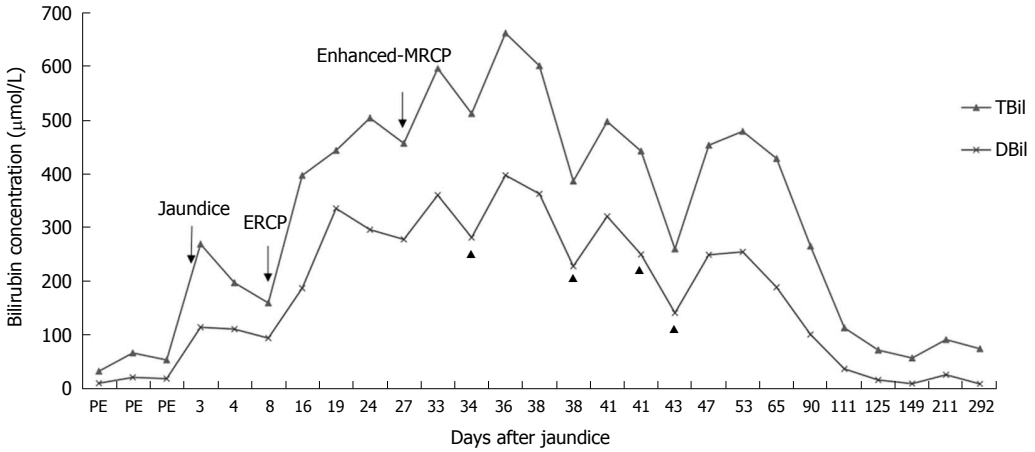

Figure 1 Bilirubin course from onset until the end of follow up. DBil: Direct bilirubin; ERCP: Endoscopic retrograde cholangiopancreatography; MRCP: Magnetic resonance cholangiopancreatography; TBil: Total bilirubin; ▲: After bilirubin adsorption treatment.

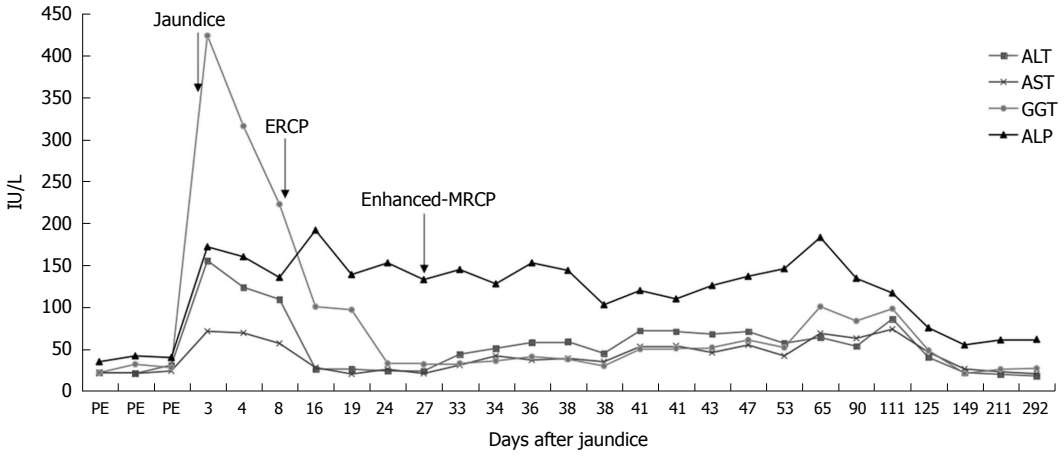

Figure 2 Liver enzyme concentrations from onset until the end of follow up. ALT: Alanine aminotransferase; ALP: Alkaline phosphatase; AST: Aspartate aminotransferase; GGT: Gamma-glutamyl transpeptidase.

inflammatory markers were normal. Gilbert gene sequencing was performed, and the analysis revealed the A(TA)^{7}TAA heterozygote [wild type: A(TA)^{6}TAA] in the promoter region (UGT1A1*28) and an UGT1A1.80:-364C>T, UGT1A1.112:-1352A>C heterozygote. A liver biopsy showed marked bilirubinostasis in zones 3 and 2, canaliculi with no evidence of portal tract inflammation or interphase hepatitis, no lesions or paucity of bile ducts, and no bile infarcts or leaks (Figures 3 and 4).

Since the age of 17, the patient had experienced intermittent yellow discoloration of the eyes with no other symptoms. Laboratory examinations revealed normal hemoglobin, reticulocyte, aminotransferases and cholestatic enzymes, while the serum TBIL level fluctuated by 32.8 μmol/L to 66.7 μmol/L, and the ratio of DBIL to TBIL was 32%. The diagnosis of congenital nonhemolytic bilirubin metabolic disorder was confirmed. The patient's family had no history of similar disorders, but his son had physiologic jaundice at birth. Before onset of the disease, the patient did not take any medications and had no history of alcohol abuse.

Combined with his history of nonhemolytic bilirubin metabolic disorder and genetic test results, the diagnosis of Gilbert syndrome was clear. Because the other potential causes of hyperbilirubinemia were ruled out and the two instances of increased bilirubin occurred postERCP and postMRCP, the use of the contrast agents iopromide and gadoterate meglumine were suspected to be the cause of the hyperbilirubinemia.

The patient was prescribed phenobarbital (60 mg three times daily) and UDCA (500 mg two times daily); prednisolone (30 mg daily) was continued, while cholestyramine (5 g three times daily) was used for symptomatic relief. In addition, with the worsening of cholestasis, bilirubin serum adsorption treatments were performed a total of four times; after each treatment, the serum bilirubin concentration decreased by 11%-23% and clinical symptoms were relieved, but the bilirubin level slightly increased again 1 to 2 d after the bilirubin serum adsorption treatment. Because the bilirubin level declined slowly, the patient was discharged after a 1-mo stay in our hospital.

In the outpatient setting, the oral prednisolone was

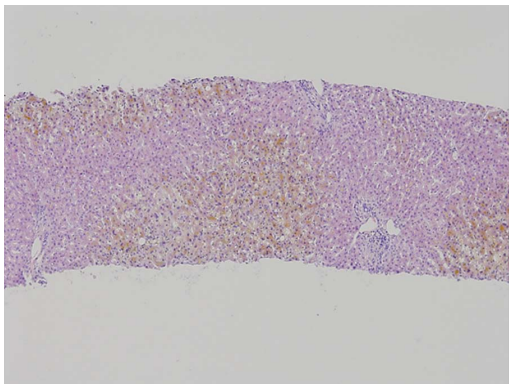

Figure 3 Cholestasis of liver tissue (hematoxylin-eosin stain, original magnification × 4).

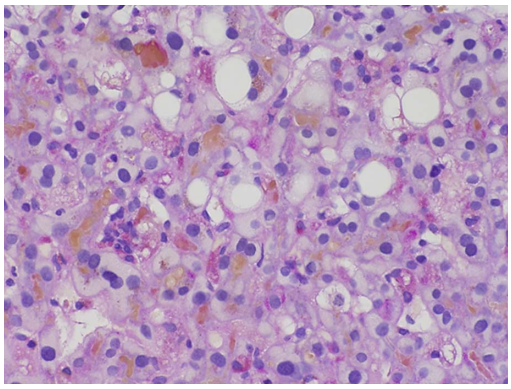

Figure 4 Liver lobular capillary bile duct cholestasis, slight inflammation, undamaged hepatocytes, and some ground-glass cytoplasm degeneration (D-PAS stain, original magnification × 60).

tapered regularly, and phenobarbital and UDCA were discontinued. At his 11-mo follow-up visit, the serum bilirubin level had slowly decreased, and as of the writing of this report, the patient's bilirubin levels had spontaneously returned to baseline levels (Figure 1).

DISCUSSION

Due to the presence of Gilbert syndrome, the patient showed prolonged jaundice postERCP, and enhanced-MRCP accentuated this effect. A liver biopsy revealed marked intrahepatic cholestasis, which may be attributed to large bile obstruction, benign recurrent intrahepatic cholestasis (BRIC) or drug-induced liver toxicity. Enhanced-MRCP had already excluded bile obstruction by stones. BRIC is a rare genetic disorder characterized by intermittent episodes of jaundice and pruritus; each episode can last for several weeks to months. A completely asymptomatic phase occurs in between attacks that can last from months to years. Liver biochemistry is characterized by conjugated hyperbilirubinemia and increased ALP levels. Serum GGT, AST and ALT levels are either normal or mildly elevated. Liver biopsy shows intrahepatic and canalicular cholestasis predominantly involving zone 3[3].

The patient's liver biopsy features were consistent with BRIC; however, genetic sequencing indicated no mutation in ATP8BI. In addition, the patient had no history of recurrent conjugated hyperbilirubinemia; therefore, the diagnosis of BRIC was not established. Because the two instances of increased bilirubin occurred after ERCP and MRCP, the use of the contrast agents iopromide and gadoterate meglumine was suspected to be the cause of the hyperbilirubinemia.

Prolonged cholestasis is a very rare complication of ERCP, and few cases of this complication are reported in the English literature[2,4-6]. The exact mechanism of this complication, however, remains unknown. Some articles consider that it may be associated with iodine contrast agents (diatrizoate or iobitridol)[2,4], while others posit that it may be caused by cefuroxime, which is one of the cephalosporins used after ERCP to prevent infections[6]. Our patient did not receive cephalosporins postERCP; therefore, the prolonged jaundice was associated with the contrast agents. Additionally, the cause-result time connection between the use of the contrast agents and bilirubin increases supported this possibility.

Gadolinium-based contrast agents (GBCAs) play an important role in enhanced-MRCP examinations. The common side effects of GBCAs include nausea, chest tightness, rash and vascular edema. Gadolinium is mainly renally excreted, although it may also be deposited in the liver, brain, muscle and other organs[7]. No cases of gadolinium-induced cholestasis have been reported in the literature. Although our patient's bilirubin level increased again after enhanced-MRCP, after his first instance of elevated bilirubin had decreased, we speculated that the gadolinium may have been involved in the cholestasis. The gadolinium used in our patient is ionic, which can lead to high osmotic pressure and dehydration of tissue cells, suggesting that the mechanism of gadolinium-induced hyperbilirubinemia may be due to the high permeability, which further aggravated the damage to the bile duct cells and affected the secretion and excretion of bile.

PostERCP jaundice has been reported to resolve after 2-4 mo, although it took approximately 1 year for this patient's bilirubin level to return to baseline levels, which may be related to the second incident of damage due to gadolinium.

The general treatment for cholestasis caused by contrast agents is UDCA, and cholestyramine can be used to relieve symptoms. If a trial of these two agents proves unsuccessful, corticosteroids may be added[8] with or without plasmapheresis[9]. In our case, UDCA (500 mg two times daily), cholestyramine (5 g three times daily) and prednisolone (30 mg daily) failed to relieve the patient's symptoms until bilirubin serum adsorption was performed, which efficiently stabilized the bilirubin level. Therefore, in the case of a poor response to traditional drug treatment methods, providers may try plasma exchange or bilirubin

adsorption, which can prevent damage to liver cells due to long-term elevated bilirubin levels.

Our patient's case illustrates a rare drug-induced liver injury due to contrast agents, which presented as prolonged cholestasis following "successful" therapeutic ERCP for an obstructing distal CBD stone and an enhanced-MRCP that excluded residual stones. Clinicians must be aware that ERCP and MRCP with the contrast agents iopromide and gadoterate meglumine may have the possibility of inducing prolonged hyperbilirubinemia.

ARTICLE HIGHLIGHTS

Case characteristics

A middle-aged male patient presented with abdominal pain, jaundice and dark urine.

Clinical diagnosis

The only physical sign of this case was a mild abdominal tenderness.

Differential diagnosis

Viral hepatitis, other viruses infection (cytomegalovirus, Epstein-Barr virus), autoimmune liver disease, IgG-4-related cholangitis, and benign recurrent intrahepatic cholestasis.

Laboratory diagnosis

The liver test results showed total bilirubin 268.7 μmol/L, direct bilirubin 114.4 μmol/L, alanine aminotransferase 155 IU/L, aspartate aminotransferase 71 IU/L, alkaline phosphatase 172 IU/L, and gamma-glutamyl transpeptidase 424 IU/L.

Imaging diagnosis

Abdominal computed tomography showed the presence of cholecystolithiasis, with features of cholecystitis and dilation of the common bile duct (CBD) and intrahepatic ducts due to a distal CBD obstruction.

Pathological diagnosis

A liver biopsy showed marked bilirubinostasis in zones 3 and 2, canaliculi with no evidence of portal tract inflammation or interphase hepatitis, no lesions or paucity of bile ducts, and no bile infarcts or leaks.

Treatment

The patient was prescribed phenobarbital, ursodeoxycholic acid, prednisolone and cholestyramine. In addition, with the worsening of cholestasis, bilirubin serum adsorption treatments were performed a total of four times.

Related reports

Prolonged cholestasis is a very rare complication of endoscopic retrograde cholangiopancreatography (ERCP), and few cases of this complication are reported in the English literature. The exact mechanism of this complication, however, remains unknown. No cases of post enhanced magnetic resonance cholangiopancreatography (MRCP)-related jaundice have been reported.

Term explanation

ERCP: Endoscopic retrograde cholangiopancreatography, which can be used for the diagnosis of cholelithiasis.

Experiences and lessons

Our patient's case illustrates a rare drug-induced liver injury due to contrast agents, which presented as prolonged cholestasis following "successful" therapeutic ERCP for an obstructing distal CBD stone and an enhanced-MRCP that excluded residual stones. Clinicians must be aware that ERCP and MRCP with the contrast agents iopromide and gadoterate meglumine may have the possibility of inducing prolonged hyperbilirubinemia.

REFERENCES

1 **Aiso M**, Yagi M, Tanaka A, Miura K, Miura R, Arizumi T, Takamori Y, Nakahara S, Maruo Y, Takikawa H. Gilbert Syndrome with Concomitant Hereditary Spherocytosis Presenting with Moderate Unconjugated Hyperbilirubinemia. *Intern Med* 2017; **56**: 661-664 [PMID: 28321066 DOI: 10.2169/internalmedicine.56.7362]

2 **Tziatzios G**, Gkolfakis P, Papanikolaou IS, Dimitriadis G, Triantafyllou K. An unusual case of prolonged post-endoscopic retrograde cholangiopancreatography jaundice. *Hepatobiliary Pancreat Dis Int* 2016; **15**: 220-222 [PMID: 27020640]

3 **Luketic VA**, Shiffman ML. Benign recurrent intrahepatic cholestasis. *Clin Liver Dis* 2004; **8**: 133-149, vii [PMID: 15062197 DOI: 10.1016/S1089-3261(03)00133-8]

4 **Dourakis SP**, Mayroyannis C, Alexopoulou A, Hadziyannis SJ. Prolonged cholestatic jaundice after endoscopic retrograde cholangiography. *Hepatogastroenterology* 1997; **44**: 677-680 [PMID: 9222670]

5 **Chavalitdhamrong D**, Donepudi S, Pu L, Draganov PV. Uncommon and rarely reported adverse events of endoscopic retrograde cholangiopancreatography. *Dig Endosc* 2014; **26**: 15-22 [PMID: 24118211 DOI: 10.1111/den.12178]

6 **Niriella MA**, Kumarasena RS, Dassanayake AS, Pathirana A, de Silva Hewavisenthi J, de Silva HJ. Worsening cholestasis and possible cefuroxime-induced liver injury following "successful" therapeutic endoscopic retrograde cholangiopancreatography for a distal common bile duct stone: a case report. *J Med Case Rep* 2016; **10**: 371 [PMID: 28003028 DOI: 10.1186/s13256-016-1123-0]

7 **Ramalho J**, Ramalho M, Jay M, Burke LM, Semelka RC. Gadolinium toxicity and treatment. *Magn Reson Imaging* 2016; **34**: 1394-1398 [PMID: 27693607 DOI: 10.1016/j.mri.2016.09.005]

8 **Lee HM**, Bonis PA, Kaplan MM. Persistent cholestatic jaundice after ERCP. *Am J Gastroenterol* 2006; **101**: 204-205 [PMID: 16405561 DOI: 10.1111/j.1572-0241.2006.00393_7.x]

9 **Saritas U**, Aydin B, Ustundag Y. Plasmapheresis and corticosteroid treatment for persistent jaundice after successful drainage of common bile duct stones by endoscopic retrograde cholangiography. *World J Gastroenterol* 2007; **13**: 4152-4153 [PMID: 17696241 DOI: 10.3748/wjg.v13.i30.4152]

P- Reviewer: Gkekas I, Isaji S, Kitamura K **S- Editor**: Ma YJ
L- Editor: Filipodia **E- Editor**: Huang Y

Published by **Baishideng Publishing Group Inc**
7901 Stoneridge Drive, Suite 501, Pleasanton, CA 94588, USA
Telephone: +1-925-223-8242
Fax: +1-925-223-8243
E-mail: bpgoffice@wjgnet.com
Help Desk: http://www.f6publishing.com/helpdesk
http://www.wjgnet.com

ISSN 1007-9327

ISSN 1007-9327 (print)
ISSN 2219-2840 (online)

World Journal of *Gastroenterology*

World J Gastroenterol 2018 April 14; 24(14): 1491-1582

Published by Baishideng Publishing Group Inc

World Journal of Gastroenterology

Contents

Weekly Volume 24 Number 14 April 14, 2018

ABOUT COVER

Editorial board member of *World Journal of Gastroenterology*, Maria Gazouli, PhD, Associate Professor, Basic Medical Science, School of Medicine, National and Kapodistrian University of Athens, Athens 11527, Greece

AIMS AND SCOPE

World Journal of Gastroenterology (*World J Gastroenterol*, *WJG*, print ISSN 1007-9327, online ISSN 2219-2840, DOI: 10.3748) is a peer-reviewed open access journal. *WJG* was established on October 1, 1995. It is published weekly on the 7th, 14th, 21st, and 28th each month. The *WJG* Editorial Board consists of 642 experts in gastroenterology and hepatology from 59 countries.

The primary task of *WJG* is to rapidly publish high-quality original articles, reviews, and commentaries in the fields of gastroenterology, hepatology, gastrointestinal endoscopy, gastrointestinal surgery, hepatobiliary surgery, gastrointestinal oncology, gastrointestinal radiation oncology, gastrointestinal imaging, gastrointestinal interventional therapy, gastrointestinal infectious diseases, gastrointestinal pharmacology, gastrointestinal pathophysiology, gastrointestinal pathology, evidence-based medicine in gastroenterology, pancreatology, gastrointestinal laboratory medicine, gastrointestinal molecular biology, gastrointestinal immunology, gastrointestinal microbiology, gastrointestinal genetics, gastrointestinal translational medicine, gastrointestinal diagnostics, and gastrointestinal therapeutics. *WJG* is dedicated to become an influential and prestigious journal in gastroenterology and hepatology, to promote the development of above disciplines, and to improve the diagnostic and therapeutic skill and expertise of clinicians.

INDEXING/ABSTRACTING

World Journal of Gastroenterology (*WJG*) is now indexed in Current Contents®/Clinical Medicine, Science Citation Index Expanded (also known as SciSearch®), Journal Citation Reports®, Index Medicus, MEDLINE, PubMed, PubMed Central and Directory of Open Access Journals. The 2017 edition of Journal Citation Reports® cites the 2016 impact factor for *WJG* as 3.365 (5-year impact factor: 3.176), ranking *WJG* as 29th among 79 journals in gastroenterology and hepatology (quartile in category Q2).

NAME OF JOURNAL
World Journal of Gastroenterology

ISSN
ISSN 1007-9327 (print)
ISSN 2219-2840 (online)

LAUNCH DATE
October 1, 1995

FREQUENCY
Weekly

EDITORIAL OFFICE
Ze-Mao Gong, Director
World Journal of Gastroenterology
Baishideng Publishing Group Inc
7901 Stoneridge Drive, Suite 501,
Pleasanton, CA 94588, USA
Telephone: +1-925-2238242
Fax: +1-925-2238243
E-mail: editorialoffice@wjgnet.com
Help Desk: http://www.f6publishing.com/helpdesk
http://www.wjgnet.com

PUBLISHER
Baishideng Publishing Group Inc
7901 Stoneridge Drive, Suite 501,
Pleasanton, CA 94588, USA
Telephone: +1-925-2238242
Fax: +1-925-2238243
E-mail: bpgoffice@wjgnet.com
Help Desk: http://www.f6publishing.com/helpdesk
http://www.wjgnet.com

PUBLICATION DATE
April 14, 2018

INSTRUCTIONS TO AUTHORS
Full instructions are available online at http://www.wjgnet.com/bpg/gerinfo/204

ONLINE SUBMISSION
http://www.f6publishing.com

World Journal of Gastroenterology

Submit a Manuscript: http://www.f6publishing.com

World J Gastroenterol 2018 April 14; 24(14): 1491-1506

DOI: 10.3748/wjg.v24.i14.1491

ISSN 1007-9327 (print) ISSN 2219-2840 (online)

REVIEW

Nonalcoholic fatty liver disease and liver transplantation - Where do we stand?

Ivana Mikolasevic, Tajana Filipec-Kanizaj, Maja Mijic, Ivan Jakopcic, Sandra Milic, Irena Hrstic, Nikola Sobocan, Davor Stimac, Patrizia Burra

Ivana Mikolasevic, Ivan Jakopcic, Sandra Milic, Davor Stimac, Department of Gastroenterology, UHC Rijeka, School of Medicine, University of Rijeka, Rijeka 51000, Croatia

Tajana Filipec-Kanizaj, Maja Mijic, Nikola Sobocan, Department of Gastroenterology, University Hospital Merkur, School of Medicine, University of Zagreb, Zagreb 10000, Croatia

Irena Hrstic, Department of Internal medicine, General Hospital Pula, Pula, School of Medicine, University of Rijeka and Zagreb, Pula 52100, Croatia

Patrizia Burra, Multivisceral Transplant Unit, Department of Surgery, Oncology and Gastroenterology, Padua University Hospital, Padua 35128, Italy

ORCID number: Ivana Mikolasevic (0000-0001-9676-0642); Tajana Filipec-Kanizaj (0000-0002-9828-8916); Maja Mijic (0000-0002-8355-1013); Ivan Jakopcic (0000-0003-0740-3171); Sandra Milic (0000-0002-6635-5360); Irena Hrstic (0000-0003-4962-2276); Nikola Sobocan (0000-0001-6721-9232); Davor Stimac (0000-0001-8243-2453); Patrizia Burra (0000-0002-8791-191X).

Author contributions: Mikolasevic I researched the database, analyzed data, wrote the manuscript, and is the guarantor of this work; Filipec-Kanizaj T, Mijic M, Jakopcic I, Milic S, Hrstic I, Sobocan N, Stimac D and Burra P contributed to the discussion and reviewed/edited the manuscript.

Conflict-of-interest statement: The authors declare no conflicts of interest.

Manuscript source: Invited manuscript

Correspondence to: Ivana Mikolasevic, MD, PhD, Assistant Professor, Department of Gastroenterology, UHC Rijeka, Rijeka, Croatia, School of Medicine, University of Rijeka, 51000, Rijeka, Croatia. ivana.mikolasevic@gmail.com
Telephone: +385-51-658122
Fax: +385-51-658122

Received: February 18, 2019
Peer-review started: February 19, 2019
First decision: March 14, 2018
Revised: March 19, 2018
Accepted: March 25, 2018
Article in press: March 25, 2018
Published online: April 14, 2018

Abstract

Nonalcoholic fatty liver disease/nonalcoholic steatohepatitis (NAFLD/NASH) is a challenging and multisystem disease that has a high socioeconomic impact. NAFLD/NASH is a main cause of macrovesicular steatosis and has multiple impacts on liver transplantation (LT), on patients on the waiting list for transplant, on post-transplant setting as well as on organ donors. Current data indicate new trends in the area of chronic liver disease. Due to the increased incidence of metabolic syndrome (MetS) and its components, NASH cirrhosis and hepatocellular carcinoma caused by NASH will soon become a major indication for LT. Furthermore, due to an increasing incidence of MetS and, consequently, NAFLD, there will be more steatotic donor livers and less high quality organs available for LT, in addition to a lack of available liver allografts. Patients who have NASH and are candidates for LT have multiple comorbidities and are unique LT candidates. Finally, we discuss long-term grafts and patient survival after LT, the recurrence of NASH

and NASH appearing *de novo* after transplantation. In addition, we suggest topics and areas that require more research for improving the health care of this increasing patient population.

Key words: Nonalcoholic steatohepatitis; Chronic liver disease; Liver transplantation; Nonalcoholic fatty liver disease; Outcome

Core tip: Nonalcoholic fatty liver disease/nonalcoholic steatohepatitis (NAFLD/NASH) is a challenging and multisystem disease that has a high socioeconomic impact. NAFLD/NASH is a primary cause of macrovesicular steatosis and has several impacts on liver transplantation (LT), which is transmitted to transplant recipients and organ donors. Current data indicate a new trend in the area of chronic liver disease. Due to the increased incidence of metabolic syndrome (MetS) and its components, NASH cirrhosis and hepatocellular carcinoma caused by NASH will soon become a major indication for LT.

Mikolasevic I, Filipec-Kanizaj T, Mijic M, Jakopcic I, Milic S, Hrstic I, Sobocan N, Stimac D, Burra P. Nonalcoholic fatty liver disease and liver transplantation - Where do we stand? *World J Gastroenterol* 2018; 24(14): 1491-1506 Available from: URL: http://www.wjgnet.com/1007-9327/full/v24/i14/1491.htm DOI: http://dx.doi.org/10.3748/wjg.v24.i14.1491

INTRODUCTION

Parallel to the increasing prevalence of diabetes mellitus type 2 (T2DM) and obesity and a close relationship with insulin resistance (IR) and metabolic risk factors, nonalcoholic fatty liver disease (NAFLD) has become the most common chronic liver disease (CLD) in the world over the past 30 years, with an estimated prevalence of 10%-40%[1,2]. NAFLD is characterized by increased fat depositions in the liver with clinical-histological phenotypes that range from a simple steatosis (present in > 5% of hepatocytes, as shown in histological analysis or magnetic resonance spectroscopy) to nonalcoholic steatohepatitis (NASH). NASH is a more aggressive form of the disease and includes a histological presentation of steatosis, ballooning hepatocytes and lobular inflammation that leads to advanced fibrosis and, finally, cirrhosis and hepatocellular carcinoma (HCC)[1,3]. Given the growing prevalence of NAFLD, several studies have attempted to determine the clinical course and progression of the disease, but the exact prognosis remains unclear. A recently published Swedish retrospective study was the largest biopsy-proven NAFLD study to provide insight on the long-term prognosis and outcomes of the disease, with a follow-up period of up to 40 years[4]. In that report, NAFLD patients had an increased risk for mortality and liver-related morbidity (12% of the patients developed severe liver disease, which is defined as liver failure, compensated or decompensated liver cirrhosis and HCC). Interestingly, the presence of NASH did not significantly increase the risk for liver-related morbidity or overall mortality. The fibrosis stage was highly predictive of the risk of developing sever liver disease, with a hazard ratio that ranged from 1.9 in F0 to 104.9 in F4. The primary high fibrosis stages (F3-F4) predicted overall mortality[4], which is similar to previous published research[5,6]. Compared to other etiologies of chronic liver disease, NAFLD has a slower fibrosis progression, with an estimated time for developing severe liver disease at 22-26 years for F0-1, 9.3 years for F2, 2.3 years for F3 and 0.9 years for F4 (for decompensation)[4]. The clinical burden of NAFLD extends beyond the liver, with evidence indicating that NAFLD is a multisystem disease that is closely related to cardiovascular disease (CVD), chronic kidney disease (CKD) and T2DM. It is still not clear whether NAFLD is only a risk factor or is an important component of the pathophysiological mechanisms in the development and progression of those diseases[7]. In addition, a major cause of morbidity and mortality in NAFLD patients is CVD, followed by malignancies and liver-related diseases (cirrhosis and HCC) as the third cause[7]. HCC is the sixth most common cancer in the world that is predisposed with the presence of cirrhosis, but emerging data suggest that HCC can evolve in non-cirrhotic NAFLD and is strongly associated with metabolic syndrome (MetS)[8]. The HCC that is associated with NAFLD/NASH has a distinct phenotype. It is often diagnosed at an older age and in the advanced stages of liver disease, and, compared with the HCC in viral hepatitis, is less aggressive and therefore more commonly missed on routine scans for malignancies[9]. With the continuous increase in the incidence of obesity, T2DM and MetS in United States (US) and Europe, it is predicted that NAFLD/NASH will become the most common cause of HCC in the Western world. NAFLD/NASH has already become the second leading cause of liver transplantation (LT) in the US and, importantly, the number of patients who have NAFLD/NASH and are on the waiting list for transplantation increased by 170% from 2004 to 2013. Thus, end-stage liver disease (ESLD) due to NAFLD/NASH will become the most common indicator for LT in the near future[10].

We expect groundbreaking changes in the area of LT. Therefore, this review discusses the multiple impacts of NAFLD on LT. First, due to the aging of the population and an increasing incidence of MetS and

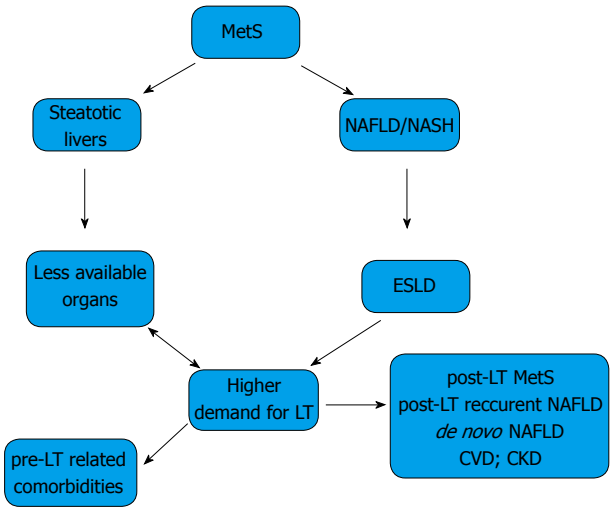

Figure 1 Higher incidence of metabolic syndrome and its complications leads to a higher incidence of nonalcoholic steatohepatitis/nonalcoholic fatty liver disease and, consequently, to more patients who have end-stage liver disease. At the same time, due to MetS and its components, we will have more steatotic livers, *i.e.*, more organs of lower quality that are available for LT. Therefore, in the future, since NAFLD will affect both the demand for LT and the supply of available organs. Patients who have NASH and are candidates for LT have several comorbidities and are unique LT candidates. Post-LT, there are several challenging issues for NAFLD: recurrent NAFLD, de novo NAFLD and the risk for CVD and CKD. MetS: Metabolic syndrome; NAFLD: Nonalcoholic fatty liver disease; NASH: Nonalcoholic steatohepatitis; ESLD: End-stage liver disease; LT: Liver transplantation; CVD: Cardiovascular diseases; CKD: Chronic kidney disease.

its liver manifestation (*i.e.*, NAFLD/NASH), ESLD as a consequence of NASH will become a primary driver of LT in the near future. Furthermore, due to the increasing incidence of obesity, and, consequently MetS, the prevalence of NAFLD in the population will also increase[1,2] As such, owing to the growing incidence of NAFLD, we can expect that there will be more steatotic donor livers and fewer high quality organs available for LT. Therefore, NAFLD affects both the demand for LT and the supply of available donors.Moreover, patients who have NASH and are candidates for LT have several comorbidities, such as obesity, T2DM and other MetS components, as well as CVD and CKD. These patients are uniquely challenging LT candidates, and transplantation specialists are continuously exposed to the challenges of transplantation from obese donors, as well as the NASH recipients with their often multiple comorbidities. Finally, we discuss long term grafts and patient survival after LT, the recurrence of NASH and NASH appearing *de novo* after transplantation[11,12] Figure 1. In addition, we suggest topics and areas for further research for improving health care for this increasing patient population.

For this Review, we identified references using PubMed and the terms "NAFLD", "NASH", and "liver transplantation." We only reviewed articles that were published in English. The references were selected based on originality and their relevance to the domain of this Review.

NAFLD RELATED END-STAGE LIVER DISEASE AND HCC AS INDICATIONS FOR LIVER TRANSPLANTATION

NAFLD patients can necessitate the need for LT in two primary ways: developing cirrhosis that manifests with decreased synthetic/excretion function(s) and signs of portal hypertension and HCC development. It is estimated that approximately one-third of the current population in industrialized countries has NAFLD as a consequence of the liver's involvement in the context of MetS. As mentioned above and according to many authors, it is clear that over the next ten or twenty years, the prevalence of NAFLD will increase due to the epidemic rise in obesity, T2DM, arterial hypertension and the prevalence of MetS, as well as people living longer[10-13]. Consequently, NAFLD-related liver disease is currently the most rapidly increasing indication for LT in the US, and it is anticipated that NAFLD-related liver disease will become the leading indication for LT in the near future[14,15]. In the context of the increasing incidence of NAFLD as an indication for LT, it is important to highlight several facts. First, due to the development of direct antiviral agents (DAA) for hepatitis C (HCV), the incidences of cirrhosis and HCC due to HCV as indications for LT will decrease over time. Three years ago, Wong *et al*[10] analyzed the United Network for Organ Sharing and Organ Procurement and Transplantation Network's (UNOS/OPTN) registry data from 2004 to 2013. There were four groups of registrants who were on the liver transplant waitlist: patients who had an HCV infection, NASH, alcoholic liver disease (ALD), or a combination of HCV infection and ALD. Over a period of nine years, the numbers of new patients on the waitlist who had NASH, ALD, and HCV increased by 170%, 45% and 14%, respectively. Moreover, the percentage of registrants who had HCV and ALD decreased by 9% (from 880 to 803)[10].

A recent study by Goldberg *et al*[16] analyzed the prevalence of HCV from 2010 to 2014 from National Health and Nutrition Examination Survey (NHANES) data. They also collected data from patients who had cirrhosis and chronic liver failure (LF) from 2006 to 2014 and were in the Health Core Integrated Research Database. In addition, they analyzed data from liver transplant recipients from UNOS from 2003 to 2015. By combining data from these three databases, the study investigated current changes in liver disease(s); HCV, alcoholic liver disease (ALD) and NAFLD/NASH through the course of liver disease; CLD - compensated cirrhosis, decompensated cirrhosis and HCC; and the waiting list for LT and LT recipients. The study authors found that there were significant changes in CLD etiology that were associated with important alterations

in the occurrence of HCV, ALD and NAFLD/NASH as indications for liver transplantation. They demonstrated that active HCV infection decreased as an indication for LT after DAA use. Subsequently, there was a decrease in the incidence of cirrhosis due to HCV in the larger population with CLD[16]. In contrast, among patients who were on the waiting list and LT recipients, NAFLD became more common. Another interesting finding from this study was that the incidence of ALD as an indication for LT increased more than NASH[16]. A retrospective study by Cholankeril *et al*[17] had similar findings after analyzing the UNOS/OPTN database from 2003 to 2014. The authors discovered that the number of LT that is secondary to NASH increased by 162% from 2003 to 2014, while the number of LT secondary to HCV increased by 33%, and the number of LT secondary to ALD increased by 55%[17].

Recently, there has been a trend of an increased incidence of HCC in developed countries, and according to the literature, this increase is most likely due to an increased incidence of MetS[8,18]. The large Bridge study included 18031 HCC patients from 2005-2012. NAFLD was one of the major risk factors for HCC development, and NAFLD was the cause of chronic liver disease for approximately 10%-12% of patients[19,20]. Similarly, a recently published US study found that HCC as a consequence of NASH is the fastest growing indication for LT. The authors of this study reported that NASH related HCC as an indication for LT had an almost fourfold increase since 2002; on the other hand, HCC that results from HCV, doubled[13,21].

In the context of LT and NAFLD, it is concerning that a recent discovery found that HCC may appear in NAFLD patients who do not have liver cirrhosis or advanced liver fibrosis[8]. Mittal *et al*[22] published data on 13% of patients who had HCC and, at the time of diagnosis, did not have cirrhosis. The primary risk factor for developing HCC was the presence of NAFLD or MetS. In addition, in a study by a group of German authors, 41.7% of the patients with NAFLD/NASH HCC previously had no diagnosis of cirrhosis[23]. Similar findings were also reported by other authors[24,25].

Another concerning issue in the context of NASH and LT is the increase in the incidence of NAFLD in children and young adults (up to age 40). Feldstein *et al*[26] analyzed long-term outcomes and survival for children who had NAFLD. In this study, children who had NAFLD had a 13.8-fold higher risk of requiring LT or dying than the general population of the same age and sex[26]. Recently, Alkhouri *et al*[27] analyzed LT in children and young adults and the frequency of NASH as an indicator for LT. They found an increased incidence of NASH as an indicator for LT in young patients. More than 100 recipients had LT before they were 34 years old, while most patients received their liver transplant closer to the age of 40 years[27].

Current guidelines do not recommend regular screenings for HCC in NAFLD patients who have no signs of liver cirrhosis or advanced fibrosis. According to recent research, NAFLD patients who have not developed cirrhosis have a risk of developing HCC; however, there are no studies that examine the cost-benefit of screening in this population of patients. However, the current data on the increasing incidence of NAFLD combined with the growing incidence of MetS and NAFLD in young people indicate that there will be a need for LT in the context of NAFLD related decompensated cirrhosis and NAFLD related HCC[13,20,21].

Due to the substantial increase in the proportion of transplants due to NAFLD, as well as new waitlist registrants with NAFLD cirrhosis complications, NAFLD/NASH cirrhosis and related HCC are the most rapidly growing indications for LT.

NAFLD PATIENTS ON THE WAITLIST FOR LIVER TRANSPLANTATION

Every CLF patient has unique characteristics and needs an individual approach in the context of LT, and the same individual approach is necessary for patients who have NASH. The risk factors for poor postoperative and long-term outcomes are age the presence of MetS components (especially T2DM and obesity), coronary artery disease (CAD) and chronic kidney disease (CKD). Patients who have NASH on the waitlist often have several or all of these risk factors. For NASH patients on the waiting list there are two problems: patient comorbidities and lower MELD than other etiologies of CLD[28].

First, NAFLD is the liver manifestation of MetS and NAFLD patients on the LT waiting list frequently have one or more components of MetS. They are often obese and have T2DM, hypertension and hyperlipidemia. In addition, NASH recipients are older than recipients who have a different CLD[28]. According to Wong *et al*[10] compared to patients who had an alcoholic, viral or alcoholic/viral etiology of CLD who were on the waitlist for LT, patients with NASH had decreased renal function, were more obese and were more likely to have T2DM. There was higher morbidity and mortality in obese patients who underwent surgical procedures. However, in the context of obesity and LT, the results were not consistent. Several studies reported worse outcomes for obese patients, while other authors found similar risks and outcomes for both obese and non-obese patient groups[28]. For example, Leonard *at al*[29] had similar results for all body mass index (BMI) categories for early and late patients and graft survival. In contrast, La Mattina *et al*[30] found that obese patients had a longer operative time, intensive care unit length of stay, and more infectious and biliary complications that required intervention. There was no significant difference in patient or graft survival for overweight Class Ⅰ and obese Class Ⅲ recipients compared to normal weight recipients. However, patients who had Class Ⅱ obesity experienced decreased patient and

allograft survival[29]. Not long ago, Conzen *et al*[31] found that morbid obesity had negative effects on long-term outcomes regardless of the short-term results. In other words, there were no differences in operative time, intensive care unit or hospital length of stay or perioperative complications. Over 3 years, recipient and graft survival rates were similar across groups. Compared to the non-obese, recipients who had a BMI > 40 kg/m^2 experienced a significantly decreased 5-year graft (49.0% *vs* 75.8%; $P < 0.02$) and recipient (51.3% *vs* 78.8%; $P < 0.01$) survival. Although between group comparisons is difficult given the different endpoints and BMIs between cohorts, in general, obese patients have increased complication rates and more resource utilization compared to non-obese recipients[19]. Given the increase in the incidence of overweight patients and MetS, we can expect an increase in the number of patients with NASH cirrhosis or HCC in NASH with high BMI who are on the transplant list in the future. In addition, the bariatric surgery (BS) methods will become more important in the context of treating obesity for the morbid obesity of NASH patients. There are promising research findings for BS in these patients. There are studies with a small number of patients who were experiencing LT and some form of BS[28]. For example, Heimbach *et al*[32] conducted a small study that combined LT with a sleeve gastrectomy, which resulted in significant weight loss for patients who were not successful with medical treatment. In addition, there were less post-LT metabolic complications[32].

Recently, 11 studies with 56 patients were analyzed in a systematic review[33]. Two studies reported that BS had been previously performed, while two studies performed it during and seven after LT. The most common procedure was the sleeve gastrectomy, while the Roux-en-Y gastric bypass, biliopancreatic diversion and gastric banding were performed in a slightly smaller number of patients. There was no mortality in the early postoperative period, with a 5.3% rate during the first postoperative year. The reoperation rate was 12.2%. Although mortality and morbidity are higher in this population, the authors agreed that BS appears to be possible[33].

In the future, there is a need for randomized studies to determine which patients on the transplant list will benefit from BS, the optimal time for BS (before, during or after LT) and the optimal type of BS. It is important to note that patients who have decompensated cirrhosis have a higher mortality rate after BS than those who have compensated cirrhosis or no chronic liver disease; thus, it is extremely important to optimize the time at which patients should undergo BS[28,34]. Future studies are also needed to demonstrate the long-term impact of BS on liver transplant recipients and graft outcomes[28].

Patients who have NASH and are on the waitlist for LT often have T2DM. Pre-transplant T2DM is a strong predictor of poor short and long-term patient and graft survival. The poor outcomes are primarily attributed to an increased incidence of postoperative infectious complications, CVD complications and kidney failure[35,36]. A recent study by Hoehn *et al*[36] indicated that recipients with pre-LT diabetes in the post-transplant period had a longer hospital length of stay, as well as higher peri-transplant mortality and 30-d readmission rates. In addition, they are less likely to be discharged home and, finally, have lower graft and patient survival than recipients who do not have diabetes[36].

For the above observations, NASH recipients often have one or more and often multiple, comorbidities that significantly affect the CVD risk in these patients so CVD risk assessment in NAFLD recipients is one of the largest problems in context of LT. According to the guidelines from European Association for the Study of the Liver (EASL), aside from obligatory electrocardiogram and transthoracic echocardiography in pre-LT evaluation, further tests need to be done to exclude asymptomatic ischemic heart disease (cardiopulmonary exercise test and if necessary in high risk patients even coronary angiography)[37]. Wray *et al*[38] showed that if coronary artery disease (CAD) is treated effectively before LT, survival after LT is not significantly different between patients with or without obstructive CAD.

Currently, many authors agree that NAFLD is a liver as well as a multisystem disease that is commonly associated with CVD, T2DM and CKD[39]. Research has shown that NAFLD is associated with an increased risk of adverse CVD events[39-42]. It is not clear whether the risk for CVD is increased in NAFLD patients due to coexisting dysmetabolic traits or whether NAFLD is actively involved in the pathogenesis of cardiovascular disease[35,39]. Previous research has shown that patients who have NASH related ESLD, compared to other ESLD recipients, have a higher CVD risk, specifically soon after LT[36]. For example, Patel *et al*[43] analyzed 420 ESLD patients that were assessed for LT: 125 had alcohol-related ESLD, and 295 had non-alcohol-related ESLD. The incidence of severe coronary artery disease (CAD) (defined by a > 70% diameter stenosis) was 13% in the non-alcohol-related ESLD group ($P < 0.005$) and 2% in the alcohol-related ESLD group. Moreover, a retrospective cohort study by Vanwagner *et al*[44] analyzed 242 LT recipients (127 alcohol-related and 115 NASH ESLD) at a post-transplant follow-up that was more than 12 mo. After controlling for recipient sex, age, smoking status, CVD, pre-transplant diabetes and the presence of MetS, the multivariate analyses shown that NASH patients were more likely to have a CVD event than alcohol-related ESLD recipients in the first year after LT. Most of the (70%) CVD events occurred in the perioperative period, and 50% of the mortality was related to the occurrence of a CVD event. However, there were no differences between the two groups in graft and patient survival[44].

According to these observations, it is important to screen all LT candidates for the presence of MeS and/or risk of CVD, especially when they have NASH related ESLD. Prospective studies are needed to answer these important questions and to provide a foundation for a

standardized approach to CVD risk assessment in the population of LT candidates[35].

An additional risk factor in the context of NAFLD is CKD, which is also a well-known CVD risk factor. Previous research has shown that patients who have NAFLD have a higher prevalence of CKD than patients who do not have NAFLD[39,45]. A recent study by Singal *et al*[46] confirmed that the most rapidly increasing indication for simultaneous liver-kidney (SLK) transplantation is NASH, which has poor renal outcomes. The authors of this study found that SLK significantly increased in the group of patients who had NASH and cryptogenic cirrhosis compared to ESLD that was related to other etiologies; the incidence increased from 6.3% from 2002 to 2003 to 19.2% from 2010 to 2011. Five-year LT recipient and graft survival rates did not differ between recipients who had NASH or cryptogenic cirrhosis and those with other etiologies of ESLD. On the other hand, in the group of patients who had NASH and cryptogenic cirrhosis, the risks for a kidney graft loss was more than 1.5-fold higher. Compared to recipients who had ESLD that was related to alcohol, primary biliary cirrhosis or primary sclerosing cholangitis, the estimated glomerular filtration rate remained lower in in the recipients who had NASH/cryptogenic ESLD[46].

When selecting LT candidates who have NASH, the largest challenge is merging these risk factors into one risk stratification tool. As such, a multi-disciplinary approach is needed to evaluate these candidates for LT.

Importantly, in the context of NASH related ESLD candidates for LT, there is an association between NASH and macrovascular venous thrombosis, especially portal vein thrombosis (PVT)[47]. In NASH patients who have cirrhosis, there is a hypercoagulable state that is characterized by increased levels of plasminogen activator inhibitor 1 and factor VIII, while anticoagulant levels of protein C are decreased in patients with cirrhosis due to NASH[47,48]. Stine *et al*[47] recently analyzed 33368 patients who have ESLD and received LT. Of these, 2096 (6.3%) patients had PVT and 12% had NASH. A comparison of NASH related ESLD recipients with all other causes of cirrhosis revealed a higher prevalence of PVT, with 10.1% in the first group versus 6% for those without NASH ($P < 0.001$). NASH cirrhosis was the strongest risk factor that was independently related to PVT in a multivariable analysis. Although the clinical significance of PVT is not entirely clear, especially whether anticoagulant therapy should be used, individual studies have shown that PVT is associated with adverse outcomes in patients who have ESLD. Specifically, several authors have shown that PVT is associated with increased pre- and post-transplant mortality, as well as with technical challenges during the transplant procedure[47,49-51]. However, the connections among NASH and PVT with hypercoagulation state is an ever-expanding field of clinical research. Additional studies on this topic are needed because there will be a significantly higher number of patients who have ESLD due to NASH on the waitlist for LT in the future, and, possibly, a higher number of thromboembolic incidents in these patients, including PVT[47].

The second important issue in the context of NASH patients who are on the waitlist for LT is competition for liver allograft allocations due to a lower MELD than other etiologies of CLD. According to current reports, patients who have ESLD due to NASH and are on the waitlist for LT have better liver functioning and, consequently, lower MELD scores than other etiologies of liver cirrhosis. In addition, these patients have a slower progression of disease[18,28]. A study by O´Leary *et al*[52] compared the data for 218 patients who had NASH or cryptogenic cirrhosis (CC) and underwent LT between 2002 and 2008, with 646 patients transplanted due to ESLD that resulted from HCV infection. Among patients who had NASH and CC, the median progression rate was 1.3 MELD points per year, and in the group of patients who had HCV, it was 3.2 MELD points per year ($P = 0.003$)[52]. Compared to patients who have HCV-related cirrhosis, patients who had NASH/CC and MELD scores $\leqslant$ 15 had fewer chances of receiving LT. They also had a higher risk of dying and a two-times higher risk of rejection or removal from the waiting list due to no suitable operative procedure given the progression of the liver disease or complications with their comorbidities. However, all patients who had MELD scores that were higher than 15 were more likely to undergo LT despite their diagnosis[52]. According to the findings from this study, the aggressive treatment of associated comorbidities is highly important; the components of MetS (hypertension, T2DM, dyslipidemia and obesity) in patients who have low MELD scores can prevent the progression of their comorbid conditions that are likely to cause death or make the patient ineligible for LT[52]. In addition, a recent study by Wong *et al*[10] demonstrated that NASH patients, compared to HCV, ALD or HCV/ALD related ESLD, are less likely to receive LT in the first 90 days on the waitlist. Another interesting finding from this study is that the one-year waiting list survival rate for ESDL patients due to NASH declined over the study period from 42.8% to 25.6%. In contrast, patients who had HCC due to NASH, compared to other etiologies of CLD with HCC, had better liver functioning and lower MELD or Child Pugh scores[18]. Taken together, these data suggest that LT candidates who have NAFLD/NASH related ESLD pose a specific challenge for the transplant community given their longer LT waiting time and associated comorbidities.

NAFLD IN DONOR LIVERS

Another challenge in the context of NASH in LT is liver allograft steatosis. Specifically, the epidemic increase in the incidence of NAFLD/NASH in the general population has a direct influence on the increased prevalence of NAFLD in deceased and living liver donors[11,28]. Based on predictions that the prevalence of MetS and its liver manifestations (*i.e.*, NAFLD) will increase in coming

years, we can expect more donors with NAFLD/NASH. We know that the availability of donor livers depends the success of the LT program. There is a global lack of organs for transplantation, as the gap between patient "demand" and organ "supply" continues to grow[53]. As such, transplant centers must use livers from "extended criteria donors" (ECD). Due to higher risk for ischemia-reperfusion injury (IRI), the severity of liver steatosis is related to a higher risk for graft failure and/or impaired graft function. Upon reperfusion, steatosis can cause microcirculatory and cellular changes in the liver graft that can lead to hepatocyte necrosis. In contrast, there is an impaired potential for regenerating steatotic livers[11,28,54-56]. For donors whose livers are more than 60% steatotic, this is almost a universal scenario; however, for those who are 30%-60% steatotic, there are controversial outcomes for donor livers[11,28,54,55]. For example, Spitzer *et al*[57] have shown that macrovesicular steatosis is an independent risk factor for graft survival. Recently, Chu *et al*[55] published a systematic review that analyzed 34 articles. The authors found that steatotic grafts that were > 60% were associated with an increased risk for poor graft functioning, while grafts that were > 30% of steatosis were related to decreased graft survival rates[55]. The lack of a standardized definition for primary non-functioning or impaired primary functioning and descriptions of the types of steatosis in research are the primary flaw in these studies. With more common utilization of ECD livers, using liver allografts that have less than 30% macrovesicular steatosis should be harmless for recipients[11,28,54,55].

There is no standardized procedure for estimating liver steatosis in potential donors; thus, evaluation procedures of liver grafts for steatosis and the use of steatotic livers for LT differ across transplant centers. Although some centers perform liver biopsies in high risk donors (abnormal liver tests, associated comorbidities, diabetes mellitus, high body mass index, older age, hepatitis B or C infections), others evaluate all potential donors[11,54,58]. Liver biopsies are the "gold standard" for detecting and assessing for steatosis. As an invasive procedure, liver biopsies can damage the organ. Moreover, it can only sample 1/50000 of the liver; thus, there is the potential for significant sampling error and limits in the numbers and sizes of biopsies. In addition, there is significant inter-observer variability for evaluating the degree of steatosis. These disadvantages place the procedure in the "silver standard" position; however, because there is not a better referential method, biopsy is still viewed as the "gold standard". Additionally, waiting for the liver biopsy results before deciding whether to accept the organ extends the cold ischemia time. Therefore, there is a need for simple, rapid and non-invasive methods for detecting steatosis in the donor[11,54,59]. Imaging methods such as ultrasonography, magnetic resonance and computed tomography are not sensitive or exact in detecting steatosis that is below 30%. Moreover, these methods cannot differentiate between micro-vesicular and macro-vesicular steatosis[11,54,58,59]. Recently, elastographic methods have been intensively investigated in the context of the noninvasive assessment of liver steatosis and fibrosis. One of the most investigated is transient elastography (TE), with a controlled attenuation parameter (CAP). In the context of donor livers, Mancia *et al*[60] examined 23 brain-dead potential donors. They analyzed TE with its CAP and reviewed liver stiffness measurements (LSM) to objectively assess liver steatosis and fibrosis. The implementation of TE with both CAP and LSM demonstrated good preoperative assessment for the histological condition and stage of the donors' liver steatosis[60]. Recently, Hong *et al*[61] investigated the usefulness of CAP as a screening tool for detecting liver steatosis in living donor livers. The author found that area under the receiver operator characteristic curve for diagnosing steatosis ($\geqslant$ S2) with CAP was 0.88, with a cutoff value of 276 dB/m. According to the findings from this study, CAP could be an adequate noninvasive method for excluding significant liver steatosis (> 33%) in liver donors[61]. There is a need for more research on using TE with CAP to evaluate steatosis and fibrosis in possible donors. A higher incidence of NAFLD/NASH in the general population will lead to a higher risk of donors who have NAFLD, which will influence on number of suitable organs from both living and deceased donors. Given the increasing incidence of NAFLD, we will face an even greater lack of LT organs or will be forced to accept liver donors that have NAFLD/NASH and are lower quality, with a high risk for poor outcomes after LT[15,54].

LIVER TRANSPLANTATION OUTCOMES FOR NAFLD PATIENTS

Although patients who are transplanted because of ESLD that is related to NASH have several comorbidities and are often older in age, post-LT survival is comparable to other etiologies of ESLD. Multiple, single-center studies of survival in ESLD related to NASH patients who had an LT, as well as several large studies were conducted over the years[28]. The studies that assess post-LT outcomes for NASH are summarized in Table 1.

One of the first studies to report outcomes for NASH patients after LT was conducted by Malik *et al*[62] and was published almost 10 years ago. This was the first study to analyze patients who had a histopathological diagnosis of NASH in the context of LT. The authors analyzed the post-LT outcomes for 98 NASH patients *vs* 686 with other etiologies, including primary biliary cirrhosis/primary sclerosing cholangitis (PBC/PSC), ALD, HCV and cryptogenic cirrhosis (CC). In 71 NASH patients, the diagnosis of NASH was based on pre-LT biopsies, and in 27 patients, the diagnosis of NASH was confirmed upon explant. The five-year survival rates

Table 1 Post liver transplantation outcomes for patients who have nonalcoholic fatty liver disease

Ref.	Study size	NASH group survival (%)	Non-NASH group survival (%)	Study period
Malik *et al*[62]	98 NASH	30-d - 93.9	30-d - 94.4-98.0	1997-2008
	686 Non-NASH group (PBC/PSC, ALD, HCV, CC)	1-yr - 79.6	1-yr - 81.6-87.2	
		5-yr - 72.4	5-yr - 65.3-80.6	
Bhagat *et al*[63]	71 NASH	1-yr - 82	1-yr - 92	1997-2007
	83 ALD	5-yr - 75	5-yr - 86	
		9-yr - 62	9-yr - 76	
Barritt *et al*[64]	21 NAFLD	30-d - 80.9	30-d - 97	2004-2007
	83 Non-NAFLD (ALD, HCV, HBV, PBC/PSC, AIH)	1-yr - 76.2	1-yr - 89.5	
		3-yr - 76.2	3-yr - 83.5	
Agopian *et al*[65]	144 NASH	90-d - 90	90-d - 90-96	1993-2011
	1150 Non-NASH (HBV, HCV, ALD, CC, PBC/PSC)	1-yr - 84	1-yr - 79-87	
		5-yr - 75	5-yr - 54-70	
Kennedy *et al*[66]	129 NASH	1-yr - 90	1-yr - 92	1999-2009
	775 Non-NASH - etiologies not defined	3-yr - 88	3-yr - 86	
		5-yr - 85	5-yr - 80	
Park *et al*[67]	71 NASH	1-yr - 78	1-yr - 87	1998-2008
	472 Non-NASH	2-yr - 78	2-yrs - 85	
Vanwagner *et al*[44]	115 NASH	1-yr - 81.3	1-yr - 88.1	1993-2010
	127 ALD	3-yr - 73.3	3-yr - 85.3	
		5-yr - 60.3	5-yr - 68.8	
Afazali *et al*[68]	1810 NASH	1-yr - 87.6	Variable	1997-2010
	3843 CC	3-yr - 82.2		
	48.085 Non-NASH	5-yr - 76.7		
Charlton *et al*[14]	1959 NASH	1-yr - 84	1-yr - 87	2001-2009
	33822 Non-NASH	3-yr - 78	3-yr - 78	

NAFLD: Nonalcoholic fatty liver disease; ALD: Alcoholic liver disease; HCV: Hepatitis C virus; HBV: Hepatitis B virus; CC: Cryptogenic cirrhosis; PBC: Primary biliary cirrhosis; PSC: Primary sclerosing cholangitis.

after the LT were similar between the patients who were transplanted for NASH and the patients who were transplanted for other etiologies of ESLD. On the other hand, there was a tendency for higher mortality soon after the LT (30-d mortality was 6.1%), and one year after the LT (21.4%). NASH patients who were older (⩾ 60 years), obese (BMI > 30 kg/m^2), and had pre-LT hypertension and pre-LT T2DM had a higher risk for poor post-LT outcomes. Another important finding was that infection was the most common cause of death in the NASH patients compared to the controls[62]. In 2009, Bhagat *et al*[63] published a retrospective study that reported the post-LT outcomes for the NASH and ALD groups of patients who underwent LT. The authors found that overall survival and death rates due to CVD events was higher in the NASH group, but this difference was not significant. Interestingly, acute rejection crises and recurrent steatohepatitis occurred significantly more often in the NASH group but did not lead to higher rates of re-transplantation[63]. Two years later, Barritt *et al*[64] published another retrospective, but small, study. The primary finding of this study was that NASH, as an indication for LT, was the independent factor that influenced early post-LT mortality[28,64]. In 2012, Agopian *et al*[65] published a large, single-center study and found that the frequency of ESLD due to NASH as an indication for LT increased from 3% in 2002 to 19% in 2011. They reported that patients who were transplanted for NASH had a longer operative time, more operative blood loss and a longer post-LT length of stay. On the other hand, recipient and graft survival rates at one, three and five years were comparable to patients who were transplanted for other causes of ESLD. The predictors of poor outcomes for the recipient and its graft were pre-LT obesity and pre-LT hemodialysis[28,65]. Early postoperative mortality due to infections and CVD events in the recipients who were transplanted for ESLD due to NASH was reported in Kennedy *et al*[66]. This study also highlighted that an older age (> 60 years), pre-LT obesity, hypertension and T2DM were associated with lower five-year survival rates after LT. However, the overall survival rates at one, three and five years were comparable to other etiologies of ESLD[28,66]. VanWagner *et al*[44] discovered that NASH recipients had an increased risk for adverse CVD events in the first year after the LT compared to recipients who had ALD. The presence of MetS before LT was the most important risk factor[42]. One of the largest national US studies that addressed the outcomes of LT for ESLD due to NASH was published by Afazali *et al*[67]. The author used the UNOS database and analyzed 1810 LT recipients who had ESLD due to NASH, 3843 recipients who had ESLD due to CC, and 48085 recipients who had ESLD due to other etiologies of ESLD. The author reported an increased proportion of LTs for NASH patients; from 1.2% in 1997-2003 to 7.4% in 2010. NASH and CC recipients had good survival rates that were comparable to other etiologies of CLD. Consistent with other studies, there was a higher rate of early mortality in the NASH patients. In addition, in line with earlier, small studies, an older age, pre-LT T2DM, obesity and pre-LT hypertension were risk factors

for higher mortality rates in the first year after LT[68]. Another large national US study that used the SRTR database and was performed by Charlaton *et al*[14] had similar findings.

Finally, a meta-analysis that was published four years ago by Wang *et al*[69] showed that similar number of patients with and without NASH survived for 1, 3, and 5 years after LT; however, those who had NASH were more likely to die due to adverse CVD events or sepsis[69].

In most studies, patients who were transplanted for ESLD related to NASH had very good survival rates. One-year survival rates were between 85% and 90%, while five-year survival ranged from 70% to 80% in most studies. In addition, patients who underwent LT due to NASH-related ESLD had almost the same outcomes as other etiologies of CLD. It is interesting that NASH recipients, despite multiple comorbidities, have survival comparable to that of other etiologies of CLD. One possible explanations is that the rate of NASH and cirrhosis recurrence is lower than the recurrence of HBV or HCV[35,68]. Another consideration is that these patients undergo a very extensive pre-transplantation screening for risk evaluation and cardiovascular status, thus; those who have significant cardiovascular morbidity are excluded from the transplant list. However, according to the results, overall survival after LT is good in the NASH recipient group, and a higher incidence of post LT CVD events are noted in NASH recipients. However, infections (sepsis) were observed more frequently in this group of recipients. When selecting NASH patients for LT, there is a need for more attention and careful consideration combined with the radical management of sepsis and CVD complications after LT[11,68,69].

NONALCOHOLIC FATTY LIVER DISEASE AFTER LIVER TRANSPLANTATION

Progress in surgical techniques for transplant surgery, as well as the development of immunosuppressive therapy, led to decreased early post-LT mortality and, consequently, to improved survival rates after LT, with a 90% survival rate at the first year and a survival rate of more than 70% five years after LT. The development of metabolic comorbidities, combined with this higher post-LT survival, contributes to morbidity and mortality rates. Subsequently, the focus of research is changing to long-term complications, such as CVD[70-72]. CVD can be initiated with every insulin resistance (IR) associated component of MetS. Furthermore, the clinical features and prevalence of MetS, such as T2DM, hypertension, rapid weight gain and dyslipidemia, often deteriorate in the post-LT period based on transplant specific factors, for example, adverse events in immunosuppression. They are also related to the recipients' morbidity and mortality[70,72]. For metabolic balance, for hyperglycemia, weight gain, hypertension and hyperlipidemia, immunosuppressant drugs, such as corticosteroids, calcineurin inhibitors (CNIs) (cyclosporine (CSA), tacrolimus (TAC)) and mammalian target of rapamycin inhibitors (mTORs) (such as sirolimus (SIR) and everolimus), have a crucial role. Corticosteroids stimulate gluconeogenesis. CNI stimulates the post-LT occurrence of new-onset diabetes (NOD) that is more likely related to TAC use compared to CSA. CNI also initiates the development of post-LT hypertension, and it appears that CSA is highly related to the development of hypertension after LT. For dyslipidemia, CSA has a higher risk of causing dyslipidemia than TAC. Finally, for dyslipidemia, mTORs are the most unfavorable immunosuppressive drugs. These groups of immunosuppressive drugs may, to an extent, affect the development of CVD through metabolic complications[70-72]. Most transplanted patients become obese after LT, with the highest increase in weight occurring after the first six months, as well as one and three years after LT[70,72,73]. Of the liver recipients, 10%-64% develop T2DM, 45%-69% experience hyperlipidemia, and approximately 50%-100% develop hypertension after LT[70-72]. Thus, a significant number of liver recipients met the criteria for MetS, which indicates that these patients have a higher risk for CVD[70-72]. Based on the literature, MetS is present in approximately 50%-60% of transplant patients[71]. Therefore, MetS is an important post transplantation problem. Because NAFLD is a liver manifestation of MetS, it is not surprising that both recurrent and *de novo* NAFLD can be found after LT[70-72]. According to the abovementioned observations, MetS components (*i.e*., NAFLD risk factors) may persist or worsen after LT due to the high incidence of MetS after LT. NAFLD can affect the post-LT course in two ways. First, post-transplant NAFLD can develop as a recurrence of a pre-LT condition, and can progress to cirrhosis and lead to ESLD when re-transplantation is necessary. Second, due to the high incidence of MetS components after LT, NAFLD can also occur *de novo* and complicate the course of the recipients who are transplanted for other etiologies of CLD[28,70-72,74]. More than 25 years ago, Burke *et al*[75] were the first to describe recurrent NAFLD, and authors from San Francisco, CA, United States, reported the first case series of *de novo* NAFLD in 2003[76].

According to the literature, recurrent NAFLD is a relatively common diagnosis after LT. Across reports, the rates of recurring steatosis and NASH range from 30%-100%[28]. For example, Bhagat *et al*[70] found that 33% of patients who were transplanted due to NASH cirrhosis had steatohepatitis in biopsy specimens during the first six months after the LT. On the other hand, none of these patients developed cirrhosis or required re-transplantation during the 10-year follow-up period[70]. A group of Dallas authors[77] conducted a retrospective study and analyzed post-LT outcomes for 257 patients undergoing LT for CC or NASH cirrhosis.

After comparing patients who had NASH/CC with patients who underwent LT due to other etiologies of CLD, they found that more NASH/CC patients developed graft steatosis at one, two, five and 10 years post-LT (8.2%, 13.6%, 24.9% and 32.9%) than those who were transplanted for other etiologies (3.1%, 5.9%, 9.6% and 10%). Of the 257 NASH/CC patients, 13 developed NASH, and 5% and 10% developed bridging fibrosis or cirrhosis after 5 and 10 years. This outcome was more common in patients who had NASH than in those who developed steatosis per se or had no fat (3%). The survival rate during the 10-year follow-up was similar for patients who underwent LT for CC or NASH or LT for other indications. However, the cause of death differed between those two groups, as the NASH group had more adverse CVD events[77]. Moreover, Dureja *et al*[78] evaluated 88 liver transplant recipients that underwent LT due to NAFLD-related cirrhosis from 1993 to 2007. There was recurrent NAFLD in 34 liver transplants, isolated steatosis in 9 and steatohepatitis in 25 recipients, while there was advanced fibrosis in 3 recipients. The survival rate after LT was not affected by NAFLD recurrence, but a higher number of CVD and infectious complications were reported in this group[78]. Recently, Sourianarayanane *et al*[79] published a retrospective study and analyzed data from NASH and ALD transplant recipients between 2001 and 2006. The authors found that NASH recipients had a higher incidence of steatosis and inflammation after LT; however, the progression of fibrosis was slower in NASH than in ALD recipients[79]. Recently, Bhati *et al*[80] analyzed 103 patients who were transplanted for NASH in whom TE and liver biopsies were used to assess steatosis and fibrosis. Of 103 total patients, 56 had TE, while 34 had a liver biopsy. Implementing TE with CAP demonstrated that 87.5% of the patients who had steatosis also had recurrent NAFLD. Most patients had LSM with no fibrosis (42.9%) or F1-F2 fibrosis (30.4%). Overall, 26.8% of the patients had advanced fibrosis, while 5.4% developed cirrhosis. Of the patients who underwent a liver biopsy, 88.2% had recurrent NAFLD, while almost half (41.2%) had NASH. Bridging fibrosis was noted in 20.6% of patients; however, none of the patients had cirrhosis. In most patients, cancer (25%) or infectious complications (25%) were the cause of death in combination with CVD (21.9%). Graft cirrhosis only caused 9% of the deaths. According to this recent study, recurrent NAFLD commonly occurs after LT (88% of all patients), while nearly a quarter of the patients developed advanced fibrosis[80]. An interesting observation was published on the genetic predisposition for NAFLD recurrence. The presence of the rs738409-G allele of the Patatin-like phospholipase in LT recipients is an independent risk factor for post-LT steatosis, as well as obesity and T2DM[72,81].

Most research that investigates the prevalence of recurrent NASH in post-LT patients have shown that the incidence of recurrent NASH is between 20% and 40%, while the incidence largely depends on NASH detection methods, including liver enzymes, imaging techniques or liver biopsies. Most of the studies that investigated the incidence of recurrent NASH were retrospective, without a standard post-LT interval biopsy protocol. In addition, the histological criteria that was used for defining the diagnosis of recurrent NAFLD varied among published studies[74,81,82]. Therefore, there is a need for prospective studies that show the actual incidence and progression for recurrent NAFLD after LT. Also, it is not clear is NAFLD a primitive process, to which follows MetS, or is it just the opposite. Further research on this topic are needed.

A recently published study investigated the incidence of NASH in children and young adults as indications for LT in addition to post-LT patients and graft outcomes. Alkhouri *et al*[27] found that approximately 4% (13) of patients who were transplanted for NASH cirrhosis needed re-transplantation due to NASH recurrence.

Based on the literature, approximately one-third of patients who were transplanted for non-NASH indications developed IR and MetS (risk factors for NAFLD) in the three years post-LT. As such, researchers have attended to understanding the development of *de novo* NAFLD in recipients who underwent LT for indications other than NASH[11]. Ten years ago, Seo *et al*[83] retrospectively analyzed data from 68 recipients who experienced LT due to ESLD that was related to non-NASH indications. They reported that 18% of the recipients developed *de novo* NAFLD, while 9% developed *de novo* NASH. The data analysis showed that the utilization of angiotensin-converting enzyme inhibitors (ACE-I) was related to a decreased risk for developing NAFLD after LT. In contrast, an increased BMI of more than 10% after LT was a risk factor for NAFLD after LT[83]. The observation related to the protective effect of ACE-I in the context of *de novo* NAFLD after LT is interesting given preliminary findings that renin-angiotensin (RAAS) inhibitors have a beneficial effect on the regression of NAFLD in non-transplanted patients[84]. Recently, we have shown that using the RAAS inhibitor is associated with a lower rate of NAFLD as defined by TE with CAP in the population of renal transplant recipients[85]. However, additional research is needed on the benefits of using RAAS inhibitors to prevent the occurrence or progression of NAFLD in post-LT patients[85]. A few years ago, Dumortier *et al*[86] published a retrospective study that analyzed the prevalence of NAFLD in post-LT liver biopsies from 421 recipients who were transplanted for non-NASH indications. Histological evidence of steatosis occurred in 131 (31.1%) patients; and 53% had grade 1, 31% grade 2 and 16% grade 3 steatosis. Interestingly, 51.1% of those with steatosis had normal liver enzymes. There was perisinusoidal fibrosis in 38 patients (29.0%), while 5 patients (3.8%) were diagnosed with NASH. In contrast, there was cirrhosis or extensive fibrosis in 2.25% of recipients at the end of the follow-up. The authors noted that post-LT obesity, tacrolimus-based regimen, hyperlipidemia, hypertension, diabetes mellitus, and alcoholic cirrhosis

were the primary indications for the LT and, combined with pre-transplant liver graft steatosis, were risk factors for steatosis after transplantation[86]. This is the first study that showed an association between the presence of steatosis in the donor liver and the development of new NAFLD after the LT[28,86]. Recently, Kim *et al*[87] showed that preexisting donor graft steatosis is associated with a threefold increased risk for developing post-LT NAFLD (OR = 3.147, P = 0.022). Although the impact of donor steatosis on graft and patient outcomes remains an insufficiently explored area, the growing incidence of NAFLD in general population indicates an urgent need for further investigations on this topic[13].

Another interesting topic in the context of NAFLD after LT is the difference between recurrent and *de novo* NAFLD after LT. Vallin *et al*[88] published the first longitudinal study four years ago with a small number of patients. The authors analyzed the characteristics of 91 patients who experienced LT between 2000 and 2010. They compared biological, clinical, and histological markers for patients who had recurrent NAFLD and patients who had *de novo* NAFLD. During the study, 91 patients were given a diagnosis of post-LT NAFLD: 11 cases were classified as recurrent NAFLD, and 80 cases were classified as *de novo* NAFLD. There were no differences in sex, age and the prevalence of obesity, hypercholesterolemia or hypertension. However, in patients with recurrent NAFLD, there was a higher prevalence of diabetes mellitus (100% *vs* 37.5%). Severe fibrosis (stage 3 or 4) and steatohepatitis at 5 years had a higher incidence in patients who had recurrent NAFLD than in patients with *de novo* NAFLD [71.4% *vs* 12.5% (P < 0.01) and 71.4% *vs* 17.2% (P < 0.01), respectively]. Additionally, after 1 year, NAFLD was diagnosed in 67% of patients who had *de novo* NAFLD, while it was present in all patients who had recurrent NAFLD. For the liver biopsy, steatosis disappeared in 18 patients (22.5%) who had *de novo* NAFLD and in no patients who had recurrent NAFLD[88]. Although this was a small study, it is important to note that recurrent and *de novo* NAFLD after LT are different entities and recurrent NAFLD appears to be a more severe and irreversible condition with an earlier onset[88].

Although many drugs have been examined for treating NAFLD/NASH in the general population, there is still no efficient therapy for NAFLD. Thus, there are no studies that examine treatment options for preventing or treating the development or recurrence of NAFLD/NASH after LT. Because NAFLD is a liver manifestation of MetS, we need to prevent and treat all MetS components in post-LT patients. Given the metabolic effects of immunosuppressive drugs that are used in liver transplant recipients, this can often be challenging. For now, we can attempt to prevent and manage hypertension, dyslipidemia, diabetes and obesity, as well as individualize immunosuppressive therapy in post-LT patients to prevent NAFLD recurrence/development and CVD complications in all recipients[28,70,72].

NAFLD AND CHRONIC KIDNEY DISEASE AFTER LIVER TRANSPLANTATION

CKD is another important area and potential challenge in the context of NAFLD and LT. The survival of the graft and patient as well as the success of LT directly depends on kidney functions. Unfortunately, it is almost impossible to prevent the development of CKD after LT. For the occurrence of CKD after LT, there are three primary risk factors: pre-LT kidney disease, using immunosuppressive drugs and recipient comorbidities. Several authors reported that a risk factor for the development and progression of CVD and CKD is NAFLD[70,72,89-91]. Musso *et al*[89] performed a meta-analysis that included 33 studies 4 years ago. The study showed that NAFLD was related to an increased incidence and prevalence of CKD. There is a close relation between NAFLD and risk factors for CVD and CKD, which makes it difficult to determine whether NAFLD is only a risk marker for CVD and/or CKD or a causal factor[71,90,91]. Park *et al*[67] reported similar results for NASH patients who were on the waitlist. Patients who had ESLD due to NASH on the waiting list had significantly higher levels of serum creatinine than patients who had other etiologies of ESLD, despite similar MELD scores[67]. Moreover, NASH is also important in the context of CKD for the post-LT setting. The first study that highlighted this association was by Houlihan *et al*[91]. They demonstrated that patients who underwent LT for ESLD related to NASH developed worse renal functioning than patients who had ESLD due to other etiologies. Compared to non-NASH patients, three months after LT, NASH patients had a significantly lower estimated glomerular filtration rate (eGFR). During the next two years 31.2% of the NASH patients (15/48) developed stage IIIb CKD, which only occurred in 8.3% of the non-NASH patients (4/48)[91]. Three years later, Fussner *et al*[92] reported that female gender and NASH were independent predictors of $\geqslant$ stage 3 CKD development at 5 years post-LT.

Given the increase in the incidence of ESLD due to NASH, and based on the MELD allocation system, which favors LT for patients with higher creatinine (kidney injury), the incidence of CKD after LT is also likely to increase. In order to prevent pre- and post-LT CKD, more effective methods of treatment are needed, such as, delayed usage of CNIs or immunosuppressive protocols without CNIs which may be effective way for saving kidney function after LT. Therefore, immunosuppressive protocols should be considered in the context of LT and NASH, and more pro-perspective studies are needed on this topic[28,91,93].

CONCLUSION

NAFLD/NASH is a challenging and multisystem disease

that has a high socioeconomic impact. NAFLD/NASH, as a primary cause of macrovesicular steatosis, has several impacts on LT; on patients on the waiting list for transplant, on post-transplant setting as well as on organ donors. Current data indicate a new trend in the area of CLD. Because of the increased incidence of T2DM and obesity, *i.e.*, the growing incidence of MetS, there is a parallel rise in the HCC incidence[13,19,25,54,94]. Consequently, NASH cirrhosis and HCC due to NASH will soon become the major indications for LT. Importantly, recent investigations and observations indicate that HCC can occur in patients who have NAFLD without liver cirrhosis. Because screening for HCC is not a part of standard approach for a patient with NAFLD without cirrhosis, HCC is often diagnosed in advanced stages. One of the primary goals of health care practitioners should be to increase awareness of NAFLD/NASH and to develop and conduct useful screening programs for this increasing patient population[13,19,25,54].

An increased incidence of MetS and, consequently, NAFLD/NASH effects the demand for LT and the supply of available donors. Thus, we can expect that there will be a higher number of steatotic livers for LT in the future. The lack of organs is a global problem and could result in one of two possible scenarios. We will either choose low quality organs that have a greater risk for post-transplantation complications and, consequently, a higher risk for worse outcome of LT. The second option is that we will decrease steatotic livers but the time on the waiting list will become longer and, consequently, there will be an increase in wait-list mortality. To develop appropriate method for optimizing the allocation of steatotic grafts prior to LT, research needs to examine procedures to protect it from IRI or primary graft non-functioning and to expand the pool of available donors. Moreover, future research should identify new non-invasive diagnostic methods for the exact detection and quantification of steatosis in donor organs. In addition, more data on other potential risk factors that are associated with the development of steatotic livers is necessary[28,54].

There are two problems with keeping NASH patients on the waiting list: their comorbidities and lower MELD scores compared to other etiologies of CLD. These patients often have different metabolic risk factors and coexisting CVD and/or CKD, which makes managing these patients complicated and demanding. As such, there is a need for more detailed and personalized screening and evaluations of NAFLD/NASH patients, particularly for assessing CVD. According to available research, there are no universal guidelines or clear recommendations for the optimal screening method for CVD in patients who have NASH related ESLD and are candidates for LT. We need new prospective studies that will answer this important question and provide a basis for a standardized approach to assessing CVD risk in this population of LT candidates[13,28,35] In addition, randomized studies are needed to determine which NASH patients on the transplant list will benefit from treatment with BS, the optimal time for BS (before LT, during LT, after LT) and the type of BS to apply[28,34]. Future research is also needed to demonstrate the long-term impact of BS on LT recipients[28].

Patients who have ESLD due to NASH and underwent LT have similar post-transplant outcomes as other etiologies of CLD[35,68]. However, according to research, the total survival rates after LT are good, but NASH recipients have a higher incidence of CVD events after LT. Interestingly, infections (sepsis) were also more frequently observed in this group of recipients. The NASH LT recipients should be viewed as population at high risk for CVD, thus, there is a need for more studies on how to follow and treat these patients[11,68,69].

The prevalence of MetS clinical features, such as T2DM, hypertension, rapid weight gain and dyslipidemia, are often higher in the period after LT, are frequently caused by transplant specific factors, including immunosuppression, and can be valuable predictors of recipients' morbidity and mortality. Immunosuppressant drugs, such as corticosteroids, CNIs and mTORs, have a specific role in metabolic balance and favor hyperglycemia, weight gain, hypertension and hyperlipidemia. These groups of immunosuppressive drugs may, to an extent, contribute to the formation of CVD by affecting metabolic complications[70,72]. Most studies that examine the prevalence of recurrent NASH in the post-LT setting have shown that the incidence of recurrent NASH is between 20% and 40%, but the incidence largely depends on NASH detection methods, such as liver enzymes, imaging techniques or liver biopsies. Most of the studies that investigated the incidence of recurrent NASH have been retrospective, without the standard Post-LT interval biopsy protocol. In addition, the histological criteria that are used for the diagnosis of recurrent NAFLD varied in the published studies[74,81]. Therefore, prospective studies with well-defined biopsy protocols are needed to show the actual incidence and progression of recurrent NAFLD after LT. According to the literature, in one-third of patients who were transplanted for non-NASH indications, IR and MetS developed within three years post-LT. As such, more research has focused on understanding the development of *de novo* NAFLD in recipients who underwent LT for indications other than NASH[11]. Another interesting topic in the context of NAFLD after LT is the difference between recurrent and *de novo* NAFLD after LT. Although the results from previous studies were conducted with a small number of patients, it is important to note that recurrent NAFLD and *de novo* NAFLD after LT are different entities and that recurrent NAFLD appears to be much more severe and irreversible and has an earlier onset[88].

Preliminary data indicated that preexisting donor graft steatosis is associated with a threefold increase in the risk for developing post-LT NAFLD. However, the influence of donor steatosis on the graft and patient outcomes has been minimally explored, and given the growing incidence of NAFLD in the general population,

there is an urgent need for further investigations on this topic[13,87].

NASH is important in the context of CKD and in the post-LT setting. Preliminary data outline that NASH is an independent predictor of ⩾ stage 3 CKD development after LT[91,92]. Given the increase in the incidence of ESLD due to NASH, there is also likely to be an increase in the incidence of CKD after LT. The transplant society will have to identify a more useful approach to these patients to prevent pre- and post-LT CKD. The delayed use of CNIs or immunosuppressive protocols without CNIs may be an effective way for saving kidney function after LT. Therefore, immunosuppressive protocols should be considered in the context of LT and NASH, and more pro-perspective studies are needed on this topic[28,91,93].

REFERENCES

1 **Younossi ZM**, Koenig AB, Abdelatif D, Fazel Y, Henry L, Wymer M. Global epidemiology of nonalcoholic fatty liver disease-Meta-analytic assessment of prevalence, incidence, and outcomes. *Hepatology* 2016; **64**: 73-84 [PMID: 26707365 DOI: 10.1002/hep.28431]

2 **Brunt EM**, Wong VW, Nobili V, Day CP, Sookoian S, Maher JJ, Bugianesi E, Sirlin CB, Neuschwander-Tetri BA, Rinella ME. Nonalcoholic fatty liver disease. *Nat Rev Dis Primers* 2015; **1**: 15080 [PMID: 27188459 DOI: 10.1038/nrdp.2015.80]

3 **European Association for the Study of the Liver (EASL)**; European Association for the Study of Diabetes (EASD); European Association for the Study of Obesity (EASO). EASL-EASD-EASO Clinical Practice Guidelines for the management of non-alcoholic fatty liver disease. *J Hepatol* 2016; **64**: 1388-1402 [PMID: 27062661 DOI: 10.1016/j.jhep.2015.11.004]

4 **Hagström H**, Nasr P, Ekstedt M, Hammar U, Stål P, Hultcrantz R, Kechagias S. Fibrosis stage but not NASH predicts mortality and time to development of severe liver disease in biopsy-proven NAFLD. *J Hepatol* 2017; **67**: 1265-1273 [PMID: 28803953 DOI: 10.1016/j.jhep.2017.07.027]

5 **Ekstedt M**, Hagström H, Nasr P, Fredrikson M, Stål P, Kechagias S, Hultcrantz R. Fibrosis stage is the strongest predictor for disease-specific mortality in NAFLD after up to 33 years of follow-up. *Hepatology* 2015; **61**: 1547-1554 [PMID: 25125077 DOI: 10.1002/hep.27368]

6 **Angulo P**, Kleiner DE, Dam-Larsen S, Adams LA, Bjornsson ES, Charatcharoenwitthaya P, Mills PR, Keach JC, Lafferty HD, Stahler A, Haflidadottir S, Bendtsen F. Liver Fibrosis, but No Other Histologic Features, Is Associated With Long-term Outcomes of Patients With Nonalcoholic Fatty Liver Disease. *Gastroenterology* 2015; **149**: 389-397.e10 [PMID: 25935633 DOI: 10.1053/j.gastro.2015.04.043]

7 **Byrne CD**, Targher G. NAFLD: a multisystem disease. *J Hepatol* 2015; **62**: S47-S64 [PMID: 25920090 DOI: 10.1016/j.jhep.2014.12.012]

8 **Baffy G**, Brunt EM, Caldwell SH. Hepatocellular carcinoma in non-alcoholic fatty liver disease: an emerging menace. *J Hepatol* 2012; **56**: 1384-1391 [PMID: 22326465 DOI: 10.1016/j.hep.2011.10.027]

9 **Guzman G**, Brunt EM, Petrovic LM, Chejfec G, Layden TJ, Cotler SJ. Does nonalcoholic fatty liver disease predispose patients to hepatocellular carcinoma in the absence of cirrhosis? *Arch Pathol Lab Med* 2008; **132**: 1761-1766 [PMID: 18976012 DOI: 10.1043/1543-2165-132.11.1761]

10 **Wong RJ**, Aguilar M, Cheung R, Perumpail RB, Harrison SA, Younossi ZM, Ahmed A. Nonalcoholic steatohepatitis is the second leading etiology of liver disease among adults awaiting liver transplantation in the United States. *Gastroenterology* 2015; **148**: 547-555 [PMID: 25461851 DOI: 10.1053/j.gastro.2014.11.039]

11 **Zezos P**, Renner EL. Liver transplantation and non-alcoholic fatty liver disease. *World J Gastroenterol* 2014; **20**: 15532-15538 [PMID: 25400437 DOI: 10.3748/wjg.v20.i42.15532]

12 **Udompap P**, Kim D, Kim WR. Current and Future Burden of Chronic Nonmalignant Liver Disease. *Clin Gastroenterol Hepatol* 2015; **13**: 2031-2041 [PMID: 26291665 DOI: 10.1016/j.cgh.2015.08.015]

13 **Canbay A**, Sowa JP, Syn WK, Treckmann J. NASH Cirrhosis - the New Burden in Liver Transplantation: How Should It Be Managed? *Visc Med* 2016; **32**: 234-238 [PMID: 27722159 DOI: 10.1159/000446379]

14 **Charlton MR**, Burns JM, Pedersen RA, Watt KD, Heimbach JK, Dierkhising RA. Frequency and outcomes of liver transplantation for nonalcoholic steatohepatitis in the United States. *Gastroenterology* 2011; **141**: 1249-1253 [PMID: 21726509 DOI: 10.1053/j.gastro.2011.06.061]

15 **Heimbach J**. Debate: A bridge too far--liver transplantation for nonalcoholic steatohepatitis will overwhelm the organ supply. *Liver Transpl* 2014; **20** Suppl 2: S32-S37 [PMID: 25155244 DOI: 10.1002/lt.23980]

16 **Goldberg D**, Ditah IC, Saeian K, Lalehzari M, Aronsohn A, Gorospe EC, Charlton M. Changes in the Prevalence of Hepatitis C Virus Infection, Nonalcoholic Steatohepatitis, and Alcoholic Liver Disease Among Patients With Cirrhosis or Liver Failure on the Waitlist for Liver Transplantation. *Gastroenterology* 2017; **152**: 1090-1099.e1 [PMID: 28088461 DOI: 10.1053/j.gastro.2017.01.003]

17 **Cholankeril G**, Wong RJ, Hu M, Perumpail RB, Yoo ER, Puri P, Younossi ZM, Harrison SA, Ahmed A. Liver Transplantation for Nonalcoholic Steatohepatitis in the US: Temporal Trends and Outcomes. *Dig Dis Sci* 2017; **62**: 2915-2922 [PMID: 28744836 DOI: 10.1007/s10620-017-4684-x]

18 **Weinmann A**, Alt Y, Koch S, Nelles C, Düber C, Lang H, Otto G, Zimmermann T, Marquardt JU, Galle PR, Wörns MA, Schattenberg JM. Treatment and survival of non-alcoholic steatohepatitis associated hepatocellular carcinoma. *BMC Cancer* 2015; **15**: 210 [PMID: 25884354 DOI: 10.1186/s12885-015-1197-x]

19 **Degasperi E**, Colombo M. Distinctive features of hepatocellular carcinoma in non-alcoholic fatty liver disease. *Lancet Gastroenterol Hepatol* 2016; **1**: 156-164 [PMID: 28404072 DOI: 10.1016/S2468-1253(16)30018-8]

20 **Park JW**, Chen M, Colombo M, Roberts LR, Schwartz M, Chen PJ, Kudo M, Johnson P, Wagner S, Orsini LS, Sherman M. Global patterns of hepatocellular carcinoma management from diagnosis to death: the BRIDGE Study. *Liver Int* 2015; **35**: 2155-2166 [PMID: 25752327 DOI: 10.1111/liv.12818]

21 **Wong RJ**, Cheung R, Ahmed A. Nonalcoholic steatohepatitis is the most rapidly growing indication for liver transplantation in patients with hepatocellular carcinoma in the U.S. *Hepatology* 2014; **59**: 2188-2195 [PMID: 24375711 DOI: 10.1002/hep.26986]

22 **Mittal S**, El-Serag HB, Sada YH, Kanwal F, Duan Z, Temple S, May SB, Kramer JR, Richardson PA, Davila JA. Hepatocellular Carcinoma in the Absence of Cirrhosis in United States Veterans is Associated With Nonalcoholic Fatty Liver Disease. *Clin Gastroenterol Hepatol* 2016; **14**: 124-131.e1 [PMID: 26196445 DOI: 10.1016/j.cgh.2015.07.019]

23 **Yasui K**, Hashimoto E, Komorizono Y, Koike K, Arii S, Imai Y, Shima T, Kanbara Y, Saibara T, Mori T, Kawata S, Uto H, Takami S, Sumida Y, Takamura T, Kawanaka M, Okanoue T; Japan NASH Study Group, Ministry of Health, Labour, and Welfare of Japan. Characteristics of patients with nonalcoholic steatohepatitis who develop hepatocellular carcinoma. *Clin Gastroenterol Hepatol* 2011; **9**: 428-433; quiz e50 [PMID: 21320639 DOI: 10.1016/j.cgh.2011.01.023]

24 **Kawada N**, Imanaka K, Kawaguchi T, Tamai C, Ishihara R, Matsunaga T, Gotoh K, Yamada T, Tomita Y. Hepatocellular carcinoma arising from non-cirrhotic nonalcoholic steatohepatitis. *J Gastroenterol* 2009; **44**: 1190-1194 [PMID: 19672551 DOI: 10.1007/s00535-009-0112-0]

25 **Perumpail RB**, Wong RJ, Ahmed A, Harrison SA. Hepatocellular Carcinoma in the Setting of Non-cirrhotic Nonalcoholic Fatty Liver Disease and the Metabolic Syndrome: US Experience. *Dig Dis Sci* 2015; **60**: 3142-3148 [PMID: 26250831 DOI: 10.1007/s10620-015-3821-7]

26 **Feldstein AE**, Charatcharoenwitthaya P, Treeprasertsuk S, Benson JT, Enders FB, Angulo P. The natural history of non-alcoholic fatty liver disease in children: a follow-up study for up to 20 years. *Gut* 2009; **58**: 1538-1544 [PMID: 19625277 DOI: 10.1136/gut.2008.171280]

27 **Alkhouri N**, Hanouneh IA, Zein NN, Lopez R, Kelly D, Eghtesad B, Fung JJ. Liver transplantation for nonalcoholic steatohepatitis in young patients. *Transpl Int* 2016; **29**: 418-424 [PMID: 26402655 DOI: 10.1111/tri.12694]

28 **Patel YA**, Berg CL, Moylan CA. Nonalcoholic Fatty Liver Disease: Key Considerations Before and After Liver Transplantation. *Dig Dis Sci* 2016; **61**: 1406-1416 [PMID: 26815171 DOI: 10.1007/s10620-016-4035-3]

29 **Leonard J**, Heimbach JK, Malinchoc M, Watt K, Charlton M. The impact of obesity on long-term outcomes in liver transplant recipients-results of the NIDDK liver transplant database. *Am J Transplant* 2008; **8**: 667-672 [PMID: 18294163 DOI: 10.1111/j.1600-6143.2007.02100.x]

30 **LaMattina JC**, Foley DP, Fernandez LA, Pirsch JD, Musat AI, D' Alessandro AM, Mezrich JD. Complications associated with liver transplantation in the obese recipient. *Clin Transplant* 2012; **26**: 910-918 [PMID: 22694047 DOI: 10.1111/j.1399-0012.2012.01669.x]

31 **Conzen KD**, Vachharajani N, Collins KM, Anderson CD, Lin Y, Wellen JR, Shenoy S, Lowell JA, Doyle MB, Chapman WC. Morbid obesity in liver transplant recipients adversely affects longterm graft and patient survival in a single-institution analysis. *HPB* (Oxford) 2015; **17**: 251-257 [PMID: 25322849 DOI: 10.1111/hpb.12340]

32 **Heimbach JK**, Watt KD, Poterucha JJ, Ziller NF, Cecco SD, Charlton MR, Hay JE, Wiesner RH, Sanchez W, Rosen CB, Swain JM. Combined liver transplantation and gastric sleeve resection for patients with medically complicated obesity and end-stage liver disease. *Am J Transplant* 2013; **13**: 363-368 [PMID: 23137119 DOI: 10.1111/j.1600-6143.2012.04318.x]

33 **Lazzati A**, Iannelli A, Schneck AS, Nelson AC, Katsahian S, Gugenheim J, Azoulay D. Bariatric surgery and liver transplantation: a systematic review a new frontier for bariatric surgery. *Obes Surg* 2015; **25**: 134-142 [PMID: 25337867 DOI: 10.1007/s11695-014-1430-8]

34 **Mosko JD**, Nguyen GC. Increased perioperative mortality following bariatric surgery among patients with cirrhosis. *Clin Gastroenterol Hepatol* 2011; **9**: 897-901 [PMID: 21782772 DOI: 10.1016/j.cgh.2011.07.007]

35 **Malhi H**, Allen AM, Watt KD. Nonalcoholic fatty liver: optimizing pretransplant selection and posttransplant care to maximize survival. *Curr Opin Organ Transplant* 2016; **21**: 99-106 [PMID: 26825357 DOI: 10.1097/MOT.0000000000000283]

36 **Hoehn RS**, Singhal A, Wima K, Sutton JM, Paterno F, Steve Woodle E, Hohmann S, Abbott DE, Shah SA. Effect of pretransplant diabetes on short-term outcomes after liver transplantation: a national cohort study. *Liver Int* 2015; **35**: 1902-1909 [PMID: 25533420 DOI: 10.1111/liv.12770]

37 **European Association for the Study of the Liver.** EASL Clinical Practice Guidelines: Liver transplantation. *J Hepatol* 2016; **64**: 433-485 [PMID: 26597456 DOI: 10.1016/j.jhep.2015.10.006]

38 **Wray C**, Scovotti JC, Tobis J, Niemann CU, Planinsic R, Walia A, Findlay J, Wagener G, Cywinski JB, Markovic D, Hughes C, Humar A, Olmos A, Sierra R, Busuttil R, Steadman RH. Liver transplantation outcome in patients with angiographically proven coronary artery disease: a multi-institutional study. *Am J Transplant* 2013; **13**: 184-191 [PMID: 23126562 DOI: 10.1111/j.1600-6143.2012.04293.x]

39 **Mikolasevic I**, Milic S, Turk Wensveen T, Grgic I, Jakopcic I, Stimac D, Wensveen F, Orlic L. Nonalcoholic fatty liver disease - A multisystem disease? *World J Gastroenterol* 2016; **22**: 9488-9505 [PMID: 27920470 DOI: 10.3748/wjg.v22.i43.9488]

40 **Mikolasevic I**, Orlic L, Milic S, Zaputovic L, Lukenda V, Racki S. Non-alcoholic fatty liver disease proven by transient elastography in hemodialysis patients: is it a new risk factor for adverse cardiovascular events? *Blood Purif* 2014; **37**: 259-265 [PMID: 24993140 DOI: 10.1159/000360270]

41 **Kim D**, Kim WR, Kim HJ, Therneau TM. Association between noninvasive fibrosis markers and mortality among adults with nonalcoholic fatty liver disease in the United States. *Hepatology* 2013; **57**: 1357-1365 [PMID: 23175136 DOI: 10.1002/hep.26156]

42 **Targher G**, Arcaro G. Non-alcoholic fatty liver disease and increased risk of cardiovascular disease. *Atherosclerosis* 2007; **191**: 235-240 [PMID: 16970951 DOI: 10.1016/j.atherosclerosis.2006.0]

43 **Patel S**, Kiefer TL, Ahmed A, Ali ZA, Tremmel JA, Lee DP, Yeung AC, Fearon WF. Comparison of the frequency of coronary artery disease in alcohol-related versus non-alcohol-related endstage liver disease. *Am J Cardiol* 2011; **108**: 1552-1555 [PMID: 21890080 DOI: 10.1016/j.amjcard.2011.07.013]

44 **Vanwagner LB**, Bhave M, Te HS, Feinglass J, Alvarez L, Rinella ME. Patients transplanted for nonalcoholic steatohepatitis are at increased risk for postoperative cardiovascular events. *Hepatology* 2012; **56**: 1741-1750 [PMID: 22611040 DOI: 10.1002/hep.25855]

45 **Jia G**, Di F, Wang Q, Shao J, Gao L, Wang L, Li Q, Li N. Non-Alcoholic Fatty Liver Disease Is a Risk Factor for the Development of Diabetic Nephropathy in Patients with Type 2 Diabetes Mellitus. *PLoS One* 2015; **10**: e0142808 [PMID: 26566287 DOI: 10.1371/journal.pone.0142808]

46 **Singal AK**, Hasanin M, Kaif M, Wiesner R, Kuo YF. Nonalcoholic Steatohepatitis is the Most Rapidly Growing Indication for Simultaneous Liver Kidney Transplantation in the United States. *Transplantation* 2016; **100**: 607-612 [PMID: 26479282 DOI: 10.1097/TP.0000000000000945]

47 **Stine JG**, Shah NL, Argo CK, Pelletier SJ, Caldwell SH, Northup PG. Increased risk of portal vein thrombosis in patients with cirrhosis due to nonalcoholic steatohepatitis. *Liver Transpl* 2015; **21**: 1016-1021 [PMID: 25845711 DOI: 10.1002/lt.24134]

48 **Tripodi A**, Fracanzani AL, Primignani M, Chantarangkul V, Clerici M, Mannucci PM, Peyvandi F, Bertelli C, Valenti L, Fargion S. Procoagulant imbalance in patients with non-alcoholic fatty liver disease. *J Hepatol* 2014; **61**: 148-154 [PMID: 24657400 DOI: 10.1016/j.jhep.2014.03.013]

49 **Englesbe MJ**, Kubus J, Muhammad W, Sonnenday CJ, Welling T, Punch JD, Lynch RJ, Marrero JA, Pelletier SJ. Portal vein thrombosis and survival in patients with cirrhosis. *Liver Transpl* 2010; **16**: 83-90 [PMID: 20035521 DOI: 10.1002/lt.21941]

50 **Stine JG**, Argo CK, Pelletier SJ, Maluf DG, Caldwell SH, Northup PG. Advanced non-alcoholic steatohepatitis cirrhosis: A high-risk population for pre-liver transplant portal vein thrombosis. *World J Hepatol* 2017; **9**: 139-146 [PMID: 28217250 DOI: 10.4254/wjh.v9.i3.139]

51 **Ponziani FR**, Zocco MA, Senzolo M, Pompili M, Gasbarrini A, Avolio AW. Portal vein thrombosis and liver transplantation: implications for waiting list period, surgical approach, early and late follow-up. *Transplant Rev* (Orlando) 2014; **28**: 92-101 [PMID: 24582320 DOI: 10.1016/j.trre.2014.01.003]

52 **O'Leary JG**, Landaverde C, Jennings L, Goldstein RM, Davis GL. Patients with NASH and cryptogenic cirrhosis are less likely than those with hepatitis C to receive liver transplants. *Clin Gastroenterol Hepatol* 2011; **9**: 700-704.e1 [PMID: 21570483 DOI: 10.1016/j.cgh.2011.04.007]

53 **Saidi RF**, Hejazii Kenari SK. Challenges of organ shortage for transplantation: solutions and opportunities. *Int J Organ Transplant Med* 2014; **5**: 87-96 [PMID: 25184029]

54 **Mikolasevic I**, Milic S, Filipec-Kanizaj T. Fatty liver allografts are associated with primary graft non-function and high mortality after transplantation. *Liver Int* 2017; **37**: 1113-1115 [PMID: 28710818 DOI: 10.1111/liv.13453]

55 **Chu MJ**, Dare AJ, Phillips AR, Bartlett AS. Donor Hepatic Steatosis and Outcome After Liver Transplantation: a Systematic Review. *J Gastrointest Surg* 2015; **19**: 1713-1724 [PMID:

25917535 DOI: 10.1007/s11605-015-2832-1]
56 **Gehrau RC**, Mas VR, Dumur CI, Suh JL, Sharma AK, Cathro HP, Maluf DG. Donor Hepatic Steatosis Induce Exacerbated Ischemia-Reperfusion Injury Through Activation of Innate Immune Response Molecular Pathways. *Transplantation* 2015; **99**: 2523-2533 [PMID: 26285018 DOI: 10.1097/TP.0000000000000857]
57 **Spitzer AL**, Lao OB, Dick AA, Bakthavatsalam R, Halldorson JB, Yeh MM, Upton MP, Reyes JD, Perkins JD. The biopsied donor liver: incorporating macrosteatosis into high-risk donor assessment. *Liver Transpl* 2010; **16**: 874-884 [PMID: 20583086 DOI: 10.1002/lt.22085]
58 **Jun MJ**, Shim JH, Kim SY, Seo N, Kim KM, Lim YS, Lee HC, Yu E, Lee SG. Clinical implications of preoperative and intraoperative liver biopsies for evaluating donor steatosis in living related liver transplantation. *Liver Transpl* 2014; **20**: 437-445 [PMID: 24478019 DOI: 10.1002/lt.23832]
59 **Kulik U**, Lehner F, Klempnauer J, Borlak J. Primary non-function is frequently associated with fatty liver allografts and high mortality after re-transplantation. *Liver Int* 2017; **37**: 1219-1228 [PMID: 28267886 DOI: 10.1111/liv.13404]
60 **Mancia C**, Loustaud-Ratti V, Carrier P, Naudet F, Bellissant E, Labrousse F, Pichon N. Controlled Attenuation Parameter and Liver Stiffness Measurements for Steatosis Assessment in the Liver Transplant of Brain Dead Donors. *Transplantation* 2015; **99**: 1619-1624 [PMID: 25719261 DOI: 10.1097/TP.0000000000000652]
61 **Hong YM**, Yoon KT, Cho M, Chu CW, Rhu JH, Yang KH, Lee JW. Clinical usefulness of controlled attenuation parameter to screen hepatic steatosis for potential donor of living donor liver transplant. *Eur J Gastroenterol Hepatol* 2017; **29**: 805-810 [PMID: 28379854 DOI: 10.1097/MEG.0000000000000876]
62 **Malik SM**, deVera ME, Fontes P, Shaikh O, Ahmad J. Outcome after liver transplantation for NASH cirrhosis. *Am J Transplant* 2009; **9**: 782-793 [PMID: 19344467 DOI: 10.1111/j.1600-6143.2009.02590.x]
63 **Bhagat V**, Mindikoglu AL, Nudo CG, Schiff ER, Tzakis A, Regev A. Outcomes of liver transplantation in patients with cirrhosis due to nonalcoholic steatohepatitis versus patients with cirrhosis due to alcoholic liver disease. *Liver Transpl* 2009; **15**: 1814-1820 [PMID: 19938128 DOI: 10.1002/lt.21927]
64 **Barritt AS 4th**, Dellon ES, Kozlowski T, Gerber DA, Hayashi PH. The influence of nonalcoholic fatty liver disease and its associated comorbidities on liver transplant outcomes. *J Clin Gastroenterol* 2011; **45**: 372-378 [PMID: 20733515 DOI: 10.1097/MCG.0b013e3181eeaff0]
65 **Agopian VG**, Kaldas FM, Hong JC, Whittaker M, Holt C, Rana A, Zarrinpar A, Petrowsky H, Farmer D, Yersiz H, Xia V, Hiatt JR, Busuttil RW. Liver transplantation for nonalcoholic steatohepatitis: the new epidemic. *Ann Surg* 2012; **256**: 624-633 [PMID: 22964732 DOI: 10.1097/SLA.0b013e31826b4b7e]
66 **Kennedy C**, Redden D, Gray S, Eckhoff D, Massoud O, McGuire B, Alkurdi B, Bloomer J, DuBay DA. Equivalent survival following liver transplantation in patients with non-alcoholic steatohepatitis compared with patients with other liver diseases. *HPB* (Oxford) 2012; **14**: 625-634 [PMID: 22882200 DOI: 10.1111/j.1477-2574.2012.00497.x]
67 **Park CW**, Tsai NT, Wong LL. Implications of worse renal dysfunction and medical comorbidities in patients with NASH undergoing liver transplant evaluation: impact on MELD and more. *Clin Transplant* 2011; **25**: E606-E611 [PMID: 21958082 DOI: 10.1111/j.1399-0012.2011.01497.x]
68 **Afzali A**, Berry K, Ioannou GN. Excellent posttransplant survival for patients with nonalcoholic steatohepatitis in the United States. *Liver Transpl* 2012; **18**: 29-37 [PMID: 21932374 DOI: 10.1002/lt.22435]
69 **Wang X**, Li J, Riaz DR, Shi G, Liu C, Dai Y. Outcomes of liver transplantation for nonalcoholic steatohepatitis: a systematic review and meta-analysis. *Clin Gastroenterol Hepatol* 2014; **12**: 394-402.e1 [PMID: 24076414 DOI: 10.1016/j.cgh.2013.09.023]
70 **Mikolasevic I**, Orlic L, Hrstic I, Milic S. Metabolic syndrome and non-alcoholic fatty liver disease after liver or kidney transplantation. *Hepatol Res* 2016; **46**: 841-852 [PMID: 26713425 DOI: 10.1111/hepr.12642]
71 **Watt KD**, Charlton MR. Metabolic syndrome and liver transplantation: a review and guide to management. *J Hepatol* 2010; **53**: 199-206 [PMID: 20451282 DOI: 10.1016/j.jhep.2010.01.040]
72 **Gitto S**, Villa E. Non-Alcoholic Fatty Liver Disease and Metabolic Syndrome after Liver Transplant. *Int J Mol Sci* 2016; **17**: 490 [PMID: 27049380 DOI: 10.3390/ijms17040490]
73 **Richards J**, Gunson B, Johnson J, Neuberger J. Weight gain and obesity after liver transplantation. *Transpl Int* 2005; **18**: 461-466 [PMID: 15773968 DOI: 10.1111/j.1432-2277.2004.00067.x]
74 **Patil DT**, Yerian LM. Evolution of nonalcoholic fatty liver disease recurrence after liver transplantation. *Liver Transpl* 2012; **18**: 1147-1153 [PMID: 22740341 DOI: 10.1002/lt.23499]
75 **Burke GW 3rd**, Cirocco R, Hensley G, Ranjan D, Reddy R, Jeffers L, Schiff E, Miller J. Liver transplantation for cirrhosis following jejuno-ileal bypass--regional cytokine differences associated with pathological changes in the transplant liver. *Transplantation* 1992; **54**: 374-377 [PMID: 1496549]
76 **Poordad F**, Gish R, Wakil A, Garcia-Kennedy R, Martin P, Yao FY. De novo non-alcoholic fatty liver disease following orthotopic liver transplantation. *Am J Transplant* 2003; **3**: 1413-1417 [PMID: 14525603]
77 **Yalamanchili K**, Saadeh S, Klintmalm GB, Jennings LW, Davis GL. Nonalcoholic fatty liver disease after liver transplantation for cryptogenic cirrhosis or nonalcoholic fatty liver disease. *Liver Transpl* 2010; **16**: 431-439 [PMID: 20373454 DOI: 10.1002/lt.22004]
78 **Dureja P**, Mellinger J, Agni R, Chang F, Avey G, Lucey M, Said A. NAFLD recurrence in liver transplant recipients. *Transplantation* 2011; **91**: 684-689 [PMID: 21248661 DOI: 10.1097/TP.0b013e31820b6b84]
79 **Sourianarayanane A**, Arikapudi S, McCullough AJ, Humar A. Nonalcoholic steatohepatitis recurrence and rate of fibrosis progression following liver transplantation. *Eur J Gastroenterol Hepatol* 2017; **29**: 481-487 [PMID: 28253211 DOI: 10.1097/MEG.0000000000000820]
80 **Bhati C**, Idowu MO, Sanyal AJ, Rivera M, Driscoll C, Stravitz RT, Kohli DR, Matherly S, Puri P, Gilles H, Cotterell A, Levy M, Sterling RK, Luketic VA, Lee H, Sharma A, Siddiqui MS. Long-term Outcomes in Patients Undergoing Liver Transplantation for Nonalcoholic Steatohepatitis-Related Cirrhosis. *Transplantation* 2017; **101**: 1867-1874 [PMID: 28296807 DOI: 10.1097/TP.0000000000001709]
81 **Finkenstedt A**, Auer C, Glodny B, Posch U, Steitzer H, Lanzer G, Pratschke J, Biebl M, Steurer M, Graziadei I, Vogel W, Zoller H. Patatin-like phospholipase domain-containing protein 3 rs738409-G in recipients of liver transplants is a risk factor for graft steatosis. *Clin Gastroenterol Hepatol* 2013; **11**: 1667-1672 [PMID: 23872669 DOI: 10.1016/j.cgh.2013.06.025]
82 **Burra P**, Germani G. Orthotopic liver transplantation in non-alcoholic fatty liver disease patients. *Rev Recent Clin Trials* 2014; **9**: 210-216 [PMID: 25514913]
83 **Seo S**, Maganti K, Khehra M, Ramsamooj R, Tsodikov A, Bowlus C, McVicar J, Zern M, Torok N. De novo nonalcoholic fatty liver disease after liver transplantation. *Liver Transpl* 2007; **13**: 844-847 [PMID: 17029282]
84 **Hirata T**, Tomita K, Kawai T, Yokoyama H, Shimada A, Kikuchi M, Hirose H, Ebinuma H, Irie J, Ojiro K, Oikawa Y, Saito H, Itoh H, Hibi T. Effect of Telmisartan or Losartan for Treatment of Nonalcoholic Fatty Liver Disease: Fatty Liver Protection Trial by Telmisartan or Losartan Study (FANTASY). *Int J Endocrinol* 2013; **2013**: 587140 [PMID: 23997767 DOI: 10.1155/2013/587140]
85 **Orlic L**, Mikolasevic I, Lukenda V, Anic K, Jelic I, Racki S. Nonalcoholic fatty liver disease and the renin-angiotensin system blockers in the patients with chronic kidney disease. *Wien Klin Wochenschr* 2015; **127**: 355-362 [PMID: 25412597 DOI: 10.1007/s00508-014-0661-y]
86 **Dumortier J**, Giostra E, Belbouab S, Morard I, Guillaud O, Spahr L, Boillot O, Rubbia-Brandt L, Scoazec JY, Hadengue A. Non-

alcoholic fatty liver disease in liver transplant recipients: another story of "seed and soil". *Am J Gastroenterol* 2010; **105**: 613-620 [PMID: 20040915 DOI: 10.1038/ajg.2009.717]

87 **Kim H**, Lee K, Lee KW, Yi NJ, Lee HW, Hong G, Choi Y, You T, Suh SW, Jang JJ, Suh KS. Histologically proven non-alcoholic fatty liver disease and clinically related factors in recipients after liver transplantation. *Clin Transplant* 2014; **28**: 521-529 [PMID: 24579874 DOI: 10.1111/ctr.12343]

88 **Vallin M**, Guillaud O, Boillot O, Hervieu V, Scoazec JY, Dumortier J. Recurrent or de novo nonalcoholic fatty liver disease after liver transplantation: natural history based on liver biopsy analysis. *Liver Transpl* 2014; **20**: 1064-1071 [PMID: 24961607 DOI: 10.1002/lt.23936]

89 **Musso G**, Gambino R, Tabibian JH, Ekstedt M, Kechagias S, Hamaguchi M, Hultcrantz R, Hagström H, Yoon SK, Charatcharoenwitthaya P, George J, Barrera F, Hafliðadóttir S, Björnsson ES, Armstrong MJ, Hopkins LJ, Gao X, Francque S, Verrijken A, Yilmaz Y, Lindor KD, Charlton M, Haring R, Lerch MM, Rettig R, Völzke H, Ryu S, Li G, Wong LL, Machado M, Cortez-Pinto H, Yasui K, Cassader M. Association of non-alcoholic fatty liver disease with chronic kidney disease: a systematic review and meta-analysis. *PLoS Med* 2014; **11**: e1001680 [PMID: 25050550 DOI: 10.1371/journal.pmed.1001680]

90 **Bonora E**, Targher G. Increased risk of cardiovascular disease and chronic kidney disease in NAFLD. *Nat Rev Gastroenterol Hepatol* 2012; **9**: 372-381 [PMID: 22565095 DOI: 10.1038/nrgastro.2012.79]

91 **Houlihan DD**, Armstrong MJ, Davidov Y, Hodson J, Nightingale P, Rowe IA, Paris S, Gunson BK, Bramhall SB, Mutimer DJ, Neuberger JM, Newsome PN. Renal function in patients undergoing transplantation for nonalcoholic steatohepatitis cirrhosis: time to reconsider immunosuppression regimens? *Liver Transpl* 2011; **17**: 1292-1298 [PMID: 21761549 DOI: 10.1002/lt.22382]

92 **Fussner LA**, Charlton MR, Heimbach JK, Fan C, Dierkhising R, Coss E, Watt KD. The impact of gender and NASH on chronic kidney disease before and after liver transplantation. *Liver Int* 2014; **34**: 1259-1266 [PMID: 24262002 DOI: 10.1111/liv.12381]

93 **Neuberger JM**, Mamelok RD, Neuhaus P, Pirenne J, Samuel D, Isoniemi H, Rostaing L, Rimola A, Marshall S, Mayer AD; ReSpECT Study Group. Delayed introduction of reduced-dose tacrolimus, and renal function in liver transplantation: the 'ReSpECT' study. *Am J Transplant* 2009; **9**: 327-336 [PMID: 19120077 DOI: 10.1111/j.1600-6143.2008.02493.x]

94 **Scalera A**, Tarantino G. Could metabolic syndrome lead to hepatocarcinoma via non-alcoholic fatty liver disease? *World J Gastroenterol* 2014; **20**: 9217-9228 [PMID: 25071314 DOI: 10.3748/wjg.v20.i28.9217]

P- Reviewer: Peltec A, Tarantino G, Tziomalos K
S- Editor: Gong ZM **L- Editor**: A **E- Editor**: Huang Y

World Journal of Gastroenterology

Submit a Manuscript: http://www.f6publishing.com

World J Gastroenterol 2018 April 14; 24(14): 1507-1520

DOI: 10.3748/wjg.v24.i14.1507

ISSN 1007-9327 (print) ISSN 2219-2840 (online)

REVIEW

Hepatitis B virus pre-S/S variants in liver diseases

Bing-Fang Chen

Bing-Fang Chen, School of Medicine, Fu-Jen Catholic University, New Taipei City 24205, Taiwan

ORCID number: Bing-Fang Chen (0000-0002-3697-1533).

Author contributions: Chen BF wrote the paper.

Supported by the grant from the National Science Council (NSC 96-2320-B-030-004-MY3), Executive Yuan, Taiwan.

Conflict-of-interest statement: No potential conflicts of interest.

Manuscript source: Invited manuscript

Correspondence to: Bing-Fang Chen, PhD, Professor, School of Medicine, Fu-Jen Catholic University, 510 Chung-Cheng Road, Hsin-Chuang Dist, New Taipei City 24205, Taiwan. nurs1018@mail.fju.edu.tw
Telephone: +886-2-29053428
Fax: +886-2-29052096

Received: March 8, 2018
Peer-review started: March 9, 2018
First decision: March 21, 2018
Revised: March 29, 2018
Accepted: March 31, 2018
Article in press: March 31, 2018
Published online: April 14, 2018

Abstract

Chronic hepatitis B is a global health problem. The clinical outcomes of chronic hepatitis B infection include asymptomatic carrier state, chronic hepatitis (CH), liver cirrhosis (LC), and hepatocellular carcinoma (HCC). Because of the spontaneous error rate inherent to viral reverse transcriptase, the hepatitis B virus (HBV) genome evolves during the course of infection under the antiviral pressure of host immunity. The clinical significance of pre-S/S variants has become increasingly recognized in patients with chronic HBV infection. Pre-S/S variants are often identified in hepatitis B carriers with CH, LC, and HCC, which suggests that these naturally occurring pre-S/S variants may contribute to the development of progressive liver damage and hepatocarcinogenesis. This paper reviews the function of the pre-S/S region along with recent findings related to the role of pre-S/S variants in liver diseases. According to the mutation type, five pre-S/S variants have been identified: pre-S deletion, pre-S point mutation, pre-S1 splice variant, C-terminus S point mutation, and pre-S/S nonsense mutation. Their associations with HBV genotype and the possible pathogenesis of pre-S/S variants are discussed. Different pre-S/S variants cause liver diseases through different mechanisms. Most cause the intracellular retention of HBV envelope proteins and induction of endoplasmic reticulum stress, which results in liver diseases. Pre-S/S variants should be routinely determined in HBV carriers to help identify individuals who may be at a high risk of less favorable liver disease progression. Additional investigations are required to explore the molecular mechanisms of the pre-S/S variants involved in the pathogenesis of each stage of liver disease.

Key words: Hepatitis B virus; Pre-S/S mutant; Pre-S deletion; Splice variant; spPS1; Chronic hepatitis; Liver cirrhosis; Hepatocellular carcinoma

Core tip: Naturally occurring hepatitis B virus (HBV) pre-S/S variants have been identified and associated with progressive liver diseases. In this review, the author discusses five pre-S/S variants: pre-S deletion,

pre-S point mutation, pre-S1 splice variant, C-terminus S point mutation, and pre-S/S nonsense mutation. Their associations with HBV genotype and the possible pathogenesis of pre-S/S variants are also discussed. Different pre-S/S variants cause liver diseases through different mechanisms. Most cause the intracellular retention of HBV envelope proteins and induction of endoplasmic reticulum stress, resulting in liver diseases. The exact pathogenesis of pre-S/S variants requires further investigation.

Chen BF. Hepatitis B virus pre-S/S variants in liver diseases. *World J Gastroenterol* 2018; 24(14): 1507-1520 Available from: URL: http://www.wjgnet.com/1007-9327/full/v24/i14/1507.htm DOI: http://dx.doi.org/10.3748/wjg.v24.i14.1507

INTRODUCTION

Hepatitis B virus (HBV) infection, which causes acute and chronic liver diseases, is a global health concern. The majority of acute HBV infections are self-limited, whereas chronic HBV infection usually results in a lifelong course. Chronic HBV infection can result in numerous clinical conditions, including asymptomatic HBV carrier (ASC), chronic hepatitis (CH), liver cirrhosis (LC), and hepatocellular carcinoma (HCC)[1,2]. More than 350 million people worldwide are estimated to have chronic HBV infection, and more than 25% of the chronically infected patients in Asia die because of HBV-related chronic diseases. The outcomes of HBV infection vary, which is likely because of differences in the host and viral factors.

To date, 10 HBV genotypes, designated as genotypes A to J, have been identified based on a divergence of > 8% over the entire genomic sequence. These 10 HBV genotypes are distributed in specific geographical locations[3,4]. Genotypes A (HBV/A) and D (HBV/D) are prevalent in Africa, Europe, and the Americas; genotypes B (HBV/B) and C (HBV/C) in Asia; genotype E (HBV/E) in sub-Saharan Africa; genotypes F and H in Southern and Central America; genotype G in France, Germany, and the United States; genotype I in Vietnam and Laos; and genotype J in Japan's Ryukyu islands. All genotypes can lead to progressive liver disease, but the clinical implications of each genotype differ. For example, patients infected by the HBV/C or HBV/D strain have a higher frequency of basal core promoter mutations, a lower response rate to interferon therapy, and a more rapid progression to liver fibrosis and HCC than those infected by the HBV/B or HBV/A strain[3,4]. In addition, carriers infected by HBV/C have a higher rate of pre-S deletions than those infected by HBV/B[5,6]. Collectively, these data indicate pathogenic and therapeutic differences among the HBV genotypes[3,4].

HBV is a small (42 nm) enveloped DNA virus, whose genome consists of partially double-stranded circular DNA that is 3182-3248 bp in length (varying with the genotype). Four genes - pre-S/S, precore (PC)/core (C), Pol, and X - encode seven polypeptides, including the structural proteins of the virion envelope and core, a small transcriptional transactivator, and a large polymerase protein with reverse transcriptase (RT) and RNase H (RH) activity (Figure 1). The pre-S/S gene has three in-frame initiation codons and encodes the small (S) envelope proteins as well as the middle (M) and large (L) envelope proteins, which contain pre-S2 and pre-S (pre-S1 and pre-S2) sequences, respectively (Figure 2A). The PC/C gene has two in-frame initiation codons and encodes the core antigen plus HBe protein, which is processed to produce soluble hepatitis B e antigen[1]. HBV replicates through the reverse transcription of an RNA intermediate, but because the RT lacks a proofreading function, errors in HBV DNA replication occur at a much higher rate than for other DNA viruses. The estimated rate of nucleotide substitution is approximately 1.4-3.2 × 10^{-5} per site per year[7]. These naturally occurring mutants evolve during the course of infection under the antiviral pressure of the host immune system or exogenous factors, including immunization or specific therapy[8]. Such HBV mutants display alteration of epitopes vital to host immune recognition, enhanced virulence with increased replication of HBV, and resistance to antiviral therapies

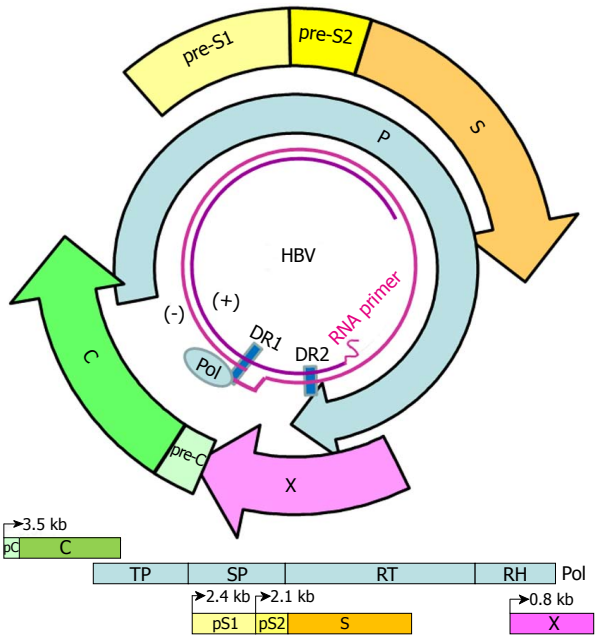

Figure 1 Genome structure and organization of hepatitis B virus. The relaxed-circular DNA genome of HBV with a complete minus strand and incomplete plus strand is shown (inner circle), along with the four main open reading frames (ORFs): pre-S/S; precore/core (pC/C); Pol, including four domains: TP, SP, reverse transcriptase (RT), and RNase H (RH); and X. The minus (-) and plus (+) DNA strands are marked. The HBV Pol and capped mRNA oligomer at the 5' end of the (-) and (+) strands as well as the DR-1 and DR-2 are illustrated. The space between the DR-1 and DR-2 is the "cohesive overlap region." The (+) strand is typically incomplete.

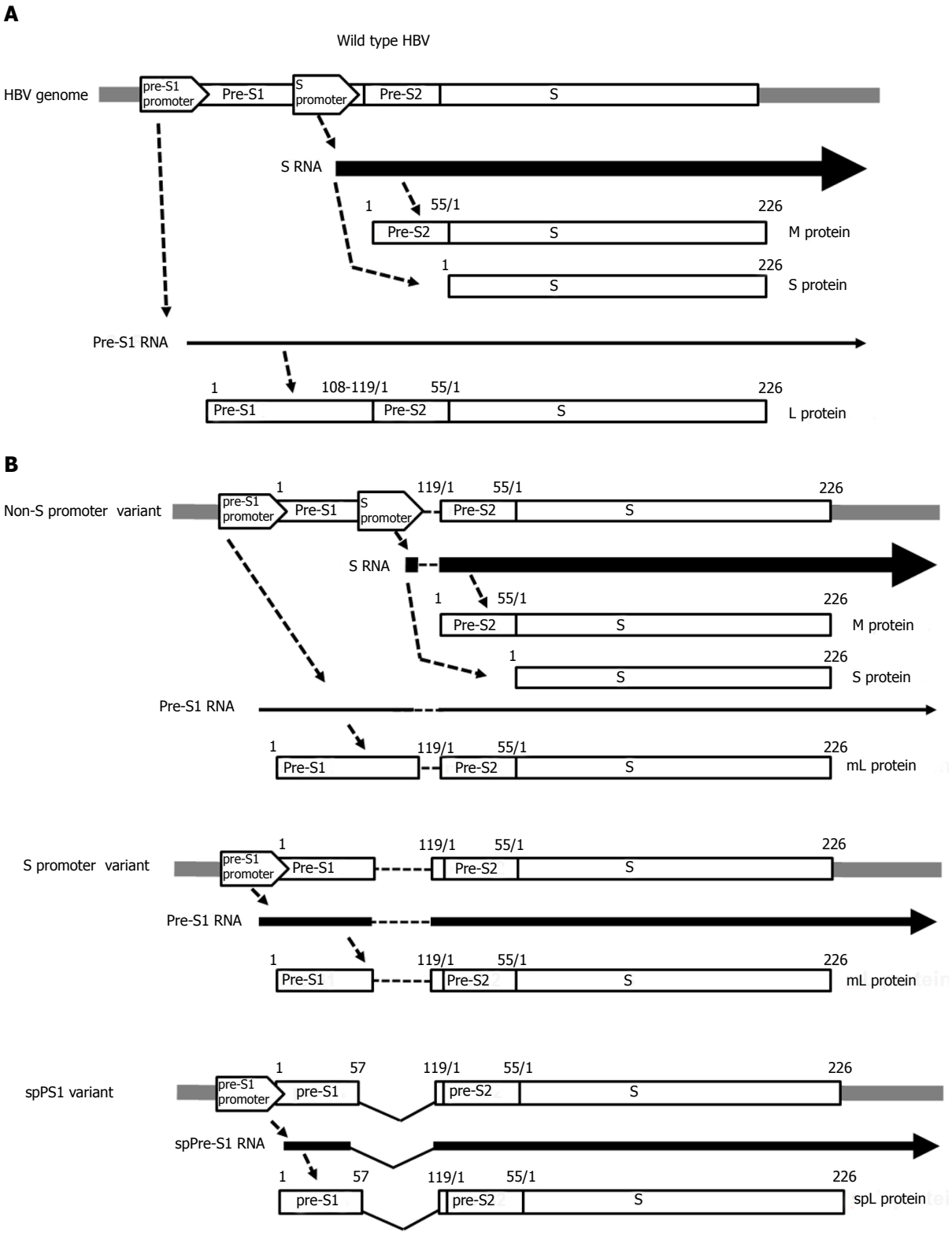

Figure 2 Gene expression of the pre-S/S gene in (A) wild-type hepatitis B virus and (B) pre-S/S variants: non-S promoter, S promoter, and spPS1.

while facilitating cell attachment or penetration[9,10]. These viral mutants, including basal core promoter, PC mutation, pre-S deletion, pre-S mutation, S mutants, and splice variants[5,6,11-27], have been associated with an increased risk of liver diseases.

The clinical significance of these naturally occurring mutants has become increasingly recognized in patients with both acute and chronic HBV infections[8-10,21,26,27]. In this article, the function of the pre-S/S region and recent findings related to the role of pre-S/S variants on

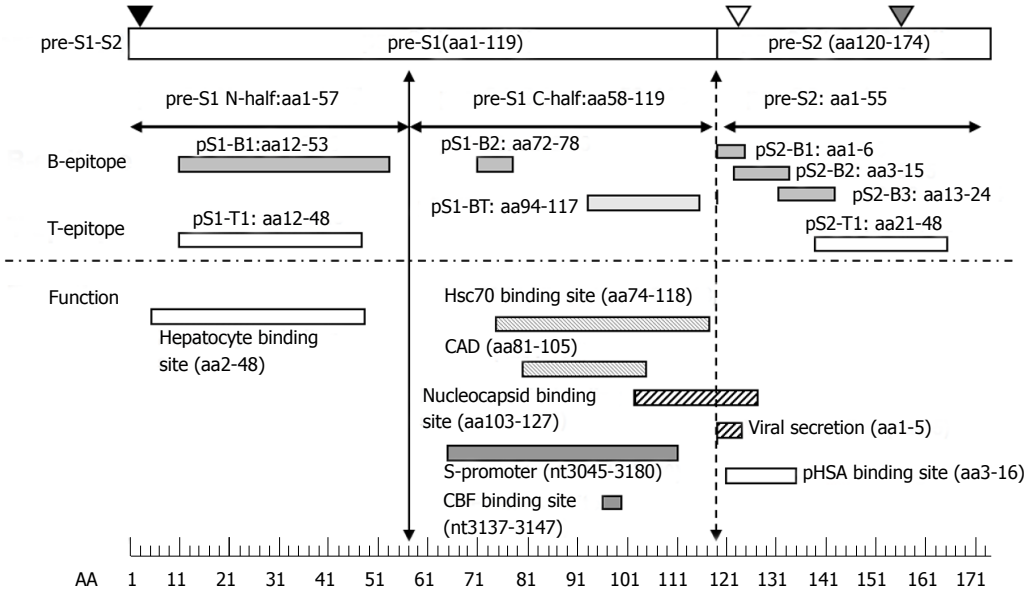

Figure 3 Immune epitopes and functional domains within the hepatitis B virus pre-S region. The pre-S region consists of the pre-S1 and pre-S2 regions. The pre-S1 region contains 119 amino acids in HBV genotypes B or C and is further divided into two parts: the N half (amino acids 1-57) and C half (amino acids 58-119). The pre-S2 region contains 55 amino acids. The pre-S domain contains many B- or T-epitopes and exerts multiple functions, as illustrated. The N-half of pre-S1 contains a hepatocyte binding site essential for infection. The C-half of pre-S1 contains a heat-shock protein 70 (Hsc70) binding site and cytosolic anchorage determinant (CAD) vital for dual topology of L proteins as well as a nucleocapsid binding site (NBS) for virion morphogenesis. The C-half of pre-S1 also contains an S-promoter and CCAAT binding factor (CBF) binding site necessary for expression of the S gene. The pre-S2 region has a polymerized human serum albumin (pHSA) binging site and viral secretion (VS) site. Black triangle, myristylation at second amino acid; white triangle, N-link glycosylation at N-4 of the M protein; gray triangle, O-link glycosylation at T-37 of the M protein. B-epitopes: pS1-B1, pS1-B2, pS2-B1, pS2-B2, and pS2-B3. T-epitopes: pS1-T1 and pS2-T1. B- and T-epitope: pS1-BT.

liver diseases is discussed and reviewed.

THE BIOLOGICAL FUNCTION OF THE PRE-S/S REGION

The pre-S/S gene has three open reading frames (ORFs) that encode three forms of hepatitis B surface antigen (HBsAg): the L, M, and S structural proteins of the viral envelope. However, these proteins are translated from different mRNAs: the L protein is translated from a long 2.4 kb pre-S1 RNA transcript, whereas the M and S proteins are translated from a slightly shorter 2.1 kb S RNA transcript (Figure 2A). The S protein consists of 226 amino acids (aa). The M protein is an extension of the S protein, with an additional 55 aa (*i.e.*, pre-S2 region). The L protein is an extension of the M protein, with an additional 108-119 aa depending on the genotype (*i.e.*, pre-S1 region). The aa sequence present at the C termini of the L and M proteins is identical to the S protein and is referred to as the S region. The pre-S (pre-S1 and pre-S2) region of the L protein is crucial for viral replication. It contains several functional sites: the hepatocyte binding site, which is essential for the attachment of HBV to liver cells; the S promoter and the CCAAT binding factor binding site, which is essential for S RNA transcription; the heat-shock protein 70 (Hsc70) binding site and the cytosolic anchorage determinant (CAD), which are essential for the dual topology (T) of L proteins; the nucleocapsid binding site (NBS), which is essential for virion morphogenesis; the site for viral secretion (VS); and the site for polymerized human albumin (pHSA) (Figure 3)[28-33].The pre-S region also plays an essential role in the interaction with the immune responses because it contains both B- and T-cell epitopes (Figure 3)[34-39]. By contrast, the biological role of M protein in the viral life cycle has been controversial. *In vitro* studies have suggested that M protein is not essential for viral replication, virion morphogenesis, or infectivity. Huang *et al*[40] defined a novel regulatory role for M protein, which may undergo a proteolytic process to generate an MHBs^{au} (aa 1-57 of M protein) species to upregulate the transcription of S promoter. In addition, the pre-S2 region of M protein binds to pHSA (aa 3-16), but the significance of this binding is unknown[34]. The S proteins are required for virion morphogenesis and secretion, and they also contain both B- and T-cell epitopes[26,41].

HBV envelope proteins are synthesized at the endoplasmic reticulum (ER). HBV envelope proteins have an unusual feature; they have multiple transmembrane domains that span the ER with loops of amino acids internal and external to the cytosol (Figure 4A)[41]. The S protein spans the ER membrane through four transmembrane domains (TM 1-4) that are linked by internal and external loops[41]. The loop of amino acids linking TM2 and TM3 is external to the ER and comprises aa 99-169. This loop is known as the "a" determinant (aa 122-148), and it is of vital virological and clinical significance as it is a major antigenic determinant of HBV. The transmembrane topology of

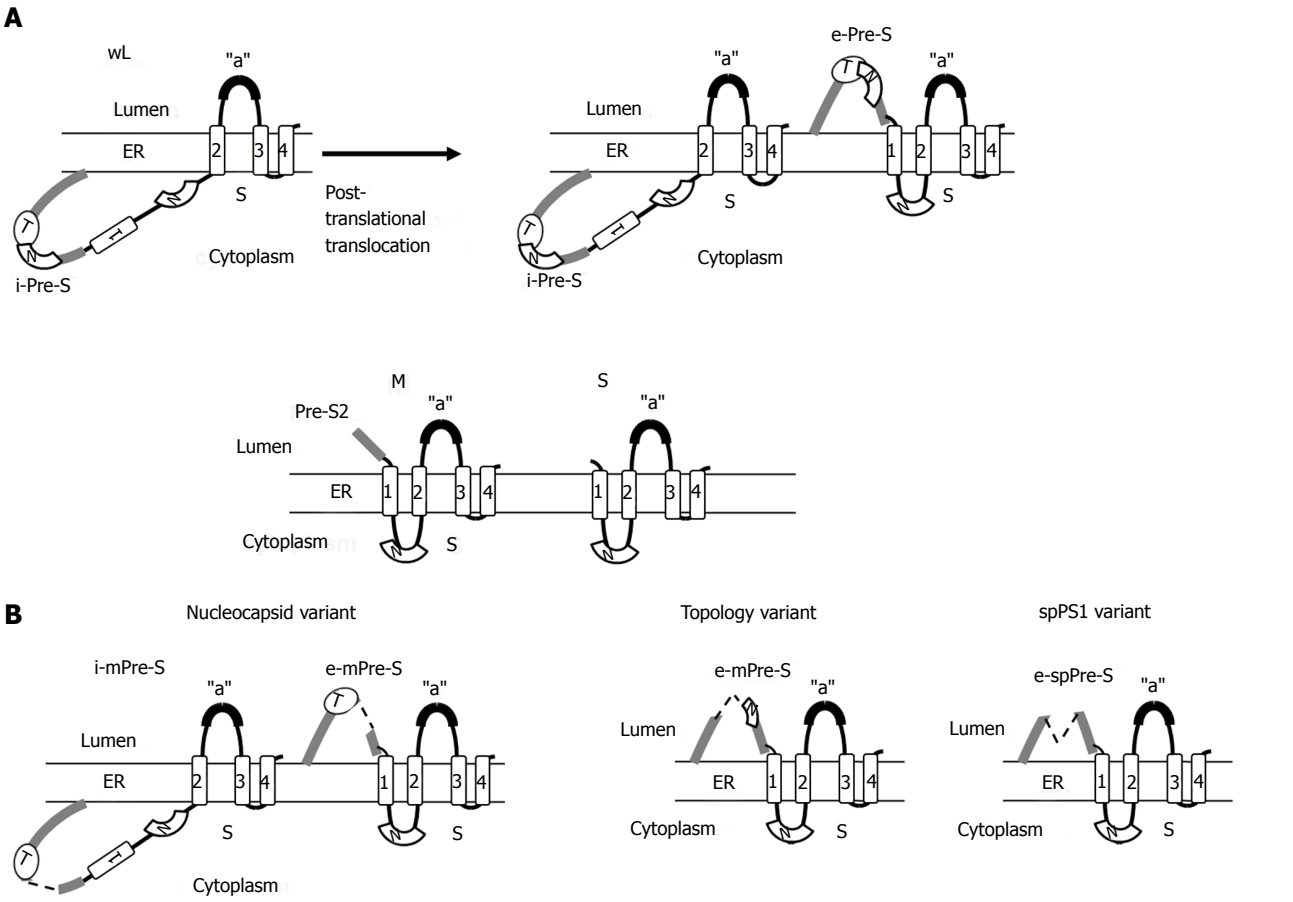

Figure 4 Topology of wild-type small (S), medium (M), and large (L) envelope proteins. The predicted four membrane-spanning segments (indicated by rectangular boxes) of S project their N and C termini into the endoplasmic reticulum lumen (A). The M proteins exhibit a topology similar to the S protein with their N-terminal pre-S2 domain protruding into the endoplasmic reticulum (ER) lumen, whereas the L proteins display a dual topology. Upon cotranslational membrane integration, the pre-S domains of L proteins are initially located on the cytosolic side of the ER membrane (i-Pre-S); they are controlled by the dual topology site (indicated by an oval). During maturation (marked by the arrow), nearly half of mature L-protein molecules posttranslationally translocate their pre-S region to the luminal space (e-Pre-S). The nucleocapsid (N) binding sites in the pre-S and S region are indicated by the white curved box. (B) The L-protein topology of pre-S/S variants. The nucleocapsid variant demonstrates a dual topology, and the topology variants and spPS1 variants display a uniform topology. The broken line indicates deletion, and "a" indicates "a" determinant.

the M protein is identical to the S protein. By contrast, the L protein has two transmembrane topologies. On biogenesis, the CAD of the pre-S1 region interacts with the cognate heat-shock protein Hsc70, thereby preventing cotranslational pre-S translocation to remain the pre-S domain of L cytosolic[42,43]. During maturation, approximately half of the L molecules posttranslationally translocate their pre-S region into the ER, thereby generating a dual topology (Figure 4A)[41-43]. The L protein serves its topological opposing functions in the virus life cycle by orientating the pre-S domain at both the cytosolic (i-Pre-S, inside the virus) and luminal (e-Pre-S, outside the virus) locations, i-Pre-S for capsid envelopment and e-Pre-S for receptor binding[41].

ASSOCIATION BETWEEN HBV PRE-S/S VARIANTS AND LIVER DISEASES

Owing to the spontaneous error rate of viral reverse transcription, naturally occurring HBV mutants arise during the course of a patient's infection under the pressure of host immunity or specific therapy[8]. Recently, many investigations have reported that pre-S/S variants are associated with the development of liver diseases[5,6,11-14,26,27]. Here, according to the mutation type, five pre-S/S variants-pre-S deletion, pre-S point mutation, pre-S1 splice variant, C-terminus S point mutation, and pre-S/S nonsense mutation-are reviewed. The pre-S region is the most variable sequence of the viral genome and changes with the genotype. The HBV genotype may influence the emergence of different pre-S variants; thus, it is also reviewed.

Pre-S deletion and genotype

Many studies have demonstrated that pre-S deletions are associated with progressive liver diseases[5,6,11-14,26,27]. Pre-S deletion is frequently found at the C-terminal half (aa 58-119) of pre-S1 and the N-terminus (aa 1-23) of pre-S2. Most are in-frame deletions[6,11-14,26,27]. Mapping of the pre-S region has revealed that all deletion regions encompassed T- and B-cell epitopes, and most of them lost one or more functional sites, including

the S promoter, T site, NBS, start codon of M, VS site, and pHSA site[6,44]. Most reports have focused on the relationship between pre-S deletion and HCC and have indicated that pre-S2 deletion is associated with HCC development in adults[5,6,11-14,21,26,27,44]. Two reports have revealed a high prevalence of HBV pre-S deletion mutation, with the mutation being recognized in 27 of 30 (90%) and 9 of 19 (47.4%) examined childhood cases of HCC[45,46]. Pre-S2 deletion also occurred frequently (20/27, 74%; 8/9, 88.8%)[45,46]. Other studies have reported a high rate of pre-S1 deletion in HBV/C-infected HCC cases[47,48]. These differences might result from the prevalence of different genotypes (or subgenotypes) in different countries. Biswas *et al*[49] investigated the association of types of pre-S mutations with HBV genotypes from 25 cases and revealed that pre-S1 deletion (5/9, 55.56%) was common in HBV/D, pre-S2 start codon mutation (5/9, 55.56%) was frequent in HBV/A, and pre-S2 deletions (3/7, 42.85%) were frequent in HBV/C. Recently, we enrolled 43 HBV/B and 43 HBV/C-infected carriers with pre-S deletion to examine the prevalence of different pre-S deletions and their associations with HBV genotypes[50]. The results showed the frequencies of some types of pre-S deletion differed between the HBV/B and HBV/C groups, whereas the frequencies of other types of pre-S deletion were similar in both genotypes[50]. Sequence alignment analysis indicated that both genotypes possessed a high frequency of deletion in the C-terminus half of the pre-S1 region and N-terminus of the pre-S2 region (86.0% and 79.1% in the HBV/B group; 69.8% and 72.1% in the HBV/C group, respectively). Epitope mapping revealed that deletion in several epitope sites was frequent in both genotypes, particularly pS1-BT and pS2-B2. Conversely, the frequency of pS2-B1 deletion was significantly higher in the HBV/B group (72.1% *vs* 37.2%, $P = 0.002$), and the frequency of pS2-T deletion was significantly higher in the HBV/C group (48.8% *vs* 25.6%, $P = 0.044$). Functional mapping revealed that the frequency of deletion in three functional sites (NBS, the start codon of M, and VS site) located in the border between the pre-S1 and pre-S2 region (aa 103-127) was significantly higher in the HBV/B group ($P < 0.05$). One variety of N-terminus pre-S1 deletion mutation demonstrating deletion of the start codon of the L protein was frequently observed in the HBV/C group (20.9% *vs* 9.3%, $P = 0.228$). The correlation of different pre-S deletion with the HBV genotype was further examined according to different clinical outcomes. Significant differences were observed between the HBV/B- and HBV/C-infected patients with LC-HCC. Deletion in the N-terminus of the pre-S2 region - including two epitope sites (pS2-B1 and pS2-B2) and three functional sites (the start codon of M, VS, and pHSA) - was significantly more frequent in the HBV/B-infected LC-HCC patients ($P < 0.05$). In Asia, HBV/B and HBV/C commonly coexist. However, their distribution differs by country[3,4]. Pre-S2 deletion has been associated with the development of HCC in Taiwan[27,45,51]. This finding may be due to HBV/B being more prevalent than HBV/C in Taiwan. HBV/C is predominant in Korea, where the N-terminus pre-S1 deletion mutant with deletion of the start codon of the L protein has been correlated with the development of HCC[47,48]. These results indicate that the tendency of different pre-S deletion varies across HBV genotypes. Therefore, the difference in genotype (or subgenotype) prevalence in different countries may influence the pattern of pre-S deletion associated with HCC.

The association of specific types of pre-S deletion with CH and LC development remains unknown. Our studies have revealed that deletion in the C-terminal half of the pre-S1 region is frequent among CH and LC patients[25,50], which is in contrast to HCC patients, who demonstrated a significantly higher frequency of deletion in the pre-S2 region[11-14,26,27,44-46]. Functional mapping showed that deletion in the S promoter was significantly frequent in CH and LC patients compared with that in ASCs[25,50]. The correlation among different pre-S deletion mutants with HBV genotypes in CH and LC patients was investigated, and deletion in the S promoter and the C-terminal half of pre-S1 was frequently observed in both genotypes[50]. In the CH patients, deletion in the pS1-BT and four functional sites (S promoter, Hsc70, CAD, and NBS), which are located in the C-terminal half of the pre-S1 region, was frequent in both genotypes. Conversely, deletion in the pHSA was more frequent in the HBV/B group than in the HBV/C group (88.9% *vs* 36.4%, $P = 0.028$). In the LC patients, no significant differences were observed between the HBV/B and HBV/C groups, except that deletion in the start codon of L was more frequent in the HBV/C group (42.9% *vs* 12.5%, $P = 0.193$)[50].

To understand the characteristics of these pre-S deletion mutants, five naturally occurring pre-S deletion mutants - namely one pre-S1 C-terminus half deletion mutant (dps1), two pre-S1/2 deletion mutants with deletion spanning pre-S1 and pre-S2 (dpS12a and dpS12b), and two pre-S2 deletion mutants (dpS2a and dpS2b) - were analyzed *in vitro*[52]. Functional analyses indicated that they could be divided into two groups: S promoter (dpS1 and dpS12a) and non-S promoter (dpS12b, dpS2a, and dpS2b) deletion mutants. Northern blot analysis revealed that S RNA could be transcribed in non-S-promoter deletion mutants and that the ratio of pre-S1 RNA to S RNA was similar to that in wild-type (WT) HBV transfected cells (Figure 2). Conversely, S promoter deletion mutants could not transcribe S RNA efficiently and had a higher level of pre-S1 RNA, causing an inverse ratio of pre-S1 RNA to S RNA (Figure 2). Western blot and ELISA analyses indicated that intracellular accumulation of envelope proteins was present in all pre-S deletion mutant transfected cells, especially in the S promoter deletion mutant transfected cells. Immunofluorescence analysis revealed that the mutant L proteins, unlike the WT L

proteins, exhibited granular staining in the S promoter deletion variants and a perinuclear staining pattern in the non-S-promoter deletion variants[52]; other studies have reported similar findings[12,26,27,53-56]. Two types of ground glass hepatocytes (GGHs) have been defined and associated with liver diseases in chronic HBV infection[27]. These GGHs contain pre-S deletion mutants that are accumulated in the ER and induce ER stress. Type I GGHs that harbor pre-S1 deletion variants display a globular or inclusion-like immunostaining pattern of HBsAg and are typical of the high viral-replicative phase of chronic HBV infection. Type Ⅱ GGHs that harbor pre-S2 deletion variants with or without point mutations at the start codon of M proteins demonstrate marginal staining patterns of HBsAg, are distributed in large clusters because of their higher proliferative activity, and are characteristic of the advanced stages of chronic liver diseases[27]. Pre-S deletion mutants have been observed to induce the ER stress response, leading to the enhanced expression of vascular endothelial growth factor-A and the activation of Akt/mammalian target of rapamycin signaling in GGHs[57]. In addition, pre-S2 deletion mutants may elicit the aberrant cyclin A expression and centrosome overduplication through ER stress induction and result in cell cycle progression, cell proliferation, and anchorage-independent growth[58-60]. In addition to the induction of ER stress signals, pre-S2 deletion L proteins may directly interact with the Jun activation domain-binding protein 1, thus triggering cyclin-dependent kinase inhibitor p27 degradation, retinoblastoma hyperphosphorylation, and cell cycle progression[61]. These studies all suggest that pre-S deletion mutants may cause the intracellular retention of HBV envelope proteins, resulting in liver diseases.

Pre-S point mutant and genotype

The pathogenic role of pre-S point mutation has been the subject of fewer studies. Chen *et al*[62] reported that, compared with control patients, patients with HCC had higher frequencies of pre-S deletions and amino acid substitutions at codon 4 (W4P/R), 7 (K7T/N), and 81 (A81T) in the pre-S1 regions; and at the start codon (M1V/I/A) in the pre-S2 regions. By contrast, patients had a lower frequency of amino acid substitution at codon2 (Q2K/R) in the pre-S2 regions compared with control patients. The correlation between different pre-S point mutation with HBV genotype was further examined; compared with patients with HBV/B infection, patients with HBV/C infection were found to have higher frequencies of amino acid substitutions at codon 4 (17 of 79 *vs* 0 of 159; $P < 0.001$), codon 7 (14 of 79 *vs* 3 of 159; $P < 0.001$), and codon 81 (16 of 79 *vs* 2 of 159; $P < 0.001$) in pre-S1 genes[62]. Zhang *et al*[44] also reported that compared with the HCC-free group, higher frequencies of pre-S deletions and point mutations at 11 codons - 4, 27, 51, 54, 60, 62, 100, 125, 137, 166, and 167 - were observed in the HCC group ($P < 0.05$) with either HBV/B or HBV/C. Multiple logistic regression analysis revealed that pre-S deletions and point mutations at codon 51 and 167 were independent factors associated with HCC. Longitudinal observation indicated that pre-S deletions and the majority of the 11 HCC-associated pre-S point mutations existed at least 10 years before HCC development, and they were more prevalent preceding HCC development in patients from the HCC groups than the HCC-free group[44]. Five amino acid sites (codon 27, 35, 54, 137, and 167) that were under positive selection pressure were identified in the HBV/C sequences, whereas no positive selection codon was detected for HBV/B[44]. Zhang *et al*[63] later used deep sequencing to examine the dynamics of HBV quasi-species and their relationship to HCC development. In total, 32 chronic hepatitis B (CHB) patients with HCC (HCC group) and 32 matched controls were recruited[63]. HCC patients were found to have a higher intrapatient prevalence of pre-S deletions and point mutations at codons 4, 27, and 167 compared with the control patients (all $P < 0.05$). Longitudinal observation in the sera of 14 HCC patients determined that quasi-species complexity ($P = 0.027$ and 0.024 at the nucleotide level and the amino acid level, respectively) and diversity ($P = 0.035$ and 0.031 at the nucleotide level and the amino acid level, respectively) increased as the disease progressed to HCC[63]. Another study in patients with either HBV/B or HBV/C indicated that point mutation C2964A, A2962G, and C3116T in the pre-S1 region; C7A and T53C in the pre-S2 region; and pre-S2 start codon mutation are associated with an increased risk of HCC, and a novel mutation C105T in the pre-S2 region is inversely associated with the risk of HCC[64]. Functional studies investigating pre-S point mutants have been conducted. Mun *et al*[65] demonstrated that amino acid substitution F141L in the pre-S2 region increases the risk of HCC in HBV/C-infected subjects. An *in vitro* study demonstrated that F141L-LHBs can induce cell cycle progression by down-regulating the p53 and p21 pathways and up-regulating cyclin-dependent kinase 4 and cyclin A. In a colony-forming assay, the colony-forming frequencies in cell lines expressing F141L-LHBs were approximately twice as high as those of the WTs[65]. This suggests that F141L-LHBs may have a vital role in the pathogenesis of HCC by inducing cell proliferation and transformation[65]. Zhang *et al*[63] proposed that these pre-S point mutants may cause imbalanced envelope protein production and intracellular retention of HBsAg, leading to ER stress and tumorigenesis. These studies were conducted in patients infected with HBV/B or HBV/C. Additional studies are required to evaluate whether these mutations exist in other HBV genotypes and whether the conclusions of previous studies are valid.

Pre-S1 splice variant and genotype

RNA splice donor and acceptor sites can be detected throughout the HBV genome. Thus, RNA splicing can occur and involve deletions of nucleotides at specific

Table 1 Putative 5′ splice donor and 3′ splice acceptor sites in hepatitis B virus used to generate the splice variant spPS1

Genotype	Position (nt)	type	Potential splice donor site	Position (nt)	Type	Potential splice acceptor site	Ref.
A	3024/3025	Donor	CAG/gtagga	3207/3208	Acceptor	tcatcctcag/GC	
B	3018/3019	Donor	AAG/gtggga	3201/3202	Acceptor	tcatcctcag/GC	[25,73]
C	3018/3019	Donor	CAG/gtagga	3201/3202	Acceptor	tcatcctcag/GC	[25,72,74]
D	2985/2986	Donor	AAG/gtagga	3168/3169	Acceptor	tcatcctcag/GC	[53,71,76]
E	3015/3016	Donor	AAG/gtagga	3198/3199	Acceptor	tcatcctcag/GC	
F	3018/3019	Donor	AAG/gtagga	3201/3202	Acceptor	acatcctcag/GC	
G	3051/3052	Donor	AAG/gtagga	3234/3235	Acceptor	tcatcctcag/GC	
H	3018/3019	Donor	AAG/gtagga	3201/3202	Acceptor	acatccacag/GC	

sites. To date, 14 types of spliced HBV genomes have been identified and isolated from the sera and liver tissues of HBV-infected patients[23,24,66,67]. Different introns are removed in different splicing variants, and the splicing variants vary by genotype. The splice sites of the HBV genome are not random: the five common splice donor sites are at nucleotide positions 2067, 2447, 2471, 2985, and 2087, and the five common splice acceptor sites are at nucleotide positions 489, 2350, 2236, 2902, and 282 (these nucleotide positions are based on HBV/D). These variants can be reverse transcribed and packaged with the help of WT virus to provide the necessary proteins[68,69]. Several studies have reported that spliced HBV variants enhance WT virus replication in patients with CH; these variants have been associated with advanced liver disease[23,24]. The most frequently detected splice variant, SP1, can encode a novel protein - the hepatitis B spliced protein - which has been associated with viral replication and liver fibrosis[24] and may induce cell apoptosis[70].

To investigate the mechanism of the generation of pre-S deletion-that is, whether these pre-S deletion mutants are generated through RNA splicing or sporadic events-the splice donor and acceptor sites of the pre-S region have been searched, and only one type of pre-S1 deletion mutant was determined to have splice donor (nt 3018) and acceptor (nt 3202)(the nucleotide positions are based on HBV/B and HBV/C) site-specific sequences at the deletion boundaries. This suggests that these pre-S1 deletion mutants (spPS1) were derived from spliced pgRNA (Figure 2B)[25]. The splice donor site was at the existing position 3018 (nucleotide position 2985 based on HBV/D), whereas the splice acceptor site at position 3202 (nucleotide position 3169 based on HBV/D) was new (Table 1). Splice mapping revealed that the splice donor and splice acceptor residues critical for spPS1 were conserved across HBV genotypes A-H (Table 1). This phenomenon explains why this splice variant is frequently found during persistent viral infection[25,53,71-76].

The molecular characteristics of the novel splice variant spPS1 are mostly unknown. The splicing event of spPS1 results in a 183-nucleotide deletion in the C-terminal half of the pre-S1 region, complete deletion of two functional sites (the S promoter and site for dual topology), partial deletion of the NBS, and generation of a spliced L protein (spL, deletion of 61 amino acids, aa 58-118) (Figure 2B). S promoter deletion should lead to a reduction in S RNAs (consequently resulting in a low level or absence of M and S proteins) and an increase in pre-S1 RNAs (consequently resulting in relative overexpression of the spL surface protein). The removal of sites for dual topology and nucleocapsid binding in the spPS1 variant leads to uniform (e-Pre-S) conformation of spL proteins (Figure 4B) and decreased secretion of HBsAg and viral particles. Our *in vitro* study revealed that spPS1 (previously named dpS1) has a defect in S RNA transcription and secretion of envelope proteins[52]. Other studies have also demonstrated that spPS1 possesses a defect in secretion of envelope proteins, viral packaging, and subsequent virion secretion[53,71,72]. Western blot analysis showed that intracellular spL proteins exhibited a heterogeneous pattern, and additional spL proteins with a higher molecular weight were detected[52]. Immunofluorescence staining revealed that spL proteins were accumulated within the ER and displayed a granular staining pattern[52].

The clinical significance of the spPS1variant remains largely unknown. This variant has been found in an occult HBV-infected child[73] and numerous chronically HBV-infected patients worldwide, and it has frequently been found in the sera of individuals with CH and cirrhosis[53,71,72,74-76]. Clinical follow-up studies conducted over a period of 10-14 years indicate that after this variant occurs, acute exacerbation of CHB occurs, which is followed by the development of liver fibrosis[71,72]. A study demonstrated that the prevalence of spPS1 was higher in CH patients (7 of 55, 12.7% *vs* 1 of 55, 1.8%; $P = 0.06$) and LC patients (8 of 55, 14.5% *vs* 1 of 55, 1.8%; $P = 0.032$) than in ASCs[25]. Logistic regression analysis revealed that spPS1 variants were highly related to CH ($P = 0.058$) and significantly related to LC ($P = 0.040$). Thus, these clinical studies strongly suggest that the spPS1 variant could cause acute exacerbation of CHB, liver inflammation, and fibrosis.

C-terminus S mutant and genotype

The C-terminus S domain (aa 179-226) is hydrophobic and assumed to be inserted in the ER membrane (Figure 4A). This domain is involved in mediating

the transit of envelope glycoproteins across the endoplasmic reticulum[77]. Mutations in this domain can result in a stable, glycosylated, but nonsecreted chain, thus affecting the biogenesis and secretion of subviral particles[77]. Two C-terminus S mutations were found and significantly correlated with HCC: P203Q (4/23, 17.4% in HCC *vs* 1/105, 1.0 in non-HCC, P = 0.004); S210R (8/23, 34.8% in HCC *vs* 4/105, 3.8% in non-HCC, $P < 0.001$); P203Q + S210R (4/23, 17.4% in HCC *vs* 0/110, 0 in non-HCC, $P = 0.001$)[78]. *In vitro* experiments revealed that P203Q, S210R, and P203Q+S210R significantly reduced the ratio of secreted and intracellular HBsAg compared with WT at each time point analyzed ($P < 0.05$); P203Q and P203Q+S210R increased the percentage of cells in S-phase compared with WT (P203Q: 26% ± 13%; P203Q+S210R: 29% ± 14%; WT: 18% ± 9%, $P < 0.01$); S210R increased the percentage of cells in the G2/M-phase (33% ± 6% for S210R *vs* 26% ± 8% for WT, $P < 0.001$)[78]. These results show that these two C-terminus S mutations, P203Q and S210R, hamper HBsAg secretion and are associated with increased cellular proliferation, supporting their involvement in HCC development. This study was conducted in patients infected with HBV/D or HBV/A. Additional studies are required to evaluate whether these mutations exist in other HBV genotypes and whether the conclusions of previous studies are valid.

Pre-S/S nonsense mutation

Pre-S nonsense mutations were also found in patients with progressive liver diseases[6]; the pathogenic impacts of these naturally occurring mutants remain unknown. Such pre-S nonsense mutations result in the occurrence of pre-S stop codon mutants and the synthesis of C terminally truncated M (MHBs^t) and L (LHBs^t) proteins. Studies have reported that MHBs^t and LHBs^t function as a transcriptional activator and result in an increased hepatocyte proliferation rate[79-81]. Results from experiments conducted on transgenic mice and hepatoma cell cultures have revealed that MHBs^t proteins retained in the ER can trigger a PKC dependent activation of the c-Raf-1/Erk2 signaling cascade, which leads to the induction of AP-1 and nuclear factor-kappa B (NF-κB) transcription factors as well as to enhanced proliferative activity of hepatocytes[82,83]. By contrast, Yeh *et al*[18] demonstrated that five patients who carried stop codons (nonsense mutation) in the pre-S region had a more favorable disease-free prognosis following multivariate analysis.

S nonsense mutations can arise as result of mutations in the P ORF that are generally caused by exposure to antivirals, a phenomenon commonly called antiviral drug-associated S gene mutations[84-87]. These mutations can cause the occurrence of S stop codon mutants and the synthesis of C terminally truncated L, M, and S proteins. For example, the HBV mutation that encodes rtA181T is selected in the viral polymerase during antiviral drug therapy and can also encode a stop codon in the overlapping S gene at amino acid 172 (sW172*), resulting in truncation of the last 55 amino acids of the C-terminal hydrophobic region of the S domain. *In vitro* study revealed that the sW172* variant had a secretory defect and exerted a dominant negative effect on WT HBV virion secretion[85]. In addition, sW172* transgenic mice developed HCC in an *in vivo* study[86]. Other S nonsense mutants such as sC69*, sL95*, sW182*, and sL216* were identified in HCC tumors[87,88]. Functional studies of sL95*, sW182*, and sL216* demonstrated that they had higher cell proliferation activities and transformation abilities than WT S, especially sW182*[87]. The sW182* mutant in HBV/C was also shown to be associated with liver cirrhosis[89].

Possible pathogenesis of pre-S/S variants

On the basis of the previous studies investigating pre-S/S variants, a model to explain the occurrences of the pre-S/S variants and the possible role of these mutants in progressive liver diseases is proposed (Figure 5). After persistent HBV infection, under the pressure of immune responses and antiviral drugs, immune epitope deletion and mutation occur along with drug-resistant mutants. Different pre-S deletion and pre-S/S mutants use different routes to cause liver diseases. Most cause the intracellular retention of HBV envelope proteins and induction of ER stress, resulting in liver diseases. Based on the region mutated, at least six pre-S/S variants occurred.

Type Ⅰ - pre-S deletion in the N-terminal pre-S1 region causes deletion of the start codon of L proteins. *In vitro* study demonstrated that the L-start codon deletion mutant resulted in the absence of L proteins and increased levels of intracellular viral mRNA and extracellular HBsAg[56]. The accumulated intracellular viral mRNA might activate the intracellular toll-like receptors, leading to the subsequent activation of NF-κB pathways, chronic inflammation, and carcinogenesis[56].

Type Ⅱ - pre-S deletion in the C-terminal half of the pre-S1 region can be separated into two groups characterized by S promoter: (Ⅱ-a) S promoter deletion variants and (Ⅱ-b) non-S promoter deletion variants (Figure 2B). (Ⅱ-a) The S promoter deletion variants that cannot transcribe S RNA efficiently result in no synthesis or reduction of the M and S proteins. Because the L protein cannot be secreted from cells efficiently when expressed by itself, it must complex with the S and M proteins to form subviral particles or mature virions, bud from intracellular post-ER pre-Golgi membranes, and be released from the cell through secretion[41]. A low level or absence of M and S proteins results in the accumulation of mutant L proteins in the ER. *In vitro* studies have revealed severe intracellular retention of mutant L proteins in S promoter deletion

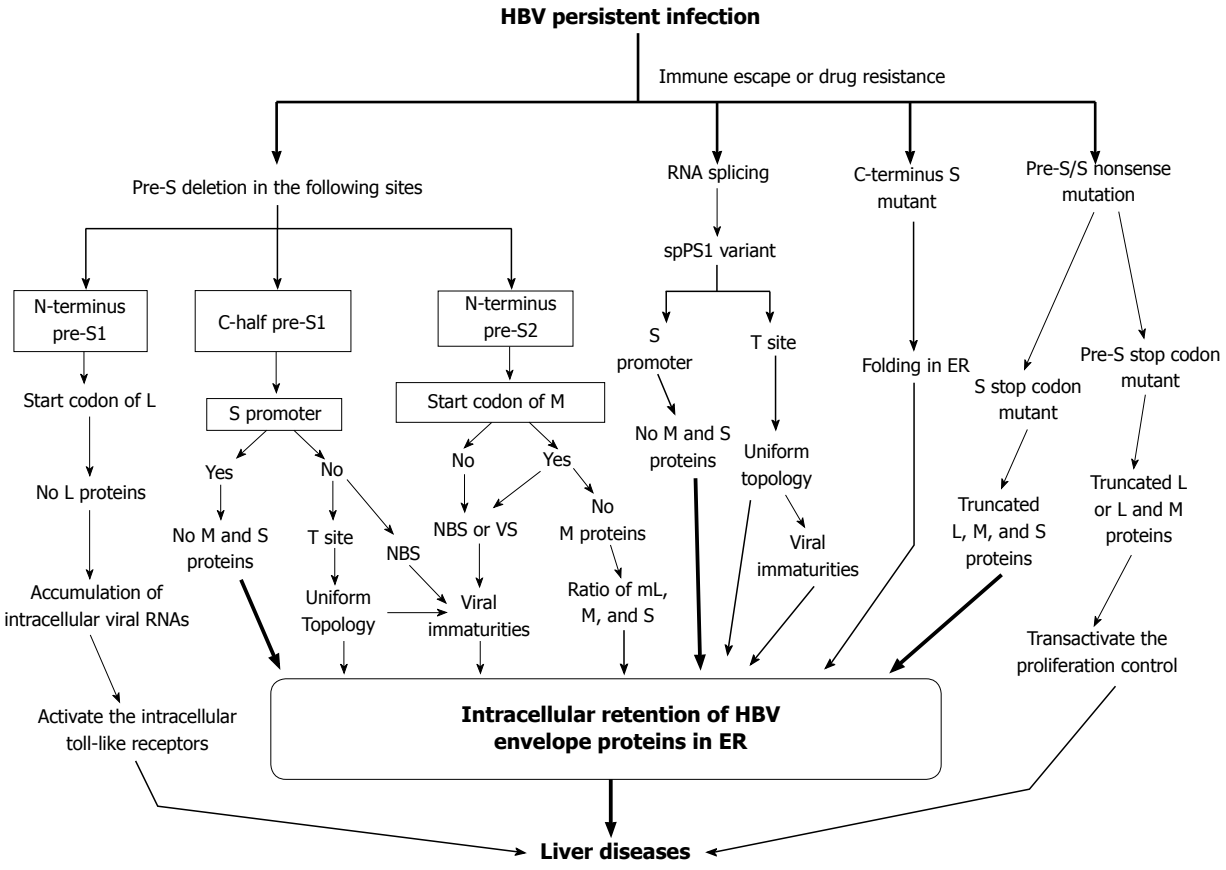

Figure 5 Proposed model for the generation of pre-S/S variants and their possible roles in liver damage and carcinogenesis. HBV: Hepatitis B virus; ER: Endoplasmic reticulum; NBS: Nucleocapsid binding site; VS: Viral secretion.

variant transfected cells[52-55]. (Ⅱ-b) The non-S promoter deletion variants can transcribe S RNA efficiently and synthesize the M and S proteins (Figure 2B), but the mutant L proteins may delete the T site to maintain a e-Pre-S form (Figure 4B, Topology variant) or delete the NBS site (Figure 4B, Nucleocapsid variant), leading to inefficient assembly of the nucleocapsid, viral immaturities, and mild intracellular retention[52].

Type Ⅲ - N-terminus pre-S2 deletion mutants can also be separated into two groups by the start codon of the M protein: (Ⅲ-a) non-M start codon deletion variants; (Ⅲ-b) M start codon deletion variants. (Ⅲ-a) non-M start codon variants with internal deletion of M proteins but the mutant L proteins may lose the NBS or VS site, resulting in viral immaturities, and slight intracellular retention[52,90]. (Ⅲ-b) The M start codon deletion variants with no M proteins change the ratio of mutant L, M, and S proteins, and lead to intracellular retention of mutant L proteins[52]. Because the M start codon is located in the NBS and VS sites, these variants may produce mutant L proteins such as the nucleocapsid variant that cannot assemble the nucleocapsid efficiently, leading to viral immaturities and slight intracellular retention of HBsAg[52].

Type Ⅳ - spPS1 variants are generated through RNA splicing of HBV pregenomic RNA. The splicing event results in a 183-nucleotide deletion in the C-terminal half of the pre-S1 region, complete deletion of two functional sites (the S promoter and T sites), partial deletion of the NBS site, and generation of spL (Figures 2B and 4B). S promoter deletion leads to absence of M and S proteins and severe intracellular retention of spL proteins[52]. T-site deletion results in uniform conformation of spL proteins (Figure 4B) and loss of i-Pre-S form for capsid envelopment, which causes viral immaturities and intracellular retention of spL proteins.

Type Ⅴ-C-terminus S mutants influence protein folding in the ER membrane, thus impairing HBsAg release, resulting in its accumulation in specific intracellular compartments (presumably represented by the ER and Golgi apparatus) and in turn contributing to cell proliferation[78]. An *in vitro* study revealed that C-terminus S mutants can also activate the proliferation control[78].

Type Ⅵ - pre-S/S nonsense mutations can be separated into two groups: (Ⅵ-a) Pre-S nonsense mutation and (Ⅵ-b) S nonsense mutation. (Ⅵ-a) Pre-S nonsense mutations can create C' truncated L and M proteins, leading to transactivation of proliferation control and causing liver diseases[79-81]. (Ⅵ-b) S nonsense mutation can create C' truncated L, M, and S proteins. *In vitro* study revealed that a stop codon in the C-terminal hydrophobic region of the S region results in truncated envelope proteins that are less glycosylated

and are defective in secretion of viral particles, causing intracellular retention of envelope proteins and liver diseases[85]. *In vitro* and *in vivo* studies have also demonstrated that these S stop codon mutants have higher cell proliferation activity[86,87].

CONCLUSION

Naturally occurring pre-S/S variants are frequently found in chronically HBV-infected patients and have been identified as influencing liver disease progression. From a review of relevant studies, pre-S/S variants should be routinely determined in HBV carriers to help identify those who may be at a higher risk of a less favorable liver disease progression. In the future, further studies are required exploring the molecular mechanisms of the pre-S/S variants involved in the pathogenesis of each stage of liver disease.

REFERENCES

1 **Seeger C**, Mason WS. Hepatitis B virus biology. *Microbiol Mol Biol Rev* 2000; **64**: 51-68 [PMID: 10704474]
2 **Kao JH**, Chen DS. Global control of hepatitis B virus infection. *Lancet Infect Dis* 2002; **2**: 395-403 [PMID: 12127351]
3 **Liu CJ**, Kao JH. Global perspective on the natural history of chronic hepatitis B: role of hepatitis B virus genotypes A to J. *Semin Liver Dis* 2013; **33**: 97-102 [PMID: 23749665 DOI: 10.1055/s-0033-1345716]
4 **Lin CL**, Kao JH. The clinical implications of hepatitis B virus genotype: Recent advances. *J Gastroenterol Hepatol* 2011; **26** Suppl 1: 123-130 [PMID: 21199523 DOI: 10.1111/j.1440-1746.2010.06541]
5 **Sugauchi F**, Ohno T, Orito E, Sakugawa H, Ichida T, Komatsu M, Kuramitsu T, Ueda R, Miyakawa Y, Mizokami M. Influence of hepatitis B virus genotypes on the development of preS deletions and advanced liver disease. *J Med Virol* 2003; **70**: 537-544 [PMID: 12794715]
6 **Chen BF**, Liu CJ, Jow GM, Chen PJ, Kao JH, Chen DS. High prevalence and mapping of pre-S deletion in hepatitis B virus carriers with progressive liver diseases. *Gastroenterology* 2006; **130**: 1153-1168 [PMID: 16618410]
7 **Okamoto H**, Imai M, Kametani M, Nakamura T, Mayumi M. Genomic heterogeneity of hepatitis B virus in a 54-year-old woman who contracted the infection through materno-fetal transmission. *Jpn J Exp Med* 1987; **57**: 231-236 [PMID: 3430800]
8 **Günther S**, Fischer L, Pult I, Sterneck M, Will H. Naturally occurring variants of hepatitis B virus. *Adv Virus Res* 1999; **52**: 25-137 [PMID: 10384235]
9 **Locarnini S**, McMillan J, Bartholomeusz A. The hepatitis B virus and common mutants. *Semin Liver Dis* 2003; **23**: 5-20 [PMID: 12616447 DOI: 10.1055/s-2003-37587]
10 **Hunt CM**, McGill JM, Allen MI, Condreay LD. Clinical relevance of hepatitis B viral mutations. *Hepatology* 2000; **31**: 1037-1044 [PMID: 10796877 DOI: 10.1053/he.2000.6709]
11 **Pollicino T**, Zanetti AR, Cacciola I, Petit MA, Smedile A, Campo S, Sagliocca L, Pasquali M, Tanzi E, Longo G, Raimondo G. Pre-S2 defective hepatitis B virus infection in patients with fulminant hepatitis. *Hepatology* 1997; **26**: 495-499 [PMID: 9252165 DOI: 10.1002/hep.510260235]
12 **Fan YF**, Lu CC, Chen WC, Yao WJ, Wang HC, Chang TT, Lei HY, Shiau AL, Su IJ. Prevalence and significance of hepatitis B virus (HBV) pre-S mutants in serum and liver at different replicative stages of chronic HBV infection. *Hepatology* 2001; **33**: 277-286 [PMID: 11124846 DOI: 10.1053/jhep.2001.21163]
13 **Chen CH**, Hung CH, Lee CM, Hu TH, Wang JH, Wang JC, Lu SN, Changchien CS. Pre-S deletion and complex mutations of hepatitis B virus related to advanced liver disease in HBeAg-negative patients. *Gastroenterology* 2007; **133**: 1466-1474 [PMID: 17915220 DOI: 10.1053/j.gastro.2007.09.002]
14 **Yeung P**, Wong DK, Lai CL, Fung J, Seto WK, Yuen MF. Association of hepatitis B virus pre-S deletions with the development of hepatocellular carcinoma in chronic hepatitis B. *J Infect Dis* 2011; **203**: 646-654 [PMID: 21227916 DOI: 10.1093/infdis/jiq096]
15 **Kao JH**, Chen PJ, Lai MY, Chen DS. Basal core promoter mutations of hepatitis B virus increase the risk of hepatocellular carcinoma in hepatitis B carriers. *Gastroenterology* 2003; **124**: 327-334 [PMID: 12557138 DOI: 10.1053/gast.2003.50053]
16 **Liu CJ**, Chen BF, Chen PJ, Lai MY, Huang WL, Kao JH, Chen DS. Role of hepatitis B viral load and basal core promoter mutation in hepatocellular carcinoma in hepatitis B carriers. *J Infect Dis* 2006; **193**: 1258-1265 [PMID: 16586363 DOI: 10.1086/502978]
17 **Chen CJ**, Yang HI, Su J, Jen CL, You SL, Lu SN, Huang GT, Iloeje UH; REVEAL-HBV Study Group. Risk of hepatocellular carcinoma across a biological gradient of serum hepatitis B virus DNA level. *JAMA* 2006; **295**: 65-73 [PMID: 16391218 DOI: 10.1001/jama.295.1.65]
18 **Yeh CT**, So M, Ng J, Yang HW, Chang ML, Lai MW, Chen TC, Lin CY, Yeh TS, Lee WC. Hepatitis B virus-DNA level and basal core promoter A1762T/G1764A mutation in liver tissue independently predict postoperative survival in hepatocellular carcinoma. *Hepatology* 2010; **52**: 1922-1933 [PMID: 20814897 DOI: 10.1002/hep.23898]
19 **Lin CL**, Kao JH. Risk stratification for hepatitis B virus related hepatocellular carcinoma. *J Gastroenterol Hepatol* 2013; **28**: 10-17 [PMID: 23094699 DOI: 10.1111/jgh.12010]
20 **Liu S**, Zhang H, Gu C, Yin J, He Y, Xie J, Cao G. Associations between hepatitis B virus mutations and the risk of hepatocellular carcinoma: a meta-analysis. *J Natl Cancer Inst* 2009; **101**: 1066-1082 [PMID: 19574418 DOI: 10.1093/jnci/djp180]
21 **Zhang ZH**, Wu CC, Chen XW, Li X, Li J, Lu MJ. Genetic variation of hepatitis B virus and its significance for pathogenesis. *World J Gastroenterol* 2016; **22**: 126-144 [PMID: 26755865 DOI: 10.3748/wjg.v22.i1.126]
22 **Lee D**, Lyu H, Chung YH, Kim JA, Mathews P, Jaffee E, Zheng L, Yu E, Lee YJ, Ryu SH. Genomic change in hepatitis B virus associated with development of hepatocellular carcinoma. *World J Gastroenterol* 2016; **22**: 5393-5399 [PMID: 27340355 DOI: 10.3748/wjg.v22.i23.5393]
23 **Soussan P**, Pol J, Garreau F, Schneider V, Le Pendeven C, Nalpas B, Lacombe K, Bonnard P, Pol S, Kremsdorf D. Expression of defective hepatitis B virus particles derived from singly spliced RNA is related to liver disease. *J Infect Dis* 2008; **198**: 218-225 [PMID: 18532883 DOI: 10.1086/589623]
24 **Soussan P**, Tuveri R, Nalpas B, Garreau F, Zavala F, Masson A, Pol S, Brechot C, Kremsdorf D. The expression of hepatitis B spliced protein (HBSP) encoded by a spliced hepatitis B virus RNA is associated with viral replication and liver fibrosis. *J Hepatol* 2003; **38**: 343-348 [PMID: 12586301]
25 **Lin YM**, Chen BF. A putative hepatitis B virus splice variant associated with chronic hepatitis and liver cirrhosis. *Virology* 2017; **510**: 224-233 [PMID: 28750326 DOI: 10.1016/j.virol.2017.07.025]
26 **Pollicino T**, Cacciola I, Saffioti F, Raimondo G. Hepatitis B virus PreS/S gene variants: pathobiology and clinical implications. *J Hepatol* 2014; **61**: 408-417 [PMID: 24801416 DOI: 10.1016/j.jhep.2014.04.041]
27 **Su IJ**, Wang HC, Wu HC, Huang WY. Ground glass hepatocytes contain pre-S mutants and represent preneoplastic lesions in chronic hepatitis B virus infection. *J Gastroenterol Hepatol* 2008; **23**: 1169-1174 [PMID: 18505413 DOI: 10.1111/j.1440-1746.2008.05348.x]
28 **Neurath AR**, Kent SB, Strick N, Parker K. Identification and

chemical synthesis of a host cell receptor binding site on hepatitis B virus. *Cell* 1986; **46**: 429-436 [PMID: 3015414]
29 **Pontisso P**, Ruvoletto MG, Gerlich WH, Heermann KH, Bardini R, Alberti A. Identification of an attachment site for human liver plasma membranes on hepatitis B virus particles. *Virology* 1989; **173**: 522-530 [PMID: 2480688]
30 **Le Seyec J**, Chouteau P, Cannie I, Guguen-Guillouzo C, Gripon P. Role of the pre-S2 domain of the large envelope protein in hepatitis B virus assembly and infectivity. *J Virol* 1998; **72**: 5573-5578 [PMID: 9621015]
31 **Poisson F**, Severac A, Hourioux C, Goudeau A, Roingeard P. Both pre-S1 and S domains of hepatitis B virus envelope proteins interact with the core particle. *Virology* 1997; **228**: 115-120 [PMID: 9024817]
32 **Bruss V**. A short linear sequence in the pre-S domain of the large hepatitis B virus envelope protein required for virion formation. *J Virol* 1997; **71**: 9350-9357 [PMID: 9371594]
33 **Bock CT**, Kubicka S, Manns MP, Trautwein C. Two control elements in the hepatitis B virus S-promoter are important for full promoter activity mediated by CCAAT-binding factor. *Hepatology* 1999; **29**: 1236-1247 [PMID: 10094970]
34 **Sobotta D**, Sominskaya I, Jansons J, Meisel H, Schmitt S, Heermann KH, Kaluza G, Pumpens P, Gerlich WH. Mapping of immunodominant B-cell epitopes and the human serum albumin-binding site in natural hepatitis B virus surface antigen of defined genosubtype. *J Gen Virol* 2000; **81**: 369-378 [PMID: 10644835]
35 **Milich DR**, Jones JE, McLachlan A, Bitter G, Moriarty A, Hughes JL. Importance of subtype in the immune response to the pre-S(2) region of the hepatitis B surface antigen. II. Synthetic Pre-S(2) immunogen. *J Immunol* 1990; **144**: 3544-3551 [PMID: 1691763]
36 **Park JH**, Cho EW, Lee YJ, Shin SY, Kim KL. Determination of the protective effects of neutralizing anti-hepatitis B virus (HBV) immunoglobulins by epitope mapping with recombinant HBV surface-antigen proteins. *Microbiol Immunol* 2000; **44**: 703-710 [PMID: 11021401]
37 **Kuroki K**, Floreani M, Mimms LT, Ganem D. Epitope mapping of the PreS1 domain of the hepatitis B virus large surface protein. *Virology* 1990; **176**: 620-624 [PMID: 1693249]
38 **Maeng CY**, Ryu CJ, Gripon P, Guguen-Guillouzo C, Hong HJ. Fine mapping of virus-neutralizing epitopes on hepatitis B virus PreS1. *Virology* 2000; **270**: 9-16 [PMID: 10772975]
39 **Ferrari C**, Cavalli A, Penna A, Valli A, Bertoletti A, Pedretti G, Pilli M, Vitali P, Neri TM, Giuberti T. Fine specificity of the human T-cell response to the hepatitis B virus preS1 antigen. *Gastroenterology* 1992; **103**: 255-263 [PMID: 1377142]
40 **Huang TJ**, Lu CC, Tsai JC, Yao WJ, Lu X, Lai MD, Liu HS, Shiau AL. Novel autoregulatory function of hepatitis B virus M protein on surface gene expression. *J Biol Chem* 2005; **280**: 27742-27754 [PMID: 15899887 DOI: 10.1074/jbc.M502209200.]
41 **Bruss V**. Hepatitis B virus morphogenesis. *World J Gastroenterol* 2007; **13**: 65-73 [PMID: 17206755 DOI: 10.3748/wjg.v13.i1.65]
42 **Lambert C**, Prange R. Chaperone action in the posttranslational topological reorientation of the hepatitis B virus large envelope protein: Implications for translocational regulation. *Proc Natl Acad Sci U S A* 2003; **100**: 5199-5204 [PMID: 12697898 DOI: 10.1073/pnas.0930813100]
43 **Löffler-Mary H**, Werr M, Prange R. Sequence-specific repression of cotranslational translocation of the hepatitis B virus envelope proteins coincides with binding of heat shock protein Hsc70. *Virology* 1997; **235**: 144-152 [PMID: 9300046 DOI: 10.1006/viro.1997.8689]
44 **Zhang AY**, Lai CL, Huang FY, Seto WK, Fung J, Wong DK, Yuen MF. Evolutionary changes of hepatitis B virus pre-S mutations prior to development of hepatocellular carcinoma. *PLoS One* 2015; **10**: e0139478 [PMID: 26421619 DOI: 10.1371/journal.pone.0139478.]
45 **Huang HP**, Hsu HY, Chen CL, Ni YH, Wang HY, Tsuei DJ, Chiang CL, Tsai YC, Chen HL, Chang MH. Pre-S2 deletions of hepatitis B virus and hepatocellular carcinoma in children. *Pediatr Res* 2010; **67**: 90-94 [PMID: 19816238 DOI: 10.1203/PDR.0b013e3181c1b0b7]
46 **Abe K**, Thung SN, Wu HC, Tran TT, Le Hoang P, Truong KD, Inui A, Jang JJ, Su IJ. Pre-S2 deletion mutants of hepatitis B virus could have an important role in hepatocarcinogenesis in Asian children. *Cancer Sci* 2009; **100**: 2249-2254 [PMID: 19719772 DOI: 10.1111/j.1349-7006.2009.01309.x]Plos]
47 **Mun HS**, Lee SA, Jee Y, Kim H, Park JH, Song BC, Yoon JH, Kim YJ, Lee HS, Hyun JW, Hwang ES, Kook YH, Kim BJ. The prevalence of hepatitis B virus preS deletions occurring naturally in Korean patients infected chronically with genotype C. *J Med Virol* 2008; **80**: 1189-1194 [PMID: 18461612 DOI: 10.1002/jmv.21208]
48 **Ahn SH**, Yuen L, Han KH, Littlejohn M, Chang HY, Damerow H, Ayres A, Heo J, Locarnini S, Revill PA. Molecular and clinical characteristics of hepatitis B virus in Korea. *J Med Virol* 2010; **82**: 1126-1134 [PMID: 20513074 DOI: 10.1002/jmv.21844]
49 **Biswas A**, Panigrahi R, Banerjee A, Pal M, De BK, Chakrabarti S, Chakravarty R. Differential pattern of pre-S mutations/deletions and its association with hepatitis B virus genotypes in Eastern India. *Infect Genet Evol* 2012; **12**: 384-391 [PMID: 22266243 DOI: 10.1016/j.meegid.2012.01.007]
50 **Chen BF**. Different pre-S deletion patterns and their association with hepatitis B virus genotypes. *World J Gastroenterol* 2016; **22**: 8041-8049 [PMID: 27672298 DOI: 10.3748/wjg.v22.i35.8041.]
51 **Kao JH**, Liu CJ, Jow GM, Chen PJ, Chen DS, Chen BF. Fine mapping of hepatitis B virus pre-S deletion and its association with hepatocellular carcinoma. *Liver Int* 2012; **32**: 1373-1381 [PMID: 22676233]
52 **Lin CM**, Wang GM, Jow GM, Chen BF. Functional analysis of hepatitis B virus pre-s deletion variants associated with hepatocellular carcinoma. *J Biomed Sci* 2012; **19**: 17 [PMID: 22313590 DOI: 10.1186/1423-0127-19-17]
53 **Melegari M**, Scaglioni PP, Wands JR. The small envelope protein is required for secretion of a naturally occurring hepatitis B virus mutant with pre-S1 deleted. *J Virol* 1997; **71**: 5449-5454 [PMID: 9188617]
54 **Bock CT**, Tillmann HL, Maschek HJ, Manns MP, Trautwein C. A preS mutation isolated from a patient with chronic hepatitis B infection leads to virus retention and misassembly. *Gastroenterology* 1997; **113**: 1976-1982 [PMID: 9394738]
55 **Xu Z**, Yen TS. Intracellular retention of surface protein by a hepatitis B virus mutant that releases virion particles. *J Virol* 1996; **70**: 133-140 [PMID: 8523517]
56 **Kim BK**, Choi SH, Ahn SH, Chung AR, Park YK, Han KH, Kim S, Kim HS, Park JH, Kim KS, Lee HS, Cho YS, Kim KH, Ahn SH. Pre-S mutations of hepatitis B virus affect genome replication and expression of surface antigens. *J Gastroenterol Hepatol* 2014; **29**: 843-850 [PMID: 24783251]
57 **Yang JC**, Teng CF, Wu HC, Tsai HW, Chuang HC, Tsai TF, Hsu YH, Huang W, Wu LW, Su IJ. Enhanced expression of vascular endothelial growth factor-A in ground glass hepatocytes and its implication in hepatitis B virus hepatocarcinogenesis. *Hepatology* 2009; **49**: 1962-1971 [PMID: 19475690 DOI: 10.1002/hep.22889]
58 **Wang HC**, Chang WT, Chang WW, Wu HC, Huang W, Lei HY, Lai MD, Fausto N, Su IJ. Hepatitis B virus pre-S2 mutant upregulates cyclin A expression and induces nodular proliferation of hepatocytes. *Hepatology* 2005; **41**: 761-770 [PMID: 15726643 DOI: 10.1002/hep.20615]
59 **Wang LH**, Huang W, Lai MD, Su IJ. Aberrant cyclin A expression and centrosome overduplication induced by hepatitis B virus pre-S2 mutants and its implication in hepatocarcinogenesis. *Carcinogenesis* 2012; **33**: 466-472 [PMID: 22159224 DOI: 10.1093/carcin/bgr296]
60 **Hung JH**, Su IJ, Lei HY, Wang HC, Lin WC, Chang WT, Huang W, Chang WC, Chang YS, Chen CC, Lai MD. Endoplasmic reticulum stress stimulates the expression of cyclooxygenase-2 through activation of NF-kappaB and pp38 mitogen-activated protein kinase. *J Biol Chem* 2004; **279**: 46384-46392 [PMID: 15319438 DOI: 10.1074/jbc.M403568200]

61 **Hsieh YH**, Su IJ, Wang HC, Tsai JH, Huang YJ, Chang WW, Lai MD, Lei HY, Huang W. Hepatitis B virus pre-S2 mutant surface antigen induces degradation of cyclin-dependent kinase inhibitor p27Kip1 through c-Jun activation domain-binding protein 1. *Mol Cancer Res* 2007; **5**: 1063-1072 [PMID: 17951406 DOI: 10.1158/1541-7786.MCR-07-0098]

62 **Chen CH**, Changchien CS, Lee CM, Hung CH, Hu TH, Wang JH, Wang JC, Lu SN. Combined mutations in pre-s/surface and core promoter/precore regions of hepatitis B virus increase the risk of hepatocellular carcinoma: a case-control study. *J Infect Dis* 2008; **198**: 1634-1642 [PMID: 18939932 DOI: 10.1086/592990]

63 **Zhang AY**, Lai CL, Huang FY, Seto WK, Fung J, Wong DK, Yuen MF. Deep sequencing analysis of quasispecies in the HBV pre-S region and its association with hepatocellular carcinoma. *J Gastroenterol* 2017; **52**: 1064-1074 [PMID: 28353014 DOI: 10.1007/s00535-017-1334-1.]

64 **Zhang Q**, Cao G. Genotypes, mutations, and viral load of hepatitis B virus and the risk of hepatocellular carcinoma: HBV properties and hepatocarcinogenesis. *Hepat Mon* 2011; **11**: 86-91 [PMID: 22087123]

65 **Mun HS**, Lee SA, Kim H, Hwang ES, Kook YH, Kim BJ. Novel F141L pre-S2 mutation in hepatitis B virus increases the risk of hepatocellular carcinoma in patients with chronic genotype C infections. *J Virol* 2011; **85**: 123-132 [PMID: 20962085 DOI: 10.1128/JVI.01524-10.]

66 **Bayliss J**, Lim L, Thompson AJ, Desmond P, Angus P, Locarnini S, Revill PA. Hepatitis B virus splicing is enhanced prior to development of hepatocellular carcinoma. *J Hepatol* 2013; **59**: 1022-1028 [PMID: 23811301 DOI: 10.1016/j.jhep.2013.06.018]

67 **Günther S**, Sommer G, Iwanska A, Will H. Heterogeneity and common features of defective hepatitis B virus genomes derived from spliced pregenomic RNA. *Virology* 1997; **238**: 363-371 [PMID: 9400609 DOI: 10.1006/viro.1997.8863]

68 **Ma ZM**, Lin X, Wang YX, Tian XC, Xie YH, Wen YM. A double-spliced defective hepatitis B virus genome derived from hepatocellular carcinoma tissue enhanced replication of full-length virus. *J Med Virol* 2009; **81**: 230-237 [PMID: 19107969 DOI: 10.1002/jmv.21393]

69 **Abraham TM**, Lewellyn EB, Haines KM, Loeb DD. Characterization of the contribution of spliced RNAs of hepatitis B virus to DNA synthesis in transfected cultures of Huh7 and HepG2 cells. *Virology* 2008; **379**: 30-37 [PMID: 18657840 DOI: 10.1016/j.virol.2008.06.021]

70 **Soussan P**, Garreau F, Zylberberg H, Ferray C, Brechot C, Kremsdorf D. In vivo expression of a new hepatitis B virus protein encoded by a spliced RNA. *J Clin Invest* 2000; **105**: 55-60 [PMID: 10619861 DOI: 10.1172/JCI8098]

71 **Gerner P**, Schäfer HM, Prange R, Pravitt D, Wirth S. Functional analysis of a rare HBV deletion mutant in chronically infected children. *Pediatr Res* 2003; **53**: 891-897 [PMID: 12646724 DOI: 10.1203/01.PDR.0000064906.63939.72]

72 **Kajiya Y**, Hamasaki K, Nakata K, Nakagawa Y, Miyazoe S, Takeda Y, Ohkubo K, Ichikawa T, Nakao K, Kato Y, Eguchi K. Full-length sequence and functional analysis of hepatitis B virus genome in a virus carrier: a case report suggesting the impact of pre-S and core promoter mutations on the progression of the disease. *J Viral Hepat* 2002; **9**: 149-156 [PMID: 11876799 DOI: 10.1046/j.1365-2893.2002.00335.x]

73 **Mu SC**, Lin YM, Jow GM, Chen BF. Occult hepatitis B virus infection in hepatitis B vaccinated children in Taiwan. *J Hepatol* 2009; **50**: 264-272 [PMID: 19070923 DOI: 10.1016/j.jhep.2008.09.017]

74 **Nakajima E**, Minami M, Ochiya T, Kagawa K, Okanoue T. PreS1 deleted variants of hepatitis B virus in patients with chronic hepatitis. *J Hepatol* 1994; **20**: 329-335 [PMID: 7516949]

75 **Takayanagi M**, Kakumu S, Ishikawa T, Higashi Y, Yoshioka K, Wakita T. Comparison of envelope and precore/core variants of hepatitis B virus (HBV) during chronic HBV infection. *Virology* 1993; **196**: 138-145 [PMID: 8356791 DOI: 10.1006/viro.1993.1462]

76 **Gerner PR**, Friedt M, Oettinger R, Lausch E, Wirth S. The hepatitis B virus seroconversion to anti-HBe is frequently associated with HBV genotype changes and selection of preS2-defective particles in chronically infected children. *Virology* 1998; **245**: 163-172 [PMID: 9614877]

77 **Bruss V**, Ganem D. Mutational analysis of hepatitis B surface antigen particle assembly and secretion. *J Virol* 1991; **65**: 3813-3820 [PMID: 2041095]

78 **Salpini R**, Surdo M, Warner N, Cortese MF, Colledge D, Soppe S, Bellocchi MC, Armenia D, Carioti L, Continenza F, Di Carlo D, Saccomandi P, Mirabelli C, Pollicita M, Longo R, Romano S, Cappiello G, Spanò A, Trimoulet P, Fleury H, Vecchiet J, Iapadre N, Barlattani A, Bertoli A, Mari T, Pasquazzi C, Missale G, Sarrecchia C, Orecchini E, Michienzi A, Andreoni M, Francioso S, Angelico M, Verheyen J, Ceccherini-Silberstein F, Locarnini S, Perno CF, Svicher V. Novel HBsAg mutations correlate with hepatocellular carcinoma, hamper HBsAg secretion and promote cell proliferation in vitro. *Oncotarget* 2017; **8**: 15704-15715 [PMID: 28152517 DOI: 10.18632/oncotarget.14944]

79 **Kim HS**, Ryu CJ, Hong HJ. Hepatitis B virus preS1 functions as a transcriptional activation domain. *J Gen Virol* 1997; **78**: 1083-1086 [PMID: 9152426 DOI: 10.1099/0022-1317-78-5-1083]

80 **Hildt E**, Urban S, Hofschneider PH. Characterization of essential domains for the functionality of the MHBst transcriptional activator and identification of a minimal MHBst activator. *Oncogene* 1995; **11**: 2055-2066 [PMID: 7478525]

81 **Hildt E**, Saher G, Bruss V, Hofschneider PH. The hepatitis B virus large surface protein (LHBs) is a transcriptional activator. *Virology* 1996; **225**: 235-239 [PMID: 8918553 DOI: 10.1006/viro.1996.0594]

82 **Hildt E**, Munz B, Saher G, Reifenberg K, Hofschneider PH. The PreS2 activator MHBs(t) of hepatitis B virus activates c-raf-1/Erk2 signaling in transgenic mice. *EMBO J* 2002; **21**: 525-535 [PMID: 11847101 DOI: 10.1093/emboj/21.4.525]

83 **Lupberger J**, Hildt E. Hepatitis B virus-induced oncogenesis. *World J Gastroenterol* 2007; **13**: 74-81 [PMID: 17206756 DOI: 10.3748/wjg.v13.i1.74]

84 **Kamili S**, Sozzi V, Thompson G, Campbell K, Walker CM, Locarnini S, Krawczynski K. Efficacy of hepatitis B vaccine against antiviral drug-resistant hepatitis B virus mutants in the chimpanzee model. *Hepatology* 2009; **49**: 1483-1491 [PMID: 19274751 DOI: 10.1002/hep.22796]

85 **Warner N**, Locarnini S. The antiviral drug selected hepatitis B virus rtA181T/sW172* mutant has a dominant negative secretion defect and alters the typical profile of viral rebound. *Hepatology* 2008; **48**: 88-98 [PMID: 18537180 DOI: 10.1002/hep.22295]

86 **Lai MW**, Liang KH, Lin WR, Huang YH, Huang SF, Chen TC, Yeh CT. Hepatocarcinogenesis in transgenic mice carrying hepatitis B virus pre-S/S gene with the sW172* mutation. *Oncogenesis* 2016; **5**: e273 [PMID: 27918551 DOI: 10.1038/oncsis.2016.77.]

87 **Huang SF**, Chen YT, Lee WC, Chang IC, Chiu YT, Chang Y, Tu HC, Yuh CH, Matsuura I, Shih LY, Lai MW, Wu HD, Chen MF, Yeh CT. Identification of transforming hepatitis B virus S gene nonsense mutations derived from freely replicative viruses in hepatocellular carcinoma. *PLoS One* 2014; **9**: e89753 [PMID: 24587012 DOI: 10.1371/journal.pone.0089753]

88 **Shirvani-Dastgerdi E**, Winer BY, Celià-Terrassa T, Kang Y, Tabernero D, Yagmur E, Rodríguez-Frías F, Gregori J, Luedde T, Trautwein C, Ploss A, Tacke F. Selection of the highly replicative and partially multidrug resistant rtS78T HBV polymerase mutation during TDF-ETV combination therapy. *J Hepatol* 2017; **67**: 246-254 [PMID: 28392234 DOI: 10.1016/j.jhep.2017.03.027]

89 **Lee SA**, Kim K, Kim H, Kim BJ. Nucleotide change of codon 182 in the surface gene of hepatitis B virus genotype C leading to truncated surface protein is associated with progression of liver

diseases. *J Hepatol* 2012; **56**: 63-69 [PMID: 21827734 DOI: 10.1016/j.jhep.2011.06.028]
90 **Tai PC**, Suk FM, Gerlich WH, Neurath AR, Shih C. Hypermodification and immune escape of an internally deleted middle-envelope (M) protein of frequent and predominant hepatitis B virus variants. *Virology* 2002; **292**: 44-58 [PMID: 11878907]

P- Reviewer: El-Shabrawi MHF, Komatsu H, Rodriguez-Frias F, Takahashi T
S- Editor: Gong ZM **L- Editor**: A **E- Editor**: Huang Y

World Journal of Gastroenterology

Submit a Manuscript: http://www.f6publishing.com

World J Gastroenterol 2018 April 14; 24(14): 1521-1530

DOI: 10.3748/wjg.v24.i14.1521

ISSN 1007-9327 (print) ISSN 2219-2840 (online)

MINIREVIEWS

Extra-intestinal manifestations of non-celiac gluten sensitivity: An expanding paradigm

Giuseppe Losurdo, Mariabeatrice Principi, Andrea Iannone, Annacinzia Amoruso, Enzo Ierardi, Alfredo Di Leo, Michele Barone

Giuseppe Losurdo, Mariabeatrice Principi, Andrea Iannone, Annacinzia Amoruso, Enzo Ierardi, Alfredo Di Leo, Michele Barone, Section of Gastroenterology, Department of Emergency and Organ Transplantation, University "Aldo Moro" of Bari, Bari 70124, Italy

ORCID number: Giuseppe Losurdo (0000-0001-7038-3287); Mariabeatrice Principi (0000-0003-0545-5656); Andrea Iannone (0000-0002-5468-9515); Annacinzia Amoruso (0000-0002-4161-3378); Enzo Ierardi (0000-0001-7275-5080); Alfredo Di Leo (0000-0003-2026-1200); Michele Barone (0000-0003-2026-1200).

Author contributions: Losurdo G, Barone M and Di Leo A planned the study; Principi M, Iannone A, Amoruso A and Barone M collected the data; Losurdo G and Ierardi E wrote the paper; Barone M and Di Leo A revised the article; Losurdo G and Principi M contributed equally and are co-first authors.

Conflict-of-interest statement: None declared.

Manuscript source: Invited manuscript

Correspondence to: Giuseppe Losurdo, MD, Doctor, Section of Gastroenterology, Department of Emergency and Organ Transplantation, University "Aldo Moro" of Bari, Piazza Giulio Cesare 11, Bari 70124, Italy. giuseppelos@alice.it
Telephone: +39-80-5593452
Fax: +39-80-5593088

Received: March 8, 2018
Peer-review started: March 9, 2018
First decision: March 14, 2018
Revised: March 27, 2018
Accepted: March 31, 2018
Article in press: March 31, 2018
Published online: April 14, 2018

Abstract

Non celiac gluten sensitivity (NCGS) is a syndrome characterized by a cohort of symptoms related to the ingestion of gluten-containing food in subjects who are not affected by celiac disease (CD) or wheat allergy. The possibility of systemic manifestations in this condition has been suggested by some reports. In most cases they are characterized by vague symptoms such as 'foggy mind', headache, fatigue, joint and muscle pain, leg or arm numbness even if more specific complaints have been described. NCGS has an immune-related background. Indeed there is a strong evidence that a selective activation of innate immunity may be the trigger for NCGS inflammatory response. The most commonly autoimmune disorders associated to NCGS are Hashimoto thyroiditis, dermatitis herpetiformis, psoriasis and rheumatologic diseases. The predominance of Hashimoto thyroiditis represents an interesting finding, since it has been indirectly confirmed by an Italian study, showing that autoimmune thyroid disease is a risk factor for the evolution towards NCGS in a group of patients with minimal duodenal inflammation. On these bases, an autoimmune stigma in NCGS is strongly supported; it could be a characteristic feature that could help the diagnosis and be simultaneously managed. A possible neurological involvement has been underlined by NCGS association with gluten ataxia, gluten neuropathy and gluten encephalopathy. NCGS patients may show even psychiatric diseases such as depression, anxiety and psychosis. Finally, a link with functional disorders (irritable bowel syndrome and fibromyalgia) is a topic under discussion. In conclusion, the novelty of this matter has generated an expansion of literature data with the unavoidable consequence that some

reports are often based on low levels of evidence. Therefore, only studies performed on large samples with the inclusion of control groups will be able to clearly establish whether the large information from the literature regarding extra-intestinal NCGS manifestations could be supported by evidence-based agreements.

Key words: Non celiac gluten sensitivity; Celiac disease; Gluten; Gluten ataxia; Autoimmunity; Gluten-related disorders; Thyroiditis; Extra-intestinal

Core tip: Non celiac gluten sensitivity is an expanding field of investigation within gluten-related disorders. Similarly to celiac disease, it shows a systemic involvement, therefore several extra-intestinal manifestations have been hypothesized and investigated in many studies. They may involve many districts and have neurological/psychiatric, dermatological, rheumatologic and nutritional implications. Moreover, the possibility of association with other autoimmune diseases should not be underestimated. However, the large data amount from the literature often requires to be supported by evidence-based agreements.

Losurdo G, Principi M, Iannone A, Amoruso A, Ierardi E, Di Leo A, Barone M. Extra-intestinal manifestations of non-celiac gluten sensitivity: An expanding paradigm. *World J Gastroenterol* 2018; 24(14): 1521-1530 Available from: URL: http://www.wjgnet.com/1007-9327/full/v24/i14/1521.htm DOI: http://dx.doi.org/10.3748/wjg.v24.i14.1521

INTRODUCTION

Non celiac gluten sensitivity (NCGS) is a syndrome characterized by a set of symptoms related to the ingestion of gluten-containing food in subjects who are not affected by celiac disease (CD) or wheat allergy[1]. Despite it has been included in the spectrum of gluten related disorders, it shows a peculiar picture with some elements resembling CD, *i.e.*, immunological involvement and response to gluten free diet, and some features close to irritable bowel syndrome[2].

In detail, NCGS is distinguished by symptoms that typically take place soon after gluten ingestion, withdraw with gluten exclusion, and relapse following gluten challenge within hours or days. The "classical" clinical picture of NCGS is a combination of irritable bowel syndrome-like manifestations, such as abdominal pain, bloating, diarrhea or alterations in bowel habit with alternation of constipation and loose stools.

However, the possibility of systemic manifestations in this condition has been suggested by some reports. In most cases they are characterized by vague symptoms such as 'foggy mind', headache, fatigue, joint and muscle pain, leg or arm numbness even if more specific complaints have been described, such as dermatitis, (eczema or skin rash), depression, neurological symptoms and anemia[3-8]. Moreover, the possibility of association with other autoimmune diseases has been hypothesized. Indeed, similarly to CD, NCGS can be considered as an immune system-related disease and this aspect should be of relevance.

In conclusion, the spectrum of NCGS extra-intestinal manifestations is constantly expanding with new reports. Therefore, we aimed to summarize the main extra-intestinal manifestations of NCGS in a narrative review. In particular, in this review we focused on the associations supported by an evidence-based link more than single case reports, where it is difficult to differentiate a casual association from a real relationship. For this reason we searched in PubMed database in February 2018 using the following terms: gluten sensitivity, extra-intestinal, autoimmune, thyroid, neurology, psychiatry, rheumatology, skin, dermatology, nutrition, irritable bowel syndrome and fibromyalgia. In this way, 880 articles were found, and, as reported in the flow chart in Figure 1, we selected 86 studies for this review. Other studies which were not focused on NCGS or reporting an unclear definition of NCGS, or in which results about extra-intestinal manifestation were not listed have been excluded. Additionally, we graded the level of evidence on the association between NCGS and systemic manifestations using the Oxford consensus[9].

ASSOCIATION WITH AUTOIMMUNE DISEASES

On the base of convincing evidence, NCGS has an immune-related background. Indeed it has been demonstrated that a selective activation of innate immunity may be the trigger for NCGS inflammatory response[10,11]. It is unclear whether gliadin is the real responsible for the autoimmune event onset, since some other components of wheat, such as amylase-trypsin inhibitors or fermentable oligo-di-mono-saccharides and polyols (FODMAPs) have been invoked[12-14]. For this reason some Authors consider the term "non celiac wheat sensitivity" more appropriate than the current one[15].

CD, which is the most common and studied gluten-related disorder, is often associated to several other autoimmune diseases, such as type 1 diabetes, autoimmune thyroiditis or dermatitis herpetiformis[16]. For this reason it is conceivable that also patients with NCGS could show autoimmune disorders. In a cohort of 131 NCGS patients[17], the prevalence of autoimmune disease (29%) was found to be higher than in control group (4%, $P < 0.001$). Moreover, anti-nucleus antibody (ANA) positivity, a well-known marker of autoimmune setting, was present in the 46% of NCGS subjects, compared to the 2% of controls, and ANA positivity

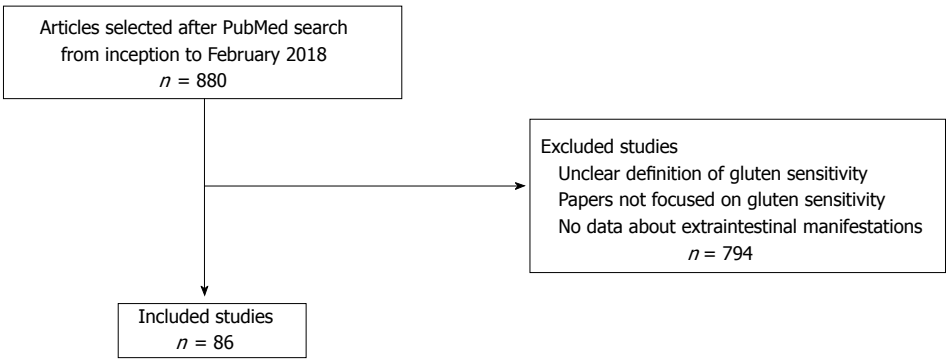

Figure 1 Flowchart summarizing the process of study selection.

correlated with DQ2/8 haplotypes. In detail, the most frequently reported NCGS-associated autoimmune disorder was Hashimoto thyroiditis (29 patients). Other diseases were psoriasis (4 cases), type 1 diabetes (4 cases), mixed connective tissue disease (1 case) and ankylosing spondylitis (1 case). The predominance of autoimmune thyroiditis represents an interesting finding, since it was indirectly confirmed by an Italian experience[18], showing that autoimmune thyroiditis is a risk factor for the evolution towards NCGS in a group of patients with minimal duodenal inflammation[19].

On these bases, an autoimmune stigma in NCGS is strongly supported; it could be a characteristic feature that could help the diagnosis and be simultaneously managed.

NEUROLOGIC AND PSYCHIATRIC MANIFESTATIONS

Recently, many studies explored the bond between the ingestion of gluten-containing food and the onset of neurologic and psychiatric disorders or symptoms such as ataxia, peripheral neuropathy, schizophrenia, autism, depression, anxiety, and hallucinations[20].

In patients with CD, a neurological involvement could be the only clinical manifestation of the disease. The production of autoantibodies directed against the tissue transglutaminase isoform 6 (expressed selectively in brain tissue) has been found in up to the 85% of these patients[21,22]. Anti-gliadin antibodies (AGA) frequently occur in such cases[21,22]. It is unclear whether the production of these antibodies takes place in the brain or in the gut mucosa, but these antibodies are considered to be the etiologic agent of neurological manifestations of CD. Finally, an inflammatory infiltrate of T lymphocytes resembling IELs in the white matter or in perivascular cuff of nerves is an important finding suggesting a specific pathogenetic mechanism of gluten-induced neuropathies[23].

Three main diseases have been described in the spectrum of gluten-related neurologic manifestations: gluten ataxia, gluten neuropathy and gluten encephalopathy[23].

Gluten ataxia has the strongest relationship with gluten-related disorders. It encompasses about the 20% of all causes of ataxia. This is mainly characterized by pure cerebellar ataxia and, rarely, by ataxia combined with myoclonus, palatal tremor, opsoclonus, or chorea. Gaze-evoked nystagmus and other ocular marks of cerebellar dysfunction are observed in about the 80%. All subjects show gait ataxia and most of them have limb ataxia[24]. A frequent finding at magnetic resonance imaging is cerebellar atrophy, secondary to necrosis of Purkinje cells[25]. Less than 10% of patients with gluten ataxia complain of gastrointestinal symptoms. A gluten free diet is able to reverse symptoms, however an early diagnosis significantly improves the prognosis, since gluten free diet may stop the loss of Purkinje cells. Therefore, a late diagnosis may be associated with an irreversible damage[26].

Gluten neuropathy is a form of peripheral neuronal damage, in which there is a serological evidence of CD positivity in the absence of alternative aetiologies. The most common type is a symmetrical sensorimotor axonal peripheral neuropathy, but other types have also been described (asymmetrical neuropathy, pure motor neuropathy or autonomic neuropathy)[27]. Gluten neuropathy occurs in the sixth decade and slowly progresses with a 9 year mean latency time between the diagnosis of neuropathy and that of CD. A third of patients shows duodenal inflammation on biopsy, however the presence or absence of enteropathy does not influence the effect of a gluten-free diet[28]. The most common histopathological feature of gluten neuropathy is lymphocyte infiltration of peri-neural vessels[29].

Gluten encephalopathy is a central nervous system disease characterized by focal abnormalities of the white matter (usually area of low perfusion) in presence of AGA or anti-transglutaminase 2 antibodies[30]. The most common symptom is migraine. It has been demonstrated that a gluten free diet improves the headaches and stops the progression of cerebral alterations detected at magnetic resonance imaging[31].

Some reports about the direct relationship between the above cited diseases and NCGS have been

published in the last years. Hadjivassiliou *et al*[32] have retrospectively evaluated 562 patients with gluten-related disorders (228 CD and 334 NCGS) and concomitant neurological involvement. In NCGS the most frequent disorder was peripheral neuropathy (54%) followed by ataxia (46%) and encephalopathy, while in CD, ataxia was the most frequent one (41%). In all cases a deep linkage with AGA positivity was recorded. Additionally, the severity of ataxia was similar in both conditions (CD and NCGS), while patients with CD exhibited more frequently severe forms of neuropathy. Rodrigo *et al*[33] found, in a cohort of 31 subjects with gluten ataxia, AGA positivity rate of 100%; this value was more similar to NCGS (89%) than CD (48%) and was associated to Marsh 1 duodenal histological picture. On the bases of such results, they concluded that gluten ataxia shows a strict affinity to NCGS more than CD.

Headache is a very frequent finding in NCGS. However, no study has so far analyzed in depth the nature of this association. The available data relies mainly on observational studies aiming to elucidate the prevalence of this condition, which ranges around the 25%[3-8,34,35]. However, the lack of case-control studies is a serious limitation to ascertain the reliability of the association. Moreover there are no studies investigating possible pathogenetic mechanisms.

The association with other neurologic diseases such as epilepsy[36], miopathy[37] and demyelinating disease[38], is anecdotal or based on a non conventional diagnosis of NCGS, therefore it is not possible to draw solid conclusions.

Among the psychiatric diseases, depression and anxiety have been hypothesized as systemic manifestations of NCGS. In an Australian study[39], a group of patients with established diagnosis of NCGS underwent a double blind crossover study with a placebo versus oral gluten supplementation after a gluten free diet. Results showed that gluten induced depression scale worsening when compared to placebo, while other symptoms (anxiety, curiosity and anger) were not influenced by the diet. However, the mechanism by which gluten may induce these changes is not yet clear. Depression is indeed a frequent finding in Western society, and it could be a distinctive mood tract of personality rather than an extra-intestinal manifestation of NCGS. However, in another study NCGS patients did not exhibit a tendency for general somatization. Additionally, personality and quality of life did not differ between NCGS and CD patients and were mostly similar to healthy controls[40].

Some authors have invoked a role of gluten for some psychiatric diseases like schizophrenia or bipolar disorder[41], but there are no studies exploring these entities in NCGS. On the other hand, some cases of "gluten psychosis" in patients with NCGS have been described[42]. In these patients, hallucinations, crying spells, relevant confusion, ataxia, severe anxiety and paranoid delirium occurred shortly after gluten ingestion and disappeared within one week of gluten free diet.

Finally, the relationship between autism and gluten is an hot topic. It has been shown that children with autism have more frequently IgG-AGA positivity than healthy children (24% *vs* 7%)[43], but currently there are no studies in which a solid diagnosis of NCGS has been achieved in autistic subjects. A gluten free diet is often proposed to these children in an empiric setting, since it has been demonstrated that it improves behavioral scores[44,45]. However, at present there are no evidence-based reasons to look for gluten sensitivity in autism and to advise an exclusion diet[46].

SKIN MANIFESTATIONS

The association between CD and skin diseases, in particular dermatitis herpetiformis, is well known[47]. Similarly to CD, the possibility of a skin involvement in the 18% of NCGS has been reported[4]. In the published case series[3-8], undefined dermatitis, rash and eczema were the most common skin manifestations in NCGS. The possibility of an association with skin autoimmune diseases such as psoriasis has been above mentioned[17]. A case report has shown that even dermatitis herpetiformis may occur[48].

Some reports have been mainly focused on the characteristics of skin lesions in NCGS from a dermatological point of view. In a series of 17 NCGS patients with skin lesions, the most common ones were very similar to dermatitis herpetiformis or subacute eczema (erythematous, excoriated papular-vesicular and extremely itchy)[49]. Some patients had also hyperkeratotic scaly lesions resembling psoriasis. The most common skin location was the extensor surfaces of upper limbs, in the 94%, alike dermatitis herpetiformis. The histological analysis showed complement C3 deposits at dermoepidermal junction in the 82%. Finally, in all patients a gluten free diet was able to lead to lesions disappearance within one month, much faster than in dermatitis herpetiformis.

Some Authors have claimed that an allergic sensitivity to food allergens other than gluten could underlie NCGS[50]. Indeed, an Italian study found that the 10% of NCGS patients suffered from nickel allergy with contact dermatitis and this prevalence was higher than in control group (5%, $P = 0.04$). However, NCGS subjects referred onset of dermatitis after wheat ingestion[51].

RHEUMATOLOGIC MANIFESTATIONS

As we already mentioned, NCGS shows the tendency to cluster autoimmune diseases. Some reports about its coexistence with rheumatologic diseases are available. The first evidence demonstrated that in a group of 30 subjects with ankylosing spondylitis, 11 had AGA positivity, while no patient in a control group exhibited this finding[52]. Isasi *et al*[53] reported 4 cases of axial spondyloarthritis (2 ankylosing spondylitis and 1

Table 1 Studies reporting the prevalence of people avoiding gluten-containing foods

Ref.	Country	Population	Sample size	Avoidance rate of gluten-based products
Tanpowpong *et al*[60], 2012	New Zealand	Pediatric	916	5.2%
Rubio-Tapia *et al*[61], 2013	United States	Pediatric	7798	0.7%
DiGiacomo *et al*[62], 2013	United States	National Health and Nutrition Examination Survey	7762	0.6%
Lis *et al*[63], 2014	Australia	Adults	910	41.2%
Golley *et al*[64], 2015	Australia	Adults	1184	10.6%
Mardini *et al*[65], 2015	United States	Pediatric	14701	1%
Aziz *et al*[59], 2014	United Kingdom	Adults	1002	3.7%
Van Gils *et al*[8], 2016	The Netherlands	Adults	785	6.2%
Carroccio *et al*[7], 2017	Italy	Adolescents	548	2.9%

psoriatic spondyloarthritis) with a microscopic enteritis picture at duodenal biopsy. They all underwent a gluten free diet, and in all cases an improvement or remission of back pain was reported, with a recrudescence after wheat challenge. The same result was recorded in another group of patients with systemic sclerosis, Raynaud's phenomenon, symmetric polyarthritis and Sjogren's syndrome[53].

However, despite such reports, the evidence for NCGS/rheumatologic association is weak, since case reports represent only a low level of evidence and case-control studies are necessary.

FIBROMYALGIA AND OTHER FUNCTIONAL DISORDERS

Fibromyalgia is a disease characterized by widespread pain, often accompanied by fatigue, memory problems, sleep disturbances, depression or irritable bowel syndrome[54]. In many case series, several NCGS patients complain of chronic muscle or joint pain, leg numbness, fatigue and headache[3-8], therefore it is possible that an underlying undiagnosed fibromyalgia could be present. Indeed, starting from some case reports demonstrating this association[55], further studies have analyzed in depth this relationship. In a Spanish series[56] of 246 fibromyalgia patients undergoing gluten free diet, 90 showed clinical symptom improvement. Additionally, Authors described the features of 20 out of such 90 patients. They had a mean duration of fibromyalgia of 12 years, and 17 had also gastrointestinal symptoms. Eighteen had a DQ2/8 haplotype and all showed an increase in duodenal IELs. After a mean gluten free diet period of 16.4 mo, 15 of them (75%) experienced a full remission of pain and in 8 of them gluten challenge led to symptom re-appearance. In another trial, gluten free diet was able to induce a decrease in some scales evaluating fibromyalgia symptoms[57]. On these bases, it is possible to hypothesize that the link between these two disorders is quite strong, but the role of microscopic enteritis in this setting should be tested in other controlled trials.

Fibromyalgia is frequently recognized as a functional disease. In this regard, NCGS has a tight bond with irritable bowel syndrome (IBS)[58]. Many patients with IBS often identify some foods that they believe to be more offending, and wheat is often invoked. Furthermore, a certain symptom overlap between NCGS and IBS-type symptoms exists[4,59]. For this reason, many patients tend to exclude gluten from their diet on their own, without medical advice, as summarized in Table 1[7,8,59-65]. The basic difference between the two conditions is that patients with NCGS assert that symptoms take place when they eat wheat so that they believe to have identified gluten as the culprit. Some experimental investigations have shown that gliadin can alter the integrity of the small intestinal mucosa, as shown by the appearance of epithelial leaks/gaps and widened inter-villous spaces detected by using confocal laser endomicroscopy[66]. Based on these assumptions, some clinical trials have demonstrated that a gluten free diet may lead to improvement of gastrointestinal symptoms in IBS, as reported in Table 2[5,67-73]. However it is not clear whether gluten is really the responsible for such symptoms. Indeed wheat contains FODMAPs as well, which are considered as a possible trigger for IBS itself, and FODMAP restriction demonstrated an improvement in IBS symptoms in up to the 74%[74]. Additionally, one trial underlined that subjects with self-reported NCGS (and IBS-like symptoms) had benefits by a low FODMAP diet despite they were still consuming a gluten free diet[75]. Based on these evidences, the link between IBS and NCGS seems to be strict even if quite nebulous. Is it possible that IBS and NCGS should be considered as the two sides of the same coin? Such fascinating question needs to be answered by well designed studies for this purpose.

NUTRITIONAL IMPAIRMENT IN NCGS

CD is often disclosed by nutritional impairments, such as vitamin D or iron deficiency, anemia or alterations in bone mineralization[76,77].

Anemia prevalence value ranges between 15% and 23% in NCGS[3,4]. Nevertheless, studies enclosing a control group are lacking, therefore it is not possible to establish which is the real relationship between anemia and NCGS. Additionally, folate deficiency has

Table 2 Main studies exploring the effect of gluten free diet in irritable bowel syndrome

Ref.	Country	Population	Outcome
Wahnschaffe *et al*[67], 2001	Germany	102 IBS-D	Stool frequency/bowel movement improved in DQ2-8 positive subjects
Aziz *et al*[68], 2016	United Kingdom	40 IBS-D	A 6-wk GFD reduced symptoms in 70%
Vazquez-Roque *et al*[69], 2013	United States	45 IBS-D	Stool frequency/bowel movement reduced in patients under GFD
Di Sabatino *et al*[5], 2015	Italy	59 IBS with self-diagnosis of NCGS	A challenge with 4 g/d of gluten worsened symptoms compared to placebo
Shahbazkhani *et al*[70], 2015	Iran	72 IBS	Worsening of intestinal symptoms with gluten compared to placebo
Zanwar *et al*[71], 2016	India	60 IBS	A 4-wk GFD improved a visual-analogue scale of symptoms
Elli *et al*[72], 2016	Italy	140 IBS with self-diagnosis of NCGS	Only the 14% showed a response to GFD as well as challenge test
Barmeyer *et al*[73], 2017	Germany	34 IBS	The 34% showed clinical improvement to GFD and continued for one year

GFD: Gluten free diet; IBS-D: Irritable bowel syndrome, diarrhea subtype; NCGS: Non celiac gluten sensitivity.

Table 3 Main extra-intestinal manifestations of non-celiac gluten sensitivity and associated disorders

Manifestations	Extra-intestinal manifestations	Level of evidence	Associated disorders	Level of evidence
General symptoms	Tiredness	4	Aphthous stomatitis	4
	Lack of wellbeing	4		
	Foggy mind	4		
	Joint or muscle pain	4		
	Arm/leg numbness	4		
Neurologic manifestations			Ataxia	3b
			Neuropathy	3b
			Encephalopathy	3b
			Epilepsy	4
			Miopathy	4
			Myelopathy	4
			Demyelinating disease	4
Psychiatric manifestations	Depression	1c	Bipolar disorder	4
	Anxiety	1c	Gluten psychosis	4
			Autism	2b
			Schizophrenia	4
Other autoimmune diseases and rheumatologic diseases			Psoriasis	2b
			Autoimmune thyroiditis	2b
			Rheumatoid arthritis	4
			Scleroderma	4
			Sjogren syndrome	4
			Raynaud phenomenon	4
Skin diseases			Dermatitis herpetiformis	2b
			Contact dermatitis	2b
			Rash and undetermined dermatitis	2b
Functional disorders			Fibromyalgia	1c
			Irritable bowel syndrome	1c
Nutritional imbalance	Anemia	4		
	Osteoporosis	2b		
Other			Interstitial cystitis	4
			Ingrown hairs	4
			Rhinitis, asthma	4
			Postural tachycardia syndrome	2b
			Oligo- or polymenorrhea	4

The level of evidence was expressed according to the Oxford consensus[85]

been reported in NCGS with solid evidence and it has been even described as a predictive factor for its development[18].

An Italian study illustrated that NCGS carries a risk of osteopenia similar to CD[78]. Low bone mineral density measured by Dual-energy X-ray absorptiometry was found in 28% of NCGS subjects, *vs* 6% of IBS as well as an influence of body mass index on mineralization was observed. This result has been explained by a lower calcium dietary intake (only 615 mg/d, while

recommended dose is 1000 mg/d).

This last observation may suggest that NCGS patients could experience an alteration in macro- and micronutrients intake due to dietary self-restrictions. Indeed Zingone *et al*[79] evaluated diet habits of 29 NCGS subjects and discovered that they ingested lower mean amounts of carbohydrates, proteins, fiber, and polyunsaturated fatty acids. Patients with NCGS reported avoiding fruit, vegetables, milk, and dairy products as well as snacks and mixed spices when compared to a control population.

NCGS is characterized by absent or minimal duodenal inflammation and, therefore, cannot be associated to nutrient deficiencies linked to malabsorption. However, an inflammatory status of duodenal mucosa, witnessed by increased expression of interferon gamma, may not be overlooked[33,80-82]. Finally, alterations in dietary pattern should not be underestimated. Gluten free diet itself can lead to an inadequate balance in macronutrients assumption[83-85].

CONCLUSION

Data from literature about extra-intestinal manifestations of NCGS strongly suggests that this condition could have a systemic involvement, similarly to CD. However, the novelty of this topic has generated an expansion of literature data with the unavoidable consequence that some reports are often based on low levels of evidence, as summarized in Table 3, with a grading of evidence according to the Oxford classification[9]. Therefore, only studies performed on large samples with the addition of control groups will be able to clearly establish whether the large information from the literature regarding extra-intestinal NCGS manifestations could be supported by evidence-based agreements.

REFERENCES

1 **Catassi C**, Bai JC, Bonaz B, Bouma G, Calabrò A, Carroccio A, Castillejo G, Ciacci C, Cristofori F, Dolinsek J, Francavilla R, Elli L, Green P, Holtmeier W, Koehler P, Koletzko S, Meinhold C, Sanders D, Schumann M, Schuppan D, Ullrich R, Vécsei A, Volta U, Zevallos V, Sapone A, Fasano A. Non-Celiac Gluten sensitivity: the new frontier of gluten related disorders. *Nutrients* 2013; **5**: 3839-3853 [PMID: 24077239 DOI: 10.3390/nu5103839]

2 **Sapone A**, Bai JC, Ciacci C, Dolinsek J, Green PH, Hadjivassiliou M, Kaukinen K, Rostami K, Sanders DS, Schumann M, Ullrich R, Villalta D, Volta U, Catassi C, Fasano A. Spectrum of gluten-related disorders: consensus on new nomenclature and classification. *BMC Med* 2012; **10**: 13 [PMID: 22313950 DOI: 10.1186/1741-7015-10-13]

3 **Volta U**, Tovoli F, Cicola R, Parisi C, Fabbri A, Piscaglia M, Fiorini E, Caio G. Serological tests in gluten sensitivity (nonceliac gluten intolerance). *J Clin Gastroenterol* 2012; **46**: 680-685 [PMID: 22138844 DOI: 10.1097/MCG.0b013e3182372541]

4 **Volta U**, Bardella MT, Calabrò A, Troncone R, Corazza GR; Study Group for Non-Celiac Gluten Sensitivity. An Italian prospective multicenter survey on patients suspected of having non-celiac gluten sensitivity. *BMC Med* 2014; **12**: 85 [PMID: 24885375 DOI: 10.1186/1741-7015-12-85]

5 **Di Sabatino A**, Volta U, Salvatore C, Biancheri P, Caio G, De Giorgio R, Di Stefano M, Corazza GR. Small Amounts of Gluten in Subjects With Suspected Nonceliac Gluten Sensitivity: A Randomized, Double-Blind, Placebo-Controlled, Cross-Over Trial. *Clin Gastroenterol Hepatol* 2015; **13**: 1604-1612.e3 [PMID: 25701700 DOI: 10.1016/j.cgh.2015.01.029]

6 **Carroccio A**, Mansueto P, Iacono G, Soresi M, D'Alcamo A, Cavataio F, Brusca I, Florena AM, Ambrosiano G, Seidita A, Pirrone G, Rini GB. Non-celiac wheat sensitivity diagnosed by double-blind placebo-controlled challenge: exploring a new clinical entity. *Am J Gastroenterol* 2012; **107**: 1898-1906; quiz 1907 [PMID: 22825366 DOI: 10.1038/ajg.2012.236]

7 **Carroccio A**, Giambalvo O, Blasca F, Iacobucci R, D'Alcamo A, Mansueto P. Self-Reported Non-Celiac Wheat Sensitivity in High School Students: Demographic and Clinical Characteristics. *Nutrients* 2017; **9**: pii: E771 [PMID: 28753927 DOI: 10.3390/nu9070771]

8 **van Gils T**, Nijeboer P, IJssennagger CE, Sanders DS, Mulder CJ, Bouma G. Prevalence and Characterization of Self-Reported Gluten Sensitivity in The Netherlands. *Nutrients* 2016; **8**: pii: E714 [PMID: 27834802 DOI: 10.3390/nu8110714]

9 **Centre for Evidence-Based Medicine**. Oxford Centre for Evidence-based Medicine – Levels of Evidence (March 2009). Accessed March 17, 2018 Available from: URL: https://www.cebm.net/2009/06/oxford-centre-evidence-based-medicine-levels-evidence-march-2009/

10 **Caio G**, Riegler G, Patturelli M, Facchiano A, DE Magistris L, Sapone A. Pathophysiology of non-celiac gluten sensitivity: where are we now? *Minerva Gastroenterol Dietol* 2017; **63**: 16-21 [PMID: 27808487 DOI: 10.23736/S1121-421X.16.02346-1]

11 **Sapone A**, Lammers KM, Casolaro V, Cammarota M, Giuliano MT, De Rosa M, Stefanile R, Mazzarella G, Tolone C, Russo MI, Esposito P, Ferraraccio F, Cartenì M, Riegler G, de Magistris L, Fasano A. Divergence of gut permeability and mucosal immune gene expression in two gluten-associated conditions: celiac disease and gluten sensitivity. *BMC Med* 2011; **9**: 23 [PMID: 21392369 DOI: 10.1186/1741-7015-9-23]

12 **Zevallos VF**, Raker V, Tenzer S, Jimenez-Calvente C, Ashfaq-Khan M, Rüssel N, Pickert G, Schild H, Steinbrink K, Schuppan D. Nutritional Wheat Amylase-Trypsin Inhibitors Promote Intestinal Inflammation via Activation of Myeloid Cells. *Gastroenterology* 2017; **152**: 1100-1113.e12 [PMID: 27993525 DOI: 10.1053/j.gastro.2016.12.006]

13 **Skodje GI**, Sarna VK, Minelle IH, Rolfsen KL, Muir JG, Gibson PR, Veierød MB, Henriksen C, Lundin KEA. Fructan, Rather Than Gluten, Induces Symptoms in Patients With Self-Reported Non-Celiac Gluten Sensitivity. *Gastroenterology* 2018; **154**: 529-539.e2 [PMID: 29102613 DOI: 10.1053/j.gastro.2017.10.040]

14 **De Giorgio R**, Volta U, Gibson PR. Sensitivity to wheat, gluten and FODMAPs in IBS: facts or fiction? *Gut* 2016; **65**: 169-178 [PMID: 26078292 DOI: 10.1136/gutjnl-2015-309757]

15 **Carroccio A**, Rini G, Mansueto P. Non-celiac wheat sensitivity is a more appropriate label than non-celiac gluten sensitivity. *Gastroenterology* 2014; **146**: 320-321 [PMID: 24275240 DOI: 10.1053/j.gastro.2013.08.061]

16 **Leffler DA**, Green PH, Fasano A. Extraintestinal manifestations of coeliac disease. *Nat Rev Gastroenterol Hepatol* 2015; **12**: 561-571 [PMID: 26260366 DOI: 10.1038/nrgastro.2015.131]

17 **Carroccio A**, D'Alcamo A, Cavataio F, Soresi M, Seidita A, Sciumè C, Geraci G, Iacono G, Mansueto P. High Proportions of People With Nonceliac Wheat Sensitivity Have Autoimmune Disease or Antinuclear Antibodies. *Gastroenterology* 2015; **149**: 596-603.e1 [PMID: 26026392 DOI: 10.1053/j.gastro.2015.05.040]

18 **Losurdo G**, Piscitelli D, Giangaspero A, Principi M, Buffelli F, Giorgio F, Montenegro L, Sorrentino C, Amoruso A, Ierardi E, Di Leo A. Evolution of nonspecific duodenal lymphocytosis over 2 years of follow-up. *World J Gastroenterol* 2015; **21**: 7545-7552 [PMID: 26140001 DOI: 10.3748/wjg.v21.i24.7545]

19 **Ierardi E**, Losurdo G, Iannone A, Piscitelli D, Amoruso A, Barone M, Principi M, Pisani A, Di Leo A. Lymphocytic duodenitis or microscopic enteritis and gluten-related conditions: what needs

to be explored? *Ann Gastroenterol* 2017; **30**: 380-392 [PMID: 28655974 DOI: 10.20524/aog.2017.0165]
20 **Jackson JR**, Eaton WW, Cascella NG, Fasano A, Kelly DL. Neurologic and psychiatric manifestations of celiac disease and gluten sensitivity. *Psychiatr Q* 2012; **83**: 91-102 [PMID: 21877216 DOI: 10.1007/s11126-011-9186-y]
21 **Hadjivassiliou M**, Aeschlimann P, Strigun A, Sanders DS, Woodroofe N, Aeschlimann D. Autoantibodies in gluten ataxia recognize a novel neuronal transglutaminase. *Ann Neurol* 2008; **64**: 332-343 [PMID: 18825674 DOI: 10.1002/ana.21450]
22 **Zis P**, Rao DG, Sarrigiannis PG, Aeschlimann P, Aeschlimann DP, Sanders D, Grünewald RA, Hadjivassiliou M. Transglutaminase 6 antibodies in gluten neuropathy. *Dig Liver Dis* 2017; **49**: 1196-1200 [PMID: 28886934 DOI: 10.1016/j.dld.2017.08.019]
23 **Hadjivassiliou M**, Sanders DS, Grünewald RA, Woodroofe N, Boscolo S, Aeschlimann D. Gluten sensitivity: from gut to brain. *Lancet Neurol* 2010; **9**: 318-330 [PMID: 20170845 DOI: 10.1016/S1474-4422(09)70290-X]
24 **Hadjivassiliou M**, Sanders DS, Woodroofe N, Williamson C, Grünewald RA. Gluten ataxia. *Cerebellum* 2008; **7**: 494-498 [PMID: 18787912 DOI: 10.1007/s12311-008-0052-x]
25 **Wilkinson ID**, Hadjivassiliou M, Dickson JM, Wallis L, Grünewald RA, Coley SC, Widjaja E, Griffiths PD. Cerebellar abnormalities on proton MR spectroscopy in gluten ataxia. *J Neurol Neurosurg Psychiatry* 2005; **76**: 1011-1013 [PMID: 15965215]
26 **Pellecchia MT**, Scala R, Perretti A, De Michele G, Santoro L, Filla A, Ciacci C, Barone P. Cerebellar ataxia associated with subclinical celiac disease responding to gluten-free diet. *Neurology* 1999; **53**: 1606-1608 [PMID: 10534283]
27 **Chin RL**, Sander HW, Brannagan TH, Green PH, Hays AP, Alaedini A, Latov N. Celiac neuropathy. *Neurology* 2003; **60**: 1581-1585 [PMID: 12771245]
28 **Hadjivassiliou M**, Kandler RH, Chattopadhyay AK, Davies-Jones AG, Jarratt JA, Sanders DS, Sharrack B, Grünewald RA. Dietary treatment of gluten neuropathy. *Muscle Nerve* 2006; **34**: 762-766 [PMID: 17013890]
29 **Hadjivassiliou M**, Grünewald RA, Kandler RH, Chattopadhyay AK, Jarratt JA, Sanders DS, Sharrack B, Wharton SB, Davies-Jones GA. Neuropathy associated with gluten sensitivity. *J Neurol Neurosurg Psychiatry* 2006; **77**: 1262-1266 [PMID: 16835287]
30 **Hadjivassiliou M**, Grünewald RA, Lawden M, Davies-Jones GA, Powell T, Smith CM. Headache and CNS white matter abnormalities associated with gluten sensitivity. *Neurology* 2001; **56**: 385-388 [PMID: 11171906]
31 **Serratrice J**, Disdier P, de Roux C, Christides C, Weiller PJ. Migraine and coeliac disease. *Headache* 1998; **38**: 627-628 [PMID: 11398309]
32 **Hadjivassiliou M**, Rao DG, Grìnewald RA, Aeschlimann DP, Sarrigiannis PG, Hoggard N, Aeschlimann P, Mooney PD, Sanders DS. Neurological Dysfunction in Coeliac Disease and Non-Coeliac Gluten Sensitivity. *Am J Gastroenterol* 2016; **111**: 561-567 [PMID: 26832652 DOI: 10.1038/ajg.2015.434]
33 **Rodrigo L**, Hernández-Lahoz C, Lauret E, Rodriguez-Peláez M, Soucek M, Ciccocioppo R, Kruzliak P. Gluten ataxia is better classified as non-celiac gluten sensitivity than as celiac disease: a comparative clinical study. *Immunol Res* 2016; **64**: 558-564 [PMID: 26676361 DOI: 10.1007/s12026-015-8750-1]
34 **Losurdo G**, Giorgio F, Piscitelli D, Montenegro L, Covelli C, Fiore MG, Giangaspero A, Iannone A, Principi M, Amoruso A, Barone M, Di Leo A, Ierardi E. May the assessment of baseline mucosal molecular pattern predict the development of gluten related disorders among microscopic enteritis? *World J Gastroenterol* 2016; **22**: 8017-8025 [PMID: 27672296 DOI: 10.3748/wjg.v22.i35.8017]
35 **Losurdo G**, Piscitelli D, Pezzuto F, Fortarezza F, Covelli C, Marra A, Iannone A, Amoruso A, Principi M, Ierardi E, Di Leo A. T Helper Lymphocyte and Mast Cell Immunohistochemical Pattern in Nonceliac Gluten Sensitivity. *Gastroenterol Res Pract* 2017; **2017**: 5023680 [PMID: 29362561 DOI: 10.1155/2017/5023680]
36 **Bruni O**, Dosi C, Luchetti A, Della Corte M, Riccioni A, Battaglia D, Ferri R. An unusual case of drug-resistant epilepsy in a child with non-celiac gluten sensitivity. *Seizure* 2014; **23**: 674-676 [PMID: 24813861 DOI: 10.1016/j.seizure.2014.04.005]
37 **Hadjivassiliou M**, Chattopadhyay AK, Grünewald RA, Jarratt JA, Kandler RH, Rao DG, Sanders DS, Wharton SB, Davies-Jones GA. Myopathy associated with gluten sensitivity. *Muscle Nerve* 2007; **35**: 443-450 [PMID: 17143894]
38 **Jacob S**, Zarei M, Kenton A, Allroggen H. Gluten sensitivity and neuromyelitis optica: two case reports. *J Neurol Neurosurg Psychiatry* 2005; **76**: 1028-1030 [PMID: 15965221]
39 **Peters SL**, Biesiekierski JR, Yelland GW, Muir JG, Gibson PR. Randomised clinical trial: gluten may cause depression in subjects with non-coeliac gluten sensitivity - an exploratory clinical study. *Aliment Pharmacol Ther* 2014; **39**: 1104-1112 [PMID: 24689456 DOI: 10.1111/apt.12730]
40 **Brottveit M**, Vandvik PO, Wojniusz S, Løvik A, Lundin KE, Boye B. Absence of somatization in non-coeliac gluten sensitivity. *Scand J Gastroenterol* 2012; **47**: 770-777 [PMID: 22519894 DOI: 10.3109/00365521.2012.679685]
41 **Casella G**, Pozzi R, Cigognetti M, Bachetti F, Torti G, Cadei M, Villanacci V, Baldini V, Bassotti G. Mood disorders and non-celiac gluten sensitivity. *Minerva Gastroenterol Dietol* 2017; **63**: 32-37 [PMID: 27647538 DOI: 10.23736/S1121-421X.16.02325-4]
42 **Lionetti E**, Leonardi S, Franzonello C, Mancardi M, Ruggieri M, Catassi C. Gluten Psychosis: Confirmation of a New Clinical Entity. *Nutrients* 2015; **7**: 5532-5539 [PMID: 26184290 DOI: 10.3390/nu7075235]
43 **Lau NM**, Green PH, Taylor AK, Hellberg D, Ajamian M, Tan CZ, Kosofsky BE, Higgins JJ, Rajadhyaksha AM, Alaedini A. Markers of Celiac Disease and Gluten Sensitivity in Children with Autism. *PLoS One* 2013; **8**: e66155 [PMID: 23823064 DOI: 10.1371/journal.pone.0066155]
44 **Ghalichi F**, Ghaemmaghami J, Malek A, Ostadrahimi A. Effect of gluten free diet on gastrointestinal and behavioral indices for children with autism spectrum disorders: a randomized clinical trial. *World J Pediatr* 2016; **12**: 436-442 [PMID: 27286693 DOI: 10.1007/s12519-016-0040-z]
45 **El-Rashidy O**, El-Baz F, El-Gendy Y, Khalaf R, Reda D, Saad K. Ketogenic diet versus gluten free casein free diet in autistic children: a case-control study. *Metab Brain Dis* 2017; **32**: 1935-1941 [PMID: 28808808 DOI: 10.1007/s11011-017-0088-z]
46 **Cruchet S**, Lucero Y, Cornejo V. Truths, Myths and Needs of Special Diets: Attention-Deficit/Hyperactivity Disorder, Autism, Non-Celiac Gluten Sensitivity, and Vegetarianism. *Ann Nutr Metab* 2016; **68** Suppl 1: 43-50 [PMID: 27356007 DOI: 10.1159/000445393]
47 **Collin P**, Salmi TT, Hervonen K, Kaukinen K, Reunala T. Dermatitis herpetiformis: a cutaneous manifestation of coeliac disease. *Ann Med* 2017; **49**: 23-31 [PMID: 27499257 DOI: 10.1080/07853890.2016.1222450]
48 **Philips C**, Paramaguru R, Indiran DA, Augustine P. Dermatitis Herpetiformis as the Initial Presentation of Primary Biliary Cholangitis in a Male with Gluten Sensitivity. *Cureus* 2017; **9**: e1247 [PMID: 28630805 DOI: 10.7759/cureus.1247]
49 **Bonciolini V**, Bianchi B, Del Bianco E, Verdelli A, Caproni M. Cutaneous Manifestations of Non-Celiac Gluten Sensitivity: Clinical Histological and Immunopathological Features. *Nutrients* 2015; **7**: 7798-7805 [PMID: 26389946 DOI: 10.3390/nu7095368]
50 **Mansueto P**, D'Alcamo A, Seidita A, Carroccio A. Food allergy in irritable bowel syndrome: The case of non-celiac wheat sensitivity. *World J Gastroenterol* 2015; **21**: 7089-7109 [PMID: 26109796 DOI: 10.3748/wjg.v21.i23.7089]
51 **D'Alcamo A**, Mansueto P, Soresi M, Iacobucci R, Blasca F, Geraci G, Cavataio F, Fayer F, Arini A, Di Stefano L, Iacono G, Bosco L, Carroccio A. Contact Dermatitis Due to Nickel Allergy in Patients Suffering from Non-Celiac Wheat Sensitivity. *Nutrients* 2017; **9**: pii: E103 [PMID: 28157173 DOI: 10.3390/nu9020103]
52 **Toğrol RE**, Nalbant S, Solmazgül E, Ozyurt M, Kaplan M, Kiralp MZ, Dinçer U, Sahan B. The significance of coeliac disease antibodies in patients with ankylosing spondylitis: a case-controlled

study. *J Int Med Res* 2009; **37**: 220-226 [PMID: 19215694 DOI: 10.1177/147323000903700127]
53 **Isasi C**, Tejerina E, Morán LM. Non-celiac gluten sensitivity and rheumatic diseases. *Reumatol Clin* 2016; **12**: 4-10 [PMID: 25956352 DOI: 10.1016/j.reuma.2015.03.001]
54 **Clauw DJ**. Fibromyalgia: a clinical review. *JAMA* 2014; **311**: 1547-1555 [PMID: 24737367 DOI: 10.1001/jama.2014.3266]
55 **Isasi C**, Tejerina E, Fernandez-Puga N, Serrano-Vela JI. Fibromyalgia and chronic fatigue syndrome caused by non-celiac gluten sensitivity. *Reumatol Clin* 2015; **11**: 56-57 [PMID: 25047419 DOI: 10.1016/j.reuma.2014.06.005]
56 **Isasi C,** Colmenero I, Casco F, Tejerina E, Fernandez N, Serrano-Vela JI, Castro MJ, Villa LF. Fibromyalgia and non-celiac gluten sensitivity: a description with remission of fibromyalgia. *Rheumatol Int* 2014; **34**: 1607-1612 [PMID: 247280274 DOI: 10.1007/s00296-014-2990-6]
57 **Slim M**, Calandre EP, Garcia-Leiva JM, Rico-Villademoros F, Molina-Barea R, Rodriguez-Lopez CM, Morillas-Arques P. The Effects of a Gluten-free Diet Versus a Hypocaloric Diet Among Patients With Fibromyalgia Experiencing Gluten Sensitivity-like Symptoms: A Pilot, Open-Label Randomized Clinical Trial. *J Clin Gastroenterol* 2017; **51**: 500-507 [PMID: 27548732 DOI: 10.1097/MCG.0000000000000651]
58 **Verdu EF**, Armstrong D, Murray JA. Between celiac disease and irritable bowel syndrome: the "no man's land" of gluten sensitivity. *Am J Gastroenterol* 2009; **104**: 1587-1594 [PMID: 19455131 DOI: 10.1038/ajg.2009.188]
59 **Aziz I**, Lewis NR, Hadjivassiliou M, Winfield SN, Rugg N, Kelsall A, Newrick L, Sanders DS. A UK study assessing the population prevalence of self-reported gluten sensitivity and referral characteristics to secondary care. *Eur J Gastroenterol Hepatol* 2014; **26**: 33-39 [PMID: 24216570 DOI: 10.1097/01.meg.0000435546.87251.f7]
60 **Tanpowpong P**, Ingham TR, Lampshire PK, Kirchberg FF, Epton MJ, Crane J, Camargo CA Jr; New Zealand Asthma and Allergy Cohort Study Group. Coeliac disease and gluten avoidance in New Zealand children. *Arch Dis Child* 2012; **97**: 12-16 [PMID: 22075107 DOI: 10.1136/archdischild-2011-300248]
61 **Rubio-Tapia A**, Ludvigsson JF, Brantner TL, Murray JA, Everhart JE. The prevalence of celiac disease in the United States. *Am J Gastroenterol* 2012; **107**: 1538-44; quiz 1537, 1545 [PMID: 22850429 DOI: 10.1038/ajg.2012.219]
62 **DiGiacomo DV**, Tennyson CA, Green PH, Demmer RT. Prevalence of gluten-free diet adherence among individuals without celiac disease in the USA: results from the Continuous National Health and Nutrition Examination Survey 2009-2010. *Scand J Gastroenterol* 2013; **48**: 921-925 [PMID: 23834276 DOI: 10.3109/00365521.2013.809598]
63 **Lis DM**, Stellingwerff T, Shing CM, Ahuja KD, Fell JW. Exploring the popularity, experiences, and beliefs surrounding gluten-free diets in nonceliac athletes. *Int J Sport Nutr Exerc Metab* 2015; **25**: 37-45 [PMID: 24901744 DOI: 10.1123/ijsnem.2013-0247]
64 **Golley S**, Corsini N, Topping D, Morell M, Mohr P. Motivations for avoiding wheat consumption in Australia: results from a population survey. *Public Health Nutr* 2015; **18**: 490-499 [PMID: 24739252 DOI: 10.1017/S1368980014000652]
65 **Mardini HE**, Westgate P, Grigorian AY. Racial Differences in the Prevalence of Celiac Disease in the US Population: National Health and Nutrition Examination Survey (NHANES) 2009-2012. *Dig Dis Sci* 2015; **60**: 1738-1742 [PMID: 25577269 DOI: 10.1007/s10620-014-3514-7]
66 **Fritscher-Ravens A**, Schuppan D, Ellrichmann M, Schoch S, Röcken C, Brasch J, Bethge J, Böttner M, Klose J, Milla PJ. Confocal endomicroscopy shows food-associated changes in the intestinal mucosa of patients with irritable bowel syndrome. *Gastroenterology* 2014; **147**: 1012-1020.e4 [PMID: 25083606 DOI: 10.1053/j.gastro.2014.07.046]
67 **Wahnschaffe U**, Ullrich R, Riecken EO, Schulzke JD. Celiac disease-like abnormalities in a subgroup of patients with irritable bowel syndrome. *Gastroenterology* 2001; **121**: 1329-1338 [PMID: 11729112]
68 **Aziz I**, Trott N, Briggs R, North JR, Hadjivassiliou M, Sanders DS. Efficacy of a Gluten-Free Diet in Subjects With Irritable Bowel Syndrome-Diarrhea Unaware of Their HLA-DQ2/8 Genotype. *Clin Gastroenterol Hepatol* 2016; **14**: 696-703.e1 [PMID: 26748221 DOI: 10.1016/j.cgh.2015.12.031]
69 **Vazquez-Roque MI**, Camilleri M, Smyrk T, Murray JA, Marietta E, O'Neill J, Carlson P, Lamsam J, Janzow D, Eckert D, Burton D, Zinsmeister AR. A controlled trial of gluten-free diet in patients with irritable bowel syndrome-diarrhea: effects on bowel frequency and intestinal function. *Gastroenterology* 2013; **144**: 903-911.e3 [PMID: 23357715 DOI: 10.1053/j.gastro.2013.01.049]
70 **Shahbazkhani B**, Sadeghi A, Malekzadeh R, Khatavi F, Etemadi M, Kalantri E, Rostami-Nejad M, Rostami K. Non-Celiac Gluten Sensitivity Has Narrowed the Spectrum of Irritable Bowel Syndrome: A Double-Blind Randomized Placebo-Controlled Trial. *Nutrients* 2015; **7**: 4542-4554 [PMID: 26056920 DOI: 10.3390/nu7064542]
71 **Zanwar VG**, Pawar SV, Gambhire PA, Jain SS, Surude RG, Shah VB, Contractor QQ, Rathi PM. Symptomatic improvement with gluten restriction in irritable bowel syndrome: a prospective, randomized, double blinded placebo controlled trial. *Intest Res* 2016; **14**: 343-350 [PMID: 27799885]
72 **Elli L**, Tomba C, Branchi F, Roncoroni L, Lombardo V, Bardella MT, Ferretti F, Conte D, Valiante F, Fini L, Forti E, Cannizzaro R, Maiero S, Londoni C, Lauri A, Fornaciari G, Lenoci N, Spagnuolo R, Basilisco G, Somalvico F, Borgatta B, Leandro G, Segato S, Barisani D, Morreale G, Buscarini E. Evidence for the Presence of Non-Celiac Gluten Sensitivity in Patients with Functional Gastrointestinal Symptoms: Results from a Multicenter Randomized Double-Blind Placebo-Controlled Gluten Challenge. *Nutrients* 2016; **8**: 84 [PMID: 26867199 DOI: 10.3390/nu8020084]
73 **Barmeyer C**, Schumann M, Meyer T, Zielinski C, Zuberbier T, Siegmund B, Schulzke JD, Daum S, Ullrich R. Long-term response to gluten-free diet as evidence for non-celiac wheat sensitivity in one third of patients with diarrhea-dominant and mixed-type irritable bowel syndrome. *Int J Colorectal Dis* 2017; **32**: 29-39 [PMID: 27695975 DOI: 10.1007/s00384-016-2663-x]
74 **Shepherd SJ**, Gibson PR. Fructose malabsorption and symptoms of irritable bowel syndrome: guidelines for effective dietary management. *J Am Diet Assoc* 2006; **106**: 1631-1639 [PMID: 17000196 DOI: 10.1016/j.jada.2006.07.010]
75 **Biesiekierski JR**, Peters SL, Newnham ED, Rosella O, Muir JG, Gibson PR. No effects of gluten in patients with self-reported non-celiac gluten sensitivity after dietary reduction of fermentable, poorly absorbed, short-chain carbohydrates. *Gastroenterology* 2013; **145**: 320-8.e1-3 [PMID: 23648697 DOI: 10.1053/j.gastro.2013.04.051]
76 **Abenavoli L**, Delibasic M, Peta V, Turkulov V, De Lorenzo A, Medić-Stojanoska M. Nutritional profile of adult patients with celiac disease. *Eur Rev Med Pharmacol Sci* 2015; **19**: 4285-4292 [PMID: 26636515]
77 **García-Manzanares A**, Lucendo AJ. Nutritional and dietary aspects of celiac disease. *Nutr Clin Pract* 2011; **26**: 163-173 [PMID: 21447770 DOI: 10.1177/0884533611399773]
78 **Carroccio A**, Soresi M, D'Alcamo A, Sciumè C, Iacono G, Geraci G, Brusca I, Seidita A, Adragna F, Carta M, Mansueto P. Risk of low bone mineral density and low body mass index in patients with non-celiac wheat-sensitivity: a prospective observation study. *BMC Med* 2014; **12**: 230 [PMID: 25430806 DOI: 10.1186/s12916-014-0230-2]
79 **Zingone F**, Bartalini C, Siniscalchi M, Ruotolo M, Bucci C, Morra I, Iovino P, Ciacci C. Alterations in Diets of Patients With Nonceliac Gluten Sensitivity Compared With Healthy Individuals. *Clin Gastroenterol Hepatol* 2017; **15**: 63-68.e2 [PMID: 27552857 DOI: 10.1016/j.cgh.2016.08.017]
80 **Ierardi E**, Amoruso A, Giorgio F, Principi M, Losurdo G, Piscitelli D, Buffelli F, Fiore MG, Mongelli A, Castellaneta NM, Giangaspero A, De Francesco V, Montenegro L, Di Leo A. Mucosal molecular pattern of tissue transglutaminase and interferon gamma in suspected seronegative celiac disease at marsh

1 and 0 stages. *Saudi J Gastroenterol* 2015; **21**: 379-385 [PMID: 26655133 DOI: 10.4103/1319-3767.167189]
81 **Dinu M**, Macchia D, Pagliai G, Gori AM, Cesari F, Marcucci R, Sofi F, Casini A. Symptomatic efficacy of buckwheat products in Non-Celiac Gluten Sensitivity (NCGS). *Asia Pac J Clin Nutr* 2017; **26**: 630-636 [PMID: 28582812 DOI: 10.6133/apjcn.072016.07]
82 **Brottveit M**, Beitnes AC, Tollefsen S, Bratlie JE, Jahnsen FL, Johansen FE, Sollid LM, Lundin KE. Mucosal cytokine response after short-term gluten challenge in celiac disease and non-celiac gluten sensitivity. *Am J Gastroenterol* 2013; **108**: 842-850 [PMID: 23588237 DOI: 10.1038/ajg.2013.91]
83 **Vici G**, Belli L, Biondi M, Polzonetti V. Gluten free diet and nutrient deficiencies: A review. *Clin Nutr* 2016; **35**: 1236-1241 [PMID: 27211234 DOI: 10.1016/j.clnu.2016.05.002]
84 **Barone M**, Della Valle N, Rosania R, Facciorusso A, Trotta A, Cantatore FP, Falco S, Pignatiello S, Viggiani MT, Amoruso A, De Filippis R, Di Leo A, Francavilla R. A comparison of the nutritional status between adult celiac patients on a long-term, strictly gluten-free diet and healthy subjects. *Eur J Clin Nutr* 2016; **70**: 23-27 [PMID: 26173865 DOI: 10.1038/ejcn.2015.114]
85 **Shepherd SJ**, Gibson PR. Nutritional inadequacies of the gluten-free diet in both recently-diagnosed and long-term patients with coeliac disease. *J Hum Nutr Diet* 2013; **26**: 349-358 [PMID: 23198728 DOI: 10.1111/jhn.12018]

P- Reviewer: Jadallah KA, Rostami-Nejad M, Sergi CM
S- Editor: Gong ZM **L- Editor**: A **E- Editor**: Huang Y

World Journal of Gastroenterology

Submit a Manuscript: http://www.f6publishing.com

World J Gastroenterol 2018 April 14; 24(14): 1531-1539

DOI: 10.3748/wjg.v24.i14.1531

ISSN 1007-9327 (print) ISSN 2219-2840 (online)

ORIGINAL ARTICLE

Basic Study

Punctual mutations in *23S rRNA* gene of clarithromycin-resistant *Helicobacter pylori* in Colombian populations

Andrés Jenuer Matta, Diana Carolina Zambrano, Alvaro Jairo Pazos

Andrés Jenuer Matta, Registro Poblacional de Cáncer de Cali, Department of Pathology, School of Medicine, Universidad del Valle, Cali 760043, Colombia

Andrés Jenuer Matta, Diana Carolina Zambrano, Faculty of Education and Sports Sciences, Institución Universitaria Escuela Nacional del Deporte, Cali 760043, Colombia

Alvaro Jairo Pazos, Department of Biology, Universidad de Nariño, Pasto 520002, Colombia

ORCID number: Andrés Jenuer Matta (0000-0002-9637-1812); Diana Carolina Zambrano (0000-0002-8636-1629); Alvaro Jairo Pazos (0000-0001-5603-7898).

Author contributions: All authors that were involved in the acquisition and interpretation of the results read and approved the final manuscript; Matta AJ, Zambrano DC and Pazos AJ conducted the microbiological and molecular tests and analyzed the data; Matta AJ, Zambrano DC, Pazos AJ wrote, edited, and revised the manuscript.

Supported by Administrative Department of Science and Innovation of the Republic of Colombia - COLCIENCIAS, No. RC-1106-408-20549; Institución Universitaria Escuela Nacional del Deporte; and Registro Poblacional de Cáncer de Cali, Universidad del Valle, Cali, Colombia.

Institutional review board statement: All procedures involving human participants were reviewed and approved by the Ethics Committee at Universidad del Valle, Cali, Colombia.

Conflict-of-interest statement: The authors declare that there is no conflict of interest related to this study.

Manuscript source: Unsolicited manuscript

Correspondence to: Andrés Jenuer Matta, MSc, PhD, Registro Poblacional de Cáncer de Cali, Department of Pathology, School of Medicine, Universidad del Valle, Street 4B No 36-00, Building 116, Floor 4, Cali 760043, Colombia. andres.matta@correounivalle.edu.co
Telephone: +57-2-5185623
Fax: +57-2-3212100-4101

Received: January 20, 2018
Peer-review started: January 22, 2018
First decision: February 6, 2018
Revised: February 25, 2018
Accepted: March 18, 2018
Article in press: March 18, 2018
Published online: April 14, 2018

Abstract

AIM

To characterize punctual mutations in *23S rRNA* gene of clarithromycin-resistant *Helicobacter pylori* (*H. pylori*) and determine their association with therapeutic failure.

METHODS

PCR products of *23S rRNA* gene V domain of 74 *H. pylori* isolates; 34 resistant to clarithromycin (29 from a low-risk gastric cancer (GC) population: Tumaco-Colombia, and 5 from a high-risk population: Tuquerres-Colombia) and 40 from a susceptible population (28 from Tumaco and 12 from Túquerres) were sequenced using capillary electrophoresis. The concordance between mutations of V domain *23S rRNA* gene of *H. pylori* and therapeutic failure was determined using the *Kappa* coefficient and McNemar's test was performed to determine the relationship between *H. pylori* mutations

and clarithromycin resistance.

RESULTS

23S rRNA gene from *H. pylori* was amplified in 56/74 isolates, of which 25 were resistant to clarithromycin (20 from Tumaco and 5 from Túquerres, respectively). In 17 resistant isolates (13 from Tumaco and 4 from Túquerres) the following mutations were found: A1593T1, A1653G2, C1770T, C1954T1, and G1827C in isolates from Tumaco, and A2144G from Túquerres. The mutations T2183C, A2144G and C2196T in *H. pylori* isolates resistant to clarithromycin from Colombia are reported for the first time. No association between the *H. pylori* mutations and *in vitro* clarithromycin resistance was found. However, therapeutic failure of eradication treatment was associated with mutations of *23S rRNA* gene in clarithromycin-resistant *H. pylori* (κ = 0.71).

CONCLUSION

The therapeutic failure of eradication treatment in the two populations from Colombia was associated with mutations of the *23S rRNA* gene in clarithromycin-resistant *H. pylori*.

Key words: Clarithromycin; *In vitro* resistance; Point mutation; *Helicobacter pylori*; Gastric cancer; *23S rRNA*

Core tip: Mutations in *23S rRNA* gene V domain of *Helicobacter pylori* (*H. pylori*) were studied in order to determine their association with therapeutic failure. In clarithromycin-resistant *H. pylori* isolated from individuals at high-risk of gastric cancer (GC) in Túquerres-Colombia and at low-risk of GC in Tumaco-Colombia, mutations A1593T1, A1653G2, C1770T, C1954T1, and G1827C in isolates from Tumaco, and A2144G from Túquerres were found. Mutations T2183C and C2196T from both cities were not associated with clarithromycin resistance. However, therapeutic failure of eradication treatment in the sampled Colombian populations was associated with mutations of *23S rRNA* gene in clarithromycin-resistant *H. pylori*.

Matta AJ, Zambrano DC, Pazos AJ. Punctual mutations in *23S rRNA* gene of clarithromycin-resistant *Helicobacter pylori* in Colombian populations. *World J Gastroenterol* 2018; 24(14): 1531-1539 Available from: URL: http://www.wjgnet.com/1007-9327/full/v24/i14/1531.htm DOI: http://dx.doi.org/10.3748/wjg.v24.i14.1531

INTRODUCTION

Eradication of *Helicobacter pylori* (*H. pylori*) from the gastric mucosa is the current treatment for conditions such as chronic gastritis, peptic ulcer, atrophic gastritis, dysplasia, and metaplasia[1]. The first line scheme for the eradication of *H. pylori* is triple therapy, which includes a proton pump inhibitor and two antibiotics such as amoxicillin and clarithromycin. This treatment aims to eradicate infection in at least 90% of patients. However, therapeutic failure is inherent and can be due to multiple factors (human and bacterial), including improper drug dose, short treatment duration, early treatment discontinuation, drug activity associated with the use of other substances, quick reinfection of successfully treated patients, and the presence of antibiotic-resistant strains[1-4]. Among the main causes of resistance to clarithromycin in *H. pylori* are mutations in the V domain of *23S rRNA* gene, this domain is the binding site for macrolide-type antibiotics. The most frequent mutations are A2143G (69.8%), A2142G (11.7%), and A2142C (2.6%). In addition, mutations A2115G, G2141A, C2147G, T2190C, C2195T, A2223G and C2694A have also been reported, but their role in resistance to clarithromycin is not yet clear[3].

In Latin America and worldwide, *H. pylori* resistance to antibiotics has been documented, with eradication being negatively affected by clarithromycin resistance[2]. In Colombia, resistance to this macrolide is estimated to be 17.2%[5]. Geographical conditions have also been documented to influence the risk of gastric cancer (GC). Coastal regions such as Tumaco have a low risk of GC, while Andean regions such as Túquerres have a high risk of GC. Hence, these geographical differences offer unique opportunities for the study of mutations of *23S rRNA* gene in *H. pylori*. This study characterized the mutations of *23S rRNA* gene V domain in *H. pylori* and their association with clarithromycin resistance and with therapeutic failure in patients from two Colombian populations (Tumaco and Túquerres) who were at different risk of developing GC.

MATERIALS AND METHODS

Subjects and samples

The subjects in this study included adult men and women with dyspepsia symptoms from Tumaco (n = 203) and from Túquerres (n = 206). Four gastric mucosal biopsies were obtained from each patient; two from the antrum and two from the gastric body, in order to isolate *H. pylori*, and determine *in vitro* susceptibility of the isolates to clarithromycin and amoxicillin using agar dilution and molecular biology procedures.

For *H. pylori* culture and genotyping, the gastric mucosa biopsies were preserved in 25% thioglycollate and glycerol. The biopsies were frozen in liquid nitrogen and later placed in dry ice and stored at -70 ℃ for analysis at the Microbiology Laboratory and Histopathology Laboratory of the Department of Pathology of the Universidad del Valle, in Cali, Colombia. This study was supported by the CIREH (Human Ethics Committee) of the Universidad del Valle. All study subjects signed an informed consent form.

After the antimicrobial susceptibility microbiological study, 74 *H. pylori* isolates were obtained, of which

34 (46%) were *in vitro* clarithromycin resistant and 40 (54%) were susceptible to the antibiotic. 39.2% (29/34) of the resistant isolates and 37.8% (30/42) of the susceptible isolates were taken from patients in Tumaco. In addition, the sequences of *23S rRNA* gene V domain of strains ATCC 43502 and ATCC 700392 were amplified and used as positive controls. DNA extraction was carried out by salting out[6] and susceptibility tests were performed using the agar dilution method[7].

Amplification of 23S rRNA gene V domain of H. pylori

The amplification of *23S rRNA* gene V domain of *H. pylori* by PCR was carried out using a thermal cycler (Swift MiniProTM, Esco, Cincinnati, OH, United States), and the following reagents were added to a 0.2 mL tube: buffer 1× (Buffer green 5× Promega®), $MgCl_2$ 1 μmol/L (Promega®), DMSO 10%, dNTPs 0.288 mmol/L (Promega®), 50 pmol/μL of each primer (starting position 1585, 5´-GATTGGAGGGAAGGCAAT-3´/3´-CTCCATAAGAGCCAAAGCCC-5´ final position 2247), 0.5 U of GoTaq DNA polymerase (Promega®); and 25 ng of *H. pylori* genomic DNA in a final volume of 50 μL. The thermal cycle consisted in an initial denaturation at 95 ℃/2 min, followed by 35 cycles [95 ℃/1 min, 54 ℃/1 min, 59 ℃/1 min and 72 ℃/1 min] and a final extension at 72 ℃/15 min[8].

The amplification fragments were detected by 2% agarose gel electrophoresis (Sigma®), stained with 1 μL of ethidium bromide (Invitrogen, Carlsbad, CA, United States) (0.5 μg/mL), with an EC-105 power source (Thermo Fisher Scientific Inc., Asheville, NC, United States), at 75 V for 60 min, using a horizontal chamber (Spectroline bio-o-visión®). The DNA bands were visualized in UV light (260/280 nm), using a transilluminator (Spectroline bio-o-visión®). The size of the amplified fragment was approximately 662 pb (expected fragment by *in silico* analysis)[8].

Sequencing and identification of mutations

The amplified fragments were sequenced in two directions (forward and reverse), using a genetic analyzer (ABI 3130 Applied Biosystem®) and the *Big Dye Terminator* methodology (Applied Biosystem®), following standardized conditions at Vanderbilt Genetic Institute Core Facilities, United States. The edition and alignment of the sequences was carried out using Bioedit software V 7.1.11® (Hall, 1999). Changes in sequences were matched by local alignment, with the reference sequence for *23S rRNA* gene, code GenBank: U27270.1[8].

Statistical analysis

For categorical variables, McNemar's Test was used for matching data, in order to identify significant differences between clarithromycin resistant and clarithromycin susceptible genotypes and the punctual mutations detected before treatment. The concordance correlation coefficient *Kappa* (*k*) was used to determine the concordance between the mutations of *23S rRNA* gene V domain and *in vitro* clarithromycin resistance such as the concordance of mutations of *23S rRNA* gene V domain with therapeutic failure in patients evaluated using the [^{13}C]-Urea breath test (UBT), 45 d after completing *H. pylori* eradication treatment. The anti-*H. pylori* treatment included omeprazole (Genfar®) 20 mg, clarithromycin (Genfar®) 500 mg, and amoxicillin (Genfar®) 1000 mg, for 14 d in accordance with the recommendations of the Maastricht Consensus[9]. Therapeutic failure was considered in patients with a positive UBT. All data were analyzed using statistical software SPSS version 15.0 for Windows. Statistical significance was estimated at $P < 0.05$.

Ethical considerations

This study was approved by the Institutional Committee for Human Ethics Revision (CIREH) of the Faculty of Health of the Universidad del Valle, regulated by Resolution 008430 of October 4/1993, issued by the Colombian Ministry of Health.

RESULTS

The prevalence of *H. pylori* infection, which was diagnosed by histopathology, was higher in the low-risk GC population from Tumaco (88.77%), than in the high-risk GC population from Túquerres (85.4%), without a statistically significant difference. However, the prevalence of *H. pylori* resistance to clarithromycin and amoxicillin was significantly higher in the low-risk GC population from Tumaco, than in the high-risk GC population from Túquerres (20.5%, 22.8%) *vs* (3.4%, 5.4%), respectively, $P < 0.05$. Efficacy of the anti-*H. pylori* treatment was similar in both populations. Of 169 infected and treated patients from Tumaco, 130 (76.9%) were cured, and of 165 infected and treated patients from Tuquerres, infection was resolved in 123 (74.6%).

PCR amplification of the 23S rRNA gene of H. pylori

The amplification and sequencing of a fragment of 662 bp (Figure 1) between nucleotides 1585 and 2247 of *23S rRNA* gene V domain of *H. pylori*, was carried out in 56 (76%) of the isolates, of which 39 (69.6%) were from Tumaco patients; of these, 20 (35.7%) were resistant and 19 (33.9%) were susceptible to clarithromycin under *in vitro* conditions. Five (8.9%) of the amplified isolates from Túquerres were resistant to clarithromycin and 12 (21.4%) were susceptible (Table 1).

Table 1, shows the number of *H. pylori* isolates at baseline, which were susceptible and resistant to clarithromycin *in vitro*. The total number of *H. pylori* isolates from both populations and those used to amplify *23S rRNA* gene V domain were evaluated; the number of *H. pylori* isolates amplified from both populations represents fragment amplification where possible. The total number of isolates is represented

Table 1 PCR frequencies of *23S rRNA* gene V domain from *Helicobacter pylori* according to the risk of gastric cancer *n* (%)

Helicobacter pylori isolates	Risk of gastric cancer		Total
	Low risk-Tumaco	High risk-Túquerres	
Evaluated			
Susceptible	28 (37.8)	12 (16.2)	40 (54)
Resistant	29 (39.2)	5 (6.8)	34 (46)
Total	57 (77)	17 (23)	74 (100)
Amplified			56 (76)
Susceptible	19 (33.93)	12 (21.43)	31 (55.4)
Resistant	20 (35.7)	5 (8.93)	25 (44.6)
Total	39 (69.6)	17 (30.4)	56 (100)

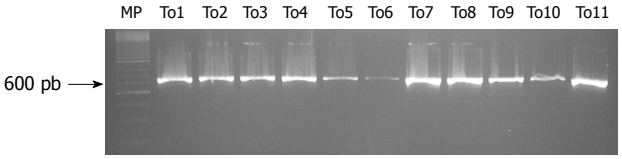

Figure 1 Electrophoretic pattern of PCR products of *23S rRNA* gene V domain in Colombian *Helicobacter pylori* isolates. Electrophoresis of PCR amplification products of *23S rRNA* gene V domain of *Helicobacter pylori* isolates was performed using 2% agarose gel. MP corresponds to the molecular weight marker of 100 bp; the arrow indicates the band corresponding to 600 bp; lanes To1 to To11, correspond to DNA of the isolates resistant to clarithromycin from the Colombian population with a low risk of gastric cancer (Tumaco).

by bold typeface.

Mutations in the 23S rRNA gene of H. pylori and resistance to clarithromycin

At least one mutation was identified in the sequences of 31 (55.3%) *H. pylori* isolates, with 17 (33.3%) resistant and 14 (25%) susceptible to clarithromycin. Of the resistant isolates, 13 (23.2%) were from Túmaco patients and 4 (7.1%) were from Túquerres patients. In addition, 9 (16.1%) of the resistant isolates did not show any mutations in their sequence; of these, 8 (14.3%) were isolated from Tumaco patients and 1 (1.8%) was isolated from Túquerres patients. The *Kappa* coefficients (κ = 0.17) and (κ = 0.23) for the low risk and high risk GC populations, respectively, suggest that there was no relationship between the presence of mutations and *in vitro* resistance to clarithromycin. Similarly, there was no association between the lack of mutations in *23S rRNA* gene and *in vitro* susceptibility to clarithromycin in both populations, $P > 0.05$ (Table 2).

Characterization of mutations in the 23S rRNA gene of H. pylori

Twenty different mutations were characterized in 33 sequences of *H. pylori* evaluated. Mutations T2183C and C2196T were present only in resistant isolates in both populations; the first mutation was observed in 2 isolates from the low risk GC population (Tumaco) and in 1 isolate from the high risk GC population (Túquerres). The second mutation was observed in 1 isolate in each population. Similarly, mutations A1593T, A1653G, C1770T, C1954T, and G1827C, were observed only in resistant isolates in Tumaco patients. Conversely, mutation A2144G was present only in 1 isolate from Túquerres (Tables 3 and 4).

Tables 3 and 4 show the changes in the sequences of *23S rRNA* gene V domain of *H. pylori* in high-risk and low-risk GC patients according to susceptibility or resistance to clarithromycin. Column MIC shows the minimum inhibitory concentration at μg/mL, which was evaluated using the agar dilution method. In Column mutations, the punctual changes in the nucleotides of *23S rRNA* gene observed in the sequence of each isolate are shown.

It was found that the mutations of *H. pylori* susceptible to clarithromycin were located in domain IV of *23S rRNA* gene, nucleotides 1562-1931, except for mutation G2221A which was located in domain V of an isolate susceptible to clarithromycin. In contrast, mutations in domain V, nucleotides 1932-2541, were mainly present in resistant isolates, except for changes C1770T, A1593T and G1827C, which were associated with mutations in domain IV (Table 5).

Mutations in the 23S rRNA gene and therapeutic failure of anti-H. pylori treatment

Although the mutations in isolates resistant to clarithromycin were observed mainly in *23S rRNA* gene V domain of *H. pylori*, no relationship was found between them and *in vitro* resistance to clarithromycin ($P > 0.05$, Tables 2-5). Punctual mutations in domain IV of the target gene were found in susceptible isolates (Table 5). However, the *Kappa* coefficient κ = 0.64 and κ = 0.69 shows that there was a good level of concordance between the mutations in *23S rRNA* gene and therapeutic failure in patients unsuccessfully treated, both in the high-risk and low-risk GC populations, respectively, and the two populations together, κ = 0.71, as shown by the positive UBT, which was performed 45 d after the end of *H. pylori* eradication treatment (Table 6).

DISCUSSION

Research on the prevalence of clarithromycin resistance and characterization of the mutations of *23S rRNA* gene, which may be associated with *in vitro* resistance in *H. pylori,* is scarce in Colombia. In general, research has focused on evaluating the frequency of mutations already

Table 2 Frequencies of mutations in *23S rRNA* gene of *Helicobacter pylori* according to susceptibility to clarithromycin and risk of gastric cancer *n* (%)

Susceptibility	Risk of gastric cancer							
	Low risk *n* = 39				High risk *n* = 17			
	Mutant		Non mutant		Mutant		Non mutant	
Resistant	13 (23.2)		8 (14.3)		4 (7.1)		1 (1.8)	
Susceptible	8 (14.3)		10 (17.8)		6 (10.7)		6 (10.7)	
Kappa-P	*k* = 0.17		*P* = 0.28		*k* = 0.23		*P* = 0.25	
Total	21	37.5	18	32.1	10	17.8	7	12.5

Table 3 Punctual mutations in *23S rRNA* gene of *Helicobacter pylori* from the population at low-risk of gastric cancer, according to susceptibility or resistance to clarithromycin

Resistant *n* = 13			Susceptible *n* = 8		
Patient ID	Mutations	MIC	Patient ID	Mutations	MIC
138	A1593G [1]T2183C	1	17	A1822G/G1827A/G1941A/T1831C	< 0.25
64	A1653G	2	94	T1645C	< 0.25
60		4			
4	A1739G [1]C1954T/G1695A	4	96	A1739G	< 0.25
65	A1739G [1]C2196T [1]G1827C	1	97	T1645C	< 0.25
42	A1822G/G1827A/T1831C	1	98	C1632T	< 0.25
102		2			
174		1			
88	C1632T	> 4	101	A1822G/G1827A/T1645C/T1831C	< 0.25
107	[1]C1770T	1	103	C1632T	< 0.25
38	T1645C	1	107	A1667G/T1668C	< 0.25
36		2			
6	[1]T2183C/A1593T/A1822G/G1827A/T1831C	4			
ATCC 700392	A1593G		ATCC 43504	A1667G/T1668C	

[1]Unique mutations of *Helicobacter pylori* resistant to clarithromycin. MIC: Minimum inhibitory concentration (μg/mL).

Table 4 Punctual mutations in *23S rRNA* gene of *Helicobacter pylori* from the population at high-risk of gastric cancer, according to susceptibility or resistance to clarithromycin

Resistant *n* = 4			Susceptible *n* = 6		
Patient ID	Mutations	MIC	Patient ID	Mutations	MIC
323	A1593G/A1822G/G1827A/T1645C/T1831C/[1]T2183C	1	351	A1822G/G1827A/T1831C	< 0.25
336	A1593G/[1]C2196T	2	377	A1822G/G1827A/G2221A/T1645C/T1831C	< 0.25
339	[1]A2144G/G1827A	4	394	A1593G	< 0.25
440	A1822G/G1827A/G2221A/T1831C	4	457	A1822G/G1827A/G2221A/T1831C	< 0.25
			467	A1739G/G1695A	< 0.25
			513	A1822G/G1827A/T1831C	< 0.25
ATCC 700392	A1593G		ATCC 43504	A1667G/T1668C	

[1]Unique mutations of *Helicobacter pylori* resistant to clarithromycin. MIC: Minimum inhibitory concentration (μg/mL).

reported and the most frequently observed mutations , such as mutations A2142G, A2143G y A2142C[3].

In Colombia, studies carried out in Risaralda, Quindío, and Cauca have reported frequencies between 1.85% and 7.3% for mutation A2142G, and between 2.2% and 2.46% for mutation A2143G in *H. pylori isolates* resistant to *in vitro* clarithromycin[10-12]. In our study, no *H. pylori* isolate which was resistant or susceptible to clarithromycin *in vitro* and exhibited these mutations was detected.

Among the mutations studied in *H. pylori* isolates resistant to clarithromycin was C2196T with a frequency of 0.05% (1/21) and 0.2% (1/5) in isolates from Tumaco and Túquerres patients, respectively. This change was reported in a study carried out in the Province of Guiyang (China), which found resistance of 30% (13/42) to *in vitro* clarithromycin, this study also reported mutation C2196T in a resistant and in a susceptible isolate, and mutation A2143G in susceptible isolates[13]. In contrast to this, mutation C2196T was found only in resistant isolates in our study, with a similar frequency. However, it was not linked to other mutations with such

Table 5 Position of mutations according to the domains of *23S rRNA* gene of *Helicobacter pylori* resistant or susceptible to clarithromycin

Domain-Region	Tumaco		Túquerres	
	Resistant position	Susceptible position	Resistant position	Susceptible position
Domain IV 1562-1931	C1770T	A1593G		A1593G
	A1593T	A1667G		A1667G
	G1827C	A1739G		A1739G
		A1822G		A1822G
		C1632T		C1632T
		G1695A		G1695A
		G1827A		G1827A
		G1941A		G1941A
		T1645C		T1645C
		T1668C		T1668C
		T1831C		T1831C
Domain V 1932-2541	C1954T	G2221A	C2196T	G2221A
	T2183C		T2183C	
	C2196T		A2144G	
	A1653G			
	C2196T			

Table 6 Concordance between mutations in *23S rRNA* gene and success or failure of anti-*Helicobacter pylori* treatment in the studied populations

Breath test [^{13}C]-urea	Population at risk of gastric cancer				Total	
	Low risk n = 39		High risk n = 17			
	Mutant	No mutant	Mutant	No mutant	Mutant	No mutant
Positive						
Therapeutic failure	18	3	8	1	26	4
Negative						
Therapeutic Success	3	15	2	6	5	21
Total	21	18	10	7	31	25
Kappa	k = 0.69		k = 0.64		k = 0.71	

resistance, but it is important to consider the proximity of a nucleotide to mutation C2195T, associated with resistance[3].

Mutation T2183C exhibited frequencies of 0.09 (2/21) and 0.2 (1/5) in resistant isolates from high-risk and low-risk GC patients from Túquerres and Tumaco, respectively. Similar results were reported in studies carried out in *H. pylori* isolates from Korean dyspepsia patients, where the frequency of this mutation was between 0.25 (1/4)[14] and 0.35 (5/14)[15]. Although this mutation is found in domain V and occurred only in isolates resistant to *in vitro* clarithromycin, some researchers believe that its relationship with clarithromycin resistance is not yet clear, as it may be found in isolates both resistant and susceptible to this drug[16,17]. However, its presence in isolates growing at MIC $\geqslant$ 1 μg/mL of clarithromycin, suggests its capability to inhibit the effect of the antibiotic, at least as reported in this study.

Mutation A2144G was found in an *H. pylori* isolate from Túquerres, with a frequency of 0.25 (1/4), which corroborates findings which suggest that the mutation is clearly associated with *in vitro* clarithromycin resistance[18-20]. It was found that the frequency in the sampled population in this study, is in line with the frequencies reported in other regions, 0.01 (1/73)[21] and 0.81(9/11)[20-23]. This mutation was first reported in *H. pylori* isolates resistant to clarithromycin in Colombia, which indicates that it may be associated with the inclusion of strains from high frequency countries such as South Korea (frequency of 0.57)[15]; Japan (frequency of 0.7)[24] and Turkey (frequency between 0.29 and 0.81[20,22].

The mutations associated with clarithromycin resistance in the *H. pylori* isolates described in this study (A2144G, C2196T, and T2183C), are located in *23S rRNA* gene V domain, as reported in the current literature[3]. Inhibition of the action of the macrolide may be due to spatial alterations in the V domain of *23S rRNA* gene, which inhibit the target, as seen in transversion mutations A2143G, A2142G, A2142C[3], A2144G[18,19,22], where a nitrogenous base with two H groups (Adenine) is changed for another with three H groups (Guanine and Cytosine), with the inherent spatial alteration of the molecular structure, a phenomenon similar in transitions C2196T and T2183C[17].

This study found that there was no concordance between the presence of punctual mutations of *H. pylori* and *in vitro* resistance to clarithromycin and no association between the absence of mutations

in the *23S rRNA* gene and *in vitro* susceptibility to clarithromycin in both populations. These findings and the absence of mutations in 36% of the isolates resistant to *in vitro* clarithromycin may be explained by the occurrence of mutations outside the amplified region, a fragment located between positions 1585-2224. Among the changes associated with clarithromycin resistance, which are located outside this fragment, are A2223G, C2694A[3], T2711C[21], T2288C[24], and T2289C[25], and these mutations may explain the discrepancy of the results on the presence of punctual mutations in the amplified region, the *in vitro* resistance to clarithromycin and the good level of concordance between punctual mutations in the *23S rRNA* gene of *H. pylori* with therapeutic failure in patients with unsuccessful eradication treatment. Clarithromycin resistance may be mediated by flow pumps that help *H. pylori* resist concentrations higher than 1 μg/mL of clarithromycin[23,26]. The presence of these mechanisms in *H. pylori* isolates in the high-risk and low-risk GC populations in Colombia was not evaluated in this study.

H. pylori resistance to clarithromycin is the main cause of failed eradication treatment; thus, the characterization of resistance is fundamental to validate gold standard methodology, such as the microbiological method of dilution in agar; however, this is a technically difficult and time-consuming method. It is worth mentioning that in our study, the sequencing method of the amplified *H. pylori* fragments of *23S rRNA* gene by PCR and the detection of their punctual mutations were consistent with the UBT, a method used to diagnose therapeutic failure in patients with unsuccessful treatment, (κ = 0.64, κ = 0.69), both for high-risk and low-risk GC populations (κ = 0.71). These results may be reproducible in future studies, improve *H. pylori* infection eradication regimens and and may be applicable in clinical practice in Colombia. However the UBT is used to evaluate the follow-up of *H. pylori* treatments and its effectiveness should be an additional test in clinical practice and in the programs and policies for the prevention of GC in Colombia.

Although two first-line antibiotics were used in the anti-*H. pylori* treatment regimen, the results of resistance mechanisms in *H. pylori* to amoxicillin were not reported in this study. It is important to emphasize that *H. pylori* resistance to clarithromycin is mainly due to mutations in *23S rRNA* gene V domain and is the main cause of first-line eradication treatment failure[2].

Other techniques that require less time for the identification of resistance include the E-test (sensibility of 45% and specificity of 95%) and DNA-based techniques, such as FISH (sensibility of 97% and specificity of 94%), PNA-FISH (sensibility of 80% and specificity of 93%), *Line Probe Test* (sensibility of 100% and specificity of 82.2%), and PCR (sensibility of 98% and specificity of 92%)[3], which require specific methods for each mutation (FISH; PNA-FISH, *Line Probe Test*) or sequencing of the amplified fragment (PCR). The efficiency of these tests is subject to knowledge of the mutations associated with clarithromycin resistance in *H. pylori* strains.

This study demonstrated that the resistant isolates from these two contrasting populations involved in the development of GC, mutations A2143G, A2142G, and A2142C, which are usually reported as the most frequent, were not found in the isolates evaluated. With regard to the design of these tests, the changes A2144G, T2183C and C2196T found in these populations should be considered for use in fast-diagnostic methods of clarithromycin resistance in clinical practice. These mutations associated with *H. pylori* resistance to clarithromycin are the first to be reported in Colombia.

It may be concluded that in *H. pylori* isolates resistant to clarithromycin in patients from both Colombian populations, no high-frequency mutation was observed in *23S rRNA* gene V domain, but there was high genotypic variation among the isolates.

No relationship between the mutations in *23S rRNA* gene V domain of *H. pylori* and *in vitro* resistance was found, contrary to that seen in other *H. pylori* non-mutant isolates resistant to clarithromycin, which may be explained by mutations outside the evaluated fragment or by the existence of flow pumps. However, the failure of eradication treatment in the Colombian populations in this study was associated with punctual mutations in *23S rRNA* gene of *H. pylori* resistant to clarithromycin.

In the Colombian populations studied, it was difficult to use a fast-resistance detection test for specific mutations, as information is scarce and the mutations reported exhibited a low frequency.

ARTICLE HIGHLIGHTS

Research background

Infection by *Helicobacter pylori* (*H. pylori*) is the leading risk factor for the development of gastric adenocarcinoma, especially in individuals infected with strains resistant to antibiotics used in primary treatment regimens. The eradication of *H. pylori* infection is a valid primary prevention strategy for gastric lesions, atrophy, and gastric cancer (GC). However, resistance of this microorganism to clarithromycin is associated with therapeutic failure and a major risk of GC in Colombia. Thus, although significant improvements in the efficacy of treatment regimens have been made, none of these regimens successfully eradicate the infection. A few studies have focused on the evaluation of clarithromycin-resistance mechanisms, particularly mutations of *23S rRNA* gene of the infecting strains in Colombia, which are associated with treatment failure and early subsequent prevention of GC.

Research motivation

Taking into account that GC prevention programs are focused on the eradication of *H. pylori*, it is important to know the specific treatment regimens for each country seeking to apply this strategy. In Colombia, the efficacy of standard triple therapy which includes clarithromycin, amoxicillin, and a proton pump inhibitor is currently being questioned. However, there are insufficient multicenter studies suggesting alternative regimens and basic studies on antibiotic resistance mechanisms in *H. pylori*. Mutations in *H. pylori 23S rRNA* gene V domain were studied to evaluate *in vitro* resistance to clarithromycin. This study identified mutations not documented in the current literature, which although are not associated with *in vitro* resistance to clarithromycin, they are

linked to the therapeutic failure of triple therapy. Punctual mutations in the Colombian strains could be useful in future studies focusing on diagnostic methods for antibiotic susceptibility and in the therapeutic efficacy of GC prevention schemes in Colombia.

Research objectives

In this study, the researchers characterized mutations in domain V of *23S rRNA* gene in clarithromycin-resistant *H. pylori* and determined their association with therapeutic failure in a high-risk gastric cancer population from Tuquerres, Colombia, and in a low-risk gastric cancer population from Tumaco, Colombia. A very interesting basic study clearly showed that therapeutic failure of eradication treatment in the sampled Colombian populations was associated with mutations of *23S rRNA* gene in clarithromycin-resistant *H. pylori*. Hopefully, these findings will help to further improve treatment success and may be applied in the future for the fast diagnosis of therapeutic failure. This study found no concordance between the presence of punctual mutations in *H. pylori* and *in vitro* resistance to clarithromycin and there was no association between the absence of mutations in the *23S rRNA* gene and *in vitro* susceptibility to clarithromycin in both populations. These findings and the absence of mutations in 36% of the isolates resistant to *in vitro* clarithromycin may be explained by the occurrence of mutations outside the amplified region, a fragment located between positions 1585-2224. Among the changes associated with clarithromycin resistance, which are located outside this fragment, are A2223G, C2694A T2711C, T2288C, and T2289C, mutations that may explain the discrepancy between the presence of punctual mutations in the amplified region and *in vitro* resistance to clarithromycin

Research methods

To achieve the objectives of this study, we used the capillary electrophoresis sequencing method of the amplified DNA fragments of the *H. pylori 23S rRNA* gene and the detection of its punctual mutations, which were concordant with the [^{13}C]-Urea breath test. This method was used in a novel way to diagnose the therapeutic failure of anti-*H. pylori* treatment *in vivo*. The [^{13}C]-Urea breath test was used during the follow-up period to evaluate the effectiveness of *H. pylori* treatments.

Research results

This study demonstrated that the resistant isolates from these two contrasting populations involved in the development of GC, mutations A2143G, A2142G, and A2142C, which are usually reported as the most frequent, were not found in the isolates evaluated. With regard to the design of tests, the changes A2144G, T2183C and C2196T found in these populations should be considered for use in fast-diagnostic methods of clarithromycin resistance in clinical practice.

These results are important in the definition of treatments for gastroduodenal diseases caused by *H. pylori*. They suggest that the failure of anti-*H. pylori* treatment is mainly due to mutations in *23S rRNA* gene V domain. The application of these findings could be complemented by studies on the genetics and virulence of the microorganism, as individuals with similar ancestry may not require anti-*H. pylori* treatment. In contrast individuals infected with strains of different evolutionary origins than their host, would benefit from additional studies on antibiotic susceptibility. These advances in basic studies tend to elucidate the African enigma, and indicate that human-*H. pylori* coevolution and virulence of the bacterium could explain the contrast in risk of disease observed in our study populations. These findings may contribute to the future identification of individuals at higher risk of GC and require antibiotic susceptibility studies prior to treatment of the infection and early GC prevention.

Research conclusions

In this investigation, mutations A2144G, C2196T and T2183C were observed in *23S rRNA* gene V domain of *H. pylori* resistant to clarithromycin and were associated with failure of eradication treatment. The mutations T2183C, A2144G and C2196T in *23S rRNA* gene V domain are reported for the first time in clarithromycin-resistant isolates of *H. pylori* in Colombia. This study demonstrated that the therapeutic failure of *H. pylori* eradication treatment in high and low risk GC populations from Colombia was associated with mutations of the *23S rRNA* gene of clarithromycin-resistant *H. pylori*. The sequencing method for the detection of punctual mutations of DNA amplified *23S rRNA* gene fragments is proposed to predict therapeutic failure induced by clarithromycin-resistant *H. pylori*. This new knowledge allows us to propose the design of a rapid detection test for *H. pylori* resistance to clarithromycin where mutations A2144G, T2183C and C2196T should be considered and can be applied in clinical practice to predict therapeutic failure of anti-*H. pylori* treatment.

Research perspectives

Following therapeutic failure, reinfection may occur in patients as well as medication with antagonistic drugs or others such as proton pump inhibitors, which allow the appearance of false positives. In this study, adherence to treatment and self-medication were taken into account during the follow-up period. Characterization of the mutations in the *23S rRNA* gene in a larger number of Colombian populations is required, in order to confirm the mutations associated with clarithromycin resistance in *H. pylori* and to determine, from multicenter studies, the optimal treatment regimen in Colombia. The molecular analysis of *23S rRNA* gene V domain of *H. pylori* and other candidate genes is required, in order predict therapeutic failure. It is possible to reproduce the method in future investigations using total DNA from gastric mucosa biopsies and validate the presence of mutations found in this study. The [^{13}C]-Urea breath test is recommended during follow-up to evaluate the effectiveness of anti-*H. pylori* treatment.

ACKNOWLEDGMENTS

We would like to thank the Microbiology and Molecular Biology Laboratory, and the Histopathology Laboratory of the Pathology Department of Universidad del Valle, for use of their facilities during this study. We are also grateful to Hospital San Andres de Tumaco and the Hospital San Jose de Túquerres, for use of their facilities for clinical sampling and isolation of the *H. pylori* fragments used in this study.

REFERENCES

1 **Wu W**, Yang Y, Sun G. Recent Insights into Antibiotic Resistance in Helicobacter pylori Eradication. *Gastroenterol Res Pract* 2012; **2012**: 723183 [PMID: 22829809 DOI: 10.1155/2012/723183]
2 **Camargo MC**, García A, Riquelme A, Otero W, Camargo CA, Hernandez-García T, Candia R, Bruce MG, Rabkin CS. The problem of Helicobacter pylori resistance to antibiotics: a systematic review in Latin America. *Am J Gastroenterol* 2014; **109**: 485-495 [PMID: 24589670 DOI: 10.1038/ajg.2014.24]
3 **Thung I**, Aramin H, Vavinskaya V, Gupta S, Park JY, Crowe SE, Valasek MA. Review article: the global emergence of Helicobacter pylori antibiotic resistance. *Aliment Pharmacol Ther* 2016; **43**: 514-533 [PMID: 26694080 DOI: 10.1111/apt.13497]
4 **Ghotaslou R**, Leylabadlo HE, Asl YM. Prevalence of antibiotic resistance in Helicobacter pylori: A recent literature review. *World J Methodol* 2015; **5**: 164-174 [PMID: 26413490 DOI: 10.5662/wjm.v5.i3.164]
5 **Trespalacios AA,** Otero W, Marcela M. Helicobacter pylori resistance to metronidazole, clarithromycin and amoxicillin in Colombian patients. *Rev Colomb Gastroenterol* 2010; **25**: 31-38
6 **Ho SA**, Hoyle JA, Lewis FA, Secker AD, Cross D, Mapstone NP, Dixon MF, Wyatt JI, Tompkins DS, Taylor GR. Direct polymerase chain reaction test for detection of Helicobacter pylori in humans and animals. *J Clin Microbiol* 1991; **29**: 2543-2549 [PMID: 1723072]
7 **Bustamante-Rengifo JA**, Matta AJ, Pazos A, Bravo LE. In vitro effect of amoxicillin and clarithromycin on the 3' region of cagA gene in Helicobacter pylori isolates. *World J Gastroenterol* 2013; **19**: 6044-6054 [PMID: 24106405 DOI: 10.3748/wjg.v19.i36.6044]
8 **Taylor DE**, Ge Z, Purych D, Lo T, Hiratsuka K. Cloning and sequence analysis of two copies of a 23S rRNA gene from Helicobacter pylori and association of clarithromycin resistance with 23S rRNA mutations. *Antimicrob Agents Chemother* 1997;

41: 2621-2628 [PMID: 9420030]
9 **Malfertheiner P**, Megraud F, O'Morain CA, Gisbert JP, Kuipers EJ, Axon AT, Bazzoli F, Gasbarrini A, Atherton J, Graham DY, Hunt R, Moayyedi P, Rokkas T, Rugge M, Selgrad M, Suerbaum S, Sugano K, El-Omar EM; European Helicobacter and Microbiota Study Group and Consensus panel. Management of Helicobacter pylori infection-the Maastricht V/Florence Consensus Report. *Gut* 2017; **66**: 6-30 [PMID: 27707777 DOI: 10.1136/gutjnl-2016-312288]
10 **Isaza MC,** Henao BJ, Alvarez A, Moncayo JI, Santacruz JJ, Meisel E, Salazar F, Giraldo D. Comparación de dos protocolos de erradicación de Helicobacter pylori. *Rev Médica Risaralda* 2007; **13**: 1-8
11 **Alvarez A**, Moncayo JI, Santacruz JJ, Corredor LF, Reinosa E, Martínez JW, Beltrán L. [Antimicrobial susceptibility of Helicobacter pylori strains isolated in Colombia]. *Rev Med Chil* 2009; **137**: 1309-1314 [PMID: 20011937]
12 **Acosta CP**, Hurtado FA, Trespalacios AA. [Determination of single nucleotide mutations in the 23S rRNA gene of Helicobacter pylori related to clarithromycin resistance in a population from Cauca, Colombia]. *Biomedica* 2014; **34** Suppl 1: 156-162 [PMID: 24968047 DOI: 10.7705/biomedica.v34i0.1649]
13 **Boyanova L**, Markovska R, Yordanov D, Gergova G, Mitov I. Clarithromycin Resistance Mutations in Helicobacter pylori in Association with Virulence Factors and Antibiotic Susceptibility of the Strains. *Microb Drug Resist* 2016; **22**: 227-232 [PMID: 26618567 DOI: 10.1089/mdr.2015.0199]
14 **Yoon KH**, Park SW, Lee SW, Kim BJ, Kim JG. Clarithromycin-based standard triple therapy can still be effective for Helicobacter pylori eradication in some parts of the Korea. *J Korean Med Sci* 2014; **29**: 1240-1246 [PMID: 25246742 DOI: 10.3346/jkms.2014.29.9.1240]
15 **Sung J**, Kim N, Park YH, Hwang YJ, Kwon S, Na G, Choi JY, Kang JB, Kim HR, Kim JW, Lee DH. Rifabutin-based Fourth and Fifth-line Rescue Therapy in Patients with for Helicobacter pylori Eradication Failure. *Korean J Gastroenterol* 2017; **69**: 109-118 [PMID: 28239079 DOI: 10.4166/kjg.2017.69.2.109]
16 **Hwang TJ**, Kim N, Kim HB, Lee BH, Nam RH, Park JH, Lee MK, Park YS, Lee DH, Jung HC, Song IS. Change in antibiotic resistance of Helicobacter pylori strains and the effect of A2143G point mutation of 23S rRNA on the eradication of H. pylori in a single center of Korea. *J Clin Gastroenterol* 2010; **44**: 536-543 [PMID: 20179610 DOI: 10.1097/MCG.0b013e3181d04592]
17 **Teh X**, Khosravi Y, Lee WC, Leow AH, Loke MF, Vadivelu J, Goh KL. Functional and molecular surveillance of Helicobacter pylori antibiotic resistance in Kuala Lumpur. *PLoS One* 2014; **9**: e101481 [PMID: 25003707 DOI: 10.1371/journal.pone.0101481]
18 **Momynaliev KT**, Selezneva OV, Kozlova AA, Vereshchagin VA, Il'ina EN, Govorun VM. [A2144G is the main mutation in the 23S rRNA gene of Helicobacter pylori associated with clarithromycin resistance]. *Genetika* 2005; **41**: 1338-1344 [PMID: 16316005]
19 **Sezgin O**, Aslan G, Altintaş E, Tezcan S, Serin MS, Emekdaş G. Detection of point mutations on 23S rRNA of Helicobacter pylori and resistance to clarithromycin with PCR-RFLP in gastric biopsy specimens in Mersin, Turkey. *Turk J Gastroenterol* 2008; **19**: 163-167 [PMID: 19115151]
20 **Caliskan R**, Tokman HB, Erzin Y, Saribas S, Yuksel P, Bolek BK, Sevuk EO, Demirci M, Yılmazli O, Akgul O, Kalayci F, Cakan H, Salih B, Bal K, Kocazeybek B. Antimicrobial resistance of Helicobacter pylori strains to five antibiotics, including levofloxacin, in Northwestern Turkey. *Rev Soc Bras Med Trop* 2015; **48**: 278-284 [PMID: 26108005 DOI: 10.1590/0037-8682-0027-2015]
21 **Toracchio S**, Aceto GM, Mariani-Costantini R, Battista P, Marzio L. Identification of a novel mutation affecting domain V of the 23S rRNA gene in Helicobacter pylori. *Helicobacter* 2004; **9**: 396-399 [PMID: 15361077 DOI: 10.1111/j.1083-4389.2004.00267.x]
22 **Tajbakhsh S,** Falahi J, Motamed N, Tabib SM, Bahador A, Gharibi S. Prevalence of A2143G and A2144G point mutations responsible for clarithromycin resistance among Helicobacter pylori strains in Bushehr, Iran. *Avicenna J Clin Microb Infec* 2016; **3**: e36521 [DOI: 10.17795/ajcmi-36521]
23 **Kim JM**, Kim JS, Jung HC, Kim N, Kim YJ, Song IS. Distribution of antibiotic MICs for Helicobacter pylori strains over a 16-year period in patients from Seoul, South Korea. *Antimicrob Agents Chemother* 2004; **48**: 4843-4847 [PMID: 15561865 DOI: 10.1128/AAC.48.12.4843-4847.2004]
24 **Rimbara E**, Noguchi N, Kijima H, Yamaguchi T, Kawai T, Sasatsu M. Mutations in the 23S rRNA gene of clarithromycin-resistant Helicobacter pylori from Japan. *Int J Antimicrob Agents* 2007; **30**: 250-254 [PMID: 17590317 DOI: 10.1016/j.ijantimicag.2007.04.009]
25 **Hao Q**, Li Y, Zhang ZJ, Liu Y, Gao H. New mutation points in 23S rRNA gene associated with Helicobacter pylori resistance to clarithromycin in northeast China. *World J Gastroenterol* 2004; **10**: 1075-1077 [PMID: 15052698 DOI: 10.3748/wjg.v10.i7.1075]
26 **Hirata K**, Suzuki H, Nishizawa T, Tsugawa H, Muraoka H, Saito Y, Matsuzaki J, Hibi T. Contribution of efflux pumps to clarithromycin resistance in Helicobacter pylori. *J Gastroenterol Hepatol* 2010; **25** Suppl 1: S75-S79 [PMID: 20586871 DOI: 10.1111/j.1440-1746.2009.06220.x]

P- Reviewer: Chuah SK, Tarnawski AS **S- Editor**: Ma YJ
L- Editor: Webster JR **E- Editor**: Huang Y

World Journal of Gastroenterology

Submit a Manuscript: http://www.f6publishing.com

World J Gastroenterol 2018 April 14; 24(14): 1540-1549

DOI: 10.3748/wjg.v24.i14.1540

ISSN 1007-9327 (print) ISSN 2219-2840 (online)

ORIGINAL ARTICLE

Retrospective Study

Post-polypectomy bleeding and thromboembolism risks associated with warfarin *vs* direct oral anticoagulants

Naohiro Yanagisawa, Naoyoshi Nagata, Kazuhiro Watanabe, Tatsuhiro Iida, Mariko Hamada, Sakurako Kobayashi, Takuro Shimbo, Junichi Akiyama, Naomi Uemura

Naohiro Yanagisawa, Naoyoshi Nagata, Kazuhiro Watanabe, Tatsuhiro Iida, Mariko Hamada, Sakurako Kobayashi, Junichi Akiyama, Department of Gastroenterology and Hepatology, National Center for Global Health and Medicine, Tokyo 162-8655, Japan

Takuro Shimbo, Ohta Nishinouchi Hospital, Fukushima 963-8022, Japan

Naomi Uemura, Department of Gastroenterology and Hepatology, National Center for Global Health and Medicine, Kohnodai Hospital, Chiba 272-8516, Japan

ORCID number: Naohiro Yanagisawa (0000-0003-0517-5830); Naoyoshi Nagata (0000-0002-7255-4024); Kazuhiro Watanabe (0000-0002-9980-859X); Tatsuhiro Iida (0000-0003-2636-2926); Mariko Hamada (0000-0002-2823-5595); Sakurako Kobayashi (0000-0003-2658-7463); Takuro Shimbo (0000-0002-6346-0771); Junichi Akiyama (0000-0001-9728-3921); Naomi Uemura (0000-0003-2436-1233).

Author contributions: Yanagisawa N collected the clinical data and drafted the manuscript; Nagata N designed the study and is equally a first author; Shimbo T was responsible for statistical analysis; Yanagisawa N, Iida T, Hamada M and Kobayashi S performed data collection and are the main authors of the manuscript; Watanabe K and Akiyama J assisted with treatment; Akiyama J and Uemura N edited the manuscript; all authors read and approved the submitted version of the manuscript.

Supported by Grant-in-Aid for Research from the National Center for Global Health and Medicine (29-2001) partly. The funding agency played no role in the study design, data collection and analysis, decision to publish, or preparation of the manuscript.

Institutional review board statement: The study design was approved by the ethics committee of the National Center for Global Health and Medicine (Approval No. 2176).

Informed consent statement: This study was a retrospective observational study, and informed consent to participate was obtained by the opt-out method at our institution.

Conflict-of-interest statement: The authors have no conflicts of interest to declare.

Manuscript source: Unsolicited manuscript

Correspondence to: Naoyoshi Nagata, MD, PhD, Doctor, Department of Gastroenterology and Hepatology, National Center for Global Health and Medicine, 1-21-1 Toyama, Shinjuku-ku, Tokyo 162-8655, Japan. nnagata_ncgm@yahoo.co.jp
Telephone: +81-3-32027181
Fax: +81-3-32071038

Received: February 20, 2018
Peer-review started: February 21, 2018
First decision: March 9, 2018
Revised: March 15, 2018
Accepted: March 25, 2018
Article in press: March 25, 2018
Published online: April 14, 2018

Abstract

AIM

To verify the validity of the endoscopy guidelines for patients taking warfarin or direct oral anticoagulants (DOAC).

METHODS

We collected data from 218 patients receiving oral anticoagulants (73 DOAC users, 145 warfarin users) and 218 patients not receiving any antithrombotics (age- and sex-matched controls) who underwent polypectomy. (1) We evaluated post-polypectomy bleeding (PPB) risk in patients

receiving warfarin or DOAC compared with controls; (2) we assessed the risks of PPB and thromboembolism between three AC management methods: Discontinuing AC with heparin bridge (HPB) (endoscopy guideline recommendation), continuing AC, and discontinuing AC without HPB.

RESULTS

PPB rate was significantly higher in warfarin users and DOAC users compared with controls (13.7% and 13.7% *vs* 0.9%, $P < 0.001$), but was not significantly different between rivaroxaban (13.2%), dabigatran (11.1%), and apixaban (13.3%) users. Two thromboembolic events occurred in warfarin users, but none in DOAC users. Compared with the continuing anticoagulant group, the discontinuing anticoagulant with HPB group (guideline recommendation) had a higher PPB rate (10.8% *vs* 19.6%, $P = 0.087$). These findings were significantly evident in warfarin but not DOAC users. One thrombotic event occurred in the discontinuing anticoagulant with HPB group and the discontinuing anticoagulant without HPB group; none occurred in the continuing anticoagulant group.

CONCLUSION

PPB risk was similar between patients taking warfarin and DOAC. Thromboembolism was observed in warfarin users only. The guideline recommendations for HPB should be re-considered.

Key words: High-risk endoscopic procedures; Novel oral anticoagulants; Endoscopic guideline validation; Post-procedure gastrointestinal bleeding

Core tip: First, we found that anticoagulant (AC) users were at higher risk of post-polypectomy bleeding (PPB) than controls. Second, PPB risk was similar between warfarin users and direct oral anticoagulant users, whereas thromboembolism risk was observed only in warfarin users. Third, PPB risk was not significantly different between rivaroxaban, dabigatran, and apixaban users. Fourth, the strategy of discontinuing AC with heparin bridge as recommended in the endoscopy guidelines showed a higher bleeding rate than continuing AC alone and had one thrombotic event, thus indicating that heparin bridge increased bleeding and may not prevent thromboembolism.

Yanagisawa N, Nagata N, Watanabe K, Iida T, Hamada M, Kobayashi S, Shimbo T, Akiyama J, Uemura N. Post-polypectomy bleeding and thromboembolism risks associated with warfarin *vs* direct oral anticoagulants. *World J Gastroenterol* 2018; 24(14): 1540-1549 Available from: URL: http://www.wjgnet.com/1007-9327/full/v24/i14/1540.htm DOI: http://dx.doi.org/10.3748/wjg.v24.i14.1540

INTRODUCTION

The number of oral anticoagulants (AC) used for prophylaxis or treatment of thromboembolic events is expected to increase as the population ages[1,2]. Along with this, the number of colonoscopic polypectomies, the most common high-risk endoscopic procedure, is also expected to increase in patients receiving AC[3-5]. Physicians are thus confronted with the issue of striking a balance between performing procedures with bleeding risk, such as polypectomy, and temporarily discontinuing AC agents to mitigate thromboembolic risk[4,6-8]. Among the AC agents commonly prescribed, warfarin requires careful and complex management because of its intricate pharmacodynamics and narrow therapeutic range[2,9], whereas direct oral anticoagulants (DOAC) offer easier management because of the rapid onset of anticoagulation and short half-lives[10]. However, whether post-polypectomy bleeding (PPB) or thromboembolic risk differs between warfarin and DOAC users remains unknown.

Several endoscopy guidelines recommend that warfarin be discontinued and replaced by heparin bridge (HPB) in patients at high thromboembolic risk during polypectomy[6-8]. In one study, DOAC were also stopped in one-third of patients who underwent HPB for a high-risk endoscopic procedure[11]. As yet however, the guideline recommendation on AC management for polypectomy has not been confirmed by a validation study. In addition, the situation is further complicated in the real-world clinical setting as some physicians may choose to continue the AC agent or to discontinue it without HPB in the peri-endoscopic period[11]. Previous data suggest that patients undergoing HPB are at higher risk of procedural-related bleeding than those not undergoing HPB or continuing their warfarin[12,13]. Therefore, continuing the AC strategy without HPB may be acceptable for polypectomy. However, there are currently no data available on the comparative risks of bleeding and thromboembolism between patients discontinuing AC with HPB, continuing AC, or discontinuing AC without HPB.

To address these gaps in our knowledge, in this study we first evaluated PPB risk in patients receiving warfarin or DOAC compared with patients not receiving any antithrombotics (controls). Second, we assessed the risks of PPB and thromboembolism between the three AC management methods mentioned above, discontinuing AC with HPB (guideline recommendation), continuing AC, and discontinuing AC without HPB.

MATERIALS AND METHODS

Study design, setting, and participants

We conducted a retrospective cohort study at the Department of Gastroenterology, National Center for Global Health and Medicine (NCGM), Japan. NCGM, with 900 beds, is the largest emergency hospital in the Tokyo

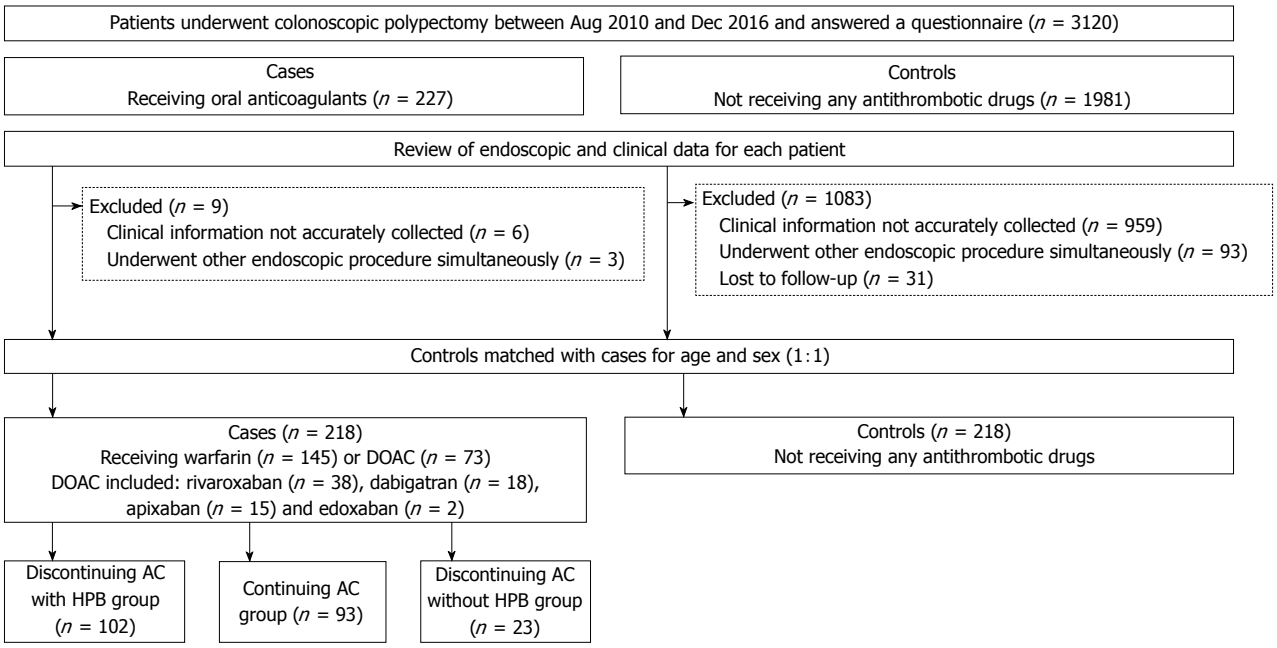

Figure 1 Patient selection and flow. AC: Anticoagulants; DOAC: Direct oral anticoagulants; HPB: Heparin bridge.

metropolitan area. We collected clinical and endoscopic data using an electronic medical database (MegaOak online imaging system, NEC, Japan) and an electronic endoscopic database (SolemioEndo, Olympus, Japan). Physicians or nurses input all findings immediately after clinical evaluation or endoscopy into the electronic medical and endoscopic reports. Staff also completed a detailed questionnaire that included patient background factors and medication information during a face-to-face interview with each patient at the endoscopy unit on the same day as pre-colonoscopy[14,15]. Patient selection and the study flow are shown in Figure 1. From the databases, we identified 5950 patients who underwent colonoscopic polypectomy at our institution between August 2010 and December 2016. Of these, 3120 provided responses to the questionnaire during the interview. We identified 227 patients receiving oral AC (cases) and 1981 patients not receiving any antithrombotics (controls). Then, we reviewed the clinical and endoscopic data for each patient and excluded the following patients: among cases, 6 patients whose clinical information could not be accurately collected and 3 patients who underwent polypectomy plus endoscopic submucosal dissection (ESD) simultaneously; among controls, 959 patients whose clinical information could not be accurately collected, 93 patients who underwent polypectomy plus another endoscopic procedure simultaneously, and 31 patients who were lost to follow-up. Then, controls (non-users of antithrombotics) were randomly selected from the cases (AC users) matched for decennial age and sex at a ratio of 1:1. Ultimately, data from a total of 436 patients (218 AC users and 218 controls) were analyzed.

This study was approved by the institutional review board of NCGM and patient consent was waived as this was a retrospective study (approval number 2176).

Patient characteristics

Using the electronic database and prospectively collected questionnaire results, we assessed the following factors: height, weight, body mass index (BMI), alcohol, smoking, 14 comorbidities or past history (diabetes mellitus, hypertension, dyslipidemia, chronic kidney disease, abnormal liver function, stroke, bleeding past history, chronic heart disease, vascular disease, acute coronary syndrome, pulmonary embolism, peripheral arterial disease, deep vein disease and advanced cancer), and medication [warfarin, rivaroxaban, dabigatran, apixaban, edoxaban, antiplatelet, and non-steroidal anti-inflammatory drugs (NSAIDs)]. We also evaluated laboratory data before colonoscopy [platelet count, prothrombin time-international normalized ratio (PT-INR), and creatinine clearance (Ccr)] and calculated the HAS-BLED[16] and CHA2DS2-VASc2[17] scores. During hospitalization, data were collected on the following AC management factors: HPB use, HPB duration, drug continuation/discontinuation, and use of reversal agent (vitamin K).

Endoscopic factors

After full bowel preparation, polypectomies were done with or without local injection of saline using a high-resolution colonoscope (CF260AI or CF260AZI, Olympus Co., Tokyo, Japan), snare (SnareMaster, Olympus Co.), and electrosurgical device (ERBE ICC-350, Somo Technology Inc., Tokyo, Japan or ESG-100, Olympus Co.). After polypectomy, patients routinely underwent prophylactic clipping. Number of polyps and polyp size were evaluated from data in the endoscopic database. Advanced ade-

noma was defined as adenoma ⩾ 1 cm with villous components (tubulovillous or villous) or high-grade or severe dysplasia[18].

AC management and heparin bridge

American, European, and Asian guidelines[6-8] recommend that patients discontinue AC and be bridged with heparin before polypectomy, and to confirm the validity of this strategy, we classified patients during the peri-endoscopic period into three main AC management groups: (1) Discontinuing AC with HPB (as recommended by the guidelines); (2) continuing AC alone (*i.e.*, without HPB) before endoscopy; and (3) discontinuing AC for > 24 h without HPB before endoscopy. Which of these strategies was adopted was at the discretion of the treating physician.

For HPB, patients received prophylactic unfractionated heparin infusion intravenously (because low-molecular-weight heparin is not covered by Japan's health care insurance system[8,19]), with the exception of 1 patient who received low-molecular-weight heparin because of heparin-induced thrombocytopenia.

In our institution, we carry out anticoagulant management during high-risk endoscopy in accordance with the Japanese Endoscopy Guidelines[8]; warfarin was stopped 3-5 d before endoscopy and DOAC was stopped 24-48 h after endoscopy. Heparin was administered after cessation of anticoagulants[8]. INR value before polypectomy was set at < 1.5 in warfarin users[8]. In these users, heparin was continued until INR was optimal after polypectomy. Because the guidelines do not recommend HPB for DOAC users[8], some DOAC users continued heparin for one day and others did not use heparin after polypectomy. The HPB period included the entire period before and after polypectomy.

Clinical outcomes

The main outcomes of interest were PPB within 30 d of polypectomy. PPB was defined as massive, continuous, or frequent hematochezia after polypectomy[20]. Not all patients underwent additional colonoscopy when PPB occurred, but those with unstable vital signs or in need of transfusion tended to undergo colonoscopy. Major bleeding was defined according to the International Society on Thrombosis and Haemostasis (ISTH) bleeding scale as (1) fatal bleeding; and/or (2) symptomatic bleeding in a critical area or organ, such as intracranial, intraspinal, intraocular, retroperitoneal, intra-articular or pericardial, or intramuscular with compartment syndrome; and/or (3) bleeding causing a fall in hemoglobin level of 20 g/L (1.24 mmol/L) or more, or leading to transfusion of two or more units of whole blood or red cells[21]. In addition, we defined late PPB as bleeding occurring more than 24 h after polypectomy and all other cases as early PPB[22]. We defined a thromboembolic event as the occurrence of acute coronary syndrome, stroke, transient ischemic attack, pulmonary embolism, deep vein thrombosis, or arterial thromboembolism. We also evaluated mortality at 30 d after polypectomy. Date and cause of death were ascertained from the electronic medical records and death certificates.

Statistical analysis

Pearson's chi-squared test or Fisher's exact test was used for categorical data to assess the difference in risk factors between subjects. Continuous data were compared with Mann-Whitney *U* test. Risk factors were examined by univariate and multivariate analysis. Odds ratios (OR) and 95% confidence intervals (CI) were estimated.

First, we compared baseline characteristics and clinical outcomes between AC users and controls. Second, we compared baseline characteristics and clinical outcomes between the following groups: discontinuing AC with HPB and continuing AC group alone and between discontinuing AC with HPB group and discontinuing AC without HPB group. These comparisons were also evaluated for the subgroups of warfarin and DOAC users.

Third, to determine the risk factors for PPB, we conducted univariate and multivariate analysis. In multivariate analysis, we developed multivariate models adjusting for propensity score for each strategy. Although there are four different propensity score methods-matching, stratification, inverse probability treatment weighting, and covariates adjustment[23,24]-we used propensity score as a covariate rather than perform a regression adjustment with all of the covariates (traditional covariate adjustment[25]), because many covariates were associated with a small number of bleeding outcomes in this study and we did not want to lose the observations of patients as typically occurs in matching. Propensity score as a covariate method allows for a large number of baseline variables to be included in the regression model, which are not adequately adjusted for when there are insufficient numbers of outcomes[23,24]. To estimate the propensity score, we employed a logistic regression model including potentially clinically important variables. Some of these were shown to differ ($P < 0.10$) between groups. We evaluated the area under the receiver operating characteristic (ROC) curve for each propensity score in each group.

A P value of < 0.05 was considered statistically significant. All statistical analyses were conducted using STATA version 14 software (StataCorp, College Station, TX, United States).

RESULTS

Baseline characteristics and outcomes of AC users and controls

There were some significant differences in baseline characteristics between AC users and controls (Table 1). In terms of outcomes, there were 32 patients with PPB and only 2 patients with major bleeding, both of whom were warfarin users and received HPB. Four patients had early PPB (bleeding within 24 h) and 28 with late PPB: 9 cases at day 2, 9 cases at day 3, 6 cases at day

Table 1 Baseline characteristics of oral anticoagulant users, warfarin users, direct oral anticoagulants users, and controls not taking any antithrombotic drugs (*n* = 436) *n* (%)

Factors	Controls (*n* = 218)	AC users (*n* = 218)	*P* value Control *vs* AC users	Warfarin users (*n* = 145)	*P* value Control *vs* warfarin users	DOAC users (*n* = 73)	*P* value Control *vs* DOAC users
Age ⩾ 75 yr	104 (47.1)	113 (51.8)	0.389	79 (54.5)	0.206	34 (46.6)	0.867
Male	157 (72.0)	157 (72.0)	1.000	103 (71.0)	0.839	54 (74.0)	0.746
BMI ⩾ 25	54 (24.8)	69 (31.7)	0.110	44 (30.3)	0.241	25 (34.2)	0.115
Drinker	119 (54.6)	131 (62.1)	0.115	77 (55.4)	0.881	54 (75.0)	0.002
Smoker	36 (16.5)	32 (14.8)	0.626	21 (14.6)	0.622	11 (15.3)	0.805
Laboratory data							
Platelet < 10×10^4 μL	6 (2.8)	5 (2.3)	1.000	3 (2.1)	1.000	2 (2.7)	1.000
Ccr < 30 mL/min	9 (4.1)	24 (11.0)	0.007	20 (13.8)	0.001	4 (5.48)	0.743
Comorbidities							
Diabetes mellitus	45 (20.6)	52 (23.9)	0.420	39 (26.9)	0.166	13 (17.8)	0.600
Hypertension	121 (55.5)	148 (67.9)	0.008	94 (64.8)	0.077	54 (74.0)	0.005
Dyslipidemia	74 (33.9)	102 (46.8)	0.006	67 (46.2)	0.019	35 (48.0)	0.037
Chronic kidney disease	49 (22.5)	37 (17.0)	0.149	32 (22.1)	0.927	5 (6.9)	0.003
Abnormal liver function	15 (6.9)	8 (3.7)	0.134	3 (2.1)	0.047	5 (6.9)	0.993
Stroke	10 (4.6)	47 (21.6)	< 0.001	29 (20.0)	< 0.001	18 (24.7)	< 0.001
Bleeding past history	21 (9.6)	13 (6.0)	0.153	10 (6.9)	0.361	3 (4.1)	0.217
Chronic heart failure	1 (0.5)	56 (25.7)	< 0.001	46 (31.7)	< 0.001	10 (13.7)	< 0.001
Vascular disease	6 (2.8)	56 (25.7)	< 0.001	49 (33.8)	< 0.001	7 (9.6)	0.014
Acute coronary syndrome	6 (2.8)	34 (15.6)	< 0.001	28 (19.3)	< 0.001	6 (8.2)	0.042
Pulmonary embolism	0 (0.0)	7 (3.2)	0.008	6 (4.1)	0.004	1 (1.4)	0.251
Peripheral arterial disease	0 (0.0)	7 (3.2)	0.008	6 (4.1)	0.004	1 (1.4)	0.251
Deep vein thrombosis	0 (0.0)	14 (6.4)	< 0.001	14 (9.7)	< 0.001	0	NA
Advanced carcinoma	7 (3.2)	33 (15.1)	< 0.001	21 (14.5)	< 0.001	12 (16.4)	< 0.001
Medications							
Antiplatelet	0 (0.0)	53 (24.3)	< 0.001	43 (30.0)	< 0.001	10 (13.7)	< 0.001
Low-dose aspirin	0 (0.0)	40 (18.4)	< 0.001	33 (22.8)	< 0.001	7 (9.6)	< 0.001
Thienopyridine[1]	0 (0.0)	5 (2.3)	0.025	5 (3.5)	0.006	0 (0.0)	NA
Other antiplatelets[2]	0 (0.0)	11 (5.1)	0.001	8 (5.5)	< 0.001	3 (4.1)	0.003
NSAIDs	21 (9.6)	7 (3.2)	0.006	3 (2.1)	0.004	4 (5.5)	0.341
Endoscopic factors							
Number of polyps	2.0 ± 1.4	8.3 ± 5.3	0.019	2.4 ± 1.8	0.063	2.5 ± 1.8	0.041
Number of polyps ⩾ 5	13 (6.0)	28 (12.8)	0.014	17 (11.7)	0.078	11 (15.1)	0.014
Polyp size	6.0 ± 3.3	6.3 ± 3.4	< 0.001	8.7 ± 5.9	< 0.001	7.4 ± 3.7	0.001
Polyp size ⩾ 10 mm	28 (12.8)	69 (31.7)	< 0.001	47 (32.4)	< 0.001	22 (30.1)	0.001
Advanced adenoma[3]	27 (12.4)	64 (29.4)	< 0.001	43 (29.7)	< 0.001	21 (28.8)	0.001

[1]Thienopyridine includes ticlopidine, clopidogrel, and prasugrel; [2]Other antiplatelets are antiplatelets other than low-dose aspirin and thienopyridine; [3]Advanced adenoma is adenoma ⩾ 1 cm with villous components (tubulovillous or villous) or high-grade or severe dysplasia. Values in parentheses are percentages. Values presented with a plus/minus sign are means ± SD. Bold type indicates statistical significance ($P < 0.05$). AC: Anticoagulant; DOAC: Direct oral anticoagulants; BMI: Body mass index; Ccr: Creatinine clearance; NSAIDs: Non-steroidal anti-inflammatory drugs.

4, 1 case at day 5, 2 cases at day 6, and 1 case at day 8. The 4 patients with early PPB were all warfarin users. Compared with controls, there were a significantly higher rate among AC users of PPB (13.7% *vs* 0.9%, $P < 0.001$; Figure 2). Adjusting for propensity score between groups, AC users had a significantly increased PPB risk (adjusted OR = 18.9, $P < 0.001$; Table 2). Two thromboembolic events occurred in AC users, but none in controls. Thromboembolism occurred in 2 warfarin users and no DOAC users. No mortality events were noted in either group.

Warfarin users vs DOAC users

In the subgroup analysis of warfarin users, there were some significant differences in baseline characteristics with controls (Table 1). In terms of outcomes, warfarin users had a significantly higher rate of PPB (13.7% *vs* 0.9%, $P < 0.001$; Figure 2); a significantly increased PPB risk when adjusting for propensity score (adjusted OR = 18.6, $P < 0.001$; Table 2). In the subgroup analysis of DOAC users, there were also some significant differences in baseline characteristics with controls (Table 1). As for outcomes, DOAC users had a significantly higher rate of PPB (13.8% *vs* 0.9%, $P < 0.001$; Figure 2); significantly increased PPB risk when adjusting for propensity score (adjusted OR = 17.8, $P = 0.001$; Table 2). PPB rates did not differ significantly between rivaroxaban, dabigatran, and apixaban users (Figure 2).

Differences in baseline characteristics and clinical outcomes between the three AC management strategies

Discontinuing AC with HPB (guideline recommendation) *vs* continuing AC: There were some significant differences in baseline characteristics between strategies (Supplementary Table 1). The discontinuing AC with HPB group showed a higher rate of PPB (19.6%

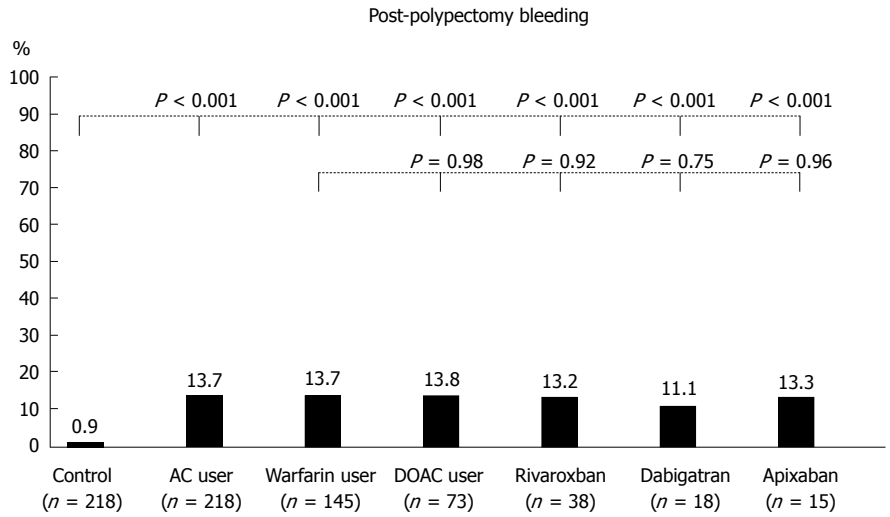

Figure 2 Thirty-day post-polypectomy bleeding in controls (*n* = 218), anticoagulants users (*n* = 218) and subgroups of warfarin (*n* = 145) and direct oral anticoagulants users [*n* = 73: rivaroxaban (*n* = 38), dabigatran (*n* = 18), and apixaban (*n* = 15)]. *P*-values for comparison of each group with controls and for comparison of direct oral anticoagulants users with warfarin users. AC: Anticoagulants; DOAC: Direct oral anticoagulants.

Table 2 Crude and adjusted odds ratios for post-polypectomy bleeding in controls (*n* = 218), anticoagulant users (*n* = 218), warfarin users (*n* = 145), and direct oral anticoagulants users (*n* = 73)

Subjects	Crude OR (95%CI)	*P* value	Propensity score-adjusted OR[1] (95%CI)	*P* value
Controls	1 (referent)		1 (referent)	
AC users	17.2 (4.1-73.1)	< 0.001	18.9 (4.2-85.5)	< 0.001
Warfarin users	17.3 (4.0-75.2)	< 0.001	18.6 (3.8-89.9)	< 0.001
DOAC users	17.1 (3.7-80.3)	< 0.001	17.8 (3.2-98.8)	0.001

[1]Propensity score estimations. Values in parentheses are percentages. Values presented with a plus/minus sign are means ± SD; bold type indicates statistical significance ($P < 0.05$). AC users *vs* controls: Logistic regression model included 17 factors that are potentially clinically important variables; area under the receiver operating characteristic (ROC) curve for propensity scores for AC users was 0.81 (95%CI: 0.77-0.85); Warfarin users *vs* controls: Logistic regression model included 18 factors that are potentially clinically important variables; area under the ROC curve for propensity scores for warfarin users was 0.83 (95%CI: 0.78-0.88); DOAC users *vs* controls: Logistic regression model included 14 factors that are potentially clinically important variables; area under the ROC curve for DOAC user propensity scores was 0.85 (95%CI: 0.80-0.90). NA: Not applicable; AC: Anticoagulants; DOAC: Direct oral anticoagulants; HPB: Heparin bridge; OR: Odds ratio.

vs 10.8%, $P = 0.087$; Figure 3A); a higher PPB risk when adjusting for propensity score (adjusted OR = 2.2, $P = 0.069$; Table 3).

In the warfarin subgroups, the discontinuing warfarin with HPB group showed a significantly higher rate of PPB (21.7% *vs* 4.7%, $P = 0.013$; Figure 3B); increased PPB risk on multivariate analysis (Table 3). In the subgroup of DOAC users, there were no significant differences between the two groups in PPB risk (Figure 3C), and multivariate models adjusted for propensity score also revealed no significant difference (Table 3).

Discontinuing AC with HPB (guideline recommendation) *vs* discontinuing AC without HPB: The discontinuing AC with HPB group showed a significantly higher rate of PPB (19.6% *vs* 0.0%, $P = 0.020$; Figure 3A); increased PPB risk on univariate analysis (OR = 7.7, $P = 0.023$; Table 3).

In the warfarin subgroups, the discontinuing AC with HPB group had a significantly higher rate of PPB (21.7% *vs* 0%, $P = 0.025$; Figure 3B); increased PPB risk on univariate analysis (OR = 7.2, $P = 0.033$; Table 3). In the DOAC subgroups, there were no significant differences in PPB risk between the two subgroups (Table 3).

Association of rate of PPB with HPB duration and INR value at endoscopy

The rate of PPB increased significantly with longer duration of HPB ($P = 0.015$ for trend; Figure 4). This trend was also found in warfarin and DOAC users (Figure 4). Rate of PPB was 18.7% for INR < 1.5, 0% for INR 1.5-1.9, 25% for INR 2.0-2.4, and 0% for INR > 2.5. INR value at pre-endoscopy did not predict PPB ($P = 0.431$ for trend; Supplementary Figure 1).

DISCUSSION

The four main findings of the study are as follows: (1) AC users were at higher risk of PPB than controls; (2) PPB risk was similar between warfarin users and DOAC users, whereas thromboembolism risk was observed only in warfarin users; (3) PPB risk was not significantly different

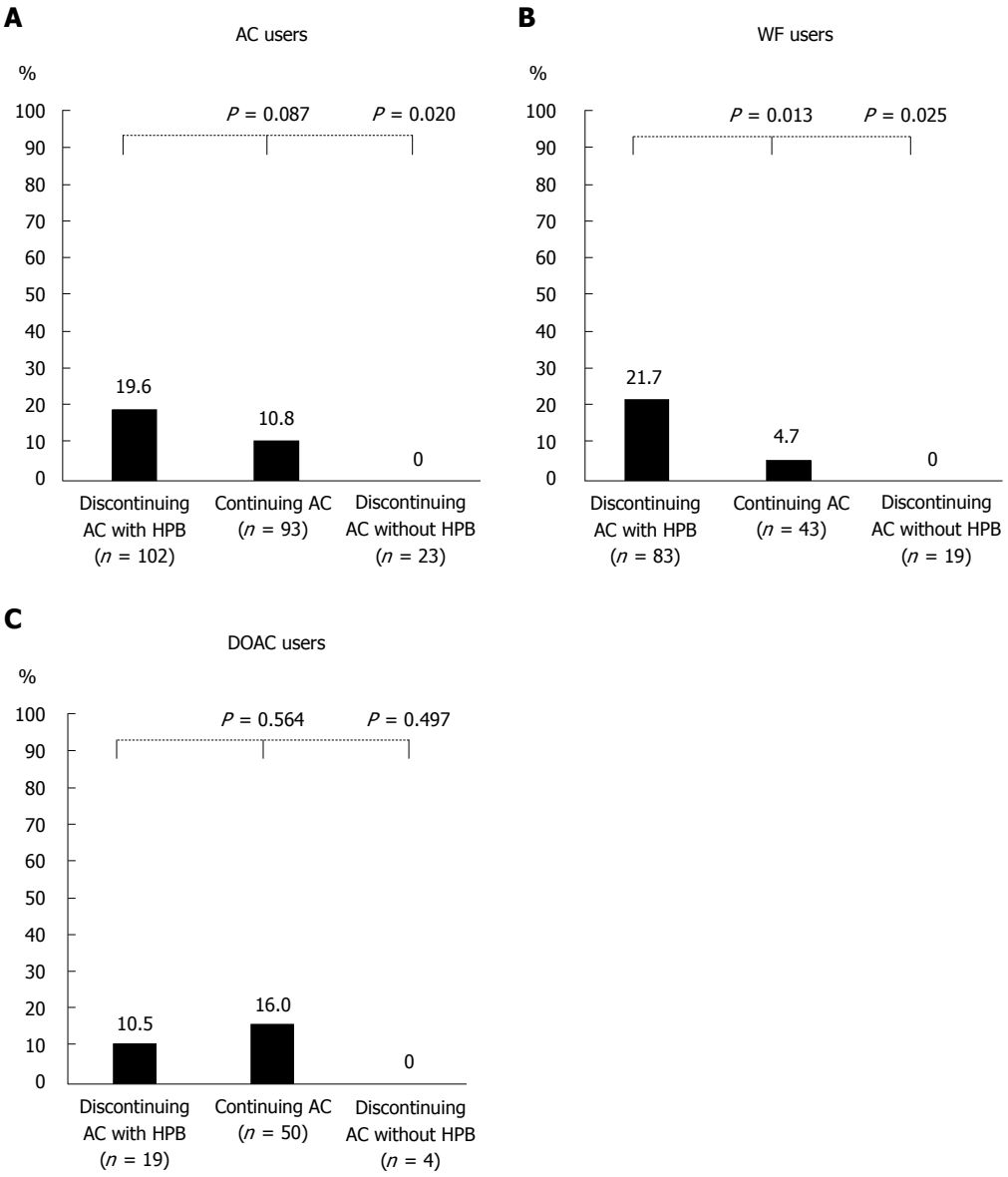

Figure 3 Post-polypectomy bleeding according to the three main anticoagulants management strategies in anticoagulants (A), warfarin (B), and direct oral anticoagulants (C) users. For the 218 patients, 102 patients (46.8%) in the discontinuing anticoagulants with heparin bridge group, 93 (42.7%) in the continuing anticoagulants group, and 23 (10.6%) in the discontinuing anticoagulants without heparin bridge group. AC: Anticoagulants; DOAC: Direct oral anticoagulants; HPB: Heparin bridge.

between rivaroxaban, dabigatran, and apixaban users; and (4) the recommended strategy of discontinuing AC with HPB showed a higher bleeding rate than continuing AC alone and had one thrombotic event, indicating that HPB increased bleeding and may not prevent thromboembolism. These findings were significantly evident in warfarin users compared with DOAC users.

In agreement with past studies, our AC users had a significantly higher OR for PPB than did controls (adjusted OR = 18.9). Witt *et al*[26] reported that PPB occurred more often in AC users than non-AC users (adjusted OR = 11.6). Hui *et al*[27] demonstrated that warfarin use was an independent risk factor for PPB (adjusted OR = 13.4). The ORs in these studies were lower than ours because their control subjects included antiplatelet users.

We revealed for the first time in this study that PPB risk was similar between warfarin and DOAC users compared with controls. A meta-analysis study indicated a higher risk of non-procedural-related bleeding in DOAC users than in warfarin users[28]. Thus, bleeding risk might be different between procedure-related and non-procedure-related bleeding. Only limited data are available on differences in post-endoscopic bleeding between DOAC and warfarin users. In this study, we found that 14% of DOAC and warfarin users had PPB. In agreement with this, Nagata *et al*[29] showed that 14% of DOAC users had PPB and 16.9% of warfarin users had PPB (P = 0.324). However, post-polypectomy-related bleeding differ according to site of the bleed in the upper or lower GI tract, because upper GI polypectomy-related bleeding was higher in warfarin users than in DOAC users (P = 0.06)[29].

Several endoscopy guidelines recommend that AC be discontinued with HPB[6-8]. However, in our study, following

Table 3 Crude and adjusted odds ratios for post-polypectomy bleeding in anticoagulant users (*n* = 218), warfarin users (*n* = 145), and direct oral anticoagulants users (*n* = 73)

AC management during peri-endoscopic period	Crude OR (95%CI)	*P* value	Propensity score-adjusted OR[1] (95%CI)	*P* value
AC users				
Discontinuing AC with HPB *vs* continuing AC	2.0 (0.9-4.6)	0.091	2.2 (0.9-5.2)	0.069
Discontinuing AC with HPB *vs* discontinuing AC without HPB	7.7 (1.3-Inf)	0.023	NA	NA
Warfarin users				
Discontinuing warfarin with HPB *vs* continuing warfarin	5.7 (1.3-25.8)	0.024	4.7 (1.0-22.1)	0.049
Discontinuing warfarin with HPB *vs* discontinuing warfarin without HPB	7.2 (1.1-Inf)	0.033	NA	NA
DOAC users				
Discontinuing DOAC with HPB *vs* continuing DOAC	0.6 (0.1-3.2)	0.567	0.7 (0.1-4.5)	0.664
Discontinuing DOAC with HPB *vs* discontinuing DOAC without HPB	0.5 (0.4-Inf)	1.000	NA	NA

[1]Propensity score estimations. Values in parentheses are percentages. Values presented with a plus/minus sign are means ± SD; bold type indicates statistical significance ($P < 0.05$). Continuing AC group *vs* standard group: Logistic regression model included 8 factors that are potentially clinically important variables; area under the ROC curve for propensity scores for the continuing AC group was 0.71 (95%CI: 0.63-0.79); standard group *vs* continuing warfarin group: Logistic regression model included 6 factors that are potentially clinically important variables; area under the ROC curve for propensity scores for the continuing warfarin group was 0.63 (95%CI: 0.53-0.73); standard group *vs* continuing DOAC group: Logistic regression model included 6 factors that are potentially clinically important variables; area under the ROC curve for propensity scores for the continuing DOAC group was 0.90 (95%CI: 0.82-0.98). NA: Not applicable; AC: Anticoagulants; CI: Confidential interval; DOAC: Direct oral anticoagulants; HPB: Heparin bridge; Inf: Infinity; OR: Odds ratio.

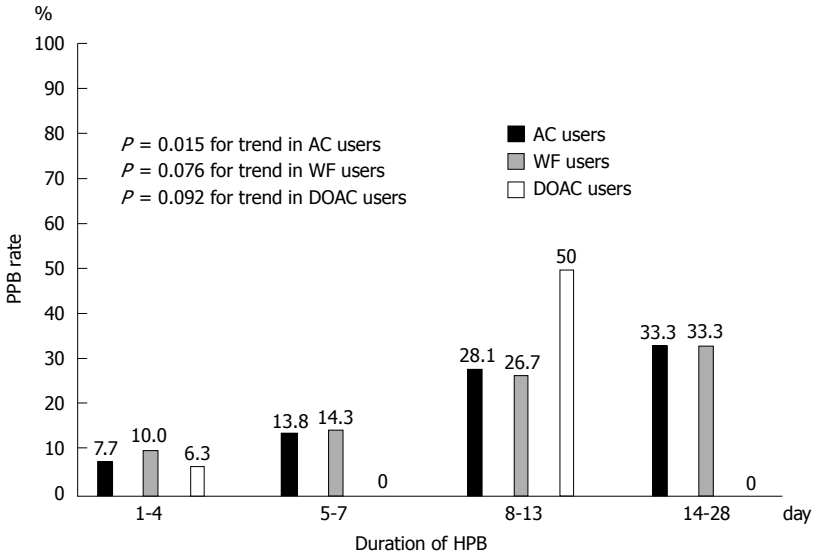

Figure 4 Association of post-polypectomy bleeding rate with duration of heparin bridge in anticoagulants, warfarin, and direct oral anticoagulants users. AC: Anticoagulants; WF: Warfarin; DOAC: Direct oral anticoagulants; HPB: Heparin bridge; PPB: Post-polypectomy bleeding.

this guideline strategy showed a higher bleeding risk and longer hospital stay compared with the continuing AC strategy, and one thrombotic event occurred with the guideline strategy and none in the continuing AC strategy. These findings suggest that continuing oral AC might be acceptable for polypectomy.

Consistent with our results, a meta-analysis[30] showed that HPB was associated with a higher rate of PPB and did not prevent thromboembolism. A randomized study[13] found that post-procedural bleeding risk was higher in patients with HPB than in those without it, and thromboembolic risk was similar in both groups. Taken together, the evidence suggests that the recommendation of several endoscopic guidelines[6-8] should be re-evaluated.

It is not clear why following the guideline strategy was associated with increased PPB risk in warfarin users but not DOAC users. One possible explanation is that in warfarin users, it takes several days for the anticoagulant effect to be sufficient, whereas onset is rapid with DOAC and therapeutic anticoagulation is achieved in a few hours[31]. The criterion for discontinuing heparin in warfarin users is that INR reaches the effective range, but the time to reach this range varies among patients. Therefore, heparin may need to be used for a long time after the procedure; the time is much shorter in DOAC users. Also, simultaneously administering warfarin and heparin (double anticoagulation effect) can increase bleeding risk. From these considerations, GI bleeding risk is high when HPB is performed in warfarin users compared with DOAC users. These prior findings, together with ours here, suggest that warfarin should be switched to DOAC before high-risk endoscopic procedures are performed.

One of the strengths of our study was the analysis of detailed clinical and endoscopic data that was collected and that we could adjust for propensity score by including these factors in the multivariate models. Another was that we identified a difference in clinical outcomes between the three main AC management strategies investigated. We also recognize limitations. First, this was a retrospective study conducted at a single site. Second, the AC users were heterogeneous and included those with atrial fibrillation, valvular disease, or with low or high thromboembolic risk. Third, we have no data on subcutaneous heparin because intravenous heparin is used in Japan. However, a previous study reported a similar incidence of major bleeding between patients treated with subcutaneous unfractionated heparin and those treated with intravenous unfractionated heparin (OR 0.91).

In conclusion, patients receiving oral AC had higher risks of bleeding after colonoscopic polypectomy compared with patients not receiving any antithrombotics. PPB risk was similar between warfarin and DOAC users, whereas thromboembolism risk was observed in warfarin users only. HPB increased bleeding risk, and may not prevent thromboembolism and therefore the current guideline recommendation should be re-considered. Continuing oral AC may be acceptable for polypectomy.

ARTICLE HIGHLIGHTS

Research background

The number of oral anticoagulants (AC) used increases as the population ages, and the number of colonoscopic polypectomies is expected to increase in patients receiving AC.

Research motivation

Whether post-polypectomy bleeding (PPB) or thromboembolic risk differs between warfarin and direct oral anticoagulant (DOAC) users remains unknown.

Research objectives

We evaluated PPB risk in patients receiving warfarin or DOAC compared with patients not receiving any antithrombotics (controls). We also assessed the risks of PPB and thromboembolism between the three AC management methods mentioned above, discontinuing AC with heparin bridge (guideline recommendation), continuing AC, and discontinuing AC without heparin bridge.

Research methods

We conducted a retrospective cohort study and collected data from 218 patients receiving oral anticoagulants (73 DOAC users, 145 warfarin users) and 218 patients not receiving any antithrombotics (age- and sex-matched controls) who underwent polypectomy.

Research results

PPB rate was significantly higher in both warfarin users and DOAC users compared with controls. Two thromboembolic events occurred in warfarin users, but none in DOAC users. Compared with the continuing anticoagulant group, the discontinuing anticoagulant with heparin bridge group (guideline recommendation) had a higher PPB rate. One thrombotic event occurred in the discontinuing anticoagulant with heparin bridge group and the discontinuing anticoagulant without heparin bridge group; none occurred in the continuing anticoagulant group.

Research conclusions

Patients receiving oral anticoagulant had higher risks of bleeding after colonoscopic polypectomy compared with patients not receiving any antithrombotics. PPB risk was similar between warfarin and DOAC users, whereas thromboembolism risk was observed in warfarin users only. Heparin bridge increased bleeding risk, and may not prevent thromboembolism.

Research perspectives

The current guideline recommendation for heparin bridge should be re-considered, and continuing oral anticoagulant may be acceptable for polypectomy.

ACKNOWLEDGMENTS

The authors thank clinical research coordinators Kuniko Miki, Kenko Yoshida, Eiko Izawa, and Hisae Kawashiro, for their help with data collection.

REFERENCES

1 **Mozaffarian D**, Benjamin EJ, Go AS, Arnett DK, Blaha MJ, Cushman M, de Ferranti S, Després JP, Fullerton HJ, Howard VJ, Huffman MD, Judd SE, Kissela BM, Lackland DT, Lichtman JH, Lisabeth LD, Liu S, Mackey RH, Matchar DB, McGuire DK, Mohler ER 3rd, Moy CS, Muntner P, Mussolino ME, Nasir K, Neumar RW, Nichol G, Palaniappan L, Pandey DK, Reeves MJ, Rodriguez CJ, Sorlie PD, Stein J, Towfighi A, Turan TN, Virani SS, Willey JZ, Woo D, Yeh RW, Turner MB; American Heart Association Statistics Committee and Stroke Statistics Subcommittee. Heart disease and stroke statistics--2015 update: a report from the American Heart Association. *Circulation* 2015; **131**: e29-322 [PMID: 25520374 DOI: 10.1161/CIR.0000000000000152]

2 **Humbert X**, Roule V, Chequel M, Fedrizzi S, Brionne M, Lelong-Boulouard V, Milliez P, Alexandre J. Non-vitamin K oral anticoagulant treatment in elderly patients with atrial fibrillation and coronary heart disease. *Int J Cardiol* 2016; **222**: 1079-1083 [PMID: 27514627 DOI: 10.1016/j.ijcard.2016.07.212]

3 **Abraham NS**, Castillo DL. Novel anticoagulants: bleeding risk and management strategies. *Curr Opin Gastroenterol* 2013; **29**: 676-683 [PMID: 24100724 DOI: 10.1097/MOG.0b013e328365d415]

4 **Baron TH**, Kamath PS, McBane RD. Management of antithrombotic therapy in patients undergoing invasive procedures. *N Engl J Med* 2013; **368**: 2113-2124 [PMID: 23718166 DOI: 10.1056/NEJMra1206531]

5 **Kwok A**, Faigel DO. Management of anticoagulation before and after gastrointestinal endoscopy. *Am J Gastroenterol* 2009; **104**: 3085-3097; quiz 3098 [PMID: 19672250 DOI: 10.1038/ajg.2009.469]

6 **Veitch AM**, Vanbiervliet G, Gershlick AH, Boustiere C, Baglin TP, Smith LA, Radaelli F, Knight E, Gralnek IM, Hassan C, Dumonceau JM. Endoscopy in patients on antiplatelet or anticoagulant therapy, including direct oral anticoagulants: British Society of Gastroenterology (BSG) and European Society of Gastrointestinal Endoscopy (ESGE) guidelines. *Endoscopy* 2016; **48**: 385-402 [PMID: 26890676 DOI: 10.1055/s-0042-102652]

7 **ASGE Standards of Practice Committee.**, Acosta RD, Abraham NS, Chandrasekhara V, Chathadi KV, Early DS, Eloubeidi MA, Evans JA, Faulx AL, Fisher DA, Fonkalsrud L, Hwang JH, Khashab MA, Lightdale JR, Muthusamy VR, Pasha SF, Saltzman JR, Shaukat A, Shergill AK, Wang A, Cash BD, DeWitt JM. The management of antithrombotic agents for patients undergoing GI endoscopy. *Gastrointest Endosc* 2016; **83**: 3-16 [PMID: 26621548 DOI: 10.1016/j.gie.2015.09.035]

8 **Fujimoto K**, Fujishiro M, Kato M, Higuchi K, Iwakiri R, Sakamoto C, Uchiyama S, Kashiwagi A, Ogawa H, Murakami K, Mine T, Yoshino J, Kinoshita Y, Ichinose M, Matsui T; Japan Gastroenterological Endoscopy Society. Guidelines for gastroenterological endoscopy in patients undergoing antithrombotic treatment. *Dig Endosc* 2014; **26**: 1-14 [PMID: 24215155 DOI: 10.1111/den.12183]

9 **Phillips KW**, Ansell J. Outpatient management of oral vitamin K antagonist therapy: defining and measuring high-quality management. *Expert Rev Cardiovasc Ther* 2008; **6**: 57-70 [PMID:

18095907 DOI: 10.1586/14779072.6.1.57]
10 **Burnett AE**, Mahan CE, Vazquez SR, Oertel LB, Garcia DA, Ansell J. Guidance for the practical management of the direct oral anticoagulants (DOACs) in VTE treatment. *J Thromb Thrombolysis* 2016; **41**: 206-232 [PMID: 26780747 DOI: 10.1007/s11239-015-1310-7]
11 **Heublein V**, Pannach S, Daschkow K, Tittl L, Beyer-Westendorf J. Gastrointestinal endoscopy in patients receiving novel direct oral anticoagulants: results from the prospective Dresden NOAC registry. *J Gastroenterol* 2018; **53**: 236-246 [PMID: 28493007 DOI: 10.1007/s00535-017-1346-x]
12 **Li HK**, Chen FC, Rea RF, Asirvatham SJ, Powell BD, Friedman PA, Shen WK, Brady PA, Bradley DJ, Lee HC, Hodge DO, Slusser JP, Hayes DL, Cha YM. No increased bleeding events with continuation of oral anticoagulation therapy for patients undergoing cardiac device procedure. *Pacing Clin Electrophysiol* 2011; **34**: 868-874 [PMID: 21410724 DOI: 10.1111/j.1540-8159.2011.03049.x]
13 **Douketis JD**, Spyropoulos AC, Kaatz S, Becker RC, Caprini JA, Dunn AS, Garcia DA, Jacobson A, Jaffer AK, Kong DF, Schulman S, Turpie AG, Hasselblad V, Ortel TL; BRIDGE Investigators. Perioperative Bridging Anticoagulation in Patients with Atrial Fibrillation. *N Engl J Med* 2015; **373**: 823-833 [PMID: 26095867 DOI: 10.1056/NEJMoa1501035]
14 **Nagata N**, Niikura R, Aoki T, Shimbo T, Kishida Y, Sekine K, Tanaka S, Okubo H, Watanabe K, Sakurai T, Yokoi C, Akiyama J, Yanase M, Mizokami M, Uemura N. Lower GI bleeding risk of nonsteroidal anti-inflammatory drugs and antiplatelet drug use alone and the effect of combined therapy. *Gastrointest Endosc* 2014; **80**: 1124-1131 [PMID: 25088922 DOI: 10.1016/j.gie.2014.06.039]
15 **Nagata N**, Niikura R, Aoki T, Shimbo T, Sekine K, Okubo H, Watanabe K, Sakurai T, Yokoi C, Yanase M, Akiyama J, Uemura N. Association between colonic diverticulosis and bowel symptoms: A case-control study of 1629 Asian patients. *J Gastroenterol Hepatol* 2015; **30**: 1252-1259 [PMID: 25777157 DOI: 10.1111/jgh.12941]
16 **Pisters R**, Lane DA, Nieuwlaat R, de Vos CB, Crijns HJ, Lip GY. A novel user-friendly score (HAS-BLED) to assess 1-year risk of major bleeding in patients with atrial fibrillation: the Euro Heart Survey. *Chest* 2010; **138**: 1093-1100 [PMID: 20299623 DOI: 10.1378/chest.10-0134]
17 **Lip GY**, Nieuwlaat R, Pisters R, Lane DA, Crijns HJ. Refining clinical risk stratification for predicting stroke and thromboembolism in atrial fibrillation using a novel risk factor-based approach: the euro heart survey on atrial fibrillation. *Chest* 2010; **137**: 263-272 [PMID: 19762550 DOI: 10.1378/chest.09-1584]
18 **Brenner H**, Hoffmeister M, Stegmaier C, Brenner G, Altenhofen L, Haug U. Risk of progression of advanced adenomas to colorectal cancer by age and sex: estimates based on 840,149 screening colonoscopies. *Gut* 2007; **56**: 1585-1589 [PMID: 17591622]
19 **Ono K**, Hidaka H, Koyama Y, Ishii K, Taguchi S, Kosaka M, Okazaki N, Tanimoto W, Katayama A. Effects of heparin bridging anticoagulation on perioperative bleeding and thromboembolic risks in patients undergoing abdominal malignancy surgery. *J Anesth* 2016; **30**: 723-726 [PMID: 27206420 DOI: 10.1007/s00540-016-2187-0]
20 **Feagins LA**, Iqbal R, Harford WV, Halai A, Cryer BL, Dunbar KB, Davila RE, Spechler SJ. Low rate of postpolypectomy bleeding among patients who continue thienopyridine therapy during colonoscopy. *Clin Gastroenterol Hepatol* 2013; **11**: 1325-1332 [PMID: 23403011 DOI: 10.1016/j.cgh.2013.02.003]
21 **Schulman S**, Kearon C; Subcommittee on Control of Anticoagulation of the Scientific and Standardization Committee of the International Society on Thrombosis and Haemostasis. Definition of major bleeding in clinical investigations of antihemostatic medicinal products in non-surgical patients. *J Thromb Haemost* 2005; **3**: 692-694 [PMID: 15842354]
22 **Park SK**, Seo JY, Lee MG, Yang HJ, Jung YS, Choi KY, Kim H, Kim HO, Jung KU, Chun HK, Park DI. Prospective analysis of delayed colorectal post-polypectomy bleeding. *Surg Endosc* 2018; **17**: Epub ahead of print [PMID: 29344790 DOI: 10.1007/s00464-018-6048-9]
23 **Austin PC**. An Introduction to Propensity Score Methods for Reducing the Effects of Confounding in Observational Studies. *Multivariate Behav Res* 2011; **46**: 399-424 [PMID: 21818162 DOI: 10.1080/00273171.2011.568786]
24 **Kurth T**, Walker AM, Glynn RJ, Chan KA, Gaziano JM, Berger K, Robins JM. Results of multivariable logistic regression, propensity matching, propensity adjustment, and propensity-based weighting under conditions of nonuniform effect. *Am J Epidemiol* 2006; **163**: 262-270 [PMID: 16371515]
25 **Elze MC**, Gregson J, Baber U, Williamson E, Sartori S, Mehran R, Nichols M, Stone GW, Pocock SJ. Comparison of Propensity Score Methods and Covariate Adjustment: Evaluation in 4 Cardiovascular Studies. *J Am Coll Cardiol* 2017; **69**: 345-357 [PMID: 28104076]
26 **Witt DM**, Delate T, McCool KH, Dowd MB, Clark NP, Crowther MA, Garcia DA, Ageno W, Dentali F, Hylek EM, Rector WG; WARPED Consortium. Incidence and predictors of bleeding or thrombosis after polypectomy in patients receiving and not receiving anticoagulation therapy. *J Thromb Haemost* 2009; **7**: 1982-1989 [PMID: 19719825 DOI: 10.1111/j.1538-7836.2009.03598.x]
27 **Hui AJ**, Wong RM, Ching JY, Hung LC, Chung SC, Sung JJ. Risk of colonoscopic polypectomy bleeding with anticoagulants and antiplatelet agents: analysis of 1657 cases. *Gastrointest Endosc* 2004; **59**: 44-48 [PMID: 14722546]
28 **Holster IL**, Valkhoff VE, Kuipers EJ, Tjwa ET. New oral anticoagulants increase risk for gastrointestinal bleeding: a systematic review and meta-analysis. *Gastroenterology* 2013; **145**: 105-112.e15 [PMID: 23470618 DOI: 10.1053/j.gastro.2013.02.041]
29 **Nagata N**, Yasunaga H, Matsui H, Fushimi K, Watanabe K, Akiyama J, Uemura N, Niikura R. Therapeutic endoscopy-related GI bleeding and thromboembolic events in patients using warfarin or direct oral anticoagulants: results from a large nationwide database analysis. *Gut* 2017; pii: gutjnl-2017-313999 [PMID: 28874418]
30 **Jaruvongvanich V**, Assavapongpaiboon B, Wijarnpreecha K, Ungprasert P. Heparin-bridging therapy and risk of post-polypectomy bleeding: Meta-analysis of data reported by Japanese colonoscopists. *Dig Endosc* 2017; **29**: 743-748 [PMID: 28370508 DOI: 10.1111/den.12882]
31 **Desai J**, Granger CB, Weitz JI, Aisenberg J. Novel oral anticoagulants in gastroenterology practice. *Gastrointest Endosc* 2013; **78**: 227-239 [PMID: 23725876 DOI: 10.1016/j.gie.2013.04.179]

P- Reviewer: Chuah SK, Cui J, Qi XS, Zuniga VL
S- Editor: Wang XJ **L- Editor**: A **E- Editor**: Huang Y

World Journal of Gastroenterology

Submit a Manuscript: http://www.f6publishing.com

World J Gastroenterol 2018 April 14; 24(14): 1550-1561

DOI: 10.3748/wjg.v24.i14.1550

ISSN 1007-9327 (print) ISSN 2219-2840 (online)

ORIGINAL ARTICLE

Randomized Controlled Trial

Maintenance for healed erosive esophagitis: Phase Ⅲ comparison of vonoprazan with lansoprazole

Kiyoshi Ashida, Katsuhiko Iwakiri, Naoki Hiramatsu, Yuuichi Sakurai, Tetsuharu Hori, Kentarou Kudou, Akira Nishimura, Eiji Umegaki

Kiyoshi Ashida, Department of Gastroenterology, Rakuwakai Otowa Hospital, Kyoto 607-8062, Japan

Katsuhiko Iwakiri, Department of Gastroenterology, Nippon Medical School Graduate School of Medicine, Tokyo 113-8603, Japan

Naoki Hiramatsu, Department of Gastroenterology and Hepatology, Osaka Rosai Hospital, Sakai, Osaka 591-8025, Japan

Yuuichi Sakurai, Tetsuharu Hori, Kentarou Kudou, Akira Nishimura, Takeda Pharmaceutical Company Limited, Osaka 540-8645, Japan

Eiji Umegaki, Department of Gastroenterology, Kobe University Graduate School of Medicine, Kobe, Hyogo 650-0017, Japan

ORCID number: Kiyoshi Ashida (0000-0002-5072-9399); Katsuhiko Iwakiri (0000-0002-5558-6104); Naoki Hiramatsu (0000-0002-8803-4488); Yuuichi Sakurai (0000-0003-3337-8213); Tetsuharu Hori (0000-0003-0638-6664); Kentarou Kudou (0000-0003-0125-6174); Akira Nishimura (0000-0001-6085-6829); Eiji Umegaki (0000-0003-3353-8096).

Author contributions: Ashida K, Sakurai Y, Hori T and Nishimura A were involved in study conception and design; Hiramatsu N served as Medical Expert; Umegaki E, Iwakiri K and Ashida K served as the Central Adjudication Committee; Kudou K conducted statistical analyses; all authors were involved in the drafting and critical revision of the manuscript, and approved the final version, including the authorship list.

Institutional review board statement: The study was reviewed and approved by the institutional review board of each participating site.

Clinical trial registration statement: This study is registered at ClinicalTrials.gov. The registration identification number is NCT01459367.

Informed consent statement: All study participants provided written informed consent prior to study enrollment.

Conflict-of-interest statement: Kiyoshi Ashida has received fees and honoraria from Takeda Pharmaceutical Company Limited and Otsuka Pharmaceutical Company Limited; Katsuhiko Iwakiri has received grants, fees, and honoraria from Takeda Pharmaceutical Company Limited, and fees from Otsuka Pharmaceutical Company Limited; Yuuichi Sakurai, Tetsuharu Hori, Kentarou Kudou, and Akira Nishimura are full-time employees of Takeda Pharmaceutical Company Limited; Naoki Hiramatsu and Eiji Umegaki have no conflicts of interest to declare.

Data-sharing statement: No additional data are available.

Manuscript source: Unsolicited manuscript

Correspondence to: Kiyoshi Ashida, MD, PhD, Department of Gastroenterology, Rakuwakai Otowa Hospital, 2 Otowachinji-cho, Yamashina-ku, Kyoto 607-8062, Japan. rakuwadr1185@rakuwadr.com
Telephone: +81-75-5934111
Fax: +81-75-5934160

Received: November 30, 2017
Peer-review started: December 1, 2017
First decision: December 13, 2017
Revised: February 6, 2018
Accepted: March 7, 2018
Article in press: March 6, 2018
Published online: April 14, 2018

Abstract

AIM

To compare vonoprazan 10 and 20 mg *vs* lansoprazole 15 mg as maintenance therapy in healed erosive esophagitis (EE).

METHODS

A total of 607 patients aged ⩾ 20 years, with endoscopically-confirmed healed EE following 8 wk of treatment with vonoprazan 20 mg once daily, were randomized 1:1:1 to receive lansoprazole 15 mg (*n* = 201), vonoprazan 10 mg (*n* = 202), or vonoprazan 20 mg (*n* = 204), once daily. The primary endpoint of the study was the rate of endoscopically-confirmed EE recurrence during a 24-wk maintenance period. The secondary endpoint was the EE recurrence rate at Week 12 during maintenance treatment. Additional efficacy endpoints included the incidence of heartburn and acid reflux, and the EE healing rate 4 wk after the initiation of maintenance treatment. Safety endpoints comprised adverse events (AEs), vital signs, electrocardiogram findings, clinical laboratory results, serum gastrin and pepsinogen Ⅰ/Ⅱ levels, and gastric mucosa histopathology results.

RESULTS

Rates of EE recurrence during the 24-wk maintenance period were 16.8%, 5.1%, and 2.0% with lansoprazole 15 mg, vonoprazan 10 mg, and vonoprazan 20 mg, respectively. Vonoprazan was shown to be non-inferior to lansoprazole 15 mg ($P < 0.0001$ for both doses). In a *post-hoc* analysis, EE recurrence at Week 24 was significantly reduced with vonoprazan at both the 10 mg and the 20 mg dose *vs* lansoprazole 15 mg (5.1% *vs* 16.8%, $P = 0.0002$, and 2.0% *vs* 16.8%, $P < 0.0001$, respectively); by contrast, the EE recurrence rate did not differ significantly between the two doses of vonoprazan ($P = 0.1090$). The safety profiles of vonoprazan 10 and 20 mg were similar to that of lansoprazole 15 mg in patients with healed EE. Treatment-related AEs were reported in 11.4%, 10.4%, and 10.3% of patients in the lansoprazole 15 mg, vonoprazan 10 mg, and vonoprazan 20 mg arms, respectively.

CONCLUSION

Our findings confirm the non-inferiority of vonoprazan 10 and 20 mg to lansoprazole 15 mg as maintenance therapy for patients with healed EE.

Key words: Gastroesophageal reflux disease; Erosive esophagitis; Lansoprazole; Potassium-competitive acid blockers; Vonoprazan; Maintenance therapy

Core tip: Proton pump inhibitors (PPIs), including lansoprazole, are widely used to maintain healing of erosive esophagitis (EE) in patients with gastroesophageal reflux disease; however, symptoms of reflux persist in significant numbers of patients treated with PPIs. We compared two doses of the novel potassium-competitive acid blocker vonoprazan (10 and 20 mg once daily) with lansoprazole at its approved dose of 15 mg once daily as maintenance therapy for healed EE in 607 Japanese patients. Vonoprazan was shown to be non-inferior to lansoprazole 15 mg at both investigated doses, while demonstrating a similar safety profile.

Ashida K, Iwakiri K, Hiramatsu N, Sakurai Y, Hori T, Kudou K, Nishimura A, Umegaki E. Maintenance for healed erosive esophagitis: Phase Ⅲ comparison of vonoprazan with lansoprazole. *World J Gastroenterol* 2018; 24(14): 1550-1561 Available from: URL: http://www.wjgnet.com/1007-9327/full/v24/i14/1550.htm DOI: http://dx.doi.org/10.3748/wjg.v24.i14.1550

INTRODUCTION

Gastroesophageal reflux disease (GERD) is a common gastric acid-related disorder that is characterized by heartburn and/or acid regurgitation caused by the reflux of gastric contents[1]. The spectrum of GERD ranges from non-erosive to erosive or complicated disease (ulcer, columnar metaplasia, and stricture), each of which is thought likely to progress if either left untreated or not treated adequately[2]. The main goals for the clinical management of GERD consist of symptom relief, healing of erosive esophagitis (EE), prevention of recurrences and complications, and overall improvement of patients' quality of life[1,3].

Owing to their superior ability to inhibit gastric acid secretion compared with H_2 receptor antagonists (H_2RAs), proton pump inhibitors (PPIs) remain the mainstay of long-term therapy for GERD[1,3-5]. However, resolution of GERD symptoms with PPIs appears to have a less predictable outcome than esophageal mucosal inflammation[4-6], with reflux symptoms persisting in up to 60% of patients treated with PPIs in randomized controlled clinical trials[7] and observational studies[5]. Proposed underlying mechanisms for PPI failure include drug- and patient-related factors, such as low bioavailability, nocturnal acid breakthrough, rapid metabolism (CYP2C19 extensive metabolizer genotype), and poor compliance with the prescribed regimen[6]. The slow cumulative onset of PPI action at therapeutic doses may also be a contributing factor[8-10]. These limitations have led to a renewed interest in alternative treatment modalities for the management of patients with GERD[1,4].

Discovered and developed by Takeda Pharmaceutical Company Limited, Japan, vonoprazan fumarate (TAK-438) belongs to a novel class of acid suppressants known as potassium-competitive acid blockers (P-CABs)[11]. Like PPIs, vonoprazan inhibits gastric H^+, K^+-ATPase,

an enzyme that catalyzes the final step in the acid secretion pathway. However, unlike PPIs, vonoprazan inhibits the enzyme in a K^+-competitive and reversible manner[12], with its inhibitory effects (pKa 9.4) on gastric acid secretion largely unaffected by ambient pH, as it accumulates in parietal cells under both acidic and resting conditions[12,13]. In animal studies, vonoprazan produced more potent and sustained suppression of gastric acid secretion than lansoprazole[11-14]. In healthy volunteers, single doses of vonoprazan 1-120 mg were well tolerated, and produced rapid, prolonged, and dose-related suppression of 24-h gastric acid secretion[15]. In another study in healthy volunteers, these effects were maintained with multiple dosing (10-40 mg once daily) over 7 d, and were also dose-related[16].

Lansoprazole 30 mg once daily is the recommended dosage for healing EE, while its step-down dose of 15 mg once daily is recommended for the maintenance treatment of healed EE, providing well-balanced efficacy and safety over the long term[17]. The current study aimed to demonstrate that vonoprazan 20 mg and its step-down dose of 10 mg once daily were non-inferior to lansoprazole 15 mg once daily in preventing EE recurrence during a 24-wk maintenance period in Japanese patients who achieve EE healing after 2, 4, or 8 wk treatment with vonoprazan 20 mg.

MATERIALS AND METHODS

Study design

This was a multicenter, randomized, double-blind, parallel-group, phase Ⅲ clinical study, which was designed and conducted to demonstrate the non-inferiority of vonoprazan 20 and 10 mg to lansoprazole 15 mg as maintenance therapy in Japanese patients with healed EE. During the initial treatment period, patients with EE Los Angeles (LA) Classification grades A to D received vonoprazan 20 mg once daily for up to 8 wk. All patients in whom endoscopic healing of EE was confirmed 2, 4, or 8 wk after the start of the study medication were immediately stratified by baseline endoscopic LA Classification grade (A/B or C/D), and subsequently randomized in a 1:1:1 ratio to receive maintenance therapy with vonoprazan 10 mg, vonoprazan 20 mg, or lansoprazole 15 mg given once daily after breakfast for 24 wk. All patients in whom endoscopic healing of EE was not confirmed at Week 8 completed the study without entering the maintenance phase. All patients in whom EE recurrence was endoscopically confirmed during maintenance treatment were withdrawn from the study and handled as 'completed cases'.

Registered at ClinicalTrials.gov with the identifier NCT01459367, the study was conducted at 55 sites in Japan between November 2011 and March 2013. The study protocol was reviewed and approved by the Institutional Review Board at each study site, and was conducted in accordance with the Declaration of Helsinki, the International Council for Harmonization of Technical Requirements for Pharmaceuticals for Human Use (ICH) Harmonized Tripartite Guideline for Good Clinical Practice, and Japanese regulatory requirements. All patients provided written informed consent prior to undergoing any study procedures.

Patients

Male or female outpatients aged ⩾ 20 years, who presented with endoscopically-confirmed healed EE (no mucosal breaks) after up to 8 wk of treatment with vonoprazan 20 mg once daily, entered the maintenance phase of the study. Main exclusion criteria included: esophageal complications (*e.g.,* eosinophilic esophagitis, esophageal varices, scleroderma, infection, esophageal stenosis); acute upper gastrointestinal bleeding; gastric or duodenal ulcer characterized by mucosal defects; hypersecretion disorders, such as Zollinger-Ellison syndrome; serious neurologic, cardiovascular, pulmonary, hepatic [alanine aminotransferase (ALT) or aspartate aminotransferase (AST) > 2.5 × the upper limit of normal (ULN)], renal (serum creatinine > 2 mg/dL), metabolic, gastrointestinal, urologic, endocrinologic, or hematologic disorders; need for surgery; history of drug (including alcohol) abuse; HIV or hepatitis; history of malignancy; and pregnancy or lactation in females. Any sexually active female of childbearing potential was required to use adequate contraceptive measures. Excluded concomitant medications included PPIs, H_2RAs, muscarinic M_3 receptor antagonists, gastrointestinal motility stimulants, anticholinergic drugs, prostaglandins, acid suppressants, anti-gastrin drugs, mucosal protective agents, *H. pylori* eradication therapies, atazanavir sulfate, and any other investigational drug. As the exclusion of non-steroidal anti-inflammatory drugs (NSAIDs) would have been difficult for patients eligible for inclusion in this study, their use was permitted; however, changes to NSAID regimens during the study were prohibited.

Treatment, randomization, and blinding

Patients were randomized to treatment groups in a 1:1:1 ratio according to a computer-generated randomization schedule prepared by independent randomization personnel. The independent randomization personnel managed the randomization process, and stored the randomization schedule in a secure area. The randomization schedule incorporated LA Classification grades as a stratification factor (A/B or C/D), to ensure that treatment groups were balanced with respect to disease severity. A double-dummy method, using matched vonoprazan placebo tablets and lansoprazole placebo capsules, was employed to ensure that the double-blind conditions were maintained throughout the study.

Procedures

Maintenance treatment was initiated on the day of randomization. Clinic visits were scheduled at Weeks

4, 12, and 24, or upon early withdrawal from the study (discontinuation/recurrence). Endoscopic examinations were performed at Weeks 12 and 24. A central adjudication committee (CAC), composed of independent experts, was established to perform standardized and consistent reviews of endoscopic EE grading by investigators, while all decisions about patient eligibility and withdrawal owing to EE recurrence were made by the investigators, irrespective of the CAC's assessment. Safety assessments were conducted at Weeks 4, 12, and 24. Histopathologic examinations of the gastric mucosa were performed at the start of treatment (baseline) and at Week 24 for subjects enrolled at designated study sites only. All biopsy specimens were full mucosal layer samples taken from the greater curvature of the upper gastric corpus during endoscopic procedures. Samples were fixed in 20% neutral buffered formalin and embedded in paraffin. Five slices were taken from each paraffin block, and were stained with hematoxylin and eosin, Grimelius, chromogranin, synaptophysin, and Ki-67 (MIB-1). For the CYP2C19 genotyping, a single 2 mL blood sample was collected at Week 4, and was analyzed to obtain information on genotypes that affect the pharmacokinetics of lansoprazole. G681A (*2) and G636A (*3) of CYP2C19 were detected using an Invader® assay. Both the histopathologic testing and CYP2C19 genotyping were carried out by Mitsubishi Chemical Medience Corporation, Tokyo, Japan. The gastric mucosa histopathology findings reported by the company were reviewed by an independent assessment committee, which assessed specimens for distribution patterns of Grimelius-positive cells, chromogranin A-positive cells, synaptophysin-positive cells, and Ki-67-positive cells. Treatment compliance was assessed in all patients on the basis of returned tablet/capsule counts at each study site visit.

Although no evidence has been reported of vonoprazan-associated liver function test abnormalities[18], drug-related hepatic changes have previously been reported with another member of the P-CAB drug class[19]. Liver function abnormalities (ALT or AST > 3 × ULN, or total bilirubin > 2 × ULN in two consecutive measurements) were therefore classified as special-interest adverse events (SIAEs) in the present study, and were monitored throughout.

The primary study endpoint was the rate of recurrence of endoscopically-confirmed EE at Week 24 of the maintenance period. The secondary endpoint was the rate of EE recurrence at Week 12 of the maintenance period. Safety endpoints included adverse events (AEs), vital signs, electrocardiogram (ECG) findings, clinical laboratory test values (hematology, serum chemistry, and urinalysis), serum gastrin and pepsinogen Ⅰ/Ⅱ levels, and gastric mucosa histopathologic findings.

Statistical analyses

A double-blind, controlled study of lansoprazole as maintenance therapy for patients with healed EE reported EE recurrence rates of 30% and 14% with lansoprazole 15 mg and 30 mg, respectively, over 24 wk[20]. It was therefore assumed that the endoscopic EE recurrence rate with vonoprazan 20 mg in the present study would be 14%, while the EE recurrence rate with vonoprazan 10 mg would be 22% - that is, halfway between the rates observed with lansoprazole 15 mg and 30 mg in the study mentioned above. It was assumed that the EE recurrence rate with lansoprazole 15 mg would again be 30%. Based on these assumptions, a sample size of 148 patients per treatment group would provide > 90% power to confirm the non-inferiority of the two vonoprazan doses to lansoprazole, with respect to the EE recurrence rate at Week 24, with a non-inferiority margin of 10% utilizing a two-sided 95% confidence interval (CI). Assuming a dropout rate of 15% during maintenance therapy, 174 randomized patients would be required for each treatment group. We therefore set the randomization target at 200 patients per treatment group, to enable evaluation of the long-term safety of vonoprazan in a sufficient number of patients.

For the primary endpoint of EE recurrence rate at Week 24 of maintenance treatment, frequency, point estimates, and corresponding 95%CIs were calculated by treatment group for the full analysis set (FAS), defined as all randomized patients who received at least one dose of study drug during the maintenance period. Vonoprazan 10 mg and 20 mg were evaluated for non-inferiority to lansoprazole 15 mg using the Farrington and Manning test[21] with a non-inferiority margin of 10%. The same analyses were performed for the secondary endpoint.

AEs (including their frequency, severity, investigator-assessed causality, and seriousness) and concomitant medications were monitored throughout the study. Treatment-emergent adverse events (TEAEs) were coded using the Medical Dictionary for Regulatory Activities (MedDRA) version 16.0. All TEAEs were summarized descriptively by treatment group, time of onset, and severity, and were categorized by System Organ Class and Preferred Term. All drug-related TEAEs were summarized by severity, while TEAEs leading to study discontinuation and serious TEAEs were summarized by treatment group.

The statistical methods of this study were prepared and conducted by Kentarou Kudou of Takeda Pharmaceutical Company Limited, and were reviewed and approved by Takamasa Hashimoto of Takeda Pharmaceutical Company Limited, Osaka, Japan.

RESULTS

Patients

In total, 737 patients signed the informed consent form. Of these 737 patients, 627 were enrolled into the treatment phase, with 611 patients completing up to 8 wk treatment for EE with vonoprazan 20 mg. Of the 611 who completed treatment, 607, who represented both the FAS and the safety analysis set (SAS), were

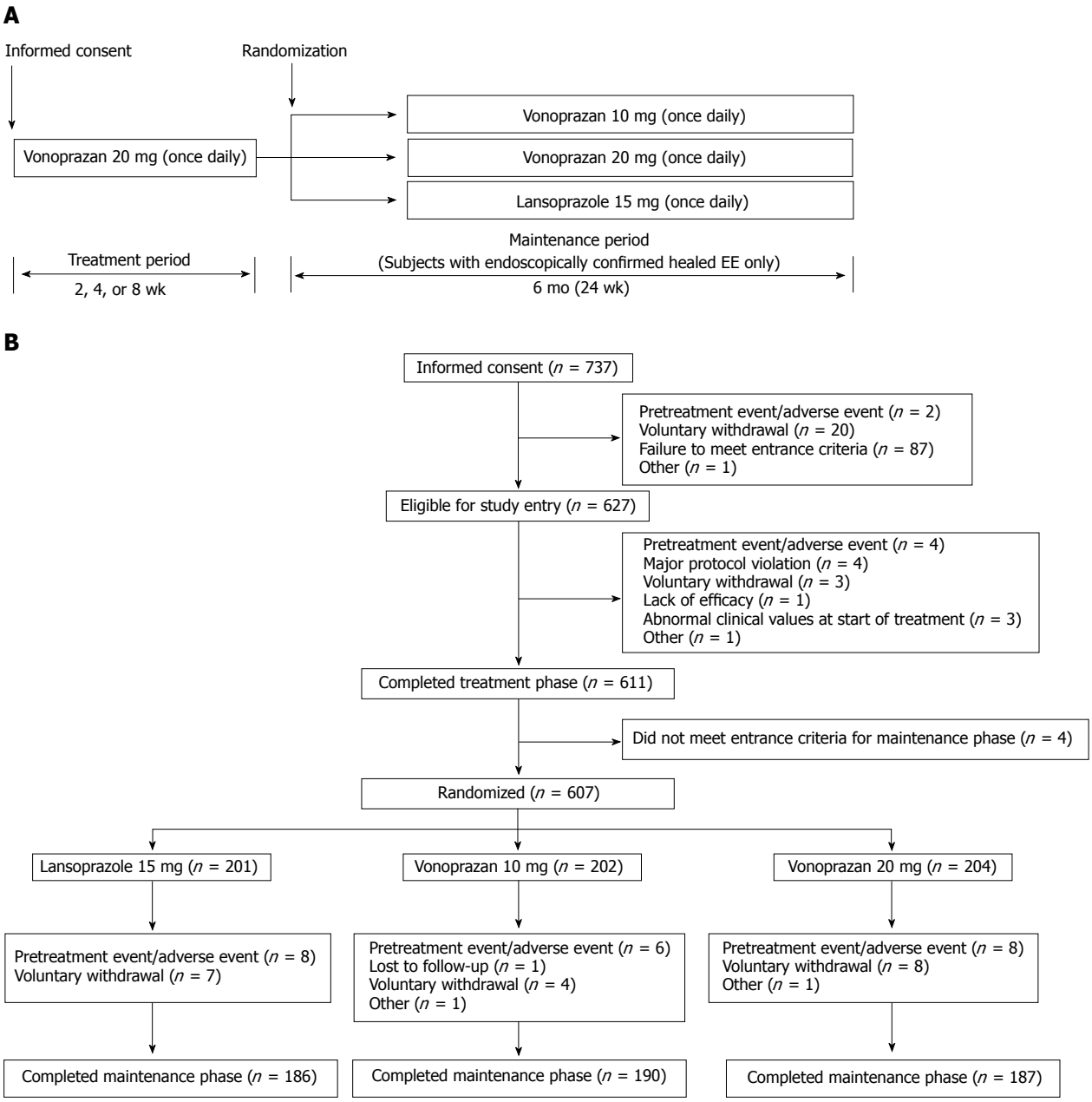

Figure 1 Study design (A) and patient disposition (B). EE: Erosive esophagitis.

randomized to maintenance therapy with lansoprazole 15 mg (n = 201), vonoprazan 10 mg (n = 202), or vonoprazan 20 mg (n = 204) (Figure 1). Five hundred sixty-three patients (92.8%) completed maintenance treatment. The main reasons for premature study discontinuation were pretreatment events/AEs (n = 22) and voluntary withdrawals (n = 19). The first informed consent form was signed on 21 November 2011, and the last follow-up visit took place on 7 March 2013.

The three maintenance groups were well matched in terms of demographic and other baseline characteristics (Table 1), and had similar baseline EE severities and medical histories. The mean treatment compliance rate was > 97% in each treatment group.

Efficacy

The rate of EE recurrence at 24 wk of maintenance therapy (primary endpoint) was 16.8%, 5.1%, and 2.0% with lansoprazole 15 mg, vonoprazan 10 mg, and vonoprazan 20 mg, respectively. Point estimates of differences in EE recurrence between the maintenance treatment groups and 95%CIs are shown in Table 2. Vonoprazan 10 mg and 20 mg were both found to be non-inferior to lansoprazole 15 mg in the FAS (both $P < 0.0001$), with the upper limits of 95%CIs for the differences between vonoprazan 10 mg or 20 mg and lansoprazole 15 mg being < 0, thus indicating a statistically significant difference. In a *post-hoc* analysis performed using the Fisher exact test, a statistically significant difference in the rate of EE recurrence was demonstrated between vonoprazan 10 mg or 20 mg and lansoprazole 15 mg ($P = 0.0002$ and $P < 0.0001$, respectively, *vs* lansoprazole 15 mg), but not between the two vonoprazan doses ($P = 0.1090$).

Table 1 Demographic and other baseline characteristics in the randomized set (n = 607)[1]

Characteristic	LPZ 15 mg (n = 201)	VPZ 10 mg (n = 202)	VPZ 20 mg (n = 204)
Age, yr	57.8 ± 12.9	55.5 ± 13.8	56.8 ± 13.6
Gender, male	140 (69.7)	160 (79.2)	160 (78.4)
Height, cm	163.5 ± 10.2	165.5 ± 9.3	165.6 ± 9.3
Weight, kg	67.0 ± 13.4	68.2 ± 12.3	69.0 ± 13.1
Erosive esophagitis grade, investigator-assessed			
LA Grade A/B	160 (79.6)	162 (80.2)	161 (78.9)
LA Grade C/D	41 (20.4)	40 (19.8)	43 (21.1)
Esophageal hiatal hernia			
⩾ 2 cm	31 (15.4)	45 (22.3)	46 (22.5)
< 2 cm	105 (52.2)	100 (49.5)	113 (55.4)
None	65 (32.3)	57 (28.2)	44 (21.6)
H. pylori infection status			
Positive	29 (14.4)	37 (18.3)	23 (11.3)
Negative	172 (85.6)	165 (81.7)	181 (88.7)
CYP2C19 genotype			
Extensive metabolizers	162 (80.6)	169 (84.1)	169 (83.3)
Poor metabolizers	39 (19.4)	32 (15.9)	34 (16.7)

[1]Values expressed as mean ± SD, or n (%). LA: Los Angeles; LPZ: Lansoprazole; SD: Standard deviation; VPZ: Vonoprazan.

Table 2 Recurrence rate of erosive esophagitis: Intergroup differences and non-inferiority test

Endpoint	LPZ 15 mg	VPZ 10 mg	VPZ 20 mg
Week 24 (primary endpoint)[1]	16.8% (33/196)	5.1% (10/197)	2.0% (4/201)
Week 12 (secondary endpoint)[1]	12.2% (24/196)	2.5% (5/197)	1.0% (2/201)
Comparison	Difference and 95%CI (%)	Non-inferiority, P value	Fisher exact test, P value[2]
Week 24 (primary endpoint)			
VPZ 10 mg *vs* LPZ 15 mg	-11.8 [-17.83, -5.69]	< 0.0001	0.0002
VPZ 20 mg *vs* LPZ 15 mg	-14.8 [-20.43, -9.26]	< 0.0001	< 0.0001
VPZ 10 mg *vs* VPZ 20 mg	-3.1 [-6.71, 0.54]	N/A	0.1090
Week 12 (secondary endpoint)			
VPZ 10 mg *vs* LPZ 15 mg	-9.7 [-14.80, -4.62]	< 0.0001	N/A
VPZ 20 mg *vs* LPZ 15 mg	-11.2 [-16.04, -6.46]	< 0.0001	N/A
VPZ 10 mg *vs* VPZ 20 mg	-1.5 [-4.13, 1.05]	N/A	N/A

[1]Values expressed as percentages with number of subjects in parentheses; [2]*Post hoc* analysis. CI: Confidence interval; LPZ: Lansoprazole; VPZ: Vonoprazan; N/A: Not applicable.

The intergroup differences in EE recurrence rate at Week 12 of the maintenance period (secondary endpoint) are shown in Table 2. Vonoprazan 10 mg and 20 mg were both shown to be non-inferior to lansoprazole 15 mg in the FAS; the upper limits of 95%CIs for the differences between vonoprazan 10 mg or 20 mg and lansoprazole 15 mg were < 0, thus consistently indicating a statistical difference.

Subgroup analyses were conducted on the EE recurrence rates during the 24-wk maintenance period according to age, sex, smoking classification, disease severity, extent of CYP2C19 metabolism, and *H. pylori* infection status. Post-hoc analyses confirmed that the differences in recurrence rates following treatment with vonoprazan 10 mg or 20 mg versus lansoprazole 15 mg were significant among: patients who were: aged < 65 years; of either sex; never smokers; had any LA classification grade; CYP2C19 extensive metabolizers; or *H. pylori*-negative (Table 3).

Safety

The incidence of TEAEs during the 24-wk maintenance period was comparable between the maintenance treatment groups (Table 4). All-cause TEAEs during maintenance therapy were reported in 51.2%, 54.0%, and 58.8% of patients treated with lansoprazole 15 mg, vonoprazan 10 mg, and vonoprazan 20 mg, respectively. Nasopharyngitis was the most commonly reported TEAE in each treatment group (13.9%, 16.8%, and 13.2%, respectively; 14.7% of patients overall). The only other TEAE occurring in > 5% of patients in any treatment group was diarrhea, which was reported in 5.5% of those treated with lansoprazole 15 mg. TEAEs were mostly mild in severity. The incidence of drug-related TEAEs was 11.4%, 10.4%, and 10.3% with lansoprazole 15 mg, vonoprazan 10 mg and vonoprazan 20 mg, respectively. Very few serious TEAEs were reported with lansoprazole 15 mg, vonoprazan 10 mg, or vonoprazan 20 mg (4, 5, and 4

Table 3 Recurrence rate of erosive esophagitis within 24 wk: sub-group analysis according to baseline characteristics

	LPZ 15 mg	VPZ 10 mg			VPZ 20 mg		
	Estimate (%)[1]	Estimate (%)[1]	Difference[2] and 95%CI (%)	Fisher exact test, *P* value[3]	Estimate (%)[1]	Difference[2] and 95%CI (%)	Fisher exact test, *P* value[3]
Age (yr)							
< 65	14.4 (19/132)	4.3 (6/139)	-10.1 [-16.95, -3.20]	0.0056	0.0 (0/136)	-14.4 [-20.38, -8.41]	< 0.0001
⩾ 65 to < 75	21.7 (10/46)	7.0 (3/43)	-14.8 [-28.91, -0.62]	0.0711	7.0 (3/43)	-14.8 [-28.91, -0.62]	0.0711
⩾ 75	22.2 (4/18)	6.7 (1/15)	-15.6 [-38.54, 7.43]	0.3457	4.5 (1/22)	-17.7 [-38.76, 3.41]	0.1554
Sex							
Male	13.9 (19/137)	6.3 (10/159)	-7.6 [-14.49, -0.67]	0.0321	1.3 (2/159)	-12.6 [-18.65, -6.57]	< 0.0001
Female	23.7 (14/59)	0.0 (0/38)	-23.7 [-34.58, -12.87]	0.0007	4.8 (2/42)	-19.0 [-31.59, -6.35]	0.0120
Smoking classification							
Never smoked	22.4 (17/76)	1.9 (1/54)	-20.5 [-30.55, -10.48]	0.0006	5.0 (3/60)	-17.4 [-28.24, -6.50]	0.0062
Current smoker	20.0 (8/40)	6.6 (4/61)	-13.4 [-27.31, 0.42]	0.0588	0.0 (0/57)	-20.0 [-32.40, -7.60]	0.0005
Ex-smoker	10.0 (8/80)	6.1 (5/82)	-3.9 [-12.27, 4.47]	0.3998	1.2 (1/84)	-8.8 [-15.78, -1.84]	0.0160
Erosive esophagitis grade[4]							
LA Grade A/B	11.0 (17/155)	3.1 (5/159)	-7.8 [-13.44, -2.21]	0.0075	1.3 (2/158)	-9.7 [-14.92, -4.48]	0.0002
LA Grade C/D	39.0 (16/41)	13.2 (5/38)	-25.9 [-44.26, -7.47]	0.0114	4.7 (2/43)	-34.4 [-50.58, -18.17]	0.0001
CYP2C19 genotype							
Extensive metabolizers	19.6 (31/158)	5.4 (9/166)	-14.2 [-21.28, -7.11]	0.0001	1.8 (3/168)	-17.8 [-24.34, -11.33]	< 0.0001
Poor metabolizers	5.3 (2/38)	3.2 (1/31)	-2.0 [-11.48, 7.40]	1.0000	3.0 (1/33)	-2.2 [-11.43, 6.97]	1.0000
H. pylori infection status							
Positive	3.7 (1/27)	2.7 (1/37)	-1.0 [-9.84, 7.83]	1.0000	0.0 (0/27)	-3.7 [-10.83, 3.42]	1.0000
Negative	18.9 (32/169)	5.6 (9/160)	-13.3 [-20.21, -6.41]	0.0003	2.2 (4/179)	-16.7 [-22.99. -10.41]	< 0.0001

[1]Data expressed as percentages with number of subjects in parentheses; [2]Calculated for difference between VPZ group and LPZ 15 mg group; [3]*Post hoc* analysis; [4]LA Classification Grade of erosive esophagitis by principal investigator at baseline. CI: Confidence interval; LA: Los Angeles; LPZ: Lansoprazole; VPZ: Vonoprazan.

Table 4 Summary of treatment-emergent adverse events during maintenance treatment *n* (%)

	LPZ 15 mg (*n* = 201)		VPZ 10 mg (*n* = 202)		VPZ 20 mg (*n* = 204)	
	Events	Patients	Events	Patients	Events	Patients
Any TEAE	166	103 (51.2)	220	109 (54.0)	212	120 (58.8)
Drug-related TEAE	30	23 (11.4)	26	21 (10.4)	23	21 (10.3)
TEAE leading to study discontinuation	10	8 (4.0)	5	5 (2.5)	8	8 (3.9)
Any serious TEAE	4	4 (2.0)	5	5 (2.5)	4	4 (2.0)
Death	0	0 (0.0)	0	0 (0.0)	0	0 (0.0)
TEAEs reported in ⩾ 2% of patients in any group, irrespective of causal relationship to study medication, during maintenance treatment.						
TEAE (preferred term)	LPZ 15 mg		VPZ 10 mg		VPZ 20 mg	
Nasopharyngitis	28 (13.9)		34 (16.8)		27 (13.2)	
Diarrhea	11 (5.5)		6 (3.0)		5 (2.5)	
Upper respiratory tract inflammation	3 (1.5)		8 (4.0)		4 (2.0)	
Elevated blood creatinine phosphokinase	2 (1.0)		4 (2.0)		6 (2.9)	
Elevated blood triglycerides	6 (3.0)		1 (0.5)		5 (2.5)	
Fall	1 (0.5)		8 (4.0)		2 (1.0)	
Gastroenteritis	1 (0.5)		5 (2.5)		5 (2.5)	
Back pain	1 (0.5)		3 (1.5)		5 (2.5)	
Constipation	4 (2.0)		2 (1.0)		3 (1.5)	
Elevated ALT[1]	1 (0.5)		3 (1.5)		4 (2.0)	
Contusion	1 (0.5)		5 (2.5)		2 (1.0)	
Seasonal allergy	2 (1.0)		4 (2.0)		2 (1.0)	
Bronchitis	2 (1.0)		5 (2.5)		0 (0.0)	
Dizziness	1 (0.5)		4 (2.0)		2 (1.0)	
Abnormal liver function test[2]	1 (0.5)		2 (1.0)		4 (2.0)	
Abnormal hepatic function[2]	1 (0.5)		0 (0.0)		4 (2.0)	
Periodontitis	0 (0.0)		4 (2.0)		1 (0.5)	

[1]Recorded as a special-interest adverse event (SIAE) if ALT > 3 × the upper limit of normal (ULN); [2]Recorded as a SIAE if total bilirubin > 2 × ULN in two consecutive measurements. ALT: Alanine aminotransferase; LPZ: Lansoprazole; TEAE: Treatment-emergent adverse event; VPZ: Vonoprazan.

TEAEs, respectively); of the TEAEs reported, one case of atrial fibrillation and abnormal liver function test [elevated ALT and AST (303 U/L and 228 U/L, respectively)] in the vonoprazan 20 mg group were considered to be possibly related to the study drug. The abnormal liver function test was reported in a patient with a prior history of alcoholic hepatic steatosis, and led to his premature withdrawal from the study. As no specific cause was identified, a possible causal relationship with the study drug could not be ruled out.

With regard to SIAEs, one case each of abnormal liver function test [elevated ALT (179 IU/L) and AST (209 IU/L) owing to fenofibrate treatment for dyslipidemia and elevated ALT (137 IU/L), which was not associated with any symptoms and was considered possibly related to the study medication] were reported in the lansoprazole 15 mg group, while two cases of abnormal liver function test were reported in the vonoprazan 10 mg group [elevated ALT (467 IU/L) and AST (571 IU/L) in one patient, which were considered possibly related to the study medication; and elevated ALT (326 IU/L) and AST (127 IU/L) that occurred in a patient with concurrent hepatic steatosis and were considered unrelated to the study drug]. In the vonoprazan 20 mg group, elevated ALT (86 IU/L) and AST (47 IU/L) were reported at the final study visit in a patient with concurrent hyperlipidemia and hepatic steatosis. Having completed the study, the patient began to receive lansoprazole as maintenance treatment for EE. Four weeks after the patient had completed the study, a further ALT elevation (139 IU/L) was reported, which qualified as a SIAE. Two days later, dark urine and itching were reported. The patient's condition remained unresolved 2 mo later but, owing to the invasive nature of blood sampling, the investigator decided that further follow-up was unnecessary, and that the patient should receive routine medical care and further treatment as required. As the initial ALT and AST elevations had occurred during the maintenance period of the study, the possibility of a causal relationship with the study medication could not be ruled out. Also in the vonoprazan 20 mg group, elevated ALT (138 IU/L, which was considered to have been caused by pre-existing hepatic steatosis) was reported in one patient, and two cases of abnormal liver function test were noted; the first in a patient with ALT elevated to 161 IU/L following the consumption of a large quantity of alcohol, and the second being the case that is described above as a serious TEAE. All the SIAEs were considered resolved or resolving, with the exception of the case of abnormal hepatic function in the vonoprazan 20 mg group. This patient was followed up with routine medical care and treated as required.

Mean levels of serum gastrin, pepsinogen Ⅰ, and pepsinogen Ⅱ increased in all three groups after the start of maintenance therapy; as shown in Figure 2, the increases were greatest with vonoprazan 20 mg and least with lansoprazole 15 mg. Histopathologic examinations showed that the observed increases in serum gastrin were not associated with clinically significant effects on the gastric mucosa. Similar slight increases in the number and density of Grimelius-positive cells were observed from baseline to Week 24 in all treatment groups (Table 5), leading to increased ratios of Grimelius-positive cells to epithelial cells. No clinically significant treatment-related changes were noted in gastric mucosal cell density, or in the percentage and density of chromogranin A-, synaptophysin-, and Ki-67-positive cells (Table 5).

No clinically significant changes were observed in clinical laboratory test values, vital signs, or ECG findings in any group during maintenance treatment.

DISCUSSION

The findings of this study demonstrate the non-inferiority of once-daily maintenance therapy with vonoprazan 10 mg or 20 mg to lansoprazole 15 mg for the prevention of EE recurrence in Japanese patients with healed EE. The upper limits of 95%CI for the differences in EE recurrence rate between vonoprazan 10 mg or 20 mg and lansoprazole 15 mg at 24 wk of maintenance treatment were below 0, indicating a statistically significant difference.

The prevalence of EE has increased in Japan over the past few decades, owing to factors such as the adoption of a westernized lifestyle, the aging of the population, and the decreasing incidence of *H. pylori* infection[22]. Moreover, endoscopic EE remission rates after healing following PPI treatment have been shown to be markedly lower in patients with more severe (LA grades C/D) *vs* milder disease[23]. In the current study, recurrence rates in patients with baseline LA grade C/D EE were significantly reduced with vonoprazan 10 mg (13.2%) and 20 mg (4.7%) *vs* lansoprazole 15 mg (39.0%) (P = 0.0114 and P = 0.0001, respectively). In addition, treatment with both vonoprazan 10 mg and 20 mg reduced recurrence rates compared with lansoprazole 15 mg among CYP2C19 extensive metabolizers (5.4% and 1.8%, respectively, *vs* 19.6%). These findings support the hypothesis that vonoprazan provides clinical benefits through potent and sustained gastric suppression in difficult-to-treat EE subgroups with more severe disease, as well as in those with milder disease.

The doses of vonoprazan and lansoprazole selected for evaluation in this study were consistent with the doses of acid suppressants commonly used for the maintenance of healed EE. PPIs are well-established in this indication, typically being approved for administration at either the same or half the dose approved for the healing of EE[24-26]. As vonoprazan is an acid suppressant, we decided to evaluate both the clinically recommended dose for EE healing and half that dose as maintenance regimens in this study. Our group previously carried out a phase Ⅱ dose-ranging study of vonoprazan in 732 Japanese patients with EE[27]. Vonoprazan, administered at once-daily doses of 5-40 mg, was found to be non-inferior to lansoprazole 30 mg once daily with respect to the rate of endoscopically-confirmed EE healing after 4 wk of treatment. Moreover, the rate of EE healing in patients with LA grade C/D EE was > 95% with vonoprazan doses of ⩾ 20 mg, *vs* 87% with lansoprazole 30 mg. The safety profile of vonoprazan at all administered doses was similar to that of lansoprazole 30 mg. On

Table 5 Histopathology of gastric mucosa: neuroendocrine cell density (/mm^2)

	LPZ 15 mg		VPZ 10 mg		VPZ 20 mg	
	n	Mean (SD)	*n*	Mean (SD)	*n*	Mean (SD)
Epithelial cells (× 10^3)						
Baseline	28	1.58 (0.4831)	29	1.82 (0.3188)	28	1.74 (0.3943)
Week 24	24	1.63 (0.2689)	26	1.71 (0.4304)	28	1.54 (0.4744)
Grimelius-positive cells (× 10^2)						
Baseline	28	0.716 (0.3997)	29	0.705 (0.5562)	28	0.656 (0.3778)
Week 24	24	1.06 (0.2676)	26	1.07 (0.3858)	28	0.943 (0.4260)
Chromogranin A-positive cells (× 10^2)						
Baseline	28	1.35 (0.6625)	29	1.25 (0.7250)	28	1.35 (0.7073)
Week 24	24	1.35 (0.2962)	26	1.31 (0.4595)	28	1.20 (0.5041)
Synaptophysin-positive cells (× 10^2)						
Baseline	28	1.73 (0.7005)	29	1.73 (0.8123)	28	1.83 (0.9076)
Week 24	24	1.58 (0.3716)	26	1.55 (0.4490)	28	1.45 (0.6173)
Ki-67-positive cells (× 10^2)						
Baseline	28	1.44 (0.8192)	29	1.10 (0.6624)	28	1.32 (0.5513)
Week 24	24	1.14 (0.5037)	26	1.09 (0.4075)	28	1.05 (0.4853)

LPZ: Lansoprazole; SD: Standard deviation; VPZ: Vonoprazan.

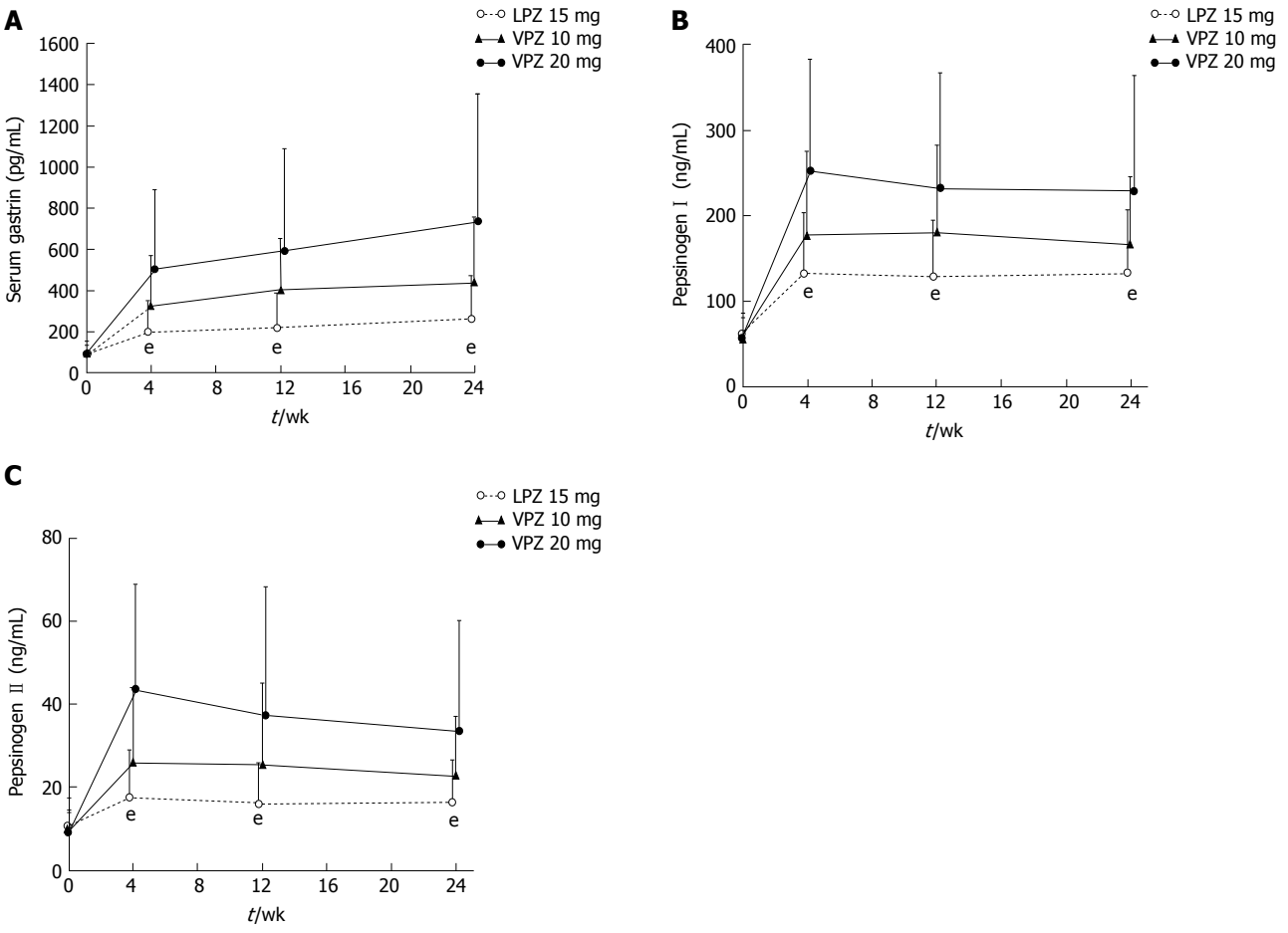

Figure 2 Time course of serum gastrin, pepsinogen Ⅰ, and pepsinogen Ⅱ concentrations. Data expressed as arithmetic mean ± SD. $^e P < 0.0001$ for VPZ 10 mg or 20 mg *vs* LPZ 15 mg. LPZ: Lansoprazole; SD: Standard deviation; VPZ: Vonoprazan.

the basis of these findings, 20 mg once daily was established as the clinically recommended dose of vonoprazan for the treatment of EE[27]. Therefore, the doses of vonoprazan evaluated as maintenance therapy in the present study were 20 and 10 mg once daily - representing the clinically recommended dose for the treatment of EE and half that dose. Lansoprazole was evaluated at the 15 mg dose that is approved for the maintenance of healed EE[26].

Vonoprazan 10 and 20 mg demonstrated similar safety profiles to lansoprazole 15 mg during the 24-wk maintenance period. All three investigated maintenance

regimens were well tolerated overall, with only a small number of TEAE-related withdrawals reported in each group. No new safety signals were identified for vonoprazan during the study. The increase in serum gastrin that we observed was not associated with clinically significant effects on the gastric mucosa. This, as well as the observed increases in pepsinogen Ⅰ and Ⅱ, were likely a negative feedback effect caused by the increase in intragastric pH that resulted from treatment with lansoprazole or vonoprazan. Histopathology of the gastric mucosa revealed no notable effects of the study drugs on neuroendocrine cells between baseline and Week 24, although the study was too short to rule out the possibility of clinically significant histopathologic changes occurring in the gastric mucosa over the long term. Thus, longer-term studies (> 1 year) are required to monitor any potential effects of vonoprazan on gastric mucosa.

This study was limited by its relatively short duration; nevertheless, the findings reported in this paper build on those from prior studies by our group, which investigated the efficacy and safety of vonoprazan in patients with acid-related disorders. In addition to the aforementioned phase Ⅱ dose-ranging study, which demonstrated the non-inferiority of vonoprazan 5-40 mg once daily to lansoprazole 30 mg once daily in terms of rates of EE healing over 4 wk[27], a recent phase Ⅲ trial confirmed the non-inferiority of vonoprazan 20 mg to lansoprazole 30 mg in the same indication within an 8-wk period[18]. Vonoprazan was found to be highly effective even among CYP2C19 extensive metabolizers and patients with baseline EE of LA Classification grade C/D. Other studies have also shown promising results with vonoprazan in the treatment of gastric or duodenal ulcers[28], and in the prevention of recurrent ulcers of these types in patients receiving low-dose aspirin or NSAIDs (ClinicalTrials.gov. identifiers NCT01452763, NCT01456247, NCT01452750, and NCT01456260).

While the primary objective of the present study was to verify the non-inferiority of vonoprazan to lansoprazole, the two-sided 95%CI for the difference between each vonoprazan group and the lansoprazole group were calculated as pre-planned for the primary analysis. A *post-hoc* Fisher's exact test was also performed as a sensitivity analysis to further support the results of the primary assessment using the CIs. These analyses confirmed that vonoprazan provided more consistent maintenance of EE healing at doses of 10 mg and 20 mg than lansoprazole 15 mg, even among CYP2C19 extensive metabolizers and patients with LA grade C/D EE. These findings suggest that vonoprazan may represent a viable alternative to PPIs in maintaining EE healing, with two doses being available for physicians to choose from.

In conclusion, this phase Ⅲ trial confirmed the non-inferiority of vonoprazan 10 mg and 20 mg to lansoprazole 15 mg once daily in preventing EE recurrence during 24 wk of maintenance treatment in Japanese patients. The safety profile of vonoprazan at the administered doses was similar to that of lansoprazole 15 mg.

ARTICLE HIGHLIGHTS

Research background

Proton-pump inhibitors (PPIs) such as lansoprazole are widely accepted as the treatment of choice for acid-related disorders, including erosive esophagitis (EE). Nevertheless, agents of this class are associated with notable shortcomings, which include: significant inter-individual variability in the time to onset of action; reduced night-time efficacy in preventing acid regurgitation, leading to nocturnal acid breakthrough; and differences in plasma concentrations and acid-inhibitory effects in extensive versus poor CYP2C19 metabolizers.

Vonoprazan fumarate (TAK-438) belongs to a relatively new class of acid suppressants known as potassium-competitive acid blockers (P-CABs), which, by virtue of their novel mechanism of action, offer a number of potential advantages over PPIs in the treatment of acid-related disorders. In animal studies, vonoprazan provided more potent and sustained suppression of gastric acid secretion than lansoprazole, while studies in healthy human volunteers demonstrated rapid, sustained, and dose-related suppression of 24-h gastric acid secretion. The present study adds to these earlier findings by confirming that vonoprazan is non-inferior to lansoprazole in preventing EE recurrence in Japanese patients with healed EE.

Research motivation

As a result of the increasingly widespread adoption of a westernized lifestyle and the general aging of the population, EE is now the most common acid-related disorder in Japan. Typical symptoms of EE include heartburn, acid reflux, difficulty swallowing, and sore throat, which can negatively impact patients' quality of life. In Japan, as elsewhere, PPIs remain the mainstay of treatment for EE and other acid-related disorders; however, in view of the limitations of PPIs mentioned above, there is a need for new treatment modalities that offer greater efficacy and more consistent outcomes. Any treatments that improve outcomes in EE may also be beneficial in gastroesophageal reflux disease, duodenal ulcer, and other acid-related disorders, and could become the focus of a new area of research.

Research objectives

The main objective of the research described in this paper was to demonstrate that the efficacy of vonoprazan in preventing EE recurrence is comparable to that of lansoprazole at its established maintenance dose. This objective was realized, with the results obtained confirming that vonoprazan, at doses of 10 and 20 mg once daily, is non-inferior to lansoprazole 15 mg once daily as maintenance therapy for healed EE. In addition, the safety profile of vonoprazan was shown to be similar to that of lansoprazole at the doses investigated. These findings suggest that vonoprazan may be a viable alternative to PPIs in the maintenance of EE healing, and provide a basis for future clinical trials to establish the optimal positioning of this new agent in the treatment of acid-related disorders.

Research methods

To establish the non-inferiority of vonoprazan 10 and 20 mg to lansoprazole 15 mg as maintenance therapy in Japanese patients with endoscopically-confirmed healed EE, we designed and conducted a multicenter, double-blind, randomized, phase Ⅲ clinical trial. Eligible patients received vonoprazan 10 or 20 mg, or lansoprazole 15 mg, once daily for 24 wk. The primary and secondary endpoints were the rate of EE recurrence at Weeks 24 and 12, respectively; safety outcomes were also evaluated. Based on EE recurrence rates in previous studies, it was calculated that 174 patients per treatment group would be required to provide > 90% power to confirm the non-inferiority of vonoprazan 10 and 20 mg to lansoprazole 15 mg.

Research results

We found that vonoprazan, administered at a dose of 10 or 20 mg once daily, is non-inferior to lansoprazole 15 mg once daily in maintaining EE healing in Japanese patients over a period of 24 wk, and demonstrates a comparable safety profile. Post-hoc analyses also confirmed that both doses of vonoprazan

investigated provide more consistent EE healing than lansoprazole, even in patients who are CYP2C19 extensive metabolizers and those with severe (Los Angeles grade C/D) EE. These results add to our previous findings that vonoprazan 5-40 mg once daily is non-inferior to lansoprazole 30 mg once daily in terms of EE healing rates over a 4-wk period, and that vonoprazan 20 mg once daily is non-inferior to lansoprazole 30 mg once daily in terms of 8-wk EE healing rates. As the maintenance period in this study was relatively short, further studies are needed to establish the long-term efficacy and safety characteristics of vonoprazan in the maintenance of EE healing.

Research conclusions

To our knowledge, this study is the first to confirm that vonoprazan is non-inferior to lansoprazole once daily in maintaining EE healing in Japanese patients. Importantly, it is also the first to show that vonoprazan is more consistent in maintaining EE healing, even in extensive CYP2C19 metabolizers and patients with more severe disease. These findings appear to confirm that the novel mechanism of action of vonoprazan is associated with advantages versus PPIs in the treatment of acid-related disorders, and suggest that vonoprazan could be an important new addition to the range of treatment options available to clinicians.

Research perspectives

This study confirms that vonoprazan demonstrates efficacy comparable with that of lansoprazole not only in healing EE, but also in maintaining the healing of EE over 24 wk. Future research should focus on evaluating the longer-term efficacy and safety of vonoprazan in this indication. In addition to randomized controlled trials, observational studies should be undertaken to gather valuable real-life data and inform decisions regarding the optimal positioning of vonoprazan in the management of EE.

ACKNOWLEDGMENTS

The authors acknowledge all participating patients and their families, as well as all staff at the 55 investigational sites. The authors also acknowledge Sandralee Lewis PhD, working on behalf of FireKite (an Ashfield Company, part of UDG Healthcare plc), who provided medical writing assistance during the development of this manuscript, which was funded by Takeda Pharmaceutical Company Limited and complied with Good Publication Practice 3 ethical guidelines (Battisti *et al*. *Ann Intern Med* 2015; 163: 461-4 [PMID: 26259067]). The results of the study were previously presented at the Digestive Disease Week (DDW) 2014, and at the Japanese Digestive Disease Week (JDDW) 2014.

REFERENCES

1 **Maradey-Romero C**, Fass R. New and future drug development for gastroesophageal reflux disease. *J Neurogastroenterol Motil* 2014; **20**: 6-16 [PMID: 24466441 DOI: 10.5056/jnm.2014.20.1.6]
2 **Pace F**, Tonini M, Pallotta S, Molteni P, Porro GB. Systematic review: maintenance treatment of gastro-oesophageal reflux disease with proton pump inhibitors taken 'on-demand'. *Aliment Pharmacol Ther* 2007; **26**: 195-204 [PMID: 17593065 DOI: 10.1111/j.1365-2036.2007.03381.x]
3 **Hershcovici T**, Fass R. Gastro-oesophageal reflux disease: beyond proton pump inhibitor therapy. *Drugs* 2011; **71**: 2381-2389 [PMID: 22117130 DOI: 10.2165/11597300-000000000-00000]
4 **Fass R**. Alternative therapeutic approaches to chronic proton pump inhibitor treatment. *Clin Gastroenterol Hepatol* 2012; **10**: 338-345; quiz e39-40 [PMID: 22178462 DOI: 10.1016/j.cgh.2011.12.020]
5 **Hungin AP**, Hill C, Molloy-Bland M, Raghunath A. Systematic review: Patterns of proton pump inhibitor use and adherence in gastroesophageal reflux disease. *Clin Gastroenterol Hepatol* 2012; **10**: 109-116 [PMID: 21782770 DOI: 10.1016/j.cgh.2011.07.008]
6 **Fass R**, Shapiro M, Dekel R, Sewell J. Systematic review: proton-pump inhibitor failure in gastro-oesophageal reflux disease--where next? *Aliment Pharmacol Ther* 2005; **22**: 79-94 [PMID: 16011666 DOI: 10.1111/j.1365-2036.2005.02531.x]
7 **El-Serag H**, Becher A, Jones R. Systematic review: persistent reflux symptoms on proton pump inhibitor therapy in primary care and community studies. *Aliment Pharmacol Ther* 2010; **32**: 720-737 [PMID: 20662774 DOI: 10.1111/j.1365-2036.2010.04406.x]
8 **Andersson K**, Carlsson E. Potassium-competitive acid blockade: a new therapeutic strategy in acid-related diseases. *Pharmacol Ther* 2005; **108**: 294-307 [PMID: 16000224 DOI: 10.1016/j.pharmthera.2005.05.005]
9 **Cederberg C**, Lind T, Röhss K, Olbe L. Comparison of once-daily intravenous and oral omeprazole on pentagastrin-stimulated acid secretion in duodenal ulcer patients. *Digestion* 1992; **53**: 171-178 [PMID: 1291405 DOI: 10.1159/000200992]
10 **Dammann HG**, Burkhardt F. Pantoprazole versus omeprazole: influence on meal-stimulated gastric acid secretion. *Eur J Gastroenterol Hepatol* 1999; **11**: 1277-1282 [PMID: 10563540]
11 **Shin JM**, Inatomi N, Munson K, Strugatsky D, Tokhtaeva E, Vagin O, Sachs G. Characterization of a novel potassium-competitive acid blocker of the gastric H,K-ATPase, 1-[5-(2-fluorophenyl)-1-(pyridin-3-ylsulfonyl)-1H-pyrrol-3-yl]-N-methylmethanamine monofumarate (TAK-438). *J Pharmacol Exp Ther* 2011; **339**: 412-420 [PMID: 21828261 DOI: 10.1124/jpet.111.185314]
12 **Hori Y**, Imanishi A, Matsukawa J, Tsukimi Y, Nishida H, Arikawa Y, Hirase K, Kajino M, Inatomi N. 1-[5-(2-Fluorophenyl)-1-(pyridin-3-ylsulfonyl)-1H-pyrrol-3-yl]-N-methylmethanamine monofumarate (TAK-438), a novel and potent potassium-competitive acid blocker for the treatment of acid-related diseases. *J Pharmacol Exp Ther* 2010; **335**: 231-238 [PMID: 20624992 DOI: 10.1124/jpet.110.170274]
13 **Matsukawa J**, Hori Y, Nishida H, Kajino M, Inatomi N. A comparative study on the modes of action of TAK-438, a novel potassium-competitive acid blocker, and lansoprazole in primary cultured rabbit gastric glands. *Biochem Pharmacol* 2011; **81**: 1145-1151 [PMID: 21371447 DOI: 10.1016/j.bcp.2011.02.009]
14 **Hori Y**, Matsukawa J, Takeuchi T, Nishida H, Kajino M, Inatomi N. A study comparing the antisecretory effect of TAK-438, a novel potassium-competitive acid blocker, with lansoprazole in animals. *J Pharmacol Exp Ther* 2011; **337**: 797-804 [PMID: 21411494 DOI: 10.1124/jpet.111.179556]
15 **Sakurai Y**, Nishimura A, Kennedy G, Hibberd M, Jenkins R, Okamoto H, Yoneyama T, Jenkins H, Ashida K, Irie S, Täubel J. Safety, Tolerability, Pharmacokinetics, and Pharmacodynamics of Single Rising TAK-438 (Vonoprazan) Doses in Healthy Male Japanese/non-Japanese Subjects. *Clin Transl Gastroenterol* 2015; **6**: e94 [PMID: 26111126 DOI: 10.1038/ctg.2015.18]
16 **Jenkins H**, Sakurai Y, Nishimura A, Okamoto H, Hibberd M, Jenkins R, Yoneyama T, Ashida K, Ogama Y, Warrington S. Randomised clinical trial: safety, tolerability, pharmacokinetics and pharmacodynamics of repeated doses of TAK-438 (vonoprazan), a novel potassium-competitive acid blocker, in healthy male subjects. *Aliment Pharmacol Ther* 2015; **41**: 636-648 [PMID: 25707624 DOI: 10.1111/apt.13121]
17 **Lauritsen K**, Devière J, Bigard MA, Bayerdörffer E, Mózsik G, Murray F, Kristjánsdóttir S, Savarino V, Vetvik K, De Freitas D, Orive V, Rodrigo L, Fried M, Morris J, Schneider H, Eklund S, Larkö A. Esomeprazole 20 mg and lansoprazole 15 mg in maintaining healed reflux oesophagitis: Metropole study results. *Aliment Pharmacol Ther* 2003; **17** Suppl 1: 24; discussion 25-24; discussion 27 [PMID: 12614304 DOI: 10.1046/j.1365-2036.17.s1.7.x]
18 **Ashida K**, Sakurai Y, Hori T, Kudou K, Nishimura A, Hiramatsu N, Umegaki E, Iwakiri K. Randomised clinical trial: vonoprazan, a novel potassium-competitive acid blocker, vs. lansoprazole for the healing of erosive oesophagitis. *Aliment Pharmacol Ther* 2016; **43**: 240-251 [PMID: 26559637 DOI: 10.1111/apt.13461]

19 **Kahrilas PJ**, Dent J, Lauritsen K, Malfertheiner P, Denison H, Franzén S, Hasselgren G. A randomized, comparative study of three doses of AZD0865 and esomeprazole for healing of reflux esophagitis. *Clin Gastroenterol Hepatol* 2007; **5**: 1385-1391 [PMID: 17950677 DOI: 10.1016/j.cgh.2007.08.014]
20 **Endo M**, Sugihara K. [Long-term maintenance treatment of reflux esophagitis resistant to H2-RA with PPI (lansoprazole)]. *Nihon Rinsho* 2000; **58**: 1865-1870 [PMID: 11004817]
21 **Farrington CP**, Manning G. Test statistics and sample size formulae for comparative binomial trials with null hypothesis of non-zero risk difference or non-unity relative risk. *Stat Med* 1990; **9**: 1447-1454 [PMID: 2281232 DOI: 10.1002/sim.4780091208]
22 **Fujiwara Y**, Arakawa T. Epidemiology and clinical characteristics of GERD in the Japanese population. *J Gastroenterol* 2009; **44**: 518-534 [PMID: 19365600 DOI: 10.1007/s00535-009-0047-5]
23 **Higuchi K**, Joh T, Nakada K, Haruma K. Is proton pump inhibitor therapy for reflux esophagitis sufficient?: a large real-world survey of Japanese patients. *Intern Med* 2013; **52**: 1447-1454 [PMID: 23812190 DOI: 10.2169/internalmedicine.52.0349]
24 **AstraZeneca Company**. NEXIUM prescribing information. Accessed July 12, 2017 Available from: URL: http://www.info.pmda.go.jp/go/pack/2329028F1023_1_28/
25 **Eisai Company Limited**. Pariet prescribing information. Accessed July 12, 2017 Available from: URL: http://www.info.pmda.go.jp/go/pack/2329029M1027_1_09/
26 **Takeda Pharmaceutical Company Limited**. Takepron prescribing information. Accessed July 12, 2017 Available from: URL: http://www.info.pmda.go.jp/go/pack/2329023M1020_1_23/
27 **Ashida K**, Sakurai Y, Nishimura A, Kudou K, Hiramatsu N, Umegaki E, Iwakiri K, Chiba T. Randomised clinical trial: a dose-ranging study of vonoprazan, a novel potassium-competitive acid blocker, vs. lansoprazole for the treatment of erosive oesophagitis. *Aliment Pharmacol Ther* 2015; **42**: 685-695 [PMID: 26201312 DOI: 10.1111/apt.13331]
28 **Miwa H**, Uedo N, Watari J, Mori Y, Sakurai Y, Takanami Y, Nishimura A, Tatsumi T, Sakaki N. Randomised clinical trial: efficacy and safety of vonoprazan vs. lansoprazole in patients with gastric or duodenal ulcers - results from two phase 3, non-inferiority randomised controlled trials. *Aliment Pharmacol Ther* 2017; **45**: 240-252 [PMID: 27891632 DOI: 10.1111/apt.13876]

P- Reviewer: Chiba T, Esmat S, Kim GH, Jonaitis LV, Shimatani T
S- Editor: Gong ZM **L- Editor**: A **E- Editor**: Huang Y

World Journal of Gastroenterology

Submit a Manuscript: http://www.f6publishing.com

World J Gastroenterol 2018 April 14; 24(14): 1562-1578

DOI: 10.3748/wjg.v24.i14.1562

ISSN 1007-9327 (print) ISSN 2219-2840 (online)

META-ANALYSIS

Application of enhanced recovery after gastric cancer surgery: An updated meta-analysis

Liu-Hua Wang, Ren-Fei Zhu, Cheng Gao, Shou-Lin Wang, Li-Zong Shen

Liu-Hua Wang, Ren-Fei Zhu, Cheng Gao, Li-Zong Shen, Division of Gastrointestinal Surgery, Department of General Surgery, First Affiliated Hospital, Nanjing Medical University, Nanjing 210029, Jiangsu Province, China

Liu-Hua Wang, Department of General Surgery, Yizheng People's Hospital, Yangzhou 211400, Jiangsu Province, China

Shou-Lin Wang, School of Public Health, Nanjing Medical University, Nanjing 211166, Jiangsu Province, China

ORCID number: Liu-Hua Wang (0000-0003-1124-0707); Ren-Fei Zhu (0000-0003-1351-0096); Cheng Gao (0000-0001-5549-1327); Shou-Lin Wang (0000-0003-3070-7560); Li-Zong Shen (0000-0002-9046-6140).

Author contributions: Wang LH, Zhu RF and Gao C contributed equally to this work; Wang LH and Shen LZ conceived and designed the updated meta-analysis; Wang LH, Zhu RF and Gao C carried out the literature search, data extraction and statistical analysis, and drafted this manuscript; Wang SL and Shen LZ were responsible for retrieval strategy and assessment of the risk of bias, and provided critical supervision and revision of this article; all authors conducted detailed review and revision for the data and approved the final version of the manuscript.

Supported by the National Natural Science Foundation of China, No. 81272711 to Shen LZ; the Priority Academic Program Development of Jiangsu Higher Education Institutions, No. JX10231801 to Shen LZ; and the Key Medical Talents Program of Jiangsu Province, No. ZDRCA2016014 to Shen LZ.

Conflict-of-interest statement: The authors declare that they have no conflicts of interest.

PRISMA 2009 Checklist statement: All authors have read the PRISMA 2009 Checklist, and the manuscript was carefully prepared and revised based on the PRISMA 2009 Checklist.

Manuscript source: Unsolicited manuscript

Correspondence to: Li-Zong Shen, MD, PhD, Chief Doctor, Professor, Division of Gastrointestinal Surgery, Department of General Surgery, First Affiliated Hospital, Nanjing Medical University, 300 Guangzhou Road, Nanjing 210029, Jiangsu Province, China. shenlz@njmu.edu.cn

Telephone: +86-25-83724440

Received: February 5, 2018
Peer-review started: February 6, 2018
First decision: February 26, 2018
Revised: March 3, 2018
Accepted: March 7, 2018
Article in press: March 6, 2018
Published online: April 14, 2018

Abstract

AIM

To provide an updated assessment of the safety and efficacy of enhanced recovery after surgery (ERAS) protocols in elective gastric cancer (GC) surgery.

METHODS

PubMed, Medline, EMBASE, World Health Organization International Trial Register, and Cochrane Library were searched up to June 2017 for all available randomized controlled trials (RCTs) comparing ERAS protocols and standard care (SC) in GC surgery. Thirteen RCTs, with a total of 1092 participants, were analyzed in this study, of whom 545 underwent ERAS protocols and 547 received SC treatment.

RESULTS

No significant difference was observed between ERAS and control groups regarding total complications (P = 0.88), mortality (P = 0.50) and reoperation (P = 0.49).

The incidence of pulmonary infection was significantly reduced (P = 0.03) following gastrectomy. However, the readmission rate after GC surgery nearly tripled under ERAS (P = 0.009). ERAS protocols significantly decreased the length of postoperative hospital stay (P < 0.00001) and medical costs (P < 0.00001), and accelerated bowel function recovery, as measured by earlier time to the first flatus (P = 0.0004) and the first defecation (P < 0.0001). Moreover, ERAS protocols were associated with a lower level of serum inflammatory response, higher serum albumin, and superior short-term quality of life (QOL).

CONCLUSION

Collectively, ERAS results in accelerated convalescence, reduction of surgical stress and medical costs, improved nutritional status, and better QOL for GC patients. However, high-quality multicenter RCTs with large samples and long-term follow-up are needed to more precisely evaluate ERAS in radical gastrectomy.

Key words: Enhanced recovery after surgery; Safety; Gastric cancer; Efficacy; Meta-analysis

Core tip: Enhanced recovery after surgery (ERAS) has emerged as an optimal perioperative strategy for improving clinical outcomes in gastric cancer surgery. However, numerous controversies exist with regard to ERAS practice after gastrectomy. To our knowledge, this study is the largest meta-analysis of randomized controlled trials to date, incorporating 1092 participants, of whom 545 received ERAS protocols and 547 received standard care, to assess the role of ERAS for radical gastrectomy. Our review clarified that ERAS results in accelerated convalescence, reduction of surgical stress and medical costs, improved nutritional status, and better quality of life for gastric cancer patients.

Wang LH, Zhu RF, Gao C, Wang SL, Shen LZ. Application of enhanced recovery after gastric cancer surgery: An updated meta-analysis. *World J Gastroenterol* 2018; 24(14): 1562-1578 Available from: URL: http://www.wjgnet.com/1007-9327/full/v24/i14/1562.htm DOI: http://dx.doi.org/10.3748/wjg.v24.i14.1562

INTRODUCTION

Enhanced recovery after surgery (ERAS), or fast-track surgery program, which was pioneered by Kehlet and Wilmore in the late 1990s, intends to attenuate surgical stress and accelerate postoperative functional recovery[1,2]. ERAS protocols involve a series of perioperative evidence-based interventions, the core elements of which include preoperative short fasting and carbohydrate-loaded fluids, intraoperative epidural anesthesia, minimally invasive procedures and fluid restriction, postoperative pain management, nutritional care and early ambulation[3-5]. Multimodal optimizing perioperative procedures were explored initially in the setting of elective colorectal resections, resulting in a significant reduction in overall hospital stay from 8-12 d to 2-5 d under the standard discharge criteria for conventional care[6,7]. Since then, ERAS concepts have become widely recognized and applied gradually to clinical practice. Currently, accumulating evidence highlights that the implementation of ERAS protocols in multiple surgical disciplines significantly reduces morbidity and mortality, while improving clinical outcomes without compromising patient safety[8-10].

Gastric cancer (GC) remains a major health problem in China and worldwide, and radical gastrectomy remains the most likely approach to cure GC. However, conventional perioperative care is associated with a high risk of morbidity after radical surgery, ranging from 12.5% to 39%[11-13]. Moreover, due to malnutrition of patients with gastric neoplasms and chronic comorbidities, perioperative mortality can reach up to 8.8%[14]. Postoperative complications result in prolonged inflammatory response, which is considered to have a negative influence not only on the overall survival (OS) but also on the disease-specific mortality of patients undergoing gastrectomy, even if the carcinoma is radically resected[15].

Given the strong evidence and recommendations for colorectal cancer, the application of ERAS protocols for gastrectomy procedures has been investigated in several studies[16-19]. ERAS principles combined with laparoscopic treatment for GC lead to satisfactory clinical outcomes[20-22], even in elderly patients[23,24]. Several meta-analyses have revealed that ERAS pathways in GC patients reduce the duration of hospital stay and medical costs without significantly increasing complications and hospital readmission[25-28], and the ERAS Society issued consensus guidelines for perioperative care after elective gastrectomy for GC in 2014[29].

However, there still remain numerous controversies, limitations and difficulties in ERAS practice after gastrectomy. Following the recent publication of two related high-level randomized controlled trials (RCTs)[22,30], we conducted an updated systematic review and meta-analysis to thoroughly assess the safety and efficacy of ERAS application in GC patients.

MATERIALS AND METHODS

Literature search

A comprehensive literature search in PubMed, Medline, EMBASE, World Health Organization International Trial Registry platform, and Cochrane Library was performed, until June 2017, independently to identify all available publications comparing the ERAS program with standard perioperative care (SC) for GC patients undergoing gastrectomy. The medical subject heading (MeSH) terms and free text terms searched

for, individually and in combination, were as follows: "fast track surgery" OR "accelerated rehabilitation" OR "enhanced recovery" OR "ERAS" OR "multimodal perioperative care" AND "gastric cancer" OR "stomach carcinoma" OR "gastrectomy" OR "gastric resection." This search strategy was able to identify all potential publications involving humans, without language restriction. Reference lists of all eligible articles were also scrutinized to identify any other related studies. Furthermore, bibliographies of systematic reviews or meta-analyses on this issue were hand-searched for additional articles that the electronic retrieval failed to capture.

Inclusion and exclusion criteria

The inclusion criteria for this study were: (1) evaluation of ERAS in comparison with traditional SC; (2) RCTs; (3) detailed patient data and outcomes available; (4) ERAS protocols composed of at least eight elements from consensus guidelines[29]; and (5) follow-up for at least 14 d after discharge. When more than one study reporting the same patient cohort was included in several publications, only the most recent or complete study was included.

The exclusion criteria were as follows: (1) non-comparative studies; (2) case-controlled trials, cohort studies, or retrospective studies; (3) application of less than eight items of ERAS; (4) no follow-up after discharge; and (5) other documentations that did not meet the inclusion criteria.

Study selection and data extraction

Following identification of citations from all potentially eligible studies, two investigators independently retrieved the full-text articles according to the inclusion criteria. Any discrepancies or divergences concerning inclusion were settled through discussion with a third reviewer until consensus was reached.

Data were extracted using a double-extraction method from each eligible study by the two investigators. Outcomes included morbidity, mortality, rates of readmission and reoperation, length of postoperative hospital stay (POHS), duration of flatus and defecation, medical costs, and postoperative inflammatory response and nutritional status, such as determined by serum C-reactive protein (CRP), interleukin-6 (IL-6) and serum albumin (ALB) concentrations.

Assessment of risk of bias

Another two investigators separately assessed the quality of identified RCTs using the criteria addressed in the Cochrane Collaboration[31]. The evaluation indices contained several aspects across randomization, allocation concealment, blinding of participants and personnel, blinding of outcome assessment, incomplete outcome data, selective outcome reporting, and other bias. Risk of bias in each domain listed was graded as "high risk," "low risk," or "unclear."

Statistical analysis

Statistical analysis was performed using the software package Review Manager Version 5.3.3 (Nordic Cochrane Centre, The Cochrane Collaboration, Copenhagen, Denmark) and STATA version 12 (Stata Corp LP, College Station, TX, United States). Pooled risk ratio (RR) with 95% confidence interval (CI) was utilized to analyze dichotomous data, while continuous data were analyzed as mean differences (MDs) with 95%CIs. Heterogeneity was evaluated using the chi-square test, for which $P < 0.1$ was considered statistically significant. The I^2 value was used to quantify the impact of heterogeneity on each analysis. If the test of heterogeneity was statistically significant, the random-effects model was used; otherwise, a fixed-effects model was used. When the study did not report specific values for mean and standard deviation (SD), these were estimated using median and range based on the methods previously described[32]. In short, the median was used as a substitute for the mean. When the sample size was greater than 70, SD was estimated as range/6, and when the sample size was 15-69, SD was calculated as range/4. In the case where the interquartile range (IQR) was available, the range was estimated to be the median ± IQR.

RESULTS

Included studies

The flow chart for the selection of literature according to the predefined retrieval strategies is shown in Figure 1. Ten studies[21-24,30,33-37] published between 2010 and 2017 met the inclusion criteria. Two studies[24,34] consisted of four groups comparing ERAS protocols and SC in laparoscopic or open radical gastrectomy, respectively, for stomach cancer, while another[23] comprised four groups comparing ERAS protocols and SC in adults (aged 45-74 years) or elderly individuals (aged 75-89 years) undergoing open gastrectomy for GC. These three studies were considered to be six independent studies with reference to previous reports[26,28]. Consequently, 13 RCTs from these 10 studies were included in the current systematic review and meta-analysis.

Characteristics and methodological quality

The main characteristics of the included studies are detailed in Table 1. All studies were from a single center involving a total of 1092 participants, of whom 545 underwent the ERAS protocol and 547 received SC treatment. The sample size ranged from 41 to 256, and four studies contained more than 100 patients[22,23,30,33]. Table 2 lists the relevant elements involved in these studies regarding the implementation of ERAS pathways based on the consensus conducted in RCTs. Surgical procedures for GC with curative intent involved proximal gastrectomy, distal gastrectomy, and total gastrectomy. These included studies were implemented predominantly in Asia (China, South

Table 1 Main characteristics of the included studies

Study	Year	Sample size		Age in yr		Sex, male/female		Approach	Neoadjuvant chemotherapy	Follow-up (d)
		ERAS	SC	ERAS	SC	ERAS	SC			
Abdikarim *et al*[21]	2015	30	31	63 ± 12	62 ± 11	21/9	20/11	Lap	No	30
Bu *et al*[23]-Adult	2015	64	64	62.4 ± 7.8	63.0 ± 7.4	31/33	35/29	Open	No	30
Bu *et al*[23]-Elderly	2015	64	64	80.1 ± 4.0	79.6 ± 3.5	37/27	40/24	Open	No	30
Chen Hu *et al*[34]-Lap	2012	19	22	59 (49-71)	62.5 (45-72)	10/9	10/12	Lap	No	28
Chen Hu *et al*[34]-Open	2012	21	20	62.5 (45-72)	64.5 (49-75)	9/12	12/8	Open	No	28
Feng *et al*[33]	2013	59	60	55.0 ± 11.4	55.8 ± 10.1	41/18	44/16	Open	No	28
Kim *et al*[35]	2012	22	22	52.6 ± 11.6	57.5 ± 14.5	13/9	15/7	Lap	-	14
Liu *et al*[36]	2010	33	30	60.7 ± 9.7	61.9 ± 8.3	18/15	16/14	Open	No	30
Liu *et al*[24]-Lap	2016	21	21	69.2 ± 5.1	70.3 ± 5.8	10/11	12/9	Lap	No	30
Liu *et al*[24]-Open	2016	21	21	67.8 ± 3.9	68.6 ± 4.9	9/12	11/10	Open	No	30
Mingjie *et al*[22]	2017	73	76	61 (40-75)	63 (35-75)	48/25	50/26	Lap	No	30
Tanaka *et al*[30]	2017	73	69	68 (29-85)	67 (44-85)	49/24	49/20	Lap/Open	No	30
Wang *et al*[37]	2010	45	47	58.8 ± 9.7	56.9 ± 9.1	32/13	29/18	Open	No	28

ERAS: Enhanced recovery after surgery; Lap: laparoscopic surgery; Open: Open surgery; SC: Standard care.

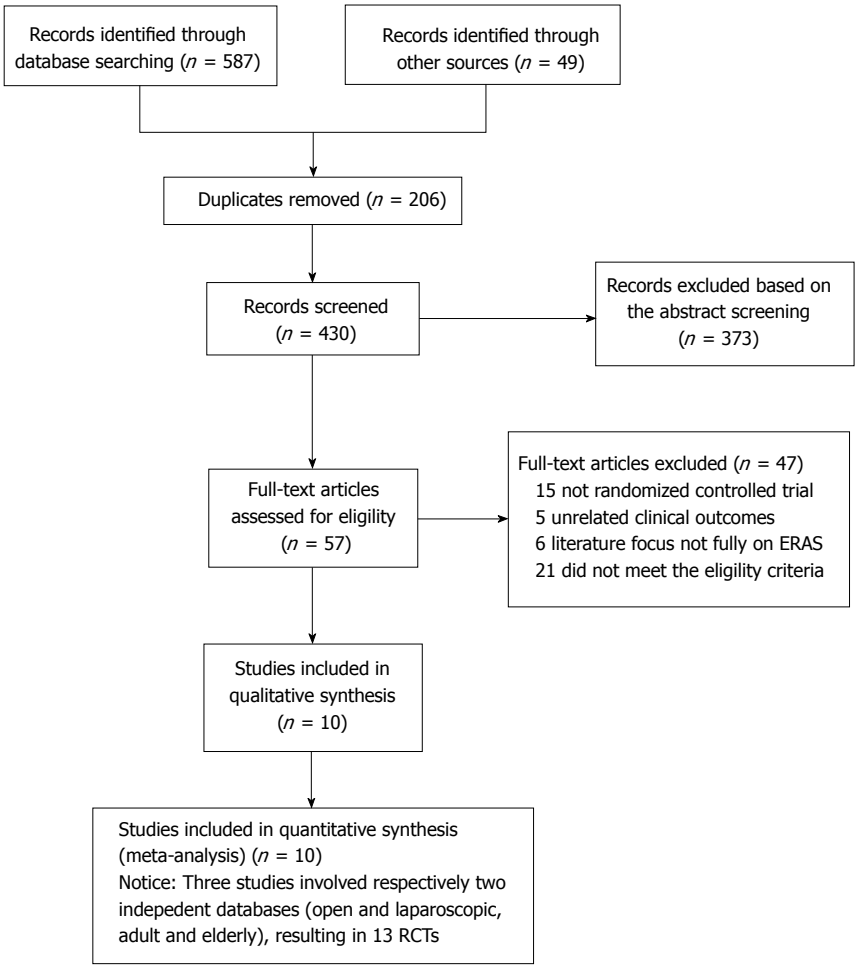

Figure 1 Study flow diagram: Enhanced recovery after surgery in gastric cancer. ERAS: Enhanced recovery after surgery; RCTs: Randomized controlled trials.

Korea, and Japan). Assessment of the risk of bias across all included studies is presented in Figure 2, most of which were of moderate quality. Blinding was the main risk of bias among these RCTs, as it was not easy to comply with double blinding in such procedural trials.

Postoperative morbidity and short-term mortality

Total complications: No significant difference was demonstrated between ERAS and the control group in the 13 RCTs regarding the incidence of total complications following gastrectomy (RR: 1.03, 95%CI: 0.73-1.44, P = 0.88) (Figure 3 and Table 3), but there

Table 2 Elements of enhanced recovery after surgery protocol applied in the included studies

Study	Year	No bowel preparation	Carbohydrate loading	No routine use of abdominal drainage	Fluid restriction	Pain management	Early mobilization	Early feeding	Others	No. of ERAS elements
Abdikarim *et al*[21]	2015	Yes	Yes	Yes	Yes	Yes	Yes	Yes	Yes	11
Bu *et al*[23]	2015	Yes	Yes	Yes	Yes	Yes	Yes	Yes	Yes	14
Chen Hu *et al*[34]	2012	Yes	Yes	Yes	Yes	Yes	Yes	Yes	Yes	13
Feng *et al*[33]	2013	-	Yes	Yes	Yes	Yes	Yes	Yes	Yes	9
Kim *et al*[35]	2012	Yes	Yes	-	-	Yes	Yes	Yes	Yes	10
Liu *et al*[36]	2010	Yes	Yes	Yes	Yes	Yes	Yes	Yes	Yes	12
Liu *et al*[24]	2016	Yes	Yes	-	Yes	Yes	Yes	Yes	Yes	11
Mingjie *et al*[22]	2017	Yes	Yes	Yes	Yes	Yes	Yes	Yes	Yes	13
Tanaka *et al*[30]	2017	Yes	Yes	Yes	-	Yes	Yes	Yes	Yes	22
Wang *et al*[37]	2010	Yes	Yes	Yes	Yes	Yes	Yes	Yes	Yes	14

ERAS: Enhanced recovery after surgery.

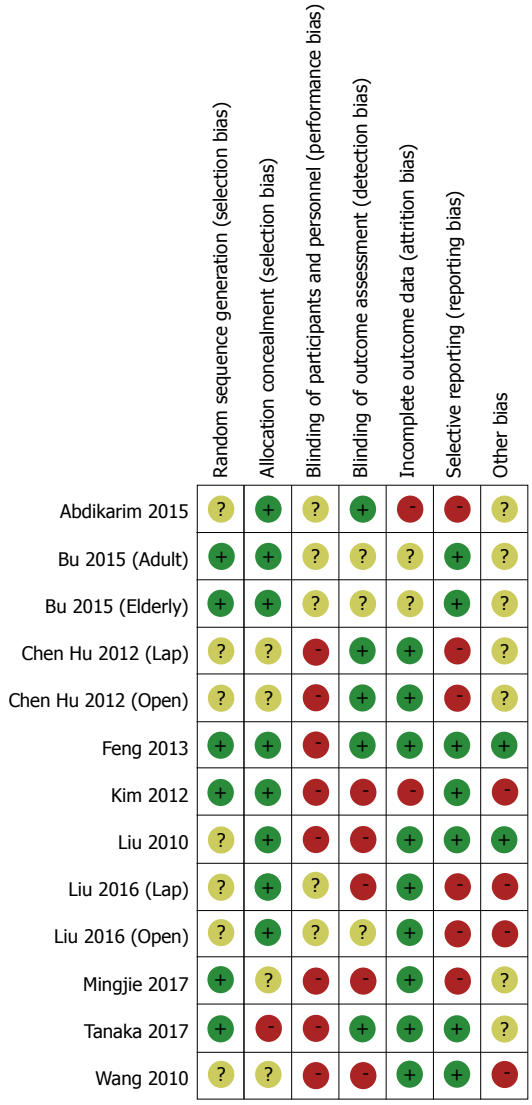

Figure 2 Risk of bias summary: Review of authors' judgments concerning each risk-of-bias item for each included study.

was significant heterogeneity among these studies (χ^2 = 47.12, I^2 = 75%, P < 0.00001). In five RCTs reporting a laparoscopic approach for GC[21,22,24,34,35], no significant difference in postoperative morbidity was found between the ERAS and SC groups (RR: 1.44, 95%CI: 0.93-2.23, P = 0.10), and no heterogeneity was observed (χ^2 = 2.18, P = 0.70; I^2 = 0). Similarly, in the open surgery RCTs[23,24,33,34,36,37], ERAS pathways did not increase the surgical complications (RR: 1.05, 95%CI: 0.68-1.63, P = 0.81), and significant heterogeneity was observed (χ^2 = 31.10, P < 0.0001; I^2 = 81%). However, three RCTs in the elderly[23,24] demonstrated that the incidence of complications was significantly higher in the ERAS arm than in the SC arm (RR: 1.45, 95%CI: 1.23-1.70, P < 0.00001), and no heterogeneity was found in the elderly (χ^2 = 1.51, P = 0.47; I^2 = 0).

Anastomotic leak: Ten RCTs[21-23,30,33,34,36,37] (964 patients) provided data on anastomotic leaks, whereby 2.3% (11/481 patients) in the ERAS group and 1.7% (8/483) in the SC group had an anastomotic leak. Pooling the results indicated that ERAS did not increase the incidence of anastomotic leaks compared with conventional care (RR: 1.36, 95%CI: 0.54-3.45, P = 0.51) (Figure 3), and heterogeneity was excluded among these trials (χ^2 = 2.35, P = 0.50; I^2 = 0).

Ileus: Twelve RCTs[21-24,30,33,34,36,37] (1048 patients) provided data regarding ileus: 3.3% (17/523 patients) in the ERAS group, and 1.9% (10/525) in the SC group had ileus. Pooling the results indicated that ERAS did not increase ileus compared with SC (RR: 1.62, 95%CI: 0.75-3.52, P = 0.22) (Figure 3), and no heterogeneity was observed among these trials (χ^2 = 5.76, P = 0.57; I^2 = 0).

Incision infection: Eleven RCTs[21-24,30,33,34,36,37] (1007 patients) reported incision infection, amounting to 2.8% (14/504 patients) in the ERAS group and 3.6% (18/503) in the SC group. Pooling the results indicated that ERAS did not increase incision infection compared with conventional care (RR: 0.79, 95%CI: 0.39-1.60, P = 0.52) (Figure 3), and there was no heterogeneity among these studies (χ^2 = 4.52, P = 0.87; I^2 = 0).

Urinary tract infection: Nine RCTs[23,24,33-37] (699 patients) provided data regarding urinary tract infection, which was observed in 2.6% (9/350 patients) in the

Table 3 Evaluation of the complications or outcomes in enhanced recovery after surgery *vs* standard care groups in the included studies

Subgroup	Studies, *n*	Participants, *n*	Statistical method	Effect estimate	Heterogeneity	
					I^2	*P* value
Total complications	13	1092	Risk ratio (M-H, random, 95%CI)	1.03 [0.73, 1.44]	75%	< 0.00001
Anastomotic leak	10	964	Risk ratio (M-H, random, 95%CI)	1.36 [0.54, 3.45]	0	0.50
Ileus	12	1048	Risk ratio (M-H, random, 95%CI)	1.62 [0.75, 3.52]	0	0.57
Incision infection	11	1007	Risk ratio (M-H, random, 95%CI)	0.79 [0.39, 1.60]	0	0.87
Urinary tract infection	9	699	Risk ratio (M-H, random, 95%CI)	0.53 [0.26, 1.08]	0	0.99
Pulmonary infection	9	775	Risk ratio (M-H, random, 95%CI)	0.52 [0.28, 0.94]	0	0.99
Postoperative hospital stay	13	1092	Mean difference (IV, random, 95%CI)	-1.65 [-2.09, -1.21]	89%	< 0.00001
Duration of first flatus	11	882	Mean difference (IV, random, 95%CI)	-12.70 [-19.71, -5.69]	92%	< 0.00001
Duration of first defecation	4	471	Mean difference (IV, random, 95%CI)	-28.07 [-41.48, -14.67]	90%	< 0.00001
Medical costs	10	819	Mean difference (IV, random, 95%CI)	-0.50 [-0.69, -0.30]	85%	< 0.00001
CRP						
POD1	8	514	Mean difference (IV, random, 95%CI)	-14.81 [-21.42, -8.21]	72%	0.0007
POD4	6	378	Mean difference (IV, random, 95%CI)	-19.81 [-29.64, -9.98]	64%	0.02
POD7	5	258	Mean difference (IV, random, 95%CI)	-21.36 [-28.81, -13.91]	74%	0.004
IL-6						
POD1	4	239	Mean difference (IV, random, 95%CI)	-61.22 [-114.58, -7.86]	99%	< 0.00001
POD4	3	147	Mean difference (IV, random, 95%CI)	-31.50 [-55.63, -7.38]	96%	< 0.00001
POD7	3	176	Mean difference (IV, random, 95%CI)	-26.62 [-34.23, -19.01]	89%	0.0001
ALB						
POD1	2	84	Mean difference (IV, random, 95%CI)	0.24 [-0.89, 1.36]	0	0.79
POD4	4	166	Mean difference (IV, random, 95%CI)	3.27 [2.24, 4.30]	23%	0.27
POD7	4	166	Mean difference (IV, random, 95%CI)	5.68 [3.31, 8.05]	83%	0.0005
Readmission	8	777	Risk ratio (M-H, Fixed, 95%CI)	2.86 [1.31, 6.24]	0	0.92
Reoperation	3	517	Risk ratio (M-H, Fixed, 95%CI)	0.62 [0.17, 2.35]	33%	0.22
Quality of life	2	136	Std. mean difference (IV, Fixed, 95%CI)	-0.46 [-0.80, -0.12]	36%	0.21

ALB: Serum albumin; CRP: C-reactive protein; IL-6: Interleukin-6; IV: Inverse Variance; M-H: Mantel-Haenszel; POD: Postoperative day.

ERAS group and 5.4% (19/349) in the SC group. Pooling the results indicated that ERAS did not increase urinary tract infection compared with conventional care (RR: 0.53, 95%CI: 0.26-1.08, $P = 0.08$) (Figure 3), and heterogeneity was excluded among these studies ($\chi^2 = 1.61$, $P = 0.99$; $I^2 = 0$).

Pulmonary infection: Nine RCTs[23,24,30,33,34,37] (775 patients) reported pulmonary infection, which affected 3.4% (13/387 patients) in the ERAS group and 7.2% (28/388) in the SC group. Pooling the results indicated that ERAS decreased significantly the incidence of pulmonary infection compared with conventional care (RR: 0.52, 95%CI: 0.28-0.94, $P = 0.03$) (Figure 3), and there was no heterogeneity among these studies ($\chi^2 = 1.09$, $P = 0.99$; $I^2 = 0$).

Short-term mortality

All studies reported short-term mortality after GC surgery; one patient (1/64) died of severe abdominal cavity infection in the elderly group[23]. No cases of death associated with surgery occurred in other studies during short-term follow-up. Pooling the results suggested that ERAS did not increase mortality compared with conventional care (RR: 3.0, 95%CI: 0.12-72.29, $P = 0.50$) (Figure 4).

Length of postoperative hospital stay

All included RCTs (1092 patients) reported POHS. Ten of these studies reported a significant reduction of POHS in the ERAS group, and three reported no significant difference. The elderly group in Bu's report[23], the laparoscopic group in Chen Hu's study[34], and the open group of Liu's report[24] demonstrated that patients receiving rapid rehabilitation care had POHS similar to that of the traditional care protocol. Meta-analysis revealed a significant reduction in POHS by 1.65 d with the application of the ERAS schemes compared with traditional perioperative care in pooled analysis (MD: -1.65, 95%CI: -2.09 to -1.21, $P < 0.00001$) (Figure 5), and the heterogeneity was significant among these studies ($\chi^2 = 105.17$, $P < 0.00001$; $I^2 = 89\%$). Laparoscopic surgery combined with ERAS[21,22,24,34,35] markedly reduced POHS compared with laparoscopic surgery alone (MD: -1.49, 95%CI: -2.25 to -0.74, $P < 0.0001$), and the heterogeneity was significant ($\chi^2 = 18.21$, $P = 0.001$; $I^2 = 78\%$). Similarly, there was a significant reduction in POHS observed in open surgery with ERAS[23,24,33,34,36,37] compared with open surgery alone (MD: -1.89, 95%CI: -2.69 to -1.09, $P < 0.00001$), and the heterogeneity was also significant ($\chi^2 = 61.54$, $P < 0.00001$; $I^2 = 90\%$).

Duration of intestinal function recovery

Eleven RCTs[23,24,30,33-37] (882 patients) analyzed the duration of first flatus. Recovery of gut function was earlier in ERAS groups, as shown by shorter duration of the first flatus and first defecation. The MD for duration of first flatus was -12.70 (95%CI: -19.71 to -5.69, $P = 0.0004$), but the heterogeneity was significant among

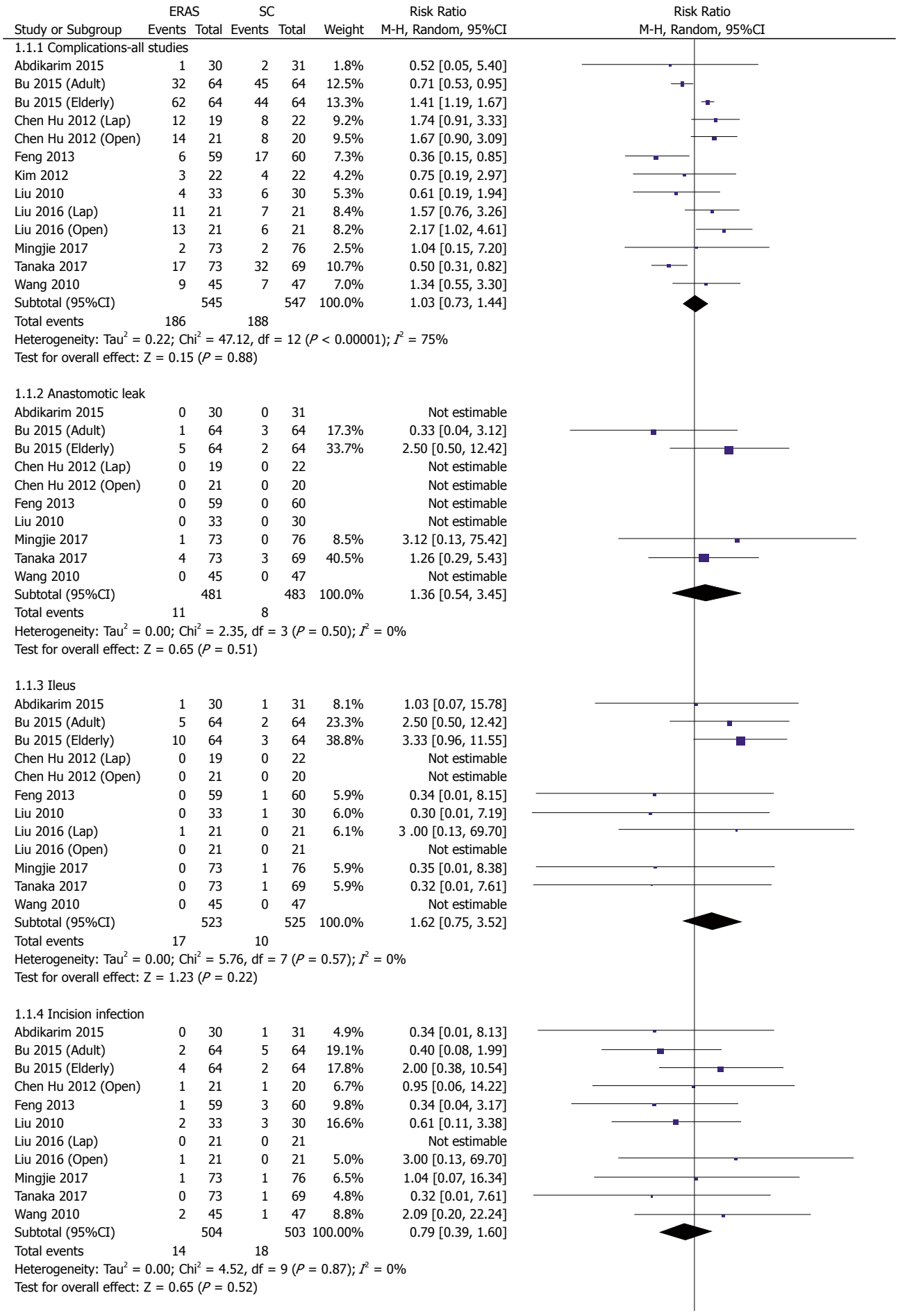
ERAS
SC
Risk Ratio
Risk Ratio
Study or Subgroup Events Total Events Total Weight M-H, Random, 95%CI
M-H, Random, 95%CI
1.1.1 Complications-all studies
Abdikarim 2015 1 30 2 31 1.8% 0.52 [0.05, 5.40]
Bu 2015 (Adult) 32 64 45 64 12.5% 0.71 [0.53, 0.95]
Bu 2015 (Elderly) 62 64 44 64 13.3% 1.41 [1.19, 1.67]
Chen Hu 2012 (Lap) 12 19 8 22 9.2% 1.74 [0.91, 3.33]
Chen Hu 2012 (Open) 14 21 8 20 9.5% 1.67 [0.90, 3.09]
Feng 2013 6 59 17 60 7.3% 0.36 [0.15, 0.85]
Kim 2012 3 22 4 22 4.2% 0.75 [0.19, 2.97]
Liu 2010 4 33 6 30 5.3% 0.61 [0.19, 1.94]
Liu 2016 (Lap) 11 21 7 21 8.4% 1.57 [0.76, 3.26]
Liu 2016 (Open) 13 21 6 21 8.2% 2.17 [1.02, 4.61]
Mingjie 2017 2 73 2 76 2.5% 1.04 [0.15, 7.20]
Tanaka 2017 17 73 32 69 10.7% 0.50 [0.31, 0.82]
Wang 2010 9 45 7 47 7.0% 1.34 [0.55, 3.30]
Subtotal (95%CI) 545 547 100.0% 1.03 [0.73, 1.44]
Total events 186 188
Heterogeneity: Tau² = 0.22; Chi² = 47.12, df = 12 (P < 0.00001); I² = 75%
Test for overall effect: Z = 0.15 (P = 0.88)
1.1.2 Anastomotic leak
Abdikarim 2015 0 30 0 31 Not estimable
Bu 2015 (Adult) 1 64 3 64 17.3% 0.33 [0.04, 3.12]
Bu 2015 (Elderly) 5 64 2 64 33.7% 2.50 [0.50, 12.42]
Chen Hu 2012 (Lap) 0 19 0 22 Not estimable
Chen Hu 2012 (Open) 0 21 0 20 Not estimable
Feng 2013 0 59 0 60 Not estimable
Liu 2010 0 33 0 30 Not estimable
Mingjie 2017 1 73 0 76 8.5% 3.12 [0.13, 75.42]
Tanaka 2017 4 73 3 69 40.5% 1.26 [0.29, 5.43]
Wang 2010 0 45 0 47 Not estimable
Subtotal (95%CI) 481 483 100.0% 1.36 [0.54, 3.45]
Total events 11 8
Heterogeneity: Tau² = 0.00; Chi² = 2.35, df = 3 (P = 0.50); I² = 0%
Test for overall effect: Z = 0.65 (P = 0.51)
1.1.3 Ileus
Abdikarim 2015 1 30 1 31 8.1% 1.03 [0.07, 15.78]
Bu 2015 (Adult) 5 64 2 64 23.3% 2.50 [0.50, 12.42]
Bu 2015 (Elderly) 10 64 3 64 38.8% 3.33 [0.96, 11.55]
Chen Hu 2012 (Lap) 0 19 0 22 Not estimable
Chen Hu 2012 (Open) 0 21 0 20 Not estimable
Feng 2013 0 59 1 60 5.9% 0.34 [0.01, 8.15]
Liu 2010 0 33 1 30 6.0% 0.30 [0.01, 7.19]
Liu 2016 (Lap) 1 21 0 21 6.1% 3 .00 [0.13, 69.70]
Liu 2016 (Open) 0 21 0 21 Not estimable
Mingjie 2017 0 73 1 76 5.9% 0.35 [0.01, 8.38]
Tanaka 2017 0 73 1 69 5.9% 0.32 [0.01, 7.61]
Wang 2010 0 45 0 47 Not estimable
Subtotal (95%CI) 523 525 100.0% 1.62 [0.75, 3.52]
Total events 17 10
Heterogeneity: Tau² = 0.00; Chi² = 5.76, df = 7 (P = 0.57); I² = 0%
Test for overall effect: Z = 1.23 (P = 0.22)
1.1.4 Incision infection
Abdikarim 2015 0 30 1 31 4.9% 0.34 [0.01, 8.13]
Bu 2015 (Adult) 2 64 5 64 19.1% 0.40 [0.08, 1.99]
Bu 2015 (Elderly) 4 64 2 64 17.8% 2.00 [0.38, 10.54]
Chen Hu 2012 (Open) 1 21 1 20 6.7% 0.95 [0.06, 14.22]
Feng 2013 1 59 3 60 9.8% 0.34 [0.04, 3.17]
Liu 2010 2 33 3 30 16.6% 0.61 [0.11, 3.38]
Liu 2016 (Lap) 0 21 0 21 Not estimable
Liu 2016 (Open) 1 21 0 21 5.0% 3.00 [0.13, 69.70]
Mingjie 2017 1 73 1 76 6.5% 1.04 [0.07, 16.34]
Tanaka 2017 0 73 1 69 4.8% 0.32 [0.01, 7.61]
Wang 2010 2 45 1 47 8.8% 2.09 [0.20, 22.24]
Subtotal (95%CI) 504 503 100.00% 0.79 [0.39, 1.60]
Total events 14 18
Heterogeneity: Tau² = 0.00; Chi² = 4.52, df = 9 (P = 0.87); I² = 0%
Test for overall effect: Z = 0.65 (P = 0.52)

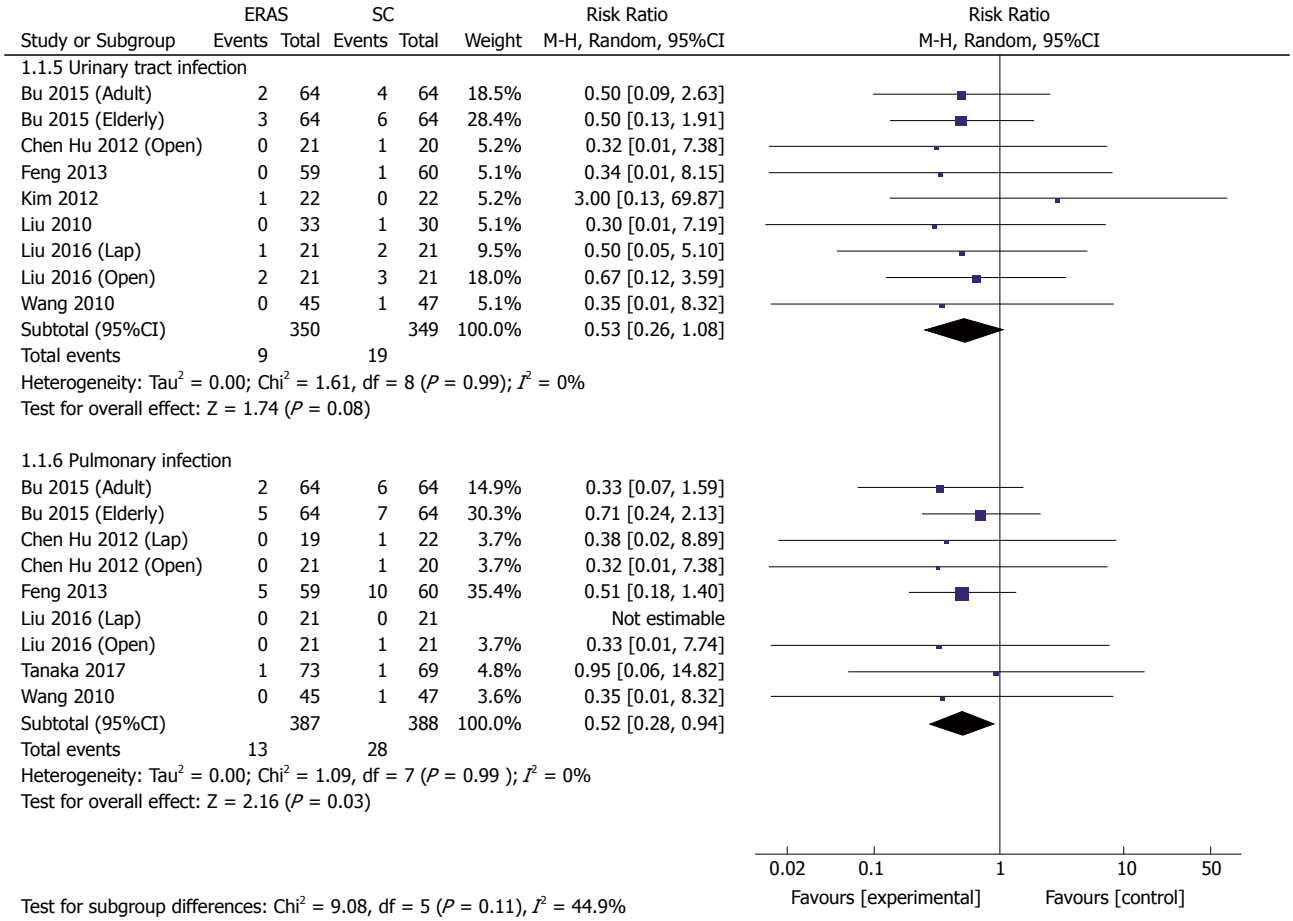

Figure 3 Forest plot evaluating the relative risk of surgical complications: Enhanced recovery after surgery *vs* standard care. ERAS: Enhanced recovery after surgery; SC: Standard care.

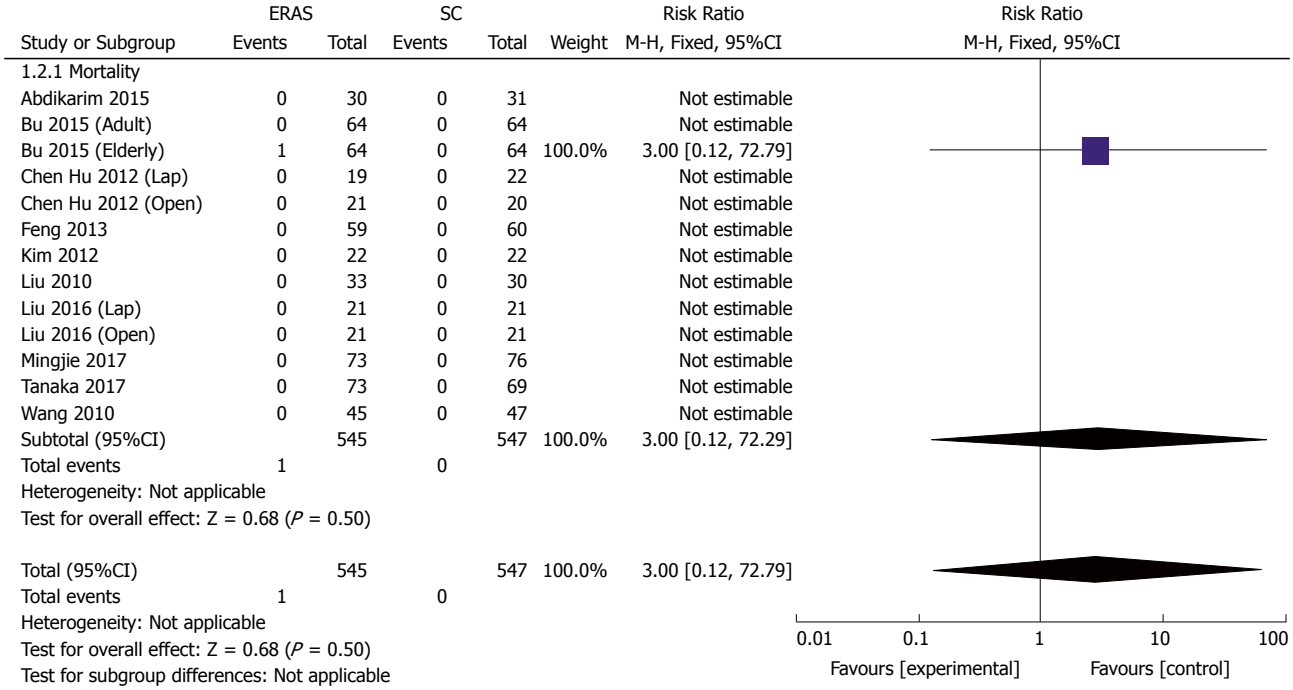

Figure 4 Forest plot evaluating the relative risk of short-term mortality: Enhanced recovery after surgery *vs* standard care. ERAS: Enhanced recovery after surgery; SC: Standard care.

these studies (χ^2 = 119.74, I^2 = 92%, P < 0.0001) (Figure 6). In the patients undergoing laparoscopic gastrectomy[24,34,35], the duration of the first flatus of patients in the ERAS group was 7.20 h less than

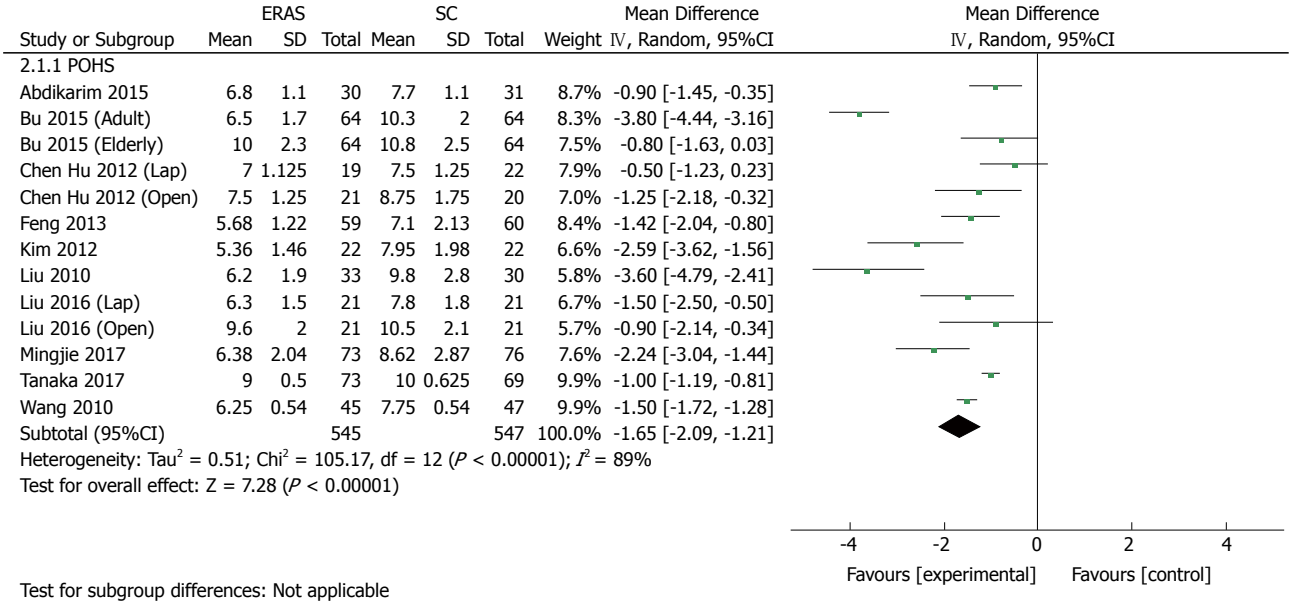

Figure 5 Forest plot evaluating the length of postoperative hospital stay: Enhanced recovery after surgery *vs* standard care. ERAS: Enhanced recovery after surgery; SC: Standard care.

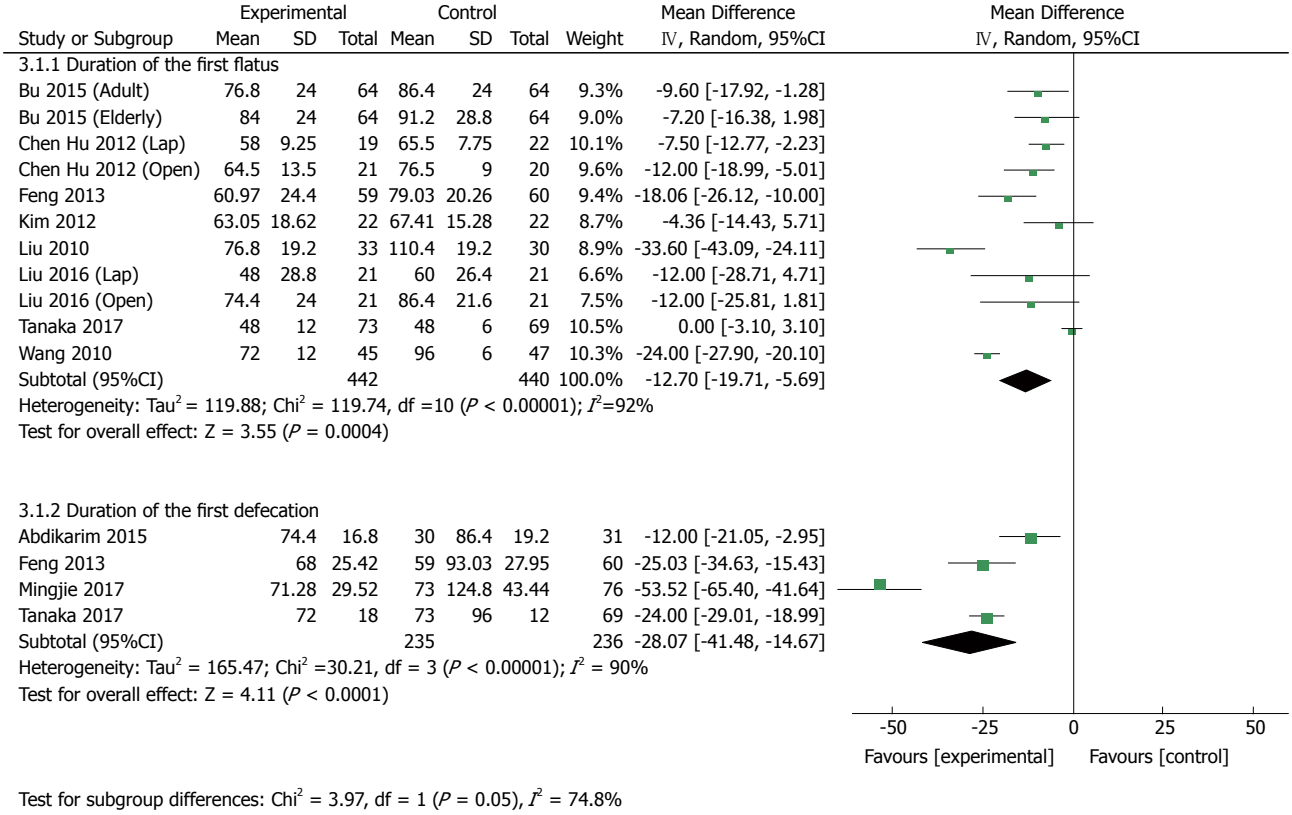

Figure 6 Forest plot evaluating the duration of intestinal function recovery: Enhanced recovery after surgery *vs* standard care. ERAS: Enhanced recovery after surgery; SC: Standard care.

that in the control group (MD: -7.20, 95%CI: -11.70 to -2.70, P = 0.002), and there was no heterogeneity among these studies (χ^2 = 0.64, P = 0.73; I^2 = 0). Similarly, the first flatus was significantly earlier in the ERAS group than in the SC group (MD: -14.47, 95%CI: -23.61 to -5.33, P = 0.002) among patients undergoing open surgery[23,24,33,34,36,37], but the heterogeneity was significant (χ^2 = 116.69, P < 0.00001; I^2 = 94%). Four RCTs[21,22,30,33] (471 patients) reported the duration of first defecation. The MD was -28.07 (95%CI: -41.48 to -14.67, P < 0.0001) (Figure 6), and there was significant heterogeneity among the studies (χ^2 = 30.21, P < 0.00001; I^2 = 90%).

Medical costs

Ten RCTs[23,24,30,33-35,37] (819 patients) provided data

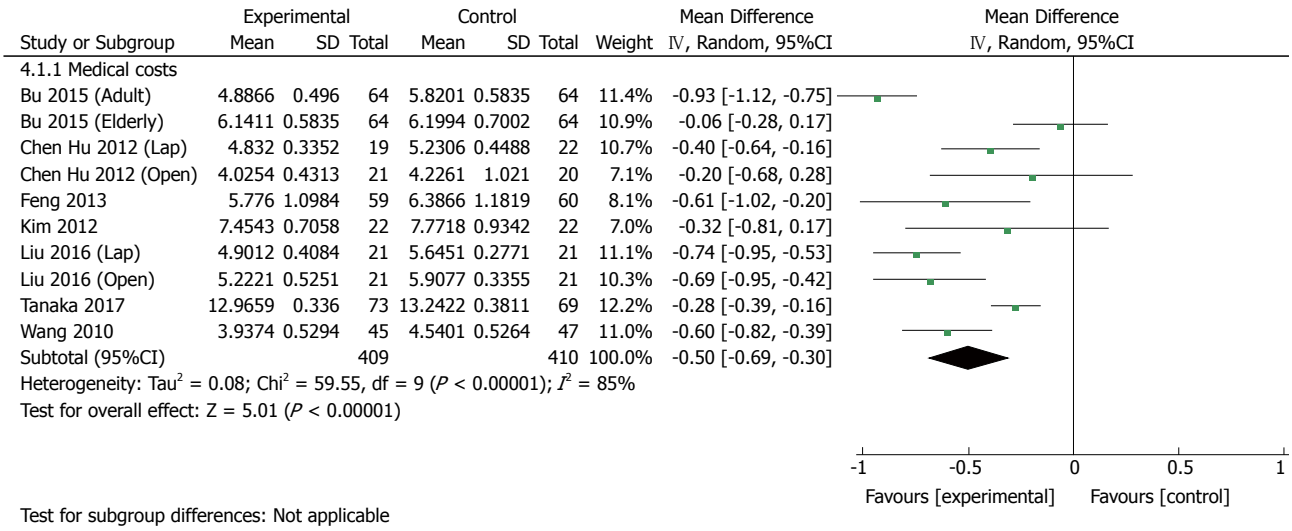

Figure 7 Forest plot evaluating the difference in total medical costs: Enhanced recovery after surgery *vs* standard care. ERAS: Enhanced recovery after surgery; SC: Standard care.

regarding medical costs. The costs of hospitalization were reported in US dollars (USD) in one trial[37], Japanese yen in one trial[30], and Chinese renminbi (RMB) in six trials. All of the medical care expenses were converted to USD (http://www.xe.com) by use of the exchange rates of the aforementioned currencies on June 28, 2017. The medical costs were significantly lower with ERAS than with traditional care (MD: -5000 USD, 95%CI: -6900 to -3000, $P < 0.00001$) (Figure 7), and there was significant heterogeneity among trials by using the random-effects model ($\chi^2 = 59.55$, $P < 0.00001$; $I^2 = 85\%$). In laparoscopic groups[24,34,35], ERAS significantly decreased the medical costs compared with traditional care (MD: -5200 USD, 95%CI: -8000 to -2500, $P = 0.0002$), and the heterogeneity was significant ($\chi^2 = 5.58$, $P = 0.06$; $I^2 = 64\%$). Similarly, there was a significant reduction in medical costs in open surgery with ERAS[23,24,33,34,37] compared with open surgery alone (MD: -5300, 95%CI: -8300 to -2300, $P = 0.0005$), and significant heterogeneity was observed ($\chi^2 = 37.63$, $P < 0.00001$; $I^2 = 87\%$).

Readmission

Eight RCTs[21,23,30,34-37] (777 patients) reported data concerning the readmission rate after discharge, whereby 5.6% (22/390) from ERAS groups and 1.8% (7/387) from SC groups had to be readmitted. A higher readmission rate was perceived in the ERAS group than in the control group (RR: 2.86, 95%CI: 1.31-6.24, $P = 0.009$) (Figure 8). There was no significant heterogeneity observed among these studies ($\chi^2 = 1.44$, $P = 0.92$; $I^2 = 0$). However, sensitivity analysis showed no significant difference in readmission (RR: 2.17, 95%CI: 0.77-6.14, $P = 0.14$) when excluding the elderly group in Bu's study[23], and no heterogeneity was observed ($\chi^2 = 0.85$, $P = 0.93$; $I^2 = 0$).

Reoperation

Three RCTs[23,30,36] (517 patients) reported reoperation rates after discharge. Two patients (0.8%) in ERAS groups and four patients (1.6%) in the conventional protocol groups had to undergo reoperation because of serious complications including abdominal infection, intraabdominal bleeding, and pancreatic fistula. There was no statistical difference in the rate of reoperation between the two groups (RR: 0.62, 95%CI: 0.17-2.35, $P = 0.49$) (Figure 8). Heterogeneity among these studies remained moderate ($\chi^2 = 3.01$, $P = 0.22$; $I^2 = 33\%$).

Inflammatory response indicators and nutritional status

Eight RCTs[22,24,34-37] (514 patients) and four RCTs[24,36,37] (239 patients) reported CRP and IL-6 levels after gastrectomy, respectively. As markers of surgical stress-associated response, levels of CRP and IL-6 were significantly elevated after surgery. Compared with patients in the conventional care group, a milder acute-phase response was detected in the ERAS group after gastrectomy. The pooled MD using a random-effects model for serum CRP was -14.81 (95%CI: -21.42 to -8.21, $P < 0.0001$), -19.81 (95%CI: -29.64 to -9.98, $P < 0.0001$), and -21.36 (95%CI: -28.81 to -13.91, $P < 0.00001$) on days 1, 4 and 7 after surgery, respectively (Figure 9), and significant heterogeneity was observed among these studies ($I^2 = 72\%$, 64%, and 74% on day 1, 4 and 7 after surgery, respectively). The level of pooled MD for IL-6 was -61.22 (95%CI: -114.58 to -7.86, $P = 0.02$), -31.50 (95%CI: -55.63 to -7.38, $P = 0.01$) and -26.62 (95%CI: -34.23 to -19.01, $P < 0.0001$) on days 1, 4 and 7 after surgery, respectively (Figure 10), and there was a high degree of heterogeneity among these studies ($I^2 = 99\%$, 96% and 89% on day 1, 4 and 7 after surgery, respectively).

Four RCTs[24,32] reported serum ALB. In general, ALB concentration dropped significantly compared with preoperative parameters. On postoperative day (POD) 1, there was no significant difference regarding the level of ALB between the ERAS and conventional care groups (MD 0.24, 95%CI: -0.89 to 1.36, $P = 0.68$) (Figure 11). On

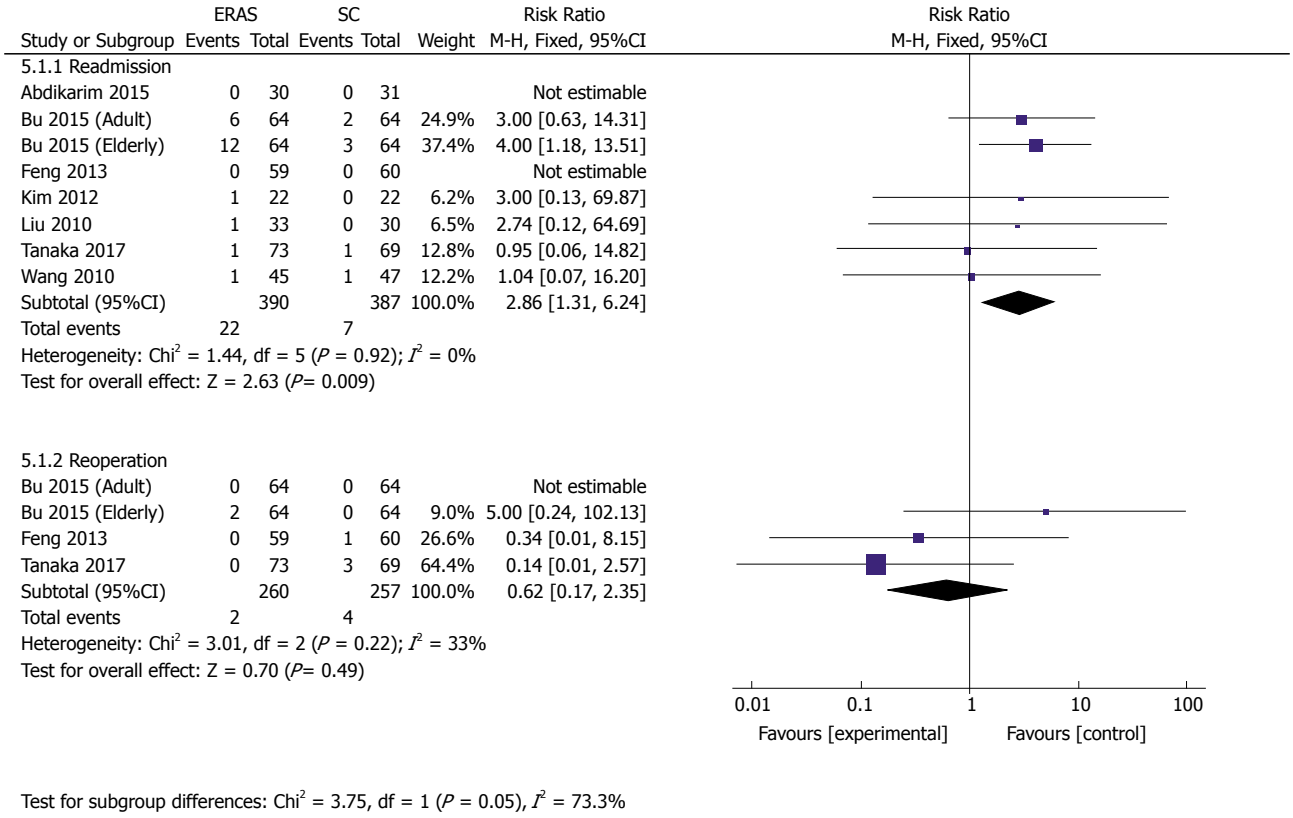

Figure 8 Forest plot evaluating the incidence of readmission and reoperation within 30 d: Enhanced recovery after surgery *vs* standard care. ERAS: Enhanced recovery after surgery; SC: Standard care.

PODs 4 and 7, the level of ALB was higher in the ERAS group than in the control group (MD: 3.27, 95%CI: 2.24-4.30, $P < 0.00001$; MD: 5.68, 95%CI: 3.31-8.05, $P < 0.00001$, respectively). Mild heterogeneity was detected on POD 4 ($\chi^2 = 3.90$, $P = 0.27$; $I^2 = 23\%$). However, there was significant heterogeneity in the outcomes on POD 7 ($\chi^2 = 17.54$, $P = 0.0005$; $I^2 = 83\%$) (Figure 11).

Quality of life

Health-related QOL was reported in two trials[35,37]. One trial checked health-related QOL with the European Organization for Research and Treatment of Cancer quality-of-life questionnaire C-30 and STO-22 at 14 d after discharge[35], while the other measured the QOL score using questionnaires at the time of discharge[37]. A significant superiority was found in the fast-track surgery protocol group compared with the conventional care program group in terms of short-term QOL using the fixed-effects model. The pooled standardized MD was -0.46 (95%CI: -0.80 to -0.12, $P = 0.008$) (Figure 12), and there was a mild degree of heterogeneity in the outcomes ($\chi^2 = 1.56$, $P = 0.21$; $I^2 = 36\%$).

Publication bias

Potential publication bias was appraised graphically by using funnel plots, Begg's test and Egger's test. No obvious asymmetry was revealed by visual indication of the Begg's funnel plot for postoperative total complications including all studies (Figure 13), and Begg's test and Egger's test indicated no significant bias was associated with publication for this meta-analysis ($P = 0.55$ and $P = 0.435$, respectively).

DISCUSSION

ERAS protocols have been gradually accepted as being able to optimize clinical outcomes, value and experience for patients with GC[22-29]. The present study is the largest meta-analysis to date, incorporating 13 RCTs enrolling 1092 participants, of whom 545 received ERAS protocols and 547 received SC for GC. Our results demonstrated that the optimized multimodal strategies significantly expedite bowel function recovery, shorten the length of POHS and reduce medical costs, and that ERAS pathways maintain comparable total complications, reoperation rates and mortality rates. The present analysis indicates that the implementation of ERAS approaches accelerates recovery, and is feasible and safe for patients with GC undergoing radical gastrectomy.

The core mechanism of ERAS is that multimodal interventions may lead to a major reduction in the undesirable sequelae of surgical injury, and stress-free surgery is the key goal of ERAS[1]. Robust evidence suggested that ERAS played an important role in attenuating the surgical stress response and accelerating the return to baseline in colorectal cancer surgery[38,39], which was afforded eloquent proof in GC surgery. The inflammatory

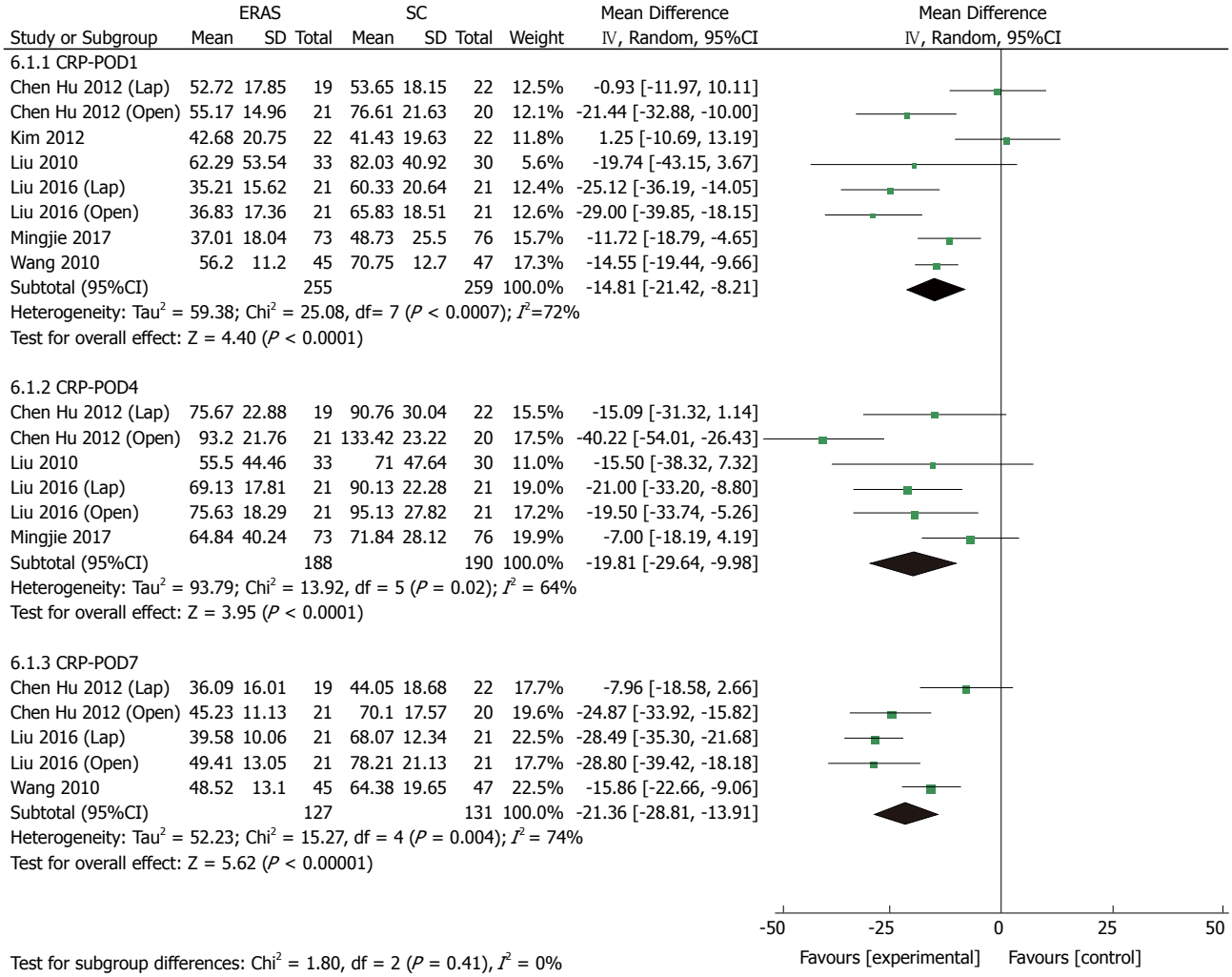

Figure 9 Forest plot evaluating the postoperative level of C-reactive protein: Enhanced recovery after surgery *vs* standard care. CRP: C-reactive protein; ERAS: Enhanced recovery after surgery; SC: Standard care.

factors, such as CRP, IL-6 and tumor necrosis factor α, are related to the extent of tissue injury caused by surgery[40,41]. In the present study, the ERAS approaches significantly reduced the concentration of CRP and IL-6 in comparison with SC on days 1, 4 and 7 after gastrectomy for GC, which was consistent with accelerated recovery. More importantly, our study suggests that the level of serum ALB after surgery in ERAS patients was significantly higher and steadier than that in SC patients, which fully demonstrates that the ERAS program could serve to improve the nutritional status of patients with GC. Good nutritional status and rapid rehabilitation after surgery allow patients to receive early postoperative multimodality therapy, including chemotherapy, thereby potentially improving their oncological outcome.

The main characteristic of ERAS is faster post-operative recovery and early discharge. However, it is noteworthy that this accelerated recovery does not come at the cost of increased medical expense. In our study, 10 RCTs reported data on medical costs and identified a mean reduction of 5000 USD in the ERAS group. If the trials with mean and imputed SD were excluded, medical expenses would be reduced by 5300 USD. Therefore, implementation of ERAS appears to have an advantage when combining clinical efficacy and cost effectiveness, which is consistent with previous reports[42,43].

More importantly, our study shows that ERAS pathways increased the readmission rate for GC patients after gastrectomy, a radically different result from previous meta-analyses[25-27]. However, sensitivity analysis, excluding the elderly patients in Bu's study[23], indicated that there was no significant difference in readmission rates between ERAS and SC groups. To date, the evidence on the application of ERAS procedures in elderly patients with GC, especially if older than 75 years, is sparse. Only two RCTs have reported ERAS care in elderly patients with GC to date, and the age criterion for inclusion was inconsistent. Liu *et al*[24] confirmed that the use of ERAS in elderly patients (60-80 years) was safe and feasible, effectively reducing the stress response, speeding up the recovery of intestinal function, and improving postoperative nutritional status without increasing the complications. However, Bu *et al*[23] showed that

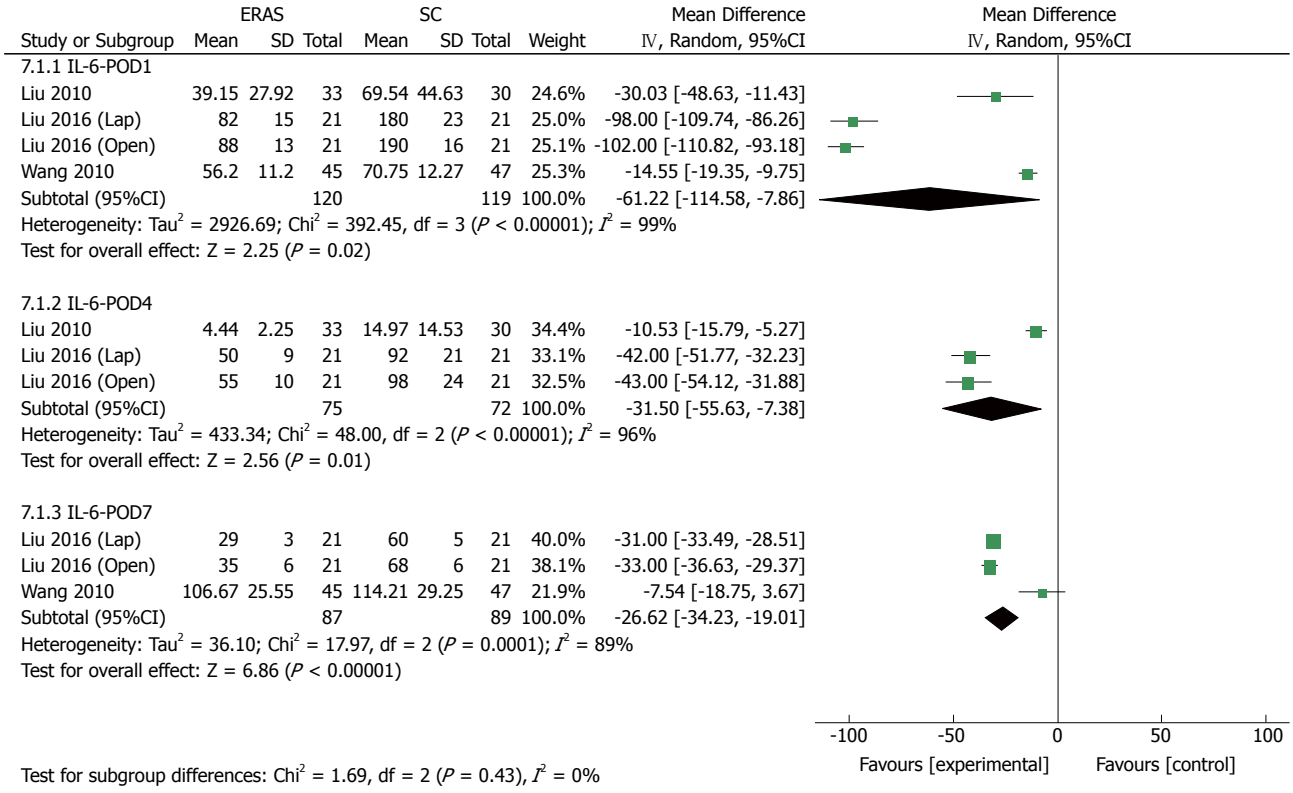

Figure 10 Forest plot evaluating the postoperative level of IL-6: Enhanced recovery after surgery *vs* standard care. ERAS: Enhanced recovery after surgery; IL: Interleukin; SC: Standard care.

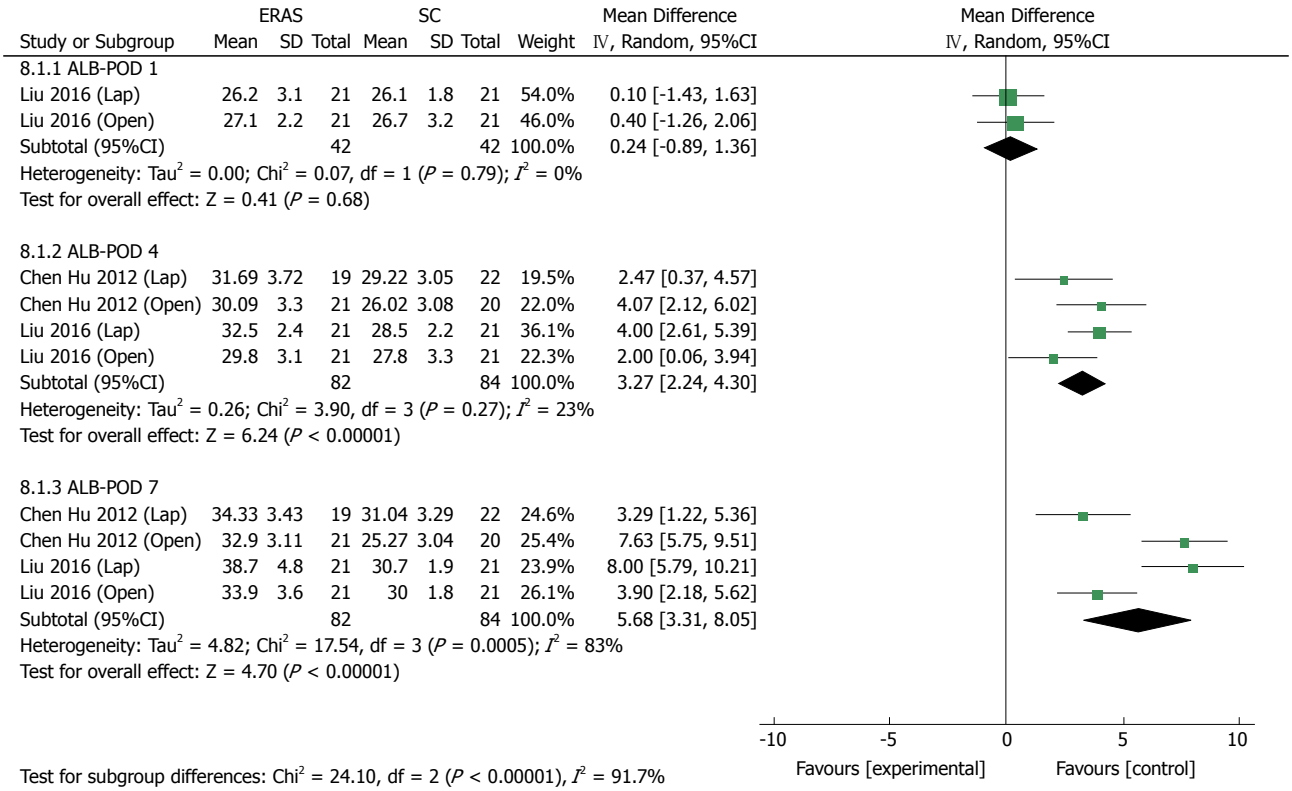

Figure 11 Forest plot evaluating the postoperative level of serum albumin: Enhanced recovery after surgery *vs* standard care. ALB: Albumin; ERAS: Enhanced recovery after surgery; SC: Standard care.

implementation of the multimodal procedure in older patients (75-89 years) undergoing distal or total gastrectomy increased significantly the incidence of nausea and vomiting, gastric retention and ileus, as well as the readmission rate, in comparison with the SC group. These inconsistent results may be due to

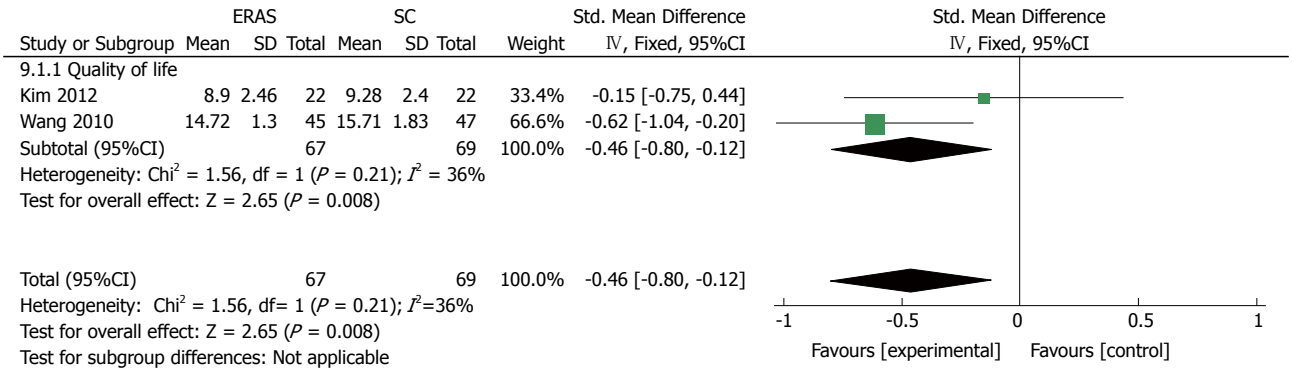

Figure 12 Forest plot evaluating health-related quality of life: Enhanced recovery after surgery *vs* standard care. ERAS: Enhanced recovery after surgery; SC: Standard care.

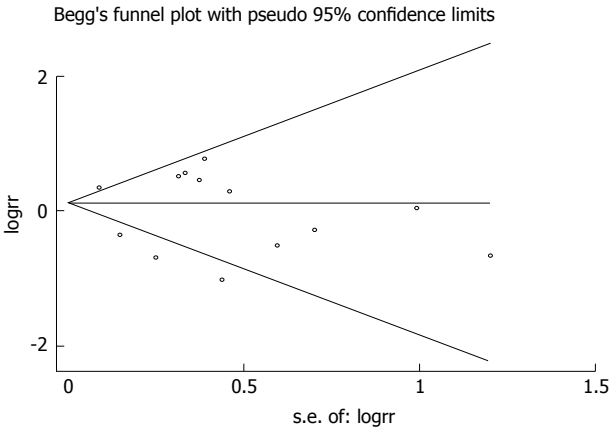

Figure 13 Begg's funnel plot to explore publication bias of all the included studies.

inclusion of age criterion, surgical type, and element selection.

Gerontal patients often experience underlying comorbidities and low physiological reserve, usually resulting in a high incidence of complications and delayed convalescence. Therefore, tailored perioperative care should be conducted in such a specific patient population. It was reported that a high degree of ERAS compliance was associated with fewer complications and shorter hospital stay[44,45]. Feroci *et al*[46] reported that male sex, advanced age (> 75 years), and American Society of Anesthesiologists' score of grade 3 and above were correlated with lower compliance to enhanced recovery with specific reference to early removal of the urethral catheter, early oral feeding, and early ambulation in patients undergoing colorectal surgery. In our study, protocol compliance was only mentioned in studies by Feng *et al*[33] and Liu *et al*[24]. Whether the compliance of elderly GC patients with ERAS regimens affects the outcomes remains to be further investigated, although several studies have indicated that ERAS in colorectal surgery was safe and feasible, with postoperative outcomes similar to those of the younger group[47-49].

In our meta-analysis, two RCTs provided QOL data at the time of discharge[37] or 14 d after discharge[35], whereby ERAS approaches showed significant superiority in QOL over SC groups. However, many investigators prefer postoperative recovery to assess the efficacy of ERAS, which begins at the time of surgery and is complete only when the patient returns (recovers) to their baseline function or to population norms[50]. Therefore, functional status and QOL attracts more interest.

The introduction of laparoscopic surgery has dramatically lessened the impact of surgical traumas on patients and accelerated their recovery. In the past 2 decades, minimally invasive surgery and the implementation of ERAS have been considered two major revolutions in elective major abdominal surgery, both intending to minimize the surgical stress and improve patient outcomes[51]. Meta-analyses of RCTs in laparoscopic colorectal surgery have demonstrated that application of the ERAS approaches is associated with fewer complications, faster recovery of bowel function and shorter hospitalization, without increased readmissions[52,53]. Laparoscopic surgery has been recommended in the guidelines for enhanced recovery after gastrectomy[29]. In this study, we observed that laparoscopic surgery combined with ERAS markedly reduced POHS and medical costs, and speeded up the return of intestinal function in patients with GC; however, laparoscopic surgery with ERAS did not increase total complications compared with laparoscopic surgery alone.

There are undoubtedly several limitations in the present study. First, several included RCTs were smaller in size, although the total sample size of the study was greater than 1000, and a multicenter trial was lacking. Second, among the included studies there was considerable heterogeneity. No remarkable heterogeneity was found with regard to the incidence of complications (including anastomotic leaks, ileus, incision infection, urinary tract infection, and pulmonary infection), rates of readmission and reoperation, and postoperative serum ALB level (POD 1 and POD 4) and QOL. However, there was significant heterogeneity for overall complications, POHS, intestinal function recovery, medical costs, and inflammatory response indicators (I^2 = 64%-99%). This substantial heterogeneity may be attributable to the clinical heterogeneity, including technical status of each institution, inclusion criteria,

surgical approach, inconsistent evaluation of the outcomes, and ERAS elements used. Third, most studies excluded patients receiving neoadjuvant chemotherapy, which may increase the potential bias to a certain extent.

In conclusion, this updated meta-analysis and systematic review provides a comprehensive assessment of ERAS following gastrectomy, and demonstrates that ERAS protocols lead to accelerated recovery, reduction of surgical stress and medical costs, improved nutritional status, and better health-related QOL for GC patients. However, it appears to be associated with increased readmission rates. Further high-quality, large-sample, multicenter RCTs with long-term follow-up are needed to more precisely evaluate ERAS pathways in GC surgery.

ARTICLE HIGHLIGHTS

Research background

Enhanced recovery after surgery (ERAS) has emerged as an optimal perioperative strategy for improving clinical outcomes in elective gastric cancer (GC) surgery. However, numerous controversies exist with regard to ERAS practice after radical gastrectomy.

Research motivation

Accumulating studies highlight that implementation of ERAS protocols reduces overall hospital stay, morbidity and mortality significantly, without compromising patient safety in multiple surgical disciplines. However, the safety and feasibility of applying ERAS in its current form in radical gastrectomy still remains to be proven by performing an updated meta-analysis.

Research objectives

This meta-analysis aims to provide an updated assessment of the safety and efficacy of ERAS protocols in GC surgery.

Research methods

A comprehensive literature search in PubMed, Medline, EMBASE, World Health Organization International Trial Registry platform, and Cochrane Library until June 2017 was performed independently to identify all available randomized controlled trials (RCTs) comparing the ERAS program with standard perioperative care (SC) in GC surgery. Non-comparative studies, case-controlled trials, cohort studies, retrospective studies, items of ERAS applied being less than four, and no follow-up after discharge were excluded.

Research results

Thirteen RCTs, with a total of 1092 participants, were analyzed in this study, of whom 545 underwent ERAS protocols and 547 received SC treatment. ERAS protocols significantly decreased the length of postoperative hospital stay and medical costs, and accelerated bowel function recovery. Moreover, ERAS protocols were associated with a lower level of serum inflammatory response, higher serum albumin, and superior short-term quality of life. There were no significant differences regarding the incidence of total complications, mortality and reoperation following gastrectomy. However, the readmission rate after GC surgery nearly tripled under ERAS.

Research conclusions

ERAS results in accelerated convalescence, reduction of surgical stress and medical costs, improved nutritional status, and better quality of life for GC patients, but increased the readmission rate. Furthermore, the significant heterogeneity of some results is a major limitation of this study. ERAS investigators need to proceed with caution as far as ERAS is concerned beyond colorectal cancer surgery.

Research perspectives

This study provides an updated assessment of ERAS in GC surgery and is expected to provide guidance and reference for clinical practice, and also to provide high-level evidence for evidence-based medicine. High-quality multicenter RCTs with large samples and long-term follow-up are needed to more precisely evaluate ERAS in radical gastrectomy.

ACKNOWLEDGMENTS

We would like to thank Dr. Mu-long Du, a member of the Biostatistic Service from the School of Public Health, Nanjing Medical University, for reviewing the statistical methods in this study.

REFERENCES

1 **Kehlet H**. Multimodal approach to control postoperative pathophysiology and rehabilitation. *Br J Anaesth* 1997; **78**: 606-617 [PMID: 9175983]
2 **Wilmore DW**, Kehlet H. Management of patients in fast track surgery. *BMJ* 2001; **322**: 473-476 [PMID: 11222424]
3 **Lassen K**, Soop M, Nygren J, Cox PB, Hendry PO, Spies C, von Meyenfeldt MF, Fearon KC, Revhaug A, Norderval S, Ljungqvist O, Lobo DN, Dejong CH; Enhanced Recovery After Surgery (ERAS) Group. Consensus review of optimal perioperative care in colorectal surgery: Enhanced Recovery After Surgery (ERAS) Group recommendations. *Arch Surg* 2009; **144**: 961-969 [PMID: 19841366 DOI: 10.1001/archsurg.2009.170]
4 **Ramírez JM**, Blasco JA, Roig JV, Maeso-Martínez S, Casal JE, Esteban F, Lic DC; Spanish working group on fast track surgery. Enhanced recovery in colorectal surgery: a multicentre study. *BMC Surg* 2011; **11**: 9 [PMID: 21489315 DOI: 10.1186/1471-2482-11-9]
5 **Kehlet H**. Fast-track colonic surgery: status and perspectives. *Recent Results Cancer Res* 2005; **165**: 8-13 [PMID: 15865015]
6 **Kehlet H**. Fast-track colorectal surgery. *Lancet* 2008; **371**: 791-793 [PMID: 18328911 DOI: 10.1016/S0140-6736(08)60357-8]
7 **Kehlet H**, Dahl JB. Anaesthesia, surgery, and challenges in postoperative recovery. *Lancet* 2003; **362**: 1921-1928 [PMID: 14667752 DOI: 10.1016/S0140-6736(03)14966-5]
8 **Faucheron JL**, Trilling B. Laparoscopy in combination with fast-track management is the best surgical strategy in patients undergoing colorectal resection for cancer. *Tech Coloproctol* 2015; **19**: 379-380 [PMID: 25995151 DOI: 10.1007/s10151-015-1309-2]
9 **Muallem MZ**, Dimitrova D, Pietzner K, Richter R, Feldheiser A, Scharfe I, Schmeil I, Hösl TM, Mustea A, Wimberger P, Burges A, Kimmig R, Sehouli J. Implementation of Enhanced Recovery After Surgery (ERAS) Pathways in Gynecologic Oncology. A NOGGO-AGO* survey of 144 Gynecological Departments in Germany. *Anticancer Res* 2016; **36**: 4227-4232 [PMID: 27466536]
10 **Auyong DB**, Allen CJ, Pahang JA, Clabeaux JJ, MacDonald KM, Hanson NA. Reduced Length of Hospitalization in Primary Total Knee Arthroplasty Patients Using an Updated Enhanced Recovery After Orthopedic Surgery (ERAS) Pathway. *J Arthroplasty* 2015; **30**: 1705-1709 [PMID: 26024988 DOI: 10.1016/j.arth.2015.05.007]
11 **Bösing NM**, Goretzki PE, Röher HD. Gastric cancer: which patients benefit from systematic lymphadenectomy? *Eur J Surg Oncol* 2000; **26**: 498-505 [PMID: 11016473 DOI: 10.1053/ejso.1999.0930]
12 **Sano T**, Sasako M, Yamamoto S, Nashimoto A, Kurita A, Hiratsuka M, Tsujinaka T, Kinoshita T, Arai K, Yamamura Y, Okajima K. Gastric cancer surgery: morbidity and mortality results from a prospective randomized controlled trial comparing D2 and extended para-aortic lymphadenectomy--Japan Clinical Oncology Group study 9501. *J Clin Oncol* 2004; **22**: 2767-2773 [PMID: 15199090 DOI: 10.1200/JCO.2004.10.184]
13 **Kim HH**, Han SU, Kim MC, Hyung WJ, Kim W, Lee HJ, Ryu SW, Cho GS, Song KY, Ryu SY. Long-term results of laparoscopic gastrectomy for gastric cancer: a large-scale case-control and case-matched Korean multicenter study. *J Clin Oncol* 2014; **32**: 627-633 [PMID: 24470012 DOI: 10.1200/JCO.2013.48.8551]
14 **Damhuis RA**, Wijnhoven BP, Plaisier PW, Kirkels WJ, Kranse R, van Lanschot JJ. Comparison of 30-day, 90-day and in-hospital

postoperative mortality for eight different cancer types. *Br J Surg* 2012; **99**: 1149-1154 [PMID: 22718521 DOI: 10.1002/bjs.8813]
15 **Kubota T**, Hiki N, Sano T, Nomura S, Nunobe S, Kumagai K, Aikou S, Watanabe R, Kosuga T, Yamaguchi T. Prognostic significance of complications after curative surgery for gastric cancer. *Ann Surg Oncol* 2014; **21**: 891-898 [PMID: 24254205 DOI: 10.1245/s10434-013-3384-9]
16 **Grantcharov TP**, Kehlet H. Laparoscopic gastric surgery in an enhanced recovery programme. *Br J Surg* 2010; **97**: 1547-1551 [PMID: 20665480 DOI: 10.1002/bjs.7184]
17 **Yamada T**, Hayashi T, Cho H, Yoshikawa T, Taniguchi H, Fukushima R, Tsuburaya A. Usefulness of enhanced recovery after surgery protocol as compared with conventional perioperative care in gastric surgery. *Gastric Cancer* 2012; **15**: 34-41 [PMID: 21573918 DOI: 10.1007/s10120-011-0057-x]
18 **Yamada T**, Hayashi T, Aoyama T, Shirai J, Fujikawa H, Cho H, Yoshikawa T, Rino Y, Masuda M, Taniguchi H, Fukushima R, Tsuburaya A. Feasibility of enhanced recovery after surgery in gastric surgery: a retrospective study. *BMC Surg* 2014; **14**: 41 [PMID: 25001198 DOI: 10.1186/1471-2482-14-41]
19 **Liu XX**, Pan HF, Jiang ZW, Zhang S, Wang ZM, Chen P, Zhao Y, Wang G, Zhao K, Li JS. "Fast-track" and "Minimally Invasive" Surgery for Gastric Cancer. *Chin Med J* (Engl) 2016; **129**: 2294-2300 [PMID: 27647187 DOI: 10.4103/0366-6999.190659]
20 **Fang F**, Gao J, Bi X, Han F, Wang HJ. Effect and clinical significance of fast-track surgery combined with laparoscopic radical gastrectomy on the plasma level of vascular endothelial growth factor in gastric antrum cancer. *Springerplus* 2016; **5**: 50 [PMID: 26835230 DOI: 10.1186/s40064-016-1699-2]
21 **Abdikarim I**, Cao XY, Li SZ, Zhao YQ, Taupyk Y, Wang Q. Enhanced recovery after surgery with laparoscopic radical gastrectomy for stomach carcinomas. *World J Gastroenterol* 2015; **21**: 13339-13344 [PMID: 26715818 DOI: 10.3748/wjg.v21.i47.13339]
22 **Mingjie X**, Luyao Z, Ze T, YinQuan Z, Quan W. Laparoscopic Radical Gastrectomy for Resectable Advanced Gastric Cancer Within Enhanced Recovery Programs: A Prospective Randomized Controlled Trial. *J Laparoendosc Adv Surg Tech A* 2017; **27**: 959-964 [PMID: 27875094 DOI: 10.1089/lap.2016.0057]
23 **Bu J**, Li N, Huang X, He S, Wen J, Wu X. Feasibility of Fast-Track Surgery in Elderly Patients with Gastric Cancer. *J Gastrointest Surg* 2015; **19**: 1391-1398 [PMID: 25943912 DOI: 10.1007/s11605-015-2839-7]
24 **Liu G**, Jian F, Wang X, Chen L. Fast-track surgery protocol in elderly patients undergoing laparoscopic radical gastrectomy for gastric cancer: a randomized controlled trial. *Onco Targets Ther* 2016; **9**: 3345-3351 [PMID: 27330314 DOI: 10.2147/OTT.S107443]
25 **Chen ZX**, Liu AH, Cen Y. Fast-track program *vs* traditional care in surgery for gastric cancer. *World J Gastroenterol* 2014; **20**: 578-583 [PMID: 24574728 DOI: 10.3748/wjg.v20.i2.578]
26 **Beamish AJ**, Chan DS, Blake PA, Karran A, Lewis WG. Systematic review and meta-analysis of enhanced recovery programmes in gastric cancer surgery. *Int J Surg* 2015; **19**: 46-54 [PMID: 26004350 DOI: 10.1016/j.ijsu.2015.05.021]
27 **Chen S**, Zou Z, Chen F, Huang Z, Li G. A meta-analysis of fast track surgery for patients with gastric cancer undergoing gastrectomy. *Ann R Coll Surg Engl* 2015; **97**: 3-10 [PMID: 25519256 DOI: 10.1308/rcsann.2015.97.1.3]
28 **Ding J**, Sun B, Song P, Liu S, Chen H, Feng M, Guan W. The application of enhanced recovery after surgery (ERAS)/fast-track surgery in gastrectomy for gastric cancer: a systematic review and meta-analysis. *Oncotarget* 2017; **8**: 75699-75711 [PMID: 29088903 DOI: 10.18632/oncotarget.18581]
29 **Mortensen K**, Nilsson M, Slim K, Schäfer M, Mariette C, Braga M, Carli F, Demartines N, Griffin SM, Lassen K; Enhanced Recovery After Surgery (ERAS®) Group. Consensus guidelines for enhanced recovery after gastrectomy: Enhanced Recovery After Surgery (ERAS®) Society recommendations. *Br J Surg* 2014; **101**: 1209-1229 [PMID: 25047143 DOI: 10.1002/bjs.9582]
30 **Tanaka R**, Lee SW, Kawai M, Tashiro K, Kawashima S, Kagota S, Honda K, Uchiyama K. Protocol for enhanced recovery after surgery improves short-term outcomes for patients with gastric cancer: a randomized clinical trial. *Gastric Cancer* 2017; **20**: 861-871 [PMID: 28062937 DOI: 10.1007/s10120-016-0686-1]
31 **Higgins JP**, Altman DG, Gøtzsche PC, Jüni P, Moher D, Oxman AD, Savovic J, Schulz KF, Weeks L, Sterne JA; Cochrane Bias Methods Group; Cochrane Statistical Methods Group. The Cochrane Collaboration's tool for assessing risk of bias in randomised trials. *BMJ* 2011; **343**: d5928 [PMID: 22008217 DOI: 10.1136/bmj.d5928]
32 **Hozo SP**, Djulbegovic B, Hozo I. Estimating the mean and variance from the median, range, and the size of a sample. *BMC Med Res Methodol* 2005; **5**: 13 [PMID: 15840177 DOI: 10.1186/1471-2288-5-13]
33 **Feng F**, Ji G, Li JP, Li XH, Shi H, Zhao ZW, Wu GS, Liu XN, Zhao QC. Fast-track surgery could improve postoperative recovery in radical total gastrectomy patients. *World J Gastroenterol* 2013; **19**: 3642-3648 [PMID: 23801867 DOI: 10.3748/wjg.v19.i23.3642]
34 **Chen Hu J**, Xin Jiang L, Cai L, Tao Zheng H, Yuan Hu S, Bing Chen H, Chang Wu G, Fei Zhang Y, Chuan Lv Z. Preliminary experience of fast-track surgery combined with laparoscopy-assisted radical distal gastrectomy for gastric cancer. *J Gastrointest Surg* 2012; **16**: 1830-1839 [PMID: 22854954 DOI: 10.1007/s11605-012-1969-4]
35 **Kim JW**, Kim WS, Cheong JH, Hyung WJ, Choi SH, Noh SH. Safety and efficacy of fast-track surgery in laparoscopic distal gastrectomy for gastric cancer: a randomized clinical trial. *World J Surg* 2012; **36**: 2879-2887 [PMID: 22941233 DOI: 10.1007/s00268-012-1741-7]
36 **Liu XX**, Jiang ZW, Wang ZM, Li JS. Multimodal optimization of surgical care shows beneficial outcome in gastrectomy surgery. *JPEN J Parenter Enteral Nutr* 2010; **34**: 313-321 [PMID: 20467014 DOI: 10.1177/0148607110362583]
37 **Wang D**, Kong Y, Zhong B, Zhou X, Zhou Y. Fast-track surgery improves postoperative recovery in patients with gastric cancer: a randomized comparison with conventional postoperative care. *J Gastrointest Surg* 2010; **14**: 620-627 [PMID: 20108171 DOI: 10.1007/s11605-009-1139-5]
38 **Ren L**, Zhu D, Wei Y, Pan X, Liang L, Xu J, Zhong Y, Xue Z, Jin L, Zhan S, Niu W, Qin X, Wu Z, Wu Z. Enhanced Recovery After Surgery (ERAS) program attenuates stress and accelerates recovery in patients after radical resection for colorectal cancer: a prospective randomized controlled trial. *World J Surg* 2012; **36**: 407-414 [PMID: 22102090 DOI: 10.1007/s00268-011-1348-4]
39 **Carli F**. Physiologic considerations of Enhanced Recovery After Surgery (ERAS) programs: implications of the stress response. *Can J Anaesth* 2015; **62**: 110-119 [PMID: 25501695 DOI: 10.1007/s12630-014-0264-0]
40 **Feng J**, Li K, Li L, Wang X, Huang M, Yang J, Hu Y. The effects of fast-track surgery on inflammation and immunity in patients undergoing colorectal surgery. *Int J Colorectal Dis* 2016; **31**: 1675-1682 [PMID: 27517680 DOI: 10.1007/s00384-016-2630-6]
41 **Mari G**, Crippa J, Costanzi A, Mazzola M, Rossi M, Maggioni D. ERAS Protocol Reduces IL-6 Secretion in Colorectal Laparoscopic Surgery: Results From a Randomized Clinical Trial. *Surg Laparosc Endosc Percutan Tech* 2016; **26**: 444-448 [PMID: 27783027 DOI: 10.1097/SLE.0000000000000324]
42 **Stowers MD**, Lemanu DP, Hill AG. Health economics in Enhanced Recovery After Surgery programs. *Can J Anaesth* 2015; **62**: 219-230 [PMID: 25391739 DOI: 10.1007/s12630-014-0272-0]
43 **Nelson G**, Kiyang LN, Chuck A, Thanh NX, Gramlich LM. Cost impact analysis of Enhanced Recovery After Surgery program implementation in Alberta colon cancer patients. *Curr Oncol* 2016; **23**: e221-e227 [PMID: 27330358 DOI: 10.3747/co.23.2980]
44 **ERAS Compliance Group.** The Impact of Enhanced Recovery Protocol Compliance on Elective Colorectal Cancer Resection: Results From an International Registry. *Ann Surg* 2015; **261**: 1153-1159 [PMID: 25671587 DOI: 10.1097/SLA.0000000000001029]

45 **Alcántara-Moral M**, Serra-Aracil X, Gil-Egea MJ, Frasson M, Flor-Lorente B, Garcia-Granero E; E.B.S.Q.-C on behalf of the collaborative Group of Coloproctology Section of The Spanish Association of Surgeons. Observational cross-sectional study of compliance with the fast track protocol in elective surgery for colon cancer in Spain. *Int J Colorectal Dis* 2014; **29**: 477-483 [PMID: 24435243 DOI: 10.1007/s00384-013-1825-3]

46 **Feroci F**, Lenzi E, Baraghini M, Garzi A, Vannucchi A, Cantafio S, Scatizzi M. Fast-track surgery in real life: how patient factors influence outcomes and compliance with an enhanced recovery clinical pathway after colorectal surgery. *Surg Laparosc Endosc Percutan Tech* 2013; **23**: 259-265 [PMID: 23751989 DOI: 10.1097/SLE.0b013e31828ba16f]

47 **Bardram L**, Funch-Jensen P, Kehlet H. Rapid rehabilitation in elderly patients after laparoscopic colonic resection. *Br J Surg* 2000; **87**: 1540-1545 [PMID: 11091243 DOI: 10.1046/j.1365-2168.2000.01559.x]

48 **Pawa N**, Cathcart PL, Arulampalam TH, Tutton MG, Motson RW. Enhanced recovery program following colorectal resection in the elderly patient. *World J Surg* 2012; **36**: 415-423 [PMID: 22146943 DOI: 10.1007/s00268-011-1328-8]

49 **Baek SJ**, Kim SH, Kim SY, Shin JW, Kwak JM, Kim J. The safety of a "fast-track" program after laparoscopic colorectal surgery is comparable in older patients as in younger patients. *Surg Endosc* 2013; **27**: 1225-1232 [PMID: 23232990 DOI: 10.1007/s00464-012-2579-7]

50 **Neville A**, Lee L, Antonescu I, Mayo NE, Vassiliou MC, Fried GM, Feldman LS. Systematic review of outcomes used to evaluate enhanced recovery after surgery. *Br J Surg* 2014; **101**: 159-170 [PMID: 24469616 DOI: 10.1002/bjs.9324]

51 **Feldman LS**, Delaney CP. Laparoscopy plus enhanced recovery: optimizing the benefits of MIS through SAGES 'SMART' program. *Surg Endosc* 2014; **28**: 1403-1406 [PMID: 24651892 DOI: 10.1007/s00464-013-3415-4]

52 **Lei QC**, Wang XY, Zheng HZ, Xia XF, Bi JC, Gao XJ, Li N. Laparoscopic Versus Open Colorectal Resection Within Fast Track Programs: An Update Meta-Analysis Based on Randomized Controlled Trials. *J Clin Med Res* 2015; **7**: 594-601 [PMID: 26124904 DOI: 10.14740/jocmr2177w]

53 **Zhao JH**, Sun JX, Huang XZ, Gao P, Chen XW, Song YX, Liu J, Cai CZ, Xu HM, Wang ZN. Meta-analysis of the laparoscopic versus open colorectal surgery within fast track surgery. *Int J Colorectal Dis* 2016; **31**: 613-622 [PMID: 26732262 DOI: 10.1007/s00384-015-2493-2]

P- Reviewer: Aoyagi K, Bona S, Dai ZJ, Muhammad JS
S- Editor: Wang XJ **L- Editor**: Filipodia **E- Editor**: Huang Y

World Journal of Gastroenterology

Submit a Manuscript: http://www.f6publishing.com

World J Gastroenterol 2018 April 14; 24(14): 1579-1582

DOI: 10.3748/wjg.v24.i14.1579

ISSN 1007-9327 (print) ISSN 2219-2840 (online)

LETTERS TO THE EDITOR

Should hot biopsy forceps be abandoned for polypectomy of diminutive colorectal polyps?

Vasileios Panteris, Antonios Vezakis, JK Triantafillidis

Vasileios Panteris, Department of Gastroenterology, Sismanogleio-A.Fleming General Hospital, Attiki, Athens 15126, Greece

Antonios Vezakis, Department of Surgery, Aretaieio Hospital, Attiki, Athens 11528, Greece

JK Triantafillidis, Department of Gastroenterology, Iaso General Hospital, Attiki, Athens 15562, Greece

ORCID number: Vasileios Panteris (0000-0003-1165-8927); Antonios Vezakis (0000-0003-0958-7664); JK Triantafillidis (0000-0002-9115-232X).

Author contributions: All authors were involved in the article conception and design; Panteris V drafted the article; Vezakis A and Triantafillidis JK provided final approval of the article.

Conflict-of-interest statement: The authors declare that there are no conflicts of interest related to this study.

Manuscript source: Unsolicited manuscript

Correspondence to: Vasileios Panteris, MD, FEBG, Consultant, Doctor, Staff Physician, Department of Gastroenterology, Sismanogleio-A.Fleming General Hospital, Sismanogliou 37, Attiki, Athens 15126, Greece. vasileios.panteris@gmail.com
Telephone: +30-6937383262

Received: March 8, 2018
Peer-review started: March 9, 2018
First decision: March 14, 2018
Revised: March 19, 2018
Accepted: March 25, 2018
Article in press: March 25, 2018
Published online: April 14, 2018

Abstract

Standardized approach to polypectomy of diminutive colorectal polyps (DCPs) is lacking since cold biopsy forceps have been associated with high levels of recurrence, hot biopsy forceps are considered inadequate and risky and cold snaring is currently under investigation for its efficacy and safety. This has led to confusion and a gap in clinical practice. This article discusses the usefulness and contemporary practical applicability of hot biopsy forceps and provides well-intentioned criticism of the new European guidelines for the treatment of DCPs. Diminutive colorectal polyps are a source of frustration for the endoscopist since their small size is accompanied by a considerable risk of premalignant neoplasia and a small but non-negligible risk of advanced neoplasia and even cancer. Since the proportion of diminutive colorectal polyps is substantial and exceeds that of larger polyps, their effective removal poses a considerable workload and a therapeutic challenge. During the last decade, the introduction of cold snaring to routine endoscopy practice has attempted to overcome the use of prior techniques, such as hot biopsy forceps. It is important to recognize that with the exception of endoscopic methods that are obviously unsafe and inadequate to serve their purpose, all other interventional endoscopic methods are operator-dependent in the sense that specific expertise and training are obligatory for the success of any therapeutic intervention. Since relevant publications on hot biopsy forceps are still in favor of its careful use, as it has not yet demonstrated inferiority compared with newer techniques, it would be prudent

for any medical practitioner to evaluate the available tools and judge any new proposed technique based on the evidence before it is adopted.

Key words: Hot forceps; Polypectomy; Endoscopy; Colon neoplasia; Diminutive polyps

Core tip: Selection of the appropriate endoscopic method for the removal of diminutive colorectal polyps (DCPs), according to the prospective prevention of colorectal cancer, is still a debatable topic. The new recommendation released by ESGE (European Society of Gastrointestinal Endoscopy, 2017) concerning the use of hot biopsy forceps (HBF) is expected to create a shift in daily clinical practice since this technique is still popular and viable for the removal of DCPs. In this letter, the authors request reconsideration of this policy in response to published data referring on the efficacy and safety of HBF and recommend a more cautious approach and transition to prevent the premature acceptance of alternative techniques.

Panteris V, Vezakis A, Triantafillidis JK. Should hot biopsy forceps be abandoned for polypectomy of diminutive colorectal polyps? *World J Gastroenterol* 2018; 24(14): 1579-1582 Available from: URL: http://www.wjgnet.com/1007-9327/full/v24/i14/1579.htm DOI: http://dx.doi.org/10.3748/wjg.v24.i14.1579

TO THE EDITOR

In a recent article[1], European Society of Gastrointestinal Endoscopy has released guidelines for colorectal polypectomy, which include a strong recommendation against the use of hot biopsy forceps (HBF) based on the GRADE system of clinical evidence. The release of guidelines by professional medical societies is acknowledged by the medical community as policy that functions as a deterrent to specific practices. With respect to that notion, the abandonment of a useful technique such HBF, which for many decades, has contributed to the polypectomy of diminutive colorectal polyps (DCPs), should be considered in an appropriate conscientious and judicious manner.

The reasons for the negative criticism are based on the following: (1) unacceptably high risks of adverse events (AEs); (2) inadequate tissue sampling for histopathology (ITSH); and (3) high incomplete resection rates (IRR). The studies cited in support of the recommendation are 4 human studies (1 RCT non-blinded with a small number of patients[2], one anecdotal report[3] and 2 observational studies[4,5]), 3 of which have already been determined to be of low quality, and 2 animal studies[6,7] (Table 1). The overall quality of evidence was graded as high. Actually, apart from the methodological quality of the individual studies and the questionable generalizability, these studies are heterogeneous in terms of ITSH and IRR. Moreover, all studies are consistent with respect to the absence of perforations, and the few bleeding episodes (0.36%) in one of the studies occured in patients taking antiplatelets[5].

Table 1 List of articles presented in support of European Society of Gastrointestinal Endoscopy guidelines

Ref.	Study design Intervention	No of polyps and patients	Level of evidence
Paspatis *et al*[2], 2005	Randomised trial Bipolar electro-coagulation *vs* HBF	38 *vs* 37 rectal DCPs among 50 patients	High quality
Peluso *et al*[3], 1991	Anecdotal report HBF	62 DCPs among 39 patients	Low quality
Yasar *et al*[4], 2015	Observational study HBF *vs* JBF	237 DCPs among 179 patients	Low quality
Weston *et al*[5], 1995	Observational study HBF *vs* CBF	1964 DCPs among 687 patients	Low quality
Savides *et al*[6], 1995	Animal study Canine model	231 biopsies in 16 right colotomies of 8 mongrel dogs	Not rated in Grade system
Metz *et al*[7], 2013	Animal study Porcine model	82 artificial polyps, sized 5-8 mm	Not rated in Grade system

JBF: Jumbo biopsy forceps; CBF: Cold biopsy forceps; DCPs: Diminutive colorectal polyps; HBF: Hot biopsy forceps.

HBF is considered an alternative method for the removal of DCPs (≤ 5 mm). According to different surveys, it seems that HBF is still a viable option that is preferred by 30%-50% of endoscopists[8-10]. The two studies, with the largest number of patients and polyps[11,12] showed no complications. The study by Wadas *et al*[13], which reports a 0.38% major bleeding rate and a 0.05% perforation rate, refers to a questionnaire-type survey from an era (1988) when the HBF technique was not standardized. Even this perforation rate is lower than the reported 0.15% for therapeutic colonoscopies[14]. The rate of AEs is also lower compared with that for snare polypectomies (3.3 *vs* 4.5/1000), and AEs are more likely to occur when low- volume endoscopists use HBF than when high-volume endoscopists (> 300 polypectomies/year) use the technique[15].

HBF has been reported to have a 17% IRR when white coagulum is present[16] and a variable rate of ITSH that ranges from 0.19%-13%-26.7% in studies with different mean polyp sizes[11,17,18]. It is acknowledged that a significant predictor of histological misinterpretation is decreasing polyp size with a cut off limit of 2

mm. It is important to mention that even in studies with high reported rates of cautery artifacts[4], the results showed that histological diagnosis could indeed have been reached in all specimens.

The new rival of HBF, namely, the cold snare polypectomy (CSP), has thus far presented disparate results for IRR at 3.4%-40%, retrieval failure at 1%-13%, and bleeding rates of 1.2%-20% for DCPs[19-24]. In the sole non-blinded RCT, in which HBF and CSP are directly compared, the IRR in the ITT analysis was 29.9% for CSP, which is still unacceptably high. However, the bleeding rates were statistically insignificant at 8.1% *vs* 8.8% for HBF and CSP, respectively, and no perforations were observed in either study arm[25].

In conclusion, it seems that available evidence is not adequate to exclude hot biopsy forceps from the routine endoscopy practice. We either need more prospective studies exhibiting beneficial comparisons with new techniques or we need to focus on proper utilization of HBF by more experienced endoscopists.

REFERENCES

1 **Ferlitsch M**, Moss A, Hassan C, Bhandari P, Dumonceau JM, Paspatis G, Jover R, Langner C, Bronzwaer M, Nalankilli K, Fockens P, Hazzan R, Gralnek IM, Gschwantler M, Waldmann E, Jeschek P, Penz D, Heresbach D, Moons L, Lemmers A, Paraskeva K, Pohl J, Ponchon T, Regula J, Repici A, Rutter MD, Burgess NG, Bourke MJ. Colorectal polypectomy and endoscopic mucosal resection (EMR): European Society of Gastrointestinal Endoscopy (ESGE) Clinical Guideline. *Endoscopy* 2017; **49**: 270-297 [PMID: 28212588 DOI: 10.1055/s-0043-102569]

2 **Paspatis GA**, Vardas E, Charoniti I, Papanikolaou N, Barbatzas C, Zois E. Bipolar electrocoagulation vs conventional monopolar hot biopsy forceps in the endoscopic treatment of diminutive rectal adenomas. *Colorectal Dis* 2005; **7**: 138-142 [PMID: 15720350 DOI: 10.1111/j.1463-1318.2004.00725.x]

3 **Peluso F**, Goldner F. Follow-up of hot biopsy forceps treatment of diminutive colonic polyps. *Gastrointest Endosc* 1991; **37**: 604-606 [PMID: 1756918]

4 **Yasar B**, Kayadibi H, Abut E, Benek D, Kochan K, Gonen C. The histological quality and adequacy of diminutive colorectal polyps resected using jumbo versus hot biopsy forceps. *Dig Dis Sci* 2015; **60**: 217-225 [PMID: 25112723 DOI: 10.1007/s10620-014-3320-2]

5 **Weston AP**, Campbell DR. Diminutive colonic polyps: histopathology, spatial distribution, concomitant significant lesions, and treatment complications. *Am J Gastroenterol* 1995; **90**: 24-28 [PMID: 7801943]

6 **Savides TJ**, See JA, Jensen DM, Jutabha R, Machicado GA, Hirabayashi K. Randomized controlled study of injury in the canine right colon from simultaneous biopsy and coagulation with different hot biopsy forceps. *Gastrointest Endosc* 1995; **42**: 573-578 [PMID: 8674930 DOI: 10.1016/S0016-5107(95)70013-7]

7 **Metz AJ**, Moss A, McLeod D, Tran K, Godfrey C, Chandra A, Bourke MJ. A blinded comparison of the safety and efficacy of hot biopsy forceps electrocauterization and conventional snare polypectomy for diminutive colonic polypectomy in a porcine model. *Gastrointest Endosc* 2013; **77**: 484-490 [PMID: 23199650 DOI: 10.1016/j.gie.2012.09.014]

8 **Din S**, Ball AJ, Taylor E, Rutter M, Riley SA, Johal S. Polypectomy practices of sub-centimeter polyps in the English Bowel Cancer Screening Programme. *Surg Endosc* 2015; **29**: 3224-3230 [PMID: 25591413 DOI: 10.1007/s00464-015-4064-6]

9 **Singh N**, Harrison M, Rex DK. A survey of colonoscopic polypectomy practices among clinical gastroenterologists. *Gastrointest Endosc* 2004; **60**: 414-418 [PMID: 15332033 DOI: 10.1016/S0016-5107(04)01808-5]

10 **Carter D**, Beer-Gabel M, Zbar A, Avidan B, Bardan E. A survey of colonoscopic polypectomy practice amongst Israeli gastroenterologists. *Ann Gastroenterol* 2013; **26**: 135-140 [PMID: 24714780]

11 **Waye JD**, Lewis BS, Frankel A, Geller SA. Small colon polyps. *Am J Gastroenterol* 1988; **83**: 120-122 [PMID: 3341333]

12 **Mann NS**, Mann SK, Alam I. The safety of hot biopsy forceps in the removal of small colonic polyps. *Digestion* 1999; **60**: 74-76 [PMID: 9892802 DOI: 10.1159/000007592]

13 **Wadas DD**, Sanowski RA. Complications of the hot biopsy forceps technique. *Gastrointest Endosc* 1988; **34**: 32-37 [PMID: 3258260 DOI: 10.1016/S0016-5107(88)71226-2]

14 **Panteris V**, Haringsma J, Kuipers EJ. Colonoscopy perforation rate, mechanisms and outcome: from diagnostic to therapeutic colonoscopy. *Endoscopy* 2009; **41**: 941-951 [PMID: 19866393 DOI: 10.1055/s-0029-1215179]

15 **Chukmaitov A**, Bradley CJ, Dahman B, Siangphoe U, BouHaidar D, Warren JL. Polypectomy techniques, endoscopist characteristics, and serious gastrointestinal adverse events. *J Surg Oncol* 2014; **110**: 207-213 [PMID: 24706376 DOI: 10.1002/jso.23615.Epub]

16 **Vanagunas A**, Jacob P, Vakil N. Adequacy of "hot biopsy" for the treatment of diminutive polyps: a prospective randomized trial. *Am J Gastroenterol* 1989; **84**: 383-385 [PMID: 2648816]

17 **Goldstein NS**, Watts JC, Neill JS, Vogel LM, Barkel D, Kadro O, Priest S, Klein S. The effect of electrothermal cautery-assisted resection of diminutive colonic polyps on histopathologic diagnosis. *Am J Clin Pathol* 2001; **115**: 356-361 [PMID: 11242791 DOI: 10.1309/0KPE-1RG6-KA78-R49Y]

18 **Mönkemüller KE**, Fry LC, Jones BH, Wells C, Mikolaenko I, Eloubeidi M. Histological quality of polyps resected using the cold versus hot biopsy technique. *Endoscopy* 2004; **36**: 432-436 [PMID: 15100953 DOI: 10.1055/s-2004-814321]

19 **Horiuchi A**, Hosoi K, Kajiyama M, Tanaka N, Sano K, Graham DY. Prospective, randomized comparison of 2 methods of cold snare polypectomy for small colorectal polyps. *Gastrointest Endosc* 2015; **82**: 686-692 [PMID: 25922251 DOI: 10.1016/j.gie.2015.02.012]

20 **Komeda Y**, Suzuki N, Sarah M, Thomas-Gibson S, Vance M, Fraser C, Patel K, Saunders BP. Factors associated with failed polyp retrieval at screening colonoscopy. *Gastrointest Endosc* 2013; **77**: 395-400 [PMID: 23211749 DOI: 10.1016/j.gie.2012.10.007]

21 **Repici A**, Hassan C, Vitetta E, Ferrara E, Manes G, Gullotti G, Princiotta A, Dulbecco P, Gaffuri N, Bettoni E, Pagano N, Rando G, Strangio G, Carlino A, Romeo F, de Paula Pessoa Ferreira D, Zullo A, Ridola L, Malesci A. Safety of cold polypectomy for <10mm polyps at colonoscopy: a prospective multicenter study. *Endoscopy* 2012; **44**: 27-31 [PMID: 22125197 DOI: 10.1055/s-0031-1291387]

22 **Takeuchi Y**, Yamashina T, Matsuura N, Ito T, Fujii M, Nagai K, Matsui F, Akasaka T, Hanaoka N, Higashino K, Iishi H, Ishihara R, Thorlacius H, Uedo N. Feasibility of cold snare polypectomy in Japan: A pilot study. *World J Gastrointest Endosc* 2015; **7**: 1250-1256 [PMID: 26634041 DOI: 10.4253/wjge.v7.i17.1250]

23 **Lee CK**, Shim JJ, Jang JY. Cold snare polypectomy vs. Cold forceps polypectomy using double-biopsy technique for removal of diminutive colorectal polyps: a prospective randomized study. *Am J Gastroenterol* 2013; **108**: 1593-1600 [PMID: 24042189 DOI: 10.1038/ajg.2013.302]

24 **Matsuura N**, Takeuchi Y, Yamashina T, Ito T, Aoi K, Nagai K, Kanesaka T, Matsui F, Fujii M, Akasaka T, Hanaoka N, Higashino K, Tomita Y, Ito Y, Ishihara R, Iishi H, Uedo N. Incomplete resection rate of cold snare polypectomy: a prospective single-arm observational study. *Endoscopy* 2017; **49**: 251-257 [PMID:

28192823 DOI: 10.1055/s-0043-100215]

25 **Komeda Y**, Kashida H, Sakurai T, Tribonias G, Okamoto K, Kono M, Yamada M, Adachi T, Mine H, Nagai T, Asakuma Y, Hagiwara S, Matsui S, Watanabe T, Kitano M, Chikugo T, Chiba Y, Kudo M. Removal of diminutive colorectal polyps: A prospective randomized clinical trial between cold snare polypectomy and hot forceps biopsy. *World J Gastroenterol* 2017; **23**: 328-335 [PMID: 28127206 DOI: 10.3748/wjg.v23.i2.328]

P- Reviewer: Bujanda L, Facciorusso A, Velayos B
S- Editor: Gong ZM **L- Editor**: A **E- Editor**: Huang Y

Published by **Baishideng Publishing Group Inc**
7901 Stoneridge Drive, Suite 501, Pleasanton, CA 94588, USA
Telephone: +1-925-223-8242
Fax: +1-925-223-8243
E-mail: bpgoffice@wjgnet.com
Help Desk: http://www.f6publishing.com/helpdesk
http://www.wjgnet.com

ISSN 1007-9327

ISSN 1007-9327 (print)
ISSN 2219-2840 (online)

World Journal of *Gastroenterology*

World J Gastroenterol 2018 April 21; 24(15): 1583-1678

Published by Baishideng Publishing Group Inc

World Journal of Gastroenterology

Contents

Weekly Volume 24 Number 15 April 21, 2018

Contents

World Journal of Gastroenterology
Volume 24 Number 15 April 21, 2018

ABOUT COVER

Editorial board member of *World Journal of Gastroenterology*, Frank I Tovey, FRCS(Hon), Honorary Research Felllow, Department of Surgery, University College London, London W1W 7EJ, United Kingdom

AIMS AND SCOPE

World Journal of Gastroenterology (*World J Gastroenterol*, *WJG*, print ISSN 1007-9327, online ISSN 2219-2840, DOI: 10.3748) is a peer-reviewed open access journal. *WJG* was established on October 1, 1995. It is published weekly on the 7th, 14th, 21st, and 28th each month. The *WJG* Editorial Board consists of 642 experts in gastroenterology and hepatology from 59 countries.

The primary task of *WJG* is to rapidly publish high-quality original articles, reviews, and commentaries in the fields of gastroenterology, hepatology, gastrointestinal endoscopy, gastrointestinal surgery, hepatobiliary surgery, gastrointestinal oncology, gastrointestinal radiation oncology, gastrointestinal imaging, gastrointestinal interventional therapy, gastrointestinal infectious diseases, gastrointestinal pharmacology, gastrointestinal pathophysiology, gastrointestinal pathology, evidence-based medicine in gastroenterology, pancreatology, gastrointestinal laboratory medicine, gastrointestinal molecular biology, gastrointestinal immunology, gastrointestinal microbiology, gastrointestinal genetics, gastrointestinal translational medicine, gastrointestinal diagnostics, and gastrointestinal therapeutics. *WJG* is dedicated to become an influential and prestigious journal in gastroenterology and hepatology, to promote the development of above disciplines, and to improve the diagnostic and therapeutic skill and expertise of clinicians.

INDEXING/ABSTRACTING

World Journal of Gastroenterology (*WJG*) is now indexed in Current Contents®/Clinical Medicine, Science Citation Index Expanded (also known as SciSearch®), Journal Citation Reports®, Index Medicus, MEDLINE, PubMed, PubMed Central and Directory of Open Access Journals. The 2017 edition of Journal Citation Reports® cites the 2016 impact factor for *WJG* as 3.365 (5-year impact factor: 3.176), ranking *WJG* as 29th among 79 journals in gastroenterology and hepatology (quartile in category Q2).

NAME OF JOURNAL
World Journal of Gastroenterology

ISSN
ISSN 1007-9327 (print)
ISSN 2219-2840 (online)

LAUNCH DATE
October 1, 1995

FREQUENCY
Weekly

EDITORIAL OFFICE
Ze-Mao Gong, Director
World Journal of Gastroenterology
Baishideng Publishing Group Inc
7901 Stoneridge Drive, Suite 501,
Pleasanton, CA 94588, USA
Telephone: +1-925-2238242
Fax: +1-925-2238243
E-mail: editorialoffice@wjgnet.com
Help Desk: http://www.f6publishing.com/helpdesk
http://www.wjgnet.com

PUBLISHER
Baishideng Publishing Group Inc
7901 Stoneridge Drive, Suite 501,
Pleasanton, CA 94588, USA
Telephone: +1-925-2238242
Fax: +1-925-2238243
E-mail: bpgoffice@wjgnet.com
Help Desk: http://www.f6publishing.com/helpdesk
http://www.wjgnet.com

PUBLICATION DATE
April 21, 2018

INSTRUCTIONS TO AUTHORS
Full instructions are available online at http://www.wjgnet.com/bpg/gerinfo/204

ONLINE SUBMISSION
http://www.f6publishing.com

World Journal of Gastroenterology

Submit a Manuscript: http://www.f6publishing.com

World J Gastroenterol 2018 April 21; 24(15): 1583-1590

DOI: 10.3748/wjg.v24.i15.1583

ISSN 1007-9327 (print) ISSN 2219-2840 (online)

REVIEW

Ultrasound findings in autoimmune hepatitis

Yi Dong, Andrej Potthoff, Christoph Klinger, Ana Paula Barreiros, Dariusz Pietrawski, Christoph F Dietrich

Yi Dong, Department of Ultrasound, Zhongshan Hospital, Fudan University, Shanghai 200032, China

Andrej Potthoff, Department of Gastroenterology, Hepatology and Endocrinology, Medizinische Hochschule Hannover, Hannover D-30625, Germany

Christoph Klinger, Department of Internal Medicine 1, Klinikum Ludwigsburg, Ludwigsburg D-71634, Germany

Ana Paula Barreiros, German Organ Transplantation Foundation, Region Mitte, Mainz D-55131, Germany

Dariusz Pietrawski, Christoph F Dietrich, Department of Internal Medicine 2, Caritas-Krankenhaus Bad Mergentheim, Bad Mergentheim D-97980, Germany

ORCID number: Yi Dong (0000-0002-0212-1477); Andrej Potthoff (0000-0002-2985-7281); Christoph Klinger (0000-0001-7680-8477); Ana Paula Barreiros (0000-0003-2529-6779); Dariusz Pietrawski (0000-0003-2399-2252); Christoph F Dietrich (0000-0001-6015-6347).

Author contributions: All authors equally contributed to this paper with conception and design of the study, literature review and analysis, drafting and critical revision and editing, and final approval of the final version.

Conflict-of-interest statement: No potential conflicts of interest. No financial support.

Manuscript source: Unsolicited manuscript

Correspondence to: Christoph F Dietrich, MD, PhD, MBA, Professor, Department of Internal Medicine 2, Caritas-Krankenhaus Bad Mergentheim, Uhlandstr. 7, Bad Mergentheim D-97980, Germany. christoph.dietrich@ckbm.de

Telephone: +49-793158-2201/2200
Fax: +49-793158-2290

Received: February 1, 2018
Peer-review started: February 2, 2018
First decision: February 24, 2018
Revised: March 20, 2018
Accepted: March 30, 2018
Article in press: March 30, 2018
Published online: April 21, 2018

Abstract

Ultrasound findings in autoimmune hepatitis (AIH) have not been reported systematically so far. The use of reliable and accurate noninvasive methods for determining fibrosis stage is important in evaluation of treatment efficacy and fibrosis regression in AIH. Imaging plays an important role in detection of complications and ruling out other possible causes of chronic liver diseases. Ultrasound elastography cut-off values in AIH patients are not the same as those in patients with chronic viral hepatitis or non-alcoholic fatty liver disease. AIH is characterized by wide fluctuations in inflammatory activity. Here we report on current knowledge of ultrasound findings in AIH.

Key words: Autoimmune hepatitis; Fibrosis stage; Ultrasound; Elastography; Chronic liver diseases

Core tip: Accurate noninvasive imaging to determine fibrosis stages is of importance in the evaluation of treatment efficacy and fibrosis regression in autoimmune hepatitis (AIH). The cut-off values in AIH patients are not the same as those in patients with chronic viral hepatitis or non-alcoholic fatty liver disease.

Dong Y, Potthoff A, Klinger C, Barreiros AP, Pietrawski D, Dietrich CF. Ultrasound findings in autoimmune hepatitis. *World*

J Gastroenterol 2018; 24(15): 1583-1590 Available from: URL: http://www.wjgnet.com/1007-9327/full/v24/i15/1583.htm DOI: http://dx.doi.org/10.3748/wjg.v24.i15.1583

INTRODUCTION

Autoimmune hepatitis (AIH) is a chronic immune mediated liver disease of unknown etiology[1,2]. About one-third of the patients already have developed advanced fibrosis and liver cirrhosis at the time of diagnosis. AIH mainly affects women and is usually characterized by chronic inflammation of the liver, hypergammaglobulinemia with increased immunoglobulin G (IgG) levels and circulating autoantibodies associated with human leukocyte antigens DR3 or DR4, typical liver histology with interface hepatitis[3], and a favorable response to immunosuppressive treatment[1,2,4]. Once other liver diseases such as viral hepatitis have been excluded, the diagnosis of AIH can be made by serological and histological findings. AIH can range from a mild or severe course to fulminant hepatic failure. Despite corticosteroid therapy, hepatic fibrosis develops in 25% of patients with AIH[5]. To find reliable and accurate noninvasive imaging methods for determining fibrosis stages is of importance in the evaluation of treatment efficacy and fibrosis regression in AIH[6]. Here we report on ultrasound findings in AIH.

CLASSIFICATION OF AIH

AIH has a global distribution. It is considered as a rare disease affecting all ages and ethnic groups with a female predominance (F:M ratio 3.6:1). The incidence of AIH is around 1 per 100000 persons per year[7]. In 1992, the International AIH Group (IAIHG) reported diagnostic criteria[8], which were remarkably simplified in 2008[9]. AIH is classified into two major types: AIH type 1 (AIH-1) and AIH type 2 (AIH-2). Antinuclear antibodies (ANA) and/or smooth muscle autoantibodies (SMA) could be detected in AIH-1. Also perinuclear anti-neutrophil cytoplasmic antibodies (p-ANCA) could be detected in 60%-90% of AIH-1 patients[4,5,9,10]. AIH-2 is characterized by the detection of anti-liver/kidney microsomal antibody type 1 or anti-LKM type 3[4,10] and/or antibodies against liver cytosol type 1 antigen[1,4]. AIH-1 accounts for about 75%-80% of all patients, however, AIH-2 is more frequently seen in children and young patients, which might present with acute onset and severe histological changes at time of diagnosis. Poor treatment prognosis, recurrence after treatment and need for lifelong treatment are more common in AIH-2[4,11]. AIH-1 patients might also show antibodies against soluble liver/liver-pancreas-antigen SLA/LP-[12,13].

PATHOGENESIS

According to the dominant pathogenetic hypothesis, AIH develops in genetically susceptible individuals by several triggers. The liver is attacked through mechanisms of "molecular mimicry", and is promoted by down regulation of regulatory T-cells[3, 4].

AIH may develop after the use of some drugs and biological agents or after viral infections and other events, including *de novo* after orthotopic liver transplantation[14-16]. AIH may first develop during pregnancy and after delivery.

CLINICAL MANIFESTATIONS

Clinically AIH is characterized by fluctuation of disease activity. Its clinical symptoms range from no obvious manifestations to severe and acute hepatitis [4,17]. Clinical manifestations range from merely elevated transaminases to liver cirrhosis and/or fulminant liver failure requiring liver transplantation[18]. Acute AIH presents in approximately 25% patients with similar symptoms as patients suffering from acute toxic or viral hepatitis[19]. At time of diagnosis, about one third of patients have established cirrhosis[3]. A specific and common clinical characteristic of AIH is its association with other autoimmune diseases including first degree relatives[20]. Concurrent extrahepatic autoimmune conditions mostly affect the thyroid gland (10%-23%)[13]. Clinical presentation of AIH might be similar to primary biliary cirrhosis (PBC) and primary sclerosing cholangitis (PSC). These diseases may coexist leading to overlap or variant syndromes[21,22].

DIAGNOSIS

Due to the absence of specific diagnostic features and diversity of clinical manifestations, serological and histological features, AIH diagnosis may be a challenge[3]. According to the International Autoimmune Hepatitis Group (IAIHG), the clinical diagnosis of AIH is based on biochemical, immunological, and histological features. Viral hepatitis should be excluded[9]. The simplified diagnostic criteria of IAIHG for AIH is based mainly on four parameters, including autoantibodies detection, serum IgG levels, absence of viral hepatitis markers and liver histology[9]. Histological changes including interface hepatitis, and hepatic rosette formation and emperipolesis[9]. Autoantibodies detectionis regarded as the hallmark for a timely diagnosis although not pathognomonic[3].

LABORATORY ASSESSMENTS AND LIVER BIOPSY

Liver biochemistry is not characteristic in most of AIH patients, with elevated bilirubin and transaminases. In most patients, polyclonal hypergammaglobulinemia with particular elevated level of serum IgG is observed. However, it should be mentioned that 15%-25% of patients (especially children, elderly and acute cases) have normal IgG levels. Therefore, AIH diagnosis

should not be excluded depending on a normal IgG testing[3]. The standard laboratory assessments include elevated LFTs, hypergammaglobulinemia, and the detection of autoantibodies (ANA, anti-SMA, and anti-LKM).

Liver biopsy is strongly recommended to confirm AIH[13], first to make the diagnosis and second to determine the stage of disease. The diagnostic histological features of AIH include moderate to severe interface hepatitis without biliary lesions or well-defined granulomas. However, it must be noted that pathognomonic histologically characteristics for AIH are missing. Regular assessment of hepatic fibrosis is important in patients with AIH because progressive fibrosis ultimately leads to cirrhosis and liver failure[23]. It has been recommended that clinical decisions about duration of treatment or immunosuppressive therapy should be based on clinical remission and histological features[2].

NON-INVASIVE MARKERS OF LIVER FIBROSIS

Laboratory methods can differentiate liver cirrhosis from non-cirrhosis, but their accuracy in distinguishing changes of AIH in histological stages is uncertain. Biochemical markers can reflect the therapeutic response during treatment, but they cannot reflect the severity of liver fibrosis[5]. Many non-invasive markers for assessing liver fibrosis and cirrhosis have been applied in clinical practice[24,25]. However, their ability to detect early stages of liver fibrosis and cirrhosis in AIH patients is still uncertain[26]. All calculated non-invasive markers are not specific. However, it has been consider feasible to predict the degree of liver fibrosis in patients with AIH using laboratory parameters. Platelet count as well as AAR could be used to predict the presence of advanced fibrosis[27,28].

DIFFERENTIAL DIAGNOSIS

Differential diagnosis of AIH includes chronic viral hepatitis (B and C), primary sclerosing cholangitis, alpha-1 antitrypsin deficiency, primary biliary cirrhosis, hemochromatosis, Wilson's disease and drug induced hepatitis (*e.g.*, minocycline, nitrofurantoin, isoniazid, methyldopa). However, to differentiate AIH from drug-induced liver injury (DILI) might be a challenge in cholestatic and severe clinical presentations, in particular when circulating liver autoantibodies are detectable in serum[2] Elevated IgG serum-levels and the histological presence of plasma cells can be found as well in a significant proportion of DILI patients[29].

Treatment

In order to prevent progressive liver fibrosis/cirrhosis, treatment aims on complete biochemical (defined by normalization of aminotransferases and IgG level) and histological remission[13,30]. Most patients respond well to immunosuppressive therapy, which usually results in an excellent prognosis[1,31,32]. Steroids are used as initial therapy leading to a treatment response in 80% of patients with AIH[33-35]. In adults, Azathioprine is effective as maintenance therapy[5,10,30]. Treatment should be continued until normalization of laboratory tests and liver histology[36]. Incomplete response and treatment failure occur in 14%[37] and 7% of patients[38], respectively[36,39,40]. Treatment failure is characterized by a missing decrease of aminotransferase levels and, in some patients, rapid progression to cirrhosis. Consequently, alternative therapeutic regimens have to be considered[5,41,42]. In cases of treatment failure, overlap with other etiologies should be considered. In those patients with liver failure, liver transplantation might be indicated and carries a 10-year survival rate exceeding 70%[1]. Future anti-fibrotic therapies and monitoring fibrosis progression are essential in patients with in AIH.

ULTRASOUND IMAGING

B-mode ultrasound and contrast-enhanced ultrasound

No characteristic conventional ultrasound imaging features of AIH have been described. For initial diagnosis of AIH, ultrasound, computed tomography (CT), and magnetic resonance imaging (MRI) are valuable methods to detect liver cirrhosis and its complications. Imaging of AIH play a role in the detection of complications[21]. Enlarged perihepatic lymph nodes are a typical ultrasound feature, similar to virus hepatitis C[43-46] (Figure 1), PBC[47,48], PSC[49], sarcoidosis[50,51] and other inflammatory liver diseases[50] in adults and children[46,50] (Figures 1 and 2). These enlarged inflammatory perihepatic lymph nodes show typical contrast behavior and elastographic architecture[52-59] (Figure 3).

About 1%-9% of AIH patients with liver cirrhosis develop HCC. Therefore, ultrasound follow-up examinations are recommended every six month[60]. Characteristically, involvement of the biliary tract is absent or minimal in AIH. Magnetic resonance cholangiography (MRC) is recommended in all children and adult patients with elevated markers of cholestasis in order to detect concurrent overlap syndromes, particularly PSC.

Ultrasound elastography

Non-invasive liver ultrasound elastography methods are useful for detection and staging of liver fibrosis initially as well as during clinical follow-up. Transient elastography (TE) has been introduced first to assess liver stiffness in patients with chronic liver diseases[61,62]. Other newer ultrasound-elastography methods include point shear-wave elastography (pSWE) and two-dimensional shear-wave elastography (2D-SWE)[63]. These tools are integrated in standard ultrasound devices.

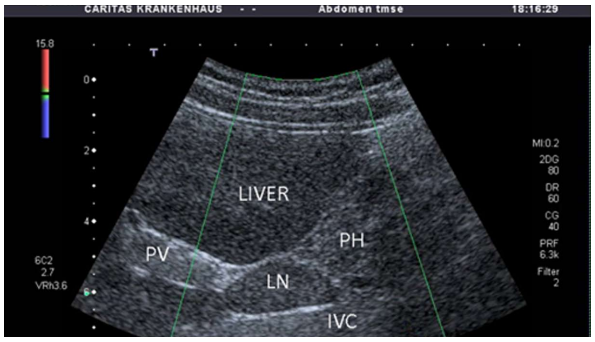

Figure 1 Enlarged perihepatic lymph nodes dorsal in the hepatoduodenal ligament between the portal vein and inferior vena cava is a typical sonographic sign of autoimmune hepatitis. PV: Portal vein; PH: Pancreatic head; ICV: Inferior vena cava.

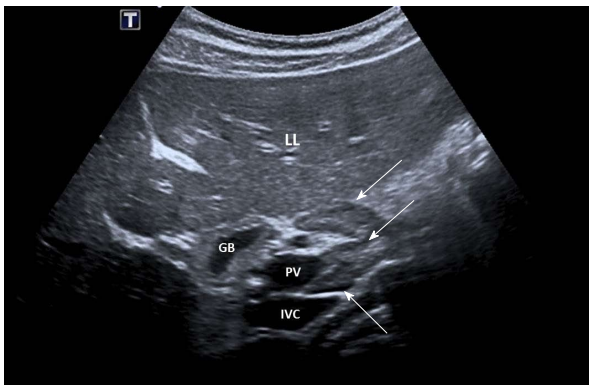

Figure 2 Enlarged perihepatic lymph nodes ventral and dorsal in the hepatoduodenal ligament between the portal vein and inferior vena cava (white arrows). LL: Liver; GB: Galbladder; PV: Portal vein; ICV: Inferior vena cava.

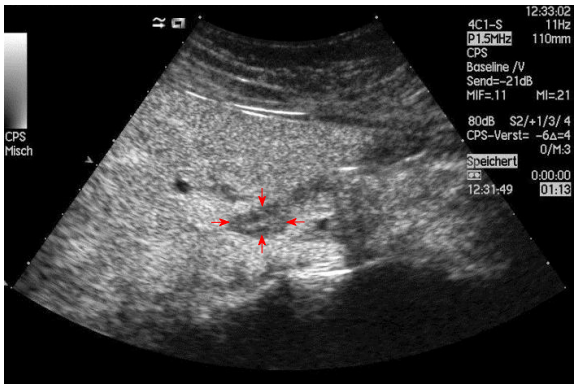

Figure 3 Enlarged perihepatic lymph nodes dorsal in the hepatoduodenal ligament is a typical sonographic sign of autoimmune hepatitis. Contrast enhanced ultrasound shows normal lymph node architecture (in between arrows).

Ultrasound elastography methods are proved to be accurate and reliable in the diagnosis of advanced fibrosis and cirrhosis, however, the diagnostic performances may be compromised by inflammation, congestion, biliary obstruction and obesity[63]. Magnetic resonance elastography (MRE) has excellent performance parameters for all histological stages in diverse liver diseases[64], which represents to be a reliable alternative to SWE. MRE is less influenced by body habitus and inflammatory activity in the evaluation of fibrosis in AIH[65-67] but its availability is limited and the investigation is more expensive.

Transient elastography

The cut-off values in AIH patients are not the same as those in patients with chronic viral hepatitis. A recent study which enrolled 108 AIH patients who underwent liver biopsies, AUROC value of liver stiffness measurement (LSM) was 0.885 for stage F2 (n = 24), 0.897 for stage F3 (n = 30), and 0.878 for stage F4 (n = 24). The optimal LSM cut-off value was 6.27 kPa for stage F2, 8.18 kPa for F3, and 12.67 kPa for F4[68]. LSM was superior to other non-invasive markers in differentiating the stages of fibrosis in AIH patients[68]. Liver stiffness measured by TE correlated significantly with the stage of liver fibrosis in a study which compared accuracy of TE and liver biopsy in AIH patients. TE correlated better than non-invasive laboratory markers[69,70]. This study demonstrated similar cut-off values, with LSM cut-off values of 6.45 kPa for F2, 8.75 kPa for F3, and 12.5 kPa for F4[70].

A previous study[70] evaluated the accuracy of LSM, APRI, and FIB-4 in 100 AIH patients. TE outperformed the other non-invasive markers. LSM was proven to be closely associated with fibrosis stages (r = 0.752, P < 0.01). Patients with more advanced fibrosis stages are associated with higher LSM values. Of importance, serum ALT levels had minor effect on LSM values and hepatic inflammatory activity had no significant effect on LSM determination.

TE proved also to be more accurate than APRI score in study published by Halasz *et al*[71] including 22 cases of AIH.

Wang *et al*[69] conducted a retrospective study with 36 histologically confirmed AIH patients (19 treated and 17 untreated). They reported that TE was accurate for distinguishing hepatic fibrosis in AIH between stages F0-F2 and F3-F4.

While comparing to other etiologies, the higher LSM values for different Ishak stages in AIH patients are in line with the results in the literature[69,72-74]. In a pediatric study of Behairy *et al*[6], a total of 90 children (HCV n = 50, AIH n = 20, Wilson´s disease n = 20) were included and underwent LSM using TE. AIH patients had both higher values of LSM and (necro) inflammation scores compared to patients with HCV and Wilson´s disease. Inflammatory activity accompanying with increased serum aminotransferase levels, can increase liver stiffness may be misinterpreted as fibrosis[75,76]. Therefore, the higher grade of (necro-) inflammatory activity in AIH patients compared to other etiologies could be a possible explanation[2,3].

Long-term treatment with mono corticosteroids or in combination with azathioprine is proposed when the AIH diagnosis is established. The effect of treatment on the diagnostic performance of LSM has been studied

as well. Hartl *et al*[77] reported that performance of TE in the detection of cirrhosis is better for AIH patients who received longer treatment compared to treatment-naïve patients and patients with shorter duration of treatment. Using the cut-off of 16 kPa, the diagnostic accuracy for cirrhosis was excellent in patients (n = 36) under immunosuppressive treatment for 6 months or longer[77]. A non-invasive inflammatory score has been proposed to discriminate patients with and without significant hepatic inflammation[78]. Those scores are easy to calculate, however, they would be only suitable to patients without co-morbidities and not for patients with low inflammatory activity[79]. Weight gain is a common consequence of corticosteroid treatment[80,81].

Acoustic radiation force impulse imaging

Acoustic radiation force impulse imaging (ARFI) can help to distinguish liver fibrosis patients with autoimmune liver diseases from healthy subjects[82,83]. In AIH patients after at least 2 years of biochemical remission, ARFI allowed to differentiate significant (F ≥ 2) from non-significant liver fibrosis (F < 2) (2.28 ± 0.68 m/s *vs* 1.20 ± 0.24 m/s, P = 0.002)[23]. Although large studies on ARFI elastography in AIH patients are still lacking preliminary data indicate that ARFI is a promising non-invasive method for detection and staging of fibrosis also in AIH patients.

2D-SWE

SuperSonic shear wave imaging (SuperSonic Imagine, Aix-en-Provence, France) had higher values in liver fibrosis with AIH of stages S2-S4[84] similar to the results with ARFI[82]. The shear moduli were 9.41 ± 2.5 kPa in S0 stage; 10.42 ± 5.1kPa in S1 stage; 13.25 ± 5.6 kPa in S2 stage; 19.03 ± 7.8 kPa in S3 stage and 24.99 ± 9.5 kPa in S4 stage[84].

Real-time elastography

In an animal based study, Hao *et al*[85] investigated the inflammation effect on fibrosis staging by measuring quantitative elasticity parameters in AIH rats (HiVision Preirus, Hitachi Medical Systems Co, Ltd, Tokyo, Japan). The grade of inflammation will influence the accuracy of Real-time elastography (RTE) measurements. The liver fibrosis index had the highest correlation with inflammation grading (r = 0.766; P< 0.05).

LIMITATIONS

Currently, ultrasound findings in AIH have been limited use so far. No characteristic ultrasound imaging features of AIH have been described in the literature. There is a need for studies to determine the better use of ultrasound in AIH patients.

CONCLUSION

In conclusion, AIH is characterized by wide fluctuations in inflammatory activity, Thus, stage of fibrosis can be overestimated by transient elastography[86] due to concomitant hepatic necroinflammatory activity. It can be also concluded that LSM using TE reflects the stages of liver fibrosis and correlates better than non-invasive laboratory markers in patients with treated AIH[77,87,88]. Other non-invasive ultrasound based techniques as ARFI, 2D-SWE or Real Time Elastography are not well investigated in the population of AIH patients yet. Further studies are needed. However, current non-invasive markers/methods for the evaluation of liver fibrosis in AIH could not replace liver biopsy, especially in differentiating mild from severe stages of fibrosis[87].

REFERENCES

1 **Manns MP**, Lohse AW, Vergani D. Autoimmune hepatitis--Update 2015. *J Hepatol* 2015; **62**: S100-S111 [PMID: 25920079 DOI: 10.1016/j.jhep.2015.03.005]

2 **Liwinski T**, Schramm C. Autoimmune hepatitis - update on clinical management in 2017. *Clin Res Hepatol Gastroenterol* 2017; **41**: 617-625 [PMID: 28882739 DOI: 10.1016/j.clinre.2017.07.002]

3 **Gatselis NK**, Zachou K, Koukoulis GK, Dalekos GN. Autoimmune hepatitis, one disease with many faces: etiopathogenetic, clinico-laboratory and histological characteristics. *World J Gastroenterol* 2015; **21**: 60-83 [PMID: 25574080 DOI: 10.3748/wjg.v21.i1.60]

4 **Zachou K**, Muratori P, Koukoulis GK, Granito A, Gatselis N, Fabbri A, Dalekos GN, Muratori L. Review article: autoimmune hepatitis -- current management and challenges. *Aliment Pharmacol Ther* 2013; **38**: 887-913 [PMID: 24010812 DOI: 10.1111/apt.12470]

5 **Manns MP**, Czaja AJ, Gorham JD, Krawitt EL, Mieli-Vergani G, Vergani D, Vierling JM; American Association for the Study of Liver Diseases. Diagnosis and management of autoimmune hepatitis. *Hepatology* 2010; **51**: 2193-2213 [PMID: 20513004 DOI: 10.1002/hep.23584]

6 **Behairy Bel-S**, Sira MM, Zalata KR, Salama el-SE, Abd-Allah MA. Transient elastography compared to liver biopsy and morphometry for predicting fibrosis in pediatric chronic liver disease: Does etiology matter? *World J Gastroenterol* 2016; **22**: 4238-4249 [PMID: 27122674 DOI: 10.3748/wjg.v22.i16.4238]

7 **Jepsen P**, Grønbæk L, Vilstrup H. Worldwide Incidence of Autoimmune Liver Disease. *Dig Dis* 2015; **33** Suppl 2: 2-12 [PMID: 26641102 DOI: 10.1159/000440705]

8 **Krawitt EL**. Can you recognize autoimmune hepatitis? *Postgrad Med* 1998; **104**: 145-149, 152 [PMID: 9721584]

9 **Hennes EM**, Zeniya M, Czaja AJ, Parés A, Dalekos GN, Krawitt EL, Bittencourt PL, Porta G, Boberg KM, Hofer H, Bianchi FB, Shibata M, Schramm C, Eisenmann de Torres B, Galle PR, McFarlane I, Dienes HP, Lohse AW; International Autoimmune Hepatitis Group. Simplified criteria for the diagnosis of autoimmune hepatitis. *Hepatology* 2008; **48**: 169-176 [PMID: 18537184 DOI: 10.1002/hep.22322]

10 **Gleeson D**, Heneghan MA; British Society of Gastroenterology. British Society of Gastroenterology (BSG) guidelines for management of autoimmune hepatitis. *Gut* 2011; **60**: 1611-1629 [PMID: 21757447 DOI: 10.1136/gut.2010.235259]

11 **Liberal R**, Grant CR, Mieli-Vergani G, Vergani D. Autoimmune hepatitis: a comprehensive review. *J Autoimmun* 2013; **41**: 126-139 [PMID: 23218932 DOI: 10.1016/j.jaut.2012.11.002]

12 **Manns M**, Gerken G, Kyriatsoulis A, Staritz M, Meyer zum Büschenfelde KH. Characterisation of a new subgroup of autoimmune chronic active hepatitis by autoantibodies against a soluble liver antigen. *Lancet* 1987; **1**: 292-294 [PMID: 2880112]

13 **Deutsche Gesellschaft für Gastroenterologie**, Verdauungs- und Stoffwechselkrankheiten (DGVS) (federführend). Deutsche

Gesellschaft für Innere Medizin (DGIM); Deutsche M. Crohn/ Colitis ulcerosa Vereinigung (DCCV); Deutsche Leberhilfe e.V; Deutsche Gesellschaft für Ultraschall in der Medizin (DEGUM); Deutsche Gesellschaft für Endoskopie und Bildgebende Verfahren (DGE-BV); Deutsche Gesellschaft für Kinder- und Jugendmedizin (DGKJ); Gesellschaft für Pädiatrische Gastroenterologie (GPGE); Deutsche Gesellschaft für Rheumatologie (DGRh); Deutsche Röntgengesellschaft (DRG); Deutsche Transplantationsgesellschaft (DTG); Deutsche Gesellschaft für Pathologie (DGP) und Bundesverband Deutscher Pathologen (BDP); Österreichische Gesellschaft für Gastroenterologie (ÖGG); Schweizer Gastroenterologische Gesellschaft (SGG); Authors; Collaborators:; Externe Begutachtung durch:. [Practice guideline autoimmune liver diseases - AWMF-Reg. No. 021-27]. *Z Gastroenterol* 2017; **55**: 1135-1226 [PMID: 29141269 DOI: 10.1055/s-0043-120199]

14 **Westbrook RH**, Yeoman AD, Kriese S, Heneghan MA. Outcomes of pregnancy in women with autoimmune hepatitis. *J Autoimmun* 2012; **38**: J239-J244 [PMID: 22261501 DOI: 10.1016/j.jaut.2011.12.002]

15 **Castiella A**, Zapata E, Lucena MI, Andrade RJ. Drug-induced autoimmune liver disease: A diagnostic dilemma of an increasingly reported disease. *World J Hepatol* 2014; **6**: 160-168 [PMID: 24799984 DOI: 10.4254/wjh.v6.i4.160]

16 **Björnsson E**, Talwalkar J, Treeprasertsuk S, Kamath PS, Takahashi N, Sanderson S, Neuhauser M, Lindor K. Drug-induced autoimmune hepatitis: clinical characteristics and prognosis. *Hepatology* 2010; **51**: 2040-2048 [PMID: 20512992 DOI: 10.1002/hep.23588]

17 **Stravitz RT**, Lefkowitch JH, Fontana RJ, Gershwin ME, Leung PS, Sterling RK, Manns MP, Norman GL, Lee WM; Acute Liver Failure Study Group. Autoimmune acute liver failure: proposed clinical and histological criteria. *Hepatology* 2011; **53**: 517-526 [PMID: 21274872 DOI: 10.1002/hep.24080]

18 **Acharya GK**, Liao HI, Frunza-Stefan S, Patel R, Khaing M. Autoimmune Hepatitis: Diagnostic Dilemma When It Is Disguised as Iron Overload Syndrome. *J Clin Exp Hepatol* 2017; **7**: 269-273 [PMID: 28970716 DOI: 10.1016/j.jceh.2017.03.006]

19 **Takahashi H**, Zeniya M. Acute presentation of autoimmune hepatitis: Does it exist? A published work review. *Hepatol Res* 2011; **41**: 498-504 [PMID: 21595804 DOI: 10.1111/j.1872-034X.2011.00808.x]

20 **Teufel A**, Weinmann A, Kahaly GJ, Centner C, Piendl A, Wörns M, Lohse AW, Galle PR, Kanzler S. Concurrent autoimmune diseases in patients with autoimmune hepatitis. *J Clin Gastroenterol* 2010; **44**: 208-213 [PMID: 20087196 DOI: 10.1097/MCG.0b013e3181c74e0d]

21 **Malik N**, Venkatesh SK. Imaging of autoimmune hepatitis and overlap syndromes. *Abdom Radiol* (NY) 2017; **42**: 19-27 [PMID: 27999888 DOI: 10.1007/s00261-016-1019-x]

22 **Weiler-Normann C**, Lohse AW. Variant Syndromes of Autoimmune Liver Diseases: Classification, Diagnosis and Management. *Dig Dis* 2016; **34**: 334-339 [PMID: 27170386 DOI: 10.1159/000444472]

23 **Efe C**, Gungoren MS, Ozaslan E, Akbiyik F, Kav T. Acoustic Radiation Force Impulse (ARFI) for Fibrosis Staging in Patients with Autoimmune Hepatitis. *Hepatogastroenterology* 2015; **62**: 670-672 [PMID: 26897951]

24 **Kim WR**, Berg T, Asselah T, Flisiak R, Fung S, Gordon SC, Janssen HL, Lampertico P, Lau D, Bornstein JD, Schall RE, Dinh P, Yee LJ, Martins EB, Lim SG, Loomba R, Petersen J, Buti M, Marcellin P. Evaluation of APRI and FIB-4 scoring systems for non-invasive assessment of hepatic fibrosis in chronic hepatitis B patients. *J Hepatol* 2016; **64**: 773-780 [PMID: 26626497 DOI: 10.1016/j.jhep.2015.11.012]

25 **Vallet-Pichard A**, Mallet V, Nalpas B, Verkarre V, Nalpas A, Dhalluin-Venier V, Fontaine H, Pol S. FIB-4: an inexpensive and accurate marker of fibrosis in HCV infection. comparison with liver biopsy and fibrotest. *Hepatology* 2007; **46**: 32-36 [PMID: 17567829 DOI: 10.1002/hep.21669]

26 **Abdollahi M**, Pouri A, Ghojazadeh M, Estakhri R, Somi M. Non-invasive serum fibrosis markers: A study in chronic hepatitis. *Bioimpacts* 2015; **5**: 17-23 [PMID: 25901293 DOI: 10.15171/bi.2015.05]

27 **Anastasiou J**, Alisa A, Virtue S, Portmann B, Murray-Lyon I, Williams R. Noninvasive markers of fibrosis and inflammation in clinical practice: prospective comparison with liver biopsy. *Eur J Gastroenterol Hepatol* 2010; **22**: 474-480 [PMID: 19887952 DOI: 10.1097/MEG.0b013e328332dd0a]

28 **Lüth S**, Herkel J, Kanzler S, Frenzel C, Galle PR, Dienes HP, Schramm C, Lohse AW. Serologic markers compared with liver biopsy for monitoring disease activity in autoimmune hepatitis. *J Clin Gastroenterol* 2008; **42**: 926-930 [PMID: 18645526 DOI: 10.1097/MCG.0b013e318154af74]

29 **de Boer YS**, Kosinski AS, Urban TJ, Zhao Z, Long N, Chalasani N, Kleiner DE, Hoofnagle JH; Drug-Induced Liver Injury Network. Features of Autoimmune Hepatitis in Patients With Drug-induced Liver Injury. *Clin Gastroenterol Hepatol* 2017; **15**: 103-112.e2 [PMID: 27311619 DOI: 10.1016/j.cgh.2016.05.043]

30 **European Association for the Study of the Liver**. EASL Clinical Practice Guidelines: Autoimmune hepatitis. *J Hepatol* 2015; **63**: 971-1004 [PMID: 26341719 DOI: 10.1016/j.jhep.2015.06.030]

31 **Lamers MM**, van Oijen MG, Pronk M, Drenth JP. Treatment options for autoimmune hepatitis: a systematic review of randomized controlled trials. *J Hepatol* 2010; **53**: 191-198 [PMID: 20400196 DOI: 10.1016/j.jhep.2010.01.037]

32 **Terziroli Beretta-Piccoli B**, Mieli-Vergani G, Vergani D. Autoimmune hepatitis: Standard treatment and systematic review of alternative treatments. *World J Gastroenterol* 2017; **23**: 6030-6048 [PMID: 28970719 DOI: 10.3748/wjg.v23.i33.6030]

33 **Jothimani D**, Cramp ME, Mitchell JD, Cross TJ. Treatment of autoimmune hepatitis: a review of current and evolving therapies. *J Gastroenterol Hepatol* 2011; **26**: 619-627 [PMID: 21073674 DOI: 10.1111/j.1440-1746.2010.06579.x]

34 **Chen J**, Eslick GD, Weltman M. Systematic review with meta-analysis: clinical manifestations and management of autoimmune hepatitis in the elderly. *Aliment Pharmacol Ther* 2014; **39**: 117-124 [PMID: 24261965 DOI: 10.1111/apt.12563]

35 **Roberts SK**, Therneau TM, Czaja AJ. Prognosis of histological cirrhosis in type 1 autoimmune hepatitis. *Gastroenterology* 1996; **110**: 848-857 [PMID: 8608895]

36 **Czaja AJ**. Review article: the management of autoimmune hepatitis beyond consensus guidelines. *Aliment Pharmacol Ther* 2013; **38**: 343-364 [PMID: 23808490 DOI: 10.1111/apt.12381]

37 **Czaja AJ**. Rapidity of treatment response and outcome in type 1 autoimmune hepatitis. *J Hepatol* 2009; **51**: 161-167 [PMID: 19446908 DOI: 10.1016/j.jhep.2009.02.026]

38 **Montano-Loza AJ**, Carpenter HA, Czaja AJ. Features associated with treatment failure in type 1 autoimmune hepatitis and predictive value of the model of end-stage liver disease. *Hepatology* 2007; **46**: 1138-1145 [PMID: 17668882 DOI: 10.1002/hep.21787]

39 **Grønbæk L**, Vilstrup H, Jepsen P. Autoimmune hepatitis in Denmark: incidence, prevalence, prognosis, and causes of death. A nationwide registry-based cohort study. *J Hepatol* 2014; **60**: 612-617 [PMID: 24326217 DOI: 10.1016/j.jhep.2013.10.020]

40 **Muratori L**, Muratori P, Lanzoni G, Ferri S, Lenzi M. Application of the 2010 American Association for the study of liver diseases criteria of remission to a cohort of Italian patients with autoimmune hepatitis. *Hepatology* 2010; **52**: 1857; author reply 1857-1857; author reply 1858 [PMID: 20931560 DOI: 10.1002/hep.23924]

41 **Hübener S**, Oo YH, Than NN, Hübener P, Weiler-Normann C, Lohse AW, Schramm C. Efficacy of 6-Mercaptopurine as Second-Line Treatment for Patients With Autoimmune Hepatitis and Azathioprine Intolerance. *Clin Gastroenterol Hepatol* 2016; **14**: 445-453 [PMID: 26492846 DOI: 10.1016/j.cgh.2015.09.037]

42 **Hennes EM**, Oo YH, Schramm C, Denzer U, Buggisch P, Wiegard C, Kanzler S, Schuchmann M, Boecher W, Galle PR, Adams DH, Lohse AW. Mycophenolate mofetil as second line therapy in autoimmune hepatitis? *Am J Gastroenterol* 2008; **103**: 3063-3070 [PMID: 18853972 DOI: 10.1111/j.1572-0241.2008.02180.x]

43 **Dietrich CF**, Lee JH, Herrmann G, Teuber G, Roth WK, Caspary WF, Zeuzem S. Enlargement of perihepatic lymph nodes in relation

to liver histology and viremia in patients with chronic hepatitis C. *Hepatology* 1997; **26**: 467-472 [PMID: 9252160 DOI: 10.1002/hep.510260230]
44 **Dietrich CF**, Stryjek-Kaminska D, Teuber G, Lee JH, Caspary WF, Zeuzem S. Perihepatic lymph nodes as a marker of antiviral response in patients with chronic hepatitis C infection. *AJR Am J Roentgenol* 2000; **174**: 699-704 [PMID: 10701612 DOI: 10.2214/ajr.174.3.1740699]
45 **Dietrich CF**, Viel K, Braden B, Caspary WF, Zeuzem S. Mediastinal lymphadenopathy: an extrahepatic manifestation of chronic hepatitis C? *Z Gastroenterol* 2000; **38**: 143-152 [PMID: 10721169 DOI: 10.1055/s-2000-14852]
46 **Schreiber-Dietrich D**, Pohl M, Cui XW, Braden B, Dietrich CF, Chiorean L. Perihepatic lymphadenopathy in children with chronic viral hepatitis. *J Ultrason* 2015; **15**: 137-150 [PMID: 26676184 DOI: 10.15557/JoU.2015.0012]
47 **Dietrich CF**, Leuschner MS, Zeuzem S, Herrmann G, Sarrazin C, Caspary WF, Leuschner UF. Peri-hepatic lymphadenopathy in primary biliary cirrhosis reflects progression of the disease. *Eur J Gastroenterol Hepatol* 1999; **11**: 747-753 [PMID: 10445795]
48 **Braden B**, Faust D, Ignee A, Schreiber D, Hirche T, Dietrich CF. Clinical relevance of perihepatic lymphadenopathy in acute and chronic liver disease. *J Clin Gastroenterol* 2008; **42**: 931-936 [PMID: 18645531 DOI: 10.1097/MCG.0b013e31811edcf7]
49 **Hirche TO**, Russler J, Braden B, Schuessler G, Zeuzem S, Wehrmann T, Seifert H, Dietrich CF. Sonographic detection of perihepatic lymphadenopathy is an indicator for primary sclerosing cholangitis in patients with inflammatory bowel disease. *Int J Colorectal Dis* 2004; **19**: 586-594 [PMID: 15088111 DOI: 10.1007/s00384-004-0598-0]
50 **Barreiros AP**, Chiorean L, Braden B, Dietrich CF. Ultrasound in rare diffuse liver disease. *Z Gastroenterol* 2014; **52**: 1247-1256 [PMID: 25390211 DOI: 10.1055/s-0034-1384996]
51 **Tana C**, Silingardi M, Dietrich CF. New trends in ultrasound of hepatosplenic sarcoidosis. *Z Gastroenterol* 2015; **53**: 283-284 [PMID: 25860577 DOI: 10.1055/s-0034-1399122]
52 **Dietrich CF**. Contrast-enhanced endobronchial ultrasound: Potential value of a new method. *Endosc Ultrasound* 2017; **6**: 43-48 [PMID: 28218200 DOI: 10.4103/2303-9027.200215]
53 **Hocke M**, Ignee A, Dietrich C. Role of contrast-enhanced endoscopic ultrasound in lymph nodes. *Endosc Ultrasound* 2017; **6**: 4-11 [PMID: 28218194 DOI: 10.4103/2303-9027.190929]
54 **Chiorean L**, Barr RG, Braden B, Jenssen C, Cui XW, Hocke M, Schuler A, Dietrich CF. Transcutaneous Ultrasound: Elastographic Lymph Node Evaluation. Current Clinical Applications and Literature Review. *Ultrasound Med Biol* 2016; **42**: 16-30 [PMID: 26489365 DOI: 10.1016/j.ultrasmedbio.2015.09.005]
55 **Dietrich CF**, Jenssen C, Arcidiacono PG, Cui XW, Giovannini M, Hocke M, Iglesias-Garcia J, Saftoiu A, Sun S, Chiorean L. Endoscopic ultrasound: Elastographic lymph node evaluation. *Endosc Ultrasound* 2015; **4**: 176-190 [PMID: 26374575 DOI: 10.4103/2303-9027.162995]
56 **Dietrich CF**, Annema JT, Clementsen P, Cui XW, Borst MM, Jenssen C. Ultrasound techniques in the evaluation of the mediastinum, part I: endoscopic ultrasound (EUS), endobronchial ultrasound (EBUS) and transcutaneous mediastinal ultrasound (TMUS), introduction into ultrasound techniques. *J Thorac Dis* 2015; **7**: E311-E325 [PMID: 26543620 DOI: 10.3978/j.issn.2072-1439.2015.09.40]
57 **Jenssen C**, Annema JT, Clementsen P, Cui XW, Borst MM, Dietrich CF. Ultrasound techniques in the evaluation of the mediastinum, part 2: mediastinal lymph node anatomy and diagnostic reach of ultrasound techniques, clinical work up of neoplastic and inflammatory mediastinal lymphadenopathy using ultrasound techniques and how to learn mediastinal endosonography. *J Thorac Dis* 2015; **7**: E439-E458 [PMID: 26623120 DOI: 10.3978/j.issn.2072-1439.2015.10.08]
58 **Cui XW**, Hocke M, Jenssen C, Ignee A, Klein S, Schreiber-Dietrich D, Dietrich CF. Conventional ultrasound for lymph node evaluation, update 2013. *Z Gastroenterol* 2014; **52**: 212-221 [PMID: 24526406 DOI: 10.1055/s-0033-1356153]
59 **Dietrich CF**, Jenssen C, Herth FJ. Endobronchial ultrasound elastography. *Endosc Ultrasound* 2016; **5**: 233-238 [PMID: 27503154 DOI: 10.4103/2303-9027.187866]
60 **Czaja AJ**. Hepatocellular carcinoma and other malignancies in autoimmune hepatitis. *Dig Dis Sci* 2013; **58**: 1459-1476 [PMID: 23306849 DOI: 10.1007/s10620-012-2525-5]
61 **Sandrin L**, Fourquet B, Hasquenoph JM, Yon S, Fournier C, Mal F, Christidis C, Ziol M, Poulet B, Kazemi F, Beaugrand M, Palau R. Transient elastography: a new noninvasive method for assessment of hepatic fibrosis. *Ultrasound Med Biol* 2003; **29**: 1705-1713 [PMID: 14698338]
62 **Castéra L**, Vergniol J, Foucher J, Le Bail B, Chanteloup E, Haaser M, Darriet M, Couzigou P, De Lédinghen V. Prospective comparison of transient elastography, Fibrotest, APRI, and liver biopsy for the assessment of fibrosis in chronic hepatitis C. *Gastroenterology* 2005; **128**: 343-350 [PMID: 15685546]
63 **Dietrich CF**, Bamber J, Berzigotti A, Bota S, Cantisani V, Castera L, Cosgrove D, Ferraioli G, Friedrich-Rust M, Gilja OH, Goertz RS, Karlas T, de Knegt R, de Ledinghen V, Piscaglia F, Procopet B, Saftoiu A, Sidhu PS, Sporea I, Thiele M. EFSUMB Guidelines and Recommendations on the Clinical Use of Liver Ultrasound Elastography, Update 2017 (Long Version). *Ultraschall Med* 2017; **38**: e16-e47 [PMID: 28407655 DOI: 10.1055/s-0043-103952]
64 **Czaja AJ**. Review article: The prevention and reversal of hepatic fibrosis in autoimmune hepatitis. *Aliment Pharmacol Ther* 2014; **39**: 385-406 [PMID: 24387318 DOI: 10.1111/apt.12592]
65 **Cui J**, Heba E, Hernandez C, Haufe W, Hooker J, Andre MP, Valasek MA, Aryafar H, Sirlin CB, Loomba R. Magnetic resonance elastography is superior to acoustic radiation force impulse for the Diagnosis of fibrosis in patients with biopsy-proven nonalcoholic fatty liver disease: A prospective study. *Hepatology* 2016; **63**: 453-461 [PMID: 26560734 DOI: 10.1002/hep.28337]
66 **Imajo K**, Kessoku T, Honda Y, Tomeno W, Ogawa Y, Mawatari H, Fujita K, Yoneda M, Taguri M, Hyogo H, Sumida Y, Ono M, Eguchi Y, Inoue T, Yamanaka T, Wada K, Saito S, Nakajima A. Magnetic Resonance Imaging More Accurately Classifies Steatosis and Fibrosis in Patients With Nonalcoholic Fatty Liver Disease Than Transient Elastography. *Gastroenterology* 2016; **150**: 626-637.e7 [PMID: 26677985 DOI: 10.1053/j.gastro.2015.11.048]
67 **Wang J**, Malik N, Yin M, Smyrk TC, Czaja AJ, Ehman RL, Venkatesh SK. Magnetic resonance elastography is accurate in detecting advanced fibrosis in autoimmune hepatitis. *World J Gastroenterol* 2017; **23**: 859-868 [PMID: 28223730 DOI: 10.3748/wjg.v23.i5.859]
68 **Guo L**, Zheng L, Hu L, Zhou H, Yu L, Liang W. Transient Elastography (FibroScan) Performs Better Than Non-Invasive Markers in Assessing Liver Fibrosis and Cirrhosis in Autoimmune Hepatitis Patients. *Med Sci Monit* 2017; **23**: 5106-5112 [PMID: 29073121]
69 **Wang QX**, Shen L, Qiu DK, Bao H, Chen XY, Zeng MD, Mao YM, Ma X. [Validation of transient elastography (Fibroscan) in assessment of hepatic fibrosis in autoimmune hepatitis]. *Zhonghua Gan Zang Bing Za Zhi* 2011; **19**: 782-784 [PMID: 22409854 DOI: 10.3760/cma.j.issn.1007-3418.2011.10.015]
70 **Xu Q**, Sheng L, Bao H, Chen X, Guo C, Li H, Ma X, Qiu D, Hua J. Evaluation of transient elastography in assessing liver fibrosis in patients with autoimmune hepatitis. *J Gastroenterol Hepatol* 2017; **32**: 639-644 [PMID: 27505153 DOI: 10.1111/jgh.13508]
71 **Halász T**, Horváth G, Kiss A, Pár G, Szombati A, Gelley F, Nemes B, Kenessey I, Piurkó V, Schaff Z. Evaluation of Histological and non-Invasive Methods for the Detection of Liver Fibrosis: The Values of Histological and Digital Morphometric Analysis, Liver Stiffness Measurement and APRI Score. *Pathol Oncol Res* 2016; **22**: 1-6 [PMID: 26189126 DOI: 10.1007/s12253-015-9964-1]
72 **Fitzpatrick E**, Quaglia A, Vimalesvaran S, Basso MS, Dhawan A. Transient elastography is a useful noninvasive tool for the evaluation of fibrosis in paediatric chronic liver disease. *J Pediatr Gastroenterol Nutr* 2013; **56**: 72-76 [PMID: 22922372 DOI: 10.1097/MPG.0b013e31826f2760]

73 **Wilder J**, Patel K. The clinical utility of FibroScan(®) as a noninvasive diagnostic test for liver disease. *Med Devices* (Auckl) 2014; **7**: 107-114 [PMID: 24833926 DOI: 10.2147/MDER.S46943]

74 **Abdalla AF**, Zalata KR, Ismail AF, Shiha G, Attiya M, Abo-Alyazeed A. Regression of fibrosis in paediatric autoimmune hepatitis: morphometric assessment of fibrosis versus semiquantiatative methods. *Fibrogenesis Tissue Repair* 2009; **2**: 2 [PMID: 19341455 DOI: 10.1186/1755-1536-2-2]

75 **Sagir A**, Erhardt A, Schmitt M, Häussinger D. Transient elastography is unreliable for detection of cirrhosis in patients with acute liver damage. *Hepatology* 2008; **47**: 592-595 [PMID: 18098325 DOI: 10.1002/hep.22056]

76 **Kim SU**, Kim DY, Park JY, Lee JH, Ahn SH, Kim JK, Paik YH, Lee KS, Chon CY, Choi EH, Song KJ, Park YN, Han KH. How can we enhance the performance of liver stiffness measurement using FibroScan in diagnosing liver cirrhosis in patients with chronic hepatitis B? *J Clin Gastroenterol* 2010; **44**: 66-71 [PMID: 19609218 DOI: 10.1097/MCG.0b013e3181a95c7f]

77 **Hartl J**, Denzer U, Ehlken H, Zenouzi R, Peiseler M, Sebode M, Hübener S, Pannicke N, Weiler-Normann C, Quaas A, Lohse AW, Schramm C. Transient elastography in autoimmune hepatitis: Timing determines the impact of inflammation and fibrosis. *J Hepatol* 2016; **65**: 769-775 [PMID: 27238753 DOI: 10.1016/j.jhep.2016.05.023]

78 **Gutkowski K**, Hartleb M, Kacperek-Hartleb T, Kajor M, Mazur W, Zych W, Walewska-Zielecka B, Habior A, Sobolewski M. Laboratory-based scoring system for prediction of hepatic inflammatory activity in patients with autoimmune hepatitis. *Liver Int* 2013; **33**: 1370-1377 [PMID: 23651331 DOI: 10.1111/liv.12198]

79 **Fabbri A**, Lenzi M. Non-invasive markers of inflammation in autoimmune hepatitis. *Liver Int* 2013; **33**: 1295-1297 [PMID: 24011359 DOI: 10.1111/liv.12251]

80 **Czaja AJ**. Safety issues in the management of autoimmune hepatitis. *Expert Opin Drug Saf* 2008; **7**: 319-333 [PMID: 18462189 DOI: 10.1517/14740338.7.3.319]

81 **Sporea I**, Bota S, Jurchis A, Sirli R, Grădinaru-Tascău O, Popescu A, Ratiu I, Szilaski M. Acoustic radiation force impulse and supersonic shear imaging versus transient elastography for liver fibrosis assessment. *Ultrasound Med Biol* 2013; **39**: 1933-1941 [PMID: 23932281 DOI: 10.1016/j.ultrasmedbio.2013.05.003]

82 **Righi S**, Fiorini E, De Molo C, Cipriano V, Cassani F, Muratori L, Lenzi M, Morselli Labate AM, Serra C. ARFI elastography in patients with chronic autoimmune liver diseases: A preliminary study. *J Ultrasound* 2012; **15**: 226-231 [PMID: 23730386 DOI: 10.1016/j.jus.2012.10.002]

83 **Bota S**, Sporea I, Peck-Radosavljevic M, Sirli R, Tanaka H, Iijima H, Saito H, Ebinuma H, Lupsor M, Badea R, Fierbinteanu-Braticevici C, Petrisor A, Friedrich-Rust M, Sarrazin C, Takahashi H, Ono N, Piscaglia F, Marinelli S, D'Onofrio M, Gallotti A, Salzl P, Popescu A, Danila M. The influence of aminotransferase levels on liver stiffness assessed by Acoustic Radiation Force Impulse Elastography: a retrospective multicentre study. *Dig Liver Dis* 2013; **45**: 762-768 [PMID: 23510533 DOI: 10.1016/j.dld.2013.02.008]

84 **Sun LL**, Chang W, Jiao LQ, Cui X, Dong G. Hepatic fibrosis and supersonic shear imaging in patients with different etiological chronic hepatic diseases. *J Biol Regul Homeost Agents* 2016; **30**: 761-765 [PMID: 27655494]

85 **Hao L**, Tu JZ, Wang XH, Shi Y, Liu XL, Zhang HH. Effect of Inflammation on Fibrosis Staging Measured by Quantitative Elasticity Parameters in Rats With Immune Hepatitis. *J Ultrasound Med* 2016; **35**: 1223-1231 [PMID: 27126399 DOI: 10.7863/ultra.15.03001]

86 **Romanque P**, Stickel F, Dufour JF. Disproportionally high results of transient elastography in patients with autoimmune hepatitis. *Liver Int* 2008; **28**: 1177-1178 [PMID: 18783552 DOI: 10.1111/j.1478-3231.2008.01743.x]

87 **E Anastasiou O**, Büchter M, A Baba H, Korth J, Canbay A, Gerken G, Kahraman A. Performance and Utility of Transient Elastography and Non-Invasive Markers of Liver Fiibrosis in Patients with Autoimmune Hepatitis: A Single Centre Experience. *Hepat Mon* 2016; **16**: e40737 [PMID: 28070199 DOI: 10.5812/hepatmon.40737]

88 **Hartl J**, Ehlken H, Sebode M, Peiseler M, Krech T, Zenouzi R, von Felden J, Weiler-Normann C, Schramm C, Lohse AW. Usefulness of biochemical remission and transient elastography in monitoring disease course in autoimmune hepatitis. *J Hepatol* 2017; Epub ahead of print [PMID: 29180000 DOI: 10.1016/j.jhep.2017.11.020]

P- Reviewer: Gatselis NK, Tai DI, Trifan A **S- Editor**: Ma YJ
L- Editor: A **E- Editor**: Huang Y

World Journal of Gastroenterology

Submit a Manuscript: http://www.f6publishing.com

World J Gastroenterol 2018 April 21; 24(15): 1591-1600

DOI: 10.3748/wjg.v24.i15.1591

ISSN 1007-9327 (print) ISSN 2219-2840 (online)

REVIEW

Nutrition status and *Helicobacter pylori* infection in patients receiving hemodialysis

Mitsushige Sugimoto, Hideo Yasuda, Akira Andoh

Mitsushige Sugimoto, Division of Digestive Endoscopy, Shiga University of Medical Science Hospital, Shiga 520-2192, Japan

Hideo Yasuda, First Department of Medicine, Hamamatsu University School of Medicine, Shizuoka 431-3192, Japan

Akira Andoh, Department of Gastroenterology, Shiga University of Medical Science Hospital, Shiga 520-2192, Japan

ORCID number: Mitsushige Sugimoto (0000-0002-9184-7392); Hideo Yasuda (0000-0002-2574-8002); Akira Andoh (0000-0001-8533-2669).

Author contributions: Sugimoto M, Yasuda H and Andoh A wrote the paper.

Conflict-of-interest statement: No potential conflicts of interest.

Manuscript source: Invited manuscript

Correspondence to: Mitsushige Sugimoto MD, PhD, Associate Professor, Division of Digestive Endoscopy, Shiga University of Medical Science Hospital, Seta Tsukinowa-cho, Shiga 520-2192, Japan. sugimo@belle.shiga-med.ac.jp
Telephone: +81-77-5482618
Fax: +81-77-5482618

Received: February 23, 2018
Peer-review started: February 23, 2018
First decision: March 15, 2018
Revised: March 18, 2018
Accepted: March 25, 2018
Article in press: March 25, 2018

Published online: April 21, 2018

Abstract

Chronic kidney disease (CKD) patients receiving hemodialysis (HD) often develop gastrointestinal abnormalities over their long treatment period. In general, prognosis in such patients is poor due to the development of protein-energy wasting (PEW). Therefore, it is important to clarify the etiology of PEW and to establish better strategies to deal with this condition. Chronic *Helicobacter pylori* (*H. pylori*) infection in the gastric mucosa has a close association with not only the development of peptic ulcer disease and gastric cancer, but is also associated with abnormal plasma and gastric mucosal ghrelin levels that are seen in malnutrition. It is unclear whether *H. pylori* infection of the gastric mucosa is directly associated with prognosis in HD patients by affecting ghrelin levels. Recent studies show that the prevalence of *H. pylori* infection in HD patients is significantly lower than in subjects with normal renal function. In the natural history of *H. pylori* infection in HD patients, the prevalence of infection decreases as the length of time on HD increases. The severity of gastric mucosal atrophy has been suggested as the major determinant of ghrelin levels in these patients, and eradication therapy of *H. pylori* improves nutritional status by increasing serum cholinesterase and cholesterol levels, especially in patients with mild-to-moderate gastric mucosal atrophy. Prompt *H. pylori* eradication to inhibit the progress of gastric atrophy may be required to prevent this decrease in ghrelin levels and subsequent PEW and improve the prognosis of HD patients by improving their nutritional status.

Key words: *Helicobacter pylori*; Hemodialysis; Ghrelin; Gastric mucosa; Anti-bacterial agents

Core tip: Hemodialysis (HD) patients have a poor prognosis related in part to protein-energy wasting (PEW), associated with low levels of ghrelin. The severity of gastric mucosal atrophy has been suggested as the major determinant of ghrelin levels. Eradication of *Helicobacter pylori* (*H. pylori*) improves nutritional status, with serum cholinesterase and cholesterol levels stimulated by rising ghrelin levels and appetite, especially in *H. pylori* infection-positive patients with severe gastric mucosal atrophy. Although infection rates of *H. pylori* have been decreasing in HD patients, it would be preferable to eradicate *H. pylori* promptly before progression of gastric atrophy for prevention of gastric cancer and PEW.

Sugimoto M, Yasuda H, Andoh A. Nutrition status and *Helicobacter pylori* infection in patients receiving hemodialysis. *World J Gastroenterol* 2018; 24(15): 1591-1600 Available from: URL: http://www.wjgnet.com/1007-9327/full/v24/i15/1591.htm DOI: http://dx.doi.org/10.3748/wjg.v24.i15.1591

INTRODUCTION

With ongoing progress in medical and dialysis machine techniques, the number of chronic renal failure patients receiving hemodialysis (HD) is increasing at a rate of 7% per year. At least 2.9 million Asians require dialysis, including Japanese, who live in an aging society and experience changes in their living environment[1,2]. HD patients often experience gastrointestinal symptoms (*e.g.*, nausea, abdominal pain, and constipation) caused by elevated urea levels, decreased gastrointestinal motility, amyloid protein deposition, and sensory disturbances, and are at increased risk of developing gastrointestinal diseases (*e.g.*, peptic ulcer disease, gastric antral vascular ectasia, gastroesophageal reflux disease, and gastric cancer)[3-7]. The risk of gastric mucosal damage is elevated in this population, in association with high ammonia levels[8], systemic and/or local chronic circulatory failure[9,10], and hypergastrinemia[11]. Gastroduodenal diseases such as peptic ulcer and gastric cancer have been linked to chronic *Helicobacter pylori* (*H. pylori*) infection[12-15]. In HD patients, the role of chronic *H. pylori* infection in their prognosis and quality of life (QOL) has not been defined.

In general, QOL in HD patients is poor. This affects their nutritional status, and thereby contributes to the development of malnutrition, which is a potent predictor of morbidity and mortality[16,17]. The state of metabolic and nutritional derangement called protein-energy wasting (PEW) has a major impact on mortality in HD patients[16,17]. Improving the prognosis of HD patients with PEW requires determination of its etiology and the development of prophylactic strategies[18,19].

The complex interactions of gastroduodenal disease, nutritional status, and *H. pylori* infection in HD patients (which tends to decrease with increasing time on dialysis[20]) remain to be elucidated. Here, we review the association between *H. pylori* infection and HD, and the relationship between *H. pylori* and nutritional status in this population. Finally, we review the effects of *H. pylori* eradication therapy in *H. pylori*-positive HD patients on nutritional status and plasma ghrelin levels.

H. PYLORI INFECTION IN HD PATIENTS

H. pylori is a spiral-shaped, microaerophilic Gram-negative flagellate bacterium isolated in 1983 from gastric biopsy specimens of patients with chronic atrophic gastritis[21]. The gastric mucosa of approximately 50% of the world's population is infected with *H. pylori*, and the infection levels exceed 70% in some developing areas[15,22-24].

Previously, we reported that the prevalence of *H. pylori* infection in 539 Japanese HD patients with a mean treatment period of 8.4 ± 0.3 year in 1997 was 48.6% (95%CI: 44.3%-52.9%). This was significantly lower than that in dyspepsia patients with normal renal function [78.5% (74.1%-82.4%), $P < 0.001$] and individuals receiving annual health checks [69.4% (60.3%-77.5%), $P < 0.001$][20]. In a meta-analysis of reports investigating the prevalence of *H. pylori* in dialysis patients before 2009, the prevalence in patients receiving HD and continuous ambulatory peritoneal dialysis (CAPD) was 43.9% [(95%CI: 42.2%-45.6%), 1435/3272] and 34.8% [(29.6%-40.2%), 113/325], respectively, which was again significantly lower than that in individuals with normal renal function [49.8% (48.0%-51.7%), 1476/2961, $P < 0.001$][25]. Although infection rates differ among different geographic populations, in East Asian countries where the prevalence of *H. pylori* infection and incidence of gastric cancer is relatively high, the latest statistics show the infection rate in HD patients to be 44.5% (41.55%-47.6%, 474/1065), which is significantly lower than that in individuals with normal renal function [54.0% (50.9%-57.1%), 560/1038, $P < 0.001$][25]. Importantly, the prevalence in individuals with normal renal function is similar in patients receiving HD treatment for < 1 year[20]. HD treatment, but not uremia from chronic renal failure, may play an important role in the decreased prevalence of *H. pylori* infection.

Recently, infection rates of *H. pylori* have been decreasing. A large-scale Japanese epidemiological study showed that the infection rate in Japanese has declined to 30%-50%, especially in younger patients[26]. Supporting this phenomenon, an investigation of 500 Japanese HD patients with a mean treatment duration of 6.9 ± 6.6 years (2015) reported that the prevalence of infection had dramatically decreased, to 15.0% (95%CI: 12.0-18.4)[27]. Although it has not yet been proven, decreasing rates of *H. pylori* infection suggest

Table 1 Hemodialysis treatment duration and *Helicobacter pylori* infection status in hemodialysis patients[27], %

	< 1 yr	1-3 yr	3-10 yr	> 10 yr	*P* value
H. pylori infection rate	23.8 (15/63)	16.7 (18/108)	15.0 (34/226)	7.8 (8/13)	0.043
Rate of *H. pylori* negatives	55.5 (35/63)	62.0 (67/108)	68.1 (154/226)	68.9 (71/103)	> 0.05

that the incidence of peptic ulcer disease and gastric cancer is expected to be decreasing in HD patients and that QOL in HD patients has improved due to decreases in *H. pylori*-related gastrointestinal disease.

TREATMENT PERIODS OF HD AND *H. PYLORI* INFECTION

There is an inverse relationship between *H. pylori* infection and dialysis treatment duration (Table 1)[20,27-31]. We showed that the duration of HD treatment in *H. pylori*-positive patients was 4.6 ± 3.8 years, which is significantly shorter than that in *H. pylori*-negatives (7.3 ± 6.9 years, $P = 0.001$)[27]. Interestingly, the finding of decreased *H. pylori* infection is characteristic of the prevalence of infection decreasing when the treatment period is ⩾ 2 year[28], and the infection rate gradually decreases up to four years after the initiation of HD and is followed by a plateau[20]. In a 4-year follow-up survey of *H. pylori*-positive patients, the prevalence of infection was 51.6% at 1 year, 42.9% at 2 year, and 38.3% at 4 year in the absence of eradication therapy. In other words, 26.7% of patients were naturally cured of *H. pylori* infection over four years[20].

It is unknown why HD patients have a lower prevalence of *H. pylori* infection. One hypothesis is that HD patients have higher levels of pro-inflammatory cytokines[32]. As a result, gastric atrophy progresses, and finally *H. pylori* are not able to live in the gastric mucosa[33-35]. Another hypothesis is that elevated blood urea and urea nitrogen levels may inhibit *H. pylori* growth[36]. A third hypothesis is that *H. pylori* may be cured with incidental antibiotic treatment, because most HD patients suffer from an increased incidence of bacterial infections, and because plasma levels of antimicrobial agents may be higher in HD patients than in individuals with normal renal function[37].

PEPSINOGEN IN HD PATIENTS

Human pepsinogens (PGs) are proenzymes that act on pepsin. Serum PG levels reflect the status of the gastric mucosa, and decreased PG secretion is a marker of gastric mucosal atrophy. In patients without renal dysfunction, measurements of serum PG levels are used in screening for gastric cancer and gastric mucosal atrophy[38]. In addition, serum PG levels and the PG I/PG II ratio are useful in determining the level of gastric acid secretion[39]. Recently in Japan, a combination of the serum PG level and *H. pylori*-IgG level, namely the ABC method, has been commonly used at health screenings as a useful marker for gastric cancer[40]. Because PG is eliminated *via* the kidney, serum PG levels are elevated in patients with renal dysfunction[41]. The value of serum PG levels as a biomarker of gastric atrophy and the capacity of gastric acid secretion in HD patients was heretofore unknown.

A recent report has demonstrated that PG I and II levels and PG I/PG II ratios in *H. pylori*-negative HD patients are significantly higher than those in *H. pylori*-positives and that PG I levels positively correlate with PG II levels and PG I/PG II ratio in *H. pylori*-negative HD patients ($|R| = 0.849$ and $|R| = 0.569$), past-infection patients ($|R| = 0.870$ and $|R|=0.575$) and current-infection patients ($|R| = 0.784$ and $|R| = 0.517$)[26,42]. In addition, a receiver operating characteristic curve using a cut-off value of 7.75 demonstrated that the sensitivity and specificity of PG I/PG II ratio in predicting the absence of *H. pylori* were 88.7% and 84.0%, respectively[26]. Therefore, serum PG I/PG II ratio may be a valid marker for *H. pylori* infection status and gastric mucosal atrophy in HD patients. Further large-scale studies are needed to verify this.

NECESSITY OF *H. PYLORI* ERADICATION THERAPY FOR HD PATIENTS

The incidence rates of peptic ulcer and gastric cancer in HD patients are higher than those in individuals with normal renal function[7,43]. In addition, because most HD patients receive anti-thrombotic therapy and/or non-steroidal anti-inflammatory drugs (NSAIDs), the development of drug-induced ulcers and hemorrhage from gastroduodenal lesions easily occurs and often causes fatal blood loss. Therefore, prompt *H. pylori* eradication therapy is necessary for *H. pylori*-infected HD patients[12,13], especially in HD patients with a higher risk of disease development, such as those with a past history of peptic ulcer, gastroduodenal hemorrhage, or use of anticoagulants and/or NSAIDs.

To reduce the risk of gastric cancer, the Japanese health insurance system in 2012 began covering *H. pylori* eradication therapy for all patients with endoscopic gastritis as well for peptic ulcers, gastric mucosa-associated-lymphoid tissue (MALT) lymphoma, post-endoscopic resection of early gastric cancer, and idiopathic thrombocytopenic purpura (ITP)[44-49]. In Japan, first-line eradication therapy is limited to a regimen that employs a standard dose of vonoprazan

or proton pump inhibitor (PPI) administered twice daily, amoxicillin (AMPC) 750 mg twice daily, and clarithromycin (CAM) 200 mg or 400 mg twice daily for 1 wk. Unfortunately, because the prevalence of CAM-resistant *H. pylori* strains in Japan is increasing (> 30%), the eradication rate is gradually decreasing[14,50-53]. Eradication therapy is more challenging in HD patients since they have many exposures to antimicrobial agents due to immune system impairment[54,55]. In fact, 36.4% of patients with chronic renal failure are reported to be infected with CAM-resistant strains, which is significantly higher than in patients with normal renal function (15.2%)[54]. Our recent data published in 2017 shows that rate of CAM-resistant strains in HD patients is 40.5% of infected patients[55]. Alternative regimens may be designed to use *H. pylori*-susceptible antimicrobial agents, increased dosages of antimicrobial agents and PPIs, increased dosing frequency, and longer treatment periods, according to international treatment guidelines[13,52,56-60].

There is no optimal *H. pylori* eradication regimen in HD patients yet (Table 2). Some antimicrobial agents, especially AMPC, are known to exacerbate renal dysfunction. The maximum drug concentration of AMPC in patients with renal failure is 2-4 times higher than in patients with normal renal function, and the half-life is 5-20 times as long as that in healthy individuals[37]. Although several previous reports showed no severe adverse effects of AMPC in HD patients receiving eradication therapy[4,11,30,61-65], the Japanese guidelines for *H. pylori* eradication therapy in the Japanese Society of Helicobacter Research recommends a reduction in AMPC dosage for HD patients[12] and the Japanese drug prescribing guidelines accordingly recommend that the dosage of AMPC for patients with renal failure should be reduced by 70%. In fact, the toxic effects of AMPC in HD patients have been reported in various studies[66-68]; for example, Sheu *et al*[68] reported that patients with a lansoprazole-CAM-metronidazole regimen had a lower risk of acute renal failure than those with a lansoprazole-CAM-AMPC regimen (2% *vs* 18%; relative risk, 0.128, 95%CI: 0.016-0.979) for chronic renal failure non-dialysis patients. Overdose of drugs has to be carefully prevented. Although an optimal regimen for dosage and periods of AMPC in HD patients is not described in the Japanese guidelines for eradication[12], an AMPC-reduced regimen may be appropriate in HD patients.

Recently, we have adopted a regimen composed of PPI and CAM, both at conventional dosage, and a dose of AMPC that is one-third of the conventional dosage (250 mg twice daily), and investigated the efficacy and safety of this regimen[55]. This regimen in HD patients provided equivalent efficacy as the standard dose in conventional therapy for non-dialysis patients in Japan (82.4% and 82.4%, respectively)[55]. Although this suggests that AMPC-reduced triple therapy is effective and safe for HD patients[55,69,70], the sample number of these reports is small, and it is necessary to set an optimal regimen in HD using a larger number of subjects.

Although the eradication rate with the Japanese standard triple therapy was first reported as approximately 85%-91%, it has gradually decreased year by year because of increased prevalence of CAM-resistant strains of *H. pylori*. Because the eradication rates with tailored treatments based only on CAM susceptibility are not very high (71.9%-94.3%), more advanced tailored treatment considering other factors (*e.g.*, different doses of antibiotics and PPIs, different dosages and treatment period) are required to achieve high eradication rates. A tailored *H. pylori* eradication regimen based on CAM susceptibility and maintaining acid secretion (rabeprazole, 10 mg, q.i.d.) is useful because it can achieve an eradication rate exceeding 95%, irrespective of eradication history, thus overcoming differences among CYP2C19 genotypes[52]. However, there was no report to investigate efficacy of tailored regimen in HD patients.

H. PYLORI INFECTION AND NUTRITION STATUS IN HD PATIENTS

HD patients have many risk factors that affect mortality, such as chronic inflammation and metabolic and nutritional derangement[16,17,71]. PEW is defined as a state of decreased body stores of protein and energy fuels (body protein and fat mass) and is diagnosed if three features are present: (1) Abnormal nutrition markers (*i.e.*, low serum levels of albumin, transthyretin or cholesterol); (2) reduced body mass (*i.e.*, low or reduced body or fat mass or weight loss with reduced intake of protein and energy); and (3) reduced muscle mass (*i.e.*, muscle wasting or sarcopenia, and reduced mid-arm muscle circumference)[72].

Ghrelin, an orexigenic peptide released primarily from endocrine cells in the stomach, is important in the pathogenesis of PEW in HD patients[71,73,74]. Ghrelin has multiple functions, including enhancement of the orexigenic effect, protein anabolism, anti-inflammatory action, and cardiovascular protection[74,75,76]. Plasma ghrelin levels increase after fasting and decrease after eating. Ghrelin levels are elevated in patients with a lean body[77]. Plasma ghrelin levels have been found to be associated with malnutrition in patients with advanced-stage cancer and anorexia nervosa[76]. In HD patients, a low ghrelin level increases the risk of cardiovascular mortality and morbidity[78], and the utility of monitoring plasma ghrelin at fixed intervals has been proven as a biomarker for mortality in HD patients[71].

H. pylori infections affect ghrelin levels. *H. pylori*-positive patients have lower gastric mucosal and plasma ghrelin levels and a smaller population of ghrelin-positive cells in the gastric mucosa[79]. Although subjects with normal renal function show a correlation between plasma ghrelin level and the severity of gastric mucosal atrophy[79], the association between ghrelin and *H. pylori* infection and between ghrelin and gastric

Table 2 *Helicobacter pylori* eradication therapy for chronic renal failure patients

Year	Author	Country	*n*	Regimen	Treatment period	Eradication rate (%)	Analytic methods
1997	Tamura *et al*[61]	Japan	14	LPZ (30) oid/ 8 wk, AMPC (500) oid/ 3 wk, plaunotol (80) tid/ 24 wk	21 d	78.6	RUT, Culture, Histology
1998	Munos de Bustillo E *et al*[30]	Spain	23	OPZ (20) bid, AMPC (500) tid	14 d	60.8	UBT
			23	plus OPZ (20) bid, CAM (500) bid	14 d	82.6	
1998	Tokushima *et al*[62]	Japan	17	LPZ (30) oid/ 8 wk, AMPC (500)	21 d	76.5	RUT, Culture, Histology
			10	LPZ (30) oid, AMPC (250), MNZ (250) bid/	7 d	90	
1999	Araki *et al*[63]	Japan	17	OPZ (20) oid/ 8 wk, AMPC (250) oid, CAM (200) oid/ 3 wk, polaprizinc (0.5) bid/ 24 wk	21 d	88.2	IgG, Histology
1999	Gur *et al*[11]	Turkey	25	FAM (40) oid, CAM (500) bid, MNZ (250) bid	15 d	80	Histology, RUT
2001	Wang *et al*[64]	China	38	OPZ (20), AMPC (1000), CAM (500) bid	7 d	86.8	Stool
2002	Mak *et al*[91]	China	21 (CRF)	OPZ (20), AMPC (1000), CAM (500) bid	7 d	90.5	RUT
2002	Tsukada *et al*[65]	Japan	39	OPZ (30) bid, AMPC (500) tid, CAM (400) bid	7 d	82.1	UBT
2003	Mak *et al*[92]	China	25 (CRF)	OPZ (20) or LPZ (30), AMPC (1000), CAM (500) bid	7 d	96	Histology
2003	Sheu *et al*[67]	China	38 (CRF)	LPZ (30), AMPC (750), CAM (500) bid	7 d	76.3	
			40 (CRF)	LPZ (30), CAM (500), MNZ (500) bid	7 d	92.5	Stool
2004	Sezer *et al*[4]	Turkey	17	OPZ (20), AMPC (1000), CAM (500) bid/	14 d	94.1	Endoscopy
2007	Tseng *et al*[93]	China	34 (CRF)	ESO (40) or OPZ (20) bid, AMPC (1000) bid, CAM (500) bid	7 d	94.1	UBT
2007	Itatsu *et al*[69]	Japan	11	LPZ (60), AMPC (750), CAM (400)	7 d	72.7	RUT
			9	LPZ (60), CAM (400)	7 d	33.3	
2010	Change *et al*[70]	Korea	12	OPZ (20), AMPC (250), CAM (250), bid	7 d	83.4	RUT, Histology
2010	Jalalzadeh *et al*[94], Falaknazi *et al*[95]	Iran	37	OPZ (20), AMPC (1000), CAM (250), bid	14 d	81.1	IgG, UBT, Stool
2012	Seyyedmajidi *et al*[96], Jalalzadeh *et al*[97,98] Vafaeimanesh *et al*[99]	Iran	17	OPZ (20), AMPC (500), CAM (250), bid	14 d	82.4	UBT, Stool
			20	OPZ (40), AMPC (500), azithromycin (250), bid	14 d	80	
2014	Makhlough *et al*[100]	Iran	21	PPZ (40), AMPC (500), CAM (250), bid	14 d	66.7	RUT, Histology
			24	Sequential therapy (PPT [40] 10 d, AMPC (500) bid, 5 d and CAM (250), tinidazole (500), bid, 5 d	10 d	84	
2016	Makhlough *et al*[101]	Iran	20	PPZ (40), AMPC (500), CAM (500), bid	14 d	70	RUT, Stool
			20	Hybrid regimen PPZ (40), AMPC (500), bid, 7 d + PPZ (40), AMPC (500), CAM (500), tinidazole (500), bid, 7 d	14 d	100	
2018	Sahara *et al*[55]	Japan	18	ESO (20), AMPC (750), CAM (200) bid	7 d	77.8	IgG
			19	ESO (20), AMPC (250), CAM (200) bid	7 d	84.2	

AMPC: Amoxicillin; CAM: Clarithromycin; ESO: Esomeprazole; FAM: Famotidine; LPZ: Lansoprazole; MNZ: Metronidazole; NA: Not available; OPZ: Omeprazole; PPZ: Pantoprazole; RUT: Rapid urease test; UBT: Urea breath test; bid: Twice-daily dosing; tid: Three-times-daily dosing.

mucosal atrophy in HD patients is less well understood. In an analysis using 78 HD patients and 51 non-dialysis patients with chronic renal disease, des-acyl ghrelin levels in HD patients were significantly higher than those in non-dialysis patients, and ghrelin levels decreased with the progress of endoscopic gastric mucosal atrophy in HD patients (Table 3)[19]. Importantly, acyl-ghrelin levels in the non-*H. pylori* infection HD group (39.4 ± 23.0 fmol/mL) were significantly higher than in patients with current (24.6 ± 17.5 fmol/mL, $P = 0.022$) and past *H. pylori* infection (23.4 ± 19.9 fmol/mL, $P = 0.007$) (Table 4)[18], suggesting that the severity of serological and endoscopic gastric mucosal atrophy is a major determinant of ghrelin levels (Table 3). In fact, multiple regression analysis shows a significant positive correlation between acyl ghrelin and PG I levels ($\beta = 0.738$, $P < 0.001$) and significant negative correlations between ghrelin and age, albumin, and creatinine levels[19]. Therefore, PG level is the most influential determinant of plasma acyl and des-acyl ghrelin levels in HD patients. This suggests that plasma and gastric mucosal ghrelin levels are influenced by not only long-standing enhanced gastric mucosal inflammation induced by *H. pylori* infection but also by gastric mucosal atrophy[79]. Because plasma and gastric ghrelin levels depend on the number of ghrelin immunoreactive cells in the gastric mucosa[79-81], plasma ghrelin levels may be influenced more by the severity of atrophy than current *H. pylori* infection in HD patients. Therefore, it is important to consider methods to prevent progression of gastric mucosal atrophy in HD patients.

HD patients with gastric mucosal atrophy have a lower normalized protein catabolic rate (nPCR) than non-atrophy patients[19]. Chronic persistent damage to the gastric mucosa and gastric mucosal atrophy in *H. pylori*-positive HD patients may contribute to

Table 3 Clinical characteristics in hemodialysis patients between patients with and without gastric mucosal atrophy[19]

	Atrophy (-)	Atrophy (+)	*P*-value
N (Male/Female)	28 (17/11)	50 (33/17)	-
Age	67.7 ± 12.3	71.6 ± 11.0	0.155
Dialysis periods (yr)	7.5 (2.4-16.8)	7.7 (3.1-12.7)	0.681
Acyl-ghrelin	38.0 (23.5-57.0)	18.0 (12.0-26.3)	< 0.001
Desacyl-ghrelin	303 (248-533)	200 (137-277)	< 0.001
BMI (kg/m^2)	19.8 ± 3.2	19.6 ± 2.8	0.773
Albumin (g/dL)	3.5 ± 0.3	3.4 ± 0.4	0.273
Total cholesterol (mg/dL)	166 ± 37	154 ± 36	0.165
Cholinesterase (U/L)	245 ± 111	219 ± 68.7	0.205
Intact PTH (pg/mL)	351 ± 294	247 ± 192	0.062
Ferritin (ng/mL)	128 ± 118	128 ± 221	0.989
PG Ⅰ (ng/mL)	416.2 (314.2-783.7)	196.0 (73.8-358.8)	< 0.001
PG Ⅱ (ng/mL)	42.3 (31.6-60.0)	28.4 (16.8-45.7)	0.003
PG Ⅰ / Ⅱ ratio	10.89 (9.11-13.38)	7.31 (4.17-11.08)	0.001
nPCR (g/kg/d)	0.94 ± 0.14	0.85 ± 0.16	0.022

BMI: Body mass index; BUN: Blood urea nitrogen; PTH: Parathyroid hormone; CRP: C-reactive protein; PG: Pepsinogen; ABI: Ankle-brachial pressure index; nPCR: Normalized protein catabolic rate.

Table 4 Plasma acyl-ghrelin and desacyl-ghrelin levels according to *Helicobacter pylori* status in hemodialysis patients[18]

	Non-infection (n = 29)	Past-infection (n = 27)	Present infection (n = 17)
Plasma acyl-ghrelin (fmol/mL)	39.4 ± 23.0	23.4 ± 19.9[a]	24.6 ± 17.5[a]
Plasma desacyl-ghrelin (fmol/mL)	353.2 ± 190.2	242.1 ± 139.6[a]	236.3 ± 143.6[a]

[a]$P < 0.05$ *vs* Non-infection group.

decreased protein intake, PEW, and decreased body weight *via* decreased ghrelin production. Because ghrelin level is associated with mortality related to cardiovascular disease and PEW in HD patients, alternative management, such as *H. pylori* eradication therapy, before the progression of gastric mucosal atrophy might be necessary to prevent the decrease in ghrelin level in HD patients[74,78].

H. PYLORI ERADICATION THERAPY AND NUTRITION STATUS IN HD PATIENTS

H. pylori infection affects the incident rate of gastroduodenal disease and nutritional status[20,25]. *H. pylori* eradication therapy often causes individuals with normal renal function to develop hyperlipidemia and hyperproteinaemia, along with an increase of body weight and BMI[80]. This phenomenon is considered to be due to increases in plasma ghrelin level followed by increased appetite and food intake after *H. pylori* eradication therapy[82,83] In CAPD patients, *H. pylori* eradication therapy significantly improves anorexia, inflammation, and malnutrition[84]. After *H. pylori* eradication, CAPD patients with anorexia showed a significant increase in markers of nutrition and in VAS scores for almost all questions. Significant differences were also found in lymphocyte count, nPCR, prealbumin, albumin, CRP, before-lunch desire to eat, after-lunch desire to eat, hunger before lunch, hunger after lunch, fullness before lunch, consumption after lunch, and palatability[85]. However, it is unclear whether nutritional disorders in HD patients improve after eradication therapy. It is important to answer this clinical question to improve the poor prognosis in HD patients.

At 1 year after eradication therapy, serum cholinesterase levels significantly increase compared with the level before eradication (303.2 ± 76.0 *vs* 287.3 ± 68.1 IU/L, $P = 0.029$). In particular, cholesterol (before, 196.6 ± 23.2 mg/dL; after, 206.1 ± 25.9 mg/dL, $P = 0.042$) and cholinesterase levels (before, 296.9 ± 70.8 IU/L; after, 316.4 ± 73.8 IU/L, $P = 0.049$) increase more in patients with mild-moderate gastric mucosal atrophy than in those with severe atrophy. This observation suggests that eradication therapy has contributed to improvement of PEW in HD patients. We therefore recommend that HD patients be checked for *H. pylori* infection and that eradication therapy should be initiated before the progression of gastric atrophy.

It is possible that the improvement in nutritional status and increase in BMI after eradication therapy depends not only on an increase in ghrelin levels but also on another biological mechanism(s), such as an improvement in gastrointestinal motility[86], change in gut microbiome profile[87], and/or increase in absorption ability[88]. Betrapally *et al*[87] reported that alterations to the intestinal microbiota affect the development of nonalcoholic steatohepatitis by influencing digestion, development of obesity, immune response, and production of gut hormones. *H. pylori* eradication therapy changes the gastrointestinal microbiota[89]. A study to examine

whether the long-term prognosis of HD patients is improved by the effect of eradication therapy on the microbiota will be required to investigate this hypothesis further.

H. PYLORI AND ANEMIA IN HEMODIALYSIS PATIENTS

H pylori has been identified as a possible cause of vitamin B12 and iron deficiency in the general population. Trimarchi *et al*[90] reported that *H. pylori*-positive HD patients may present with lower vitamin B12 blood levels and that *H. pylori* should be suspected in HD patients when low or low-normal vitamin B12 levels or macrocytosis exist.

CONCLUSION

Chronic renal failure patients receiving HD have a low prevalence of *H. pylori* infection. More than one-third of patients receiving < 4 year of dialysis had naturally cured *H. pylori* infection within the 4 year observation period. However, because chronic renal failure patients have a higher risk of gastroduodenal disorders, all HD patients are recommended to receive endoscopic check-ups to reduce the chance of developing peptic ulcer disease. Moreover, patients with *H. pylori* infection should also receive eradication therapy including AMPC 250 mg twice daily to prevent peptic ulcer, gastric cancer, and hemorrhage from gastroduodenal lesions. QOL in HD patients is usually poor and affects their nutritional status. Severity of gastric atrophy is shown to be the major determinant of ghrelin levels in HD patients and eradication treatment of *H. pylori* improves nutrition status by increasing serum cholinesterase and cholesterol levels. *H. pylori* eradication before progress of gastric atrophy may be required to prevent a decrease in ghrelin levels and improve prognosis of HD patients in relation to poor nutritional status.

REFERENCES

1 **Prasad N**, Jha V. Hemodialysis in Asia. *Kidney Dis* (Basel) 2015; **1**: 165-177 [PMID: 27536677 DOI: 10.1159/000441816]
2 **Lysaght MJ**. Maintenance dialysis population dynamics: current trends and long-term implications. *J Am Soc Nephrol* 2002; **13** Suppl 1: S37-S40 [PMID: 11792760]
3 **Ala-Kaila K**. Upper gastrointestinal findings in chronic renal failure. *Scand J Gastroenterol* 1987; **22**: 372-376 [PMID: 3296137]
4 **Sezer S**, Ibiş A, Ozdemir BH, Ozdemir FN, Külah E, Boyacioğlu S, Haberal M. Association of helicobacter pylori infection with nutritional status in hemodialysis patients. *Transplant Proc* 2004; **36**: 47-49 [PMID: 15013297]
5 **Sotoudehmanesh R**, Ali Asgari A, Ansari R, Nouraie M. Endoscopic findings in end-stage renal disease. *Endoscopy* 2003; **35**: 502-505 [PMID: 12783348 DOI: 10.1055/s-2003-39672]
6 **Tsai CJ**, Hwang JC. Investigation of upper gastrointestinal hemorrhage in chronic renal failure. *J Clin Gastroenterol* 1996; **22**: 2-5 [PMID: 8776085]
7 **Khedmat H**, Ahmadzad-Asl M, Amini M, Lessan-Pezeshki M, Einollahi B, Pourfarziani V, Naseri MH, Davoudi F. Gastroduodenal lesions and Helicobacter pylori infection in uremic patients and renal transplant recipients. *Transplant Proc* 2007; **39**: 1003-1007 [PMID: 17524875 DOI: 10.1016/j.transproceed.2007.03.034]
8 **Neithercut WD**, Rowe PA, el Nujumi AM, Dahill S, McColl KE. Effect of Helicobacter pylori infection on intragastric urea and ammonium concentrations in patients with chronic renal failure. *J Clin Pathol* 1993; **46**: 544-547 [PMID: 8331178]
9 **Block GA**, Raggi P, Bellasi A, Kooienga L, Spiegel DM. Mortality effect of coronary calcification and phosphate binder choice in incident hemodialysis patients. *Kidney Int* 2007; **71**: 438-441 [PMID: 17200680]
10 **Nakamura S**, Sasaki O, Nakahama H, Inenaga T, Kawano Y. Clinical characteristics and survival in end-stage renal disease patients with arteriosclerosis obliterans. *Am J Nephrol* 2002; **22**: 422-428 [PMID: 12381939]
11 **Gür G**, Boyacioglu S, Gül C, Turan M, Gürsoy M, Baysal C, Ozdemir N. Impact of Helicobacter pylori infection on serum gastrin in haemodialysis patients. *Nephrol Dial Transplant* 1999; **14**: 2688-2691 [PMID: 10534513]
12 **Asaka M**, Kato M, Takahashi S, Fukuda Y, Sugiyama T, Ota H, Uemura N, Murakami K, Satoh K, Sugano K; Japanese Society for Helicobacter Research. Guidelines for the management of Helicobacter pylori infection in Japan: 2009 revised edition. *Helicobacter* 2010; **15**: 1-20 [PMID: 20302585]
13 **Malfertheiner P**, Megraud F, O'Morain CA, Gisbert JP, Kuipers EJ, Axon AT, Bazzoli F, Gasbarrini A, Atherton J, Graham DY, Hunt R, Moayyedi P, Rokkas T, Rugge M, Selgrad M, Suerbaum S, Sugano K, El-Omar EM; European Helicobacter and Microbiota Study Group and Consensus panel. Management of Helicobacter pylori infection-the Maastricht V/Florence Consensus Report. *Gut* 2017; **66**: 6-30 [PMID: 27707777 DOI: 10.1136/gutjnl-2016-312288]
14 **Suzuki H**, Mori H. World trends for H. pylori eradication therapy and gastric cancer prevention strategy by H. pylori test-and-treat. *J Gastroenterol* 2018; **53**: 354-361 [PMID: 29138921 DOI: 10.1007/s00535-017-1407-1]
15 **Pellicano R**, Ribaldone DG, Fagoonee S, Astegiano M, Saracco GM, Mégraud F. A 2016 panorama of Helicobacter pylori infection: key messages for clinicians. *Panminerva Med* 2016; **58**: 304-317 [PMID: 27716738]
16 **Ikizler TA**, Cano NJ, Franch H, Fouque D, Himmelfarb J, Kalantar-Zadeh K, Kuhlmann MK, Stenvinkel P, TerWee P, Teta D, Wang AY, Wanner C; International Society of Renal Nutrition and Metabolism. Prevention and treatment of protein energy wasting in chronic kidney disease patients: a consensus statement by the International Society of Renal Nutrition and Metabolism. *Kidney Int* 2013; **84**: 1096-1107 [PMID: 23698226 DOI: 10.1038/ki.2013.147]
17 **Kovesdy CP**, George SM, Anderson JE, Kalantar-Zadeh K. Outcome predictability of biomarkers of protein-energy wasting and inflammation in moderate and advanced chronic kidney disease. *Am J Clin Nutr* 2009; **90**: 407-414 [PMID: 19535427 DOI: 10.3945/ajcn.2008.27390]
18 **Ichikawa H**, Sugimoto M, Sakao Y, Sahara S, Ohashi N, Kato A, Sugimoto K, Furuta T, Andoh A, Sakao T, Yasuda H. Relationship between ghrelin, Helicobacter pylori and gastric mucosal atrophy in hemodialysis patients. *World J Gastroenterol* 2016; **22**: 10440-10449 [PMID: 28058025 DOI: 10.3748/wjg.v22.i47.10440]
19 **Sakao Y**, Sugimoto M, Ichikawa H, Sahara S, Tsuji T, Ohashi N, Kato A, Fujigaki Y, Sugimoto K, Furuta T, Sakao T, Yasuda H. Severity of Gastric Mucosal Atrophy Is the Major Determinant of Plasma Ghrelin Level in Hemodialysis Patients. *Am J Nephrol* 2016; **44**: 224-233 [PMID: 27578611 DOI: 10.1159/000449019]
20 **Sugimoto M**, Sakai K, Kita M, Imanishi J, Yamaoka Y. Prevalence of Helicobacter pylori infection in long-term hemodialysis patients. *Kidney Int* 2009; **75**: 96-103 [PMID: 18843261]
21 **Marshall BJ**, Warren JR. Unidentified curved bacilli in the stomach of patients with gastritis and peptic ulceration. *Lancet* 1984; **1**: 1311-1315 [PMID: 6145023]

22 **Perez-Perez GI**, Taylor DN, Bodhidatta L, Wongsrichanalai J, Baze WB, Dunn BE, Echeverria PD, Blaser MJ. Seroprevalence of Helicobacter pylori infections in Thailand. *J Infect Dis* 1990; **161**: 1237-1241 [PMID: 2345304]

23 **Sugimoto M**, Yamaoka Y. The association of vacA genotype and Helicobacter pylori-related disease in Latin American and African populations. *Clin Microbiol Infect* 2009; **15**: 835-842 [PMID: 19392900 DOI: 10.1111/j.1469-0691.2009.02769.x]

24 **Sugimoto M**, Zali MR, Yamaoka Y. The association of vacA genotypes and Helicobacter pylori-related gastroduodenal diseases in the Middle East. *Eur J Clin Microbiol Infect Dis* 2009; **28**: 1227-1236 [PMID: 19551413 DOI: 10.1007/s10096-009-0772-y]

25 **Sugimoto M**, Yamaoka Y. Review of Helicobacter pylori infection and chronic renal failure. *Ther Apher Dial* 2011; **15**: 1-9 [PMID: 21272246 DOI: 10.1111/j.1744-9987.2010.00851.x]

26 **Hirayama Y**, Kawai T, Otaki J, Kawakami K, Harada Y. Prevalence of Helicobacter pylori infection with healthy subjects in Japan. *J Gastroenterol Hepatol* 2014; **29** Suppl 4: 16-19 [PMID: 25521727 DOI: 10.1111/jgh.12795]

27 **Sugimoto M**, Sahara S, Ichikawa H, Sakao Y, Ohashi N, Sugimoto K, Yasuda H, Furuta T, Andoh A. Natural Course of Helicobacter pylori Infection in Japanese Hemodialysis Patients. *Digestion* 2017; **95**: 302-309 [PMID: 28521319 DOI: 10.1159/000475659]

28 **Nakajima F**, Sakaguchi M, Amemoto K, Oka H, Kubo M, Shibahara N, Ueda H, Katsuoka Y. Helicobacter pylori in patients receiving long-term dialysis. *Am J Nephrol* 2002; **22**: 468-472 [PMID: 12381945]

29 **Yildiz A**, Beşişik F, Akkaya V, Sever MS, Bozfakioğlu S, Yilmaz G, Ark E. Helicobacter pylori antibodies in hemodialysis patients and renal transplant recipients. *Clin Transplant* 1999; **13**: 13-16 [PMID: 10081629]

30 **Muñoz de Bustillo E**, Sánchez Tomero JA, Sanz JC, Moreno JA, Jiménez I, López-Brea M, Pajares JM, Traver JA. Eradication and follow-up of Helicobacter pylori infection in hemodialysis patients. *Nephron* 1998; **79**: 55-60 [PMID: 9609463]

31 **Nakajima F**, Sakaguchi M, Oka H, Kawase Y, Shibahara N, Inoue T, Ueda H, Katsuoka Y. Prevalence of Helicobacter pylori antibodies in long-term dialysis patients. *Nephrology* (Carlton) 2004; **9**: 73-76 [PMID: 15056265]

32 **Hwang IR**, Kodama T, Kikuchi S, Sakai K, Peterson LE, Graham DY, Yamaoka Y. Effect of interleukin 1 polymorphisms on gastric mucosal interleukin 1beta production in Helicobacter pylori infection. *Gastroenterology* 2002; **123**: 1793-1803 [PMID: 12454835]

33 **Wesdorp RI**, Falcao HA, Banks PB, Martino J, Fischer JE. Gastrin and gastric acid secretion in renal failure. *Am J Surg* 1981; **141**: 334-338 [PMID: 7011077]

34 **El-Omar EM**, Carrington M, Chow WH, McColl KE, Bream JH, Young HA, Herrera J, Lissowska J, Yuan CC, Rothman N, Lanyon G, Martin M, Fraumeni JF Jr, Rabkin CS. Interleukin-1 polymorphisms associated with increased risk of gastric cancer. *Nature* 2000; **404**: 398-402 [PMID: 10746728]

35 **Sugimoto M**, Furuta T, Shirai N, Nakamura A, Xiao F, Kajimura M, Sugimura H, Hishida A. Different effects of polymorphisms of tumor necrosis factor-alpha and interleukin-1 beta on development of peptic ulcer and gastric cancer. *J Gastroenterol Hepatol* 2007; **22**: 51-59 [PMID: 17201881 DOI: 10.1111/j.1440-1746.2006.04442.x]

36 **Gladziwa U**, Haase G, Handt S, Riehl J, Wietholtz H, Dakshinamurty KV, Glöckner WM, Sieberth HG. Prevalence of Helicobacter pylori in patients with chronic renal failure. *Nephrol Dial Transplant* 1993; **8**: 301-306 [PMID: 8390002]

37 **Francke EL**, Appel GB, Neu HC. Kinetics of intravenous amoxicillin in patients on long-term dialysis. *Clin Pharmacol Ther* 1979; **26**: 31-35 [PMID: 445959]

38 **Yoshimura T**, Shimoyama T, Fukuda S, Tanaka M, Axon AT, Munakata A. Most gastric cancer occurs on the distal side of the endoscopic atrophic border. *Scand J Gastroenterol* 1999; **34**: 1077-1081 [PMID: 10582756]

39 **Iijima K**, Koike T, Abe Y, Shimosegawa T. Cutoff serum pepsinogen values for predicting gastric acid secretion status. *Tohoku J Exp Med* 2014; **232**: 293-300 [PMID: 24717778]

40 **Masuyama H**, Yoshitake N, Sasai T, Nakamura T, Masuyama A, Zuiki T, Kurashina K, Mieda M, Sunada K, Yamamoto H, Togashi K, Terano A, Hiraishi H. Relationship between the degree of endoscopic atrophy of the gastric mucosa and carcinogenic risk. *Digestion* 2015; **91**: 30-36 [PMID: 25632914 DOI: 10.1159/000368807]

41 **Nakahama H**, Tanaka Y, Shirai D, Nishihara F, Takamitsu Y, Nakanishi T, Sugita M. Elevated serum pepsinogens in chronic renal failure patients. *Nephron* 1995; **70**: 211-216 [PMID: 7566306]

42 **Moriyama T**, Matsumoto T, Hirakawa K, Ikeda H, Tsuruya K, Hirakata H, Iida M. Helicobacter pylori status and esophagogastroduodenal mucosal lesions in patients with end-stage renal failure on maintenance hemodialysis. *J Gastroenterol* 2010; **45**: 515-522 [PMID: 20084526 DOI: 10.1007/s00535-009-0196-6]

43 **Ota K**, Yamashita N, Suzuki T, Agishi T. Malignant tumours in dialysis patients: a nationwide survey. *Proc Eur Dial Transplant Assoc* 1981; **18**: 724-730 [PMID: 7329999]

44 **Uemura N**, Okamoto S, Yamamoto S, Matsumura N, Yamaguchi S, Yamakido M, Taniyama K, Sasaki N, Schlemper RJ. Helicobacter pylori infection and the development of gastric cancer. *N Engl J Med* 2001; **345**: 784-789 [PMID: 11556297]

45 **Wong BC**, Lam SK, Wong WM, Chen JS, Zheng TT, Feng RE, Lai KC, Hu WH, Yuen ST, Leung SY, Fong DY, Ho J, Ching CK, Chen JS; China Gastric Cancer Study Group. Helicobacter pylori eradication to prevent gastric cancer in a high-risk region of China: a randomized controlled trial. *JAMA* 2004; **291**: 187-194 [PMID: 14722144]

46 **Hopkins RJ**, Girardi LS, Turney EA. Relationship between Helicobacter pylori eradication and reduced duodenal and gastric ulcer recurrence: a review. *Gastroenterology* 1996; **110**: 1244-1252 [PMID: 8613015]

47 **Uemura N**, Mukai T, Okamoto S, Yamaguchi S, Mashiba H, Taniyama K, Sasaki N, Haruma K, Sumii K, Kajiyama G. Effect of Helicobacter pylori eradication on subsequent development of cancer after endoscopic resection of early gastric cancer. *Cancer Epidemiol Biomarkers Prev* 1997; **6**: 639-642 [PMID: 9264278]

48 **Wotherspoon AC**, Doglioni C, de Boni M, Spencer J, Isaacson PG. Antibiotic treatment for low-grade gastric MALT lymphoma. *Lancet* 1994; **343**: 1503 [PMID: 7911202]

49 **Sugimoto M**, Kajimura M, Shirai N, Furuta T, Kanaoka S, Ikuma M, Sato Y, Hishida A. Outcome of radiotherapy for gastric mucosa-associated lymphoid tissue lymphoma refractory to Helicobacter pylori eradication therapy. *Intern Med* 2006; **45**: 405-409 [PMID: 16617193]

50 **Asaka M**, Sugiyama T, Kato M, Satoh K, Kuwayama H, Fukuda Y, Fujioka T, Takemoto T, Kimura K, Shimoyama T, Shimizu K, Kobayashi S. A multicenter, double-blind study on triple therapy with lansoprazole, amoxicillin and clarithromycin for eradication of Helicobacter pylori in Japanese peptic ulcer patients. *Helicobacter* 2001; **6**: 254-261 [PMID: 11683930]

51 **Murakami K**, Sato R, Okimoto T, Nasu M, Fujioka T, Kodama M, Kagawa J, Sato S, Abe H, Arita T. Eradication rates of clarithromycin-resistant Helicobacter pylori using either rabeprazole or lansoprazole plus amoxicillin and clarithromycin. *Aliment Pharmacol Ther* 2002; **16**: 1933-1938 [PMID: 12390102]

52 **Sugimoto M**, Uotani T, Sahara S, Ichikawa H, Yamade M, Sugimoto K, Furuta T. Efficacy of tailored Helicobacter pylori eradication treatment based on clarithromycin susceptibility and maintenance of acid secretion. *Helicobacter* 2014; **19**: 312-318 [PMID: 24690010 DOI: 10.1111/hel.12128]

53 **Sugimoto M**, Sahara S, Ichikawa H, Kagami T, Ban H, Otsuka T, Andoh A, Furuta T. Four-times-daily Dosing of Rabeprazole with Sitafloxacin, High-Dose Amoxicillin, or Both for Metronidazole-Resistant Infection with Helicobacter pylori in Japan. *Helicobacter* 2017; **22** [PMID: 27213463 DOI: 10.1111/hel.12319]

54 **Aydemir S**, Boyacioglu S, Gur G, Demirbilek M, Can FK, Korkmaz M, Yilmaz U. Helicobacter pylori infection in hemodialysis patients: susceptibility to amoxicillin and clarithromycin. *World J Gastroenterol* 2005; **11**: 842-845 [PMID: 15682477]

55 **Sahara S,** Sugimoto M, Ichikawa H, Kagami T, Sakao Y, Ohashi

N, Horio Y, Sugimoto K, Kato A, Furuta T, Yasuda H. Efficacy of reduced dosage of amoxicillin in an eradication therapy for Helicobacter pylori infection in patients on hemodialysis: a randomized controlled trial. *Digestion* 2018; **97:** 163-169[PMID: 29310119 DOI: 10.1159/000484981]

56 **Sharara AI**, Chaar HF, Aoun E, Abdul-Baki H, Araj GF, Kanj SS. Efficacy and safety of rabeprazole, amoxicillin, and gatifloxacin after treatment failure of initial Helicobacter pylori eradication. *Helicobacter* 2006; **11**: 231-236 [PMID: 16882325]

57 **Murakami K**, Sato R, Okimoto T, Nasu M, Fujioka T, Kodama M, Kagawa J. Efficacy of triple therapy comprising rabeprazole, amoxicillin and metronidazole for second-line Helicobacter pylori eradication in Japan, and the influence of metronidazole resistance. *Aliment Pharmacol Ther* 2003; **17**: 119-123 [PMID: 12492740]

58 **Kawakami E**, Machado RS, Ogata SK, Langner M, Fukushima E, Carelli AP, Bonucci VC, Patricio FR. Furazolidone-based triple therapy for H pylori gastritis in children. *World J Gastroenterol* 2006; **12**: 5544-5549 [PMID: 17006997]

59 **Sugimoto M**, Sahara S, Ichikawa H, Kagami T, Uotani T, Furuta T. High Helicobacter pylori cure rate with sitafloxacin-based triple therapy. *Aliment Pharmacol Ther* 2015; **42**: 477-483 [PMID: 26075959 DOI: 10.1111/apt.13280]

60 **Siddique O**, Ovalle A, Siddique AS, Moss SF. Helicobacter pylori Infection: an Update for the Internist in the Age of Increasing Global Antibiotic Resistance. *Am J Med* 2018; Epub ahead of print [PMID: 29353050 DOI: 10.1016/j.amjmed.2017.12.024]

61 **Tamura H**, Tokushima H, Murakawa M, Matsumura O, Itoyama S, Sekine S, Hirose H, Mitarai T, Isoda K. Eradication of Helicobacter pylori in patients with end-stage renal disease under dialysis treatment. *Am J Kidney Dis* 1997; **29**: 86-90 [PMID: 9002534]

62 **Tokushima H**, Tamura H, Murakawa M, Matsumura O, Itakura Y, Itoyama S, Mitarai T, Isoda K. Eradication of Helicobacter pylori restores elevation of serum gastrin concentrations in patients with end-stage renal disease. *Intern Med* 1998; **37**: 435-439 [PMID: 9652896]

63 **Araki H**, Miyazaki R, Matsuda T, Gejyo F, Koni I. Significance of serum pepsinogens and their relationship to Helicobacter pylori infection and histological gastritis in dialysis patients. *Nephrol Dial Transplant* 1999; **14**: 2669-2675 [PMID: 10534510]

64 **Wang YL**, Sheu BS, Huang JJ, Yang HB. Noninvasive stool antigen assay can effectively screen Helicobacter pylori Infection and assess success of eradication therapy in hemodialysis patients. *Am J Kidney Dis* 2001; **38**: 98-103 [PMID: 11431188]

65 **Tsukada K**, Miyazaki T, Katoh H, Masuda N, Ojima H, Fukai Y, Nakajima M, Manda R, Fukuchi M, Kuwano H, Tsukada O. Seven-day triple therapy with omeprazole, amoxycillin and clarithromycin for Helicobacter pylori infection in haemodialysis patients. *Scand J Gastroenterol* 2002; **37**: 1265-1268 [PMID: 12465723]

66 **Arancibia A**, Drouguett MT, Fuentes G, González G, González C, Thambo S, Palombo G. Pharmacokinetics of amoxicillin in subjects with normal and impaired renal function. *Int J Clin Pharmacol Ther Toxicol* 1982; **20**: 447-453 [PMID: 7141752]

67 **Jones DP**, Gaber L, Nilsson GR, Brewer ED, Stapleton FB. Acute renal failure following amoxicillin overdose. *Clin Pediatr* (Phila) 1993; **32**: 735-739 [PMID: 8275607]

68 **Sheu BS**, Huang JJ, Yang HB, Huang AH, Wu JJ. The selection of triple therapy for Helicobacter pylori eradication in chronic renal insufficiency. *Aliment Pharmacol Ther* 2003; **17**: 1283-1290 [PMID: 12755841]

69 **Itatsu T**, Miwa H, Nagahara A, Kubota M, Miyazaki A, Sato N, Hayashida Y. Eradication of Helicobacter pylori in hemodialysis patients. *Ren Fail* 2007; **29**: 97-102 [PMID: 17365917]

70 **Chang WC**, Jo YI, Park HS, Jegal J, Park JH, Lee JH, Jin CJ. Helicobacter pylori eradication with a 7-day low-dose triple therapy in hemodialysis patients. *Clin Exp Nephrol* 2010; **14**: 469-473 [PMID: 20632062 DOI: 10.1007/s10157-010-0319-7]

71 **Mak RH**, Cheung WW. Is ghrelin a biomarker for mortality in end-stage renal disease? *Kidney Int* 2011; **79**: 697-699 [PMID: 21403653 DOI: 10.1038/ki.2010.520]

72 **Fouque D**, Kalantar-Zadeh K, Kopple J, Cano N, Chauveau P, Cuppari L, Franch H, Guarnieri G, Ikizler TA, Kaysen G, Lindholm B, Massy Z, Mitch W, Pineda E, Stenvinkel P, Treviño-Becerra A, Wanner C. A proposed nomenclature and diagnostic criteria for protein-energy wasting in acute and chronic kidney disease. *Kidney Int* 2008; **73**: 391-398 [PMID: 18094682 DOI: 10.1038/sj.ki.5002585]

73 **Kojima M**, Hosoda H, Date Y, Nakazato M, Matsuo H, Kangawa K. Ghrelin is a growth-hormone-releasing acylated peptide from stomach. *Nature* 1999; **402**: 656-660 [PMID: 10604470 DOI: 10.1038/45230]

74 **Carrero JJ**, Nakashima A, Qureshi AR, Lindholm B, Heimbürger O, Bárány P, Stenvinkel P. Protein-energy wasting modifies the association of ghrelin with inflammation, leptin, and mortality in hemodialysis patients. *Kidney Int* 2011; **79**: 749-756 [PMID: 21178976 DOI: 10.1038/ki.2010.487]

75 **Pradhan G**, Samson SL, Sun Y. Ghrelin: much more than a hunger hormone. *Curr Opin Clin Nutr Metab Care* 2013; **16**: 619-624 [PMID: 24100676 DOI: 10.1097/MCO.0b013e328365b9be]

76 **Akamizu T**, Kangawa K. Ghrelin for cachexia. *J Cachexia Sarcopenia Muscle* 2010; **1**: 169-176 [PMID: 21475698 DOI: 10.1007/s13539-010-0011-5]

77 **Ariyasu H**, Takaya K, Tagami T, Ogawa Y, Hosoda K, Akamizu T, Suda M, Koh T, Natsui K, Toyooka S, Shirakami G, Usui T, Shimatsu A, Doi K, Hosoda H, Kojima M, Kangawa K, Nakao K. Stomach is a major source of circulating ghrelin, and feeding state determines plasma ghrelin-like immunoreactivity levels in humans. *J Clin Endocrinol Metab* 2001; **86**: 4753-4758 [PMID: 11600536 DOI: 10.1210/jcem.86.10.7885]

78 **Chou CC**, Bai CH, Tsai SC, Wu MS. Low serum acylated ghrelin levels are associated with the development of cardiovascular disease in hemodialysis patients. *Intern Med* 2010; **49**: 2057-2064 [PMID: 20930430]

79 **Osawa H**, Nakazato M, Date Y, Kita H, Ohnishi H, Ueno H, Shiiya T, Satoh K, Ishino Y, Sugano K. Impaired production of gastric ghrelin in chronic gastritis associated with Helicobacter pylori. *J Clin Endocrinol Metab* 2005; **90**: 10-16 [PMID: 15483107 DOI: 10.1210/jc.2004-1330]

80 **Osawa H**, Kita H, Ohnishi H, Nakazato M, Date Y, Bowlus CL, Ishino Y, Watanabe E, Shiiya T, Ueno H, Hoshino H, Satoh K, Sugano K. Changes in plasma ghrelin levels, gastric ghrelin production, and body weight after Helicobacter pylori cure. *J Gastroenterol* 2006; **41**: 954-961 [PMID: 17096064 DOI: 10.1007/s00535-006-1880-4]

81 **Suzuki H**, Masaoka T, Hosoda H, Ota T, Minegishi Y, Nomura S, Kangawa K, Ishii H. Helicobacter pylori infection modifies gastric and plasma ghrelin dynamics in Mongolian gerbils. *Gut* 2004; **53**: 187-194 [PMID: 14724148]

82 **Furuta T**, Shirai N, Xiao F, Takashima M, Hanai H. Effect of Helicobacter pylori infection and its eradication on nutrition. *Aliment Pharmacol Ther* 2002; **16**: 799-806 [PMID: 11929399]

83 **Jang EJ**, Park SW, Park JS, Park SJ, Hahm KB, Paik SY, Sin MK, Lee ES, Oh SW, Park CY, Baik HW. The influence of the eradication of Helicobacter pylori on gastric ghrelin, appetite, and body mass index in patients with peptic ulcer disease. *J Gastroenterol Hepatol* 2008; **23** Suppl 2: S278-S285 [PMID: 19120912 DOI: 10.1111/j.1440-1746.2008.05415.x]

84 **Kawashima J**, Ohno S, Sakurada T, Takabayashi H, Kudo M, Ro S, Kato S, Yakabi K. Circulating acylated ghrelin level decreases in accordance with the extent of atrophic gastritis. *J Gastroenterol* 2009; **44**: 1046-1054 [PMID: 19701601 DOI: 10.1007/s00535-009-0120-0]

85 **Aguilera A**, Codoceo R, Bajo MA, Diéz JJ, del Peso G, Pavone M, Ortiz J, Valdez J, Cirugeda A, Fernández-Perpén A, Sánchez-Tomero JA, Selgas R. Helicobacter pylori infection: a new cause of anorexia in peritoneal dialysis patients. *Perit Dial Int* 2001; **21** Suppl 3: S152-S156 [PMID: 11887811]

86 **Zhang CL**, Geng CH, Yang ZW, Li YL, Tong LQ, Gao P, Gao YQ. Changes in patients' symptoms and gastric emptying after Helicobacter pylori treatment. *World J Gastroenterol* 2016; **22**: 4585-4593 [PMID: 27182168 DOI: 10.3748/wjg.v22.i18.4585]

87 **Betrapally NS**, Gillevet PM, Bajaj JS. Changes in the Intestinal Microbiome and Alcoholic and Nonalcoholic Liver Diseases: Causes or Effects? *Gastroenterology* 2016; **150**: 1745-1755.e3 [PMID: 26948887 DOI: 10.1053/j.gastro.2016.02.073]

88 **Serin E**, Gümürdülü Y, Ozer B, Kayaselçuk F, Yilmaz U, Koçak R. Impact of Helicobacter pylori on the development of vitamin B12 deficiency in the absence of gastric atrophy. *Helicobacter* 2002; **7**: 337-341 [PMID: 12485119]

89 **Li L**, Zhou X, Xiao S, Ye F, Zhang G. The Effect of Helicobacter pylori Eradication on the Gastrointestinal Microbiota in Patients with Duodenal Ulcer. *J Gastrointestin Liver Dis* 2016; **25**: 139-146 [PMID: 27308643 DOI: 10.15403/jgld.2014.1121.252.hpe]

90 **Trimarchi H**, Forrester M, Schropp J, Pereyra H, Freixas EA. Low initial vitamin B12 levels in Helicobacter pylori--positive patients on chronic hemodialysis. *Nephron Clin Pract* 2004; **96**: c28-c32 [PMID: 14752251 DOI: 10.1159/000075569]

91 **Mak SK**, Loo CK, Wong AM, Wong PN, Lo KY, Tong GM, Lam EK, Wong AK. Efficacy of a 1-week course of proton-pump inhibitor-based triple therapy for eradicating Helicobacter pylori in patients with and without chronic renal failure. *Am J Kidney Dis* 2002; **40**: 576-581 [PMID: 12200810]

92 **Mak SK**, Loo CK, Wong PN, Lo KY, Tong GM, Lam EK, Wong AK. A retrospective study on efficacy of proton-pump inhibitor-based triple therapy for eradication of Helicobacter pylori in patients with chronic renal failure. *Singapore Med J* 2003; **44**: 74-78 [PMID: 14503780]

93 **Tseng GY**, Lin HJ, Fang CT, Yang HB, Tseng GC, Wang PC, Hung TL, Deng YC, Cheng YT, Huang CH. Recurrence of peptic ulcer in uraemic and non-uraemic patients after Helicobacter pylori eradication: a 2-year study. *Aliment Pharmacol Ther* 2007; **26**: 925-933 [PMID: 17767477]

94 **Jalalzadeh M**, Saber HR, Vafaeimanesh J, Mirzamohammadi F, Falaknazi K. Association of Helicobacter pylori infection and serum albumin in patients on hemodialysis. *Iran J Kidney Dis* 2010; **4**: 312-316 [PMID: 20852373]

95 **Falaknazi K**, Jalalzadeh M, Vafaeimanesh J. Noninvasive stool antigen assay for screening of Helicobacter pylori infection and assessing success of eradication therapy in patients on hemodialysis. *Iran J Kidney Dis* 2010; **4**: 317-321 [PMID: 20852374]

96 **Seyyedmajidi M**, Falaknazi K, Mirsattari D, Zojaji H, Roshani M, Lahmi F, Orimi PG, Hadizadeh M, Zali M. Correlation between creatinine clearance and Helicobacter pylori infection eradication with sequential and triple therapeutic regimens: A randomised clinical trial. *Arab J Gastroenterol* 2011; **12**: 150-153 [PMID: 22055594 DOI: 10.1016/j.ajg.2011.07.004]

97 **Jalalzadeh M**, Ghadiani MH, Mousavinasab N. Association between helicobacter pylori infection and body mass index, before and after eradication of infection in hemodialysis batients. *J Nephropathol* 2012; **1**: 170-176 [PMID: 24475411 DOI: 10.5812/nephropathol.8115]

98 **Jalalzadeh M**, Nazarian M, Vafaeimanesh J, Mirzamohammadi F. Comparison of azithromycin and clarithromycin triple therapy regimens for helicobacter pylori eradication in hemodialysis patients. *Nephrourol Mon* 2012; **4**: 571-577 [PMID: 23573488 DOI: 10.5812/numonthly.2794]

99 **Vafaeimanesh J**, Jalalzadeh M, Nazarian M. Expression comparison of azithromycin and clarithromycin in triple-therapy regimens for eradication of Helicobacter pylori in hemodialysis patients. *Saudi J Kidney Dis Transpl* 2014; **25**: 53-57 [PMID: 24434382]

100 **Makhlough A**, Fakheri H, Farkhani AR, Seddighi O, Hossieni SV, Khademloo M, Bari Z. A comparison between standard triple therapy and sequential therapy on eradication of Helicobacter pylori in uremic patients: A randomized clinical trial. *Adv Biomed Res* 2014; **3**: 248 [PMID: 25590026 DOI: 10.4103/2277-9175.146372]

101 **Makhlough A**, Fakheri H, Hojati S, Hosseini V, Bari Z. A Comparison between Hybrid Therapy and Standard Triple Therapy for Helicobacter pylori Eradication in Patients with Uremia: A Randomized Clinical Trial. *Middle East J Dig Dis* 2016; **8**: 39-43 [PMID: 26933480 DOI: 10.15171/mejdd.2016.05]

P- Reviewer: Papamichail K, Paoluzi OA, Pellicano R, Slomiany BL
S- Editor: Wang XJ **L- Editor**: A **E- Editor**: Huang Y

World Journal of Gastroenterology

Submit a Manuscript: http://www.f6publishing.com

World J Gastroenterol 2018 April 21; 24(15): 1601-1615

DOI: 10.3748/wjg.v24.i15.1601

ISSN 1007-9327 (print) ISSN 2219-2840 (online)

MINIREVIEWS

Multiomics biomarkers for the prediction of nonalcoholic fatty liver disease severity

Carlos J Pirola, Silvia Sookoian

Carlos J Pirola, Department of Genetics and Molecular Biology of Complex Diseases. University of Buenos Aires, Institute of Medical Research A Lanari, Buenos Aires, Argentina, National Scientific and Technical Research Council-University of Buenos Aires. Institute of Medical Research (IDIM), CABA 1427, Argentina

Silvia Sookoian, Clinical and Molecular Hepatology, University of Buenos Aires, Institute of Medical Research A Lanari, Buenos Aires, Argentina, National Scientific and Technical Research Council-University of Buenos Aires. Institute of Medical Research (IDIM), CABA 1427, Argentina

ORCID number: Carlos J Pirola (0000-0001-8234-4058); Silvia Sookoian (0000-0001-5929-5470).

Author contributions: All authors equally contributed to this paper with conception and design of the study, literature review and analysis, drafting and critical revision and editing, and final approval of the final version.

Supported by Agencia Nacional de Promoción Científicay Tecnológica, No. PICT 2014-0432, No. PICT 2014-1816 and No. PICT 2015-0551.

Conflict-of-interest statement: No potential conflicts of interest.

Manuscript source: Invited manuscript

Correspondence to: Silvia Sookoian, MD, PhD, Senior Scientist, Clinical and Molecular Hepatology, University of Buenos Aires, Institute of Medical Research A Lanari, Buenos Aires, Argentina, National Scientific and Technical Research Council-University of Buenos Aires. Institute of Medical Research, Combatientes de Malvinas 3150, CABA 1427, Argentina. sookoian.silvia@lanari.fmed.uba.ar
Telephone: +54-11-52873905

Received: January 1, 2018
Peer-review started: February 1, 2018
First decision: February 24, 2018
Revised: March 13, 2018
Accepted: March 31, 2018
Article in press: March 31, 2018
Published online: April 21, 2018

Abstract

This review intends to uncover how information from large-scale genetic profiling (whole genome sequencing, and whole exome sequencing) of nonalcoholic fatty liver disease (NAFLD), as well as information from circulating transcriptomics (cell-free miRNAs) and metabolomics, contributes to the understanding of NAFLD pathogenesis. A further aim is to address the question of whether OMICs information is ready to be implemented in the clinics. The available evidence suggests that any new knowledge pertaining to molecular signatures associated with NAFLD and nonalcoholic steatohepatitis should be promptly translated into the clinical setting. Nevertheless, rigorous steps that must include validation and replication are mandatory before utilizing OMICs biomarkers in diagnostics to identify patients at risk of advanced disease, including liver cancer.

Key words: Nonalcoholic steatohepatitis; Fibrosis; Liver biopsy; Genetics; *PNPLA3*; *TM6SF2*; Metabolomics; Proteomics; Transcriptomics; Nonalcoholic fatty liver disease; miR122

Core tip: It is expected that, in the near future, nonalcoholic fatty liver disease patients can be diagnosed and treated according to their own "molecular signature". Specific focus should be placed on prevention and early diagnosis through the application of biomarkers of disease risk. Selection of "personalized drugs" as well as tailored therapy according to the specific molecular signature should be further guaranteed.

Pirola CJ, Sookoian S. Multiomics biomarkers for the prediction of nonalcoholic fatty liver disease severity. *World J Gastroenterol* 2018; 24(15): 1601-1615 Available from: URL: http://www.wjgnet.com/1007-9327/full/v24/i15/1601.htm DOI: http://dx.doi.org/10.3748/wjg.v24.i15.1601

INTRODUCTION

Nonalcoholic fatty liver disease (NAFLD) is a chronic liver disease that affects adult and children populations around the world, with prevalence reaching alarming levels[1,2].

NAFLD may progress from a benign histological disease stage characterized by plain fat accumulation, usually referred to as simple steatosis or nonalcoholic fatty liver (NAFL), to a more severe histological form characterized by liver cell injury, a mixed inflammatory lobular infiltrate, and variable fibrosis named nonalcoholic steatohepatitis (NASH)[3,4].

Precise histological diagnosis, including disease stages (NAFL and NASH), is commonly based on liver biopsy[2]. Nevertheless, because this method imposes certain limitations, including potential complications such as bleeding and patients' abdominal discomfort, and needs to be performed in a special setting, noninvasive approaches are favored and have gained considerable attention. It is also noteworthy that the histological diagnosis of the severity of NAFLD might be potentially biased if a small portion of hepatic tissue is sampled.

Hence, significant clinical and research efforts are currently being directed toward the search for reliable biomarkers aimed at the prediction of the disease severity and prognosis.

Knowledge in the field of liver diseases, particularly NAFLD, has benefitted in the last ten years from the rapid development of high-throughput technologies, including genomics, transcriptomics, proteomics and metabolomics. This review intends to uncover how information from large-scale genetic profiling (whole genome sequencing and whole exome sequencing) of NAFLD, as well as information from transcriptomics and metabolomics, and the interplay of these personal characteristics with dietary factors may contribute to the diagnosis and risk prediction of NAFLD progression. In addition, the question of whether OMICs information is ready to be implemented in the clinics will be addressed.

A brief description of OMICs signatures, including their main applications as biomarkers in clinical practice, is provided in Figure 1. OMICs biomarkers may be considered either for screening purposes to assess the disease risk or exposure, or for the assessment of the disease severity and prognosis, and/or for monitoring treatment response (Figure 1).

ROLE OF GENETIC MARKERS IN THE PREDICTION OF NAFLD RISK AND DISEASE SEVERITY

Although the pathogenesis of NAFLD is not understood fully, a growing body of evidence indicates that the disease develops from a complex process involving many factors, including genetic susceptibility and environmental insults[5,6].

In fact, the results yielded by the first genome-wide association study on NAFLD[7] on the role of rs738409 C/G -a variant nonsynonymous single nucleotide polymorphism (SNP) of *PNPLA3* (patatin-like phospholipase domain containing 3, also known as adiponutrin or calcium-independent phospholipase A2-epsilon) have significantly contributed to the knowledge of the genetic component of NAFLD. This finding was subsequently widely replicated around the world, confirming that the G allele in the forward strand is significantly associated not only with an increased risk of fatty liver but the histological disease severity as well[8,9] (OR 1.88 per G allele). In fact, rs738409 explains about 5.3% of the total variance in NAFLD[9].

Furthermore, results of the first exome-wide association study of liver fat content indicate that rs58542926 (E167K), a nonsynonymous variant located in *TM6SF2* (Transmembrane 6 Superfamily Member 2), is significantly associated with increased liver fat content[10]. Nevertheless, in contrast to the effect of the variant located in *PNPLA3*, the rs58542926 exerts a moderate effect on the risk of NAFLD (odds ratio: 2.13)[11]. Subsequent studies have also revealed an association of rs58542926 with the disease severity[12-14], as well as dual and opposite role in cardiovascular disease prevention[11,12,15].

Thus, it is reasonable to speculate that genetic markers, particularly the 738409-G risk allele, may be used for individual risk assessment either alone or as a part of multi-score biomarkers (Figure 2). For example, Kotronen and coworkers evaluated the performance of rs738409 in predicting the risk of NAFLD by combining routine clinical and laboratory data and the rs738409 genotypes[16]. The authors observed a sensitivity of 86% and a specificity of 71% in the estimation of increased liver fat content[16]. Surprisingly, addition of the genetic information to the score improved the accuracy of NAFLD prediction by less than 1%.

The incorporation of genetic markers into noni-

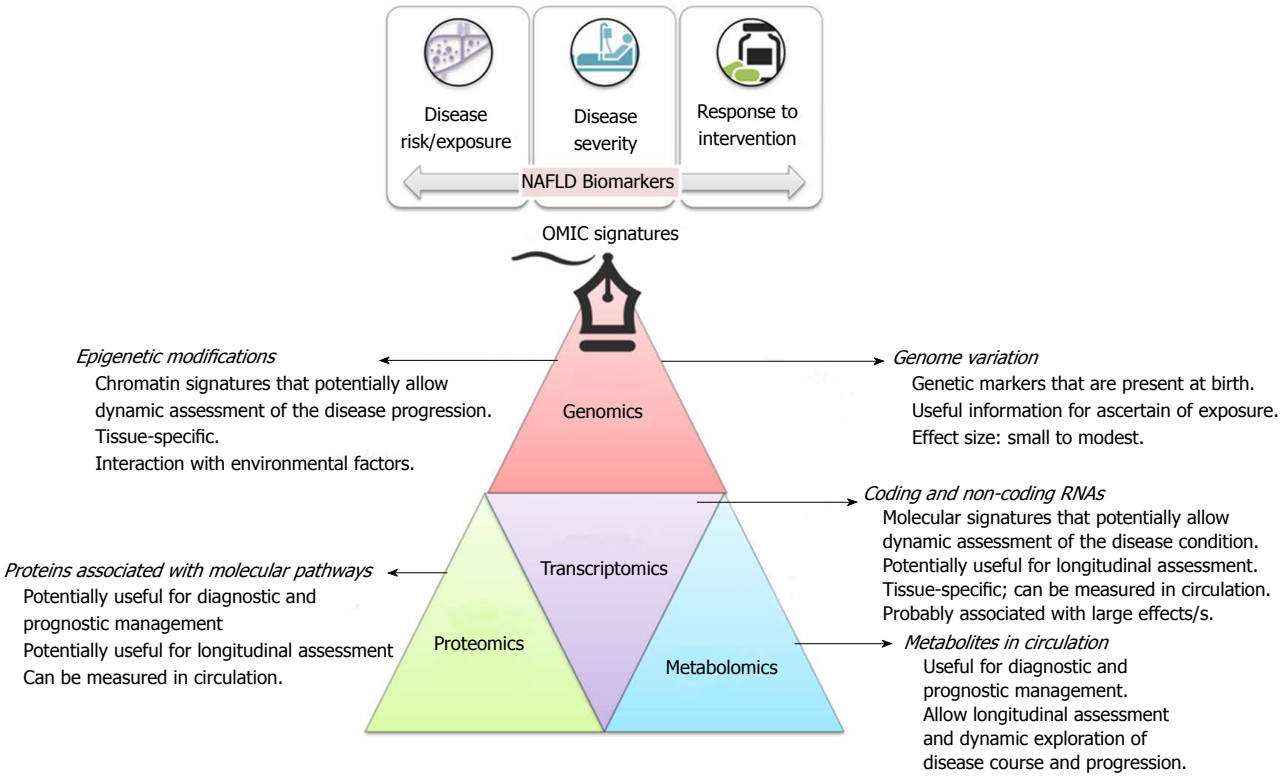

Figure 1 Brief description of OMICs signatures, including their main applications as biomarkers in clinical practice.

nvasive tests that discriminate between NAFL and NASH results in a more challenging strategy; despite these difficulties, there have been some interesting attempts. For instance, a risk score comprising of both clinical and genetic (*PNPLA3* rs738409 C>G, *SOD2* rs4880 C>T, *KLF6* rs3750861 G>A, and *LPIN1* rs13412852 C>T) risk factors resulted in an AUROC (Area Under the Receiver Operating Characteristic) of 0.80 to predict NASH in obese children with increased levels of liver enzymes[17], as shown in Figure 2.

Other examples include the *NASH Clin Score* that combines laboratory tests (AST, fasting insulin) and rs738409 genotypes, and the NASH ClinLipMet Score that combines laboratory test (AST, fasting insulin), circulating metabolites (glutamate, isoleucine, glycine, lyso PC 16:0; PE 40:6) and rs738409 genotypes[18], as depicted in Figure 2.

Furthermore, promising results have been reported on the use of genetic markers in predicting NAFLD-intervention response, as summarized in Figure 2. For example, it was observed that genetic variation in *PNPLA3* might confer sensitivity to liver fat content decrease in obese patients undergoing weight loss[19]. The findings yielded by this study, though based on a small number of subjects, suggested that weight loss was more effective in decreasing liver fat in subjects who were homozygous for the rs738409-G allele[19]. Likewise, rs738409 correlated with changes in metabolic profile and intrahepatic triglyceride content (IHTG) as measured by proton magnetic resonance spectroscopy in patients enrolled in a lifestyle modification program[20]. Concordant results were reported regarding greater improvement in hepatic steatosis after bariatric surgery in the risk-G-rs738409 allele carriers[21] (Figure 2).

A different approach to the use of genetic testing based on single base variations in the DNA sequence requires search for variants in mitochondrial DNA (mtDNA). Mitochondria contain their own genetic information in the mtDNA (16.5 kb), which is maternally inherited; the 13 mtDNA-encoded proteins are all components of the oxidative phosphorylation (OXPHOS). A comprehensive exploration of the complete liver mtDNA-mutation spectrum in patients with NAFLD during different stages of the disease by next generation sequencing showed that the disease severity is associated with an increased liver mtDNA mutational burden, including point mutations in OXPHOS-genes that showed high degrees of heteroplasmy[22]. Given that the variability in the mt-genomes observed in NAFLD and NASH seems to originate from a common germline source, rather than from tissue-specific mutations, point mutations can also be assessed in samples of peripheral blood mononuclear cells[22].

ROLE OF EPIGENETIC MODIFICATIONS AS NONINVASIVE BIOMARKERS OF NAFLD AND NASH

The dynamic nature of epigenetic modifications is not only an ideal frame to explain the cross-talk between NAFLD and related phenotypes, including

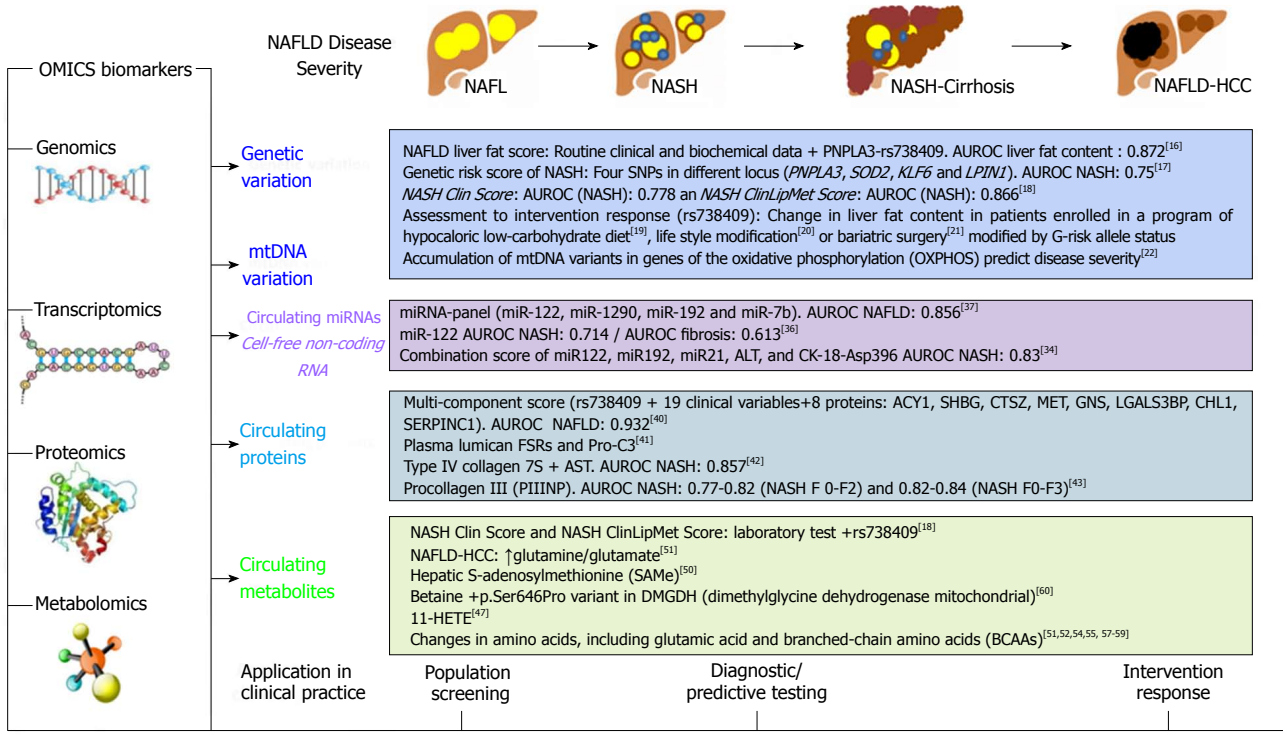

Figure 2 Summary of OMICs biomarkers in the prediction of nonalcoholic fatty liver disease severity.

insulin resistance[23], but is also an attractive target for therapeutic intervention[24]. Treatment-induced epigenetic remodeling of liver tissue was observed in a cohort of obese patients with NAFLD who underwent bariatric surgery[24]. In addition, changes in DNA methylation could be used as a target of a biomarker that allows monitoring, for instance, effectiveness of pharmacotherapy. Interesting results have been reported in the context of other non-cancer complex diseases, including rheumatoid arthritis[25], pediatric asthma[26] or anxiety disorders[27].

It is worth noting that epigenetic modifications, *i.e.* DNA methylation, are not restricted to the nuclear genome, but can also be found in mt-genomes[28]. In fact, we found for the first time that hepatic methylation and transcriptional activity of the MT-ND6 (mt genome-encoded NADH deshydrogenase 6, a member of the OXPHOS complex 1) are associated with the histological severity of NAFLD[29]. This epigenetic change to mtDNA is potentially reversible by lifestyle interventional programs, as physical activity could modulate the methylation status of MT-ND6[29].

CELL-FREE DNA AND RNA AS NONINVASIVE BIOMARKERS OF NASH

Circulating molecular biomarkers, particularly cell-free DNA (cfDNA) and cell-free RNA (cfRNA) are focus of intensive research; however, the strategies employed in these studies are not necessarily novel. In fact, the first description of cell-free nucleic acids (cfNAs) was provided by Mandel and Métais in 1948[30]; indeed, these authors introduced the concept of liquid biopsy.

Basically, cfNAs refer to molecules of nucleic acids that circulate free of cells in the bloodstream and the source of which is primarily dying cells from distant tissues.

Considerable efforts have been dedicated to the use cfDNA for the prediction of liver fibrosis associated with NASH and alcoholic liver disease[31]; however, the preliminary results indicate substantial lack of specificity, as they can be completely unrelated to NASH-biology[32]. Furthermore, the fact that cfDNA circulates not only at very low concentrations but is also highly fragmented imposes analytical and technical challenges that are very difficult to overcome[33].

Conversely, detection of microRNAs (miRNAs), which are highly conserved noncoding small RNAs, has demonstrated quite robust performance, particularly in the circulating compartment. In addition, unlike cfDNA, cfmiRNAs are resistant to degradation as well as to several freeze–thaw cycles, making them ideal biomarkers for use in the clinical setting.

The circulating miRNA signature of NAFLD has been extensively explored in case-control studies, including patients with liver biopsy[34-37], Figure 2. Studies in which liver and circulating miRNA levels were compared demonstrated that cfmiRNAs are good predictors of NAFLD-disease stages[36]. Specifically, circulating miR122 and miR192 not only mirror histological and molecular events occurring in the liver, but have a reliable predictive power in differentiating simple steatosis from NASH[36]. Thus, it can be posited

that cfmiRNAs are reliable candidates for incorporation into multi-panel scores for the prediction of NAFLD and NASH (Figure 2).

For example, a miRNA panel, composed by the detection of miR122-5p, miR1290, miR27b-3p, and miR192-5p) showed a high diagnostic accuracy for NAFLD[37] (Figure 2). A combination score that included miR122, miR192, miR21, ALT, and CK-18-Asp396 exhibited an AUROC of 0.83 for the prediction of NASH[34] (Figure 2).

ROLE OF CIRCULATING PROTEINS IN THE PREDICTION OF NASH SEVERITY

The use of proteins that circulate in serum or plasma for predicting liver-related histological outcomes, specifically liver fibrosis, has been largely relegated probably because such approaches are technically challenging, while offering low performance and poor accuracy. The most remarkable example of this strategy is based on the use of plasma caspase-generated cytokeratin-18 fragments (CK-18) as a noninvasive alternative biomarker of NASH. Results from a large multicenter study showed that plasma CK-18 has relatively good specificity for NAFLD (AUROC: 0.77), NASH (0.65) and fibrosis (0.68). Nevertheless, the overall sensitivity for NAFLD (63%), NASH (58%) and fibrosis (54%) is limited, making this test inadequate for use as a single noninvasive screening test[38].

Interesting attempts to develop multi-component tests that integrate clinical and laboratory data, including circulating proteins, have also been made. For example, we have tested a diagnostic model based on a composite index using clinical and laboratory data, including circulating biomarkers such as soluble intercellular adhesion molecule-1 (sICAM-1), which was able to differentiate between patients with simple steatosis and NASH with a post-test probability for NASH of 99.5% when all positive tests were present[39].

There are similar proposals - though restricted to the prediction of NAFLD but not NASH - based on OMICs-derived data, including genetic information (rs738409), clinical variables, and measurement of different proteins (ACY1, SHBG, CTSZ, MET, GNS, LGALS3BP, CHL1, SERPINC1), which - if combined - seem to be quite reliable in disease risk identification (AUROC for steatosis 0.935)[40]. Nevertheless, it seems that this approach has limited cost-effectiveness for NAFLD-screening programs.

Latest advancements in this field focus directly on disease phenotypes, for example liver fibrosis, which target the detection of excess collagen synthesis rate both directly in liver tissue and noninvasively in blood[41].

The combination of type IV collagen 7S and aspartate aminotransferase (AST) in a multi-test for the prediction of NASH-fibrosis showed promising results[42]. Likewise, measurement of circulating procollagen III (PIIINP) has been quite accurate in the prediction of NASH (AUROC 0.77-0.82) and NASH-fibrosis (0.82-0.84)[43].

Unfortunately, proteomic analysis using state of the art technology is currently poorly developed in the field of NAFLD. In fact, robust attempts to refine, replicate and follow-up on putative discovered proteins have not been done, even though some promising studies have been carried out. For example, using MALDI TOF/TOF and western blot analysis of coupled tissue and serum samples allowed the identification of two interesting protein candidates, including the mitochondrial enzyme CPS1 (Carbamoyl-Phosphate Synthase 1) and GRP78, also known as heat shock protein family A (Hsp70) member 5, which could stratify the different phenotypes associated with the disease severity[44]. Results obtained by using similar approaches, including SELDI-TOF mass spectrometry[45] and matrix-assisted laser desorption ionization time-of-flight mass spectrometry (MALDI TOF-MS)[46] have been published. Still, the identified peaks require validation, replication and large-scale testing.

CIRCULATING METABOLITES IN NASH PREDICTION

Initial case-control studies on plasma metabolomics of NAFLD have been performed years ago by Puri *et al*[47], who conducted a comprehensive analysis of plasma lipids and eicosanoid metabolites quantified by mass spectrometry. The authors reported a stepwise increase in lipoxygenase (LOX) metabolites, 5(S)-hydroxyeicosatetraenoic acid (5-HETE), 8-HETE and 15-HETE that characterized the progression from normal liver to NAFL to NASH[47]. Puri and colleagues found that the level of 11-HETE, a nonenzymatic oxidation product of arachidonic (20:4) acid, was significantly and specifically increased in NASH but not in NAFL patients[47]. Subsequent studies that included untargeted global metabolomic analysis revealed marked changes in bile salts and glutathione-related metabolites, as well as higher levels of branched-chain amino acids, phosphocholine, carbohydrates (glucose, mannose), lactate and pyruvate, in subjects with severe NAFLD[48]. Regarding bile salts, a recent study indicated that total conjugated primary bile acids were significantly higher in NASH[49].

A novel study in which the authors combined metabolomic data from experimental animals and human samples introduced the interesting concept that NASH might be sub-classified into two major subtypes according to the circulating pattern of triglycerides, diglycerides, fatty acids, ceramides and oxidized fatty acids[50].

As mentioned earlier, interesting strategies that combine clinical, genetic and lipidomic-derived variables into a multi-score have shown good predictive values in differentiating NAFL from NASH. Specifically, Zhou and coworkers reported on the performance of the *NASH*

Table 1 List of pathways involved in nonalcoholic fatty liver disease selected from significant *Q*-values that dependent on both genes and metabolites analyzed jointly

Pathway name	Q-joint
Solute carriers -mediated transmembrane transport	1.23E-12
Transmembrane transport of small molecules	9.66E-12
Transport of glucose and other sugars bile salts and organic acids metal ions and amine compounds	8.40E-10
Leukotriene biosynthesis	8.71E-10
Transport of glucose and other sugars bile salts and organic acids metal ions and amine compounds	1.91E-09
Transport of inorganic cations-anions and amino acids-oligopeptides	4.27E-09
Amino acid and oligopeptide SLC transporters	1.10E-08
Transport of inorganic cations/anions and amino acids/oligopeptides	2.40E-08
tRNA Aminoacylation	3.03E-08
Gamma-glutamyl cycle	3.61E-08
tRNA charging	5.96E-08
mRNA protein and metabolite induction pathway by cyclosporine A	8.47E-08
Class I MHC mediated antigen processing & presentation	1.73E-07
Na^+/Cl^- dependent neurotransmitter transporters	3.10E-07
Amino acid transport across the plasma membrane	3.72E-07
S-methyl-5-thio-alpha;-D-ribose 1-phosphate degradation	6.17E-07
Amine compound solute carrier transporters	6.17E-07
Protein digestion and absorption - homo sapiens (human)	2.13E-06
Amino acid interconversion	2.21E-06
Biochemical pathways part I	2.34E-06
Amino acid metabolism	3.96E-06
Aminoacyl-tRNA biosynthesis - homo sapiens (human)	6.88E-06
Metabolism of amino acids and derivatives	8.72E-06
Mineral absorption - homo sapiens (human)	1.47E-05
Cytosolic tRNA aminoacylation	2.86E-05
Mitochondrial tRNA aminoacylation	2.86E-05
tRNA Aminoacylation	2.86E-05
Histidine, lysine, phenylalanine, tyrosine, proline and tryptophan catabolism	0.000159
Gene expression	0.000181
Tryptophan catabolism	0.000275
Phase Ⅱ conjugation	0.000426
Phenylalanine and tyrosine catabolism	0.003
Glutamine and glutamate metabolism - homo sapiens (human)	0.00376
Glutaminolysis and cancer	0.00493
Glycine metabolism	0.0052
Glutamate glutamine metabolism	0.00665
Recycling of bile acids and salts	0.00669
Glycine serine alanine and threonine metabolism	0.0101
Branched-chain amino acid catabolism	0.0103

OMICs-integrative analysis was performed using the IMPaLA (integrated molecular pathway level analysis, http://impala.molgen.mpg.de)[67] platform. A joined adjusted *P*-value (*Q*-value) was calculated to control for multiple testing by false discovery rate.

Clin Score, obtained through backward stepwise logistic regression analyses of biochemical variables (glutamate, isoleucine, glycine, lysophosphatidylcholine 16:0, phosphoethanolamine 40:6, AST, and fasting insulin), along with rs738409 genotypes[18]; this score identified patients with NASH with an AUROC of 0.866 (Figure 2).

Recent explorations on changes in liver metabolism during NASH development[51,52], along with the findings from high-throughput circulating profiling of patients with metabolic syndrome[53] suggest that elevated levels of alanine (ALT) and aspartate (AST) aminotransaminases in patients with NAFLD are the consequence of impaired liver metabolism of amino acids, including glutamate and aromatic amino acids, rather than a mere biomarker of liver injury[14,52,54]. This observation is consistent with the fact that NASH is associated with changes in the level of circulating amino acids[55], including L-glutamic acid, 2-hydroxyglutarate and alanine / pyruvate ratio, which are significantly associated with NAFLD-disease severity[52,56]. Changes in the level of branched-chain amino acids were described in pediatric population[57], and these findings were replicated in studies on adults as well[58].

Interestingly, alterations in multiple aminoacids, gamma-glutamyl dipeptides and lipids may be related to common genetic variations associated with NAFLD, as observed in earlier *in vitro* studies based on knocking down or over-expression of the pIle148Met (rs738409) isoforms[59].

Finally, a two-stage multicenter case-control study that combined results of NAFLD-histological variables, levels of circulating metabolites and genetic markers indicated that NASH is associated with decreased levels of betaine in circulation. Furthermore, the disease severity is associated with genotypes of the missense variant p.Ser646Pro (rs1805074) in *DMGDH* gene,

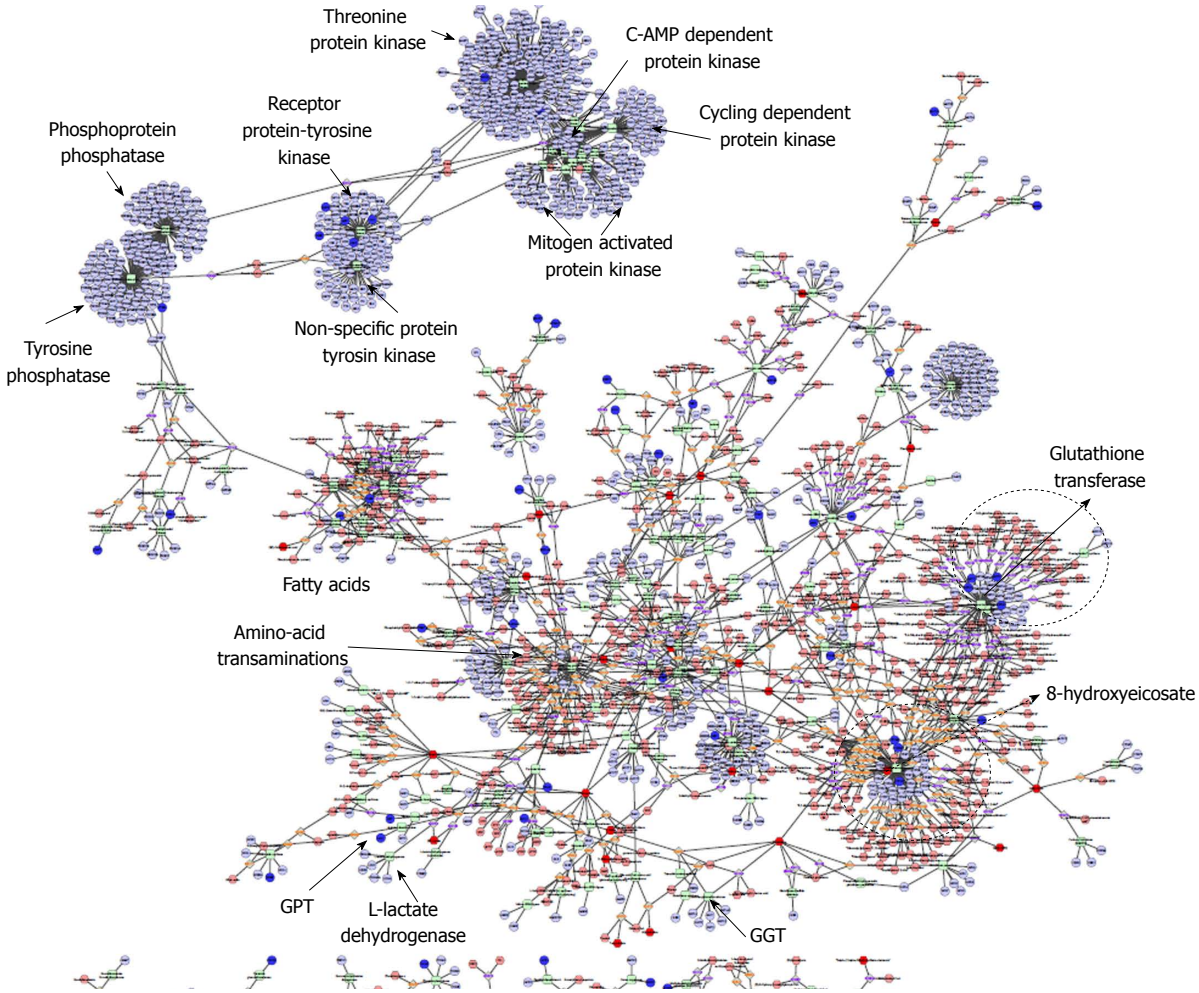
Threonine protein kinase
C-AMP dependent protein kinase
Receptor protein-tyrosine kinase
Cycling dependent protein kinase
Phosphoprotein phosphatase
Mitogen activated protein kinase
Non-specific protein tyrosin kinase
Tyrosine phosphatase
Glutathione transferase
Fatty acids
Amino-acid transaminations
8-hydroxyeicosate
GPT
L-lactate dehydrogenase
GGT

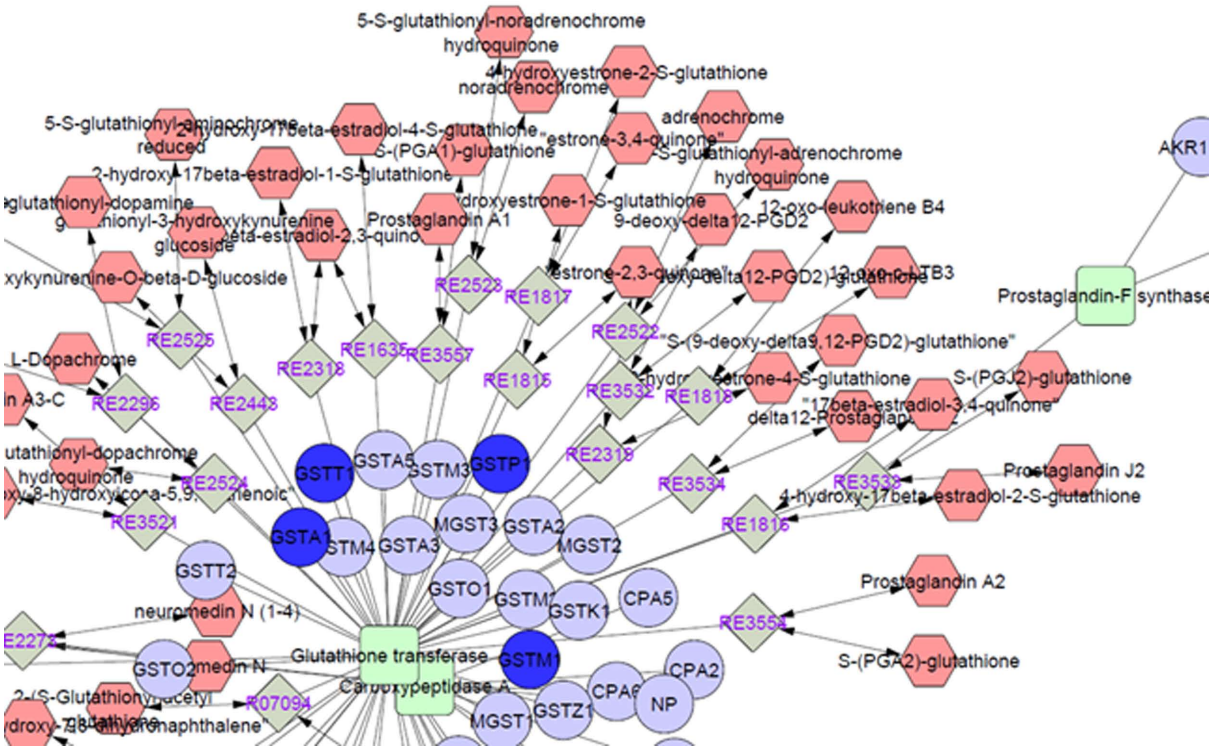
5-S-glutathionyl-noradrenochrome hydroquinone
4-hydroxyestrone-2-S-glutathione
noradrenochrome
adrenochrome
2-hydroxy-17beta-estradiol-4-S-glutathione
S-(PGA1)-glutathione
2-hydroxy-17beta-estradiol-1-S-glutathione
S-glutathionyl-adrenochrome hydroquinone
Prostaglandin A1
9-deoxy-delta12-PGD2
12-oxo-leukotriene B4
glucoside
RE2523
RE1817
RE2522
RE2525
RE1635
RE3557
RE2318
RE1815
RE3532
RE1818
RE2296
RE2443
RE2319
RE3534
RE2524
RE3521
RE1816
GSTT1
GSTA5
GSTM3
GSTP1
GSTA1
GSTM4
GSTA3
MGST3
GSTA2
MGST2
GSTT2
GSTO1
GSTM2
GSTK1
CPA5
neuromedin N (1-4)
RE3554
Glutathione transferase
GSTM1
GSTO2
medin N
CPA2
CPA6
NP
GSTZ1
MGST1
R07094
AKR1
Prostaglandin-F synthase
S-(9-deoxy-delta9,12-PGD2)-glutathione
S-(PGJ2)-glutathione
Prostaglandin J2
4-hydroxy-17beta-estradiol-2-S-glutathione
Prostaglandin A2
S-(PGA2)-glutathione

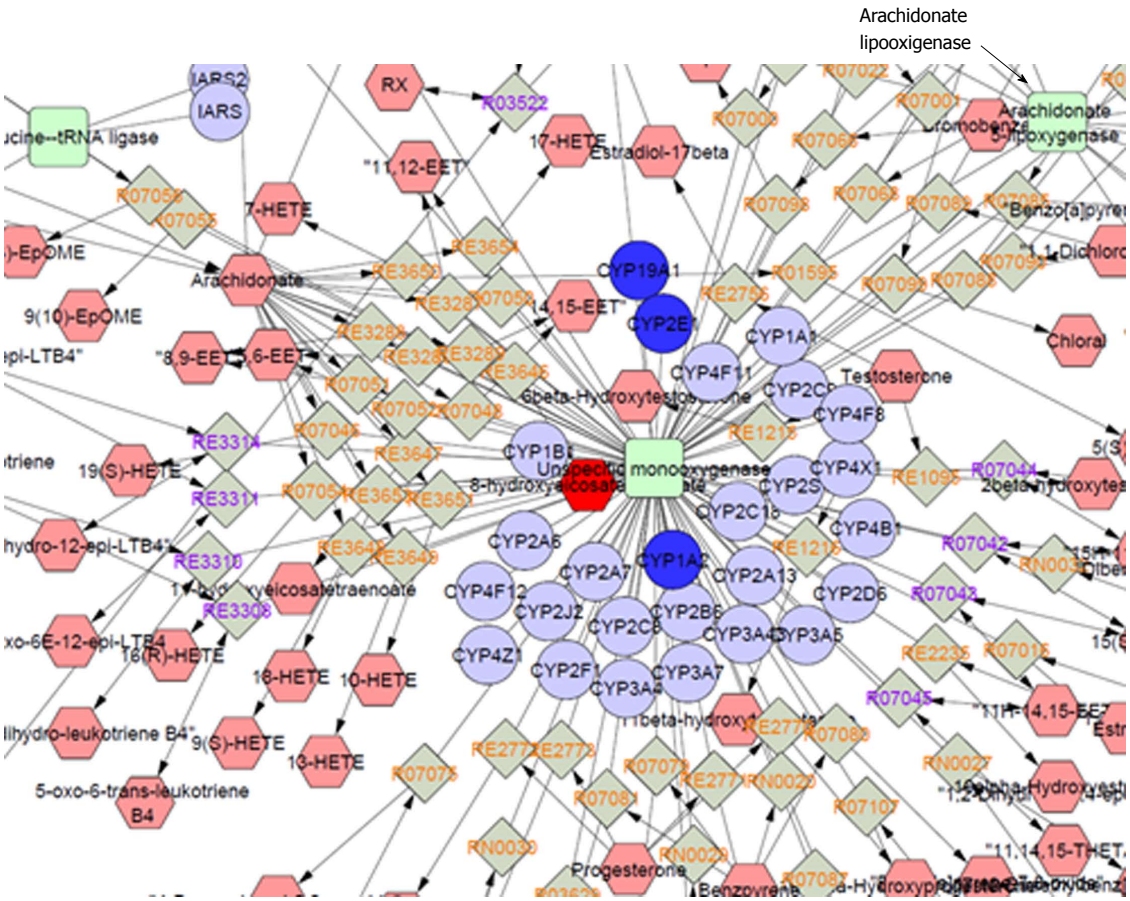

Figure 3 Whole interactome of compounds (hexagons), chemical reactions (diamonds), enzymes (squares) and genes (circles) associated with nonalcoholic fatty liver disease. Details on the set of genes and metabolites that were included in the analysis can be found in the main text; terms were filtered according to the ones already found in the databases. The interactome was built using Metscape[73], a plug-in for the widely used network analysis software Cytoscape[74] that supports calculation, analysis and visualization of gene-to-metabolite networks in the context of metabolism.

which encodes for the mitochondrial dimethylglycine dehydrogenase[60]. Betaine (N,N,N-trimethylglicine) performs a critical function in the pathway of methylogenesis by controlling the serum methionine levels; thus, the results of the aforementioned study[61] might be used to tailor therapeutic interventions based on metabolites that modulate the liver methylome.

INTEGRATION OF DATA DERIVED FROM GENOMICS/PROTEOMICS/ TRANSCRIPTOMICS AND METABOLOMICS TO PREDICT BIOMARKERS ASSOCIATED WITH NAFLD AND NASH

Integration of analyses carried out across multiple biological measurements or OMIC-platforms represents an emerging approach aimed at addressing the challenges imposed by the complex biochemical regulation processes[62].

For example, application of Systems Biology approaches, *i.e.* Gene Set Enrichment Analysis (GSEA)[63], to the field of genomic data has rendered novel knowledge of shared disease-pathways between alcoholic and nonalcoholic liver disease[64]. Likewise, integration of genomic data has highlighted the shared genetic basis of metabolic syndrome and NAFLD[5].

A similar approach can be employed in the field of metabolomics to analyze the enrichment of metabolites that are overrepresented (ORA) in a query-sample against the whole set of metabolites in metabolic pathways. In this context, metabolite set enrichment analysis (MSEA) is the metabolomic counterpart of gene set enrichment. Such analysis, which can be performed by using either commercial or freely available software[65], has been applied to demonstrate alterations in metabolic pathways associated with NAFLD[66].

As a proof of principle, as a part of this work, we performed OMICs-integrative analysis using the IMPaLA (Integrated Molecular Pathway Level Analysis, http://impala.molgen.mpg.de)[67] platform. Briefly, the analysis was conducted by integrating the information on metabolites, genes and proteins, allowing the joint adjusted P-value (Q-value) to be calculated.

Specifically, we selected a list of genes previously associated with NAFLD[5,64], and metabolites that are known to be altered in NAFLD/NASH[68]. Names on metabolites were curated using the compound ID conversion of the web-based MetaboAnalyst tool

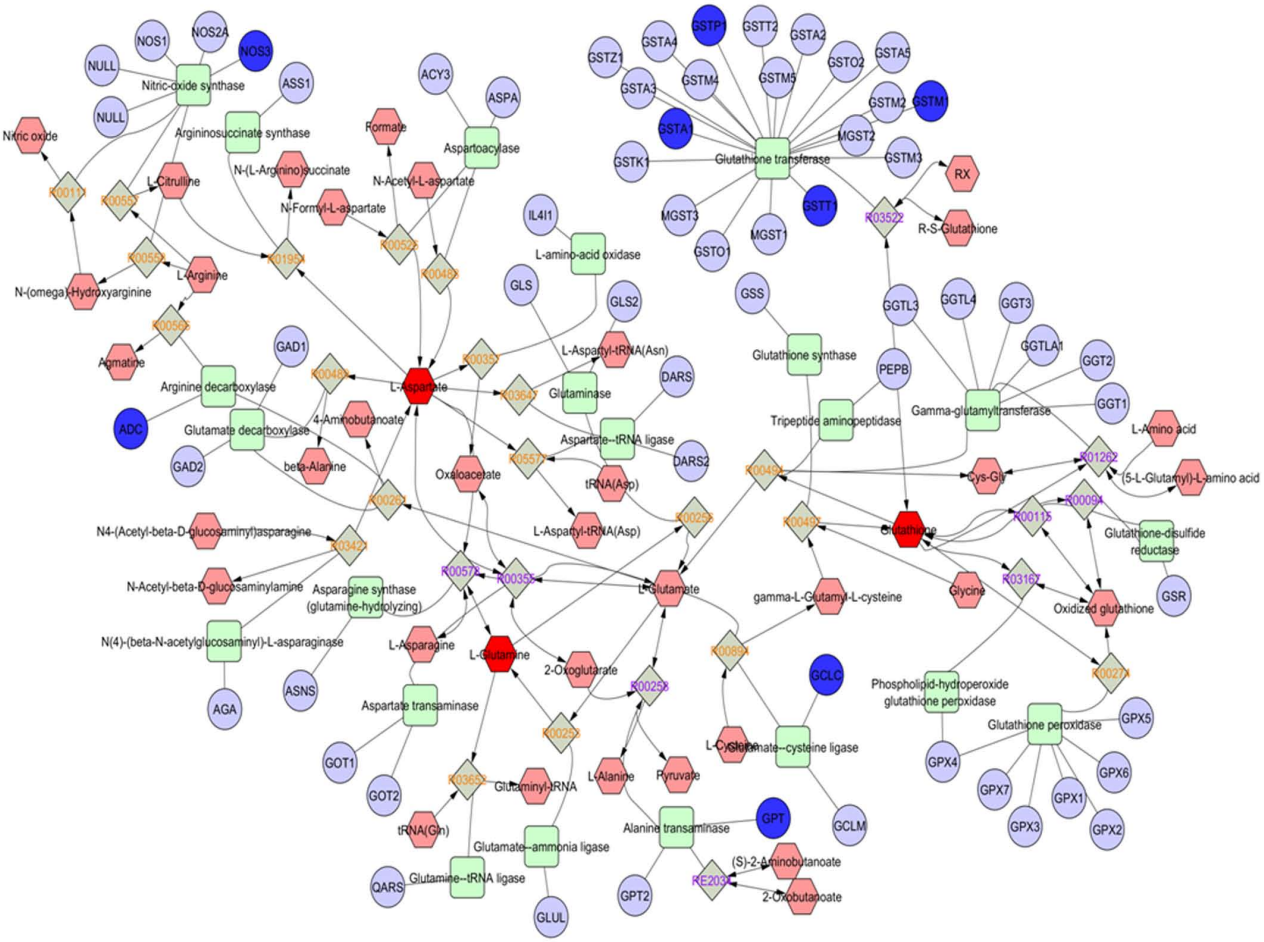

Figure 4 The urea-cycle, glutamate, and branched-chain amino acids in the biology of nonalcoholic fatty liver disease. Sub-network analysis showing the urea-cycle and metabolism of amino acids (L-arginine, L-proline, L-glutamate, L-aspartate and L-asparagine) that were extracted from the interactome shown in Figure 3. Compounds (common names in the Human Metabolome Database, http://www.hmdb.ca), chemical reactions, enzymes (KEGG database) and genes (HUGO symbols) are represented by hexagons, diamonds, squares and circles, respectively.

(http://www.metaboanalyst.ca/)[69,70]. We found 2,827 pathways; however, only 219 of 347 input gene-identifiers were mapped to 219 distinct physical entities found in these pathways (with a gene background size of 12655). Similarly, only 32 of 51 input metabolite-identifiers were mapped to 32 distinct physical entities found in the pathways (with a metabolite background size of 5340). Relevant findings, excluding data that was exclusively and heavily dependent on genes or metabolites, are shown in Table 1; pathways and the Q-values for gene and/or metabolite enrichment were jointly calculated.

It is interesting to highlight and discuss a few examples in more detail. For instance, in the pathway "SLC-mediated transmembrane transport" (Reactome database), the overlapping genes and metabolites are *CALM1* (Calmodulin 1), *G6PC* (Glucose-6-Phosphatase Catalytic Subunit), *FGF21* (Fibroblast Growth Factor 21), *GCK* (Glucokinase) and *GCKR* (Glucokinase Regulator), and taurocholic acid, D-mannose, creatinine, L-lactic acid, L-valine, L-isoleucine, L-phenylalanine, L-aspartic acid, L-tyrosine, carnitine, betaine, L-glutamine, linoleic acid, oleic acid, L-leucine and glycocholic acid, respectively.

Another interesting example is the pathway "Transmembrane transport of small molecules" (Reactome database), in which the overlapping genes and metabolites are *G6PC*, *CALM1*, *ATP1A1* (ATPase Na+/K+ Transporting Subunit Alpha 1), *TF* (Transferrin), *ABCC1* (ATP Binding Cassette Subfamily C Member 1), *FGF21*, *GCK*, *GCKR*, *HMOX1* (Heme Oxygenase 1), *ABCB1* (ATP Binding Cassette Subfamily B Member 1), *ABCC2* (ATP Binding Cassette Subfamily C Member 2), *ABCC3* (ATP Binding Cassette Subfamily C Member 3) and *ABCG2* ATP Binding Cassette Subfamily G Member 2), and L-glutamine, D-mannose, creatinine, L-lactic acid, L-valine, L-isoleucine, L-phenylalanine, taurocholic acid, L-aspartic acid, L-tyrosine, carnitine, betaine, linoleic acid, oleic acid, L-leucine and glycocholic acid, respectively.

Finally, in the pathway "Central carbon metabolism in cancer -Homo sapiens (human)" (KEGG database), the overlapping genes and metabolites are *PTEN* (Phosphatase and Tensin Homolog), *EGFR* (Epidermal Growth Factor Receptor), *MET* (MET Proto-Oncogene, Receptor Tyrosine Kinase), *PIK3CA* (Phosphatidylinositol-

Table 2 List of pathways involved in nonalcoholic fatty liver disease selected from significant *Q*-values independently on whether they represent the effect of gene/s or metabolite/s only

Pathway name	Pathway source	Q-joint
Adipogenesis	Wikipathways	2.00E-17
Non-alcoholic fatty liver disease (NAFLD) - homo sapiens (human)	KEGG	2.33E-17
Metabolism	Reactome	3.72E-17
AGE-RAGE pathway	Wikipathways	4.22E-17
Vitamin B12 Metabolism	Wikipathways	5.24E-17
Hepatitis B - homo sapiens (human)	KEGG	1.79E-16
Folate metabolism	Wikipathways	1.29E-15
Selenium micronutrient network	Wikipathways	3.87E-15
TNF signaling pathway - homo sapiens (human)	KEGG	5.77E-15
JAK-STAT-core	Signalink	1.99E-14
Adipocytokine signaling pathway - homo sapiens (human)	KEGG	7.07E-14
Nuclear receptors meta-pathway	Wikipathways	1.26E-13
IL1 and megakaryocytes in obesity	Wikipathways	2.73E-13
AGE-RAGE signaling pathway in diabetic complications - homo sapiens (human)	KEGG	3.79E-13
Spinal cord injury	Wikipathways	5.44E-13
Malaria - homo sapiens (human)	KEGG	7.09E-13
Metabolism of lipids and lipoproteins	Reactome	7.09E-13
SLC-mediated transmembrane transport	Reactome	1.23E-12
Pathways in cancer - homo sapiens (human)	KEGG	1.41E-12
Inflammatory bowel disease (IBD) - homo sapiens (human)	KEGG	2.25E-12
Lung fibrosis	Wikipathways	2.63E-12
Integrated pancreatic cancer pathway	Wikipathways	3.10E-12
PI3K-Akt signaling pathway - homo sapiens (human)	KEGG	3.28E-12
Chagas disease (American trypanosomiasis) - homo sapiens (human)	KEGG	4.67E-12
HIF-1 signaling pathway - homo sapiens (human)	KEGG	4.67E-12
AMPK signaling pathway - homo sapiens (human)	KEGG	9.56E-12
Transmembrane transport of small molecules	Reactome	9.66E-12
Central carbon metabolism in cancer - homo sapiens (human)	KEGG	1.41E-11
Jak-STAT signaling pathway - homo sapiens (human)	KEGG	5.75E-11
DNA damage response (only ATM dependent)	Wikipathways	7.27E-11
Cytokine-cytokine receptor interaction - homo sapiens (human)	KEGG	1.01E-10
Longevity regulating pathway - homo sapiens (human)	KEGG	1.02E-10
Toll-like receptor signaling pathway	Wikipathways	2.12E-10
Toll-like receptor signaling pathway - homo sapiens (human)	KEGG	3.94E-10
Toxoplasmosis - homo sapiens (human)	KEGG	4.73E-10
ABC transporters - homo sapiens (human)	KEGG	5.94E-10
Transport of glucose and other sugars bile salts and organic acids metal ions and amine compounds	Wikipathways	8.40E-10
Leukotriene biosynthesis	HumanCyc	8.71E-10
Insulin resistance - homo sapiens (human)	KEGG	1.14E-09
Transport of glucose and other sugars bile salts and organic acids metal ions and amine compounds	Reactome	1.91E-09
Sudden infant death syndrome (SIDS) susceptibility pathways	Wikipathways	2.12E-09
Cytokines and inflammatory response	Wikipathways	2.17E-09
AP-1 transcription factor network	PID	2.22E-09
FoxO signaling pathway - homo sapiens (human)	KEGG	3.05E-09
Leptin signaling pathway	Wikipathways	3.57E-09
Transport of inorganic cations-anions and amino acids-oligopeptides	Wikipathways	4.27E-09
Oncostatin M signaling pathway	Wikipathways	5.72E-09
Focal adhesion-PI3K-Akt-mTOR-signaling pathway	Wikipathways	6.53E-09
Amino acid and oligopeptide SLC transporters	Reactome	1.10E-08
Apoptosis	Wikipathways	1.41E-08
Apoptotic signaling pathway	Wikipathways	1.41E-08
Photodynamic therapy-induced NF-kB survival signaling	Wikipathways	1.84E-08
JAK STAT molecularvariation 1	INOH	2.04E-08
MAPK signaling pathway	Wikipathways	2.04E-08
Aryl hydrocarbon receptor	Wikipathways	2.35E-08
Transport of inorganic cations/anions and amino acids/oligopeptides	Reactome	2.40E-08
tRNA aminoacylation	Wikipathways	3.03E-08
gamma-glutamyl cycle	HumanCyc	3.61E-08
Glucose homeostasis	Wikipathways	4.08E-08
Validated transcriptional targets of AP1 family members Fra1 and Fra2	PID	4.13E-08
Hepatitis C and hepatocellular carcinoma	Wikipathways	4.26E-08
Calcineurin-regulated NFAT-dependent transcription in lymphocytes	PID	4.29E-08
Prostate cancer - homo sapiens (human)	KEGG	4.29E-08
Tuberculosis - homo sapiens (human)	KEGG	4.45E-08
Apoptosis - homo sapiens (human)	KEGG	4.54E-08

tRNA charging	HumanCyc	5.96E-08
Transcription factor regulation in adipogenesis	Wikipathways	6.27E-08
Sterol regulatory element-binding proteins (SREBP) signalling	Wikipathways	6.27E-08
Integrated lung cancer pathway	Wikipathways	6.43E-08
TNF related weak inducer of apoptosis (TWEAK) signaling pathway	Wikipathways	8.14E-08
mRNA protein and metabolite induction pathway by cyclosporin A	Wikipathways	8.47E-08
PPAR signaling pathway	Wikipathways	9.54E-08
Immune system	Reactome	9.57E-08
Regulation of lipid metabolism by peroxisome proliferator-activated receptor alpha (PPARalpha)	Wikipathways	1.13E-07
AMP-activated protein kinase (AMPK) signaling	Wikipathways	1.34E-07
Photodynamic therapy-induced NFE2L2 (NRF2) survival signaling	Wikipathways	1.52E-07
Leptin insulin overlap	Wikipathways	1.65E-07
Class I MHC mediated antigen processing and presentation	Wikipathways	1.73E-07
Caspase cascade in apoptosis	PID	1.99E-07
Overview of nanoparticle effects	Wikipathways	2.17E-07
Alpha6Beta4Integrin	NetPath	2.29E-07
VEGFA-VEGFR2 signaling pathway	Wikipathways	2.30E-07
HIV-1 Nef: Negative effector of Fas and TNF-alpha	PID	2.65E-07
Innate immune system	Reactome	2.69E-07
Na^+/Cl^- dependent neurotransmitter transporters	Reactome	3.10E-07
Colorectal cancer - homo sapiens (human)	KEGG	3.42E-07
Regulation of toll-like receptor signaling pathway	Wikipathways	3.64E-07
stress induction of hsp regulation	BioCarta	3.64E-07
Amino acid transport across the plasma membrane	Reactome	3.72E-07
Programmed cell death	Reactome	3.85E-07
Apoptosis modulation and signaling	Wikipathways	4.42E-07
SREBF and miR33 in cholesterol and lipid homeostasis	Wikipathways	4.84E-07
JAK STAT pathway and regulation	INOH	5.42E-07

OMICs-integrative analysis was performed using the IMPaLA (Integrated Molecular Pathway Level Analysis, http://impala.molgen.mpg.de)[67] platform. A joined adjusted *P*-value (*Q*-value) was calculated to control for multiple testing by false discovery rate.

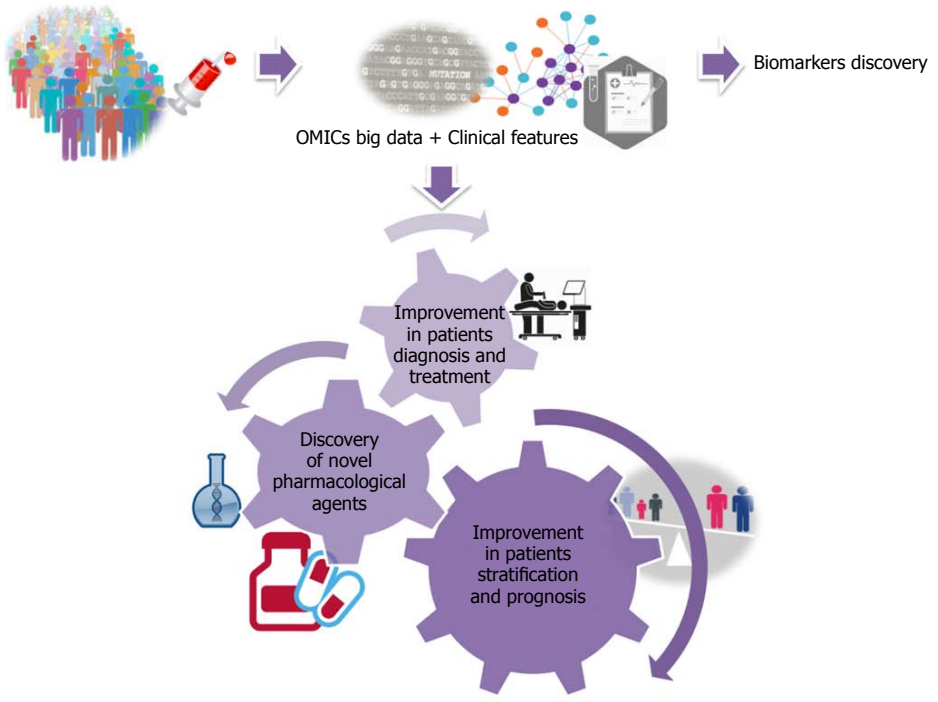

Figure 5 What to expect for the near future. A personalized nonalcoholic fatty liver disease approach by integrating OMICs big data with clinical information.

4,5-Bisphosphate 3-Kinase Catalytic Subunit Alpha), *MTOR* (Mechanistic Target Of Rapamycin Kinase), *AKT2* (AKT Serine/Threonine Kinase 2) and *GCK*, and L-glutamine, L-lactic acid, L-valine, L-isoleucine, L-phenylalanine, L-aspartic acid, L-tyrosine and L-leucine, respectively.

From these few examples, we may conclude that some pathways such as solute carrier (SLC) transporters should be further explored; in fact, available experimental data, while limited, support the participation of ABCC-family in NAFLD pathophysiology[71].

Nonetheless, the findings discussed above do not

necessarily indicate that no other important pathways are potentially involved in the biology of NAFLD. In fact, Table 2 illustrates the myriad of processes involved in the pathogenesis of a complex disease such as NAFLD. In addition, Figure 3 depicts the complexity of the interactome among the whole set of genes, enzymes, chemical reactions and metabolites associated with NAFLD. Figure 4 shows a sub-network emphasizing the importance of the urea-cycle and metabolism of L-arginine, L-proline, L-glutamate, L-aspartate and L-asparagine. Specifically, features in Figure 4 highlight the central role played by aminotransferases and gamma-glutamyl transferases in the frame of altered L-glutamine/L-glutamate, glutathione and BCAA levels, as already mentioned.

Finally, additional biomarkers that target immunity-related pathways, for example circulating levels of cytokines/chemokines, antibodies *etc*. might be useful in predicting NASH progression toward advanced phases[72].

CONCLUSION

Implementation of OMICs-derived biomarkers in the management and treatment of patients with NAFLD is still under extensive evaluation. Knowledge gained on genetic signatures associated with NAFLD and NASH, as well as the role of circulating cfmiRNAs and plasma metabolites, should be promptly translated into the clinical setting. Nevertheless, rigorous steps that must include validation and replication are mandatory before OMICs biomarkers are ready for use as diagnostic markers to identify patients at risk of advanced disease, including liver cancer.

What to expect for the near future: A personalized NAFLD approach by integration of OMICs - big data and clinical information (Figure 5): (1) It is expected that, in the near future, NAFLD patients can be diagnosed and treated according to their own "molecular signature"; (2) Specific focus should be placed on prevention and early diagnosis by the application of biomarkers of disease risk; (3) Selection of "personalized drugs" as well as tailored therapy should be made according to the specific molecular signature; and (4) Personalized lifestyle intervention is desirable but it is envisioned that the basic and general recommendations about alcohol restriction, healthy diet and exercise would remain the foundation of prevention and therapy.

REFERENCES

1 **Brunt EM**, Wong VW, Nobili V, Day CP, Sookoian S, Maher JJ, Bugianesi E, Sirlin CB, Neuschwander-Tetri BA, Rinella ME. Nonalcoholic fatty liver disease. *Nat Rev Dis Primers* 2015; **1**: 15080 [PMID: 27188459 DOI: 10.1038/nrdp.2015.80]

2 **Chalasani N**, Younossi Z, Lavine JE, Charlton M, Cusi K, Rinella M, Harrison SA, Brunt EM, Sanyal AJ. The diagnosis and management of nonalcoholic fatty liver disease: Practice guidance from the American Association for the Study of Liver Diseases. *Hepatology* 2018; **67**: 328-357 [PMID: 28714183 DOI: 10.1002/hep.29367]

3 **Brunt EM**. Histopathology of non-alcoholic fatty liver disease. *Clin Liver Dis* 2009; **13**: 533-544 [PMID: 19818303 DOI: 10.1016/j.cld.2009.07.008]

4 **Brunt EM**. Pathology of nonalcoholic fatty liver disease. *Nat Rev Gastroenterol Hepatol* 2010; **7**: 195-203 [PMID: 20195271 DOI: 10.1038/nrgastro.2010.21]

5 **Sookoian S**, Pirola CJ. Nonalcoholic fatty liver disease and metabolic syndrome: Shared genetic basis of pathogenesis. *Hepatology* 2016; **64**: 1417-1420 [PMID: 27480050 DOI: 10.1002/hep.28746]

6 **Sookoian S**, Pirola CJ. Genetic predisposition in nonalcoholic fatty liver disease. *Clin Mol Hepatol* 2017; **23**: 1-12 [PMID: 28268262 DOI: 10.3350/cmh.2016.0109]

7 **Romeo S**, Kozlitina J, Xing C, Pertsemlidis A, Cox D, Pennacchio LA, Boerwinkle E, Cohen JC, Hobbs HH. Genetic variation in PNPLA3 confers susceptibility to nonalcoholic fatty liver disease. *Nat Genet* 2008; **40**: 1461-1465 [PMID: 18820647 DOI: 10.1038/ng.257]

8 **Sookoian S**, Castaño GO, Burgueño AL, Gianotti TF, Rosselli MS, Pirola CJ. A nonsynonymous gene variant in the adiponutrin gene is associated with nonalcoholic fatty liver disease severity. *J Lipid Res* 2009; **50**: 2111-2116 [PMID: 19738004 DOI: 10.1194/jlr.P900013-JLR200]

9 **Sookoian S**, Pirola CJ. Meta-analysis of the influence of I148M variant of patatin-like phospholipase domain containing 3 gene (PNPLA3) on the susceptibility and histological severity of nonalcoholic fatty liver disease. *Hepatology* 2011; **53**: 1883-1894 [PMID: 21381068 DOI: 10.1002/hep.24283]

10 **Kozlitina J**, Smagris E, Stender S, Nordestgaard BG, Zhou HH, Tybjærg-Hansen A, Vogt TF, Hobbs HH, Cohen JC. Exome-wide association study identifies a TM6SF2 variant that confers susceptibility to nonalcoholic fatty liver disease. *Nat Genet* 2014; **46**: 352-356 [PMID: 24531328 DOI: 10.1038/ng.2901]

11 **Pirola CJ**, Sookoian S. The dual and opposite role of the TM6SF2-rs58542926 variant in protecting against cardiovascular disease and conferring risk for nonalcoholic fatty liver: A meta-analysis. *Hepatology* 2015; **62**: 1742-1756 [PMID: 26331730 DOI: 10.1002/hep.28142]

12 **Dongiovanni P**, Petta S, Maglio C, Fracanzani AL, Pipitone R, Mozzi E, Motta BM, Kaminska D, Rametta R, Grimaudo S, Pelusi S, Montalcini T, Alisi A, Maggioni M, Kärjä V, Borén J, Käkelä P, Di Marco V, Xing C, Nobili V, Dallapiccola B, Craxi A, Pihlajamäki J, Fargion S, Sjöström L, Carlsson LM, Romeo S, Valenti L. Transmembrane 6 superfamily member 2 gene variant disentangles nonalcoholic steatohepatitis from cardiovascular disease. *Hepatology* 2015; **61**: 506-514 [PMID: 25251399 DOI: 10.1002/hep.27490]

13 **Liu YL**, Reeves HL, Burt AD, Tiniakos D, McPherson S, Leathart JB, Allison ME, Alexander GJ, Piguet AC, Anty R, Donaldson P, Aithal GP, Francque S, Van Gaal L, Clement K, Ratziu V, Dufour JF, Day CP, Daly AK, Anstee QM. TM6SF2 rs58542926 influences hepatic fibrosis progression in patients with non-alcoholic fatty liver disease. *Nat Commun* 2014; **5**: 4309 [PMID: 24978903 DOI: 10.1038/ncomms5309]

14 **Sookoian S**, Pirola CJ. Liver enzymes, metabolomics and genome-wide association studies: from systems biology to the personalized medicine. *World J Gastroenterol* 2015; **21**: 711-725 [PMID: 25624707 DOI: 10.3748/wjg.v21.i3.711]

15 **Sookoian S**, Castaño GO, Scian R, Mallardi P, Fernández Gianotti T, Burgueño AL, San Martino J, Pirola CJ. Genetic variation in transmembrane 6 superfamily member 2 and the risk of nonalcoholic fatty liver disease and histological disease severity. *Hepatology* 2015; **61**: 515-525 [PMID: 25302781 DOI: 10.1002/hep.27556]

16 **Kotronen A**, Peltonen M, Hakkarainen A, Sevastianova K, Bergholm R, Johansson LM, Lundbom N, Rissanen A, Ridderstråle M, Groop L, Orho-Melander M, Yki-Järvinen H. Prediction of non-alcoholic fatty liver disease and liver fat using metabolic and genetic factors. *Gastroenterology* 2009; **137**: 865-872 [PMID:

19524579 DOI: 10.1053/j.gastro.2009.06.005]
17 **Nobili V**, Donati B, Panera N, Vongsakulyanon A, Alisi A, Dallapiccola B, Valenti L. A 4-polymorphism risk score predicts steatohepatitis in children with nonalcoholic fatty liver disease. *J Pediatr Gastroenterol Nutr* 2014; **58**: 632-636 [PMID: 24345846 DOI: 10.1097/MPG.0000000000000279]
18 **Zhou Y**, Orešič M, Leivonen M, Gopalacharyulu P, Hyysalo J, Arola J, Verrijken A, Francque S, Van Gaal L, Hyötyläinen T, Yki-Järvinen H. Noninvasive Detection of Nonalcoholic Steatohepatitis Using Clinical Markers and Circulating Levels of Lipids and Metabolites. *Clin Gastroenterol Hepatol* 2016; **14**: 1463-1472.e6 [PMID: 27317851 DOI: 10.1016/j.cgh.2016.05.046]
19 **Sevastianova K**, Kotronen A, Gastaldelli A, Perttilä J, Hakkarainen A, Lundbom J, Suojanen L, Orho-Melander M, Lundbom N, Ferrannini E, Rissanen A, Olkkonen VM, Yki-Järvinen H. Genetic variation in PNPLA3 (adiponutrin) confers sensitivity to weight loss-induced decrease in liver fat in humans. *Am J Clin Nutr* 2011; **94**: 104-111 [PMID: 21525193 DOI: 10.3945/ajcn.111.012369]
20 **Shen J**, Wong GL, Chan HL, Chan RS, Chan HY, Chu WC, Cheung BH, Yeung DK, Li LS, Sea MM, Woo J, Wong VW. PNPLA3 gene polymorphism and response to lifestyle modification in patients with nonalcoholic fatty liver disease. *J Gastroenterol Hepatol* 2015; **30**: 139-146 [PMID: 25040896 DOI: 10.1111/jgh.12656]
21 **Krawczyk M**, Jiménez-Agüero R, Alustiza JM, Emparanza JI, Perugorria MJ, Bujanda L, Lammert F, Banales JM. PNPLA3 p.I148M variant is associated with greater reduction of liver fat content after bariatric surgery. *Surg Obes Relat Dis* 2016; **12**: 1838-1846 [PMID: 27576208 DOI: 10.1016/j.soard.2016.06.004]
22 **Sookoian S**, Flichman D, Scian R, Rohr C, Dopazo H, Gianotti TF, Martino JS, Castaño GO, Pirola CJ. Mitochondrial genome architecture in non-alcoholic fatty liver disease. *J Pathol* 2016; **240**: 437-449 [PMID: 27577682 DOI: 10.1002/path.4803]
23 **Sookoian S**, Rosselli MS, Gemma C, Burgueño AL, Fernández Gianotti T, Castaño GO, Pirola CJ. Epigenetic regulation of insulin resistance in nonalcoholic fatty liver disease: impact of liver methylation of the peroxisome proliferator-activated receptor γ coactivator 1α promoter. *Hepatology* 2010; **52**: 1992-2000 [PMID: 20890895 DOI: 10.1002/hep.23927]
24 **Ahrens M**, Ammerpohl O, von Schönfels W, Kolarova J, Bens S, Itzel T, Teufel A, Herrmann A, Brosch M, Hinrichsen H, Erhart W, Egberts J, Sipos B, Schreiber S, Häsler R, Stickel F, Becker T, Krawczak M, Röcken C, Siebert R, Schafmayer C, Hampe J. DNA methylation analysis in nonalcoholic fatty liver disease suggests distinct disease-specific and remodeling signatures after bariatric surgery. *Cell Metab* 2013; **18**: 296-302 [PMID: 23931760 DOI: 10.1016/j.cmet.2013.07.004]
25 **Plant D**, Webster A, Nair N, Oliver J, Smith SL, Eyre S, Hyrich KL, Wilson AG, Morgan AW, Isaacs JD, Worthington J, Barton A. Differential Methylation as a Biomarker of Response to Etanercept in Patients With Rheumatoid Arthritis. *Arthritis Rheumatol* 2016; **68**: 1353-1360 [PMID: 26814849 DOI: 10.1002/art.39590]
26 **Zhang X**, Biagini Myers JM, Yadagiri VK, Ulm A, Chen X, Weirauch MT, Khurana Hershey GK, Ji H. Nasal DNA methylation differentiates corticosteroid treatment response in pediatric asthma: A pilot study. *PLoS One* 2017; **12**: e0186150 [PMID: 29028809 DOI: 10.1371/journal.pone.0186150]
27 **Roberts S**, Lester KJ, Hudson JL, Rapee RM, Creswell C, Cooper PJ, Thirlwall KJ, Coleman JR, Breen G, Wong CC, Eley TC. Serotonin transporter [corrected] methylation and response to cognitive behaviour therapy in children with anxiety disorders. *Transl Psychiatry* 2014; **4**: e444 [PMID: 25226553 DOI: 10.1038/tp.2014.109]
28 **Shock LS**, Thakkar PV, Peterson EJ, Moran RG, Taylor SM. DNA methyltransferase 1, cytosine methylation, and cytosine hydroxymethylation in mammalian mitochondria. *Proc Natl Acad Sci U S A* 2011; **108**: 3630-3635 [PMID: 21321201 DOI: 10.1073/pnas.1012311108]
29 **Pirola CJ**, Gianotti TF, Burgueño AL, Rey-Funes M, Loidl CF, Mallardi P, Martino JS, Castaño GO, Sookoian S. Epigenetic modification of liver mitochondrial DNA is associated with histological severity of nonalcoholic fatty liver disease. *Gut* 2013; **62**: 1356-1363 [PMID: 22879518 DOI: 10.1136/gutjnl-2012-302962]
30 **MANDEL P**, METAIS P. [Not Available]. *C R Seances Soc Biol Fil* 1948; **142**: 241-243 [PMID: 18875018]
31 **Hardy T**, Zeybel M, Day CP, Dipper C, Masson S, McPherson S, Henderson E, Tiniakos D, White S, French J, Mann DA, Anstee QM, Mann J. Plasma DNA methylation: a potential biomarker for stratification of liver fibrosis in non-alcoholic fatty liver disease. *Gut* 2017; **66**: 1321-1328 [PMID: 27002005 DOI: 10.1136/gutjnl-2016-311526]
32 **Yiğit B**, Boyle M, Özler O, Erden N, Tutucu F, Hardy T, Bergmann C, Distler JHW, Adalı G, Dayangaç M, Mann DA, Zeybel M, Mann J. Plasma cell-free DNA methylation: a liquid biomarker of hepatic fibrosis. *Gut* 2018; Epub ahead of print [PMID: 29353249 DOI: 10.1136/gutjnl-2017-315668]
33 **Sookoian S**, Pirola CJ. Cell-free DNA methylation as liquid biopsy for the assessment of fibrosis in patients with nonalcoholic steatohepatitis: a gap between innovation and implementation. *Hepatobiliary Surg Nutr* 2017; **6**: 117-121 [PMID: 28503559 DOI: 10.21037/hbsn.2017.01.07]
34 **Becker PP**, Rau M, Schmitt J, Malsch C, Hammer C, Bantel H, Müllhaupt B, Geier A. Performance of Serum microRNAs -122, -192 and -21 as Biomarkers in Patients with Non-Alcoholic Steatohepatitis. *PLoS One* 2015; **10**: e0142661 [PMID: 26565986 DOI: 10.1371/journal.pone.0142661]
35 **Cermelli S**, Ruggieri A, Marrero JA, Ioannou GN, Beretta L. Circulating microRNAs in patients with chronic hepatitis C and non-alcoholic fatty liver disease. *PLoS One* 2011; **6**: e23937 [PMID: 21886843 DOI: 10.1371/journal.pone.0023937]
36 **Pirola CJ**, Fernández Gianotti T, Castaño GO, Mallardi P, San Martino J, Mora Gonzalez Lopez Ledesma M, Flichman D, Mirshahi F, Sanyal AJ, Sookoian S. Circulating microRNA signature in non-alcoholic fatty liver disease: from serum non-coding RNAs to liver histology and disease pathogenesis. *Gut* 2015; **64**: 800-812 [PMID: 24973316 DOI: 10.1136/gutjnl-2014-306996]
37 **Tan Y**, Ge G, Pan T, Wen D, Gan J. A pilot study of serum microRNAs panel as potential biomarkers for diagnosis of nonalcoholic fatty liver disease. *PLoS One* 2014; **9**: e105192 [PMID: 25141008 DOI: 10.1371/journal.pone.0105192]
38 **Cusi K**, Chang Z, Harrison S, Lomonaco R, Bril F, Orsak B, Ortiz-Lopez C, Hecht J, Feldstein AE, Webb A, Louden C, Goros M, Tio F. Limited value of plasma cytokeratin-18 as a biomarker for NASH and fibrosis in patients with non-alcoholic fatty liver disease. *J Hepatol* 2014; **60**: 167-174 [PMID: 23973932 DOI: 10.1016/j.jhep.2013.07.042]
39 **Sookoian S**, Castaño G, Burgueño AL, Gianotti TF, Rosselli MS, Pirola CJ. A diagnostic model to differentiate simple steatosis from nonalcoholic steatohepatitis based on the likelihood ratio form of Bayes theorem. *Clin Biochem* 2009; **42**: 624-629 [PMID: 19071103 DOI: 10.1016/j.clinbiochem.2008.11.005]
40 **Wood GC**, Chu X, Argyropoulos G, Benotti P, Rolston D, Mirshahi T, Petrick A, Gabrielson J, Carey DJ, DiStefano JK, Still CD, Gerhard GS. A multi-component classifier for nonalcoholic fatty liver disease (NAFLD) based on genomic, proteomic, and phenomic data domains. *Sci Rep* 2017; **7**: 43238 [PMID: 28266614 DOI: 10.1038/srep43238]
41 **Decaris ML**, Li KW, Emson CL, Gatmaitan M, Liu S, Wang Y, Nyangau E, Colangelo M, Angel TE, Beysen C, Cui J, Hernandez C, Lazaro L, Brenner DA, Turner SM, Hellerstein MK, Loomba R. Identifying nonalcoholic fatty liver disease patients with active fibrosis by measuring extracellular matrix remodeling rates in tissue and blood. *Hepatology* 2017; **65**: 78-88 [PMID: 27706836 DOI: 10.1002/hep.28860]
42 **Okanoue T**, Ebise H, Kai T, Mizuno M, Shima T, Ichihara J, Aoki M. A simple scoring system using type IV collagen 7S and aspartate aminotransferase for diagnosing nonalcoholic steatohepatitis and related fibrosis. *J Gastroenterol* 2018; **53**: 129-139 [PMID: 28589339 DOI: 10.1007/s00535-017-1355-9]
43 **Tanwar S**, Trembling PM, Guha IN, Parkes J, Kaye P, Burt AD,

Ryder SD, Aithal GP, Day CP, Rosenberg WM. Validation of terminal peptide of procollagen III for the detection and assessment of nonalcoholic steatohepatitis in patients with nonalcoholic fatty liver disease. *Hepatology* 2013; **57**: 103-111 [PMID: 22930399 DOI: 10.1002/hep.26030]

44 **Rodriguez-Suarez E**, Mato JM, Elortza F. Proteomics analysis of human nonalcoholic fatty liver. *Methods Mol Biol* 2012; **909**: 241-258 [PMID: 22903720 DOI: 10.1007/978-1-61779-959-4_16]

45 **Younossi ZM**, Baranova A, Ziegler K, Del Giacco L, Schlauch K, Born TL, Elariny H, Gorreta F, VanMeter A, Younoszai A, Ong JP, Goodman Z, Chandhoke V. A genomic and proteomic study of the spectrum of nonalcoholic fatty liver disease. *Hepatology* 2005; **42**: 665-674 [PMID: 16116632 DOI: 10.1002/hep.20838]

46 **Ulukaya E**, Yilmaz Y, Moshkovskii S, Karpova M, Pyatnitskiy M, Atug O, Dolar E. Proteomic analysis of serum in patients with non-alcoholic steatohepatitis using matrix-assisted laser desorption ionization time-of-flight mass spectrometry. *Scand J Gastroenterol* 2009; **44**: 1471-1476 [PMID: 19883279 DOI: 10.3109/00365520903353379]

47 **Puri P**, Wiest MM, Cheung O, Mirshahi F, Sargeant C, Min HK, Contos MJ, Sterling RK, Fuchs M, Zhou H, Watkins SM, Sanyal AJ. The plasma lipidomic signature of nonalcoholic steatohepatitis. *Hepatology* 2009; **50**: 1827-1838 [PMID: 19937697 DOI: 10.1002/hep.23229]

48 **Kalhan SC**, Guo L, Edmison J, Dasarathy S, McCullough AJ, Hanson RW, Milburn M. Plasma metabolomic profile in nonalcoholic fatty liver disease. *Metabolism* 2011; **60**: 404-413 [PMID: 20423748 DOI: 10.1016/j.metabol.2010.03.006]

49 **Puri P**, Daita K, Joyce A, Mirshahi F, Santhekadur PK, Cazanave S, Luketic VA, Siddiqui MS, Boyett S, Min HK, Kumar DP, Kohli R, Zhou H, Hylemon PB, Contos MJ, Idowu M, Sanyal AJ. The presence and severity of nonalcoholic steatohepatitis is associated with specific changes in circulating bile acids. *Hepatology* 2017; Epub ahead of print [PMID: 28696585]

50 **Alonso C**, Fernández-Ramos D, Varela-Rey M, Martínez-Arranz I, Navasa N, Van Liempd SM, Lavín Trueba JL, Mayo R, Ilisso CP, de Juan VG, Iruarrizaga-Lejarreta M, delaCruz-Villar L, Mincholé I, Robinson A, Crespo J, Martín-Duce A, Romero-Gómez M, Sann H, Platon J, Van Eyk J, Aspichueta P, Noureddin M, Falcón-Pérez JM, Anguita J, Aransay AM, Martínez-Chantar ML, Lu SC, Mato JM. Metabolomic Identification of Subtypes of Nonalcoholic Steatohepatitis. *Gastroenterology* 2017; **152**: 1449-1461.e7 [PMID: 28132890 DOI: 10.1053/j.gastro.2017.01.015]

51 **Sunny NE**, Parks EJ, Browning JD, Burgess SC. Excessive hepatic mitochondrial TCA cycle and gluconeogenesis in humans with nonalcoholic fatty liver disease. *Cell Metab* 2011; **14**: 804-810 [PMID: 22152305 DOI: 10.1016/j.cmet.2011.11.004]

52 **Sookoian S**, Castaño GO, Scian R, Fernández Gianotti T, Dopazo H, Rohr C, Gaj G, San Martino J, Sevic I, Flichman D, Pirola CJ. Serum aminotransferases in nonalcoholic fatty liver disease are a signature of liver metabolic perturbations at the amino acid and Krebs cycle level. *Am J Clin Nutr* 2016; **103**: 422-434 [PMID: 26791191 DOI: 10.3945/ajcn.115.118695]

53 **Shin SY**, Fauman EB, Petersen AK, Krumsiek J, Santos R, Huang J, Arnold M, Erte I, Forgetta V, Yang TP, Walter K, Menni C, Chen L, Vasquez L, Valdes AM, Hyde CL, Wang V, Ziemek D, Roberts P, Xi L, Grundberg E; Multiple Tissue Human Expression Resource (MuTHER) Consortium, Waldenberger M, Richards JB, Mohney RP, Milburn MV, John SL, Trimmer J, Theis FJ, Overington JP, Suhre K, Brosnan MJ, Gieger C, Kastenmüller G, Spector TD, Soranzo N. An atlas of genetic influences on human blood metabolites. *Nat Genet* 2014; **46**: 543-550 [PMID: 24816252 DOI: 10.1038/ng.2982]

54 **Yin X**, Subramanian S, Willinger CM, Chen G, Juhasz P, Courchesne P, Chen BH, Li X, Hwang SJ, Fox CS, O'Donnell CJ, Muntendam P, Fuster V, Bobeldijk-Pastorova I, Sookoian SC, Pirola CJ, Gordon N, Adourian A, Larson MG, Levy D. Metabolite Signatures of Metabolic Risk Factors and their Longitudinal Changes. *J Clin Endocrinol Metab* 2016; **101**: 1779-1789 [PMID: 26908103 DOI: 10.1210/jc.2015-2555]

55 **Sookoian S**, Pirola CJ. NAFLD. Metabolic make-up of NASH: from fat and sugar to amino acids. *Nat Rev Gastroenterol Hepatol* 2014; **11**: 205-207 [PMID: 24566880 DOI: 10.1038/nrgastro.2014.25]

56 **Sookoian S**, Pirola CJ. The nonalcoholic steatohepatitis metabotype: Imbalance of circulating amino acids and transamination reactions reflect impaired mitochondrial function. *Hepatology* 2018; **67**: 1177-1178 [PMID: 29205411 DOI: 10.1002/hep.29705]

57 **Goffredo M**, Santoro N, Tricò D, Giannini C, D'Adamo E, Zhao H, Peng G, Yu X, Lam TT, Pierpont B, Caprio S, Herzog RI. A Branched-Chain Amino Acid-Related Metabolic Signature Characterizes Obese Adolescents with Non-Alcoholic Fatty Liver Disease. *Nutrients* 2017; **9**: pii: E642 [PMID: 28640216 DOI: 10.3390/nu9070642]

58 **Gaggini M**, Carli F, Rosso C, Buzzigoli E, Marietti M, Della Latta V, Ciociaro D, Abate ML, Gambino R, Cassader M, Bugianesi E, Gastaldelli A. Altered amino acid concentrations in NAFLD: Impact of obesity and insulin resistance. *Hepatology* 2018; **67**: 145-158 [PMID: 28802074 DOI: 10.1002/hep.29465]

59 **Min HK**, Sookoian S, Pirola CJ, Cheng J, Mirshahi F, Sanyal AJ. Metabolic profiling reveals that PNPLA3 induces widespread effects on metabolism beyond triacylglycerol remodeling in Huh-7 hepatoma cells. *Am J Physiol Gastrointest Liver Physiol* 2014; **307**: G66-G76 [PMID: 24763554 DOI: 10.1152/ajpgi.00335.2013]

60 **Sookoian S**, Puri P, Castaño GO, Scian R, Mirshahi F, Sanyal AJ, Pirola CJ. Nonalcoholic steatohepatitis is associated with a state of betaine-insufficiency. *Liver Int* 2017; **37**: 611-619 [PMID: 27614103 DOI: 10.1111/liv.13249]

61 **Wanichthanarak K**, Fan S, Grapov D, Barupal DK, Fiehn O. Metabox: A Toolbox for Metabolomic Data Analysis, Interpretation and Integrative Exploration. *PLoS One* 2017; **12**: e0171046 [PMID: 28141874]

62 **Wanichthanarak K**, Fahrmann JF, Grapov D. Genomic, Proteomic, and Metabolomic Data Integration Strategies. *Biomark Insights* 2015; **10**: 1-6 [PMID: 26396492 DOI: 10.4137/BMI.S29511]

63 **Subramanian A**, Tamayo P, Mootha VK, Mukherjee S, Ebert BL, Gillette MA, Paulovich A, Pomeroy SL, Golub TR, Lander ES, Mesirov JP. Gene set enrichment analysis: a knowledge-based approach for interpreting genome-wide expression profiles. *Proc Natl Acad Sci USA* 2005; **102**: 15545-15550 [PMID: 16199517 DOI: 10.1073/pnas.0506580102]

64 **Sookoian S**, Pirola CJ. Systems biology elucidates common pathogenic mechanisms between nonalcoholic and alcoholic-fatty liver disease. *PLoS One* 2013; **8**: e58895 [PMID: 23516571]

65 **Cambiaghi A**, Ferrario M, Masseroli M. Analysis of metabolomic data: tools, current strategies and future challenges for omics data integration. *Brief Bioinform* 2017; **18**: 498-510 [PMID: 27075479]

66 **Dumas ME**, Kinross J, Nicholson JK. Metabolic phenotyping and systems biology approaches to understanding metabolic syndrome and fatty liver disease. *Gastroenterology* 2014; **146**: 46-62 [PMID: 24211299 DOI: 10.1053/j.gastro.2013.11.001]

67 **Kamburov A**, Cavill R, Ebbels TM, Herwig R, Keun HC. Integrated pathway-level analysis of transcriptomics and metabolomics data with IMPaLA. *Bioinformatics* 2011; **27**: 2917-2918 [PMID: 21893519 DOI: 10.1093/bioinformatics/btr499]

68 **Safaei A**, Arefi Oskouie A, Mohebbi SR, Rezaei-Tavirani M, Mahboubi M, Peyvandi M, Okhovatian F, Zamanian-Azodi M. Metabolomic analysis of human cirrhosis, hepatocellular carcinoma, non-alcoholic fatty liver disease and non-alcoholic steatohepatitis diseases. *Gastroenterol Hepatol Bed Bench* 2016; **9**: 158-173 [PMID: 27458508]

69 **Xia J**, Sinelnikov IV, Han B, Wishart DS. MetaboAnalyst 3.0--making metabolomics more meaningful. *Nucleic Acids Res* 2015; **43**: W251-W257 [PMID: 25897128 DOI: 10.1093/nar/gkv380]

70 **Xia J**, Wishart DS. Using MetaboAnalyst 3.0 for Comprehensive Metabolomics Data Analysis. *Curr Protoc Bioinformatics* 2016; **55**: 14.10.1-14.10.91 [PMID: 27603023 DOI: 10.1002/cpbi.11]

71 **Tanaka N**, Matsubara T, Krausz KW, Patterson AD, Gonzalez FJ. Disruption of phospholipid and bile acid homeostasis in mice with nonalcoholic steatohepatitis. *Hepatology* 2012; **56**: 118-129 [PMID:

22290395 DOI: 10.1002/hep.25630]
72 **Sutti S**, Jindal A, Bruzzì S, Locatelli I, Bozzola C, Albano E. Is there a role for adaptive immunity in nonalcoholic steatohepatitis? *World J Hepatol* 2015; **7**: 1725-1729 [PMID: 26167244 DOI: 10.4254/wjh.v7.i13.1725]
73 **Karnovsky A**, Weymouth T, Hull T, Tarcea VG, Scardoni G, Laudanna C, Sartor MA, Stringer KA, Jagadish HV, Burant C, Athey B, Omenn GS. Metscape 2 bioinformatics tool for the analysis and visualization of metabolomics and gene expression data. *Bioinformatics* 2012; **28**: 373-380 [PMID: 22135418 DOI: 10.1093/bioinformatics/btr661]
74 **Shannon P**, Markiel A, Ozier O, Baliga NS, Wang JT, Ramage D, Amin N, Schwikowski B, Ideker T. Cytoscape: a software environment for integrated models of biomolecular interaction networks. *Genome Res* 2003; **13**: 2498-2504 [PMID: 14597658 DOI: 10.1101/gr.1239303]

P- Reviewer: Arslan N, Enomoto H, Jarcuska P, Sutti S, Toshikuni N
S- Editor: Ma YJ **L- Editor**: A **E- Editor**: Huang Y

World Journal of Gastroenterology

Submit a Manuscript: http://www.f6publishing.com

World J Gastroenterol 2018 April 21; 24(15): 1616-1621

DOI: 10.3748/wjg.v24.i15.1616

ISSN 1007-9327 (print) ISSN 2219-2840 (online)

MINIREVIEWS

Autonomic nervous system network and liver regeneration

Kenya Kamimura, Ryosuke Inoue, Takuro Nagoya, Norihiro Sakai, Ryo Goto, Masayoshi Ko, Yusuke Niwa, Shuji Terai

Kenya Kamimura, Ryosuke Inoue, Takuro Nagoya, Norihiro Sakai, Ryo Goto, Masayoshi Ko, Yusuke Niwa, Shuji Terai, Division of Gastroenterology and Hepatology, Graduate School of Medical and Dental Sciences, Niigata University, Niigata 951-8510, Japan

ORCID number: Kenya Kamimura (0000-0001-7182-4400); Ryosuke Inoue (0000-0002-3409-4119); Takuro Nagoya (0000-0002-4000-9558); Norihiro Sakai (0000-0003-4332-4681); Ryo Goto (0000-0002-3736-329X); Masayoshi Ko (0000-0002-0792-0868); Yusuke Niwa (0000-0002-8655-421X); Shuji Terai (0000-0002-5439-635X).

Author contributions: Kamimura K wrote the manuscript; Inoue R, Nagoya T, Sakai N, Goto R, Ko M, Niwa Y, and Terai S collected information and performed experiments; all authors read and approved the final version of the manuscript.

Supported by the Brain Research Institute Grant, Niigata University.

Institutional review board statement: The study was reviewed and approved by the Institutional Review Board of Niigata University. All animal experiments were approved by and conducted in full compliance with the regulations of the Institutional Animal Care and Use Committee at Niigata University, Niigata, Japan.

Conflict-of-interest statement: The authors declare that they have no current financial arrangement or affiliation with any organization that may have a direct influence on their work.

Manuscript source: Invited manuscript

Correspondence to: Kenya Kamimura, MD, PhD, Lecturer, Division of Gastroenterology and Hepatology, Graduate School of Medical and Dental Sciences, Niigata University, 1-757 Asahimachido-ri, Chuo-ku, Niigata 951-8510, Japan. kenya-k@med.niigata-u.ac.jp
Telephone: +81-25-2272207
Fax: +81-25-2270776

Received: March 13, 2018
Peer-review started: March 14, 2018
First decision: March 30, 2018
Revised: April 1, 2018
Accepted: April 16, 2018
Article in press: April 16, 2018
Published online: April 21, 2018

Abstract

To date, various signal transducers, cytokines, growth factors, and hormones have been reported to play an important role in homeostasis of various organs. Various cells and organs are involved in the hepatic regeneration process, which proceeds as a result of the coordination of many factors. While these factors are well known to be involved in the liver regeneration after the liver injury, however, as the details of such mechanisms have not been sufficiently elucidated, the practical applicability of hepatic regeneration based on the action of these and cytokines growth factors is still unclear. In terms of the involvement of the autonomic nervous system in hepatic regeneration, cell proliferation resulting from direct signal transduction to the liver has also been reported and recent studies focusing on the inter-organ communication *via* neural network opened a novel aspect of this field for therapeutic applicability. Therefore, the appropriate understanding of the relationship between autonomic neural network and liver regeneration through various organs including brain, afferent nerve, efferent nerve, *etc*. is essential. This mini-review explains the principle of neural system involved in the inter-organ communication and its contribution on the liver regeneration upon the liver

injury reviewing recent progress in this field.

Key words: Autonomic nerve; Neural network; Liver regeneration; Hormone

Core tip: The review of the relationship between autonomic neural network and liver regeneration shows that an inter-organ communication is functioning in a coordinated manner through the autonomic nervous system as a biological mechanism for hepatic regeneration and functional maintenance when the liver is damaged. Therefore, this mini-review presents how autonomic nerve fibers affect hepatic regeneration including the results of our most recent research.

Kamimura K, Inoue R, Nagoya T, Sakai N, Goto R, Ko M, Niwa Y, Terai S. Autonomic nervous system network and liver regeneration. *World J Gastroenterol* 2018; 24(15): 1616-1621 Available from: URL: http://www.wjgnet.com/1007-9327/full/v24/i15/1616.htm DOI: http://dx.doi.org/10.3748/wjg.v24.i15.1616

INTRODUCTION

Many studies on the mechanisms of hepatic regeneration have led to the identification of cytokines, growth factors, and signal transducers that are produced by Kupffer cells and other cell types[1-17] which may play an important role in homeostasis of the liver (Table 1). These cytokines and growth factors are thought to cause cells enlargement and proliferation, resulting in functional recovery. However, as the details of such mechanisms have not been sufficiently elucidated, the practical applicability of hepatic regeneration based on the action of cytokines and growth factors is still unclear. Various cells and organs are involved in the hepatic regeneration process, which proceeds as a result of the coordination of many factors.

Moreover, in terms of the involvement of the autonomic nervous system in hepatic regeneration, cell proliferation resulting from direct signal transduction to the liver has also been reported[18-20].

More specifically, this refers to actions accompanying the activation of the parasympathetic nervous system, which mediates the hepatic branch of the vagus nerve. The autonomic nervous system was first described by John N Langley in 1916[21] as an important mechanism that maintains homeostasis in organisms. These nerves are distributed internally within the blood vessels, heart, lungs, gastrointestinal tract, liver[22,23], and reproductive organs and are controlled by a feedback system that is mainly situated in the brain. While the functions of the sympathetic and parasympathetic nerves comprising the autonomic nervous system have been considered as antagonistic, they are now believed to play an important organ-related role as part of a network that maintains homeostasis in organisms. This inter-organ communication is very important in various pathologies. For example, intestinal bacterial flora have been found to be strongly involved in Parkinson's disease[24] and autism[25], and a system to control blood sugar has been discovered in which pancreatic beta cells proliferate *via* autonomic nervous system signaling following a hepatectomy[26,27-29].

These results suggest that an inter-organ network functions in a coordinated manner through the autonomic nervous system as a biological mechanism for hepatic regeneration and functional maintenance when the liver is damaged[30]. This mini-review describes how autonomic nerve fibers affect hepatic regeneration based on our recent research results.

Table 1 Factors related to the liver regeneration

Factors related to liver regeneration	Ref.
Tumour necrosis factor	[3]
Interleukin 6	[3]
NF-kappa B	[4]
Oncostatin M	[5]
Signal transducers and activator of transcription 3	[6]
Hepatocyte growth factor	[7-9,11,16]
Epidermal growth factor	[10]
Transforming growth factor alpha	[10,14]
Epidermal growth factor receptor	[12,13]
Platelets	[15,16]
Insulin-like growth factor 1	[16]
Lymphotoxin beta receptor	[17]
Insulin	[38]
Glucagon	[38]
Epidermal growth factor	[38]
Serotonin	[41,43,45,47]
Serotonin S2 receptor	[33]
Beta-catenin	[2]
Autonomic nervous system (direct feedback)	[18,20,31,32]

IMPACT OF AUTONOMIC NERVE FIBERS DISTRIBUTED IN THE LIVER ON HEPATIC REGENERATION

Reportedly, in addition to humoral factors, the autonomic nervous system is also involved in the hepatic regeneration process. Most studies have examined direct feedback relationship between the liver and brain. Signals starting in the liver are transmitted *via* the afferent sympathetic nervous system to the ventromedial region of the hypothalamus and then to the lateral region of the hypothalamus; they then pass through the dorsal nucleus of the vagus nerve of the medulla oblongata after which they return to the liver[18,19]. Kiba *et al*[20]. reported that in rats that had undergone partial hepatectomy, hepatic regeneration was slow when the hepatic branch of the vagus nerve

was resected. In addition, they demonstrated that when the ventromedial region of the hypothalamus, which is the center of the sympathetic nervous system, was destroyed, vagus nerve signal transduction became excessive, thereby promoting post-hepatectomy hepatic regeneration[31,32]. This phenomenon occurred even if hepatectomy was not performed, and chronological evaluation showed that cell proliferation in the hepatic regeneration process peaked on day 3[33].

Thus, autonomic nervous system feedback throughout the liver is involved in hepatocyte proliferation. Kiba *et al*[34] also demonstrated that when the ventromedial hypothalamus, the center of the efferent sympathetic nervous system, was destroyed, pancreatic beta cells and extrapancreatic secretory cells proliferated, activating the growth of epithelial cells in the gastrointestinal tract[35]. These results demonstrated the importance of the efferent vagus nerve in the activation of cell proliferation in various organs and suggested that when the liver is injured, neural signals relayed from the liver to various organs through the brain and efferent vagus nerve might contribute to homeostasis maintenance in the body.

IMPACT OF INTER-ORGAN NETWORKS MEDIATING HEPATIC REGENERATION *VIA* THE AUTONOMIC NERVOUS SYSTEM

Based on the suspected contribution of the neural network on hepatic regeneration after liver injury, we focused on the effect of various organs on liver regeneration after liver injury with respect to this network. While no reports on liver regeneration have focused on this neural network, several studies so far have focused on the pancreas as an organ controlled by the autonomic nervous system[26,27-29,36]. Briefly, marked proliferation of beta cells was noted in the pancreas following partial hepatectomy in response to signal transduction through the afferent sympathetic nervous system, brain, and efferent vagus nerve[27]. Additionally, similar results were obtained when gene transfer promoted the afferent signal transduction by ERK activation[26]. These results provide evidence that the autonomic nervous system is important in maintaining for blood sugar homeostasis after severe liver damage.

It appears that this autonomic nervous system first activates the afferent sympathetic nerve in the damaged liver, which transduces the signal to the center of the autonomic nervous system in the brain and then to the efferent vagus nerve; this results in the activation of cell proliferation in various organs inside the abdominal cavity, such as the liver, gastrointestinal tract organs, and pancreas. However, no study has focused on the effect of this system on liver regeneration. Therefore, here, we focus on this system as an effector of liver regeneration. While various factors might be involved, GI hormones are known to play an important role in hepatic regeneration.

Fujita *et al*[37] administered various gastrointestinal and pancreatic hormones, including glucagon, secretin, and cholecystokinin, to mice that had undergone partial hepatectomy and investigated their effects on hepatic regeneration based on weight changes and histological findings. They found that the mice exhibited liver weight increases of approximately 50% following glucagon and insulin administration and suggested that this effect was mainly due to hypertrophy of the remaining cells. Lai *et al*[38] also reported that the combined administration of glucagon and insulin was effective for hepatic regeneration in rats that had undergone partial hepatectomy. These results demonstrated that gastrointestinal hormones may play an important role in hepatic regeneration.

Many gastrointestinal hormones assist in the maintenance of homeostasis in living organisms. Among these, serotonin, which is emitted by chromaffin cells in the intestines, has been known to encourage proliferation of liver cells[39,40]. Serotonin is a monoamine neurotransmitter that is synthesized by the enzyme tryptophan hydroxylase 1 in chromaffin cells[41] and is released in the intestine[26,27] when the parasympathetic nervous system is activated[42]. Platelet granules also contain serotonin, which is released when platelets come into contact with liver cells, after which it functions as a growth factor for liver cells[40,41,43] through the 5-HT_2 receptors. Moreover, it has been reported that mice deficient in tryptophan hydroxylase 1 exhibit poor liver regeneration after hepatectomy[41].

In addition, Matondo *et al*[44] reported that although serotonin transporter depletion disturbed biological homeostasis, a small amount of serotonin in the liver was sufficient for liver regeneration. Mechanistically, DNA synthesis in primary rat hepatocytes cultures was induced by serotonin[33], but it was arrested by 5-HT2 receptor blockade at G_1/S transition[15,45]. In the pathophysiological state, reduction of serotonin reuptake transporter function caused insulin resistance and hepatic steatosis independent of the food intake[46]; serotonin protected mouse liver from cholestatic injury by stabilizing the bile salt pool after bile duct ligation through adaptation of renal transporters in cholestasis[47].

Thus, while serotonin has been reported to act as a growth factor, no analyses of an intra-organ network, focusing on increased serotonin production in the small intestine through the afferent sympathetic nervous system and the efferent vagus nerve branch, or the promotion of hepatic regeneration have been reported.

These reports provide evidence that gastrointestinal hormones may function as growth factors upon hepatic injury. Therefore, recent studies are focusing on inter-organ communication between the liver and GI tract upon liver injury. We have reported that the effect of serotonin on liver regeneration following liver injury is mediated through this neural relay, which

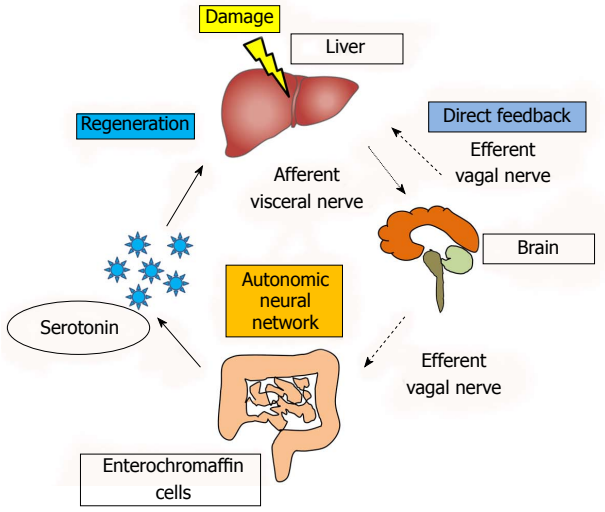

Figure 1 Involvement of neural signals in liver regeneration. This figure is partly reused and modified with updated information from Figure 1 in reference 49 with their permission.

begins in the liver and passes through the brain and GI tract and then returns to the liver[48,49]. Our results demonstrated that the partial hepatectomy increases the serotonin release from the GI tract contributing to the liver regeneration which were evidenced by the proliferating cell nuclear antigen, BrdU incorporation and liver weight-to-body weight ratio[48,49] (see details in reference 48). In addition, this activation was blocked by neuronal blockade of the afferent visceral nerve by capsaicin suggesting that the activation of the afferent visceral nerve from the liver to the efferent vagal nerve through the brain is important[48]. Therefore, the neural relay significantly contributes in the liver regeneration upon the liver injury by activating the release of GI tract hormones as a part of maintenance of homeostasis. A summary of our studies and the reported effects of the autonomic nervous system are shown in Figure 1. This figure illustrate that while the traditionally studies have shown the direct feedback between the liver and brain have been reported, neural relay signal communicating various organs is also important, which starts from the damaged liver to the GI tract through the afferent visceral nervous system, brain, and the efferent vagal nervous system contributes to activate and release the serotonin from enterochromaffin cells to promote liver regeneration. As various factors are related to the liver regeneration (Table 1), it is obvious however, further studies are necessary to clarify the relationship between the factors.

CONCLUSION

The review of the relationship between autonomic neural network and liver regeneration shows that an inter-organ network is functioning in a coordinated manner through the autonomic nervous system as a biological mechanism for hepatic regeneration and functional maintenance when the liver is damaged. We believe that this study may represent a step toward the development of essential therapeutics to promote liver regeneration.

ACKNOWLEDGMENTS

The authors would like to thank Takao Tsuchida, Division of Gastroenterology and Hepatology, Niigata University for his excellent assistance in preparing the figure.

REFERENCES

1 **Tan X**, Behari J, Cieply B, Michalopoulos GK, Monga SP. Conditional deletion of beta-catenin reveals its role in liver growth and regeneration. *Gastroenterology* 2006; **131**: 1561-1572 [PMID: 17101329 DOI: 10.1053/j.gastro.2006.08.042]
2 **Sekine S**, Gutiérrez PJ, Lan BY, Feng S, Hebrok M. Liver-specific loss of beta-catenin results in delayed hepatocyte proliferation after partial hepatectomy. *Hepatology* 2007; **45**: 361-368 [PMID: 17256747 DOI: 10.1002/hep.21523]
3 **Iwai M**, Cui TX, Kitamura H, Saito M, Shimazu T. Increased secretion of tumour necrosis factor and interleukin 6 from isolated, perfused liver of rats after partial hepatectomy. *Cytokine* 2001; **13**: 60-64 [PMID: 11145844 DOI: 10.1006/cyto.2000.0797]
4 **Yang L**, Magness ST, Bataller R, Rippe RA, Brenner DA. NF-kappaB activation in Kupffer cells after partial hepatectomy. *Am J Physiol Gastrointest Liver Physiol* 2005; **289**: G530-G538 [PMID: 15905413 DOI: 10.1152/ajpgi.00526.2004]
5 **Nakamura K**, Nonaka H, Saito H, Tanaka M, Miyajima A. Hepatocyte proliferation and tissue remodeling is impaired after liver injury in oncostatin M receptor knockout mice. *Hepatology* 2004; **39**: 635-644 [PMID: 14999682 DOI: 10.1002/hep.20086]
6 **Moh A**, Iwamoto Y, Chai GX, Zhang SS, Kano A, Yang DD, Zhang W, Wang J, Jacoby JJ, Gao B, Flavell RA, Fu XY. Role of STAT3 in liver regeneration: survival, DNA synthesis, inflammatory reaction and liver mass recovery. *Lab Invest* 2007; **87**: 1018-1028 [PMID: 17660847 DOI: 10.1038/labinvest.3700630]
7 **Nakamura T**, Nishizawa T, Hagiya M, Seki T, Shimonishi M, Sugimura A, Tashiro K, Shimizu S. Molecular cloning and expression of human hepatocyte growth factor. *Nature* 1989; **342**: 440-443 [PMID: 2531289 DOI: 10.1038/342440a0]
8 **Nakamura T**, Sakai K, Nakamura T, Matsumoto K. Hepatocyte growth factor twenty years on: Much more than a growth factor. *J Gastroenterol Hepatol* 2011; **26** Suppl 1: 188-202 [PMID: 21199531 DOI: 10.1111/j.1440-1746.2010.06549.x]
9 **Fujiwara K**, Nagoshi S, Ohno A, Hirata K, Ohta Y, Mochida S, Tomiya T, Higashio K, Kurokawa K. Stimulation of liver growth by exogenous human hepatocyte growth factor in normal and partially hepatectomized rats. *Hepatology* 1993; **18**: 1443-1449 [PMID: 8244271]
10 **Block GD**, Locker J, Bowen WC, Petersen BE, Katyal S, Strom SC, Riley T, Howard TA, Michalopoulos GK. Population expansion, clonal growth, and specific differentiation patterns in primary cultures of hepatocytes induced by HGF/SF, EGF and TGF alpha in a chemically defined (HGM) medium. *J Cell Biol* 1996; **132**: 1133-1149 [PMID: 8601590]
11 **Patijn GA**, Lieber A, Schowalter DB, Schwall R, Kay MA. Hepatocyte growth factor induces hepatocyte proliferation in vivo and allows for efficient retroviral-mediated gene transfer in mice. *Hepatology* 1998; **28**: 707-716 [PMID: 9731563 DOI: 10.1002/hep.510280317]
12 **Alroy I**, Yarden Y. The ErbB signaling network in embryogenesis and oncogenesis: signal diversification through combinatorial ligand-receptor interactions. *FEBS Lett* 1997; **410**: 83-86 [PMID: 9247128]
13 **Linggi B**, Carpenter G. ErbB receptors: new insights on mechanisms and biology. *Trends Cell Biol* 2006; **16**: 649-656

[PMID: 17085050 DOI: 10.1016/j.tcb.2006.10.008]
14 **Mead JE**, Fausto N. Transforming growth factor alpha may be a physiological regulator of liver regeneration by means of an autocrine mechanism. *Proc Natl Acad Sci USA* 1989; **86**: 1558-1562 [PMID: 2922399]
15 **Murata S**, Ohkohchi N, Matsuo R, Ikeda O, Myronovych A, Hoshi R. Platelets promote liver regeneration in early period after hepatectomy in mice. *World J Surg* 2007; **31**: 808-816 [PMID: 17354025 DOI: 10.1007/s00268-006-0772-3]
16 **Matsuo R**, Ohkohchi N, Murata S, Ikeda O, Nakano Y, Watanabe M, Hisakura K, Myronovych A, Kubota T, Narimatsu H, Ozaki M. Platelets Strongly Induce Hepatocyte Proliferation with IGF-1 and HGF In Vitro. *J Surg Res* 2008; **145**: 279-286 [PMID: 17688880 DOI: 10.1016/j.jss.2007.02.035]
17 **Anders RA**, Subudhi SK, Wang J, Pfeffer K, Fu YX. Contribution of the lymphotoxin beta receptor to liver regeneration. *J Immunol* 2005; **175**: 1295-1300 [PMID: 16002734]
18 **Kiba T**. The role of the autonomic nervous system in liver regeneration and apoptosis--recent developments. *Digestion* 2002; **66**: 79-88 [PMID: 12428066 DOI: 10.1159/000065594]
19 **Hendrickse MT**, Thuluvath PJ, Triger DR. Natural history of autonomic neuropathy in chronic liver disease. *Lancet* 1992; **339**: 1462-1464 [PMID: 1351136]
20 **Kiba T**, Tanaka K, Numata K, Hoshino M, Inoue S. Facilitation of liver regeneration after partial hepatectomy by ventromedial hypothalamic lesions in rats. *Pflugers Arch* 1994; **428**: 26-29 [PMID: 7971158]
21 **Langley JN**. Sketch of the progress of discovery in the eighteenth century as regards the autonomic nervous system. *J Physiol* 1916; **50**: 225-258 [PMID: 16993339]
22 **Berthoud HR**. Anatomy and function of sensory hepatic nerves. *Anat Rec A Discov Mol Cell Evol Biol* 2004; **280**: 827-835 [PMID: 15382018 DOI: 10.1002/ar.a.20088]
23 **Sawchenko PE**, Friedman MI. Sensory functions of the liver--a review. *Am J Physiol* 1979; **236**: R5-20 [PMID: 373465 DOI: 10.1152/ajpregu.1979.236.1.R5]
24 **Sampson TR**, Debelius JW, Thron T, Janssen S, Shastri GG, Ilhan ZE, Challis C, Schretter CE, Rocha S, Gradinaru V, Chesselet MF, Keshavarzian A, Shannon KM, Krajmalnik-Brown R, Wittung-Stafshede P, Knight R, Mazmanian SK. Gut Microbiota Regulate Motor Deficits and Neuroinflammation in a Model of Parkinson's Disease. *Cell* 2016; **167**: 1469-1480.e12 [PMID: 27912057 DOI: 10.1016/j.cell.2016.11.018]
25 **Lynch SV**, Pedersen O. The Human Intestinal Microbiome in Health and Disease. *N Engl J Med* 2016; **375**: 2369-2379 [PMID: 27974040 DOI: 10.1056/NEJMra1600266]
26 **Imai J**, Katagiri H, Yamada T, Ishigaki Y, Suzuki T, Kudo H, Uno K, Hasegawa Y, Gao J, Kaneko K, Ishihara H, Niijima A, Nakazato M, Asano T, Minokoshi Y, Oka Y. Regulation of pancreatic beta cell mass by neuronal signals from the liver. *Science* 2008; **322**: 1250-1254 [PMID: 19023081 DOI: 10.1126/science.1163971]
27 **Moreau F**, Seyfritz E, Toti F, Sigrist S, Bietigier W, Pinget M, Kessler L. Early effects of liver regeneration on endocrine pancreas: in vivo change in islet morphology and in vitro assessment of systemic effects on β-cell function and viability in the rat model of two-thirds hepatectomy. *Horm Metab Res* 2014; **46**: 921-926 [PMID: 25376550 DOI: 10.1055/s-0034-1389995]
28 **Araújo TG**, Oliveira AG, Saad MJ. Partial-Hepatectomized (70%) Model Shows a Correlation between Hepatocyte Growth Factor Levels and Beta-Cell Mass. *Front Endocrinol* (Lausanne) 2015; **6**: 20 [PMID: 25762981 DOI: 10.3389/fendo.2015.00020]
29 **Araújo TG**, Oliveira AG, Carvalho BM, Guadagnini D, Protzek AO, Carvalheira JB, Boschero AC, Saad MJ. Hepatocyte growth factor plays a key role in insulin resistance-associated compensatory mechanisms. *Endocrinology* 2012; **153**: 5760-5769 [PMID: 23024263 DOI: 10.1210/en.2012-1496]
30 **Higgins GM,** Anderson RM. Experimental pathology of liver. I. Restoration of liver of white rat following partial surgical removal. *Arch Pathol* 1931; **12**: 186-202
31 **Kiba T**, Tanaka K, Endo O, Inoue S. Role of vagus nerve in increased DNA synthesis after hypothalamic ventromedial lesions in rat liver. *Am J Physiol* 1992; **262**: G483-G487 [PMID: 1550237 DOI: 10.1152/ajpgi.1992.262.3.G483]
32 **Kiba T**, Tanaka K, Numata K, Saito S, Sekihara H. Hepatocyte proliferation in rats after ventromedial hypothalamic lesions: immunoreactivity patterns of proliferating cell nuclear antigen (PCNA). *J Gastroenterol* 1998; **33**: 523-528 [PMID: 9719236]
33 **Balasubramanian S**, Paulose CS. Induction of DNA synthesis in primary cultures of rat hepatocytes by serotonin: possible involvement of serotonin S2 receptor. *Hepatology* 1998; **27**: 62-66 [PMID: 9425918 DOI: 10.1002/hep.510270111]
34 **Kiba T**, Tanaka K, Numata K, Hoshino M, Misugi K, Inoue S. Ventromedial hypothalamic lesion-induced vagal hyperactivity stimulates rat pancreatic cell proliferation. *Gastroenterology* 1996; **110**: 885-893 [PMID: 8608899]
35 **Kiba T**, Tanaka K, Endo O, Inoue S. Ventromedial hypothalamic lesions increase gastrointestinal DNA synthesis through vagus nerve in rats. *Gastroenterology* 1993; **104**: 475-484 [PMID: 8425690]
36 **Imai J**, Oka Y, Katagiri H. Identification of a novel mechanism regulating β-cell mass: neuronal relay from the liver to pancreatic β-cells. *Islets* 2009; **1**: 75-77 [PMID: 21084852 DOI: 10.4161/isl.1.1.8615]
37 **Fujita T**. [Development of concept of gastro-entero-pancreatic endocrine system]. *Nihon Rinsho* 1974; **32**: 668-673 [PMID: 4603459]
38 **Lai HS**, Chung YC, Chen WJ, Chen KM. Rat liver regeneration after partial hepatectomy: effects of insulin, glucagon and epidermal growth factor. *J Formos Med Assoc* 1992; **91**: 685-690 [PMID: 1360295]
39 **Gershon MD**. 5-Hydroxytryptamine (serotonin) in the gastrointestinal tract. *Curr Opin Endocrinol Diabetes Obes* 2013; **20**: 14-21 [PMID: 23222853 DOI: 10.1097/MED.0b013e32835bc703]
40 **Ruddell RG**, Mann DA, Ramm GA. The function of serotonin within the liver. *J Hepatol* 2008; **48**: 666-675 [PMID: 18280000 DOI: 10.1016/j.jhep.2008.01.006]
41 **Lesurtel M**, Graf R, Aleil B, Walther DJ, Tian Y, Jochum W, Gachet C, Bader M, Clavien PA. Platelet-derived serotonin mediates liver regeneration. *Science* 2006; **312**: 104-107 [PMID: 16601191 DOI: 10.1126/science.1123842]
42 **Berger M**, Gray JA, Roth BL. The expanded biology of serotonin. *Annu Rev Med* 2009; **60**: 355-366 [PMID: 19630576 DOI: 10.1146/annurev.med.60.042307.110802]
43 **Nocito A**, Georgiev P, Dahm F, Jochum W, Bader M, Graf R, Clavien PA. Platelets and platelet-derived serotonin promote tissue repair after normothermic hepatic ischemia in mice. *Hepatology* 2007; **45**: 369-376 [PMID: 17256748 DOI: 10.1002/hep.21516]
44 **Matondo RB**, Punt C, Homberg J, Toussaint MJ, Kisjes R, Korporaal SJ, Akkerman JW, Cuppen E, de Bruin A. Deletion of the serotonin transporter in rats disturbs serotonin homeostasis without impairing liver regeneration. *Am J Physiol Gastrointest Liver Physiol* 2009; **296**: G963-G968 [PMID: 19246633 DOI: 10.1152/ajpgi.90709.2008]
45 **Papadimas GK**, Tzirogiannis KN, Panoutsopoulos GI, Demonakou MD, Skaltsas SD, Hereti RI, Papadopoulou-Daifoti Z, Mykoniatis MG. Effect of serotonin receptor 2 blockage on liver regeneration after partial hepatectomy in the rat liver. *Liver Int* 2006; **26**: 352-361 [PMID: 16584399 DOI: 10.1111/j.1478-3231.2005.01230.x]
46 **Chen X**, Margolis KJ, Gershon MD, Schwartz GJ, Sze JY. Reduced serotonin reuptake transporter (SERT) function causes insulin resistance and hepatic steatosis independent of food intake. *PLoS One* 2012; **7**: e32511 [PMID: 22412882 DOI: 10.1371/journal.pone.0032511]
47 **Jang JH**, Rickenbacher A, Humar B, Weber A, Raptis DA, Lehmann K, Stieger B, Moritz W, Soll C, Georgiev P, Fischer D, Laczko E, Graf R, Clavien PA. Serotonin protects mouse liver from cholestatic injury by decreasing bile salt pool after bile duct ligation. *Hepatology* 2012; **56**: 209-218 [PMID: 22290718 DOI: 10.1002/hep.25626]
48 **Inoue R**, Kamimura K, Nagoya T, Sakai N, Yokoo T, Goto R,

Ogawa K, Shinagawa-Kobayashi Y, Watanabe-Mori Y, Sakamaki A, Abe S, Kamimura H, Miyamura N, Nishina H, Terai S. Effect of a neural relay on liver regeneration in mice: activation of serotonin release from the gastrointestinal tract. *FEBS Open Bio* 2018; **8**: 449-460 [PMID: 29511622 DOI: 10.1002/2211-5463.12382]

49 **Kamimura K**, Inoue R, Nagoya T. The effect of autonomic nervous system on liver regeneration. *Kan-tan-sui* (Japan) 2017; **75**: 967-972

P- Reviewer: Boscá L, Ilangumaran S, Nagaya M **S- Editor**: Wang XJ
L- Editor: A **E- Editor**: Huang Y

World Journal of Gastroenterology

Submit a Manuscript: http://www.f6publishing.com

World J Gastroenterol 2018 April 21; 24(15): 1622-1631

DOI: 10.3748/wjg.v24.i15.1622

ISSN 1007-9327 (print) ISSN 2219-2840 (online)

ORIGINAL ARTICLE

Basic Study

Evaluation of safety for hepatectomy in a novel mouse model with nonalcoholic-steatohepatitis

Yusuke Ozawa, Takafumi Tamura, Yohei Owada, Yoshio Shimizu, Akira Kemmochi, Katsuji Hisakura, Takashi Matsuzaka, Hitoshi Shimano, Hiroko Isoda, Nobuhiro Ohkohchi

Yusuke Ozawa, Takafumi Tamura, Yohei Owada, Yoshio Shimizu, Akira Kemmochi, Katsuji Hisakura, Nobuhiro Ohkohchi, Department of Gastrointestinal and Hepato-Biliary-Pancreatic Surgery, Faculty of Medicine, University of Tsukuba, Tsukuba 305-8575, Japan

Takashi Matsuzaka, Hitoshi Shimano, Department of Endocrinology and Metabolism, Faculty of Medicine, University of Tsukuba, Tsukuba 305-8575, Japan

Hiroko Isoda, Faculty of Life and Environmental Sciences, University of Tsukuba, Tsukuba 305-8572, Japan

ORCID number: Yusuke Ozawa (0000-0002-5436-2272); Takafumi Tamura (0000-0003-0396-2291); Yohei Owada (0000-0003-4979-7236); Yoshio Shimizu (0000-0003-1853-7386); Akira Kemmochi (0000-0002-4970-3706); Katsuji Hisakura (0000-0001-9256-7140); Takashi Matsuzaka (0000-0002-5898-3463); Hitoshi Shimano (0000-0002-5562-5572); Hiroko Isoda (0000-0002-1399-9541); Nobuhiro Ohkohchi (0000-0003-2779-1247).

Author contributions: Ozawa Y and Tamura T designed the study and wrote the initial draft of the manuscript; Ozawa Y, Owada Y, Shimizu Y and Kemmochi A performed the animal experiments, the biochemical analysis and gene expression analysis; Ozawa Y, Tamura T, Matsuzaka T and Shimano H contributed to the analysis and interpretation of the data; all of the other authors have critically reviewed the manuscript; the final version of the manuscript was approved by all of the authors.

Supported by Ministry of Education, Culture, Sports, Science, and Technology of Japan, KAKENHI, No. 26861059 and No. 16K10489.

Institutional review board statement: Animal experiments were performed in accordance with the university's Regulations for Animal Experiments and Fundamental Guidelines for Proper Conduct of Animal Experiment and Related Activities in Academic Research Institutions, under the jurisdiction of the Japanese Ministry of Education, Culture, Sports, Science, and Technology.

Institutional animal care and use committee statement: Animal experiments were performed in human manner after receiving approval from Institutional University Experiment Committee of University of Tsukuba (protocol number: 17-312).

Conflict-of-interest statement: The authors report no relevant conflicts of interest.

Data sharing statement: No data are available.

ARRIVE guidelines statement: The authors have read the ARRIVE guidelines, and the manuscript was prepared and revised according to the ARRIVE guidelines.

Manuscript source: Unsolicited manuscript

Correspondence to: Nobuhiro Ohkohchi, MD, PhD, Professor, Surgeon, Department of Gastrointestinal and Hepato-Biliary-Pancreatic Surgery, Faculty of Medicine, University of Tsukuba, 1-1-1 Tennodai, Tsukuba 305-8575, Japan. nokochi3@md.tsukuba.ac.jp
Telephone: +81-29-8533221
Fax: +81-29-8533222

Received: February 14, 2018
Peer-review started: February 14, 2018
First decision: March 9, 2018
Revised: March 16, 2018
Accepted: March 25,2018
Article in press: March 25,2018
Published online: April 21, 2018

Abstract

AIM

To investigate whether the liver resection volume in a newly developed nonalcoholic steatohepatitis (NASH) model influences surgical outcome.

METHODS

For establishment of a NASH model, mice were fed a high-fat diet for 4 wk, administered CCl_4 for the last 2 wk, and administered T0901317 for the last 5 d. We divided these mice into two groups: A 30% partial hepatectomy (PH) of NASH liver group and a 70% PH of NASH liver group. In addition, a 70% PH of normal liver group served as the control. Each group was evaluated for survival rate, regeneration, apoptosis, necrosis and DNA expression after PH.

RESULTS

In the 70% PH of NASH group, the survival rate was significantly decreased compared with that in the control and 30% PH of NASH groups ($P < 0.01$). 10 of 32 mice in the NASH 70% PH group died within 48 h after PH. Serum aspartate aminotransferase (AST) levels and total bilirubin (T-Bil) in the NASH 70% PH group were significantly higher than the levels in the other two groups (AST: $P < 0.05$, T-Bil: $P < 0.01$). In both PH of NASH groups, signaling proteins involved in regeneration were expressed at lower levels than those in the control group ($P < 0.01$). The 70% PH of NASH group also exhibited a lower number of Ki-67-positive cells and higher rates of apoptosis and necrosis than the NASH 30% PH group ($P < 0.01$). In addition, DNA microarray assays showed differences in gene expression associated with cell cycle arrest and apoptosis.

CONCLUSION

The function of the residual liver is impaired in fatty liver compared to normal liver. A larger residual volume is required to maintain liver functions in mice with NASH.

Key words: Hepatectomy; Liver regeneration; Residual liver; Liver proliferation; Nonalcoholic steatohepatitis

Core tip: We report whether the liver resection volume in the nonalcoholic steatohepatitis (NASH) model influences surgical outcome. The population of patients with NASH has been increasing. However, few animal models fully reflect both the histopathology and pathophysiology of NASH in humans. We established a novel experimental NASH model that exhibited the same characteristics as NASH in humans. This study elucidates the metabolism of the residual liver after a hepatectomy with NASH. Compared with normal liver, the residual NASH liver function is impaired, especially its regenerative ability. Therefore, a larger residual volume is required to maintain liver function in NASH liver after partial hepatectomy.

Ozawa Y, Tamura T, Owada Y, Shimizu Y, Kemmochi A, Hisakura K, Matsuzaka T, Shimano H, Isoda H, Ohkohchi N. Evaluation of safety for hepatectomy in a novel mouse model with nonalcoholic-steatohepatitis. *World J Gastroenterol* 2018; 24(15): 1622-1631 Available from: URL: http://www.wjgnet.com/1007-9327/full/v24/i15/1622.htm DOI: http://dx.doi.org/10.3748/wjg.v24.i15.1622

INTRODUCTION

Nonalcoholic fatty liver disease (NAFLD) is observed in 20%-40% of the general population, and its incidence continues to increase in industrialized countries[1,2]. NAFLD includes several diseases, such as simple liver steatosis, nonalcoholic steatohepatitis (NASH), and cirrhosis. NASH is characterized by hepatic steatosis, lobular inflammation, and abnormal glucose tolerance. In NASH, continuous inflammation contributes to hepatocellular carcinoma (HCC)[3,4]. The cause of HCC is frequently infection with hepatitis B virus and hepatitis C virus (HCV). New antiviral medications for hepatitis are currently being used in clinics; therefore, the number of patients with virus-related HCC is expected to decrease in the future[5-9]. By contrast, the number of patients with NASH-related HCC has been increasing recently, and this trend is expected to continue because no effective treatments are available[10].

Steatosis is a risk factor for postoperative liver failure[11,12]. A number of clinical studies revealed that steatosis caused severe mortality and morbidity after liver resection compared with normal liver following liver resection[11,12]. In experimental models, hepatectomy of fatty livers resulted in suppressed liver regeneration and survival rates[13-16]. However, the influence of hepatectomy on NASH livers has not been extensively evaluated.

Hepatectomy is a standard and most effective therapy for HCC patients. Postoperative liver failure is a serious complication after hepatectomy, and its occurrence correlates with the volume and function of the residual liver[17-20]. To prevent liver failure after hepatectomy, the liver resection volume is limited according to preoperative liver function[21-23]. For promotion of regeneration and maintaining liver function preserving sufficient residual liver volume enables the prevention of liver failure[24,25]. Thus, the degree of liver regeneration is dependent on the volume of the residual liver. Although several NASH models, such as the methionine- and choline-deficient (MCD) model and high-fat (HF) diet model, have been reported, few models completely reflect the histopathology and pathophysiology of NASH in humans[26,27]. The disadvantages of the MCD model are that MCD mice exhibit severe body weight loss with the absence of insulin resistance. The HF diet model is not suitable for researching the pathogenesis of NASH because a longer period of time is required for presentation of NASH characteristics, and hepatic fibrosis is weaker than that observed in human NASH.

Thus, the ability of regeneration in the NASH liver has not yet been assessed in an experimental model. For the same reasons, the effect of hepatectomy on NASH liver has not been clearly elucidated in previous reports. We established a novel experimental NASH model that indicates similar histopathological and pathophysiological characteristics as those of NASH in humans[28]. The aim of this study was to investigate whether a difference in liver resection volume in a novel NASH model influences surgical outcomes.

MATERIALS AND METHODS

Animals

Six-week-old male C57BL/6J mice were obtained from Charles River Laboratories Japan, Inc. (Kanagawa, Japan) and were acclimated for one week before the start of the experiment. Mice were maintained under a 12-h light-dark cycle and had free access to standard chow and tap water. The animal experiments were performed in a humane manner after receiving approval from the Institutional University Experiment Committee of the University of Tsukuba and in accordance with the Regulations for Animal Experiments at the university and Fundamental Guidelines for Proper Conduct of Animal Experiment and Related Activities in Academic Research Institutions under the jurisdiction of the Ministry of Education, Culture, Sports, Science, and Technology.

NASH mouse model protocol

NASH mice were fed an HF diet (60 kcal% fat; D12492, Research Diets, Inc., New Brunswick, NJ, United States) for 4 wk, intraperitoneally injected with CCl_4 (Wako Pure Chemical Industries, Ltd., Osaka, Japan) twice a week for the final 2 wk, and intraperitoneally injected with T0901317 (Cayman Chemical Co., Ann Arbor, MI, United States) solubilized in DMSO for the final 5 d. The CCl_4 dose was 0.1 mL/kg, and the T0901317 dose was 2.5 mg/kg[28].

Surgical procedure and anesthesia

We categorized the mice into three groups: (1) 70% partial hepatectomy (PH) of normal liver mice as the control; (2) 30% PH of NASH liver group; and (3) 70% PH of NASH liver group. The normal liver mice have been not added any reagent and the histology and pathology have been not change. In 30% PH and 70% PH of the NASH liver group, liver specimens were evaluated by an experienced pathologist in a blinded fashion, the histology and pathology finding in the NASH severity of each groups have resulted in no difference in the NAFLD activity scores[28]. All mice received the hepatectomy 48 h after the final administration of CCl_4 and T0901317. In the 70% PH groups, the left and middle lobes of the liver were removed by using a single ligature, whereas only the left lobe was removed in the 30% PH group[29]. Hepatectomy was performed under ether anesthesia.

Liver tissue collection

Blood samples were collected from the orbital capillary and centrifuged at 3000 rpm for 10 min to isolate the serum. Each sample was stored at -80 ℃ until analysis. Mice of each group were sacrificed at 6 h and 12 h after PH. Then, the liver was quickly removed and weighed. The liver specimen was immediately fixed in 10% neutral-buffered formalin for further histological examination. Survival rates were evaluated in the NASH 70% PH group (n = 32) and NASH 30% PH group (n = 27).

Histology and immunohistochemistry

Fixed liver tissues were processed and embedded in paraffin using standard methods. Then, liver tissues were sliced into 2-μm thick paraffin sections and stained with hematoxylin and eosin (HE) to evaluate necrosis. Necrotic areas were detected by morphological features, and the ratio of necrosis/total area was calculated in 20 random intralobular fields. Liver proliferation was assessed by Ki-67 staining. Apoptosis was detected by TUNEL staining. TUNEL staining and Ki-67 staining were performed using an antibody kit (New History Science Laboratory Co., Ltd., Tokyo, Japan). The ratio of positive/total hepatocytes was calculated in 20 random intralobular fields.

Immunoblotting

Liver tissue extracts were prepared from specimens that were frozen in liquid nitrogen. We evaluated the expression of signaling proteins involved in liver regeneration, including AKT, STAT3, and ERK1/2, by western blotting. We compared the expression levels of these proteins in each group 6 h after PH. Immunoblots were developed using polyclonal antibodies against phospho-AKT (9271), total AKT (9272), phospho-STAT3 (9131), total STAT3 (9132), phospho-ERK1/2 (9101), and total ERK1/2 (9102) (Cell Signaling Technology, Beverly, MA, United States).

Gene expression analysis

Liver tissue samples were freshly collected and immediately frozen at -30 ℃ until investigation. Frozen liver samples were homogenized, and total RNA was isolated from whole cells using a NucleoSpin® RNA kit (Takara Bio, Inc., Otsu, Japan). RNA concentrations were determined by measuring the absorbance at 260/280 nm with a NanoDrop Spectrophotometer (Thermo Fisher Scientific, Inc., Wilmington, DE, United States). Synthesis of complementary DNA was performed using AMV Reverse Transcriptase (Promega, Corp., Madison, WI, United States) and random primers (Takara Bio, Inc., Otsu, Japan). Briefly, a mixture of 1 mmol/L dNTPs (Fermentas Life Sciences, Inc., Burlington, ON, Canada), 0.025 μg/mL random primers, 0.25 U/mL reverse transcriptase, and 500 ng of total RNA was incubated at 30 ℃ for 10 min, 37 ℃ for 60 min, 95 ℃ for 5 min and

Table 1 Serum parameters of normal liver and nonalcoholic steatohepatitis groups after partial hepatectomy

	6 h after PH				12 h after PH			
	AST	ALT	T-Bil	IL-6	AST	ALT	T-Bil	IL-6
Normal 70%PH	2343.3 ± 6160.4	1828.3 ± 990.4	1.43 ± 0.5	2036.0 ± 1470.9	2976.7 ± 1395.7	2053.3 ± 886.2	2.0 ± 0.9	731.5 ± 483.7
NASH 30%PH	1610.0 ± 3700.6	1507.1 ± 563.5	0.76 ± 0.2	1511.5 ± 284.8	1841.3 ± 619.1	1522.9 ± 537.9	0.9 ± 0.7	692.8 ± 211.1
NASH 70%PH	3064.3 ± 1289.8[a]	2422.9 ± 1194.8	2.57 ± 1.36[b]	3026.2 ± 2127.5	4067.5 ± 2059.2[a]	2403.8 ± 1111.8	3.85 ± 0.96[b]	987.9 ± 550.7

Data are presented as the mean ± SD (n = 5-7). [a]P < 0.05, [b]P < 0.01 *vs* other groups. NASH: Nonalcoholic steatohepatitis; ALT: Alanine aminotransferase; AST: Aspartate aminotransferase; PH: Partial hepatectomy; T-Bil: Total bilirubin; IL-6: Interleukin-6.

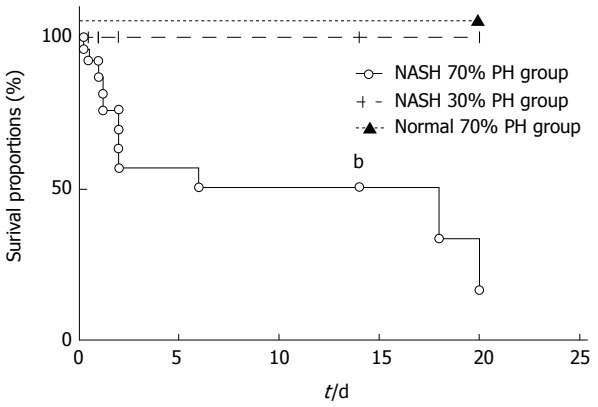

Figure 1 Survival rate after partial hepatectomy. Survival rates of the 30% PH and 70% PH groups were evaluated by the Kaplan-Meier method. All mice in the 30% PH group survived. In contrast, 80% of the NASH 70% PH group died by 20 d. n = 27 in NASH 30% PH group; n = 32 in NASH 70% PH group. [b]P < 0.01. PH: partial hepatectomy; NASH: nonalcoholic steatohepatitis.

4 ℃ before storage at -80 ℃.

RT-PCR primers were designed using Primer Express Software for Real-time PCR ver. 3.0 (Applied Biosystems, Inc., Foster City, CA, United States) based on the sequences available in GenBank. Primers were purchased from Takara Bio, Inc. (Otsu, Japan). *GADD45A* primer sequences were 5′-CCTGCACTGTGTGCTGGTGA-3′ and 5′-CCACTGATCCATGTAGCGACTTTC-3′. *PDE4B* primer sequences were 5′-CCCATCAGCAGTTAAGGACAGGA-3′ and 5′-TGGGCAGAACTAGGGACTCAAGA-3′.

Glyceraldehyde-3-phosphate dehydrogenase (*GAPDH*) was used as an endogenous control. RT-PCR was performed using SYBR-Green Real-Time PCR Master Mix-Plus (Toyobo Co., Ltd., Osaka, Japan) and an Applied Biosystems 7300 real-time PCR system (Applied Biosystems, Inc., Foster City, CA, United States) as recommended by the manufacturer's instructions[28].

Microarray analysis

DNA microarray analysis was conducted on RNA samples isolated from liver tissue in the control group and novel NASH model group. Labeled cRNA was synthesized from 100 ng of total RNA using a GeneChip® 3′ IVT Plus Reagent Kit (Affymetrix, Inc., Santa Clara, CA, United States) according to the manufacturer's protocol. Fragmented and labeled cRNA (7.5 μg) was hybridized to an Affymetrix Mouse MG-430 PM Array Strip (Affymetrix) for 16 h at 45 ℃. The strips were washed and stained using a GeneAtlas Fluidics Station 400 (Affymetrix), and the resulting images were scanned using a GeneAtlas Imaging Station (Affymetrix). Probe-level analysis, including background subtraction and quantile normalization, was conducted using a robust multiarray average algorithm (RMA) using Affymetrix Expression Console Software 1.4 (Affymetrix). The gene expression profile of the novel NASH model was compared with the HF group. Genes exhibiting differences in expression with an increase of greater than 1.4-fold and a decrease of less than 0.65-fold were classified as differentially expressed genes[28].

Statistical analysis

All data are expressed as the mean ± SD. Statistical analyses were conducted using PRISM. Mann-Whitney *U* test was used for comparing between two groups. *P*-values less than 0.05 were considered significant. The Kaplan-Meier estimator was used for survival rate evaluation.

RESULTS

Survival rate

The survival rate of the NASH 70% PH group was significantly lower than that of the NASH 30% PH group (P < 0.01) (Figure 1), and 10 of 32 mice in the NASH 70% PH group died within 48 h after PH. On the other hand, all mice in the NASH 30% PH group survived.

Liver function

At 6 and 12 h after PH, serum aspartate aminotransferase (AST) and alanine aminotransferase (ALT) levels were high in all three groups. AST levels in the NASH 70% PH group were significantly higher than the levels in the other two groups (AST: P < 0.05). Total bilirubin (T-Bil) in the normal liver and NASH 30% PH groups did not change, but the values only significantly increased in the NASH 70% PH group (P < 0.01) (Table 1).

Liver proliferation assay

Many more Ki-67-positive hepatocytes were observed in the NASH 30% PH group than in the preoperative NASH liver (P < 0.05). On the other hand, fewer Ki-67-positive cells were noted in the NASH 70% PH group than in the preoperative NASH liver (P < 0.01). Additionally, significantly fewer Ki-67-positive cells were noted in the 70% PH group than in the NASH 30% PH

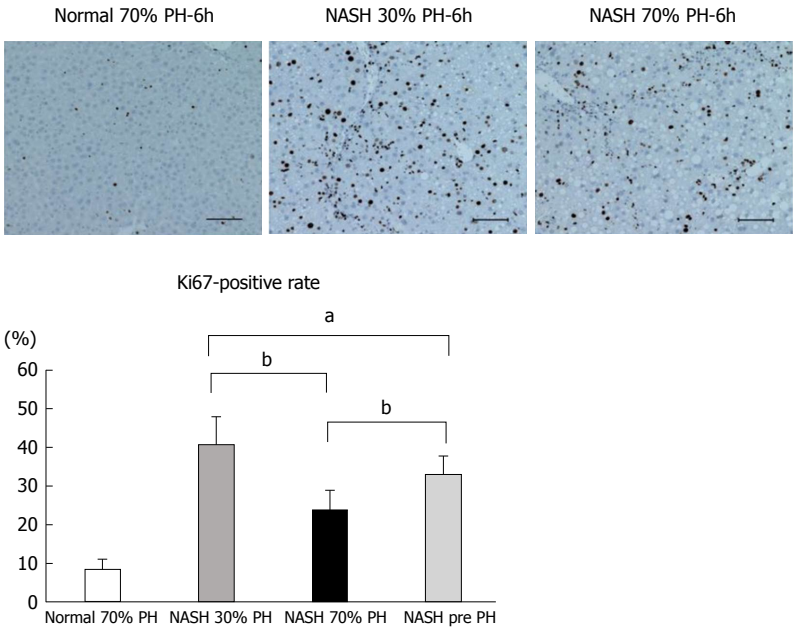

Figure 2 Ki-67 staining and proliferation score. Proliferation was evaluated by Ki-67 staining. We compared preoperative nonalcoholic steatohepatitis (NASH) groups with NASH 30% PH and NASH 70% PH groups 6 h after PH. Ratios of Ki-67-positive/total hepatocytes were calculated. Significantly fewer Ki-67-positive cells were noted in the 70% PH group than in the NASH 30% PH group. Ratios (%) are expressed as the mean ± SD. n = 2 per groups, 10 fields per sample. $^{a}P < 0.05$; $^{b}P < 0.01$. Scale bar: 100 μm. PH: partial hepatectomy; NASH: nonalcoholic steatohepatitis.

group ($P < 0.01$) (Figure 2).

Liver regeneration signal

In the normal 70% PH liver group, *i.e.*, the control group, expression of AKT, STAT3, and ERK1/2 phosphorylation was observed. In the both NASH 30% PH and 70% groups, phosphorylation of AKT, STAT3, and ERK1/2 was significantly lower than in the control group ($P < 0.01$) (Figure 3).

Histological assay

The number of TUNEL-positive cells in the NASH 70% PH group was significantly higher than in the other groups ($P < 0.01$). The TUNEL-positive rate of normal liver was significantly higher than that in the NASH 30% PH group ($P < 0.01$) (Figure 4A). The area of necrosis in the NASH 70% PH group was significantly larger than that in the NASH 30% PH group ($P < 0.01$). In both NASH groups, the necrotic area was significantly larger than that in the normal liver group ($P < 0.01$) (Figure 4B).

Microarray assay

mRNAs in the NASH 70% PH group with the highest fold-change (> 1.4 or < 0.70) in expression and with *P*-values <0.05 were selected and compared with those in the NASH 30% PH group (Table 2). *PDE4B*, *SLC20A1*, *CXADR*, *GADD45A*, *ZSWIM6*, and *C15orf39* were expressed at higher levels in the NASH 70% PH group. *PDE4B* and *GADD45A* are associated with cell cycle arrest and apoptosis. Using qPCR, *GADD45A* and *PDE4B* mRNA expression was significantly different between the two groups (*GADD45A*: $P < 0.01$, *PDE4B*: $P < 0.05$) (Figure 5).

DISCUSSION

NAFLD/NASH is a common hepatic disorder that causes HCC[1-4]. Recently, the population of patients with NASH and NASH-related HCC has been increasing[1,2,10]. Hepatectomy is the first-line treatment for patients with HCC[21]. After hepatectomy, the incidences of mortality and morbidity are dependent on the volume and function of the residual liver[17-20]. Previous reports have demonstrated that steatosis impaired liver regeneration and caused liver dysfunction after hepatectomy[11,12]. NASH has been proposed to cause liver failure rather than steatosis because NASH presents with not only steatosis but also fibrosis, inflammation, and insulin resistance. However, regarding NASH animal models, few models completely reflect the histopathology and pathophysiology of NASH in humans. Therefore, the effect on the residual liver under NASH conditions has not been appropriately evaluated[26,27]. In our previous study, we established a novel experimental NASH model that exhibited histopathological and pathophysiological findings similar to that of NASH in humans[28]. In this study, new NASH mice were received 30% PH or 70% PH, and the influence of liver resection volume on the residual liver function in NASH liver was investigated. Our results indicated that the survival rate after PH in NASH liver strongly correlated with resected liver volume and was attributed to the proliferative ability and the rates of apoptosis and necrosis compared

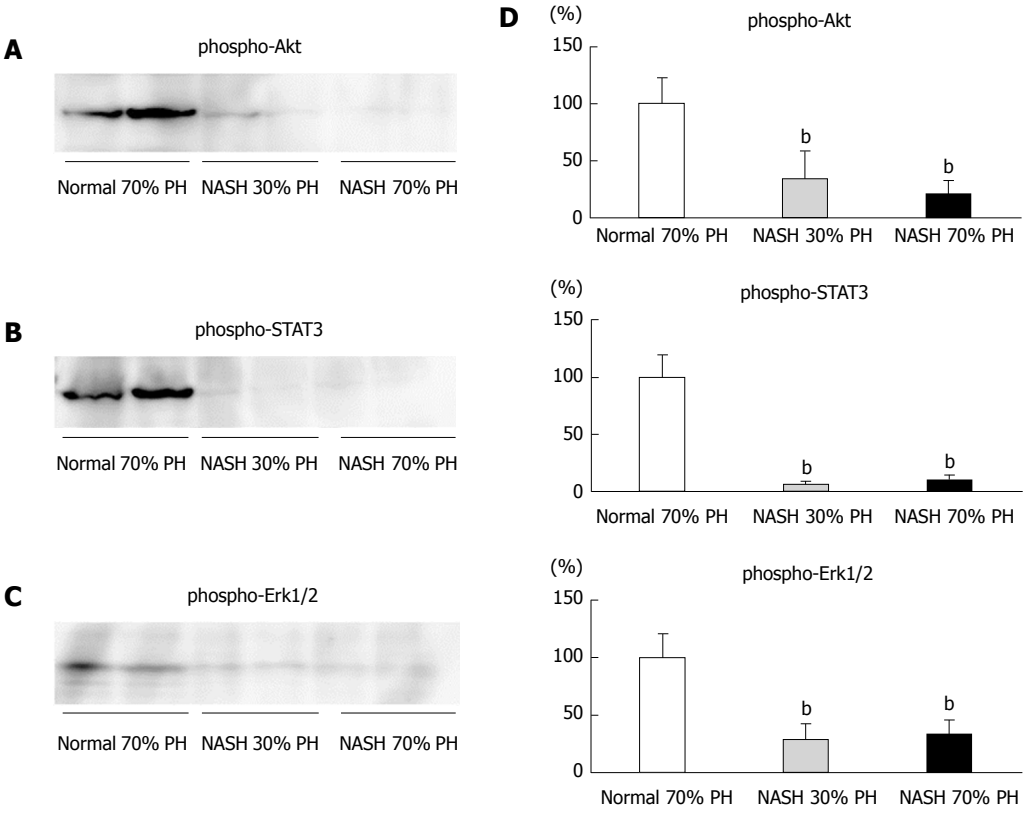

Figure 3 Protein assay. Expression of phosphorylated (A) Akt, (B) STAT3, and (C) ERK1/2 in normal and nonalcoholic steatohepatitis liver groups 6 h after PH. Expression levels were detected by western blot analysis. Ratios of densitometry were calculated by each score/score of control 70% PH (D). Data are expressed as the mean ± SD. n = 5-7 per groups. $^{b}P < 0.01$ *vs* other groups.

with those in the normal liver. Even 30% of PH NASH residual liver could not offer sufficient liver function, and the volume of the functional residual liver significantly decreased due to less cell proliferation, apoptosis and necrosis after hepatectomy. Based on these results, we hypothesized that the residual liver volume that can support sufficient function in a normal liver could not maintain liver function in NASH. Our results suggested that to avoid liver dysfunction after hepatectomy in NASH, resection volume should be carefully determined and not the same as that in patients with normal liver.

In patients with PH, fatty liver causes a high rate of mortality and morbidity compared with normal liver[11]. In NAFLD patients, postoperative complications also increase in a manner that is similar to patients with fatty liver[12,30]. In animal models with PH, the survival rate of a fatty liver model decreased compared with a normal liver even with the same residual volume[13,15,16,31]. In this study, the survival rate after PH remarkably decreased in the NASH 70% PH group, and 30% of the deaths occurred within the first 48 h after PH. This result supported the previous reports, *i.e.*, outcome of PH significantly influences the survival rate of fatty mice[13,15,16,31]. In NASH liver, it was assumed that other characteristics, *i.e.*, fibrosis, inflammation, and insulin resistance, caused increased liver function deterioration. It was hypothesized that the residual liver volume of the small group, *i.e.*, 30% of residual volume of the NASH liver, could not maintain sufficient liver function for survival after PH.

Liver regeneration occurred in cases with acute injury and/or liver resection[19]. In normal liver after PH, cell proliferation was observed in a small residual liver but not in a large residual liver[24]. Large residual livers have sufficient volume to maintain liver function, whereas small residual livers are unable to maintain liver function. Therefore, promotion of cell proliferation occurs in the small residual liver[24]. Ki-67 protein is expressed during the G1, G2, and S phases of cell division[32,33]. In this study, the number of Ki-67-positive cells in the residual liver in the 30% PH of NASH liver group was higher than in the preoperative NASH liver. On the other hand, the number of Ki-67-positive cells in the residual liver of the 70% PH of NASH liver group was significantly decreased. These results suggested that NASH hepatocytes would not have insufficient proliferation ability after large amount of PH, such as 70%.

Signaling pathways of liver regeneration are promoted by cytokines, *i.e.*, interleukin (IL)-6 and tumor necrosis factor (TNF)-alpha, and growth factors[20]. The expression of AKT, STAT3, and ERK1/2 protein play an important role in liver regeneration, and the IL-6/STAT3 signaling pathway accelerates liver proliferation[16,24,34-36]. STAT3 was expressed at high levels in a liver with steatosis; however, these phenomena did not induce liver regeneration[37]. The NASH liver received continuous

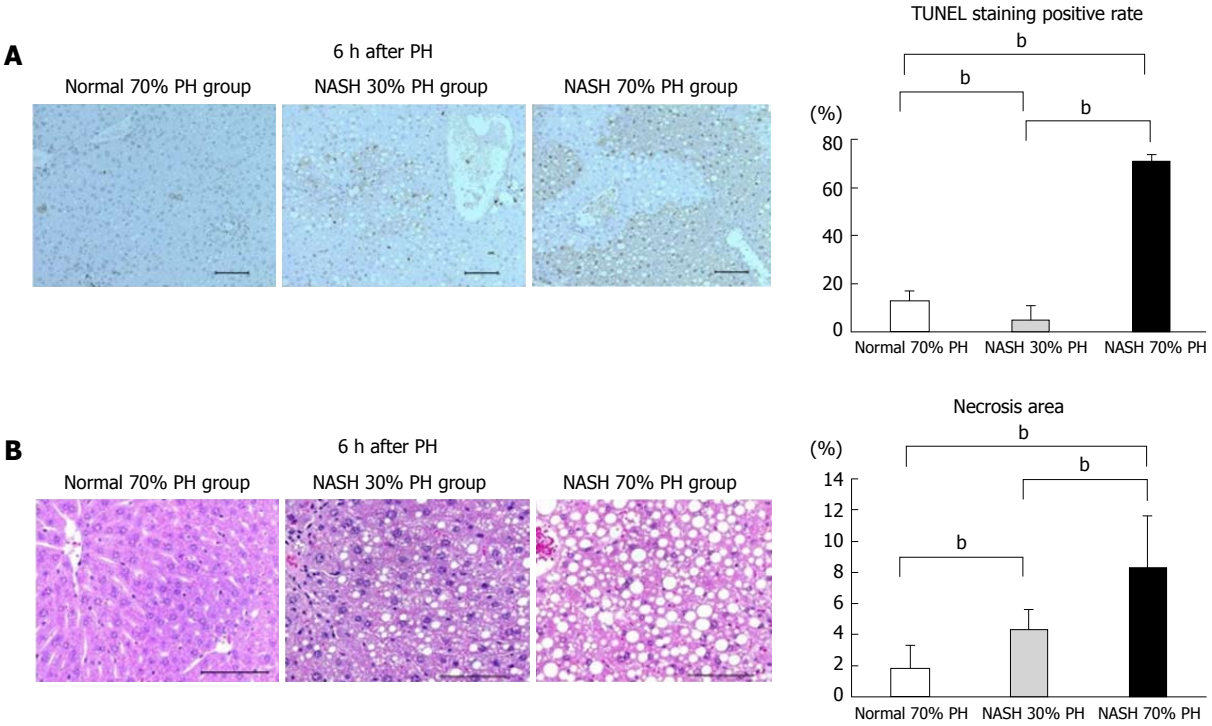

Figure 4 Histopathological findings. A: Apoptosis was evaluated by TUNEL staining. Ratios of TUNEL-positive/total hepatocytes were calculated; B: Necrosis was evaluated by HE staining. Ratios of necrosis morphological feature/total area were calculated. Apoptosis and necrosis were higher in the NASH 70% PH group than in the other groups. Data are expressed as the mean ± SD. n = 2 per groups, 10 fields per sample. $^{b}P < 0.01$. Scale bar: 100 μm. PH: Partial hepatectomy; NASH: Nonalcoholic steatohepatitis.

Table 2 Gene expression microarray

Function	Gene name	Gene abbreviation	Fold-change (> 1.4)	*P* value (< 0.05)
Regulate the cellular concentrations of cyclic nucleotides	Phosphodiesterase 4B, cAMP-specific	*PDE4B*	2.102691211	0.0063
Growth arrest	Growth arrest and DNA-damage-inducible, alpha	*GADD45A*	1.672778704	0.013
Signal transduction	Coronin 1C	*CORO1C*	1.489851976	0.031
Stimulates expression of cytokines, including IL6, MIF and VEGFA	Hypoxia inducible lipid droplet associated	*HILPDA*	1.481465541	0.011
EGF-like growth factor	Heparin binding EGF-like growth factor	*HBEGF*	1.432049736	0.043
Cell-cell junctions	Membrane associated guanylate kinase, WW And PDZ domain containing 1	*MAGI1*	1.430522907	0.0222
Innate immune system	Ankyrin repeat and SOCS box containing 13	*ASB13*	0.515175325	0.0042
Apoptosis and autophagy	TIA1 cytotoxic granule-associated RNA binding protein-like 1	*TIAL1*	0.609948905	0.027
Gene expression	Nucleic acid binding protein 1	*NABP1*	0.6558797325	0.042
Cell cycle	S-phase kinase-associated protein 2, E3 ubiquitin protein ligase	*SKP2*	0.6588204077	0.044
Mitochondrial metabolism	Translocase of inner mitochondrial membrane 9 homolog (yeast)	*TIMM9*	0.6598542503	0.042
Cytokine signaling in immune system	B-cell CLL/lymphoma 6	*BCL6*	0.6760241074	0.0097
Cell cycle	Mutated in colorectal cancers	*MCC*	0.6761191711	0.0076
Gene expression	Zinc finger protein 519	*ZNF519*	0.6864230003	0.028
Gene expression	RNA binding motif protein, X-linked	*RBMX*	0.6983542235	0.012

In total, 6 genes were overexpressed greater than 1.4-fold in the nonalcoholic steatohepatitis (NASH) 70% PH group compared with their expression in the NASH 30% PH group, and 7 genes were downregulated by less than 0.70-fold in the NASH PH group compared with their expression in the NASH 30% PH group (n = 2). PH: Partial hepatectomy.

damage and stress *via* inflammatory cytokines and cells; therefore, NASH liver was considered to exhibit limited proliferation, which was only induced by hepatectomy[38]. In this study, the expression of transcriptional factors induced by cytokines for liver regeneration was not recognized in the residual livers of the NASH PH groups. No significant difference was noted in the activation of these proteins in both NASH PH groups, but liver cell proliferation was significantly higher in the 30% PH NASH liver group than in the 70% PH NASH liver group.

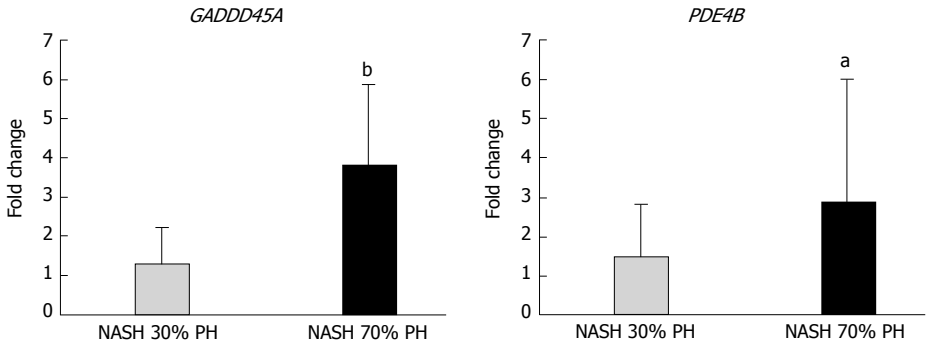

Figure 5 Gene expression of microarray. *GADD45A* and *PDE4B* expression correlated with the cell cycle. RT-PCR demonstrated a significant difference between the groups. Data are expressed as the mean ± SD. n = 5-7 per groups. [a]$P < 0.05$; [b]$P < 0.01$. PH: partial hepatectomy; NASH: nonalcoholic steatohepatitis.

Although we need to confirm these findings in future studies, the consistent decrease in liver proliferation exists, especially in the 70% PH of NASH liver group, *i.e.*, a large hepatectomy volume, which reduces the survival rate.

In general, the stress of liver resection promotes apoptosis in the residual liver[13,39], and liver damage after hepatectomy is considered to be the result of apoptosis to some degree[38]. The degree of liver damage also depends on the extent of the liver resection volume[37,39]. The STAT3 and AKT signaling pathways not only promote liver regeneration but also inhibit apoptosis[38]. In this study, STAT3 and AKT expression was significantly suppressed, and the number of TUNEL-positive cells was higher in the NASH PH groups than in the control. These results suggest that the difference in the expression of regenerative signaling proteins affected the degree of apoptosis. Resection of a large volume of the liver also enhanced necrosis[38]. In this study, microarray analysis revealed *GADD45A* upregulation in the NASH 70% PH group. *GADD45A* promotes apoptosis and cell cycle arrest[13]. The differences in the survival rate between 30% or 70% PH in the NASH groups are inversely proportional to the incidence of Ki-67-positive cells, apoptosis, and necrosis. *GADD45A* upregulation correlates with the differences between the NASH groups and the low survival rate in small residual NASH liver after 70% PH.

In conclusion, residual NASH liver dysfunction after hepatectomy is attributed to a reduction in liver regeneration and cell proliferation. These findings suggest that the resection volume is a more limiting factor in patients with NASH than in those with a normal liver. Regarding liver surgery, the risk of complications for patients diagnosed with NASH by liver biopsy should be determined before hepatectomy. Further studies are needed to clarify therapeutic agents for NASH using our novel NASH model.

ARTICLE HIGHLIGHTS

Research background

The population of patients with nonalcoholic steatohepatitis (NASH) and NASH-related hepatocellular carcinoma (HCC) has been increasing. However, few animal models fully reflect both the histopathology and pathophysiology of NASH in humans, therefore, the metabolism of the residual liver after a hepatectomy with NASH has not been clarified. We succeeded to establish a novel experimental NASH model that had same characteristics of histopathology and pathophysiology of NASH in humans.

Research motivation

In NASH, continuous inflammation contributes to HCC. The cause of HCC is frequently infection with hepatitis B virus and hepatitis C virus (HCV). New antiviral medications for hepatitis are currently being used in clinics; therefore, the number of patients with virus-related HCC is expected to decrease in the future. By contrast, the number of patients with NASH-related HCC has been increasing recently, and this trend is expected to continue because no effective treatments are available

Research objectives

The aim of this study was to investigate whether a difference in liver resection volume in a novel NASH model influences surgical outcomes.

Research methods

To establishment of a NASH model, mice were fed a high-fat diet for 4 wk, administered CCl_4 for the last 2 wk and administered T0901317 for the last 5 d. These mice were divided into two groups: A 30% partial hepatectomy (PH) of NASH liver group and a 70% PH of NASH liver group (control). Evaluate the survival rate, regeneration, apoptosis, necrosis and DNA expression level after PH.

Research results

In the 70% PH of NASH group, the survival rate was significantly decreased compared with that in the control and 30% PH of NASH groups ($P < 0.01$). 10 of 32 mice in the NASH 70% PH group died within 48 h after PH. serum aspartate aminotransferase (AST) levels and total bilirubin (T-Bil) in the NASH 70% PH group were significantly higher than the levels in the other two groups (AST: $P < 0.05$, T-Bil: $P < 0.01$). In both PH of NASH groups, signaling proteins involved in regeneration were expressed at lower levels than those in the control group ($P < 0.01$). The 70% PH of NASH group also exhibited a lower number of Ki-67-positive cells and higher rates of apoptosis and necrosis than the NASH 30% PH group ($P < 0.01$). In addition, DNA microarray assays showed differences in gene expression associated with cell cycle arrest and apoptosis.

Research conclusions

The residual NASH liver dysfunction after hepatectomy is attributed to a reduction in liver regeneration and cell proliferation. A larger residual volume is required to maintain liver functions in mice with NASH.

Research perspectives

This study suggests that the resection volume is a more limiting factor in patients with NASH than in those with a normal liver. Regarding liver surgery, the risk of complications for patients diagnosed with NASH by liver biopsy

should be determined before hepatectomy. Further studies are needed to clarify therapeutic agents for NASH using our novel NASH model.

REFERENCES

1 **Chitturi S**, Farrell GC, George J. Non-alcoholic steatohepatitis in the Asia-Pacific region: future shock? *J Gastroenterol Hepatol* 2004; **19**: 368-374 [PMID: 15012772]

2 **Browning JD**, Szczepaniak LS, Dobbins R, Nuremberg P, Horton JD, Cohen JC, Grundy SM, Hobbs HH. Prevalence of hepatic steatosis in an urban population in the United States: impact of ethnicity. *Hepatology* 2004; **40**: 1387-1395 [PMID: 15565570 DOI: 10.1002/hep.20466]

3 **White DL**, Kanwal F, El-Serag HB. Association between nonalcoholic fatty liver disease and risk for hepatocellular cancer, based on systematic review. *Clin Gastroenterol Hepatol* 2012; **10**: 1342-1359.e2 [PMID: 23041539 DOI: 10.1016/j.cgh.2012.10.001]

4 **Younossi ZM**, Otgonsuren M, Henry L, Venkatesan C, Mishra A, Erario M, Hunt S. Association of nonalcoholic fatty liver disease (NAFLD) with hepatocellular carcinoma (HCC) in the United States from 2004 to 2009. *Hepatology* 2015; **62**: 1723-1730 [PMID: 26274335 DOI: 10.1002/hep.28123]

5 **Yokosuka O**, Takaguchi K, Fujioka S, Shindo M, Chayama K, Kobashi H, Hayashi N, Sato C, Kiyosawa K, Tanikawa K, Ishikawa H, Masaki N, Seriu T, Omata M. Long-term use of entecavir in nucleoside-naïve Japanese patients with chronic hepatitis B infection. *J Hepatol* 2010; **52**: 791-799 [PMID: 20409606 DOI: 10.1016/j.jhep.2009.12.036]

6 **Parkin DM**. The global health burden of infection-associated cancers in the year 2002. *Int J Cancer* 2006; **118**: 3030-3044 [PMID: 16404738 DOI: 10.1002/ijc.21731]

7 **Nishiguchi S**, Kuroki T, Nakatani S, Morimoto H, Takeda T, Nakajima S, Shiomi S, Seki S, Kobayashi K, Otani S. Randomised trial of effects of interferon-alpha on incidence of hepatocellular carcinoma in chronic active hepatitis C with cirrhosis. *Lancet* 1995; **346**: 1051-1055 [PMID: 7564784]

8 **Yoshida H**, Shiratori Y, Moriyama M, Arakawa Y, Ide T, Sata M, Inoue O, Yano M, Tanaka M, Fujiyama S, Nishiguchi S, Kuroki T, Imazeki F, Yokosuka O, Kinoyama S, Yamada G, Omata M. Interferon therapy reduces the risk for hepatocellular carcinoma: national surveillance program of cirrhotic and noncirrhotic patients with chronic hepatitis C in Japan. IHIT Study Group. Inhibition of Hepatocarcinogenesis by Interferon Therapy. *Ann Intern Med* 1999; **131**: 174-181 [PMID: 10428733]

9 **Liaw YF**, Sung JJ, Chow WC, Farrell G, Lee CZ, Yuen H, Tanwandee T, Tao QM, Shue K, Keene ON, Dixon JS, Gray DF, Sabbat J; Cirrhosis Asian Lamivudine Multicentre Study Group. Lamivudine for patients with chronic hepatitis B and advanced liver disease. *N Engl J Med* 2004; **351**: 1521-1531 [PMID: 15470215 DOI: 10.1056/NEJMoa033364]

10 **Tateishi R,** Okanoue T, Fujiwara N, Okita K, Kiyosawa K, Omata M, Kumada H, Hayashi N, Koike K. Clinical characteristics, treatment, and prognosis of non-B, non-C hepatocellular carcinoma: a large retrospective multicenter cohort study. *J Gastroenterol* 2015; **50**: 350-360 [PMID: 24929638 DOI: 10.1007/s00535-014-0973-8]

11 **Veteläinen R,** van Vliet A, Gouma DJ, van Gulik TM. Steatosis as a risk factor in liver surgery. *Ann Surg* 2007; **245**: 20-30 [PMID: 17197961 DOI: 10.1097/01.sla.0000225113.88433.cf]

12 **Molla NW**, Hassanain MM, Fadel Z, Boucher LM, Madkhali A, Altahan RM, Alrijraji EA, Simoneau EB, Alamri H, Salman A, Gao Z, Metrakos PP. Effect of non-alcoholic liver disease on recurrence rate and liver regeneration after liver resection for colorectal liver metastases. *Curr Oncol* 2017; **24**: e233-e243 [PMID: 28680292 DOI: 10.3747/co.24.3133]

13 **Inaba Y**, Furutani T, Kimura K, Watanabe H, Haga S, Kido Y, Matsumoto M, Yamamoto Y, Harada K, Kaneko S, Oyadomari S, Ozaki M, Kasuga M, Inoue H. Growth arrest and DNA damage-inducible 34 regulates liver regeneration in hepatic steatosis in mice. *Hepatology* 2015; **61**: 1343-1356 [PMID: 25420998 DOI: 10.1002/hep.27619]

14 **Haga S,** Ozawa T, Yamada Y, Morita N, Nagashima I, Inoue H, Inaba Y, Noda N, Abe R, Umezawa K, Ozaki M. p62/SQSTM1 plays a protective role in oxidative injury of steatotic liver in a mouse hepatectomy model. *Antioxid Redox Signal* 2014; **21**: 2515-2530 [PMID: 24925527 DOI: 10.1089/ars.2013.5391]

15 **Murata H,** Yagi T, Iwagaki H, Ogino T, Sadamori H, Matsukawa H, Umeda Y, Haga S, Takaka N, Ozaki M. Mechanism of impaired regeneration of fatty liver in mouse partial hepatectomy model. *J Gastroenterol Hepatol* 2007; **22**: 2173-2180 [PMID: 18031377 DOI: 10.1111/j.1440-1746.2006.04798.x]

16 **Aoyama T**, Ikejima K, Kon K, Okumura K, Arai K, Watanabe S. Pioglitazone promotes survival and prevents hepatic regeneration failure after partial hepatectomy in obese and diabetic KK-A(y) mice. *Hepatology* 2009; **49**: 1636-1644 [PMID: 19205029 DOI: 10.1002/hep.22828]

17 **Helling TS**. Liver failure following partial hepatectomy. *HPB* (Oxford) 2006; **8**: 165-174 [PMID: 18333270 DOI: 10.1080/13651820510035712]

18 **Bernal W**, Lee WM, Wendon J, Larsen FS, Williams R. Acute liver failure: A curable disease by 2024? *J Hepatol* 2015; **62**: S112-S120 [PMID: 25920080 DOI: 10.1016/j.jhep.2014.12.016]

19 **Michalopoulos GK**, DeFrances MC. Liver regeneration. *Science* 1997; **276**: 60-66 [PMID: 9082986]

20 **Forbes SJ,** Newsome PN. Liver regeneration-mechanisms and models to clinical application. *Nat Rev Gastroenterol Hepatol* 2016; **13**: 473-485 [PMID: 27353402 DOI: 10.1038/nrgastro.2016.97]

21 **Shirabe K**, Shimada M, Gion T, Hasegawa H, Takenaka K, Utsunomiya T, Sugimachi K. Postoperative liver failure after major hepatic resection for hepatocellular carcinoma in the modern era with special reference to remnant liver volume. *J Am Coll Surg* 1999; **188**: 304-309 [PMID: 10065820]

22 **Seyama Y**, Kokudo N. Assessment of liver function for safe hepatic resection. *Hepatol Res* 2009; **39**: 107-116 [PMID: 19208031 DOI: 10.1111/j.1872-034X.2008.00441.x]

23 **Millet G**, Truant S, Leteurtre E, Hebbar M, Zerbib P, Huet G, Boleslawski E, Pruvot FR. Volumetric analysis of remnant liver regeneration after major hepatectomy in bevacizumab-treated patients: a case-matched study in 82 patients. *Ann Surg* 2012; **256**: 755-761; discussion 761-762 [PMID: 23095619 DOI: 10.1097/SLA.0b013e31827381ca]

24 **Meier M**, Andersen KJ, Knudsen AR, Nyengaard JR, Hamilton-Dutoit S, Mortensen FV. Liver regeneration is dependent on the extent of hepatectomy. *J Surg Res* 2016; **205**: 76-84 [PMID: 27621002 DOI: 10.1016/j.jss.2016.06.020]

25 **Guglielmi A,** Ruzzenente A, Conci S, Valdegamberi A, Iacono C. How much remnant is enough in liver resection? *Dig Surg* 2012; **29**: 6-17 [PMID: 22441614 DOI: 10.1159/000335713]

26 **Nakagawa H**. Recent advances in mouse models of obesity- and nonalcoholic steatohepatitis-associated hepatocarcinogenesis. *World J Hepatol* 2015; **7**: 2110-2118 [PMID: 26301053 DOI: 10.4254/wjh.v7.i17.2110]

27 **Takahashi Y**, Soejima Y, Fukusato T. Animal models of nonalcoholic fatty liver disease/nonalcoholic steatohepatitis. *World J Gastroenterol* 2012; **18**: 2300-2308 [PMID: 22654421 DOI: 10.3748/wjg.v18.i19.2300]

28 **Owada Y,** Tamura T, Tanoi T, Ozawa Y, Shimizu Y, Hisakura K, Matsuzaka T, Shimano H, Nakano N, Sakashita S, Matsukawa T, Isoda H, Ohkohchi N. Novel non-alcoholic steatohepatitis model with histopathological and insulin-resistant features. *Pathol Int* 2018; **68**: 12-22 [PMID: 29154469 DOI: 10.1111/pin.12612]

29 **Rashidi B**, An Z, Sun FX, Sasson A, Gamagammi R, Moossa AR, Hoffman RM. Minimal liver resection strongly stimulates the growth of human colon cancer in the liver of nude mice. *Clin Exp Metastasis* 1999; **17**: 497-500 [PMID: 10763915 DOI: 10.1023/A:1006693224835]

30 **Wakai T,** Shirai Y, Sakata J, Korita PV, Ajioka Y, Hatakeyama K. Surgical outcomes for hepatocellular carcinoma in nonalcoholic fatty liver disease. *J Gastrointest Surg* 2011; **15**: 1450-1458 [PMID:

21512848 DOI: 10.1007/s11605-011-1540-8]
31 **Ninomiya M**, Shirabe K, Terashi T, Ijichi H, Yonemura Y, Harada N, Soejima Y, Taketomi A, Shimada M, Maehara Y. Deceleration of regenerative response improves the outcome of rat with massive hepatectomy. *Am J Transplant* 2010; **10**: 1580-1587 [PMID: 20642684 DOI: 10.1111/j.1600-6143.2010.03150.x]
32 **Gerlach C**, Sakkab DY, Scholzen T, Dassler R, Alison MR, Gerdes J. Ki-67 expression during rat liver regeneration after partial hepatectomy. *Hepatology* 1997; **26**: 573-578 [PMID: 9303485 DOI: 10.1002/hep.510260307]
33 **Scholzen T**, Gerdes J. The Ki-67 protein: from the known and the unknown. *J Cell Physiol* 2000; **182**: 311-322 [PMID: 10653597 DOI: 10.1002/(SICI)1097-4652(200003)182:3<311::AID-JCP1>3.0.CO;2-9]
34 **Sydor S**, Gu Y, Schlattjan M, Bechmann LP, Rauen U, Best J, Paul A, Baba HA, Sowa JP, Gerken G, Canbay A. Steatosis does not impair liver regeneration after partial hepatectomy. *Lab Invest* 2013; **93**: 20-30 [PMID: 23069937 DOI: 10.1038/labinvest.2012.142]
35 **Nakamura Y**, Mizuguchi T, Tanimizu N, Ichinohe N, Ooe H, Kawamoto M, Meguro M, Hirata K, Mitaka T. Preoperative hepatocyte transplantation improves the survival of rats with nonalcoholic steatohepatitis-related cirrhosis after partial hepatectomy. *Cell Transplant* 2014; **23**: 1243-1254 [PMID: 25330059 DOI: 10.3727/096368913X668645]
36 **Myronovych A**, Murata S, Chiba M, Matsuo R, Ikeda O, Watanabe M, Hisakura K, Nakano Y, Kohno K, Kawasaki T, Hashimoto I, Shibasaki Y, Yasue H, Ohkohchi N. Role of platelets on liver regeneration after 90% hepatectomy in mice. *J Hepatol* 2008; **49**: 363-372 [PMID: 18602717 DOI: 10.1016/j.jhep.2008.04.019]
38 **Fujiyoshi M**, Ozaki M. Molecular mechanisms of liver regeneration and protection for treatment of liver dysfunction and diseases. *J Hepatobiliary Pancreat Sci* 2011; **18**: 13-22 [PMID: 20607568 DOI: 10.1007/s00534-010-0304-2]
39 **Kubota T,** Takabe K, Yang M, Sekido H, Endo I, Ichikawa Y, Togo S, Shimada H. Minimum sizes for remnant and transplanted livers in rats. *J Hep Bil Pancr Surg* 1997; **4**: 398-404 [DOI: 10.1007/bf02488972]

P- Reviewer: Lin GM, Tarantino G, Ulasoglu C **S- Editor**: Wang XJ
L- Editor: A **E- Editor**: Huang Y

World Journal of Gastroenterology

Submit a Manuscript: http://www.f6publishing.com

World J Gastroenterol 2018 April 21; 24(15): 1632-1640

DOI: 10.3748/wjg.v24.i15.1632

ISSN 1007-9327 (print) ISSN 2219-2840 (online)

ORIGINAL ARTICLE

Retrospective Study

Endoscopic submucosal dissection for early esophageal neoplasms using the stag beetle knife

Toshio Kuwai, Toshiki Yamaguchi, Hiroki Imagawa, Ryoichi Miura, Yuki Sumida, Takeshi Takasago,Yuki Miyasako, Tomoyuki Nishimura, Sumio Iio, Atsushi Yamaguchi, Hirotaka Kouno, Hiroshi Kohno, Sauid Ishaq

Toshio Kuwai, Toshiki Yamaguchi, Hiroki Imagawa, Ryoichi Miura, Yuki Sumida, Takeshi Takasago, Yuki Miyasako, Tomoyuki Nishimura, Sumio Iio, Atsushi Yamaguchi, Hirotaka Kouno, Hiroshi Kohno, Department of Gastroenterology, National Hospital Organization, Kure Medical Center and Chugoku Cancer Center, Kure 737-0023, Japan

Sauid Ishaq, Department of Gastroenterology, DGH, SGU, WI, Birmingham City University, Birmingham B4 7BD, United Kingdom

ORCID number: Toshio Kuwai (0000-0001-9956-1358); Toshiki Yamaguchi (0000-0002-6984-1639); Hiroki Imagawa (0000-0003-0623-6594); Ryoichi Miura (0000-0002-3643-7293); Yuki Sumida (0000-0003-2204-2319); Takeshi Takasago (0000-0003-1585-8555); Yuki Miyasako (0000-0002-4940-5549); Tomoyuki Nishimura (0000-0003-3531-1944); Sumio Iio (0000-0002-7853-4761); Atsushi Yamaguchi (0000-0002-4573-5241); Hirotaka Kouno (0000-0003-0041-2462); Hiroshi Kohno (0000-0002-6292-9996); Sauid Ishaq (0000-0003-1458-4708).

Author contributions: Kuwai T designed the research; Yamaguchi T, Imagawa H, Yamaguchi A, Kouno H, Kohno H and Ishaq S contributed by providing critical intellectual input for the revised manuscript; Kuwai T, Miura R, Sumida Y, Takasago T, Miyasako Y, Nishimura T and Iio S analyzed the data; Kuwai T wrote the article.

Institutional review board statement: This study was approved by the National Hospital Organization Kure Medical Center and the Chugoku Cancer Center Institutional Review Board Ethics Committee on 3 October 2016, the study incorporated good clinical practice, conforming to Declaration of Helsinki principles.

Informed consent statement: All patients were informed of the risks and benefits of ESD and provided written informed consent.

Conflict-of-interest statement: All authors declare no conflicts-of-interest related to this article.

Data sharing statement: No additional data are available.

Manuscript source: Invited manuscript

Correspondence to: Toshio Kuwai, MD, PhD, Chief Doctor, Department of Gastroenterology, National Hospital Organization Kure Medical Center and Chugoku Cancer Center, 3-1 Aoyama-cho, Kure 737-0023, Japan. kuwait@kure-nh.go.jp

Telephone: +81-823-223111

Fax: +81-823-210478

Received: February 9, 2018

Peer-review started: February 11, 2018

First decision: March 9, 2018

Revised: March 16, 2018

Accepted: March 31, 2018

Article in press: March 30, 2018

Published online: April 21, 2018

Abstract

AIM

To determine short- and long-term outcomes of endoscopic submucosal dissection (ESD) using the stag beetle (SB) knife, a scissor-shaped device.

METHODS

Seventy consecutive patients with 96 early esophageal neoplasms, who underwent ESD using a SB knife at

Kure Medical Center and Chugoku Cancer Center, Japan, between April 2010 and August 2016, were retrospectively evaluated. Clinicopathological characteristics of lesions and procedural adverse events were assessed. Therapeutic success was evaluated on the basis of *en bloc*, histologically complete, and curative or non-curative resection rates. Overall and tumor-specific survival, local or distant recurrence, and 3- and 5-year cumulative overall metachronous cancer rates were also assessed.

RESULTS

Eligible patients had dysplasia/intraepithelial neoplasia (22%) or early cancers (squamous cell carcinoma, 78%). The median procedural time was 60 min and on average, the lesions measured 24 mm in diameter, yielding 33-mm tissue defects. The *en bloc* resection rate was 100%, with 95% and 81% of dissections deemed histologically complete and curative, respectively. All procedures were completed without accidental incisions/perforations or delayed bleeding. During follow-up (mean, 35 ± 23 mo), no local recurrences or metastases were observed. The 3- and 5-year survival rates were 83% and 70%, respectively, with corresponding rates of 85% and 75% for curative resections and 74% and 49% for non-curative resections. The 3- and 5-year cumulative rates of metachronous cancer in the patients with curative resections were 14% and 26%, respectively.

CONCLUSION

ESD procedures using the SB knife are feasible, safe, and effective for treating early esophageal neoplasms, yielding favorable short- and long-term outcomes.

Key words: Neoplasms; Stag beetle knife; Esophageal; Endoscopic submucosal dissection;Outcome measures

Core tip: Various devices designed for endoscopic submucosal dissection (ESD) are currently under investigation for their usefulness in the treatment of early esophageal neoplasms. This study aimed to evaluate the short- and long-term outcomes of ESD using the stag beetle (SB) knife, a scissor-shaped device. Seventy-four patients with 101 esophageal lesions underwent resection via SB-knife ESD. Rates of en bloc, histologically complete, and curative resections were 100%, 95%, and 81%, respectively. The 3- and 5-year survival rates were 83% and 70%, respectively. The SB knife allows safe and effective ESD of early esophageal neoplasms.

Kuwai T, Yamaguchi T, Imagawa H, Miura R, Sumida Y, Takasago T, Miyasako Y, Nishimura T, Iio S, Yamaguchi A, Kouno H, Kohno H, Ishaq S. Endoscopic submucosal dissection for early esophageal neoplasms using the stag beetle knife. World J Gastroenterol 2018; 24(15): 1632-1640 Available from: URL: http://www.wjgnet.com/1007-9327/full/v24/i15/1632.htm DOI: http://dx.doi.org/10.3748/wjg.v24.i15.1632

INTRODUCTION

Esophageal carcinoma is the eighth most common cancer worldwide and the sixth leading cause of cancer-related deaths globally[1,2]. Squamous cell carcinoma (SCC) is the commonest histotype of esophageal cancer in Japan and worldwide[1,3]. Despite advances in diagnosis and treatment, outcomes in these patients remain poor, with five-year survival rates of 15%-20%[4,5]. Aggressive use of enhanced imaging for screening and advanced magnification endoscopy systems have aided in early diagnosis. However, given the many possible comorbidities in patients undergoing conventional treatments (such as esophagectomy) and the greater likelihood of incomplete resection through endoscopic mucosal resection, researchers are now actively investigating endoscopic submucosal dissection (ESD) of superficial esophageal neoplasms[6-8].

A number of conventional ESD devices (*i.e.*, dual, flush, insulated-tip, and hook knives) have been utilized for esophageal ESD[9-14]. Compared to those of the stomach, the thin wall (with no serosa) and narrow lumen of the esophagus make ESD inherently more challenging. The endoscopic maneuverability difficulties imposed by conventional ESD devices are also problematic, particularly the lack of fixation to targets and the fact that these devices are partially or entirely uninsulated. Constraints of this sort are conducive to unintentional incisions, increasing the potential risk of adverse events such as perforation and mediastinal emphysema[15-18].

On the other hand, the stag beetle (SB) knife (Sumitomo Bakelite Co., Ltd., Akita, Japan), with its ability to grasp, assess, and then cut targeted tissue, allows endoscopists to maintain adequate dissection planes, preventing inadvertent injury to the muscular layer and promoting safe ESD[19-23]. Although early experiences at selected institutions suggest that the SB knife is safe and effective, no large series of patients or long-term outcomes have been reported to date[21-24]. The aim of this study was to investigate use of the SB knife for ESD of early esophageal neoplasms, assessing both feasibility and safety. Subsequent short- and long-term clinical outcomes were examined as well.

MATERIALS AND METHODS

Study design

A single-center retrospective review of collected data was conducted, examining 74 consecutive patients with 101 esophageal lesions who underwent resection *via* SB-knife ESD between April 2010 and August 2016 at Kure Medical Center and Chugoku Cancer Center,

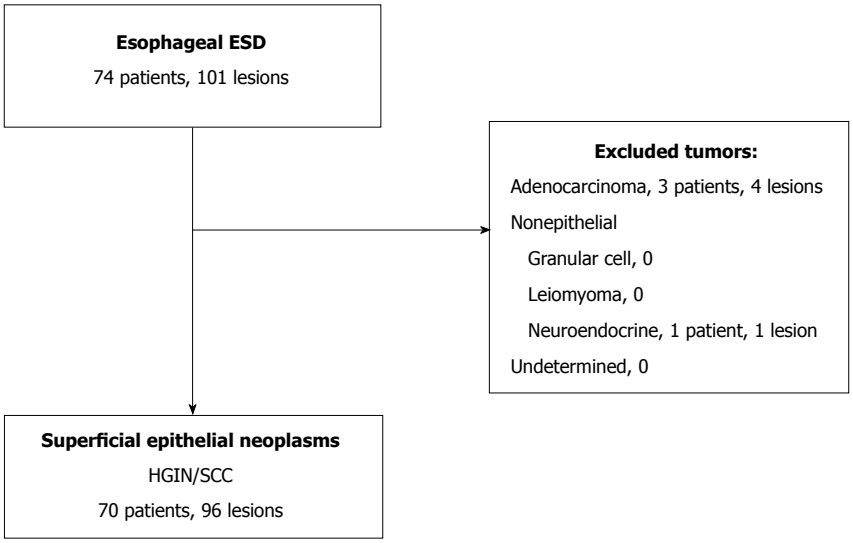

Figure 1 Study design, evaluating the use of the stag beetle knife for esophageal endoscopic submucosal dissection. ESD: Endoscopic submucosal dissection; HGIN: High-grade intraepithelial neoplasia; SCC: Squamous cell carcinoma.

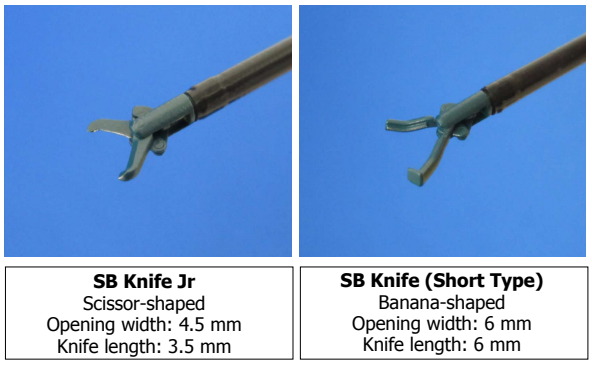

Figure 2 Features of the stag beetle Knife Jr and short devices.

Japan (Figure 1). All patients underwent resection using only SB-knife ESD during this time period. Approved by the National Hospital Organization Kure Medical Center and the Chugoku Cancer Center Institutional Review Board Ethics Committee on 3 October 2016, the study incorporated good clinical practice, conforming to Declaration of Helsinki principles. All lesions were diagnosed preoperatively during chromoendoscopy, identifying areas for biopsy through narrow-band imaging or iodine staining. Inclusion criteria were patients with superficial esophageal neoplasms (SENs), consisting of high-grade intraepithelial neoplasia or SCC. Exclusion criteria included patients with adenocarcinoma, non-epithelial tumors (*i.e.*, granular cell tumors, leiomyomas, and neuroendocrine tumors) or undetermined tumors.

All patients were informed of the risks and benefits of ESD and provided written informed consent. ESD was contraindicated in patients with serious comorbidities, distant metastasis, or massive submucosal invasion.

ESD procedure

ESD procedures were performed by four board-certified endoscopists of the Japan Gastroenterological Endoscopy Society, three with no previous conventional esophageal ESD experience and one with low experience (10 cases). Patients received intravenous nitrazepam for sedation, and cardiorespiratory function was monitored throughout the procedure. A single-channel endoscope equipped with a water jet (GIF-H260Z; Olympus Corp, Tokyo, Japan) and attached transparent tip hood was routinely used, along with carbon dioxide insufflation. Initially, the outside margin of each lesion was marked using argon plasma coagulation in forced coagulation mode; the esophageal mucosa was injected with 0.4% sodium hyaluronate (MucoUp; Seikagaku Corp., Tokyo, Japan) mixed with a small amount of indigo carmine. Circumferential excision was then carried out with the SB Knife Jr (4.5-mm opening width, 3.5-mm length; Sumitomo Bakelite Co.) (Figure 2). For submucosal dissection, the SB Knife Short (6-mm opening width, 6-mm length) (Figure 2) was often preferred, because detachment/peeling of the submucosa was faster, and it was less likely to engage the muscular layer, given the curved shape of the blade. The SB knife allowed grasping of the targeted segment, which was then cut using a high-frequency generator (VIO300D; ERBE, Tubingen, Germany) in the endo-cut Q mode (effect 1) for incising mucosa and dissecting submucosa. The soft coagulation mode (effect 5.40 W) was used for hemostasis. If repeated coagulation was required, hemostatic forceps (Coagrasper; Olympus Corp.) were applied to facilitate endoscopic hemostasis. The procedure was continued until resection was completed (Figure 3).

In instances of semi-circumferential or circumferential ESD, intralesional diluted triamcinolone acetonide injected on postoperative day 2 [Kenacort (40-80 mg); Bristol-Myers Squibb Co., New York, NY, United States] or oral prednisolone (30 mg/d) was prescribed and tapered gradually over several weeks[25] to prevent

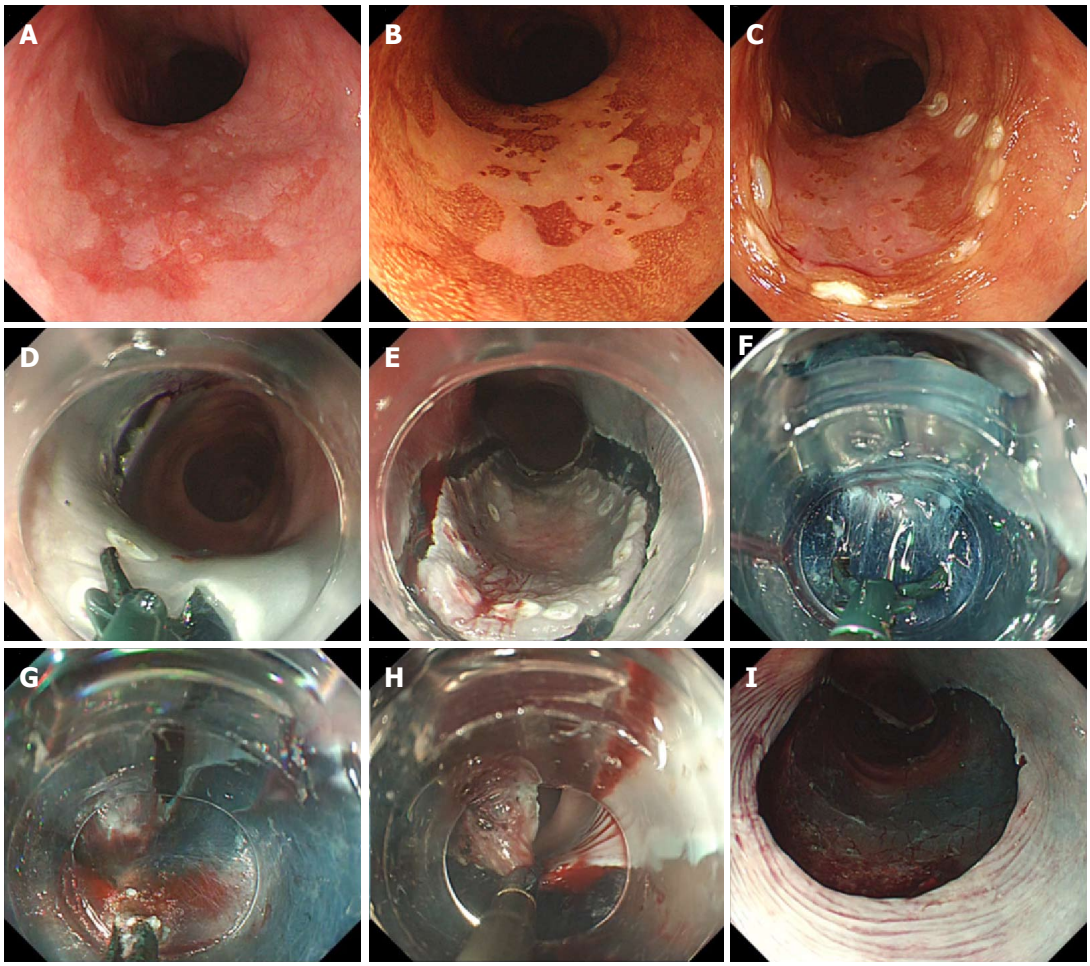

Figure 3 Stag beetle knife used for esophageal endoscopic submucosal dissection in a 79-year-old man. Endoscopic appearance of a 35-mm, depressed lesion in the middle one-third of the esophagus (A) under white light (B) on a scatter image with Lugol's iodine applied (C) with argon plasma coagulation markings; D and E: Use of the SB Knife Jr for full-circumferential incision; use of the SB Knife Short for (F) submucosal dissection and (G) hemostasis; H: *En bloc* resection of the lesion; I: Ulcer floor after resection.

postoperative stricture[26,27].

Histopathology and short-term outcomes

Resected specimens were immediately fixed in 10% buffered formalin, with samples later selected for routine processing, embedding in paraffin, and slide preparation (3-4 μm, hematoxylin & eosin stain). The histotype, depth of invasion, and resection margins (vertical and lateral) of the lesions were assessed microscopically (Figure 4) using an optical micrometer to measure invasive areas. The tumor size, anatomic location (upper one-third, middle one-third, or lower one-third of the esophagus), and extent (%) of esophageal circumferential involvement were documented. Rates of *en bloc* resection, histologically complete resection (*i.e.*, *en bloc* resection with negative lateral and vertical margins), and curative or non-curative resection served as indices of therapeutic success. Curative resection was defined as complete tumor resection with invasion $\leqslant$ 200 μm below the deep border of the lamina muscularis mucosae and no lymphovascular involvement[8].

Adverse events

Immediate adverse events such as perforation, delayed bleeding, and postoperative pneumonia and delayed adverse events such as esophageal stricture were recorded.

Long-term outcomes

To monitor patients, esophagogastroduodenoscopy was performed 3-6 mo and 1 year following ESD and annually thereafter; computed tomography was also performed annually. Three- and 5-year overall survival rates were assessed for the entire study cohort. SENs detected > 1 year after curative resection by ESD were considered metachronous cancers. Cumulative overall metachronous cancer rates during the 3- and 5-year periods were also assessed.

Statistical analysis

Continuous variables were expressed as a mean ± standard deviation or median and range, as appropriate, and categorical variables as frequency or number of

Table 1 Study demographics and clinicopathologic characteristics *n* (%)

Characteristics	Value
Number of patients	70
Number of lesions	96
Age, mean ± SD (range), yr	67 ± 10 (43-87)
Sex	
Male	59 (84)
Female	11 (16)
Location of the tumor in the esophagus	
Upper one-third	11 (11)
Middle one-third	53 (55)
Lower one-third	33 (34)
Gross appearance	
Depressed	86 (90)
Elevated	7 (7)
Flat	2 (2)
Mixed	1 (1)
Resected specimen size, mean ± SD (range), mm	33 ± 14 (9-75)
Resected tumor size, mean ± SD (range), mm	24 ± 13 (1-64)
Luminal extent	
< 1/2	59 (61)
⩾ 1/2, < 2/3	20 (21)
⩾ 2/3	17 (18)
Histopathologic features	
Dysplasia/intraepithelial neoplasia	21 (22)
Squamous cell carcinoma	75 (78)
Epithelial lining	15 (20)
Lamina propria mucosae	31 (41)
Muscularis mucosae	13 (17)
Submucosa (SM1)	2 (3)
Submucosa (SM2 or deeper)	14 (19)

Table 2 Short-term outcomes and adverse events of esophageal endoscopic submucosal dissection, *n* %

	95%CI
Procedure duration, median (range)	60 (25-305)
En bloc resection	96 (100) [96.2-100]
Complete resection with negative margins	91 (95) [88.4-97.8]
Curative resection	78 (81) [72.3-87.8]
Adverse events	
Perforation	0 (0) [0-3.9]
Delayed bleeding	0 (0) [0-3.9]
Pneumonia	3 (3) [1.1-8.8]
Esophageal stricture	7 (7) [3.6-14.3]

occurrences. Kaplan-Meier curves were generated to analyze survival and metachronous cancer rates. A log-rank test was used to evaluate the significance of differences between curves, and a *P* value of less than 5% was considered significant. All statistical analyses were performed using JMP software (SAS Institute, Inc., Cary, NC, United States).

RESULTS

Demographic and clinicopathologic characteristics

A total of 96 SENs in 70 patients qualified for analysis. One subject was excluded, having received a final diagnosis of nonepithelial tumor, and 4 subjects were excluded, having received a final diagnosis of adenocarcinoma (Figure 1). Fifteen patients had multiple lesions, harboring two (*n* = 9), three (*n* = 3), four (*n* = 1), or five (*n* = 2) lesions. Mean age of the study population (*n* = 70; 84% men) was 67 ± 10 years (Table 1). By location, 11% of lesions involved the upper one-third of the esophagus, 55% the middle one-third, and 34% the lower one-third. Macroscopically, majority of the lesions were depressed (90%) rather than elevated (7%) or flat (2%).

Resected specimens measured 33 ± 14 mm on average, with a mean tumor size of 24 ± 13 mm. Most tumors (61%) involved < one-half of the esophageal luminal circumference. Histopathological diagnoses were as follows: dysplasia/intraepithelial neoplasia (22%), or SCC (78%). Typically, invasive SCCs were limited to the lamina propria mucosae (41%), with SM2 or deeper infiltration accounting for 19% (Table 1).

Short-term outcomes

Short-term outcomes are summarized in Table 2. The median procedural time was 60 min (range, 25-305 min). Rates of *en bloc* resection, histologically complete resection, and curative resection were 100%, 95%, and 81%, respectively.

Adverse events

All lesions were safely resected without any unintentional incisions/perforations or delayed bleeding episodes. Pneumonia was observed in 3% of patients and managed through antibiotic treatment. To prevent postoperative stricture after semi-circumferential ESD, intralesional injection of triamcinolone acetonide (3 patients) or oral prednisolone (7 patients) was administered. Esophageal strictures were encountered in seven patients, one requiring balloon dilatation (Table 2).

Long-term outcomes

Curative resection was achieved in 57 patients, three of whom received additional chemoradiotherapy (CRT). One of these three patients later developed metachronous cancer. Seven of the 54 patients who were given no additional treatment also developed metachronous cancers. The 3- and 5-year cumulative rates of metachronous cancer in patients with curative resections were 14% and 26%, respectively (Figure 5A). Non-curative resection was achieved in 13 patients, seven of whom underwent additional treatment, either surgery (*n* = 4), chemotherapy (*n* = 1), or CRT (*n* = 2). No instances of local recurrence or metastasis were observed in any patient during the mean follow-up period of 35 ± 23 mo.

Survival analysis

Three- and 5-year overall survival rates for the study cohort were 83% and 70%, respectively (Figure 5B), with corresponding rates of 85% and 75% in curative resections, and 74% and 49% in non-curative resections (Figure 5C). However, the difference in survival between curative and non-curative resections

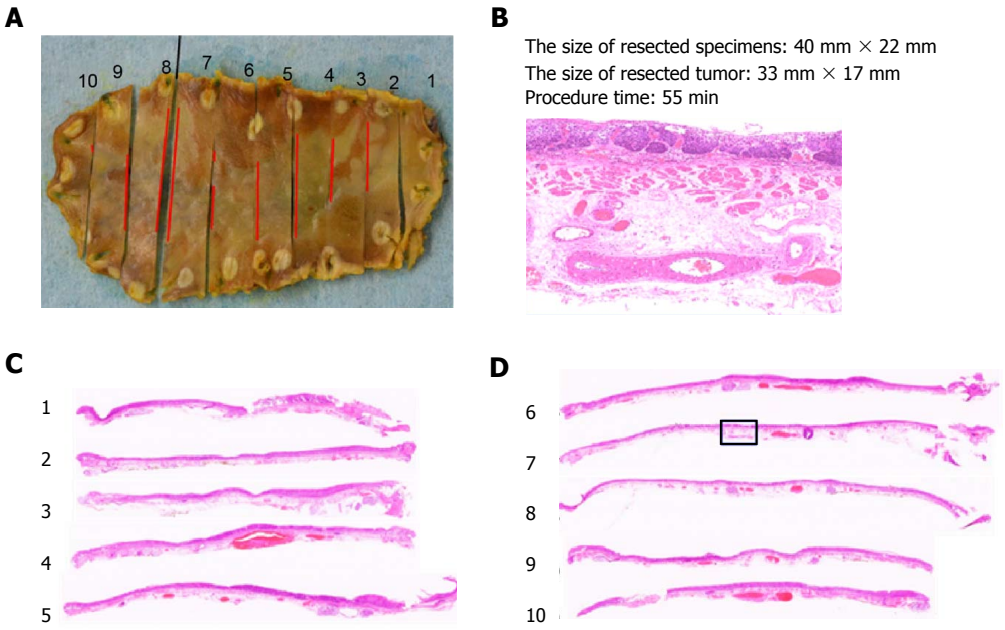

Figure 4 Formalin-fixed specimen sliced at 2-mm intervals for routine processing and slide preparation (A); Evaluation of the histotype, invasion depth, and vertical/lateral resection margins (B-D).

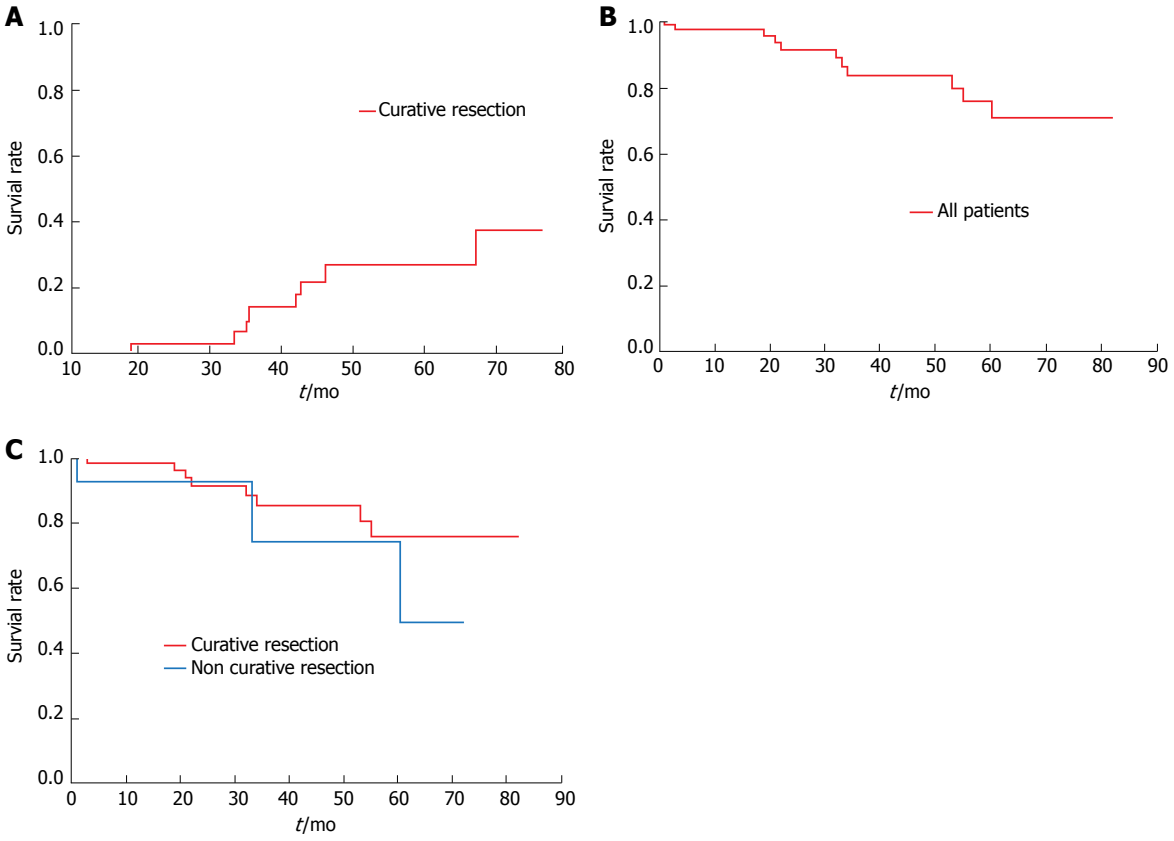

Figure 5 Long-term outcomes and survival analysis. A: Cumulative metachronous cancer rates in patients with curative resection; B: Kaplan-Meier analysis of overall survival rates in all patients; C: Patients grouped according to curative and non-curative resection.

by ESD was not statistically significant. Eleven of 70 patients (curative resections, 8/57; non-curative resections, 3/13) died during follow-up. In patients with curative resections, causes of death included isolated instances of unknown primary cancer, hepatocellular carcinoma, lung cancer, pharyngeal carcinoma, drowning, and aspiration pneumonia, as well as two instances of interstitial pneumonia. Causes of death after non-curative resection were oropharyngeal carcinoma, liver cirrhosis, and aspiration pneumonia,

each a single occurrence. None of the deaths was directly attributable to esophageal neoplasms.

DISCUSSION

Our study suggests that the SB knife is safe and effective when used for ESD of early esophageal neoplasms. This technique resulted in high rates of *en bloc* resection (100%), histologically complete resection (95%), and curative resection (81%), with a low incidence of procedural adverse events, despite three of the certified endoscopists having either limited or no experience of esophageal ESD. Specifically, there were no unintentional incisions/perforations or delayed bleeding events. Furthermore, no patient experienced local recurrences or metastases in the long term, and the overall survival rates were highly favorable and similar to those for other devices[8,28,29].

Data reported here are consistent with those of a previous study demonstrating the safety and efficacy of the SB knife as a means of esophageal ESD in 15 patients[23]. Importantly, overall adverse events for the SB knife are relatively low[10-14]. Its unique scissor-action allows surgeons to grasp and pull the targeted tissue away from the muscularis and then inspect the area before cutting for more controlled resection and avoidance of perforation. Unlike other devices[30,31], no complex adjustments or special endoscopic techniques are required. This facilitated the acquisition of implementation skills by even general endoscopists[19,30] and shortened the training process[31-34], and we obtained good results from the first case itself. The notable absence of perforation reflects the safe and easy use of the SB knife in this setting, despite cyclic respiratory and cardiac fluctuations encountered during esophageal ESD. This tool also acts as a hemostatic clamp, eliminating the need for separate hemostatic forceps, making the procedure simple and cost-effective, and encouraging high resectability rates.

We would like to emphasize that no tumors recurred when the SB knife was used for esophageal ESD. Earlier studies have already reported positive short-term treatment outcomes (*i.e.*, resection rates) using the SB knife in small series[23,24]. The present results indicate for the first time, in the largest series reported to date, that use of the SB knife offers excellent short- and long-term outcomes in treating early esophageal neoplasms. The high resection rates achieved and absence of local recurrence or metastasis during 35 ± 23 mo of follow-up constitute a new paradigm shift in the treatment of SEN[14,16,17,28,35]. Consistent with other published studies[36], several of our patients with curative resections (8/57) developed metachronous lesions, including one of three who received additional CRT. This finding underscores the need for follow-up monitoring on a regular basis.

On analyzing longer-term patient outcomes, 3- and 5-year survival rates tended to be slightly, but not significantly, poorer if resections were non-curative (74% and 49%, respectively) rather than curative (85% and 75%, respectively). Although non-curatively resected esophageal cancer is typically associated with a poor prognosis, none of the deaths recorded in the present study were a direct result of esophageal cancer. The aforementioned trend may then have a singular explanation. As ESD ordinarily is not indicated in patients with SM-level invasive cancer, such patients who agreed to undergo ESD for excisional biopsy (the goal being localized control) were included in the non-curative resection group. Consequently, it appears that achieving local control of esophageal cancer *via* ESD is quite feasible in elderly patients and in those with serious underlying diseases, who ultimately may die from other causes. By seemingly benefitting from the safe performance of esophageal ESD, we have thereby demonstrated the efficacy of the SB knife in a high-risk population.

Contrary to earlier concerns that the use of the SB knife might prolong ESD procedures[16,18], we found that it greatly expedited ESD. The median time needed to complete ESD was 60 min (mean, 78 min), approximating the time required for conventionally performed ESD (median, 90 min) in one large multicenter study[8].

Our study has three limitations. It is retrospective, although data were collected from consecutive patients, it was conducted at a single center; and no comparison with another device was attempted. However, strengths of the study include the sizeable patient population and the extended follow-up period, both providing valuable data on the feasibility, safety, and efficacy of SB knife usage for esophageal ESD.

In conclusion, ESD procedures using the SB knife are feasible, safe, and effective for treating early esophageal neoplasms, yielding favorable short- and long-term outcomes. No perforation occurred in our study population, attesting to the innovative design of the SB knife, which allows better control for safer dissection. The availability of this tool may promote widespread adoption of ESD to treat early-stage cancers of the esophagus. There is need to conduct RCT studies to compare this new innovative device with established devices.

ARTICLE HIGHLIGHTS

Research background

Several conventional endoscopic submucosal dissection (ESD) devices have been utilized for esophageal ESD. The thin wall with no serosa and narrow lumen of the esophageal wall make ESD more challenging in the esophagus. The restricted endoscopic maneuvering required with conventional ESD devices is also problematic owing to lack of fixation to targets and the fact that these devices are partially or entirely uninsulated. These factors can lead to unintentional incisions, increasing the potential risk of adverse events such as perforation and mediastinal emphysema.

Research motivation

The stag beetle (SB) knife, with its ability to grasp, assess, and then cut the targeted tissue allows endoscopists to maintain adequate dissection planes, preventing inadvertent injury to the muscular layer for safe ESD. Because of these advantages, the SB Knife is gaining acceptance, but relevant long-term

outcome data is limited.

Research objectives

The aim of this study was to investigate use of the SB knife for ESD of early esophageal neoplasms, assessing both feasibility and safety. The subsequent short- and long-term clinical outcomes were examined as well.

Research methods

We retrospectively reviewed 70 consecutive patients with 96 early esophageal neoplasms (HGIN/SCC) treated using ESD. An SB knife was used routinely in all procedures. Clinicopathologic characteristics of the lesions and rates of procedural adverse events, *en bloc* and histologically complete resection, overall and tumor-specific survival, and local or distant recurrence were assessed.

Research results

The *en bloc* resection rate was 100%, with 95% and 81% of dissections deemed histologically complete and curative, respectively. All procedures were completed without accidental incisions/perforations or delayed bleeding. During follow-up (mean, 35 ± 23 mo), no local recurrences or metastases were observed. The 3- and 5-year survival rates were 83% and 70%, respectively. The 3- and 5-year cumulative rates of metachronous cancer in the patients with curative resections were 14% and 26%, respectively.

Research conclusions

ESD procedures using the SB knife are feasible, safe, and effective for treating early esophageal neoplasms, yielding favorable short- and long-term outcomes. No perforation occurred in our study population, attesting to the innovative design of the SB knife, which allows better control for safer dissection.

Research perspectives

The availability of this tool may promote widespread adoption of ESD to treat early-stage cancers of the esophagus. There is a need to conduct RCT studies to compare this new innovative device with established devices.

ACKNOWLEDGMENTS

Writing support was provided by Cactus Communications. The authors extend thanks to Naoko Matsumoto for data collection and administrative assistance.

REFERENCES

1 **Giri S**, Pathak R, Aryal MR, Karmacharya P, Bhatt VR, Martin MG. Incidence trend of esophageal squamous cell carcinoma: an analysis of Surveillance Epidemiology, and End Results (SEER) database. *Cancer Causes Control* 2015; **26**: 159-161 [PMID: 25376829 DOI: 10.1007/s10552-014-0485-0]

2 **Yamamoto M**, Weber JM, Karl RC, Meredith KL. Minimally invasive surgery for esophageal cancer: review of the literature and institutional experience. *Cancer Control* 2013; **20**: 130-137 [PMID: 23571703 DOI: 10.1177/107327481302000206]

3 **Napier KJ**, Scheerer M, Misra S. Esophageal cancer: A Review of epidemiology, pathogenesis, staging workup and treatment modalities. *World J Gastrointest Oncol* 2014; **6**: 112-120 [PMID: 24834141 DOI: 10.4251/wjgo.v6.i5.112]

4 **Kosugi S**, Sasamoto R, Kanda T, Matsuki A, Hatakeyama K. Retrospective review of surgery and definitive chemoradiotherapy in patients with squamous cell carcinoma of the thoracic esophagus aged 75 years or older. *Jpn J Clin Oncol* 2009; **39**: 360-366 [PMID: 19389794 DOI: 10.1093/jjco/hyp030]

5 **Allen JW**, Richardson JD, Edwards MJ. Squamous cell carcinoma of the esophagus: a review and update. *Surg Oncol* 1997; **6**: 193-200 [PMID: 9775405 DOI: 10.1016/s0960-7404(98)00003-6]

6 **Takahashi H**, Arimura Y, Masao H, Okahara S, Tanuma T, Kodaira J, Kagaya H, Shimizu Y, Hokari K, Tsukagoshi H, Shinomura Y, Fujita M. Endoscopic submucosal dissection is superior to conventional endoscopic resection as a curative treatment for early squamous cell carcinoma of the esophagus (with video). *Gastrointest Endosc* 2010; **72**: 255-264, 264.e1-264.e2 [PMID: 20541198 DOI: 10.1016/j.gie.2010.02.040]

7 **Martelli MG**, Duckworth LV, Draganov PV. Endoscopic Submucosal Dissection Is Superior to Endoscopic Mucosal Resection for Histologic Evaluation of Barrett's Esophagus and Barrett's-Related Neoplasia. *Am J Gastroenterol* 2016; **111**: 902-903 [PMID: 27249992 DOI: 10.1038/ajg.2016.124]

8 **Tsujii Y**, Nishida T, Nishiyama O, Yamamoto K, Kawai N, Yamaguchi S, Yamada T, Yoshio T, Kitamura S, Nakamura T, Nishihara A, Ogiyama H, Nakahara M, Komori M, Kato M, Hayashi Y, Shinzaki S, Iijima H, Michida T, Tsujii M, Takehara T. Clinical outcomes of endoscopic submucosal dissection for superficial esophageal neoplasms: a multicenter retrospective cohort study. *Endoscopy* 2015; **47**: 775-783 [PMID: 25826277 DOI: 10.1055/s-0034-1391844]

9 **Fukami N**, Ryu CB, Said S, Weber Z, Chen YK. Prospective, randomized study of conventional versus HybridKnife endoscopic submucosal dissection methods for the esophagus: an animal study. *Gastrointest Endosc* 2011; **73**: 1246-1253 [PMID: 21316668 DOI: 10.1016/j.gie.2010.12.004]

10 **Hirasawa D**, Oyama T. [Hook knife method of ESD for early esophageal cancer]. *Nihon Rinsho* 2011; **69** Suppl 6: 248-254 [PMID: 22471026]

11 **Motohashi O**, Nishimura K, Nakayama N, Takagi S, Yanagida N. Endoscopic submucosal dissection (two-point fixed ESD) for early esophageal cancer. *Dig Endosc* 2009; **21**: 176-179 [PMID: 19691765 DOI: 10.1111/j.1443-1661.2009.00881.x]

12 **Oyama T**, Tomori A, Hotta K, Morita S, Kominato K, Tanaka M, Miyata Y. Endoscopic submucosal dissection of early esophageal cancer. *Clin Gastroenterol Hepatol* 2005; **3**: S67-S70 [PMID: 16013002 DOI: 10.1016/s1542-3565(05)00291-0]

13 **Fujishiro M**, Kodashima S, Goto O, Ono S, Niimi K, Yamamichi N, Oka M, Ichinose M, Omata M. Endoscopic submucosal dissection for esophageal squamous cell neoplasms. *Dig Endosc* 2009; **21**: 109-115 [PMID: 19691785 DOI: 10.1111/j.1443-1661.2009.00837.x]

14 **Higuchi K**, Tanabe S, Azuma M, Katada C, Sasaki T, Ishido K, Naruke A, Katada N, Koizumi W. A phase II study of endoscopic submucosal dissection for superficial esophageal neoplasms (KDOG 0901). *Gastrointest Endosc* 2013; **78**: 704-710 [PMID: 23680178 DOI: 10.1016/j.gie.2013.04.182]

15 **Zhong H**, Ma L, Zhang Y, Shuang J, Qian Y, Sheng Y, Wang X, Miao L, Fan Z. Nonsurgical treatment of 8 cases with esophageal perforations caused by ESD. *Int J Clin Exp Med* 2015; **8**: 21760-21764 [PMID: 26885139]

16 **Oyama T**. Esophageal ESD: technique and prevention of complications. *Gastrointest Endosc Clin N Am* 2014; **24**: 201-212 [PMID: 24679232 DOI: 10.1016/j.giec.2013.12.001]

17 **Toyonaga T**, Man-i M, East JE, Nishino E, Ono W, Hirooka T, Ueda C, Iwata Y, Sugiyama T, Dozaiku T, Hirooka T, Fujita T, Inokuchi H, Azuma T. 1,635 Endoscopic submucosal dissection cases in the esophagus, stomach, and colorectum: complication rates and long-term outcomes. *Surg Endosc* 2013; **27**: 1000-1008 [PMID: 23052530 DOI: 10.1007/s00464-012-2555-2]

18 **Cao Y**, Liao C, Tan A, Gao Y, Mo Z, Gao F. Meta-analysis of endoscopic submucosal dissection versus endoscopic mucosal resection for tumors of the gastrointestinal tract. *Endoscopy* 2009; **41**: 751-757 [PMID: 19693750 DOI: 10.1055/s-0029-1215053]

19 **Oka S**, Tanaka S, Takata S, Kanao H, Chayama K. Usefulness and safety of SB knife Jr in endoscopic submucosal dissection for colorectal tumors. *Dig Endosc* 2012; **24** Suppl 1: 90-95 [PMID: 22533760 DOI: 10.1111/j.1443-1661.2012.01255.x]

20 **Kuwai T,** Yamaguchi T Imagawa H, Sumida Y, Takasago T, Miyasako Y, Nishimura T, Iio S, Yamaguchi A, Kouno H, Kohno H, Ishaq S. Endoscopic submucosal dissection of early colorectal neoplasms with a monopolar scissors-type knife: short- to long-term outcomes. *Endoscopy* 2017; **49**: 913-918 [PMID: 28743145 DOI: 10.1055/s-0043-113631]

21 **Yamaguchi T**, Kuwai T, Iio S, Tsuboi A, Mori T, Boda K,

Yamashita K, Yamaguchi A, Kouno H, Kohno H. Endoscopic submucosal dissection using a stag beetle knife for early esophageal cancer in lower esophageal diverticula. *Gastrointest Endosc* 2015; **82**: 566-567 [PMID: 25975528 DOI: 10.1016/j.gie.2015.04.009]

22 **Takasago T,** Kuwai T, Yamaguchi T, Kohno H, Ishaq S. Endoscopic submucosal dissection with a scissors-type knife for post-EMR recurrence tumor involving the colon diverticulum (with video). *GIE* 2017; **2**: 211–212 [DOI: 10.1016/j.vgie.2017.05.002]

23 **Nishimura T,** Kuwai T, Yamaguchi T, Kohno H, Ishaq S. Usefulness and safety of a scissors-type knife in endoscopic submucosal dissection for non-ampullary duodenal epithelial tumors (with video). *GIE* 2017 [DOI: 10.1016/j.vgie.2017.06.012]

24 **Fujinami H**, Hosokawa A, Ogawa K, Nishikawa J, Kajiura S, Ando T, Ueda A, Yoshita H, Sugiyama T. Endoscopic submucosal dissection for superficial esophageal neoplasms using the stag beetle knife. *Dis Esophagus* 2014; **27**: 50-54 [PMID: 23442212 DOI: 10.1111/dote.12039]

25 **Yamaguchi N**, Isomoto H, Nakayama T, Hayashi T, Nishiyama H, Ohnita K, Takeshima F, Shikuwa S, Kohno S, Nakao K. Usefulness of oral prednisolone in the treatment of esophageal stricture after endoscopic submucosal dissection for superficial esophageal squamous cell carcinoma. *Gastrointest Endosc* 2011; **73**: 1115-1121 [PMID: 21492854 DOI: 10.1016/j.gie.2011.02.005]

26 **Ono S**, Fujishiro M, Niimi K, Goto O, Kodashima S, Yamamichi N, Omata M. Predictors of postoperative stricture after esophageal endoscopic submucosal dissection for superficial squamous cell neoplasms. *Endoscopy* 2009; **41**: 661-665 [PMID: 19565442 DOI: 10.1055/s-0029-1214867]

27 **Mizuta H**, Nishimori I, Kuratani Y, Higashidani Y, Kohsaki T, Onishi S. Predictive factors for esophageal stenosis after endoscopic submucosal dissection for superficial esophageal cancer. *Dis Esophagus* 2009; **22**: 626-631 [PMID: 19302207 DOI: 10.1111/j.1442-2050.2009.00954.x]

28 **Ono S**, Fujishiro M, Niimi K, Goto O, Kodashima S, Yamamichi N, Omata M. Long-term outcomes of endoscopic submucosal dissection for superficial esophageal squamous cell neoplasms. *Gastrointest Endosc* 2009; **70**: 860-866 [PMID: 19577748 DOI: 10.1016/j.gie.2009.04.044]

29 **Joo DC**, Kim GH, Park DY, Jhi JH, Song GA. Long-term outcome after endoscopic submucosal dissection in patients with superficial esophageal squamous cell carcinoma: a single-center study. *Gut Liver* 2014; **8**: 612-618 [PMID: 25368748 DOI: 10.5009/gnl13130]

30 **Homma K**, Otaki Y, Sugawara M, Kobayashi M. Efficacy of novel SB knife Jr examined in a multicenter study on colorectal endoscopic submucosal dissection. *Dig Endosc* 2012; **24** Suppl 1: 117-120 [PMID: 22533765 DOI: 10.1111/j.1443-1661.2012.01266.x]

31 **Shiga H**, Kuroha M, Endo K, Kimura T, Kakuta Y, Kinouchi Y, Kayaba S, Shimosegawa T. Colorectal endoscopic submucosal dissection (ESD) performed by experienced endoscopists with limited experience in gastric ESD. *Int J Colorectal Dis* 2015; **30**: 1645-1652 [PMID: 26243470 DOI: 10.1007/s00384-015-2334-3]

32 **Jeon HH**, Lee HS, Youn YH, Park JJ, Park H. Learning curve analysis of colorectal endoscopic submucosal dissection (ESD) for laterally spreading tumors by endoscopists experienced in gastric ESD. *Surg Endosc* 2016; **30**: 2422-2430 [PMID: 26423415 DOI: 10.1007/s00464-015-4493-2]

33 **Ohata K**, Nonaka K, Misumi Y, Tsunashima H, Takita M, Minato Y, Tashima T, Sakai E, Muramoto T, Matsuyama Y, Hiejima Y, Matsuhashi N. Usefulness of training using animal models for colorectal endoscopic submucosal dissection: is experience performing gastric ESD really needed? *Endosc Int Open* 2016; **4**: E333-E339 [PMID: 27004253 DOI: 10.1055/s-0042-101022]

34 **Imai K**, Hotta K, Yamaguchi Y, Kakushima N, Tanaka M, Takizawa K, Kawata N, Matsubayashi H, Shimoda T, Mori K, Ono H. Preoperative indicators of failure of en bloc resection or perforation in colorectal endoscopic submucosal dissection: implications for lesion stratification by technical difficulties during stepwise training. *Gastrointest Endosc* 2016; **83**: 954-962 [PMID: 26297870 DOI: 10.1016/j.gie.2015.08.024]

35 **Jin XF**, Chai TH, Gai W, Chen ZS, Guo JQ. Multiband Mucosectomy Versus Endoscopic Submucosal Dissection for Treatment of Squamous Intraepithelial Neoplasia of the Esophagus. *Clin Gastroenterol Hepatol* 2016; **14**: 948-955 [PMID: 27108794 DOI: 10.1016/j.cgh.2016.04.018]

36 **Ikeda A**, Hoshi N, Yoshizaki T, Fujishima Y, Ishida T, Morita Y, Ejima Y, Toyonaga T, Kakechi Y, Yokosaki H, Azuma T. Endoscopic Submucosal Dissection (ESD) with Additional Therapy for Superficial Esophageal Cancer with Submucosal Invasion. *Intern Med* 2015; **54**: 2803-2813 [PMID: 26567992 DOI: 10.2169/internalmedicine.54.3591]

P- Reviewer: Chetty R, Sugimoto M **S- Editor**: Wang XJ
L- Editor: A **E- Editor**: Huang Y

World Journal of Gastroenterology

Submit a Manuscript: http://www.f6publishing.com

World J Gastroenterol 2018 April 21; 24(15): 1641-1649

DOI: 10.3748/wjg.v24.i15.1641

ISSN 1007-9327 (print) ISSN 2219-2840 (online)

ORIGINAL ARTICLE

Retrospective Study

Analysis of aggressiveness factors in hepatocellular carcinoma patients undergoing transarterial chemoembolization

Yossi Ventura, Brian I Carr, Issac Kori, Vito Guerra, Oren Shibolet

Yossi Ventura, Oren Shibolet, Liver Unit, Department of Gastroenterology and Hepatology, Tel-Aviv Medical Center, Tel-Aviv 62431, Israel

Yossi Ventura, Oren Shibolet, Sackler faculty of Medicine, Tel-Aviv University, Tel-Aviv 69978, Israel

Brian I Carr, Izmir Biomedicine and Genome Center, Dokuz Eylul University, Izmir 35340, Turkey

Issac Kori, Interventional Radiology, Division of Imaging Tel Aviv Medical Center, Tel-Aviv 62431, Israel

Vito Guerra, Department of Clinical Trials and Epidemiology, IRCCS de Bellis, Castellana Grotte 70013, Italy

ORCID number: Yossi Ventura (0000-0003-2975-8627); Brian I Carr (0000-0002-6111-5077); Issac Kori (0000-0002-9716-4719); Vito Guerra (0000-0001-7827-1909); Oren Shibolet (0000-0003-6111-5067).

Author contributions: All authors equally contributed to this manuscript.

Institutional review board statement: The Tel-Aviv medical center database management conforms to Israeli legislation on privacy and this study was approved by the institutional research committee in Tel-Aviv Medical Center (Approval number: 0528-16-TLV) in accordance with the ethical standards of the 1964 Helsinki Declaration and its later amendments or comparable ethical standards.

Informed consent statement: Our manuscript is a retrospective study, therefore an informed consent waver was given by the IRB. Data was anonymized to prevent identification.

Conflict-of-interest statement: Professor Shibolet has nothing to disclose.

Data sharing statement: Technical appendix, statistical code, and dataset available from the corresponding author at orensh@tlvmc.gov.il. Consent was not obtained but the presented data are anonymized and there is no risk of patient identification. The potential benefits of sharing these data outweigh the potential harms because of its possible application in improving future identification and treatment of HCC.

Manuscript source: Unsolicited manuscript

Correspondence to: Oren Shibolet, MD, Liver Unit, Department of Gastroenterology and Hepatology, Tel-Aviv Medical Center, 14 Weizman Street, Tel-Aviv 62431, Israel. orensh@tlvmc.gov.il
Telephone: +972-3-6973984
Fax: +972-3-6974622

Received: January 3, 2018
Peer-review started: January 4, 2018
First decision: January 16, 2018
Revised: March 10, 2018
Accepted: March 25, 2018
Article in press: March 25, 2018
Published online: April 21, 2018

Abstract

AIM

To investigate novel predictors of survival in hepatocellular carcinoma (HCC) patients following transarterial chemoembolization (TACE).

METHODS

One hundred sixty seven patients with un-resectable HCC were retrospectively analyzed to identify factors that might contribute to their HCC biology and aggre-

ssiveness. We correlated routine laboratory results (total bilirubin, AST, ALKP, GGTP, albumin *etc*.) to maximum tumor diameter, number of tumor nodules, portal vein thrombosis and blood alpha-fetoprotein levels. These 4 parameters were previously combined to form an aggressiveness index (AgI). We used The Wilcoxon rank-sum (Mann-Whitney), to test the correlation between the AgI categories and liver function parameters. The Cox proportional hazards model was applied to evaluate the categories of AgI associated with overall survival.

RESULTS

The AgI was strongly correlated with survival in this novel patient population. Three year survival probability for AgI > or < 4 was 42.4% *vs* 61.8%; $P < 0.0863$ respectively. Several factors independently correlated with AgI using univariate multiple logistic regression of AgI with 8 laboratory parameters. Lower albumin levels had an OR of 2.56 (95%CI: 1.120-5.863 $P < 0.026$), elevated Alkaline phosphatase and gamma glutamyl transpeptidase (GGTP) had ORs of 1.01 (95%CI: 1.003-1.026, $P < 0.017$) and 0.99 (95%CI: 0.99-1.00, $P < 0.053$) respectively. In a Cox proportional hazard model combining mortality for AgI score and liver function parameters, only GGTP levels and the AgI were independently associated with survival. An AgI > 4 had HR for mortality of 2.18 (95%CI: 1.108-4.310, $P < 0.024$). GGTP's single unit change had a HR for mortality of 1.003 (95%CI: 1.001-1.006, $P < 0.016$). These were considered in the final multivariate model with the total cohort. An AgI > 4 had a HR for mortality of 2.26 (95%CI: 1.184-4.327, $P < 0.016$). GGTP had a HR of 1.003 (95%CI: 1.001-1.004, $P < 0.001$).

CONCLUSION

Our study validates the AgI in a new population with un-resectable HCC patients undergoing TACE. The analysis establishes a correlation between GGTP and the AgI.

Key words: Hepatocellular carcinoma; Aggressiveness index; Liver function; Transarterial chemoembolization; Survival

Core tip: Our cohort's population included patients with multiple underlying liver diseases and can be widely generalized. The aggressiveness index (AgI) was correlated with survival. AgI > 4 was associated with decreased survival. Combining the AgI with elevated GGTP and ALKP levels improved its prognostic yield in our patient population. We validated the AgI as a prognostic tool to predict overall survival in a novel population of hepatocellular carcinoma patients undergoing transarterial chemoembolization.

Ventura Y, Carr BI, Kori I, Guerra V, Shibolet O. Analysis of aggressiveness factors in hepatocellular carcinoma patients undergoing transarterial chemoembolization. *World J Gastroenterol* 2018; 24(15): 1641-1649 Available from: URL: http://www.wjgnet.com/1007-9327/full/v24/i15/1641.htm DOI: http://dx.doi.org/10.3748/wjg.v24.i15.1641

INTRODUCTION

Hepatocellular carcinoma (HCC) is the fourth most common cancer and the third leading cause of cancer-related deaths in the world[1]. In the last several decades the incidence of HCC in developed countries has been rising, secondary to an increased incidence of HCV and non alcoholic steatohepatitis (NASH) associated cirrhosis[2]. The annual Nation Cancer Report of the United States published in 2016, noted that between 2003 and 2012, in contrast to the general decline in cancer incidence rates, HCC incidence continues to rise. Most cases of HCC arise on the background of chronic liver disease. Patients are usually asymptomatic until late in their disease, when symptoms and signs related to their cirrhosis are manifested. Early detection of HCC can be accomplished by screening populations at risk. The recommended surveillance of cirrhotic patients is abdominal ultrasound every six-months[3]. Measuring levels of alpha fetoprotein (AFP) a serum marker for HCC can be used together with ultrasonography. However, due to its low sensitivity and specificity it was recently omitted from clinical practice guidelines[4]. A staging system introduced by the Barcelona Clinic Liver Cancer (BCLC), is currently recommended as the best method for HCC staging and treatment allocation. The system incorporates the dimensions of the primary lesion, vascular invasion, extra-hepatic spread, performance status, general symptoms and the degree of severity of the underlying liver disease according to the Child-Pugh-Turcot score[5].

Trans-arterial chemoembolization (TACE) is performed by catheterization of tumor feeding branches of the hepatic artery and injecting chemotherapy with Lipidol. After the injection, the artery is embolized by particles. The TACE procedure is the treatment of choice for non-operable, intermediate stage HCC according to the BCLC classification[6]. Survival after the procedure varies and ranges between 12 to 34 mo[7]. Given the complexity of TACE and the variability in response, there is an urgent need to identify prognostic indices to predict overall survival in HCC patients undergoing the procedure[8]. Current prognostic indices include different inflammation scores such as the Glasgow prognostic score (GPS), neutrophil to lymphocyte ratio (NLR) and staging systems such as Barcelona Clinic Liver Cancer (BCLC), and Cancer of the Liver Italian Program (CLIP) scores. The GPS score was demonstrated as an independent marker of poor prognosis in patients with HCC and as a prognostic score predicting survival for patients with HBV related HCC after TACE[9-14]. All these indices have their shortcomings with some lacking strong

prognostic power (even when combined), and others lacking validation and or limited to specific populations.

An "HCC Aggressiveness" scoring system was recently described, which incorporates 4 tumor-related parameters: maximum tumor diameter (MTD), number of tumor nodules, portal vein thrombosis (PVT) and serum AFP levels. The score was shown to predict survival in HCC patients[15-17].

We retrospectively analyzed laboratory and clinical data from 167 patients with HCC that underwent TACE in Tel-Aviv medical Center in order to identify novel biomarkers to predict survival following TACE. These, 167 patients, were diagnosed predominantly through screening and thus at an earlier stage in their disease and some underwent the procedure as bridging for transplantation.

MATERIALS AND METHODS

Patients and data collection

We retrospectively analyzed prospectively-collected data from manual and computerized medical records of 167 HCC patients at Tel-Aviv Medical center, a tertiary center with a liver transplantation service, who underwent the TACE procedure between the years 2000 and 2015. We excluded patients with fibrolamellar HCC, mixed cholangio-hepatocellular carcinoma and sarcomatous type HCC.

Data was collected for 161 patients (6 patients were excluded because of missing data) during the 3 mo period before the first TACE procedure. Baseline tumor parameters including: maximum tumor diameter, number of tumor nodules and presence of PVT - were gathered from imaging reports carried out at Tel-Aviv medical center. Labs including: blood count; routine liver function tests, (total bilirubin, AST, ALKP, GGTP, albumin) and plasma AFP levels; demographics and overall survival information. The Tel-Aviv medical center database management conforms to Israeli legislation on privacy and this study was approved by the institutional research committee in Tel-Aviv Medical Center (Approval number: 0528-16-TLV) in accordance with the ethical standards of the 1964 Helsinki Declaration and its later amendments or comparable ethical standards. We collected data to conform to the previously described aggressiveness index (AgI): including the following four parameters: Maximum Tumor dimension, AFP, presence or absence of PVT, and the number of tumor nodules. The AgI score was calculated as follows: MTD (in tertiles): MTD < 4.5; 4.5 $\leqslant$ MTD $\leqslant$ 9.6; MTD > 9.6; scores 1, 2, 3 respectively. AFP (cut-off): AFP < 100; 100 $\leqslant$ AFP $\leqslant$ 1000; AFP > 1000 ng/mL; scores 1, 2, 3 respectively. PVT (No/Yes): PVT (No); PVT (Yes); scores 1, 3 respectively. Tumor Nodule (number): Nodules $\leqslant$ 3; Nodules > 3; scores 1, 3 respectively. The AgI score was divided into three categories for Cox analysis (Table 1): a, score - < 4; b, 4 < score $\leqslant$ 7; and c, score $\geqslant$ 8.

TACE technique

The TACE procedure was first introduced in 1974 by Doyon *et al*[18] and was performed in our institute with the following modifications. In brief: Classical Seldinger catheterization with an end-hole angiographic catheter was used. Arteriography of the celiac trunk or the superior mesenteric artery was obtained to visualize the arterial vascularization of the liver. The same catheter was used for both drug injection and embolization. Selective injection was performed unless technical difficulties prevented selective catheterization. If the hepatic artery was occluded, an attempt was made to catheterize extrahepatic collaterals supplying the liver such as the inferior diaphragmatic, gastro-duodenal and left gastric arteries. The therapeutic emulsion contained Adriamycin and Lipiodol. The emulsion was injected into the hepatic artery distal to the gastroduodenal artery origin. Gelatin sponge particles, 1-2 mm in diameter, were then utilized to embolize the feeding vessels until a markedly reduced flow was observed. Particle size and arterial slow-down intensity) as evaluated fluoroscopically) were adapted to the status of the hepatic portal perfusion, being less aggressive (larger particles and lesser degree of arterial slowdown) in cases of poor hepatic portal perfusion. Patients received 1.5 L/d of intravenous fluid from 24 h before to 48 h after treatment. Cefamezin (1 g) and Dexamethasone (10-20 mg) was given 1 h before the procedure. Patients underwent repeated TACE procedures according to tumor viability and clinical condition as assessed by a multi-disciplinary team.

Statistical analysis

Mean and SD for continuous variables were used as indices of centrality and dispersion of the distribution. For non-normally distributed values it was necessary to use a non-parametric methods, The Wilcoxon rank-sum (Mann-Whitney) test, was used for continuous variables, to test the comparisons between the AgI categories of liver function parameters. The Cox proportional hazards model was applied to evaluate the predictive factors as categories of AgI score associated with overall survival. The results were presented as HR with 95%CI. Unconditional multiple logistic regression model was used to evaluate the Odds-Ratio of the AgI score ($\geqslant$ 4) on the dichotomized Gamma Glutamyl-Transpeptidase (GGTP). All variables were included together in the model. The results were presented as OR with 95%CI. In all models, Cox regression and Logistic regression, the HR and the OR respectively, represent the risk for one-unit variation of the predictor variable considered as dummy variables. Patient survival between the two categories of AgI score was estimated with the Kaplan-Meier method and comparison of survival was made with the Breslow (generalized Wilcoxon) test. The log rank test was used, due to the small proportion of patients who died early. When testing the hypothesis of significant association, *P*-value was < 0.05, two tailed

Table 1 Multiple logistic regression of aggressiveness index (score = 4/score > 4) on liver function parameter

All models in total cohort	OR	se(OR)	*P* value	95%CI
Variables included together in the model				
Total Bilirubin (mg/dL)	2.044	0.875	0.095	0.883 to 4.729
ALKP (IU/mL)	1.013	0.006	0.046	1.000 to 1.025
GGTP (IU/mL)	0.995	0.002	0.045	0.990 to 0.999
AST (IU/L)	1.002	0.003	0.442	0.996 to 1.009
Albumin (g/dL)	3.197	1.74	0.033	0.101 to 9.288
Platelets (× 10^9/L)	1.014	0.008	0.056	1.000 to 1.029
WBC (× 10^9/L)	0.811	0.121	0.158	0.606 to 1.085
Lymphocyte (× 10^9/L)	1.311	0.354	0.315	0.773 to 2.227
Final model from stepwise method in backward				
ALKP (IU/mL)	1.014	0.006	0.017	1.003 to 1.026
GGTP (IU/mL)	0.996	0.002	0.053	0.991 to 1.000
Albumin (g/dL)	2.562	1.082	0.026	1.120 to 5.863

Aggressiveness index (sum of scores): MTD (in tertiles): MTD < 4.5; 4.5 ⩽ MTD ⩽ 9.6; MTD > 9.6; scores 1, 2, 3 respectively; AFP (cut-off): AFP < 100; 100 ⩽ AFP ⩽ 1000; AFP > 1000; scores 1, 2, 3 respectively; PVT (no/yes): PVT (no); PVT (yes); scores 1, 3 respectively; nodules (number): Nodules ⩽ 3; nodules > 3; scores 1, 3 respectively. AFP: Alpha-fetoprotein; MTD: Maximum tumor diameter; PVT: Portal vein thrombosis; ALKP: Alkaline phosphatase; GGTP: Gamma glutamyl transpeptidae; AST: Aspartate aminotransaminase; Hb: Haemoglobin; Plt: Platelet count; WBC: White blood cell.

Table 2 Characteristics of patients in the total cohort

Parameter[1]	Value
Age (yr)	64.24 ± 10.35
Sex (M) (%)	124 (74.25)
Cirrhosis (yes) (%)	134 (80.24)
AFP (ng/dL)	1769.49 ± 7297.65
AFP (median, range)	53.80 (1-66000)
AFP > 100 (%)	54 (40.60)
Number nodules	1.95 ± 1.39
MTD (cm)	4.45 ± 2.64
PVT (yes) (%)	24 (14.37)
Aggressiveness index score (%)	
Score > 4	75 (63.56)
Total bilirubin (mg/dL)	1.23 ± 0.80
ALKP (IU/mL)	133.29 ± 74.74
GGTP (IU/mL)	152.26 ± 152.80
AST (IU/L)	104.68 ± 110.73
ALT (IU/L)	77.85 ± 88.25
Albumin (g/dL)	3.63 ± 1.93
Platelet count (× 10^9/L)	113.78 ± 82.70
WBC (× 10^9/L)	5.46 ± 2.59
Lymphocyte (× 10^9/L)	1.41 ± 0.98
Survival time (median, range)	38 (3-175)

[1]All values: mean ± SD for continuous variables; Aggressiveness Index (sum of scores): MTD (in tertiles): MTD < 4.5; 4.5 ⩽ MTD ⩽ 9.6; MTD > 9.6; scores 1, 2, 3 respectively; AFP (cut-off): AFP < 100; 100 ⩽ AFP ⩽ 1000; AFP > 1000; scores 1, 2, 3 respectively; PVT (no/yes): PVT (no); PVT (yes); scores 1, 3 respectively; Nodules (number): Nodules ⩽ 3; Nodules > 3; scores 1, 3 respectively. AFP: Alpha-fetoprotein; MTD: Maximum tumor diameter; PVT: Portal vein thrombosis; ALKP: Alkaline phosphatase; GGTP: Gamma glutamyl transpeptidae; AST: Aspartate aminotransaminase; ALT: Alanina amminotransferasi; Hb: Haemoglobin; WBC: White blood cell.

for all analyses. Statistical analysis was performed with State Corp 2007 State Statistical Software: release 10. College Station, TX: StataCorp LP.

RESULTS

Patients' characteristics

A total of 167 patients were included in this study. Six patients were omitted because of missing data, leaving 161 patients in the final analysis. Sixty seven patients were under surveillance for their underlying liver disease. The median age was 64.24 ± 10.35 years, the majority were males (*n* = 124, 74.25%) and 80.24% had cirrhosis with complications, including ascites (*n* = 40), varices (*n* = 67), encephalopathy (*n* = 20), and abdominal pain (*n* = 34) at diagnosis. Etiologies of the underlying liver disease included: HCV (*n* = 91); HBV (*n* = 35); NASH (*n* = 17); cryptogenic cirrhosis (*n* = 17); HCV and HBV (*n* = 3); ASH and HCV (*n* = 2); Autoimmune hepatitis (*n* = 1), Alcoholic steatohepatitis (*n* = 1). The mean AFP levels were 53.8 (range: 1-66000). Mean number of tumor nodules was 1.95 + 1.39 and the MTD was 4.45 ± 2.65 cm. Twenty four patients (14.37%) had PVT. Mean serum ALKP, GGTP, bilirubin and albumin levels were 104.68 ± 110.73 IU, 152.26 ± 152.8 IU, 1.23 ± 0.80 (mg/dL) and 3.63 ± 1.93 (g/dL) respectively (Table 2).

Survival analysis and AgI

Median survival from the time of HCC diagnosis to death or transplantation was 38 mo (range 3-175 mo) (Table 2). Seventy five (63.5%) patients had a score of > 4 on the AgI (Table 2). The AgI was correlated with survival. The 3-year survival probability for AgI of > 4 *vs* < 4 was 42.4% *vs* 61.8%; *P* < 0.0863, from the time of diagnosis by Kaplan-Meier plot (Figure 1). Moreover, according to the univariate Cox proportional hazard model for mortality with AgI score of > 4, there was a HR of 2.18 (95%CI: 1.108-4.310, *P* < 0.024) (Table 3).

Correlation of AgI with other parameters

A univariate multiple logistic regression of AgI with 8 laboratory parameters was obtained and two baseline laboratory parameters were found to independently correlate with the AgI score (Table 1). Albumin's single unit change was associated with an OR of 3.19

Table 3 Cox proportional hazard model for death on aggressiveness index score and liver function parameters

All models in total cohort	HR	se(HR)	*P* value	95%CI
Variables included together in the model				
Aggressiveness Index				
Score = 4 [Ref. category]	1	-	-	-
Score > 4	2.185	0.757	0.024	1.108 to 4.310
Total bilirubin (mg/dL)	0.985	0.154	0.925	0.725 to 1.339
ALKP (IU/mL)	0.999	0.003	0.793	0.993 to 1.005
GGTP (IU/mL)	1.003	0.001	0.016	1.001 to 1.006
AST (IU/L)	0.999	0.002	0.511	0.995 to 1.003
Albumin (g/dL)	0.793	0.250	0.462	0.427 to 1.472
Platelets ($\times 10^9$/L)	1.002	0.002	0.161	0.999 to 1.006
Final model from stepwise method in backward				
Aggressiveness Index				
Score = 4 [Ref. category]	1	-	-	-
Score > 4	2.263	0.748	0.013	1.184 to 4.327
GGTP (IU/mL)	1.003	0.001	0.001	1.001 to 1.004

Aggressiveness index (sum of scores): MTD (in tertiles): MTD < 4.5; 4.5 ⩽ MTD ⩽ 9.6; MTD > 9.6; scores 1, 2, 3 respectively; AFP (cut-off): AFP < 100; 100 ⩽ AFP ⩽ 1000; AFP > 1000; scores 1, 2, 3 respectively; PVT (no/yes): PVT (no); PVT (yes); scores 1, 3 respectively; nodules (number): Nodules ⩽ 3; nodules > 3; scores 1, 3 respectively. AFP: Alpha-fetoprotein; MTD: Maximum tumor diameter; PVT: Portal vein thrombosis; ALKP: Alkaline phosphatase; GGTP: gamma glutamyl transpeptidae; AST: Aspartate aminotransaminase; Hb: Haemoglobin; Plt: Platelet count.

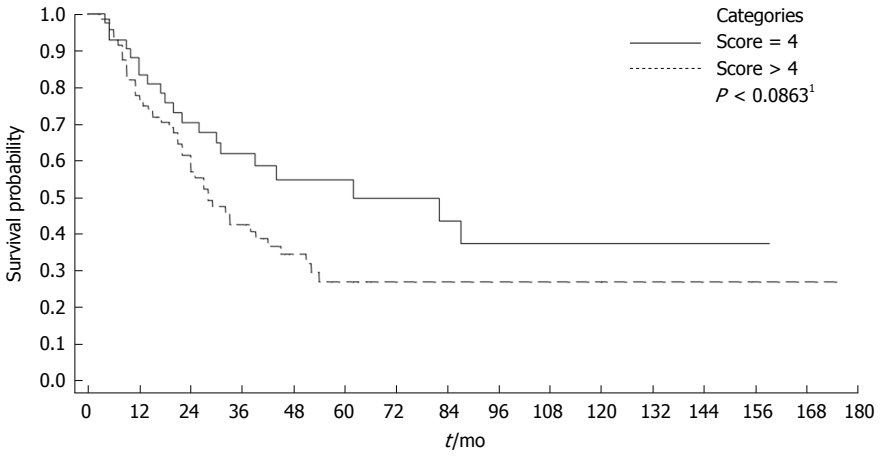

	Survival probability (%)		
Categories	1 yr	2 yr	3 yr
Score = 4	83.3	70.4	61.8
Score > 4	76.3	56.9	42.4

Figure 1 Kaplan-Meier survival plots between categories of aggressiveness Index, in total cohort. Aggressiveness index as sum of scores, MTD (in tertiles): MTD < 4.5; 4.5 ⩽ MTD ⩽ 9.6; MTD > 9.6; scores 1, 2, 3 respectively; AFP (cut-off): AFP < 100; 100 ⩽ AFP ⩽ 1000; AFP > 1000 ng/mL; scores 1, 2, 3 respectively; PVT (no/yes): PVT (no); PVT (yes); scores 1, 3 respectively; Tumor nodules (number): Nodules ⩽ 3; nodules > 3; scores 1, 3 respectively. [1]Wilcoxon (breslow) test. MTD: Maximum tumor diameter; AFP: Alpha-fetoprotein; PVT: Portal vein thrombosis.

(95%CI: 0.101-9.299), followed by ALKP with an OR of 1.01 (95%CI: 1.000-1.025) (Table 1). These two parameters were then assessed in a multivariate multiple logistic regression to a final model which showed the following correlation: Albumin with an OR of 2.56 (95%CI: 1.120-5.863) followed by ALKP with an OR of 1.01 (95%CI: 1.003-1.026) (Table 1).

A univariate Cox proportional hazard model for mortality with AgI score and liver function parameters was performed. We found that only GGTP levels and the AgI were independently associated with survival of the HCC patients following TACE (Table 3). We used our cohort to validate the previously described AgI. An AgI with the score > 4 had HR for mortality of 2.18 (95%CI: 1.108-4.310, $P < 0.024$). GGTP's single unit change had an HR for mortality of 1.003 (95%CI: 1.001-1.006, $P < 0.016$). We considered them in the final multivariate model with the total cohort. An AgI with the score > 4 had an HR for mortality of 2.26 (95%CI: 1.184-4.327, $P < 0.016$). GGTP had an HR of 1.003 (95%CI: 1.001-1.004, $P < 0.001$) (Table 3).

Comparison of GGTP level groups

We then compared the HCC patients (Table 4) dichotomized by GGTP levels of 100IU/L (< 100/> 100) based on a previous finding that there is a marked

Table 4 Comparisons in hepatocellular carcinoma patients among dichotomization of gamma glutamyl transpeptidase (⩽ 100/> 100 IU/L), in the total cohort

Parameter[1]	GGTP (IU/L)		P^2 value
	⩽ 100 (n = 81) (50.31%)	> 100 (n = 80) (49.69%)	
Total bilirubin (mg/dL)	1.25 ± 0.75	1.19 ± 0.87	0.17
ALKP (IU/mL)	104.55 ± 42.06	160.92 ± 89.79	< 0.0001
GGTP (IU/mL)	55.44 ± 24.46	250.29 ± 165.35	< 0.0001
AST (IU/L)	93.61 ± 79.10	115.45 ± 137.27	0.06
Albumin (g/dL)	3.70 ± 2.68	3.56 ± 0.57	0.13
Platelets (× 10^9/L)	100.14 ± 61.45	129.60 ± 100.06	0.02
Aggressiveness index (%)			
Score > 4	33 (56.90)	42 (75.00)	0.04[3]
Survival at time (%)			
1 yr	68 (87.18)	54 (70.13)	0.01[3]
2 yr	52 (66.67)	37 (48.05)	0.02[3]
3 yr	39 (50.00)	25 (32.47)	0.03[3]

[1]All values: mean ± SD; [2]Wilcoxon rank-sum (Mann-Whitney) test; [3]Test Z for proportions. Aggressiveness index (sum of scores): MTD (in tertiles): MTD < 4.5; 4.5 ⩽ MTD ⩽ 9.6; MTD > 9.6; scores 1, 2, 3 respectively; AFP (cut-off): AFP < 100; 100 ⩽ AFP ⩽ 1000; AFP > 1000; scores 1, 2, 3 respectively; PVT (no/yes): PVT(no); PVT(yes); scores 1, 3 respectively; nodules (number): Nodules ⩽ 3; nodules > 3; scores 1, 3 respectively. AFP: Alpha-fetoprotein; MTD: Maximum tumor diameter; PVT: Portal vein thrombosis; ALKP: Alkaline phosphatase; GGTP: Gamma glutamyl transpeptidae; AST: Aspartate aminotransaminase; Hb: Haemoglobin; Plt: Platelet count.

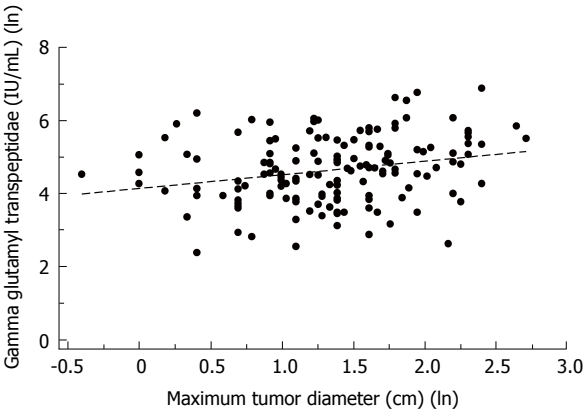

Figure 2 Scatterplots between maximum tumor diameter (cm) and gamma glutamyl transpeptidae (IU/mL) (Spearman's rho = 0.2604, P = 0.0012), together with linear regression line of gamma glutamyl transpeptidae on maximum tumor diameter, in total cohort. All transformed into natural logarithm. ln, natural logarithm; Fitted values (-------).

difference in survival of patients with HCC between these values[19]. The GGT*P* < 100 group had 81 patients and the GGTP > 100 had 80 patients. The GGTP > 100 group had higher liver enzyme levels: ALKP = 160.92 + 89.79 *vs* 104.55 + 42.06; respectively (P < 0.0001) (Table 4). The 1 and 3 year survival was 17% higher in the GGTP (< or =) 100 group (87.18% *vs* 70.1% and 50% *vs* 32.47%, P = 0.01 and P = 0.03, respectively) (Table 4). We also assessed correlation between laboratory parameters and MTD. Gamma-glutamyl-transpeptidase levels (IU/mL) and the Maximum Tumor Diameter (cm) showed a low positive correlation with a Spearman's coefficient of r = 0.2604 and a P-value of 0.0012 with a linear regression line (Figure 2).

DISCUSSION

Tumor factors and liver function parameters were shown to have prognostic value in predicting survival of HCC patients. Our goal was to validate the usefulness of the recently-described HCC AgI, in a novel HCC cohort and to assess its usefulness in patients that underwent TACE while trying to identify additional laboratory serum parameters to improve its accuracy. We excluded patients with fibrolamellar HCC, mixed cholangio-hepatocellular carcinoma and sarcomatous type HCC, because of their rarity and their variant clinical course which may be different then "regular" HCC.

The AgI was recently reported and includes the following tumor parameters: maximum tumor diameter, number of tumor nodules and presence of PVT and plasma AFP levels.

Our cohort included patients with multiple underlying liver diseases and can be widely generalized, in contrast to the original cohort, where the underlying etiology of the liver disease was not specified.

HCC tumor parameters were previously shown to have prognostic value and were used in various staging systems[20]. In a 2011 paper by Hu *et al*[7], analyzing data from 362 patients undergoing TACE, all 4 of the AgI parameters were found to be independently significant predictors of patient's survival. Maximal tumor size (HR = 1.66, P < *0*.002), Portal vein invasion (HR = 2.39, P < *0*.001), Tumor nodule number (HR = 1.92, P < *0*.001), and AFP value (HR = 1.54, P < *0*. 003). Portal vein invasion was associated with a marked decrease in patients' survival, while the other parameters had only a modest effect on survival. However, combining them in the AgI increased their predictive power considerably. Furthermore, in their original paper the authors used single categories for each parameter, whereas the AgI divides each parameter into tertiles refining the scoring. We similarly show that combining these parameters in our specific population of patients that underwent TACE increases

their predictive power.

Our patients had smaller tumors and longer survival time for both of the < 4 and > 4 score groups compared to previously reported groups[21-23]. The fact that most of the patients had an underlying liver disease and 40% were under a strict surveillance program made it possible to detect HCC at an early stage.

We found a significant increase in HR for death in patients with an AgI > 4, thus expanding the original observation to our patient population (Table 3).

Our second goal was to examine possible correlation between the AgI and other laboratory parameters of liver function (Table 1). We focused on 8 parameters that were previously shown to be associated with prognosis in HCC patients. Included were albumin and bilirubin which are part of the CPT score. Also included were markers of liver damage such as AST, ALK and GGTP[15]. Finally we looked at the hematologic parameters; platelets that were previously shown to be associated with tumor aggressiveness[16] and WBC and Lymphocytes, that were considered because Neutrophils to Lymphocytes ratio predicted overall survival in HBV-related HCC patients after TACE[13].

Other parameters that may better predict liver function or tumor aggressiveness such as Indocyanine Green (ICG) clearance[24] and Des-Gamma carboxyprothrombin (DCP) were excluded because they were not routinely utilized in our center and are not in wide clinical use[25,26].

In contrast to previous reports[10,11,27], and although albumin was correlated to AgI, we were unable to show that albumin is an independent predictor of survival in our cohort. We attribute this discrepancy to the fact that in a large portion of our cohort the tumor was discovered early when tumor parameters were favorable and liver function relatively preserved. Therefore, most of the patients (n = 110) had Albumin levels within the normal range.

Similar to previous reports[15,16] we also found elevated GGTP, to be an independent risk factor for mortality (HR = 1.003; 95%CI: 1.001-1.004; P < 0.001). In earlier publications, elevated levels of GGTP were found to be a poor prognostic factor after liver transplantation and before liver resection as they were associated with advanced tumor stage and aggressive tumor behaviors[28,29]. This factor can now be used as a predictor of prognosis in the population of TACE treated HCC patients.

We divided GGTP into two groups with a cutoff of 100IU/L (< 100/> 100). The group with the higher GGTP (> 100) had higher AgI score (52.5% compared with 40.7%) and lower survival at 1 and 3 years. (87.18% *vs* 70.1% and 50% *vs* 32.47%, P = 0.01, 0.03 respectively). In a recently published paper by Barman *et al*[30], focusing on patients undergoing TACE, it was noted that survival was higher among those patients with well-preserved liver synthetic function.

We were unable to show that other laboratory parameters associated with CPT (Bilirubin and INR-data not shown) were independently associated with prognosis. Other studies assessing these factors, show conflicting results. A previously published study found that elevated bilirubin (HR = 4.2; 95%CI: 2.2-7.9; P < 0.001) was a significant independent risk factor for mortality in 84 consecutive patients with HCC treated with TACE as first-line or second-line treatment that were enrolled between 2004 to 2009[31]. In contrast, a study of 109 patients who underwent TACE from 2006 to 2012 in a veterans hospital in the United States, did not show any single component of Child-Pugh score to be a predictor of survival[30]. The authors explain their results stating that their population was mostly males with HCV and dissimilar to previously published studies in which the population was mostly Asian with HBV and preserved liver function. These discrepancies suggest that different factors may predict tumor aggressiveness in different patient populations.

We concluded that the AgI is a validated tool to predict overall survival in unresectable HCC patients undergoing the TACE procedure. We further suggest that it can be combined with elevated GGTP levels, elevated levels of ALKP and decreased levels of albumin to improve its prognostic yield in this patient population.

ARTICLE HIGHLIGHTS

Research background

Hepatocellular carcinoma (HCC) is a common and deadly cancer. Transterial chemoembolization (TACE) is the treatment of choice for non-operable, intermediate stage HCC.

Research motivation

There is a need to identify prognostic indices in HCC patients undergoing TACE. An "HCC aggressiveness index (AgI)" incorporates 4 tumor-related parameters: maximum tumor diameter (MTD), number of tumor nodules, portal vein thrombosis (PVT) and serum alpha fetoprotein (AFP) levels. This score predicts survival in HCC patients.

Research objective

To identify novel biomarkers to predict survival following TACE and combine them with the AgI.

Research methods

We retrospectively analyzed data from 167 patients with HCC that underwent TACE at Tel-Aviv Medical center from 2000 to 2015. Baseline tumor parameters including: maximum tumor diameter, number of tumor nodules and presence of PVT; labs including: blood count; routine liver function tests and plasma AFP levels; demographics and overall survival information were all collected. The Cox proportional hazards model was applied to identify the correlation of AgI with overall survival and analyze laboratory factors' associated with the AgI.

Research results

The AgI was correlated with survival. The 3-year survival probability for AgI of > 4 *vs* < 4 was 42.4% *vs* 61.8%; P < 0.0863, from the time of diagnosis by Kaplan-Meier plot. Moreover, According to the univariate Cox proportional hazard model for mortality with AgI score of > 4, there was a HR of 2.18 (95%CI: 1.108-4.310, P < 0.024). We found that only GGTP levels and the AgI were independently associated with survival of the HCC patients following TACE.

Research conclusions

AgI was validated as a useful predictor of survival in HCC patients undergoing TACE. Combining the AgI with liver function parameters may improve its prognostic yield in this patient population.

Research prospective

This novel score can be used to assess prognosis in HCC undergoing TACE.

REFERENCES

1 **Mlynarsky L**, Menachem Y, Shibolet O. Treatment of hepatocellular carcinoma: Steps forward but still a long way to go. *World J Hepatol* 2015; **7**: 566-574 [PMID: 25848480 DOI: 10.4254/wjh.v7.i3.566]

2 **Jemal A**, Bray F, Center MM, Ferlay J, Ward E, Forman D. Global cancer statistics. *CA Cancer J Clin* 2011; **61**: 69-90 [PMID: 21296855 DOI: 10.3322/caac.20107]

3 **Bolondi L**. Screening for hepatocellular carcinoma in cirrhosis. *J Hepatol* 2003; **39**: 1076-1084 [PMID: 14642630 DOI: 10.1016/S0168-8278(03)00349-0]

4 **Crissien AM**, Frenette C. Current management of hepatocellular carcinoma. *Gastroenterol Hepatol* (N Y) 2014; **10**: 153-161 [PMID: 24829542]

5 **Llovet JM**, Brú C, Bruix J. Prognosis of hepatocellular carcinoma: the BCLC staging classification. *Semin Liver Dis* 1999; **19**: 329-338 [PMID: 10518312 DOI: 10.1055/s-2007-1007122]

6 **Forner A**, Gilabert M, Bruix J, Raoul JL. Treatment of intermediate-stage hepatocellular carcinoma. *Nat Rev Clin Oncol* 2014; **11**: 525-535 [PMID: 25091611 DOI: 10.1038/nrclinonc.2014.122]

7 **Hu HT**, Kim JH, Lee LS, Kim KA, Ko GY, Yoon HK, Sung KB, Gwon DI, Shin JH, Song HY. Chemoembolization for hepatocellular carcinoma: multivariate analysis of predicting factors for tumor response and survival in a 362-patient cohort. *J Vasc Interv Radiol* 2011; **22**: 917-923 [PMID: 21571545 DOI: 10.1016/j.jvir.2011.03.005]

8 **Kadalayil L**, Benini R, Pallan L, O'Beirne J, Marelli L, Yu D, Hackshaw A, Fox R, Johnson P, Burroughs AK, Palmer DH, Meyer T. A simple prognostic scoring system for patients receiving transarterial embolisation for hepatocellular cancer. *Ann Oncol* 2013; **24**: 2565-2570 [PMID: 23857958 DOI: 10.1093/annonc/mdt247]

9 **Kinoshita A**, Onoda H, Imai N, Iwaku A, Oishi M, Fushiya N, Koike K, Nishino H, Tajiri H. Comparison of the prognostic value of inflammation-based prognostic scores in patients with hepatocellular carcinoma. *Br J Cancer* 2012; **107**: 988-993 [PMID: 22878374 DOI: 10.1038/bjc.2012.354]

10 **McMillan DC**. An inflammation-based prognostic score and its role in the nutrition-based management of patients with cancer. *Proc Nutr Soc* 2008; **67**: 257-262 [PMID: 18452641 DOI: 10.1017/S0029665108007131]

11 **Pinato DJ**, Stebbing J, Ishizuka M, Khan SA, Wasan HS, North BV, Kubota K, Sharma R. A novel and validated prognostic index in hepatocellular carcinoma: the inflammation based index (IBI). *J Hepatol* 2012; **57**: 1013-1020 [PMID: 22732513 DOI: 10.1016/j.jhep.2012.06.022]

12 **Ishizuka M**, Kubota K, Kita J, Shimoda M, Kato M, Sawada T. Usefulness of a modified inflammation-based prognostic system for predicting postoperative mortality of patients undergoing surgery for primary hepatocellular carcinoma. *J Surg Oncol* 2011; **103**: 801-806 [PMID: 21240991 DOI: 10.1002/jso.21857]

13 **Zhou DS**, Xu L, Luo YL, He FY, Huang JT, Zhang YJ, Chen MS. Inflammation scores predict survival for hepatitis B virus-related hepatocellular carcinoma patients after transarterial chemoembolization. *World J Gastroenterol* 2015; **21**: 5582-5590 [PMID: 25987783 DOI: 10.3748/wjg.v21.i18.5582]

14 **Li X**, Chen ZH, Xing YF, Wang TT, Wu DH, Wen JY, Chen J, Lin Q, Dong M, Wei L, Ruan DY, Lin ZX, Wu XY, Ma XK. Platelet-to-lymphocyte ratio acts as a prognostic factor for patients with advanced hepatocellular carcinoma. *Tumour Biol* 2015; **36**: 2263-2269 [PMID: 25409616 DOI: 10.1007/s13277-014-2833-9]

15 **Carr BI**, Guerra V. A Hepatocellular Carcinoma Aggressiveness Index and Its Relationship to Liver Enzyme Levels. *Oncology* 2016; **90**: 215-220 [PMID: 26974336 DOI: 10.1159/000444394]

16 **Carr BI**, Guerra V, Giannini EG, Farinati F, Ciccarese F, Rapaccini GL, Di Marco M, Benvegnù L, Zoli M, Borzio F, Caturelli E, Masotto A, Trevisani F. A Liver Index and its Relationship to Indices of HCC Aggressiveness. *J Integr Oncol* 2016; **5**: pii: 178 [PMID: 28580457 DOI: 10.4172/2329-6771.1000178]

17 **Carr BI**, Guerra V, Giannini EG, Farinati F, Ciccarese F, Ludovico Rapaccini G, Di Marco M, Benvegnù L, Zoli M, Borzio F, Caturelli E, Chiaramonte M, Trevisani F; Italian Liver Cancer (ITA.LI.CA) Group. Association of abnormal plasma bilirubin with aggressive hepatocellular carcinoma phenotype. *Semin Oncol* 2014; **41**: 252-258 [PMID: 24787296 DOI: 10.1053/j.seminoncol.2014.03.006]

18 **Doyon D**, Mouzon A, Jourde AM, Regensberg C, Frileux C. [Hepatic, arterial embolization in patients with malignant liver tumours (author's transl)]. *Ann Radiol* (Paris) 1974; **17**: 593-603 [PMID: 4142843]

19 **Carr BI**, Guerra V, Pancoska P. Thrombocytopenia in relation to tumor size in patients with hepatocellular carcinoma. *Oncology* 2012; **83**: 339-345 [PMID: 23006937 DOI: 10.1159/000342431]

20 **Tandon P**, Garcia-Tsao G. Prognostic indicators in hepatocellular carcinoma: a systematic review of 72 studies. *Liver Int* 2009; **29**: 502-510 [PMID: 19141028 DOI: 10.1111/j.1478-3231.2008.01957.x]

21 **Carr BI**, Kondragunta V, Buch SC, Branch RA. Therapeutic equivalence in survival for hepatic arterial chemoembolization and yttrium 90 microsphere treatments in unresectable hepatocellular carcinoma: a two-cohort study. *Cancer* 2010; **116**: 1305-1314 [PMID: 20066715 DOI: 10.1002/cncr.24884]

22 **Ebied OM**, Federle MP, Carr BI, Pealer KM, Li W, Amesur N, Zajko A. Evaluation of responses to chemoembolization in patients with unresectable hepatocellular carcinoma. *Cancer* 2003; **97**: 1042-1050 [PMID: 12569604 DOI: 10.1002/cncr.11111]

23 **Carr BI**, Irish W, Federle MP. Chemoembolization for unresectable hepatocellular carcinoma in patients with or without portal vein thrombosis. *Hepatogastroenterology* 2010; **57**: 1375-1381 [PMID: 21443089]

24 **Sheng QS**, Lang R, He Q, Yang YJ, Zhao DF, Chen DZ. Indocyanine green clearance test and model for end-stage liver disease score of patients with liver cirrhosis. *Hepatobiliary Pancreat Dis Int* 2009; **8**: 46-49 [PMID: 19208514]

25 **Zakhary NI**, Khodeer SM, Shafik HE, Abdel Malak CA. Impact of PIVKA-II in diagnosis of hepatocellular carcinoma. *J Adv Res* 2013; **4**: 539-546 [PMID: 25685463 DOI: 10.1016/j.jare.2012.10.004]

26 **Okuda H**, Nakanishi T, Takatsu K, Saito A, Hayashi N, Takasaki K, Takenami K, Yamamoto M, Nakano M. Serum levels of des-gamma-carboxy prothrombin measured using the revised enzyme immunoassay kit with increased sensitivity in relation to clinicopathologic features of solitary hepatocellular carcinoma. *Cancer* 2000; **88**: 544-549 [PMID: 10649245]

27 **Brown DB**, Fundakowski CE, Lisker-Melman M, Crippin JS, Pilgram TK, Chapman W, Darcy MD. Comparison of MELD and Child-Pugh scores to predict survival after chemoembolization for hepatocellular carcinoma. *J Vasc Interv Radiol* 2004; **15**: 1209-1218 [PMID: 15525739 DOI: 10.1097/01.RVI.0000128123.04554.C1]

28 **Wu SJ**, Lin YX, Ye H, Xiong XZ, Li FY, Cheng NS. Prognostic value of alkaline phosphatase, gamma-glutamyl transpeptidase and lactate dehydrogenase in hepatocellular carcinoma patients treated with liver resection. *Int J Surg* 2016; **36**: 143-151 [PMID: 27793641 DOI: 10.1016/j.ijsu.2016.10.033]

29 **Fu SJ**, Zhao Q, Ji F, Chen MG, Wu LW, Ren QQ, Guo ZY, He XS. Elevated Preoperative Serum Gamma-glutamyltranspeptidase Predicts Poor Prognosis for Hepatocellular Carcinoma after Liver Transplantation. *Sci Rep* 2016; **6**: 28835 [PMID: 27381639 DOI: 10.1038/srep28835]

30 **Barman PM**, Sharma P, Krishnamurthy V, Willatt J, McCurdy H, Moseley RH, Su GL. Predictors of mortality in patients

with hepatocellular carcinoma undergoing transarterial chemoembolization. *Dig Dis Sci* 2014; **59**: 2821-2825 [PMID: 24973040 DOI: 10.1007/s10620-014-3247-7]

31 **Cabibbo G**, Genco C, Di Marco V, Barbara M, Enea M, Parisi P, Brancatelli G, Romano P, Craxì A, Cammà C. Predicting survival in patients with hepatocellular carcinoma treated by transarterial chemoembolisation. *Aliment Pharmacol Ther* 2011; **34**: 196-204 [PMID: 21564144 DOI: 10.1111/j.1365-2036.2011.04694.x]

P- Reviewer: Hashimoto N, Kang KJ **S- Editor**: Ma YJ
L- Editor: A **E- Editor**: Huang Y

World Journal of Gastroenterology

Submit a Manuscript: http://www.f6publishing.com

World J Gastroenterol 2018 April 21; 24(15): 1650-1657

DOI: 10.3748/wjg.v24.i15.1650

ISSN 1007-9327 (print) ISSN 2219-2840 (online)

ORIGINAL ARTICLE

Observational Study

Development and predictive validity of the cirrhosis-associated ascites symptom scale: A cohort study of 103 patients

Agnete Nordheim Riedel, Nina Kimer, Anne-Sofie Houlberg Jensen, Emilie Kristine Dahl, Mads Israelsen, Luise Aamann, Lise Lotte Gluud

Agnete Nordheim Riedel, Nina Kimer, Anne-Sofie Houlberg Jensen, Emilie Kristine Dahl, Lise Lotte Gluud, Gastro Unit, Medical Davison, Copenhagen University Hospital Hvidovre, Hvidovre 2650, Denmark

Nina Kimer, Abdominal Center K, Medical Section, Copenhagen University Hospital Bispebjerg, København 2400, Denmark

Anne-Sofie Houlberg Jensen, Department of Gastroenterology and Hepatology, University Hospital Zealand Slagelse, Slagelse 4200, Denmark

Luise Aamann, Department of Hepatology and Gastroenterology, Aarhus University Hospital, Aarhus C 8000, Denmark

Mads Israelsen, Department of Gastroenterology and Hepatology, Odense University Hospital, Odense C 5000, Denmark

ORCID number: Agnete Nordheim Riedel (0000-0002-3532-1272); Nina Kimer (0000-0002-4807-1575); Anne-Sofie Houlberg Jensen (0000-0002-5982-8684); Emilie Kristine Dahl (0000-0002-1383-5619); Mads Israelsen (0000-0001-9443-5846); Luise Aamann (0000-0003-0046-887X);Lise Lotte Gluud (0000-0002-9462-4468).

Author contributions: Gluud LL designed the study and drafted the protocol; Gluud LL, Jensen AS and Dahl EK collected questionnaires and conducted interviews for the pilot-testing of the cirrhosis-associated ascites symptom (CAS); Riedel AN, Jensen AS, Dahl EK, Gluud LL, Aamann L, Israelsen M and Kimer N collected questionnaires for the validation of CAS; Riedel AN and Gluud LL performed the analyses; Kimer N, Riedel AN and Gluud LL drafted the first version of the manuscript. All authors critically revised and approved of the final version of the manuscript.

Institutional review board statement: The study was approved by the Danish Data protection Agency, journal no: 04054, ID: AHH-2015-075.

Informed consent statement: All participants signed an informed consent.

Conflict-of-interest statement: The authors declare no conflicts of interest.

Data sharing statement: No additional data are available.

Manuscript source: Unsolicited manuscript

Correspondence to: Lise Lotte Gluud, DSc, MD, Associate Professor, Chief Doctor, Research Fellow, Gastro Unit, Medical Division, Copenhagen University Hospital Hvidovre, Kettegaard Alle 30, Hvidovre 2650, Denmark. lise.lotte.gluud.01@regionh.dk
Telephone: +45-31-353212

Received: November 28, 2017
Peer-review started: November 29, 2017
First decision: December 13, 2017
Revised: December 20, 2017
Accepted: January 18, 2018
Article in press: January 18, 2018
Published online: April 21, 2018

Abstract

AIM

To develop a scale of domains associated with the health-related quality-of-life (HRQOL) in patients with cirrhosis-related ascites.

METHODS

We initially undertook literature searches and a qualitative study in order to design a cirrhosis-associated ascites symptom (CAS) scale describing symptoms with a potential detrimental impact on health related quality of life (HRQL) (the higher the score, the worse the symptoms). Discriminatory validity was assessed in a validation cohort including cirrhotic patients with (1) tense/severe; (2) moderate/mild; or (3) no ascites (controls). Patients also completed chronic liver disease questionnaire (CLDQ) and the EuroQoL 5-Dimensions 5-Level (EQ-5D-5L) questionnaire evaluating HRQL. The relation between scale scores was analysed using Spearman correlations.

RESULTS

The final CAS scale included 14 items. The equivalent reliability was high (Chronbach's alpha 0.88). The validation cohort included 103 patients (72% men, mean age 62.4 years). The mean scores for each question in the CAS scale were higher for patients with severe/tense ascites than for mild/moderate ascites and controls. Compared with controls (mean = 9.9 points), the total CAS scale score was higher for severe/tense ascites (mean = 23.8 points) as well as moderate/mild ascites (mean = 18.6 points) ($P < 0.001$ both groups). We found a strong correlation between the total CAS and CLDQ score (rho = 0.82, $P < 0.001$) and a moderate correlation between the CAS and the EQ-5D-5L score (0.67, $P < 0.001$).

CONCLUSION

The CAS is a valid tool, which reflects HRQOL in patients with ascites.

Key words: Health-related quality-of-life; Cirrhosis; Symptom burden; Symptom assessment

Core tip: This paper presents a newly generated cirrhosis-associated ascites symptom scale consisting of 14 items. The questionnaire addresses relevant questions of symptom burden of cirrhosis-associated ascites, takes only five minutes to complete and correlates strongly with chronic liver disease questionnaire score in patients with cirrhosis and ascites.

Riedel AN, Kimer N, Jensen AS, Dahl EK, Israelsen M, Aamann L, Gluud LL. Development and predictive validity of the cirrhosis-associated ascites symptom scale: A cohort study of 103 patients. *World J Gastroenterol* 2018; 24(15): 1650-1657 Available from: URL: http://www.wjgnet.com/1007-9327/full/v24/i15/1650.htm DOI: http://dx.doi.org/10.3748/wjg.v24.i15.1650

INTRODUCTION

Ascites is a serious complication to cirrhosis[1,2]. Without liver transplantation, only about 55% of patients with cirrhosis and ascites are alive, five years after the initial diagnosis. In addition, the severity of symptoms associated with ascites may have a detrimental impact on health-related quality of life (HRQL). Five previous studies have evaluated the HRQL in patients with cirrhosis using generic questionnaires including the Medical Outcome Study Short Form 36 (SF-36), the Nottingham Health Profile and the Sickness Impact Profile[3-7]. All studies found that cirrhosis is associated with a detrimental effect on HRQL. None of the studies were designed to evaluate the association between ascites severity and the quality of life. However, one study found that disease progression, including development of ascites, is associated with an impaired HRQL[7]. Disease-specific questionnaires developed for the assessment of HRQL in patients with liver disease and cirrhosis have reached similar conclusions[8,9]. The questionnaires include aspects that are of particular relevance to patients with cirrhosis, such as concerns about complications and liver transplantation. The 29 item chronic liver disease questionnaire (CLDQ) was used to evaluate HRQL in 204 patients representing all stages of various liver diseases[10]. The scale correlates with the severity of the underlying liver disease and is also associated with active medical and psychiatric comorbidity. Liver failure, development of minimal hepatic encephalopathy, malnutrition, abdominal pain, fatigue, and anxiety may also affect HRQL[11,12].

None of previous studies specifically evaluated the association between the severity of ascites related symptoms and HRQL. However, it is likely that the severity of symptoms is important.

In clinical trials of medical interventions, HRQL as well as symptom management are important parameters in the assessment of intervention benefits and harms[4,5,13,14]. A study including 212 outpatients with cirrhosis found that the management of cirrhosis-related complications is associated with improved HRQOL assessed using the Medical Outcomes Study Form, SF-36 and CLDQ questionnaires. The study found that ascites as well as a decrease in haemoglobin and previous hepatic encephalopathy predicted the HRQOL[15].

We therefore developed and evaluated the predictive ability of a scale specifically made to assess symptoms related to cirhosis-associated ascites. We subsequently undertook a multicenter cohort study to evaluate the association between our scale and a disease specific scale (CLDQ) as well as a generic HRQL questionnaire (EQ-5D-5L).

MATERIALS AND METHODS

The present study was conducted as a multi-center study, with participation of three university hospitals in Denmark: Copenhagen University Hospital Hvidovre, Odense University Hospital and Aarhus University Hospital. The study was approved by the Danish Data protection Agency, journal no: 04054, ID: AHH-2015-075.

The development of the cirrhosis-associated ascites symptom (CAS) scale included a literature review and a

Table 1 Cirrhosis-associated ascites symptom scale in Danish

Please answer the following questions with a cross or tick with regards to how you have felt in the past four weeks.				
	Nej *No*	**Sjældent** *Rarely*	**Indimellem** *Sometimes*	**Ofte** *Often*
1 Har du ondt i maven? *Do you have stomach ache?*				
2 Har du ømhed i maven? *Does your stomach feel sore?*				
3 Har du kvalme? *Do you feel nauseous?*				
4 Har du madlede? *Do you feel an aversion for food?*				
5 Har du nedsat appetit? *Do you experience a loss of appetite?*				
6 Har du ændret afføring? *Have you experienced a change in your stool?*				
7 Har du følt dig utilpas? *Have you felt uncomfortable?*				
8 Er du træt? *Are you tired?*				
9 Har du åndenød? *Do you experience a shortness of breath?*				
10 Har du svært ved at trække vejret helt igennem? *Do you feel troubled when breathing deeply?*				
11 Har du svært ved at få tøj eller sko på? *Are you disabled when dressing or putting on shoes?*				
12 Har du svært ved at komme rundt derhjemme? *Do you experience difficulties in mobility at home?*				
13 Har du svært ved at gå? *Do you experience trouble walking?*				
14 Har du ondt i benene? *Do your legs hurt?*				

qualitative study to evaluate face and content validity as well as discriminatory ability.

We initially searched for previously validated scales in MEDLINE and EMBASE ('ascites' AND ('quality of life [Mesh]' OR 'life quality' OR 'health-related quality of life' OR 'health related quality of life' OR 'symptoms') AND ('cirrhosis' OR 'end-stage liver disease'). The searches were combined with manual searches of reference lists in potentially relevant articles and conference proceedings. None of our searches identified questionnaires evaluating symptoms associated with ascites.

We then proceeded with a qualitative study. Initially, the study group and ten independent experts identified and listed what they believed were the most important symptoms with an expected negative impact on HRQL (six hepatologists and four nurses with clinical experience in the management of patients with ascites from Gastro Unit, medical division, Copenhagen University Hospital Hvidovre, were interviewed). In our selection of symptoms (domains), we decided that they should occur frequently or be severe enough to have substantial impact on daily function in order to be considered for our scale.

After the selection of domains, we first conducted open interviews followed by structured interviews of ten patients with cirrhosis and moderate (n = 4) or severe ascites (n = 6). The interviews took place in a quiet room in the hospital ward. The selected domains were initially presented and patients were asked to rate them (Supplementary Table 1) according to the patient's perceived 'importance', on the extent to which the symptom had bothered them. Each patient was then asked to complete the preliminary questionnaire themselves and to answer a debriefing form with the questions: (1) How long did it take to complete the questionnaire? (2) Did you need assistance from others to fill out the questionnaire? (3) Did you find any items confusing or difficult to respond to (and if so, list the items)? (4) Did you find any items upsetting? (5) Were any important items missing? and (6) Do you have any additional comments?

We revised the questionnaire instrument based on the answers. One question, which patients found upsetting and two questions, which patients found to be irrelevant or unimportant were removed. Revisions were decided by consensus among investigators.

Validation of the CAS scale (known group comparison)

After the development of the questionnaire, we prospectively enrolled a validation cohort (known group comparison) consisting of patients with cirrhosis of any aetiology and (1) severe/tense ascites; (2) mild/moderate ascites; and (3) no ascites as determined through a combination of clinical assessments and abdominal ultrasound. All gave their informed consent to participate. Subjects were attending out-patient clinics or were admitted to hospital ward with ascites as their

Table 2 Patient characteristics according to degree of ascites *n* (%)

	Control group, no ascites (*n* = 31)	Mild/moderate (*n* = 27)	Tense (*n* = 45)	Total (*n* = 103)
Age: mean (SD)	61.5 (8.4)	62.3 (10.2)	63.1 (11.3)	62.4 (10.1)
Gender: Males	23 (74)	19 (70)	32 (71)	74 (72)
Etiology				
Alcohol	28 (90)	22 (81)	38 (86)	88 (86)
Viral	1 (3)	2 (7)	3 (7)	6 (6)
Alcohol and viral	1 (3)	1 (4)	3 (7)	5 (5)
Other	3 (10)	4 (15)	6 (13)	13 (13)
MELD score: mean (SD)	10.1 (3.3)	14.8 (6.2)	15.9 (6.3)	13.8 (6.0)
Child PUGH: mean (SD)	6.2 (1.8)	8.1 (1.3)	9.1 (1.4)	7.9 (1.9)
Class A	19 (61)	4 (15)	-	23 (22)
Class B	7 (23)	17 (63)	27 (60)	51 (50)
Class C	2 (6)	2 (7)	12 (27)	16 (16)
Laboratory values (SD)				
Hemoglobin (mmol/L)	8.4 (1.4)	7.1 (1.2)	6.4 (1.4)	7.2 (1.6)
White blood cells ($\times 10^9$/L)	6.9 (2.6)	7.2 (3.9)	7.3 (3.5)	7.1 (3.3)
Platelets (mmol/L)	145 (65)	158 (95)	160 (87)	155 (83)
Albumin (g/L)	35 (5.8)	29 (5.9)	30 (14)	31 (10)
Cogulation factor Ⅱ, Ⅶ, X (INR)	1.3 (0.3)	1.4 (0.3)	1.5 (0.5)	1.4 (0.4)
Creatinine (μmol/L)	74 (17)	87 (29)	94 (48)	86 (37)
Sodium (mmol/L)	138 (3.6)	134 (5.9)	132 (6.9)	135 (6.3)
Potassium (mmol/L)	4.1 (0.4)	4.3 (0.5)	4.2 (0.7)	4.2 (0.6)

There were no patients in Child Pugh Class A with tense ascites.

primary problem. Subjects with hepatic encephalopathy or other cognitive disability were excluded.

Subjects completed the following scales and questionnaires: (1) CAS scale; (2) Chronic Liver Disease Questionnaire[9]; and (3) EQ-5D-5L questionnaire[16,17].

Statistical analysis

Statistics were calculated using STATA IC v14 R2 and GraphPad Prism v6. We used the Crohnbach's alpha to assess equivalent reliability. We defined *discriminant validity* as the ability of the questionnaire to discriminate between the severity of ascites. Discriminant validity was evaluated using Dunnett's test to adjust for multiple comparisons. The severe and mild ascites groups (assuming that this group has fewer and less severe symptoms than patients with severe ascites) were compared with the control group and *P*-values < 0.05 were considered significant. We originally planned to evaluate convergent validity with previously validated scales assessing symptoms or HRQOL associated with ascites. Since no previous scales were identified, we used the CLDQ and the EQ-5D-5L. We compared scale scores using Spearman correlation and included the (1) CAS scale; (2) CLDQ; (3) CLDQ subscale parameters; and (4) EQ-5D-5L. The CLDQ subscale parameters are defined domains consisting of specific questions in the CLDQ questionnaire. These domains include fatigue, emotional function, worry, activity, abdominal symptoms and systemic symptoms[9].

Correlations higher than 0.70 were considered strong and values below 0.40 were interpreted as poor.

RESULTS

The final scale included 14 items (Table 1). Chronbach's alpha was 0.88 for the total score, which we considered as acceptable. The validation cohort included 103 patients.

Demographic data are stated in Table 2. Seventy-four were male (72%) and mean age was 62.4 years (range 38-85). The proportion of patients with Child Pugh A was 24%, Child Pugh B: 58% and Child Pugh C: 19%. Forty-four percent had severe/tense ascites and 27% had mild/moderate ascites. A control group of 31 patients (30%) had no ascites.

Discriminant validity

The mean scores for each question in the CAS scale suggested that symptoms were worse for patients with severe/tense ascites than for controls (Figure 1).

Symptoms also appeared worse for patients with mild/moderate ascites. Accordingly, the CAS scale score found that patients with severe/tense ascites or moderate/mild ascites had significantly worse scores compared with controls ($P < 0.001$ and $P < 0.001$; Figure 2).

As expected, patients with severe/tense ascites had the worst symptoms scores. Based on the CLDQ questionnaire, tense/severe ascites had a detrimental impact on HRQOL compared with controls ($P < 0.001$) as did moderate/mild ascites ($P = 0.002$). The EQ-5D-5L also found a lower HRQOL in patients with severe/tense ascites ($P = 0.002$) or moderate/mild ascites ($P = 0.038$).

Convergent validity

We found a strong correlation between the CAS and the CLDQ total score (Spearman's rho = 0.82, $P < 0.001$) as well as the CLDQ subscores; fatigue (0.78, $P < 0.001$), activity (0.81, $P < 0.001$) and systemic

Table 3 Correlation between cirrhosis-associated ascites symptom score, EuroQoL 5-Dimensions 5-Level scale questionnaire and chronic liver disease questionnaire total score and subscores

	Rho	*P* value
Total EQ-5D-5L	-0.67	< 0.001
Total CLDQ score	-0.82[1]	< 0.001
Fatigue	-0.78[1]	< 0.001
Emotional function	-0.55	< 0.001
Worry	-0.47	< 0.001
Abdominal symptoms	-0.66	< 0.001
Activity	-0.81[1]	< 0.001
Systemic symptoms	-0.77[1]	< 0.001

[1]Strong correlations. CLDQ: Chronic liver disease questionnaire; EQ-5D-5L: EuroQoL 5-Dimensions 5-Level scale questionnaire.

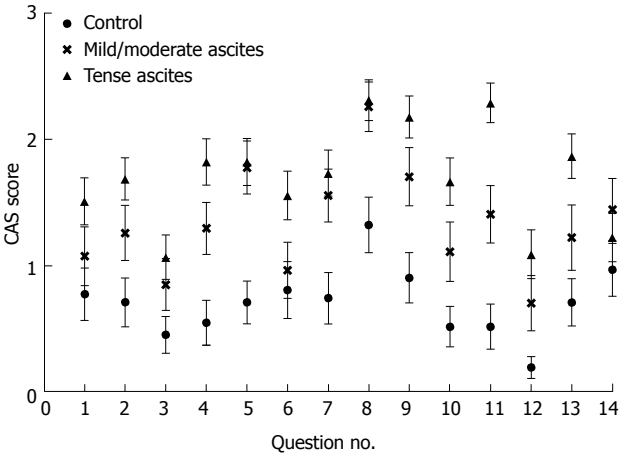

Figure 1 Mean cirrhosis-associated ascites symptom scores by question number and ascites severity.

symptoms (0.77, $P < 0.001$) (Table 3). The CAS correlation with the generic scale (EQ-5D-5L) was moderate (0.67, $P < 0.001$).

DISCUSSION

We found that the developed CAS scale is effective in discriminating between various severities of ascites. It takes five minutes to perform and is easily implemented in daily practice. Moreover the CAS scale correlates strongly with the well-developed liver disease-specific HRQL instrument, CLDQ[9]. This suggests that our symptom assessment scale reflects the perceived HRQL of patients with cirrhosis and ascites. The CLDQ subparameters: fatigue, activity and systemic symptoms were likewise strongly correlated with the CAS scale suggesting that these domains are influential symptoms or functional limitations for patient with ascites. Surprisingly, the subparameter abdominal symptoms was not associated with the CAS scale. This may be due to use of words or inaccuracy of the questions, and will need further investigations for clarification. The total CLDQ was better correlated with CAS than each subparameter. This may be due to the impact of low quality of life affecting all aspects of life, allowing a total low score higher statistical significance. The CAS versus EQ-5D-5L correlation was moderate. The EQ-5D-5L is a generic scale which aims at examining non-disease specific HRQL[16,18,19], and specific symptoms related to cirrhosis and ascites may be undetected by this questionnaire. On the contrary, the CLDQ is created for patients with chronic liver disease, and it includes questions concerning ascites related symptoms and gains a stronger correlation with the CAS score.

To our knowledge, no previous study has developed and validated a questionnaire specifically aimed at evaluating HRQL in patients with ascites. However, previous literature describes correlations between disease severity in chronic liver disease and HRQL[7,12,20]. One study found that ascites had significant effects on self-related disease progression in cirrhosis[7]. Another showed that ascites was not a predictor for HRQL[12] and two studies found that management of ascites may improve HRQL[15,21]. In a study evaluating the impact of the Medical Outcomes Study Short Form (SF-36) on HRQL in 523 patients with cirrhosis and ascites, a strong association between the physical component score (PCS) and leg edema, history of previous hepatic encephalopathy, severe ascites and low serum sodium levels were found[22]. The PCS includes questions on physical role, physical functioning, and body pain and general health. Also, a lower mental component score in the SF-36 was associated with low levels of serum sodium and treatment with lactulose. Hence, several factors influence HRQL when measured by SF36 and the impact of ascites was not clearly established by this study.

The CAS score comprises only 14 questions with high compliance to answering, takes only five minutes to complete and is readily implemented in daily clinic. The present study supports the results implying correlation between ascites severity and HRQL assuming that the CAS scale is valid and reliable. Progression in liver disease (*e.g.,* measured by Child Pugh score which includes presence of ascites) is associated with ascites severity grade. This argues that our results support previous literature finding a correlation between liver disease severity and HRQL.

Our study has some considerable weaknesses. The relatively small sample size is one of the main limitations. Moreover, the majority of patients had cirrhosis due to alcohol. Dependency of alcohol, concomitant diseases related to alcohol use or cirrhosis that may impact physical health was not assessed in our cohort. Malnutrition is a serious complication to cirrhosis with impact on HRQL[23]. Also, impact of socioeconomic factors may influence quality of life substantially[24,25]. Future studies may address the synergy between various factors affecting quality of life in cirrhosis and ascites. The CAS scale is a specific scale evaluating the impact of symptoms related to ascites. When assessing overall quality of life on chronic liver disease or the impact of

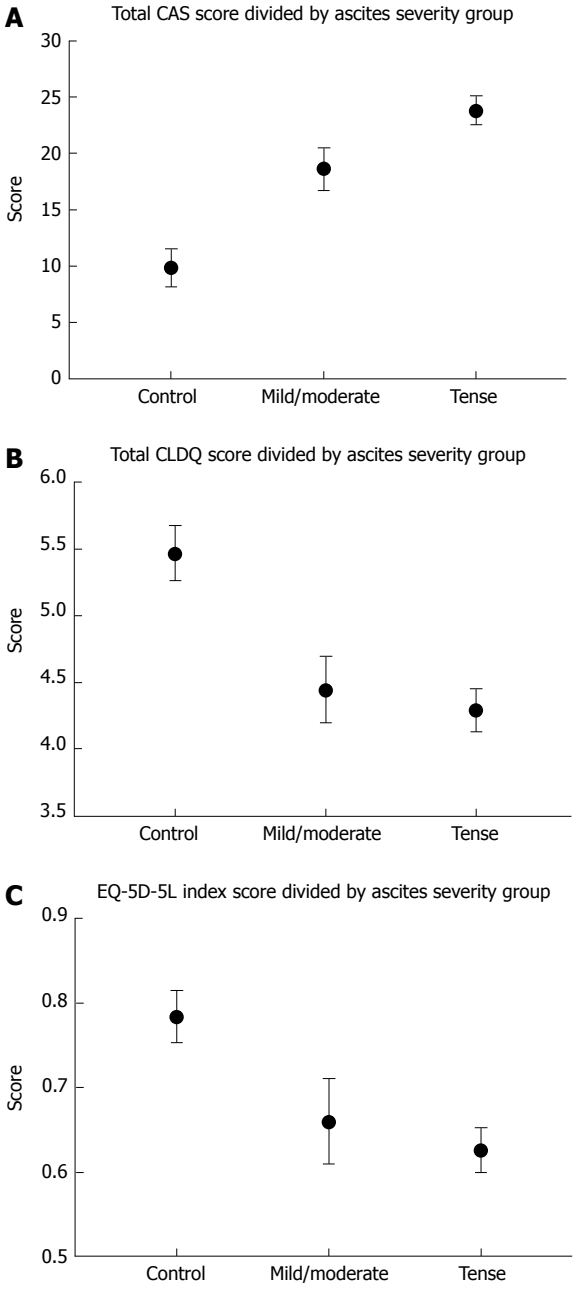

Figure 2 Median test scores with SEM divided by control, mild/moderate and tense ascites respectively. A: CAS scale. Control *vs* mild/moderate, $P < 0.001$; control *vs* tense, $P < 0.001$; B: CLDQ. Control *vs* mild/moderate $P = 0.002$; Control *vs* tense, $P < 0.001$; C: EQ-5D-5L. Control *vs* mild/moderate, $P = 0.038$; Control *vs* tense, $P = 0.002$. CAS: Cirrhosis-associated ascites symptom scale; CLDQ: Chronic liver disease questionnaire; EQ-5D-5L: EuroQoL 5-Dimensions 5-Level scale questionnaire.

multi-morbidity in cirrhosis; validated and recommended scores such as SF36 or CLDQ should be used, with the CAS scale as a supplement[9]. Consequently, CAS scale validation also requires further research on larger sample size and applied on standardized groups of subjects. An interesting study setup would be to test the CAS scale on patients with cirrhosis presented with ascites before and after treatment. Further, the CAS scale ought to be tested as a monitoring tool for efficacy in intervention trials, compared with CLDQ and SF-36 questionnaires.

In conclusion, the present construction and validation of the CAS scale seems promising for future research in the area of ascites symptom management and HRQL. Initially the scale requires testing in other study setups in order to clarify the quality and practicability of the questionnaire. In future perspectives an optimized and/or further validated version of the CAS scale can be used as a monitoring tool in interventional trials and to assess the effects of standardized treatment. Ultimately the CAS scale can contribute to gaining further knowledge on how to treat ascites effectively and consequently improve patients' quality of life.

ARTICLE HIGHLIGHTS

Research background

Cirrhosis is associated with a detrimental effect on health related quality of life (HRQL). Disease-specific questionnaires have been developed for the assessment of HRQL in patients with liver disease and cirrhosis. The questionnaires include aspects that are of particular relevance to patients with cirrhosis, such as concerns about complications and liver transplantation.

Research motivation

No previous studies have specifically evaluated the association between the severity of ascites related symptoms and HRQL. However, it is likely that the severity of symptoms is important.

Research objectives

We therefore developed and evaluated the predictive ability of a symptom assessment scale specifically made to assess symptoms related to cirhosis-associated ascites. We subsequently undertook a multicenter cohort study to evaluate the association between our scale and a disease specific scale (CLDQ) as well as a generic HRQL questionnaire (EQ-5D-5L).

Research methods

Development of the cirrhosis-associated ascites symptom (CAS) scale included a literature review, and a qualitative study to evaluate face and content validity as well as discriminatory ability. We initially searched for previously validated scales in MEDLINE and EMBASE. The searches were combined with manual searches of reference lists in potentially relevant articles and conference proceedings. We then proceeded with a qualitative study, where ten independent experts identified and listed what they believed were the most important symptoms with an expected negative impact on HRQL. Symptoms should occur frequently or be severe enough to have substantial impact on daily function in order to be considered for our scale.

We then conducted open interviews followed by structured interviews of ten patients with cirrhosis and moderate ($n = 4$) or severe ascites ($n = 6$). The selected domains were initially presented and patients were asked to rate them according to the patient's perceived 'importance', on the extent to which the symptom had bothered them.

We revised the questionnaire instrument based on the answers.

After the development of the questionnaire, we prospectively enrolled a validation cohort consisting of patients with cirrhosis of any aetiology and severe, moderate or no ascites. All gave their informed consent to participate.

Subjects completed the following scales and questionnaires: CAS scale; Chronic Liver Disease Questionnaire; and EQ-5D-5L questionnaire.

We used the Crohnbach's alpha to assess equivalent reliability. *Discriminant validity* was evaluated using Dunnett's test to adjust for multiple comparisons. We originally planned to evaluate *convergent validity* with previously validated scales assessing symptoms or HRQOL associated with ascites. Since no previous scales were identified, we used the CLDQ and the EQ-5D-5L. We compared scale scores using Spearman correlation and included the CAS scale, CLDQ, CLDQ subscale parameters, and EQ-5D-5L. Correlations higher than 0.70 were considered strong and values below 0.40 were interpreted as poor.

Research results

The final scale included 14 items. Chronbach's alpha was 0.88 for the total score, which we considered as acceptable. The validation cohort included 103 patients.

The proportion of patients with Child Pugh A was 24%, Child Pugh B: 58% and Child Pugh C: 19%. Fourty-four percent had severe ascites and 27 percent had moderate ascites. A control group of 30 percent had no ascites. The mean scores for each question in the CAS scale suggested that symptoms were worse for patients with severe ascites than for controls. The CAS scale score found that patients with severe ascites or moderate ascites had significantly worse scores compared with controls. Based on the CLDQ questionnaire, severe ascites had a detrimental impact on HRQOL compared with controls as did moderate ascites. The EQ-5D-5L also found a lower HRQOL in patients with severe or moderate ascites. We found a strong correlation between the CAS and the CLDQ total score as well as the CLDQ subscores; fatigue, activity and systemic symptoms.

Research conclusions

This study has developed and tested a symptom assessment scale for the impact of ascites in cirrhosis. The CAS scale is easy to use and correlates well with more extensive QoL questionnaires.

Research perspectives

This study has brought focus to the impact and importance of effective management of ascites in chronic liver disease.

The CAS scale should be tested in larger clinical and interventional trials, preferably in combination with CLDQ or other generic health related quality of life questionnaires.

The CAS scale should be tested in larger cohorts with various etiologies for chronic liver disease and ascites, also in malignant ascites. The CAS scale should also be tested in interventional trials in which the effect of a given intervention on the CAS scale is evaluated, to demonstrate whether the CAS scale is applicable as a monitoring tool in ascites.

ACKNOWLEDGMENTS

The authors would like to thank the health care professionals at the Gastro Unit, Copenhagen University Hospital Hvidovre, who participated in the qualitative study, thereby contributing to the design of the CAS scale. We also wish to thank medical professor Per Bech and senior doctor Finn Zierau for valuable feedback on statistical issues.

REFERENCES

1 **Ginès P**, Cárdenas A, Arroyo V, Rodés J. Management of cirrhosis and ascites. *N Engl J Med* 2004; **350**: 1646-1654 [PMID: 15084697 DOI: 10.1056/NEJMra035021]

2 **Ginés P**, Quintero E, Arroyo V, Terés J, Bruguera M, Rimola A, Caballería J, Rodés J, Rozman C. Compensated cirrhosis: natural history and prognostic factors. *Hepatology* 1987; **7**: 122-128 [PMID: 3804191 DOI: 10.1002/hep.1840070124]

3 **Haraguchi M**, Miyaaki H, Ichikawa T, Shibata H, Honda T, Ozawa E, Miuma S, Taura N, Takeshima F, Nakao K. Glucose fluctuations reduce quality of sleep and of life in patients with liver cirrhosis. *Hepatol Int* 2017; **11**: 125-131 [PMID: 27624504 DOI: 10.1007/s12072-016-9762-1]

4 **Maharshi S**, Sharma BC, Sachdeva S, Srivastava S, Sharma P. Efficacy of Nutritional Therapy for Patients With Cirrhosis and Minimal Hepatic Encephalopathy in a Randomized Trial. *Clin Gastroenterol Hepatol* 2016; **14**: 454-460.e3; quiz e33 [PMID: 26453952 DOI: 10.1016/j.cgh.2015.09.028]

5 **Prasad S**, Dhiman RK, Duseja A, Chawla YK, Sharma A, Agarwal R. Lactulose improves cognitive functions and health-related quality of life in patients with cirrhosis who have minimal hepatic encephalopathy. *Hepatology* 2007; **45**: 549-559 [PMID: 17326150 DOI: 10.1002/hep.21533]

6 **Navasa M**, Forns X, Sánchez V, Andreu H, Marcos V, Borràs JM, Rimola A, Grande L, García-Valdecasas JC, Granados A, Rodés J. Quality of life, major medical complications and hospital service utilization in patients with primary biliary cirrhosis after liver transplantation. *J Hepatol* 1996; **25**: 129-134 [PMID: 8878772 DOI: 10.1016/S0168-8278(96)80064-X]

7 **Marchesini G**, Bianchi G, Amodio P, Salerno F, Merli M, Panella C, Loguercio C, Apolone G, Niero M, Abbiati R; Italian Study Group for quality of life in cirrhosis. Factors associated with poor health-related quality of life of patients with cirrhosis. *Gastroenterology* 2001; **120**: 170-178 [PMID: 11208726 DOI: 10.1053/gast.2001.21193]

8 **Häuser W**, Schnur M, Steder-Neukamm U, Muthny FA, Grandt D. Validation of the German version of the Chronic Liver Disease Questionnaire. *Eur J Gastroenterol Hepatol* 2004; **16**: 599-606 [PMID: 15167163 DOI: 10.1097/00042737-200406000-00014]

9 **Younossi ZM**, Guyatt G, Kiwi M, Boparai N, King D. Development of a disease specific questionnaire to measure health related quality of life in patients with chronic liver disease. *Gut* 1999; **45**: 295-300 [PMID: 10403745 DOI: 10.1136/gut.45.2.295]

10 **Häuser W**, Holtmann G, Grandt D. Determinants of health-related quality of life in patients with chronic liver diseases. *Clin Gastroenterol Hepatol* 2004; **2**: 157-163 [PMID: 15017621 DOI: 10.1016/S1542-3565(03)00315-X]

11 **Ahluwalia V**, Heuman DM, Feldman G, Wade JB, Thacker LR, Gavis E, Gilles H, Unser A, White MB, Bajaj JS. Correction of hyponatraemia improves cognition, quality of life, and brain oedema in cirrhosis. *J Hepatol* 2015; **62**: 75-82 [PMID: 25111174 DOI: 10.1016/j.jhep.2014.07.033]

12 **Thiele M**, Askgaard G, Timm HB, Hamberg O, Gluud LL. Predictors of health-related quality of life in outpatients with cirrhosis: results from a prospective cohort. *Hepat Res Treat* 2013; **2013**: 479639 [PMID: 24490061 DOI: 10.1155/2013/479639]

13 **Ong JP**, Oehler G, Krüger-Jansen C, Lambert-Baumann J, Younossi ZM. Oral L-ornithine-L-aspartate improves health-related quality of life in cirrhotic patients with hepatic encephalopathy: an open-label, prospective, multicentre observational study. *Clin Drug Investig* 2011; **31**: 213-220 [PMID: 21208014 DOI: 10.2165/11586700-000000000-00000]

14 **Sidhu SS**, Goyal O, Mishra BP, Sood A, Chhina RS, Soni RK. Rifaximin improves psychometric performance and health-related quality of life in patients with minimal hepatic encephalopathy (the RIME Trial). *Am J Gastroenterol* 2011; **106**: 307-316 [PMID: 21157444 DOI: 10.1038/ajg.2010.455]

15 **Les I**, Doval E, Flavià M, Jacas C, Cárdenas G, Esteban R, Guardia J, Córdoba J. Quality of life in cirrhosis is related to potentially treatable factors. *Eur J Gastroenterol Hepatol* 2010; **22**: 221-227 [PMID: 19794311 DOI: 10.1097/MEG.0b013e3283319975]

16 **Linde L**, Sørensen J, Ostergaard M, Hørslev-Petersen K, Hetland ML. Health-related quality of life: validity, reliability, and responsiveness of SF-36, 15D, EQ-5D [corrected] RAQoL, and HAQ in patients with rheumatoid arthritis. *J Rheumatol* 2008; **35**: 1528-1537 [PMID: 18484697]

17 **Søgaard R**, Christensen FB, Videbaek TS, Bünger C, Christiansen T. Interchangeability of the EQ-5D and the SF-6D in long-lasting low back pain. *Value Health* 2009; **12**: 606-612 [PMID: 19900258 DOI: 10.1111/j.1524-4733.2008.00466.x]

18 **EuroQol Group**. EuroQol--a new facility for the measurement of health-related quality of life. *Health Policy* 1990; **16**: 199-208 [PMID: 10109801 DOI: 10.1016/0168-8510(90)90421-9]

19 **Herdman M**, Gudex C, Lloyd A, Janssen M, Kind P, Parkin D, Bonsel G, Badia X. Development and preliminary testing of the new five-level version of EQ-5D (EQ-5D-5L). *Qual Life Res* 2011; **20**: 1727-1736 [PMID: 21479777 DOI: 10.1007/s11136-011-9903-x]

20 **Younossi ZM**, Boparai N, Price LL, Kiwi ML, McCormick M, Guyatt G. Health-related quality of life in chronic liver disease: the impact of type and severity of disease. *Am J Gastroenterol* 2001; **96**: 2199-2205 [PMID: 11467653 DOI: 10.1111/j.1572-0241.2001.03956.x]

21 **Bhanji RA**, Carey EJ, Watt KD. Review article: maximising

quality of life while aspiring for quantity of life in end-stage liver disease. *Aliment Pharmacol Ther* 2017; **46**: 16-25 [PMID: 28464346 DOI: 10.1111/apt.14078]

22 **Solà E**, Watson H, Graupera I, Turón F, Barreto R, Rodríguez E, Pavesi M, Arroyo V, Guevara M, Ginès P. Factors related to quality of life in patients with cirrhosis and ascites: relevance of serum sodium concentration and leg edema. *J Hepatol* 2012; **57**: 1199-1206 [PMID: 22824819 DOI: 10.1016/j.jhep.2012.07.020]

23 **Rojas-Loureiro G**, Servín-Caamaño A, Pérez-Reyes E, Servín-Abad L, Higuera-de la Tijera F. Malnutrition negatively impacts the quality of life of patients with cirrhosis: An observational study. *World J Hepatol* 2017; **9**: 263-269 [PMID: 28261383 DOI: 10.4254/wjh.v9.i5.263]

24 **Bajaj JS**, Wade JB, Gibson DP, Heuman DM, Thacker LR, Sterling RK, Stravitz RT, Luketic V, Fuchs M, White MB, Bell DE, Gilles H, Morton K, Noble N, Puri P, Sanyal AJ. The multi-dimensional burden of cirrhosis and hepatic encephalopathy on patients and caregivers. *Am J Gastroenterol* 2011; **106**: 1646-1653 [PMID: 21556040 DOI: 10.1038/ajg.2011.157]

25 **Scalone L**, Fagiuoli S, Ciampichini R, Gardini I, Bruno R, Pasulo L, Lucà MG, Fusco F, Gaeta L, Del Prete A, Cesana G, Mantovani LG. The societal burden of chronic liver diseases: results from the COME study. *BMJ Open Gastroenterol* 2015; **2**: e000025 [PMID: 26462277 DOI: 10.1136/bmjgast-2014-000025]

P- Reviewer: Jarcuska P, Jin B, Maruyama M, Niu ZS, Shimizu Y
S- Editor: Wang JL **L- Editor**: A **E- Editor**: Huang Y

World Journal of Gastroenterology

Submit a Manuscript: http://www.f6publishing.com

World J Gastroenterol 2018 April 21; 24(15): 1658-1665

DOI: 10.3748/wjg.v24.i15.1658

ISSN 1007-9327 (print) ISSN 2219-2840 (online)

META-ANALYSIS

Platelet-to-lymphocyte ratio in the setting of liver transplantation for hepatocellular cancer: A systematic review and meta-analysis

Quirino Lai, Fabio Melandro, Zoe Larghi Laureiro, Francesco Giovanardi, Stefano Ginanni Corradini, Flaminia Ferri, Redan Hassan, Massimo Rossi, Gianluca Mennini

Quirino Lai, Fabio Melandro, Zoe Larghi Laureiro, Francesco Giovanardi, Redan Hassan, Massimo Rossi, Gianluca Mennini, Hepato-bilio-pancreatic and Liver Transplant Unit, Department of Surgery, Sapienza University of Rome, Rome 00161, Italy

Stefano Ginanni Corradini, Flaminia Ferri, Division of Gastroenterology, Department of Clinical Medicine, Sapienza University of Rome, Rome 00161, Italy

ORCID number: Quirino Lai (0000-0003-1487-3235); Fabio Melandro (0000-0003-4056-9245); Zoe Larghi Laureiro (0000-0003-4183-2017); Francesco Giovanardi (0000-0002-8395-2722); Stefano Ginanni Corradini (0000-0002-0839-1961); Flaminia Ferri (0000-0001-8553-5589); Redan Hassan (0000-0003-2925-8972); Massimo Rossi (0000-0001-5105-4656); Gianluca Mennini (0000-0002-6412-6863).

Author contributions: Lai Q contributed to conception and design of the study; Lai Q, Melandro F, Giovanardi F, Ferri F and Hassan R contributed to acquisition of data; Lai Q and Melandro F analysed and interpreted the data; Lai Q drafted the article; Ginanni Corradini S, Rossi M and Mennini G critically revised the manuscript; and all authors approved the final version.

Conflict-of-interest statement: The authors have no conflicts of interest to declare.

PRISMA 2009 Checklist statement: The authors have read the PRISMA 2009 Checklist, and the manuscript was prepared and revised according to the PRISMA 2009 Checklist.

Manuscript source: Invited manuscript

Correspondence to: Quirino Lai, MD, PhD, Senior Lecturer, Hepato-bilio-pancreatic and Liver Transplant Unit, Department of Surgery, Sapienza University of Rome, Umberto I Policlinic of Rome, Viale del Policlinico 155, Rome 00161, Italy. lai.quirino@libero.it.
Telephone: +39-3493020126
Fax: +39-06499701

Received: March 9, 2018
Peer-review started: March 10, 2018
First decision: March 29, 2018
Revised: April 2, 2018
Accepted: April 9, 2018
Article in press: April 9, 2018
Published online: April 21, 2018

Abstract

AIM

To perform a systematic review and meta-analysis on platelet-to-lymphocyte ratio (PLR) as a risk factor for post-transplant hepatocellular cancer (HCC) recurrence.

METHODS

A systematic literature search was performed using PubMed. Participants of any age and sex, who underwent liver transplantation for HCC were considered following these criteria: (1) studies comparing pre-transplant low *vs* high PLR values; (2) studies reporting post-transplant recurrence rates; and (3) if more than one study was reported by the same institute, only the most recent was included. The primary outcome measure was set for HCC recurrence after transplantation.

RESULTS

A total of 5 articles, published between 2014 and 2017, fulfilled the selection criteria. As for the quality of the reported studies, all the investigated articles presented

an overall high quality. A total of 899 cases were investigated: 718 cases (80.0%) were males. Three studies coming from European countries and one from Japan presented HCV as the main cause of cirrhosis. On the opposite, one Chinese study presented a greater incidence of HBV-related cirrhotic cases. In all the studies apart one, the PLR cut-off value of 150 was reported. At meta-analysis, high PLR value was associated with a significant increase in recurrence after transplantation (OR = 3.33; 95%CI: 1.78-6.25; $P < 0.001$). A moderate heterogeneity was observed among the identified studies according to the Higgins I^2 statistic value.

CONCLUSION

Pre-transplant high PLR values are connected with an increased risk of post-operative recurrence of hepatocellular cancer. More studies are needed for better clarify the biological mechanisms of this results.

Key words: Recurrence; Inflammation; Hepatocellular cancer; Liver transplantation; Platelet-to-lymphocyte ratio

Core tip: Poor data exist on the role of the inflammatory marker platelet-to-lymphocyte ratio (PLR) and hepatocellular cancer (HCC) recurrence after liver transplantation. This is the first systematic review and meta-analysis specifically investigating the role of PLR in the setting of liver transplant for HCC. Pre-transplant high PLR values confirmed their utility as predictors of recurrence, being connected with a 3.33-fold increased risk of post-transplant HCC recurrence.

Lai Q, Melandro F, Larghi Laureiro Z, Giovanardi F, Ginanni Corradini S, Ferri F, Hassan R, Rossi M, Mennini G. Platelet-to-lymphocyte ratio in the setting of liver transplantation for hepatocellular cancer: A systematic review and meta-analysis. *World J Gastroenterol* 2018; 24(15): 1658-1665 Available from: URL: http://www.wjgnet.com/1007-9327/full/v24/i15/1658.htm DOI: http://dx.doi.org/10.3748/wjg.v24.i15.1658

INTRODUCTION

Liver transplantation (LT) represents the best therapy for the treatment of hepatocellular cancer (HCC)[1]. However, LT represents a scarce resource. As a consequence, a careful selection of HCC patients must be done preoperatively, with the intent to minimize the risk of post-LT recurrence[2] It is, in fact, clear that transplanting too advanced tumors is connected with a higher risk of poor post-LT outcomes[3]. Moreover, an error in the selection process corresponds to a "futile transplant", avoiding to transplant another patient in the waiting list[4].

After the introduction of the Milan Criteria (MC) in 1996, several other scores have been proposed in the last decades with the intent to refine the selection of HCC patients waiting for LT[5-8]. Apart from tumor morphology, also biology has been integrated into prognostic scores in the last years: Thus, the markers alpha-fetoprotein and des-gamma-carboxy-prothrombin, the radiological response after locoregional therapies or the tumor behaviour at PET scan have been largely investigated[9-13]. Recently, also systemic inflammation has been added as a possible value to add in the complex "mainframe" of HCC selection[14]. Among the different evaluated markers, the neutrophil-to-lymphocyte ratio (NLR) has been proposed as the most promising predictor of HCC recurrence[15,16]. NLR has been also integrated into several scores aimed at better select HCC patients waiting for LT[17,18]. However, another less intensely investigated ratio, namely the platelet-to-lymphocyte ratio (PLR), has also reported interesting results[19,20].

The main aim of the present study is to report a systematic review of the literature and a meta-analysis focused on investigating the role of PLR in the setting of liver transplantation as a useful predictor of HCC recurrence.

MATERIALS AND METHODS

Search strategy

A systematic search was done in relation to relevant studies focusing on the role of PLR in HCC patients undergoing LT. The search strategy was done in accordance with the Preferred Reporting Items for Systemic Reviews and Meta-Analysis (PRISMA) guidelines, as well as PRISMA for abstracts[21]. A search of the electronic databases MEDLINE-PubMed, Cochrane Library and EMBASE was conducted using the following research terms: (liver transplant*[tw]) AND (platelet-to-lymphocyte ratio[tw] OR PLR[tw]). Text word [tw] was preferred respect to MeSH words with the intent to identify In Process citations. Studies published before March 6, 2018, were taken into consideration.

Screening process

The present qualitative systematic review included a priori search criteria of journal articles among adult (age $\geqslant$ 18 years) human patients. Studies were limited to the English language. We defined as enrollable all the studies based on HCC patients having received LT in which pre-operative PLR values were correlated with the risk of post-LT HCC recurrence. Investigated time to recurrence was set at 5 years after LT.

Exclusion criteria were: (1) papers lacking sufficient details; (2) review articles; (3) nonclinical studies; (4) expert opinions; (5) letters; (6) conference summaries; and (7) case reports.

Study selection

Two reviewers (QL and FM) independently screened the identified studies and their extracted data. In case

Table 1 Quality of studies evaluated by the modified Newcastle-Ottawa scale

Ref.	Selection				Comparability		Outcome		Quality score
	Case definition	Representativeness	Selection of controls	Definition of controls	Comparable for therapy	Comparable for etiology	Assessment of outcomes	Integrity of follow-up	
Xia *et al*[24]	Yes	Yes	No	Yes	Yes	Yes	Yes	Yes	★★★★ ★★★★
Lai *et al*[25]	Yes	Yes	No	Yes	Yes	Yes	Yes	Yes	★★★★ ★★★★
Parisi *et al*[26]	Yes	Yes	No	Yes	Yes	Yes	Yes	Yes	★★★★ ★★★★
Nicolini *et al*[27]	Yes	Yes	No	Yes	Yes	Yes	Yes	Yes	★★★★ ★★★★
Harimoto *et al*[28]	Yes	Yes	No	Yes	Yes	Yes	Yes	Yes	★★★★ ★★★★

of disagreement, the paper was discussed by all the authors.

Quality assessment

Selected studies were reviewed based on the representativeness of the study population, comparability of cohorts, adequate assessment of outcomes, sufficient length of follow-up, adequacy of follow-up, and source of study funding. The quality of the papers was assessed using the Newcastle-Ottawa Quality Assessment Scale (NOS): studies with scores > 6 were defined as high-quality studies[22].

NOS details of each selected study were reported in Table 1. The characteristics coming from each study were collected in Table 2. The following features were collected: first author's name, reference number, number of patients, patient age, patient gender, waiting time duration in months, model for end-stage liver disease, underlying liver pathology, the diameter of the major lesion and the number of tumors at the moment of LT, the MC-OUT status at the moment of LT, AFP value ⩾ 200 ng/mL, any type of locoregional treatment (LRT), the PLR cut-off used in the article, the area under the receiver operator curve (ROC) for the diagnosis of recurrence, the number of post-LT recurrences and the 5-year tumor-free survival (TFS).

Statistical analysis

Different PLR cut-offs were observed among the identified studies. TFS end-point in the different studies corresponded to 5 years after LT. Summary measures were extracted from each study and used to generate a pooled odds ratio (OR). Higgins I^2 statistic was used to assess heterogeneity. Higgins I^2 statistic values of 0%-25%, 25%-50%, and > 50% were considered as indicative of homogeneity, moderate heterogeneity, and high heterogeneity, respectively. Only the random-effects model was used, starting from the assumption that a common OR was unreliable in the analyzed studies due to the broad eligibility criteria and the different used PLR cut-off values. OR was considered statistically significant when the *P*-value was < 0.05. OR and 95% confidence intervals (CI) > 1 revealed that the patients with high PLR values had poor prognoses (higher risk of recurrence), whereas a result < 1 had the opposite meaning. The analysis was performed using OpenMEE software (http://www.cebm.brown.edu/openmee/index.html).

RESULTS

The selection process of the articles is explained in Figure 1.

As for the selection process according to the PRISMA guidelines, the various examined databases provided a total of 39 articles to screen. After removing the duplicates and reading the title and the abstract, 28 articles were removed. Of the remaining 11 papers, 6 were not considered eligible after full-text evaluation. Two studies coming from Hangzhou China were performed on the same population, so only one of these studies was selected for the last analysis[23,24].

Eventually, 5 articles were identified, with a total of 899 investigated cases (Table 2)[24-28].

As for the quality of the reported studies, all the investigated articles were retrospective cohort studies all presenting the excellent NOS value of eight, thus reporting the overall high quality of the studies focused on this topic (Table 1).

In the selected series, median/mean age ranged 49-58 years. As for patient gender, 718 cases (80.0%) were males. Three studies coming from European countries and one from Japan presented HCV as the main reason for underlying cirrhotic liver disease (298/556 cases; 53.6%). On the opposite, one Chinese study presented a greater incidence of HBV-related cirrhotic cases (320/343 cases; 93.3%).

Last radiology before LT was available in only three studies, showing a median diameter of the major lesion ranging 1.3-2.7 cm and a median single lesion (range 0-2). MC-OUT status was observed in 309 (34.4) patients: interestingly enough, a great discrepancy was observed among the reported studies, with one series coming from Europe showing no cases exceeding the MC, and the study coming from China presenting 58.0% of MC-OUT individuals. Different AFP cut-offs

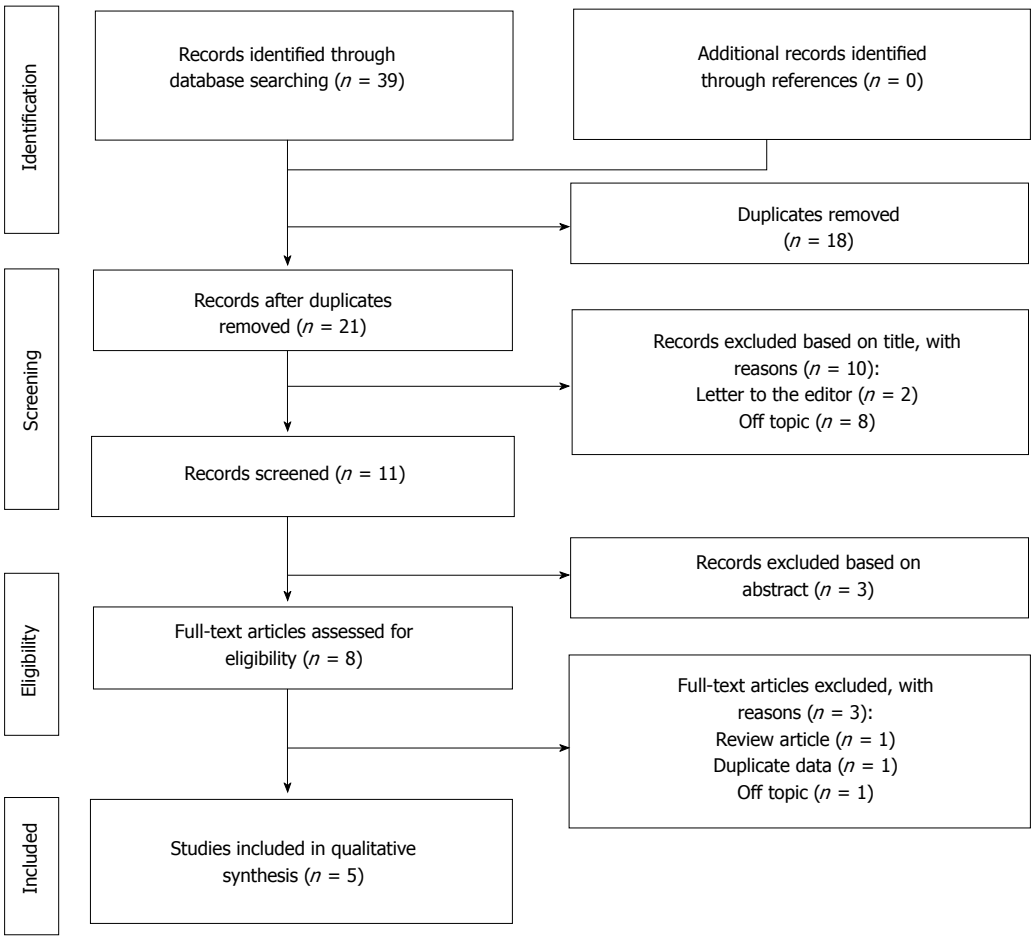

Figure 1 PRISMA flowchart of the literature search and study selection.

were reported in the studies (200/300/400 ng/mL). Also in this case, great discrepancies were observed among the study coming from Hangzhou and the other ones in terms of cases exceeding the reported threshold values (48.1% *vs* 5.5%-15.8%). When reported, LRT were performed in 47.3%-100.0% of cases.

Specifically investigating the PLR values, the cut-off of 150 was reported in all the series apart from the study from Fukuoka Japan, in which the median value of 70.4 was investigated. When the diagnostic power of PLR in terms of HCC recurrence was investigated, an area under the ROC curve of 0.63-0.70 was observed, showing an acceptable-to-good ability of this variable to diagnose post-transplant recurrence. A total of 180 (20.0%) cases exceeded the proposed threshold values, with a percentage ranging 7.1%-51.1% in the various series.

Five-year tumor-free survivals were reported in four studies. In all of them, patients presenting high PLR values had worse results, with a value ranging 81%-25% respect to the ones reported in patients with low PLR values (95%-52%).

The binary random-effects meta-analysis showed a strong relationship between poor TFS and elevated PLR values (OR = 3.33, 95%CI: 1.78-6.25; $P < 0.001$). Higgins I^2 statistic presented a value = 26.8% (P = 0.24), showing a moderate heterogeneity among the examined studies (Figure 2).

DISCUSSION

Until now, few data have been reported on the predictive role of PLR as a risk factor for HCC recurrence after liver transplant. Indeed, only five studies have been identified in the present systematic review, the first of whom published in 2014[24-28]. However, although the number of reported cases is relatively limited (n = 899), the biological effect of PLR looks to be clear, with a strong correlation between high PLR values and a greater risk for recurrence. According to the results of the meta-analysis, subjects having pre-LT high PLR values present a 3.33-fold increased risk of experiencing HCC recurrence after LT.

Interestingly enough, the only study in which the PLR failed to be a prognostic tool for recurrence was the sole in which only patients meeting the MC were transplanted[26]. Such an evidence should represent a possible explanation for the observed results. It is, in fact, possible that a direct correlation may exist between higher PLR values and a progressively increasing tumor aggressiveness (*i.e.*, higher AFP and greater tumor burden). As a possible confirmation of

Table 2 Demographic and clinical aspects of the selected studies

Ref.	*n*	Age	Male gender (%)	waiting time (mo)	MELD	Underlying disease	Major lesion diam (cm)	Number lesions	MC-OUT (%)	AFP ⩾ 200 ng/mL (%)	LRT (%)	Cut-off	AUROC	> cut-off (%)	Recurr (%)	5-yr TFS
Xia *et al*[24]	343	49 ± 10	308 (90)	NA	13 ± 6	HBV = 320 Other = 23	> 5:110	> 3:91	199 (58)	165 (48)	222 (65)	150	0.63	33 (10)	NA	< 150: 52 ⩾ 150:25
Lai *et al*[25]	146	58 (54-63)	116 (80)	8 (3-10)	11 (8-11)	HCV = 63 HBV = 26 Other = 57	2.5 (1.7-3.5)	1 (1-2)	32 (22)	8 (6)	136 (93)	150	0.66	28 (19)	14 (10)	< 150:92 ⩾ 150:81
Parisi *et al*[26]	150	54 ± 7	125 (83)	2 (0-12)	NA	HCV = 60 HBV = 34 Other = 56	2.7	1	0 (-)	13 (9)	71 (47)	150	NA	17 (11)	19 (13)	NA
Nicolini *et al*[27]	70	57 (51-62)	62 (89)	NA	11 (7-15)	HCV = 41 HBV = 15 Other = 14	1.3 (0.0-2.1)	1 (0-2)	12 (17)	6 (9)[1]	70 (100)	150	NA	5 (7)	8 (11)	< 150:89 ⩾ 150:50
Harimoto *et al*[28]	190	⩾ 59:97	107 (56)	NA	⩾ 15:60	HCV = 134 Other = 56	> 5:8	> 3:41	66 (35)	30 (16)[2]	NA	70.4	0.70	97 (51)	28 (15)	< 70.4:95 ⩾ 70.4:76

[1]AFP ⩾ 400 ng/mL; [2]AFP ⩾ 300 ng/mL. MELD: Model for end-stage liver disease; MC: Milan Criteria; AFP: Alpha-fetoprotein; LRT: Locoregional treatment; AUROC: Area under the receiver operator curve; TFS: Tumor-free survival; HCV: Hepatitis C virus; HBV: Hepatitis B virus; NA: Not available.

these data, all the series reported in the present study showed a gradient among PLR values, patients exceeding the MC and worse survival results.

This evidence has been observed also in an ITA.L.I.C.A. study in which a direct correlation between tumor dimension and the absolute number of platelets was reported[29]. Another study from Taiwan performed on more than 3000 HCC patients showed that platelets count efficaciously predicted extrahepatic metastases, even better than AFP did[30].

The link between HCC and platelets has been recently documented also in a Korean study only investigating absolute platelets count and HCC recurrence. A platelets value > 75 × 10^9/L was connected with higher 5-year recurrence rates (28.2% *vs* 13.2% in patients with lower count; $P = 0.002$). Similarly, at multivariable analysis, a significantly greater recurrence risk was confirmed in the high platelets group (HR = 1.90; 95%CI: 1.02-3.54; $P = 0.04$). Of interest, platelets count remained significant as a risk factor for recurrence even when it was introduced in a multivariable model comprehending aspects of tumor biology and morphology. Thus, we can postulate that platelets present an independent role in favouring tumor progression[31].

As a confirmation of this result, it has been well established that platelets are effector cells directly interacting with tumor cells in the metastatic cascade[32,33]. During total hepatectomy for LT, some tumor cells may be observed in the bloodstream due to HCC manipulation, only needing a few hours to days to complete the metastatic cascade[33]. Platelets favour some of the mechanisms required for metastatic dissemination: For example, they favour tumor cell surviving in the bloodstream, extravasation, initial seeding and tumor re-growth[34].

All these considerations present great repercussions from a clinical point of view: In fact, platelets might provide a potential therapeutic target for anti-hepatoma treatments. Of interest, sorafenib already represents an anti-HCC drug directly acting against cellular pathways mediated by platelet-derived growth factors (*i.e.*, vascular endothelial growth factor and platelet-derived growth factor)[35]. Other therapies including cyclooxygenase inhibitors, protease-activated receptor inhibitors, and glycoprotein IIb/IIIa inhibitors may further play an underestimated role in this phenomenon[36].

However, although the reported data suggest an effective biological correlation between platelets and tumor aggressive behaviour, we should underline that further clinical studies trying to univocally demonstrate the biological role of platelets in the HCC oncogenesis are needed. Indeed, the present meta-analysis was in fact affected by several potential shortcomings. First, moderate heterogeneity was observed among the studies investigated, as clearly shown by the reported Higgins I^2 statistic value (26.8%). Such a phenomenon was surely caused by the broad eligibility criteria for HCC and the different PLR cut-off values used in the different centers. It is, in

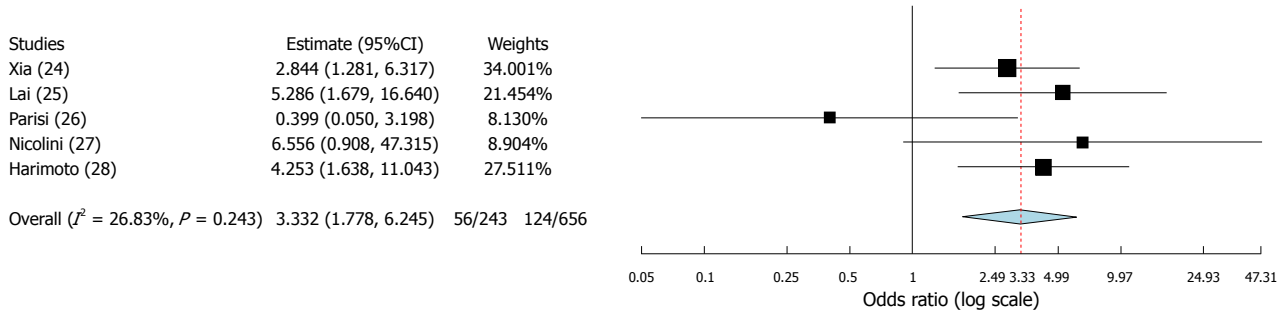

Figure 2 Forest plot of odds ratios and 95% confidence intervals for the association between platelet-to-lymphocyte ratio and recurrence in hepatocellular cancer patients undergoing liver transplantation. Weights are from binary random-effect analysis.

fact, clear that a meta-regression weighted for the geographical area, HCV *vs* HBV as the main cause of liver failure, living-donor *vs* deceased-donor LT, and markers of tumor aggressiveness should represent a more accurate way for better clarify the role of PLR in this setting. Unfortunately, the limited number of cases reported did not consent us to perform more sophisticated analyses. Secondly, no information was reported in the different series on the presence and grade of portal hypertension, a very well known cause of thrombocytopenia in cirrhosis[37].

In conclusion, platelet-to-lymphocyte ratio is an easy and cheap value to use for selecting patients with hepatocellular cancer waiting for liver transplantation. A direct correlation between PLR values and tumor aggressiveness has been observed in several studies. High pre-transplant PLR values cause a 3.3-fold increased risk for post-transplant recurrence. More studies aimed at better understanding biological and clinical mechanisms of the link between PLR and HCC are needed.

ARTICLE HIGHLIGHTS

Research background

Liver transplantation is the best curative therapy in case of hepatocellular cancer (HCC). However, it represents a scarce resource due to the reduced number of donors. Thus, a careful selection of HCC patients must be done preoperatively, with the intent to minimize the risk of futile transplants (*i.e.*, post-operative cancer recurrence). As a consequence, new and easy-to-use predictors of recurrence are needed.

Research motivation

Recently, several biological aspects of HCC have been investigated, with the intent to identify scores aimed at improving the prediction of poor post-transplant outcomes. Among them, the inflammatory marker platelet-to-lymphocyte ratio (PLR) has been only marginally investigated, although it should represent a potentially excellent and cheap marker to use.

Research objectives

The main objective of the present study is to evaluate the role of PLR as a possible selection tool for the risk of HCC recurrence in the setting of liver transplantation.

Research methods

A systematic review and a meta-analysis have been performed with the intent to evaluate the role of PLR. The PRISMA Guidelines have been used for performing the systematic research of studies focused on PLR, HCC and LT.

Research results

Five articles coming from Europe and Asia have been identified, with a total of 899 subjects investigated. At meta-analysis, high PLR value was associated with a significant increase in recurrence after transplantation (OR = 3.33; 95%CI: 1.78-6.25; P < 0.001).

Research conclusions

A direct correlation between PLR values and tumor aggressiveness has been observed. High pre-transplant PLR values cause a 3.3-fold increased risk for post-transplant recurrence. Platelet-to-lymphocyte ratio is an easy and cheap value to use for selecting patients with hepatocellular cancer waiting for liver transplantation. PLR should be taken into account in the creation of new selection scores for HCC.

Research perspectives

More studies aimed at better understanding biological and clinical mechanisms of the link between PLR and HCC are necessary.

REFERENCES

1 **Mazzaferro V**, Regalia E, Doci R, Andreola S, Pulvirenti A, Bozzetti F, Montalto F, Ammatuna M, Morabito A, Gennari L. Liver transplantation for the treatment of small hepatocellular carcinomas in patients with cirrhosis. *N Engl J Med* 1996; **334**: 693-699 [PMID: 8594428 DOI: 10.1056/NEJM199603143341104]
2 **Lai Q**, Lerut JP. Hepatocellular cancer: how to expand safely inclusion criteria for liver transplantation. *Curr Opin Organ Transplant* 2014; **19**: 229-234 [PMID: 24811435 DOI: 10.1097/MOT.0000000000000085]
3 **Mazzaferro V**. Results of liver transplantation: with or without Milan criteria? *Liver Transpl* 2007; **13**: S44-S47 [PMID: 17969068 DOI: 10.1002/lt.21330]
4 **Lai Q**, Vitale A, Iesari S, Finkenstedt A, Mennini G, Spoletini G, Hoppe-Lotichius M, Vennarecci G, Manzia TM, Nicolini D, Avolio AW, Frigo AC, Graziadei I, Rossi M, Tsochatzis E, Otto G, Ettorre GM, Tisone G, Vivarelli M, Agnes S, Cillo U, Lerut J; European Hepatocellular Cancer Liver Transplant Study Group. Intention-to-treat survival benefit of liver transplantation in patients with hepatocellular cancer. *Hepatology* 2017; **66**: 1910-1919 [PMID: 28653750 DOI: 10.1002/hep.29342]
5 **Mazzaferro V**, Bhoori S, Sposito C, Bongini M, Langer M, Miceli R, Mariani L. Milan criteria in liver transplantation for hepatocellular carcinoma: an evidence-based analysis of 15 years of experience. *Liver Transpl* 2011; **17** Suppl 2: S44-S57 [PMID: 21695773 DOI: 10.1002/lt.22365]
6 **Yao FY**, Ferrell L, Bass NM, Watson JJ, Bacchetti P, Venook A, Ascher NL, Roberts JP. Liver transplantation for hepatocellular carcinoma: expansion of the tumor size limits does not adversely impact survival. *Hepatology* 2001; **33**: 1394-1403 [PMID: 11391528 DOI: 10.1053/jhep.2001.24563]

7 **Mazzaferro V**, Llovet JM, Miceli R, Bhoori S, Schiavo M, Mariani L, Camerini T, Roayaie S, Schwartz ME, Grazi GL, Adam R, Neuhaus P, Salizzoni M, Bruix J, Forner A, De Carlis L, Cillo U, Burroughs AK, Troisi R, Rossi M, Gerunda GE, Lerut J, Belghiti J, Boin I, Gugenheim J, Rochling F, Van Hoek B, Majno P; Metroticket Investigator Study Group. Predicting survival after liver transplantation in patients with hepatocellular carcinoma beyond the Milan criteria: a retrospective, exploratory analysis. *Lancet Oncol* 2009; **10**: 35-43 [PMID: 19058754 DOI: 10.1016/S1470-2045(08)70284-5]

8 **Gao T**, Xia Q, Qiu DK, Feng YY, Chi JC, Wang SY, Xi ZF, Zhang JJ, Xu N, Chen SY, Qiu YL, Shen LW, Zhou TT, Dong XJ, Li QG, Li H. Comparison of survival and tumor recurrence rates in patients undergoing liver transplantation for hepatitis B-related hepatocellular carcinoma using Milan, Shanghai Fudan and Hangzhou criteria. *J Dig Dis* 2013; **14**: 552-558 [PMID: 23782458 DOI: 10.1111/1751-2980.12083]

9 **Lai Q**, Avolio AW, Manzia TM, Sorge R, Agnes S, Tisone G, Berloco PB, Rossi M. Combination of biological and morphological parameters for the selection of patients with hepatocellular carcinoma waiting for liver transplantation. *Clin Transplant* 2012; **26**: E125-E131 [PMID: 22192083 DOI: 10.1111/j.1399-0012.2011.01572.x]

10 **Duvoux C**, Roudot-Thoraval F, Decaens T, Pessione F, Badran H, Piardi T, Francoz C, Compagnon P, Vanlemmens C, Dumortier J, Dharancy S, Gugenheim J, Bernard PH, Adam R, Radenne S, Muscari F, Conti F, Hardwigsen J, Pageaux GP, Chazouillères O, Salame E, Hilleret MN, Lebray P, Abergel A, Debette-Gratien M, Kluger MD, Mallat A, Azoulay D, Cherqui D; Liver Transplantation French Study Group. Liver transplantation for hepatocellular carcinoma: a model including α-fetoprotein improves the performance of Milan criteria. *Gastroenterology* 2012; **143**: 986-994.e3; quiz e14-15 [PMID: 22750200 DOI: 10.1053/j.gastro.2012.05.052]

11 **Lai Q**, Iesari S, Levi Sandri GB, Lerut J. Des-gamma-carboxy prothrombin in hepatocellular cancer patients waiting for liver transplant: a systematic review and meta-analysis. *Int J Biol Markers* 2017; **32**: e370-e374 [PMID: 28561879 DOI: 10.5301/ijbm.5000276]

12 **Lai Q**, Avolio AW, Graziadei I, Otto G, Rossi M, Tisone G, Goffette P, Vogel W, Pitton MB, Lerut J; European Hepatocellular Cancer Liver Transplant Study Group. Alpha-fetoprotein and modified response evaluation criteria in solid tumors progression after locoregional therapy as predictors of hepatocellular cancer recurrence and death after transplantation. *Liver Transpl* 2013; **19**: 1108-1118 [PMID: 23873764 DOI: 10.1002/lt.23706]

13 **Kornberg A**, Freesmeyer M, Bärthel E, Jandt K, Katenkamp K, Steenbeck J, Sappler A, Habrecht O, Gottschild D, Settmacher U. 18F-FDG-uptake of hepatocellular carcinoma on PET predicts microvascular tumor invasion in liver transplant patients. *Am J Transplant* 2009; **9**: 592-600 [PMID: 19191771 DOI: 10.1111/j.1600-6143.2008.02516.x]

14 **Pinato DJ**, Stebbing J, Ishizuka M, Khan SA, Wasan HS, North BV, Kubota K, Sharma R. A novel and validated prognostic index in hepatocellular carcinoma: the inflammation based index (IBI). *J Hepatol* 2012; **57**: 1013-1020 [PMID: 22732513 DOI: 10.1016/j.jhep.2012.06.022]

15 **Halazun KJ**, Hardy MA, Rana AA, Woodland DC 4th, Luyten EJ, Mahadev S, Witkowski P, Siegel AB, Brown RS Jr, Emond JC. Negative impact of neutrophil-lymphocyte ratio on outcome after liver transplantation for hepatocellular carcinoma. *Ann Surg* 2009; **250**: 141-151 [PMID: 19561458 DOI: 10.1097/SLA.0b013e3181a77e59]

16 **Xu ZG**, Ye CJ, Liu LX, Wu G, Zhao ZX, Wang YZ, Shi BQ, Wang YH. The pretransplant neutrophil-lymphocyte ratio as a new prognostic predictor after liver transplantation for hepatocellular cancer: a systematic review and meta-analysis. *Biomark Med* 2018; **12**: 189-199 [PMID: 29327595 DOI: 10.2217/bmm-2017-0307]

17 **Halazun KJ**, Najjar M, Abdelmessih RM, Samstein B, Griesemer AD, Guarrera JV, Kato T, Verna EC, Emond JC, Brown RS Jr. Recurrence After Liver Transplantation for Hepatocellular Carcinoma: A New MORAL to the Story. *Ann Surg* 2017; **265**: 557-564 [PMID: 27611615 DOI: 10.1097/SLA.0000000000001966]

18 **Lai Q**, Nicolini D, Inostroza Nunez M, Iesari S, Goffette P, Agostini A, Giovagnoni A, Vivarelli M, Lerut J. A Novel Prognostic Index in Patients With Hepatocellular Cancer Waiting for Liver Transplantation: Time-Radiological-response-Alpha-fetoprotein-INflammation (TRAIN) Score. *Ann Surg* 2016; **264**: 787-796 [PMID: 27429025 DOI: 10.1097/SLA.0000000000001881]

19 **Zheng J**, Cai J, Li H, Zeng K, He L, Fu H, Zhang J, Chen L, Yao J, Zhang Y, Yang Y. Neutrophil to Lymphocyte Ratio and Platelet to Lymphocyte Ratio as Prognostic Predictors for Hepatocellular Carcinoma Patients with Various Treatments: a Meta-Analysis and Systematic Review. *Cell Physiol Biochem* 2017; **44**: 967-981 [PMID: 29179180 DOI: 10.1159/000485396].]

20 **Li X**, Chen ZH, Xing YF, Wang TT, Wu DH, Wen JY, Chen J, Lin Q, Dong M, Wei L, Ruan DY, Lin ZX, Wu XY, Ma XK. Platelet-to-lymphocyte ratio acts as a prognostic factor for patients with advanced hepatocellular carcinoma. *Tumour Biol* 2015; **36**: 2263-2269 [PMID: 25409616 DOI: 10.1007/s13277-014-2833-9]

21 **Hutton B**, Salanti G, Caldwell DM, Chaimani A, Schmid CH, Cameron C, Ioannidis JP, Straus S, Thorlund K, Jansen JP, Mulrow C, Catalá-López F, Gøtzsche PC, Dickersin K, Boutron I, Altman DG, Moher D. The PRISMA extension statement for reporting of systematic reviews incorporating network meta-analyses of health care interventions: checklist and explanations. *Ann Intern Med* 2015; **162**: 777-784 [PMID: 26030634 DOI: 10.7326/M14-2385]

22 **Stang A**. Critical evaluation of the Newcastle-Ottawa scale for the assessment of the quality of nonrandomized studies in meta-analyses. *Eur J Epidemiol* 2010; **25**: 603-605 [PMID: 20652370 DOI: 10.1007/s10654-010-9491-z]

23 **Xia W**, Ke Q, Guo H, Wang W, Zhang M, Shen Y, Wu J, Xu X, Yan S, Yu J, Zhang M, Zheng S. Expansion of the Milan criteria without any sacrifice: combination of the Hangzhou criteria with the pre-transplant platelet-to-lymphocyte ratio. *BMC Cancer* 2017; **17**: 14 [PMID: 28056901 DOI: 10.1186/s12885-016-3028-0]

24 **Xia W**, Ke Q, Wang Y, Wang W, Zhang M, Shen Y, Wu J, Xu X, Zheng S. Predictive value of pre-transplant platelet to lymphocyte ratio for hepatocellular carcinoma recurrence after liver transplantation. *World J Surg Oncol* 2015; **13**: 60 [PMID: 25885777 DOI: 10.1186/s12957-015-0472-2]

25 **Lai Q**, Castro Santa E, Rico Juri JM, Pinheiro RS, Lerut J. Neutrophil and platelet-to-lymphocyte ratio as new predictors of dropout and recurrence after liver transplantation for hepatocellular cancer. *Transpl Int* 2014; **27**: 32-41 [PMID: 24118272 DOI: 10.1111/tri.12191]

26 **Parisi I**, Tsochatzis E, Wijewantha H, Rodríguez-Perálvarez M, De Luca L, Manousou P, Fatourou E, Pieri G, Papastergiou V, Davies N, Yu D, Luong T, Dhillon AP, Thorburn D, Patch D, O'Beirne J, Meyer T, Burroughs AK. Inflammation-based scores do not predict post-transplant recurrence of hepatocellular carcinoma in patients within Milan criteria. *Liver Transpl* 2014; **20**: 1327-1335 [PMID: 25088400 DOI: 10.1002/lt.23969]

27 **Nicolini D**, Agostini A, Montalti R, Mocchegiani F, Mincarelli C, Mandolesi A, Robertson NL, Candelari R, Giovagnoni A, Vivarelli M. Radiological response and inflammation scores predict tumour recurrence in patients treated with transarterial chemoembolization before liver transplantation. *World J Gastroenterol* 2017; **23**: 3690-3701 [PMID: 28611522 DOI: 10.3748/wjg.v23.i20.3690]

28 **Harimoto N**, Yoshizumi T, Shimagaki T, Nagatsu A, Motomura T, Harada N, Okabe H, Itoh S, Ikegami T, Uchiyama H, Soejima Y, Maehara Y. Inflammation-based Prognostic Score in Patients with Living Donor Liver Transplantation for Hepatocellular Carcinoma. *Anticancer Res* 2016; **36**: 5537-5542 [PMID: 27798927 DOI: 10.21873/anticanres.11137]

29 **Carr BI**, Guerra V, Giannini EG, Farinati F, Ciccarese F, Rapaccini GL, Di Marco M, Benvegnù L, Zoli M, Borzio F, Caturelli E, Chiaramonte M, Trevisani F; Italian Liver Cancer Group. Significance of platelet and AFP levels and liver function

parameters for HCC size and survival. *Int J Biol Markers* 2014; **29**: e215-e223 [PMID: 24526315 DOI: 10.5301/jbm.5000064]
30 **Lee CH**, Lin YJ, Lin CC, Yen CL, Shen CH, Chang CJ, Hsieh SY. Pretreatment platelet count early predicts extrahepatic metastasis of human hepatoma. *Liver Int* 2015; **35**: 2327-2336 [PMID: 25752212 DOI: 10.1111/liv.12817]
31 **Han S**, Lee S, Yang JD, Leise MD, Ahn JH, Kim S, Jung K, Gwak MS, Kim GS, Ko JS. Risk of posttransplant hepatocellular carcinoma recurrence is greater in recipients with higher platelet counts in living donor liver transplantation. *Liver Transpl* 2018; **24**: 44-55 [PMID: 29024412 DOI: 10.1002/lt.24961]
32 **Leslie M**. Cell biology. Beyond clotting: the powers of platelets. *Science* 2010; **328**: 562-564 [PMID: 20430990 DOI: 10.1126/science.328.5978.562]
33 **Bihari C**, Rastogi A, Shasthry SM, Bajpai M, Bhadoria AS, Rajesh S, Mukund A, Kumar A, Sarin SK. Platelets contribute to growth and metastasis in hepatocellular carcinoma. *APMIS* 2016; **124**: 776-786 [PMID: 27457354 DOI: 10.1111/apm.12574]
34 **Liu D**, Zhang Y, Wei Y, Liu G, Liu Y, Gao Q, Zou L, Zeng W, Zhang N. Activation of AKT pathway by Nrf2/PDGFA feedback loop contributes to HCC progression. *Oncotarget* 2016; **7**: 65389-65402 [PMID: 27588483 DOI: 10.18632/oncotarget.11700]
35 **Nishida N**, Kitano M, Sakurai T, Kudo M. Molecular Mechanism and Prediction of Sorafenib Chemoresistance in Human Hepatocellular Carcinoma. *Dig Dis* 2015; **33**: 771-779 [PMID: 26488287 DOI: 10.1159/000439102]
36 36 **Hossain MA**, Kim DH, Jang JY, Kang YJ, Yoon JH, Moon JO, Chung HY, Kim GY, Choi YH, Copple BL, Kim ND. Aspirin induces apoptosis in vitro and inhibits tumor growth of human hepatocellular carcinoma cells in a nude mouse xenograft model. *Int J Oncol* 2012; **40**: 1298-1304 [PMID: 22179060 DOI: 10.3892/ijo.2011.1304]
37 **Zhang Z**, Zhang Y, Wang W, Hua Y, Liu L, Shen S, Peng B. Thrombocytopenia and the outcomes of hepatectomy for hepatocellular carcinoma: a meta-analysis. *J Surg Res* 2017; **210**: 99-107 [PMID: 28457347 DOI: 10.1016/j.jss.2016.11.002]

P- Reviewer: Boin IF, Gencdal G, Ramia JM, Zheng SS
S- Editor: Gong ZM **L- Editor**: A **E- Editor**: Huang Y

World Journal of Gastroenterology

Submit a Manuscript: http://www.f6publishing.com

World J Gastroenterol 2018 April 21; 24(15): 1666-1678

DOI: 10.3748/wjg.v24.i15.1666

ISSN 1007-9327 (print) ISSN 2219-2840 (online)

META-ANALYSIS

Impact of enhanced recovery after surgery programs on pancreatic surgery: A meta-analysis

Hai-Bin Ji, Wen-Tao Zhu, Qiang Wei, Xiao-Xiao Wang, Hai-Bin Wang, Qiang-Pu Chen

Hai-Bin Ji, Wen-Tao Zhu, Qiang Wei, Xiao-Xiao Wang, Hai-Bin Wang, Department of Hepatobiliary Surgery, Affiliated Hospital of Binzhou Medical University, Binzhou 256603, Shandong Province, China

Qiang-Pu Chen, Department of Hepatobiliary Surgery, Clinical Nutrition Support Center, Affiliated Hospital of Binzhou Medical University; Clinical Nutrition and Metabolism Key Laboratory of Shandong Province, Binzhou 256603, Shandong Province, China

ORCID number: Hai-Bin Ji (0000-0001-6606-4929); Wen-Tao Zhu (0000-0002-3432-0606); Qiang Wei (0000-0003-0668-6579); Xiao-Xiao Wang (0000-0002-9402-9685); Hai-Bin Wang (0000-0002-6525-6846); Qiang-Pu Chen (0000-0002-1941-3572).

Author contributions: Zhu WT, Wei Q, and Chen QP designed the research; Ji HB, Wei Q, Wang XX, and Wang HB performed the research; Ji HB, Zhu WT, and Wei Q analyzed the data; Ji HB, Wang XX, and Chen QP wrote the paper.

Conflict-of-interest statement: The authors deny any conflict of interest.

PRISMA 2009 Checklist: The authors have read and revised according to the PRISMA 2009 Checklist.

Manuscript source: Unsolicited manuscript.

Correspondence to: Qiang-Pu Chen, MS, professor, Chief, Department of Hepatobiliary Surgery, Clinical Nutrition Support Center, Affiliated Hospital of Binzhou Medical University, Clinical Nutrition and Metabolism Key Laboratory of Shandong Province, NO.661 of the 2nd Huanghe Road, Binzhou 256603, Shandong Province, China. drcqp_med@163.com.
Telephone: +86-543-3258597
Fax: +86-543-3257792

Received: February 5, 2018
Peer-review started: February 6, 2018
First decision: February 24, 2018
Revised: March 8, 2018
Accepted: March 18, 2018
Article in press: March 18, 2018
Published online: April 21, 2018

Abstract

AIM

To evaluate the impact of enhanced recovery after surgery (ERAS) programs on postoperative complications of pancreatic surgery.

METHODS

Computer searches were performed in databases (including PubMed, Cochrane Library and Embase) for randomized controlled trials or case-control studies describing ERAS programs in patients undergoing pancreatic surgery published between January 1995 and August 2017. Two researchers independently evaluated the quality of the studies' extracted data that met the inclusion criteria and performed a meta-analysis using RevMan5.3.5 software. Forest plots, demonstrating the outcomes of the ERAS group *vs* the control group after pancreatic surgery, and funnel plots were used to evaluate potential publication bias.

RESULTS

Twenty case-control studies including 3694 patients, published between January 1995 and August 2017, were selected for the meta-analysis. This study included the ERAS group (n = 1886) and the control group (n = 1808), which adopted the traditional perioperative management. Compared to the control group, the ERAS group had lower delayed gastric emptying rates [odds ratio (OR) = 0.58, 95% confidence interval

(CI): 0.48-0.72, $P < 0.00001$], lower postoperative complication rates (OR = 0.57, 95%CI: 0.45-0.72, $P < 0.00001$), particularly for the mild postoperative complications (Clavien-Dindo Ⅰ-Ⅱ) (OR = 0.71, 95%CI: 0.58-0.88, $P = 0.002$), lower abdominal infection rates (OR = 0.70, 95%CI: 0.54-0.90, $P = 0.006$), and shorter postoperative length of hospital stay (PLOS) (WMD = -4.45, 95%CI: -5.99 to -2.91, $P < 0.00001$). However, there were no significant differences in complications, such as, postoperative pancreatic fistulas, moderate to severe complications (Clavien-Dindo Ⅲ-Ⅴ), mortality, readmission and unintended reoperation, in both groups.

CONCLUSION

The perioperative implementation of ERAS programs in pancreatic surgery is safe and effective, can decrease postoperative complication rates, and can promote recovery for patients.

Key words: Pancreatic surgery; Enhanced recovery after surgery; Postoperative complication; Meta-analysis

Core tip: Enhanced recovery after surgery (ERAS) programs have been launched in a variety of surgical fields, including colorectal, orthopedics, urology, esophageal and gynecology, demonstrating favorable outcomes. Pancreatic surgery is considered a high-risk abdominal surgery, due to increased surgical trauma and high incidence of postoperative complications. In this meta-analysis we aimed to evaluate the impact of ERAS on complications of pancreatic surgery. The present study demonstrates that ERAS could reduce complication rates, especially of mild complications, delayed gastric emptying, abdominal infection and postoperative length of hospital stay, while not affecting the rates of postoperative pancreatic fistulas, reoperation, readmission and mortality during the perioperative period.

Ji HB, Zhu WT, Wei Q, Wang XX, Wang HB, Chen QP. Impact of enhanced recovery after surgery programs on pancreatic surgery: A meta-analysis. *World J Gastroenterol* 2018; 24(15): 1666-1678 Available from: URL: http://www.wjgnet.com/1007-9327/full/v24/i15/1666.htm DOI: http://dx.doi.org/10.3748/wjg.v24.i15.1666

INTRODUCTION

Enhanced recovery after surgery (ERAS; also called 'fast-track surgery') was first introduced by Kehlet H, a Danish surgeon, in 1997[1]. ERAS is a multidisciplinary and evidence-based framework developed to decrease perioperative surgical stress, accelerate postoperative recovery and significantly reduce the postoperative length of hospital stay (PLOS). ERAS programs were initially implemented in colorectal surgery and have been shown to be effective for reducing PLOS and complications[2]. Subsequently, ERAS programs have been published in numerous areas of surgery, such as orthopedics, urology, esophageal, gynecology, breast and hepatobiliary[3-8].

An array of studies has shown that the perioperative implementation of ERAS programs can reduce PLOS without increasing complications or mortality. However, pancreatic surgery is still considered a high-risk abdominal surgery, due to the anatomical location of the pancreas and high rate of complications (30%-60%). Postoperative complications, such as postoperative pancreatic fistula (POPF), delayed gastric emptying (DGE), abdominal infection, and so on, are the main reasons for delayed recovery and the frequent need for additional interventions, without which the complications are potentially life threatening. For these reasons, the implementation of ERAS programs has lagged for pancreatic surgeries.

There had been an increasing number of ERAS programs implemented in pancreatic surgery when the ERAS group published evidence-based consensus recommendations for pancreatic surgery in 2012[9]. The benefit of implementing ERAS programs on postoperative complications in pancreatic surgery has not reached consensus. For this reason, we performed a meta-analysis of the available studies on ERAS programs compared with traditional perioperative management in patients undergoing pancreatic surgery.

MATERIALS AND METHODS

Search strategy

A search was performed by two researchers (Ji HB and Wang XX) in August 2017 of the PubMed, Cochrane Library and Embase database, spanning the period from January 1995 to August 2017. The search language was restricted to English, using the search terms "enhanced recovery after surgery", "fast track surgery", "ERAS", "clinical pathways", "pancreatectomy", "pancreatoduodenectomy" and "duodenopancreatectomy", and using the Boolean operators "AND" and "OR". Synonyms of all these terms were used in this search. The PubMed search strategy for the meta-analysis is shown in Table 1.

Inclusion/exclusion criteria

Studies meeting all of the following selection criteria were eligible for inclusion: (1) studies concerning patients undergoing pancreatic surgery; (2) the ERAS group implemented ERAS programs management, and the control group adopted traditional perioperative management; (3) measures in perioperative management were described in both groups; and (4) studies reported at least the following outcome measures, POPF, DGE, abdominal infection, mortality and PLOS, and explained their diagnostic criteria for postoperative complications.

Table 1 The search strategy for the PubMed database[1]

Search number	Description	Number of publications
1	Enhanced recovery after surgery [Title/Abstract] OR ERAS [Title/Abstract] OR fast track surgery [Title/Abstract]	3333
2	Clinical pathways [MeSH Terms]	5848
3	1 OR 2	9130
4	Pancreatectomy [MeSH Terms] OR Pancreatectomy* [Title/Abstract] OR Pancreatoduodenectomy [MeSH Terms] OR Pancreatoduodenectom* [Title/Abstract] OR duodenopancreatectomy [MeSH Terms] OR duodenopancreatectom* [Title/Abstract]	21497
5	3 AND 4 NOT (animals[mh] NOT humans[mh])	69
6	5 limited to English	68

[1]Date of search: August 1, 2017.

Exclusion criteria were (1) sample size of less than 10; (2) comments, guidelines, reviews, case reports, abstracts, letters and non-comparative studies; (3) repeated publication of the same study population; and (4) incomplete clinical data.

Outcomes of interest

The outcomes of interest were POPF, DGE, PLOS, abdominal infection, mortality, readmission, unintended reoperation and occurrence of any complication within a postoperative period of 30 d. POPF was defined using the International Study Group of Pancreatic Fistula (ISGPF) guidelines describing a drain output of any measurable volume of fluid on or after postoperative day (POD) 3, with an amylase content greater than three times the serum amylase activity or as defined by the study's authors[10]. DGE was defined according to the International Study Group of Pancreatic Surgery's (ISGPS) recommendation that patients needing maintenance of a nasogastric tube (NGT) for > 3 d, needing to reinsert the NGT for persistent vomiting after POD 3, or unable to tolerate a solid diet by POD 7, should be considered DGE. In addition, there are another two widely used definitions for DGE after pancreatic resection (1) Yeo defined DGE as an NGT left in place for ≥ 10 d plus one of the following, or for < 10 d plus two of the following (a) repeated emesis after removal of the NGT, (b) need for prokinetic agents after POD 10, (c) need for reinsertion of the NGT, or (d) failure to progress with the diet. (2) Van Berge Henegouwen *et al*[11] defined DGE as gastric stasis requiring NGT for ≥ 10 d or the inability to tolerate a regular diet after POD 14. PLOS was defined as the span from the day of surgery to the day of actual discharge from the hospital. Abdominal infection was defined by the study's authors. Mortality was defined as the range from the day of hospitalization to the first 30 d after actual discharge. Readmission was defined as the patient needing medical attention again within 30 d after discharge. Overall postoperative complications included any complication from the time of surgery to discharge, or within 30 d, with severity grading and classification relying on the Clavien-Dindo system[12]. Unintended reoperation was defined as patients with complications or other reasons that required reoperation within 30 d after discharge.

Data extraction

Data were extracted from each study by two authors (Ji HB and Wei Q) independently. The main parameters included common information (time of study publication, country, study type, and authors), characteristics of the study population (sex and age), elements of ERAS programs, and postoperative outcomes (overall complications, POPF, DGE, abdominal infection, PLOS, mortality, readmission, and unintended reoperation). All continuous outcome variables were described using the means and standard deviations for this meta-analysis. We needed to estimate means and standard deviations via the methodologies reported by Hozo *et al*[13] if the original data were expressed as medians or ranges.

Quality assessment

The quality assessment of each study was done by two authors (Zhu WT and Ji HB) independently via the Methodological Index for Non-Randomized Studies (MINORS) checklist. It was then summarized by a French surgeon, and if there was a disagreement, the third researcher was involved in the negotiation or adjudication, until a consensus was achieved. The MINORS checklist includes eight methodological items for non-comparative studies and an additional four items for comparative studies. The items are scored 0 (not reported), 1 (reported but inadequate), or 2 (reported and adequate). The overall ideal scores were 24 for comparative studies.

Statistical analysis

The meta-analysis was performed using RevMan5.3.5 software (Ji HB and Wang HB). Continuous and categorical variables were calculated as weighted mean differences (WMDs) or odds ratios (ORs) with their corresponding 95% confidence interval (CI), respectively. Heterogeneity was assessed using a chi-square test, where $P > 0.05$ was considered non-significant. I^2 values were used for the evaluation of statistical heterogeneity, and the I^2 value of 50% or more indicated the presence

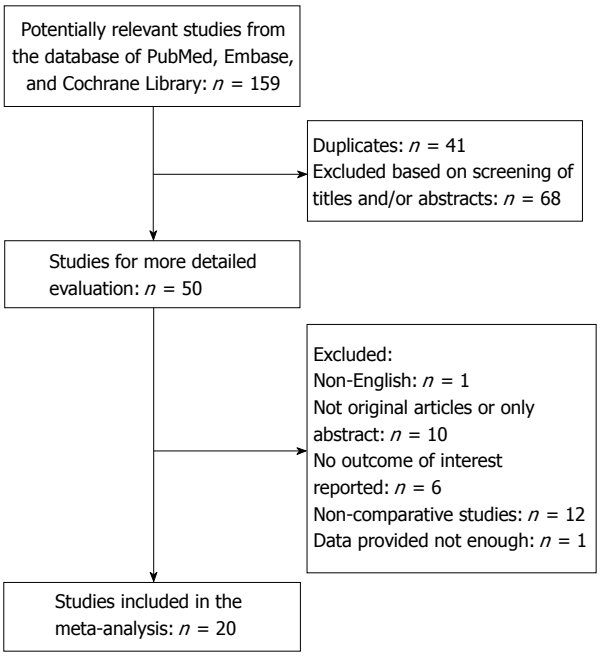

Figure 1 The diagram of selected studies for this meta-analysis.

of heterogeneity. The fixed-effects model was used for studies of homogeneity (I^2 < 50%), and the random-effects model was applied when studies indicated heterogeneity ($I^2 \geqslant$ 50%). In addition, funnel plots were used to evaluate potential publication bias based on the incidence of POPF and mortality.

Eligible studies

The search strategy initially identified 159 relevant studies. No randomized control trials were identified. Figure 1 shows the process of selecting the studies for meta-analysis. After removing duplicates, the titles and abstracts of 118 studies were reviewed. Of these, 68 studies were not related to ERAS in pancreatic surgery, 12 studies did not have a control group, 6 studies did not have the outcomes of interest reported, 10 studies only had an abstract or we were unable to get the full text, 1 study did not have enough data, and 1 study was published in a language other than English. A total of 20 studies met the inclusion criteria for the meta-analysis.

Study characteristics and quality assessment

The characteristics and quality assessments of the included studies are shown in Table 2[14-33]. All studies clearly described an ERAS program. The major components are summarized in Table 2. All of the studies used a retrospective case-control model, and of those, there were 16 studies that had sample sizes greater than 100. A total of 3694 patients were included, of which there were 1886 patients and 1808 patients included in the ERAS group and control group, respectively. In addition, there were 17 studies with MINORS scores > 12.

RESULTS

Pancreatic fistula

Eighteen studies reported the rates of POPF. The overall results (OR = 0.87, 95%CI: 0.74-1.03, *P* = 0.10; Figure 2), or only those using the ISGPF definition (OR = 0.90, 95%CI: 0.76-1.07, *P* = 0.24), showed that there were no significant differences present in either group. Furthermore, there was no significant difference in A (OR = 1.05, 95%CI: 0.81-1.36, *P* = 0.71), B (OR = 1.13, 95%CI: 0.85-1.51, *P* = 0.40), and C (OR = 0.90, 95%CI: 0.60-1.33, *P* = 0.59) grade of POPF between the ERAS group and control group.

DGE

Eighteen studies reported the rates of DGE. Compared to the control group, the ERAS group had a lower incidence of DGE (OR = 0.58, 95%CI: 0.48-0.72, *P* < 0.00001; Figure 3). The difference persisted when including only studies that adopted the ISGPS definition (OR = 0.50, 95%CI: 0.39-0.65, *P* < 0.00001).

Postoperative complications

The rate of overall postoperative complications was lower in the ERAS group (OR = 0.57, 95%CI: 0.45-0.72, *P* < 0.00001; Figure 4). Additionally, the incidence of mild postoperative complications (Clavien-Dindo I-II), which relies on the Clavien-Dindo definition of severity and classification, was lower in the ERAS group (OR = 0.71, 95%CI: 0.58-0.88, *P* = 0.002; Figure 5). There were no statistical differences in the moderate to severe complication rates (Clavien-DindoⅢ-Ⅴ) between the ERAS group and control group (OR = 0.90, 95%CI: 0.73-1.11, *P* = 0.32).

Abdominal infection

A total of 12 studies reported the rates of abdominal infection. The incidence of abdominal infection was lower (OR = 0.70, 95%CI: 0.54-0.90, *P* = 0.006; Figure 6) in the ERAS group.

PLOS

A total of 13 studies reported the PLOS, and they showed that the ERAS group had shorter PLOS (WMD = -4.45, 95%CI: -5.99 to -2.91, *P* < 0.00001; Figure 7) than the control group.

In addition, there were no significant differences in rates of mortality (OR = 0.85, 95%CI: 0.54-1.36, *P* = 0.51; Figure 8), readmission (OR = 1.04, 95%CI: 0.83-1.30, *P* = 0.75; Figure 9), and unintended reoperation (OR = 0.87, 95%CI: 0.63-1.20, *P* = 0.40; Figure 10).

Subgroup analysis

The subgroup analysis, which included only larger

Table 2 Study Characteristics and Quality Assessment.

Study	Year	Country	Study design	Sample size		ERAS programs[1]	MINORS Score
				ERAS group	Control group		
Kennedy *et al*[14]	2007	United States	Case-control	91	44	e, f, g, h	16/24
Vanounou *et al*[15]	2007	United States	Case-control	145	64	c, d, g, h	15/24
Balzano *et al*[16]	2008	Italy	Case-control	252	252	d, e, f, g, h	13/24
Kennedy *et al*[17]	2009	United States	Case-control	71	40	d, e, f, g, h	11/24
Abu Hilal *et al*[18]	2013	Britain	Case-control	20	24	b, e, f, g, h	15/24
Braga *et al*[19]	2014	Italy	Case-control	115	115	a, b, c, d, e, f, g, h	17/24
Pillai *et al*[20]	2014	India	Case-control	20	20	c, d, e, f, g, h	17/24
Coolsen *et al*[21]	2014	Holland	Case-control	86	97	b, c, d, e, f, g, h	12/24
Nussbaum *et al*[22]	2014	United States	Case-control	100	142	c, e, f, g, h	11/24
Yui *et al*[23]	2014	Japan	Case-control	57	52	e, g, h	13/24
Nussbaum *et al*[24]	2014	United States	Case-control	50	100	c, e, f, g, h	16/24
Kobayashi *et al*[25]	2014	Japan	Case-control	100	90	a, e, g, h	13/24
Shao *et al*[26]	2015	China	Case-control	325	310	d, e, f, g, h	15/24
Joliat *et al*[27]	2015	Switzerland	Case-control	74	87	a, b, c, d, e, f, g, h	15/24
Partelli *et al*[28]	2015	Italy	Case-control	22	66	a, c, d, e, f, g, h	13/24
Williamsson *et al*[29]	2015	Sweden	Case-control	50	50	c, d, e, f, g, h	17/24
Morales Soriano *et al*[30]	2015	Spain	Case-control	41	44	a, b, c, d, e, f, g, h	17/24
Bai *et al*[31]	2016	China	Case-control	124	63	a, d, e, f, g, h	15/24
Zouros *et al*[32]	2016	Greece	Case-control	75	50	a, b, c, d, e, f, g, h	16/24
Dai *et al*[33]	2017	China	Case-control	68	98	a, b, c, e, f, g, h	15/24

[1]ERAS programs: a: No bowel preparation in the preoperative period; b: Clear fluids until 2-3 h before surgery; c: Restrictive policy of intravenous fluids in the intra-operative period; d: Multimodal analgesia of the postoperative period; e: Clear fluids or food intakes in the early period; f: Enhanced mobilization in the early period; g: Removal of the drainage tube; h: Others. ERAS: enhanced recovery after surgery; MINORS score: Methodological Index for Non-Randomized Studies checklist.

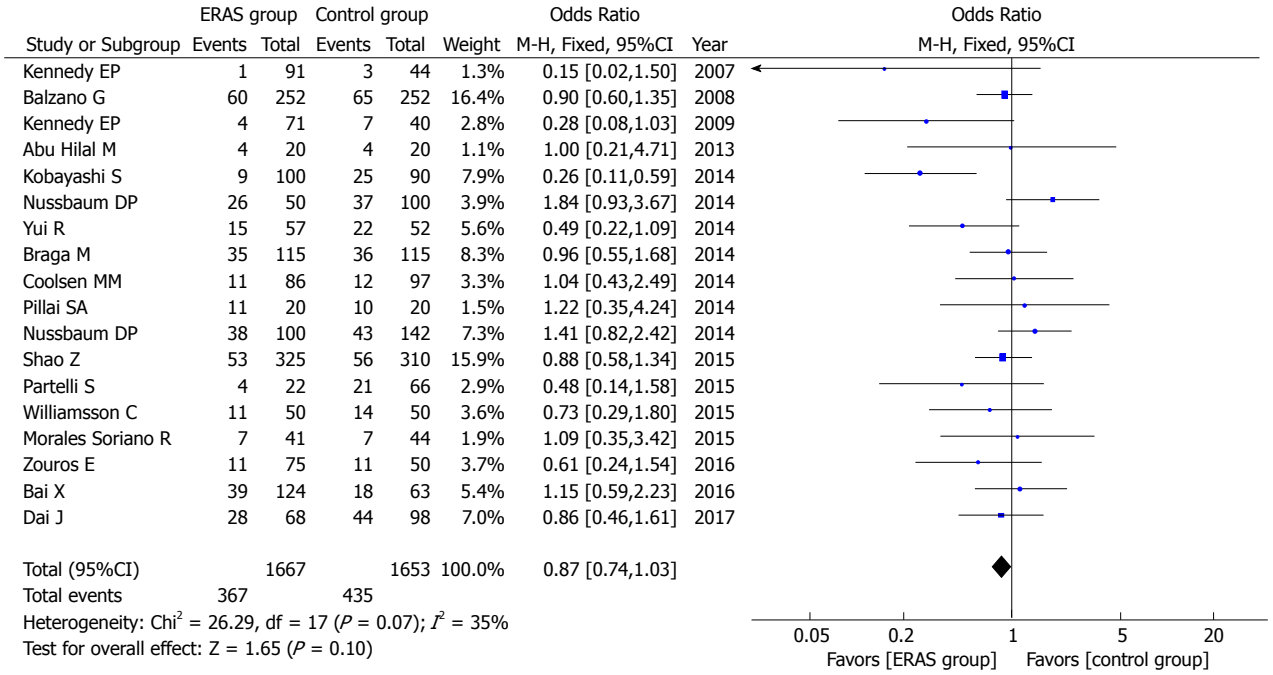

Figure 2 Forest plots demonstrating the outcomes of postoperative pancreatic fistula.

size studies ($n \geqslant 100$) generated similar results in postoperative outcomes (Table 3). Furthermore, the analysis of only high-quality studies (MINORS score > 12) also yielded parallel results in postoperative outcomes (Table 3). However, the heterogeneity for overall complications and PLOS still exists in larger studies and high-quality studies.

Sensitivity analysis

We aimed to investigate the influence of a single study on the overall results by omitting one study in each turn. This analysis revealed that no single study generated an

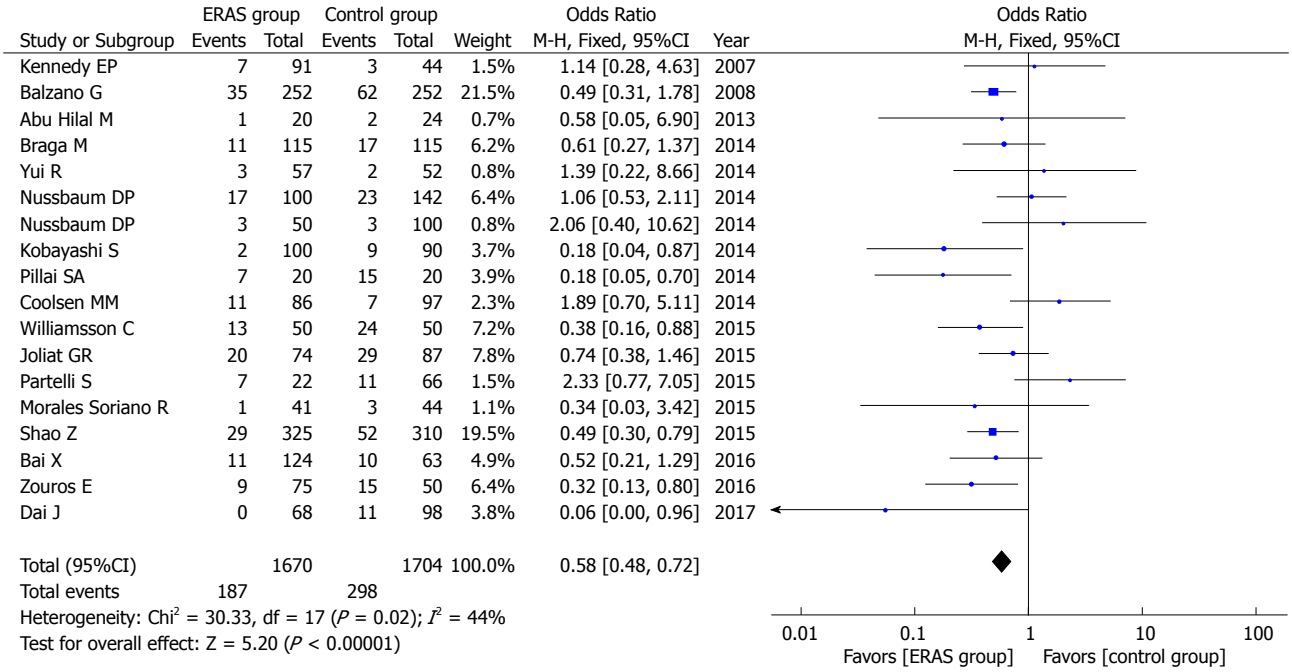

Figure 3 Forest plots demonstrating the outcomes of delayed gastric emptying.

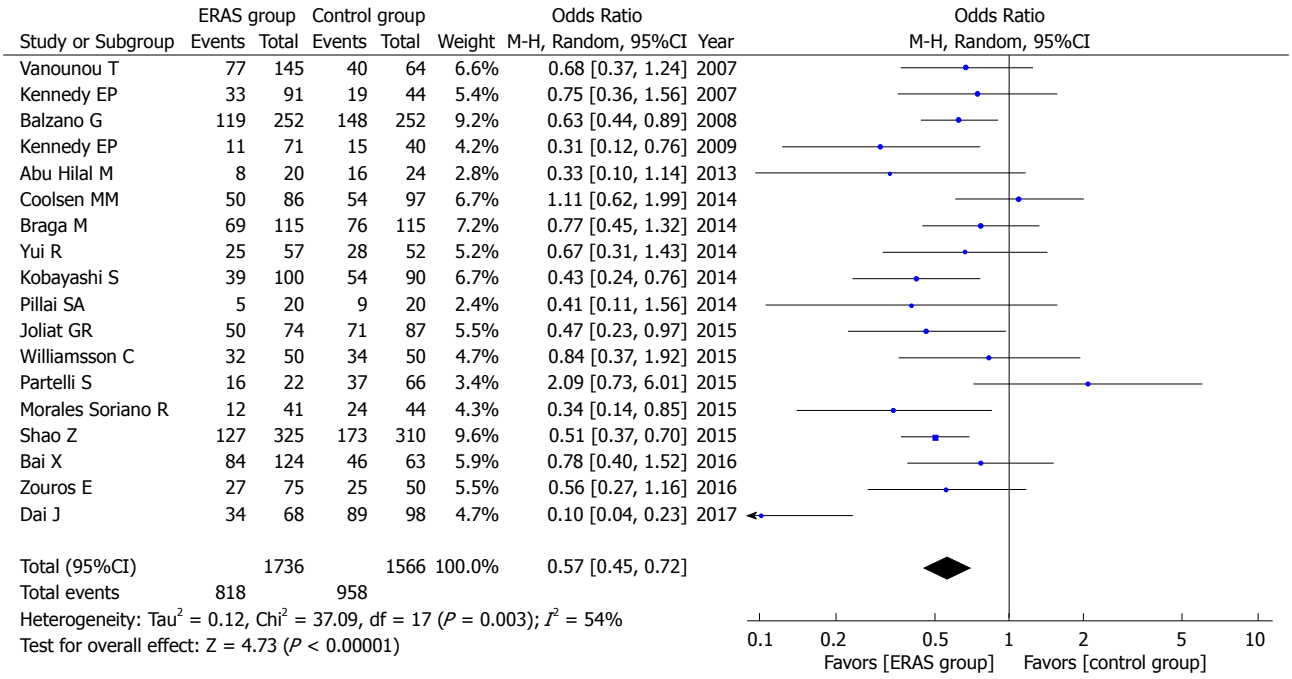

Figure 4 Forest plots demonstrating the outcomes of overall complications.

especially strong influence on the results, with estimates ranging from an OR of 0.54 to 0.62 (Table 4).

Publication bias

Funnel plots based on the incidence of POPF and mortality were used to evaluate potential publication bias in this study (Figure 11). There was no evidence of publication bias of POPF, mortality or other outcomes of this study (other figures not shown).

DISCUSSION

ERAS requires surgical, nursing, anesthesia, nutritionist and other specialties to work together and uses a series of optimal and evidence-based management measures to lessen perioperative surgical stress while promoting the recovery of organ function in the early postoperative period[34,35]. ERAS programs were initially implemented in colorectal surgery, with recommendations for each step

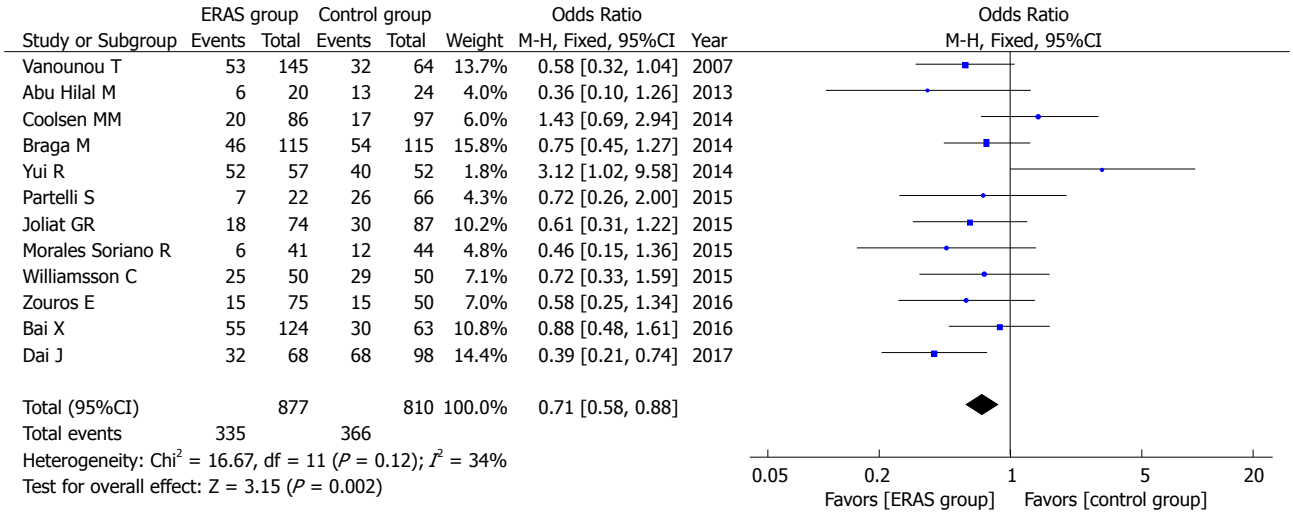

Figure 5 Forest plots demonstrating the outcomes of mild complications.

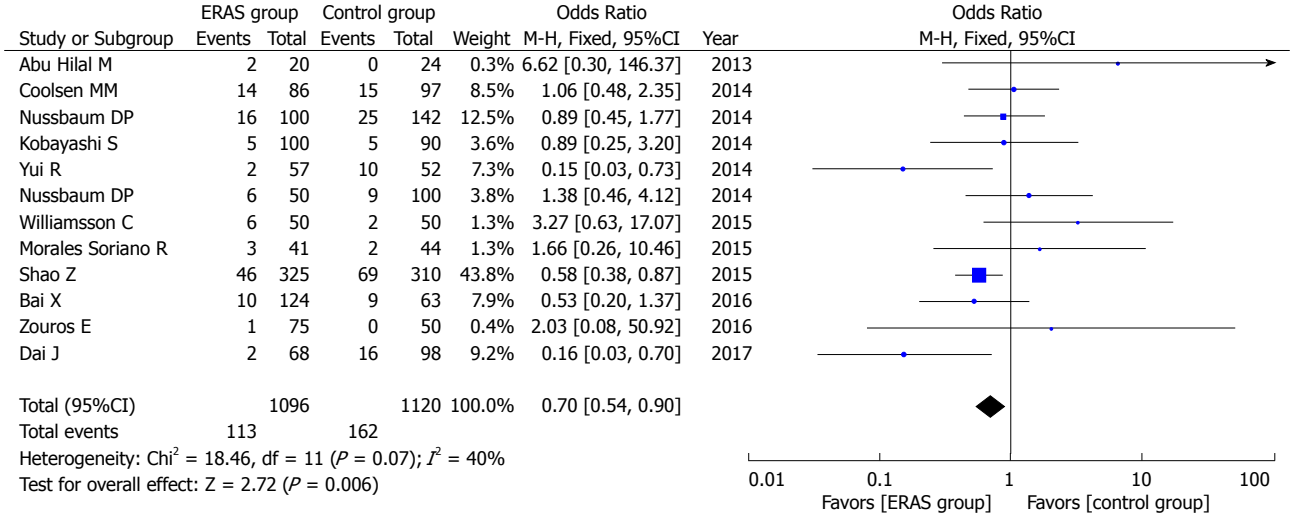

Figure 6 Forest plots demonstrating the outcomes of abdominal infection.

to achieve optimal perioperative care[36]. Subsequently, ERAS programs had been launched in numerous fields of surgery, such as orthopedics, urology, esophageal and gynecology.

The literature from these disciplines has suggested that standardizing ERAS measures could reduce the incidence of complications, accelerate recovery for patients, reduce hospitalization costs and save medical resources in perioperative care[3,4,7,8]. Pancreatic surgery is an effective treatment of pancreatic tumors, periampullary tumors, duodenal tumors and distal bile duct tumors. Currently, despite surgical techniques, anesthesia, and preoperative imaging assessment making great progress and the mortality of the procedure dropping to approximately 2% in high-volume medical centers, it is still considered a complicated and high-risk abdominal surgery[37].

Coolsen *et al*[38] analyzed 8 studies, which related to pancreatic surgery, and suggested that the ERAS group had shorter PLOS and lower postoperative complication rates; however, there were no significant differences in rates of DGE, POPF, readmission, and mortality. Kagedan *et al*[39] analyzed 10 studies suggesting that the ERAS group had only shorter PLOS and no differences in other complications. As mentioned above, we may reasonably conclude that the influence of ERAS programs on the postoperative complications of pancreatic surgery is controversial. Hence, the application of ERAS programs in the perioperative period of pancreatic surgery is still being explored in our practices.

The main measures of the ERAS programs include no bowel preparation and clear fluids until 2-3 h before surgery, multimodal analgesia of postoperative, clear fluids or food intakes, enhanced mobilization and removal of the drainage tube in early period**.** The ERAS group has reduced time of fasting in the preoperative period, which can decrease the insulin resistance in the postoperative period. We adopted multimodal

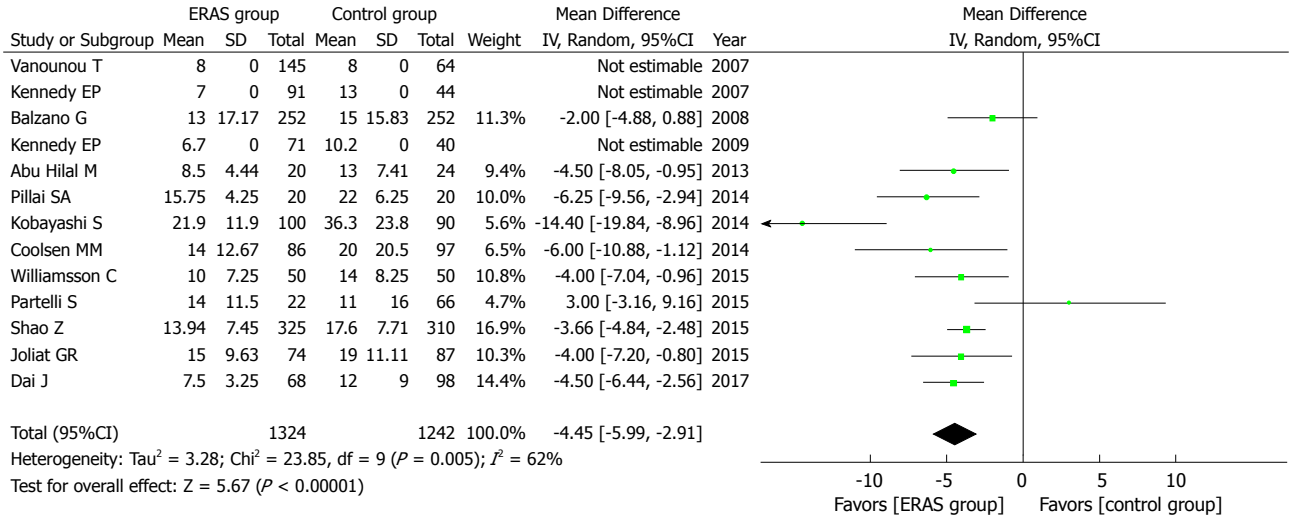

Figure 7 Forest plots demonstrating the outcomes of postoperative length of hospital stay.

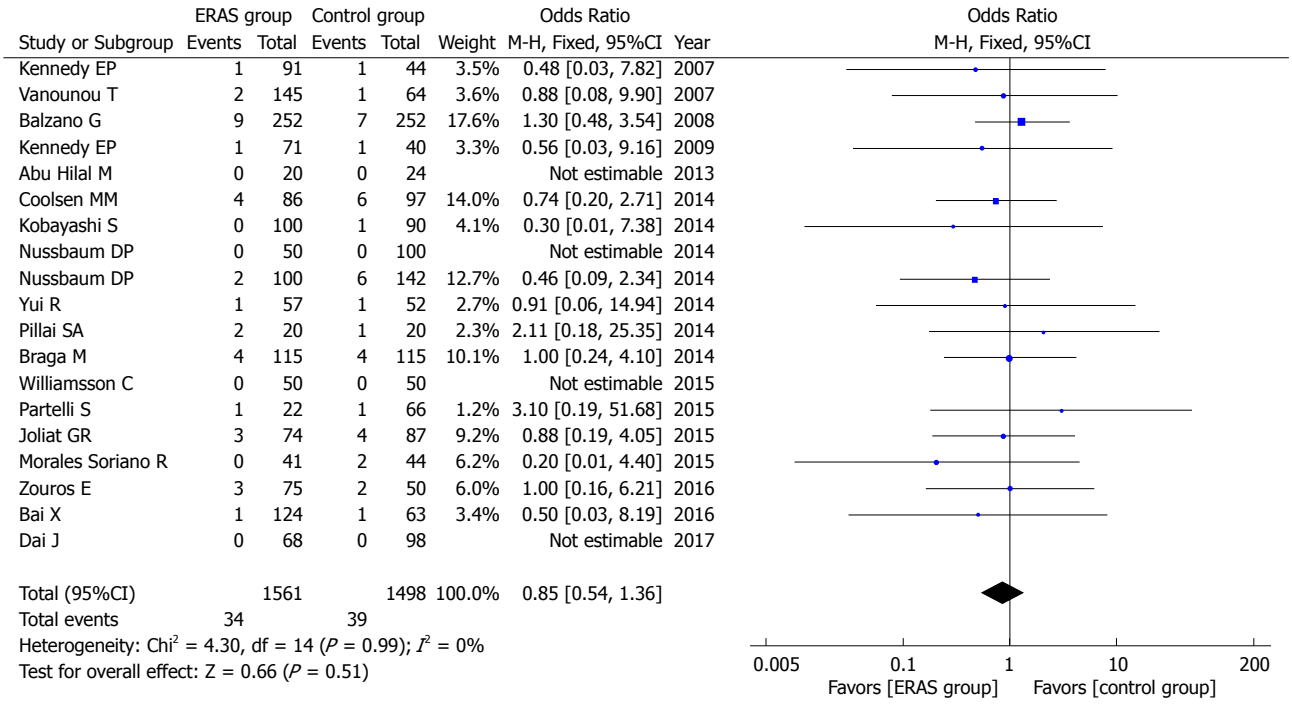

Figure 8 Forest plots demonstrating the outcomes of mortality.

analgesia in the postoperative period, which was able to reduce the stress caused by pain. The programs, such as, no bowel preparation before surgery, clear fluids or food intakes, enhanced mobilization in the early postoperative period which may promote rehabilitation of gastrointestinal function[40].

The ERAS programs aimed to reduce the incidence of complications and accelerate recovery for patients. Among them, gastrointestinal function rehabilitation is an important part of the rapid recovery in abdominal surgery. In addition, the early postoperative oral feeding, which may play an important role in the gastrointestinal function rehabilitation in the postoperative period. This is because early postoperative oral feeding is more in line with human physiology of the digestive tract, and which may have a beneficial effect on immunological, inflammatory and nutritional status. In addition, early postoperative oral feeding can promote the recovery of gastrointestinal motility, protect the gastrointestinal mucosal barrier, shorten time to gas and stools passage, and reduce the incidence of complications.

A total of 20 studies and 3694 patients were included in our meta-analysis. Compared with the control group, the ERAS group had lower rates of DGE, lower postoperative complication rates, particularly lower mild postoperative complication rates, lower abdominal infection rates, and shorter PLOS. However, no significant differences existed in POPF, moderate

Study or Subgroup	ERAS group Events	Total	Control group Events	Total	Weight	Odds Ratio M-H, Fixed, 95%CI	Year
Kennedy EP	7	91	3	44	2.5%	1.14 [0.28, 4.63]	2007
Vanounou T	13	145	4	64	3.4%	1.48 [0.46, 4.72]	2007
Balzano G	18	252	16	252	10.1%	1.13 [0.56, 2.28]	2008
Kennedy EP	5	71	10	40	8.1%	0.23 [0.07, 0.72]	2009
Abu Hilal M	1	20	2	24	1.2%	0.58 [0.05, 6.90]	2013
Coolsen MM	11	86	14	97	7.8%	0.87 [0.37, 2.03]	2014
Braga M	14	115	12	115	7.1%	1.19 [0.52, 2.70]	2014
Nussbaum DP	31	100	36	142	13.9%	1.32 [0.75, 2.33]	2014
Nussbaum DP	15	50	20	100	6.3%	1.71 [0.79, 3.73]	2014
Pillai SA	0	20	0	20		Not estimable	2014
Shao Z	43	325	44	310	26.5%	0.92 [0.59, 1.45]	2015
Partelli S	3	22	11	66	3.2%	0.79 [0.20, 3.14]	2015
Morales Soriano R	4	41	4	44	2.4%	1.08 [0.25, 4.64]	2015
Zouros E	5	75	3	50	2.3%	1.12 [0.26, 4.91]	2016
Bai X	11	124	2	63	1.6%	2.97 [0.64, 13.83]	2016
Dai J	0	68	6	98	3.6%	0.10 [0.01, 1.88]	2017
Total (95%CI)		1605		1529	100.0%	1.04 [0.83, 1.30]	
Total events	181		187				

Heterogeneity: Chi^2 = 14.49, df = 14 (P = 0.41); I^2 = 3%
Test for overall effect: Z = 0.31 (P = 0.75)

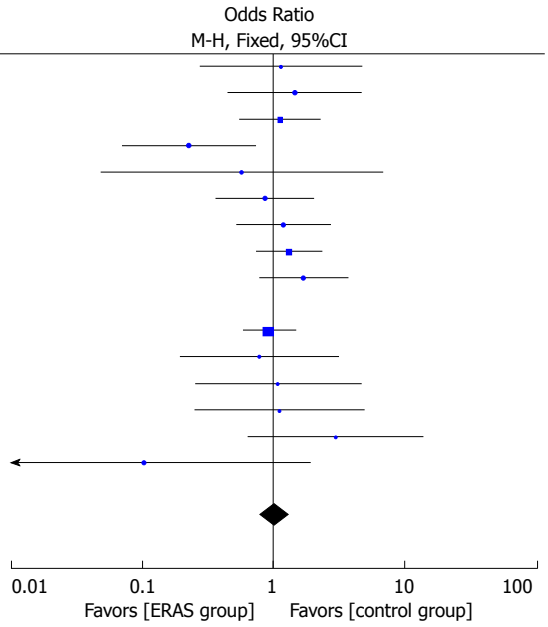

Figure 9 Forest plots demonstrating the outcomes of readmission.

Study or Subgroup	ERAS group Events	Total	Control group Events	Total	Weight	Odds Ratio M-H, Fixed, 95%CI	Year
Vanounou T	7	145	4	64	6.8%	0.76 [0.21, 2.70]	2007
Balzano G	17	252	20	252	24.1%	0.84 [0.43, 1.64]	2008
Abu Hilal M	0	20	3	24	4.0%	0.15 [0.01, 3.08]	2013
Nussbaum DP	10	100	18	142	17.3%	0.77 [0.34, 1.74]	2014
Yui R	1	57	1	52	1.3%	0.91 [0.06, 14.94]	2014
Pillai SA	3	20	1	20	1.1%	3.35 [0.32, 35.36]	2014
Coolsen MM	7	86	13	97	14.5%	0.57 [0.22, 1.51]	2014
Braga M	14	115	12	115	13.6%	1.19 [0.52, 2.70]	2014
Morales Soriano R	5	41	5	44	5.5%	1.08 [0.29, 4.05]	2015
Partelli S	1	22	3	66	1.9%	1.00 [0.10, 10.14]	2015
Zouros E	4	75	2	50	2.9%	1.35 [0.24, 7.68]	2016
Bai X	4	124	1	63	1.7%	2.07 [0.23, 18.89]	2016
Dai J	2	68	5	98	5.1%	0.56 [0.11, 2.99]	2017
Total (95%CI)		1125		1087	100.0%	0.87 [0.63, 1.20]	
Total events	75		88				

Heterogeneity: Chi^2 = 5.20, df = 12 (P = 0.95); I^2 = 0%
Test for overall effect: Z = 0.84 (P = 0.40)

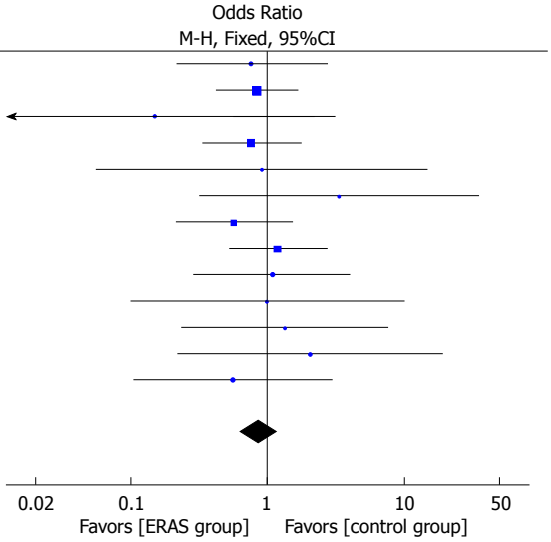

Figure 10 Forest plots demonstrating the outcomes of unintended reoperation.

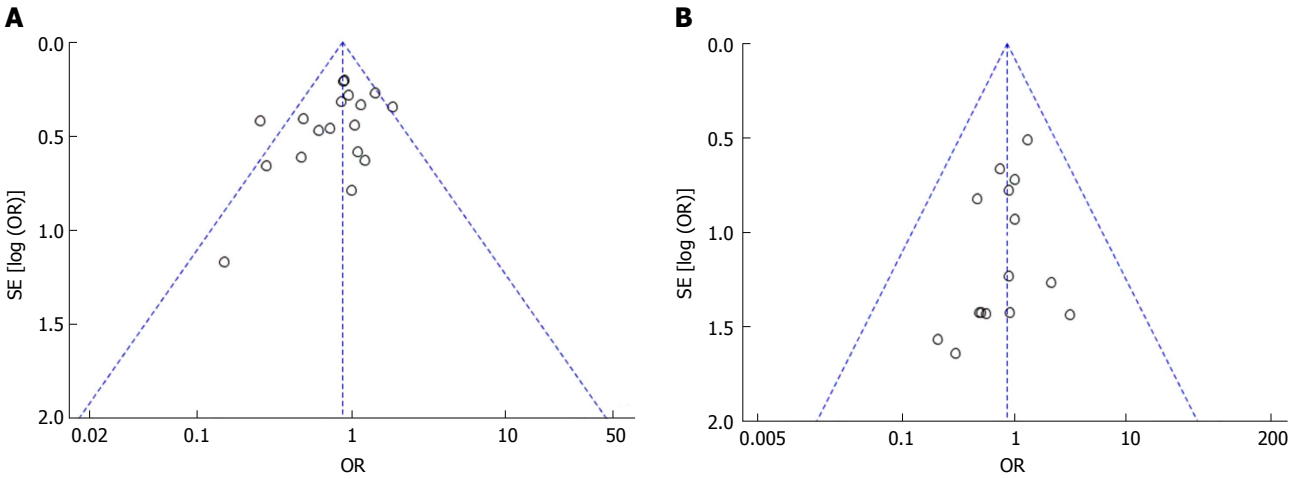

Figure 11 The funnel plots were used to evaluate potential publication bias. A: POPF; B: Mortality.

Table 3 Results of Subgroup Analysis

Outcomes of interest	Studies	Patients	OR/WMD	95%CI	*P*-value	Heterogeneity *P*-value	I^2, %
Studies with cases ⩾ 100							
POPF	14	3067	0.87	0.73-1.03	0.11	0.02	48
DGE	14	3117	0.58	0.47-0.71	< 0.00001	0.07	39
Overall complications	14	3045	0.57	0.45-0.72	< 0.00001	0.006	55
Mild complications	9	1470	0.74	0.59-0.93	0.009	0.06	46
Abdominal infection	10	2087	0.67	0.51-0.87	0.003	0.07	42
PLOS	10	2394	-4.64	-6.37 to -2.91	< 0.00001	0.009	65
Mortality	15	2802	0.83	0.51-1.37	0.47	1	0
Readmission	12	2877	1.05	0.83-1.33	0.68	0.23	22
Unintended reoperation	9	1955	0.85	0.60-1.21	0.38	0.96	0
MINORS score > 12							
POPF	15	2784	0.84	0.70-1.00	0.05	0.13	30
DGE	16	2949	0.52	0.42-0.64	< 0.00001	0.12	31
Overall complications	16	3008	0.56	0.44-0.71	< 0.00001	0.01	51
Mild complications	11	1504	0.67	0.54-0.83	0.0003	0.24	21
Abdominal infection	10	1791	0.63	0.46-0.85	0.002	0.05	46
PLOS	11	2272	-4.35	-5.97 to -2.72	< 0.00001	0.003	66
Mortality	16	2523	0.96	0.56-1.65	0.89	0.99	0
Readmission	13	2598	1.09	0.84-1.43	0.52	0.82	0
Unintended reoperation	11	1787	0.96	0.65-1.41	0.83	0.94	0

CI: Confidence interval; DGE: Delayed gastric emptying; MINORS score: Methodological Index for Non-Randomized Studies checklist; OR: Odds ratio; PLOS: Postoperative length of hospital stay; POPF: Postoperative pancreatic fistula; WMD: Weighted mean difference.

Table 4 Results of sensitivity analysis by omitting one study in each turn

Studies	OR	95%CI	*P*-value
Omitting Vanounou *et al*[15]	0.56	0.44-0.72	< 0.00001
Omitting Kennedy *et al*[14]	0.56	0.44-0.71	< 0.00001
Omitting Balzano *et al*[16]	0.56	0.43-0.73	< 0.0001
Omitting Kennedy *et al*[17]	0.58	0.46-0.74	< 0.00001
Omitting Abu Hilal *et al*[18]	0.58	0.45-0.73	< 0.00001
Omitting Yui *et al*[23]	0.56	0.44-0.72	< 0.00001
Omitting Kobayashi *et al*[25]	0.58	0.45-0.74	< 0.00001
Omitting Coolsen *et al*[21]	0.54	0.43-0.69	< 0.00001
Omitting Braga *et al*[19]	0.55	0.43-0.71	< 0.00001
Omitting Pillai *et al*[20]	0.57	0.45-0.73	< 0.00001
Omitting Joliat *et al*[27]	0.57	0.45-0.73	< 0.0001
Omitting Partelli *et al*[28]	0.55	0.44-0.68	< 0.00001
Omitting Williamsson *et al*[29]	0.56	0.44-0.71	< 0.00001
Omitting Morales Soriano *et al*[30]	0.58	0.46-0.74	< 0.00001
Omitting Shao *et al*[26]	0.57	0.44-0.74	< 0.0001
Omitting Zouros *et al*[32]	0.57	0.44-0.73	< 0.00001
Omitting Bai *et al*[31]	0.56	0.44-0.71	< 0.00001
Omitting Dai *et al*[33]	0.62	0.52-0.71	< 0.00001
Overall effect	0.57	0.45-0.72	< 0.00001

CI: Confidence interval; OR: Odds ratio.

to severe complications, mortality, readmission or unintended reoperation in both groups.

Many factors, such as age, nutritional status, and serious comorbidity, can influence patients' postoperative complication rates and the process of postoperative recovery[41, 42]. The patients' demographic data in the included studies was basically identical, so these influences may be eliminated for the outcomes in this study. In addition, all of the included studies described the diagnostic criteria for postoperative complications.

Despite our careful work on this meta-analysis of currently available evidence, some limitations should be acknowledged. First, the diagnostic criteria of some postoperative complications were not uniformly defined, though all the included studies gave a description of the diagnostic criteria. Therefore, to a certain extent, information bias was possible, because some complications did not have national criteria. Second, only retrospective case control studies were included in this analysis. Therefore, to a certain extent, the outcomes of this study may be influenced by the selection bias. Third, the degree of implementation of ERAS programs and the compliance of patients may be different between studies. Finally, there was no evidence

to indicate that major publication bias existed in these studies, and potential publication bias is impossible to completely rule out in small studies. Hence, these factors had some influence on our results.

In summary, the results from our present study demonstrate that the implementation of ERAS programs could reduce overall complication rates, especially of mild complications, DGE, rates of abdominal infection, and PLOS, while not affecting the rates of POPF, reoperation, readmission, and mortality during the perioperative period for pancreatic surgery. The perioperative period for pancreatic surgery is safe and effective to implement ERAS programs that can decrease postoperative complication rates and promote recovery. However, in the future, we need to include more high-quality and strict prospective studies to assess the contributions of individual program components.

ARTICLE HIGHLIGHTS

Research background

Enhanced recovery after surgery (ERAS) is a multidisciplinary and evidence-based framework, developed to decrease perioperative surgical stress, accelerate postoperative recovery and significantly reduce the postoperative length of hospital stay (PLOS). ERAS programs have been launched in a variety of other fields of surgery, such as colorectal, orthopedics, urology, esophageal, and gynecology, and have demonstrated favorable outcomes. The implementation of ERAS programs has lagged surrounding pancreatic surgeries because of the anatomical location of the pancreas and the high rate of postoperative complications (30%-60%). It is very important to promote the postoperative recovery for this high-risk abdominal surgery via implementing ERAS programs during the perioperational period.

Research motivation

ERAS requires surgical, nursing, anesthesia and other specialties to work together and uses a series of optimal or evidence-based management measures to lessen perioperative surgical stress while promoting the recovery of organ function in the early postoperative period. The implementation of ERAS programs may play a very important role in the perioperational period for pancreatic surgery.

Research objectives

This study evaluated the impact of ERAS programs on postoperative complications and PLOS of pancreatic surgery.

Research methods

Computer searches were performed in databases (including PubMed, Cochrane Library, and Embase) for randomized controlled trials or case-control studies describing ERAS programs in patients undergoing pancreatic surgery published between January 1995 and August 2017. Two researchers independently evaluated the quality of the studies' extracted data that met inclusion criteria and performed a meta-analysis using RevMan5.3.5 software. Forest plots, demonstrating the outcomes of the ERAS group *versus* the control group after pancreatic surgery, and funnel plots were used to evaluate potential publication bias.

Research results

Twenty case-control studies, published between January 1995 and August 2017, including 3694 patients, were selected for the meta-analysis. They included the ERAS group (n = 1886) and control group (n = 1808), which adopted the traditional perioperative management. Compared to the control group, the ERAS group had lower delayed gastric emptying (DGE) rates (odds ratio (OR) = 0.58, 95% confidence interval (CI): 0.48-0.72, P < 0.00001), lower postoperative complication rates (OR = 0.57, 95%CI: 0.45-0.72, P < 0.00001), particularly for mild postoperative complications (Clavien-Dindo Ⅰ-Ⅱ) (OR = 0.71, 95%CI: 0.58-0.88, P = 0.002), lower abdominal infection rates (OR = 0.70, 95%CI: 0.54-0.90, P = 0.006) and shorter PLOS (weighted mean difference (WMD) = -4.45, 95%CI: -5.99 to -2.91, P < 0.00001). However, there were no significant differences in postoperative pancreatic fistulas (POPF), moderate to severe complications (Clavien-Dindo Ⅲ-Ⅳ), mortality, readmission and unintended reoperation in both groups.

Research conclusions

The results from our present study demonstrate that the implementation of ERAS programs could reduce overall complication rates, especially of mild complications, DGE, rate of abdominal infection and PLOS, while not affecting the rates of POPF, reoperation, readmission and mortality during the perioperative period for pancreatic surgery. The perioperative period for pancreatic surgery is safe and effective to implement ERAS programs that can decrease postoperative complication rates and promote recovery

Research perspectives

We need to include more high-quality and strict prospective studies to assess the contributions of individual program components, such as clear fluids or food intakes in the early period, and removal of the drainage tube.

REFERENCES

1 **Kehlet H**. Multimodal approach to control postoperative pathophysiology and rehabilitation. *Br J Anaesth* 1997; **78**: 606-617 [PMID: 9175983]

2 **Basse L**, Raskov HH, Hjort Jakobsen D, Sonne E, Billesbølle P, Hendel HW, Rosenberg J, Kehlet H. Accelerated postoperative recovery programme after colonic resection improves physical performance, pulmonary function and body composition. *Br J Surg* 2002; **89**: 446-453 [PMID: 11952586 DOI: 10.1046/j.0007-1323.2001.02044.x]

3 **Barbieri A**, Vanhaecht K, Van Herck P, Sermeus W, Faggiano F, Marchisio S, Panella M. Effects of clinical pathways in the joint replacement: a meta-analysis. *BMC Med* 2009; **7**: 32 [PMID: 19570193 DOI: 10.1186/1741-7015-7-32]

4 **Azhar RA**, Bochner B, Catto J, Goh AC, Kelly J, Patel HD, Pruthi RS, Thalmann GN, Desai M. Enhanced recovery after urological surgery: a contemporary systematic review of outcomes, key elements, and research needs. *Eur Urol* 2016; **70**: 176-187 [PMID: 26970912 DOI: 10.1016/j.eururo.2016.02.051]

5 **Arsalani-Zadeh R**, ElFadl D, Yassin N, MacFie J. Evidence-based review of enhancing postoperative recovery after breast surgery. *Br J Surg* 2011; **98**: 181-196 [PMID: 21104705 DOI: 10.1002/bjs.7331]

6 **Hughes MJ**, McNally S, Wigmore SJ. Enhanced recovery following liver surgery: a systematic review and meta-analysis. *HPB* (Oxford) 2014; **16**: 699-706 [PMID: 24661306 DOI: 10.1111/hpb.12245]

7 **Pisarska M**, Małczak P, Major P, Wysocki M, Budzyński A, Pędziwiatr M. Enhanced recovery after surgery protocol in oesophageal cancer surgery: systematic review and meta-analysis. *PLoS One* 2017; **12**: e0174382 [PMID: 28350805 DOI: 10.1371/journal.pone.0174382]

8 **de Groot JJ**, Ament SM, Maessen JM, Dejong CH, Kleijnen JM, Slangen BF. Enhanced recovery pathways in abdominal gynecologic surgery: a systematic review and meta-analysis. *Acta Obstet Gynecol Scand* 2016; **95**: 382-395 [PMID: 26613531 DOI: 10.1111/aogs.12831]

9 **Lassen K**, Coolsen MM, Slim K, Carli F, de Aguilar-Nascimento JE, Schäfer M, Parks RW, Fearon KC, Lobo DN, Demartines N, Braga M, Ljungqvist O, Dejong CH; ERAS® Society; European Society for Clinical Nutrition and Metabolism; International Association for Surgical Metabolism and Nutrition. Guidelines for perioperative care for pancreaticoduodenectomy: Enhanced Recovery After Surgery (ERAS®) Society recommendations. *Clin Nutr* 2012; **31**: 817-830 [PMID: 23079762 DOI: 10.1016/

j.clnu.2012.08.011]
10 **Bassi C**, Dervenis C, Butturini G, Fingerhut A, Yeo C, Izbicki J, Neoptolemos J, Sarr M, Traverso W, Buchler M; International Study Group on Pancreatic Fistula Definition. Postoperative pancreatic fistula: an international study group (ISGPF) definition. *Surgery* 2005; **138**: 8-13 [PMID: 16003309 DOI: 10.1016/j.surg.2005.05.001]
11 **Wente MN**, Bassi C, Dervenis C, Fingerhut A, Gouma DJ, Izbicki JR, Neoptolemos JP, Padbury RT, Sarr MG, Traverso LW, Yeo CJ, Büchler MW. Delayed gastric emptying (DGE) after pancreatic surgery: a suggested definition by the International Study Group of Pancreatic Surgery (ISGPS). *Surgery* 2007; **142**: 761-768 [PMID: 17981197 DOI: 10.1016/j.surg.2007.05.005]
12 **Dindo D**, Demartines N, Clavien PA. Classification of surgical complications: a new proposal with evaluation in a cohort of 6336 patients and results of a survey. *Ann Surg* 2004; **240**: 205-213 [PMID: 15273542]
13 **Hozo SP**, Djulbegovic B, Hozo I. Estimating the mean and variance from the median, range, and the size of a sample. *BMC Med Res Methodol* 2005; **5**: 13 [PMID: 15840177 DOI: 10.1186/1471-2288-5-13]
14 **Kennedy EP**, Rosato EL, Sauter PK, Rosenberg LM, Doria C, Marino IR, Chojnacki KA, Berger AC, Yeo CJ. Initiation of a critical pathway for pancreaticoduodenectomy at an academic institution--the first step in multidisciplinary team building. *J Am Coll Surg* 2007; **204**: 917-23; discussion 923-4 [PMID: 17481510 DOI: 10.1016/j.jamcollsurg.2007.01.057]
15 **Vanounou T**, Pratt W, Fischer JE, Vollmer CM Jr, Callery MP. Deviation-based cost modeling: a novel model to evaluate the clinical and economic impact of clinical pathways. *J Am Coll Surg* 2007; **204**: 570-579 [PMID: 17382215 DOI: 10.1016/j.jamcollsurg.2007.01.025]
16 **Balzano G**, Zerbi A, Braga M, Rocchetti S, Beneduce AA, Di Carlo V. Fast-track recovery programme after pancreatico-duodenectomy reduces delayed gastric emptying. *Br J Surg* 2008; **95**: 1387-1393 [PMID: 18844251 DOI: 10.1002/bjs.6324]
17 **Kennedy EP**, Grenda TR, Sauter PK, Rosato EL, Chojnacki KA, Rosato FE Jr, Profeta BC, Doria C, Berger AC, Yeo CJ. Implementation of a critical pathway for distal pancreatectomy at an academic institution. *J Gastrointest Surg* 2009; **13**: 938-944 [PMID: 19190968 DOI: 10.1007/s11605-009-0803-0]
18 **Abu Hilal M**, Di Fabio F, Badran A, Alsaati H, Clarke H, Fecher I, Armstrong TH, Johnson CD, Pearce NW. Implementation of enhanced recovery programme after pancreatoduodenectomy: a single-centre UK pilot study. *Pancreatology* 2013; **13**: 58-62 [PMID: 23395571 DOI: 10.1016/j.pan.2012.11.312]
19 **Braga M**, Pecorelli N, Ariotti R, Capretti G, Greco M, Balzano G, Castoldi R, Beretta L. Enhanced recovery after surgery pathway in patients undergoing pancreaticoduodenectomy. *World J Surg* 2014; **38**: 2960-2966 [PMID: 24870390 DOI: 10.1007/s00268-014-2653-5]
20 **Pillai SA**, Palaniappan R, Pichaimuthu A, Rajendran KK, Sathyanesan J, Govindhan M. Feasibility of implementing fast-track surgery in pancreaticoduodenectomy with pancreaticogastrostomy for reconstruction--a prospective cohort study with historical control. *Int J Surg* 2014; **12**: 1005-1009 [PMID: 25014648 DOI: 10.1016/j.ijsu.2014.07.002]
21 **Coolsen MM**, van Dam RM, Chigharoe A, Olde Damink SW, Dejong CH. Improving outcome after pancreaticoduodenectomy: experiences with implementing an enhanced recovery after surgery (ERAS) program. *Dig Surg* 2014; **31**: 177-184 [PMID: 25097014 DOI: 10.1159/000363583]
22 **Nussbaum DP**, Penne K, Stinnett SS, Speicher PJ, Cocieru A, Blazer DG 3rd, Zani S, Clary BM, Tyler DS, White RR. A standardized care plan is associated with shorter hospital length of stay in patients undergoing pancreaticoduodenectomy. *J Surg Res* 2015; **193**: 237-245 [PMID: 25062813 DOI: 10.1016/j.jss.2014.06.036]
23 **Yui R**, Satoi S, Toyokawa H, Yanagimoto H, Yamamoto T, Hirooka S, Yamaki S, Ryota H, Michiura T, Inoue K, Matsui Y, Kwon AH. Less morbidity after introduction of a new departmental policy for patients who undergo open distal pancreatectomy. *J Hepatobiliary Pancreat Sci* 2014; **21**: 72-77 [PMID: 23804436 DOI: 10.1002/jhbp.4]
24 **Nussbaum DP**, Penne K, Speicher PJ, Stinnett SS, Perez A, White RR, Clary BM, Tyler DS, Blazer DG 3rd. The role of clinical care pathways: an experience with distal pancreatectomy. *J Surg Res* 2014; **190**: 64-71 [PMID: 24666986 DOI: 10.1016/j.jss.2014.02.026]
25 **Kobayashi S**, Ooshima R, Koizumi S, Katayama M, Sakurai J, Watanabe T, Nakano H, Imaizumi T, Otsubo T. Perioperative care with fast-track management in patients undergoing pancreaticoduodenectomy. *World J Surg* 2014; **38**: 2430-2437 [PMID: 24692004 DOI: 10.1007/s00268-014-2548-5]
26 **Shao Z**, Jin G, Ji W, Shen L, Hu X. The role of fast-track surgery in pancreaticoduodenectomy: a retrospective cohort study of 635 consecutive resections. *Int J Surg* 2015; **15**: 129-133 [PMID: 25615646 DOI: 10.1016/j.ijsu.2015.01.007]
27 **Joliat GR**, Labgaa I, Petermann D, Hübner M, Griesser AC, Demartines N, Schäfer M. Cost-benefit analysis of an enhanced recovery protocol for pancreaticoduodenectomy. *Br J Surg* 2015; **102**: 1676-1683 [PMID: 26492489 DOI: 10.1002/bjs.9957]
28 **Partelli S**, Crippa S, Castagnani R, Ruffo G, Marmorale C, Franconi AM, De Angelis C, Falconi M. Evaluation of an enhanced recovery protocol after pancreaticoduodenectomy in elderly patients. *HPB* (Oxford) 2016; **18**: 153-158 [PMID: 26902134 DOI: 10.1016/j.hpb.2015.09.009]
29 **Williamsson C**, Karlsson N, Sturesson C, Lindell G, Andersson R, Tingstedt B. Impact of a fast-track surgery programme for pancreaticoduodenectomy. *Br J Surg* 2015; **102**: 1133-1141 [PMID: 26042725 DOI: 10.1002/bjs.9856]
30 **Morales Soriano R**, Esteve Pérez N, Tejada Gavela S, Cuadrado García Á, Rodríguez Pino JC, Morón Canis JM, Molina Romero X, Muñoz Pérez J, González Argente X. Outcomes of an enhanced recovery after surgery programme for pancreaticoduodenectomy. *Cir Esp* 2015; **93**: 509-515 [PMID: 26072690 DOI: 10.1016/j.ciresp.2015.04.009]
31 **Bai X**, Zhang X, Lu F, Li G, Gao S, Lou J, Zhang Y, Ma T, Wang J, Chen W, Huang B, Liang T. The implementation of an enhanced recovery after surgery (ERAS) program following pancreatic surgery in an academic medical center of China. *Pancreatology* 2016; **16**: 665-670 [PMID: 27090583 DOI: 10.1016/j.pan.2016.03.018]
32 **Zouros E**, Liakakos T, Machairas A, Patapis P, Agalianos C, Dervenis C. Improvement of gastric emptying by enhanced recovery after pancreaticoduodenectomy. *Hepatobiliary Pancreat Dis Int* 2016; **15**: 198-208 [PMID: 27020637]
33 **Dai J**, Jiang Y, Fu D. Reducing postoperative complications and improving clinical outcome: Enhanced recovery after surgery in pancreaticoduodenectomy - a retrospective cohort study. *Int J Surg* 2017; **39**: 176-181 [PMID: 28132917 DOI: 10.1016/j.ijsu.2017.01.089]
34 **Wilmore DW**, Kehlet H. Management of patients in fast track surgery. *BMJ* 2001; **322**: 473-476 [PMID: 11222424]
35 **Kehlet H**, Wilmore DW. Multimodal strategies to improve surgical outcome. *Am J Surg* 2002; **183**: 630-641 [PMID: 12095591]
36 **Lassen K**, Soop M, Nygren J, Cox PB, Hendry PO, Spies C, von Meyenfeldt MF, Fearon KC, Revhaug A, Norderval S, Ljungqvist O, Lobo DN, Dejong CH; Enhanced Recovery After Surgery (ERAS) Group. Consensus review of optimal perioperative care in colorectal surgery: Enhanced Recovery After Surgery (ERAS) Group recommendations. *Arch Surg* 2009; **144**: 961-969 [PMID: 19841366 DOI: 10.1001/archsurg.2009.170]
37 **Barton JG**. Enhanced recovery pathways in pancreatic surgery. *Surg Clin North Am* 2016; **96**: 1301-1312 [PMID: 27865279 DOI: 10.1016/j.suc.2016.07.003]
38 **Coolsen MM**, van Dam RM, van der Wilt AA, Slim K, Lassen K, Dejong CH. Systematic review and meta-analysis of enhanced recovery after pancreatic surgery with particular emphasis on pancreaticoduodenectomies. *World J Surg* 2013; **37**: 1909-1918 [PMID: 23568250 DOI: 10.1007/s00268-013-2044-3]
39 **Kagedan DJ**, Ahmed M, Devitt KS, Wei AC. Enhanced recovery

after pancreatic surgery: a systematic review of the evidence. *HPB* (Oxford) 2015; **17**: 11-16 [PMID: 24750457 DOI: 10.1111/hpb.12265]

40 **Martos-Benítez FD**, Gutiérrez-Noyola A, Soto-García A, González-Martínez I, Betancourt-Plaza I. Program of gastrointestinal rehabilitation and early postoperative enteral nutrition: a prospective study. *Updates Surg* 2018; **70**: 105-112 [PMID: 29429053 DOI: 10.1007/s13304-018-0514-8]

41 **Garth AK**, Newsome CM, Simmance N, Crowe TC. Nutritional status, nutrition practices and post-operative complications in patients with gastrointestinal cancer. *J Hum Nutr Diet* 2010; **23**: 393-401 [PMID: 20337847 DOI: 10.1111/j.1365-277X.2010.01058.x]

42 **Kobayashi S**, Segami K, Hoshino H, Nakahara K, Katayama M, Koizumi S, Otsubo T. Risk factors for failure of early recovery from pancreatoduodenectomy despite the use of enhanced recovery after surgery protocols and a physical aging score to predict postoperative risks. *J Hepatobiliary Pancreat Sci* 2018; **25**: 231-239 [PMID: 29412516 DOI: 10.1002/jhbp.540]

P- Reviewer: Cesaretti M, Mastoraki A, Negoi I, Tang Y, Wani IA
S- Editor: Wang XJ **L- Editor**: Filipodia **E- Editor**: Huang Y

Published by **Baishideng Publishing Group Inc**
7901 Stoneridge Drive, Suite 501, Pleasanton, CA 94588, USA
Telephone: +1-925-223-8242
Fax: +1-925-223-8243
E-mail: bpgoffice@wjgnet.com
Help Desk: http://www.f6publishing.com/helpdesk
http://www.wjgnet.com

ISSN 1007-9327

ISSN 1007-9327 (print)
ISSN 2219-2840 (online)

World Journal of *Gastroenterology*

World J Gastroenterol 2018 April 28; 24(16): 1679-1824

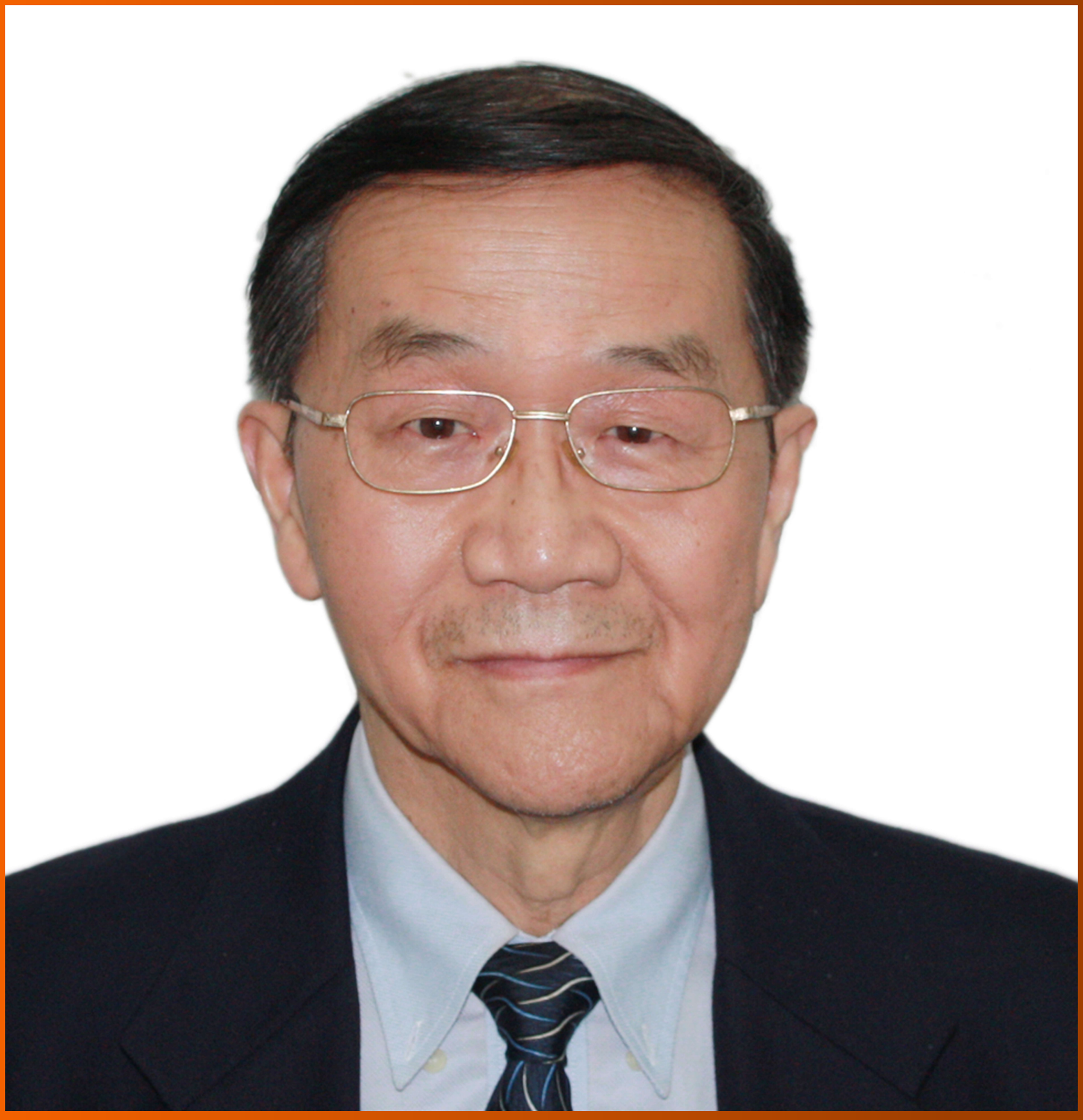

Published by Baishideng Publishing Group Inc

World Journal of Gastroenterology

Contents

Weekly Volume 24 Number 16 April 28, 2018

ABOUT COVER

Editorial board member of *World Journal of Gastroenterology*, Shu-You Peng, FRCS (Gen Surg), FRCS (Hon), MD, Professor, Surgeon, General Surgery, The Second Affiliated Hospital, College of Medicine, Zhejiang University, Hangzhou 310009, Zhejiang Province, China

AIMS AND SCOPE

World Journal of Gastroenterology (*World J Gastroenterol*, *WJG*, print ISSN 1007-9327, online ISSN 2219-2840, DOI: 10.3748) is a peer-reviewed open access journal. *WJG* was established on October 1, 1995. It is published weekly on the 7th, 14th, 21st, and 28th each month. The *WJG* Editorial Board consists of 642 experts in gastroenterology and hepatology from 59 countries.

The primary task of *WJG* is to rapidly publish high-quality original articles, reviews, and commentaries in the fields of gastroenterology, hepatology, gastrointestinal endoscopy, gastrointestinal surgery, hepatobiliary surgery, gastrointestinal oncology, gastrointestinal radiation oncology, gastrointestinal imaging, gastrointestinal interventional therapy, gastrointestinal infectious diseases, gastrointestinal pharmacology, gastrointestinal pathophysiology, gastrointestinal pathology, evidence-based medicine in gastroenterology, pancreatology, gastrointestinal laboratory medicine, gastrointestinal molecular biology, gastrointestinal immunology, gastrointestinal microbiology, gastrointestinal genetics, gastrointestinal translational medicine, gastrointestinal diagnostics, and gastrointestinal therapeutics. *WJG* is dedicated to become an influential and prestigious journal in gastroenterology and hepatology, to promote the development of above disciplines, and to improve the diagnostic and therapeutic skill and expertise of clinicians.

INDEXING/ABSTRACTING

World Journal of Gastroenterology (*WJG*) is now indexed in Current Contents®/Clinical Medicine, Science Citation Index Expanded (also known as SciSearch®), Journal Citation Reports®, Index Medicus, MEDLINE, PubMed, PubMed Central and Directory of Open Access Journals. The 2017 edition of Journal Citation Reports® cites the 2016 impact factor for *WJG* as 3.365 (5-year impact factor: 3.176), ranking *WJG* as 29th among 79 journals in gastroenterology and hepatology (quartile in category Q2).

NAME OF JOURNAL
World Journal of Gastroenterology

ISSN
ISSN 1007-9327 (print)
ISSN 2219-2840 (online)

LAUNCH DATE
October 1, 1995

FREQUENCY
Weekly

EDITORIAL OFFICE
Ze-Mao Gong, Director
World Journal of Gastroenterology
Baishideng Publishing Group Inc
7901 Stoneridge Drive, Suite 501,
Pleasanton, CA 94588, USA
Telephone: +1-925-2238242
Fax: +1-925-2238243
E-mail: editorialoffice@wjgnet.com
Help Desk: http://www.f6publishing.com/helpdesk
http://www.wjgnet.com

PUBLISHER
Baishideng Publishing Group Inc
7901 Stoneridge Drive, Suite 501,
Pleasanton, CA 94588, USA
Telephone: +1-925-2238242
Fax: +1-925-2238243
E-mail: bpgoffice@wjgnet.com
Help Desk: http://www.f6publishing.com/helpdesk
http://www.wjgnet.com

PUBLICATION DATE
April 28, 2018

INSTRUCTIONS TO AUTHORS
Full instructions are available online at http://www.wjgnet.com/bpg/gerinfo/204

ONLINE SUBMISSION
http://www.f6publishing.com

World Journal of Gastroenterology

Submit a Manuscript: http://www.f6publishing.com

World J Gastroenterol 2018 April 28; 24(16): 1679-1707

DOI: 10.3748/wjg.v24.i16.1679

ISSN 1007-9327 (print) ISSN 2219-2840 (online)

REVIEW

Beneficial effects of naringenin in liver diseases: Molecular mechanisms

Erika Hernández-Aquino, Pablo Muriel

Erika Hernández-Aquino, Pablo Muriel, Laboratory of Experimental Hepatology, Department of Pharmacology, Cinvestav-IPN, Mexico City 07000, Mexico

ORCID number: Erika Hernández-Aquino (0000-0003-4783-4240); Pablo Muriel (0000-0002-2236-6631).

Author contributions: All authors equally contributed to this paper with the conception and design of the study, the literature review and analysis, the drafting and critical revision and editing of the manuscript, and with their final approval of the final version.

Supported by National Council of Science and Technology (Conacyt) of Mexico, No. 253037.

Conflict-of-interest statement: The authors declare no conflicts of interest.

Manuscript source: Invited manuscript

Correspondence to: Pablo Muriel, PhD, Research Scientist, Laboratory of Experimental Hepatology, Department of Pharmacology, Cinvestav-IPN, Av. Instituto Politécnico Nacional 2508, Apartado postal 14-740, Mexico City 07000, Mexico. pmuriel@cinvestav.mx
Telephone: +52-55-57473303
Fax: +52-55-57473394

Received: March 7, 2018
Peer-review started: March 8, 2018
First decision: March 29, 2018
Revised: April 4, 2018
Accepted: April 16, 2018
Article in press: April 16, 2018

Published online: April 28, 2018

Abstract

Liver diseases are caused by different etiological agents, mainly alcohol consumption, viruses, drug intoxication or malnutrition. Frequently, liver diseases are initiated by oxidative stress and inflammation that lead to the excessive production of extracellular matrix (ECM), followed by a progression to fibrosis, cirrhosis and hepatocellular carcinoma (HCC). It has been reported that some natural products display hepatoprotective properties. Naringenin is a flavonoid with antioxidant, antifibrogenic, anti-inflammatory and anticancer properties that is capable of preventing liver damage caused by different agents. The main protective effects of naringenin in liver diseases are the inhibition of oxidative stress, transforming growth factor (TGF-β) pathway and the prevention of the transdifferentiation of hepatic stellate cells (HSC), leading to decreased collagen synthesis. Other effects include the inhibition of the mitogen activated protein kinase (MAPK), toll-like receptor (TLR) and TGF-β non-canonical pathways, the inhibition of which further results in a strong reduction in ECM synthesis and deposition. In addition, naringenin has shown beneficial effects on nonalcoholic fatty liver disease (NAFLD) through the regulation of lipid metabolism, modulating the synthesis and oxidation of lipids and cholesterol. Moreover, naringenin protects from HCC, since it inhibits growth factors such as TGF-β and vascular endothelial growth factor (VEGF), inducing apoptosis and regulating MAPK pathways. Naringenin is safe and acts by targeting multiple proteins. However, it possesses low bioavailability and high intestinal metabolism. In this regard, formulations, such as nanoparticles or liposomes, have been developed to improve naringenin bioavailability. We conclude that naringenin should be considered in the future as an important candidate in the treatment of different liver

diseases.

Key words: Naringenin; Transforming growth factor; Liver; Fibrosis; MAPKs; CCl_4; Flavonoids; JNK; Hepatic stellate cells; Cirrhosis; Smads; α-SMA

Core tip: Natural products such as flavonoids have been shown to display hepatoprotective properties. Naringenin possesses the ability to inhibit oxidative stress and inflammation and has anti-inflammatory and anticancer properties. Thus, naringenin should be considered in the future as an important candidate for the treatment of liver diseases.

Hernández-Aquino E, Muriel P. Beneficial effects of naringenin in liver diseases: Molecular mechanisms. *World J Gastroenterol* 2018; 24(16): 1679-1707 Available from: URL: http://www.wjgnet.com/1007-9327/full/v24/i16/1679.htm DOI: http://dx.doi.org/10.3748/wjg.v24.i16.1679

INTRODUCTION

Liver damage can be caused by alcohol intake, heavy metal intoxication, hepatitis virus infection, obstruction of the biliary tract or malnutrition. Chronic hepatic injury results in organ fibrosis characterized by an imbalance between the synthesis and degradation of extracellular matrix (ECM) derived from oxidative stress and inflammation during liver damage. After fibrosis, cirrhosis develops with tissue scars, the loss of parenchymal architecture, the disruption of hepatic blood flow and organ failure[1,2]. The main causes of fibrosis globally are NAFLD (40%), hepatitis B virus (HBV) (30%), hepatitis C virus (HCV) (15%), and harmful alcohol consumption (11%)[3]. The prevalence of cirrhosis is increasing; in 2010, 33% more people died from cirrhosis than in 1990[4].

While the elimination of the causative agent may be the best option for some cirrhotic patients, in most cases, medical intervention is required. Therefore, pharmacological strategies should be developed to prevent or reverse hepatic damage. Researchers have developed multiple therapeutic strategies to combat this disease, including transforming growth factor-β (TGF-β) inhibitors[5], antivirals[6], cell-based therapies[7], nanoparticles[8], and natural products[9-15].

Liver transplantation is an interesting option; unfortunately, the lack of sufficient donors and organ rejection restrict this surgical procedure. In recent years, the investigation on hepatoprotective properties of natural products has increased. Due to their molecular structure, many of them possess antioxidant properties and display anti-inflammatory and anticancer properties and are generally considered safe for human consumption. Among the most studied natural compounds are silymarin, quercetin, and curcumin[10,12,14], but recently, a flavonoid with very specific hepatoprotective properties has emerged: naringenin.

Naringenin has been studied in various *in vivo* and *in vitro* liver damage models, using hepatic damage agents such as carbon tetrachloride (CCl_4), alcohol, N-methyl-N-nitro-Nitroguanidine, lipopolysaccharide (LPS), and heavy metals, among others, displaying a good hepatoprotective activity due to its antioxidant capacity as well as its ability to inhibit inflammatory and profibrotic signaling pathways. However, despite the importance of naringenin in liver diseases, there is no detailed review of the effects of naringenin on hepatic pathologies.

Therefore, our objective was to document the effects of naringenin on liver diseases and to highlight the importance of this flavonoid in the therapeutic of pathologies of this organ.

LITERATURE SEARCH

A systematic literature search was conducted using PubMed, Scopus and EMBASE.

ABSORPTION, METABOLISM AND DISTRIBUTION OF NARINGENIN

Naringenin (4′,5,7-trihydroxy flavanone) is a flavonoid, specifically a flavanone, and is the aglycone of naringin (naringenin-7-rhamnoglucoside)[16]; naringenin can also be found as narirutin (naringenin- 7-O-rutinoside) or naringenin-glucoside (naringenin-7-O-glucoside), depending on the sugar motive (Figure 1)[11].

This review is focused on the effects of naringenin (aglycone); the reader interested in glycosylated molecules is referred to another review[11]. Because naringenin is found mostly in citrus fruits, natural intake occurs orally. Due to its chemical structure, naringenin is very lipophilic; thus, it is readily absorbed through the intestinal epithelium by passive diffusion into enterocytes. Once inside the intestinal cells, it can enter the general circulation by multidrug resistance-associated proteins (Mrp1) or can be transported by active efflux protein carriers P-glycoprotein (P-gp) and Mrp2 back to the intestinal lumen, out of the enterocytes, repeating the cycle[17] (Figure 2).

On the other hand, small intestine, colonic epithelium, and liver metabolize naringenin *via* phase II conjugation by UDP-glucuronosyl transferase (UGT), sulfotransferase, and catechol-O-methyltransferase[18-20]. Naringenin-glucuronides leave the cells by Mrp2 protein or pass into blood *via* breast cancer-resistant protein (Bcrp1)[21]. Moreover, naringenin can be cleaved by β-glucuronidases (GUSB) located in tissues and liver[22]. This deconjugation results in release of the aglycone, which in turn can be absorbed by passive transcellular diffusion or undergo efflux by Mrp2 and P-gp[19]. Then,

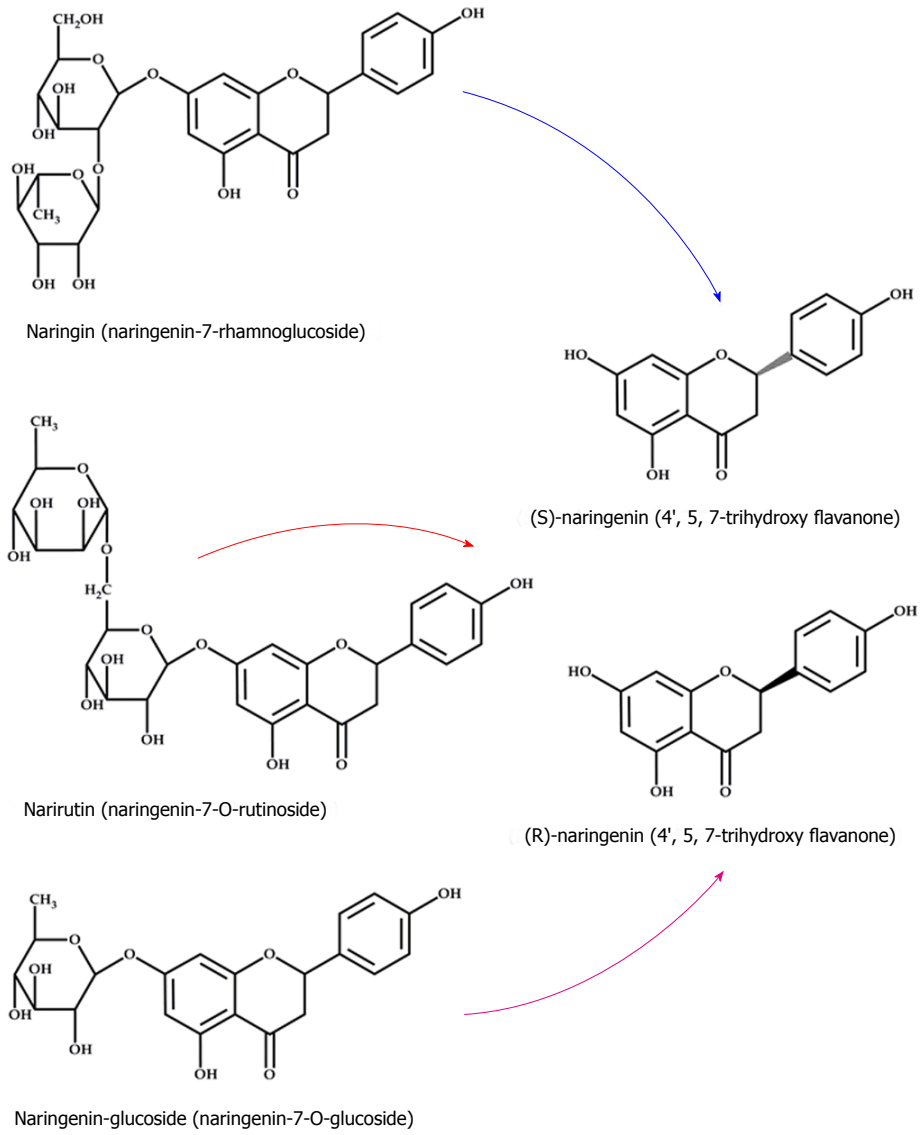

Figure 1 Chemical structure of naringenin, naringin, narirutin, and naringenin-glucoside. The flavonoid naringenin exists in two forms: Glycosylated (naringin, narirutin and naringenin-glucoside) and aglycone (naringenina). There are three types of naringenin glycosides depending of sugar moiety bound to the flavonoid: Naringin (rhamnose), narirutin (rutinose) and naringenin-glucoside (glucose); when the sugar moiety is cleaved by specific enzymes, the aglycone (naringenin) is released.

naringenin is metabolized in the lower intestine by *Streptococcus S-2*, *Lactobacillus L-2*, and *Bacteroides JY-6* to generate a series of low molecular weight aromatic acids[11] (Figure 2).

With respect to naringenin distribution, it has been found in the stomach, small intestine, liver, kidney, trachea, lung, heart, fat, muscle, testis, ovary, spleen, brain, and urine[20,23-25]. Furthermore, naringenin and its metabolites are bound to plasma proteins such as albumin[26-28].

ANTIOXIDANT EFFECTS OF NARINGENIN, BEYOND THE STRUCTURE ACTIVITY RELATIONSHIP

Normally, flavonoid antioxidant activity has been attributed to the structure-activity relationship of flavonoids. However, in addition to a direct antioxidant property by free radical scavenging activity, naringenin possesses the ability to induce the endogenous antioxidant system.

Classically, naringenin's antioxidant effect is due to its hydroxyl substituents (OH), which have high reactivity against reactive oxygen species (ROS) and reactive nitrogen species (RNS). In general, the antioxidant capacity of a given molecule increases in function with the number of OH radicals in the molecule, which, in the case of naringenin, is 3. Then, OH can donate its H to free radicals ($R^{\bullet}$), and later, naringenin can be stabilized by resonance[29,30] (Figure 3). Within the typical structure of flavonoids, the B ring is very important because when OH groups are in the ring, flavonoids can stabilize hydroxyl ($OH^{\bullet}$), peroxyl ($ROO^{\bullet}$), and peroxynitrite ($ONOO^{\bullet}$) radicals, producing a relatively stable flavonoid radical. On the other hand, 5-OH substitution and a 5,7-*m*-dihydroxy arrangement

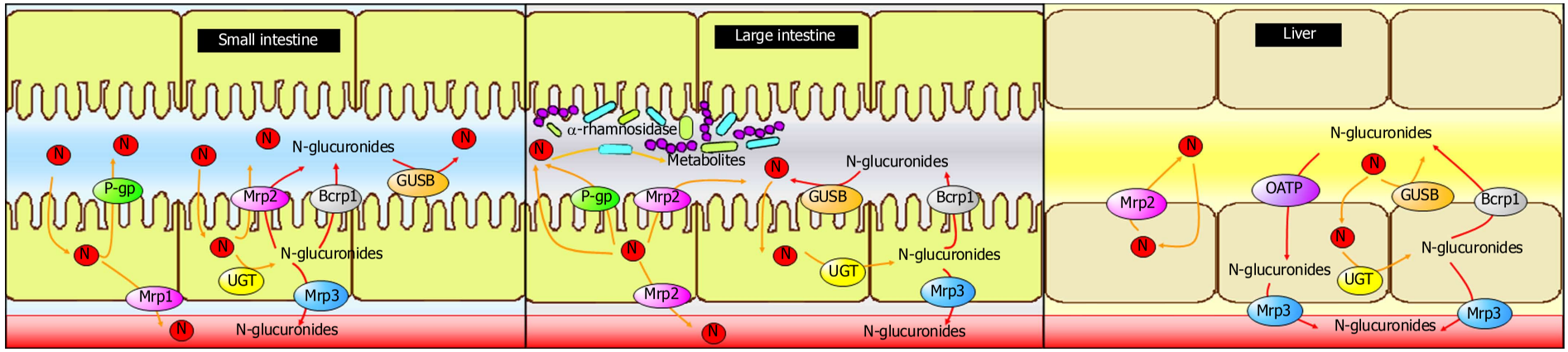

Figure 2 Absorption and metabolism of naringenin. Small intestine: Naringenin (N, orange arrows) is absorbed through the intestinal epithelium by passive diffusion into enterocytes; then, it can pass to general circulation by multidrug resistance associated proteins (Mrp1) or transported by active efflux protein carriers P-glycoprotein (P-gp) and Mrp2, back to the intestinal lumen, out of the enterocytes. Inside the enterocyte, naringenin is glucuronized by UDP-glucuronosyl transferase (UGT), and after that, naringenin-glucuronides (red arrows) leave cells by Mrp2 protein or pass into blood via breast cancer-resistant protein (Bcrp1). Moreover, naringenin-glucuronides can be cleaved by β-glucuronidases (GUSB), resulting in release of the aglycone. Large intestine: Naringenin undergoes same processes as in small intestine but also is highly metabolized by *Streptococcus S-2*, *Lactobacillus L-2*, and *Bacteroides JY-6* to generate a series of low molecular weight aromatic acids. Liver: Naringenin is highly conjugated to form naringenin-glucuronides, which allows it to pass into circulation. On the other hand, naringenin-glucuronides reach the liver from intestine and enter into hepatocytes *via* organic anion transporting protein-B (OATP), and then, they are transported by Mrp3 into the circulation.

in the A-ring is an important feature of naringenin that makes it an antioxidant and, at the same time, serves to stabilize the structure after donating H to the R$^{\bullet}$. Finally, the association between 5-OH and 4-oxo substituents contributes to the ability of naringenin to chelate compounds such as heavy metals[29] (Figure 3).

An important phenomenon during liver damage is lipid peroxidation (LP); it can be defined as the abstraction of hydrogen from fatty acid that initiates a complex series of reactions that terminate in the complete disintegration of the polyunsaturated fatty acid (PUFA) molecules with the formation of aldehydes, such as malondialdehyde (MDA), other carbonyls, and alkanes. LP may be initiated by R$^{\bullet}$. Therefore, maintaining the normal redox balance with antioxidants during liver damage is important to prevent the deleterious effects of LP[31].

Naringenin trolox equivalent antioxidant activity is 1.53 mmol/L, which is a small value compared with that of quercetin, which is 4.7 mmol/L[30]. In a model of nonenzymatic LP induction by ascorbic acid, naringenin showed 21%-44% inhibition of MDA formation in a dose-dependent manner; however, quercetin was able to prevent 70%-85% of the MDA formation at doses from 0.1 mmol/L to 4.0 mmol/L[32]. During a di(phenyl)-(2,4,6-trinitrophenyl) iminoazanium (DPPH) assay, naringenin had an ID_{50} of 225 μmol/L at 2 h, and the number of molecules of DPPH scavenged/naringenin molecule was 0.5, while the ID_{50} of quercetin was 12.5 μmol/L of DPPH scavenged/quercetin molecule. In addition, naringenin showed a lower effect than quercetin in an LP model in liver and lung with an ID_{50} of more than 1000 μmol/L and 35 μmol/L, respectively[33]. Moreover, naringenin's effect on LP induced by iron-ascorbate in hepatic microsomes revealed that naringenin (5 μmol/L and 25 μmol/L) increases LP, unlike quercetin, which almost completely inhibited LP at the same dose. In this same study, a modest effect of naringenin (25 μmol/L) against LP induced by Fe^{3+}-ADP/NADPH or TBH assay was observed. In contrast, naringenin strongly protected hepatocytes from TBH-cytotoxicity, suggesting that naringenin did not exert its cytoprotective effects through purely direct antioxidant mechanisms[34].

Although several reports show that naringenin displays poor antioxidant capacity compared to other flavonoids such as quercetin, the results obtained in the 2,2′-azinobis-(3-ethylbenzothiazoline-6-sulfonic acid (ABTS) assay showed that naringenin had an IC_{50} of 7.9 μmol/L, and when the determination of superoxide radical ($O_2^{\bullet}$) scavenger activity was performed by the nitro blue tetrazolium (NBT) method and the Xanthine oxidase/cytochrome c (CYPc) method, naringenin had an IC_{50} of 94.7 and 4.4 μmol/L, respectively. Moreover, naringenin had an IC_{50} of 1.06 and 1.55 μmol/L with EDTA and without EDTA on OH$^{\bullet}$ scavenger activity, respectively; in addition, the IC_{50}

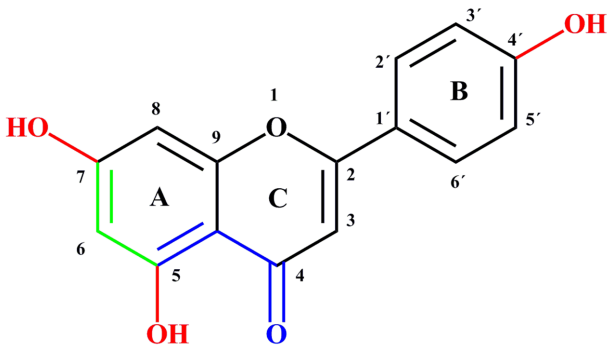

Figure 3 Naringenin antioxidant activity-structure relationship. In red: Hydroxyl substituents (OH) that have high reactivity against reactive oxygen species and reactive nitrogen species. In green: 5,7-*m*-dihydroxy arrangement in the A-ring serves to stabilize the structure after donating electrons to free radicals. In blue: The association between 5-OH and 4-oxo substituents contributes to the chelation of compounds such as heavy metals.

of naringenin on liver LP in the presence of $HO_2^{\bullet}$ or $OH^{\bullet}$ was 1.21 and 0.23 mmol/L, respectively[35].

As seen, the antioxidant effect of naringenin can be considered ambiguous, and it may depend on the radical formed and the model used and the flavonoid concentration. Even though naringenin has fewer antioxidant functional groups than quercetin, it shows other properties due to its structure-activity relationship, as it has been reported that naringenin is able to accumulate in cell membranes[36] and biomembranes[37,38]. Interaction with membranes is favored because flavonoids form reversible bonds with the polar heads of the phospholipids[39], and this interaction may be possible due to naringenin's solubility, since it is highly lipophilic because of its structure (Figure 4).

Interestingly, it has been shown that naringenin decreases membrane fluidity. Membrane fluidity is the relative motional freedom of the lipid molecules in the membrane bilayer, and naringenin accumulates in the membrane hydrophobic core, where it modifies lipid packing order leading to decreased membrane fluidity in a concentration-dependent manner. Therefore, by increasing the rigidity of membranes, naringenin can reduce the interaction between $R^{\bullet}$ and lipids; as a result, LP may be attenuated[38]. In conclusion, in addition to its antioxidant capacity, naringenin can block LP by reducing membrane fluidity[40] (Figure 4).

Although antioxidant assays are important, *in vitro* and *in vivo* model systems offer much more information since normal functions of a complete system are preserved. Either by its antioxidant activity or by protection of lipid membranes, naringenin offers protection against ROS and other $R^{\bullet}$ in *in vitro* and *in vivo* models. Naringenin protects against ROS in a model of neuronal damage, since it reduces their levels in neurons and decreases mitochondrial dysfunction and increases mitochondrial membrane potential[41]. In addition, naringenin inhibits KO_2-induced oxidative stress in a pain model in mice by inhibiting LP and $O_2^{\bullet}$ production[42]. On the other hand, naringenin exerts antioxidant effects against paraquat-induced toxicity in human bronchial epithelial cells, since it decreases intracellular ROS generation[43]. Moreover, this flavanone significantly decreased thiobarbituric acid reactive substances (TBARS) and improved membrane phospholipid composition in favor of n-3 PUFAs and the n-6/n-3 PUFAs ratio in the liver of old-aged Wistar rats[44].

Naringenin has shown the ability of combating LP in many organs, tissues and cells, for example, in lung[45], ankle joints (arthritis model)[46], retina of streptozotocin-induced diabetic rats[47], SH-SY5Y cells[48], cardiomyoblast cells[49], skin[50], testis[51] and, interestingly, in liver[44,52,53]. It can be concluded that, in contrast to the results obtained in chemical antioxidant assays, the beneficial effects of naringenin against LP in systems involving living organisms or cells, the flavanone shows strong activity. This characteristic is very important for the treatment of hepatic diseases, since LP constitutes one of the main causative agents that triggers liver damage.

In the studies where a reduction in LP by naringenin was demonstrated, a relationship between reduced glutathione (GSH) and flavonoid levels is observed. In fact, it has been observed that naringenin improves GSH levels during oxidative stress[44,47-52]. Improvement of GSH levels by naringenin is associated with the beneficial properties of this flavonoid on the liver because oxidative stress plays a causative role in hepatic disorders[54].

The effect of naringenin on GSH levels deserves further explanation. GSH is a tripeptide (L-γ-glutamyl-L-cysteinyl-glycine) that serves several essential functions within the cell. The main functions of GSH are antioxidant, detoxification of oxygen-derived free radicals, thiol disulfide exchange and storage/transfer of cysteine. GSH is formed in two steps: in the first (rate-limiting) step, cysteine and glutamate form c-glutamyl cysteine by the enzyme glutamyl cysteinyl ligase (GCL); in the second step, GSH forms from c-glutamyl cysteine and glycine by GSH synthetase (GSS) catalysis[55-57] (Figure 4). It has been observed that naringenin possesses the ability to increase total and mitochondrial GSH levels during hydrogen peroxide (H_2O_2)-induced liver damage[48,49,51], as well total hepatic GSH[52,58,59] and total GSH in other organs[60,61]. These effects can be explained because naringenin increases the expression of the GCLC catalytic subunit and the GCL modulatory subunit at both the protein and mRNA levels[60-62].

The tripeptide can directly scavenge $R^{\bullet}$ or function as a co-substrate of the internal antioxidant system enzymes. For example, GSH is the co-substrate of glutathione peroxidase (GPx) in H_2O_2 reduction and of glutathione transferase (GST), which catalyzes xenobiotics biotransformation in the liver[56,57]. In either case, GSH is oxidized to GSSG, which leads to consumption of GSH. Therefore, there are mechanisms in charge of maintaining the GSH/GSSG balance; for example, glutathione reductase (GR or GSR) is responsible of GSSG reduction to the disulfide form (GSH) at the

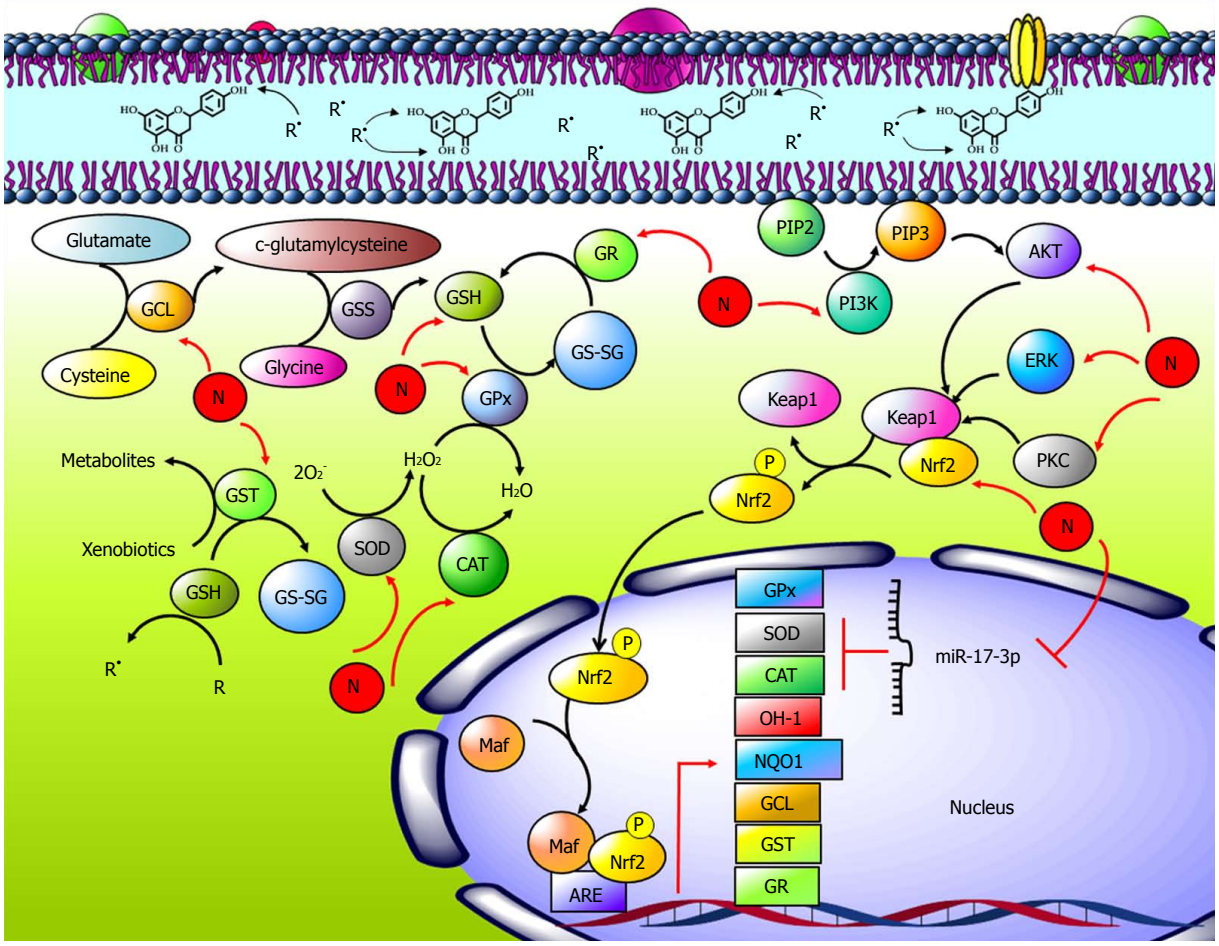

Figure 4 Antioxidant effects of naringenin. Naringenin (N) accumulates in cell membranes, where it provides rigidity to the lipid bilayer; naringenin can reduce the interaction between free radicals ($R^{\bullet}$) and the cell membrane, as well as reduce membrane phospholipid attack and prevent lipid peroxidation (LP). Glutathione (GSH) is formed when cysteine and glutamate form c-glutamyl cysteine by the enzyme glutamyl cysteinyl ligase (GCL); then, glycine and c-glutamyl cysteine form GSH by GSH synthetase (GSS). Naringenin increases GCLC protein and mRNA levels as well as GSH levels. Naringenin increases activity and protein and mRNA of superoxide dismutase (SOD), catalase (CAT), glutathione peroxidase (GPx), glutathione transferase (GST) and glutathione reductase (GR), enzymes that are part of the endogenous antioxidant system. Naringenin decreases the expression level of *miR-17-3p*; its targets genes are *SOD* and *GPx*. The nuclear factor-erythroid 2-related factor 2 (Nrf2) is an oxidative stress regulator; it stimulates antioxidant enzyme expression as well as heme oxygenase (OH-1) and NADPH quinone oxidoreductase (NQO1). Naringenin upregulates the Nrf2 pathway by increasing its activation, nucleus translocation, and protein and mRNA levels through PI3K/AKT, ERK and PKC.

expense of NADPH[55-57]. It has been reported that naringenin increased the GSH/GSSG ratio[59,61] by improving GR mRNA levels and activity in the liver[44,63-66] and in other organs[67,68] (Figure 4).

Naringenin can influence cellular antioxidant balance not only through its own chemical structure but also by inducing the cell antioxidant system. In this regard, it has been reported that naringenin upregulates important antioxidant enzymes, such as superoxide dismutase (SOD), catalase (CAT), GPx and GST.

SOD catalyzes the reaction in which $O_2^{\bullet}$ is converted to H_2O_2, a more stable species but that at high concentrations is harmful to cells; in turn, CAT eliminates excess H_2O_2, generating water[69]. Naringenin significantly increases SOD enzyme activity in different models of liver damage induced by oxidative stress[44,50,52,62-65,67,70-74]. This effect is associated with the ability of this flavonoid to increase enzyme protein levels in the liver and other organs[58,59,68]. Naringenin can prevent CAT activity decrement after damage to several tissues[44,49,50,52,62-65,67,70-74] by increasing protein[58,59,68] and mRNA levels[43].

SOD and CAT, together with GPx and GST, are diminished during oxidative stress. It is worth noting that naringenin has been reported to upregulate these enzymes[44,63-66] (Figure 4). There are some reports trying to explain the mechanism of naringenin to increase GPx activity. One report indicates that the flavanone produces an increment in GPx mRNA levels[43], while others indicate that it increases the protein content[58,59,68]. Another hypothesis postulates that during cell damage, GSH is almost depleted and, thus, cannot be utilized by GPx as a cofactor, leading to decreased enzyme activity; in this situation, naringenin acts by improving GSH levels and, as a consequence, enzyme activity[44,49,50,52,63-65,71-74]. Further experiments are needed to clarify this point.

Naringenin preserves GST activity under prooxidant conditions associated with several illnesses[49-51,63-65,70,72,74].

It has been demonstrated that the flavanone acts by increasing mRNA levels of GST[61,63], which in turn induces the transduction of the corresponding functional protein[68]. The specific action mechanism by which naringenin produces these effects remains to be elucidated (Figure 4).

As it has been previously described, naringenin has very important effects on endogenous antioxidant system enzymes, in contrast to its own weak antioxidant properties in comparison to those of other natural compounds, such as quercetin. This low antioxidant activity suggests that naringenin's effects are not only a result of its structural activity relationship but also due to other properties. In this regard, it is worth noting that naringenin influences microRNAs (miRNAs) and nuclear factor-erythroid 2 related factor 2 (Nrf2).

miRNAs are noncoding or nonmessenger RNAs that are approximately 22 nucleotides in length that regulate gene expression because they bind to target mRNA, inhibiting protein synthesis[75]. *miR-17-3p* is involved in oxidative stress, and its targets are mRNAs coding for SOD and GPx, thereby preventing the expression of these proteins[76]. Naringenin decreased the expression level of *miR-17-3p*, which is in agreement with increased levels of target mRNAs coding for *SOD* and *GPx2*[77]. As noted, this reduction in *miR-17-3p* expression may be a mechanism by which naringenin modulates antioxidant enzymes; however, more research is needed on the role of naringenin in miRNA and its effect on the endogenous antioxidant system (Figure 4).

Nrf2 interacts with the actin binding protein, Kelch-like ECH associating protein 1 (Keap1), inactivating Nrf2 in the cytoplasm. Nrf2 must be released from Keap1 to be active. Its release can occur either by MAPK phosphorylation or by conformational changes in Keap1 due to ROS. Once free, Nrf2 translocates to the nucleus, where it forms a dimer with the musculoaponeurotic fibrosarcoma (Maf) family proteins. Nrf2-Maf dimer is a transcription factor that binds to the antioxidant response element (ARE) sequence, resulting in transcriptional activation of detoxification proteins such as NADPH quinone oxidoreductase (NQO1), GST, and aldo-keto reductase (AKR), antioxidant enzymes such as thioredoxin (TXN1), thioredoxin reductase 1(TXNR), peroxiredoxin 1 (PRDX1), GPx, GCL, GR, CAT and SOD, and heme and iron metabolism proteins such as heme oxygenase (OH-1) and ferro chelatase (FECH)[78-80] (Figure 4).

Interestingly, there are reports indicating that naringenin upregulates Nrf2 in various models. In a model of UVB irradiation-induced skin inflammation and oxidative damage in hairless mice, naringenin significantly increased *Nrf2* mRNA levels compared with those in the damaged group[66]. Moreover, in a model of KO_2-induced inflammatory pain in mice, naringenin inhibited the KO_2-induced decrease in *Nrf2* mRNA expression[42]. In addition, naringenin upregulated the mRNA expression of *Nrf2* in complete Freund's adjuvant-induced rats[46], and naringenin increased Nrf2 mRNA expression in a model of oxidative stress induced by H_2O_2[49].

The induction of *Nrf2* mRNA may propitiate Nrf2 protein levels to increase. It has been reported that naringenin is capable of increasing Nrf2 protein levels in CCl_4-induced hepatic damage[63]. In addition, the flavonoid protected SH-SY5Y cells against 6-OHDA neurotoxicity *via* Nrf2 because it improved the levels of this protein[60]. Moreover, one mechanism to explain why naringenin prevented CCl_4-induced acute liver injury in mice is by preserving Nrf2 levels[59]. In addition, naringenin improved intracellular Nrf2 levels in LPS-induced apoptosis of PC12 cells[81] and reduced oxidative stress by increasing Nrf2 protein levels in neurons[41].

Increased Nrf2 protein levels do not necessarily correlate with increases in Nrf2 activity. Nrf2 must dissociate from Keap1 to translocate to the nucleus and to induce proteins of the antioxidant system. Naringenin activates Nrf2 because it promotes its translocation from the cytoplasm to the nucleus[43,61-63,82].

Phosphorylation of Nrf2 by extracellular signal-regulated protein kinase (ERK) triggers the dissociation of Nrf2-Keap1 and inhibits the reassociation of Nrf2-Keap1 complexes[83,84]. Other important proteins involved in the activation of Nrf2 are 5′ AMP-activated protein kinase (AMPK)[85], phosphatidylinositol-3-kinase (PI3K/AKT), and protein kinase C (PKC)[86]. Notably, it has been observed that naringenin upregulated phosphorylated ERK1/2, leading to nuclear translocation of Nrf2 in doxorubicin-induced toxicity in H9c2 cardiomyocytes[62]. In another report, after treatment with 40 μg/mL of naringenin, nuclear Nrf2 increased at 0.25 h and remained elevated until 3 h after naringenin treatment to H9c2 cells[82]. In addition, naringenin increased the phosphorylation levels of ERK1/2, PKCδ, and AKT, but this increase was prevented by chemical inhibitors of AKT (LY294002), ERK1/2 (PD98059), and PKCα (rottlerin), which suppressed Nrf2 activation induced by naringenin[82]. These results suggest that the naringenin-induced activation of Nrf2 signaling may be mediated by the phosphorylation of ERK1/2, PKCδ, and AKT[82] (Figure 4).

Nrf2 activation and its translocation to the nucleus lead to its union with Maf; Nrf2-Maf dimer, in turn, binds to ARE sequence, which results in transcriptional activation of detoxification and antioxidant proteins. Naringenin not only activates Nrf2 but also increases the mRNA and protein levels of target genes such as NQO1, GPx, GCL, GR, OH-1, and GST[43,46,49,59-63,66,81,82,87]. To corroborate this effect, experiments have been carried out to silence Nrf2. A small interfering RNA (siRNA) study revealed that the knockdown of *Nrf2* can abrogate naringenin-mediated protection of the BEAS-2B cells from paraquat-induced cellular toxicity[43]. Another report showed that naringenin fails to block 6-OHDA neurotoxicity if *Nrf2* siRNA is administered[60]. Moreover, naringenin prevented mitochondrial depolarization is inhibited by *Nrf2* siRNA[87]; in addition, the naringenin-

induced upregulation of GCL and HO-1 proteins was significantly inhibited by *Nrf2*-siRNA transfection in H9c2 cells[82]. Finally, silencing of *Nrf2* suppressed naringenin-induced cytoprotection and mitochondrial protection in SH-SY5Y cells exposed to H_2O_2[48] (Figure 4).

Due to the important regulatory effects of naringenin on endogenous antioxidant system, the flavonoid takes great importance as a possible hepatoprotector, since one of the main mechanisms of liver damage is oxidative stress[54]. In addition, this antioxidant is different from others, since in addition to its direct effect as an antioxidant, it induces the expression of endogenous antioxidants.

NARINGENIN PREVENTS LIVER DAMAGE CAUSED BY ALCOHOL

Liver damage induced by excessive alcohol consumption is a worldwide problem[3]. It has been reported that an intake of 80 g/day by men and 40 g/day by women between 10-20 years may lead to fibrosis[88-90]. Therefore, it is important to find a drug that prevents or reverses the effects of alcohol abuse in the population.

Liver alcohol metabolism consists of the following steps: (1) In the cytosol, alcohol is converted into acetaldehyde by the enzyme alcohol dehydrogenase (ADH) using NAD^+ to generate NADH; acetaldehyde is also formed in microsomes by CYP2E1 and in peroxisomes by CAT; and (2) In the mitochondria, acetaldehyde dehydrogenase (ALDH) transforms acetaldehyde to acetate[91-93] (Figure 5). During these reactions, secondary harmful products to hepatocytes are generated; among the most important of these harmful products is MDA, which forms adducts with proteins and is also an important indicator of LP[91-93]. Moreover, ROS, such as H_2O_2 and $O_2^{\bullet}$, are generated during the metabolism of alcohol by CYP2E1. Additionally, alcohol metabolism induces fatty liver disease by increasing the $NADH/NAD^+$ ratio. In general, these processes induce hepatocyte damage, leading to an inflammatory environment that activates endothelial cells, Kupffer cells and HSCs[91-93].

The evidence indicates that naringin, the naringenin-glycoside, significantly lowered ethanol concentration in plasma in a dose-dependent manner[94]. Ethanol administration resulted in higher ADH and lower ALDH activities, resulting in toxic acetaldehyde accumulation. Naringin increased the activities of both enzymes, resulting in efficient alcohol elimination *via* acetaldehyde and its conversion to acetate, preventing the accumulation of acetaldehyde, and resulting in the rapid clearance of alcohol from the serum[94]. In agreement with these findings, naringenin administration to alcohol-treated rats increased ADH and ALDH enzyme activities[70]. In addition, ethanol increased the activity of cytochrome CYP2E1, while this effect was reversed by naringenin[70] (Figure 5).

Ethanol consumption modifies the phase I and phase II xenobiotic metabolism enzymes. During phase I metabolism, enzymes catalyze reactions of oxidation, reduction, and hydrolysis of xenobiotics to increase their polarity and improve their excretion. On the other hand, phase II reactions are glucuronidation, acetylation, S-methylation, and glutathione- or sulfo-conjugation of xenobiotics. These reactions are carried out on phase I products for their better excretion, since tissue damage occurs if the products of phase I are not eliminated by the enzymes of phase II[95]. It has been reported that alcohol intake raises the activity of phase I enzymes such as CYP450, cytochrome b5, NADH-cytochrome b5 reductase and NADPH-CYP450 reductase. In contrast, ethanol injection decreases the activity of phase II enzymes such as GST and DT-diaphorase[70,96]. Interestingly, naringenin was able to reverse these effects caused by alcohol in both types of enzymes, leading to efficient elimination of alcohol metabolism products and reestablishment of the $NADH/NAD^+$ ratio[70] (Figure 5).

Due to acetaldehyde accumulation during alcohol metabolism, oxidative stress is generated. This is characterized by LP, increased $R^{\bullet}$ and endogenous antioxidant system dysfunction[97]. During ethanol administration *in vivo*, significantly elevated levels of TBARS, lipid hydroperoxides (LOOH), conjugated dienes (CD), protein carbonyl content and significantly lowered activities of SOD, GPx, CAT, GR and GST, and lowered levels of GSH have been observed[64,70,94].

As discussed above, naringenin displays antioxidant effects at different levels, and this was evident when the administration of naringin or naringenin prevented and reverted oxidative stress caused by ethanol, normalizing levels of TBARS, LOOH, CD, protein carbonyl content, antioxidant enzymes activity and GSH levels[64,70,94] (Figure 5).

If oxidative stress is constant and the antioxidant system has failed, liver damage is generated; this liver damage is marked by increases in liver damage markers such as alkaline phosphatase (AP), aspartate aminotransferase (AST), alanine aminotransaminase (ALT), γ-glutamyl transferase (GGT) and lactate dehydrogenase (LDH) activities or by the elevation of serum bilirubins and aspartate levels. However, naringenin administration during ethanol-induced hepatic damage decreases the activity/levels of liver damage markers, demonstrating that naringenin protects hepatocytes against necrosis, cholestasis and membrane permeation[64,70,98] (Figure 5).

After hepatocyte damage occurs, an inflammatory reaction is produced that is characterized by increases in cytokines and proteins that mediate the immune response. It has been reported that rats that received 20% ethanol equivalent to 6 g/kg body weight (bw) every day for a period of 60 days showed significantly elevated mRNA levels of tumor necrosis factor-alpha (TNF-α), interleukin-6 (IL-6), nuclear factor-kappa

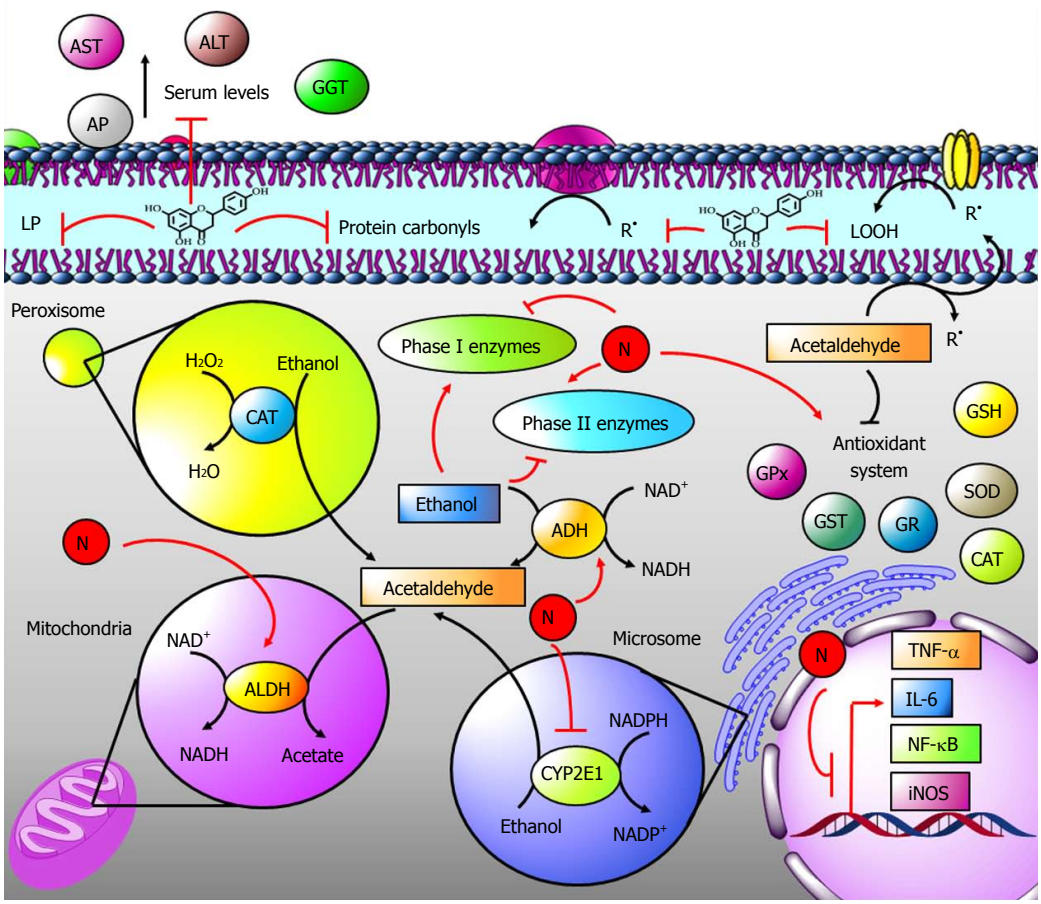

Figure 5 The role of naringenin in alcohol-induced liver damage. Alcohol metabolism: In the cytosol, alcohol is converted into acetaldehyde by alcohol dehydrogenase (ADH); it is also formed in microsomes by CYP2E1 and in peroxisomes by catalase (CAT). In mitochondria, acetaldehyde dehydrogenase (ALDH) transforms acetaldehyde to acetate. Ethanol elevates ADH and CYP2E1 activities but decreases ALDH activity, resulting in toxic acetaldehyde accumulation, free radical ($R^{\cdot}$) formation in the form of lipid hydroperoxides (LOOH) or protein carbonyls and resulting in the elevation of lipid peroxidation (LP). Naringenin (N) increases the activities of all those enzymes, which results in alcohol efficient elimination leading to endogenous antioxidant system restoration, oxidative stress prevention and balance of phase Ⅰ and phase Ⅱ xenobiotic metabolism enzymes. Naringenin also prevents increased levels of alkaline phosphatase (AP), aspartate aminotransferase (AST), alanine aminotransaminase (ALT), and γ-glutamyl transferase (GGT) as well as inflammation during alcohol-mediated liver damage.

B (NF-κB), cyclooxygenase-2 (COX-2), macrophage inflammatory protein 2 (MIP-2) and CD14, as well as increased staining for inducible nitric oxide synthase (iNOS) protein adducts in the liver. Notably, when naringenin (50 mg/kg p.o.) was administered every day during the last 30 d of alcohol intoxication, the flavanone decreased the mRNA levels of all inflammatory markers[98], indicating the potent anti-inflammatory properties of naringenin (Figure 5).

One of the main effects of alcohol abuse on the liver is lipid accumulation in hepatocytes. Even though fatty liver is a reversible condition, it can progress to inflammation and fibrosis. During alcohol consumption, there is a deregulation of pathways that regulate lipid synthesis, oxidation and very-low density lipoprotein (VLDL) exportation that leads to the accumulation of triglycerides and fatty acids in the liver[93]. In a study performed to investigate the effect of naringin supplements on lipid metabolism in ethanol-treated rats, the results showed that the concentrations of plasma/liver total cholesterol and plasma/liver total triglyceride were significantly higher in the ethanol-treated rats and, conversely, decreased the high-density lipoprotein (HDL)-cholesterol level and HDL-cholesterol/total-cholesterol ratio, while naringin reestablished normal levels of all measured lipid parameters. Another interesting effect of the glycoside was a decreased number of hepatic cells containing lipid droplets compared to the alcohol-group, where many of these cells were observed. It was concluded, therefore, that naringin is able to prevent lipid accumulation in liver caused by alcohol[94].

In another study, serum insulin was diminished, glucose/insulin ratio and liver triglycerides were increased in ethanol-drinking rats; however, naringenin co-administration partially protected rats from these effects produced by alcohol intoxication. Unfortunately, naringenin was not able to protect from alterations in serum glucose, triglycerides, total, free and esterified cholesterol or HDL cholesterol, or from liver and muscle triglycerides or glycogen[99].

Naringenin has effects on several steps of ethanol

metabolism, as well as on liver damage by this xenobiotic, suggesting that it can be used in the prevention and reversion of alcohol-induced liver damage. However, more studies are necessary to further investigate naringenin's mechanism of action in alcohol-induced hepatic injury and whether it is able to protect from fibrosis induced by alcohol abuse.

EFFECT OF NARINGENIN ON CCl_4-INDUCED LIVER DAMAGE

CCl_4 is a haloalkane widely used to induce liver damage[100]. To induce liver damage, CCl_4 must be activated by CYP2E1, CYP2B1 or CYP2B2, and CYP3A, to form the trichloromethyl radical ($CCl_3^{\bullet}$). This radical reacts with oxygen to form the trichloromethylperoxy radical ($CCl_3OO^{\bullet}$), a highly reactive species. These two species are highly reactive; they can bind to cellular molecules, for example, nucleic acids, proteins or lipids. $CCl_3OO^{\bullet}$ initiates the chain reaction of LP, which attacks and destroys PUFAs, those associated with phospholipids in cell membranes as the mitochondrial or the reticulum membranes. This membrane damage leads to hepatocyte damage, which in turn activates Kupffer cells and HSC, regulating fibrosis and cirrhosis[31,101] (Figure 6).

Facino *et al*[102] were pioneers to study the effectiveness of naringenin against CCl_4 damage. In this study, a glycosidic fraction (containing naringenin-glycoside) and naringenin-glycoside extracted from the flowering tops of *Helichrysum italicum* G. Don were utilized to investigate the effect of these flavonoids on CCl_4-induced rat microsomes, finding that microsomal LP was reduced by the glycosidic fraction and by naringenin-glycoside[102]. Another study showed that CCl_4-induced liver damage was decreased by concomitant administration of an aqueous extract of the rhizomes of *Sansevieria liberica*, containing 5.99% naringenin, since AP, AST and ALT activities and fatty degeneration of hepatocytes were prevented[103]. Finally, another report investigated the effect of an aqueous extract of *Trifolium pratense L*. (Leguminosae) leaves on CCl_4-induced liver damage; it was observed that naringenin in the extract was able to reduce LP levels and xanthine oxidase (XOD) activity[104].

On the basis that natural extracts containing naringenin had positive effects against injury induced by CCl_4, different protocols have been carried out to evaluate naringenin hepatoprotective capacity. In 2009, Yen *et al*[16] evaluated the ability of naringenin to prevent acute liver failure induced by CCl_4 in rats. Naringenin (100 mg/kg) was administered during three consecutive days, and then on the fourth day, CCl_4 was intraperitoneally (i.p.) administered with a single dose (3 mL/kg, olive oil: CCl_4, 1:1). The flavonoid was able to prevent AST, ALT and LP elevations and the reduction of SOD, CAT and GPx levels, and it significantly suppressed the activation of caspase (Cas)3 and Cas9 induced by CCl_4 administration[16].

Later, Hermenean *et al*[105] published an experiment in which acute liver damage was induced in mice with CCl_4 (1.0 mL/kg, olive oil: CCl_4, 1:1, i.p.), and naringenin (50 mg/kg) pretreatment for seven days was evaluated. The elevation of serum AST, ALT and LP levels as well as the reduction of CAT, SOD and GPx activities and GSH levels in livers from rats intoxicated with CCl_4 were all significantly prevented by naringenin. Moreover, naringenin prevented necrotic changes of hepatocytes, fatty degeneration, sinusoidal dilatation, mild fibrosis, and inflammatory cell infiltration and retained the normal ultrastructure of the hepatocytes, including mild restoration of normal bile canaliculi configuration filled with microvilli[105].

The action mechanism of naringenin on acute liver damage induced by CCl_4 can be explained by different mechanisms. CCl_4 is activated in hepatocytes by CYP2E1; therefore, the $R^{\bullet}$ formed attacks membranes of these cells, generating LP. During CCl_4 administration, the expression of CYP2E1 is elevated; however, it has been reported that naringin strongly inhibited this cytochrome; therefore, one possible mechanism of hepatoprotection is the inhibition of CYP2E1 by the flavanone, preventing bioactivation of CCl_4[59] (Figure 6). Another mechanism is associated with the ability of naringenin to induce the endogenous antioxidant system by upregulating Nrf2. It was reported that the administration of 50 mg/kg of naringenin to rats significantly increased Nrf2 protein levels in the cytoplasm and nucleus, elevating mRNA levels of its target genes, such as *HO-1*, *NQO1* and *GST*[63]; in addition, naringenin can prevent the decrease in Nrf2, HO-1 and SOD protein levels exerted by CCl_4 treatment in mice[59] (Figure 6).

In addition to oxidative stress, inflammation plays a crucial role in the development of liver damage. During fibrosis produced by CCl_4 chronic administration, there is a proinflammatory environment generated by Kupffer cells and HSCs. In these cells, inflammatory signaling pathways, mainly NF-κB-related signaling pathways, are activated. This pathway starts when TLRs are activated; then, intermediaries lead to inhibitor κB (IKB) phosphorylation by IκB kinase (IKK) and NF-κB release into the cytoplasm. NF-κB then translocates into nucleus to induce the transcription of target genes. NF-κB regulates proinflammatory protein expression of TNF-α, IL-1β and IL-6[59,31,106]. In addition, NF-κB binds to *iNOS* and *COX-2* gene promoters, activating the transcription of these genes; iNOS catalyzes the production of nitric oxide (NO), which is a highly oxidizing product[107,108]. On the other hand, during the NF-κB pathway, the intermediate TGF-β-activated kinase 1(TAK1) is activated. Additionally, through MAPKs, NF-κB activates activator protein 1 (AP-1), a factor that promotes the transcription of genes related to inflammation[106,109]. Moreover, high mobility group box 1 (HMGB1) is widely involved in proinflammatory processes through its

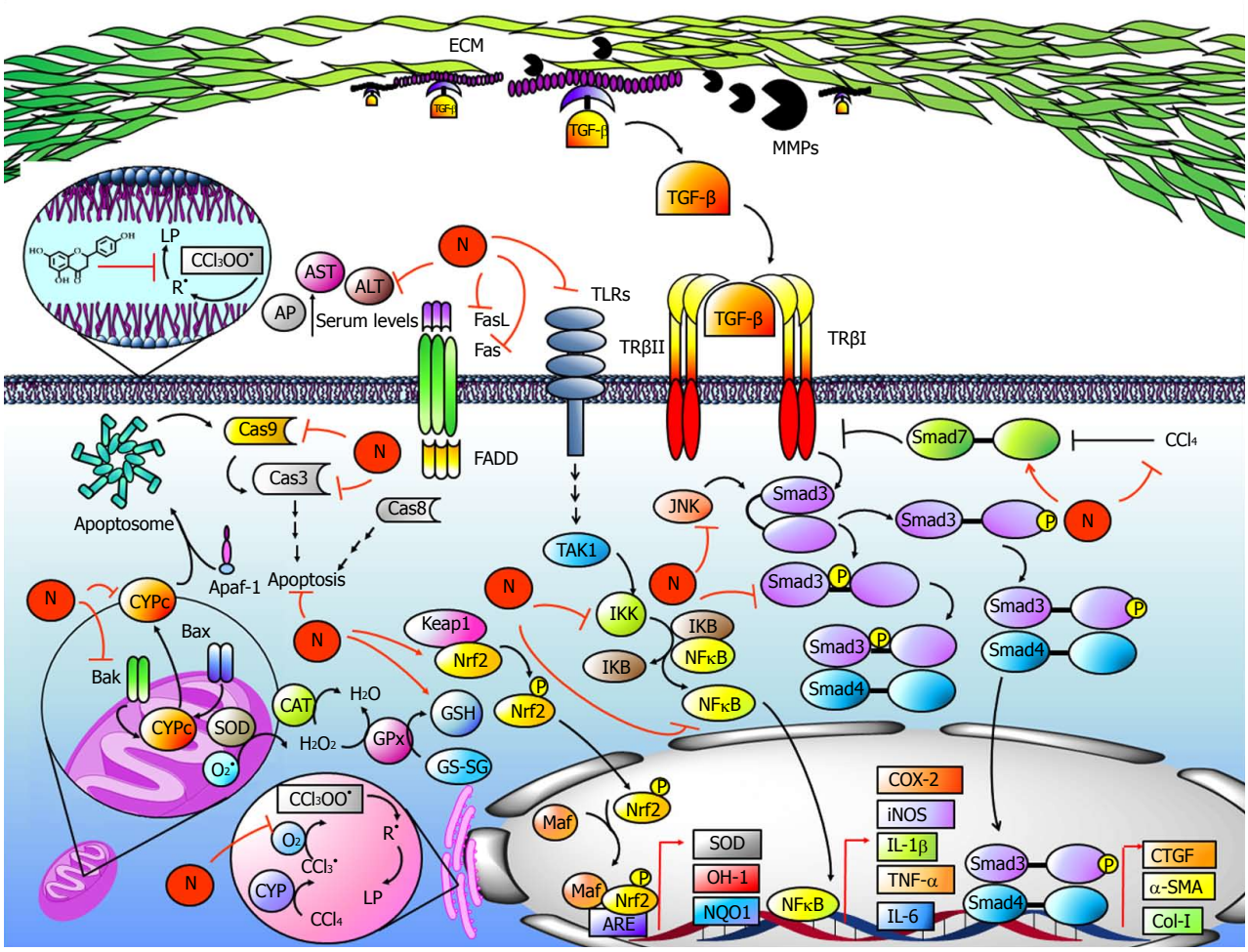

Figure 6 Naringenin prevents acute and chronic CCl_4-induced liver damage. Carbon tetrachloride (CCl_4) is activated by CYP2E1, CYP2B1, CYP2B2, and CYP3A (CYP) to form the trichloromethyl radical ($CCl_3^{\bullet}$); then, it reacts with the oxygen-forming trichloromethylperoxy radical ($CCl_3OO^{\bullet}$). The $CCl_3OO^{\bullet}$ initiates lipid peroxidation (LP), free radical ($R^{\bullet}$) generation, and imbalance of the endogenous antioxidant system formed by superoxide dismutase (SOD), catalase (CAT), glutathione peroxidase (GPx), glutathione (GSH), heme oxygenase (OH-1), NADPH quinone oxidoreductase (NQO1) and nuclear factor-erythroid 2 related factor 2 (Nrf2). Naringenin prevents CCl_4 metabolism, LP and imbalance of the antioxidant system. Naringenin also prevents increased levels of alkaline phosphatase (AP), aspartate aminotransferase (AST), alanine aminotransaminase (ALT), and γ-glutamyl transferase (GGT). On the other hand, CCl_4 increases intrinsic and extrinsic apoptosis pathways in hepatocytes; however, naringenin prevents CYPc release, as well as BCL2-associated X protein (Bax), BCL2-antagonist/killer 1 (Bak), Caspase 3 (Cas3) and Caspase 9 (Cas9) elevation, a protein related with the intrinsic pathway. For the extrinsic apoptosis pathway, naringenin prevents Fas and Fas ligand (FasL) increases produced by CCl_4 administration. During CCl_4-induced fibrosis, there is a proinflammatory environment generated by Kupffer cells and HSCs. The NF-κB pathway starts when TLRs are activated; then, intermediates are activated leading to inhibitor κB (IKB) phosphorylation by IκB kinase (IKK) and NF-κB release. NF-κB regulates inflammatory protein expression, including tumor necrosis factor-alpha (TNF-α), interleukin-6 (IL-6), cyclooxygenase-2 (COX-2), interleukin-1 (IL-1) and inducible nitric oxide synthase (iNOS), while naringenin maintains normal levels of these proteins during CCl_4-induced liver damage. Transforming growth factor-β (TGF-β) activates receptor-activated Smad3 (Smad3), leading to transcriptional induction of α-smooth muscle actin (α-SMA), connective tissue growth factor (CTGF), and collagen-1 (Col-1). Moreover, Smad3 is also activated by JNK *via* linker domain phosphorylation. Naringenin prevents Smad3 activation and α-SMA, CTGF, and Col-1 elevation because it inhibits TGF-β elevation and JNK activation. Metalloproteases (MMPs) cleave extra cellular matrix (ECM) proteins, favoring TGF-β release as well as HSC migration to other sites, increasing fibrosis development; naringenin prevents MMPs elevation. On the other hand, CCl_4 decreases Smad7 protein levels; this protein inhibits the TGF-β signaling pathway by TGF-β receptor I (TβRI) ubiquitination, but nevertheless, naringenin maintains normal levels of Smad7 during CCl_4 treatment.

receptor for advanced glycation end product (RAGE) and TLRs; HMGB1 is released by necrotic cells and by monocytes or macrophage[110].

Because inflammation plays a pivotal role in the establishment and perpetuation of liver diseases, naringenin has been evaluated as an anti-inflammatory therapeutic agent. In this context, a recent paper reported that naringenin (30, 60 and 120 mg/kg) administration to mice treated with CCl_4 (0.3% CCl_4, 10 mL/kg, dissolved in olive oil) showed that at a dose of 120 mg/kg, the flavonoid dramatically downregulated the expressions of TLR4, TNF-α, IL-1β, IL-6, iNOS, AP-1, COX-2, HMGB-1 and NF-κB[59]. Another report of a study carried out in rats that were acutely intoxicated with CCl_4 indicates that naringenin (50 mg/kg) prevents the CCl_4-induced increases in TNF-α and elevations in iNOS, COX-2 protein and mRNA[63]. Figure 6 shows that naringin and naringenin possess important anti-inflammatory properties by blocking the NF-κB signaling pathway.

During hepatic damage, hepatocytes may undergo apoptosis mediated by intrinsic or extrinsic pathways.

In the intrinsic pathway, BCL2-associated X protein (Bax) and BCL2-antagonist/killer 1 (Bak) are activated by proapoptotic stimuli, resulting in the release of electron transport protein CYPc from the mitochondria to the cytoplasm; then, this protein binds to Apaf-1, forming the apoptosome. In turn, the apoptosome activates Cas9, which cleaves procaspase 3 zymogens, amplifying the cell death cascade[11].

The administration of CCl_4 induces apoptosis in hepatocytes as well as DNA fragmentation, increases the mRNA levels of Bax, Bak, Cas3 and Cas9 and increases CYPc release[59,31,101]. It has been reported that glycosylated naringenin (naringin) effectively prevented CCl_4-induced DNA fragmentation, apoptosis and mitochondrial injury by attenuating the release of CYPc, therefore inhibiting apoptosis initiation. Another explanation is that naringin significantly increased the expression of antiapoptotic proteins B-cell CLL/lymphoma 2 (Bcl-2) and BCL2-like 1 (Bcl-xL) but decreased Bax, Bak, Cas3 and Cas9 mRNA levels[59] (Figure 6).

Through the extrinsic pathway, Fas is activated by Fas ligand (FasL), which then binds to Fas-associated protein with a death domain (FADD). The Fas-FADD complex activates procaspase 8, which in turn activates other Cas, leading to apoptosis[111]. After CCl_4-induced acute liver damage, the mRNA levels of Fas, FasL, and proapoptotic protein p53 are increased, but preventive administration of naringin inhibited this increase and reduced apoptosis in liver[59] (Figure 6).

While there are some reports indicating evidence of the beneficial effects of naringenin on acute liver damage induced by CCl_4, there is little information on the effect of this flavanone on chronic treatment. Recently, we have demonstrated that naringenin effectively prevents liver cirrhosis induced by chronic administration of CCl_4 in the rat[112]. Moreover, we studied the molecular mechanisms involved in the hepatoprotective effects of naringenin on CCl_4-induced liver fibrosis. Our results indicate that naringenin prevented necrosis and cholestasis and improved liver biosynthetic capacity in CCl_4-treated rats since the flavonoid completely prevented the increase in ALT, AP and GGT serum activity and hepatic glycogen depletion. In addition, naringenin inhibited oxidative stress caused by chronic liver damage, maintaining normal levels of MDA, GSH and GPx activity. Moreover, inflammation was prevented by naringenin since the levels of NF-κB, IL-1β and IL-6 were preserved within normal values despite CCl_4 administration[112].

Perhaps the most important feature of chronic liver damage is the deposition of scar tissue in the hepatic parenchyma, leading to fibrosis and cirrhosis. In general, livers of rats treated with CCl_4 presented macro nodular fibrosis; the tissue showed liver parenchymal disruption, steatosis, hyperchromatic nuclear hepatocytes, and atypical pleomorphic nuclei. In addition, cirrhotic rats presented large amounts of collagen around fibrotic nodules. In contrast, rats treated with naringenin had livers without macro nodular fibrosis; collagen accumulation as well as regenerative nodules were prevented, and it was found that total collagen and collagen-I (Col-I) accumulation was prevented by naringenin. One of the main profibrogenic signaling molecules is TGF-β, which exerts its effects by activating receptor-activated Smads (R-Smads), leading to transcriptional induction of α-smooth muscle actin (α-SMA), the main marker of transdifferentiation of HSCs, and connective tissue growth factor (CTGF), a TGF-β downstream signal amplifier[113,114]. Notably, naringenin was able to maintain basal levels of TGF-β, as well as α-SMA, CTGF and Col-I, in rats treated with CCl_4. In addition to being activated by TGF-β, MAPKs also activate R-Smads in an alternative pathway (non-canonical), where the linker domain is phosphorylated instead of the carboxyl domain in R-Smads molecules[115,116]. After the administration of CCl_4 for 8 wk, activated JNK levels increased significantly, as well as total and phosphorylated Smad3 in the linker domain (pSmad3L); however, naringenin was able to prevent these effects, providing another explanation for the antifibrotic effect of the flavonoid (Figure 6). Moreover, metalloproteases (MMPs), produced by the activated HSCs, cleave TGF-β, leading to further activation and proliferation of HSCs and collagen fiber formation; consequently, fibrosis ensues. In agreement with these findings, we noticed that chronic CCl_4 administration produced increased MMP2, MMP9 and MMP13; notably, we found for the first time that naringenin treatment preserved normal levels of these MMPs[117] (Figure 6).

Furthermore, CCl_4 decreased Smad7 protein levels; Smad7 inhibits the TGF-β profibrogenic signaling pathway by TGF-β receptor I (TβRI) ubiquitination[118]. Nevertheless, naringenin was able to maintain normal levels of Smad7 during CCl_4 treatment, therefore preserving the normal/physiological antifibrotic pathway and, thus, blocking ECM deposition in the hepatic parenchyma (Figure 6).

Our working group recently showed that naringenin also has effects on the reversion of a previously established fibrosis (unpublished data). CCl_4 was given for 12 weeks to male Wistar rats (400 mg/kg, 3 times/wk); however, naringenin (100 mg/kg/two times a day, p.o.) was administered at the beginning of week 9 of CCl_4 treatment to determine its ability to reverse established experimental cirrhosis. Different techniques demonstrated that naringenin had the ability to reverse elevated liver damage biochemical markers and to restore GSH and glycogen levels. Additionally, the high levels of TGF-β and α-SMA (protein and mRNA) observed during CCl_4 treatment were diminished by naringenin administration. The protein levels of CTGF, Col-1 and MMP13, as well as the activity of MMP2 and MMP9, proteins involved in MEC remodeling, were restored by the flavonoid. The protein levels of NF-κB, IL-1β and IL-10 were elevated during CCl_4 intoxication; however, naringenin reversed this effect. Naringenin also reversed

JNK activation and Smad3 phosphorylation in the linker domain, as well as total protein and total Smad3 mRNA. The results demonstrate that naringenin blocks TGF-β-Smad3 and JNK-Smad3 pathways, and thereby, it has antifibrotic effects, making it a good candidate for properly performed clinical studies. In summary, these results show that naringenin not only reduces CCl_4-induced acute liver damage but also reduces fibrosis. The action mechanism of naringenin to protect the liver from chronic liver damage covers several fronts. This flavonoid displays important effects on the endogenous antioxidant system, blocks the main proinflammatory factor, NF-κB, and inhibits many profibrogenic pathways. These actions make this flavonoid an effective compound to not only to prevent but also to reverse chronic hepatic damage induced by CCl_4.

ANTICANCER ACTIVITY OF NARINGENIN IN THE LIVER

HCC is one of the most frequent tumor types worldwide. It is the fifth most common cancer in men and the ninth in women, with approximately 500000 and 200000 new cases per year, respectively[119].

HCC is a genetically heterogeneous tumor. Hepatocarcinogenesis is complex and, therefore, requires several genetic and epigenetic alterations. Several etiological factors of HCC have been defined, including HBV, HCV, excessive alcohol consumption, obesity, and aflatoxins, and the prevalence/contribution of these risk factors vary by region[120]. In Western countries, the increasing prevalence of nonalcoholic steatohepatitis (NASH), known as the manifestation of the metabolic syndrome, is becoming the most prevalent risk cause for liver failure and HCC[3].

HCC is strongly associated with oxidative stress[121]; hepatic virus infection, the deposition of heavy metals, and fatty liver disease are closely associated with chronic inflammation, which in turn can induce oxidative stress in hepatocytes[122]. Alterations in cell structure and mitochondria can generate electron leakage from the mitochondria, resulting in the activation of pro-oncogenic pathways[123]. In addition, Kupffer cell activation during inflammation produces ROS that are liberated in the liver tissue, inducing damage to the hepatocyte membrane[124].

Elevated levels of intracellular ROS induce the accumulation of many genetic and epigenetic modifications that may play a pivotal role in the induction of many proinflammatory, onco-suppressor- and onco-promoter-related genes that participate in HCC development[125]. When ROS are increased for prolonged periods of time, the antioxidant defense capacity and the repair systems of the cells can be insufficient and lead to lipid, protein and DNA damage, altering different cellular pathways and influencing gene expression, cell adhesion, cell metabolism, the cell cycle, and cell death[126]. In general, ROS have negative effects; they are potential carcinogens because of their role in mutagenesis and the consequential chromosomal aberrations[127], as well as in the regulation of tumor promotion and progression[128]. It is worth noting that ROS have been linked to the hepatocarcinogenic process because they are implicated in the activation of cellular signaling pathways, such as those mediated by MAPKs, NF-kB, PI3K, p53, and b-catenin/Wnt, which are associated with mutagenesis, angiogenesis, tumor promotion, and progression[129,130] (Figure 7).

Abundant evidence from humans and experimental animals has shown that a high intake of natural products rich in antioxidants is associated with a decreased risk of many cancers[131-135]. Flavonoids have diverse biological activities because of their antiallergic, anti-inflammatory, antioxidant, and anticancer properties without significant systemic toxicity[134,135]. Naringenin has been found to exhibit antioxidant, antimutagenic and anticarcinogenic effects[65,136,137] and acts as chemopreventive agent against colon carcinogenesis *in vitro* and *in vivo*[138,139]. It is worth noting that naringenin inhibits cell proliferation *via* the downregulation of NF-κB, VEGF, and MMPs and induces apoptosis *via* Bcl-2, Bax and Cas in a rat model of hepatocarcinogenesis by N-nitrosodiethylamine (NDEA)[140]. Arul and Subramanian demonstrated that naringenin attenuates NDEA-induced hepatocarcinogenesis; they postulated that the flavanone aids in liver cell regeneration, leading to the protection of hepatic cells and membrane integrity by scavenging $R^{\bullet}$ and enhancing the antioxidant status, thus hindering the process of carcinogenesis[141]. A growing body of evidence indicates that naringenin prevents liver damage in chemically induced hepatotoxicity by inhibiting $R^{\bullet}$ and LP and by enhancing the antioxidant system of the cell[65,112,142-144]. Accordingly, the administration of naringenin effectively suppressed NDEA-hepatocarcinogenesis and preneoplastic lesions by modulating antioxidant enzymes and attenuating LP through the scavenging of free radicals, thus enhancing the antioxidant status[141]. Taken together, naringenin can markedly modulate oxidative stress by its activation of the antioxidant defense system. Thus, naringenin appears to be an attractive candidate as an antioxidant supplement for HCC prevention (Figure 7).

In another study, naringenin was found to inhibit the growth of Hep G2 cells in a concentration-dependent manner[145]. The activation of p53 has been implicated in triggering cell cycle arrest, including both G1 and G2 phases of the cell cycle. Notably, naringenin induced a rapid accumulation of p53 in a dose-dependent manner, which might account for the naringenin-induced G0/G1 and G2/M phase arrests in Hep G2 cells[145] (Figure 7).

In addition, evidence has shown that the anti-proliferative effect of natural products is associated with the induction of apoptosis[146,147]. In agreement, naringenin was found to exert antiproliferative effects by inducing apoptosis, as evidenced by the nuclei damage of Hep G2 cells[148,149]. The dysregulation of the cell cycle

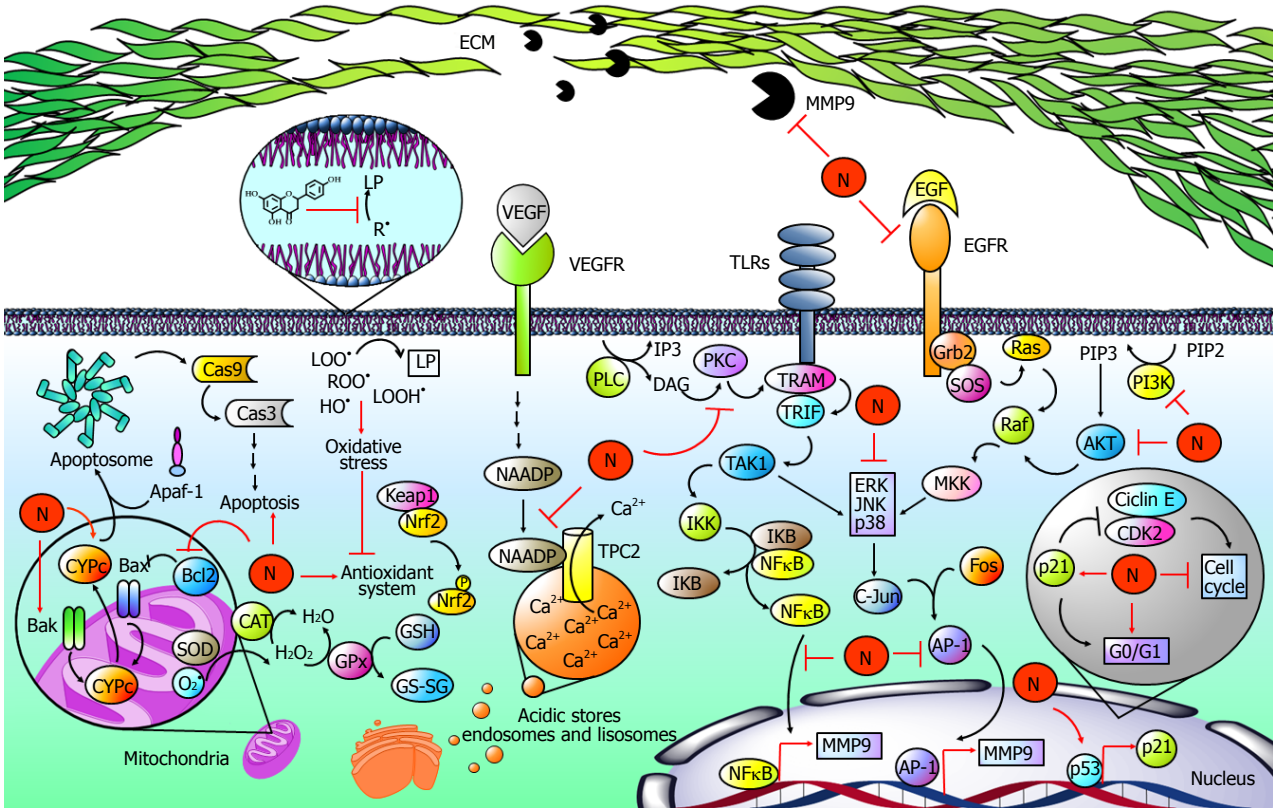

Figure 7 Naringenin in cancer development. Hepatocellular carcinoma is strongly associated with elevated levels of free radicals such as lipid hydroperoxides (LOOH•), peroxyl radicals (ROO•), and hydroxyl radicals (OH•), leading to the development of lipid peroxidation (LP), oxidative stress and finally to an imbalance of the endogenous antioxidant system. Naringenin (N) inhibits oxidative stress by its intrinsic antioxidant properties and by improving the endogenous antioxidant system. Notably, oxidative stress has been linked to the hepatocarcinogenic process because it is implicated in the activation of mitogen activated protein kinases (MAPKs), nuclear factor-kappa B (NF-κB), or phosphatidylinositol-3-kinase (PI3K/AKT) pathways, increasing the production and activity of metalloprotease 9 (MMP9), which is involved in migration and invasion processes. When toll-like receptors (TLRs) are activated, TRAMP is recruited to activate TRIF; in turn, it promotes transforming growth factor beta-activated kinase 1 (TAK1) activation, which phosphorylates IκB kinase (IKK). Then, IKK promotes NF-κB release *via* inhibitor κB (IKB) phosphorylation. On the other hand, phospholipase C (PLC) catalyzes phospholipid hydrolysis, generating inositol triphosphate (IP3) and diacylglycerol (DAG); the latter is an activator of protein kinase C (PKC), which can induce the NF-κB pathway in a TRAMP-dependent manner. Then, NF-κB induces the expression of MMP9. Epidermal growth factor (EGF) is highly involved in carcinogenic pathways; it binds to epidermal growth factor receptor (EGFR) promoting Grb2, SOS, Ras, Raf and mitogen-activated protein kinase kinase (MKK) activation, which participates in extracellular signal-regulated protein kinase (ERK), c-Jun N-terminal kinase (JNK) and p38 (MAPK) phosphorylation and activation. Then, MAPKs promote activator protein 1 (AP-1) activation by c-Jun and Fos dimerization. After that, AP-1 induces the expression of MMP9. Alternatively, MAPKs are activated *via* PI3K/AKT. PI3K produces phosphatidylinositol (3, 4, 5)-trisphosphate (PIP3) from phosphatidylinositol 4,5-bisphosphate (PIP2); PIP3 activates AKT, which promotes MAPK activation in a Ras-dependent pathway. It has been reported that naringenin inhibits MM9 expression and secretion through diminution of p38, JNK, ERK, IKB, and PI3K/AKT phosphorylation as well as NF-κB and AP-1-DNA binding. In addition, naringenin inhibits PKC cytoplasm-to-membrane translocation. Notably, naringenin induces p53 accumulation, leading to p21 expression. Then, p21 inhibits cyclin E/cyclin-dependent kinase 2 (CDK2) complex, which participates in proliferation. p53 accumulation results in naringenin-induced G0/G1 phase arrests. An important mechanism for the elimination of cancer cells is apoptosis. Naringenin induces apoptosis by increased cytochrome c (CYPc) release, as well as BCL2-associated X protein (Bax), BCL2-antagonist/killer 1 (Bak) and Caspase 3 (Cas3) elevation. Additionally, naringenin inhibited B-cell CLL/lymphoma 2 (Bcl-2) an antiapoptotic protein. Two-pore channels (TPCs) are members of the voltage-gated ion channel superfamily localized in acidic calcium (Ca^{2+}) stores and have been implicated in angiogenic processes. Vascular endothelial growth factor (VEGF) and its receptor vascular endothelial growth factor receptor (VEGFR) promotes TPC activation *via* nicotinic acid adenine dinucleotide phosphate (NAADP); then, Ca^{2+} is transported to the cytoplasm through TPCs, activating angiogenic signals. Naringenin inhibits VEGF angiogenesis induction blocking NAADP activation and NAADP/TPC association.

mechanism and the induction of cancer cell apoptosis are recognized as important targets in cancer therapy. In this sense, naringenin is known to induce apoptosis through the modification of Bcl-2 family of proteins involved in the apoptotic mitochondrial pathway, and the results from HepG2 cells showed that naringenin increases the activity of Cas3[145]. Additionally, flow cytometry with Annexin V-FITC/PI staining demonstrated that the flavonoid increased apoptotic cells, confirming that naringenin induced apoptosis in HepG2 cells[145]. The accumulated data suggest that naringenin, as well as other compounds derived from plants, may induce apoptosis through the mitochondria-initiated death pathway[148,150,151] (Figure 7).

On the other hand, two-pore channels (TPCs), are members of the voltage-gated ion channel superfamily and localize in acidic Ca^{2+} stores and have been implicated in different pathophysiological processes[152,153]; TPC2 is expressed predominantly in late endosomes and lysosomes[154]. It has been found that naringenin impairs TPC2-dependent biological activities, leading to antiangiogenic effects mediated by VEGF. Overall, these

data suggest that naringenin inhibition of TPC2 activity and the observed inhibition of the angiogenic response to VEGF are linked by impaired intracellular calcium signaling[155]. Therefore, TPC2 inhibition is emerging as a key therapeutic step in the progression and metastatic potential of malignant cells. The identification of naringenin as an inhibitor of TPC2-mediated signaling provides a novel and potentially relevant tool for the advancement of anticancer research (Figure 7).

12-O-tetradecanoylphorbol-13-acetate (TPA) is widely utilized for studying the mechanisms of carcinogenesis[156]. TPA upregulated MMP9 expression *via* PKC-dependent activation of the Ras/ERK signaling pathway, increasing invasiveness in cell lines[157] and tumor metastasis[158]. Importantly, Yen *et al*[159] demonstrated that naringenin possesses a strong antiinvasive and antimigratory effect in TPA-activated hepatoma cells *via* the downregulation of PKC, epidermal growth factor (EGF), MAPK and PI3K/Akt signaling pathways, and NF-κB, AP-1 and MMP9 activities (Figure 6).

In conclusion, naringenin is highly effective in inhibiting cell proliferation and inducing apoptotic cell death in HepG2 cells and reducing invasion and metastasis. Therefore, it may be a promising candidate for hepatocarcinogenesis treatment.

NARINGENIN PROTECTS FROM LIVER DAMAGE INDUCED BY HEAVY METALS

Heavy metals can be classified according to their mechanism of action in redox-active metals or redox-inactive metals. Redox-active metals such as iron (Fe), copper (Cu), chromium (Cr), cobalt (Co), among others, develop redox cycling reactions, and they produce $R^{\bullet}$ in biological systems, producing oxidative stress, LP, DNA damage and other deleterious effects. Meanwhile, redox inactive metals such as cadmium (Cd), arsenic (As) and lead (Pb) bind to proteins and sulfhydryl groups and induce GSH depletion[160].

In this section, liver damage caused by redox-active and -inactive metals will be discussed.

Iron

Iron is an indispensable micronutrient for living organisms; it participates in oxygen transport, DNA synthesis and host defense, among others. Total body iron content ranges from 3 to 5 g, but its level increases due to diseases or intoxication[161]. The liver is the main iron depot; thus, it is highly susceptible to damage induced by iron overload[161,162].

Iron is captured by hepatocytes through transferrin receptor 1 (TfR1); during iron overload, its transcript is degraded and its synthesis is inhibited; however, iron uptake can be mediated by TfR2 even with high iron levels[161,162]. When iron binding capacity or transferrin saturation is exceeded, non-transferrin bound iron (NTBI) is elevated, and then it is transported into hepatocytes through divalent metal transporter 1 (DMT1). In hepatocytes, iron is incorporated into the ferritin molecule that preserves iron bioavailability[162] (Figure 8).

One of the most reactive $R^{\bullet}$ is $O_2^{\bullet}$; under normal conditions, it is produced in the respiratory chain by NADP oxidase, and then, it is neutralized by SOD, generating H_2O_2. Intracellular iron is released from ferritin by $O_2^{\bullet}$; next, free iron reacts with H_2O_2 in the Fenton reaction, generating high amounts of $OH^{\bullet}$, and in turn, $OH^{\bullet}$ attracts the double bonds of DNA bases. In the case of lipids, free iron produced LP forming $ROO^{\bullet}$[160]. These processes produce hepatocyte damage, such as mitochondrial dysfunction and apoptosis, which results in the recruitment of Kupffer cells that phagocyte damaged hepatocytes, leading to the release of proinflammatory and profibrogenic cytokines that activate HSCs; as a result, hepatic fibrosis ensues[161-163].

The Fenton reaction is inhibited by flavonoids with 3′,4′-catechol, 4-oxo, and 5-OH arrangements. Chelating complexes with cations may form between the 5-OH and 4-oxo group or between the 3′- and 4′-OH[29]. Using an electrospray mass spectrometry study, it was observed that naringenin can form complexes with Fe(III) through its 4-oxo and 5-OH groups; in addition, this flavonoid is oxidized in the presence of metal ions, which are consequently reduced[164]. Furthermore, naringenin was investigated for its ability to suppress the Fenton reaction characteristic of the iron-ATP complex; the flavanone interfered with the voltammetry catalytic wave associated with the iron-ATP complex in the presence of H_2O_2 because it has the arrangement of 4-oxo and 5-OH that is indispensable for this inhibition[165] (Figure 8).

In an experiment where the modulation of DNA integrity in Fenton's system by naringin was studied, it was shown that the glycoside protected DNA from damage caused by $OH^{\bullet}$ generated during the Fenton reaction; naringin blocks the Fenton reaction by iron chelation rather than by antioxidant mechanisms or reduction of Fe(III) to Fe(II), and as a result, damage is prevented[166]. In another study, the isolated mouse liver mitochondrial fraction was incubated with naringin before Fe(III) loading, generating elevations in LP, protein carbonyl content and DNA oxidation, while iron overload decreased GSH levels and GST, GPx, CAT and SOD activities; however, pretreatment with naringin inhibited these iron effects[167]. Iron exposure in HepG2 cells caused a decline in cell survival, a time-dependent increase in DNA oxidation, an elevation in DNA strand breaks, a high level of LP, and a depletion of GSH as well as decreases in GPx, CAT and SOD levels. Notably, the pretreatment of HepG2 cells with naringin resulted in cell survival induction, DNA damage prevention, improvement in the antioxidant system and the inhibition of iron-mediated cellular damage[168] (Figure 8).

Regarding naringenin's effects on iron-induced damage *in vivo*, it has been reported that the flavanone protected against iron-induced neurotoxicity in the

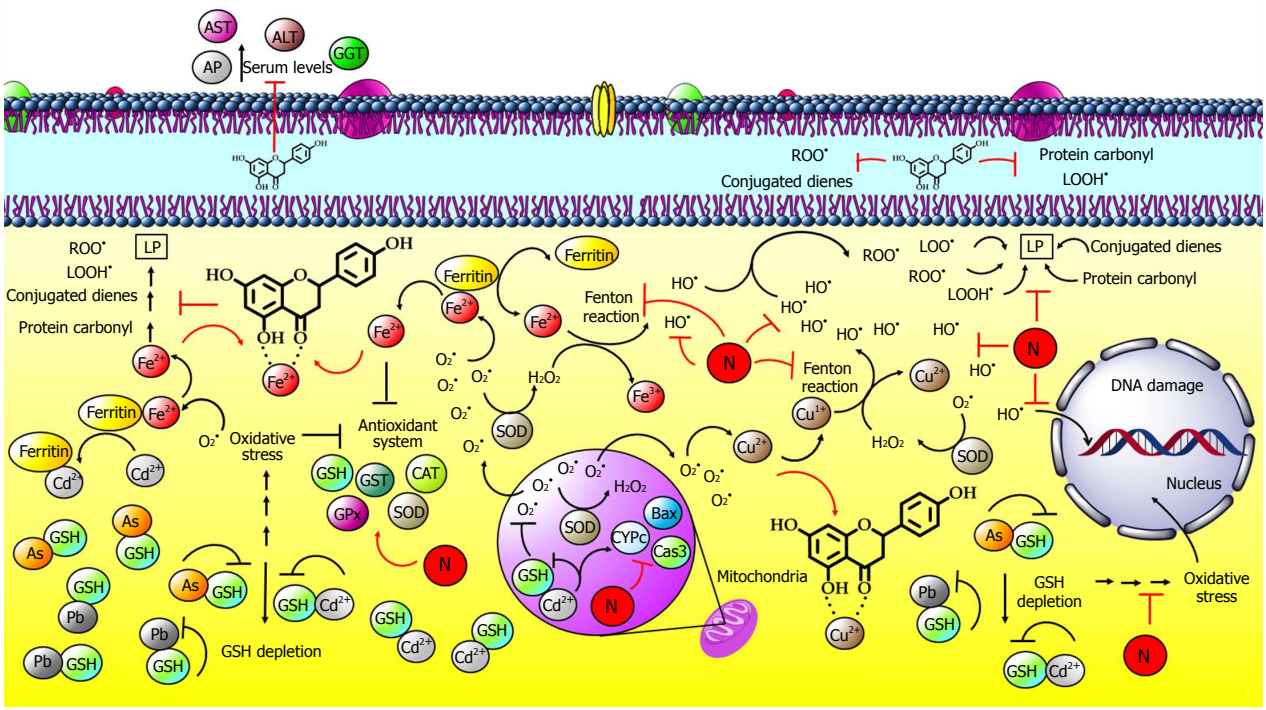

Figure 8 Naringenin inhibits hepatic damage induced by heavy metals. Heavy metals can be classified according to the mechanism of action in redox-active metals such as iron (Fe) and copper (Cu) or redox-inactive metals such as cadmium (Cd), arsenic (As) and lead (Pb). One of the main free radicals is superoxide radical ($O_2^{\bullet}$); normally, it is produced by NADP oxidase, and then, it is neutralized by superoxide dismutase (SOD), generating hydrogen peroxide (H_2O_2). Intracellular Fe is releases from ferritin by $O_2^{\bullet}$; next, free Fe reacts with H_2O_2 in the Fenton reaction, generating high amounts of hydroxyl radicals ($OH^{\bullet}$). After that, $OH^{\bullet}$ attacks double bonds of DNA bases. In the case of lipids, free Fe produces lipid peroxidation (LP) through peroxyl radicals ($ROO^{\bullet}$), producing lipid hydroperoxides ($LOOH^{\bullet}$), conjugated dienes and protein carbonyl. Regarding Cu, once inside the hepatocyte, Cu ion (Cu^{2+}), can be reduced to cuprous ion (Cu^{1+}) when reacting with $O_2^{\bullet}$; then, it mediates H_2O_2 decomposition in $OH^{\bullet}$ *via* the Fenton reaction. These processes result in hepatocyte and liver damage. Naringenin can chelate these metals, preventing their participation in the Fenton reaction; naringenin also inhibits oxidative stress by its antioxidant capacity and by promoting the endogenous antioxidant system. On the other hand, redox-inactive metals such as Cd, arsenic (As) and lead (Pb) form complexes with thiol groups, such as glutathione (GSH), in the cytoplasm and mitochondria. GSH level reduction, GSH inactivation, and GSH system deregulation increase metal toxicity. In addition, Cd can replace Fe and Cu in ferritin or apoferritin; thus, free Fe and Cu ions cause oxidative stress *via* the Fenton reactions and elevation of BCL2-associated X protein (Bax), Caspase 3 (Cas3) and cytochrome (CYPc) proapoptotic proteins. Naringenin improves the antioxidant system by increasing SOD, catalase (CAT), glutathione peroxidase (GPx), glutathione transferase (GST) enzymes and GSH levels.

cerebral cortex of Wistar rats. After four weeks of iron administration, LP and protein oxidation were increased, but SOD, CAT, total thiols and ascorbic acid were decreased. Significant decreases in acetylcholinesterase and Na+/K+-ATPase activities were also shown, along with a substantial rise in NO levels. Co-administration with naringenin blocked the development of oxidative stress and improved antioxidant enzyme activities in the cerebral cortex[169]. In another work, the effect of naringenin on iron-induced hippocampus damage was investigated: iron administration for 28 d induced an impairment of the anxiogenic-like behavior and induced purinergic and cholinergic dysfunctions with oxidative stress-related disorders on mitochondrial function in the rat hippocampus, but naringenin was able to restore those parameters[170] (Figure 8).

As seen, naringenin and naringin have the ability to block iron-induced oxidative stress; these natural compounds are able to chelate metal ions such as iron; thus, free iron is not available for the Fenton reaction, and therefore, $OH^{\bullet}$ generation is blocked, as is oxidative stress. The chelation capacity is given in the naringenin molecule by the 4-oxo and 5-OH groups, which probably represent the place where an iron ion is conjugated. In the absence of this arrangement, some flavonoids do not have chelating capacity or are less effective[164-166]. This structure-activity relationship indicates that naringenin and naringin can act as antioxidants or as chelators, depending on the hepatotoxic agent employed.

Copper

Copper is a redox active metal, and an imbalance in its metabolism produces disorders such as Wilson´s disease, Indian childhood cirrhosis or endemic Tyrolean infantile cirrhosis, which share the common end of cirrhosis due to excessive copper accumulation; another problem is copper toxicity caused by copper poisoning or dietary copper toxicity[160,171,172]. Like iron, copper exerts its hepatotoxic effects by oxidative stress generation; this is a consequence of its redox reactivity, triggering events that end in liver damage.

Like iron, copper is stored in the liver; it is introduced into the hepatocyte through the high-affinity human copper transporter (hCtr1)[173]. Once inside the hepatocyte, cupric ion (Cu(II)), can be reduced to cuprous ion (Cu(I)) when reacting with $O_2^{\bullet}$, ascorbic

acid or GSH; meanwhile, Cu(I) mediates H_2O_2 decomposition in $OH^•$ *via* the Fenton reaction[160]. The formed $OH^•$ reacts with lipids, proteins and DNA, as well as with practically any biological molecule, generating lipid radicals, protein carbonyls or DNA strand breaks and oxidation of bases; in fact, copper is more powerful that iron in enhancing DNA breakage[160,174]. Furthermore, copper binds directly to free thiols of cysteines, which can result in oxidation and subsequent crosslinks between proteins, leading to impaired activity of target enzymes[171]. In addition, copper induces LP and 4-hydroxy-2-nonenal (HNE) formation. Importantly, HNE may increase the phosphorylation of JNK and p38, AP-1 activity and the expression of Col-I and TGF-β[160], resulting in the exacerbation of fibrosis (Figure 8).

As previously mentioned, naringenin may act as a metal chelator. In this regard, two studies have reported the chelating capacity of the flavonoid on copper. Fernández *et al*[164] showed that naringenin, at various stoichiometries (metal: flavonoid) with copper, 1:1, 1:2, 2:2 and 2:3, produces several complexes, preferably with Cu(II). Additionally, comparing the 4-oxo and 5-OH arrangement with the 4-oxo and 3-OH arrangement, the first one seems to favor cooper chelation[164]. Meanwhile, Mira *et al*[175] reported that naringenin has higher reducing capacity for copper ions than for iron ions. Additionally, the copper reducing activity seems to depend largely on the number of OH groups. In addition, naringenin chelates Cu^{2+} at pH 7.4 and pH 5.5 between the 5-OH and the 4-oxo groups, producing 7.1 ± 1.1 mmol Cu^+/mmol naringenin, indicating that a large number of copper ions per molecule of flavonoid were chelated[175] (Figure 8).

It has been shown that copper induces the oxidation of low-density lipoproteins (LDL); as a consequence, PUFAs in the lipoprotein are rapidly converted to LOOH and aldehydic breakdown products[160,176,177]. It has been reported that when freshly isolated human LDL (50 μg protein/mL) was incubated with 2 μmol/L Cu^{2+} at 37 ℃, naringenin (25 μmol/L) slightly inhibited LDL oxidation, but prenylflavanones (25 μmol/L) such as 8-geranylnaringenin, 6-prenylnaringenin, 8-prenylnaringenin and 6,8-diprenylnaringenin effectively inhibit LDL oxidation dienes formation. Then, Cu^{2+}-mediated LDL oxidation was evaluated by measuring TBARS levels; the results showed that prenylflavanones significantly inhibited TBARS formation and were ranked as follows: 8-geranylnaringenin > 6,8-diprenylnaringenin, 6-geranylnaringenin, 8-prenylnaringenin > 6-prenylnaringenin[177] (Figure 8).

As seen, naringenin and its derivatives can inhibit the first steps of copper-induced damage by preventing the Fenton reaction and by preventing lipid and protein oxidation.

Cadmium

Unlike iron and copper, cadmium is a redox inactive metal; although it does not directly form $R^•$, it can induce oxidative stress in other ways. In addition, there is no mechanism for cadmium excretion in humans; thus, cadmium accumulates in tissues indefinitely[160,178].

Cadmium is absorbed though the intestines, and in the liver, DMT1, ZIP8 and ZIP14 are responsible for Cd uptake into hepatocytes[178]. Once inside hepatic cells, cadmium follows two pathways to exert liver damage: (1) Cadmium forms complexes with thiol groups of proteins or small peptides, such as GSH, in the cytoplasm and mitochondria. GSH is the first line of defense against cadmium-induced damage; thus, GSH level reduction, inactivation, and GSH system deregulation increase cadmium toxicity. In mitochondria, thiol group inactivation causes oxidative stress, mitochondrial permeability transition, and mitochondrial dysfunction[178,179]. And (2) Cadmium can replace iron and copper in ferritin or apoferritin; thus, free iron and copper ions readily cause oxidative stress *via* the Fenton reaction[160,178]. Thereby, although cadmium is unable to generate $R^•$ directly, indirect formation of ROS, $O_2^•$, $OH^•$ and NO has been reported. In addition, increased LP levels and antioxidant system deregulation has been observed during cadmium liver damage[160,178,179]. Because of oxidative stress induced from cadmium intoxication, Kupffer and HSCs cells can be activated, and thus, a large number of inflammatory and cytotoxic mediators can be produced[178,179] (Figure 8).

One of the first reports on the beneficial effect of naringenin on damage induced by cadmium was performed in kidney, and after 4 wk of $CdCl_2$ administration (5 mg/kg/d), TBARS, LOOH and protein carbonyl levels were elevated. Conversely, total sulfhydryl groups, GSH, vitamin C and vitamin E levels, as well as SOD, CAT, GPx, GST and GR, and glutathione-6-phosphate dehydrogenase (G6PD) activities were decreased. Co-administration of naringenin (25 and 50 mg/kg daily) resulted in the prevention of Cd-induced LP and in the restoration of the endogenous antioxidant system. Histopathological analysis showed that naringenin markedly reduced $CdCl_2$ toxicity and preserved the normal histological architecture of renal tissue[180].

Later, Renugadevi *et al*[65] reported that cadmium (5 mg/kg) administered orally for 4 wk induced liver damage. Increased activities of serum AST, ALT, AP, LDH, GGT and bilirubin were found. Furthermore, LP and protein carbonyl contents were elevated. Antioxidant enzymes such as SOD, CAT, GPx, and GST as well as GSH, vitamin C and vitamin E concentrations were diminished. Naringenin (50 mg/kg) significantly prevented the elevation of serum hepatic marker enzymes. Additionally, the flavonoid significantly reduced LP and restored antioxidant defense levels. The histopathological studies showed that naringenin preserved normal histological architecture of the tissue[65]. The same working group reported that naringenina plus vitamins C and E improved the altered biochemical and histopathological changes in the liver of Cd-intoxicated

rats to a greater extent than naringenin or vitamins alone[72] (Figure 8).

In another work, naringenin (4 and 8 mg/kg) was orally administered to mice 30 min before oral administration of $CdCl_2$ (12 mg/kg) for 11 consecutive days. Cotreatment with naringenin significantly prevented disarrangement in body and organ weights, hematological profiles, serum and hepatic altered biochemical parameters in Cd-intoxicated mice[181].

Naringin also displays protective effects in cadmium-induced damage to HepG2 cells, where the glycoside maintained redox homeostasis, mitochondrial membrane potential, reduced Cas3 and CYPc and reduced apoptosis by regulating the Bax/Bcl2 ratio. Moreover, naringin prevented diminution of protein thiol levels, SOD, GST and CAT activities, and LP development through increasing Nrf2 and metallothionein (MT)[182] (Figure 8).

Most evidence concurs that naringenin prevents cadmium-induced liver damage by protecting enzymatic and non-enzymatic antioxidant systems and by safe-guarding GSH thiol groups. The antioxidant actions of naringenin may also be associated with its ability to chelate heavy metals, thus preventing the formation of ROS and with its ability to increase Nrf2. These data show that naringenin is effective in preventing damage induced by cadmium.

Arsenic

Arsenic is a highly distributed metal that is found in organic and inorganic forms; both forms are toxic, although inorganic arsenic is more toxic than organic arsenic[160]. This metal is metabolized by reduction and methylation reactions, which are catalyzed by glutathione-S-transferase omega-1(GSTO1) and arsenic (III) methyltransferase (AS3MT); it has been reported that during arsenic metabolism, high amounts of reactive species are generated[160,183].

Like cadmium, arsenic induces cellular damage through binding to sulfhydryl groups and inducing mitochondrial dysfunction. Cadmium produces oxidative stress-generating species such as $O_2^{\bullet}$, singlet oxygen ($^1O_2$), $ROO^{\bullet}$, NO, H_2O_2, dimethylarsinic peroxyl radical [$(CH_3)_2AsOO^{\bullet}$] and dimethylarsinic radical [$(CH_3)_2As^{\bullet}$][160,184]. In general, an oxidative environment results in GSH depletion, LP elevation, protein oxidation, DNA damage, morphologic changes in mitochondrial integrity and a rapid decline of mitochondrial membrane potential[160,184,185]. Oxidative stress induces hepatocyte apoptosis as well as total bilirubin, ALT, and AST elevation and liver damage [183] (Figure 8).

Since arsenic induces damage *via* oxidative stress, naringenin has been studied in arsenic-induced liver damage. Arsenic administration (2 mg/kg) for 28 d to rats or 14 d (3 mg/kg) to mice produced elevations in AST, ALT and AP activities, high LP markers, hepatic GSH depletion and reductions in SOD, CAT, GPx, GST and GR activities. In addition, arsenic exposure produced DNA fragmentation. However, the simultaneous administration of naringenin prevented hepatic injury by arsenic[68,74].

Jain *et al*[73] reported that $NaAsO_2$ administration (8 mo) to male Wistar rats induced high levels of ROS in blood and liver and increased levels of hepatic LP; simultaneously, the endogenous antioxidant system was attenuated, leading to a reduction of GSH levels and to the inhibition of GPx, GST, SOD and CAT activities in liver. Once liver damage was established, naringenin was administered for two weeks; the flavanone was able to reverse oxidative stress, since ROS and TBARS levels were diminished. Moreover, the enzymatic antioxidant system was restored by naringenin[73].

Naringin also has been shown to prevent liver and kidney damage induced by $NaAsO_2$ (5 mg/kg); the glycoside inhibited increased serum levels of ALT and AST as well as prevented SOD and GSH depletion. In addition, naringin downregulated the expression of TGF-β, Cas3 and TNF-α in kidney[186] (Figure 8).

In summary, naringenin and naringin display hepatoprotective effects in arsenic-induced liver injury mainly by improving the endogenous antioxidant system and probably by their chelating effect.

Lead

The mechanism of action of lead toxicity is similar to those of cadmium and arsenic. This heavy metal does not generate free radicals directly; instead, lead deactivates antioxidant pools by binding to sulfhydryl groups of protein or peptides. For instance, lead-GSH interaction inactivates GSH antioxidant activity; moreover, lead reduces GSH levels bay blocking GR, GSG and δ-aminolevulinic acid dehydratase (ALAD), an enzyme in charge of preserving the GSH/GSSG balance[160,187-189]. The inhibition of the antioxidant GSH system produces $R^{\bullet}$ such as $O_2^{\bullet}$, $^1O_2$ and $ROO^{\bullet}$, which destabilize cellular membranes through LP processes, resulting in mitochondria and DNA damage leading to p53 upregulation, an imbalance of Bax/Bcl-2 and apoptosis. After oxidative damage caused by lead, proinflammatory pathways are activated, exacerbating preexisting liver damage[187,188] (Figure 8).

Two reports have been published dealing with naringenin's effects on lead-induced liver injury. Wang *et al*[58] and Ozkaya *et al*[144] reported that rats treated with lead acetate in drinking water showed significant increases in MDA and depletion of GSH levels and GPx activity. Elevated levels of ALT and AST in serum and decreased SOD activity in liver were also shown[58]. Furthermore, histopathological results showed that the livers of lead-intoxicated rats had periportal cell infiltration, sinusoidal congestion, hepatic steatosis, and capsular fibrosis[144]. Naringenin administration (50 mg/kg) prevented the disarrangement of most parameters studied, and histopathological abnormalities such as necrosis, hydropic degeneration, and hepatic cord disorganization were attenuated by naringenin treatment[58,144] (Figure 8).

These studies show that naringenin has hepatoprotective effects against lead-induced liver damage; however, more studies are needed to further understand the naringenin mechanism of action.

ANTIVIRAL PROPERTIES OF NARINGENIN

The study of hepatovirus has been an important issue in hepatology research in the last four decades. HBV and HCV are most studied, as they produce chronic liver damage, leading to cirrhosis and HCC[190]. As global causes of liver cirrhosis, HBV accounts for 30%, HCV for 28%, alcohol for 27% and others for 14% of cirrhosis cases. The etiology of liver cancer is HBV (45%), HCV (26%), alcohol (20%), and others (39%)[3]. Therefore, research on treatment for these infections is important for the prevention/reversion of chronic liver diseases.

HCV is a virus belonging to the Flaviviridae family; its genome consists of a positive-sense single-stranded RNA. Hepatocytes are the major site of HCV replication, but peripheral blood mononuclear cells and lymph nodes are also natural HCV targets[3,191,192].

HSC machinery processes three structural HCV proteins (core, E1 and E2), an ion channel protein (p7) and six non-structural proteins (NS) (NS2, NS3A, NS4A, NS4B, NS5A and NS5B)[191]. HCV adopts an icosahedral structure with a lipid envelope and glycoproteins E1 and E2 immersed in the envelope. Underneath the envelope is the nucleocapsid, composed of multiple copies of core forming the internal viral coat that encapsulates the genomic RNA[192] (Figure 9).

E1 and E2 are responsible for receptor binding and HCV entry into hepatocytes. Among the receptors for HCV, CD81 is probably the best characterized; low-density lipoprotein receptor (LDLR), scavenger receptor class B type I (SR-B1), human scavenger receptor, and glycosaminoglycans may also act as receptors for HCV[191,192]. After binding to its receptor, HCV endocytosis is activated, leading to the uptake of HCV particles across the cell plasma membrane[191]. After endocytosis, nucleocapsids are deposited into the cytoplasm *via* a low pH dependent mechanism; then, the nucleocapsids are uncoated, and their RNA is released[191,192] (Figure 9).

Genomic RNA translation is mediated by an internal ribosome entry site (IRES) binding to the ribosome; then, the HCV polyprotein is produced in the rough endoplasmic reticulum (RER) membrane, and after that, viral proteins remain associated with intracellular membranes and gave rise to a seemingly ER-derived membranous web where NS proteins form the replication complex (RC)[191,192]. Within the RC, the positive-stranded RNA genome is used as a template for synthesis of negative-stranded RNA, which in turn serves as a template for new positive-stranded synthesis. New viral RNA is encapsulated within multiple copies of the core to form the nucleocapsid, and then, it acquires envelope; HCV virions are exported out the cell ready to infect healthy hepatocytes[192] (Figure 9).

An interesting phenomenon is that HCV circulates in the blood in the form of a lipoprotein complex called lipoviroparticle (LVP); it has been reported that HCV may be associated with lipoproteins such as VLDL and low-density lipoprotein (LDL). Notably, the binding of lipoviroparticle to receptors as LDLR or SR-B1 enables the infectivity of HCV and its escape from the humoral immune response[190-193]. A relationship between the virion production process and lipoproteins, cholesterol, triglycerides and fatty acids has been suggested. HCV assembly appears to occur on lipid droplets, and the core protein clearly coats the surface of this organelle, but the lipid droplet not only serves as a site for viral assembly but also supplies lipoproteins that complex with HCV particles[191] (Figure 9).

It has been reported that HCV core protein is bound to apolipoprotein (Apo) B-100 and, therefore, to VLDL in HCV secreted by infected cells in the JFH1/Huh7.5.1 full viral life-cycle model. In addition, the HCV-VLDL complex is actively secreted by the cells; moreover, the colocalization of HCV's core and ApoB100 was found in the cytoplasm of infected cells. Interestingly, silencing ApoB production by a SureSilencing shRNA in the cell downregulates HCV core protein secretion and HCV-positive strand RNA secretion[193] (Figure 9).

Naringenin was used as an ApoB100 inhibitor because the flavonoid reduces microsomal triglyceride transfer protein (MTP) and enzyme acyl-coenzyme A (CoA): cholesterol acyltransferase (ACAT) activity, whose expression is indispensable for ApoB synthesis[11,193]. The results showed that naringenin inhibits the secretion of HCV core and HCV-positive stranded RNA, as well as HCV secretion, more than ApoB10 silencing by the SureSilencing shRNA. Nevertheless, intracellular levels of HCV-positive strand RNA and intracellular HCV core protein expression remained unchanged; despite this, the ability of the secreted virus to infect cells was strongly inhibited following naringenin treatment. This inhibition by naringenin was mediated by a reduction in MTP activity and by the transcriptional inhibition of 3-hydroxy-3-methylglutaryl CoA reductase (HMGCR) and acyl-coenzyme A: Cholesterol acyltransferase (ACAT2)[193] (Figure 9).

Inhibition of HCV secretion by naringenin is mediated by a reduction in ApoB100 synthesis because naringenin regulates proteins related with ApoB. Normally, cholesterol is synthetized in an HMGCR-dependent pathway which is the rate-limiting enzyme for cholesterol synthesis; then, cholesterol is converted to cholesteryl esters (CEs) by ACAT. CEs are very important to VLDL and LDL assembly. Another important element to VLDL and LDL assembly is MTP, which plays a key role in ApoB100 secretion by catalyzing the transfer of lipids to the nascent ApoB100; if ApoB-MTP binding is inhibited, ApoB is predicted to undergo degradation[11].

Naringenin improves metabolic imbalance by reducing the activity and mRNA levels of HMGCR, which explains

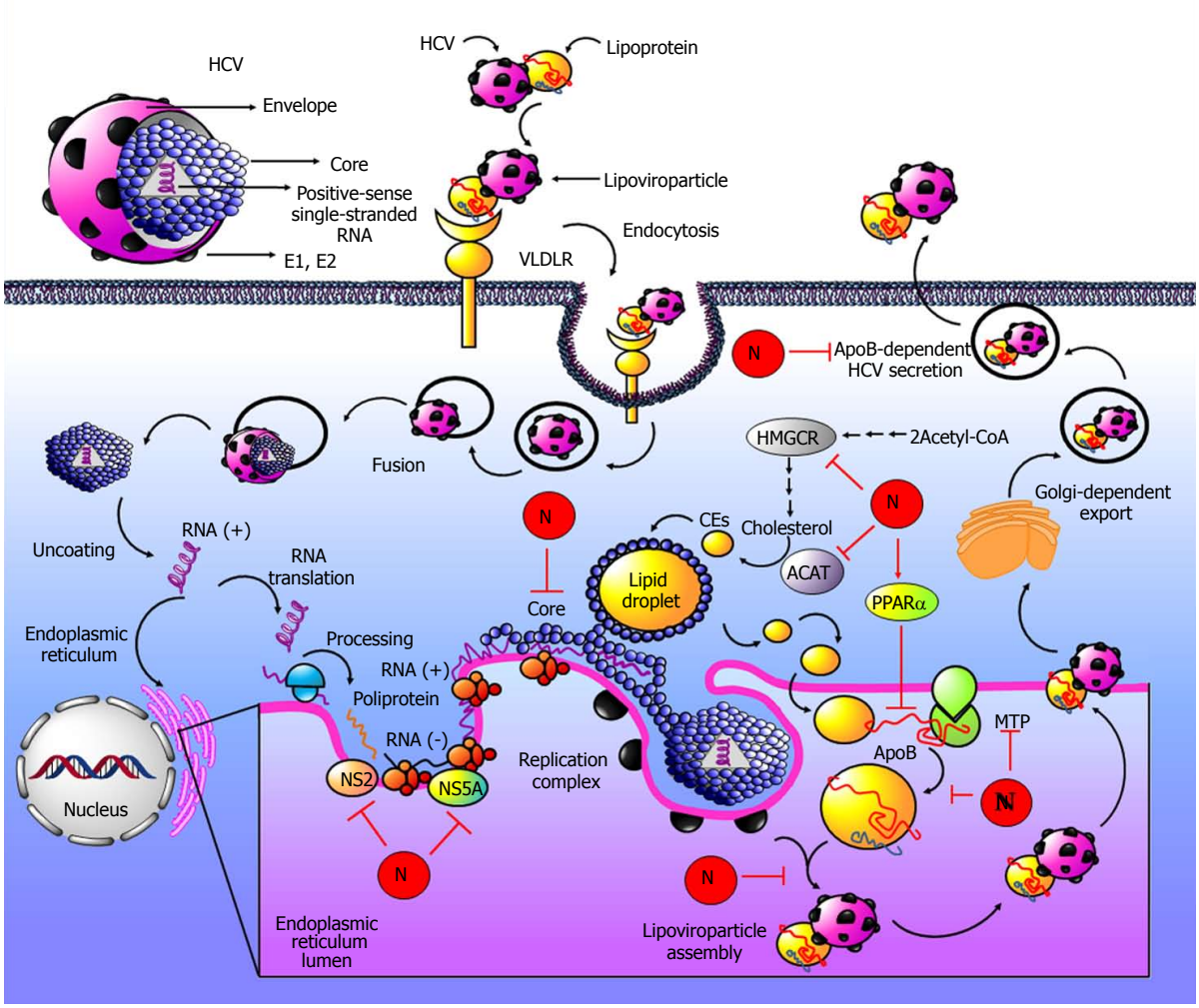

Figure 9 Antiviral properties of naringenin. The Hepatitis C virus (HCV) genome consists of a positive-sense single-stranded RNA. HCV adopts an icosahedral structure with a lipid envelope and glycoproteins E1 and E2 immersed in the envelope. Underneath the envelope is the nucleocapsid, which is composed of multiple copies of core forming the internal viral coat that encapsulates the genomic RNA. HCV may be associated with lipoproteins such as very-low density lipoprotein (VLDL), forming a lipoprotein complex called lipoviroparticle. Binding of lipoviroparticle to very-low density lipoprotein receptor (VLDLR) results in virus endocytosis; after that, nucleocapsids are deposited into the cytoplasm. Then, nucleocapsids are uncoated, and the RNA is released. The genomic RNA is translated to the endoplasmic reticulum when HCV polyprotein is produced. The positive-stranded RNA genome is used as a template for synthesis of negative-stranded RNA; this new viral RNA is encapsulated within multiple copies of the core to form the nucleocapsid, and then, it acquires envelope and HCV virions, which are exported out of the cell in a Golgi-dependent manner. Naringenin inhibits the secretion and assembly of HCV through regulating lipid metabolism *via* 3-hydroxy-3-methylglutaryl CoA reductase (HMGCR), and acyl-coenzyme A: cholesterol acyltransferase (ACAT) inhibition. Cholesterol is synthetized in an HMGCR-dependent pathway; it is the rate limiting enzyme for cholesterol synthesis, and then, cholesterol is converted to cholesteryl esters (CEs) by ACAT. CEs are very important to VLDL assembly. In addition, microsomal triglyceride transfer protein (MTP) catalyzes the transfer of lipids to the apolipoprotein (Apo) B-100 ApoB100; if the ApoB-MTP binding is inhibited, VLDL assembly in inhibited. Reduction in the bioavailability of CEs, triglycerides and cholesterol by naringenin reduces MTP activity and apoB-MTP binding. In addition, naringenin decreased intracellular triglycerides through peroxisome proliferator activated receptor alpha (PPARα), a regulator of lipid metabolism. Through these mechanisms, naringenin leads to a reduction in VLDL assembly and to the inhibition of ApoB-dependent HCV secretion. Additionally, naringenin inhibits viral NS5A protein, a multifunctional HCV nonstructural protein. Furthermore, naringenin could be an NS2 protease and core protein inhibitor.

the finding that the flavanone can decrease hepatic cholesterol. In addition, naringenin possesses the ability to reduce the CE mass and cholesterol esterification by decreasing ACAT1 and ACAT2 activity[11,194-196]. The mRNA levels of MTP are significantly reduced by naringenin; therefore, ApoB-MTP binding is inhibited, and consequently, ApoB is degraded. In addition, although ApoB mRNA levels are not affected by naringenin, the protein does not accumulate in hepatocytes, suggesting that naringenin promotes the degradation of ApoB. Thereby, the reduction in the bioavailability of CEs, triglycerides and cholesterol by naringenin reduces MTP activity and ApoB-MTP binding, leading to ApoB degradation[11,197-203] (Figure 9). This seems to be the primary mechanism by which naringenin blocks ApoB secretion and VLDL and LDL assembly and, therefore, the inhibition of ApoB–dependent HCV secretion.

In addition, the same group[204] reported that naringenin treatment did not lead to the intracellular accumulation of infectious HCV particles compared with brefeldin A (BFA), a toxin known to disrupt HCV mature Golgi-dependent export; hence, naringenin blocks the assembly of HCV prior to viral egress. The inhibition of MTP and BFA treatment in JFH1-infected Huh7.5.1 cells

blocks the accumulation of intracellular infectious HCV particles, indicating that MTP activity is essential for HCV assembly. Treatment of JFH1-infected Huh7.5.1 cells with naringenin (MTP inhibitor) and BFA decreased the accumulation of infectious particles, suggesting that the flavonoid inhibits the assembly of HCV LVP[204] (Figure 9).

MTP inhibition can lead to lipid accumulation and steatosis; however, treatment with naringenin decreased intracellular triglycerides, and this was mediated by activation of peroxisome proliferator-activated receptor alpha (PPARα), a regulator of lipid metabolism. Naringenin and WY14643 (a classical PPARα agonist) were compared to reduce ApoB and virus production in the HCV model. The results showed that both the flavonoid and the PPARα agonist caused a significant inhibition of MTP activity and ApoB secretion, as well as a significant inhibition of HCV RNA secretion without affecting the intracellular levels of the HCV core protein. In addition, the treatment with naringenin led to a rapid 1.4 log reduction in secreted HCV in cell culture, but this effect was reversible by PPARα inhibitor treatment[204]. In summary, naringenin inhibits the assembly and long-term production of infectious HCV particles through a PPARα-mediated mechanism that includes the inhibition of MTP and the inhibition of lipid accumulation (Figure 9).

Interestingly, Khachatoorian *et al*[205] compared the antiviral effects of naringenin, quercetin and catechin. The evidence demonstrated that in an HCV system, naringenin significantly reduced intracellular viral protein translation as well as viral protein production during one viral life cycle; however, quercetin showed better results, but the infectious virion secretion was not inhibited by any flavonoid. Naringenin significantly blocked infectious virion assembly; in this case, naringenin was more effective than quercetin[205].

NS5A is a multifunctional NS protein and viral RC component; it participates in HCV genome replication, viral protein translation, virion assembly, and viral secretion[191,192,205]. NS5A mRNA and protein levels were measured, finding that naringenin reduced both parameters. Then, in a cell culture-based bicistronic reporter system, catechin, naringenin, and quercetin were tested to measure levels of viral IRES-mediated translation; all bioflavonoids significantly decreased IRES-mediated translation, but quercetin completely blocked NS5A-augmented IRES activity in contrast to catechin and naringenin, which demonstrated only mild inhibition. According to these results, quercetin demonstrated a marked decrease in HSP70 expression in treated cells. A slight decrease in HSP70 was seen with naringenin and catechin treatments. The complex of HSP70 with NS5A, NS5A-HSP70, is important for viral protein production; therefore, the disruption of this complex results in a marked decrease of viral protein synthesis[206,207] (Figure 9).

On the other hand, *in silico* studies have been carried out to evaluate naringenin activity on the HCV particle. Mathew *et al*[208] in 2014 reported a docking interaction study between the 3D structure of capsid core protein of HCV-genotype 3 (G3) (Q68867) and its subtypes 3b (Q68861) and 3g (Q68865) from north India and naringenin. The results indicated that the flavonoid exhibited five, seven and nine H-bond interactions within the core protein of HCV-G3, subtypes 3b and 3g, respectively. In HCV-G3, naringenin formed H-bonds individually with GLU69 and ASN115 and three H-bonds, with SER103 exhibiting the highest interaction energy (-129.636 kcal/mole). In the case of HCV-3b, naringenin formed three H-bonds with TRP90, two with GLN86, and one with GLY84 and TRP93, with an interaction energy of -145.682 kcal/mole. Finally, the flavanone binds to HCV-3g through two H-bonds with TRP73 and GLY77 and individually with ASN85, TYR78 and TRP73 with an interaction energy of -159.483 kcal/mole[208]. These results suggest that naringenin binds to the core protein of three important HCV genotypes in India, especially to HCV-3 based on their interaction energies; this ability of naringenin to bind core protein could be involved in the inhibition of viral particle assembly that was previously reported. Naturally, *in vivo* studies are needed to confirm predictions suggested by this docking study (Figure 9).

NS2 is a transmembrane protein of 21-23 kDa that is not required for RNA replication but that is vital to produce infectious viruses *in vitro*, and it acts as an apoptosis inhibitor[191,209]. Using a docking analysis, it has been identified that naringenin could be an NS2 protease inhibitor. Molecular rigid docking of the modeled NS2 protease was performed with the naringenin molecule. The flavanone had a binding energy of -7.97 kcal/mol when interacting with amino acids such as LEU9, VAL27, LEU54, ASP6, ALA5, ILE31, ALA30, LEU2, PHE33, ILE34, VAL44, ALA47, ALA43, and LEU46. In addition, naringenin possesses lower binding energy than the commercially available drugs such as eltrombopag (-5.07 kcal/mol), ribavirin (-5.89), and telbivudine (-6.39 kcal/mol)[209] (Figure 9). Therefore, naringenin appears to be a strong NS2 protein inhibitor and, thus, prevents efficient HCV infection.

More *in vivo* and *in vitro* studies are needed to further investigate the effectiveness of naringenin to fight virus infection in the liver and to elucidate the action(s) mechanism(s) involved in such protection.

ANTIDIABETIC EFFECT OF NARINGENIN

In addition to its antioxidant, scavenger, anti-inflammatory, antiviral and antifibrotic properties, naringenin possesses antidiabetic effects. It has been reported that, in diabetic rats, the flavonoid reduced diabetic markers through PPARγ and glucose transporter type 4 (GLUT4) and increased their gene and protein expression levels in pancreas[210]. In the liver, naringenin increased glycogen content, decrease activities of glycogen phosphorylase and glucose-6- phosphatase[211] and ameliorated diabetes-induced hepatotoxicity[212,213]. For more information see

Nyane *et al*[214].

NARINGENIN SAFETY AND TOXICITY

The first study about the toxicity of naringenin was carried out in 1996, and it was found that in a model system of isolated rat liver nuclei, the flavonoid induced a concentration-dependent peroxidation of nuclear membrane lipids concurrent with DNA strand breaks[215]. It has been reported that the flavonoid can be oxidized to form naringenin phenoxyl radicals[216] and that the medium lethal dose (LD50) is > 5000 mg/kg[217]. Interestingly, embryos exposed to naringenin with hydroxyurea were significantly protected from growth and developmental retardation, and abnormalities induced by hydroxyurea[218]. Only a few studies on the safety, teratogenicity and toxicity of naringenin have been published, therefore use of this flavonoid in the clinical setting should be cautious.

CONCLUSION

Naringenin displays poor direct antioxidant properties as a free radical scavenger; however, due to its ability to induce the endogenous antioxidant system by upregulating Nrf2, this flavanone exerts important effects to maintain the normal redox of the cell, even in disease conditions where free radicals are generated as a mechanism of damage. In this scenario, throughout this review, we have described the benefits of this flavonoid in many types of liver damage in which oxidative stress plays a crucial role as causative agent. Of note, the anti-inflammatory activity of naringenin by blocking NF-κB, affords protection or relief to liver pathologies as inflammation is a common cause of damage. Moreover, naringenin displays a multitarget effect to fight fibrosis through both canonical and non-canonical TGF-β pathways and by regulating metalloproteinase activity. Additionally, this abundant citrus flavonoid has shown anticancer and antiviral activities. Even though NAR has disadvantages such as its low bioavailability, there are pharmaceutical formulations that can solve this problem. Given the evidence provided in this review, it is concluded that naringenin is a useful natural product for the treatment of many liver diseases by its antioxidant capacity, anti-inflammatory abilities, antifibrogenic properties, fibrolytic actions and anticancer and antiviral properties. However, more basic and clinical studies are needed to further support the use of this flavonoid in humans.

REFERENCES

1 **Bataller R**, Brenner DA. Liver fibrosis. *J Clin Invest* 2005; **115**: 209-218 [PMID: 15690074 DOI: 10.1172/JCI24282]

2 **Pellicoro A**, Ramachandran P, Iredale JP. Reversibility of liver fibrosis. *Fibrogenesis Tissue Repair* 2012; **5**: S26 [PMID: 23259590 DOI: 10.1186/1755-1536-5-S1-S26]

3 **Muriel P**. The liver: General aspects and epidemiology. In Muriel P. Liver pathophysiology: therapies & antioxidants. Waltham, MA: Elsevier, 2017: 3-22

4 **Lozano R**, Naghavi M, Foreman K, Lim S, Shibuya K, Aboyans V, Abraham J, Adair T, Aggarwal R, Ahn SY, Alvarado M, Anderson HR, Anderson LM, Andrews KG, Atkinson C, Baddour LM, Barker-Collo S, Bartels DH, Bell ML, Benjamin EJ, Bennett D, Bhalla K, Bikbov B, Bin Abdulhak A, Birbeck G, Blyth F, Bolliger I, Boufous S, Bucello C, Burch M, Burney P, Carapetis J, Chen H, Chou D, Chugh SS, Coffeng LE, Colan SD, Colquhoun S, Colson KE, Condon J, Connor MD, Cooper LT, Corriere M, Cortinovis M, de Vaccaro KC, Couser W, Cowie BC, Criqui MH, Cross M, Dabhadkar KC, Dahodwala N, De Leo D, Degenhardt L, Delossantos A, Denenberg J, Des Jarlais DC, Dharmaratne SD, Dorsey ER, Driscoll T, Duber H, Ebel B, Erwin PJ, Espindola P, Ezzati M, Feigin V, Flaxman AD, Forouzanfar MH, Fowkes FG, Franklin R, Fransen M, Freeman MK, Gabriel SE, Gakidou E, Gaspari F, Gillum RF, Gonzalez-Medina D, Halasa YA, Haring D, Harrison JE, Havmoeller R, Hay RJ, Hoen B, Hotez PJ, Hoy D, Jacobsen KH, James SL, Jasrasaria R, Jayaraman S, Johns N, Karthikeyan G, Kassebaum N, Keren A, Khoo JP, Knowlton LM, Kobusingye O, Koranteng A, Krishnamurthi R, Lipnick M, Lipshultz SE, Ohno SL, Mabweijano J, MacIntyre MF, Mallinger L, March L, Marks GB, Marks R, Matsumori A, Matzopoulos R, Mayosi BM, McAnulty JH, McDermott MM, McGrath J, Mensah GA, Merriman TR, Michaud C, Miller M, Miller TR, Mock C, Mocumbi AO, Mokdad AA, Moran A, Mulholland K, Nair MN, Naldi L, Narayan KM, Nasseri K, Norman P, O'Donnell M, Omer SB, Ortblad K, Osborne R, Ozgediz D, Pahari B, Pandian JD, Rivero AP, Padilla RP, Perez-Ruiz F, Perico N, Phillips D, Pierce K, Pope CA 3rd, Porrini E, Pourmalek F, Raju M, Ranganathan D, Rehm JT, Rein DB, Remuzzi G, Rivara FP, Roberts T, De León FR, Rosenfeld LC, Rushton L, Sacco RL, Salomon JA, Sampson U, Sanman E, Schwebel DC, Segui-Gomez M, Shepard DS, Singh D, Singleton J, Sliwa K, Smith E, Steer A, Taylor JA, Thomas B, Tleyjeh IM, Towbin JA, Truelsen T, Undurraga EA, Venketasubramanian N, Vijayakumar L, Vos T, Wagner GR, Wang M, Wang W, Watt K, Weinstock MA, Weintraub R, Wilkinson JD, Woolf AD, Wulf S, Yeh PH, Yip P, Zabetian A, Zheng ZJ, Lopez AD, Murray CJ, AlMazroa MA, Memish ZA. Global and regional mortality from 235 causes of death for 20 age groups in 1990 and 2010: a systematic analysis for the Global Burden of Disease Study 2010. *Lancet* 2012; **380**: 2095-2128 [PMID: 23245604 DOI: 10.1016/S0140-6736(12)61728-0s]

5 **Mehal WZ**, Schuppan D. Antifibrotic therapies in the liver. *Semin Liver Dis* 2015; **35**: 184-198 [PMID: 25974903 DOI: 10.1055/s-0035-1550055]

6 **Schuppan D**. Liver fibrosis: Common mechanisms and antifibrotic therapies. *Clin Res Hepatol Gastroenterol* 2015; **39** Suppl 1: S51-S59 [PMID: 26189980 DOI: 10.1016/j.clinre.2015.05.005]

7 **Huebert RC**, Rakela J. Cellular therapy for liver disease. *Mayo Clin Proc* 2014; **89**: 414-424 [PMID: 24582199 DOI: 10.1016/j.mayocp.2013.10.023]

8 **Poilil Surendran S**, George Thomas R, Moon MJ, Jeong YY. Nanoparticles for the treatment of liver fibrosis. *Int J Nanomedicine* 2017; **12**: 6997-7006 [PMID: 29033567 DOI: 10.2147/IJN.S145951]

9 **Girish C**, Pradhan SC. Herbal drugs on the liver. In: Muriel P. Liver pathophysiology: therapies & antioxidants. Waltham, MA: Elsevier, 2017: 605-620

10 **Abenavoli L**, Milic N. Silymarin for liver disease. In: Muriel P. Liver pathophysiology: therapies & antioxidants. Waltham, MA: Elsevier, 2017: 621-631

11 **Hernández-Aquino E**, Muriel P. Naringenin and the liver. In: Muriel P. Liver pathophysiology: therapies & antioxidants. Waltham, MA: Elsevier, 2017: 633-651

12 **Vázquez-Flores LF**, Casas-Grajales S, Hernández-Aquino E, Vargas-Pozada EE, Muriel P. Antioxidant antiinflammatory and antifibrotic properties of quercetin in the liver. In: Muriel P. Liver pathophysiology: therapies & and antioxidants. Waltham, MA: Elsevier, 2017: 653-674

13 **Arauz J**, Ramos-Tovar E, Muriel P. Coffee and the liver. In: Muriel P. Liver pathophysiology: therapies & antioxidants. Waltham, MA: Elsevier, 2017: 675-685
14 **Reyes-Gordillo K**, Shah R, Lakshman, Flores-Beltrán RE, Muriel P. Hepatoprotective properties of curcumin. In: Muriel P. Liver pathophysiology: therapies & antioxidants. Waltham, MA: Elsevier, 2017: 687-704
15 **Ramos-Tovar E**, Muriel P. Stevia as a putative hepatoprotector. In: Muriel P. Liver pathophysiology: therapies & antioxidants. Waltham, MA: Elsevier, 2017: 715-727
16 **Yen FL**, Wu TH, Lin LT, Cham TM, Lin CC. Naringenin-loaded nanoparticles improve the physicochemical properties and the hepatoprotective effects of naringenin in orally-administered rats with CCl_4-induced acute liver failure. *Pharm Res* 2009; **26**: 893-902 [PMID: 19034626 DOI: 10.1007/s11095-008-9791-0]
17 **Nait Chabane M**, Al Ahmad A, Peluso J, Muller CD, Ubeaud G. Quercetin and naringenin transport across human intestinal Caco-2 cells. *J Pharm Pharmacol* 2009; **61**: 1473-1483 [PMID: 19903372 DOI: 10.1211/jpp/61.11.0006]
18 **Bredsdorff L**, Nielsen IL, Rasmussen SE, Cornett C, Barron D, Bouisset F, Offord E, Williamson G. Absorption, conjugation and excretion of the flavanones, naringenin and hesperetin from alpha-rhamnosidase-treated orange juice in human subjects. *Br J Nutr* 2010; **103**: 1602-1609 [PMID: 20100371 DOI: 10.1017/S0007114509993679]
19 **Scalbert A**, Morand C, Manach C, Rémésy C. Absorption and metabolism of polyphenols in the gut and impact on health. *Biomed Pharmacother* 2002; **56**: 276-282 [PMID: 12224598 DOI: 10.1016/S0753-3322(02)00205-6]
20 **Simons AL**, Renouf M, Murphy PA, Hendrich S. Greater apparent absorption of flavonoids is associated with lesser human fecal flavonoid disappearance rates. *J Agric Food Chem* 2010; **58**: 141-147 [PMID: 19921837 DOI: 10.1021/jf902284u]
21 **Xu H**, Kulkarni KH, Singh R, Yang Z, Wang SW, Tam VH, Hu M. Disposition of naringenin via glucuronidation pathway is affected by compensating efflux transporters of hydrophilic glucuronides. *Mol Pharm* 2009; **6**: 1703-1715 [PMID: 19736994 DOI: 10.1021/mp900013d]
22 **Mata-Bilbao Mde L**, Andrés-Lacueva C, Roura E, Jáuregui O, Escribano E, Torre C, Lamuela-Raventós RM. Absorption and pharmacokinetics of grapefruit flavanones in beagles. *Br J Nutr* 2007; **98**: 86-92 [PMID: 17391560 DOI: 10.1017/S0007114507707262]
23 **Zou W**, Yang C, Liu M, Su W. Tissue distribution study of naringin in rats by liquid chromatography-tandem mass spectrometry. *Arzneimittelforschung* 2012; **62**: 181-186 [PMID: 22270844 DOI: 10.1055/s-0031-1299746]
24 **Choudhury R**, Chowrimootoo G, Srai K, Debnam E, Rice-Evans CA. Interactions of the flavonoid naringenin in the gastrointestinal tract and the influence of glycosylation. *Biochem Biophys Res Commun* 1999; **265**: 410-415 [PMID: 10558881 DOI: 10.1006/bbrc.1999.1695]
25 **El Mohsen MA**, Marks J, Kuhnle G, Rice-Evans C, Moore K, Gibson G, Debnam E, Srai SK. The differential tissue distribution of the citrus flavanone naringenin following gastric instillation. *Free Radic Res* 2004; **38**: 1329-1340 [PMID: 15763957 DOI: 10.1080/10715760400017293]
26 **Bolli A**, Marino M, Rimbach G, Fanali G, Fasano M, Ascenzi P. Flavonoid binding to human serum albumin. *Biochem Biophys Res Commun* 2010; **398**: 444-449 [PMID: 20599706 DOI: 10.1016/j.bbrc.2010.06.096]
27 **Hu YJ,** Wang Y, Ou-Yang Y, Zhou J, Liu Y. Characterize the interaction between naringenin and bovine serum albumin using spectroscopic approach. *J Lumin* 2010; **130**: 1394-1399 [DOI: 10.1016/j.jlumin.2010.02.053]
28 **Khan MK**, Rakotomanomana N, Dufour C, Dangles O. Binding of citrus flavanones and their glucuronides and chalcones to human serum albumin. *Food Funct* 2011; **2**: 617-626 [PMID: 21952533 DOI: 10.1039/c1fo10077g]
29 **Heim KE**, Tagliaferro AR, Bobilya DJ. Flavonoid antioxidants: chemistry, metabolism and structure-activity relationships. *J Nutr Biochem* 2002; **13**: 572-584 [PMID: 12550068 DOI: 10.1016/S0955-2863(02)00208-5]
30 **Rice-Evans CA**, Miller NJ, Paganga G. Structure-antioxidant activity relationships of flavonoids and phenolic acids. *Free Radic Biol Med* 1996; **20**: 933-956 [PMID: 8743980 DOI: 10.1016/0891-5849(95)02227-9]
31 **Weber LW**, Boll M, Stampfl A. Hepatotoxicity and mechanism of action of haloalkanes: carbon tetrachloride as a toxicological model. *Crit Rev Toxicol* 2003; **33**: 105-136 [PMID: 12708612 DOI: 10.1080/713611034]
32 **Ratty AK**, Das NP. Effects of flavonoids on nonenzymatic lipid peroxidation: structure-activity relationship. *Biochem Med Metab Biol* 1988; **39**: 69-79 [PMID: 3355718 DOI: 10.1016/0885-4505(88)90060-6]
33 **Khanduja KL**, Bhardwaj A. Stable free radical scavenging and antiperoxidative properties of resveratrol compared in vitro with some other bioflavonoids. *Indian J Biochem Biophys* 2003; **40**: 416-422 [PMID: 22900369]
34 **Rodriguez RJ**, Miranda CL, Stevens JF, Deinzer ML, Buhler DR. Influence of prenylated and non-prenylated flavonoids on liver microsomal lipid peroxidation and oxidative injury in rat hepatocytes. *Food Chem Toxicol* 2001; **39**: 437-445 [PMID: 11313109 DOI: 10.1016/S0278-6915(00)00159-9]
35 **Cavia-Saiz M**, Busto MD, Pilar-Izquierdo MC, Ortega N, Perez-Mateos M, Muñiz P. Antioxidant properties, radical scavenging activity and biomolecule protection capacity of flavonoid naringenin and its glycoside naringin: a comparative study. *J Sci Food Agric* 2010; **90**: 1238-1244 [PMID: 20394007 DOI: 10.1002/jsfa.3959]
36 **van Acker FA**, Schouten O, Haenen GR, van der Vijgh WJ, Bast A. Flavonoids can replace alpha-tocopherol as an antioxidant. *FEBS Lett* 2000; **473**: 145-148 [PMID: 10812062 DOI: 10.1016/S0014-5793(00)01517-9]
37 **Saija A**, Scalese M, Lanza M, Marzullo D, Bonina F, Castelli F. Flavonoids as antioxidant agents: importance of their interaction with biomembranes. *Free Radic Biol Med* 1995; **19**: 481-486 [PMID: 7590397 DOI: 10.1016/0891-5849(94)00240-K]
38 **Arora A**, Byrem TM, Nair MG, Strasburg GM. Modulation of liposomal membrane fluidity by flavonoids and isoflavonoids. *Arch Biochem Biophys* 2000; **373**: 102-109 [PMID: 10620328 DOI: 10.1006/abbi.1999.1525]
39 **Bombardelli E**, Spetta M. Phospholipid-polyphenol complexes: a new concept in skin care ingredients. *Cosm Toil* 1991; **106**: 69-76
40 **Kaneko T**, Kaji K, Matsuo M. Protection of linoleic acid hydroperoxide-induced cytotoxicity by phenolic antioxidants. *Free Radic Biol Med* 1994; **16**: 405-409 [PMID: 8063204]
41 **Wang K**, Chen Z, Huang L, Meng B, Zhou X, Wen X, Ren D. Naringenin reduces oxidative stress and improves mitochondrial dysfunction via activation of the Nrf2/ARE signaling pathway in neurons. *Int J Mol Med* 2017; **40**: 1582-1590 [PMID: 28949376 DOI: 10.3892/ijmm.2017.3134]
42 **Manchope MF**, Calixto-Campos C, Coelho-Silva L, Zarpelon AC, Pinho-Ribeiro FA, Georgetti SR, Baracat MM, Casagrande R, Verri WA Jr. Naringenin inhibits superoxide anion-induced inflammatory pain: role of oxidative stress, cytokines, Nrf-2 and the NO-cGMP-PKG-KATP channel signaling pathway. *PLoS One* 2016; **11**: e0153015 [PMID: 27045367 DOI: 10.1371/journal.pone.0153015]
43 **Podder B**, Song HY, Kim YS. Naringenin exerts cytoprotective effect against paraquat-induced toxicity in human bronchial epithelial BEAS-2B cells through NRF2 activation. *J Microbiol Biotechnol* 2014; **24**: 605-613 [PMID: 24561720 DOI: 10.4014/jmb.1402.02001]
44 **Miler M**, Živanović J, Ajdžanović V, Oreščanin-Dušić Z, Milenković D, Konić-Ristić A, Blagojević D, Milošević V, Šošić-Jurjević B. Citrus flavanones naringenin and hesperetin improve antioxidant status and membrane lipid compositions in the liver of old-aged Wistar rats. *Exp Gerontol* 2016; **84**: 49-60 [PMID: 27587005 DOI: 10.1016/j.exger.2016.08.014]
45 **Ali R**, Shahid A, Ali N, Hasan SK, Majed F, Sultana S.

Amelioration of benzo[a]pyrene-induced oxidative stress and pulmonary toxicity by naringenin in Wistar rats: a plausible role of COX-2 and NF-κB. *Hum Exp Toxicol* 2017; **36**: 349-364 [PMID: 27206700 DOI: 10.1177/0960327116650009]

46 **Fan R**, Pan T, Zhu AL, Zhang MH. Anti-inflammatory and anti-arthritic properties of naringenin via attenuation of NF-κB and activation of the heme oxygenase (HO)-1/related factor 2 pathway. *Pharmacol Rep* 2017; **69**: 1021-1029 [PMID: 28943290 DOI: 10.1016/j.pharep.2017.03.020]

47 **Al-Dosari DI**, Ahmed MM, Al-Rejaie SS, Alhomida AS, Ola MS. Flavonoid naringenin attenuates oxidative stress, apoptosis and improves neurotrophic effects in the diabetic rat retina. *Nutrients* 2017; **9**: [PMID: 29064407 DOI: 10.3390/nu9101161]

48 **de Oliveira MR**, Brasil FB, Andrade CMB. Naringenin attenuates H_2O_2-induced mitochondrial dysfunction by an Nrf2-dependent mechanism in SH-SY5Y Cells. *Neurochem Res* 2017; **42**: 3341-3350 [PMID: 28786049 DOI: 10.1007/s11064-017-2376-8]

49 **Ramprasath T**, Senthamizharasi M, Vasudevan V, Sasikumar S, Yuvaraj S, Selvam GS. Naringenin confers protection against oxidative stress through upregulation of Nrf2 target genes in cardiomyoblast cells. *J Physiol Biochem* 2014; **70**: 407-415 [PMID: 24526395 DOI: 10.1007/s13105-014-0318-3]

50 **Al-Roujayee AS**. Naringenin improves the healing process of thermally-induced skin damage in rats. *J Int Med Res* 2017; **45**: 570-582 [PMID: 28415935 DOI: 10.1177/0300060517692483]

51 **Sahin Z**, Ozkaya A, Cuce G, Uckun M, Yologlu E. Investigation of the effect of naringenin on oxidative stress-related alterations in testis of hydrogen peroxide-administered rats. *J Biochem Mol Toxicol* 2017; **31**: [PMID: 28467669 DOI: 10.1002/jbt.21928]

52 **Pari L**, Gnanasoundari M. Influence of naringenin on oxytetracycline mediated oxidative damage in rat liver. *Basic Clin Pharmacol Toxicol* 2006; **98**: 456-461 [PMID: 16635103 DOI: 10.1111/j.1742-7843.2006.pto_351.x]

53 **Bodas R**, Prieto N, Jordán MJ, López-Campos O, Giráldez FJ, Morán L, Andrés S. The liver antioxidant status of fattening lambs is improved by naringin dietary supplementation at 0.15% rates but not meat quality. *Animal* 2012; **6**: 863-870 [PMID: 22558934 DOI: 10.1017/S175173111100214X]

54 **Casas-Grajales S**, Muriel P. The liver, oxidative stress and antioxidants. In: Muriel P. Liver pathophysiology: therapies & antioxidants. Waltham, MA: Elsevier, 2017: 583-604

55 **DeLeve LD**, Kaplowitz N. Glutathione metabolism and its role in hepatotoxicity. *Pharmacol Ther* 1991; **52**: 287-305 [PMID: 1820580 DOI: 10.1016/0163-7258(91)90029-L]

56 **Kretzschmar M**. Regulation of hepatic glutathione metabolism and its role in hepatotoxicity. *Exp Toxicol Pathol* 1996; **48**: 439-446 [PMID: 8765689 DOI: 10.1016/S0940-2993(96)80054-6]

57 **Yuan L**, Kaplowitz N. Glutathione in liver diseases and hepatotoxicity. *Mol Aspects Med* 2009; **30**: 29-41 [PMID: 18786561 DOI: 10.1016/j.mam.2008.08.003]

58 **Wang J**, Yang Z, Lin L, Zhao Z, Liu Z, Liu X. Protective effect of naringenin against lead-induced oxidative stress in rats. *Biol Trace Elem Res* 2012; **146**: 354-359 [PMID: 22109809 DOI: 10.1007/s12011-011-9268-6]

59 **Dong D**, Xu L, Yin L, Qi Y, Peng J. Naringenin prevents carbon tetrachloride-induced acute liver injury in mice. *J Funct Foods* 2015; **12**: 179-191 [DOI: 10.1016/j.jff.2014.11.020]

60 **Lou H**, Jing X, Wei X, Shi H, Ren D, Zhang X. Naringenin protects against 6-OHDA-induced neurotoxicity via activation of the Nrf2/ARE signaling pathway. *Neuropharmacology* 2014; **79**: 380-388 [PMID: 24333330 DOI: 10.1016/j.neuropharm.2013.11.026]

61 **Gopinath K**, Sudhandiran G. Naringin modulates oxidative stress and inflammation in 3-nitropropionic acid-induced neurodegeneration through the activation of nuclear factor-erythroid 2-related factor-2 signalling pathway. *Neuroscience* 2012; **227**: 134-143 [PMID: 22871521 DOI: 10.1016/j.neuroscience.2012.07.060]

62 **Han X**, Pan J, Ren D, Cheng Y, Fan P, Lou H. Naringenin-7-O-glucoside protects against doxorubicin-induced toxicity in H9c2 cardiomyocytes by induction of endogenous antioxidant enzymes. *Food Chem Toxicol* 2008; **46**: 3140-3146 [PMID: 18652870 DOI: 10.1016/j.fct.2008.06.086]

63 **Esmaeili MA**, Alilou M. Naringenin attenuates CCl_4 -induced hepatic inflammation by the activation of an Nrf2-mediated pathway in rats. *Clin Exp Pharmacol Physiol* 2014; **41**: 416-422 [PMID: 24684352 DOI: 10.1111/1440-1681.12230]

64 **Jayaraman J**, Veerappan M, Namasivayam N. Potential beneficial effect of naringenin on lipid peroxidation and antioxidant status in rats with ethanol-induced hepatotoxicity. *J Pharm Pharmacol* 2009; **61**: 1383-1390 [PMID: 19814872 DOI: 10.1211/jpp/61.10.0016]

65 **Renugadevi J**, Prabu SM. Cadmium-induced hepatotoxicity in rats and the protective effect of naringenin. *Exp Toxicol Pathol* 2010; **62**: 171-181 [PMID: 19409769 DOI: 10.1016/j.etp.2009.03.010]

66 **Martinez RM**, Pinho-Ribeiro FA, Steffen VS, Silva TC, Caviglione CV, Bottura C, Fonseca MJ, Vicentini FT, Vignoli JA, Baracat MM, Georgetti SR, Verri WA Jr, Casagrande R. Topical formulation containing naringenin: efficacy against ultraviolet B irradiation-induced skin inflammation and oxidative stress in mice. *PLoS One* 2016; **11**: e0146296 [PMID: 26741806 DOI: 10.1371/journal.pone.0146296]

67 **Shakeel S**, Rehman MU, Tabassum N, Amin U, Mir MUR. Effect of naringenin (a naturally occurring flavanone) against pilocarpine-induced status epilepticus and oxidative stress in mice. *Pharmacogn Mag* 2017; **13**: S154-S160 [PMID: 28479741 DOI: 10.4103/0973-1296.20397]

68 **Roy A**, Das A, Das R, Haldar S, Bhattacharya S, Haldar PK. Naringenin, a citrus flavonoid, ameliorates arsenic-induced toxicity in Swiss albino mice. *J Environ Pathol Toxicol Oncol* 2014; **33**: 195-204 [PMID: 25272058 DOI: 10.1615/JEnvironPatholToxicolOncol.2014010317]

69 **Davies KJ**. Oxidative stress, antioxidant defenses, and damage removal, repair, and replacement systems. *IUBMB Life* 2000; **50**: 279-289 [PMID: 11327322 DOI: 10.1080/713803728]

70 **Jayaraman J**, Namasivayam N. Naringenin modulates circulatory lipid peroxidation, anti-oxidant status and hepatic alcohol metabolizing enzymes in rats with ethanol induced liver injury. *Fundam Clin Pharmacol* 2011; **25**: 682-689 [PMID: 21105911 DOI: 10.1111/j.1472-8206.2010.00899]

71 **Hermenean A**, Ardelean A, Stan M, Herman H, Mihali CV, Costache M, Dinischiotu A. Protective effects of naringenin on carbon tetrachloride-induced acute nephrotoxicity in mouse kidney. *Chem Biol Interact* 2013; **205**: 138-147 [PMID: 23845967 DOI: 10.1016/j.cbi.2013.06.016]

72 **Prabu SM**, Shagirtha K, Renugadevi J. Naringenin in combination with vitamins C and E potentially protects oxidative stress-mediated hepatic injury in cadmium-intoxicated rats. *J Nutr Sci Vitaminol* (Tokyo) 2011; **57**: 177-185 [PMID: 21697638 DOI: 10.3177/jnsv.57.177]

73 **Jain A**, Yadav A, Bozhkov AI, Padalko VI, Flora SJ. Therapeutic efficacy of silymarin and naringenin in reducing arsenic-induced hepatic damage in young rats. *Ecotoxicol Environ Saf* 2011; **74**: 607-614 [PMID: 20719385 DOI: 10.1016/j.ecoenv.2010.08.002]

74 **Mershiba SD**, Dassprakash MV, Saraswathy SD. Protective effect of naringenin on hepatic and renal dysfunction and oxidative stress in arsenic intoxicated rats. *Mol Biol Rep* 2013; **40**: 3681-3691 [PMID: 23283742 DOI: 10.1007/s11033-012-2444-8]

75 **Ambros V**. The functions of animal microRNAs. *Nature* 2004; **431**: 350-355 [PMID: 15372042 DOI: 10.1038/nature02871]

76 **Xu Y**, Fang F, Zhang J, Josson S, St Clair WH, St Clair DK. miR-17* suppresses tumorigenicity of prostate cancer by inhibiting mitochondrial antioxidant enzymes. *PLoS One* 2010; **5**: e14356 [PMID: 21203553 DOI: 10.1371/journal.pone.0014356]

77 **Curti V**, Di Lorenzo A, Rossi D, Martino E, Capelli E, Collina S, Daglia M. Enantioselective modulatory effects of naringenin enantiomers on the expression levels of miR-17-3p involved in endogenous antioxidant defenses. *Nutrients* 2017; **9**: pii: E215 [PMID: 28264488 DOI: 10.3390/nu9030215]

78 **Tebay LE**, Robertson H, Durant ST, Vitale SR, Penning TM, Dinkova-Kostova AT, Hayes JD. Mechanisms of activation of

the transcription factor Nrf2 by redox stressors, nutrient cues, and energy status and the pathways through which it attenuates degenerative disease. *Free Radic Biol Med* 2015; **88**: 108-146 [PMID: 26122708 DOI: 10.1016/j.freeradbiomed.2015.06.021]
79 **Ooi BK**, Goh BH, Yap WH. Oxidative stress in cardiovascular diseases: involvement of Nrf2 antioxidant redox signaling in macrophage foam cells formation. *Int J Mol Sci* 2017; **18**: pii: E2336 [PMID: 29113088 DOI: 10.3390/ijms18112336.]
80 **Tang W**, Jiang YF, Ponnusamy M, Diallo M. Role of Nrf2 in chronic liver disease. *World J Gastroenterol* 2014; **20**: 13079-13087 [PMID: 25278702 DOI: 10.3748/wjg.v20.i36.13079]
81 **Wang H**, Xu YS, Wang ML, Cheng C, Bian R, Yuan H, Wang Y, Guo T, Zhu LL, Zhou H. Protective effect of naringin against the LPS-induced apoptosis of PC12 cells: implications for the treatment of neurodegenerative disorders. *Int J Mol Med* 2017; **39**: 819-830 [PMID: 28260042 DOI: 10.3892/ijmm.2017.2904]
82 **Chen RC**, Sun GB, Wang J, Zhang HJ, Sun XB. Naringin protects against anoxia/reoxygenation-induced apoptosis in H9c2 cells via the Nrf2 signaling pathway. *Food Funct* 2015; **6**: 1331-1344 [PMID: 25773745 DOI: 10.1039/c4fo01164c]
83 **Cullinan SB**, Zhang D, Hannink M, Arvisais E, Kaufman RJ, Diehl JA. Nrf2 is a direct PERK substrate and effector of PERK-dependent cell survival. *Mol Cell Biol* 2003; **23**: 7198-7209 [PMID: 14517290 DOI: 10.1128/MCB.23.20.7198-7209.2003]
84 **Zipper LM**, Mulcahy RT. Erk activation is required for Nrf2 nuclear localization during pyrrolidine dithiocarbamate induction of glutamate cysteine ligase modulatory gene expression in HepG2 cells. *Toxicol Sci* 2003; **73**: 124-134 [PMID: 12657749 DOI: 10.1093/toxsci/kfg083]
85 **Liu XM**, Peyton KJ, Shebib AR, Wang H, Korthuis RJ, Durante W. Activation of AMPK stimulates heme oxygenase-1 gene expression and human endothelial cell survival. *Am J Physiol Heart Circ Physiol* 2011; **300**: H84-H93 [PMID: 21037234 DOI: 10.1152/ajpheart.00749]
86 **Lee SE**, Yang H, Jeong SI, Jin YH, Park CS, Park YS. Induction of heme oxygenase-1 inhibits cell death in crotonaldehyde-stimulated HepG2 cells via the PKC-δ-p38-Nrf2 pathway. *PLoS One* 2012; **7**: e41676 [PMID: 22848562 DOI: 10.1371/journal.pone.0041676]
87 **Wang K**, Chen Z, Huang J, Huang L, Luo N, Liang X, Liang M, Xie W. Naringenin prevents ischaemic stroke damage via anti-apoptotic and anti-oxidant effects. *Clin Exp Pharmacol Physiol* 2017; **44**: 862-871 [PMID: 28453191 DOI: 10.1111/1440-1681.12775]
88 **Liu JD**, Leung KW, Wang CK, Liao LY, Wang CS, Chen PH, Chen CC, Yeh EK. Alcohol-related problems in Taiwan with particular emphasis on alcoholic liver diseases. *Alcohol Clin Exp Res* 1998; **22**: 164S-169S [PMID: 9622397 DOI: 10.1097/00000374-199803001-00019]
89 **Mandayam S**, Jamal MM, Morgan TR. Epidemiology of alcoholic liver disease. *Semin Liver Dis* 2004; **24**: 217-232 [PMID: 15349801 DOI: 10.1055/s-2004-832936]
90 **Teli MR**, Day CP, Burt AD, Bennett MK, James OF. Determinants of progression to cirrhosis or fibrosis in pure alcoholic fatty liver. *Lancet* 1995; **346**: 987-990 [PMID: 7475591]
91 **Boye A**, Zou YH, Yang Y. Metabolic derivatives of alcohol and the molecular culprits of fibro-hepatocarcinogenesis: Allies or enemies? *World J Gastroenterol* 2016; **22**: 50-71 [PMID: 26755860 DOI: 10.3748/wjg.v22.i1.50]
92 **Rocco A**, Compare D, Angrisani D, Sanduzzi Zamparelli M, Nardone G. Alcoholic disease: liver and beyond. *World J Gastroenterol* 2014; **20**: 14652-14659 [PMID: 25356028 DOI: 10.3748/wjg.v20.i40.14652]
93 **Ceni E**, Mello T, Galli A. Pathogenesis of alcoholic liver disease: role of oxidative metabolism. *World J Gastroenterol* 2014; **20**: 17756-17772 [PMID: 25548474 DOI: 10.3748/wjg.v20.i47.17756]
94 **Seo HJ**, Jeong KS, Lee MK, Park YB, Jung UJ, Kim HJ, Choi MS. Role of naringin supplement in regulation of lipid and ethanol metabolism in rats. *Life Sci* 2003; **73**: 933-946 [PMID: 12798418 DOI: 10.1016/S0024-3205(03)00358-8]
95 **Deenen MJ**, Cats A, Beijnen JH, Schellens JH. Part 2: pharmacogenetic variability in drug transport and phase I anticancer drug metabolism. *Oncologist* 2011; **16**: 820-834 [PMID: 21632461 DOI: 10.1634/theoncologist.2010-0259]
96 **Porta EA**. Dietary modulation of oxidative stress in alcoholic liver disease in rats. *J Nutr* 1997; **127**: 912S-915S [PMID: 9164262]
97 **French SW**. The pathophysiology of alcoholic liver disease. In: Muriel P. Liver pathophysiology: therapies & antioxidants. Waltham, MA: Elsevier, 2017: 141-157
98 **Jayaraman J**, Jesudoss VA, Menon VP, Namasivayam N. Anti-inflammatory role of naringenin in rats with ethanol induced liver injury. *Toxicol Mech Methods* 2012; **22**: 568-576 [PMID: 22900548 DOI: 10.3109/15376516.2012.707255]
99 **Szkudelska K**, Nogowski L, Nowicka E, Szkudelski T. In vivo metabolic effects of naringenin in the ethanol consuming rat and the effect of naringenin on adipocytes in vitro. *J Anim Physiol Anim Nutr* (Berl) 2007; **91**: 91-99 [PMID: 17355338 DOI: 10.1111/j.1439-0396.2006.00647.x]
100 **Muriel P**, Ramos-Tovar E, Montes-Páez G, Buendía-Montaño LD. Experimental models of liver damage mediated by oxidative stress. In: Muriel P. Liver pathophysiology: therapies & antioxidants. Waltham, MA: Elsevier, 2017: 529-546
101 **Ingawale DK**, Mandlik SK, Naik SR. Models of hepatotoxicity and the underlying cellular, biochemical and immunological mechanism(s): a critical discussion. *Environ Toxicol Pharmacol* 2014; **37**: 118-133 [PMID: 24322620 DOI: 10.1016/j.etap.2013.08.015]
102 **Facino RM**, Carini M, Franzoi L, Pirola O, Bosisio E. Phytochemical characterization and radical scavenger activity of flavonoids from Helichrysum italicum G. Don (Compositae). *Pharmacol Res* 1990; **22**: 709-721 [PMID: 2075159]
103 **Ikewuchi JC**, Ikewuchi CC, Igboh NM, Mark-Balm T. Protective effect of aqueous extract of the rhizomes of Sansevieria liberica Gérôme and Labroy on carbon tetrachloride induced hepatotoxicity in rats. *EXCLI J* 2011; **10**: 312-321 [PMID: 29033712]
104 **Kaurinovic B**, Popovic M, Vlaisavljevic S, Schwartsova H, Vojinovic-Miloradov M. Antioxidant profile of Trifolium pratense L. *Molecules* 2012; **17**: 11156-11172 [PMID: 22990457 DOI: 10.3390/molecules170911156]
105 **Hermenean A**, Ardelean A, Stan M, Hadaruga N, Mihali CV, Costache M, Dinischiotu A. Antioxidant and hepatoprotective effects of naringenin and its β-cyclodextrin formulation in mice intoxicated with carbon tetrachloride: a comparative study. *J Med Food* 2014; **17**: 670-677 [PMID: 24611872 DOI: 10.1089/jmf.2013.0007]
106 **Kawai T**, Akira S. TLR signaling. *Cell Death Differ* 2006; **13**: 816-825 [PMID: 16410796 DOI: 10.1038/sj.cdd.4401850]
107 **Yamanishi R**, Yoshigai E, Okuyama T, Mori M, Murase H, Machida T, Okumura T, Nishizawa M. The anti-inflammatory effects of flavanol-rich lychee fruit extract in rat hepatocytes. *PLoS One* 2014; **9**: e93818 [PMID: 24705335 DOI: 10.1371/journal.pone.0093818]
108 **O'Neill LA**, Kaltschmidt C. NF-κB: a crucial transcription factor for glial and neuronal cell function. *Trends Neurosci* 1997; **20**: 252-258 [PMID: 9185306]
109 **Czaja MJ**. The future of GI and liver research: editorial perspectives. III. JNK/AP-1 regulation of hepatocyte death. *Am J Physiol Gastrointest Liver Physiol* 2003; **284**: G875-G879 [PMID: 12736142 DOI: 10.1152/ajpgi.00549.2002]
110 **Wang X**, Xiang L, Li H, Chen P, Feng Y, Zhang J, Yang N, Li F, Wang Y, Zhang Q, Li F, Cao F. The role of HMGB1 signaling pathway in the development and progression of hepatocellular carcinoma: a review. *Int J Mol Sci* 2015; **16**: 22527-22540 [PMID: 26393575 DOI: 10.3390/ijms160922527]
111 **Pollard TD**, Earnshaw WC, Lippincott-Schwartz J. Cell Biology. 2th edition. Philadelphia: Elsevier, 2008: 433-435
112 **Hernández-Aquino E**, Zarco N, Casas-Grajales S, Ramos-Tovar E, Flores-Beltrán RE, Arauz J, Shibayama M, Favari L, Tsutsumi V, Segovia J, Muriel P. Naringenin prevents experimental liver fibrosis by blocking TGFβ-Smad3 and JNK-Smad3 pathways. *World J Gastroenterol* 2017; **23**: 4354-4368 [PMID: 28706418

DOI: 10.3748/wjg.v23.i24.4354]
113 **Kisseleva T**, Brenner DA. Role of hepatic stellate cells in fibrogenesis and the reversal of fibrosis. *J Gastroenterol Hepatol* 2007; **22** Suppl 1: S73-S78 [PMID: 17567473 DOI: 10.1111/j.1440-1746.2006.04658.x]
114 **Arauz J**, Moreno MG, Cortés-Reynosa P, Salazar EP, Muriel P. Coffee attenuates fibrosis by decreasing the expression of TGF-β and CTGF in a murine model of liver damage. *J Appl Toxicol* 2013; **33**: 970-979 [PMID: 22899499 DOI: 10.1002/jat.2788]
115 **Matsuzaki K**. Smad phospho-isoforms direct context-dependent TGF-β signaling. *Cytokine Growth Factor Rev* 2013; **24**: 385-399 [PMID: 23871609 DOI: 10.1016/j.cytogfr.2013.06.002]
116 **Yoshida K**, Murata M, Yamaguchi T, Matsuzaki K, Okazaki K. Reversible human TGF-β signal shifting between tumor suppression and fibro-carcinogenesis: implications of smad phospho-isoforms for hepatic epithelial-mesenchymal transitions. *J Clin Med* 2016; **5**: [PMID: 26771649 DOI: 10.3390/jcm5010007]
117 **Hemmann S**, Graf J, Roderfeld M, Roeb E. Expression of MMPs and TIMPs in liver fibrosis - a systematic review with special emphasis on anti-fibrotic strategies. *J Hepatol* 2007; **46**: 955-975 [PMID: 17383048 DOI: 10.1016/j.jhep.2007.02.003]
118 **Imamura T**, Oshima Y, Hikita A. Regulation of TGF-β family signalling by ubiquitination and deubiquitination. *J Biochem* 2013; **154**: 481-489 [PMID: 24165200 DOI: 10.1093/jb/mvt097]
119 **Bray F**, Ren JS, Masuyer E, Ferlay J. Global estimates of cancer prevalence for 27 sites in the adult population in 2008. *Int J Cancer* 2013; **132**: 1133-1145 [PMID: 22752881 DOI: 10.1002/ijc.27711]
120 **Tarocchi M**, Polvani S, Marroncini G, Galli A. Molecular mechanism of hepatitis B virus-induced hepatocarcinogenesis. *World J Gastroenterol* 2014; **20**: 11630-11640 [PMID: 25206269 DOI: 10.3748/wjg.v20.i33.11630]
121 **Tarocchi M**, Galli A. Oxidative stress as a mechanism for hepatocellular carcinoma. In: Muriel P. Liver pathophysiology: therapies & antioxidants. Waltham, MA: Elsevier, 2017: 279-287
122 **Beasley RP**, Hwang LY, Lin CC, Chien CS. Hepatocellular carcinoma and hepatitis B virus. A prospective study of 22 707 men in Taiwan. *Lancet* 1981; **2**: 1129-1133 [PMID: 6118576]
123 **Higgs MR**, Chouteau P, Lerat H. 'Liver let die': oxidative DNA damage and hepatotropic viruses. *J Gen Virol* 2014; **95**: 991-1004 [PMID: 24496828 DOI: 10.1099/vir.0.059485-0]
124 **Fisher AB**. Redox signaling across cell membranes. *Antioxid Redox Signal* 2009; **11**: 1349-1356 [PMID: 19061438 DOI: 10.1089/ars.2008.2378]
125 **El-Serag HB**, Rudolph KL. Hepatocellular carcinoma: epidemiology and molecular carcinogenesis. *Gastroenterology* 2007; **132**: 2557-2576 [PMID: 17570226 DOI: 10.1053/j.gastro.2007.04.061]
126 **Perry G**, Raina AK, Nunomura A, Wataya T, Sayre LM, Smith MA. How important is oxidative damage? Lessons from Alzheimer's disease. *Free Radic Biol Med* 2000; **28**: 831-834 [PMID: 10754280]
127 **Niu D**, Zhang J, Ren Y, Feng H, Chen WN. HBx genotype D represses GSTP1 expression and increases the oxidative level and apoptosis in HepG2 cells. *Mol Oncol* 2009; **3**: 67-76 [PMID: 19383368 DOI: 10.1016/j.molonc.2008.10.002]
128 **Dröge W**. Oxidative stress and aging. *Adv Exp Med Biol* 2003; **543**: 191-200 [PMID: 14713123]
129 **Ha HL**, Shin HJ, Feitelson MA, Yu DY. Oxidative stress and antioxidants in hepatic pathogenesis. *World J Gastroenterol* 2010; **16**: 6035-6043 [PMID: 21182217 DOI: 10.3748/wjg.v16.i48.6035]
130 **Scott TL**, Rangaswamy S, Wicker CA, Izumi T. Repair of oxidative DNA damage and cancer: recent progress in DNA base excision repair. *Antioxid Redox Signal* 2014; **20**: 708-726 [PMID: 23901781 DOI: 10.1089/ars.2013.5529]
131 **Khan N**, Afaq F, Mukhtar H. Cancer chemoprevention through dietary antioxidants: progress and promise. *Antioxid Redox Signal* 2008; **10**: 475-510 [PMID: 18154485 DOI: 10.1089/ars.2007.1740]
132 **Valko M**, Leibfritz D, Moncol J, Cronin MT, Mazur M, Telser J. Free radicals and antioxidants in normal physiological functions and human disease. *Int J Biochem Cell Biol* 2007; **39**: 44-84 [PMID: 16978905 DOI: 10.1016/j.biocel.2006.07.001]
133 **Valko M**, Rhodes CJ, Moncol J, Izakovic M, Mazur M. Free radicals, metals and antioxidants in oxidative stress-induced cancer. *Chem Biol Interact* 2006; **160**: 1-40 [PMID: 16430879 DOI: 10.1016/j.cbi.2005.12.009]
134 **Kandaswami C**, Middleton E Jr. Free radical scavenging and antioxidant activity of plant flavonoids. *Adv Exp Med Biol* 1994; **366**: 351-376 [PMID: 7771265]
135 **Russo M**, Spagnuolo C, Tedesco I, Russo GL. Phytochemicals in cancer prevention and therapy: truth or dare? *Toxins (Basel)* 2010; **2**: 517-551 [PMID: 22069598 DOI: 10.3390/toxins2040517]
136 **Francis AR**, Shetty TK, Bhattacharya RK. Modulating effect of plant flavonoids on the mutagenicity of N-methyl-N'-nitro-N-nitrosoguanidine. *Carcinogenesis* 1989; **10**: 1953-1955 [PMID: 2676226]
137 **Ekambaram G**, Rajendran P, Magesh V, Sakthisekaran D. Naringenin reduces tumor size and weight lost in N-methyl-N'-nitro-N-nitrosoguanidine-induced gastric carcinogenesis in rats. *Nutr Res* 2008; **28**: 106-112 [PMID: 19083396 DOI: 10.1016/j.nutres.2007.12.002]
138 **Leonardi T**, Vanamala J, Taddeo SS, Davidson LA, Murphy ME, Patil BS, Wang N, Carroll RJ, Chapkin RS, Lupton JR, Turner ND. Apigenin and naringenin suppress colon carcinogenesis through the aberrant crypt stage in azoxymethane-treated rats. *Exp Biol Med* (Maywood) 2010; **235**: 710-717 [PMID: 20511675 DOI: 10.1258/ebm.2010.009359]
139 **Yoon H**, Kim TW, Shin SY, Park MJ, Yong Y, Kim DW, Islam T, Lee YH, Jung KY, Lim Y. Design, synthesis and inhibitory activities of naringenin derivatives on human colon cancer cells. *Bioorg Med Chem Lett* 2013; **23**: 232-238 [PMID: 23177257 DOI: 10.1016/j.bmcl.2012.10.130]
140 **Subramanian P**, Arul D. Attenuation of NDEA-induced hepatocarcinogenesis by naringenin in rats. *Cell Biochem Funct* 2013; **31**: 511-517 [PMID: 23172681 DOI: 10.1002/cbf.2929]
141 **Arul D**, Subramanian P. Inhibitory effect of naringenin (citrus flavonone) on N-nitrosodiethylamine induced hepatocarcinogenesis in rats. *Biochem Biophys Res Commun* 2013; **434**: 203-209 [PMID: 23523793 DOI: 10.1016/j.bbrc.2013.03.039]
142 **Taha MM**, Abdul AB, Abdullah R, Ibrahim TA, Abdelwahab SI, Mohan S. Potential chemoprevention of diethylnitrosamine-initiated and 2-acetylaminofluorene-promoted hepatocarcinogenesis by zerumbone from the rhizomes of the subtropical ginger (Zingiber zerumbet). *Chem Biol Interact* 2010; **186**: 295-305 [PMID: 20452335 DOI: 10.1016/j.cbi.2010.04.029]
143 **Lee MH**, Yoon S, Moon JO. The flavonoid naringenin inhibits dimethylnitrosamine-induced liver damage in rats. *Biol Pharm Bull* 2004; **27**: 72-76 [PMID: 14709902]
144 **Ozkaya A**, Sahin Z, Dag U, Ozkaraca M. Effects of naringenin on oxidative stress and histopathological changes in the liver of lead acetate administered Rats. *J Biochem Mol Toxicol* 2016; **30**: 243-248 [PMID: 26929248 DOI: 10.1002/jbt.21785]
145 **Arul D**, Subramanian P. Naringenin (citrus flavonone) induces growth inhibition, cell cycle arrest and apoptosis in human hepatocellular carcinoma cells. *Pathol Oncol Res* 2013; **19**: 763-770 [PMID: 23661153 DOI: 10.1007/s12253-013-9641-1]
146 **Zhong Z**, Chen X, Tan W, Xu Z, Zhou K, Wu T, Cui L, Wang Y. Germacrone inhibits the proliferation of breast cancer cell lines by inducing cell cycle arrest and promoting apoptosis. *Eur J Pharmacol* 2011; **667**: 50-55 [PMID: 21497161 DOI: 10.1016/j.ejphar.2011.03.041]
147 **Giono LE**, Manfredi JJ. The p53 tumor suppressor participates in multiple cell cycle checkpoints. *J Cell Physiol* 2006; **209**: 13-20 [PMID: 16741928 DOI: 10.1002/jcp.20689]
148 **Alshatwi AA**, Shafi G, Hasan TN, Al-Hazzani AA, Alsaif MA, Alfawaz MA, Lei KY, Munshi A. Apoptosis-mediated inhibition of human breast cancer cell proliferation by lemon citrus extract. *Asian Pac J Cancer Prev* 2011; **12**: 1555-1559 [PMID: 22126498]
149 **Park HS**, Kim GY, Nam TJ, Deuk Kim N, Hyun Choi Y. Antiproliferative activity of fucoidan was associated with the induction of apoptosis and autophagy in AGS human gastric cancer cells. *J Food Sci* 2011; **76**: T77-T83 [PMID: 21535865 DOI:

10.1111/j.1750-3841.2011.02099.x]
150 **Tan AC**, Konczak I, Ramzan I, Sze DM. Native Australian fruit polyphenols inhibit cell viability and induce apoptosis in human cancer cell lines. *Nutr Cancer* 2011; **63**: 444-455 [PMID: 21391128 DOI: 10.1080/01635581.2011.535953]
151 **Chidambara Murthy KN**, Jayaprakasha GK, Kumar V, Rathore KS, Patil BS. Citrus limonin and its glucoside inhibit colon adenocarcinoma cell proliferation through apoptosis. *J Agric Food Chem* 2011; **59**: 2314-2323 [PMID: 21338095 DOI: 10.1021/jf104498p]
152 **Patel S**. Function and dysfunction of two-pore channels. *Sci Signal* 2015; **8**: re7 [PMID: 26152696 DOI: 10.1126/scisignal.aab3314]
153 **Scholz-Starke J**, Carpaneto A, Gambale F. On the interaction of neomycin with the slow vacuolar channel of Arabidopsis thaliana. *J Gen Physiol* 2006; **127**: 329-340 [PMID: 16505151 DOI: 10.1085/jgp.200509402]
154 **Calcraft PJ**, Ruas M, Pan Z, Cheng X, Arredouani A, Hao X, Tang J, Rietdorf K, Teboul L, Chuang KT, Lin P, Xiao R, Wang C, Zhu Y, Lin Y, Wyatt CN, Parrington J, Ma J, Evans AM, Galione A, Zhu MX. NAADP mobilizes calcium from acidic organelles through two-pore channels. *Nature* 2009; **459**: 596-600 [PMID: 19387438 DOI: 10.1038/nature08030]
155 **Pafumi I**, Festa M, Papacci F, Lagostena L, Giunta C, Gutla V, Cornara L, Favia A, Palombi F, Gambale F, Filippini A, Carpaneto A. Naringenin impairs two-pore channel 2 activity and inhibits VEGF-induced angiogenesis. *Sci Rep* 2017; **7**: 5121 [PMID: 28698624 DOI: 10.1038/s41598-017-04974-1]
156 **Fürstenberger G**, Berry DL, Sorg B, Marks F. Skin tumor promotion by phorbol esters is a two-stage process. *Proc Natl Acad Sci U S A* 1981; **78**: 7722-7726 [PMID: 6801661]
157 **Liu JF**, Crépin M, Liu JM, Barritault D, Ledoux D. FGF-2 and TPA induce matrix metalloproteinase-9 secretion in MCF-7 cells through PKC activation of the Ras/ERK pathway. *Biochem Biophys Res Commun* 2002; **293**: 1174-1182 [PMID: 12054499 DOI: 10.1016/S0006-291X(02)00350-9]
158 **Lee KH**, Yeh MH, Kao ST, Hung CM, Liu CJ, Huang YY, Yeh CC. The inhibitory effect of hesperidin on tumor cell invasiveness occurs via suppression of activator protein 1 and nuclear factor-kappaB in human hepatocellular carcinoma cells. *Toxicol Lett* 2010; **194**: 42-49 [PMID: 20138977 DOI: 10.1016/j.toxlet.2010.01.021]
159 **Yen HR**, Liu CJ, Yeh CC. Naringenin suppresses TPA-induced tumor invasion by suppressing multiple signal transduction pathways in human hepatocellular carcinoma cells. *Chem Biol Interact* 2015; **235**: 1-9 [PMID: 25866363 DOI: 10.1016/j.cbi.2015.04.003]
160 **Jomova K**, Valko M. Advances in metal-induced oxidative stress and human disease. *Toxicology* 2011; **283**: 65-87 [PMID: 21414382 DOI: 10.1016/j.tox.2011.03.001]
161 **Pietrangelo A**. Iron and the liver. *Liver Int* 2016; **36** Suppl 1: 116-123 [PMID: 26725908 DOI: 10.1111/liv.13020]
162 **Sikorska K**, Bernat A, Wroblewska A. Molecular pathogenesis and clinical consequences of iron overload in liver cirrhosis. *Hepatobiliary Pancreat Dis Int* 2016; **15**: 461-479 [PMID: 27733315]
163 **Arthur MJ**. Iron overload and liver fibrosis. *J Gastroenterol Hepatol* 1996; **11**: 1124-1129 [PMID: 9034931]
164 **Fernandez MT**, Mira ML, Florêncio MH, Jennings KR. Iron and copper chelation by flavonoids: an electrospray mass spectrometry study. *J Inorg Biochem* 2002; **92**: 105-111 [PMID: 12459155]
165 **Cheng IF**, Breen K. On the ability of four flavonoids, baicilein, luteolin, naringenin, and quercetin, to suppress the Fenton reaction of the iron-ATP complex. *Biometals* 2000; **13**: 77-83 [PMID: 10831228]
166 **Benherlal PS**, Arumughan C. Studies on modulation of DNA integrity in Fenton's system by phytochemicals. *Mutat Res* 2008; **648**: 1-8 [PMID: 18824181 DOI: 10.1016/j.mrfmmm.2008.09.001]
167 **Jagetia GC**, Reddy TK. Alleviation of iron induced oxidative stress by the grape fruit flavanone naringin in vitro. *Chem Biol Interact* 2011; **190**: 121-128 [PMID: 21345335 DOI: 10.1016/j.cbi.2011.02.009]
168 **Jagetia GC**, Reddy TK, Venkatesha VA, Kedlaya R. Influence of naringin on ferric iron induced oxidative damage in vitro. *Clin Chim Acta* 2004; **347**: 189-197 [PMID: 15313158 DOI: 10.1016/j.cccn.2004.04.022]
169 **Chtourou Y**, Fetoui H, Gdoura R. Protective effects of naringenin on iron-overload-induced cerebral cortex neurotoxicity correlated with oxidative stress. *Biol Trace Elem Res* 2014; **158**: 376-383 [PMID: 24682942 DOI: 10.1007/s12011-014-9948-0]
170 **Chtourou Y**, Slima AB, Gdoura R, Fetoui H. Naringenin mitigates iron-induced anxiety-like behavioral impairment, mitochondrial dysfunctions, ectonucleotidases and acetylcholinesterase alteration activities in rat hippocampus. *Neurochem Res* 2015; **40**: 1563-1575 [PMID: 26050208 DOI: 10.1007/s11064-015-1627-9]
171 **Uriu-Adams JY**, Keen CL. Copper, oxidative stress, and human health. *Mol Aspects Med* 2005; **26**: 268-298 [PMID: 16112185 DOI: 10.1016/j.mam.2005.07.015]
172 **Johncilla M**, Mitchell KA. Pathology of the liver in copper overload. *Semin Liver Dis* 2011; **31**: 239-244 [PMID: 21901654 DOI: 10.1055/s-0031-1286055]
173 **Zhou B**, Gitschier J. hCTR1: a human gene for copper uptake identified by complementation in yeast. *Proc Natl Acad Sci U S A* 1997; **94**: 7481-7486 [PMID: 9207117]
174 **Moriwaki H**, Osborne MR, Phillips DH. Effects of mixing metal ions on oxidative DNA damage mediated by a Fenton-type reduction. *Toxicol In Vitro* 2008; **22**: 36-44 [PMID: 17869055 DOI: 10.1016/j.tiv.2007.07.011]
175 **Mira L**, Fernandez MT, Santos M, Rocha R, Florêncio MH, Jennings KR. Interactions of flavonoids with iron and copper ions: a mechanism for their antioxidant activity. *Free Radic Res* 2002; **36**: 1199-1208 [PMID: 12592672]
176 **Esterbauer H**, Gebicki J, Puhl H, Jürgens G. The role of lipid peroxidation and antioxidants in oxidative modification of LDL. *Free Radic Biol Med* 1992; **13**: 341-390 [PMID: 1398217]
177 **Miranda CL**, Stevens JF, Ivanov V, McCall M, Frei B, Deinzer ML, Buhler DR. Antioxidant and prooxidant actions of prenylated and nonprenylated chalcones and flavanones in vitro. *J Agric Food Chem* 2000; **48**: 3876-3884 [PMID: 10995285]
178 **Rani A**, Kumar A, Lal A, Pant M. Cellular mechanisms of cadmium-induced toxicity: a review. *Int J Environ Health Res* 2014; **24**: 378-399 [PMID: 24117228 DOI: 10.1080/09603123.2013.835032]
179 **Rikans LE**, Yamano T. Mechanisms of cadmium-mediated acute hepatotoxicity. *J Biochem Mol Toxicol* 2000; **14**: 110-117 [PMID: 10630425]
180 **Renugadevi J**, Prabu SM. Naringenin protects against cadmium-induced oxidative renal dysfunction in rats. *Toxicology* 2009; **256**: 128-134 [PMID: 19063931 DOI: 10.1016/j.tox.2008.11.012]
181 **Das A**, Roy A, Das R, Bhattacharya S, Haldar PK. Naringenin alleviates cadmium-induced toxicity through the abrogation of oxidative stress in swiss albino mice. *J Environ Pathol Toxicol Oncol* 2016; **35**: 161-169 [PMID: 27481493 DOI: 10.1615/JEnvironPatholToxicolOncol.2016015892]
182 **Rathi VK**, Das S, Parampalli Raghavendra A, Rao BSS. Naringin abates adverse effects of cadmium-mediated hepatotoxicity: An experimental study using HepG2 cells. *J Biochem Mol Toxicol* 2017; **31**: [PMID: 28422390 DOI: 10.1002/jbt.21915]
183 **Singh AP**, Goel RK, Kaur T. Mechanisms pertaining to arsenic toxicity. *Toxicol Int* 2011; **18**: 87-93 [PMID: 21976811 DOI: 10.4103/0971-6580.84258]
184 **Jomova K**, Jenisova Z, Feszterova M, Baros S, Liska J, Hudecova D, Rhodes CJ, Valko M. Arsenic: toxicity, oxidative stress and human disease. *J Appl Toxicol* 2011; **31**: 95-107 [PMID: 21321970 DOI: 10.1002/jat.1649]
185 **Liu J**, Waalkes MP. Liver is a target of arsenic carcinogenesis. *Toxicol Sci* 2008; **105**: 24-32 [PMID: 18566022 DOI: 10.1093/toxsci/kfn120]
186 **Adil M**, Kandhare AD, Visnagri A, Bodhankar SL. Naringin ameliorates sodium arsenite-induced renal and hepatic toxicity in rats: decisive role of KIM-1, Caspase-3, TGF-β, and TNF-α. *Ren Fail* 2015; **37**: 1396-1407 [PMID: 26337322 DOI: 10.3109/08860

22X.2015.1074462]
187 **Kim HC**, Jang TW, Chae HJ, Choi WJ, Ha MN, Ye BJ, Kim BG, Jeon MJ, Kim SY, Hong YS. Evaluation and management of lead exposure. *Ann Occup Environ Med* 2015; **27**: 30 [PMID: 26677413 DOI: 10.1186/s40557-015-0085-9]
188 **Matović V**, Buha A, Đukić-Ćosić D, Bulat Z. Insight into the oxidative stress induced by lead and/or cadmium in blood, liver and kidneys. *Food Chem Toxicol* 2015; **78**: 130-140 [PMID: 25681546 DOI: 10.1016/j.fct.2015.02.011]
189 **Pal M**, Sachdeva M, Gupta N, Mishra P, Yadav M, Tiwari A. Lead exposure in different organs of mammals and prevention by curcumin-nanocurcumin: a review. *Biol Trace Elem Res* 2015; **168**: 380-391 [PMID: 26005056 DOI: 10.1007/s12011-015-0366-8]
190 **Fierro NA**, Gonzalez-Aldaco K, Roman S, Panduro A. The immune system and viral hepatitis. In Muriel P. Liver pathophysiology: therapies & antioxidants. Waltham, MA: Elsevier, 2017: 129-139
191 **Tang H**, Grisé H. Cellular and molecular biology of HCV infection and hepatitis. *Clin Sci (Lond)* 2009; **117**: 49-65 [PMID: 19515018 DOI: 10.1042/CS20080631]
192 **Penin F**, Dubuisson J, Rey FA, Moradpour D, Pawlotsky JM. Structural biology of hepatitis C virus. *Hepatology* 2004; **39**: 5-19 [PMID: 14752815 DOI: 10.1002/hep.20032]
193 **Nahmias Y**, Goldwasser J, Casali M, van Poll D, Wakita T, Chung RT, Yarmush ML. Apolipoprotein B-dependent hepatitis C virus secretion is inhibited by the grapefruit flavonoid naringenin. *Hepatology* 2008; **47**: 1437-1445 [PMID: 18393287 DOI: 10.1002/hep.22197]
194 **Bok SH**, Shin YW, Bae KH, Jeong TS, Kwon YK, Park YB, Choi MS. Effects of naringin and lovastatin on plasma and hepatic lipids in high-fat and high-cholesterol fed rats. *Nutr Res* 2000; **20**: 1007-1015 [DOI: 10.1016/S0271-5317(00)00191-3]
195 **Kim SY**, Kim HJ, Lee MK, Jeon SM, Do GM, Kwon EY, Cho YY, Kim DJ, Jeong KS, Park YB, Ha TY, Choi MS. Naringin time-dependently lowers hepatic cholesterol biosynthesis and plasma cholesterol in rats fed high-fat and high-cholesterol diet. *J Med Food* 2006; **9**: 582-586 [PMID: 17201649 DOI: 10.1089/jmf.2006.9.582]
196 **Lee CH**, Jeong TS, Choi YK, Hyun BH, Oh GT, Kim EH, Kim JR, Han JI, Bok SH. Anti-atherogenic effect of citrus flavonoids, naringin and naringenin, associated with hepatic ACAT and aortic VCAM-1 and MCP-1 in high cholesterol-fed rabbits. *Biochem Biophys Res Commun* 2001; **284**: 681-688 [PMID: 11396955 DOI: 10.1006/bbrc.2001.5001]
197 **Mulvihill EE**, Allister EM, Sutherland BG, Telford DE, Sawyez CG, Edwards JY, Markle JM, Hegele RA, Huff MW. Naringenin prevents dyslipidemia, apolipoprotein B overproduction, and hyperinsulinemia in LDL receptor-null mice with diet-induced insulin resistance. *Diabetes* 2009; **58**: 2198-2210 [PMID: 19592617 DOI: 10.2337/db09-0634]
198 **Wilcox LJ**, Borradaile NM, de Dreu LE, Huff MW. Secretion of hepatocyte apoB is inhibited by the flavonoids, naringenin and hesperetin, via reduced activity and expression of ACAT2 and MTP. *J Lipid Res* 2001; **42**: 725-734 [PMID: 11352979]
199 **Borradaile NM**, de Dreu LE, Barrett PH, Behrsin CD, Huff MW. Hepatocyte apoB-containing lipoprotein secretion is decreased by the grapefruit flavonoid, naringenin, via inhibition of MTP-mediated microsomal triglyceride accumulation. *Biochemistry* 2003; **42**: 1283-1291 [PMID: 12564931 DOI: 10.1021/bi026731o]
200 **Borradaile NM**, de Dreu LE, Barrett PH, Huff MW. Inhibition of hepatocyte apoB secretion by naringenin: enhanced rapid intracellular degradation independent of reduced microsomal cholesteryl esters. *J Lipid Res* 2002; **43**: 1544-1554 [PMID: 12235187]
201 **Borradaile NM**, de Dreu LE, Huff MW. Inhibition of net HepG2 cell apolipoprotein B secretion by the citrus flavonoid naringenin involves activation of phosphatidylinositol 3-kinase, independent of insulin receptor substrate-1 phosphorylation. *Diabetes* 2003; **52**: 2554-2561 [PMID: 14514640]
202 **Allister EM**, Borradaile NM, Edwards JY, Huff MW. Inhibition of microsomal triglyceride transfer protein expression and apolipoprotein B100 secretion by the citrus flavonoid naringenin and by insulin involves activation of the mitogen-activated protein kinase pathway in hepatocytes. *Diabetes* 2005; **54**: 1676-1683 [PMID: 15919788]
203 **Allister EM**, Mulvihill EE, Barrett PH, Edwards JY, Carter LP, Huff MW. Inhibition of apoB secretion from HepG2 cells by insulin is amplified by naringenin, independent of the insulin receptor. *J Lipid Res* 2008; **49**: 2218-2229 [PMID: 18587069 DOI: 10.1194/jlr.M800297-JLR200]
204 **Goldwasser J**, Cohen PY, Lin W, Kitsberg D, Balaguer P, Polyak SJ, Chung RT, Yarmush ML, Nahmias Y. Naringenin inhibits the assembly and long-term production of infectious hepatitis C virus particles through a PPAR-mediated mechanism. *J Hepatol* 2011; **55**: 963-971 [PMID: 21354229 DOI: 10.1016/j.jhep.2011.02.011]
205 **Khachatoorian R**, Arumugaswami V, Raychaudhuri S, Yeh GK, Maloney EM, Wang J, Dasgupta A, French SW. Divergent antiviral effects of bioflavonoids on the hepatitis C virus life cycle. *Virology* 2012; **433**: 346-355 [PMID: 22975673 DOI: 10.1016/j.virol.2012.08.029]
206 **Gonzalez O**, Fontanes V, Raychaudhuri S, Loo R, Loo J, Arumugaswami V, Sun R, Dasgupta A, French SW. The heat shock protein inhibitor quercetin attenuates hepatitis C virus production. *Hepatology* 2009; **50**: 1756-1764 [PMID: 19839005 DOI: 10.1002/hep.23232]
207 **Khachatoorian R**, Arumugaswami V, Ruchala P, Raychaudhuri S, Maloney EM, Miao E, Dasgupta A, French SW. A cell-permeable hairpin peptide inhibits hepatitis C viral nonstructural protein 5A-mediated translation and virus production. *Hepatology* 2012; **55**: 1662-1672 [PMID: 22183951 DOI: 10.1002/hep.25533]
208 **Mathew S**, Faheem M, Archunan G, Ilyas M, Begum N, Jahangir S, Qadri I, Qahtani MA, Mathew S. In silico studies of medicinal compounds against hepatitis C capsid protein from north India. *Bioinform Biol Insights* 2014; **8**: 159-168 [PMID: 25002815 DOI: 10.4137/BBI.S15211]
209 **Lulu SS**, Thabitha A, Vino S, Priya AM, Rout M. Naringenin and quercetin--potential anti-HCV agents for NS2 protease targets. *Nat Prod Res* 2016; **30**: 464-468 [PMID: 25774442 DOI: 10.1080/14786419.2015.1020490]
210 **Singh AK**, Raj V, Keshari AK, Rai A, Kumar P, Rawat A, Maity B, Kumar D, Prakash A, De A, Samanta A, Bhattacharya B, Saha S. Isolated mangiferin and naringenin exert antidiabetic effect via PPARγ/GLUT4 dual agonistic action with strong metabolic regulation. *Chem Biol Interact* 2018; **280**: 33-44 [PMID: 29223569 DOI: 10.1016/j.cbi.2017.12.007]
211 **Ahmed OM**, Hassan MA, Abdel-Twab SM, Abdel Azeem MN. Navel orange peel hydroethanolic extract, naringin and naringenin have anti-diabetic potentials in type 2 diabetic rats. *Biomed Pharmacother* 2017; **94**: 197-205 [PMID: 28759757 DOI: 10.1016/j.biopha.2017.07.094]
212 **Sirovina D**, Oršolić N, Gregorović G, Končić MZ. Naringenin ameliorates pathological changes in liver and kidney of diabetic mice: a preliminary study. *Arh Hig Rada Toksikol* 2016; **67**: 19-24 [PMID: 27092635 DOI: 10.1515/aiht-2016-67-2708]
213 **Kapoor R**, Kakkar P. Naringenin accords hepatoprotection from streptozotocin induced diabetes in vivo by modulating mitochondrial dysfunction and apoptotic signaling cascade. *Toxicol Rep* 2014; **1**: 569-581 [PMID: 28962270 DOI: 10.1016/j.toxrep.2014.08.002]
214 **Nyane NA**, Tlaila TB, Malefane TG, Ndwandwe DE, Owira PMO. Metformin-like antidiabetic, cardio-protective and non-glycemic effects of naringenin: Molecular and pharmacological insights. *Eur J Pharmacol* 2017; **803**: 103-111 [PMID: 28322845 DOI: 10.1016/j.ejphar.2017.03.042]
215 **Sahu SC**, Gray GC. Lipid peroxidation and DNA damage induced by morin and naringenin in isolated rat liver nuclei. *Food Chem Toxicol* 1997; **35**: 443-447 [PMID: 9216742]
216 **Galati G**, Moridani MY, Chan TS, O'Brien PJ. Peroxidative metabolism of apigenin and naringenin versus luteolin and quercetin: glutathione oxidation and conjugation. *Free Radic Biol*

Med 2001; **30**: 370-382 [PMID: 11182292]
217 **Ortiz-Andrade RR**, Sánchez-Salgado JC, Navarrete-Vázquez G, Webster SP, Binnie M, García-Jiménez S, León-Rivera I, Cigarroa-Vázquez P, Villalobos-Molina R, Estrada-Soto S. Antidiabetic and toxicological evaluations of naringenin in normoglycaemic and NIDDM rat models and its implications on extra-pancreatic glucose regulation. *Diabetes Obes Metab* 2008; **10**: 1097-1104 [PMID: 18355329 DOI: 10.1111/j.1463-1326.2008.00869.x]
218 **Pérez-Pastén R**, Martínez-Galero E, Chamorro-Cevallos G. Quercetin and naringenin reduce abnormal development of mouse embryos produced by hydroxyurea. *J Pharm Pharmacol* 2010; **62**: 1003-1009 [PMID: 20663034 DOI: 10.1111/j.2042-7158.2010.01118.x]

P- Reviewer: Abenavoli L, Chiu KW, Shimizu Y, Tarantino G
S- Editor: Gong ZM **L- Editor**: A **E- Editor**: Huang Y

World Journal of Gastroenterology

Submit a Manuscript: http://www.f6publishing.com

World J Gastroenterol 2018 April 28; 24(16): 1708-1724

DOI: 10.3748/wjg.v24.i16.1708

ISSN 1007-9327 (print) ISSN 2219-2840 (online)

REVIEW

Naturally occurring hepatitis B virus reverse transcriptase mutations related to potential antiviral drug resistance and liver disease progression

Yu-Min Choi, So-Young Lee, Bum-Joon Kim

Yu-Min Choi, So-Young Lee, Bum-Joon Kim, Department of Microbiology and Immunology, Biomedical Sciences, Liver Research Institute and Cancer Research Institute, Seoul National University, College of Medicine, Seoul 110799, South Korea

ORCID number: Yu-Min Choi (0000-0003-4709-3155); So-Young Lee (0000-0002-9638-893X); Bum-Joon Kim (0000-0003-0085-6709).

Author contributions: Kim BJ conceived participated in its design and coordination; Choi YM and Lee SY analyzed and interpreted the data.

Supported by the Korea Health Technology R&D Project through the Korea Health Industry Development Institute and the Ministry of Health and Welfare, South Korea, No. HI14C0955.

Conflict-of-interest statement: There was no conflict of interest.

Manuscript source: Invited manuscript

Correspondence to: Bum-Joon Kim, PhD, Professor, Department of Biomedical Sciences, Microbiology and Immunology, and Liver Research Institute, Seoul National University College of Medicine, 103, Daehak-ro, Jongno-gu, Seoul 110799, South Korea. kbumjoon@snu.ac.kr
Telephone: +82-2-7408316
Fax: +82-2-7430881

Received: March 27, 2018
Peer-review started: March 27, 2018
First decision: April 3, 2018
Revised: April 10, 2018
Accepted: April 16, 2018

Article in press: April 16, 2018
Published online: April 28, 2018

Abstract

The annual number of deaths caused by hepatitis B virus (HBV)-related disease, including cirrhosis and hepatocellular carcinoma (HCC), is estimated as 887000. The reported prevalence of HBV reverse transcriptase (RT) mutation prior to treatment is varied and the impact of preexisting mutations on the treatment of naïve patients remains controversial, and primarily depends on geographic factors, HBV genotypes, HBeAg serostatus, HBV viral loads, disease progression, intergenotypic recombination and co-infection with HIV. Different sensitivity of detection methodology used could also affect their prevalence results. Several genotype-dependent HBV RT positions that can affect the emergence of drug resistance have also been reported. Eight mutations in RT (rtL80I, rtD134N, rtN139K/T/H, rtY141F, rtM204I/V, rtF221Y, rtI224V, and rtM309K) are significantly associated with HCC progression. HBeAg-negative status, low viral load, and genotype C infection are significantly related to a higher frequency and prevalence of preexisting RT mutations. Preexisting mutations are most frequently found in the A-B interdomain of RT which overlaps with the HBsAg "a" determinant region, mutations of which can lead to simultaneous viral immune escape. In conclusion, the presence of baseline RT mutations can affect drug treatment outcomes and disease progression in HBV-infected populations via modulation of viral fitness and host-immune responses.

Key words: Polymerase; Hepatocellular carcinoma; Reverse transcriptase; Preexisting mutations; Hepatitis B virus

Core tip: The prevalence of preexisting reverse transcriptase (RT) mutations in treatment-naïve patients largely depends on geographic factors, HBV genotypes, HBeAg serostatus, hepatitis B virus (HBV) viral loads, disease progression, intergenotypic recombination, co-infection with HIV and the method used for detecting the mutation. Genotype-dependent polymorphic amino acid substitutions in RT may affect the emergence of drug resistance, and genotype C exhibits relatively elevated spontaneous RT mutation rates. HBeAg-negative status and low viral loads are significantly associated with a higher frequency and prevalence of HBV preexisting RT mutations. Preexisting mutations are most frequently found in the A-B interdomain of RT, mutations of which can lead to simultaneous viral immune escape.

Choi YM, Lee SY, Kim BJ. Naturally occurring hepatitis B virus reverse transcriptase mutations related to potential antiviral drug resistance and liver disease progression. *World J Gastroenterol* 2018; 24(16): 1708-1724 Available from: URL: http://www.wjgnet.com/1007-9327/full/v24/i16/1708.htm DOI: http://dx.doi.org/10.3748/wjg.v24.i16.1708

INTRODUCTION

Although an effective and safe vaccine against hepatitis B virus (HBV) has been available since 1982[1], approximately 257 million people are chronic carriers of the virus. The annual number of deaths caused by HBV related diseases, including cirrhosis and hepatocellular carcinoma (HCC), was estimated as 887000 in 2015 (WHO, 2017)[2].

Reverse transcriptase (RT) conducts the major enzymatic activity required for viral replication. Nucleos(t)ide analogs (NAs) such as lamivudine[3], adefovir dipivoxil[4], entecavir[5], telbivudine[6], and tenofovir[7], for treatment of HBV infection, mainly target RT and function as reverse transcriptase inhibitors by mimicking natural nucleosides and integrating within the DNA molecules to interfere with viral replication[8,9]. However, due to the lack of proof reading ability of RT, the error rate for viral genome replication is as high as 10^{-7} per nucleotide, which is 10-fold greater than that of other DNA viruses[10], resulting in the emergence of antiviral-drug resistance mutations[11-15]. These NA-resistant (NAr) mutants are the greatest challenge for treatment of HBV because they change the conformational structure of RT and lower the effectiveness of NAs by impeding their binding[16]. In addition, RT partially overlaps with HBV surface antigen (HBsAg) and RT mutation may simultaneously generate HBsAg mutations, which can alter the antigenicity, immune recognition, replication capacity, and virulence of HBV[17-19].

The reported prevalence of preexisting HBV polymerase RT mutations is varied and the impact of preexisting RT mutations on treatment-naïve patients remains controversial. In addition, the relationship between preexisting RT mutations and advanced liver diseases, such as cirrhosis and HCC, has not been fully investigated[20]. Therefore, this review focuses primarily on factors affecting the prevalence and types of preexisting RT mutations in treatment-naïve patients and the relationship between these mutations and disease progression.

DISTRIBUTION OF PREEXISTING HBV NAR MUTATIONS IN SAMPLES FROM TREATMENT-NAÏVE PATIENTS

Liu *et al*[21] identified pre-existing HBV RT mutations in 42 potential NAr RT positions from 192 treatment-naïve Chinese patients and arranged them into following four mutation categories: primary drug resistance (Category 1); secondary/compensatory mutation (Category 2); putative NAr (Category 3); and pretreatment (Category 4) (Table 1). To understand the global prevalence of these 42 naturally occurring NAr resistance mutations of RT, we reviewed a total of 50 previous studies[12,20-68] and collated their results (Figure 1). These include 32 articles published from institutions based in Asia (12 published from China, four from Iran, four from Turkey, four from India, three from Japan, two from Taiwan, and one each from Korea, Jordan, and Indonesia), 11 articles published from institutions based in Europe (six from Italy, two from Germany, and one each from Austria, Ireland, and Spain), four articles published from institutions based in North America (three from United States and one from Canada), two articles published from institutions based in South America (both from Brazil), and one article published from an institution in South Africa (Supplementary Table 1). Among the 50 studies, 36[12,20,21,32-58,60-65] used direct PCR sequencing methods, 11[22-28,59,66-68] used the INNO-LiPA line assay, and 3[29-31] detected RT mutations by ultra-deep pyrosequencing (UDPS). Seventeen articles[21,26,27,30,31,34,35,37-39,42,43,46-48,53,58] included treatment-naïve patients infected with genotypes B and C, one study[32] with genotypes A and D, eleven studies[22,28,29,36,50,51,55,56,60,63,68] with genotype D, one study[33] with genotype C, and fifteen studies[20,23-25,40,41,44,45,52,54,57,61,64,65,67] with more than three genotypes (*e.g.*, A, C, and D or A, B, C, and D). In five studies, genotypes of patients were not mentioned. Our literature-based study demonstrated that preexisting RT mutations were also found in treatment-naïve patients at 40 of 42 preciously identified NAr RT positions, the two exceptions were rtF242A, a pretreatment mutation and rtF166L, a lamivudine (LMV)-associated putative mutation. The distribution and overall incidence of RT mutations is presented in Figures 1 and 2.

Primary drug resistance mutations are amino acid changes that cause direct NA resistance by decreasing viral susceptibility to NAs[69-71]. Mutated RT positions known to induce primary drug resistance are rt169,

Table 1 Distribution of preexisting RT mutation in 42 potential NAr regions in treatment naïve patients

Mutation	RT mutation type	Change in HBsAg[3]	Drug resistance	Genotype	Location	Ref.
Primary[1]	I169T		ETV	B, C	China	[20,53]
	A181T/V	sW172 stop	LMV, LdT, ADV, TNF	A, B, C, D	Canada, Italy, China, United States	[24,25,30,39,45,51,53]
	T184A/C/F/G/I/L/M/S		ETV, LMV	A, B, C, D	Canada, China, South Korea	[24,27,33]
	A194T	no change in HBsAg	ADV, TNF	B, C, D	Indonesia, Italy	[38,51]
	S202C/G/I		ETV, LMV	A, B, C, D	Canada, China, Spain, Italy	[24,27,30,57,59]
	M204I/V/S	V-sI195M, I- sW196S/L/Stop	LMV, LdT, ADV, TNF, ETV	A, B, C, D	Canada, Italy, South Korea, China, Indonesia, United States, Turkey	[24,25,27,30,33-36,38, 39,47,52,53]
	N236T		ADV, TNF	B, C	China	[27,30,47]
	M250I/L/V		ETV	A, B, C, D	Canada, Italy, China, United States	[24,25,27,45]
Secondary[1]	L80I/V	no change in HBsAg	LMV	A, B, C, D	Canada, Italy, South Korea, Indonesia, China	[24,25,33,38,47,53]
	V173L	sE164D	LMV	A, B, C, D	China, Canada, Italy	[20,24,25,30,39,47]
	L180M	no change in HBsAg	LMV, ETV, LdT	A, B, C, D	Canada, South Korea, China, Italy, Indonesia	[24,25,27,30,33,38, 39,47,53]
Putative[2]	S53N		LMV	B, C	China, South Korea	[21,33,58]
	T54N	sP46T	ADV	A, B, C, D	Italy	[83]
	L82M		LMV	C	South Korea	[33]
	V84M, S85A		ADV	B, C	South Korea, China	[33,53,127]
	I91L	no change in HBsAg	LMV	B, C, D	China, Indonesia, India	[21,38,54,58]
	Y126C/R/H	C-sT118A	ADV	A, B, C, D	South Korea, China, India	[33,54,58]
	T128I, T128N	N-sG145R, I-sP120S	LMV	B, C, D	Indonesia, China, India	[38,53,54,58]
	N139D/E/Q			A	India	[54]
	W153Q/R/E	Q- sP120T/ sG145R, E-sD144E/G145R	LMV	B, C, D	South Korea, Indonesia, China, India	[33,38,54,58]
	F166L	sF158Y	LMV			
	V191I	sW182 stop	LMV, ADV	B, C, D	South Korea, China, Italy	[33,39,51,58]
	A200V	sL192F	LMV	B, C	South Korea, China	[27,33,42]
	V207I	sW199 stop, sM198I	LMV	A, B, C, D	Germany, China, Italy	[27,32,39,83]
	S213T		LMV, ETV	A, B, C, D	China, India	[39,40,42,58]
	V214A	T-sS204R	ADV	B, C, D	South Korea, Italy, China,	[30,33,53,83]
	Q215E/H/P/S		LMV, ADV	A, B, C, D	China, Italy, India, Turkey	[30,39,51,53-55]
	L217R, E218D, F221Y	D-sS210I/T	ADV	A, B, C, D	South Korea, China	[21,33,42,58]
	L229G/V/W		LMV	B, C	South Korea, China	[33,42,58]
	L229F	F-sC221L, V-sF220L	LMV	B, C, D	China, India	[54,58,128]
	I233V		ADV	A, C, D	Indonesia, Italy, India, China, South Korea, Germany	[25,38,40,58,78,79]
	P237H, N238D/S/T, Y245H	N/A	ADV	B, C	South Korea, China	[21,33,39,58]
	S/C256G		LMV, ETV	B, C	China, Indonesia	[21,38,58]
Pretreatment[2]	T38A, T38K	K-sQ30K		B, C	South Korea, China	[33,58]
	Y124H/D/N			B, C,	China, South Korea	[21,33,58]
	D134E/N	sI126S/N		B, C, D	China, South Korea, Indonesia	[21,33,38,58]
	N139K/H	K-sT131N, T-sT131P, H-sG139N		A, B, C	South Korea, India, Indonesia, China	[33,38,54,58]
	I224V	No change in HBsAg		B, C,	China, South Korea	[21,33,39,58]
	R242A					

[1]Well known NA resistance mutations (primary and secondary) with phenotypic data; [2]Putative and pretreatment mutations relevant to NA resistance but not experimentally confirmed; [3]Changes in HBsAg, reported in Sheldon *et al*[17], Liu *et al*[21], Locarnini *et al*[72], and Yang *et al*[77]. Rt139 is shared in both Categories 3 (N139D/E/Q) and 4 (N139K/H). Overall, 42 positions in the RT region were studied. ADV: Adefovir dipivoxil; ETV: Entecavir; Ldt: Telbivudine; LMV: Lamivudine; TNF: Tenofovir.

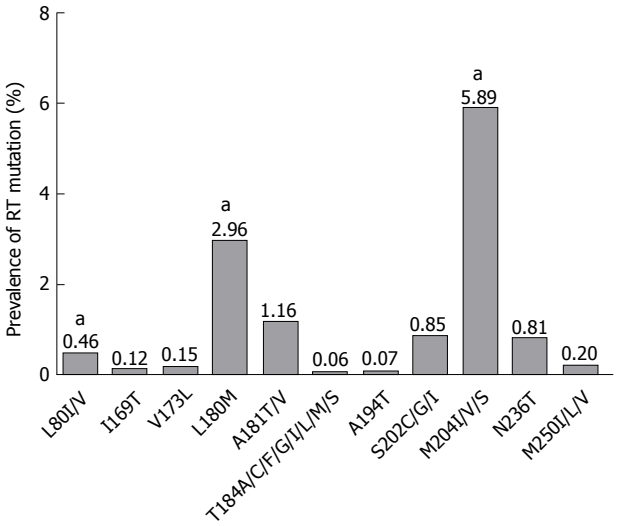

Figure 1 Pooled incidence and distribution of preexisting primary and secondary reverse transcriptase mutations compiled using data from 50 previous studies. The distribution and overall incidence of RT region is presented; numbers indicate the pooled incidence rate of the RT mutation in a total of 8,435 treatment-naïve patients. [a]Pre-existing RT mutation associated with the progression of HCC in treatment-naïve patients.

rt181, rt184, rt194, rt202, rt204, rt236, and rt250. The mutations rtA181T/V, rtM204I, and rtM204V also cause the simultaneous HBsAg mutations, sW172 stop, sW196S/L/Stop, and sI195M, respectively[17,72] (Table 1). Our literature based pooled incidence data showed that of primary drug resistance mutations, M204I/V is the most frequently encountered in treatment-naïve patients[14,28,33] (5.89%), which was far more than the pooled mutation rate of rtA181T/V, rtS202C/G/I and rtN236T (incidence: 1.16%, 0.85% and 0.81%, respectively). Mutation of rtI169T (0.12%), rtT184G (0.06%), rtA194T (0.07%), and rtM250V/L (0.20%) had a very low pooled incidence (Figure 1). A systematic review by Zhang *et al*[73] revealed that the global incidence of rtM204I/V/S is 4.85%. Several other studies[24,28,34-37] have also reported the frequent incidence of rtM204I/V/S in treatment-naïve patients. For examples, Kobayashi *et al*[34], Lee *et al*[35], Tuncbilek *et al*[36], Fung *et al*[24], and Huang *et al*[37] reported rtM204I/V/S mutation frequencies in Japanese, Taiwanese, Turkish, Canadian, and Chinese treatment-naïve patients reached of 27.8%, 57%, 7.8%, 12%, and 26.9%, respectively.

Secondary, or compensatory, mutations refer to amino acid substitutions that compensate for replication defects caused by primary drug resistance mutations and may reduce drug susceptibility by restoring viral replication fitness[38,69,74]. The mutations rtL80I/V, rtV173L, rtL180M are known for secondary resistance mutations. Our literature based incidence data showed that rtL180M had the highest natural incidence (2.96%), which was higher than the pooled mutation rate of rtL80I/V and V173L (incidence:0.46% and 0.15%, respectively) (Figure 1). Similarly, Zhang *et al*[73] reported that the overall frequency of rtL180M mutation is 2.67%. Other studies, including Fung *et al*[24], Yamani *et al*[38], and Mirandola *et al*[25] reported that the prevalence rates of rtL180M were 10.0%, 2.08%, and 1.18% in Chinese, Indonesian, and Italian HBV carriers, respectively. The rtL80I/V mutation also occurs frequently in treatment-naïve patients. Yamani *et al*[38], Kim *et al*[33], and Mirandola *et al*[25] found pre-existing rtL80I/V mutation frequencies of 1.07%, 3.82%, and 0.78%, respectively. Notably, Kim *et al*[33] reported that rtL80I/V was the most frequently encountered preexisting mutation of secondary drug resistance mutations in South Korea (3.8%, 5/131 patients), even higher than rtL180M frequency (2.3%, 3/131 patients). Another compensatory RT mutation, rtV173L, was also detected in several studies of treatment-naïve patients, where Zheng *et al*[20], Wang *et al*[39], and Mirandola *et al*[25] reported that it occurred in 0.6%, 0.56%, and 0.39% of their patients, respectively.

RT mutations which have been identified as associated with drug resistance, but have not been confirmed experimentally *in vitro*, are defined as putative NA resistant mutations[75-77]. A total of 26 types of RT mutations, including rtS53N, rtT54N, rtL82M, rtV84M, rtS85A, rtI91L, rtY126C, rtT128I/N, rtN139D, rtW153Q, rtF166L, rtV191I, rtA200V, rtV207I, rtS213T, rtV214A, rtQ215P/S, rtL217R, rtE218D, rtF221Y, rtL229G/V/W, rtI233V, rtP237H, rtN238D/S/T, rtY245H, and rtS/C256G, are considered putative drug resistance mutations (Category 3) (Table 1)[21]. Other amino acid substitutions, which were detected before treatment, but for which the association between their occurrence and drug resistance has not been evaluated, are defined as pretreatment mutations, these include rtT38A, rtY124H, rtD134E/N, rtN139K/H, rtI224V, and rtR242A (Category 4) (Table 1)[21,38].

Recently, it has been proven through in vitro and in vivo experiments that several putative or pretreatment mutations, including rtL229F, rtS13T, and rtI233V, can also contribute to the development of drug resistance[40,78,79]. In addition, several studies have reported that treatment-naïve patients with only putative RT mutations, and without primary or secondary changes, developed drug resistance since treatment initiation[41]. Our literature based pooled incidence data showed that several putative or pretreatment mutations, including rtI91L, mutations in 6 positions of A-B interdomain (rtY124H, rtY126C/R/H, rtT128I/N, rtD134E/N, rtN139D/E/H/K/Q and rtW153Q/R/E), rtF221Y and rtI224V, were encountered with high frequency from the treatment naïve patients[20,21,33,38,39,42]. Of these, a RT mutation in the A-B interdomain, rtD134E/N, which also cause a simultaneous sI126N/S mutation of the HBsAg "a" determinant, was found to have the highest frequency in treatment-naïve patients (1.70%) (Figure 2). Of note, the following four putative or pretreatment mutations found in treatment naïve patients, rtD134E/N, rtN139D/E/H/K/Q, rtF221Y, and rtI224V, are also reported as associated with progression of severe liver diseases, such as HCC and cirrhosis (described below).

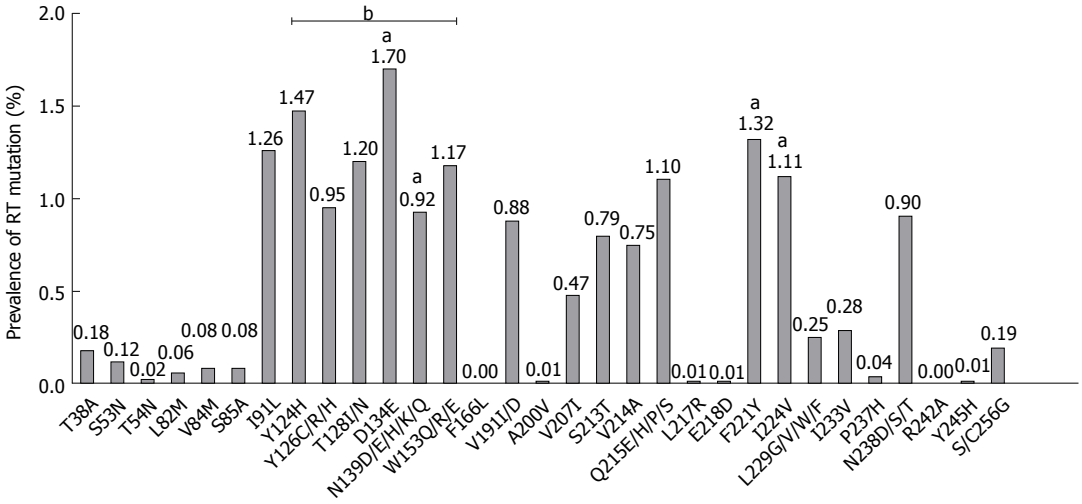

Figure 2 Pooled incidence and distribution of preexisting putative and pretreatment reverse transcriptase mutations compiled using data from 50 previous studies. The distribution and overall incidence of RT region is presented; numbers indicate the pooled incidence rate of the RT mutation in a total of 8435 treatment-naïve patients. [a]Pre-existing RT mutation associated with the progression of HCC in treatment-naïve patients; [b]A-B interdomain region.

Moreover, some of these mutations also overlapped with genotype-dependent polymorphic sites, as described in the next section.

DISTRIBUTION OF GENOTYPE-DEPENDENT AMINO ACID POLYMORPHIC SITES IN TREATMENT-NAÏVE PATIENTS

To date, a total of 10 HBV genotypes (A-J) and several sub-genotypes have been identified; genotypes are separated from each other by sequence differences of more than 8% by phylogenetic analysis, based on whole genome sequences[80,81]. HBV genotypes, including genotypes A-J and the various sub-genotypes, are associated with several distinct traits, including geographical distribution, host ethnicity, and pathogenicity[82]. Since specific mutational patterns of mutation can be restricted by structural/functional constraints to particular genotypes, HBV genotype can influence the evolution frequency, or types, of mutations associated with NAr in treatment-naïve patients, as described by Liu *et al*[21]. Moreover, HBV genotypes can affect LAM-resistant mutations in the YMDD motif of viral RT in patients with chronic infections after long term drug treatment[42,43,83]. Two recent studies[83,84] reported that genotype A favors the rtM204V mutation, while HBV-B, C, and D select for rtM204I at higher rates, compared with rtM204V. Moreover, Liu *et al*[21] identified eight genotype-dependent AA polymorphic positions, (*i.e.*, rt53, rt91, rt124, rt134, rt221, rt224, rt238, and rt256) useful as signature for B- and C-genotypes with mutations at the 42 positions associated with NAr, and which are important for the distinction between mutations and mere polymorphisms during genotypic mutation analysis of samples from infected patients. These specific, genotype-dependent AA polymorphic positions in RT functional domains, (*i.e.*, rt91 in domain A, rt238 in domain D and rt256 in domain E) affect drug treatment outcomes[21,85]. Liu *et al*[21] also showed that rtL91 and rtI91 were generally favored by genotypes B and C, respectively, and that rtS256 was prevalent in both genotypes, with rtC256 more common in genotype C than in genotype B. rtL91 and rtC256 were also more closely correlated with failure of extended LMV therapy, compared with other polymorphisms (rtI91and rtS256) leading to the suggestion that they may represent potential pretreatment markers[86].

Mirandola *et al*[83] further extended the eight genotype dependent polymorphic-sites suggested by Liu *et al*[21] into a total of 27 polymorphic-sites potentially affecting treatment, *via* sequence analysis of 200 treatment-naïve chronically infected patients from north-east Italy, infected with the six HBV genotypes; A, B, C, D, E, and F. In this study, substitutions at residues rt53, rt54, and rt91 of the 27 genotype-dependent polymorphic sites were the most frequent single AA substitutions, and HBV-DNA levels of patients with these mutations were significantly lower than those of patients with no mutations, suggesting that these changes contributed to reducing viral fitness during infections. The authors also found that patients with multiple mutations were mainly infected with genotype D, rather than other genotypes (A, B, C, E, or F), strongly supporting previous results indicating that HBV-D may have the highest genetic variability among all HBV-genotypes[87].

Yamani *et al*[38] demonstrated that the distribution of primary and secondary drug resistance mutations was not significantly different between genotypes B and C; however, significant differences were identified in some genotype-dependent polymorphic sites. For example, rtL91I and rtY221F were more common in genotype C, compared to genotype B ($P < 0.001$) (Table 2). Moreover, some genotype dependent mutations, such as rtM129L, rtD134N, rtM145L, and rtE263H/D/Q,

Table 2 Genotype-dependent amino acid polymorphic sites and reverse transcriptase mutations in treatment-naïve patients

RT position	Drug resistance	Mutations in RT region of four genotypes[1]				Polymorphism	Ref.
		A	B	C	D		
38		T (4.4)[4]			T (14.0)[4]	A/T/T/A	[83]
53	LMV		D/T (1.8)[4]			I/N/S/N	[21]
54	ADV	N (2.2)[2]				T/T/T/H	[83]
84				I (0.5)[2]		V	[127]
				I (1.5)[2]			[21]
85				T (0.6)[2]		S	[127]
91	LMV		I (20.0)[4]	L (23.5)[2]	I (16.7)[4]	I/L/I/L	[83]
					I (14.3)[2]		[44]
103		I (100)[3]			I (1.67)[3]	V	[40]
122		H (47.0)[2]			H (6.66)[2]	F	[40]
					L/V/I(25.0)[2]		[44]
124		H (2.2)[3]	H (20.0)[3]	H (11.8)[3]		N/N/Y/H	[83]
			H (3.6)[3]	H (6.6)[3]			[21]
			D (5.5)[3]				
126		H (6.7)[4]			R (23.7)[4]	Y/H/H/H	[83]
					R (17.9)[4]		[44]
					Y (1.4)[4] Q (0.5)[4]		[83]
128	LMV	N (2.2)[2]			N (1.4)[2] I (1.4)[2]	T	[83]
			I (1.9)[2]				[38]
129				L (60.0)[2]	L (21.4)[2]	M	[44]
			L (1.9)[2]	L (26.2)[2]			[38]
		L (100.0)[2]		L (9.0)[2]	L (3.3)[2]		[40]
134				N (40.5)[2]		D/N/D/D	[38,54]
				E (23.1)[3]	E (5.0)[3]		[21,54]
			I/S (1.8)[3]	E (5.8)[3]			[21]
139	LMV		K (3.7)[2]		K (11.9)[2]	Q/N/N/N	[38]
					K (2.3)[3]		[83]
				K (1.5)[3]			[21]
145			L (3.7)[2]	L (40.5)[2]		M	[83]
153	LMV	Q (100)[2]				W/R/R/R	[40]
191	LMV			V (8.3)[2]		V/I/I/V	[39]
		I (4.6)[2]		F (7.7)[2]			[54]
200	LMV	V (2.2)[2]				A	[83]
207	LMV		M (6.0)[2] L (2.3)[2]			V	[26]
				I (5.9)[2]			[83]
				I/L/G (2.1)[2]			[39]
214	LMV/ADV			A (5.9)[2]	A (2.3)[2]	V	[83]
		A (0.5)[2] I (0.5)[2]		I (0.6)[2]	A (0.8)[2] E (0.7)[2]		[127]
215	ADV			E (7.7)[2]	H (5.0)[2] S (5.0)[2]	Q	[54]
			H (0.9)[2]		H (3.0)[2] S (4.3)[2]		[127]
					P (2.8)[2] S (4.2)[2]		[83]
217		L (6.7)[4]			R (0.9)[2]	R/L/L/L	[83]
221	ADV			F (40.5)[2]		Y/Y//F/F	[38]
					Y (5.1)[2]		[83]
226			H/T (33.3)[2]	H/T (2.4)[2]		N	[38]
237					T (6.4)[2]	P	[127]
238	LMV, ETV	H(1.0)[2] W(1.0)[2]	Q (3.9)[2]	T (8.7)[2]	H (2.3)[2]	N/H/N/N	[127]
			Q (1.82)[2]	S (2.19)[2] T (0.73)[2]			[21]
				T (3.87)[2]			[39]
		D (2.2)[2] T (2.2)[2]			D (1.4)[2]		[83]
245					H (1.4)[2]	Y	[83]
248	ADV		H (7.4)[3]	H (4.8)[3]		N	[38]
256	LMV			G (40.0)[2]	G (10.7)[2]	S/S/S/C	[44]
			G (20.0)[2]		G (3.7)[2]		[83]
			G (5.45)[2]				[21]
					G (3.7)[2]		[26]

A total of 29 reported genotype-dependent amino acid polymorphic sites in the RT region in treatment-naïve patients are shown. The first column contains the RT positions and the second column details the relationship between mutations and drug resistance. Column three to six indicate the prevalence of each mutation as percentages, according genotype. Consensus amino acids are presented in column seven. [1]Incidence (%) of mutations in the RT region; [2]Putative mutation; [3]Pretreatment mutation; [4]Novel mutation. ADV: Adefovir dipivoxil; ETV: Entecavir; Ldt: Telbivudine; LMV: Lamivudine; TNF: Tenofovir.

were more frequent in in genotype C than genotype B viruses ($P < 0.001$). Notably, rtN226H/T was the only pretreatment mutation, which is more common in genotype B than genotype C ($P < 0.001$). Singla *et al*[44]

Table 3 Positive relationships between HBeAg negative serostatus and preexisting reverse transcriptase mutation frequency in the treatment- naïve patients

HBeAg-positive		HBeAg-negative		HBV genotype (%)	Location	Ref.
Mutations[1]	HBV-DNA[2]	Mutations[1]	HBV-DNA[2]			
3/14 (21.4)	7.8	11/14 (78.6)	5.7	B, C, E	California	[26]
6/24 (25.0)	5.5	18/24 (75.0)	3.9	B, C, B-C	China	[27]
0/4 (0.0)	7.2	4/4 (100.0)	4.7	A, B, C, D, F	California	[45]
3/6 (50.0)	8.0	3/6 (50.0)	3.2	D	Turkey	[36]
8/12 (67.0)	7.9	4/12 (33.0)	6.9	NA	Taiwan, China	[35]
27/43 (62.8)	5.7	16/43 (37.2)	4.7	B, C	China	[46]
8/13 (61.5)	6.3	5/13 (38.5)	5.4	B, C	China	[47]
0/5 (0.0)	NA	5/5 (100.0)	NA	NA	Japan	[34]
0/4 (0.0)	NA	4/4 (100.0)	NA	NA	Japan	[88]

[1]Number of patients with RT mutation (%); [2]HBV-DNA level (log_{10} IU/mL).

also showed that rtL91I and rtM129L are more common in samples from genotype C, than genotype D, infected patients. Overall, these findings indicate that distribution of genotype dependent polymorphic sites in treatment-naive patients could affect drug treatment outcomes via modulation of viral fitness or replication. The distribution of the 29 genotype-dependent polymorphic-sites in the HBV RT region among treatment naïve patients identified in other reports is summarized in Table 2.

GENOTYPE DISTRIBUTION OF PRIMARY RT MUTATIONS IN TREATMENT-NAÏVE PATIENTS

Mirandola *et al*[25] identified the different genotype different distributions of antiviral drug resistant RT mutations using INNO LiPA line probe analysis of samples from treatment-naïve patients; RT mutations were detected in 13 (5%) of 255 HBV infected patients. Of these, 10 patients had mutations associated with primary resistance or reduced sensitivity, including three cases with a YMDD mutation (rtM204V), three with the mutation, rtM250L/V, which is associated with ETV resistance, and four with the mutation rtI233V, which is associated with reduced sensitivity to ADV. Notably all the three patients with the rtM204V mutation also had coexisting L180M compensatory mutations, and all were infected with HBV-C genotype viruses, suggesting that naturally occurring LMV-resistant HBV may be more frequent in patients infected with genotype C virus. This hypothesis is strongly supported by the recent report of Kim *et al*[33] of the high frequency of the YMDD mutation, (rtM204V/I) (6.87%, 9/131 patients), in Korean treatment-naïve patients with HBV genotype C2 infections. Wang *et al*[39] also reported that RT mutations were only found in genotype C treatment-naïve patients; however, no primary or secondary RT mutations were found in genotype B patients. In addition, a systemic meta-analysis review by Zhang *et al*[73] showed that rtM204V/I had the highest incidence of 4.89% (95%CI: 4.13%-5.65%) among primary and secondary RT mutations. These authors also found, *via* the subgroup analysis by genotype, that HBV genotype C had a tendency of toward a higher spontaneous YMDD mutation frequency (19.32%) than genotype B (15.01%) or D (14.79%). The increased spontaneous mutations in the viral genome of HBV genotype C could translate to a higher risk of primary NA resistance in HBV endemic areas, where genotype C infections are prevalent, including China and South Korea.

CLINICAL FACTORS (HBEAG SEROSTATUS AND HBV VIRAL LOADS) AFFECTING INCIDENCE OF PREEXISTING RT MUTATIONS IN TREATMENT-NATIVE PATIENTS

The majority of studies have consistently reported a significant association between the prevalence of preexisting RT mutations and lower HBV DNA loads, or HBeAg-negative status, in treatment-naïve patients[26,27,34-36,45-47,88] (Table 3). Vutien *et al*[26] reported that treatment-naïve patients with HBeAg-negative status had higher RT mutation frequencies (78.57%), compared with HBeAg-positive patients (21.42%). These authors also showed that HBeAg-negative patients had significantly lower HBV DNA viral loads compared with HBeAg-positive patients (5.65 log_{10} IU/mL *vs* 7.82 log_{10} IU/mL, respectively). Zhao *et al*[27] also reported similar results showing that 75% of patients with RT mutations were HBeAg-negative and had lower HBV DNA levels (3.92 log_{10} IU/mL) whereas 25% of patients with RT mutations were HBeAg-positive with higher HBV DNA loads (5.54 log_{10} IU/mL). Similarly, Zhu *et al*[89] found that Chinese patients with chronic HBV carrying preexisting RT mutations had significantly decreased serum baseline HBV DNA loads (P = 0.0363) and blood platelet counts (P = 0.0181) compared with those without RT mutations.

Several other studies[34,45,88] also found RT mutations only in HBeAg-negative patients, and the patients were also more likely to have decreased HBV DNA levels compared with those who were HBeAg-positive[45].

Kobayashi *et al*[34] reported that all asymptomatic HBV carriers with YMDD mutation were HBeAg-negative and eAb-positive, suggesting that sustained host immune pressure may be a major force driving potential NAr mutations. Zhang *et al*[73] also reported a systemic meta-analysis finding that patients with chronic hepatitis B (CHB) and genotype C infections, who were male and HBeAg-negative tended to have higher spontaneous mutation rates in subgroup analysis. Xu *et al*[46] reported no significant correlation between pre-existing mutations and the majority of clinical factors including gender, age, HBV genotype, ALT, HBeAg, and HBV DNA loads, in a Chinese population; however, subgroup analysis indicated that pre-existing mutations were strongly associated with lower HBV DNA levels in HBeAg sero-negative, but not HBeAg sero-positive, patients (HBeAg+ *vs* HBeAg-: 5.74 $\log_{10}$ IU/mL *vs* 4.72 $\log_{10}$ IU/mL, $P = 0.0112$). These findings suggest that preexisting RT mutations might lead to lower HBV viral loads in treatment-naïve patients with HBeAg-negative serostatus. Several other studies have reported similar positive associations between the frequency of pre-existing RT mutations and decreased HBV viral loads[33,42,83].

Taken together, there appears to be a clear causal link between preexisting RT mutations and HBeAg-negative status, decreased HBV DNA load, or liver disease progression. This may be because mutations in the RT active domain, could impair enzyme activity, particularly at the HBeAg negative immune clearance stage, thus decreasing the efficacy of virus replication and, resulting in liver disease progression and poor treatment outcomes[17,42,90,91].

GENOTYPE DISTRIBUTION AND GEOGRAPHICAL FACTOR AFFECTING THE INCIDENCE OF PREEXISTING RT MUTATIONS

Reports of the incidence of preexisting RT mutations in treatment-naïve patients are highly variable, ranging from 0% to 57%[25,26,28,32-35,48,92,93]. This huge discrepancy among studies may be due to differences in factors such as the geographical or ethnic backgrounds of studied patients, sample size, and viral genotype[27]. A number of studies have reported prevalence rate of preexisting RT mutations (primary and secondary RT mutations) of more than 5% in treatment-naïve patients (Table 4). Fung *et al*[24] found a higher rate of baseline RT mutations (12% M204I/V, 10% L180M) by using the INNO-LIPA v.3 assay. In this study, many patients, most of whom were infected with genotype D, carried rtL180M, rtM204V/I, and rtL80V/I mutations. In addition, Nishijima *et al*[94] identified a high mutation rate (35.7%) in 14 treatment-naive patients in Japan, using UDPS. Also, a recent study using direct sequencing[33] of samples from 131 treatment-naïve patients infected with genotype C2 reported an overall rate of 12.98% for primary (rtT184A/C/F and rtM204I/V) or compensatory (rtL80I and rtL180M) mutations. According to a systemic meta-analysis review conducted by Zhang *et al*[73], the overall prevalence of spontaneous mutations among treatment-naïve patients worldwide was 5.73%. The highest pooled prevalence (8.00%) was identified in samples from China, followed by Japan, Turkey, Korea, South America, and Europe at 6.62%, 6.43%, 5.72%, 3.89%, and 2.53%, respectively. Another study of 325 genotype D infected treatment-naïve patients using direct PCR sequencing[50] reported overall incidence of 15.69% for primary and secondary drug resistance mutations, including L80V/I, L180M, M204I/V, and S213T/N.

In contrast, several studies have reported prevalence rates of less than 5 % for pre-existing RT mutations (primary and secondary RT mutations) in treatment-naïve patients (Table 4). For example, using direct sequencing of samples from treatment-naïve patients from the United States, Nguyen *et al*[45] demonstrated that only four (0.9%) of 472 patients were infected with viruses with primary and secondary mutations (rtA181A/S, rtA194S, and rtM250I). Similarly, Zollner *et al*[32] screened a total of 96 patients infected with HBV genotypes A and D (52.08% and 47.92%, respectively) using a direct sequencing assay, but found no primary or secondary resistance mutations. Another study by Salpini *et al*[51] using the direct sequencing method reported that, of 140 treatment-naïve patients infected with genotype D, only 1.4% had primary drug resistance mutations, while 2.1% carried secondary mutations.

Overall, preexisting RT mutation prevalence clearly reflects the geographical distribution of HBV infection. For example, China is an area with high levels of endemic area of HBV infection (8%, according to a national survey in 2006) and also has higher prevalence of pre-existing RT mutations[73]. Meanwhile, in Europe, which has low levels of endemic HBV infection (approximately 2%), there is a low incidence of spontaneous mutations (2.53%)[73]. Since the HBV geographic distribution has also a close relationship with the genotype distribution, the majority of countries in Asia with prevalent genotype B and C infections have high rates of spontaneous RT mutation ($\geqslant$ 5%)[27,33-35,39,47,73], whereas countries in Europe, where genotype A and D infections are dominant, tended to have low incidences ($\leqslant$ 5%)[32,49,51].

HBV INTERGENOTYPIC RECOMBINATION AND COINFECTION WITH HIV AFFECTING THE INCIDENCE OF PREEXISTING RT MUTATIONS

HBV intergenotypic recombination between different

Table 4 Variation in the prevalence of preexisting reverse transcriptase mutations according to mutation detection methods, genotype, and geographic distribution

Prevalence	Location	No. of cases	Genotype	HBV DNA loads (log_{10} IU/mL)	RT mutations prevalence	Mutation detecting methods	Ref.
HBV DNA RT mutations ≥ 5%	Italy	255	A, C, D	5.0	5.0% mutations overall	INNO-Lipa HBV DR v.3	[25]
	China	269	B, C, B-C	4.9	8.9% mutations overall	INNO-Lipa HBV DR v.3	[27]
	Canada	209	A, B, C, D	7.0	12% M204I/V, 10% L180M, 9% L80V/I, 3%V173L	INNO-Lipa HBV DR v.3	[24]
	Turkey	71	NA	NA	18.3% YMDD mutations	INNO-Lipa HBV DR v.1	[28]
	South Korea	131	C2	6.5	12.98% mutations overall	Direct Sequencing	[33]
	Turkey	77	D	7.3	7.8% YMDD mutations	Direct Sequencing	[36]
	China	213	B, C	6.2	6.1% mutations overall	Direct Sequencing	[47]
	China	104	B, C, B-C	4.5	26.9% YMDD mutations	Direct Sequencing	[93]
	Japan	18	NA	NA	27.8% YMDD mutations	Direct Sequencing	[34]
	Iran	325	D	NA	15.69% mutations overall	Direct Sequencing	[50]
	Taiwan, China	28	NA	7.5	57% YMDD mutations	Direct Sequencing	[35]
	China	357	B, C	6.3	16.8% mutations overall	Direct Sequencing	[39]
	Meta-analysis (China)	8156	B, C, D	NA	8.00% mutations overall	Record screening	[73]
	Japan	14	B, C	4.9	35.7% YMDD mutations	Ultra-deep sequencing	[94]
HBV DNA RT mutations < 5%	Iran	147	D	NA	None	Direct sequencing	[56]
	China	328	B, C	6.9	3.6% mutations overall	Direct sequencing	[53]
	Japan	20	NA	NA	None	Direct sequencing	[48]
	California	472	A, B, C, D, F	5.3	< 1% mutations overall	Direct sequencing	[45]
	Italy	100	NA	NA	None	Direct sequencing	[49]
	Italy	140	D	4.0	3.5% mutations overall	Direct sequencing	[51]
	Germany	96	A, D	NA	None	Direct sequencing	[32]
	Brazil	189	A, C, D, F	3.2	overall 6.0% in Northeast/ 0% in North	Direct sequencing	[41]
	California	198	B, C	4.2	1% mutations in polymerase	INNO-Lipa HBV DR v.3	[26]

genotypes is regarded as an important strategy for HBV genetic diversity and may impose challenges on vaccine designation and antiviral therapy strategies[95,96]. In particular, the high prevalence of vertical infections in HBV endemic areas, such as Asia or Africa, could lead to a life-long chronic infection[97], resultantly leading to a high probability of co-infection and a high risk for virus recombination[96,98-101]. Previous studies on HBV recombination have identified different types of intergenotypic recombinants in HBV RT, most of which have recombination in RT/S overlapping region[96,98-103]. Of note, a recent study conducted by Liu *et al*[100] demonstrated that, through full-length HBV RT sequences analysis from 201 Chinese chronic hepatitis B (CHB) patients, 38.10% (24/63) infected with genotype B had recombination with genotype C in the 3'-terminal RT sequences. These authors also showed that these intergenotypic recombinants were associated with enhanced viral DNA load and higher RT point mutation rates, compared with their parental genotype B or C, highlighting the importance of monitoring intergenotypic RT recombinants in HBV endemic areas to ensure optimal management.

Approximately, 10% of HIV-infected persons worldwide are chronically infected with HBV, and co-infection of two viruses is most frequently identified (up to 25%) in sub-Saharan Africa and Asia[104]. HBV and HIV co-infection is a major cause of morbidity and mortality because it could contribute to an increased risk of liver cirrhosis and HCC[105]. In general, previous studies showed a predominance of HBV genotype A in HIV infected individuals, compared with other genotypes[106,107]. In particular, Makondo *et al*[108] reported that the ratio of genotype A to non-A (97% to 3%) was higher in the HBV/HIV co-infected Southern Africa patients compared with mono-infected individuals. These authors also showed that 10 percent, 3 out of 29 patients prior to the initiation of antiretroviral therapy (ART), had drug resistance mutations rtV173L, rtL180M+rtM204V, and rtV214A. In South Africa, rtM204I has been mainly detected in treatment-naïve HBV/HIV co-infected individuals[12] with rtM204V in treated HBV mono-infected participants[109], suggesting HIV co-infection could affect HBV preexisting RT mutation pattern. A study of South African patients conducted by Selabe *et al*[12] demonstrated that HBV lamivudine - resistant strains were detected in three out of 15 treatment-naïve mono - infected chronic hepatitis B patients,

Table 5 Relationship of preexisting reverse transcriptase mutations with disease severity

Type of mutation in RT	Chang in HBsAg	Genotype	Location	Disease progression	*P* value	Ref.
rtL80I[2]	NC	C	South Korea	HCC	0.036	[33]
rtD134N[4]	sI126S/N	B, C	China	HCC	0.007	[114]
rtN139K/T/H[4]	sT131N/P	C	South Korea	HCC	0.008	[33]
rtY141F[5]	sM307T	Ce	Taiwan	HCC	0.029	[37]
rtM204I/V[1]	sW196L/S/W	C	South Korea	HCC	0.021	[33]
rtF221Y[3]	NA	B,C,D	China	HCC, poor survival rate	0.028/0.004	[20,115]
rtI224V[4]	NC	C	China	HCC	0.005	[116]
rtM309K[5]	NA	C	China	HCC	0.007	[116]

HBV polymerase RT mutation; [1]Primary; [2]Secondary; [3]Putative; [4]Pretreatment; [5]Novel RT mutation. HCC: Hepatocellular carcinoma; NA: Not available; NC: Not changed; RT: Reverse transcriptase.

whereas detected in 10 out of 20 treatment-naïve HBV/HIV-coinfected patients. In contrast, a multinational study of HIV/HBV-coinfected individuals carried out by Thio *et al*[110] demonstrated that no subject had preexisting RT mutations in the majority population of the quasispecies, suggesting no need for HBV drug-resistance testing prior to starting anti-HBV therapy in HIV-HBV co-infected individuals. It is also supported by a recent study of Ghana patients conducted by Archampong *et al*[111]. Taken together, geographical factors and HBV genotypes could have effects on the preexisting HBV RT mutation in treatment-naïve HBV/HIV-coinfected patients.

DIFFERENT SENSITIVITY OF DETECTION METHODOLOGY USED CAN AFFECT THE REPORTED PREVALENCE OF PREEXISTING RT MUTATIONS: LIMITATION OF THE STUDIES IN PREEXISTING RT MUTATIONS

The detection methods used can also have a profound effect on the reported incidence results of preexisting RT mutations. The majority of studies have used direct sequencing methods, which can lead to the underestimation of preexisting RT mutations, due to the relative low sensitivity of these assays. Wang *et al*[39] reported that the sensitivity of direct sequencing-based protocols declined when circulating viral subspecies (AA substitutions) levels were at ratio below 20%-25%. Similarly, there were several studies have reported discordance in the incidence of pre-existing RT mutations detected by direct sequencing and other screening methods, such as the INNO-LiPA assay, or UDPS. For example, Margeridon-Thermet *et al*[52] reported that direct sequencing found an average of 5.9 mutations per sample, while UDPS identified an additional 4.6 mutations per sample, which could not be detected by direct sequencing. In that study, two of 17 treatment-naïve patients had mutations which were detected only by UDPS, but not by direct sequencing; one rtM204I mutation with (1.3% mutant ratio) and the other an rtA181T mutation (1.0% ratio). Similarly, Aberle *et al*[66] also compared the detection efficacies for preexisting RT mutations between the INNO-LiPA assay and direct sequencing. The former identified additional mutations in 8 (14%) of 56 patient samples, which could not be detected using the latter method, indicating the superiority of the former over the latter for RT mutation detection. Overall, these data demonstrate that the method used for detecting the mutations can affect the prevalence estimates of preexisting RT mutations in treatment-naïve patients, which may cause discrepancies among the results of different studies.

PREEXISTING RT MUTATIONS ARE RELATED TO THE PROGRESSION OF LIVER DISEASES

Although the clear association between preexisting RT mutations and advanced liver disease has not been fully investigated, several types of HBV mutations in RT have previously been reported as related to the progression of liver diseases, such as cirrhosis and HCC (Table 5). Kim *et al*[33] compared types and frequencies of pre-existing RT mutations between CHB and HCC treatment-naïve patients. These authors found a significantly higher rate of RT mutations in HCC patients than in those with chronic hepatitis (3.17% *vs* 2.09%, $P = 0.003$) and also identified a total of three NAr mutations (rtL80I, rtN139K/T/H, and rtM204I/V) significantly associated with HCC progression. RT mutations rtN139K/T/H and rtM204I/V also cause simultaneous mutations in the overlapped HBsAg coding sequence (sT131N/P and sI195M, or sW196S/L/Stop)[17,21,72]. Of these, the YMDD-motif mutation (rtM204I/V) was found in 9 patients of 131 patients (8 HCC and 1 CHB) with the other two types of mutation, rt204I and rt204V, in 8 and 1 patients, respectively. The other HCC-related mutation (rtL80I) was first identified as a compensatory mutation associated with LMV resistance[69,112]. Its relationship with clinical deterioration is also corroborated by other reports that it was associated with increased viral loads, accompanied by an elevation in serum aminotransferase activity, and exacerbation of liver disease in every

Table 6 Distribution of preexisting reverse transcriptase mutations among reverse transcriptase domains

Mutation frequency (%)[1]			*P* value[5]	Ref.
Domains[2]	A-B interdomain[3]	Non-A-B interdomains[4]		
1.45	3.51	2.58	< 0.001	[38]
1.37	4.4	3.77	< 0.001	[20]
1.07	7.5	3.16	0.008	[33]
0.43	3.82	0.52	0.0014	[21]

[1]Mutation frequency was calculated as the number of mutations found in a specific RT domain divided by the total number of sites in the domain; [2]Domain including RT mutation sites; rt38, rt84, rt207, rt233, rt238, and rt256; [3]A-B interdomain including RT mutations sites: rt53, rt191, rt213, rt218, rt229, and rt242; [4]Non-A-B interdomains including RT mutation sites: rt124, rt126, rt128, rt134, rt139, and rt153; [5]*P*-values of comparisons of mutation frequencies between A-B interdomain and other functional domains.

case[113]. Interestingly, Kim *et al*[33] also showed that rtL80I was combined with the rtM204I/V mutation in five of nine rtM204I/V cases, and that patients with L80I had increased HBV replication compared with those without this mutation, suggesting that, together with rtM204I/V, it may contribute to HCC generation in treatment-naïve patients by compensating for the defective replication of caused by rtM204I/V.

In another study, Yin *et al*[114] analyzed the association of the mutations of HBV polymerase with postoperative survival in 92 patients with HBV-related HCC using direct sequencing. They discovered three nucleotide sites, one (31st nucleotide) in a spacer region and two [529th (P = 0.007) and 1078th (P = 0.038)] in the RT region, which could be considered independent predictors of postoperative survival in HBV-related HCC. Of the two sites in RT related to HCC outcomes, rtD134N (mutation G529A) was associated with lamivudine resistance, further supporting previous findings of potential correlation between resistance to the anti-HBV nucleoside analog, lamivudine, and HCC prognosis[114]. Since rtD134N also causes an amino acid change in HBsAg (sI126N/V), it can induce changes in the antigenic properties of HBsAg. Further functional studies are necessary to determine whether the rtD134N mutation can induce HCC via modulation of RT activity or through its effects on HBV replication.

Huang *et al*[37] found seven viral single nucleotide polymorphisms (SNPs) in HBV polymerase, which enhance viral replication and liver disease progression in HBeAg negative subjects. Of these SNPs, rtY141F (Y487F), which is located in the RT region of HBV polymerase was associated with increased viral load and HCC (P = 0.0291). Moreover, rtY141F, a genotype C-related SNP, also led to a simultaneous amino acid change in the overlapping 'a' determinant region of HBsAg (sM307T). In addition, Li *et al*[115] and Zheng *et al*[20] reported that the rtF221Y mutation was strongly related to HCC prognosis after liver resection (hazard ratio, 2.345; P = 0.001). Moreover, the rtF221Y mutation was also associated with poor overall survival (hazard ratio, 2.557; P = 0.004), suggesting that it is a potential independent risk factor and viral marker for HCC. Those results were consistent with the report of Li *et al*[115], which identified the rtF221Y mutant as an independent risk factor for recurrence of HCC and poor overall survival (P = 0.001 and P = 0.004, respectively). Wu *et al*[116] also investigated preexisting RT mutations potentially related to HCC in Chinese patients and identified rtI224V and rtM309K as significant risk factors for HCC (P = 0.005 and P = 0.007, respectively).

In addition, the number of RT mutations is associated with the liver disease progression. Zhu *et al*[89] revealed that patients with multiple RT mutant sites showed a significantly higher rate of liver fibrosis (P = 0.0128), suggesting a link between viral mutation and clinical progression of chronic hepatitis, and also highlighting that the natural accumulation of RT mutations is a process involved in viral survival during chronic liver fibrosis.

Overall, eight mutations in the RT region, namely rtL80I, rtD134N, rtN139K/T/H, rtY141F, rtM204I/V, rtF221Y, rtI224V, and rtM309K, are significantly related to liver disease progression. The majority of HCC-related RT mutations were reported from studies of treatment-naïve patients infected with genotype C HBV. This supports previous reports that HBV genotype C is more likely to lead to severe and aggressive liver disease than other HBV genotypes[112,117-122]. Of note, association of the following three mutations, rtM204V, rtL80I, and rtD134N, with disease progression provides a likely explanation for the positive relationship between lamivudine resistance and liver disease progression.

DISTRIBUTION AND FREQUENCY OF PREEXISTING RT MUTATIONS IN DIFFERENT RT REGIONS

HBV RT consists of seven functional domains (G, F, A, B, C, D, and E) and five inter-domains (F-A, A-B, B-C, C-D, and D-E) which link the functional domains[18,31,123]. Previous studies[20,21,33,38] reported a higher frequency of preexisting RT mutations in the A-B inter-domain, compared with other regions.

Liu *et al*[21] revealed that all six sites in the A-B interdomain, rt124, rt126, rt128, rt134, rt139, and rt153, exhibit mutations (6/6, prevalence 100%), indicating high genetic variability of this region compared with other sites within RT domains (sites with mutations: 6/22, 27.27%; P = 0.0014). In this study, the mutation frequency of the A-B inter-domain (44/1152, 3.82%) was also significantly higher than those in other RT domains (Table 6). This result is in line with that reported by Zheng *et al*[20], who demonstrated that A-B interdomain exhibits higher mutation frequencies (4.3%, 5.3%, 3.6%) than those of other RT domains (1.4%, 1.4%, 1.3%) in Chinese

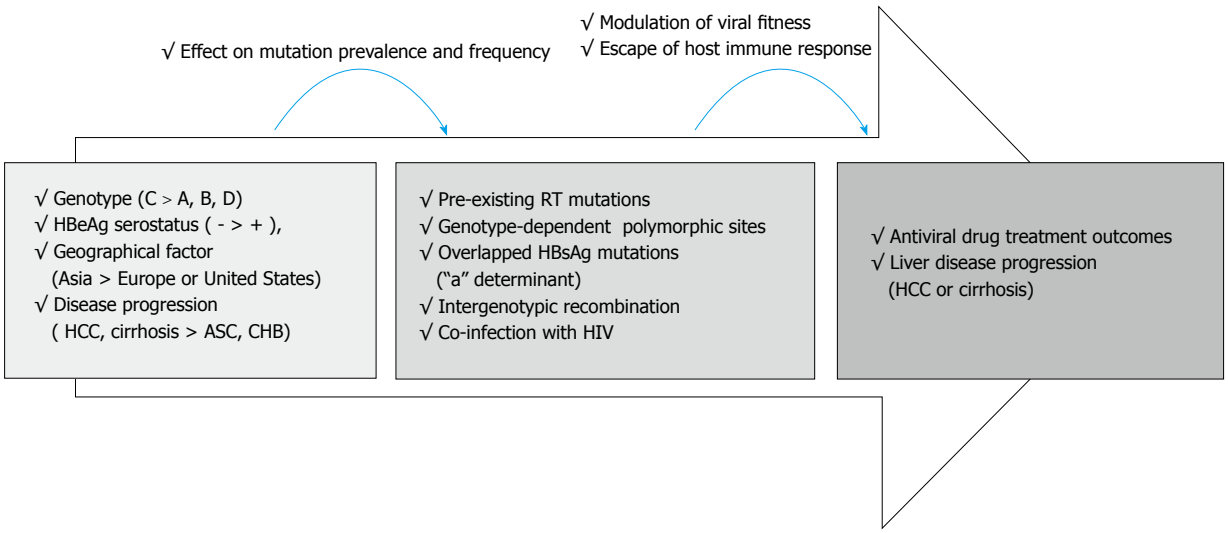

Figure 3 Schematic representation indicating the role of preexisting hepatitis B virus reverse transcriptase mutations in liver disease progression and treatment outcomes. HBV: Hepatitis B virus; HCC: Hepatocellular carcinoma; ASC: Asymptomatic carriers; CHB: Chronic hepatitis B; HIV: Human immunodeficiency virus.

treatment-naive patients with CHB, cirrhosis, and HCC. Specifically, they found that there was a clear tendency toward frequent mutations of the A-B interdomain in patients with cirrhosis suggesting a relationship between mutations in the A-B inter-domain and the development of this condition.

Similarly, Yamani *et al*[38] also reported that the A-B interdomain had the highest mutation prevalence and frequency (3.51% ± 2.53%) compared with functional domains and non-A-B interdomains (1.45% ± 1.05% and 2.58% ± 0.51%, respectively) in Indonesian treatment-naïve patients (Table 6). Moreover, they found that genotype C had substantially higher mutations rates in the A-B interdomain than genotype B ($P < 0.001$). Kim *et al*[33] also revealed that mutations within the A-B interdomain were most frequent in treatment-naïve Korean patients infected with genotype C2, compared with other domains, with 46 of 79 patients (58.22%) with preexisting RT mutations having changes in the A-B inter-domain. In this study, rtD134E/N/C was the most frequently encountered hot spot site among the six A-B inter-domain sites and was mutated in 12/79 patients (15.2%). The authors also showed that the mutation frequency of A-B interdomain (59/786, 7.50%) was higher than that of non A-B interdomain (3.16%) (Table 6). Our pooled incidence also supported the previous notion of higher frequency of persisting RT mutations in A-B interdomain compared with other region in RT (Figure 2).

RT and HBsAg mutations can occur simultaneously, due to the overlap of RT region and HBsAg gene sequences[19,124]. Liu *et al*[21] reported that 14 of 18 mutated positions in RT overlapped with HBsAg, and that RT mutations at 12 out of 14 RT positions (except those at rt124 and rt126) also led to simultaneous HBsAg mutations of 19 types in 16.67% (32/192) of isolates (Figure 1). Notably, these authors also found that RT mutations in the A-B interdomain could lead to simultaneous AA substitutions sI126A/N/S/, sG130N, sT131N/P, and sG145R of the overlapped 'a' determinant of HBsAg, including the most frequently described immune-escape mutation sG145R (1/192, 0.52%)[125,126]. Similarly, Kim *et al*[33] demonstrated that RT mutations at 10 of 42 NAr positions could lead to 15 types of simultaneous overlapped HBsAg mutations in 32.06% (42/131) patients. Of interest, they also found that the RT mutations at 3 NAr positions (rt134, rt139, and rt153) located in the overlapped HBsAg "a" determinant region from 22 treatment-naïve patients also had simultaneous "a" determinant mutations in two positions, S126 and S131, in 15 patients (15/22, 68.2%) (12 patients with mutations at rt134, leading to 10 changes of AA S126, and 8 patients with mutations at rt139, leading to 5 alterations of AA S131).

Overall, preexisting RT mutations are distributed in a non-random manner, and most frequently found in the A-B interdomain, overlapped with the HBsAg "a" determinant region, than in other domains. Moreover, the A-B interdomain also contains the most abundant mutations, indicating that these positions might be preexisting mutation hotspots in treatment-naïve patients. Of six positions' mutation in the A-B interdomain, three RT mutations, rtD134E/N, rtN139D/E/H/K/Q, and rtW153E/Q/R, that overlap with HBsAg "a" determinant region are hotspots found most frequently in treatment-naïve patients, which could contribute to HBV viral persistence via generation of immune escape "a" determinant mutants proteins. In general, A-B interdomain mutations are prevalent in patients with genotype C2 infections and could contribute to HBV-associated disease, such as HCC and cirrhosis.

CONCLUSION

Preexisting HBV RT mutations in treatment-naïve

patients are related to potential drug resistance and progression of liver disease, such as HCC or cirrhosis. In addition, genotype-dependent polymorphic amino acid substitution in RT can also affect the emergence of drug resistance and treatment outcomes. The reported prevalence of spontaneous RT mutations in treatment-naïve patients is varied, and largely depends on geographic factors, HBV genotypes, HBeAg serostatus, HBV viral loads, disease progression, intergenoytpic recombination, and co-infection with HIV. Different sensitivity of detection methodology used could also affect their prevalence results. The INNO-LiPA assay and UDPS method detect higher prevalence rates of preexisting RT mutations compared with direct PCR sequencing in treatment-naïve patients. Genotype C infection, HBeAg-negative status, and low viral loads are significantly associated with higher frequencies and prevalence rate of pre-existing HBV RT mutations. Higher frequencies of preexisting RT mutations were also generally associated with liver disease progression, including of HCC and cirrhosis. Eight mutations in RT region, rtL80I, rtD134N, rtN139K/T/H, rtY141F, rtM204I/V, rtF221Y, rtI224V, and rtM309K were significantly associated with progression of HCC in treatment-naïve patients. Of RT domains, preexisting RT mutations occur most frequently in the A-B interdomain which overlaps with the HBsAg "a" determinant region, in which mutations can lead to simultaneous viral immune escape (Figure 3). In conclusion, the presence of baseline preexisting RT mutations can affect drug treatment outcomes and disease progression in populations by modulation of viral fitness and host-immune responses.

REFERENCES

1 **Beasley RP**, Hwang LY, Lee GC, Lan CC, Roan CH, Huang FY, Chen CL. Prevention of perinatally transmitted hepatitis B virus infections with hepatitis B immune globulin and hepatitis B vaccine. *Lancet* 1983; **2**: 1099-1102 [PMID: 6138642 DOI: 10.1016/S0140-6736(83)90624-4]

2 **GBD 2013 Mortality and Causes of Death Collaborators**. Global, regional, and national age-sex specific all-cause and cause-specific mortality for 240 causes of death, 1990-2013: a systematic analysis for the Global Burden of Disease Study 2013. *Lancet* 2015; **385**: 117-171 [PMID: 25530442 DOI: 10.1016/S0140-6736(14)61682-2]

3 **Nevens F**, Main J, Honkoop P, Tyrrell DL, Barber J, Sullivan MT, Fevery J, De Man RA, Thomas HC. Lamivudine therapy for chronic hepatitis B: a six-month randomized dose-ranging study. *Gastroenterology* 1997; **113**: 1258-1263 [PMID: 9322520 DOI: 10.1053/gast.1997.v113.pm9322520]

4 **Marcellin P**, Chang TT, Lim SG, Tong MJ, Sievert W, Shiffman ML, Jeffers L, Goodman Z, Wulfsohn MS, Xiong S, Fry J, Brosgart CL; Adefovir Dipivoxil 437 Study Group. Adefovir dipivoxil for the treatment of hepatitis B e antigen-positive chronic hepatitis B. *N Engl J Med* 2003; **348**: 808-816 [PMID: 12606735 DOI: 10.1056/NEJMoa020681]

5 **Rivkin A**. Entecavir: a new nucleoside analogue for the treatment of chronic hepatitis B. *Drugs Today (Barc)* 2007; **43**: 201-220 [PMID: 17460784 DOI: 10.1358/dot.2007.43.4.1037479]

6 **Matthews SJ**. Telbivudine for the management of chronic hepatitis B virus infection. *Clin Ther* 2007; **29**: 2635-2653 [PMID: 18201580 DOI: 10.1016/j.clinthera.2007.12.032]

7 **Jenh AM**, Thio CL, Pham PA. Tenofovir for the treatment of hepatitis B virus. *Pharmacotherapy* 2009; **29**: 1212-1227 [PMID: 19792994 DOI: 10.1592/phco.29.10.1212]

8 **Song ZL**, Cui YJ, Zheng WP, Teng DH, Zheng H. Diagnostic and therapeutic progress of multi-drug resistance with anti-HBV nucleos(t)ide analogues. *World J Gastroenterol* 2012; **18**: 7149-7157 [PMID: 23326119 DOI: 10.3748/wjg.v18.i48.7149]

9 **Shi H**, Han Z, Liu J, Xue J, Zhang S, Zhu Z, Xia J, Huang M. Comparing Efficacy of Lamivudine, Adefovir Dipivoxil, Telbivudine, and Entecavir in Treating Nucleoside Analogues Naïve for HBeAg-Negative Hepatitis B with Medium Hepatitis B Virus (HBV) DNA Levels. *Med Sci Monit* 2017; **23**: 5230-5236 [PMID: 29095799 DOI: 10.12659/MSM.903382]

10 **Nowak MA**, Bonhoeffer S, Hill AM, Boehme R, Thomas HC, McDade H. Viral dynamics in hepatitis B virus infection. *Proc Natl Acad Sci U S A* 1996; **93**: 4398-4402 [PMID: 8633078 DOI: 10.1073/pnas.93.9.4398]

11 **Caligiuri P**, Cerruti R, Icardi G, Bruzzone B. Overview of hepatitis B virus mutations and their implications in the management of infection. *World J Gastroenterol* 2016; **22**: 145-154 [PMID: 26755866 DOI: 10.3748/wjg.v22.i1.145]

12 **Selabe SG**, Lukhwareni A, Song E, Leeuw YG, Burnett RJ, Mphahlele MJ. Mutations associated with lamivudine-resistance in therapy-naïve hepatitis B virus (HBV) infected patients with and without HIV co-infection: implications for antiretroviral therapy in HBV and HIV co-infected South African patients. *J Med Virol* 2007; **79**: 1650-1654 [PMID: 17854040 DOI: 10.1002/jmv.20974]

13 **Rodriguez C**, Chevaliez S, Bensadoun P, Pawlotsky JM. Characterization of the dynamics of hepatitis B virus resistance to adefovir by ultra-deep pyrosequencing. *Hepatology* 2013; **58**: 890-901 [PMID: 23505208 DOI: 10.1002/hep.26383]

14 **Tenney DJ**, Rose RE, Baldick CJ, Pokornowski KA, Eggers BJ, Fang J, Wichroski MJ, Xu D, Yang J, Wilber RB, Colonno RJ. Long-term monitoring shows hepatitis B virus resistance to entecavir in nucleoside-naïve patients is rare through 5 years of therapy. *Hepatology* 2009; **49**: 1503-1514 [PMID: 19280622 DOI: 10.1002/hep.22841]

15 **Zhang Y**, Lian JQ, Li Y, Wang JP, Huang CX, Bai XF, Wang JP. Telbivudine plus adefovir therapy for chronic hepatitis B patients with virological breakthrough or genotypic resistance to telbivudine. *Eur J Gastroenterol Hepatol* 2013; **25**: 814-819 [PMID: 23406845 DOI: 10.1097/MEG.0b013e32835ee516]

16 **Strasfeld L**, Chou S. Antiviral drug resistance: mechanisms and clinical implications. *Infect Dis Clin North Am* 2010; **24**: 809-833 [PMID: 20674805 DOI: 10.1016/j.idc.2010.07.001]

17 **Sheldon J**, Rodès B, Zoulim F, Bartholomeusz A, Soriano V. Mutations affecting the replication capacity of the hepatitis B virus. *J Viral Hepat* 2006; **13**: 427-434 [PMID: 16792535 DOI: 10.1111/j.1365-2893.2005.00713.x]

18 **Stuyver LJ**, Locarnini SA, Lok A, Richman DD, Carman WF, Dienstag JL, Schinazi RF. Nomenclature for antiviral-resistant human hepatitis B virus mutations in the polymerase region. *Hepatology* 2001; **33**: 751-757 [PMID: 11230757 DOI: 10.1053/jhep.2001.22166]

19 **Sheldon J**, Soriano V. Hepatitis B virus escape mutants induced by antiviral therapy. *J Antimicrob Chemother* 2008; **61**: 766-768 [PMID: 18218641 DOI: 10.1093/jac/dkn014]

20 **Zheng J**, Zeng Z, Zhang D, Yu Y, Wang F, Pan CQ. Prevalence and significance of Hepatitis B reverse transcriptase mutants in different disease stages of untreated patients. *Liver Int* 2012; **32**: 1535-1542 [PMID: 22882650 DOI: 10.1111/j.1478-3231.2012.02859.x]

21 **Liu BM**, Li T, Xu J, Li XG, Dong JP, Yan P, Yang JX, Yan L, Gao ZY, Li WP, Sun XW, Wang YH, Jiao XJ, Hou CS, Zhuang H. Characterization of potential antiviral resistance mutations in hepatitis B virus reverse transcriptase sequences in treatment-naïve Chinese patients. *Antiviral Res* 2010; **85**: 512-519 [PMID: 20034521 DOI: 10.1016/j.antiviral.2009.12.006]

22 **Solmone M**, Vincenti D, Prosperi MC, Bruselles A, Ippolito G, Capobianchi MR. Use of massively parallel ultradeep pyrosequencing to characterize the genetic diversity of hepatitis B virus in drug-resistant and drug-naive patients and to detect

minor variants in reverse transcriptase and hepatitis B S antigen. *J Virol* 2009; **83**: 1718-1726 [PMID: 19073746 DOI: 10.1128/JVI.02011-08]

23 **Tan YW**, Ge GH, Zhao W, Gan JH, Zhao Y, Niu ZL, Zhang DJ, Chen L, Yu XJ, Yang LJ. YMDD motif mutations in chronic hepatitis B antiviral treatment naïve patients: a multi-center study. *Braz J Infect Dis* 2012; **16**: 250-255 [PMID: 22729192 DOI: 10.1016/S1413-8670(12)70319-7]

24 **Fung SK**, Mazzulli T, El-Kashab M, Sherman M, Popovic V, Sablon E. Lamivudine-Resistant Mutation among Treatment-Naive Hepatitis B Patients Is Common and May Be Associated with Treatment Failure. *Hepatology* 2008; **48**: 703a-703a

25 **Mirandola S**, Campagnolo D, Bortoletto G, Franceschini L, Marcolongo M, Alberti A. Large-scale survey of naturally occurring HBV polymerase mutations associated with anti-HBV drug resistance in untreated patients with chronic hepatitis B. *J Viral Hepat* 2011; **18**: e212-e216 [PMID: 21692935 DOI: 10.1111/j.1365-2893.2011.01435.x]

26 **Vutien P**, Trinh HN, Garcia RT, Nguyen HA, Levitt BS, Nguyen K, da Silveira E, Daugherty T, Ahmed A, Garcia G, Lutchman GA, Nguyen MH. Mutations in HBV DNA polymerase associated with nucleos(t)ide resistance are rare in treatment-naive patients. *Clin Gastroenterol Hepatol* 2014; **12**: 1363-1370 [PMID: 24342744 DOI: 10.1016/j.cgh.2013.11.036]

27 **Zhao Y**, Wu J, Sun L, Liu G, Li B, Zheng Y, Li X, Tao J. Prevalence of mutations in HBV DNA polymerase gene associated with nucleos(t)ide resistance in treatment-naive patients with Chronic Hepatitis B in Central China. *Braz J Infect Dis* 2016; **20**: 173-178 [PMID: 26876337 DOI: 10.1016/j.bjid.2015.12.006]

28 **Akarsu M**, Sengonul A, Tankurt E, Sayiner AA, Topalak O, Akpinar H, Abacioglu YH. YMDD motif variants in inactive hepatitis B carriers detected by Inno-Lipa HBV DR assay. *J Gastroenterol Hepatol* 2006; **21**: 1783-1788 [PMID: 17074014 DOI: 10.1111/j.1440-1746.2006.04567.x]

29 **Ciftci S**, Keskin F, Cakiris A, Akyuz F, Pinarbasi B, Abaci N, Dincer E, Badur S, Kaymakoglu S, Ustek D. Analysis of potential antiviral resistance mutation profiles within the HBV reverse transcriptase in untreated chronic hepatitis B patients using an ultra-deep pyrosequencing method. *Diagn Microbiol Infect Dis* 2014; **79**: 25-30 [PMID: 24630522 DOI: 10.1016/j.diagmicrobio.2014.01.005]

30 **Zhang X**, Li M, Xi H, Zhang R, Chen J, Zhang Y, Xu X. Pre-existing mutations related to tenofovir in chronic hepatitis B patients with long-term nucleos(t)ide analogue drugs treatment by ultra-deep pyrosequencing. *Oncotarget* 2016; **7**: 70264-70275 [PMID: 27602500 DOI: 10.18632/oncotarget.11840]

31 **Wasityastuti W**, Yano Y, Widasari DI, Yamani LN, Ratnasari N, Heriyanto DS, Okada R, Tanahashi T, Murakami Y, Azuma T, Hayashi Y. Different Variants in Reverse Transcriptase Domain Determined by Ultra-deep Sequencing in Treatment-naïve and Treated Indonesian Patients Infected with Hepatitis B Virus. *Kobe J Med Sci* 2016; **62**: E1-E8 [PMID: 27492206]

32 **Zöllner B**, Sterneck M, Wursthorn K, Petersen J, Schröter M, Laufs R, Feucht HH. Prevalence, incidence, and clinical relevance of the reverse transcriptase V207I mutation outside the YMDD motif of the hepatitis B virus polymerase during lamivudine therapy. *J Clin Microbiol* 2005; **43**: 2503-2505 [PMID: 15872296 DOI: 10.1128/JCM.43.5.2503-2505.2005]

33 **Kim JE**, Lee SY, Kim H, Kim KJ, Choe WH, Kim BJ. Naturally occurring mutations in the reverse transcriptase region of hepatitis B virus polymerase from treatment-naïve Korean patients infected with genotype C2. *World J Gastroenterol* 2017; **23**: 4222-4232 [PMID: 28694662 DOI: 10.3748/wjg.v23.i23.4222]

34 **Kobayashi S**, Ide T, Sata M. Detection of YMDD motif mutations in some lamivudine-untreated asymptomatic hepatitis B virus carriers. *J Hepatol* 2001; **34**: 584-586 [PMID: 11394659 DOI: 10.1016/S0168-8278(00)00023-4]

35 **Lee CZ**, Lee HS, Huang GT, Yang PM, Sheu JC. Detection of YMDD mutation using mutant-specific primers in chronic hepatitis B patients before and after lamivudine treatment. *World J Gastroenterol* 2006; **12**: 5301-5305 [PMID: 16981258 DOI: 10.3748/wjg.v12.i33.5301]

36 **Tunçbilek S**, Köse S, Elaldi A, Akman S. Lamivudine resistance in untreated chronic hepatitis B patients in Turkey. *Turk J Gastroenterol* 2008; **19**: 99-103 [PMID: 19110664]

37 **Huang CJ**, Wu CF, Lan CY, Sung FY, Lin CL, Liu CJ, Liu HF, Yu MW. Impact of genetic heterogeneity in polymerase of hepatitis B virus on dynamics of viral load and hepatitis B progression. *PLoS One* 2013; **8**: e70169 [PMID: 23936156 DOI: 10.1371/journal.pone.0070169]

38 **Yamani LN**, Yano Y, Utsumi T, Wasityastuti W, Rinonce HT, Widasari DI, Juniastuti, Lusida MI, Soetjipto, Hayashi Y. Profile of Mutations in the Reverse Transcriptase and Overlapping Surface Genes of Hepatitis B Virus (HBV) in Treatment-Naïve Indonesian HBV Carriers. *Jpn J Infect Dis* 2017; **70**: 647-655 [PMID: 29093313 DOI: 10.7883/yoken.JJID.2017.078]

39 **Wang LP**, Han FZ, Duan HL, Ji F, Yan XB, Fan YC, Wang K. Hepatitis B virus pre-existing drug resistant mutation is related to the genotype and disease progression. *J Infect Dev Countr* 2017; **11**: 727-732 [DOI: 10.3855/jidc.9021]

40 **Ismail AM**, Samuel P, Eapen CE, Kannangai R, Abraham P. Antiviral resistance mutations and genotype-associated amino acid substitutions in treatment-naïve hepatitis B virus-infected individuals from the Indian subcontinent. *Intervirology* 2012; **55**: 36-44 [PMID: 21311172 DOI: 10.1159/000323521]

41 **Pacheco SR**, Dos Santos MIMA, Stocker A, Zarife MAS, Schinoni MI, Paraná R, Dos Reis MG, Silva LK. Genotyping of HBV and tracking of resistance mutations in treatment-naïve patients with chronic hepatitis B. *Infect Drug Resist* 2017; **10**: 201-207 [PMID: 28740410 DOI: 10.2147/IDR.S135420]

42 **Fan J**, Zhang Y, Xiong H, Wang Y, Guo X. Nucleotide analogue-resistant mutations in hepatitis B viral genomes found in hepatitis B patients. *J Gen Virol* 2015; **96**: 663-670 [PMID: 25481755 DOI: 10.1099/jgv.0.000010]

43 **Li X**, Liu Y, Zhao P, Wang Y, Chen L, Xin S, Zhang XX, Xu D. Investigation into drug-resistant mutations of HBV from 845 nucleoside/nucleotide analogue-naive Chinese patients with chronic HBV infection. *Antivir Ther* 2015; **20**: 141-147 [PMID: 24992206 DOI: 10.3851/IMP2813]

44 **Singla B**, Chakraborti A, Sharma BK, Kapil S, Chawla YK, Arora SK, Das A, Dhiman RK, Duseja A. Hepatitis B virus reverse transcriptase mutations in treatment Naïve chronic hepatitis B patients. *J Med Virol* 2013; **85**: 1155-1162 [PMID: 23918533 DOI: 10.1002/jmv.23608]

45 **Nguyen MH**, Garcia RT, Trinh HN, Nguyen HA, Nguyen KK, Nguyen LH, Levitt B. Prevalence of hepatitis B virus DNA polymerase mutations in treatment-naïve patients with chronic hepatitis B. *Aliment Pharmacol Ther* 2009; **30**: 1150-1158 [PMID: 19785624 DOI: 10.1111/j.1365-2036.2009.04151.x]

46 **Xu J**, Wu B, Wang JH, Huang L, Wang DY, Zhao L, Zhao GP, Wang Y. Pre-existing mutations in reverse transcriptase of hepatitis B virus in treatment-naive Chinese patients with chronic hepatitis B. *PLoS One* 2015; **10**: e0117429 [PMID: 25821965 DOI: 10.1371/journal.pone.0117429]

47 **Qian F**, Zou W, Qin J, Li D. Naturally occurring genotypic drug-resistant mutations of HBV in Huzhou, China: a single-center study. *Infect Drug Resist* 2017; **10**: 507-509 [PMID: 29276396 DOI: 10.2147/IDR.S149992]

48 **Matsuda M**, Suzuki F, Suzuki Y, Tsubota A, Akuta N, Hosaka T, Someya T, Kobayashi M, Saitoh S, Arase Y, Satoh J, Takagi K, Kobayashi M, Ikeda K, Kumada H. Low rate of YMDD motif mutations in polymerase gene of hepatitis B virus in chronically infected patients not treated with lamivudine. *J Gastroenterol* 2004; **39**: 34-40 [PMID: 14767732 DOI: 10.1007/s00535-003-1242-4]

49 **Pollicino T**, Isgrò G, Di Stefano R, Ferraro D, Maimone S, Brancatelli S, Squadrito G, Di Marco V, Craxì A, Raimondo G. Variability of reverse transcriptase and overlapping S gene in hepatitis B virus isolates from untreated and lamivudine-resistant chronic hepatitis B patients. *Antivir Ther* 2009; **14**: 649-654 [PMID: 19704167]

50 **Mahabadi M**, Norouzi M, Alavian SM, Samimirad K, Azad TM, Saberfar E, Mahmoodi M, Ramezani F, Karimzadeh H, Malekzadeh R, Montazeri G, Nejatizadeh A, Ziaee M, Abedi F, Ataei B, Yaran M, Sayad B, Hossein Somi M, Sarizadeh G, Sanei-Moghaddam I, Mansour-Ghanaei F, Rafatpanah H, Pourhosseingholi MA, Keyvani H, Kalantari E, Saberifiroozi M, Ali Judaki M, Ghamari S, Daram M, Fazeli Z, Goodarzi Z, Khedive A, Moradi A, Jazayeri SM. Drug-related mutational patterns in hepatitis B virus (HBV) reverse transcriptase proteins from Iranian treatment-naïve chronic HBV patients. *Hepat Mon* 2013; **13**: e6712 [PMID: 23596461 DOI: 10.5812/hepatmon.6712]

51 **Salpini R**, Svicher V, Cento V, Gori C, Bertoli A, Scopelliti F, Micheli V, Cappiello T, Spanò A, Rizzardini G, De Sanctis GM, Sarrecchia C, Angelico M, Perno CF. Characterization of drug-resistance mutations in HBV D-genotype chronically infected patients, naïve to antiviral drugs. *Antiviral Res* 2011; **92**: 382-385 [PMID: 21920388 DOI: 10.1016/j.antiviral.2011.08.013]

52 **Margeridon-Thermet S**, Shulman NS, Ahmed A, Shahriar R, Liu T, Wang C, Holmes SP, Babrzadeh F, Gharizadeh B, Hanczaruk B, Simen BB, Egholm M, Shafer RW. Ultra-deep pyrosequencing of hepatitis B virus quasispecies from nucleoside and nucleotide reverse-transcriptase inhibitor (NRTI)-treated patients and NRTI-naive patients. *J Infect Dis* 2009; **199**: 1275-1285 [PMID: 19301976 DOI: 10.1086/597808]

53 **Han Y**, Huang LH, Liu CM, Yang S, Li J, Lin ZM, Kong XF, Yu DM, Zhang DH, Jin GD, Lu ZM, Gong QM, Zhang XX. Characterization of hepatitis B virus reverse transcriptase sequences in Chinese treatment naive patients. *J Gastroenterol Hepatol* 2009; **24**: 1417-1423 [PMID: 19486254 DOI: 10.1111/j.1440-1746.2009.05864.x]

54 **Panigrahi R**, Biswas A, De BK, Chakrabarti S, Chakravarty R. Characterization of antiviral resistance mutations among the Eastern Indian Hepatitis B virus infected population. *Virol J* 2013; **10**: 56 [PMID: 23409946 DOI: 10.1186/1743-422X-10-56]

55 **Altindis M**, Aslan FG, Koroglu M, Eren A, Demir L, Uslan MI, Aslan S, Ozdemir M, Baykan M. Hepatitis B Virus Carrying Drug-resistance Compensatory Mutations in Chronically Infected Treatment-naive Patients. *Viral Hepat J* 2016; **22**: 103-107 [DOI: 10.4274/vhd.07830]

56 **Amini-Bavil-Olyaee S**, Hosseini SY, Sabahi F, Alavian SM. Hepatitis B virus (HBV) genotype and YMDD motif mutation profile among patients infected with HBV and untreated with lamivudine. *Int J Infect Dis* 2008; **12**: 83-87 [PMID: 17698384 DOI: 10.1016/j.ijid.2007.05.001]

57 **Jardi R**, Rodriguez-Frias F, Schaper M, Ruiz G, Elefsiniotis I, Esteban R, Buti M. Hepatitis B virus polymerase variants associated with entecavir drug resistance in treatment-naive patients. *J Viral Hepat* 2007; **14**: 835-840 [PMID: 18070286 DOI: 10.1111/j.1365-2893.2007.00877.x]

58 **Li XG**, Liu BM, Xu J, Liu XE, Ding H, Li T. Discrepancy of potential antiviral resistance mutation profiles within the HBV reverse transcriptase between nucleos(t)ide analogue-untreated and -treated patients with chronic hepatitis B in a hospital in China. *J Med Virol* 2012; **84**: 207-216 [PMID: 22170539 DOI: 10.1002/jmv.23182]

59 **Lampertico P**, Vigano M, Facchetti F, Puoti M, Minola E, Suter F, Brunetto M, Coco B, Fargion S, Fotta E, Del Poggio P, Pozzi M, Milanese M, Colloredo G, Fagiuoti S, Colombol M, Pasulo L. Effectiveness of entecavir for the treatment of NUC-naive chronic hepatitis B patients: A large multicenter cohort study in clinical practice. *Hepatology* 2008; **48**: 707A-708A

60 **Ramezani A**, Velayati AA, Roshan MR, Gachkar L, Banifazl M, Keyvani H, Aghakhani A. Rate of YMDD motif mutants in lamivudine-untreated Iranian patients with chronic hepatitis B virus infection. *Int J Infect Dis* 2008; **12**: 252-255 [PMID: 17954033 DOI: 10.1016/j.ijid.2007.08.003]

61 **Ghosh S**, Mondal RK, Banerjee P, Nandi M, Sarkar S, Das K, Santra A, Banerjee S, Chowdhury A, Datta S. Tracking the naturally occurring mutations across the full-length genome of hepatitis B virus of genotype D in different phases of chronic e-antigen-negative infection. *Clin Microbiol Infect* 2012; **18**: E412-E418 [PMID: 22827722 DOI: 10.1111/j.1469-0691.2012.03975.x]

62 **Ludwig AD**, Goebel T, Adams O, Baumann N, Hauck K, Fey H, Hengel H, Haussinger D, Erhardt A. Primary Resistance Mutations against Nucleos(t)ide Analogues in Treatment Name Patients with HBV-Infection. *Hepatology* 2008; **48**: 701A-701A

63 **Hamidi-Fard M**, Makvandi M, Samarbaf-Zadeh A, Hajiani E, Shayesteh A, Masjedizadeh A. Mutation analysis of hepatitis B virus reverse transcriptase region among untreated chronically infected patients in Ahvaz city (South-West of Iran). *Indian J Med Microbiol* 2013; **31**: 360-365 [PMID: 24064642 DOI: 10.4103/0255-0857.118882]

64 **Villa E**, Lei B, Taliani G, Graziosi A, Critelli R, Luongo M, Gennari W, Bianchini M, Ferretti I. Pretreatment with pegylated interferon prevents emergence of lamivudine mutants in lamivudine-naive patients: a pilot study. *Antivir Ther* 2009; **14**: 1081-1087 [PMID: 20032538 DOI: 10.3851/IMP1465]

65 **Mantovani N**, Cicero M, Santana LC, Silveira C, do Carmo EP, Abrão PR, Diaz RS, Caseiro MM, Komninakis SV. Detection of lamivudine-resistant variants and mutations related to reduced antigenicity of HBsAg in individuals from the cities of Santos and São Paulo, Brazil. *Virol J* 2013; **10**: 320 [PMID: 24165277 DOI: 10.1186/1743-422X-10-320]

66 **Aberle SW**, Kletzmayr J, Watschinger B, Schmied B, Vetter N, Puchhammer-Stöckl E. Comparison of sequence analysis and the INNO-LiPA HBV DR line probe assay for detection of lamivudine-resistant hepatitis B virus strains in patients under various clinical conditions. *J Clin Microbiol* 2001; **39**: 1972-1974 [PMID: 11326026 DOI: 10.1128/JCM.39.5.1972-1974.2001]

67 **Feeney F**, Fanning LJ, Horgan M. Baseline genotypic resistance in untreated hepatitis B virus infection. *Gastroenterology* 2007; **132**: 35A

68 **Masaadeh HA**, Hayajneh WA, Alqudah EA. Hepatitis B virus genotypes and lamivudine resistance mutations in Jordan. *World J Gastroenterol* 2008; **14**: 7231-7234 [PMID: 19084939 DOI: 10.3748/wjg.14.7231]

69 **Lok AS**, Zoulim F, Locarnini S, Bartholomeusz A, Ghany MG, Pawlotsky JM, Liaw YF, Mizokami M, Kuiken C; Hepatitis B Virus Drug Resistance Working Group. Antiviral drug-resistant HBV: standardization of nomenclature and assays and recommendations for management. *Hepatology* 2007; **46**: 254-265 [PMID: 17596850 DOI: 10.1002/hep.21698]

70 **Shaw T**, Bartholomeusz A, Locarnini S. HBV drug resistance: mechanisms, detection and interpretation. *J Hepatol* 2006; **44**: 593-606 [PMID: 16455151 DOI: 10.1016/j.jhep.2006.01.001]

71 **Langley DR**, Walsh AW, Baldick CJ, Eggers BJ, Rose RE, Levine SM, Kapur AJ, Colonno RJ, Tenney DJ. Inhibition of hepatitis B virus polymerase by entecavir. *J Virol* 2007; **81**: 3992-4001 [PMID: 17267485 DOI: 10.1128/JVI.02395-06]

72 **Locarnini S**. Primary resistance, multidrug resistance, and cross-resistance pathways in HBV as a consequence of treatment failure. *Hepatol Int* 2008; **2**: 147-151 [PMID: 19669299 DOI: 10.1007/s12072-008-9048-3]

73 **Zhang Q**, Liao Y, Cai B, Li Y, Li L, Zhang J, An Y, Wang L. Incidence of natural resistance mutations in naïve chronic hepatitis B patients: a systematic review and meta-analysis. *J Gastroenterol Hepatol* 2015; **30**: 252-261 [PMID: 25318660 DOI: 10.1111/jgh.12831]

74 **Lai CL**, Leung N, Teo EK, Tong M, Wong F, Hann HW, Han S, Poynard T, Myers M, Chao G, Lloyd D, Brown NA; Telbivudine Phase II Investigator Group. A 1-year trial of telbivudine, lamivudine, and the combination in patients with hepatitis B e antigen-positive chronic hepatitis B. *Gastroenterology* 2005; **129**: 528-536 [PMID: 16083710 DOI: 10.1016/j.gastro.2005.05.053]

75 **Fu L**, Cheng YC. Role of additional mutations outside the YMDD motif of hepatitis B virus polymerase in L(-)SddC (3TC) resistance. *Biochem Pharmacol* 1998; **55**: 1567-1572 [PMID: 9633992 DOI: 10.1016/S0006-2952(98)00050-1]

76 **Wakil SM**, Kazim SN, Khan LA, Raisuddin S, Parvez MK, Guptan RC, Thakur V, Hasnain SE, Sarin SK. Prevalence and

profile of mutations associated with lamivudine therapy in Indian patients with chronic hepatitis B in the surface and polymerase genes of hepatitis B virus. *J Med Virol* 2002; **68**: 311-318 [PMID: 12226816 DOI: 10.1002/jmv.10205]

77 **Yang H**, Westland CE, Delaney WE 4th, Heathcote EJ, Ho V, Fry J, Brosgart C, Gibbs CS, Miller MD, Xiong S. Resistance surveillance in chronic hepatitis B patients treated with adefovir dipivoxil for up to 60 weeks. *Hepatology* 2002; **36**: 464-473 [PMID: 12143057 DOI: 10.1053/jhep.2002.34740]

78 **Ahn SH**, Park YK, Park ES, Kim JH, Kim DH, Lim KH, Jang MS, Choe WH, Ko SY, Sung IK, Kwon SY, Kim KH. The impact of the hepatitis B virus polymerase rtA181T mutation on replication and drug resistance is potentially affected by overlapping changes in surface gene. *J Virol* 2014; **88**: 6805-6818 [PMID: 24696492 DOI: 10.1128/JVI.00635-14]

79 **Schildgen O**, Sirma H, Funk A, Olotu C, Wend UC, Hartmann H, Helm M, Rockstroh JK, Willems WR, Will H, Gerlich WH. Variant of hepatitis B virus with primary resistance to adefovir. *N Engl J Med* 2006; **354**: 1807-1812 [PMID: 16641397 DOI: 10.1056/NEJMoa051214]

80 **Kramvis A**, Kew M, François G. Hepatitis B virus genotypes. *Vaccine* 2005; **23**: 2409-2423 [PMID: 15752827 DOI: 10.1016/j.vaccine.2004.10.045]

81 **Schaefer S**. Hepatitis B virus taxonomy and hepatitis B virus genotypes. *World J Gastroenterol* 2007; **13**: 14-21 [PMID: 17206751 DOI: 10.3748/wjg.v13.i1.14]

82 **Sunbul M**. Hepatitis B virus genotypes: global distribution and clinical importance. *World J Gastroenterol* 2014; **20**: 5427-5434 [PMID: 24833873 DOI: 10.3748/wjg.v20.i18.5427]

83 **Mirandola S**, Sebastiani G, Rossi C, Velo E, Erne EM, Vario A, Tempesta D, Romualdi C, Campagnolo D, Alberti A. Genotype-specific mutations in the polymerase gene of hepatitis B virus potentially associated with resistance to oral antiviral therapy. *Antiviral Res* 2012; **96**: 422-429 [PMID: 23026293 DOI: 10.1016/j.antiviral.2012.09.014]

84 **Damerow H**, Yuen L, Wiegand J, Walker C, Bock CT, Locarnini S, Tillmann HL. Mutation pattern of lamivudine resistance in relation to hepatitis B genotypes: hepatitis B genotypes differ in their lamivudine resistance associated mutation pattern. *J Med Virol* 2010; **82**: 1850-1858 [PMID: 20872711 DOI: 10.1002/jmv.21902]

85 **Colonno RJ**, Rose R, Baldick CJ, Levine S, Pokornowski K, Yu CF, Walsh A, Fang J, Hsu M, Mazzucco C, Eggers B, Zhang S, Plym M, Klesczewski K, Tenney DJ. Entecavir resistance is rare in nucleoside naïve patients with hepatitis B. *Hepatology* 2006; **44**: 1656-1665 [PMID: 17133475 DOI: 10.1002/hep.21422]

86 **Ciancio A**, Smedile A, Rizzetto M, Lagget M, Gerin J, Korba B. Identification of HBV DNA sequences that are predictive of response to lamivudine therapy. *Hepatology* 2004; **39**: 64-73 [PMID: 14752824 DOI: 10.1002/hep.20019]

87 **Chu CJ**, Keeffe EB, Han SH, Perrillo RP, Min AD, Soldevila-Pico C, Carey W, Brown RS Jr, Luketic VA, Terrault N, Lok AS; U.S. HBV Epidemiology Study Group. Prevalence of HBV precore/core promoter variants in the United States. *Hepatology* 2003; **38**: 619-628 [PMID: 12939588 DOI: 10.1053/jhep.2003.50352]

88 **Kirishima T**, Okanoue T, Daimon Y, Itoh Y, Nakamura H, Morita A, Toyama T, Minami M. Detection of YMDD mutant using a novel sensitive method in chronic liver disease type B patients before and during lamivudine treatment. *J Hepatol* 2002; **37**: 259-265 [PMID: 12127432 DOI: 10.1016/S0168-8278(02)00145-9]

89 **Zhu B**, Wang T, Wei X, Zhuo Y, Liu A, Zhang G. Accumulation of mutations in reverse transcriptase of hepatitis B virus is associated with liver disease severity in treatment-naïve Chinese patients with chronic hepatitis B. *Adv Clin Exp Med* 2017; **26**: 1123-1129 [PMID: 29211361 DOI: 10.17219/acem/63998]

90 **Fukai K**, Zhang KY, Imazeki F, Kurihara T, Mikata R, Yokosuka O. Association between lamivudine sensitivity and the number of substitutions in the reverse transcriptase region of the hepatitis B virus polymerase. *J Viral Hepat* 2007; **14**: 661-666 [PMID: 17697019 DOI: 10.1111/j.1365-2893.2007.00852.x]

91 **Wang YX**, Xu X, Luo C, Ma ZM, Jiang HL, Ding JP, Wen YM. A putative new domain target for anti-hepatitis B virus: residues flanking hepatitis B virus reverse transcriptase residue 306 (rtP306). *J Med Virol* 2007; **79**: 676-682 [PMID: 17457904 DOI: 10.1002/jmv.20835]

92 **Pollicino T**, Cacciola I, Saffioti F, Raimondo G. Hepatitis B virus PreS/S gene variants: pathobiology and clinical implications. *J Hepatol* 2014; **61**: 408-417 [PMID: 24801416 DOI: 10.1016/j.jhep.2014.04.041]

93 **Huang ZM**, Huang QW, Qin YQ, He YZ, Qin HJ, Zhou YN, Xu X, Huang MJ. YMDD mutations in patients with chronic hepatitis B untreated with antiviral medicines. *World J Gastroenterol* 2005; **11**: 867-870 [PMID: 15682483 DOI: 10.3748/wjg.v11.i6.867]

94 **Nishijima N**, Marusawa H, Ueda Y, Takahashi K, Nasu A, Osaki Y, Kou T, Yazumi S, Fujiwara T, Tsuchiya S, Shimizu K, Uemoto S, Chiba T. Dynamics of hepatitis B virus quasispecies in association with nucleos(t)ide analogue treatment determined by ultra-deep sequencing. *PLoS One* 2012; **7**: e35052 [PMID: 22523569 DOI: 10.1371/journal.pone.0035052]

95 **Sugauchi F**, Orito E, Ichida T, Kato H, Sakugawa H, Kakumu S, Ishida T, Chutaputti A, Lai CL, Ueda R, Miyakawa Y, Mizokami M. Hepatitis B virus of genotype B with or without recombination with genotype C over the precore region plus the core gene. *J Virol* 2002; **76**: 5985-5992 [PMID: 12021331 DOI: 10.1128/JVI.76.12.5985-5992.2002]

96 **Yang J**, Xing K, Deng R, Wang J, Wang X. Identification of Hepatitis B virus putative intergenotype recombinants by using fragment typing. *J Gen Virol* 2006; **87**: 2203-2215 [PMID: 16847116 DOI: 10.1099/vir.0.81752-0]

97 **Rehermann B**, Nascimbeni M. Immunology of hepatitis B virus and hepatitis C virus infection. *Nat Rev Immunol* 2005; **5**: 215-229 [PMID: 15738952 DOI: 10.1038/nri1573]

98 **Shi W**, Carr MJ, Dunford L, Zhu C, Hall WW, Higgins DG. Identification of novel inter-genotypic recombinants of human hepatitis B viruses by large-scale phylogenetic analysis. *Virology* 2012; **427**: 51-59 [PMID: 22374235 DOI: 10.1016/j.virol.2012.01.030]

99 **Shi W**, Zhu C, Zheng W, Carr MJ, Higgins DG, Zhang Z. Subgenotype reclassification of genotype B hepatitis B virus. *BMC Gastroenterol* 2012; **12**: 116 [PMID: 22925657 DOI: 10.1186/1471-230X-12-116]

100 **Liu B**, Yang JX, Yan L, Zhuang H, Li T. Novel HBV recombinants between genotypes B and C in 3'-terminal reverse transcriptase (RT) sequences are associated with enhanced viral DNA load, higher RT point mutation rates and place of birth among Chinese patients. *Infect Genet Evol* 2018; **57**: 26-35 [PMID: 29111272 DOI: 10.1016/j.meegid.2017.10.023]

101 **Lee SY**, Lee SH, Kim JE, Kim H, Kim K, Kook YH, Kim BJ. Identification of Novel A2/C2 Inter-Genotype Recombinants of Hepatitis B Virus from a Korean Chronic Patient Co-Infected with Both Genotype A2 and C2. *Int J Mol Sci* 2017; **18**: pii: E737 [PMID: 28358313 DOI: 10.3390/ijms18040737]

102 **Pan D**, Zhou B, Yang J, Hou J. [Identification of hepatitis B virus intergenotype recombination in Chinese patients]. *Nan Fang Yi Ke Da Xue Xue Bao* 2014; **34**: 1436-1442 [PMID: 25345938]

103 **Simmonds P**, Midgley S. Recombination in the genesis and evolution of hepatitis B virus genotypes. *J Virol* 2005; **79**: 15467-15476 [PMID: 16306618 DOI: 10.1128/JVI.79.24.15467-15476.2005]

104 **Burnett RJ**, François G, Kew MC, Leroux-Roels G, Meheus A, Hoosen AA, Mphahlele MJ. Hepatitis B virus and human immunodeficiency virus co-infection in sub-Saharan Africa: a call for further investigation. *Liver Int* 2005; **25**: 201-213 [PMID: 15780040 DOI: 10.1111/j.1478-3231.2005.01054.x]

105 **Thio CL**, Seaberg EC, Skolasky R Jr, Phair J, Visscher B, Muñoz A, Thomas DL; Multicenter AIDS Cohort Study. HIV-1, hepatitis B virus, and risk of liver-related mortality in the Multicenter Cohort Study (MACS). *Lancet* 2002; **360**: 1921-1926 [PMID: 12493258 DOI: 10.1016/S0140-6736(02)11913-1]

106 **Audsley J**, Arrifin N, Yuen LK, Ayres A, Crowe SM, Bartholomeusz A, Locarnini SA, Mijch A, Lewin SR, Sasadeusz J. Prolonged use

of tenofovir in HIV/hepatitis B virus (HBV)-coinfected individuals does not lead to HBV polymerase mutations and is associated with persistence of lamivudine HBV polymerase mutations. *HIV Med* 2009; **10**: 229-235 [PMID: 19178592 DOI: 10.1111/j.1468-1293.2008.00675.x]

107 **Quarleri J**, Moretti F, Bouzas MB, Laufer N, Carrillo MG, Giuliano SF, Pérez H, Cahn P, Salomon H. Hepatitis B virus genotype distribution and its lamivudine-resistant mutants in HIV-coinfected patients with chronic and occult hepatitis B. *AIDS Res Hum Retroviruses* 2007; **23**: 525-531 [PMID: 17506609 DOI: 10.1089/aid.2006.0172]

108 **Makondo E**, Bell TG, Kramvis A. Genotyping and molecular characterization of hepatitis B virus from human immunodeficiency virus-infected individuals in southern Africa. *PLoS One* 2012; **7**: e46345 [PMID: 23029487 DOI: 10.1371/journal.pone.0046345]

109 **Selabe SG**, Song E, Burnett RJ, Mphahlele MJ. Frequent detection of hepatitis B virus variants associated with lamivudine resistance in treated South African patients infected chronically with different HBV genotypes. *J Med Virol* 2009; **81**: 996-1001 [PMID: 19382250 DOI: 10.1002/jmv.21479]

110 **Thio CL**, Smeaton L, Saulynas M, Hwang H, Saravanan S, Kulkarni S, Hakim J, Nyirenda M, Iqbal HS, Lalloo UG, Mehta AS, Hollabaugh K, Campbell TB, Lockman S, Currier JS. Characterization of HIV-HBV coinfection in a multinational HIV-infected cohort. *AIDS* 2013; **27**: 191-201 [PMID: 23032418 DOI: 10.1097/QAD.0b013e32835a9984]

111 **Archampong TN**, Boyce CL, Lartey M, Sagoe KW, Obo-Akwa A, Kenu E, Blackard JT, Kwara A. HBV genotypes and drug resistance mutations in antiretroviral treatment-naive and treatment-experienced HBV-HIV-coinfected patients. *Antivir Ther* 2017; **22**: 13-20 [PMID: 27167598 DOI: 10.3851/IMP3055]

112 **Warner N**, Locarnini S, Kuiper M, Bartholomeusz A, Ayres A, Yuen L, Shaw T. The L80I substitution in the reverse transcriptase domain of the hepatitis B virus polymerase is associated with lamivudine resistance and enhanced viral replication in vitro. *Antimicrob Agents Chemother* 2007; **51**: 2285-2292 [PMID: 17438047 DOI: 10.1128/AAC.01499-06]

113 **Shi YH**, Shi CH. Molecular characteristics and stages of chronic hepatitis B virus infection. *World J Gastroenterol* 2009; **15**: 3099-3105 [PMID: 19575488 DOI: 10.3748/wjg.15.3099]

114 **Yin F**, Xie Y, Fan H, Zhang J, Guo Z. Mutations in hepatitis B virus polymerase are associated with the postoperative survival of hepatocellular carcinoma patients. *PLoS One* 2017; **12**: e0189730 [PMID: 29287068 DOI: 10.1371/journal.pone.0189730]

115 **Li H**, Jia J, Wang M, Wang H, Gu X, Fang M, Gao C. F221Y mutation in hepatitis B virus reverse transcriptase is associated with hepatocellular carcinoma prognosis following liver resection. *Mol Med Rep* 2017; **15**: 3292-3300 [PMID: 28339094 DOI: 10.3892/mmr.2017.6362]

116 **Wu Y**, Gan Y, Gao F, Zhao Z, Jin Y, Zhu Y, Sun Z, Wu H, Chen T, Wang J, Sun Y, Fan C, Xiang Y, Qian G, Groopman JD, Gu J, Tu H. Novel natural mutations in the hepatitis B virus reverse transcriptase domain associated with hepatocellular carcinoma. *PLoS One* 2014; **9**: e94864 [PMID: 24788140 DOI: 10.1371/journal.pone.0094864]

117 **Kao JH**, Chen PJ, Lai MY, Chen DS. Hepatitis B genotypes correlate with clinical outcomes in patients with chronic hepatitis B. *Gastroenterology* 2000; **118**: 554-559 [PMID: 10702206 DOI: 10.1016/S0016-5085(00)70261-7]

118 **Lee CM**, Chen CH, Lu SN, Tung HD, Wang JH, Chen TM, Huang CC. Hepatitis B virus genotypes and the progression of chronic liver disease. *J Hepatol* 2002; **36**: 238 [DOI: 10.1016/S0168-8278(02)80854-6]

119 **Fujie H**, Moriya K, Shintani Y, Yotsuyanagi H, Iino S, Koike K. Hepatitis B virus genotypes and hepatocellular carcinoma in Japan. *Gastroenterology* 2001; **120**: 1564-1565 [PMID: 11339239 DOI: 10.1053/gast.2001.24501]

120 **Tsubota A**, Arase Y, Ren F, Tanaka H, Ikeda K, Kumada H. Genotype may correlate with liver carcinogenesis and tumor characteristics in cirrhotic patients infected with hepatitis B virus subtype adw. *J Med Virol* 2001; **65**: 257-265 [PMID: 11536231 DOI: 10.1002/jmv.2028]

121 **Zhong YW**, Li J, Song HB, Duan ZP, Dong Y, Xing XY, Li XD, Gu ML, Han YK, Zhu SS, Zhang HF. Virologic and clinical characteristics of HBV genotypes/subgenotypes in 487 Chinese pediatric patients with CHB. *BMC Infect Dis* 2011; **11**: 262 [PMID: 21961963 DOI: 10.1186/1471-2334-11-262]

122 **Chan HL**, Hui AY, Wong ML, Tse AM, Hung LC, Wong VW, Sung JJ. Genotype C hepatitis B virus infection is associated with an increased risk of hepatocellular carcinoma. *Gut* 2004; **53**: 1494-1498 [PMID: 15361502 DOI: 10.1136/gut.2003.033324]

123 **Kwon H**, Lok AS. Hepatitis B therapy. *Nat Rev Gastroenterol Hepatol* 2011; **8**: 275-284 [PMID: 21423260 DOI: 10.1038/nrgastro.2011.33]

124 **Datta S**, Chatterjee S, Veer V, Chakravarty R. Molecular biology of the hepatitis B virus for clinicians. *J Clin Exp Hepatol* 2012; **2**: 353-365 [PMID: 25755457 DOI: 10.1016/j.jceh.2012.10.003]

125 **Avellón A**, Echevarria JM. Frequency of hepatitis B virus 'a' determinant variants in unselected Spanish chronic carriers. *J Med Virol* 2006; **78**: 24-36 [PMID: 16299725 DOI: 10.1002/jmv.20516]

126 **Svicher V**, Gori C, Trignetti M, Visca M, Micheli V, Bernassola M, Salpini R, Gubertini G, Longo R, Niero F, Ceccherini-Silberstein F, De Sanctis GM, Spanò A, Cappiello G, Perno CF. The profile of mutational clusters associated with lamivudine resistance can be constrained by HBV genotypes. *J Hepatol* 2009; **50**: 461-470 [PMID: 19041149 DOI: 10.1016/j.jhep.2008.07.038]

127 **Rhee SY**, Margeridon-Thermet S, Nguyen MH, Liu TF, Kagan RM, Beggel B, Verheyen J, Kaiser R, Shafer RW. Hepatitis B virus reverse transcriptase sequence variant database for sequence analysis and mutation discovery. *Antiviral Res* 2010; **88**: 269-275 [PMID: 20875460 DOI: 10.1016/j.antiviral.2010.09.012]

128 **Ji D**, Liu Y, Li L, Xu Z, Si LL, Dai JZ, Li X, Wang L, Yao Z, Xin SJ, Chen GF, Xu D. The rtL229 substitutions in the reverse transcriptase region of hepatitis B virus (HBV) polymerase are potentially associated with lamivudine resistance as a compensatory mutation. *J Clin Virol* 2012; **54**: 66-72 [PMID: 22398037 DOI: 10.1016/j.jcv.2012.02.003]

P- Reviewer: Quarleri J, Tamori A **S- Editor**: Gong ZM
L- Editor: A **E- Editor**: Huang Y

World Journal of Gastroenterology

Submit a Manuscript: http://www.f6publishing.com

World J Gastroenterol 2018 April 28; 24(16): 1725-1733

DOI: 10.3748/wjg.v24.i16.1725

ISSN 1007-9327 (print) ISSN 2219-2840 (online)

MINIREVIEWS

Nucleotide-binding oligomerization domain 1 and *Helicobacter pylori* infection: A review

Kosuke Minaga, Tomohiro Watanabe, Ken Kamata, Naoki Asano, Masatoshi Kudo

Kosuke Minaga, Tomohiro Watanabe, Ken Kamata, Masatoshi Kudo, Department of Gastroenterology and Hepatology, Kindai University Faculty of Medicine, Osaka 589-8511, Japan

Naoki Asano, Division of Gastroenterology, Tohoku University Graduate School of Medicine, Miyagi 980-8574, Japan

ORCID number: Kosuke Minaga (0000-0001-5407-7925); Tomohiro Watanabe (0000-0001-7781-6305); Ken Kamata (0000-0003-1568-0769); Naoki Asano (0000-0003-4452-8459); Masatoshi Kudo (0000-0002-4102-3474).

Author contributions: Minaga K and Watanabe T wrote the manuscript draft and prepared the figures; Kamata K, Asano N and Kudo M assisted in writing the manuscript and reviewed the final version.

Conflict-of-interest statement: None of the authors has any conflict of interests related to this manuscript.

Manuscript source: Invited manuscript

Correspondence to: Tomohiro Watanabe, MD, PhD, Associate Professor, Department of Gastroenterology and Hepatology, Kindai University Faculty of Medicine, 377-2 Ohno-Higashi, Osaka-Sayama, Osaka 589-8511, Japan. tomohiro@med.kindai.ac.jp
Telephone: +81-72-366-0221
Fax: +81-72-367-2880

Received: March 6, 2018
Peer-review started: March 6, 2018
First decision: March 29, 2018
Revised: April 3, 2018
Accepted: April 9, 2018
Article in press: April 9, 2018

Published online: April 28, 2018

Abstract

Nucleotide-binding oligomerization domain 1 (NOD1) is an intracellular innate immune sensor for small molecules derived from bacterial cell components. NOD1 activation by its ligands leads to robust production of pro-inflammatory cytokines and chemokines by innate immune cells, thereby mediating mucosal host defense systems against microbes. Chronic gastric infection due to *Helicobacter pylori* (*H. pylori*) causes various upper gastrointestinal diseases, including atrophic gastritis, peptic ulcers, and gastric cancer. It is now generally accepted that detection of *H. pylori* by NOD1 expressed in gastric epithelial cells plays an indispensable role in mucosal host defense systems against this organism. Recent studies have revealed the molecular mechanism by which NOD1 activation caused by *H. pylori* infection is involved in the development of chronic gastritis and gastric cancer. In this review, we have discussed and summarized how sensing of *H. pylori* by NOD1 mediates the prevention of chronic gastritis and gastric cancer.

Key words: Nucleotide-binding oligomerization domain 1; *Helicobacter pylori*, Gastritis; Gastric cancer

Core tip: Nucleotide-binding oligomerization domain 1 (NOD1), an intracellular innate immune sensor, plays a role in mucosal host defense systems against *Helicobacter pylori* (*H. pylori*) infection. NOD1 activation is involved in the generation of T helper type 1 responses against *H. pylori* through activation of type I IFN signaling pathways. NOD1 activation prevents gastric carcinogenesis through negative regulation of caudal-related homeobox 2 expression.

Minaga K, Watanabe T, Kamata K, Asano N, Kudo M. Nucleotide-binding oligomerization domain 1 and *Helicobacter pylori* infection: A review. *World J Gastroenterol* 2018; 24(16): 1725-1733 Available from: URL: http://www.wjgnet.com/1007-9327/full/v24/i16/1725.htm DOI: http://dx.doi.org/10.3748/wjg.v24.i16.1725

INTRODUCTION

Helicobacter pylori (*H. pylori*) is a Gram negative bacterium that preferentially colonizes the human gastric mucosa[1,2]. Infection due to this organism is usually established during childhood[1,2], which then causes various upper gastrointestinal (GI) disorders, including atrophic gastritis, peptic ulcers, gastric mucosa-associated lymphoid tissue lymphoma, and gastric cancer. Thus, it is now generally accepted that persistent *H. pylori* infection in the gastric mucosa is the highest risk factor for the development of the aforementioned diseases[3]. This notion is supported by recent studies indicating that successful eradication of *H. pylori* prevents the development of gastric cancer[4,5].

Colonization of the human stomach by *H. pylori* triggers innate and adaptive immune responses. As in the cases of other microbial infections, sensing of *H. pylori* by pattern recognition receptors (PRRs) expressed in innate immune cells, such as epithelial cells (ECs) and antigen-presenting cells (APCs), is an initial step for eradicating this organism. Toll-like receptors (TLRs) and nucleotide-binding oligomerization domain (NOD)-like receptors (NLRs) are the prototypical PRRs and represent the first line of defense against *H. pylori*[6,7]. Indeed, gastric epithelial cells and APCs express functional TLRs and lipopolysaccharide (LPS)-mediated TLR4 activation is involved in the development of gastric mucosal inflammatory responses[8]. However, the ability to stimulate TLRs by *H. pylori*-derived antigens is much lower than that by other pathogenic bacteria. For example, *H. pylori*-derived LPS and flagellin exhibit low stimulatory activity toward TLR4 and TLR5[9,10]. Thus, *H. pylori* might evade the major innate immune system molecules, TLRs, to establish persistent gastric infection. Therefore, it is possible that PRRs other than TLRs might play a major role in mucosal host defense systems against *H. pylori* although roles played by TLRs need to be determined in future studies.

NOD1 is a prototypical innate immune receptor belonging to the NLR protein family, which detects small molecules derived from Gram-negative bacteria[7,11]. NOD1 activation induced by intestinal microflora is associated with lymphoid tissue genesis[12] and development of pancreatitis[13-15]. In 2004, Viala *et al*[16]. demonstrated that gastric mucosal host defense against *H. pylori* depends on the activation of NOD1 in gastric ECs. Many efforts have been made by gastroenterologists, microbiologists, and immunologists to elucidate the molecular mechanisms by which colonization of the human stomach by *H. pylori* induces the activation of NOD1 and such NOD1 activation mediates antimicrobial immune responses[11]. In this review, we have summarized and discussed how sensing of *H. pylori* by NOD1 mediates the prevention of chronic gastritis and gastric cancer.

CYTOKINE AND CHEMOKINE RESPONSES IN THE GASTRIC MUCOSA HARBORING *H. PYLORI* INFECTION

Gastric inflammation caused by chronic *H. pylori* infection is mediated by gastric mucosal T helper type 1 (Th1) and Th17 cells producing IFN-γ and IL-17, respectively[17]. Initial studies addressing the role of IFN-γ in *H. pylori*-induced gastritis revealed that lack of chronic gastritis in IFN-γ-deficient mice is associated with higher colonization of the gastric mucosa by this organism than in IFN-γ-intact mice[18]. In addition, gastric mucosal $CD4^+$ T cells isolated from *H. pylori*-infected patients have been reported to produce a high level of IFN-γ[19]. Thus, gastric mucosa harboring chronic *H. pylori* infection is characterized by Th1 responses that are involved in both eradication and inflammation[20]. In addition to a well-established role played by Th1 cells, recent studies have highlighted the importance of another type of Th cells, Th17 cells, producing IL-17[20]. The development of chronic gastritis is significantly attenuated in IL-17-deficient mice in long-term *H. pylori* infection[20]. Moreover, treatment of mice with a neutralizing anti-IL-17 antibody reduced the *H. pylori* burden and inflammation in the stomach[21]. In line with these experimental studies, Serrano *et al*[22]. provided evidence that downregulation of Th17 responses is associated with reduced gastritis in *H. pylori*-infected patients. Therefore, both Th1 and Th17 cells are involved in the development of chronic gastritis caused by persistent *H. pylori* infection in the gastric mucosa.

Differentiation of Th1 and Th17 cells requires cytokines produced by APCs such as dendritic cells and macrophages[23]. Differentiation of Th1 cells depends on IL-12, whereas that of Th17 cells depends on IL-1β, IL-6, and IL-23. Expression of IFN-γ and IL-17 in the gastric mucosa of mice challenged with *H. pylori* was accompanied by IL-12 and IL-23 expression, derived from APCs[21]. Furthermore, the levels of APC-derived pro-inflammatory cytokines in the gastric mucosa, including IL-1β, IL-6 and TNF-α were significantly higher in *H. pylori*-positive patients than in *H. pylori*-negative patients[24]. Thus, it is likely that pro-inflammatory cytokines produced by APCs contribute to *H. pylori*-induced gastric pathology through differentiation of Th1 and Th17 cells. Consistent with this idea, the exposure of human APCs to *H. pylori* results in robust production of IL-6, IL-12, and TNF-α[25,26].

ECs are an important source of chemokines that attract immune cells to the lesions[27,28]. Yamaoka *et al*[28]. assessed chemokine responses in the gastric mucosa

of patients with *H. pylori* infection and found that *H. pylori* infection is associated with increased expression of C-X-C motif chemokine ligand 8 (CXCL8) and chemokine (C-C motif) ligand 5 (CCL5). In addition to CXCL8 and CCL5, the gastric mucosa of *H. pylori*-positive patients exhibited enhanced expression of CXCL9 and CXCL10[29]. Given the fact that CXCL8 is a strong attractant for neutrophils and that CXCL9 and CXCL10 are strong attractants for Th1 cells[28,29], these results suggest that EC-derived chemokines are also involved in the development of chronic gastritis caused by persistent *H. pylori* infection. Taken together, these findings suggest that cytokines and chemokines produced by immune cells and ECs play a substantial role in the development of *H. pylori*-induced gastric pathology.

TYPE IV SECRETION SYSTEM OF *H. PYLORI* AND NOD1 ACTIVATION

NOD1 is expressed in the cytosolic regions of innate immune cells, such as APCs and ECs[7,11]. Peptidoglycan (PGN) is a polymer consisting of sugars and amino acids that constitute the cell wall of both Gram-positive and Gram-negative bacteria[7]. Small peptides derived from the PGN layer of Gram-negative bacteria activate intracellular NOD1[7,11]. γ-D-glutamyl-meso-diaminopimelic acid (iE-DAP) is considered as the minimal motif of the NOD1 ligand, and NOD1-deficient mice exhibit impaired responses to iE-DAP[30]. Two models have been proposed by which *H. pylori* activates intracellular NOD1.

H. pylori is classified into two types according to the expression of cag pathogenicity island (*cag*PAI)[1]. *cag*PAI is a gene locus necessary to assemble type IV secretion system (T4SS), a syringe and needle-like structure[1,31]. The primary function of T4SS, encoded by *cag*PAI, is the injection of pathogenic factors, such as cytotoxin-associated gene A (CagA) into the host gastric ECs upon attachment to the epithelium[1,31]. Thus, *cag*PAI-positive *H. pylori* can cause gastric mucosal injury through injection of CagA mediated by T4SS. Hence, T4SS may enable *H. pylori* to deliver its cell wall components, such as PGN, into the host ECs. Viala *et al*[16]. addressed this possibility and demonstrated that intracellular NOD1 expressed in gastric ECs sense *H. pylori*-derived PGN delivered to the cytosolic region through T4SS. NOD1 activation is not observed in gastric ECs upon exposure to *H. pylori* harboring non-functional *cag*PAI, which supports the idea that NOD1 functions as an intracellular innate immune sensor for *cag*PAI-positive *H. pylori*. Interestingly, *H. pylori* burden in the stomach was much higher in NOD1-deficient mice than in the NOD1-intact ones, when they were orally challenged with *cag*PAI-positive *H. pylori*[16]. In contrast, *H. pylori* burden in the stomach was comparable between NOD1-intact and NOD1-deficient mice when mice were orally challenged with *cag*PAI-mutated *H. pylori.* Thus, these studies showed that NOD1 is an intracellular receptor for *cag*PAI-positive *H. pylori* and that NOD1 activation is necessary for eradication of this organism.

OUTER MEMBRANE VESICLE OF *H. PYLORI* AND NOD1 ACTIVATION

Outer membrane vesicles (OMVs), which are released by Gram-negative bacteria during normal growth, contain bacterial cell components, including PGN[32]. Kaparakis *et al*[33]. addressed the possibility that OMVs released from *H. pylori* activate cytosolic NOD1 through intracellular delivery of PGN. OMVs isolated from *H. pylori* activate nuclear factor kappa B (NF-κB) in AGS cells, a gastric cancer cell line, in a *cag*PAI-independent manner. Importantly, knockdown of NOD1 expression by siRNA abrogated CXCL8 production in AGS cells upon exposure to *H. pylori*-derived OMVs. Furthermore, intragastrically delivered OMVs efficiently induced gastric mucosal expression of CXCL2, a murine chemoattractant for neutrophils, and antibody responses against OMVs. These innate and adaptive responses to OMVs depend on NOD1 activation because NOD1-deficient mice exhibit defective CXCL2 expression and OMV-specific antibody responses. Thus, these data suggest that intracellular delivery of PGN as a form of OMVs activates NOD1 in gastric ECs in a *cag*PAI-independent manner.

A study has highlighted the role of autophagy to address the molecular mechanisms accounting for OMV-mediated NOD1 activation[34]. Irving *et al*[34]. first found that *H. pylori*-derived OMVs induce autophagy in ECs. Consistent with autophagy induction, mouse embryonic fibroblasts (MEFs) deficient in *ATG5*, a critical molecule for autophagy, exhibited diminished production of CXCL2 compared with *ATG5*-intact MEFs upon exposure to *H. pylori*-derived OMVs. Autophagosome formation was diminished in NOD1-knockdown AGS cells stimulated with *H. pylori*-derived OMVs, suggesting the involvement of NOD1 activation in autophagy induction. Fluorescent labeling studies clearly demonstrated that EEA1 (early endosome antigen 1)-positive early endosomes containing both OMVs and PGN recruit NOD1 and its downstream kinase, receptor interacting protein 2 (RIP2). Such endosomal interactions between *H. pylori*-derived OMVs, NOD1, and RIP2 are necessary for chemokine production and autophagy induction, as RIP2 inhibitor efficiently blocks these responses. Collectively, these studies provide the evidence that NOD1 recognizes *H. pylori*-derived PGN within $EEA1^+$ early endosomes and subsequently activates RIP2 to induce autophagy and pro-inflammatory chemokine responses[34]. However, it should be noted that involvement of RIP2 in the induction of NOD1-mediated autophagy requires future studies, as it has been previously observed that NOD1 activation induces RIP2-independent autophagy in case of *Shigella flexneri* infection[35].

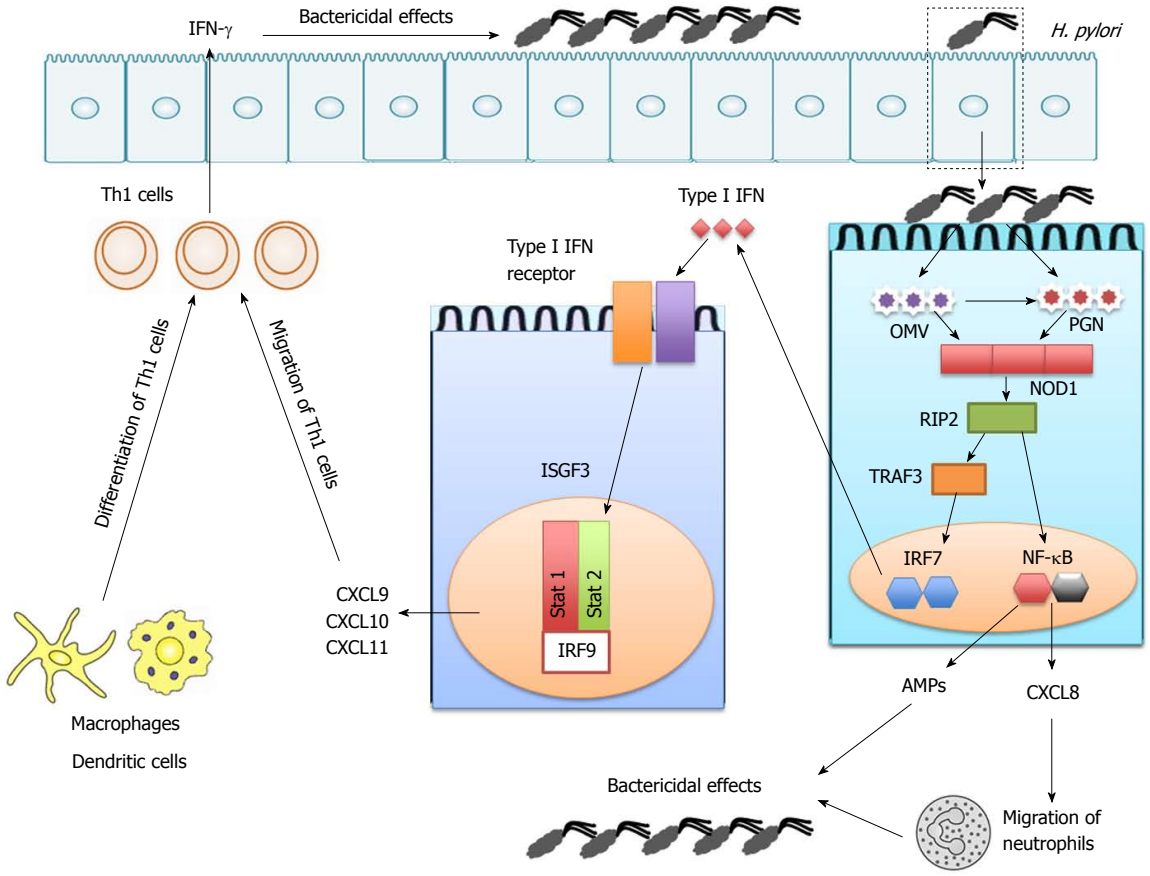

Figure 1 Nucleotide-binding oligomerization domain 1-mediated mucosal host defense against *Helicobacter pylori* infection. Nucleotide-binding oligomerization domain 1 (NOD1) recognizes *Helicobacter pylori* (*H. pylori*)-derived peptidoglycan (PGN) or outer membrane vesicles (OMVs). Sensing of *H. pylori*-derived PGN or OMVs by intracellular NOD1 in the gastric epithelial cells induces production of type I IFN and C-X-C motif chemokine ligand 10 (CXCL10) through the receptor interacting protein 2 (RIP2)-TNF receptor-associated factor 3 (TRAF3)-interferon regulatory factor 7(IRF7)-IFN-stimulated gene factor 3 (ISGF3) pathway, thereby promoting T helper type 1 (Th1) responses. ISGF3 is a heterotrimeric complex composed of signal transduction and activator of transcription 1 (Stat1), Stat2, and IRF9. NOD1 activation also induces production of anti-microbial peptides (AMPs) through nuclear translocation of nuclear factor-kappa B (NF-κB) subunits. IFN-γ and AMPs exert bactericidal effects.

CYTOKINE AND CHEMOKINE RESPONSES AGAINST *H. PYLORI* BY NOD1 ACTIVATION

NOD1 senses *H. pylori*-derived PGN that is delivered to the cytosolic region of gastric ECs *via* T4SS and/or OMV transport. The next question is how NOD1 activation leads to the induction of Th1 and Th17 responses, both of which are characteristics of chronic *H. pylori* infection (Figure 1).

NOD1 activation leads to the physical interaction between NOD1 and RIP2, its downstream effector molecule[7,11]. NOD1-induced RIP2 activation triggers the pro-inflammatory signaling cascade through nuclear translocation of NF-κB subunits[7,11]. In addition to NF-κB, the interaction between NOD1 and RIP2 leads to the activation of mitogen-activated kinases (MAPKs), including extracellular signal-regulated kinase, c-JUN N-terminal kinase, and p38[7,11]. Thus, one major outcome of NOD1-mediated signaling pathways is the activation of NF-κB and MAPKs[7,11]. Activation of NF-κB and MAPKs as well as production of CXCL8 is induced in gastric ECs, such as AGS cells, upon exposure to *H. pylori*[36-38]. However, it remains controversial whether activation of NF-κB/MAPKs and production of CXCL8 are dependent upon the recognition of *H. pylori* by NOD1. Grubman *et al*[36] established a stable AGS cell line with diminished expression of NOD1 (NOD1 knockdown, NOD1 KD cells), and found that NF-κB activation and CXCL8 production are markedly reduced in NOD1 KD cells than in AGS cells with intact NOD1 expression. Moreover, *H. pylori*-induced CXCL8 production by gastric ECs is partially mediated by MAPK activation following the recognition of this organism by NOD1, as knockdown of NOD1 expression by siRNA results in reduced activation of MAPKs and MAPKs inhibitors efficiently blocks CXCL8 production[39]. These reports support the idea that activation of NF-κB/MAPK and production of CXCL8 induced by exposure to *H. pylori* are dependent on NOD1. On the other hand, Hirata *et al*[38] reported that knockdown of NOD1 or RIP2 expression by specific siRNAs did not affect *H. pylori*-induced NF-κB/MAPK activation or CXCL8 production in AGS cells. Future *in vitro* studies are required to determine the contribution of NOD1 in NF-κB activation

in response to *H. pylori* infection.

Human gastric mucosa with persistent *H. pylori* infection is characterized by Th1 responses. CXCL9, CXCL10, and CXCL11 are EC-derived chemokines that play a pivotal role in the generation of Th1 responses through the attraction of Th1 cells expressing C-X-C chemokine receptor type 3 (CXCR3)[40]. High expression of CXCL9 and CXCL10 in the human gastric mucosa with chronic *H. pylori* infection strongly suggests that CXCL9 and CXCL10 contribute to the generation of Th1 responses[29,41]. We discerned from previous studies that stimulation of colon and gastric cancer cell lines (HT-29 and AGS cells) with NOD1 ligands lead to the robust production of CXCL9, CXCL10, and CXCL11[11,27,42]. Surprisingly, NOD1-induced CXCL10 production by colonic and gastric ECs is not dependent on NF-κB or MAPK activation, because blockade of these pathways by specific pharmacological inhibitors or siRNA transfection did not alter the production of CXCL10[11,27,42]. Instead, NOD1-induced CXCL10 production is markedly decreased by the addition of type I IFN receptor antibody, suggesting that type I IFN production is one of the major outcomes following NOD1 activation. Indeed, HT-29 cells produce a large amount of type I IFN upon stimulation with NOD1 ligand.

Next, we focused on identifying the signaling pathways involved in type I IFN production through NOD1 activation. Detailed knockdown and over-expression studies revealed the involvement of TNF receptor-associated factor 3 (TRAF3) in the induction of type I IFN[11,27,42]. The interaction between NOD1 and RIP2 initiates recruitment of TRAF3 to this complex and leads to the activation of downstream signaling molecules, TANK-binding kinase 1 (TBK1) and IκB kinase ε (IKKε), both of which play an indispensable role in the induction of type I IFN responses through nuclear translocation of interferon regulatory factor 3 (IRF3) and IRF7[43,44]. Indeed, the RIP2-TRAF3-TBK1-IKKε-IRF7 axis plays a key role in inducing the production of type I IFN by ECs[27,42]. Furthermore, NOD1-mediated type I IFN production promotes the transcription of CXCL10 through nuclear translocation of the heterotrimeric complex, IFN-stimulated gene factor 3 (ISGF3), composed of signal transduction and activator of transcription 1 (Stat1), Stat2, and IRF9, because gene silencing of Stat1 or Stat2 by siRNA leads to a marked reduction in CXCL10 production. Thus, these data suggest that NOD1 activation induces the production of type I IFN and CXCL10 through activation of the RIP2-TRAF3-TBK1-IKKε-IRF7-ISGF3 pathway[11,27,42].

The relevance of NOD1-mediated type I IFN responses was examined in animal studies in which NOD1-intact and NOD1-deficient mice were challenged with *H. pylori*. As expected, NOD1-deficient mice exhibited a higher bacterial burden in the stomach two weeks after the infection, and the effects were accompanied by reduced expression of type I IFN-related factors, such as IFN-β, IFN-γ and CXCL10, rather than NF-κB-related factors, such as TNF-α and CXCL2[11,27,42]. Reduced expression of phospho-Stat1 (p-Stat1) and p-Stat2 is observed in the gastric mucosa of NOD1-deficient mice, when compared with that in NOD1-intact mice. However, comparable levels of NF-κB activation are observed in both mice. Finally, the blockade of type I IFN signaling pathways by Stat1 siRNA increased bacterial burden in the stomach upon oral infection with *H. pylori* in NOD1-intact mice. Its effects were accompanied by reduced expression of IFN-γ and CXCL10 in the stomach. In contrast, blockade of NF-κB signaling pathways by NF-κB decoy oligonucleotide did not alter the bacterial burden or expression of IFN-γ or CXCL10 in the stomach, although these treatments reduced the gastric expression of TNF-α and CXCL2. Collectively, these data suggest that sensing of *H. pylori*-derived PGN by intracellular NOD1 in gastric ECs induces production of type I IFN and CXCL10 through the RIP2-TRAF3-TBK1-IKKε-IRF7-ISGF3 pathway and thereby promotes Th1 responses. Because IFN-γ produced by Th1 cells enhances the expression of NOD1[27,42,45], we propose that the type I IFN-CXCL10-IFN-γ axis induced by NOD1 activation forms a positive feedback loop for the generation of Th1 responses in the gastric mucosa with persistent *H. pylori* infection.

Little is known about the molecular mechanisms accounting for NOD1-mediated Th17 responses in *H. pylori* infection. In this regard, a recent study has highlighted the importance of NOD1 activation in non-hematopoietic cells, *i.e.* ECs, in the generation of Th17 responses[46]. Therefore, it is possible that the sensing of *H. pylori*-derived PGN or OMVs by intracellular NOD1 in gastric ECs is involved in Th17 responses.

RESPONSE OF ANTI-MICROBIAL PEPTIDES AGAINST *H. PYLORI* BY NOD1 ACTIVATION

Antimicrobial peptides (AMPs) constitute a part of the innate host defense system[47]. AMPs released by APCs and ECs rapidly act to eradicate invading microorganisms[47]. Grubman *et al*[36] reported that AGS cells release β-defensins upon exposure to *cag*PAI-positive *H. pylori*. Production of β-defensins by AGS cells is dependent on NOD1 activation, because stable NOD1-knockdown AGS cells exhibit reduced production of AMPs. Moreover, AMPs induced by exposure to *H. pylori* exhibit potent *H. pylori* eradicating activity. Consistent with this, the expression of β-defensin 4 in the stomach is markedly decreased in NOD1-deficient mice than in NOD1-intact mice following *H. pylori* infection[48]. Collectively, these *in vitro* and *in vivo* studies suggest the possible involvement of NOD1-dependent production of AMPs in the mucosal host

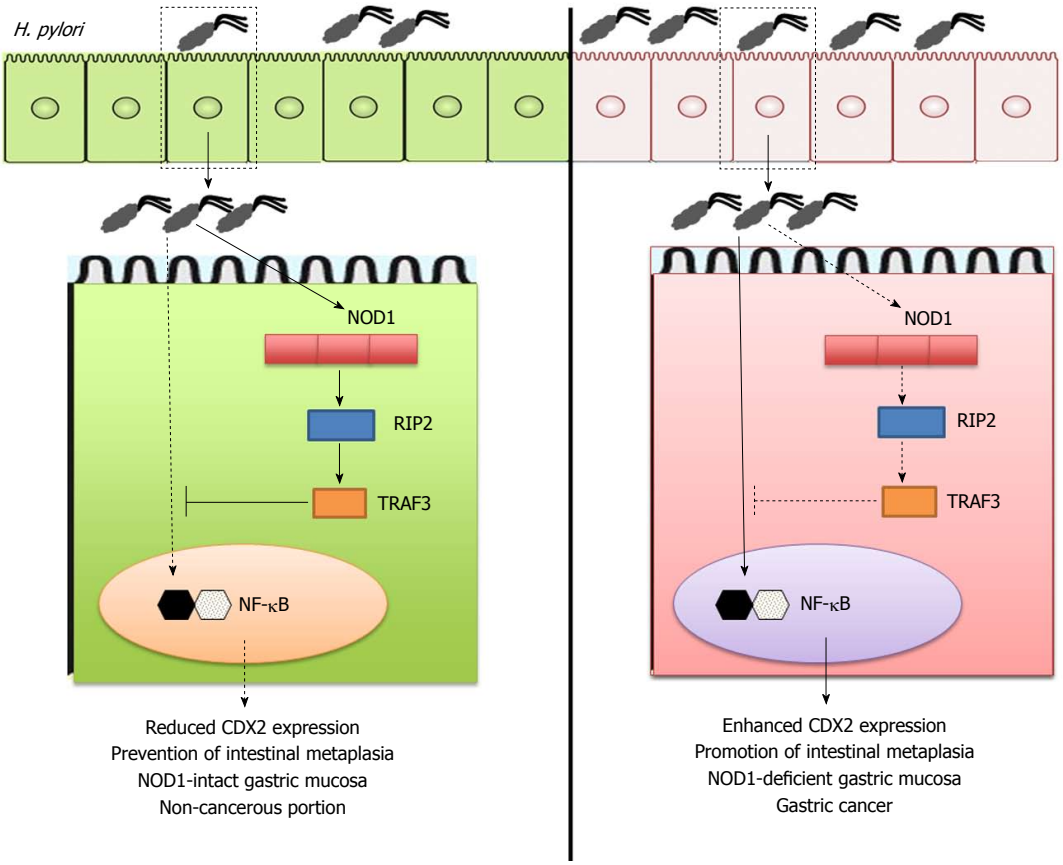

Figure 2 Prevention of gastric cancer development by nucleotide-binding oligomerization domain 1. Sensing of *Helicobacter pylori* (*H. pylori*)-derived peptidoglycan (PGN) by intracellular nucleotide-binding oligomerization domain 1 (NOD1) in gastric epithelial cells induces activation of TNF receptor associated factor 3 (TRAF3) as mentioned in Figure 1. TRAF3 activation by NOD1 negatively regulates expression of caudal-related homeobox 2 (Cdx2) via the inhibition of nuclear factor-kappa B (NF-κB) activation to prevent intestinal metaplasia and gastric cancer (left panel). On the other hand, lack of NOD1-mediated negative regulation on Cdx2 expression promotes the development of gastric cancer (right panel).

defenses against *H. pylori* infection (Figure 1).

NOD1 POLYMORPHISMS AND UPPER GASTROINTESTINAL DISEASES

Several reports have suggested an association between NOD1 gene polymorphisms and upper GI diseases[49-51]. Wang *et al*[51] identified the NOD1 rs7789045 TT genotype as an increased risk for gastric cancer in a Chinese population. Another Chinese cohort study reported that the risk of gastric cancer is high in *H. pylori*-infected subjects carrying the NOD1 rs 2709800 TT genotype[52]. Moreover, Hofner *et al*[53] reported that the G796A NOD1 polymorphism is associated with peptic ulcers in *H. pylori*-infected patients. Although these studies support the correlation between NOD1 polymorphisms and upper GI disorders caused by *H. pylori*, the mechanisms by which NOD1 polymorphisms lead to the development of *H. pylori*-associated diseases remain unknown. Because NOD1 deficiency increases gastric *H. pylori* burden in animals and its expression is lower in the cancerous tissues of the stomach than in the non-cancerous tissues[54], it would be interesting to study whether NOD1 function is impaired or enhanced in the presence of such polymorphisms associated with gastric cancer.

PREVENTION OF GASTRIC CANCER BY NOD1 ACTIVATION

NOD1 activation is required for mucosal host defense against *H. pylori* infection. This protective effect is partially mediated by the activation of type I IFN signaling pathways following the molecular interaction between NOD1 and TRAF3[11,27]. Suarez *et al*[54] have addressed the clinical relevance of NOD1-TRAF3 interaction in human *H. pylori*-associated diseases. They reported that expression levels of NOD1 and TRAF3 are much weaker in gastric cancer tissues than in non-cancerous tissues. Thus, these studies utilizing human gastric cancer samples strongly suggest that impaired activation of NOD1 and TRAF3 is involved in the pathogenesis of gastric cancer and that NOD1-TRAF3 interaction may play a protective role in the development of gastric cancer (Figure 2).

Thus, after confirming the possible involvement of NOD1 activation in the development of human gastric cancer, the next question is how NOD1 serves

as a protective factor for gastric cancer development. Intestinal metaplasia, wherein the gastric mucosa exhibits an intestinal phenotype, is a pre-neoplastic lesion of gastric cancer[55]. Aberrant expression of caudal-related homeobox 2 (Cdx2)[55], a transdifferentiation factor, in the gastric tissue induces intestinal metaplasia and gastric carcinogenesis. We hypothesized that NOD1 activation inhibits the development of gastric cancer through negative regulation of Cdx2[37]. To address this question, we performed a long-term infection study in which NOD1-intact and NOD1-deficient mice were challenged with *cag*PAI-positive *H. pylori*. Interestingly, formation of gastric intestinal metaplasia was observed in NOD1-deficient mice, eight months after initial challenge with *H. pylori,* but not in NOD1-intact mice. This effect was accompanied with higher expression of Cdx2 in the gastric mucosa of NOD1-deficient mice than in the NOD1-intact mice. On the contrary, expression of TRAF3 was lower in the gastric mucosa of NOD1-deficient mice than in NOD1-intact mice. Furthermore, development of gastric intestinal metaplasia in the absence of intact NOD1 signaling pathways is associated with enhanced activation of NF-κB, because most gastric ECs are positive for nuclear p65 staining. Detection of *H. pylori* in gastric mucosa exhibiting intestinal metaplasia is difficult in human samples[56]. Consistent with this, *H. pylori* burden in the gastric mucosa was much lower in NOD1-deficient mice than in the NOD1-intact mice[37]. Thus, the results of our long-term *H. pylori* infection study support the data[54] obtained from human gastric cancer samples, demonstrating that impaired activation of NOD1-TRAF3 signaling pathways is involved in the development of intestinal metaplasia[37].

Regarding the molecular mechanisms by which NOD1 activation prevents the development of intestinal metaplasia and gastric cancer, we provided evidence that NOD1 activation upon exposure to *H. pylori* negatively regulates Cdx2 expression through activation of TRAF3[37]. Exposure to *H. pylori* upregulates Cdx2 expression in gastric cancer cell lines, and the effects are enhanced or diminished by gene silencing of NOD1 by siRNA or over-expression of TRAF3, respectively[37]. Furthermore, promoter gene and gel shift assays revealed that interaction between NOD1 and TRAF3 inhibits the expression of Cdx2 through negative regulation of NF-κB activation. Thus, these *in vitro* studies have elucidated a part of the molecular mechanisms accounting for the prevention of intestinal metaplasia followed by gastric cancer *via H. pylori*-induced NOD1 activation. Collectively, these two recent studies strongly suggest that NOD1 activation by *H. pylori* infection plays a protective role in the development of gastric cancer.

CONCLUSION

NOD1 contributes to mucosal host defense against *H. pylori* infection through the activation of type I IFN signaling pathways and production of AMPs. In addition, NOD1 activation negatively regulates Cdx2 expression, and thereby inhibits the development of gastric cancer. Molecules involved in NOD1-mediated signaling pathways might be new therapeutic targets for treating chronic gastric diseases and gastric cancer.

REFERENCES

1 **Hatakeyama M**. Helicobacter pylori CagA and gastric cancer: a paradigm for hit-and-run carcinogenesis. *Cell Host Microbe* 2014; **15**: 306-316 [PMID: 24629337 DOI: 10.1016/j.chom.2014.02.008]

2 **Amieva M**, Peek RM Jr. Pathobiology of Helicobacter pylori-Induced Gastric Cancer. *Gastroenterology* 2016; **150**: 64-78 [PMID: 26385073 DOI: 10.1053/j.gastro.2015.09.004]

3 **Chiba T**, Marusawa H, Ushijima T. Inflammation-associated cancer development in digestive organs: mechanisms and roles for genetic and epigenetic modulation. *Gastroenterology* 2012; **143**: 550-563 [PMID: 22796521 DOI: 10.1053/j.gastro.2012.07.009]

4 **Fukase K**, Kato M, Kikuchi S, Inoue K, Uemura N, Okamoto S, Terao S, Amagai K, Hayashi S, Asaka M; Japan Gast Study Group. Effect of eradication of Helicobacter pylori on incidence of metachronous gastric carcinoma after endoscopic resection of early gastric cancer: an open-label, randomised controlled trial. *Lancet* 2008; **372**: 392-397 [PMID: 18675689 DOI: 10.1016/S0140-6736(08)61159-9]

5 **Uemura N**, Okamoto S, Yamamoto S, Matsumura N, Yamaguchi S, Yamakido M, Taniyama K, Sasaki N, Schlemper RJ. Helicobacter pylori infection and the development of gastric cancer. *N Engl J Med* 2001; **345**: 784-789 [PMID: 11556297 DOI: 10.1056/NEJMoa001999]

6 **Akira S**, Takeda K. Toll-like receptor signalling. *Nat Rev Immunol* 2004; **4**: 499-511 [PMID: 15229469 DOI: 10.1038/nri1391]

7 **Strober W**, Murray PJ, Kitani A, Watanabe T. Signalling pathways and molecular interactions of NOD1 and NOD2. *Nat Rev Immunol* 2006; **6**: 9-20 [PMID: 16493424 DOI: 10.1038/nri1747]

8 **Slomiany BL**, Slomiany A. Role of LPS-elicited signaling in triggering gastric mucosal inflammatory responses to H. pylori: modulatory effect of ghrelin. *Inflammopharmacology* 2017; **25**: 415-429 [PMID: 28516374 DOI: 10.1007/s10787-017-0360-1]

9 **Andersen-Nissen E**, Smith KD, Strobe KL, Barrett SL, Cookson BT, Logan SM, Aderem A. Evasion of Toll-like receptor 5 by flagellated bacteria. *Proc Natl Acad Sci USA* 2005; **102**: 9247-9252 [PMID: 15956202 DOI: 10.1073/pnas.0502040102]

10 **Ferrero RL**. Innate immune recognition of the extracellular mucosal pathogen, Helicobacter pylori. *Mol Immunol* 2005; **42**: 879-885 [PMID: 15829277 DOI: 10.1016/j.molimm.2004.12.001]

11 **Watanabe T**, Asano N, Kudo M, Strober W. Nucleotide-binding oligomerization domain 1 and gastrointestinal disorders. *Proc Jpn Acad Ser B Phys Biol Sci* 2017; **93**: 578-599 [PMID: 29021509 DOI: 10.2183/pjab.93.037]

12 **Bouskra D**, Brézillon C, Bérard M, Werts C, Varona R, Boneca IG, Eberl G. Lymphoid tissue genesis induced by commensals through NOD1 regulates intestinal homeostasis. *Nature* 2008; **456**: 507-510 [PMID: 18987631 DOI: 10.1038/nature07450]

13 **Tsuji Y**, Watanabe T, Kudo M, Arai H, Strober W, Chiba T. Sensing of commensal organisms by the intracellular sensor NOD1 mediates experimental pancreatitis. *Immunity* 2012; **37**: 326-338 [PMID: 22902233 DOI: 10.1016/j.immuni.2012.05.024]

14 **Watanabe T**, Kudo M, Strober W. Immunopathogenesis of pancreatitis. *Mucosal Immunol* 2017; **10**: 283-298 [PMID: 27848953 DOI: 10.1038/mi.2016.101]

15 **Watanabe T**, Sadakane Y, Yagama N, Sakurai T, Ezoe H, Kudo M, Chiba T, Strober W. Nucleotide-binding oligomerization domain 1 acts in concert with the cholecystokinin receptor agonist, cerulein, to induce IL-33-dependent chronic pancreatitis. *Mucosal Immunol* 2016; **9**: 1234-1249 [PMID: 26813347 DOI: 10.1038/mi.2015.144]

16 **Viala J**, Chaput C, Boneca IG, Cardona A, Girardin SE, Moran AP, Athman R, Mémet S, Huerre MR, Coyle AJ, DiStefano PS, Sansonetti PJ, Labigne A, Bertin J, Philpott DJ, Ferrero RL. Nod1

responds to peptidoglycan delivered by the Helicobacter pylori cag pathogenicity island. *Nat Immunol* 2004; **5**: 1166-1174 [PMID: 15489856 DOI: 10.1038/ni1131]
17 **Moyat M**, Velin D. Immune responses to Helicobacter pylori infection. *World J Gastroenterol* 2014; **20**: 5583-5593 [PMID: 24914318 DOI: 10.3748/wjg.v20.i19.5583]
18 **Sawai N**, Kita M, Kodama T, Tanahashi T, Yamaoka Y, Tagawa Y, Iwakura Y, Imanishi J. Role of gamma interferon in Helicobacter pylori-induced gastric inflammatory responses in a mouse model. *Infect Immun* 1999; **67**: 279-285 [PMID: 9864227]
19 **Itoh T**, Wakatsuki Y, Yoshida M, Usui T, Matsunaga Y, Kaneko S, Chiba T, Kita T. The vast majority of gastric T cells are polarized to produce T helper 1 type cytokines upon antigenic stimulation despite the absence of Helicobacter pylori infection. *J Gastroenterol* 1999; **34**: 560-570 [PMID: 10535482]
20 **Gray BM**, Fontaine CA, Poe SA, Eaton KA. Complex T cell interactions contribute to Helicobacter pylori gastritis in mice. *Infect Immun* 2013; **81**: 740-752 [PMID: 23264048 DOI: 10.1128/IAI.01269-12]
21 **Shi Y**, Liu XF, Zhuang Y, Zhang JY, Liu T, Yin Z, Wu C, Mao XH, Jia KR, Wang FJ, Guo H, Flavell RA, Zhao Z, Liu KY, Xiao B, Guo Y, Zhang WJ, Zhou WY, Guo G, Zou QM. Helicobacter pylori-induced Th17 responses modulate Th1 cell responses, benefit bacterial growth, and contribute to pathology in mice. *J Immunol* 2010; **184**: 5121-5129 [PMID: 20351183 DOI: 10.4049/jimmunol.0901115]
22 **Serrano C**, Wright SW, Bimczok D, Shaffer CL, Cover TL, Venegas A, Salazar MG, Smythies LE, Harris PR, Smith PD. Downregulated Th17 responses are associated with reduced gastritis in Helicobacter pylori-infected children. *Mucosal Immunol* 2013; **6**: 950-959 [PMID: 23299619 DOI: 10.1038/mi.2012.133]
23 **Strober W**, Fuss IJ. Proinflammatory cytokines in the pathogenesis of inflammatory bowel diseases. *Gastroenterology* 2011; **140**: 1756-1767 [PMID: 21530742 DOI: 10.1053/j.gastro.2011.02.016]
24 **Yamaoka Y**, Kita M, Kodama T, Sawai N, Kashima K, Imanishi J. Induction of various cytokines and development of severe mucosal inflammation by cagA gene positive Helicobacter pylori strains. *Gut* 1997; **41**: 442-451 [PMID: 9391240]
25 **Amedei A**, Cappon A, Codolo G, Cabrelle A, Polenghi A, Benagiano M, Tasca E, Azzurri A, D'Elios MM, Del Prete G, de Bernard M. The neutrophil-activating protein of Helicobacter pylori promotes Th1 immune responses. *J Clin Invest* 2006; **116**: 1092-1101 [PMID: 16543949 DOI: 10.1172/JCI27177]
26 **Kranzer K**, Eckhardt A, Aigner M, Knoll G, Deml L, Speth C, Lehn N, Rehli M, Schneider-Brachert W. Induction of maturation and cytokine release of human dendritic cells by Helicobacter pylori. *Infect Immun* 2004; **72**: 4416-4423 [PMID: 15271898 DOI: 10.1128/IAI.72.8.4416-4423.2004]
27 **Watanabe T**, Asano N, Fichtner-Feigl S, Gorelick PL, Tsuji Y, Matsumoto Y, Chiba T, Fuss IJ, Kitani A, Strober W. NOD1 contributes to mouse host defense against Helicobacter pylori via induction of type I IFN and activation of the ISGF3 signaling pathway. *J Clin Invest* 2010; **120**: 1645-1662 [PMID: 20389019 DOI: 10.1172/JCI39481]
28 **Yamaoka Y**, Kita M, Kodama T, Sawai N, Tanahashi T, Kashima K, Imanishi J. Chemokines in the gastric mucosa in Helicobacter pylori infection. *Gut* 1998; **42**: 609-617 [PMID: 9659152]
29 **Eck M**, Schmausser B, Scheller K, Toksoy A, Kraus M, Menzel T, Müller-Hermelink HK, Gillitzer R. CXC chemokines Gro(alpha)/IL-8 and IP-10/MIG in Helicobacter pylori gastritis. *Clin Exp Immunol* 2000; **122**: 192-199 [PMID: 11091274]
30 **Chamaillard M**, Hashimoto M, Horie Y, Masumoto J, Qiu S, Saab L, Ogura Y, Kawasaki A, Fukase K, Kusumoto S, Valvano MA, Foster SJ, Mak TW, Nuñez G, Inohara N. An essential role for NOD1 in host recognition of bacterial peptidoglycan containing diaminopimelic acid. *Nat Immunol* 2003; **4**: 702-707 [PMID: 12796777 DOI: 10.1038/ni945]
31 **Varga MG**, Peek RM. DNA Transfer and Toll-like Receptor Modulation by Helicobacter pylori. *Curr Top Microbiol Immunol* 2017; **400**: 169-193 [PMID: 28124154 DOI: 10.1007/978-3-319-50520-6_8]
32 **Kuehn MJ**, Kesty NC. Bacterial outer membrane vesicles and the host-pathogen interaction. *Genes Dev* 2005; **19**: 2645-2655 [PMID: 16291643 DOI: 10.1101/gad.1299905]
33 **Kaparakis M**, Turnbull L, Carneiro L, Firth S, Coleman HA, Parkington HC, Le Bourhis L, Karrar A, Viala J, Mak J, Hutton ML, Davies JK, Crack PJ, Hertzog PJ, Philpott DJ, Girardin SE, Whitchurch CB, Ferrero RL. Bacterial membrane vesicles deliver peptidoglycan to NOD1 in epithelial cells. *Cell Microbiol* 2010; **12**: 372-385 [PMID: 19888989 DOI: 10.1111/j.1462-5822.2009.01404.x]
34 **Irving AT**, Mimuro H, Kufer TA, Lo C, Wheeler R, Turner LJ, Thomas BJ, Malosse C, Gantier MP, Casillas LN, Votta BJ, Bertin J, Boneca IG, Sasakawa C, Philpott DJ, Ferrero RL, Kaparakis-Liaskos M. The immune receptor NOD1 and kinase RIP2 interact with bacterial peptidoglycan on early endosomes to promote autophagy and inflammatory signaling. *Cell Host Microbe* 2014; **15**: 623-635 [PMID: 24746552 DOI: 10.1016/j.chom.2014.04.001]
35 **Travassos LH**, Carneiro LA, Ramjeet M, Hussey S, Kim YG, Magalhães JG, Yuan L, Soares F, Chea E, Le Bourhis L, Boneca IG, Allaoui A, Jones NL, Nuñez G, Girardin SE, Philpott DJ. Nod1 and Nod2 direct autophagy by recruiting ATG16L1 to the plasma membrane at the site of bacterial entry. *Nat Immunol* 2010; **11**: 55-62 [PMID: 19898471 DOI: 10.1038/ni.1823]
36 **Grubman A**, Kaparakis M, Viala J, Allison C, Badea L, Karrar A, Boneca IG, Le Bourhis L, Reeve S, Smith IA, Hartland EL, Philpott DJ, Ferrero RL. The innate immune molecule, NOD1, regulates direct killing of Helicobacter pylori by antimicrobial peptides. *Cell Microbiol* 2010; **12**: 626-639 [PMID: 20039881 DOI: 10.1111/j.1462-5822.2009.01421.x]
37 **Asano N**, Imatani A, Watanabe T, Fushiya J, Kondo Y, Jin X, Ara N, Uno K, Iijima K, Koike T, Strober W, Shimosegawa T. Cdx2 Expression and Intestinal Metaplasia Induced by H. pylori Infection of Gastric Cells Is Regulated by NOD1-Mediated Innate Immune Responses. *Cancer Res* 2016; **76**: 1135-1145 [PMID: 26759244 DOI: 10.1158/0008-5472.CAN-15-2272]
38 **Hirata Y**, Ohmae T, Shibata W, Maeda S, Ogura K, Yoshida H, Kawabe T, Omata M. MyD88 and TNF receptor-associated factor 6 are critical signal transducers in Helicobacter pylori-infected human epithelial cells. *J Immunol* 2006; **176**: 3796-3803 [PMID: 16517750]
39 **Allison CC**, Kufer TA, Kremmer E, Kaparakis M, Ferrero RL. Helicobacter pylori induces MAPK phosphorylation and AP-1 activation via a NOD1-dependent mechanism. *J Immunol* 2009; **183**: 8099-8109 [PMID: 20007577 DOI: 10.4049/jimmunol.0900664]
40 **Antonelli A**, Ferrari SM, Giuggioli D, Ferrannini E, Ferri C, Fallahi P. Chemokine (C-X-C motif) ligand (CXCL)10 in autoimmune diseases. *Autoimmun Rev* 2014; **13**: 272-280 [PMID: 24189283 DOI: 10.1016/j.autrev.2013.10.010]
41 **Allison CC**, Ferrand J, McLeod L, Hassan M, Kaparakis-Liaskos M, Grubman A, Bhathal PS, Dev A, Sievert W, Jenkins BJ, Ferrero RL. Nucleotide oligomerization domain 1 enhances IFN-γ signaling in gastric epithelial cells during Helicobacter pylori infection and exacerbates disease severity. *J Immunol* 2013; **190**: 3706-3715 [PMID: 23460743 DOI: 10.4049/jimmunol.1200591]
42 **Watanabe T**, Asano N, Kitani A, Fuss IJ, Chiba T, Strober W. Activation of type I IFN signaling by NOD1 mediates mucosal host defense against Helicobacter pylori infection. *Gut Microbes* 2011; **2**: 61-65 [PMID: 21637021 DOI: 10.4161/gmic.2.1.15162]
43 **Kawai T**, Akira S. Signaling to NF-kappaB by Toll-like receptors. *Trends Mol Med* 2007; **13**: 460-469 [PMID: 18029230 DOI: 10.1016/j.molmed.2007.09.002]
44 **Honda K**, Yanai H, Takaoka A, Taniguchi T. Regulation of the type I IFN induction: a current view. *Int Immunol* 2005; **17**: 1367-1378 [PMID: 16214811 DOI: 10.1093/intimm/dxh318]
45 **Hisamatsu T**, Suzuki M, Podolsky DK. Interferon-gamma augments CARD4/NOD1 gene and protein expression through interferon regulatory factor-1 in intestinal epithelial cells. *J Biol Chem* 2003; **278**: 32962-32968 [PMID: 12813035 DOI: 10.1074/

jbc.M304355200]
46 **Fritz JH**, Le Bourhis L, Sellge G, Magalhaes JG, Fsihi H, Kufer TA, Collins C, Viala J, Ferrero RL, Girardin SE, Philpott DJ. Nod1-mediated innate immune recognition of peptidoglycan contributes to the onset of adaptive immunity. *Immunity* 2007; **26**: 445-459 [PMID: 17433730 DOI: 10.1016/j.immuni.2007.03.009]
47 **Roudi R**, Syn NL, Roudbary M. Antimicrobial Peptides As Biologic and Immunotherapeutic Agents against Cancer: A Comprehensive Overview. *Front Immunol* 2017; **8**: 1320 [PMID: 29081781 DOI: 10.3389/fimmu.2017.01320]
48 **Boughan PK**, Argent RH, Body-Malapel M, Park JH, Ewings KE, Bowie AG, Ong SJ, Cook SJ, Sorensen OE, Manzo BA, Inohara N, Klein NJ, Nuñez G, Atherton JC, Bajaj-Elliott M. Nucleotide-binding oligomerization domain-1 and epidermal growth factor receptor: critical regulators of beta-defensins during Helicobacter pylori infection. *J Biol Chem* 2006; **281**: 11637-11648 [PMID: 16513653 DOI: 10.1074/jbc.M510275200]
49 **Castaño-Rodríguez N**, Kaakoush NO, Mitchell HM. Pattern-recognition receptors and gastric cancer. *Front Immunol* 2014; **5**: 336 [PMID: 25101079 DOI: 10.3389/fimmu.2014.00336]
50 **Rosenstiel P**, Hellmig S, Hampe J, Ott S, Till A, Fischbach W, Sahly H, Lucius R, Fölsch UR, Philpott D, Schreiber S. Influence of polymorphisms in the NOD1/CARD4 and NOD2/CARD15 genes on the clinical outcome of Helicobacter pylori infection. *Cell Microbiol* 2006; **8**: 1188-1198 [PMID: 16819970 DOI: 10.1111/j.1462-5822.2006.00701.x]
51 **Wang P**, Zhang L, Jiang JM, Ma D, Tao HX, Yuan SL, Wang YC, Wang LC, Liang H, Zhang ZS, Liu CJ. Association of NOD1 and NOD2 genes polymorphisms with Helicobacter pylori related gastric cancer in a Chinese population. *World J Gastroenterol* 2012; **18**: 2112-2120 [PMID: 22563200 DOI: 10.3748/wjg.v18.i17.2112]
52 **Li ZX**, Wang YM, Tang FB, Zhang L, Zhang Y, Ma JL, Zhou T, You WC, Pan KF. NOD1 and NOD2 Genetic Variants in Association with Risk of Gastric Cancer and Its Precursors in a Chinese Population. *PLoS One* 2015; **10**: e0124949 [PMID: 25933107 DOI: 10.1371/journal.pone.0124949]
53 **Hofner P**, Gyulai Z, Kiss ZF, Tiszai A, Tiszlavicz L, Tóth G, Szõke D, Molnár B, Lonovics J, Tulassay Z, Mándi Y. Genetic polymorphisms of NOD1 and IL-8, but not polymorphisms of TLR4 genes, are associated with Helicobacter pylori-induced duodenal ulcer and gastritis. *Helicobacter* 2007; **12**: 124-131 [PMID: 17309748 DOI: 10.1111/j.1523-5378.2007.00481.x]
54 **Suarez G**, Romero-Gallo J, Piazuelo MB, Wang G, Maier RJ, Forsberg LS, Azadi P, Gomez MA, Correa P, Peek RM Jr. Modification of Helicobacter pylori Peptidoglycan Enhances NOD1 Activation and Promotes Cancer of the Stomach. *Cancer Res* 2015; **75**: 1749-1759 [PMID: 25732381 DOI: 10.1158/0008-5472.CAN-14-2291]
55 **Camilo V**, Barros R, Sousa S, Magalhães AM, Lopes T, Mário Santos A, Pereira T, Figueiredo C, David L, Almeida R. Helicobacter pylori and the BMP pathway regulate CDX2 and SOX2 expression in gastric cells. *Carcinogenesis* 2012; **33**: 1985-1992 [PMID: 22791809 DOI: 10.1093/carcin/bgs233]
56 **Yabuki N**, Sasano H, Tobita M, Imatani A, Hoshi T, Kato K, Ohara S, Asaki S, Toyota T, Nagura H. Analysis of cell damage and proliferation in Helicobacter pylori-infected human gastric mucosa from patients with gastric adenocarcinoma. *Am J Pathol* 1997; **151**: 821-829 [PMID: 9284831]

P- Reviewer: Day AS, Ozen H, Slomiany BL **S- Editor**: Gong ZM
L- Editor: A **E- Editor**: Huang Y

World Journal of Gastroenterology

Submit a Manuscript: http://www.f6publishing.com

World J Gastroenterol 2018 April 28; 24(16): 1734-1747

DOI: 10.3748/wjg.v24.i16.1734

ISSN 1007-9327 (print) ISSN 2219-2840 (online)

MINIREVIEWS

Diversion colitis and pouchitis: A mini-review

Kentaro Tominaga, Kenya Kamimura, Kazuya Takahashi, Junji Yokoyama, Satoshi Yamagiwa, Shuji Terai

Kentaro Tominaga, Kenya Kamimura, Kazuya Takahashi, Junji Yokoyama, Satoshi Yamagiwa, Shuji Terai, Division of Gastroenterology and Hepatology, Graduate School of Medical and Dental Sciences, Niigata University, Niigata 951-8510, Japan

ORCID number: Kentaro Tominaga (0000-0001-6792-1005); Kenya Kamimura (0000-0001-7182-4400); Kazuya Takahashi (0000-0002-3097-9841); Junji Yokoyama (0000-0002-1810-7709); Satoshi Yamagiwa (0000-0003-4791-6107); Shuji Terai (0000-0002-5439-635X).

Author contributions: Tominaga K and Kamimura K wrote the manuscript; Takahashi K, Yokoyama J, Yamagiwa S and Terai S collected information; all authors read and approved the final version of the manuscript.

Conflict-of-interest statement: The authors declare that they have no current financial arrangement or affiliation with any organization that may have a direct influence on their work.

Manuscript source: Invited manuscript

Correspondence to: Kenya Kamimura, MD, PhD, Lecturer, Division of Gastroenterology and Hepatology, Graduate School of Medical and Dental Sciences, Niigata University, 1-757 Asahimachi-dori, Chuo-ku, Niigata 951-8510, Japan. kenya-k@med.niigata-u.ac.jp
Telephone: +81-25-2272207
Fax: +81-25-2270776

Received: March 12, 2018
Peer-review started: March 13, 2018
First decision: March 30, 2018
Revised: April 1, 2018
Accepted: April 16, 2018
Article in press: April 16, 2018

Published online: April 28, 2018

Abstract

Diversion colitis is characterized by inflammation of the mucosa in the defunctioned segment of the colon after colostomy or ileostomy. Similar to diversion colitis, diversion pouchitis is an inflammatory disorder occurring in the ileal pouch, resulting from the exclusion of the fecal stream and a subsequent lack of nutrients from luminal bacteria. Although the vast majority of patients with surgically-diverted gastrointestinal tracts remain asymptomatic, it has been reported that diversion colitis and pouchitis might occur in almost all patients with diversion. Surgical closure of the stoma, with reestablishment of gut continuity, is the only curative intervention available for patients with diversion disease. Pharmacologic treatments using short-chain fatty acids, mesalamine, or corticosteroids are reportedly effective for those who are not candidates for surgical reestablishment; however, there are no established assessment criteria for determining the severity of diversion colitis, and no management strategies to date. Therefore, in this mini-review, we summarize and review various recently-reported treatments for diversion disease. We are hopeful that the information summarized here will assist physicians who treat patients with diversion colitis and pouchitis, leading to better case management.

Key words: Diversion colitis; Diversion pouchitis; Ileitis; Inflammatory bowel disease

Core tip: Diversion colitis is characterized by inflammation of the mucosa in the defunctioned segment of the colon after colostomy or ileostomy. The vast majority of diverted patients remain asymptomatic,

however diversion colitis occurs in almost all diverted patients. Pharmacologic treatment using short-chain fatty acids, mesalamine, or corticosteroids are reportedly effective for those who are not candidates for surgical reestablishment; however, there are no established assessment criteria for determining the severity of diversion colitis, and no management strategies to date. In this mini-review, we summarize and review various recently-reported diversion disease treatments. We hope this review will be useful for future treatment.

Tominaga K, Kamimura K, Takahashi K, Yokoyama J, Yamagiwa S, Terai S. Diversion colitis and pouchitis: A mini-review. *World J Gastroenterol* 2018; 24(16): 1734-1747 Available from: URL: http://www.wjgnet.com/1007-9327/full/v24/i16/1734.htm DOI: http://dx.doi.org/10.3748/wjg.v24.i16.1734

INTRODUCTION

Diversion colitis was first described by Morson *et al*[1] in 1974 as a non-specific inflammation in the diverted colon. Glotzer *et al*[2] labeled this inflammation "diversion colitis" in 1981. Since then, the disease has been reported in both retrospective[3-20] and prospective studies[21-27] which have described the characteristic clinical, endoscopic, and pathological findings. Surprisingly, the prospective study reported that almost all cases exhibit colitis, evidenced by endoscopic analyses, 3 to 36 mo after the colostomy[21]. Symptomatic cases make up only around 30% of all cases diagnosed *via* endoscopic studies, and the precise pathogenesis of this condition remains unclarified. Although a wide range of symptoms are reportedly associated with the disease, including abdominal discomfort, tenesmus, anorectal pain, mucous discharge, and rectal bleeding[3,4], there are no established diagnostic criteria for assessing disease severity. Diversion pouchitis is similar to diversion colitis, featuring inflammation of the ileal pouch that results from fecal stream exclusion and the subsequent lack of nutrients from luminal bacteria. Therefore, the difference between the pouchitis and diversion puchitis is whether the lesion is exposed to the fecal stream or not. Patients generally present with varying symptoms such as tenesmus, bloody or mucus-like discharge, and abdominal pain[28]. The incidence of diversion pouchitis is unknown; however, it appears more commonly in patients with underlying inflammatory bowel disease (IBD). Nonsurgical approaches for the treatment of diversion pouchitis include the use of short chain fatty acids (SCFA), topical 5-aminosalicylic acids, and topical glucocorticoids. Unfortunately, efficacy study outcomes are conflicting, and the only curative approach is surgical re-anastomosis with the reestablishment of gut continuity[28-30].

In their 1989 examination of non-surgical treatment options procedure, Harig *et al*[5] reported the efficacy of short-chain fatty acids. The usefulness of the 5-ASA enema in patients with diversion colitis was reported for the first time by Triantafillidis *et al*[31] in 1991; Glotzer *et al*[2] reported the efficacy of steroid enemas in patients with diversion colitis in 1984, and similar results were subsequently reported by Lim *et al*[32] and Jowett *et al*[33]. Nonsurgical treatments include short-chain fatty acids, 5-aminosalicylic acids, glucocorticoids, antibiotics, and so on. However, due to the lack established assessment methods, the efficacy of these treatments has not been clearly confirmed. Consequently, surgical re-anastomosis remains the most reliable and effective treatment option. There is an unmet need for a summary of these therapeutic options and information regarding the disease assessment, and this need informed the present literature review. We believe that the information summarized in this mini-review will help physicians treat cases and, by increasing the number of treated cases, we will support the establishment of novel criteria for disease assessments and therapeutic decision trees.

LITERATURE ANALYSIS

A literature search was conducted using PubMed and Ovid, with the terms "diversion colitis" or "diversion proctitis" and "diversion pouchitis" used to extract studies published over the preceding 45 years. All appropriate English-language publications from relevant journals were selected. We summarized the available information on demographics, clinical symptoms, endoscopic and histological findings, treatment, and the clinical course.

CLINICAL CHARACTERS

Epidemiology

A total of 69 articles, including 25 case reports, were matched to our definition of diversion colitis and pouchitis assessment; this information is summarized in Tables 1 and 2. Based on our review, the prevalence estimates of these conditions appear extremely high, reaching almost the entire population of interest if the phenomenon is followed prospectively, beginning at 3 to 36 mo after colostomy[21]. In a recent study, Szczepkowski *et al*[3] described more than 90% incidence of diversion colitis on endoscopy in a series of 145 patients. The study further reported that there were no significant associations between diversion colitis and age, sex, type of stoma, or mode of surgery performed. The frequency of disease occurrence ranged from 70%-74% in patients without pre-existing IBD[22] and 91% in patients with pre-existing IBD[6,21]. In patients with histories of Crohn's disease chronic severe inflammation, often with transmural disease, has been described after defunctioning colostomies[34]. It has also been hypothesized that diversion colitis may be a risk factor for ulcerative colitis in predisposed individuals, and that ulcerative colitis can be triggered by anatomically discontinuous inflammation in the large bowel[35]. Among the 46 reported cases of diversion colitis and

Table 1 Clinical characteristics of case report

Case (No)	Reference	Reporting yr	Country	Age (yr)	Gender (male/female)	Primary illness (reason for diversion)	Type of diversion (surgical procedure)	Period of up to diagnosis from operation	Symptoms	Endoscopy findings	Pathological findings	Diagnosis
1	Glotzer *et al*[2]	1981	United States	49	M	Free perforation sigmoid diverticulum	Loop sigmoid colostomy	2.5 mo	No symptoms	Erythema, friability, petechiae, atrophy	Crypt abscess, surface epithelial cell degeneration, acute inflammation, chronic inflammation, regeneration	Diversion colitis
				56	F	Adenocarcinoma. Protect low anastomosis	Loop transverse colostomy	3 mo	No symptoms	Erythema, friability, petechiae	Normal	Diversion colitis
				78	M	Sigmoid diverticulitis with perforation	Loop sigmoid colostomy	6 mo	No symptoms	Erythema, friability, granularity	No biopsy	Diversion colitis
				70	F	Sigmoid diverticulitis found at pelvic operation	Loop sigmoid colostomy	3 mo	No symptoms	Erythema, friability, nodularity	Regeneration	Diversion colitis
				43	F	Sigmoid diverticulitis with perforation	Loop sigmoid colostomy	8 mo	No symptoms	Erythema, friability	Crypt abscess, acute inflammation.	Diversion colitis
				41	F	Fecal incontinence secondary to cordotomy for pain	Loop sigmoid colostomy	18 mo	No symptoms	Erythema, friability, petechiae	No biopsy	Diversion colitis
				65	M	Sigmoid diverticulitis with perforation	Loop transverse colostomy	3 yr	No symptoms	Erythema, friability, granularity, petechiae, inflammatory polyp	Crypt abscess, surface epithelial cell degeneration, chronic inflammation, regeneration.	Diversion colitis
				83	M	Sigmoid diverticulitis with perforation	Loop transverse colostomy	6 mo	No symptoms	Erythema, friability, granularity	Crypt abscess	Diversion colitis
				26	M	Fecal incontinence after T9-10 cord transection	Loop transverse colostomy	7 yr	Rectal discharge	Erythema, friability, petechiae	Surface epithelial cell degeneration, chronic inflammation.	Diversion colitis
				70	M	Colonic ileus secondary to anticholinergics for Parkinson's disease	Loop transverse colostomy	4 mo	No symptoms	Erythema, friability, petechiae, inflammatory polyp	Crypt abscess	Diversion colitis
2	lusk *et al*[39]	1984	United States	28	M	Perforated sigmoid colon for gunshot	Loop sigmoid colostomy	6 wk	No symptoms	Red granular rectum with aphthous ulcers	Moderate loss of goblet cells with focal edema and lymphocytosis of the lamina propria.	Diversion colitis
				68	M	Sigmoid carcinoma	Loop transverse colostomy	6 wk	No symptoms	Multiple aphthae	Not obtained	Diversion colitis
3	Scott *et al*[46]	1984	United States	21	M	Gunshot	Loop transverse colostomy	2 mo	No symptoms	Multiple, small, polypoid lesions in the rectum and sigmoid colon up to the cutaneous part of the mucous fistula.	Mucosal biopsies of the rectal lesions were interpreted as "chronic nonspecific colitis with pseudopolyps, probably from diversion colitis".	Diversion colitis
4	Korelitz *et al*[42]	1984	United States	22	F	Crohn's Disease	Ileostomy and subtotal colectomy	2 yr	No symptoms	Friable, nodular	Not obtained	Diversion colitis

				34	F	Crohn's ileitis	Ileocolic anastomosis and Loop ileostomy	2 yr	No symptoms	Exudate	Focal chronic inflammation, edema, erosions, and an increased number of lymphoid follicles.	Diversion colitis
				31	M	Crohn's ileitis	Ileocolic anastomosis and Loop ileostomy	1 yr	No symptoms	Aphthous lesions	Chronic inflammation	Diversion colitis
				32	M	Crohn's ileitis	Ileocolic anastomosis and Loop ileostomy	1 yr	No symptoms	Friable, exudate	Not obtained	Perforation due to complication of barium enema and diversion colitis
5	Fernand *et al*[40]	1985	United States	67	F	Perforated sigmoid diverticulum	Loop sigmoid colostomy	22 yr	Rectal bleeding	N/A	Diffuse multiple superficial ulcerations and intense inflammatory infiltrates composed mainly of plasma cells, lymphocytes, and some eosinophils.	Diversion colitis
6	Frank *et al*[13]	1987	United States	38	M	Perineal laceration as result of a motor vehicle accident	End sigmoid colostomy	1 yr	Rectal bleeding	Diffuse nodularity and ulceration	Moderate to severe nonspecific inflammation.	Diversion colitis
7	Harig *et al*[5]	1989	United States	63	M	Neurogenic fecal incontinence	Mucus fistula	13 mo	Bloody discharge	Endoscopic index of 10	Inflammatory infiltrate of both acute and chronic cells in the lamina propria and the crypt abscess. Lining epithelial cells show decreased mucin secretion.	Diversion colitis
				63	F	Irradiation of rectum	Mucus fistula	2 wk	Bloody discharge	Endoscopic index of 10	Erosions, surface exudate, crypt abscesses, edema.	Diversion colitis
				54	M	Perianal fistulas	Rectosigmoid pouch	35 mo	Bloody discharge	Endoscopic index of 9	Lymph follicles	Diversion colitis
				56	M	Diverticulitis	Mucus fistula	N/A	N/A	Endoscopic index of 8	N/A	Diversion colitis
8	Triantafillidis *et al*[31]	1991	Greece	64	F	Diverticula with perforation	Hartman's type of operation laparotomy	16 mo	Bloody rectal discharge	Endoscopic index of 9 (quite inflamed with friability and erythema)	Severe inflammatory infiltration, formation of lymph follicles, surface erosions, edema, and crypt abnormalities.	Diversion colitis
9	Tripodi *et al*[43]	1992	United States	85	F	Small bowel perforation with a ruptured chronic pelvic abscess secondary to diverticular disease	End transverse colostomy	10 wk	Bloody rectal discharge	Erythematous and friable, with diffuse exudation, petechiae, and ulceration	Acute and chronic inflammation with cryptitis.	Diversion colitis
10	Lu *et al*[38]	1995	United States	45	F	Chronic constipation	Loop transverse colostomy	25 yr	Sepsis(no symptoms such as rectal bleeding)	Large ulcers with overlying pseudomembrane	Infiltration primarily with plasma cells and lymphocytes was noted, as well as a moderate numbers of polymorphonuclear cells, large lymphoid aggregates were seen in the lamina propria	Diversion colitis

11	Lai *et al*[47]	1997	United States	49	M	Intractable ileus,C6 ASIAB tetraplegic	Colostomy	10 yr	Rectal pain and bleeding.	Partial stricture 70 cm proximally to the rectum. The colonic mucosa appeared granular and friable with evidence of linear ulceration.	Extravasation of erythrocytes, lymphocytic and neutrophilic cells infiltrates, and edema were present within the lamina propria. No evidence of malignancy and glandular dysplasia was found. Pathologic report was consistent with chronic colitis.	Diversion colitis
12	Lim *et al*[32]	1999	United Kingdom	60	F	Faecal incontinence for DM	End sigmoid colostomy	6 mo	Blood and mucus per rectum	Edematous mucosa with bloodstained mucopurulent exudate	Active chronic colitis with focal cryptitis and crypt abscesses.	Diversion colitis → UC
				16	M	Imperforate anus	Ileostomy and colostomy	6 mo	Blood and mucus per rectum	Granular, erythematous mucosa with contact bleeding	Active inflammation with polymorphs infiltrating crypts and a diffuse increase in lymphocytes and plasma cells in the lamina propria.	Diversion colitis → UC
13	Jowett *et al*[33]	2000	United Kingdom	75	F	Faecal incontinence	End colostomy	8 mo	Blood and mucus per rectum	Granular, congested, and oedematous mucosa with contact bleeding	Mixed inflammatory cell infiltrate with distortion of the crypt architecture and cryptitis.	Diversion colitis (→ UC)
14	Lim *et al*[35]	2000	United Kingdom	66	M	Sigmoid carcinoma	Hartmann's procedure with colostomy.	18 mo	No symptoms	Mildly inflamed	Active colitis	Diversion colitis (→ UC)
15	Kiely *et al*[36]	2001	United Kingdom	6	M	Ulcerative colitis	Total colectomy and ileostomy	9 mo	Rectal bleeding	Endoscopic index of 8	Lymphoid hyperplasia, lymphoplasmacytosis, crypt abscesses and moderate mucosal architectural disruption.	Diversion proctocolitis
				3	M	Perforated typhoid disease	Subtotal colectomy and ileostomy	5 mo	Rectal bleeding and abdominal pains	Endoscopic index of 8	Lymphoplasmacytic infiltration of lamina propria, and architectural disruption.	Diversion proctocolitis
				8	F	Aplastic anemia, a large solitary rectal ulcer	Loop sigmoid colostomy	4 mo	Rectal discharge	Endoscopic index of 9	Lymphoplasmacytic and neurophilic infiltrate in the lamina propria, mucin depletion, and Paneth cell metaplasia.	Diversion proctocolitis
				3	M	Hirschsprung's disease	ileostomy	N/A	Rectal bleeding	Florid colitis	Lymphoid hyperplasia, lymphoplasmacytosis and mucin depletion,	Diversion proctocolitis
				10	M	Rectovesical fistula	Loop sigmoid colostomy	N/A	Rectal discharge	Florid colitis	Lymphoid hyperplasia, lymphoplasmacytosis.	Diversion proctocolitis
16	Komuro *et al*[41]	2003	Japan	46	M	Ascending colon diverticular perforation (systemic lupus erythematosus and chronic renal failure)	Loop transverse colostomy	N/A (On surveillance colonoscopy)	No symptoms	Mild colitis with a decreased vascular pattern, oedema and mucosal tear	N/A	Diversion colitis

17	Tsironi *et al*[48]	2006	United Kingdom	40	M	UC pancolitis-type	Rectal stump and ileostomy, subtotal colectomy and ileostomy	5 mo	Blood and mucus per rectum	Severe chronic inflammation with ulceration and numerous inflammatory polyps	Diffuse chronic inflammation with patchy cryptitis	Divesion collitis with caused by clostridium difficile infection.
18	Boyce *et al*[37]	2008	United Kingdom	29	M	Life-long constipation	Subtotal colectomy	15 yr	Rectal bleeding and anal pain	The mucosa of the rectal stump was found to be chronically inflamed and ulcerated.	Inflammatory change	Diversion pouchitis
19	Haugen *et al*[49]	2008	United States	36	F	Faecal incontinence due to spina bifida	Laparoscopic sigmoid colostomy and creation of a Hartmann's pouch	N/A	Rectal discharge	N/A	N/A	Diversion colitis
20	Talisetti *et al*[50]	2009	United States	19	F	Megacystis-microcolon-intestinal hypoperistalsis syndrome (MMIHS)	Gastrostomy and ileostomy	4 yr	Abdominal pain and rectal bleeding	Friable mucosa with areas of pinpoint hemorrhage from the anal verge to 30 cm proximally	Acute cryptitis and scattered crypt abscesses, consistent with diversion colitis.	Diversion colitis
21	Kominami *et al*[51]	2013	Japan	84	M	Angiodysplasia S/O	Subtotal colectomy and ileostomy	5 yr	Blood in the stool	Granular, edematous mucosa with contact bleeding	Lymphoplasmacytic and neurophilic infiltrate in the lamina propria.	Diversion colitis
22	Watanabe *et al*[44]	2014	Japan	76	F	UC	3-stage pancolectomy with construction of an IPAA	13 yr	Bloody purulent rectal discharge	Severely active pouchitis with large erosions	N/A	Diversion pouchitis
23	Gundling *et al*[45]	2015	Germany	75	F	Chronic constipation	Permanent end-colostomy	N/A	Tenesmus and severe rectal pain	Severe DC was seen on colonoscopy	Confirmed histologically	Diversion colitis
24	Matsumoto *et al*[52]	2016	Japan	65	M	UC pancolitis-type	Subtotal colectomy and ileostomy	4 mo	Rectal bleeding	Moderate mucosal inflammation	Ulcer, granulation tissue and epithelial defect	Diversion colitis or exacerbation of UC was suspected.
25	Custon *et al*[29]	2017	United States	44	M	UC complicated by colitis-associated low-grade dysplasia	Total proctocolectomy with 2-stage IPAA	7 yr	Blood in the stool	Edematous and coated with old and fresh blood	N/A	Severe diversion pouchitis

pouchitis, there was a slight male predominance (28 males, 18 females), and the age of the patients ranged from 3 to 85 years old[2,5,13,29,31-33,35-52]. The period from diagnosis to surgical treatment was a median of 8 mo, ranging from 2 wk to 25 years (Table 1). The types of diversions included: 9 cases of loop sigmoid colostomy; 3 cases of end sigmoid colostomy; 9 cases of loop transverse colostomy; 4 cases of loop ileostomy; 7 cases of ileostomy and colostomy; 3 cases of proctocolectomy; 2 cases of Hartmann's type with colostomy; and only one case of other operations (Table 1).

Pathogenesis

The basic mechanisms underlying diversion colitis are still unclear. Glotzer hypothesized that it might be the result of bacterial overgrowth, the presence of harmful bacteria,

Table 2 Clinical course of case reports

Case (No)	Ref.	Age (yr)	Gender (male/female)	Ineffective treatment	Effective treatment	Prognosis
1	Glotzer *et al*[2]	49	M	N/A	Closure 4 mo post-diversion	Asymptomatic. Proctoscopy and biopsy normal 2.5 and 30 mo postclosure.
		56	F	N/A	Closure 3 mo post-diversion	Recurrent Ca. Mucosa not inflamed grossly or microscopically 18 mo post closure.
		78	M	N/A	Closure 6 mo post-diversion	Asymptomatic 1 yr postclosure.
		70	F	N/A	Closure 5 mo post-diversion	Asymptomatic. Normal sigmoidoscopy 2 mo postclosure.
		43	F	N/A	Closure 2 yr post-diversion	Asymptomatic. Normal sigmoidoscopy 3 yr postclosure.
		41	F	N/A	None	Asymptomatic 2 yr after ileostomy.
		65	M	N/A	None	Abdominal cramps purulent rectal discharge. Continued inflammation 8 yr after colostomy.
		83	M	N/A	None	Asymptomatic. Continued mild inflammation 4.5 yr after colostomy.
		26	M	N/A	Steroid enemas	Inproved. Continued 8 yr after colostomy.
		70	M	N/A	Steroid enemas	Tenesmus, discharge and fever 4 yr after colostomy. Resolved with steroid enemas. Continued inflammation at 8 yr.
2	Lusk *et al*[39]	28	M	-	Colostomy closure	Normal at 16 mo follow-up.
		68	M	-	Colostomy closure	Normal at 7 wk after clousure.
3	Scott *et al*[46]	21	M	-	Colostomy closure	One month later, the patient was examined by flexible sigmoidoscopy, which demonstrated normal mucosa throughout with no sign of pseudopolyps.
4	Korelitz *et al*[42]	22	F	Steroid enemas	Ileocolic reanastomosis (ileostomy closure)	3 mo (interval from reanastomosis to normal sigmoidoscopy), 7 yr (duration normal).
		34	F	-	Ileostomy closure	1 mo (interval from reanastomosis to normal sigmoidoscopy), 2 yr (duration normal).
		31	M	-	Ileostomy closure	3 mo (interval from reanastomosis to normal sigmoidoscopy), 18 mo (duration normal).
		32	M	-	Ileostomy closure	2 mo (interval from reanastomosis to normal sigmoidoscopy), 14 mo (duration normal).
5	Fernand *et al*[40]	67	F	-	Left hemicolectomy and left salpingo-oophorectomy	She recoverd well and discharged 9 d later.
6	Frank *et al*[13]	38	M	Oral and topical steroids	Abdominoperineal resection of the diverted loop and permanent colostomy	No evidence of inflammatory bowel disease has developed. Barium study of the small bowel was normal 1 yr after surgery.
7	Harig *et al*[5]	63	M	N/A	Short-chain-fatty acid irrigation	N/A
		63	F	N/A	Short-chain-fatty acid irrigation	N/A
		54	M	N/A	Short-chain-fatty acid irrigation	N/A
		56	M	N/A	Short-chain-fatty acid irrigation	N/A
8	Triantafillidis *et al*[31]	64	F	-	5 aminosalicylic acid enemas comparison with Betamethasone enemas	There were no differences in the degree of clinical improvement, or in the endoscopic and histologic scores seen at the end of the trials, between betamethasone and 5-ASA.
9	Tripodi *et al*[43]	85	F	-	5-aminosalicylic acid enemas	Clinically asymptomatic at a 6-mo follow-up.
10	Lu *et al*[38]	45	F	Intravenous metronidazole	Colectomy of the diverted segment	Without complications and has been doing well postoeratively.
11	Lai *et al*[47]	49	M	-	Daily 5-ASA suppository and total parenteral nutrition	6 wk of treatment with 5-ASA, the patient had decreased rectal pain and bleeding.
12	Lim *et al*[32]	60	F	-	Oral prednisolone, oral mesalazine, and mesalazine enemas	PSL was tapered off over four months and she remained well.
		0	M	Closure of the loop ileostomy→ oral prednisolone, oral olsalazine and oral metronidazole →sigmoid loop colostomy	The defunctioned rectosigmoid was partially removed, leaving the lower rectum and anal canal; the loop colostomy was refashioned into an end colostomy→colectomy and removal of residual rectal stump and anal canal was performed and an end ileostomy fashioned	He subsequently made a good recovery and steroid therapy was discontinued.
13	Jowett *et al*[33]	75	F	-	Topical steroid enemas.	UC
14	Lim *et al*[35]	66	M	-	Steroid enemas	6 mo later he developed ulcerative colitis.

15	Kiely *et al*[36]	6	M	PSL and AZA	SCFA	Oral PSL was continued at the reduced rate of 5mg on alternate days until he underwent an uneventful rectal excision and J-pouch anal anastomosis 1 mo later. Two months after this, his ileostomy was closed.
		3	M	Salazopyrine	SCFA	His ileostomy was closed 3 mo later, and he was remained symptom free.
		8	F	-	SCFA	Her ulceration was virtually healed and showed a reduction in endoscopic index from 9 to 3. Treatment was maintained until her colostomy was reversed a month later. After stoma closure, SCFAs were discontinued with no further recurrence of symptoms.
		3	M	N/A	SCFA	For redo pull-through
		10	M	N/A	SCFA	Rectal excision
16	Komuro *et al*[41]	46	M	-	-	The post endoscopic course was uneventful without any treatment.
17	Tsironi *et al*[48]	40	M	Mesalazine suppository and steroid enemas	Metronidazole suppository	Improved quickly and remains well and asymptomatic 12 wk after treatment.
18	Boyce *et al*[37]	29	M	-	Completion proctectomy	Completion proctectomy was uneventful and from which the patient made an unremarkable recovery.
19	Haugen *et al*[49]	36	F	The water and vinegar solution enema, steroid enema, bismuth subsalicylate (standard treatment SCFA enmas was not option due to insurance and spina bifida)	Antegrade irrigations of her distal bowel with tap water	Weekly to twice weekly irrigations completely stopped the malodorous and troublesome discharge.
20	Talisetti *et al*[50]	19	F	SCFA enema, steroids, metronidazole	Colectomy(entire colon was ultimately resected, Since only 15 cm of jejunum appeared healthy, her mid and distal small bowel was also resected up to 15 cm from the ligament of Treitz)	N/A
21	Kominami *et al*[51]	84	M	Short-chain fatty acid enema	5-aminosalicylic acid enemas	Undergoing 5-aminosalicylic acid enemas maintenance therapy.
22	Watanabe *et al*[44]	76	F	Oral mesalazine, corticosteroid, metronidazole, and ciprofloxacin	Leukocytapheresis, following low dose of metronidazole and ciprofloxacin	After 18 mo, her condition remains stable without the need for medication.
23	Gundling *et al*[45]	75	F	Enemas containing 5-aminosalicylic acid and steroids and antibiotic therapy	Autologous fecal transplantation	All symptoms improved dramatically within 5 d after the first treatment. Colonoscopy 28 d after the first treatment showed no major signs of inflammation in the colonic stump.
24	Matsumoto *et al*[52]	65	M	Corticosteroid and mesalazine enemas, prednisolone injections.	A combined mesalazine plus corticosteroid enema	Finally proctectomy and ileal pouch-anal anastomosis were successfully performed.
25	Custon *et al*[29]	44	M	-	Dextrose(hypertonic glucose) spray endoscopically	The patient did not experience further episodes of recurrent bleeding during the 6-mo follow-up. No prescribed medicines were given after the endoscopic therapy.

nutritional deficiencies, toxins, or disturbance in the symbiotic relationship between luminal bacteria and the mucosal layer[2]. Reportedly, concentrations of carbohydrate-fermenting anaerobic bacteria and pathogenic bacteria are reduced in de-functioned colons[5,23,53] and these reports indicate that the overgrowth of anaerobic bacteria or a pathogenic bacterium is unlikely to be an important etiological factor. On the other hand, there is an increase of nitrate-reducing bacteria in patients with diversion colitis[7] and nitrate-reducing bacteria produce nitric oxide (NO) which plays a protective role in low concentrations, but at higher levels it becomes toxic to the colonic tissue[54]. Thus, it has been suggested that increases in nitrate-reducing bacteria may result in toxic levels of NO, leading to the diversion colitis.

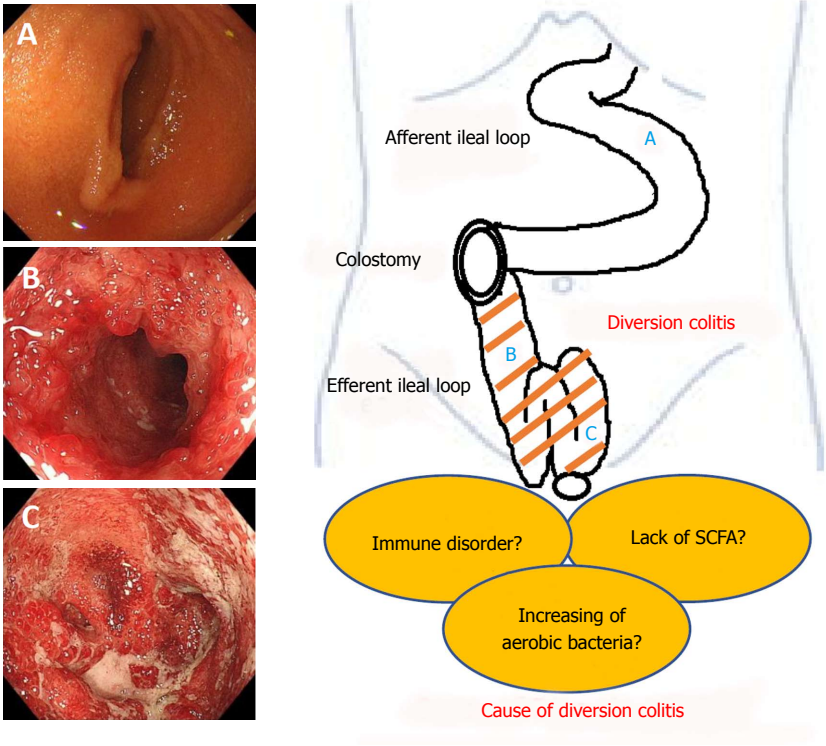

Figure 1 Schematic presentation of diversion colitis and pouchitis.

Recently, ischemia has been proposed as a cause of diversion colitis[8]. The explanation surely lies in changes to the luminal flora consequent to fecal stream interruption. Normal luminal bacteria produce SCFA, such as butyric acid. Butyrate is the principal oxidative substrate for colonocytes[55] and patients with diversion colitis may improve following topical treatment with SCFA, especially with butyrate enemas[5,36]. This hypothesis is based on evidence that suggests SCFA relax vascular smooth muscle and that butyrate deficiencies may induce increased tone in the pelvic arteries, therefore leading to relative ischemia of the colorectal mucosa and intestinal wall[5]. It is obvious that additional, basic research is necessary in order to discern disease mechanisms. We have summarized the pathogenesis of this disease entity in Figure 1.

Symptoms

Most patients are asymptomatic[22], however about one third of patients may exhibit symptoms of diversion colitis[2,3,6,9]. Patients generally present with varying symptoms such as abdominal discomfort, tenesmus, anorectal pain, mucous discharge, and rectal bleeding. The most common symptoms include bloody, serous, or mucous discharge in 40% of the population, and abdominal pain and tenesmus in 15% of the population[3]. There have been several reports of severe rectal bleeding[24,29,56]. There is a report of massive rectal distension causing bilateral ureteric obstruction[37] and a case report of diversion colitis causing severe sepsis requiring a colectomy[38]. These symptoms can start within 1 mo to 3 years after surgery[22,24]. Our review also showed that clinical symptoms of rectal bleeding were seen in 25 cases, abdominal pain in 3 cases, anal pain in 3 cases, and sepsis in 1 case[38]. On the other hand, 21 of 46 cases had no symptoms (Table 1), as previously reported[24]. Additionally, in the presence of Crohn's disease and ulcerative colitis, the number of symptomatic patients rises to 33% and 87% respectively[53]. Our review showed cases with primary illness of diverticula with perforation (n = 11), fecal incontinence (n = 6), chronic constipation or ileus (n = 5), ulcerative colitis (n = 5), Crohn's disease (n = 4), carcinoma (n = 3), and various other diseases (Table 1).

Macroscopic findings

Macroscopically, diversion colitis may involve the whole de-functioned colon or isolated segments. These findings include erythema, diffuse granularity, and blurring of vascular pattern in about 90% of the population. It is also associated with mucosal friability (80%) edema (60%), apthous ulceration, and bleeding, to varying degrees[2,3,8-12,39,40]. There is a case report of diversion colitis causing mucosal tears within the defunctioned colon[41]. Recently, Hundorfean *et al*[57] reported a first description and *in vivo* diagnosis of diversion colitis after surgery, by virtual chromoendoscopy and fluorescein-guided confocal laser endomicroscopy. Our literature review showed that endoscopic findings were evidenced in 44 out of 46 cases, and severe inflammation with ulceration (endoscopic index $\geqslant$ 8) in 17 cases.

Microscopic findings

The pathological finding of diversion colitis and pouchitis

usually vary with degree of severity, therefore, no specific microscopic findings have been noted. The histological features of diversion colitis can mimic those of IBD, even when a pre-existing IBD has not been documented[10,11,13-15]. The most notable feature often seen in diversion colitis is lymphoid follicular hyperplasia[9,14,58]. Atrophy, crypt branching, mucin depletion, crypt distortion, regenerative hyperplasia, paneth cell metaplasia, thickening of muscularis mucosa, diffuse active mucosal inflammation with crypt abscesses, ulceration, and vacuolar and epithelial degeneration along with features of chronic inflammation (usually confined to the mucosa) are seen with varying degrees of severity[9-12,14,16,17,59]. More recently, features of ischemia, such as superficial coagulative necrosis and fibrosis, have been described[8]. Our review showed that 37 out of 46 cases exhibited pathological findings including 15 cases of crypt abscess or cryptitis[2], and 14 cases of lymphoid follicular hyperplasia (which was not previously identified as a feature of diversion colitis). These features are non-specific and, to date, no characteristic feature or features of diversion colitis have been identified.

Treatment

Because of the small number of patients and the unknown etiology, there is no established standard therapy for diversion colitis and pouchitis. Szczepkowski *et al*[4] proposed a management strategy for patients with de-functioned distal stomas. He divided patients with diversion colitis into three groups based on a study of 145 patients. These groups consisted of Group 1 (no clinical, morphological or endoscopic evidence of diversion colitis), Group 2, (mild or moderate signs of diversion colitis), and Group 3 (severe diversion colitis). Group 1 can be treated conservatively, Group 2 can be treated using conservative management prior to restoration of colonic continuity and Group 3 should ideally undergo restoration of colonic continuity. If a surgical option is not feasible, pharmacologic treatment options should be tried to resolve the inflammation. A summary of the clinical courses of case reports is shown in Table 2.

Surgery

Treatment of diversion colitis should be primarily directed at restoring bowel continuity to restore the luminal flow. This will resolve the symptoms and assist the bowel to return to normal. Re-anastomosis has proven to be consistently effective in halting the symptoms of diversion colitis in a number of studies[2,10,25,39,42]. Re-anastomosis of diverted segments in patients with preexisting inflammatory bowel disease is a more difficult decision because inflammation in the diverted segment could represent inflammatory bowel disease or diversion colitis, each of which dictate different courses of action[3,21,42]. Resection is not typically required. Indications for resection include uncontrolled perianal sepsis, perianal fistulous disease, anal incontinence, and uncontrolled symptoms related to diversion colitis.

Diet and lifestyle

Nutritional imbalance in the excluded colon is likely responsible for the pathologic changes and symptoms of diversion colitis. However, current evidence does not support the effectiveness of lifestyle modifications or nutritional imbalance[60].

Pharmacologic treatment is generally indicated for the temporary control of symptoms in preparation for surgery. It is used occasionally for patients who are not considered surgical candidates because of severe medical comorbidities, poor sphincter function, or reasons of technical difficulty.

Short-chain-fatty acid

Short-chain fatty acids, mainly butyrate, are the major fuel source for the epithelium. Their absence in the diverted tract may produce mucosal atrophy and inflammation. Bacteria produce SCFAs as byproducts of carbohydrate fermentation in the colonic lumen, and SCFAs provide the primary energy source for colonic mucosal cells[13]. In human neutrophils, SCFAs reduce the production of reactive oxygen species, which are the agents of oxidative tissue damage[61]. Treatment of diversion colitis with SCFA or butyrate has shown inconsistent results. Harig successfully improved symptoms and endoscopic inflammatory change by SCFA[5]. Komorowski *et al*[10] reported similar results in four patients with diversion colitis with SCFA irrigation. However, Guillmot *et al*[16,28]. failed to demonstrate either histological or endoscopic improvement The differences in response may be partially accounted for by disease groupings. In recent years, several studies on the usefulness of SCFA, including of butyrate, are reported[19,62]. Cristina *et al*[27] proposed that butyrate enemas may prevent the atrophy of the diverted colon/rectum, thus improving the recovery of tissue integrity.

5-aminosalicylic acid

Usefulness of 5-aminosalicylic acid (5-ASA) enemas in diversion colitis was reported for the first time by Triantafillidis *et al*[31] in 1991. Tripodi *et al*[43] has also reported similar results in 1992. Caltabiano *et al*[63] reported that 5-ASA enema reduces oxidative DNA damage in colonic mucosa and reduces mucosal damage using rats in a diversion colitis model. It is considered that the mucosal disorder may be improved by protective action against oxidative DNA damage and the anti-inflammatory action of 5ASA[64].

Corticosteroids

Glotzer reported on several patients with diversion colitis treated by steroid enemas in 1984[2]. Lim and Jowett also reported the efficacy of the steroid enemas in 2000[32,33]. Corticosteroids are first-line agents for symptomatic diversion colitis, with varying effectiveness.

Table 3 Summary of pharmacologic treatments

Treatment	Ref.	Procedure/standard dosage	Efficacy	Complications/main side effects
Surgical anastomosis	[2,3,10,21,25,39,42]	Mobilization of both ends of the bowel with either sutured or stapled anastomosis.	The most effective method of eliminating the signs and symptoms	Bleeding, infection, anastomotic leak, anastomotic stricture, anesthetic risks
Corticosteroids	[2,32,33]	Hydrocortisone (100 mg per 60 mL bottle) enema is administered once daily for up to 3 wk. Occasional treatment may be given for 2 to 3 mo depending on clinical response.	Response to treatment is generally seen in 3 to 5 d.	Local pain and burning, occasionally rectal bleeding. Prolonged treatment may result in systemic absorption, causing systemic side effects.
5-aminosalicylic acid (5-ASA) enemas	[31,43,63,64]	4 g of mesalazine in 60 mL suspensions, administered rectally once-daily dose for 4 to 5 wk.	Varying effect	Occasionally produces acute intolerance manifested by cramping, acute abdominal pain, bloody diarrhea, fever, headache, and rash.
Short-chain-fatty acid (SCFA)	[5,10,13,18,19,26,27,61,62]	SCFA enema rectally twice a day for 2 wk, and then tapered according to response over 2 to 4 wk.	Varying effect	None
Irrigation with Fibers	[65,66]	Solution containing 5% fibers (10 g/d) for 7 d.	The endoscopic score which is used to quantify the intensity of the inflammation at the mucosa at the diverted colon diminished after treatment.	Probably none
Leukocytapheresis	[44]	Leukocytapheresis, at flow rate of 40 mL/min for 60 min, once weekly for 5 wk, following low dose of metronidazole and ciprofloxacin, another set of weekly leukocytapheresis was added.	Significant improvement in her pouchitis disease activity index (PDAI) from 14 to 1.	The common side effects were nausea, vomiting, fever, chills, and nasal obstruction.
Autologous fecal transplantation	[45]	Feces were collected from the colostomy bag, diluted with 600 ml of sterile saline (0.9 %), stirred and filtered three times using an ordinary coffee filter, irrigation endoscopically. This procedure was repeated 3 times within 4 wk (on day 0, day 10 and day 28).	All symptoms improved dramatically within 5 d after the first treatment. Colonoscopy 28 d after the first treatment showed no major signs of inflammation in the colonic stump	None, patient's tolerance required.
Dextrose spray (hypertonic glucose)	[29]	Endoscopically sprayed with 150 mL 50% dextrose via a catheter.	Follow-up pouchoscopy 2 wk after the dextrose spray showed normal pouch mucosa with no evidence of bleeding or mucosal friability.	It has a very low chance of causing transient hyperglycemia because there is no direct injection of the hypertonic solution into blood vessels.

SCFA: Short chain fatty acids; 5-ASA: 5-aminosalicylic acid.

Irrigation with fibers

Resolution of diversion colitis, based on endoscopic and histologic examination, has been reported following irrigation of the diverted segment of the colon with fibers[65,66]. Joaquim *et al*[66] investigated the effect of irrigating the colorectal mucosa of patients with a colostomy using a solution of fibers. In 11 patients with loop colostomies, the diverted colorectal segment was irrigated with a solution containing 5% fibers (10 g/d) for 7 d. Irrigation with fibers improves inflammation within the defunctionalized colon, so this therapy may play a role in the preoperative management of colostomies, potentially decreasing the high incidence of diarrhea after reestablishment of the intestinal transit.

Leukocytapheresis

Watanabe *et al*[44] reported successful treatment of leukocytapheresis in a patient with chronic antibiotic-refractory diversion pouchitis following IPAA for UC with diverting ileostomy. The mucosa of the diverted pouch is less exposed to the fecal stream and pathogens. Therefore, altered immunity likely plays a major role in the maintenance of diversion pouchitis. Leukocytapheresis to address the altered immunity would seem a reasonable approach for antibiotic-refractory pouchitis following IPAA for UC with diverting ileostomy, and its effectiveness in the case suggests that altered immunity may be a key contributing factor compared with dysbiosis, bacterial pathogens, and ischemia.

Autologous fecal microbiota transplantation

Fecal microbiota transplantation (FMT), which consists of transferring stool from a healthy donor to the patient's colon, is an effective treatment for some diseases of the

colon such as Crohn's disease and recurrent Clostridium difficile infections[67]. Gundling *et al*[45] presented that autologous FMT might be an effective and safe option for relapsing DC after standard therapies have failed. Since the interruption of the fecal stream is central to the development of DC, FMT seems to be a hopeful treatment.

Dextrose spray

Custon *et al*[29] presented a patient with ulcerative colitis with severe hematochezia and diffuse mucosal bleeding in a diverted ileal pouch, which was successfully treated with endoscopic spray of hypertonic glucose (50% dextrose). Hypertonic glucose may work thorough osmotic dehydration and sclerosant effects, inducing long-term mural necrosis and fibrotic obliteration of mucosal vessels[68,69]. Glucose spray is safe and inexpensive, and it carries a very low risk of complications. The approach has the potential to reduce recurrent bleeding and need for surgical interventions.

SUMMARY OF PHARMACOLOGIC TREATMENTS

The goal of treatment is the reduction or elimination of symptoms. Patients who desire stoma closure and have acceptable risks should undergo surgery to re-establish intestinal continuity. In their prospective study, Son *et al*[20] reported that the severity of DC is related to diarrhea after an ileostomy reversal and may adversely affect quality of life. Pharmacologic treatments are needed for symptomatic patients with permanent stomas and patients who are unable to undergo stoma closure for reasons of technical difficulty, poor anal sphincter function, or persistent perianal sepsis. In our review, SCFA[5,10,18,19,26,27,36,62], 5-ASA enemas[31,43,47,51], steroid enemas[21,32,33], and irrigation with fibers[65,66] have been tried with various efficacies for mucosal inflammation. Only case reports of therapy involving leukocytapheresis[44], autologous fecal microbiota transplantation (FMT)[45] and dextrose (hypertonic glucose) spray[29] have been tried with some effect. We have summarized the method, advantages and disadvantages of each pharmacologic treatment in Table 3.

CONCLUSION

The vast majority of diverted patients remain asymptomatic, however diversion colitis occurs in almost all diverted patients. It generally resolves following colostomy closure. However, those patients with significant symptoms or histories of colitis or diarrhea should undergo a complete proximal and distal colonic evaluation prior to stoma closure, and some treatments need not be delayed in these patients. Patients with permanent diversions should undergo periodic pharmacologic treatment. This review of various treatments for diversion colitis will hopefully be useful for determining future treatments.

REFERENCES

1 **Morson BC**, Dawson IMP. Gastrointestinal Pathology, first ed., Blackwellfic Publications, London, 1972
2 **Glotzer DJ**, Glick ME, Goldman H. Proctitis and colitis following diversion of the fecal stream. *Gastroenterology* 1981; **80**: 438-441 [PMID: 7450438]
3 **Mudretsova-Viss KA**, Gabriél'iants GM. [Enterococcal survival in forcemeat preserved in polymer films and in cutlets made from it]. *Vopr Pitan* 1975; **1**: 68-72 [PMID: 1906]
4 **Ma CK**, Gottlieb C, Haas PA. Diversion colitis: a clinicopathologic study of 21 cases. *Hum Pathol* 1990; **21**: 429-436 [PMID: 2318485]
5 **Harig JM**, Soergel KH, Komorowski RA, Wood CM. Treatment of diversion colitis with short-chain-fatty acid irrigation. *N Engl J Med* 1989; **320**: 23-28 [PMID: 2909876 DOI: 10.1056/NEJM198901053200105]
6 **Frisbie JH**, Ahmed N, Hirano I, Klein MA, Soybel DI. Diversion colitis in patients with myelopathy: clinical, endoscopic, and histopathological findings. *J Spinal Cord Med* 2000; **23**: 142-149 [PMID: 10914356]
7 **Neut C**, Guillemot F, Colombel JF. Nitrate-reducing bacteria in diversion colitis: a clue to inflammation? *Dig Dis Sci* 1997; **42**: 2577-2580 [PMID: 9440640]
8 **Villanacci V**, Talbot IC, Rossi E, Bassotti G. Ischaemia: a pathogenetic clue in diversion colitis? *Colorectal Dis* 2007; **9**: 601-605 [PMID: 17824976 DOI: 10.1111/j.1463-1318.2006.01182.x]
9 **Roe AM**, Warren BF, Brodribb AJ, Brown C. Diversion colitis and involution of the defunctioned anorectum. *Gut* 1993; **34**: 382-385 [PMID: 8472988]
10 **Komorowski RA**. Histologic spectrum of diversion colitis. *Am J Surg Pathol* 1990; **14**: 548-554 [PMID: 2337203]
11 **Geraghty JM**, Talbot IC. Diversion colitis: histological features in the colon and rectum after defunctioning colostomy. *Gut* 1991; **32**: 1020-1023 [PMID: 1916483]
12 **Winslet MC**, Poxon V, Youngs DJ, Thompson H, Keighley MR. A pathophysiologic study of diversion proctitis. *Surg Gynecol Obstet* 1993; **177**: 57-61 [PMID: 8322151]
13 **Murray FE**, O'Brien MJ, Birkett DH, Kennedy SM, LaMont JT. Diversion colitis. Pathologic findings in a resected sigmoid colon and rectum. *Gastroenterology* 1987; **93**: 1404-1408 [PMID: 3678755]
14 **Yeong ML**, Bethwaite PB, Prasad J, Isbister WH. Lymphoid follicular hyperplasia--a distinctive feature of diversion colitis. *Histopathology* 1991; **19**: 55-61 [PMID: 1916687]
15 **Asplund S**, Gramlich T, Fazio V, Petras R. Histologic changes in defunctioned rectums in patients with inflammatory bowel disease: a clinicopathologic study of 82 patients with long-term follow-up. *Dis Colon Rectum* 2002; **45**: 1206-1213 [PMID: 12352238 DOI: 10.1097/01.DCR.0000027037.66166.F3]
16 **Haque S**, West AB. Diversion colitis--20 years a-growing. *J Clin Gastroenterol* 1992; **15**: 281-283 [PMID: 1294631]
17 **Vujanić GM**, Dojcinov SD. Diversion colitis in children: an iatrogenic appendix vermiformis? *Histopathology* 2000; **36**: 41-46 [PMID: 10632750]
18 **Neut C**, Guillemot F, Gower-Rousseau C, Biron N, Cortot A, Colombel JF. [Treatment of diversion colitis with short-chain fatty acids. Bacteriological study]. *Gastroenterol Clin Biol* 1995; **19**: 871-875 [PMID: 8746044]
19 **Pal K**, Tinalal S, Al Buainain H, Singh VP. Diversion proctocolitis and response to treatment with short-chain fatty acids--a clinicopathological study in children. *Indian J Gastroenterol* 2015; **34**: 292-299 [PMID: 26243588 DOI: 10.1007/s12664-015-0577-0]
20 **Son DN**, Choi DJ, Woo SU, Kim J, Keom BR, Kim CH, Baek SJ, Kim SH. Relationship between diversion colitis and quality of life in rectal cancer. *World J Gastroenterol* 2013; **19**: 542-549 [PMID: 23382634 DOI: 10.3748/wjg.v19.i4.542]
21 **Korelitz BI**, Cheskin LJ, Sohn N, Sommers SC. The fate of the rectal segment after diversion of the fecal stream in Crohn's disease: its implications for surgical management. *J Clin*

Gastroenterol 1985; **7**: 37-43 [PMID: 3980962]
22 **Ferguson CM**, Siegel RJ. A prospective evaluation of diversion colitis. *Am Surg* 1991; **57**: 46-49 [PMID: 1796797]
23 **Baek SJ**, Kim SH, Lee CK, Roh KH, Keum B, Kim CH, Kim J. Relationship between the severity of diversion colitis and the composition of colonic bacteria: a prospective study. *Gut Liver* 2014; **8**: 170-176 [PMID: 24672659 DOI: 10.5009/gnl.2014.8.2.170]
24 **Whelan RL**, Abramson D, Kim DS, Hashmi HF. Diversion colitis. A prospective study. *Surg Endosc* 1994; **8**: 19-24 [PMID: 8153859]
25 **Orsay CP**, Kim DO, Pearl RK, Abcarian H. Diversion colitis in patients scheduled for colostomy closure. *Dis Colon Rectum* 1993; **36**: 366-367 [PMID: 8458263]
26 **Guillemot F**, Colombel JF, Neut C, Verplanck N, Lecomte M, Romond C, Paris JC, Cortot A. Treatment of diversion colitis by short-chain fatty acids. Prospective and double-blind study. *Dis Colon Rectum* 1991; **34**: 861-864 [PMID: 1914718]
27 **Luceri C**, Femia AP, Fazi M, Di Martino C, Zolfanelli F, Dolara P, Tonelli F. Effect of butyrate enemas on gene expression profiles and endoscopic/histopathological scores of diverted colorectal mucosa: A randomized trial. *Dig Liver Dis* 2016; **48**: 27-33 [PMID: 26607831 DOI: 10.1016/j.dld.2015.09.005]
28 **Fazio VW**, Ziv Y, Church JM, Oakley JR, Lavery IC, Milsom JW, Schroeder TK. Ileal pouch-anal anastomoses complications and function in 1005 patients. *Ann Surg* 1995; **222**: 120-127 [PMID: 7639579]
29 **Nyabanga CT**, Shen B. Endoscopic Treatment of Bleeding Diversion Pouchitis with High-Concentration Dextrose Spray. *ACG Case Rep J* 2017; **4**: e51 [PMID: 28377939 DOI: 10.14309/crj.2017.51]
30 **Gorgun E**, Remzi FH. Complications of ileoanal pouches. *Clin Colon Rectal Surg* 2004; **17**: 43-55 [PMID: 20011284 DOI: 10.1055/s-2004-823070]
31 **Triantafillidis JK**, Nicolakis D, Mountaneas G, Pomonis E. Treatment of diversion colitis with 5-aminosalicylic acid enemas: comparison with betamethasone enemas. *Am J Gastroenterol* 1991; **86**: 1552-1553 [PMID: 1928058]
32 **Lim AG**, Langmead FL, Feakins RM, Rampton DS. Diversion colitis: a trigger for ulcerative colitis in the in-stream colon? *Gut* 1999; **44**: 279-282 [PMID: 9895391]
33 **Jowett SL**, Cobden I. Diversion colitis as a trigger for ulcerative colitis. *Gut* 2000; **46**: 294 [PMID: 10712080]
34 **Burman JH**, Thompson H, Cooke WT, Williams JA. The effects of diversion of intestinal contents on the progress of Crohn's disease of the large bowel. *Gut* 1971; **12**: 11-15 [PMID: 5543369]
35 **Lim AG**, Lim W. Diversion colitis: a trigger for ulcerative colitis in the instream colon. *Gut* 2000; **46**: 441 [PMID: 10733317]
36 **Kiely EM**, Ajayi NA, Wheeler RA, Malone M. Diversion procto-colitis: response to treatment with short-chain fatty acids. *J Pediatr Surg* 2001; **36**: 1514-1517 [PMID: 11584399 DOI: 10.1053/jpsu.2001.27034]
37 **Boyce SA**, Hendry WS. Diversion colitis presenting with massive rectal distension and bilateral ureteric obstruction. *Int J Colorectal Dis* 2008; **23**: 1143-1144 [PMID: 18443804 DOI: 10.1007/s00384-008-0491-3]
38 **Lu ES**, Lin T, Harms BL, Gaumnitz EA, Singaram C. A severe case of diversion colitis with large ulcerations. *Am J Gastroenterol* 1995; **90**: 1508-1510 [PMID: 7661179]
39 **Lusk LB**, Reichen J, Levine JS. Aphthous ulceration in diversion colitis. Clinical implications. *Gastroenterology* 1984; **87**: 1171-1173 [PMID: 6479539]
40 **Ona FV**, Boger JN. Rectal bleeding due to diversion colitis. *Am J Gastroenterol* 1985; **80**: 40-41 [PMID: 3871305]
41 **Komuro Y**, Watanabe T, Hata K, Nagawa H. Diversion colitis with a mucosal tear on endoscopic insufflation. *Gut* 2003; **52**: 1388-1389 [PMID: 12912883]
42 **Korelitz BI**, Cheskin LJ, Sohn N, Sommers SC. Proctitis after fecal diversion in Crohn's disease and its elimination with reanastomosis: implications for surgical management. Report of four cases. *Gastroenterology* 1984; **87**: 710-713 [PMID: 6745620]
43 **Tripodi J**, Gorcey S, Burakoff R. A case of diversion colitis treated with 5-aminosalicylic acid enemas. *Am J Gastroenterol* 1992; **87**: 645-647 [PMID: 1595655]
44 **Watanabe C**, Hokari R, Miura S. Chronic antibiotic-refractory diversion pouchitis successfully treated with leukocyteapheresis. *Ther Apher Dial* 2014; **18**: 644-645 [PMID: 24571541 DOI: 10.1111/1744-9987.12175]
45 **Gundling F**, Tiller M, Agha A, Schepp W, Iesalnieks I. Successful autologous fecal transplantation for chronic diversion colitis. *Tech Coloproctol* 2015; **19**: 51-52 [PMID: 25300242 DOI: 10.1007/s10151-014-1220-2]
46 **Scott RL**, Pinstein ML. Diversion colitis demonstrated by double-contrast barium enema. *AJR Am J Roentgenol* 1984; **143**: 767-768 [PMID: 6332481 DOI: 10.2214/ajr.143.4.767]
47 **Lai JM**, Chuang TY, Francisco GE, Strayer JR. Diversion colitis: a cause of abdominal discomfort in spinal cord injury patients with colostomy. *Arch Phys Med Rehabil* 1997; **78**: 670-671 [PMID: 9196478]
48 **Tsironi E**, Irving PM, Feakins RM, Rampton DS. "Diversion" colitis caused by Clostridium difficile infection: report of a case. *Dis Colon Rectum* 2006; **49**: 1074-1077 [PMID: 16729217 DOI: 10.1007/s10350-006-0577-3]
49 **Haugen V**, Rothenberger DA, Powell J. Antegrade irrigations of a surgically reconstructed Hartmann's pouch to treat intractable diversion colitis. *J Wound Ostomy Continence Nurs* 2008; **35**: 231-232 [PMID: 18344801 DOI: 10.1097/01.WON.0000313649.90612.a1]
50 **Talisetti A**, Longacre T, Pai RK, Kerner J. Diversion colitis in a 19-year-old female with megacystis-microcolon-intestinal hypoperistalsis syndrome. *Dig Dis Sci* 2009; **54**: 2338-2340 [PMID: 19582576 DOI: 10.1007/s10620-009-0882-5]
51 **Kominami Y**, Ohe H, Kobayashi S, Higashi R, Uchida D, Morimoto Y, Nakarai A, Numata N, Hirao K, Ogawa T, Ueki T, Nakagawa M, Araki Y, Mizuno M, Chayama K. [Classification of the bleeding pattern in colonic diverticulum is useful to predict the risk of bleeding or re-bleeding after endoscopic treatment]. *Nihon Shokakibyo Gakkai Zasshi* 2012; **109**: 393-399 [PMID: 22398904]
52 **Matsumoto S**, Mashima H. Efficacy of Combined Mesalazine Plus Corticosteroid Enemas for Diversion Colitis after Subtotal Colectomy for Ulcerative Colitis. *Case Rep Gastroenterol* 2016; **10**: 157-160 [PMID: 27403119 DOI: 10.1159/000445868]
53 **Neut C**, Colombel JF, Guillemot F, Cortot A, Gower P, Quandalle P, Ribet M, Romond C, Paris JC. Impaired bacterial flora in human excluded colon. *Gut* 1989; **30**: 1094-1098 [PMID: 2767506]
54 **McCafferty DM**, Mudgett JS, Swain MG, Kubes P. Inducible nitric oxide synthase plays a critical role in resolving intestinal inflammation. *Gastroenterology* 1997; **112**: 1022-1027 [PMID: 9041266]
55 **Velázquez OC**, Lederer HM, Rombeau JL. Butyrate and the colonocyte. Production, absorption, metabolism, and therapeutic implications. *Adv Exp Med Biol* 1997; **427**: 123-134 [PMID: 9361838]
56 **Bosshardt RT**, Abel ME. Proctitis following fecal diversion. *Dis Colon Rectum* 1984; **27**: 605-607 [PMID: 6468202]
57 **Hundorfean G**, Chiriac MT, Siebler J, Neurath MF, Mudter J. Confocal laser endomicroscopy for the diagnosis of diversion colitis. *Endoscopy* 2012; **44** Suppl 2 UCTN: E358-E359 [PMID: 23012020 DOI: 10.1055/s-0032-1310019]
58 **Lechner GL**, Frank W, Jantsch H, Pichler W, Hall DA, Waneck R, Wunderlich M. Lymphoid follicular hyperplasia in excluded colonic segments: a radiologic sign of diversion colitis. *Radiology* 1990; **176**: 135-136 [PMID: 2353081 DOI: 10.1148/radiology.176.1.2353081]
59 **Edwards CM**, George B, Warren B. Diversion colitis--new light through old windows. *Histopathology* 1999; **34**: 1-5 [PMID: 9934577]
60 **Eggenberger JC**, Farid A. Diversion Colitis. *Curr Treat Options Gastroenterol* 2001; **4**: 255-259 [PMID: 11469982]
61 **Liu Q**, Shimoyama T, Suzuki K, Umeda T, Nakaji S, Sugawara K. Effect of sodium butyrate on reactive oxygen species generation

by human neutrophils. *Scand J Gastroenterol* 2001; **36**: 744-750 [PMID: 11444474]
62 **Schauber J**, Bark T, Jaramillo E, Katouli M, Sandstedt B, Svenberg T. Local short-chain fatty acids supplementation without beneficial effect on inflammation in excluded rectum. *Scand J Gastroenterol* 2000; **35**: 184-189 [PMID: 10720118]
63 **Caltabiano C**, Máximo FR, Spadari AP, da Conceição Miranda DD, Serra MM, Ribeiro ML, Martinez CA. 5-aminosalicylic acid (5-ASA) can reduce levels of oxidative DNA damage in cells of colonic mucosa with and without fecal stream. *Dig Dis Sci* 2011; **56**: 1037-1046 [PMID: 21042854 DOI: 10.1007/s10620-010-1378-z]
64 **Grisham MB**, Granger DN. Neutrophil-mediated mucosal injury. Role of reactive oxygen metabolites. *Dig Dis Sci* 1988; **33**: 6S-15S [PMID: 2831016]
65 **Agarwal VP**, Schimmel EM. Diversion colitis: a nutritional deficiency syndrome? *Nutr Rev* 1989; **47**: 257-261 [PMID: 2689929]
66 **de Oliveira-Neto JP**, de Aguilar-Nascimento JE. Intraluminal irrigation with fibers improves mucosal inflammation and atrophy in diversion colitis. *Nutrition* 2004; **20**: 197-199 [PMID: 14962686 DOI: 10.1016/j.nut.2003.10.006]
67 **van Nood E**, Vrieze A, Nieuwdorp M, Fuentes S, Zoetendal EG, de Vos WM, Visser CE, Kuijper EJ, Bartelsman JF, Tijssen JG, Speelman P, Dijkgraaf MG, Keller JJ. Duodenal infusion of donor feces for recurrent Clostridium difficile. *N Engl J Med* 2013; **368**: 407-415 [PMID: 23323867 DOI: 10.1056/NEJMoa1205037]
68 **Chang KY**, Wu CS, Chen PC. Prospective, randomized trial of hypertonic glucose water and sodium tetradecyl sulfate for gastric variceal bleeding in patients with advanced liver cirrhosis. *Endoscopy* 1996; **28**: 481-486 [PMID: 8886633 DOI: 10.1055/s-2007-1005527]
69 **Tian C**, Mehta P, Shen B. Endoscopic Therapy of Bleeding from Radiation Enteritis with Hypertonic Glucose Spray. *ACG Case Rep J* 2014; **1**: 181-183 [PMID: 26157869 DOI: 10.14309/crj.2014.45]

P- Reviewer: De Silva AP, Triantafillidis JK, Tandon RK
S- Editor: Wang XJ **L- Editor**: A **E- Editor**: Huang Y

World Journal of Gastroenterology

Submit a Manuscript: http://www.f6publishing.com

World J Gastroenterol 2018 April 28; 24(16): 1748-1765

DOI: 10.3748/wjg.v24.i16.1748

ISSN 1007-9327 (print) ISSN 2219-2840 (online)

ORIGINAL ARTICLE

Basic Study

Nonalcoholic steatohepatitis severity is defined by a failure in compensatory antioxidant capacity in the setting of mitochondrial dysfunction

Michelle L Boland, Stephanie Oldham, Brandon B Boland, Sarah Will, Jean-Martin Lapointe, Silvia Guionaud, Christopher J Rhodes, James L Trevaskis

Michelle L Boland, Stephanie Oldham, Brandon B Boland, Sarah Will, Christopher J Rhodes, James L Trevaskis, Cardiovascular and Metabolic Diseases, MedImmune LLC, Gaithersburg, MD 20878, United States

Jean-Martin Lapointe, Pathology, MedImmune Ltd., Cambridge CB21 6GH, United Kingdom

Silvia Guionaud, Pathology, Drug Safety and Metabolism, IMED Biotech Unit, AstraZeneca, Cambridge CB22 3AT, United Kingdom

ORCID number: Michelle L Boland (0000-0002-9920-2088); Stephanie Oldham (0000-0002-0295-1921); Brandon B Boland (0000-0003-1280-9547); Sarah Will (0000-0001-9408-9234); Jean-Martin Lapointe (0000-0003-0141-4603); Silvia Guionaud (0000-0003-1929-6094); Christopher J Rhodes (0000-0002-4852-516X); James L Trevaskis (0000-0002-5356-6118).

Author contributions: Boland ML and Trevaskis JL conceived of the project; Boland ML, Rhodes CJ and Trevaskis JL designed and interpreted experiments; Boland ML, Oldham S, Boland BB, Will S, Lapointe JM and Guionaud S acquired and analyzed data; Boland ML, Boland BB, Rhodes CJ and Trevaskis JL wrote and edited the manuscript.

Supported by MedImmune.

Institutional animal care and use committee statement: All animal experiments were conducted in accordance with policies of the NIH Guide for the Care and Use of Laboratory Animals and the Institutional Animal Care and Use Committee (IACUC) of MedImmune, LLC. Specific protocols used in this study were approved by the MedImmune IACUC, protocol number MI-16-0034.

Conflict-of-interest statement: All authors are current employees and/or stockholders of MedImmune/AstraZeneca.

ARRIVE guidelines statement: The authors have read the ARRIVE guidelines, and the manuscript was prepared and revised according to the ARRIVE guidelines

Manuscript source: Unsolicited manuscript

Correspondence to: James L Trevaskis, PhD, Principal Scientist, Cardiovascular and Metabolic Diseases, MedImmune, LLC, Gaithersburg, MD 20878, United States. trevaskisj@medimmune.com

Telephone: +1-301-3986695

Received: January 17, 2018
Peer-review started: January 17, 2018
First decision: February 11, 2018
Revised: February 22, 2018
Accepted: February 26, 2018
Article in press: February 25, 2018
Published online: April 28, 2018

Abstract

AIM

To comprehensively evaluate mitochondrial (dys) function in preclinical models of nonalcoholic steatohepatitis (NASH).

METHODS

We utilized two readily available mouse models of nonalcoholic fatty liver disease (NAFLD) with or without

progressive fibrosis: *Lep*^{ob}/*Lep*^{ob} (*ob/ob*) and FATZO mice on high *trans*-fat, high fructose and high cholesterol (AMLN) diet. Presence of NASH was assessed using immunohistochemical and pathological techniques, and gene expression profiling. Morphological features of mitochondria were assessed *via* transmission electron microscopy and immunofluorescence, and function was assessed by measuring oxidative capacity in primary hepatocytes, and respiratory control and proton leak in isolated mitochondria. Oxidative stress was measured by assessing activity and/or expression levels of *Nrf1*, *Sod1*, *Sod2*, catalase and 8-OHdG.

RESULTS

When challenged with AMLN diet for 12 wk, *ob/ob* and FATZO mice developed steatohepatitis in the presence of obesity and hyperinsulinemia. NASH development was associated with hepatic mitochondrial abnormalities, similar to those previously observed in humans, including mitochondrial accumulation and increased proton leak. AMLN diet also resulted in increased numbers of fragmented mitochondria in both strains of mice. Despite similar mitochondrial phenotypes, we found that *ob/ob* mice developed more advanced hepatic fibrosis. Activity of superoxide dismutase (SOD) was increased in *ob/ob* AMLN mice, whereas FATZO mice displayed increased catalase activity, irrespective of diet. Furthermore, 8-OHdG, a marker of oxidative DNA damage, was significantly increased in *ob/ob* AMLN mice compared to FATZO AMLN mice. Therefore, antioxidant capacity reflected as the ratio of catalase:SOD activity was similar between FATZO and C57BL6J control mice, but significantly perturbed in *ob/ob* mice.

CONCLUSION

Oxidative stress, and/or the capacity to compensate for increased oxidative stress, in the setting of mitochondrial dysfunction, is a key factor for development of hepatic injury and fibrosis in these mouse models.

Key words: Nonalcoholic steatohepatitis; Steatosis; Fibrosis; Mitochondrial function; Oxidative stress

Core tip: *ob*/*ob* and FATZO mice developed nonalcoholic fatty liver disease/nonalcoholic steatohepatitis (NASH) when fed a high *trans*-fat, high fructose and high cholesterol diet, in the context of obesity and insulin resistance, but showed differences in liver disease severity including collagen deposition and monocyte/macrophage infiltration. Mitochondrial dysfunction and increased numbers of mitochondria were observed in both models, similar to that reported in human NASH. Oxidative damage and antioxidant capacity were associated with disease severity. FATZO mice displayed increased catalase activity and reduced oxidative DNA damage compared to *ob*/*ob* mice, which may explain their lower disease burden.

Boland ML, Oldham S, Boland BB, Will S, Lapointe JM, Guionaud S, Rhodes CJ, Trevaskis JL. Nonalcoholic steatohepatitis severity is defined by a failure in compensatory antioxidant capacity in the setting of mitochondrial dysfunction. *World J Gastroenterol* 2018; 24(16): 1748-1765 Available from: URL: http://www.wjgnet.com/1007-9327/full/v24/i16/1748.htm DOI: http://dx.doi.org/10.3748/wjg.v24.i16.1748

INTRODUCTION

Non-alcoholic fatty liver disease (NAFLD), now the most common liver disease, encompasses a spectrum of disorders from benign simple fatty liver to the more severe non-alcoholic steatohepatitis (NASH) that can progress to liver cirrhosis and hepatocellular carcinoma. Given the strong association of NAFLD with obesity, type Ⅱ diabetes and other aspects of the metabolic syndrome, the current estimated NAFLD prevalence of 20%-40% worldwide is expected to increase[1-3]. While no FDA-approved pharmacotherapies for NAFLD/NASH currently exist, more than 100 clinical trials are now targeting this highly significant unmet medical need.

Insulin resistance is a major pathophysiological factor that underlies the strong association between obesity/type Ⅱ diabetes and NAFLD. Increased circulating free fatty acids and *de novo* lipogenesis lead to excess lipid storage in the hepatocyte, and accumulation of intrahepatic lipid is linked to pathogenic insulin resistance and subsequent onset of type 2 diabetes. This lipid overload also places a unique burden on the mitochondria and promotes mitochondrial dysfunction *in vitro* and in animal models. Data from multiple studies suggest that while TCA cycle activity is increased in NAFLD, mitochondrial respiratory chain inefficiencies lead to increased generation of reactive oxygen species (ROS) and lipotoxic intermediates that further promote oxidative damage and inflammation[4-7]. Importantly, while increased hepatic mitochondrial respiration was observed in obese patients with and without fatty liver, this increase was lost in obese patients with NASH and was associated with increased mitochondrial content, proton leakage and oxidative stress[8].

While dysregulated mitochondrial metabolism has been implicated in NALFD pathogenesis and progression, the specific contribution to disease etiology remains an active area of investigation[9,10]. Multiple lines of evidence suggest that therapeutically targeting the mechanisms leading to mitochondrial dysfunction may improve liver disease[10,11]. The use of pre-clinical models that mimic human pathology in the context of known risk factors, including obesity and insulin resistance, are necessary to understand the clinical translatability of pharmacological interventions given the difficulty of studying humans with a slow progressing disease that cannot be confirmed non-invasively[12].

Hepatic mitochondrial function and oxidative stress in metabolically-relevant, pre-clinical models of simple fatty liver *vs* NASH have not been fully assessed. Here,

two pre-clinical mouse models of simple steatosis and NASH were investigated: *ob/ob* mice on NASH-inducing AMLN diet[13], and the recently described polygenic FATZO mouse which develops high-fat diet-induced obesity and impaired glucose tolerance and which retains an intact leptin axis[14,15]. Importantly, these models are readily available and rapidly and consistently develop clinically relevant disease. We characterized the contribution of mitochondria and oxidative stress to disease phenotype and demonstrate that a reduced ability to combat oxidative stress in the setting of mitochondrial dysfunction is associated with the progression to NASH with advanced fibrosis. These data highlight the utility of these models to dissect the underlying pathobiology of NAFLD disease progression and to predict pharmacological efficacy.

MATERIALS AND METHODS

Animals

Animal studies were conducted in accordance with protocols approved by the Institutional Animal Care and Use Committee (IACUC) at MedImmune and in compliance with the applicable national laws and regulations concerning use of laboratory animals and the AstraZeneca Animal Welfare and Bioethics policies. Eight-week old male C57BL6J or *Lep*^{ob}/*Lep*^{ob} (*ob*/*ob*) mice (Jackson labs, Bar Harbor, ME, United States) and 8-week-old male FATZO mice (Crown Bioscience, Indianapolis, IN, United States) were housed in standard caging at 22 ℃ in a 12-h light: 12-h dark cycle at standard temperature and humidity conditions with *ad libitum* access to water and food. Mice were maintained on test diets for 12 wk. The following test diets were used: 2018 Tekland rodent diet (Envigo, United States), low-fat diet (LFD; 10% kcal/fat; D09100304, Research Diets, New Brunswick, NJ, United States) and the Amylin Liver NASH (AMLN) diet high in fat (40% kcal), fructose (22% by weight), and cholesterol (2% by weight) (D09100301 Research Diets). Study groups comprised C57BL6J chow fed (lean) mice (n = 6), *ob*/*ob* mice on LFD (n = 8) and *ob*/*ob* mice on AMLN diet (n = 10), or C57BL6J lean mice, FATZO mice on LFD, or FATZO mice on AMLN diet (all n = 5 per group).

Measurement of plasma ALT

Terminal blood was collected in EDTA-coated tubes and centrifuged at 10000 × g for 10 min. The plasma was collected and analyzed for ALT levels using a biochemistry analyzer (Cobas c-111, Roche Diagnostics, Indianapolis, IN, United States).

Liver lipid quantification

Total lipids were measured in liver samples using a Bruker LF-90 minispec system (Bruker Biospin Corporation, Billerica, MA, United States). The data are expressed as the percent lipid relative to the total tissue mass.

Plasma insulin and pancreatic insulin content

To isolate pancreatic insulin, the tissue was incubated in a 1.5% HCl/70% EtOH solution overnight at -20 ℃. The tissue was homogenized and frozen again overnight at -20 ℃. Following centrifugation at 2000 rpm for 15 min, the aqueous layer was transferred to a new tube and neutralized upon the addition of 1 mol/L Tris, pH 7.5 at a 1:1 ratio. Plasma and pancreatic insulin levels were measured *via* immunoassay (K152BZC, MesoScale Diagnostics, Rockville, MD, United States).

Histological analysis and quantification of liver tissue

Livers were fixed in 10% neutral buffered formalin for 24 h. Paraffin-embedded tissue sections were stained with hematoxylin and eosin using standard procedures. Histological assessments were conducted by a pathologist under blinded conditions. A modified scoring system, based on the Brunt and Kleiner NAFLD activity score, previously developed and validated to enable a more reproducible and semi-quantitative assessment of murine liver was used to quantify various parameters of liver phenotype[16]. The following parameters were graded to generate the overall NASH score: macrovesicular steatosis (0: < 5%, 1: 5%-33%, 2: 34%-66%, 3: > 66%); ballooning degeneration (0 = absent, 1 = present); lobular inflammation (0 = no foci, 1 = rare foci, 2 = occasional foci, 3 = frequent foci); biliary hyperplasia (0 = none, 1 = mild, 2 = prominent); CD68 immunoreactivity (0 = normal, 1 = minimal increased, 2 = more than minimal increase).

Customized algorithms (Definiens, Munich, Germany) were applied to the liver sections to quantify macrosteatosis per liver area, total collagen area and number of CD68-positive cells. White spaces, non-native liver tissues, large blood vessels and bile ducts were excluded from the analyses.

Immunohistochemistry

Immunohistochemistry was performed using a Ventana Discovery ULTRA Staining Module (Ventana Medical Systems, Tucson, AZ, United States). Formalin-fixed, paraffin embedded liver sections were stained with anti-CD68 (ab125212 Abcam, Cambridge, MA, United States), anti-collagen type 1 A1 (1310-01 Southern Biotech, Birmingham, AL, United States), or anti-catalase (PA5-29183, ThermoFisher).

Transmission electron microscopy

Freshly isolated liver was chemically fixed in 0.1 mol/L cacodylate buffer containing 4% paraformaldehyde and 2% glutaraldehyde. Samples were resin-embedded, sectioned, and stained as previously described[17]. Samples were imaged using the FEI Tecnai G2 SPIRIT electron microscope equipped with a CCD camera (Pleasanton, CA, United States) at 120000 V. Images were acquired using GATAN digital micrograph software (Warrendale, PA, United States). Electron micrographs

were viewed in a blinded fashion using 3Dmod software[18] on a Wacom Cintiq 22HD art tablet (Vancouver, WA, United States). Mitochondrial area and number were quantified per total cytoplasmic area from ⩾ 10 electron micrographs per group *via* manual tracing using the art tablet as previously described (N ⩾ 3 biological replicates, ⩾ 1.5 mm^2 total cytoplasmic area)[19].

Immunofluorescence

FFPE liver sections were deparaffinized followed by blocking of endogenous peroxidases. Antigen retrieval was carried out by heating samples at 119 C for 6.5 min in citrate buffer solution (Dako Target Retrieval Solution, Agilent Technologies, Santa Clara, CA, United States). After blocking with 1.5% horse serum, slides were incubated overnight in anti-HSP60 (D6F1, Cell Signaling Technology, Danvers, MA, United States) in Dako antibody diluent (S3022, Agilent Technologies). Secondary antibody incubation with goat anti-rabbit Alexa 488 (ThermoFisher) was carried out at room temperature for 1 h. Slides were mounted using Prolong Gold plus DAPI (ThermoFisher). Slides were imaged using a Leica TCS SP5 X confocal microscope. Confocal images were viewed in a blinded fashion using 3Dmod software on a Wacom Cintiq 22HD art tablet (Vancouver, WA, United States). Mitochondrial length and number per total cytoplasmic area were quantified from ⩾ 15 images per group (n ⩾ 3 biological replicates) *via* manual tracing of cell boundaries, nuclei, lipid droplets and mitochondria. Total cytoplasmic area was calculated as area within the cell boundary minus the nuclei and lipid droplet areas.

Primary hepatocyte isolation

Murine primary hepatocytes were isolated using a modified two-step non-recirculating perfusion method as previously described[20]. All assays were carried out within 18-24 h post-plating.

Mitochondrial oxygen consumption

Mitochondrial oxygen consumption was measured using the Seahorse Xfe96 analyzer (Agilent Technologies). Primary hepatocytes were plated at a density of 7500 cells per well and allowed to recover overnight. The medium was exchanged (DMEM containing 5 mmol/L glucose, 4 mmol/L L-glutamine, 2 mmol/L sodium pyruvate, pH 7.4) and the plate was placed in a CO_2-free incubator for 30 min prior to being placed in the analyzer. The following compounds were used in the mitochondrial stress test: 1 μmol/L oligomycin (Sigma, St Louis, MO, United States), 0.5 μmol/L FCCP (Sigma), and 5 μmol/L antimycin A (Sigma). The data represent the average of three independent experiments each with a minimum of 8 replicates per group.

Mitochondrial coupling and proton leak

The respiratory control ratio (RCR) and leak control ratio (LCR) were quantified using freshly isolated hepatic mitochondria as an index of mitochondrial coupling and proton leak, respectively[8]. Briefly, 5 μg of mitochondria were loaded per well of the seahorse plate in assay medium (70 mmol/L sucrose, 220 mmol/L mannitol, 10 mmol/L KH_2PO_4, 5 mmol/L $MgCl_2$, 2 mmol/L HEPES, 1 mmol/L EGTA, 0.2% (w/v) fatty acid-free BSA, pH 7.2 supplemented with complex Ⅱ substrate succinate at 10 mmol/L). The following injections were performed: 4 mmol/L ADP (state 3), 1 μmol/L oligomycin (state 3_o), 1 μmol/L FCCP (state 3_U) and 4 μmol/L antimycin A/ 2 μmol/L rotenone. RCR is represented by the ratio of ADP-stimulated respiration (state 3) to respiration in the presence of oligomycin (state 3_o), and LCR is represented by the ratio of respiration in the presence of oligomycin (State 3_o) to FCCP-stimulated respiration (state 3_U).

Citrate synthase activity

Mitochondrial content was quantified by citrate synthase activity (CSA) of freshly isolated primary hepatocytes or liver mitochondria using the Citrate Synthase Activity Colorimetric Assay Kit (BioVision, Milpitas, CA, United States) according to the manufacturer's instructions and normalized to total protein assessed by the Pierce BCA protein assay kit (ThermoFisher).

Isolation of liver mitochondria

Excised liver was rinsed in several changes of PBS and homogenized in ice cold isolation buffer (70 mmol/L sucrose, 210 mmol/L mannitol, 5 mmol/L HEPES, 1 mmol/L EGTA, 0.5% w/v fatty acid-free BSA, pH 7.2) using a Wheaton™ Dounce Tissue Grinder (Fisher Scientific). After centrifugation at 800 x g for 10 min at 4 ℃, the supernatants were collected and centrifuged at 8000 × g for 10 min at 4 ℃. The resulting mitochondrial pellet was washed two times and resuspended in a minimal volume of isolation buffer. The isolated mitochondria were kept on ice until use. Protein concentration was determined using the Pierce BCA Protein Assay Kit (ThermoFisher).

RNA isolation and real-Time PCR

Total liver RNA and genomic DNA were isolated using standard procedures. Qiagen RNeasy® columns (Qiagen, United States) were used for RNA purification according to the manufacturer's protocol, including an on-column DNA digestion using DNaseI. Equal amounts of RNA were reverse transcribed to cDNA using SuperScript Ⅲ First Strand cDNA synthesis kit (Invitrogen, Carlsbad, CA, United States) according to the manufacturer's instructions. Real-Time PCR was performed on a QuantStudio-7 Flex System (Applied Biosystems, Foster City, CA, United States) using Applied Biosystems TaqMan Fast Universal PCR Master Mix and TaqMan probes. Each sample was assayed in triplicate and quantified using the ΔΔCT method normalized to endogenous control *Ppia* (mRNA) or nuclear encoded gene β-globin (gDNA). The following Taqman probes were used in qPCR assays: collagen type 1 alpha 1 (Col1a1, Mm00801666_g1), collagen type 1 alpha 2

(Col1a2, Mm00483888_m1), TIMP metallopeptidase inhibitor 1 (Timp1, Mm01341361_m1), interleukin 1 beta (Il1b, Mm00434228_m1), cluster of differentiation 68 (Cd68, Mm03047343_m1), tumor necrosis factor alpha (Tnf, Mm00443258_m1), PPARG coactivator 1 alpha (Ppargc1a, Mm01208835_m1), nuclear respiratory factor 1 (Nrf1, Mm01135606_m1), transcription factor A, mitochondrial (Tfam, Mm00447485_m1), superoxide dismutase 1, soluble (Sod1, Mm1344233_g1), superoxide dismutase 2, mitochondrial (Sod2, Mm01313000_m1), catalase (Cat, Mm00437992_m1), glutathione peroxidase (Gpx1, Mm00656767_g1), and peptidylprolyl isomerase A (Ppia, Mm02342430_g1).

Oxidative stress assays

Superoxide dismutase activity (7501-500-K, Trevigen, Gaithersburg, MD, United States) and catalase activity (707002, Cayman Chemical, Ann Arbor, MI, United States) were measured in freshly prepared liver homogenates according to the manufacturer's protocols. The levels of 8-hydroxydeoxyguanosine (8-OHdG) were measured *via* ELISA using approximately 20 μg of total hepatic genomic DNA (4380-096-K, Trevigen).

Statistical analysis

All statistical analyses were carried out using GraphPad Prism 7 (GraphPad Software, San Diego, CA, United States). The data were analyzed *via* one-way or two-way ANOVA and Tukey's post-test. Data are shown as the mean ± SE. Values of $P \leq 0.05$ were considered significant.

RESULTS

Ob/ob mice develop NASH with fibrosis in the setting of obesity and insulin resistance

NASH induction was assessed in *ob/ob* mice, a proposed NASH model when challenged with AMLN diet. C57BL6J mice served as healthy age-matched controls (lean) and were compared to *ob/ob* mice maintained on LFD (*ob/ob* LFD) or AMLN diet (*ob/ob* AMLN) for 12 wk. After the 12-wk disease induction period, *ob/ob* LFD and *ob/ob* AMLN mice weighed significantly more than lean controls ($P < 0.0001$), but did not significantly differ from one another (Figure 1A). While non-fasting blood glucose was slightly reduced in *ob/ob* AMLN animals compared to lean controls (132 mg/dL *vs* 186 mg/dL, $P < 0.05$; Figure 1B), plasma insulin levels ($P < 0.05$; Figure 1C) and pancreatic insulin content ($P < 0.01$; Figure 1D) were concomitantly increased.

We measured markers associated with NAFLD including liver weight, liver lipid, and plasma alanine aminotransferase (ALT). Liver weight was significantly greater in *ob/ob* LFD *vs* lean animals (8.6% *vs* 4.5%, $P < 0.0001$), and was further increased in *ob/ob* AMLN animals (12.7%, $P < 0.0001$; Figure 2A). Similarly, *ob/ob* AMLN livers contained approxiately 34% intrahepatic lipid, which was significantly greater than livers from *ob/ob* LFD (25% lipid, $P < 0.0001$) and lean animals (5% lipid, $P < 0.0001$; Figure 2B). Plasma ALT was also significantly increased in *ob/ob* LFD *vs* lean animals (771 U/L *vs* 160 U/L, $P < 0.0001$) and was further elevated in *ob/ob* AMLN animals (1160 U/L, $P < 0.001$ *vs ob/ob* LFD; Figure 2C).

Macrovesicular steatosis was prominent in both *ob/ob* LFD (60%) and *ob/ob* AMLN animals (67%, $P < 0.001$ *vs ob/ob* LFD; Figure 2D). Hepatic fibrosis assessed by quantification of type 1 collagen stained area was significantly greater in *ob/ob* LFD *vs* lean livers ($P < 0.01$) and even greater in *ob/ob* AMLN liver ($P < 0.0001$ *vs ob/ob* LFD) (Figure 2E). Immunolabeling with the monocyte/macrophage marker CD68 was also markedly elevated in *ob/ob* AMLN livers compared to *ob/ob* LFD and lean controls ($P < 0.0001$ *vs ob/ob* LFD; Figure 2F).

We analyzed hepatic transcript levels of genes involved in fibrosis and inflammation that differentiate the more benign disease observed in *ob/ob* LFD liver histopathology from the steatohepatitis observed in *ob/ob* AMLN livers. Transcripts encoding the most abundant form of liver collagen, type 1 (*Col1a1* and *Col1a2*), in addition to type 3 collagen (*Col3a1*) were significantly elevated in *ob/ob* AMLN livers *vs* lean and *ob/ob* LFD livers ($P < 0.001$, $P < 0.01$, $P < 0.0001$, respectively, *vs ob/ob* LFD; Figure 2G). *Timp1*, another gene associated with increased extracellular matrix turnover, was significantly elevated in *ob/ob* AMLN compared to *ob/ob* LFD and lean livers ($P < 0.001$ *vs ob/ob* LFD; Figure 2G). The expression of cytokines including *Tgfb*, *Tnf*, *Il1b*, and *Il10*, and chemokines including *Ccl2*, *Ccl3*, and *Ccl11* were similarly upregulated in *ob/ob* AMLN livers compared to *ob/ob* LFD and lean controls ($P < 0.01$, $P < 0.05$, $P < 0.05$, $P = 0.2$; $P < 0.01$, $P < 0.001$, $P < 0.01$, respectively, *vs ob/ob* LFD; Figure 2H). Additionally, *Lgals3*, a marker associated with multiple inflammatory cell types and thought to contribute to fibrogenesis, was highly expressed in the livers of *ob/ob* AMLN but not lean or *ob/ob* LFD mice (30-fold induction *vs* lean controls, $P < 0.001$ *vs ob/ob* LFD; Figure 2H).

The steatosis grade was significantly higher in *ob/ob* LFD (grade 2.5, $P < 0.0001$) and *ob/ob* AMLN (grade 3, $P < 0.0001$) compared to lean livers (grade 0; Figure 3A). A significant increase in the number of inflammatory foci (Figure 3B), biliary hyperplasia (Figure 3C) and CD68-positive cells (Figure 3D) was observed in *ob/ob* AMLN *vs* lean ($P < 0.0001$) and *ob/ob* LFD livers ($P < 0.0001$). Ballooned hepatocytes were only observed in *ob/ob* AMLN livers (Figure 3E). An integrated NASH score was generated by combining the grades of steatosis, inflammation, biliary hyperplasia, CD68 positive cells, and ballooning degeneration (Figure 3F), which reflected the clear distinction between *ob/ob* LFD and *ob/ob* AMLN liver histopathology.

Fragmented mitochondria in ob/ob AMLN hepatocytes

We examined mitochondrial ultrastructure in livers from lean, *ob/ob* LFD and *ob/ob* AMLN mice by transmission

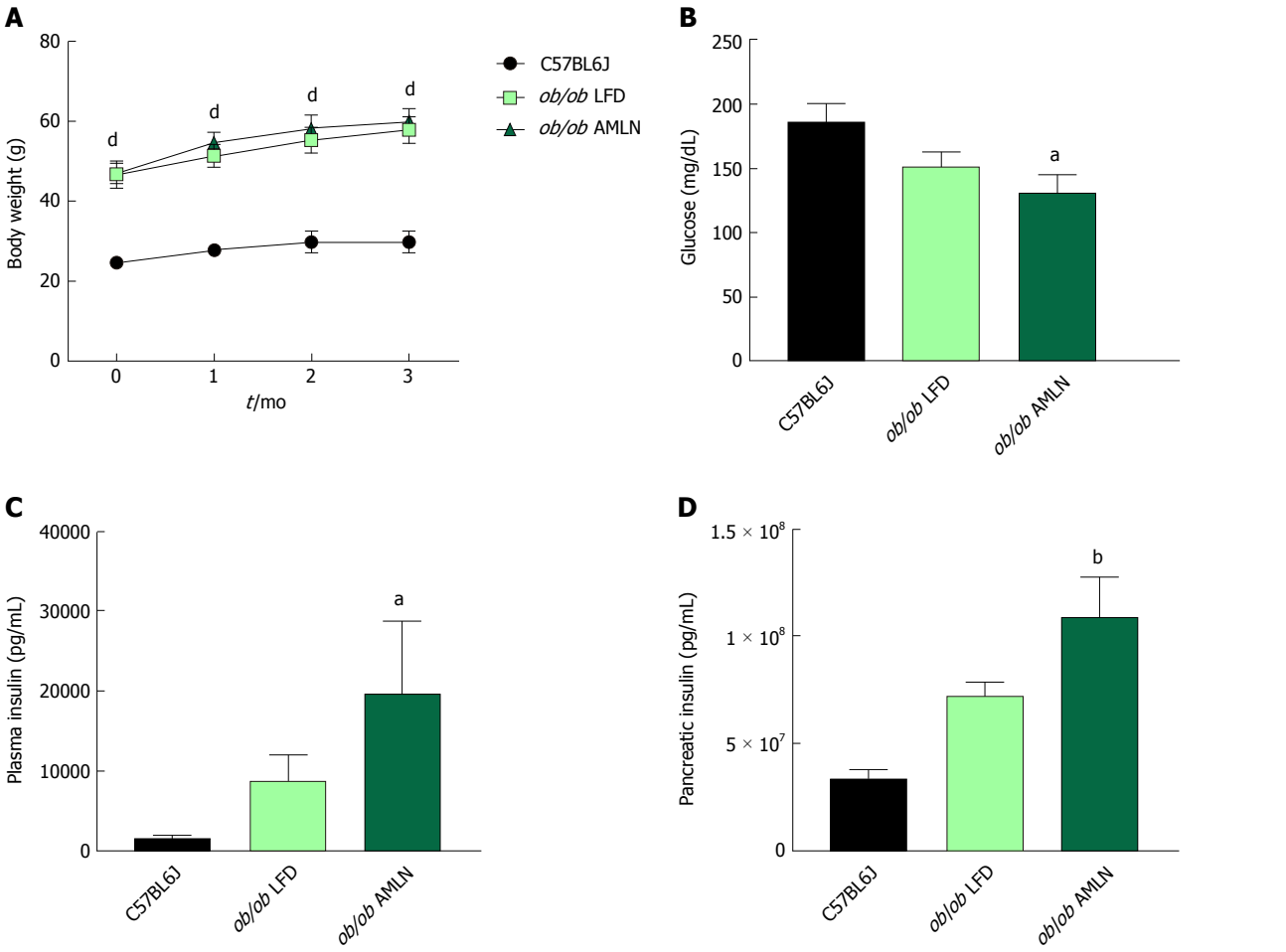

Figure 1 Obese *ob/ob* mice display increased hyperinsulinemia on AMLN diet. (A): Average body weight over 12-wk disease induction period; (B): Terminal non-fasting blood glucose levels; (C): Terminal non-fasting plasma insulin levels; (D): Pancreatic insulin content. $^{a}P \leq 0.05$, $^{b}P \leq 0.01$, $^{d}P \leq 0.0001$ *vs* C57BL6J. LFD: Low-fat diet.

electron micrography (TEM; Figure 4A). Quantitative assessment of TEM images showed *ob/ob* AMLN hepatocytes had increased numbers of mitochondria (approximately 1.5-fold, $P < 0.001$ *vs ob/ob* LFD; Figure 4B). While lean and *ob/ob* LFD hepatocytes contained a mixture of elongated and fragmented mitochondria, *ob/ob* AMLN hepatocytes contained smaller, more fragmented mitochondria (average area = 70 μm^2 for lean controls *vs* 45 μm^2 for *ob/ob* AMLN, $P < 0.01$; Figure 4C); however, no overt defects in outer membrane integrity or cristae formation were observed. Similarly, quantification of mitochondrial length and number from HSP60 immunostained liver sections revealed increased numbers of mitochondria overall in *ob/ob* AMLN livers ($P < 0.005$ *vs* lean controls; Figure 4D) and a significant increase in shorter, more fragmented mitochondria (Figure 4E). Citrate synthase activity (CSA), another measure of mitochondrial content, was increased over 2-fold in primary hepatocytes isolated from *ob/ob* AMLN mice *vs* lean controls ($P < 0.05$; Figure 4F). In line with smaller mitochondria in *ob/ob* AMLN hepatocytes, the expression of proteins required for mitochondrial fusion, mitofusin 1 (*Mfn1*) and dynamin-like 120 kDa protein, mitochondrial (*Opa1*), was significantly decreased in *ob/ob* AMLN livers compared to lean controls ($P < 0.01$ and $P < 0.05$, respectively; Supplementary Figure 4G).

To assess whether this increase in mitochondrial number was due to increased biogenesis, we quantified the expression of transcription factors required for mitochondrial biogenesis and components of the electron transport chain (ETC). While the expression of PPARγ-coactivator 1a (*Ppargc1a*) was slightly increased in *ob/ob* LFD livers (1.4-fold, $P = 0.06$ *vs* lean controls), it was unchanged in *ob/ob* AMLN *vs* lean livers (data not shown). Similarly, nuclear respiratory factor 1 (*Nrf1*) and mitochondrial transcription factor A (*Tfam*) mRNA levels were unchanged in *ob/ob* AMLN *vs* lean and *ob/ob* LFD livers (data not shown). Additionally, expression of mitochondrial autophagy genes *Bnip3*, *Park2* and *Pink1* was not different between groups (Figure 4G). Although *ob/ob* AMLN hepatocytes displayed increased mitochondrial number, they contained significantly less mitochondrial DNA (mtDNA) as assessed by the expression of mitochondrially-encoded genes *Cytb* and *Nd-1* relative to the expression of nuclear encoded β-globin (approximately 30% reduction, $P < 0.05$ *vs* lean controls; Supplementary Figure 4H).

Hepatic ob/ob AMLN mitochondria have reduced respiratory capacity and increased proton leak

To assess mitochondrial function, oxygen consumption of intact primary hepatocytes from lean, *ob/ob* LFD

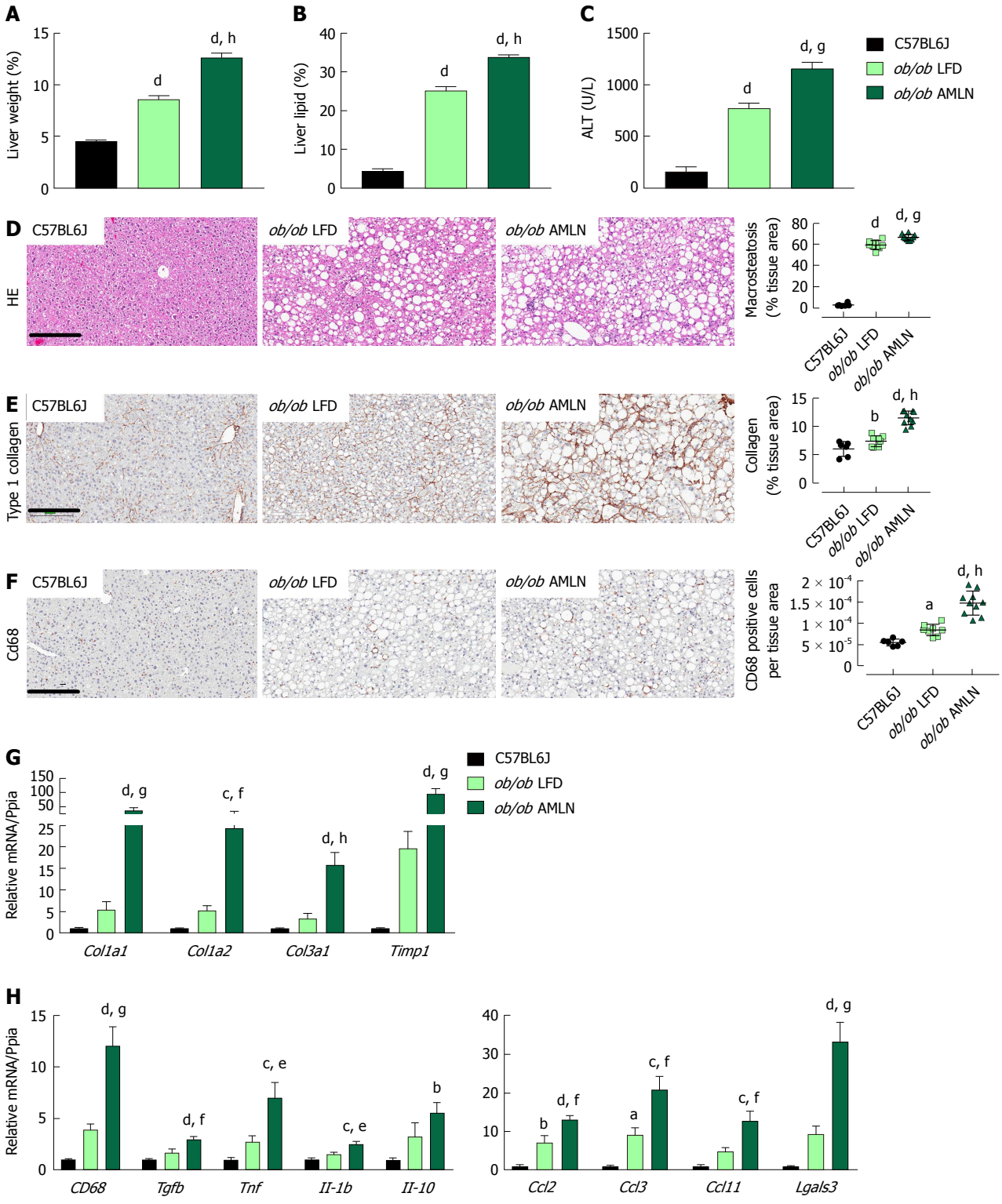

Figure 2 Comparison of metabolic and hepatic abnormalities associated with diet-induced nonalcoholic fatty liver disease/nonalcoholic steatohepatitis in *ob/ob* mice. Liver weight (A), liver lipid (B), and plasma alanine aminotransferase (ALT) levels (C) of lean (C57BL6J) and *ob/ob* mice maintained on control low-fat diet (*ob/ob* LFD) or AMLN diet (*ob/ob* AMLN) for 12 wk; (D): Representative hematoxylin and eosin stained liver sections and quantification of percentage of liver area containing macrosteatosis; (E): Representative collagen type 1 alpha 1 stained liver sections and quantification of collagen area. Scale bar = 200 μm; (F): Representative CD68-stained liver sections and quantification of CD68-positive cells; G, H: Relative expression of genes associated with fibrosis and inflammation. $^{a}P \leq 0.05$, $^{b}P \leq 0.01$, $^{c}P \leq 0.001$, $^{d}P \leq 0.0001$ *vs* C57BL6J; $^{e}P \leq 0.05$, $^{f}P \leq 0.01$, $^{g}P \leq 0.001$, $^{h}P \leq 0.0001$ *vs* LFD. LFD: Low-fat diet.

and *ob/ob* AMLN animals was measured (Figure 5A). *ob/ob* AMLN hepatocytes displayed significantly reduced basal respiration that was approximately 50% lower compared to lean ($P < 0.01$) and *ob/ob* LFD hepatocytes ($P < 0.05$) (Figure 5B). Maximal mitochondrial respiratory capacity was significantly

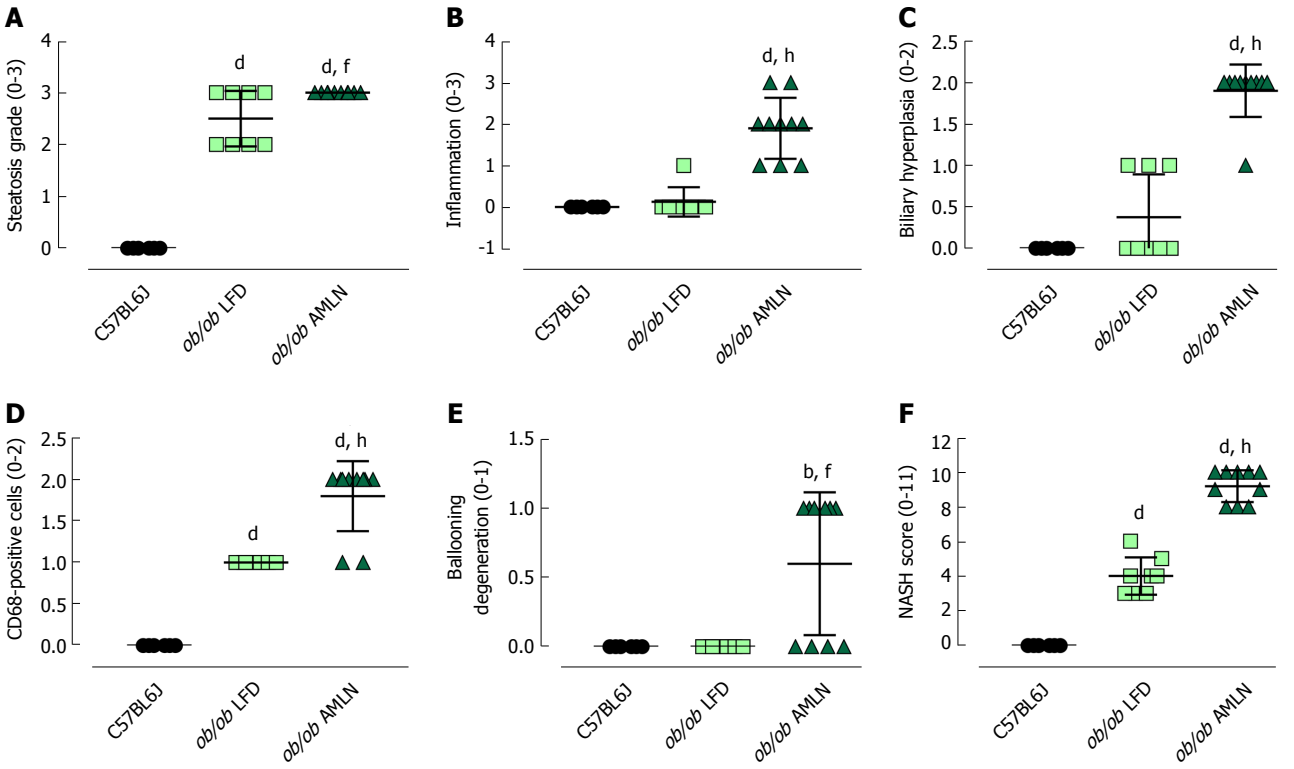

Figure 3 Histopathological grading of C57BL6J, *ob/ob* low-fat diet and *ob/ob* AMLN liver. Individual grades of steatosis (A), inflammation (B), biliary hyperplasia (C), CD68-positive cells (D) and ballooning degeneration (E) are shown; (F): Comparison of the total NASH scores representing the sum of all histologic parameters. $^{b}P \leqslant 0.01$, $^{d}P \leqslant 0.0001$ *vs* C57BL6J; $^{f}P \leqslant 0.01$, $^{h}P \leqslant 0.0001$ *vs* LFD. LFD: Low-fat diet.

increased in *ob/ob* LFD compared to lean hepatocytes (+45%, $P < 0.05$; Figure 5B). In contrast, *ob/ob* AMLN hepatocytes displayed significantly reduced maximal respiration compared to lean (-45%, $P < 0.05$) and *ob/ob* LFD hepatocytes (-60%, $P < 0.001$; Figure 5B).

We also assessed mitochondrial coupling and proton leak. The mitochondrial respiratory control ratio (RCR) and leak control ratio (LCR) were quantified using isolated mitochondria from lean, *ob/ob* LFD and *ob/ob* AMLN livers. Mitochondria from *ob/ob* mouse liver displayed slightly increased proton leak without a significant decrease in respiratory control[21], and AMLN diet further increased proton leak and reduced RCR. Mitochondrial coupling was decreased in *ob/ob* AMLN mice compared to mitochondria from lean mice (4.2 *vs* 5.6; Figure 5C), although this difference did not reach statistical significance. *ob/ob* AMLN mitochondria also displayed a higher LCR compared to lean controls (0.35 *vs* 0.23, $P = 0.06$; Figure 5D), indicating increased proton leak.

FATZO mice fed AMLN diet display enhanced microvesicular steatosis and lobular inflammation but minimal fibrosis

While the *ob/ob* mouse exhibits key aspects of human metabolic disease and, importantly, develops diet-induced NASH with consistent grade 2-3 fibrosis, most humans with NAFLD/NASH are likely hyperleptinemic as opposed to leptin-deficient. We therefore investigated the FATZO mouse, an inbred polygenic cross of AKR/J and C57BL6J strains with a predisposition to obesity and insulin resistance, but intact leptin axis[14,15].

After 12 wk on diet, FATZO mice fed LFD (FATZO LFD) weighed significantly more than lean (C57BL6J) controls (43 g *vs* 35 g, $P < 0.0001$), while FATZO mice fed AMLN diet (FATZO AMLN) weighed significantly more than both FATZO LFD and lean controls (50 g, $P < 0.001$ *vs* FATZO LFD; Figure 6A). Plasma glucose was slightly elevated in FATZO LFD (271 mg/dL) and FATZO AMLN mice (236 mg/dL) compared to lean controls (186 mg/dL; Figure 6B). FATZO AMLN mice displayed severe hyperinsulinemia with average plasma insulin levels that were significantly greater compared to FATZO LFD and lean controls ($P < 0.01$ for *ob/ob* AMLN *vs* lean controls; Figure 6C). Both FATZO LFD and FATZO AMLN mice had increased pancreatic insulin content, which was significantly greater in FATZO AMLN mice compared to lean controls (+50%, $P < 0.05$; Figure 6D).

Markers of liver disease including hepatomegaly, hepatic steatosis and elevated plasma ALT levels were present in both FATZO LFD and FATZO AMLN mice. Relative liver weight was significantly increased in FATZO LFD *vs* lean animals (7.3% *vs* 4.4%, $P < 0.0001$), and was further increased in FATZO AMLN animals (10.6%, $P < 0.001$ *vs* FATZO LFD) (Figure 7A). Similarly, hepatic lipid content was significantly greater in FATZO LFD compared to lean controls (20% *vs* 6%) and was greatest in FATZO AMLN mice (30%, $P < 0.0001$ *vs* FATZO LFD; Figure 7B). Plasma ALT was also significantly increased in FATZO LFD *vs* lean animals

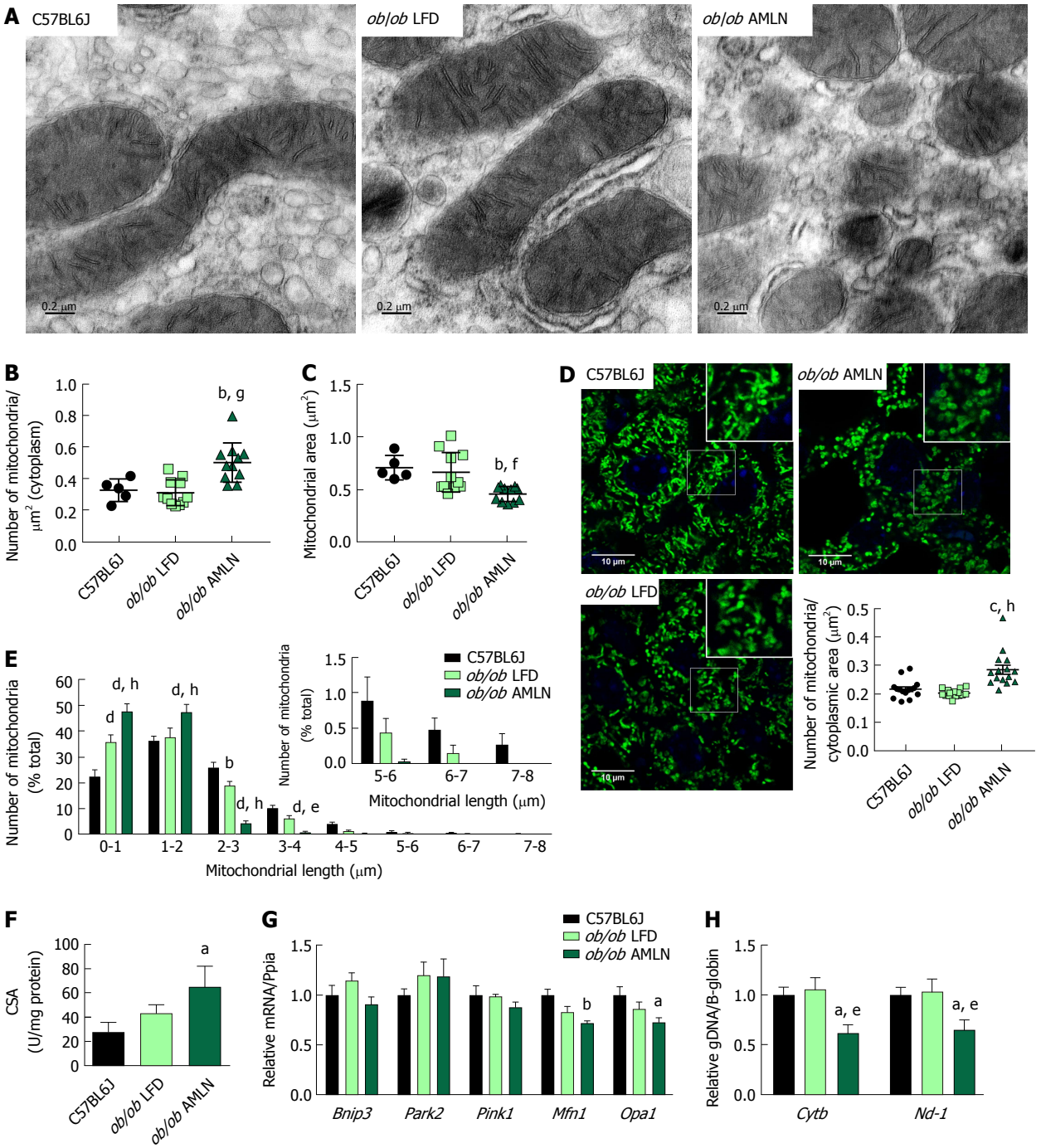

Figure 4 ***ob/ob*** **AMLN hepatocytes display increased numbers of fragmented mitochondria.** (A) Transmission electron micrographs (TEM) showing mitochondrial morphology and ultrastructure in the liver. Scale bar = 0.2 μm. Quantification of the number of mitochondria (B) and mitochondrial area (C) from TEM images; (D): Confocal images of HSP60 stained liver sections and quantification of mitochondrial number per cytoplasmic area. Scale bar = 10 μm; (E): Histogram depicting the number of mitochondria per binned mitochondrial length as a percentage of total mitochondria per cell; (F): Mitochondrial content measured by citrate synthase activity in isolated primary hepatocytes; (G): Relative hepatic expression of genes associated with mitophagy; (H): Quantification of mitochondrial genome-encoded *CytB* or *Nd1* relative to nuclear-encoded β-globin from total genomic DNA extracted from the liver. $^{a}P \leq 0.05$, $^{b}P \leq 0.01$, *vs* C57BL6J; $^{e}P \leq 0.05$, $^{f}P \leq 0.01$, $^{g}P \leq 0.001$, $^{h}P \leq 0.0001$ *vs* LFD. LFD: Low-fat diet.

(260 U/L *vs* 50 U/L, $P < 0.0001$) and was further elevated in FATZO AMLN animals (370 U/L, $P < 0.01$ *vs* FATZO LFD; Figure 7C), but was nonetheless still much lower than levels observed in *ob/ob* AMLN mice (>1100 U/L, Figure 1C).

Assessment of HE-stained liver samples revealed the presence of prominent steatosis, both micro- and macrovesicular, in both FATZO LFD and FATZO AMLN animals (Figure 7D). Increased macrophage/monocyte infiltration was also observed in FATZO LFD and FATZO AMLN mice (Figure 7E), paralleled by increased expression of hepatic *Cd68* (3.5-fold in FATZO LFD and 5.2-fold in FATZO AMLN; $P < 0.05$ FATZO LFD *vs* FATZO AMLN; Figure 7H). Mild collagen deposition was also

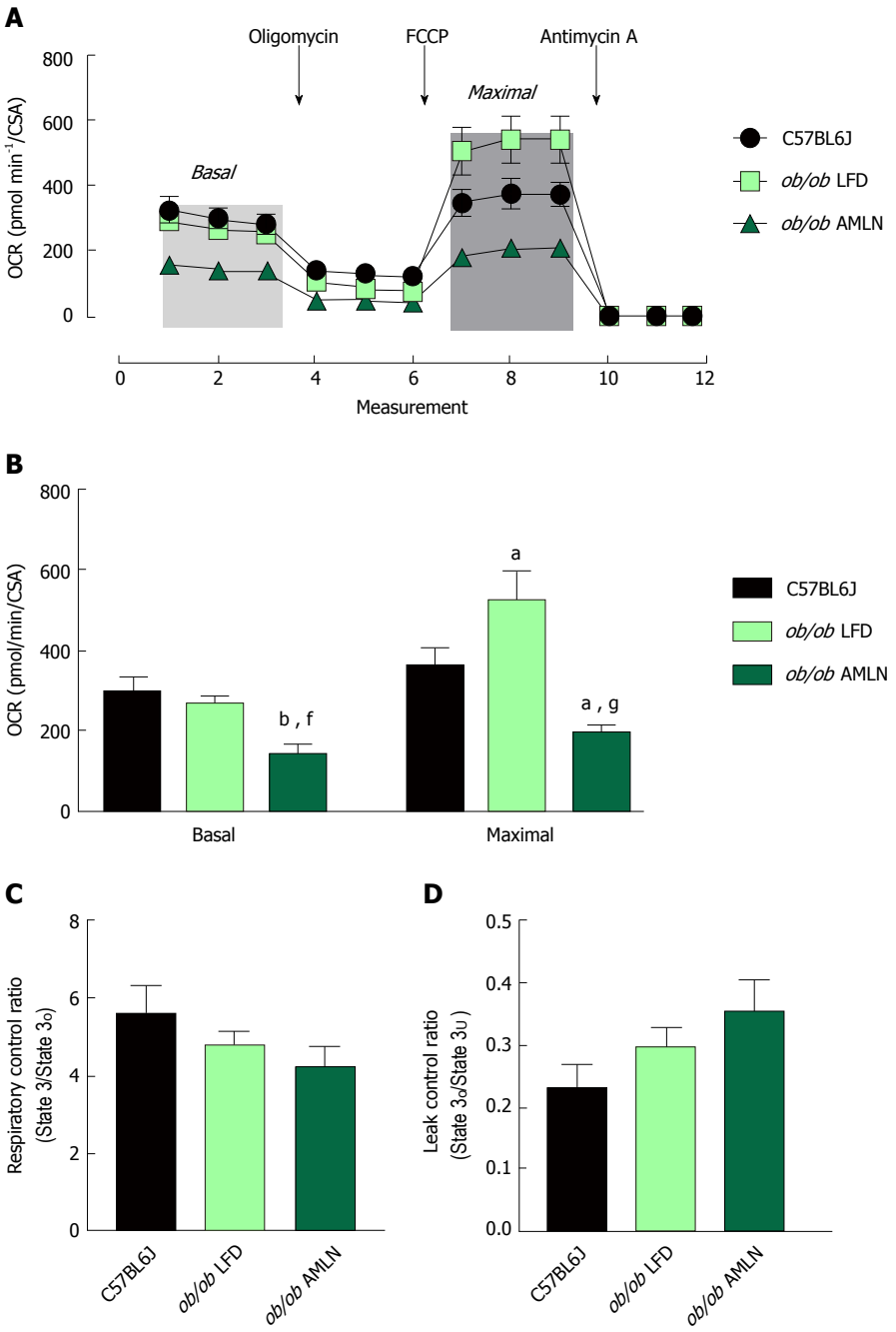

Figure 5 Mitochondria from *ob/ob* AMLN livers display reduced respiratory capacity and increased proton leak. (A): Oxygen consumption of primary hepatocytes isolated from C57BL6J, *ob/ob* LFD and *ob/ob* AMLN livers normalized to mitochondrial content (citrate synthase activity, CSA). Changes in mitochondrial respiration in response to oligomycin, FCCP and antimycin A are shown. Light grey box = basal respiration, dark grey box = maximal uncoupled respiration; (B): Quantification of baseline oxygen consumption (basal respiration) and FCCP-stimulated oxygen consumption (maximal respiration) normalized to CSA; (C): Mitochondrial respiratory control ratio, a measure of mitochondrial coupling, defined as state 3/ state o respiration of mitochondria isolated from the livers of C57BL6J, *ob/ob* LFD and *ob/ob* AMLN mice; (D): Mitochondrial leaking control ratio, a measure of proton leak, defined as state o/ state 3_U respiration. $^{a}P \leqslant 0.05$, $^{b}P \leqslant 0.01$, *vs* C57BL6J; $^{f}P \leqslant 0.01$, $^{g}P \leqslant 0.001$, *vs* LFD. LFD: Low-fat diet.

apparent in FATZO animals but did not worsen upon AMLN diet feeding (Figure 7F).

Transcriptional profiling of genes involved in hepatic fibrosis and inflammation revealed additional evidence of active liver disease in FATZO mice. Collagens including *Col1a1*, *Col1a2* and *Col3a1* were increased in FATZO LFD livers compared to lean controls (approximately 6-8-fold for each), and were further induced in FATZO AMLN livers (Figure 7G). All cytokines assayed including *Tgfb*, *Tnf*, *Il1b*, and *Il10*, and chemokines including *Ccl2*, *Ccl3*, and *Ccl11* were similarly upregulated in FATZO LFD livers compared to lean controls and even further induced in FATZO AMLN livers (Figure 7H). Additional fibrosis related genes *Timp1* and *Lgals3* were significantly elevated in FATZO LFD livers compared to lean controls, with even further induction observed in FATZO AMLN livers (Figure 7G, H). Integrated NASH scores generated from combining

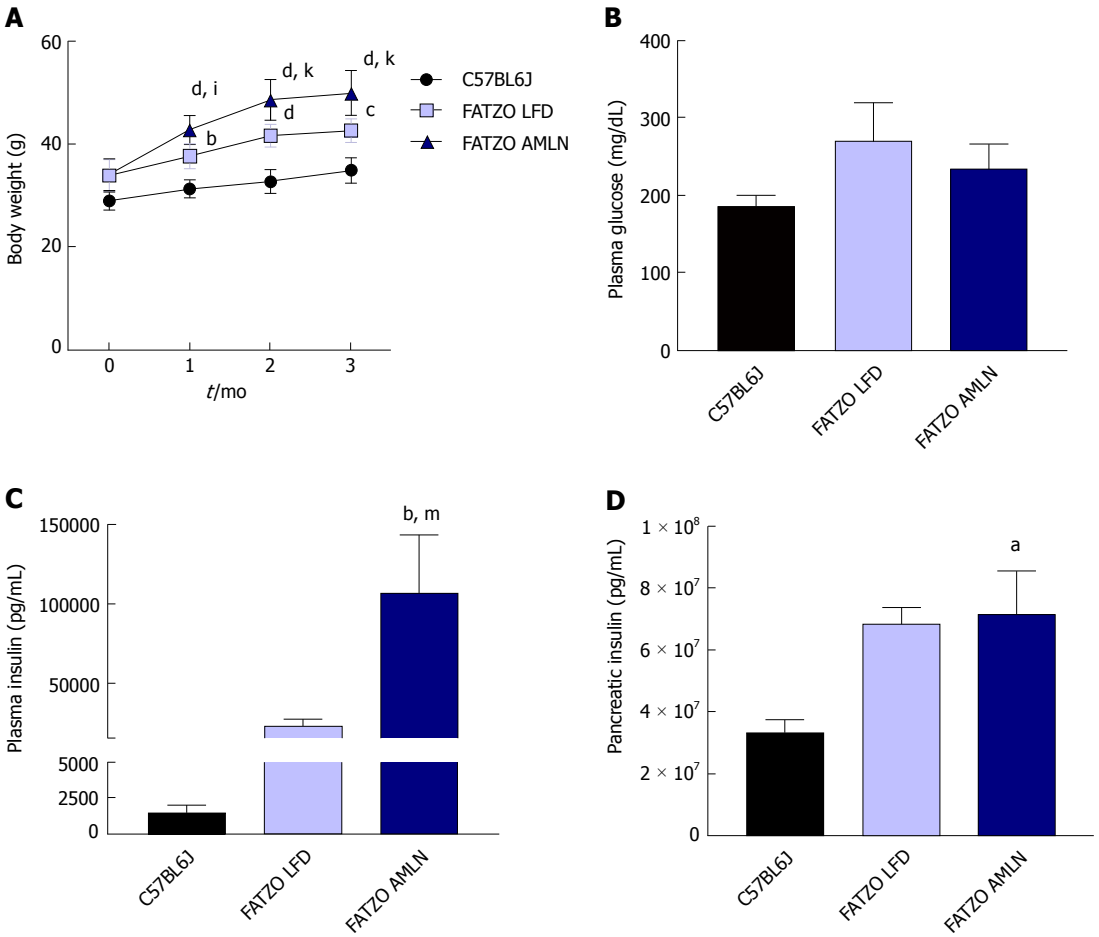

Figure 6 AMLN diet exacerbates obesity and hyperinsulinemia in FATZO mice. (A): Average body weight over 12-wk disease induction period; (B): Terminal non-fasting blood glucose levels; (C): Terminal non-fasting plasma insulin levels; (D): Pancreatic insulin content. $^{a}P \leq 0.05$, $^{b}P \leq 0.01$, $^{c}P \leq 0.001$, $^{d}P \leq 0.0001$ *vs* C57BL6J; $^{i}P \leq 0.05$, $^{k}P \leq 0.001$, FATZO LFD; $^{m}P \leq 0.05$, FATZO AMLN unless noted otherwise. LFD: Low-fat diet.

grades of steatosis (Figure 8A), inflammation (Figure 8B), biliary hyperplasia (Figure 8C), CD68-positive cells (Figure 8D) and hepatocyte ballooning (Figure 8E) were significantly greater for FATZO LFD and FATZO AMLN mice compared to lean controls, but did not significantly differ from one another (Figure 8F).

Increased mitochondrial fragmentation in FATZO mice is associated with mild mitochondrial dysfunction

Similar to *ob/ob* mice, FATZO AMLN mice displayed significantly increased numbers of fragmented mitochondria (Figure 9A, B) and hepatic CSA (Figure 9C) compared to FATZO LFD and lean controls. In contrast, this increase was associated with a significant induction of mitochondrial biogenesis genes in FATZO mice. *Nrf1* was consistently induced in both FATZO LFD and FATZO AMLN livers compared to lean controls ($P <$ 0.01 for FATZO LFD, $P < 0.0001$ for FATZO AMLN *vs* lean), *Ppargc1a* was significantly induced in FATZO LFD livers compared to lean controls (1.75-fold, $P < 0.001$) and *Tfam* was significantly induced in FATZO AMLN livers *vs* lean controls 1.4-fold, $P < 0.01$; Figure 9D). Additionally, decreased mitophagy may contribute to increased mitochondrial content, although only *Bnip3* expression was significantly reduced in FATZO LFD and FATZO AMLN livers compared to lean controls (-40%, $P < 0.05$ for FATZO LFD, -25%, $P = 0.08$ for FATZO AMLN *vs* lean) with no changes observed in *Park2* or *Pink1* expression (Supplementary Figure 9E). No differences in the mitochondrial:nuclear DNA ratio were observed (Figure 9F), suggesting that mtDNA replication is occurring normally in contrast to that observed in the *ob/ob* AMLN model.

To assess hepatic mitochondrial function in the FATZO mice we measured mitochondrial coupling and proton leak in isolated mitochondria. While there was a trend for reduced RCR in FATZO AMLN mitochondria compared to lean controls, this reduction was small and did not reach statistical significance (4.1 *vs* 4.9, $P = 0.5$; Figure 9G). Similar to the *ob/ob* models, both FATZO LFD and FATZO AMLN mitochondria displayed a trend for increased proton leak compared to lean controls (0.43 for both FATZO LFD and AMLN *vs* 0.32 for lean controls; $P = 0.08$ and $P = 0.07$, respectively; Figure 9H).

Ob/ob mice display a reduced ability to manage oxidative stress compared to FATZO mice

The oxidative stress responsive transcription factor *Nrf2* was significantly induced in both *ob/ob* and

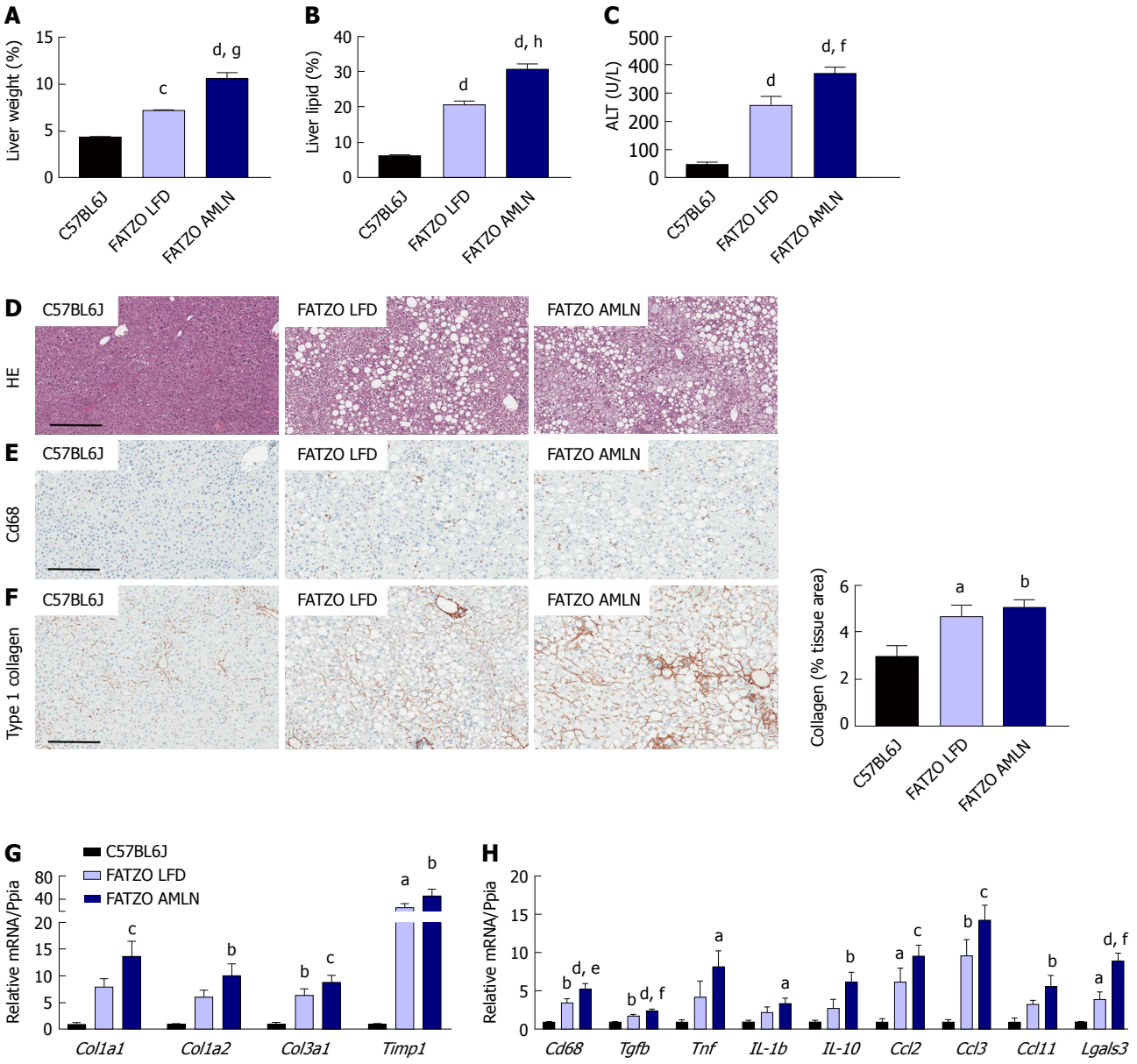

Figure 7 Comparison of metabolic and hepatic abnormalities associated with diet-induced nonalcoholic fatty liver disease/nonalcoholic steatohepatitis in FATZO mice. Liver weight (A), liver lipid (B), and plasma alanine aminotransferase (ALT) levels (C) of lean (C57BL6J) and FATZO mice maintained on control LFD (FATZO LFD) or AMLN diet (FATZO AMLN) for 12 wk; (D): Representative hematoxylin and eosin stained liver sections and quantification of percentage of liver area containing macrosteatosis; (E): Representative CD68-stained liver sections; (F): Representative collagen type 1 alpha 1 stained liver sections and quantification of collagen area; (G, H): Hepatic expression of genes associated with fibrosis and inflammation. $^{a}P \leqslant 0.05$, $^{b}P \leqslant 0.01$, $^{c}P \leqslant 0.001$, $^{d}P \leqslant 0.0001$ *vs* C57BL6J; $^{e}P \leqslant 0.05$, $^{f}P \leqslant 0.01$, $^{g}P \leqslant 0.001$, $^{h}P \leqslant 0.0001$ *vs* LFD. LFD: Low-fat diet.

FATZO mice on LFD and further induced by AMLN diet, indicating that the antioxidant response system was induced. Interestingly, when we quantified the expression levels of antioxidant enzymes that are collectively required for ROS detoxification, including superoxide dismustase 1 (*Sod1*), superoxide dismutase 2 (*Sod2*) and catalase (*Cat*), we detected unchanged or reduced hepatic expression in all diseased livers. *Sod1* mRNA was significantly reduced in both *ob/ob* LFD and *ob/ob* AMLN livers compared to lean controls (-25%, $P < 0.001$ for both; Figure 6A), while *Sod2* expression was significantly reduced in *ob/ob* AMLN livers compared to lean controls (-25%, $P < 0.05$; Figure 10A). All diseased livers displayed significantly reduced *Cat* expression compared to lean controls (-50%, $P < 0.0001$ for *ob/ob* LFD and AMLN *vs* lean controls; -20%, $P < 0.05$ for FATZO LFD and AMLN *vs* lean controls; Figure 10A). FATZO AMLN livers, however, did display significantly increased glutathione peroxidase (*Gpx1*) mRNA levels (+50%, $P < 0.01$ *vs* C57BL6J, Figure 10A).

Despite reduced (*ob/ob* mice) or unchanged (FATZO mice) *Sod1* and *Sod2* mRNA, there was a trend for increased hepatic superoxide dismutase activity for *ob/ob* and FATZO mice compared to lean controls ($P < 0.05$ *ob/ob* AMLN *vs* lean; Figure 10B). Catalase activity was increased approximately 2-fold in both FATZO LFD ($P < 0.001$) and FATZO AMLN livers ($P < 0.01$), but unchanged in *ob/ob* LFD and *ob/ob* AMLN

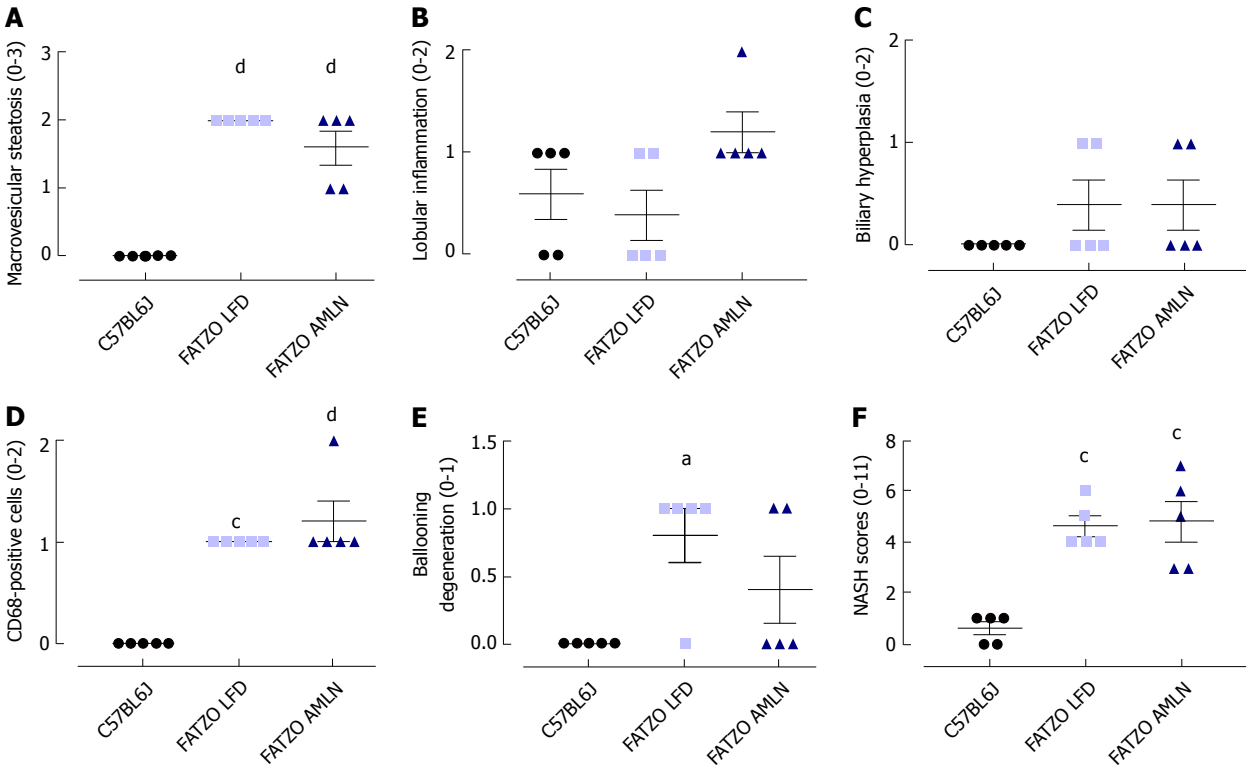

Figure 8 Histopathological scoring of FATZO mice. Individual grades of macrovesicular steatosis (A), lobular inflammation (B), biliary hyperplasia (C), CD68-positive cells (D) and ballooning degeneration. (E) Composite NASH scores. $^{a}P \leq 0.05$, $^{c}P \leq 0.001$, $^{d}P \leq 0.0001$ *vs* C57BL6J.

livers compared to lean controls (Figure 10C). We also detected increased catalase expression in liver sections from FATZO LFD and FATZO AMLN mice compared to lean controls (Figure 10D). Further, the ratio of hepatic catalase:SOD activity was reduced in *ob/ob* LFD mice and worsened by AMLN diet, but unchanged in FATZO animals compared to lean controls (Figure 10E). Hepatic 8-hydroxydeoxyguanosine (8-OHdG), a marker of oxidative DNA damage, tended to be higher in *ob/ob* LFD animals compared to both lean controls and FATZO LFD mice (Figure 10F). In *ob/ob* AMLN mice, hepatic 8-OHdG levels were significantly higher than both FATZO mice and lean controls (2.5-fold, $P < 0.01$ *vs* lean; Figure 10E). Additionally, we observed a negative correlation between catalase activity and hepatic 8-OHdG levels (Figure 10G). Taken together these data suggest that a reduced ability to manage ROS may be a key mechanism underlying the more severe liver phenotype observed in *ob/ob* AMLN mice.

DISCUSSION

The increasing health and economic burden and lack of FDA-approved therapies underscore the importance of appropriate pre-clinical models for NAFLD/NASH[22]. Surprisingly, only a handful of animal models are available that reflect human disease with respect to metabolic status and liver pathology[23,24]. These models are similar in that their genetic background predisposes to diet-induced NASH, and include the DIAMOND model[25], the *ob/ob* mouse[13,26], and the LDLR knockout mouse[27]. To a lesser extent, C57BL6J mice fed a high-fat (AMLN) diet will also develop NASH when given enough time (> 24 wk), but this model does not develop as advanced fibrosis[28,29]. Other reported models of liver disease do not develop liver inflammation, such as the APOE2 knock-in mouse[27], or lack metabolic context, such as the CCl_4 and MCDD models.

We report herein that both the leptin-deficient *ob/ob* mouse and hyperleptinemic FATZO mouse develop steatohepatitis within 12 wk of AMLN diet feeding. Despite similar levels of liver lipid and less severe hyperinsulinemia, *ob/ob* AMLN mice displayed a worse liver phenotype with increased inflammation and more advanced fibrosis relative to FATZO mice. Notably, hepatic expression of macrophage markers and related inflammatory chemokines were more prominently upregulated in *ob/ob* AMLN compared to FATZO AMLN mice, but were similar in *ob/ob* LFD and FATZO LFD animals, suggesting that the baseline inflammatory status and matrix deposition of the livers is similar in these models and that leptin deficiency *per se* does not predispose the liver to inflammation and fibrosis, but nonetheless may contribute to a proinflammatory, profibrotic phenotype upon dietary challenge.

While the precise pathophysiology of NASH remains to be fully determined, one aspect that has emerged in recent years is the role of mitochondrial (dys)function in hepatocytes associated with NAFLD/NASH. Evidence from human studies has recently emerged[8,30], however similar analyses in mouse models of NASH has not

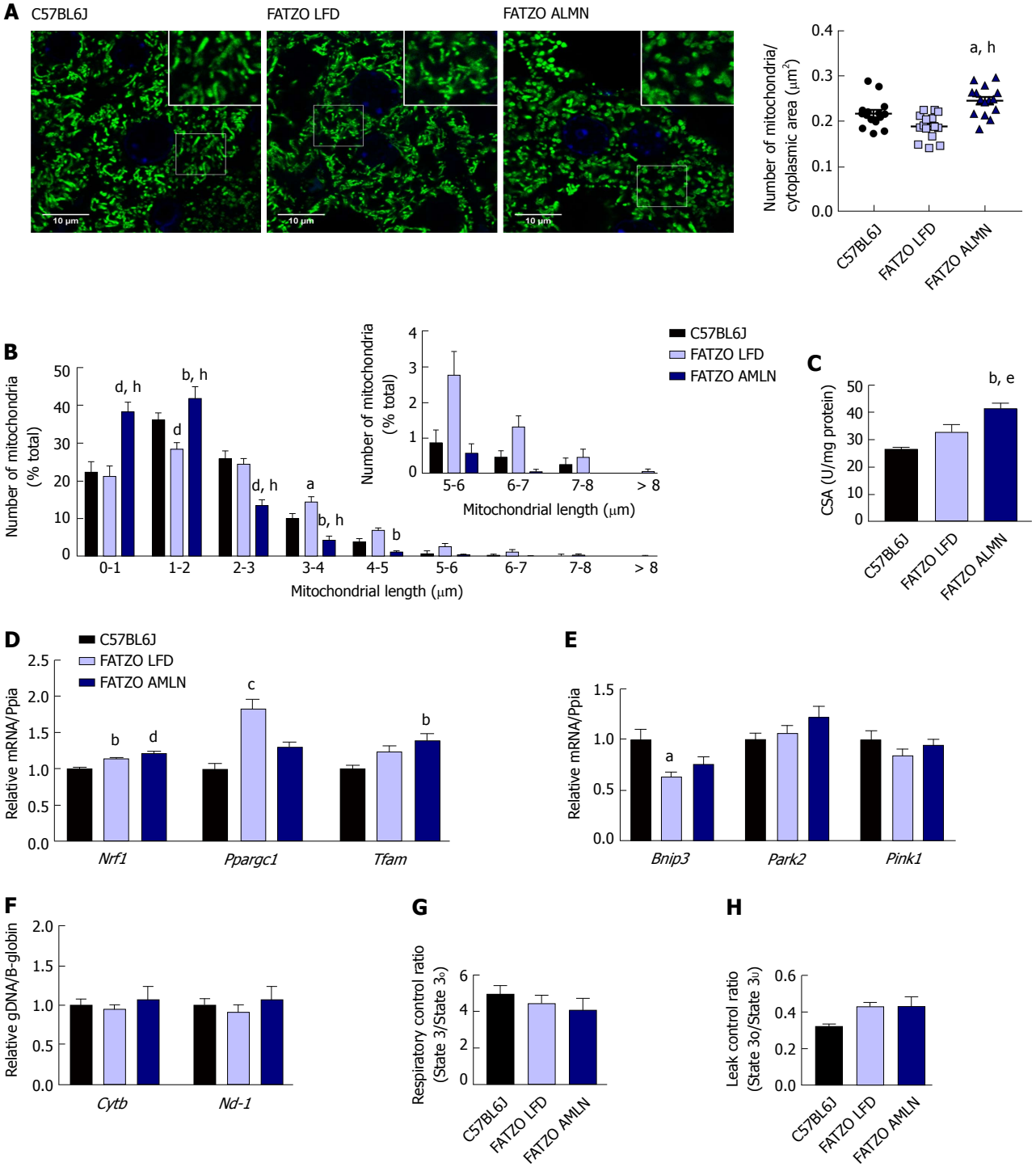

Figure 9 Mitochondrial content alterations in FATZO mice are associated with increased biogenesis and elevated proton leak. (A): Confocal images of HSP60 stained liver sections with quantification of mitochondrial number per cytoplasmic area. Scale bar = 10 μm; (B): Histogram depicting the number of mitochondria per binned mitochondrial length as a percentage of total mitochondria per cell; (C): Mitochondrial content measured by citrate synthase activity of isolated hepatic mitochondria; (D): Expression of hepatic mitochondrial biogenesis genes; (E): Relative hepatic expression of mitophagy-associated genes; (F): Quantification of mitochondrial genome-encoded *CytB* or *Nd1* relative to nuclear-encoded β- globin from total genomic DNA extracted from the liver; (G): Mitochondrial respiratory control ratio; (H): Mitochondrial leak control ratio. $^{a}P \leqslant 0.05$, $^{b}P \leqslant 0.01$, $^{c}P \leqslant 0.001$, $^{d}P \leqslant 0.0001$ *vs* C57BL6J; $^{e}P \leqslant 0.05$, $^{h}P \leqslant 0.0001$ *vs* LFD. LFD: Low-fat diet.

been reported. Multiple interconnected facets of mitochondrial biology including morphology, overall content (numbers and size), and respiratory capacity influence mitochondrial function. Our data show that *ob/ob* AMLN mice developed NASH associated with increased numbers of fragmented mitochondria with reduced respiratory capacity but without overt defects in mitochondrial membrane integrity or cristae structure. Similarly, FATZO AMLN mice displayed fragmented mitochondria with a trend for reduced respiratory control, but nonetheless better responded to oxidative damage and presented less overall fibrosis.

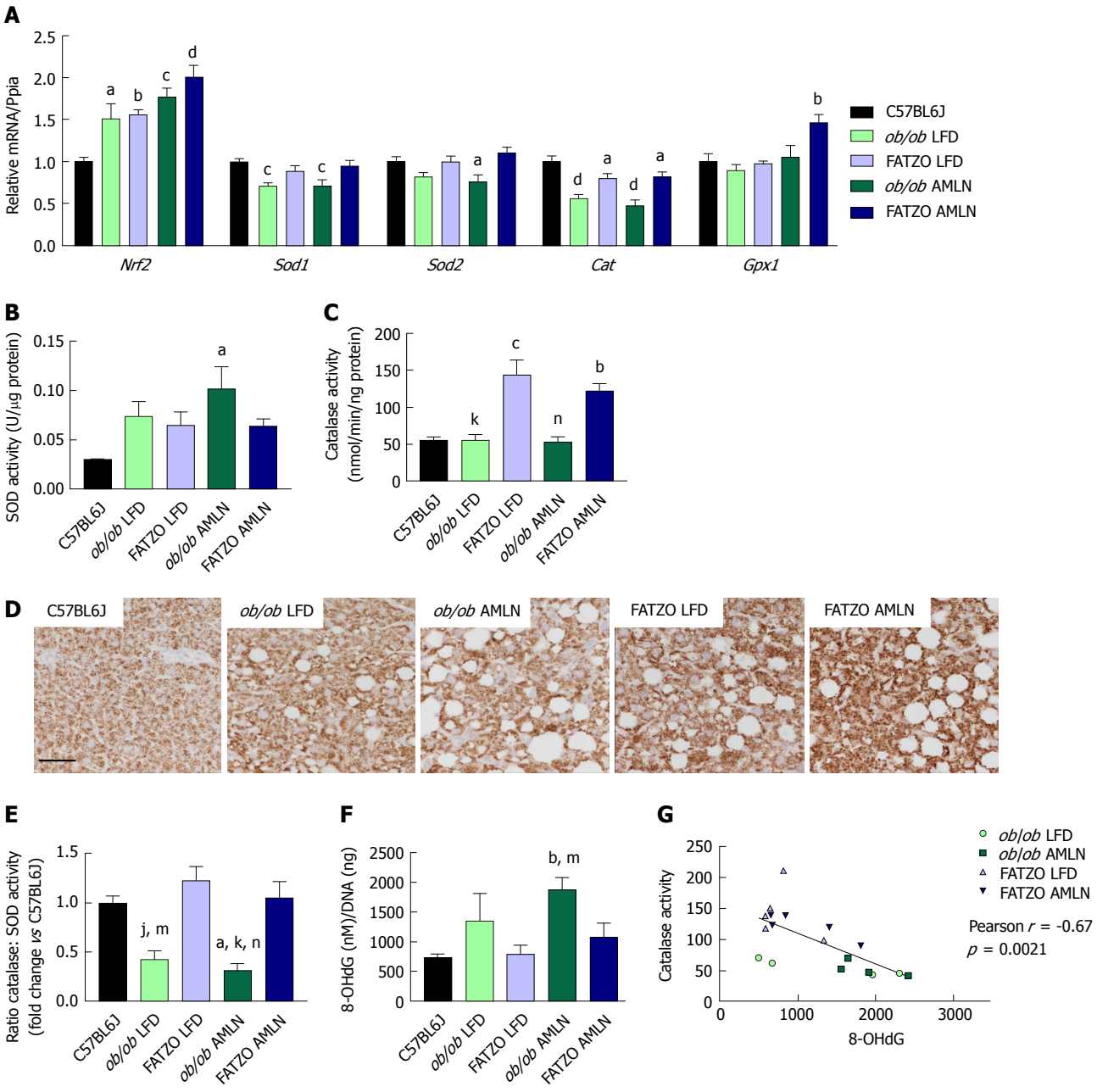

Figure 10 Hepatic oxidative stress is mitigated by increased catalase activity in FATZO but not *ob/ob* mice. (A): Expression of antioxidant genes *Nrf2*, *Sod1*, *Sod2*, *Cat* and *Gpx1* in *ob/ob* LFD, FATZO LFD, *ob/ob* AMLN and FATZO AMLN livers relative to lean controls. Superoxide dismutase activity (B) and catalase activity (C) in hepatic lysates from C57BL6J, *ob/ob* LFD, FATZO LFD, *ob/ob* AMLN and FATZO AMLN animals; (D): Representative images of catalase stained liver sections. Scale bar represents 100 μm; (E): Ratio of catalase: SOD activities; (F): Levels of 8-hydroxydeoxyguanosine (8-OHdG) in genomic DNA isolated from C57BL6J, *ob/ob* LFD, FATZO LFD, *ob/ob* AMLN and FATZO AMLN livers; (G): Pearson's correlation of catalase activity and 8-OHdG levels in *ob/ob* and FATZO livers. $^{a}P \leqslant 0.05$, $^{b}P \leqslant 0.01$, $^{c}P \leqslant 0.001$, $^{d}P \leqslant 0.0001$ *vs* C57BL6J; $^{j}P \leqslant 0.01$, $^{k}P \leqslant 0.001$, FATZO LFD; $^{m}P \leqslant 0.05$, $^{n}P \leqslant 0.01$, FATZO AMLN unless noted otherwise. LFD: Low-fat diet.

Mitochondrial morphology is appreciated to play an active role in regulating energy metabolism and cell death and can therefore influence NASH development at numerous stages[31,32]. Leptin has previously been shown to alter mitochondrial morphology and function. In primary mouse hepatocytes, leptin treatment induced mitochondrial fusion through induction of *Ppargc1a* and *Mfn1* and was associated with protection from high-glucose induced fatty acid accumulation[33]. Complementary work demonstrated that inhibition of mitochondrial fission reduced steatosis and development of NAFLD[34]. *Mfn1* and *Opa1* expression were significantly reduced in *ob/ob* mice when fed AMLN diet. Consistent with transcript levels, we observed smaller but more numerous mitochondria in both *ob/ob* AMLN and FATZO AMLN hepatocytes. Increased mitochondrial fragmentation and uncoupling have been proposed as adaptive mechanisms to reduce ROS levels and maintain energy balance by limiting ATP production in states of excess substrate supply which may explain the more fragmented, leaky mitochondria in *ob/ob* AMLN and FATZO AMLN livers.

Reduced mitochondrial function assessed by coupling efficiency and proton leak was also observed in both models; however, only *ob/ob* AMLN livers displayed significantly reduced mtDNA levels, similar to patients with NAFLD[35,36], which may affect other aspects of mitochondrial function including ATP generation and ROS production. Moreover, ROS itself may promote mtDNA mutation and degradation[37], leading to a feed-forward loop of continuous oxidative damage that leads to hepatocyte cell death, inflammation and fibrosis development. As such, targeting hepatic oxidative stress driven by chronic overnutrition could be an important therapeutic target for NASH prevention.

The capacity to manage oxidative stress was dissimilar between *ob/ob* and FATZO mice. Multiple antioxidant molecules within the cell are regulated by the transcription factor NRF2. While hepatic *Nrf2* expression was significantly upregulated in both *ob/ob* and FATZO livers, indicative of increased oxidative stress, oxidative DNA damage was only detected in *ob/ob* livers. Increased hepatic superoxide dismutase activity was detected in both *ob/ob* and FATZO animals, suggestive of elevated hydrogen peroxide in these livers, but concomitantly increased catalase activity and *Gpx1* expression was detected only in FATZO liver. Increased hepatic hydrogen peroxide levels have been reported for humans with NASH and correlated with catalase activity and oxidative DNA damage[8]. In line with these human studies, hepatic catalase activity was indeed negatively correlated with 8-OHdG levels.

In the clinic, single antioxidant therapy has shown mixed efficacy. Among these agents, vitamin E (despite its limited antioxidant efficacy) is the most investigated[38,39]. While the majority of studies showed improvements in select features, including steatosis, serum ALT and histopathology, none have demonstrated improvement in fibrosis, the key feature linked to disease progression[40]. Strategies to enhance antioxidant defenses are also being actively explored. One such target is NRF2, which can be activated by numerous natural products, including resveratrol and synthetic compounds[41]. Combination strategies that include the oxidant scavenging effects with an anti-fibrotic molecule such as the anti-galectin 3 drug GR-MD-02, currently in Phase 2 trials[42] may be informative.

In summary, we have described convenient mouse models of NAFLD/NASH that accurately reflect human disease context (obesity and insulin resistance) and liver pathology (steatosis, ballooning degeneration, inflammation and fibrosis). Additionally, both models appear to mimic reported aspects of mitochondrial phenotype in human NASH, including elevated mitochondrial numbers and increased proton leak. The unanticipated differences in disease severity may in part be due to an increased ability to manage oxidative stress in the FATZO mouse. These models may better predict therapeutic efficacy of putative NASH treatments in the clinic, particularly for agents targeting mitochondrial/oxidative pathways.

ARTICLE HIGHLIGHTS

Research background

Non-alcoholic steatohepatitis (NASH) is an unmet medical need with no approved therapies. Studies here characterize the hepatic phenotype of two different diet-induced mouse models of NASH with a focus on mitochondrial function and ability to regulate oxidative damage.

Research motivation

Emerging evidence from cross-sectional human studies suggests a role for mitochondrial function in the development of NASH. As the pathogenesis of NASH remains largely unknown it is imperative to characterize potential therapeutic agents in a relevant preclinical model.

Research objectives

The primary objective was to characterize NASH histopathology (*e.g.*, NASH activity score for steatosis, inflammation, ballooning and fibrosis) and function with a focus on mitochondrial biology and capacity to respond to oxidative stress. We contrast these endpoints in two distinct mouse strains (genetically obese Lep^{ob}/Lep^{ob} (*ob/ob*) and polygenic obesity-prone FATZO mice) on a previously validated NASH-inducing diet that is high in *trans*-fat, fructose and cholesterol (AMLN diet).

Research methods

Development of NASH was assessed using blinded qualitative (HE stained sections) and quantitative (% collagen-stained area) methods. Mitochondria were assessed via transmission electron micrography and immunofluorescent detection of HSP60. Mitochondrial function was assessed in primary hepatocytes using Seahorse. Activity of superoxide dismutase and catalase were measured from whole liver tissue homogenates. Candidate genes from total liver RNA were measured using quantitative PCR.

Research results

Both *ob/ob* and FATZO mice developed NASH with concomitant obesity and hyperinsulinemia when challenged with AMLN diet for 12 wk, and was associated with mitochondrial accumulation and reduced function. The degree of hepatic fibrosis, however, was markedly greater in *ob/ob* mice and was associated with increased activity of superoxide dismutase (SOD), whereas FATZO mice displayed increased catalase activity. Antioxidant capacity, reflected as the ratio of catalase: SOD activity, was significantly perturbed in *ob/ob* mice with diet-induced NASH.

Research conclusions

Both of these commonly available mouse models develop AMLN diet-induced NASH after 12 wk, associated with reduced mitochondrial function and perturbed morphology. The intrinsic capacity of the FATZO mice to increase antioxidant capacity in the face of impaired mitochondrial function/increased oxidative damage due to diet may be contributory towards the reduced level of fibrosis in that model.

Research perspectives

The AMLN mouse model of NASH is gaining widespread academic and industry acceptance as a translatable model of NASH. These studies extend previous observations in the model to highlight mitochondrial dysfunction thus confirming the model as relevant for prosecution of therapeutic agents targeting improvement in mitochondrial function for NASH. Furthermore, the contrasting fibrosis between *ob/ob* and FATZO mice implicates the capacity to adapt to oxidative damage as a key regulator of liver fibrosis in diet-induced NASH.

ACKNOWLEDGMENTS

We gratefully acknowledge the assistance of Sally Lee, Holly Koelkebeck, Wanda King, Kenesha Riley and Charles Brown (MedImmune, Gaithersburg, MD, United

States) for expert technical assistance with tissue processing and immunohistochemistry. We thank Lorenz Rognoni and Farzad Sekhavati (Definiens, Germany) for tissue image analysis. We also thank Donna Goldsteen, Krystal Nacel and the Laboratory Animal Resource staff (MedImmune, Gaithersburg, MD) for their assistance with animal husbandry and care.

REFERENCES

1 **Younossi ZM**, Blissett D, Blissett R, Henry L, Stepanova M, Younossi Y, Racila A, Hunt S, Beckerman R. The economic and clinical burden of nonalcoholic fatty liver disease in the United States and Europe. *Hepatology* 2016; **64**: 1577-1586 [PMID: 27543837 DOI: 10.1002/hep.28785]

2 **Younossi ZM**, Koenig AB, Abdelatif D, Fazel Y, Henry L, Wymer M. Global epidemiology of nonalcoholic fatty liver disease-Meta-analytic assessment of prevalence, incidence, and outcomes. *Hepatology* 2016; **64**: 73-84 [PMID: 26707365 DOI: 10.1002/hep.28431]

3 **Kabbany MN**, Conjeevaram Selvakumar PK, Watt K, Lopez R, Akras Z, Zein N, Carey W, Alkhouri N. Prevalence of Nonalcoholic Steatohepatitis-Associated Cirrhosis in the United States: An Analysis of National Health and Nutrition Examination Survey Data. *Am J Gastroenterol* 2017; **112**: 581-587 [PMID: 28195177 DOI: 10.1038/ajg.2017.5]

4 **Patterson RE**, Kalavalapalli S, Williams CM, Nautiyal M, Mathew JT, Martinez J, Reinhard MK, McDougall DJ, Rocca JR, Yost RA, Cusi K, Garrett TJ, Sunny NE. Lipotoxicity in steatohepatitis occurs despite an increase in tricarboxylic acid cycle activity. *Am J Physiol Endocrinol Metab* 2016; **310**: E484-E494 [PMID: 26814015 DOI: 10.1152/ajpendo.00492.2015]

5 **Satapati S**, Kucejova B, Duarte JA, Fletcher JA, Reynolds L, Sunny NE, He T, Nair LA, Livingston KA, Fu X, Merritt ME, Sherry AD, Malloy CR, Shelton JM, Lambert J, Parks EJ, Corbin I, Magnuson MA, Browning JD, Burgess SC. Mitochondrial metabolism mediates oxidative stress and inflammation in fatty liver. *J Clin Invest* 2016; **126**: 1605 [PMID: 27035816 DOI: 10.1172/JCI86695]

6 **Begriche K**, Massart J, Robin MA, Bonnet F, Fromenty B. Mitochondrial adaptations and dysfunctions in nonalcoholic fatty liver disease. *Hepatology* 2013; **58**: 1497-1507 [PMID: 23299992 DOI: 10.1002/hep.26226]

7 **Satapati S**, Sunny NE, Kucejova B, Fu X, He TT, Méndez-Lucas A, Shelton JM, Perales JC, Browning JD, Burgess SC. Elevated TCA cycle function in the pathology of diet-induced hepatic insulin resistance and fatty liver. *J Lipid Res* 2012; **53**: 1080-1092 [PMID: 22493093 DOI: 10.1194/jlr.M023382]

8 **Koliaki C**, Szendroedi J, Kaul K, Jelenik T, Nowotny P, Jankowiak F, Herder C, Carstensen M, Krausch M, Knoefel WT, Schlensak M, Roden M. Adaptation of hepatic mitochondrial function in humans with non-alcoholic fatty liver is lost in steatohepatitis. *Cell Metab* 2015; **21**: 739-746 [PMID: 25955209 DOI: 10.1016/j.cmet.2015.04.004]

9 **Auger C**, Alhasawi A, Contavadoo M, Appanna VD. Dysfunctional mitochondrial bioenergetics and the pathogenesis of hepatic disorders. *Front Cell Dev Biol* 2015; **3**: 40 [PMID: 26161384 DOI: 10.3389/fcell.2015.00040]

10 **Sunny NE**, Bril F, Cusi K. Mitochondrial Adaptation in Nonalcoholic Fatty Liver Disease: Novel Mechanisms and Treatment Strategies. *Trends Endocrinol Metab* 2017; **28**: 250-260 [PMID: 27986466 DOI: 10.1016/j.tem.2016.11.006]

11 **Gusdon AM**, Song KX, Qu S. Nonalcoholic Fatty liver disease: pathogenesis and therapeutics from a mitochondria-centric perspective. *Oxid Med Cell Longev* 2014; **2014**: 637027 [PMID: 25371775 DOI: 10.1155/2014/637027]

12 **Machado MV**, Michelotti GA, Xie G, Almeida Pereira T, Boursier J, Bohnic B, Guy CD, Diehl AM. Mouse models of diet-induced nonalcoholic steatohepatitis reproduce the heterogeneity of the human disease. *PLoS One* 2015; **10**: e0127991 [PMID: 26017539 DOI: 10.1371/journal.pone.0127991]

13 **Trevaskis JL**, Griffin PS, Wittmer C, Neuschwander-Tetri BA, Brunt EM, Dolman CS, Erickson MR, Napora J, Parkes DG, Roth JD. Glucagon-like peptide-1 receptor agonism improves metabolic, biochemical, and histopathological indices of nonalcoholic steatohepatitis in mice. *Am J Physiol Gastrointest Liver Physiol* 2012; **302**: G762-G772 [PMID: 22268099 DOI: 10.1152/ajpgi.00476.2011]

14 **Droz BA**, Sneed BL, Jackson CV, Zimmerman KM, Michael MD, Emmerson PJ, Coskun T, Peterson RG. Correlation of disease severity with body weight and high fat diet in the FATZO/Pco mouse. *PLoS One* 2017; **12**: e0179808 [PMID: 28640904 DOI: 10.1371/journal.pone.0179808]

15 **Peterson RG**, Jackson CV, Zimmerman KM, Alsina-Fernandez J, Michael MD, Emmerson PJ, Coskun T. Glucose dysregulation and response to common anti-diabetic agents in the FATZO/Pco mouse. *PLoS One* 2017; **12**: e0179856 [PMID: 28640857 DOI: 10.1371/journal.pone.0179856]

16 **Kleiner DE**, Brunt EM, Van Natta M, Behling C, Contos MJ, Cummings OW, Ferrell LD, Liu YC, Torbenson MS, Unalp-Arida A, Yeh M, McCullough AJ, Sanyal AJ; Nonalcoholic Steatohepatitis Clinical Research Network. Design and validation of a histological scoring system for nonalcoholic fatty liver disease. *Hepatology* 2005; **41**: 1313-1321 [PMID: 15915461 DOI: 10.1002/hep.20701]

17 **Alarcon C**, Boland BB, Uchizono Y, Moore PC, Peterson B, Rajan S, Rhodes OS, Noske AB, Haataja L, Arvan P, Marsh BJ, Austin J, Rhodes CJ. Pancreatic β-Cell Adaptive Plasticity in Obesity Increases Insulin Production but Adversely Affects Secretory Function. *Diabetes* 2016; **65**: 438-450 [PMID: 26307586 DOI: 10.2337/db15-0792]

18 **Kremer JR,** Mastronarde DN, McIntosh JR. Computer visualization of three-dimensional image data using IMOD. Journal of Structural Biology 1996; **116**: 71-76 [PMID: 8742726 DOI: 10.1006/jsbi.1996.0013]

19 **Boland BB**, Brown C Jr., Alarcon C, Demozay D, Grimsby JS, Rhodes CJ. β-Cell Control of Insulin Production During Starvation-Refeeding in Male Rats. *Endocrinology* 2018; **159**: 895-906 [PMID: 29244064 DOI: 10.1210/en.2017-03120]

20 **Glick D**, Zhang W, Beaton M, Marsboom G, Gruber M, Simon MC, Hart J, Dorn GW 2nd, Brady MJ, Macleod KF. BNip3 regulates mitochondrial function and lipid metabolism in the liver. *Mol Cell Biol* 2012; **32**: 2570-2584 [PMID: 22547685 DOI: 10.1128/MCB.00167-12]

21 **Chavin KD**, Yang S, Lin HZ, Chatham J, Chacko VP, Hoek JB, Walajtys-Rode E, Rashid A, Chen CH, Huang CC, Wu TC, Lane MD, Diehl AM. Obesity induces expression of uncoupling protein-2 in hepatocytes and promotes liver ATP depletion. *J Biol Chem* 1999; **274**: 5692-5700 [PMID: 10026188]

22 **Abdelmalek MF**. NAFLD: The clinical and economic burden of NAFLD: time to turn the tide. *Nat Rev Gastroenterol Hepatol* 2016; **13**: 685-686 [PMID: 27826139 DOI: 10.1038/nrgastro.2016.178]

23 **Hansen HH**, Feigh M, Veidal SS, Rigbolt KT, Vrang N, Fosgerau K. Mouse models of nonalcoholic steatohepatitis in preclinical drug development. *Drug Discov Today* 2017; **22**: 1707-1718 [PMID: 28687459 DOI: 10.1016/j.drudis.2017.06.007]

24 **Larter CZ**, Yeh MM. Animal models of NASH: getting both pathology and metabolic context right. *J Gastroenterol Hepatol* 2008; **23**: 1635-1648 [PMID: 18752564 DOI: 10.1111/j.1440-1746.2008.05543.x]

25 **Asgharpour A**, Cazanave SC, Pacana T, Seneshaw M, Vincent R, Banini BA, Kumar DP, Daita K, Min HK, Mirshahi F, Bedossa P, Sun X, Hoshida Y, Koduru SV, Contaifer D Jr, Warncke UO, Wijesinghe DS, Sanyal AJ. A diet-induced animal model of non-alcoholic fatty liver disease and hepatocellular cancer. *J Hepatol* 2016; **65**: 579-588 [PMID: 27261415 DOI: 10.1016/j.jhep.2016.05.005]

26 **Clapper JR**, Hendricks MD, Gu G, Wittmer C, Dolman CS, Herich J, Athanacio J, Villescaz C, Ghosh SS, Heilig JS, Lowe C, Roth JD.

Diet-induced mouse model of fatty liver disease and nonalcoholic steatohepatitis reflecting clinical disease progression and methods of assessment. *Am J Physiol Gastrointest Liver Physiol* 2013; **305**: G483-G495 [PMID: 23886860 DOI: 10.1152/ajpgi.00079.2013]

27 **Bieghs V**, Van Gorp PJ, Wouters K, Hendrikx T, Gijbels MJ, van Bilsen M, Bakker J, Binder CJ, Lütjohann D, Staels B, Hofker MH, Shiri-Sverdlov R. LDL receptor knock-out mice are a physiological model particularly vulnerable to study the onset of inflammation in non-alcoholic fatty liver disease. *PLoS One* 2012; **7**: e30668 [PMID: 22295101 DOI: 10.1371/journal.pone.0030668]

28 **Liedtke C**, Luedde T, Sauerbruch T, Scholten D, Streetz K, Tacke F, Tolba R, Trautwein C, Trebicka J, Weiskirchen R. Experimental liver fibrosis research: update on animal models, legal issues and translational aspects. *Fibrogenesis Tissue Repair* 2013; **6**: 19 [PMID: 24274743 DOI: 10.1186/1755-1536-6-19]

29 **Kristiansen MN**, Veidal SS, Rigbolt KT, Tølbøl KS, Roth JD, Jelsing J, Vrang N, Feigh M. Obese diet-induced mouse models of nonalcoholic steatohepatitis-tracking disease by liver biopsy. *World J Hepatol* 2016; **8**: 673-684 [PMID: 27326314 DOI: 10.4254/wjh.v8.i16.673]

30 **Hyötyläinen T**, Jerby L, Petäjä EM, Mattila I, Jäntti S, Auvinen P, Gastaldelli A, Yki-Järvinen H, Ruppin E, Orešič M. Genome-scale study reveals reduced metabolic adaptability in patients with non-alcoholic fatty liver disease. *Nat Commun* 2016; **7**: 8994 [PMID: 26839171 DOI: 10.1038/ncomms9994]

31 **Westermann B**. Mitochondrial fusion and fission in cell life and death. *Nat Rev Mol Cell Biol* 2010; **11**: 872-884 [PMID: 21102612 DOI: 10.1038/nrm3013]

32 **Wai T**, Langer T. Mitochondrial Dynamics and Metabolic Regulation. *Trends Endocrinol Metab* 2016; **27**: 105-117 [PMID: 26754340 DOI: 10.1016/j.tem.2015.12.001]

33 **Hsu WH**, Lee BH, Pan TM. Leptin-induced mitochondrial fusion mediates hepatic lipid accumulation. *Int J Obes* (Lond) 2015; **39**: 1750-1756 [PMID: 26119995 DOI: 10.1038/ijo.2015.120]

34 **Galloway CA**, Lee H, Brookes PS, Yoon Y. Decreasing mitochondrial fission alleviates hepatic steatosis in a murine model of nonalcoholic fatty liver disease. *Am J Physiol Gastrointest Liver Physiol* 2014; **307**: G632-G641 [PMID: 25080922 DOI: 10.1152/ajpgi.00182.2014]

35 **Sookoian S**, Rosselli MS, Gemma C, Burgueño AL, Fernández Gianotti T, Castaño GO, Pirola CJ. Epigenetic regulation of insulin resistance in nonalcoholic fatty liver disease: impact of liver methylation of the peroxisome proliferator-activated receptor γ coactivator 1α promoter. *Hepatology* 2010; **52**: 1992-2000 [PMID: 20890895 DOI: 10.1002/hep.23927]

36 **Sookoian S**, Flichman D, Scian R, Rohr C, Dopazo H, Gianotti TF, Martino JS, Castaño GO, Pirola CJ. Mitochondrial genome architecture in non-alcoholic fatty liver disease. *J Pathol* 2016; **240**: 437-449 [PMID: 27577682 DOI: 10.1002/path.4803]

37 **Shokolenko I**, Venediktova N, Bochkareva A, Wilson GL, Alexeyev MF. Oxidative stress induces degradation of mitochondrial DNA. *Nucleic Acids Res* 2009; **37**: 2539-2548 [PMID: 19264794 DOI: 10.1093/nar/gkp100]

38 **Al-Busafi SA**, Bhat M, Wong P, Ghali P, Deschenes M. Antioxidant therapy in nonalcoholic steatohepatitis. *Hepat Res Treat* 2012; **2012**: 947575 [PMID: 23227320 DOI: 10.1155/2012/947575]

39 **Sanyal AJ**, Chalasani N, Kowdley KV, McCullough A, Diehl AM, Bass NM, Neuschwander-Tetri BA, Lavine JE, Tonascia J, Unalp A, Van Natta M, Clark J, Brunt EM, Kleiner DE, Hoofnagle JH, Robuck PR; NASH CRN. Pioglitazone, vitamin E, or placebo for nonalcoholic steatohepatitis. *N Engl J Med* 2010; **362**: 1675-1685 [PMID: 20427778 DOI: 10.1056/NEJMoa0907929]

40 **Hagström H**, Nasr P, Ekstedt M, Hammar U, Stål P, Hultcrantz R, Kechagias S. Fibrosis stage but not NASH predicts mortality and time to development of severe liver disease in biopsy-proven NAFLD. *J Hepatol* 2017; **67**: 1265-1273 [PMID: 28803953 DOI: 10.1016/j.jhep.2017.07.027]

41 **Musso G**, Cassader M, Gambino R. Non-alcoholic steatohepatitis: emerging molecular targets and therapeutic strategies. *Nat Rev Drug Discov* 2016; **15**: 249-274 [PMID: 26794269 DOI: 10.1038/nrd.2015.3]

42 **Harrison SA**, Marri SR, Chalasani N, Kohli R, Aronstein W, Thompson GA, Irish W, Miles MV, Xanthakos SA, Lawitz E, Noureddin M, Schiano TD, Siddiqui M, Sanyal A, Neuschwander-Tetri BA, Traber PG. Randomised clinical study: GR-MD-02, a galectin-3 inhibitor, vs. placebo in patients having non-alcoholic steatohepatitis with advanced fibrosis. *Aliment Pharmacol Ther* 2016; **44**: 1183-1198 [PMID: 27778367 DOI: 10.1111/apt.13816]

P- Reviewer: Garcia-Fernandez MI, Novo E, Streba LAM
S- Editor: Ma YJ **L- Editor**: A **E- Editor**: Huang Y

World Journal of Gastroenterology

Submit a Manuscript: http://www.f6publishing.com

World J Gastroenterol 2018 April 28; 24(16): 1766-1778

DOI: 10.3748/wjg.v24.i16.1766

ISSN 1007-9327 (print) ISSN 2219-2840 (online)

ORIGINAL ARTICLE

Basic Study

Mucosa repair mechanisms of Tong-Xie-Yao-Fang mediated by CRH-R2 in murine, dextran sulfate sodium-induced colitis

Shan-Shan Gong, Yi-Hong Fan, Shi-Yi Wang, Qing-Qing Han, Bin Lv, Yi Xu, Xi Chen, Yao-Er He

Shan-Shan Gong, Shi-Yi Wang, Qing-Qing Han, Xi Chen, Yao-Er He, The First Clinical Medical College of Zhejiang Chinese Medical University, Hangzhou 310053, Zhejiang Province, China

Yi-Hong Fan, Bin Lv, Yi Xu, Department of Gastroenterology, The First Affiliated Hospital of Zhejiang Chinese Medical University, Hangzhou 310006, Zhejiang Province, China

ORCID number: Shan-Shan Gong (0000-0001-5483-720X); Yi-Hong Fan (0000-0001-8217-9793); Shi-Yi Wang (0000-0002-2134-3892); Qing-Qing Han (0000-0002-3155-3746); Bin Lv (0000-0002-6247-571X); Yi Xu (0000-0002-3265-9534); Xi Chen (0000-0002-6236-6345); Yao-Er He (0000-0003-3511-8554).

Author contributions: Gong SS and Wang SY performed the experiments, analyzed the data and wrote the paper; Fan YH and Han QQ designed the research, revised the paper and contributed equally to this study; Xu Y and Lv B performed parts of the experiments and provided valuable suggestions for this study; Chen X and He YE contributed new analytic tools; All authors have read and approved the final manuscript.

Supported by National Natural Science Foundation of China, No. 81473506; Natural Science Foundation of Zhejiang Province, No.LY13H030011 and No. LY17H290009; State Administration of Traditional Chinese Medicine of Zhejiang Province, No. 2013ZB050; Department of Zhejiang Province to Build Funded Project, No. WKJ-ZJ-1531; Zhejiang TCM Science and Technology Project, No. 2016ZB047, No. 2017ZA056 and No. 2018ZB046.

Institutional review board statement: The study was reviewed and approved by the Institutional Review Board of Zhejiang Chinese Medical University.

Institutional animal care and use committee statement: All procedures involving animals were reviewed and approved by the Institutional Animal Care and Use Committee of Zhejiang Chinese Medical University.

Conflict-of-interest statement: No potential conflicts of interest exist.

Data sharing statement: No additional data are available.

Manuscript source: Unsolicited manuscript

Correspondence to: Yi-Hong Fan, PhD, Associate Professor, Department of Gastroenterology, The First Affiliated Hospital of Zhejiang Chinese Medical University, No. 54, Youdian Road, Shangcheng District, Hangzhou 310006, Zhejiang Province, China. yhfansjr@163.com
Telephone: +86-571-87608001
Fax: +86-571-87608001

Received: February 12, 2018
Peer-review started: February 13, 2018
First decision: March 9, 2018
Revised: March 14, 2018
Accepted: March 31, 2018
Article in press: March 31, 2018
Published online: April 28, 2018

Abstract

AIM

To explore the significance of corticotropin-releasing hormone (CRH)-receptor (R)2 in mucosal healing of dextran sulfate sodium (DSS)-induced colitis and the effect of Tong-Xie-Yao-Fang (TXYF) on CRH-R2 expression and regulation.

METHODS

Ulcerative colitis was induced in mice by administration of 3% (w/v) DSS for 7 d. Once the model was established,

mice were administered urocortin-2 (30 μg/kg), a peptide which binds exclusively to CRH-R2, or various doses of aqueous TXYF extracts (2.8-11.2 g/kg), a CRH-R2 antagonist Astressin (Ast)2B (20 μg/kg), Ast2B + Ucn2, or Ast2B with various doses of aqueous TXYF extracts for 9 d. Colonic mucosal permeability was then evaluated by measuring the fluorescence intensity in serum. The colitis disease activity index (DAI), histology, body weight loss and colon length were assessed to evaluate the condition of colitis. Terminal deoxynucleotidyl transferase dUTP nick-end labeling was used to detect apoptosis of the intestinal epithelial cells. The expression level of Ki-67 represented the proliferation of colonic epithelial cells and was detected by immunohistochemistry. The expression levels of inflammation cytokines IL-6, TNF-α and CXCL-1 were examined in colon tissues using real-time PCR and ELISA kits.

RESULTS

Compared with the DSS group, mice treated with the CRH-R2 antagonist Ast2B showed greater loss of body weight, shorter colon lengths (4.90 ± 0.32 *vs* 6.21 ± 0.34 cm, $P < 0.05$), and higher DAI (3.61 ± 0.53 *vs* 2.42 ± 0.32, $P < 0.05$) and histological scores (11.50 ± 1.05 *vs* 8.33 ± 1.03, $P < 0.05$). Additionally, the Ast2B group showed increased intestinal permeability (2.76 ± 0.11 μg/mL *vs* 1.47 ± 0.11 μg/mL, $P < 0.001$), improved secretion of inflammatory cytokines in colon tissue, and reduced colonic epithelial cell proliferation (4.97 ± 4.25 *vs* 22.51 ± 8.22, $P < 0.05$). Increased apoptosis (1422.39 ± 90.71 *vs* 983.01 ± 98.17, $P < 0.001$) was also demonstrated. The Ucn2 group demonstrated lower DAI (0.87 ± 0.55 *vs* 2.42 ± 0.32, $P < 0.001$) and histological scores (4.33 ± 1.50 vs 8.33 ± 1.03, $P < 0.05$). Diminished weight loss, longer colon length (9.58 ± 0.62 *vs* 6.21 ± 0.34 cm, $P < 0.001$), reduced intestinal permeability (0.75 ± 0.07 *vs* 1.47 ± 0.11 μg/mL, $P < 0.001$), inhibited secretion of inflammatory cytokines in colon tissue and increased colonic epithelial cell proliferation (90.04 ± 15.50 *vs* 22.51 ± 8.22, $P < 0.01$) were all observed. Reduced apoptosis (149.55 ± 21.68 *vs* 983.01 ± 98.17, $P < 0.05$) was also observed. However, significant statistical differences in the results of the Ast2B group and Ast2B + Ucn2 group were observed. TXYF was also found to ameliorate symptoms of DSS-induced colitis in mice and to promote mucosal repair like Ucn2. There were significant differences between the Ast2B + TXYF groups and the TXYF groups.

CONCLUSION

CRH-R2 activates the intestinal mucosal antiinflammatory response by regulating migration, proliferation and apoptosis of intestinal epithelial cells in colitis-induced mice, and plays an important antiinflammatory role. TXYF promotes mucosal repair in colitis mice by regulating CRH-R2.

Key words: Tong-Xie-Yao-Fang; Aqueous extracts; Corticotropin-releasing hormone receptor 2; Urocortin 2; Astressin 2B; Mucosal healing; Ulcerative colitis

Core tip: Mucosal healing is a desired therapeutic endpoint in the treatment of inflammatory bowel disease. However, it is difficult to treat inflammatory bowel disease thoroughly, and there are some adverse reactions. Studies have shown that corticotropin-releasing hormone (CRH)-receptor (R)2 can activate the inflammatory response of intestinal mucosa and exert an antiinflammatory effect. Our preliminary study found that Tong-Xie-Yao-Fang could reduce the expression of CRH-R1, increase CRH-R2, and participate in reconstruction of the intestinal barrier. The aim of this study was to explore the significance of CRH-R2 in the mucosal healing of dextran sulfate sodium-induced colitis and study the effect of Tong-Xie-Yao-Fang on CRH-R2 expression and regulation.

Gong SS, Fan YH, Wang SY, Han QQ, Lv B, Xu Y, Chen X, He YE. Mucosa repair mechanisms of Tong-Xie-Yao-Fang mediated by CRH-R2 in murine, dextran sulfate sodium-induced colitis. *World J Gastroenterol* 2018; 24(16): 1766-1778 Available from: URL: http://www.wjgnet.com/1007-9327/full/v24/i16/1766.htm DOI: http://dx.doi.org/10.3748/wjg.v24.i16.1766

INTRODUCTION

Inflammatory bowel diseases (IBD), including Crohn's disease and ulcerative colitis (UC), are a group of chronic inflammatory disorders of the gastrointestinal tract, characterized by intestinal inflammation and mucosal damage[1]. In traditional Chinese medicine theory, UC is known as the "changpi" and chronic dysentery[2]. Characterized by chronic mucosal inflammation and damage of the colon, UC presents with bloody diarrhea, tenesmus, abdominal pain, weight loss, anemia, and even toxic megacolon. Intestinal perforation, intestinal obstruction, intestinal bleeding and cancer are also observed, thus affecting an individual's quality of life[3].

Treatment targets for IBD have changed over the recent years. Previous therapeutic strategies focusing on induction and maintenance of clinical remission have shown no effect on the natural course of the disease[4,5]. However, in the late 1990s, the advent of biologic agents for the treatment of IBD showed that while patients may be in clinical remission, ongoing mucosal inflammation may still be present, resulting in structural damage[6-11].

This finding has led to the concept of mucosal healing as a more meaningful therapeutic target in clinical practice. Indeed, emerging data suggests that mucosal healing is strongly associated with a reduction in steroid use, complications, hospitalizations, and surgeries[12].

Mucosal repair of the intestinal barrier is a tightly coordinated response to injury that preserves homeostasis and limits the adverse effects of inflammation. After damage to the epithelial tissue, intestinal epithelial cells migrate to the site of injury in a critical process known as epithelial restitution[13-15]. Restitution is followed by epithelial cell proliferation and differentiation which is regulated by factors that promote cell viability and limit apoptosis[14,16]. IBD is a chronic relapsing inflammatory disorder that involves a defective epithelial barrier[17].

Corticotropin-releasing hormone (CRH), the primary mediator of the stress response, is expressed in both the central nervous system and the periphery, including the intestine[18]. The CRH family of peptides interacts with a variety of cell types in the intestinal mucosa, including epithelial cells, enteric neurons, and immune cells[19]. In addition to CRH, three distinct peptides known as urocortins (Ucn1, Ucn2, and Ucn3) bind to two types of G protein-coupled receptors to exert their effects, CRH receptor (R)1 and CRH-R2. Yet, Ucn1 has greater affinity for CRH-R2 than CRH-R1, and Ucn2 and Ucn3 bind exclusively to CRH-R2[20]. Interactions between CRH-Rs and their ligands modulate several functional and pathophysiologic responses within the gut, including stress-induced alterations in motility, ion secretion, and visceral pain, and the development and maintenance of intestinal inflammation[21].

Studies from others have found that CRH may be involved in the maintenance of intestinal barrier integrity by regulating autophagy in the intestinal epithelial cells[18]. Our previous studies have also found that CRH could cause an increase in intercellular permeability in the intestinal epithelium[22]. Some studies have found that CRH-R2 can activate the antiinflammatory response of intestinal mucosa and exert an antiinflammatory effect[23]. In addition, activation of CRH-R2 can promote the migration and proliferation of colon cancer cells and gastric mucosa cells[24,25]. Furthermore, the expression of CRH-R2 was found to be down-regulated in the biopsy specimens of UC patients[26] and CRH-deficient mice are unable to initiate healing responses after acute experimental colitis[27], suggesting a role for the CRH peptide family, especially CRH-R2, in mucosal repair mechanisms.

Tong-Xie-Yao-Fang (TXYF) is a prescription in traditional Chinese medicine, used for relieving abdominal pain and diarrhea. TXYF has also been shown to be involved in the reconstruction of the intestinal epithelial barrier and to promote the healing of mucosa in UC[28,29]. While the mechanism is not understood, it is thought to target and intervene with CRH-R2. This regulates the migration, proliferation and apoptosis of epithelial cells, like the role of Ucn2[30,31].

The overall aim of the present investigation was to determine whether CRH-R2 regulates mucosal repair on dextran sulfate sodium (DSS)-induced colitis in mice and to examine the relationship between TXYF and CRH-R2 signaling.

Table 1 Criteria for disease activity index

Score	Weight loss, %	Stool consistency	Bloodstain or gross bleeding
0	None	Normal	Negative
1	1-5	-	-
2	5-10	Loose stool	Positive
3	10-15	-	-
4	> 15	Diarrhea	Gross bleeding

MATERIALS AND METHODS

TXYF composition and dosage preparation

TXYF was prepared with large head atractylodes rhizome (*Rhizoma Atractylodis Macrocephalae*), white peony root (*Radix Paeoniae Alba*), dried tangerine peel (*Pericarpium Citri Reticulatae*) and divaricate saposhnikovia root (*Radix Saposhnikoviae*)[32], which were used in a 15:12:6:10 proportion. Raw components were soaked in an 8-fold volume of distilled water for 1 h and boiled twice for 0.5 h each time. Two of the boiled ingredients were filtered, mixed together, concentrated at a 1:1 ratio (100% concentration), and stored at 4 ℃ for later use.

Animal modeling and drug treatment

Male CD-1(ICR) mice (8-10 wk old) were purchased from Shanghai Xipuer-bikai Experimental Animal Co., Ltd., (Shanghai, China) and housed 1 wk under a 12 h light/dark cycle at 22-24 ℃ with 50%-60% humidity and a noise level < 50 d. Prior to experimentation, mice were allowed free access to food and tap water. All the procedures involving animals were conducted in accordance with the ethical principles adopted by the Animal Experimental Center of Zhejiang Chinese Medical University and were approved by the Ethics Committee on Animal Experiments at Zhejiang Chinese Medical University.

Mice (n = 110) were randomized into 11 assigned groups as follows: control group (n = 10), DSS group (n = 10), DSS + Astressin (Ast)2B group (Ast2B group; n = 10), DSS + Ucn2 group (Ucn2 group; n = 10), DSS + Ast2B + Ucn2 group (Ast2B + Ucn2 group; n = 10), DSS + Ast2B + low-dose (2.8 g/kg•d) aqueous TXYF extract group (Ast2B + TXYF-L group; n = 10), DSS + Ast2B + medium-dose (5.6 g/kg•d) aqueous TXYF extract group (Ast2B + TXYF-M group; n = 10), DSS + Ast2B + high-dose (11.2 g/kg•d) aqueous TXYF extract group (Ast2B + TXYF-H group; n = 10), DSS + low-dose (2.8 g/kg•d) aqueous TXYF extract group (TXYF-L group; n = 10), DSS + medium-dose (5.6 g/kg•d) aqueous TXYF extract group (TXYF-M group; n = 10), and DSS + high-dose (11.2 g/kg•d) aqueous TXYF extract group (TXYF-H group; n = 10). Colitis was induced in mice by administering 3% (w/v) DSS (MP Biomedicals, Inc., Aurora, OH, United States) in

Table 2 Histological score to quantify the degree of colitis

Score	Inflammation	Depth of lesions	Destruction of crypt	Width of lesions, %
0	None	None	None	
1	Slight	Mucosa	Basal 1/3 damaged	1-25
2	Moderate	Mucosa and submucosa	Basal 2/3 damaged	26-50
3	Severe	Transmural	Intact epithelium only	51-75
4	-	-	Total crypt and epithelium	76-100

their drinking water for 7 d. On days 8 to 16, mice were switched to normal water. Additionally, the mice treated with Ast2B were injected daily with the CRH-R2 antagonist Ast2B (Sigma-Aldrich, St. Louis, MO, United States) administered intraperitoneally (20 μg/kg). The mice treated with Ucn2 received an intraperitoneal injection of Ucn2 (Peptide Institute Inc., Osaka, Japan) (30 μg/kg). The mice treated with TXYF were administered the aqueous TXYF extract. The doses of 2.8 g/kg•d, 5.6 g/kg•d, and 11.2 g/kg•d aqueous TXYF extract represented an equivalent of 0.5 ×, 1.0 × and 2.0 × for the human adult dosage.

Disease activity index

Intestinal disease activity was assessed based on weight loss, the presence of diarrhea accompanied by blood and mucus, and colonic shortening[33]. DAI was calculated by scoring weight loss, diarrhea and rectal bleeding, based on a previous scoring system (Table 1) described by Murthy *et al*[34] with little modification. Weight loss was defined as the difference between the initial and final weights. Diarrhea was defined by the absence of fecal pellet formation and the presence of continuous fluid fecal material in the colon. Rectal bleeding was assessed based on the presence of diarrhea containing visible blood and on the presence of gross rectal bleeding, and was scored as diarrhea. Disease activity index (DAI) values were calculated using the following formula: DAI = [(weight loss score) + (diarrhea score) + (rectal bleeding score)]/3. The clinical parameters used in the present study were chosen to represent the subjective clinical symptoms observed in human UC.

Histological process

Sections of colon fixed in 10% formalin, paraffin-embedded and stained with hematoxylin and eosin were used for histological scoring. The sections were graded by two blinded investigators, using a range from 0 to 3 as to amount of inflammation (acute and chronic) and depth of inflammation and with a range from 0 to 4 as to the amount of crypt damage or regeneration, as indicated in Table 2[35]. These changes were also quantified as to the percent involvement by the disease process: (1) 1%-25%; (2) 26%-50%; (3) 51%-75%; (4) 76%-100%. Histological score was calculated using the following formula: histological colitis score = inflammation + depth of lesions + destruction of crypt + width of lesions.

Immunohistochemistry and imaging

Formalin-fixed, paraffin-embedded colons were sectioned (1 μm) and stained with a Ki-67 antigen (dilution 1:100; AF0198; Affinity Biosciences, Cincinnati, OH, United States) or terminal deoxynucleotidyl transferase dUTP nick-end labeling (TUNEL) with the Apop-Tag Plus Peroxidase *in situ* cell death detection kit, POD (11684817910; Roche, Basel, Switzerland) according to the manufacturer's instructions. To quantify Ki-67 immunoreactivity and TUNEL, pixel-based quantification of staining intensity was performed with Image-ProPlus 6.0 software. Stained sections were observed under a 40 × objective lens.

In vivo intestinal permeability

The intestinal permeability was measured by determination of the amount of FITC-dextran (molecular weight 4.0 kDa; Sigma-Aldrich) in blood after oral administration, as described previously[36]. Briefly, mice were fasted overnight and FITC-dextran solution (4 kDa, 600 mg/kg) was administered. Blood samples were obtained after 3 h, centrifuged at 10000× rpm for 5 min, and serum was collected. Serum levels of FITC were read at 483 nm and 525 nm on a full wavelength multifunctional enzyme spectrometer (Varioskan Flash, Thermo Fisher Scientific, Waltham, MA, United States).

Real-time quantitative PCR

RNAiso Plus (9108; Takara Bio, Inc., Shiga, Japan) was used to extract RNA from frozen tissue samples, and the concentration of RNA was measured using a trace nucleic acid analyzer (Thermo Fisher Scientific). RNA was reverse-transcribed to cDNA using a PrimeScript RT reverse transcription kit (RR036A; Takara Bio, Inc.). Quantitative real-time PCR was carried out by ABI 7500 real-time PCR system (7500; Applied Biosystems of Thermo Fisher Scientific). Primers were designed and synthesized by Shenggong Biology and Engineering Co., Ltd. (Shanghai, China) (Table 3). β-actin was used as the normalization control, and the $2^{-\Delta\Delta CT}$ method was used to calculate the relative expression of target genes.

TNF-α, CXCL-1 and IL-6 measurement

CXCL-1 level and IL-6 level were measured by mouse TNF-α enzyme-linked immunosorbent assay (ELISA) kit, mouse CXCL-1 ELISA kit and Mouse IL-6 ELISA kit (Shanghai WesTang Bio-Tech Co., Ltd., Shanghai,

Table 3 Primer sequences and amplification length

Gene	Primer sequences	Amplification length
TNF-α	Forward: 5′-GCCTATGTCTCAGCCTCTTCTC-3′	22
	Reverse: 5′-TGGTGGTTTGCTACGACGTG-3′	20
CXCL-1	Forward: 5′-TCACCTCAAGAACATCCAGAGC-3′	22
	Reverse: 5′-ACTTGGGGACACCTTTTAGCAT-3′	22
IL-6	Forward: 5′-TCTCTGCAAGAGACTTCCATCC-3′	22
	Reverse: 5′-TTCCACGATTTCCCAGAGAACA-3′	22
β-*actin*	Forward: 5′-AGATCAAGATCATTGCTCCTCC-3′	22
	Reverse: 5′-GGTGTAAAACGCAGCTCAGTAA-3′	22

TNF-α: Tumor necrosis factor-alpha; CXCL-1: Chemokine (C-X-C motif) ligand-1; IL-6: Interleukin-6; β-actin: Beta-actin.

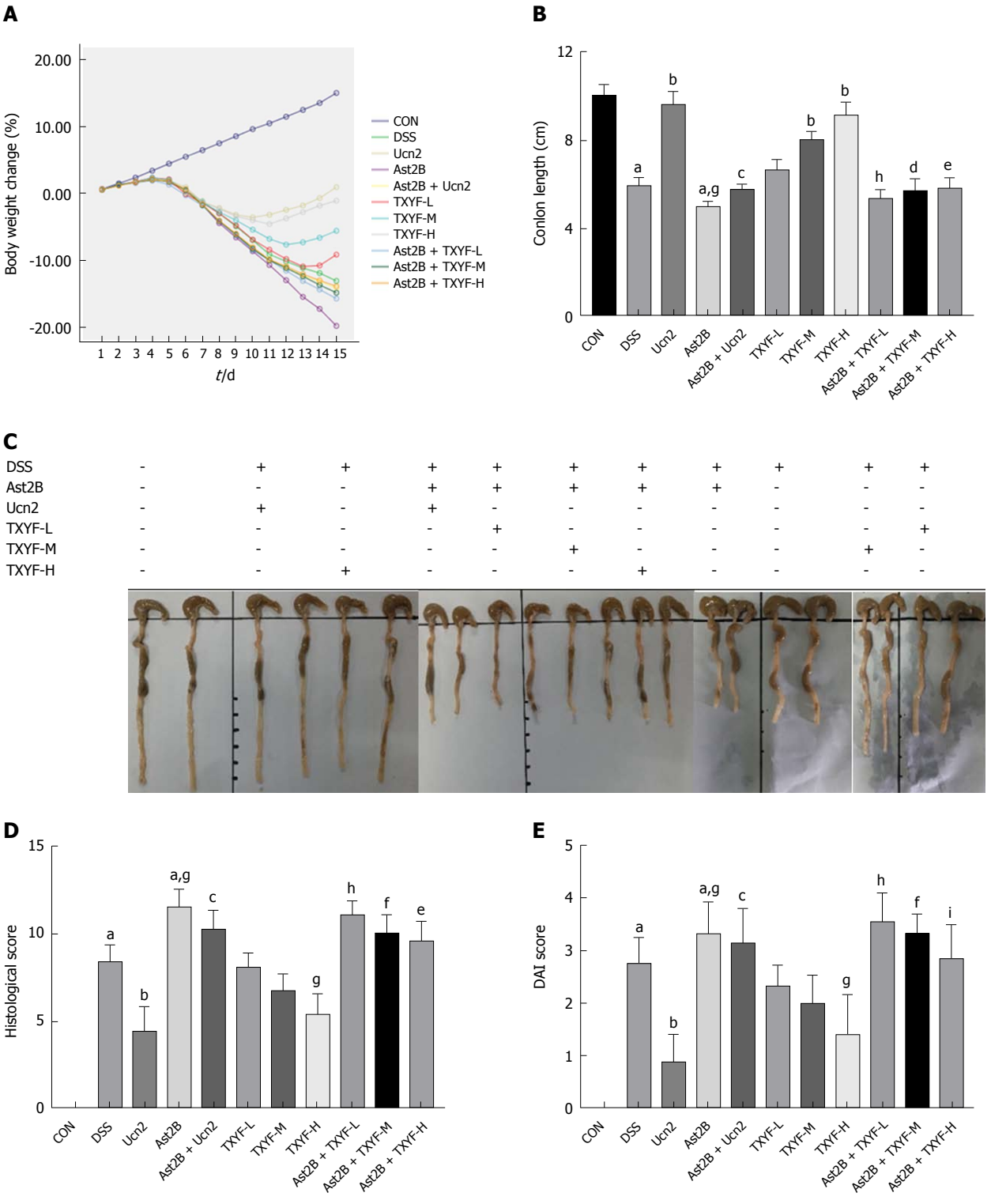

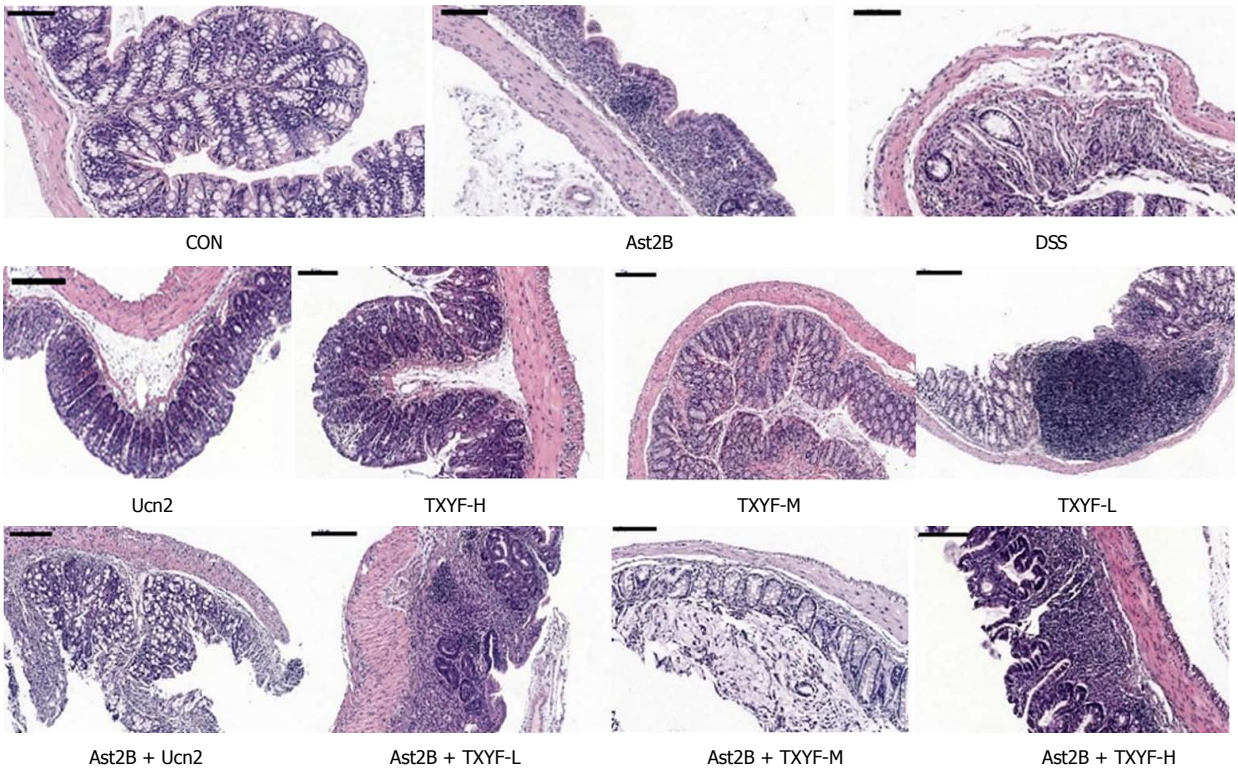

Figure 1 Inhibition of CRH-R2 signaling aggravates symptoms of DSS-induced colitis in mice. A: Mice body weights measured for 16 d, and shown as percentage of weight change; B: Colon length; C: Representative photographs of colon lengths; D: DAI; E: Histological scores were evaluated on the 16th day; F: Representative images of hematoxylin-eosin staining histology. Data are presented as mean ± standard deviation, n = 6-10 per group, scale bar = 200 μm. $^{a}P < 0.001$ *vs* control group; $^{g}P < 0.05$, $^{b}P < 0.001$ *vs* DSS group; $^{c}P < 0.001$ *vs* Ucn2 group; $^{h}P < 0.05$ *vs* TXYF-L group; $^{f}P < 0.01$, $^{d}P < 0.001$ *vs* TXYF-M group; $^{i}P < 0.05$, $^{e}P < 0.001$ *vs* TXYF-H group. CRH-R2: Corticotropin-releasing hormone-receptor 2; DAI: Disease activity index; DSS: Dextran sulfate sodium; TXYF: Tong-Xie-Yao-Fang.

China), respectively. All assays were conducted by following the manufacturer's instruction.

Statistical analysis

All analyses were performed using SPSS 24.0 statistical software (IBM Corp., Armonk, NY, United States). Comparisons between groups were performed using one-way analysis of variance (ANOVA), followed by Scheffe post hoc test for multiple comparisons, otherwise a Dunnett's T3 method was used. All data are expressed as the mean ± SD. $P < 0.05$ was considered statistically significant.

RESULTS

Inhibition of CRH-R2 signaling aggravates the symptoms of DSS-induced colitis in mice

We first assessed the involvement of CRH-R2 signaling in mucosal repair after colitis by administering the CRH-R2 antagonist Ast2B to mice after induction of DSS colitis. Mice received an intraperitoneal injection of Ast2B daily for 9 d after withdrawal of DSS, and body weight loss, DAI, colon length and histological score were monitored.

Compared with the DSS group, mice treated with the CRH-R2 antagonist Ast2B showed more body weight loss ($P < 0.05$) (Figure 1A) and shorter colon lengths (4.90 ± 0.32 cm *vs* 6.21 ± 0.34 cm, $P < 0.05$) (Figure 1B). DAI score and histological score were used to evaluate the severity of UC in mice. The mice in the Ast2B group exhibited significantly higher DAI scores (3.61 ± 0.53 *vs* 2.42 ± 0.32, $P < 0.05$) (Figure 1D) and histological scores (11.50 ± 1.05 *vs* 8.33 ± 1.03, $P < 0.05$) (Figure 1E) compared to the mice in the DSS group.

Interestingly, mice treated with Ucn2 after DSS-induced colitis showed a smaller degree of body weight loss ($P < 0.001$) (Figure 1A), longer colon length (9.58 ± 0.62 cm *vs* 6.21 ± 0.34 cm, $P < 0.001$) (Figure 1B), lower DAI (0.87 ± 0.55 *vs* 2.42 ± 0.32, $P < 0.001$) (Figure 1D) and improved histological scores (4.33 ± 1.50 *vs* 8.33 ± 1.03, $P < 0.05$) (Figure 1E) compared to the mice in the DSS group. However, a significant statistical difference was found between the Ast2B + Ucn2 group and the Ucn2 group (Figure 1A-F).

Inhibition of CRH-R2 signaling increases secretion of inflammatory cytokines in colon tissues of DSS-induced UC mice

The levels of proinflammatory factors such as TNF-α, CXCL-1 and IL-6 in mouse colon tissues were detected by real time-PCR and ELISA. Compared with the DSS group, the Ast2B group showed significantly up-regulated mRNA expression of TNF-α (6.19 ± 0.51 *vs* 3.87 ± 0.98, $P < 0.05$) (Figure 2A), CXCL-1 (10.77 ± 2.55 *vs* 5.08 ± 0.76, $P < 0.05$) (Figure 2B),and IL-6

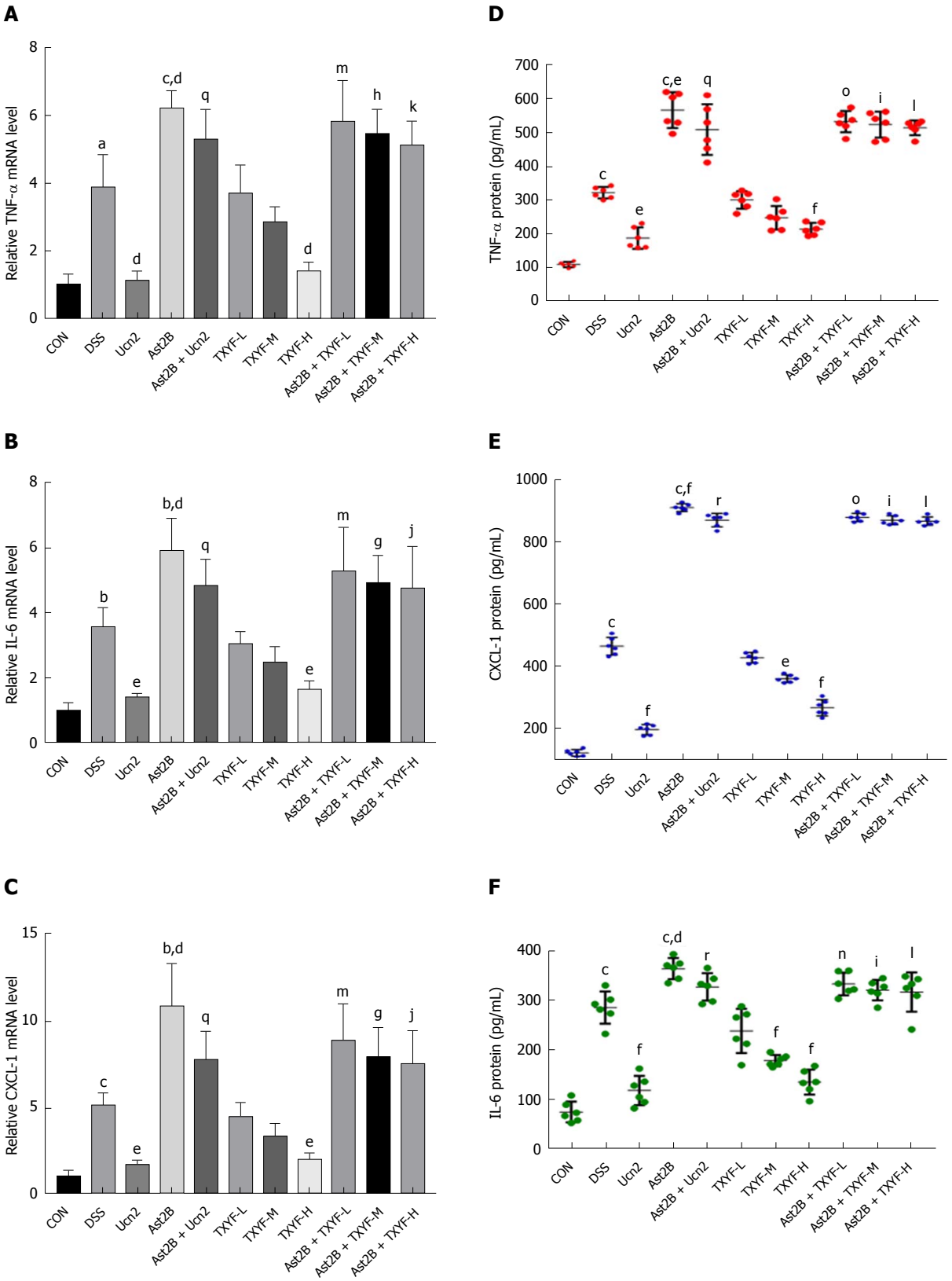

Figure 2 Inhibition of CRH-R2 signaling increases secretion of inflammatory cytokines in colon tissues of DSS-induced ulcerative colitis mice. A-C: Real time-PCR-assessed mRNA level of TNF α (A), CXCL-1 (B) and IL 6 (C) in colon tissues. The mRNA level in each group was determined relative to the level in the control group (defined as 100%); E-F: Enzyme-linked immunosorbent assay-detected protein levels of TNF α (D), CXCL-1 (E) and IL 6 (F) in colon tissues. Data are presented as mean ± standard deviation, $n = 6$ per group. $^{b}P < 0.01$, $^{c}P < 0.001$ *vs* control group; $^{d}P < 0.05$, $^{e}P < 0.01$, $^{f}P < 0.001$ *vs* DSS group; $^{q}P < 0.01$, $^{r}P < 0.001$ *vs* Ucn2 group; $^{m}P < 0.05$, $^{n}P < 0.01$, $^{o}P < 0.001$ *vs* TXYF-L group; $^{g}P < 0.05$, $^{h}P < 0.01$, $^{i}P < 0.001$ *vs* TXYF-M group; $^{j}P < 0.05$, $^{k}P < 0.01$, $^{l}P < 0.001$ *vs* TXYF-H group. CRH-R2: Corticotropin-releasing hormone-receptor 2; DSS: Dextran sulfate sodium; TXYF: Tong-Xie-Yao-Fang.

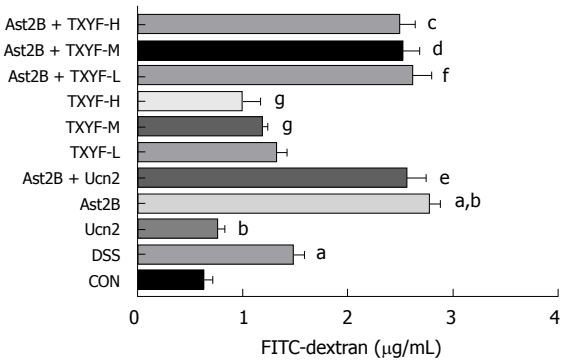

Figure 3 Inhibition of CRH-R2 signaling promotes intestinal permeability in DSS-induced colitis. The FITC-dextran levels in serum were determined. Data are presented as mean ± standard deviation, $n = 6$ per group. $^{a}P < 0.001$ *vs* control group; $^{g}P < 0.05$, $^{b}P < 0.001$ *vs* DSS group; $^{e}P < 0.001$ *vs* Ucn2 group; $^{f}P < 0.001$ *vs* TXYF-L group; $^{d}P < 0.001$ *vs* TXYF-M group; $^{c}P < 0.001$ *vs* TXYF-H group. CRH-R2: Corticotropin-releasing hormone-receptor 2; DSS: Dextran sulfate sodium; TXYF: Tong-Xie-Yao-Fang.

(5.93 ± 0.99 *vs* 3.55 ± 0.62, $P < 0.05$) (Figure 2C). Meanwhile, the protein expression levels of TNF-α (Figure 2D), CXCL-1 (Figure 2E) and IL-6 (Figure2F) were increased markedly in the Ast2B group.

However, compared with the DSS group, the Ucn2 group showed significantly decreased mRNA expression of TNF-α (Figure 2A), CXCL-1 (Figure 2B) and IL-6 (Figure 2C). Simultaneously, the Ucn2 group demonstrated reduced protein expression of TNF-α (Figure 2D), CXCL-1 (Figure 2E) and IL-6 (Figure 2F). Interestingly, the Ast2B + Ucn2 group showed drastically increased mRNA and protein expression of TNF-α, CXCL-1 and IL-6 compared with the Ucn2 group ($P < 0.05$ for all).

Inhibition of CRH-R2 signaling promotes intestinal permeability in DSS induced colitis

To determine the effect of CRH-R2 signaling on epithelial permeability, we analyzed intestinal permeability in DSS-induced colitis model by measuring the concentration of the serum FITC. The concentration of serum FITC-dextran was higher in the Ast2B group than DSS group (2.76 ± 0.11 μg/mL *vs* 1.47 ± 0.11 μg/mL, $P < 0.05$) (Figure 3). However, the concentration of serum FITC-dextran in the Ucn2 group was lower than DSS group (0.75 ± 0.07 μg/mL *vs* 1.47 ± 0.11 μg/mL, $P < 0.05$) (Figure 3). An obvious difference was observed between the Ast2B+Ucn2 group and the Ucn2 group.

Inhibition of CRH-R2 signaling promotes colonic epithelial cell apoptosis and reduces epithelial cell proliferation

The effect of Ast2B on cell proliferation and cell death was then determined. TUNEL staining was significantly increased in the Ast2B group compared with the DSS group (1422.39 ± 90.71 *vs* 983.01 ± 98.17, $P < 0.001$) (Figure 4L). At the same time, the Ast2B group showed significantly decreased cell proliferation (4.97 ± 4.25 *vs* 22.51 ± 8.22, $P < 0.05$) (Figure 5L). Interestingly, the Ucn2 group showed promoted colonic epithelial cell proliferation (Figure 5L) and reduced epithelial cell apoptosis (Figure 4L). However, significant statistical differences were found between the Ucn2 group and the Ast2B + Ucn2 group with regards to colonic epithelial cell apoptosis and proliferation ($P < 0.01$ for both).

TXYF promotes mucosal repair in colitis mice by regulating CRH-R2 signaling

To obtain insight into the underlying mechanism responsible for promoting mucosal repair of TXYF, DSS-induced colitis mice were pretreated with the CRH-R2 antagonist Ast2B, and later treated with various doses of aqueous TXYF extracts.

Compared with the DSS group, the TXYF-H groups had lower DAI scores (Figure 1D) and histological scores (Figure 1E), and decreased body weight loss (Figure 1A). TXYF-M,H groups, on the other hand, had longer colon length (Figure 1B) and improved intestinal permeability (Figure 3). Furthermore, TXYF inhibited secretion of inflammatory cytokines in colon tissues (Figure 2A-F) and promoted colonic epithelial cell proliferation (Figure 5L), along with reducing apoptosis (Figure 4L). However, the Ast2B + TXYF groups showed significant statistical difference in DAI, body weight loss, colon length and histological scores, when compared with the TXYF groups. As for inhibiting secretion of inflammatory cytokines, the Ast2B + TXYF groups demonstrated significant differences within the TXYF groups. Additionally, the Ast2B + TXYF groups showed markedly improved intestinal permeability in DSS-induced colitis compared with the TXYF groups, respectively. In addition, the Ast2B + TXYF groups demonstrated significant differences with the TXYF groups in promoting colonic epithelial cell proliferation and reducing epithelial cell apoptosis.

These results further confirm the idea that CRH-R2 signaling is the main mechanism of TXYF-mediated mucosal repair in DSS-induced colitis in mice.

DISCUSSION

Mucosal healing is a desired therapeutic end-point in the treatment of IBD; interventions that promote restoration of the epithelial barrier are needed to limit inflammation and to prevent future injury. Mucosal healing consists of two processes[15]. Firstly, intact cells in the adjacent region migrate to the injured area; then, the cells compensate for damaged cells by proliferation and help to maintain normal thickness of the intestinal epithelium. Therefore, the migration and proliferation of intestinal epithelial cells are the key mechanisms for the healing of epithelial defects after mucosal injury. In addition, inhibiting apoptosis of intestinal epithelial cells can promote the healing process of mucosa[37]. It is well known that intestinal epithelial barrier defects are

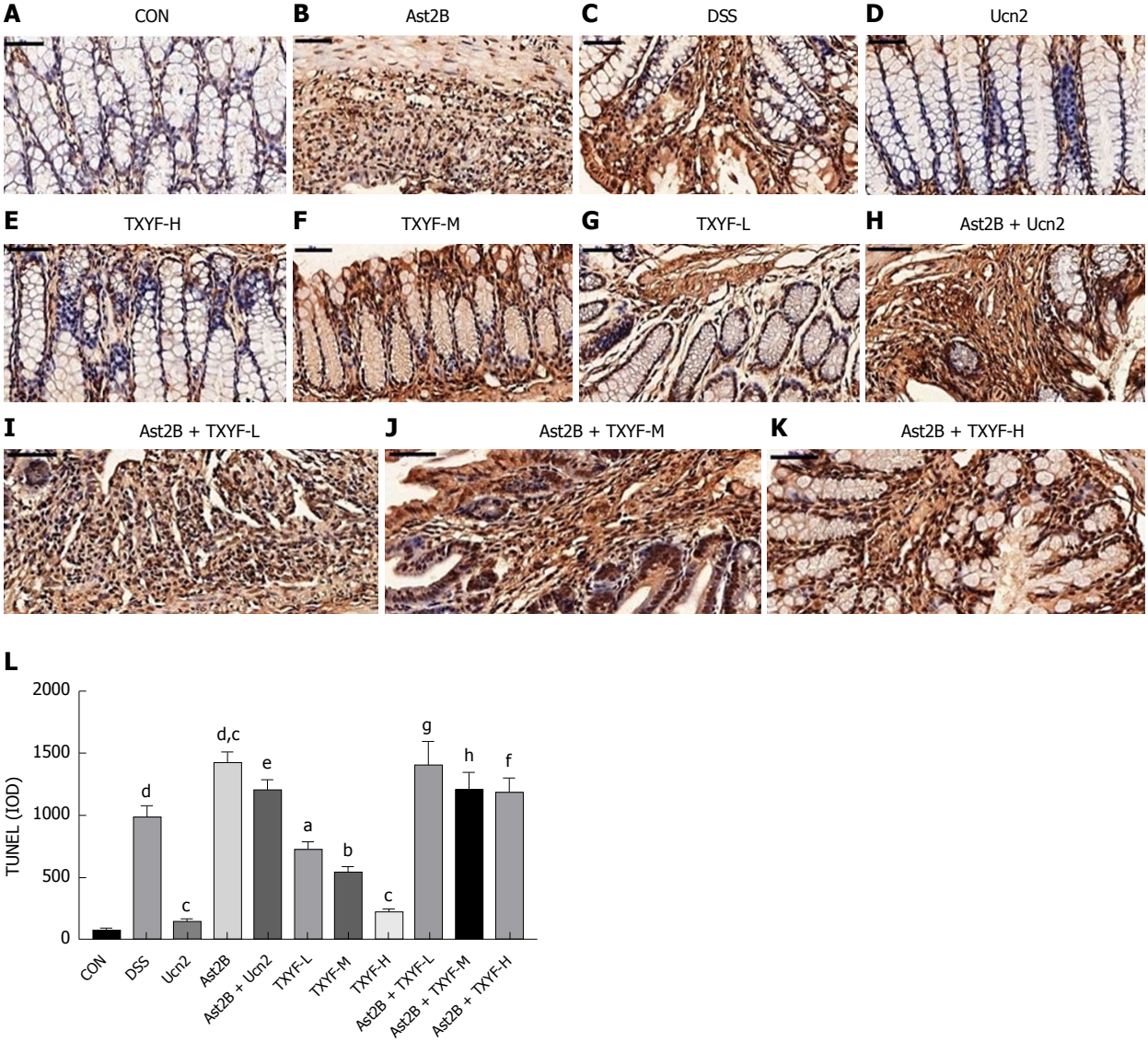

Figure 4 Inhibition of CRH-R2 signaling promotes colonic epithelial cell apoptosis in DSS-induced colitis. A-K: Representative images from TUNEL sections; L: Quantification of TUNEL data. Data are presented as mean ± standard deviation, $n = 6$ per group, scale bar = 50 μm. $^{d}P < 0.001$ *vs* control group; $^{a}P < 0.05$, $^{b}P < 0.01$, $^{c}P < 0.001$ *vs* DSS group; $^{e}P < 0.001$ *vs* Ucn2 group; $^{g}P < 0.01$ *vs* TXYF-L group; $^{h}P < 0.01$ *vs* TXYF-M group; $^{f}P < 0.001$ *vs* TXYF-H group. CRH-R2: Corticotropin-releasing hormone-receptor 2; DSS: Dextran sulfate sodium; TUNEL: Terminal deoxynucleotidyl transferase dUTP nick-end labeling; TXYF: Tong-Xie-Yao-Fang.

characterized by increased intestinal permeability.

In the present study, it was found that selective inhibition of CRH-R2 signaling can aggravate symptoms of DSS-induced colitis, destroy the impaired intestinal barrier function, promote colonic epithelial cell apoptosis and reduce epithelial cell proliferation. After treatment with Ucn2 and TXYF, DSS-induced mice demonstrated ameliorated symptoms of DSS-induced colitis, improved impaired intestinal barrier function, promoted colonic epithelial cell proliferation and reduced epithelial cell apoptosis. Moreover, Ucn2 and TXYF reduced the expression of the proinflammatory factors TNF-α, CXCL-1, and IL-6 in colon tissues.

Cytokines play a central role in the regulation of both intestinal inflammation and mucosal repair mechanisms[38]. Treatments that neutralize the proinflammatory actions of TNF-α promote mucosal healing and are a standard of current IBD treatment paradigms[7,38]. In addition, production of the key proinflammatory cytokine IL-6 correlates with the degree of active intestinal inflammation in IBD patients[39], further supporting the concept that therapeutic interventions that modulate cytokine production and/or release may promote mucosal repair after inflammation. Taken together, these results indicate that Ucn2 and TXYF promote mucosal repair.

Studies from others have found that CRH may be involved in the maintenance of intestinal barrier integrity by regulating autophagy in the intestinal epithelial cells[18]. Our previous studies also found that CRH could induce an increase in intercellular permeability in the intestinal epithelium[22]. Some studies have also found that CRH-R2 can activate the antiinflammatory response of intestinal mucosa and exert an antiinflammatory effect[23]. In addition, activation of CRH-R2 can promote

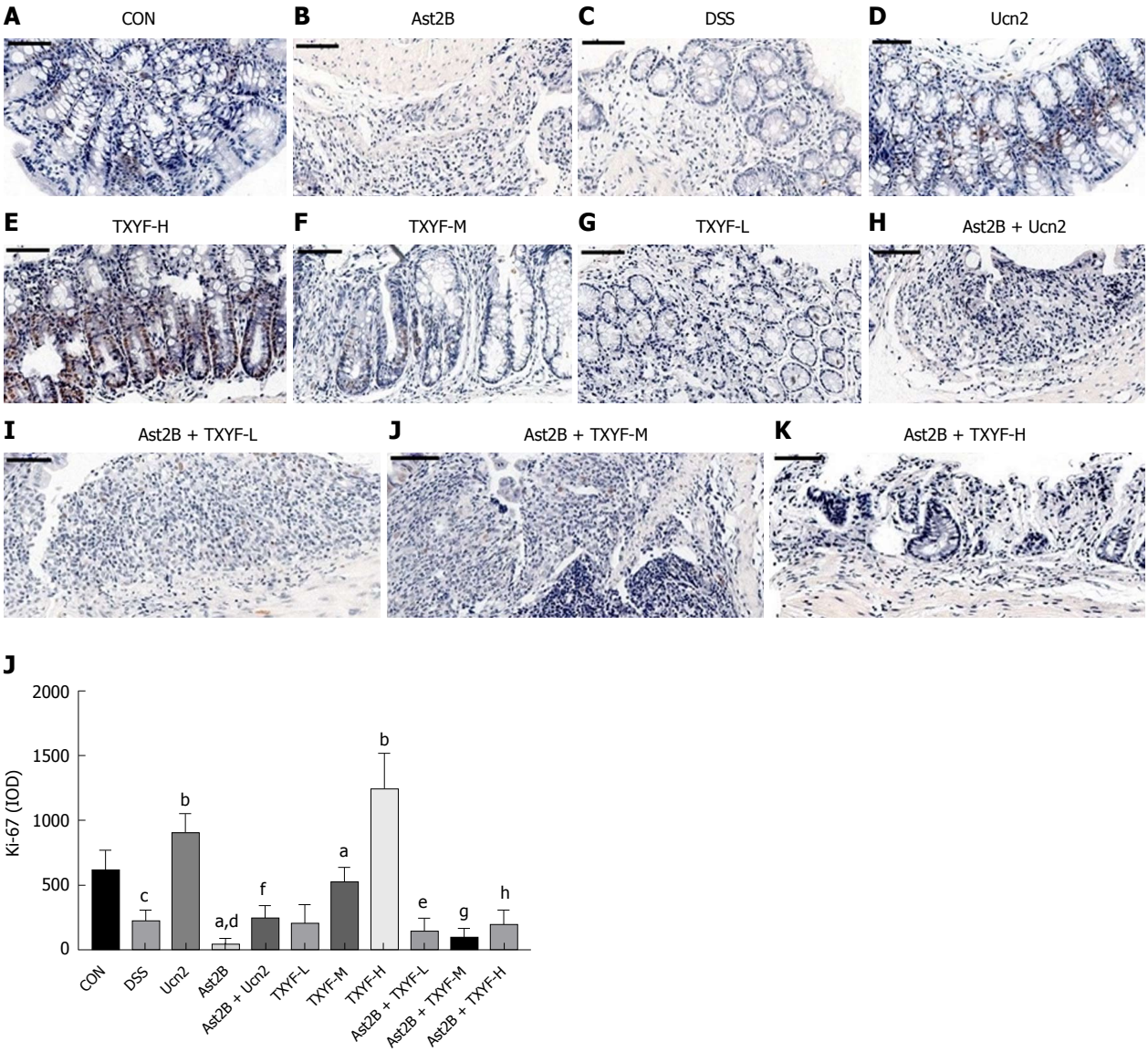

Figure 5 Inhibition of CRH-R2 signaling reduces epithelial cell proliferation in DSS-induced colitis. A-K: Representative images from Ki-67 immunoreactive sections; L: Quantification of Ki-67 immunohistochemistry data. Data presented as mean ± standard deviation, $n = 6$ per group, scale bar = 50 μm. $^{c}P < 0.05$, $^{d}P < 0.01$ *vs* control group; $^{a}P < 0.05$, $^{b}P < 0.01$ *vs* DSS group. $^{f}P < 0.01$ *vs* Ucn2 group; $^{e}P < 0.05$ *vs* TXYF-L group; $^{g}P < 0.01$ *vs* TXYF-M group; $^{h}P < 0.01$ *vs* TXYF-H group. CRH-R2: Corticotropin-releasing hormone-receptor 2; DSS: Dextran sulfate sodium; TXYF: Tong-Xie-Yao-Fang.

the migration and proliferation of colon cancer cells and gastric mucosa cells[24,25]. Furthermore, the expression of CRH-R2 has been reported as down-regulated in biopsy specimens of UC patients[26] and CRH-deficient mice have been reported as unable to initiate healing responses after acute experimental colitis[27].

These results suggest a role for the CRH peptide family, especially CRH-R2, in mucosal repair mechanisms. It is known that Ucn2 is a peptide which binds exclusively to CRH-R2. Significant statistical differences were found between the Ast2B group and the Ast2B + Ucn2 group. Thus, a conclusion can be made that CRH-R2 activated the intestinal mucosal antiinflammatory response by regulating the migration, proliferation and apoptosis of intestinal epithelial cells in colitis mice.

Subsequently, the efficacy of TXYF was assessed. According to the theory of traditional Chinese medicine, IBD belongs to "diarrhea, dysentery". The principle of treatment is focused on relieving pain and eliminating dampness and diarrhea. TXYF is a classic formula in the Jing yue quan shu (Jingyue's Complete Book), which consists of atractylodes rhizome (*Rhizoma Atractylodis Macrocephalae*) head groups, white peony root (*Radix Paeoniae Alba*), dried tangerine peel (*Pericarpium Citri Reticulatae*), and divaricate saposhnikovia root (*Radix Saposhnikoviae*). TXYF has been believed to be effective in improving disorders of the digestive system and alleviating abdominal pain, diarrhea, and has been used widely as a medication to treat inflammatory bowel syndrome and UC clinically, without inducing hepatomegaly or splenomegaly[40-42].

TXYF has also been shown to improve reconstruction

of the intestinal epithelial barrier and promote the healing of mucosa in UC[28,29]. Our previous study found that TXYF down-regulated CRH-R1 and up-regulated CRH-R2. While the mechanism underlying TXYF promotion of mucosal repair is not well understood, it is thought to intervene using CRH-R2 and to regulate the migration, proliferation and apoptosis of epithelial cells, like the role of Ucn2[30,31].

Herein, we describe the selective inhibition of CRH-R2 signaling in the intestinal mucosa of mice after experimental colitis, along with TXYF treatment, leading to exacerbated symptoms of DSS-induced colitis, delayed healing, increased expression of proinflammatory factors TNF-α, CXCL-1 and IL-6 in colon tissues, decreased epithelial cell proliferation and promoted cell apoptosis. These results suggest that TXYF promoted the mucosal repair process of colitis mice by regulating CRH-R2.

In conclusion, CRH-R2 activates the intestinal mucosal antiinflammatory response by regulating the migration, proliferation and apoptosis of intestinal epithelial cells in colitis mice, and exerts an antiinflammatory effect. The effects of TXYF on the mucosal repair process are focused on regulating CRH-R2 in colitis mice.

ARTICLE HIGHLIGHTS

Research background

Mucosal healing is a desired therapeutic end-point in the treatment of inflammatory bowel disease (IBD). However, thorough treatment of IBD is difficult and there are some adverse reactions. According to studies, corticotropin-releasing hormone (CRH)-receptor (R)2 can activate the inflammatory response of intestinal mucosa. Our preliminary study found that Tong-Xie-Yao-Fang could lower CRH-R1, increase the expression of CRH-R2, and participates in reconstruction of the intestinal barrier.

Research motivation

Mucosal healing is a desired therapeutic end-point in the treatment of IBD. However, the mechanism of mucosal healing is still unclear.

Research objectives

To explore the significance of CRH-R2 in the mucosal healing of dextran sulfate sodium (DSS)-induced colitis and study the effect of Tong-Xie-Yao-Fang (TXYF) on CRH-R2.

Research methods

Ulcerative colitis (UC) was induced in mice by administration of 3% (w/v) DSS for 7 d. Then, mice were administered urocortin (Ucn)-2 or various doses of aqueous TXYF extracts, the CRH-R2 antagonist Astressin (Ast)2B, Ast2B + Ucn2, or Ast2B with various doses of aqueous TXYF extracts for 9 d. The colitis disease activity index (DAI) was assessed to evaluate the condition of colitis. The expression level of Ki-67 represented the proliferation of colonic epithelial cells. The expression levels of inflammation cytokines IL-6, TNF-α and CXCL-1 were examined by PCR and enzyme-linked immunosorbent assay.

Research results

Compared with the DSS group, mice treated with the CRH-R2 antagonist Ast2B showed greater loss of body weight, shorter colon lengths, and higher DAI and histological scores. Additionally, the Ast2B group showed increased intestinal permeability, improved secretion of inflammatory cytokines in colon tissue and reduced colonic epithelial cell proliferation. Increased apoptosis was also demonstrated. The Ucn2 group demonstrated lower DAI and histological scores. Diminished weight loss, longer colon length, reduced intestinal permeability, inhibited secretion of inflammatory cytokines in colon tissue and increased colonic epithelial cell proliferation were all observed. Reduced apoptosis was also observed.

Research conclusions

CRH-R2 activates the intestinal mucosal antiinflammatory response and plays an important antiinflammatory role. TXYF promotes the mucosal repair process in colitis mice.

Research perspectives

The CRH-R2 signaling pathway plays a pivotal role in mucosal healing in experimental UC in mice. Mucosal healing is a desired therapeutic end-point in the treatment of IBD. Thus, the findings of this study indicate a new potential mechanism by which CRH-R2 treats UC. TXYF, which has fewer side effects than other medicines, promotes the mucosal repair process of colitis mice by regulating CRH-R2. Therefore, TXYF can be used in patients with UC to promote their mucosal repair.

ACKNOWLEDGMENTS

We would like to thank our colleagues in the Institute of Digestive Disease affiliated the First Clinical Medical College of Zhejiang Chinese Medical University for their help and support in this research.

REFERENCES

1 **Norouzinia M**, Chaleshi V, Alizadeh AHM, Zali MR. Biomarkers in inflammatory bowel diseases: insight into diagnosis, prognosis and treatment. *Gastroenterol Hepatol Bed Bench* 2017; **10**: 155-167 [PMID: 29118930]

2 **Jin F L,** Yi-Ping L I. Progress in the traditional Chinese medicine treatment of ulcerative colitis. *China Modern Medicine* 2016

3 **Ouyang Q**, Xue LY. Inflammatory bowel disease in the 21(st) century in China: turning challenges into opportunities. *J Dig Dis* 2012; **13**: 195-199 [PMID: 22435503 DOI: 10.1111/j.1751-2980.2012.00579.x]

4 **Bernstein CN**, Loftus EV Jr, Ng SC, Lakatos PL, Moum B; Epidemiology and Natural History Task Force of the International Organization for the Study of Inflammatory Bowel Disease (IOIBD). Hospitalisations and surgery in Crohn's disease. *Gut* 2012; **61**: 622-629 [PMID: 22267595 DOI: 10.1136/gutjnl-2011-301397]

5 **Magro F**, Rodrigues A, Vieira AI, Portela F, Cremers I, Cotter J, Correia L, Duarte MA, Tavares ML, Lago P, Ministro P, Peixe P, Lopes S, Garcia EB. Review of the disease course among adult ulcerative colitis population-based longitudinal cohorts. *Inflamm Bowel Dis* 2012; **18**: 573-583 [PMID: 21793126 DOI: 10.1002/ibd.21815]

6 **Baars JE**, Nuij VJ, Oldenburg B, Kuipers EJ, van der Woude CJ. Majority of patients with inflammatory bowel disease in clinical remission have mucosal inflammation. *Inflamm Bowel Dis* 2012; **18**: 1634-1640 [PMID: 22069022 DOI: 10.1002/ibd.21925]

7 **van Dullemen HM**, van Deventer SJ, Hommes DW, Bijl HA, Jansen J, Tytgat GN, Woody J. Treatment of Crohn's disease with anti-tumor necrosis factor chimeric monoclonal antibody (cA2). *Gastroenterology* 1995; **109**: 129-135 [PMID: 7797011 DOI: 10.1016/0016-5085(95)90277-5]

8 **Rutgeerts P**, D'Haens G, Targan S, Vasiliauskas E, Hanauer SB, Present DH, Mayer L, Van Hogezand RA, Braakman T, DeWoody KL, Schaible TF, Van Deventer SJ. Efficacy and safety of retreatment with anti-tumor necrosis factor antibody (infliximab) to maintain remission in Crohn's disease. *Gastroenterology* 1999; **117**: 761-769 [PMID: 10500056 DOI: 10.1016/S0016-5085(99)70332-X]

9 **Rutgeerts P**, Diamond RH, Bala M, Olson A, Lichtenstein GR, Bao W, Patel K, Wolf DC, Safdi M, Colombel JF, Lashner B, Hanauer SB. Scheduled maintenance treatment with infliximab is superior to episodic treatment for the healing of mucosal ulceration associated with Crohn's disease. *Gastrointest Endosc* 2006; **63**: 433-442; quiz 464 [PMID: 16500392 DOI: 10.1016/j.gie.2005.08.011]

10 **Hanauer SB**, Feagan BG, Lichtenstein GR, Mayer LF, Schreiber S, Colombel JF, Rachmilewitz D, Wolf DC, Olson A, Bao W, Rutgeerts P; ACCENT I Study Group. Maintenance infliximab for Crohn's disease: the ACCENT I randomised trial. *Lancet* 2002; **359**: 1541-1549 [PMID: 12047962 DOI: 10.1016/S0140-6736(02)08512-4]

11 **Sands BE**, Anderson FH, Bernstein CN, Chey WY, Feagan BG, Fedorak RN, Kamm MA, Korzenik JR, Lashner BA, Onken JE, Rachmilewitz D, Rutgeerts P, Wild G, Wolf DC, Marsters PA, Travers SB, Blank MA, van Deventer SJ. Infliximab maintenance therapy for fistulizing Crohn's disease. *N Engl J Med* 2004; **350**: 876-885 [PMID: 14985485 DOI: 10.1056/NEJMoa030815]

12 **Römkens TE**, Gijsbers K, Kievit W, Hoentjen F, Drenth JP. Treatment Targets in Inflammatory Bowel Disease: Current Status in Daily Practice. *J Gastrointestin Liver Dis* 2016; **25**: 465-471 [PMID: 27981302 DOI: 10.15403/jgld.2014.1121.254.ken]

13 **Taupin D**, Podolsky DK. Trefoil factors: initiators of mucosal healing. *Nat Rev Mol Cell Biol* 2003; **4**: 721-732 [PMID: 14506475 DOI: 10.1038/nrm1203]

14 **Sturm A**, Dignass AU. Epithelial restitution and wound healing in inflammatory bowel disease. *World J Gastroenterol* 2008; **14**: 348-353 [PMID: 18200658 DOI: 10.3748/wjg.14.348]

15 **Neurath MF**. New targets for mucosal healing and therapy in inflammatory bowel diseases. *Mucosal Immunol* 2014; **7**: 6-19 [PMID: 24084775 DOI: 10.1038/mi.2013.73]

16 **Neurath MF**, Travis SP. Mucosal healing in inflammatory bowel diseases: a systematic review. *Gut* 2012; **61**: 1619-1635 [PMID: 22842618 DOI: 10.1136/gutjnl-2012-302830]

17 **Laukoetter MG**, Nava P, Nusrat A. Role of the intestinal barrier in inflammatory bowel disease. *World J Gastroenterol* 2008; **14**: 401-407 [PMID: 18200662]

18 **Giannogonas P**, Apostolou A, Manousopoulou A, Theocharis S, Macari SA, Psarras S, Garbis SD, Pothoulakis C, Karalis KP. Identification of a novel interaction between corticotropin releasing hormone (Crh) and macroautophagy. *Sci Rep* 2016; **6**: 23342 [PMID: 26987580 DOI: 10.1038/srep23342]

19 **Bonaz BL**, Bernstein CN. Brain-gut interactions in inflammatory bowel disease. *Gastroenterology* 2013; **144**: 36-49 [PMID: 23063970 DOI: 10.1053/j.gastro.2012.10.003]

20 **Hillhouse EW**, Grammatopoulos DK. The molecular mechanisms underlying the regulation of the biological activity of corticotropin-releasing hormone receptors: implications for physiology and pathophysiology. *Endocr Rev* 2006; **27**: 260-286 [PMID: 16484629 DOI: 10.1210/er.2005-0034]

21 **Hoffman JM**, Baritaki S, Ruiz JJ, Sideri A, Pothoulakis C. Corticotropin-Releasing Hormone Receptor 2 Signaling Promotes Mucosal Repair Responses after Colitis. *Am J Pathol* 2016; **186**: 134-144 [PMID: 26597886 DOI: 10.1016/j.ajpath.2015.09.013]

22 **Wang X T,** Hu Y, Li M, Lv B. Study on the role of stress through CRF up regulation of CK8 mediated change of close connexin in the pathogenesis of irritable bowel syndrome. The national association of Chinese and western medicine on digestive system disease academic conference, 2015

23 **Im E**, Rhee SH, Park YS, Fiocchi C, Taché Y, Pothoulakis C. Corticotropin-releasing hormone family of peptides regulates intestinal angiogenesis. *Gastroenterology* 2010; **138**: 2457-2467, 2467.e1-2467.e5 [PMID: 20206175 DOI: 10.1053/j.gastro.2010.02.055]

24 **Ducarouge B**, Pelissier-Rota M, Lainé M, Cristina N, Vachez Y, Scoazec JY, Bonaz B, Jacquier-Sarlin M. CRF2 signaling is a novel regulator of cellular adhesion and migration in colorectal cancer cells. *PLoS One* 2013; **8**: e79335 [PMID: 24260200 DOI: 10.1371/journal.pone.0079335]

25 **Chatzaki E**, Lambropoulou M, Constantinidis TC, Papadopoulos N, Taché Y, Minopoulos G, Grigoriadis DE. Corticotropin-releasing factor (CRF) receptor type 2 in the human stomach: protective biological role by inhibition of apoptosis. *J Cell Physiol* 2006; **209**: 905-911 [PMID: 16972272 DOI: 10.1002/jcp.20792]

26 **Chatzaki E**, Anton PA, Million M, Lambropoulou M, Constantinidis T, Kolios G, Taché Y, Grigoriadis DE. Corticotropin-releasing factor receptor subtype 2 in human colonic mucosa: down-regulation in ulcerative colitis. *World J Gastroenterol* 2013; **19**: 1416-1423 [PMID: 23539366 DOI: 10.3748/wjg.v19.i9.1416]

27 **Chaniotou Z**, Giannogonas P, Theoharis S, Teli T, Gay J, Savidge T, Koutmani Y, Brugni J, Kokkotou E, Pothoulakis C, Karalis KP. Corticotropin-releasing factor regulates TLR4 expression in the colon and protects mice from colitis. *Gastroenterology* 2010; **139**: 2083-2092 [PMID: 20732324 DOI: 10.1053/j.gastro.2010.08.024]

28 **Stanisic V**, Quigley EM. The overlap between IBS and IBD: what is it and what does it mean? *Expert Rev Gastroenterol Hepatol* 2014; **8**: 139-145 [PMID: 24417262 DOI: 10.1586/17474124.2014.876361]

29 **Quigley EM**. Overlapping irritable bowel syndrome and inflammatory bowel disease: less to this than meets the eye? *Therap Adv Gastroenterol* 2016; **9**: 199-212 [PMID: 26929782 DOI: 10.1177/1756283X15621230]

30 **Chao G**, Lv B, Meng L, Zhang S, Zahng L, Guo Y. [Influence of tongxie prescription on CRF expression in spinal cord and brain of hypersensitive viscera rats]. *Zhongguo Zhong Yao Za Zhi* 2010; **35**: 2012-2016 [PMID: 20931858]

31 **Ding Y**, Lv B, Meng L N, Fan Y H, Shen Y. Effect of Tongxieyaofang on Colonic Mucosal Protein Expression Profile in Rats with Visceral Hypersensitivity. *Chinese Journal of Gastroenterology* 2012; **17**: 660-664 [DOI: 10.3969/j.issn.1008-7125.2012.11.005]

32 **Yang C**, Xiong Y, Zhang SS, An FM, Sun J, Zhang QL, Zhan Q. Regulating effect of TongXie-YaoFang on colonic epithelial secretion via Cl- and HCO3- channel. *World J Gastroenterol* 2016; **22**: 10584-10591 [PMID: 28082810 DOI: 10.3748/wjg.v22.i48.10584]

33 **Hendrickson BA**, Gokhale R, Cho JH. Clinical aspects and pathophysiology of inflammatory bowel disease. *Clin Microbiol Rev* 2002; **15**: 79-94 [PMID: 11781268]

34 **Murthy SN**, Cooper HS, Shim H, Shah RS, Ibrahim SA, Sedergran DJ. Treatment of dextran sulfate sodium-induced murine colitis by intracolonic cyclosporin. *Dig Dis Sci* 1993; **38**: 1722-1734 [PMID: 8359087]

35 **Dieleman LA**, Palmen MJ, Akol H, Bloemena E, Peña AS, Meuwissen SG, Van Rees EP. Chronic experimental colitis induced by dextran sulphate sodium (DSS) is characterized by Th1 and Th2 cytokines. *Clin Exp Immunol* 1998; **114**: 385-391 [PMID: 9844047]

36 **Nguyen HT**, Dalmasso G, Torkvist L, Halfvarson J, Yan Y, Laroui H, Shmerling D, Tallone T, D'Amato M, Sitaraman SV, Merlin D. CD98 expression modulates intestinal homeostasis, inflammation, and colitis-associated cancer in mice. *J Clin Invest* 2011; **121**: 1733-1747 [PMID: 21490400 DOI: 10.1172/JCI44631]

37 **Seidelin JB**, Larsen S, Linnemann D, Vainer B, Coskun M, Troelsen JT, Nielsen OH. Cellular inhibitor of apoptosis protein 2 controls human colonic epithelial restitution, migration, and Rac1 activation. *Am J Physiol Gastrointest Liver Physiol* 2015; **308**: G92-G99 [PMID: 25394657 DOI: 10.1152/ajpgi.00089.2014]

38 **Neurath MF**. Cytokines in inflammatory bowel disease. *Nat Rev Immunol* 2014; **14**: 329-342 [PMID: 24751956 DOI: 10.1038/nri3661]

39 **Suzuki Y**, Saito H, Kasanuki J, Kishimoto T, Tamura Y, Yoshida S. Significant increase of interleukin 6 production in blood mononuclear leukocytes obtained from patients with active inflammatory bowel disease. *Life Sci* 1990; **47**: 2193-2197 [PMID: 2266787]

40 **Fan H**, Qiu MY, Mei JJ, Shen GX, Liu SL, Chen R. Effects of four regulating-intestine prescriptions on pathology and ultrastructure

of colon tissue in rats with ulcerative colitis. *World J Gastroenterol* 2005; **11**: 4800-4806 [PMID: 16097047]
41 **Hu X**, Zhang X, Han B, Bei W. The inhibitory effect of tongxieyaofang on rats with post infectious irritable bowel syndrome through regulating colonic par-2 receptor. *BMC Complement Altern Med* 2013; **13**: 246 [PMID: 24088410 DOI: 10.1186/1472-6882-13-246]
42 **Lu X**, Zhang S, Yang C, Wang Z, Zhao L, Wu Z, Xie J. Effect of TongXie-YaoFang on Cl(-) and HCO3 (-) Transport in Diarrhea-Predominant Irritable Bowel Syndrome Rats. *Evid Based Complement Alternat Med* 2016; **2016**: 7954982 [PMID: 27403199 DOI: 10.1155/2016/7954982]

P- Reviewer: Gassler N, Ozen H, Tarnawski AS **S- Editor**: Wang XJ
L- Editor: Filipodia **E- Editor**: Huang Y

World Journal of Gastroenterology

Submit a Manuscript: http://www.f6publishing.com

World J Gastroenterol 2018 April 28; 24(16): 1779-1794

DOI: 10.3748/wjg.v24.i16.1779

ISSN 1007-9327 (print) ISSN 2219-2840 (online)

ORIGINAL ARTICLE

Basic Study

Sodium chloride exacerbates dextran sulfate sodium-induced colitis by tuning proinflammatory and antiinflammatory lamina propria mononuclear cells through p38/MAPK pathway in mice

Hong-Xia Guo, Nan Ye, Ping Yan, Min-Yue Qiu, Ji Zhang, Zi-Gang Shen, Hai-Yang He, Zhi-Qiang Tian, Hong-Li Li, Jin-Tao Li

Hong-Xia Guo, Jin-Tao Li, Department of Microbiology, Third Military Medical University (Army Medical University), District Shapingba, Chongqing 400038, China

Hong-Xia Guo, Nan Ye, Min-Yue Qiu, Jin-Tao Li, Institute of Tropical Medicine, Third Military Medical University (Army Medical University), District Shapingba, Chongqing 400038, China

Ping Yan, Department of Obstetrics and Gynecology, Southwest Hospital, Third Military Medical University (Army Medical University), Chongqing 400038, China

Ji Zhang, Zi-Gang Shen, Hai-Yang He, Zhi-Qiang Tian, Institute of Immunology, Third Military Medical University (Army Medical University), District Shapingba, Chongqing 400038, China

Hong-Li Li, Department of Histology and Embryology, College of Basic Medicine, Third Military Medical University (Army Medical University), Chongqing 400038, China

ORCID number: Hong-Xia Guo (0000-0003-4476-3141); Nan Ye (0000-0001-8929-7813); Ping Yan (0000-0001-7984-9880); Min-Yue Qiu (0000-0002-7718-3111); Ji Zhang (0000-0002-6444-3949); Zi-Gang Shen (0000-0001-5224-5315); Hai-Yang He (0000-0002-2862-3600); Zhi-Qiang Tian (0000-0003-4609-6637); Hong-Li Li (0000-0003-0851-2310); Jin-Tao Li (0000-0003-3637-2386).

Author contributions: Li JT designed the research; Guo HX, Ye N, Li HL and Qiu MY performed the research; Yan P, Zhang J, Shen ZG, He HY and Tian ZQ contributed reagents and analytic tools; Ye N contributed to the statistical analysis; Guo HX and Li JT wrote the manuscript and carried out the critical revision of the manuscript; all authors provided final approval of the article.

Supported by National Natural Science Foundation of China, No. 81271813 and No. 81570497.

Institutional review board statement: This study was reviewed and approved by the Third Military Medical University (Army Medical University) Institutional Review Board.

Institutional animal care and use committee statement: All procedures involving the care and use of animals were approved by The Institutional Animal Care and Use Committee of the Third Military Medical University (Army Medical University).

Conflict-of-interest statement: All authors declared there were no conflicts of interests.

Data sharing statement: No additional data are available.

ARRIVE guidelines statement: The authors have read the ARRIVE guidelines, and the manuscript was prepared and revised according to the ARRIVE guidelines.

Manuscript source: Unsolicited manuscript

Correspondence to: Jin-Tao Li, PhD, Professor, Institute of Tropical Medicine, Third Military Medical University (Army Medical University), Gaotanyan Street 30, Chongqing 400038, China. ljtqms@tmmu.edu.cn
Telephone: +86-23-68752329
Fax: +86-23-68752329

Received: January 25, 2018
Peer-review started: January 26, 2018

First decision: February 24, 2018
Revised: March 11, 2018
Accepted: March 18, 2018
Article in press: March 18, 2018
Published online: April 28, 2018

Abstract

AIM

To investigate the influence of high salt on dextran sulfate sodium (DSS)-induced colitis in mice and explore the underlying mechanisms of this effect.

METHODS

DSS and NaCl were used to establish the proinflammatory animal model. We evaluated the colitis severity. Flow cytometry was employed for detecting the frequencies of Th1, macrophages and Tregs in spleen, mesenteric lymph node and lamina propria. The important role of macrophages in the promotion of DSS-induced colitis by NaCl was evaluated by depleting macrophages with clodronate liposomes. Activated peritoneal macrophages and lamina propria mononuclear cells (LPMCs) were stimulated with NaCl, and proteins were detected by western blotting. Cytokines and inflammation genes were analyzed by enzyme-linked immunosorbent assay and RT-PCR, respectively.

RESULTS

The study findings indicate that NaCl up-regulates the frequencies of $CD11b^+$ macrophages and $CD4^+$IFN-γ^+IL-17^+ T cells in lamina propria in DSS-treated mice. $CD3^+CD4^+CD25^+Foxp3^+$ T cells, which can secrete high levels of IL-10 and TGF-β, increase through feedback in NaCl- and DSS-treated mice. Furthermore, clodronate liposomes pretreatment significantly alleviated DSS-induced colitis, indicating that macrophages play a vital role in NaCl proinflammatory activity. NaCl aggravates peritoneal macrophage inflammation by promoting the expressions of interleukin (IL)-1, IL-6 and mouse inducible nitric oxide synthase. Specifically, high NaCl concentrations promote p38 phosphorylation in lipopolysaccharide- and IFN-γ-activated LPMCs mediated by SGK1.

CONCLUSION

Proinflammatory macrophages may play an essential role in the onset and development of NaCl-promoted inflammation in DSS-induced colitis. The underlining mechanism involves up-regulation of the p38/MAPK axis.

Key words: Inflammatory bowel disease; Macrophage; NaCl; $CD4^+$IFN-γ^+IL-17^+ T cell; p38/MAPK

Core tip: NaCl, as an indispensable environmental factor, evokes both innate and adaptive immune proinflammation cell activation in mice affected by dextran sulfate sodium (DSS)-induced colitis. Proinflammatory $CD4^+$ cells in DSS- and NaCl-treated mice are mainly double-positive IL-17^+IFN-γ^+ T cells. Macrophage depletion significantly alleviates DSS-induced colitis. M1 macrophages play an important role in the proinflammatory effect of NaCl in the mouse gut. NaCl promotes M1 proinflammatory gene expression in lipopolysaccharide-activated peritoneal macrophage. The mechanism by which NaCl promotes DSS-induced colitis involves up-regulation of the p38/MAPK axis.

Guo HX, Ye N, Yan P, Qiu MY, Zhang J, Shen ZG, He HY, Tian ZQ, Li HL, Li JT. Sodium chloride exacerbates dextran sulfate sodium-induced colitis by tuning proinflammatory and antiinflammatory lamina propria mononuclear cells through p38/MAPK pathway in mice. *World J Gastroenterol* 2018; 24(16): 1779-1794 Available from: URL: http://www.wjgnet.com/1007-9327/full/v24/i16/1779.htm DOI: http://dx.doi.org/10.3748/wjg.v24.i16.1779

INTRODUCTION

Inflammatory bowel disease (IBD) is a chronic and recurrent disease, usually manifesting as ulcerative colitis and Crohn's disease (CD)[1]. IBD is a high-risk factor for colorectal cancer and it is a serious threat to the human health globally. Although its etiology is presently unclear, findings yielded by extant studies indicate that IBD is a complex process involving heredity, environment and immunity[2-5].

Innate and adaptive immune cells play different roles in IBD pathogenesis. Results obtained in a large number of studies have shown that Th17, Th1, regulatory T cells (Tregs) and macrophages play important roles in IBD pathogenesis. For instance, the number of Th17 cells increases significantly in mucosa lamina propria (LP) of colitis patients, whereby interleukin (IL)-17 is produced, resulting in mucosal damage and enhancing disease activity[6,7]. Th1 polarization is related to colonic inflammation, through its induction of IFN-γ and TNF-α production, whereas the differential propensity to develop colitis is linked to the inherent tendency of the immune system to give rise to Th1 or Th17/Treg responses[8]. Tregs, which are very important regulatory T cells, express IL-10 highly and inhibit inflammation in IBD[9]. Macrophages in the intestinal mucosa of colitis patients can secrete the cytokines TNF-α, IL-1 and IL-6[10]. Intestinal macrophages are the major population of antigen presenting cells in intestinal mucosa and they shape the types of T cell response to luminal antigens[11].

Sodium chloride mediates the inflammatory effects of immune cells that are very important to IBD. NaCl exacerbates experimental autoimmune encephalomyelitis in mice by promoting Th17 cell differentiation[12]. High salt content strengthens the lipopolysaccharides (LPS)-induced macrophage activation by activating

signaling pathways of p38 and ERK1 to induce the production of proinflammatory factors[13]. Extant studies have shown that the high-salt diet promotes Th17 cell activation in LP and exacerbates experimental colitis in mice[14,15]. However, high-salt diet effect on other immune cells, such as Th1, Tregs and macrophages, which are also associated with pathopoiesis in IBD, is still unclear. Macrophage activation plays a pivotal role in inflammation initiation and progression in diverse pathological conditions. Findings obtained in our previous research indicate that, in mice treated with clodronate liposomes (MDP), gut macrophages were successfully depleted. Macrophage depletion could protect mice against colitis induced by dextran sulfate sodium (DSS), suggesting that the macrophages play an important role in colitis pathogenesis.

In the present study, we hypothesized that NaCl promotes the onset and course of DSS-induced colitis, as well as sustains the disease. The promotion effect may be due to monocyte-macrophages shifting the T cell response toward Th17, Th1 and Treg cells. We tested this hypothesis in a DSS-induced colitis mouse model, which shares many characteristics with human ulcerative colitis[16,17]. We found that NaCl promoted both macrophages and $CD4^+$ proinflammatory cell immune response, whereby $CD4^+$ proinflammatory cells were mainly $CD4^+IFN\text{-}\gamma^+IL\text{-}17^+$ T cells. NaCl enhanced the proinflammatory gene expression and cytokine secretion in the colons of mice affected by colitis. Depletion of gut macrophages significantly alleviated DSS-induced colitis, suggesting that macrophages play a vital role in the NaCl proinflammation process. High NaCl enhanced M1 proinflammation gene expression in LPS-activated peritoneal macrophages. Therefore, colitis promoted by high NaCl levels may be a result of M1 macrophage polarization. M1 polarization shifts T cell response toward proinflammatory $CD4^+IFN\text{-}\gamma^+IL\text{-}17^+$ T cells. High NaCl proinflammation in LPS- and IFN-γ-activated lamina propria mononuclear cells (LPMCs) relies on up-regulation of the p38 mitogen-activated protein kinase (p38/MAPK) axis.

MATERIALS AND METHODS

Animal treatment

For this study, 8- to 10-wk-old female C57BL/6J mice were purchased from the Animal Center of Third Military Medical University (Army Medical University). Mice were housed at 24 ℃, under light-controlled cycle (12 h) and with free access to standard laboratory water and food. All processes were supported by the Committee on Use and Care of Laboratory Animals at Third Military Medical University (Army Medical University).

Establishment of the animal model with DSS and NaCl

Mice purchased from the Animal Center were allowed at least 7 d to adapt to the environment before being randomly divided into four groups. They received water containing 2% NaCl (Sinopharm Chemical Reagent, China) and/or water containing 2.5% DSS (160110; MP Biomedicals, United States) for 10 d. The intestinal macrophages were depleted using MDP (van Rooijen and van Kesteren-Hendrikx, 2003, clodronateliposomes.org, Holland)[18]. Briefly, 200 μL MDP was injected i.p. into mice 4 d prior to the onset of inflammation and on days -1, 1, 3 and 5 during the 2.5% DSS and 2% NaCl treatment. The disease activity index (DAI), which was used for the clinical scoring of stool consistency, bleeding and weight loss, served as the measure of colitis severity. The criteria for grading the DAI were adopted from elsewhere[19].

Cell isolation

Spleen (SP) and mesenteric lymph node (MLN) cells from each mouse in all groups were separated by grinding on filters. SP red blood cells were lysed using red blood cell lysis buffer (C3702; Beyotime, China). Single cell suspensions of SP and MLN were obtained through filters. Cells were washed twice with phosphate-buffered saline (PBS) (Zhongshanjinqiao, China) containing 2% fetal calf serum (FBS; as 2% FBS/PBS) (Gibco, Life Technologies, United States) through centrifugation.

Cell pellets were resuspended in the 2% FBS/PBS and were kept on ice for later use. Intestinal LPMCs were isolated in accordance with the Lamina Propria Dissociation Kit instructions (130-097-410; Miltenyi Biotec, Germany). Cell pellets were resuspended in 40% percoll (Ruitaibio, China) and added slowly to the upper part of centrifuge tubes, which had 5 mL of 80% percoll at the bottoms. LPMCs were obtained by washing twice with 2% FBS/PBS after density gradient centrifuging at 420 *g* for 20 min.

Flow analysis

The isolated cells from SP, MLN and LP from each experimental group were cultured in 96-well U plates in 0.2 mL 1640 medium containing 1% penicillin-streptomycin (C0222; Beyotime) and 10% FBS with ionomycin (I) (1 μg/mL) (S1672; Beyotime), phorbol 12-myristate 13-acetate (PMA) (25 ng/mL) (S1819; Beyotime) and Brefeldin A (BFA) (10 μg/mL) (51-2092KZ; BD Bioscience, United States) for 6 h. The cells were collected and preblocked by Fc receptors for 20 min. Cell-surface staining was performed using PE-, FITC-, APC- or percp-conjugated anti-CD4, CD3, CD25 or CD11b (eBioscience, United States). Intracellular staining was performed using the FITC-conjugated anti-mouse IFN-γ, PE-conjugated anti-mouse IL-17 or Foxp3 (eBioscience). The intracellular or nuclear staining for IFN-γ, IL-17 and Foxp3 analysis was performed according to the BD Bioscience protocol.

LPMC stimulation

Isolated LPMCs were cultured at a concentration of 5×10^6 cells/mL for 24 h, after which the culture

supernatants were collected and cytokine levels were analyzed by enzyme-linked immunosorbent assay (ELISA) or were stimulated using different NaCl concentrations (5, 10, 20, 40, 60 or 80 mmol/L) in the presence of 100 ng/mL LPS (Sigma, United States) and 20 ng/mL IFN-γ (Sigma) with SB20358 (p38 inhibitor) or DMSO (ST038; Beyotime) for 24 h. The cells were detected by western blot (WB) or real time-PCR (RT-PCR).

Mouse peritoneal macrophage preparation

Mice were injected intraperitoneally with 2 mL of 4% sterile thioglycollate medium (Becton Dickinson, United States)[20]. Peritoneal macrophages were obtained by washing the peritoneal cavity with 8 mL PBS containing 1% penicillin-streptomycin per mouse. Peritoneal macrophages were centrifuged and resuspended in DMEM (Gibco, Thermo Fisher Scientific, United States) containing 10% FBS and 1% penicillin-streptomycin. Next, peritoneal macrophages were seeded in 24-well plates (Corning, United States) and nonadherent cells were removed 4 h after seeding by washing with medium[21]. Once adhered to the culture plates, cells were stimulated with NaCl (10, 20, 40, 60 or 80 mmol/L) and 100 ng/mL LPS for 24 h. Finally, cells were collected for gene expression evaluation.

Colon culture

Colon tissues were cultured as previously described[22,23]. Briefly, after cutting longitudinally, colon tissues were washed with PBS for removing intestinal contents and were cut into 1-cm segments. These pieces were cultured in 24-well plates in 2 mL of RPMI1640 medium (Gibco, Life Technology, Shanghai, China) containing 1% penicillin-streptomycin for 24 h. Supernatant was obtained by centrifuging at 10000 *g* at 4 ℃ for 10 min and was immediately stored at -80 ℃ until required for further ELISA detection.

RNA isolation and RT-PCR

RNAs of cells and tissues were extracted by Trizol (Ambion, Life Technology, United States). RNA was transcribed into cDNA using reverse transcription kits (RR047A; Takara, Japan). Quantitative RT-PCR was performed using Bio-Rad instruments (United States) in duplicates with the reagent SYBR Green (RR820A; Takara) to measure the products. Gene expression was analyzed using the comparative Ct method and was normalized to GAPDH, which served as internal control. The primer sequences are shown in Table 1.

ELISA

Cytokine content was expressed in pg/mL. Abs, including purified and biotinylated antimouse, and related reagents were purchased from eBioscience. Briefly, 2 μg/mL capture antibody diluted with coat buffering was incubated at 4 ℃ overnight in 96-well plates (Corning) and was blocked with 5% bovine serum albumin (BSA) (Sigma) at 37 ℃ for 2 h. Samples were incubated at 37 ℃ for 2 h after being washed three times with PBS containing 0.05% Tween-20 (PBST). Biotinylated antibodies were incubated at 37 ℃ for 1 h after being washed with PBST three times. Horseradish peroxidase-conjugated antibody was incubated at 37 ℃ for 30 min after being washed with PBST five times. The reaction of detection reagent at 37 ℃ required 15 min after the unbounded antibody was removed by washing with PBST five times. The plate was analyzed at 450 nm wavelength after terminating the reaction with the stop solution.

Histology and immunohistochemistry

Colon tissues were fixed with 4% paraformaldehyde before being embedding in paraffin. To assess inflammation, colon tissue cross sections were stained with hematoxylin and eosin (HE). Sections were incubated with rabbit anti-mouse inducible nitric oxide synthase (iNOS) antibody labeled with FITC (orb14179; Biorbyt, United Kingdom) and rabbit anti-mouse F4/80 antibody labeled with PE (123109; Biolegend). All immunofluorescence images were taken by a fluorescence microscope (Leica, Germany) under the same exposure and intensity settings.

Western blotting

Proteins were extracted by RIPA lysis buffer containing protease inhibitor cocktail. The protein concentration was detected using the Protein Concentration Kits (P0012; Beyotime) and the samples were boiled for 5 min at 98 ℃. Then, 30 μg of protein for each sample was separated with SDS-PAGE. Next, proteins were electrotransferred onto a nitrocellulose membrane (GE Healthcare, Sweden) and were blocked with 5% BSA in TBS-0.05% Tween-20 (TBST) at room temperature for 2 h. The membrane was subsequently incubated with GAPDH (1:1000) (Santa Cruz Biotechnologies, United States), p38 or phosphorylated p38 (1:250) (Abcam, United States) at 4 ℃ for 16 h. The membrane was washed with TBST before being incubated at room temperature for 1 h with antibody conjugated with horseradish peroxidase (1:2000) (Zhongshanjinqiao, China). Antibody binding was detected with the ECL substrate (170-5060; Bio-Rad) after washing with TBST. The optical density of bands was analyzed using ImageJ 1.42 software (United States).

Statistical analysis

All data were expressed as mean ± SD. GraphPad Prism 5.00 software for Windows (United States) was used for data analysis. Statistical results were evaluated using unpaired Student's *t*-test or ANOVA, and $P < 0.05$ was considered statistically significant.

RESULTS

NaCl aggravates DSS-induced colitis in mice

To determine the influence of NaCl on enteritis, mice

Table 1 Primers used in the real time-PCR

Gene name		Primer sequences
GAPDH	Sense	5′-AGGTCGGTGTGAACGGATT-3′
	Anti-sense	5′-AATCTCCACTTTGCCACTGC-3′
IL-1β	Sense	5′-TGGTGTGTGACGTTCCCATTA-3′
	Anti-sense	5′-CAGCACGAGGCTTTTTTGTTG-3′
IL-1α	Sense	5′-CGCCAATGACTCAGAGGAAGA-3′
	Anti-sense	5′-GGCGTCATTCAGGATGAATTC-3′
IL-6	Sense	5′-ACAACCACGGCCTTCCCTACTT-3′
	Anti-sense	5′-CACGATTTCCCAGAGAACATGTG-3′
IFN-γ	Sense	5′-CTGCTGATGGGAGGAGATGT-3′
	Anti-sense	5′-ATTTGTCATTCGGGTGTAGTCA-3′
Arg1	Sense	5′-CTCCAAGCCAAAGTCCTTAGAG-3′
	Anti-sense	5′-GGAGCTGTCATTAGGGACATCA-3′
iNOS	Sense	5′-ACATCGACCCGTCCACAGTAT-3′
	Anti-sense	5′-CAGAGGGGTAGGCTTGTCTC-3′
IL-10	Sense	5′-GCTCTTACTGACTGGCATGAG-3′
	Anti-sense	5′-CGCAGCTCTAGGAGCATGTG-3′
TNF-α	Sense	5′-CTGAACTTCGGGGTGATCGG-3′
	Anti-sense	5′-GGCTTGTCACTCGAATTTTGAGA-3′
IL-17α	Sense	5′-TGTGAAGGTCAACCTCAAAGTCT-3′
	Anti-sense	5′-GAGGGATATCTATCAGGGTCTTCAT-3′
SGK1	Sense	5′-CTGCTCGAAGCACCCTTACC-3′
	Anti-sense	5′-TCCTGAGGATGGGACATTTTCA-3′

were given 2.5% DSS and/or 2% NaCl. Mice that received both NaCl and DSS started losing weight from day 5 and subsequently exhibited greater weight loss compared to the DSS group (Figure 1A). Moreover, the death rate in the DSS + NaCl group was markedly higher than in the DSS group (Figure 1B). Compared to other groups, colons of mice in the DSS + NaCl group became shorter (Figure 1C). HE staining displayed obvious inflammatory cell infiltration in both groups, but the DSS + NaCl group exhibited more inflammatory cell infiltration in colon tissues than the DSS group (Figure 1D). These findings suggest that NaCl aggravated inflammation in DSS-induced colitis.

NaCl up-regulates the frequency of CD4$^+$IFN-γ$^+$IL17$^+$ T cells and promotes the secretion of inflammatory cytokines in mice with DSS-induced colitis

Increasing evidence indicates that CD4$^+$ T cells play a crucial role in the pathogenesis of chronic intestinal inflammation, and related cytokines (such as IFN-γ, IL-6, IL-17A and TNF) are highly expressed in the inflamed mucosa of IBD patients[24,25]. To explore the influence of NaCl on CD4$^+$ T cells in colitis-affected mice, the CD4$^+$IFN-γ$^+$IL-17$^+$ T cell subsets were detected. Compared to the DSS group, the flow cytometry analysis indicated that frequencies of CD4$^+$IL-17$^+$ and CD4$^+$IFN-γ$^+$ T cell subsets were markedly up-regulated in the DSS + NaCl group (Figure 2A). NaCl promotion of the DSS-induced colitis development is associated with both CD4$^+$IL-17$^+$ and CD4$^+$IFN-γ$^+$ T cells in LP, MLN and SP. In addition, the frequencies of inflammatory CD4$^+$ T cells (IL-17$^+$ and IFN-γ$^+$ single-positive T cells and IFN-γ$^+$IL-17$^+$ double-positive T cells) in the DSS + NaCl group were higher than in the DSS group. It is also noteworthy that the frequency of CD4$^+$IFN-γ$^+$ T cells was up-regulated the most (Figure 2B). These findings suggest that CD4$^+$IFN-γ$^+$IL-17$^+$ T cells are crucial in the inflammation promotion by NaCl in DSS-treated mice.

Cytokines IFN-γ, IL-17α, IL-1α, IL-6 and TNF-α secreted by colon tissues were detected by ELISA, and the gene expression of colon tissues from the animal model was measured by RT-PCR. Compared to the DSS group, IFN-γ, IL-17α, IL-1α, IL-1β, IL-6 and TNF-α were all higher in the DSS + NaCl group (Figure 2C and D). Therefore, high NaCl levels up-regulate inflammation gene expression and promote the secretion of multiple proinflammatory cytokines in mice affected by DSS-induced colitis.

NaCl up-regulates macrophage frequency in DSS-treated mice

Macrophages play a crucial role in the Th1 and Th17 responses, and are also important regulators of salt homeostasis[26]. To determine the effect of NaCl on macrophages in mice affected by colitis, we detected the frequency of CD11b$^+$ macrophages in mice that received DSS and/or NaCl by flow cytometry. We observed that the macrophages increased significantly in the LP, MLN and SP of the DSS + NaCl group compared to those of the DSS group (Figure 3A). The increased CD11b$^+$ macrophages were mainly located in intestinal LP and MLN (Figure 3B). These findings indicate that the macrophages also participate in the NaCl proinflammation activities in DSS-induced colitis.

Tregs increase through feedback in the development of NaCl aggravating inflammation associated with DSS-induced colitis

Tregs play an important role in the maintenance of intestinal mucosal homeostasis by suppressing

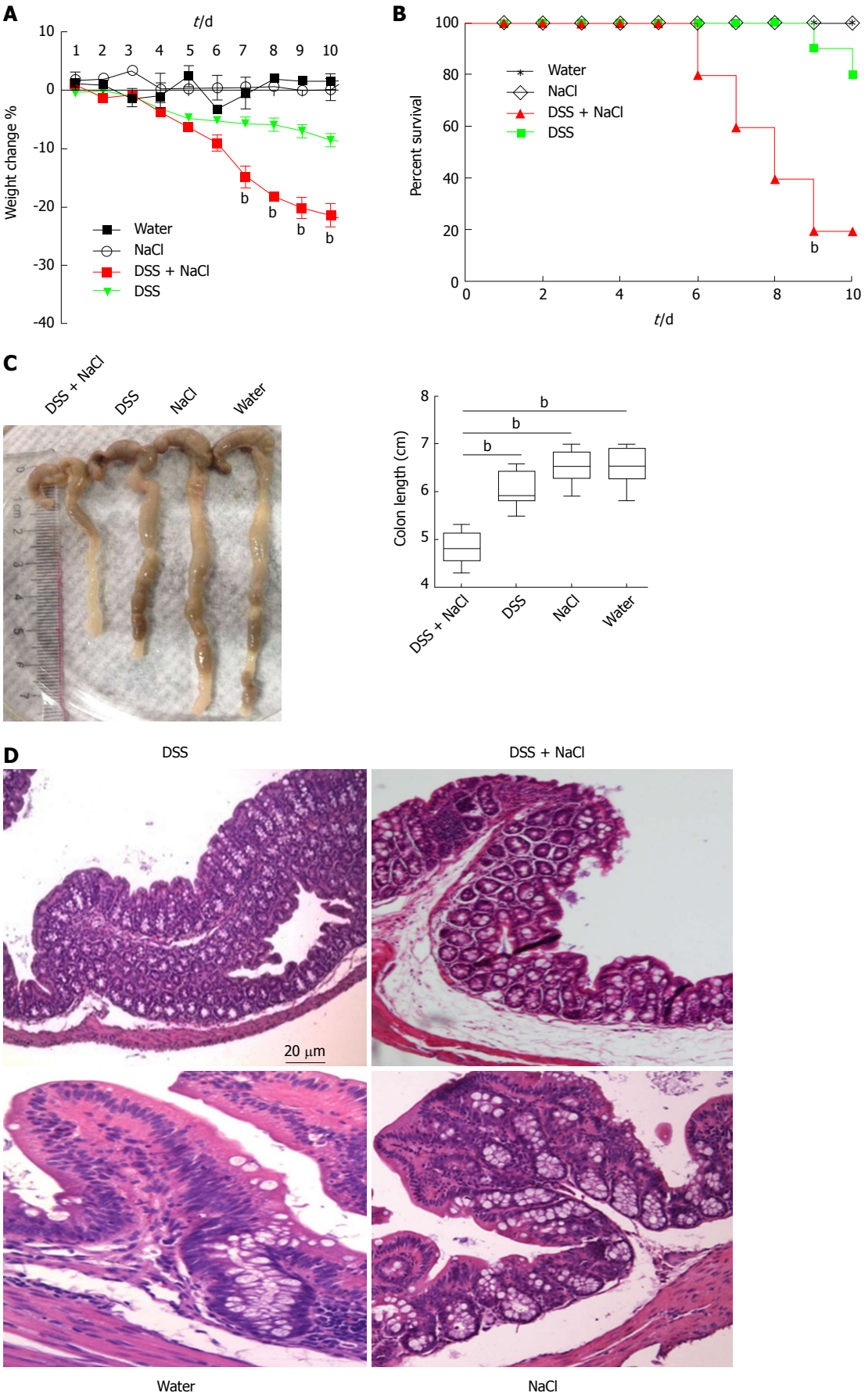

Figure 1 Mice treated with DSS and NaCl develop more severe colitis. A: Mice were given DSS and/or NaCl, and were weighed daily; B: Death status was recorded daily; C: Colonic tissues were collected from four groups of mice and colonic length was measured; D: Histological analyses show sections of the colon stained with HE for DSS- or NaCl-treated mice. In all the panels, data indicate three separate experiments, whereby 10 mice per group were used in each experiment. $^{a}P < 0.05$; $^{b}P < 0.01$; $^{c}P < 0.001$. DSS: Dextran sulfate sodium.

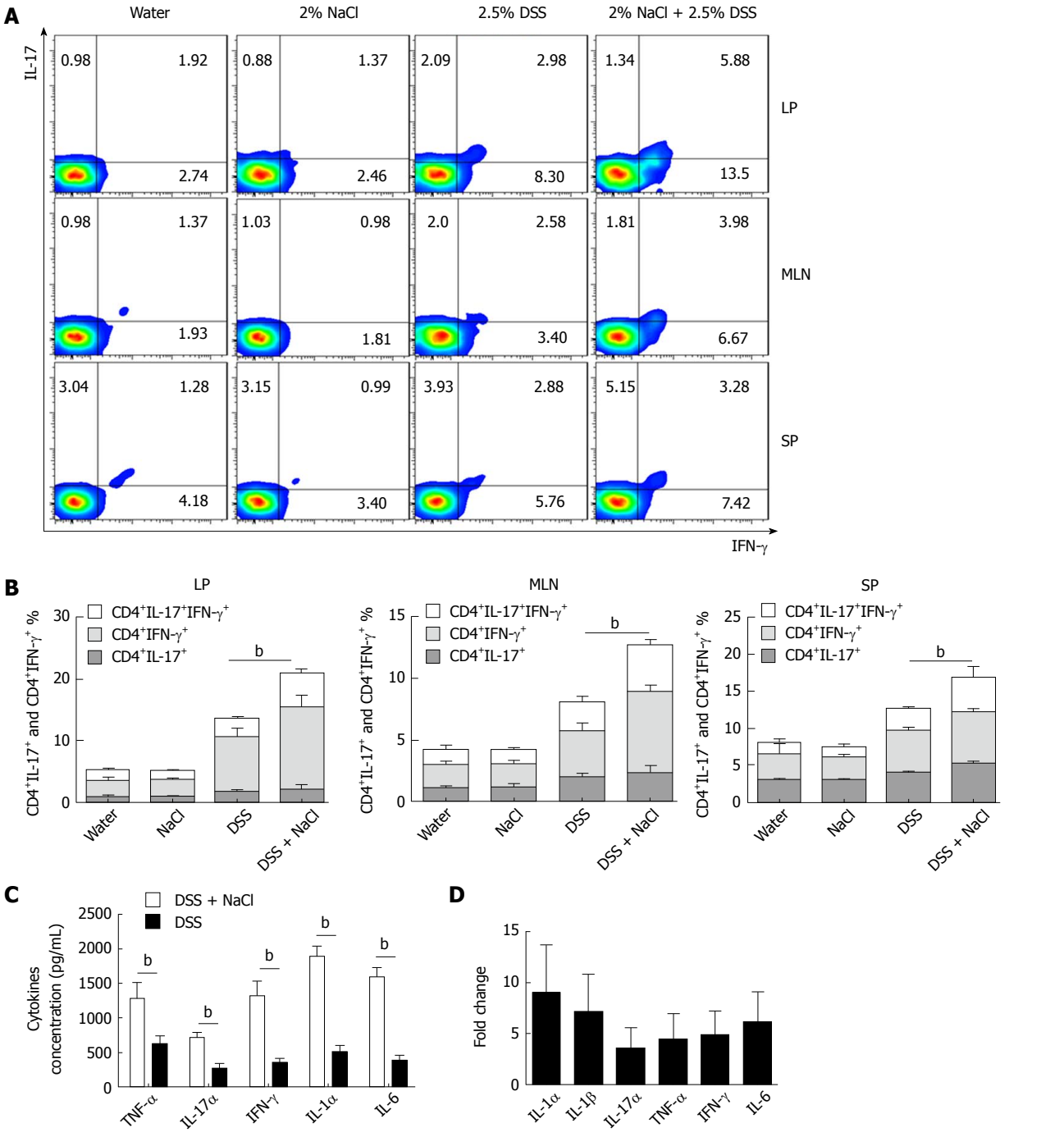

Figure 2 NaCl promotes CD4$^+$IFN-γ$^+$IL-17$^+$ T cell increase and inflammatory cytokine secretion in DSS-treated mice. A: The CD4$^+$IFN-γ$^+$IL-17$^+$ T cells in LP, MLN and SP from mice treated with NaCl and/or DSS were detected by flow cytometry; B: Combined flow cytometry data of CD4$^+$IL-17$^+$, CD4$^+$IFN-γ$^+$ and CD4$^+$IFN-γ$^+$IL-17$^+$ T cell subsets distribution in LP, MLN and SP; C: Colon tissues collected from mice treated with DSS or DSS + NaCl, which were washed with phosphate-buffered saline and cultured for 24 h, and the supernatants were collected and detected by enzyme-linked immunosorbent assay; D: Colon tissues collected from mice treated with NaCl and DSS (or only DSS) were detected by RT-PCR. The relative fold-change in DSS + NaCl-treated mice *vs* DSS-treated mice. In all the panels, data indicate three separate experiments, whereby 3 mice per group were used in each experiment. $^aP < 0.05$; $^bP < 0.01$; $^cP < 0.001$. DSS: Dextran sulfate sodium; LP: Lamina propria; MLN: Mesenteric lymph node; SP: Spleen.

abnormal immune response against dietary antigens or commensal flora[8]. To explore the changes in Tregs in the mice that received DSS and NaCl, we detected CD3$^+$CD4$^+$CD25$^+$Forp3$^+$ T cells by flow cytometry and observed that their levels were higher in the DSS + NaCl group than in the DSS group (Figure 4A). The increased Tregs were mainly distributed in the LP and MLN, while their prevalence in SP did not change significantly (Figure 4B). To explore the influence of NaCl on Tregs in DSS-induced colitis, we evaluated cytokine levels in culture supernatants of LPMCs by ELISA. The results yielded by the analyses indicate that NaCl induces LPMCs to secrete TNF-α, IL-1α, IL-6 and IL-17, which are critical Th17 cell-related cytokines. Moreover, NaCl promotes

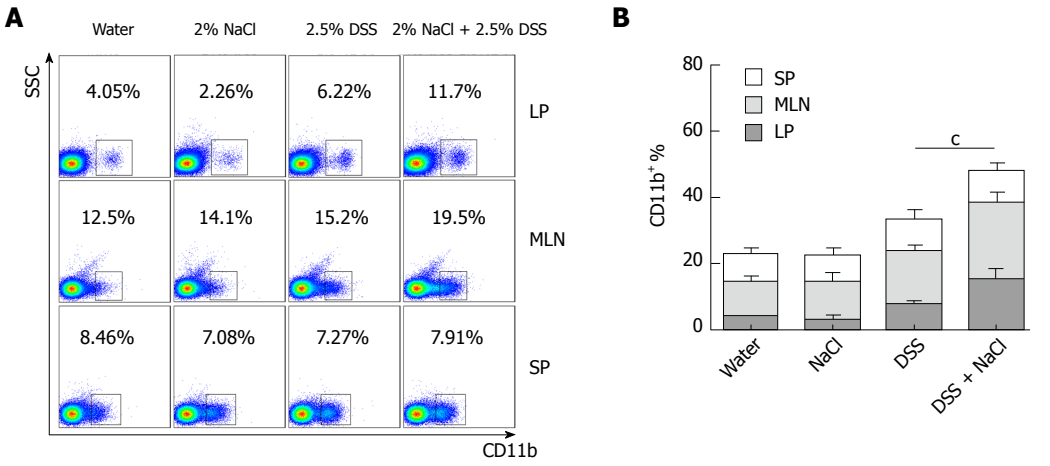

Figure 3 CD11b$^+$ macrophages are increased in DSS- and NaCl-treated mice. A: The CD11b$^+$ cells in LP, MLN and SP from the four groups were detected by flow cytometry; B: Quantification of the flow cytometry data indicates the CD11b$^+$ cell distribution in LP, MLN and SP. In the panels, data indicate three separate experiments, whereby 3 mice per group were used in each experiment. $^aP < 0.05$; $^bP < 0.01$; $^cP < 0.001$. DSS: Dextran sulfate sodium; LP: Lamina propria; MLN: Mesenteric lymph node; SP: Spleen.

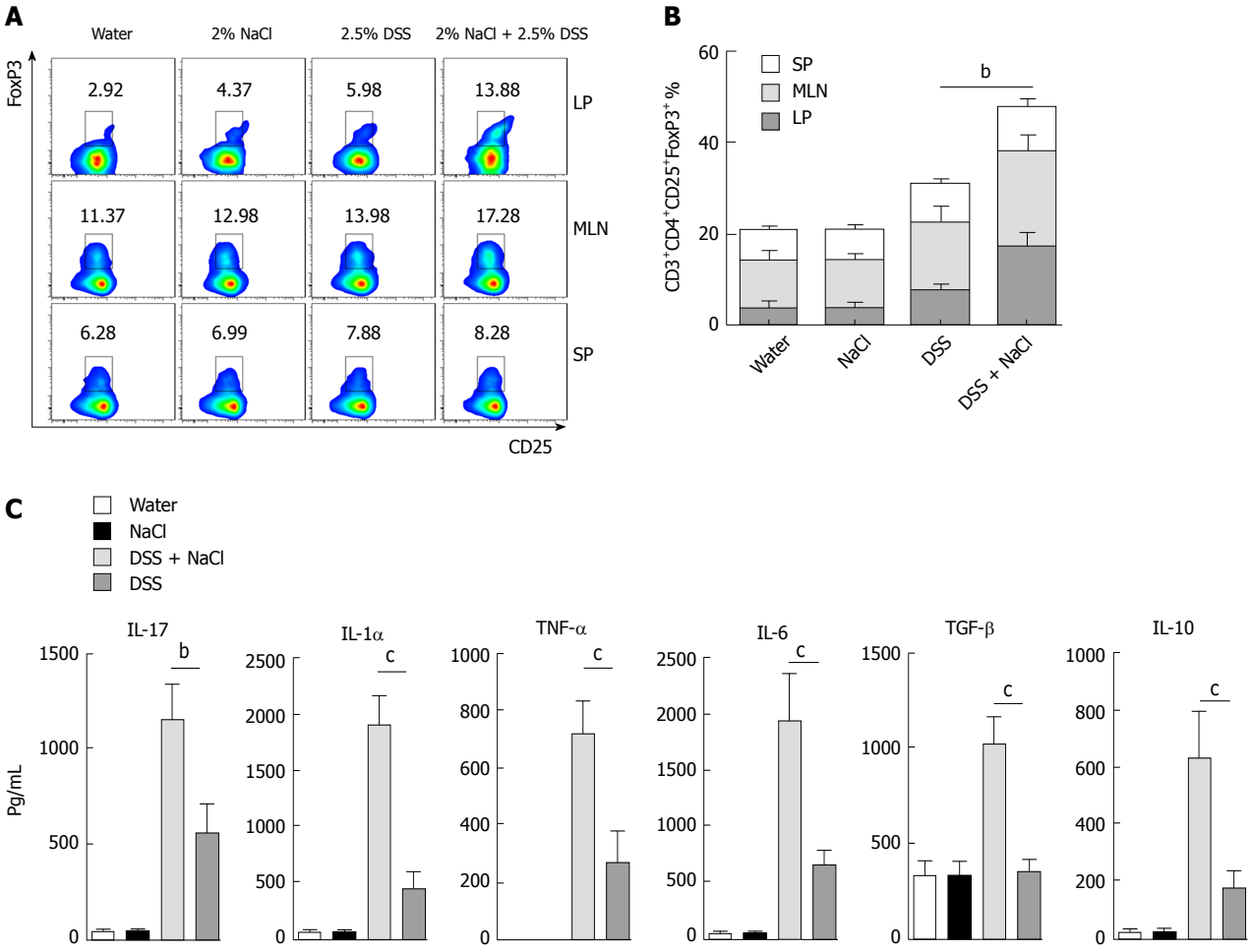

Figure 4 CD3$^+$CD4$^+$CD25$^+$Foxp3$^+$ T cells are increased in mice treated with DSS and NaCl. A: CD3$^+$CD4$^+$CD25$^+$Foxp3$^+$ T cells in LP, MLN and SP from animal models were detected by flow cytometry; B: A summary of the percentages of CD3$^+$CD4$^+$CD25$^+$Foxp3$^+$ T cell distribution in LP, MLN and SP; C: LPMCs from the four groups were isolated and cultured for 24 h, and the levels of cytokines in the culture supernatants were collected and analyzed by enzyme-linked immunosorbent assay. In all the panels, data indicate three separate experiments, whereby 3 mice per group were used in each experiment. $^aP < 0.05$; $^bP < 0.01$; $^cP < 0.001$ *vs* the DSS group. DSS: Dextran sulfate sodium; LMPCs: Lamina propria mononuclear cells; LP: Lamina propria; MLN: Mesenteric lymph node; SP: Spleen.

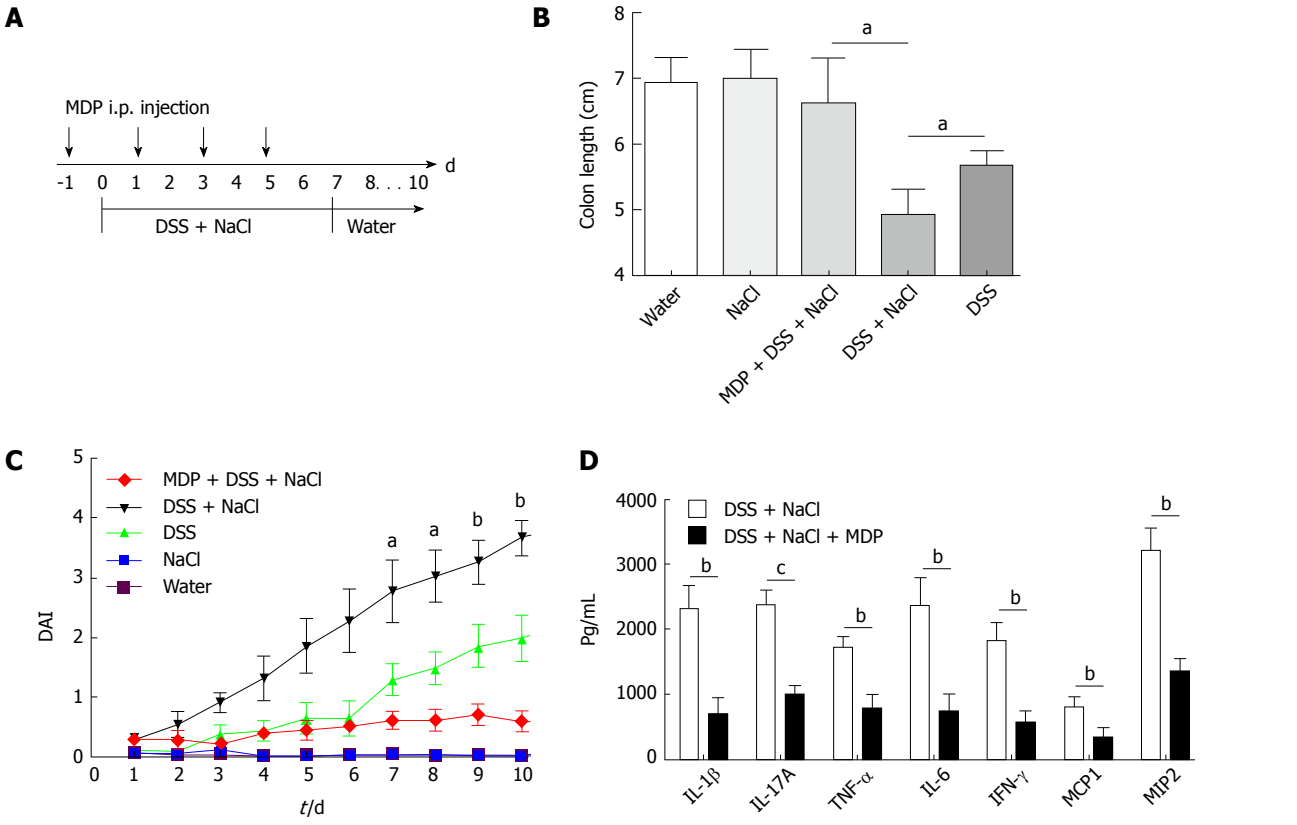

Figure 5 Depletion of macrophages reduces the severity of DSS-induced colitis promoted by NaCl. A: Clodronate liposomes (denoted as MDP) or control PBS-liposomes (denoted as PBS) were administrated intravenously to all mice, as the schematic protocol indicated during DSS and NaCl treatment; B: The disease activity index was monitored daily; C: Colon length was measured in each group of mice (n = 10); D: Colon explants were cultured for 24 h and the inflammatory cytokines in supernatants were detected by enzyme-linked immunosorbent assay (n = 3). $^{a}P < 0.05$; $^{b}P < 0.01$; $^{c}P < 0.001$ (clodronate liposomes + DSS + NaCl *vs* DSS + NaCl). DSS: Dextran sulfate sodium.

the secretion of TGF-β and IL-10, which are significant antiinflammatory cytokines secreted by Tregs (Figure 4C). These findings show that Tregs' levels also increase as a result of inflammation promotion by NaCl in mice with DSS-induced colitis.

Macrophages play a critical role in NaCl aggravating DSS-induced colitis

Extant studies have shown that MDP can deplete macrophages in mice[27]. We used MDP to deplete the macrophages in mice during the DSS and NaCl treatments to determine their role in the promotion of DSS-induced colitis by NaCl (Figure 5A). We observed that macrophage depletion by MDP could prevent colon shortening in the mice treated with NaCl and DSS (Figure 5B). The DAI also showed that macrophage depletion alleviated inflammation in NaCl proinflammatory processes (Figure 5C). The levels of inflammatory cytokines IFN-γ, TNF-α, IL-1β, IL-17A, IL-6, MCP1 and MIP2 secreted by colon tissues were reduced in MDP-treated mice (Figure 5D). The colon tissues from the DSS + NaCl group contained a greater number of F4/80^{+}iNOS^{+} macrophages compared to the DSS group. In addition, the MDP-treated mice had fewer F4/80^{+}iNOS^{+} macrophages compared to the DSS + NaCl group (Figure 6). Thus, we posit that macrophage depletion can reduce colitis severity in mice.

High NaCl promotes M1 macrophage polarization in vitro

Macrophages in both peritoneal cavity and gastrointestinal tract are linked to IBD[28]. Different NaCl concentrations (10, 20, 40, 60 and 80 mmol/L) were used to stimulate the macrophages from the abdominal cavity and the gene expression was detected by RT-PCR. Our findings indicate that IL-1β, IL-6 and iNOS, which usually exhibit proinflammatory roles, gradually increased as the NaCl concentration increased (Figure 7A-C). It is worth noting that IL-10 and Arg1, which are M2 macrophage markers, increased modestly at low NaCl concentrations, whereas their expression markedly increased at 40 mmol/L and above (Figure 7D and E). These results display that high NaCl levels promote LPS-activated peritoneal macrophages toward M1 polarization.

NaCl promotes the inflammation response in LP, whereas LPS and IFN-γ activated LPMCs rely on p38/MAPK

p38/MAPK is related to both IBD and hyperosmotic

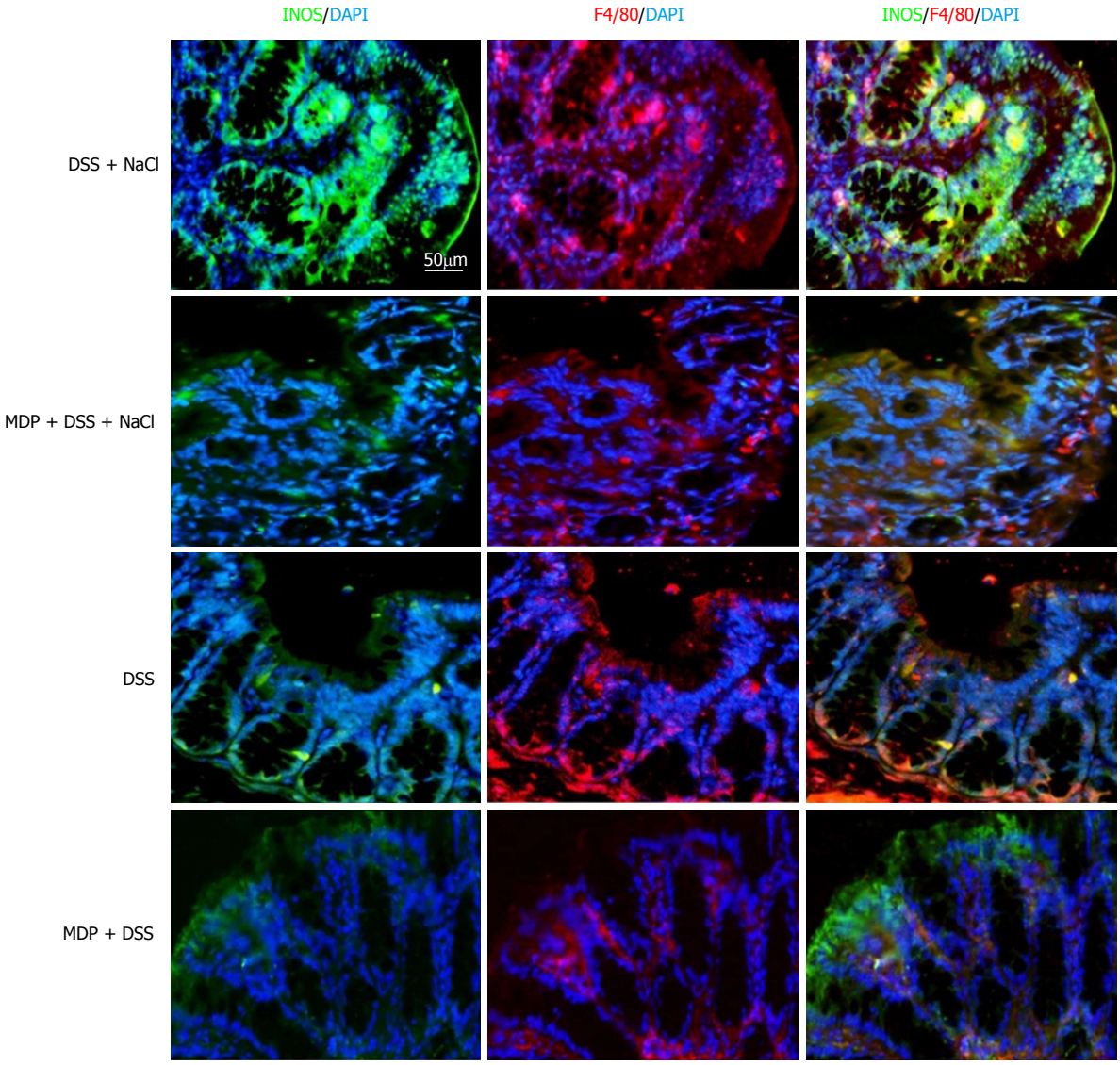

Figure 6 iNOS$^+$F4/80$^+$ macrophages increase in the colon of DSS- and NaCl-treated mice. Macrophages in colon tissue obtained from mice injected intraperitoneally with PBS-containing liposomes (denoted as PBS), or clodronate liposomes (denoted as MDP) during the NaCl and DSS treatment were analyzed. The sections were stained with antibodies of anti-F4/80 (red) and anti-iNOS (green). Nuclei were stained with DAPI (blue). Laser confocal microscopy was used to detect fluorescence. (Scale bar = 50 μm). DSS: Dextran sulfate sodium; iNOS: inducible nitric oxide synthase.

stress[29,30]. Western blot analysis revealed that high NaCl levels significantly up-regulated phosphorylated-p38 of LPMCs stimulated with LPS and IFN-γ for different time periods (1 h, 6 h, 12 h, 24 h); however, they did not affect the total level of p38, and p38 phosphorylation reached the highest level after 12 h (Figure 8A). LPMCs were treated with NaCl at different concentrations (5, 10, 20, 40, 60 and 80 mmol/L) in the presence of LPS and IFN-γ for 24 h. The western blotting revealed that p38 phosphorylation increased in a dose-dependent manner (Figure 8B). Serum glucocorticoid regulated kinase 1 (SGK1) increased in LPMCs activated by LPS and IFN-γ due to NaCl stimulation (Figure 8C). The results further indicated that p38 inhibitor can decrease high NaCl-promoted p38 phosphorylation in LPMCs (Figure 8D). These findings confirmed that NaCl promotes inflammatory response in the LPS and IFN-γ activated LPMCs, and the proinflammation effect depends on p38/MAPK phosphorylation mediated by SGK1.

DISCUSSION

NaCl has been shown to exert a proinflammatory effect in many diseases, including experimental colitis, experimental autoimmune encephalomyelitis and cardiovascular disease[31-33]. In the present study, we observed that macrophages play an important role in the promotion of DSS-induced colitis by NaCl. Macrophages, as antigen-presenting cells, are important in regulating innate and adaptive immune responses and have a crucial role in resolving tissue injury and promoting tissue repair in IBD[34,35]. Even though the cause of IBD remains unclear, mice with lymphocyte deficiency developed more severe inflammation,

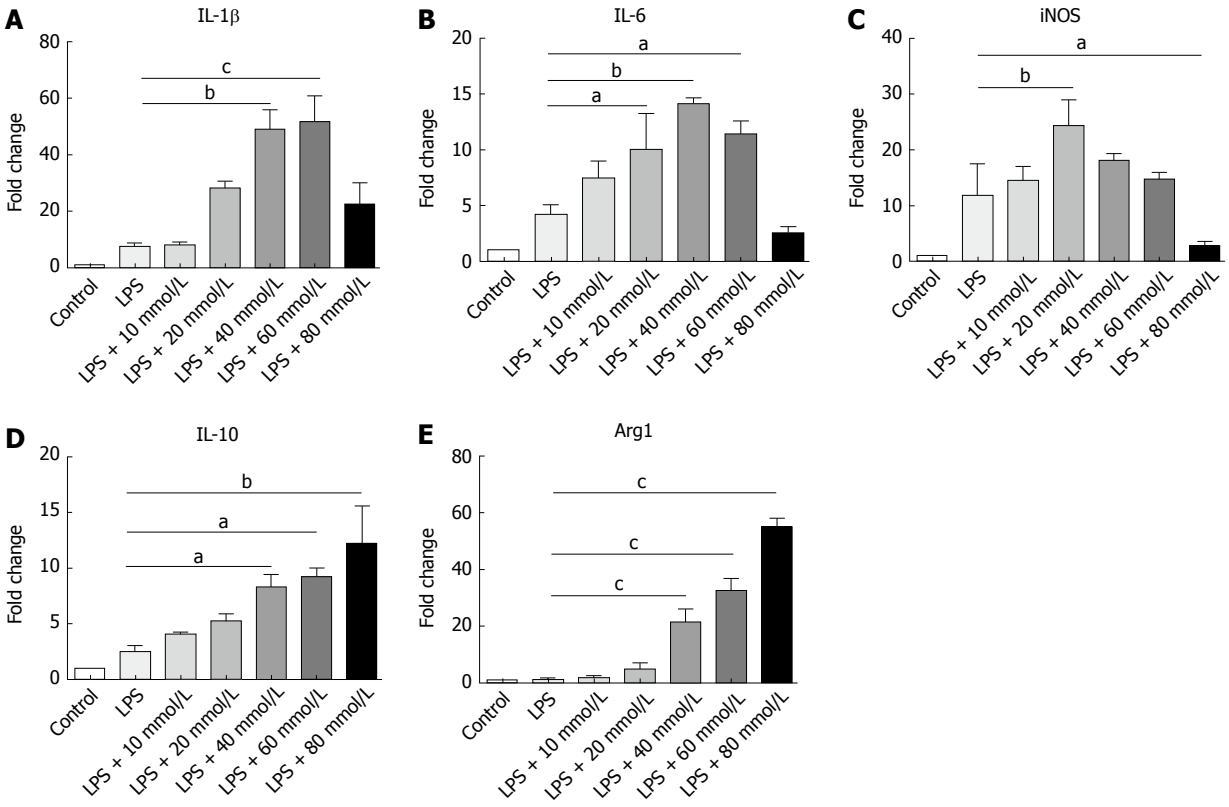

Figure 7 High NaCl levels enhance proinflammation gene expression in LPS-activated peritoneal macrophage. A-E: Peritoneal macrophages were stimulated with different NaCl concentrations (10-80 mmol/L) in the presence of LPS for 24 h. mRNA expression was measured by RT-PCR for the indicated genes. In all the panels, data indicate three separate experiments. $^{a}P < 0.05$; $^{b}P < 0.01$; $^{c}P < 0.001$. LPS: Lipopolysaccharide.

suggesting that innate immune cells are capable of triggering the onset and development of disease[36]. Activation of the innate immune system is regarded as the most direct cause of IBD because it can recruit cells of the adaptive immune system to the inflammatory site, thus resulting in inflammation[37].

Findings yielded by the present study further indicated that NaCl promoted the increase in the $CD4^+$ T cell count, especially the IFN-γ^+IL-17^+ double-positive T cells in DSS-treated mice. Extant research indicates that high-salt diet promotes the differentiation of $CD4^+$ T cells into Th17 as well as Th1[32]. However, Wei *et al*[38] showed that, in 2,4,6-trinitrobenzene sulfonic acid (TNBS)-induced colitis, NaCl promoted Th17 polarization, but not Th1 polarization[15]. DSS and TNBS may involve different pathogenic mechanisms. Wei *et al*[38] used TNBS to induce colitis, which mainly simulated CD. However, we used DSS to induce colitis, which mainly simulated ulcerative colitis. In both CD and ulcerative colitis patients, activation and mucosal infiltration of $CD4^+$ T lymphocytes has been reported[39].

Extant studies have revealed that blocking $CD4^+$ T cell activation was capable of limiting the development of mucosal inflammation in experimental colitis models[40]. $CD4^+$ IFN-γ^+IL-17^+ T cells, as an intermediate form between Th17 and Th1, are an easily observable crossover subset promoted by IL-12 signaling beyond IL-17[41,42]. Th17 cells play an important role in colitis pathogenesis by directly giving rise to Th1-like cell response[43]. Empirical evidence indicates that IBD is characterized by Th1 cell activation and subsequent over-expression of cytokines such as TNF-α, IL-6 and IL-1β[44,45]. In addition, findings yielded by extant research suggest that Th1 cytokines are important promoters of continuous mucosal inflammation in DSS-induced colitis[46,47].

The results obtained in the present work confirmed the important role of $CD4^+$IFN-γ^+IL-17^+ T cells in the promotion of inflammation by NaCl in DSS-treated mice. High NaCl content up-regulates inflammation gene expression and promotes the secretion of multiple proinflammatory cytokines for promoting intestinal inflammation in mice affected by DSS-induced colitis.

IL-6 and IL-17 are critical Th17 cell-related cytokines that are involved in inflammatory responses during IBD development[7,48]. In contrast, antiinflammatory TGF-β and IL-10, are mainly produced by Tregs[49]. Wei and colleagues[15] demonstrated that, while high-salt diet did not change Tregs' percentage, it did inhibit the secretion of IL-10 and the suppressive function of Tregs in TNBS-induced colitis. In our study, NaCl promoted an increase in Tregs' frequency in MLN and LP, as well as enhanced IL-10 and TGF-β expression, in DSS-induced colitis. Tregs, as immune suppressing cells, are essential in maintaining intestinal homeostasis[50].

In DSS-treated beta7-deficient mice, in which colonic Tregs were depleted, excessive macrophage infiltration in colons occurred by up-regulation of colonic epithelial intercellular ICAM1, which promoted proinflammatory cytokine expression, aggravating DSS-induced colitis[51].

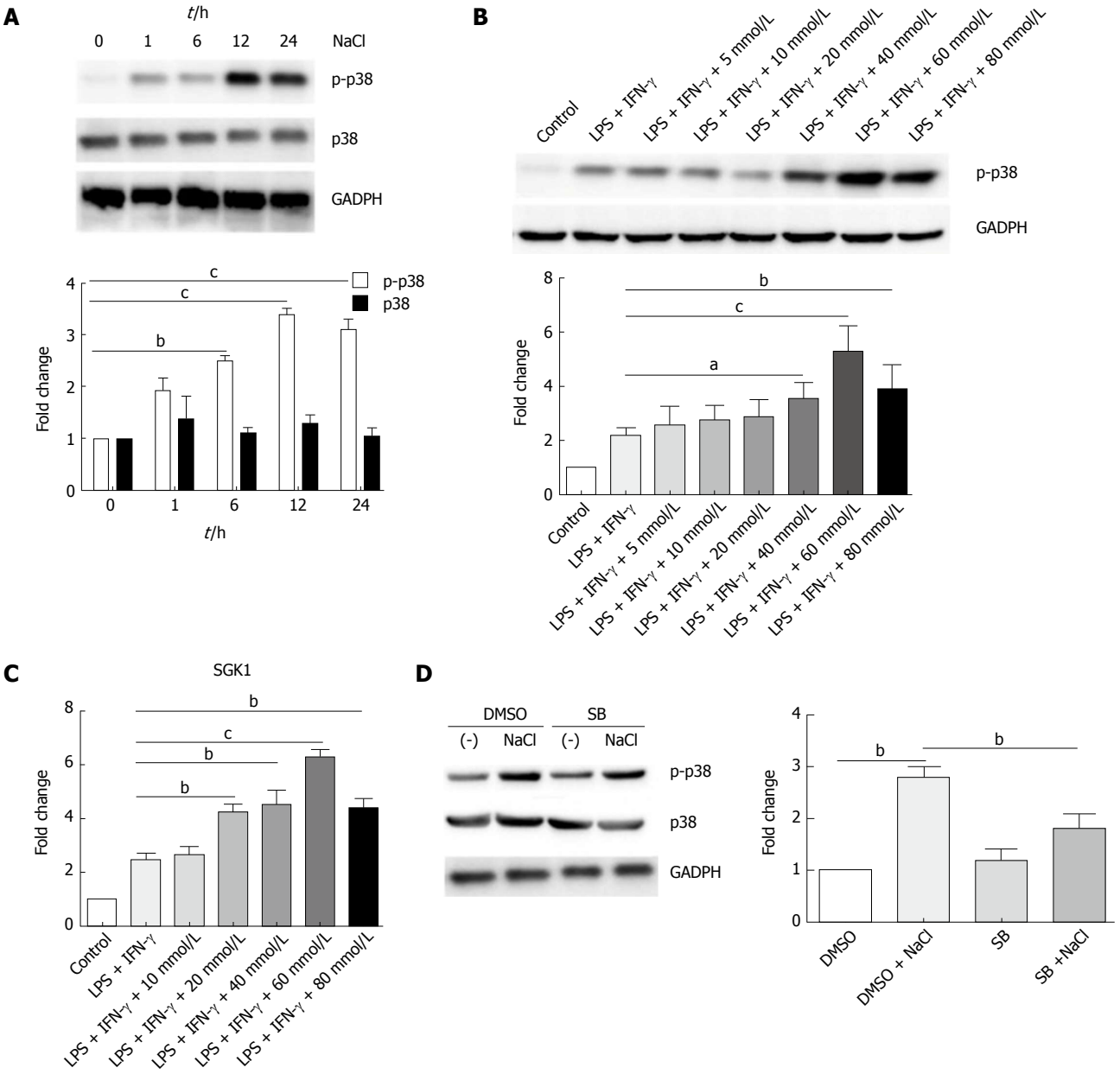

Figure 8 NaCl promotion of inflammation relies on the p38/MAPK pathway. A: LPMCs were stimulated with 60 mmol/L NaCl in the presence of 100 ng/mL LPS and 20 ng/mL IFN-γ for 1 h, 6 h, 12 h and 24 h, and the p38 and phosphorylated-p38 proteins were detected by western blot; B: LPMCs were stimulated with different NaCl concentrations in the presence of 100 ng/mL LPS and 20 ng/mL IFN-γ for 24 h and phosphorylated p38 protein was detected by western blot; C: LPMCs were stimulated with different NaCl concentrations in the presence of LPS and IFN-γ, and the mRNA expression of SGK1 was measured by RT-PCR; D: LPMCs were pretreated with 10 μmol/L SB or DMSO for 2 h and were subsequently stimulated with 60 mmol/L NaCl along with 100 ng/mL LPS and 20 ng/mL IFN-γ in the presence of DMSO or 10 μmol/L SB for 24 h and the proteins of p38 and phosphorylated-p38 were detected by western blot. In all the panels, data indicate three separate experiments. $^{a}P < 0.05$; $^{b}P < 0.01$; $^{c}P < 0.001$. DSS: Dextran sulfate sodium; LMPCs: Lamina propria mononuclear cells; LP: Lamina propria; LPS: Lipopolysaccharide; MLN: Mesenteric lymph node; SB: SB20358; SP: Spleen.

Disruption in balance may allow T cells to proliferate in an increased fashion, thereby promoting chronic intestinal inflammatory development[52]. Therefore, continuous Tregs' differentiation and trafficking in the gut is required to dampen immune responses to dietary antigens and commensal bacteria[53].

We also found that NaCl promoted an increase in $CD11b^+$ cells in the LP and MLN from mice treated with DSS. Denning *et al*[54] have shown that $CD11b^+F4/80^+CD11c^-$ macrophages in LP could induce $Foxp3^+$ Tregs' differentiation, while $CD11b^+$ dendritic cells in LP elicited responses of IL-17-producing T cells[54]. Empirical evidence indicates that the intake of high dietary salt could boost Th17 response through activating the caspase-1 in macrophages[15,55]. Moreover, in reaction to NaCl, macrophages with enhanced expression of immune-stimulatory molecules promote proinflammatory cytokine production and T cell proliferation[10,56].

Human monocyte-derived granulocyte-macrophage colony-stimulating factors exhibit potent antigen-presenting functions, produce IL-12p40 and IL-23p19, and promote development of Th1 immunity[57,58]. In our study, inflammation was relieved when the intestinal macrophages were depleted by MDP, which indicated

that the activation of Th17 and Th1 cells required macrophage participation.

Peritoneal macrophages from mice are among the best-studied macrophage populations and their role in the regulation of inflammatory responses and mucosal immunity is well understood[59,60]. Macrophages in peritoneal cavity, which are crucial in the regulation of inflammatory pathologies, are also related to IBD[28,61]. In the present study, we have shown that high NaCl content enhanced the expression of proinflammation genes for IL-1β, IL-6 and iNOS and antiinflammation genes for Arg1 and IL-10 in macrophages from the abdominal cavity of mice.

Macrophages can be polarized to either classically activated (M1) or alternatively activated (M2) macrophages[62]. M1 macrophages are proinflammatory cells due to their high capacity for producing proinflammatory cytokines, such as IL-23, IL-12, IL-1β, TNF-α and iNOS[63,64]. M2 macrophages highly express IL-10 and Arg1, which are involved in antiinflammatory, antimicrobial response[62,65]. These cytokines promote the activation of the adaptive immune and T cell response[66].

In the present study, high NaCl content was found to boost M1 polarization and up-regulate expression of proinflammatory genes to promote inflammation. Under low NaCl concentrations, IL-1, IL-6 and iNOS mainly produced by M1 macrophages were up-regulated, while the negative adjustment factor expressions were low. When the NaCl concentration rose to a certain dose, high levels of proinflammatory factors IL-1, IL-6 and iNOS induced the cell protective response through feedback, and caused the up-regulation of negative adjustment factors IL-10 and Arg1. Thus, when the inflammation continues to worsen, the M2 macrophages will respond to balance inflammation with protective immunity, and inhibit the expression of proinflammatory factors.

We explored the influence of NaCl on LPS- and IFN-γ-activated LPMCs and demonstrated that high NaCl enhanced phosphorylation of p38, as inflammation and salt intake are both linked to p38/MAPK. The p38/MAPK signaling pathway is important in IBD and the inhibition of p38/MAPK can effectively suppress the production of inflammatory mediators[29]. Available evidence indicates that p38/MAPK mediates intestinal inflammation gene expression, such as TNF-α, IL-1 and IL-6, and this up-regulation occurs in multiple types of cells, especially monocytes and macrophages[67]. In addition, p38/MAPK can regulate the SGK1 activation[30].

High NaCl concentration promotes p38/MAPK phosphorylation and activates SGK1[32]. SGK1 has been shown to control Na(+) transport and NaCl homeostasis in cells, and could trigger Th17 responses and promote tissue inflammation[12]. Human LPMCs exposed to high NaCl concentrations highly express IL-17A, IL-23R and TNF-α, and pharmacological inhibition of p38/MAPK has been shown to abrogate the effect of NaCl on LPMC-derived cytokines[14]. In the present study, high NaCl content was shown to promote inflammation in LPS- and IFN-γ-activated LPMCs. However, this process relies on the up-regulation of p38/MAPK and SGK1.

In summary, the study findings reported here indicate that NaCl induces alterations to both the innate and acquired immune system in mice with DSS-induced colitis. NaCl promotes M1 macrophage polarization, and M1 polarization may shift T cell response toward the proinflammatory $CD4^+IFN\text{-}\gamma^+IL\text{-}17^+$ T cells' aggravating colitis. The mechanism by which high NaCl concentrations promote inflammation relies on the up-regulation of p38/MAPK and SGK1. Although results obtained in the present study indicate that excessive NaCl intake can promote the inflammation in mice with the DSS-induced colitis, the causality of high-salt diet and IBD still needs to be confirmed by further investigations. More clinical and experimental studies are required to fully clarify the role of salt in IBD.

ARTICLE HIGHLIGHTS

Research background

At present, most diets are characterized by high salt content. Extant studies have shown that high salt intake contributes to inflammatory bowel disease (IBD) incidence and pathogenesis. However, the mechanism underlying these effects remains unclear.

Research motivation

NaCl mediates the inflammatory effects of immune cells. Both innate and adaptive immune proinflammatory cells play important roles in IBD. Studies have shown the high salt intake promotes the activation of Th17 cells in lamina propria (LP) and exacerbates experimental colitis in mice. However, the influence of high salt content in diet on other immune cells is still unclear. The present study explored the influence of high NaCl concentration on immune cell subsets and the underlying mechanisms.

Research objectives

The aim of the present study was to determine the impact of high NaCl concentration on dextran sulfate sodium (DSS)-induced colitis in mice and explore its influence on other immune cells, such as T helper 1 cells, regulatory T cells and macrophages, while attempting to elucidate the mechanism underlying this effect.

Research methods

DSS and NaCl were used to establish a proinflammatory animal model. The immune cell subsets were detected by flow cytometry in order to determine the target cells of NaCl. Cytokines secreted by intestinal tissue were detected. In the present study, clodronate liposomes treatment was used to deplete macrophages to further delineate their vital role in the promotion of DSS-induced colitis in mice by NaCl. In cell experiments, NaCl at different concentrations acted directly on lamina propria mononuclear cells (LPMCs) and macrophages. mRNA levels of inflammation genes and p38/MAPK proteins were determined by RT-PCR and western blot, respectively.

Research results

High NaCl concentration exacerbated the DSS-induced colitis. Intestinal $CD4^+IFN\text{-}\gamma^+IL\text{-}17^+$ T cells and macrophages both play crucial roles in the promotion of inflammation by NaCl in mice with colitis. NaCl promotes M1 proinflammatory gene expression in lipopolysaccharide (LPS)-activated peritoneal macrophages. High NaCl concentrations promote the up-regulation of the p38/MAPK axis in the LPS and IFN-γ-activated LPMCs.

Research conclusions

NaCl evokes both innate and adaptive immune proinflammatory cell activation in mice affected by colitis. Colitis may be promoted by high NaCl levels, by

NaCl initially by acting on macrophages, pushing them towards M1 polarization. Then, M1 polarization shifts the T cell response toward proinflammatory $CD4^+IFN\text{-}\gamma^+IL\text{-}17^+$ T cells. Inflammation promotion by NaCl in LPS- and IFN-γ-activated LPMCs relies on the up-regulation of the p38/MAPK axis.

Research perspectives

Although results in this study indicate that high NaCl intake can promote the inflammation in mice with DSS-induced colitis, the causality of high-salt diet and IBD still needs to be confirmed by further investigations. More clinical and experimental studies are inspired to fully clarify the role of salt in IBD.

REFERENCES

1 **Vasovic M**, Gajovic N, Brajkovic D, Jovanovic M, Zdravkovaic N, Kanjevac T. The relationship between the immune system and oral manifestations of inflammatory bowel disease: a review. *Cent Eur J Immunol* 2016; **41**: 302-310 [PMID: 27833449 DOI: 10.5114/ceji.2016.63131]

2 **Boedeker EC**. Gut microbes, the innate immune system and inflammatory bowel disease: location, location, location. *Curr Opin Gastroenterol* 2007; **23**: 1-3 [PMID: 17133076 DOI: 10.1097/MOG.0b013e328011b837]

3 **Van Limbergen J**, Russell RK, Nimmo ER, Ho GT, Arnott ID, Wilson DC, Satsangi J. Genetics of the innate immune response in inflammatory bowel disease. *Inflamm Bowel Dis* 2007; **13**: 338-355 [PMID: 17206667 DOI: 10.1002/ibd.20096]

4 **Reinisch W**. Fecal Microbiota Transplantation in Inflammatory Bowel Disease. *Dig Dis* 2017; **35**: 123-126 [PMID: 28147375 DOI: 10.1159/000449092]

5 **Dutta AK**, Chacko A. Influence of environmental factors on the onset and course of inflammatory bowel disease. *World J Gastroenterol* 2016; **22**: 1088-1100 [PMID: 26811649 DOI: 10.3748/wjg.v22.i3.1088]

6 **Jiang W**, Su J, Zhang X, Cheng X, Zhou J, Shi R, Zhang H. Elevated levels of Th17 cells and Th17-related cytokines are associated with disease activity in patients with inflammatory bowel disease. *Inflamm Res* 2014; **63**: 943-950 [PMID: 25129403 DOI: 10.1007/s00011-014-0768-7]

7 **Hundorfean G**, Neurath MF, Mudter J. Functional relevance of T helper 17 (Th17) cells and the IL-17 cytokine family in inflammatory bowel disease. *Inflamm Bowel Dis* 2012; **18**: 180-186 [PMID: 21381156 DOI: 10.1002/ibd.21677]

8 **Yang F**, Wang D, Li Y, Sang L, Zhu J, Wang J, Wei B, Lu C, Sun X. Th1/Th2 Balance and Th17/Treg-Mediated Immunity in relation to Murine Resistance to Dextran Sulfate-Induced Colitis. *J Immunol Res* 2017; **2017**: 7047201 [PMID: 28584821 DOI: 10.1155/2017/7047201]

9 **Groux H**, O'Garra A, Bigler M, Rouleau M, Antonenko S, de Vries JE, Roncarolo MG. A CD4+ T-cell subset inhibits antigen-specific T-cell responses and prevents colitis. *Nature* 1997; **389**: 737-742 [PMID: 9338786 DOI: 10.1038/39614]

10 **Kamada N**, Hisamatsu T, Okamoto S, Chinen H, Kobayashi T, Sato T, Sakuraba A, Kitazume MT, Sugita A, Koganei K, Akagawa KS, Hibi T. Unique CD14 intestinal macrophages contribute to the pathogenesis of Crohn disease via IL-23/IFN-gamma axis. *J Clin Invest* 2008; **118**: 2269-2280 [PMID: 18497880 DOI: 10.1172/JCI34610]

11 **Mahida YR**. The key role of macrophages in the immunopathogenesis of inflammatory bowel disease. *Inflamm Bowel Dis* 2000; **6**: 21-33 [PMID: 10701146]

12 **Wu C**, Yosef N, Thalhamer T, Zhu C, Xiao S, Kishi Y, Regev A, Kuchroo VK. Induction of pathogenic TH17 cells by inducible salt-sensing kinase SGK1. *Nature* 2013; **496**: 513-517 [PMID: 23467085 DOI: 10.1038/nature11984]

13 **Zhang WC**, Zheng XJ, Du LJ, Sun JY, Shen ZX, Shi C, Sun S, Zhang Z, Chen XQ, Qin M, Liu X, Tao J, Jia L, Fan HY, Zhou B, Yu Y, Ying H, Hui L, Liu X, Yi X, Liu X, Zhang L, Duan SZ. High salt primes a specific activation state of macrophages, M(Na). *Cell Res* 2015; **25**: 893-910 [PMID: 26206316 DOI: 10.1038/cr.2015.87]

14 **Monteleone I**, Marafini I, Dinallo V, Di Fusco D, Troncone E, Zorzi F, Laudisi F, Monteleone G. Sodium chloride-enriched Diet Enhanced Inflammatory Cytokine Production and Exacerbated Experimental Colitis in Mice. *J Crohns Colitis* 2017; **11**: 237-245 [PMID: 27473029 DOI: 10.1093/ecco-jcc/jjw139]

15 **Wei Y**, Lu C, Chen J, Cui G, Wang L, Yu T, Yang Y, Wu W, Ding Y, Li L, Uede T, Chen Z, Diao H. High salt diet stimulates gut Th17 response and exacerbates TNBS-induced colitis in mice. *Oncotarget* 2017; **8**: 70-82 [PMID: 27926535 DOI: 10.18632/oncotarget.13783]

16 **Ko JK**, Auyeung KK. Inflammatory bowel disease: etiology, pathogenesis and current therapy. *Curr Pharm Des* 2014; **20**: 1082-1096 [PMID: 23782147]

17 **Li K**, Wang B, Sui H, Liu S, Yao S, Guo L, Mao D. Polymorphisms of the macrophage inflammatory protein 1 alpha and ApoE genes are associated with ulcerative colitis. *Int J Colorectal Dis* 2009; **24**: 13-17 [PMID: 18762952 DOI: 10.1007/s00384-008-0575-0]

18 **Weisser SB**, van Rooijen N, Sly LM. Depletion and reconstitution of macrophages in mice. *J Vis Exp* 2012; **1**: 4105 [PMID: 22871793 DOI: 10.3791/4105]

19 **Li YH**, Xiao HT, Hu DD, Fatima S, Lin CY, Mu HX, Lee NP, Bian ZX. Berberine ameliorates chronic relapsing dextran sulfate sodium-induced colitis in C57BL/6 mice by suppressing Th17 responses. *Pharmacol Res* 2016; **110**: 227-239 [PMID: 26969793 DOI: 10.1016/j.phrs.2016.02.010]

20 **Nam TG**, Lim TG, Lee BH, Lim S, Kang H, Eom SH, Yoo M, Jang HW, Kim DO. Comparison of Anti-Inflammatory Effects of Flavonoid-Rich Common and Tartary Buckwheat Sprout Extracts in Lipopolysaccharide-Stimulated RAW 264.7 and Peritoneal Macrophages. *Oxid Med Cell Longev* 2017; **2017**: 9658030 [PMID: 28928906 DOI: 10.1155/2017/9658030]

21 **He G**, Zhang X, Chen Y, Chen J, Li L, Xie Y. Isoalantolactone inhibits LPS-induced inflammation via NF-κB inactivation in peritoneal macrophages and improves survival in sepsis. *Biomed Pharmacother* 2017; **90**: 598-607 [PMID: 28407580 DOI: 10.1016/j.biopha.2017.03.095]

22 **Rakoff-Nahoum S**, Paglino J, Eslami-Varzaneh F, Edberg S, Medzhitov R. Recognition of commensal microflora by toll-like receptors is required for intestinal homeostasis. *Cell* 2004; **118**: 229-241 [PMID: 15260992 DOI: 10.1016/j.cell.2004.07.002]

23 **Siegmund B**, Lehr HA, Fantuzzi G, Dinarello CA. IL-1 beta -converting enzyme (caspase-1) in intestinal inflammation. *Proc Natl Acad Sci USA* 2001; **98**: 13249-13254 [PMID: 11606779 DOI: 10.1073/pnas.231473998]

24 **Zhou R**, Chang Y, Liu J, Chen M, Wang H, Huang M, Liu S, Wang X, Zhao Q. JNK Pathway-Associated Phosphatase/DUSP22 Suppresses $CD4^+$ T-Cell Activation and Th1/Th17-Cell Differentiation and Negatively Correlates with Clinical Activity in Inflammatory Bowel Disease. *Front Immunol* 2017; **8**: 781 [PMID: 28725226 DOI: 10.3389/fimmu.2017.00781]

25 **Strober W**, Fuss IJ. Proinflammatory cytokines in the pathogenesis of inflammatory bowel diseases. *Gastroenterology* 2011; **140**: 1756-1767 [PMID: 21530742 DOI: 10.1053/j.gastro.2011.02.016]

26 **Machnik A**, Neuhofer W, Jantsch J, Dahlmann A, Tammela T, Machura K, Park JK, Beck FX, Müller DN, Derer W, Goss J, Ziomber A, Dietsch P, Wagner H, van Rooijen N, Kurtz A, Hilgers KF, Alitalo K, Eckardt KU, Luft FC, Kerjaschki D, Titze J. Macrophages regulate salt-dependent volume and blood pressure by a vascular endothelial growth factor-C-dependent buffering mechanism. *Nat Med* 2009; **15**: 545-552 [PMID: 19412173 DOI: 10.1038/nm.1960]

27 **Zhao A**, Urban JF Jr, Anthony RM, Sun R, Stiltz J, van Rooijen N, Wynn TA, Gause WC, Shea-Donohue T. Th2 cytokine-induced alterations in intestinal smooth muscle function depend on alternatively activated macrophages. *Gastroenterology* 2008; **135**: 217-225.e1 [PMID: 18471439 DOI: 10.1053/j.gastro.2008.03.077]

28 **Gross M**, Salame TM, Jung S. Guardians of the Gut - Murine Intestinal Macrophages and Dendritic Cells. *Front Immunol* 2015; **6**: 254 [PMID: 26082775 DOI: 10.3389/fimmu.2015.00254]

29 **Feng YJ**, Li YY. The role of p38 mitogen-activated protein

kinase in the pathogenesis of inflammatory bowel disease. *J Dig Dis* 2011; **12**: 327-332 [PMID: 21955425 DOI: 10.1111/j.1751-2980.2011.00525.x]

30 **Bell LM**, Leong ML, Kim B, Wang E, Park J, Hemmings BA, Firestone GL. Hyperosmotic stress stimulates promoter activity and regulates cellular utilization of the serum- and glucocorticoid-inducible protein kinase (Sgk) by a p38 MAPK-dependent pathway. *J Biol Chem* 2000; **275**: 25262-25272 [PMID: 10842172 DOI: 10.1074/jbc.M002076200]

31 **Tubbs AL**, Liu B, Rogers TD, Sartor RB, Miao EA. Dietary Salt Exacerbates Experimental Colitis. *J Immunol* 2017; **199**: 1051-1059 [PMID: 28637899 DOI: 10.4049/jimmunol.1700356]

32 **Kleinewietfeld M**, Manzel A, Titze J, Kvakan H, Yosef N, Linker RA, Muller DN, Hafler DA. Sodium chloride drives autoimmune disease by the induction of pathogenic TH17 cells. *Nature* 2013; **496**: 518-522 [PMID: 23467095 DOI: 10.1038/nature11868]

33 **Zidek W**. [High salt consumption increases cardiovascular risk in hypertonic patients]. *Dtsch Med Wochenschr* 2016; **141**: 1524 [PMID: 27750335 DOI: 10.1055/s-0042-117074]

34 **Gren ST**, Grip O. Role of Monocytes and Intestinal Macrophages in Crohn's Disease and Ulcerative Colitis. *Inflamm Bowel Dis* 2016; **22**: 1992-1998 [PMID: 27243595 DOI: 10.1097/MIB.0000000000000824]

35 **Steinbach EC**, Plevy SE. The role of macrophages and dendritic cells in the initiation of inflammation in IBD. *Inflamm Bowel Dis* 2014; **20**: 166-175 [PMID: 23974993 DOI: 10.1097/MIB.0b013e3182a69dca]

36 **Kim TW**, Seo JN, Suh YH, Park HJ, Kim JH, Kim JY, Oh KI. Involvement of lymphocytes in dextran sulfate sodium-induced experimental colitis. *World J Gastroenterol* 2006; **12**: 302-305 [PMID: 16482634]

37 **Katakura K**, Watanabe H, Ohira H. Innate immunity and inflammatory bowel disease: a review of clinical evidence and future application. *Clin J Gastroenterol* 2013; **6**: 415-419 [PMID: 26182129 DOI: 10.1007/s12328-013-0436-4]

38 **Alex P**, Zachos NC, Nguyen T, Gonzales L, Chen TE, Conklin LS, Centola M, Li X. Distinct cytokine patterns identified from multiplex profiles of murine DSS and TNBS-induced colitis. *Inflamm Bowel Dis* 2009; **15**: 341-352 [PMID: 18942757 DOI: 10.1002/ibd.20753]

39 **Fantini MC**, Monteleone G, Macdonald TT. New players in the cytokine orchestra of inflammatory bowel disease. *Inflamm Bowel Dis* 2007; **13**: 1419-1423 [PMID: 17712836 DOI: 10.1002/ibd.20212]

40 **Elson CO**, Cong Y, Brandwein S, Weaver CT, McCabe RP, Mähler M, Sundberg JP, Leiter EH. Experimental models to study molecular mechanisms underlying intestinal inflammation. *Ann N Y Acad Sci* 1998; **859**: 85-95 [PMID: 9928372]

41 **Annunziato F**, Romagnani S. Do studies in humans better depict Th17 cells? *Blood* 2009; **114**: 2213-2219 [PMID: 19494349 DOI: 10.1182/blood-2009-03-209189]

42 **Li J**, Ueno A, Iacucci M, Fort Gasia M, Jijon HB, Panaccione R, Kaplan GG, Beck PL, Luider J, Barkema HW, Qian J, Gui X, Ghosh S. Crossover Subsets of CD^4 T Lymphocytes in the Intestinal Lamina Propria of Patients with Crohn's Disease and Ulcerative Colitis. *Dig Dis Sci* 2017; **62**: 2357-2368 [PMID: 28573508 DOI: 10.1007/s10620-017-4596-9]

43 **Harbour SN**, Maynard CL, Zindl CL, Schoeb TR, Weaver CT. Th17 cells give rise to Th1 cells that are required for the pathogenesis of colitis. *Proc Natl Acad Sci U S A* 2015; **112**: 7061-7066 [PMID: 26038559 DOI: 10.1073/pnas.1415675112]

44 **Fuss IJ**, Neurath M, Boirivant M, Klein JS, de la Motte C, Strong SA, Fiocchi C, Strober W. Disparate CD4+ lamina propria (LP) lymphokine secretion profiles in inflammatory bowel disease. Crohn's disease LP cells manifest increased secretion of IFN-gamma, whereas ulcerative colitis LP cells manifest increased secretion of IL-5. *J Immunol* 1996; **157**: 1261-1270 [PMID: 8757634]

45 **Yamamoto M**, Yoshizaki K, Kishimoto T, Ito H. IL-6 is required for the development of Th1 cell-mediated murine colitis. *J Immunol* 2000; **164**: 4878-4882 [PMID: 10779797]

46 **Fichtner-Feigl S**, Fuss IJ, Preiss JC, Strober W, Kitani A. Treatment of murine Th1- and Th2-mediated inflammatory bowel disease with NF-kappa B decoy oligonucleotides. *J Clin Invest* 2005; **115**: 3057-3071 [PMID: 16239967 DOI: 10.1172/JCI24792]

47 **Dieleman LA**, Palmen MJ, Akol H, Bloemena E, Peña AS, Meuwissen SG, Van Rees EP. Chronic experimental colitis induced by dextran sulphate sodium (DSS) is characterized by Th1 and Th2 cytokines. *Clin Exp Immunol* 1998; **114**: 385-391 [PMID: 9844047]

48 **Li L**, Shi QG, Lin F, Liang YG, Sun LJ, Mu JS, Wang YG, Su HB, Xu B, Ji CC, Huang HH, Li K, Wang HF. Cytokine IL-6 is required in Citrobacter rodentium infection-induced intestinal Th17 responses and promotes IL-22 expression in inflammatory bowel disease. *Mol Med Rep* 2014; **9**: 831-836 [PMID: 24430732 DOI: 10.3892/mmr.2014.1898]

49 **Ma L**, Liang Y, Fang M, Guan Y, Si Y, Jiang F, Wang F. The cytokines (IFN-gamma, IL-2, IL-4, IL-10, IL-17) and Treg cytokine (TGF-beta1) levels in adults with immune thrombocytopenia. *Pharmazie* 2014; **69**: 694-697 [PMID: 25272942]

50 **Geng X**, Xue J. Expression of Treg/Th17 cells as well as related cytokines in patients with inflammatory bowel disease. *Pak J Med Sci* 2016; **32**: 1164-1168 [PMID: 27882014 DOI: 10.12669/pjms.325.10902]

51 **Zhang HL**, Zheng YJ, Pan YD, Xie C, Sun H, Zhang YH, Yuan MY, Song BL, Chen JF. Regulatory T-cell depletion in the gut caused by integrin β7 deficiency exacerbates DSS colitis by evoking aberrant innate immunity. *Mucosal Immunol* 2016; **9**: 391-400 [PMID: 26220167 DOI: 10.1038/mi.2015.68]

52 **Gibson DJ**, Ryan EJ, Doherty GA. Keeping the bowel regular: the emerging role of Treg as a therapeutic target in inflammatory bowel disease. *Inflamm Bowel Dis* 2013; **19**: 2716-2724 [PMID: 23899545 DOI: 10.1097/MIB.0b013e31829ed7df]

53 **Curotto de Lafaille MA**, Lafaille JJ. Natural and adaptive foxp3+ regulatory T cells: more of the same or a division of labor? *Immunity* 2009; **30**: 626-635 [PMID: 19464985 DOI: 10.1016/j.immuni.2009.05.002]

54 **Denning TL**, Wang YC, Patel SR, Williams IR, Pulendran B. Lamina propria macrophages and dendritic cells differentially induce regulatory and interleukin 17-producing T cell responses. *Nat Immunol* 2007; **8**: 1086-1094 [PMID: 17873879 DOI: 10.1038/ni1511]

55 **Ip WK**, Medzhitov R. Macrophages monitor tissue osmolarity and induce inflammatory response through NLRP3 and NLRC4 inflammasome activation. *Nat Commun* 2015; **6**: 6931 [PMID: 25959047 DOI: 10.1038/ncomms7931]

56 **Hausmann M**, Kiessling S, Mestermann S, Webb G, Spöttl T, Andus T, Schölmerich J, Herfarth H, Ray K, Falk W, Rogler G. Toll-like receptors 2 and 4 are up-regulated during intestinal inflammation. *Gastroenterology* 2002; **122**: 1987-2000 [PMID: 12055604]

57 **Akagawa KS**. Functional heterogeneity of colony-stimulating factor-induced human monocyte-derived macrophages. *Int J Hematol* 2002; **76**: 27-34 [PMID: 12138892]

58 **Verreck FA**, de Boer T, Langenberg DM, Hoeve MA, Kramer M, Vaisberg E, Kastelein R, Kolk A, de Waal-Malefyt R, Ottenhoff TH. Human IL-23-producing type 1 macrophages promote but IL-10-producing type 2 macrophages subvert immunity to (myco)bacteria. *Proc Natl Acad Sci USA* 2004; **101**: 4560-4565 [PMID: 15070757 DOI: 10.1073/pnas.0400983101]

59 **Ghosn EE**, Cassado AA, Govoni GR, Fukuhara T, Yang Y, Monack DM, Bortoluci KR, Almeida SR, Herzenberg LA, Herzenberg LA. Two physically, functionally, and developmentally distinct peritoneal macrophage subsets. *Proc Natl Acad Sci USA* 2010; **107**: 2568-2573 [PMID: 20133793 DOI: 10.1073/pnas.0915000107]

60 **Wynn TA**, Chawla A, Pollard JW. Macrophage biology in development, homeostasis and disease. *Nature* 2013; **496**: 445-455 [PMID: 23619691 DOI: 10.1038/nature12034]

61 **Asano K**, Takahashi N, Ushiki M, Monya M, Aihara F, Kuboki E,

Moriyama S, Iida M, Kitamura H, Qiu CH, Watanabe T, Tanaka M. Intestinal CD169(+) macrophages initiate mucosal inflammation by secreting CCL8 that recruits inflammatory monocytes. *Nat Commun* 2015; **6**: 7802 [PMID: 26193821 DOI: 10.1038/ncomms8802]

62 **Lawrence T**, Natoli G. Transcriptional regulation of macrophage polarization: enabling diversity with identity. *Nat Rev Immunol* 2011; **11**: 750-761 [PMID: 22025054 DOI: 10.1038/nri3088]

63 **Mosser DM**, Edwards JP. Exploring the full spectrum of macrophage activation. *Nat Rev Immunol* 2008; **8**: 958-969 [PMID: 19029990 DOI: 10.1038/nri2448]

64 **Cibiček N**, Roubalová L, Vrba J, Zatloukalová M, Ehrmann J, Zapletalová J, Večeřa R, Křen V, Ulrichová J. Protective effect of isoquercitrin against acute dextran sulfate sodium-induced rat colitis depends on the severity of tissue damage. *Pharmacol Rep* 2016; **68**: 1197-1204 [PMID: 27657482 DOI: 10.1016/j.pharep.2016.07.007]

65 **Mills CD**, Kincaid K, Alt JM, Heilman MJ, Hill AM. M-1/M-2 macrophages and the Th1/Th2 paradigm. *J Immunol* 2000; **164**: 6166-6173 [PMID: 10843666]

66 **Cassado Ados A**, D'Império Lima MR, Bortoluci KR. Revisiting mouse peritoneal macrophages: heterogeneity, development, and function. *Front Immunol* 2015; **6**: 225 [PMID: 26042120 DOI: 10.3389/fimmu.2015.00225]

67 **Scaldaferri F**, Correale C, Gasbarrini A, Danese S. Molecular signaling blockade as a new approach to inhibit leukocyte-endothelial interactions for inflammatory bowel disease treatment. *Cell Adh Migr* 2009; **3**: 296-299 [PMID: 19571660]

P- Reviewer: Chiba T, Day AS, De Ponti F, Triantafillidis JK
S- Editor: Gong ZM **L- Editor**: Filipodia **E- Editor**: Huang Y

World Journal of Gastroenterology

Submit a Manuscript: http://www.f6publishing.com

World J Gastroenterol 2018 April 28; 24(16): 1795-1802

DOI: 10.3748/wjg.v24.i16.1795

ISSN 1007-9327 (print) ISSN 2219-2840 (online)

ORIGINAL ARTICLE

Retrospective Cohort Study

High tacrolimus intra-patient variability is associated with graft rejection, and *de novo* donor-specific antibodies occurrence after liver transplantation

Arnaud Del Bello, Nicolas Congy-Jolivet, Marie Danjoux, Fabrice Muscari, Laurence Lavayssière, Laure Esposito, Anne-Laure Hebral, Julie Bellière, Nassim Kamar

Arnaud Del Bello, Laurence Lavayssière, Laure Esposito, Anne-Laure Hebral, Julie Bellière, Nassim Kamar, Department of Nephrology and Organ Transplantation, CHU Rangueil, Toulouse 31000, France

Arnaud Del Bello, Nicolas Congy-Jolivet, Fabrice Muscari, Julie Bellière, Nassim Kamar, Université Paul Sabatier, Toulouse 31000, France

Julie Bellière, Molecular Immunogenetics Laboratory, Faculté de Médecine Purpan, IFR150 (INSERM), Montréal H3G 1Y6, France

Nicolas Congy-Jolivet, Department of Immunology, CHU de Toulouse, Hôpital de Rangueil, CHU de Toulouse, Toulouse 31000, France

Marie Danjoux, Department of Pathology, Institut Universitaire du Cancer, CHU Toulouse 31000, France

Fabrice Muscari, Department of Surgery and Liver Transplantation, Toulouse 31000, France

Nassim Kamar, INSERM, IFR-BMT, CHU Purpan, Toulouse 31000, France

ORCID number: Arnaud Del Bello (0000-0003-3115-868X); Nicolas Congy-Jolivet (0000-0002-2441-6145); Fabrice Muscari (0000-0001-6754-1686);Julie Bellière (0000-0002-4229-8584); Nassim Kamar (0000-0003-1930-8964).

Author contributions: Del Bello A and Kamar N designed research; Del Bello A, Congy-Jolivet N, Danjoux M, Muscari F, Lavayssière L, Esposito L, Hebral AL, Bellière J and Kamar N followed patients and performed research; Del Bello A, Bellière J, and Kamar N contributed analytic tools; Del Bello A and Kamar N analysed data; Del Bello A and Kamar N wrote the paper.

Institutional review board statement: The study was reviewed and approved for publication by our Institutional Reviewer.

Conflict-of-interest statement: All the authors have no conflict of interest related to the manuscript.

Data sharing statement: No additional data are available.

Manuscript source: Unsolicited manuscript

Correspondence to: Arnaud Del Bello, MD, Doctor, Department of Nephrology and Organ Transplantation, CHU Rangueil, TSA 50032, Cedex 9, Toulouse 31059, France. delbello.a@chu-toulouse.fr
Telephone: +33-5-61323923
Fax: +33-5-61323989

Received: December 5, 2017
Peer-review started: December 5, 2017
First decision: January 18, 2018
Revised: March 6, 2018
Accepted: March 31, 2018
Article in press: March 30, 2018
Published online: April 28, 2018

Abstract

AIM

To investigate the role of tacrolimus intra-patient variability (IPV) in adult liver-transplant recipients.

METHODS

We retrospectively assessed tacrolimus variability in a cohort of liver-transplant recipients and analyzed its effect on the occurrence of graft rejection and *de novo* donor-specific antibodies (*dn*DSAs), as well as graft

survival during the first 2 years posttransplantation. Between 02/08 and 06/2015, 116 patients that received tacrolimus plus mycophenolate mofetil (with or without steroids) were included.

RESULTS

Twenty-two patients (18.5%) experienced at least one acute-rejection episode (BPAR). Predictive factors for a BPAR were a tacrolimus IPV of > 35% [OR = 3.07 95%CI (1.14-8.24), *P* = 0.03] or > 40% [OR = 4.16 (1.38-12.50), *P* = 0.01), and a tacrolimus trough level of < 5 ng/mL [OR=3.68 (1.3-10.4), *P* =0.014]. Thirteen patients (11.2%) developed at least one *dn*DSA during the follow-up. Tacrolimus IPV [coded as a continuous variable: OR = 1.1, 95%CI (1.0-1.12), *P* = 0.006] of > 35% [OR = 4.83, 95%CI (1.39-16.72), *P* = 0.01] and > 40% [OR = 9.73, 95%CI (2.65-35.76), *P* = 0.001] were identified as predictors to detect *dn*DSAs. IPV did not impact on patient- or graft-survival rates during the follow-up.

CONCLUSION

Tacrolimus-IPV could be a useful tool to identify patients with a greater risk of graft rejection and of developing a *de novo* DSA after liver transplantation

Key words: Variability; Liver transplantation; Donor-specific antibodies; Immunosuppression

Core tip: Tacrolimus intra-patient variability (Tac IPV) was associated with kidney-graft rejection and worse long-term outcomes, but until now, was not well studied after liver transplantation in adult recipients. We found that the coefficient of variability-IPV of tacrolimus was a predictive factor for acute rejection and the occurrence of *de novo* donor-specific antibodies (DSA) after liver transplantation in a retrospective cohort of 116 recipients treated with tacrolimus and mycophenolate mofetil. This could be a useful tool to identify patients with a greater risk of graft rejection and of developing a *de novo* DSA after liver transplantation.

Del Bello A, Congy-Jolivet N, Danjoux M, Muscari F, Lavayssière L, Esposito L, Hebral AL, Bellière J, Kamar N. High tacrolimus intra-patient variability is associated with graft rejection, and *de novo* donor-specific antibodies occurrence after liver transplantation. *World J Gastroenterol* 2018; 24(16): 1795-1802 Available from: URL: http://www.wjgnet.com/1007-9327/full/v24/i16/1795.htm DOI: http://dx.doi.org/10.3748/wjg.v24.i16.1795

INTRODUCTION

Tacrolimus (Tac) is considered a cornerstone within immunosuppression protocols to prevent T-cell and antibody-mediated rejection after liver transplantation[1-3] However, this treatment presents a narrow therapeutic index: overexposure can lead to clinically serious events[4] thus necessitating regular therapeutic drug monitoring, whereas underexposure can lead to acute or chronic graft rejection[4-6] Inter-individual variability from Tac therapy may be explained by the polymorphism of cytochromes P450 3A4 and 5 (responsible for biotransformation of Tac)[7] and the drug transporter ABCB1[8], circadian rhythms[9] and also drug-drug interactions[10]. In addition to inter-individual variability, the pharmacokinetics of Tac can vary within individual patients. The concept of intra-patient variability (IPV) refers to the fluctuations in Tac blood concentrations (and consequently episodes of over- and under-immunosuppression) that some patients experience over time[11].

Several non-modifiable and modifiable factors contribute to Tac IPV (*e.g.*, polymorphism in CYP3A genes, the circadian rhythm of Tac exposure, gastrointestinal events such as diarrhea, cholestasis, changes in protein levels, anemia, but also drug-drug interactions with macrolides or azole anti-fungal treatments, foods, or changes in formulation or generic substitution)[11], but non-adherence to Tac seems to be the main cause of IPV[12,13]. It was previously suggested that higher degree of Tac IPV was associated with kidney-graft rejection and worse long-term outcomes after kidney transplantation[14,15]. Similar limited data have been reported after liver transplantation[16,17], mainly in pediatric cohorts. Moreover, little is known concerning the relationship between Tac variability and the occurrence of donor-specific antibodies (DSAs). Herein, we retrospectively assessed the variability of Tac in a cohort of liver-transplant recipients and analyzed its impact on the number of acute rejections, the occurrence of *de novo* DSAs, and patient- and graft-survival rates.

MATERIALS AND METHODS

Patients

Between February 2008 (*i.e.*, the date when the solid-phase Luminex assay was set up in our institution) and June 2015, a total of 298 adult patients received a liver transplant from deceased donors (DDLT) in our center. Patients excluded from the study were those that died within the first month posttransplantation (*n* = 34), those that needed a re-transplant during the first month (*n* = 2), and those that received a transplant with a preformed DSA (mean fluorescence intensity cut-off > 1000) directed against human leukocyte antigen (HLA) A, B, Cw, DR, DQ, or DP (*n* = 37). In order to avoid confounding factors associated with others immunosuppressive treatments, only patients that received and were maintained under Tac and mycophenolate mofetil (MMF) (with or without steroids) were included in this study (Figure 1). All patients but five received Tac given twice daily (Prograf®). The other five received Tac once daily (Advagraf®). We excluded patients that had Tac or MMF withdrawn.

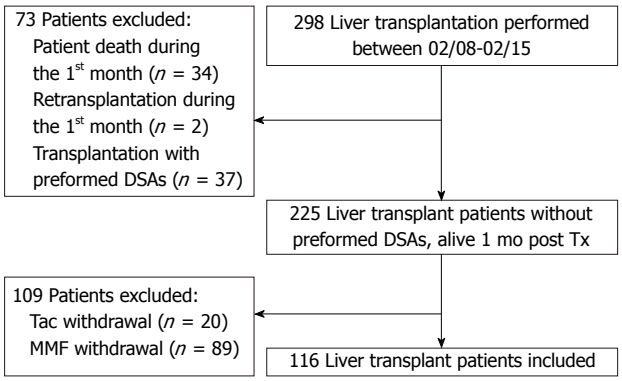

Figure 1 Flow chart.

Moreover, to calculate intra-patient variability, at least three trough levels of Tac had to be available. Hence, 116 patients with a functioning liver allograft at 1 mo posttransplantation were included in this study after having given their informed consent and after we had obtained Toulouse University IRB approval.

The target concentration of Tac trough level was 7-10 ng/mL during the first 3 mo, and 5-10 ng/mL thereafter during the follow-up. Each participant was followed for 2 years or until re-transplantation (n = 3) or death (n = 6). The median follow-up was 24 mo (range: 6-24). All rejection episodes were biopsy proven. Biopsies were only performed for cause during the study period and were analyzed according to the Banff criteria[18-20]. Graft failure was defined as the need for re-transplantation or as death from liver failure.

Detection of cytomegalovirus was performed using real-time PCR, as previously described[21], at month 3, 6, 12, and 24, and at any other time if clinically indicated.

Intra-patient variability

Tac trough levels were routinely assessed using high-performance liquid chromatography-linked tandem mass spectrometry (HPLC-MS) at discharge, then monthly between months 1-6, and thereafter at months 9, 12, 15, 18, and 24. To calculate the IPV of Tac, at least three Tac trough levels from each patient had to be available. The median number of available Tac measurements was 10 (range: 4-12).

Tac IPV was estimated using the coefficient of variability (CV). The CV-IPV was calculated as follows: CV-IPV (%) = (standard deviation/mean Tac trough-level concentration) × 100. Because all patients received the same drug dose between discharge and M24, the obtained levels were corrected for the corresponding daily dose of tacrolimus (CV C_0/D-IPV). In addition, because some patients were converted from one formulation to another during the follow-up, we calculated CV and CV C_0/D-IPV after excluding the Tac trough levels obtained during the adjustment dose period, *i.e.*, the month following a switch.

To compare IPV with the two formulations of Tac, the Tac twice-daily CV-IPV was calculated using Tac trough levels obtained from patients that had received Tac twice daily since transplantation until last follow-up and those obtained in patients switched for Tac once daily before the switch. The Tac once-daily CV-IPV was calculated using Tac trough levels from patients that received Tac once daily since transplantation until the last follow-up, and those obtained from patients that were later switched from twice- to a once-daily formulation after the switch (this excluded Tac trough levels obtained in the month following the switch).

Immunological analyses

All patients were screened for anti-HLA DSAs at transplantation, and at month 3 and 12, and annually thereafter. Additional screening was performed in case of graft dysfunction. Luminex® assays were used to determine the specificity of class Ⅰ HLAs in A/B/Cw and class Ⅱ in DR/DQ/DP IgG antibodies in the recipients' sera (centrifuged at 10000 *g* for 10 min) using Labscreen single Ag HLA class-Ⅰ and class-Ⅱ detection tests (One Lambda, Canoga Park, CA, United States), according to the manufacturer's instructions. The presence and specificity of antibodies were then detected using a Labscan 100®, and the mean fluorescence (baseline) value for each sample in each bead was evaluated. The baseline value was calculated as follows: [raw sample mean fluorescence intensity (MFI)-raw negative serum control MFI-negative-bead raw MFI sample-negative-bead raw MFI negative serum control]. A baseline value of > 1000 was considered positive.

Statistical analyses

Categorical variables are expressed as percentages and comparisons between groups were made using the chi-squared test or, if appropriate, Fisher's exact test. Continuous variables were expressed as medians and ranges, and compared using the Mann-Whitney test. Logistic regression analysis was used to determine the predictors for acute-rejection episodes and the occurrence of *de novo* anti-HLA DSAs. Variables with a $P < 0.1$ in the univariate analyses were included in the stepwise multivariable analyses. $P < 0.05$ was considered statistically significant.

RESULTS

The patients' characteristics at transplantation are presented in Table 1. All liver transplantations performed in this study were performed from DDLT. The mean DDLT age was 51 ± 17 years. To note, one DDLT was < 18 years, and 4 DDLT were > 80 years.

Tacrolimus levels and variability

During the follow-up, 44 (38%) patients were switched from Tac immediate-release given twice a day (Prograf®), to Tac once a day to improve quality of life. The switch was performed at a mean of 15 (range: 1-18) mo post-

Table 1 Characteristics of the liver-transplant recipients

Variable	*n* = 116
Donors' age at transplantation, yr (range)	53 (9-85)
Recipients' age at transplantation, yr (range)	57 (18-72)
Recipients' gender: male, *n* (%)	96 (83)
Initial liver disease, *n* (%)	
Alcohol	49 (43)
Viral (HCV, HBV)	36 (31)
Autoimmune disease (AIH, PSC, PBC)	13 (11)
Other[1]	18 (17)
Median MELD score at transplantation (range) (%)	22 (6-40)
Positive HCV RNA at transplantation, *n* (%)	21 (18)
Re-transplantation, yes (%)	3 (3)
Induction therapy, yes: *n* (%)	87 (75)
Polyclonal antibodies, *n* (%)	9 (8)
Interleukin-2 receptor blocker, *n* (%)	78 (67)
Conversion during the follow-up from twice-daily to once daily tacrolimus, *n* (%)	42 (36)
Number of patients receiving tacrolimus once daily, *n* (%)	5 (4)
At discharge	
Month 1	8 (7)
Month 3	9 (8)
Month 6	12 (10)
Month 9	18 (16)
Month 12	26 (31)
Month 18	39 (34)
Month 24	47 (41)
Tacrolimus trough level (ng/mL)	7.6 ± 3
At discharge	
Month 1	8 ± 3
Month 3	8.4 ± 3
Month 6	8.4 ± 3
Month 9	7.4 ± 3
Month 12	7.8 ± 3
Month 18	7.5 ± 2
Month 24	6.9 ± 3
Mycophenolate mofetil dose (mg/d)	1700 ± 600
At discharge	
Month 3	1250 ± 550
Month 6	1100 ± 450
Month 12	1000 ± 300
Month 24	1000 ± 300
Steroids (mg/d)	
At discharge: Yes (%)	116 (100)
Dose (mg/d)	20 ± 12
Month 3: Yes (%)	114 (98)
Dose (mg/d)	8 ± 4
Month 6: Yes (%)	110 (95)
Dose (mg/d)	7 ± 5
Month 12: Yes (%)	104 (90)
Dose (mg/d)	6 ± 6
Month 24: Yes (%)	97 (84)
Dose (mg/d)	5 ± 2

[1]Polycystic disease (*n* = 7), NASH syndrome (*n* = 4), Wilson disease (*n* = 2), bile duct atrophia (*n* = 1), drug intoxication (*n* = 2), and cryptogenic cirrhosis (*n* = 1). HBV: Hepatitis B virus; HCV: Hepatitis C virus; AIH: Auto-immune hepatitis; PSC: Primary sclerosing cholangitis; PBC: Primary biliary cirrhosis.

transplantation.

Mean tacrolimus trough level was 8 ± 3 ng/mL during the follow-up (Table 1). The mean dose of Tac was 6.8, 6.7, 6.4, 5.9, 5.4, 5.1, 4.8, and 4.6 mg/d, respectively, at discharge and at months 1, 3, 6, 9, 12, 18, and 24. Forty-five (38.8%) patients presented with a Tac trough level of < 5 ng/mL at least once during the follow-up. The overall mean Tac CV- IPV was 32 ± 12% [median CV-IPV 30.5% (7.6-80.6)]. Tac CV-IPV distribution is presented in Figure 2. The 1th, 2th, 3th, and 4th quartiles were, respectively, 25%, 30.5%, 36.5%, and 80.6%. The mean Tac CV-IPV was 30% ± 11% in patients given Tac once daily and was 32% ± 12% in patients that received Tac twice daily (P = 0.10). The mean Tac CV- IPV in the five patients that had received Tac once-daily since transplantation was 30% ± 7%. In the 44 patients that were converted from Tac twice-daily to once daily, the mean values of Tac CV-IPV were 32.3% ± 12% and 30% ± 12% before and after the switch, respectively (P = 0.21).

Table 2 Risk factors for a graft-rejection episode

Variable	Univariate analyses			Multivariate analyses		
	OR	95%CI	*P* value	OR	95%CI	*P* value
MELD score > 30 (n = 31)	0.55	0.12-1.90	0.42		-	
Initial liver disease						
(1) Alcohol cirrhosis (n = 49) *vs* (2, 3, 4)	0.58	0.18-1.68	0.34		-	
(2) Viral disease (n = 36) *vs* (1, 3, 4)	1.34	0.44-3.90	0.61		-	
(3) Auto-immune ILD (n = 13) *vs* (1, 2,4)	3.12	0.71-12.47	0.07	1.00	0.51-1.15	0.210
(4) Other (n = 18) *vs* (1, 2, 3)	0.49	0.05-2.37	0.52		-	
Induction therapy, yes (n = 87)	0.66	0.22-2.15	0.42		-	
Polyclonal antibodies (*vs* other)	3.89	0.70-20.13	0.06	2.87	0.61-13.47	0.180
IL2R blockers (*vs* other)	0.40	0.14-1.70	0.08	0.52	0.185-1.50	0.230
Donors' age > 50 yr (n = 69)	0.98	0.35-2.88	1.00		-	
Recipients' age > 50 yr (n = 92)	0.61	0.20-2.01	0.41		-	
HCV-RNA + At transplantation (n = 21)	1.96	0.54-6.45	0.22		-	
Steroid withdrawal during the FU (n = 19)	2.30	0.63-7.82	0.20		-	
De novo DSAs during the FU (n = 13)	2.80	0.64-11.19	0.13		-	
Tacrolimus trough level < 5 ng/mL (n = 34)	3.00	1.05-8.96	0.02	3.68	1.30-10.41	0.014
CV-IPV tacrolimus (continuous variable)	2.70	1.88-13.45	0.01	1.10	1.01-1.11	0.008
CV-IPV > 35%	3.05	1.05-8.96	0.03	3.07	1.14-8.24	0.030
CV-IPV > 0%	2.97	0.91-9.30	0.04	4.16	1.38-12.50	0.010
CV-C_0/d-IPV	1.89	0.67-5.74	0.24		-	

FU: Follow-up; ILD: Initial liver disease; HCV: Hepatitis C virus; CV-IPV: Coefficient of variability-intra-patient variability; CV-C_0/d-IPV: Coefficient of variability corrected for the corresponding daily dose-intra-patient variability.

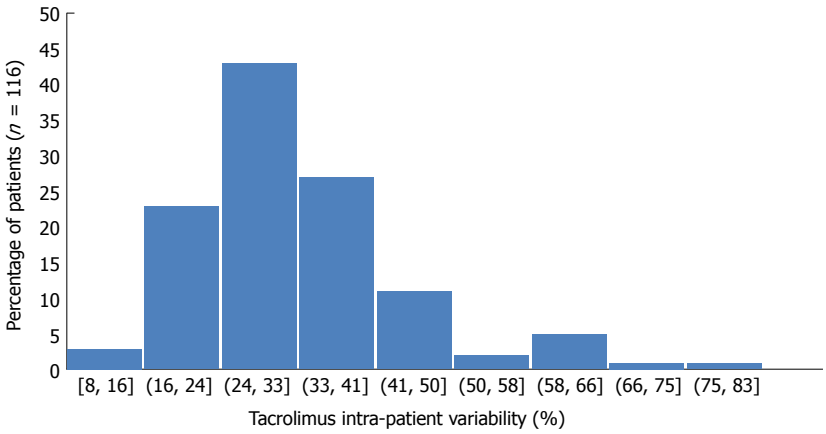

Figure 2 Distribution of tacrolimus according to intra-patient variability.

Overall mean CV C_0/d- IPV was 73% ± 43%. It was 69% ± 29% with Tac twice-daily compared to 79% ± 50% for Tac given once daily (P = 0.9).

Incidence of acute rejection and de novo donor-specific antibodies

During the follow-up, 22 patients (19%) presented with at least one episode of acute rejection. The time between transplantation and a diagnosis of acute rejection (*i.e.*, the date of the biopsy) was 3.5 mo (range: 0.5-12). Fourteen patients (12%) experienced a T-cell steroid-sensitive acute rejection, and six patients (5%) presented with a T-cell steroid-resistant acute rejection, which was treated with polyclonal antibodies. One patient presented with an acute antibody-mediated rejection at 4 mo posttransplantation. The Tac CV-IPV in this patient was high: CV-IPV of 63.2% and CV C_0/d- IPV = 68.2%. The risk factors for acute rejection after liver transplantation are presented in Table 2. The predictive factors for a biopsy-proven acute rejection were a Tac trough level of < 5 ng/mL [OR = 3.68; 95%CI (1.30-10.41), P = 0.014], the Tac CV-IPV (coded as a continuous variable) [OR = 1.1; 95%CI (1.01-1.11), P = 0.008], a CV-IPV of > 35% [OR = 3.07; 95%CI (1.14-8.24), P = 0.03], and a CV-IPV of > 40% [OR = 4.16; 95%CI (1.38-12.50), P = 0.01]. Twenty-one of the 22 patients that presented with an acute-rejection episode were receiving Tac twice daily when the rejection was diagnosed.

Thirteen patients (11.2%) presented with at least one *de novo* DSA during the posttransplantation follow-up (nine anti-HLA class Ⅱ, three anti-HLA class Ⅰ, one anti-HLA class Ⅰ and Ⅱ). Only one of these patients developed an antibody-mediated rejection. The median time between transplantation and detection of a *de novo* DSA was 3.5 mo (range: 1-12). The risk

Table 3 Risk factors for developing *de novo* donor-specific antibodies after liver transplantation.

Variable	Univariate analyses			Multivariate analyses		
	OR	95%CI	*P* value	OR	95%CI	*P* value
MELD score > 30 (n = 31)	1.84	0.43-7.10	0.33		-	
Initial liver disease						
(1) Alcohol cirrhosis (n = 49) *vs* (2, 3, 4)	0.58	0.12-2.22	0.55		-	
(2) Viral disease (n = 36) *vs* (1, 3, 4)	0.98	0.21-3.86	1.0		-	
(3) Autoimmune ILD (n = 13) *vs* (1, 2, 4)	1.51	0.14-8.46	0.64		-	
(4) Other (n = 18) *vs* (1, 2, 3)	2.79	0.55-11.83	0.64		-	
Induction therapy, yes (n = 87)	1.61	0.41-7.61	0.55		-	
Polyclonal antibodies (*vs* other)	0.59	0.70-18.00	0.60		-	
IL2R blockers (*vs* other)	1.1	0.28-5.28	1.0		-	
Donors' age > 50 yr (n = 69)	0.78	0.20-3.00	0.77		-	
Recipients' age > 50 yr (n = 92)	0.36	0.09-1.58	0.10	0.2	0.07-0.85	0.3
HCV RNA + at transplantation (n = 21)	1.41	0.23-6.23	0.70		-	
Steroid withdrawal during the FU (n = 19)	0.39	0.01-3.01	0.69		-	
Tacrolimus trough level < 5 ng/mL (n = 34)	1.59	0.38-6.05	0.52		-	
CV-IPV tacrolimus (continuous variable)	1.92	-1.28-21.39	0.08	1.1	1.0-1.12	0.006
CV-IPV > 35%	4.66	1.22-19.82	0.02	4.83	1.39-16.72	0.01
CV-IPV > 40%	9.10	2.28-40.63	< 0.001	9.73	2.65-35.76	0.001
CV-C_0/d-IPV	3.15	5.47-27.31	0.005	1.0	0.97-1.02	0.09

FU: Follow-up; ILD: Initial liver disease; HCV: Hepatitis C virus; CV-IPV: Coefficient of variability-intra-patient variability; CV-C_0/d-IPV: Coefficient of variability corrected for the corresponding daily dose-intra-patient variability.

factors for a *de novo* DSA are presented in Table 3. The Tac CV-IPV [coded as a continuous variable: OR = 1.1, 95%CI (1.0-1.12), P = 0.006), and a CV-IPV of > 35% [OR = 4.83, 95%CI (1.39-16.72), P = 0.01] or of > 40% [OR = 9.73, 95%CI (2.65-35.76), P = 0.001] were identified as predictors for the occurrence of *de novo* DSAs detection.

Survival of patients

During the follow-up, six patients died [at a mean of 13 mo (range: 6-23) posttransplantation]. The causes of death were infections (n = 3), cardiovascular (n = 2), and neoplastic (n = 1) complications. No difference in Tac CV- IPV was observed between patients that died during the follow-up (CV-IPV 33% ± 6%) and those that did not (CV-IPV 32% ± 12%; P = 0.70). Three patients required re-transplantation at month 5, 10, and 14, respectively, for ischemic cholangitis that occurred posttransplantation. During the follow-up, 24 patients presented with posttransplant replication of cytomegalovirus. No difference in Tac CV-IPV was observed between patients with replication of cytomegalovirus (CV-IPV 32% ± 9%) and those without replication (32% ± 12%, P = 0.90).

DISCUSSION

High IPV has been previously associated with a greater risk of graft rejection, an accelerated progression of chronic histological lesions, and worse long-term survival after kidney transplantation[11,14,22,23]. In pediatric liver-transplants, Tac variability was associated with late acute rejection[16]. In the present study, we investigated the impact of Tac variability in 116 adult liver-transplant recipients. In order to avoid confounding factors, we focused on patients that received a graft without preformed DSAs and that had received Tac associated with MMF. Although the mean Tac trough level was 8 ± 3 ng/mL during the study period, nearly 40% of patients had a Tac trough level of < 5 ng/mL at least once during the follow-up. Tac CV-IPV varied from 7.6%-80.6% (median 30.5%), and median Tac CV C_0/d-IPV was 62% (18-147). Almost one-third of patients presented with a Tac CV-IPV of > 35%. This high value is similar to those reported in previous studies, mainly after kidney transplantation[24,25]. In kidney-transplant[13,25] and pediatric liver-transplant patients[16], high CV-IPV was associated with an increased risk of acute rejection. In the present study, we found that a Tac trough level of < 5 ng/mL, the Tac CV-IPV (coded as a continuous variable), a CV-IPV of > 35%, and a CV-IPV > 40% were independent predictive factors for a biopsy-proven graft rejection.

Posttransplant positive DSAs were associated with decreased graft survival and increased acute or chronic graft rejections[2,3,26]. It has been previously suggested that iterative transplantation, low levels of calcineurin inhibitors, the use of cyclosporine (compared to Tac), and non-adherence can promote the development of a *de novo* DSA after liver transplantation[2]. Herein, we found that the Tac CV-IPV (coded as a continuous variable), a CV-IPV of > 35%, and CV-IPV > 40% were independent predictive factors for the occurrence of a *de novo* DSA. Similar data, reported after kidney transplantation[24], from a cohort of 310 adult kidney-transplant patients given Tac twice-daily during the first year posttransplant, showed that a history of acute rejection, re-transplantation and a Tac CV greater than 30% were associated with the occurrence of a *de novo* DSA. In our study, one patient presented with an acute antibody-mediated rejection associated with an anti-class Ⅱ *de novo* DSA at 3 mo after liver transplantation.

Interestingly, this patient had high tacrolimus variability (CV-IPV 63.2%, CV C_0/d-IPV 68.2%). None of the other 12 patients that developed a DSA experienced an acute antibody-mediated rejection. However, it was suggested that patients with positive DSAs would present lower graft survival, consecutive to chronic antibody mediated rejection[27] rather than to acute antibody-mediated rejection episodes.

In several studies, but not all, the use of once-daily tacrolimus compared to a twice daily formulation has been found to improve adherence and to reduce IPV[11,28-31]. In the present study, no difference between Tac formulations was observed.

This study has several limitations. Because of its retrospective design, we could not evaluate the cause of Tac variability. It has been suggested previously that non-adherence is the main cause of Tac variability[11]. However, in our study, adherence was not evaluated using objective methods, such as those previously reported using electronic devices[28]. Moreover, we did not evaluate MMF variability in our study because we do not perform this analysis routinely in our center. Of note, conflicting results have been reported concerning the use of MMF variability after solid-organ transplantation[14,25]. It was also previously suggested that pre-transplant determination of CYP3A5 and MDR1 polymorphisms[32] allows more rapid achievement of therapeutic Tac trough level. However, no association between the pharmacogenomics parameters and Tac intra-patient variability is expected and was reported.

In conclusion, we found that the CV-IPV of Tac was a predictive factor for acute rejection and the occurrence of a *de novo* DSA after liver transplantation. This could be a useful tool to identify patients with a greater risk of graft rejection and of developing a *de novo* DSA after liver transplantation. Future studies should investigate the role of Tac IPV on long-term outcomes, on chronic graft rejection, and over-immunosuppression-related diseases (cancer, and related immunocompromised infections).

ARTICLE HIGHLIGHTS

Research background

Tacrolimus (Tac) is considered a cornerstone within immunosuppression protocols to prevent T-cell and antibody-mediated rejection after liver transplantation. However, this treatment presents a narrow therapeutic index: overexposure can lead to clinically serious events, thus necessitating regular therapeutic drug monitoring, whereas underexposure can lead to acute or chronic graft rejection. The concept of intra-patient variability (IPV) refers to the fluctuations in Tac blood concentrations (and consequently episodes of over- and under-immunosuppression) that some patients experience over time.

Research motivation

Tac-IPV is an inexpensive assay to explore fluctuations in Tac blood concentrations. We investigated the potential usefulness of Tac-IPV to predict the incidence of donor specific antibodies and graft rejection episodes.

Research objectives

Our aim was to investigate the role of tacrolimus IPV in adult liver-transplant recipients.

Research methods

We retrospectively assessed tacrolimus variability and analyzed its effect on the occurrence of graft rejection and *de novo* donor-specific antibodies.

Research results

Twenty-two patients experienced at least one acute-rejection episode (BPAR). Predictive factors for a BPAR were a tacrolimus IPV of > 35% or > 40%, and a tacrolimus trough level of < 5 ng/mL. Thirteen patients developed at least one *dn*DSA during the follow-up. Tacrolimus IPV and tacrolimus IPV of > 35%, and > 40% were identified as predictors to detect *dn*DSAs. IPV did not impact on patient- or graft-survival rates during the follow-up.

Research conclusions

In our study higher Tac-IPV was associated with graft rejection and occurrence of DSAs.

Research perspective

Tacrolimus-IPV could be a useful tool to identify patients with a greater risk of graft rejection and of developing a *de novo* DSA after liver transplantation.

REFERENCES

1 **Price DC**. Radioisotopic evaluation of the thyroid and the parathyroids. *Radiol Clin North Am* 1993; **31**: 991-1015 [PMID: 8362060 DOI: 10.1002/14651858.CD011639.pub2]

2 **Kaneku H**, O'Leary JG, Banuelos N, Jennings LW, Susskind BM, Klintmalm GB, Terasaki PI. De novo donor-specific HLA antibodies decrease patient and graft survival in liver transplant recipients. *Am J Transplant* 2013; **13**: 1541-1548 [PMID: 23721554 DOI: 10.1111/ajt.12212]

3 **European Association for the Study of the Liver.** EASL Clinical Practice Guidelines: Liver transplantation. *J Hepatol* 2016; **64**: 433-485 [PMID: 26597456 DOI: 10.1016/j.jhep.2015.10.006]

4 **de Mare-Bredemeijer EL**, Metselaar HJ. Optimization of the use of Calcineurin inhibitors in liver transplantation. *Best Pract Res Clin Gastroenterol* 2012; **26**: 85-95 [PMID: 22482528 DOI: 10.1016/j.bpg.2012.01.017]

5 **Rodríguez-Perálvarez M**, Germani G, Papastergiou V, Tsochatzis E, Thalassinos E, Luong TV, Rolando N, Dhillon AP, Patch D, O' Beirne J, Thorburn D, Burroughs AK. Early tacrolimus exposure after liver transplantation: relationship with moderate/severe acute rejection and long-term outcome. *J Hepatol* 2013; **58**: 262-270 [PMID: 23023010 DOI: 10.1016/j.jhep.2012.09.019]

6 **Del Bello A**, Congy-Jolivet N, Muscari F, Lavayssière L, Esposito L, Cardeau-Desangles I, Guitard J, Dörr G, Suc B, Duffas JP, Alric L, Bureau C, Danjoux M, Guilbeau-Frugier C, Blancher A, Rostaing L, Kamar N. Prevalence, incidence and risk factors for donor-specific anti-HLA antibodies in maintenance liver transplant patients. *Am J Transplant* 2014; **14**: 867-875 [PMID: 24580771 DOI: 10.1111/ajt.12651]

7 **Staatz CE**, Tett SE. Clinical pharmacokinetics and pharmacodynamics of tacrolimus in solid organ transplantation. *Clin Pharmacokinet* 2004; **43**: 623-653 [PMID: 15244495 DOI: 10.1007/s40262-015-0282-2]

8 **Hesselink DA**, Bouamar R, Elens L, van Schaik RH, van Gelder T. The role of pharmacogenetics in the disposition of and response to tacrolimus in solid organ transplantation. *Clin Pharmacokinet* 2014; **53**: 123-139 [PMID: 24249597 DOI: 10.1007/s40262-013-0120-3]

9 **Tada H**, Satoh S, Iinuma M, Shimoda N, Murakami M, Hayase Y, Kato T, Suzuki T. Chronopharmacokinetics of tacrolimus in kidney transplant recipients: occurrence of acute rejection. *J Clin Pharmacol* 2003; **43**: 859-865 [PMID: 12953343 DOI: 10.1177/0091270003254797]

10 **van Gelder T**. Drug interactions with tacrolimus. *Drug Saf* 2002; **25**: 707-712 [PMID: 12167066 DOI: 10.2165/00002018-200225100-00003]

11 **Shuker N**, van Gelder T, Hesselink DA. Intra-patient variability

in tacrolimus exposure: causes, consequences for clinical management. *Transplant Rev* (Orlando) 2015; **29**: 78-84 [PMID: 25687818 DOI: 10.1016/j.trre.2015.01.002]

12 **Shemesh E**, Shneider BL, Savitzky JK, Arnott L, Gondolesi GE, Krieger NR, Kerkar N, Magid MS, Stuber ML, Schmeidler J, Yehuda R, Emre S. Medication adherence in pediatric and adolescent liver transplant recipients. *Pediatrics* 2004; **113**: 825-832 [PMID: 15060234 DOI: 10.1542/peds.113.4.825]

13 **Pollock-Barziv SM**, Finkelstein Y, Manlhiot C, Dipchand AI, Hebert D, Ng VL, Solomon M, McCrindle BW, Grant D. Variability in tacrolimus blood levels increases the risk of late rejection and graft loss after solid organ transplantation in older children. *Pediatr Transplant* 2010; **14**: 968-975 [PMID: 21040278 DOI: 10.1111/j.1399-3046.2010.01409.x]

14 **Borra LC**, Roodnat JI, Kal JA, Mathot RA, Weimar W, van Gelder T. High within-patient variability in the clearance of tacrolimus is a risk factor for poor long-term outcome after kidney transplantation. *Nephrol Dial Transplant* 2010; **25**: 2757-2763 [PMID: 20190242 DOI: 10.1093/ndt/gfq096]

15 **Ro H**, Min SI, Yang J, Moon KC, Kim YS, Kim SJ, Ahn C, Ha J. Impact of tacrolimus intraindividual variability and CYP3A5 genetic polymorphism on acute rejection in kidney transplantation. *Ther Drug Monit* 2012; **34**: 680-685 [PMID: 23149441 DOI: 10.1097/FTD.0b013e3182731809]

16 **Shemesh E**, Bucuvalas JC, Anand R, Mazariegos GV, Alonso EM, Venick RS, Reyes-Mugica M, Annunziato RA, Shneider BL. The Medication Level Variability Index (MLVI) Predicts Poor Liver Transplant Outcomes: A Prospective Multi-Site Study. *Am J Transplant* 2017; **17**: 2668-2678 [PMID: 28321975 DOI: 10.1111/ajt.14276]

17 **Christina S**, Annunziato RA, Schiano TD, Anand R, Vaidya S, Chuang K, Zack Y, Florman S, Shneider BL, Shemesh E. Medication level variability index predicts rejection, possibly due to nonadherence, in adult liver transplant recipients. *Liver Transpl* 2014; **20**: 1168-1177 [PMID: 24931127 DOI: 10.1002/lt.23930]

18 Banff schema for grading liver allograft rejection: an international consensus document. *Hepatology* 1997; **25**: 658-663 [PMID: 9049215 DOI: 10.1002/hep.510250328]

19 **Demetris A**, Adams D, Bellamy C, Blakolmer K, Clouston A, Dhillon AP, Fung J, Gouw A, Gustafsson B, Haga H, Harrison D, Hart J, Hubscher S, Jaffe R, Khettry U, Lassman C, Lewin K, Martinez O, Nakazawa Y, Neil D, Pappo O, Parizhskaya M, Randhawa P, Rasoul-Rockenschaub S, Reinholt F, Reynes M, Robert M, Tsamandas A, Wanless I, Wiesner R, Wernerson A, Wrba F, Wyatt J, Yamabe H. Update of the International Banff Schema for Liver Allograft Rejection: working recommendations for the histopathologic staging and reporting of chronic rejection. An International Panel. *Hepatology* 2000; **31**: 792-799 [PMID: 10706577 DOI: 10.1002/hep.510310337]

20 **Demetris AJ**, Bellamy C, Hübscher SG, O'Leary J, Randhawa PS, Feng S, Neil D, Colvin RB, McCaughan G, Fung JJ, Del Bello A, Reinholt FP, Haga H, Adeyi O, Czaja AJ, Schiano T, Fiel MI, Smith ML, Sebagh M, Tanigawa RY, Yilmaz F, Alexander G, Baiocchi L, Balasubramanian M, Batal I, Bhan AK, Bucuvalas J, Cerski CTS, Charlotte F, de Vera ME, ElMonayeri M, Fontes P, Furth EE, Gouw ASH, Hafezi-Bakhtiari S, Hart J, Honsova E, Ismail W, Itoh T, Jhala NC, Khettry U, Klintmalm GB, Knechtle S, Koshiba T, Kozlowski T, Lassman CR, Lerut J, Levitsky J, Licini L, Liotta R, Mazariegos G, Minervini MI, Misdraji J, Mohanakumar T, Mölne J, Nasser I, Neuberger J, O'Neil M, Pappo O, Petrovic L, Ruiz P, Sağol Ö, Sanchez Fueyo A, Sasatomi E, Shaked A, Shiller M, Shimizu T, Sis B, Sonzogni A, Stevenson HL, Thung SN, Tisone G, Tsamandas AC, Wernerson A, Wu T, Zeevi A, Zen Y. 2016 Comprehensive Update of the Banff Working Group on Liver Allograft Pathology: Introduction of Antibody-Mediated Rejection. *Am J Transplant* 2016; **16**: 2816-2835 [PMID: 27273869 DOI: 10.1111/ajt.13909]

21 **Mengelle C**, Sandres-Sauné K, Pasquier C, Rostaing L, Mansuy JM, Marty M, Da Silva I, Attal M, Massip P, Izopet J. Automated extraction and quantification of human cytomegalovirus DNA in whole blood by real-time PCR assay. *J Clin Microbiol* 2003; **41**: 3840-3845 [PMID: 12904398 DOI: 10.1128/JCM.41.8.3840-3845.2003]

22 **Taber DJ**, Su Z, Fleming JN, McGillicuddy JW, Posadas-Salas MA, Treiber FA, Dubay D, Srinivas TR, Mauldin PD, Moran WP, Baliga PK. Tacrolimus Trough Concentration Variability and Disparities in African American Kidney Transplantation. *Transplantation* 2017; **101**: 2931-2938 [PMID: 28658199 DOI: 10.1097/TP.0000000000001840]

23 **Vanhove T**, Vermeulen T, Annaert P, Lerut E, Kuypers DRJ. High Intrapatient Variability of Tacrolimus Concentrations Predicts Accelerated Progression of Chronic Histologic Lesions in Renal Recipients. *Am J Transplant* 2016; **16**: 2954-2963 [PMID: 27013142 DOI: 10.1111/ajt.13803]

24 **Rodrigo E**, Segundo DS, Fernández-Fresnedo G, López-Hoyos M, Benito A, Ruiz JC, de Cos MA, Arias M. Within-Patient Variability in Tacrolimus Blood Levels Predicts Kidney Graft Loss and Donor-Specific Antibody Development. *Transplantation* 2016; **100**: 2479-2485 [PMID: 26703349 DOI: 10.1097/TP.0000000000001040]

25 **Hsiau M**, Fernandez HE, Gjertson D, Ettenger RB, Tsai EW. Monitoring nonadherence and acute rejection with variation in blood immunosuppressant levels in pediatric renal transplantation. *Transplantation* 2011; **92**: 918-922 [PMID: 21857278 DOI: 10.1097/TP.0b013e31822dc34f]

26 **O'Leary JG**, Kaneku H, Jennings LW, Bañuelos N, Susskind BM, Terasaki PI, Klintmalm GB. Preformed class II donor-specific antibodies are associated with an increased risk of early rejection after liver transplantation. *Liver Transpl* 2013; **19**: 973-980 [PMID: 23780820 DOI: 10.1002/lt.23687]

27 **O'Leary JG**, Cai J, Freeman R, Banuelos N, Hart B, Johnson M, Jennings LW, Kaneku H, Terasaki PI, Klintmalm GB, Demetris AJ. Proposed Diagnostic Criteria for Chronic Antibody-Mediated Rejection in Liver Allografts. *Am J Transplant* 2016; **16**: 603-614 [PMID: 26469278 DOI: 10.1111/ajt.13476]

28 **Kuypers DR**, Peeters PC, Sennesael JJ, Kianda MN, Vrijens B, Kristanto P, Dobbels F, Vanrenterghem Y, Kanaan N; ADMIRAD Study Team. Improved adherence to tacrolimus once-daily formulation in renal recipients: a randomized controlled trial using electronic monitoring. *Transplantation* 2013; **95**: 333-340 [PMID: 23263559 DOI: 10.1097/TP.0b013e3182725532]

29 **van Hooff J**, Van der Walt I, Kallmeyer J, Miller D, Dawood S, Moosa MR, Christiaans M, Karpf C, Undre N. Pharmacokinetics in stable kidney transplant recipients after conversion from twice-daily to once-daily tacrolimus formulations. *Ther Drug Monit* 2012; **34**: 46-52 [PMID: 22249344 DOI: 10.1097/FTD.0b013e318244a7fd]

30 **Wehland M**, Bauer S, Brakemeier S, Burgwinkel P, Glander P, Kreutz R, Lorkowski C, Slowinski T, Neumayer HH, Budde K. Differential impact of the CYP3A5*1 and CYP3A5*3 alleles on pre-dose concentrations of two tacrolimus formulations. *Pharmacogenet Genomics* 2011; **21**: 179-184 [PMID: 20818295 DOI: 10.1097/FPC.0b013e32833ea085]

31 **Shuker N**, Cadogan M, van Gelder T, Roodnat JI, Kho MM, Weimar W, Hesselink DA. Conversion from twice-daily to once-daily tacrolimus does not reduce intrapatient variability in tacrolimus exposure. *Ther Drug Monit* 2015; **37**: 262-269 [PMID: 25265255 DOI: 10.1097/FTD.0000000000000136]

32 **Tang JT**, Andrews LM, van Gelder T, Shi YY, van Schaik RH, Wang LL, Hesselink DA. Pharmacogenetic aspects of the use of tacrolimus in renal transplantation: recent developments and ethnic considerations. *Expert Opin Drug Metab Toxicol* 2016; **12**: 555-565 [PMID: 27010623 DOI: 10.1517/17425255.2016.1170808]

P- Reviewer: Chiu KW, Sergi CM, Sugawara Y **S- Editor**: Wang XJ
L- Editor: A **E- Editor**: Huang Y

World Journal of Gastroenterology

Submit a Manuscript: http://www.f6publishing.com

World J Gastroenterol 2018 April 28; 24(16): 1803-1811

DOI: 10.3748/wjg.v24.i16.1803

ISSN 1007-9327 (print) ISSN 2219-2840 (online)

ORIGINAL ARTICLE

Randomized Clinical Trial

Papillary fistulotomy *vs* conventional cannulation for endoscopic biliary access: A prospective randomized trial

Carlos Kiyoshi Furuya, Paulo Sakai, Fabio Ramalho Tavares Marinho, Jose Pinhata Otoch, Spencer Cheng, Lívia Lemes Prudencio, Eduardo Guimarães Hourneaux de Moura, Everson Luiz de Almeida Artifon

Carlos Kiyoshi Furuya, Paulo Sakai, Fabio Ramalho Tavares Marinho, Spencer Cheng, Eduardo Guimarães Hourneaux de Moura, Department of Gastrointestinal Endoscopy Unit, University of Sao Paulo, Sao Paulo 05409001, Brazil

Jose Pinhata Otoch, Lívia Lemes Prudencio, Department of Surgery, University of Sao Paulo, Sao Paulo 05403000, Brazil

Everson Luiz de Almeida Artifon, Department of Gastroenterology and Radiology, University of Sao Paulo, Sao Paulo 04107-030, Brazil

ORCID number: Carlos Kiyoshi Furuya (0000-0002-6512-5029); Paulo Sakai (0000-0003-3088-9210); Fabio Ramalho Tavares Marinho (0000-0002-7509-7113); Jose Pinhata Otoch (0000-0002-8293-1508); Spencer Cheng (0000-0001-9584-203X); Lívia Lemes Prudencio (0000-0002-8256-9035); Eduardo Guimarães Hourneaux de Moura (0000-0003-1215-5731); Everson Luiz de Almeida Artifon (0000-0003-1900-8777).

Author contributions: Furuya CK designed and performed the research; Sakai P, Marinho FRT and Prudencio LL wrote the paper; Otoch JP and de Moura EGH analyzed the data; Artifon EL performed the research and analyzed the data.

Institutional review board statement: The study was reviewed and approved by Ethics Committee for Research Project Analysis of Clinics Hospital, University of Sao Paulo and UNILUS Ethics Subcommittee.

Informed consent statement: All study participants, or their legal guardian, provided informed written consent prior to study enrollment.

Conflict-of-interest statement: All authors declare no potential conflicting interests related to this paper.

Data sharing statement: No additional data are available.

Manuscript source: Unsolicited manuscript

Correspondence to: Carlos Kiyoshi Furuya, MD, PhD, Medical Assistant, Department of Gastrointestinal Endoscopy Unit, University of Sao Paulo, Av. Dr. Eneas de Carvalho Aguiar, 255 Predio dos Ambulatorios-6 andar-Bloco 3, Sao Paulo 5409001, Brazil. carloskfjr@gmail.com
Telephone: +55-11-30697579

Received: February 25, 2018
Peer-review started: February 26, 2018
First decision: March 9, 2018
Revised: March 12, 2018
Accepted: March 25, 2018
Article in press: March 25, 2018
Published online: April 28, 2018

Abstract

AIM

To compare the cannulation success, biochemical profile, and complications of the papillary fistulotomy technique *vs* catheter and guidewire standard access.

METHODS

From July 2010 to May 2017, patients were prospectively randomized into two groups: Cannulation with a catheter and guidewire (Group Ⅰ) and papillary fistulotomy (Group Ⅱ). Amylase, lipase and C-reactive protein at T0, as well as 12 h and 24 h after endoscopic retrograde cholangiopancreatography, and complications (pancreatitis, bleeding, perforation) were recorded.

RESULTS

We included 102 patients (66 females and 36 males, mean age 59.11 ± 18.7 years). Group Ⅰ and Group Ⅱ had 51 patients each. The successful cannulation rates were 76.5% and 100%, respectively (P = 0.0002). Twelve patients (23.5%) in Group Ⅰ had a difficult cannulation and underwent fistulotomy, which led to successful secondary biliary access (Failure Group). The complication rate was 13.7% (2 perforations and 5 mild pancreatitis) *vs* 2.0% (1 patient with perforation and pancreatitis) in Groups Ⅰ and Ⅱ, respectively (P = 0.0597).

CONCLUSION

Papillary fistulotomy was more effective than guidewire cannulation, and it was associated with a lower profile of amylase and lipase. Complications were similar in both groups.

Key words: Catheterization; Complications; Endoscopic retrograde cholangiopancreatography; Therapeutic use; Common bile duct

Core tip: Biliary cannulation is the first step of therapeutic endoscopic retrograde cholangiopancreatography and can determine several complications. There are small numbers of papers regarding comparison between conventional cannulation *vs* fistulotomy. Our study is a well-designed approach in its matter. In fact, we compare the cannulation success, biochemical profile and complications of the papillary fistulotomy technique *versus* catheter and guidewire standard access. Papillary fistulotomy was more effective than guidewire cannulation, and it was associated with a lower profile of amylase and lipase, as the routine endoscopic access to the biliary tree, including difficult cases. Complications were similar in both groups.

Furuya CK, Sakai P, Marinho FR, Otoch JP, Cheng S, Prudencio LL, de Moura EG, Artifon EL. Papillary fistulotomy *vs* conventional cannulation for endoscopic biliary access: A prospective randomized trial. *World J Gastroenterol* 2018; 24(16): 1803-1811 Available from: URL: http://www.wjgnet.com/1007-9327/full/v24/i16/1803.htm DOI: http://dx.doi.org/10.3748/wjg.v24.i16.1803

INTRODUCTION

Biliary tract cannulation is the critical step in diagnosis and treatment of biliopancreatic diseases during endoscopic retrograde cholangiopancreatography (ERCP). Catheter introduction through the papillary ostium fails in 5% to 20% of the patients[1,2]. Several alternatives can be used for difficult cases, such as double-guidewire, pancreatic stent, rendezvous, precut papillotomy, transpancreatic sphincterotomy and papillary fistulotomy (PF) techniques. Acute pancreatitis after ERCP is the most feared complication. It is also one of the most frequent, with an incidence of 1% up to 10% or more, and a mortality of 0.1%-1%[3].

Selective cannulation of the biliary tract, thereby avoiding the pancreatic duct, can curb the mechanisms that trigger pancreatitis, and therefore prevent its occurrence. The precut sphincterotomy has been identified as an independent risk factor of postERCP pancreatitis (PEP). It is unclear whether prolonged cannulation attempts, or precut incisions are to blame. Studies suggest that an early precut is a protective factor, compared to persistent attempts at cannulation[4,5]. However, all protocols that found a lower risk of PEP with a precut technique were performed at specialized centers, and the use of pancreatic stents was limited and inconsistent.

There are few investigations in which the precut and PF techniques were initially employed, to access the biliary tract[6-8]. The PF technique is based on accessing the bile duct far from the pancreatic duct, by sectioning the papilla proximally, and thus avoiding the ostium (proximal half of the papilla). PF was initially described by Osnes *et al*[9]. These authors observed a spontaneous choledochoduodenal fistula during ERCP. Contrast injection through the fistula detected bile duct stones. After enlargement of the fistula with a diathermic snare, the patients were observed for a few days with the spontaneous exit of the stones. Sakai *et al*[10] reported a pancreatitis occurrence rate of 7.6% in 2001, particularly in the setting of previous manipulation of the papilla, and trauma to the pancreatic duct, after several frustrated attempts at biliary tract cannulation.

The main objective of this study was to evaluate the success of the PF technique, in the cannulation of the biliary tract. The secondary objective was to assess the enzyme profile and ensuing complications, in comparison with direct cannulation.

MATERIALS AND METHODS

From July 2010 to May 2017, candidates for ERCP due to choledocolithiasis were recruited at Ana Costa Santos Hospital and the Endoscopy Unit of the Clinical Hospital, Faculty of Medicine, University of Sao Paulo. Enrolled patients were randomized for conventional cannulation with a catheter and guidewire (Group Ⅰ) and PF (Group Ⅱ).

Inclusion criteria were adult (both sexes) with choledocholithiasis and diagnosis by abdominal ultrasound, computed tomography (CT), cholangio resonance, or intraoperative cholangiography. Exclusion criteria were Billroth Ⅱ gastrectomy, duodenal obstruction, coagulopathy or anticoagulant use, pregnancy or lactation, acute pancreatitis, myocardial infarction in the last 6 mo, previous papillotomy, or refusal to participate in the study.

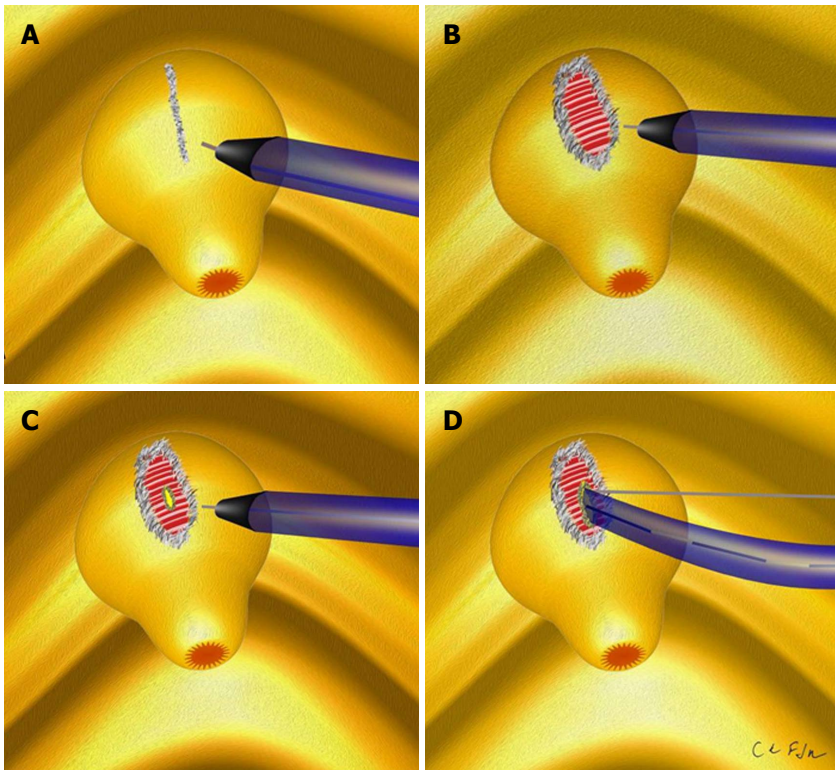

Figure 1 Schematic sequence of papillary fistulotomy. A and B: Dissection of the major papilla; C: Sphincterotome in the bile duct; D: Radiological image.

The protocol was approved by the institutional Ethical Committee, and also registered as a randomized trial at the University of Sao Paulo Registry-MA3: 014/2010 and 0671/09. Informed consent was signed by all participants. Side-view endoscopes (Pentax ED-3670TK, Olympus TJF-160, or Fujinon ED-250XT5) were used during the ERCP. WEM SS-200E, Erbe ICC 200 and ValleyLab Force FX electrosurgical units were employed.

Group I

Cannulation of the papillary ostium was performed using a 4.4 Fr sphincterotome (TRUEtome; Boston Scientific) with a 0.035-inch guidewire (Jagwire; Boston Scientific). A pure cut current (50 watts), applied in short-duration pulses, was adopted to perform papillotomy. A 30-watt pure cut current was indicated for intradiverticular papillae, and the complementation of fistulotomies (Figures 1 and 2).

A difficult cannulation was recognized if it took > 10 min, required > 5 cannulation attempts, or when > 2 pancreatic duct penetrations occurred. Difficult cases were referred to PF. Pancreatic plastic stents were placed in case of prolonged procedure.

Group II

Incision was made on the mucosa, using a needle-knife catheter (MicroKnife XL; Boston Scientific), in distal to proximal direction, aiming at the papillary apex. It involved the proximal two-thirds of the papillary protuberance, and above the papillary orifice (approximately 5 mm far from the ostium). A pure cutting current (30 watts) was used to section the mucosa and the choledochal sphincter. The dissection was stopped when biliary secretion, open bile duct mucosa, or bulging of the bile duct mucosa was identified. The fistula was cannulated into the bile duct with a guidewire and sphincterotome, and it was enlarged by cutting the sphincter, to the limit of the transverse mucosal fold.

The PF procedure was stopped when there were signs of perforation, false route, major bleeding, loss of anatomy, or if cannulation of the bile duct was not achieved within 15 min. In these cases, the procedure was repeated after 5 to 7 d.

Enzymatic abnormalities (serum amylase and lipase) were documented up to 24 h before the examination (T0), as well as 12 h and 24 h after the endoscopic procedure. The diagnosis of acute pancreatitis was based on persistent or worsening abdominal pain 24 h following ERCP and abnormal laboratory data, complemented by imaging methods. An amylase or lipase concentration of more than three times the upper limit of normal was considered diagnostic[11].

Hyperamylasemia was defined as amylase and/or lipase 3 times the upper limit of normal (> 300 U/L), without clinical features of pancreatitis. Inflammatory changes were monitored by serum C-reactive protein, collected at the same times.

A duodenal perforation was defined as gas or contrast accumulation in the retroperitoneum detected by simple X-ray of the abdomen. Endoscopic evidence, and clinical-laboratory findings consistent with bleeding were carefully monitored. These included bloody vomit or stools.

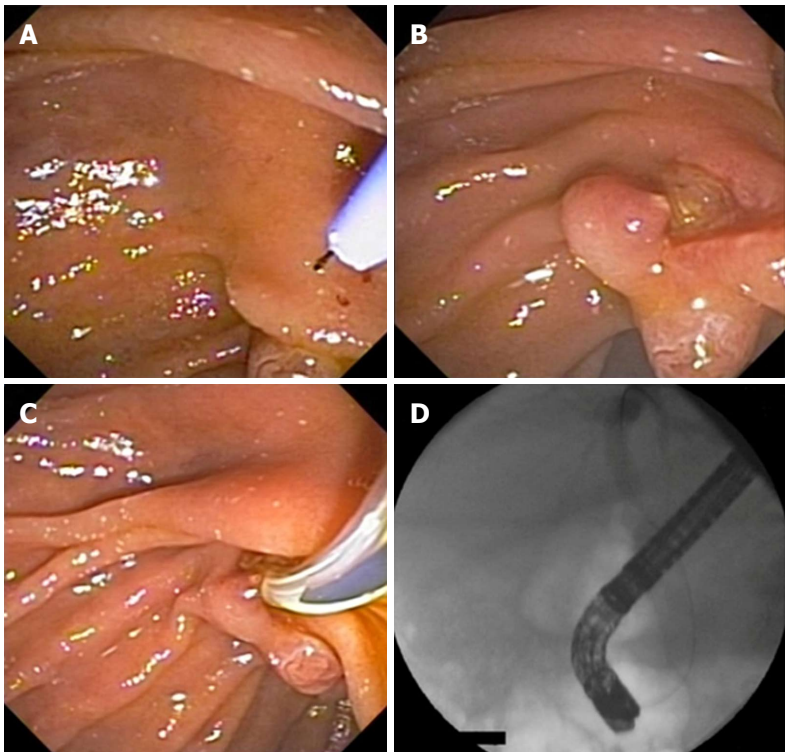

Figure 2 Sequence of papillary fistulotomy. A and B: Dissection of the major papilla; D: Sphincterotome in the bile duct; D: Radiological image.

Whenever the problem was suspected, hemoglobin concentration was serially measured, starting at 12 h after the intervention, and compared with preprocedure values, with hemoglobin drop of 2 g/dL.

Patients were admitted for 24 h after the endoscopic procedure and under fasting condition. Asymptomatic patients without laboratorial or radiological signs of pancreatitis or other complications were discharged after 24 h and contacted by phone call 36 h and 48 h after discharge to ensure there were no symptoms. Any symptomatic patient would be referred to the hospital for clinical and laboratorial assessment. If a complication occurred, the patient remained hospitalized until complete recovery was observed. All complications were managed using a multidisciplinary approach and according to international guidelines, with consensus between the Endoscopist and Surgeon.

Sample size calculation

Calculations were based on similar studies, reporting a biliary cannulation failure rate of 5% to 20%[1,2]. Adopting a 95% confidence interval of 3.65, a total population of 90 patients, and a minimum method failure rate of 2% (total ERCP success of 98% as maximum), 35 patients were deemed necessary per group. For safety, 51 patients were allocated to each group.

Statistical analysis

Analyses were performed with IBM SPSS for Windows version 20.0. The significance level was 5%. Randomization employed sealed envelopes, and descriptive statistics comprised mean ± SD as well as median, minimum and maximum, whenever appropriate. Student's *t* test and Mann-Whitney test were used for comparisons, depending on initial normality assessment. Qualitative characteristics were informed as absolute and relative frequencies, and compared by means of chi-square, Fisher's exact test, and likelihood ratio test[12]. Pancreatic enzyme curves were compared by generalized estimating equations (GEE), with gamma marginal distribution and identity link function, within a first order autoregressive correlation matrix between the evaluation times.

RESULTS

A total of 102 patients were selected and randomized into Group Ⅰ (51 patients) and Group Ⅱ (51 patients). There were no post hoc exclusions. Table 1 demonstrates that the demographic and preliminary clinical findings were comparable ($P > 0.05$).

As informed in Table 2, choledocholithiasis was confirmed in 80.4% and 62.7% of Groups Ⅰ and Ⅱ, respectively ($P = 0.048$). The success rate for biliary duct cannulation was higher in Group Ⅱ (100%) than in Group Ⅰ (76.48%) ($P = 0.0002$). PF was performed in a single session. Dilated intrahepatic and extrahepatic bile ducts, and placement of biliary stents, were not different between the groups ($P > 0.05$). No difference in the risk of pancreatitis could be accounted to either intrahepatic or extrahepatic dilatation.

Intra- or peridiverticular papillae were observed in 15.7% and 3.9% of the populations, respectively ($P = 0.046$). Twelve cannulations (23.5%) were classified

Table 1 Patient characteristics and baseline laboratory tests

Variable	Group Ⅰ, *n* = 51	Group Ⅱ, *n* = 51	Total, *n* = 102	*P* value
Age in yr				0.343[1]
Mean ± σ	57.4 ± 19.3	60.9 ± 18.1	59.1 ± 18.7	
Median (min; max)	56 (19; 91)	64 (22; 95)	58 (19; 95)	
Sex, *n* (%)				> 0.999[2]
Female	33 (64.7)	33 (64.7)	66 (64.7)	
Male	18 (35.3)	18 (35.3)	36 (35.3)	
AST				0.680
Mean ± σ	116.3 ± 143.4	124.3 ± 168.3	120.1 ± 155.1	
Median (min; max)	44 (8; 691)	60 (13; 762)	50 (8; 762)	
ALT				0.873
Mean ± σ	163.6 ± 191.6	154.1 ± 169.3	159 ± 180.4	
Median (min; max)	83 (9; 776)	104 (11; 662)	90 (9; 776)	
AP				0.585
Mean ± σ	267.8 ± 329.7	301.9 ± 320.4	284.3 ± 323.9	
Median (min; max)	153.5 (8; 1567)	173 (32; 1320)	162 (8; 1567)	
GGT				0.821
Mean ± σ	532 ± 454.3	543.4 ± 578.2	537.5 ± 515.1	
Median (min; max)	466.5 (39; 1684)	284 (11; 2269)	382 (11; 2269)	
Total bilirubin				0.994
Mean ± σ	4.1 ± 4.9	5.3 ± 7.5	4.7 ± 6.3	
Median (min; max)	2 (0.1; 23.4)	2.1 (0.2; 29.2)	2.1 (0.1; 29.2)	
Direct bilirubin				0.683
Mean ± σ	3.6 ± 4.4	4.2 ± 6.3	3.9 ± 5.4	
Median (min; max)	1.6 (0.1; 20.9)	1.1 (0.1; 22.4)	1.5 (0.1; 22.4)	

[1]Student's *t*-test; [2]Chi-square test, Mann-Whitney test. AST: Aspartate transaminase; ALT: Alanine transaminase; AP: Alkaline phosphatase; GGT: Gamma-glutamyl transpeptidase; σ: Standard deviation.

Table 2 Endoscopic retrograde cholangiopancreatography findings and complications *n* (%)

Variable	Group Ⅰ, *n* = 51	Group Ⅱ, *n* = 51	Total, *n* = 102	*P* value
Choledocolithiasis				0.048
No	10 (19.6)	19 (37.3)	29 (28.4)	
Yes	41 (80.4)	32 (62.7)	73 (71.6)	
Intrahepatic dilatation				0.6572
No	36 (70.6)	38 (74.5)	74 (72.6)	
Yes	15 (29.4)	13 (25.5)	28 (27.4)	
Extrahepatic dilatation				0.5512
No	25 (49.02)	22 (43.1)	47 (46.1)	
Pancreatitis	2 (3.9)	1 (1.9))	3 (2.9)	1[1]
Yes	26 (50.98)	29 (56.9)	55 (53.9)	
Pancreatitis	3	0	3 (2.9)	0.0991[1]
Intra- or peridiverticular papilla				0.046
No	43 (84.3)	49 (96.1)	92 (90.2)	
Yes	8 (15.7)	2 (3.9)	10 (9.8)	
Prosthesis				0.236
No	42 (82.4)	37 (72.6)	79 (77.5)	
Yes	9 (17.6)	14 (27.4)	23 (22.5)	
Biliary prosthesis				0.463
No	42 (82.4)	39 (76.5)	81(79.4)	
Yes	9 (17.6)	12 (23.5)	21 (20.6)	
Cholangitis				0.678[1]
No	49 (96.1)	47 (92.2)	96 (94.1)	
Yes	2 (3.9)	4 (7.9)	6 (5.9)	
Biliary access				
No	12 (23.5)	0		0.0002[1]
Yes	39 (76.5)	51 (100)		
Complications,pancreatitis, bleeding or perforation				0.0537[1]
No	44 (86.3)	50 (98)	94 (92.2)	
Yes	7 (13.7)	1 (2)	8 (7.8)	
Pancreatitis	5	1		
Perforation	2	1		
Bleeding	0	0		

Data are presented as *n* (%). [1]Fisher's exact test; Chi-square test.

Table 3 Endoscopic retrograde cholangiopancreatography findings and complications according to group and subgroup

Variable	Groups			Total, *n* = 102	*P* value
	Group Ⅰ, *n* = 51		Group Ⅱ, *n* = 51		
	GWC, *n* = 39	Difficult cannulation, *n* = 12			
Complications, pancreatitis, bleeding or perforation					0.062
No	34 (87.2)	10 (83.3)	50 (98)	94 (92.2)	
Yes	5 (12.8)	2 (16.7)	1 (2)	8 (7.8)	
Number of cannulations					< 0.001[1]
Mean ± σ	3.3 ± 1.9	7.5 ± 2.8		4.3 ± 2.8	
Median (min.; max.)	3 (1; 10)	8.5 (3; 10)		3 (1; 10)	

[1]Mann-Whitney test, Likelihood ratio test. GWC: Guidewire cannulation; σ: Standard deviation.

Table 4 Lipase, amylase and C-reactive protein measurements at the different evaluation times

Variable	Group Ⅰ, *n* = 51			Group Ⅱ, *n* = 51			*P* value	*P* value for time	*P* value for interaction
	Pre	12 h	24 h	Pre	12 h	24 h			
Lipase							0.006	< 0.001	0.026
mean ± σ	69.4 ± 102.1	439.0 ± 1064.8	199.5 ± 528.3	41.4 ± 37.2	100.6 ± 183.3	85.2 ± 189.1			
median (min; max)	38 (9; 611)	52 (10; 5014)	48 (8; 3000)	32 (0; 239)	42.5 (8; 968)	40 (5; 1334)			
Amylase							0.003	< 0.001	0.013
mean ± σ	76.4 ± 57.8	453.5 ± 1287.4	304.0 ± 979.3	59.6 ± 36.2	98.1 ± 94.3	85.8 ± 102.6			
median (min; max)	59 (12; 310)	80 (14; 7900)	70 (13; 6721)	50 (14; 236)	69 (21; 624)	67.5 (12; 732)			
C-reactive protein							0.189	0.070	0.353
mean ± σ	126.6 ± 539.7	49.5 ± 89.7	45.4 ± 70.5	58.6 ± 104.8	41.4 ± 62.0	38.8 ± 52.9			
median (min; max)	11.1 (0.1; 3813)	15.5 (0.3; 486.1)	19.16 (0.5; 340.9)	12 (0.2; 549)	13.8 (0.3; 271)	16.6 (0.5; 223.1)			

GEE with gamma distribution and identity link function. Not all patients were evaluated at all times. GEE: Generalized estimating equations; σ: Standard deviation.

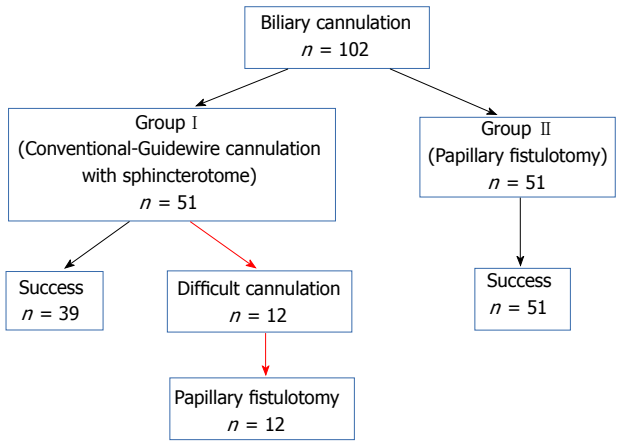

Figure 3 Flowchart showing the sequence of procedures performed in the study.

as difficult, thus migrating to the PF technique (Figure 3). Groups Ⅰ and Ⅱ had complication rates of 13.7% and 2.0%, respectively, which barely failed to reach significance (P = 0.0597). Two perforations and five cases of pancreatitis were observed in the first group, compared to a single case of retroperitoneal perforation and pancreatitis in the second one.

Table 3 reveals that the number of cannulations, as expected, was significantly different in the difficult cannulation group (P < 0.001), unlike ERCP findings, stent placement or complications (P > 0.05).

In Table 4 it can be appreciated that both lipase and amylase differed between the groups and over time (P = 0.026 and P = 0.013, respectively). In contrast, no discrepancy for C-reactive protein was detected regarding groups (P = 0.189) or time (P = 0.07).

Figures 4-6 depict the amylase and lipase elevations in Group Ⅰ patients. C-reactive protein, as alluded to, failed to exhibit discriminant patterns.

DISCUSSION

Pancreatitis is the most frequent complication of ERCP, occurring in as many as 15.1% of the patients[6-8,13,14]. It is associated with considerable morbidity and mortality. Precut techniques have been associated with a high risk of PEP in previous studies[7,8,15-17].

A difficult cannulation is an independent risk factor[18,19]. The failure rate of primary biliary tract cannulation, with the use of a sphincterotome, was calculated as 2.5%-24% without a guidewire[20-23] and 1.5%-10%[21,23,24] adopting the wire. The American Society for Gastrointestinal Endoscopy benchmark for cannulation success during ERCP procedures of low to moderate complexity is > 90% for all indications[25].

In this study, the primary success rate was 76.5%, with 9.8% of PEP. Difficult cannulation occurred in 12 patients, yet access was achieved *via* PF in all these individuals. The high failure rate (23.5%) may be explained by the participation of fellows, who are less experienced, thus making additional attempts by endoscopists with greater expertise required.

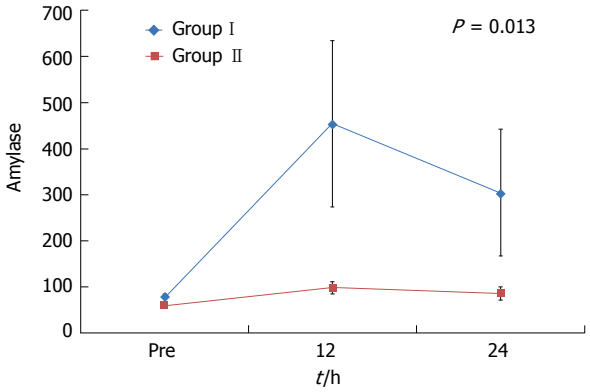

Figure 4 Amylase profile after the procedure.

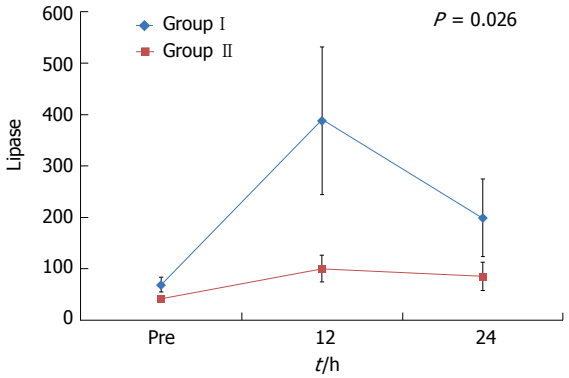

Figure 5 Lipase profile for the two groups.

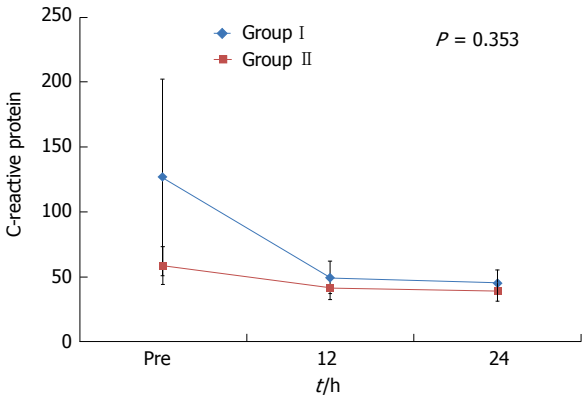

Figure 6 Evolution of C-reactive protein.

Nevertheless, papillary trauma eventually inflicted during the first intervention may hinder subsequent access, thus compromising the overall success rate.

Common bile duct stones were not found in all cases during ERCP, possibly on account of the long period that had elapsed since the original diagnosis in the primary care institution. It is important to mention that per protocol, PF was conducted directly, without prior manipulation by conventional techniques. Cannulation of the bile duct using PF was accomplished in all patients in Group Ⅱ. Three previous studies with a similar design displayed 89.3%-96.5% success rates for fistulotomy[26-28]. In the control group (conventional technique), the corresponding values were 70.6% and 88%[26-28].

The mean diameter of the common bile duct in this experience was 8.7 mm (5-18.2 mm). Sakai *et al*[10] in 2001, suggested that PF be reserved mainly for patients with a dilated common bile duct. Jin *et al*[27] concluded in 2016, based on 55 interventions, that a bile duct < 9 mm was a risk factor. Yet Khatibian *et al*[26] reported in 2008 that the diameter of the common bile duct was not relevant for need of PF.

In the current series, PF (Group Ⅱ and Failures) was performed in 28 of 63 patients (44.4%; P = 0.834); for each, being performed through the common bile duct without dilatation. No difference in the risk of pancreatitis emerged when considering the caliber of the intra- and extrahepatic biliary tracts. Bile duct stones could not be removed in the first attempt in 20.8% of the cases, due to large size; therefore, in these cases, a biliary stent was placed.

Hyperamylasemia was observed in 2 patients in Group Ⅰ (P = 0.49). Transient asymptomatic elevations in amylase, lipase, or both, range from 0 to 64% in the literature[29-31]. Asymptomatic hyperamylasemia, defined as amylase levels > 5 times the upper limit at 24 h after ERCP, has been reported in approximately 27% of the cases[32].

In our study, the number of cannulation attempts significantly correlated with increased lipase and amylase levels, at 12 h and 24 h after the procedure. In a series of 907 patients, the rates of PEP were 0.6%, 3.1%, 6.1% and 11.9% following one, two, three to four, and more than five primary cannulation attempts that led to success, respectively. PEP risk increased to 11.5% if the primary cannulation method failed[19]. In our study, PEP occurred following the guidewire cannulation (GWC) technique in 5 patients (9.8%), of which 2 (3.9%) exhibited a difficult papillary access, which was only achieved by means of PF.

No significant increase in pancreatic enzymes was observed, and the incidence of PEP was not greater in the group that underwent PF as the initial procedure; neither did the 12 patients with PF as a rescue procedure exhibit a different pattern. This demonstrates the safety of PF, whenever performed or supervised by experienced physicians. In 2016, Zagalsky *et al*[33] compared early precut (PCP) techniques and use of a pancreatic duct stent in 101 patients who suffered difficult cannulations. The success rates of biliary cannulation (98% and 96%), and the occurrence of PEP (4% and 3.92%) were similar between the early PCP and stent groups, respectively. Two perforations and bleeds occurred in the early PCP group, which also demonstrates the safety of the procedure compared to standard PEP prevention technique after a failed GWC.

Other recent studies have shown that precut techniques lead to an increased rate of successful deep biliary tract access and that their early use by experienced endoscopists results in a decrease in PEP[4,27,34]. Weerth *et al*[2] compared primary PCP and GWC for bile duct access and reported a success rate at the first attempt of 100% and 71%, respectively.

They observed mild to moderate PEP in 2.1% and 2.9% ($P > 0.05$), after primary PCP or GWC, respectively. Only 1 patient (in the GWC group) suffered from postpapillotomy bleeding. In our experience, a single patient presented a retroperitoneal perforation and pancreatitis in Group Ⅱ, both of which were conservatively managed.

There were two perforations (3.9%) in Group Ⅰ, and the one (1.9%) in Group Ⅱ already alluded to, which were always conservatively treated. No bleeding was observed. The negligible incidence of bleeding is consistent with previous precut studies (0-3.4%)[2,17,26,28,35]. In regards to perforation (0-1.8%), our results are also quite acceptable[2,17,26,28,35].

In conclusion, PF was more effective than GWC, and it was associated with a lower profile of amylase and lipase, as the routine endoscopic access to the biliary tree, including difficult cases. Complications were similar in both groups.

ARTICLE HIGHLIGHTS

Research background

Successfully cannulating the biliary tract is important in the diagnosis and treatment of biliopancreatic diseases with endoscopic retrograde cholangiopancreatography (ERCP), but it can be associated with severe complications and mortality.

Research motivation

The number of papers regarding comparison between conventional cannulation *versus* fistulotomy is small. Our study is a well-designed approach in its matter.

Research objectives:

To compare the cannulation success, biochemical profile, and complications of the papillary fistulotomy technique *versus* catheter and guidewire standard access.

Research methods

Patients were prospectively randomized into two groups: cannulation with a catheter and guidewire (Group Ⅰ) and papillary fistulotomy (Group Ⅱ). Amylase, lipase and C-reactive protein at T0 as well as 12 h and 24 h after ERCP, and complications (pancreatitis, bleeding, perforation) were recorded. Comparison was made of the cannulation success, biochemical profile and complications of the papillary fistulotomy technique *vs* catheter and guidewire standard access.

Research results

We included 102 patients, and Groups Ⅰ and Ⅱ had 51 patients each. The successful cannulation rates were 76.5% and 100%, respectively ($P = 0.0002$). Twelve patients (23.5%) in Group Ⅰ had a difficult cannulation and underwent fistulotomy, which led to successful secondary biliary access (Failure Group). The complication rate was 13.7% (2 perforations and 5 mild pancreatitis) in Group Ⅰ *versus* 2.0% (1 patient with perforation and pancreatitis) in Group Ⅱ ($P = 0.0597$).

Research conclusions

Papillary fistulotomy was more effective than guidewire cannulation, and it was associated with a lower profile of amylase and lipase. Complications were similar in both groups.

Research perspectives

The fistulotomy demonstrated safety similar to conventional cannulation and less local trauma into the ampulla, according to the levels of the amylase, lipase and C-reactive protein.

REFERENCES

1 **Abu-Hamda EM**, Baron TH, Simmons DT, Petersen BT. A retrospective comparison of outcomes using three different precut needle knife techniques for biliary cannulation. *J Clin Gastroenterol* 2005; **39**: 717-721 [PMID: 16082283]

2 **de Weerth A**, Seitz U, Zhong Y, Groth S, Omar S, Papageorgiou C, Bohnacker S, Seewald S, Seifert H, Binmoeller KF, Thonke F, Soehendra N. Primary precutting versus conventional over-the-wire sphincterotomy for bile duct access: a prospective randomized study. *Endoscopy* 2006; **38**: 1235-1240 [PMID: 17163325 DOI: 10.1055/s-2006-944962]

3 **Freeman ML**, Guda NM. ERCP cannulation: a review of reported techniques. *Gastrointest Endosc* 2005; **61**: 112-125 [PMID: 15672074]

4 **Sundaralingam P**, Masson P, Bourke MJ. Early Precut Sphincterotomy Does Not Increase Risk During Endoscopic Retrograde Cholangiopancreatography in Patients With Difficult Biliary Access: A Meta-analysis of Randomized Controlled Trials. *Clin Gastroenterol Hepatol* 2015; **13**: 1722-1729.e2 [PMID: 26144018 DOI: 10.1016/j.cgh.2015.06.035]

5 **Mariani A**, Di Leo M, Giardullo N, Giussani A, Marini M, Buffoli F, Cipolletta L, Radaelli F, Ravelli P, Lombardi G, D'Onofrio V, Macchiarelli R, Iiritano E, Le Grazie M, Pantaleo G, Testoni PA. Early precut sphincterotomy for difficult biliary access to reduce post-ERCP pancreatitis: a randomized trial. *Endoscopy* 2016; **48**: 530-535 [PMID: 26990509 DOI: 10.1055/s-0042-102250]

6 **Freeman ML**, Nelson DB, Sherman S, Haber GB, Herman ME, Dorsher PJ, Moore JP, Fennerty MB, Ryan ME, Shaw MJ, Lande JD, Pheley AM. Complications of endoscopic biliary sphincterotomy. *N Engl J Med* 1996; **335**: 909-918 [PMID: 8782497 DOI: 10.1056/NEJM199609263351301]

7 **Mavrogiannis C**, Liatsos C, Romanos A, Petoumenos C, Nakos A, Karvountzis G. Needle-knife fistulotomy versus needle-knife precut papillotomy for the treatment of common bile duct stones. *Gastrointest Endosc* 1999; **50**: 334-339 [PMID: 10462652 DOI: 10.1053/ge.1999.v50.98593]

8 **Zhou W**, Li Y, Zhang Q, Li X, Meng W, Zhang L, Zhang H, Zhu K, Zhu X. Risk factors for postendoscopic retrograde cholangiopancreatography pancreatitis: a retrospective analysis of 7,168 cases. *Pancreatology* 2011; **11**: 399-405 [PMID: 21894057 DOI: 10.1016/S1424-3903(11)80094-3]

9 **Osnes M**, Kahrs T. Endoscopic choledochoduodenostomy for choledocholithiasis through choledochoduodenal fistula. *Endoscopy* 1977; **9**: 162-165 [PMID: 913369 DOI: 10.1055/s-0028-1098510]

10 **Sakai P**, Artifon ELA, Maluf Filho F. Fistulopapilotomia Endoscópica: Uma Alternativa à Papila de Difícil Cateterização. *GED* 2001; **20**: 208-212

11 **Lerch MM**. Classifying an unpredictable disease: the revised Atlanta classification of acute pancreatitis. *Gut* 2013; **62**: 2-3 [PMID: 23220948 DOI: 10.1136/gutjnl-2012-303724]

12 **Kirkwood B,** JAC S. Essential Medical Statistics. 2nd ed. Massachusetts, United States: Blackwell Science; 2006

13 **Cheng CL**, Sherman S, Watkins JL, Barnett J, Freeman M, Geenen J, Ryan M, Parker H, Frakes JT, Fogel EL, Silverman WB, Dua KS, Aliperti G, Yakshe P, Uzer M, Jones W, Goff J, Lazzell-Pannell L, Rashdan A, Temkit M, Lehman GA. Risk factors for post-ERCP pancreatitis: a prospective multicenter study. *Am J Gastroenterol* 2006; **101**: 139-147 [PMID: 16405547 DOI: 10.1111/j.1572-0241.2006.00380.x]

14 **Bailey AA**, Bourke MJ, Williams SJ, Walsh PR, Murray MA, Lee EY, Kwan V, Lynch PM. A prospective randomized trial of cannulation technique in ERCP: effects on technical success and post-ERCP pancreatitis. *Endoscopy* 2008; **40**: 296-301 [PMID: 18389448 DOI: 10.1055/s-2007-995566]

15 **Bailey AA**, Bourke MJ, Kaffes AJ, Byth K, Lee EY, Williams SJ. Needle-knife sphincterotomy: factors predicting its use and the

relationship with post-ERCP pancreatitis (with video). *Gastrointest Endosc* 2010; **71**: 266-271 [PMID: 20003969 DOI: 10.1016/j.gie.2009.09.024]
16 **Halttunen J**, Keränen I, Udd M, Kylänpää L. Pancreatic sphincterotomy versus needle knife precut in difficult biliary cannulation. *Surg Endosc* 2009; **23**: 745-749 [PMID: 18649101 DOI: 10.1007/s00464-008-0056-0]
17 **O'Connor HJ**, Bhutta AS, Redmond PL, Carruthers DA. Suprapapillary fistulosphincterotomy at ERCP: a prospective study. *Endoscopy* 1997; **29**: 266-270 [PMID: 9255529 DOI: 10.1055/s-2007-1004187]
18 **Freeman ML**, DiSario JA, Nelson DB, Fennerty MB, Lee JG, Bjorkman DJ, Overby CS, Aas J, Ryan ME, Bochna GS, Shaw MJ, Snady HW, Erickson RV, Moore JP, Roel JP. Risk factors for post-ERCP pancreatitis: a prospective, multicenter study. *Gastrointest Endosc* 2001; **54**: 425-434 [PMID: 11577302 DOI: 10.1067/mge.2001.117550]
19 **Halttunen J**, Meisner S, Aabakken L, Arnelo U, Grönroos J, Hauge T, Kleveland PM, Nordblad Schmidt P, Saarela A, Swahn F, Toth E, Mustonen H, Löhr JM. Difficult cannulation as defined by a prospective study of the Scandinavian Association for Digestive Endoscopy (SADE) in 907 ERCPs. *Scand J Gastroenterol* 2014; **49**: 752-758 [PMID: 24628493 DOI: 10.3109/00365521.2014.894120]
20 **Laasch HU**, Tringali A, Wilbraham L, Marriott A, England RE, Mutignani M, Perri V, Costamagna G, Martin DF. Comparison of standard and steerable catheters for bile duct cannulation in ERCP. *Endoscopy* 2003; **35**: 669-674 [PMID: 12929062 DOI: 10.1055/s-2003-41515]
21 **Lella F**, Bagnolo F, Colombo E, Bonassi U. A simple way of avoiding post-ERCP pancreatitis. *Gastrointest Endosc* 2004; **59**: 830-834 [PMID: 15173796]
22 **Schwacha H**, Allgaier HP, Deibert P, Olschewski M, Allgaier U, Blum HE. A sphincterotome-based technique for selective transpapillary common bile duct cannulation. *Gastrointest Endosc* 2000; **52**: 387-391 [PMID: 10968855 DOI: 10.1067/mge.2000.107909]
23 **Artifon EL**, Sakai P, Cunha JE, Halwan B, Ishioka S, Kumar A. Guidewire cannulation reduces risk of post-ERCP pancreatitis and facilitates bile duct cannulation. *Am J Gastroenterol* 2007; **102**: 2147-2153 [PMID: 17581267 DOI: 10.1111/j.1572-0241.2007.01378.x]
24 **Zhou PH**, Yao LQ, Xu MD, Zhong YS, Gao WD, He GJ, Zhang YQ, Chen WF, Qin XY. Application of needle-knife in difficult biliary cannulation for endoscopic retrograde cholangiopancreatography. *Hepatobiliary Pancreat Dis Int* 2006; **5**: 590-594 [PMID: 17085348]
25 **Adler DG**, Lieb JG 2nd, Cohen J, Pike IM, Park WG, Rizk MK, Sawhney MS, Scheiman JM, Shaheen NJ, Sherman S, Wani S. Quality indicators for ERCP. *Gastrointest Endosc* 2015; **81**: 54-66 [PMID: 25480099 DOI: 10.1016/j.gie.2014.07.056]
26 **Khatibian M**, Sotoudehmanesh R, Ali-Asgari A, Movahedi Z, Kolahdoozan S. Needle-knife fistulotomy versus standard method for cannulation of common bile duct: a randomized controlled trial. *Arch Iran Med* 2008; **11**: 16-20 [PMID: 18154417]
27 **Jin YJ**, Jeong S, Lee DH. Utility of needle-knife fistulotomy as an initial method of biliary cannulation to prevent post-ERCP pancreatitis in a highly selected at-risk group: a single-arm prospective feasibility study. *Gastrointest Endosc* 2016; **84**: 808-813 [PMID: 27102829 DOI: 10.1016/j.gie.2016.04.011]
28 **Ayoubi M**, Sansoè G, Leone N, Castellino F. Comparison between needle-knife fistulotomy and standard cannulation in ERCP. *World J Gastrointest Endosc* 2012; **4**: 398-404 [PMID: 23125897 DOI: 10.4253/wjge.v4.i9.398]
29 **Tanaka R**, Itoi T, Sofuni A, Itokawa F, Kurihara T, Tsuchiya T, Tsuji S, Ishii K, Ikeuchi N, Umeda J, Tonozuka R, Honjo M, Mukai S, Moriyasu F. Is the double-guidewire technique superior to the pancreatic duct guidewire technique in cases of pancreatic duct opacification? *J Gastroenterol Hepatol* 2013; **28**: 1787-1793 [PMID: 23800118 DOI: 10.1111/jgh.12303]
30 **Nishino T**, Toki F, Oyama H, Shiratori K. More accurate prediction of post-ercp pancreatitis by 4-h serum lipase levels than amylase levels. *Dig Endosc* 2008; **20**: 169-177
31 **Dumonceau JM**, Devière J, Cremer M. A new method of achieving deep cannulation of the common bile duct during endoscopic retrograde cholangiopancreatography. *Endoscopy* 1998; **30**: S80 [PMID: 9826155]
32 **Testoni PA**, Testoni S, Giussani A. Difficult biliary cannulation during ERCP: how to facilitate biliary access and minimize the risk of post-ERCP pancreatitis. *Dig Liver Dis* 2011; **43**: 596-603 [PMID: 21377432 DOI: 10.1016/j.dld.2011.01.019]
33 **Zagalsky D**, Guidi MA, Curvale C, Lasa J, de Maria J, Ianniccillo H, Hwang HJ, Matano R. Early precut is as efficient as pancreatic stent in preventing post-ERCP pancreatitis in high-risk subjects - A randomized study. *Rev Esp Enferm Dig* 2016; **108**: 258-562 [PMID: 27604474 DOI: 10.17235/reed.2016.4348/2016]
34 **Cennamo V**, Fuccio L, Zagari RM, Eusebi LH, Ceroni L, Laterza L, Fabbri C, Bazzoli F. Can early precut implementation reduce endoscopic retrograde cholangiopancreatography-related complication risk? Meta-analysis of randomized controlled trials. *Endoscopy* 2010; **42**: 381-388 [PMID: 20306386 DOI: 10.1055/s-0029-1243992]
35 **Huibregtse K**, Katon RM, Tytgat GN. Precut papillotomy via fine-needle knife papillotome: a safe and effective technique. *Gastrointest Endosc* 1986; **32**: 403-405 [PMID: 3803839]

P- Reviewer: Kahraman A, Ker CG **S- Editor**: Wang XJ
L- Editor: Filipodia **E- Editor**: Huang Y

World Journal of Gastroenterology

Submit a Manuscript: http://www.f6publishing.com

World J Gastroenterol 2018 April 28; 24(16): 1812-1824

DOI: 10.3748/wjg.v24.i16.1812

ISSN 1007-9327 (print) ISSN 2219-2840 (online)

META-ANALYSIS

Compared efficacy of preservation solutions on the outcome of liver transplantation: Meta-analysis

Ágnes Lilla Szilágyi, Péter Mátrai, Péter Hegyi, Eszter Tuboly, Daniella Pécz, András Garami, Margit Solymár, Erika Pétervári, Márta Balaskó, Gábor Veres, László Czopf, Bastian Wobbe, Dorottya Szabó, Juliane Wagner, Petra Hartmann

Ágnes Lilla Szilágyi, Eszter Tuboly, Daniella Pécz, Petra Hartmann, Institute of Surgical Research, University of Szeged, Szeged H-6720, Hungary

Péter Mátrai, Institute of Bioanalysis, University of Pécs, Pécs H-7624, Hungary

Péter Hegyi, András Garami, Margit Solymár, Erika Pétervári, Márta Balaskó, Institute for Translational Medicine and First Department of Medicine, University of Pécs, Pécs H-7624, Hungary

Péter Hegyi, MTA-SZTE Translational Gastroenterology Research Group, Szeged H-6720, Hungary

Péter Hegyi, János Szentágothai Research Center, University of Pécs, Pécs H-7624, Hungary

Gábor Veres, 1st Department of Paediatrics, University of Semmelweis, Budapest H-1085, Hungary

László Czopf, Bastian Wobbe, Dorottya Szabó, Juliane Wagner, Department of Cardiology, 1st Department of Medicine, University of Pécs, Pécs H-7624, Hungary

ORCID number: Ágnes Lilla Szilágyi (0000-0003-1584-5906); Péter Mátrai (0000-0001-5144-0733); Péter Hegyi (0000-0002-4333-265X); Eszter Tuboly (0000-0003-0333-6952); Daniella Pécz (0000-0002-0214-8389); András Garami (0000-0003-2493-0571); Margit Solymár (0000-0001-6667-6263); Erika Pétervári (0000-0002-3673-8491); Márta Balaskó (0000-0003-4377-9758); Gábor Veres (0000-0002-0911-1941); László Czopf (0000-0001-9565-0732); Bastian Wobbe (0000-0002-7278-1470); Dorottya Szabó (0000-0001-7351-2929); Juliane Wagner (0000-0002-7762-0377); Petra Hartmann (0000-0002-4746-9792).

Author contributions: Szilágyi ÁL, Garami A, Solymár M, Pétervári E, Balaskó M and Hartmann P designed the study; Szilágyi ÁL, Tuboly E, Pécz D, Veres G, Szabó D and Wagner J collected and analyzed the data; Mátrai P performed the statistical analysis; Hartmann P drafted and wrote the manuscript; Wobbe B performed language editing; Hegyi P and Czopf L revised the manuscript critically for intellectual content; and all the authors provided intellectual input for the study and approved the final version of the manuscript.

Supported by grants from the National Research Development and Innovation Office, NKFI K120232; Hungarian Science Research Fund, No. GINOP 2.3.2-15-2016-00015 and No. EFOP -3.6.2-16-2017-00006; and New National Excellence Program of the Ministry of Human Capacities, No. UNKP-17-4.

Conflict-of-interest statement: None of the authors has any conflict of interests related to this manuscript.

Data sharing statement: No additional data are available.

Manuscript source: Unsolicited manuscript

Correspondence to: Petra Hartmann, MD, PhD, Assistant Professor, Institute of Surgical Research, University of Szeged, Szőkefalvi-Nagy Béla street 6, Szeged H-6720, Hungary. hartmann.petra@med.u-szeged.hu
Telephone: +36-62-545103
Fax: +36-62-545743

Received: January 31, 2018
Peer-review started: January 31, 2018
First decision: February 24, 2018
Revised: April 2, 2018
Accepted: April 9, 2018
Article in press: April 9, 2018

Published online: April 28, 2018

Abstract

AIM

To compare the effects of the four most commonly used preservation solutions on the outcome of liver transplantations.

METHODS

A systematic literature search was performed using MEDLINE, Scopus, EMBASE and the Cochrane Library databases up to January 31st, 2017. The inclusion criteria were comparative, randomized controlled trials (RCTs) for deceased donor liver (DDL) allografts with adult and pediatric donors using the gold standard University of Wisconsin (UW) solution or histidine-tryptophan-ketoglutarate (HTK), Celsior (CS) and Institut Georges Lopez (IGL-1) solutions. Fifteen RCTs (1830 livers) were included; the primary outcomes were primary non-function (PNF) and one-year post-transplant graft survival (OGS-1).

RESULTS

All trials were homogenous with respect to donor and recipient characteristics. There was no statistical difference in the incidence of PNF with the use of UW, HTK, CS and IGL-1 (RR = 0.02, 95%CI: 0.01-0.03, P = 0.356). Comparing OGS-1 also failed to reveal any difference between UW, HTK, CS and IGL-1 (RR = 0.80, 95%CI: 0.80-0.80, P = 0.369). Two trials demonstrated higher PNF levels for UW in comparison with the HTK group, and individual studies described higher rates of biliary complications where HTK and CS were used compared to the UW and IGL-1 solutions. However, the meta-analysis of the data did not prove a statistically significant difference: the UW, CS, HTK and IGL-1 solutions were associated with nearly equivalent outcomes.

CONCLUSION

Alternative solutions for UW yield the same degree of safety and effectiveness for the preservation of DDLs, but further well-designed clinical trials are warranted.

Key words: Liver transplantation; Preservation solution; Primary non-function; One-year post-transplant graft survival; Systematic review; Meta-analysis

Core tip: The University of Wisconsin (UW) solution is the gold standard for static cold storage in liver transplantation. Numerous clinical trials have investigated the potential benefit of the most frequently used alternative solutions, histidine-tryptophan-ketoglutarate, Celsior and Institut Georges Lopez, but their results have been variable. This meta-analysis has reviewed the current evidence and found no significant differences in risk of transplant outcomes: primary non-function (RR = 0.02, 95%CI: 0.01-0.03, P = 0.36) and one-year post-transplant graft survival (RR = 0.80, 95%CI: 0.80-0.80, P = 0.37) between UW and the other examined solutions.

Szilágyi ÁL, Mátrai P, Hegyi P, Tuboly E, Pécz D, Garami A, Solymár M, Pétervári E, Balaskó M, Veres G, Czopf L, Wobbe B, Szabó D, Wagner J, Hartmann P. Compared efficacy of preservation solutions on the outcome of liver transplantation: Meta-analysis. *World J Gastroenterol* 2018; 24(16): 1812-1824 Available from: URL: http://www.wjgnet.com/1007-9327/full/v24/i16/1812.htm DOI: http://dx.doi.org/10.3748/wjg.v24.i16.1812

INTRODUCTION

Organ transplantation is inevitably associated with ischemia-reperfusion (IR) injury; several methods have thus been formulated to reduce IR-related morbidity and to maintain the viability of tissues[1,2]. The introduction of the University of Wisconsin (UW) solution in 1987 has led to significant clinical progress and increased cold ischemic tolerance and has become the most widely used, gold standard preservation solution for liver transplantation[3]. Nevertheless, in spite of the clinical success, it has many potential shortcomings (Table 1). UW is an intracellular colloid solution with high potassium and low sodium concentration that inhibits activity of Na-K-adenosine triphosphatase and the resultant depletion of adenosine triphosphate stores. However, its low sodium content promotes the accumulation of calcium during ischemia, resulting in calcium-dependent endothelial dysfunction in renal glomeruli and in bile ducts during reperfusion[4,5]. Additionally, the high potassium increases the risk for hyperkalemia-induced cardiac arrest, requiring liver flushing before reperfusion. Moreover, low temperature storage in the container bag may result in the formation of adenosine crystals[6]. Therefore, the use of UW has been intensively challenged, and alternative solutions with potentially more benefits were developed. Among them, histidine-tryptophan-ketoglutarate (HTK), Celsior (CS) and Institut George Lopez (IGL-1) are the most commonly used preservation solutions in transplantation centers[7].

A number of prospective trials have investigated the effects of these preservation solutions on liver transplant outcomes over many years with variable results. HTK, also known as Bretschneider's solution, is mostly used in European liver transplantation centers, especially in Germany. It has very low viscosity, which is based on a histidine buffer system with two additional substrates (tryptophan and ketoglutarate). A lower index of viscosity allows faster cooling and, theoretically, an

Table 1 Ingredients in the investigated preservation solutions

	UW	HTK	CS	IGL-1
HES	0.25	-	-	-
PEG-35	-	-	-	0.03
Na^+	27	15	100	120
K^+	125	10	15	25

Concentrations are expressed in mmol/L. HES: Hydroxyethyl starch; PEG-35: Polyethylene glycol 35 kDa.

improved washout of blood cells from the graft[8]. UW was first compared to HTK in a randomized fashion in liver transplantation in 1994, and these solutions were found to have similar outcomes in terms of initial non-function of the graft and 30-mo patient survival[9]. However, more recent studies with a larger liver transplant population from Europe and North America have provided different conclusions[10,11].

CS has initially been applied in heart transplantation and then for kidney and liver transplantation as well, with the idea of providing preservation for all organs with a single solution[12]. The use of CS is based on similar principles to those of UW and HTK, but certain aspects are different. CS and HTK are categorized as extracellular preservation fluids; however, their buffering systems and substrates, which provide high-energy phosphates, are different. With its high sodium (above 70 mmol/L) and low potassium content, CS is specifically designed to limit calcium overload (Table 1). It contains reduced glutathione concentration together with the addition of mannitol and histidine to prevent reactive oxygen species-induced oxidative injury. Like HTK, CS is devoid of colloids, therefore resulting in decreased viscosity and improved perfusability, it is thus unnecessary to the liver prior to reperfusion[13]. Due to its characteristically low viscosity, high sodium, low potassium and antioxidant properties, CS is considered particularly suitable for preserving liver grafts.

There are promising preliminary reports on the recently introduced Institut Georges Lopez (IGL-1) solution, also known as the UW-polyethylene glycol (PEG) solution. IGL-1 combines a cationic inversion (lower concentration of potassium) and replacement of hydroxyethyl starch with PEG. These properties could improve hepatic microcirculatory changes, thereby decreasing IR- injury[14].

The aim of our study was to provide a systematic review of this topic. The goal was to update current knowledge and compare data evidence on the effectiveness of the most frequently used preservation solutions. The primary endpoint of the study was primary non-function (PNF) of the graft after liver transplantation. PNF is the most common cause of early graft loss, and it has been shown that the organ preservation method is an independent predictive factor of PNF[15]. The secondary endpoint was one-year post-transplant graft survival (OGS-1), this being an appropriate period to evaluate the effect of the preservation solutions according to an expert consensus opinion[16]. Other outcomes, such as primary dysfunction (PDF), early retransplantation rate (RT), post-transplant death within 30 d (POD) and one-year post-transplant patient survival (OPS-1) were also evaluated together with donors and recipient characteristics.

It should be added that three previous systematic reviews and two registry data analyses have explored this topic, each with limitations[10,16-19]. In 2015, Adam *et al*[10] analyzed the efficacy of the four most commonly used preservation solutions based on the European Liver Transplant Registry (ELTR) database. The largest and most comprehensive study in recent times was performed by analyzing outcomes of 42869 (first) liver transplantations, including living and deceased donors, as well as partial liver graft transplantations. Although the study population in this registry data analysis was relatively large, non-selective groups of donors were included[10,18,20]. Two systematic reviews lacked sufficient sample sizes and therefore were underpowered to identify clinically relevant differences in important outcomes, such as PNF of the graft.[16,17] A systematic review by O'Callaghan *et al*[19] chose 16 RCTs for analysis; however, it included unpublished data and conference abstracts as well. Since then, new prospective trials have also been published, especially with the IGL-1 solution[8,21].

Therefore, the aim of this systematic review was to evaluate, compare and update the evidence obtained in randomized controlled trials (RCTs) on the efficacy of the four most frequently used preservation solutions for static cold storage of deceased donor liver (DDL) allografts.

MATERIALS AND METHODS

This study was conducted in accordance with the PRISMA (Preferred Reporting Items in Systematic Reviews and Meta-Analysis) statement[22]. The review protocol was registered with the National Institute for Health Research PROSPERO system on January 12th, 2017, and can be found online (Registration No. CRD42017054908)[23].

Literature search

A systematic literature search was performed using EMBASE/MEDLINE, PubMed, Scopus and Cochrane. Database searches were conducted with MeSH key-words, combined with various terms for organ transplantation and organ preservation solutions (Figure 1). No language limitation was applied. The end date for the literature search was January 31st, 2017.

Inclusion criteria

Inclusion criteria specified any RCT comparing two or more preservation solutions for the static cold storage of DDLs, from both adult and pediatric donors. Living

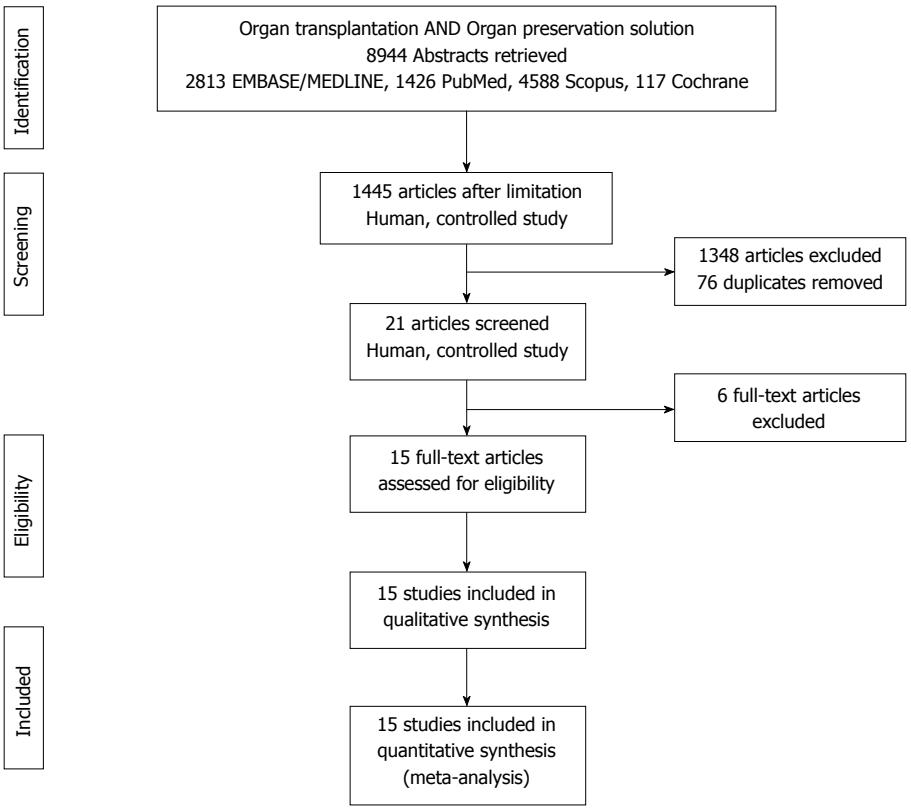

Figure 1 PRISMA flowchart of search strategy with inclusions and exclusions.

donor transplantation, multiple organ transplantation, retransplantation, nonhuman and uncontrolled studies were excluded. Abstracts for inclusion were independently reviewed by two authors, and disagreements were resolved by discussion with a third author (Figure 1).

Outcomes

The primary outcome was PNF of the liver grafts. PNF is a life-threatening condition after transplantation that leads to death or to the need for retransplantation within seven days of transplantation. It is characterized by hepatic cytolysis, elevated fasting transaminase levels, diminishing or absent bile production, coalgulation deficit related to severely impaired liver function, high lactate levels, hypoglycemia, respiratory failure requiring ventilatory support, circulatory failure requiring catecholamines, and the onset of renal and multi-organ failure[15].

The secondary outcome was OGS-1, since the one-year post-transplant time point was considered by an expert consensus opinion as most suitable to evaluate the effect of the preservation solutions[16].

Data extraction

Demographic, quality and outcome data were extracted independently into Microsoft Excel by two authors. Data were collected from all articles describing the studies; in the case of discrepancies, the article with the largest number of patients was used. Any questions in data extraction were settled by discussion with a third author.

Statistical analysis

The statistical analysis for this study was conducted by Péter Mátrai, Institute of Bioanalysis, University of Pécs, H-7624 Pécs, Hungary. Risk ratios (RR) from individual studies were pooled statistically by random effect model using the DerSimonian-Laird estimator and were displayed on forest plots. As RR allows for the comparison of two samples, the Celsior and HTK solutions were compared to UW. Summary RRs were calculated with 95% confidence intervals (CI) and p values to test if summary RR = 1 can be rejected. $P < 0.05$ was defined as a significant difference between solutions. In the analysis of outcomes for PNF and PDF, we used a computational correction recommended in the Cochrane Handbook and proposed by Sweeting *et al*[24]. to overcome the difficulty of dividing by 0. Statistical heterogeneity was tested using the I^2 statistic and the chi-square test to obtain probability-values; $P < 0.05$ was defined to indicate significant heterogeneity. All statistical calculations were performed using Stata 11 SE (Stata Corp) and Comprehensive Meta-analysis Software (Version 3, Biostat, Englewood). We sought signs of a small study effect with the funnel plot. To identify potential sources of heterogeneity, we defined a priori subgroup analyses with the model of end-stage

Table 2 Primary non-function rate in included studies

Study	Solution 1				Solution 2				RR	*P* value
		N	*n*	%		N	*n*	%		
Cavallari *et al*[13], 2003	UW	90	1	1.100	CS	83	0	0.000	2.77	0.53
Lopez-Andujar *et al*[26], 2009	UW	104	2	1.900	CS	92	2	2.200	0.88	0.90
García-Gil *et al*[33], 2006	UW	40	0	0.000	CS	40	0	0.000	1.00	1.00
Nardo *et al*[27], 2001	UW	60	2	3.333	CS	53	0	0.000	4.43	0.33
Duca *et al*[28], 2010	UW	51	0	0.000	CS	51	0	0.000	1.00	1.00
García-Gil *et al*[35], 2011	UW	51	4	11.100	CS	51	4	11.100	1.00	1.00
Lama *et al*[29], 2002	UW	10	0	0.000	CS	10	0	0.000	1.00	1.00
Rayya *et al*[30], 2008	UW	68	1	1.471	HTK	69	1	1.449	1.01	0.99
Meine *et al*[32], 2006	UW	65	2	3.070	HTK	37	1	3.030	1.14	0.91
Erhard *et al*[9], 1994	UW	30	2	6.660	HTK	30	0	0.000	5.00	0.29
Mangus *et al*[31], 2008	UW	98	5	5.102	HTK	111	3	2.703	1.89	0.38
Dondéro *et al*[37], 2010	UW	92	4	4.350	IGL-1	48	1	2.080	2.09	0.51
Meine *et al*[8], 2015	HTK	65	2	3.100	IGL-1	113	3	2.700	1.16	0.87
Wiederkehr *et al*[21], 2014	HTK	125	1	0.700	IGL-1	53	0	0.000	1.29	0.88
Nardo *et al*[12], 2005	HTK	20	1	5.000	CS	20	0	0.000	3.00	0.49

Studies are grouped by preservation solutions. PNF: Primary non-function; N: Indicates number in group; *n*: Number of PNF; RR: Relative risk; UW: University of Wisconsin solution; HTK: Histidine-tryptophan-ketoglutarate solution; CS: Celsior solution; IGL-1: Institut Georges Lopez solution.

Table 3 One-year post-transplant graft survival rate in included studies

Study	Solution 1				Solution 2				RR	*P* value
		N	*n*	%		N	*n*	%		
Cavallari *et al*[13], 2003	UW	90	75	83.0	CS	83	71	85.0	0.97	0.69
Lopez-Andujar *et al*[26], 2009	UW	104	83	80.0	CS	92	75	81.0	0.98	0.76
García-Gil *et al*[33], 2006	UW	40	26	66.1	CS	40	31	78.0	0.84	0.22
Nardo *et al*[27], 2001	UW	60	54	90.0	CS	53	48	90.6	0.99	0.92
Duca *et al*[28], 2010	UW	51	31	60.6	CS	51	37	73.5	0.84	0.21
Rayya *et al*[30], 2008	UW	68	53	78.0	HTK	69	49	71.0	1.01	0.35
Meine *et al*[32], 2006	UW	65	61	94.0	HTK	37	35	94.0	0.99	0.88
Mangus *et al*[31], 2008	UW	98	82	84.0	HTK	111	95	86.0	0.98	0.70
Dondéro *et al*[37], 2010	UW	92	73	79.1	IGL-1	48	19	39.8	2.00	0.00
Meine *et al*[8], 2015	HTK	65	54	83.0	IGL-1	113	96	85.0	0.98	0.74
Nardo *et al*[12], 2005	HTK	20	15	75.0	CS	20	18	90.0	0.83	0.22

Studies are grouped by preservation solutions. OGS-1: One-year post-transplant graft survival; N: Number in group; *n*: Number of OGS-1; RR: Relative risk; UW: University of Wisconsin solution; HTK: Histidine-tryptophan-ketoglutarate solution; CS: Celsior solution; IGL-1: Institut Georges Lopez solution.

liver disease (MELD) score and cold ischemia time (CIT). All other outcomes related to the solutions were also investigated by subgroup analysis.

RESULTS

Demographic and clinical characteristics of donors and recipients were homogenous in all trials (Supplementary Tables 1-3).

MELD score

The MELD score incorporates parameters of recipients (such as abnormal coagulation, creatinine and serum bilirubin levels and the etiology of cirrhosis) and serves as a predictor of mortality after liver transplantation[25]. MELD scores were reported in five studies (Supplementary Table 2). Subgroup analysis showed no significant difference in MELD score between the four solutions (RR = 18.6, 95%CI: 15.7-21.5, P = 0.379) (Supplementary Figure 1A).

CIT

CIT (time interval from the clamping of the donor aorta to the anastomosis of the organ to the recipient's vascular system or organs disposal) was reported in five studies (Supplementary Table 3). Subgroup analysis showed no significant difference in risk of CIT between the four solutions (RR = 484.7, 95%CI: 445.4-524.0, P = 0.1) (Supplementary Figure 1B).

PNF

PNF rates were reported in 15 studies (Table 2)[8,9,12,13,21,26-35]. In four studies, PNF was defined as patient death or retransplantation in the first week. In eleven studies, PNF was undefined. Overall rates of PNF were very low (range 0-13.7%). Our meta-analysis showed no significant difference in risk of PNF between the UW and CS solutions (z = 0.41, P = 0.680) and between UW and HTK (z = 1.07, P = 0.284) (Figure 2A). We found only one RCT that dealt with IGL-1, which was not sufficient for a meta-analysis to compare IGL-1 with the UW

A

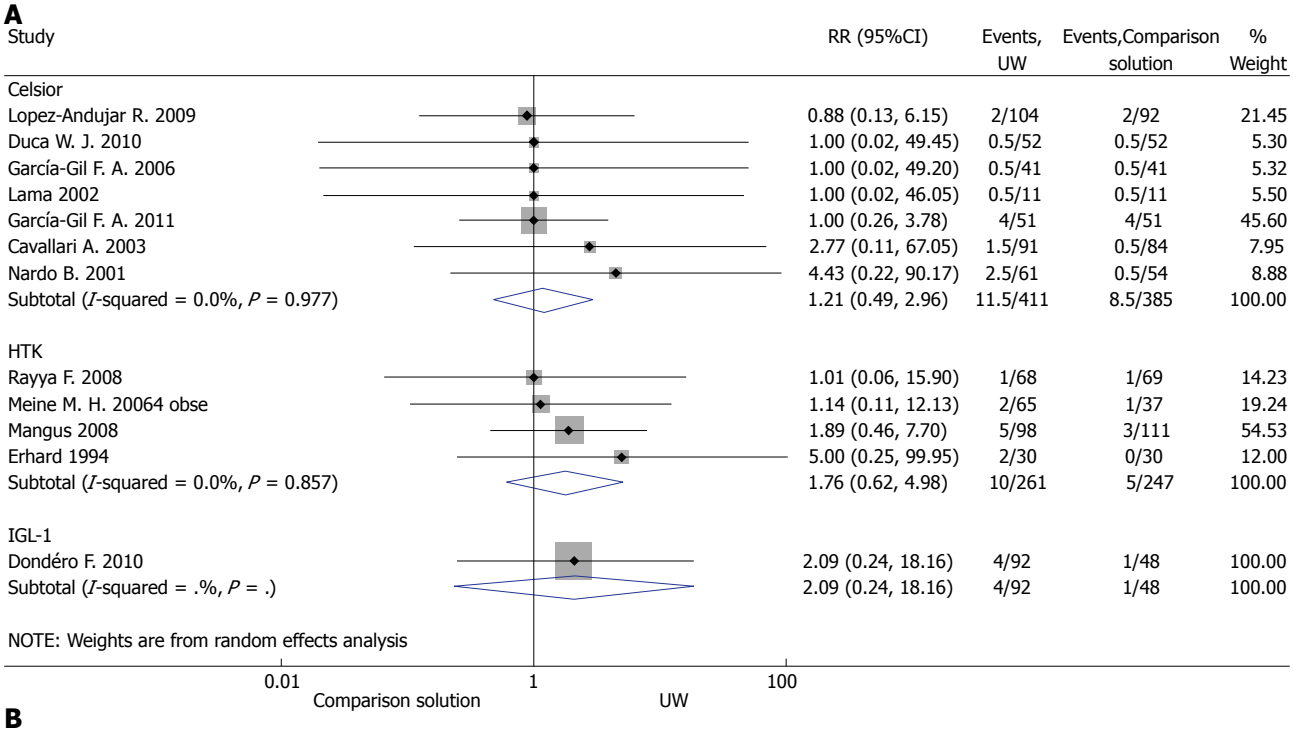
Study
RR (95%CI)
Events, UW
Events,Comparison solution
% Weight
Celsior
Lopez-Andujar R. 2009 0.88 (0.13, 6.15) 2/104 2/92 21.45
Duca W. J. 2010 1.00 (0.02, 49.45) 0.5/52 0.5/52 5.30
García-Gil F. A. 2006 1.00 (0.02, 49.20) 0.5/41 0.5/41 5.32
Lama 2002 1.00 (0.02, 46.05) 0.5/11 0.5/11 5.50
García-Gil F. A. 2011 1.00 (0.26, 3.78) 4/51 4/51 45.60
Cavallari A. 2003 2.77 (0.11, 67.05) 1.5/91 0.5/84 7.95
Nardo B. 2001 4.43 (0.22, 90.17) 2.5/61 0.5/54 8.88
Subtotal (I-squared = 0.0%, P = 0.977) 1.21 (0.49, 2.96) 11.5/411 8.5/385 100.00
HTK
Rayya F. 2008 1.01 (0.06, 15.90) 1/68 1/69 14.23
Meine M. H. 20064 obse 1.14 (0.11, 12.13) 2/65 1/37 19.24
Mangus 2008 1.89 (0.46, 7.70) 5/98 3/111 54.53
Erhard 1994 5.00 (0.25, 99.95) 2/30 0/30 12.00
Subtotal (I-squared = 0.0%, P = 0.857) 1.76 (0.62, 4.98) 10/261 5/247 100.00
IGL-1
Dondéro F. 2010 2.09 (0.24, 18.16) 4/92 1/48 100.00
Subtotal (I-squared = .%, P = .) 2.09 (0.24, 18.16) 4/92 1/48 100.00
NOTE: Weights are from random effects analysis
0.01
1
100
Comparison solution
UW

B

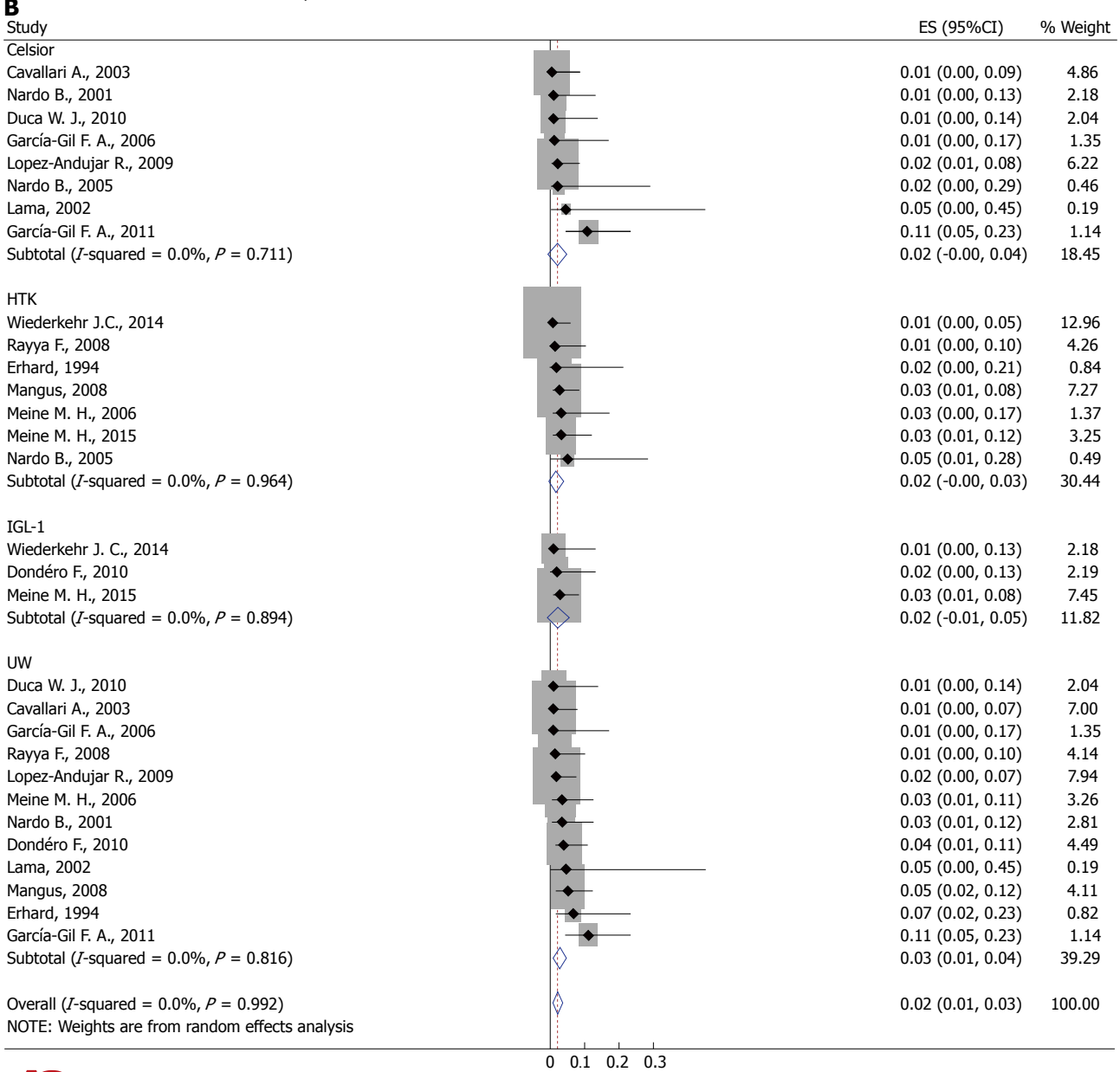
Study
ES (95%CI)
% Weight
Celsior
Cavallari A., 2003 0.01 (0.00, 0.09) 4.86
Nardo B., 2001 0.01 (0.00, 0.13) 2.18
Duca W. J., 2010 0.01 (0.00, 0.14) 2.04
García-Gil F. A., 2006 0.01 (0.00, 0.17) 1.35
Lopez-Andujar R., 2009 0.02 (0.01, 0.08) 6.22
Nardo B., 2005 0.02 (0.00, 0.29) 0.46
Lama, 2002 0.05 (0.00, 0.45) 0.19
García-Gil F. A., 2011 0.11 (0.05, 0.23) 1.14
Subtotal (I-squared = 0.0%, P = 0.711) 0.02 (-0.00, 0.04) 18.45
HTK
Wiederkehr J.C., 2014 0.01 (0.00, 0.05) 12.96
Rayya F., 2008 0.01 (0.00, 0.10) 4.26
Erhard, 1994 0.02 (0.00, 0.21) 0.84
Mangus, 2008 0.03 (0.01, 0.08) 7.27
Meine M. H., 2006 0.03 (0.00, 0.17) 1.37
Meine M. H., 2015 0.03 (0.01, 0.12) 3.25
Nardo B., 2005 0.05 (0.01, 0.28) 0.49
Subtotal (I-squared = 0.0%, P = 0.964) 0.02 (-0.00, 0.03) 30.44
IGL-1
Wiederkehr J. C., 2014 0.01 (0.00, 0.13) 2.18
Dondéro F., 2010 0.02 (0.00, 0.13) 2.19
Meine M. H., 2015 0.03 (0.01, 0.08) 7.45
Subtotal (I-squared = 0.0%, P = 0.894) 0.02 (-0.01, 0.05) 11.82
UW
Duca W. J., 2010 0.01 (0.00, 0.14) 2.04
Cavallari A., 2003 0.01 (0.00, 0.07) 7.00
García-Gil F. A., 2006 0.01 (0.00, 0.17) 1.35
Rayya F., 2008 0.01 (0.00, 0.10) 4.14
Lopez-Andujar R., 2009 0.02 (0.00, 0.07) 7.94
Meine M. H., 2006 0.03 (0.01, 0.11) 3.26
Nardo B., 2001 0.03 (0.01, 0.12) 2.81
Dondéro F., 2010 0.04 (0.01, 0.11) 4.49
Lama, 2002 0.05 (0.00, 0.45) 0.19
Mangus, 2008 0.05 (0.02, 0.12) 4.11
Erhard, 1994 0.07 (0.02, 0.23) 0.82
García-Gil F. A., 2011 0.11 (0.05, 0.23) 1.14
Subtotal (I-squared = 0.0%, P = 0.816) 0.03 (0.01, 0.04) 39.29
Overall (I-squared = 0.0%, P = 0.992) 0.02 (0.01, 0.03) 100.00
NOTE: Weights are from random effects analysis
0
0.1
0.2
0.3

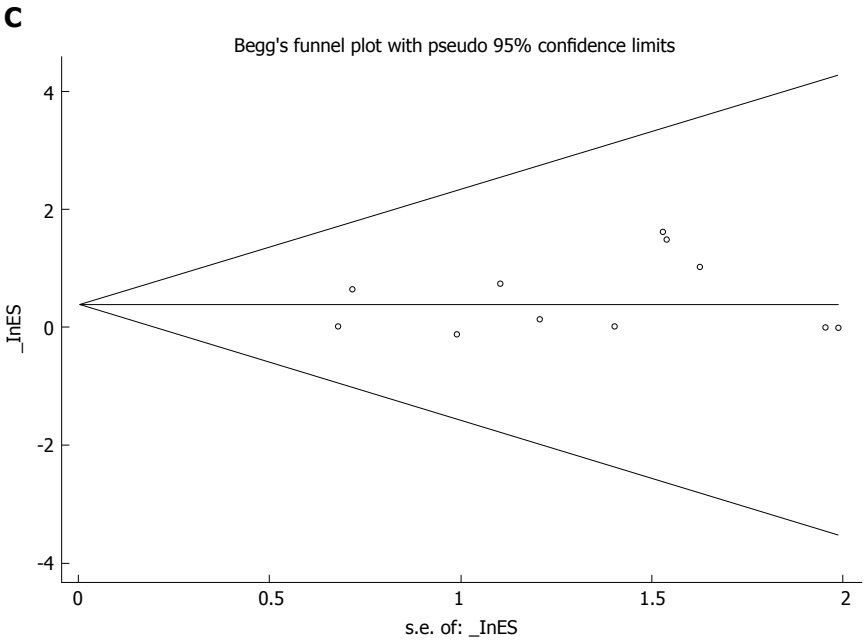

Figure 2 Effects of preservation solutions on primary non-function. A: Meta-analysis of the relative risk (-RR-) of PNF comparing studies using different preservation solutions: UW *vs* Celsior and UW *vs* HTK; B: Forest plot for subgroup analysis of PNF; and C: Funnel plot for PNF in studies. Squares represent individual study effects, with the size of the box relating to the weight of the study in the meta-analysis. Each diamond represents a summary effect from meta-analysis. Horizontal bars represent 95% CIs. There is no evidence of a small study effect in the test or the formal plot. PNF: Primary non-function; RCTs: Randomized controlled trials; ES: Effect size; UW: University of Wisconsin solution; HTK: Histidine-tryptophan-ketoglutarate solution; CS: Celsior solution; IGL-1: Institut Georges Lopez solution.

solution. We performed a subgroup analysis to compare the four solutions in the context of PNF. There was no significant difference between solutions (RR = 0.02, 95%CI: 0.01-0.03, P = 0.356) (Figure 2B). We found no evidence of a small study effect using the funnel plot analysis of the meta-analyses for the primary outcome (P = 0.846) (Figure 2C).

OGS-1

OGS-1 was reported in eleven studies (Table 3). No study was individually powered for small differences in graft survival, and no study reported a difference related to the preservation fluid used. Meta-analysis of the data showed no significant difference in the risk of OGS-1 between the UW and CS solutions (z = 0.30, P = 0.763) (Figure 3A) or between the UW and HTK solutions (z = 0.01, P = 0.991) (Figure 3A). We also performed a subgroup analysis to compare all four solutions, including IGL-1. There was no significant difference between the solutions (RR = 0.80, 95%CI: 0.80-0.80, P = 0.369) (Figure 3B). We found no evidence of a small study effect using the funnel plot analysis from either of the meta-analyses for the OGS-1 (P = 0.397) (Figure 3C).

PDF

PDF rates were reported in six studies: five of them compared UW with CS, and one compared UW with HTK (Supplementary Table 4). Overall rates of PDF were very low (range 0-15.5%). The difference in PDF rate was found higher with the use of UW solutions in one study[32]. However, the subgroup analysis showed no increased risk of PDF in the UW group (RR = 0.1, 95%CI: 0.0-0.1, P = 0.582) (Supplementary Figure 2).

Early RT

Early RT was reported in seven studies and ranged from 0.9% to 20% (Supplementary Table 4). None of the studies found a significant difference in early RT between groups; however, they were underpowered to detect such a low incidence outcome. Similarly, subgroup analysis showed no increased risk of early RT in the UW group (RR = 0.0, 95%CI: 0.0-0.1, P = 0.698) (Supplementary Figure 3).

POD

POD rates were reported in seven studies (Supplementary Table 4). Overall rates of POD were very low (range 1.7%-14.4%). The difference in POD rate was higher with the use of the CS solution compared with the UW solution in two studies[12,33]; however, subgroup analysis showed no increased risk (Supplementary Figure 4). In contrast, there was a significant difference when UW was compared to HTK or IGL-1 (RR = 0.07, 95%CI: 0.04-0.09, P < 0.01).

OPS-1

OPS-1 rates were reported in ten studies (Supplementary Table 4). No study was individually powered for small differences in graft survival, and no study reported

A

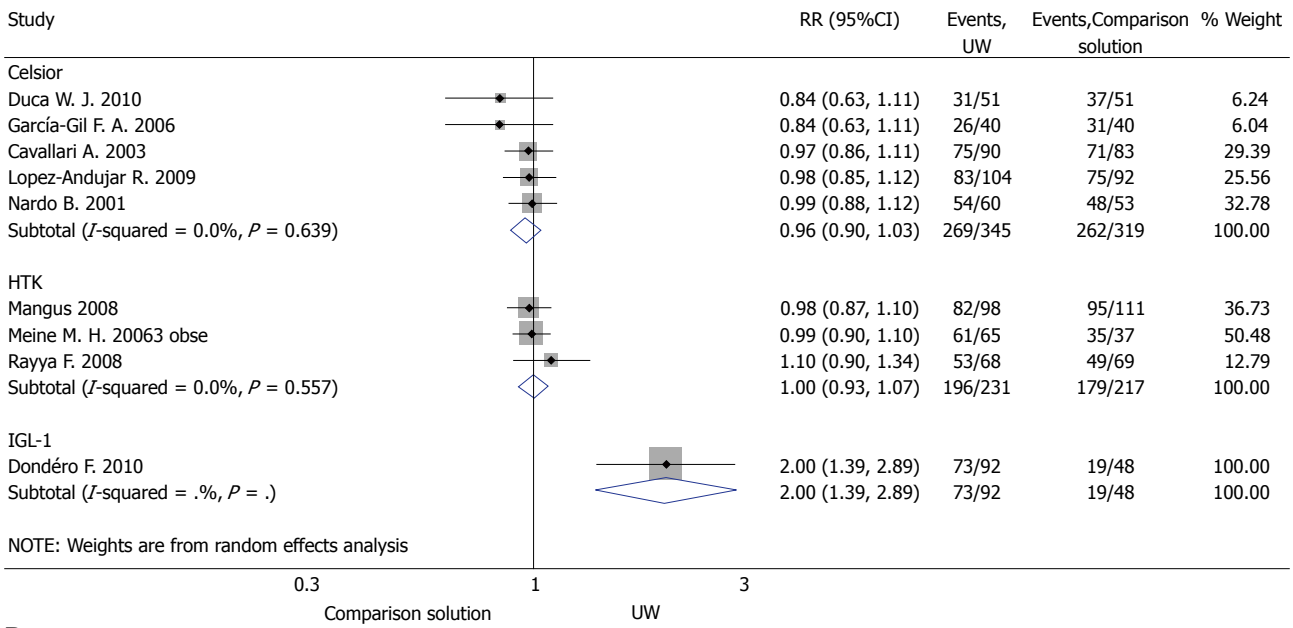
Study
RR (95%CI)
Events, UW
Events,Comparison solution
% Weight
Celsior
Duca W. J. 2010 0.84 (0.63, 1.11) 31/51 37/51 6.24
García-Gil F. A. 2006 0.84 (0.63, 1.11) 26/40 31/40 6.04
Cavallari A. 2003 0.97 (0.86, 1.11) 75/90 71/83 29.39
Lopez-Andujar R. 2009 0.98 (0.85, 1.12) 83/104 75/92 25.56
Nardo B. 2001 0.99 (0.88, 1.12) 54/60 48/53 32.78
Subtotal (I-squared = 0.0%, P = 0.639) 0.96 (0.90, 1.03) 269/345 262/319 100.00
HTK
Mangus 2008 0.98 (0.87, 1.10) 82/98 95/111 36.73
Meine M. H. 20063 obse 0.99 (0.90, 1.10) 61/65 35/37 50.48
Rayya F. 2008 1.10 (0.90, 1.34) 53/68 49/69 12.79
Subtotal (I-squared = 0.0%, P = 0.557) 1.00 (0.93, 1.07) 196/231 179/217 100.00
IGL-1
Dondéro F. 2010 2.00 (1.39, 2.89) 73/92 19/48 100.00
Subtotal (I-squared = .%, P = .) 2.00 (1.39, 2.89) 73/92 19/48 100.00
NOTE: Weights are from random effects analysis
0.3
1
3
Comparison solution
UW

B

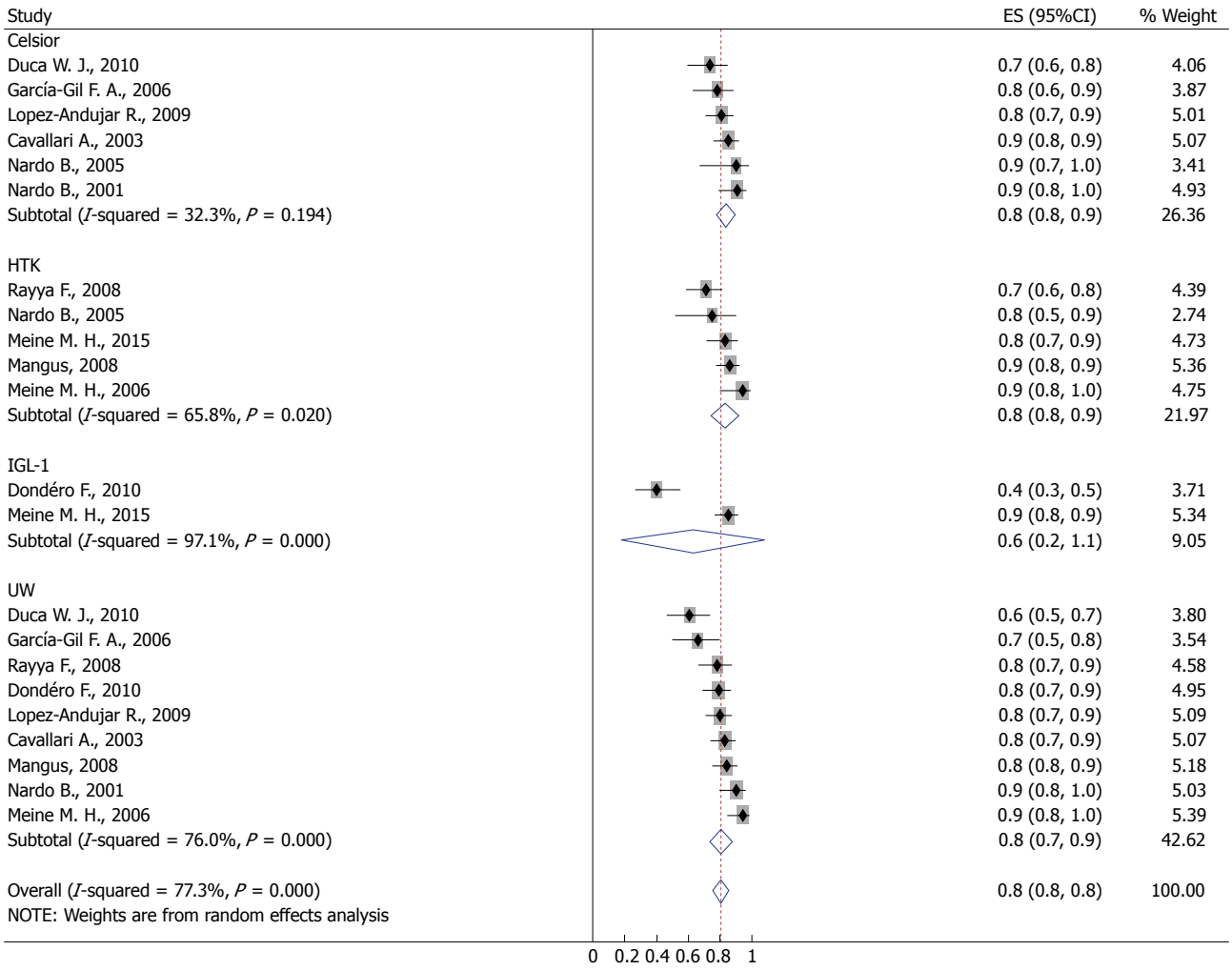
Study
ES (95%CI)
% Weight
Celsior
Duca W. J., 2010 0.7 (0.6, 0.8) 4.06
García-Gil F. A., 2006 0.8 (0.6, 0.9) 3.87
Lopez-Andujar R., 2009 0.8 (0.7, 0.9) 5.01
Cavallari A., 2003 0.9 (0.8, 0.9) 5.07
Nardo B., 2005 0.9 (0.7, 1.0) 3.41
Nardo B., 2001 0.9 (0.8, 1.0) 4.93
Subtotal (I-squared = 32.3%, P = 0.194) 0.8 (0.8, 0.9) 26.36
HTK
Rayya F., 2008 0.7 (0.6, 0.8) 4.39
Nardo B., 2005 0.8 (0.5, 0.9) 2.74
Meine M. H., 2015 0.8 (0.7, 0.9) 4.73
Mangus, 2008 0.9 (0.8, 0.9) 5.36
Meine M. H., 2006 0.9 (0.8, 1.0) 4.75
Subtotal (I-squared = 65.8%, P = 0.020) 0.8 (0.8, 0.9) 21.97
IGL-1
Dondéro F., 2010 0.4 (0.3, 0.5) 3.71
Meine M. H., 2015 0.9 (0.8, 0.9) 5.34
Subtotal (I-squared = 97.1%, P = 0.000) 0.6 (0.2, 1.1) 9.05
UW
Duca W. J., 2010 0.6 (0.5, 0.7) 3.80
García-Gil F. A., 2006 0.7 (0.5, 0.8) 3.54
Rayya F., 2008 0.8 (0.7, 0.9) 4.58
Dondéro F., 2010 0.8 (0.7, 0.9) 4.95
Lopez-Andujar R., 2009 0.8 (0.7, 0.9) 5.09
Cavallari A., 2003 0.8 (0.7, 0.9) 5.07
Mangus, 2008 0.8 (0.8, 0.9) 5.18
Nardo B., 2001 0.9 (0.8, 1.0) 5.03
Meine M. H., 2006 0.9 (0.8, 1.0) 5.39
Subtotal (I-squared = 76.0%, P = 0.000) 0.8 (0.7, 0.9) 42.62
Overall (I-squared = 77.3%, P = 0.000) 0.8 (0.8, 0.8) 100.00
NOTE: Weights are from random effects analysis
0 0.2 0.4 0.6 0.8 1

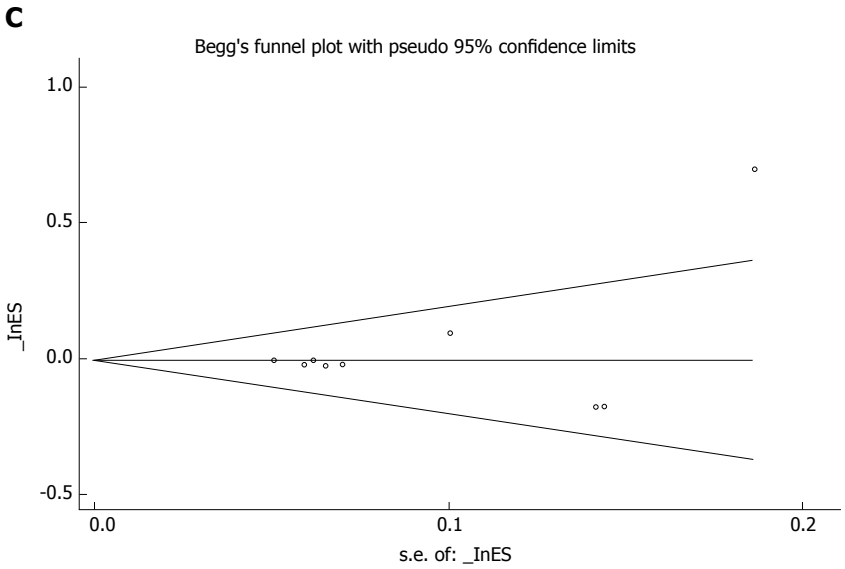

Figure 3 Effects of preservation solutions on one-year post-transplant graft survival. A: Meta-analysis of the relative risk (-RR-) of OGS-1 comparing studies using different preservation solutions: UW *vs* Celsior and UW *vs* HTK; B: Forest plot for subgroup analysis of OGS-1; and C: Funnel plot for OGS-1 in studies. Squares represent individual study effects, with the size of the box relating to the weight of the study in the meta-analysis. Each diamond represents a summary effect from meta-analysis. Horizontal bars represent 95% CIs. There is no evidence of a small study effect in the test or the formal plot. OGS-1: One-year post-transplant graft survival; RR: Relative risk; RCTs: Randomized controlled trials; ES: Effect size; UW: University of Wisconsin solution; HTK: Histidine-tryptophan-ketoglutarate solution; CS: Celsior solution; IGL-1: Institut Georges Lopez solution.

a difference related to the preservation fluid used. Subgroup analysis showed no significant difference in risk of OPS-1 between the four solutions (RR = 0.9, 95%CI: 0.8-0.9, P = 0.786) (Supplementary Figure 5).

DISCUSSION

This study reviews the current evidence and updates knowledge on four frequently used preservation solutions for static cold storage of DDLs for transplantation. The treatment groups were homogenous in terms of donor and recipient characteristics; the prediction of primary and secondary outcomes (*i.e.*, PNF and OGS-1) was thus likely independent of individual risk variables, patient selection or the overall severity of the disease at liver transplantation. More importantly, the analysis of outcome parameters (*i.e.*, PNF and OGS-1) provided good evidence that UW is not outperformed by CS, HTK and IGL-1 solutions in maintaining organ function and viability of liver grafts in cold storage.

PNF mainly depends on the organ preservation method[15]. It occurs in 2%-6% of transplants and is unrelated to any direct surgical, immunologic or other complications[34]. Our meta-analysis included eleven trials that evaluated the effectiveness of the UW solution as compared to either the CS or HTK solution. In accordance with the literature, the overall rates of PNF were very low, except in one trial (13%)[35]. When analyzing the single studies, we found two trials with a higher incidence of PNF in the UW group than in the HTK group[9,36], but the difference did not reach statistical significance upon meta-analysis. It should be added that a recent analysis of the ELTR database demonstrated that use of HTK represented an individual risk factor for the development of PNF when compared to the UW solution[10]. The contradictory conclusions can be explained with the selection bias of the database analysis[20]. In either case, we found no difference between UW and the other solutions with regard to the risk of PNF. As regards IGL-1 and HTK, two prospective randomized clinical studies with 356 patients reported identical results[8,21]. Similar outcome was detected in a single-center study with 140 patients that compared IGL-1 and UW solutions[37]. This was confirmed in the current study, since IGL-1 showed a similar PNF risk to that of UW and HTK in our subgroup analyses.

In our study, OGS-1 was the secondary endpoint. Graft survival rates were evaluated one, three and five years after liver transplantation in single studies. The one-year term was chosen as an appropriate period to evaluate the effect of the preservation solutions because other factors could have a greater impact on this outcome parameter after this time. A retrospective analysis of the ELTR database demonstrated that HTK preservation was independently associated with higher mortality than UW, CS and IGL-1 in a multivariate analysis[10]. Another analysis of a large national registry database (United Network for Organ Sharing, UNOS) has also demonstrated differences in graft survival rate between the HTK and UW solutions[18]. However, important risk factors among donors were not considered in the ELTR analysis[20], and selected groups of transplant patients were not homogenous in the

other analysis: HTK was utilized in allografts with more favorable recipient traits, as well as shorter CIT and less local and national export[18]. In accordance with the findings from numerous clinical trials, the meta-analyses and subgroup analyses in this study did not show a significant difference in risk of OGS-1 between UW and any of the examined solutions. Similarly, there was no evidence for a difference between IGL-1 and UW solutions and between IGL-1 and HTK in the subgroup analyses.

Apart from the preservation methods used to protect the organ from IR injury, the final outcome of transplantation can also be linked to factors such as donor age, general condition and CIT[38]. A recent UNOS study showed a more pronounced risk for graft loss with longer CIT and donors over 70 years[18]. In our study, subgroup analysis showed that the included trials did not vary significantly and that the mean CITs were beyond the critical 12 h[39]. Several experimental studies demonstrated that the use of the UW solution allows for longer CITs with better graft preservation; however, it remains to be determined whether any of the alternative solutions is better than UW when CIT is prolonged over 12 h.

Recipient morbidity and MELD scores are also important contributing factors to the outcome of liver transplantation. Recipient parameters are incorporated into the MELD score, which indicates the state of health of the recipient; the MELD score-based organ allocation algorithm could thus significantly influence the graft survival rate[40]. In the present study, there was no significant difference between the preservation solutions in the context of the MELD score and other recipient characteristics.

In recent times, the crisis in organ supply has made it necessary to extend the scope of potential donors by using extended criteria donors (ECD). Although there is no precise definition of ECD, frequently cited characteristics are donor age, steatosis, donation after cardiac death (DCD), donors with increased risk of disease transmission and transplantation after prolonged CIT, as well as the use of partial grafts (split grafts and living donor liver transplantation)[41]. Unfortunately, higher rates of graft failure were documented in this class of extended allograft; in addition, very little data is available on the influence of preservation solutions on their post-transplant outcomes[42]. A single-center study by Mangus *et al*[30] failed to find statistically significant differences in overall graft survival when they compared UW to HTK in ECD transplantations. However, they suggested that HTK may be protective against biliary complications. In contrast, in 2009, the UNOS database analysis reported that HTK was associated with an increased risk of graft loss and early graft loss[18]. More recently, Adam *et al*[10] compared the four most frequently used preservation solutions and concluded that HTK is an independent risk factor for graft loss after ECD liver transplantations. The remaining three solutions, UW, CE and IGL-1, provided similar results in post-transplant outcomes after ECD transplantations. In the special condition of using a partially deceased donor liver graft, IGL-1 offered the best graft outcome[10]. In another study, it was suggested that IGL-1 was superior to other solutions for preserving fatty livers by protecting against PNF and early allograft dysfunction[43]. However, a prospective randomized study could not show any significant improvement in the subgroup of patients receiving IGL-1-preserved grafts[36]. In living donor liver transplantations, risk-adjusted analyses of single- and double-center studies consistently reported that UW and HTK were equally effective and safe for cold preservation[44-47]. There is currently no evidence-based recommendation on the optimal preservation solution in ECD liver transplantations because the number and quality of RCTs are not sufficient. However, based on the above data, differences in the indications of various preservation solutions are expected.

This study has some limitations. There are so far only three small RCTs that compare IGL-1 with UW or IGL-1 with HTK. Therefore, we could not run a meta-analysis to compare IGL-1 with any of the solutions. In order to compare the risk of the four solutions for PNF, we had to perform a subgroup analysis. In addition, surgery time and hemoderivative transfusions due to recipient coagulation problems are often not cited in the literature as predictors of poor outcome[36]. This factor was not considered in the selected trials. Moreover, different trials presented some differences as regards the operative procedure. Furthermore, the included RCTs were homogenous with regard to donor and recipient parameters. On the one hand, this provided the possibility to exclude selection bias, but, on the other hand, the effects of preservation solutions in the case of longer CIT and involvement of expanded criteria donors could not be evaluated.

In conclusion, elucidation of the role of preservation solutions in the outcome of liver transplantation is complicated by the intrinsic complexity of the clinical procedure, which is made up of many different, but interacting phases. This review evaluated the best available evidence from comparisons of the four most frequently used preservation fluids in DDL transplantation. A direct meta-analysis comparison was made and the sample size of included trials was large enough to estimate the risk of low-incidence outcomes such as PNF or OGS-1 correctly. Based on our results, there is good evidence that the UW, CS, HTK and IGL-1 solutions are associated with nearly equivalent outcomes. Additional studies on larger patient populations including marginal donors, longer cold ischemia time, multi-organ transplantations and economic aspects are needed to evaluate the superiority of any alternative solution over UW.

ARTICLE HIGHLIGHTS

Research background

The introduction of the University of Wisconsin (UW) solution for static cold storage of liver grafts was a breakthrough and has remained the conventional method of organ preservation. However, many alternative preservation solutions exist, and each is thought to offer an advantage over UW solution.

Research motivation

At present, 98% of liver transplantations use the UW, histidine-tryptophan-ketoglutarate (HTK), Celsior (CS) or Institute Georges Lopez (IGL-1) solution for the cold preservation of grafts. Previously, prospective trials have investigated their effects on liver transplant outcomes, but with contradictory results. Furthermore, no systematic review reports the effect of IGL-1, which was first used by 2003, as compared to other solutions.

Research objectives

To provide an update and to compare the latest findings from clinical trials on the effects of the four most frequently used preservation solutions on liver transplant outcomes.

Research methods

A systematic review and meta-analysis were conducted on randomized controlled trials of deceased donor liver transplantations using UW and either HTK, CS or IGL-1 for cold storage of allografts. Primary and secondary outcomes were primary non-function (PNF) and one-year post-transplant graft survival (OGS-1).

Research results

In spite of differences found in individual studies, a meta-analysis of PNF and OGS-1 showed no statistical difference between groups. Subgroup analysis showed no increased risk for other outcomes, such as primary dysfunction, early retransplantation rate, post-transplantation death and one-year post-transplant patient survival.

Research conclusions

This meta-analysis provided evidence that UW and alternative solutions are associated with almost the same transplant outcome. Further studies are needed with extended criteria donors to ascertain the superiority of any alternative solution over UW.

REFERENCES

1 **Jia JJ**, Li JH, Jiang L, Lin BY, Wang L, Su R, Zhou L, Zheng SS. Liver protection strategies in liver transplantation. *Hepatobiliary Pancreat Dis Int* 2015; **14**: 34-42 [PMID: 25655288 DOI: 10.1016/S1499-3872(15)60332-0]

2 **Brisson H**, Arbelot C, Monsel A, Parisot C, Girard M, Savier E, Vezinet C, Lu Q, Vaillant JC, Golmard JL, Gorochov G, Langeron O, Rouby JJ; Members of the Pitié-Salpêtrière Liver Transplantation Study Group. Impact of graft preservation solutions for liver transplantation on early cytokine release and postoperative organ dysfunctions. A pilot study. *Clin Res Hepatol Gastroenterol* 2017; **41**: 564-574 [PMID: 28330599 DOI: 10.1016/j.clinre.2016.12.011]

3 **Stewart ZA**. UW solution: still the "gold standard" for liver transplantation. *Am J Transplant* 2015; **15**: 295-296 [PMID: 25612481 DOI: 10.1111/ajt.13062]

4 **Sanchez-Urdazpal L**, Gores GJ, Ward EM, Maus TP, Wahlstrom HE, Moore SB, Wiesner RH, Krom RA. Ischemic-type biliary complications after orthotopic liver transplantation. *Hepatology* 1992; **16**: 49-53 [PMID: 1618482 DOI: 10.1002/hep.1840160110]

5 **Cutrin JC**, Cantino D, Biasi F, Chiarpotto E, Salizzoni M, Andorno E, Massano G, Lanfranco G, Rizzetto M, Boveris A, Poli G. Reperfusion damage to the bile canaliculi in transplanted human liver. *Hepatology* 1996; **24**: 1053-1057 [PMID: 8903374 DOI: 10.1002/hep.510240512]

6 **Tullius SG**, Filatenkow A, Horch D, Mehlitz T, Reutzel-Selke A, Pratschke J, Steinmüller T, Lun A, Al-Abadi H, Neuhaus P. Accumulation of crystal deposits in abdominal organs following perfusion with defrosted University of Wisconsin solutions. *Am J Transplant* 2002; **2**: 627-630 [PMID: 12201363 DOI: 10.1034/j.1600-6143.2002.20707.x]

7 **Fridell JA**, Rogers J, Stratta RJ. The pancreas allograft donor: current status, controversies, and challenges for the future. *Clin Transplant* 2010; **24**: 433-449 [PMID: 20384731 DOI: 10.1111/j.1399-0012.2010.01253.x]

8 **Meine MH**, Leipnitz I, Zanotelli ML, Schlindwein ES, Kiss G, Martini J, de Medeiros Fleck A Jr, Mucenic M, de Mello Brandão A, Marroni CA, Craco Cantisani GP. Comparison Between IGL-1 and HTK Preservation Solutions in Deceased Donor Liver Transplantation. *Transplant Proc* 2015; **47**: 888-893 [PMID: 26036479 DOI: 10.1016/j.transproceed.2015.03.033]

9 **Erhard J**, Lange R, Scherer R, Kox WJ, Bretschneider HJ, Gebhard MM, Eigler FW. Comparison of histidine-tryptophan-ketoglutarate (HTK) solution versus University of Wisconsin (UW) solution for organ preservation in human liver transplantation. A prospective, randomized study. *Transpl Int* 1994; **7**: 177-181 [PMID: 8060466]

10 **Adam R**, Delvart V, Karam V, Ducerf C, Navarro F, Letoublon C, Belghiti J, Pezet D, Castaing D, Le Treut YP, Gugenheim J, Bachellier P, Pirenne J, Muiesan P; ELTR contributing centres, the European Liver, Intestine Transplant Association (ELITA). Compared efficacy of preservation solutions in liver transplantation: a long-term graft outcome study from the European Liver Transplant Registry. *Am J Transplant* 2015; **15**: 395-406 [PMID: 25612492 DOI: 10.1111/ajt.13060]

11 **Fridell JA**, Agarwal A, Milgrom ML, Goggins WC, Murdock P, Pescovitz MD. Comparison of histidine-tryptophan-ketoglutarate solution and University of Wisconsin solution for organ preservation in clinical pancreas transplantation. *Transplantation* 2004; **77**: 1304-1306 [PMID: 15114104 DOI: 10.1097/01.TP.0000122222.93740.B2]

12 **Nardo B**, Bertelli R, Montalti R, Beltempo P, Puviani L, Pacilè V, Cavallari A. Preliminary results of a clinical randomized study comparing Celsior and HTK solutions in liver preservation for transplantation. *Transplant Proc* 2005; **37**: 320-322 [PMID: 15808630 DOI: 10.1016/j.transproceed.2004.11.028]

13 **Cavallari A**, Cillo U, Nardo B, Filipponi F, Gringeri E, Montalti R, Vistoli F, D'amico F, Faenza A, Mosca F, Vitale A, D'amico D. A multicenter pilot prospective study comparing Celsior and University of Wisconsin preserving solutions for use in liver transplantation. *Liver Transpl* 2003; **9**: 814-821 [PMID: 12884193 DOI: 10.1053/jlts.2003.50161]

14 **Tabka D**, Bejaoui M, Javellaud J, Roselló-Catafau J, Achard JM, Abdennebi HB. Effects of Institut Georges Lopez-1 and Celsior preservation solutions on liver graft injury. *World J Gastroenterol* 2015; **21**: 4159-4168 [PMID: 25892865 DOI: 10.3748/wjg.v21.i14.4159]

15 **Ploeg RJ**, D'Alessandro AM, Knechtle SJ, Stegall MD, Pirsch JD, Hoffmann RM, Sasaki T, Sollinger HW, Belzer FO, Kalayoglu M. Risk factors for primary dysfunction after liver transplantation--a multivariate analysis. *Transplantation* 1993; **55**: 807-813 [PMID: 8475556]

16 **Lema Zuluaga GL**, Serna Agudelo RE, Zuleta Tobón JJ. Preservation solutions for liver transplantation in adults: celsior versus custodiol: a systematic review and meta-analysis with an indirect comparison of randomized trials. *Transplant Proc* 2013; **45**: 25-32 [PMID: 23267794 DOI: 10.1016/j.transproceed.2012.02.031]

17 **Feng L**, Zhao N, Yao X, Sun X, Du L, Diao X, Li S, Li Y. Histidine-tryptophan-ketoglutarate solution vs. University of Wisconsin solution for liver transplantation: a systematic review. *Liver Transpl* 2007; **13**: 1125-1136 [PMID: 17665493 DOI: 10.1002/lt.21208]

18 **Stewart ZA**, Cameron AM, Singer AL, Montgomery RA, Segev

DL. Histidine-Tryptophan-Ketoglutarate (HTK) is associated with reduced graft survival in deceased donor livers, especially those donated after cardiac death. *Am J Transplant* 2009; **9**: 286-293 [PMID: 19067658 DOI: 10.1111/j.1600-6143.2008.02478.x]

19 **O'Callaghan JM**, Morgan RD, Knight SR, Morris PJ. The effect of preservation solutions for storage of liver allografts on transplant outcomes: a systematic review and meta-analysis. *Ann Surg* 2014; **260**: 46-55 [PMID: 24374537 DOI: 10.1097/SLA.0000000000000402]

20 **Nashan B**, Spetzler V, Schemmer P, Kirste G, Rahmel A. Regarding "Compared Efficacy of Preservation Solutions in Liver Transplantation: A Long-Term Graft Outcome Study From the European Liver Transplant Registry". *Am J Transplant* 2015; **15**: 3272-3273 [PMID: 26555321 DOI: 10.1111/ajt.13513]

21 **Wiederkehr JC**, Igreja MR, Nogara MS, Goncalves N, Montemezzo GP, Wiederkehr HA, Wassen MP, Nobrega HA, Zenatti KB, Mori LY, Tudisco MS. Use of IGL-1 preservation solution in liver transplantation. *Transplant Proc* 2014; **46**: 1809-1811 [PMID: 25131043 DOI: 10.1016/j.transproceed.2014.05.040]

22 **Moher D**, Liberati A, Tetzlaff J, Altman DG; PRISMA Group. Preferred reporting items for systematic reviews and meta-analyses: the PRISMA statement. *PLoS Med* 2009; **6**: e1000097 [PMID: 19621072 DOI: 10.1371/journal.pmed.1000097]

23 The University of York Centre for Reviews and Dissemination. PROSPERO Register of ongoing systematic reviews. Available from: https://www.crd.york.ac.uk/PROSPERO/display_record.asp?ID=CRD42017054908

24 **Sweeting MJ**, Sutton AJ, Lambert PC. What to add to nothing? Use and avoidance of continuity corrections in meta-analysis of sparse data. *Stat Med* 2004; **23**: 1351-1375 [PMID: 15116347 DOI: 10.1002/sim.1761]

25 **Huo TI**, Lee SD, Lin HC. Selecting an optimal prognostic system for liver cirrhosis: the model for end-stage liver disease and beyond. *Liver Int* 2008; **28**: 606-613 [PMID: 18433390 DOI: 10.1111/j.1478-3231.2008.01727.x]

26 **Lopez-Andujar R**, Deusa S, Montalvá E, San Juan F, Moya A, Pareja E, DeJuan M, Berenguer M, Prieto M, Mir J. Comparative prospective study of two liver graft preservation solutions: University of Wisconsin and Celsior. *Liver Transpl* 2009; **15**: 1709-1717 [PMID: 19938119 DOI: 10.1002/lt.21945]

27 **Nardo B**, Catena F, Cavallari G, Montalti R, Di Naro A, Faenza A, Cavallari A. Randomized clinical study comparing UW and Celsior solution in liver preservation for transplantation: preliminary results. *Transplant Proc* 2001; **33**: 870-872 [PMID: 11267110 DOI: 10.1016/S0041-1345(00)02357-5]

28 **Duca WJ**, da Silva RF, Arroyo PC Jr, Sgnolf A, Cabral CM, Ayres DC, Felício HC, da Silva RD. Liver transplantation using University of Wisconsin or Celsior preserving solutions in the portal vein and Euro-Collins in the aorta. *Transplant Proc* 2010; **42**: 429-434 [PMID: 20304157 DOI: 10.1016/j.transproceed.2010.01.035]

29 **Lama C**, Rafecas A, Figueras J, Torras J, Ramos E, Fabregat J, Busquets J, Garcia-Barrasa A, Jaurrieta E. Comparative study of Celsior and Belzer solutions for hepatic graft preservation: preliminary results. *Transplant Proc* 2002; **34**: 54-55 [PMID: 11959183 DOI: 10.1016/S0041-1345(01)02664-1]

30 **Rayya F**, Harms J, Martin AP, Bartels M, Hauss J, Fangmann J. Comparison of histidine-tryptophan-ketoglutarate solution and University of Wisconsin solution in adult liver transplantation. *Transplant Proc* 2008; **40**: 891-894 [PMID: 18555073 DOI: 10.1016/j.transproceed.2008.03.044]

31 **Mangus RS**, Fridell JA, Vianna RM, Milgrom MA, Chestovich P, Chihara RK, Tector AJ. Comparison of histidine-tryptophan-ketoglutarate solution and University of Wisconsin solution in extended criteria liver donors. *Liver Transpl* 2008; **14**: 365-373 [PMID: 18306380 DOI: 10.1002/lt.21372]

32 **Meine MH**, Zanotelli ML, Neumann J, Kiss G, de Jesus Grezzana T, Leipnitz I, Schlindwein ES, Fleck A Jr, Gleisner AL, de Mello Brandão A, Marroni CA, Cantisani GP. Randomized clinical assay for hepatic grafts preservation with University of Wisconsin or histidine-tryptophan-ketoglutarate solutions in liver transplantation. *Transplant Proc* 2006; **38**: 1872-1875 [PMID: 16908310 DOI: 10.1016/j.transproceed.2006.06.071]

33 **García-Gil FA**, Arenas J, Güemes A, Esteban E, Tomé-Zelaya E, Lamata F, Sousa R, Jiménez A, Barrao ME, Serrano MT. Preservation of the liver graft with Celsior solution. *Transplant Proc* 2006; **38**: 2385-2388 [PMID: 17097942 DOI: 10.1016/j.transproceed.2006.08.032]

34 **Uemura T**, Randall HB, Sanchez EQ, Ikegami T, Narasimhan G, McKenna GJ, Chinnakotla S, Levy MF, Goldstein RM, Klintmalm GB. Liver retransplantation for primary nonfunction: analysis of a 20-year single-center experience. *Liver Transpl* 2007; **13**: 227-233 [PMID: 17256780 DOI: 10.1002/lt.20992]

35 **García-Gil FA**, Serrano MT, Fuentes-Broto L, Arenas J, García JJ, Güemes A, Bernal V, Campillo A, Sostres C, Araiz JJ, Royo P, Simón MA. Celsior versus University of Wisconsin preserving solutions for liver transplantation: postreperfusion syndrome and outcome of a 5-year prospective randomized controlled study. *World J Surg* 2011; **35**: 1598-1607 [PMID: 21487851 DOI: 10.1007/s00268-011-1078-7]

36 **Mangus RS**, Kinsella SB, Nobari MM, Fridell JA, Vianna RM, Ward ES, Nobari R, Tector AJ. Predictors of blood product use in orthotopic liver transplantation using the piggyback hepatectomy technique. *Transplant Proc* 2007; **39**: 3207-3213 [PMID: 18089355 DOI: 10.1016/j.transproceed.2007.09.029]

37 **Dondéro F**, Paugam-Burtz C, Danjou F, Stocco J, Durand F, Belghiti J. A randomized study comparing IGL-1 to the University of Wisconsin preservation solution in liver transplantation. *Ann Transplant* 2010; **15**: 7-14 [PMID: 21183870]

38 **Stahl JE**, Kreke JE, Malek FA, Schaefer AJ, Vacanti J. Consequences of cold-ischemia time on primary nonfunction and patient and graft survival in liver transplantation: a meta-analysis. *PLoS One* 2008; **3**: e2468 [PMID: 18575623 DOI: 10.1371/journal.pone.0002468]

39 **Belle SH**, Beringer KC, Detre KM. An update on liver transplantation in the United States: recipient characteristics and outcome. *Clin Transpl* 1995; 19-33 [PMID: 8794252]

40 **Weismüller TJ**, Fikatas P, Schmidt J, Barreiros AP, Otto G, Beckebaum S, Paul A, Scherer MN, Schmidt HH, Schlitt HJ, Neuhaus P, Klempnauer J, Pratschke J, Manns MP, Strassburg CP. Multicentric evaluation of model for end-stage liver disease-based allocation and survival after liver transplantation in Germany--limitations of the 'sickest first'-concept. *Transpl Int* 2011; **24**: 91-99 [PMID: 20819196 DOI: 10.1111/j.1432-2277.2010.01161.x]

41 **Vodkin I**, Kuo A. Extended Criteria Donors in Liver Transplantation. *Clin Liver Dis* 2017; **21**: 289-301 [PMID: 28364814 DOI: 10.1016/j.cld.2016.12.004]

42 **Nemes B**, Gámán G, Polak WG, Gelley F, Hara T, Ono S, Baimakhanov Z, Piros L, Eguchi S. Extended-criteria donors in liver transplantation Part II: reviewing the impact of extended-criteria donors on the complications and outcomes of liver transplantation. *Expert Rev Gastroenterol Hepatol* 2016; **10**: 841-859 [PMID: 26831547 DOI: 10.1586/17474124.2016.1149062]

43 **Zaoualí MA**, Mosbah IB, Abdennebi HB, Calvo M, Boncompagni E, Boillot O, Peralta C, Roselló-Catafau J. New insights into fatty liver preservation using Institute Georges Lopez preservation solution. *Transplant Proc* 2010; **42**: 159-161 [PMID: 20172305 DOI: 10.1016/j.transproceed.2009.12.035]

44 **Kaltenborn A**, Gwiasda J, Amelung V, Krauth C, Lehner F, Braun F, Klempnauer J, Reichert B, Schrem H. Comparable outcome of liver transplantation with histidine-tryptophan-ketoglutarate vs. University of Wisconsin preservation solution: a retrospective observational double-center trial. *BMC Gastroenterol* 2014; **14**: 169 [PMID: 25263587 DOI: 10.1186/1471-230X-14-169]

45 **Moray G**, Sevmis S, Karakayali FY, Gorur SK, Haberal M. Comparison of histidine-tryptophan-ketoglutarate and University of Wisconsin in living-donor liver transplantation. *Transplant Proc* 2006; **38**: 3572-3575 [PMID: 17175334 DOI: 10.1016/j.transproce

ed.2006.10.174]
46 **Jain A**, Mohanka R, Orloff M, Abt P, Kashyap R, Cullen J, Lansing K, Bozorgzadeh A. University of Wisconsin versus histidine-tryptophan-ketoglutarate for tissue preservation in live-donor liver transplantation. *Exp Clin Transplant* 2006; **4**: 451-457 [PMID: 16827642]
47 **Ringe B**, Braun F, Moritz M, Zeldin G, Soriano H, Meyers W. Safety and efficacy of living donor liver preservation with HTK solution. *Transplant Proc* 2005; **37**: 316-319 [PMID: 15808629 DOI: 10.1016/j.transproceed.2004.12.009]

P- Reviewer: Bramhall S, Chiu KW, Inoue K, Rosello-Catafau J, Tsoulfas G
S- Editor: Gong ZM **L- Editor**: A **E- Editor**: Huang Y

Published by **Baishideng Publishing Group Inc**
7901 Stoneridge Drive, Suite 501, Pleasanton, CA 94588, USA
Telephone: +1-925-223-8242
Fax: +1-925-223-8243
E-mail: bpgoffice@wjgnet.com
Help Desk: http://www.f6publishing.com/helpdesk
http://www.wjgnet.com

ISSN 1007-9327